SAFETY ANALYSIS REPORT FOR PACKAGING

MODEL 9977

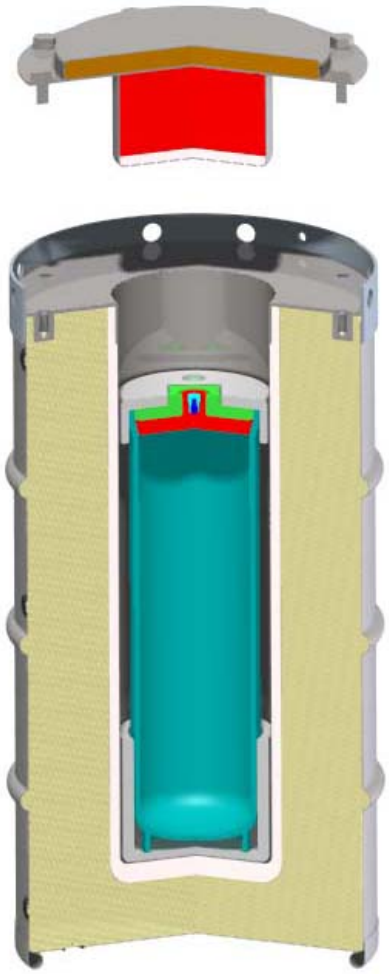

May 2006

Prepared by
Savannah River Packaging Technology
Savannah River National Laboratory

Washington Savannah River Company
Savannah River Site
Aiken, SC 29808

Prepared for the Department of Energy under Contract No. DE-AC09-96SR18500

This Page Intentionally Left Blank

APPROVALS

Signature _____ Date 5-17-06

G. A. Abramczyk 9977 Design Agency

Signature _____ Date 5-17-06

P. S. Blanton 9977 Design Authority

Signature _____ Date 5/17/06

J. S. Bellamy Manager, Savannah River Packaging Technology

This page Intentionally Left Blank

PREFACE

This Safety Analysis Report for Packaging (SARP) documents the analysis and testing performed on and for the 9977 Shipping Package, referred to as the General Purpose Fissile Package (GPFP). The performance evaluation presented in this SARP documents the compliance of the 9977 package with the regulatory safety requirements for Type B packages. Per 10 CFR 71.59, for the 9977 packages evaluated in this SARP, the value of "N" is 50, and the Transport Index based on nuclear criticality control is 1.0.

The 9977 package is designed with a high degree of single containment. The 9977 complies with 10 CFR 71 (2002), Department of Energy (DOE) Order 460.1B, DOE Order 460.2, and 10 CFR 20 (2003) for As Low As Reasonably Achievable (ALARA) principles. The 9977 also satisfies the requirements of the Regulations for the Safe Transport of Radioactive Material – 1996 Edition (Revised) - Requirements. IAEA Safety Standards, Safety Series No. TS-R-1 (ST-1, Rev.), International Atomic Energy Agency, Vienna, Austria (2000).

The 9977 package is designed, analyzed and fabricated in accordance with Section III of the American Society of Mechanical Engineers (ASME) Boiler and Pressure Vessel (B&PV) Code, 1992 edition.

This page Intentionally Left Blank

TABLE OF CONTENTS

TABLE OF CONTENTS (cont.)

TABLE OF CONTENTS (cont.)

TABLE OF CONTENTS (cont.)

TABLE OF CONTENTS (cont.)

TABLE OF CONTENTS (cont.)

TABLE OF CONTENTS (cont.)

TABLE OF CONTENTS (cont.)

TABLE OF CONTENTS (cont.)

TABLE OF CONTENTS (cont.)

This page Intentionally Left Blank

ACRONYMS AND ABBREVIATIONS

5CV	5-inch Inside Diameter Containment Vessel
6CV	6-inch Inside Diameter Containment Vessel
9977	General Purpose Fissile Package
9978	ALARA As Low As Reasonably Achievable
ANS	American Nuclear Society
ANSI	American National Standards Institute
ASME	American Society of Mechanical Engineers
ASTM	American Society for Testing Materials
AWS	American Welding Society
BPVC	Boiler and Pressure Vessel Code
CFR	Code of Federal Regulations
CG	Center of Gravity
CGOC	Center of Gravity over Corner
CMTR	Certified Material Test Report
CoC	Certificate of Compliance
CSI	Criticality Safety Index
CV	Containment Vessel, applies to both 5CV and 6CV
DBR	Design by Rule
DOE	Department of Energy
DOT	Department of Transportation
EES	Engineering Equipment and Systems
EM	Environmental Management
ESH&QA	Environment, Safety, Health and Quality Assurance
FEA	Finite Element Analysis
FSS	Field Support Services Business Unit
GS	General Support
GP3716	General Plastics FR-3716 Polyurethane Foam
GPFP	General Purpose Fissile Package (working name for the 9977)
GW	Gross Weight
HAC	Hypothetical Accident Conditions
HP	Health Protection
IAEA	International Atomic Energy Agency
ID	Inside Diameter
IR	Inside Radius
LAW	Library to Analyze Waste
LDF	Load Distribution Fixture
LLNL	Lawrence Livermore National Laboratory
MIP	Manufacturing and Inspection Plan

ACRONYMS AND ABBREVIATIONS (cont.)

M&TE	Measuring and Test Equipment
MCNP	Monte Carlo N Particle Transport Code
MNOP	Maximum Normal Operating Pressure
NCR	Nonconformance Report
NCSE	Nuclear Criticality Safety Evaluation
NCT	Normal Conditions of Transport
NDE	Nondestructive Examination
NRC	Nuclear Regulatory Commission
OD	Outside Diameter
PM	Procurement Management
QA	Quality Assurance
ref	Reference
RG	Regulatory Guide
RTG	Radioisotope Thermoelectric Generator
RTV	Room Temperature Vulcanizing
SARP	Safety Analysis Report for Packaging
SC	Safety Class
SNL	Sandia National Laboratory
SP	Single Package
SRS	Savannah River Site
SRNL	Savannah River National Laboratory
SRPT	Savannah River Packaging Technology
SS	Stainless Steel
std	Standard
STP	Standard Temperature and Pressure
ΔT	difference in temperature
TI	Transport Index
TID	Tamperproof-Indicating Device
UNS	Unified National – Special
WSMS	Washington Safety Management Solutions
WSRC	Washington Savannah River Company, LLC

DEFINITIONS

Category A Items
Subcategory of quality assurance "Q" items. Category A items are critical to safe operation.

Category B Items
Subcategory of quality assurance "Q" items. Category B items have a major impact on safety.

Category C Items
Subcategory of quality assurance "Q" items. Category C items have a minor impact on safety.

Certifying Official
The designated Headquarters official responsible for administering the DOE program for the design review of DOE packagings and the issuance of a certificate of compliance upon approval.

Compliant
Meets regulatory requirements and standards.

Conformant
To be in agreement with design, fulfills official design requirements.

Containment system
The assembly of components of the packaging intended to retain the radioactive contents during transportation.

contents
The radioactive material being packaged plus its container [RTG shell, food pack cans, convenience cans, and/or the 3013 (the Outer and Inner or Bagless Transfer Cans)], and any plastic bagging used for contamination control.

Design Authority
Person/Organization directly responsible for developing, conducting and documenting the prototype tests, producing and revising the SARP, establishing and maintaining the packaging design and design drawings, and for maintaining the package modification records.

H/X
Ratio of hydrogen to fissile atoms in the inner containment.

M&I Plan
Document produced by the packaging supplier that details how fabrications and inspections are to be performed and describes the qualifications of the suppliers and inspectors.

DEFINITIONS (cont.)

non-compliance
Does not meet regulatory requirements and standards.

non-conformant
Does not agree with certified design and/or fails to fulfill official design requirements.

Non-"Q" item
Items not related to safety and that require no formal QA program.

Owner
The organization that accepts a packaging from the manufacturer (or as a transfer from the previous owner), documents that the packaging is acceptable for use in accordance with the Certificate of Compliance, and maintains the package records as required by Chapter 9 of this SARP. The owner may delegate the performance of these responsibilities.

overpack assembly
The lower drum assembly (including the drum body, liner, top plate and internal insulation) and the closure lid (with internal insulation) that surrounds the containment vessel, Al spacers (if any), and the load distribution fixtures.

package
Contents plus packaging and any spacer materials.

packaging
The assembly of the overpack assembly, the containment vessel, Al spacers (if any), and the load distribution fixtures.

"Q" item
Quality-related item judged to have a significant impact on nuclear criticality control, off-site contamination release, or operations personnel exposure. "Q" items require a formal QA program and are subcategorized according to Nuclear Regulatory Commission Regulatory Guide 7.10 by the Design Agency. See Category A, B, C, and “Non-Q” Items above.

“shall”
Denotes actions that must be performed if the objectives of the package safety basis and the Safety Analysis are to be met.

spacer materials
The spacers (RTG components, empty food pack cans and/or aluminum foil) as specified in Section 1.2.3 for the content configuration being packaged.

This page Intentionally Left Blank

LIST OF REVISIONS

Revision	Change	Date
0	All New	May 2006

This page Intentionally Left Blank

Safety Analysis Report for Packaging

Model 9977 Type B(M)F-96

CHAPTER 1

GENERAL INFORMATION

Preface

This chapter provides the general description of the Model 9977 packaging and physical descriptions of major components and subassemblies. It also describes the radioactive material contents and content configurations. As summarized in Section 1.2.5, the packaging meets the requirements of 10 CFR 71.[1]

Note: During development of the design and testing the 9977 was referred to as the General Purpose Fissile Package, Version 1 (GPFP-1 or just GPFP). The GPFP-1/GPFP name may still appear in historical or record documents.

This Page Intentionally Left Blank

TABLE OF CONTENTS

LIST OF TABLES

Page

LIST OF FIGURES

Page

ACRONYMS AND ABBREVIATIONS

5CV	5-inch diameter Containment Vessel
6CV	6-inch diameter Containment Vessel
ANSI	American National Standards Institute
ASME	American Society of Mechanical Engineers
ASTM	American Society for Testing Materials
BPVC	Boiler and Pressure Vessel Code
CFR	Code of Federal Regulations
CV	Containment Vessel
DOE	Department of Energy
GP3716	General Plastics FR-3716 Polyurethane Foam
GPFP	General Purpose Fissile Package (working name for the 9977)
HAC	Hypothetical Accident Conditions
IAEA	International Atomic Energy Agency
ID	Inside Diameter
NCT	Normal Conditions of Transport
NRC	Nuclear Regulatory Commission
OD	Outside Diameter
QA	Quality Assurance
RG	Regulatory Guide
RTG	Radioisotope Thermoelectric Generator
SARP	Safety Analysis Report for Packaging
SNL	Sandia National Laboratory
SRNL	Savannah River National Laboratory
SS	Stainless Steel
TI	Transport Index
TID	Tamper-Indicating Device
WSRC	Washington Savannah River Company

This Page Intentionally Left Blank

1 GENERAL INFORMATION

1.1 INTRODUCTION

This Safety Analysis Report for Packaging (SARP) documents the performance of the Model 9977 shipping package in satisfying the regulatory safety requirements of the Code of Federal Regulations (CFR) 10 CFR 71 and the International Atomic Energy Agency (IAEA) Safety Series No. TS-R-1, *Regulations for the Safe Transport of Radioactive Material.*[2] The results of the package analysis and testing performed are presented in this SARP, which was prepared in accordance with U.S. Department of Energy (DOE) Order 460.1B[3] and in the format specified in the Nuclear Regulatory Commission (NRC) Regulatory Guides (RGs) 7.9 and 7.10.[4, 5]

The performance evaluation documents the compliance of the package to the regulatory safety requirements for a Type B(M)F-96 package. The 9977 is designated as "B(M)" because the package design pressure is greater than 100 lb/in^2 (700 kPa) gauge. Package contents include actinide metals and oxides in Type B quantities. Package contents can exceed 3,000 A_2 units, as defined in 10 CFR71.4, therefore, the 9977 is considered a Category I package.[6]

Limits on package contents are based on nuclear criticality, radiation shielding, and decay heat rate. The calculated nuclear Criticality Safety Index (CSI) for the package is 1.0. The transport index based on dose rate is established by measurement at the time of shipment. The package utilizes passive cooling to maintain internal temperatures below allowable limits.

Packages are shipped under *non-exclusive use* dose-rate limits in the Safe-Secure Trailer, Safe Guards Trailer, or by commercial carrier as determined by the contents and DOE Order 474.1A.[7] Package users may also ship 9977s in accordance with *exclusive use* dose-rate limits via Safe Secure Transport Safeguards Transporter as long as they have prior written approval from the DOE Office of Secure Transportation.

1.2 PACKAGE DESCRIPTION

The 9977 is designed to ship radioactive contents in three basic configurations; assemblies of Radioisotope Thermoelectric Generators (RTGs), arrangements of nested food-pack cans, or DOE-STD-3013[8] containers. These content configurations minimize contamination, simplify handling, and facilitate storage. Some of these container configurations (e.g., the RTGs and 3013s) are designed and tested to remain leaktight during handling and storage; however, their ability to remain leaktight during transport is not credited.

1.2.1 Packaging

The packaging assembly is shown in Figures 1.1 and 1.2 and in Drawings R-R1-G-00020 and R-R1-G-00021 given in Appendix 1.1. The packaging design is controlled in accordance with Section 9.3, *Design Control*. Package weights and dimensions are summarized in Table 1.1.

Table 1.1 - Package Weights and Overall Dimensions

Nominal Drum Size (gallons)	**Drum Diameter** [a] (inches)	**Drum Height** (inches)	**Nominal Packaging Weight** (lb)	**Maximum Payload Weight** [b] [c] (lb)	**Maximum Gross Weight** [d] (lb)
35	18.35	36.1	230 – 250	50 (5CV [e]) 100 (6CV [f])	300 (5CV) 350 (6CV)

a) Diameter of drum body (diameters of rim and rolling ring are 18.72 and 18.85 inches, respectively.)
b) Payload is the weight of everything placed in the Containment Vessel (CV) (i.e. the radioactive material and all packing components)
c) Limited such that the gross weight of the loaded package is equal to, or less than, the maximum allowed.
d) Provided as a shipment limit, and not for derivation of payload weight from net weight
e) 5-inch diameter containment vessel.
f) 6-inch diameter containment vessel.

1.2.1.1 Drum

The drum is designed and fabricated with a removable head in accordance with 49 CFR 178[9] but with a bolted-flange closure. The closure does not incorporate a gasket. The drum body is a closed unit consisting of a shell, top deck plate, reinforcing rim (vertical flange) and a liner assembly, with the volume between the liner assembly and drum shell filled with shock-absorbing thermal-insulating materials. The drum shell and liner are fabricated of 18-gage (0.048-inch) Type 304L stainless steel (SS). The drum shell incorporates a "sanitary" style drum bottom with a rolled "wear ring," 0.060-inch thick by ¾-inch inside diameter (ID), attached by non-structural welds. The drum's top deck plate is fabricated of $^{3}/_{16}$-inch thick Type 304L SS plate. The top portion of the drum incorporates a $^{3}/_{16}$-inch thick reinforcing rim (vertical flange) and reinforces the drum head and protects both the closure lid and the bolts during Hypothetical Accident Condition (HAC) events. The rim includes eight (8) 1-inch diameter drain holes that are qualified as package lifting and tie-down points. Drum construction details are shown on drawings R-R2-G-00017 and R-R2-G-00018. As applicable, the drum is designed, analyzed and fabricated in accordance with Section III, Subsection NF of the American Society of Mechanical

Engineers Boiler and Pressure Vessel Code (ASME BPVC), as listed in Table 9.6. The drum design is controlled in accordance with Section 9.3.

Four (4) ¾-inch diameter vent holes are drilled at locations around the drum, approximately 90° apart and at each of three elevations, for a total of twelve vent holes along the drum sidewall. Two additional holes, one 1-inch diameter fill hole and a ¾-inch diameter vent hole, are drilled into the drum bottom. All of the holes are covered with appropriately sized Caplug® fusible plastic plugs. During the HAC fire event, the plugs combust or melt, allowing the drum to vent gases generated by intumescing foam insulation. The vent holes ensure that the drum cannot be ruptured by gas pressure.

The drum closure lid is fabricated from ⅛-inch thick Type 304L SS plate. Eight (8) ⅝-inch by 1¼-inch long hex-head bolts with ⅝-inch plain, narrow Type B washers secure the lid to the top deck plate of the drum body. The closure lid incorporates chambers above and below the Lid Plate filled with shock-absorbing thermal-insulating materials. The Lid Top and Lid Bottom chambers are fabricated of 18-gage (0.048-inch) and 14-gage (0.07-inch) Type 304L SS, respectively. The top of the Lid Top chamber is approximately 0.275 inches below the top surface of the drum-head reinforcing rim. The Lid Top chamber reinforces the Lid Plate, adds thermal protection to the contents, and prevents the closure lid from shearing away from the bolts during HAC events. The Lid Bottom chamber also reinforces the Lid Plate, and provides additional thermal protection shock absorption for the containment vessel during HAC events.

Four (4) ¼-inch diameter holes through the Lid Plate allow the Lid Top and Lid Bottom volumes to exchange gases and equilibrate pressure. The Lid Top chamber is vented by four (4) ¼-inch diameter holes also covered with Caplug® fusible plastic plugs. The Caplugs prevent water from entering the lid through the vent holes under Normal Conditions of Transport (NCT). In a HAC fire event, the plugs combust or melt, allowing the lid to vent heated air from the Lid Top and Lid Bottom chambers to prevent rupture.

To simplify drum-closure operations, the threaded inserts that receive the drum-closure bolts are welded to the underside of the drum's top deck plate. During installation, the bolts are tightened to a torque value of 45 (±5) ft-lb. The hex-heads of the eight (8) bolts drilled through with a ⅛-inch hole to receive tamper-indicating devices (TIDs). Details are shown in Drawings R-R2-F-00020 and R-R2-F-00021.

1.2.1.2 Insulation

Two layers of insulation material fill the volume between the drum shell and the drum liner. First, two ½-inch thick blankets of Fiberfrax® insulation are wrapped around and attached to the sides and bottom of the liner. The Fiberfrax® is backed on both sides with fiberglass cloth held in place by fiberglass thread stitched longitudinally at 4-inch intervals. The fiberglass cloth gives the Fiberfrax® composite both mechanical strength and wear resistance and helps retard gas flow during the HAC fire event. The remaining volume between the Fiberfrax® and the drum wall is filled with General Plastics FR-3716 polyurethane foam, poured through the fill hole in the drum bottom and foamed in place. The nominal densities of Fiberfrax® and FR-3716 foam are 7-to-10 lb/ft^3 and 16 lb/ft^3, respectively. Thermal-physical properties of Fiberfrax® and FR-3716 are listed in Tables 2.9, 2.10, 3.7 and 3.8. The combined thickness of the two insulators is approximately 4.9 inches radially (i.e., between the liner and the drum shell) and

approximately four (4) inches axially (i.e., between the liner bottom and drum bottom). Details are shown in Figure 1.1 and Drawings R-R2-F-0020, R-R2-F-0021, and R-R2-F-0019.

The closure lid incorporates two chambers of insulation. The Lid Top chamber contains a disk of Thermal Ceramics Min-K 2000 insulation one (1) inch thick with a diameter if 14 inches. The Lid Bottom chamber contains a rigid disk of Thermal Ceramics TR-19 Block insulation, 4.3-inch thick by 8-inch diameter. When installed, this disk compresses two (2) 8-inch diameter by ½-inch thick blankets of Fiberfrax® insulation to a total thickness of ½-inch. The total axial thickness of the Lid Bottom chamber insulation is approximately 5.73 inches. Details are shown in Figure 1.1 and Drawing R-R2-F-00017.

1.2.1.3 6-inch Diameter Containment Vessel

The 9977 is designed to accept either of two containment vessels (CVs), with nominal IDs of either six (6) or five (5) inches. The 6-inch ID Containment Vessel (6CV) is a stainless steel pressure vessel designed, analyzed and fabricated in accordance with Section III, Subsection NB of the ASME Code, with design conditions of 800 psig at 300 °F, as listed in Table 9.5. The 6CV is illustrated in Figure 1.4. The 6CV is fabricated from 6-inch, Schedule 40, seamless, Type 304L SS pipe (0.280-inch nominal wall). A standard Schedule 40 Type 304L SS pipe cap (also 0.280-inch nominal wall) is welded to the pipe segment to form a blind end. A stayed head is machined from a 7½-inch diameter by 2¼-inch long Type 304L SS bar and welded to the open end of the pipe segment, completing the vessel body weldment. The head is machined to include 6½-12UNS-2B internal threads and an internal cone-seal surface with a 32 µin. finish. Both vessel body joints are Category B full-penetration circumferential welds. A support skirt to stand the 6CV vertically is formed from a short segment of 5-inch, Schedule 40 Type 304L SS pipe welded to the convex side of the cap. Two rectangular notches milled into the bottom edge of the skirt (180° apart) can engage a rectangular key to prevent vessel rotation during removal and installation of the closure assembly.

The 6CV closure assembly consists of a Type 304L SS cone-seal plug shaped in part like a truncated cone and a threaded cone-seal nut made from Nitronic® 60. The two closure-assembly components rotate freely relative to one another and are coupled by a snap-ring that also ensures unseating of the closure seal during disassembly. As the cone-seal nut is threaded into the stayed head of the vessel, the cone-seal plug is thrust axially against the corresponding cone-seal surface of the vessel. Both internal and external sealing surfaces are machined to identical angles so that they mate with zero clearance. To minimize the potential for thread galling, the cone-seal nut and the containment vessel body are made from dissimilar materials. Two O-ring grooves (outer and inner) are machined in the face of the external cone-seal plug with a 32 µin. finish as shown in Figure 1.4. Viton GLT O-rings fit into these grooves to complete the leaktight closure assembly.

For operator safety, a 0.094-inch diameter vent hole is located in the stayed head between the threads and the internal sealing surface. Unscrewing the cone-seal nut a few turns will unseat the cone-seal plug from the internal cone-seal surface and route any pressurized gases from the CV through the vent hole.

A leak-test port is incorporated into the cone-seal plug and connected by a drilled radial passage to the annular volume between the two O-ring grooves in cone-seal plug. The leak-test port

provides a means of verifying proper assembly of the vessel closure and is itself closed by the leak-test port plug. The vessel containment boundary is formed by the vessel body, the cone-seal plug, and the inner O-ring.

The internal volume of a closed 6CV is approximately 600 cubic inches. The nominal assembly weight is 52.2 lb and nominal overall length is 24 inches. The usable cavity of the 6CV is approximately 21.5 inches deep with a maximum diameter of six (6) inches. Details are shown in Drawing R-R2-G-00042.

1.2.1.4 5-inch Diameter Containment Vessel

The 5-inch ID Containment Vessel (5CV) is a SS pressure vessel similar to the 6CV, designed, analyzed, fabricated, and examined in accordance with Section III, Subsection NB of the ASME Code, with design conditions of 900 psig at 300 °F, as listed in Table 9.5. However, the 5CV is fabricated from 5-inch, Schedule 40, seamless, Type 304L SS pipe (0.258-inch nominal wall) with a corresponding standard Schedule 40 Type 304L SS pipe cap (also 0.258-inch nominal wall) welded at the blind end. A stayed head is machined from a 6-inch diameter by 2¼-inch long Type 304L SS bar and welded to the open end of the pipe. The head is machined to include 5½-12UNS-2B internal threads and an internal cone-seal surface with a 32 μin. finish. Both vessel-body joints are Category B with full penetration circumferential welds. A short segment of 4-inch, Schedule 40 Type 304L SS pipe is welded to the convex side of the cap to form a skirt to support the 5CV vertically. The skirt includes two rectangular notches on the bottom edge (180° apart) that can engage a rectangular key to prevent vessel rotation during removal and installation of the cone-seal closure.

The 5CV closure is identical to that of the 6CV, except for a smaller diameter. The closed 5CV has an internal volume of approximately 313 cubic inches, weighs 34 lb, and has a closed nominal length of 18.6 inches. It's usable inside cavity is approximately 15 inches deep with a minimum diameter of 5 inches. Details are shown in Drawing R-R2-G-00043.

1.2.1.5 Load Distribution Fixtures

Top and a Bottom Load Distribution Fixtures (LDFs) are made from 6061-T6 aluminum round bar and fit within the Drum Liner cavity, above and below either CV. The LDFs center the CV in the liner, stiffen the package in the radial direction, and distribute loads away from the CV, see Figures 1.1 and 1.4. The 6CV fits directly into the LDFs. Aluminum honeycomb spacers (discussed in Section 1.2.1.8) fill the volume between smaller 5CV and the LDFs. Details are shown in Drawings R-R4-G-00032 and R-R4-G-00033.

1.2.1.6 Shielding Features

Neither 9977 materials nor component geometry provides significant radiation shielding. Dose-rate attenuation is provided primarily by the distance between the source and points external to the package.

1.2.1.7 Criticality Control Features

The 9977 design does not incorporate materials specifically for the purpose of poisoning or moderating neutron radiation. Subcriticality is ensured by limiting package contents and by crediting the packaging as a means of maintaining a minimum distance between adjacent sources. These restrictions prevent criticality under NCT and under HAC-damaged package array conditions.

1.2.1.8 5CV Aluminum Honeycomb Spacers

Three aluminum honeycomb spacers center the 5CV within the LDFs. Top, Annular, and Bottom Spacers are fabricated from 3-mil minimum foil with a 3-mil thick outer sheathing and are rated for an axial compressive strength of 1500 ± 500 psi before permanent deformation. These are discussed in order of placement into the drum.

The Bottom Spacer is 6½ inches in diameter and three (3) inches thick along axis of the corrugations, with a 0.7-inch deep recess that receives the 5CV's skirt ring. The Bottom Spacer is placed into the Bottom LDF below the 5CV in part to help center the 5CV in the package. The Bottom Spacer prevents the 5CV from impacting the LDF in the event of package mishandling or a transportation accident.

The Annular Spacer separates the 5CV body from the wall of the Drum Liner and helps center the 5CV in the package. The Annular Spacer has a 5.5-inch ID, an 8-inch OD, and is 19.8 inches tall (axis of the corrugations).

The Top Spacer is seven (7) inches in diameter and 2.8 inches thick (axis of the corrugations), with a 0.6-inch deep recess that fits over the square nut on the 5CV cone-seal assembly. The Top Spacer is placed above the 5CV under the Top LDF to finish centering the 5CV in the package. The Top Spacer also prevents the 5CV from impacting the LDF in the event of package mishandling or a transportation accident. The three aluminum honeycomb spacers are illustrated in Figure 1.1 and details are shown in Drawing R-R4-G-00033.

1.2.1.9 Package Markings

An Identification Plate is welded to the drum shell with markings die stamped and filled with epoxy paint for durably and legibility. The package markings include:

- The package name "9977"
- DOE package Competent Authority and their address
- "Radioactive Material, Fissile"
- "USA/9977/B(M)F-96(DOE)"
- Year of manufacture, Serial Number, and Package Gross Weight (in units of both lb and kg)
- Radioactive material Trefoil symbol

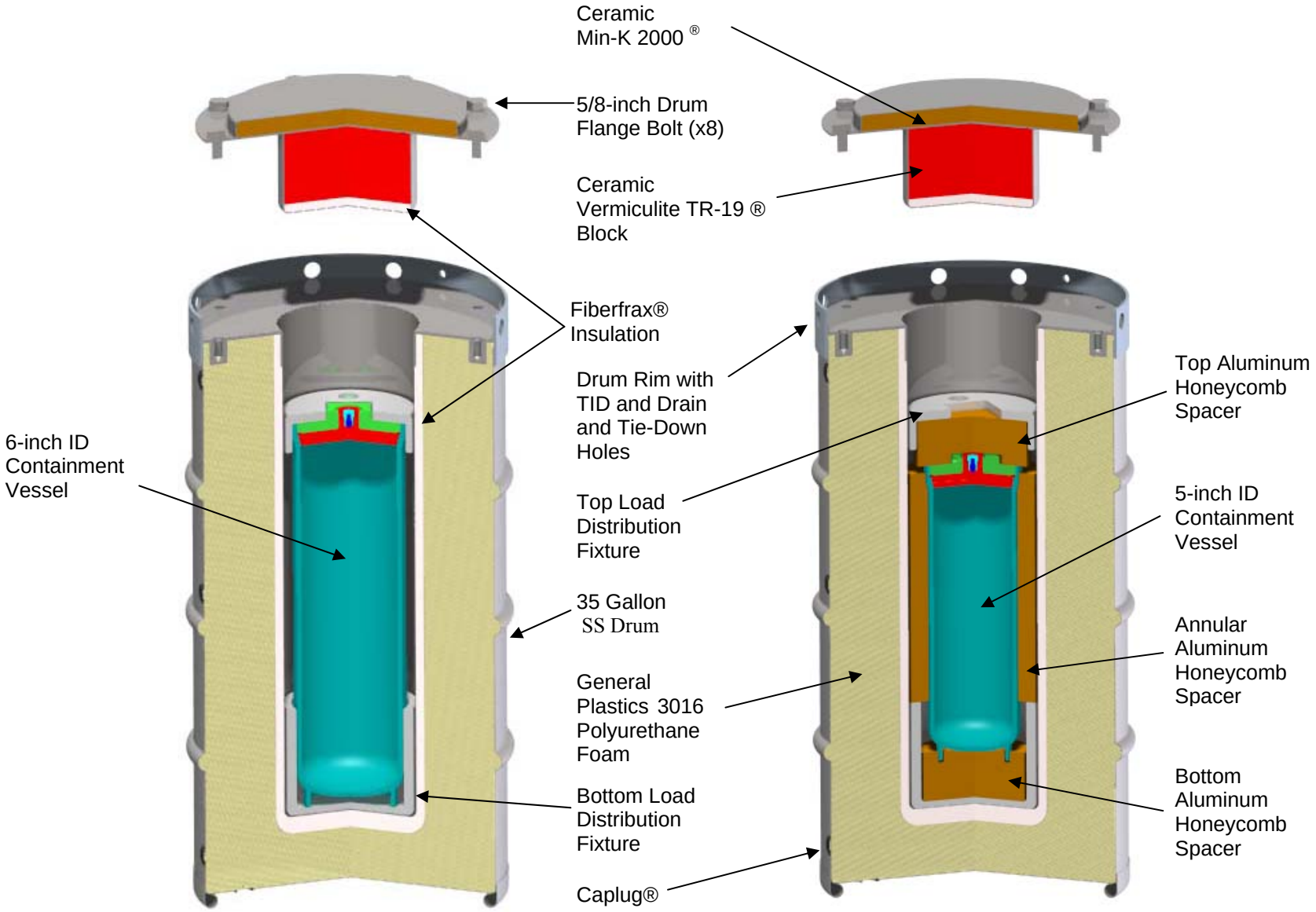

Figure 1.1 – 3-Dimensional Cut Away Illustration of the 9977 with a 5-inch and 6-inch Diameter Containment Vessels

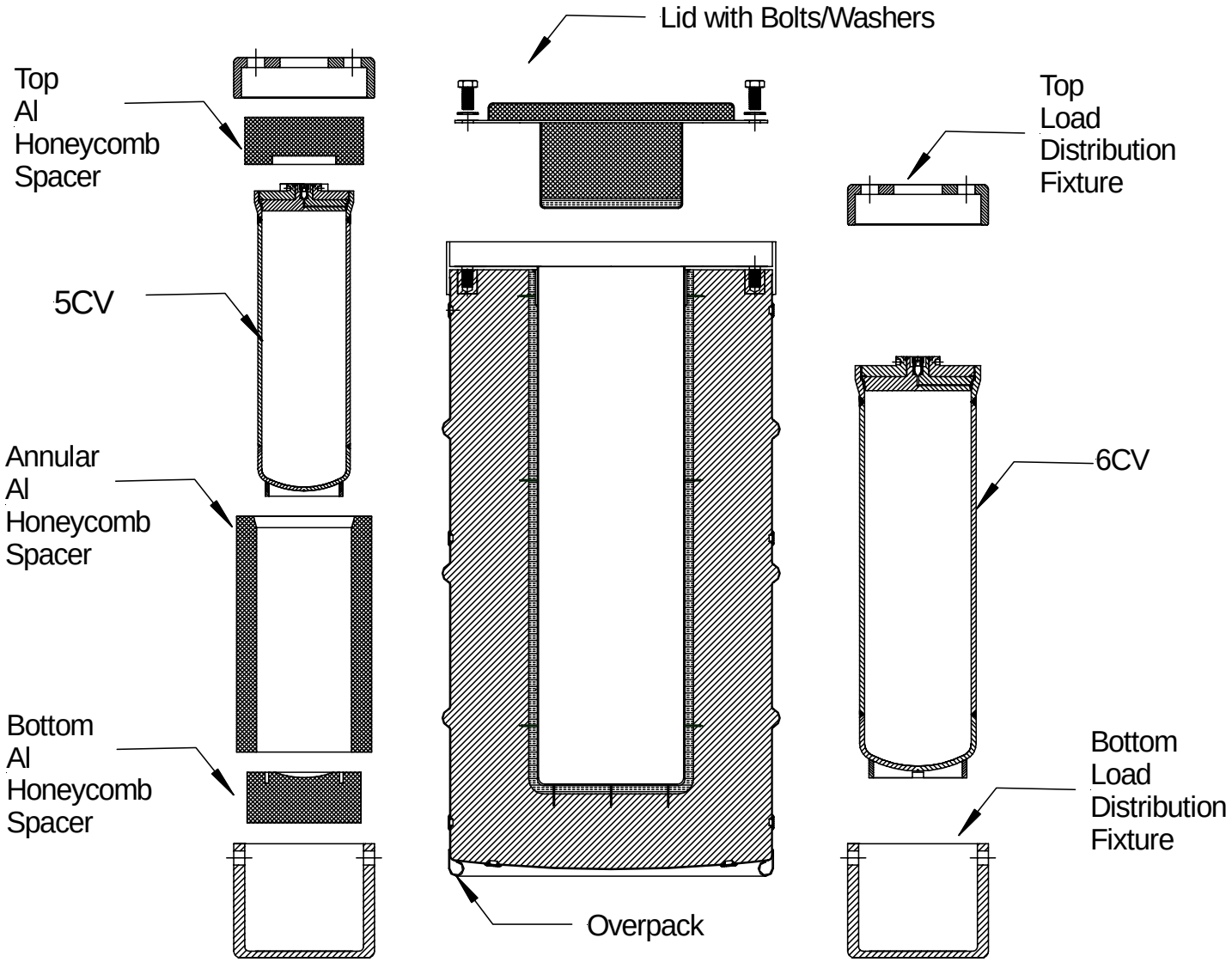

Figure 1.2 – Exploded View of the 9977 with a 5-inch and 6-inch Diameter Containment Vessels

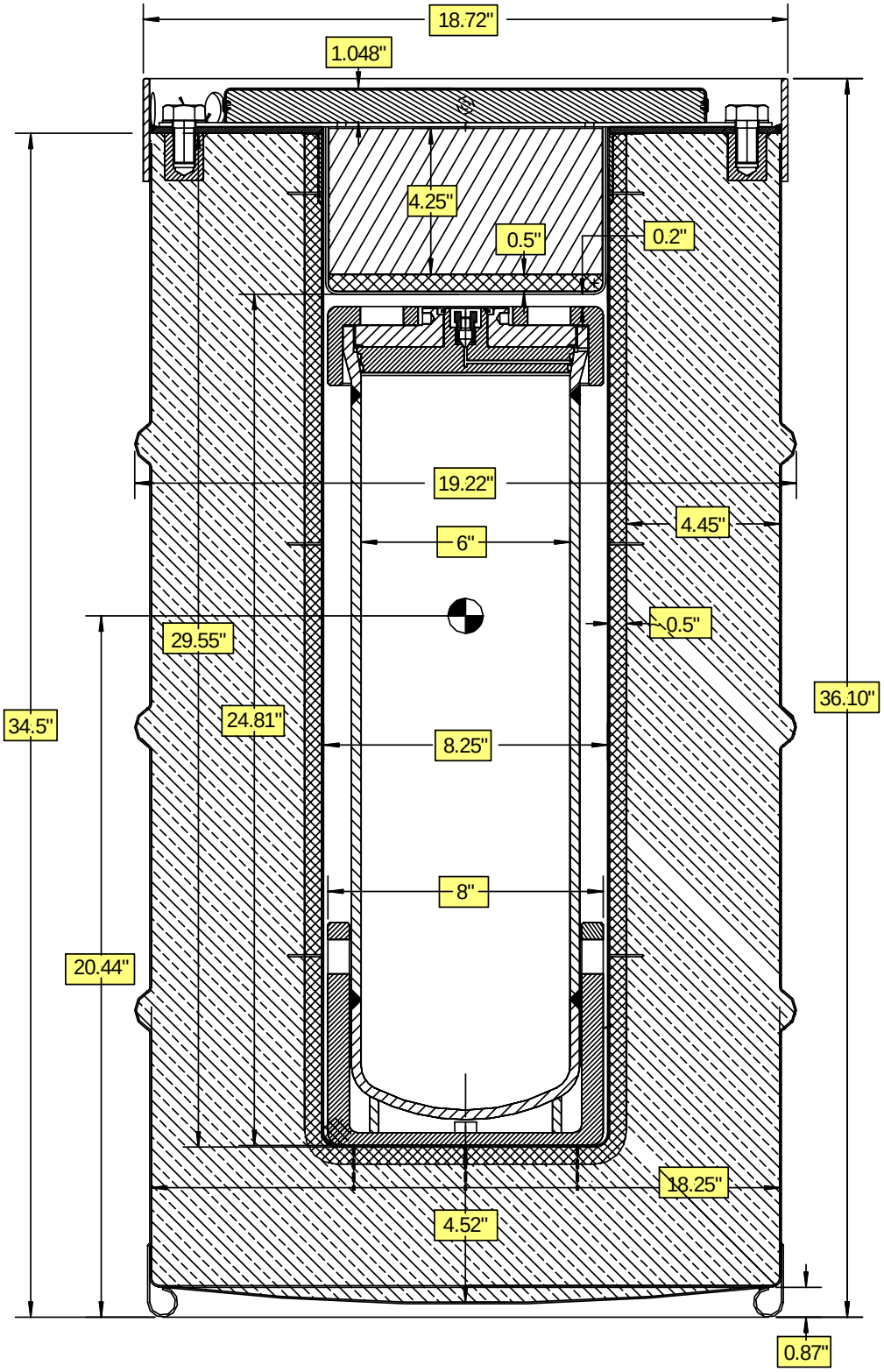

Figure 1.3 - 9977 6CV Packaging Configuration - Key Dimensions

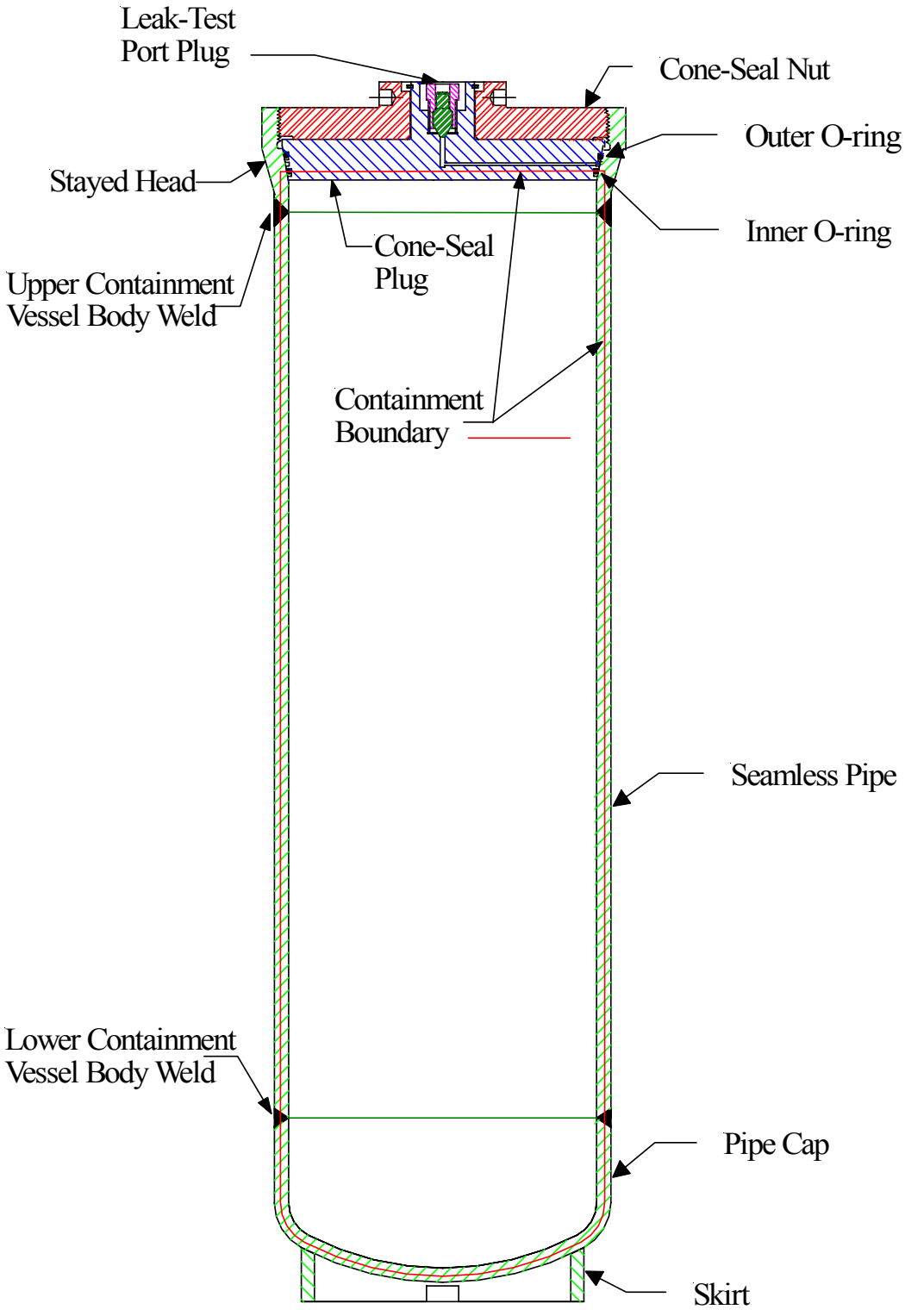

Figure 1.4 - Typical 9977 Containment Vessel

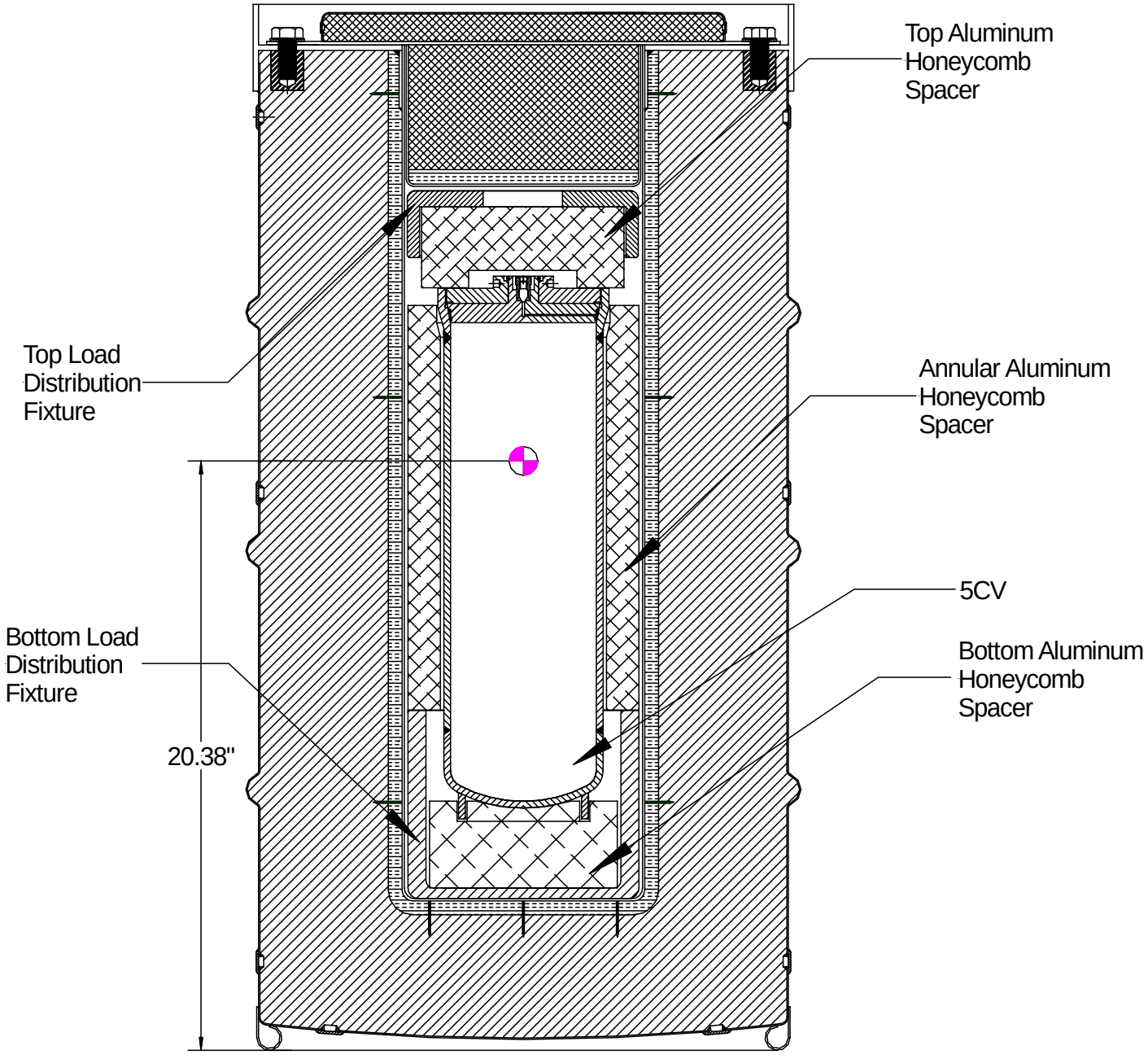

Figure 1.5 - 9977 5CV Packaging Configuration

1.2.2 Contents of Packaging

Package contents are identified as Content Envelopes C.1 through C.5 and defined in Table 1.2. The contents are in solid form as metal pieces or oxides. Contents in liquid form are not permitted.

The total content mass listed in Table 1.2 excludes material containers and packing materials (i.e., RTG containers, springs, cups and union). Contents containers and content-specific configuration requirements are listed in Sections 1.2.2.1 and 1.2.2.2, respectively. Where applicable, the material container dimensional requirements are provided.

Compatibility of the packaging materials of construction, packing materials, and the contents is discussed in Section 2.2.2. There are no material incompatibilities in the package. Since the CVs are leaktight, they may become pressurized by heating of gases contained at the time of closure and pressurized further by gases generated from the contents. The contents do not generate fission gases. The Maximum Normal Operating Pressures (MNOPs) for the 6CV and 5CV are 41.2 psig and 56.3 psig respectively. MNOPs are developed in Section 3.3.2.

Requirements common to all contents and payload configurations are the following.

- The maximum allowable radioactive decay heat rate is 19 Watts.
- Except as stated in Table 1.2, small concentrations (<1000 ppm each) of other actinides, fission products, decay products, and neutron activation products are permitted. Assessment of these impurities may be based on process knowledge.
- Except as stated in Table 1.2, inorganic material impurity quantities of less than 100 ppm each are permitted as long as the total mass is less than 0.1 weight percent of the total content mass. Assessment of these impurities may be based on process knowledge.
- The maximum weight of the payload (everything that goes into the CV, including radioactive contents, convenience cans, contamination control devices, packing materials, spacers, etc.) is not to exceed 50-lb for the 5CV and 100-lb for the 6CV.

All 9977 contents requirements are summarized in Table 1.3 by content envelope and container configuration.

Table 1.2 - Content Envelopes

	Material [a, b]	C.1 Heat Sources	C.2[c] Pu/U Metals	C.3 Pu/U Oxides
Radioisotope (weight percent)	^{238}Pu	100	2	
	^{239}Pu [d]	40	100	
	^{240}Pu [e]	13	25	
	^{241}Pu [d]	1	15	
	^{242}Pu [d]	1.5	5	
	^{232}U [d]	1.4×10^{-4}	1×10^{-7}	
	^{233}U [d]	0.2	0.5	
	^{234}U [d]	40	100	
	^{235}U [d]	40	100	
	^{236}U	16	40	
	^{238}U	40	100	
Impurities [f] (grams)	Ca	15		
	Fe	5		
	Cr	2		
Total Mass (kg)	Radioactive Materials	0.1	4.4	
	Impurities	0.02	3.08 [g]	
	All Contents	0.1	4.4	

RESERVED

Notes

a All contents shall be dry.

b Pu/U content bulk density shall be no greater than 19.84 g/cc and no less than 2.0 g/cc.

c Contents shall be stabilized in accordance with DOE-STD-3013, Section 6.1.1.

d Nuclide classified as "fissile" per DOE Good Practices Guide, Criticality Safety Good Practices Program, Guide For DOE Nonreactor Nuclear Facilities, DOE G 421.1-1, 3.79 Fissile Nuclide, 8-25-99.

e ^{240}Pu shall be greater than ^{241}Pu.

f Less than 0.005 g of (α, n) impurities {aluminum, beryllium, boron, fluorine, lithium, magnesium, and sodium} are permitted.

g The impurity limit is based on the DOE-STD-3013 requirement that plutonium plus uranium mass shall not be less than 30 weight percent of the total content mass.

Table 1.2 (continued) - Content Envelopes

	Material [a, b, c]	C.1 U Metal or Alloy	C.5 U Compounds	
		H/X = 0 [d]	H/X = 0	H/X ≤ 0.15
Radioisotope Mass (Kg)	^{233}U [e]	RESERVED		
	^{235}U [e]	13.5	4.4	4.4

Notes

a Except as permitted for compounds, all contents shall be dry. The moisture content of the compounds shall be less than 0.5 weight percent of the total content mass.

b U content bulk density shall be no greater than 19.84 g/cc and no less than 2.0 g/cc.

c H/X is the ratio of hydrogen to fissile atoms that can be mixed with the fissile material mass. The moisture content of the compounds shall be less than 0.5 weight percent of the total content mass.

d Pieces shall have a specific surface area less than 100 mm2/g. This limit may be implemented by either restricting each piece mass to at least 50 g or by performing calculations and measurements.

e Nuclide classified as “fissile” per DOE Good Practices Guide, Criticality Safety Good Practices Program, Guide For DOE Nonreactor Nuclear Facilities, DOE G 421.1-1, 3.79 Fissile Nuclide, 8-25-99.

1.2.2.1 Contents Containers

The 9977 is evaluated for shipment of radioactive contents in the following containers.

- Assemblies of Radioisotope Thermoelectric Generators (RTGs)
- 3013 storage containers, and
- Food-pack cans.

Descriptions, illustrations, and the packaging limitations of these configurations are provided in the following sections. For user convenience, a summary of the packaging requirements by contents and container configurations is provided in Table 1.3. Content-specific configuration controls and requirements are discussed in Section 1.2.2.2. The 9977 has been designed, analyzed and tested to demonstrate compliance with the requirements of 10 CFR 71 in the 6CV packaging configuration shown in Figure 1.2. The 5CV configuration given in Figure 1.1 has been shown by analysis to be bounded by the 6CV configuration. Additional packing materials are not required and any related benefit for the contents is not credited in the package safety evaluations.

1.2.2.1.1 ASSEMBLIES OF RADIOISOTOPE THERMOELECTRIC GENERATORs

RTGs provide power for remote instrumentation and experimental equipment by converting the heat generated from the radioactive decay of ^{238}Pu into electricity. Two different sizes of RTGs can be shipped within essentially a single 9977 container configuration.

The RTG assembly configuration illustrated in Figure 1.6 has been evaluated for transportation in the 6CV only. The Sandia National Laboratory (SNL) RTG Assembly components are defined in the following drawings.

Drawing Number	Title	Quantity
1A6780-00	Spring Assembly	2
1A6781-00	Union Assembly	1
1A6782-00	Finned Cup Assembly	2

The RTGs are placed within vibration-limiting and thermal-conducting assemblies. One RTG Assembly holds a maximum of four (4) RTGs. Either or both size RTGs may be shipped in the same assembly provided the general requirements listed in Section 1.2.2, above are satisfied.

1.2.2.1.2 3013 STORAGE CONTAINERS

Plutonium metal or oxide contents targeted for long-term storage must meet DOE's 3013 standard. The 3013 configuration requires a series of nested containers designed specifically for long-term storage. These include a 3013 outer storage can,[10] a 3013 inner storage can, and optional material container(s). The 3013 inner storage can and material containers are often site-specific designs. For user convenience, descriptions of typical 3013 containers and configurations are provided in Appendix 1.2.

Figure 1.7 illustrates the basic 3013 storage container configuration evaluated in this SARP. Various 3013 inner and material containers are acceptable provided the general requirements listed in Section 1.2.2 are satisfied and the requirements below are fulfilled.

- The 5CV packaging configuration must be used.
- The Reference 3013 outer storage can must be used.
- The 3013 inner and product containers meet the requirements of DOE's 3013 standard, Section 6.2, *Containers*.
- The 3013 inner and material containers must not include organic liners.
- A perforated food-pack can must be placed above the 3013 to consume otherwise open axial space.

1.2.2.1.3 FOOD-PACK CANS

The term "food-pack" can includes metal cans with crimped-seal closures, "slip-lid" closures, or site-specific "convenience containers." Crimp-sealed food-pack cans are typically fabricated in accordance with Federal Specification PPP-C-96E[11] or equivalent, and meet the size specification as defined by the Can Manufacturers Institute - Voluntary Can Standards.[12] Convenience containers are typically application-specific designs that incorporate screw thread, crimp-sealed, or welded closures. These three types of cans are made typically from tin-plated mild steel or stainless steel.

Actinide metals, oxides, and other materials may be placed inside food-pack cans prior to placing items in the packaging. If not part of a 3013-qualified storage plan, an elastomeric gasket material or polyvinyl chloride tape may be applied to the edge of the can lid. The seal material may limit the spread of contamination, but is not credited for any measure of containment within the package.

The can containing the radioactive material is typically placed inside low-density polyethylene or nylon bagging for contamination control. Multiple bags may be present, up to the mass limit for plastics. The bagged inner can is typically then nested within one or more outer cans. The nested assemblies are then placed within the 5CV.

A typical single food-pack can configuration is shown in Figure 1.7. Although shown in the figure, nesting of food-pack cans is not required (i.e., a single food-pack can is allowed). Food-pack cans may be arranged for handling convenience and contamination control into single, double, or triple-stacked configurations, provided the general requirements listed in Section 1.2.2 are satisfied and the requirement below is fulfilled.

- The 5CV configuration must be used.

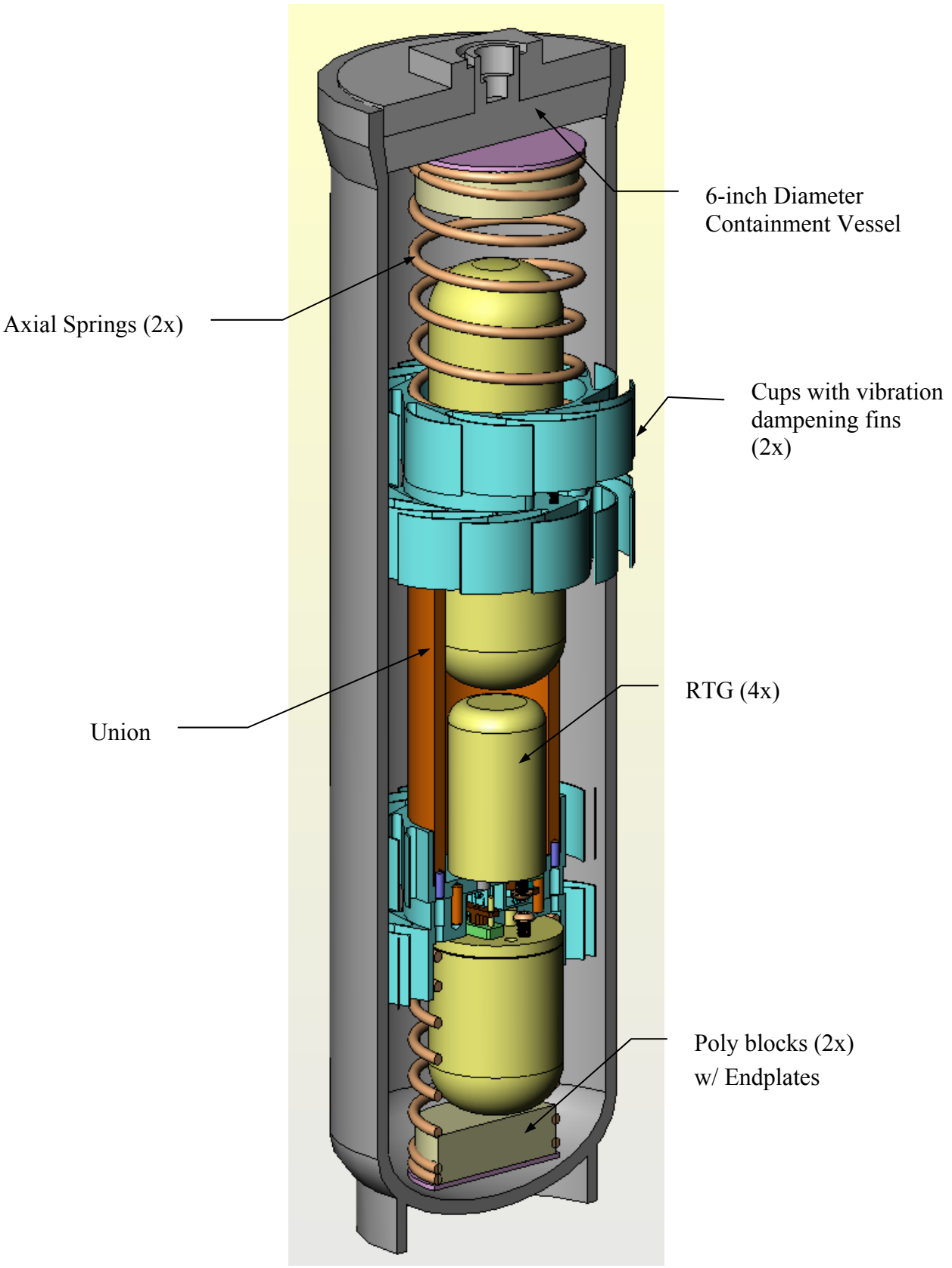

Figure 1.6 - 6CV -- Radioisotope Thermoelectric Generator (RTG) Assembly

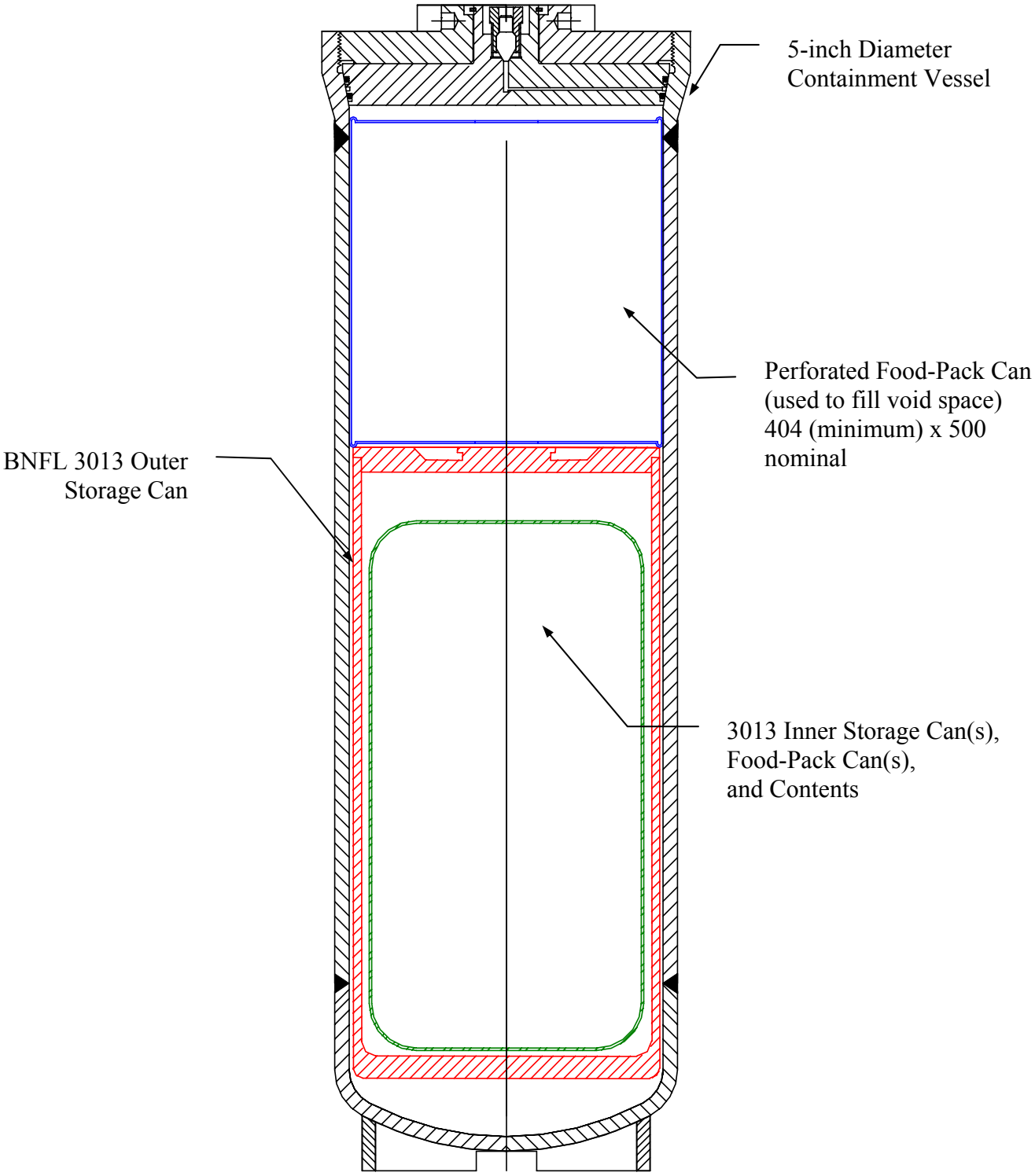

Figure 1.7 - 5CV – Typical 3013 Configuration with Contents

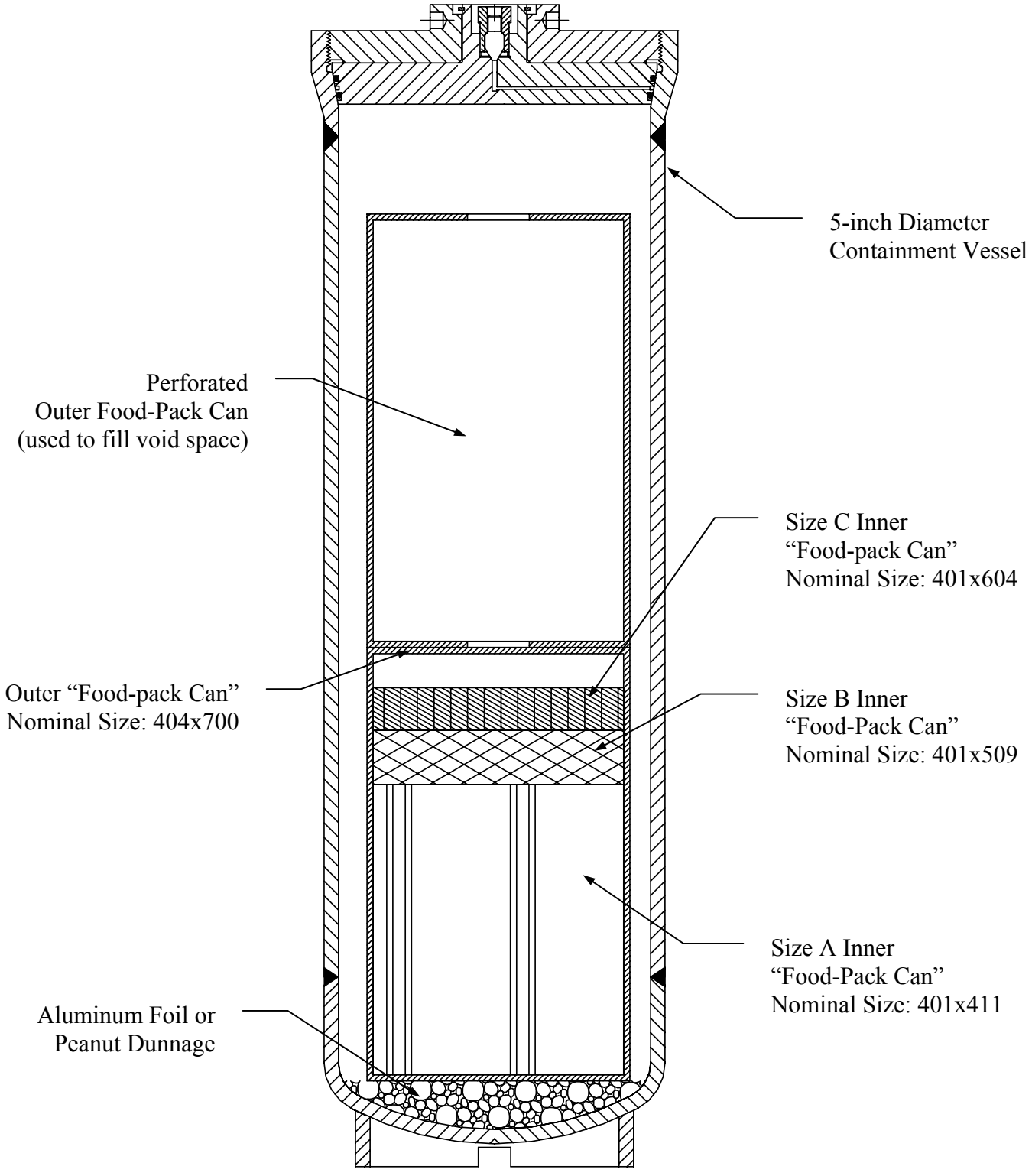

Figure 1.8 - 5CV – Typical Single Food-Pack Can Configuration with Spacer Can

1.2.2.2 Content-Specific Configuration Requirements

As described in this section, loading restrictions vary with content envelope and configuration.

1.2.2.2.1 ENVELOPE C.1 --PLUTONIUM-238 OXIDE HEAT SOURCES

RTG Configuration

The Radioisotope Thermoelectric Generators (RTGs) assembly packing configuration within the 6CV is shown in Figure 1.4. In addition to the general requirements listed in Section 1.2.2, the isotopic and chemical content restrictions in Table 1.2, Section 1.2.2.1.1 describes the only configuration acceptable for packaging RTGs in the 9977. The configuration is required only for protection of the RTGs and has no influence on the package safety evaluation. The following condition also applies:

- A total of 100 grams of plastic may be present as low-density polyethylene or nylon and/or polyvinyl chloride tape.

1.2.2.2.2 ENVELOPE C.2 -- PLUTONIUM AND URANIUM METAL

3013 Container Configurations

A typical 3013 packing configuration within the 5CV is shown in Figure 1.7. In addition to the general requirements listed in Section 1.2.2, the isotopic and chemical content restrictions in Table 1.2, and the configuration criteria listed in Section 1.2.2.1.2, a mass threshold applies. If the radionuclide content mass is greater than 3 kg per innermost material container, the following restrictions apply (no additional restrictions apply if the mass is less than 3 kg):

- The sum of the radial wall thicknesses of all cans (convenience can, 3013 inner can, and the 3013 outer can) constituting a 3013 configuration shall not exceed 0.26 inch.
- The sum of the thicknesses (tops and bottoms) of all cans constituting a 3013 configuration shall not exceed 1.77 inches.
- The innermost material container shall be at least 3.9 inches in diameter and at least 4.125 inches long (i.e., can size 315 × 402 or longer), or shall be at least 4 inches in diameter and at least 4 inches long (i.e., minimum can size 400 × 400).

Food-Pack Can Configurations

A typical food-pack can packing configuration within the 5CV is shown in Figure 1.8. In addition to the general requirements listed in Section 1.2.2, the isotopic and chemical content restrictions in Table 1.2, and the configuration criteria listed in Section 1.2.2.1.3, the following conditions apply.

- A total of 100 grams of plastic may be present as low-density polyethylene or nylon and/or polyvinyl chloride tape.

If the radionuclide content mass is equal to or greater than 3 kg per innermost material container, the following restrictions apply (no additional restrictions apply if the mass is less than 3 kg).

- The sum of the radial wall thicknesses of all nested cans shall not exceed 0.26 inch.
- The sum of the thicknesses of the tops and bottoms of all nested cans shall not exceed 1.77 inches.
- The innermost material container shall be at least 3.9 inches in diameter and at least 4.125 inches long (i.e., can size 315 × 402 or longer), or shall be at least 4 inches in diameter and at least 4 inches long (i.e., minimum can size 400 × 400).

1.2.2.2.3 ENVELOPES C.4 AND C.5 -- URANIUM METAL AND OXIDES

Food-Pack Can Configurations

The typical food-pack can packing configurations within the 5CV is shown in Figure 1.7. In addition to the general requirements listed in Section 1.2.2, the isotopic and chemical content restrictions in Table 1.2, and the configuration criteria listed in Section 1.2.2.1.3, the following conditions apply.

- A total of 100 grams of plastic may be present as low-density polyethylene or nylon and/or polyvinyl chloride tape.

If the radionuclide content mass is equal to or greater than 3 kg per innermost material container, the following restrictions apply (no additional restrictions apply if the mass is less than 3 kg).

- The sum of the radial wall thicknesses of all nested cans shall not exceed 0.26 inch.
- The sum of the thicknesses of the tops and bottoms of all nested cans shall not exceed 1.77 inches.
- The innermost material container shall be at least 3.9 inches in diameter and at least 4.125 inches long (i.e., can size 315 × 402 or longer), or shall be at least 4 inches in diameter and at least 4 inches long (i.e., minimum can size 400 × 400).

Table 1.3 - Summary of Requirements by Content and Configuration

Content Envelope	Container Configuration			
	CV	3013	Food-Pack Can	SNL RTGs
C.1	6CV only			manufactured per drawings listed packing configuration control maximum 100-g plastic
C.2	5CV Only	Ref. 3013 outer can Inner and material cans per STD-3013 No organic liners Top spacer can required if ≥ 3kg per inner/material can * sum of container walls < 0.26 inches * sum of tops & bottoms < 1.77 inches * 400 x 400 or bigger * 315 x 402 or bigger	maximum 100-g plastic if ≥ 3kg per food-pack can * sum of can walls < 0.26 inches * sum of can tops & bottoms < 1.77 inches * 400 x 400 or bigger	
C.4 & C.5			perforated spacer can used in axial void space maximum 100-g plastic maximum 200-g Al foil maximum 900-g can mass	
All	19 watts maximum radioactive decay heat rate less than 1000 ppm other radionuclides (unless otherwise stated) less than 100 ppm other inorganic impurities with total mass less than 0.1 weight percent (unless otherwise stated) 50-lb (5CV) and 100 lb (6CV) maximum content weight (radioactive contents, convenience cans, contamination control devices, packing materials, spacers, etc.)			

1.2.3 Special Requirements for Plutonium

Plutonium contents in excess of 0.74 Tbq (20 Ci) per package must be in solid form. This condition is required for all content envelopes as stated in Section 1.2.2.

1.2.4 Operational Features

In general, all components are handled manually. Therefore, the features discussed below have been incorporated into the design to assist personnel in manual operation of the package.

Rectangular notches are located in the base of the CV support skirt that can be used to prevent rotation of the vessel body while installing/removing the closure assembly. The CVs are top heavy and the user should provide a fixture or support stand to prevent tipping during loading or unloading operations.

Four (4) ¼-inch diameter by ¼-inch deep holes are located in square drive on top of the cone-seal nut to facilitate lifting the cone-seal closure assembly or the fully assembled CV. Examples of special tools that may facilitate lifting and other package operations are discussed in Appendix 7.1.

The hex-heads of the eight (8) drum-closure bolts are drilled through for insertion of a tamper-indicating device (TID). During shipment, two or more bolts are wired together in series such that removal of one of these bolts would require breaking the TID.

Threaded inserts are welded to the bottom of the drum's top deck plate to receive closure bolts and simplify closure operations.

The drum's reinforcing rim (circumferential vertical flange) includes eight (8) 1-inch diameter drain holes that are also qualified as package lifting and tie-down points.

1.2.5 Compliance with 10 CFR 71

This SARP documents that the 9977 package satisfies the regulatory safety requirements of 10 CFR 71.

The results of the structural and thermal analyses and testing performed on the package are presented in the Chapters 2 and 3 and are summarized below.

1.2.5.1 Structural and Thermal Performance Under Testing for NCT 10 CFR 71.71 and HAC 10 CFR 71.73

The package is designed, constructed and prepared for transport so that under the tests specified in 10 CFR 71.71 there is no loss or dispersal of radioactive contents, no significant increase in external surface radiation levels and no substantial reduction in the effectiveness of the packaging. Specifically, Section 2.6 demonstrates compliance with the performance requirements of 10 CFR 71.43 and 10 CFR 71.51(a). The NCT pressures and temperatures are summarized in Table 2.21.

Section 2.7 demonstrates that the package satisfies the performance requirements of 10 CFR 71.51(a)(2) under the HAC requirements given in 10 CFR 71.73, including; free drop, puncture, thermal, immersion (for both fissile material and all packages) and crush. HAC tests were conducted in a sequential application, in the order indicated, to determine their cumulative effect on a package in accordance with 10 CFR 71.73(a). The HAC regulatory limit of "no escape of radioactive material exceeding a total amount A_2 in one week" is met by demonstrating that the containment system remained leaktight. The external radiation dose requirement is met by factoring the results of the analyses and test described in Section 2.7 into the shielding evaluation described in Section 5.1. The general requirements for fissile material packages in 10 CFR 71.55 are met by factoring the results of the tests described in Section 2.7 into the criticality evaluation described in Section 6.1. The package is shown to meet the performance requirements of 10 CFR 71.73 by evaluation and by a combination of physical testing on the 9977 package, 9977 package prototypes and its predecessor packages of similar design.

1.2.5.2 General Requirements for All Packages – 10 CFR 71.43

The performance criteria for the package under NCT, from 10 CFR 71.43, General Standards for All Packages, are met, as demonstrated in Section 2.4. The package design incorporates;

a) overall dimensions greater than 4 inches;
b) provision for a Tamper Indicating Device that provide evidence that the package has not been opened;
c) a containment system that cannot be opened unintentionally or by a pressure that may arise within the package;
d) materials and contents with no significant chemical, galvanic, or other reactions;
e) no valves;
f) no pressure relief devices;
g) under the NCT conditions, no loss or dispersal of radioactive contents, no significant increase in external surface radiation levels, and no substantial reduction in the effectiveness of the packaging;
h) no accessible surface temperature exceeding 122°F in still air, at 100°F, in the shade; and
i) no venting devices.

1.2.5.3 Structural Requirements for Lifting and Tie-Down Devices – 10 CFR 71.45

The drum rim vertical flange includes eight (8) 1-inch diameter holes that are qualified as package lifting and tie-down points, as demonstrated in Section 2.5.

1.2.5.4 External Radiation Requirements – 10 CFR 71.47

The package radiation dose rate limits are met for NCT and HAC for all content envelopes as shown in Section 5.1 and listed in Table 5.1.

1.2.5.5 Requirements for Type B Packages – 10 CFR 71.51

The package is demonstrated by testing to be leaktight in accordance with American National Standards Institute (ANSI) N14.5[13] during acceptance (in accordance with Section 8.1.3) and normal operations and use (in accordance with Section 8.2.2). The analysis and testing described in Sections 2.6 and 2.7 show that there is no loss of containment during NCT and in HAC events.

1.2.5.6 Criticality Requirements – 10 CFR 71.53, 71.55, and 71.59

The criticality safety evaluation provided in Sections 6.4.3 and 6.4.4 demonstrates that the package is subcritical for all single package and array configurations. The package Criticality Safety Index is 1.

1.2.5.7 Special Requirements for Plutonium Packages – 10 CFR 71.63

All 9977 contents shall be in solid form. This restriction exceeds the "greater than 0.74 TBq (20 Ci) of plutonium" requirement of 10 CFR 71.63.

1.2.5.8 Requirements for Operating Controls and Procedures – 10 CFR 71 Subpart G

Chapter 7 provides the minimum procedural elements that ensure the package is operated in accordance with its design. The package user's implementation of the SAR procedural elements, and any requirements provided in the package Certificate of Compliance, ensures safe performance of the package under NCT and HAC.

1.2.5.9 Requirements for Quality Assurance – Subpart H

The quality assurance (QA) requirements for ensuring the safety of the package, as applied by Washington Savannah River Company at the Savannah River National Laboratory and the Savannah River Site are provided in Chapter 9. Requirements provided include the QA methodology and applicable areas of package design, purchasing, fabrication, handling, shipping, storage, cleaning, assembly, inspection, testing, operation, maintenance, repair, and component modification. Non-WSRC users of the package are responsible for implementing comparable QA programs.

This Page Intentionally Left Blank

1.3 REFERENCES

1. *Packaging and Transportation of Radioactive Material*, Code of Federal Regulations, Title 10, Part 71, Washington, DC (January 2002).

2. *Regulations for the Safe Transport of Radioactive Material – 1996 Edition (Revised) - Requirements*, IAEA Safety Standards, Safety Series No. TS-R-1 (ST-1, Rev.), International Atomic Energy Agency, Vienna, Austria (2000).

3. *Packaging and Transportation Safety.* DOE Order 460.1B, U.S. Department of Energy, Washington, DC (April 2003).

4. *Standard Format and Content of Part 71 Applications for Approval of Packaging for Radioactive Material*, Regulatory Guide 7.9, (Rev. 2), U. S. Nuclear Regulatory Commission, Washington, DC (March 2005).

5. *Establishing Quality Assurance Programs for Packaging Used in the Transport of Radioactive Material*, Regulatory Guide 7.10, (Rev. 1), U.S. Nuclear Regulatory Commission, Washington, DC (January 1980).

6. *Fracture Toughness Criteria of Base Material Ferritic Steel Shipping Cask Containment Vessels with Maximum Wall Thickness of 4 inches (0.1 m)*, Regulatory Guide 7.11, U.S. Nuclear Regulatory Commission, Washington, DC (June 1991).

7. *Control and Accountability of Nuclear Materials,* DOE Order 474.1A, U.S. Department of Energy, Washington, DC (November 2000).

8. *Stabilization, Packaging, and Storage of Plutonium-Bearing Materials,* DOE Standard, DOE-STD-3013-2004, U.S. Department of Energy, Washington, DC (April 2004).

9. *Specifications for Packagings*, Code of Federal Regulations, Title 49, Part 178, Washington, DC (October 2002).

10. *PUSPS Plutonium Stabilization and Packaging System Assembly and Details Outer Can PI No. V4003*, Drawing M-PV-F-0017 Revision 0 (July 1999).

11. PPP-C-96E, *Cans, Metal, 28 Gauge and Lighter*, GL - U.S. Army Soldier Systems Center (December 1992).

12. *Dimensional Food Can Standards*, Can Manufacturers Institute, 1730 Rhode Island Ave. Suite 1000, Washington DC 20036, www.cancentral.com.

13. *American National Standard for Radioactive Material - Leakage Tests on Packages for Shipment*, ANSI N14.5, American National Standards Institute, Inc. (1997).

This Page Intentionally Left Blank

1.4 APPENDICES

Appendix	Description
1.1	Engineering Drawing List for the 9977 Package
1.2	DOE-STD-3013 Storage Container Configurations

This Page Intentionally Left Blank

APPENDIX 1.1

DRAWING LIST

This Page Intentionally Left Blank

DRAWING LIST

Drawing Number	Rev	Title
R-R5-G-00002	0	9977 - General Purpose Fissile Packaging Drawing Tree (U)
R-R1-G-00020	0	9977 - General Purpose Fissile Packaging Assembly with 6-inch Diameter Containment Vessel (U)
R-R1-G-00021	0	9977 - General Purpose Fissile Packaging Assembly with 5-inch Diameter Containment Vessel (U)
R-R2-G-00017	0	9977 - General Purpose Fissile Packaging Drum and Liner Subassembly (U)
R-R2-G-00018	0	9977 - General Purpose Fissile Packaging Drum Lid Subassembly (U)
R-R2-G-00019	0	9977 - General Purpose Fissile Packaging Insulating Blanket Subassembly (U)
R-R2-G-00042	0	9977 - General Purpose Fissile Packaging 6-inch Diameter Containment Vessel (CV) Subassembly (U)
R-R2-G-00043	0	9977 - General Purpose Fissile Packaging 5-inch Diameter Containment Vessel (CV) Subassembly (U)
R-R4-G-00032	0	9977 - General Purpose Fissile Packaging Spacer Part Details for 6-inch Containment Vessel (U)
R-R4-G-00033	0	9977 - General Purpose Fissile Packaging Spacer Part Details for 5-inch Containment Vessel (U)

This Page Intentionally Left Blank.

APPENDIX 1.2

DOE-STD-3013 STORAGE CONTAINER CONFIGURATIONS

This Page Intentionally Left Blank

DOE-STD-3013 STORAGE CONTAINER CONFIGURATIONS

Metal or oxide contents targeted for long-term storage must meet DOE-STD-3013. [*Stabilization, Packaging, and Storage of Plutonium-Bearing Materials*, DOE Standard, DOE-STD-3013-2000, U. S. Department of Energy, Washington, D. C. (September 2000)] The 3013 configuration uses a series of nested containers specifically designed for long-term storage; an outer container, an inner container, and an optional material container. These are shipped in the 9977. Descriptions of various 3013 components and configurations that have been reviewed and approved for use within the 9977 are provided here. A summary listing of the various components and their controlling design drawing is included.

3013 Outer Storage Can

Only one design for the 3013 outer storage can has been evaluated for use in the package. The British Nuclear Fuels, Limited (BNFL) 3013 Outer is used for all 3013 configurations. The 3013 Outer has a full-penetration welded closure.

3013 Inner Storage Can and Material Containers

Individual package users typically develop site-specific 3013 inner and product containers. The material containers in the following figures facilitate packaging operations, reduce the potential for contamination during loading, and are not required by the DOE-STD-3013. All food-pack cans are manufactured in compliance with the Can Manufacturing Institute (CMI) "Voluntary Can Standards."

The 3013 Containers

	User	Designation	Designer	Closure Type	Drawing Number
"Outer"	All	3013 Outer	BNFL	Full-penetration weld	SRS: M-PV-F-0017
"Inner"	BNFL	3013 Inner	BNFL	Laser weld	SRS: M-PV-F-0016
	LANL	Aries 3013 Inner	LANL	Full-penetration weld	LANL: 90Y-219875
	Hanford	Bagless Inner 3013	Dynamic Machine Works	Resistance seam weld	DMW: 2043A
	SRS	"Short" Bagless Transfer Canister	SRS	Resistance seam weld	SRS: R-R1-F-0039
	SRS	"Tall" Bagless Transfer System Can	SRS	Resistance seam weld	SRS: R-R4-F-0107
"Material Container"	BNFL	Convenience Container	BNFL	Screw top lid	SRS: M-PV-F-0015
	Hanford	Convenience Container	Dynamic Machine Works	Screw top lid	DMW: 1911
	Rocky Flats	Convenience Container	Dynamic Machine Works	Screw top lid	DMW: 1509-02
	LLNL	Food-Pack Can	Can Manufacturers Inst.	Crimp sealed	404 × 700 or 404 × 800
	LANL	Food-Pack Can	LANL	Crimp sealed	LANL: 90Y-219959
	SRS	Bagless Convenience Can	SRS	Open top	SRS: M-FFD-F-00083
	SRS	Tall Bagless Convenience Can	SRS	Open top	SRS: M-FFD-F-00105
	SRS	Convenience Can Assembly	SRS	Screw Top	SRS: R-R1-F-0098

The 3013 storage container configurations that have been evaluated as content for the 9977 are illustrated in Figures A1.2.1 through A1.2.8, as follows:

Figure	Description
A1.2.1	BNFL oxide convenience can inside a 3013 inner storage can inside a 3013 outer storage can.
A1.2.2	A metal Rocky Flats convenience can inside a 3013 inner storage can inside a 3013 outer storage can with a button spacer.
A1.2.3	Two SRS "Bagless Transfer" cans inside a 3013 outer storage can with optional "Bagless Convenience Can Assembly".
A1.2.4	SRS Tall "Bagless Transfer" can inside a 3013 outer storage can with optional screw top "FB-Line Convenience Can Assembly".
A1.2.5	SRS Tall "Bagless Transfer" can inside a 3013 outer storage can with optional "Tall Bagless Convenience Can".
A1.2.6	LLNL convenience can inside a 3013 inner storage can inside a 3013 outer storage can.
A1.2.7	LANL/ARIES 3013 Convenience Can Configuration inside a 3013 outer storage can.
A1.2.8	Hanford convenience can inside the Hanford "bagless transfer" can inside a 3013 outer storage can.

Note: Two smaller convenience cans or a different sized single convenience can is an acceptable substitute for the single convenience can illustrated in Figure A1.2.6 so long as the minimum container size criteria specified in Section 1.2.3 are met.

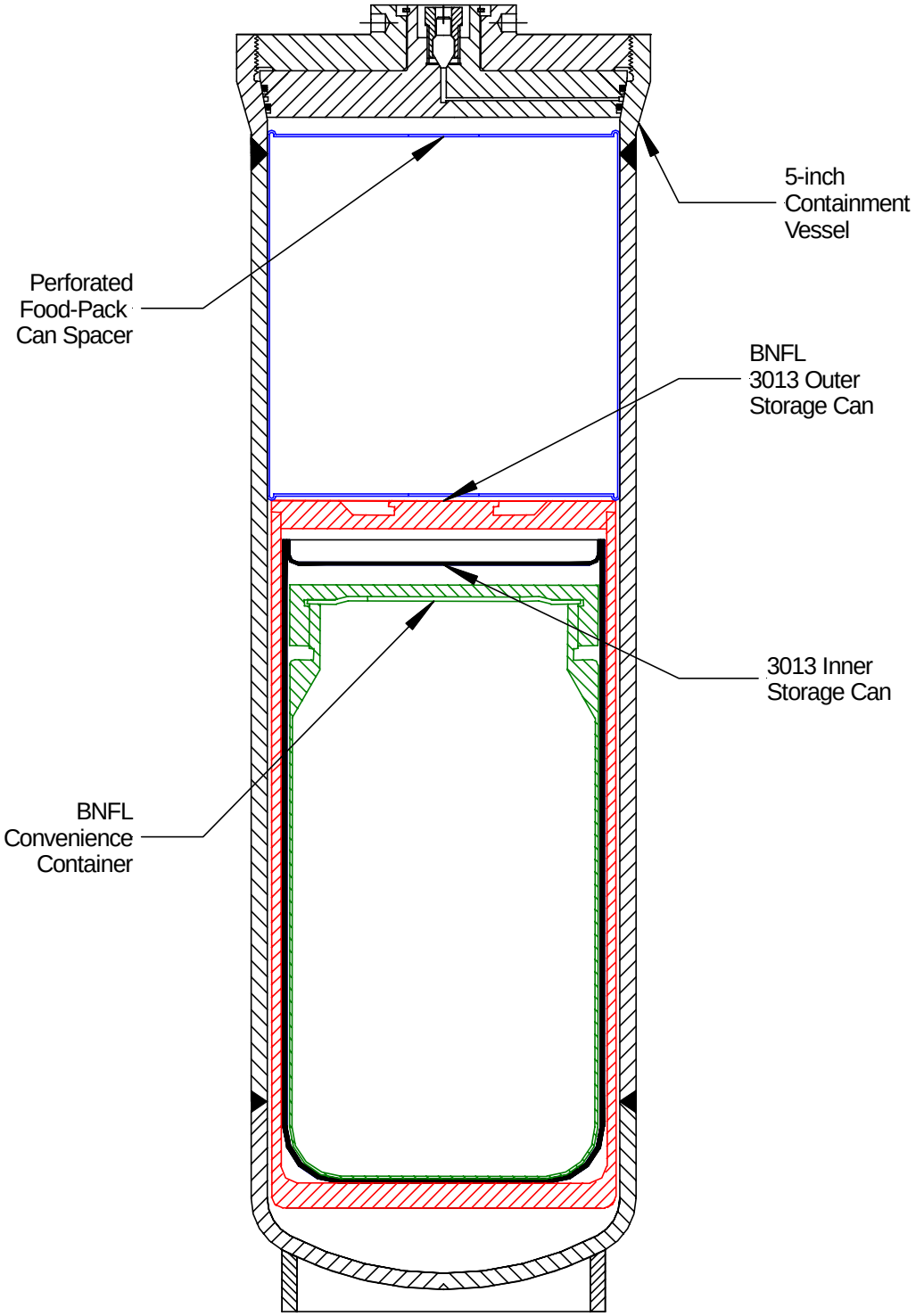

Figure A1.2.1 - 3013 Container Configuration

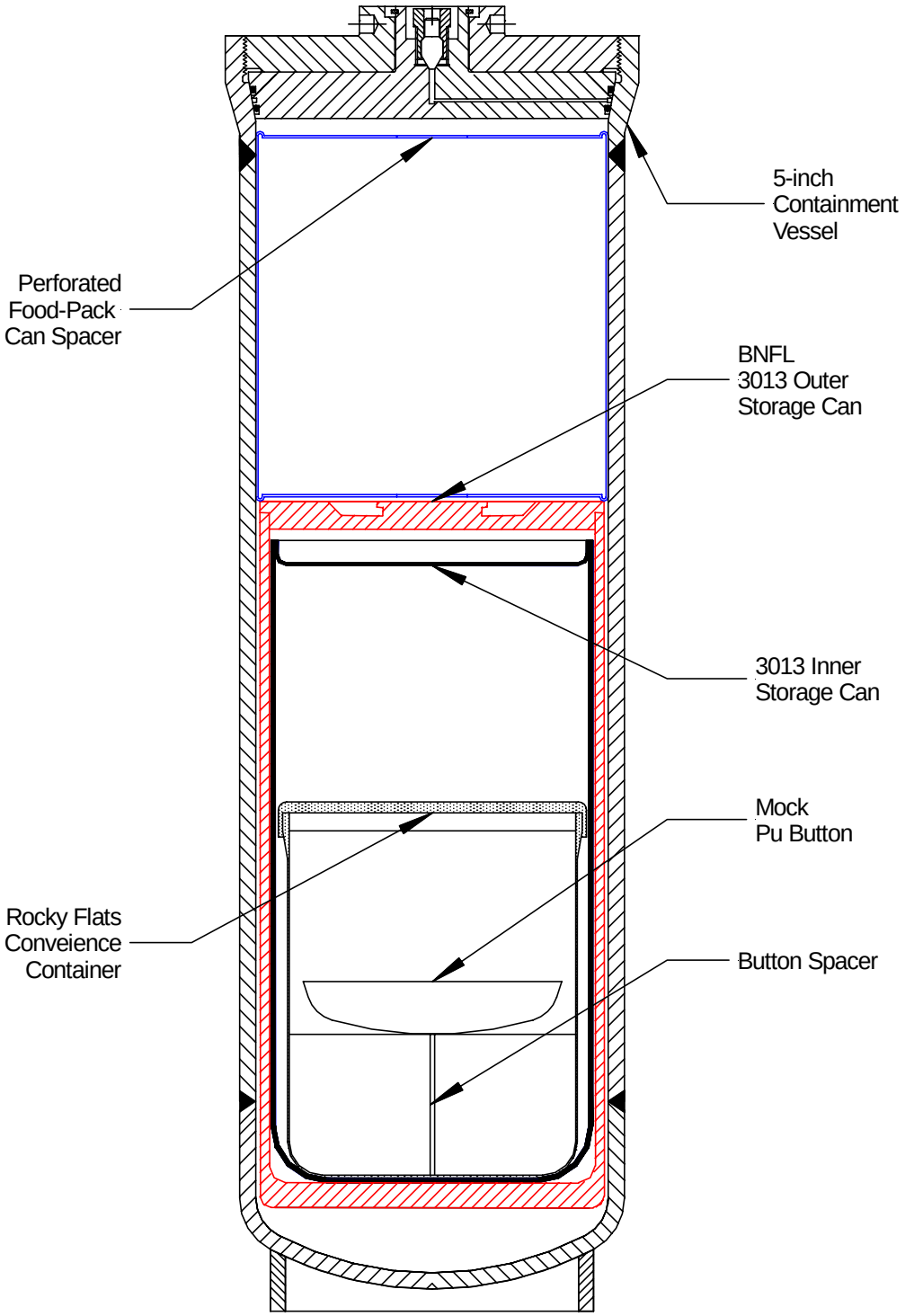

Figure A1.2.2 - Rocky Flats 3013 Convenience Container Configuration with Button Spacer

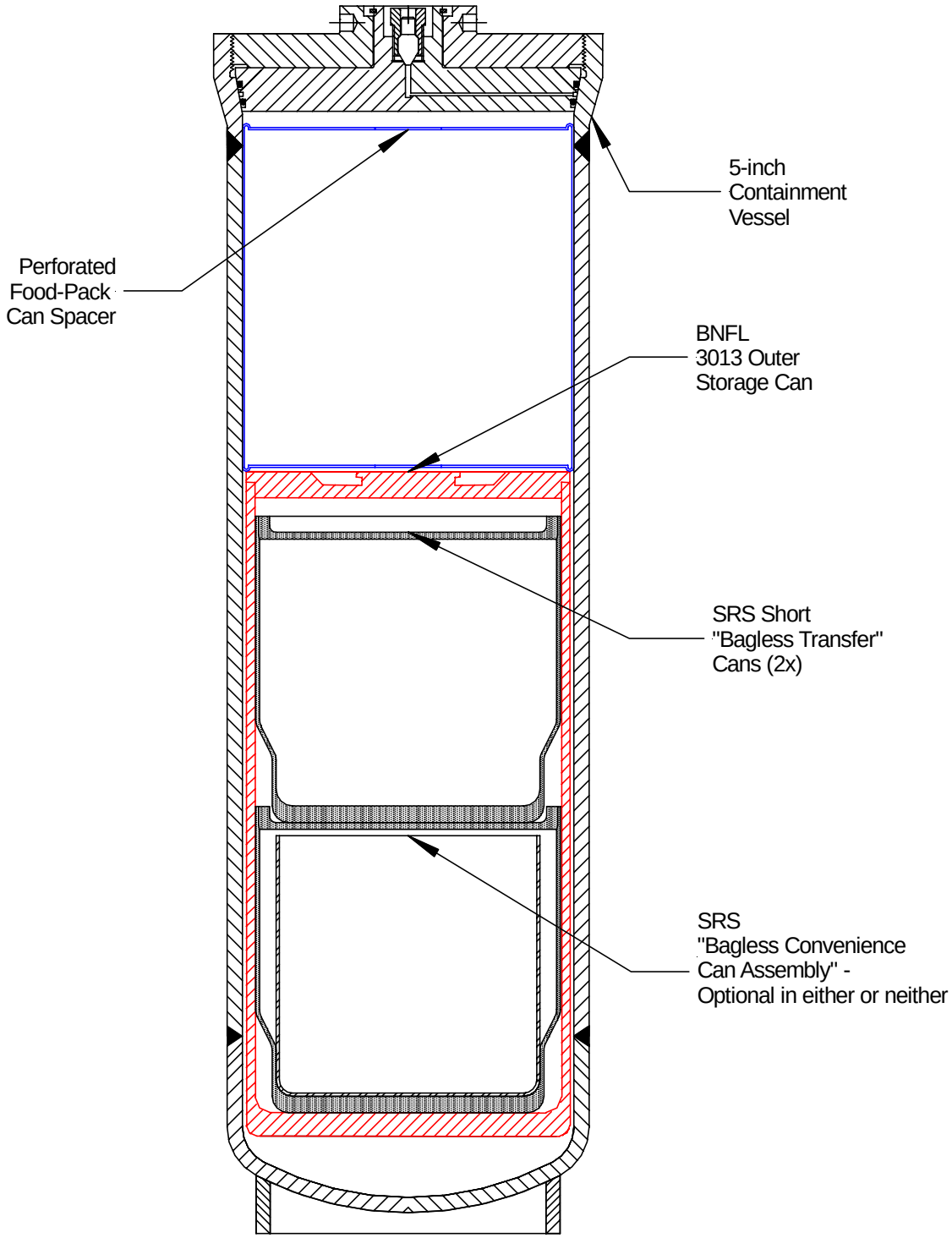

Figure A1.2.3 - SRS 3013 Configuration – Short "Bagless Transfer" Can with optional "Bagless Convenience Can Assembly"

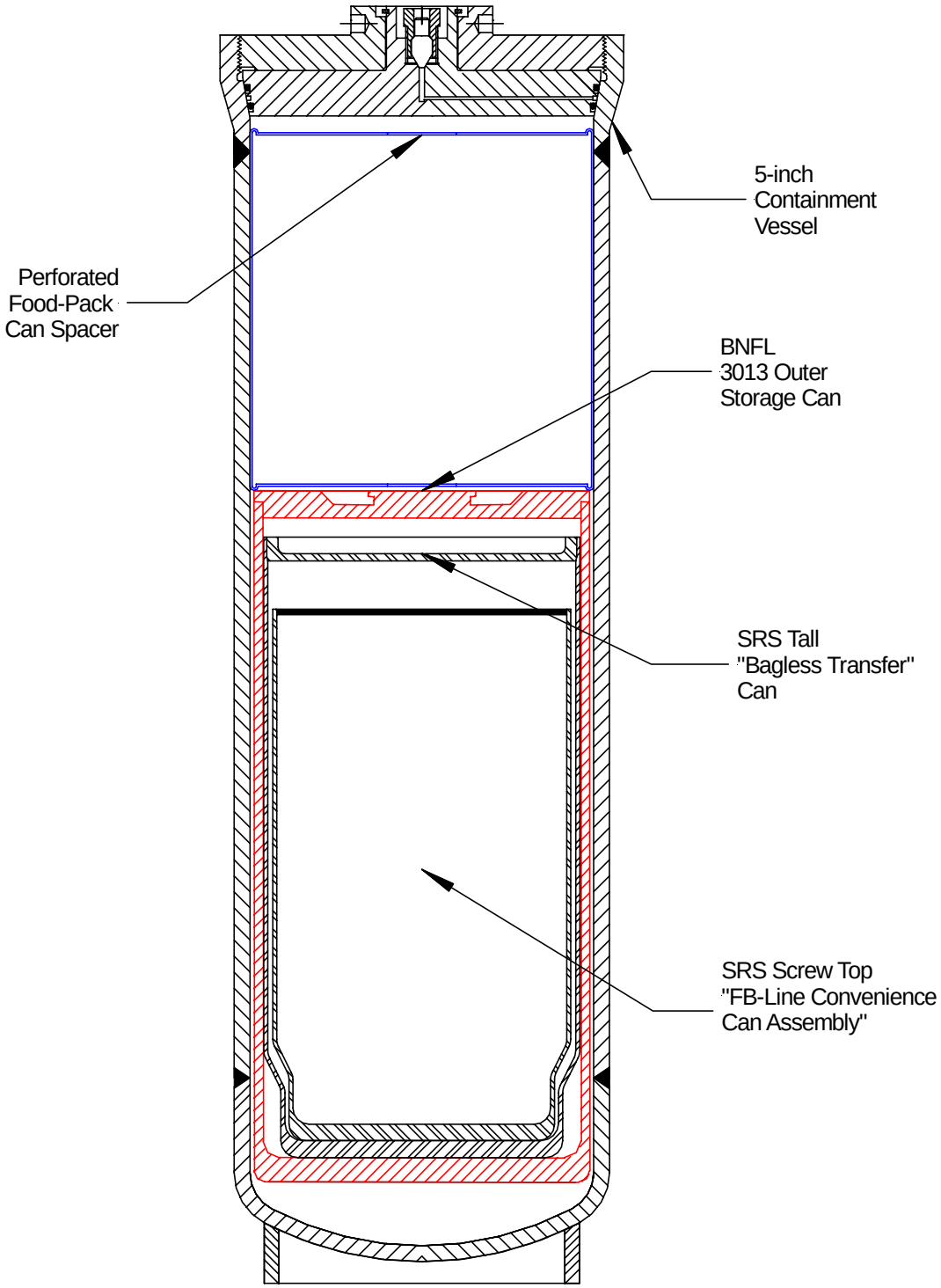

Figure A1.2.4 - SRS 3013 Configuration – Tall "Bagless Transfer" Can with optional screw top "FB-Line Convenience Can Assembly"

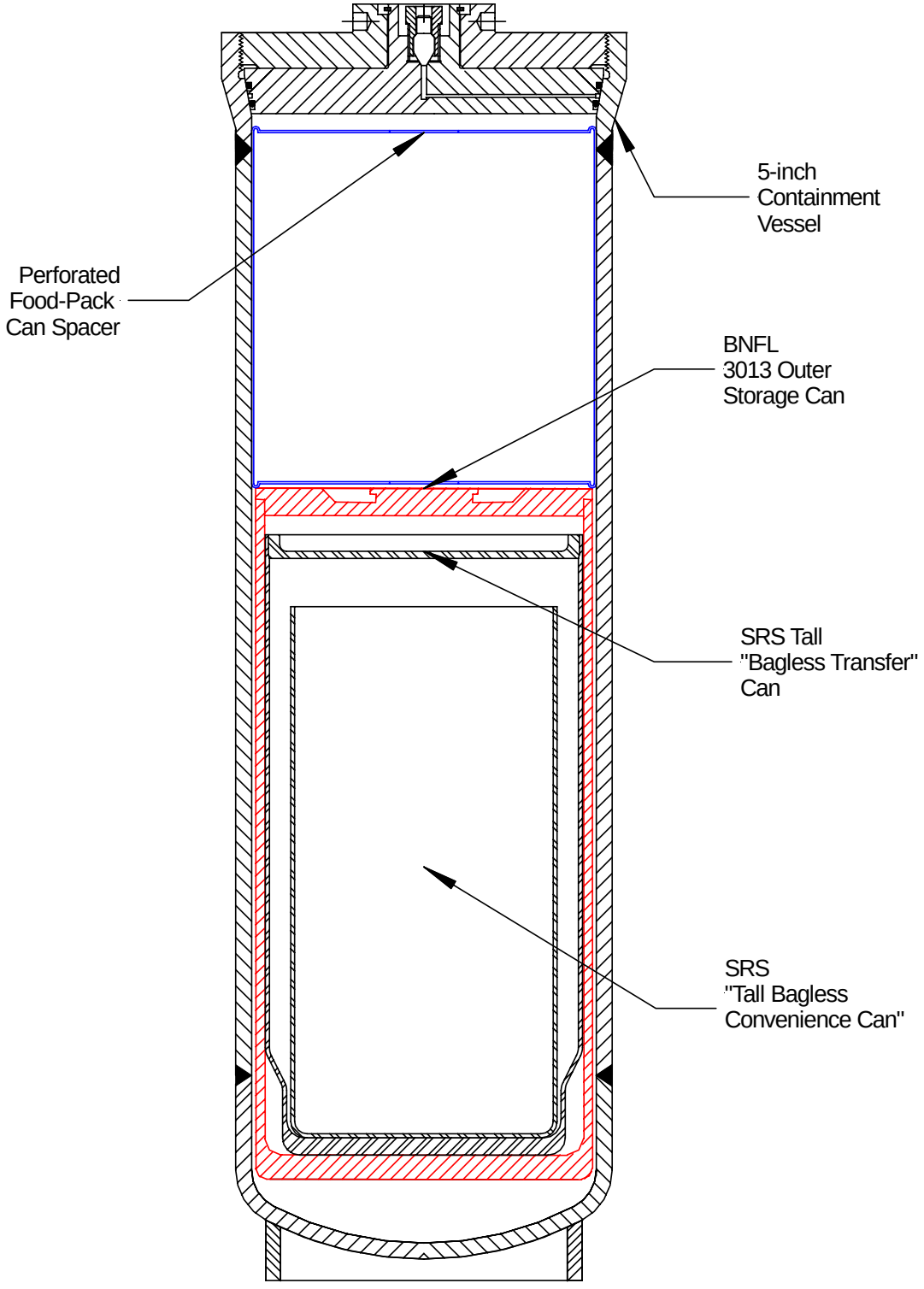

Figure A1.2.5 - SRS 3013 Configuration – Tall "Bagless Transfer" Can with optional "Tall Bagless Convenience Can"

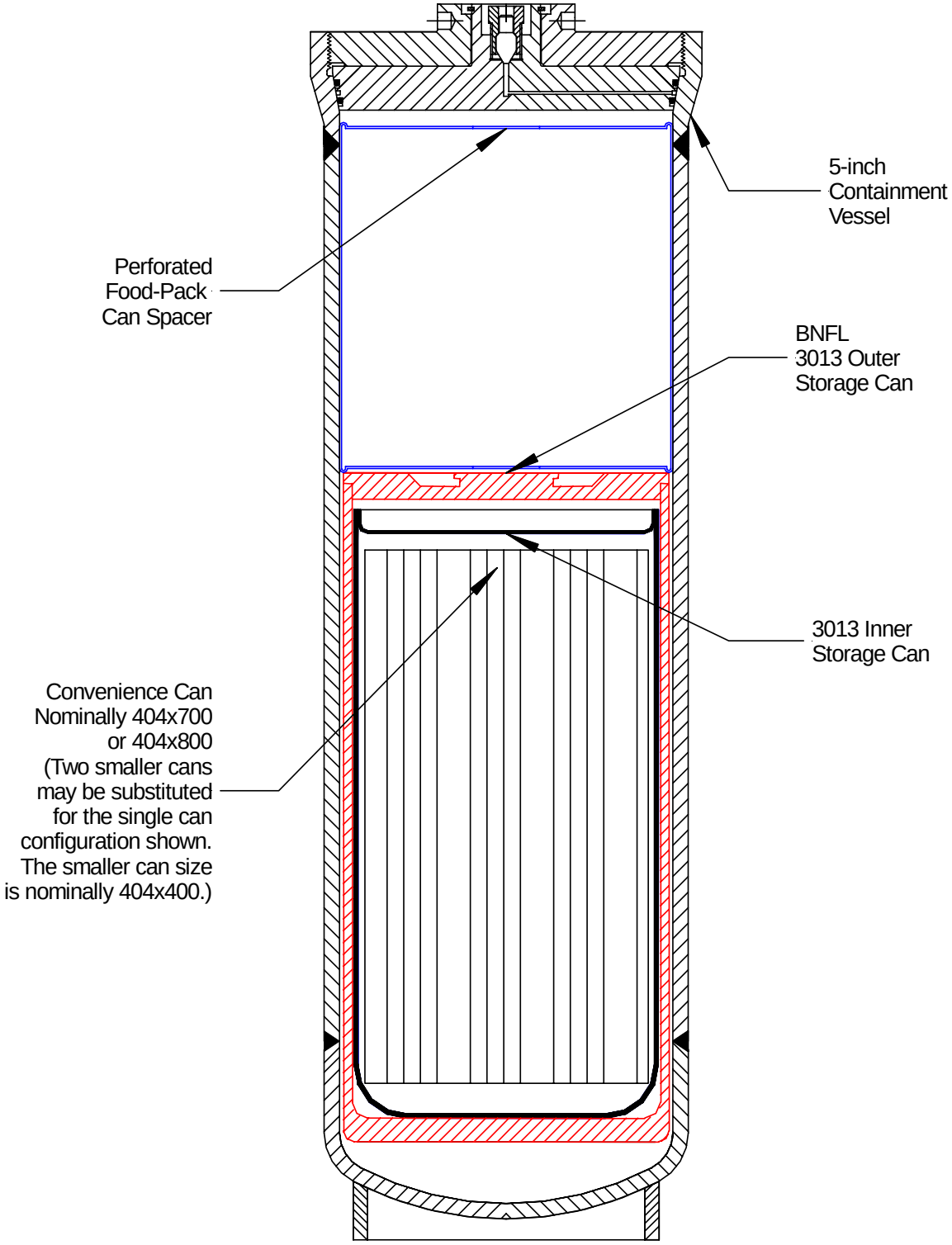

Figure A1.2.6 - LLNL 3013 Convenience Can Configuration
(Note: Food Pack Cans are according to the Can Manufacturers Institute Voluntary Can Standards)

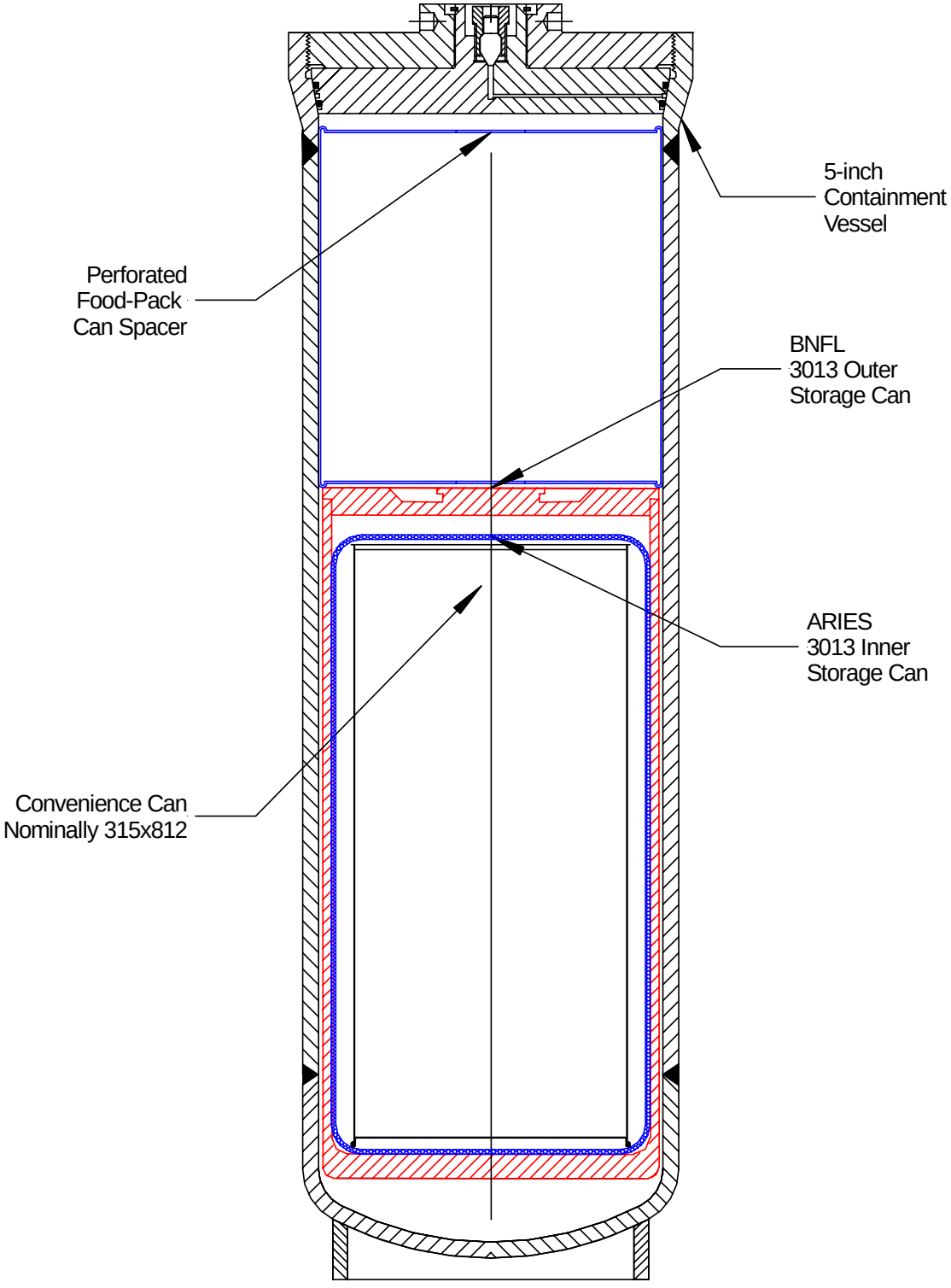

Figure A1.2.7 - LANL/ARIES 3013 Convenience Can Configuration
(Note: Food Pack Cans are according to the Can Manufacturers Institute Voluntary Can Standards)

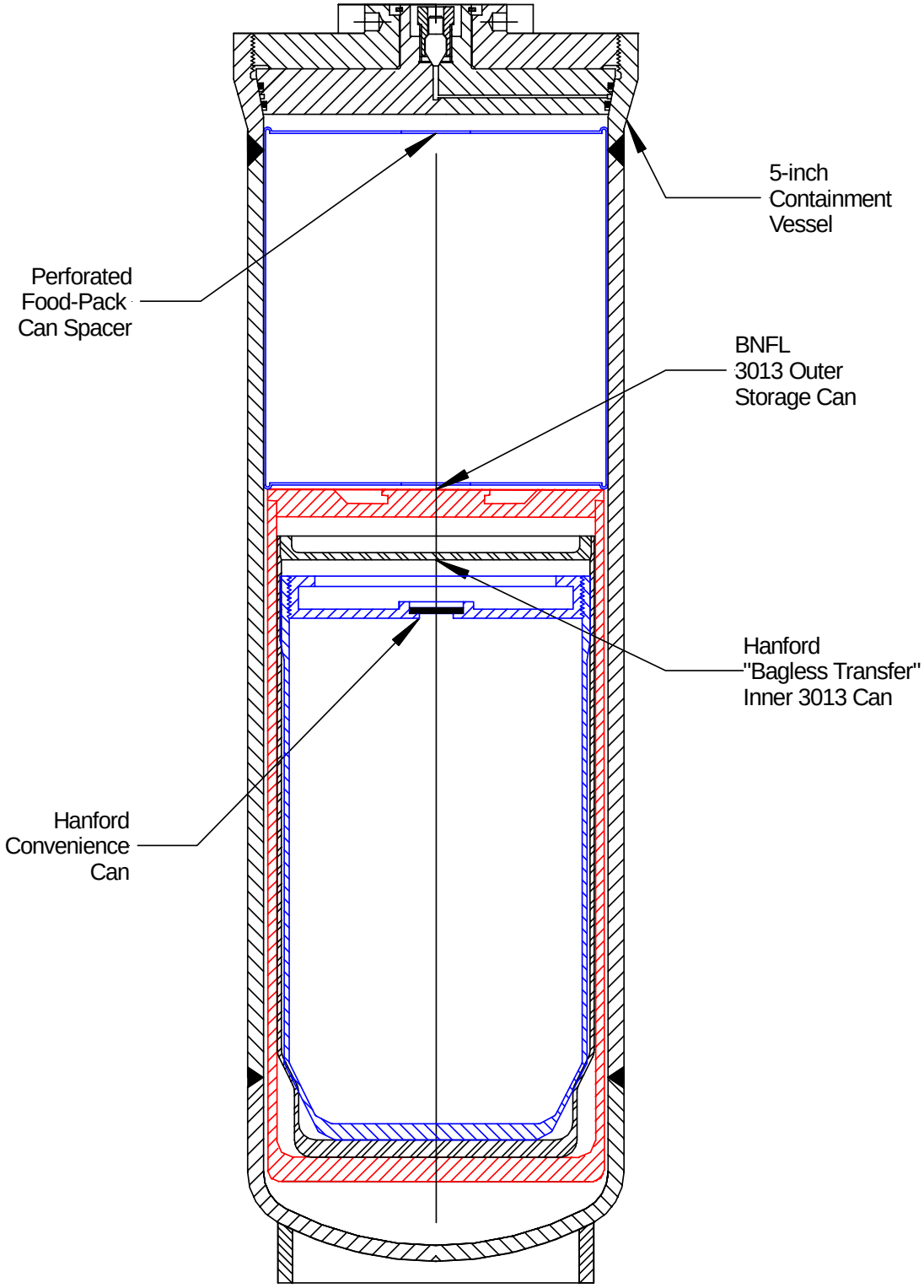

Figure A1.2.8 - Hanford 3013 Convenience Can Configuration

This Page Intentionally Left Blank

NOTES:

1. SAVANNAH RIVER NATIONAL LABORATORY'S (SRNL) SAVANNAH RIVER PACKAGING TECHNOLOGY (SRPT) ORGANIZATION IS THE DESIGN AUTHORITY FOR THE 9977 PACKAGING. ANY AND ALL PROPOSED CHANGES TO THE DESIGN AND/OR TESTING INFORMATION ON THE DESIGN DRAWINGS SHALL BE REVIEWED AND APPROVED BY SRPT.

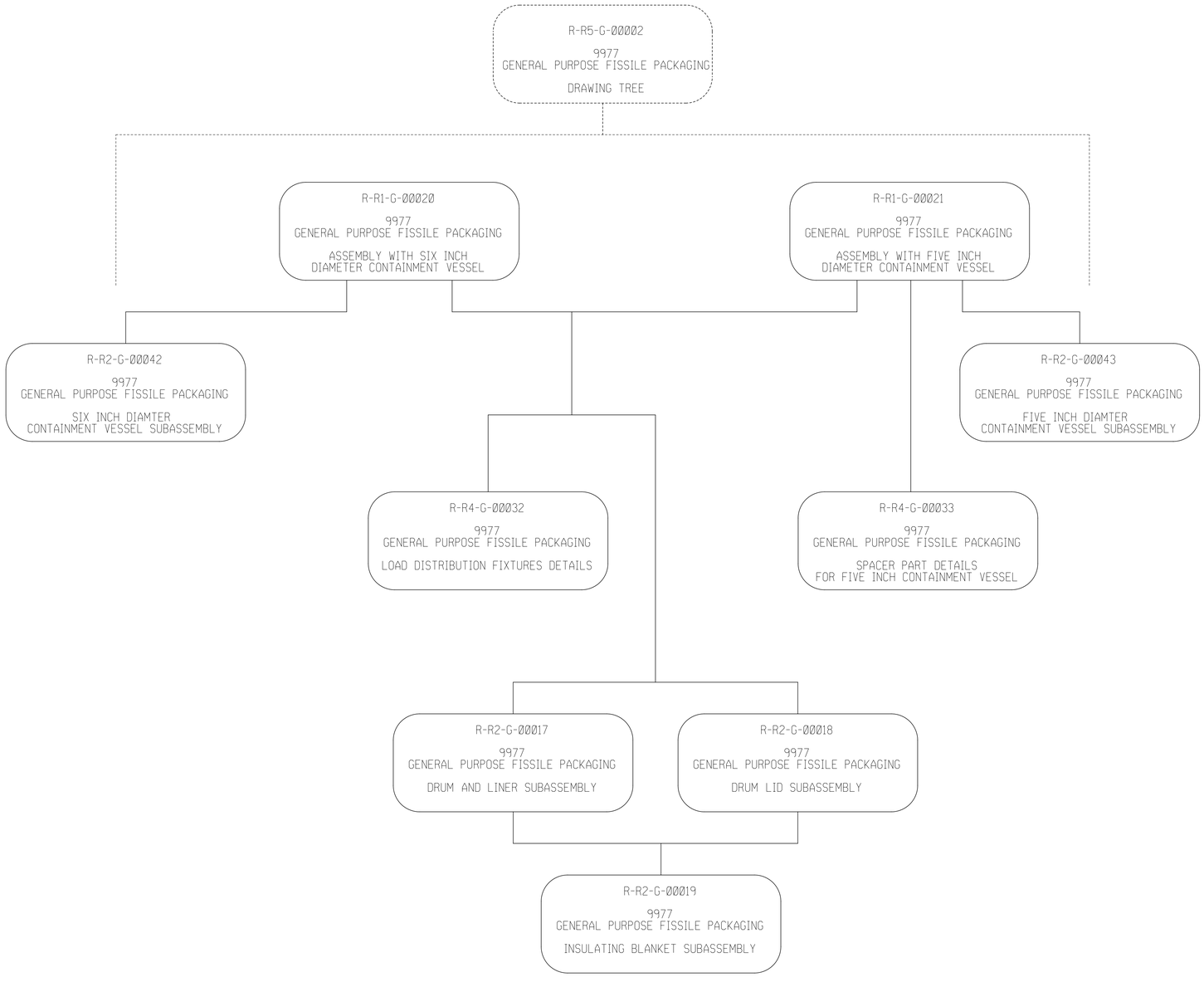

NOTE:
DRAFTING IS IN ACCORDANCE WITH ANSI 14.5, ANSI/AWS A2.4 AND ASME STANDARDS AS APPLICABLE.

ITEM	PART AND DRAWING NO.	REQD PER ASSY	DESCRIPTION

FINISH 125/ ALL MACHINED SURFACES AND BREAK ALL SHARP EDGES UNLESS OTHERWISE SPECIFIED

THE NUMBER IN THE FINISH SYMBOL √ IS THE MAXIMUM ACCEPTABLE ROUGHNESS VALUE IN AA/MICRO-INCHES.

TOLERANCES ON ALL DIMENSIONS UNLESS OTHERWISE NOTED SHALL BE:

ONE PLACE DECIMAL	±.03	FRACTIONAL	±1/16"
TWO PLACE DECIMAL	±.01	ANGULAR	±0° - 30'
THREE PLACE DECIMAL	±.005		

JOB NUMBER 23047

DRAWING NO. R-R5-G-00002 LATEST REVISION Ø

UNCLASSIFIED
DOES NOT CONTAIN UNCLASSIFIED CONTROLLED NUCLEAR INFORMATION

ADC & Reviewing Official: P. BLANTON, SRPT PGM. MGR. (Name and Title)

Date: 5/16/06

THIS DRAWING CONTAINS INFORMATION ON SHIPPING PACKAGES FOR RADIOACTIVE MATERIAL
REVISIONS REQUIRE PRIOR APPROVAL OF DESIGN AGENCY
(SRNL PACKAGING TECHNOLOGY GROUP)

THIS DRAWING IS FURNISHED FOR THE UNITED STATES DEPARTMENT OF ENERGY AT THE SAVANNAH RIVER SITE, THE INFORMATION AND KNOW-HOW THEREON MAY NOT BE USED OR REPRODUCED WITHOUT THE WRITTEN PERMISSION OF THE PRIME CONTRACTOR. ALL REPRODUCTIONS IN WHOLE OR PART, INCLUDING ANY VENDOR'S SHOP DRAWINGS, SHALL INCLUDE OR REFER TO THIS NOTE.

UNITED STATES DEPARTMENT OF ENERGY

SRNL™ SAVANNAH RIVER NATIONAL LABORATORY

We Put Science To Work

REFERENCE DRAWINGS

REFERENCE STANDARDS

BLDG NO.	SITE CLEARANCE NO.	DA NO.	DESIGN GROUP
OFFSITE	N/A	N/A	SRNL/EES

TITLE

9977
GENERAL PURPOSE FISSILE PACKAGING
DRAWING TREE
(U)

SCALE	SRS DRAWING NO.	SHEET NO.	LATEST REV
N/A	N/A	1 OF 1	Ø

RESPONSIBLE ENGINEER	KURT R. EBERL
ENGINEERING MANAGER	GLENN A. ABRAMCZYK

PROJ	REV NO.	DATE	REVISION	PRPD	ENGR	CHK'D	DEM	APPR	OTHER	OTHER	OTHER
								CUSTOMER			
N/A	Ø	5/16/06	S-SARP-G-00001 SUBMITTAL	KE	KE	PB	SB				

SRS NODE:

FILE PATH:

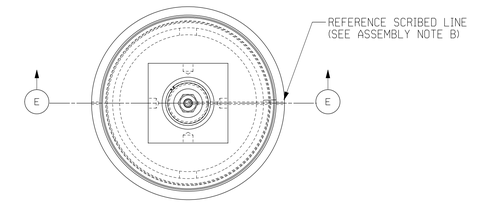

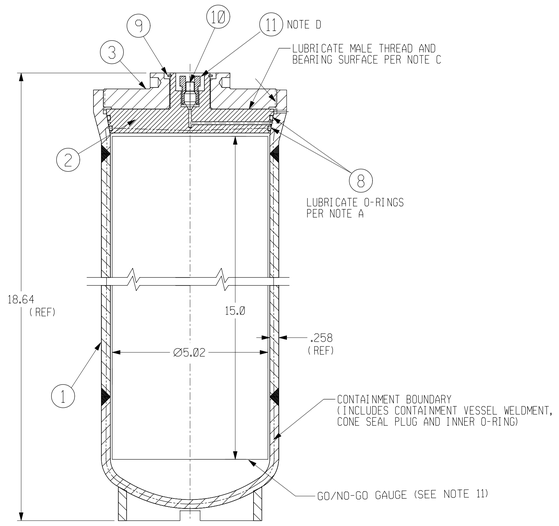

SECTION E-E

FIVE INCH DIAMETER
CONTAINMENT VESSEL SUBASSEMBLY

R-R2-G-00043-A

SCALE: 1/2

(SEE NOTE 11 & 20)

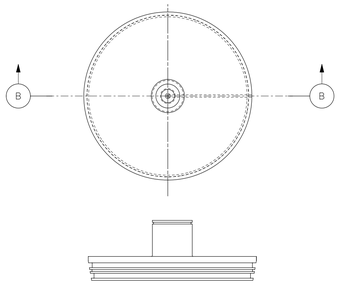

CONE SEAL PLUG

R-R2-G-00043-C

SCALE: 1/2

WEIGHT: 4.6 LBS. (NOTE 14)

(SOME HIDDEN LINES NOT SHOWN FOR CLARITY)

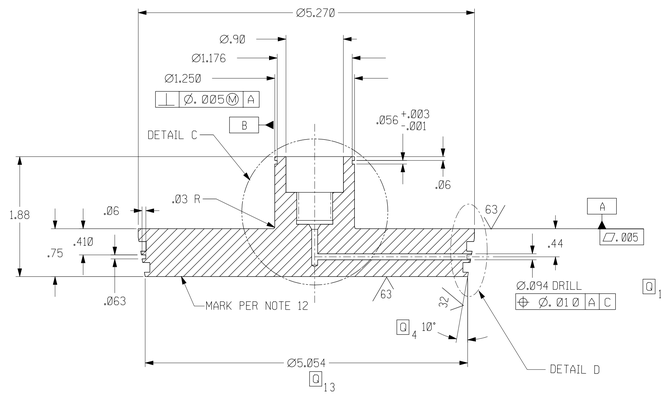

SECTION B-B

SCALE: FULL

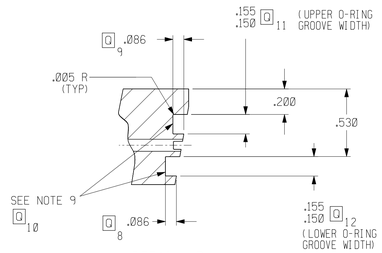

DETAIL D

SCALE: 2/1

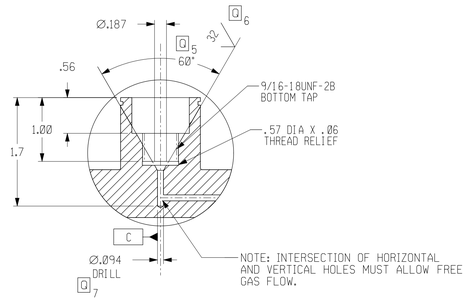

DETAIL C

SCALE: FULL

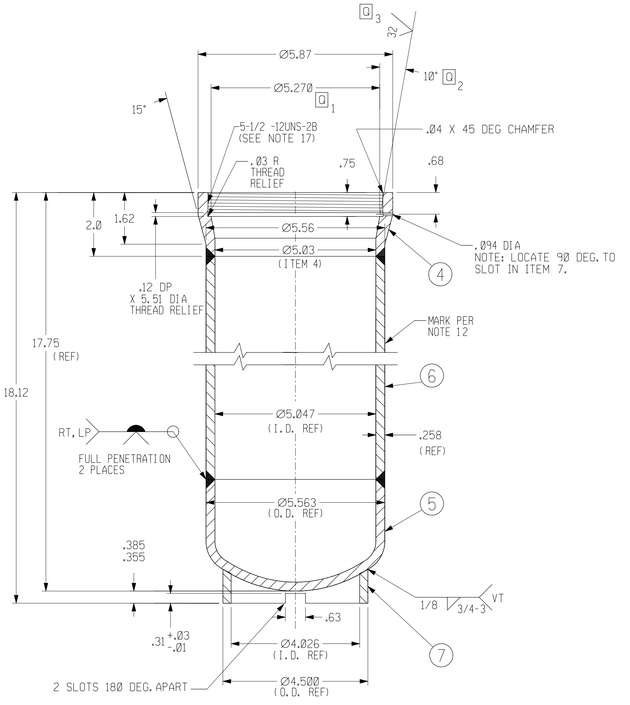

SECTION VIEW

SCALE: 1/2

CONTAINMENT VESSEL WELDMENT

R-R2-G-00043-B

WEIGHT: 23.1 LBS. (NOTE 14)

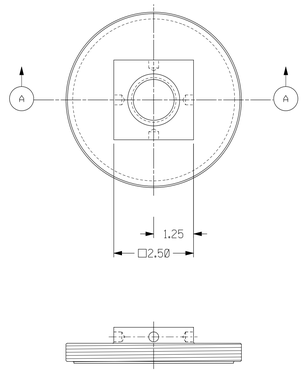

CONE SEAL NUT

R-R2-G-00043-D

SCALE: 1/2

WEIGHT: 4.4 LBS. (NOTE 14)

(SOME HIDDEN LINES NOT SHOWN FOR CLARITY)

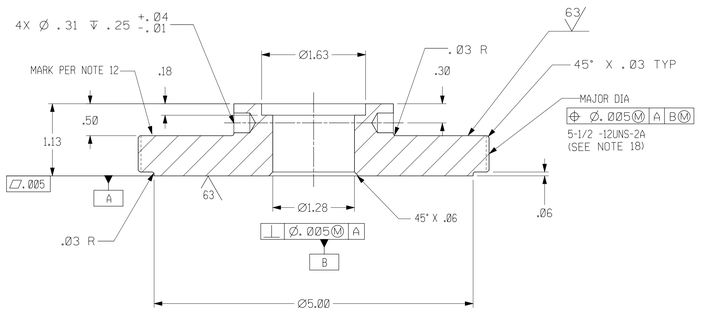

SECTION A-A

SCALE: FULL

14

FABRICATION AND TESTING NOTES:

1. ALL WELDS MUST MEET THE REQUIREMENTS OF APPLICABLE CODES AND STANDARDS AS DESCRIBED ON THIS DRAWING.
2. DRAFTING IS IN ACCORDANCE WITH ANSI, AWS AND ASME STANDARDS WHEN APPLICABLE (I.E, ANSI Y14.5, ANSI/AWS A2.4).
3. ANY ITEM SPECIFIED AS HAVING AN ACCEPTABLE EQUIVALENT MUST BE APPROVED BY THE DESIGN AGENCY SRPT.
4. STAINLESS STEEL MATERIALS TO BE IN ACCORDANCE WITH ASME B&PVC SECTION III, DIV. 1, SUBSECTION NB-2000.
5. ALL WELDS SHALL BE MADE USING FILLER METAL IN ACCORDANCE WITH ASME B&PVC SECTION III, DIV. 1, SUBSECTION NB-2400. WELDING PROCEDURES AND WELDERS SHALL BE QUALIFIED IN ACCORDANCE WITH ASME B&PVC SECTION IX. WELDING AND FABRICATION SHALL BE IN ACCORDANCE WITH ASME B&PVC SECTION III. DIV. 1, SUBSECTION NB-4000.
6. ALL WELDS SHALL BE INSPECTED IN ACCORDANCE WITH ASME B&PVC SECTION III, DIV. 1, SUBSECTION NB-5000.
7. FEATURES MARKED WITH A Q HAVE QUALITY REQUIREMENTS DEFINED IN S-SARP-G-00001.
8. THE CONTAINMENT VESSEL WELDMENT (ITEM 1) SHALL BE GLASS BEAD BLASTED WITH AE BEAD FOLLOWING ALL NDE, LEAK TESTING AND HYDROSTATIC TESTING EXCEPT THREAD AND SEALING SURFACES.
9. Q10 ENTIRE SURFACE OF UPPER AND LOWER O-RING GROOVES TO BE 32 .
10. A STANDARD WEIGHT 6 INCH SCH 40 PIPE CAP, NOMINAL .280 INCH THICK, 2:1 ELLIPTICAL HEAD, APPROX. WT. 6.4 POUNDS, SHALL BE USED. HEAVIER WEIGHT PIPE CAPS ARE NOT PERMITTED.
11. A 5.02 INCH DIA RIGHT CIRCULAR CYLINDER 15 INCHES LONG SHALL FIT IN THE INTERNAL CAVITY OF EACH ASSEMBLED AND SEALED CONTAINMENT VESSEL.
12. CONTAINMENT VESSEL WELDMENT, CONE SEAL NUT AND CONE SEAL PLUG SHALL BE MARKED ON THE SURFACES INDICATED WITH THE FOLLOWING INFORMATION: LAST FOUR DIGITS AND LETTER OF THEPART NUMBER, DRAWING REVISION AND SERIAL NUMBER (E.G., 0043-A R0 SN0001). SERIAL NUMBERS ARE TO BE FURNISHED BY THE OWNER. LETTER SIZE TO BE 5/16" HEIGHT CHARACTERS. MARKING METHOD TO BE BY ELECTRICAL CHEMICAL ETCH.
13. ALL METAL PARTS SHALL BE CLEANED AND DEGREASED PER ASTM A-380 AFTER COMPLETION OF ALL FABRICATION AND QA/QC REQUIREMENTS.
14. CALCULATED WEIGHTS ARE BASED ON NOMINAL DIMENSIONS OF PARTS.
15. THE CONTAINMENT VESSEL SHALL SATISFACTORILY PASS THE HYDROSTATIC TEST REQUIREMENTS DEFINED IN ACCORDANCE WITH ARTICLE NB-6200 OF THE 2004 ASME BOILER & PRESSURE VESSEL CODE, SECTION III. THE TEST SHALL BE CONDUCTED AT 1365 (+/- 10) PSIG.
16. THE CONTAINMENT VESSEL SHALL BE LEAK TIGHT PER ANSI N14.5.
17. INTERNAL THREADS SHALL PASS CLASS 2B TOLERANCE GO/NO-GO PLUG GAUGE.
18. EXTERNAL THREADS SHALL PASS CLASS 2A TOLERANCE GO/NO-GO RING GAUGE.
19. ITEM 4, 5 & 6 SHALL BE EXAMINED IN ACCORDANCE WITH SUBARTICLE NB-2500 OF THE 2004 ASME BOILER AND PRESSURE VESSEL CODE, SECTION III.
20. CONTAINMENT VESSEL SUBASSEMBLY SPECIFICATIONS:

NOMINAL WEIGHT (LBS) (NOTE 14)	APPROX INTERNAL VOLUME (IN 3)	DESIGN PRESSURE (PSI)	DESIGN TEMPERATURE (°F)
32	313	900	500

ASSEMBLY NOTES:

A. APPLY DOW CORNING SILICONE HIGH VACUUM GREASE OR EQUIVALENT SPARINGLY TO THE O-RINGS PRIOR TO INSTALLATION.

B. IN SERVICE CV TORQUE REQUIREMENTS: TIGHTEN CV CONE SEAL NUT (ITEM 3) TO 50 FT-LBS (+10 / Ø FT-LBS). VERIFY THAT THE SCRIBED LINE ON THE CONE SEAL NUT IS ALIGNED WITHIN 1 INCH OF THE SCRIBED REFERENCE LINE ON THE CV AS DESCRIBED IN S-SARP-G-00001.

C. CONE SEAL NUT THREADS (ITEM 3) AND CONE SEAL NUT/CONE SEAL PLUG MATING SURFACES SHALL BE LUBRICATED WITH DUPONT KRYTOX® GRADE 240AC OR EQUIVALENT.

D. IN SERVICE GLAND NUT TORQUE REQUIREMENTS: TIGHTEN GLAND NUT (ITEM 11) TO 10 FT-LBS (+5/-Ø FT-LBS).

ITEM	PART AND DRAWING NO.	REQD PER ASSY	DESCRIPTION
11	COML	1	GLAND NUT, PPI CATALOG NO. P-130-60, 316L SST, OR EQUIVALENT
10	COML	1	PLUG, PPI CATALOG NO. P-110-60, 316L SST, OR EQUIVALENT
9	COML	1	RETAINING RING, WALDES TRUARC NO. 5108-125
8	COML	2	O-RING, AS-568-252 VITON GLT, PARKER NO. V0835-75
7	R-R2-G-00042-H	1	PIPE, 5 INCH DIA SCH 40, ASME SA-312, GRADE TP-304L
6	R-R2-G-00042-G	1	PIPE, 6 INCH DIA SCH 40, ASME SA-312, GRADE TP-304L, SEAMLESS (NOTE 19)
5	R-R2-G-00042-F	1	PIPE CAP, 6 INCH, STANDARD WEIGHT, ASME SA-403, GRADE 304L WP-W (SEE NOTE 10 & 19)
4	R-R2-G-00042-E	1	STAYED HEAD, MAKE FROM BAR, 7 1/2", ASME SA-479, GRADE 304L (NOTE 19)
3	R-R2-G-00042-D	1	CONE SEAL NUT, ARMCO NITRONIC-60 SST, ASME SA-479 UNS-S21800 BAR, ANNEALED
2	R-R2-G-00042-C	1	CONE SEAL PLUG, 304L SST, ASME SA-479
1	R-R2-G-00042-B	1	CONTAINMENT VESSEL WELDMENT

FINISH 125/ √ ALL MACHINED SURFACES AND BREAK ALL SHARP EDGES UNLESS OTHERWISE SPECIFIED

THE NUMBER IN THE FINISH SYMBOL √ IS THE MAXIMUM ACCEPTABLE ROUGHNESS VALUE IN A.A.MICRO-INCHES.

TOLERANCES ON ALL DIMENSIONS UNLESS OTHERWISE NOTED SHALL BE:
ONE PLACE DECIMAL ±.03 FRACTIONAL ±1/16"
TWO PLACE DECIMAL ±.01 ANGULAR ±0° - 30'
THREE PLACE DECIMAL ±.005

JOB NUMBER 23047

DRAWING NO. R-R2-G-00043 LATEST REVISION Ø

UNCLASSIFIED
DOES NOT CONTAIN
UNCLASSIFIED CONTROLLED
NUCLEAR INFORMATION

ADC & Reviewing Official: P. BLANTON, SRPT PGM. MGR. (Name and Title) 5/16/06 (Date)

THIS DRAWING IS FURNISHED FOR THE UNITED STATES DEPARTMENT OF ENERGY AT THE SAVANNAH RIVER SITE, THE INFORMATION AND KNOW-HOW THEREON MAY NOT BE USED OR REPRODUCED WITHOUT THE WRITTEN PERMISSION OF THE PRIME CONTRACTOR. ALL REPRODUCTIONS IN WHOLE OR PART, INCLUDING ANY VENDOR'S SHOP DRAWINGS, SHALL INCLUDE OR REFER TO THIS NOTE.

UNITED STATES DEPARTMENT OF ENERGY

SRNL™ SAVANNAH RIVER NATIONAL LABORATORY
We Put Science To Work

REFERENCE DRAWINGS

R-R1-G-00021	ASSEMBLY WITH FIVE INCH DIA CV
R-R5-G-00002	DRAWING TREE

REFERENCE STANDARDS

BLDG NO.	SITE CLEARANCE NO.	DA NO.	DESIGN GROUP
OFFSITE	N/A	N/A	SRNL/EES

TITLE

9977

GENERAL PURPOSE FISSILE PACKAGING

FIVE INCH DIAMETER
CONTAINMENT VESSEL
SUBASSEMBLY
(U)

SCALE	SRS DRAWING NO.	SHEET NO.	LATEST REV
AS NOTED	N/A	1 OF 1	Ø

THIS DRAWING CONTAINS INFORMATION ON SHIPPING PACKAGES FOR RADIOACTIVE MATERIAL
REVISIONS REQUIRE PRIOR APPROVAL OF DESIGN AGENCY
(SRNL PACKAGING TECHNOLOGY GROUP)

RESPONSIBLE ENGINEER: KURT R. EBERL
ENGINEERING MANAGER: GLENN A. ABRAMCZYK

PROJ	REV NO.	DATE	REVISION	PRPD	ENGR	CHK'D	DEM	APPR CUSTOMER	OTHER	OTHER	OTHER
N/A	Ø	5/16/06	S-SARP-G-00001 SUBMITTAL	KE/MP	KE	PB	SB				

SRS NODE: FILE PATH:

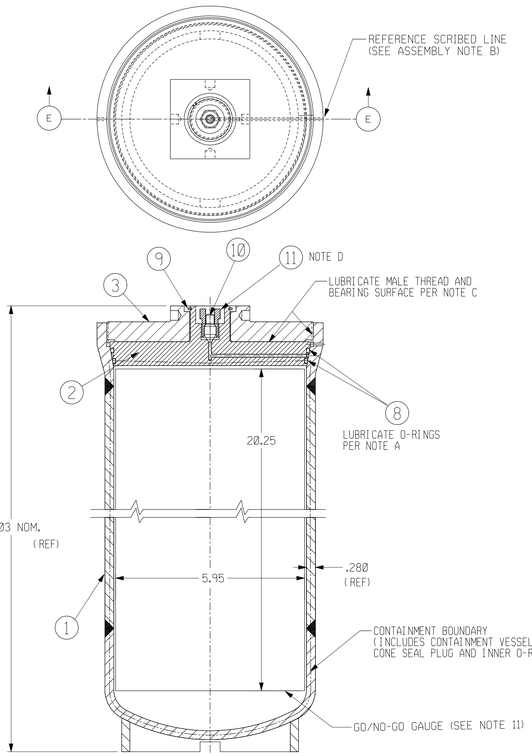

SECTION E-E

SIX INCH DIAMETER
CONTAINMENT VESSEL SUBASSEMBLY

R-R2-G-00042-A

SCALE: 1/2

(SEE NOTE 11 AND NOTE 20)

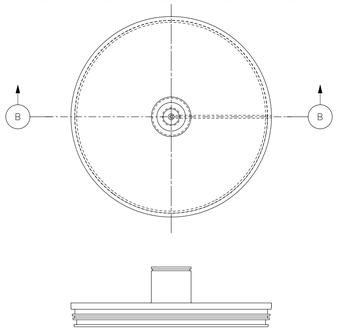

CONE SEAL PLUG

R-R2-G-00042-C

SCALE: 1/2

WEIGHT: 6.6 LBS. (NOTE 14)

(SOME HIDDEN LINES NOT SHOWN FOR CLARITY.)

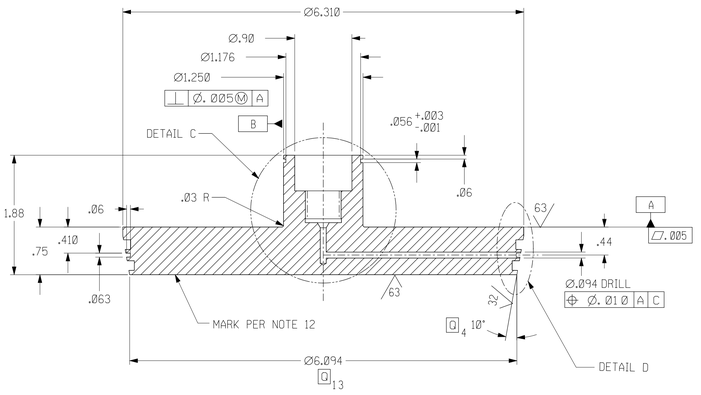

SECTION B-B

SCALE: FULL

FABRICATION AND TESTING NOTES:

1. ALL WELDS MUST MEET THE REQUIREMENTS OF APPLICABLE CODES AND STANDARDS AS DESCRIBED ON THIS DRAWING.
2. DRAFTING IS IN ACCORDANCE WITH ANSI 14.5, ANSI/AWS A2.4 AND ASME STANDARDS AS APPLICABLE.
3. ANY ITEM SPECIFIED AS HAVING AN ACCEPTABLE EQUIVALENT MUST BE APPROVED BY THE DESIGN AGENCY, SRPT.
4. STAINLESS STEEL MATERIALS TO BE IN ACCORDANCE WITH ASME B&PVC SECTION III, DIV. 1, SUBSECTION NB-2000.
5. ALL WELDS SHALL BE MADE USING FILLER METAL IN ACCORDANCE WITH ASME B&PVC SECTION III, DIV. 1, SUBSECTION NB-2400. WELDING PROCEDURES AND WELDERS SHALL BE QUALIFIED IN ACCORDANCE WITH ASME B&PVC SECTION IX. WELDING AND FABRICATION SHALL BE IN ACCORDANCE WITH ASME B&PVC SECTION III. DIV. 1, SUBSECTION NB-4000.
6. ALL WELDS SHALL BE INSPECTED IN ACCORDANCE WITH ASME B&PVC SECTION III, DIV. 1, SUBSECTION NB-5000.
7. FEATURES MARKED WITH A Q HAVE QUALITY REQUIREMENTS DEFINED IN S-SARP-G-00001.
8. THE CONTAINMENT VESSEL WELDMENT (ITEM 1) SHALL BE GLASS BEAD BLASTED WITH AE BEAD FOLLOWING ALL NDE, LEAK TESTING AND HYDROSTATIC TESTING EXCEPT THREAD AND SEALING SURFACES.
9. Q10 ENTIRE SURFACE OF UPPER AND LOWER O-RING GROOVES TO BE 32 .
10. A STANDARD WEIGHT 6 INCH SCH 40 PIPE CAP, NOMINAL .280 INCH THICK, 2:1 ELLIPTICAL HEAD, APPROX. WT. 6.4 POUNDS, SHALL BE USED. HEAVIER WEIGHT PIPE CAPS ARE NOT PERMITTED.
11. A 5.95 INCH DIA RIGHT CIRCULAR CYLINDER 20.25 INCHES LONG SHALL FIT IN THE INTERNAL CAVITY OF EACH ASSEMBLED AND SEALED CONTAINMENT VESSEL.
12. CONTAINMENT VESSEL WELDMENT, CONE SEAL NUT AND CONE SEAL PLUG SHALL BE MARKED ON THE SURFACES AS INDICATED WITH THE FOLLOWING INFORMATION: LAST FOUR DIGITS AND LETTER OF THE PART NUMBER, DRAWING REVISION AND SERIAL NUMBER (E.G., Ø042-A RØ SNØØØ1). SERIAL NUMBERS ARE TO BE FURNISHED BY THE OWNER. LETTER SIZE TO BE5/16" HEIGHT CHARACTERS. MARKING METHOD TO BE BY ELECTRICAL CHEMICAL ETCH.
13. ALL METAL PARTS SHALL BE CLEANED AND DEGREASED PER ASTM A-380 AFTER COMPLETION OF ALL FABRICATION AND QA/QC REQUIREMENTS.
14. CALCULATED WEIGHTS ARE BASED ON NOMINAL DIMENSIONS OF PARTS.
15. THE CONTAINMENT VESSEL SHALL SATISFACTORILY PASS THE HYDROSTATIC TEST REQUIREMENTS DEFINED IN ACCORDANCE WITH ARTICLE NB-6200 OF THE 2004 ASME BOILER & PRESSURE VESSEL CODE, SECTION III. THE TEST SHALL BE CONDUCTED AT 1235 (+/- 10) PSIG.
16. THE CONTAINMENT VESSEL SHALL BE LEAK TIGHT PER ANSI N14.5.
17. INTERNAL THREADS SHALL PASS CLASS 2B TOLERANCE GO/NO-GO PLUG GAUGE.
18. EXTERNAL THREADS SHALL PASS CLASS 2A TOLERANCE GO/NO-GO RING GAUGE.
19. ITEMS 4, 5 & 6 SHALL BE EXAMINED IN ACCORDANCE WITH SUBARTICLE NB-2500 OF THE 2004 ASME BOILER AND PRESSURE VESSEL CODE, SECTION III.
20. CONTAINMENT VESSEL SUBASSEMBLY SPECIFICATIONS:

NOMINAL WEIGHT (LBS.) (NOTE 14)	APPROX INTERNAL VOLUME (IN 3)	DESIGN PRESSURE (PSI)	DESIGN TEMPERATURE (°F)
52.2	608	800	300

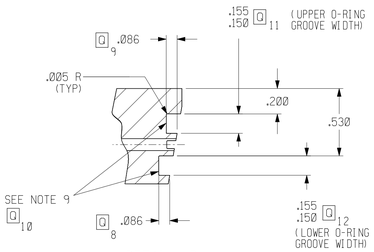

DETAIL D

SCALE: 2/1

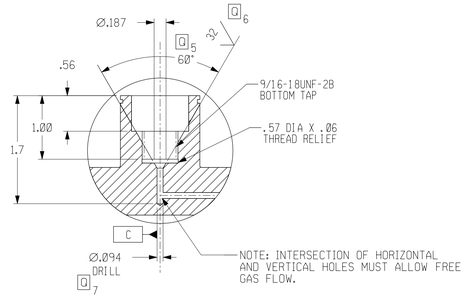

DETAIL C

SCALE: FULL

ASSEMBLY NOTES:

A. APPLY DOW CORNING SILICONE HIGH VACUUM GREASE OR EQUIVALENT SPARINGLY TO THE O-RINGS PRIOR TO INSTALLATION.

B. IN SERVICE CV TORQUE REQUIREMENTS: TIGHTEN CV CONE SEAL NUT (ITEM 3) TO 100 FT-LBS (+20 / Ø FT-LBS). VERIFY THAT THE SCRIBE LINE ON THE CONE SEAL NUT IS ALIGNED WITHIN 1 INCH OF THE SCRIBED REFERENCE LINE ON THE CV AS DESCRIBED IN S-SARP-G-00001.

C. CONE SEAL NUT THREADS (ITEM 3) AND CONE SEAL NUT/CONE SEAL PLUG MATING SURFACES SHALL BE LUBRICATED WITH DUPONT KRYTOX® GRADE 240AC OR EQUIVALENT.

D. IN SERVICE GLAND NUT TORQUE REQUIREMENTS: TIGHTEN GLAND NUT (ITEM 11) TO 10 FT-LBS (+5/-Ø FT-LBS).

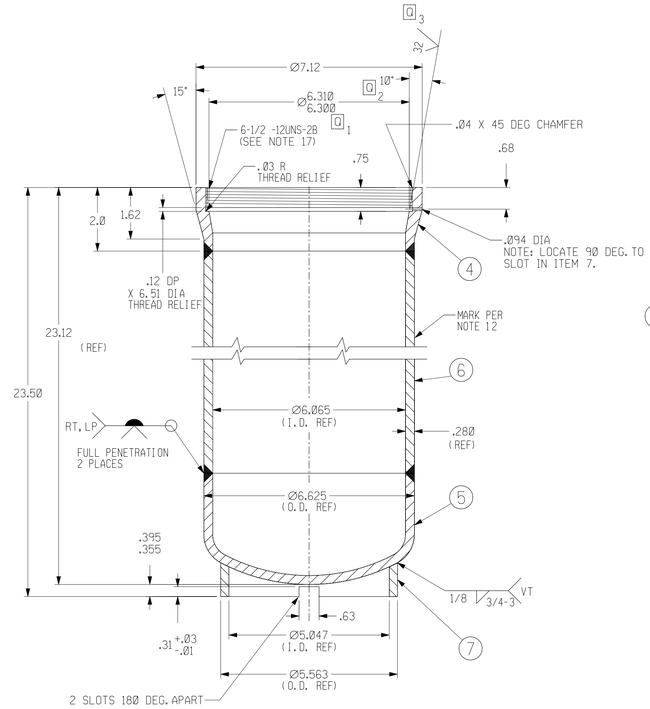

SECTION VIEW

SCALE: 1/2

CONTAINMENT VESSEL WELDMENT

R-R2-G-00042-B

WEIGHT: 40 LBS. (NOTE 14)

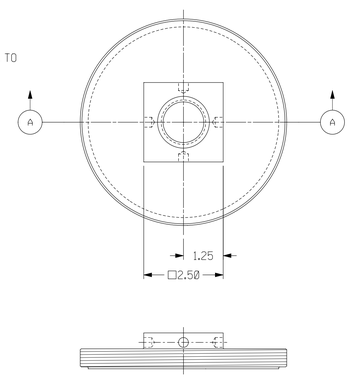

CONE SEAL NUT

R-R2-G-00042-D

SCALE: 1/2

WEIGHT: 6.1 LBS. (NOTE 14)

(SOME HIDDEN LINES NOT SHOWN FOR CLARITY.)

Q 14

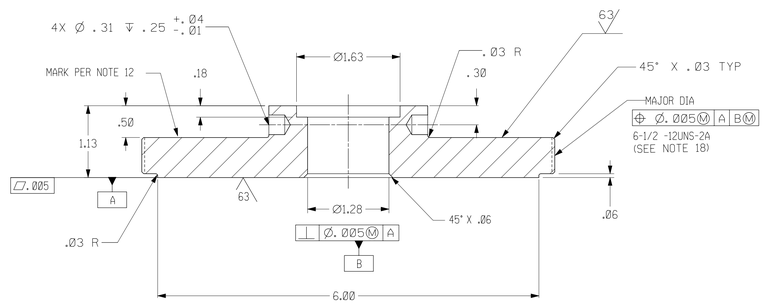

SECTION A-A

SCALE: FULL

UNCLASSIFIED
DOES NOT CONTAIN
UNCLASSIFIED CONTROLLED
NUCLEAR INFORMATION

ADC & Reviewing Official: P. BLANTON, SRPT PCM, MGR.
(Name and Title)
Date: 5/16/06

THIS DRAWING CONTAINS INFORMATION ON SHIPPING PACKAGES FOR RADIOACTIVE MATERIAL
REVISIONS REQUIRE PRIOR APPROVAL OF DESIGN AGENCY
(SRNL PACKAGING TECHNOLOGY GROUP)

RESPONSIBLE ENGINEER	KURT R. EBERL
ENGINEERING MANAGER	GLENN A. ABRAMCZYK

PROJ	REV NO.	DATE	REVISION	PPD	ENGR	CHK'D	DEM	APPR CUSTOMER	OTHER	OTHER	OTHER
N/A	Ø	5/16/06	S-SARP-G-00001 SUBMITTAL	KE/MP	KE	PB	SB				

R-R1-G-00020	ASSEMBLY WITH SIX INCH DIA CV
R-R5-G-00002	DRAWING TREE

REFERENCE STANDARDS

ITEM	PART AND DRAWING NO.	REQD PER ASSY	DESCRIPTION
11	COML	1	GLAND NUT, PPI CATALOG NO. P-130-60, 316L SST, OR EQUIVALENT
10	COML	1	PLUG, PPI CATALOG NO. P-110-60, 316L SST, OR EQUIVALENT
9	COML	1	RETAINING RING, WALDES TRUARC NO. 5108-125
8	COML	2	O-RING, AS-568-252 VITON GLT, PARKER NO. V0835-75
7	R-R2-G-00042-H	1	PIPE, 5 INCH DIA SCH 40, ASME SA-312, GRADE TP-304L
6	R-R2-G-00042-G	1	PIPE, 6 INCH DIA SCH 40, ASME SA-312, GRADE TP-304L, SEAMLESS (NOTE 19)
5	R-R2-G-00042-F	1	PIPE CAP, 6 INCH, STANDARD WEIGHT, ASME SA-403, GRADE 304L WP-W (SEE NOTE 10 & 19)
4	R-R2-G-00042-E	1	STAYED HEAD, MAKE FROM BAR, 7 1/2", ASME SA-479, GRADE 304L (NOTE 19)
3	R-R2-G-00042-D	1	CONE SEAL NUT, ARMCO NITRONIC-60 SST, ASME SA-479 UNS-S21800 BAR, ANNEALED
2	R-R2-G-00042-C	1	CONE SEAL PLUG, 304L SST, ASME SA-479
1	R-R2-G-00042-B	1	CONTAINMENT VESSEL WELDMENT

FINISH 125 ALL MACHINED SURFACES AND BREAK ALL SHARP EDGES UNLESS OTHERWISE SPECIFIED

THE NUMBER IN THE FINISH SYMBOL ✓ IS THE MAXIMUM ACCEPTABLE ROUGHNESS VALUE IN AA MICRO-INCHES.

TOLERANCES ON ALL DIMENSIONS UNLESS OTHERWISE NOTED SHALL BE:
ONE PLACE DECIMAL ±.03 FRACTIONAL ±1/16"
TWO PLACE DECIMAL ±.01 ANGULAR ±Ø° - 30'
THREE PLACE DECIMAL ±.005

JOB NUMBER 23047
DRAWING NO. R-R2-G-00042
LATEST REVISION Ø

UNITED STATES DEPARTMENT OF ENERGY

SRNL SAVANNAH RIVER NATIONAL LABORATORY™
We Put Science To Work

BLDG NO.	SITE CLEARANCE NO.	DA NO.	DESIGN GROUP
OFFSITE	N/A	N/A	SRNL/EES

TITLE

9977

GENERAL PURPOSE FISSILE PACKAGING

SIX INCH DIAMETER
CONTAINMENT VESSEL
SUBASSEMBLY
(U)

SCALE	SRS DRAWING NO.	SHEET NO.	LATEST REV
AS NOTED	N/A	1 OF 1	Ø

SRS NODE: FILE PATH:

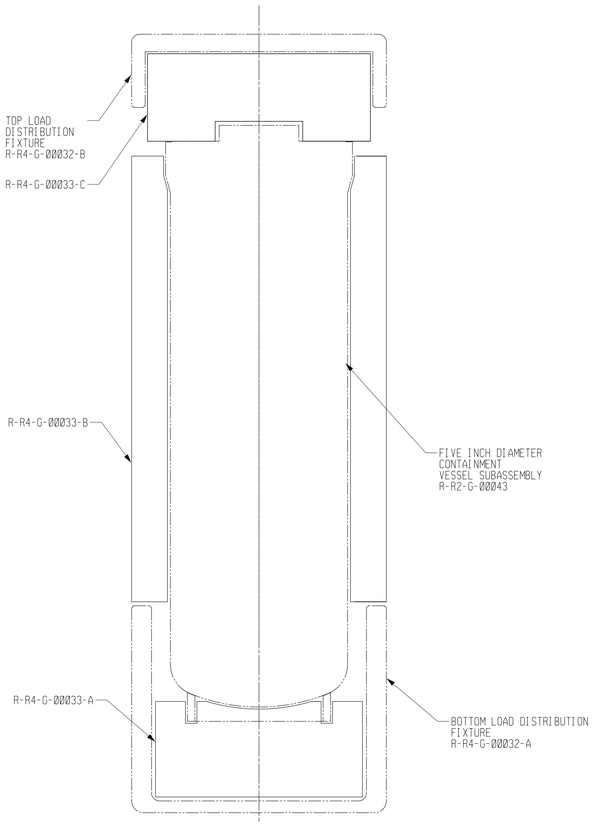

SPACER CONFIGURATION

SCALE 1/2

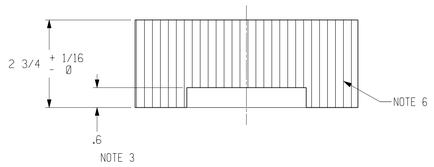

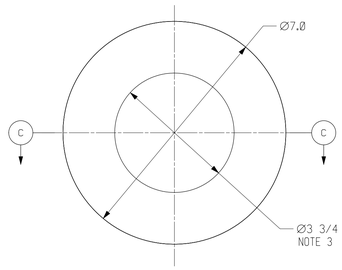

SECTION C-C

SCALE 1/2

UPPER SPACER

R-R4-G-00033-C

WEIGHT: Ø.7 LBS. (NOTE 1)

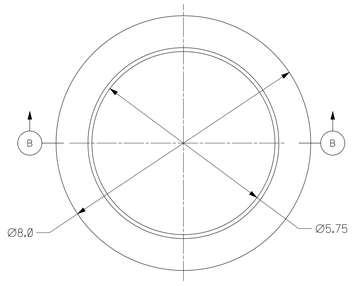

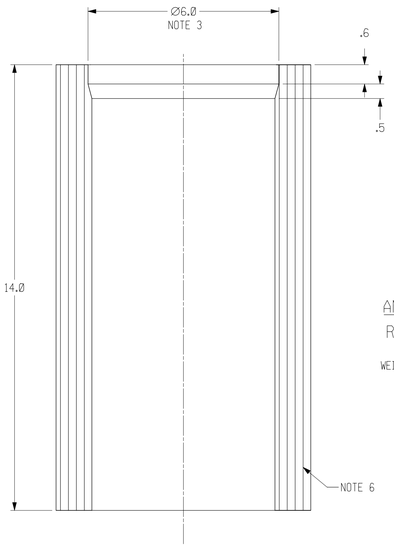

SECTION B-B

SCALE 1/2

ANNULAR SPACER

R-R4-G-00033-B

WEIGHT: 2.4 LBS. (NOTE 1)

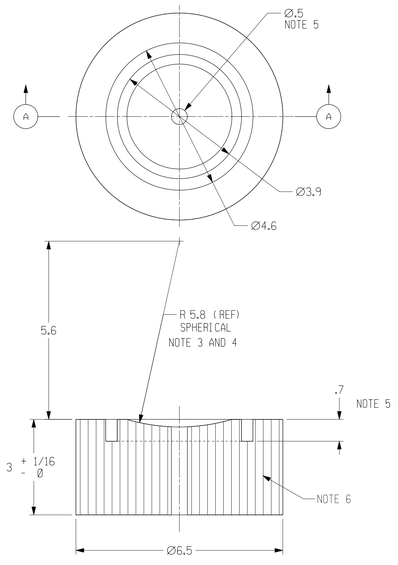

SECTION A-A

SCALE 1/2

LOWER SPACER

R-R4-G-00033-A

WEIGHT: Ø.7 LBS. (NOTE 1)

NOTES:

1. WEIGHTS ARE CALCULATED BASED ON NOMINAL DIMENSIONS OF PARTS. WEIGHTS BASED ON UNCRUSHED BULK DENSITY OF 12 PCF.
2. ALUMINUM TUBE HONEYCOMB MATERIAL (OR EQUIVALENT) SHALL BE PRECRUSHED, 3 MIL MINIMUM FOIL, CRUSH STRENGTH 1500 +/- 500 PSI.
3. CONTOUR TO BE CRUSHED TO DIMENSION SHOWN. TOLERANCE OF +/- 1/16 INCH ALLOWED FOR RECESSED FEATURES. CONTOUR MATCHES TOP OF THE CONE SEAL NUT OF 5 INCH CONTAINMENT VESSEL.
4. CONTOUR TO BE WITHIN +/- 1/16 INCH OF THE OUTSIDE BOTTOM OF THE 5 INCH CONTAINMENT VESSEL, A 5" SCHEDULE 40 PIPE CAP (R-R2-G-00043-F).
5. OPTIONAL THROUGH HOLE (.5 " DIAMETER MAX) MAY BE USED FOR EASE OF FABRICATION.
6. HONEYCOMB CELL AXIS TO BE ORIENTED IN THE DIRECTION AS SHOWN, PARALLEL TO THE AXIS OF THE CYLINDER.

NOTE:
DRAFTING IN ACCORDANCE WITH ANSI Y14.5, ANSI/AWS A2.4 AND ASME STANDARDS AS APPLICABLE.

ITEM	PART AND DRAWING NO.	REQD PER ASSY	DESCRIPTION
3	R-R4-G-00033-C	1	UPPER SPACER, ALUMINUM TUBE HONEYCOMB, ALLOY 1100 (NOTES 1 AND 2)
2	R-R4-G-00033-B	1	ANNULAR SPACER, ALUMINUM TUBE HONEYCOMB, ALLOY 1100 (NOTES 1 AND 2)
1	R-R4-G-00033-A	1	LOWER SPACER, ALUMINUM TUBE HONEYCOMB, ALLOY 1100 (NOTES 1 AND 2)

FINISH 125/ ALL MACHINED SURFACES AND BREAK ALL SHARP EDGES UNLESS OTHERWISE SPECIFIED

THE NUMBER IN THE FINISH SYMBOL √ IS THE MAXIMUM ACCEPTABLE ROUGHNESS VALUE IN AA(MICRO)-INCHES.

TOLERANCES ON ALL DIMENSIONS UNLESS OTHERWISE NOTED SHALL BE:

ONE PLACE DECIMAL	±.03	FRACTIONAL	±1/16"
TWO PLACE DECIMAL	±.01	ANGULAR	±0° - 30'
THREE PLACE DECIMAL	±.005		

JOB NUMBER 23047

DRAWING NO. R-R4-G-00033 LATEST REVISION Ø

UNCLASSIFIED
DOES NOT CONTAIN UNCLASSIFIED CONTROLLED NUCLEAR INFORMATION

ADC & Reviewing Official: P. BLANTON, SRPT PGM. MGR. (Name and Title)

Date: 5/16/06

THIS DRAWING CONTAINS INFORMATION ON SHIPPING PACKAGES FOR RADIOACTIVE MATERIAL
REVISIONS REQUIRE PRIOR APPROVAL OF DESIGN AGENCY
(SRNL PACKAGING TECHNOLOGY GROUP)

RESPONSIBLE ENGINEER	KURT R. EBERL
ENGINEERING MANAGER	GLENN A. ABRAMCZYK

PROJ	REV NO.	DATE	REVISION	PRPD	ENGR	CHK'D	DEM	APPR CUSTOMER	OTHER	OTHER	OTHER
N/A	Ø	5/16/06	S-SARP-G-00001 SUBMITTAL	KE	KE	PB	SB				

UNITED STATES DEPARTMENT OF ENERGY

SRNL SAVANNAH RIVER NATIONAL LABORATORY

We Put Science To Work

REFERENCE DRAWINGS

R-R1-G-00021	ASSEMBLY WITH FIVE INCH DIA CV
R-R5-G-00002	DRAWING TREE

REFERENCE STANDARDS

BLOG NO.	SITE CLEARANCE NO.	DA NO.	DESIGN GROUP
OFFSITE	N/A	N/A	SRNL/EES

TITLE

9977

GENERAL PURPOSE FISSILE PACKAGING

SPACER PART DETAILS FOR FIVE INCH CONTAINMENT VESSEL (U)

SCALE	SRS DRAWING NO.	SHEET NO.	LATEST REV
	N/A	1 OF 1	Ø

SRS NODE:

FILE PATH:

NOTES:

1. WEIGHTS ARE CALCULATED BASED ON NOMINAL DIMENSIONS OF PARTS.
2. MATERIAL PER ASME BOILER & PRESSURE VESSEL CODE, SECTION VIII, DIVISION 1.

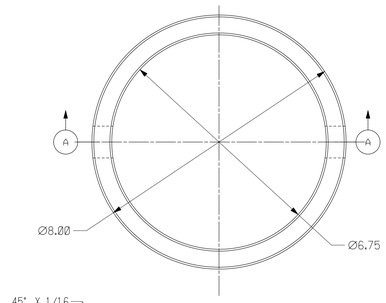

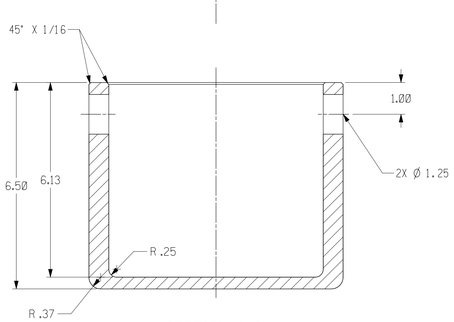

SECTION A-A

SCALE 1/2

BOTTOM LOAD DISTRIBUTION FIXTURE

R-R4-G-ØØØ32-A

WEIGHT: 1Ø.3 LBS. (NOTE 1)

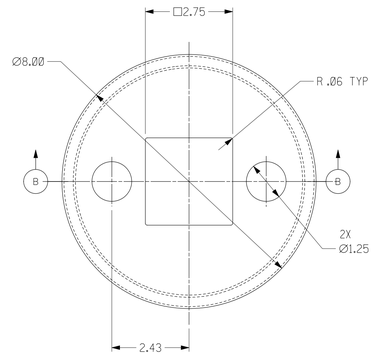

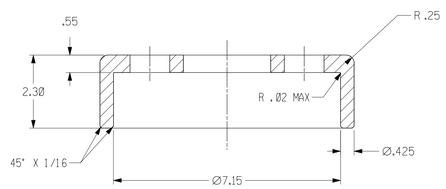

SECTION B-B

SCALE 1/2

TOP LOAD DISTRIBUTION FIXTURE

R-R4-G-ØØØ32-B

WEIGHT: 3.9 LBS. (NOTE 1)

NOTE:
DRAFTING IN ACCORDANCE WITH ANSI Y14.5, ANSI/AWS A2.4 AND ASME STANDARDS WHEN APPLICABLE.

ITEM	PART AND DRAWING NO.	REQD PER ASSY	DESCRIPTION
2	R-R4-G-ØØØ32-B	1	TOP LOAD DISTRIBUTION FIXTURE, 6061-T6 ALUMINUM PER ASME SB-221 (NOTE 2)
1	R-R4-G-ØØØ32-A	1	BOTTOM LOAD DISTRUBUTION FIXTURE, 6061-T6 ALUMINUM PER ASME SB-221 (NOTE 2)

FINISH 125/ ALL MACHINED SURFACES AND BREAK ALL SHARP EDGES UNLESS OTHERWISE SPECIFIED

THE NUMBER IN THE FINISH SYMBOL √ IS THE MAXIMUM ACCEPTABLE ROUGHNESS VALUE IN AA/MICRO-INCHES.

TOLERANCES ON ALL DIMENSIONS UNLESS OTHERWISE NOTED SHALL BE:

ONE PLACE DECIMAL ±.Ø3 FRACTIONAL ±1/16°
TWO PLACE DECIMAL ±.Ø1 ANGULAR ±Ø° - 3Ø'
THREE PLACE DECIMAL ±.ØØ5

JOB NUMBER 23Ø47

DRAWING NO. R-R4-G-ØØØ32 LATEST REVISION Ø

UNCLASSIFIED
DOES NOT CONTAIN UNCLASSIFIED CONTROLLED NUCLEAR INFORMATION

ADC & Reviewing Official: P. BLANTON, SRPT PGM. MGR. (Name and Title)

Date: 5/16/Ø6

THIS DRAWING CONTAINS INFORMATION ON SHIPPING PACKAGES FOR RADIOACTIVE MATERIAL
REVISIONS REQUIRE PRIOR APPROVAL OF DESIGN AGENCY
(SRNL PACKAGING TECHNOLOGY GROUP)

RESPONSIBLE ENGINEER	KURT R. EBERL
ENGINEERING MANAGER	GLENN A. ABRAMCZYK

PROJ	REV NO.	DATE	REVISION	PRPD	ENGR	CHK'D	DEM	APPR	OTHER	OTHER	OTHER
N/A	Ø	5/16/Ø6	S-SARP-G-ØØØØ1 SUBMITTAL	KE	KE	PB	SB	CUSTOMER			

REFERENCE DRAWINGS

R-R1-G-ØØØ2Ø	ASSEMBLY WITH SIX INCH DIA CV
R-R5-G-ØØØØ2	DRAWING TREE

REFERENCE STANDARDS

UNITED STATES DEPARTMENT OF ENERGY

SRNL™ SAVANNAH RIVER NATIONAL LABORATORY

We Put Science To Work

BLDG NO.	SITE CLEARANCE NO.	DA NO.	DESIGN GROUP
OFFSITE	N/A	N/A	SRNL/EES

TITLE

9977

GENERAL PURPOSE FISSILE PACKAGING

LOAD DISTRIBUTION FIXTURES DETAILS (U)

SCALE	SRS DRAWING NO.	SHEET NO.	LATEST REV
	N/A	1 OF 1	Ø

SRS NODE: FILE PATH:

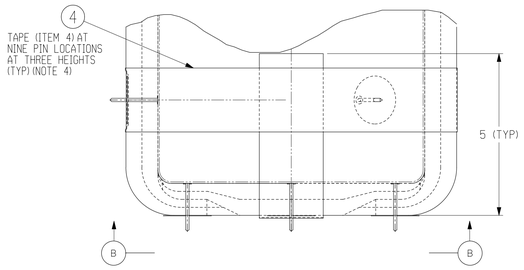

INSULATING BLANKET
TAPE INSTALLATION
DETAILS

SCALE: 1/2

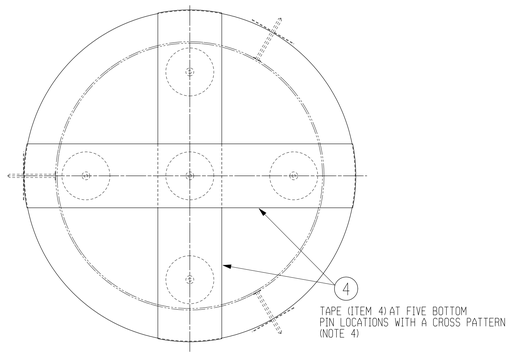

VIEW B-B

SCALE: 1/2

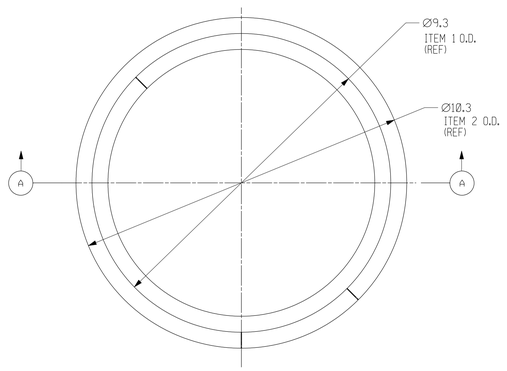

NOTES:

1. FIBERFRAX INSULATION SPECIFICATIONS MANUFACTURER: UNIFRAX CORPORATION, 2351 WHIRLPOOL ST., NIAGRA FALLS, NY PRODUCT TRADE NAME: LTC HSA SYSTEMS PRODUCT GROUP: REFRACTORY CERAMIC FIBER PRODUCT CHEMICAL NAME: VITREOUS ALUMINOSILICATE FIBER 1/2" THICK QUILTED COMPOSITE PER KCP SS-R51507 (SGT TRAILERS) DENSITY: 5-7 PCF.
2. NOMINAL WIDTH OF INSULATION ITEM 1 (TO BE WRAPPED AROUND OUTSIDE OF DRUM LINER (R-R2-G-00017-D)) IS ESTIMATED TO BE 29.4 INCHES. ENDS SHALL BUTT TOGETHER UPON WRAPPING INTO A CYLINDER.
3. NOMINAL WIDTH OF INSULATION ITEM 2 (TO BE WRAPPED AROUND OUTSIDE OF INNER SIDE INSULATION (R-R2-G-00019-B)) IS ESTIMATED TO BE 32.5 INCHES. ENDS SHALL BUTT TOGETHER UPON WRAPPING INTO A CYLINDRICAL SHAPE.
4. AFTER INSULATION (ITEMS 1, 2 AND 3) ARE WRAPPED AROUND DRUM LINER AS SHOWN AND SECURED WITH WASHERS (ITEM 14 OF R-R2-G-00017). FIBERGLASS TAPE (ITEM 4) IS TO BE USED TO TO SECURE THE INSULATION AND WASHERS IN PLACE. FIBERGLASS TAPE TO BE APPLIED AS SHOWN ON THIS DRAWING. IF REQUIRED BY THE FABRICATOR, ADDITIONAL TAPE MAY BE USED.
5. INSULATING BLANKET SUBASSEMBLY AND DETAILS ON THIS DRAWING DEPICT THE REQUIRED CONFIGURATION OF FINAL ASSEMBLY. INSTALLATION PROCEDURES SHALL BE DEVELOPED BY FABRICATOR AND REVIEWED AND APPROVED BY SRPT.

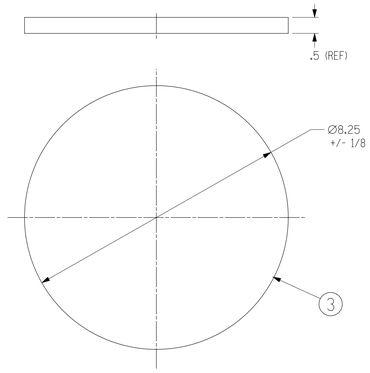

INSULATION, BOTTOM

R-R2-G-00019-D

SCALE 1/2

NOTE 1

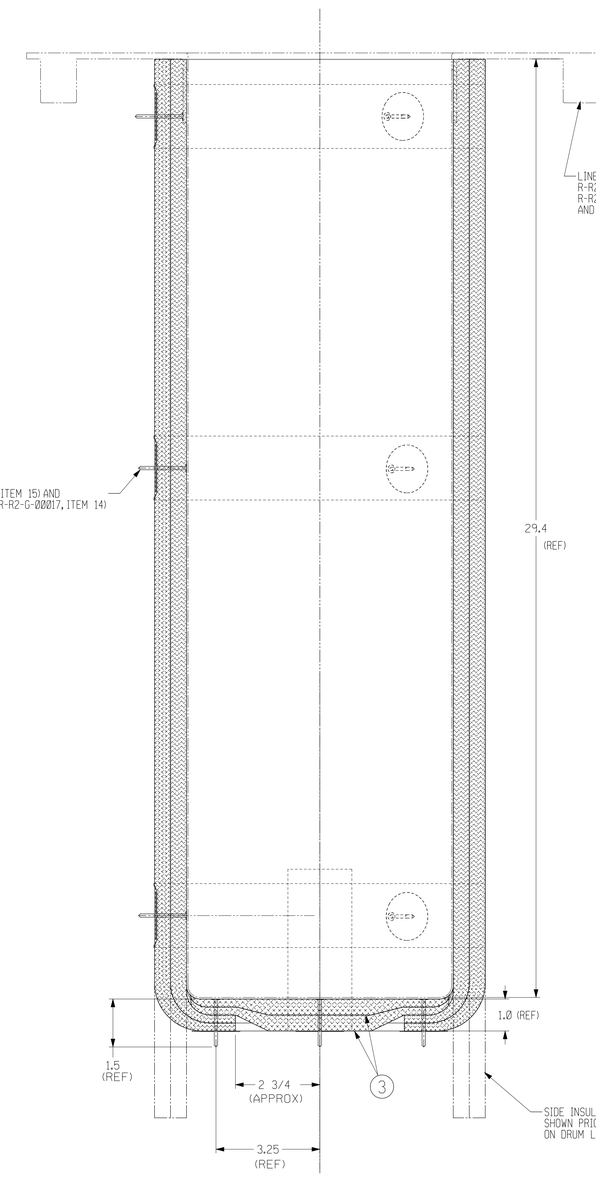

INSULATING BLANKET SUBASSEMBLY

R-R2-G-00019-A

SCALE: 1/2

(SHOWN SECTIONED THROUGH THE CENTER)

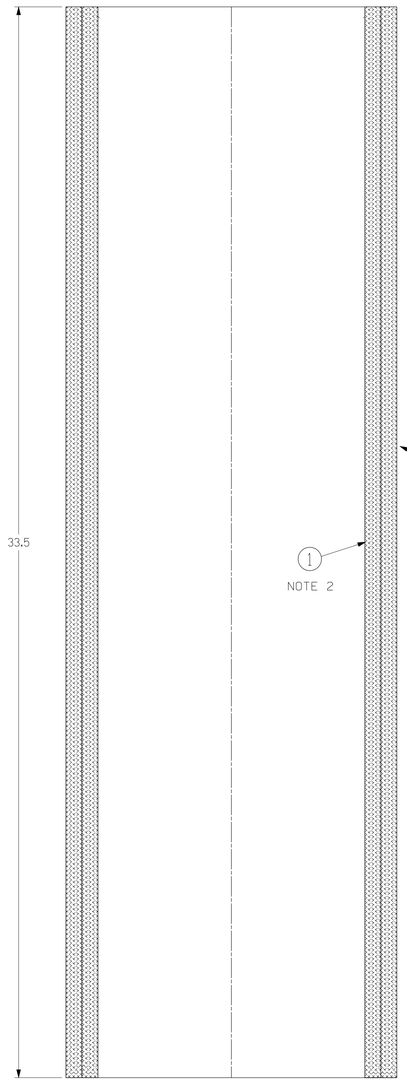

SECTION A-A

SCALE: 1/2

INSULATION, SIDE (INNER, OUTER)

R-R2-G-00019-B
R-R2-G-00019-C

NOTE 1

NOTE:
DRAFTING IS IN ACCORDANCE WITH ANSI 14.5, ANSI/AWS A2.4 AND ASME STANDARDS AS APPLICABLE.

ITEM	PART AND DRAWING NO.	REQD PER ASSY	DESCRIPTION
4	COML	AR	TAPE, 3M GLASS CLOTH TAPE 361, 2 INCH WIDE, .0075" THICK, MCMASTER PN 7742A999
3	R-R2-G-00019-D	2	INSULATION, BOTTOM (NOTE 1)
2	R-R2-G-00019-C	1	INSULATION, SIDE, OUTER (NOTE 1)
1	R-R2-G-00019-B	1	INSULATION, SIDE, INNER (NOTE 1)

FINISH 125/ ALL MACHINED SURFACES AND BREAK ALL SHARP EDGES UNLESS OTHERWISE SPECIFIED

THE NUMBER IN THE FINISH SYMBOL √ IS THE MAXIMUM ACCEPTABLE ROUGHNESS VALUE IN AA MICRO-INCHES.

TOLERANCES ON ALL DIMENSIONS UNLESS OTHERWISE NOTED SHALL BE:

ONE PLACE DECIMAL	±.03	FRACTIONAL	±1/16"
TWO PLACE DECIMAL	±.01	ANGULAR	±0° - 30'
THREE PLACE DECIMAL	±.005		

JOB NUMBER: 23047

DRAWING NO.: R-R2-G-00019 | LATEST REVISION: Ø

UNCLASSIFIED
DOES NOT CONTAIN
UNCLASSIFIED CONTROLLED
NUCLEAR INFORMATION

ADC & Reviewing Official: P. BLANTON, SRPT PGM. MGR.
(Name and Title)
Date: 5/16/06

THIS DRAWING CONTAINS INFORMATION ON SHIPPING PACKAGES FOR RADIOACTIVE MATERIAL
REVISIONS REQUIRE PRIOR APPROVAL OF DESIGN AGENCY
(SRNL PACKAGING TECHNOLOGY GROUP)

RESPONSIBLE ENGINEER	KURT R. EBERL
ENGINEERING MANAGER	GLENN A. ABRAMCZYK

PROJ	REV NO.	DATE	REVISION	PRPD	ENGR	CHK'D	DEM	APPR	OTHER	OTHER	OTHER
N/A	Ø	5/16/06	S-SARP-G-00001	KE	KE	PB	SB	CUSTOMER			

THIS DRAWING IS FURNISHED FOR THE UNITED STATES DEPARTMENT OF ENERGY AT THE SAVANNAH RIVER SITE. THE INFORMATION AND KNOW-HOW THEREON MAY NOT BE USED OR REPRODUCED WITHOUT THE WRITTEN PERMISSION OF THE PRIME CONTRACTOR. ALL REPRODUCTIONS IN WHOLE OR PART, INCLUDING ANY VENDOR'S SHOP DRAWINGS, SHALL INCLUDE OR REFER TO THIS NOTE.

UNITED STATES DEPARTMENT OF ENERGY

SRNL SAVANNAH RIVER NATIONAL LABORATORY

We Put Science To Work

REFERENCE DRAWINGS

R-R1-G-00017	DRUM AND LINER SUBASSEMBLY
R-R1-G-00018	DRUM LID SUBASSEMBLY
R-R5-G-00002	GPFP DRAWING TREE

REFERENCE STANDARDS

BLDG NO.	SITE CLEARANCE NO.	DA NO.	DESIGN GROUP
OFFSITE	N/A	N/A	SRNL/EES

TITLE

9977

GENERAL PURPOSE FISSILE PACKAGING

INSULATING BLANKET SUBASSEMBLY

(U)

SCALE	SRS DRAWING NO.	SHEET NO.	LATEST REV
	N/A	1 OF 1	Ø

SRS NODE:

FILE PATH:

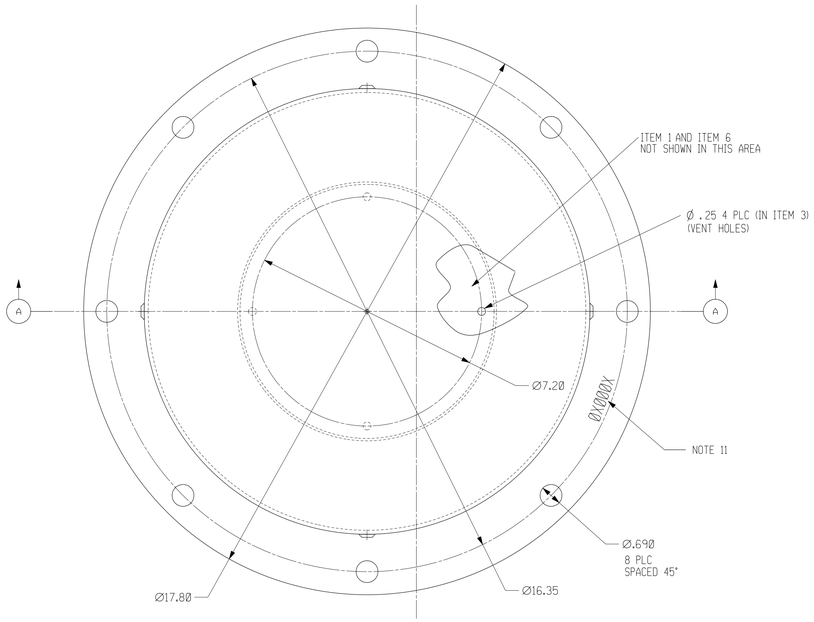

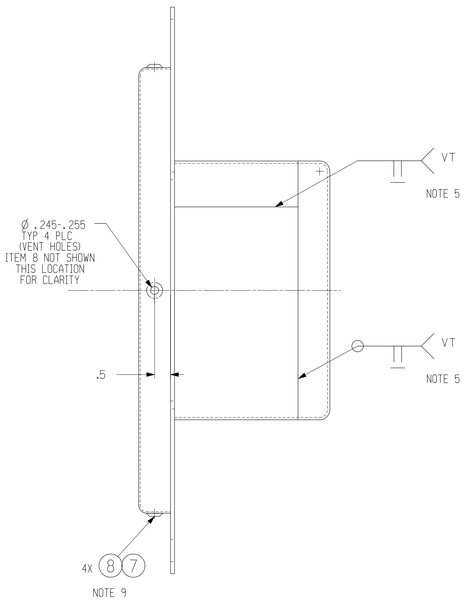

NOTES:

1. ALL WELDS MUST MEET REQUIREMENTS OF APPLICABLE CODES AND STANDARDS AS DESCRIBED ON THIS DRAWING.
2. STAINLESS STEEL MATERIALS TO BE IN ACCORDANCE WITH ASME B&PVC SECTION III, DIV. 1, SUBSECTION NF-2000.
3. ALL WELDS SHALL BE MADE USING FILLER METAL IN ACCORDANCE WITH ASME B&PVC SECTION III, DIV. 1, SUBSECTION NF-2140. WELDING PROCEDURES AND WELDERS SHALL BE QUALIFIED IN ACCORDANCE WITH ASME B&PVC SECTION IX. WELDING AND FABRICATION SHALL BE IN ACCORDANCE WITH ASME B&PVC SECTION III. DIV. 1, SUBSECTION NF-4000.
4. ALL WELDS SHALL BE VISUALLY INSPECTED IN ACCORDANCE WTH ASME B&PVC SECTION III, DIV. 1, SUBSECTION NF-5000. SURFACE POROSITY IS UNACCEPTABLE AND UNDERCUT WILL BE LIMITED TO LESS THAN 10 PERCENT OF THE THICKNESS OF THE THINNER MEMBER.
5. LID TOP (ITEM 2) AND LID BOTTOM (ITEM 3) MAY BE FABRICATED BY DRAWING/SPINNING OR BY ROLLING/WELDING.
6. INSULATION BLANKET (ITEM 4) WILL BE COMPRRESSED FROM ONE INCH NOMINALLY TO APROXIMATELY 1/2 INCH DURING ASSEMBLY OF ITEMS 2 AND 3.
7. MIN-K 2000 (ITEM 6) WILL BE COMPRESSED FROM NOMINALLY 1.0 INCH TO APPROXIMATELY .95 INCHES DURING ASSEMBLY OF ITEM 1 AND ITEM 2.
8. SEALANT (ITEM 7) SHALL BE APPLIED TO THE INSIDE OF THE SIDE WALLS OF THE LID TOP (ITEM 1) AND LID BOTTOM (ITEM 3) APPROXIMATELY AS SHOWN. CARE SHOULD BE TAKEN TO AVOID APPLYING SEALANT TO ITEMS 1 AND 3 AT WELD LOCATIONS.
9. PRIOR TO INSTALLING CAPLUGS (ITEM 8), SEALANT (ITEM 7) TO BE APPLIED TO HOLES AND AROUND PERIPHERY OF CAPLUG. AFTER CAPLUG INSERTION, REMOVE SILICONE RESIDUE FROM AROUND CAPLUG.
10. DRUM LID SUBASSEMBLY (R-R2-G-00018-A) SHALL INSERT INTO THE DRUM AND LINER SUBASSEMBLY (R-R2-G-00017) AND BE FREE TO ROTATE 360° WITHOUT BINDING.
11. PERMANENTLY MARK INFORMATION AS SHOWN. INFORMATION SHALL BE DIE STAMPED AND FILLED WITH BLACK EPOXY PAINT. ALTERNATIVE MARKING METHOD MAY BE USED IF APPROVED BY SRPT. CHARACTERS ARE 3/8 INCH HIGH AND ARE GOTHIC/LEROY TYPE. SERIAL NUMBER TO BE SUPPLIED BY PURCHASER. (0X000X INDICATES TWO DIGIT YEAR AND 4 DIGIT SERIAL NUMBER).

DRUM LID SUBASSEMBLY

R-R2-G-00018-A

SCALE: 1/2

APPROX. WT. 20 LBS.

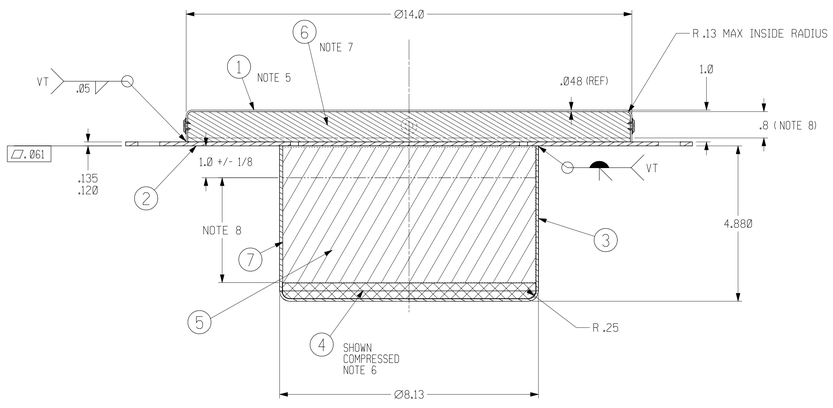

SECTION A-A

SCALE: 1/2

NOTE: DRAFTING IS IN ACCORDANCE WITH ANSI 14.5, ANSI/AWS A.4 AND ASME STANDARDS AS APPLICABLE.

ITEM	PART AND DRAWING NO.	REQD PER ASSY	DESCRIPTION
8	COML	4	CAPLUGS, "BPF- 1/4, MATERIAL: ETHYENE VINYL ACETATE
7	COML	AR	SILICONE SEALANT, DOW CORNING " 382 RTV OR EQUAL
6	COML	1	MIN-K 2000, THERMAL CERAMICS, 14 IN DIA X 1.0 IN THK
5	COML	1	TR-19 BLOCK, THERMAL CERAMICS VERMICULITE (NOM. 7-15/16 INCH DIA X 4 1/4 INCHES HIGH)
4	R-R2-G-00019-D	2	LID INSULATION BLANKET ASSY (NOMINAL 1 INCH THICK X 8-1/4 INCH O.D)
3	R-R2-G-00018-D	1	LID BOTTOM, 14 GAUGE (.075 REF), GRADE TP-304L, ASME SA-240
2	R-R2-G-00018-C	1	LID PLATE, 1/8 IN THK (NOMINAL), GRADE TP-304L, ASME SA-240
1	R-R2-G-00018-B	1	LID TOP, 18 GAUGE (.0478 REF), TP-304L, ASME SA-240

FINISH 125/ ALL MACHINED SURFACES AND BREAK ALL SHARP EDGES UNLESS OTHERWISE SPECIFIED

THE NUMBER IN THE FINISH SYMBOL √ IS THE MAXIMUM ACCEPTABLE ROUGHNESS VALUE IN AA MICRO-INCHES.

TOLERANCES ON ALL DIMENSIONS UNLESS OTHERWISE NOTED SHALL BE:

ONE PLACE DECIMAL ±.03 FRACTIONAL ±1/16"
TWO PLACE DECIMAL ±.01 ANGULAR ±0° - 30'
THREE PLACE DECIMAL ±.005

JOB NUMBER 23047

DRAWING NO. R-R2-G-00018

LATEST REVISION Ø

UNCLASSIFIED
DOES NOT CONTAIN
UNCLASSIFIED CONTROLLED
NUCLEAR INFORMATION

ADC & Reviewing Official: P. BLANTON, SRPT PGM. MGR.
(Name and Title)
Date: 5/16/06

THIS DRAWING CONTAINS INFORMATION ON SHIPPING PACKAGES FOR RADIOACTIVE MATERIAL
REVISIONS REQUIRE PRIOR APPROVAL OF DESIGN AGENCY
(SRNL PACKAGING TECHNOLOGY GROUP)

RESPONSIBLE ENGINEER	KURT R. EBERL
ENGINEERING MANAGER	GLENN A. ABRAMCZYK

PROJ	REV NO.	DATE	REVISION	PRPD	ENGR	CHK'D	DEM	APPR CUSTOMER	OTHER	OTHER	OTHER
N/A	Ø	5/16/06	S-SARP-G-00001 SUBMITTAL	KE/MP	KE	PB	SB				

UNITED STATES DEPARTMENT OF ENERGY

SRNL™ SAVANNAH RIVER NATIONAL LABORATORY

We Put Science To Work

REFERENCE DRAWINGS

R-R1-G-00020	QPFP ASSEMBLY WITH SIX INCH DIA CV
R-R1-G-00021	QPFP ASSEMBLY WITH FIVE INCH DIA CV
R-R5-G-00002	DRAWING TREE

REFERENCE STANDARDS

BLDG NO.	SITE CLEARANCE NO.	DA NO.	DESIGN GROUP
OFFSITE	N/A	N/A	SRNL/EES

TITLE

9977

GENERAL PURPOSE FISSILE PACKAGING

DRUM LID SUBASSEMBLY (U)

SCALE	SRS DRAWING NO.	SHEET NO.	LATEST REV
AS NOTED	N/A	1 OF 1	Ø

SRS NODE: FILE PATH:

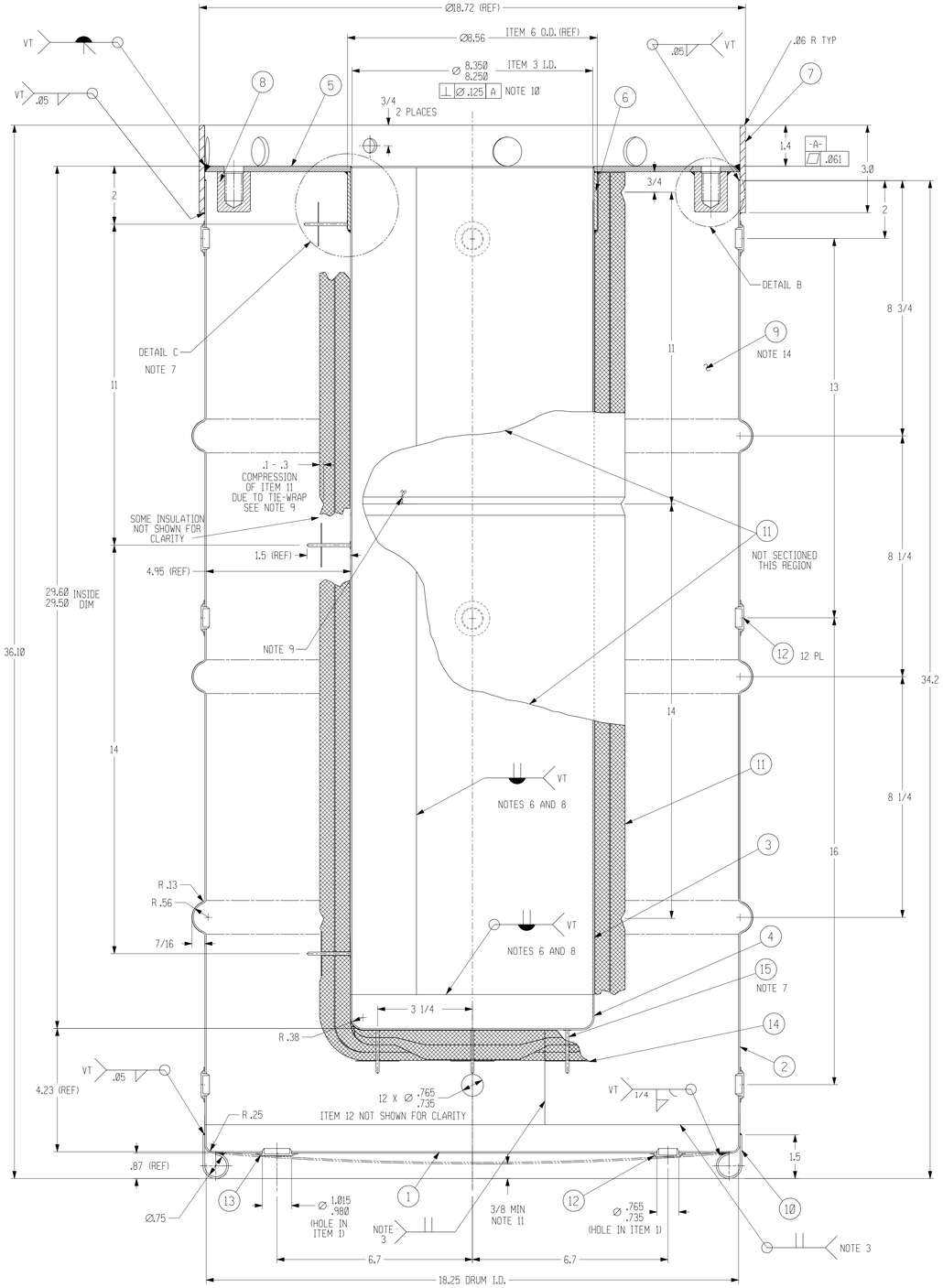

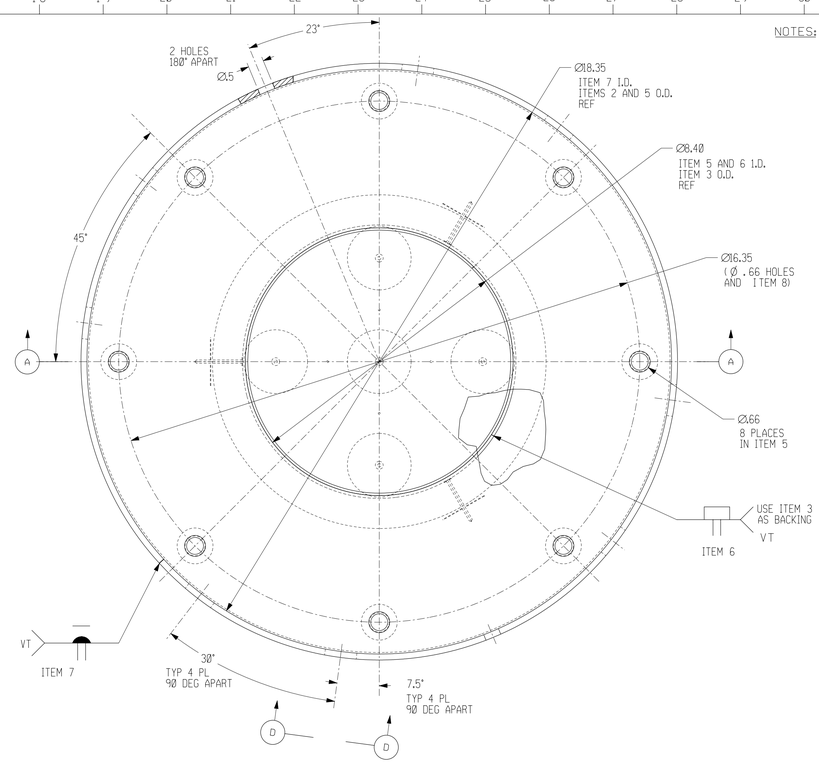

TOP VIEW

SCALE: 1/2

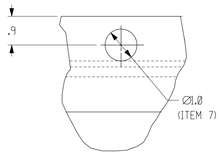

VIEW D-D

SCALE: 1/2

TYP 8 PL

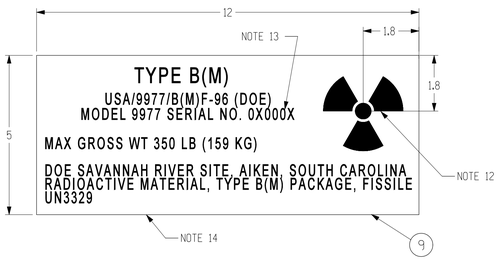

INDENTIFICATION PLATE

R-R2-G-00017-J

SCALE: 1/2

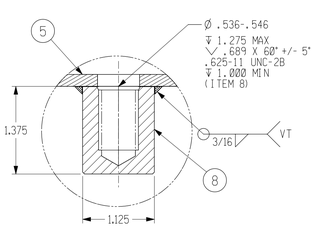

SECTION A-A

SCALE: 1/2

DRUM AND LINER SUBASSEMBLY

R-R2-G-00017-A

APPROX. WT. 75 LBS.

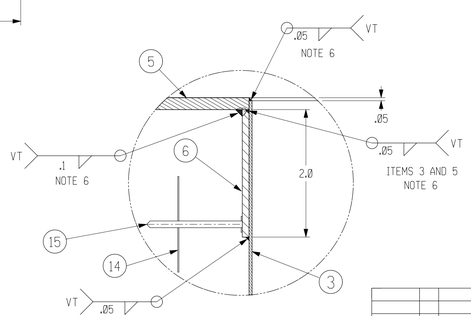

DETAIL C

SCALE: FULL

FITTING, THREADED

R-R2-G-00017-I

NOTE 15

NOTES:

1. ALL WELDS MUST MEET REQUIREMENTS OF APPLICABLE CODES AND STANDARDS AS DESCRIBED ON THIS DRAWING. USE OF ADDENDA OTHER THAN THOSE LISTED ON THIS DRAWING REQUIRE PRIOR APPROVAL OF DESIGN AUTHORITY.
2. MATERIAL TO BE IN ACCORDANCE WITH ASME BOILER & PRESSURE VESSEL CODE (B&PVC), SECTION III, DIV. 1, SUBSECTION NF-2000, 2004 EDITION.
3. DRUM BODY WELDMENT (ITEMS 1 & 2) SHALL SATISFY REQUIREMENTS OF UN 1A2/X/250/yy/USA/zzz PER 49 CFR 178 SUBPART L BEFORE INSTALLATION OF ITEMS 12 & 13. YEAR OF MANUFACTURE AND MANUFACTURER'S SYMBOL ARE INDICATED BY "yy" AND "zzz", RESPECTIVELY. UN MARKING SHALL BE .47 INCH HIGH MIN.
4. ALL WELDS SHALL BE MADE USING FILLER METAL IN ACCORDANCE WITH ASME B&PVC SECTION III, DIV. 1, SUBSECTION NF-2140 (2004). WELDING PROCEDURES AND WELDERS SHALL BE QUALIFIED IN ACCORDANCE WITH ASME B&PVC SECTION IX (2005). WELDING AND FABRICATION SHALL BE IN ACCORDANCE ASME B&PVC SECTION III, DIV. 1, SUBSECTION NF-4000 (2004).
5. ALL WELDS SHALL BE VISUALLY INSPECTED IN ACCORDANCE WITH ASME B&PVC SECTION III, DIV. 1, SUBSECTION NF-5000 (2004) EXCEPT SURFACE POROSITY IS UNACCEPTABLE AND UNDERCUT WILL BE LIMITED TO LESS THAN 10 PERCENT OF THE THICKNESS OF THE THINNER MEMBER.
6. A HYDRO-STATIC PRESSURE TEST SHALL BE PERFORMED ON THE DRUM LINER WELDMENT (ITEMS 3 THRU 6) AT 5 PSI FOR 10 MINUTES. ANY WELD LEAKS MUST BE REPAIRED AND THE TEST REPEATED. HYDROSTATIC TEST NOT REQUIRED FOR WELDS BETWEEN ITEM 5 AND ITEM 7 AND BETWEEN ITEM 2 AND ITEM 7.
7. STUDS (ITEM 15) TO BE LOCATED AS SHOWN AND TACK-WELDED IN PLACE. NINE (9) STUDS ARE LOCATED ON THE O.D. OF THE LINER SIDE AND RING APPROXIMATELY 120 DEGREES (+/- 5 DEGREES) APART AT THE THREE HEIGHT LOCATIONS. FIVE (5) STUDS ARE LOCATED ON THE LINER BOTTOM.
8. DRUM LINER (ITEMS 3 AND 4) MAY BE FABRICATED BY DRAWING/SPINNING OR BY ROLLING/WELDING.
9. SECURE INSULATION ASSY USING ONE TIE WRAP OF 22 GAUGE (.0286" REF) 304/304L WIRE IN THREE (3) LOCATIONS APPROXIMATELY AS SHOWN (+/- 3/8").
10. I.D. OF LINER (AFTER WELDING) SHALL ALLOW INSERTION OF LOAD DISTRIBUTION FIXTURE (R-R4-G-00032-A) WITHOUT BINDING, AS SHOWN ON R-R1-G-00020.
11. DRUM BOTTOM MAY BE CONVEX AS SHOWN.
12. TREFOIL SYMBOL CONFIGURATION SHALL BE IN ACCORDANCE WITH 49CFR172, APP B, MARKING. RADIUS OF CIRCLE TO BE .25 INCH. COLOR TO BE MAGENTA.
13. PERMANENTLY MARK INFORMATION AS SHOWN. INFORMATION SHALL BE DIE STAMPED AND FILLED WITH BLACK EPOXY PAINT. ALTERNATIVE MARKING METHOD MAY BE USED IF APPROVED BY SRPT. SMALL AND LARGE CHARACTERS ARE 3/8 AND 1/2 INCH HIGH, RESPECTIVELY, AND ARE GOTHIC/LEROY TYPE. SERIAL NUMBER TO BE SUPPLIED BY PURCHASER (0X000X INDICATES TWO DIGIT YEAR AND 4 DIGIT SERIAL NUMBER).
14. IDENTIFICATION PLATE SHALL BE WELDED (MIN. 1/2 INCH LONG WELDS) TO OUTSIDE OF DRUM. WELD LOCATIONS SHALL BE AT EACH CORNER AND SPACED EVERY 3 INCHES ON THE LONG EDGES AND AT THE CENTER OF THE SHORT EDGES. THE I.D. PLATE SHALL CONFORM TO THE O.D. OF THE DRUM. LOCATION TO BE CENTERED BETWEEN VENT HOLES WITH TOP EDGE OF THE ID PLATE LOCATED AT THE VENT HOLE CENTERLINE. SEE DRAWINGS R-R1-G-00020 AND R-R1-G-00021 FOR PLACEMENT.
15. ITEM 8 SHALL BE PER ASME SA-194 (2004) AND SA-320 (2004). SUPPLEMENTARY REQUIREMENT S1 OF SA-194 FOR STRAIN-HARDENING OF AUSTENETIC STEEL NUTS IS REQUIRED. ITEM 8 SHALL BE VISUALLY INSPECTED PER ASME B&PVC, SECTION III, DIV. 1, SUBSECTION NF-2581.2. ANY ADDITIONAL APPLICABLE REQUIREMENTS FOR BOLTING MATERIALS OF ASME B&PVC, SECTION III, DIV. 1, SUBSECTION NF ARE REQUIRED. DIMENSIONS PERTAINING TO ITEM 8 SUPERCEDE DIMENSIONAL REQUIREMENTS OF SA-194.

NOTE: DRAFTING IS IN ACCORDANCE WITH ANSI 14.5, ANSI/AWS A2.4 AND ASME STANDARDS AS APPLICABLE.

ITEM	PART AND DRAWING NO.	REQD PER ASSY	DESCRIPTION
15	COML	14	STUD, 4d NAIL, 12 GAUGE (.105" DIA) X 1-1/2" LONG, 316 SST, MCMASTER PN 97990A102 (NOTE 7)
14	COML	14	WASHER, PIN STYLE, MCMASTER PN 93610A410
13	COML	1	CAPLUG, BPF-1, BUTTON PLUG FLUSH TYPE HEAD
12	COML	13	CAPLUG, BPF-3/4, BUTTON PLUG FLUSH TYPE HEAD
11	R-R2-G-00019-A	1	INSULATING BLANKET SUBASSEMBLY
10	R-R2-G-00017-K	1	WEAR RING, 16 GAUGE (Ø.06 REF), 304/304L SST
9	R-R2-G-00017-J	1	IDENTIFICATION PLATE, 16 GAUGE (Ø.06 REF), 304/304L SST
8	R-R2-G-00017-I	8	FITTING, THREADED, 304 SST, GRADE 8 PER ASME SA-194 AND SA-320 (NOTE 15)
7	R-R2-G-00017-H	1	DRUM RIM, 3/16 IN THK, 304L, ASME SA-240
6	R-R2-G-00017-G	1	DRUM LINER RING, 12 GA (Ø.105 REF), 304L, ASME SA-240
5	R-R2-G-00017-F	1	DRUM TOP PLATE, 3/16 IN THK, 304L, ASME SA-240
4	R-R2-G-00017-E	1	DRUM LINER BOTTOM, 18 GA (Ø.048 REF), 304L, ASME SA-240
3	R-R2-G-00017-D	1	DRUM LINER SIDE, 18 GA (Ø.048 REF), 304L, ASME SA-240
2	R-R2-G-00017-C	1	DRUM SIDE, 18 GA (Ø.048 REF), 304L, ASME SA-240
1	R-R2-G-00017-B	1	DRUM BOTTOM, 18 GA (Ø.048 REF), 304L, ASME SA-240

FINISH 125 ALL MACHINED SURFACES AND BREAK ALL SHARP EDGES UNLESS OTHERWISE SPECIFIED

THE NUMBER IN THE FINISH SYMBOL √ IS THE MAXIMUM ACCEPTABLE ROUGHNESS VALUE IN AA MICRO-INCHES.

TOLERANCES ON ALL DIMENSIONS UNLESS OTHERWISE NOTED SHALL BE:

ONE PLACE DECIMAL	±.03	FRACTIONAL	±1/16"
TWO PLACE DECIMAL	±.01	ANGULAR	±0° - 30'
THREE PLACE DECIMAL	±.005		

JOB NUMBER

DRAWING NO. R-R2-G-00017

LATEST REVISION Ø

UNCLASSIFIED
DOES NOT CONTAIN UNCLASSIFIED CONTROLLED NUCLEAR INFORMATION

ADC & Reviewing Official: P. BLANTON, SRPT PGM. MGR. (Name and Title)

Date: 5/16/06

THIS DRAWING CONTAINS INFORMATION ON SHIPPING PACKAGES FOR RADIOACTIVE MATERIAL
REVISIONS REQUIRE PRIOR APPROVAL OF DESIGN AGENCY (SRNL PACKAGING TECHNOLOGY GROUP)

RESPONSIBLE ENGINEER	KURT R. EBERL
ENGINEERING MANAGER	GLENN A. ABRAMCZYK

PROJ	REV NO.	DATE	REVISION	KE/MP PRPD	KE ENGR	PB CHK'D	SB DEM	APPR CUSTOMER	OTHER	OTHER	OTHER
N/A	Ø	5/16/06	S-SARP-G-00001 SUBMITTAL								

REFERENCE DRAWINGS

R-R1-G-00020	ASSEMBLY WITH SIX INCH DIA CV
R-R1-G-00021	ASSEMBLY WITH FIVE INCH DIA CV
R-R5-G-00002	DRAWING TREE

REFERENCE STANDARDS

THIS DRAWING IS FURNISHED FOR THE UNITED STATES DEPARTMENT OF ENERGY AT THE SAVANNAH RIVER SITE. THE INFORMATION AND KNOW-HOW THEREON MAY NOT BE USED OR REPRODUCED WITHOUT THE WRITTEN PERMISSION OF THE PRIME CONTRACTOR. ALL REPRODUCTIONS IN WHOLE OR PART, INCLUDING ANY VENDOR'S SHOP DRAWINGS, SHALL INCLUDE OR REFER TO THIS NOTE.

UNITED STATES DEPARTMENT OF ENERGY

SRNL™ SAVANNAH RIVER NATIONAL LABORATORY

We Put Science To Work

BLOG NO.	SITE CLEARANCE NO.	QA NO.	DESIGN GROUP
OFFSITE	N/A	N/A	SRNL/EES

TITLE

9977

GENERAL PURPOSE FISSILE PACKAGING

DRUM AND LINER SUBASSEMBLY

(U)

SCALE	SRS DRAWING NO.	SHEET NO.	LATEST REV
AS NOTED	N/A	1 OF 1	Ø

SRS NODE: FILE PATH:

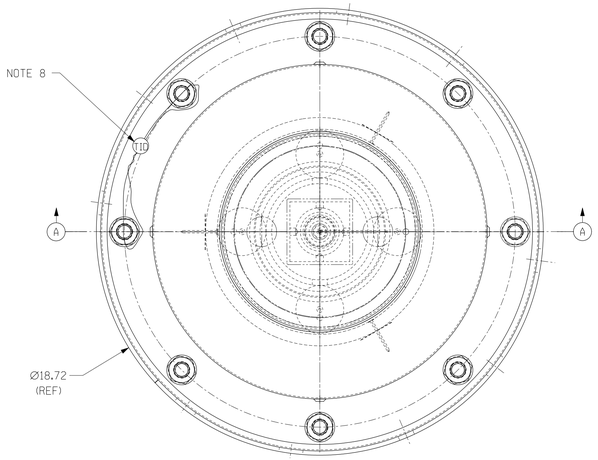

TOP VIEW

SCALE: 3/8

(SOME HIDDEN LINES NOT SHOWN FOR CLARITY)

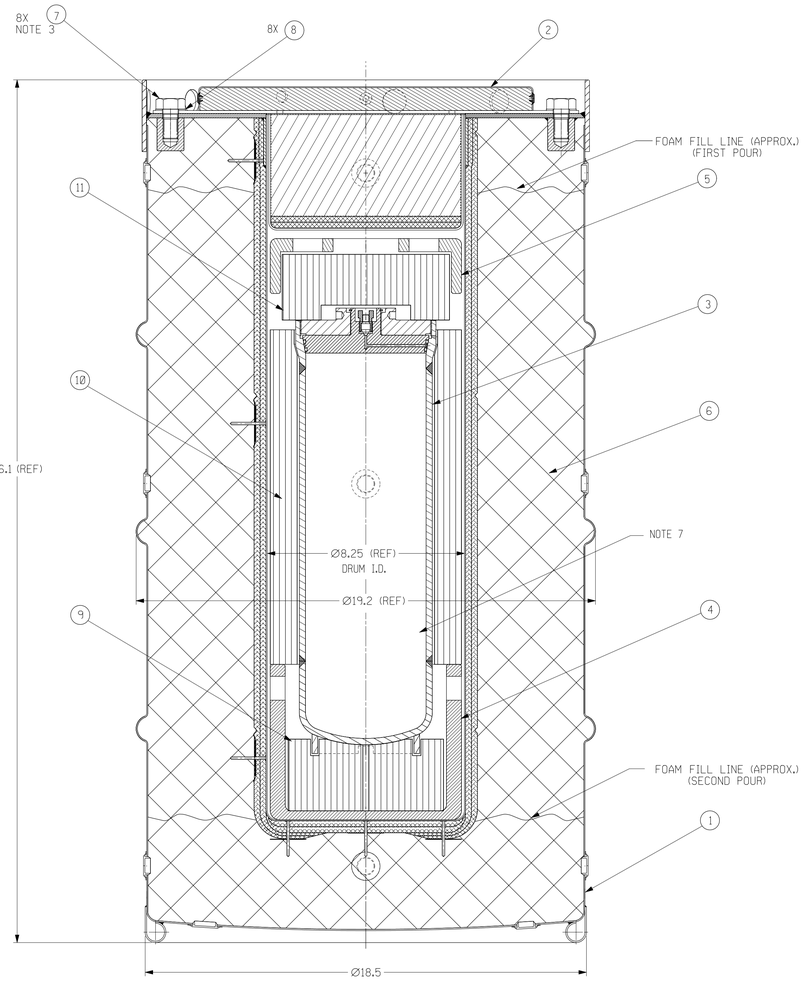

SECTION A-A

SCALE: 3/8

ASSEMBLY WITH FIVE INCH DIAMETER CONTAINMENT VESSEL

R-R2-G-00021-A

NOMINAL WT. 219 LBS.

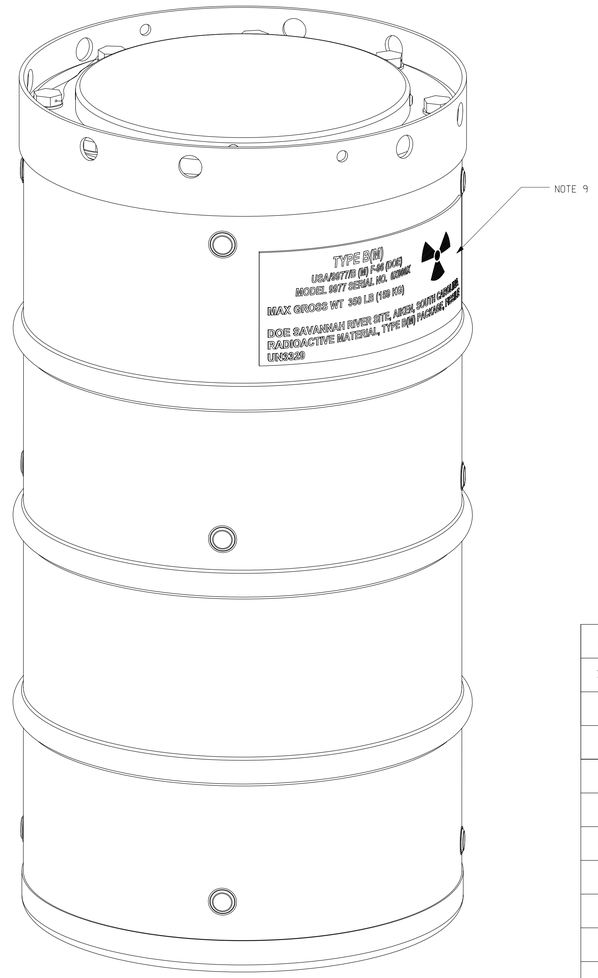

9977 GPFP DRUM ASSEMBLY

SCALE: NONE

NOTES:

1. SAVANNAH RIVER NATIONAL LABORATORY'S (SRNL) SAVANNAH RIVER PACKAGING TECHNOLOGY (SRPT) ORGANIZATION IS THE DESIGN AUTHORITY FOR THE 9977 PACKAGING. ANY AND ALL CHANGES TO THE DESIGN AND/OR TESTING INFORMATION ON THE DESIGN DRAWINGS SHALL BE REVIEWED AND APPROVED BY SRPT.
2. THE FOAM INSULATION (ITEM 6) SHALL BE POURED THROUGH THE 1 INCH DIAMETER HOLE LOCATED ON THE BOTTOM OF THE DRUM PER AN APPROVED PROCEDURE. TWO SEPARATE POUR OPERATIONS ARE REQUIRED TO FILL THE SPACE WITHIN THE DRUM COMPLETELY. THE TWO FILL LINES REPRESENT APPROXIMATE LOCATIONS OF THE TWO POURS.
3. BOLTS (ITEM 7) SHALL BE TORQUED TO 45 +/- 5 FT-LBS INCLUDING TOOL TOLERANCE. TWO TORQUING PASSES TO BE MADE FOR ALL BOLTS.
4. RE-INSTALL TWO BOTTOM CAPLUGS AFTER FOAMING OPERATION IS COMPLETE.
5. DRILL Ø.094 INCH HOLE THROUGH BOLT HEAD PER ANSI B18.21.1a -1999 TABLE E1.
6. ITEM 7 BOLTS TO BE VISUALLY INSPECTED PER ASME B&PVC, SECTION III, DIV. 1, SUBSECTION NF-2581.2.
7. MAXIMUM ALLOWABLE WEIGHT OF THE CONTENTS AND SECONDARY PACKAGING IS 100 LBS.
8. TAMPER INDICATING DEVICE (TID) AS DEFINED IN S-SARP-G-00001.
9. REFERENCE DWG. R-R2-G-00017 FOR IDENTIFICATION PLATE SPECIFICATIONS AND PLACEMENT.

NOTE: DRAFTING IS IN ACCORDANCE WITH ANSI 14.5, ANSI/AWS A2.4 AND ASME STANDARDS AS APPLICABLE.

ITEM	PART AND DRAWING NO.	REQD PER ASSY	DESCRIPTION
11	R-R4-G-00033-C	9	SPACER, UPPER
10	R-R4-G-00033-B	1	SPACER, ANNULAR
9	R-R4-G-00033-A	1	SPACER, LOWER
8	COML	8	WASHER, HARDENED, 5/8 INCH NOM., PLAIN, NARROW, TYPE B, 18-8 SST, PER ANSI B18.22.1 (R 1975)
7	COML	8	SCREW, HEAVY HEX, 5/8"-11 UNC-2A X 1-1/4 LG, 304/304L PER ASME SA-193 AND SA-320, GRADE B8, CLASS 2 (NOTES 5 & 6)
6	COML	AR	GENERAL PLASTICS LAST-A-FOAM FR 3716, 16 PCF
5	R-R4-G-00032-B	1	TOP LOAD DISTRIBUTION FIXTURE
4	R-R4-G-00032-A	1	BOTTOM LOAD DISTRIBUTION FIXTURE
3	R-R2-G-00043-A	1	FIVE INCH DIAMETER CONTAINMENT VESSEL SUBASSEMBLY
2	R-R2-G-00018-A	1	DRUM LID SUBASSEMBLY
1	R-R2-G-00017-A	1	DRUM AND LINER SUBASSEMBLY

FINISH 125/ ALL MACHINED SURFACES AND BREAK ALL SHARP EDGES UNLESS OTHERWISE SPECIFIED

THE NUMBER IN THE FINISH SYMBOL √ IS THE MAXIMUM ACCEPTABLE ROUGHNESS VALUE IN AA MICRO-INCHES.

TOLERANCES ON ALL DIMENSIONS UNLESS OTHERWISE NOTED SHALL BE:

ONE PLACE DECIMAL ±.03 FRACTIONAL ±1/16"
TWO PLACE DECIMAL ±.01 ANGULAR ±0° - 30'
THREE PLACE DECIMAL ±.005

JOB NUMBER 23047

DRAWING NO. R-R1-G-00021 LATEST REVISION A

UNITED STATES DEPARTMENT OF ENERGY

SRNL SAVANNAH RIVER NATIONAL LABORATORY™

We Put Science To Work

REFERENCE DRAWINGS

R-R5-G-00002	DRAWING TREE

REFERENCE STANDARDS

BLDG NO.	SITE CLEARANCE NO.	DA NO.	DESIGN GROUP
OFFSITE	N/A	N/A	SRNL/EES

TITLE

9977
GENERAL PURPOSE FISSILE PACKAGING

ASSEMBLY WITH FIVE INCH DIAMETER CONTAINMENT VESSEL (U)

SCALE AS NOTED | SRS DRAWING NO. N/A | SHEET NO. 1 OF 1 | LATEST REV A

UNCLASSIFIED
DOES NOT CONTAIN UNCLASSIFIED CONTROLLED NUCLEAR INFORMATION

ADC & Reviewing Official: P. BLANTON, SRPT PGM. MGR. (Name and Title)

Date: 5/16/06

THIS DRAWING CONTAINS INFORMATION ON SHIPPING PACKAGES FOR RADIOACTIVE MATERIAL
REVISIONS REQUIRE PRIOR APPROVAL OF DESIGN AGENCY
(SRNL PACKAGING TECHNOLOGY GROUP)

RESPONSIBLE ENGINEER: KURT R. EBERL
ENGINEERING MANAGER: GLENN A. ABRAMCZYK

PROJ	REV NO.	DATE	REVISION	PRPD	ENGR	CHK'D	DCM	APPR CUSTOMER	OTHER	OTHER	OTHER
N/A	0	5/16/06	S-SARP-G-00001	KE/MP	KE	PB	SB				

SRS NODE: FILE PATH:

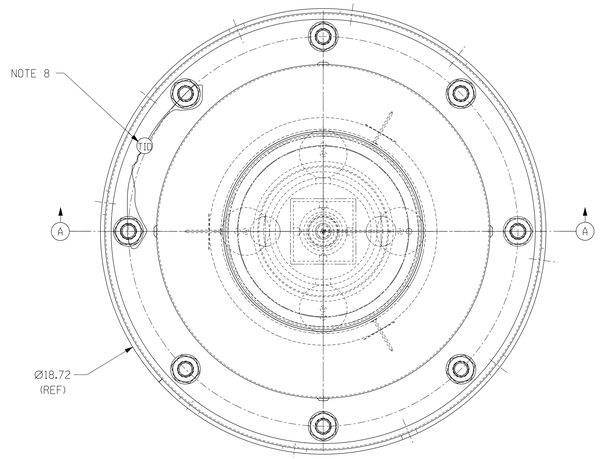

TOP VIEW

SCALE: 3/8

(SOME HIDDEN LINES NOT SHOWN FOR CLARITY)

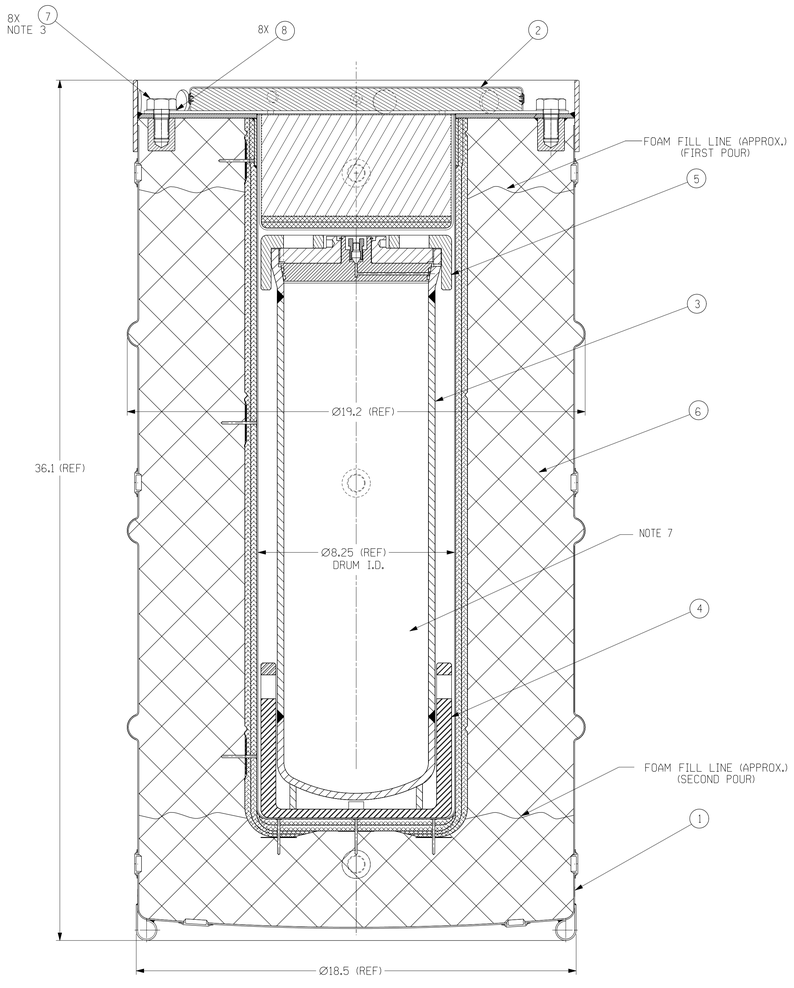

SECTION A-A

SCALE: 3/8

ASSEMBLY WITH SIX INCH DIAMETER CONTAINMENT VESSEL
R-R2-G-00020-A

NOMINAL WT. 235 LBS.

9977 GPFP DRUM ASSEMBLY

SCALE: NONE

NOTES:

1. SAVANNAH RIVER NATIONAL LABORATORY'S (SRNL) SAVANNAH RIVER PACKAGING TECHNOLOGY (SRPT) ORGANIZATION IS THE DESIGN AUTHORITY FOR THE 9977 PACKAGING. ANY AND ALL CHANGES TO THE DESIGN AND/OR TESTING INFORMATION ON THE DESIGN DRAWINGS SHALL BE REVIEWED AND APPROVED BY SRPT.
2. THE FOAM INSULATION (ITEM 6) SHALL BE POURED THROUGH THE 1 INCH DIAMETER HOLE LOCATED ON THE BOTTOM OF THE DRUM PER AN APPROVED PROCEDURE. TWO SEPARATE POUR OPERATIONS ARE REQUIRED TO FILL THE SPACE WITHIN THE DRUM COMPLETELY. THE TWO FILL LINES REPRESENT APPROXIMATE LOCATIONS OF THE TWO POURS.
3. BOLTS (ITEM 7) SHALL BE TORQUED TO 45 +/- 5 FT-LBS INCLUDING TOOL TOLERANCE. TWO TORQUING PASSES TO BE MADE FOR ALL BOLTS.
4. RE-INSTALL TWO BOTTOM CAPLUGS AFTER FOAMING OPERATION IS COMPLETE.
5. DRILL Ø .094 INCH HOLE THROUGH BOLT HEAD PER ANSI B18.21.1a -1999 TABLE E1.
6. ITEM 7 BOLTS TO BE VISUALLY INSPECTED PER ASME B&PVC, SECTION III, DIV. 1, SUBSECTION NF-2581.2.
7. MAXIMUM ALLOWABLE WEIGHT OF THE CONTENTS AND SECONDARY PACKAGING IS 100 LBS.
8. TAMPER INDICATING DEVICE (TID) AS DEFINED IN S-SARP-G-00001.
9. REFERENCE DWG. R-R2-G-00017 FOR IDENTIFICATION PLATE SPECIFICATIONS AND PLACEMENT.

NOTE: DRAFTING IS IN ACCORDANCE WITH ANSI 14.5, ANSI/AWS A2.4 AND ASME STANDARDS AS APPLICABLE.

ITEM	PART AND DRAWING NO.	REQD PER ASSY	DESCRIPTION
8	COML	8	WASHER, HARDENED, 5/8 INCH NOM., PLAIN, NARROW, TYPE B, 18-8 SST, PER ANSI B18.22.1 (R 1975)
7	COML	8	SCREW, HEAVY HEX, 5/8"-11 UNC-2A X 1-1/4 LG, 304/304L PER ASME SA-193 AND SA-320, GRADE B8, CLASS 2 (NOTES 5 & 6)
6	COML	AR	GENERAL PLASTICS LAST-A-FOAM FR 3716, 16 PCF
5	R-R4-G-00032-B	1	TOP LOAD DISTRIBUTION FIXTURE
4	R-R4-G-00032-A	1	BOTTOM LOAD DISTRIBUTION FIXTURE
3	R-R2-G-00042-A	1	SIX INCH DIAMETER CONTAINMENT VESSEL SUBASSEMBLY
2	R-R2-G-00018-A	1	DRUM LID SUBASSEMBLY
1	R-R2-G-00017-A	1	DRUM AND LINER SUBASSEMBLY

FINISH 125/ ALL MACHINED SURFACES AND BREAK ALL SHARP EDGES UNLESS OTHERWISE SPECIFIED

THE NUMBER IN THE FINISH SYMBOL √ IS THE MAXIMUM ACCEPTABLE ROUGHNESS VALUE IN AA,MICRO-INCHES.

TOLERANCES ON ALL DIMENSIONS UNLESS OTHERWISE NOTED SHALL BE:
ONE PLACE DECIMAL ±.03 FRACTIONAL ±1/16"
TWO PLACE DECIMAL ±.01 ANGULAR ±2° - 30'
THREE PLACE DECIMAL ±.005

JOB NUMBER 23047
DRAWING NO. R-R1-G-00020
LATEST REVISION A

UNITED STATES DEPARTMENT OF ENERGY

SRNL SAVANNAH RIVER NATIONAL LABORATORY

We Put Science To Work

UNCLASSIFIED
DOES NOT CONTAIN
UNCLASSIFIED CONTROLLED
NUCLEAR INFORMATION

ADC & Reviewing Official: P. BLANTON, SRPT PGM. MGR. (Name and Title)
Date: 5/16/06

THIS DRAWING CONTAINS INFORMATION ON SHIPPING PACKAGES FOR RADIOACTIVE MATERIAL
REVISIONS REQUIRE PRIOR APPROVAL OF DESIGN AGENCY
(SRNL PACKAGING TECHNOLOGY GROUP)

RESPONSIBLE ENGINEER: KURT R. EBERL
ENGINEERING MANAGER: GLENN A. ABRAMCZYK

REFERENCE DRAWINGS

R-RS-G-00002	DRAWING TREE

REFERENCE STANDARDS

PROJ	REV NO.	DATE	REVISION	PPD	ENGR	CHK'D	DEM	APPR CUSTOMER	OTHER	OTHER
N/A	Ø	5/16/06	S-SARP-G-00001	KE/MP	KE	PB	SB			

BLDG NO. OFFSITE | SITE CLEARANCE NO. N/A | DA NO. N/A | DESIGN GROUP SRNL/EES

TITLE

9977
GENERAL PURPOSE FISSILE PACKAGING

ASSEMBLY WITH SIX INCH DIAMETER CONTAINMENT VESSEL
(U)

SCALE AS NOTED | SRS DRAWING NO. N/A | SHEET NO. 1 OF 1 | LATEST REV A

SRS NODE: | FILE PATH:

Safety Analysis Report – 9977 Packaging

CHAPTER 2

STRUCTURAL EVALUATION

Preface

The Model 9977 Package is a single-containment packaging designed to ship plutonium and uranium in metal and oxide form. It features two single containment vessel shipping configurations. Each CV is designed, analyzed, fabricated, and examined in accordance with Section III of the American Society of Mechanical Engineers (ASME) Boiler and Pressure Vessel Code, 2004 Edition[1] as described in Section 9.3. The analytical evaluations and test results presented in this chapter demonstrate that the 9977 meets the requirements of Department of Energy (DOE) Order 460.1B,[2] 10 CFR 71[3] and the International Atomic Energy Agency (IAEA) Safety Series No. TS-R-1, *Regulations for the Safe Transport of Radioactive Material*.[4]

The information presented in this Chapter is in the format specified in U.S. Nuclear Regulatory Commission (NRC) Regulatory Guide (RG) 7.9.[5]

This Page Intentionally Left Blank

TABLE OF CONTENTS

LIST OF TABLES

LIST OF FIGURES

ACRONYMS AND ABBREVIATIONS

5CV	5-Inch Inside Diameter Containment Vessel
6CV	6-Inch Inside Diameter Containment Vessel
ANSI	American National Standards Institute
ASME	American Society of Mechanical Engineers
ASTM	American Society for Testing and Materials
AWS	American Welding Society
BPVC	Boiler and Pressure Vessel Code
CFR	Code of Federal Regulations
CG	Center of Gravity
CGOC	Center of Gravity over Corner
CV	Containment Vessel
DBR	Design by Rule
DOE	Department of Energy
EM	Environmental Management
FEA	Finite Element Analysis
GPFP	General Purpose Fissile Package
HAC	Hypothetical Accident Conditions
MNOP	Maximum Normal Operating Pressure
NCT	Normal Conditions of Transport
NRC	Nuclear Regulatory Commission
QA	Quality Assurance
RG	Regulatory Guide
RTV	Room Temperature Vulcanizing
SARP	Safety Analysis Report for Packaging
SS	Stainless Steel
TID	Tamper Indicating Device
UNS	Unified National - Special

This Page Intentionally Left Blank

2 STRUCTURAL EVALUATION

2.1 DESCRIPTION OF STRUCTURAL DESIGN

2.1.1 Discussion

The Model 9977 Package is designed and shown through testing and analysis to withstand the structural loads and thermal stresses from regulatory Normal Conditions of Transport (NCT), 10 CFR 71.71, and Hypothetical Accident Conditions (HAC), 10 CFR 71.73.

The principal packaging features and components that make up the 9977 are illustrated in Chapter 1, Figures 1.1 and 1.2. As shown in the Figure 1.1, the packaging consists of an overpack and either of two containment vessel (CV) configurations. The drum and closure lid are fabricated from stainless steel and are joined through an eight-bolt flange. Drum fabrication includes a welded inner liner. The liner is wrapped by an insulating blanket and the volume between the wrapped liner and drum is filled completely with polyurethane foam. The drum closure lid is fabricated from a simple plate enhanced by top and bottom chambers that are filled with thermal insulation and impact absorbing materials. Aluminum load distribution fixtures and honeycomb spacers are used to isolate the CVs within the drum liner as applicable, see Figures 1.1 and 1.2 of Chapter 1.

The drum overpack supports and protects the CV to ensure that shielding, containment and sub-criticality are maintained under both NCT and HAC. The threaded stayed head of the CV weldment receives the cone-seal closure assembly. The cone-seal plug includes two elastomer O-rings that seal the closure. The containment boundary is formed by the CV weldment, cone-seal plug and inner O–ring (Drawings R-R2-G-00042 and R-R2-G-00043). The outer O-ring serves to facilitate testing the seal provided by the inner O-ring. Table 2.1 lists the primary packaging components and their safety functions. Figure 1.3 provides nominal packaging dimensions for the 9977.

Table 2.1 - Primary 9977 Components and Functions

Component	Function for NCT and HAC
35-Gallon Drum Overpack	Provides Confinement for the Containment Vessel and acts as a form for the polyurethane insulation.
Overpack Insulation Materials	Provides impact and thermal protection for the Containment Vessel.
Containment Vessel	Provides containment for the Contents and packing materials.
CV Spacer Assemblies	Hold the Containment Vessel during shipment. The fixtures limit movement of the CV inside the Overpack liner and limit transmittal of HAC loads to the CV.

Structural details of the 9977 are given in the following subsections. As there are two containment vessel shipping configurations for the 9977, the use of the term "Containment Vessel" or its acronym "CV," is used when discussion is applicable to either 5-inch or 6-inch ID CVs. The acronyms "5CV" and "6CV" are used when discussion applies specifically to only one or the other vessel designs.

2.1.1.1 Overpack

The Overpack consists of an insulated drum and an insulated closure lid. The function of the overpack is to protect the CV and maintain payload confinement under regulatory NCT and HAC events. The drum is filled in part with a polyurethane foam that serves primarily as an impact absorber and secondarily, as a thermal insulator. The closure lid chambers are filled with ceramic materials that perform similarly as impact-absorbing thermal insulators.

2.1.1.1.1 Drum Body

The drum is fabricated of 18-gage (0.0478-inch) Type SA240-304/304L stainless steel (SS). The drum is nominally 18¾ inches in diameter and 36 inches high with a capacity of approximately 35 gallons. Drum body fabrication includes a welded "sanitary" style bottom in accordance with UN standards for open head drums. In addition, an independent wear surface consisting of a ⅞-inch diameter, 60-mil thick ring is welded to the sanitary bottom.

A strip of SA479-304/304L SS flat bar stock, three (3) inches wide by $^{3}/_{16}$ inch thick, is rolled and welded to the open head of the drum, reinforcing the rim. Fitting inside the drum shell, an 8.25-inch diameter, 29.5-inch deep-well liner welded to a $^{3}/_{16}$-inch thick top deck plate. This weldment is in turn welded to the reinforcing rim at mid-height. The deep-well liner provides the overpack with a robust protective surface that resists mechanical damage during normal loading/unloading operations and is easy to decontaminate. Together the drum and liner weldment serve as a form to confine General Plastic's polyurethane Last-A-Foam, FR-3716,[6] during the foam installation. The drum's liner and top deck plate are designed and fabricated in accordance with Section III, Subsection NF, of the American Society of Mechanical Engineers (ASME), Boiler and Pressure Vessel Code (BPVC),[7] as explained in Section 9.3.

Prior to the foaming operation, the liner is wrapped with two ½-inch thick Fiberfrax® Insulation blankets.[8] Protruding from the exterior sidewall of the liner are nine 12-gauge (0.105-inch) by 1½-inch long studs. The studs penetrate the Fiberfrax blanket as it is applied and prevent the blanket from slipping from the liner side wall while the polyurethane foam cures. The studs are located at the bottom; middle and upper portion of the liner and are spaced circumferentially every 120 degrees. In addition, 22-gauge wire is twist wrapped just above each row of studs to ensure the blankets' position. Extending from the bottom of the liner are five additional studs. These studs secure Fiberfrax disks cut to the size and fitted to the bottom of the liner. The side-wall Fiberfrax is folded over the Fiberfrax disks and held in place with a high temperature 3M glass tape. Washers are pressed onto the studs to finish securing the assembled Fiberfrax to the liner weldment. Appendix 2.5 shows a photographic sample of the studs and securing washer.

Eight (8), ⅝-inch 11UNC-2B, ASME SA-193, Grade-8 blind-threaded inserts, 1⅛ inches in diameter by 1⅜ inches long are welded to the underside of the $^{3}/_{16}$-inch thick top deck plate,

drawing R-R2-G-00017. The purpose of welding the threaded inserts is to resist bolt closure torque during packaging operation. The inserts also prevent local escape of decomposition products during the HAC fire and potential flow of hot gases under the closure lid and into the overpack liner cavity.

The maximum weight of an empty drum body without its closure lid and bolting hardware is 170 lb.

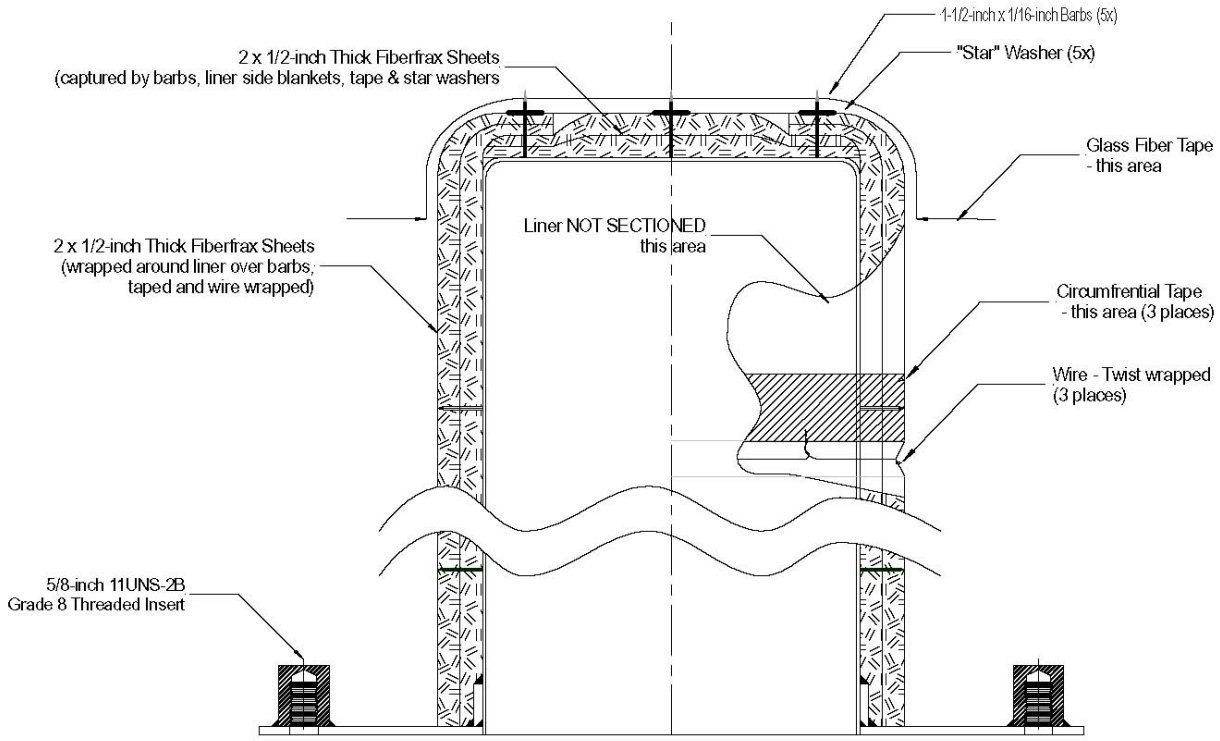

Figure 2.1 - Cross Section of Drum Liner and Fiberfrax Insulation Assembly (inverted)

The drum incorporates fourteen (14) holes that permit polyurethane combustion products to vent during the HAC fire event. Twelve of the vent holes, ¾-inch diameter, are aligned axially on the drum side wall at three elevations, and located circumferentially 90 degrees apart.. The remaining two holes, 1-inch diameter and ¾-inch diameter, are located on the bottom of the drum. The 1-inch hole and the ¾-inch hole are fill port and vent for the polyurethane foaming operations. The holes located on the drum side wall are sealed during foam installation, and all fourteen vents are plugged for normal package operation by appropriately sized plastic Caplugs®.[9]

The three-inch wide reinforcing rim welded to the top of the drum includes eight (8) 1-inch diameter drain holes, located as shown on Drawing R-R2-G-00017. These holes also qualify as lifting or tie down points during package operation or transport. The bottom of each hole is tangent to the drum top to prevent water from accumulating on the top deck plate. In addition,

two ½-inch diameter holes are drilled through the reinforcing rim, approximately 180 degrees apart to accommodate an optional Tamper Indicating Device (TID) during storage.

2.1.1.1.2 Drum Closure Lid

The drum closure lid is a single piece construction that like the drum body protects the CV under NCT and during HAC events. In addition, it provides thermal protection of the CV during the HAC thermal event. The lid is secured to the drum with eight (8), ASME SA-193-04, Grade B8M-Class 2, ⅝ × 1¼-inch long hex screws, torqued to 45 ±5 ft-lb. The lid is constructed from three SA240-304/304L SS components. A ⅛-inch thick by 17.8-inch diameter plate (the bolt flange) is welded between an 18-gauge (0.0478-inch) thick SS top chamber, 14 inches in diameter by one (1) inch deep, and a 14-gauge (0.075-inch) SS bottom chamber, 8.13 inches in diameter and 5.3 inches deep. The top chamber is filled with Thermal Ceramics Min-K 2000[10] insulation, and then inverted and welded to the lid plate. The 5.3-inch deep bottom chamber is filled with two (2) ½-inch thick by 8.13-inch diameter pieces of Fiberfrax followed by a 7.96-inch diameter × 4.3-inch high cylinder of Thermal Ceramics TR-19 Block insulation.[11] The bottom chamber is then welded to the bottom of the lid plate. A thin layer of room temperature vulcanizing adhesive RTV 382[12] is placed around the internal perimeter of both closure-lid chambers before installation of the insulation materials. The cured RTV bonds the materials in place, mitigating the effect of NCT vibration. Details are shown in Drawing R-R2-G-00018.

The Min-K 2000 and Thermal Ceramics TR-19 are both composed of vermiculite granules and high-temperature bonding materials. Min-K 2000 and TR-19 both have good high-temperature strength with minimal shrinkage up to 1,800°F and 1,900°F, respectively, even when exposed to direct flame. Appendix 2.5 shows photographic samples of the Min-K 2000 and TR-19 used in fabrication of the 9977 drum closure lid.

Fiberfrax is a lightweight batting, comprised of a mat of bulk ceramic fibers sandwiched between two layers of strong, high-temperature fiberglass cloth. The material is flexible, has excellent vibration resistance and is unaffected by moisture. The ceramic fibers, i.e., the core insulation, has an operating temperature of up to 2,300°F while the continuous-service limit for the fiberglass covering is 1,200°F.

The closure lid plate incorporates four (4) ¼-inch diameter holes that permit internal communication of gases between the top and bottom chambers. The top chamber is vented externally by four (4) ¼-inch diameter holes positioned at 90-degree intervals around the 1-inch vertical leg. Out-gassing from the ceramic materials, Fiberfrax, Min-K 2000 and TR-19 is minimal during the HAC fire event. The lid vents are included to permit out-gassing from the RTV that bonded these materials in place during fabrication. RTV 382 has continuous-service temperature range of -58°F to 500°F.

The TR-19 block insulation plus two ½-inch thick pieces of Fiberfrax are greater than the height of the bottom chamber, as specified on Drawing R-R2-G-00018. When installed into the chamber, the block insulation compresses the Fiberfrax to a final thickness of ½ inch. During inverted HAC impacts, the compressed Fiberfrax located in the bottom of the closure lid allows the steel shell of the bottom chamber to buckle axially, expand laterally and seat itself

mechanically against the wall of the drum liner. The mechanical seat mitigates any gas flow that may occur due to lid scalloping between bolts or lid bowing due to top-down oriented impacts, see Figure 2.25.

A ⅛-inch hole is drilled through opposing flats of the head of each closure bolt for installation of TID hardware.

2.1.1.2 Impact Limiters

The 9977 includes three design features that provide impact protection;

- the polyurethane foamed drum body,
- the insulation filled closure lid, and
- the aluminum load distribution fixtures and aluminum honeycomb structures that restrain the 5CV or 6CV inside the drum liner.

Each of these features is discussed in detail in the following sections.

2.1.1.2.1 Polyurethane Foamed Drum Body and Insulation Filled Closure Lid

Two layers of Fiberfrax® insulation material surround the drum liner to protect the containment vessel from the HAC thermal environment. Two (2) ½-inch thick blankets of Fiberfrax® Insulation (LTC LoCon, Grade E, 7 to 10 lb/ft^3) are wrapped around and attached to the side wall and bottom of the liner. The insulation blanket is quilted with non-combustible E-Grade Fiberglass Fabric on both sides and is rated for continuous service up to 1200°F. The HSA fibers are not prone to settling or breaking down through internal abrasion, and therefore offer high resistance to mechanical vibration. A tightly woven fiberglass fabric and the composite quilt stitching, gives the blanket its tensile strength. The material is flexible and formable providing ease of fabrication. The thermal properties are unaffected by water immersion or exposure to humidity. Appendix 2.5 shows a photograph of the composite Fiberfrax blanket material used in the 9977.

In addition, the density of the fiberous ceramic material and the four layers of densely woven fiberglass cloth resist the flow of gases through the blanket. For example, if an HAC impact should form a radial and/or axial crack through the polyurethane foam, the Fiberfrax will protect the liner from direct impingement of hot gases from the intumescing polyurethane. Though not a true vapor barrier, the material has been shown by testing to be effective in attenuating the encroachment of gases from the HAC fire event, even absence of ablative foam, see Section 2.7.4. The Fiberfrax blanket has no structural requirements except that it must remain in place during foam installation and during the HAC thermal event.

The interstitial volume between the Fiberfrax® blanket and the drum wall is filled with General Plastics (GP) Last-A-Foam®. The material is poured as a liquid through a fill hole in the bottom of the drum and sets exothermically to form rigid, closed-cell polyurethane foam of a prescribed density. The nominal densities of Fiberfrax and GP FR-3716 foam are 8.5 lb/ft3 and 16 lb/ft3, respectively. The function of the rigid foam is to protect the CV from impact damage during

NCT and HAC events. The closed cells of the foam provide thermal insulation similarly. In addition, the intumescing properties of polyurethane consume heat during phase change to help protect package internal components from the HAC fire event. Physical properties of Fiberfrax are listed in

Table 2.10. Properties of GP FR-3716 Last-A-Foam are listed in Table 2.9 and shown in Figures 2.4 and 2.5. The radial thickness of the insulation between the drum liner and drum wall is approximately 4.95 inches. The axial thickness of the insulation between the drum and liner bottoms is approximately 4.5 inches. The nominal aggregate weight of the foam and Fiberfrax drum insulation is approximately, 76.7 lb.

The polyurethane foam and the laminate formed by the polyurethane and Fiberfrax blanket are in use in radioactive material shipping package and transportation applications.

2.1.1.2.2 Load Distribution Fixtures

Two Load Distribution Fixtures (LDFs) help confine the CV within the overpack liner cavity. Both LDFs are fabricated from 6061-T6 aluminum and weigh approximately 4 lb and 10 lb, top and bottom units, respectively. The top LDF is 8 inches in diameter, 4 inches high, with $^{3}/_{8}$-inch wall and ½-inch thick top plate. The top LDF also includes a 2½-inch square opening that fits around the square drive portion of the cone-seal closure. The bottom fixture is 8 inches diameter, 7 inches high, with a ½-inch thick wall and ⅜-inch bottom plate. To facilitate installation and removal within the overpack liner, two 1¼-inch diameter finger-holes are provided in the side-wall of the bottom LDF and through the top plate of the top LDF. Figures 1.1 and 1.2 show the LDFs in place as part of the packaging. Appendix 2.5 shows a photograph of both top and bottom LDF components.

The 9977 includes two packaging configurations depending on which CV is used to contain the payload. The 6CV fits directly between the LDFs, but a trio of honeycomb spacers are required to adapt the smaller 5CV to fit the LDFs. The two packaging configurations are discussed below.

6CV

The bottom LDF is placed into the overpack liner followed directly by the 6CV, followed by the top LDF covering the cone-seal closure. The LDFs locate the CV and stiffen the thin-walled liner from within to prevent collapse from lateral HAC impacts. The LDFs also help distribute impact loads over the 6CV structure. During a bottom-down impact, the bottom LDF distributes the circular line-load from the 6CV skirt over the bottom of the liner. The top LDF distributes the load from the top-down impact over the 6CV closure. Similarly, the fixtures spread the impulse over the 6CV during corner impacts.

5CV

The bottom LDF is placed into the overpack liner followed by the bottom honeycomb spacer and then the annular honeycomb spacer. The 5CV is lowered into this protected volume followed by the top honeycomb spacer then the top LDF.

2.1.1.2.3 Aluminum Honeycomb Spacers

Because the 5CV is smaller in diameter and shorter than the 6CV, a honeycomb spacer assembly is used to center the 5CV between the two LDFs and maintain the same composite height, see Figures 1.1 and 1.2. The honeycomb assembly serves four purposes:

1) to absorb sufficient HAC impact energy such that the impulse imparted to the 5CV (5CV packaging configuration) is bounded by that associated with the 6CV (6CV packaging configuration),
2) to maintain the locations of the LDFs within the overpack liner such that impact damage to the overpack in the 6CV packaging configuration is not altered significantly by the 5CV packaging configuration,
3) to absorb sufficient HAC impact energy such that the structural loading on the 5CV (5CV packaging configuration) is less than that associated with the 6CV (6CV packaging configuration), and
4) to enhance heat transfer to the overpack liner during NCT.

The honeycomb is manufactured from 3-mil thick aluminum with nominal axial crush strength of 1,500 psi and nominal lateral crush strength of 75 psi. The honeycomb spacer details are shown on drawingsR-R4-G-00033. The bottom aluminum spacer is 3-inches long by 6.5-inch diameter and weighs nominally 0.7 lbs. One side of the spacer is embossed with the outline of the 5CV bottom configuration (i.e., cap and skirt). The middle tubular honeycomb spacer is 14-inches long with a 5¾-inch ID and 8-inch OD. The top inside ID of the tubular spacer is crushed to match the outline of the 5CV. The middle spacer weighs nominally 2.4 lbs. The top aluminum honeycomb spacer is 2¾-inch -inches long by 7-inch diameter and weighs nominally 0.7 lbs.

2.1.1.3 Containment Vessel

The containment vessel (CV) provides a structural barrier and leak-testable closure that prevents the release of the radioactive contents under regulatory NCT and HAC. The two 9977 packaging configurations include 5-inch or 6-inch diameter CV designs, both with conical sealing surfaces and a single-threaded closure, as developed originally by Gordon Chalfant. CVs are shown on drawings R-R2-F-00042 and R-R2-F-00043. Both CV designs are part of the currently certified 9975 package. The CVs are designed, fabricated, and examined in accordance with ASME B&PV Code Section III, Subsection NB, as described in Sections 2.3 and 9.3. Exceptions to NB are summarized in Section 9.3. Design pressures and temperatures are given in Tables 2.20 and 2.21. Design details are discussed below.

The 5CV and CV are designed for 900 and 800 psig at 500 ºF. Every CV is proof-tested at an internal pressure at least 50% higher than its design value. This exceeds the 10 CFR 71.85

requirements for proof-testing at 50% above the calculated maximum normal operating pressure (MNOP), see Table 2.20. It also exceeds the ASME Code pressure test requirement of 25% above the design pressure. The 5CV/6CV assemblies are also evaluated and tested for leak-tightness at an external pressure of 21 psig (50-ft head of water).

5CV Description

The 5-inch CV body is fabricated from Schedule 40S, Type 304L stainless steel (SS) seamless pipe having 0.258-inch nominal wall thickness. The pipe is terminated by a standard weight 5-inch Type 304L SS pipe cap (also 0.280-inch nominal wall) welded at one end. A stayed head welded at the other end completes the 5CV body and is fabricated from 5-inch diameter 2¼-inch long stainless steel bar stock machined to include 5½-12UNS-2B internal thread and an interior conical sealing surface. Vessel body joints are circumferential, full-penetration, Category B welds in accordance with the ASME Code. A short segment of 4-inch, Schedule 40S Type 304L SS pipe is welded to the convex side of the pipe cap, forming a skirt to support the 5CV vertically. The skirt includes two notches in the bottom edge (180° apart) to engage a rectangular key and thereby prevent vessel rotation during removal and installation of the closure. The completed 5CV weldment weighs nominally 23.5 lb.

The CV body is closed by a ¾-inch thick 304L SS cone-seal plug held in place by a 0.63-inch thick Nitronic® 60 cone-seal nut. The nut is machined to include an external 5½-12UNS-2A thread. Two parallel O-ring grooves are machined into the sealing surface of the cone-seal plug as shown in Drawing R-R2-G-00043, Appendix 1.1. The cone-seal nut threads into the stayed head of the CV, forcing metal-to-metal contact between the exterior of the cone-seal plug and the interior cone-seal surface of the CV body. Compression of the inner O-ring between the conical sealing surfaces completes the leak-tight containment boundary, as demonstrated in accordance with ANSI N14.5.

The cone-seal plug incorporates a leak-test port that sealed with a commercial gland nut and plug, manufactured by Pressure Products Industries (PPI). The outer O-ring and leak-test port on the cone-seal plug form a convenient leak-test volume for verifying the containment performance of the inner O-ring. The cone-seal plug and cone-seal nut are coupled mechanically by a retaining ring attached to the cone-seal plug as shown in Drawing R-R2-G-00043. The combined weight of the closure assembly is nominally 9 lbs. The average weight of an assembled 5CV empty is 32.2 lb.

6CV Description

The 6-inch CV is fabricated from Schedule 40S, Type 304L SS seamless pipe having a 0.280-inch nominal wall thickness. The pipe is terminated by a standard weight 6-inch Type 304L SS pipe cap (also 0.280-inch nominal wall) welded at one end. A stayed head welded at the other end completes the 6CV body and is fabricated from a 7½-inch diameter by 2¼-inch long Type 304L SS bar stock machined to include 6½-12UNS-2B interior thread and an interior conical sealing surface. Vessel body joints are circumferential, full-penetration, Category B welds in accordance with the ASME Code. A short segment of 5-inch, Schedule 40S Type 304L SS pipe is welded to the blind end cap, forming a skirt to support the 6CV vertically. The skirt

includes two notches in the bottom edge (180° apart) to engage a rectangular key and thereby prevent vessel rotation during removal and installation of the closure. The completed 6CV body weighs on average 52.2 lb.

The CV body is closed by a ¾-inch thick 304L SS cone-seal plug held in place by a 0.63-inch thick Nitronic® 60 cone-seal nut. The nut is machined to include an external 6½-12UNS-2A thread. Two parallel O-ring grooves are machined into the sealing surface of the cone-seal plug as shown in Drawing R-R2-G-00043. The cone-seal nut threads into the stayed head of the CV, forcing metal-to-metal contact between the exterior of the cone-seal plug and the interior cone-seal surface of the CV body. Compression of the inner O-ring between the conical sealing surfaces completes the leak-tight containment boundary, as demonstrated in accordance with ANSI N14.5.

The cone-seal plug incorporates a leak-test port that sealed with a commercial gland nut and plug, manufactured by Pressure Products Industries (PPI). The outer O-ring and leak-test port on the cone-seal plug form a convenient leak-test volume for verifying the containment performance of the inner O-ring. The cone-seal plug and cone-seal nut are coupled mechanically by a retaining ring attached to the cone-seal plug as shown in Drawing R-R2-F-00042. The combined weight of the closure assembly is approximately 12.7 lb. The weight of an assembled 6CV empty is about 52.2 lb.

2.1.2 Design Criteria

Design and fabrication criteria for the package comply with 71.41 through 71.51 of 10 CFR 71, 49CFR173[13] and 177, International Atomic Energy Agency (IAEA) Safety Series No. TS-R-1 and Regulatory Guide (RG) 7.11[14] and NUREG/CR-3854.[15] Structural analyses were performed in accordance with the methodology and stress criteria specified in ASME BPVC, Section III, Division 1, and NRC RGs 7.6[16] and 7.8.[17]

The structural analyses of the CV designs are based on the ASME Code Section III, Division 1, Subsection NB. Finite element analyses were performed to evaluate the CVs for the required loading conditions per RG 7.8. From the stress results, stress intensities were calculated for evaluation against the acceptance criteria specified in the ASME Code Section III, Subsection NB.

For the geometries of the containment vessels, the principal stress directions are hoop, longitudinal, and radial. Therefore, if σ_h, σ_l, and σ_r are the hoop, longitudinal, and radial stresses at any point, then the principal stresses are:

$$\sigma_1 = \sigma_h, \sigma_2 = \sigma_l, \text{ and } \sigma_3 = \sigma_r$$

Radial stresses, σ_r, are compressive and vary from the value of internal pressure at the inside surface to zero at the outside surface of the cylinder. An average value of σ_r is used to calculate the stress intensities. If S is the stress intensity, then S can be calculated as:

$$S = \text{Max} (|\sigma_1 - \sigma_2|, |\sigma_2 - \sigma_3|, |\sigma_3 - \sigma_1|)$$

Stress intensities from various loadings are combined conservatively by adding their absolute values to obtain the total stress intensity.

The overpack is designed and fabricated with a "sanitary" bottom in accordance with United Nations (UN) Drum Specification 1A2, per 49 CFR 178 Subpart L and Section III, Subsection NF of the ASME Code. The bolted closure of the overpack is evaluated against the stress criteria specified in the ASME Code, Section III, Subsection NF.

To ensure safe structural behavior of the package, RGs 7.6 and 7.8 require that the package designer consider specific initial conditions and load combinations. Table 2.2 is a summary of conditions specified in RG 7.8 and in 10 CFR 71 for NCT and HAC. Figure 2.2 shows the load combinations required by RG 7.8 and the stress intensity limits specified by RG 7.6. As specified in RG 7.6, the stress criteria applied for NCT are those specified in ASME BPVC, Section III for Level A Service Loads. Nonlinear finite element analyses were performed to simulate the dynamic response of the package during the NCT and HAC impact events. Stress criteria specified in the ASME BPVC, Section III, Appendix F for Level D service loads were used to verify that the HAC loading did not result in a CV exceeding Code-allowable limits. Based on experimental data, the maximum allowable strain limit for the stainless steel components is 30 percent at 257°F.[18] In addition, elastic buckling of the CV was evaluated in accordance with Section III, Division 1 of the ASME BPVC.

To eliminate brittle fracture of the CV under HAC events, the containment vessels are fabricated from 304L SS in accordance with the guidance provided in RG 7.11.[15] Consideration of brittle behavior is not required based on RG 7.11, which states,

> "Since austenitic stainless steels are not susceptible to brittle fracture at temperatures encountered in transport, their use in containment vessels is acceptable to the staff and no tests are needed to demonstrate resistance to brittle fracture."

The structural components of the containment vessels, and the drum, are fabricated from stainless steel, which does not experience creep below 700°F. The highest temperatures the containment vessels are exposed to during NCT remain below 300°F and 400 °F during HAC, therefore, the potential for creep is negligible. Design considerations relative to the creep failure mode are therefore satisfied.

Package analyses are based on nominal packaging component weights with maximum payload weight. Based on the maximum 6CV payload weight of 100 lb, the maximum weight of the loaded 9977 is 350 lbs. This bounds the lighter 5CV configuration with a 50 lb payload which has a maximum weight of 287.5 lbs.

Recognizing the large margins of safety quantified by analyses performed with nominal packaging component sizes, there is no design feature of the 9977 that would be compromised by analyses performed at the minimum package weight or component size. Therefore, the combination of nominal packaging weight and maximum payload weight is used to evaluate the 9977 performance under NCT and HAC loading conditions shown in Table 2.2.

Table 2.2 - Summary of Load Combinations for NCT and HAC

Applicable Initial Condition	Ambient Temperature		Insolation		Decay-Heat Rate		Internal Pressure		Fabrication Stresses
	100°F	-20°F	Max.	Zero	Max.	Zero	Max.	Min.	Note 3
NORMAL CONDITIONS									
Hot environment: 100°F ambient temperature	✓		✓		✓		✓		
Cold environment: -40°F ambient temperature				✓		✓		✓	
Increased external pressure: 20 psia		✓		✓		✓		✓	
Minimum external pressure: 3.5 psia	✓		✓		✓		✓		
Vibration and shock: normally incident to the mode of transport	✓		✓		✓		✓		
		✓		✓		✓		✓	
Free drop: 4-ft drop	✓		✓		✓			✓	
		✓		✓			✓		
Corner Drop	Note 1								
Compression	✓			✓		✓		✓	
Penetration	✓		✓		✓		✓		
ACCIDENT CONDITIONS									
Free drop: 30-ft drop impact	✓		✓		✓		✓		
		✓		✓		✓		✓	
Crush: 1,100 lb plate		✓		✓		✓		✓	
	✓		✓		✓			✓	
Puncture: 40-inch drop onto "pin"	✓		✓		✓			✓	
		✓		✓		✓		✓	
Immersion, 3 ft	Note 2								
Immersion, 50 ft				✓		✓		✓	
Thermal: 1475ºF fire event	✓		Note 4	✓	✓		✓	✓	

1. Not applicable as "this test applies to only fiberboard, wood or fissile material rectangular and cylindrical packages not exceeding 110 lbs and 220 lbs, respectively. The minimum 9977 calculated weight is 240 lb.
2. Not applicable, criticality analysis includes water inleakage.
3. Evaluation not required, as defined by RG 7.8, Regulatory Position 1.5.
4. NRC RG 7.8 identifies this as an initial condition of testing; however, NRC adopts the view of IAEA which is that package initial condition prior to the fire does not include the effects of insolation, Federal Register/Vol 60. No. 188/ Thursday, September 28, 1995/Rules and Regulations, pg 50257.

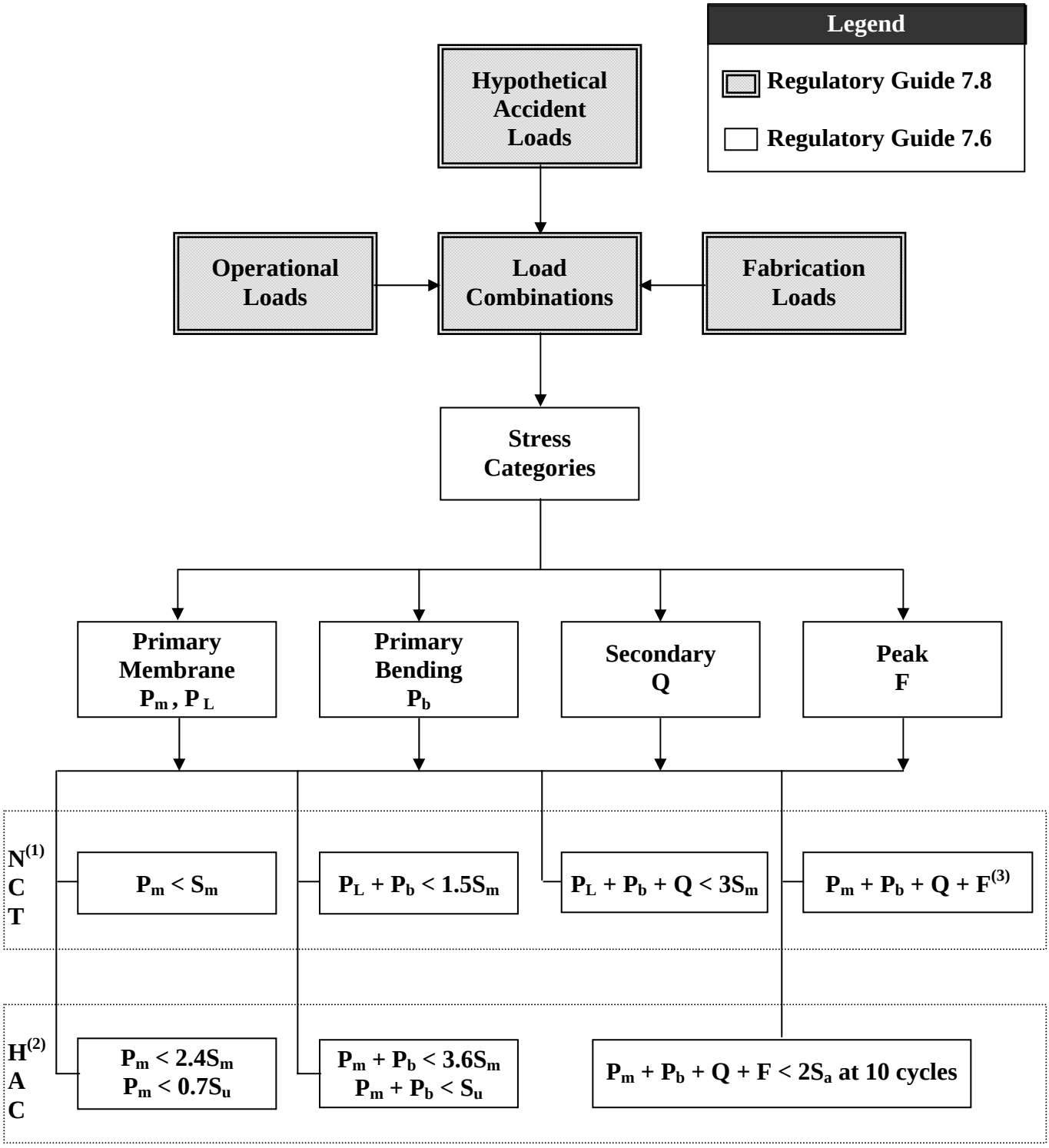

Notes – 1) Level A Service Limits for Stress
2) Level D Service Limits for Stress
3) The allowable stress intensity for the full range of fluctuations is 2 S_a per Figure NB-3222-1.

Figure 2.2 – Load Combinations and Stress Intensity Limits from Regulatory Guides 7.6 and 7.8

2.1.3 Weights and Centers of Gravity

Table 2.3 provides a summary of the 9977 package weights when fitted with the 5CV and 6CV. Minimum and maximum permissible content weight for each CV is also shown. Nominal, minimum, and maximum component weights for the 9977 are summarized in Table 2.4. Package component weights are calculated in detail in Appendix 2.3.

Table 2.3 - 9977 Loaded Package Weights

Packaging Configuration		**Weight** (lb)		
		Minimum	Nominal	Maximum
9977 with 5-inch CV	Empty Overpack w/spacers	171.9	186.6	202.8
	5CV Empty	29.7	32.2	34.7
	5CV Contents	50	50	50
	Total 5CV w/ max payload	251.6	268.8	287.5
9977 with 6-inch CV	Empty Overpack w/spacers	168.7	182.8	198.4
	6 CV Empty	48.0	52.2	56.4
	6CV contents	100	100	100
	Total 6CV w/ max payload	316.7	335.0	354.8

Table 2.4 - Packaging Component Weights

Overpack Components		**Weight** (lb)			**Comments**
		Minimum	Nominal	Maximum	
Overpack Hardware	Drum Body	62.8	70.0	83.7	SS shell, including tape, wire
	Fiberfrax	3.8	5.1	6.4	Insulation
	Last-A-Foam FR-3716	68.3	8	75.4	
	Drum Closure Lid	14.4	15	16.5	SS shell only
	Min-K 2000	1.4	1.7	1.9	
	TR-19	2.3	2.6	2.9	
	Fiberfrax	0.2	0.3	0.3	
	Drum Closure Bolts & Washers	1.9	2.0	2.1	
	Empty Overpack Total	153.3	166.5	181.3	
CV Hardware	5-inch Containment Vessel	29.7	32.2	34.7	Assembly
	6-inch Containment Vessel	48	52.2	56.4	Assembly
	5CV Honeycomb spacers	3.2	3.8	4.3	
	Load Distribution Fixtures	13.5	14.2	14.9+	

The centers of gravity (CGs) of the packaging components are all located on the longitudinal axis of the packaging. Figure 2.3 illustrates the CG's locations for an empty packaging and loaded package.

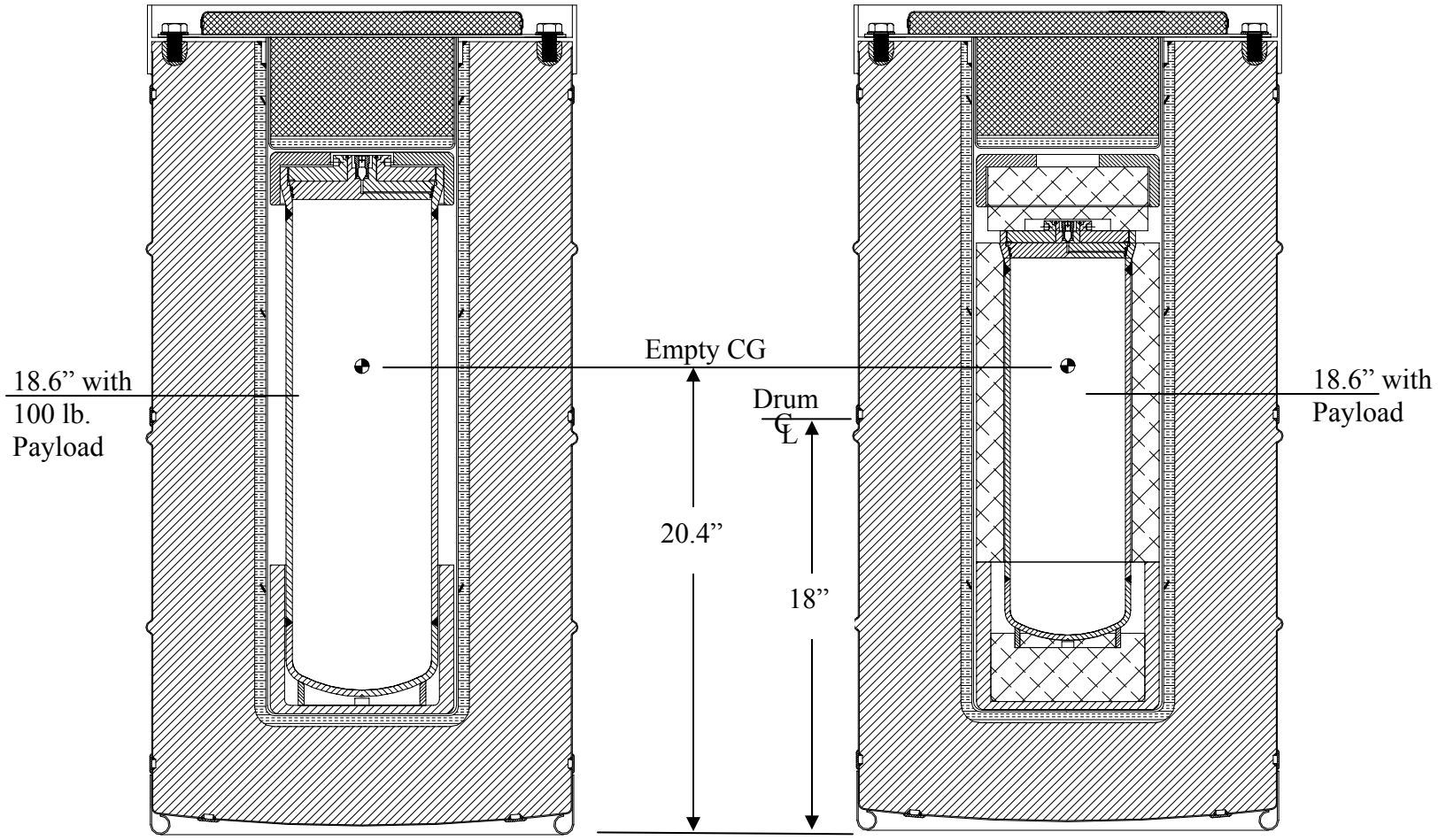

Figure 2.3 – 9977 Centers of Gravity for Empty 5CV and 6CV Packaging Configurations

2.1.4 Identification of Codes and Standards for Package Design

The packaging design criteria are based on evaluation of the maximum radiological hazard (A_2 units) and curie (Ci) content for "Normal Form" radioactive material. Based on this data, RG 7.11 and NUREG/CR-3854 are used to identify "established codes and standards for design, fabrication, assembly, testing, maintenance and use" requirements for the packaging.

The most hazardous 9977 content loading is 4.4 kg of Plutonium/Uranium, as shown in Table 1.2. The calculated hazard (in A_2 units) and total curie count are 122,000 A_2 and >69,700 Ci, respectively. Given this data, RG 7.11 specifies the radioactive material packaging design as "Category I." Applicable Codes and Standards to be used for the design, fabrication, assembly, testing and maintenance of the 9977 are specified in NUREG 3854, Table 1.1, *Summary of fabrication criteria based on the ASME Code*. The 9977 design does not incorporate active heat transfer processes, nor does it incorporate secondary seals, criticality control features or radiation shielding. The package does include features that permit lifting and tie down for transport.

Table 2.5 presents detailed ASME code criteria for fabricating 9977 metal components as Category I design entities, i.e., containment vessels. In addition, the table includes criteria for fabrication, assembly, testing and maintenance of the other features of the 9977. The table is reproduced in part from NUREG 3854, Table 4.1.

Table 2.5 - Criteria for Metallic and Non-Metallic Components for a Category I Radioactive Material Packaging - 9977

Acceptance	Component Safety										
	Containment		Criticality	Other Safety Features							
				Overpack		Impact limiters			Tie-down	Lifting	
	CV Body	Seals		Drum	Bolted closure [3]	Load Distribution Fixtures	Honeycomb Spacers	Insulation			
Design	ASME NB-3000	NB-3000	Note 1	UN 1A2	VIII, Div 1 and ASME NF-3000	Per Design	Commercial [2]	Commercial	10 CFR 71.45(b)	ANSI N14.6	
Materials	NB-2000	MIL-R-83485 Type 1		NF-2000	ASME SA-193, 194 & 320	Section VIII, Div 1	Commercial	Commercial	NF-2000	NF-2000	
Forming, Fitting and Aligning	NB-4200	Commercial		UN 1A2	NF-4200	Per Design	Commercial	Commercial	Per Design	Per Design	
Fabrication and Examinations	NB-5000	Commercial		UN 1A2	NF-4000 NF-5000	Per Design	Commercial	Commercial	Per Design	Per Design	
Acceptance Testing	NB-6000	ANSI-N14.5		UN 1A2	NF-2581.2	Per Design	Commercial	Commercial	Per Design	Per Design	

Note 1. The 9977 does not incorporate any passive or active criticality control features. Accordingly, no ASME code criteria for criticality are applicable.
2. The use of the term "Commercial" implies that specific vendor data was used to evaluate the material for use in the 9977 package.
3. The bolted closure also includes the drum flange weldment and lid construction.

2.2 MATERIALS

2.2.1 Material Properties and Specifications

Material specifications for packaging components presented in Table 2.6 were extracted from the design drawings provided in Appendix 1.1. Mechanical properties of the packaging materials are presented in Tables 2.7 through 2.14 and in Figures 2.4 and 2.5. Tables 2.7 and 2.14 present the mechanical properties of the overpack closure hardware, drum overpack and CVs. Table 2.8 presents properties of the 5CV honeycomb spacer materials.

Stainless steel components of the 9977 are unaffected by normal operating temperatures. The Fiberfrax, TR-19 and Min-K 2000 materials are rated for continuous use at temperature above 1,200°F, and are therefore unaffected by the normal operating temperatures within the 9977.

The constitutive properties of the General Plastics Last-A-Foam® FR-3716 insulation are provided in Table 2.9. Figures 2.4 and 2.5 summarize the relationship between load and deflection for the bulk polyurethane Last-A-Foam from -20°F to 300°F. The polyurethane foam has a glass transition temperature, Tg, of 279°F. The foam slowly softens at temperatures greater than Tg. If the polyurethane foam is confined and no mechanical loads are applied, it can be held at 300°F for an extended period, without degradation.[19,20] Upon cool-down, the foam fully recovers its physical properties.[21] Out-gassing and melting/oxidation is not observed below about 500°F. The foam becomes a flowing liquid just below its ignition temperature, which is above 600°F. The type of foam used in the 9977 is also used in a variety of military H-Gear. Aging studies have been performed at temperatures above and below the Tg to evaluate changes to the foam chemistry that could degrade physical properties. These studies have been performed by the Supplier (General Plastics) and by Sandia National Laboratory. Little change has been observed in the crush strength or thermal conductivity of Last-A-Foam aged up to twenty years.[21, 22, 23]

Material properties data for Fiberfrax®, Thermal Ceramics Min-K 2000 and Thermal Ceramics TR-19 insulation materials are presented in Tables 2.10, 2.12 and 2.11, respectively.

Physical and mechanical property data for Viton® GLT O-ring material is provided in Table 2.13. Mechanical properties for stainless steel given in Table 2.14 and corresponding stress limits given in Table 2.15, were obtained from the ASME BPVC, Section II, Parts A and D, 2004.[24] The ASME BPVC provides properties at temperatures -20°F and higher. The ASME values at -20°F are assumed to be conservative relative to the -40°F design temperature properties required by 10 CFR 71. Regulatory Guide 7.11 states that austenitic steels are not susceptible to brittle fracture at transport temperatures, and therefore, brittle failure of 9977 steels in service is not a safety concern.

Table 2.6 - Packaging Components and Material Specifications

Component	Material Specifications (Form, Specification, Type/Grade)
35-Gallon Drum Overpack	
Drum Body	18-gauge Sheet, ASME SA-240, Type 304L
Drum Rim	3 × $^{3}/_{16}$-inch , ASME SA-240 plate, Type 304L
Drum Top	3/16-inch thick, SA-240 plate, Type 304L
Drum Wear Ring	16-gauge Sheet, SA-240, Type 304L
Drum Liner	18-gauge Sheet, SA-240, Type 304L
Closure Lid	16-gauge Sheet, ASME SA-240, Type 304/304L
Closure Screws	⅝-11UNC-2A × 1¼ inch long, Heavy Hex Head Screw, ASME SA-193/SA-320, Grade B8, Class 2, ANSI B18.2.1 & B18.21.1a
Closure Inserts (Nut)	Threaded Fitting, ⅝-11UNC-2B, Grade 8 per ASME SA-194 and SA-320, 304 SS
Closure Washers	⅝-inch, Plain Narrow Type B, 18-8 SS, ASME/ANSI B18.22.1
Caplugs	BPF-¼ , Ethylene Vinyl Acetate, Black, Flush Button Plugs
Caplugs	BPF-3/4 and BPF-1, Low density Polyethylene, Black, Flush Button Plugs
Stud	4d Nail, 12 Gauge × 1½ Long, 316 SS, McMaster PN 97990A102
Lock Washer	Washer, Pin Style, McMaster PN 93610A410
Identification Plate	16-gauge (0.06 REF), 304/304L SS, Lettering filled with Epoxy Paint, High Temperature, Glossy Black
Overpack Insulation Materials	
Glass Cloth Tape	3M Product Number-361, 2-inches wide × 7.5 mils thick, temperature range -65°F to 450°F
Lid-Chamber Silicone	RTV-382 High Temperature Silicone
Polyurethane Insulation	General Plastics, Last-A-Foam® FR-3716, Intumescent Polyurethane Foam, 15–17 lb/ft^3 (free rise density)
Fiberfrax Insulation	½-inch thick Fiberfrax® Insulation, HSA, Grade E, 7-10 lb/ft^3, Quilted with E Grade Fiberglass Fabric (both sides), Kansas City Plant Specification[25]
Thermal Ceramics Insulation	TR-19 Block Insulation, 23 lb/ft^3
Thermal Ceramics Insulation	Thermal Ceramics item BL#31274-100, Min-K 2000, 20 lb/ft^3, 14 inches OD by 1-inch thick

Table 2.6 - Packaging Components and Material Specifications (continued)

Component	Material Specifications (Form, Specification, Type/Grade)
Containment Vessel	
Body Cylinder	5- and 6-inch diameter Schedule 40S Pipe, Seamless, ASME SA-312, Type TP304L, (product analysis, hydrostatic and UT electric test apply)
Body Closure	Bar, ASME SA-479, Type 304L
Body Bottom Pipe Cap	5- and 6-inch diameter Schedule 40S Cap ASME SA-403, Type 304L, WP-W
Body Skirt	4- and 5-inch diameter Schedule 40S Pipe, Seamless, ASME SA-312, Type TP304L
Cone Seal	Bar, ASME SA-479, Type 304L
Cone Seal Nut	Bar, ASME SA-479 Annealed Condition ARMCO Nitronic-60 SST
Gland Nut	PPI Catalog No. P-130-60, Stainless Steel
Gland Plug	PPI Catalog No. P-110-60, Stainless Steel
Retaining Ring	Waldes Truarc No. 5108-125
5-inch Diameter CV O-rings	Molded Viton "GLT," Compound No. V-0835-75, Class AN, Parker Part AS-568-244
6-inch Diameter CV O-rings	Molded Viton "GLT," Compound No. V-0835-75, Class AN, Parker Part AS-568-252
Thread and CV Closure Lubricant	Krytox® fluorinated grease, E.I. DuPont, Aerospace Grease Grade 240 AC[26]
Overpack CV Spacer Assembly	
Upper and Lower Load Distribution Fixtures	ASME SB-221, 6061-T6 Aluminum Round Bar
Axial and Lateral Honeycomb Spacers	Aluminum Tube Honeycomb, Pre-crushed, Crush Strength 1500 ±500 psi, 3-mil minimum thickness aluminum foil

Table 2.7 - Mechanical Properties of the Overpack Closure Hardware

Materials of Construction		Minimum Yield Strength, S_y (ksi)	Minimum Tensile Strength, S_u (ksi)
Heavy Hex Screw [a]	ASME SA-193/SA-320, Grade B8, Class 2	100	125
Closure Inserts (Nut) [b]	ASME SA-194/320, Grade 8	-	-
Washer [c]	18-8 hardened	c	c

a) Material properties taken from ASME BPVC Section II, Part D (Table 3, line 29, pg. 391 per Section VIII-1),

b) Specification for nuts does not include yield/tensile strength values. Grade-8M nut specifications include a hardness requirement of 60-105 Rockwell B, and a proof load of 18,080 lb based on a proof stress of 80,000 psi.

c) Washer mechanical properties are not critical to safety, and consequently no values are provided.

Table 2.8 – Mechanical and Physical Properties of the Overpack Containment Vessel Spacers

Packaging Component	Materials of Construction[a]	Property (units)	Value	Temperature (°F)
Upper and Lower Load Distribution Fixtures	SB-221, Grade 6061-T6, Aluminum	Minimum Yield Strength (psi)	35,000	--
		Minimum Tensile Strength (psi)	38,000	--
		Elongation (%)	8 - 10	--
		Poisson's Ration	0.33	--
		Density (lb/in^3)	0.098	--
		Average Thermal Expansion from 70°F (in./in./°F)	--	-100
			12.1×10^{-6}	70
			12.6×10^{-6}	100
			13.5×10^{-6}	200
			14.0×10^{-6}	300
			14.3×10^{-6}	400
			15.3×10^{-6}	500
		Modulus of Elasticity, E (psi)	10.5×10^{6}	-100
			10.0×10^{6}	70
			--	100
			9.6×10^{6}	200
			9.4×10^{6}	300
			8.7×10^{6}	400
			8.1×10^{6}	500
Hexcel Honeycomb Spacers (3-mil min. foil thickness)	Aluminum	AXIAL CRUSH STRENGTH (PSI)	1500 ± 500	--
		Lateral Crush Strength (psi)	75 ± 25	--

a) ASME Code, Section II, Parts A and D, [Error! Bookmark not defined.]
- Yield Strength, Table Y-1, pg. 563, Line 39,
- Tensile Strength, Material Group 3, Table U, pg. 456, Line 35,
- Elongation; (SB-221, 8% up to 0.249 inches thick, 10% over 0.25 inches)
- Poisson's Ratio, Table NF-1, pg. 702,
- Density, Table NF-2, Pg. 703,
- Thermal Expansion, Table TE-2, pg. 672, and

- Modulus of Elasticity, Material Group G, Table TM-1, pg. 698.

Table 2.9 - Mechanical Properties of Last-A-Foam FR-3716

Material Parameter	Property
Stress vs Strain (-20ºF to 300ºF)	See Figures 2.4 and 2.5
Poisson's Ratio	0.3
Coefficient of Liner Thermal Expansion	$3.5\text{-}5.0 \times 10^{-5}$ in/in/ºF (-320ºF to 200ºF)
Water Absorption [a]	0.011 lb/ft^2
Density (Free Rise)	15-17 lb/ft^3

a) Last-a-Foam is a closed cell structure; therefore, water absorptivity is surface (wetting) phenomena and measured in square feet.

Table 2.10 - Mechanical Properties of Quilted Fiberfrax® Lo-Con Blanket, Grade E Fabric

Materials of Construction	Material Parameter	Property
Lo-Con Blanket (Felt core)	Linear Expansion	0.5 %
	Nominal Use Temperature Limit	2300ºF
	Thickness	0.44 – 0.69
	Density	5-7 lb/ft^3
	Weight Quilted Composite	4 lb/ft^2
E-Fiberglass Textile Cloth (Quilting)	Stitching Pattern Warp Fill Weight Thickness	 Woven-plain weave 60 ends/in 58 ends/in 3.10 oz/yd^2 0.0035 inches
	Nominal Use Temperature limit	1200ºF
	Tensile Strength	n/a
	Thread	E-Fiberglass
Quilted Composite	Thickness	0.40 – 0.50
	Density	7-10 lb/ft^3
	Weight	4 lb/ft^2

Table 2.11 - Mechanical Properties of TR-19 Block Insulation

Material Parameter	Property
Modulus of Rupture (lb/in^2)	
Ambient	120
1900°F	89
Crushing Strength (lb/in^2)	
Ambient	184
1900°F	85
Nominal Density (lb/ft^3)	
Ambient	23
1900°F	23.5

Table 2.12 - Mechanical Properties of Min-K 2000 Insulation

Material Parameter	Property
Average transverse strength, minimum (lb/in^2)	55
Compressive Strength (lb/in^2)	
5% compression	110
8% compression	190
Nominal Density (lb/ft^3)	20

Table 2.13 - Mechanical Properties of O-rings

Material Parameter	Viton GLT Fluorocarbon Rubber [a]
Rubber Specification	AMS-R-83485
Parker Compound	V0835-75
Fabrication Method	Molded
Temperature Range	-40°F to 400°F
Hardness Durometer (Shore A)	70-80

a) Parker Data from O-ring Handbook, ORD-5700A[12]

Table 2.14 –Mechanical and Physical Properties of Containment Vessel and Drum Metal

Packaging Component		**Materials of Construction** [a]	
Containment Vessel			
Vessel Wall		SA-312, Grade TP-304L	
End Pipe Cap		SA-403, Grade WP-W 304L	
Stayed Head		SA-479, Type 304L	
Cone-Seal Plug		SA-479, Type 304L	
Cone-Seal Nut		Nitronic-60 SS (Annealed condition)	
Drum Body & Closure Lid		SA-240, Type 304L	
Material Properties		304L	Nitronic-60[27]
Mechanical and Physical Properties [a]	Minimum Yield Strength (psi)	25,000	50,000
	Minimum Tensile Strength (psi)	70,000	90,000
	Elongation	28% - 40%	35%
	Poisson's Ratio	0.34	0.298
	Density (lb/in^3)	0.286	0.275
	Temperature (°F)	**Average Thermal Expansion from 70°F** [b] (in./in./°F)	**Modulus of Elasticity, E** [b] (psi)
	-100	--	29.2×10^6
	70	8.5×10^{-6}	[26.2] 28.3×10^6
	100	8.6×10^{-6}	--
	200	[8.8] 8.9×10^{-6}	27.5×10^6
	300	9.2×10^{-6}	27.0×10^6
	400	[9.2] 9.5×10^{-6}	26.4×10^6
	500	9.7×10^{-6}	25.9×10^6
	600	--	25.3×10^6

a) ASME Code, Section II, Parts A and D[Error! Bookmark not defined.];
   i. Yield Strength, Table Y-1, pg. 563, Line 39,
   ii. Tensile Strength, Material Group 3, Table U, pg. 456, Line 35,
   iii. Elongation; (SA-479, 35%, UNS-21800), (SA-240, 40%), (SA-403, 28% longitudinal), (SA-312, 35% longitudinal),
   iv. Poisson's Ratio, Table NF-1, pg. 702,
   v. Thermal Expansion, Material Group 3, Table TE-1, pg. 669, Coefficient "B". 304L and Nitronic-60 (UNS #21800) are 18Cr-8Ni material property are equivalent, and
   vi. Modulus of Elasticity Material Group G, Table TM-1, pg. 696.

b) Items shown in brackets are for Nitronic-60 SS; all other values are for 304L.

Table 2.15 - Containment Vessel Allowable Stress, Yield and Tensile Strengths

Temperature (°F)	**Allowable Stress Intensity** (ksi)	**Yield Strength** (ksi)	**Tensile Strength** (ksi)
SA-312, TP-304L Seamless and Welded Pipe			
-20 to 100	16.7	25.0	70.0
200	16.7	21.4	66.1
300	16.7	19.2	61.2
400	15.8	17.5	58.7
500	14.7	16.4	57.5
SA-403, 304L WP-W Weld Fittings			
-20 to 100	16.7	25.0	70.0
200	16.7	21.4	66.1
300	16.7	19.2	61.2
400	15.8	17.5	58.7
500	14.8	16.4	57.5
SA-479, 304L Bar			
-20 to 100	16.7	25.0	70.0
200	16.7	21.4	66.1
300	16.7	19.2	61.2
400	15.8	17.5	58.7
500	14.8	16.4	57.5
SA-479, Nitronic-60, Bar, UNS-S21800			
-20 to 100	31.7	50.0	95.0
200	25.9	38.8	93.9
300	22.1	33.2	87.0
400	19.8	29.7	82.1
500	18.4	27.6	79.3

Note: Class 1 material with stress intensities based on material allowable stress intensities, S_m, from ASME Code, Section II, Part D.

SA312, TP304L	[Sm, Table 2A Page 314, Line 15], [Sy, Table Y-1, Page 568, Line 2], [Su, Table U, Page 456, Line 37]	SA-403, 304L, WP-W	[Sm, Table 2A Page 314, Line 20], [Sy, Table Y-1, Page 568, Line 4], [Su, Table U, Page 456, Line 39]
SA-479, 304L, Bar	[Sm, Table 2A Page 314, Line 21], [Sy, Table Y-1, Page 568, Line 6], [Su, Table U, Page 459, Line 2]	SA479, Nitronic-60,	[Sm, Table 2A Page 322, Line 40], [Sy, Table Y-1, Page 576, Line 5], [Su, Table U, Page 461, Line 40]

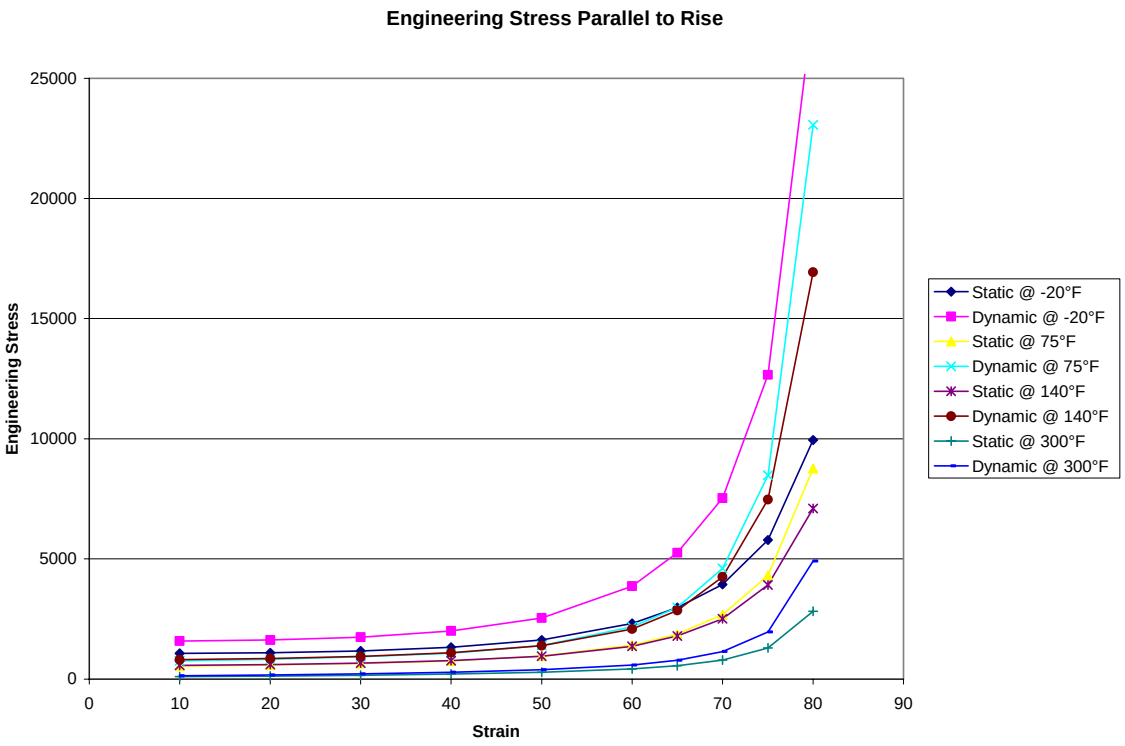

Figure 2.4 – Dynamic Engineering Stress-Strain Curve – Parallel to Rise for FR-3716 Foam

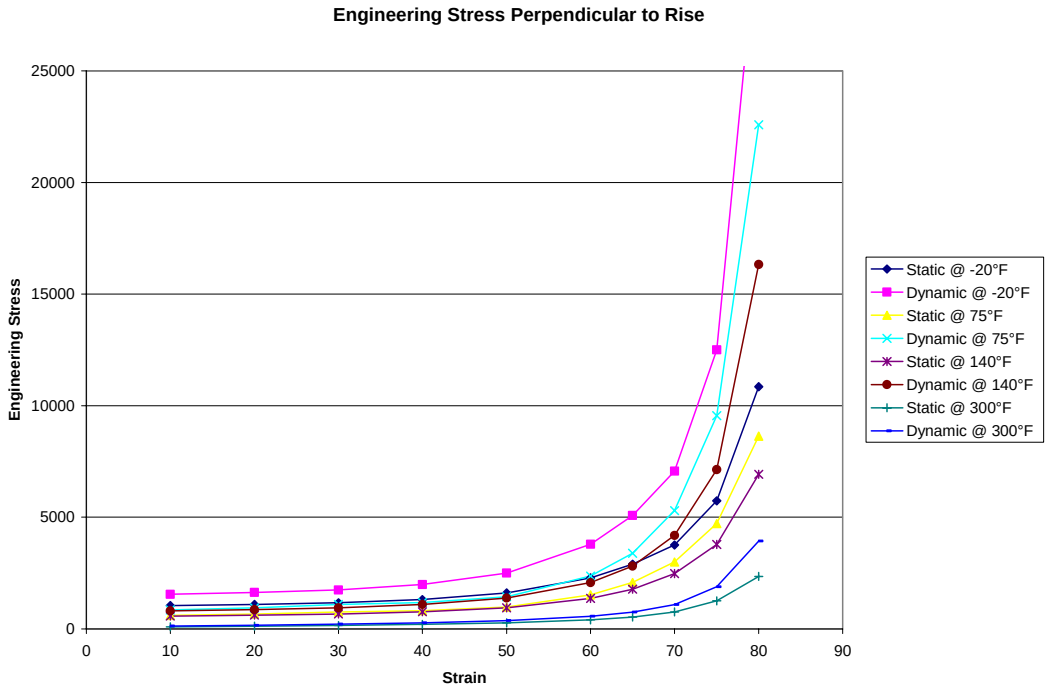

Figure 2.5 – Dynamic Engineering Stress-Strain Curve – Perpendicular to Rise for FR-3716 Foam

At small static strains, i.e., 10 to 20%, General Plastic's data indicates that Last-A-Foam FR-3700 crush strength in the direction perpendicular to rise is about 5% greater than that parallel to the rise. At the higher strain rates of dynamic loading, foam crushing behavior is essentially isotropic.

Dynamic testing of 15 lb/ft^3 FR-3700 foam by Federal Manufacturing and Technologies (FMT), indicates that the dynamic crush strength increases by about 50% over quasi-static data.[37] Figures 2.4 and 2.5 show the stress-strain relationships in the directions parallel to and perpendicular to the foam rise, respectively, for temperatures ranging from -20°F to 300°F. Application of the dynamic stress-strain properties at -20°F and 75°F in structural analyses of the packaging correlated extremely well with the damage observed in prototypes impact-tested under similar conditions. Because of this good agreement at low temperatures, extrapolation of material behavior model to elevated temperatures is expected to deliver acceptable analysis results.

2.2.2 Chemical, Galvanic, or Other Reactions

Requirement: 10 CFR 71.43(d) – A package must be made of materials and construction that assure that there will be no significant chemical, galvanic, or other reaction among the packaging components, among package contents, or between the packaging components and the package contents, including possible reaction resulting from in-leakage of water, to the maximum credible extent. Account must be taken of the behavior of materials under irradiation.

Evaluation: The 9977 packaging is designed for dry handling, transportation and storage. The required absence of liquid water from the contents significantly reduces the potential for adverse chemical and galvanic reactions. Nonetheless, the packaging is constructed of materials that would not be expected to react chemically, galvanically or otherwise with other packaging components. The combination of materials of construction present in the 9977 has been in service in other packagings for over twenty years without incident. Examples include the TRUPACT-II, AT-400R and the H-1616.

The matrix presented in Table 2.16 summarizes the material contacts within the package. The matrix presented in Table 2.17 summarizes the interactions between the radioactive contents and the materials of the CV. The packaging materials of construction, contents and potential chemical, galvanic and radiolytic reactions are discussed below. Table 2.18 presents chemical analysis of the materials used in the 9977.

Chemical and Galvanic Compatibility

The 9977 is constructed from 300-series stainless steel, various inorganic insulation materials and aluminum with a very minor presence of organic compounds as adhesives or lubricants. The 304L stainless steel used in the construction of the overpack and CVs is inherently corrosion resistant. Similarly, aluminum components (LDFs and honeycomb spacers) are also corrosion resistant. The General Plastics FR-3700 foam insulation is chemically inert and carries no detectable chlorides. The closed-cell nature of the foam precludes water absorption. Water may cling to the external surface of the foam surface but dries quickly in air. In a practical sense, the foam will not absorb water. In fact, testing to ASTM D-2842 is difficult, because water

absorption of the foam is typically less than the error inherent in the test. Therefore, corrosion within the package from the FR-3700 foam interaction shows no material incompatibilities.

The Fiberfrax sandwiched between the SS overpack liner and the Last-A-Foam, as well as the Min-K and TR-19 captured within the SS closure lid chambers, are composed primarily of alumina and silica (Al_2O_3, SiO_2) that will not react with the foam or stainless steel in either dry or wet environments. Similarly, the fiberglass textile cloth and fiberglass thread that bind the Fiberfrax blanket are non-reactive with both the stainless steel and Fiberfrax with which it is in contact. The silicone-based RTV-382 is formulated for safe use with corrosion prone metals and has no material incompatibilities when used in contact with the TR-19 and SS.[28]

The fiberglass tape[29] in contact with the Fiberfrax is resistant to high temperatures. Its adhesive is low-chloride silicone and is non-reactive with the Fiberglass textile cloth and fiberglass thread bindings.

Aluminum components are used to locate the CV inside the overpack liner. Aluminum is slightly anodic to stainless steel, and therefore, will not adversely affect the stainless steel CV or overpack liner.

No significant galvanic cell interactions exist among other package materials.[18,19] The radioactive materials are also chemically compatible with polyethylene or polyvinyl chloride bags commonly used to control the spread of radioactive contamination.

Other - Thermal Compatibility

Stainless steel components of the 9977 are unaffected by normal operating temperatures. The Fiberfrax blanket, TR-19 Block and Min-K 2000 are rated for continuous use at temperature above 1,200°F, and are therefore unaffected by the normal operating temperatures of the 9977.

The glass transition temperature of polyurethane foam is 279°F. Thermal decomposition occurs at 532°F. The maximum foam temperature is 295°F in a localized area below the drum liner (see Section 3.3). The mechanical strength of the foam is reduced at this temperature; however, there are no incompatibilities with surrounding materials.

There are no compatibility or reactivity issues associated with the gases generated by thermal decomposition of plastic bagging and the packaging or radioactive contents. The partial pressure of these gases is included in the Maximum Normal Operating Pressure (MNOP) for the CV (developed in Section 3.4.4). The MNOP is less negligible for each CV design pressure. A summary of pressures and temperatures used to calculate stress and thermal expansion of the containment system is given in Tables 2.21 and 2.22. The O-rings are Viton GLT fluoroelastomer and compatible with both the atmosphere and vacuum grease that will be in contact with them. Therefore, a chemical reaction that may affect mechanical properties used in the regulatory evaluation is not expected.[30]

Plutonium-iron compatibility issues have been identified in plutonium-handling facilities, where plutonium metal is in direct contact with stainless or carbon steel of storage containers. Plutonium and iron form a eutectic phase at 90% Pu - 10% Fe with a melting point of

approximately 770ºF. The presence of gallium can depress the eutectic point temperature to 752ºF. The postulated compatibility issue assumes that iron from the stainless steel diffuses into the plutonium to a sufficient extent that the eutectic composition is attained. If the temperature of this region were to exceed 752ºF, the affected region would melt. If the molten material alloyed with material from the container, breach of the container could occur. Several factors mitigate this phenomenon in the 9977. The presence of surface oxide layers on the plutonium metal or container provides an effective barrier preventing diffusion of iron from the container into the plutonium metal. Thermal analysis of the 9977 has shown that the maximum temperature in the contact region between a postulated point heat source and the stainless steel CV is 498ºF, well below the 752ºF eutectic temperature. Accordingly, the plutonium-iron eutectic issue is not a concern for the 9977.

Table 2.16 – Packaging Dissimilar Contacting Materials of Construction

Material	Material No.							
	1	**2**	**3**	**4**	**5**	**6**	**7**	**8**
1 Fiberfrax	--	✓	✓	✓		✓		
2 FR-3716 Foam	✓	--	✓	✓				
3 304L Stainless Steel	✓	✓	--	✓	✓	✓	✓	✓
4 E- Fiberglass	✓	✓	✓	--		✓		
5 RTV			✓		--	✓	✓	
6 TR-19	✓		✓	✓	✓	--		
7 Min-K 2000			✓		✓		--	
8 Aluminum			✓					--

☑ ≡ contacting material pairs. ⊟ ≡ same material. ☐ ≡ non-contacting surfaces.

Table 2.17 - Dissimilar Contacting Materials within the Containment Vessel

Material	Material No.					
	1	**2**	**3**	**4**	**5**	**6**
1 U/Pu	--	✓		✓		✓
2 Aluminum	✓	--		✓		✓
3 Kryotox Grease			--	✓	✓	
4 Stainless Steel	✓	✓	✓	--	✓	✓
5 Viton (O-rings)			✓	✓	--	
6 Polyethylene	✓	✓		✓		--

☑ ≡ contacting material pairs. ⊟ ≡ same material. ☐ ≡ non-contacting surfaces.

Table 2.18 - Materials of Construction - Chemical Analysis/Composition by Weight Percent

Nominal Composition	SS 304L[a]	TR-19	Fiber-frax [b]	E-glass [b]	Min-K 2000	FR-3700 Foam	Aluminum 6061
Alkalies, as, Na_2O, K_2O		2.6					
Alumina, Al_2O_3		9.1	40-54	12-16			
Aluminum							Remainder
Antimony trioxide					0-0.3		
Boron Oxide				8-13			
Calcium oxide, CaO		15		16-25			
Carbon	0.035					62.83	
Chromium	18-20						0.04-0.35
Copper							0.15-0.4
Decabromodiphenyl oxide					0-0.5		
Ferric oxide, Fe_2O_3		6.8	< 3				
Fibrous glass					5-30		
Hydrated Alumina					0-50		
Hydrogen						6.74	
Iron							0.7
Magnesium Oxide, MgO		13					
Manganese	2.0						0.8-1.2
Nickel	8-13						
Nitrogen	0.1					6.19	
Oxygen						22.21	
Phenol Formaldehyde					0-5		
Phosphorus	0.045						
Silica, SiO_2		40	46-60	52-60	35-95		
Silicon	1				0-25		0.4-0.8
Sulfur	0.030						
Sulfur trioxide, SO_3		0.4					
Titanium							0.15
Titanium oxide, TiO_2		1.2			0-25		
Zinc							0.25
Source References	[31]	[32]	[33]	[33]	[34]	[35]	[36]

a) Material composition based on minimum and maximum percentages from 304L specifications: SA-240, SA-312, SA-403, SA-479.

b) Other chemical/elements and inorganics are less than <4% for Fiberfrax and 7% for E-glass.

2.2.3 Effects of Radiation on Materials

Requirement: 10 CFR 71.43(d) – A package must be made of materials and construction that assure that there will be no significant chemical, galvanic, or other reaction among the packaging components, among package contents, or between the packaging components and the package contents, including possible reaction resulting from in-leakage of water, to the maximum credible extent. Account must be taken of the behavior of materials under irradiation.

Evaluation: The insulating materials used in the 9977 are relatively low density with no constitutive water content. None of the insulators present a significant cross-section for nuclear interaction. Radiation dose experiments performed at the University of Michigan on General Plastics Manufacturing Company polyurethane foam, which is the major insulating material within the package, has shown that foam samples subjected to 2×10^7, 4.21×10^7 and 2×10^8 rads had no effect on material compressive strength and intumescences proprieties from the radiation doses.[37] Polyurethane foams are environmentally stable materials due to their urethane polymer matrix. With the exception of ultraviolet radiation and some strong acids the foams do not degrade. The foam in the 9977 is encapsulated and is not exposed to ultraviolet radiation or harsh acids.

Radiation dose in excess of 10^7 rad is required before significant changes to physical properties of the O-ring are observed.[38] The 9975 Package utilizes containment vessels of the same design and materials as the 9977. The 9977 content envelope C.2 is similar to the 9975 content envelope C.3, both covering Pu and U Metals but has a lower dose rate because the 9975 content C.3 permits more impurities. The 9975 content C.4 (Pu/U Oxides) has a greater dose rate than the 9975 C.3 contents. Based on a calculated dose rate from the 9975 Content C.4, of approximately 0.1 rad/hr for the primary seal and a possible cumulative dose of approximately 1.8×10^4 rad for a conservative 2-year period, no significant changes in mechanical properties of the O-rings are expected.[39] This is conservative as the O-rings are limited by this SARP to a one-year service life.

No degradation or activation of the stainless steel structural components is expected at the neutron and photon dose rates as calculated in Chapter 5.

2.3 FABRICATION AND EXAMINATION

The 9977 packaging shall be constructed in accordance with the design drawings provided in Appendix 1.1, Quality Assurance requirements of Chapter 9 and the fabrication processes delineated below. Based on these data, manufactures shall develop detailed fabrication drawings and specifications that demonstrate their understanding of the requirements. No material purchases or fabrication activities shall commence until the requisite drawings and specifications have been reviewed and approved by the Packaging Design Authority.

Packaging fabrication can be divided into two categories, the manufacture of its 35 gallon overpack, and its containment vessels and the CV spacers (as applicable). Fabrication and examination of each of these components are described below.

2.3.1 Fabrication

2.3.1.1 Five-inch Containment Vessel Fabrication

The "5CV" containment vessel is comprised of a body and closure assembly. The 5CV body consists of a 5-inch Schedule 40S pipe cap, a 5-inch Schedule 40 seamless pipe and a machined interior-threaded stayed head. The 5CV closure assembly consists of a machined exterior-threaded closure nut and a truncated conical plug. The plug is machined to include a leak-test port and two O-ring grooves. The materials of fabrication and manufacturing specifications for the CV are listed in Tables 2.14 and 9.4 and follow the requirements of ASME BPVC, Section III, Division 1 for Class 1 components.

The 5CV is constructed by butt welding a 5-inch Schedule 40S, seamless, Type 304L stainless steel pipe cap to one end of the seamless pipe followed by a rough cut stayed head butt welded to the opposite end of the pipe. Both vessel body joints are circumferential full penetration Category B welds per ASME B&PV Code, Section III, Subsection NB-3350. A 4-inch, Schedule 40 Type 304L SS pipe is welded to the convex side of the cap to form a skirt which functions as a vertical support for the 5CV. The skirt includes two notches on the bottom edge (180° apart) that engage a rectangular key to prevent vessel rotation during removal and installation of the closure. The welded construction forms the CV body. The stayed head is rough-cut machined from a 6-inch diameter by 2¼-inch long Type 304L SS bar and welded to the body. Then the head is finish machined to include 5½-12UNS-2B internal thread and an interior cone-seal surface to a 32µin. finish.

Methods used to fabricate the CV weldment shall not reduce the thickness of the base materials below the minimum allowed per their material specifications. If the method used violates minimum material thickness the manufacturer shall verify that an approved manufacturing process is employed to recover.

Methods used to join the pipe to pipe cap and pipe to stayed closure head shall not reduce the wall thicknesses of the base materials below their minima as specified by their supporting material standards. If the minimum wall thickness is violated as a result of the method for joining components, the manufacturer shall verify minimum wall thickness is recovered. The go-no-go gauges required by Section 2.3.2 require the roundness and assembly of the 5CV and 6CV pipe and components to be tightly controlled. In most cases, pipe purchased to the SA-312 standard is not perfectly round and fit up of standard pipe caps not exact.

2.3.1.2 Six-inch Containment Vessel Fabrication

The "6CV" containment vessel consists of a 6-inch Schedule 40S pipe cap, a 6-inch Schedule 40 seamless pipe, a machined interior-threaded stayed head, a machined exterior-threaded closure nut and a truncated conical plug machined to hold two O-rings. The materials of fabrication and manufacturing specifications for the 6CV are listed in Tables 2.14 and 9.4 and follow the requirements of ASME BPVC, Section III, Division 1 for Class 1 components.

The 6CV is constructed by butt welding a Schedule 40S, seamless, Type 304L stainless steel pipe cap to one end of the seamless pipe followed by a rough cut stayed head butt welded to the

opposite end of the pipe. Both vessel body joints are circumferential full-penetration Category B welds per ASME B&PV Code, Section III, Subsection NB-3350. A short segment of 5-inch, Schedule 40 Type 304L SS pipe is welded to the convex side of the cap forming a skirt to support the 6CV vertically. The skirt includes two notches in the bottom edge (180° apart) to engage a rectangular key and prevent vessel rotation during removal and installation of the closure. The welded construction forms the CV body. the stayed head is rough-cut machined from a 7½-inch diameter by 2¼-inch long Type 304L SS bar and welded to the body. Then the head is finish machined to include 6½-12UNC-2B internal threads and an interior cone-seal surface to a 32µin finish.

Methods used to join the pipe to pipe cap and pipe to stayed closure head shall not reduce the wall thicknesses of the base materials below their minima as specified by their supporting material standards. If the minimum wall thickness is violated as a result of the method for joining components, the manufacturer shall verify minimum wall thickness is recovered.

2.3.1.3 Overpack Body Fabrication

The 9977 overpack is comprised of a modified UN 35-gallon drum incorporating a sanitary style bottom, a welded deck-lid/liner insert and a flanged closure lid. The drum liner insert and closure are fabricated in accordance with the drawings and specifications listed in Appendix 1.1. The materials of fabrication and manufacturing specifications for the Overpack are listed in Tables 2.14 and 9.5 and follow the requirements of ASME BPVC, Section III, subsection NF and ASME BPVC, Section VIII, Division 1. The overpack drum is procured to the UN drum specification UN/1A2.

Drum Body Fabrication

The overpack body is comprised of two metal parts; the drum body and a welded deck-lid/liner insert. Fabrication requirements for these two items are presented in Appendix 1.1. When assembled (by welding), the two parts create a form in which liquid-form polyurethane is poured. Prior to assembly (welding), the liner portion of the insert must be wrapped externally by two (2) ½-inch thick blankets of Fiberfrax®. The blankets are secured to the side wall and bottom of the liner by tape, wire and a series of studs that protrude from the liner wall. The insulated insert is then welded to the drum shell, and the volume between the liner and the drum shell is filled with foam. Details of how the Fiberfrax is installed and the foam process requirements are provided below.

Overpack Fiberfrax Installation (Drawing R-R2-G-00019)

2. Two (2) 8¼-inch diameter disks of ½-inch thick Fiberfrax blanket are cut to fit the liner bottom. See Figure 2.1. The disks are aligned and secured by impressing them unto the five (5) $^{1}/_{16}$-inch diameter studs located on the liner bottom.
3. Cut a rectangular piece of ½-inch thick Fiberfrax blanket, 33½-inches long by approximately 29½-inches wide to fit around the liner wall. Wrap the blanket securely around the wall with the end butt snugly against the drum top flange and its longitudinal seam. The wrapped blanket should extend approximately 3 inches below the installed blanket on the liner bottom. While holding the blanket seam together

apply one piece of strapping tape along the seam. Then apply three rows of tape circumferentially around the blanket where the studs protrude from the blanket. Do not compress the blanket when applying the circumferential pieces of tape. Fold the edges of the blanket around the bottom of the liner and apply strapping tape in a crisscrossing pattern across the disks and three (3) of the liner-bottom studs, running the tape up the side walls of the blanket at least 2-inches.

4. Cut a second rectangular piece of ½-inch thick Fiberfrax blanket, 33½-inches long by approximately 32½ inches wide. Repeat step 2 using this larger blanket but apply the second layer such that the longitudinal seam is approximately 180 degrees away from the first layer.
5. Impale a washer on each of the five (5) bottom liner studs capturing the four (4) layers of Fiberfrax blanket and the tape. Impale a washer on each of the nine (9) side liner studs capturing the two (2) layers of Fiberfrax blanket and the tape.
6. Wrap a length of 22-gage wire circumferentially around the blanket just below each row of liner studs and twist closed. (This assumes the drum liner is in the up-side down orientation.)

Overpack Foam Installation Steps (Drawing R-R1-G-00021)

The volume between the Fiberfrax®-insulated liner and the drum wall is filled with General Plastics Last-A-Foam® FR-3716. The liquid is poured into the volume through the 1-inch fill hole located in the bottom of the drum and sets to form rigid, closed-cell, intumescent polyurethane foam. A ¾-inch hole is also present to vent the air being displaced. The twelve ¾-inch vent holes in the drum side-wall are closed with Caplugs® during foam emplacement. Installation is done by General Plastic personnel using a proprietary process and procedure. General Plastics Corporation will permit onsite inspection of the operation and document review, but will not permit written disclosure of the process. Appendix 2.5 shows a sample of the polyurethane foam after being poured into a sample cup. In brief, the foaming operation can be described as follows.

The liquid is a two part mixture similar to an epoxy, combined just prior to a pouring. When first mixed, the viscosity of the liquid is roughly that of 30-weight motor oil, and the components begin reacting exothermically. The reaction increases the surface temperature of the overpack to about 150°F temporarily, but it drops below 120°F in about an hour. As the reaction progresses, foam rises at a rate of approximately 6 inches per minute and a skin soon forms over the rising mass. Foam installation is performed in two steps while the drum is inverted.

The first step is to meter the level of liquid accumulating in the top of the inverted drum to about three inches as shown in Figure 2.6. The foam rise from this pour will reach roughly the bottom of the drum liner. Typically, the second pour is carried out after the first installation has cooled. However, cooling is not a fabrication requirement, but permitted for the safety of the equipment operator. The mixture of the second pour is slightly different and metered to a depth of approximately one inch above the surface of the first foam mass. The fill hole is closed with a Caplug® immediately after the second pour. Foam rises until it extrudes through the vent hole, at which time this hole is closed. Restricting the foam rise during the second pour is a process

called "overpacking" and increases the final foam density to the requisite 16 lb/ft^3. The drum is weighed before and after each pour to measure the foam density.

Foam expansion exerts significant loads on any confining structure. Hence, after curing, the liner wall is inspected to verify that radial expansion loads have not affected the liner significantly, and that it has remained parallel with the drum wall. Radial loads exerted by the foam expansion from the first pour typically compress the 1-inch thick layer of Fiberfrax about 50%.

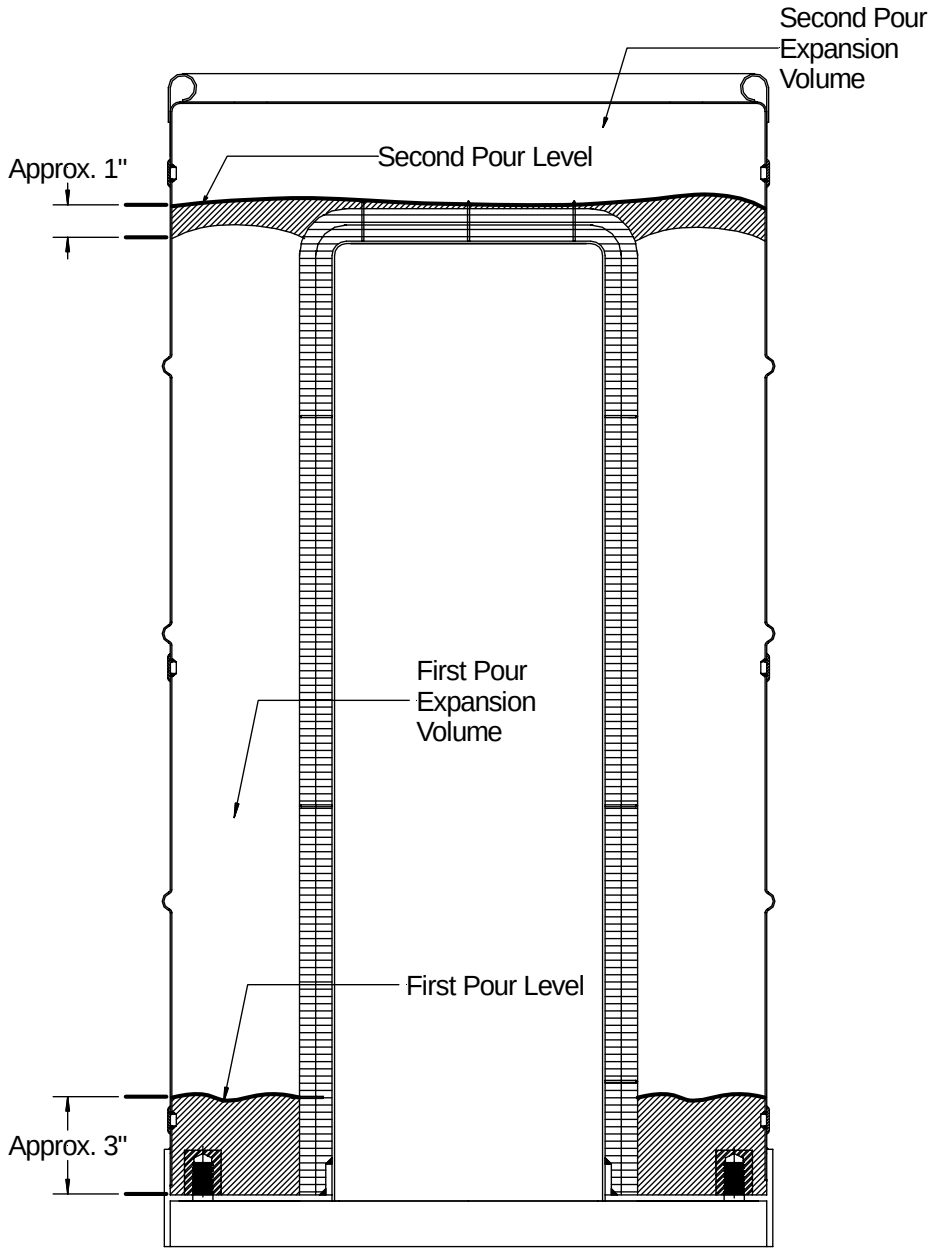

Figure 2.6 – Schematic for Emplacement of FR-3716 Foam

2.3.1.4 Overpack Closure-Lid Fabrication

The 9977 overpack closure lid (Figure 1.1) is a ⅛-inch thick, flat stainless-steel plate supplemented by sheet metal liners above and below, forming top and bottom chambers. These volumes are filled with insulation, and the sheet metal liners are welded to the plate. The outer perimeter of the plate is drilled to pass closure bolts and serves as the lid's bolted-closure flange. The center of the plate is drilled to permit venting of heated gases from decomposing insulation and RTV. When the overpack is closed, the bottom chamber of the lid plugs the liner cavity. The Overpack closure lid is fabricated in accordance with the drawings and specifications listed in Appendix 1.1. The total axial thickness of insulation in the lid is 5.8 inches.

The bottom closure lid chamber contains a single piece 4.3-inch thick by 8-inch diameter cylinder of Thermal Ceramics TR-19 insulation and two (2) ½-inch thick by 8-inch diameter blankets of Fiberfrax® Insulation. The height of the insulation exceeds the depth of the bottom chamber. The relatively incompressible block of TR-19 compresses the softer Fiberfrax® thickness from 1-inch to ½-inch during emplacement. RTV-382 is used to fill any void between the TR-19 and liner wall reducing the possibility of the TR-19 degrading due to vibrations during transport.

The top closure-lid chamber serves as both shock absorber and thermal insulator. The chamber contains a disk of Thermal Ceramics Min-K 2000 insulation 1-inch thick by 14-inches diameter. The top chamber is larger in diameter than the bottom chamber (14 versus 8 inches) to lengthen the path that heat must travel to reach (reduce the net heat transfer to) the CV. The vertical edge of the top chamber includes four (4) ¼-inch diameter vent holes to permit venting of heated gases from decomposing insulation and RTV. The holes are sealed under NCT with Room Temperature Vulcanizing (RTV-382) silicone adhesive and plugged with Caplugs to preclude moisture infiltrating the insulation. Details are shown in Drawing R-R2-G-0018.

2.3.2 Examination

2.3.2.1 Five- and Six-inch Containment Vessel Examination

The surfaces and volumes of the CVs are examined in accordance with ASME BPVC, Section III, Subsection NB as described in Section 9.3. Closed 5CV and 6CV assemblies shall accept without binding a 5.02-inch diameter by 15.0-inch long right circular cylinder and a 5.95-inch diameter by 20.25-inch long right circular cylinder, respectively, as shown in Figure 2.7.

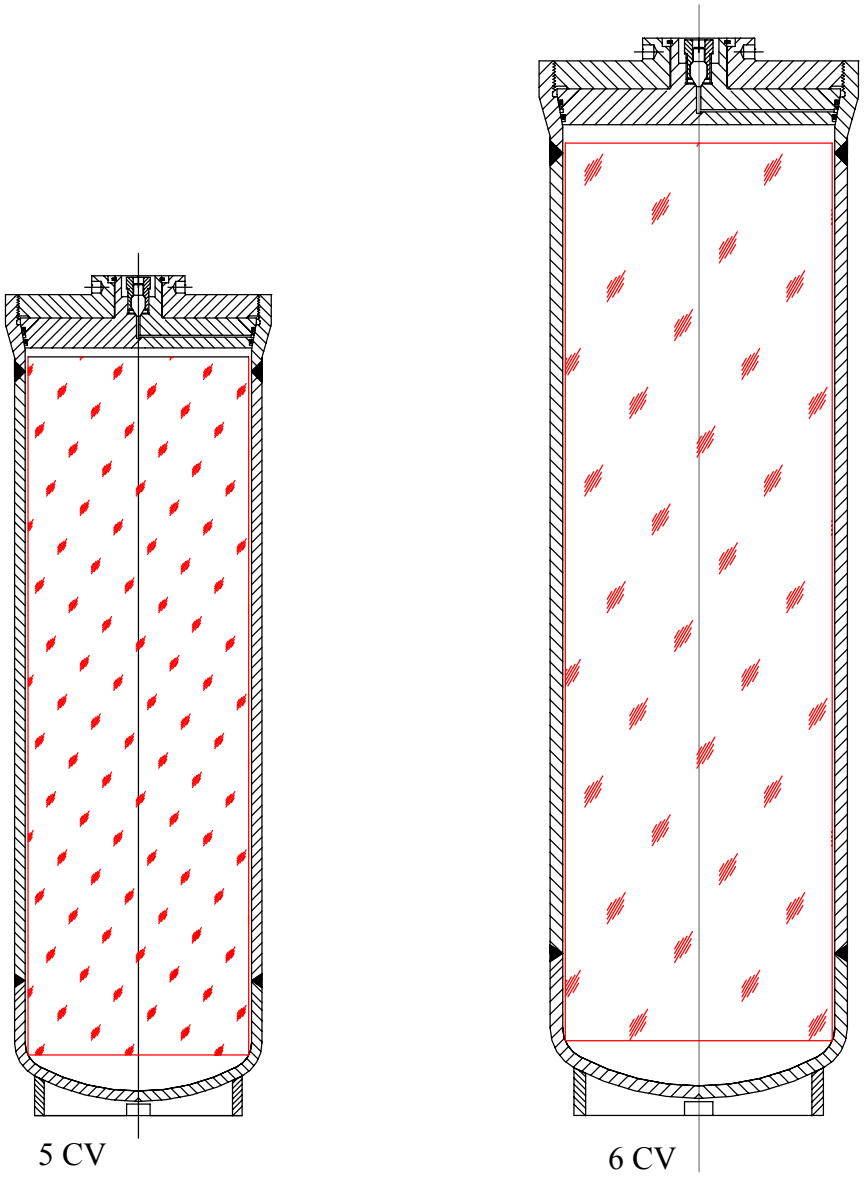

Figure 2.7 - 6CV and 5CV with Go-No-Go Gauge

2.3.2.2 Overpack Assembly Examination

Drum

The overpack drum shell procurement requires the drum to be tested and certified to be acceptable per UN1A2 standards. Drawing R-R2-G-00017 requires the drum-liner weldment to be tested hydrostatically at 5 psig for not less than ten minutes. This action is necessary to verify that the insert welds do not leak. All welds on the liner weldment (liner plus top deck plate) and its attachment to the drum shell are examined visually per ASME BPVC, Section III, Division 1, Subsection NF-5000.

Foam Installation

If confined, Last-A-Foam can produce significant mechanical loads as it expands and cures. Verification of liner perpendicularity and circularity is required after the first of two foam installation stages. Overpack dimensional checks are not required after the second (last) stage of foam installation.

Dimensional inspection following the first pour ensures the radial loads exerted by the foam as it solidifies do not significantly affect the liner positioning within the drum or its circularity. The drum liner is not permitted to move radially by more than ⅛ inch from its as assembled location. Liner circularity is demonstrated by the ability to pass a 7.8-inch diameter by 6–inch long gauge block to the bottom of the liner. The gauge block dimensions mimic the outer dimensions of the bottom load distribution fixture.

During foaming operations, samples of foam from each lot/batch are collected tested for flame intumescence, free rise density, thermal conductivity, compressive strength (parallel and perpendicular to rise) and for leachable chlorides.

2.4 GENERAL REQUIREMENTS FOR ALL PACKAGES

This section demonstrates that the 9977 meets the NCT performance criteria from 10 CFR Part 71.43(a) through (e) and (g) and (h), *General Standards for All Packages*.

2.4.1 Minimum Package Size

Requirement: 71.43(a) – The smallest overall dimension of a package shall not be less than 10 cm (4 in.).

Evaluation: The smallest overall dimension of the package (excluding fasteners and plugs) is 18.72 inches and much greater than four (4) inches; therefore, 9977 meets this requirement.

2.4.2 Tamper-Indicating Feature

Requirement: 71.43(b) – The outside of the package must incorporate a feature, such as a seal, that is not readily breakable and that, while intact, would be evident that the package has not been opened by unauthorized persons.

Evaluation: The 9977 provides for the installation of one or more tamper-indicating devices (TID). The TIDs provide physical evidence that a package has not been opened by unauthorized persons. For transport security, the flats of the head of each eight (8) ⅝-11 UNC-2B closure lid bolts are drilled through to provide a 0.094-inch hole to receive a TID. During shipping, a tamper seal consisting of a braided stainless-steel cable with a crimped closure is attached through two or more of the bolt heads. Removing the closure lid from the package would require severing the wire.

For storage security, two ½-inch through holes are provided in the drum reinforcing rim 180 degrees apart. An optional ½-inch diameter × 2-inch long bolt with a 0.31-inch diameter hole drilled through the end of the bolt shank may be attached through the rim holes for use with Radio Frequency (RF) TIDs.

2.4.3 Positive Closure

Requirement: 71.43(c) – Each package must include a containment system securely closed by a positive fastening device that cannot be opened unintentionally or by a pressure that may arise within the package.

Evaluation: The packaging includes a containment system securely closed by a positive fastening device that cannot be opened unintentionally or by a pressure that may arise within the package. The 5-inch and the 6-inch inside diameter containment vessels (5CV and 6CV) are identical (other than relative size) closures. Positive closure of the CVs during normal package operation is accomplished by threading the cone-seal closure assembly into the CV body and tightening with a minimum torque of 50 or 100 ft-lb, for the 5CV and the 6CV, respectively. These tightening torques are sufficient to provide the required seal and prevent inadvertent opening of the containment vessels during transport.

The CV is located within the drum liner, which is closed by the drum closure lid, which is held in place by eight (8) ⅝-inch diameter bolts threaded into a mating threaded inserts welded to the underside of the drum's top deck plate. The bolts are tightened to a torque of 25 ±2 ft-lb that is sufficient to prevent unintentional opening of the overpack closure during transport. Inadvertent opening of the overpack closure lid during transport would also require breaking of at least one TID between at least two of the eight closure bolts. The bottom chamber of the closure lid extends into the drum liner, and the lid can be removed only after all of the closure bolts have been removed. Therefore, unintentional opening of the package is not possible.

2.4.4 Package Valving

Requirement: 71.43(e) – A package valve or other device, the failure of which would allow radioactive contents to escape, must be protected against unauthorized operation and, except for a pressure relief device, must be provided with an enclosure to retain any leakage.

Evaluation: The 9977 design does not incorporate any valves or other appurtenances that would allow radioactive contents to escape.

2.4.5 Packaging Effectiveness

Requirement: 71.43(f) – A package must be designed, constructed, and prepared for shipment so that under the tests specified in § 71.71 (*Normal Conditions of Transport*) there would be no loss or dispersal of radioactive contents, no significant increase in external surface radiation levels, and no substantial reduction in the effectiveness of the packaging.

Evaluation: The package is designed and shown through physical testing and structural evaluation that under the NCT specified in 10 CFR 71.71 there is no release of radioactive contents, no significant increase in external surface radiation levels, and hence, no significant reduction in the effectiveness of the packaging. Structural evaluation of NCT includes thermal effects, pressure effects, vibration and shock, water spray in-leakage, drop impacts, stacking compression, and penetration impact.

2.4.6 Transportation Use

Requirement: 71.43(g) – A package must be designed, constructed, and prepared for transport so that in still air at 38°C (100°F) and in the shade, no accessible surface of a package would have a temperature exceeding 50°C (122°F) in a nonexclusive use shipment, or 85°C (185°F) in an exclusive use shipment.

Evaluation: The package design is such that with the maximum content decay heat rate thermal loading (19W) and the condition of still air at 100°F and in the shade, the maximum temperature of any accessible surfaces of the package is approximately 100°F (Section 3.1), which satisfies the 122°F limit for nonexclusive use shipment of the package.

2.4.7 Continuous Package Venting

Requirement: 71.43(h) – A package may not incorporate a feature intended to allow continuous venting during transport.

Evaluation: The 9977 design does not incorporate any feature intended to allow continuous venting during transport.

2.5 LIFTING AND TIE-DOWN STANDARDS FOR ALL PACKAGES

The 9977 package design incorporates two features for lifting and tie-down. First, a set of blind holes is drilled into the cone-seal nut specifically to receive apparatus for lifting the CV during handling operations. Second, the 9977 overpack includes a series of eight (8) holes through the reinforcing rim at the top of the drum as points for tie-down and for lifting the package. The following sections further describe these attachment points and evaluate their effect on package integrity during lifting and tie-down operations.

Not specifically evaluated are the effects on the package of industry-standard practice for handling, lifting and tie-down of drums. Acceptable package performance under routine forms of lifting and tie-down is satisfied by compliance with the requirements for acceptable performance of the package under NCT.

2.5.1 Lifting Devices

Requirement: 71.45(a) – Any lifting attachment that is a structural part of a package must be designed with a minimum safety factor of three against yielding when used to lift the package in the intended manner, and it must be designed so that failure of any lifting device under excessive load would not impair the ability of the package to meet other requirements of this subpart. Any other structural part of the package that could be used to lift the package must be capable of being rendered inoperable for lifting the package during transport, or must be designed with strength equivalent to that required for lifting attachments.

Evaluation: The 9977 package CVs are designed to be lifted using either of two sets of opposing ¼-diameter blind holes located in the cone-seal nut as depicted by the grappling fixture in Figure 2.8.[40] Examples of special tools specifically designed for lifting the CVs are shown in Appendix 7.1.

The overpack reinforcing rim is fabricated with a series of eight (8) 1-inch diameter holes around its perimeter designed to serve as tie-down attachment points. However, these openings could also be used to lift the overpack during normal operations, as depicted in Figure 2.9. Evaluation of these features as lifting points is presented below.

Containment Vessel Lifting

Design calculations provided in Appendix 2.1 show that the stress from a force equivalent to three times the weight of a maximally loaded 6CV suspended by two opposing drive-nut lifting holes is approximately 2.2 ksi. This is well below the material shear stress allowable, 4.167 ksi.

During transport, the CV is confined within the overpack, rendering the lifting holes inoperable.

Because the drive nut design for both CVs is identical and the weight of the maximally-loaded 6CV is much greater than the maximally loaded 5CV, performance of the 5CV is bounded by analysis of the 6CV.

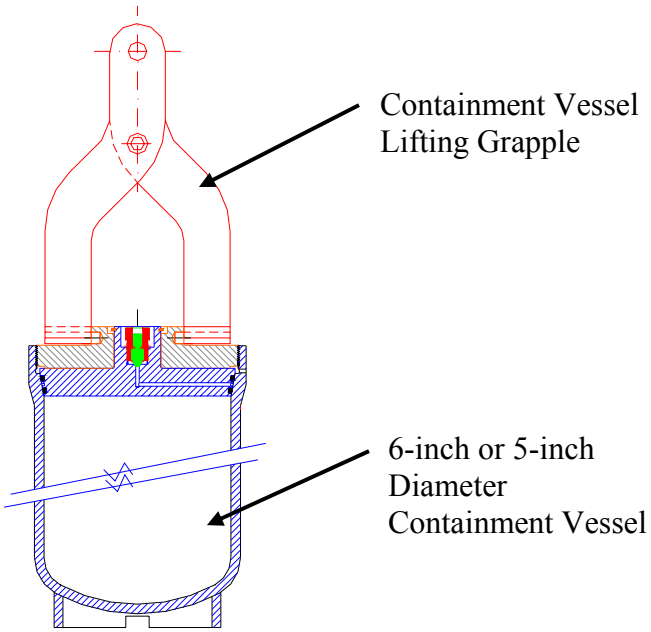

Figure 2.8 - Containment Vessel Lifting

Drum Assembly Lifting

Design calculations provided in Appendix 2.1 show the stress in any two opposing 1-inch diameter drum rim holes with a suspending force equivalent to three times a maximum loaded package, is less than 2.5 ksi, which is about half the material allowable, 4.17 ksi. If the package is lifted by a single opening the calculated stress would slightly exceed the allowable material stress limit. Based on the 3X load conservatism and reduced material strength for Code material, the single point lift may deform but would not fail the drum rim. If the lifting point was to deform or fail under a single-point lift load, the resulting ligament failure would occur in a component not associated with containment, shielding, or maintaining a sub-critical configuration. Nor would a failure of a drum lifting attachment point affect the performance of the package during NCT or HAC events.

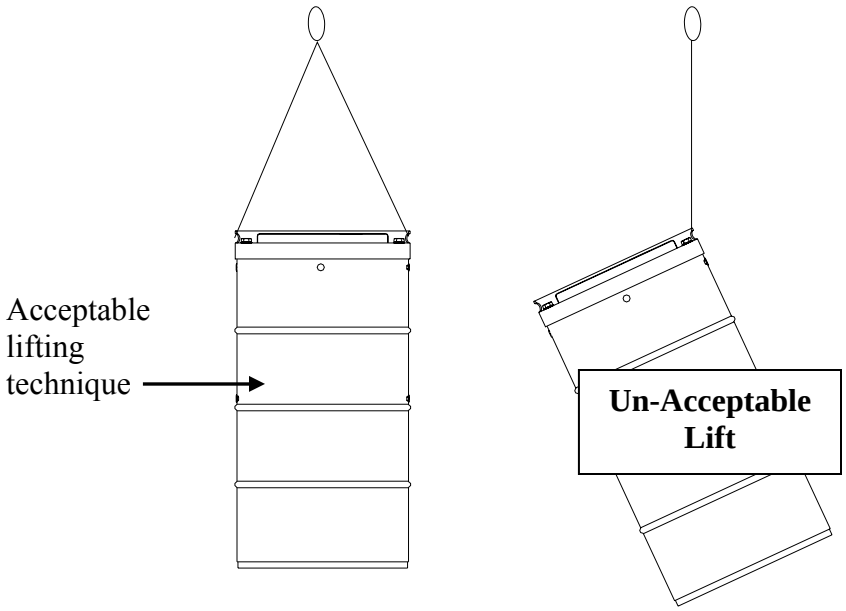

Figure 2.9 - Overpack Lifting Diagram

2.5.2 Tie-Down Devices

Requirement: 71.45(b)(1) If there is a system of tie-down devices that is a structural part of the package, the system must be capable of withstanding, without generating stress in any material of the package in excess of its yield strength, a static force applied to the center of gravity of the package having a vertical component of 2 times the weight of the package with its contents, a horizontal component along the direction in which the vehicle travels of 10 times the weight of the package with its contents, and a horizontal component in the transverse direction of 5 times the weight of the package with its contents.

(2) Any other structural part of the package that could be used to tie down the package must be capable of being rendered inoperable for tying down the package during transport, or must be designed with strength equivalent to that required for tie-down devices.

(3) Each tie-down device that is a structural part of a package must be designed so that failure of the device under excessive load would not impair the ability of the package to meet other requirements of this part.

Evaluation: The 9977 design incorporates a series of 1-inch diameter through holes along the perimeter of the drum rim that may be used as tie-down points when the drum is secured in an upright position in accordance with the tie down constraint methods for shipment in the Safeguards Safe Secure Trailer. Figure 2.10 illustrates the tie-down arrangement. The attachment points are designed to withstand design loading of 10, 5, and 2 without exceeding yield strength of the 304L stainless steel rim material.

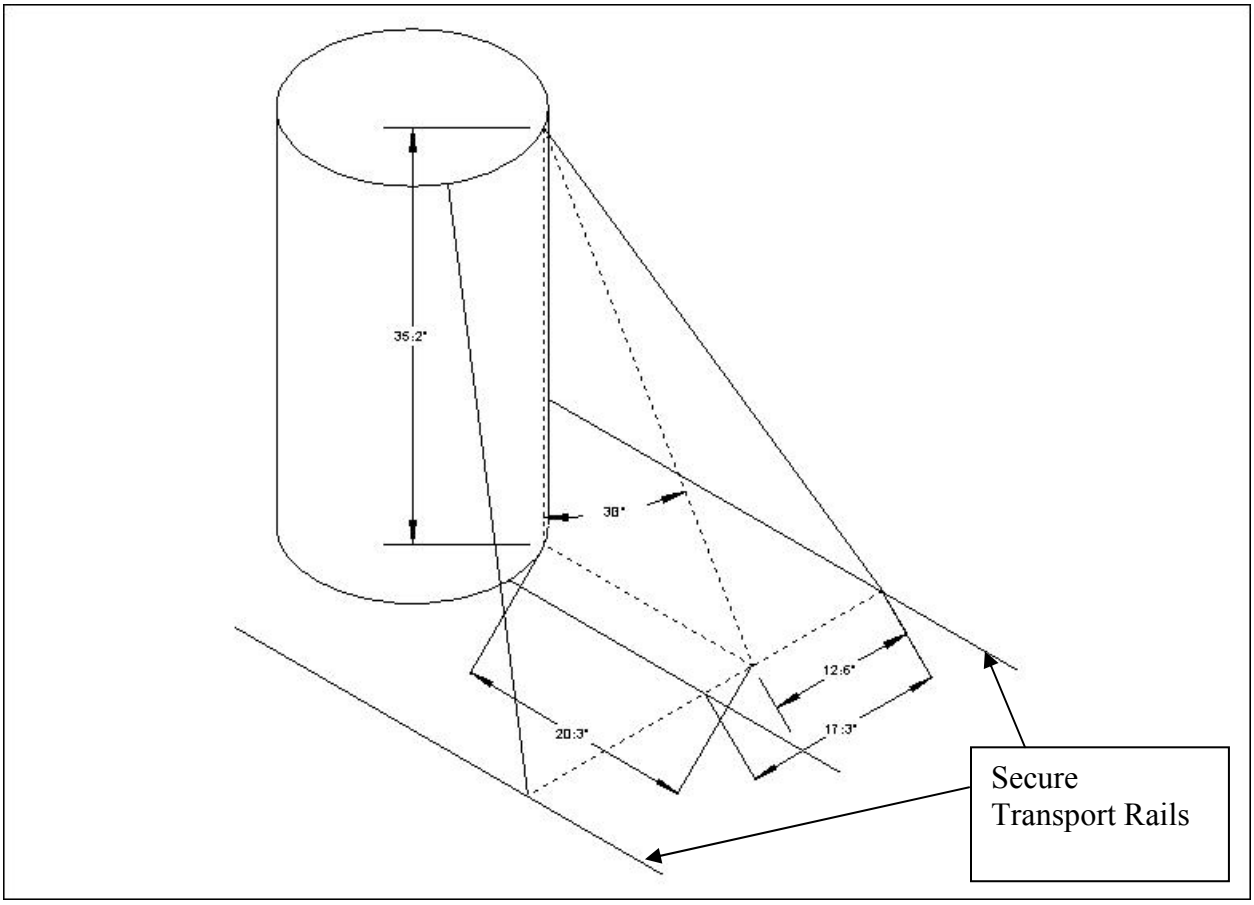

Figure 2.10 - Overpack Tie-down

2.6 NORMAL CONDITIONS OF TRANSPORT

This section demonstrates through full scale performance tests, analysis and similarity, that the 9977 package design and construction is in compliance with the performance requirements of 10 CFR 71.43(f) and 10 CFR 71.51(a)(1), (b) and (c) so that, when prepared for transport, under the test conditions specified in 10 CFR 71.71 Normal Conditions of Transport (NCT), there is no loss or dispersal of radioactive contents (as demonstrated to a sensitivity of $10^{-6}A_2$ per hr), no significant increase in external surface radiation levels and no substantial reduction in the effectiveness of the packaging. Additionally, the 9977 is shown to meet the requirements in 10 CFR 71.55(d) when subjected to the tests specified.

Structural evaluation of NCT influences includes thermal effects, pressure effects, vibration and shock, water spray in-leakage, drop impacts, stacking compression, and penetration impact. The CVs MNOP and a summary of component temperatures for NCT are provided in Tables 2.20 and 2.21, respectively. The thermal evaluation for NCT conditions is presented in Chapter 3. The mechanical consequences of thermal influences are also evaluated, including differential thermal expansion and thermal stresses from temperature gradients through containment vessel walls. The effects these conditions have on the 9977 package are presented in the following sections. Detailed evaluation for NCT conditions is provided in the attached Appendices. A summary of the NCT analyses and testing performed that demonstrate the 9977 meets 10CFR71 is provided in the Sections below.

2.6.1 Heat

Requirement: 71.71(c)(1) – Exposure to an ambient temperature of 100 ºF in still air, and insolation according to the following table.

Table 2.19 - Insolation Data

Form and location of surface	**Total Insolation for a 12-hour period** (g cal/cm^2)
Flat surfaces transported horizontally;	
Base	None
Other Surfaces	800
Flat surfaces not transported horizontally	200
Curved surfaces	400

Evaluation: Package testing and analysis are used to evaluate the effect of the maximum normal operating pressure (MNOP) on the 9977 as a result of exposure to an ambient temperature to 100°F in still air with insolation. Per 10CFR71.4, MNOP is defined as the "maximum gauge pressure that would develop in the containment system in a period of 1 year under the heat condition specified in 10 CFR7.71(c)(1)."

A prototypical 9977 package was tested under exposure to an ambient temperature of 100°F in still air with a simulated maximum content decay heat load of 19W (see Appendix 3.1). Numerical analysis was benchmarked against the prototypical test unit with identical boundary conditions, i.e., exposure to an ambient temperature of 100°F in still air and maximum internal heat load of 19W. Following agreement between the prototypical test and benchmark analysis, the benchmark analysis was appended with the insolation boundary conditions as highlighted in the Table above, (see Section 3.4 for full detailed analysis description). The results of these analyses are used to determine the average gas temperature inside the CV that is needed to determine the MNOP and to determine thermal gradients through the package. The calculated MNOP and package temperatures under NCT are listed in Tables 2.20 and 2.21. These values are used to evaluate the performance of the 9977 to NCT conditions in this section. Based on the package temperatures and calculated MNOP for the CVs, the insolation and ambient temperature exposure will have no adverse effect on the ability of the packaging, its containment vessels or contents to satisfy the requirements of NCT.

2.6.1.1 Summary of Pressures and Temperatures

The MNOP and temperatures used to calculate applicable stress and thermal expansion of the containment system and packaging features are given in Tables 2.20 and 2.21 (values extracted from Tables 3.2 and 3.3). An ambient temperature of 70°F is assumed for the packaging at assembly. Since the drum lid connection is not sealed (i.e., non-gasketed), and further, the drum incorporates fourteen (14) vent holes on its perimeter, it will not become pressurized assuming slow temperature changes during NCT. Since the containment vessels are sealed, their internal pressure will change with temperature.

Table 2.20 – Summary of Containment Vessel MNOP

Package Feature	**Gas Temperature** (^{o}F)	**MNOP** (psig)	**Design Pressure** (psig)
5CV	[535][a]	56.3	900
6CV	[535][a]	41.2	800

a. Maximum content temperature for 6CV point source used to evaluate internal pressure.

Table 2.21 - Summary of NCT Temperatures with and without Insolation

(Ambient 100°F, 19W payload)

Package Component	5CV Temperature (°F)		6CV Temperature (°F)	
	No insolation	Insolation	No insolation	Insolation
CV Contents (19W)	n/c	280	347	350
CV Wall (Mid-height)	n/c	260	220	321
CV O-ring Seals	n/c	240	198	302
Aluminum LDF	n/c	-	-	-
Foam	n/c	-	185	295
Drum Wall	n/c	-	105	203

n/c – not calculated. 6CV bounds 5CV temperatures.

The maximum pressure loading for the package under normal condition loading consists of the combination of MNOP and a 3.5 psia reduced external pressure per 10 CFR 71.71(c)(3). A reduced external pressure is equivalent to increasing the internal design pressure of each CV by the same amount. The resulting differential pressure for the 5CV (900 + 11.2 = 911.2 psig) and 6CV (800 + 11.2 = 811.2 psig) is used in evaluating the 9977 in the following Sections.

The 5CV is proof-tested prior to first use with a hydrostatic test of 1.5 times the design pressure, 900 psig, (1.5 × 900 = 1350 psig) which bounds the ASME Section III, NB-6200 proof-test requirement. The ASME proof test pressure exceeds the requirement of 10 CFR 71.85(b) for a pressure test at 1.5 times the 5CV MNOP (1.5 × 56.3 psig = 84.5 psig).

The 6CV is proof-tested prior to first use with a hydrostatic test of 1.5 times the design pressure, 800 psig, (1.5 × 800 =1200 psig) which bounds the ASME Section III, NB-6200 proof-test requirement. The ASME proof test pressure exceeds the requirement of 10 CFR 71.85(b) for a pressure test at 1.5 times the 5CV MNOP (1.5 × 41.2 psig = 61.8 psig).

2.6.1.2 Differential Thermal Expansion

The potential for interference in circumferential and axial dimensions within the package as a result of differential thermal expansion and contraction have been investigated and is documented in Appendix 2.1. For the evaluated conditions, there was no unacceptable stress or interferences in the 9977 due to expansion or contraction.

The 6CV weldment and Closure Assembly are fabricated from similar materials, 304L and Nitronic stainless steels, and expand and contract equally with temperature changes. Therefore, under the temperatures gradients reported in Chapter 3 there will be negligible stress and no interferences due to differential thermal expansion in the 6CV. By similarity of design this is also true for the 5CV.

Interference between the 6CV and its LDFs due to differential thermal contraction is evaluated in Appendix 2.1. Assuming a differential temperature of 110 °F (loading at 70 °F and cooling to -40 ºF with no content decay heat), the radial clearances provided by the design is sufficient to prevent material interference with the 6CV. The 5CV design is surrounded by crushable material and by inspection is not affected. The axial and radial clearances for the design are greater than radial clearances and are sufficient to ensure clearance at elevated temperature.

The polyurethane foam's thermal expansion is roughly an order of magnitude greater than the SS drum, Section 2.2.1. However, the ½-inch thick pliant layer of Fiberfrax adjacent to the drum liner permits free expansion and contraction of the foam, thereby, minimizing stress in the overpack and foam during NCT heating or cooling. Based upon experience utilizing poured polyurethane foams, the potential for cracking/voiding during the foaming operation and/or thermal cycling has been observed. Cracking was observed after foaming operations of the AT-400A package designs with General Plastics FR-3700 foam while none was experienced with the AL-SX. [41] This phenomenon, also has not been observed during production of the 9977 prototypes and is conjectured to be due to the thicker radial cross-section of the 9977 foam. Though post foam cracking has not been observed for the 9977 voids have been observed as seen in digital radiographs in the 9977 Test Report. Structurally, the foam remains confined within the drum annulus and is functionally unaffected by the degree of voiding observed.[42] Thermally, testing has shown that the foam provides an equivalent level of protection to high temperatures even when cubed.[43]

The SS drum shell, closure lid and bolts are fabricated from 304L SS. Since the overpack is unconstrained, contraction or expansion, due to changes in temperature will have negligible effect on the drum.

In addition to the possible effects caused by interference due to dissimilar material expansion, stresses due to temperature changes across the 5CV and 6CV walls were evaluated. The maximum through-wall temperature differential is less than 2°F (Appendix 3.1). However, a conservative value of $\Delta T = 10°F$ was used in the thermal stress calculations. Table 2.22 lists the absolute values of secondary thermal stresses of the containment vessels. The secondary thermal stresses are combined with the primary calculated stress and compared to ASME Code Level A service limits for each CV, Table 2.23. Reported CV stresses do not exceed ASME Code limits.

Table 2.22 - Maximum 5CV and 6CV Secondary (Thermal) Stresses

Component	Thermal Stress (psi)	
	5CV	6CV
Body inside	1,830	1,720
Body outside	1,960	2,070
Ellipsoidal head	1,900	1,900
Conical lid	1,900	1,900

2.6.1.3 Stress Calculations

Stress analyses were performed to calculate the stresses in the 9977 subject to normal conditions of transport, e.g., thermal loading, pressure and mechanical loads. Detailed analyses with assumptions are provided in Chapter 2 Appendices and summarized and discussed in Table 2.23 and the Sections of this chapter. Stress evaluations were performed for the 5 and 6-inch CVs to demonstrate the structural containment integrity of the design at 500 ºF at 900 psig and 800 psig, respectively. The results of these analyses show that when compared to ASME BP&VC, Section III, for Level A Service Loads, the effectiveness of the 9977 under NCT is not reduced. The residual stresses resulting from the processes used in fabrication, testing and installation were calculated and found to be negligible and, therefore, were not superimposed with any of the stress calculations. The analyzed stressed are compared with the stress criteria shown in Figure 2.2. The following summarize the containment vessel and drum liner design analyses.

The ABAQUS code [44] was used for all package dynamic and linear-elastic structural analyses. The ABAQUS program is well benchmarked and widely used. ABAQUS is verified using benchmark problems and validated in accordance with written procedures under the WSRC Quality Assurance program (see Section 9.3.2). Two types of ABAQUS models were created, one for the ASME pressure code analysis and one for the NCT/HAC structural analyses.

For the ASME BP&VC, Section III Code analysis for the pressure vessels, axisymmetric 4-node bilinear solid elements were used for the cylindrical body, ellipsoidal head, interior cone seal, exterior cone seal plug and cone seal nut. The materials library called by the ABAQUS code uses the material properties of materials as presented in Section 2.3. Approximately 10,000 discrete finite elements used in the model and were chosen to accurately approximate the stress and displacements within the packaging when subjected to the NCT and HAC structural loadings.

For the NCT/HAC structural analyses for the package, the finite-element models of the drums' cylindrical body, closure lid and bolt ring, bottom, rim and skirt are comprised of 3D shell elements (Type S4R). 3D solid elements (C3D8R) are used for the foam, the drum bolts and nuts, the containment vessel flange and its closure, fixtures and the contents. The floor, the crush plate and puncture bar are represented by the rigid elements (R3D4). Simulated bolt torque is represented by connector elements. Approximately 10,000 discrete finite elements used in the model and were chosen to accurately approximate the stress and displacements within the packaging when subjected to the NCT and HAC structural loadings.

Sensitivity studies were performed to refine the mesh density as appropriate at locations of interest for evaluating the 9977 model.

2.6.1.3.1 Containment Vessel Closure Design and Analysis

The calculations included in Appendix 2.2 show that the Cone-Seal Nut keeps the conical lid seated against the internal seal surface when the containment vessel assembly is closed in accordance with the design. The investigation determined that the 5CV closure remains seated at internal pressures up to 515 psig, and the 6CV up to 563 psig. These pressures are significantly higher than the calculated containment vessel MNOPs of 56.3 (5CV) and 41.2 psig

(6CV) listed in Table 2.20. Since the pressure necessary to unseat the Cone-Seal Plug is higher than either containment vessel MNOP, O-ring compression is assured.

At pressures higher than the calculated unseating pressure, 515 psig, the wall of the containment vessel expands radially and a theoretical gap forms between the interior cone of the containment vessel and the exterior cone of the Cone-Seal Plug. This gap remains less than 2.8 mils for internal pressure up to 5,000 psig. A review of the O-ring sealing pressure curves shows that for sealing surfaces with less than a 10 mil gap the O-ring retains its seal at pressures up to 1,000 psig (Parker O-ring Handbook[45] Figure 3.2, *Limits for Extrusion*). These calculations indicate that the seal design has a safety factor of approximately 4 against the Parker design curves.

This margin is evidenced by the hydrostatic burst test shown in Figure 2.11 where the 2R was pressurized to failure. The longitudinal vessel wall failure demonstrates that the O-rings maintained a seal while the vessel failed at greater than 7,000 psig. Parker data indicates that the O-rings should fail between 4,000 to 6,000 psig in a zero clearance design.

Figure 2.11 - Prototype 5-inch diameter Chalfont 2R (Cone-Seal Closure) after Hydrostatic Burst beside an Undamaged Containment Vessel

2.6.1.3.2 Containment Vessel Boundary Stresses

A summary of the primary stress intensities for each containment vessel subject to their design pressure is presented in Table 2.23 for the locations illustrated in Figure 2.12. The stress summaries demonstrate that containment vessel pressure-induced stresses are well below the ASME stress limits as indicated by the tabulated Safety Margins. In addition to evaluation for nominal wall thickness, detailed analyses of the 5CV and 6CV using minimum wall thicknesses based on ASME SA-312 pipe fabrication tolerances (0.226 and 0.245-inches, respectively), were evaluated for both pressure stress and buckling due to external pressure. (Appendix 2.2) Though the results listed herein are for the nominal thickness values, the minimum thickness evaluation also showed significant design margin above code stress allowables.

2.6.1.3.3 Fabrication Stresses in the Overpack Liner

The stresses in the overpack liner due to a 5 psig pressure test following fabrication have been evaluated. (See Appendix 2.1) The calculated residual stresses in the drum liner due the fabrication pressure test are negligible.

2.6.1.4 Comparison with Allowable Stresses

Table 2.23 summarize primary membrane stresses plus the primary bending stresses plus secondary stresses at the critical locations within the 5CV and 6CV at their respective design pressures from finite element analyses (FEA) documented in Appendix 2.2. Figure 2.12 shows the critical locations (Sections A-A, B-B, C-C, D-D, E-E, F-F and G-G) where the stress intensities were calculated. For conservatism, all stresses are added directly, ignoring sign and direction of application. The maximum stresses (primary plus secondary) also listed in the Table are less than the allowable stress limits defined by Regulatory Guide 7.6 and the ASME Code; therefore, the integrity of the containment vessel is assured during NCT.

Table 2.23 - Maximum Containment Vessel (Pressure) and Secondary (Thermal) Stress Combinations

NCT Stress Summary (psi) with 900 psi in 5CV and 800 psi in 6CV. Stress notations per RG 7.8.

	Primary Pressure Stresses					Thermal Stress	Total Primary + Secondary	Total Stress Range	Stress Margin % [d]
	P_m	P_m+P_b	$P_m+P_b+Q_{pr}$	$P_m+P_b+Q_{pr}+F_{pr}$	$P_{m,pure-shear}$	Q_{th}	$P_m+P_b+Q_{total}$	$P_m+P_b+Q_{total}+F_{total}$	
Stress Limit	S_m=16700	1.5S_m=25050	3S_m=50100	2S_a=338000 [a]	1.2S_m=20040	–	3S_m=50100	2S_a=338000 [a]	
5CV Body									
Section AA	9264	10092				1960	12052	12052	45
Section BB	4667		12680 [b]	15576 [c]		1960	14640	17540	71
Section CC	6116		12260 [b]	13311 [c]		1900	14160	15210	63
Section DD	9005	13938				1900	15838	15838	44
5CV Cone-Seal Plug (preload only)	53.18	1575				1900	3475	3475	93
5CV Cone-Seal Nut (e)					3636		3636	3636	82
5CV Tapered Wall Thread (f)					7868		7868		61
5CV Tapered Wall Minimum Section (gg)	6022		29,706	118824 [c]			29706	118824	41
6CV Body									
Section AA	9066	9808				2070	11878	11878	46
Section BB	4687		12899 [b]	15659 [c]		2070	14969	17729	70
Section CC	6456		12070 [b]	12807 [c]		1900	13970	14707	61
Section DD	9004	13210				1900	15110	15110	46
6CV Cone-Seal Plug (preload only)	63.86	2716				1900	4616	4616	89
6CV Cone-Seal Nut (e)					3927		3927	3927	80
6CV Tapered Wall Thread (f)					8485		8485	8485	57
6CV Tapered Wall Minimum Section (gg)	3897		17653	70613			17650	70613	65

a) S_a =169KSI from ASME III, Fig. I-9.2.1 Allowable for 1000 load cycles (=100 year design life at 10 shipments per year)
b) Includes through wall bending stresses, but not thermal stress.
c) Includes maximum surface stresses, but not thermal stress or stress concentrations where finite element analysis has been performed except at threaded portion of tapered wall. Thermal stresses are calculated separately and reported in column 7. The total primary plus secondary stress intensities, which include both bending and thermal stresses, as the secondary stresses are included in column 8. The primary plus secondary stress intensities are derived by linealizing the stress components across the vessel wall to exclude the peak stresses. The primary plus secondary stress intensities may cause structure deformation, whereas the peak stresses only cause fatigue failure. Therefore, the stress criteria defined in the ASME Code are different for these two stress categories.
d) Minimum calculated value from columns using Margin of Safety = Stress Allowable/Stress

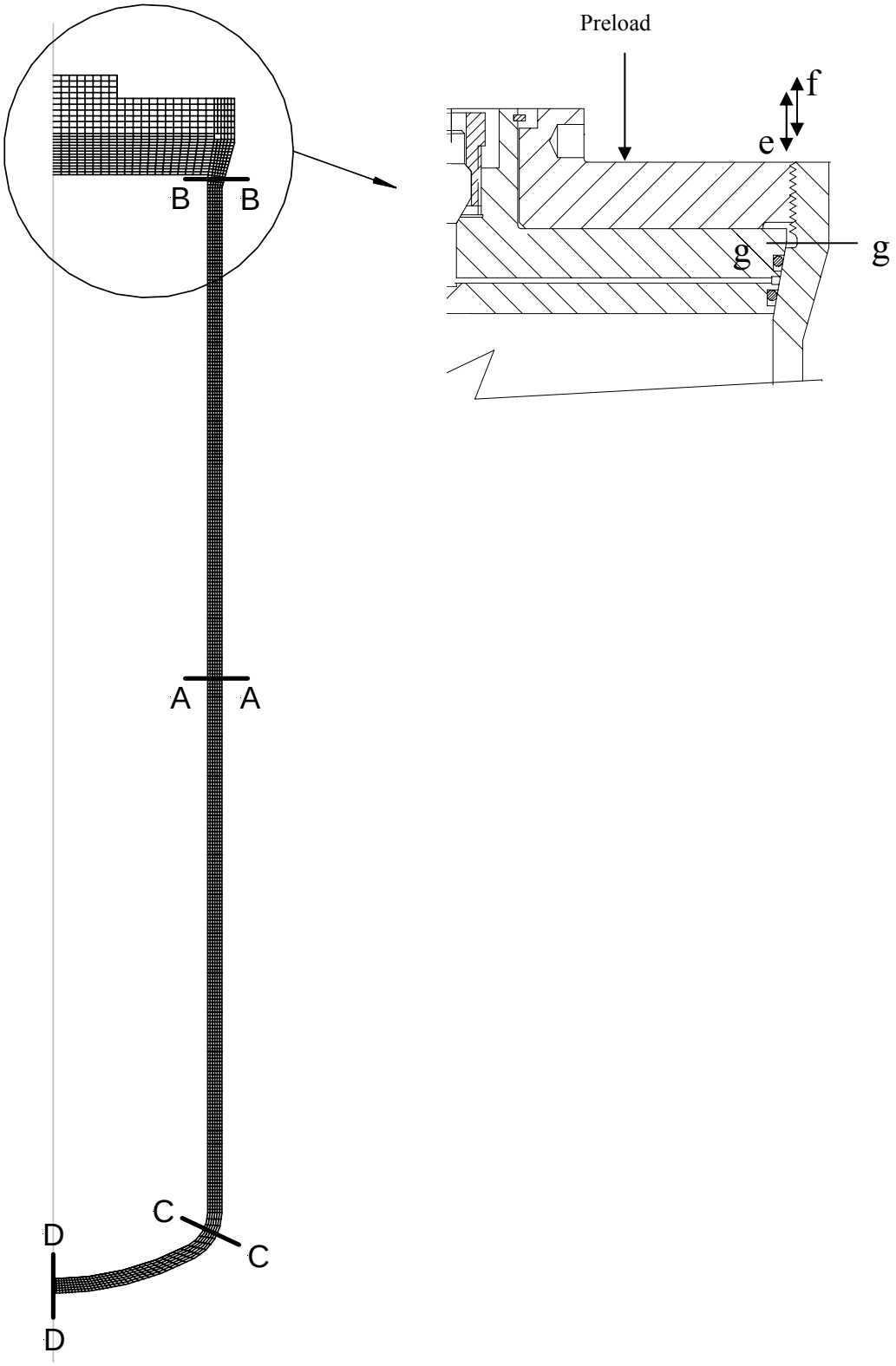

Figure 2.12 - 5CV and 6CV Boundary Stresses Locations listed in Table 2.23

2.6.2 Cold

Requirement: 71.71(c)(2) *Cold*. An ambient temperature of -40°C (-40°F) in still air and shade.

Evaluation: The packaging materials of design would not be adversely affected by an ambient temperature of -40°F.

The containment vessels assemblies and overpack drum and lid are manufactured from Type 304L austenitic stainless steel, and Nitronic-60 alloy. As stated in RG 7.11, and Section 2.1.2, stainless steel is effective at low temperatures, particularly regarding impact strength, making it a proper selection for -40°F applications. Izod impact strength, an indicator for brittle fracture, for 304L stainless steels remains constant at about 100 ft-lb from –320° to +70°F, while tensile strength increases from about 85,000 to 246,000 psi as temperature decreases from +70° to -320°F, and yield strength increases about 10% over the same range. These data demonstrate that stainless steels are satisfactory for low temperature applications.

The O-ring material selected for the 5CV and 6CV seals is a fluorocarbon elastomer, Viton GLT fluoro-elastomer Compound V0835-75, with a specified operating range -40ºF to 400ºF.[**Error! Bookmark not defined.**] (Table 2.13). The Viton GLT elastomer O-rings were tested at -40°F at minimum internal pressure, on a 5-inch diameter Model 9965 [46] CV that has an identical closure design as that used by the 9977 CVs. The CV was helium leak-rate tested per RG 7.4[47] and the bell jar method in ANSI N14.5.[48] The containment vessel was fitted with two Viton GLT O-rings and cooled to -40°F. The bell jar was evacuated and the CV was pressurized to 15 psig with helium. The test showed that the CV remained leaktight to a sensitivity less than 10^{-7} ref cm^3/sec. The test was repeated confirming the initial results. Test records are reported as indicated in Appendix 2.4. As the 9977 CV closure design is identical to the 9965 CV design the cold test results for the 9965 CV demonstrate the acceptability of the 9977 5CV. With the exception of a slightly larger diameter of the 9977 6CV the testing is also applicable for demonstrating acceptable performance of the 6CV design.

The FR-3700 thermal insulating foam due to its chemical make-up and closed-cell form does not absorb appreciable moisture and therefore would be unaffected by freezing at -40ºF. Fiberfrax is unaffected by moisture. After installation, the Fiberfrax is sealed by the FR-3700 foam which precludes water absorption from the outside of the overpack. During fabrication the inner cavity of the drum is leakage tested at 5 psig which precludes water from entering from the inside of the drum. TR-19 and MinK-2000 are vermiculites and will absorb water. These materials are sealed into welded enclosures that are closed with RTV and Caplugs which preclude the ingress of water. The effect cold has on FR-3700, TR-19, Fiberfrax and MinK-2000 has been evaluated for in the package analyses and investigated through package tests. A prototypical 9977 package was tested under exposure to an ambient temperature of -20°F (Appendix 2.8). Test and analysis results demonstrate the acceptable performance of the packaging and its insulation materials at low temperatures.

Because water ingress into the liner cavity is possible (see Section 2.6.6), water filling the liner cavity and then freezing was evaluated. See Appendix 2.1. Stress in the liner and CVs are calculated and compared against ASME Code Section III, Level A service limits. The 9977 is intended for dry service. It is extremely improbable that a package would be shipped in a

manner that water ingress into the cavity of the drum liner would occur. Therefore, the loads due to water (frozen or liquid) were not included with the NCT 4-ft drop loads or where the effects of the formation of ice or liquid water factored into the HAC drops.

An ambient temperature exposure to -40°F will have no adverse effect on the ability of the packaging, its containment vessels or contents to satisfy the requirements of NCT.

2.6.3 Reduced External Pressure

Requirement: 71.71(c)(3) *Reduced external pressure*. An external pressure of 25 kPa (3.5 lbf/in^2) absolute.

Evaluation: The overpack design incorporates multiple vent holes that are closed by plastic plugs that by design are weather proof but do not provide a gas tight seal. Since the drum lid doesn't form a gas-tight seal the liner internal pressure would equalize with the reduced external pressure. However, in the event the plugs were to form a gas-tight seal a reduced external pressure would result in an 11.2 psig differential pressure across the liner wall. Appendix 2.1 shows that the liner and drum are unaffected with this pressure differential.

The CVs have a gas-tight seal and therefore are affected by a reduced external pressure. The maximum pressure differential across each CV is the difference between the reduced pressure and containment vessel design pressures. Reducing external pressure on the CVs is equivalent to increasing the design pressure by the same amount:

6CV (800 + 11.2 = 811.2 psig),and

5CV (900 + 11.2 = 911.2 psig).

These pressures bound the *Maximum* Normal Operating Pressures (MNOPs) for the 5CV and 6CV of 56.3 psig and 41.2 psig, respectively (see Appendix 2.2) and are below the ASME Section III, Level A service limits.

A reduced external pressure will have no adverse effect on the ability of the packaging, its containment vessels or contents to satisfy the requirements of NCT.

2.6.4 Increased External Pressure

Requirement: 71.71(c)(4) *Increased external pressure*. An external pressure of 140 kPa (20 lbf/in^2) absolute.

Evaluation: The overpack assembly incorporates multiple vent holes that are closed by plastic plugs that provide a weather proof seal and could provide a gas tight seal. Generally, an increase in external pressure to 20 psia would have no affect on the overpack because the vents will permit the drum to equilibrate with an external pressure rise. However, in the event the plugs were to form a gas-tight seal an increased external pressure would result in a 5.3 psig differential pressure across the overpack wall. A 5.3 psig external pressure would have no effect on the drum which is internally supported by rigid polyurethane foam. The effect of a 5.3 psig pressure differential across the drum liner is negligible as shown in Appendix 2.1 where the liner is

evaluated for 5 psig fabrication internal pressure test. By inspection, the lid would also not be affected.

The CVs are sealed and would be affected by a rise in external pressure. Buckling analyses of the 5CV and 6CV were carried out in accordance with ASME Code, Section III, for an external pressure differential of 20 psi as given in Appendix 2.2. The analyses evaluated the effect of the increased external pressure, combined with minimum internal pressurization of the containment vessels. The analyses demonstrated that the stresses due to external pressure are very small and will not cause localized buckling of either containment vessel.

An increased external pressure will have no adverse effect on the ability of the packaging, its containment vessels or contents to satisfy the requirements of NCT.

2.6.5 Vibration

Requirement: 71.71(c)(5) Vibration normally incident to transportation..

Analysis: An analysis of random vibrations reported in Appendix 2.1, based on the power spectral density for the Safe-Secure Transport,[35] demonstrates that vibration and shock loadings are small and would not cause any fatigue concerns. The 9977 package CVs are the same in design to the 9975 and 9968 packages, which have withstood years of transport with no damage known to have occurred from vibration.

Service vibration loads are very small compared to drum closure-bolt preload, and the bolts will not loosen during normal transport (Appendix 2.1).

Test: Vibration testing was performed at Sandia National Laboratory on prototype 9977 SN-2. Sandias' vibration test report is provided in Reference 49. The 9977 prototype was subjected to shock and vibration loads representative of both truck transport and forklift handling. Following vibration tests SN-2 was subjected to sequential NCT and HAC testing. In preparation for vibration testing the 9977 is secured to a rectangular and circular metal table that is part of the vibration test equipment, Figures 2.13 and 2.14. The rectangular table is used for horizontal vibration while the circular table is used for vertical vibration testing.

Figure 2.13 - Horizontal Vibration Test of 9977 Prototype SN-2

Figure 2.14 - Vertical Vibration Test of 9977 Prototype SN-2

For the vibration and shock tests, test package, SN-2, was assembled in its heaviest configuration; the 6CV loaded with a 100 lb simulated payload. The package was subjected to a series of random vibrations and shocks that simulated over the road transport, forklift handling, and loading operations. The vibration and shock spectrum used is considered conservative in respect to that required by 10 CFR 71.71(c)(5). The prototypical package testing was run for 20 hours at the power spectral density plots shown in Reference **Error! Bookmark not defined.**. The random vibrations and shocks are conservative with respect to the power spectral density plots indicative of the SST/SGT [35] and other large truck and trailer combinations. Mil-STD-810F equates 1000 miles of transport by common carrier to 60 minutes of testing. Given this comparison the 9977 was subject to 20,000 miles of shipping. The shocks and vibration actually seen by a package in service would not be as severe as the spectrum tested.

SN-2 was X-rayed before and after testing. Figure 2.15 compares the before and after images of SN-2 at the "60 degree" orientation. The digital radiography (DR) images taken before and after testing are aligned as closely as possible so as to make objective comparisons possible. A grid has been overlaid on the images to assist with evaluation. Based on pre and post-vibration DR

examinations, there is no observable external damage to the package or material degradation inside the package. In Figure 2.15 the radiographs show voids in the foam that can occur during the overpack foaming process. The first two radiographs show SN-2 with and without the 6CV. The third radiograph is the post vibration shot. Based on comparison of radiographs taken before and after vibration/shock testing, there is no discernable change in the relative size or shape of these voids. No other vibration or shock induced damage is observable from the radiographs. Appendix 2.9 provides detailed pre/post digital radiographic images of SN-2.

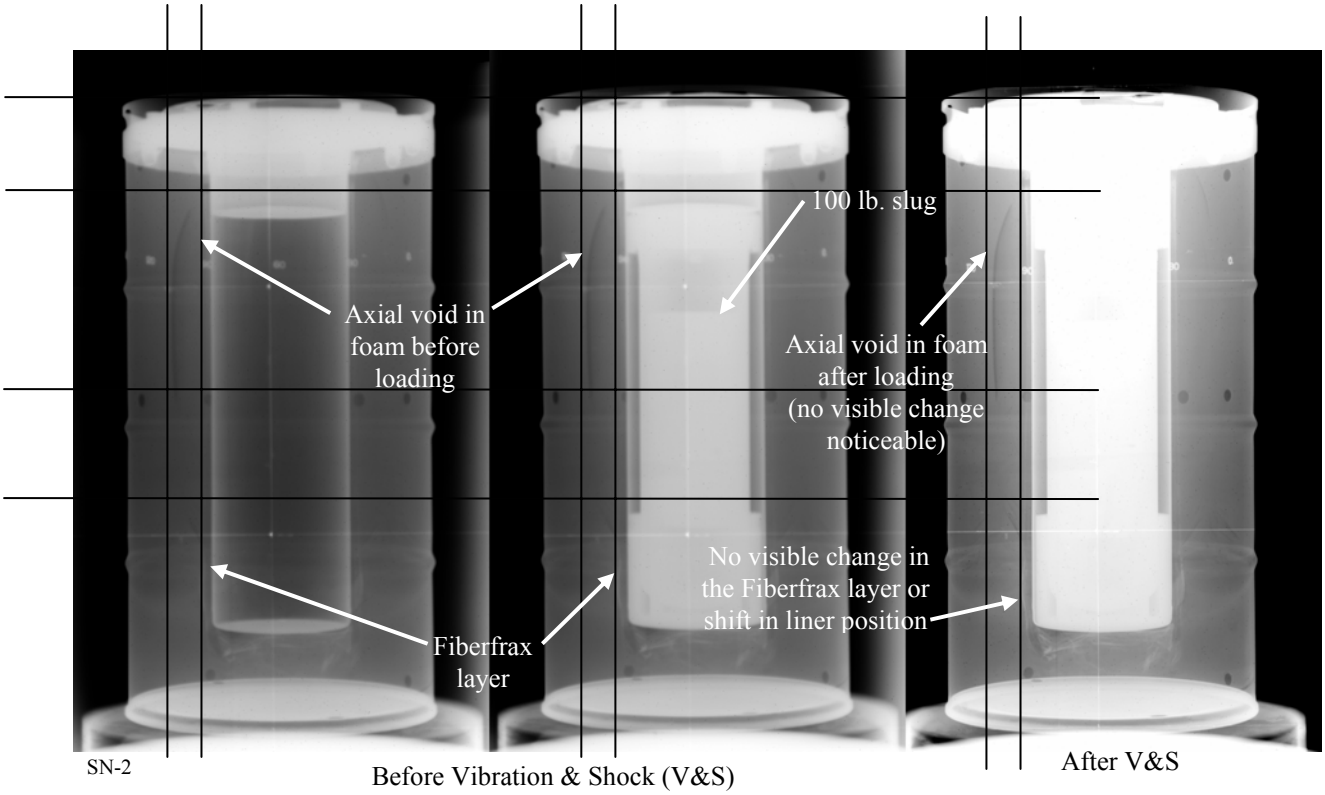

Figure 2.15 - Combined 60 Degree Digital Radiographic Images of SN-2 Before and After Shock and Vibration Testing

The drum lid and liner both include pliable layers of Fiberfrax between the lid or drum liner and more rigid insulation comprising the overpack. The Fiberfrax, because of its manufacturing, is resilient to mechanical damage and serves as a padding to mitigate the effects of vibration from the CV to the surrounding foam in the overpack and TR-19 insulation in the lid. The methods used during fabrication to secure the TR-19 and Min-K 2000 inside the overpack lid preclude their movement, this mitigates the effects of vibrations as is evident by post X-ray observations and observations of the lid post test cross-sections taken of the hardware following the fire. The overpack foam is securely locked into the drum due to expansion during curing. The only noticeable effect of the shock and vibration tests was the generation of aluminum particles by the repeated contact of the load distribution fixtures against the CV and drum liner. The scuffing that occurs was minimal. Figure 2.16 compares photographs of a non-vibrated LDF against the vibration tested LDFs.

Figure 2.16 – LDFs Before and After Shock and Vibration Testing

Based on analysis and test, vibration normally incident to transportation will have no adverse effect on the ability of the packaging, its containment vessels or contents to satisfy the requirements of NCT. Vibration has no affect on the package closure torques and only introduces superficial damage (scuffing) to the containment vessel LDFs. The superficial scuffing would not impact the design-basis performance of the 9977 in NCT and HAC events. The observed damage to the spacers does introduce the need for an investigation into changing the LDF material to a more wear resistant material, in order to eliminate the observed aluminum degradation. Degradation over time will be addressed during package maintenance. However, as the effect would not impact package performance under HAC, and the LDF is a replaceable part of the design, a revised material selection will be explored in the future.

2.6.6 Water Spray

Requirement: The package design is evaluated for the effects of water spray of approximately 2 inches/hour for at least one (1) hour as required by 10 CFR 71.71(c)(6).

Evaluation: The 9977 design was tested for the effects of water spray per 10 CFR71.71 (c)(6) as shown in Figure 2.17. Water spray did not damage the stainless steel drum. The overpack design does not incorporate a seal between the drum flange and its closure lid. Tests performed on the package showed that the lid to top deck closure does not preclude the possibility of water

ingress into the drum cavity, Reference 52. During the water spray test of SN-2, 13.6 lbs of water was found to have entered the drum cavity. The weight of water ingress shows that the liner was nearly full. Using nominal dimensions of the liner, 6CV and its load distribution fixtures the free volume in the liner excluding the annular region between the liner and drum lid was calculated to be 388 in^3, Appendix 2.1. Assuming standard conditions, the density of water is 62.4 lb/ft^3; the equivalent mass of water is 13.85 lbs. The effect of water freezing is addressed in Section 2.6.2.

The drum's 14 vent holes preclude water intrusion during NCT by plastic Caplugs. However, there would be minimal affect to the overpack if it were assumed one or more of the vent plugs were missing during the water spray test since the polyurethane foam is closed cell and will not absorb a significant amount of water. The water spray test will have no adverse effect on the ability of the package to satisfy the requirements of NCT.

Figure 2.17 - Water Spray Test

2.6.7 Free Drop

Requirement: 10 CFR 71.71(c)(7) *Free drop*. Between 1.5 and 2.5 hours after the conclusion of the water spray test, a free drop through the distance of 4-feet (for packages weighing less than 5,000 lb) onto a flat, essentially unyielding, horizontal surface, striking the surface in a position for which maximum damage is expected. Additionally, for fissile material packages the requirements of 10CFR 71.55(d)(2) and (4) is assessed. These are; 1) The geometric form of the contents would not be substantially altered; and 2) there is no more than five percent reduction in the effective volume of a packaging or spacing between the fissile contents and the outer surface of the package, and 3) no aperture in the packaging large enough to permit entry of 4-inch cube.

Evaluation: Compliance is demonstrated through prototype testing and analysis as described in the following sections.

Unyielding Surface

Requirement: 10 CFR 71.71(c)(7) and 71.73(c)(1) require that packages be dropped onto an unyielding surface. The IAEA describes an unyielding surface as a "flat, horizontal surface of such a character that any increase in its resistance to displacement or deformation upon impact by the specimen would not significantly increase damage to the specimen". (IAEA Regulations, para. 717)[4] The IAEA advisory Material further specifies an example of an unyielding target as one that includes a steel plate at least 1.57 inches thick floated to a concrete block mounted on firm soil or bedrock, where the combined mass of the steel and the concrete is at least 10 times that of the test package. (IAEA Advisory Material, para. 717.2)[50]

The NCT 4-ft drop and HAC 30-ft drop and HAC puncture test are performed on an unyielding surface in an environmentally controlled test facility located in building 723-A at the SRS. The unyielding impact surface is constructed from very high strength armor plate steel. The plate which serves as the unyielding surface is 5 ft square and 6-¼ inches thick, and is anchored in a 6-ft square by 36-inch thick reinforced concrete slab. The surrounding slab is isolated from the building concrete floor, (see Appendix 2.7). The concrete-steel monolith that serves as the impact target weighs approximately 19,475 lb. The target pad weight is greater than 50 times the weight of the 9977 and it will not deform or displace during testing. Appendix 2.7 presents the test pad design used for the NCT free drop testing.

2.6.7.1 Prototype Testing

Prototype 9977 packages were dropped in the top-down and CGOC orientations from 4-ft onto a flat unyielding surface. Testing and finite element analysis performed on various drum orientations shows minimal damage to the drum and negligible stress in the package containment vessels due to the 4-ft drop. Based on observations of drum damage from the 4-ft drops and analysis it was concluded the 9977 satisfies 10 CFR71.71(c)(7) and no further normal condition testing of the 9977 was performed. A summary of the prototype free drops is provided below.

Damage Description:

Test package SN-2 was dropped from 4 feet in a top-down vertical position. The drop orientation was estimated to produce the greatest damage to the drum closure and containment vessel closure. Prior to the free-drop, SN-2 was subjected to vibration testing and the water spray test. No precondition from these tests was noted that would affect the 9977 performance during the free drop. Appendix 2.7 presents a detailed evaluation of the preconditioning tests preceding the NCT free-drop. Figure 2.18 shows SN-2 test package elevated above the target pad preceding the 4-ft drop test.

On impact, the top of the package squarely struck along the top of the drum rim. The paper marker between the drum rim and target pad was cut where the rim of the drum squarely impacted the pad. The drum rebounded about 6 inches and came to rest on its top about 3 inches back from the point of impact, as shown by the cut paper marker, see Figure 2.18.

Figure 2.19 shows the top of the drum being evaluated for damage and digital radiographic images taken before and after the 4-ft drop test. Negligible surface damage was observed on the lid and drum rim. There was no observation of deformation in the lid plate between bolts. Placement of a straight edge across the top of drum identified that a portion of the lid pan was domed. It is uncertain rather the domed lid pan is a result of the 4-foot drop or how the pan is fabricated and installed. On close inspection of the digital radiographs taken after the 4-ft drop there was no discernible damage to the drum closure plug from the vertical impact of the Top LDF that would be expected if the lid domed due to the drop. FEA of the 4-foot top-down drop summarized in Section 2.6.7.2 and detailed in Appendix 2.3 showed there was negligible package deformation.

DP-1, an earlier 9977 prototype, was also dropped 4-ft top-down. Similar to SN-2, no significant damage was observed to the lid or the drum rim, Reference 52.

Figure 2.18 - SN-2 Elevated for 4-Foot NCT Drop

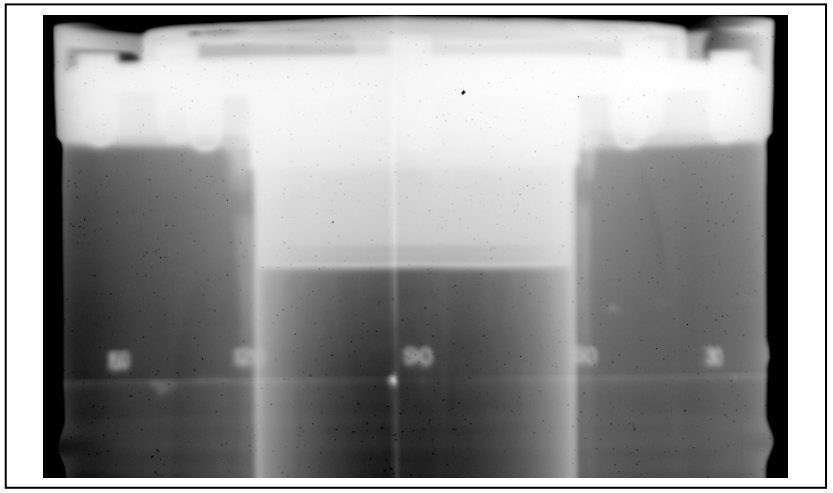

SN-2

Pre-Drop Radiograph w/o CV

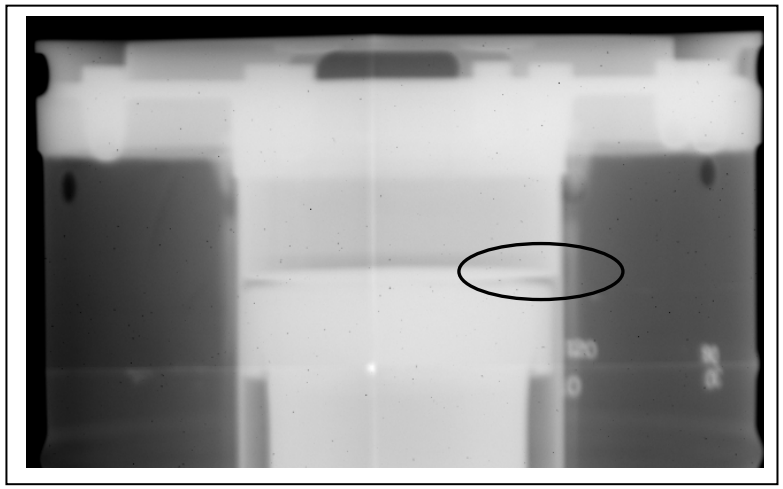

SN-2

Pre-Drop Radiograph with CV

SN-2

Post 4’ Drop Inspection of Drum Top

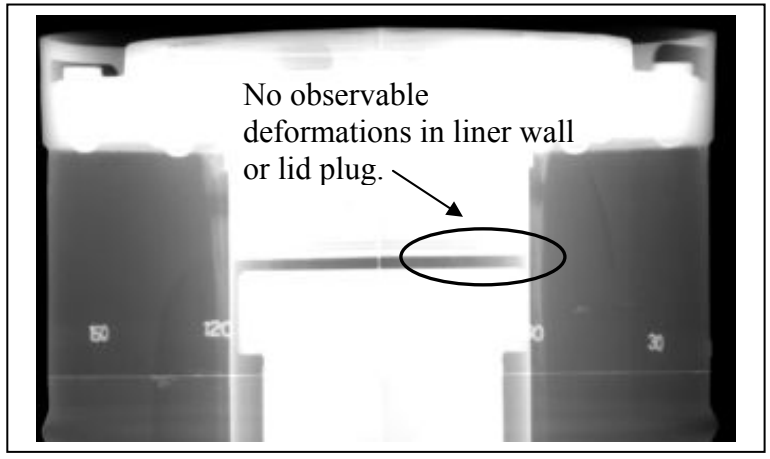

SN-2

Post Drop Radiograph Inspection of Drum Lid and Liner

Figure 2.19 - SN-2 4-Ft Top-Down Post Drop Images

2.6.7.2 Analysis

Nonlinear dynamic analyses were performed to evaluate the structural responses of the package design due to the effects of a free drop through four (4) feet onto a flat, essentially unyielding, horizontal surface. The effects the heat and cold have on the 9977 due to payload internal heat generation and a cold environment when subjected to a 4-ft impact are evaluated. Table 2.24 lists the analyzed NCT drop conditions. Five analyses were performed with the 6CV configuration and are considered to bound the lighter weight 5CV configuration. Like letters shown in the table define the analysis boundary conditions.

Production Package versus Prototype: Appendix 2.8 provides the comparison between the 9977 prototypes versus the Production model being requested by this SARP. Differences between the prototype and production model are based on lessons learned from testing. These differences are highlighted and discussed in detail in Appendix 2.8. The design modifications made to the 9977 as a result of 2nd set of prototype 9977 testing, "SN Designated Packages", are minimal. After achieving agreement between the tested package and benchmark FEA, the FEA model was revised to reflect the production model design.

Table 2.24 Normal Condition Free Drop Analysis

Applicable Initial Condition		**Ambient Temperature**		**Insolation**		**Decay-Heat Rate**		**Internal Pressure**
		100°F	-20°F	Max.	Zero	Max.	Zero	psig
Free drop: 4-ft	TD		a		a		a	Note 1
	BD	b		b		b		
	CG		c		c		c	
	horizontal	d f	e g	d f	e g	d f	e g	

Note 1: All analyses were performed at ambient pressure.

FEA Bench Mark Analysis: Appendices 2.3 and 2.6 includes the optimization of the benchmark analyses that compared the HAC model and tested prototype. After achieving agreement between the benchmark FEA and the tested prototype package, the 9977 analysis model was revised to reflect the production model design. The revised package model was then analyzed under various NCT drop orientation and conditions and compared against NCT acceptance criteria to demonstrate compliance with 10 CFR 71 NCT requirements.

As part of the benchmark analysis, model sensitivity studies (i.e., mesh density, material properties, and solution time steps) were performed to obtain agreement between the tested packages and model. The baseline model developed from the sensitivity study is used for all other models and comparisons.

Finite Element Analysis for NCT: A prototype 9977 was free dropped top-down from 4-ft unto a flat unyielding surface. Finite element analysis calculations of 4-ft drops, performed on various

drum orientations and initial conditions shows minimal damage to the drum and negligible stress in the package containment vessels. Based on these results it was concluded the top-down drop satisfies 10 CFR71.71(c)(7) and no further NCT analyses were performed.

As testing of the DP and SN packages showed no drop necessarily resulted in greater drum damage or analysis showed no significant difference in stress in the CV the top-down drop orientation was chosen to proceed HAC event testing as it was estimated to subject the 9977 to overall most severe NCT conditions. The reason for selecting the top-down drop orientation was to induce the greatest bolt loading and compression of the lid and its insulating materials prior to the HAC impacts and thermal event.

2.6.8 Corner Drop

Requirement*:* 71.71(c)(8) *Corner Drop*. A free drop onto each corner of the package in succession, or in the case of a cylindrical package onto each quarter of each rim, from a height of 0.3 m (1 ft) onto a flat, essentially unyielding, horizontal surface. This test applies only to fiberboard, wood, or fissile material rectangular packages not exceeding 50 kg (110 lbs) and fiberboard, wood, or fissile material cylindrical packages not exceeding 100 kg (220 lbs).

Evaluation: No 1-Ft corner drops were performed. Corner drop evaluation per 10 CFR 71.71(c)(8) is not applicable to the 9977, because its minimum weight of 250 lb exceeds the maximum weight requirement of 220 lb for a cylindrical fissile material package.

2.6.9 Compression

Requirement: 71.71(c)(9) *Compression*. For packages weighing up to 5000 kg (11,000 lbs), the package must be subjected, for a period of 24 hours, to a compressive load applied uniformly to the top and bottom of the package in the position in which the package would normally be transported. The compressive load must be the greater of the following:

(i) The equivalent of 5 times the weight of the package; or

(ii) The equivalent of 13 kPa (2 lbf/in^2) multiplied by the vertically projected area of the package.

Evaluation: Compliance is demonstrated through testing and analysis as described in the following sections.

2.6.9.1 Prototype Testing

In addition to performing the analysis, a compressive test load of 1,800 lb was applied to the 9977 for 24 hours. Figure 2.20 is a photograph of the 9977 with the applied test weight. There was no observable deformation to the 9977 following the 24 hour test. Appendix 2.10 provides the test results and reference to test procedures used. Results of the compression test and analysis form the basis for the conclusion that the 9977 satisfies this requirement.

SN-2

Figure 2.20 - 9977 Compression Test of SN-2

2.6.9.2 Analysis

The 9977 design was analyzed for the effects of compression as required from a vertical load equivalent to five (5) times the maximum package weight (5 × 350 lb = 1,750 lb) which bounds the load corresponding to 2 psig on the projected area of the package (554 lb). The compression strength of the 9977 drum was evaluated in Appendix 2.1 using the FEA. The yield strength for the 304L stainless steel drum is 25 ksi. The five-high stacking load resulted in an axial stress of 14 ksi in the drum. Therefore, the drum design is more than adequate to sustain the axial stress from a compressive load of five (5) times the package weight.

2.6.10 Penetration

Requirement: 71.71(c)(10) *Penetration*. Impact of the hemispherical end of a vertical steel cylinder of 3.2 cm (1.25 in) diameter and 6 kg (13 lbs) mass, dropped from a height of 1 m (40 in) onto the exposed surface of the package that is expected to be most vulnerable to puncture. The long axis of the cylinder must be perpendicular to the package surface.

Evaluation: The 9977 design was tested for the effects from an impact of a steel cylinder striking the package per 10CFR71.71(c)(10).

The 9977 overpack design is a stainless steel drum with a bolted lid that does not include any exposed valves, rupture disks or fittings. Consequently, there are no operational devices that would be affected by the impact of a steel cylinder in transport. To verify, the package design was tested to evaluate the effects of a free drop impact of a vertical steel cylinder through 40 inches onto its surface. For the 9977 the worst case impact was concluded to be the overpack closure lid which is fabricated with a 14 gauge dish welded to its top that houses a 1-inch thick disk of insulation. The remaining exposed portions of the overpack are fabricated from material thicker than 14 gauge. Note that the steel cylinder rebounded and impacted the lid multiple times before falling away from the drum. The impact points are seen in Figure 2.21. As can be seen, the small indentations to the lid will have negligible affect on the package.

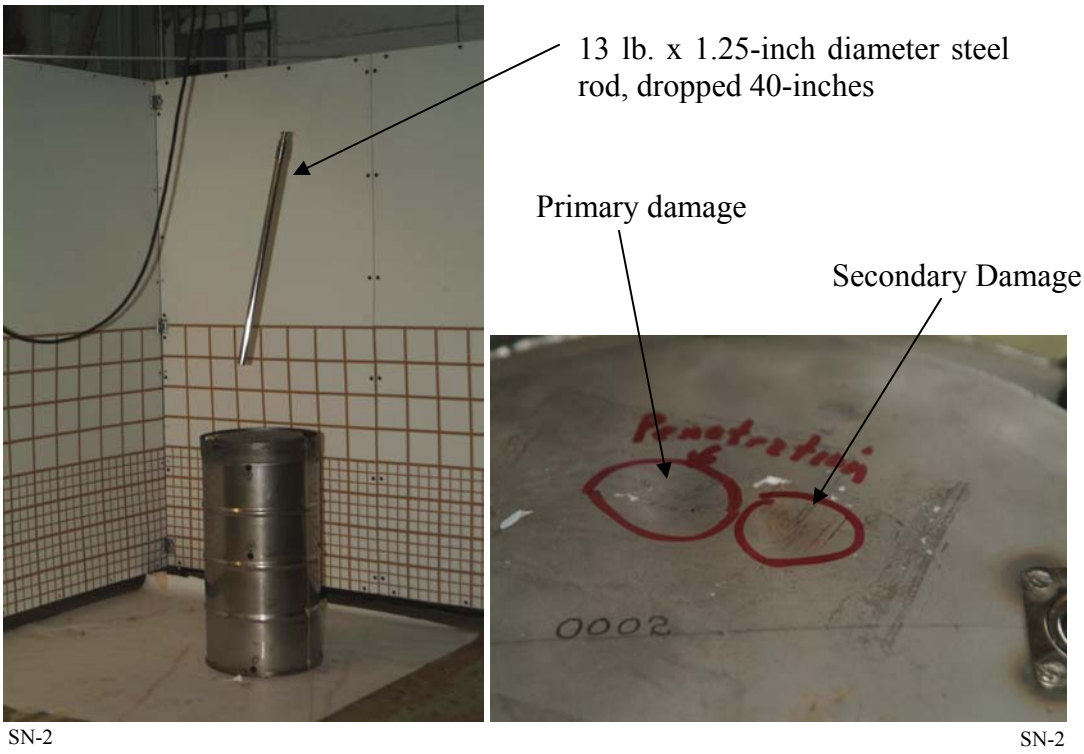

Figure 2.21 - NCT Penetration Test and Test Damage of 9977 SN-2

Results of the penetration test, with the fact that the design does not include any exposed fittings, form the basis for the conclusion that the 9977 satisfies this requirement.

In summary, the NCT tests do not challenge the 9977. With the exception of minimal deformation to the drum and lid from the 4-ft drop, superficial damage from the penetration test, and aluminum particles from the vibration tests, the package does not show any significant signs of being affected by NCT events.

2.7 HYPOTHETICAL ACCIDENT CONDITIONS

This section demonstrates that the 9977 package satisfies the performance requirements of 10 CFR 71.51(a)(2) that its design, construction and preparation for shipment, under the HAC tests given in 10 CFR 71.73, "there would be no release of krypton-85 exceeding 10-A_2 in 1-week, no escape of other radioactive material exceeding a total amount A_2 in 1-week, and external radiation dose rate exceed in 1 rem/h at 40-inches from the external surface of the package." Additionally the 9977 is shown to meet the requirements in 10 CFR 71.55(e) and 71.59(a)(2), when subjected to the tests specified.

HAC tests are conducted sequentially, per the order indicated, to determine their cumulative effect on a package in accordance with 10 CFR 71.73(a). (An exception is provided for the water immersion test for "all packages", where an undamaged package may be used. An exception is also provided for water immersion of "fissile packages" if water inleakage is assumed.)

(1) Free drop - A free drop of 30 ft onto a flat, essentially unyielding surface.

(2) Crush – A 1100 lb mass dropped 30 ft onto the drum resting on an essentially unyielding surface.

(3) Puncture - A free drop through a distance of 40 inches, striking a bar 6 inches in diameter.

(4) Thermal - Exposure to an environment of 1475°F for 30 minutes.

(5) Immersion (fissile material) - Immersion of package following the first three tests in water to a minimum depth of 3 ft for at least 8 hours.

(6) Immersion (all) - Immersion in water of an undamaged package to a minimum depth of 50 ft for at least 8 hours.

As described in the following sections, the 9977 is shown to meet the performance requirements of 10 CFR 71.73 by a combination of physical testing and analysis. Where applicable, comparison to packages of similar design is also made. Appendix 2.8 presents a detailed comparison of the 9977 with its earlier development designs. Physical testing has been performed on these development designs. Design changes made to the packages through the course of development testing are included in the final analysis models for the 9977.

Nine prototypical 9977 packages have been subjected to some or all of the HAC test sequence and are evidence of the 9977 being able to meet the performance requirements of 10 CFR 71.73. Four test packages (nearly identical to the final 9977 design) are identified by serial numbers SN-2 through -5 were sequentially subjected to the HAC; free drop, crush, puncture and thermal (pool fire) as specified in 10 CFR 71.73. Details of the tests are documented in Appendix 2.10. An additional test package, referred to as the "Practice Package", was constructed from a 9975 drum and the liner and lid from a 9977. This package is discussed in detail in Chapter 3 and Section 2.7.4, this package was only subjected to the thermal test. The remaining five test packages, earlier prototypes of the 9977, identified as DP-1, 2, 3, 5 and 6 were subjected to free

drop, crush, puncture and thermal (furnace testing), (Reference 1). Water inleakage was assumed for criticality evaluations and therefore, the 3-ft water immersion test was not performed following the thermal test. The 50 ft immersion test requirement is satisfied by referencing immersion testing performed on 9968 containment vessels which are identical in design to the 9977 containment vessels. Test results for the 9968 showed no inleakage of water or structural degradation to the containment vessels following the 50-ft immersion test.[]

Test unit SN-2 and all of the DP test packages were preconditioned with the 4-ft free drop test before the HAC sequential testing. Additionally, test package SN-2 was also subjected to the full battery of NCT tests before undergoing the HAC sequential testing.

For HAC evaluation, 10 CFR 71.73(b) requires that all tests be performed under the most unfavorable ambient temperature within the range of -20°F to 100°F. Additionally, "the initial internal pressure within the containment system must be the maximum normal operating pressure, unless a lower internal pressure, consistent with the ambient temperature assumed to precede and follow the tests, is more unfavorable." The 9977 tests were conducted with the package at a steady state temperature of either -20°F or approximately 70°F. As discussed in Section 2.3, the materials of the package are not significantly affected by temperatures ranging between 70°F and 100°F. Therefore, it is assumed that the difference in package performance over the 30°F differential is negligible and testing performed at 70°F is equivalent to testing at 100°F. The maximum normal operating pressure of the two 9977 CVs as reported in Section 3.1 is significantly below each CV design pressure. The effect of internal pressure on package performance during HAC is considered negligible and was not tested for the 9977. However, CVs in the 9975 package, of identical design to those in the 9977, were pressurized to their design pressures, 6CV 800 and 5CV 900 psig, and the package dropped 30-ft with no observed structural change to the CVs or their leak-tight capability.

FEA Bench Mark Analysis: Appendix 2.6 details the benchmarks the drop and crush dynamic analyses. Tables 2.25 and 2.27 present the matrix of HAC tests that were performed for the SN and DP Series Packages. Figure 2.23 illustrates the 9977 HAC drop and crush orientations that were tested. Figure 2.24 illustrates the HAC analyses orientations that were modeled for test benchmarking and/or for evaluating orientations not tested. Testing was performed at -20ºF and 75ºF for the SN Series.

The analyses were performed over a package material temperature range from -20ºF to 300ºF. The structural properties of stainless steel and the insulation materials in the lid and Fiberfrax around the drum liner are essentially unchanged over the temperature range of interest. However, the properties of the drum foam are temperature dependent and analysis was performed to evaluate the effect of the foam property change on performance of the package. Low temperature, -20ºF and ambient, 75ºF analysis was performed to benchmark the tested configurations. Analysis at higher temperatures, 140ºF and 300ºF, were performed to evaluate the 9977 at NCT without solar and NCT with insolation respectively. The foam was conservatively assumed to be at a uniform 140ºF based on the unmodified average model temperatures of thermocouples T0 and T27 listed in Table 3.15. The foam properties for NCT with insolation (ambient temperature 100ºF) were based on the distributed heat source at the bottom of the 6CV reported in Table 3.16. The 300ºF is not uniformly applied to the material

properties. Figure 2.22 shows the foam temperature model. The bulk of the foam is modeled at 260 ºF, only a small region around the bottom of the liner is modeled at 300 ºF. This temperature distribution is conservative and is based on Figure 17 of Appendix 3.3 "Source at Bottom of CV".

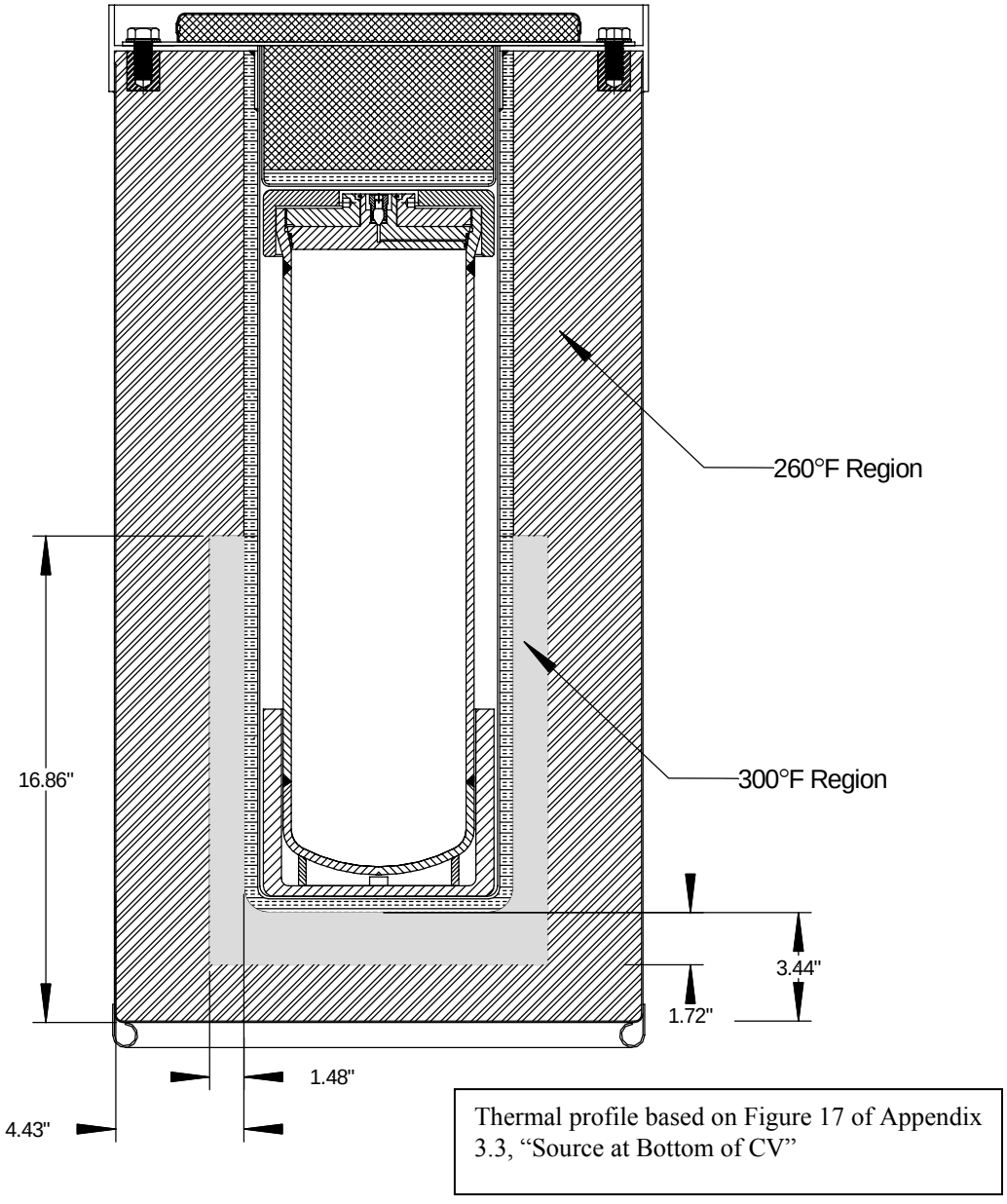

Figure 2.22 NCT Insolation Foam Temperature Model used for 9977 Structural Analysis

In summary, the 9977 through physical testing and analysis has been demonstrated to meet the package performance requirements for HAC with a large margin of safety. Specifically, the regulatory release rate limit following HAC, i.e., "no escape of radioactive material exceeding a total amount A_2 in one week." is met by demonstrating that the containment system remained

leak-tight after HAC testing as shown in Table 2.25 and containment vessel stress shown in Table 2.28 is below Code allowables. The regulatory external radiation dose requirement, i.e., dose shall not exceed 1 Rem/hour at 40-inches from the external surface of the package) is met by factoring the damage results from the tests into analyses described in the shielding evaluation (Section 5.1) and showing that calculated dose for a damaged 9977 is <<10 mRem/hour at 1-meter from the package surface. Lastly, the general requirements for fissile material packages in 10 CFR 71.55 are met by factoring the damage results of the tests as described in this section into the criticality evaluation (Section 6.1) and showing that for a N x N array of packages the 9977 array remains subcritical (K-eff < 0.9).

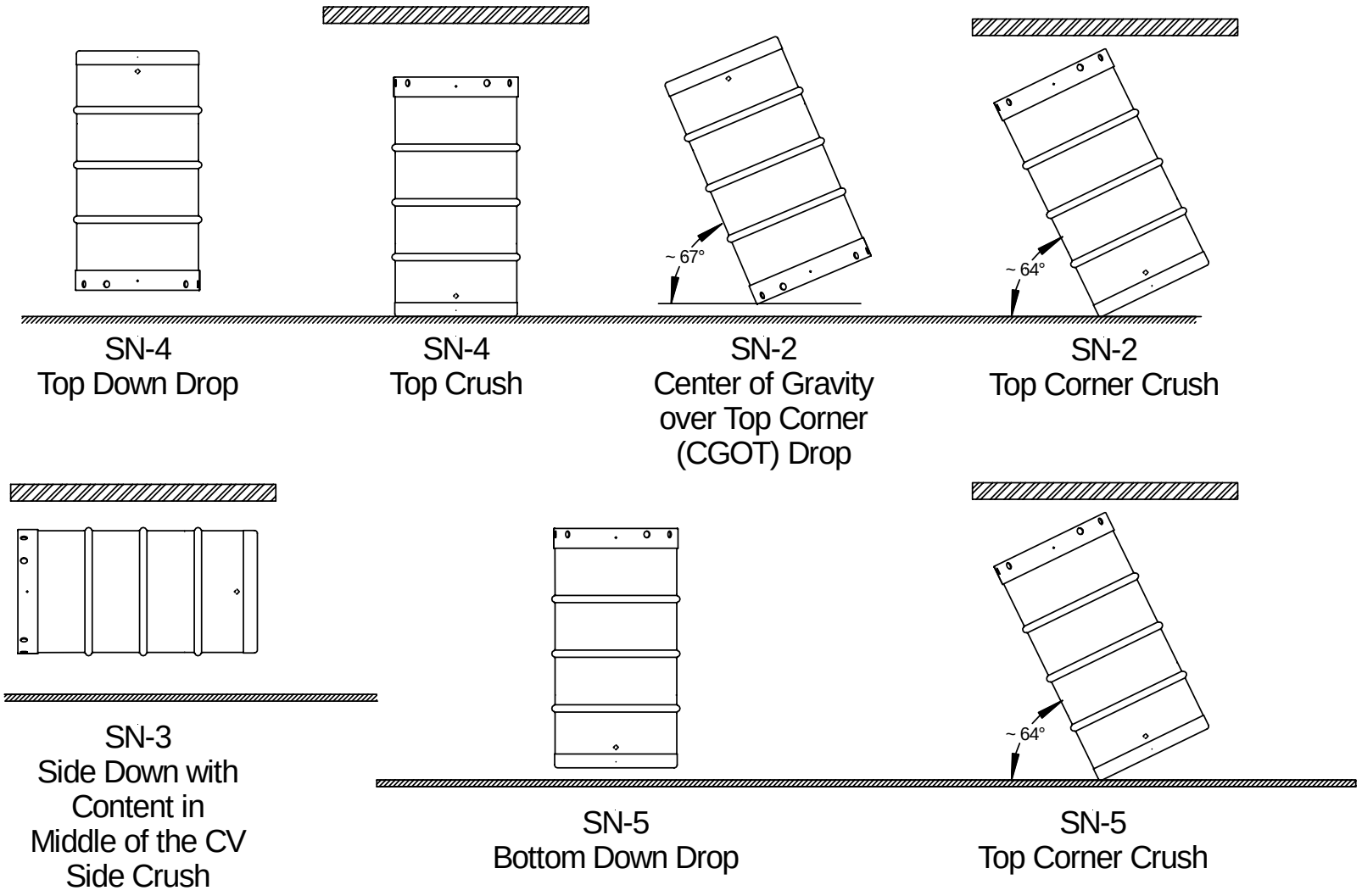

Figure 2.23 9977 HAC Prototype Testing Drop and Crush Orientations

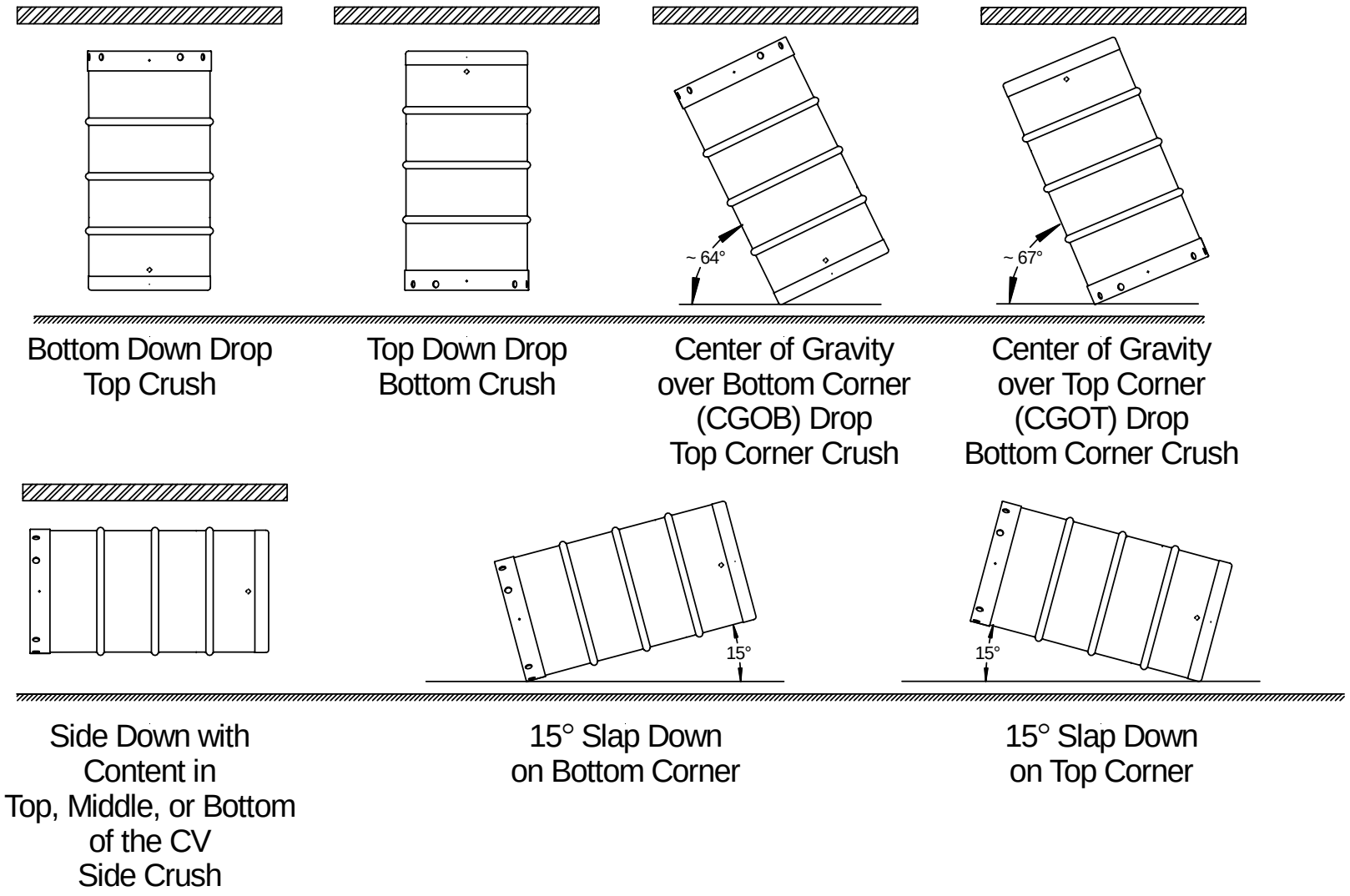

Figure 2.24 9977 HAC Analysis Drop and Crush Orientations

Table 2.25 – NCT/HAC Test and Analysis Summary for the 9977 - SN Series Prototypes

Test Unit	NCT		Hypothetical Accident Condition Testing (HAC)								CV Leak Rates (cc/sec atm)
	4-ft Drop	All other NCT	30 ft **Drop** (U.S.O. Ambient 75°F, CV pressure 1 ATM) **Crush** (U.S.O. Ambient 75°F, CV pressure 1 ATM)					Puncture Ambient (uos)	Preheat	Thermal	
			Top	CGOT	Bottom	CGOB	Side	Side	Package soak-temperature before fire (ºF)	Orientation Average-Time Temperature	Pre-Test / Post Test
SN-2	TD ✓	✓		✓				✓	200	TD 33 min 1873ºF	<1 x10^{-9} / <8.8 x 10^{-10}
				✓							
SN-3	NA						✓ -20°F	✓ & Bottom -20°F		Side 33 min 1472ºF	2 x10^{-9} / <1.8 x 10^{-9}
							✓ -20°F				
SN-4	NA		✓					✓		BD 35 min 1558ºF	<9.7 x10^{-10} / 2.1 x 10^{-9}
			✓								
SN-5	NA				✓			✓		BD 35 min 1591ºF	<1.0 x10^{-9} / <8.8 x 10^{-10}
				✓							
Practice Package	NA									BD 32 min 1857ºF	<1.1 x10^{-9} / <2.2 x 10^{-9}

Legend: ✓ - Tested Condition
Uos – unless otherwise stated

Table 2.26 – NCT/HAC Test and Analysis Summary for the 9977 - DP Prototype Packages

Test Unit	NCT		Hypothetical Accident Condition Testing (HAC)								CV Leakage Rates (cc/sec atm)
	4-ft Drop	Water spray, etc	30 ft Drop (U.S.O. Ambient 70°F, CV pressure 1 ATM) / Crush (U.S.O. Ambient 70°F, CV pressure 1 ATM)					Puncture	Preheat	Thermal	Pre-Test / Post Test
			Top Down 0º	CGOT	Bottom Down	Oblique	Side	Side	Package soak-temperature before fire (ºF)	Orientation Average-Time Temperature	
DP-1	CGOT ✓	Not tested		✓				CGOT	NA	Side 50 min 2000ºF	2.9×10^{-8} / Note 1
				✓							
DP-2	CGOT ✓		✓					Bottom		Side 55 min 2000ºF	$<1.9 \times 10^{-9}$ / Note 1
			✓								
DP-3	CGOT ✓						✓	✓		Side 45 min 2000ºF	2.4×10^{-9} / Note 1
							✓				
DP-5	CGOT✓		✓					Bottom edge of drum		Side 45 min 2000ºF	4.5×10^{-9} / Note 1
			✓								
DP-6	CGOT✓						✓	✓		Side 45 min 2000ºF	2.3×10^{-8} / Note 1
							✓				

Legend: ✓ - Tested Condition
CGOB – Center of Gravity over Bottom
CGOT – Center of Gravity over Top
BD – Bottom Down; Package with drum axis vertically oriented with bottom striking ground first
TD – Top Down; Package vertically oriented with drum axis 0-25 degrees from vertical with top striking ground first
BSD – Bottom Slap Down; Package oriented with drum axis 0-25 degrees from horizontal with bottom striking ground first
TSD – Top Slap Down; Package oriented with drum axis 0-25 degrees from horizontal with top striking ground first
Side – Package oriented with drum axis parallel to target
SAD – Shallow Angle Drop; Package oriented 25+ degrees from horizontal with top end striking ground first

Note 1: The Post-HAC test was performed only to verify no gross leakage (i.e. leakage < 1x10-3 std-cc/sec) and all the CV's passed this test. These were units were for investigation of packaging design alternatives and the CVs were not modified to perform standard helium Leak-Tight testing.

2.7.1 Free Drop

Requirement: 10 CFR 71.71 (c)(1) *Free Drop*. A free drop of the specimen through a distance of 9 m (30 ft) onto a flat, essentially unyielding, horizontal surface, striking the surface in a position for which maximum damage is expected.

Evaluation: Compliance is demonstrated through testing and dynamic finite element analysis as described in the following sections.

Free drop tests were conducted at the SRS in Building 730-A. See Section 2.6.7 for a description of the target that was used as the unyielding surface for drop tests. Testing was accomplished by hoisting packages to 30-feet and dropping with the assistance of a magnetic release.

A total of nine prototype packages were tested in the 30-ft free drop. In all but a few cases, multiple digital radiographic images were made before and after each test to enable evaluation of internal package damage in addition to typical external damage. No scale model testing was carried out to evaluate the performance of the 9977 design. Of the nine package drops only five, SN-02 through -05 and DP-1 are summarized in the following sections. The SN test units are nearly identical to the 9977 final design. The DP-1 test unit is similar to the 9977 with the exception of having a larger diameter and foamed overpack closure lid; DP-2, DP-3, DP-4 and DP-5 are referenced where valid comparisons can be made between them and the 9977. Appendix 2.10 and Reference 51 discuss in detail the prototype package testing and observed damage for the SN series and DP series development packagings, respectively. The primary differences between DP series prototypes and the aforementioned SN series prototypes are as follows:

<u>DP-2 and DP-3</u>

- increased foam density in the overpack
- foamed overpack lid
- larger diameter overpack lid
- no extension on top of lid

<u>DP-4 and DP-5</u>

- same as DP-2 and -3 plus,
- 16-inch diameter drum.

Appendix 2.8 presents a detailed description of the differences between the various prototype designs and the 9977. An explanation for each design change is also included. All HAC testing was performed with the 9977 fitted with a 6CV and maximum payload of approximately 100 lb. Analyses presented in the following section show that the 5CV loading configuration is bounded by the 6CV configuration.

The 9977 package was tested under four different drop orientations; top-down, bottom-down, center of gravity over top corner and horizontally, see Table 2.27. These configurations are considered to be the most challenging to the 9977s containment vessel and overpack. The

follow-on crush and fire were considered in each of the 30-ft drop orientations. Table 2.1 of Appendix 2.6 lists the HAC test package orientations and the primary components and or features that were being evaluated for the 30-ft free drop, crush and fire tests. The puncture test was not expected to appreciably challenge the package. One or two puncture drops were made depending on the damage observed from previous testing. The required puncture was to impact the package over its center of gravity along its longitudinal axis. An optional puncture was to strike the package in a position where an apparent weakness from the previous tests justified an additional impact.

Dynamic finite element analyses were performed to augment physical drop testing in demonstrating that the 9977 package remains in a safe configuration under 10 CFR 71, Hypothetical Accident Conditions (HAC). Specifically, these analyses determined the relative stress and deformation to the overpack and the five- and six-inch diameter containment vessels. Analysis results are compared against ASME BPVC, Section III, Appendix F for Level D Service to verify that the packaging components do not exceed Code-allowable limits.

The results of these analyses show that when compared to acceptance criteria, a large margin of safety exists and the effectiveness of the 9977 under HAC is not compromised. The HAC calculations evaluated are summarized in the following Sections. Detailed analyses with assumptions are provided in referenced Appendices.

2.7.1.1 End Drop

The effects of an end drop were evaluated on two test packages, SN-4 and SN-5. SN-4 was dropped top-down. In the follow on crush test (Section 2.7.2), the crush plate impacted the top of the drum. SN-5 was subjected to a bottom-down drop. In the follow-on crush test the crush plate impacted the drum over its top center of gravity.

2.7.1.1.1 Test – Top Down (SN-4)

Test unit SN-4 was dropped top-down with the drum axis vertical. Testing was performed indoors with the package at ambient conditions, approximately 75 ºF. The 6CV contents were simulated with a 5½-inch diameter by 13 inch long steel slug weighing 101 lbs, bringing the total weight of SN-4 to 339 lbs. The slug was loaded in the CV without dunnage, thereby eliminating any energy absorption due to cushioning during impact. The objective of this test was to evaluate the amount of crushing of the lid plug and stress in the closure bolts from the direct top-down impact. The top-down hit also results in a high loading to the CV threaded closure. Also of interest was whether the lid would deform plastically between bolts as was seen in the earlier DP-Series prototype testing. Excessive crushing of the plug, lid deformation between bolts, failure of one or more lid bolts, or overstressing the CV closure could affect the performance of the package in the subsequent crush and thermal tests.

SN-4 hit at about 3-degrees from vertical. It rebounded about 1-inch and came to rest about 1-foot from point of impact. Figure 2.25 illustrates SN-4 before and after the test. The CV and top LDF assembly impacted the bottom of the lid in a piston fashion, locally buckling the bottom of the plug and expanding it radially into the liner. The drum shell buckled just below the drum rim producing a fourth rolling hoop. When the drum rim rebounded upward the CV assembly

was still decelerating downward resulting in the closure lid top being domed out approximately ½-inch above the drum rim.

The localized buckling of the lid plug is a result of the ½-inch thick layer of Fiberfrax placed in the bottom of the plug. The Fiberfrax has no resistance to compressive loads until it reaches lock-up. Based on the DR images after the 30-ft drop, the gap between the 6CV Top LDF and the bottom of the lid plug is 0.6-inches. This is an increase of 0.4 inches from the nominal 0.20-inch design spacing, See Figure 1.3. The 0.4 inch change corresponds to the amount of compression seen in the before and after radiographic images of the Fiberfrax layer, Figure 2.25.

The lid did not significantly deform between the bolt locations as was seen in early prototype testing (Reference 52, pg 35). Figure 2.25 shows a lid deformation of about 0.2-inches. This is small compared to the ¾-inch in the DP design. The addition of the insulated top on the lid and the replacement of foam with less rigid impact absorbing materials significantly reduced the amount of load transmitted to the lid flange from top-down vertical drops. The redistribution of load path results in near elimination of scalloping effect that was seen on the previous design. Based on examination of post drop specimens and radiographic imagery, the 9977 with a maximum loaded 6CV does not appreciably challenge the drum closure.

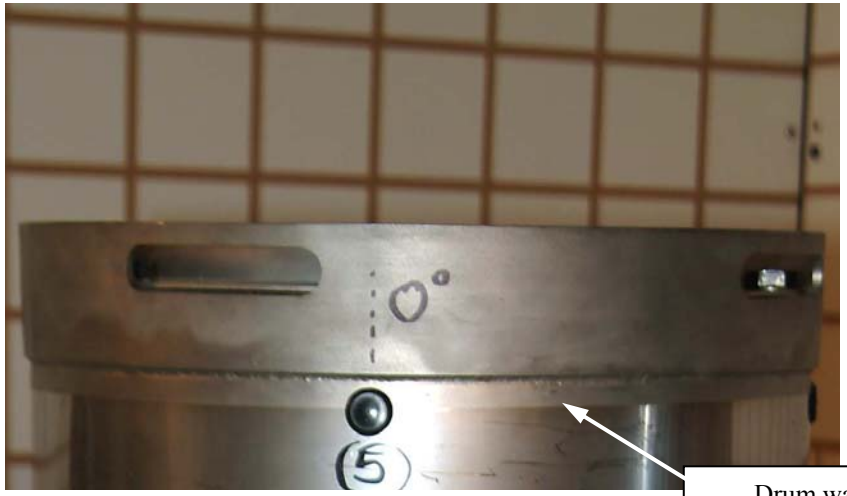

SN-4

PreDrop Configuration

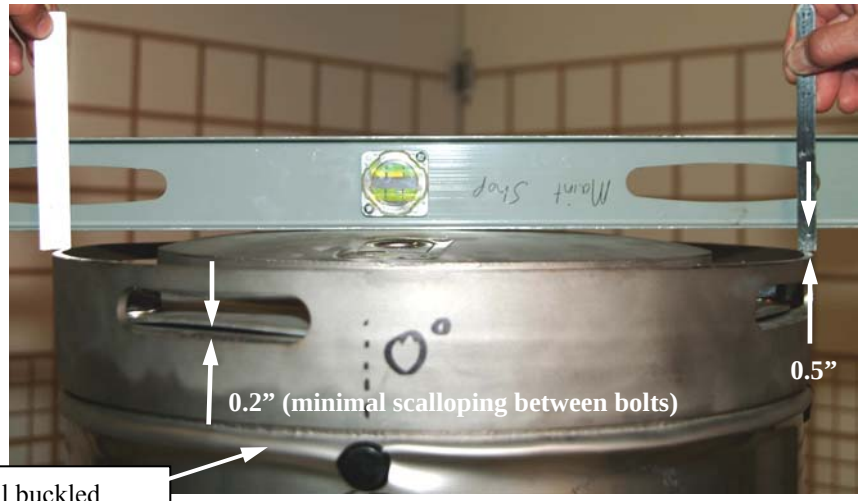

Drum wall buckled producing faux rolling hoop beneath lid flange

Post 30-ft Top Down Drop

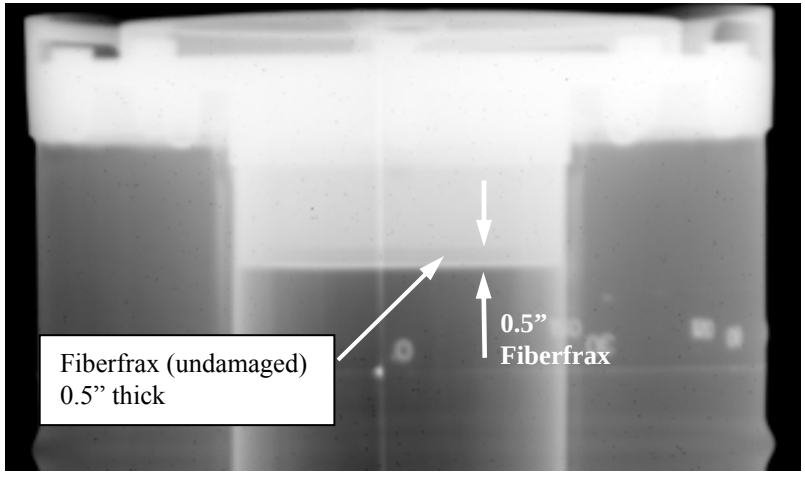

SN-4

PreDrop Radiograph

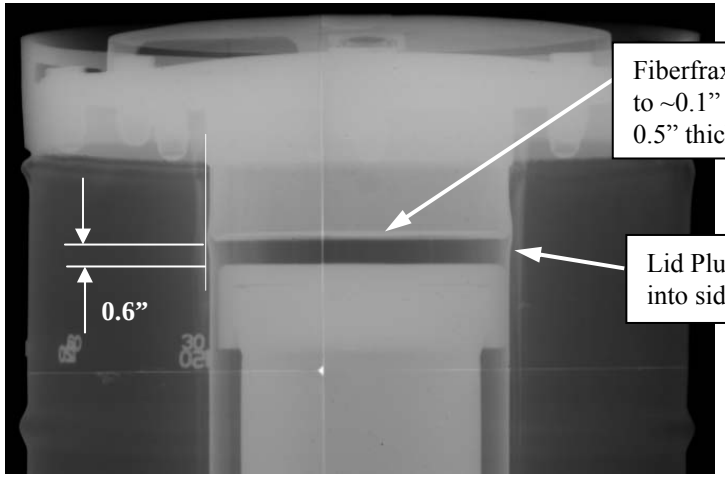

SN-4

Post 30-ft Drop Radiograph

Figure 2.25 - SN-4 / Top-Down 30-Foot Drop (Before & After Images)

2.7.1.1.2 Analysis – Top Down

Nonlinear dynamic analysis was used to evaluate the structural response of the 9977 CV design and drum overpack to the impact from a top-down 30-ft drop, Appendix 2.6. Drop analyses were performed at temperatures of 75°F and 140°F. The structural properties of stainless steel and the insulation materials in the lid are essentially unaffected over this temperature range, however, the foam properties do change with respect to temperature and analysis was performed to evaluate the effect of foam property changes on the package.

Figure 2.26 compares the FEA deformation plots at 75°F and 140°F with damage observed from test package SN-4 that was dropped vertically top-down under ambient conditions, 75°F. The radiograph shows the drum lid flange is away from the top deck of the drum at the liner by approximately 3/8-inch. The inner lid pan is crushed by about ½-inch resulting in the lower part of lid deforming into and buckling the side wall of the liner out locally about 1/10-inch.

The deformation plots for the overpack show similar damage for each analysis. The drum strains illustrated vary by about 2% between analyses, see Appendix 2.6. The lid protrudes above the top deck where it inserts into the liner by ~½-inch, which compares favorably with the SN-4, which scales to about 3/8-inch. The bottom of the lid buckles about 1/2-inch, (i.e., the depth of the Fiberfrax). The lid buckling causes the lid to expand radially forcing the side wall of the liner to also buckle. These structural deformations compare favorably to what is observed in the test package radiographic images.

The CV stress varies by about 1% between cases. This is not unexpected, since, for the top down impact the lid receives the majority of the load and its materials are relatively unaffected by temperature change. The results of top-down impact, analyses at various temperatures demonstrate the structural adequacy of the 9977 design under this HAC event. Table 2.28 lists the maximum stress for the components of interest. The component stress results are compared in Table 2.28 to allowable values from ASME Section III, Appendix F, Level D, Service loads, showing that the computed values are less than the limits.

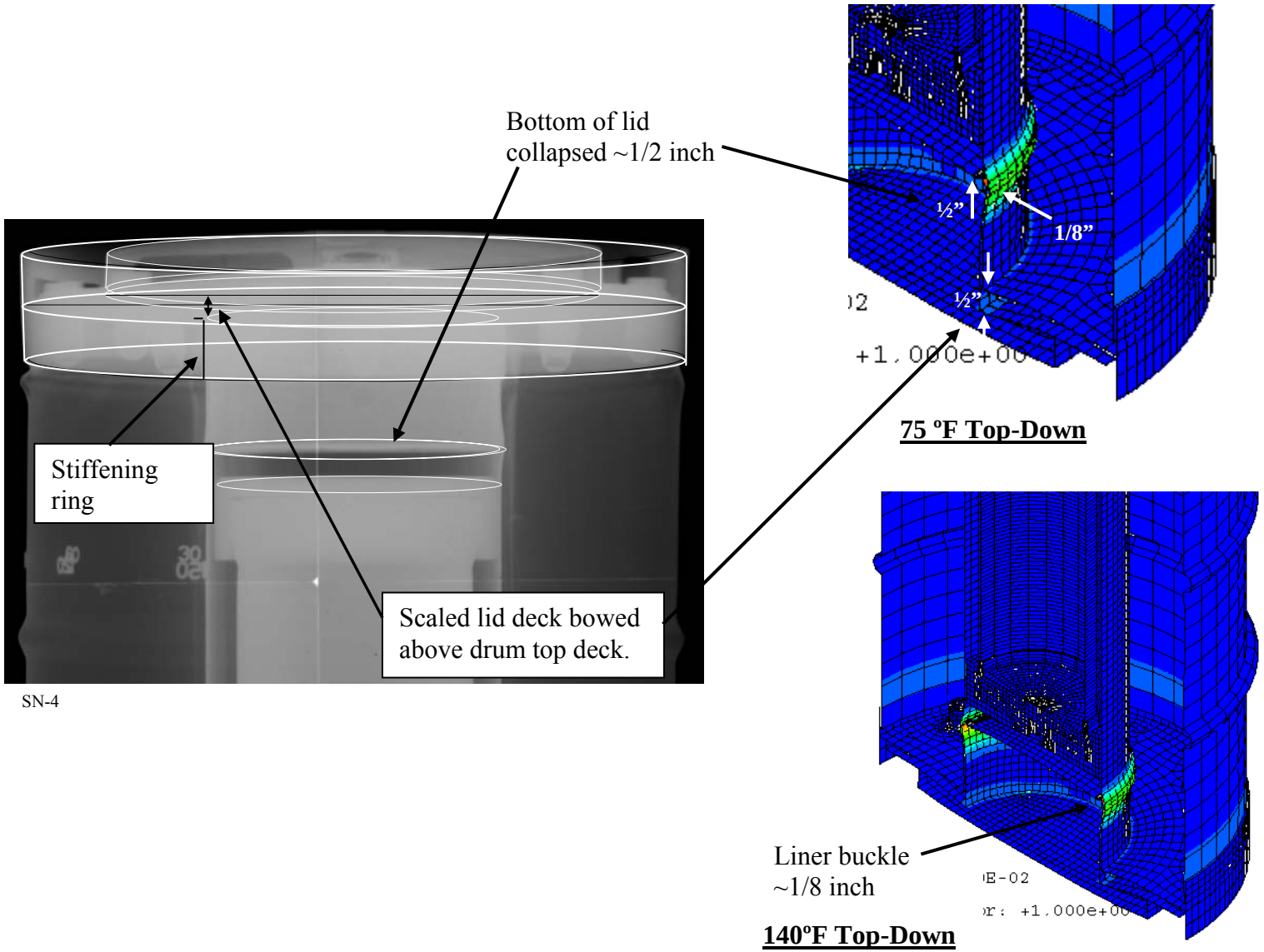

Figure 2.26 SN-4 Top-Down 30 Foot Drop at 75°F Comparison with 75°F and 140°F Analysis

2.7.1.1.3 Test – Bottom Down Drop(SN-5)

Test unit, SN-5, was dropped bottom-down with the drum axis vertical. Testing was performed with the package at ambient conditions. The 6CV content was simulated with a 5½-inch diameter by 13-inch long steel slug weighing 100 lbs, bringing the total weight of SN-5 to 341.6 lbs. The slug was loaded in the CV without dunnage, thereby eliminating any energy absorption due to cushioning during impact. The primary objective of this test was to evaluate loading to the overpack's liner bottom and its connection to the overpack's top deck. A design change was made from the DP series prototypes to the SN series packaging to add insulation around the liner (see Appendix 2.8). Rupture of the liner could affect the performance of the package in the thermal test by permitting foam decomposition products to enter into the liner, thereby increasing CV temperatures. (Thermal testing of the DP test packages showed that any opening, including at the bolt threaded connection, permit foam combustion products to pass, though no foam residue was observed.)

On impact SN-5 was a few degrees from vertical. The drum's bottom edge cleanly stamped a 350-degree circle from the paper marker positioned on the target pad (the uncut portion being the initial point of impact). SN-5 rebounded vertically approximately 6 feet and came to rest on its side with the bottom of the package coming to rest in the circle of impact. The package rebound is significantly greater than the 1-inch rebound observed in the 30-ft top-down drop. Figure 2.27 illustrates SN-5 following the drop test. The bottom of the drum was flattened by the impact which produced a buckle in the drum wall just above the chime (Figures (a) and (b)). The slightly off vertical hit produced an external buckle that varied in width from zero, where the drum first impacted point #2, to ½-inch at point #4, on the opposite side of the drum rim, Figures (c) and (d). The energetic rebound could indicate that the time it took the CV assembly to impact the liner bottom and pushed through the Fiberfrax layer until lockup was reached corresponded to the approximate time that it took to collapse the overpacks bottom chime. This resulted in the overpack and CV assembly impacting the stiffer foam in unison and thus recoil of the package was much more energetic than the top-down drop.

The secondary 6-foot drop from the rebound caused an approximately 10-degree sector of the drum rim to be dented radially approximately 3/8-inch. Minor scuffing occurred along the side of the drum. External examination revealed no other damage.

Comparison of DRs taken before and after the drop showed little variation in internal structure but external drum damage could be easily distinguished. Figure 2.28 presents the pre and post-drop DRs taken of SN-5 In the DRs the deformed drum wall just above the chime can clearly be seen. Also, imperfections in the foam, (e.g., voids and fissures) can be seen in the pre- and post-drop DRs. The imperfections were confirmed upon package disassembly. There appears to be no change in the foam imperfections following the drop.

(a) Damaged SN-05, 180º Photo, Point 3

Drum chime is flush with drum bottom following drop.

(b) Damaged SN-05, 0º Photo

(c) Damaged SN-05, 90º Photo, Point 2

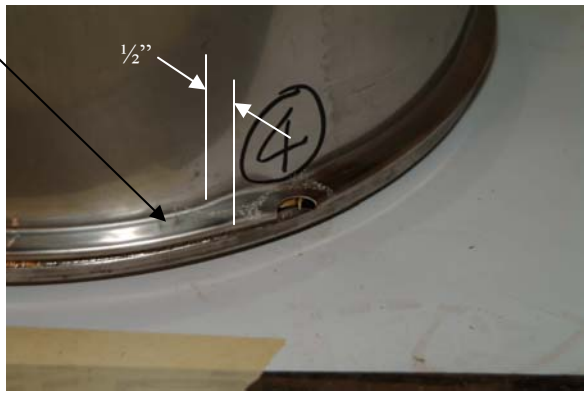

(d) Damaged SN-05, 270º Photo, Point 4

Figure 2.27 - Bottom Down 30-Ft Drop (Prototype SN-5)

Examination of the DRs in the vicinity of the liner connection to the overpack top deck was indeterminate. Resolution of the DRs in this region of the drum were insufficient to make out damage, if any occurred. (Note: had the liner failed (i.e., was breached) due to either the 30-ft drop or crush impact, foam decomposition gases would have passed through any fissures/cracks during the thermal test; no indications of liner failure was observed following the thermal event.) Based on the DR images, there appears to be little or no permanent displacement of the Fiberfrax directly beneath the liner. No visible displacement implies that the liner deformed elastically. This is in contrast to the top-down 30-ft drop where it can be clearly seen the lid plastically deformed and the lid Fiberfrax layer is permanently displaced. Foam compression appears to be negligible from the 30-ft drop. The effective change in height between the bottom

of the liner and drum bottom appears to be associated primarily with the collapse of the drum chime. Based on review of the bottom-drop DRs, the distance between the liner and drum bottom appears to be relatively unchanged from the fabrication.

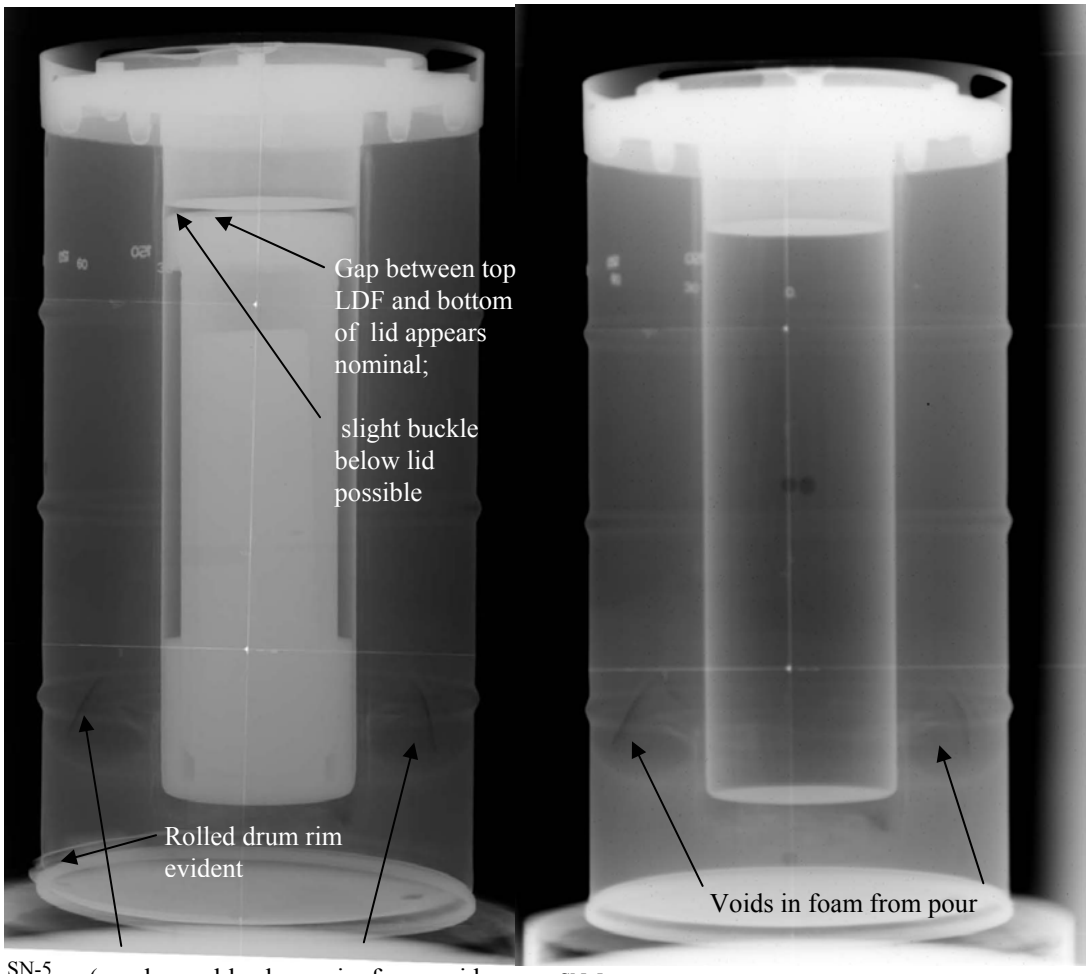

Figure 2.28 - Bottom Down 30-Ft Vertical Drop X-Ray (SN-05)

Based on examination of the packages post drop-test and of radiographic imagery, the 9977 30-ft drop does not appreciably challenge the drum or drum liner. Analysis results described in the following section shows that the stress in the overpack and CV are well within Code allowables.

2.7.1.1.4 Analysis – Bottom Down

Nonlinear dynamic analysis was used to evaluate the structural response of the 9977 6CV design and overpack to the impact from a 30-ft free drop, impacting bottom-down, Appendix 2.6. Drops were analyzed at temperatures of -20°F, 75°F (ambient), 140 °F and 300°F. Package analyses modeled the same weight and configuration as the test article. The structural properties of stainless steel and the insulation materials in the lid and Fiberfrax around the drum liner are essentially unaffected by temperature. However, the properties of the drum foam are temperature dependent and analysis was performed to evaluate the effect of the foam property change on performance of the package. Analysis demonstrates material property changes do not appreciably alter the damage from that observed to 9977s dropped under ambient conditions.

Figure 2.29 compares the FEA deformation results at 75°F, with damage observed from test package SN-5 that was dropped at ambient conditions. The analysis shows the top-deck depressed slightly where it connects to the liner. This deformation appears to be translated through slightly compressed Fiberfrax under the bottom of the liner. The radiographic images taken at this location are not detailed enough to verify the deformation illustrated by the analysis. The radiograph shown in Figure 2.29 appears to show some small necking of the liner next to the drum lid. The stiff drum chime of the test drum caused a portion of the outer drum wall to buckle on the bottom down drop. Based on the analysis, the redesigned rolled skirt is less stiff and does not buckle the drum wall. There are no significant internal or external deformation to compare between the test drum and the analysis. The bottom down drop for the most part is unremarkable.

Figure 2.30 compares the deformation results at -20°F, 75°F, 140°F and 300°F. As shown, the relative damage to the overpack is similar for all cases. The strains at the bottom of the drum liner and its connection to the top deck of the drum increase as foam strength is reduced. The strain results indicate the liner to top-deck connection deforms downward more as foam strength decreases with increasing temperature. In all cases, the relative change in strain is small. As can be seen in Figure 2.30, strain in the liner becomes more distributed as the foam becomes less stiff. The strain in the liner is 1.6% at the top deck connection at 300 °F. The strain in the drum top deck liner connection is 1.3% at -20 °F. Both strain results are well below the 35% allowable for the 304L material.

The CV stress varies by about 75% between the -20°F and 300°F analysis with the -20°F analysis estimating a maximum stress of 51 ksi. This is expected, since the foam is significantly more rigid at the lower temperature compared to the foam properties at higher temperatures. The -20°F analysis bounds the potential for worst damage to the package. The more rigid foam results in higher loads in the CV, whereas, the overpack is largely unaffected by the foam temperature variations. The containment vessel stress results are compared in Table 2.28 to allowable values from ASME Section III, Appendix F, Level D, Service loads. The computed values are less than the Code limits. The results of bottom-down impact analyses at various temperatures demonstrate the structural adequacy of the 9977 design.

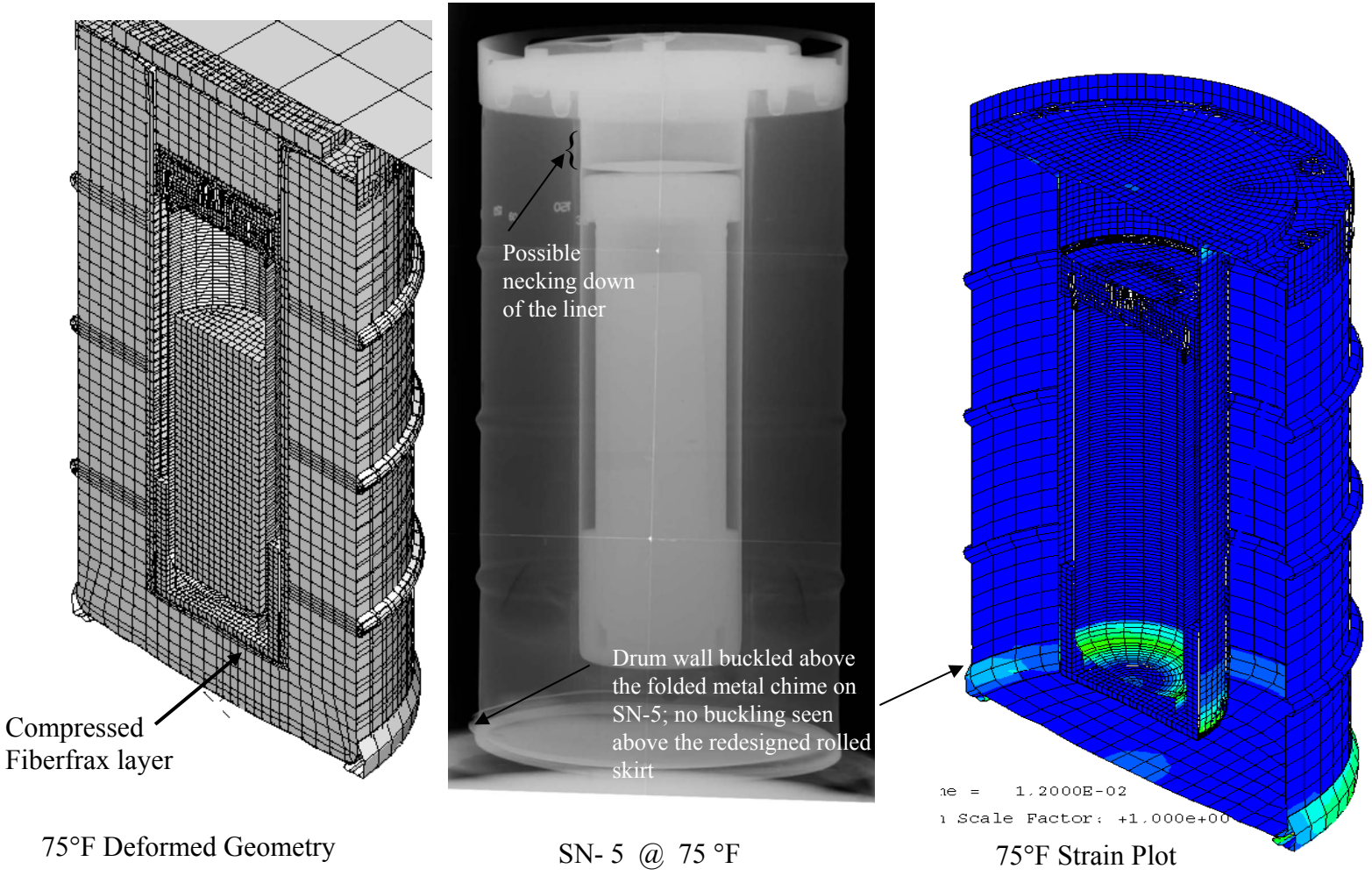

75°F Deformed Geometry

SN- 5 @ 75 °F

75°F Strain Plot

Figure 2.29 Bottom-Down 30-ft Drop Analysis Comparison to Test

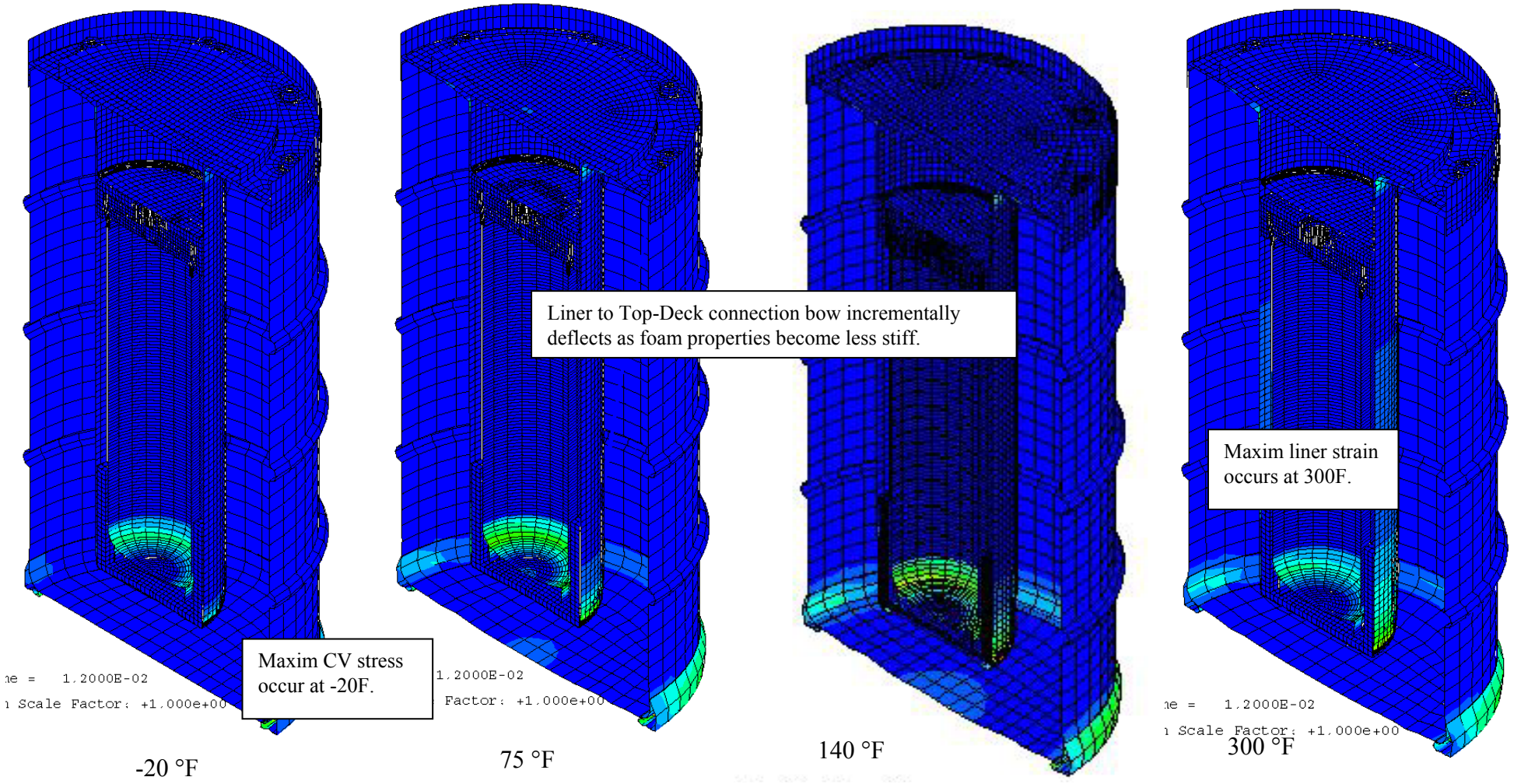

Figure 2.30 Bottom Down 30-ft Drop 9977 Strain Distribution Comparison -20 °F to 300 °F

2.7.1.2 Side Drop

2.7.1.2.1 Test - Side Drop (SN-3)

Test unit SN-3 was dropped horizontally with the package at -20ºF. The 6CV contents were simulated with a 5 ½ -inch diameter by 13 inch long steel slug weighing 100 lbs, bringing the total weight of SN-3 to 340.6 lbs. The slug was loaded in the CV without dunnage, thereby eliminating any energy absorption due to cushioning during impact. The primary objective of this test was to evaluate loading to the overpack foam, the liner connection to the overpack's top deck as a result of cantilever effect due to the addition of the pliable layer of Fiberfrax to the package from the DP design to the SN package designs (see Appendix 2.8). The liner is minimally supported at its closed end and the resulting cantilever effect in the 30-ft side drop affects the liner to drum top plate connection. A break at the liner/top plate juncture could alter the performance of the package in the thermal test by permitting foam decomposition products to enter into the liner cavity, thereby increasing CV temperatures. A liner tear would not be expected to significantly affect the package performance in the crush.

SN-3 hit at 2.3 degrees from horizontal with the top rim of the drum striking first. The drum rebounded about 3 ½ feet. The impact caused the drum to rotate a little more than 270-degrees. The rotational momentum of the drum was just enough to prevent the drum from remaining upright on its bottom and it toppled to its initial side of impact, completing a 360-degree rotation. SN-3's rebound was approximately half that of the SN-5's 6-feet, but still much greater than the 1-inch SN-4s top-down drop produced.

Figure 2.31 illustrates damage to test package SN-03 from the 30-ft side drop. As can be seen in the photographs, the external damage to the drum is unremarkable. The rim of the drum was slightly dented and forced into the lid flange. The rim was flattened over about a 15-degree arc. Damage did not extend below the drum's 3-inch high rim. The lid flange was bent slightly by the rim impact as shown. The bottom of the drum was flattened over a 30-degree sector of the drum as seen in the far right photo. The deformation extended about 5-inches along the longitudinal axis of the drum.

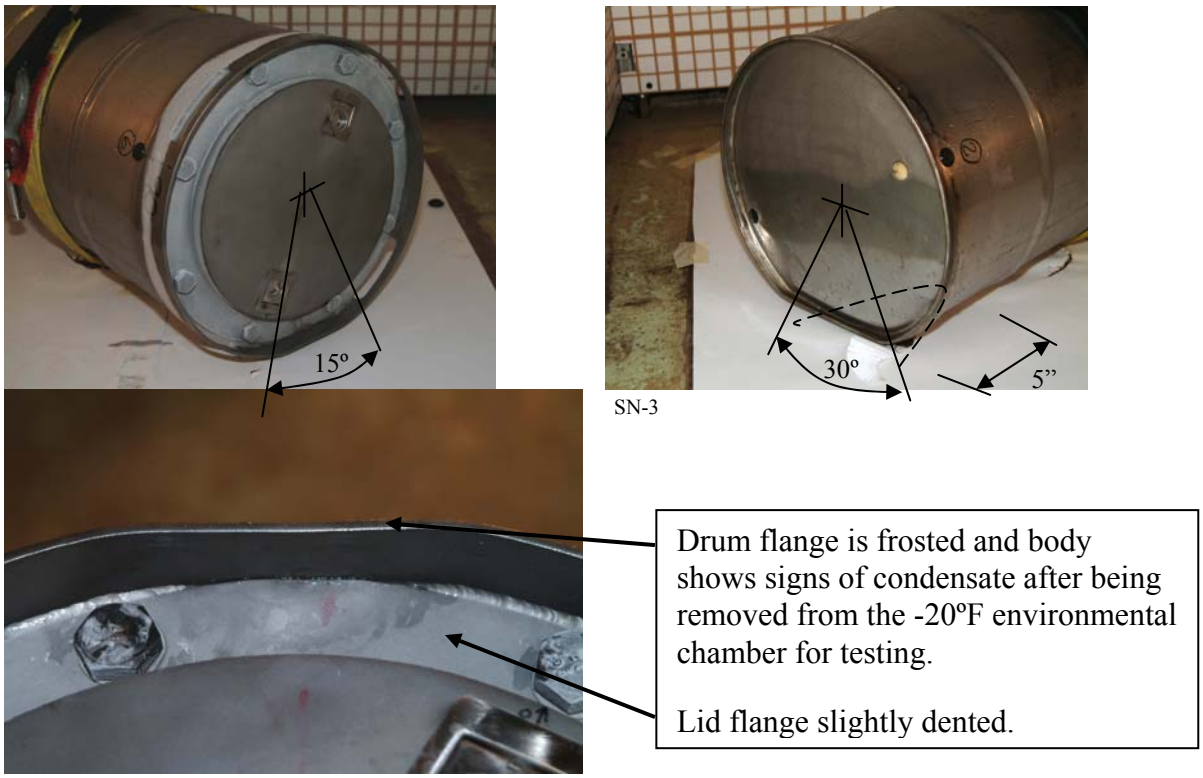

Figure 2.31 - Horizontal Drop 30-Ft (Prototype SN-3)

The secondary 3½-ft impact from the rebound produced only minor scuff marks on the drum. External examination revealed no other damage.

Digital radiographs taken of the drum after the side drop showed only the minor damage to the outer overpack as seen in the above photographs. However, DRs show pronounced damage on the inside of the package, Figure 2.32. The two DRs shown in Figure 2.32 are images of SN-3 perpendicular to and 90-degrees to the side of impact, respectively. Most noticeable in the left DR is the symmetric buckling of the liner just above the CVs lower load distribution fixture. The right DR photo is taken at 90 degrees from line of impact and the liner is stamped with the impression of the upper and lower load distribution fixtures. The far right photo shows the buckled liner following completion of HAC testing following package disassembly. The liner orientation is roughly 90-degrees from the direction of drum impact. The buckling in the liner is symmetric. The post crush DRs show no further liner deformations. Therefore, the liner condition in the photo is representative of the damage from the 30-ft drop as pictured in the DRs. The DRs were taken with the drum oriented vertically so the weight is seen at the bottom of the 6CV in the image but was approximately centered during the drop.

The liner buckles during the 30-foot drop because it acts like a cantilevered beam that can translate through the surrounding pliable layer of Fiberfrax. Similar deformation occurred in DP-3, but the damage to the liner was not as pronounced since the earlier prototype did not include a Fiberfrax layer around the liner. No apparent failure, i.e., breach, of the liner was observed from the DRs through the thermal test or the subsequent drum disassembly.

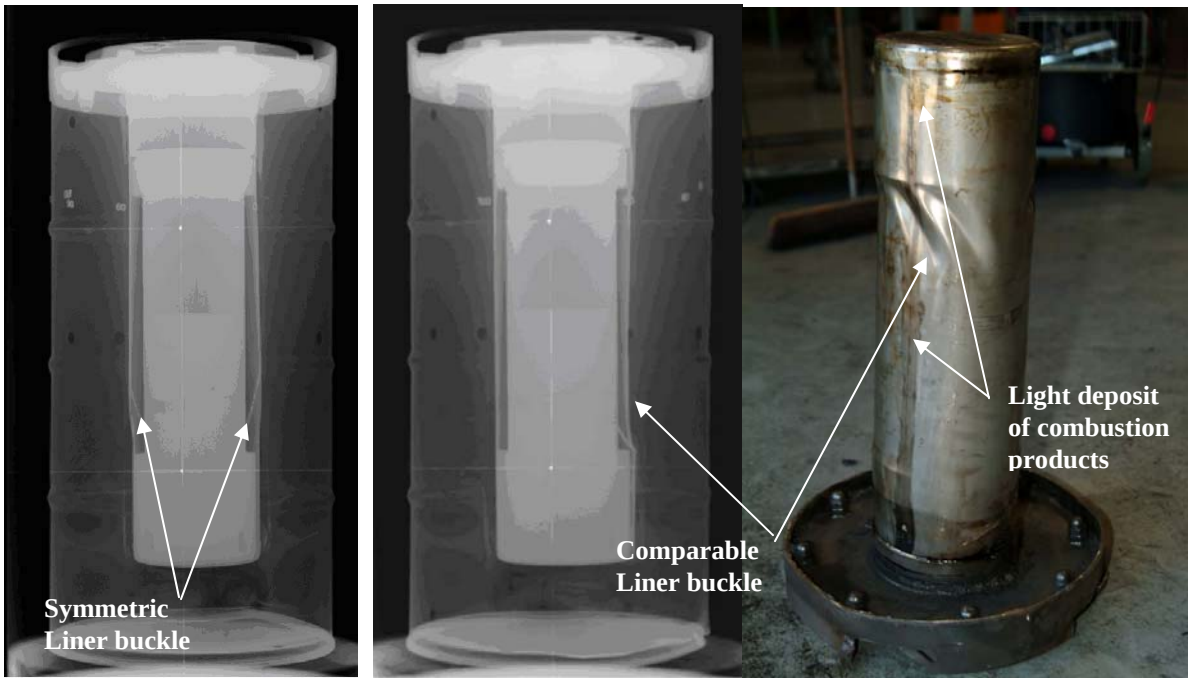

SN-3

Figure 2.32 - Side Drop 30-Ft Digital Radiographs (Prototype SN-3)

Inspection of DRs of the liner connection to the overpacks top deck was unrevealing. Resolution of the DRs at this location was insufficient to determine if any damage occurred. Examination of the overpack liner to top-deck connection following package disassembly revealed a solid connection with no damage.

Pre-drop DRs identified some small inclusions in the foam, typical of what has been seen in other foam images. Images made of the foam after the 30-ft drop tests showed no significant changes to the foam or these inclusions. The expectation was the foam may crack along the mid-section of the drum perpendicular to impact as happened in DP-3 testing. No longitudinal cracking is discernable in the DR of the foam for SN-3.

Based on visual examination of the outer drum and radiographic images of internal components, the 9977 30-ft free drop with a maximum loaded 6CV does not fail the drum or drum liner. Furthermore, no CV damage is observed. Analysis results described throughout Section 2.7 show that the stress in the overpack and CV are well within Code allowables.

2.7.1.2.2 Analysis - Side Drop

Nonlinear dynamic analyses were used to evaluate the structural response of the 9977 CV design and overpack to the impact from a 30-ft side drop. (Appendix 2.6) Drop analyses were performed of the package at temperatures of -20°F to 300°F. Package analyses assumed the same content weight as the test article. Analyses also evaluated the effect of the content weight being shifted from one end of the CV to the other. Testing was performed with the weight centered in the CV with the package cooled to -20ºF. The structural properties of stainless steel

and the insulation materials in the lid are essentially unaffected by temperature. However, the foam properties do change significantly with respect to temperature and analyses were performed to evaluate the effect of the foam property change on performance of the package.

Figure 2.33 compares the -20ºF analysis results with the damage observed from test package SN-3 that was dropped at -20°F. The deformation seen in the analysis seems to correspond very well to that observed in the test. Table 2.28 lists the maximum stress for the components of interest. The component stress results are compared to allowable values from ASME Section III, Appendix F, Level D, Service loads. The computed values are less than the Code limits.

Figure 2.34 compares the FEA horizontal drop results at -20°F, 140°F, and 300°F. As shown, the relative damage to the external overpack is similar for all cases. However, the deformation in the drum appears to be increasing at the drum top-deck and drum bottom with increasing temperature. Liner damage changes depending on the location of the weight within the CV and is worst when the weight is at the bottom. Also, the damage to the bottom of the liner is increasing with increasing temperature. However, the top of the liner (side opposite the drop) shows negligible deformation or strain in any of the analyses. The maximum strain result is 14.1% from the -20°F analysis. This is well below the 35% allowable; therefore, drum failure is not a concern.

Analysis demonstrates material property changes do not appreciably alter the damage to 9977s dropped 30-ft over the temperature range of interest, -20°F to 300°F. The CV stress remains about the same between the evaluated temperatures and content weight locations. The results of side impact analyses at various temperatures and CV weight distribution shows that the 9977 design is acceptable.

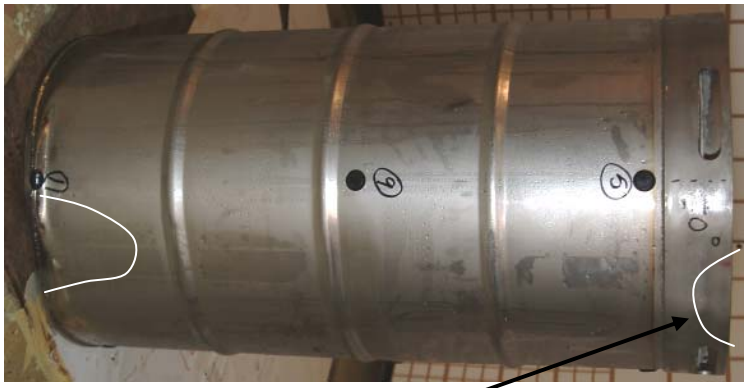

SN-3

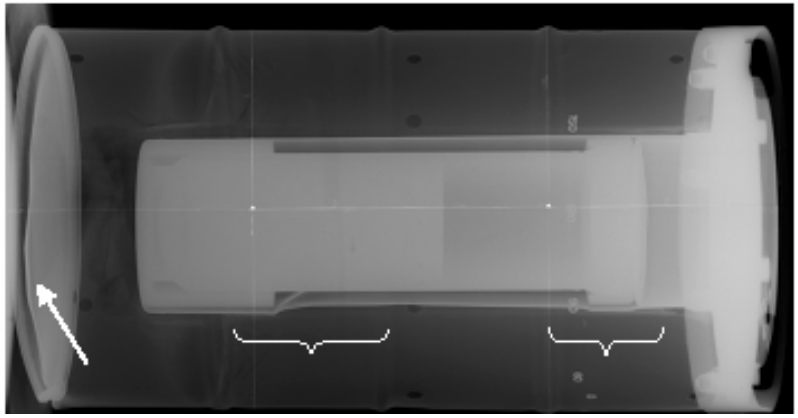

SN-3

Local deformation at drum flange observed on test package and shown in analysis (see Figure 2.34)

Greatest deformation is in liner, where buckling is visible in both the radiograph and analysis.

Analysis shows the drum rolling hoops are just slightly dented; similar deformation is also seen in test article above.

Side Drop, -20ºF,
Weight in Middle of CV not shown

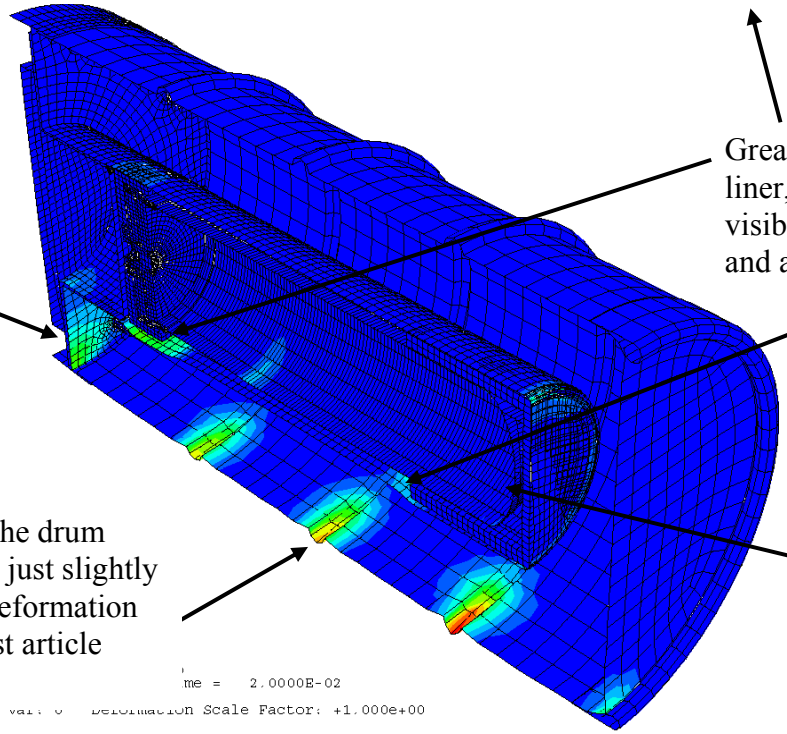

Figure 2.33 Side Drop 30-Ft Analysis Compared to Test

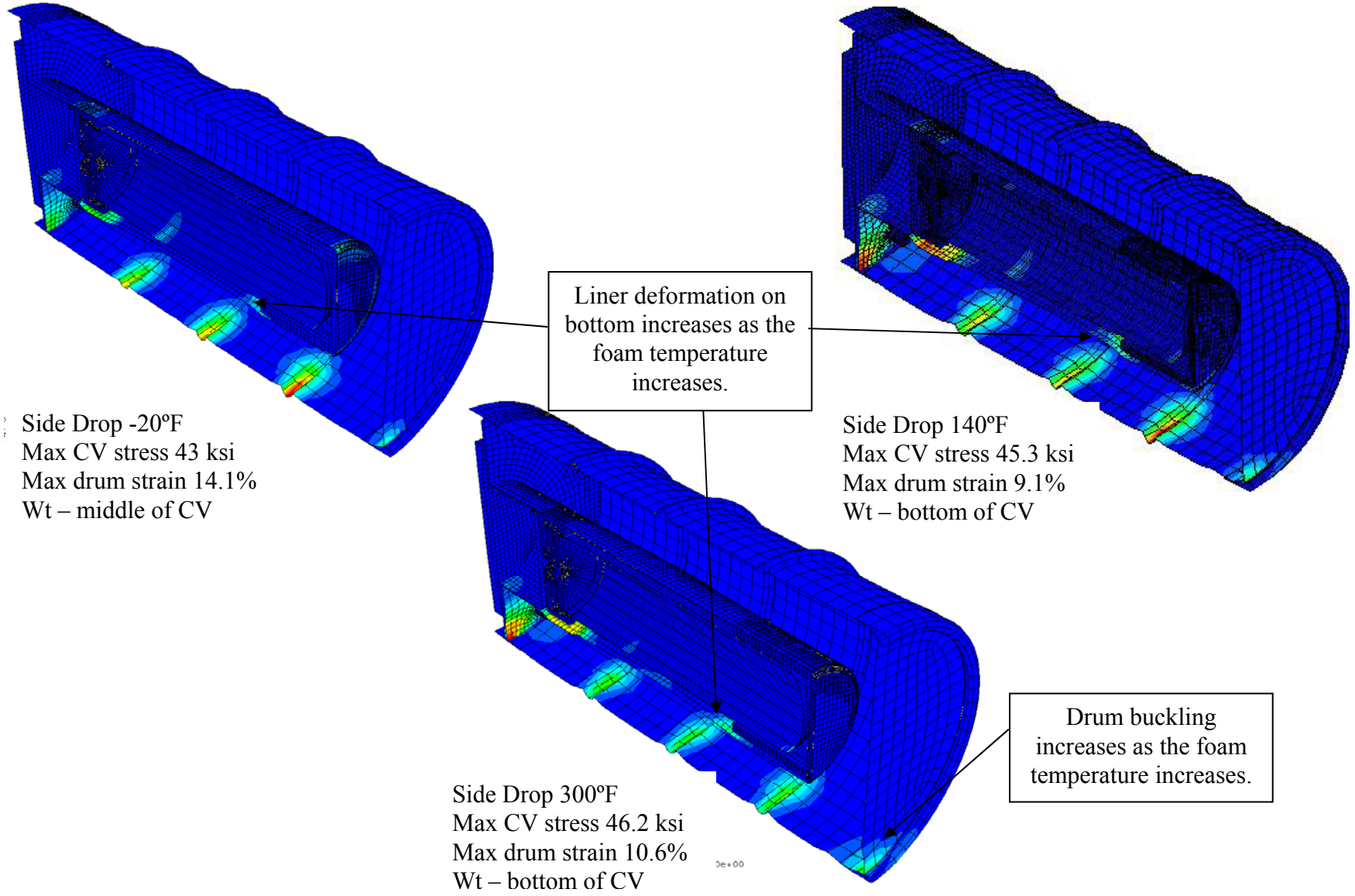

Figure 2.34 30-Ft Side Drop Analysis (Weight at CV Middle & Bottom)

2.7.1.3 Corner Drop

The effects of a center of gravity over a top corner impact of the 9977 were evaluated on two test packages, SN-2 and DP-1. SN-2 and DP-1 were dropped 30-ft onto their drum rims top-down at an angle of 67 degrees and 63 degrees from horizontal, respectively. Prior to the HAC drop, SN-2 was subjected to the full complement of NCT tests, whereas, DP-1 was preconditioned with only the NCT 4-ft drop.

2.7.1.3.1 Test - Center of Gravity over Top Corner (SN-2)

Prototype SN-2 was dropped top-down with its longitudinal axis at an angle of 67-degrees from horizontal. The package was dropped at a weight of 341.4 lbs that included the 6CV and a payload weight of 100 lb. The payload was simulated with a 5 ½ -inch diameter by 13 inch long steel slug. The slug was loaded in the CV without dunnage, thereby eliminating any energy absorption due to cushioning during impact. This test investigated the crushing of the lid plug and stress to the lid bolts from an off centerline top-down drop. The center of gravity top-down impact also results in high loading to the CV threaded closure. Also of interest was whether the lid would deform between bolts as was seen in the DP Series prototype testing. Excessive crushing of the plug, deformation of the lid between bolts, failure of one or more lid bolts or overstressing the CV closure could affect the performance of the package in the crush and thermal tests. The liner to top-plate weld was also evaluated. Failure of this juncture could affect the performance of the package in the thermal test by permitting foam decomposition products to enter into the liner cavity, thereby increasing CV temperatures.

SN-2 hit at approximately its release angle. It rebounded about 6-inches rotated 90-degrees and struck the opposite side of the overpack rim at the approximate angle of original impact before rotating in the opposite direction and coming to rest on the side of the drum that was facing up for the test. Figure 2.35 shows SN-2 before and after the test. Figure (a) shows the drum suspended on angle (67 degrees) prior to being hoisted to 30-ft for the drop. On impact, the overpack rim collapsed over a 90-degree arc and produced a series of rolled buckles in the drum shell just below the rim as shown in Figures (c&d). The lid closure flange and two of the lid closure bolts were covered by the collapsed rim Figure (b).

The CV and LDF impacted the inner lid plug in a piston fashion, locally buckling the bottom of the plug and expanding it into the liner as shown in Figure 2.36. SN-2 rebounded about half as much as DP-1, discussed in Section 2.7.1.3.2. Similar to the top-down impact of test package SN-4, the CV assembly was still decelerating toward the target plate when the drum overpack rebounded. This resulted in a reduced package rebound and a lid crown as shown in Figure (d). The top weldment to the closure lid crowned approximately 1-inch above the drum rim as shown in Figure 2.36.

Figure 2.35 – CGOT Corner 30-ft Drop at 67° (SN-2)

The localized buckling of the lid plug is again the result of the layer of Fiberfrax placed in the bottom of the plug. The Fiberfrax has no resistance to compressive loads until lock-up is reached. As seen in the DR image, the gap between the 6CV top load distribution fixture and the bottom of the lid plug is 1.1 inches. This is an increase of 0.9 inches from the nominal 0.20-inch design spacing.

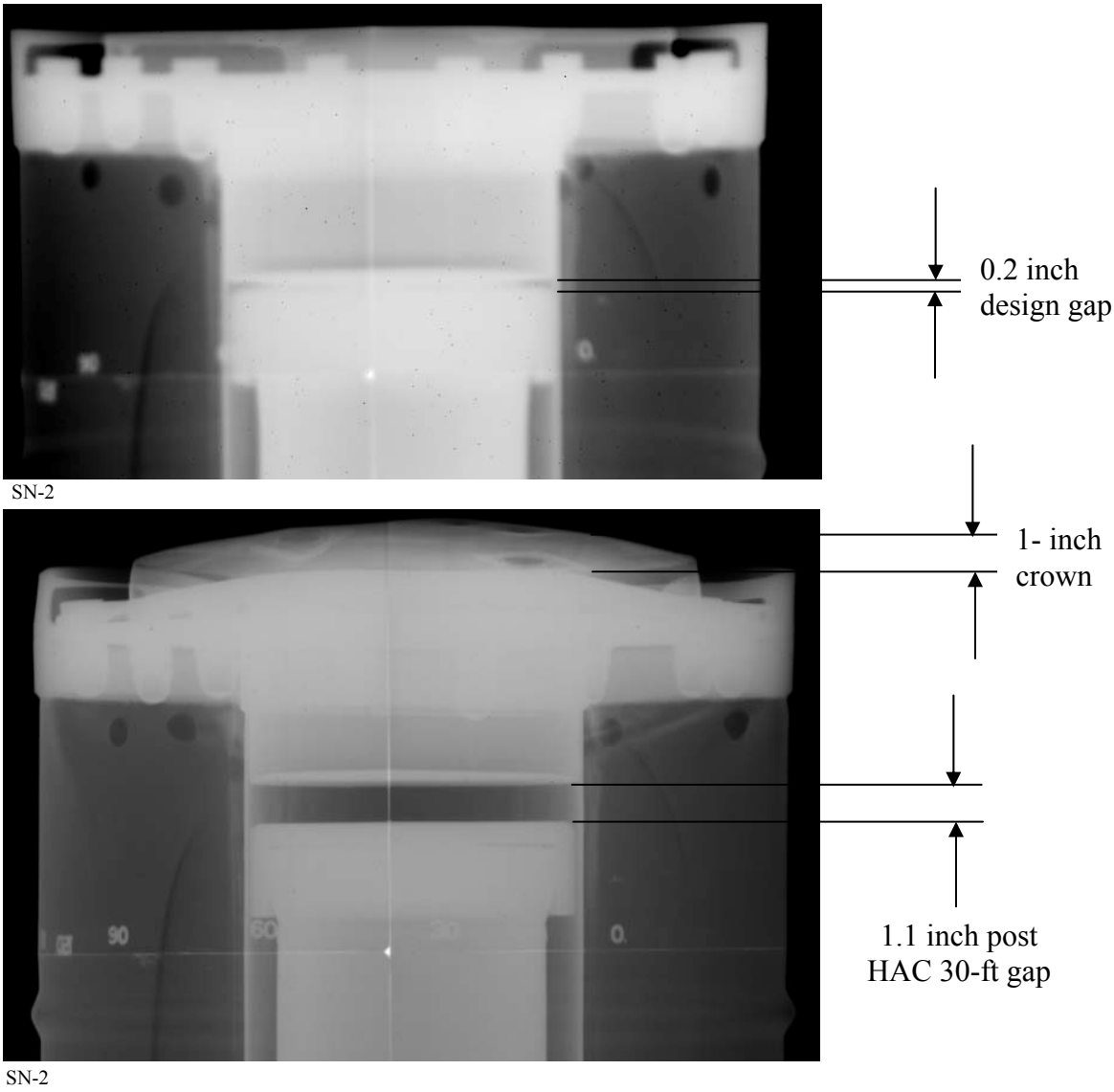

**Figure 2.36 - Test Package SN-2 Digital Radiographs
Before and After 30-ft CGOT Corner Drop**

The lid did not deform between the bolted connections as severely as was seen in earlier prototype testing. (Reference 52, pg 35) However, it was more pronounced than the direct top-down drop for test package SN-4, approximately 5/8-inch versus 1/8-inch. Based on examination of the outer drum and the radiographic images of internal components, the 9977 with a maximum loaded 6CV does not appreciably challenge the drum or its closure. No CV damage is observed. Analysis results described throughout Section 2.7 show that the stress in the overpack and CV are well within Code allowables.

2.7.1.3.2 Test - Center of Gravity over Top Corner (DP-1)

Reference 52 provides a detailed description of the DP-1 drop tests and the post drop examinations. Similar to package SN-2, the contents were simulated with a 6CV loaded with a 100lb payload. The test drop was performed at ambient conditions (approximately 70°F). The primary difference between DP-1 and SN-2 is DP-1 has a larger diameter overpack lid closure and its liner was not surrounded by the layer of Fiberfrax. Given these differences, the general test observations were very similar.

Based on examination of outer drum and radiographic images of internal components, the 30-ft free drop of the DP Series with a loaded 6CV does not overly challenge the drum or its closure. No CV damage was observed in the testing. Given the similarity in design (see Appendix 2.8) the favorable results support the production 9977.

2.7.1.3.3 Analysis - Center of Gravity over Top Corner

Nonlinear dynamic analyses evaluated the structural response of the 9977 to a 30-ft free drop impacting the drum closure with the Center of Gravity above the point of contact, Appendix 2.6. Drop analyses were performed of packages at temperatures of -20°F and 75°F (ambient). Package analysis assumed similar weighting as the test articles. The structural properties of stainless steel and the insulation materials in the lid are essentially unaffected by temperature, however, the foam properties do change with respect to temperature and analysis was performed to evaluate the effect of the foam property change on performance of the package.

Figure 2.37 compares the FEA results at -20°F and 75°F with damage observed from test package SN-2 that was dropped CGOT corner under ambient conditions. As shown, the relative damage to the outside of the overpack is similar for both cases. The drum flange is bent over in the vicinity of impact and the layer of Fiberfrax in the lid is compressed by the falling mass of the CV. Figure 2.38 compares the FEA strain deformed shapes with a CGOT DR. The damage to the liner for the two analyzed conditions is approximately the same. The most obvious damage is the collapse of the lid bottom through the Fiberfrax and the bent drum rim. The strain distribution in the side wall of the drum is relatively the same between analyses but the side wall is slightly more deformed in the 75°F analysis. Damage was seen on SN-2 after the 30-Ft drop as buckling beneath the rim. The greatest stress in the CV, 48 ksi, occurs at -20°F and is located where the CV necks down. The maximum stress at 75°F is 47 ksi.

The maximum CV stress between the two temperature analyses is less than 1%. The component stress results are compared in Table 2.28 to allowable values from ASME Section III, Appendix F, Level D, Service loads, showing that the computed values are significantly less than the limits. The results of CGOT impact analyses at various temperatures shows that the 9977 design is acceptable.

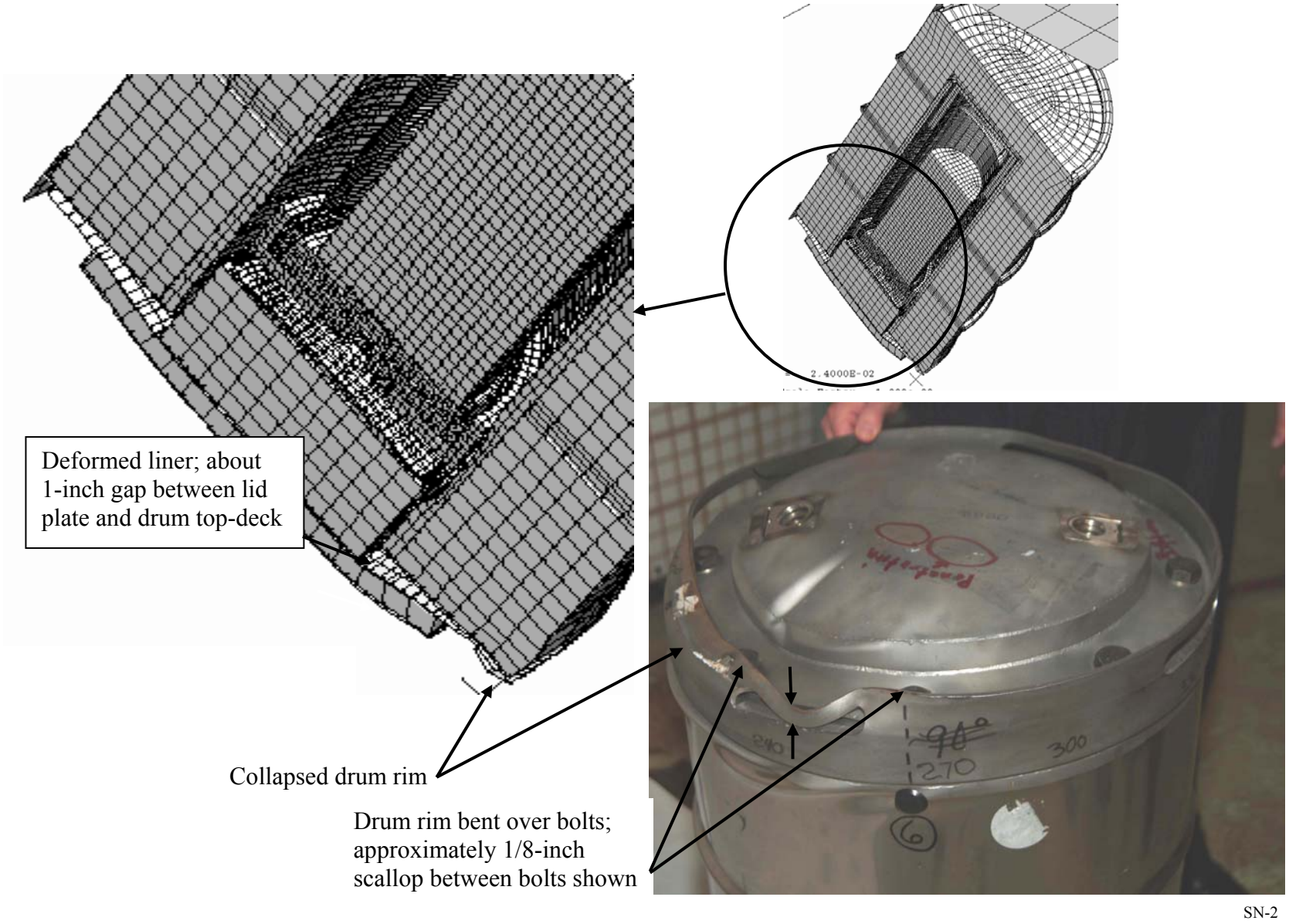

Figure 2.37 CGOT 30-Ft Drop Comparison with Analysis

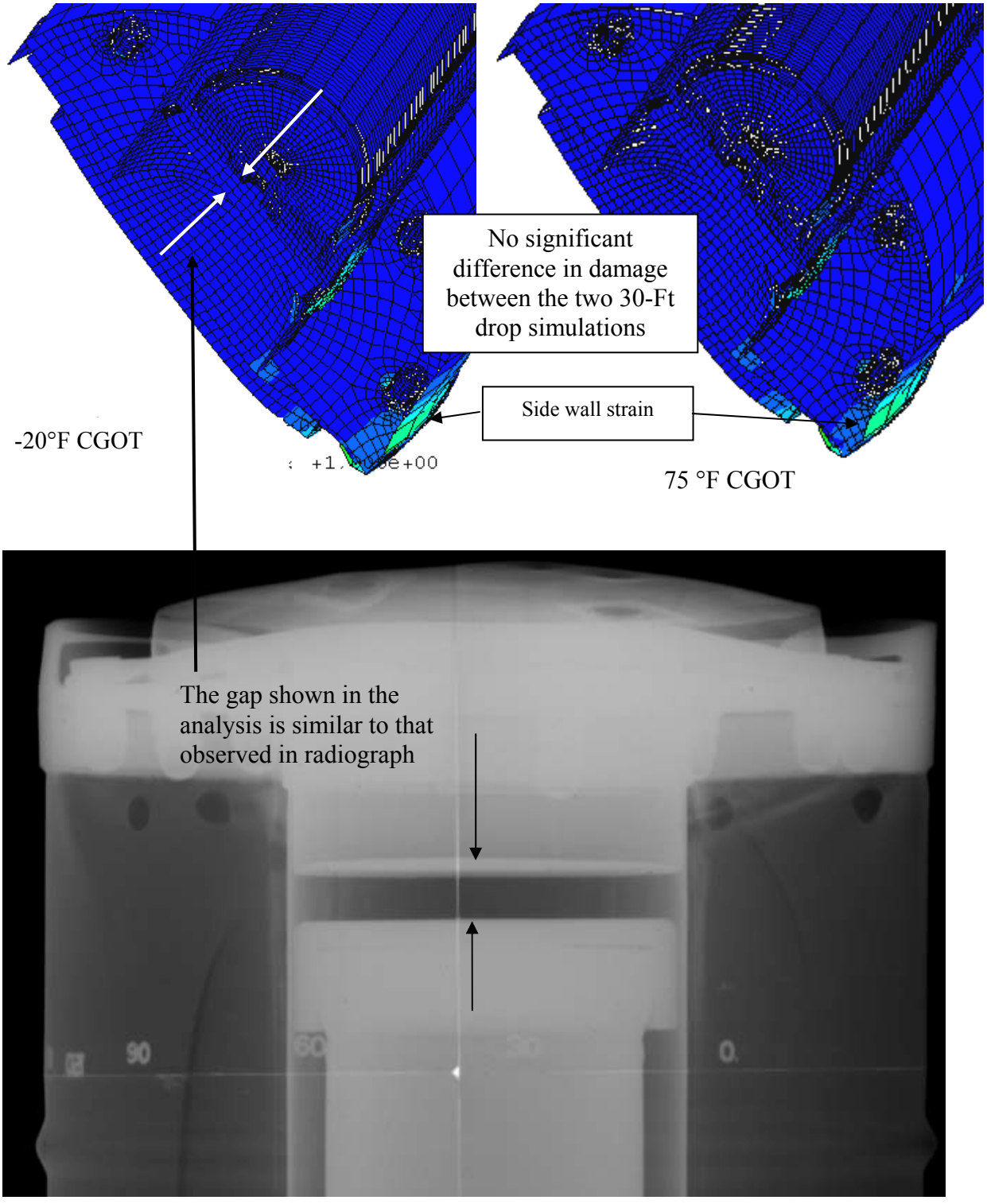

SN-2

Figure 2.38 CGOT 30-Ft Analysis Deformation Plot Comparison with Radiograph

2.7.1.4 Oblique Drops

No oblique drop tests were performed on the 9977. There are two types of oblique drops, the slap-down and shallow-angle. The tested HAC package orientations were considered to be more challenging than the oblique orientations. Confirmation of this conclusion was made by performing a series of non-linear dynamic FEA to assess package damage due to oblique drops and comparing the results to the tested packages and their analysis.

The slap-down drop, typically performed on a horizontal drum at an angle less than 15 degrees, is designed to challenge slender packages, since the secondary impact with added angular momentum can be significant. Based on the length to diameter ratio of 36 inches to 18-3/4 inches, or 1.9:1, the secondary slap-down acceleration was not considered to have a significant effect on the 9977 CV or for either end of the drum, because the bolted closure lid is captured by the drum rim and liner and the drum bottom has a sanitary closure with an attached wear ring. The slap-down will has no effect on the CV. Its uni-construction closure, i.e., the solid steel monolith it creates when closed, and its welded bottom will not be affected by oblique drops.

Shallow angle drop tests involving a horizontally oriented drum with an angle not greater than 30 degrees, were found to be important in challenging bolt/nut/ring closures.[52] The 9977 incorporates a bolted lid closure protected by a stiff outer ring welded to the drum and is not sensitive to shallow angle drops. As such, no analysis or testing was performed.

Figures 2.39 and 2.40 compare strain deformation plots of the 9977 when dropped at 15º bottom down and top down, respectively. Analyses for the bottom 15º slap down, Figure 2.39, evaluated the performance of the 9977 with foam properties at 140ºF and 300º. Figure 2.40 compares the package strain results for a top down slap at -20ºF, 140ºF and 300ºF. As shown in Table 2.28 the maximum CV stress is not as great for slap down orientations as some of the other orientations evaluated.

Hence, shallow-angle orientation is not considered to be more severe than the orientations that were tested. Finally, the stress margins calculated for the End (top-down), Side and Corner impacts are large and similar to analysis of the oblique drops and confirm that testing of additional impact orientations is not necessary.

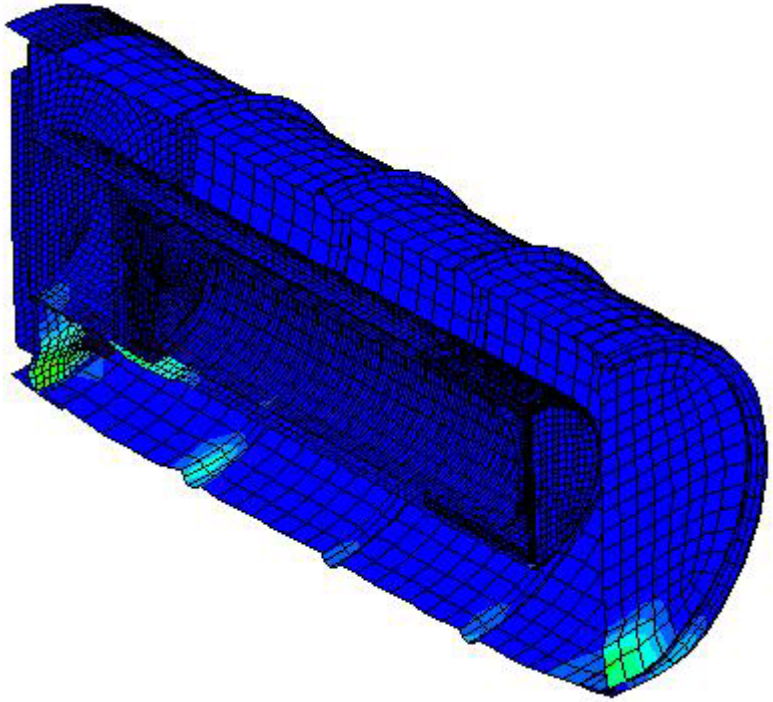

30-ft Drop onto Drum Bottom at 15° with Slap Down onto Drum Rim at 140°F

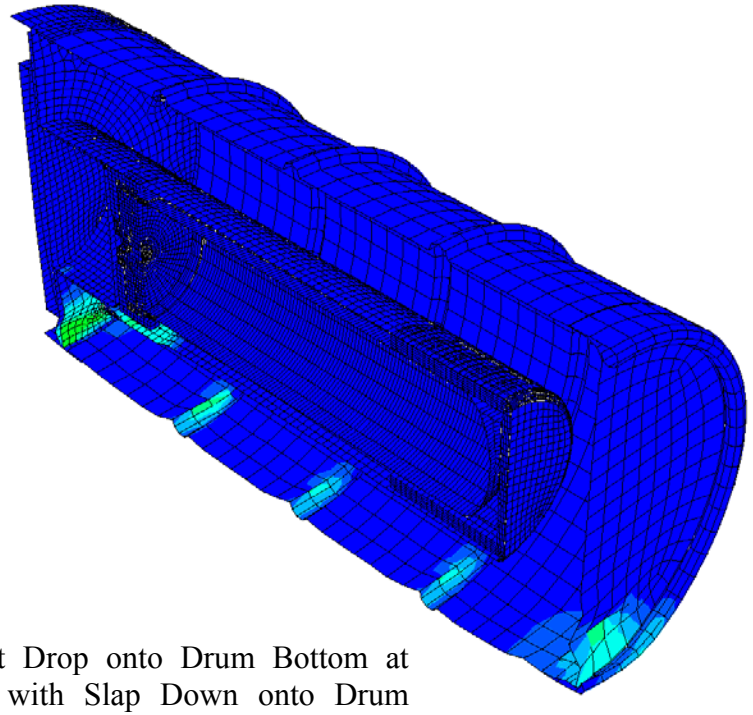

30-ft Drop onto Drum Bottom at 15° with Slap Down onto Drum Rim at 300°F

Figure 2.39 Slap Down -15° Drop onto Drum Bottom

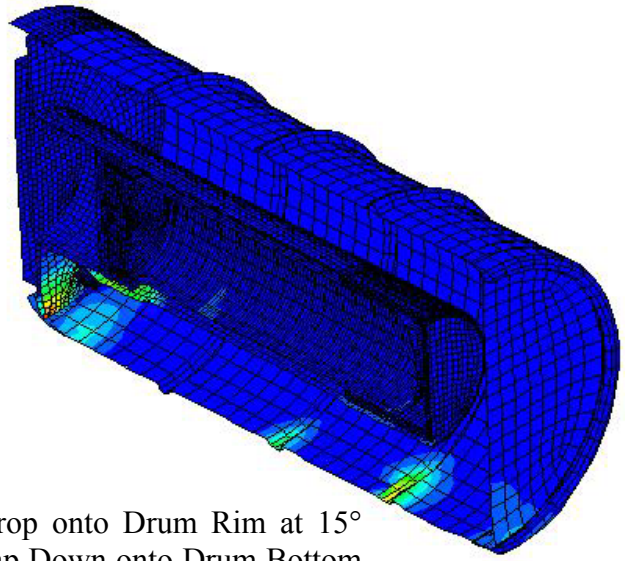

30-ft Drop onto Drum Rim at 15° with Slap Down onto Drum Bottom at -20°F

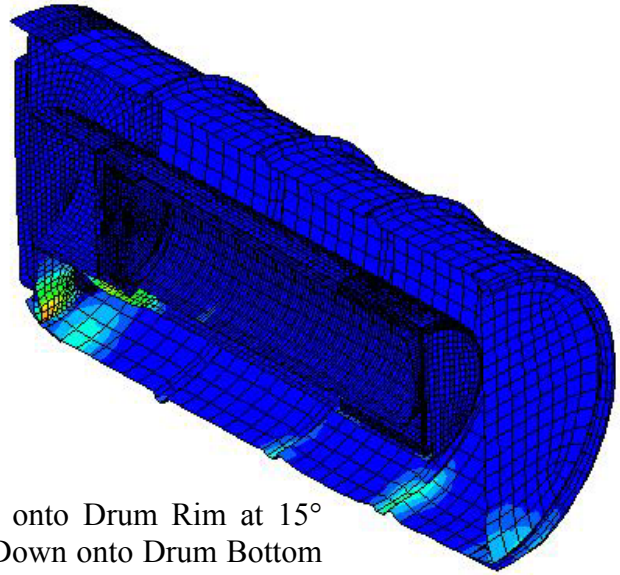

30-ft Drop onto Drum Rim at 15° with Slap Down onto Drum Bottom at 140°F

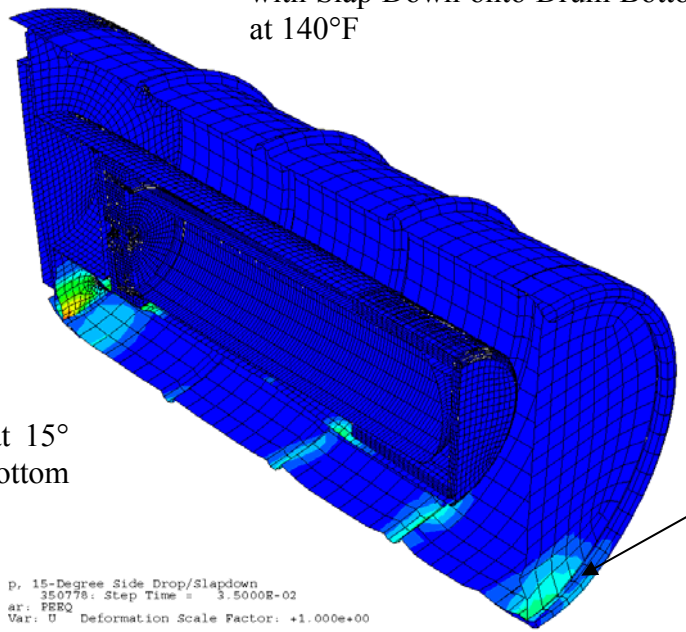

30-ft Drop onto Drum Rim at 15° with Slap Down onto Drum Bottom at 300°F

Drum bottom deformation increase as foam temperature rises.

Figure 2.40 Slap Down -15° Drop onto Drum Rim

2.7.1.5 Summary of Results

The 9977 design was evaluated both by finite element analyses and by test as summarized in the preceding sections. The evaluation has shown that damage to the 9977 from HAC free drop will not compromise the confinement performance of the drum nor the leaktight performance of its containment vessels. Therefore, the 9977 design can be expected to satisfy the performance requirements of 10 CFR 71.51(a)(2) under HAC given in 10 CFR 71.73.

Analyses of the 9977 design confirm that the overpack (drum and foam insulation) will protect the containment vessel satisfactorily during regulatory HAC events. The thermal evaluation of the 9977 is described in Section 3.5.4 and also confirms the package can withstand he regulatory thermal event.

2.7.2 Crush

Requirement: 71.73(c)(2) *Crush*. Subjection of the specimen to a dynamic crush test by positioning the specimen on a flat, essentially unyielding horizontal surface so as to suffer maximum damage by the drop of a 1,100-lb mass from 30 ft onto the specimen. The mass must consist of a solid mild steel plate 40 inches square and must fall in a horizontal attitude. The crush test is required only when the specimen has a mass not greater than 1,100 lb, an overall density not greater than 62.4 lb/ft^3 based on external dimension, and radioactive contents greater than 1000 A_2 not as special form radioactive material. For packages containing fissile material, the radioactive contents greater than 1000 A_2 criterion does not apply.

Evaluation: In accordance with 10 CFR 71.73(c)(2), the crush test is required for the 9977 as shown in Table 2.26. The 9977 design was tested and analyzed to evaluate the effects of the crush. Analysis and test demonstrate that the sequential HAC crush test will not adversely affect the performance of the package before being subjected to puncture and thermal testing

Table 2.27 - Comparison of 9977 to Crush Criteria

Regulatory Crush Criteria	9977	Test Required
Package mass < 1,100 lb	366.6 lb	yes
Package Density < 62.4 lb/ft^3	65 lb/ft^3 (6CV and maximum content mass) 53 lb/ft^3 (5CV and maximum content mass)	No (excluded) yes
Package Contents > 1000 A2, or fissile package	Fissile package, and A2 >>1,000	yes

Compliance with the regulatory crush test is demonstrated by testing and analyses. Four 9977 prototypes were struck under various orientations by a 1,170 lb steel plate dropped from 30-feet pictured in Figure 2.30.

Impact Surface and Crush Plate: The crush test is performed on an outside test pad located on an abandoned concrete foundation for Building 8343 in N-Area at the SRS. The test pad is qualified as an unyielding impact surface [] and is constructed from a steel plate grouted in place on top of the abandoned building footing. The steel plate is 4 ft square by 3 inches thick, and is floated on approximately ¾ inches of grout and anchored to the building footer by five (5) 5/8-inch diameter, 7-inch long, Hilti lag bolts one at its center and four at the plate corners. The combined weight of the base plate and concrete footer is approximately 6,000 lb.

The crush plate is fabricated from a 40-inch square by 2½-inch thick, carbon steel. The plate has a measured weight of 1,170 lb. The plate is threaded for four (4) lifting eyes located at the four plate corners. During testing the plate is magnetically released. The release mechanism is a RELEASE-A-MATIC, Model H44-3, limited to 4,500 lb safe working load. Figure 2.41 illustrates the crush test pad with the crush plate suspended above it.

Figure 2.41 - Crush Pad shown with 1,170 lb Impact Plate Suspended Above

Three package crush orientations were selected to cause the greatest package damage, center of gravity over the top (CGOT), horizontal and top-down impact. Appendix 2.6, Table 1 lists the HAC test summary for the 9977. Figure 2.24 lists the analysis configurations for the crush. Of the three crush orientations the CGOT causes the greatest external damage to the overpack and was performed on two packages. However, the initial 30-ft drop orientations preceding these two crushes varied.

2.7.2.1 Test – Crush CGOT

Test Package SN-2 that was dropped CGOT from 30-ft was crushed directly over the area of damage from the 30-ft drop, see Figure 2.42. Figure 2.43 compares the cumulative damage of the drop and crush to radiography. Figure 2.44 compares the cumulative damage resulting from analyses that were performed at 75ºF, 140ºF and at 300ºF to complement drop testing.. The crush analysis is different in that the drum was first dropped CGOB and then crushed CGOB while SN-2 dropped and crushed CGOT. Appendix 2.10 provides a detailed summary of the crush test with additional photography and radiographs. Results of the drop and crush analyses are provided in Appendix 2.6. The maximum stress calculated in the CV was 42 ksi, at 75 ºF, which is less than the Code allowable of 57.8 ksi. Drum strain was approximately 21% for all of the analyses and is less than the 35% allowable, therefore the drum will not rupture from the combined drop and crush.

SN-2 was crush tested under ambient conditions. The primary impact increased the region of circumferential damage from 18-inches, due to the drop, to 34-inches as shown in Figure 2.43. The bottom of the drum, opposite the impact, had about 28-inches of circumferential damage (180º) and was crushed in approximately 2¾ at the center of damage. The edge weld along the top of the lid pan developed a crack in the area of the crush. Scalloped areas between bolts initially opened by the 30-ft drop were closed.

SN-2

SN-2

Figure 2.42 Test - CGOT Drop/Crush Orientation

1

SN-2

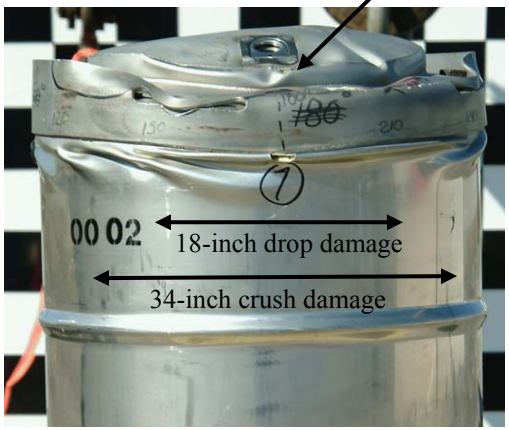

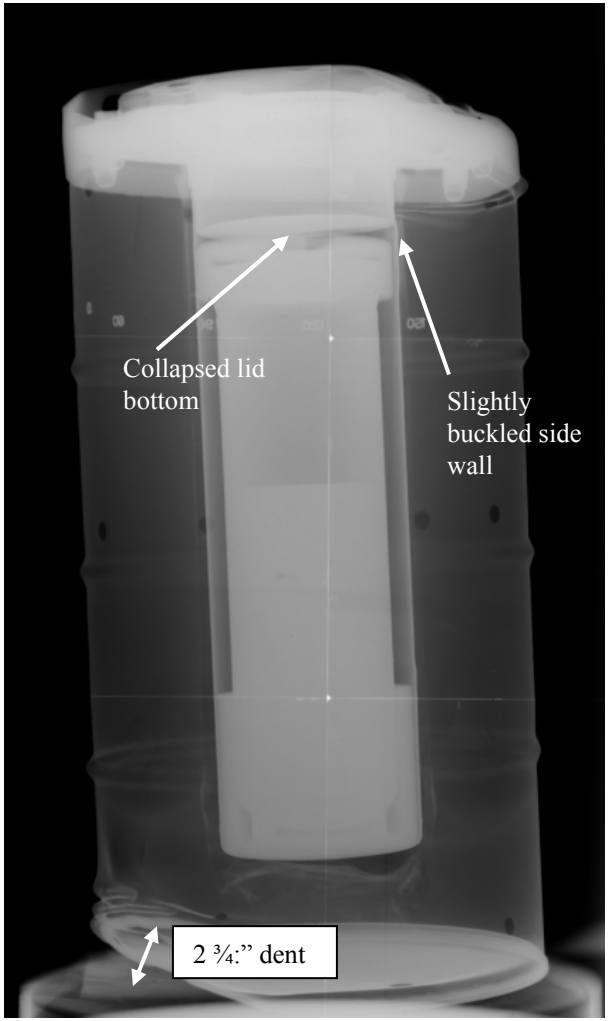

SN-2

Figure 2.43 CGOT Crush Test

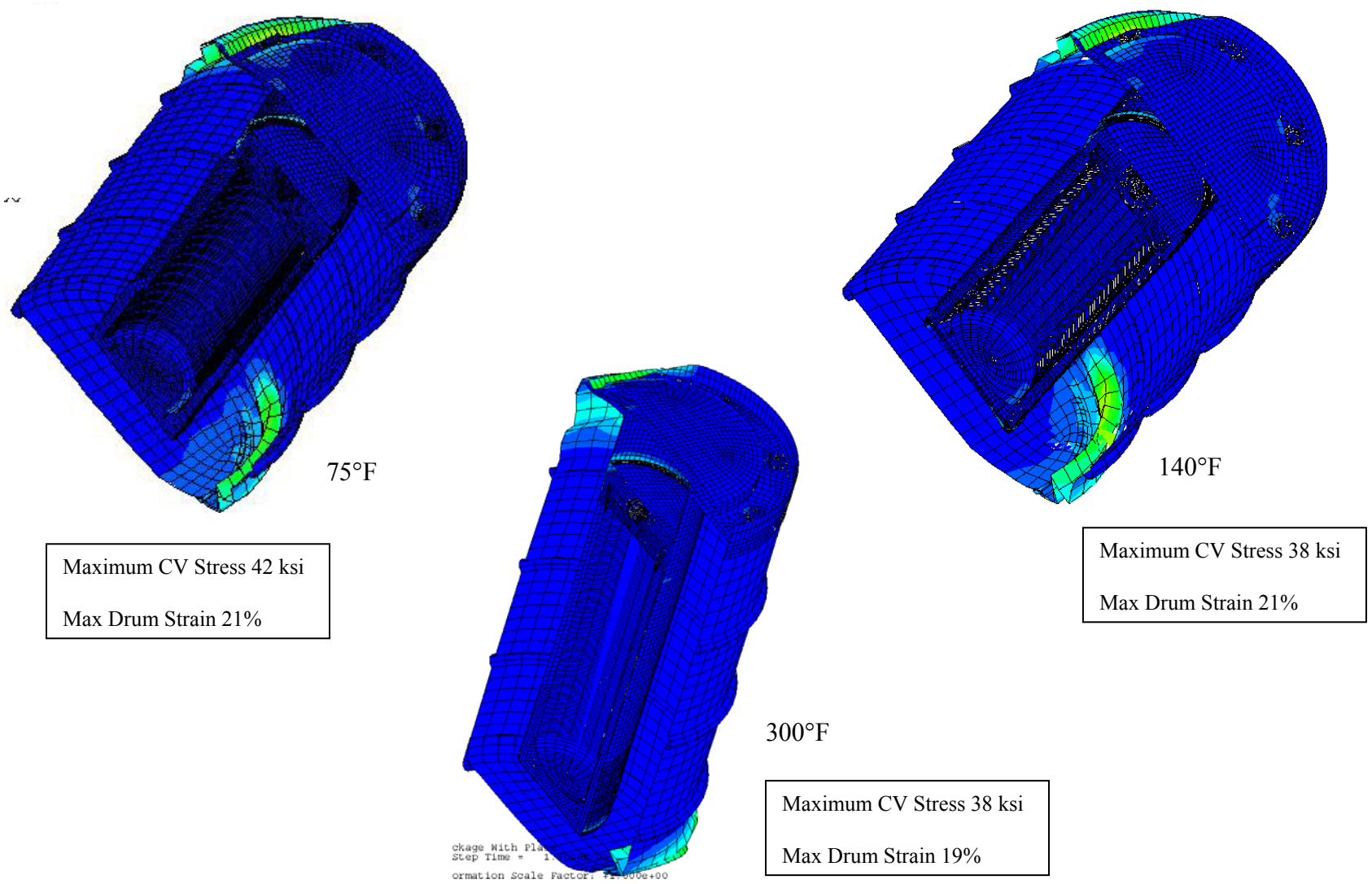

Figure 2.44 CGOB Crush Analysis Comparison at 75ºF, 140ºF and at 300ºF

2.7.2.2 Test – Side Crush

Test Package SN-3 that was dropped horizontally from 30-ft and then crushed directly over the area of damage from the 30-ft drop. Figure 2.45 shows the cumulative damage from the drop and crush. SN-3 was crush tested after chilling to less than -20ºF. The crush plate fell slightly off axis impacting the drum rim first followed by a slap down onto the bottom of the drum. The unintentional slap-down temporarily crushed the bottom of the drum to about one-third its original diameter. At the peak of drum ovalization the drum chime split open at about 90-degrees away from the point of crush plate impact. The split was 11 inches long or about 20% of the drum circumference. It is postulated the split occurred because the steel is cold worked when formed into the drum chime. Some of the foam adjacent to the split was still in the drum but was observed to be broken into a few small chunks. While there was significant damage observed at the bottom of the drum, the top of the drum experienced much less damage. Appendix 2.8 provides a detailed description of the damage. As a result of the chime split the drum bottom was redesigned with a welded sanitary closure. The crimped chime was replaced with a ¾-inch diameter rolled wear ring.

Figure 2.46 compares the cumulative drop and crush damage resulting from analyses that were performed at -20ºF, 140ºF and at 300ºF for the 6CV. Figure 2.47 shows damage for the comparable orientation for the 5CV. Because of the crush plate off angle impact, no direct comparison can be made between the -20ºF 6CV analysis and the -20ºF tested drum. The analyses are also slightly different than the prototype test as the crush plate is dropped opposite to the drop damage. By comparing the 30-Ft side drop strain plots, Figure 2.34, with the crush strain plots of Figure 2.46, it can be easily seen that as the foam becomes less rigid more of the crush load is transmitted through the foam and deforms the liner. The greatest deformation can be observed by comparing the 300°F analyses. Radiographic comparison of the pre- and post crush of SN-3, Appendix 2.10, Figure 58 appears to show some additional damage to the liner after the crush. However, on closer inspection of the DR it may be that the observed deformation was pre-existing and only appears to be an extension of the crush due to a slight rotation of the drum DR view angle. Drum strains are at least double for the crush over those calculated in the 30-ft drop. The greatest drum strain calculated is 38% for the 300 °F analysis. The maximum strain is located at a lid bolt hole and exceeds the 35% strain limit. However, the strain is local compressive strain and would not be considered to affect the package performance in the subsequent puncture and fire. The maximum strain in the liner is 10% at 300°F.

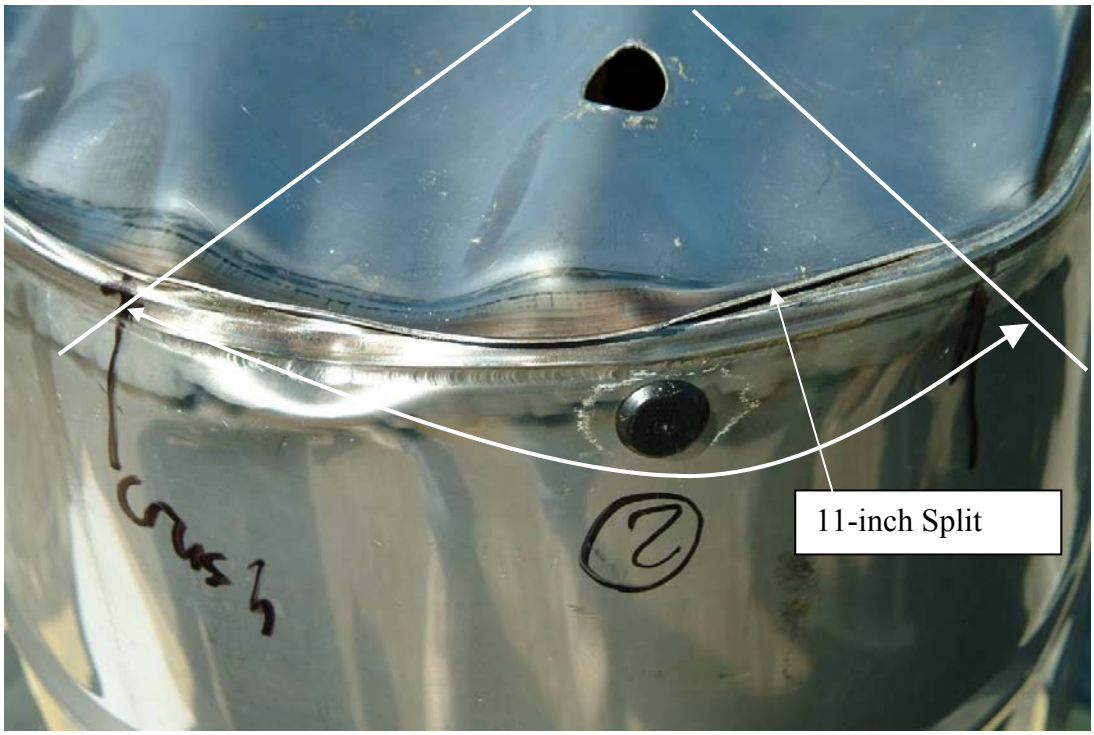

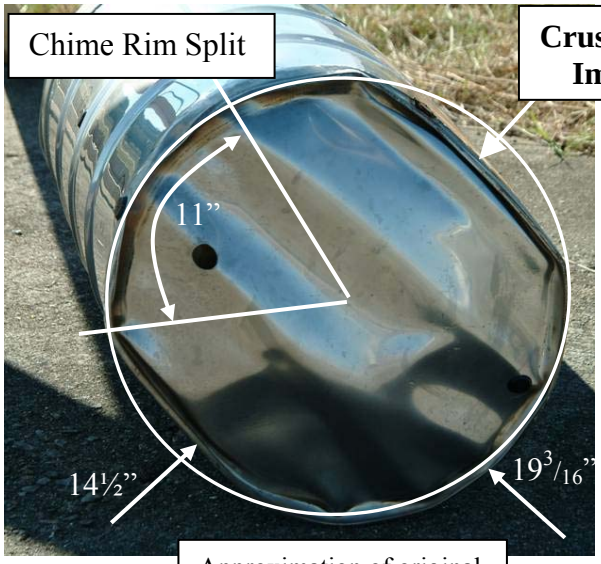

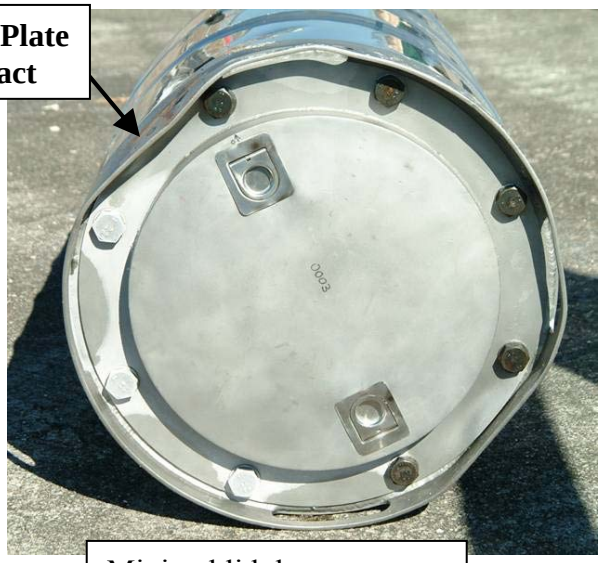

Figure 2.45 Side Drop Crush Test SN-3

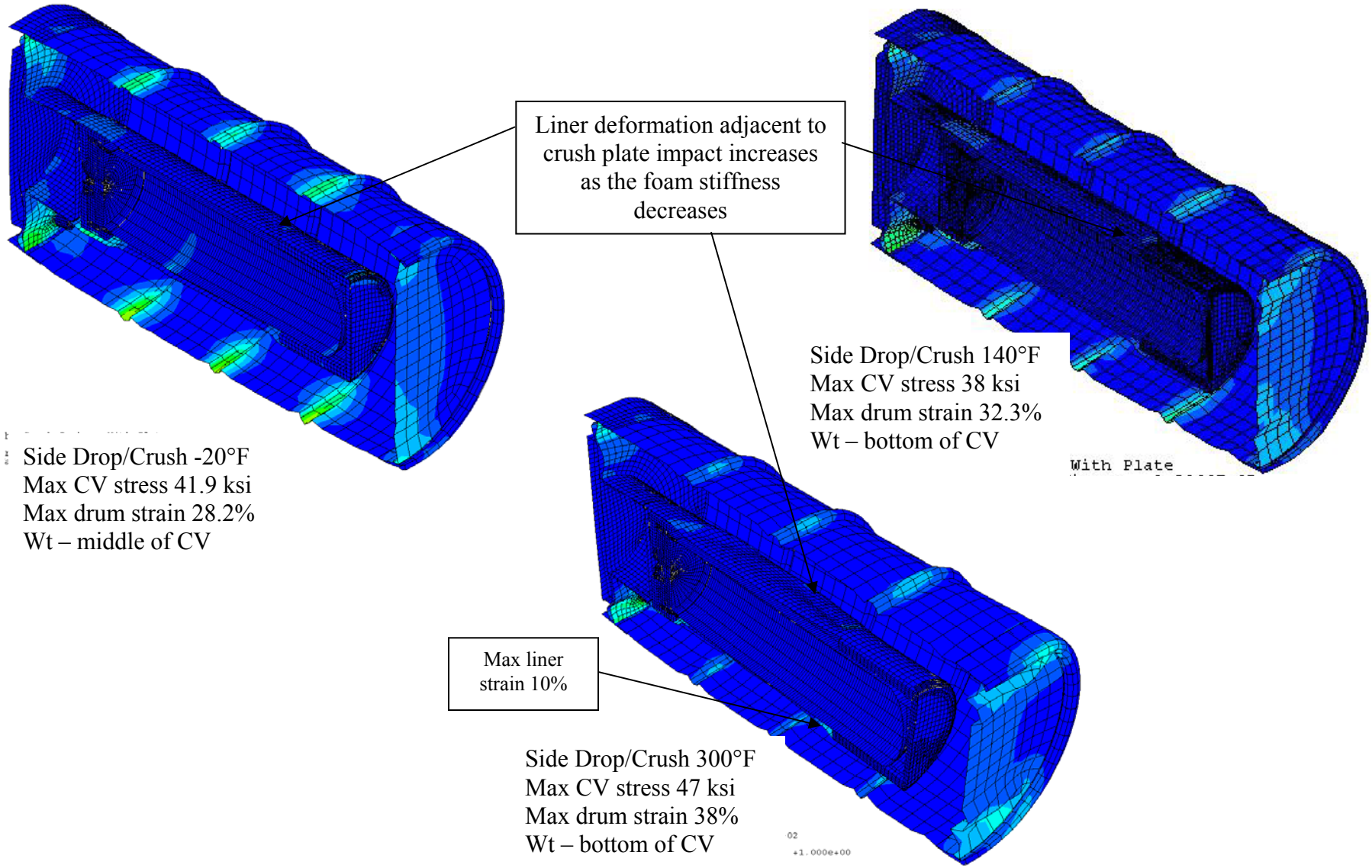

Figure 2.46 Side Drop and Crush Analysis with 6CV

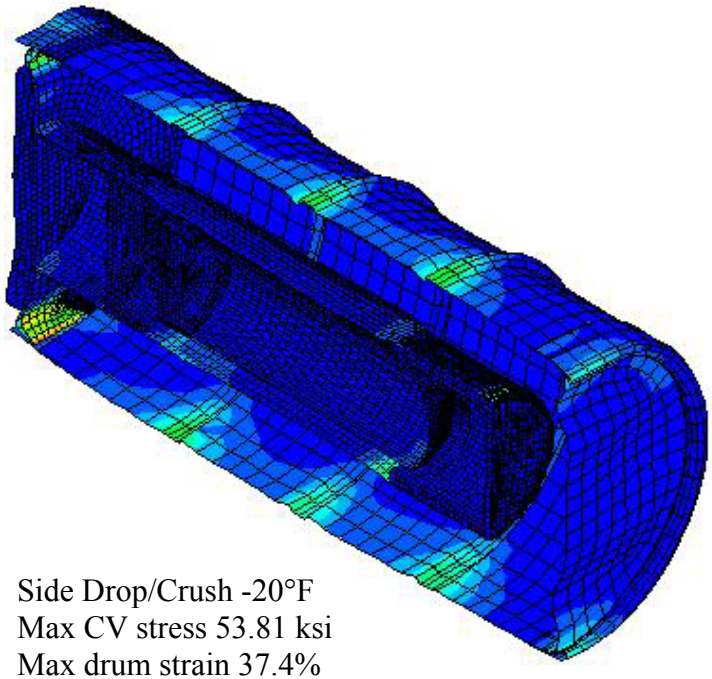

Side Drop/Crush -20°F
Max CV stress 53.81 ksi
Max drum strain 37.4%
Wt – middle of CV

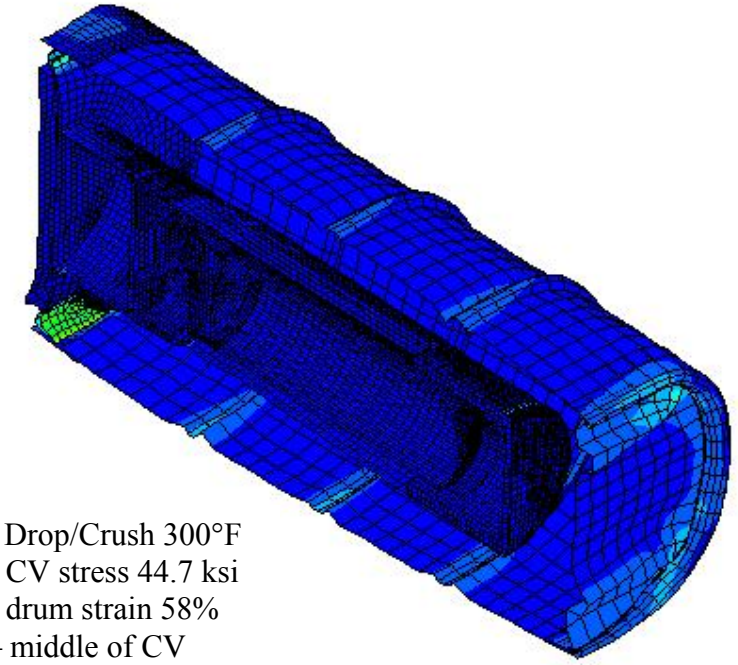

Side Drop/Crush 300°F
Max CV stress 44.7 ksi
Max drum strain 58%
Wt – middle of CV

Figure 2.47 Side Drop and Crush Analysis with 5CV

2.7.2.3 Test – Top Crush

Test Package SN-4 was dropped top-down from 30-ft and then crushed on its top over the area of damage from the 30-ft drop, see Figure 2.48. The drop and crush sequence was intended to assess damage to the top of the drum from a dual impact. Figure 2.49 shows the cumulative damage of the drop and crush. SN-4 was drop and crush tested at ambient conditions with the 6CV and 100 lb payload.

The crush plate fell slightly off axis impacting one side of the drum rim first, Figure 2.49. The off axis impact caused the drum to preferentially buckle along the side below the initial point of impact, as shown in Figure 2.49. The plate rebounded vertically and struck the drum a second time on its side as it lay horizontally. Appendix 2.8 provides a detailed summary of the test. External examination of the drum found the only damage to be the exacerbation of a buckle in the drum directly below the rim, which occurred in the 30-ft drop. Also the drum bottom rolling hoop was deformed. The top and middle rolling hoops were unaffected by the crush, see Figure 2.49. The DRs clearly show that the liner was dented radially as the crush plate pivoted the lid bottom into the liner.

30-Ft Drop Setup

SN-4

Crush Setup

SN-4

Figure 2.48 Test Drop/Crush SN-4 Package Orientation

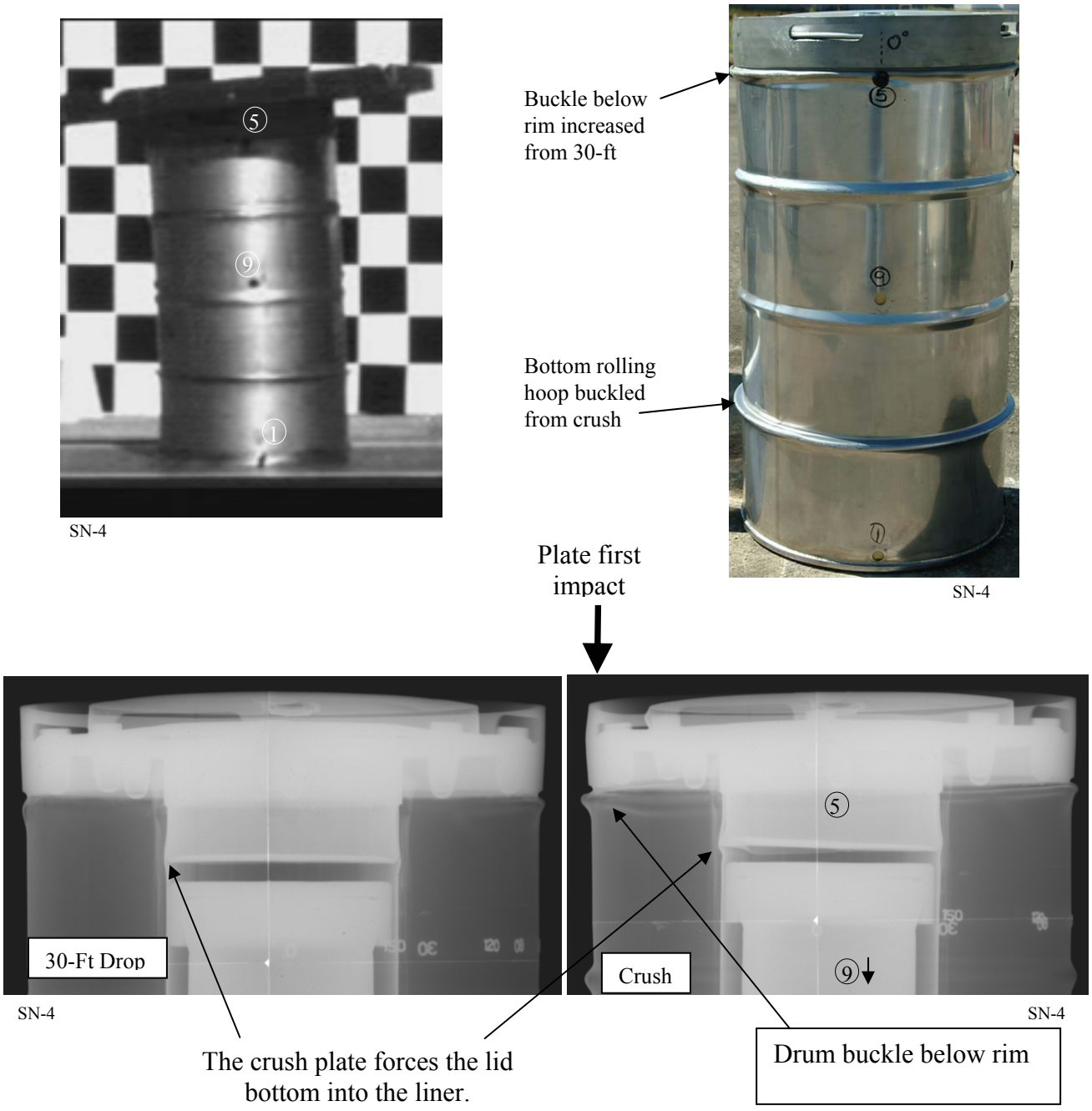

Figure 2.49 Test Top Crush Damage for SN-4

2.7.2.4 Test – CGOT Crush

Test Package SN-5 was dropped bottom-down from 30-ft and then crushed CGOT, see Figure 2.25. The drop and crush sequence was intended to challenge the liner connection to the top deck. Figure 2.50 shows the cumulative damage of the drop and crush. SN-5 was crush tested at ambient conditions with the 6CV and a 100 lb payload.

External damage to the drum as a result of the bottom down free drop was minimal, Figure 2.29. The crush causes the majority of drum damage. For this test the crush plate fell off axis as shown in Appendix 2.10 Figure 107. The crush produced roughly an equivalent level of deformation on the opposing corners of the drum, Figure 2.50. The three radiographs shown in Figure 2.51 easily identify the external damage to the drum. With the exception of some slight buckling in the liner around the Top LDF and the bottom of the Lid there is no other apparent damage inside the overpack.

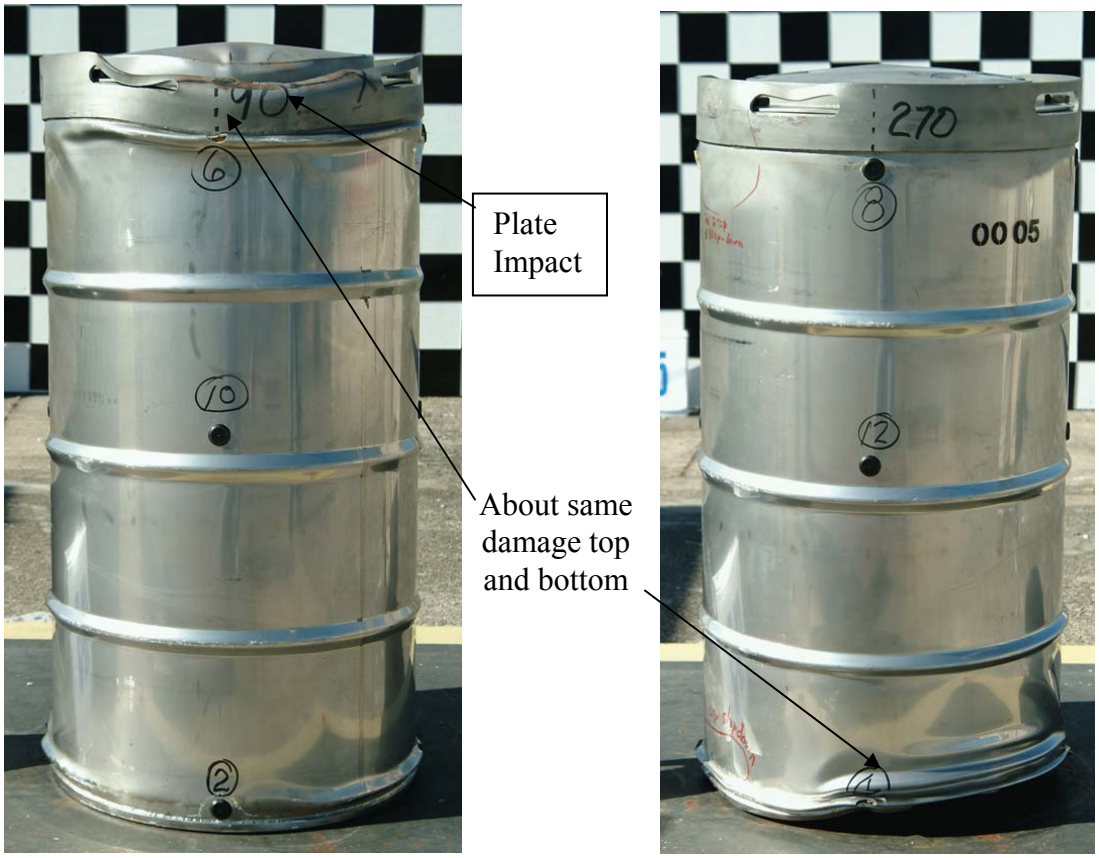

Figure 2.50 Test CGOT Crush (SN-5)

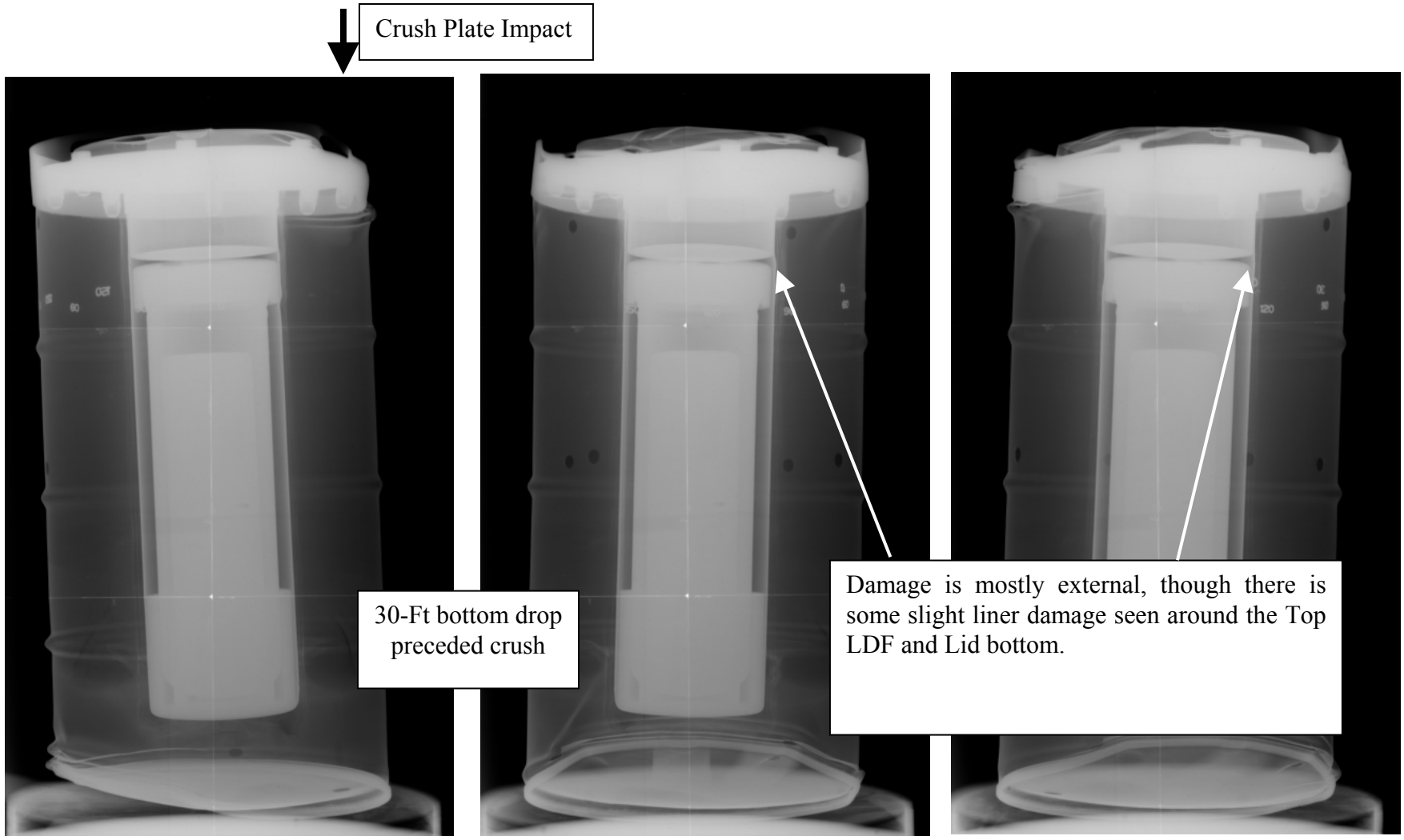

Figure 2.51 Test CGOT Post Crush Digital Radiographs (SN-5)

In addition to the Top and CGOT crush tests performed to physically evaluate damage to the 9977, complimentary FEA was performed to calculate package stress and strain.

Figure 2.52 illustrates the three axial crush analyses performed. The first illustration shows a bottom down drop followed by a top crush. This is similar to the planned test configuration for SN-4, (top down drop; top crush), as summarized in Section 2.7.2.3. 75ºF ambient foam properties were used. The strain plot shows the drum body deforming just below the rim. There is also some deformation around the bottom of the drum Lid. Deformations seen in the analysis closely resemble the damage seen in SN-4, Figure 2.49. The maximum calculated stress in the CV is 31.4 ksi. The maximum calculated strain in the drum is 9.2%. Both are within Code limits.

No testing was performed where the bottom of the drum was crushed. Analysis was used to evaluate this crush orientation. The second and third figure illustrates the drum subjected to a top down drop followed by a bottom crush. Two temperature cases were analyzed, 140ºF and 300ºF. As seen in Figure 2.52, the decrease in foam stiffness with the increased temperature results in collapse of the drum rolling hoops and lateral deformation of the liner where the piston effect of the CV/Top LDF impact has caused displacement of the lid liner bottom. For the 140ºF case, the maximum calculated strain in the drum is 12.7% and 9.5% in the liner. For this case the maximum calculated stress in the CV is 17.8 ksi. For the 30ºF case, the maximum calculated strain in the drum is 22% and 16.5% in the liner. For this case the maximum calculated stress in the CV is 37.1 ksi. All these values are within Code limits.

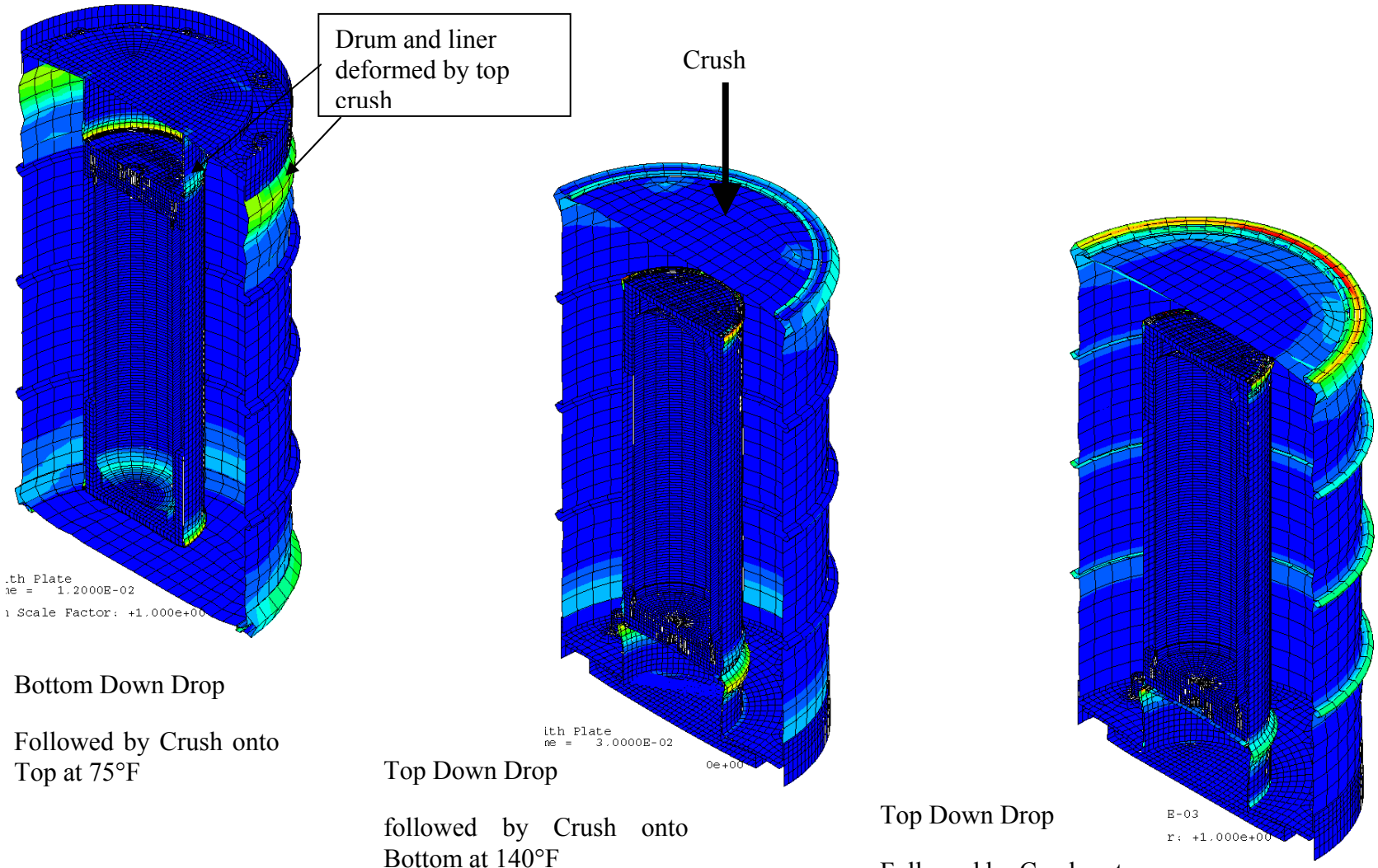

Figure 2.52 Analysis – Top and Bottom Down Drops Post Crush Strain Plots

2.7.3 Puncture

Requirement: 71.73(c)(3) *Puncture*. A free drop of the specimen through a distance of 40 inches in a position for which maximum damage is expected, onto the upper end of a solid, vertical, cylindrical, mild steel bar mounted on an essentially unyielding, horizontal surface. The bar must be 6 inches in diameter, with the top horizontal and its edge rounded to a radius of not more than 0.25 inches, and of a length as to cause maximum damage to the package, but not less than 8 inches long. The long axis of the bar must be vertical.

Evaluation: The 9977 design was tested and analyzed to evaluate the effects of puncture per 10 CFR 71.73(c)(3). Analysis and test demonstrate that the sequential HAC puncture test will not adversely affect the performance of the package before being subjected to thermal testing.

2.7.3.1 Puncture Testing

Puncture Bar: Puncture tests were performed at SRS in building 730-A. The puncture bar used for package testing is 6-inches in diameter by 40-inches long which exceeds the minimum 8-inch length.[1] Its top edge includes a machined ¼-inch radius. The bar is welded to an 18-inch square by 2-¼ inch thick steel plate. The base of the bar is also gusseted with three equally spaced 5-1/2 inch by ½-inch thick triangular steel plates. The plate is in turn welded to the target pad that is used for the NCT 4-foot drops and HAC 30-foot drops. The pad is an unyielding surface as described in Appendix 2.7. Figure 2.53 shows test package SN-4 suspended above the puncture pin in preparation for testing.

SN-4

9977 SN-4 is shown balanced and aligned over the stationary pin before being lifted 40-inches above its surface for dropping.

[1] The selection of a 40-inch bar length is based on past testing where drum packages equipped with the standard bolt-ring-nut closures were common. The bar length permitted a drum to be dropped in a vertical bottom-down orientation and strike the drum closure prior to the drum bottoming out on the ground. Present drum designs are not subject to the same damage. The current 40-inch long bar exceeds the minimum 8-inch bar length and adds conservatism into the test as the package is dropped from a height of over six (6) feet following the preceding HAC tests.

Figure 2.53 - Puncture Pin Test Setup (SN-4)

A horizontal drop over the package center of gravity was selected to do the most damage. Lesser angles over the package CG may exert more localized stress to the drum surface but because of the drum assembly's rigidity, due to the foams stiffness, the package will tend to slide and or rotate from the point of impact and therefore the full inertia of the package would not be realized at the point of impact. This glancing effect can be seen in the "half-moon" secondary impact shown in Figure 2.32. Finite element analysis was performed to determine overpack shell stress for varying drop orientations and puncture angles at both tested and untested conditions (see Section 2.7.3.2).

SN-2 through -5 were puncture tested in a horizontal position over the package center of gravity as illustrated in Figures 2.54 & 2.55. Additionally, SN-3 was subject to a bottom-down puncture test in an attempt to exploit a rip in the drum chime which occurred during its crush test. Figure 2.54 illustrates the puncture damage typical of all the packages that were dropped horizontally. The deflection of the drum surface resulting from these drops was typically an approximate1/8 inches dent. As shown, part of the drum rolling hoop is depressed where the edge of the pin contacted half of the hoop. To the right of the initial damage is secondary damage after the drum rebounded off of the pin and struck a second time. The drum impacted a third time at the top rolling hoop before coming to rest. No rupture or indication of a potential drum rupture was observed in this or any of the puncture tests.

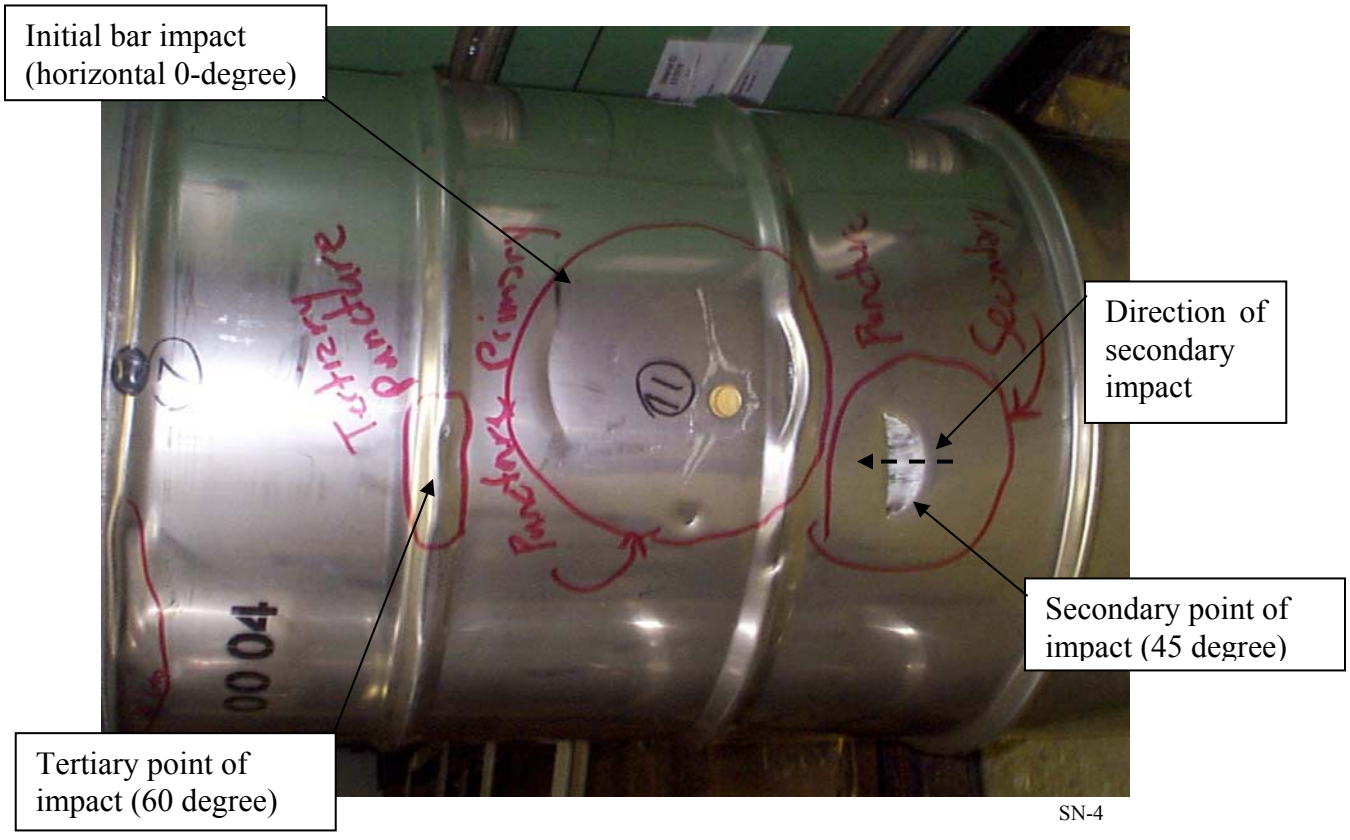

Figure 2.54 - Post Puncture Test (SN-4)

Figure 2.55 shows the radial split which occurred along SN-3s drum chime from the crush and the resultant deformation after the puncture test. The puncture test did not increase the size of the split; however, it did cause a section of it to protrude from the drum bottom exposing more of the foam. Subsequent thermal testing showed that even with the added exposure of foam, package performance was not significantly affected. As a result of the split the design for the drums bottom was revised to eliminate the standard crimp-seal chime to a fully welded sanitary drum bottom with an external skirt. A discussion of the design change is provided in Appendix 2.8.

A detailed description of all the puncture tests and a summary of the results are provided in Appendix 2.10.

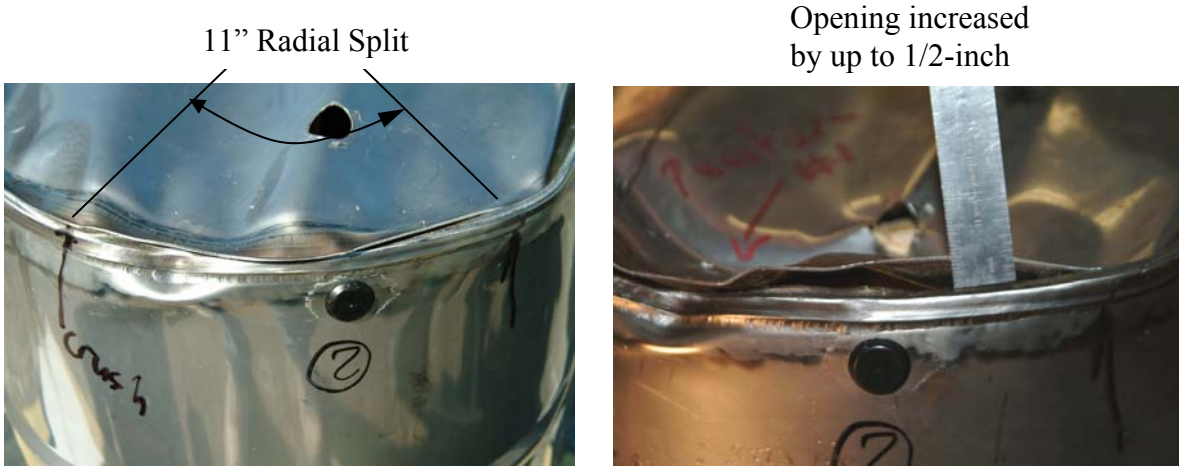

Figure 2.55 - Pre and Post Puncture Damage (SN-3)

Based on the observed test damage, the effects of the puncture drop after the free-drop and crush tests is negligible and would not affect the performance of the package in the subsequent thermal test.

2.7.3.2 Puncture Analysis

Puncture analyses were performed to demonstrate that other drop orientations, puncture angles and package conditions that were not tested, would not show an appreciably greater amount of damage than the tested configurations. This demonstrates that packages punctured at different conditions would not alter their performance in the fire test. The results for the drum puncture evaluation, Appendix 2.9, show that the strain in the drum's stainless steel wall is not greater than 20%, which is less than the 35% rupture strain of stainless steel. Therefore, the drum would not be expected to tear. The finite element analyses that were performed to determine the effects of puncture on the package did not include the cumulative damage of the initial HAC impacts (free-drop and crush). Nevertheless, these analyses complement and benchmark puncture testing

that was performed. This is considered acceptable as the observed damage from puncture testing on the 9977 was minor. With the exception of the tear in the bottom chime of the drum, damage resulting from the free-drop and crush tests does not appear to influence puncture damage.

Two puncture models were analyzed to assess shell stress for the multi-angle drops, as shown in Figure 2.56. The heavier 6CV configuration was modeled, bounding the lighter 5CV configuration. The first model assumed the drum was positioned horizontally and the pin struck at its CG, similar to testing. The second model assumed the drum was positioned top-down and pin strike was at the drums CG. Each model was then rotated 45-degrees and dropped onto the same location and resulting damage assessed. Bottom-down drop analyses were not performed as it was concluded the horizontal puncture would show similar damage. For the horizontal drops the foam properties were varied from -20 ºF to 300 ºF to simulate NCT conditions. For the top-down puncture analyses the packaging material properties were modeled at 75 ºF since the properties of the insulating materials used in the lid are not temperature sensitive over the noted range.

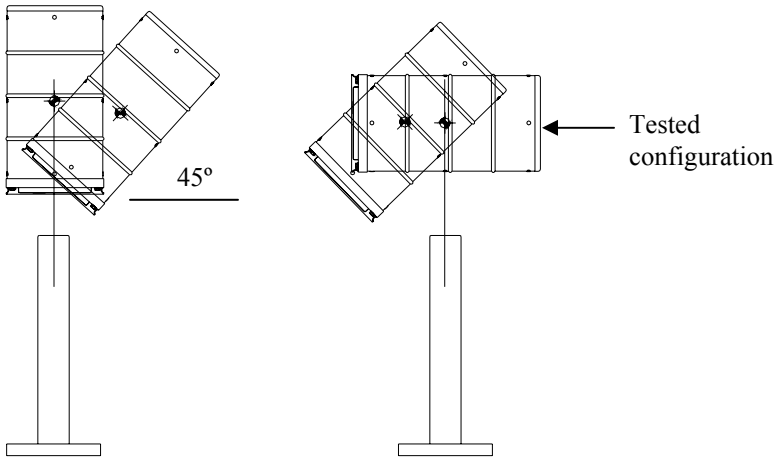

Figure 2.56 - Puncture Analysis of Horizontal and Vertical Oriented Packages

The analytical results for drum strain and CV stress are compared against their respective allowables and the allowable maximum values of the primary membrane stress intensities for the CV are shown in Appendix 2.9, Table 1. The maximum values of primary membrane stress intensities in the containment vessel is 46.55 ksi for the sided drop at -20 ºF and is within the Level D service load allowable limits specified in the ASME Code, Section III, Appendix F, 57.8 ksi. The analytical results found negligible plastic deformation in the containment vessel during the impact condition. The maximum calculated value of the effective plastic strain in the drum is 15.8% for the top down 45-degree drop onto the drum lid. This value is less than the minimum elongation of 35% for the 304L lid material. Therefore, the drum will not be ruptured by the 40-inch drop of the package onto the bar. Strain reported are maximum peak values and not averaged across the material thickness.

Based on the summary of test damage in the preceding section and the analysis, it is concluded the effects of the puncture drop following the free-drop and crush tests has a negligible effect on the subsequent thermal test.

2.7.4 Thermal

Requirement: 71.73(c)(4) *Thermal.* Exposure of the specimen fully engulfed, except for a simple support system, in a hydrocarbon fuel/air fire of sufficient extent, and in sufficiently quiescent ambient conditions, to provide an average emissivity coefficient of at least 0.9, with an average flame temperature of at least 1475°F for a period of 30 minutes. The fuel source must extend horizontally at least 40 in, but may not extend more than 10 ft, beyond any external surface of the specimen, and the specimen must be positioned 40 in above the surface of the fuel source. For purposes of calculation, the surface absorptivity coefficient must be either that value which the package may be expected to possess if exposed to the fire specified or 0.8, whichever is greater; and the convective coefficient must be that value which may be demonstrated to exist if the package were exposed to the fire specified. Artificial cooling may not be applied after cessation of external heat input, and any combustion of materials of construction, must be allowed to proceed until it terminates naturally.

Evaluation: Compliance with the thermal requirements of HAC is shown by test and thermal numerical analysis. Following the HAC drop testing, four test units were each subjected to a HAC pool fire in accordance with 10 CFR71.73(c)(4). One of these units had previously been subjected to the full suite of 10 CFR17.71 NCT tests. Prior to each pool fire, the unit being tested was preheated in an environmental chamber at 200 °F for a minimum of four (4) days. The 200 °F soak temperature was chosen based upon the calculated 6CV O-ring temperature under NCT without insolation, as analyzed in Section 3.1.3.1. The 200 °F also conservatively bounds the maximum foam temperature of 185 °F, under the same conditions. The packages were insulated when in transit from the environmental chamber to the thermal test facility and heated and insulated while at the test facility prior to beginning the thermal test.

Temperature indicating labels were used to determine the maximum temperatures reached during the fire. The temperature indicating labels (TILs) have “dots” which change from white or yellow to black when a specific temperature is reached, see Figure 2.57. Each TIL spans a specific temperature range, typically in seven (7) discrete steps, for a total of eight (8) temperatures. The set of TILs shown in Figure 2.57 cover the range from 170 °F to 500 °F. The lowest value indicator “dot” that has not turned black is conservatively used as the temperature which that component has reached. For the set of labels shown in Figure 2.57, the component reached at least 330 °F but not 340 °F, therefore, it is assumed that the component maximum temperature was 340 °F. The TILs shown are for the practice package, (i.e., only the Fiberfrax blanket surrounding the liner and insulated drum lid thermally protected the CV.) By comparison, the equivalent temperature dot for the foam insulated drums for the same location on the CV was less than 250 ºF for all of the burned drums, Appendix 2.10.

The maximum CV temperature recorded from the SN test series, with foam, was 270 ºF on the top of the cone seal nut for SN-4. Based on thermal analysis of the 4-day, 200 ºF soak, the CV temperature increased by about 90 ºF as a result of the 30-minute fire.

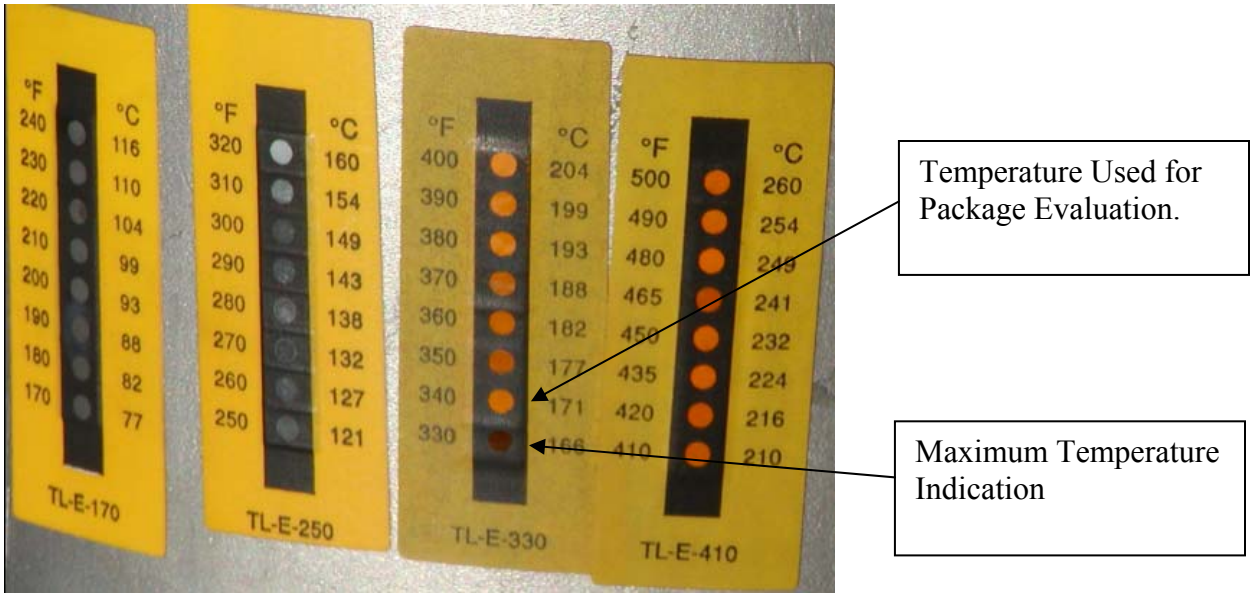

Label bank taken from "Practice Package"; located on outside bottom of CV

Figure 2-57 Typical Set of Temperature Indicating Labels

Following the thermal test each package was permitted to cool in the pool fire test structure. (See Figure 3.17). After the packages had cooled they were digitally radiographed, destructively examined, and the CVs leak tested. All CVs remained leak tight, see Table 2.26.

Destructive examination following the regulatory burn showed that the packages were consistent in regard to the residual char formation that remained from the degraded foam. Figures 2.58 through 2.61 are photographs of the four SN test drums sectioned following the fire. The char formation within each drum is essentially the same; degraded foam is replaced by an interlocked weave of various size char nodules. The char is fairly resistant to mechanical damage as the drums were handled and transported over 70-miles from the test site before being radiographed and then subjected to shocks and vibrations received during sectioning activities. Similar char formation was observed on the DP Series test packages (Reference 52, Figure 71, pg. 69).

From an outward appearance, the char in each package is similar. However, volumetrically, the percentage of un-degraded polyurethane foam varies from 27.6% to 36.8%. Though the ratio of degraded foam to un-degraded foam varies by as much as 25%, the temperatures recorded within the drum liner are relatively unaffected. Even for the "practice drum" which had no foam, the temperatures inside the liner where not significantly greater than those when foam is present. The percentage of degraded foam to un-degraded foam is likely a function of its initial pour integrity, the damage it receives (i.e., cracks, fissures, local fragmentation) from impacts and the vent area of the enclosing drum. Since the temperatures inside the liner appear independent of the percentage of foam degradation, this supports the hypothesis that the foam provides more structural than thermal protection. Nevertheless, even with the variations in foam degradation

observed, the TILs show that the foam and Fiberfrax layer keep the CV assembly well below its design temperature limits.

In addition to the foam decomposition matrix which provides thermal protection, the Fiberfrax wrap around the liner significantly impedes the direct impingement of hot gases from the intumescing polyurethane. Though not a true vapor barrier, the Fiberfrax composite material has been shown by testing to be effective in attenuating the encroachment of gases from the HAC fire event onto the liner. Figure 2.61 compares the SN series thermal test results to that of the earlier DP series which shows the mitigating effect of the Fiberfrax wrap. The average CV temperature difference between the DP and SN thermal test was 60º higher for the DP packages. The DP packages with higher temperatures still did not exceed packaging material thermal limits.

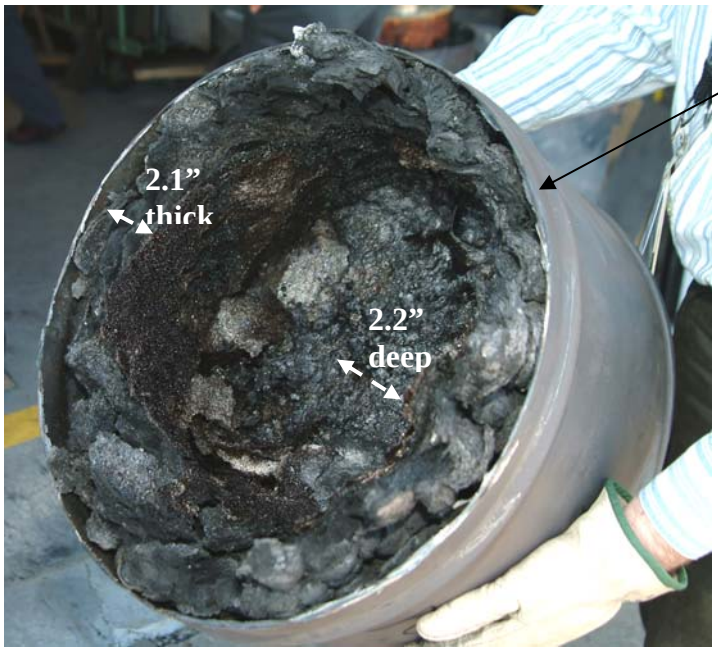

Bottom of drum following drum sectioning. Foam is securely attached to the inside of the drum bottom.

- Char depth at drum bottom is about 2.2 inches.
- Char depth around the side wall is about 2.1 inches.

SN-2

Top of SN-4 sectioned for examining char, after first cutting through the un-degraded foam and bottom of the liner to extract the CV.

Char still holds the impression of the drum chime.

Bottom of liner

SN-2

Figure 2.58 Foam Char Formation in SN-2

Bottom of SN-5 removed to extract CV from liner. Foam is securely attached to the inside of the drum bottom.

- Char depth at drum bottom is about 2.2 inches.
- Char depth around the side wall is about 2.1 inches.

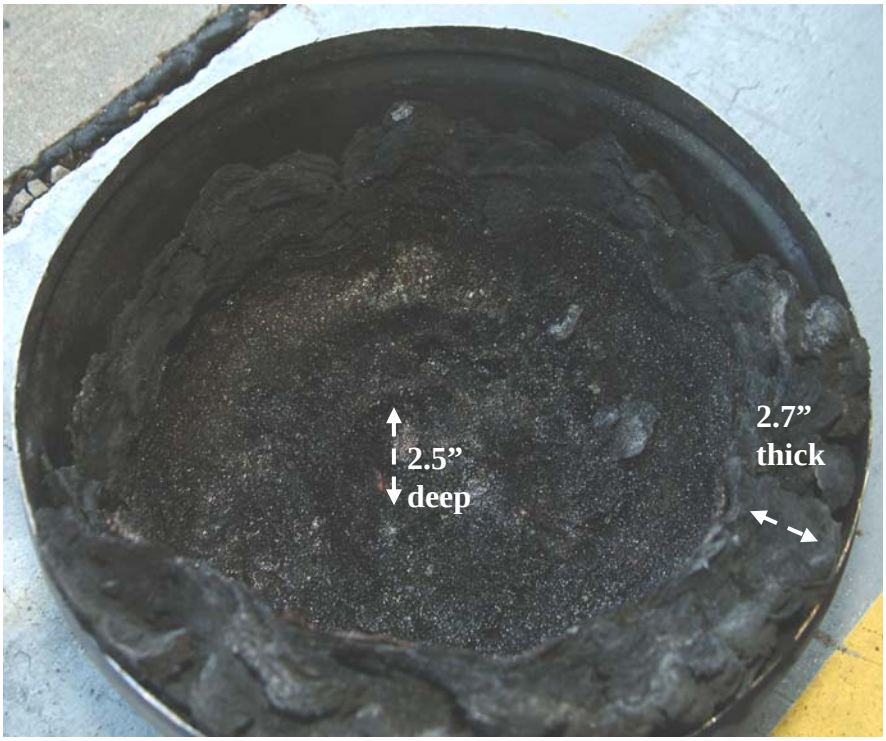

SN-5

Top of SN-5 sectioned longitudinally for continued char examination.

SN-5

Foam nodules and interlocking characteristic of char is typical to other containers inspected.

Figure 2.59 Foam Char Formation in SN-5

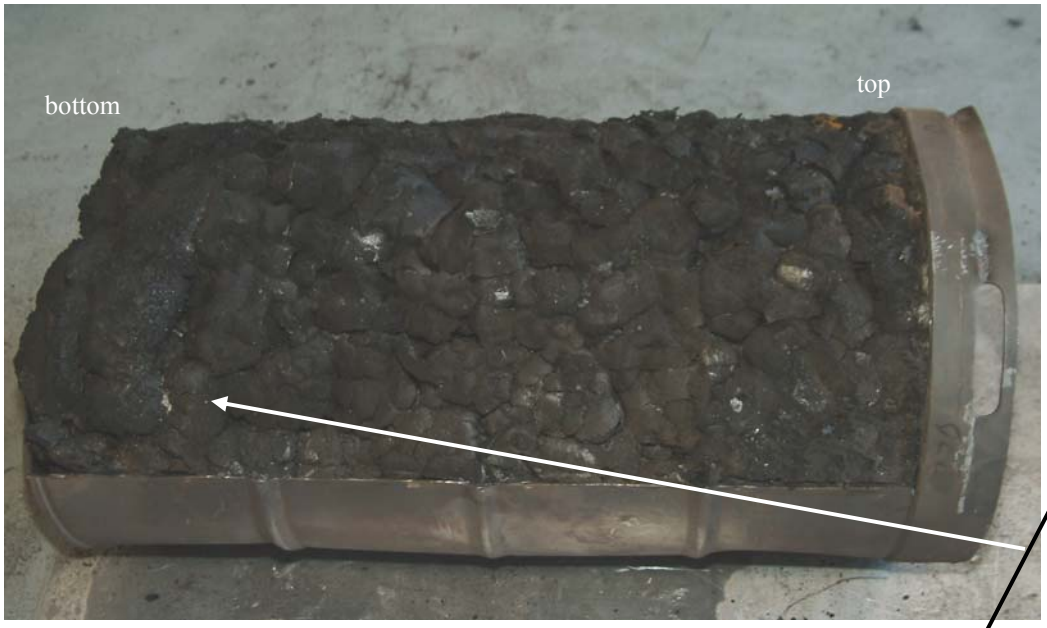

SN-3

SN-3 was initially sectioned to permit full inspection of the degraded foam.

Foam nodules are irregularly shaped and interlocked.

Not readily detectable but only char fills bottom of drum; top is half char half foam.

Figure 2.60 Foam Char Formation in SN-3

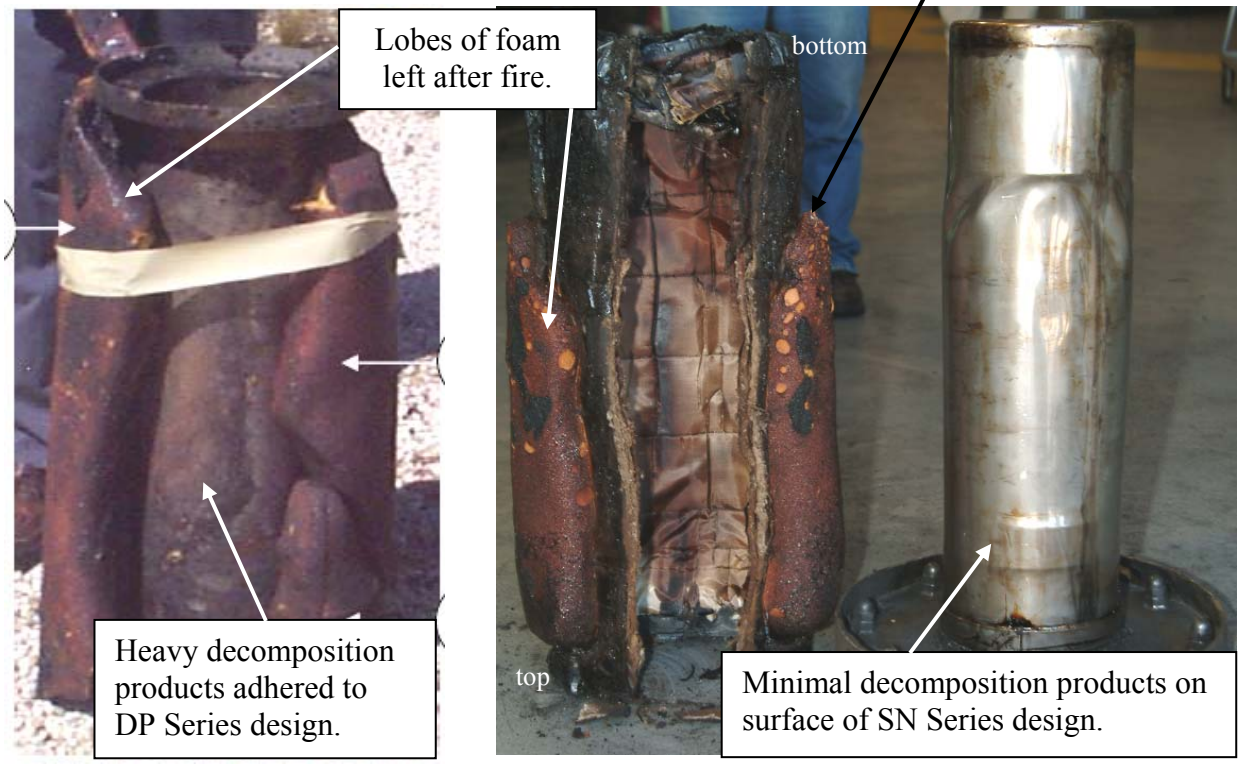

DP-3 (fig. 72, pg 70, Ref **Error! Bookmark**

SN-3

Figure 2.61 Foam Decomposition Product Comparison between DP and SN Package Designs

As shown in Table 2.25 all test packages were leak-tight following the 30 minute pool fire.

The package, with maximum internal heat load, was analyzed in a fire at 1475°F. Package temperatures reached the values shown in Table 3.2. Temperatures internal to the overpack were well below the limits for the CV and O-ring materials as given in Table 3.2. Therefore, the HAC fire event will not compromise the leaktight performance of the 9977 CV.

2.7.4.1 Summary of Pressures and Temperatures

Peak HAC temperatures and pressure are calculated in Appendix 3.1, and thermal analysis results are summarized in Table 2.27.

Table 2.28 - HAC Thermal Analysis Results for the 9977 Shipping Package

Package Component	**Calculated NCT Temperature** (°F)		**Calculated HAC Temperature** (°F)		**Calculated HAC MNOP** (psig)	
	5CV	6CV	5CV	6CV	5CV	6CV
Containment Vessel	260	321	n/c	400	48.5	35.0
Contents	280	350	n/c	425	na	na

2.7.4.2 Differential Thermal Expansion

The HAC temperatures for the containment vessel are summarized in Table 2.27 (See Section 3.3). The HAC temperatures are greater than the temperatures calculated for NCT, however, the differential thermal expansion calculation for the NCT conditions assumed 500 °F (see Section 2.6.1.2) which bounds the HAC temperatures listed in Table 2.2. Based on the NCT differential thermal calculations reported in Appendix 2.1 component thermal expansion does not affect the performance of the 9977 package.

2.7.4.3 Stress Calculations

Stresses from pressure loadings and from other primary loadings are combined for comparison to the stress limits specified in RG 7.6. However, small structural loads from the <2 ºF temperature gradient across the vessel wall produce negligible stresses and were not incorporated into the final stress results. Stresses resulting from CV design pressure and HAC thermal loadings are calculated in Appendix 2.2 and include fatigue analysis required by RG 7.6. The stress intensity totals that include fabrication, primary, and secondary stresses are shown to be less than $2S_a$ at

10 cycles based on the design fatigue curves in Appendix I of the ASME BPVC. The stresses resulting from the HAC drop and crush impacts are reported in Table 2.28, and from puncture are in Appendix 2.9, Table 1. All reported stresses are within the Level D service load allowable limits specified in the ASME Code, Section III, Appendix F, 57.8 ksi. Therefore, based upon the leak-tight performance of the CVs following the HAC fire, the 9977 satisfies the performance requirements of 10CFR71.

Table 2.29 - Summary of Calculated and Allowable Stress Intensities
6-inch and 5-inch Diameter Containment Vessel HAC (30-Foot) Drop and Crush

HAC Load Cases [c]		Calculated Maximum Values of Stress Intensities for the Containment Vessel [a, b] (ksi)							
		30-Foot Drop				Crush			
		-20 ºF ambient, zero watts	75 ºF	140 ºF	260/300 ºF	-20 ºF ambient, zero watts	75 ºF	140 ºF	260/300 ºF
6CV	Top Down		29,960	30,020	39,270			17,830	37,140
	Bottom Down	51,190	46,320	42,020	38,220		31,400		
	CGOT	47,990	47,840				42,810		
	CGOB		49,960	48,050	37,760		42,120	38,190	37,930
	Side-wt in Middle	42,820				41,970			
	Side-wt in Bottom			45,300	46,220			37,990	47,030
	Side-wt in Top			52,400	46,520				
	15° Slap on Top			43,760	42,210				
	15° Slap on Bottom	40,330		32,480	29,380				
5CV	Side-wt in Middle	44,310			43,970	53,810			44,770
	CGOT	46,000							
	15° Slap on Bottom	45,400							

a Values listed are maximum values at any location on the CV.
b The allowable true stress intensity limits are 57.8-ksi for P_m and 74.3-ksi for P_L.
c See illustration on next page of the drop orientations

2.7.4.4 Comparison with Allowable Stresses

Detailed stress calculations for the package are given in Appendix 2.6. For a simple conservative assessment of the stresses resulting from combination of NCT and HAC stresses, the minimum margin NCT stress from Table 2.15 can be added to the maximum HAC stress from Table 2.28. For NCT the maximum Primary (Membrane+Bending) stress is 13248 psi for the 5CV. The Maximum local primary membrane stress in Table 2.28 is 53,810 psi, also for the 5CV. Addition of these two maximum values results in a combined value of 68,048 psi. Comparison of this value with the true stress intensity, P_L, allowable limit, 74,300 psi, from Table 2.28, results in a code margin of 8.4%. Even with the extremely conservative combination of maximum stresses from different locations on different parts and minimum possible pipe wall thickness, the containment vessels have margin above the demand due to combination of NCT and HAC loads.

2.7.5 Immersion – Fissile Material

Requirement: 71.73(c)(5) – *Immersion--fissile material*. For fissile material subject to § 71.55, in those cases where water inleakage has not been assumed for criticality analysis, immersion under a head of water of at least 3 ft in the attitude for which maximum leakage is expected.

Evaluation: The 9977 package criticality analysis assumes water inleakage and therefore the immersion test was not performed. Though not performed, the 9977 containment vessel design is similar to other packages which utilize its design on which water immersion under a 3-ft head of water was conducted and no inleakage found. (See Section 2.7.6)

2.7.6 Water Immersion—All Packages

Requirement: 71.73(c)(6) – *Immersion--all packages*. A separate, undamaged specimen must be subjected to water pressure equivalent to immersion under a head of water of at least 50 ft. For test purposes, an external pressure of water of 21.7 lbf/in^2 gauge is considered to meet these conditions.

Evaluation: Immersion testing was not performed on the 9977. Instead the 9977 is shown by comparison to demonstrate compliance with 19 CFR 71.73(c)(6) due to its similarity with the 9966 package containment system. The 9966 package employs the identical containment vessel closure design as used in the 9977. Inspection of the tested 9966 package showed that water did not affect the containment vessels in the immersion test where the package was immersed in 52 ft of water for 24 hours.[53] Due to its similarity in containment vessel design it is concluded the 9966 package can be used to demonstrate the 9977 satisfies the 50-ft immersion test.

2.7.7 Deep Water Immersion Test (for Type B Packages Containing More Than 10^5 A_2)

Requirement: 71.61 – *Special requirements for Type B packages containing more than 10^5 A_2.* A Type B package containing more than 10^5 A_2 must be designed so that its undamaged containment system can withstand an external water pressure of 290 psi for a period of not less than 1 hour without collapse, buckling, or inleakage of water.

Evaluation: Section 4.2 shows the maximum number of A_2 in the 9977 as 122,000, which exceeds the 10^5 A_2 limit. External water pressure testing was not performed on the 9977.

Buckling analysis in Appendix 2.2 shows that stresses from external pressure on the 5CV and 6CV are negligible and will not cause local buckling. In addition, the criticality analysis shows that the package will be critically safe assuming water inleakage and worst case material configuration and therefore is not a concern.

2.7.8 Summary of Damage

The 9977 design was evaluated both by finite element analyses and by test as summarized in the preceding sections. The evaluation has shown that damage to the 9977 from HAC events will not compromise the confinement performance of the drum nor the leaktight performance of the containment vessel. Therefore, the 9977 design can be expected to satisfy the performance requirements of 10 CFR 71.51(a)(2) under HAC given in 10 CFR 71.73.

Analyses of the 9977 design confirm that the overpack (drum and foam insulation) will protect the containment vessel satisfactorily during regulatory HAC events. The thermal evaluation of the 9977 is described in Section 3.5.4 and also confirms the package can withstand he regulatory thermal event.

2.8 ACCIDENT CONDITIONS FOR AIR TRANSPORT OF PLUTONIUM

Not applicable. The 9977 has not been evaluated for the air transport of plutonium.

2.9 ACCIDENT CONDITIONS FOR FISSILE MATERIAL PACKAGES FOR AIR TRANSPORT

Not applicable. The 9977 has not been evaluated for the air transport of fissile material.

2.10 SPECIAL FORM

Not applicable. The contents shipped in the 9977 are not considered to be special form.

2.11 FUEL RODS

Not applicable. The 9977 has not evaluated for the transport of fuel rods.

2.12 REFERENCES

1. *ASME Boiler and Pressure Vessel Code Section III*, "Rules for Construction of Nuclear Power Plant Components," Division 1, American Society of Mechanical Engineers, New York, NY (2004).
2. *Packaging Transportation of Radioactive*, DOE Order 460.1B, Washington, DC (April 2004).
3. *Energy*, Code of Federal Regulations, Title 10, Part 71, *Packaging and Transportation of Radioactive Material* U.S. NRC, Washington, DC (January 2002)
4. *Regulations for the Safe Transport of Radioactive Material – 2005 Edition*, IAEA Safety Standard Series No. TS-R-1, International Atomic Energy Agency, Vienna, Austria, http://www.iaea.org/books (April 2005).
5. Standard Format and Content of Part 71 Applications for Approval of Packaging for Radioactive Material, Regulatory Guide 7.9, Rev. 2, U.S. Nuclear Regulatory Commission, Washington, DC (March 2005).
6. General Plastics Manufacturing Company, FR-3700 Last-A-Foam, Tacoma, Washington.
7. *ASME Boiler and Pressure Vessel Code Section III*, "Rules for Construction of Nuclear Power Plant Components," Division 1, Subsection NF, American Society of Mechanical Engineers, New York, NY (2004).
8. UNIFRAX Corporation, Fiberfrax® LTC HSA™ Systems, Niagara Falls, NY.
9. Caplugs LLC, www.caplugs.com.
10. Thermal Ceramics Americas, Min-K Data Recorder, Min-K 2000, August, GA.
11. Thermal Ceramics Americas, TR-19 Block Insulation, web page, August, GA
12. INTEK Adhesives Ltd, RTV 382, web page, Blyth, Northumberland.
13. *Transportation*, Code of Federal Regulations, Title 49, Part 173, *Shippers - General Requirements for Shipments and Packaging*, U.S. NRC, Washington, DC (January 2002)
14. Fracture Toughness Criteria of Base Material for Ferritic Steel Shipping Cask Containment Vessels with a Maximum Wall Thickness of 4 Inches, Regulatory Guide 7.11, United States Nuclear Regulatory Commission, Office of Nuclear Regulatory Research, Washington, DC (June 1991).
15. *Fabrication Criteria for Shipping Containers*, NUREG/CR-3854, U.S. Nuclear Regulatory Commission, Washington, DC (March 1985).
16. *Design Criteria for the Structural Analysis of Shipping Cask Containment Vessels*, Regulatory Guide 7.6, Rev. 1, U.S. NRC Office of Nuclear Regulatory Research (March 1980).
17. *Load Combinations for the Structural Analysis of Shipping Casks for Radioactive Material*. Regulatory Guide 7.8, Rev. 1, U.S. Nuclear Regulatory Commission Office of Nuclear Regulatory Research, Washington, DC (March 1989).

18. Sindelar, R.L., "Tensile Properties of Type 304/304L Stainless Steel for Impact Deformation Analysis of Nuclear Containers," SRT-MTS-93-3113, November, 1993.

19. Letter, J. Nichols, Project Engineer, General Plastics Manufacturing Company to K. Eberl, March 2006.

20. Safety Analysis Report for Type B(U) AL-SX (H1616) Reservoir Packages, Sandia Report SAND91-2205, Sandia National Laboratories, Albuquerque, NM, June 1998.

21. General Plastics Manufacturing Company, Memorandum, Dated Feb 2006 To Kurt Eberl.

22. L.A. Domeier, H1259 Container Foams: Performance Data on Aged Materials, Sandia Report, SAND2002-8113, Sandia National Laboratories, Albuquerque, NM, May 2002.

23. Rand, P.B, Weapon Foam Accelerated Aging Using Dynamic Mechanical Analysis, SAND96-0647C, Sandia National Laboratories, Albuquerque, NM.

24. *ASME Boiler and Pressure Vessel Code Section II*, "Ferrous Material Specificatins," Part A, "Properties," Part D, American Society of Mechanical Engineers, New York, NY (2004).

25. Kansas City Plant – Engineering Development Specification, *Specification for SGT Thermal Protective Insulation (U)*, SS-R51507, Issue B, June 2002.

26. DuPont, Kryton 240AC Fluorinated Grease

    http://www.dupont.com/lubricants/en/literature/pdf_files/H-58519-2.pdf

27. Nitronic-60,
    http://www.hpalloy.com/Alloys/Nitronic60/Brochure/Physical%20Properties.htm

28. RTV 382 Silicone Adhesive and Sealant, http://www.intek-uk.com/rtv382.htm.

29. 3M Glass Cloth Tape 361 from

    http://solutions.3m.com/wps/portal/3M/en_US/3M-SpecialtyTapes/
    SpcltyTape/Docs/TechnicalDataSheets?#glasscloth

30. Skidmore, T.E., *Performance Evaluation of O-ring Seals in Model 9975 Packaging Assemblies (U)*, WSRC-TR-98-00439, Savannah River Site, Aiken, SC (December 1998).

31. *ASME Boiler and Pressure Vessel Code Section II*, "Ferrous Material Specificatins," Part A, "Properties," Part D, American Society of Mechanical Engineers, New York, NY (2004).

32. TR-19 Insulating Block, http://www.thermalceramics.com/upload/pdf/1014-100.pdf

33. Fiberfrax, Kansas City Plant, Specification SS-R51507, Specification for SGT Thermal Protective Insulation (U)

34. Min-K 2000, http://www.thermalceramics.com/literature/MK201.pdf,

35. FR-3700 Foam, Email From: Zelda Iams to Paul Blanton, General Plastics Inc., 7/9/2004, FW: Answers to your 9977 foam questions

36. *ASME Boiler and Pressure Vessel Code Section II*, "Ferrous Material Specificatins," Part A, "Properties," Part D, American Society of Mechanical Engineers, New York, NY (2004).

37. Glass, R.E., AT-400A Development Report, SAND97-0118, pg. 66, Sandia National Laboratories, Albuquerque, NM, (January 29, 1999)

38. Skidmore, T.E., Radiation Resistance of Viton® GLT O-rings for model 9975 Packaging Assemblies (U), Westinghouse SRTC Memo, SRT-MTS-98-4117 (September 30, 1998).

39. Blanton, P.S., *Request for Extension to Annual Maintenance Requirement for 9975 Type B Packagings*, SRT-RMPT-2002-00009, Westinghouse Savannah River Company, Aiken, SC, (March 2002)

40. 2R Shipping Container Grapple fro 2R Shipping Containers (U), EES-22498-R1-001, Rev E, Savannah River Site, Aiken, SC.

41. Safety Analysis Report for the Type B(U) AL-SX(H1616) Reservoir Packages, SAND91-2205, pg. 44, Sandia National Laboratory, Albuquerque, NM, (June 1998).

42. F.P. Henry and C.L. Williamson, "Rigid polyurethane Foam for Impact and Thermal Protection", Presented at PATRAM '95, 11th International Conference on the Packaging and Transportation of Radioactive Materials.

43. C.L. Williamson and Z.L Iams, "Thermal Assault and Polyurethane Foam Evaluating Protective Mechanisms", Presented at PATRAM 2004, International Symposium on the Packaging and Transportation of Radioactive Materials, Berlin Germany.

44. ABAQUS Structural Analysis Code, Version 6.4, Hibbitt, Karlsson, and Sorensen, Inc., Pawtucket, Rhode Island

45. *Parker O-ring Handbook*, ORD-5700A, The Parker Seal Group, Parker Hannifin Corporation, Cleveland, OH, http://www.parker.com/o-ring. (2001).

46. 9965 Safety Analysis Report - Packages, DPSPU 83-124-1, Westinghouse Savannah River Company, June 1984.

47. *Leakage Tests on Packages for Shipment of Radioactive Materials*, Regulatory Guide 7.4, U.S. Nuclear Regulatory Commission, Washington, DC (June 1975).

48. ANSI N 14.5-1997, American National Standard for Radioactive Materials—Leakage Tests on Packages for Shipment, American Natl. Standards Institute (February 5, 1998).

49. Shock and Vibration Test Specifications and Actual Environments for the August 2005 Vibration/Shock Testing of the General Purpose Fissile Package (GPFP) Shipping Container, Email, From Mark Cranfill, SNL 2111/MS0447, Sandia National Laboratory, Albuquerque, NM, (September 14, 2005).

50. Advisory Material for the IAEA Regulations for the Safe Transport of Radioactive Material Safety Guide Details

51. Safety Standards Series No. TS-G-1.1 (ST-2), July, 19 2002.

52. Gelder, L.G., General Purpose Fissile Packaging Prototype Testing, M-TRT-A-00006, Revision 0, Westinghouse Savannah River Company, (May 2005).

53. P.S. Blanton and A.C. Smith, Response Of Conventional Ring Closures Of Drum Type Packages To Regulatory Drop Tests With Application to The 9974/9975 Package, WSRC-MS-2001-00306, Westinghouse Savannah River Company, PVP (August 2002).

54. Immersion Test of the 9966 Package, M-TSM-A-00005, Rev 0, Savannah River Site, Aiken, SC (October 2003).

This Page Intentionally Left Blank

2.13 APPENDIX

Appendix	Description
2.1	General Normal Condition Design Calculations for 9977 Packaging
2.2	General Design and ASME Calculations for the 9977 Containment Vessels
2.3	9977 General Purpose Fissile Packaging Weights
2.4	9965 Cone-Seal Closure Performance at -40°F
2.5	9977 Packaging Materials and Components of Fabrication
2.6	Hypothetical Accident Condition Analysis Drop and Crush for the Model 9977
2.7	SRS Drop Test Pad Infrastructure For Drums
2.8	9977 Packaging Comparisons with the GPFP Development Prototypes
2.9	Dynamic Analysis of the 9977 Package Puncture Strength for a 40-inch Drop onto a Steel Bar
2.10	9977 General Purpose Fissile Packaging Prototype Testing

This Page Intentionally Left Blank

Appendix 2.1

Structural Evaluation

Of

General Purpose Fissile Package

(9977 Series)

This Page is Intentionally Left Blank

Calculation Cover Sheet

Project	Calculation No.	Project No.
N/A	M-CLC-G-00357	N/A
Title Structural Evaluation of General Purpose Fissile Package (9977 Series) (U)	**Functional Classification** SS	Sheet 1 of 42
	Discipline Mechanical	
Calc Level ☒ Type 1 ☐ Type 2	**Type 1 Calc Status** ☐ Preliminary ☒ Confirmed	
Computer Program No. Abaqus NA ☐	**Version/Release No.** 6.5.3 / 2005_03_03-17.29.04 57675	

Purpose and Objective

The purpose of this calculation is to document analyses performed as part of the structural design of the 9977 series General Purpose Fissile Package (GPFP) to support generation of its Safety Analysis Report for Packaging. The load cases analyzed are delineated in Section 1.0.

Summary of Conclusion

Analyses presented in this calculation meet the design criteria required by 10 CFR 71in the evaluation of the Model 9977.

Revisions

Rev. No.	Revision Description
0	Original Issue

Sign Off

Rev. No.	Originator (Print) Sign/Date	Verification/ Checking Method	Verifier/Checker (Print) Sign/Date	Manager (Print) Sign/Date
0	R.R. Rothermel/T.T. Wu 5/17/06	Document Review	N. K. Gupta 5/17/06	J.S. Bellamy 5/17/06

Design Authority -- (Print)	Signature	Date
Release to Outside Agency -- (Print) N/A	**Signature** N/A	**Date** N/A

Security Classification of the Calculation

(U)

Calculation Continuation Sheet

Calculation No.	Sheet No.	Rev.
M-CLC-G-00357	2	**0**

OPEN ITEMS

None

Calculation Continuation Sheet

Calculation No.	Sheet No.	Rev.
M-CLC-G-00357	3	**0**

RECORD OF REVISION					
REV. NO.	PAGES SUPERSEDED	PAGES ADDED	PAGES DELETED	PAGES REVISED	DESCRIPTION OF REVISIONS
0					Original Issue

Calculation Continuation Sheet

Calculation No.	Sheet No.	Rev.
M-CLC-G-00357	4	0

Table of Contents

Calculation Continuation Sheet

Calculation No.	Sheet No.	Rev.
M-CLC-G-00357	5	**0**

1.0 Purpose

The purpose of this calculation is to document analyses performed as part of the structural design and component sizing of the 9977 shipping package to support generation of the Safety Analysis Report for Packaging (SARP). The 9977 shipping package is composed of a stainless steel pressure vessel with a dual o-ring seal that serves as the Containment Vessel (CV) for the package contents. Two shipping configurations exist for the 9977 package, namely (1) contents contained within a six-inch CV, commonly known as a 6CV, and (2) contents contained within a five-inch CV, commonly known as a 5CV. Differences between the two shipping configurations are discussed further in the calculations below.

Analysis of the package for loads related to transportation, normal operation, and lifting were completed using the guidance of ASME B&PV Code, Section III, Subsection NB, 2004 edition [6.1]. Where additional analysis guidance was required to evaluate the design, other subsections of the ASME code were utilized. References to subsections other than NB that were used are included in the analysis section of this calculation.

This calculation addresses the following specific conditions:

1. Pressure and/or structural design per ASME III.
2. Heat: Differential thermal expansion (Maximum design temperature = 300F)
3. Cold: Differential thermal expansion (Minimum design temperature = -40F)
4. Reduced external pressure (3.5 psi absolute) effects on CVs and Overpack.
5. Increased external pressure (20 psi absolute) effects on CVs and Overpack.
6. Compression (Larger of 5 times package weight or 2 psi on vertical area)
7. Containment Vessel and Overpack Lifting and Tie-down
8. Overpack lid bolting evaluation
9. Vibratory loading on drum closure-bolt preload

2.0 Input

The following Revision 0 drawings were used as input for the analyses contained herein:

R-R1-G-00020	R-R2-G-00017	R-R2-G-00019	R-R2-G-00033	R-R2-G-00043
R-R1-G-00021	R-R2-G-00018	R-R2-G-00032	R-R2-G-00042	

Tables 2.7 through 2.14 of S-SARP-G-00001 give the material properties.

3.0 Conclusions

Analysis presented in this calculation meet the design criteria required by 10 CFR 71 in the evaluation of the Model 9977.

4.0 Analysis

4.1 Stresses in Drum Closure Fasteners

The drum closure fasteners are evaluated for the stresses due to boltup. The components evaluated include the bolts and the fittings, which are the internally-threaded parts to which the bolts are assembled.

The drum closure bolts are evaluated to determine preload and the resulting stresses due to boltup. Stresses in the bolts are found using the methods prescribed in reference [6.2]. The bolts are torqued to 45 +/- 5 lb-ft per assembly drawing R-R1-G-00020 and R-R1-G-00020 at assembly. The drum closure is not subjected to pressure loads and, therefore no ASME B&PV Code evaluation of bolts for pressure loads is required.

Fastener Nomenclature:

μ_1 = thread coefficient of friction

μ_2 = collar coefficient of friction

r_t = pitch radius of threads

r_c = average radius of head contact area

θ_n = thread angle = $\tan^{-1}[(\tan \theta)(\cos \alpha)]$

θ = one-half the thread included angle (= 30 degrees for standard V-threads)

α = thread helix angle = $\tan^{-1}[L / 2\pi r_t]$

L = lead of thread

Calculation Continuation Sheet

Calculation No.	Sheet No.	Rev.
M-CLC-G-00357	7	**0**

Inputs: Maximum Preload

Torque, T: $T_{max} := 50 \cdot 12 \cdot lbf \cdot in$ $D_{nom} := 0.625 \cdot in$

From Reference [6.2]:

Preload:

$$W_{max} := \frac{T_{max}}{0.2 \cdot D_{nom}} \qquad W_{max} = 4800 lbf$$

Inputs: Minimum Preload

Torque, T: $T_{min} := 40 \cdot 12 \cdot lbf \cdot in$

Preload:

$$W_{min} := \frac{T_{min}}{0.2 \cdot D_{nom}} \qquad W_{min} = 3840 lbf$$

Calculation Continuation Sheet

Calculation No.	Sheet No.	Rev.
M-CLC-G-00357	8	**0**

Bolt Stress due to Preload:

Bolt Basic Parameters:

$n := \frac{11}{in}$ $P := \frac{1}{n}$ $P = 0.091\ in$ $d := 0.625\ in$

$d_p := d - 0.649519\ P$ $d_p = 0.5660\ in$ Pitch Diameter

$d_m := d - 1.299038\ P$ $d_m = 0.5069\ in$ Minor Diameter

Define D_{eff} as mean of pitch and minor diameters: $d_{eff} := .5 \cdot (d_p + d_m)$

$A_t := \frac{\pi}{4} \cdot (d_{eff})^2$ $A_t = 0.2260\ in^2$ Tensile Stress Area

Find Von Mises stress due to tightening:

Torque, min/max $T_{min} := 40 \cdot 12\ lbf \cdot in.$ $T_{max} := 50 \cdot 12\ . lbf \cdot in$

Area moment of inertia: $J := \frac{\pi}{32} \cdot (d_{eff})^4$ $J = 8.129\ in^{-3}$

Shear Stress due to torque: $S_{smax} := \frac{T_{max} \cdot d_{eff}}{2 \cdot J}$ $S_{smax} = 19796\ \frac{lbf}{in^2}$

Tensile Stress due to Preload: $W_{max} = 4800\ lbf$

$S_{tmax} := \frac{W_{max}}{A_t}$ $S_{tmax} = 21239\ \frac{lbf}{in^2}$

Von Mises stress, from reference [6.2]:

$S_{max} := \left(S_{tmax}^2 + 3 \cdot S_{smax}^2 \right)^{0.5}$ $S_{max} = 40333\ \frac{lbf}{in^2}$

Calculation Continuation Sheet

Calculation No.	Sheet No.	Rev.
M-CLC-G-00357	9	**0**

Shear Stress in Threads:

Find limiting member for dissimilar materials:

Bolt: A193, Gr B8, Cl 2 UTS =125,000 psi
Nut: A194 Gr 8 (304) UTS =75,000 psi

Shearout strength per inch of thread engagement:

External (Bolt) Thread:

$K_{nmax} := 0.546\,in \qquad E_{smin} := 0.5589\,in$

$$A_s := \pi \cdot n \cdot K_{nmax} \cdot \left[\frac{1}{2 \cdot n} + .57735 \left(E_{smin} - K_{nmax} \right) \right] \qquad A_s = 0.998in$$

Internal (nut) Thread:

$D_{smin} := 0.6113\,in \qquad E_{nmax} := 0.5732\,in$

$$A_n := \pi \cdot n \cdot D_{smin} \cdot \left[\frac{1}{2 \cdot n} + .57735 \left(D_{smin} - E_{nmax} \right) \right] \qquad A_n = 1.425in$$

The relative strength of the internal and external threads must be compared to determine which is weaker

$$S_{uext} := 125000 \frac{lbf}{in^2} \qquad S_{uint} := 75000 \frac{lbf}{in^2}$$

$$J := \frac{A_s \cdot S_{uext}}{A_n \cdot S_{uint}} \qquad J = 1.168$$

J>1, and the required length of engagement is determined by the following formula:

$$L_e := \frac{2 \cdot A_t \cdot J}{\pi \cdot K_{nmax} \cdot \left[0.5 + .57735 n \cdot \left(E_{smin} - K_{nmax} \right) \right]} \qquad L_e = 0.529in$$

Calculation Continuation Sheet

Calculation No.	Sheet No.	Rev.
M-CLC-G-00357	10	**0**

The actual length of engagement is found below:

Length of threads on bolt = 1.0 inch
Thickness of drum top plate = 0.188 inch
Thickness of lid = 0.125 inch
Thickness of washer = .132 inch

$L_{act} := 1.000\,in - .188\,in - .125\,in - .132\,in$

$L_{act} = 0.555in$

The length of engagement is adequate, since $L_{act} > L_e$

The 9977 package bolts do not serve a pressure boundary or sealing function, and therefore, ASME Code stress limits are not applicable. However, the bolt stresses are compared to ASME limits below.

Description	Actual Stress, psi	ASME Code NB-3232 Limit
Average Stress NB-3232.1	4,800 lbs./0.2260 = 21,250 psi	2S = 2(25,000) = 50,000 psi
Maximum Stress NB-3232.2	40, 333 psi (see above)	3S = 3(25,000) = 75,000 psi
Fatigue analysis NB-3232.3	(see below)	U < 1.0

Fatigue Evaluation of Closure Bolts

The only condition which produces cyclic loads on the closure bolts is vibration (see Section 4.11). The vibratory loads are conservatively assumed to be taken up entirely by the bolts, which is true only if there is no preload in the bolts. The vibratory load in each bolt is (28 lbs) / (8 bolts) = 3.5 lb. The bolt alternating stress is (3.5 lb) / (0.2260 sq in) = 16 psi. Assuming a theoretical stress concentration factor of 10 for the bolt threads and head/shank fillet, the bolt alternating stress is less than 200 psi. This stress level does not challenge the fatigue capability of the SA-193 Type B8, Class 2 bolting material and fatigue will not be a problem during Normal Conditions of Transport.

Evaluation of Fittings for Assembly Torque Loads

The fittings are welded to the underside of the drum top plate using 0.12-inch fillet welds. The welds are evaluated for the torsional loads resulting from application of the full bolt assembly torque at the threads, as could occur if the threads were seized.

The maximum applied torque is 50 lbf-ft. The outer diameter of the fittings is 1.125 inches. The mean diameter of the weld is 1.125 + 0.12 = 1.245 inches. From Reference 6.2, the torsional moment of inertia is found as follows:

$$J = 2 \cdot \pi \cdot b \cdot r^3$$

where b is the weld throat = 0.707 h = (0.707)(0.12) = .0848 inch, and r is the mean radius of the weld = 1.245 / 2 = 0.6225 inch. Therefore,

$$J = 2 \cdot \pi \cdot (0.0848) \cdot (0.6225)^3 = 0.1285 \text{ in}^4$$

The maximum assembly torque is (50)(12) = 600 lbf-in., and the torsional shear stress in the weld is:

$$S_s = \frac{T \cdot r_m}{J} = \frac{(600 \text{ lbf} - \text{in}) \cdot (0.6225 \text{ in})}{(0.1285 \text{ in}^4)} = 2{,}900 \text{ psi}$$

The maximum shear stress in the weld is evaluated using 304L stainless steel properties. The maximum shear stress is compared to a limit of 0.5 S_y = 0.5 (25,000 psi) = 12,500 psi. The maximum shear stress of 2,900 psi is well below the limit of 12,500 psi.

4.2 Evaluation of Reduced External Pressure on CV's and Overpack

The package is required to withstand a reduction in external pressure to 3.5 psia. This results in a differential pressure of 11.2 psi (14.7 – 3.5) across the drum shell and liner. This pressure differential exists as an internal pressure for the drum shell, and an external pressure for the drum liner. The components are evaluated for the differential pressure below.

Primary Membrane Stress

The primary membrane stresses on the drum and liner shell regions are found below:

$$P_m = \frac{P \cdot R_m}{t}$$

For the liner shell:

$$P_m = \frac{(11.2)\cdot(8.25+.048)}{2\cdot(.048)} = 970 \text{ psi}$$

For the drum shell:

$$P_m = \frac{(11.2)\cdot(18.25+.048)}{2\cdot(.048)} = 2140 \text{ psi}$$

Primary Membrane Plus Bending Stress

The primary membrane plus bending stress in the drum and liner are maximum at the junction between the shell and ends. The stresses are found from Abaqus finite element analyses of these components.

The primary membrane plus bending stress in the liner is shown in Figure 4.2-1. The maximum stress at the junction between the shell and the bottom of the liner is 28,000 psi, which slightly exceeds the yield strength of the material. The bottom of the liner exhibits significant membrane behavior, which provides a stiffening effect. The primary membrane stress in the bottom of the liner is 10,350 psi, which is well below the yield strength of the 304L material of 25,000 psi.

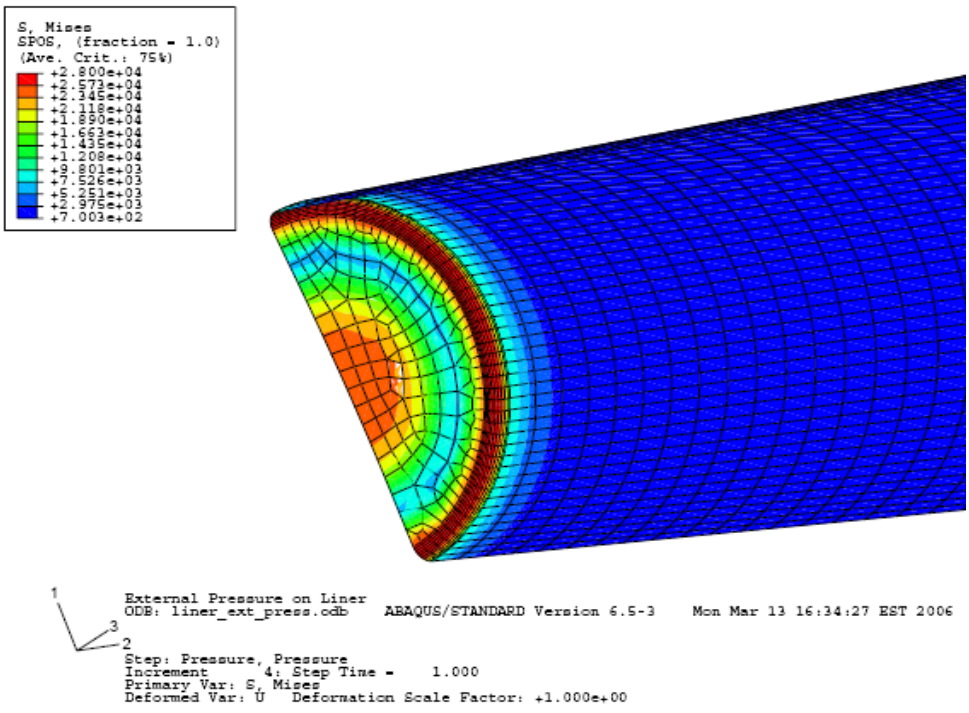

Figure 4.2-1 – Liner Primary Membrane Plus Bending Stress, 11.2 psi External Pressure

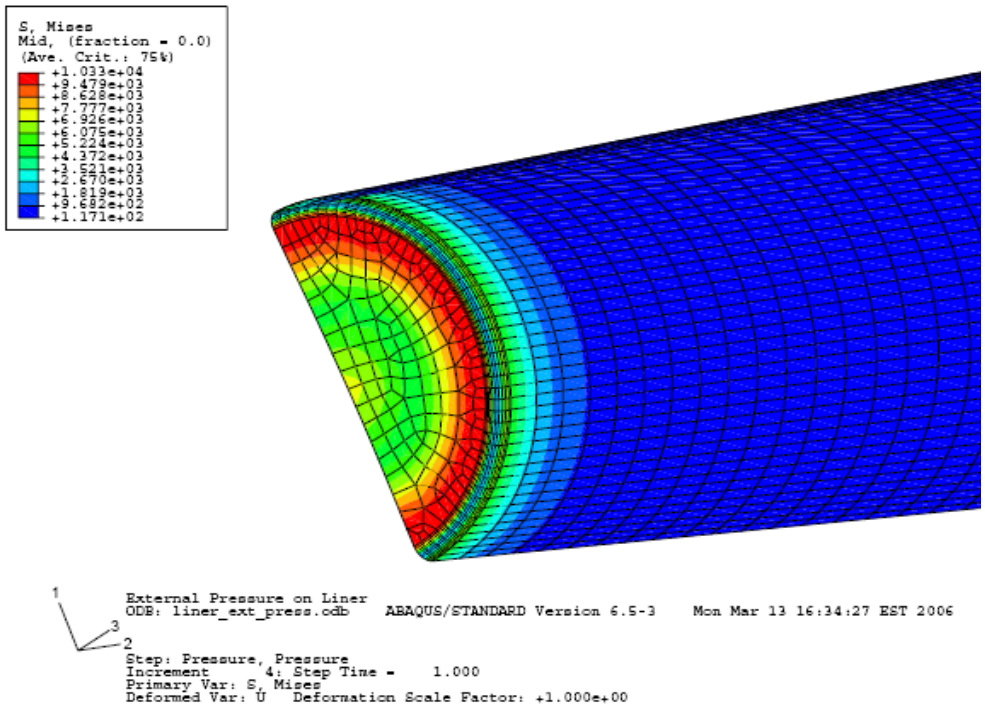

Figure 4.2-2 - Primary Membrane Stress in Liner, 11.2 psi External Pressure

The drum shell is evaluated for an internal pressure of 11.2 psi, using an Abaqus finite element analysis. The primary membrane and primary membrane plus bending stresses in the drum are shown in Figures 4.2-3 and 4.2-4 respectively. It is seen that the maximum primary membrane stress of 26,700 psi, and the primary membrane plus bending stress of 32,300 psi exceeds the minimum specified yield strength of the 304L stainless steel material of 25,000 psi. The drum shell provides sufficient load-carrying capacity even though the yield strength is exceeded, by membrane stiffening of the drum bottom, and by strain hardening of the 304L stainless steel material. The plastic strain in the drum shell at the shell to bottom junction is 0.00233 due to the internal pressurization, which is insignificant compared to the strains experienced during NCT drops and does not degrade the capability of the drum shell.

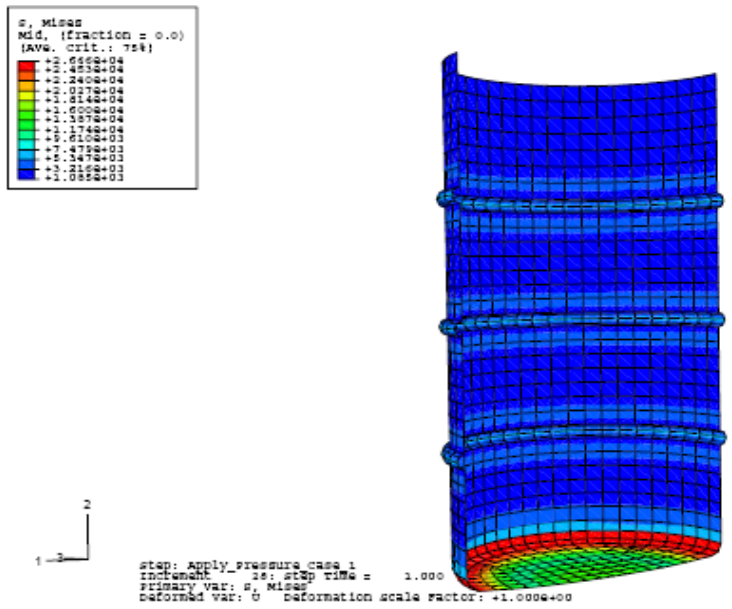

Figure 4.2-3 - Primary Membrane Stress in Drum, 11.2 psi Internal Pressure

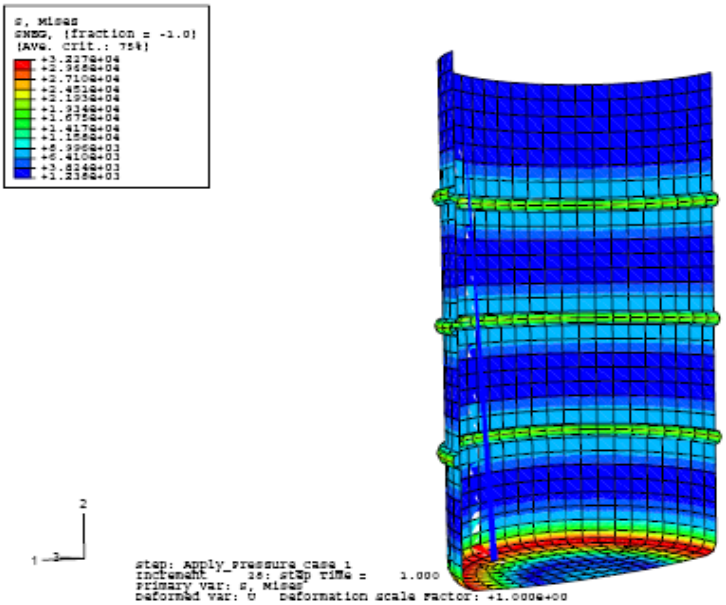

Figure 4.2-4 – Primary Membrane Plus Bending Stress in Drum, 11.2 psi Internal Pressure

Buckling of Liner

Buckling of the liner is evaluated using the method prescribed in ASME III, NB-3133.3:

Liner characteristics: $D_o = 8.25 + 2(0.048) = 8.198$ in $L = 29.5$ in $T = 0.048$ in
$D_o / T = 8.198 / 0.048 = 174$ $L / D_o = 29.5 / 8.198 = 3.53$

For SA240-304L, A = 0.00016, from ASME Section II, Part D, Subpart 3, Figure G

From Figure HA-3: B = 2300 at 100 F; B = 2000 at 400F; interpolating gives B = 2100 at 300F

The maximum allowable pressure is:

$$P_a = \frac{4 \cdot B}{3 \cdot \frac{D_o}{T}} = \frac{4 \cdot B}{3 \cdot (174)} = 0.0077 \cdot B \rightarrow P_a = 16.2 \text{ psi at 100 F, and 15.3 psi at 300 F}$$

The applied external load on the liner is less than that allowed by the ASME Code.

4.3 Evaluation of Increased External Pressure on Overpack

The package is required to withstand an increased external pressure of up to 20 psia. This imposes a possible pressure differential of 20 – 14.7 = 5.3 psid across the liner and drum. The imposed pressure differential acts external to the drum, and internal to the liner. The liner is subjected to a 5 psi pressure test during fabrication, which is bounded by the 5.3 psi condition. The effect of these loads is discussed below.

Primary Membrane Stress in Liner

The primary membrane stresses on the drum and liner shell regions are found below:

$$P_m = \frac{P \cdot R_m}{t}$$

For the liner shell:

$$P_m = \frac{(5.3) \cdot (8.25 + .048)}{2 \cdot (.048)} = 460 \text{ psi}$$

The primary membrane stress is well below the limit of S_m = 16,700 psi.

Stresses in the liner bottom for the 5.3 psi internal pressure are bounded by those determined in 4.2 above for the 11.2 psi external pressure.

Drum Shell

The overpack assembly without contents (CV and load distribution fixtures) is evaluated for an external pressure of 5.3 psi, using an Abaqus finite element analysis. This analysis credits the stiffening effect of the drum foam and fiberfrax in preventing excessive distortion of the drum and liner. The primary membrane plus bending stress for the 5.3 psi external pressure condition is 9,260 psi, which is well within the yield strength of the drum and liner 304L stainless steel material. Refer to Figure 4.3-1 for a contour plot of the primary membrane plus bending stress in the drum and liner.

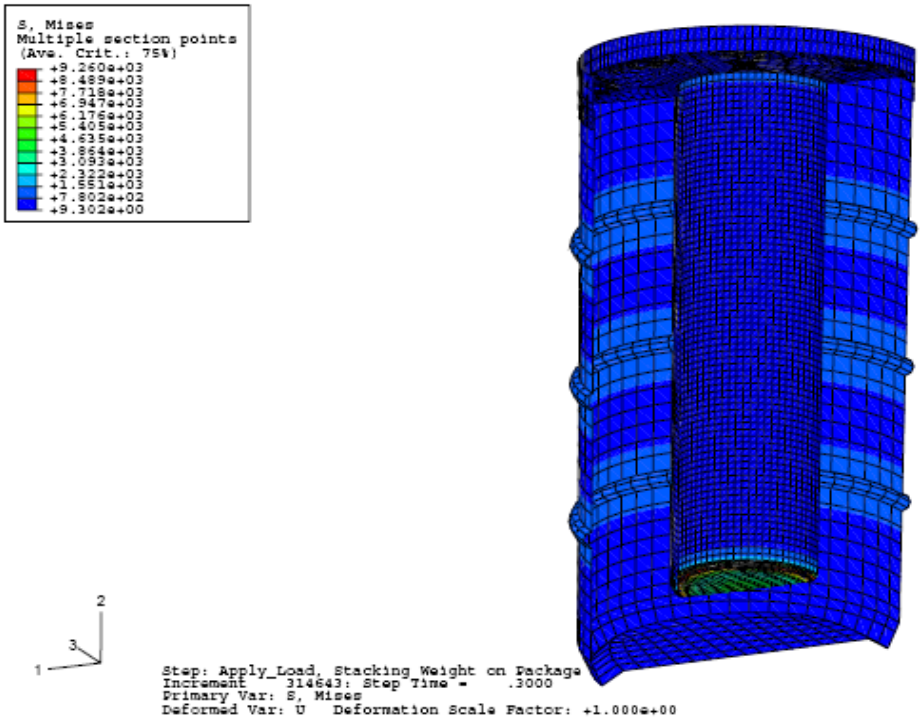

Figure 4.3-1 – Primary Membrane Plus Bending Stress for 5.3 psi External Pressure

4.4 Evaluation of Overpack for Static Compression Loading

The package must be evaluated for the greater of: (1) Five times the weight of the package, imposed on the end of the package, or (2) A load equivalent to 2 psi pressure applied over the projected area of the end of the package. For the 9977 package, these loads are (1) 5 x 350 = 1750 pounds, or (2) $2 \cdot (\pi/4) \cdot 18.5^2 = 537$ pounds. The governing case of 5 x package weight is evaluated below.

Since the drum contents provide significant stiffening of the shell, adequate capability exists to withstand the applied loads. The package, without containment vessel and other contents, is evaluated by Abaqus finite element analysis to determine stresses and deflections in the overpack for the imposed load of 1750 pounds. Drum, top plate, and liner stresses are shown in Figure 4.4-1. The

maximum primary membrane plus bending stress is found to be less than 14,000 psi, which is well below the yield strength of the 304L stainless steel material of 25,000 psi.

The maximum deflection within the drum is less than 0.04 inch, see Figure 4.4-2. The small deflection is approximately 10 percent of the axial clearance between the package contents and the drum lid, and the drum contents are therefore not loaded by the stacking conditions.

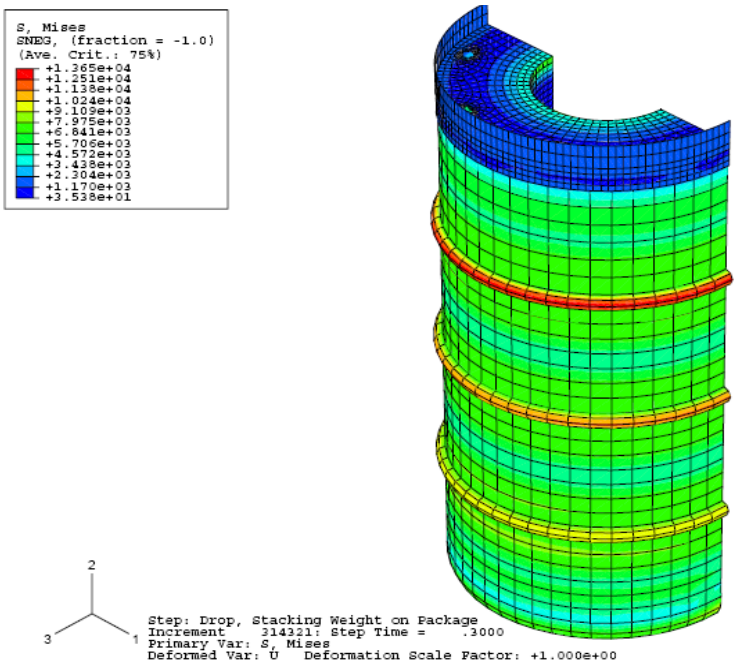

Figure 4.4-1 – Stresses in 9977 Overpack for Stacking Condition

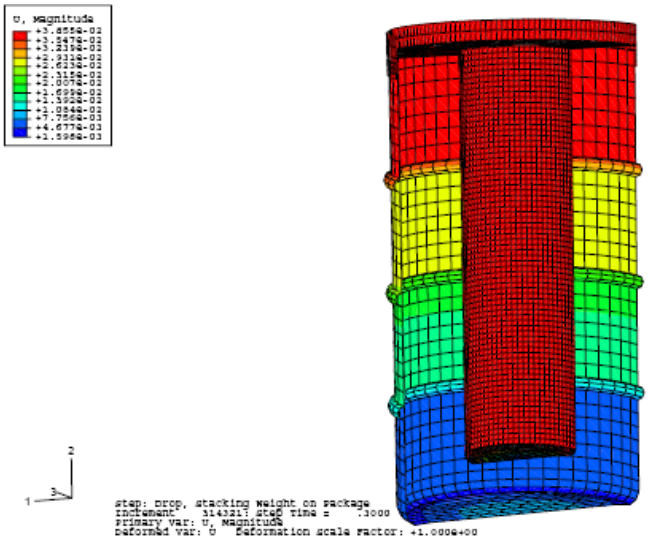

Figure 4.4-2 – Deflections in 9977 Overpack and Liner for Stacking Condition

4.5 Evaluation of Lifting Stresses on Package Components

Stresses in the 9977 package lifting features are evaluated below for the loads applied during lifting of the package and the CV subassembly. The lifting features shall withstand the maximum loads imposed during lift without exceeding a maximum stress equal to the lesser of S_y / 3 or S_u / 5 (reference 6.11). For the 304L stainless steel components, the stress limit is min (25,000 / 3, 70,000 / 5) = 8330 psi.

Lifting of 9977 Package

Lifting of the package is achieved by means of the 1-inch holes in the drum flange. Eight holes are provided, equally spaced around the periphery of the flange. The stresses in the flange ligaments are evaluated below, conservatively assuming that only two of the holes are used for lifting. It is assumed that a maximum sling angle of 15-degrees is used, consistent with good lifting practices.

Package weight = 350 lbs, reference [6.3].

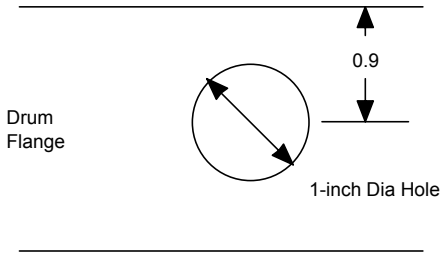

For a 15-degree sling angle, the load in each flange ligament is:

$$P_{lig} = \frac{350\ \text{lb}}{2 \cdot \cos(15)} = 182\ \text{lb}$$

Shear Stress in Ligament:

The area for double shear is 2(0.4 inch min ligament)(.1875 thick) = 0.15 sq. in. The shear stress is (182 lb) / (0.15 sq.in.) = 1220 psi. For pure shear, the stress limit is 0.5 times the limit in tension, or (0.5)(8333 psi) = 4170 psi. Adequate margin exists for shear loads.

Bearing Stress at Hole:

Assuming a ¾-inch shackle or hook is used for lifting, the bearing area is (.75)(.1875) = .1406 sq.in. The bearing stress is (182 lb) / (0.1406 sq in) = 1300 psi. The bearing stress is well with in the stress limit of 8330 psi.

Bending stresses in the flange hole ligaments are low, since the height of the ligament is approximately the same as the hole radius.

Lifting of the 5-inch and 6-inch CV Assemblies

The CV assemblies are lifted using a lift fixture which engages the blind holes in the CV closure nut. These holes are 0.31-inch diameter, 0.25-inch deep, and are centered 0.30 inch below the top of the nut. The 6CV assembly, when filled with the design weight payload (100 lbs) weighs less than 160 pounds total (Appendix 2.13). The 6CV total weight bounds that of the 5CV. Shear and bearing stresses in the ligaments above the holes are calculated below:

Shear Area = 2 (.30 - .31 / 2) (0.25) = 0.0725 sq.in

Shear Stress = (160 lb) / (0.0725 sq in) = 2206 psi

The shear stress in the ligaments is less than the shear allowable for 304L stainless steel of 4167 psi.

Bearing Stress:

Bearing area = 2 (.31) (.25) = 0.155 sq. in.

Bearing Stress = (160 lb) / (0.155 sq in) = 1032 psi

The bearing stress in the ligaments is less than the allowable stress of 8330 psi.

4.6 Evaluation of Tiedown Stresses on Package Components

4.6.1 Purpose

The purpose of this engineering calculation is to evaluate the structural integrity of the drum rim of the 9977 package subjected to the tie-down loads as required by 10CFR71.45.

4.6.2 Scope

The scope of this analysis is to evaluate the adequacy of the tie-down system of the 9977 package when subjected to the transportation loads specified in 10CFR71.45.

4.6.3 Conclusion

The maximum values of von Mises intensities and effective plastic strains are given Table 4.6-1. Although the maximum stress intensity in the local area exceeds the yield stress of stainless steel 304L, the rim will not rupture since the maximum values of the stress intensity and the equivalent plastic strain as given in Table 4.6-1 are below the rupture values.

Table 4.6-1 - Summary of Analytical Results and Material Properties

Maximum Calculated Values		Material Properties		
Stress Intensity (ksi)	Equivalent Plastic Strain	Yield Stress (ksi)	Ultimate Stress (ksi)	Rupture Strain
63.62	0.176	25.0	81.81	0.3

4.6.4 Input Data and Assumptions

Input Data

The components, weight and geometric configuration and material properties of the 9977 Package are given in Appendix 2.5.

The tie-down loads are given in References 6.6 and 6.7.

Assumptions

The following assumptions apply the retention system of the retention of the 9977 package.

1. The package is fixed to the conveyance floor with chains through four of the eight 1-inch diameter drain holes located in the drum rim. The arrangement and orientation of these chains is shown in Figures 4.6-1 and 4.6-2.

2. The bottom of the package is assumed to be blocked as recommended by IAEA Safety Series 37 (Reference 6.8), Section 2.68 and IAEA Safety Guide ST-2 (Reference 6.7).

3. The pretension loads in the chains are negligible.

Calculation Continuation Sheet

Calculation No.	Sheet No.	Rev.
M-CLC-G-00357	21	0

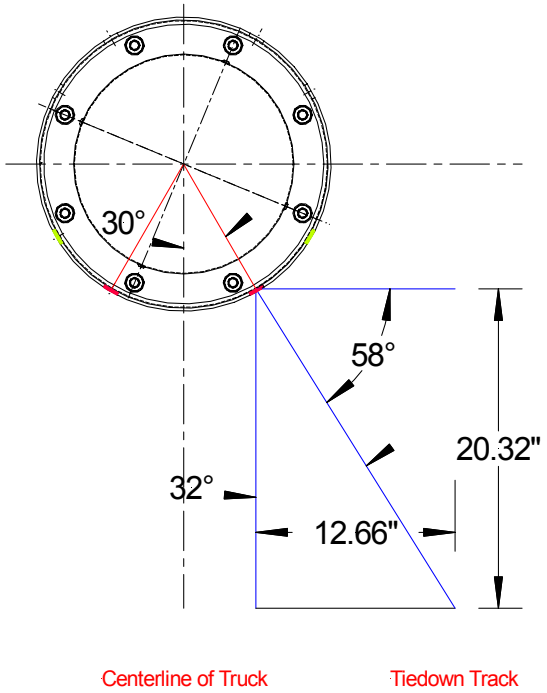

Figure 4.6-1 - Configuration of Tie-Down Chains – Top View

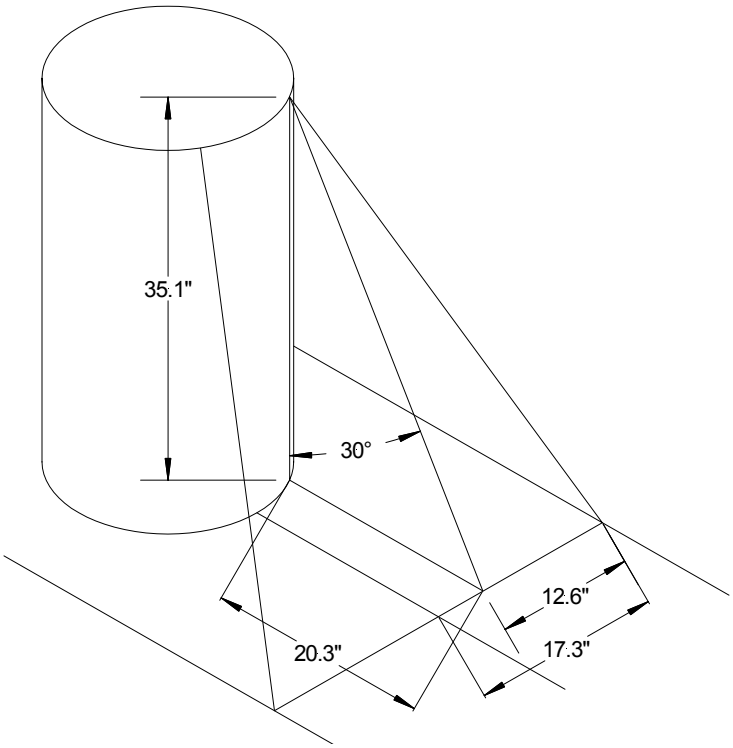

Figure 4.6-2 - Configuration of Tie-Down Chains – Isometric View

4.6.5 Discussion of Analysis

4.6.5.1 Description of Methodology

The loads defined in Reference 6.7 are given in Table 4.6-2.

Table 4.6-2 - Acceleration Factors for Type B Package Retention System

Acceleration Factors		
Longitudinal	Lateral	Vertical
10 G	5 G	2 G

Rigorous calculations of the loads in retention systems arising from accelerations are difficult because of the numerical singularities involved in solving simultaneous equations. Therefore the simplified yet conservative method discussed in Reference 6.7 is customarily used. However, in the present case, the main concern is the structural integrity of the drum rim subjected to the tie-down loads and the simplified method is not applicable in this case.

To avoid the problem of numerical singularities, the retention system subjected to the equivalent static G loads is analyzed dynamically by using explicit numerical integration. The ABAQUS/Explicit computer code, version 6.5 (Reference 6.9) was used to perform the computations. The finite-element meshes were generated using the MSC/PATRAN computer program (Reference 6.10).

4.6.5.2 Description of Finite-Element Model

The finite-element model of the entire 9977 package retention system is shown in Figure 4.6-3. It consists of a drum body, a drum rim, a drum bottom, four chains, four hooks and a truck floor and a point mass. The rim, hooks, drum bottom are modeled by 3D shell elements (Type S4R in ABAQUS computer code). The chains are represented by 3D truss elements (Type T3D2). The drum body and the truck floor are modeled using the 3D rigid elements (Type R3D4). The weight of the package is represented by a point mass (Type MASS).

Figures 4.6-4 through 4.6-6 show the finite-element models of the drum body, the drum rim and the drum bottom, respectively. Figure 4.6-7 is the blow up view of the chain hook and it also shows the connection between the rim, the hook and the chain.

Figure 4.6-8 depicts the point mass element and the applied concentrated forces. The point mass element is located at the center of gravity of the 9977 package and represents the mass of the package with the contents. The total weight of the loaded package is 350 pounds and thus its mass is:

$$MASS = \frac{350lb}{386.4in/\sec^2} = 0.9058\frac{lb-\sec^2}{in}$$

The location of the point mass element coincides with the location of the reference node for the drum-body rigid elements.

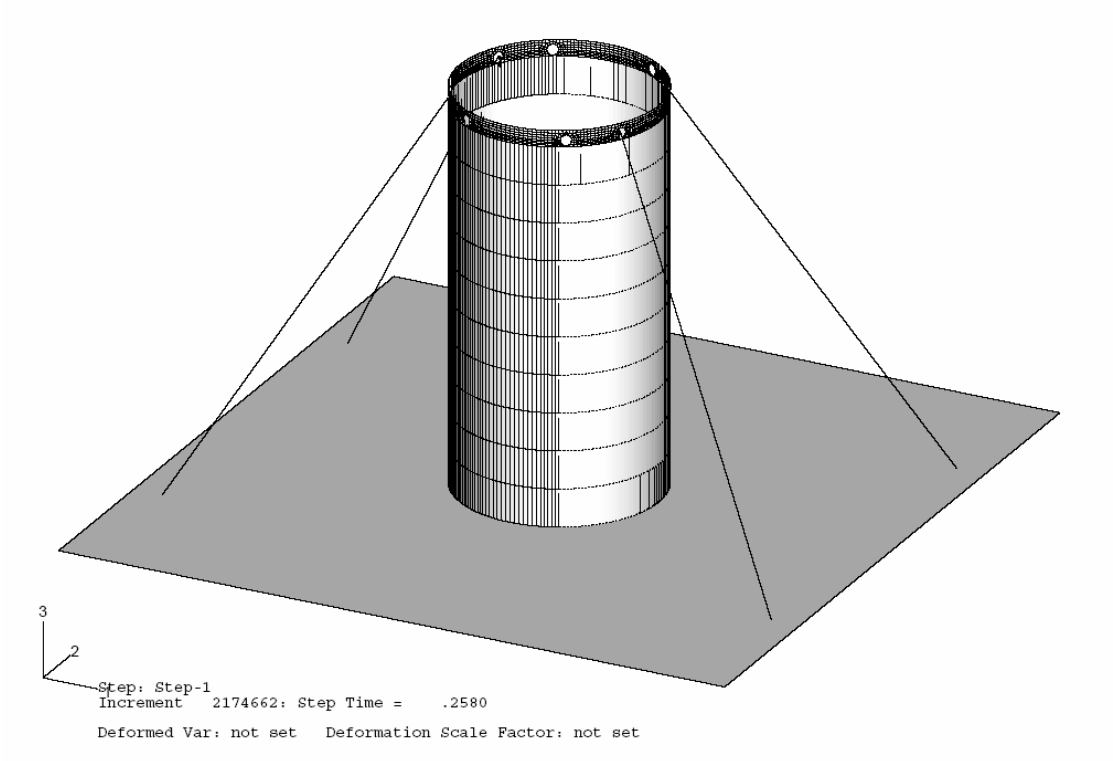

Figure 4.6-3 - Finite-Element Model of 9977 Retention System

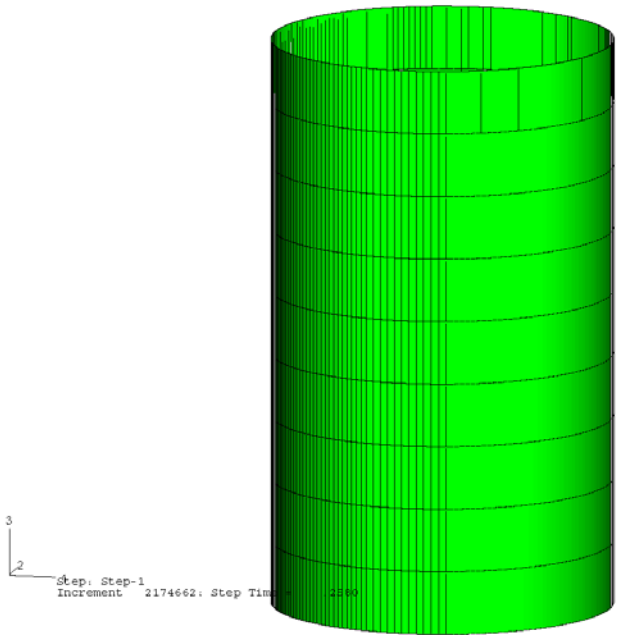

Figure 4.6-4 - Finite-Element Model of 9977 Drum Body

Calculation Continuation Sheet

Calculation No.	Sheet No.	Rev.
M-CLC-G-00357	24	**0**

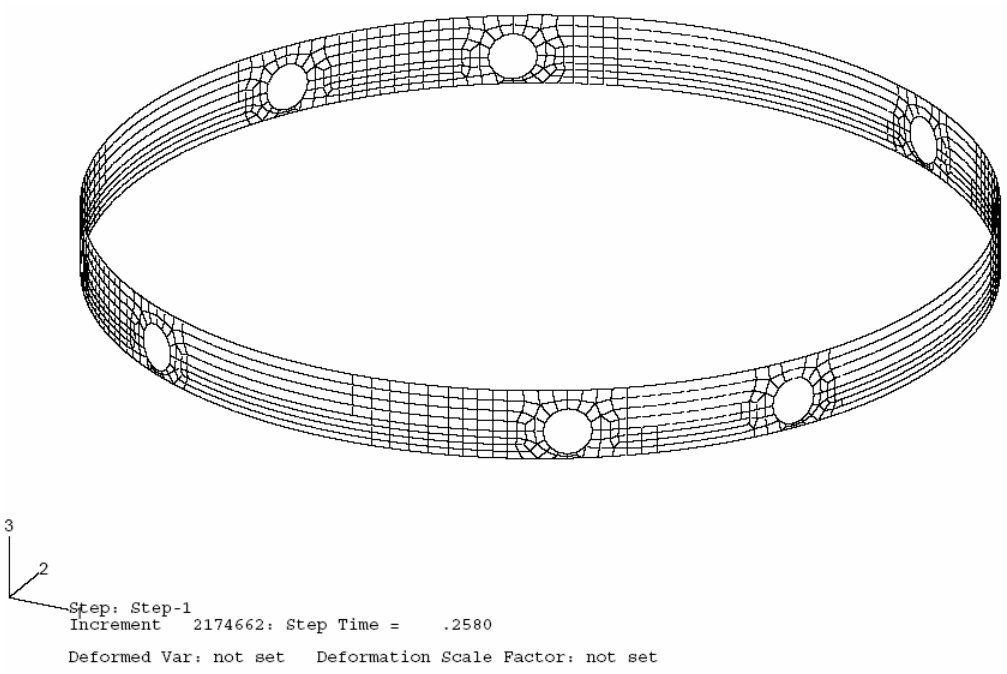

Figure 4.6-5 - Finite-Element Model of 9977 Drum Rim

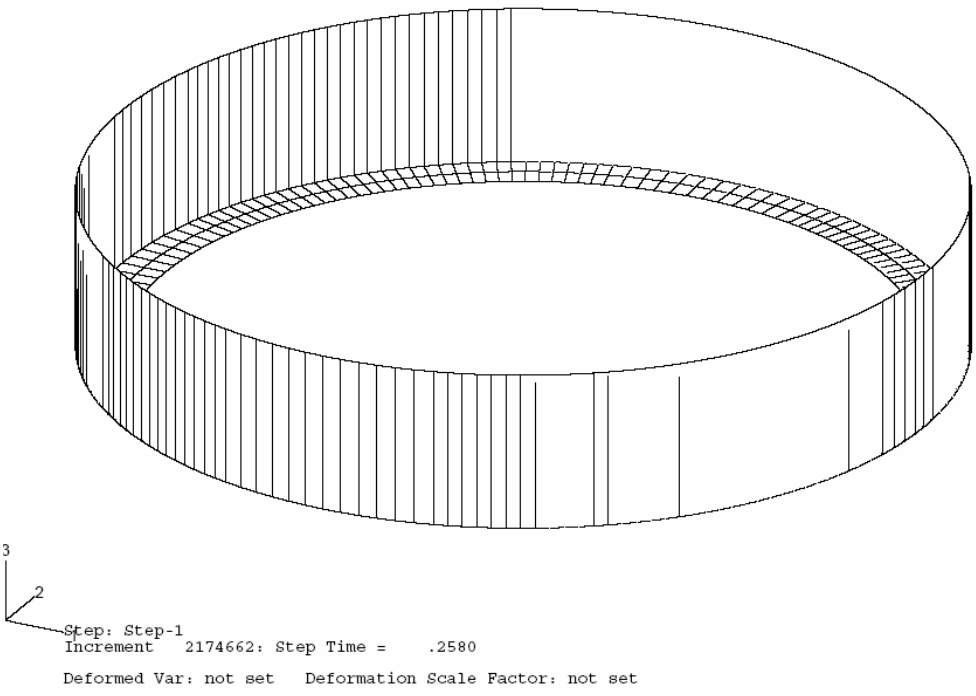

Figure 4.6-6 - Finite-Element Model of 9977 Drum Bottom

Calculation Continuation Sheet

Calculation No.	Sheet No.	Rev.
M-CLC-G-00357	25	**0**

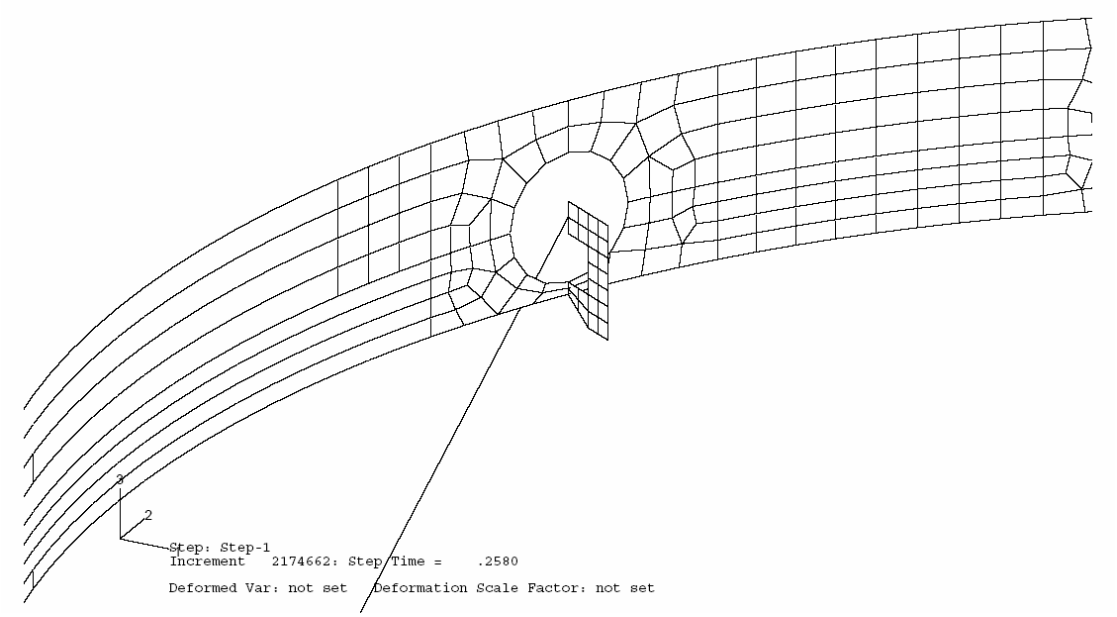

Figure 4.6-7 - Finite-Element Model of Hook-Chain-Rim Connection

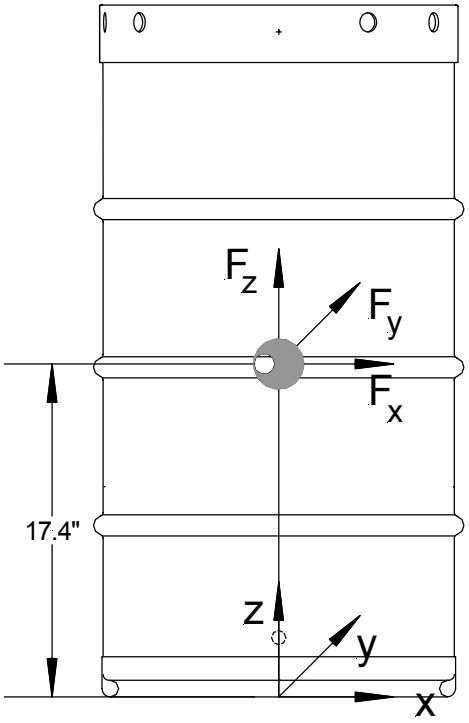

Figure 4.6-8 - Locations and Orientations of Point Mass and Applied Forces

4.6.5.3 Applied Loads

The applied concentrated forces corresponding to the tie-down loads are calculated as follows.

$F_x = 10 \times 350 = 3500 lbs$ in the longitudinal direction

$F_y = 5 \times 350 = 1750 lbs$ in the lateral direction

$F_z = (2-1) \times 350 = 350 lbs$ in the vertical direction

The gravitational load is included in F_z as a negative force. These concentrated forces are applied gradually the smooth ramp forces from 0 to 0.1 seconds to reduce the structural acceleration. These forces then remain constant form 0.1 to 0.4 seconds to ensure that there is enough time for the structure oscillation to die down. Figure 4.6-9 shows the time-history profile of the applied forces.

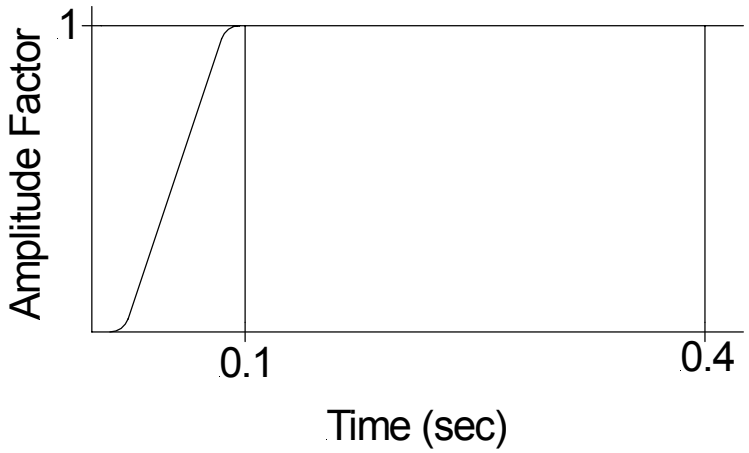

Figure 4.6-9 - Time-History of Applied Loads

4.6.5.4 Boundary Conditions

The floor rigid element and the lower ends of the chains are fixed. The node of the drum bottom model located at the x most point has zero x translation; whereas, the node of the drum model located at the y most point has zero y translation to represent the chock constraint.

4.6.5.5 Contact Conditions

The contact conditions between the drum bottom and the floor are simulated by using the general contact option available in the ABAQUS/Explicit computer program.

4.6.6 Analytical Results

4.6.6.1 Kinetic Energy of Point Mass

Figure 4.6-10 is the time-history plot of the point mass model which represents the mass of the package. At the time of 0.25 seconds after the tie-down loads are applied, the kinetic energy of the point mass approaches zero. In other words, the responses of the package nearly reach static at this instant.

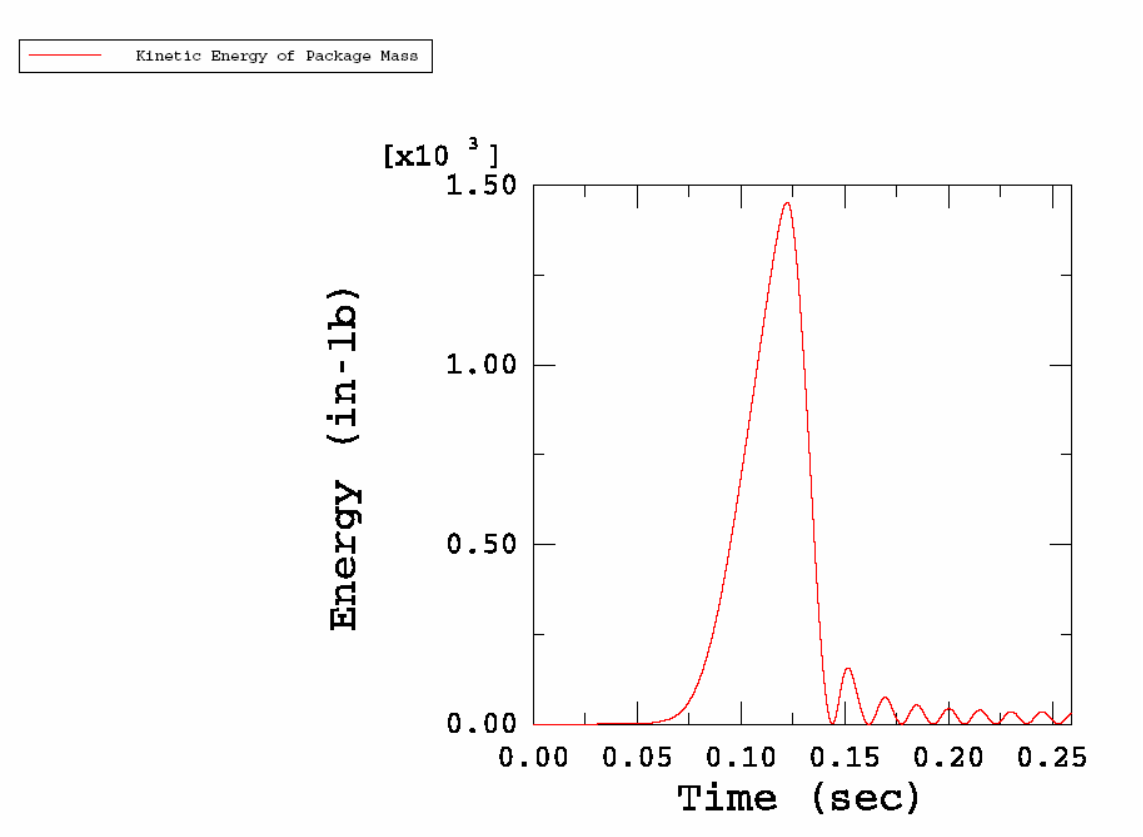

Figure 4.6-10 - Time History of Point-Mass Kinetic Energy

4.6.6.2 Stress and Strains in Drum Rim

Figure 4.6-11 shows the stress magnitudes and distribution in drum rim. The maximum value of the stress intensities is 63.62 ksi.

Figure 4.6-12 shows the magnitudes and distribution of the equivalent plastic strain in the drum rim. Figure 4.6-13 is the blowup view of the high strain region. The maximum value of the equivalent plastic strain is 0.176.

Calculation Continuation Sheet

Calculation No.	Sheet No.	Rev.
M-CLC-G-00357	28	**0**

Consequently, the analytical results show that the tie-down loads cause local yielding but the rim will not rupture. It is noted that the "hook" connection to the drum rim is conservatively modeled as a line contact. Consequently, the applied loads are concentrated when in actuality the hook will have a finite width and the associated loads distributed. The distributed loads will have a lower stress intensity and lower equivalent plastic strain.

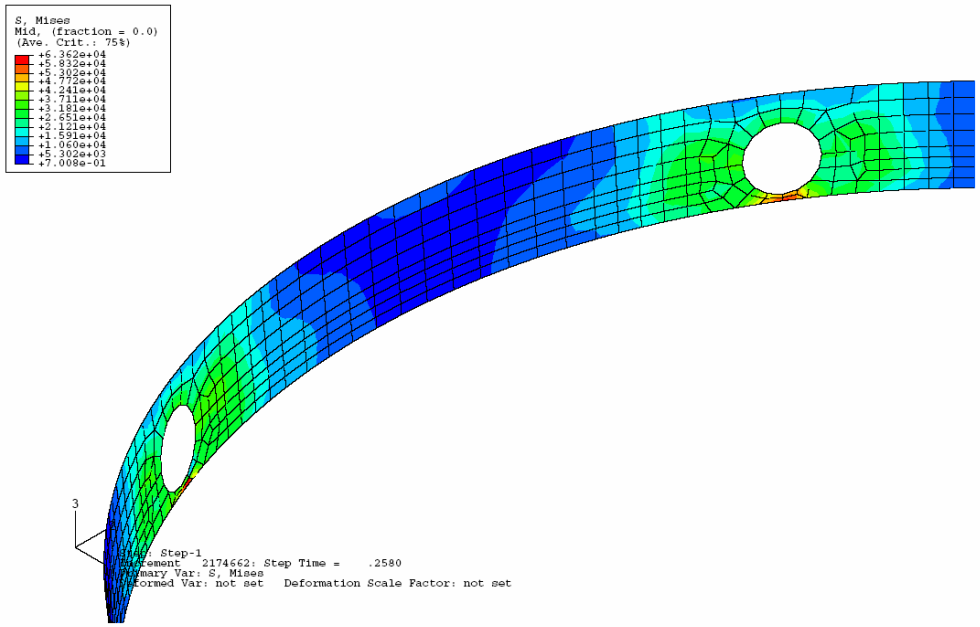

Figure 4.6-11 - Stress Intensities in Drum Rim

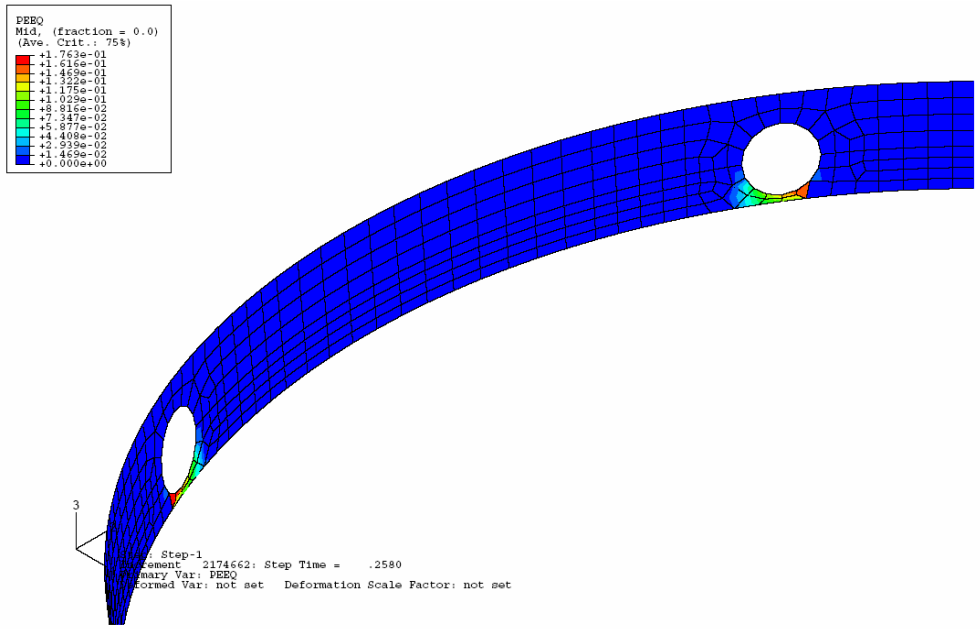

Figure 4.6-12 - Equivalent Plastic Strains in Drum Rim

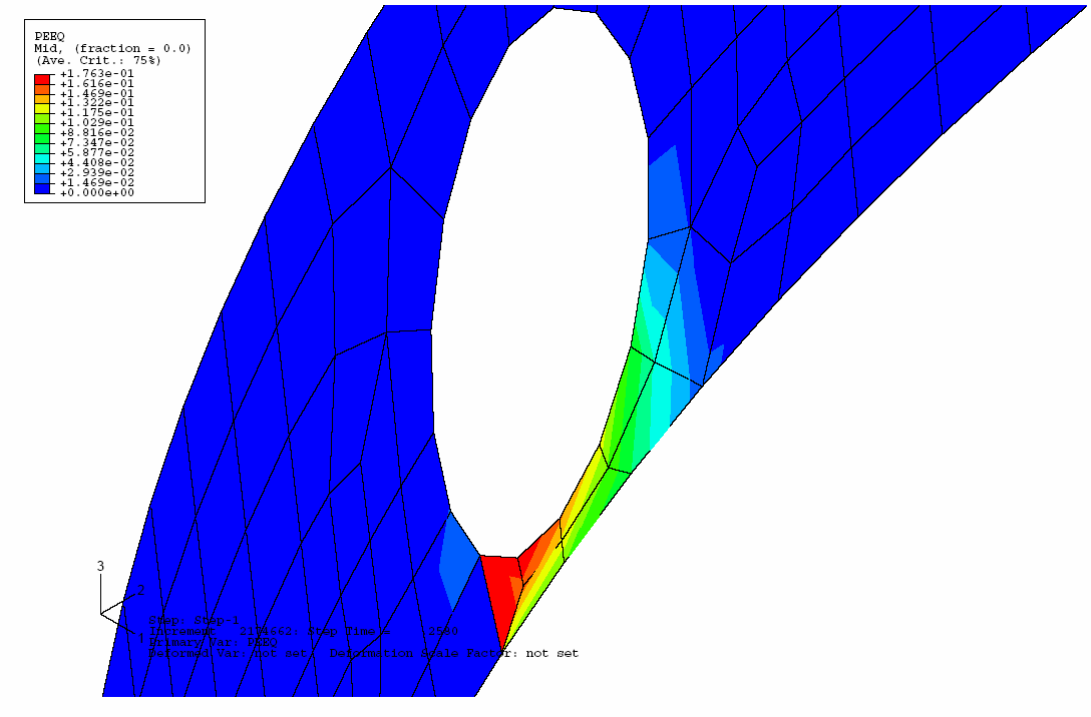

Figure 4.6-13 - Blow-Up View of Equivalent Plastic Strains in Drum Rim

4.6.6.3 Tension Forces in Chains

Figures 4.6-14 through 4.6-17 show the time-history plots of the tensile axial stresses in the chains. The stress waves in the chains propagate rapidly between anchor points and the stresses in chain 2 and 3 still oscillate over a time of 0.25 seconds after the tie-down loads are applied. Since the objective of this analysis is the structural integrity of the drum rim subjected to the tie-down loads, the chain stresses are estimated from these figures, for informational purposes only. as follows.

S11 in Chain 1 = 0.0

S11 in Chain 2 = 22,500.0 psi

S11 in Chain 3 = 26,000.0 psi

S11 in Chain 4 = 0.0

The cross section areas of the chain models are set equal to 0.1243 in^2. Thus, the tension forces in the chains are:

$P_1 = 0.0$

$P_2 = 22{,}500 \times 0.1243 = 2{,}797$ lbs

P_3 = 26,000.0 x 0.1243 = 3,232 lbs

P_4 = 0.0

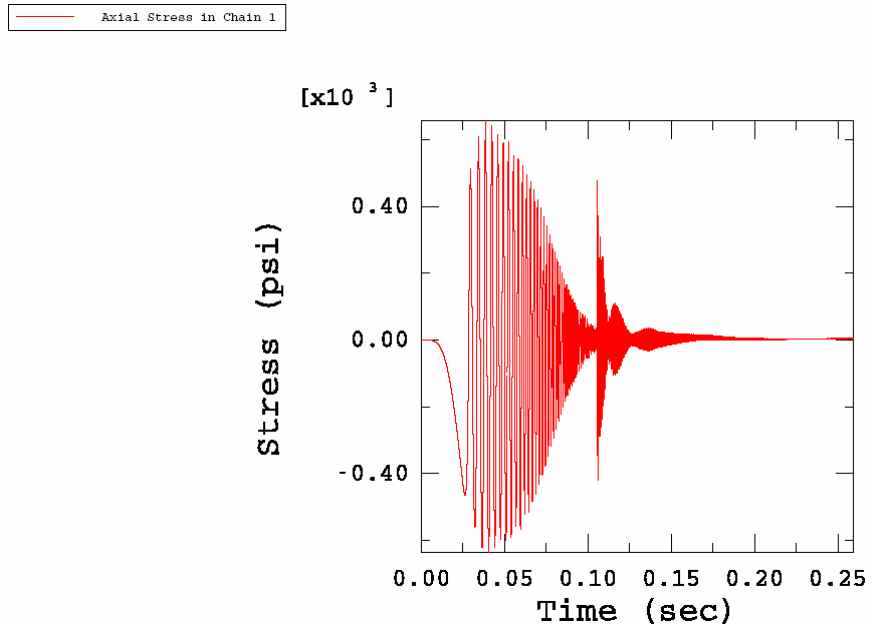

Figure 4.6-14. Time History of Stresses in Chain 1

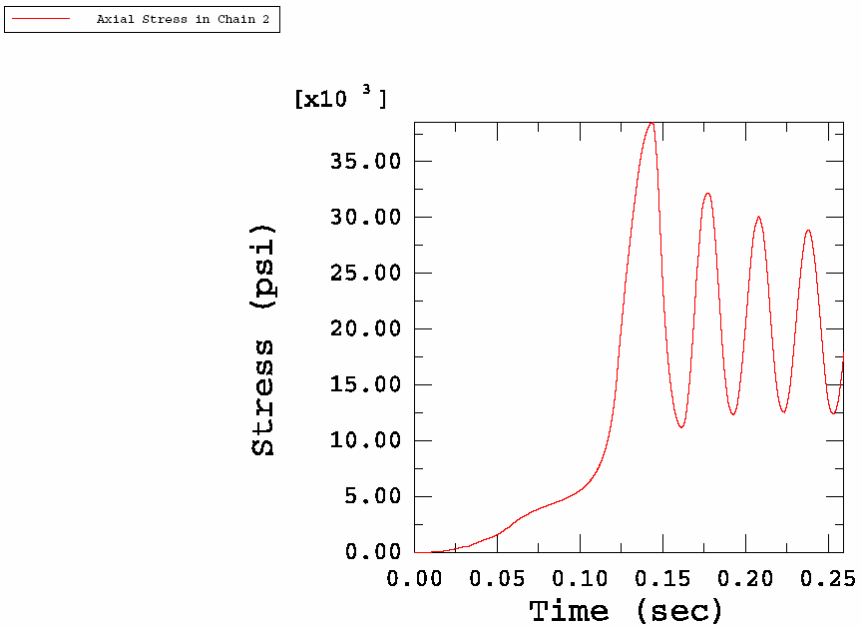

Figure 4.65-15. Time History of Stresses in Chain 2

Calculation Continuation Sheet

Calculation No.	Sheet No.	Rev.
M-CLC-G-00357	31	0

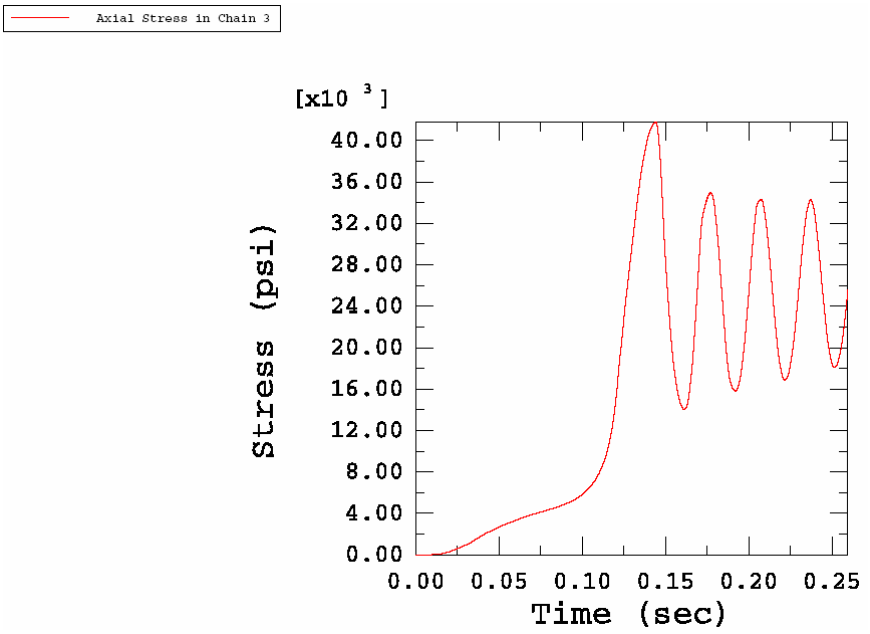

Figure 4.6-16 - Time History of Stresses in Chain 3

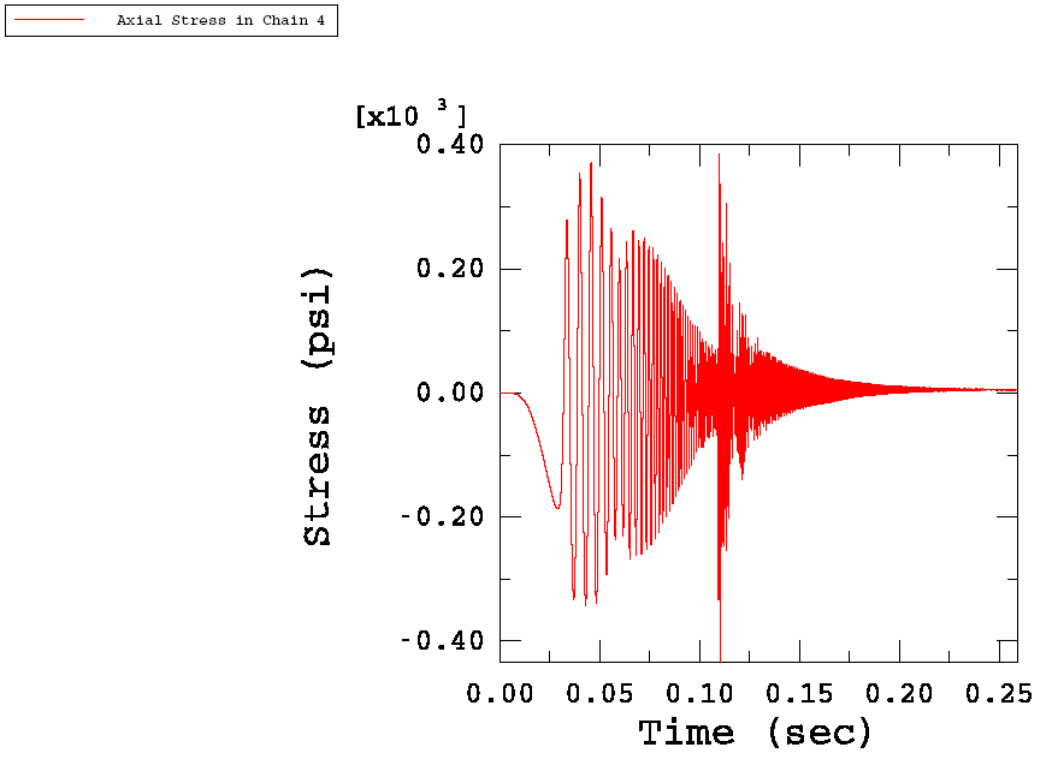

Figure 4.6-17 - Time History of Stresses in Chain 4

4.7 Evaluation of Stresses in Package Components Due to Differential Thermal Expansion

Expansion of the various components of the 9977 package as a result of temperature changes during NCT requires investigation. The thermal stresses within the containment vessels are investigated below. The design of the 9977 package accounts for thermal expansion by using similar materials with the same coefficient of thermal expansion for construction of the containment vessels, and by providing clearances that would not result in material interferences. The radial clearance between the 6CV (304L stainless steel) and load distribution fixtures (6061 aluminum) is a minimum at -40F, and is evaluated below.

Maximum OD of 6CV at Flange = 7.12 in + 0.01 tolerance = 7.13 in

Minimum ID of upper LDF = 7.15 in – 0.01 tolerance = 7.14 in

Coefficients of linear expansion (ASME Code, Section II):

304 Stainless Steel: $\alpha = 8.5 \times 10^{-6}$ in/in/°F
6061 Aluminum: $\alpha = 12.1 \times 10^{-6}$ in/in/°F

The clearance change in going from 75F to -40F is:

$$\delta = D \cdot \Delta\alpha \cdot \Delta T = (7.14) \cdot (8.5 - 12.1)(10^{-6}) \cdot \left[75 - (-40)\right] = -0.0030 \; in$$

The change in clearance is negative, so the clearance is less at -40F than at 75F. However, the initial clearance of (7.14 – 7.13 = 0.01 inch) is sufficient to prevent interference. The minimum clearance at -40F is 0.010 – 0.0030 = 0.007 inch.

The bottom load distribution fixture has a nominal clearance of (6.75 – 6.625 =) 0.125 inch diametral at room temperature. Even with tolerances taken into account, the bottom load distribution fixture has sufficient clearance with the 6CV to prevent interference at a reduced temperature of -40F.

Differential thermal expansion between the load distribution fixtures (aluminum) and the liner (304L stainless steel) is also evaluated as follows. The load distribution fixtures are nominally 8.00 inches outer diameter. The liner inner diameter is nominally 8.25 inches. Even with tolerances considered, the nominal clearance of 0.25-inch is sufficient to ensure clearance exists at elevated temperatures.

Axial clearance between the 6CV and the liner and lid is approximately 0.25-inch nominally at room temperature. This clearance is also sufficient to ensure clearance exists at elevated temperatures.

4.8 Evaluation of Freezing Water on Package Components

Calculation Continuation Sheet

Calculation No.	Sheet No.	Rev.
M-CLC-G-00357	33	**0**

Tests performed on the Prototype SN-2 showed that the lid to top deck closure does not preclude the possibility of water ingress into the drum cavity, Reference 6.12. During the water spray test 13.6 lbs of water entered the drum cavity. The weight of water ingress shows that the liner was full.

Using nominal dimensions of the liner, 6CV and its load distribution fixtures the free volume in the liner excluding the annular region between the liner and drum lid was calculated to be 384 in^3.

Liner volume below drum lid: 8.25-inch diameter by (29.6-4.88)inch deep; 1320.77 in^3

6CV external volume (Appendix 2.13): 792 in^3

Top and Bottom Load Distribution Fixtures (Appendix 2.13): (39.42+105.27)in^3 = 144.69 in^3

The available volume: (1320.77-(792.57+144.69))in^3 = 383.5 in^3

Assuming the density of water is 62.426 lb/ft^3; the equivalent mass of water is 13.85 lbs.

The configuration of the package is such that water can enter the crevices between the drum top plate and the closure lid. This water could subsequently freeze and become entrapped in the annular region between the CV and the liner. The effect of the subsequent pressure buildup on the integrity of the liner is evaluated below.

Water properties: at 4° C $\rho = 62.426 \frac{lb}{ft^3}$ $\upsilon_{water} = 0.016019 \frac{ft^3}{lb}$

Ice at 32°F: $\upsilon_{ice} = 0.01747 \frac{ft^3}{lb}$

Part dimensions: Drum Liner ID = 8.25 in Liner Thickness = 0.048 in.
C.V. OD = 6.625 in

Assuming the expansion of the water is taken up entirely by the liner, and that the expansion is all radial (no axial expansion), consider a 1-inch ring of water turning to ice:

$$V_w = \frac{\pi}{4} \cdot (D_L^2 - D_{CV}^2) \qquad V_{ice} = \frac{\pi}{4} \cdot (D_{ice}^2 - D_{CV}^2)$$

$$V_{ice} = V_{water} \cdot \frac{\upsilon_{ice}}{\upsilon_{water}}$$

$$(D_{ice}^2 - D_{CV}^2) = (D_L^2 - D_{CV}^2) \cdot \frac{\upsilon_{ice}}{\upsilon_{water}} \quad \rightarrow \quad D_{ice} = \sqrt{(D_L^2 - D_{CV}^2) \cdot \frac{\upsilon_{ice}}{\upsilon_{water}} + D_{CV}^2}$$

$$D_{ice} = \sqrt{(8.25^2 - 6.625^2) \cdot \frac{0.01747}{0.016019} + (6.625^2)} = 8.3816 \text{ in}$$

The hoop strain resulting from the stretch in the liner is:

$$\varepsilon_h = \frac{D_{ice} - D_L}{D_L} = \frac{8.3816 - 8.25}{8.25} = 0.0159$$

The above calculated strain is above the yield-strain of the 304L stainless steel liner material (≈ 25,000 / 28,300,000 + 0.002 = 0.0029 in/in), and the liner would be expected to experience yielding. The freezing condition is secondary in nature, as the yielding of the liner relieves the imposed loads. In addition, the liner does not carry any normal in-service pressure loads and therefore, the imposed secondary stresses do not act in combination with imposed primary stresses. The above calculated strain of 1.6% is well below the failure strain of the material. The liner is therefore acceptable for a one-time application of the loads associated with freezing of water within the annular region between the liner and CV.

4.9 Vibratory Loads on 9977 Package During Normal Conditions of Transport

Road induced vibrations are random vibrations. A random vibration analysis is followed to determine a root mean square (RMS) value of the acceleration felt by the package. Random vibration analysis is based on the power spectral density for the transport vehicle, given in Figure 3.30 of reference [6.4] and reproduced as Figure 4.9-1.

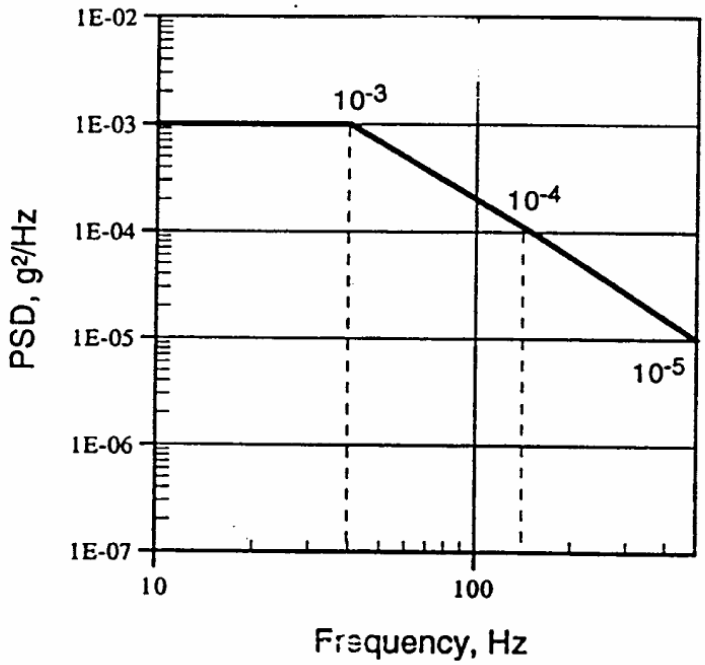

Figure 4.9-1 Safe-Secure Trailer Power Spectral Density

For a single degree of freedom and a damped system, RMS response of a mass to the broad-band random vibration input is given by (reference [6.5]):

$$G_{out} = \sqrt{\frac{\pi \cdot P \cdot f \cdot Q}{2}}$$

where:

G_{out} = acceleration response (g units)
P = power spectral density (g^2/Hz)
f = resonance frequency of the system (Hz)
Q = transmissibility at the resonance frequency

Input for the solution of the above equation are discussed and determined below:

Resonance Frequency of the Package, f

Vibratory response of the 9977 package is evaluated by assuming the natural frequency to coincide with the peak of the power spectral density curve shown in Figure 4.9-1. This corresponds to a frequency of 40 hz and a PSD of 1E-3 g^2/Hz. The degree of conservatism in the above approach, compared to standard practices in evaluating drum vibratory loads, is evaluated by considering the containment vessels with mass M associated with its contained vessel assembly, and structural stiffness k, characterized by the supporting polyurethane insulation. The natural frequency is:

$$f = \frac{1}{2 \cdot \pi} \cdot \sqrt{\frac{k \cdot g}{w}}$$

where:

k = stiffness of polyurethane insulation = A E / L
E ≈ 20,000 psi, from manufacturer's data
A = Effective area of foam, see below
L = Effective length of foam, see below
w = weight of the combined 6CV vessel assembly with maximum 100 lb payload= 155 lb
g = acceleration of gravity = 386.4 in/sec^2

The vessel assemblies are supported by the 8-inch diameter drum liner, which bears on a ≈ 4.00 inch thick layer of polyurethane. The stiffness of the supporting polyurethane, k is calculated below:

$$k = \frac{A_c \cdot E}{L_c} = \frac{\left[\pi \cdot (8)^2 / 4\right] \cdot (20{,}000)}{4.00} = 251{,}000 \ \text{lb/in.}$$

where:

A_c = area of the supporting polyurethane (taken as the diameter of the drum liner)
L_c = height of the column of polyurethane under the support plate

The natural frequency of the package is now calculated using the above relation:

$$f = \frac{1}{2 \cdot \pi} \cdot \sqrt{\frac{k \cdot g}{w}} = \frac{1}{2 \cdot \pi} \cdot \sqrt{\frac{(251{,}000) \cdot (386.4)}{155}} = 125 \text{ Hz}$$

Transmissibility, Q

From reference [6.5], the transmissibility, Q (also known as magnification factor) is determined as:

$$Q = \left[\left(1 - r^2\right)^2 + (2 \cdot r \cdot d)^2\right]^{-.5} = \left[(1 - 1^2)^2 + (2 \cdot 1 \cdot .10)^2\right]^{-.5} = 5$$

where:

d = damping coefficient = 0.10
r = frequency ratio = f / f_n = 125 / 125 = 1, where f_n = natural frequency

The package acceleration, G_{out} is now calculated below at 125 Hz:

$$G_{out} = \sqrt{\frac{\pi \cdot P \cdot f \cdot Q}{2}} = \sqrt{\frac{\pi \cdot (0.00011 g^2 / hz) \cdot (125 hz) \cdot (5)}{2}} = 0.33 \text{ g}$$

where P = 0.00011 from Figure 4.9-1 at 125 Hz. Using the low-frequency cutoff of 40 Hz in the above equations results in 0.26 g, which is lower than the acceleration at 125 Hz.

The maximum vibration of the containment vessels and contents is about 3 to 4 times the root mean square, or about 1.0 g to 1.4 g. Conservatively assuming 100% of the package mass is acting at this acceleration level yields a maximum load of less than 1000 lbs. The resistance of the container lid to this load is from the bolt pre-load, as documented in Section 4.10.

4.10 Loosening of Drum Bolts During Normal Conditions of Transport

The known mechanism for bolt loosening in the 9977 package bolts is vibration-caused motion of the lid relative to the drum and the vibration of the bolts relative to the drum lid.

Bolt Loosening due to Lid Vibration

The weight of the drum lid is approximately 20 pounds, as determined by measurement. The vibratory load tending to loosen the bolts is calculated as the product of the maximum acceleration, 1.4g (see Section 4.9) and the bolt weight, or

$$P_{max} = 1.4 \times 20 = 28 \text{ lbs}$$

The torque applied at each bolt that tends to loosen the bolt is

$$T_{loose} = 0.2 D_{nom} F_{\max} = 0.2 \times 0.625 in \times 28 lbs \times \frac{ft}{12 in} \times \frac{1}{8} = 0.0365 \text{ ft-lb}$$

Since the loosening torque is much less than the minimum torque required for the preload of 40 ft-lb, the drum bolts will not be loosen due to the vibration during the normal conditions of transport.

Bolt Loosening due to Bolt Vibration

The weight of the drum bolt is approximately 0.227 pounds. The vibratory load tending to loosen the bolts is calculated as the product of the maximum acceleration, 1.4g (see Section 4.9) and the bolt weight, or

$$P_{\max} = 1.4 \times 0.227 = 0.3178 \text{ lbs}$$

The torque that tends to loosen the bolt is

$$T_{loose} = 0.2 D_{nom} F_{\max} = 0.2 \times 0.625 in \times 0.3178 lbs \times \frac{ft}{12 in} = 0.0033 \text{ ft-lb}$$

Since the loosening torque is much less than the minimum torque required for the preload of 40 ft-lb, the drum bolts will not be loosen due to the vibration during the normal conditions of transport.

5.0 Results

Section	Evaluation	Result	Criteria
4.1	**Stresses in Drum Closure Bolts**		
	Preload in drum bolts	Min = 3,840 lb Max = 4,800 lb	Used as input for other analysis
	Average bolt stress due to preload	21,250 psi	50,000 (ref)
	Maximum stress intensity due to preload	43,500 psi	75,000 psi (ref)
	Fatigue in bolts	$U \approx 0$	$U < 1.0$
	Length of Engagement	0.555 in.	> 0.529 in
4.2	**Evaluation of Reduced External Pressure on CV's and Overpack**		
	Primary membrane stress in liner	970 psi (shell) 10,350 psi (end)	16,700 psi (ref)
	Primary membrane plus bending stress in liner at bottom (acceptable due to membrane action and strain hardening in section)	28,000 psi	25,000 psi (ref)
	Primary membrane stress in drum (acceptable due to membrane action and strain hardening in section)	26,700 psi	16,700 psi (ref)
	Primary membrane plus bending stress in drum at bottom (acceptable due to membrane action and strain hardening in section)	32,300 psi	25,000 psi (ref)
	Buckling of liner	11.2 psi	< 15.3 psi
4.3	**Evaluation of Increased External Pressure on Overpack**		
	Primary membrane stress in liner	460 psi	16,700 psi (ref)
	Primary membrane plus bending stress in liner at bottom	Bounded by evaluation in 4.2 above	
	Primary membrane plus bending stress in drum	9,260 psi	25,000 psi (ref)
4.4	**Evaluation of Overpack for Static Compression Loading**		
	Primary membrane plus bending stress in drum	14,000 psi	25,000 psi (ref)
	Reduction in internal clearances in drum (excessive deflection results in loading of CV, which would require further evaluation)	0.04 inch	≈ 0.25 inch

Calculation Continuation Sheet

Calculation No.	Sheet No.	Rev.
M-CLC-G-00357	40	**0**

Section	Evaluation	Result	Criteria
4.5	**Evaluation of Lifting Stresses on Package Components**		
	Drum flange maximum shear stress	1220 psi	4170 psi
	Drum flange maximum bearing stress	1300 psi	8330 psi
	CV Nut shear stress	2206 psi	4170 psi
	CV Nut bearing stress	1032 psi	8330 psi
4.6	**Evaluation of Tiedown Stresses on Package Components**		
	Hook Chain Rim	63620 psi	25000 psi (see Section 4.6.3)
4.7	**Evaluation of Stresses in Package Components Due to Differential Thermal Expansion**		
	No Interference		
4.8	**Evaluation of Freezing Water on Package Components**		
	Maximum strain in liner for single event (Strain judged acceptable based on secondary nature of stress and magnitude of strain low compared to failure strain)	0.0159 in / in	-
4.9	**Vibratory Loads on 9977 Package During Normal Conditions of Transport**		
	Maximum acceleration of drum (used as input to other analyses)	1.0 – 1.4 g	-
4.10	**Loosening of Drum Bolts During Normal Conditions of Transport**		
	Bolt preload frictional resistance to slippage due to lateral vibratory loads	3070 lb	> 28 lb

6.0 References

6.1 ASME Boiler & Pressure Vessel Code, Section III, Subsection NB, 2004 edition

6.2 Design of Machine Elements, M. F. Spotts; Prentice-Hall, 1971

6.3 SRNL-EDS-2006-00010 , dated 2/14/06, "GPFP Packaging Weight Compilation", L. F. Gelder

6.4 C. F. Magnuson. Manufacture-to-Stockpile Sequence. SAND83-0480, Sandia National Laboratory, Albuquerque, NM 87115 (June 1983)

6.5 Shock and Vibration Handbook, C. M. Harris and C. E. Crede; 2nd Ed; McGraw-Hill, 1976

6.6 Code of Federal Regulations, 10CFR71.45, 2005.

6.7 IAEA Safety Guide TS-G-1.1 (ST-2). Advisory Material for the IAEA Regulations for the Safe Transport of Radioactive Material, International Atomic Energy Agency, First Edition, June 2002.

6.8 IAEA Safety Series 37, Advisory Material for the Application of the IAEA Regulations, International Atomic Energy Agency, Second Edition, 1982.

6.9 ABAQUS/Explicit Computer Code, Version 6.5, Abaqus, Inc.

6.10 MSC/PTRAN, Version 2003r2, MacNeal-Schwendler Corporation.

6.11 ANSI N14.6, Special Lifting Devices for Shipping Containers Weighing 10,000 Pounds or More, p. 7, 1986.

6.12 Gelder, L.G., General Purpose Fissile Packaging Prototype Testing, M-TRT-A-00006, Revision 0, Westinghouse Savannah River Company, (May 2005).

Calculation Continuation Sheet

Calculation No.	Sheet No.	Rev.
M-CLC-G-00357	42	**0**

This Page Intentionally Left Blank

APPENDIX 2.8

9977 PACKAGING COMPARISONS WITH THE GPFP DEVELOPMENT PROTOTYPES

This Page Intentionally Left Blank

9977 PACKAGING DEVELOPMENT FROM THE DESIGN PACKAGE 1, THE PRACTICE PACKAGE, AND THE GPFP PROTOTYPE

1.0 Prototype Series 1 - Design Packages (DP) 1 through 6

The Savannah River Packaging Technology (SRPT) group designed and developed a series of General Purpose Fissile Package (GPFP) prototype units. The first series of prototype packages were referred to as the Design Package (DP) series and were fabricated in both 16 in. and 18-½ in. diameter drum overpack configurations and were filled with 16, 20, or 24 lb/ft^3 polyurethane foam. The DP units were fabricated at the Savannah River Site (SRS) in conjunction with Honeywell Federal Manufacturing & Technologies, LLC; also known as the Kansas City Plant (KCP). The DP units were subjected to 10CFR71, Type B packaging performance testing to evaluate the performance of the design.[1]

The objective of the DP Package testing was to evaluate the adequacy of this design series to meet the free drop, crush, puncture, and thermal hypothetical accident conditions specified in 10CFR71.73. The results from and evaluation of this testing provided feedback to the SRPT designers. These results also provided the DOE Program Manager(s) with data relevant to the progress and future funding of the SRPT/KCP GPFP development.

Design prototype number one (DP-1), Figures 2.8.1 and 2.8.5, was the design variation within the Series 1 family decided to have the greatest potential for further development. The design for this prototype included:

A drum with:

- 18.25-inch inside diameter
- 35 gallon capacity
- 18 gage wall thickness
- 304L stainless steel
- 16 lb/ft^3 polyurethane shock absorbing and insulating foam
- 14 gage liner
- reinforced top rim

A removable drum lid with:

- internal insulation
- bolted flange closure

Containment vessels (CV) of the Chalfant design and identical those used in the 9975.
Aluminum load distribution fixtures (above and below the CV).

Key packaging features and dimensions are listed in Table 2.8.1. Five of the six DP series developmental prototypes were subjected to the full suite of HAC sequential tests. The packages performed well in these tests and the containment vessels were verified to be leak-tight following the series. However, the package performance suggested several changes that would enhance the safety margins.

Figure 2.8.1 – DP-1

Figure 2.8.2 – Practice Package

2.0 Prototype Series 2 - Serial Numbers (SN) 1 through 7

The second series of GPFP prototypes were developed using the lessons learned from testing of the first series. See Figures 2.5.4 and 2.5.5. The major changes incorporated into the series two design included:

- Adding an insulated top to the lid, with a diameter greater than the drum liner.
- Removing the "step" from the drum liner and decreasing the diameter of the corresponding lower portion of the cap.
- Changing the insulation in the lid bottom to more thermally stable materials.
- Replacing the ½-inch of polyurethane foam immediately adjacent to the drum liner with two ½-inch blankets of Fiberfrax insulation (which get compressed by the foam to a final thickness of approximately ½-inch).
- The drum liner material was increased to 18 gage.
- Adding four (4) drain slots to the drum rim.
- Adding a third rolling ring to the drum body.
- Increasing the height of the Bottom Load Distribution Fixture.

Figure 2.8.6 illustrates the similarities and differences between the first and second series of prototypes.

3.0 Practice Package

NovaTech Innovative Technologies International (NovaTech) was contracted to perform thermal testing of the Series 2 packages in accordance with 10CFR71.73(c)(4).[2] Four thermal tests were contracted (for packages SN-2 through SN-5). This testing was performed using a modified training "prop" at the South Carolina Fire Academy. As part of their contract, NovaTech requested an additional package that could be used for a "practice" burn. The purpose of the burn was to:

- Confirm correct operation of the test facilities and the equipment added to support the burn tests;
- Practice the procedures needed to perform the burn test and provide participants with test experience; and
- Confirm that the fire conditions produced by the facility met the regulatory requirements.

This extra test presented the opportunity to expand the GPFP test matrix and investigate the effect of another variable on the performance of the design. The preliminary thermal analysis had established the difficulty in modeling polyurethane foam during the HAC Thermal phase. With the complexities of heat input, foam intumescing, mass and latent heat flow out of the package openings, and heat transfer by radiation, conduction, and convection; modeling the HAC fire event was not easily done. Therefore, it was decided to create a package with the Fiberfrax®, Min K 2000, and TR-19 Block insulation but without the polyurethane foam. The thermal performance of this "practice" package could be evaluated without benefit of the insulation provided by the polyurethane foam.

The Practice Package is shown in Figure 2.8.2. The outer drum from a previously drop-tested 9975 was used, Figure 2.8.3. A deck plate was installed that mated to the external bolt circle of the 9975 flange closure and the internal bolt circle of the 9977 lid. A 9977 drum liner was welded to the deck plate and a double layer of Fiberfrax insulating blanket (i.e. two layers each one-half inch thick) was applied around the liner. A 6-inch diameter CV with a 100-lb "content" slug was placed into the liner centered between the aluminum Top and Bottom Load Distribution Fixtures. A thermocouple (TC) was attached to the exterior of the CV adjacent to the Lower O-ring and the TC wire run out a hole made in the bottom of the liner and then out the bottom of the drum. The lid from GPFP SN-7 was installed. Because the lid fit tightly to the liner and because the package was not being drop tested, the lid was not bolted in place. Because the deck plate was flat, the SN-7 lid stands proud of the Practice Package drum rim, rather than being recessed as in the Series 2 configuration. Therefore, the Practice Package is approximately ¾-inch taller than the 9977. This increase in height and internal drum volume was judged to have minimal effect of the package performance.

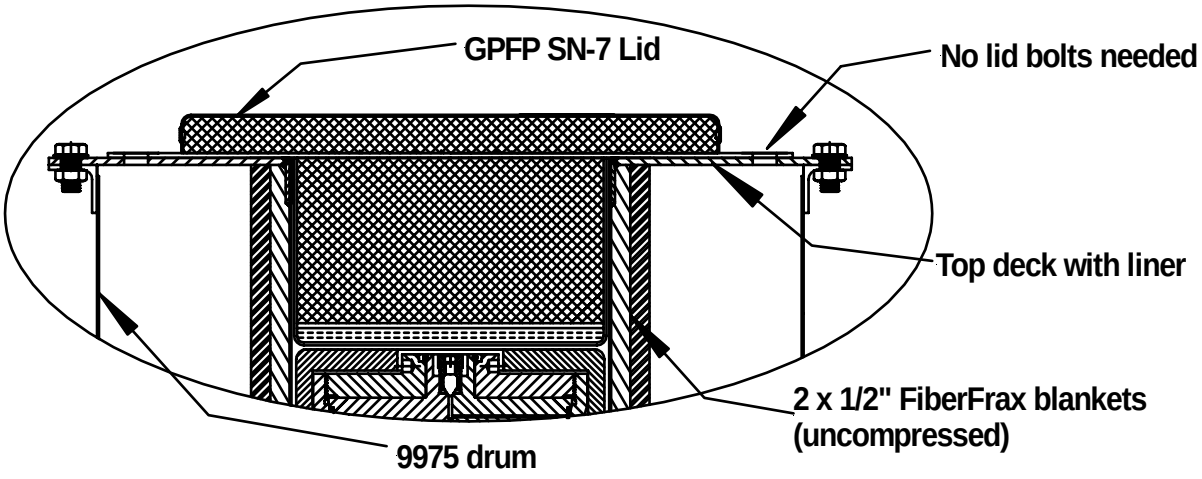

Figure 2.8.3 – Upper Portion of Practice Package

Figure 2.8.4 – GPFP Series 2 Prototypes

4.0 The 9977

The final 9977 design was developed using the lessons learned from testing of the Practice Package and the GPFP Series 2 prototypes.[3] See Figure 2.5.7. The major changes incorporated into the final design included:

- Replacing the four (4) lid drain slots with eight (8) drain holes that are also qualified for package lifting and tie-down.
- Improving the method for attaching the Fiberfrax to the drum liner.
- Changing the drum bottom design from a chimed configuration to a sanitary bottom with a wear ring.
- Replacing the Tamper Indicating Device (TID) pin with a hole drilled through each of the lid bolts. A larger through hole was also placed in the drum rim for use with facility TID systems.

Figure 2.8.7 illustrates the differences between the second prototype series and the final 9977 design.

Series 1 (Design Package – 1) Practice Package Series 2 (SN Prototypes) 9977

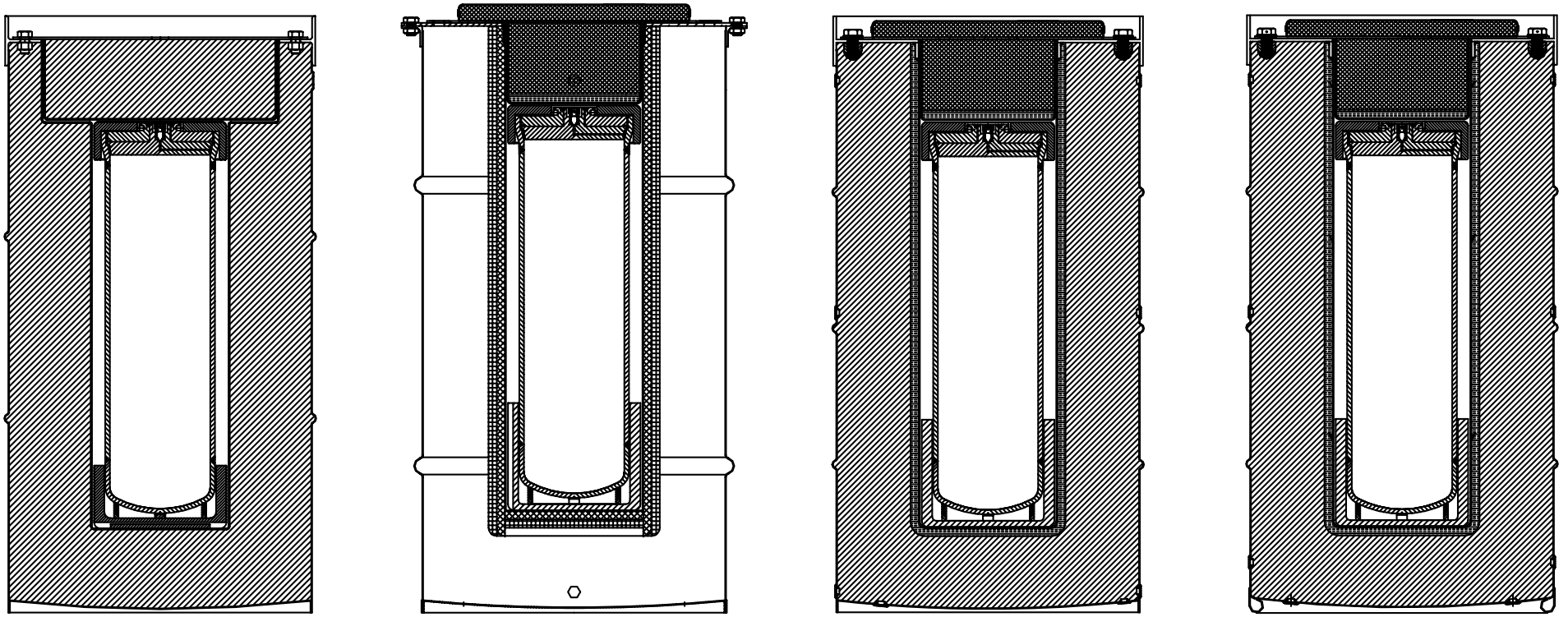

Figure 2.8.5 – 9977 Package Development

Table 2.8.1 - 9977 and Prototype Packages Comparison

Packaging Model			GPFP DP-1	Practice Package	GPFP Prototype	9977
Packaging Gross Weight			338	Not Measured	350	350
Drum	Capacity (gal)		35			
	Gauge (gage)		18			
	Material		304 Stainless Steel			
	Inside Diameter (in.)		18.25			
	Height (in.)		36	36.8	36.1	36.1
Insulation Thicknesses	Lid (in)	**Fiberfrax**	-	1 ⇒ ½ [a]	1 ⇒ ½	1 ⇒ ½
		Foam	4.80	-	-	-
		Min K 2000	-	1	1	1
		Vermiculite TR-19	-	4.3	4.3	4.3
		Total	4.80	5.80	5.80	5.80
	Bottom (in)	Fiberfrax	-	1	1 ⇒ ~ ½ [b]	1 ⇒ ~ ½
		Foam	4.86	-	4.36	4.02 [c]
		Total	4.86	1	4.86	4.52
	Radial (in)	Fiberfrax	-	1	1 ⇒ ~ ½	1 ⇒ ~ ½
		Foam	4.94	-	4.44	4.44
		Total	4.94	1	4.94	4.94

Notes:

a: "1 ⇒ ½" indicates that a 1-inch thick layer of Fiberfrax was installed and was compressed to a thickness of ½-inch.

b: "1 ⇒ ~ ½" indicates that a 1-inch thick layer of Fiberfrax was installed and was compressed by the foaming process to a thickness of approximately ½-inch.

c: Minimum thickness with a flat bottom drum. Permitted convexity of drum bottom will increase the insulation thickness in this area.

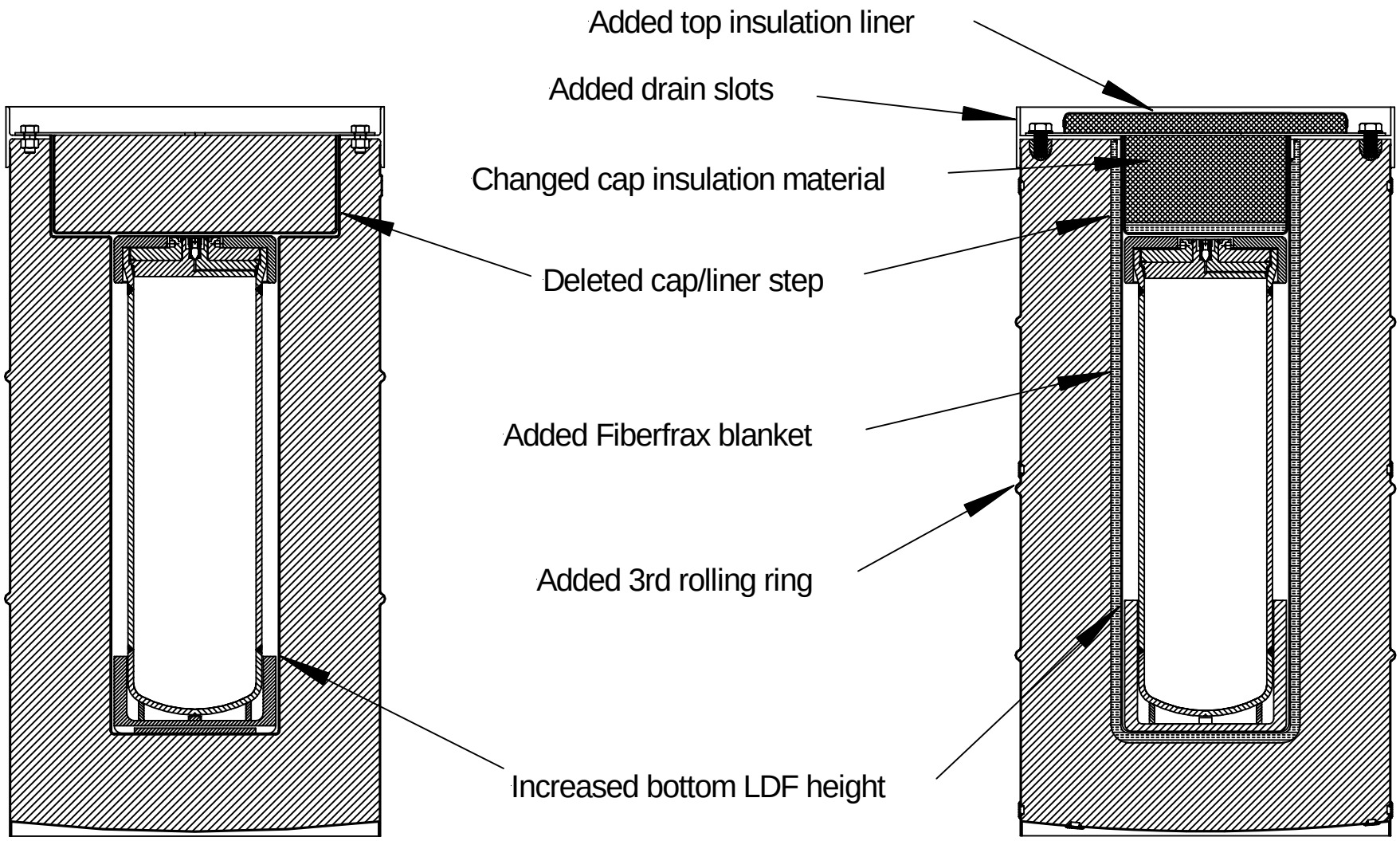

Figure 2.8.6 – Design Package 1 to GPFP Package Comparison

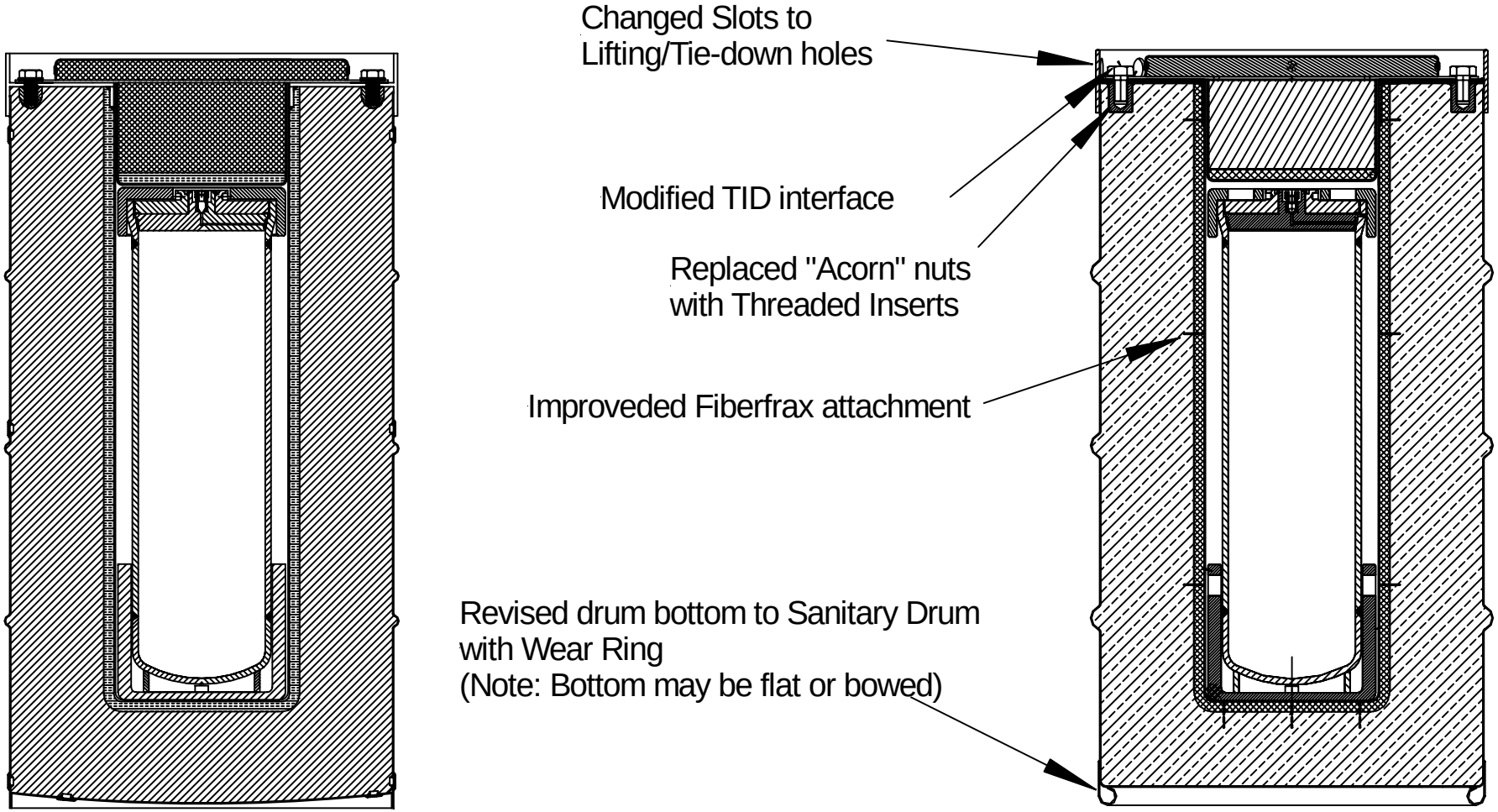

Figure 2.8.7 – GPFP Package to 9977 Comparison

5.0 Observations and Changes

When compared to the 16-inch diameter drum tested in Series one, the 18-inch diameter drum provides a greater margin of safety.

Extending the lid bolting flange diameter to almost equal that of the drum side wall restricts gas flow from the container edge to container cavity. It also "locks" the lid flange into the rim in side or top oriented impacts which prevents lid loss.

Increasing the lid bolt circle diameter reduces direct bolt loading and the deformation of lid flange (lid scalloping) between bolt holes.

Replacing the foam filled lid with non-out gassing insulators eliminated the potential for foam decomposition products from a breached lid filling the package liner.

Sealed overpack closure bolt holes. Prevent foam outgas products entering overpack liner.

Reduced liner thickness from 14 to 18 gauge. Decrease thermal flow to CV during HAC.

Added top pan filled with insulation to closure lid. Reduces load to bolted closer during HAC top-down impacts. Reduces scalloping between lid closure bolts. Added insulation reduces heat flow to CV during HAC.

6.0 REFERENCES:

1. *General Purpose Fissile Packaging Prototype Tests*, M-TRT-A-00006, Rev. 0, Savannah River Site, Aiken, SC (May 2005).
2. *SRNL Package Burn Test Report*, NT-TDR-06-101, Rev. 0, NovaTech Innovative Technologies International, (January 2005).
3. 9977 *General Purpose Fissile Packaging Prototype Testing*, M-TRT-A-00007, Rev. 0, Savannah River Site, Aiken, SC (April 2006).

APPENDIX 2.7

SRS DROP TEST PAD INFRASTRUCTURE FOR DRUMS

This Page Intentionally Left Blank

SRS 723-A DROP TEST FACILITY

Unyielding Surface

Requirement: 10 CFR 71.71(c)(7) and 71.73(c)(1) require that packages be dropped onto an unyielding surface.

The IAEA describes an unyielding surface as a "flat, horizontal surface of such a character that any increase in its resistance to displacement or deformation upon impact by the specimen would not significantly increase damage to the specimen". (TS-R-1, 2005 Edition, para. 717) The IAEA Advisory Material goes on to further specify an example of an unyielding target as one that includes a steel plate at least 4 cm (1.57 inches) thick floated to a concrete block mounted on firm soil or bedrock, where the combined mass of the steel and the concrete is at least 10 times that of the test package. (IAEA Safety Series, Advisory Material)

SRS Drop Test Pad 723-A

NCT 4-ft drop, HAC 30-ft drop and HAC puncture tests are performed on an unyielding surface in an environmentally controlled test facility located in building 723-A at the SRS. The unyielding impact surface is constructed from very high strength armor plate steel. The plate which serves as the unyielding surface is 5 ft square and 6-1/4 inches thick, and is anchored in a 6-ft square by 36-inch thick reinforced concrete slab. The surrounding slab is insulated from the building concrete floor, See Figure 1.

The concrete-steel monolith that serves as the impact target weighs approximately 19,500 lb.

Armor plate weight:

Volume 60 inch x 60 inch x 6.25 inch = 18,900 in^3

Steel Density 0.286 lb/in^3

Steel pad weight: 18,900 in^3 x 0.286 lb/in^3 = 5,386.5 lb

Concrete Isolation Pad weight:

Volume of concrete block less steel slab

Volume: 72 inch x 72 inch x 36 inch – (18,900 in^3) = 167,724 in^3

Weight = 167,724 in^3 x 0.084 lb/in^3 = 14,088.82 lb

Total Weight = 19,475 lb (less rebar reinforcement)

The target pad weight is greater than 45 times the weight of the 9977 and it will not deform of displace during testing. Figure 2 pictures the drop pad used for the NCT drop tests.

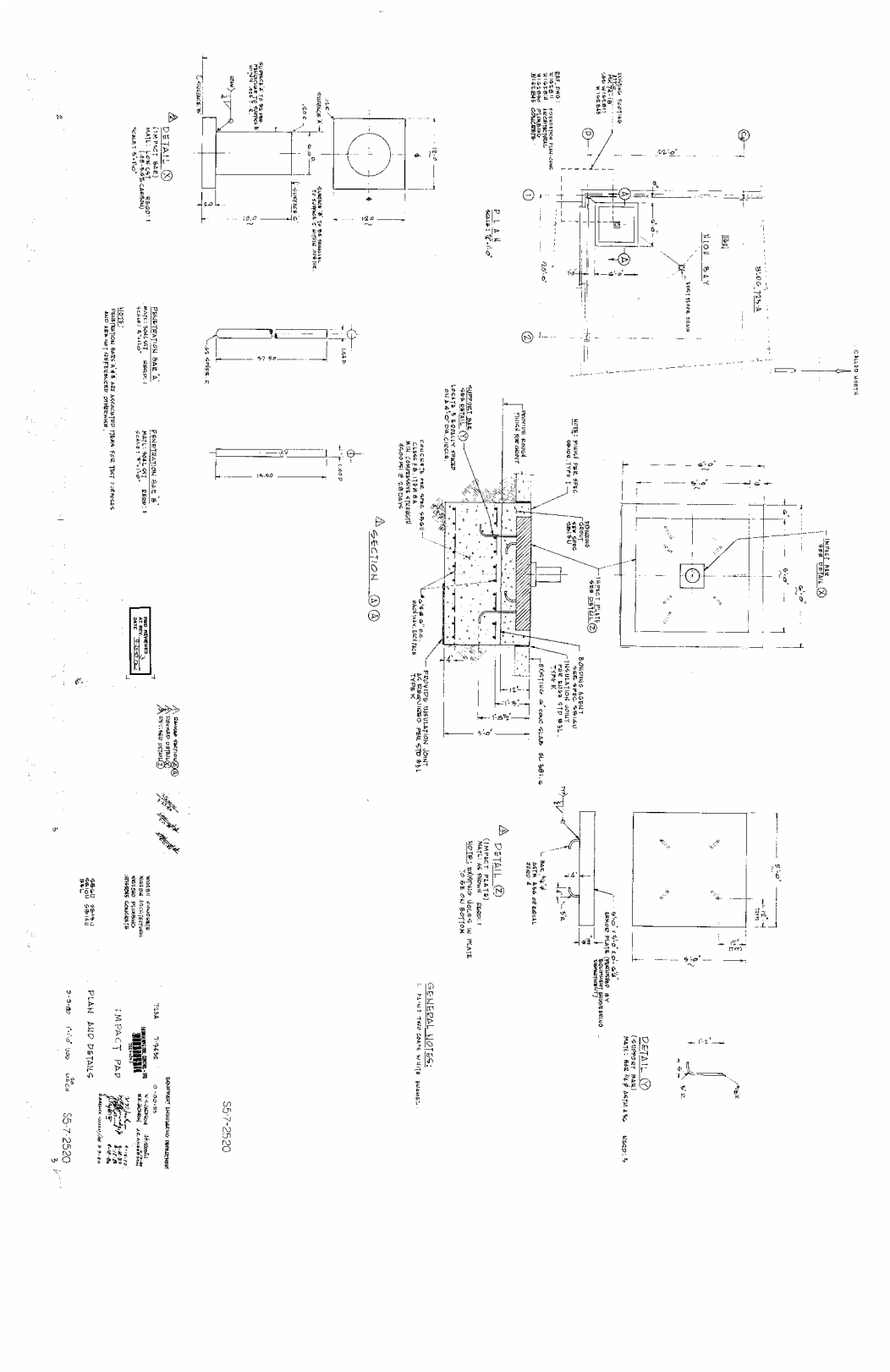

Figure 1 SRS N-Area Crush Test Pad

Figure 2 Impact Pad made from 6-1/4 inch thick battle ship armor.

SRS Crush Test Pad N-Area

HAC 30-ft crush tests are performed on steel-concrete pad that has been constructed on top of an existing building footer for building 8343 located in N-Area at SRS. The impact surface is constructed from a 4 foot square by 3 inch thick plate of A-36 steel. The steel pad is floated onto approximately 3/4-inches of grout to ensure a solid connection between the steel plate and footer. Additionally, the steel plate is anchored into the building footer by five (5) 5/8-inch diameter 7-inch long HILTI bolts, one located in the center of the plate and four at its corners. The steel plate is machined with recesses so the HILTI bolts do not protrude above the plate surface. See Figure 3.

The existing building footer is 4 foot square. Its depth is unknown. To account for this unknown and to demonstrate it as an unyielding surface a vibration study was performed to determine if it exhibited the same vibration response as a known unyielding surface. The results of this evaluation concluded that the N-Area pad is acceptable for performing crush tests. (Reference 1)

Assuming the existing concrete footer is at least 12-inches deep the concrete-steel monolith that serves as the impact target weighs approximately 19,500 lb.

Steel plate weight:

Volume 48 inch x 48 inch x 2-1/2 inch = 6,912 in^3

Steel Density 0.286 lb/in^3

Steel pad weight: 6,912 in^3 x 0.286 lb/in^3 = 1,963 lb

Concrete Grout Pad weight:

Volume of concrete block less steel slab

Volume: 48 inch x 48 inch x 3/4 inch = 1728 in^3

Weight = 1,728 in^3 x 0.084 lb/in^3 = 145 lb

Concrete Building Footer weight: (no rebar; assume 12 inches deep)

Volume of concrete block

Volume: 48 inch x 48 inch x 12 inch = 27,648 in^3

Weight = 27,648 in^3 x 0.084 lb/in^3 = 2,322 lb

Total Weight = 4,430lb (less rebar reinforcement)

Figure 3 pictures the pad used for the HAC crush impact tests. The impact plate is shown suspended above the pad being held by the magnetic release. The perimeter of the crush pad is painted light tan and picture frames a 40-inch square section of the steel plate. The 40-inch square corresponds to the dimensions of the impact plate. The painted perimeter made it easier to align the crush plate with the pad before being lifted to its 30-foot drop height. As shown in the figure, strings acting as plumb bobs were hung from the plate to assist with alignment when a drum was positioned on the pad.

Figure 3 N-Area

Reference

1 E. G. Estochen, *Removable Crush Test Pad (RCTP) Evaluation*, SRT-MTS-2004-20045, October 2004.

This Page is Intentionally Left Blank.

Appendix 2.6

Structural Evaluation of Model 9977 Package

For

HAC Drop and Crush

This Page is Intentionally Left Blank

Calculation Cover Sheet

OSR 45-24 (Rev 11-15-2004)

Project	Calculation No.	Project No.
N/A	M-CLC-G-00358	N/A
Title Structural Evaluation of Model 9977 Package for HAC Drop and Crush (U)	**Functional Classification** SS	**Sheet 1 of** ~~164~~ 168 (4A)
	Discipline Mechanical	
Calc Level ☒ Type 1 ☐ Type 2	**Type 1 Calc Status** ☐ Preliminary ☒ Confirmed	
Computer Program No. ABAQUS ☐ NA	**Version/Release No.** 6.5.3 / 2005_03_03-17.29.04 57675	

Purpose and Objective

The purpose of this calculation is to document the finite element analyses performed as part of the structural design of the Model 9977 series General Purpose Fissile Package (GPFP) to support generation of its Safety Analysis Report for Packaging

Summary of Conclusion

Analysis presented in this calculation meet the design criteria required by 10 CFR 71in the evaluation of the Model 9977.

Revisions

Rev. No.	Revision Description
0	Original Issue

Sign Off

Rev. No.	Originator (Print) Sign/Date	Verification/ Checking Method	Verifier/Checker (Print) Sign/Date	Manager (Print) Sign/Date
0	R. R. Rothermel 5/10/06	Document Review	N. K. Gupta 5/16/06	J. S. Bellamy 5/16/06

Design Authority -- (Print)	Signature	Date

Release to Outside Agency -- (Print)	Signature	Date
N/A	N/A	N/A

Security Classification of the Calculation

(U)

OPEN ITEMS

None

RECORD OF REVISION					
REV. NO.	PAGES SUPERSEDED	PAGES ADDED	PAGES DELETED	PAGES REVISED	DESCRIPTION OF REVISIONS
0					Original Issue

Table Of Contents

Figures

1.0 Purpose

The purpose of this calculation is to evaluate the structural response of the Model 9977 shipping package subjected to the impact loads that simulate hypothetical accident conditions. The simulated hypothetical accident conditions include the 30 foot drop and crush discussed in section 2.0.

2.0 Scope

The equipment evaluated is the Model 9977 shipping package. A sketch of the package cross section is shown in Figure 1. Table 1 and Reference 1 list the HAC cases analyzed for the package being dropped 30-feet onto an unyielding rigid surface and being impacted by 1,100 lb rigid plate falling 30-feet. For each case the maximum stress and strain of the containment vessels are determined. Overpack stresses are also evaluated for various drop and crush orientations.

3.0 Conclusion

Nonlinear dynamic analyses were performed for the Model 9977 shipping package to evaluate the structural responses of the two containment vessel shipping configurations and packaging to the Hypothetical Accident Conditions (HAC) defined in 10 CFR 71 (Reference 1).

For simplicity and conservatism, the maximum von Mises stresses average across the containment wall thickness (approximately equal to the Local Primary Membrane stress intensities, P_L) are used for comparison with the allowable General (P_m) and Local (P_L) Primary Membrane stress intensities specified in the ASME Code, Appendix F (Reference 2).

The computed analytical results and stress criteria are summarized in Table 2. As shown, the maximum calculated values of stress intensities in the containment vessel of the 9977 package are within the allowable limits for the Level D service load specified in the ASME Code, Section III, Appendix F.

In addition, the analytical results show that the maximum value of the equivalent plastic strain averaged across the containment vessel wall is less than the effective strain corresponding to the ultimate strength of stainless steel 304L.

Consequently, the analyses have confirmed that the containment vessel of the Model 9977 shipping package will be structurally adequate when subjected to the hypothetical accident conditions.

Table 1 HAC 5CV and 6CV 30-Foot Drop Case Matrix

Drop Configuration	Package Orientation	HAC Drop/Crush Cases (°F)				Max. CV Stress and Strain	Results (Max Stain and or Stress)				
							Drum			Lid/drum	
		-20	100/75	140	260/300		outer shell	Liner to top deck	Liner & bottom	flange	Bolt
		D/C	D/C	D/C	D/C						
30-ft drop w/6CV	Top down		1/2			**x**				**x**	**x**
	Bottom down	3	4	5/7	6/8	**x**		**x**	**x**		
	Side – wt middle	9/10		11	12	**x**					
	- wt bottom			/13	/14	**x**	**x**	**x**	**x**		
	- wt top			15	16	**x**		**x**	**x**		
	CGOT *	17	18/19			**x**				**x**	**x**
	CGOB **		/20	21/23	22/24	**x**	**x**	**x**	**x**		
	Slap 15° top			25	26	**x**					
	Slap 15° bottom	27			28	**x**		**x**	**x**	**x**	**x**
30-ft drop w/5CV	Side – wt middle	29			30/31	**x**	**x**	**x**			
	CGOT		32			**x**	**x**	**x**			**x**
	Slap 15° bottom	33				**x**					

* - Center of Gravity over the Top Corner of the package (CGOT)
* - Center of Gravity over the Bottom Corner of the package (CGOB)

Table 2 Summary of Calculated Maximum Stress Intensities

HAC Load Cases [c]		Calculated Maximum Values of Stress Intensities for the Containment Vessel [a, b] (ksi)							
		30-Foot Drop				Crush			
		-20 ºF ambient, zero watts	75 ºF	140 ºF	260/300 ºF	-20 ºF ambient, zero watts	75 ºF	140 ºF	260/300 ºF
6CV	Top Down		29,960	30,020	39,270			17,830	37,140
	Bottom Down	51,190	46,320	42,020	38,220		31,400		
	CGOT	47,990	47,840				42,810		
	CGOB		49,960	48,050	37,760		42,120	38,190	37,930
	Side-wt in Middle	42,820				41,970			
	Side-wt in Bottom			45,300	46,220			37,990	47,030
	Side-wt in Top			52,400	46,520				
	15° Slap on Top			43,760	42,210				
	15° Slap on Bottom	40,330		32,480	29,380				
5CV	Side-wt in Middle	44,310			43,970	53,810			44,770
	CGOT	46,000							
	15° Slap on Bottom	45,400							

a Values listed are maximum values at any location on the CV.
b The allowable true stress intensity limits are 57.8-ksi for P_m and 74.3-ksi for P_L.
c See illustration on next page of the drop orientations

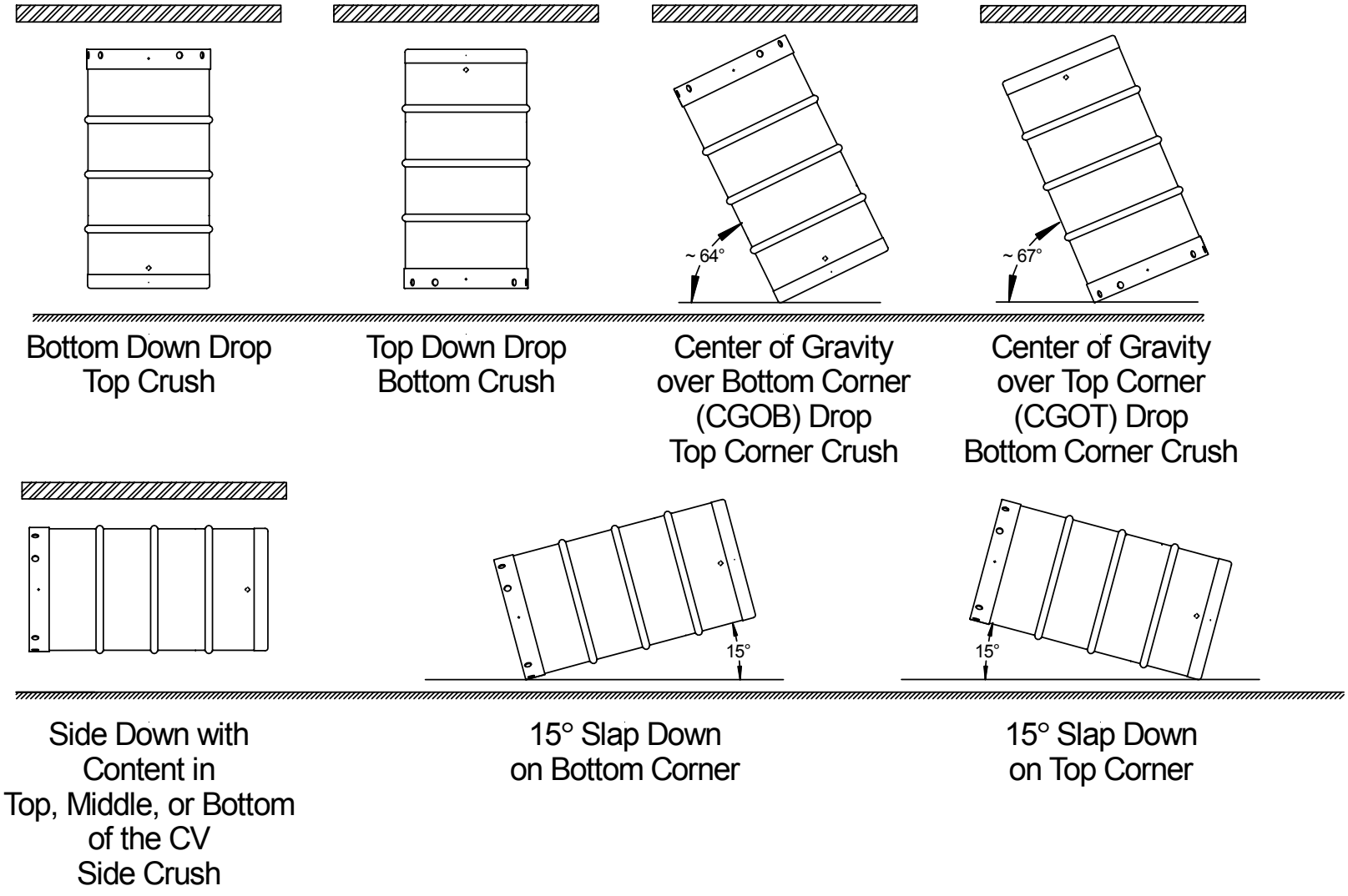

Table 2 - Footnote ‘c” - 9977 HAC Model Drop Orientations

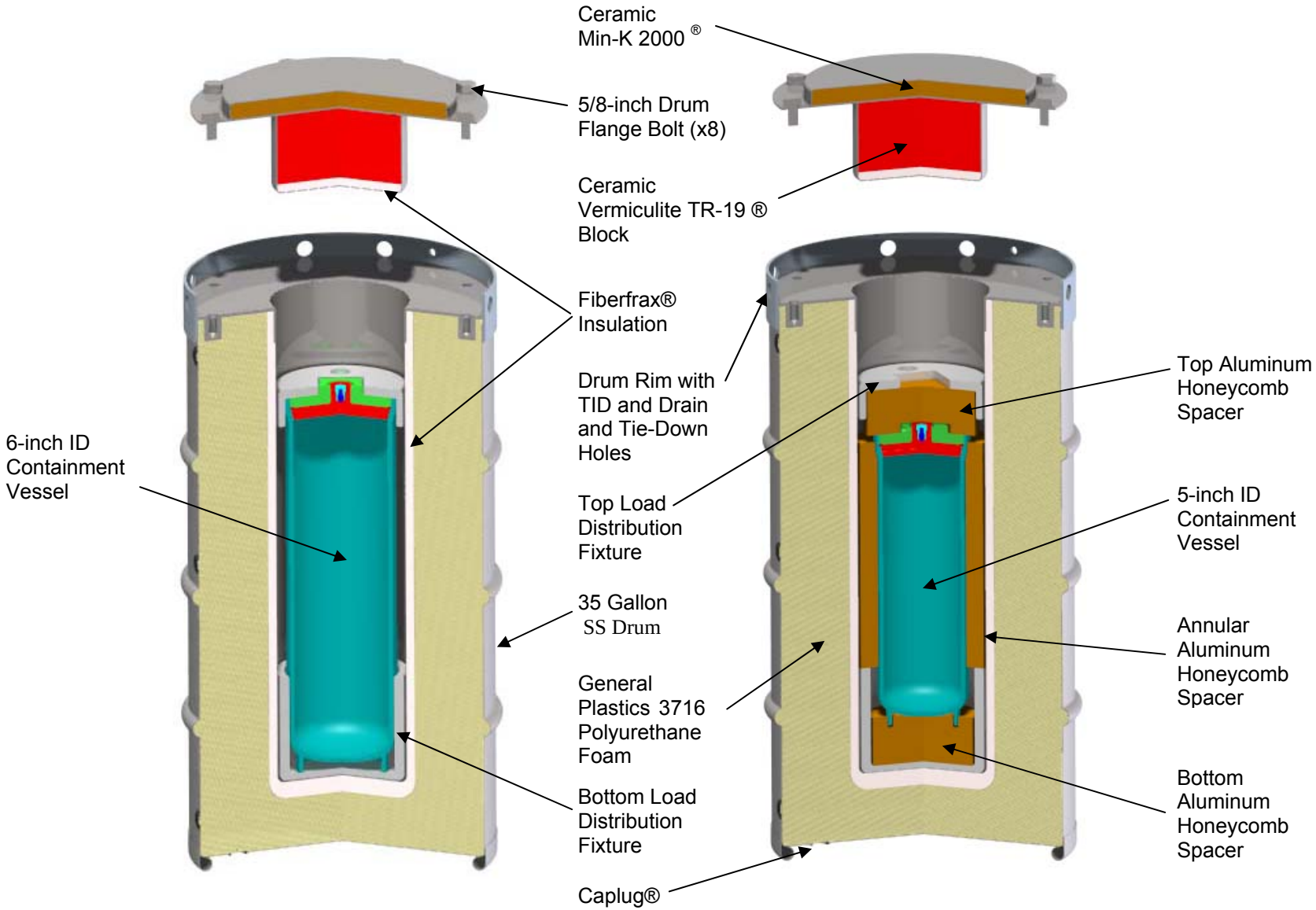

Figure 1 - 5CV and 6CV Configurations of Model 9977 Shipping Package

4.0 Input Data and Assumptions

Input Data

The following Revision 0 drawings were used as input for weight and geometric configuration of the 9977 shipping package analyses contained herein: (Reference 3)

R-R1-G-00020	R-R2-G-00017	R-R2-G-00018	R-R2-G-00019
R-R2-G-00032	R-R2-G-00033	R-R2-G-00042	R-R2-G-00043

The stress versus strain curve of stainless steel 304L is given in Appendix A. The strain curve used represents median centered properties, rather than Code minimum properties. The effect of this modeling is to conservatively overestimate the stress response level during the impact condition. The generation of the stress-strain curves of aluminum 6061-T6 and polyurethane foam materials are also presented in Appendix A.

Assumptions

The bolted flange closure connection of the drum is modeled as solid elements, therefore, preload caused by the tightening the bolts to the drum flanges is not included in the model.

5.0 Discussion of Analysis

5.1 Description of Methodology

The structural responses of the 9977 shipping package to the hypothetical accident conditions were determined by performing nonlinear dynamic finite-element analysis with explicit time integration.

The ABAQUS/Explicit Computer Code was used to perform the computations. (Reference 4) The finite-element meshes were generated using the ABAQUS Preprocessor CAE computer program (Reference 5). Modeling results were analyzed with MSC/PATRAN (Reference 6) and ABAQUS.

5.2 Description of Finite-Element Model

The basic finite element geometries of the 9977 when configured with the 5CV and 6CV are shown in Figure 1. Table 3 summarizes the principal components of the package. The material properties of the package are given in Table 4. Table 5 contains the weights of the package components.

Since the arrangement of the package components is symmetric with respect to a plane containing the axis of the package, only one half of the package components are included in the finite-element model.

The finite-element model representation of the containment vessel, drum body, lid and liner consists of three dimensional shell elements (Type S4R elements in the ABAQUS Computer Code). The containment vessel flange, plug, and nut are modeled using 3D brick elements (Type C3D8R). The unyielding target floor and the unyielding falling plate are represented by the rigid element (Type R3D4). The weight of the falling plate is modeled by a point mass (Type MASS).

Figure 2 shows the shaded plot of the finite-element model of the 5CV and 6CV package configurations for clarity. Figures 3 through 5 are the three representative finite-element models of the 5CV and 6CV configurations for (i.e., side, top-down, CGOT), of the cases described in Section 2.0.

Table 3 - 9977 Package Components

Item Number	Description	Material
1	Containment Vessel	Stainless Steel 304L
2	Load Distribution Fixtures	Aluminum 6061-T6
3	5CV Honeycomb Spacer	Aluminum 1100
4	Lid Upper Insulator	Min-K 2000
5	Lid Lower Insulator	TR-19
6	Fiberfrax Blanket	Fiberfrax (LO Con)
7	Drum / Liner / Lid	Stainless Steel 304L
8	Polyurethane Foam	FR-3716 Foam

Table 4 Material Properties of 9977 Package Components
(Elastic Properties – See App A for Plastic Regime Properties used in the Model)

Component	Material	Modulus of Elasticity (psi)	Poisson's Ratio	Density ($lb\text{-}sec^2/in^4$)
Vessel, drum, lid, liner	Stainless steel 304L	28.3E6	0.3	7.324E-4
LDF Spacer	Aluminum 6061-T6	10.0E6	0.33	2.536E-4
5CV Honeycomb Spacer	Aluminum 1100	1.0E6	0.1	4.622E-5
Lid Upper Insulator	Min-K 2000	3.0E4	0.0	2.995E-5
Lid Lower Insulator	TR-19	1.0E7	0.3	3.445E-5
Polyurethane	Foam	27,290	0.3	2.396E-5

Table 5 Weights of Package Components (See Section 4.0)

Components	Weight (lb)
Overpack	194
Containment Vessel 6CV	56
Containment Vessel 5CV	34
Contents 6CV	100
Contents 5CV	50

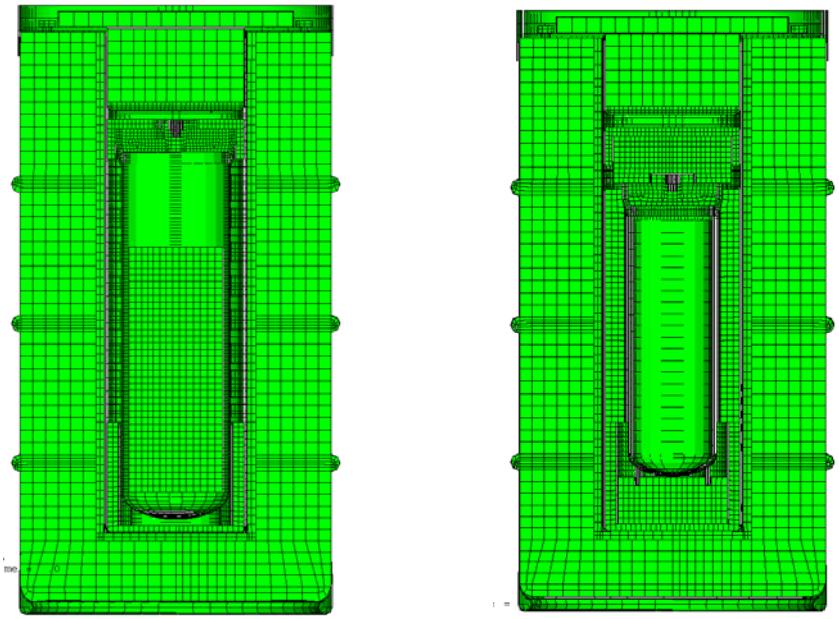

Figure 2 - Shaded View of 5CV and 6CV Package Finite-Element Models

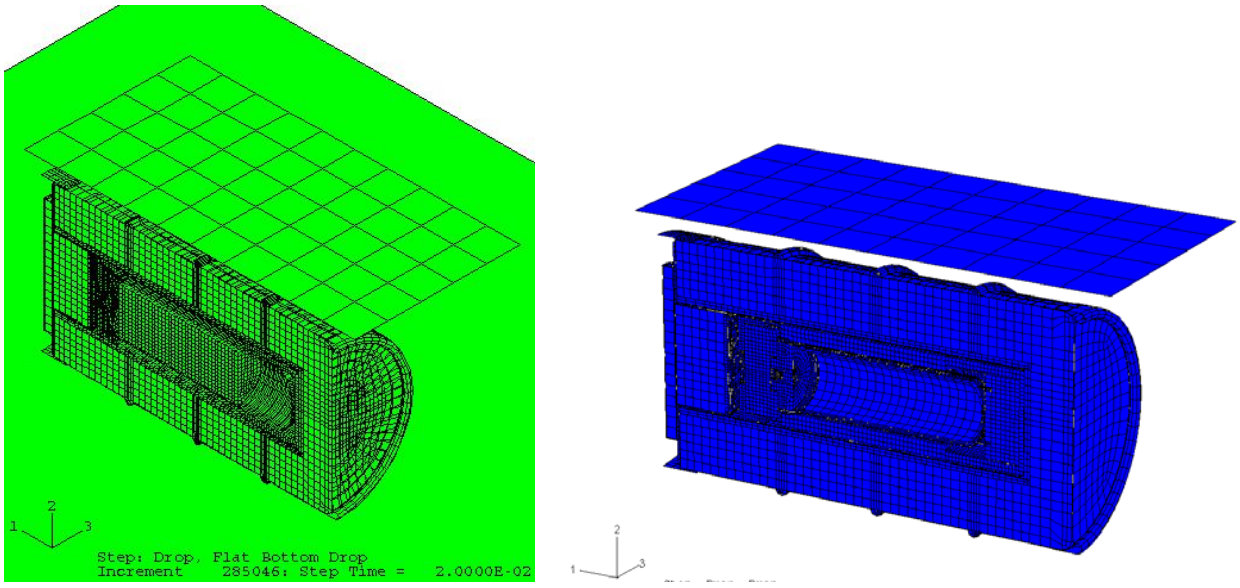

Figure 3 - Finite-Element Model of Lateral Free Drop and Crush

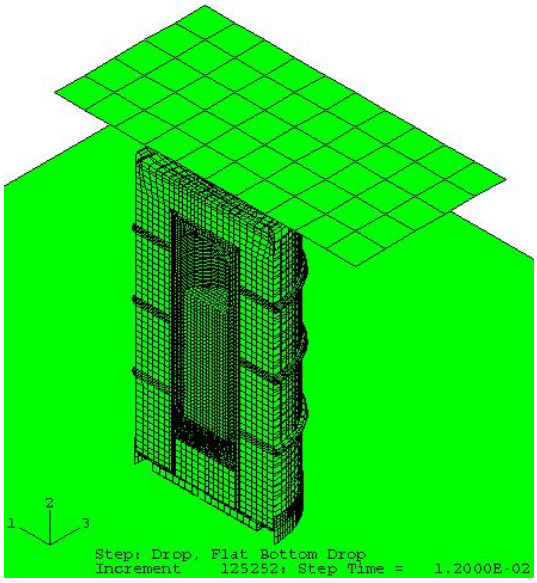

Figure 4 - Finite-Element Model of 6CV Vertical (Top-Down) 30-ft Drop and Crush

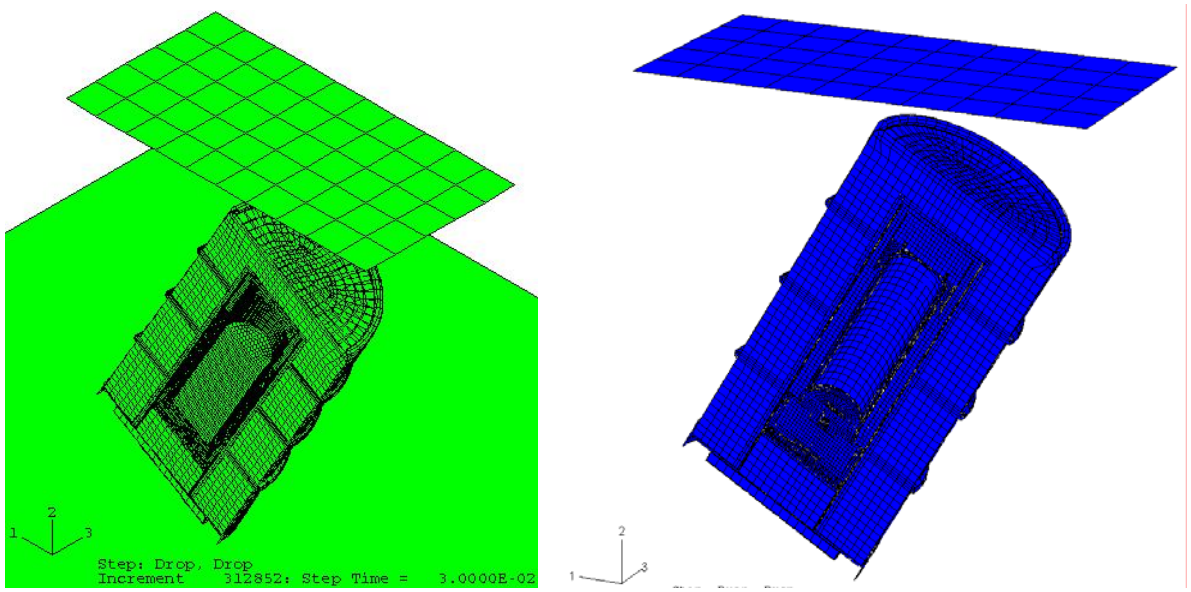

Figure 5 - Finite-Element Model of Center of Gravity over Top Corner Free Drop and Crush

5.3 Applied Loads and Initial Conditions

The applied loads and initial conditions are the same for all three cases analyzed.

Gravitational Load

The downward gravitational force of the falling package and rigid plate is represented by the gravitational load of 386.4 in/sec^2 in the negative "Z' direction of the model.

Initial Condition for 30-Foot Free Drop

During a typical analysis case, the package model is initially located near the target floor so that the initial velocity of the package model is equal to the velocity of the package after a 30-ft free fall in the negative "Z" direction of the model. Therefore, the initial velocity of the package model can be calculated as follows.

$$V_0 = \sqrt{2gh} = \sqrt{2 \times 386.4 \frac{in}{\sec^2} \times 12.0 \frac{in}{ft} \times 30\, ft} = 527.5 \frac{in}{\sec}$$

Initial Condition for 30-Foot Crush

The rigid plate model which impacts the package is initially located near the package and on the side of the package opposite to the target floor. After falling 30 feet, the plate also has the initial velocity of 527.5 in/sec as calculated above. In the dynamic simulations, the falling plate impacts the package following the initial impact of the package with the floor after 30-ft free fall. The velocity of the rigid plate at the onset of its impact with the package is defined as a velocity-type boundary condition with the amplitude varying with respect to time.

Figure 6 illustrates the methodology for specifying the velocity-type boundary condition of the plate for the case 1 analysis during the period traveling across the clearance between the plate and the package. The plate initially rests near the side of the package and then gradually increases its velocity to the value of 527.5 in/sec during the period from 0.020 seconds (at the end of the lateral 30-ft drop) to 0.0201 seconds. To preclude any unintended acceleration that might be the result of numerical calculations, the rigid plate velocity is specified as a constant value of 527.5 in/sec during the period from 0.0201 seconds to 0.0210 second prior to impact. This velocity characteristic is specified as a rigid plate boundary condition.

The total duration of 0.001 seconds is an estimated value when the rigid plate will traverse preset clearance between the plate and the package culminating impact. To verify this estimated value, the velocity of the rigid plate at the onset of impact will be calculated for each case analyzed to ensure that the initial kinetic energy of the striking plate represents a 30-ft fall.

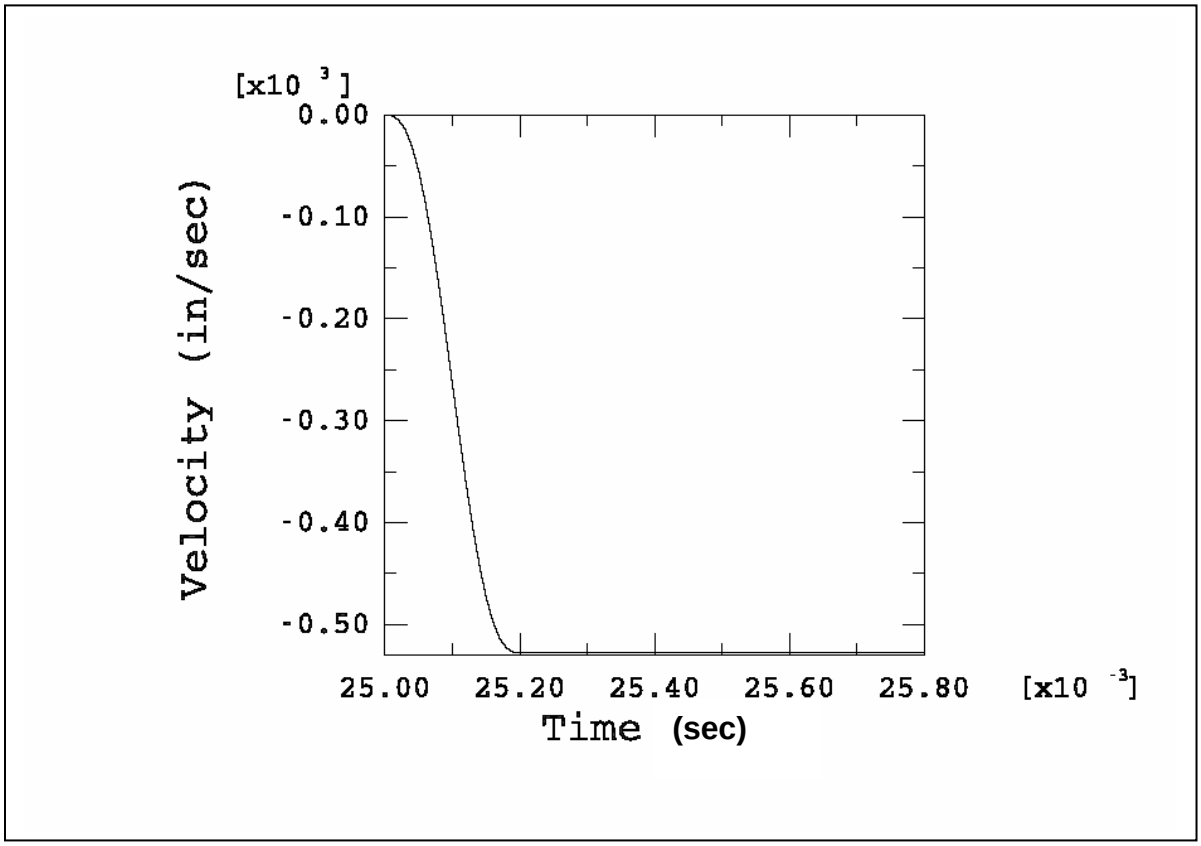

Figure 6 - Input Velocity Profile of Falling Plate

5.4 Boundary Conditions

Due to the symmetrical conditions of the geometry and loading, the following boundary conditions are applied at the nodes of the shell elements:

$$UY = 0 \qquad RX = 0 \qquad RZ = 0\,;$$

and the following boundary condition is applied at the nodes of the brick elements:

$$UY = 0$$

The target floor is fixed and thus its boundary conditions are as follows.

$$UX = UY = UZ = RX = RY = RZ = 0$$

5.5 Contact Conditions

The contact conditions between the interfaces of the package components are simulated by using the general contact options available in the ABAQUS Explicit computer code.

6.0 Stress Criteria in Accordance with ASME Code

The dynamic load associated with a the 30-ft drop or a 30-ft crush of a 9977 package is classified as a Level D Service Load defined in the ASME Code, Section III, Appendix F and the stress limits are specified as follows:

$$P_m \le 0.7 S_u$$

$$P_L \le 0.9 S_u$$

where P_m = General primary membrane stress intensity
P_L = Local primary membrane stress intensity
S_u = Ultimate strength of material

The maximum temperature under normal operating conditions is 300 ^{0}F and the minimum ultimate strength of stainless steel 304L is 61.2 ksi per ASME (Reference 7).

The results of the finite-element analysis are expressed in terms of true stresses and thus, the allowable stress limits should also be converted to true stresses. Using the minimum required engineering elongation value of 35%, (Reference 8) the true ultimate stress of the material at the failure strain is:

$S_{tu} = S_u(\varepsilon + 1) = 61.2(0.35 + 1) = 82.62$ ksi for temperature = 300 °F

where,

S_{tu} = True ultimate stress of stainless steel 304L at 300 °F
ε = Engineering strain corresponding to ultimate strength

Consequently, the stress limits in terms of true stresses are:

$P_m \le 0.7 S_{tu} = 0.7 \times 82.62 = 57.8$ ksi for temperature = 300 °F

$P_L \le 0.9 S_{tu} = 0.9 \times 82.62 = 74.3$ ksi for temperature = 300 °F

7.0 Discussion of Analytical Results

7.1 Drum Top Down Drop Followed by Crush On Bottom (75, 140 and 300 ºF)

Figure 7 shows the finite element model used for evaluating the 30-ft drum top down drop with the follow on impact of the 1,100 lb plate dropped 30-ft onto the package bottom.

7.1.1 Case 1: Drum Top Down - 30-Ft Drop (75 ºF)

Energy History
The time-history plots of energy components for the 30-ft drum top down drop simulation shown in Figure 8 indicate that the kinetic energy approaches zero at the end of the analysis. Therefore, we know that the analysis covers the entire impact duration.

Deformed Shape of Full Model
Figure 9 is the deformed shape of the overall model.

Stress and Strain Contours in Component Models
Figures 10 and 11 show the von Mises stresses and the equivalent plastic strains in the CV model. Figure 12 shows the equivalent plastic strains in the overpack shell.

Evaluations of Maximum Local Primary Membrane Stress Intensities and Maximum Equivalent Plastic Strains in Containment Vessel
The stress components across the wall thickness at the locations away from or near the geometrical discontinuities should be used to calculate the general primary membrane stress intensities (P_m) or the local primary membrane stress intensities (P_L). For simplicity, the maximum value of the von Mises stresses in the containment vessel is used as the local primary membrane stress intensity (P_L). This value is higher than the actual local primary membrane stress intensity because the latter is calculated by averaging the thru-wall stresses across the component's thickness.

The maximum value of the local primary membrane stress intensity in the containment vessel is 29.96 ksi as given in Figure 10. This value is less than the allowable value of 57.3 ksi for the

general primary membrane stress intensity and of 73.6 ksi for the local primary membrane stress intensity (as given in Section 6.0). The structural integrity of the 9977 subjected to a 30-ft drop has therefore been justified according to the ASME Code, Section III.

As shown in Figure 11, the maximum plastic strain experienced at any location within the containment vessel after the 30-ft drop is 0.97%. The maximum calculated value of the effective plastic strain at any point in the overpack is 9.55%. This value is less than the maximum average through-wall elongation of 35% for the 304L material use in the drum. Therefore, the drum will not be ruptured by the 30-ft drop impact.

7.1.2 Case 2: Drum Top Down - 30-Ft Drop (140 ºF)

Energy History

The time-history plots of energy components for the 30-ft drum top down drop simulation shown in Figure 13 indicate that the kinetic energy approaches zero at the end of the analysis. Therefore, we know that the analysis covers the entire impact duration.

Deformed Shape of Full Model

Figure 14 is the deformed shape of the overall model.

Stress and Strain Contours in Component Models

Figures 15 and 16 show the von Mises stresses and the equivalent plastic strains in the CV model. Figure 17 shows the equivalent plastic strains in the overpack shell.

Evaluations of Maximum Local Primary Membrane Stress Intensities and Maximum Equivalent Plastic Strains in Containment Vessel

The stress components across the wall thickness at the locations away from or near the geometrical discontinuities should be used to calculate the general primary membrane stress intensities (P_m) or the local primary membrane stress intensities (P_L). For simplicity, the maximum value of the von Mises stresses in the containment vessel is used as the local primary membrane stress intensity (P_L). This value is higher than the actual local primary membrane stress intensity because the latter is calculated by averaging the thru-wall stresses across the component's thickness.

The maximum value of the local primary membrane stress intensity in the containment vessel is 30.02 ksi as given in Figure 15. This value is less than the allowable value of 57.3 ksi for the general primary membrane stress intensity and of 73.6 ksi for the local primary membrane stress intensity (as given in Section 6.0). The structural integrity of the 9977 subjected to a 30-ft drop has therefore been justified according to the ASME Code, Section III.

As shown in Figure 16, the maximum plastic strain experienced at any location within the containment vessel after the 30-ft drop is 0.97%. The maximum calculated value of the effective plastic strain at any point in the overpack is 9.25%. This value is less than the maximum average through-wall elongation of 35% for the 304L material use in the drum. Therefore, the drum will not be ruptured by the 30-ft drop impact.

7.1.3 Case 3: Drum Top Down - Bottom Crush (140 ºF)

Energy History

Figure 18 depicts the kinetic energy variation of the plate during the 30-ft fall. The plot indicates that the kinetic energy approaches zero before the end of the analysis. Therefore, we know that the analysis covers the entire impact duration.

Deformed Shape of Full Model

Figure 19 shows the deformed shape of the overall model.

Stress and Strain Contours in Component Models

Figures 20 and 21 show the von Mises stresses and the equivalent plastic strains in the containment vessel and its internal components. Figure 22 shows the equivalent plastic strains in the overpack shell.

Evaluations of Maximum Local Primary Membrane Stress Intensities and Maximum Equivalent Plastic Strains in Containment Vessel

The maximum value of the local primary membrane stress intensity in the containment vessel is 17.83 ksi as shown in Figure 20. This value is less than the allowable value of 57.3 ksi for the general primary membrane stress intensity and of 73.6 ksi for the local primary membrane stress intensity (as given in Section 6.0). The structural integrity of the 9977 subjected to a 30-ft crush has therefore been verified according to the ASME Code, Section III.

As shown in Figure 21, the maximum plastic strain experienced at any location within the containment vessel after a crush is 0.97%. The maximum calculated value of the effective plastic strain at any point in the overpack is 12.74%. This value is less than the maximum average through-wall elongation of 35% for the 304L material use in the drum. Therefore, the drum will not be ruptured by the crush impact.

7.1.4 Case 4: Drum Top Down - 30-Ft Drop (300 ºF)

Energy History

The time-history plots of energy components for the 30-ft drum top down drop simulation shown in Figure 23 indicate that the kinetic energy approaches zero at the end of the analysis. Therefore, we know that the analysis covers the entire impact duration.

Deformed Shape of Full Model

Figure 24 is the deformed shape of the overall model.

Stress and Strain Contours in Component Models

Figures 25 and 26 show the von Mises stresses and the equivalent plastic strains in the CV model. Figure 27 shows the equivalent plastic strains in the overpack shell.

Evaluations of Maximum Local Primary Membrane Stress Intensities and Maximum Equivalent Plastic Strains in Containment Vessel

The stress components across the wall thickness at the locations away from or near the geometrical discontinuities should be used to calculate the general primary membrane stress intensities (P_m) or the local primary membrane stress intensities (P_L). For simplicity, the maximum value of the von Mises stresses in the containment vessel is used as the local primary membrane stress intensity (P_L). This value is higher than the actual local primary membrane stress intensity because the latter is calculated by averaging the thru-wall stresses across the component's thickness.

The maximum value of the local primary membrane stress intensity in the containment vessel is 39.27 ksi as given in Figure 25. This value is less than the allowable value of 57.3 ksi for the general primary membrane stress intensity and of 73.6 ksi for the local primary membrane stress intensity (as given in Section 6.0). The structural integrity of the 9977 subjected to a 30-ft drop has therefore been justified according to the ASME Code, Section III.

As shown in Figure 26, the maximum plastic strain experienced at any location within the containment vessel after the 30-ft drop is 0.49%. The maximum calculated value of the effective plastic strain at any point in the overpack is 9.54%. This value is less than the maximum average through-wall elongation of 35% for the 304L material use in the drum. Therefore, the drum will not be ruptured by the 30-ft drop impact.

7.1.5 Case 5: Drum Top Down - Bottom Crush (300 ºF)

Energy History

Figure 28 depicts the kinetic energy variation of the plate during the 30-ft fall. The plot indicates that the kinetic energy approaches zero before the end of the analysis. Therefore, we know that the analysis covers the entire impact duration.

Deformed Shape of Full Model

Figure 29 shows the deformed shape of the overall model.

Stress and Strain Contours in Component Models

Figures 30 and 31 show the von Mises stresses and the equivalent plastic strains in the containment vessel and its internal components. Figure 32 shows the equivalent plastic strains in the overpack shell.

Evaluations of Maximum Local Primary Membrane Stress Intensities and Maximum Equivalent Plastic Strains in Containment Vessel

The maximum value of the local primary membrane stress intensity in the containment vessel is 37.14 ksi as shown in Figure 30. This value is less than the allowable value of 57.3 ksi for the general primary membrane stress intensity and of 73.6 ksi for the local primary membrane stress intensity (as given in Section 6.0). The structural integrity of the 9977 subjected to a 30-ft crush has therefore been verified according to the ASME Code, Section III.

As shown in Figure 31, the maximum plastic strain experienced at any location within the containment vessel after the crush is 4.92%. The maximum calculated value of the effective plastic strain at any point in the overpack is 22.00%. This value is less than the maximum average

through-wall elongation of 35% for the 304L material use in the drum. Therefore, the drum will not be ruptured by the crush impact.

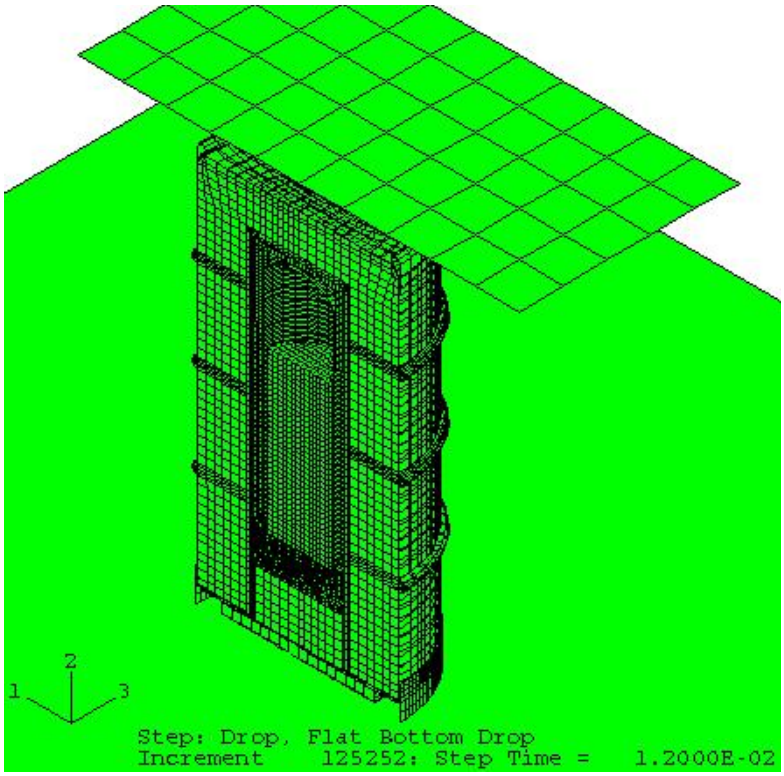

Figure 7 - Finite Element Model of the 9977 6CV Top Down Drop and Bottom Crush

(ALLKE = kinetic energy; ALLIE = internal energy; ALLPD = plastic strain energy; ALLSE = elastic strain energy; ALLAE = artificial energy)

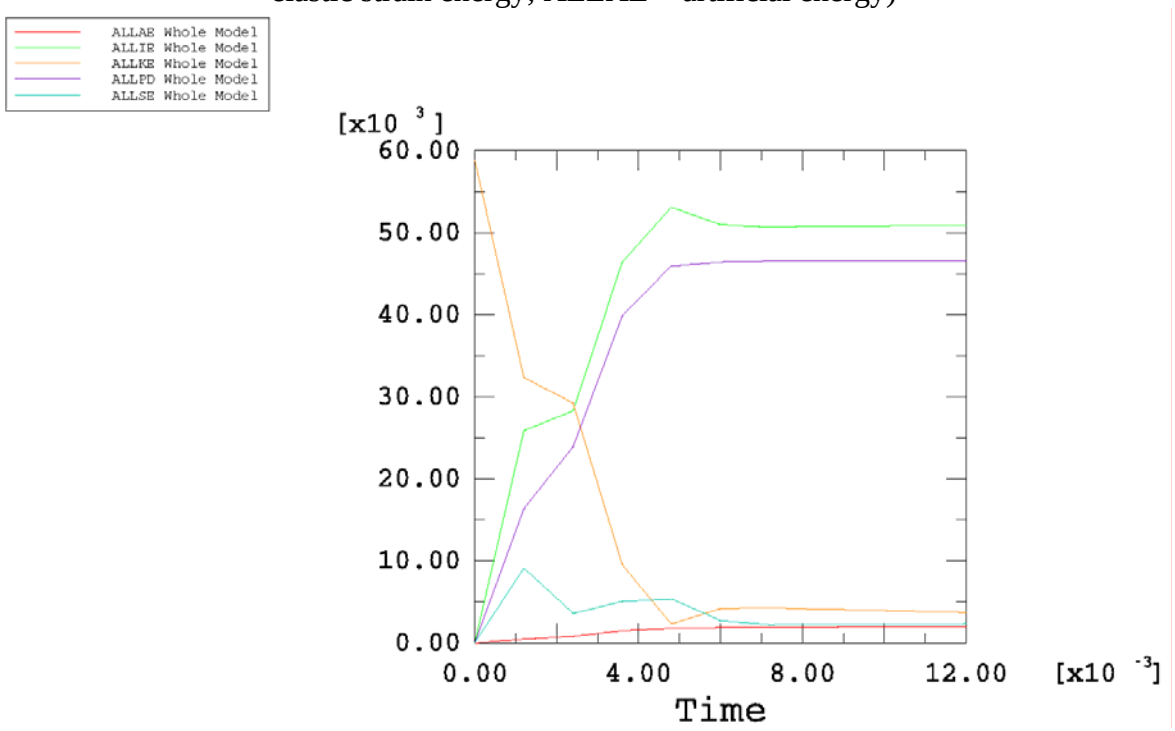

Figure 8 - Time-History Plot of Energy during Drum Top Down - 30-ft Drop Simulation (75 ºF)

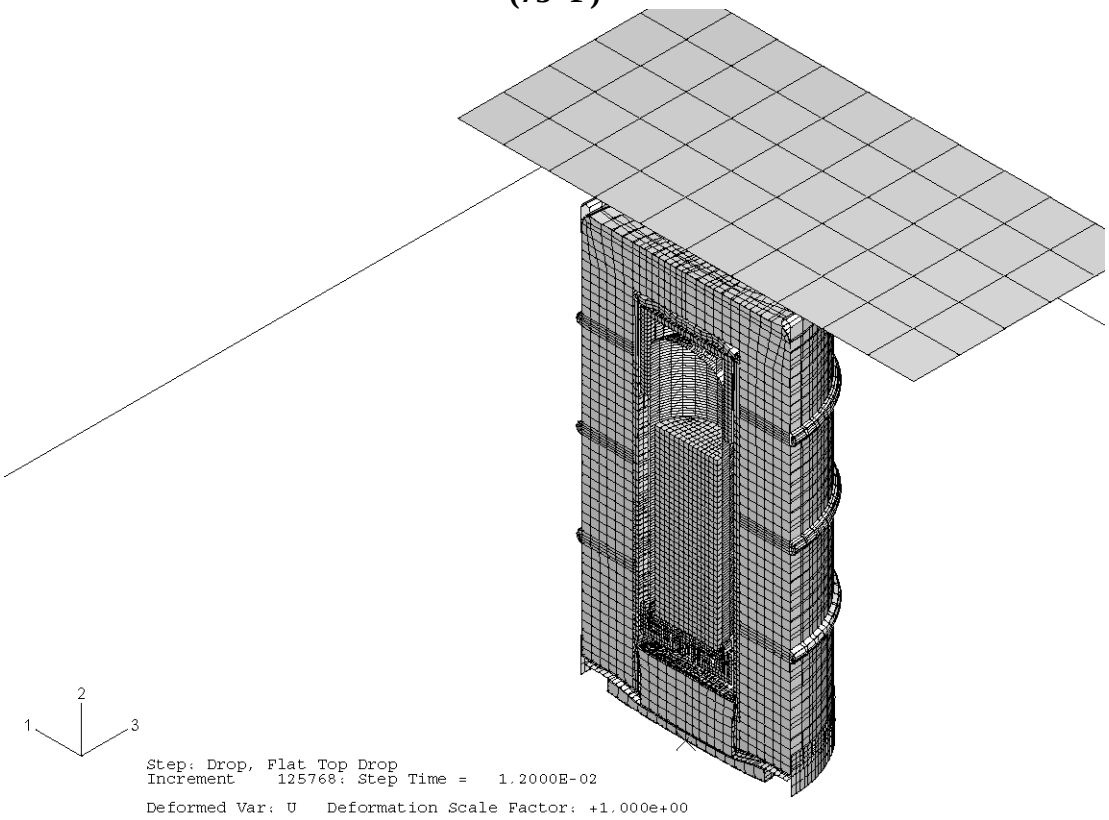

Figure 9 - Deformed Shape of 9977 with 6CV After the Drum Top Down - 30-ft Drop (75 ºF)

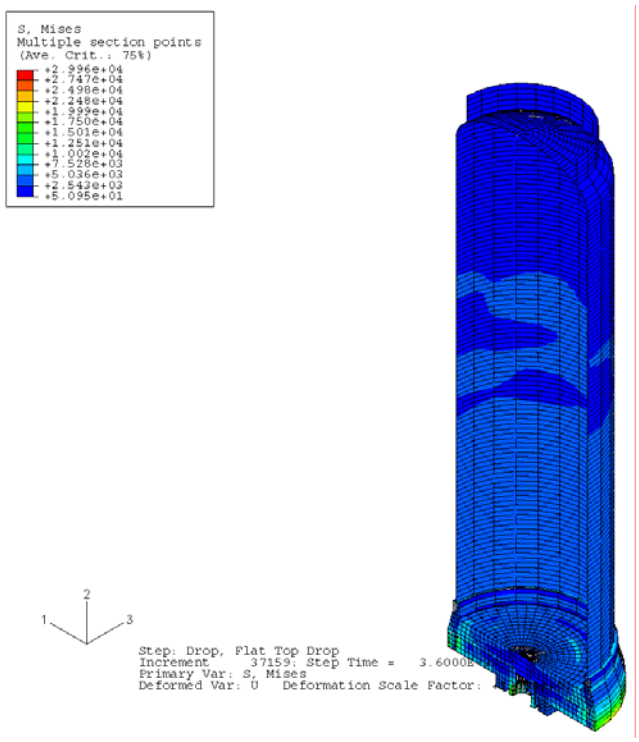

Figure 10 - Stress Distribution in the 6CV Model for Drum Top Down - 30-ft Drop (75 ºF)

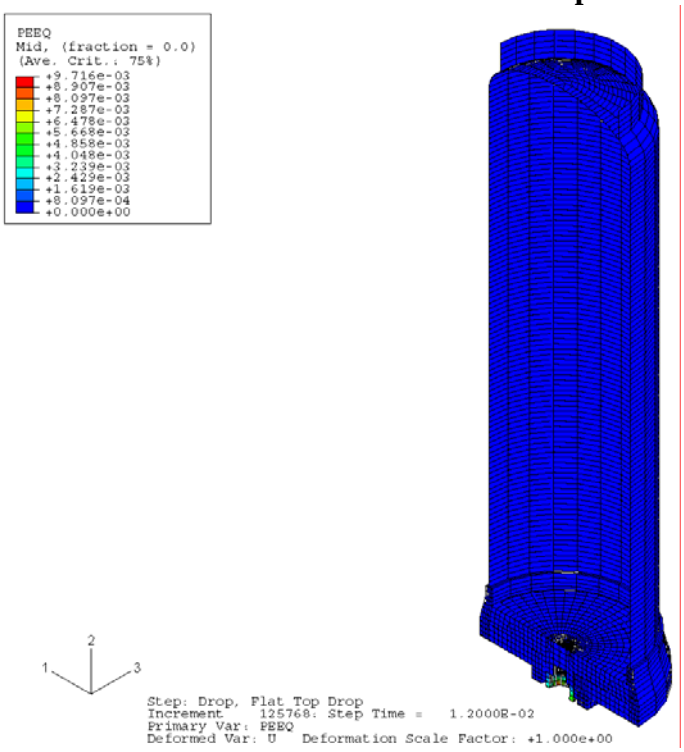

Figure 11 - Strain Distribution in 6CV Model for Drum Top Down - 30-ft Drop (75 ºF)

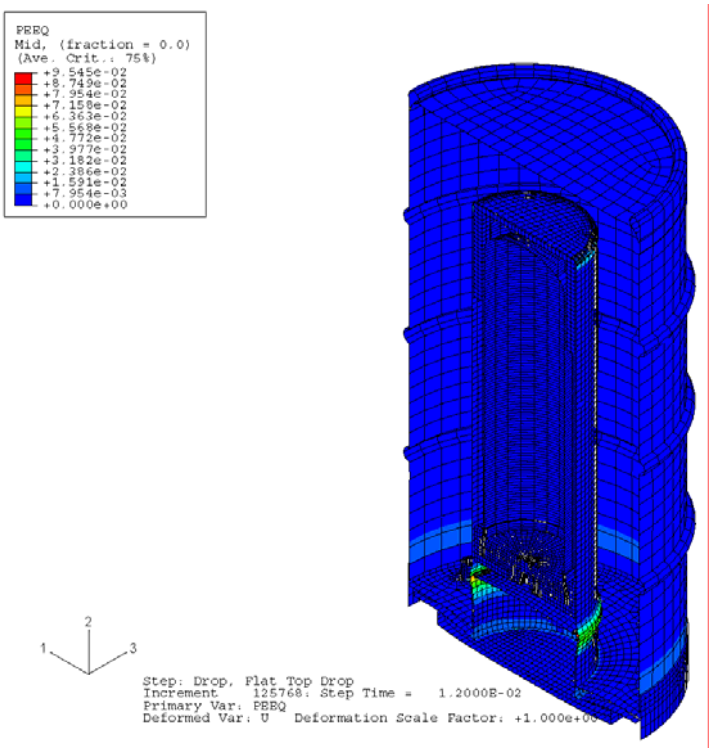

Figure 12 - Strain Distribution in Overpack for 6CV for Drum Top Down - 30-ft Drop (75 ºF)

(ALLKE = kinetic energy; ALLIE = internal energy; ALLPD = plastic strain energy; ALLSE = elastic strain energy; ALLAE = artificial energy)

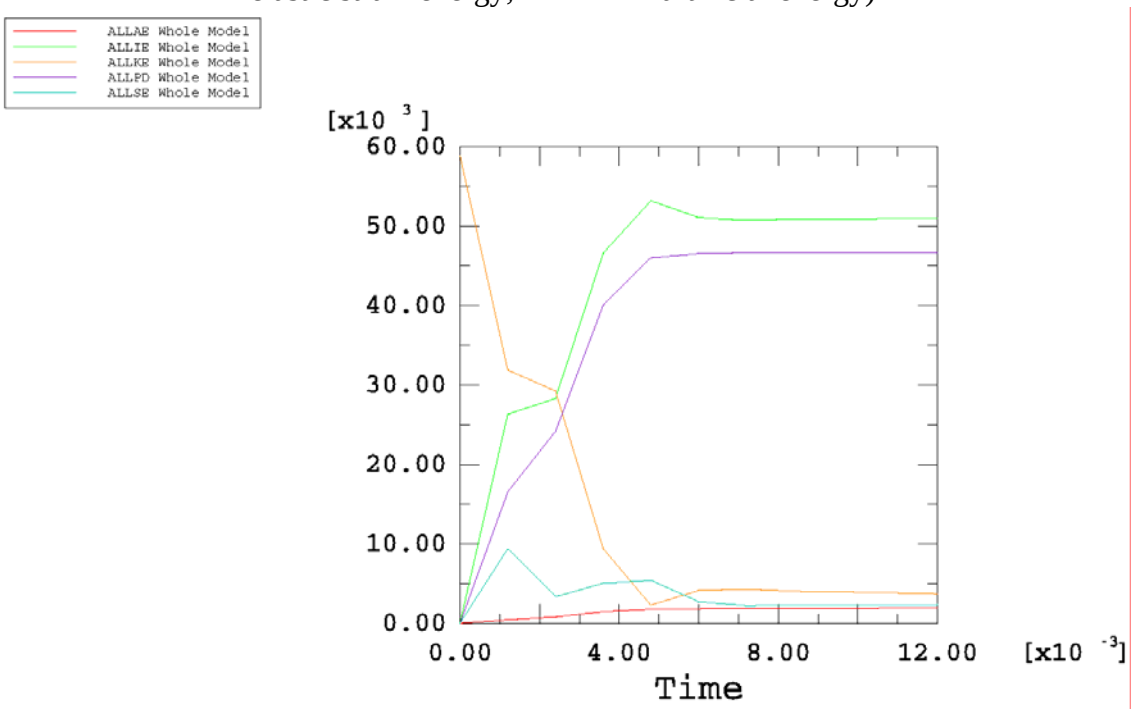

Figure 13 - Time-History Plot of Energy during Drum Top Down - 30-ft Drop Simulation (140 ºF)

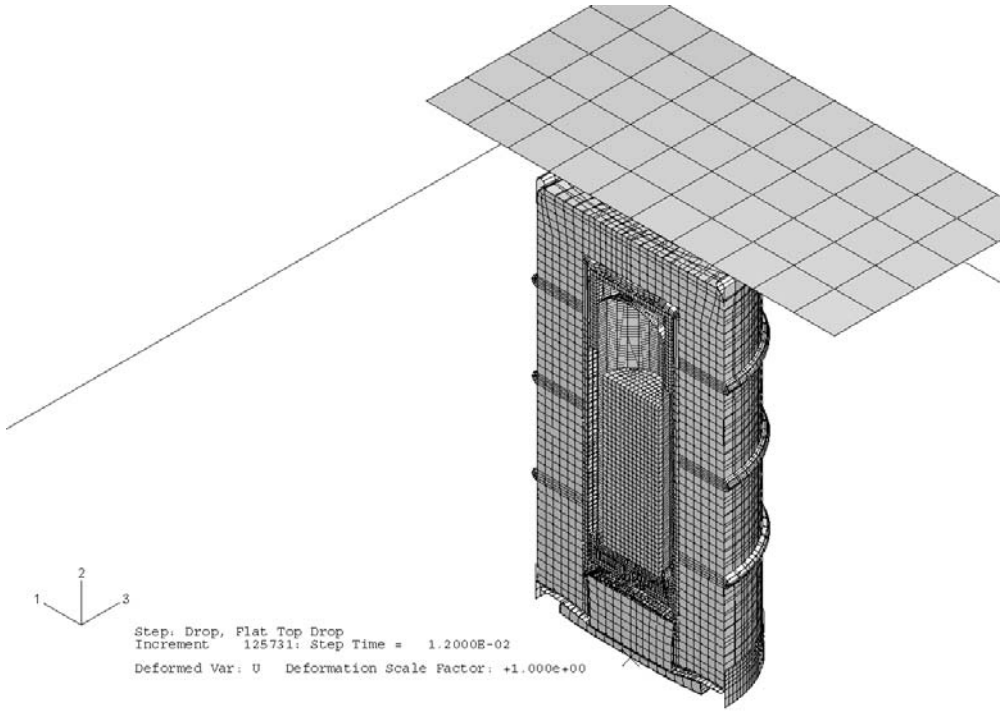

Figure 14 - Deformed Shape of 9977 with 6CV for Drum Top Down - 30-ft Drop (140 ºF)

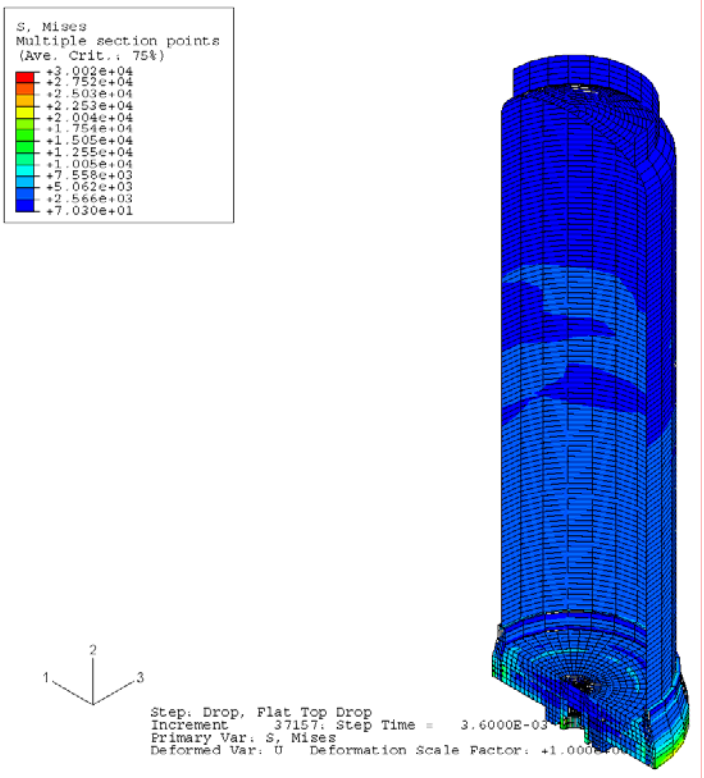

Figure 15 - Stress Distribution in 6CV Model for Drum Top Down - 30-ft Drop (140 ºF)

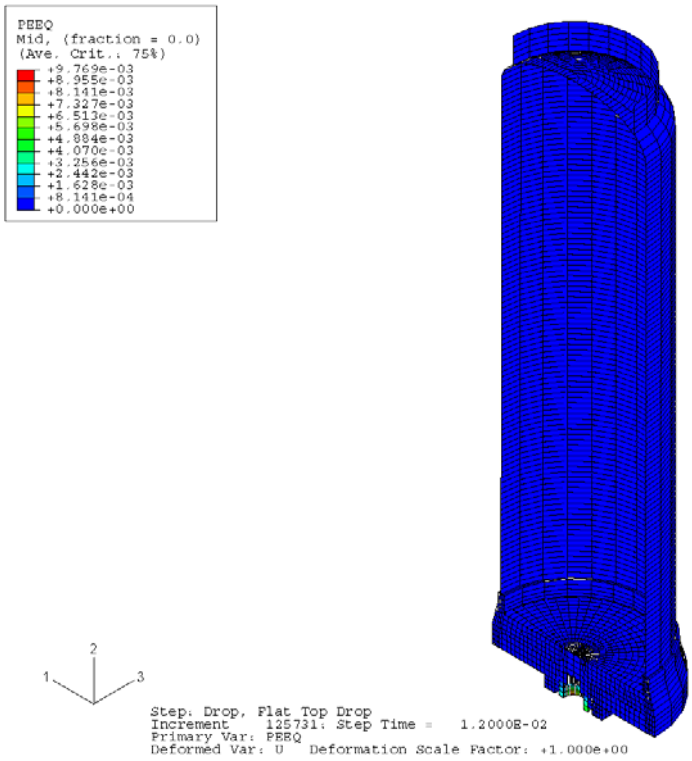

Figure 16 - Strain Distribution in 6CV Model for Drum Top Down - 30-ft Drop (140 ºF)

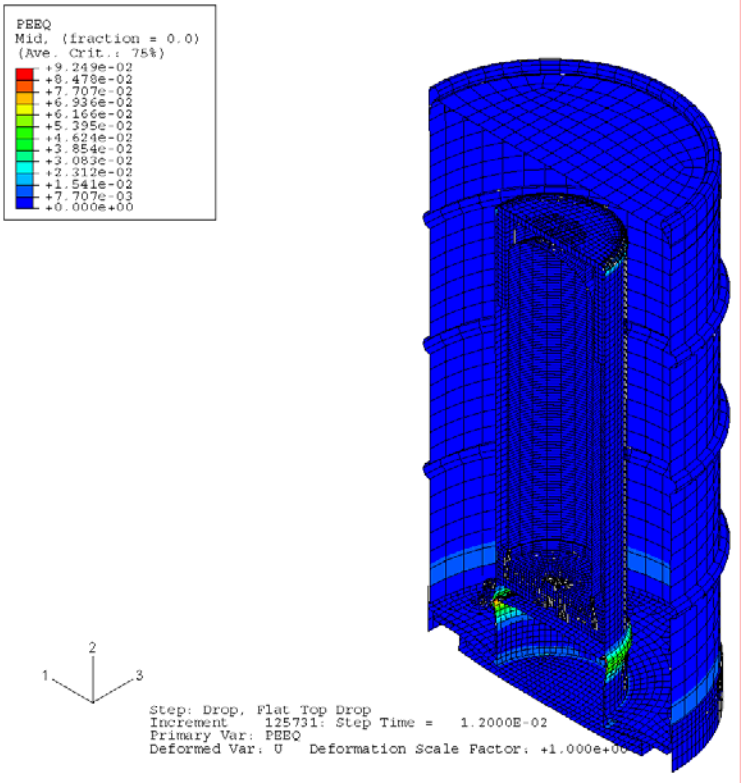

Figure 17 - Strain Distribution in Overpack for 6CV for Drum Top Down - 30-ft Drop (140 ºF)

(ALLKE = kinetic energy; ALLIE = internal energy; ALLPD = plastic strain energy; ALLSE = elastic strain energy; ALLAE = artificial energy)

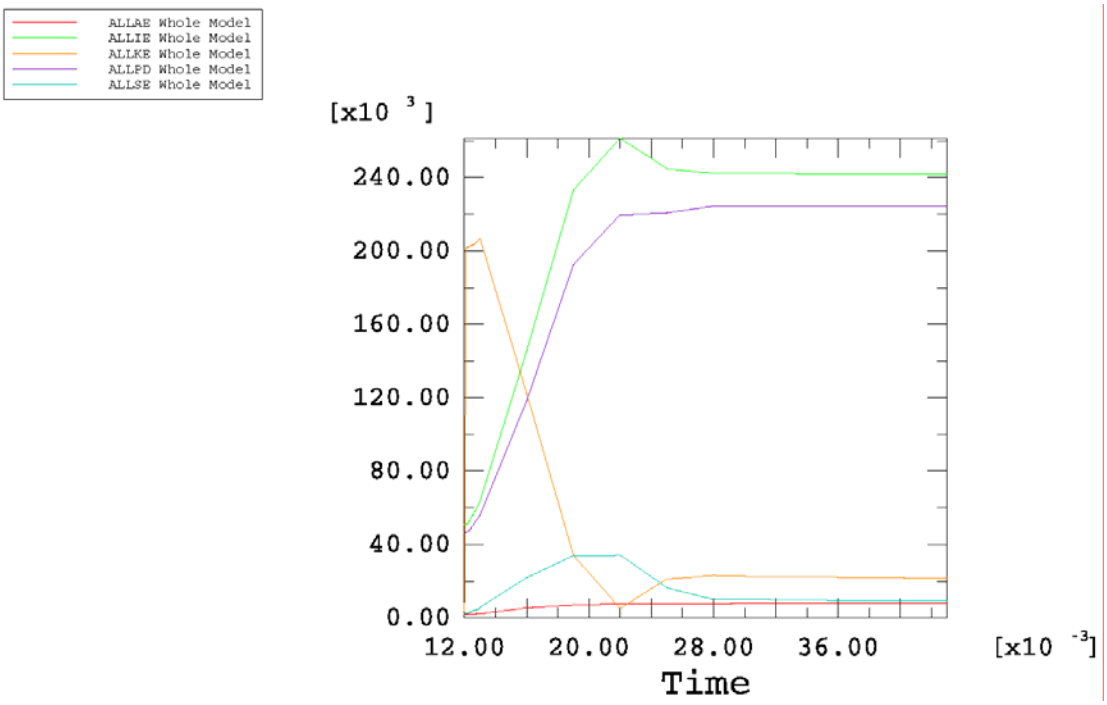

Figure 18 - Time-History Plot of Plate Energy during Drum Top-Down, 30-ft Bottom Crush Simulation (140 ºF)

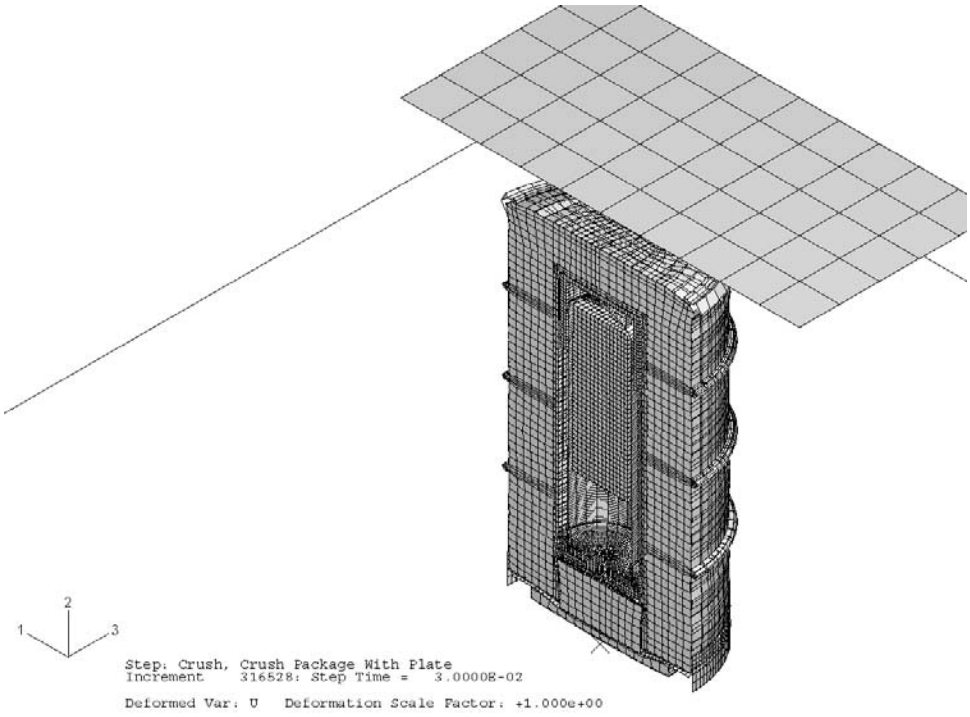

Figure 19 - Deformed Shape of 9977 with 6CV for Drum Top-Down - 30-ft Bottom Crush (140 ºF)

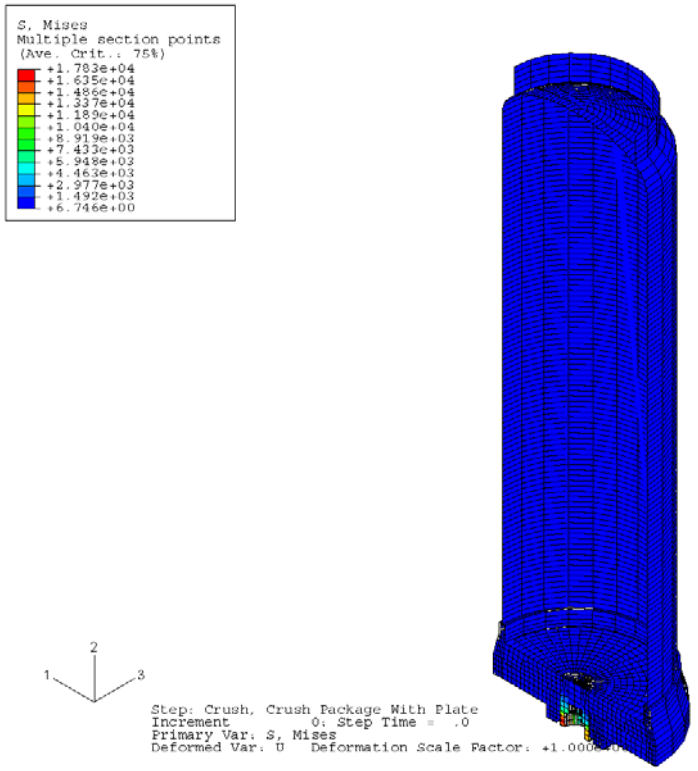

Figure 20 - Stress Distribution in 6CV Model for Drum Top-Down - 30-ft Bottom Crush (140 ºF)

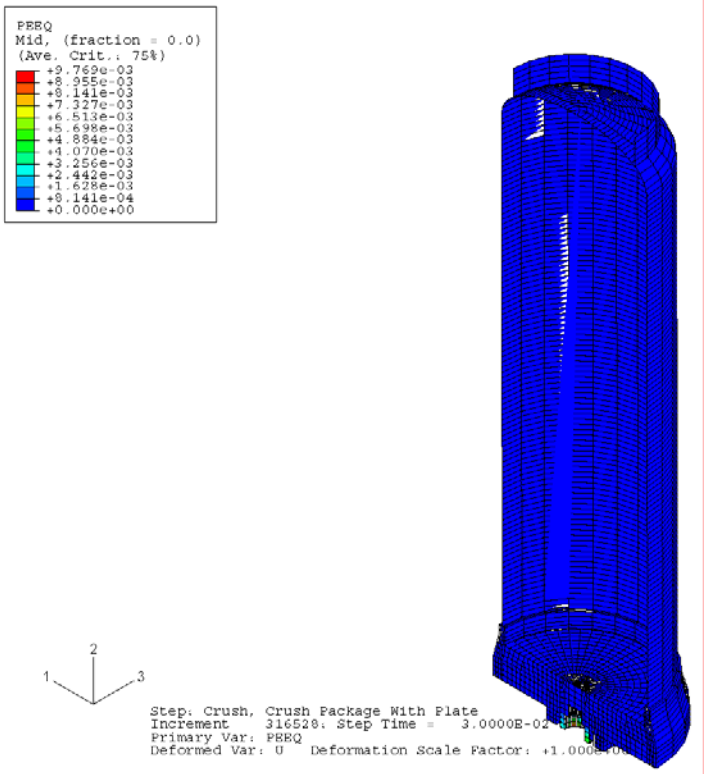

Figure 21 - Strain Distribution in 6CV Model for Drum Top-Down - 30-ft Bottom Crush (140 ºF)

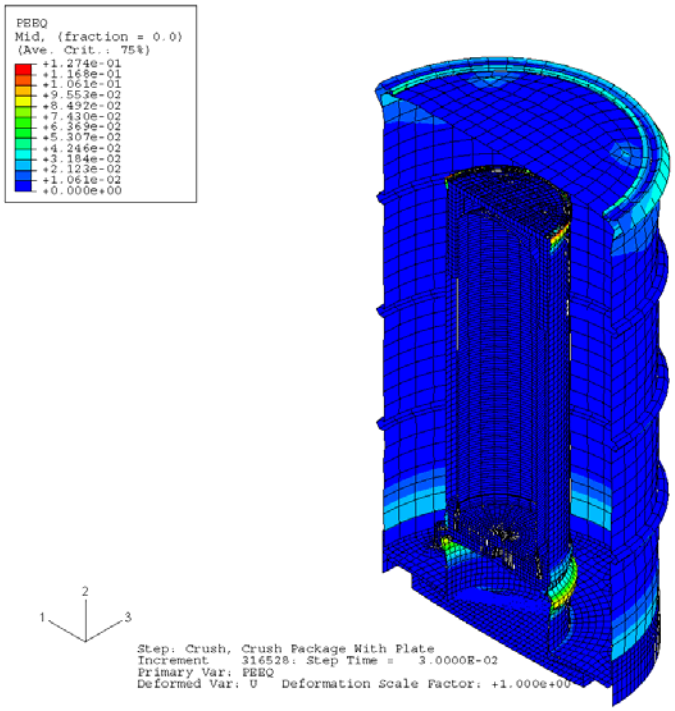

Figure 22 - Strain Distribution in Overpack for 6CV for Drum Top-Down - 30-ft Bottom Crush (140 °F)

(ALLKE = kinetic energy; ALLIE = internal energy; ALLPD = plastic strain energy; ALLSE = elastic strain energy; ALLAE = artificial energy)

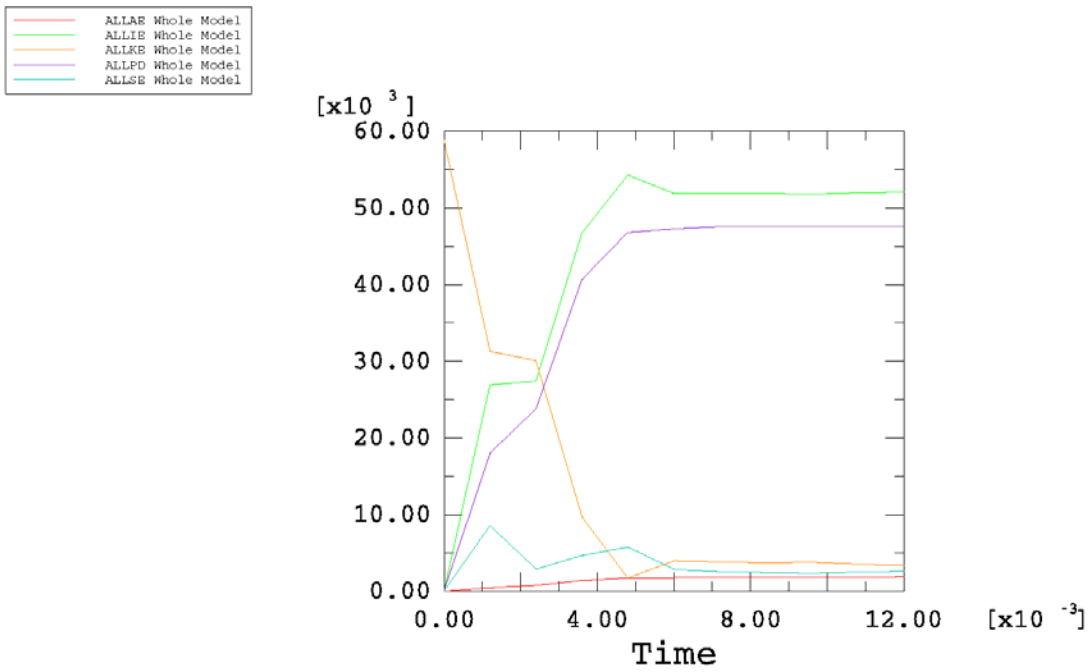

Figure 23 - Time-History Plot of Energy during Drum Top Down - 30-ft Drop Simulation (300 °F)

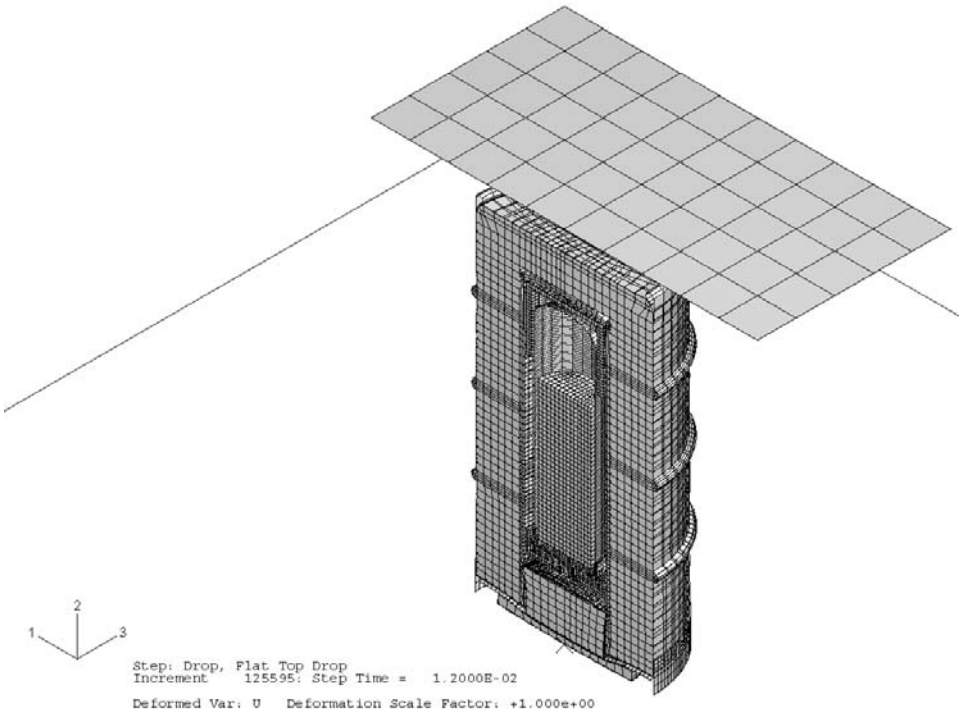

Figure 24 - Deformed Shape of 9977 with 6CV for Drum Top Down - 30-ft Drop (300 ºF)

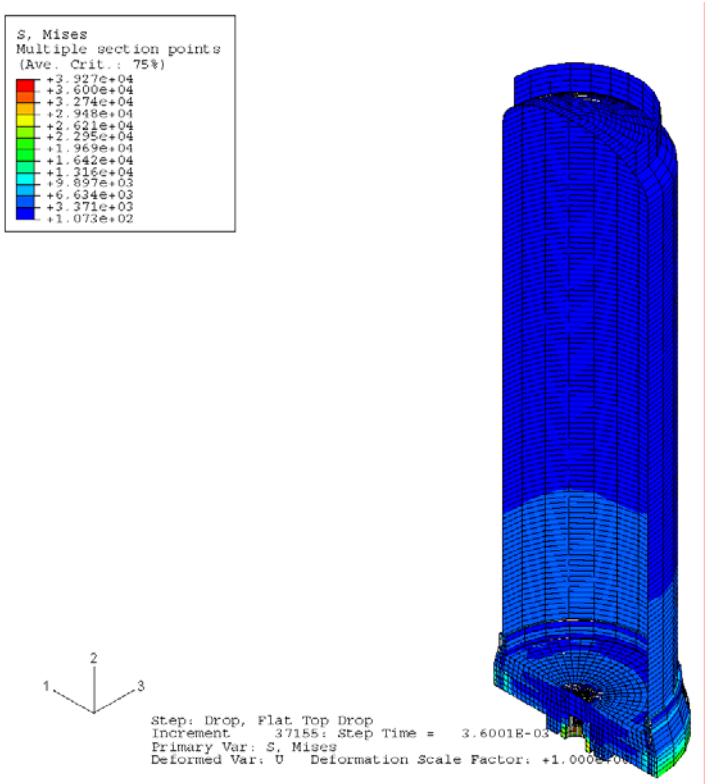

Figure 25 - Stress Distribution in 6CV Model for Drum Top Down - 30-ft Drop (300 ºF)

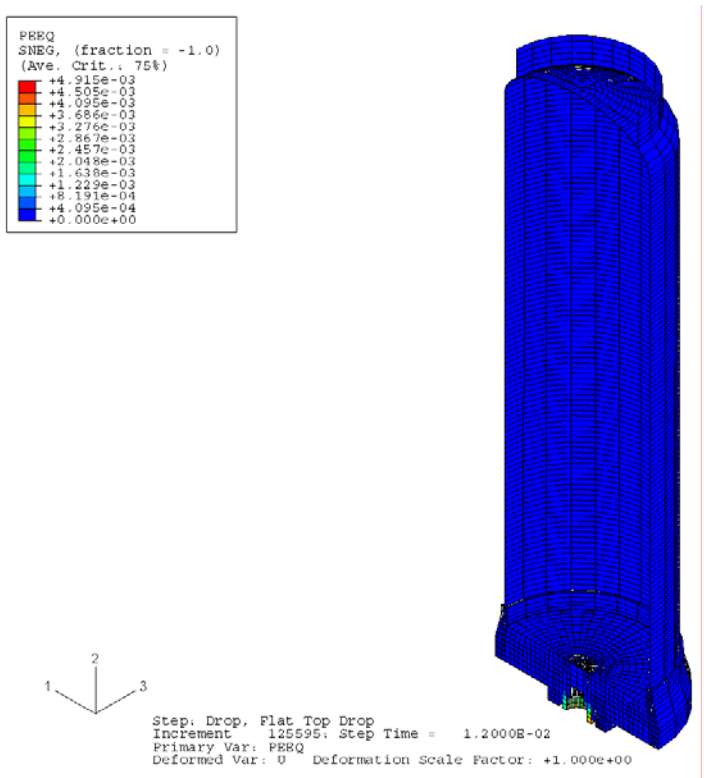

Figure 26 - Strain Distribution in 6CV Model for Drum Top Down - 30-ft Drop (300 ºF)

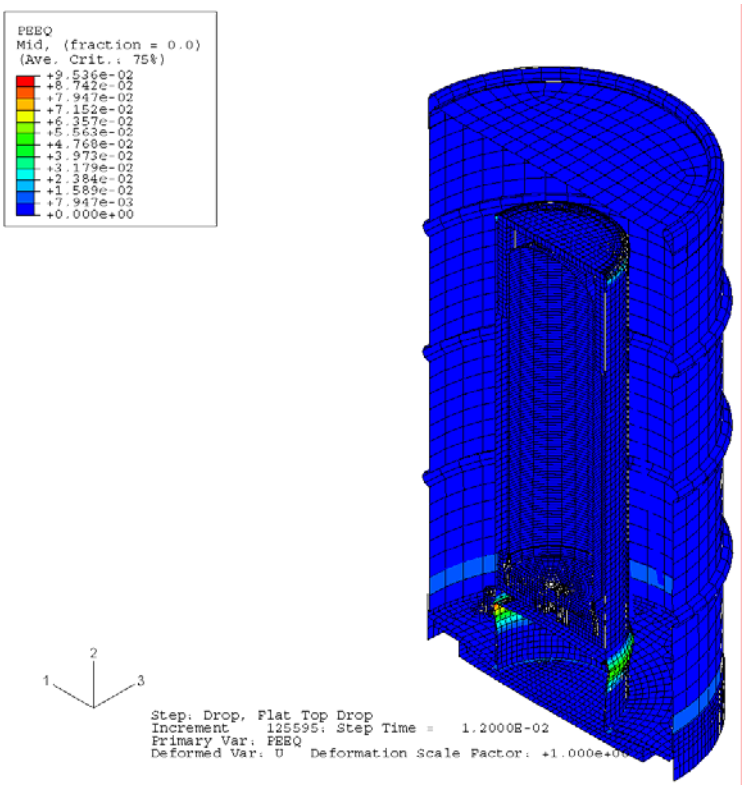

Figure 27 - Strain Distribution in Overpack for 6CV for Drum Top Down - 30-ft Drop (300 ºF)

(ALLKE = kinetic energy; ALLIE = internal energy; ALLPD = plastic strain energy; ALLSE = elastic strain energy; ALLAE = artificial energy)

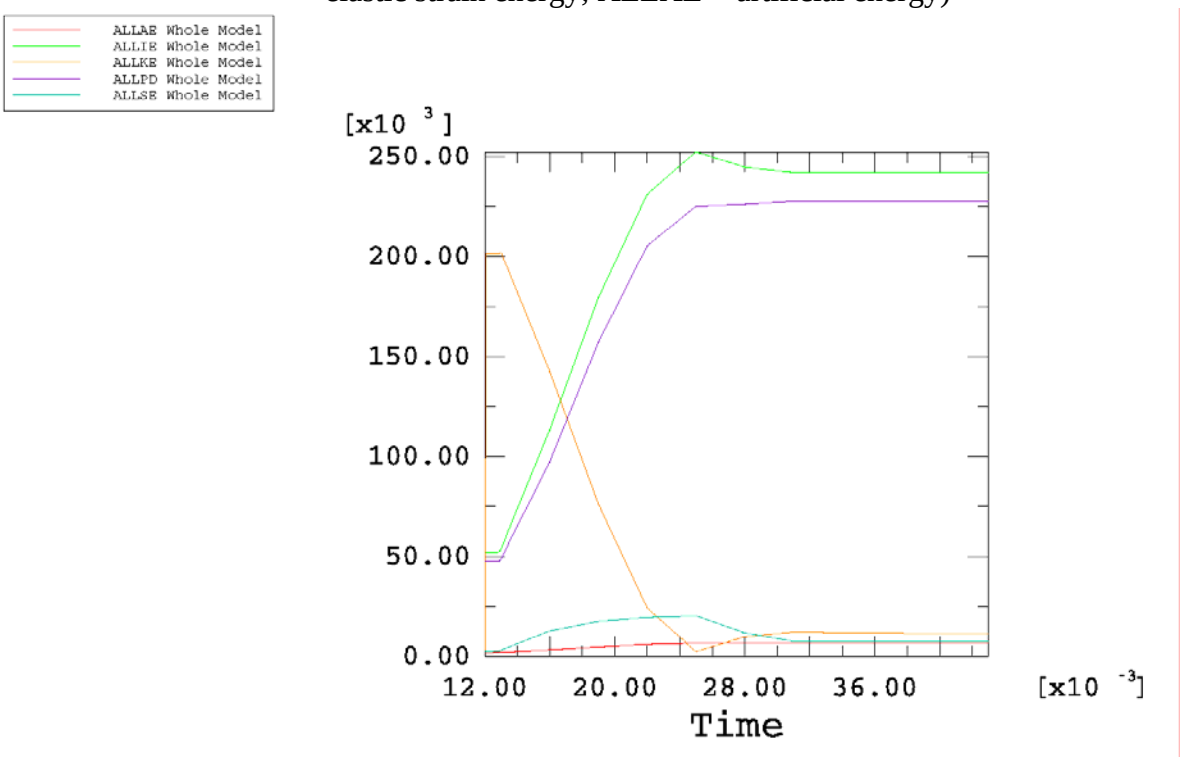

Figure 28 - Time-History Plot of Plate Energy during Drum Top Down - 30-ft Bottom Crush Simulation (300 ºF)

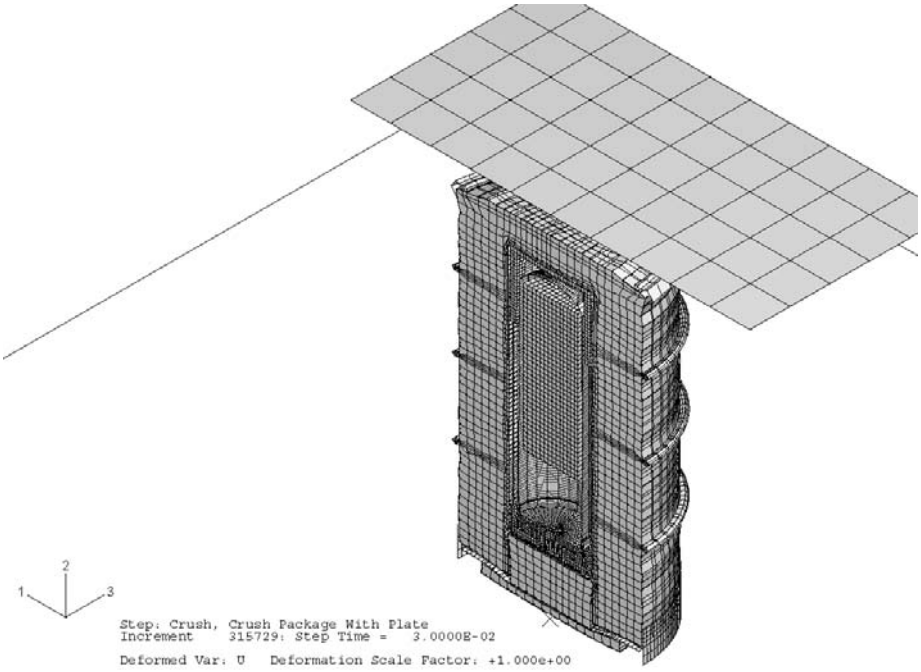

Figure 29 - Deformed Shape of 9977 with 6CV for Drum Top Down - Bottom Crush (300 ºF)

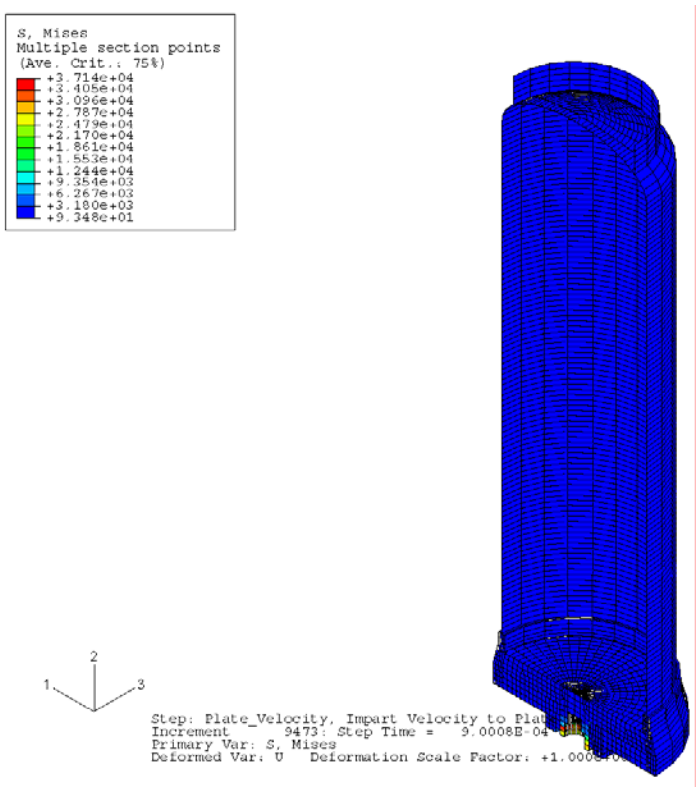

Figure 30 - Stress Distribution in 6CV Model for Drum Top Down - Bottom Crush (300 ºF)

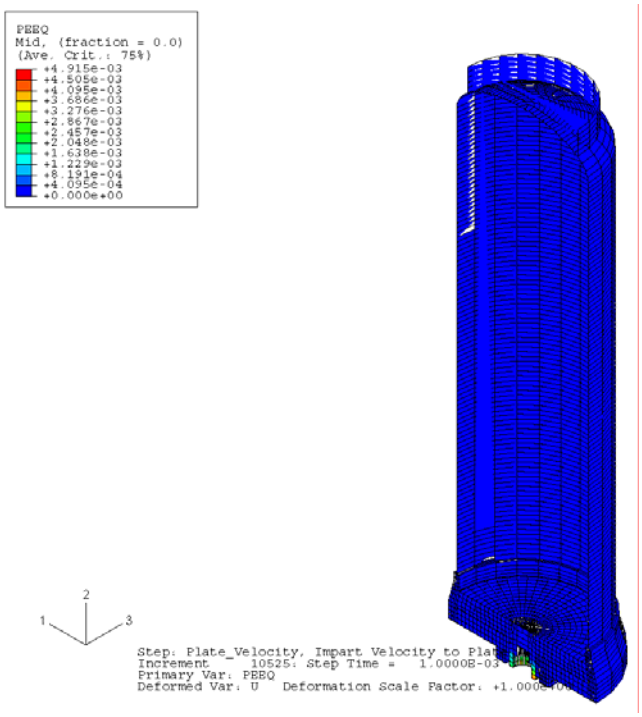

Figure 31 - Strain Distribution in 6CV Model for Drum Top Down - Bottom Crush (300 ºF)

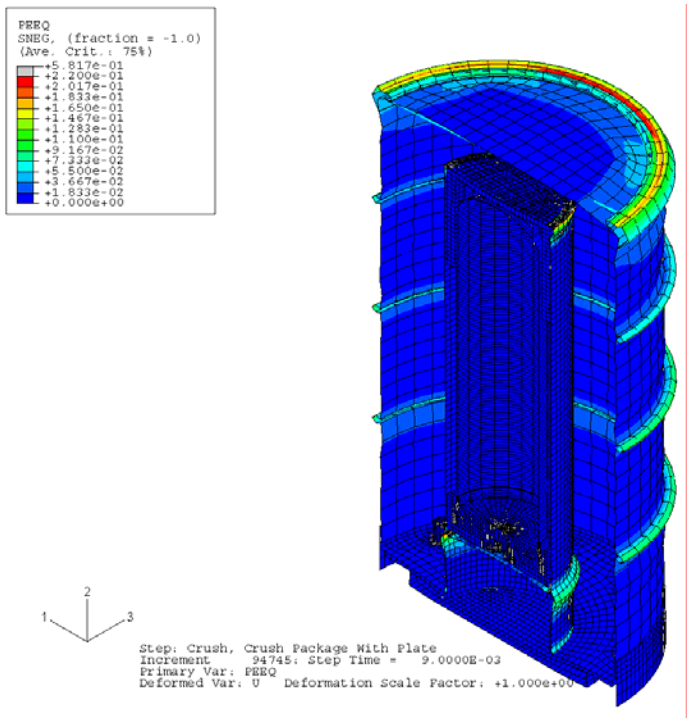

Figure 32 - Strain Distribution in Overpack for 6CV for Drum Top Down - Bottom Crush (300 ºF)

7.2 Drum Bottom Down Drop Followed by Crush On Top (-20, 75, 140 and 300 ºF)

Figure 33 shows the finite element model used for evaluating the 30-Ft bottom down drop with the follow on impact of the 1,100 lb plate dropped 30-ft onto the package bottom.

7.2.1 Case 1: Drum Bottom Down - 30-ft Drop at -20 ºF

Energy History

The time-history plots of energy components for the 30-ft drum bottom down drop simulation shown in Figure 34 indicate that the kinetic energy approaches zero at the end of the analysis. Therefore, we know that the analysis covers the entire impact duration.

Deformed Shape of Full Model

Figure 35 is the deformed shape of the overall model.

Stress and Strain Contours in Component Models

Figures 36 and 37 show the von Mises stresses and the equivalent plastic strains in the CV model. Figure 38 shows the equivalent plastic strains in the overpack shell.

Evaluations of Maximum Local Primary Membrane Stress Intensities and Maximum Equivalent Plastic Strains in Containment Vessel

The stress components across the wall thickness at the locations away from or near the geometrical discontinuities should be used to calculate the general primary membrane stress intensities (P_m) or the local primary membrane stress intensities (P_L). For simplicity, the maximum value of the von

Mises stresses in the containment vessel is used as the local primary membrane stress intensity (P_L). This value is higher than the actual local primary membrane stress intensity because the latter is calculated by averaging the thru-wall stresses across the component's thickness.

The maximum value of the local primary membrane stress intensity in the containment vessel is 51.19 ksi as given in Figure 36. This value is less than the allowable value of 57.3 ksi for the general primary membrane stress intensity and of 73.6 ksi for the local primary membrane stress intensity (as given in Section 6.0). The structural integrity of the 9977 subjected to a 30-ft drop has therefore been justified according to the ASME Code, Section III.

As shown in Figure 37, the maximum plastic strain experienced at any location within the containment vessel after the 30-ft drop is 3.24%. The maximum calculated value of the effective plastic strain at any point in the overpack is 7.74%. This value is less than the maximum average through-wall elongation of 35% for the 304L material use in the drum. Therefore, the drum will not be ruptured by the 30-ft drop impact.

7.2.2 Case 2: Drum Bottom Down - 30-ft Drop at 75 °F

Energy History

The time-history plots of energy components for the 30-ft drum bottom down drop simulation shown in Figure 39 indicate that the kinetic energy approaches zero at the end of the analysis. Therefore, we know that the analysis covers the entire impact duration.

Deformed Shape of Full Model

Figure 40 is the deformed shape of the overall model.

Stress and Strain Contours in Component Models

Figures 41 and 42 show the von Mises stresses and the equivalent plastic strains in the CV model. Figure 43 shows the equivalent plastic strains in the overpack shell.

Evaluations of Maximum Local Primary Membrane Stress Intensities and Maximum Equivalent Plastic Strains in Containment Vessel

The stress components across the wall thickness at the locations away from or near the geometrical discontinuities should be used to calculate the general primary membrane stress intensities (P_m) or the local primary membrane stress intensities (P_L). For simplicity, the maximum value of the von Mises stresses in the containment vessel is used as the local primary membrane stress intensity (P_L). This value is higher than the actual local primary membrane stress intensity because the latter is calculated by averaging the thru-wall stresses across the component's thickness.

The maximum value of the local primary membrane stress intensity in the containment vessel is 46.32 ksi as given in Figure 41. This value is less than the allowable value of 57.3 ksi for the general primary membrane stress intensity and of 73.6 ksi for the local primary membrane stress intensity (as given in Section 6.0). The structural integrity of the 9977 subjected to a 30-ft drop has therefore been justified according to the ASME Code, Section III.

As shown in Figure 42, the maximum plastic strain experienced at any location within the containment vessel after the 30-ft drop is 2.82%. The maximum calculated value of the effective

plastic strain at any point in the overpack is 4.80%. This value is less than the maximum average through-wall elongation of 35% for the 304L material use in the drum. Therefore, the drum will not be ruptured by the 30-ft drop impact.

7.2.3 Case 3: Drum Bottom Down - Crush on Drum Top at 75 ºF

Energy History

Figure 44 depicts the kinetic energy variation of the plate during the 30-ft fall. The plot indicates that the kinetic energy approaches zero before the end of the analysis. Therefore, we know that the analysis covers the entire impact duration.

Deformed Shape of Full Model

Figure 45 shows the deformed shape of the overall model.

Stress and Strain Contours in Component Models

Figures 46 and 47 show the von Mises stresses and the equivalent plastic strains in the containment vessel and its internal components. Figure 48 shows the equivalent plastic strains in the overpack shell.

Evaluations of Maximum Local Primary Membrane Stress Intensities and Maximum Equivalent Plastic Strains in Containment Vessel

The maximum value of the local primary membrane stress intensity in the containment vessel is 31.40 ksi as shown in Figure 46. This value is less than the allowable value of 57.3 ksi for the general primary membrane stress intensity and of 73.6 ksi for the local primary membrane stress intensity (as given in Section 6.0). The structural integrity of the 9977 subjected to a 30-ft crush has therefore been verified according to the ASME Code, Section III.

As shown in Figure 47, the maximum plastic strain experienced at any location within the containment vessel after a crush is 2.82%. The maximum calculated value of the effective plastic strain at any point in the overpack is 9.25%. This value is less than the maximum average through-wall elongation of 35% for the 304L material use in the drum. Therefore, the drum will not be ruptured by the crush impact.

7.2.4 Case 3: Drum Bottom Down - 30-ft Drop at 140 ºF

Energy History

The time-history plots of energy components for the 30-ft drum bottom down drop simulation shown in Figure 49 indicate that the kinetic energy approaches zero at the end of the analysis. Therefore, we know that the analysis covers the entire impact duration.

Deformed Shape of Full Model

Figure 50 is the deformed shape of the overall model.

Stress and Strain Contours in Component Models

Figures 51 and 52 show the von Mises stresses and the equivalent plastic strains in the CV model. Figure 53 shows the equivalent plastic strains in the overpack shell.

Evaluations of Maximum Local Primary Membrane Stress Intensities and Maximum Equivalent Plastic Strains in Containment Vessel

The stress components across the wall thickness at the locations away from or near the geometrical discontinuities should be used to calculate the general primary membrane stress intensities (P_m) or the local primary membrane stress intensities (P_L). For simplicity, the maximum value of the von Mises stresses in the containment vessel is used as the local primary membrane stress intensity (P_L). This value is higher than the actual local primary membrane stress intensity because the latter is calculated by averaging the thru-wall stresses across the component's thickness.

The maximum value of the local primary membrane stress intensity in the containment vessel is 40.02 ksi as given in Figure 51. This value is less than the allowable value of 57.3 ksi for the general primary membrane stress intensity and of 73.6 ksi for the local primary membrane stress intensity (as given in Section 6.0). The structural integrity of the 9977 subjected to a 30-ft drop has therefore been justified according to the ASME Code, Section III.

As shown in Figure 52, the maximum plastic strain experienced at any location within the containment vessel after the 30-ft drop is 2.62%. The maximum calculated value of the effective plastic strain at any point in the overpack is 3.82%. This value is less than the maximum average through-wall elongation of 35% for the 304L material use in the drum. Therefore, the drum will not be ruptured by the 30-ft drop impact.

7.2.5 Case 5: Drum Bottom Down - 30-ft Drop at 300 ºF

Energy History

The time-history plots of energy components for the 30-ft drum bottom down drop simulation shown in Figure 54 indicate that the kinetic energy approaches zero at the end of the analysis. Therefore, we know that the analysis covers the entire impact duration.

Deformed Shape of Full Model

Figure 55 is the deformed shape of the overall model.

Stress and Strain Contours in Component Models

Figures 56 and 57 show the von Mises stresses and the equivalent plastic strains in the CV model. Figure 58 shows the equivalent plastic strains in the overpack shell.

Evaluations of Maximum Local Primary Membrane Stress Intensities and Maximum Equivalent Plastic Strains in Containment Vessel

The stress components across the wall thickness at the locations away from or near the geometrical discontinuities should be used to calculate the general primary membrane stress intensities (P_m) or the local primary membrane stress intensities (P_L). For simplicity, the maximum value of the von Mises stresses in the containment vessel is used as the local primary membrane stress intensity (P_L). This value is higher than the actual local primary membrane stress intensity because the latter is calculated by averaging the thru-wall stresses across the component's thickness.

The maximum value of the local primary membrane stress intensity in the containment vessel is 38.22 ksi as given in Figure 56. This value is less than the allowable value of 57.3 ksi for the general primary membrane stress intensity and of 73.6 ksi for the local primary membrane stress intensity (as given in Section 6.0). The structural integrity of the 9977 subjected to a 30-ft drop has therefore been justified according to the ASME Code, Section III.

As shown in Figure 57, the maximum plastic strain experienced at any location within the containment vessel after the 30-ft drop is 1.84%. The maximum calculated value of the effective plastic strain at any point in the overpack is 4.73%. This value is less than the maximum average through-wall elongation of 35% for the 304L material use in the drum. Therefore, the drum will not be ruptured by the 30-ft drop impact.

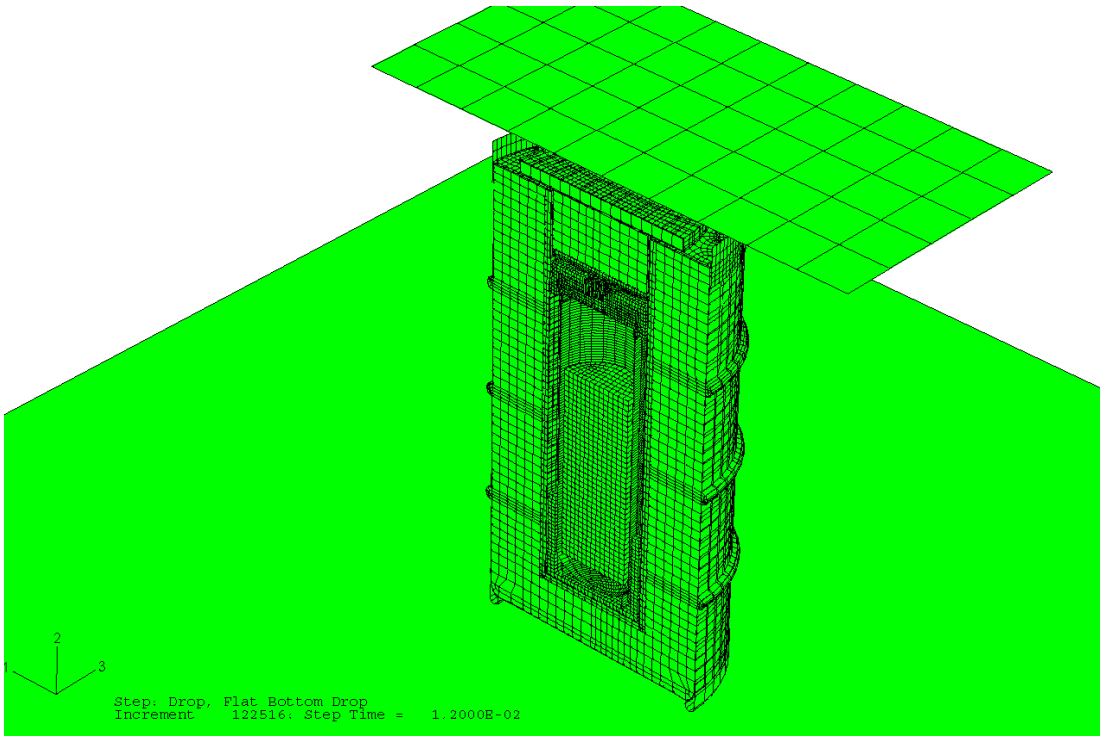

Figure 33 - Finite Element Model of the 9977 Bottom Down Drop and Top Crush

(ALLKE = kinetic energy; ALLIE = internal energy; ALLPD = plastic strain energy; ALLSE = elastic strain energy; ALLAE = artificial energy)

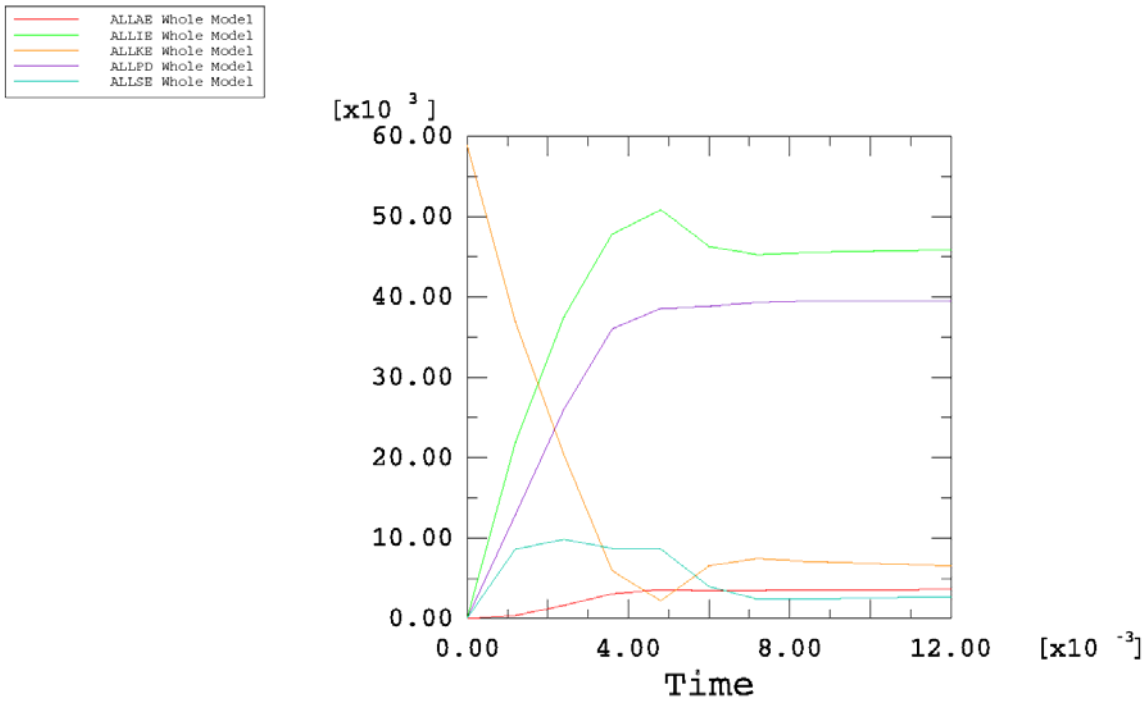

Figure 34 - Time-History Plot of Energy during Drum Bottom Down - 30-ft Drop Simulation (-20 ºF)

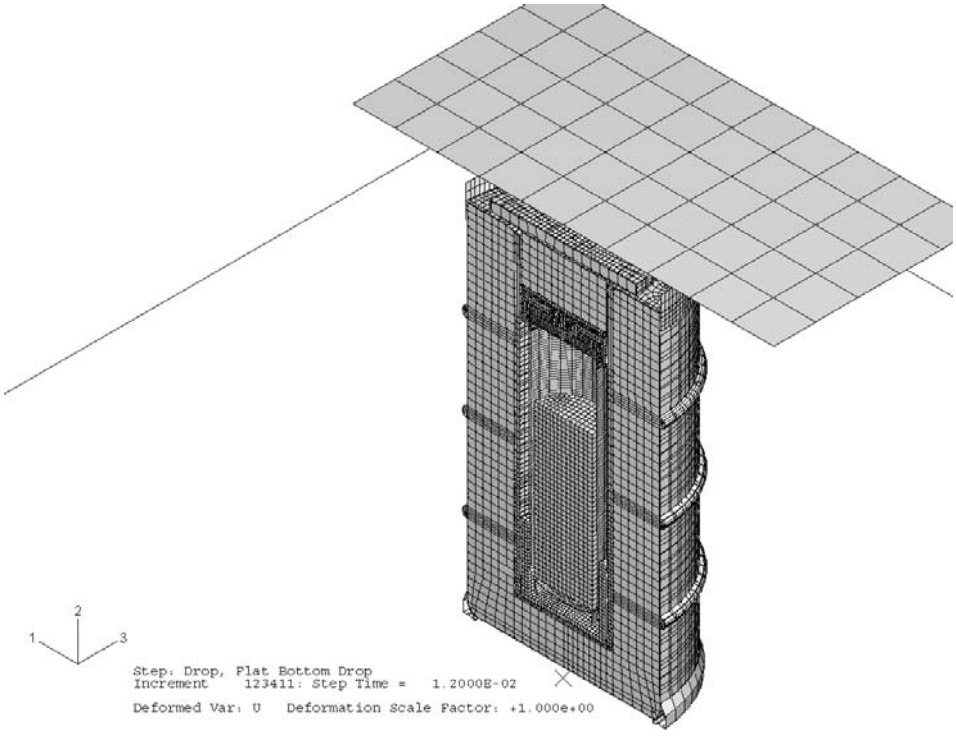

Figure 35 - Deformed Shape of 9977 with 6CV After Drum Bottom Down - 30-ft Drop (-20 ºF)

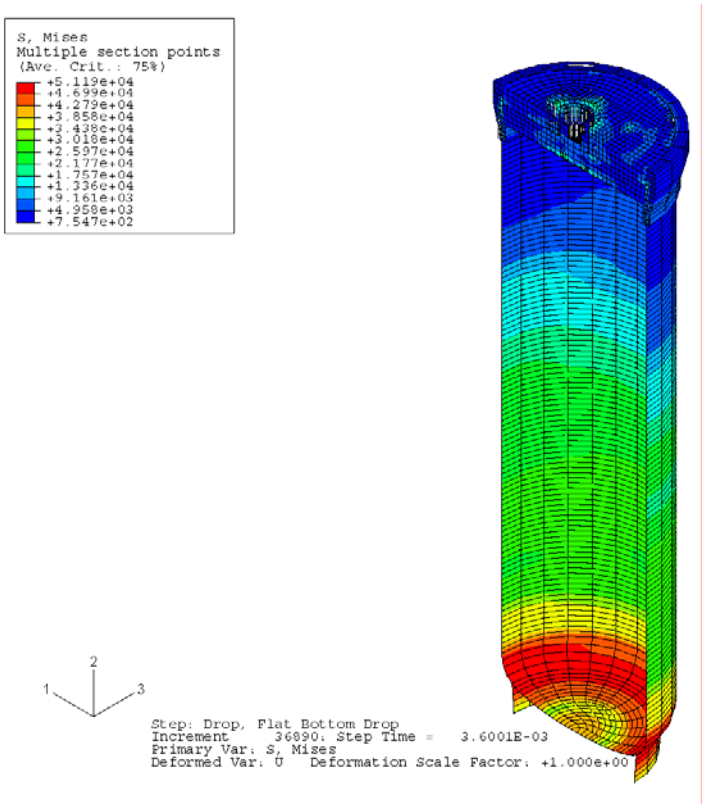

Figure 36 - Stress Distribution in the 6CV Model for Drum Bottom Down - 30-ft Drop (-20 ºF)

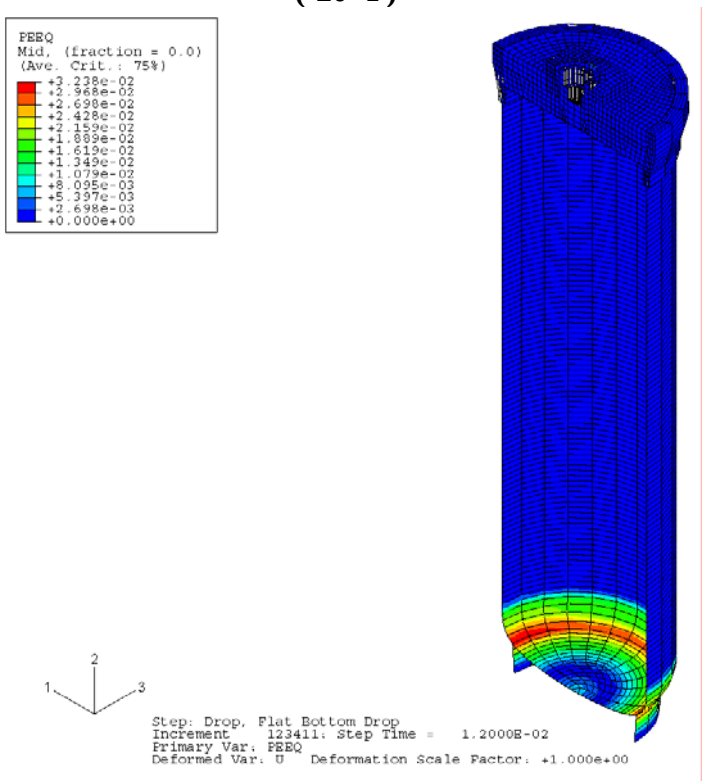

Figure 37 - Strain Distribution in 6CV Model for Drum Bottom Down - 30-ft Drop (-20 ºF)

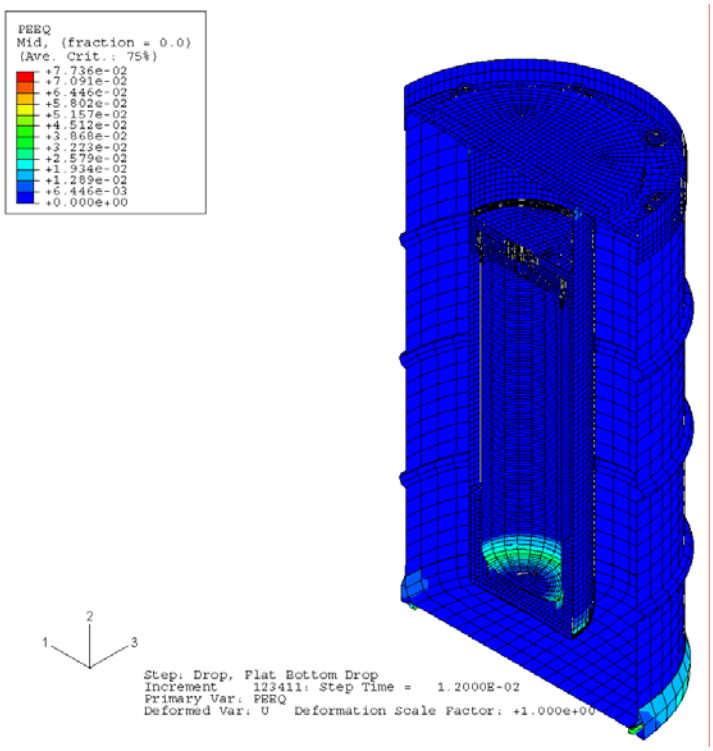

Figure 38 - Strain Distribution in Overpack for 6CV for Drum Bottom Down - 30-ft Drop (-20 ºF)

(ALLKE = kinetic energy; ALLIE = internal energy; ALLPD = plastic strain energy; ALLSE = elastic strain energy; ALLAE = artificial energy)

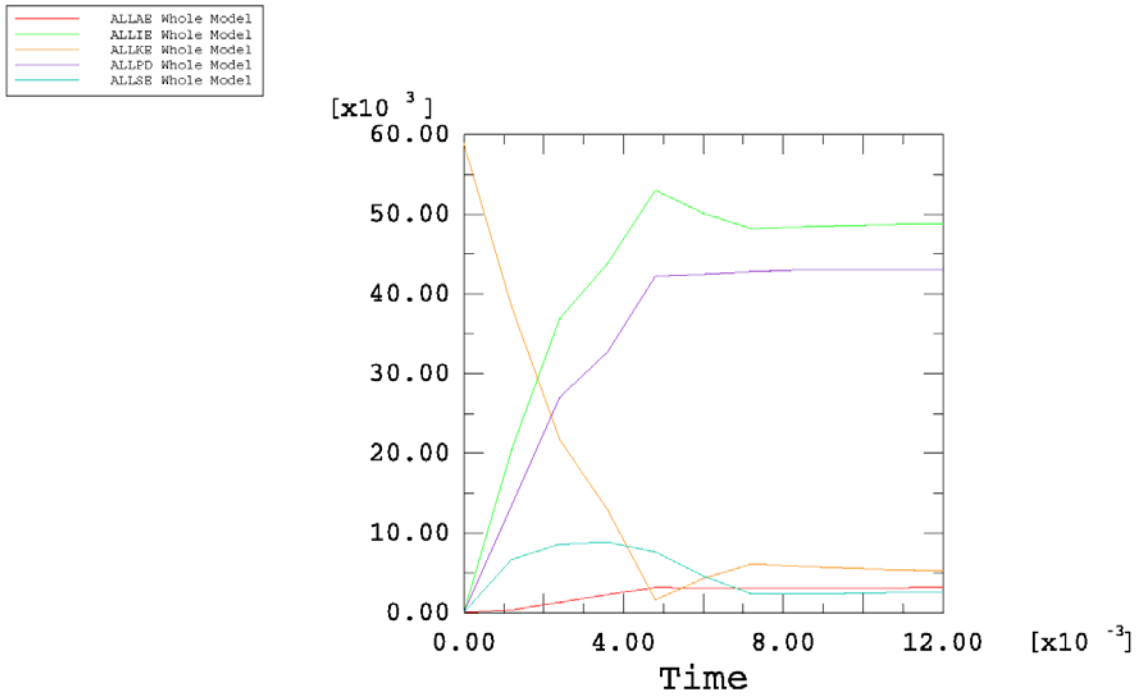

Figure 39 - Time-History Plot of Energy during Drum Bottom Down - 30-ft Drop (75 ºF)

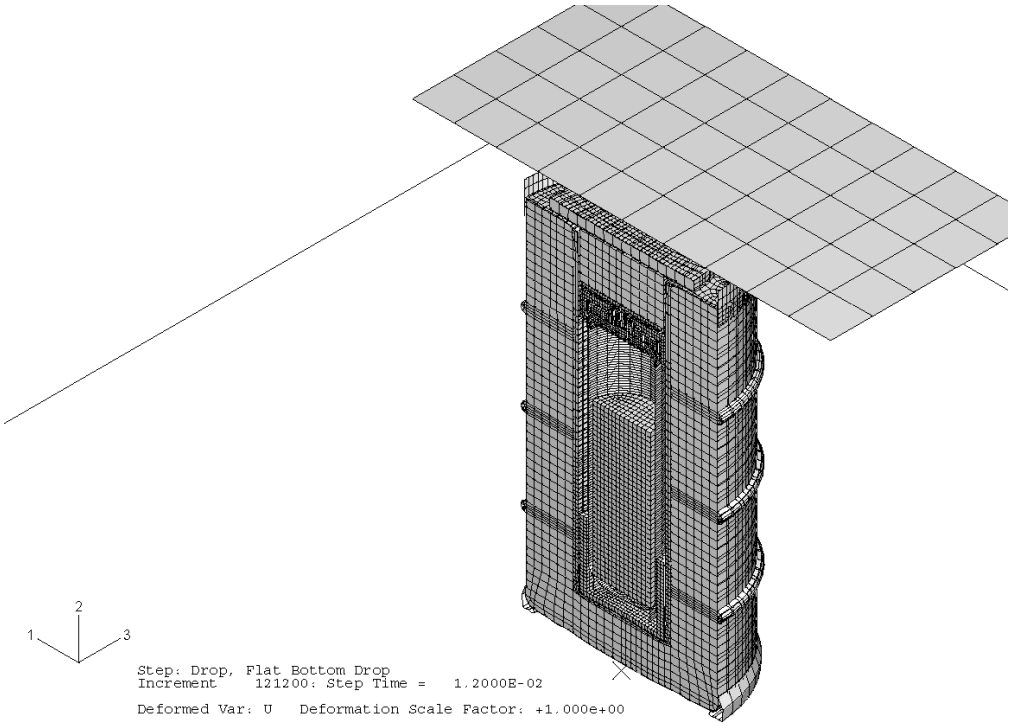

Figure 40 - Deformed Shape of 9977 with 6CV After Drum Bottom Down - 30-ft Drop (75 ºF)

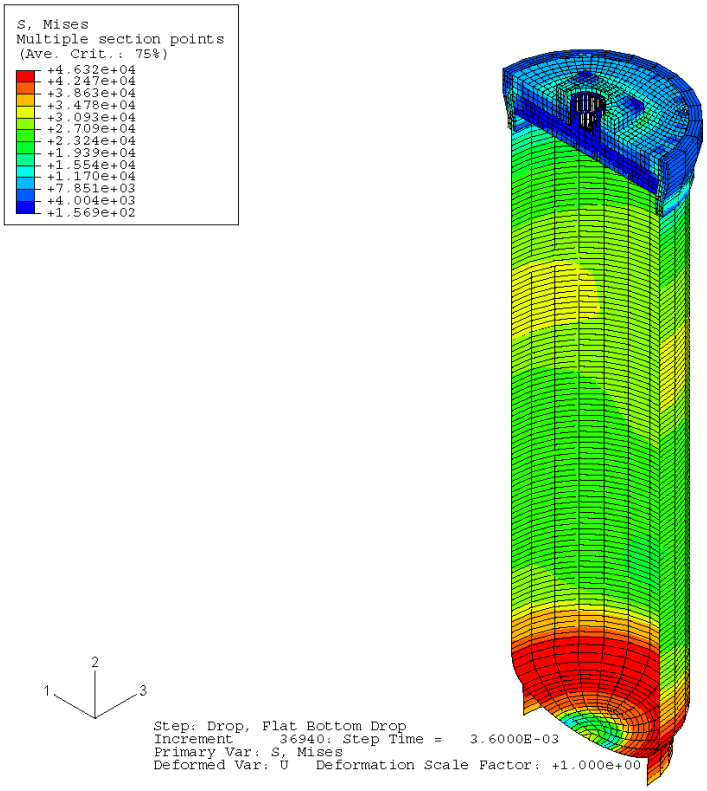

Figure 41 - Stress Distribution in the 6CV Model for Drum Bottom Down - 30-ft Drop (75 ºF)

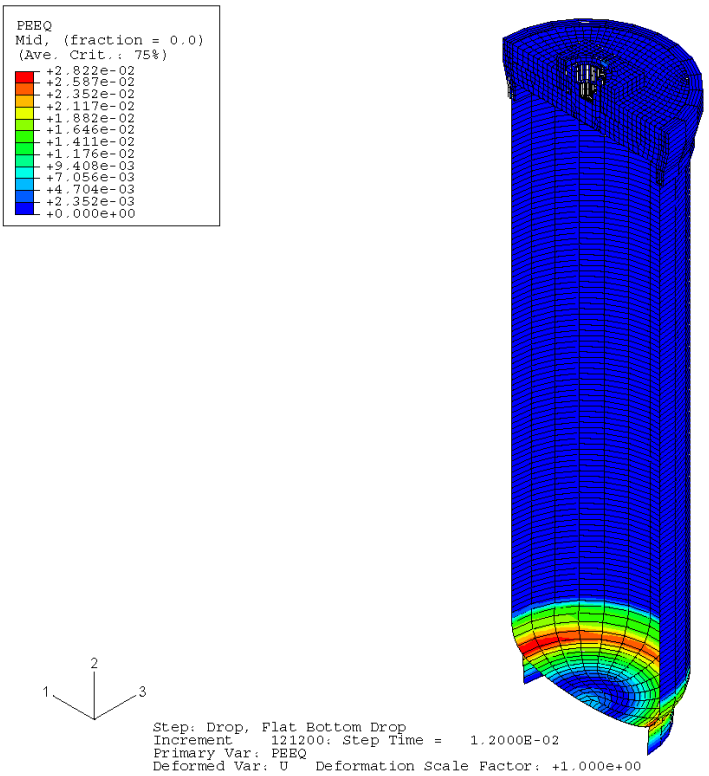

Figure 42 - Strain Distribution in 6CV Model for Drum Bottom Down - 30-ft Drop (75 ºF)

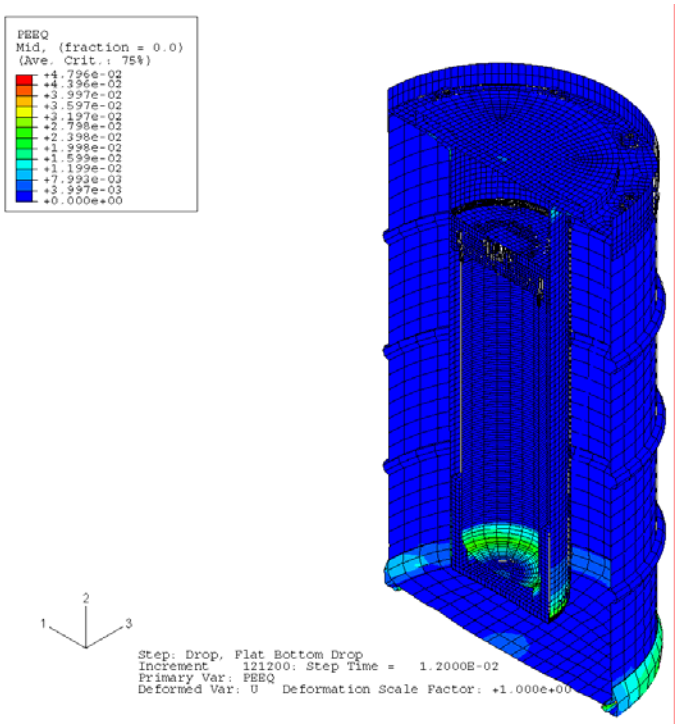

Figure 43 - Strain Distribution in Overpack for 6CV for Drum Bottom Down - 30-ft Drop (75 ºF)

(ALLKE = kinetic energy; ALLIE = internal energy; ALLPD = plastic strain energy; ALLSE = elastic strain energy; ALLAE = artificial energy)

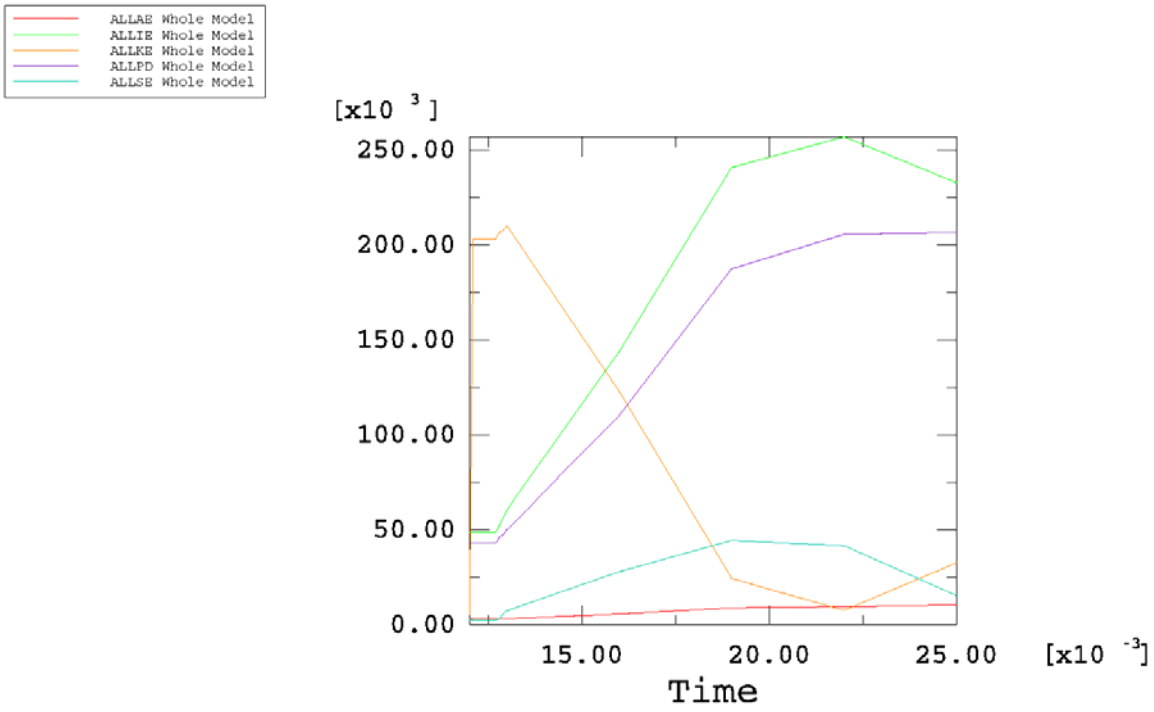

Figure 44 - Time-History Plot of Plate Energy during Drum Bottom Down - Top Crush Simulation (75 ºF)

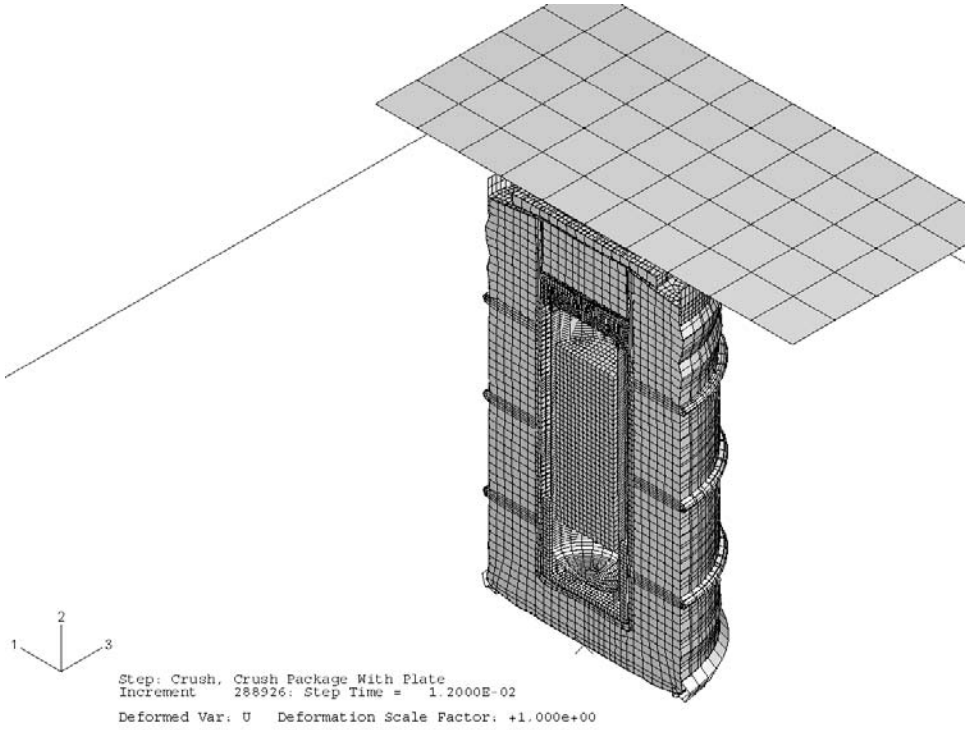

Figure 45 - Deformed Shape of 9977 with 6CV After the Drum Bottom Down - Top Crush (75 ºF)

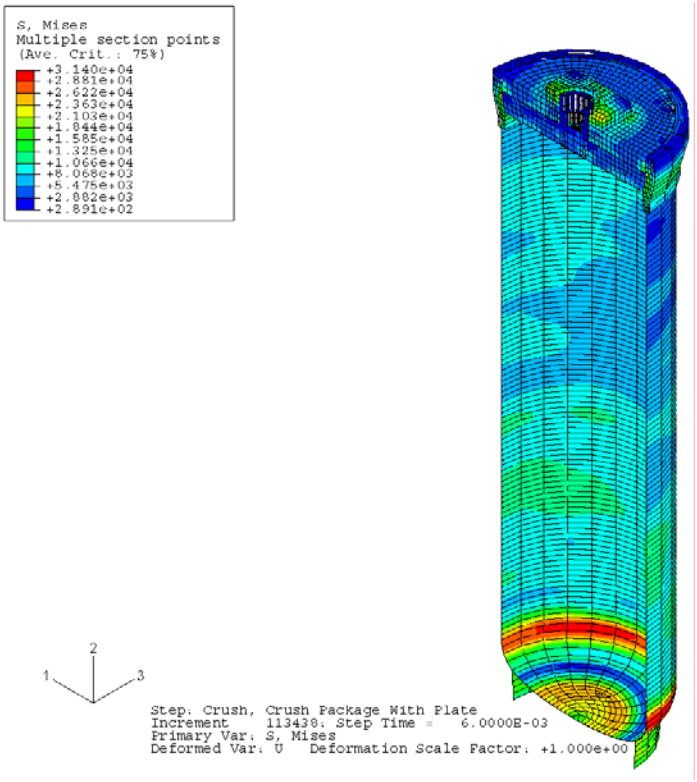

Figure 46 - Stress Distribution in the 6CV Model for Drum Bottom Down - Top Crush (75 ºF)

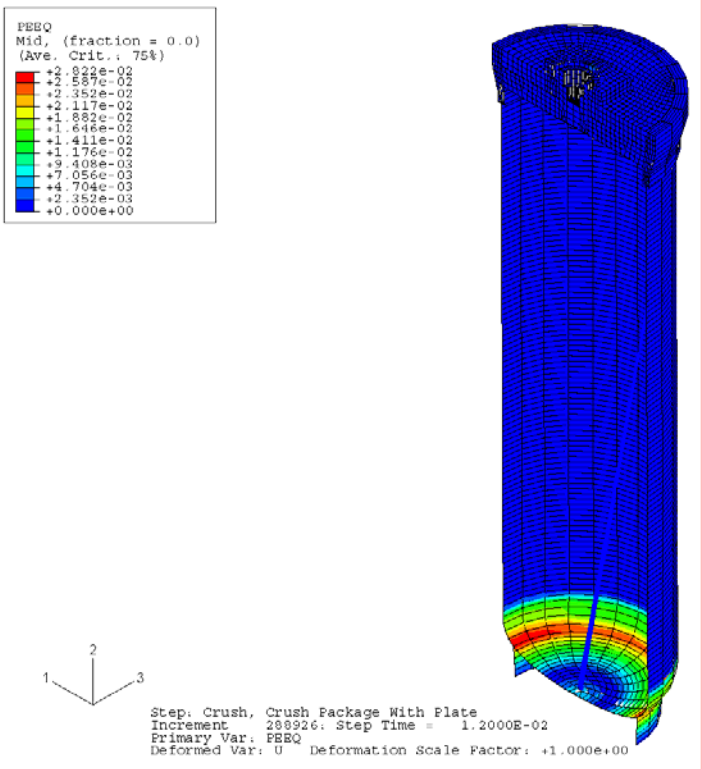

Figure 47 - Strain Distribution in 6CV Model for Drum Bottom Down - Top Crush (75 ºF)

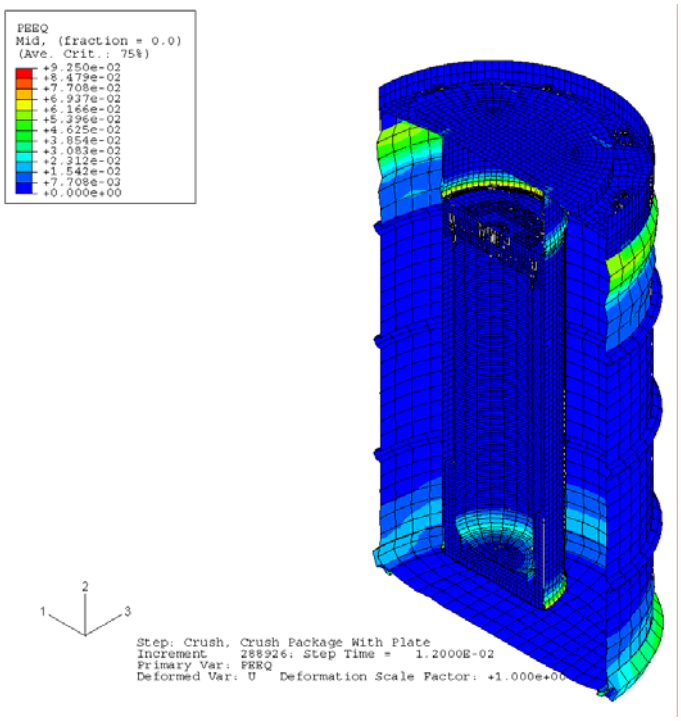

Figure 48 - Strain Distribution in Overpack for 6CV for Drum Bottom Down - Top Crush (75 ºF)

(ALLKE = kinetic energy; ALLIE = internal energy; ALLPD = plastic strain energy; ALLSE = elastic strain energy; ALLAE = artificial energy)

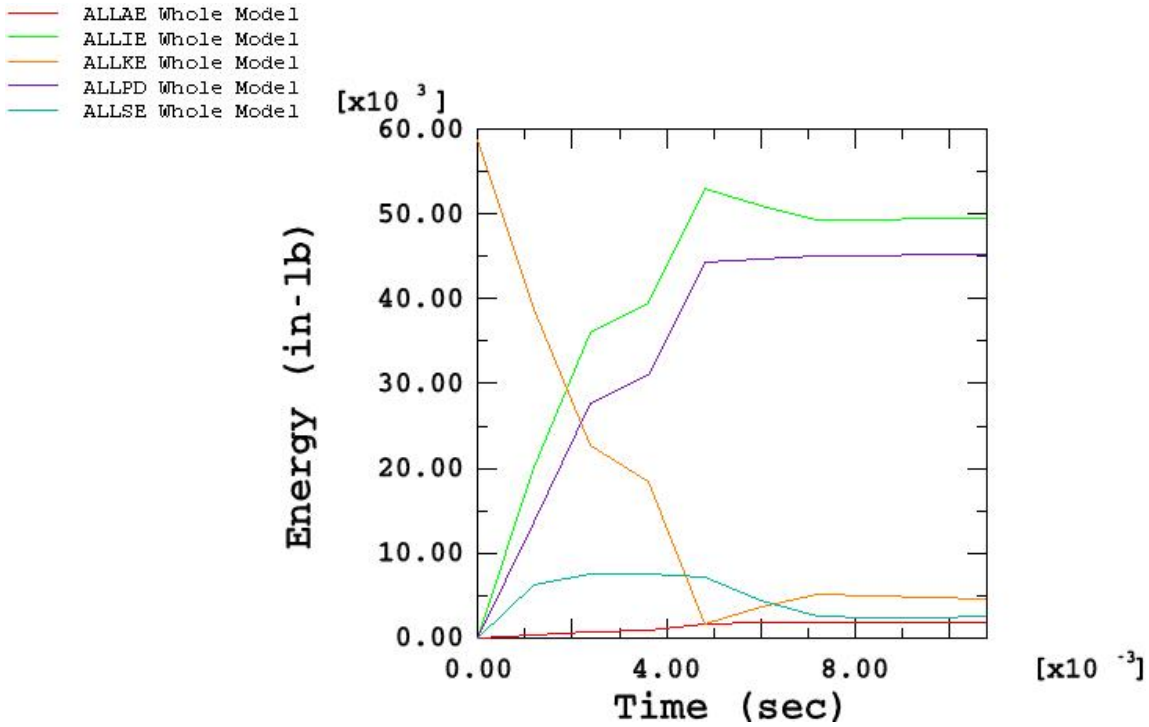

Figure 49 - Time-History Plot of Energy during Drum Bottom Down - 30-ft Drop Simulation (140 ºF)

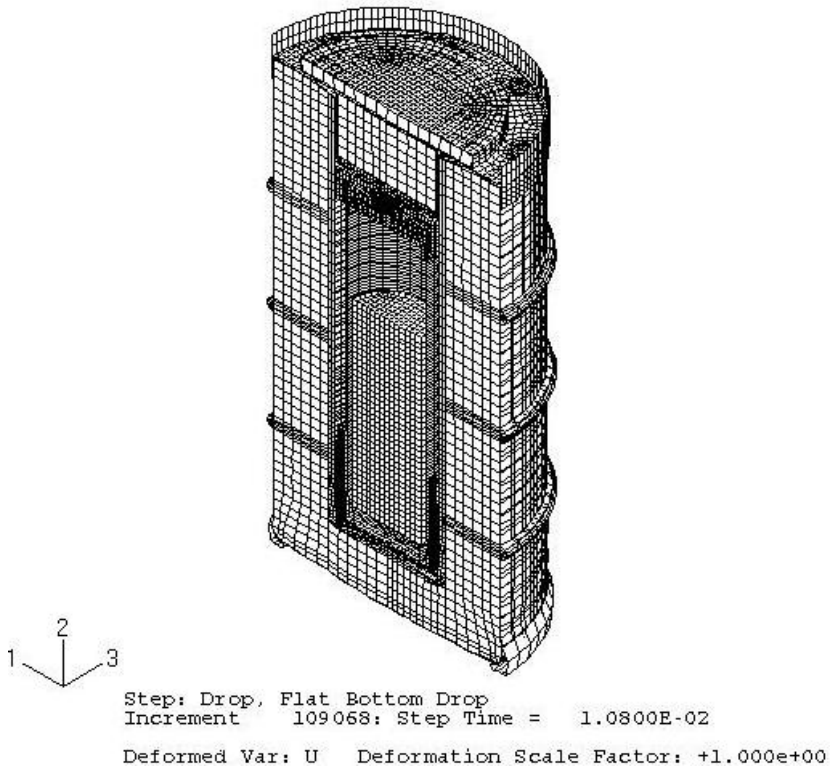

Figure 50 - Deformed Shape of 9977 with 6CV After the Drum Bottom Down - 30-ft Drop (140 ºF)

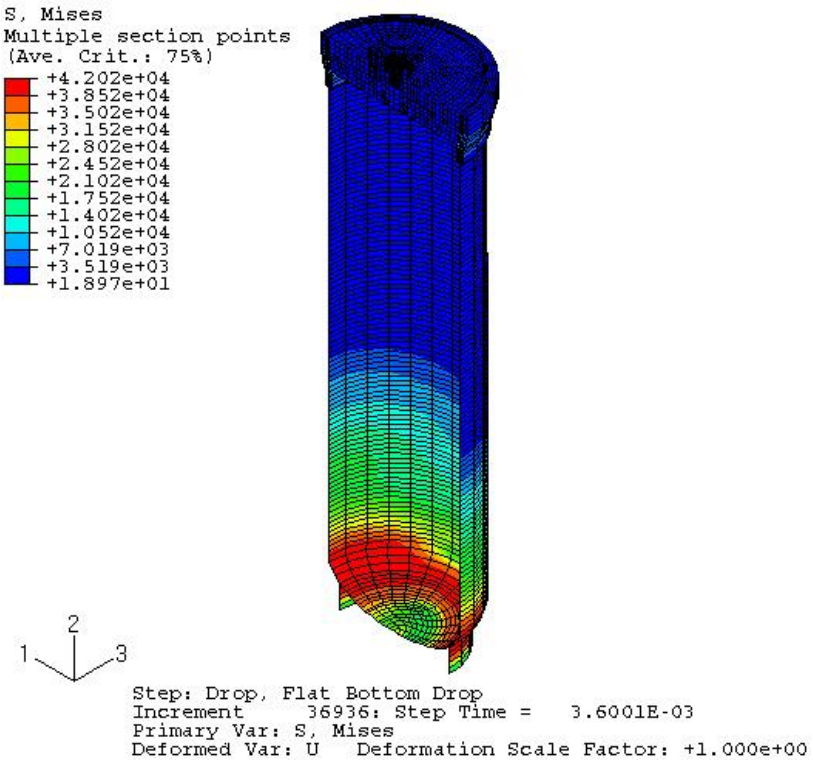

Figure 51 - Stress Distribution in the 6CV Model for Drum Bottom Down - 30-ft Drop (140 ºF)

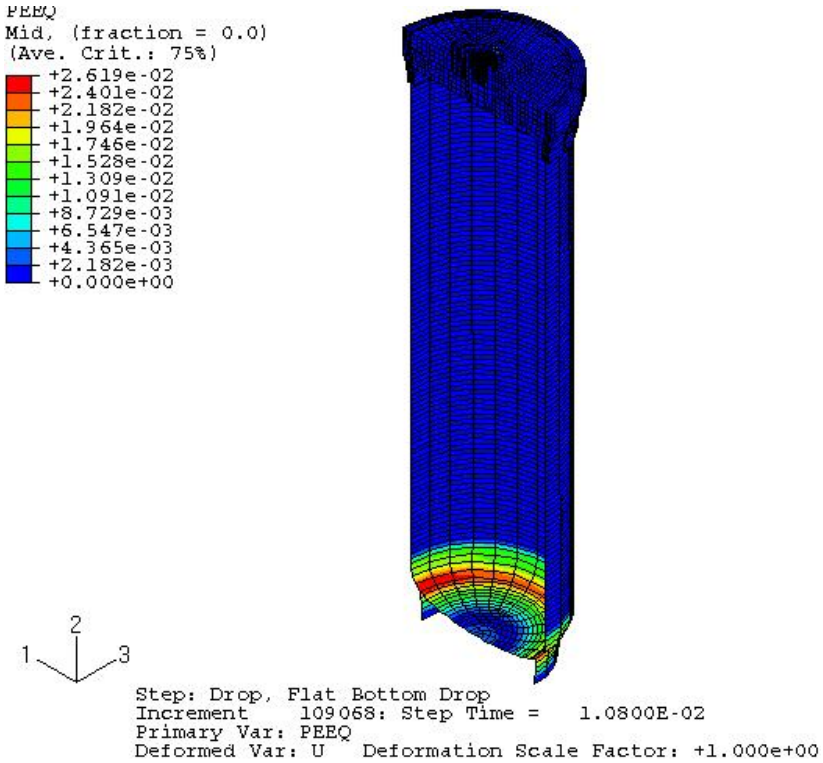

Figure 52 - Strain Distribution in 6CV Model for Drum Bottom Down - 30-ft Drop (140 ºF)

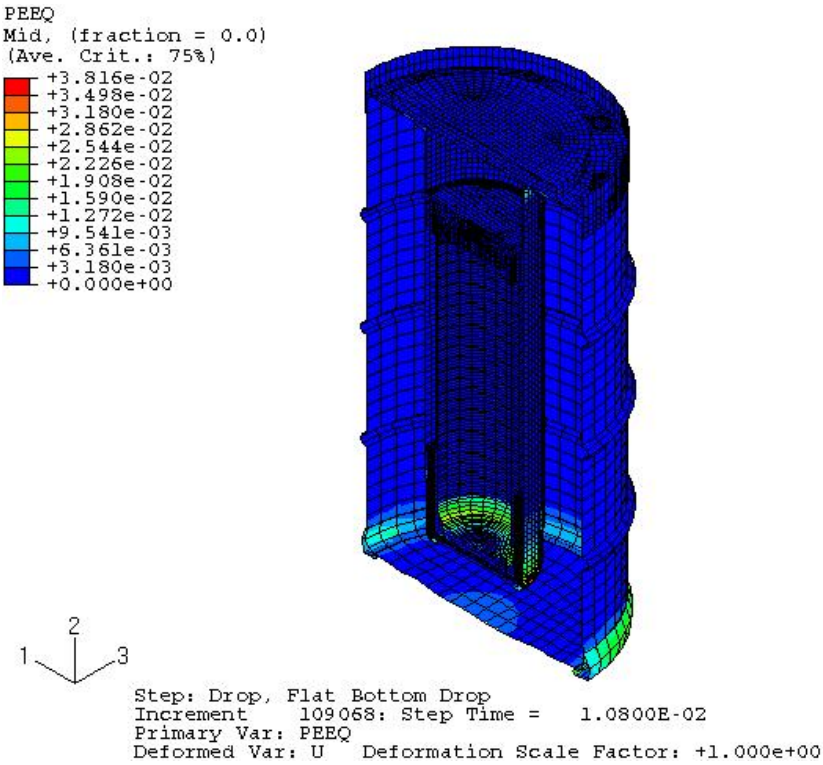

Figure 53 - Strain Distribution in Overpack for 6CV for Drum Bottom Down - 30-ft Drop (140 ºF)

(ALLKE = kinetic energy; ALLIE = internal energy; ALLPD = plastic strain energy; ALLSE = elastic strain energy; ALLAE = artificial energy)

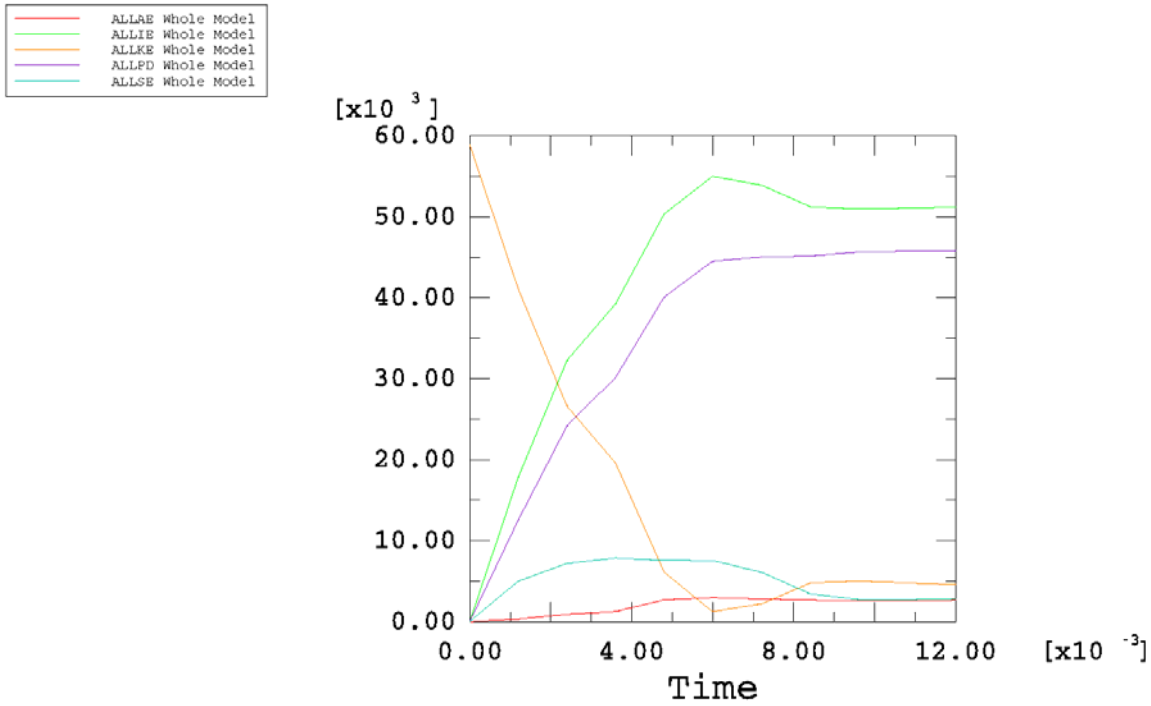

Figure 54 - Time-History Plot of Energy Drum Bottom Down - 30-ft Drop Simulation (300 ºF)

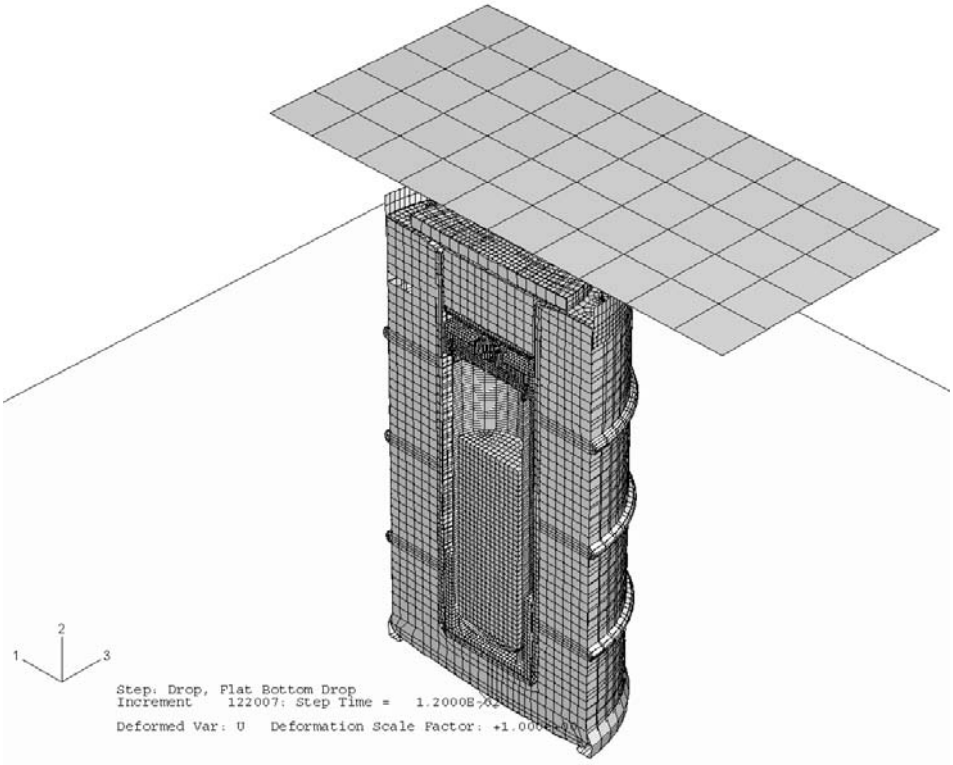

Figure 55 - Deformed Shape of 9977 with 6CV for Drum Bottom Down - 30-ft Drop (300 ºF)

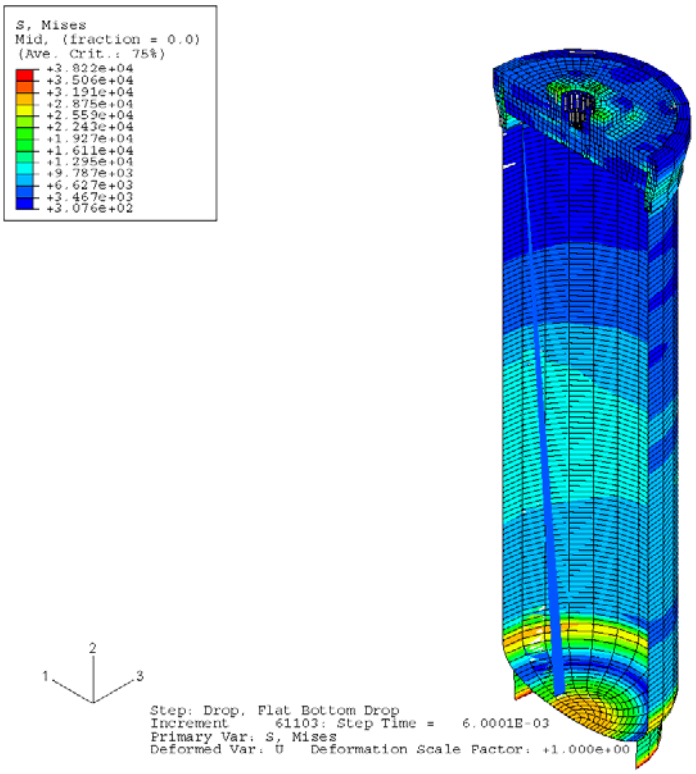

Figure 56 - Stress Distribution in 6CV Model for Drum Bottom Down - 30-ft Drop (300 ºF)

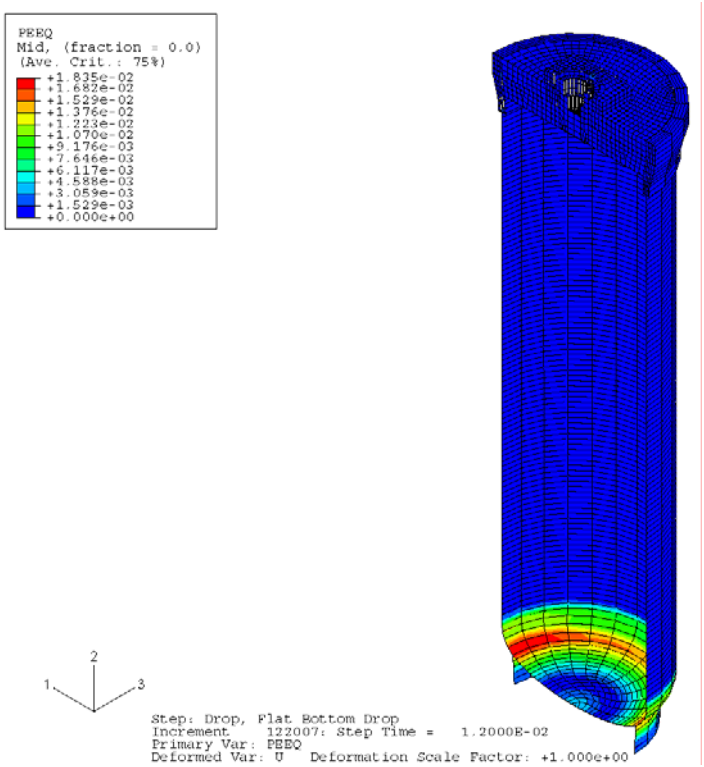

Figure 57 - Strain Distribution in 6CV Model for Drum Bottom Down - 30-ft Drop (300 ºF)

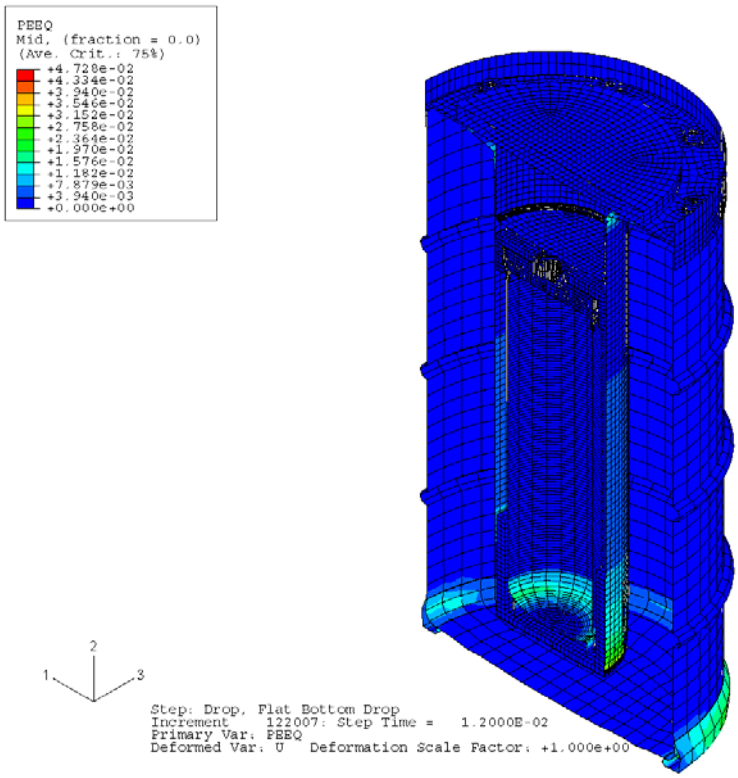

Figure 58 - Strain Distribution in Overpack for Drum Bottom Down - 30-ft Drop (300 ºF)

7.3 Side Drop Followed by Side Crush with 6CV (-20, 140 and 300 ºF)

Figure 59 shows the finite element model used for evaluating the 30-Ft side drop with the follow on impact of the 1,100 lb plate dropped 30-ft impacting the side opposite of the drop impact.

7.3.1 Case 1: Drum on Side - 30-Ft Drop with Weight in the Middle of 6CV (-20 ºF)

Energy History

The time-history plots of energy components for the 30-ft side drop simulation shown in Figure 60 indicate that the kinetic energy approaches zero at the end of the analysis. Therefore, we know that the analysis covers the entire impact duration.

Deformed Shape of Full Model

Figure 61 is the deformed shape of the overall model.

Stress and Strain Contours in Component Models

Figures 62 and 63 show the von Mises stresses and the equivalent plastic strains in the CV model. Figure 64 shows the equivalent plastic strains in the overpack shell.

Evaluations of Maximum Local Primary Membrane Stress Intensities and Maximum Equivalent Plastic Strains in Containment Vessel

The stress components across the wall thickness at the locations away from or near the geometrical discontinuities should be used to calculate the general primary membrane stress intensities (P_m) or the local primary membrane stress intensities (P_L). For simplicity, the maximum value of the von Mises stresses in the containment vessel is used as the local primary membrane stress intensity (P_L). This value is higher than the actual local primary membrane stress intensity because the latter is calculated by averaging the thru-wall stresses across the component's thickness.

The maximum value of the local primary membrane stress intensity in the containment vessel is 42.82 ksi as given in Figure 62. This value is less than the allowable value of 57.3 ksi for the general primary membrane stress intensity and of 73.6 ksi for the local primary membrane stress intensity (as given in Section 6.0). The structural integrity of the 9977 subjected to a 30-ft drop has therefore been justified according to the ASME Code, Section III.

As shown in Figure 63, the maximum plastic strain experienced at any location within the containment vessel after the 30-ft drop is 3.12%. The maximum calculated value of the effective plastic strain at any point in the overpack is 14.12%. This value is less than the minimum specified uniform elongation of 35% for the 304L material used in the drum. Therefore, the drum will not be ruptured by the 30-ft drop impact.

7.3.2 Case 2: Drum on Side - Crush with Weight in the Middle of 6CV (-20 ºF)

Energy History

Figure 65 depicts the kinetic energy variation of the plate during the 30-ft drop. The plot indicates that the kinetic energy approaches zero before the end of the analysis. Therefore, we know that the analysis covers the entire impact duration.

Deformed Shape of Full Mode
Figure 66 shows the deformed shape of the overall model.

Stress and Strain Contours in Component Models
Figures 67 and 68 show the von Mises stresses and the equivalent plastic strains in the containment vessel and its internal components. Figure 69 shows the equivalent plastic strains in the overpack shell.

Evaluations of Maximum Local Primary Membrane Stress Intensities and Maximum Equivalent Plastic Strains in Containment Vessel

The maximum value of the local primary membrane stress intensity in the containment vessel is 41.97 ksi as shown in Figure 67. This value is less than the allowable value of 57.3 ksi for the general primary membrane stress intensity and of 73.6 ksi for the local primary membrane stress intensity (as given in Section 6.0). The structural integrity of the 9977 subjected to a 30-ft crush has therefore been verified according to the ASME Code, Section III.

As shown in Figure 68, the maximum plastic strain experienced at any location within the containment vessel after the crush is 5.29%. The maximum calculated value of the effective plastic strain at any point in the overpack is 28.18%. This value is less than the maximum average through-wall elongation of 35% for the 304L material use in the drum. Therefore, the drum will not be ruptured by the crush impact.

7.3.3 Case 3: Drum on Side - 30-Ft Drop with Weight at the Bottom of 6CV (140 ºF)

Energy History
The time-history plots of energy components for the 30-ft side drop simulation shown in Figure 70 indicate that the kinetic energy approaches zero at the end of the analysis. Therefore, we know that the analysis covers the entire impact duration.

Deformed Shape of Full Model
Figure 71 is the deformed shape of the overall model.

Stress and Strain Contours in Component Models
Figures 72 and 73 show the von Mises stresses and the equivalent plastic strains in the CV model. Figure 74 shows the equivalent plastic strains in the overpack shell.

Evaluations of Maximum Local Primary Membrane Stress Intensities and Maximum Equivalent Plastic Strains in Containment Vessel
The stress components across the wall thickness at the locations away from or near the geometrical discontinuities should be used to calculate the general primary membrane stress intensities (P_m) or the local primary membrane stress intensities (P_L). For simplicity, the maximum value of the von Mises stresses in the containment vessel is used as the local primary membrane stress intensity (P_L). This value is higher than the actual local primary membrane stress intensity because the latter is calculated by averaging the thru-wall stresses across the component's thickness.

The maximum value of the local primary membrane stress intensity in the containment vessel is 45.30 ksi as given in Figure 72. This value is less than the allowable value of 57.3 ksi for the general primary membrane stress intensity and of 73.6 ksi for the local primary membrane stress intensity (as given in Section 6.0). The structural integrity of the 9977 subjected to a 30-ft drop has therefore been justified according to the ASME Code, Section III.

As shown in Figure 73, the maximum plastic strain experienced at any location within the containment vessel after the 30-ft drop is 2.20%. The maximum calculated value of the effective plastic strain at any point in the overpack is 9.14%. This value is less than the maximum average through-wall elongation of 35% for the 304L material use in the drum. Therefore, the drum will not be ruptured by the 30-ft drop impact.

7.3.4 Case 4: Drum on Side - Crush with Weight in the Bottom of 6CV (140 ºF)

Energy History

Figure 75 depicts the kinetic energy variation of the plate during the 30-ft drop. The plot indicates that the kinetic energy approaches zero before the end of the analysis. Therefore, we know that the analysis covers the entire impact duration.

Deformed Shape of Full Model

Figure 76 shows the deformed shape of the overall model.

Stress and Strain Contours in Component Models

Figures 77 and 78 show the von Mises stresses and the equivalent plastic strains in the containment vessel and its internal components. Figure 79 shows the equivalent plastic strains in the overpack shell.

Evaluations of Maximum Local Primary Membrane Stress Intensities and Maximum Equivalent Plastic Strains in Containment Vessel

The maximum value of the local primary membrane stress intensity in the containment vessel is 37.99 ksi as shown in Figure 77. This value is less than the allowable value of 57.3 ksi for the general primary membrane stress intensity and of 73.6 ksi for the local primary membrane stress intensity (as given in Section 6.0). The structural integrity of the 9977 subjected to a 30-ft crush has therefore been verified according to the ASME Code, Section III.

As shown in Figure 78, the maximum plastic strain experienced at any location within the containment vessel after a crush is 3.55%. The maximum calculated value of the effective plastic strain at any point in the overpack is 32.25%. This value is less than the maximum average through-wall elongation of 35% for the 304L material use in the drum. Therefore, the drum will not be ruptured by the crush impact.

7.3.5 Case 5: Drum on Side - 30-Ft Drop with Weight in the Bottom of 6CV (300 ºF)

Energy History

The time-history plots of energy components for the 30-ft side drop simulation shown in Figure 80 indicate that the kinetic energy approaches zero at the end of the analysis. Therefore, we know that the analysis covers the entire impact duration.

Deformed Shape of Full Model

Figure 81 is the deformed shape of the overall model.

Stress and Strain Contours in Component Models

Figures 82 and 83 show the von Mises stresses and the equivalent plastic strains in the CV model. Figure 84 shows the equivalent plastic strains in the overpack shell.

Evaluations of Maximum Local Primary Membrane Stress Intensities and Maximum Equivalent Plastic Strains in Containment Vessel

The stress components across the wall thickness at the locations away from or near the geometrical discontinuities should be used to calculate the general primary membrane stress intensities (P_m) or the local primary membrane stress intensities (P_L). For simplicity, the maximum value of the von Mises stresses in the containment vessel is used as the local primary membrane stress intensity (P_L). This value is higher than the actual local primary membrane stress intensity because the latter is calculated by averaging the thru-wall stresses across the component's thickness.

The maximum value of the local primary membrane stress intensity in the containment vessel is 46.22 ksi as given in Figure 82. This value is less than the allowable value of 57.3 ksi for the general primary membrane stress intensity and of 73.6 ksi for the local primary membrane stress intensity (as given in Section 6.0). The structural integrity of the 9977 subjected to a 30-ft drop has therefore been justified according to the ASME Code, Section III.

As shown in Figure 83, the maximum plastic strain experienced at any location within the containment vessel after the 30-ft drop is 2.41%. The maximum calculated value of the effective plastic strain at any point in the overpack is 10.06%. This value is less than the maximum average through-wall elongation of 35% for the 304L material use in the drum. Therefore, the drum will not be ruptured by the 30-ft drop impact.

7.3.6 Case 6: Drum on Side - Crush with Weight in the Bottom of 6CV (300 ºF)

Energy History

Figure 85 depicts the kinetic energy variation of the plate during the 30-ft fall. The plot indicates that the kinetic energy approaches zero before the end of the analysis. Therefore, we know that the analysis covers the entire impact duration.

Deformed Shape of Full Mode

Figure 86 shows the deformed shape of the overall model.

Stress and Strain Contours in Component Models

Figures 87 and 88 show the von Mises stresses and the equivalent plastic strains in the containment vessel and its internal components. Figure 89 shows the equivalent plastic strains in the overpack shell.

Evaluations of Maximum Local Primary Membrane Stress Intensities and Maximum Equivalent Plastic Strains in Containment Vessel

The maximum value of the local primary membrane stress intensity in the containment vessel is 47.03 ksi as shown in Figure 87. This value is less than the allowable value of 57.3 ksi for the general primary membrane stress intensity and of 73.6 ksi for the local primary membrane stress intensity (as given in Section 6.0). The structural integrity of the 9977 subjected to a 30-ft crush has therefore been verified according to the ASME Code, Section III.

As shown in Figure 88, the maximum plastic strain experienced at any location within the containment vessel after the crush is 2.61%. The maximum calculated value of the effective plastic strain at any point in the overpack is 38.03%. While this value is slightly greater than the minimum specified uniform elongation of 35% for the 304L material used in the drum, the strain is restricted to an extremely small area at the edge of a bolt hole in the drum top plate and has no effect on the drum performance. The drum will not be ruptured by the crush impact.

7.3.7 Case 7: Drum on Side - 30-Ft Drop with Weight at the Top of 6CV (140 ºF)

Energy History

The time-history plots of energy components for the 30-ft side drop simulation shown in Figure 90 indicate that the kinetic energy approaches zero at the end of the analysis. Therefore, we know that the analysis covers the entire impact duration.

Deformed Shape of Full Model

Figure 91 is the deformed shape of the overall model.

Stress and Strain Contours in Component Models

Figures 92 and 93 show the von Mises stresses and the equivalent plastic strains in the CV model. Figure 94 shows the equivalent plastic strains in the overpack shell.

Evaluations of Maximum Local Primary Membrane Stress Intensities and Maximum Equivalent Plastic Strains in Containment Vessel

The stress components across the wall thickness at the locations away from or near the geometrical discontinuities should be used to calculate the general primary membrane stress intensities (P_m) or the local primary membrane stress intensities (P_L). For simplicity, the maximum value of the von Mises stresses in the containment vessel is used as the local primary membrane stress intensity (P_L). This value is higher than the actual local primary membrane stress intensity because the latter is calculated by averaging the thru-wall stresses across the component's thickness.

The maximum value of the local primary membrane stress intensity in the containment vessel is 52.40 ksi as given in Figure 92. This value is less than the allowable value of 57.3 ksi for the general primary membrane stress intensity and of 73.6 ksi for the local primary membrane stress

intensity (as given in Section 6.0). The structural integrity of the 9977 subjected to a 30-ft drop has therefore been justified according to the ASME Code, Section III.

As shown in Figure 93, the maximum plastic strain experienced at any location within the containment vessel after the 30-ft drop is 5.29%. The maximum calculated value of the effective plastic strain at any point in the overpack is 9.70%. This value is less than the maximum average through-wall elongation of 35% for the 304L material use in the drum. Therefore, the drum will not be ruptured by the 30-ft drop impact.

7.3.8 Case 8: Drum on Side - 30-Ft Drop with Weight at the Top of 6CV (300 ºF)

Energy History

The time-history plots of energy components for the 30-ft side drop simulation shown in Figure 95 indicate that the kinetic energy approaches zero at the end of the analysis. Therefore, we know that the analysis covers the entire impact duration.

Deformed Shape of Full Model

Figure 96 is the deformed shape of the overall model.

Stress and Strain Contours in Component Models

Figures 97 and 98 show the von Mises stresses and the equivalent plastic strains in the CV model. Figure 99 shows the equivalent plastic strains in the overpack shell.

Evaluations of Maximum Local Primary Membrane Stress Intensities and Maximum Equivalent Plastic Strains in Containment Vessel

The stress components across the wall thickness at the locations away from or near the geometrical discontinuities should be used to calculate the general primary membrane stress intensities (P_m) or the local primary membrane stress intensities (P_L). For simplicity, the maximum value of the von Mises stresses in the containment vessel is used as the local primary membrane stress intensity (P_L). This value is higher than the actual local primary membrane stress intensity because the latter is calculated by averaging the thru-wall stresses across the component's thickness.

The maximum value of the local primary membrane stress intensity in the containment vessel is 46.52 ksi as given in Figure 97. This value is less than the allowable value of 57.3 ksi for the general primary membrane stress intensity and of 73.6 ksi for the local primary membrane stress intensity (as given in Section 6.0). The structural integrity of the 9977 subjected to a 30-ft drop has therefore been justified according to the ASME Code, Section III.

As shown in Figure 16, the maximum plastic strain experienced at any location within the containment vessel after the 30-ft drop is 1.99%. The maximum calculated value of the effective plastic strain at any point in the overpack is 9.59%. This value is less than the maximum average through-wall elongation of 35% for the 304L material use in the drum. Therefore, the drum will not be ruptured by the 30-ft drop impact.

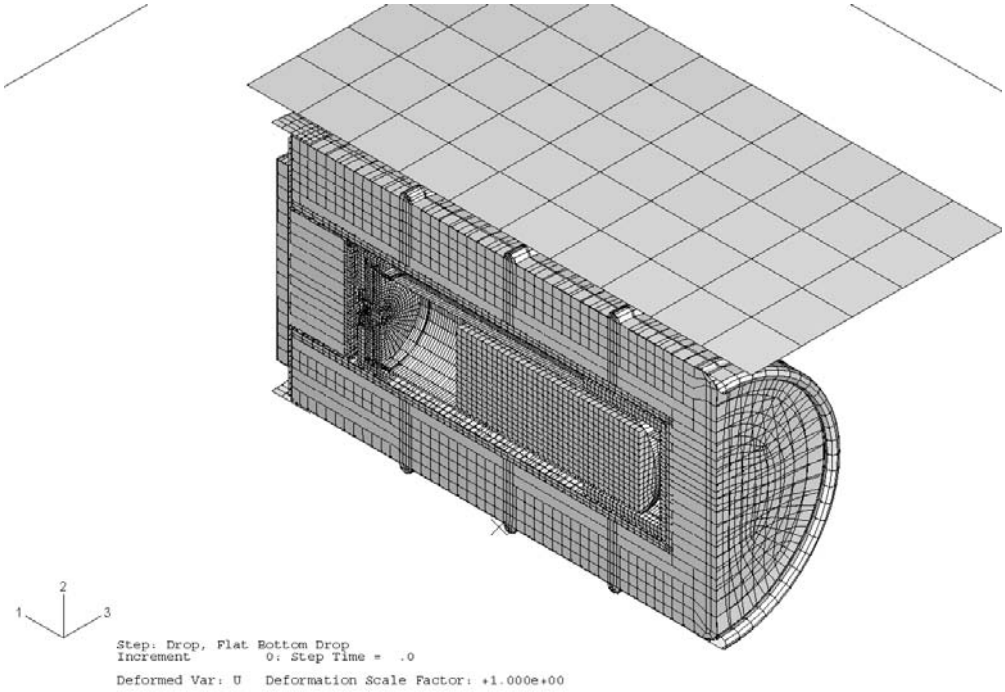

Figure 59 - Finite Element Model of the 9977 Side Drop and Side Crush (weight at bottom of 6CV)

(ALLKE = kinetic energy; ALLIE = internal energy; ALLPD = plastic strain energy; ALLSE = elastic strain energy; ALLAE = artificial energy)

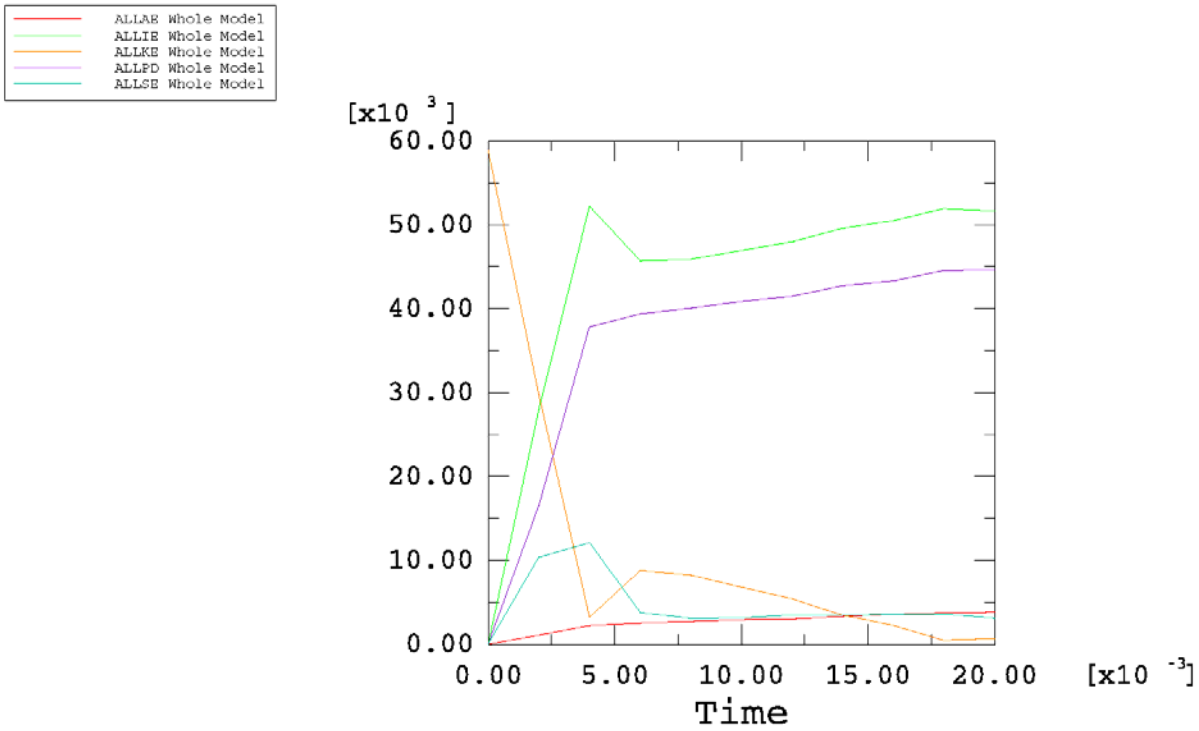

Figure 60 - Time-History Plot of Energy during Drum on Side - 30-ft Drop Simulation (-20 ºF)

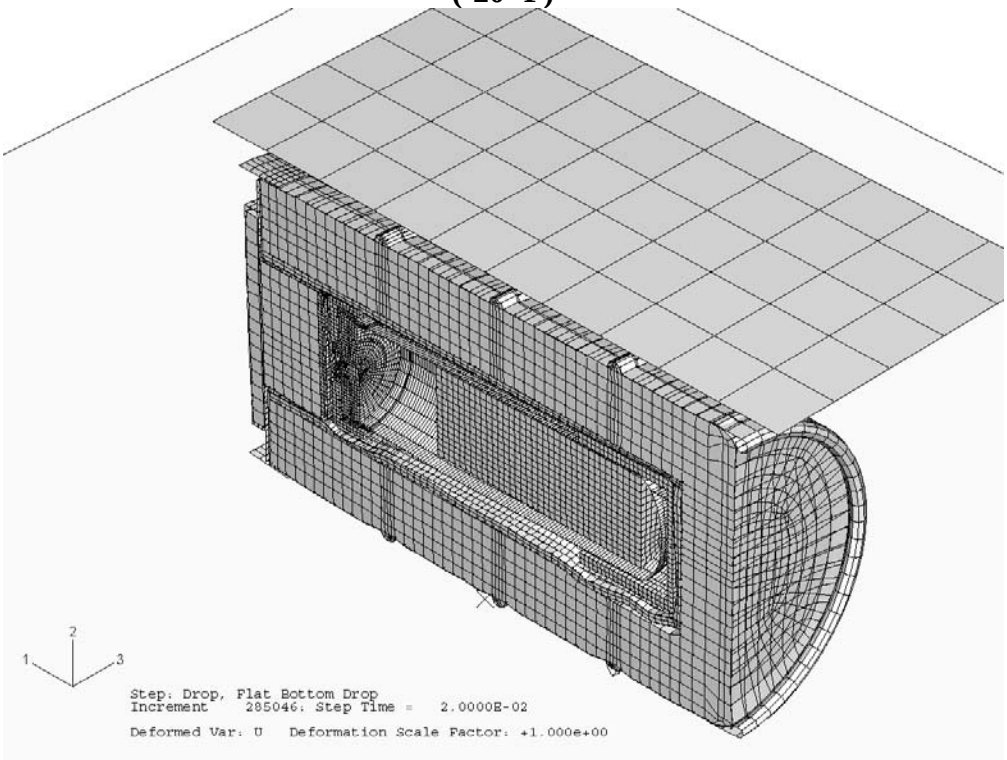

Figure 61 - Deformed Shape of 9977 with 6CV After Drum on Side - 30-ft Drop (-20 ºF)(weight in middle of CV)

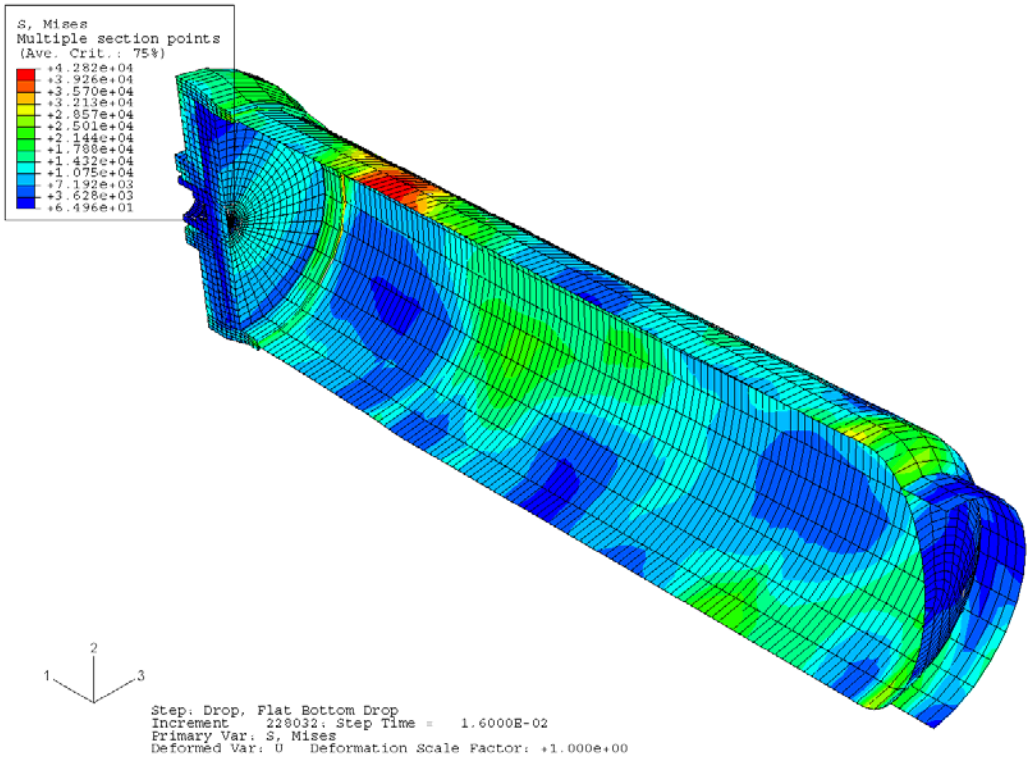

Figure 62 - Stress Distribution in the 6CV Model for Drum on Side - 30-ft Drop (-20 ºF)(weight in middle of CV)

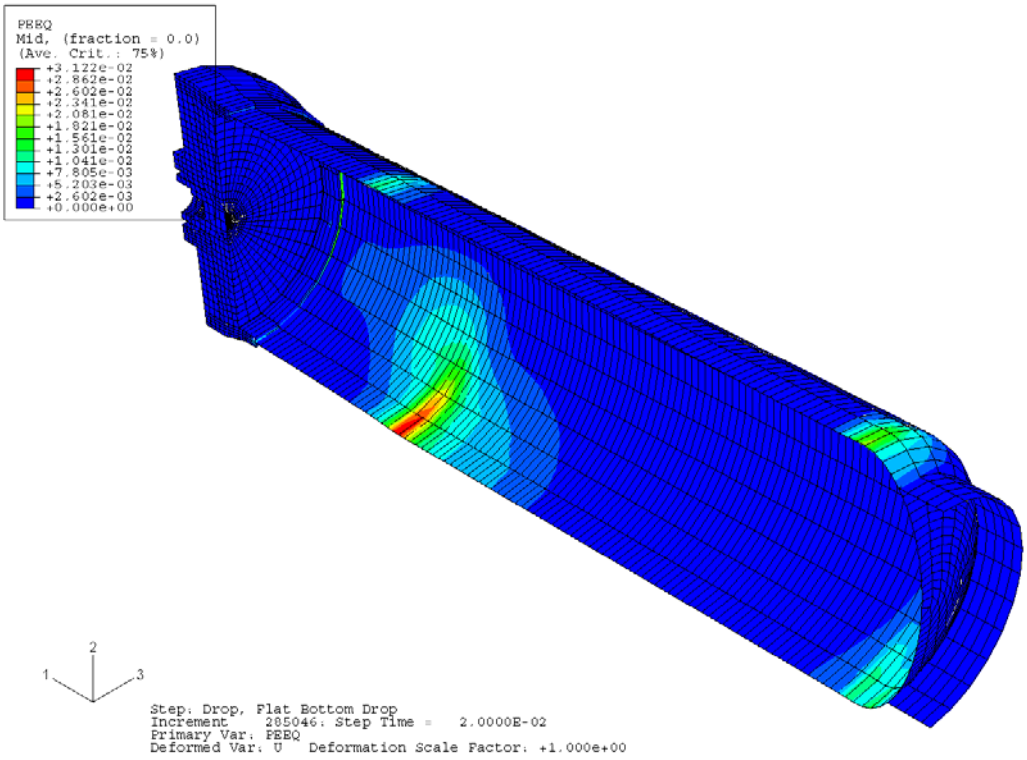

Figure 63 - Strain Distribution in 6CV Model for Drum on Side - 30-ft Drop (-20 ºF)(weight in middle of CV)

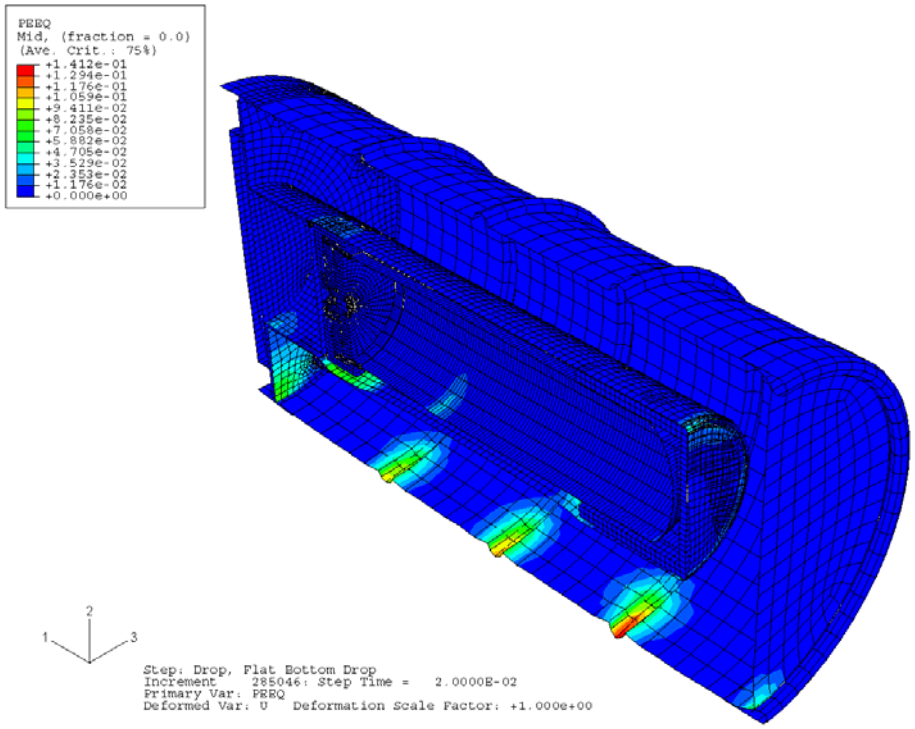

Figure 64 - Strain Distribution in Overpack for 6CV for Drum on Side - 30-ft Drop (-20 ºF)(weight in middle of CV)

(ALLKE = kinetic energy; ALLIE = internal energy; ALLPD = plastic strain energy; ALLSE = elastic strain energy; ALLAE = artificial energy)

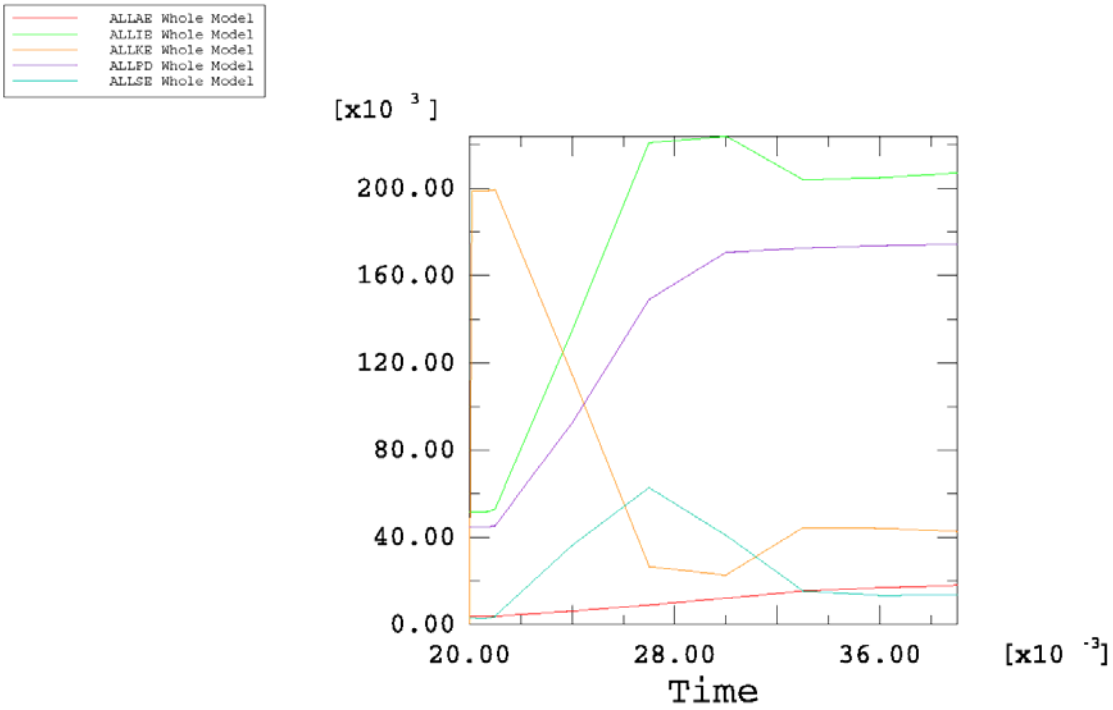

Figure 65 - Time-History Plot of Plate Energy for Drum on Side - Crush Simulation (-20 ºF)(weight in middle of CV)

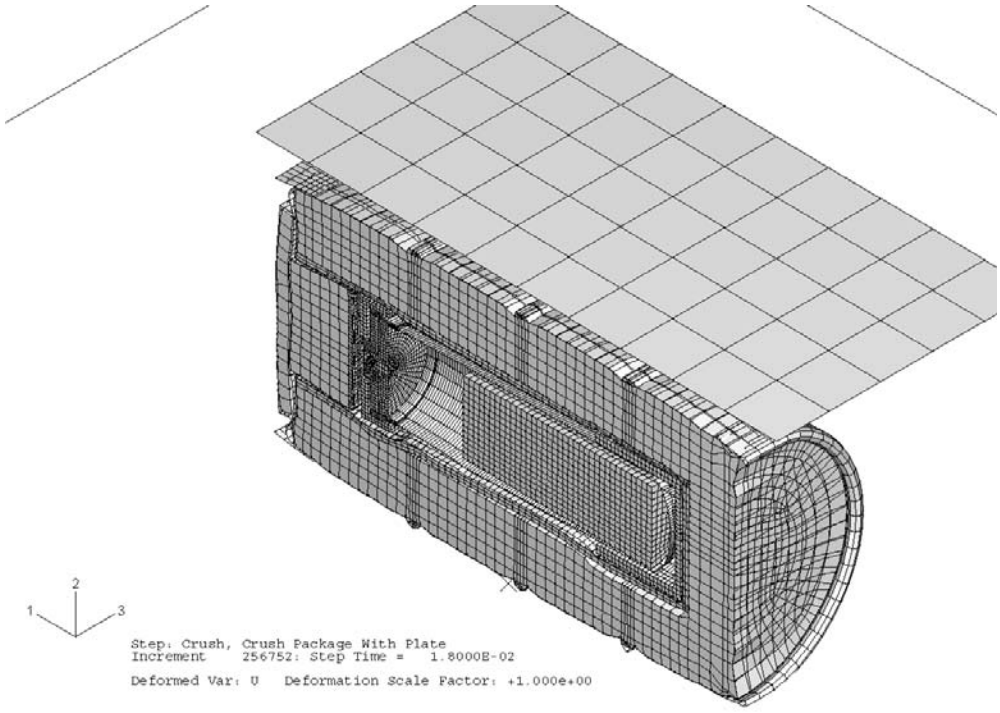

Figure 66 - Deformed Shape of 9977 with 6CV for Drum on Side - Crush (-20 ºF)(weight in middle of CV)

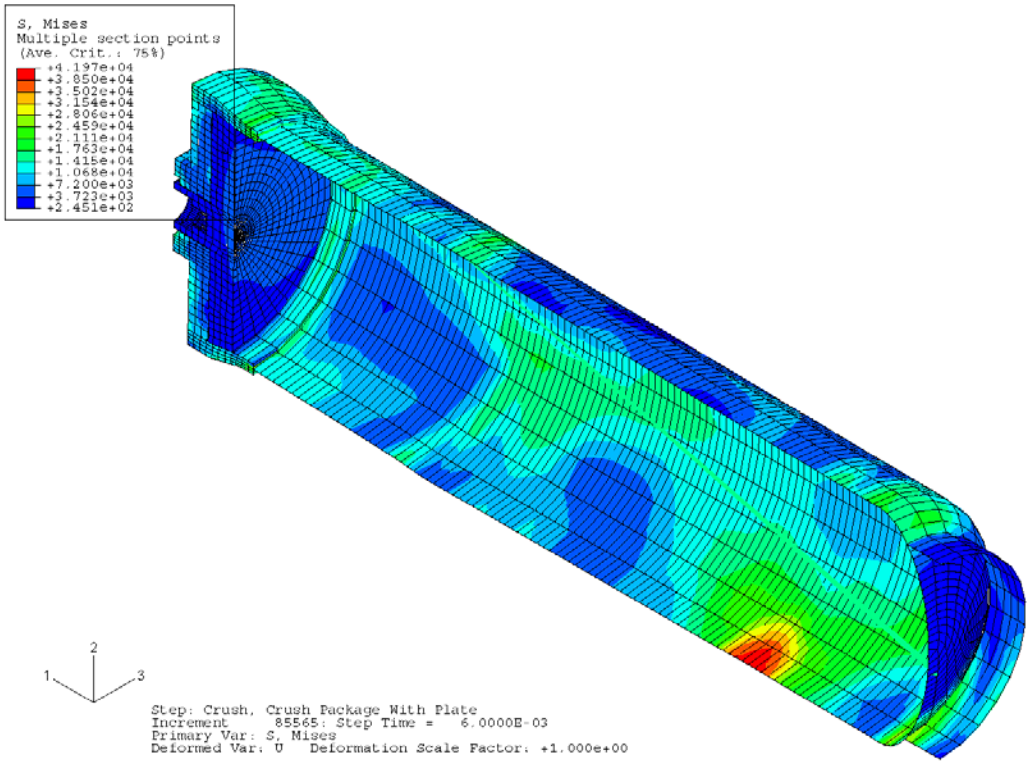

Figure 67 - Stress Distribution in 6CV Model for Drum on Side - Crush (-20 ºF)(weight in middle of CV)

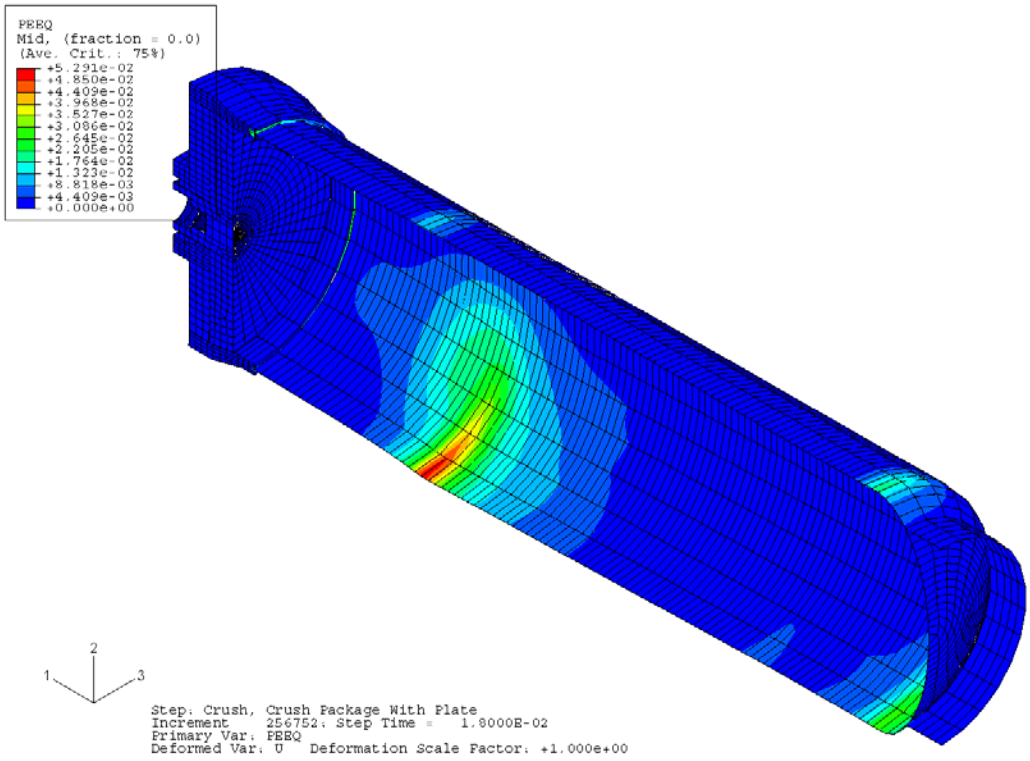

Figure 68 - Strain Distribution in 6CV Model for Drum on Side - Crush (-20 ºF)(weight in middle of CV)

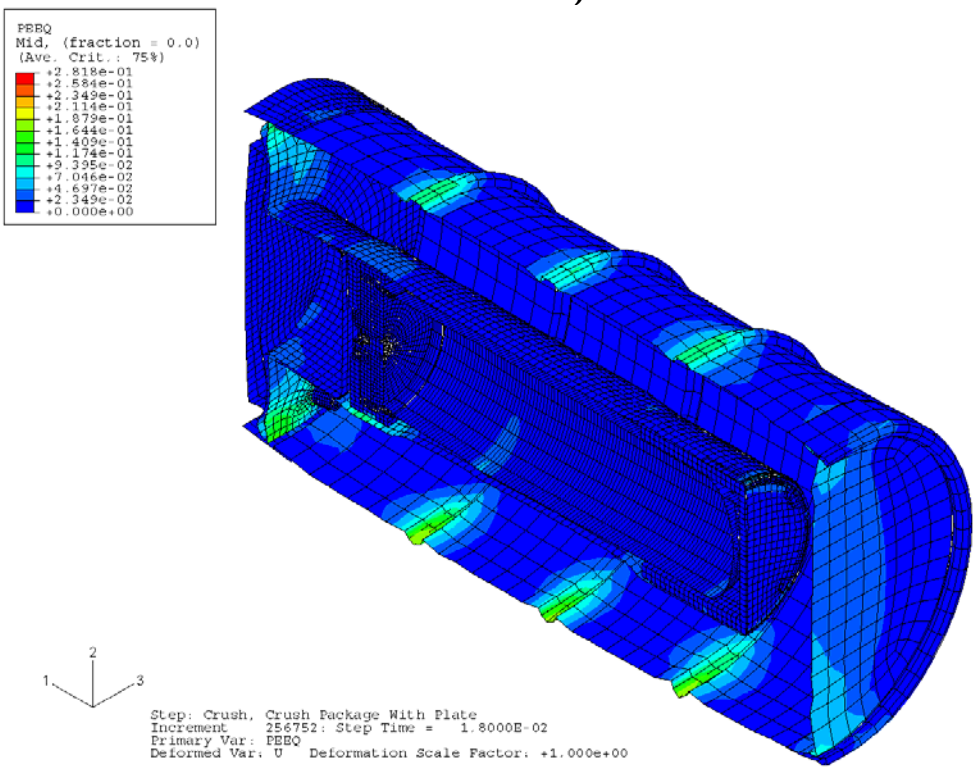

Figure 69 - Strain Distribution in Overpack for Drum on Side - Crush (-20 ºF)(weight in middle of CV)

(ALLKE = kinetic energy; ALLIE = internal energy; ALLPD = plastic strain energy; ALLSE = elastic strain energy; ALLAE = artificial energy)

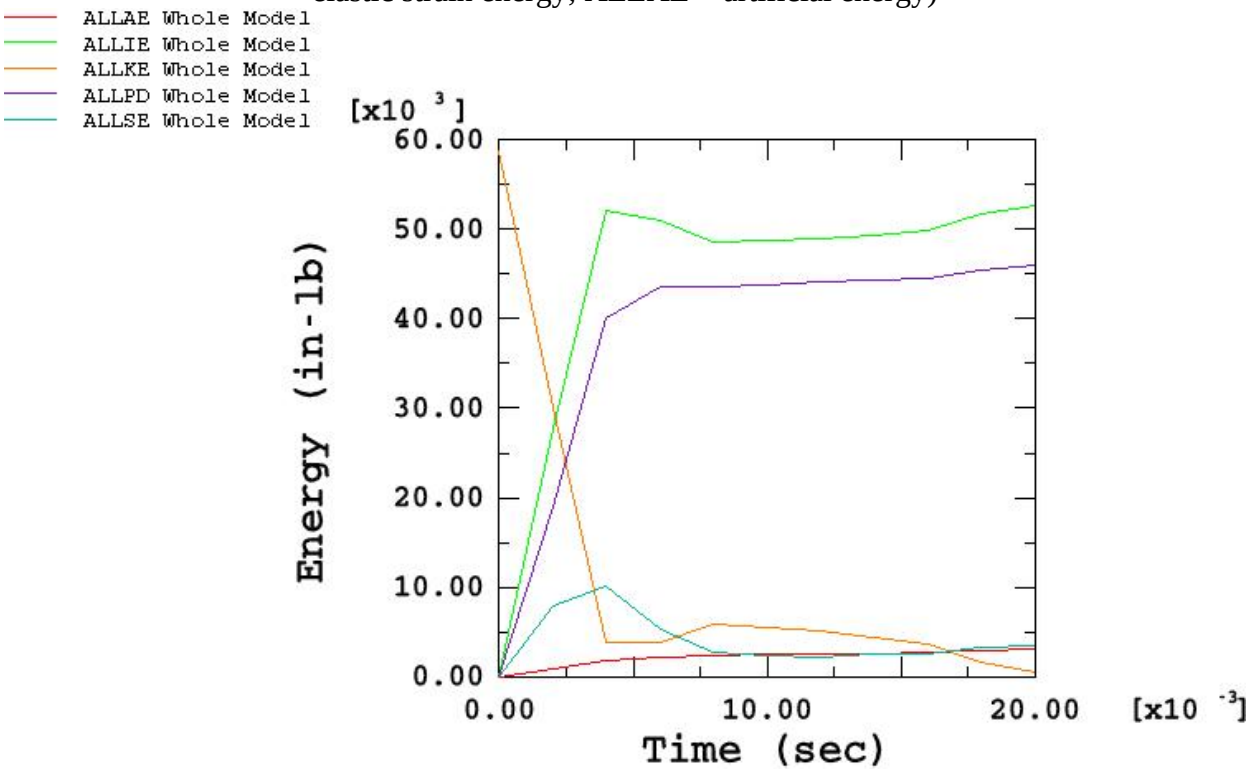

Figure 70 - Time-History Plot of Energy during Drum on Side - 30-ft Drop Simulation (140 ºF)(weight at the bottom of CV)

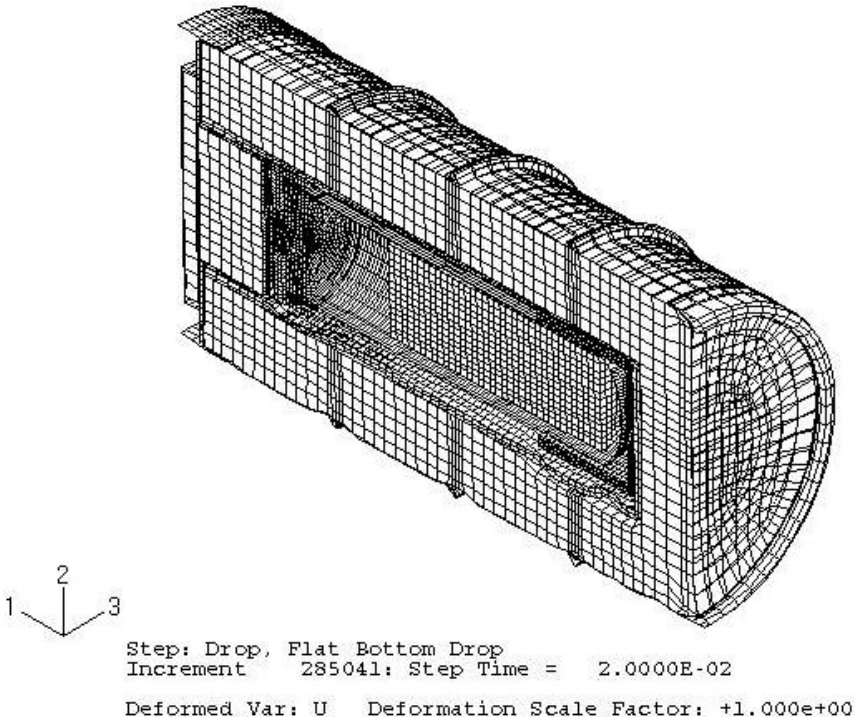

Figure 71 - Deformed Shape of 9977 with 6CV After the Drum on Side - 30-ft Drop (140 ºF)(weight at the bottom of CV)

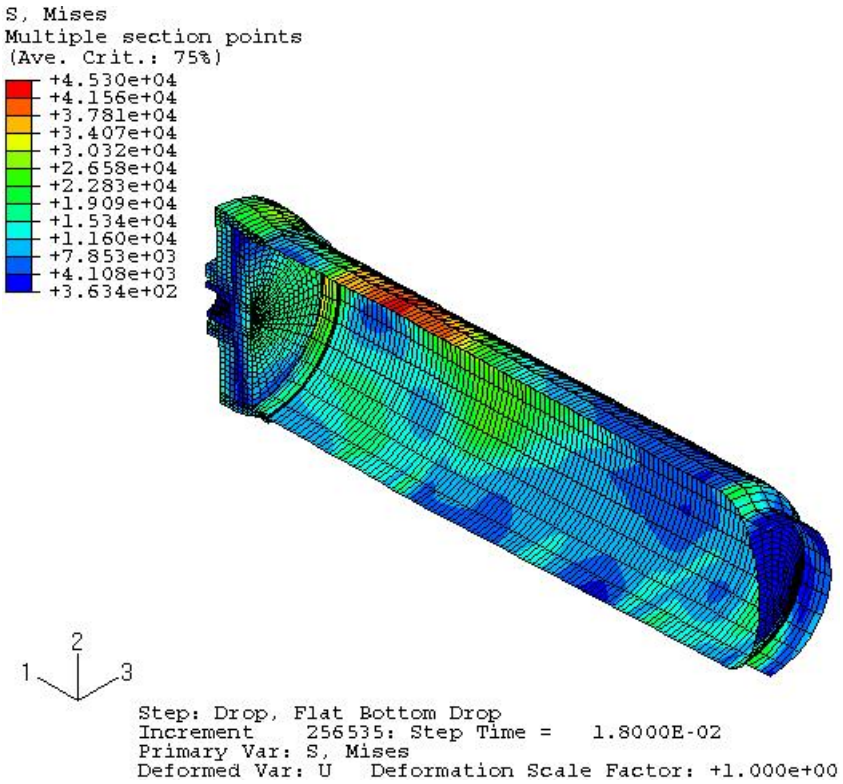

Figure 72 - Stress Distribution in the 6CV Model for Drum on Side - 30-ft Drop (140 ºF)(weight at the bottom of CV)

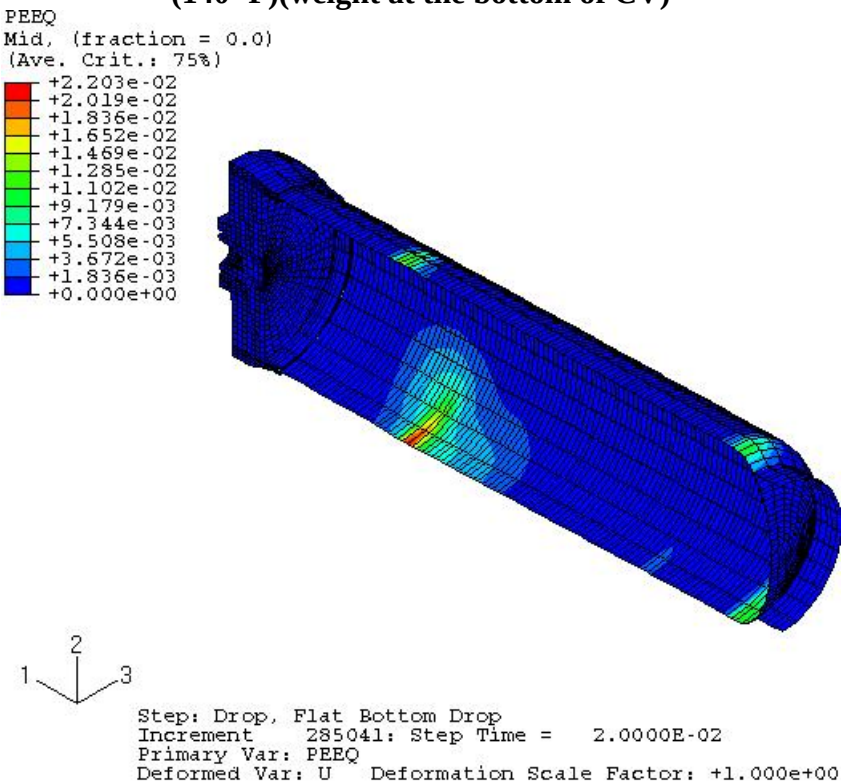

Figure 73 - Strain Distribution in 6CV Model for Drum on Side - 30-ft Drop (140 ºF)(weight at the bottom of CV)

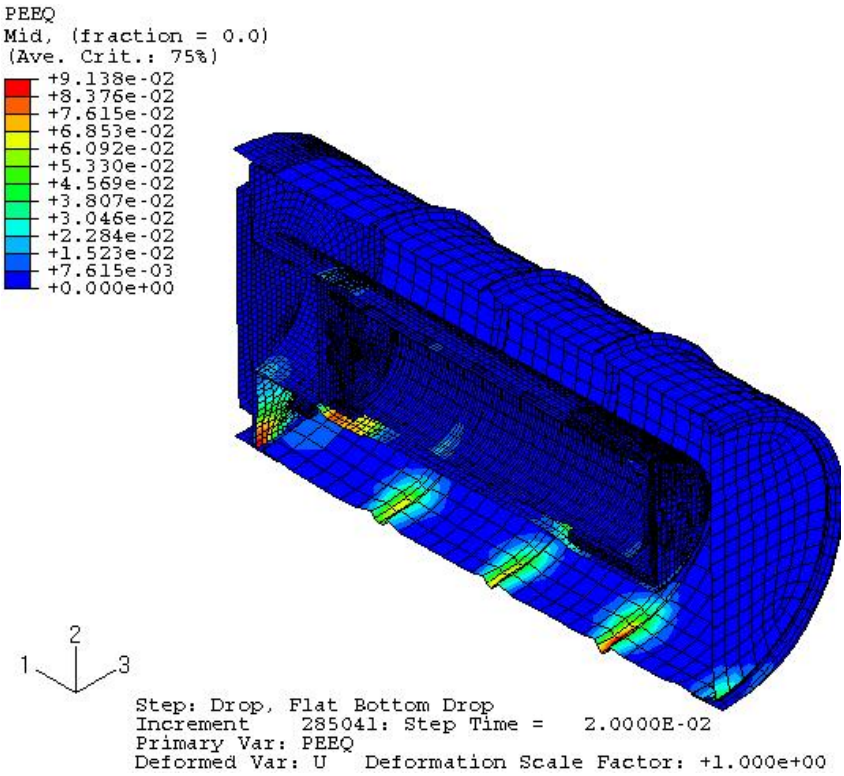

Figure 74 - Strain Distribution in Overpack for 6CV for Drum on Side - 30-ft Drop (140 ºF)(weight at the bottom of CV)

(ALLKE = kinetic energy; ALLIE = internal energy; ALLPD = plastic strain energy; ALLSE = elastic strain energy; ALLAE = artificial energy)

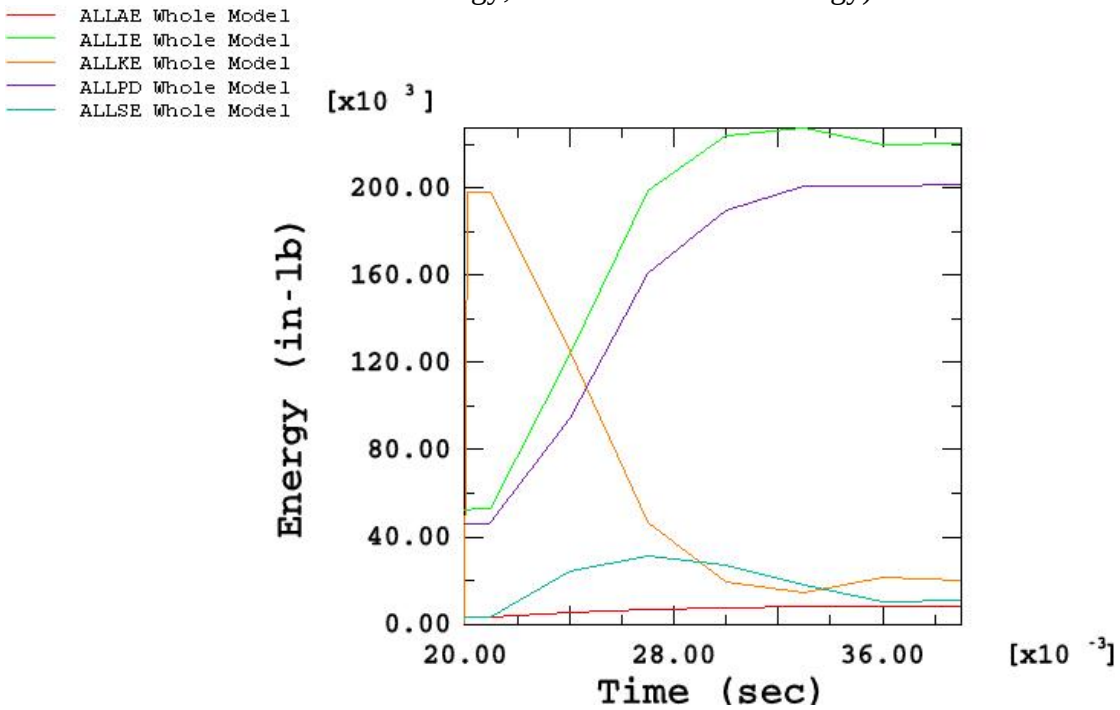

Figure 75 - Time-History Plot of Energy during Drum on Side - Crush Simulation (140 ºF)(weight at the bottom of CV)

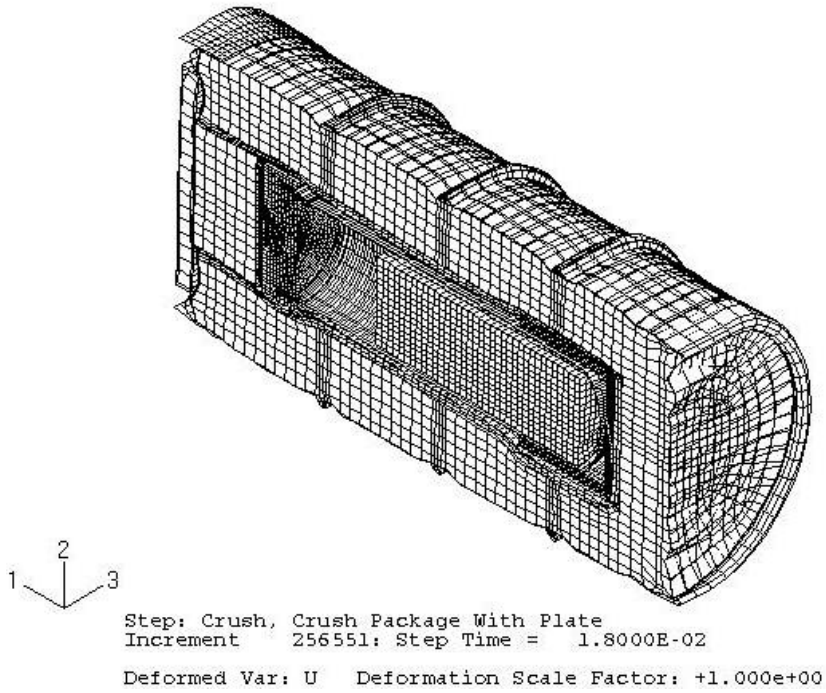

Figure 76 - Deformed Shape of 9977 with 6CV for Drum on Side - Crush (140 ºF)(weight at the bottom of CV)

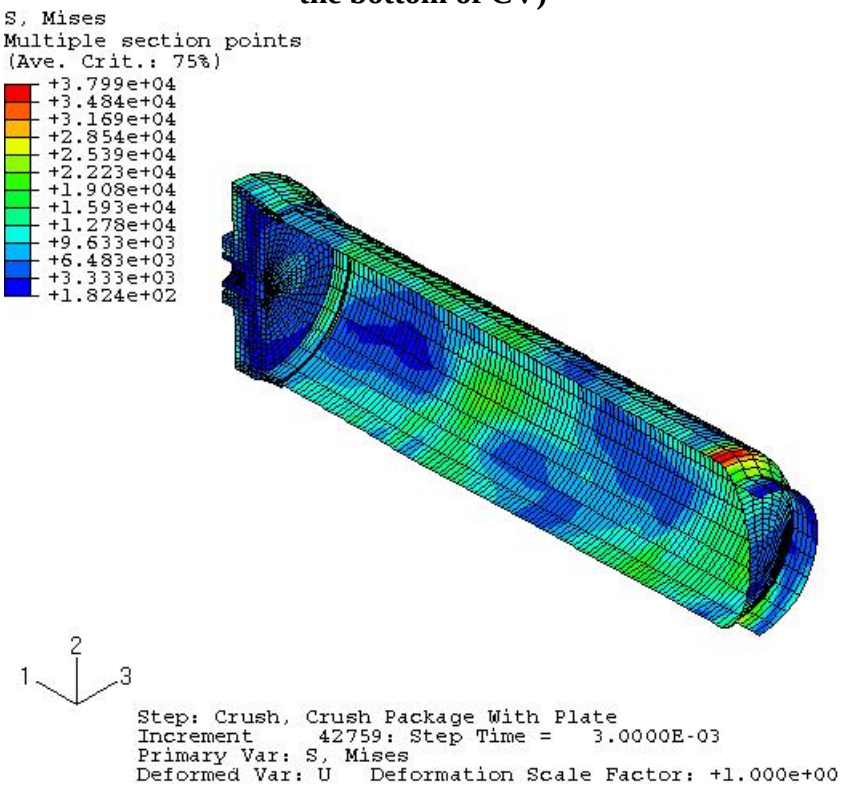

Figure 77 - Stress Distribution in 6CV Model for Drum on Side - Crush (140 ºF)(weight at the bottom of CV)

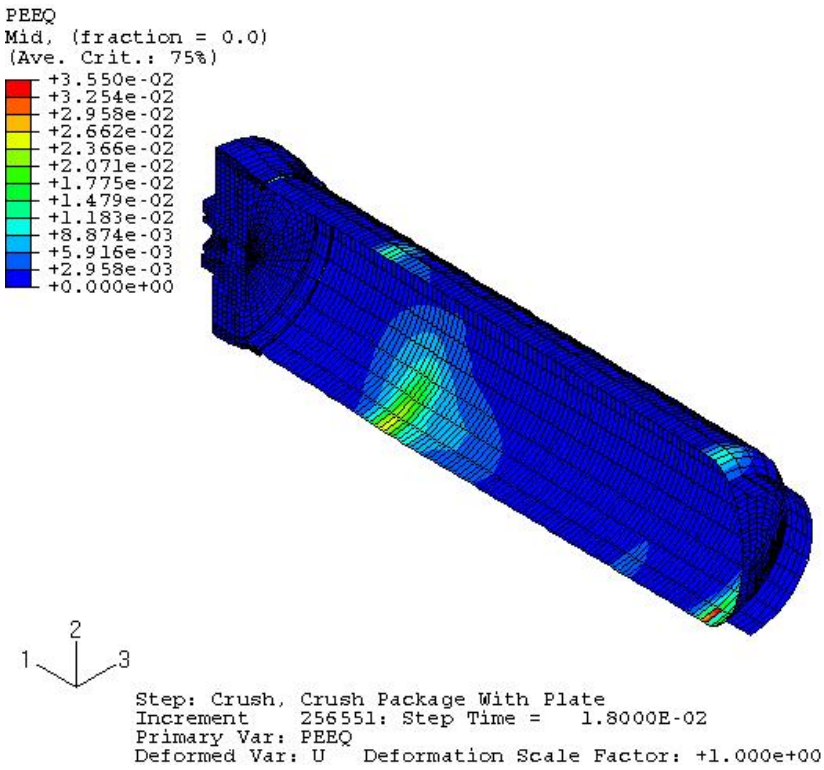

Figure 78 - Strain Distribution in 6CV Model for Drum on Side - Crush (140 ºF)(weight at the bottom of CV)

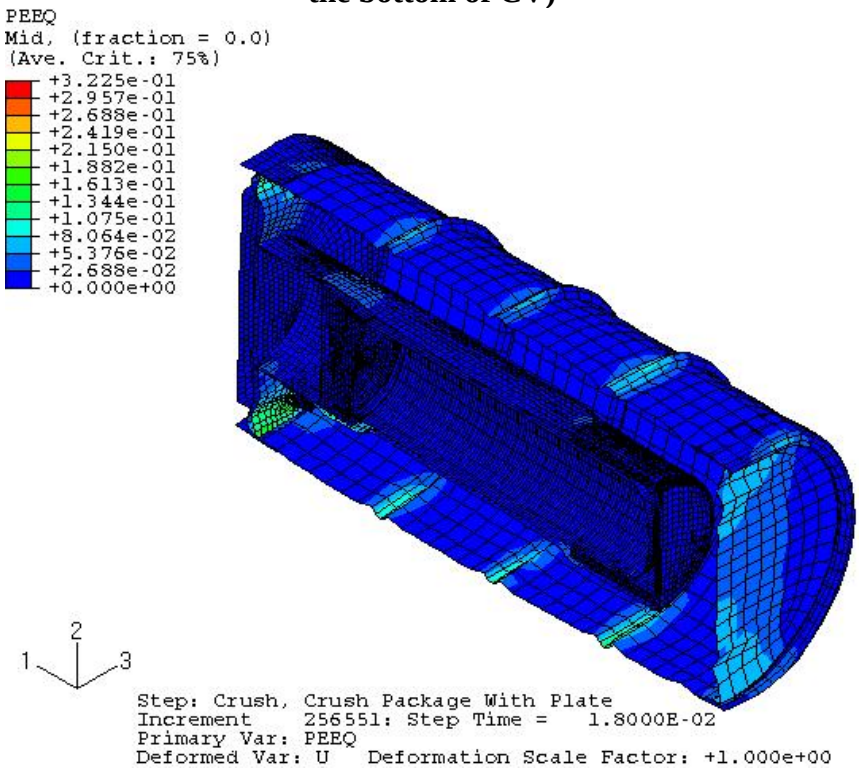

Figure 79 - Stress Distribution in Overpack for Drum on Side - Crush (140 ºF)(weight at the bottom of CV)

(ALLKE = kinetic energy; ALLIE = internal energy; ALLPD = plastic strain energy; ALLSE = elastic strain energy; ALLAE = artificial energy)

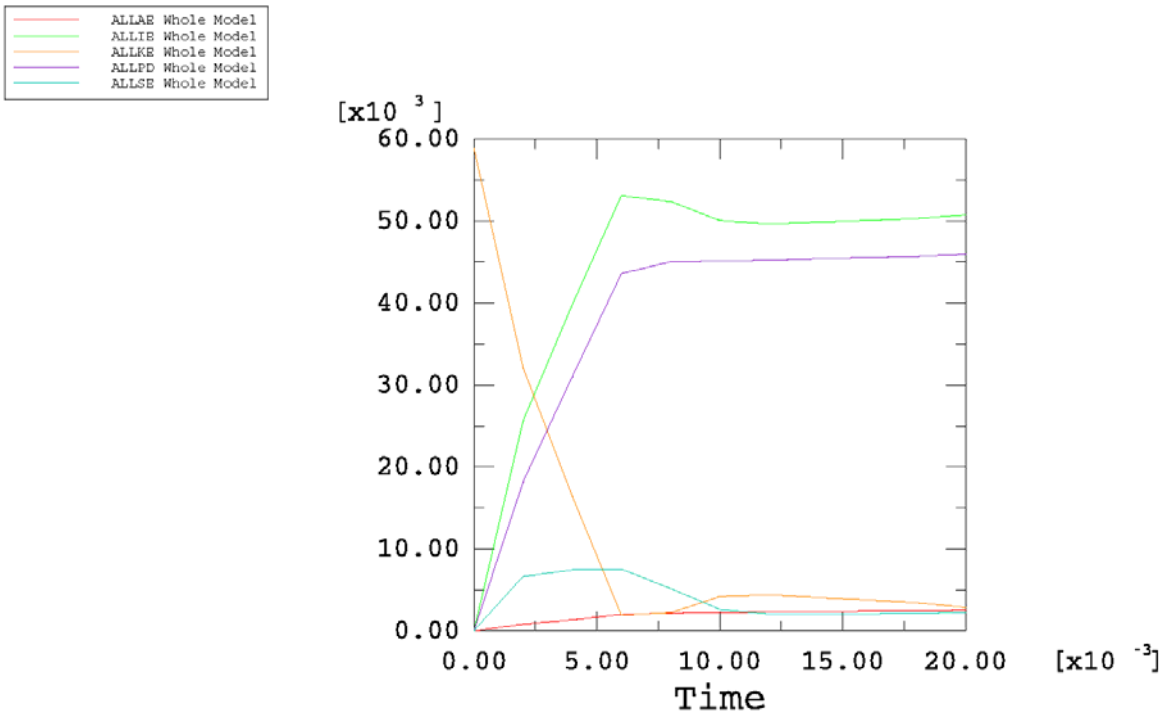

Figure 80 - Time-History Plot of Energy during Drum on Side - 30-ft Drop Simulation (300 ºF)(weight at the bottom of CV)

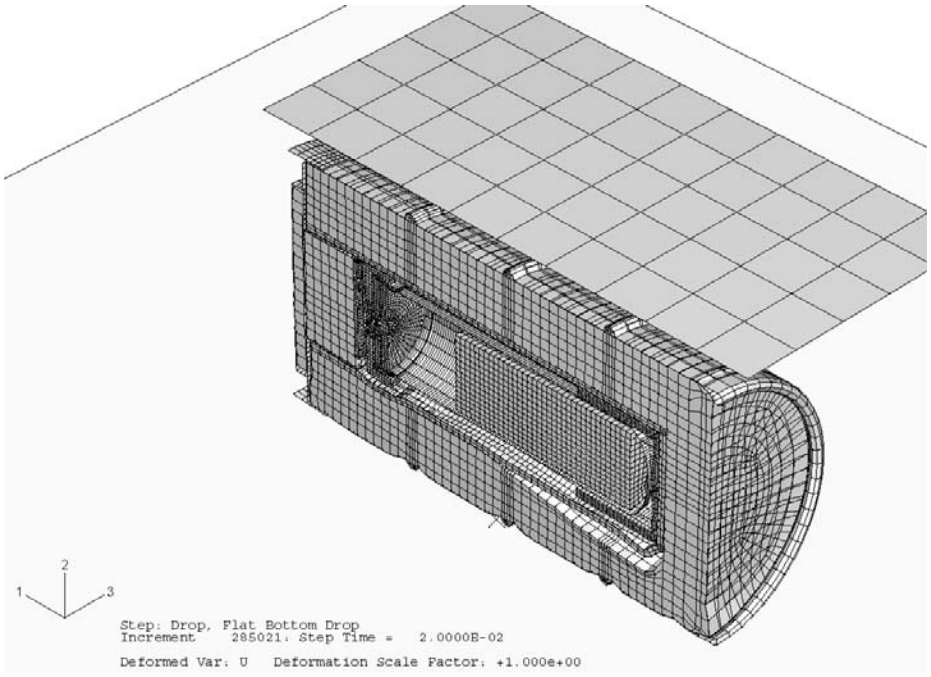

Figure 81 - Deformed Shape of 9977 with 6CV After the Drum on Side - 30-ft Drop (300 ºF)(weight at the bottom of CV)

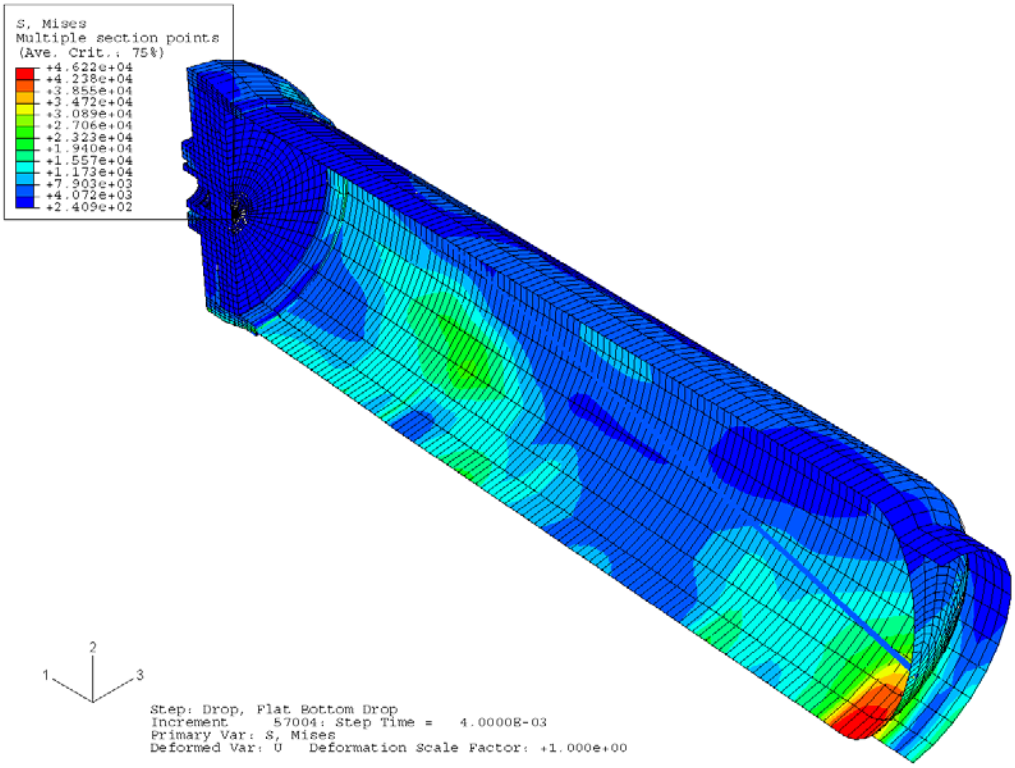

Figure 82 - Stress Distribution in the 6CV Model for Drum on Side - 30-ft Drop (300 ºF)(weight at the bottom of CV)

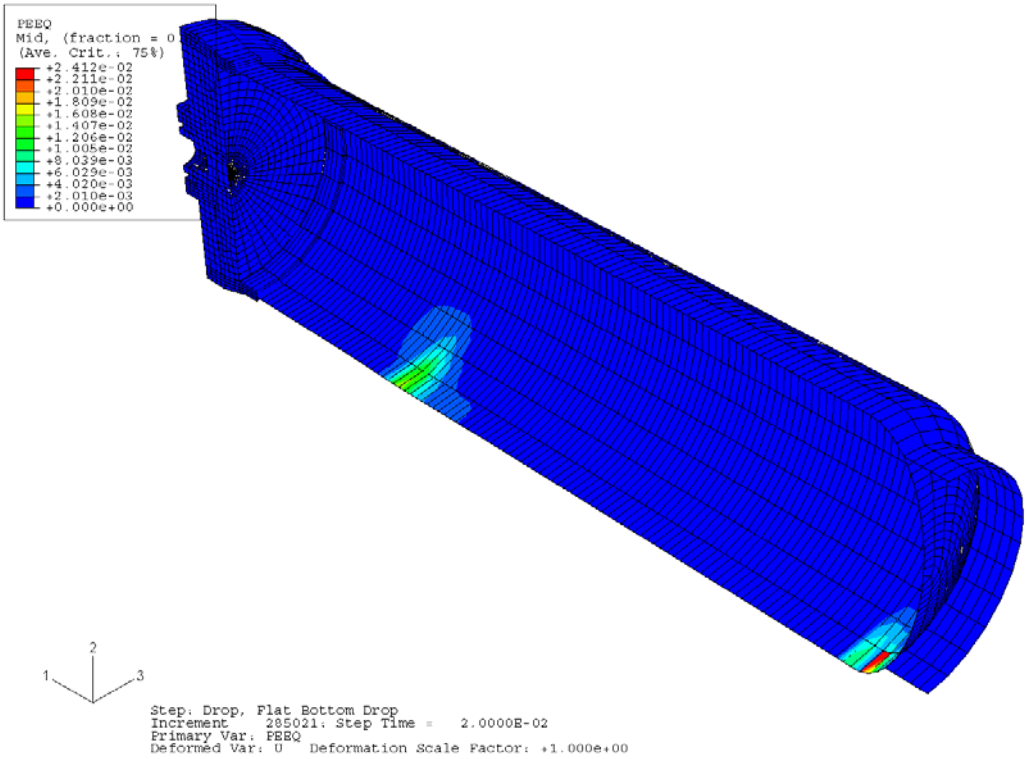

Figure 83 - Strain Distribution in 6CV Model for Drum on Side - 30-ft Drop (300 ºF)(weight at the bottom of CV)

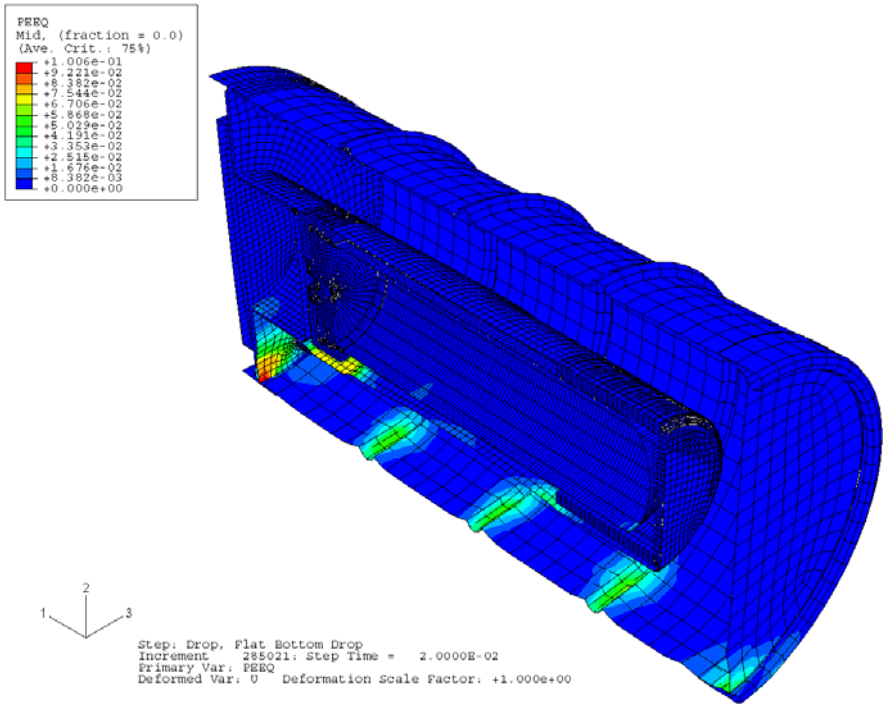

Figure 84 - Strain Distribution in Overpack for 6CV for Drum on Side - 30-ft Drop (300 ºF)(weight at the bottom of CV)

(ALLKE = kinetic energy; ALLIE = internal energy; ALLPD = plastic strain energy; ALLSE = elastic strain energy; ALLAE = artificial energy)

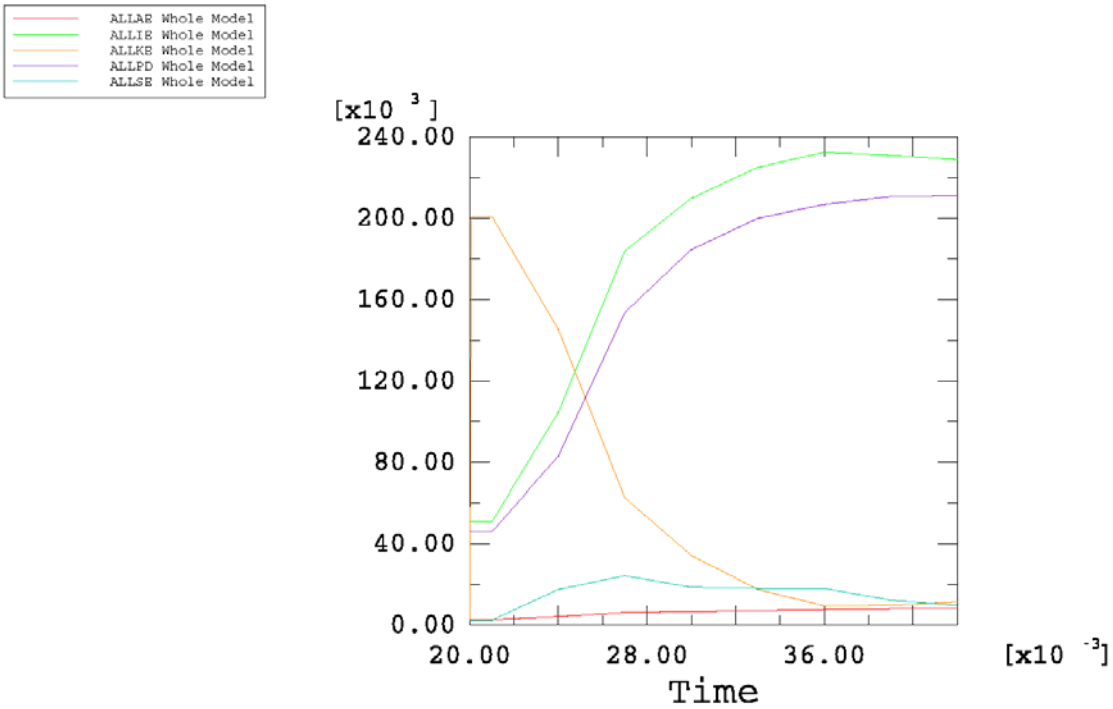

Figure 85 - Time-History Plot of Plate Energy during Drum on Side - Crush Simulation (300 ºF)(weight at the bottom of CV)

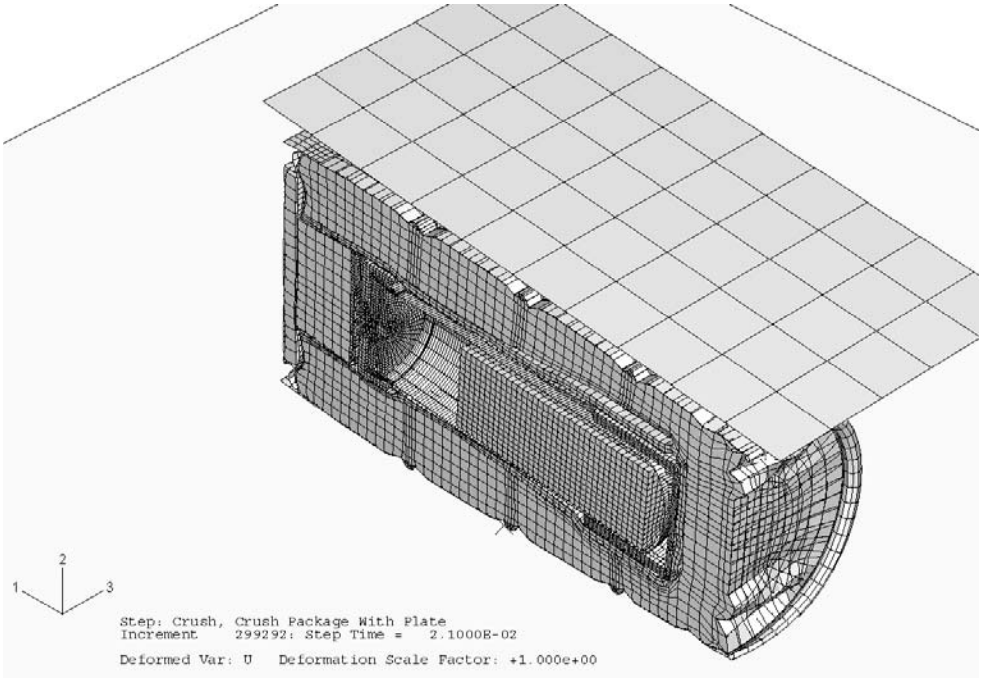

Figure 86 - Deformed Shape of 9977 with 6CV for Drum on Side - Crush (300 ºF)(weight at the bottom of CV)

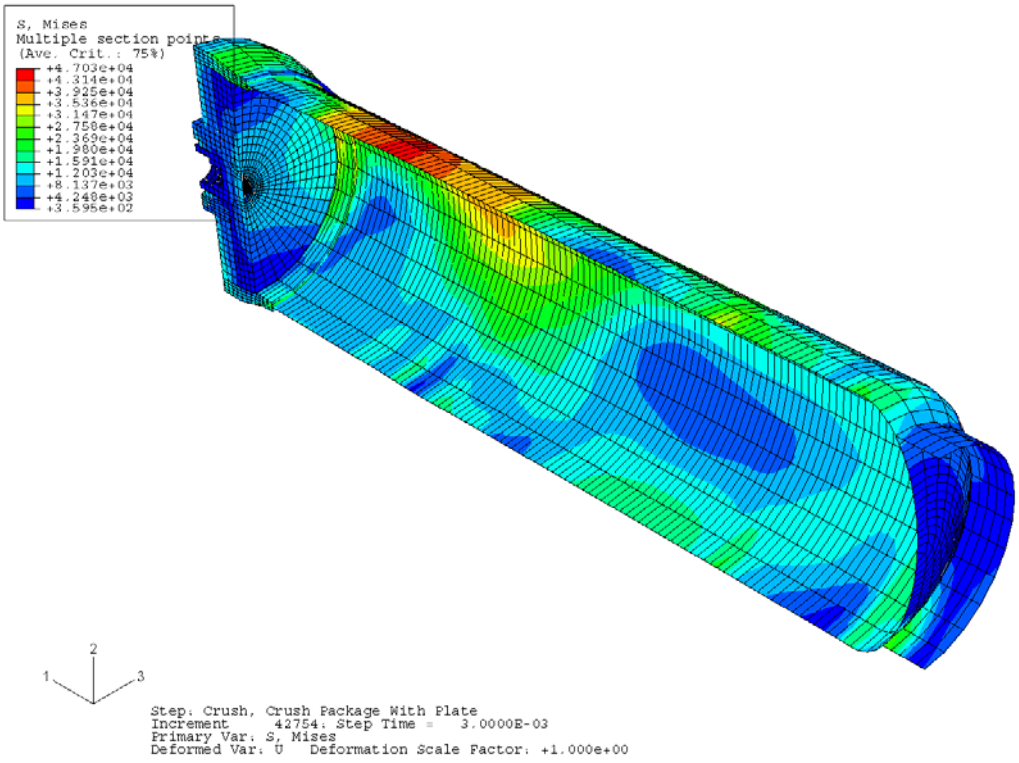

Figure 87 - Stress Distribution in 6CV Model for Drum on Side - Crush (300 ºF)(weight at the bottom of CV)

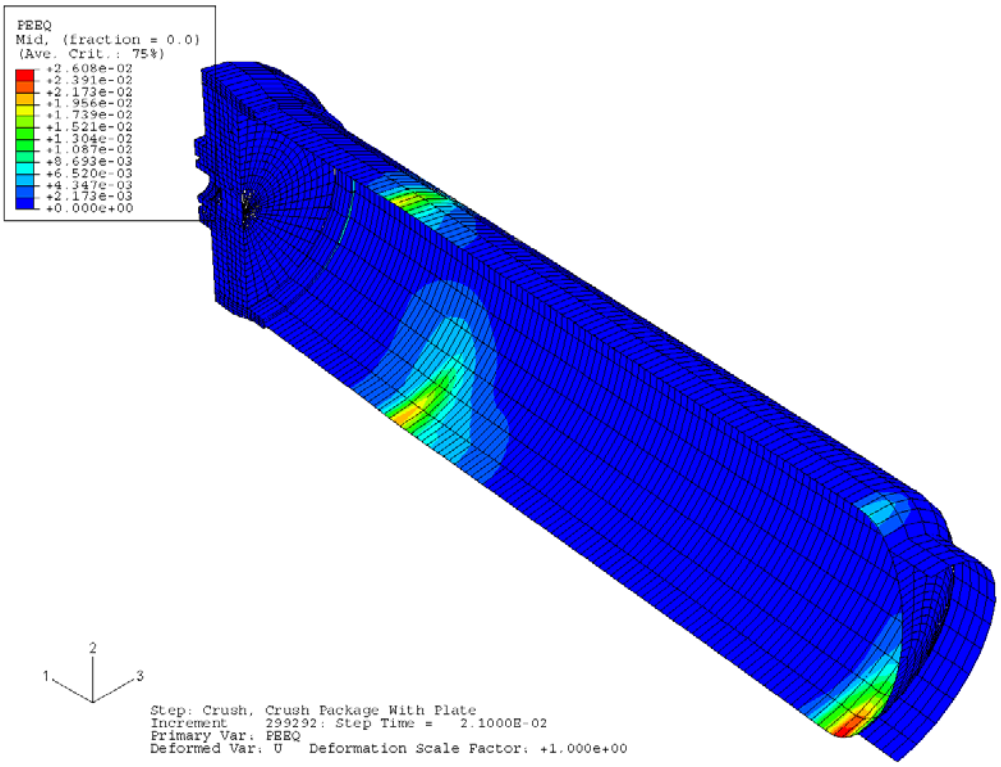

Figure 88 - Strain Distribution in 6CV Model for Drum on Side - Crush (300 ºF)(weight at the bottom of CV)

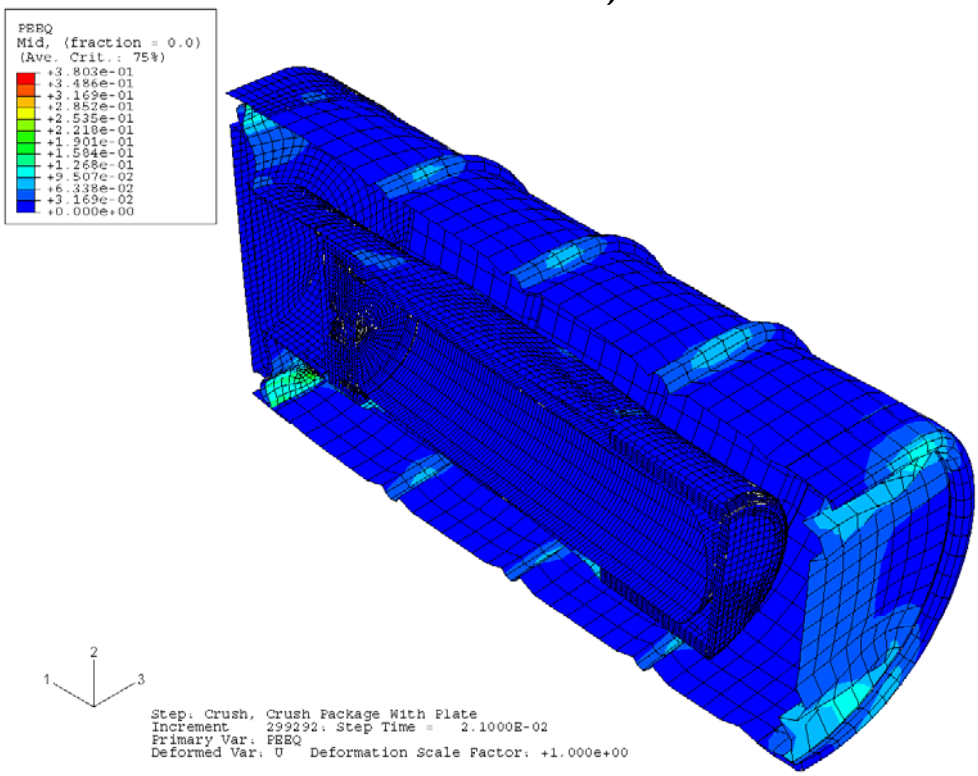

Figure 89 - Strain Distribution in Overpack for Drum on Side - Crush (300 ºF)(weight at the bottom of CV)

(ALLKE = kinetic energy; ALLIE = internal energy; ALLPD = plastic strain energy; ALLSE = elastic strain energy; ALLAE = artificial energy)

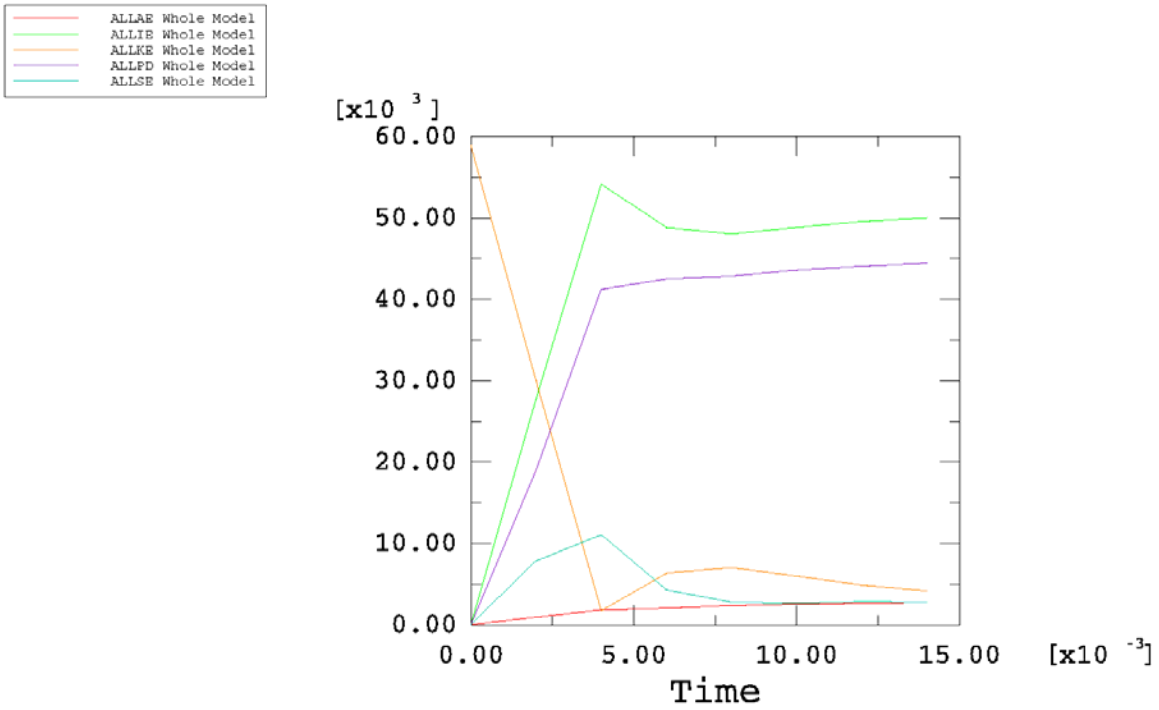

Figure 90 - Time-History Plot of Energy during Drum on Side - 30-ft Drop Simulation (140 ºF)(weight at the top of CV)

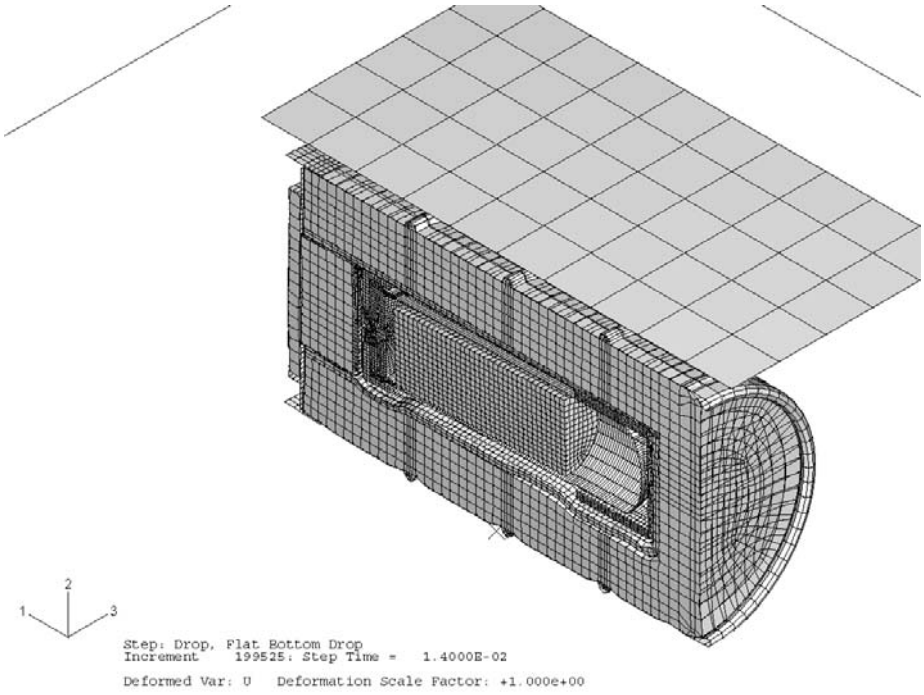

Figure 91 - Deformed Shape of 9977 with 6CV After the Drum on Side - 30-ft Drop (140 ºF)(weight at the top of CV)

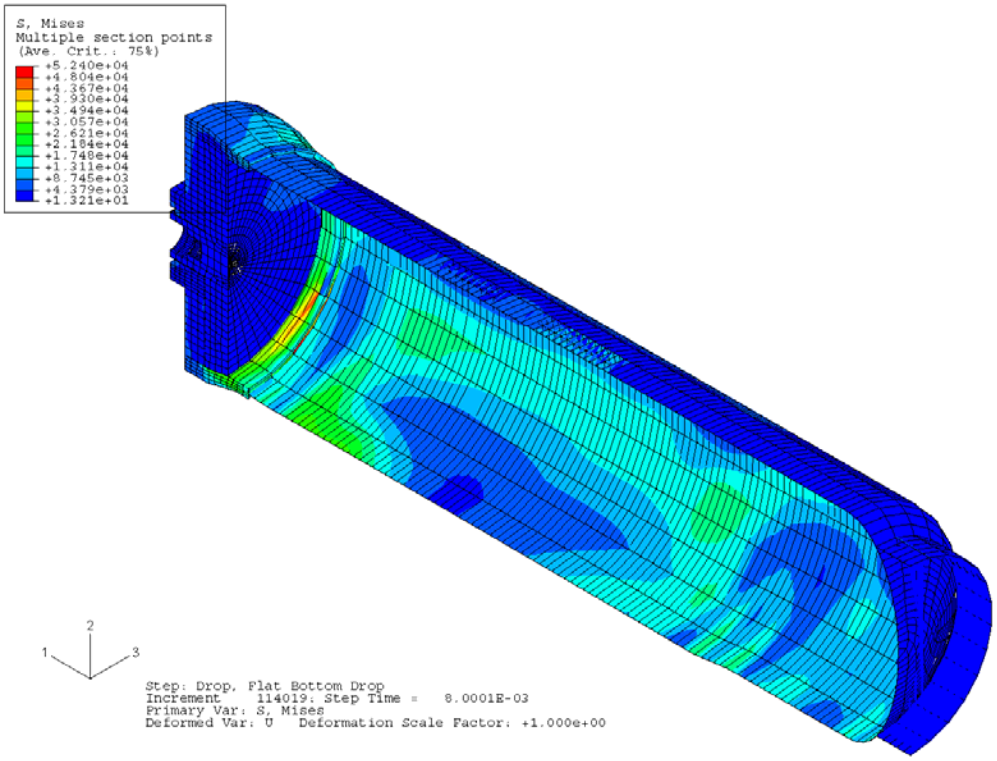

Figure 92 - Stress Distribution in the 6CV Model for Drum on Side - 30-ft Drop (140 ºF)(weight at the top of CV)

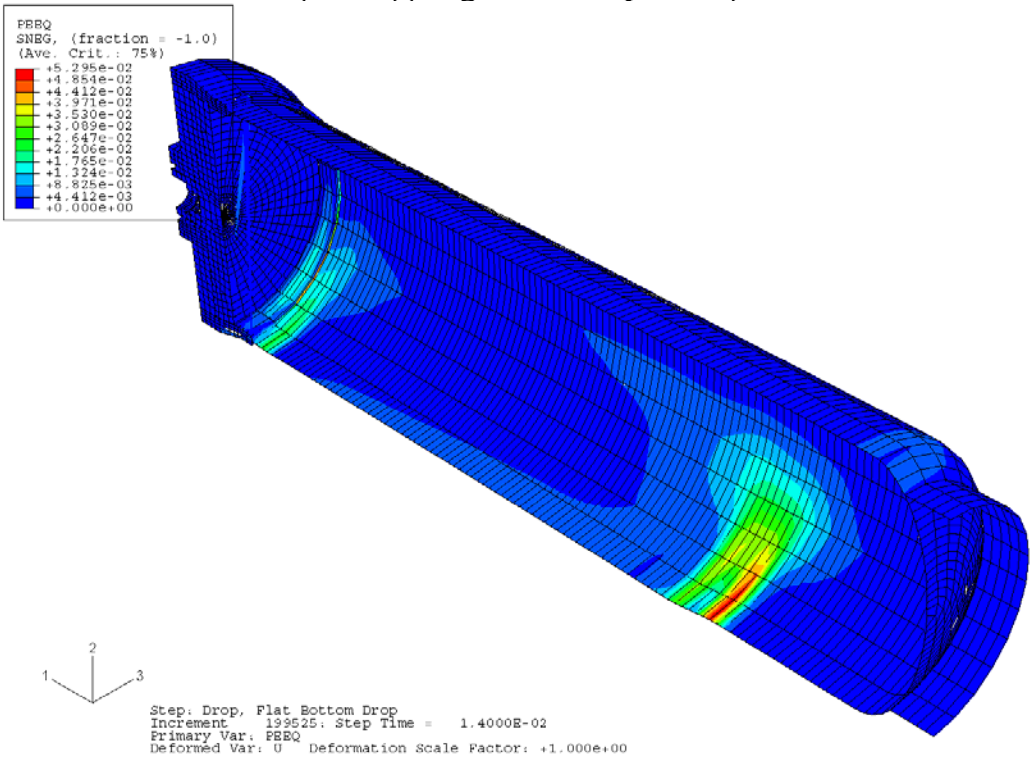

Figure 93 - Strain Distribution in 6CV Model for Drum on Side - 30-ft Drop (140 ºF)(weight at the top of CV)

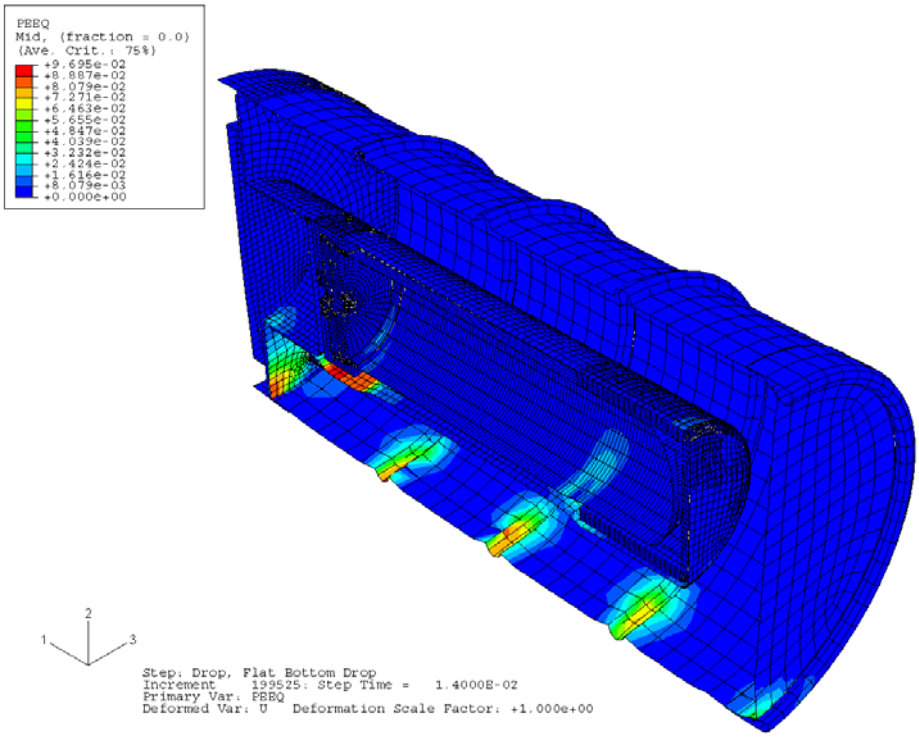

Figure 94 - Strain Distribution in Overpack for 6CV for Drum on Side - 30-ft Drop (140 ºF)(weight at the top of CV)

(ALLKE = kinetic energy; ALLIE = internal energy; ALLPD = plastic strain energy; ALLSE = elastic strain energy; ALLAE = artificial energy)

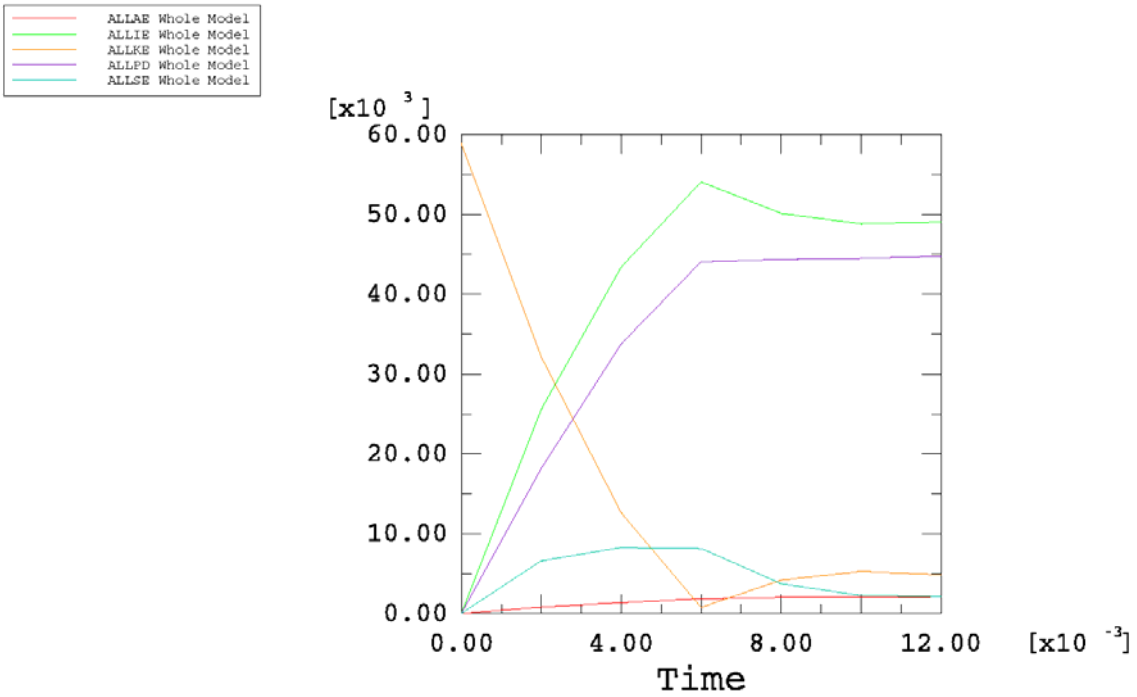

Figure 95 - Time-History Plot of Energy during Drum on Side - 30-ft Drop Simulation (300 ºF)(weight at the top of CV)

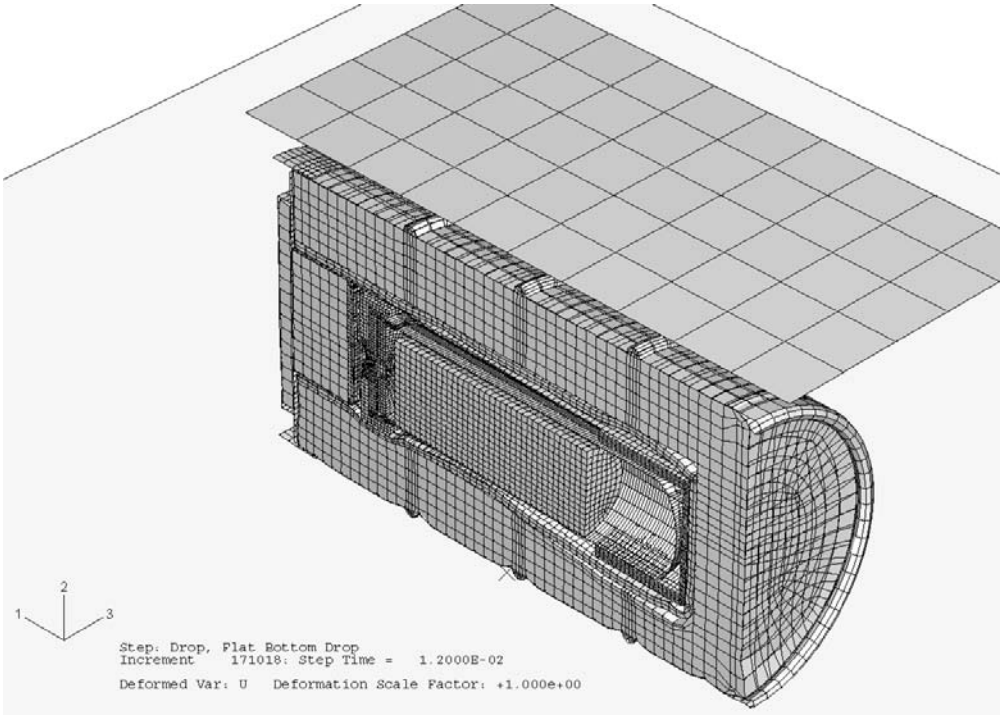

Figure 96 - Deformed Shape of 9977 with 6CV After the Drum on Side - 30-ft Drop (300 ºF)(weight at the top of CV)

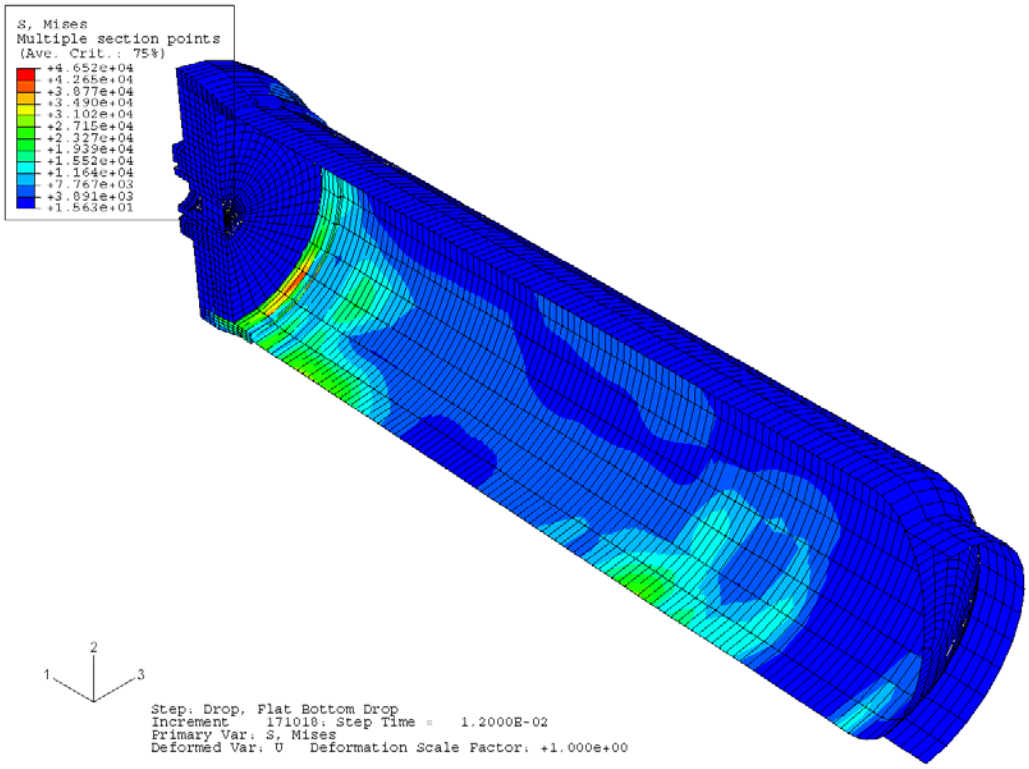

Figure 97 - Stress Distribution in the 6CV Model for Drum on Side - 30-ft Drop (300 ºF)(weight at the top of CV)

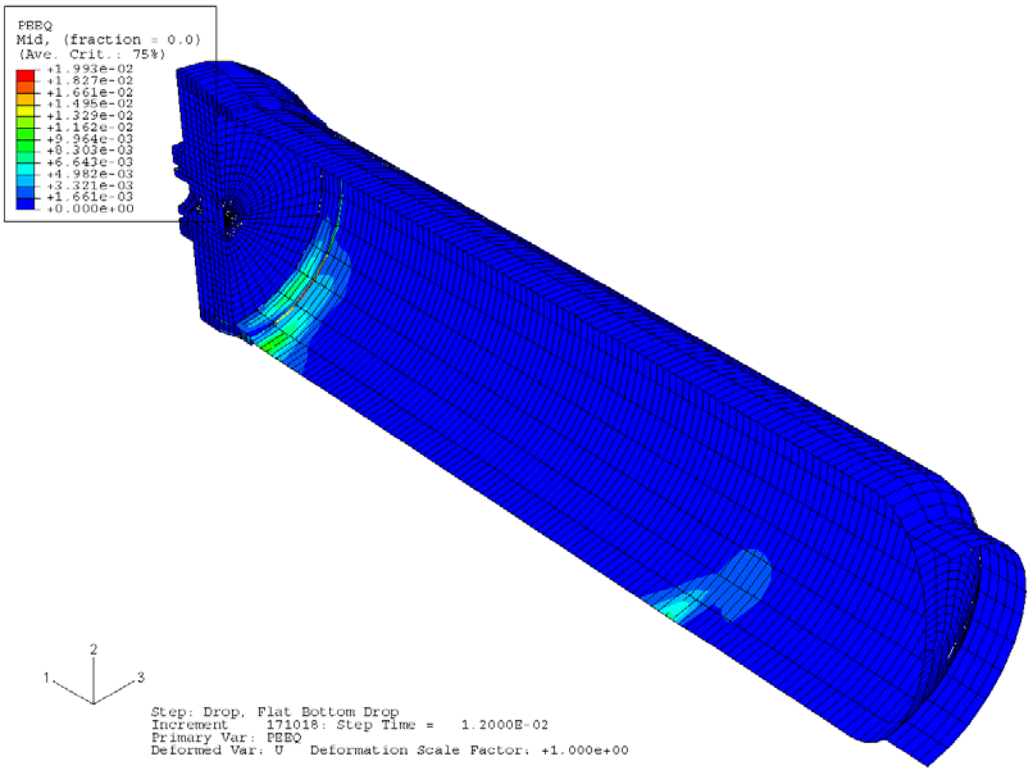

Figure 98 - Strain Distribution in 6CV Model for Drum on Side - 30-ft Drop (300 ºF)(weight at the top of CV)

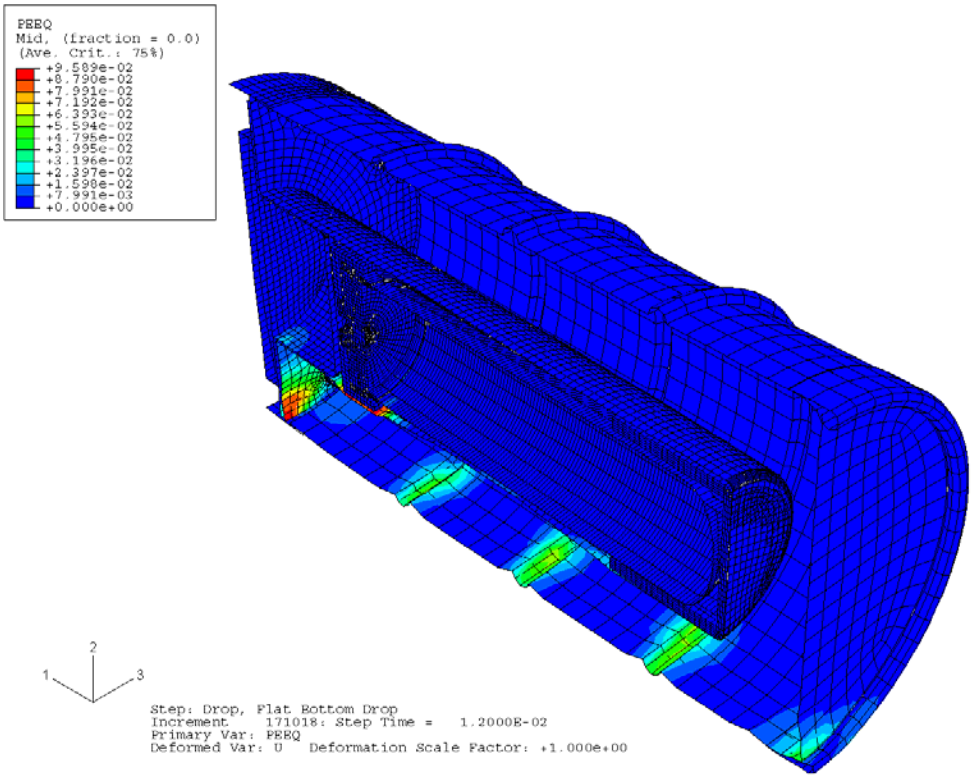

Figure 99 - Strain Distribution in 6CV Model for Drum on Side - 30-ft Drop (300 ºF)(weight at the top of CV)

7.4 Center of Gravity over Drum Top Corner - Drop Followed by Crush (-20 & 75 ºF)

Figure 100 shows the finite element model used for evaluating the 30-ft drum center of gravity over the top corner drop with the follow on impact of the 1,100 lb plate dropped 30-ft onto the package bottom.

7.4.1 Case 1: Drum CGOT - 30-Ft Drop (-20 ºF)

Energy History

The time-history plots of energy components for the 30-ft CGOT drop simulation shown in Figure 101 indicate that the kinetic energy approaches zero at the end of the analysis. Therefore, we know that the analysis covers the entire impact duration.

Deformed Shape of Full Model

Figure 102 is the deformed shape of the overall model.

Stress and Strain Contours in Component Models

Figures 103 and 104 show the von Mises stresses and the equivalent plastic strains in the CV model. Figure 105 shows the equivalent plastic strains in the overpack shell.

Evaluations of Maximum Local Primary Membrane Stress Intensities and Maximum Equivalent Plastic Strains in Containment Vessel

The stress components across the wall thickness at the locations away from or near the geometrical discontinuities should be used to calculate the general primary membrane stress intensities (P_m) or the local primary membrane stress intensities (P_L). For simplicity, the maximum value of the von Mises stresses in the containment vessel is used as the local primary membrane stress intensity (P_L). This value is higher than the actual local primary membrane stress intensity because the latter is calculated by averaging the thru-wall stresses across the component's thickness.

The maximum value of the local primary membrane stress intensity in the containment vessel is 47.99 ksi as given in Figure 103. This value is less than the allowable value of 57.3 ksi for the general primary membrane stress intensity and of 73.6 ksi for the local primary membrane stress intensity (as given in Section 6.0). The structural integrity of the 9977 subjected to a 30-ft drop has therefore been justified according to the ASME Code, Section III.

As shown in Figure 104, the maximum plastic strain experienced at any location within the containment vessel after the 30-ft drop is 3.11%. The maximum calculated value of the effective plastic strain at any point in the overpack is 17.10%. This value is less than the maximum average through-wall elongation of 35% for the 304L material use in the drum. Therefore, the drum will not be ruptured by the 30-ft drop impact.

7.4.2 Case 2: Drum CGOT - 30-Ft Drop (75 ºF)

Energy History

The time-history plots of energy components for the 30-ft CGOT drop simulation shown in Figure 106 indicate that the kinetic energy approaches zero at the end of the analysis. Therefore, we know that the analysis covers the entire impact duration.

Deformed Shape of Full Model

Figure 107 is the deformed shape of the overall model.

Stress and Strain Contours in Component Models

Figures 108 and 109 show the von Mises stresses and the equivalent plastic strains in the CV model. Figure 110 shows the equivalent plastic strains in the overpack shell.

Evaluations of Maximum Local Primary Membrane Stress Intensities and Maximum Equivalent Plastic Strains in Containment Vessel

The stress components across the wall thickness at the locations away from or near the geometrical discontinuities should be used to calculate the general primary membrane stress intensities (P_m) or the local primary membrane stress intensities (P_L). For simplicity, the maximum value of the von Mises stresses in the containment vessel is used as the local primary membrane stress intensity (P_L). This value is higher than the actual local primary membrane stress intensity because the latter is calculated by averaging the thru-wall stresses across the component's thickness.

The maximum value of the local primary membrane stress intensity in the containment vessel is 47.84 ksi as given in Figure 108. This value is less than the allowable value of 57.3 ksi for the general primary membrane stress intensity and of 73.6 ksi for the local primary membrane stress intensity (as given in Section 6.0). The structural integrity of the 9977 subjected to a 30-ft drop has therefore been justified according to the ASME Code, Section III.

As shown in Figure 16, the maximum plastic strain experienced at any location within the containment vessel after the 30-ft drop is 3.25%. The maximum calculated value of the effective plastic strain at any point in the overpack is 16.51%. This value is less than the maximum average through-wall elongation of 35% for the 304L material use in the drum. Therefore, the drum will not be ruptured by the 30-ft drop impact.

7.4.3 Case 3: Drum CGOT - Crush on Bottom Corner (75 ºF)

Energy History

Figure 111 depicts the kinetic energy variation of the plate during the 30-ft drop. The plot indicates that the kinetic energy approaches zero before the end of the analysis. Therefore, we know that the analysis covers the entire impact duration.

Deformed Shape of Full Model

Figure 112 shows the deformed shape of the overall model.

Stress and Strain Contours in Component Models

Figures 113 and 114 show the von Mises stresses and the equivalent plastic strains in the containment vessel and its internal components. Figure 115 shows the equivalent plastic strains in the overpack shell.

Evaluations of Maximum Local Primary Membrane Stress Intensities and Maximum Equivalent Plastic Strains in Containment Vessel

The maximum value of the local primary membrane stress intensity in the containment vessel is 42.81 ksi as shown in Figure 113. This value is less than the allowable value of 57.3 ksi for the general primary membrane stress intensity and of 73.6 ksi for the local primary membrane stress intensity (as given in Section 6.0). The structural integrity of the 9977 subjected to a 30-ft crush has therefore been verified according to the ASME Code, Section III.

As shown in Figure 114, the maximum plastic strain experienced at any location within the containment vessel after the crush is 3.31%. The maximum calculated value of the effective plastic strain at any point in the overpack is 28.82%. This value is less than the maximum average through-wall elongation of 35% for the 304L material use in the drum. Therefore, the drum will not be ruptured by the crush impact.

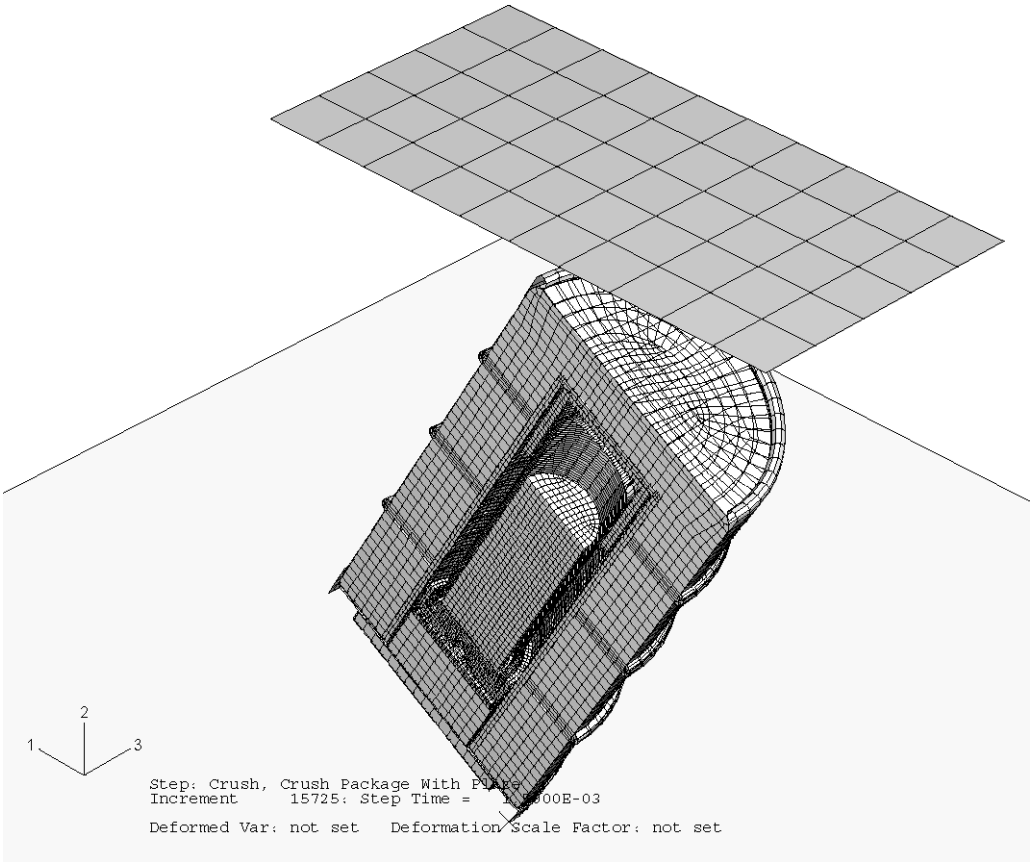

Figure 100 - Finite Element Model of the 9977 CGOT Drop and CGOT Crush

(ALLKE = kinetic energy; ALLIE = internal energy; ALLPD = plastic strain energy; ALLSE = elastic strain energy; ALLAE = artificial energy)

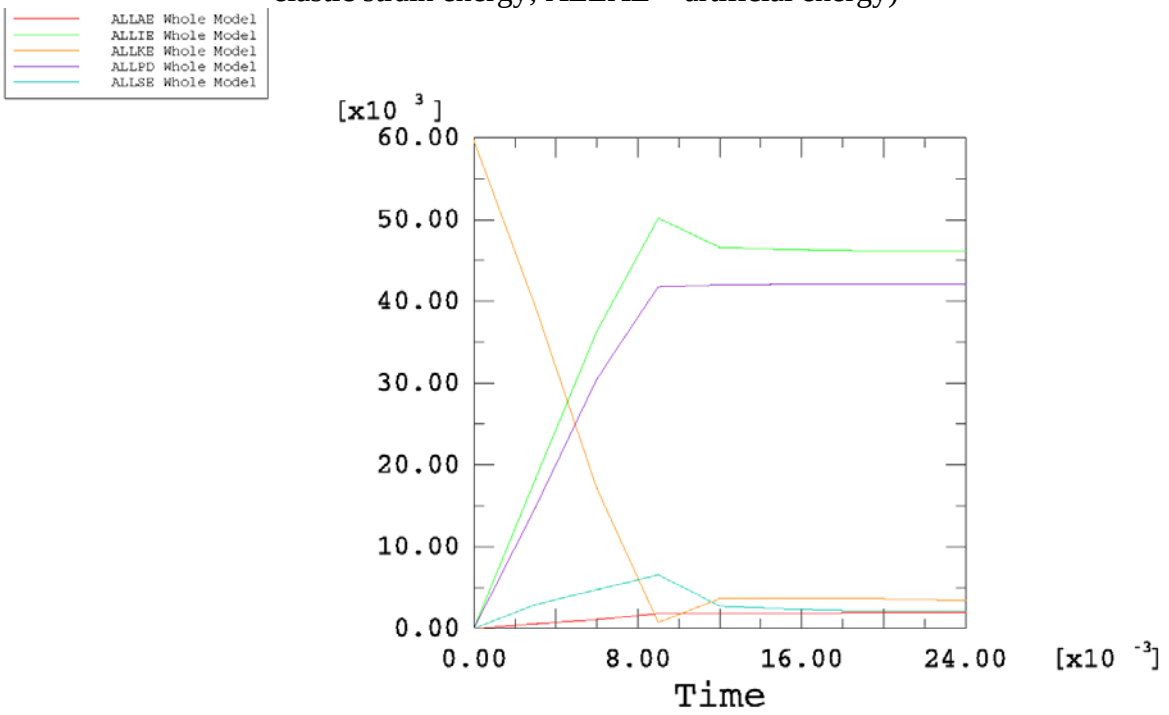

Figure 101 - Time-History Plot of Energy during Drum CGOT - 30-ft Drop simulation (-20 ºF)

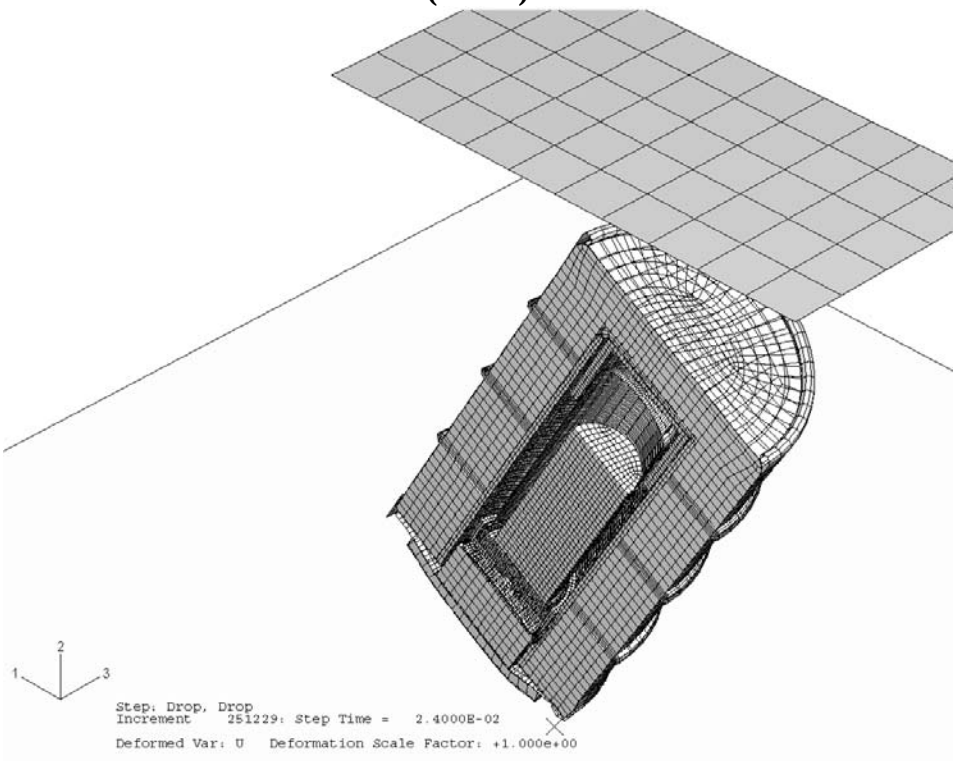

Figure 102 - Deformed Shape of 9977 with 6CV After the Drum CGOT - 30-ft Drop (-20 ºF)

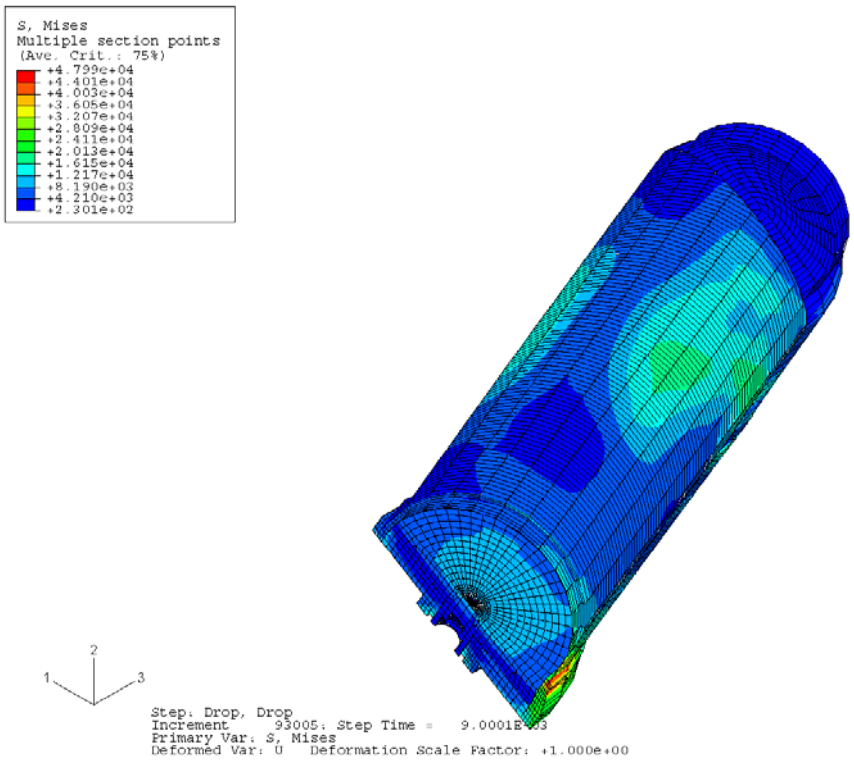

Figure 103 - Stress Distribution in the 6CV Model for Drum CGOT - 30-ft Drop (-20 ºF)

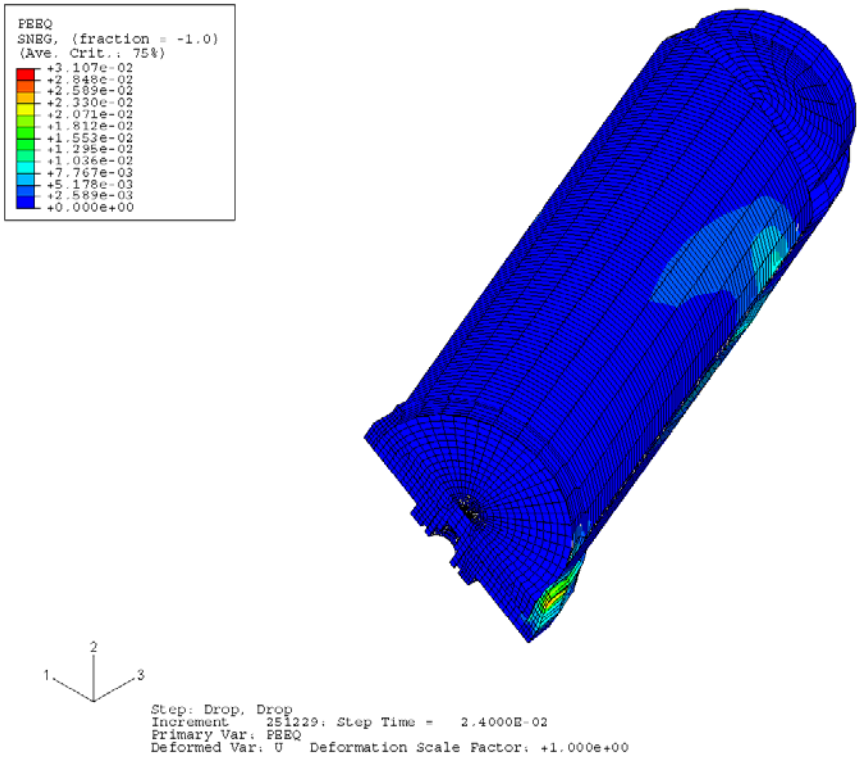

Figure 104 - Strain Distribution in 6CV Model for Drum CGOT - 30-ft Drop (-20 ºF)

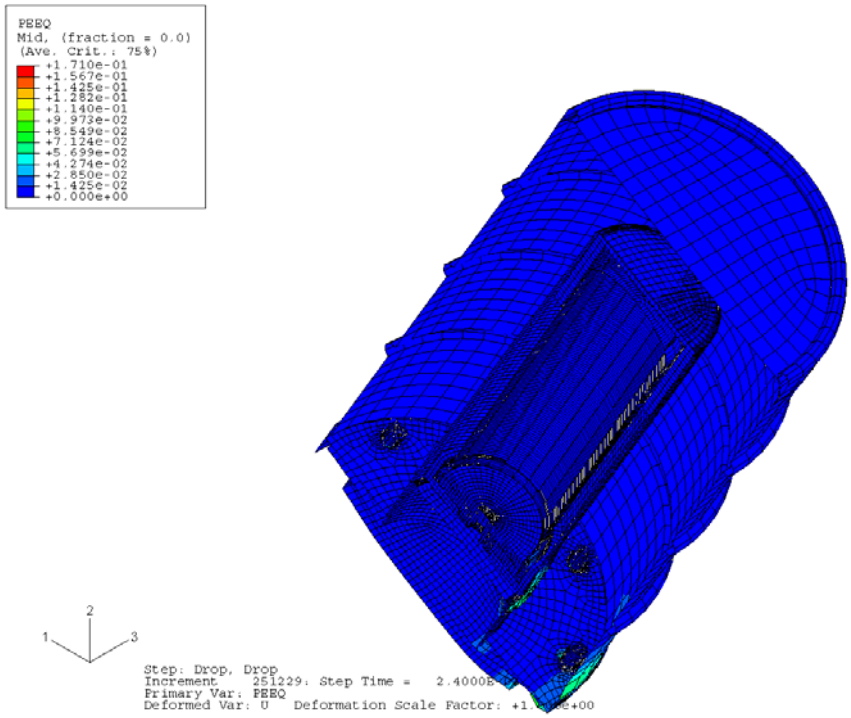

Figure 105 - Strain Distribution in Overpack for 6CV for Drum CGOT - 30-ft Drop (-20 ºF)

(ALLKE = kinetic energy; ALLIE = internal energy; ALLPD = plastic strain energy; ALLSE = elastic strain energy; ALLAE = artificial energy)

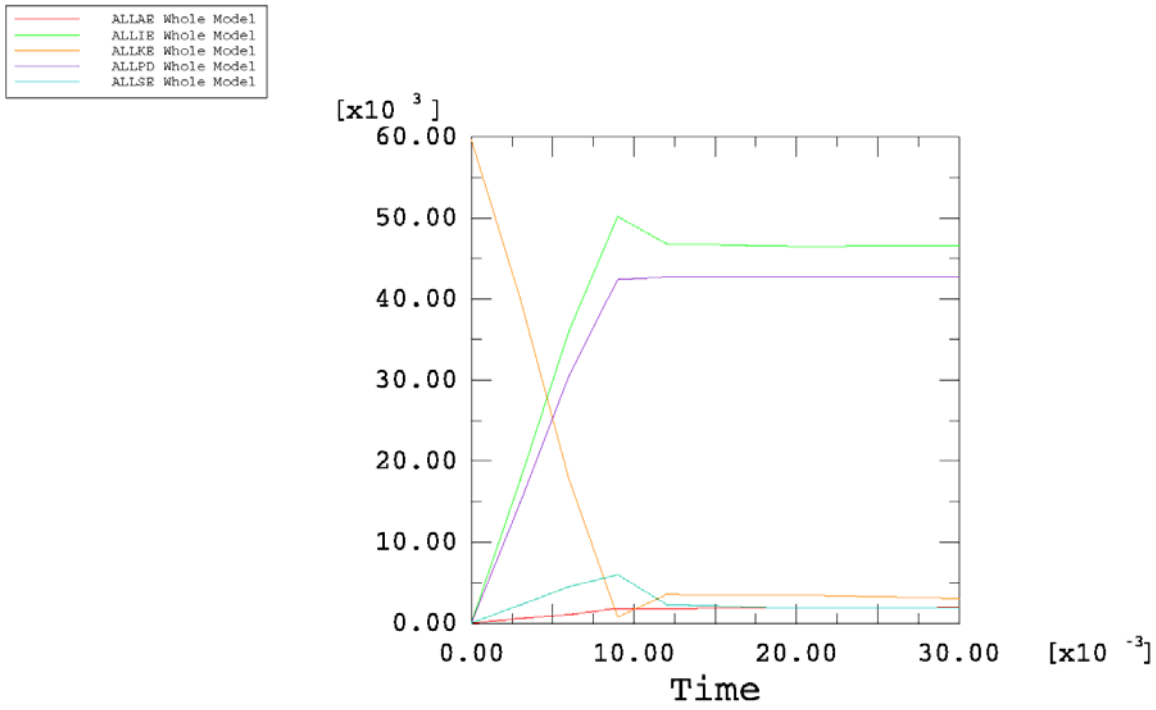

Figure 106 - Time-History Plot of Energy during Drum CGOT - 30-ft Drop Simulation (75 ºF)

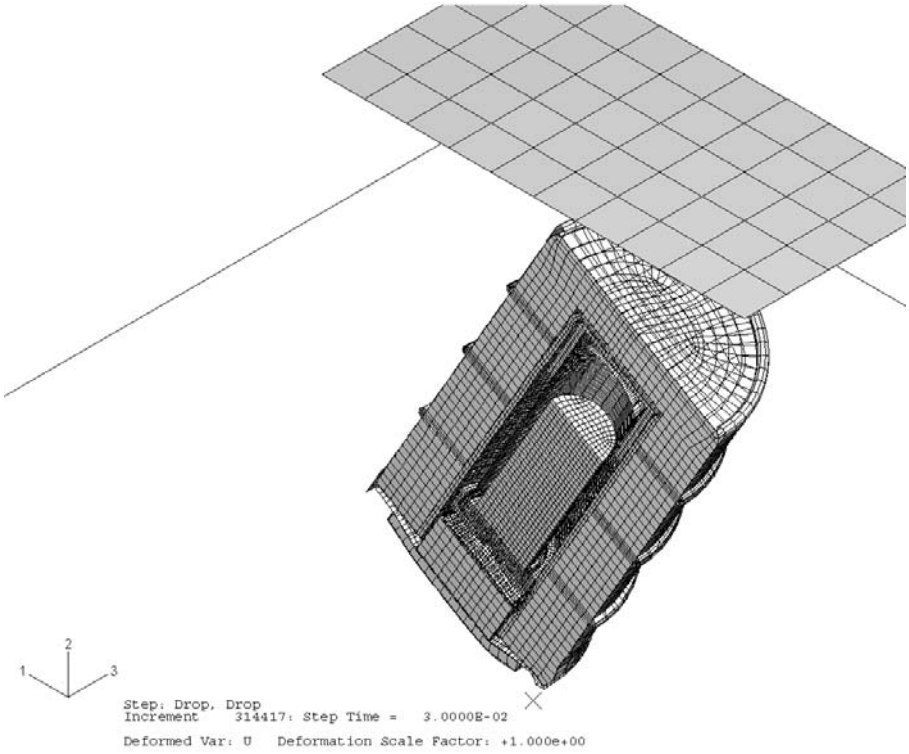

Figure 107 - Deformed Shape of 9977 with 6CV After the Drum CGOT - 30-ft Drop (75 ºF)

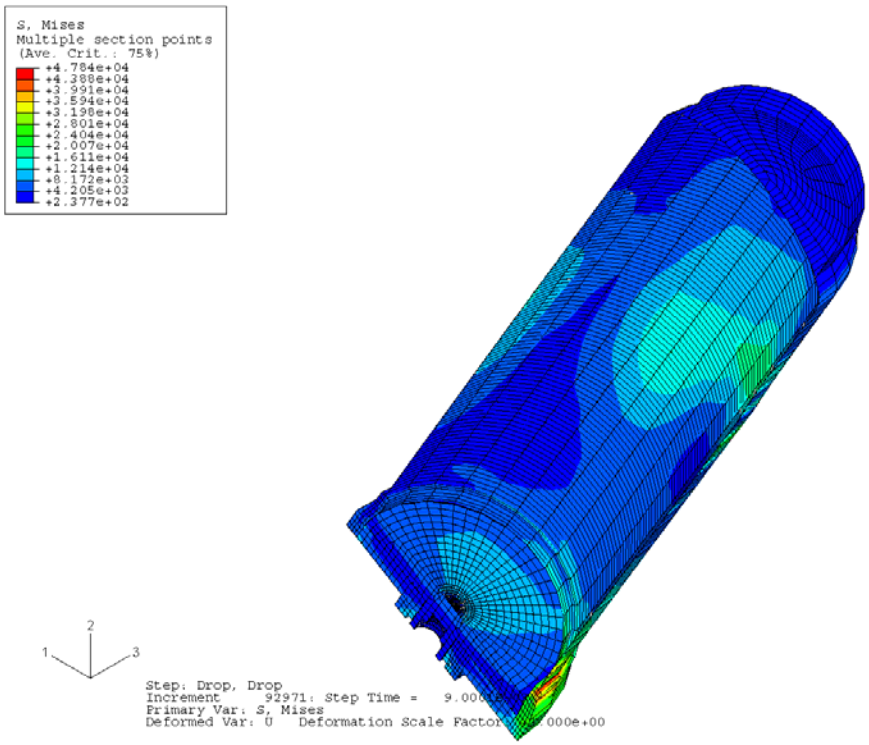

Figure 108 - Stress Distribution in the 6CV Model for Drum CGOT - 30-ft Drop (75 ºF)

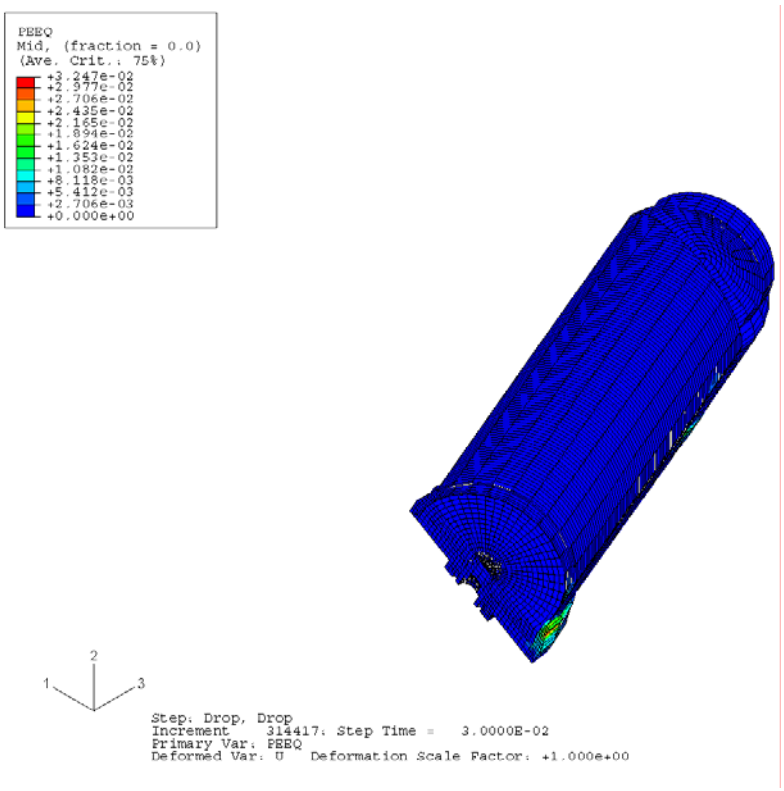

Figure 109 - Strain Distribution in 6CV Model for Drum CGOT - 30-ft Drop (75 ºF)

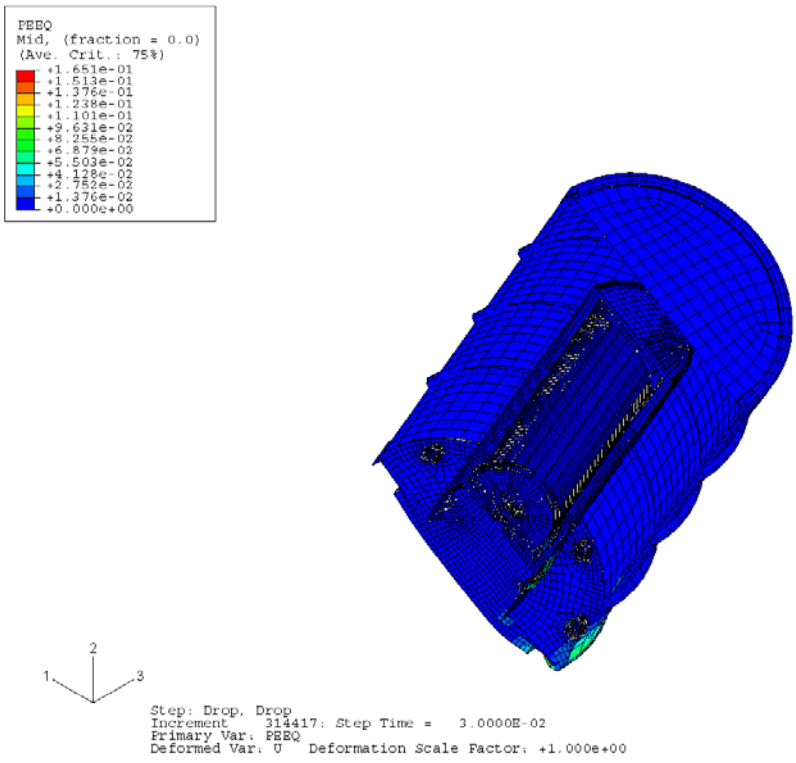

Figure 110 - Strain Distribution in Overpack for 6CV for Drum CGOT - 30-ft Drop (75 ºF)

(ALLKE = kinetic energy; ALLIE = internal energy; ALLPD = plastic strain energy; ALLSE = elastic strain energy; ALLAE = artificial energy)

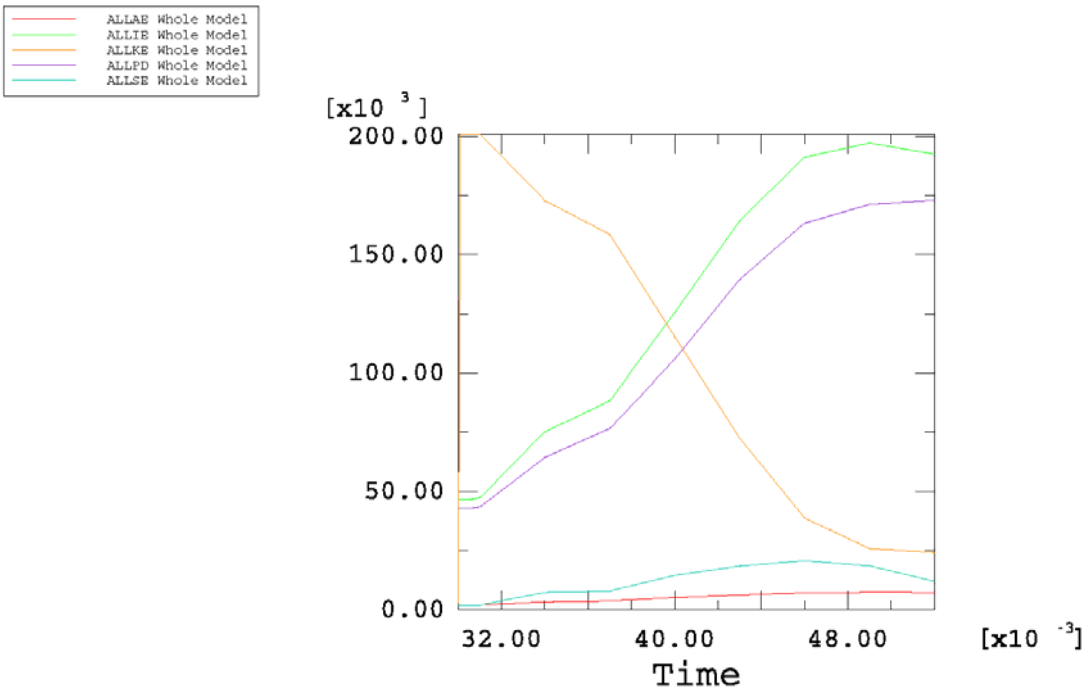

Figure 111 - Time-History Plot of Energy during Drum CGOT - Bottom Corner Crush Simulation (75 ºF)

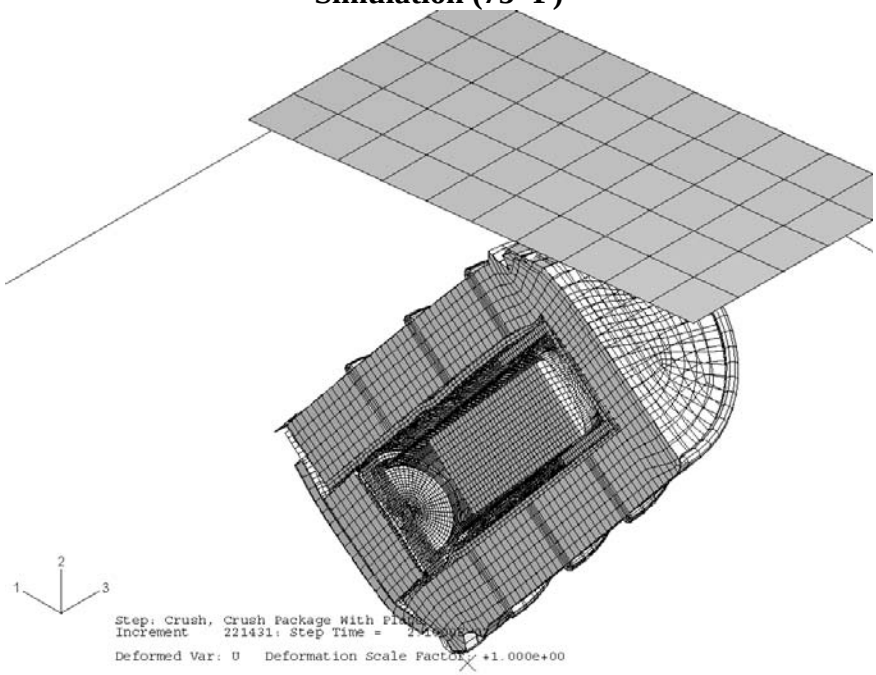

Figure 112 - Deformed Shape of 9977 with 6CV for Drum CGOT - Bottom Corner Crush (75 ºF)

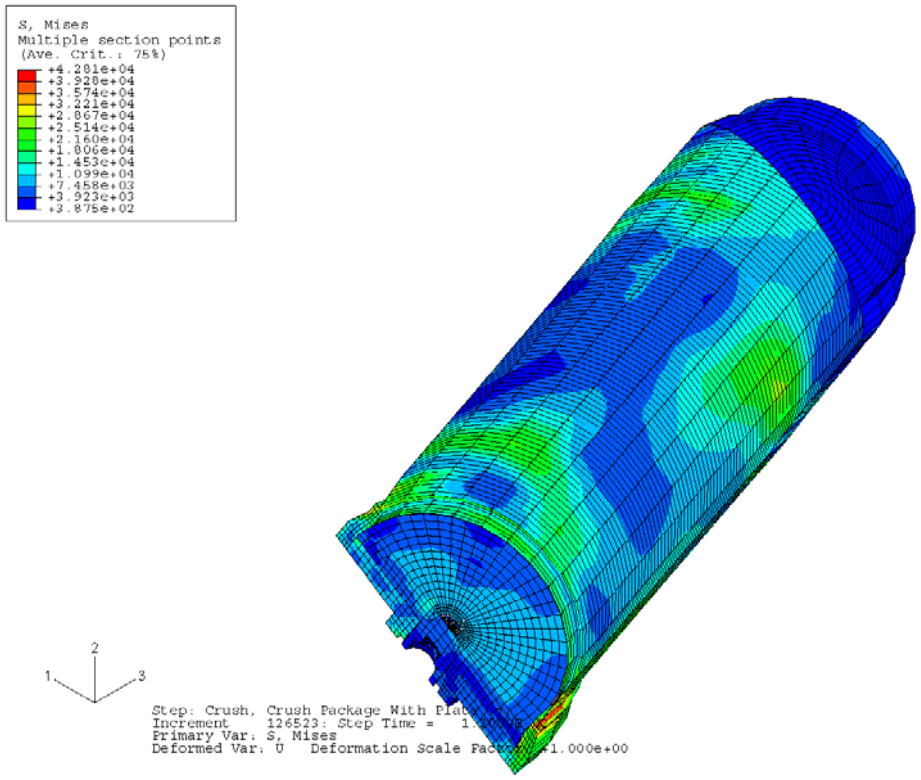

Figure 113 - Stress Distribution in 6CV Model for Drum CGOT - Bottom Corner Crush (75 ºF)

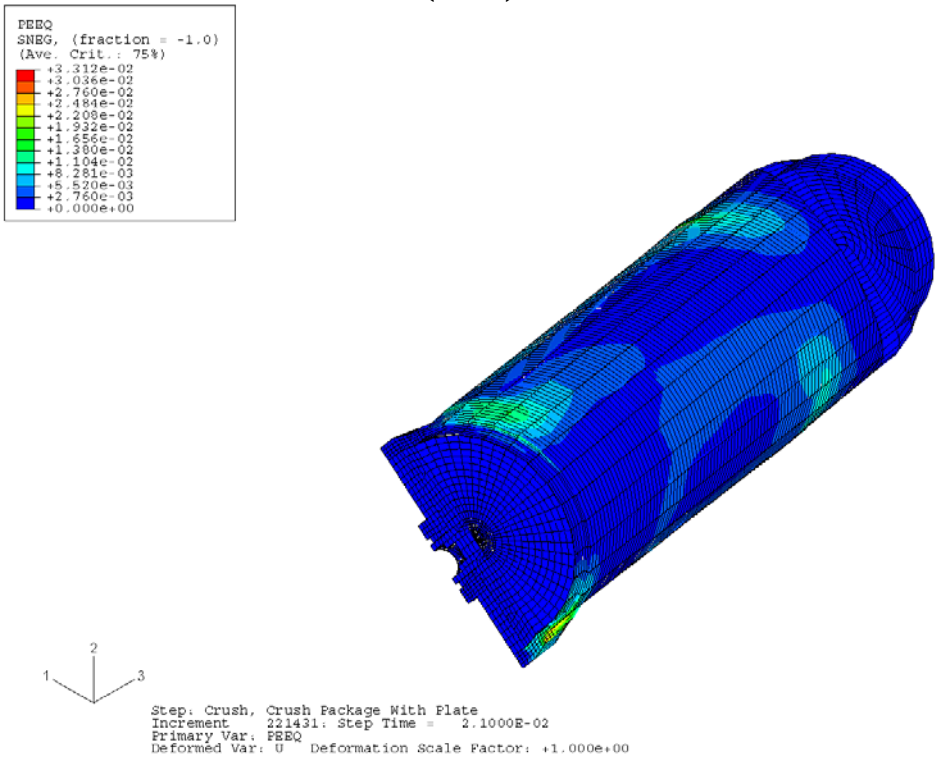

Figure 114 - Strain Distribution in 6CV Model for Drum CGOT - Bottom Corner Crush (75 ºF)

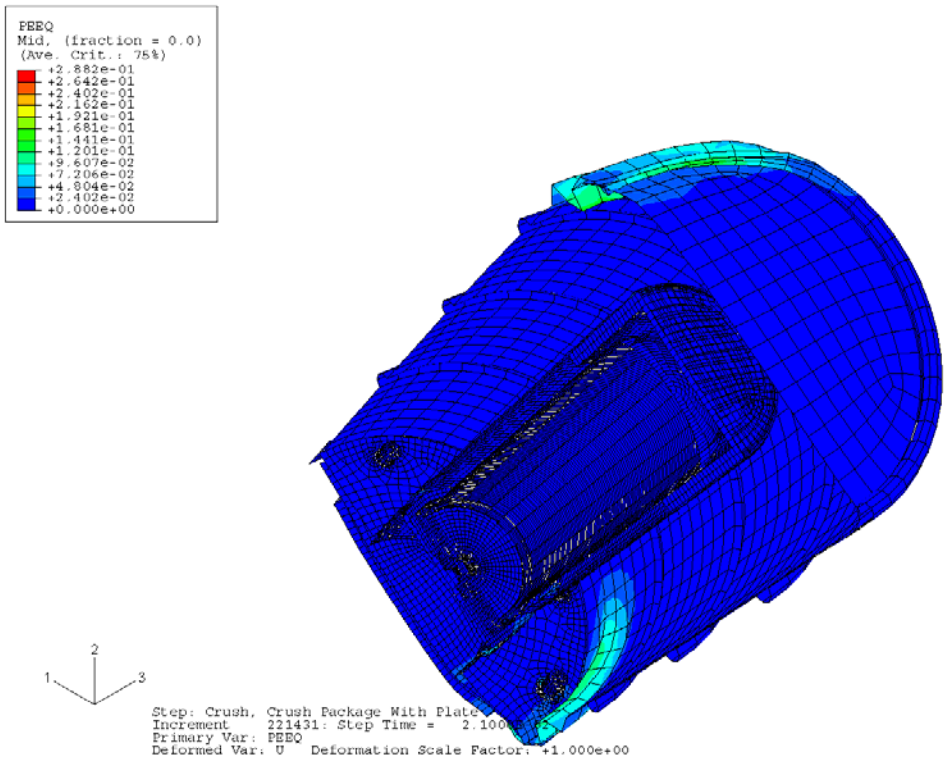

Figure 115 - Strain Distribution in Overpack for 6CV for Drum CGOT - Bottom Corner Crush (75 ºF)

7.5 Center of Gravity over Drum Bottom Drop Followed by Crush (75, 140, 300 ºF)

Figure 116 shows the finite element model used for evaluating the 30-ft drum center of gravity over the bottom corner drop with the follow on impact of the 1,100 lb plate dropped 30-ft onto the package top corner.

7.5.1 Case 1: Drum CGOB - 30-ft Drop (75 ºF)

Energy History

The time-history plots of energy components for the 30-ft CGOB drop simulation shown in Figure 117 indicate that the kinetic energy approaches zero at the end of the analysis. Therefore, we know that the analysis covers the entire impact duration.

Deformed Shape of Full Model

Figure 118 is the deformed shape of the overall model.

Stress and Strain Contours in Component Models

Figures 119 and 120 show the von Mises stresses and the equivalent plastic strains in the CV model. Figure 121 shows the equivalent plastic strains in the overpack shell.

Evaluations of Maximum Local Primary Membrane Stress Intensities and Maximum Equivalent Plastic Strains in Containment Vessel

The stress components across the wall thickness at the locations away from or near the geometrical discontinuities should be used to calculate the general primary membrane stress intensities (P_m) or the local primary membrane stress intensities (P_L). For simplicity, the maximum value of the von Mises stresses in the containment vessel is used as the local primary membrane stress intensity (P_L). This value is higher than the actual local primary membrane stress intensity because the latter is calculated by averaging the thru-wall stresses across the component's thickness.

The maximum value of the local primary membrane stress intensity in the containment vessel is 49.96 ksi as given in Figure 119. This value is less than the allowable value of 57.3 ksi for the general primary membrane stress intensity and of 73.6 ksi for the local primary membrane stress intensity (as given in Section 6.0). The structural integrity of the 9977 subjected to a 30-ft drop has therefore been justified according to the ASME Code, Section III.

As shown in Figure 120, the maximum plastic strain experienced at any location within the containment vessel after the 30-ft drop is 2.92%. The maximum calculated value of the effective plastic strain at any point in the overpack is 11.38%. This value is less than the maximum average through-wall elongation of 35% for the 304L material use in the drum. Therefore, the drum will not be ruptured by the 30-ft drop impact.

7.5.2 Case 2: Drum CGOB - Top Corner Crush (75 ºF)

Energy History

Figure 122 depicts the kinetic energy variation of the plate during the 30-ft fall. The plot indicates that the kinetic energy approaches zero before the end of the analysis. Therefore, we know that the analysis covers the entire impact duration.

Deformed Shape of Full Model

Figure 123 is the deformed shape of the overall model.

Stress and Strain Contours in Component Models

Figures 124 and 125 show the von Mises stresses and the equivalent plastic strains in the CV model. Figure 126 shows the equivalent plastic strains in the overpack shell.

Evaluations of Maximum Local Primary Membrane Stress Intensities and Maximum Equivalent Plastic Strains in Containment Vessel

The stress components across the wall thickness at the locations away from or near the geometrical discontinuities should be used to calculate the general primary membrane stress intensities (P_m) or the local primary membrane stress intensities (P_L). For simplicity, the maximum value of the von Mises stresses in the containment vessel is used as the local primary membrane stress intensity (P_L). This value is higher than the actual local primary membrane stress intensity because the latter is calculated by averaging the thru-wall stresses across the component's thickness.

The maximum value of the local primary membrane stress intensity in the containment vessel is 42.12 ksi as given in Figure 124. This value is less than the allowable value of 57.3 ksi for the general primary membrane stress intensity and of 73.6 ksi for the local primary membrane stress intensity (as given in Section 6.0). The structural integrity of the 9977 subjected to a crush has therefore been justified according to the ASME Code, Section III.

As shown in Figure 125, the maximum plastic strain experienced at any location within the containment vessel after the crush is 15.33%. The maximum calculated value of the effective plastic strain at any point in the overpack is 20.19%. This value is less than the minimum specified uniform elongation of 35% for the 304L material used in the drum. Therefore, the drum will not be ruptured by the crush impact.

7.5.3 Case 3: Drum CGOB - 30-ft Drop (140 ºF)

Energy History

The time-history plots of energy components for the 30-ft CGOB drop simulation shown in Figure 127 indicate that the kinetic energy approaches zero at the end of the analysis. Therefore, we know that the analysis covers the entire impact duration.

Deformed Shape of Full Model

Figure 128 shows the deformed shape of the overall model.

Stress and Strain Contours in Component Models

Figures 129 and 130 show the von Mises stresses and the equivalent plastic strains in the containment vessel and its internal components. Figure 131 shows the equivalent plastic strains in the overpack shell.

Evaluations of Maximum Local Primary Membrane Stress Intensities and Maximum Equivalent Plastic Strains in Containment Vessel

The maximum value of the local primary membrane stress intensity in the containment vessel is 48.05 ksi as shown in Figure 129. This value is less than the allowable value of 57.3 ksi for the general primary membrane stress intensity and of 73.6 ksi for the local primary membrane stress intensity (as given in Section 6.0). The structural integrity of the 9977 subjected to a 30-ft drop has therefore been verified according to the ASME Code, Section III.

As shown in Figure 130, the maximum plastic strain experienced at any location within the containment vessel after the 30-ft drop is 2.86%. The maximum calculated value of the effective plastic strain at any point in the overpack is 12.17%. This value is less than the maximum average through-wall elongation of 35% for the 304L material use in the drum. Therefore, the drum will not be ruptured by the 30-ft drop impact.

7.5.4 Case 4: Drum CGOB - Top Corner Crush (140 ºF)

Energy History

Figure 132 depicts the kinetic energy variation of the plate during the 30-ft fall. The plot indicates that the kinetic energy approaches zero before the end of the analysis. Therefore, we know that the analysis covers the entire impact duration.

Deformed Shape of Full Model

Figure 133 is the deformed shape of the overall model.

Stress and Strain Contours in Component Models

Figures 134 and 135 show the von Mises stresses and the equivalent plastic strains in the CV model. Figure 136 shows the equivalent plastic strains in the overpack shell.

Evaluations of Maximum Local Primary Membrane Stress Intensities and Maximum Equivalent Plastic Strains in Containment Vessel

The stress components across the wall thickness at the locations away from or near the geometrical discontinuities should be used to calculate the general primary membrane stress intensities (P_m) or the local primary membrane stress intensities (P_L). For simplicity, the maximum value of the von Mises stresses in the containment vessel is used as the local primary membrane stress intensity (P_L). This value is higher than the actual local primary membrane stress intensity because the latter is calculated by averaging the thru-wall stresses across the component's thickness.

The maximum value of the local primary membrane stress intensity in the containment vessel is 38.19 ksi as given in Figure 134. This value is less than the allowable value of 57.3 ksi for the general primary membrane stress intensity and of 73.6 ksi for the local primary membrane stress

intensity (as given in Section 6.0). The structural integrity of the 9977 subjected to a crush has therefore been justified according to the ASME Code, Section III.

As shown in Figure 135, the maximum plastic strain experienced at any location within the containment vessel after the crush is 15.56%. The maximum calculated value of the effective plastic strain at any point in the overpack is 20.83%. This value is less than the maximum average through-wall elongation of 35% for the 304L material use in the drum. Therefore, the drum will not be ruptured by the crush impact.

7.5.5 Case 5: Drum CGOB - 30-ft Drop (300 ºF)

Energy History

The time-history plots of energy components for the 30-ft CGOB drop simulation shown in Figure 137 indicate that the kinetic energy approaches zero at the end of the analysis. Therefore, we know that the analysis covers the entire impact duration.

Deformed Shape of Full Mode

Figure 138 shows the deformed shape of the overall model.

Stress and Strain Contours in Component Models

Figures 139 and 140 show the von Mises stresses and the equivalent plastic strains in the containment vessel and its internal components. Figure 141 shows the equivalent plastic strains in the overpack shell.

Evaluations of Maximum Local Primary Membrane Stress Intensities and Maximum Equivalent Plastic Strains in Containment Vessel

The maximum value of the local primary membrane stress intensity in the containment vessel is 37.76 ksi as shown in Figure 139. This value is less than the allowable value of 57.3 ksi for the general primary membrane stress intensity and of 73.6 ksi for the local primary membrane stress intensity (as given in Section 6.0). The structural integrity of the 9977 subjected to a 30-ft drop has therefore been verified according to the ASME Code, Section III.

As shown in Figure 140, the maximum plastic strain experienced at any location within the containment vessel after the 30-ft drop is 2.33%. The maximum calculated value of the effective plastic strain at any point in the overpack is 11.31%. This value is less than the maximum average through-wall elongation of 35% for the 304L material use in the drum. Therefore, the drum will not be ruptured by the 30-ft drop impact.

7.5.6 Case 6: Drum CGOB - Top Corner Crush (300 ºF)

Energy History

Figure 142 depicts the kinetic energy variation of the plate during the 30-ft fall. The plot indicates that the kinetic energy approaches zero before the end of the analysis. Therefore, we know that the analysis covers the entire impact duration.

Deformed Shape of Full Model

Figure 143 is the deformed shape of the overall model.

Stress and Strain Contours in Component Models

Figures 144 and 145 show the von Mises stresses and the equivalent plastic strains in the CV model. Figure 146 shows the equivalent plastic strains in the overpack shell.

Evaluations of Maximum Local Primary Membrane Stress Intensities and Maximum Equivalent Plastic Strains in Containment Vessel

The stress components across the wall thickness at the locations away from or near the geometrical discontinuities should be used to calculate the general primary membrane stress intensities (P_m) or the local primary membrane stress intensities (P_L). For simplicity, the maximum value of the von Mises stresses in the containment vessel is used as the local primary membrane stress intensity (P_L). This value is higher than the actual local primary membrane stress intensity because the latter is calculated by averaging the thru-wall stresses across the component's thickness.

The maximum value of the local primary membrane stress intensity in the containment vessel is 37.93 ksi as given in Figure 144. This value is less than the allowable value of 57.3 ksi for the general primary membrane stress intensity and of 73.6 ksi for the local primary membrane stress intensity (as given in Section 6.0). The structural integrity of the 9977 subjected to a crush has therefore been justified according to the ASME Code, Section III.

As shown in Figure 145, the maximum plastic strain experienced at any location within the containment vessel after the crush is 23.32%. The maximum calculated value of the effective plastic strain at any point in the overpack is 19.25%. This value is less than the maximum average through-wall elongation of 35% for the 304L material use in the drum. Therefore, the drum will not be ruptured by the crush impact.

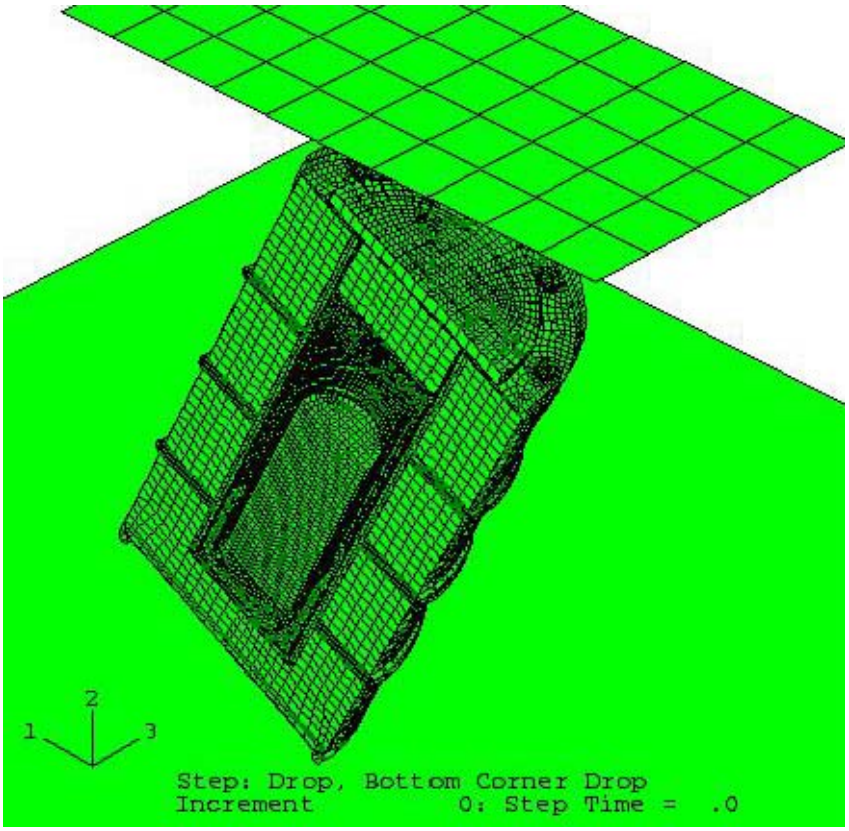

Figure 116 - Finite Element Model of the 9977 CGOB Drop and CGOB Crush

(ALLKE = kinetic energy; ALLIE = internal energy; ALLPD = plastic strain energy; ALLSE = elastic strain energy; ALLAE = artificial energy)

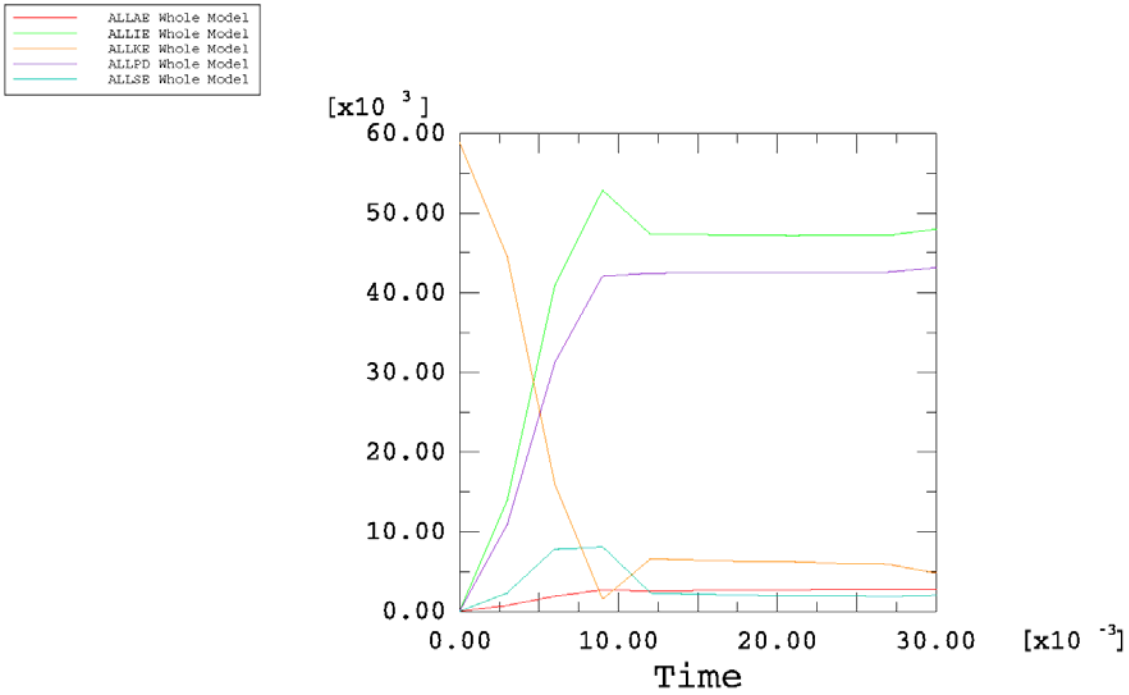

Figure 117 - Time-History Plot of Energy during Drum CGOB - 30-ft Drop Simulation (75 ºF)

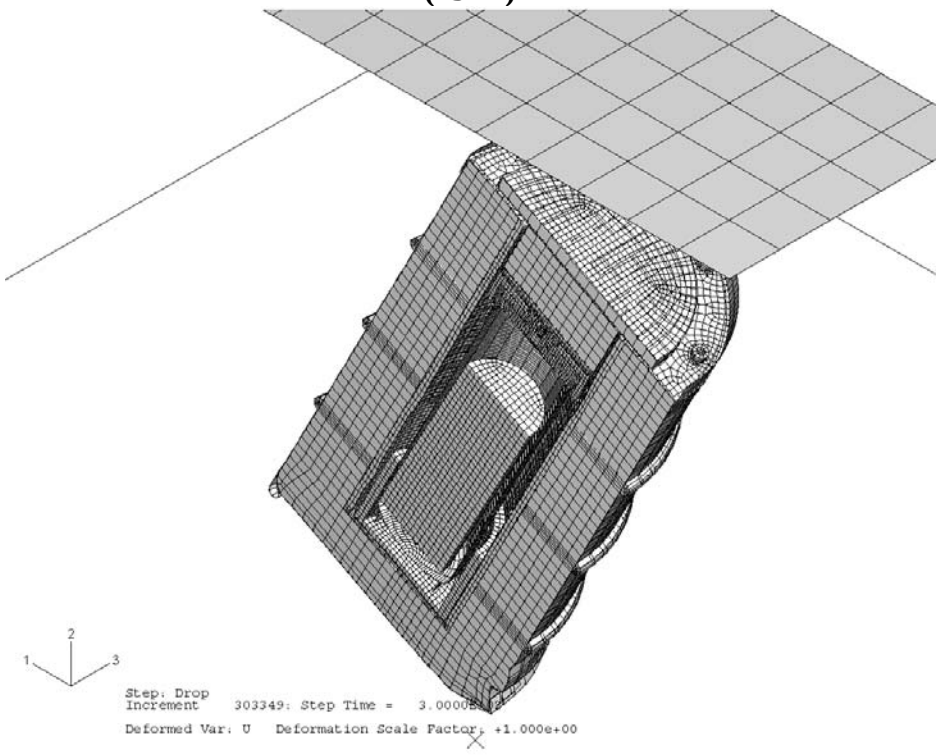

Figure 118 - Deformed Shape of 9977 with 6CV After the Drum CGOB - 30-ft Drop (75 ºF)

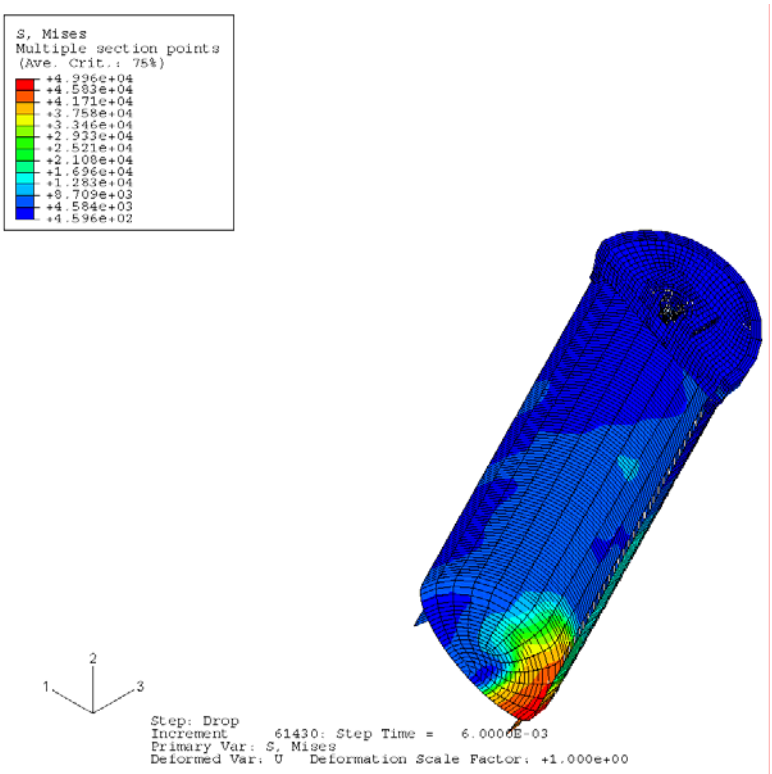

Figure 119 - Stress Distribution in the 6CV Model for Drum CGOB - 30-ft Drop (75 ºF)

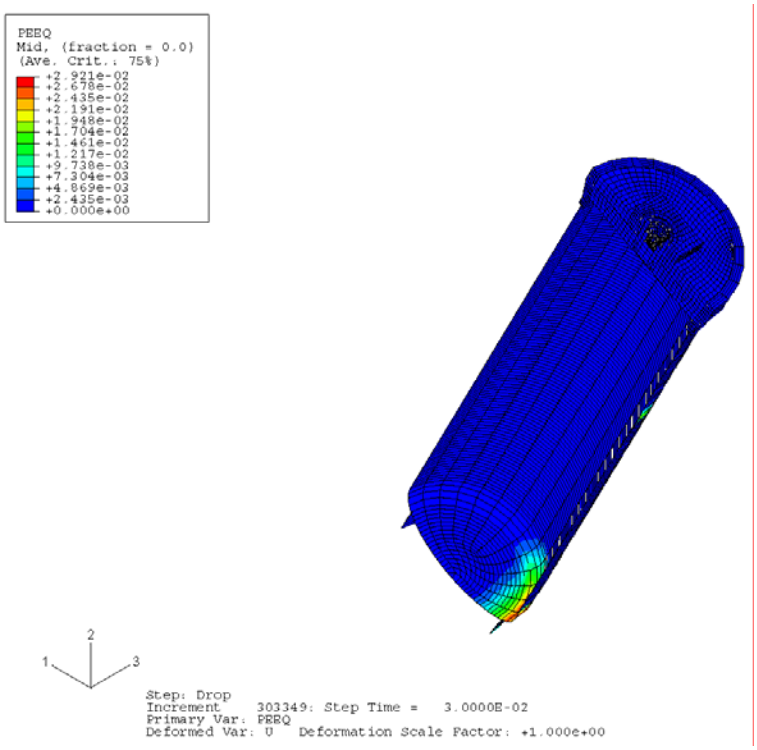

Figure 120 - Strain Distribution in 6CV Model for Drum CGOB - 30-ft Drop (75 ºF)

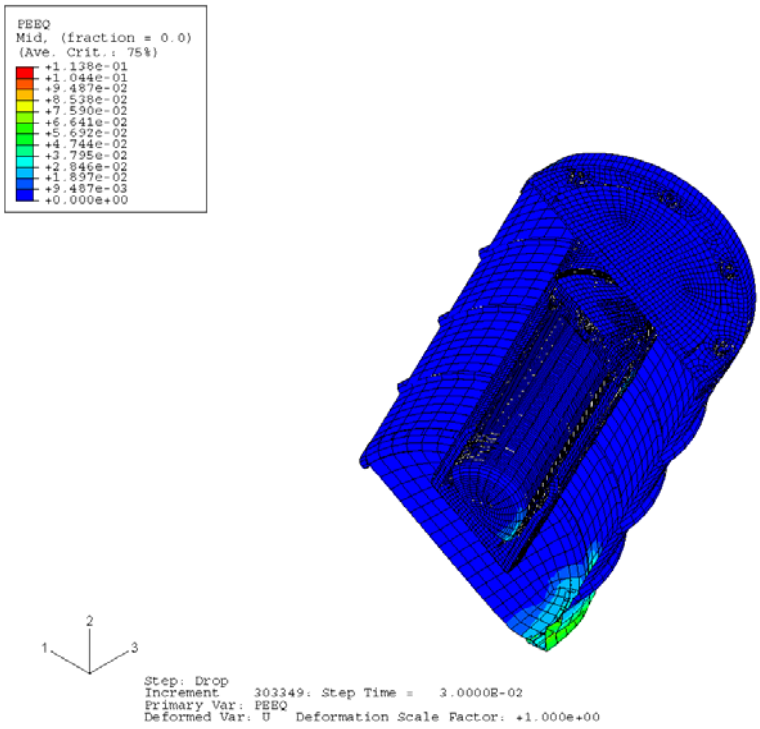

Figure 121 - Strain Distribution in Overpack for 6CV for Drum CGOB - 30-ft Drop (75 ºF)

(ALLKE = kinetic energy; ALLIE = internal energy; ALLPD = plastic strain energy; ALLSE = elastic strain energy; ALLAE = artificial energy)

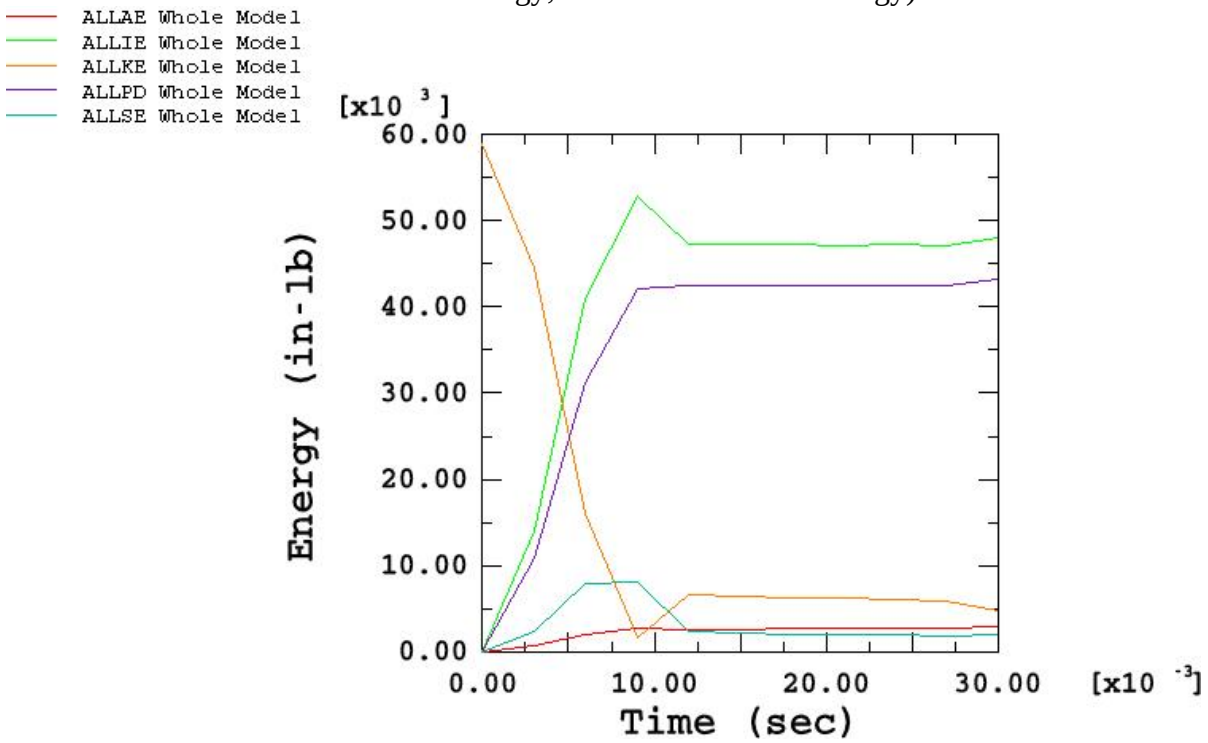

Figure 122 - Time-History Plot of Plate Energy during Drum CGOB - Top Corner Crush Simulation (75 ºF)

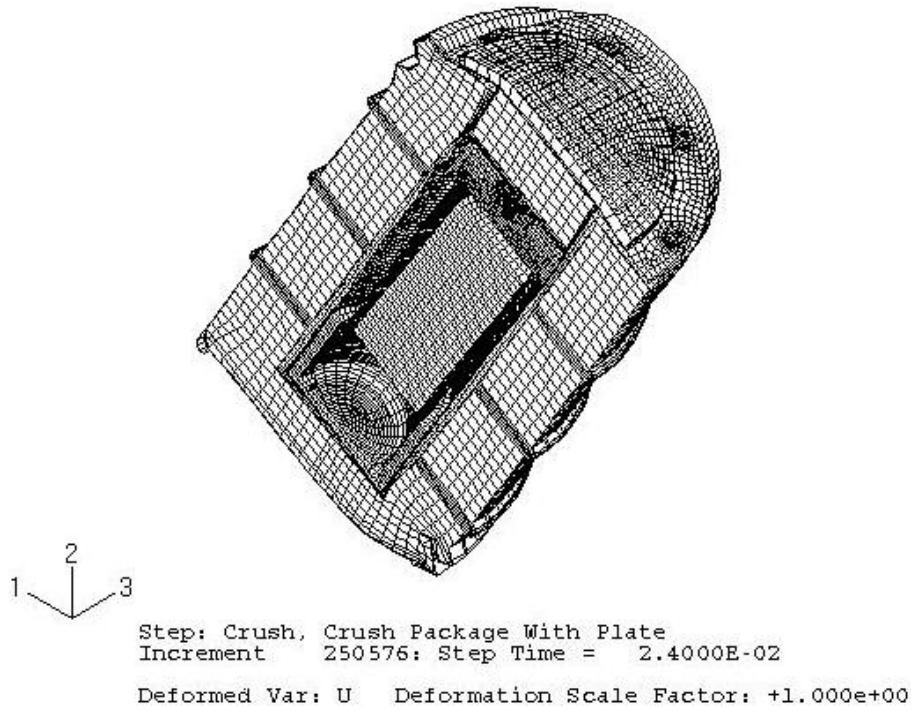

Figure 123 - Deformed Shape of 9977 with 6CV After the Drum CGOB - Top Corner Crush (75 ºF)

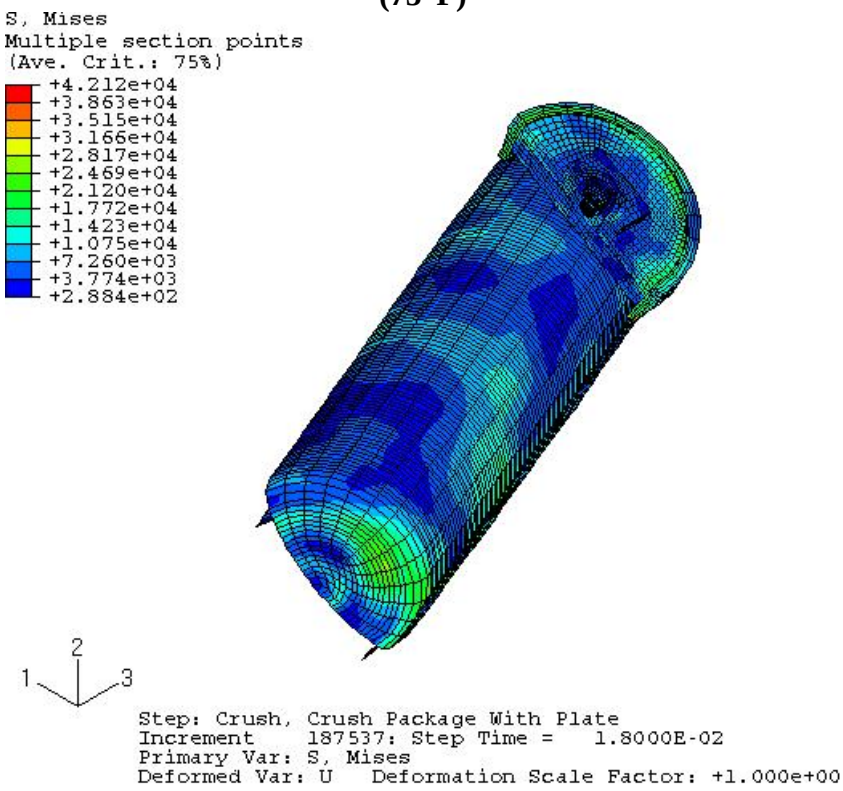

Figure 124 - Stress Distribution in the 6CV Model for Drum CGOB - Top Corner Crush (75 ºF)

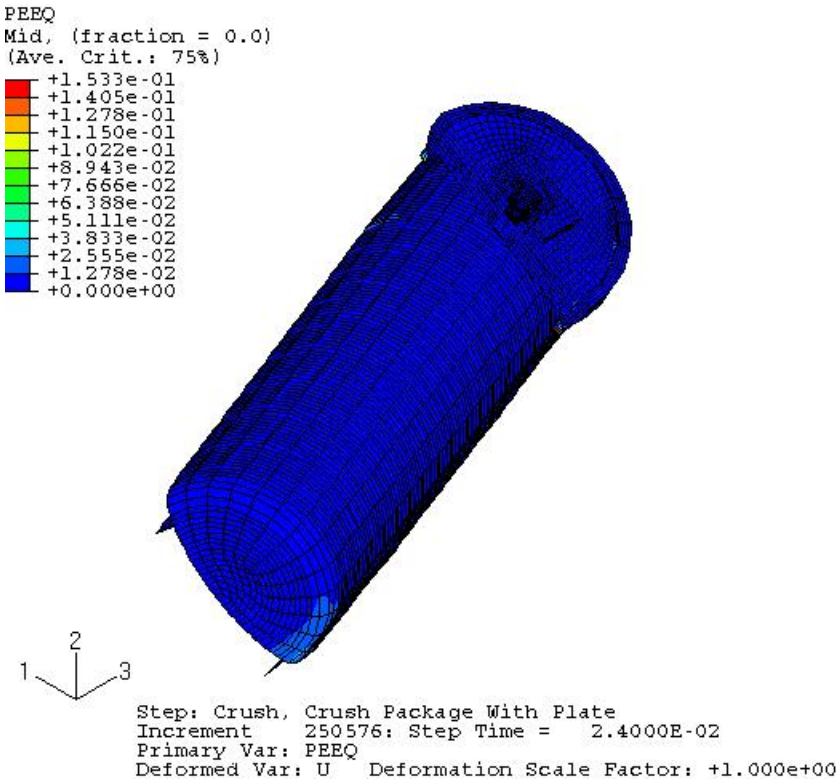

Figure 125 - Strain Distribution in 6CV Model for Drum CGOB - Top Corner Crush (75 ºF)

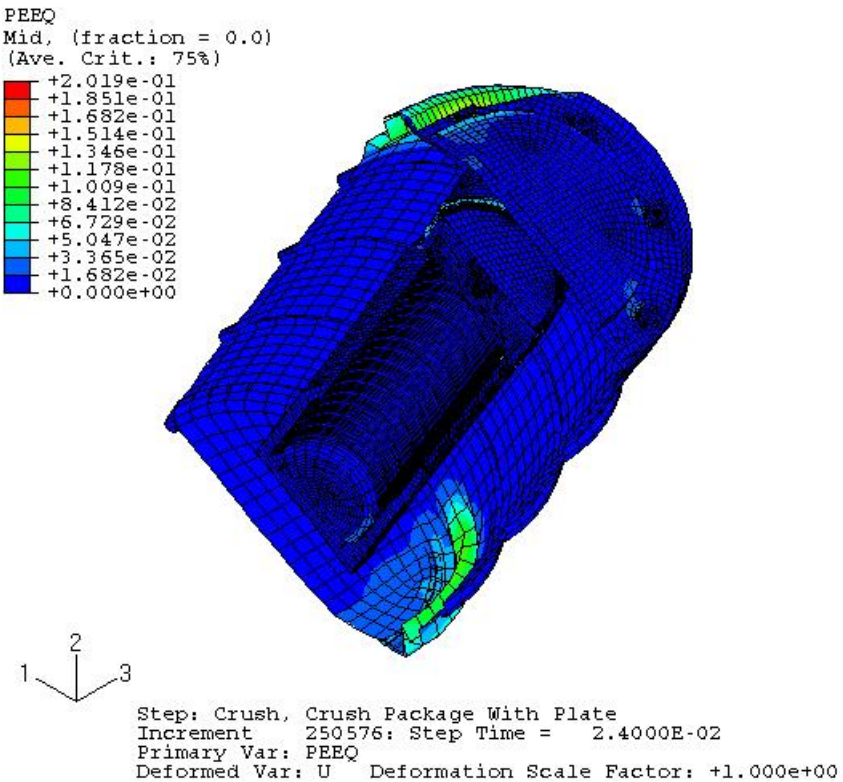

Figure 126 - Strain Distribution in Overpack for 6CV for Drum CGOB - Top Corner Crush (75 ºF)

(ALLKE = kinetic energy; ALLIE = internal energy; ALLPD = plastic strain energy; ALLSE = elastic strain energy; ALLAE = artificial energy)

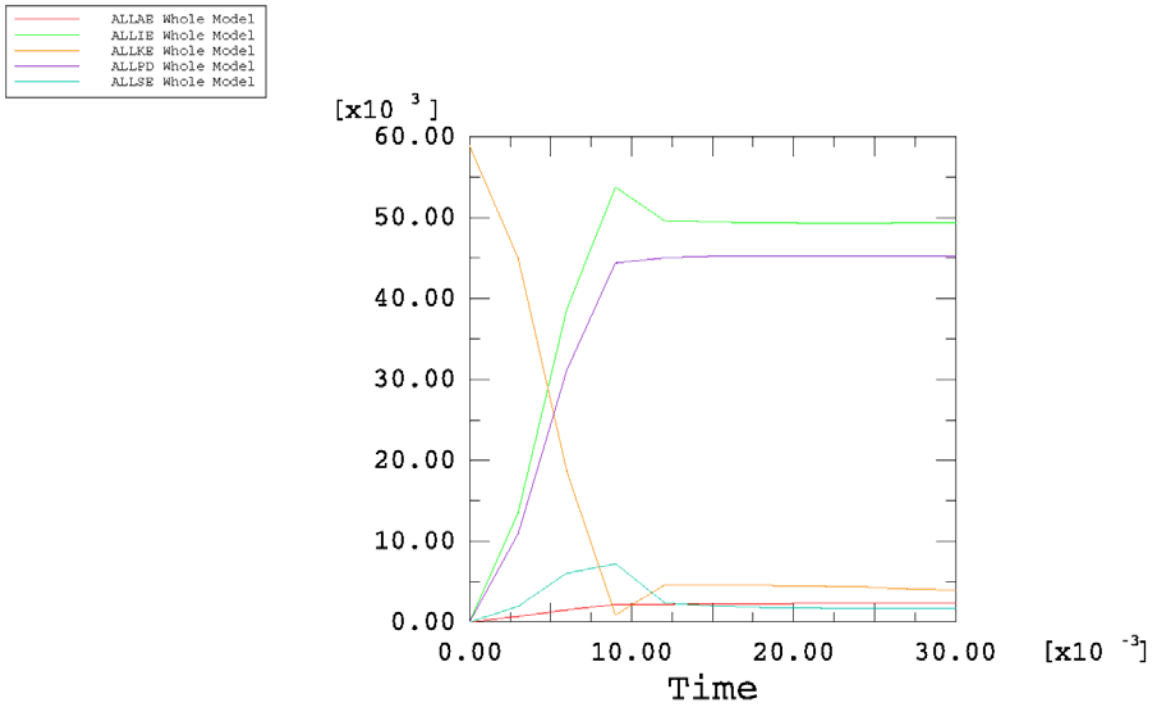

Figure 127 - Time-History Plot of Energy during Drum CGOB - 30-ft Drop Simulation (140 ºF)

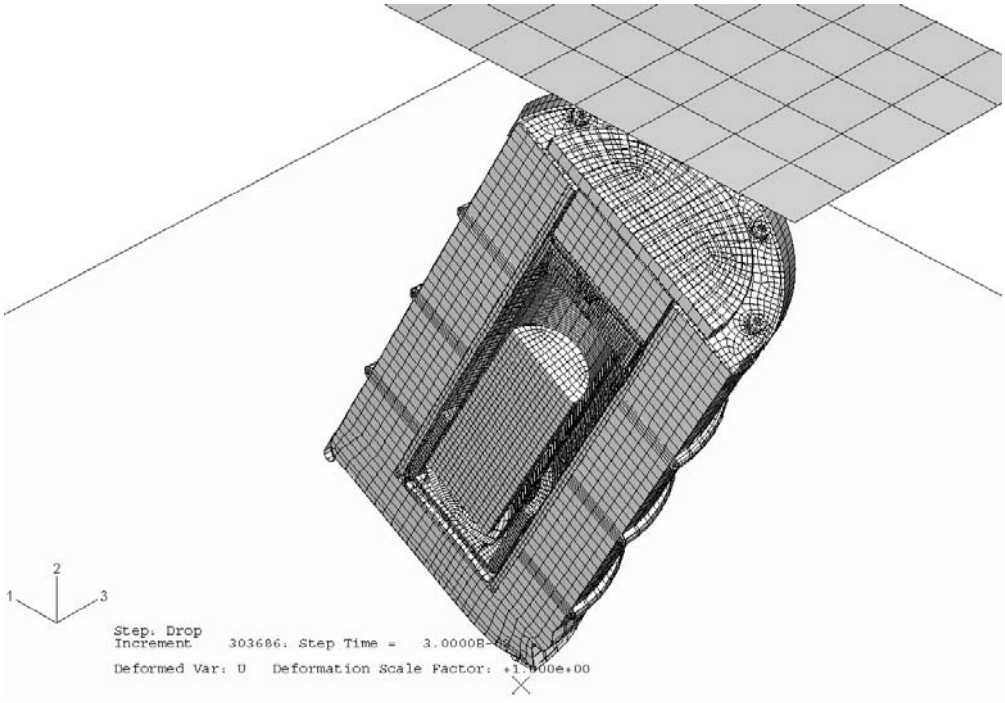

Figure 128 - Deformed Shape of 9977 with 6CV for Drum CGOB - 30-ft Drop (140 ºF)

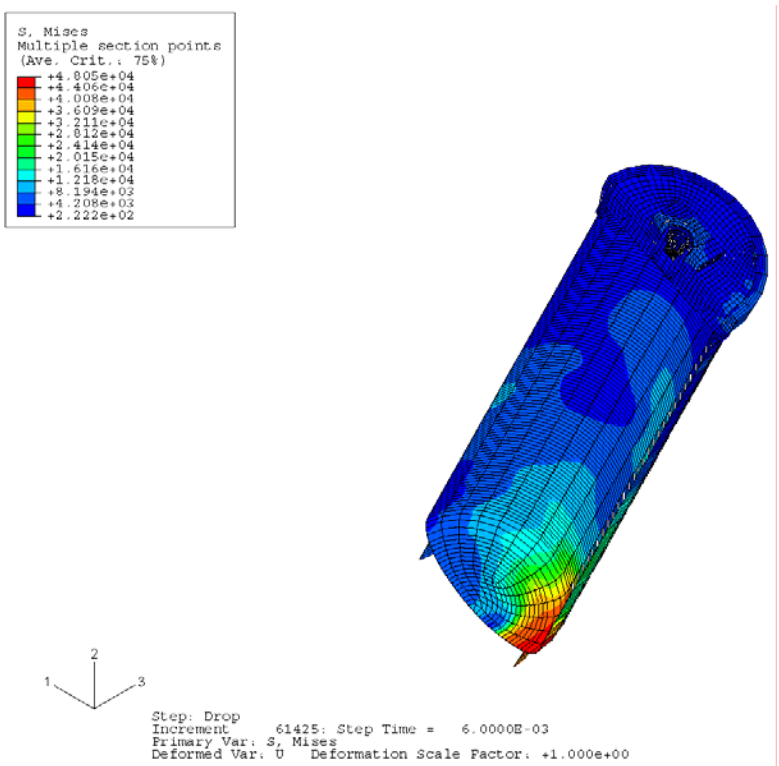

Figure 129 - Stress Distribution in 6CV Model for Drum CGOB - 30-ft Drop (140 ºF)

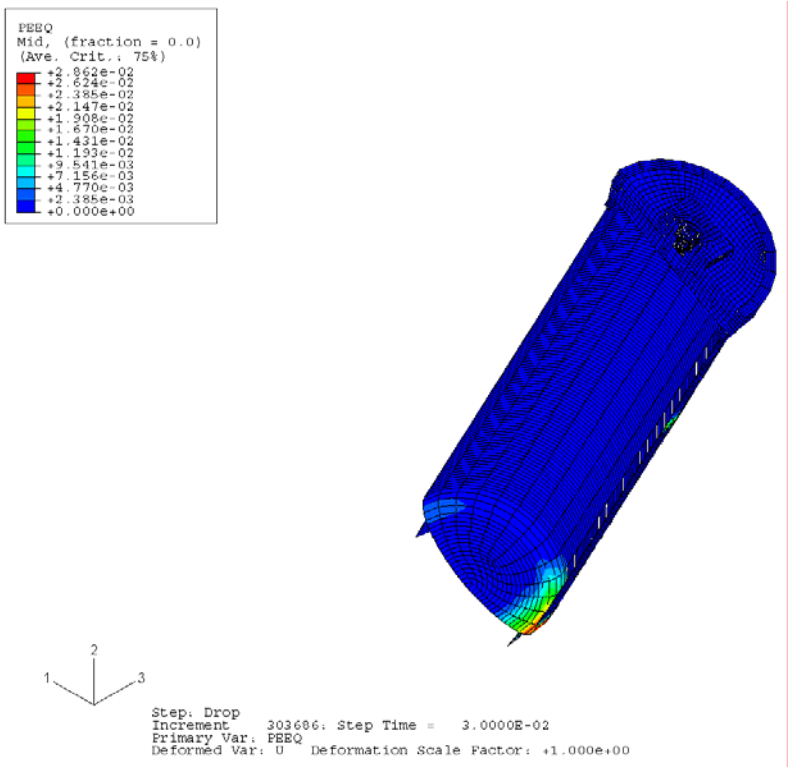

Figure 130 - Strain Distribution in 6CV Model for Drum CGOB - 30-ft Drop (140 ºF)

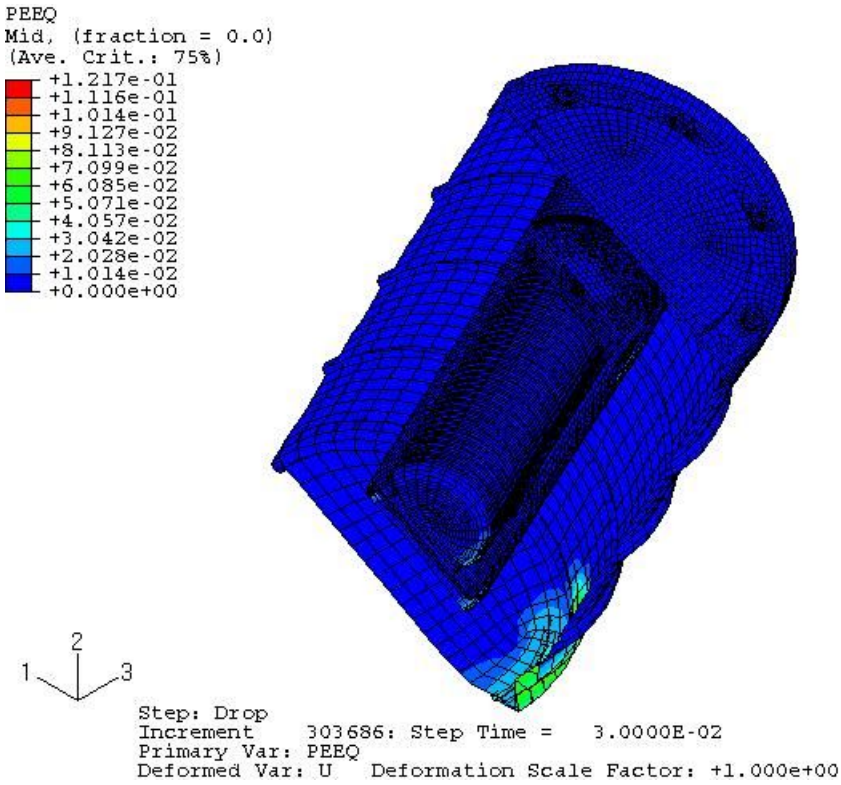

Figure 131 - Strain Distribution in Overpack for 6CV for Drum CGOB - 30-ft Drop (140 ºF)

(ALLKE = kinetic energy; ALLIE = internal energy; ALLPD = plastic strain energy; ALLSE = elastic strain energy; ALLAE = artificial energy)

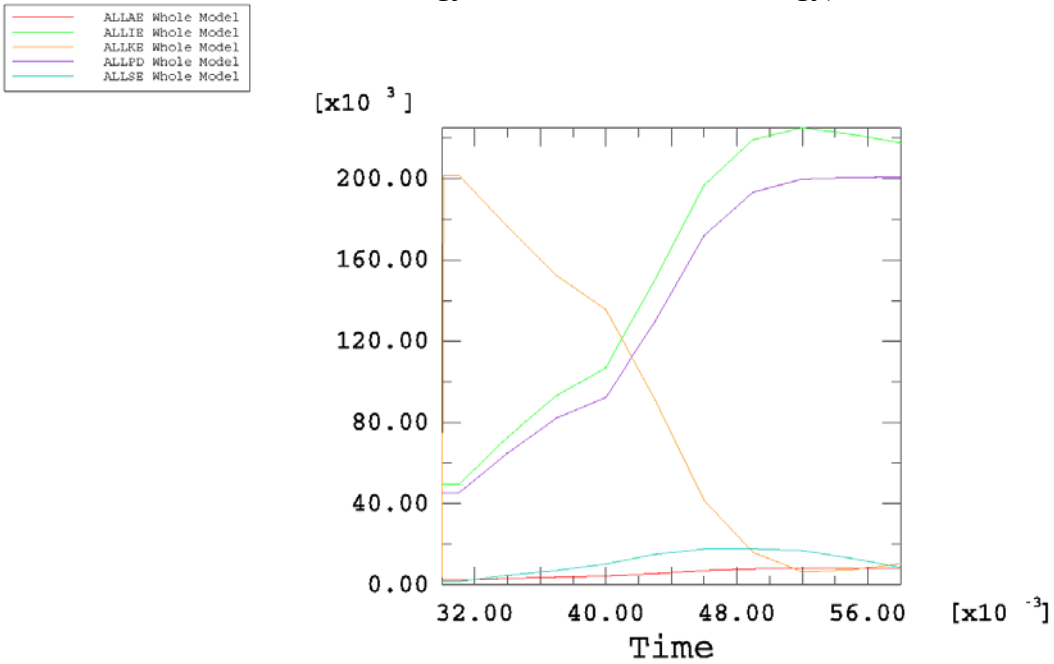

Figure 132 - Time-History Plot of Plate Energy during Drum CGOB - Top Corner Crush Simulation (140 ºF)

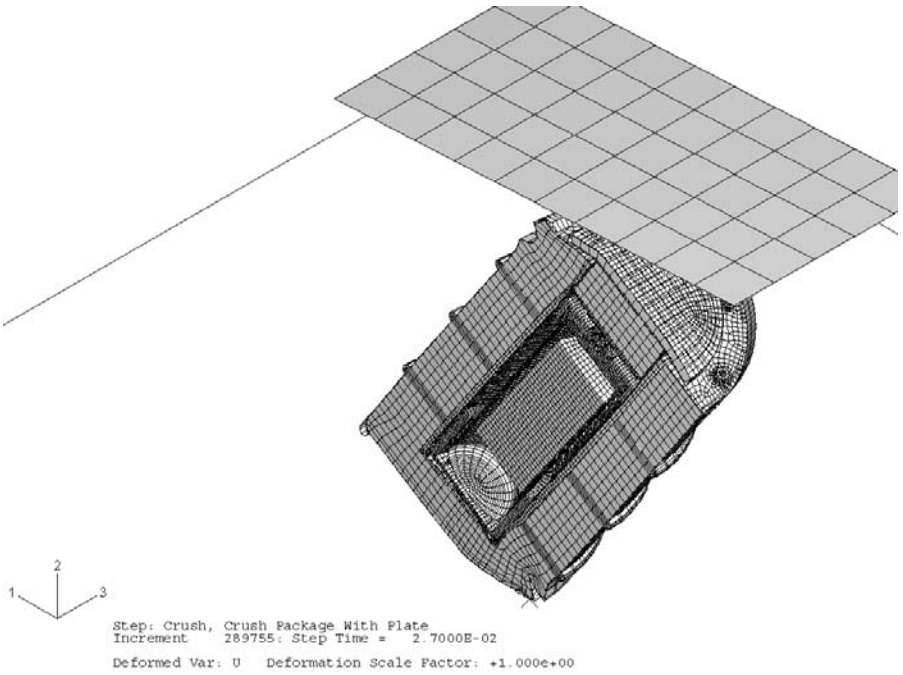

Figure 133 - Deformed Shape of 9977 with 6CV After the Drum CGOB - Top Corner Crush (140 ºF)

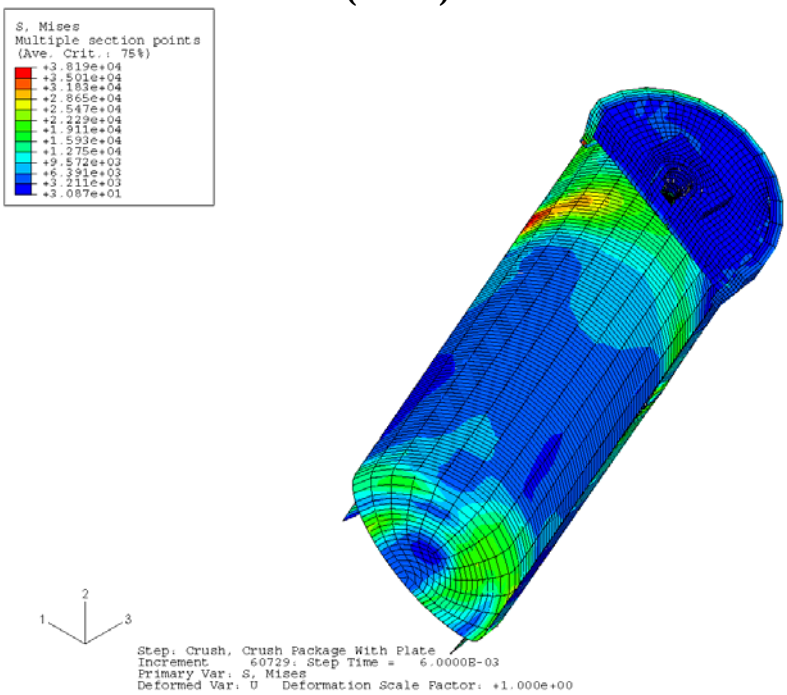

Figure 134 - Stress Distribution in the 6CV Model for Drum CGOB - Top Corner Crush (140 ºF)

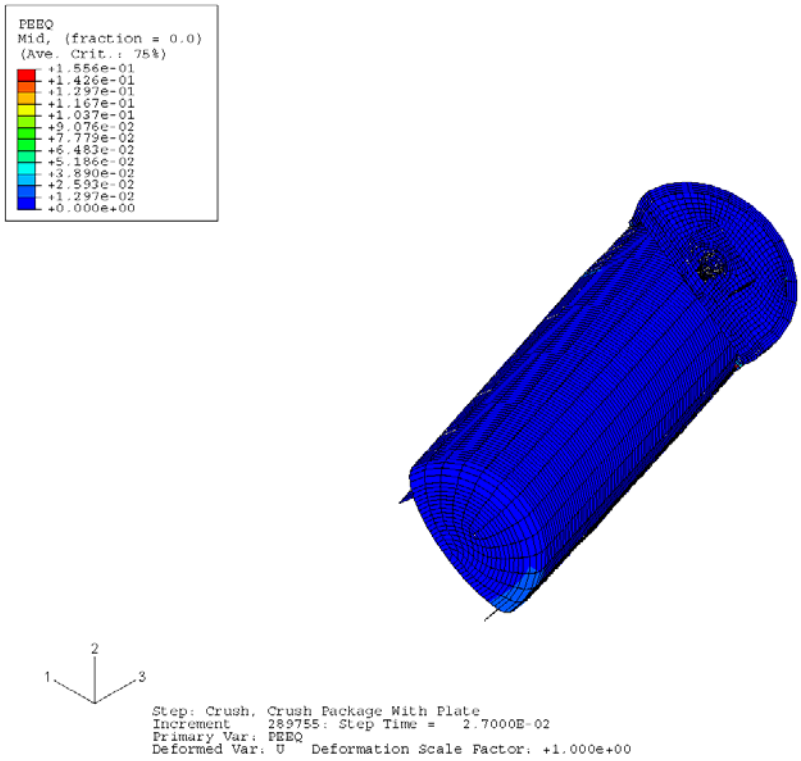

Figure 135 - Strain Distribution in 6CV Model for Drum CGOB - Top Corner Crush (140 ºF)

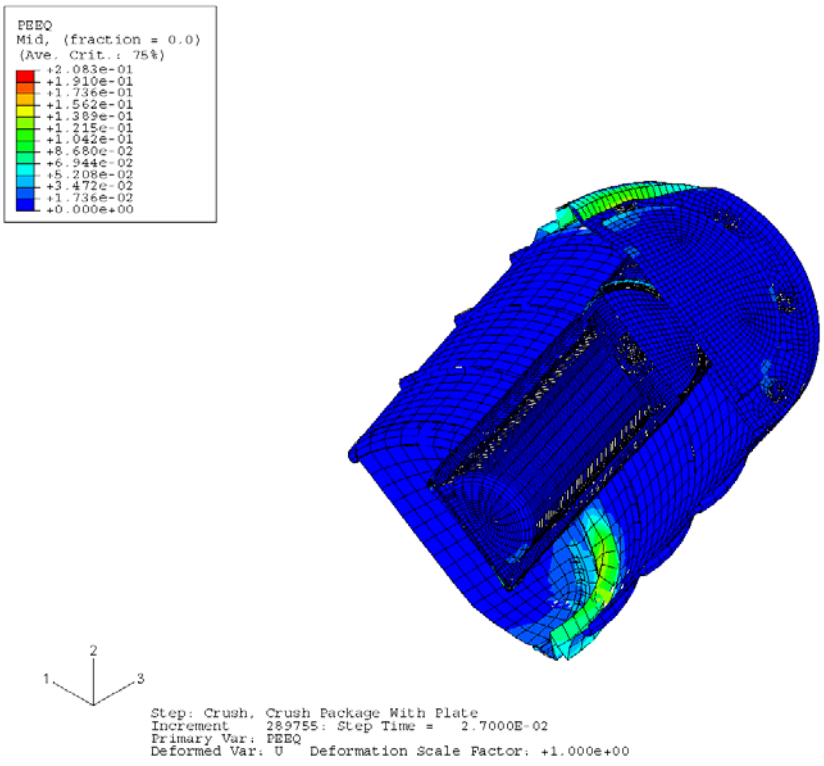

Figure 136 - Strain Distribution in Overpack for 6CV for Drum CGOB - Top Corner Crush (140 ºF)

(ALLKE = kinetic energy; ALLIE = internal energy; ALLPD = plastic strain energy; ALLSE = elastic strain energy; ALLAE = artificial energy)

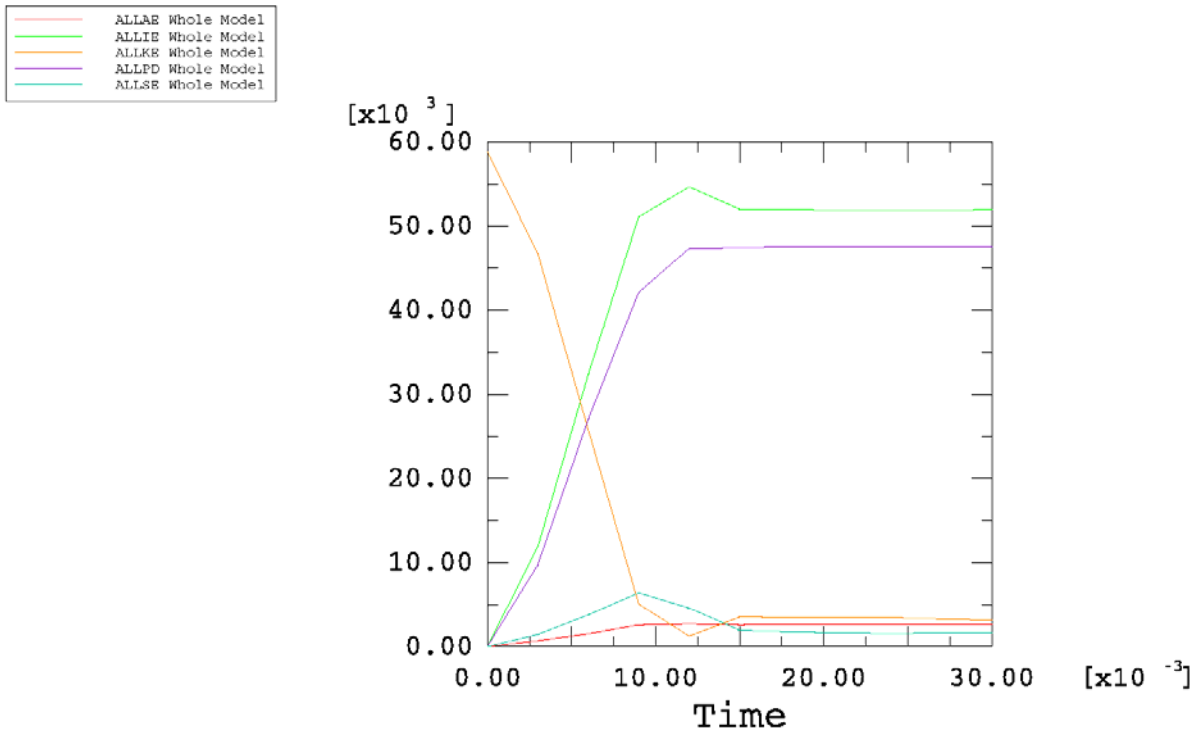

Figure 137 - Time-History Plot of Energy during Drum CGOB - 30-ft Drop Simulation (300 ºF)

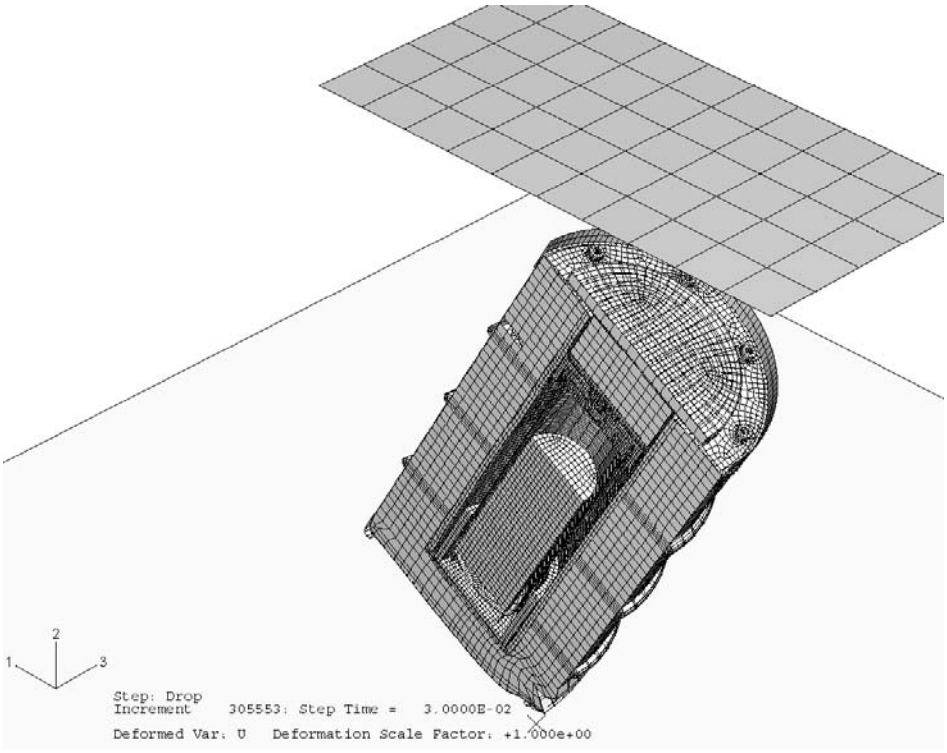

Figure 138 - Deformed Shape of 9977 with 6CV for Drum CGOB - 30-ft Drop (300 ºF)

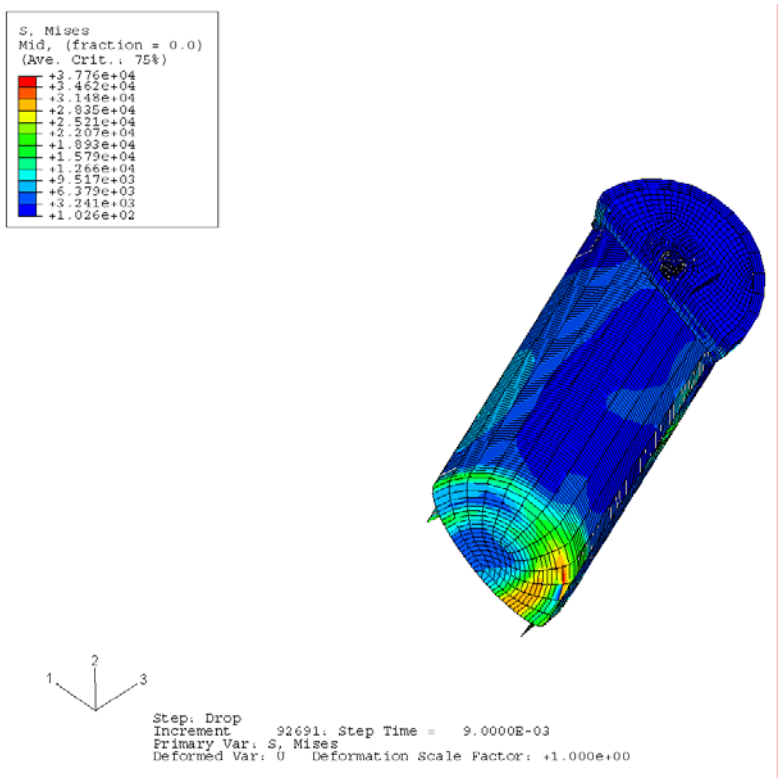

Figure 139 - Stress Distribution in 6CV Model for Drum CGOB - 30-ft Drop (300 ºF)

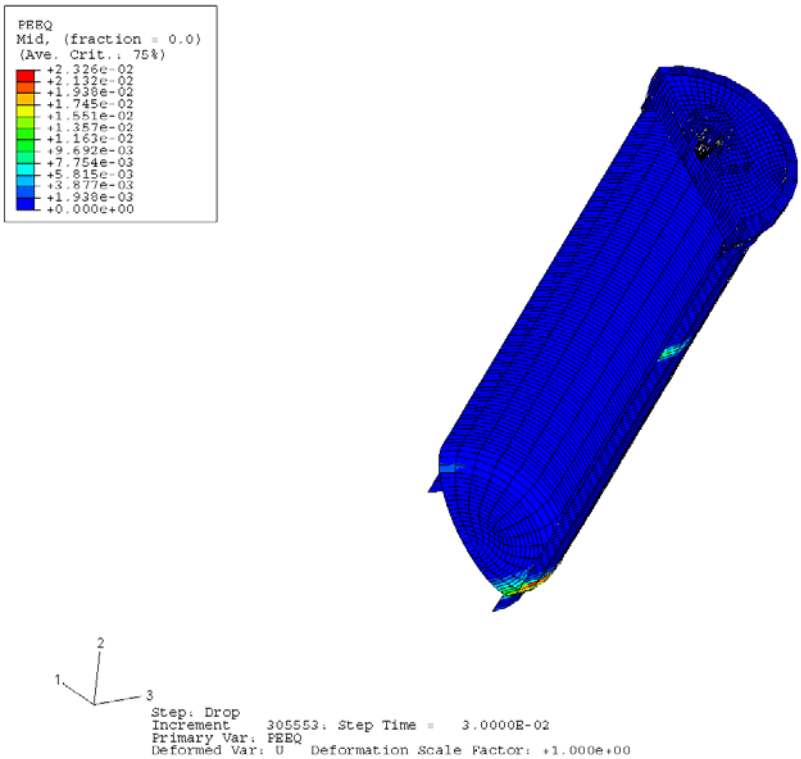

Figure 140 - Strain Distribution in 6CV Model for Drum CGOB - 30-ft Drop (300 ºF)

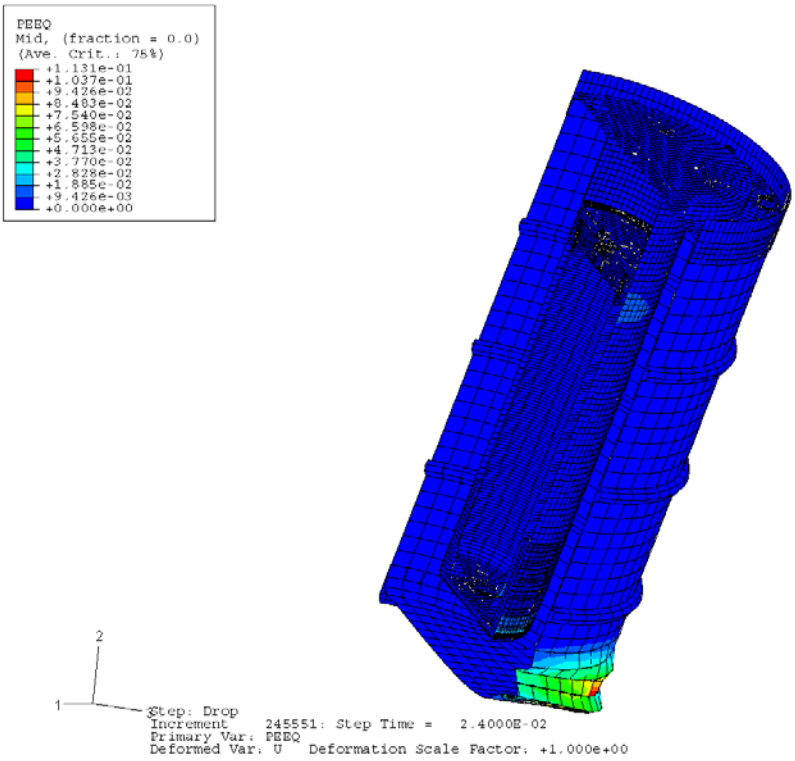

Figure 141 - Strain Distribution in Overpack for 6CV for Drum CGOB - 30-ft Drop (300 ºF)

(ALLKE = kinetic energy; ALLIE = internal energy; ALLPD = plastic strain energy; ALLSE = elastic strain energy; ALLAE = artificial energy)

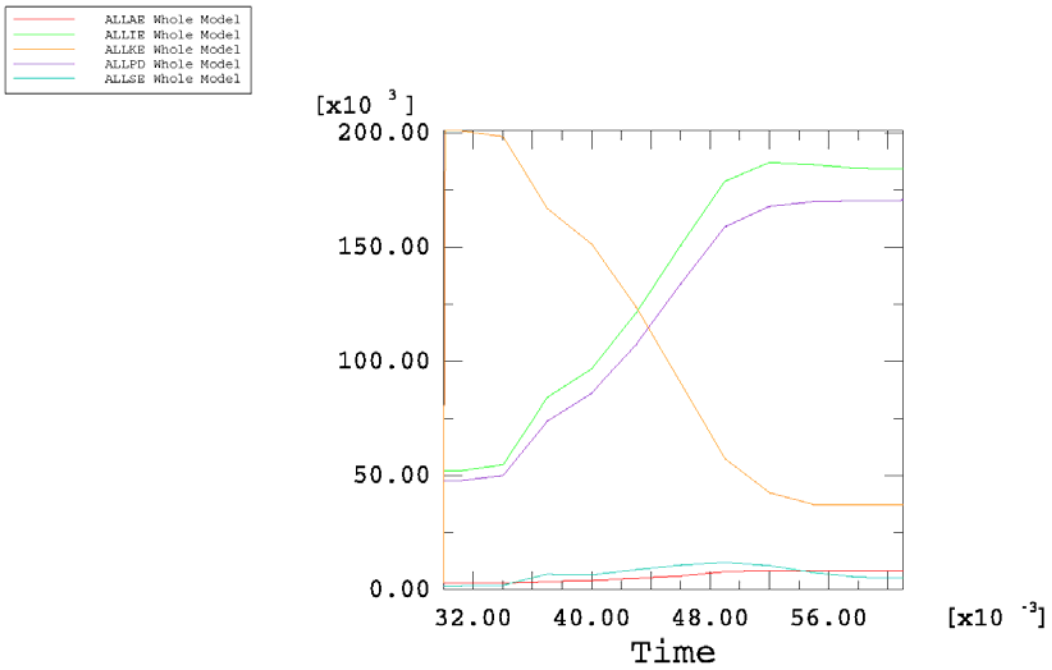

Figure 142 - Time-History Plot of Plate Energy during Drum CGOB - Top Corner Crush Simulation (300 ºF)

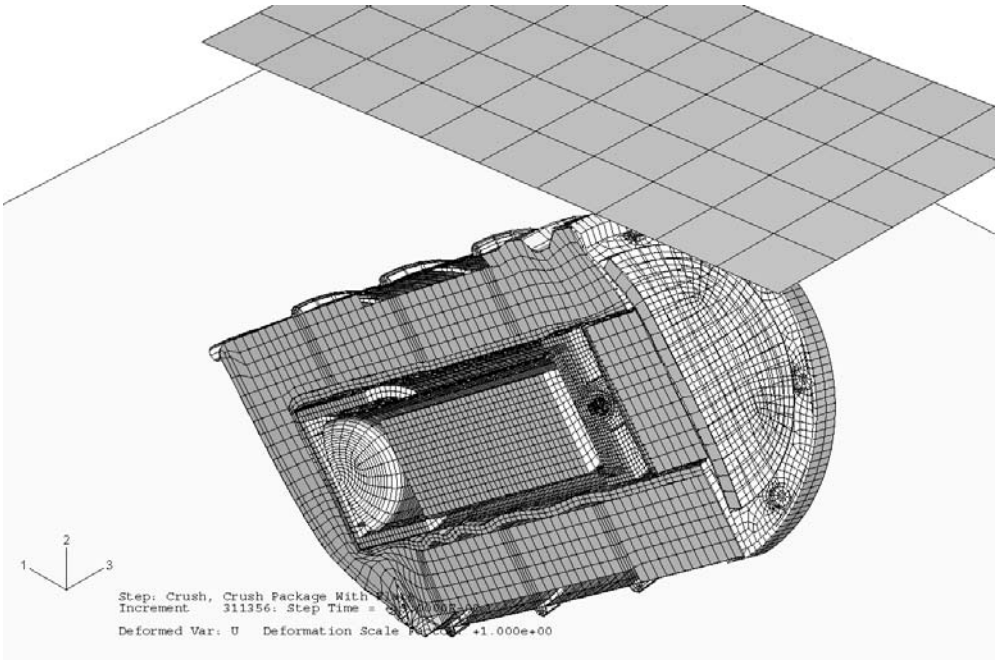

Figure 143 - Deformed Shape of 9977 with 6CV After the Drum CGOB - Top Corner Crush (300 ºF)

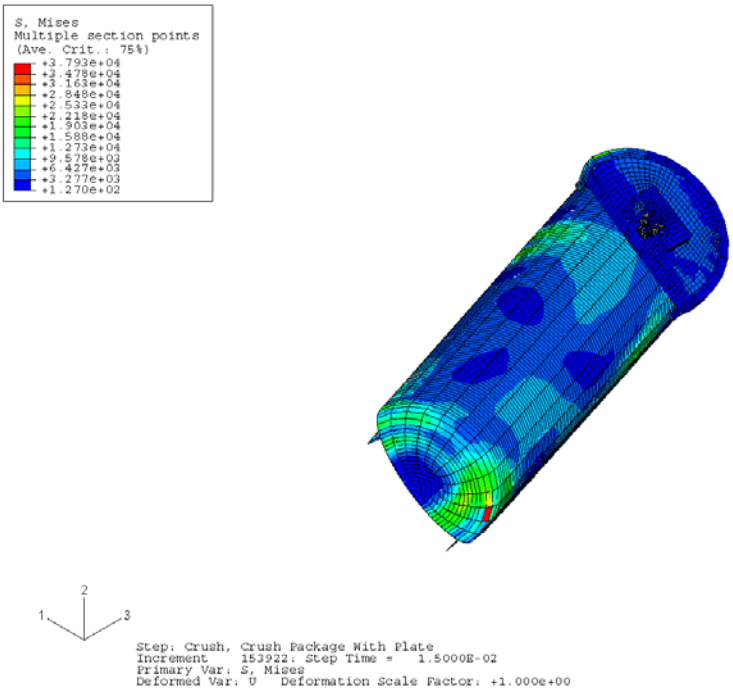

Figure 144 - Stress Distribution in the 6CV Model for Drum CGOB - Top Corner Crush (300 ºF)

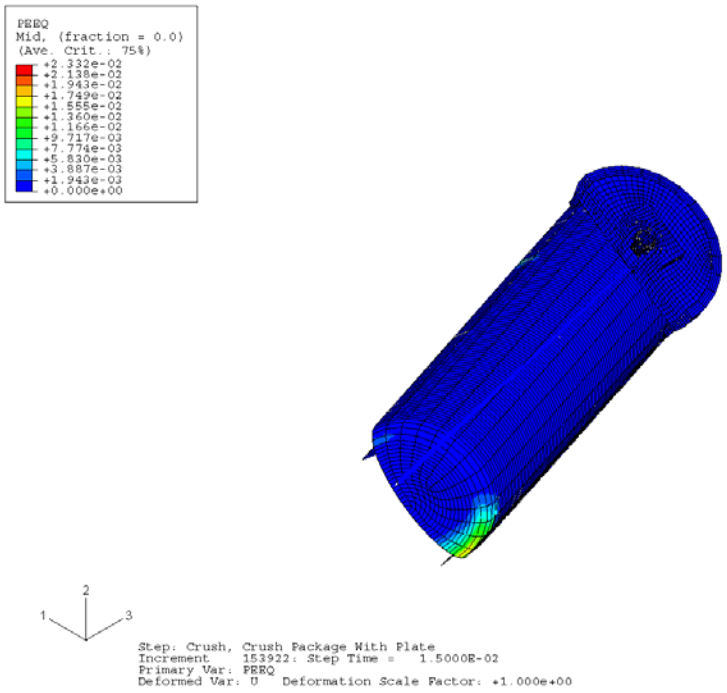

Figure 145 - Strain Distribution in 6CV Model for Drum CGOB - Top Corner Crush (300 ºF)

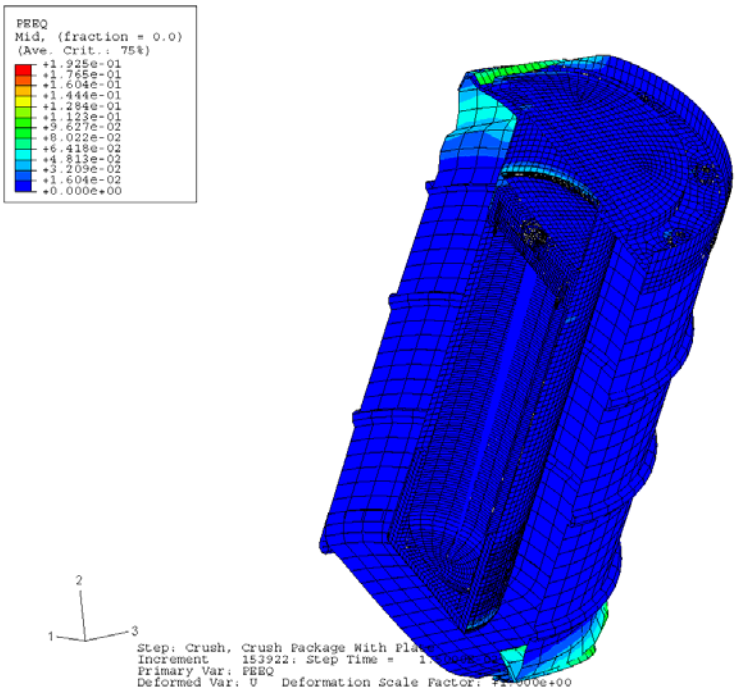

Figure 146 - Strain Distribution in Overpack for 6CV for Drum CGOB - Top Corner Crush (300 ºF)

7.6 30-ft Drop at 15º onto the Drum Bottom with Slap Down on Top (140 and 300 ºF)

Figure 147 shows the finite element model used for evaluating the 30-ft 15º slap down drop onto the drum top.

7.6.1 Case 1: 15º Slap Down onto Drum Top – 30-ft Drop onto Drum Top (140 ºF)

Energy History

The time-history plots of energy components for the 30-ft 15º slap down drop simulation shown in Figure 148 indicate that the kinetic energy approaches zero at the end of the analysis. Therefore, we know that the analysis covers the entire impact duration.

Deformed Shape of Full Model

Figure 149 is the deformed shape of the overall model.

Stress and Strain Contours in Component Models

Figures 150 and 151 show the von Mises stresses and the equivalent plastic strains in the CV model. Figure 152 shows the equivalent plastic strains in the overpack shell.

Evaluations of Maximum Local Primary Membrane Stress Intensities and Maximum Equivalent Plastic Strains in Containment Vessel

The stress components across the wall thickness at the locations away from or near the geometrical discontinuities should be used to calculate the general primary membrane stress intensities (P_m) or the local primary membrane stress intensities (P_L). For simplicity, the maximum value of the von Mises stresses in the containment vessel is used as the local primary membrane stress intensity (P_L). This value is higher than the actual local primary membrane stress intensity because the latter is calculated by averaging the thru-wall stresses across the component's thickness.

The maximum value of the local primary membrane stress intensity in the containment vessel is 43.76 ksi as given in Figure 150. This value is less than the allowable value of 57.3 ksi for the general primary membrane stress intensity and of 73.6 ksi for the local primary membrane stress intensity (as given in Section 6.0). The structural integrity of the 9977 subjected to a 30-ft drop has therefore been justified according to the ASME Code, Section III.

As shown in Figure 151, the maximum plastic strain experienced at any location within the containment vessel after the 30-ft drop is 2.06%. The maximum calculated value of the effective plastic strain at any point in the overpack is 20.71%. This value is less than the maximum average through-wall elongation of 35% for the 304L material use in the drum. Therefore, the drum will not be ruptured by the 30-ft drop impact.

7.6.2 Case 2: 15º Slap Down onto Drum Top – 30-ft Drop onto Drum Bottom (300 ºF)

Energy History

The time-history plots of energy components for the 30-ft 15º slap down drop simulation shown in Figure 153 indicate that the kinetic energy approaches zero at the end of the analysis. Therefore, we know that the analysis covers the entire impact duration.

Deformed Shape of Full Model

Figure 154 is the deformed shape of the overall model.

Stress and Strain Contours in Component Models

Figures 155 and 156 show the von Mises stresses and the equivalent plastic strains in the CV model. Figure 157 shows the equivalent plastic strains in the overpack shell.

Evaluations of Maximum Local Primary Membrane Stress Intensities and Maximum Equivalent Plastic Strains in Containment Vessel

The stress components across the wall thickness at the locations away from or near the geometrical discontinuities should be used to calculate the general primary membrane stress intensities (P_m) or the local primary membrane stress intensities (P_L). For simplicity, the maximum value of the von Mises stresses in the containment vessel is used as the local primary membrane stress intensity (P_L). This value is higher than the actual local primary membrane stress intensity because the latter is calculated by averaging the thru-wall stresses across the component's thickness.

The maximum value of the local primary membrane stress intensity in the containment vessel is 42.21 ksi as given in Figure 155. This value is less than the allowable value of 57.3 ksi for the general primary membrane stress intensity and of 73.6 ksi for the local primary membrane stress intensity (as given in Section 6.0). The structural integrity of the 9977 subjected to a 30-ft drop has therefore been justified according to the ASME Code, Section III.

As shown in Figure 156, the maximum plastic strain experienced at any location within the containment vessel after the 30-ft 15° slap down drop is 1.16%. The maximum calculated value of the effective plastic strain at any point in the overpack is 22.20%. This value is less than the maximum average through-wall elongation of 35% for the 304L material use in the drum. Therefore, the drum will not be ruptured by the 30-ft drop impact.

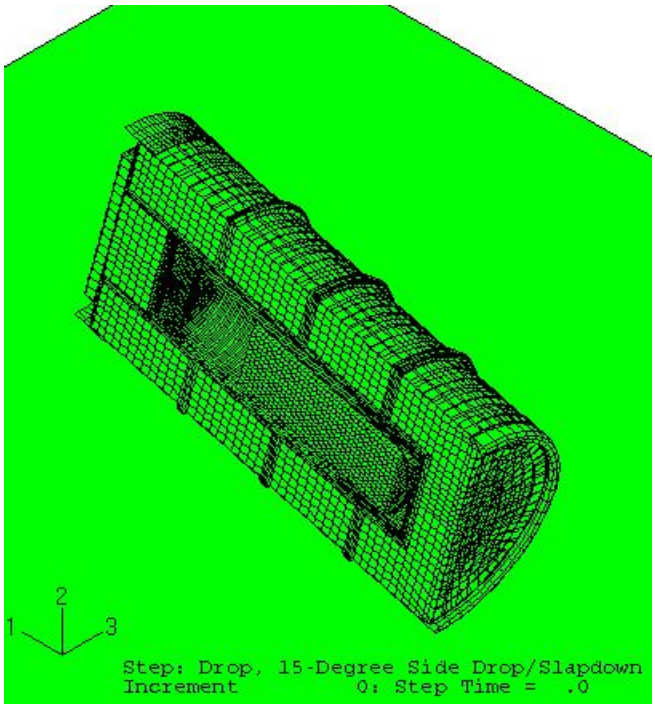

Figure 147 - Finite Element Model of the 9977 15º Slap Down onto Top - 30-ft Drop

(ALLKE = kinetic energy; ALLIE = internal energy; ALLPD = plastic strain energy; ALLSE = elastic strain energy; ALLAE = artificial energy)

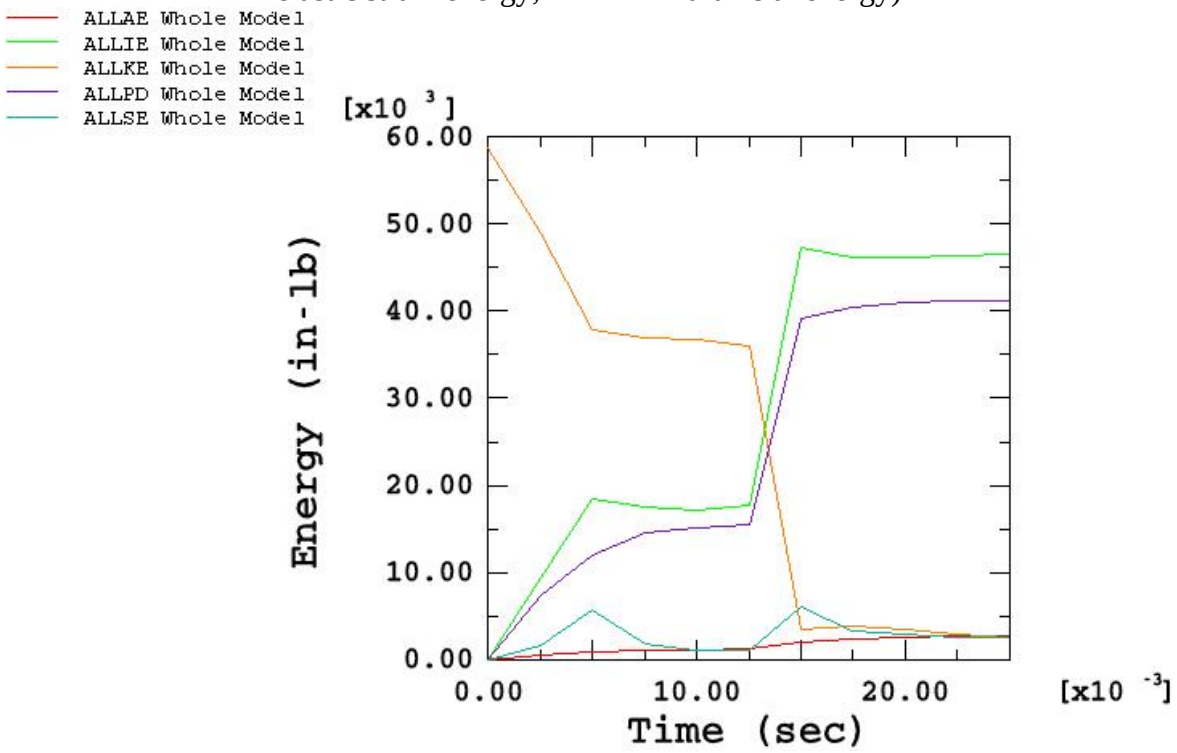

Figure 148 - Time-History Plot of Energy during Drum Top 15º Slap Down – 30-ft Drop Simulation (140 ºF)

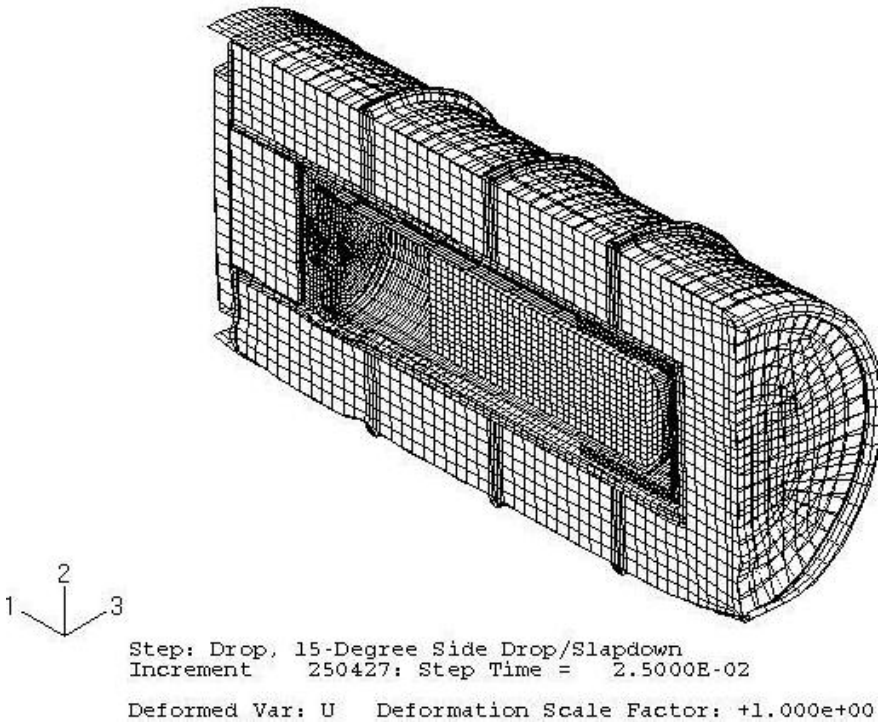

Figure 149 - Deformed Shape of 9977 with 6CV After the Drum Top 15º Slap Down – 30-ft Drop (140 ºF)

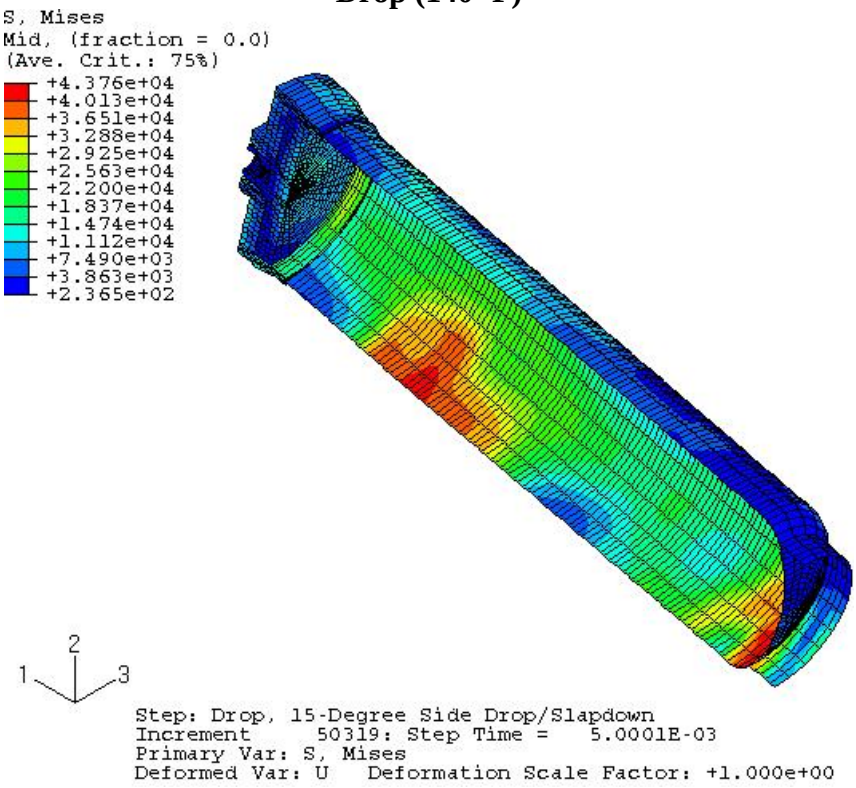

Figure 150 - Stress Distribution in the 6CV Model for Drum Top 15º Slap Down – 30-ft Drop (140 ºF)

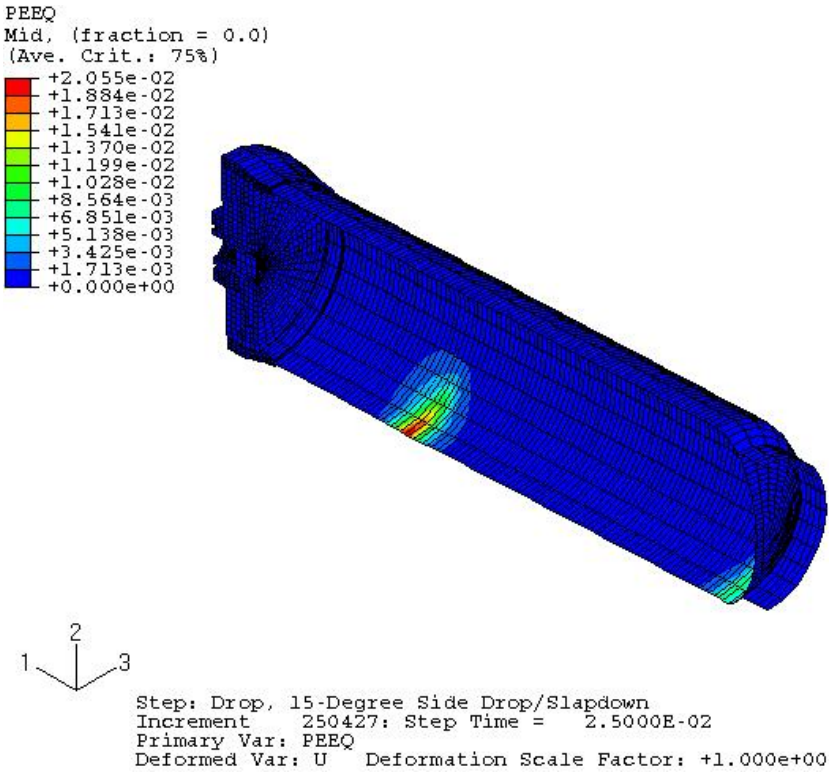

Figure 151 - Strain Distribution in 6CV Model for Drum Top 15º Slap Down – 30-ft Drop (140 ºF)

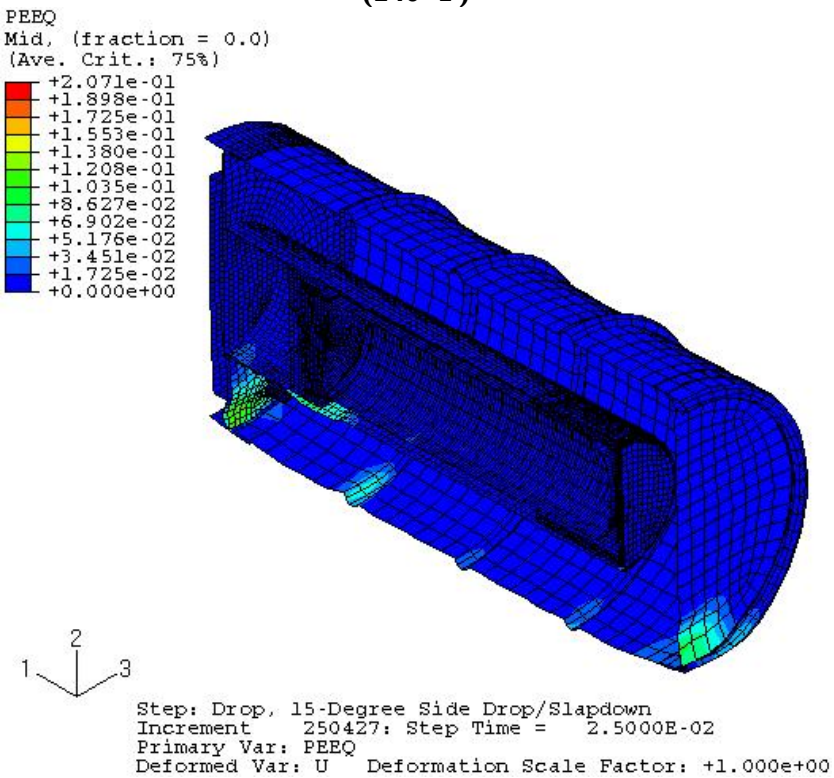

Figure 152 - Strain Distribution in Overpack for 6CV for Drum Top 15º Slap Down – 30-ft Drop (140 ºF)

(ALLKE = kinetic energy; ALLIE = internal energy; ALLPD = plastic strain energy; ALLSE = elastic strain energy; ALLAE = artificial energy)

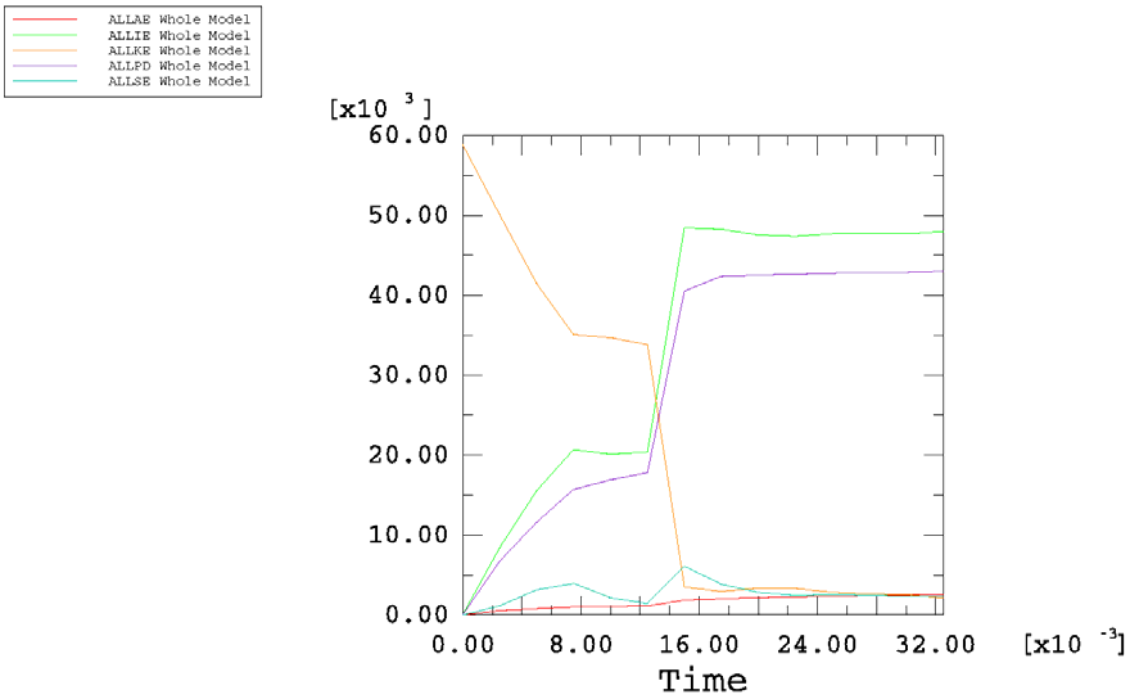

Figure 153 - Time-History Plot of Energy during 15º Slap Down – 30-ft Drop onto Drum Top Simulation (300 ºF)

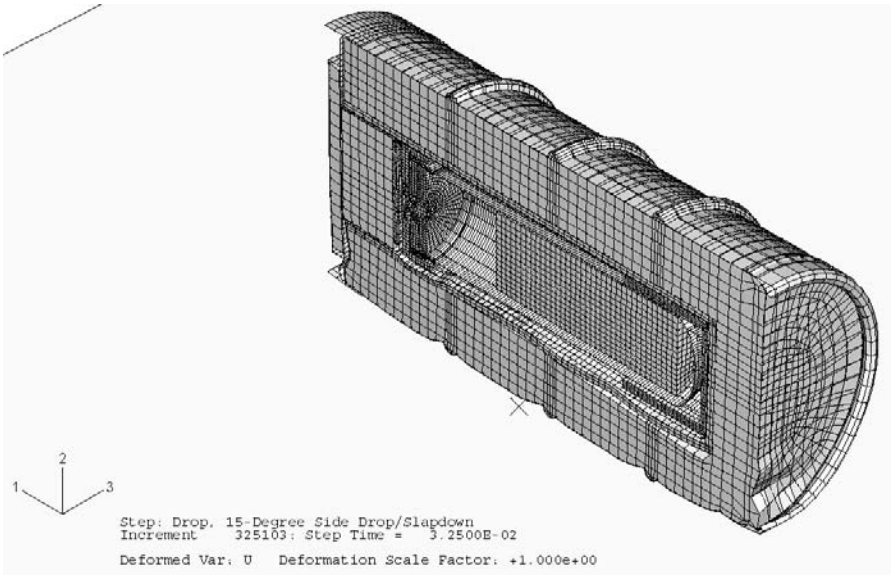

Figure 154 - Deformed Shape of 9977 with 6CV After the 15º Slap Down – 30-ft Drop onto Drum Top (300 ºF)

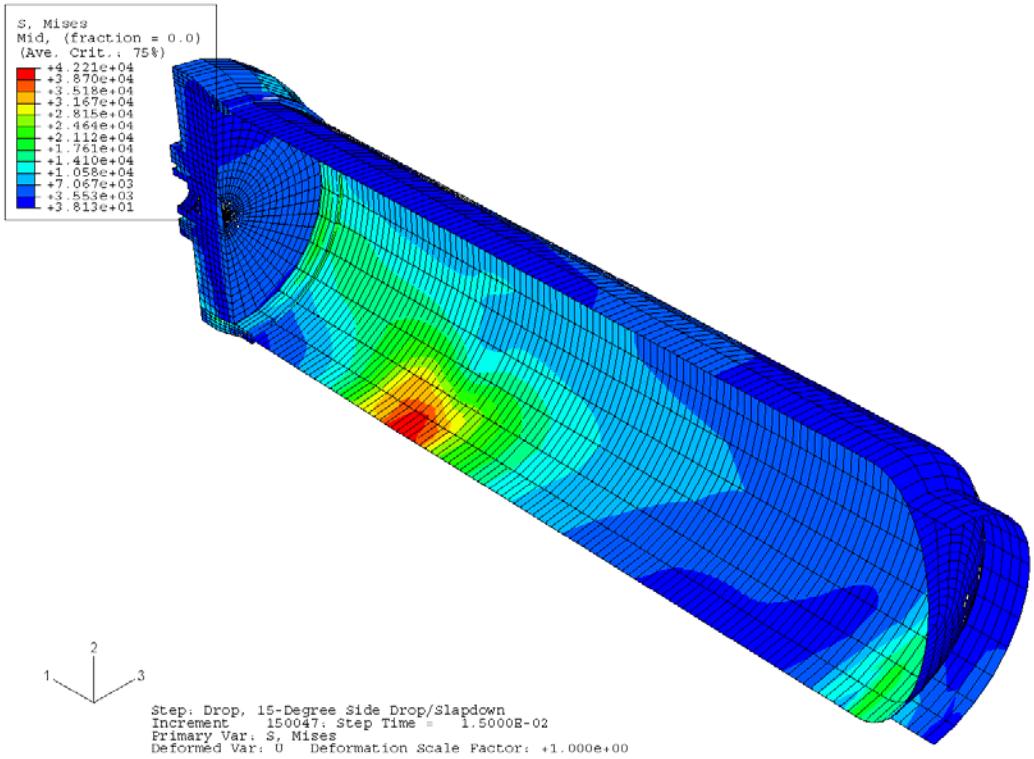

Figure 155 - Stress Distribution in the 6CV Model for 15º Slap Down – 30-ft Drop onto Drum Top (300 ºF)

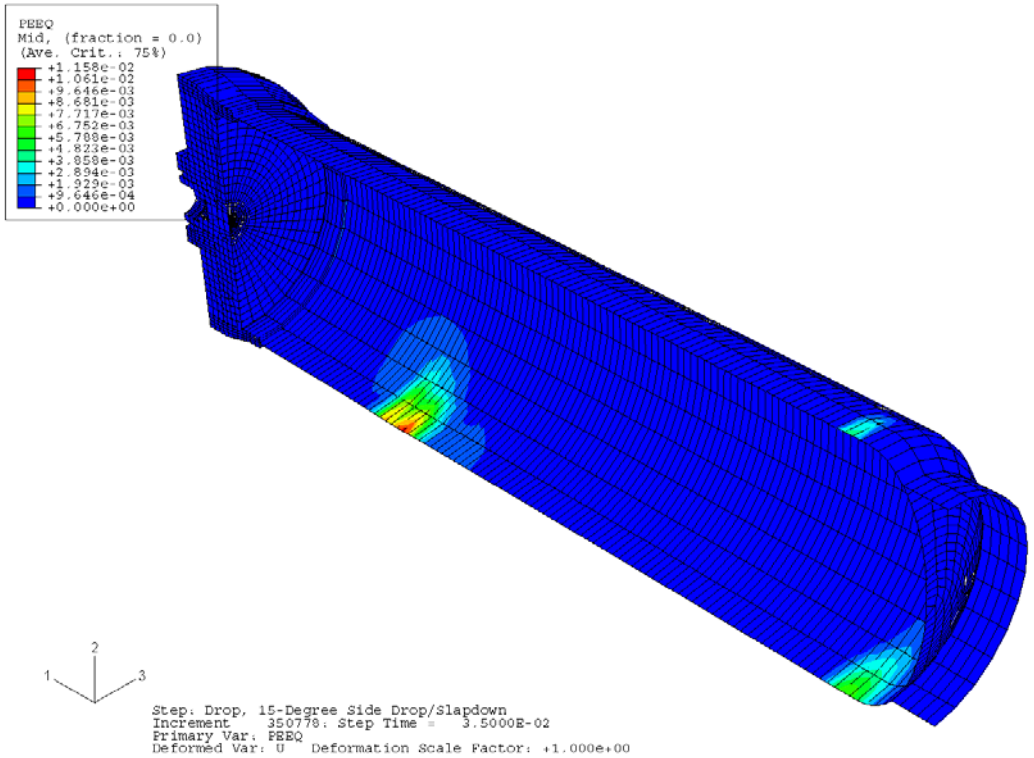

Figure 156 - Strain Distribution in 6CV Model for 15º Slap Down – 30-ft Drop onto Drum Top (300 ºF)

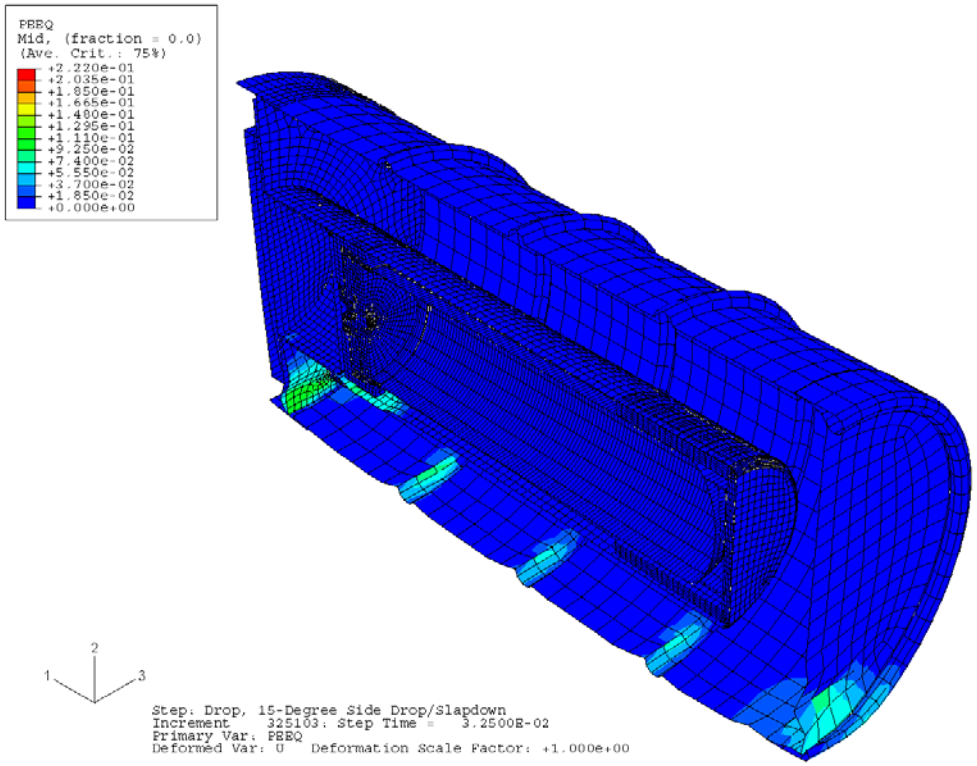

Figure 157 - Strain Distribution in Overpack for 6CV for 15º Slap Down – 30-ft Drop onto Drum Top (300 ºF)

7.7 15º Slap Down in a 30-ft Drop onto the Drum Bottom (-20, 140, & 300 ºF)

Figure 158 shows the finite element model used for evaluating the 30-ft 15º slap down drop onto the drum bottom.

7.7.1 Case 1: 15º Slap Down – 30-ft Drop onto Drum Bottom at -20 ºF

Energy History

The time-history plots of energy components for the 30-ft 15º slap down drop simulation shown in Figure 159 indicate that the kinetic energy approaches zero at the end of the analysis. Therefore, we know that the analysis covers the entire impact duration.

Deformed Shape of Full Model

Figure 160 is the deformed shape of the overall model.

Stress and Strain Contours in Component Models

Figures 161 and 162 show the von Mises stresses and the equivalent plastic strains in the CV model. Figure 163 shows the equivalent plastic strains in the overpack shell.

Evaluations of Maximum Local Primary Membrane Stress Intensities and Maximum Equivalent Plastic Strains in Containment Vessel

The stress components across the wall thickness at the locations away from or near the geometrical discontinuities should be used to calculate the general primary membrane stress intensities (P_m) or the local primary membrane stress intensities (P_L). For simplicity, the maximum value of the von Mises stresses in the containment vessel is used as the local primary membrane stress intensity (P_L). This value is higher than the actual local primary membrane stress intensity because the latter is calculated by averaging the thru-wall stresses across the component's thickness.

The maximum value of the local primary membrane stress intensity in the containment vessel is 40.33 ksi as given in Figure 161. This value is less than the allowable value of 57.3 ksi for the general primary membrane stress intensity and of 73.6 ksi for the local primary membrane stress intensity (as given in Section 6.0). The structural integrity of the 9977 subjected to a 30-ft drop has therefore been justified according to the ASME Code, Section III.

As shown in Figure 162, the maximum plastic strain experienced at any location within the containment vessel after the 30-ft drop is 2.42%. The maximum calculated value of the effective plastic strain at any point in the overpack is 15.92%. This value is less than the maximum average through-wall elongation of 35% for the 304L material use in the drum. Therefore, the drum will not be ruptured by the 30-ft drop impact.

7.7.2 Case 2: 15º Slap Down – 30-ft Drop onto Drum Bottom at 140 ºF

Energy History

The time-history plots of energy components for the 30-ft 15º slap down drop simulation shown in Figure 164 indicate that the kinetic energy approaches zero at the end of the analysis. Therefore, we know that the analysis covers the entire impact duration.

Deformed Shape of Full Model

Figure 165 is the deformed shape of the overall model.

Stress and Strain Contours in Component Models

Figures 166 and 167 show the von Mises stresses and the equivalent plastic strains in the CV model. Figure 168 shows the equivalent plastic strains in the overpack shell.

Evaluations of Maximum Local Primary Membrane Stress Intensities and Maximum Equivalent Plastic Strains in Containment Vessel

The stress components across the wall thickness at the locations away from or near the geometrical discontinuities should be used to calculate the general primary membrane stress intensities (P_m) or the local primary membrane stress intensities (P_L). For simplicity, the maximum value of the von Mises stresses in the containment vessel is used as the local primary membrane stress intensity (P_L). This value is higher than the actual local primary membrane stress intensity because the latter is calculated by averaging the thru-wall stresses across the component's thickness.

The maximum value of the local primary membrane stress intensity in the containment vessel is 32.48 ksi as given in Figure 166. This value is less than the allowable value of 57.3 ksi for the general primary membrane stress intensity and of 73.6 ksi for the local primary membrane stress intensity (as given in Section 6.0). The structural integrity of the 9977 subjected to a 30-ft drop has therefore been justified according to the ASME Code, Section III.

As shown in Figure 167, the maximum plastic strain experienced at any location within the containment vessel after a the 30-ft drop is 1.73%. The maximum calculated value of the effective plastic strain at any point in the overpack is 15.17%. This value is less than the maximum average through-wall elongation of 35% for the 304L material use in the drum. Therefore, the drum will not be ruptured by the 30-ft drop impact.

7.7.3 Case 3: 15º Slap Down – 30-ft Drop onto Drum Bottom at 300 ºF

Energy History

The time-history plots of energy components for the 30-ft 15º slap down drop simulation shown in Figure 169 indicate that the kinetic energy approaches zero at the end of the analysis. Therefore, we know that the analysis covers the entire impact duration.

Deformed Shape of Full Model

Figure 170 is the deformed shape of the overall model.

Stress and Strain Contours in Component Models

Figures 171 and 172 show the von Mises stresses and the equivalent plastic strains in the CV model. Figure 173 shows the equivalent plastic strains in the overpack shell.

Evaluations of Maximum Local Primary Membrane Stress Intensities and Maximum Equivalent Plastic Strains in Containment Vessel

The stress components across the wall thickness at the locations away from or near the geometrical discontinuities should be used to calculate the general primary membrane stress intensities (P_m) or the local primary membrane stress intensities (P_L). For simplicity, the maximum value of the von Mises stresses in the containment vessel is used as the local primary membrane stress intensity (P_L). This value is higher than the actual local primary membrane stress intensity because the latter is calculated by averaging the thru-wall stresses across the component's thickness.

The maximum value of the local primary membrane stress intensity in the containment vessel is 29.38 ksi as given in Figure 171. This value is less than the allowable value of 57.3 ksi for the general primary membrane stress intensity and of 73.6 ksi for the local primary membrane stress intensity (as given in Section 6.0). The structural integrity of the 9977 subjected to a 30-ft drop has therefore been justified according to the ASME Code, Section III.

As shown in Figure 172, the maximum plastic strain experienced at any location within the containment vessel after the 30-ft drop is 1.16%. The maximum calculated value of the effective plastic strain at any point in the overpack is 15.43%. This value is less than the minimum specified uniform elongation of 35% for the 304L material used in the drum. Therefore, the drum will not be ruptured by the 30-ft drop impact.

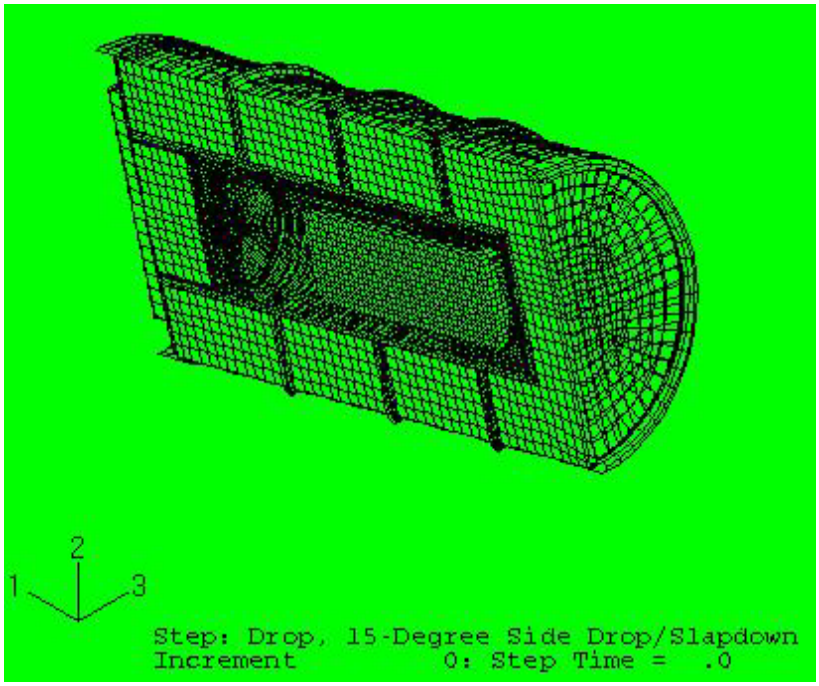

Figure 158 - Finite Element Model of the 9977 15º Slap Down onto Bottom - 30-ft Drop

(ALLKE = kinetic energy; ALLIE = internal energy; ALLPD = plastic strain energy; ALLSE = elastic strain energy; ALLAE = artificial energy)

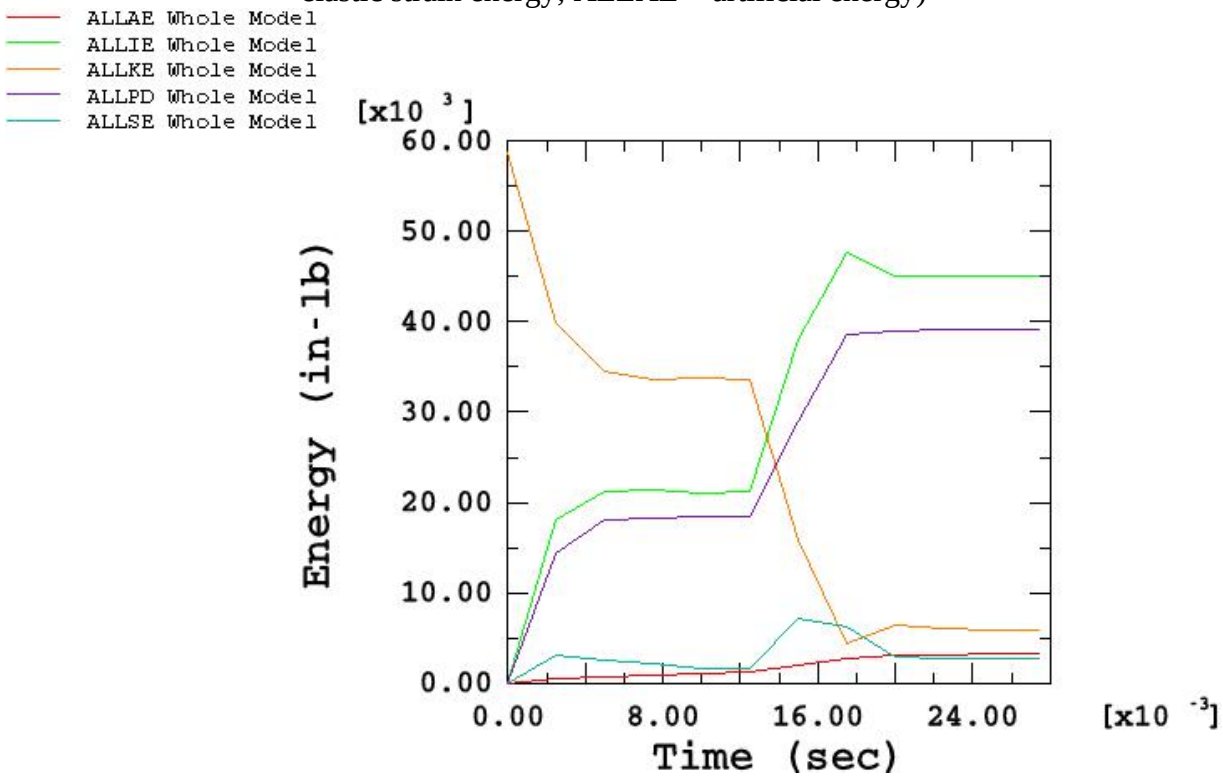

Figure 159 - Time-History Plot of Energy during 15º Slap Down - 30-ft Drop onto Drum Bottom Simulation (-20 ºF)

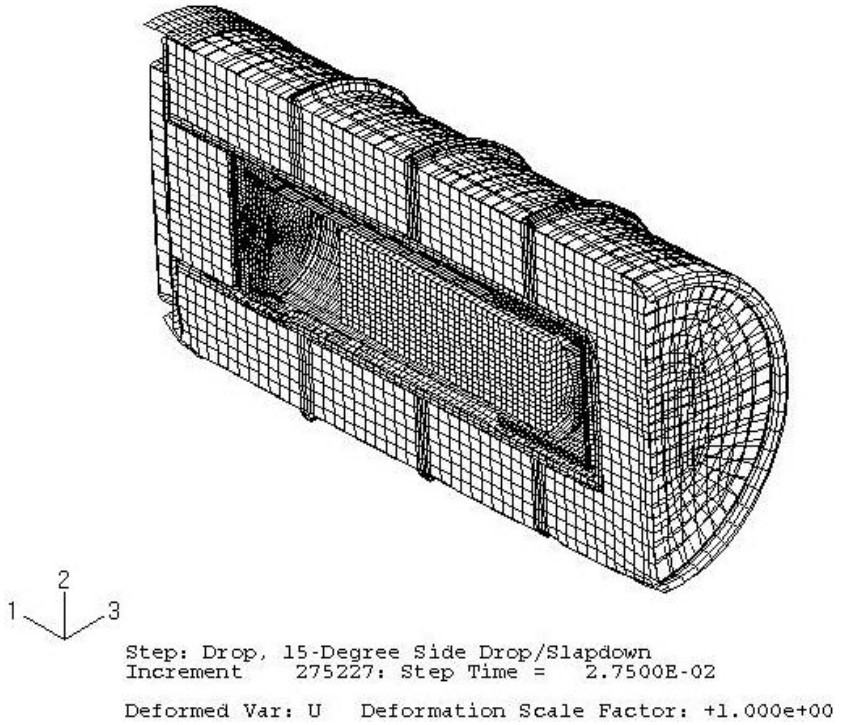

Figure 160 - Deformed Shape of 9977 with 6CV After the 15º Slap Down - 30-ft Drop onto Drum Bottom (-20 ºF)

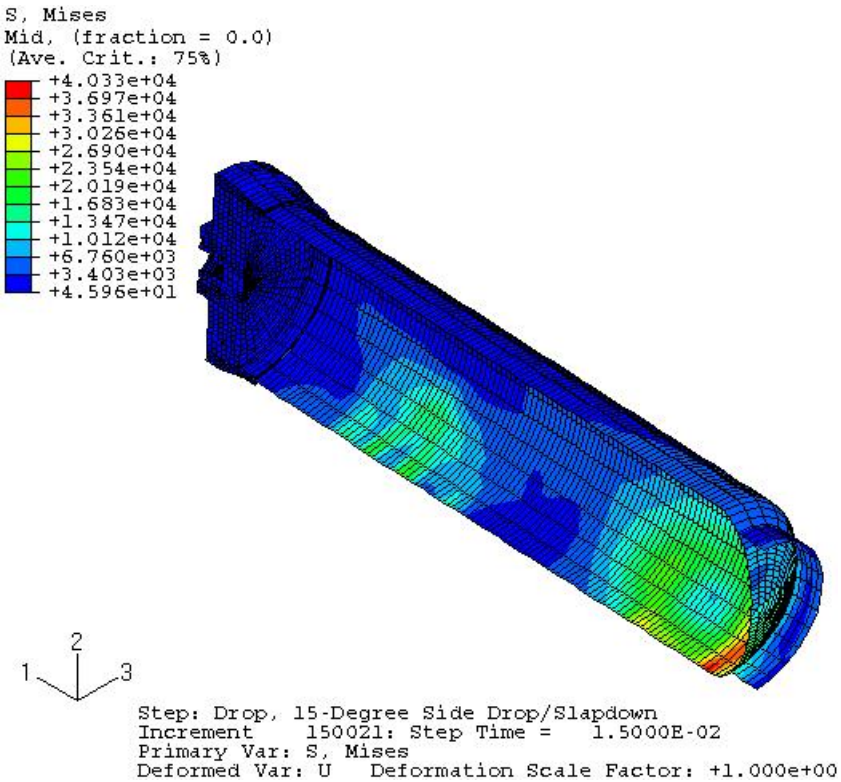

Figure 161 - Stress Distribution in the 6CV Model for 15º Slap Down - 30-ft Drop onto Drum Bottom (-20 ºF)

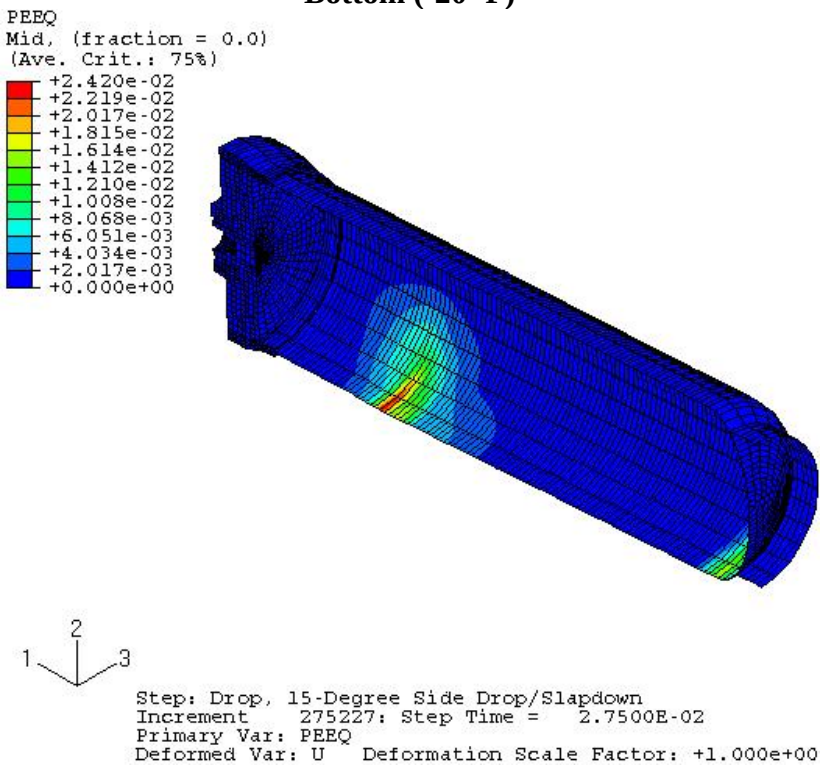

Figure 162 - Strain Distribution in 6CV Model for 15º Slap Down - 30-ft Drop onto Drum Bottom (-20 ºF)

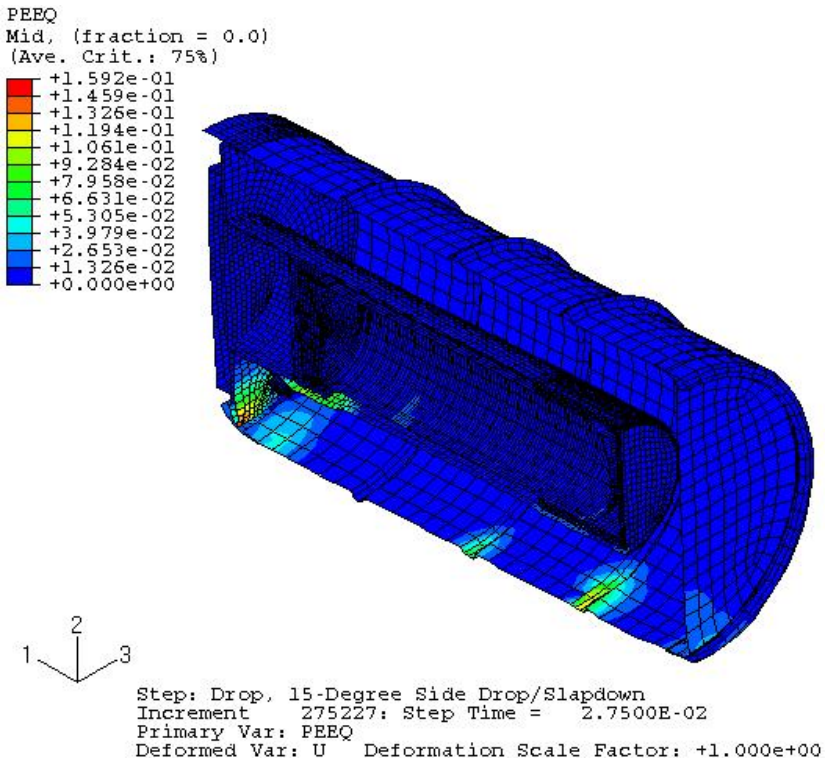

Figure 163 - Strain Distribution in Overpack for 6CV for 15º Slap Down - 30-ft Drop onto Drum Bottom (-20 ºF)

(ALLKE = kinetic energy; ALLIE = internal energy; ALLPD = plastic strain energy; ALLSE = elastic strain energy; ALLAE = artificial energy)

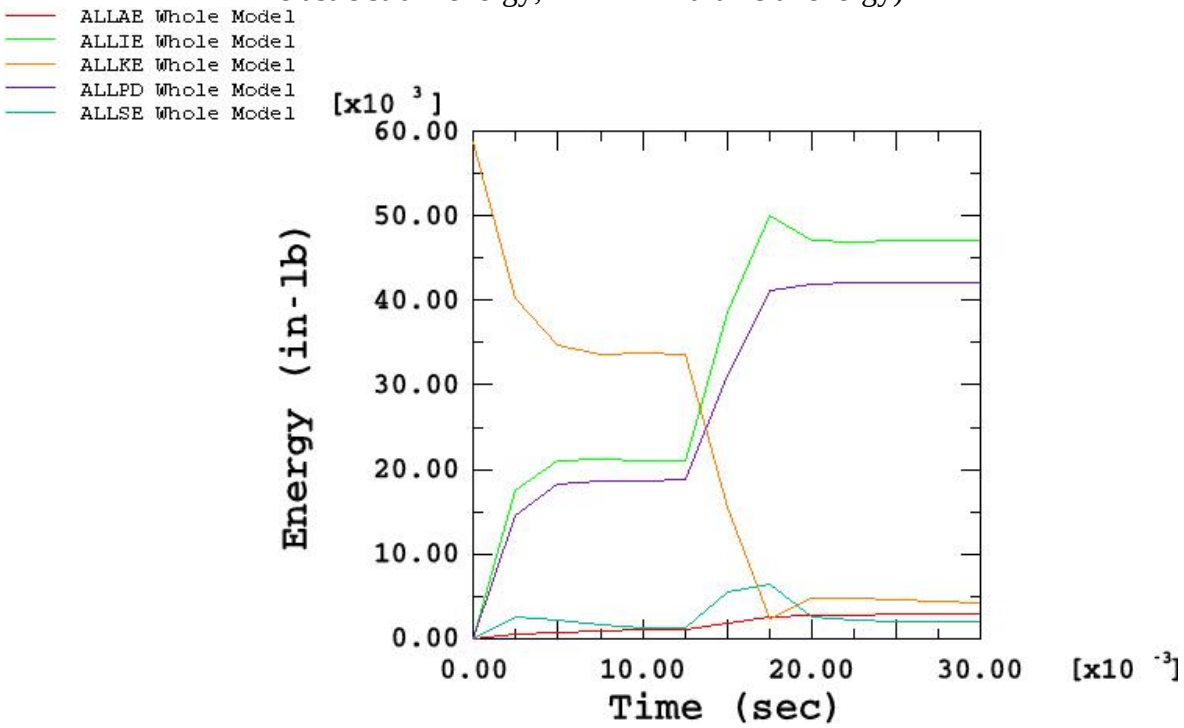

Figure 164 - Time-History Plot of Energy during 15º Slap Down - 30-ft Drop onto Drum Bottom Simulation (140 ºF)

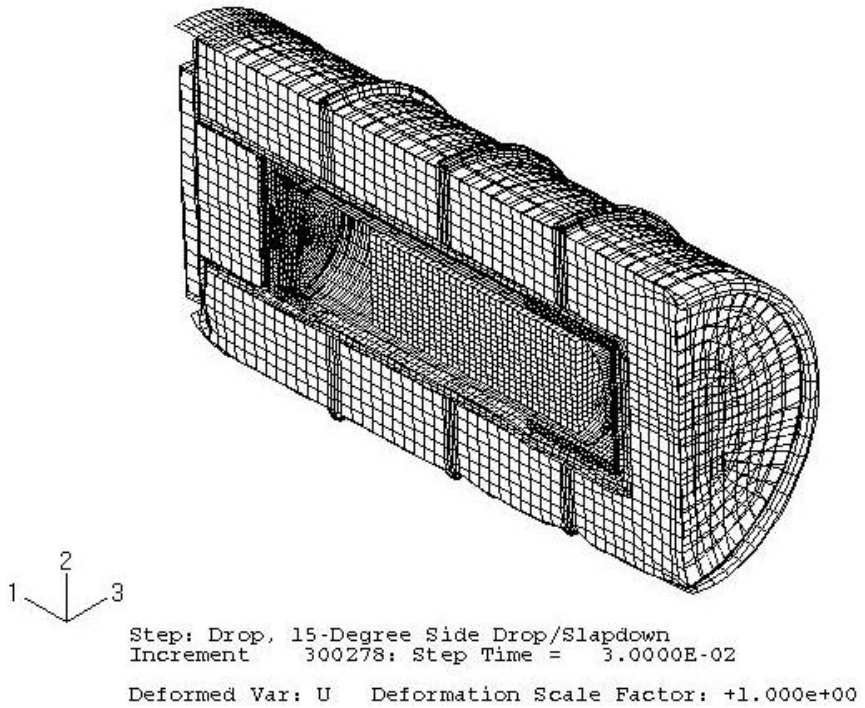

Figure 165 - Deformed Shape of 9977 with 6CV After the 15º Slap Down - 30-ft Drop onto Drum Bottom (140 ºF)

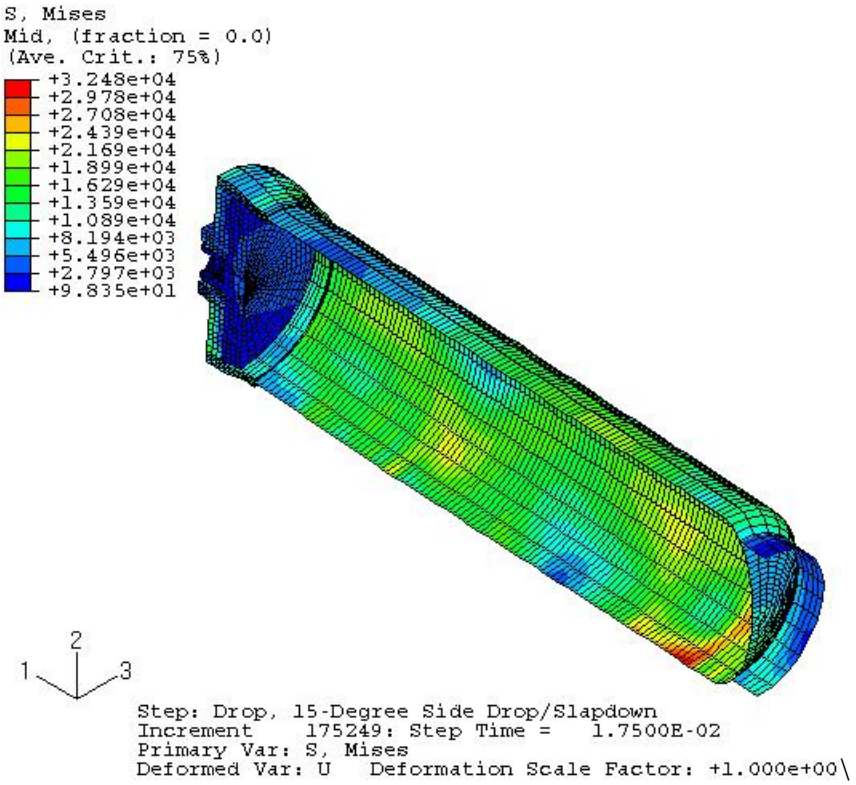

Figure 166 - Stress Distribution in the 6CV Model for 15º Slap Down - 30-ft Drop onto Drum Bottom (140 ºF)

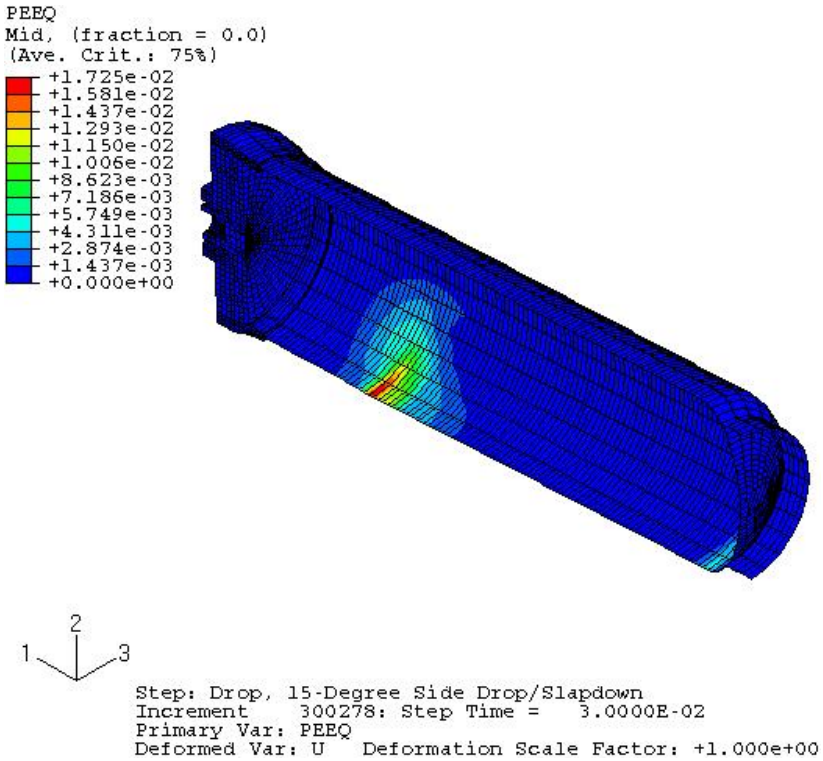

Figure 167 - Strain Distribution in 6CV Model for 15º Slap Down - 30-ft Drop onto Drum Bottom (140 ºF)

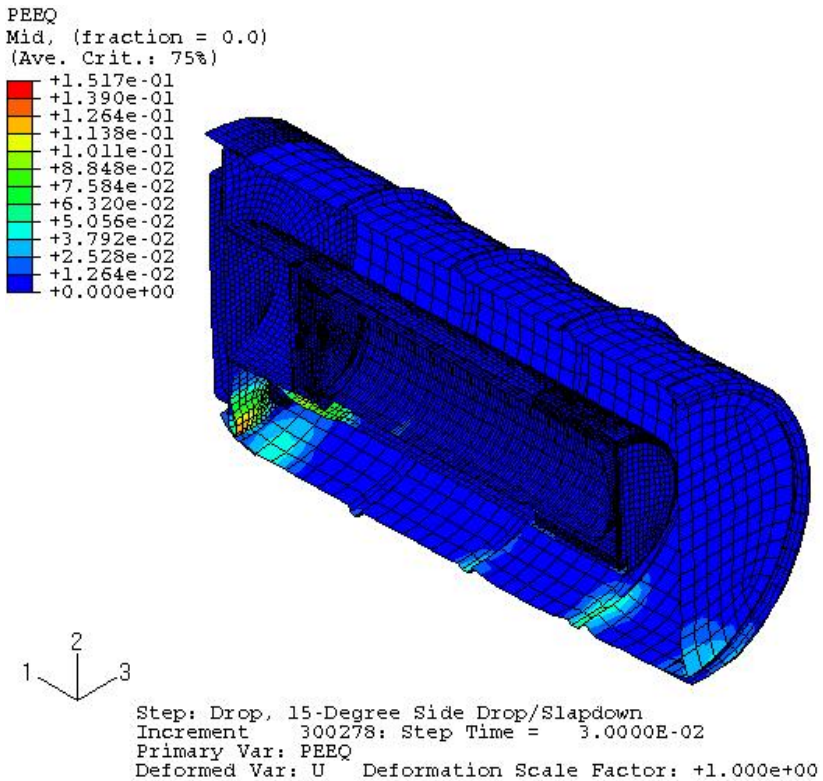

Figure 168 - Strain Distribution in Overpack for 6CV for 15º Slap Down - 30-ft Drop onto Drum Bottom (140 ºF)

(ALLKE = kinetic energy; ALLIE = internal energy; ALLPD = plastic strain energy; ALLSE = elastic strain energy; ALLAE = artificial energy)

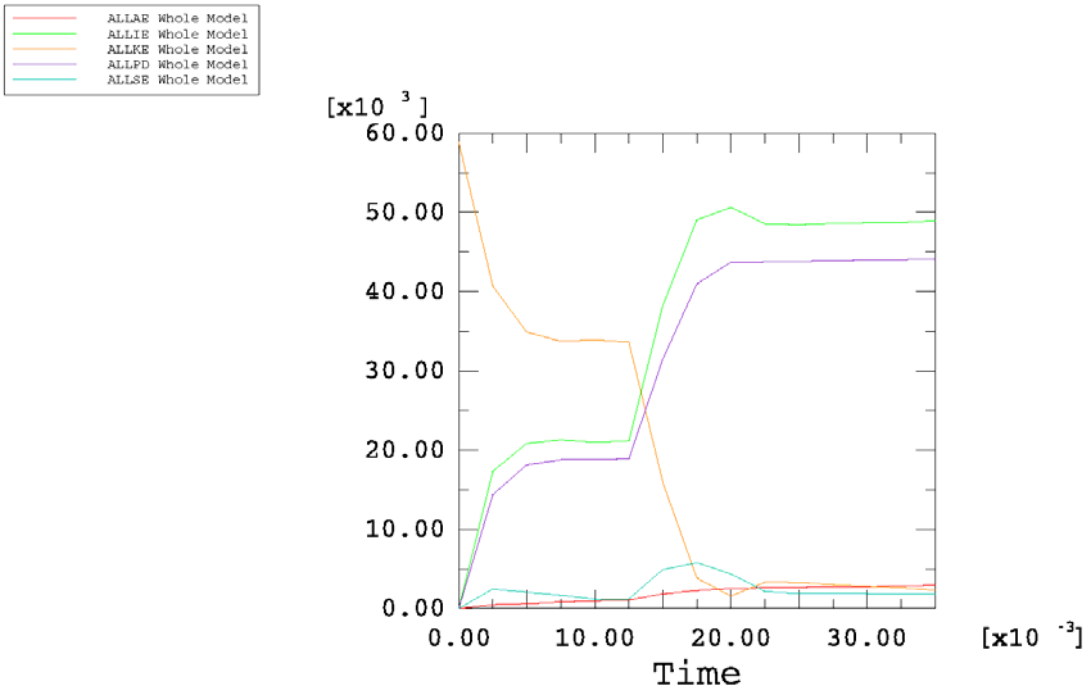

Figure 169 - Time-History Plot of Energy during 15º Slap Down - 30-ft Drop onto Drum Bottom Simulation (300 ºF)

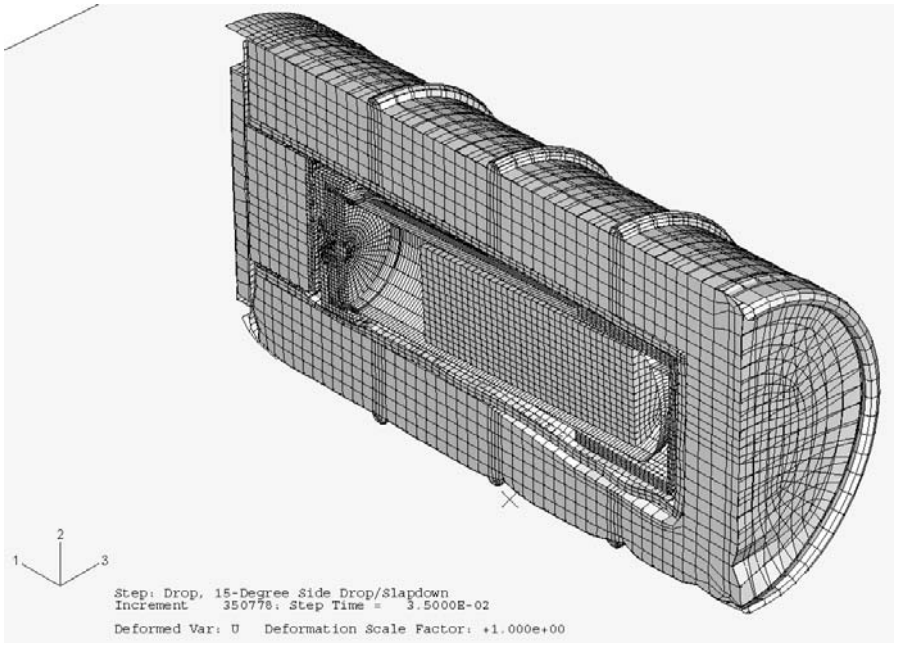

Figure 170 - Deformed Shape of 9977 with 6CV After the 15º Slap Down - 30-ft Drop onto Drum Bottom (300 ºF)

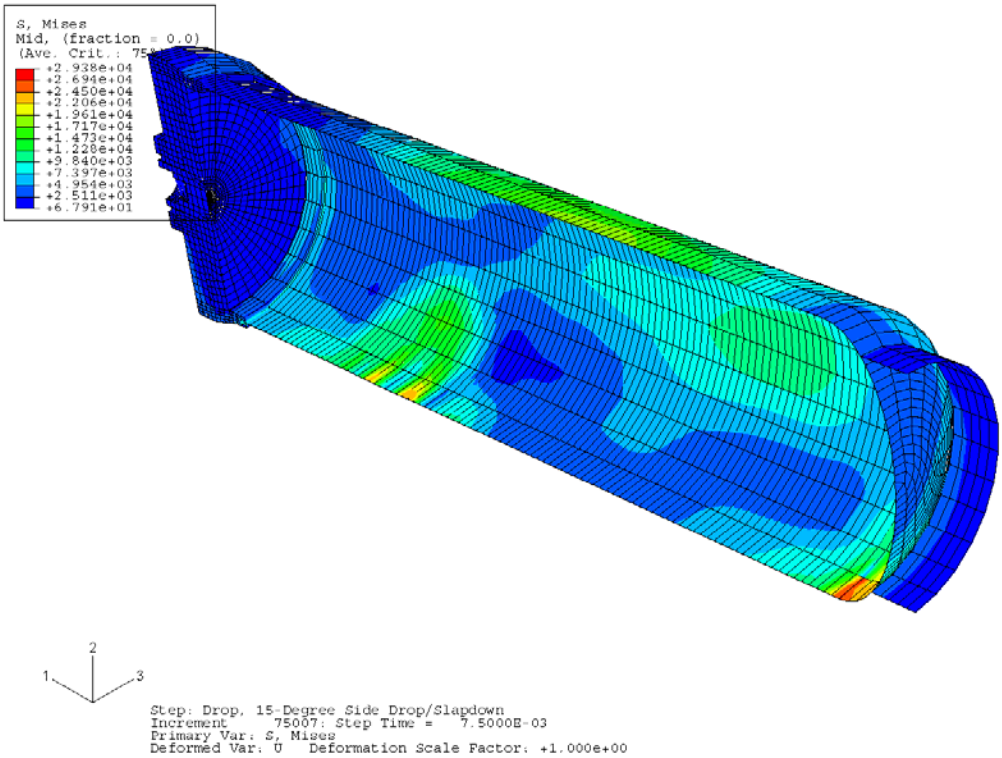

Figure 171 - Stress Distribution in the 6CV Model for 15º Slap Down - 30-ft Drop onto Drum Bottom (300 ºF)

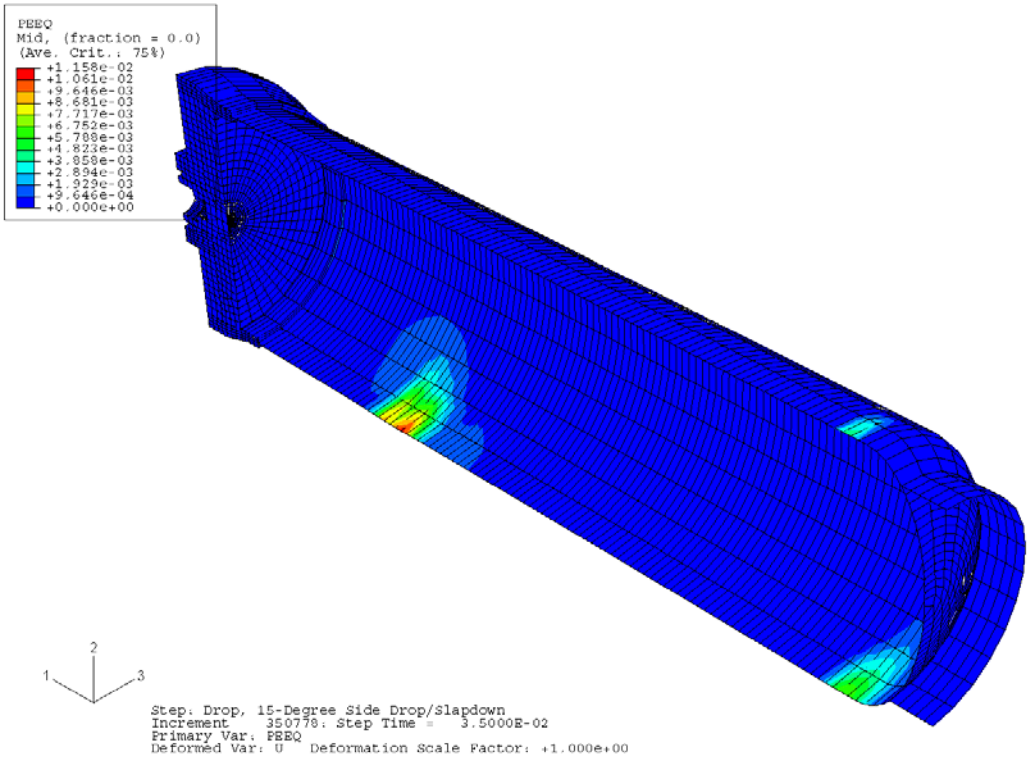

Figure 172 - Strain Distribution in 6CV Model for 15º Slap Down - 30-ft Drop onto Drum Bottom (300 ºF)

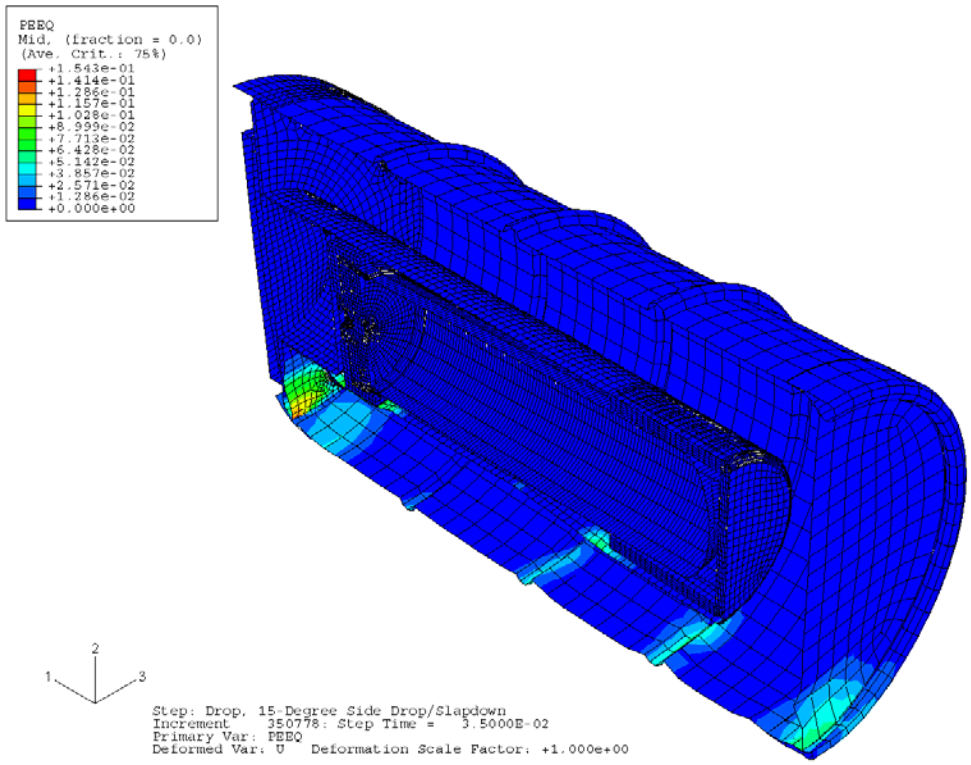

Figure 173 - Strain Distribution in Overpack for 6CV for 15º Slap Down - 30-ft Drop onto Drum Bottom (300ºF)

7.8 Side Drop Followed by Side Crush with 5CV (weight in middle)(-20, 140 and 300 ºF)

Figure 174 shows the finite element model used for evaluating the 30-Ft side drop with the 5CV. The 6CV crush was considered to bound the 5CV side crush and none were analyzed.

7.8.1 Case 1: Drum on Side - 30-ft Drop with Weight in the Middle of 5CV (-20 ºF)

Energy History

The time-history plots of energy components for the 30-ft side drop simulation shown in Figure 175 indicate that the kinetic energy approaches zero at the end of the analysis. Therefore, we know that the analysis covers the entire impact duration.

Deformed Shape of Full Model

Figure 176 is the deformed shape of the overall model.

Stress and Strain Contours in Component Models

Figures 177 and 178 show the von Mises stresses and the equivalent plastic strains in the CV model. Figure 179 shows the equivalent plastic strains in the overpack shell.

Evaluations of Maximum Local Primary Membrane Stress Intensities and Maximum Equivalent Plastic Strains in Containment Vessel

The stress components across the wall thickness at the locations away from or near the geometrical discontinuities should be used to calculate the general primary membrane stress intensities (P_m) or the local primary membrane stress intensities (P_L). For simplicity, the maximum value of the von Mises stresses in the containment vessel is used as the local primary membrane stress intensity (P_L). This value is higher than the actual local primary membrane stress intensity because the latter is calculated by averaging the thru-wall stresses across the component's thickness.

The maximum value of the local primary membrane stress intensity in the containment vessel is 44.31 ksi as given in Figure 177. This value is less than the allowable value of 57.3 ksi for the general primary membrane stress intensity and of 73.6 ksi for the local primary membrane stress intensity (as given in Section 6.0). The structural integrity of the 9977 subjected to a 30-ft drop has therefore been justified according to the ASME Code, Section III.

As shown in Figure 178, the maximum plastic strain experienced at any location within the containment vessel after the 30-ft drop is 1.53%. The maximum calculated value of the effective plastic strain at any point in the overpack is 17.57%. This value is less than the maximum average through-wall elongation of 35% for the 304L material use in the drum. Therefore, the drum will not be ruptured by the 30-ft drop impact.

7.8.2 Case 2: Drum on Side - Crush with weight in the Middle of 5CV (-20 °F)

Energy History

Figure 180 depicts the kinetic energy variation of the plate during the 30-ft fall. The plot indicates that the kinetic energy approaches zero before the end of the analysis. Therefore, we know that the analysis covers the entire impact duration.

Deformed Shape of Full Mode

Figure 181 shows the deformed shape of the overall model.

Stress and Strain Contours in Component Models

Figures 182 and 183 show the von Mises stresses and the equivalent plastic strains in the CV model. Figure 184 shows the equivalent plastic strains in the overpack shell.

Evaluations of Maximum Local Primary Membrane Stress Intensities and Maximum Equivalent Plastic Strains in Containment Vessel

The stress components across the wall thickness at the locations away from or near the geometrical discontinuities should be used to calculate the general primary membrane stress intensities (P_m) or the local primary membrane stress intensities (P_L). For simplicity, the maximum value of the von Mises stresses in the containment vessel is used as the local primary membrane stress intensity (P_L). This value is higher than the actual local primary membrane stress intensity because the latter is calculated by averaging the thru-wall stresses across the component's thickness.

The maximum value of the local primary membrane stress intensity in the containment vessel is 53.81 ksi as shown in Figure 182. This value is less than the allowable value of 57.3 ksi for the general primary membrane stress intensity and of 73.6 ksi for the local primary membrane stress intensity (as given in Section 6.0). The structural integrity of the 9977 subjected to a crush has therefore been justified according to the ASME Code, Section III.

As shown in Figure 183, the maximum plastic strain experienced at any location within the containment vessel after the crush is 10.59%. The maximum calculated value of the effective plastic strain at any point in the overpack is 37.39%. While this value is slightly greater than the minimum specified uniform elongation of 35% for the 304L material used in the drum, this compressive strain is restricted to an extremely small area at a bolt hole in the drum top plate and has no effect on the drum performance. The drum will not be ruptured by the crush impact.

Case 3: Drum on Side - 30-ft Drop with Weight in the Middle of 5CV (300 °F)

Energy History

The time-history plots of energy components for the 30-ft side drop simulation shown in Figure 185 indicate that the kinetic energy approaches zero at the end of the analysis. Therefore, we know that the analysis covers the entire impact duration.

Deformed Shape of Full Model

Figure 186 is the deformed shape of the overall model.

Stress and Strain Contours in Component Models

Figures 187 and 18893 show the von Mises stresses and the equivalent plastic strains in the CV model. Figure 189 shows the equivalent plastic strains in the overpack shell.

Evaluations of Maximum Local Primary Membrane Stress Intensities and Maximum Equivalent Plastic Strains in Containment Vessel

The stress components across the wall thickness at the locations away from or near the geometrical discontinuities should be used to calculate the general primary membrane stress intensities (P_m) or the local primary membrane stress intensities (P_L). For simplicity, the maximum value of the von Mises stresses in the containment vessel is used as the local primary membrane stress intensity (P_L). This value is higher than the actual local primary membrane stress intensity because the latter is calculated by averaging the thru-wall stresses across the component's thickness.

The maximum value of the local primary membrane stress intensity in the containment vessel is 43.97 ksi as given in Figure 192. This value is less than the allowable value of 57.3 ksi for the general primary membrane stress intensity and of 73.6 ksi for the local primary membrane stress intensity (as given in Section 6.0). The structural integrity of the 9977 subjected to a 30-ft drop has therefore been justified according to the ASME Code, Section III.

As shown in Figure 188, the maximum plastic strain experienced at any location within the containment vessel after the 30-ft drop is 1.34%. The maximum calculated value of the effective plastic strain at any point in the overpack is 19.58%. This value is less than the minimum specified uniform elongation of 35% for the 304L material used in the drum. Therefore, the drum will not be ruptured by the 30-ft drop impact.

7.8.3 Case 4: Drum on Side - Crush with weight in the Middle of 5CV (300 ºF)

Energy History

Figure 190 depicts the kinetic energy variation of the plate during the 30-ft fall. Therefore, we know that the analysis covers the entire impact duration.

Deformed Shape of Full Mode

Figure 191 shows the deformed shape of the overall model.

Stress and Strain Contours in Component Models

Figures 192 and 193 show the von Mises stresses and the equivalent plastic strains in the containment vessel and its internal components. Figure 194 shows the equivalent plastic strains in the overpack shell.

Evaluations of Maximum Local Primary Membrane Stress Intensities and Maximum Equivalent Plastic Strains in Containment Vessel

The maximum value of the local primary membrane stress intensity in the containment vessel is 44.77 ksi as shown in Figure 192. This value is less than the allowable value of 57.3 ksi for the general primary membrane stress intensity and of 73.6 ksi for the local primary membrane stress

intensity (as given in Section 6.0). The structural integrity of the 9977 subjected to a crush has therefore been verified according to the ASME Code, Section III.

As shown in Figure 193, the maximum plastic strain experienced at any location within the containment vessel after the crush is 1.61%. The maximum calculated value of the effective plastic strain at any point in the overpack is 58.11%. This value is less than the minimum specified uniform elongation of 35% for the 304L material used in the drum. Therefore, the drum will not be ruptured by the crush impact.

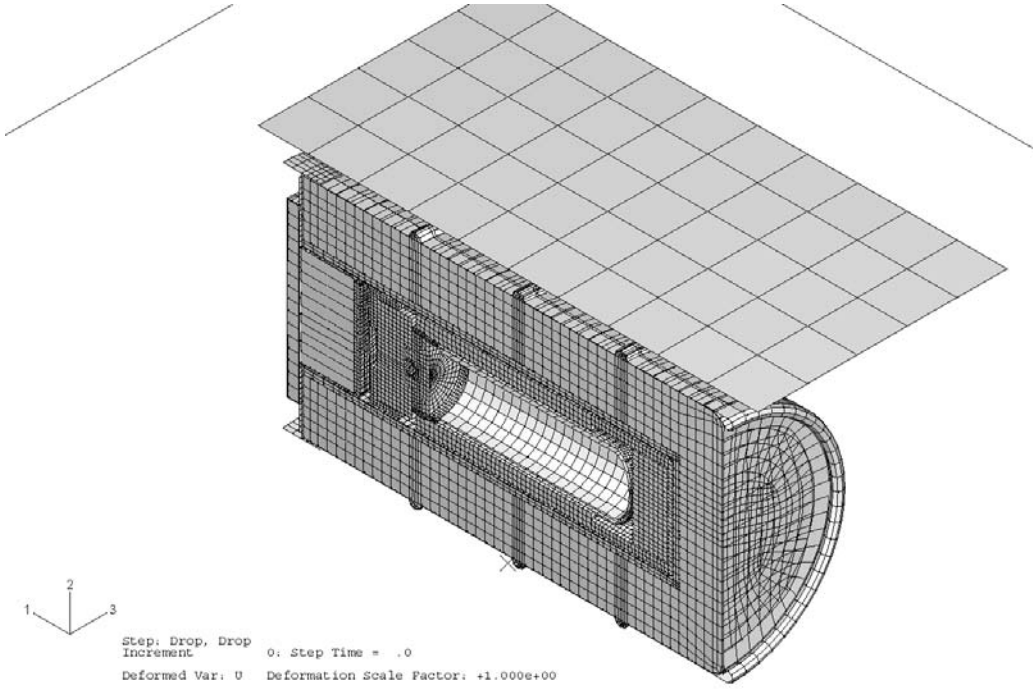

Figure 174 - Finite Element Model of the 9977 Side Drop with 5CV

(ALLKE = kinetic energy; ALLIE = internal energy; ALLPD = plastic strain energy; ALLSE = elastic strain energy; ALLAE = artificial energy)

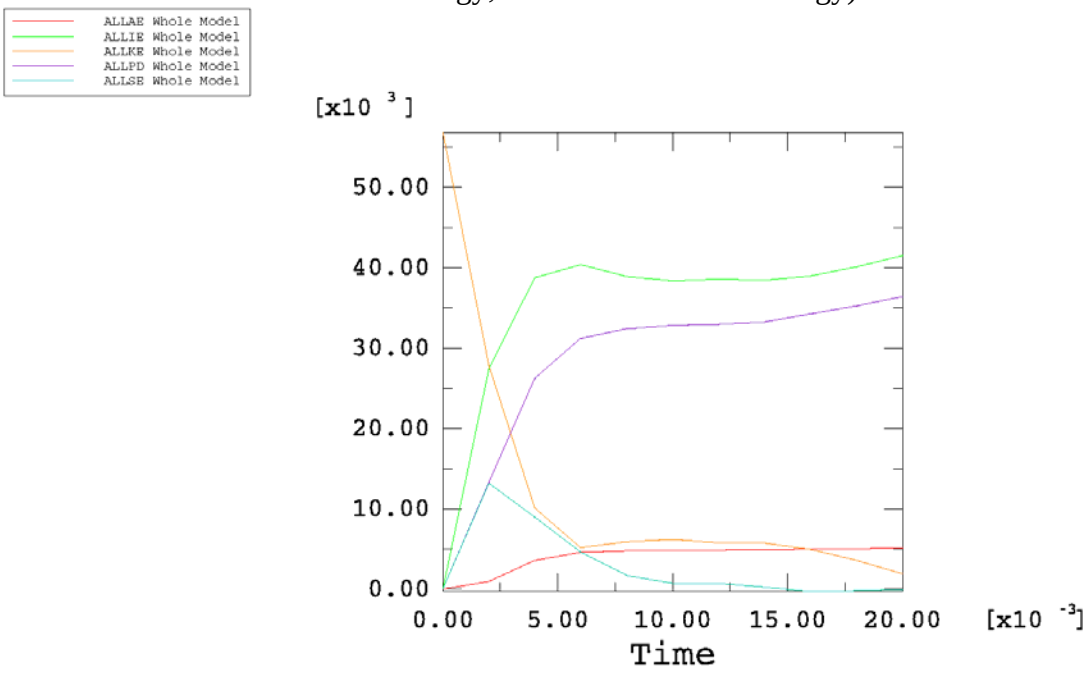

Figure 175 - Time-History Plot of Energy during the 30 foot Side Drop simulation with 5CV (-20 ºF)(Weight in Middle of CV)

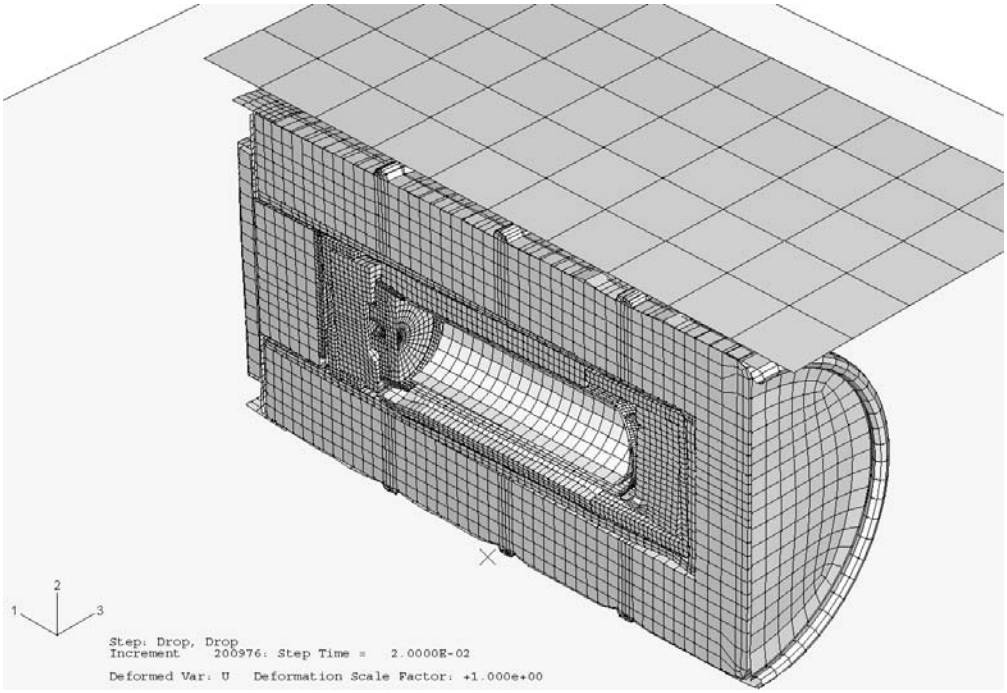

Figure 176 - Deformed Shape of 9977 with 5CV After Drum on Side - 30-ft Side Drop (-20 ºF)(Weight in Middle of CV)

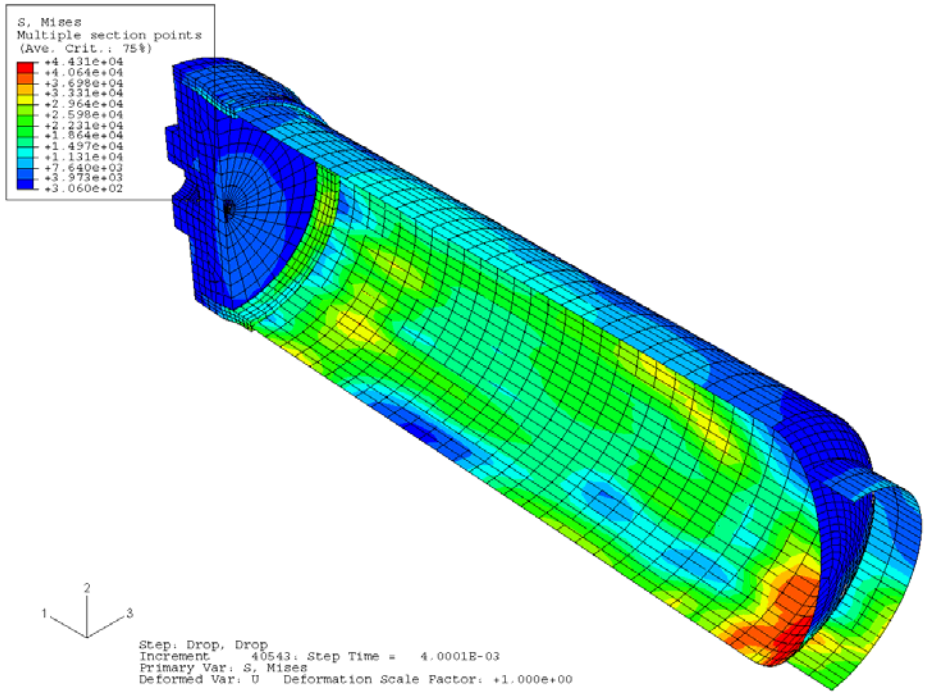

Figure 177 - Stress Distribution in the 5CV Model for Drum on Side - 30-ft Drop (-20 ºF)(Weight in Middle of CV)

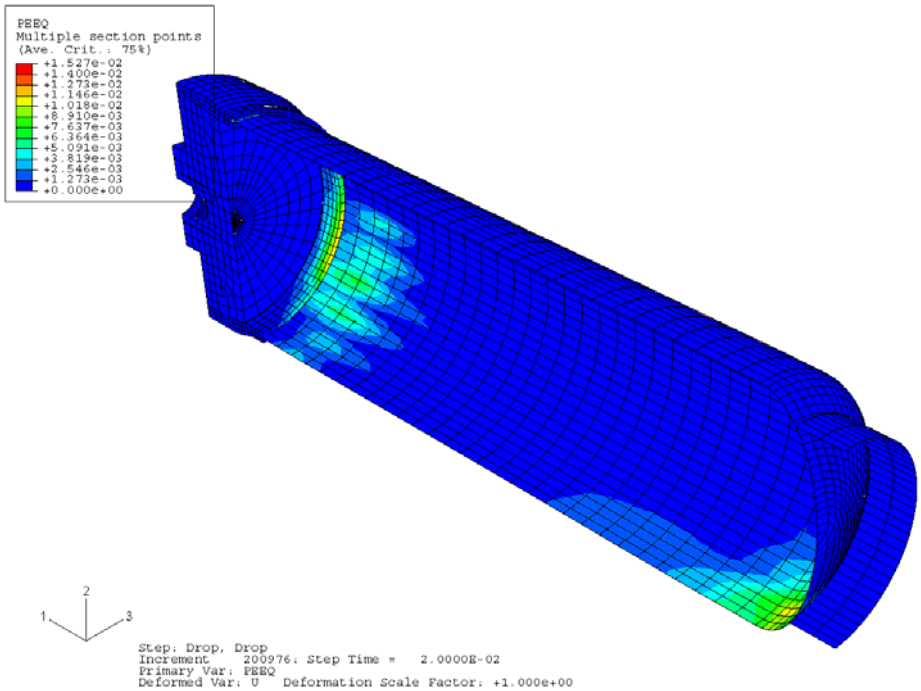

Figure 178 - Strain Distribution in 5CV Model for Drum on Side - 30-ft Drop (-20 ºF)(Weight in Middle of CV)

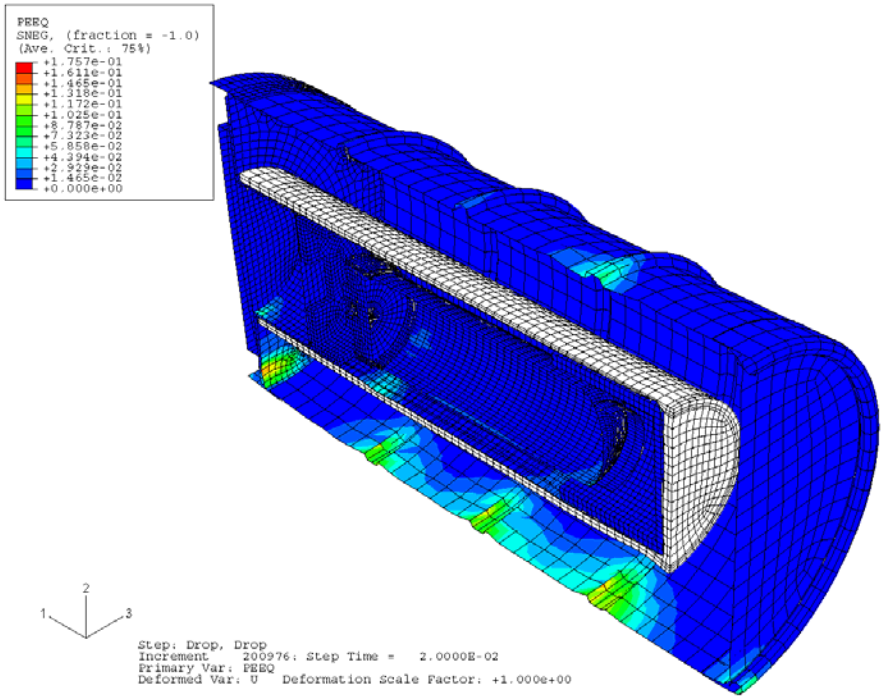

Figure 179 - Strain Distribution in Overpack for 5CV Model Drum on Side - 30-ft Drop (-20 ºF)(Weight in Middle of CV)

(ALLKE = kinetic energy; ALLIE = internal energy; ALLPD = plastic strain energy; ALLSE = elastic strain energy; ALLAE = artificial energy)

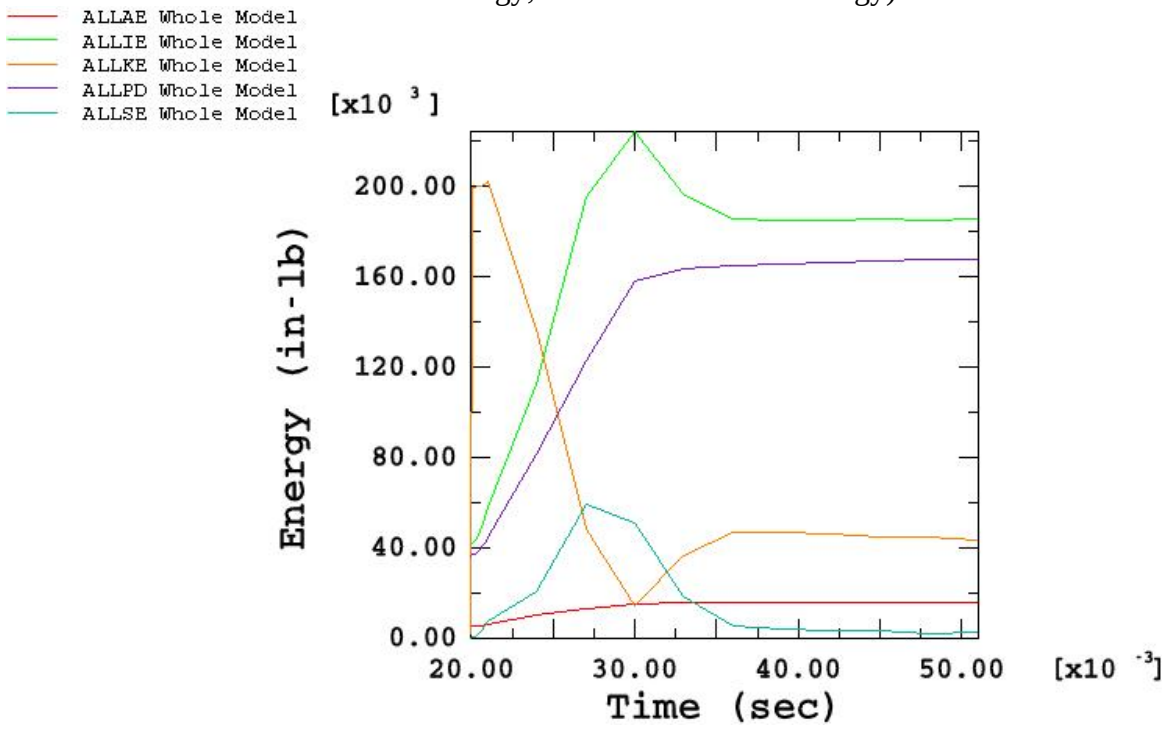

Figure 180 - Time-History Plot of Plate Energy during the 30 ft Side Drop simulation with 5CV (-20 ºF)

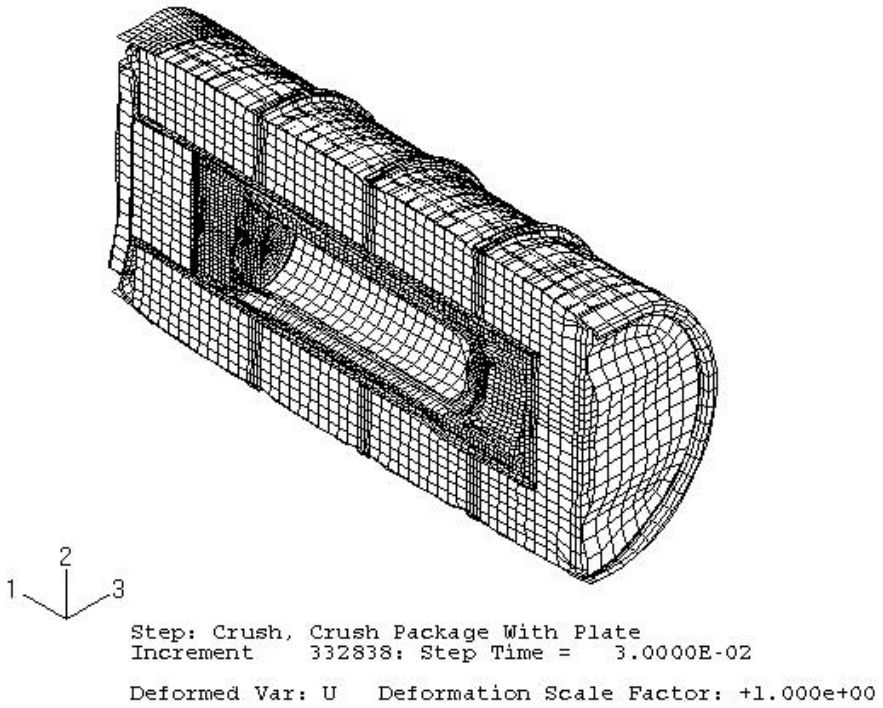

Figure 181 - Deformed Shape of 9977 with 6CV for Drum on Side - Crush (-20 ºF)(weight in middle of CV)

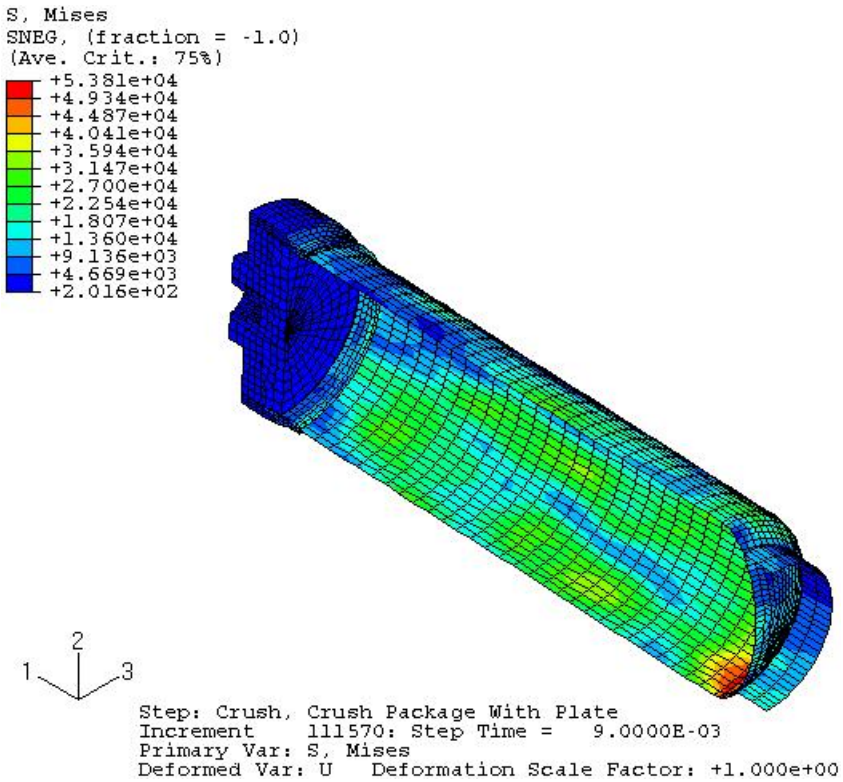

Figure 182 - Stress Distribution in 5CV Model for Drum on Side - Crush (-20 ºF)(weight in middle of CV)

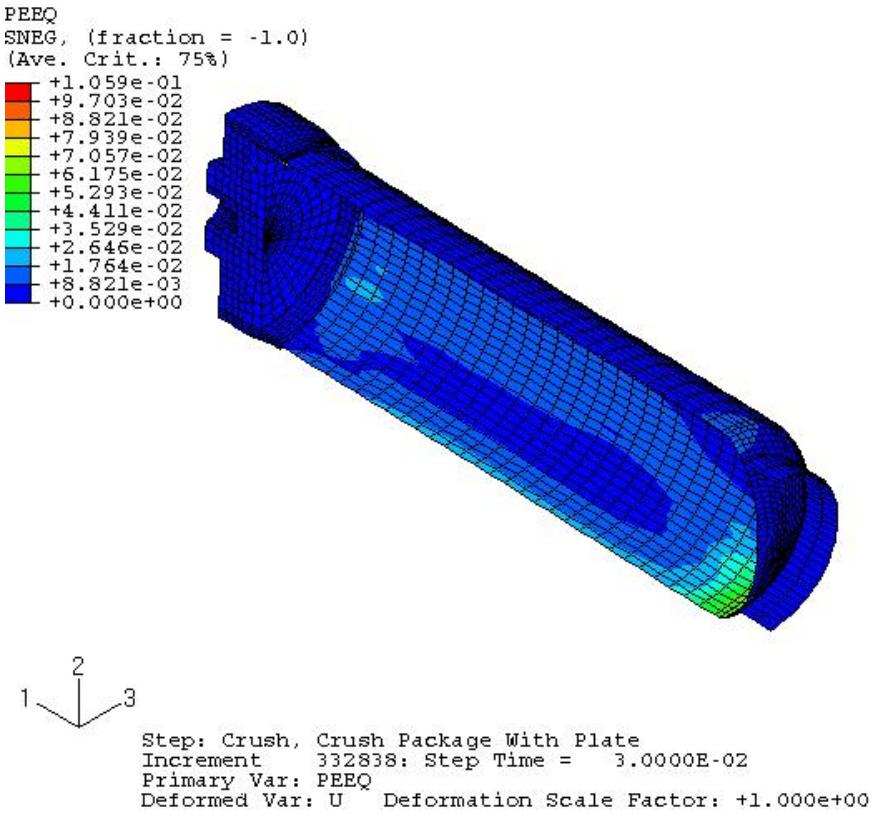

Figure 183 - Strain Distribution in 6CV Model for Drum on Side - Crush (-20 ºF)(weight in middle of CV)

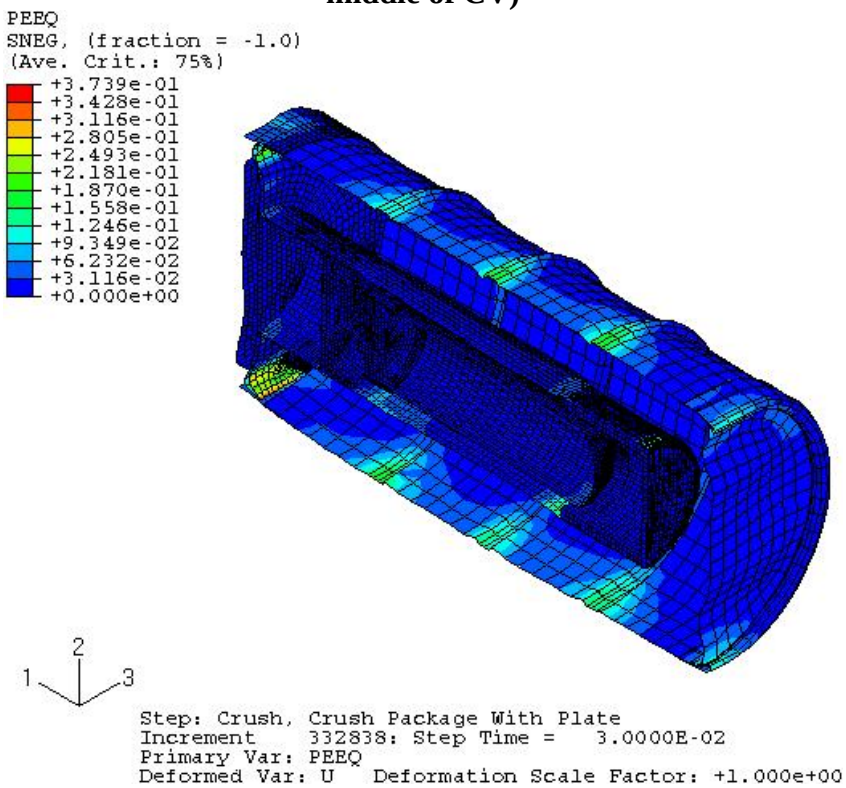

Figure 184 - Strain Distribution in Overpack for Drum on Side - Crush (-20 ºF)(weight in middle of CV)

(ALLKE = kinetic energy; ALLIE = internal energy; ALLPD = plastic strain energy; ALLSE = elastic strain energy; ALLAE = artificial energy)

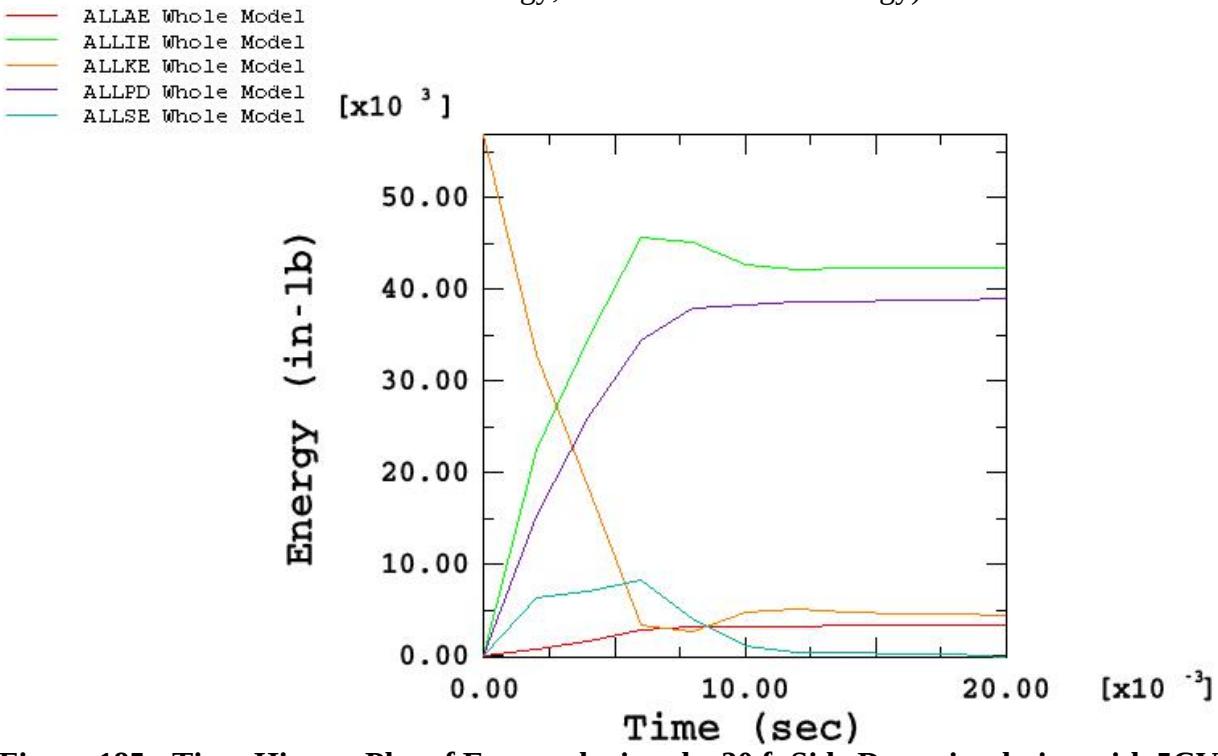

Figure 185 - Time-History Plot of Energy during the 30 ft Side Drop simulation with 5CV (300 ºF)

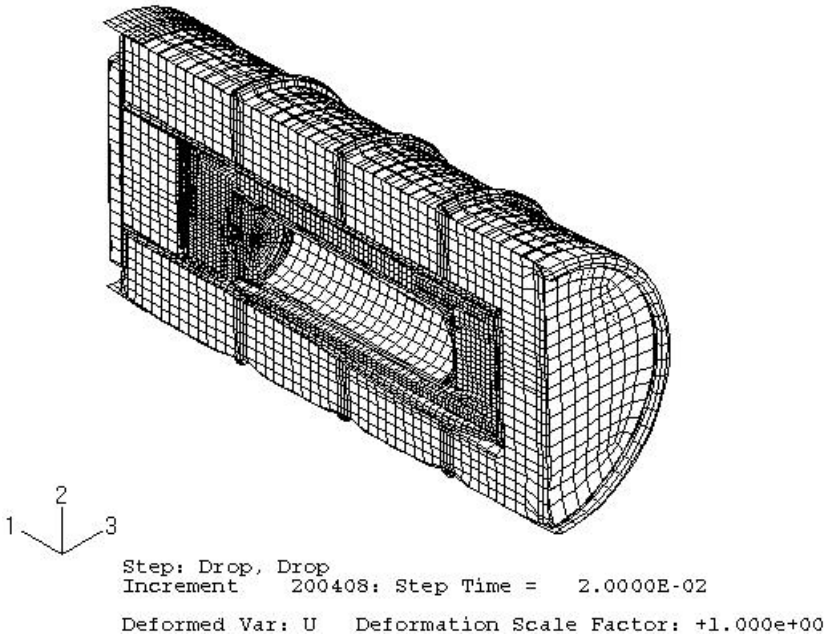

Figure 186 - Deformed Shape of 9977 with 6CV for Drum on Side - 30-ft Drop (300 ºF)(weight in middle of CV)

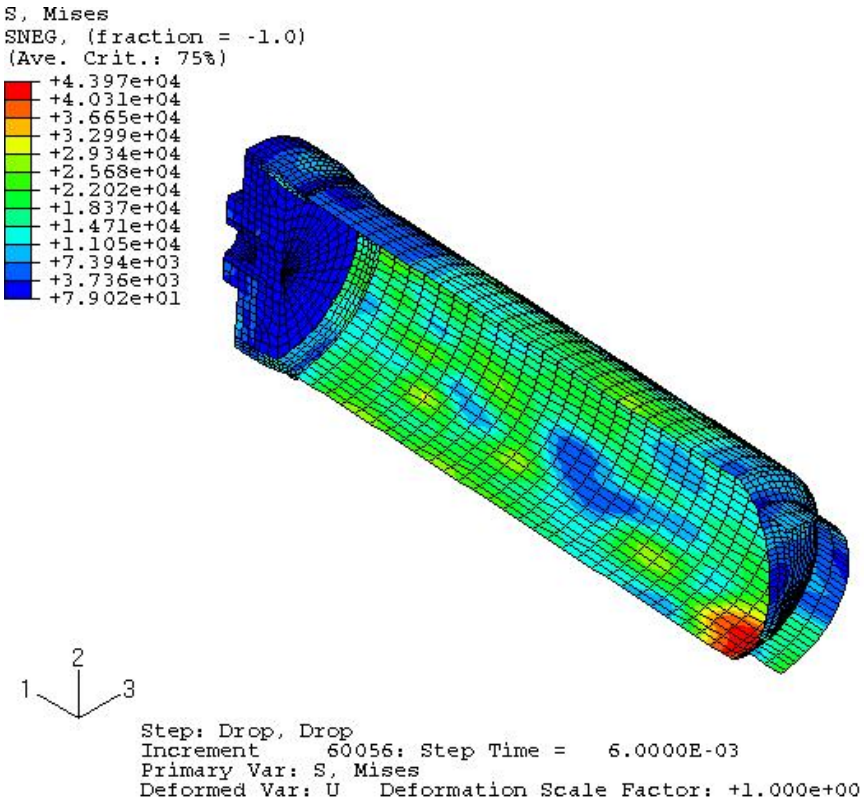

Figure 187 - Stress Distribution in 5CV Model for Drum on Side - Crush (300 ºF)(weight in middle of CV)

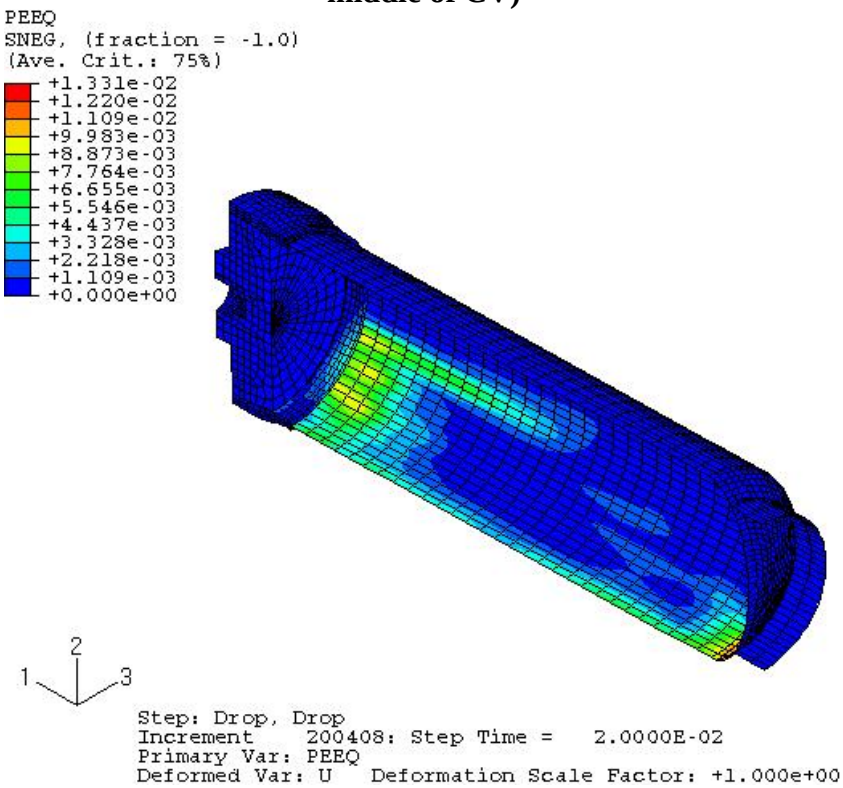

Figure 188 - Strain Distribution in 6CV Model for Drum on Side - Crush (300 ºF)(weight in middle of CV)

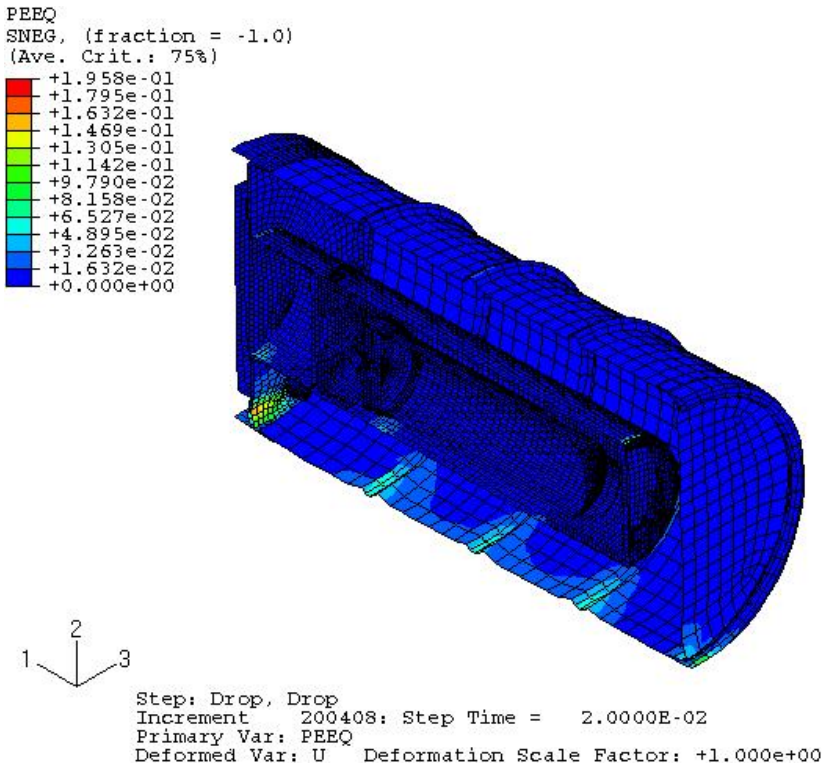

Figure 189 - Strain Distribution in Overpack for 5CV Model Drum on Side - 30-ft Drop (300 ºF)(Weight in Middle of CV)

(ALLKE = kinetic energy; ALLIE = internal energy; ALLPD = plastic strain energy; ALLSE = elastic strain energy; ALLAE = artificial energy)

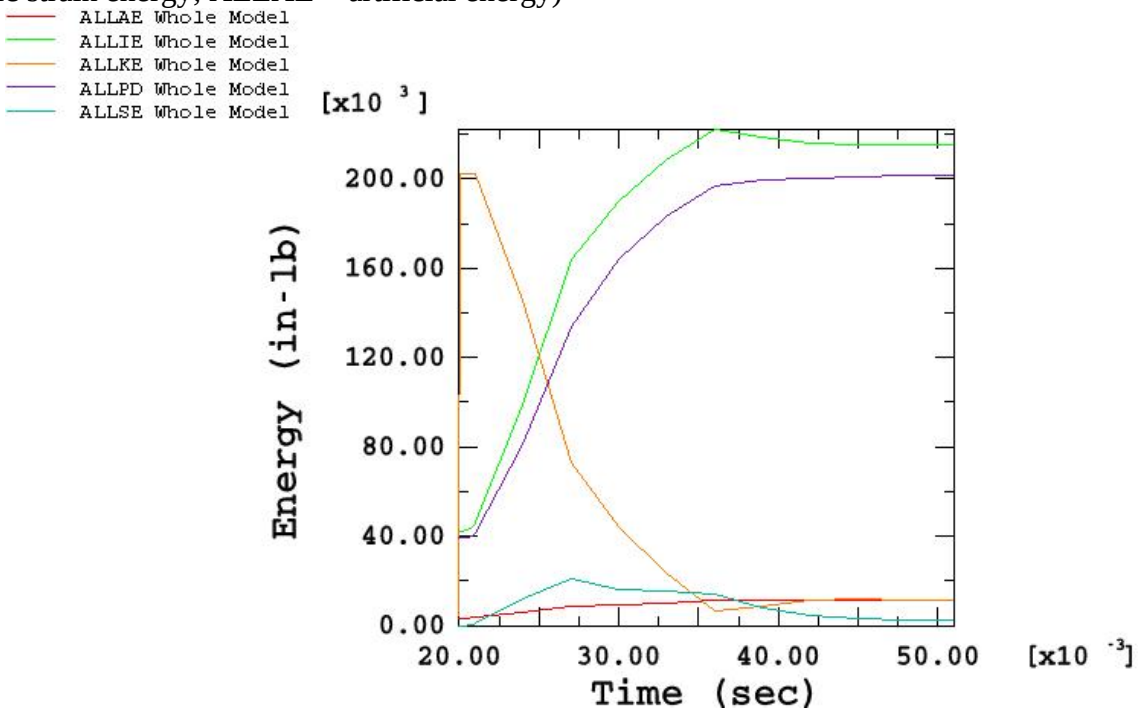

Figure 190 - Time-History Plot of Plate Energy during the 30 ft Side Drop simulation with 5CV (300 ºF)

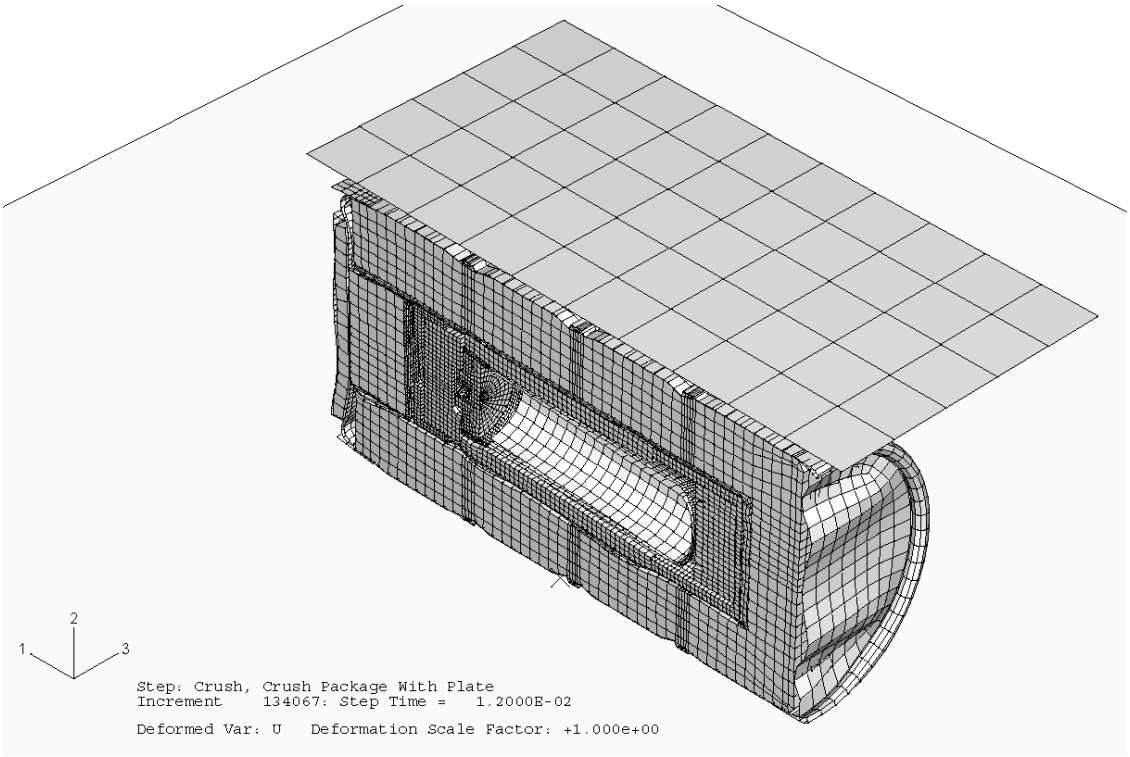

Figure 191 - Deformed Shape of 9977 with 6CV for Drum on Side - Crush (300 ºF)(weight in middle of CV)

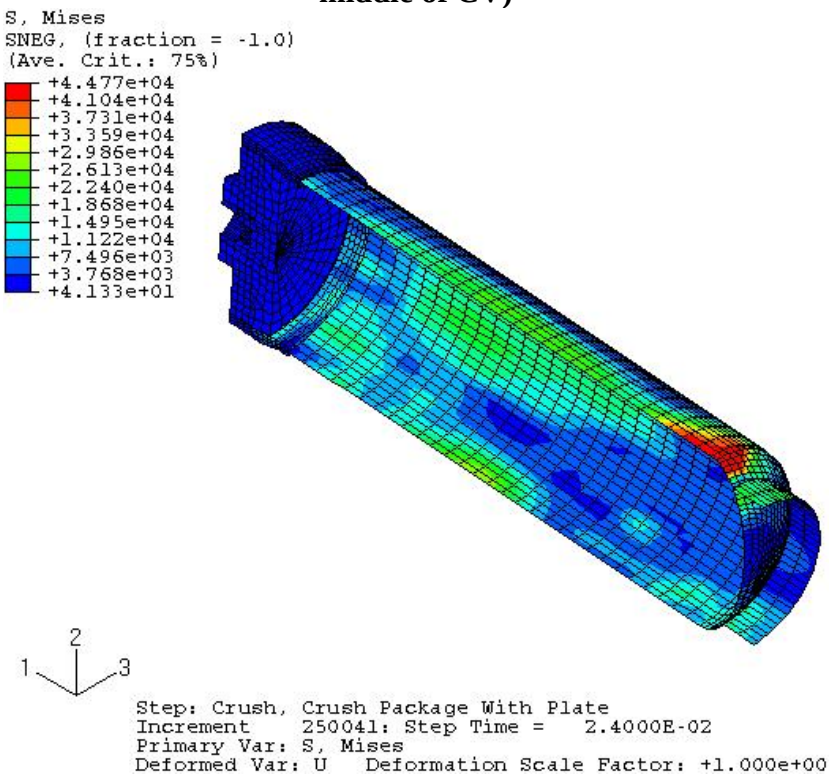

Figure 192 - Stress Distribution in 5CV Model for Drum on Side - Crush (30 °F)(weight in middle of CV)

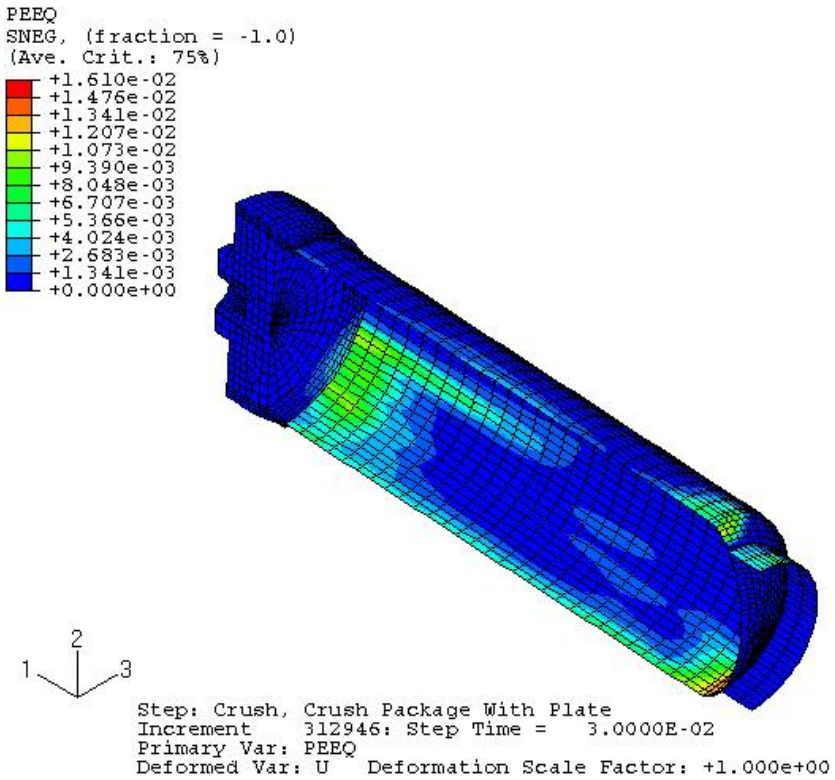

Figure 193 - Strain Distribution in 5CV Model for Drum on Side - Crush (300 ºF)(weight in middle of CV)

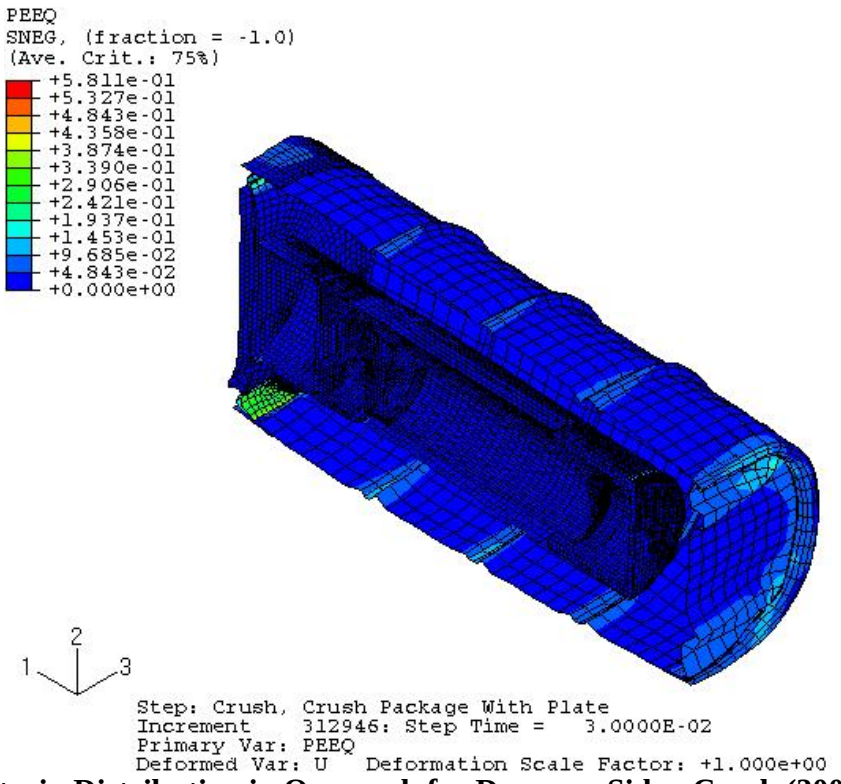

Figure 194 - Strain Distribution in Overpack for Drum on Side - Crush (300 ºF)(weight in middle of CV)

7.9 Center of Gravity over Top Drop with 5CV (75 ºF)

Figure 195 shows the finite element model used for evaluating the 30-ft center of gravity over top corner of the package drop. The Crush was not evaluated as it is considered to be bounded by the 6CV evaluation.

7.9.1 Case 1: Center of Gravity over Top Drop 5CV (75 ºF)

Energy History

The time-history plots of energy components for the 30-ft CGOT drop simulation shown in Figure 196 indicate that the kinetic energy approaches zero at the end of the analysis. Therefore, we know that the analysis covers the entire impact duration.

Deformed Shape of Full Model

Figure 197 is the deformed shape of the overall model.

Stress and Strain Contours in Component Models

Figures 198 and 199 show the von Mises stresses and the equivalent plastic strains in the CV model. Figure 200 shows the equivalent plastic strains in the overpack shell.

Evaluations of Maximum Local Primary Membrane Stress Intensities and Maximum Equivalent Plastic Strains in Containment Vessel

The stress components across the wall thickness at the locations away from or near the geometrical discontinuities should be used to calculate the general primary membrane stress intensities (P_m) or the local primary membrane stress intensities (P_L). For simplicity, the maximum value of the von Mises stresses in the containment vessel is used as the local primary membrane stress intensity (P_L). This value is higher than the actual local primary membrane stress intensity because the latter is calculated by averaging the thru-wall stresses across the component's thickness.

The maximum value of the local primary membrane stress intensity in the containment vessel is 46.00 ksi as given in Figure 198. This value is less than the allowable value of 57.3 ksi for the general primary membrane stress intensity and of 73.6 ksi for the local primary membrane stress intensity (as given in Section 6.0). The structural integrity of the 9977 subjected to a 30-ft drop has therefore been justified according to the ASME Code, Section III.

As shown in Figure 199, the maximum plastic strain experienced at any location within the containment vessel after the 30-ft drop is 2.00%. The maximum calculated value of the effective plastic strain at any point in the overpack is 11.00%. This value is less than the minimum specified uniform elongation of 35% for the 304L material used in the drum. Therefore, the drum will not be ruptured by the 30-ft drop impact.

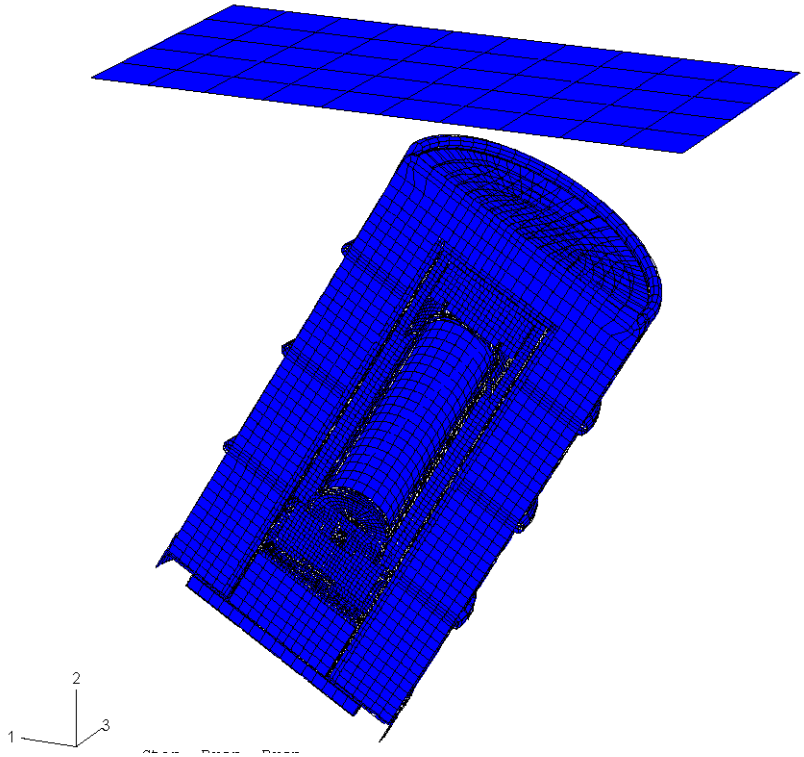

Figure 195 - Finite Element Model of the 9977 CGOT Drop with 5CV

(ALLKE = kinetic energy; ALLIE = internal energy; ALLPD = plastic strain energy; ALLSE = elastic strain energy; ALLAE = artificial energy)

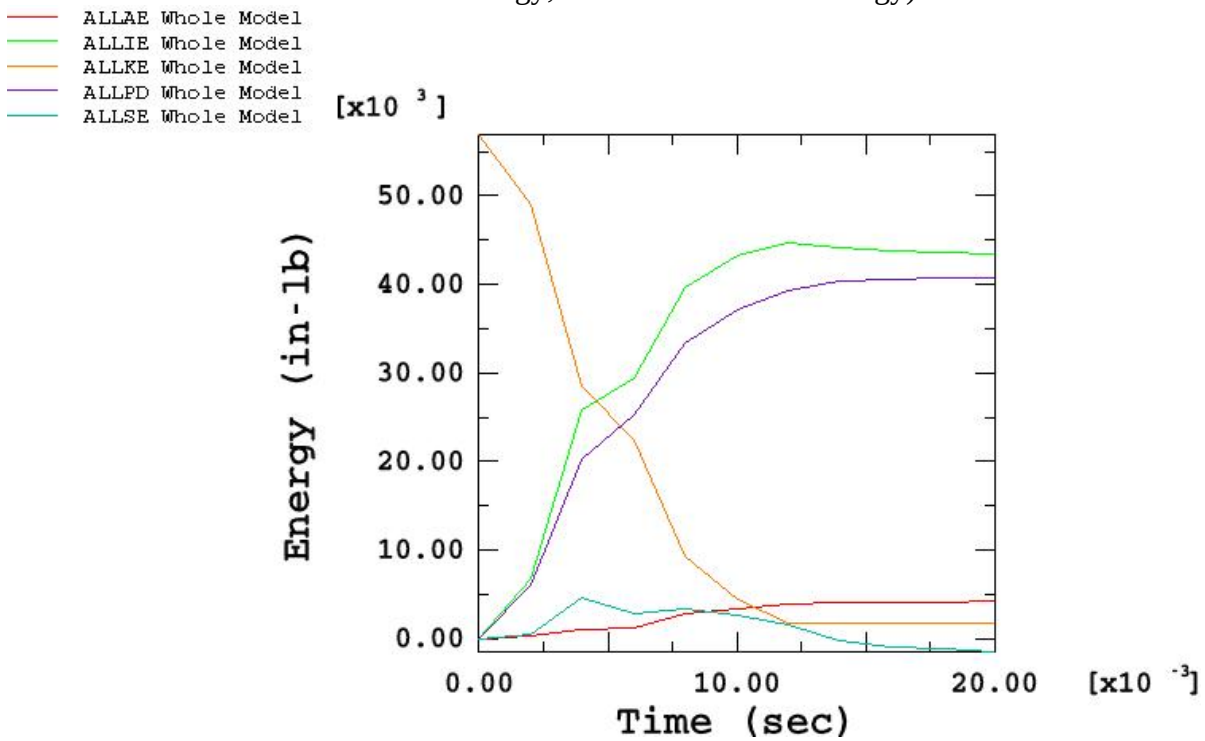

Figure 196 - Time-History Plot of Energy during Drum CGOT - 30-ft Drop Simulation with 5CV (75 ºF)

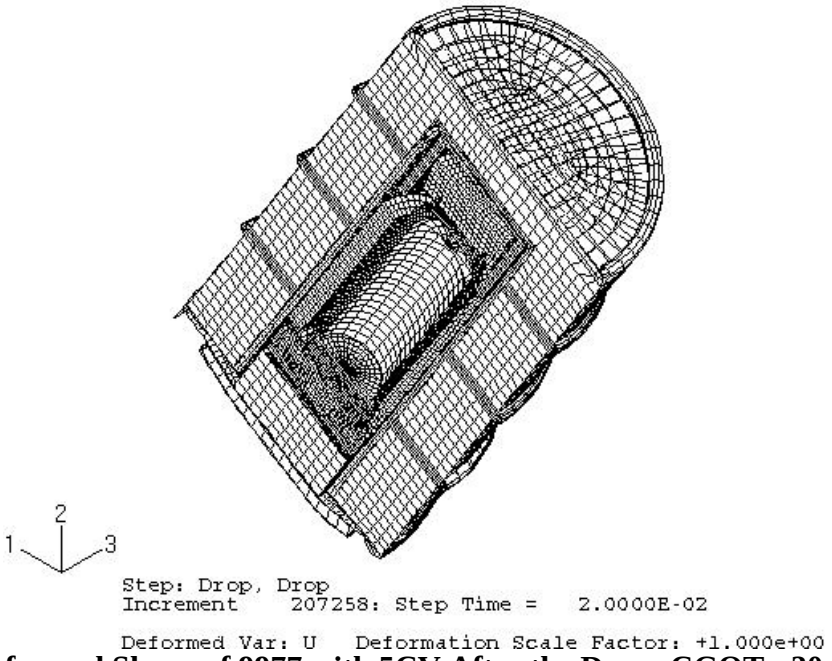

Figure 197 - Deformed Shape of 9977 with 5CV After the Drum CGOT - 30-ft Drop (75 ºF)

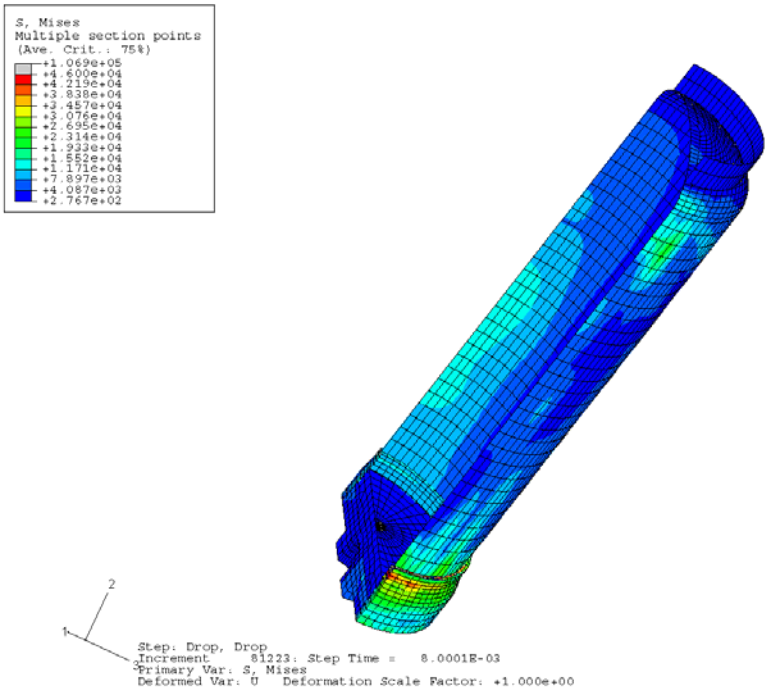

Figure 198 - Stress Distribution in the 5CV Model for Drum CGOT - 30-ft Drop (75 ºF)

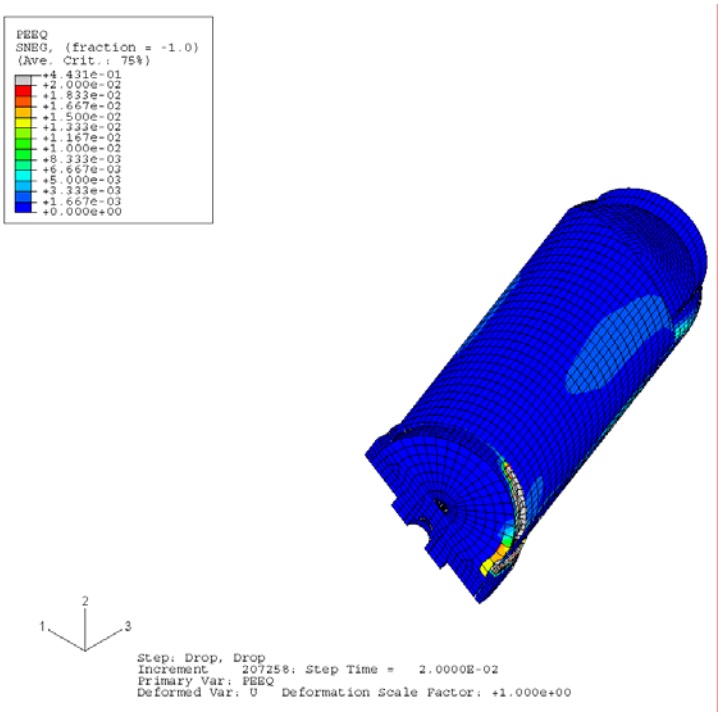

Figure 199 - Strain Distribution in 5CV Model for Drum CGOT - 30-ft Drop (75 ºF)

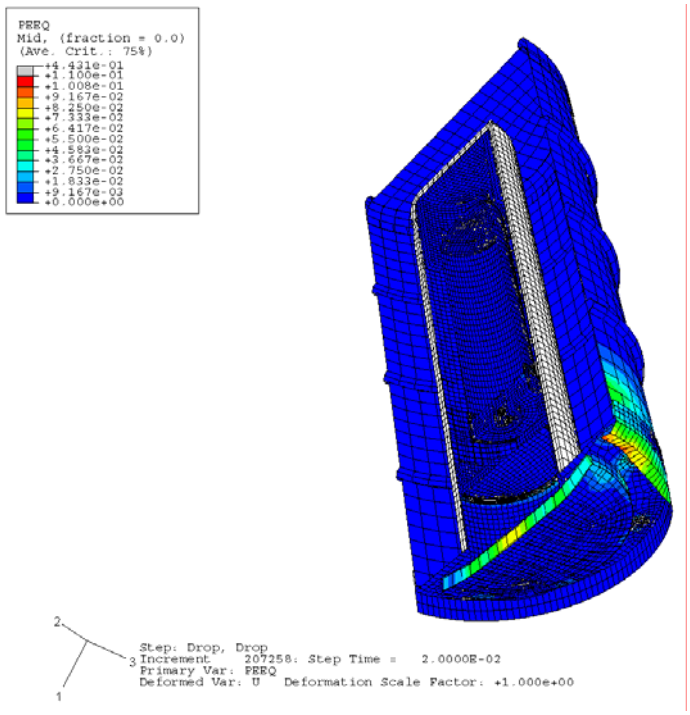

Figure 200 - Strain Distribution in Overpack for 5CV for Drum CGOT - 30-ft Drop (75 ºF)

7.10 15º Slap Down - 30-ft Drop onto Drum Top with Slap onto Bottom with 5CV (-20 ºF)

Figure 201 shows the finite element model used for evaluating the 30-ft slap down 15º bottom down drop.

7.10.1 Case 1: 15º Slap Down - 30-ft Drop onto Drum Top with Slap onto Bottom with 5CV (-20 ºF)

Energy History

The time-history plots of energy components for the 30-ft 15º slap down drop simulation shown in Figure 202 indicate that the kinetic energy approaches zero at the end of the analysis. Therefore, we know that the analysis covers the entire impact duration.

Deformed Shape of Full Model

Figure 203 is the deformed shape of the overall model.

Stress and Strain Contours in Component Models

Figures 204 and 205 show the von Mises stresses and the equivalent plastic strains in the CV model. Figure 206 shows the equivalent plastic strains in the overpack shell.

Evaluations of Maximum Local Primary Membrane Stress Intensities and Maximum Equivalent Plastic Strains in Containment Vessel

The stress components across the wall thickness at the locations away from or near the geometrical discontinuities should be used to calculate the general primary membrane stress intensities (P_m) or the local primary membrane stress intensities (P_L). For simplicity, the maximum value of the von Mises stresses in the containment vessel is used as the local primary membrane stress intensity (P_L). This value is higher than the actual local primary membrane stress intensity because the latter is calculated by averaging the thru-wall stresses across the component's thickness.

The maximum value of the local primary membrane stress intensity in the containment vessel is 45.54 ksi as given in Figure 204. This value is less than the allowable value of 57.3 ksi for the general primary membrane stress intensity and of 73.6 ksi for the local primary membrane stress intensity (as given in Section 6.0). The structural integrity of the 9977 subjected to a 30-ft drop has therefore been justified according to the ASME Code, Section III.

As shown in Figure 205, the maximum plastic strain experienced at any location within the containment vessel after the 30-ft drop is 3.99%. The maximum calculated value of the effective plastic strain at any point in the overpack is 26.23%. This value is less than the maximum average through-wall elongation of 35% for the 304L material use in the drum. Therefore, the drum will not be ruptured by the 30-ft drop impact.

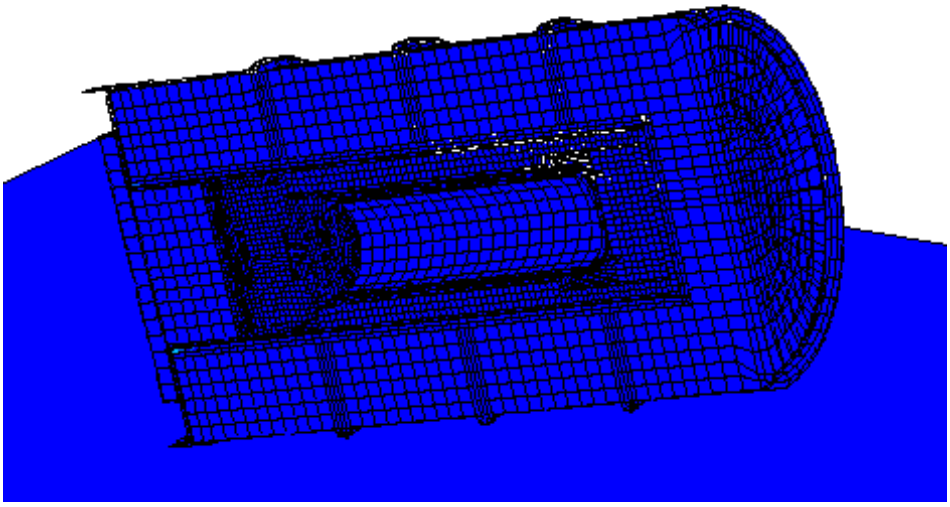

Figure 201 - Finite Element Model of the 9977 with 5CV 15º Slap Down – 30-ft Drop onto Bottom

(ALLKE = kinetic energy; ALLIE = internal energy; ALLPD = plastic strain energy; ALLSE = elastic strain energy; ALLAE = artificial energy)

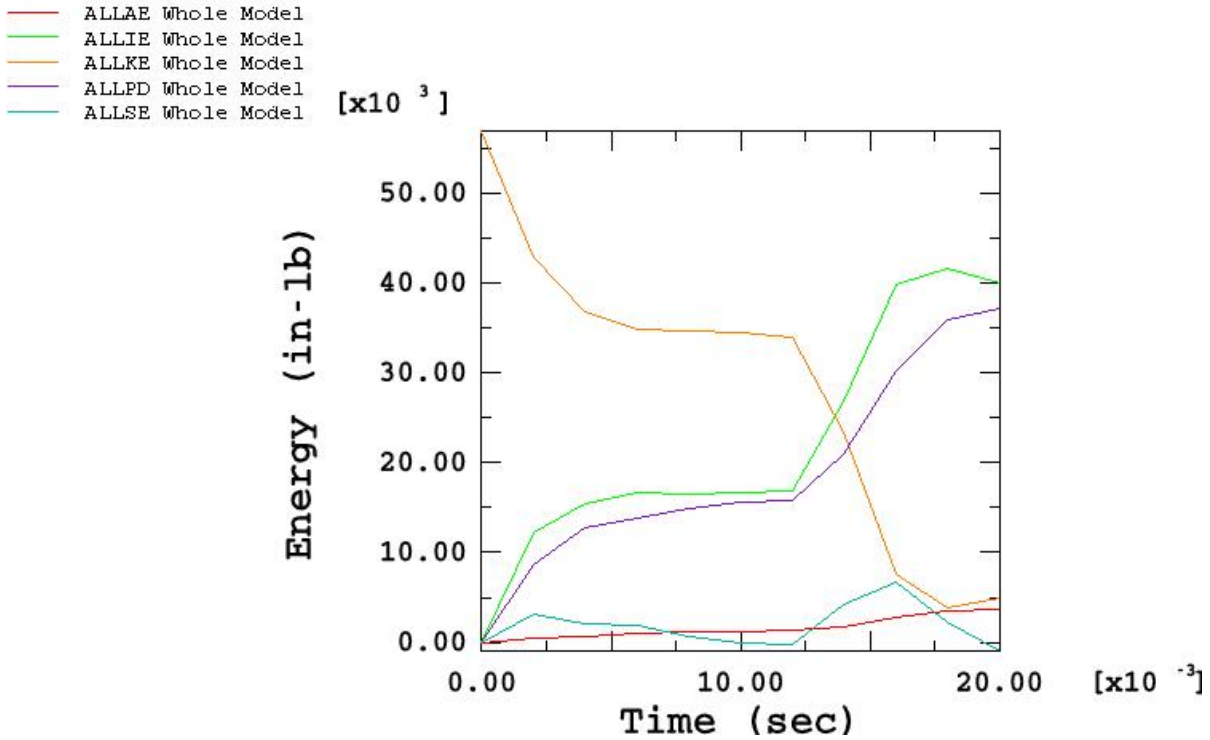

Figure 202 - Time-History Plot of Energy during 15º Slap Down – 30-ft Drop onto Bottom Simulation with 5CV (-20 ºF)

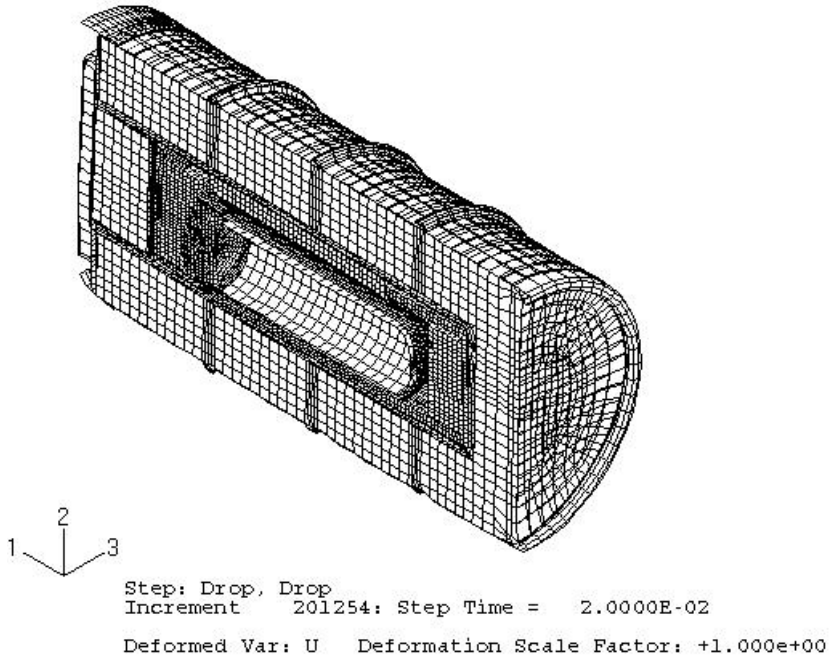

Figure 203 - Deformed Shape of 9977 with 5CV After the 15º Slap Down – 30-ft Drop onto Bottom (-20 ºF)

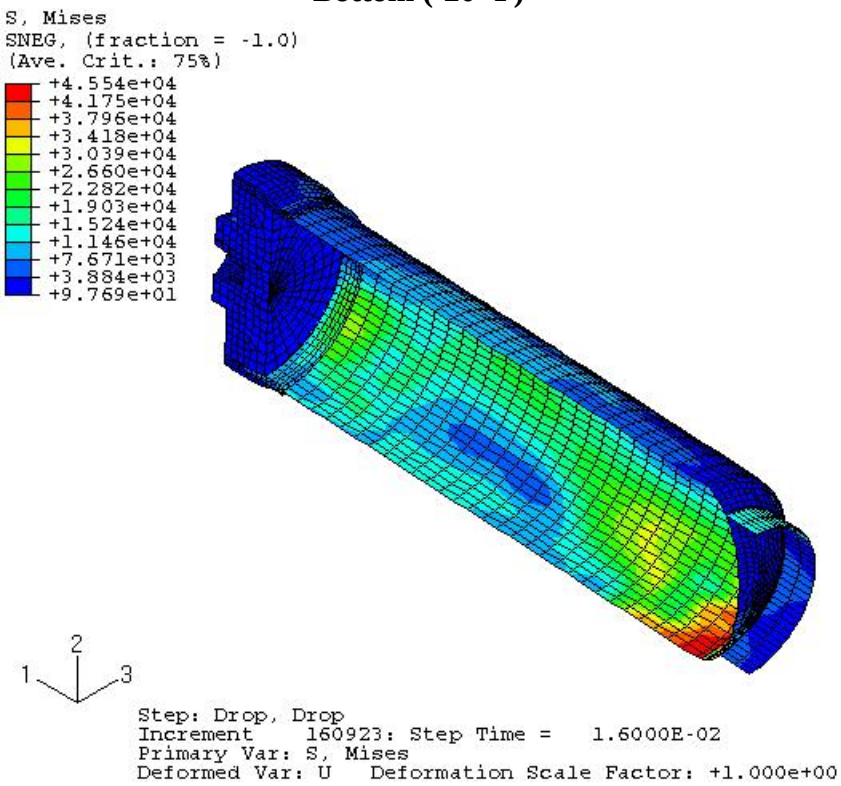

Figure 204 - Stress Distribution in the 5CV Model for 15º Slap Down – 30-ft Drop onto Bottom (-20 ºF)

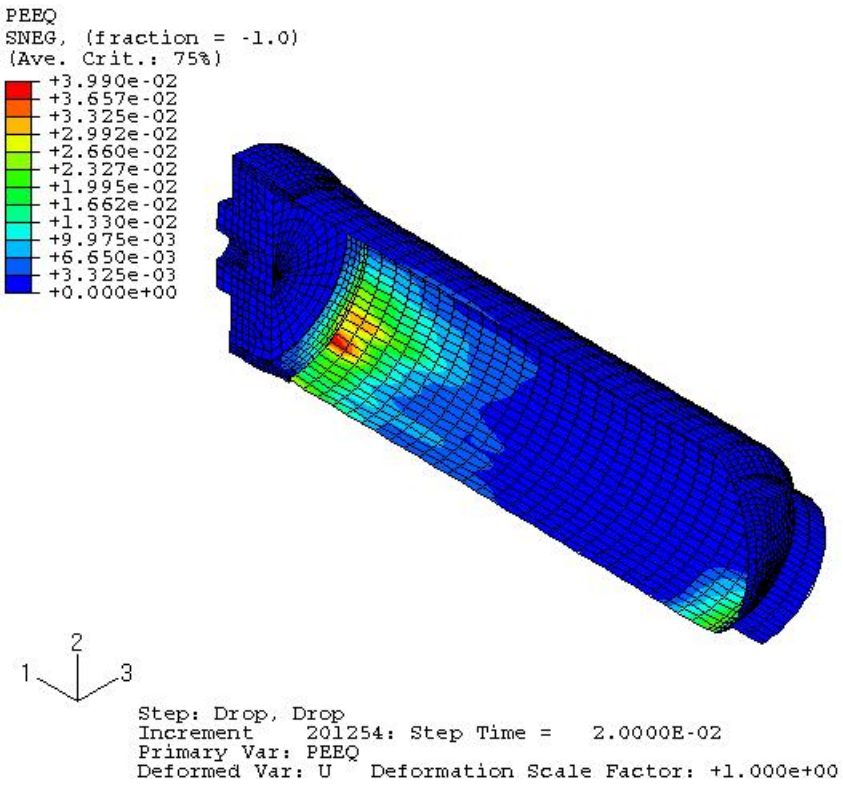

Figure 205 - Strain Distribution in 5CV Model for 15º Slap Down – 30-ft Drop onto Bottom (-20 ºF)

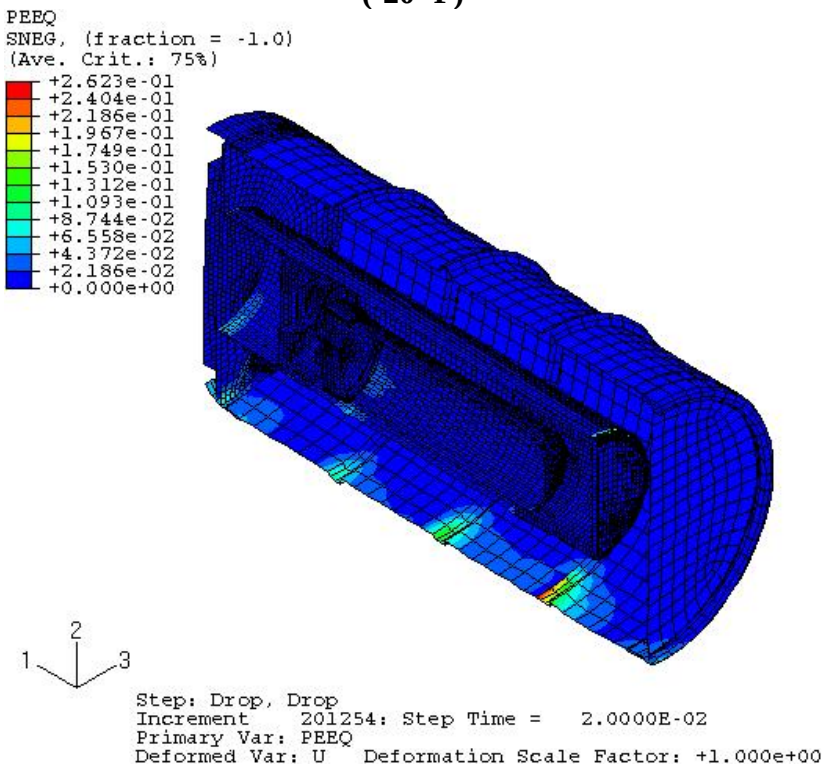

Figure 206 - Strain Distribution in Overpack for 5CV for 15º Slap Down – 30-ft Drop onto Bottom (-20 ºF)

8.0 References

Appendix A

Material Property Data

A.1 Stress-Strain Relationship of Stainless Steel 304L

Figure A1 shows the stress-strain curve of stainless steel 304L (Sindelar).

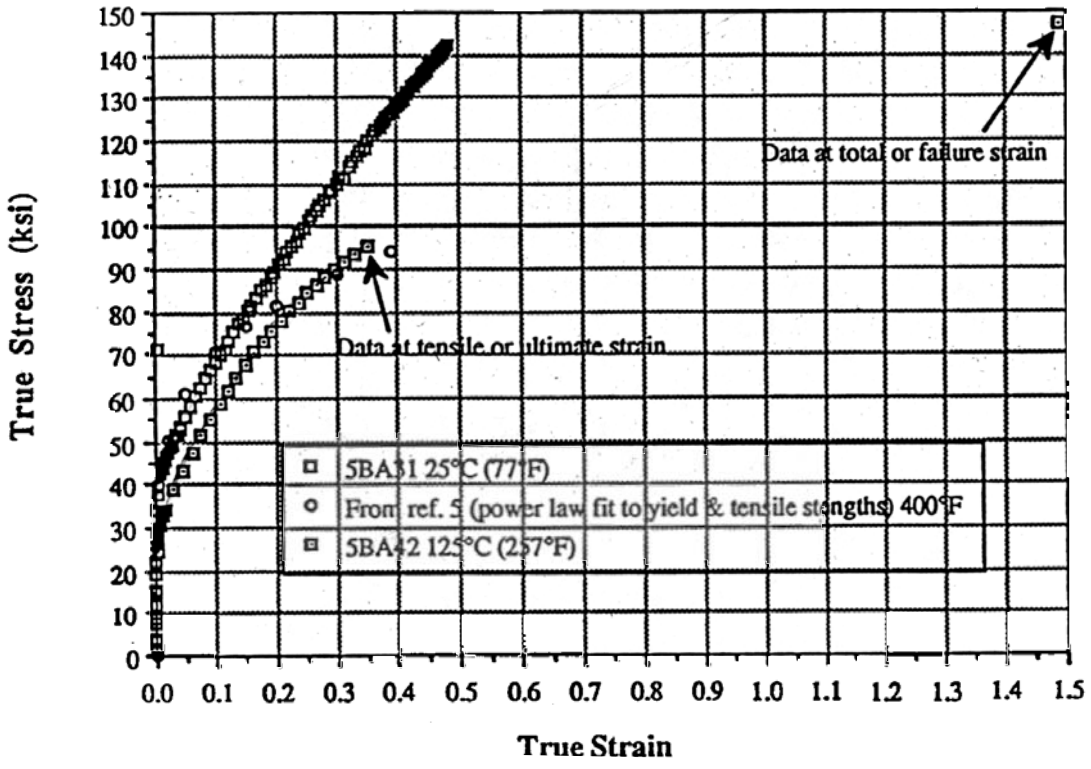

Figure A-1. Stress vs. Strain Curve of Stainless Steel 304L

A.2 Stress-Strain Relationship of Aluminum 6061-T6.

The material properties for aluminum are given as follows.

Nominal yield Stress, σ_y = 32,000.0 psi
Nominal ultimate strength, σ_u = 38,000.0 psi
Uniform elongation to maximum load, $\varepsilon_u = 0.17$
Young's modulus, E = 10.0E6 psi
Poisson ration, ν = 0.33
Density, ρ = 0.098 lb/in^3

From the values given above, we can calculate the following values.

Yield strain, $\varepsilon_y = \frac{\sigma_y}{E} = \frac{3200.0}{10 \times 10^6} = 0.0032$

True ultimate strain, $\varepsilon_{u,t} = \ln(1+\varepsilon_u) = \ln(1+0.17) = 0.157$

True ultimate stress, $\sigma_{u,t} = \sigma_u(\varepsilon_u + 1) = 38000.0(0.17+1) = 44{,}460.0$ psi

Density, $\rho = \frac{0.098\frac{lb}{in^3}}{386.4\frac{in}{\sec^2}} = 2.536 \times 10^{-4}\frac{lb - \sec^2}{in^4}$

The flow curve of aluminum 6061-T6 in the region of uniform plastic deformation can be expressed by the following power curve relation (Reference 9).

$$\sigma_t = K\varepsilon_t^{\,n} \qquad \text{(A-1)}$$

where η is the strain-hardening exponent and K is the strength coefficient; σ_t and ε_t are true stress and true strain, respectively.

At the ultimate strain where metal necking occurs, the following relationship is valid (Reference 9).

$$\varepsilon_{u,t} = \eta \qquad \text{(A-2)}$$

The strength coefficient, K, can be calculated from Equations (A-1) and (A-2) as follows.

$$\sigma_{u,t} = K\varepsilon_{u,t}^{n}$$

$$44{,}460.0 = K(0.157)^{0.157} = 0.74775K$$

Then,

$$K = 59{,}458.0$$

Substituting the values of K and η into Equation (A-1), we obtain the flow curve equation of aluminum 6061-T6 as follows.

$$\sigma_t = 59458\varepsilon_t^{0.157} \qquad \text{(A-3)}$$

Based on the above equation together with the values of Young's modulus and the yield stress, we are able to generate the stress-strain curve of aluminum 6061-T6 as shown in Figure A-2.

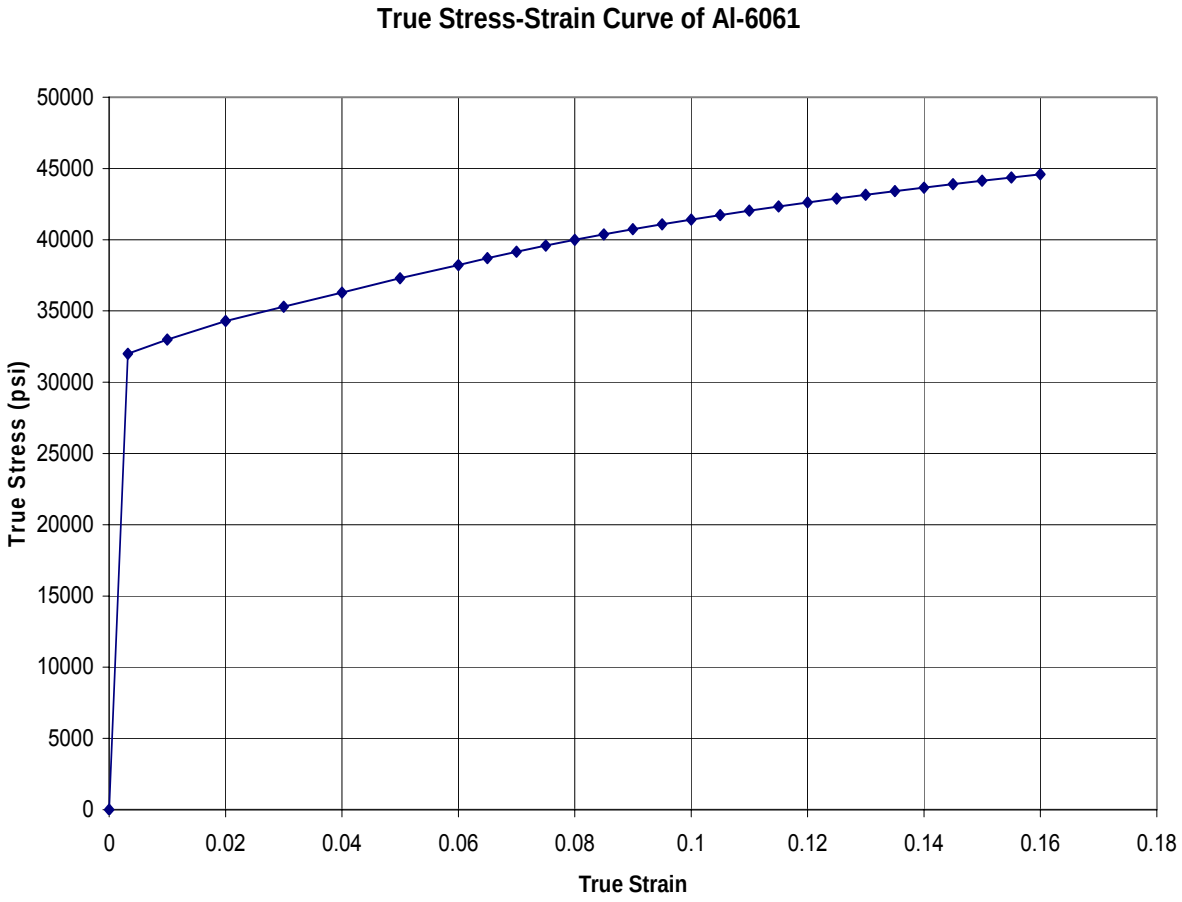

Figure A-2. True Stress vs. True Strain Curve of Aluminum 6061-T6

A.3 Stress-Strain Relationship of FR-3716 Polyurethane Foam

The stress-strain curve of FR-3716 polyurethane foam parallel and perpendicular to rise for dynamic compression is shown below in Figure A-3.

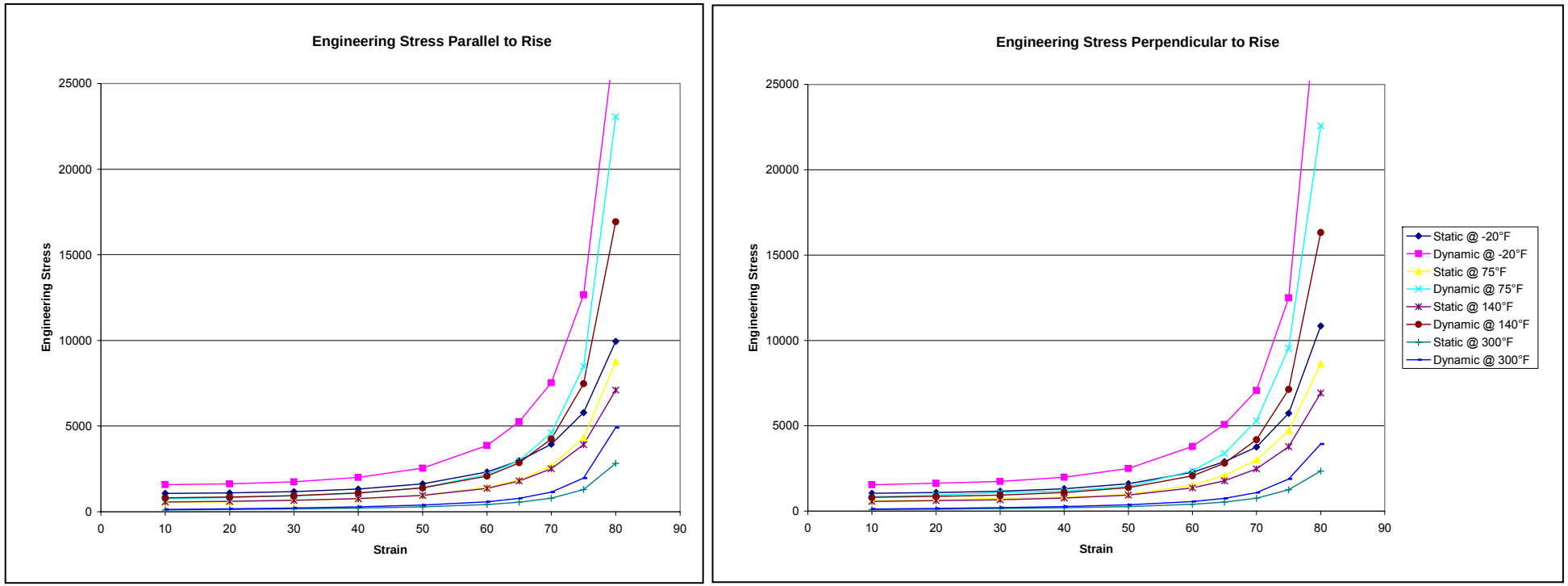

Figure A-3 Engineering Stress vs. Engineering Strain Curve for FR-3716 Foam – Parallel and Perpendicular to Rise

REFERENCES:

1 Code of Federal Regulations, 10CFR 71, January 2002.

2 ASME Boiler and Pressure Vessel Code, Section III, Appendix F, January 2004.

3 Safety Analysis Report for Packaging – Model 9977 (U), S-SARP-G-00001, May 2006.

4 ABAQUS/Explicit Computer Code, Version 6.4, ABAQUS, Inc., Providence, RI.

5 ABAQUS/CAE, Version 6.5-3, ABAQUS, Inc. Build ID:2005:03_03-17.29.04 57675, Providence, RI.

6 MSC/PATRAN, Version 2003r2, MacNeal-Schwendler Corporation.

7 ASME Boiler and Pressure Vessel Code, Section II, Part D, Properties, (2004).

8 Sindelar, R.L., “Tensile Properties of Type 304/304L SS for Impact Deformation Analyses of Nuclear Containers”, SRT-MTS-93-3113, November 1993.

This Page Intentionally Left Blank

APPENDIX 2.5

9977 PACKAGING MATERIALS & COMPONENTS OF FABRICATION

This Page Intentionally Left Blank

9977 PACKAGING MATERIALS & COMPONENTS OF FABRICATION

The Savannah River Packaging Technology (SRPT) group designed and developed the Model 9977 prototype units. These units were fabricated at the Savannah River Site (SRS) in conjunction with Honeywell Federal Manufacturing & Technologies, LLC; also known as the Kansas City Plant (KCP). Several of the materials of fabrication used in the 9977 are not routinely used in the construction of radioactive material packagings or are used in novel applications in the 9977. These materials are illustrated and specific design features are annotated in the figures below.

The materials and or components discussed in this appendix are:

- Polyurethane Last-A-Foam,
- Fiberfrax blanket,
- Min-K 2000,
- TR-19, and
- Retaining Studs and Washers.

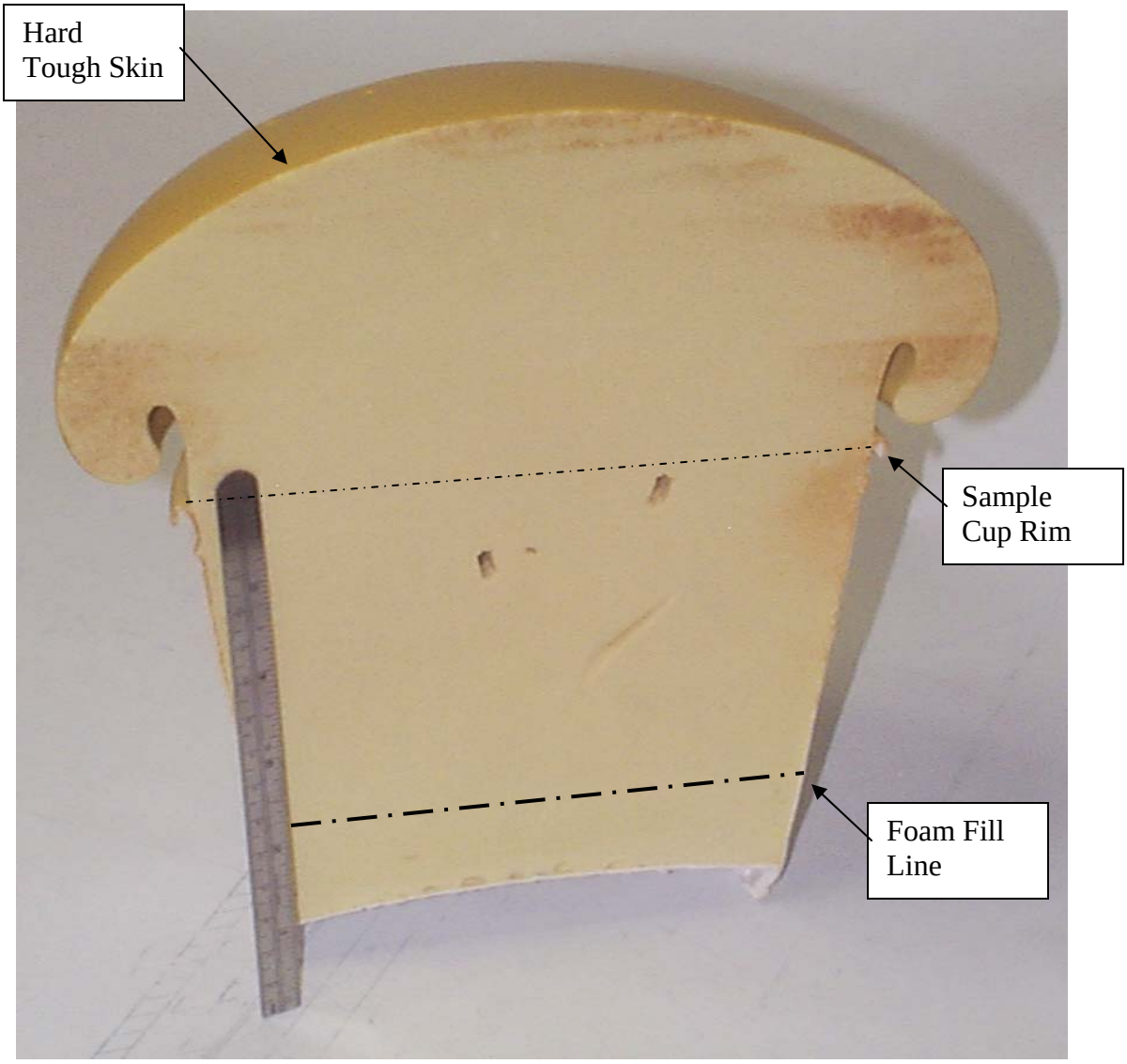

- Polyurethane Foam Sample Cup

Last-A-Foam polyurethane foam: General Plastics Manufacturing Co.

The sample cup pictured above is not filled with the FR-3716 polyurethane used in the 9977. However, its appearance and forming process is the equivalent to the FR-3716.

The foam is produced as a two part liquid which when mixed has a viscosity roughly the same as 30-weight motor oil. The photograph above shows the approximate liquid fill for this sample. When the mix was first placed into the cup it generated and released gasses for approximately a minute and then rose to form the muffing shape shown. The foam took several minutes to completely solidify. As the foam rises it forms a smooth and relatively tough outer "skin." The chemical reaction which created the foam is exothermic, and resulted in the foam having a surface temperature above 150°F. The

foam sample pictured, while still warm to the touch, could be easily handled after about 10 minutes. If the foam had been formed in a confined structure, it would have placed a tensile load on the structure and would have produced a more dense section than that formed with free expansion. The foam pictured is roughly a 6 lb/ft^3. The discoloration of the foam shown is the result of sectioning the sample cup with a dirty hack saw. The foam is typically a uniform cream/tan color. The indentions seen in the center of the foam in the photograph were made with a screw driver. Considerable force was used to stab the foam with the flat blade of screw driver, which penetrated approximately 1-inch.

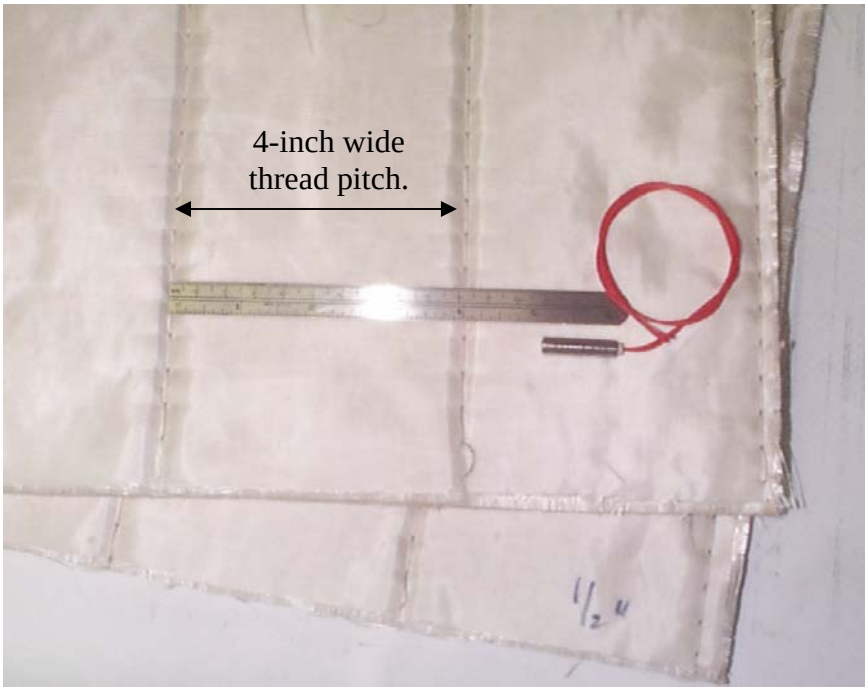

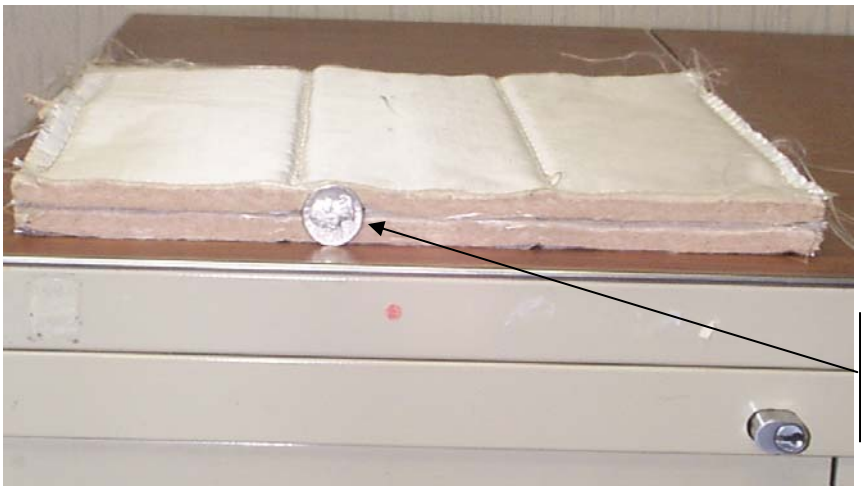

Fiberfrax Insulation ½-inch thick

Fiberfrax® Insulation (Lo-Con Felt), with Grade E Fiberglass Fabric on Both Sides, 7-10 lb/ft^3: Unifrax Corporation

The Fiberfrax is a lightweight batting, comprised of bulk ceramic fibers sandwiched between strong, high temperature fiberglass-cloth. The material is flexible, has excellent vibration resistance and is unaffected by moisture. The core insulation (i.e. the ceramic fibers) has an operating temperature of up to 2,300°F while the fiberglass E-cloth covering can be used continuously without degrading up to 1,200°F.

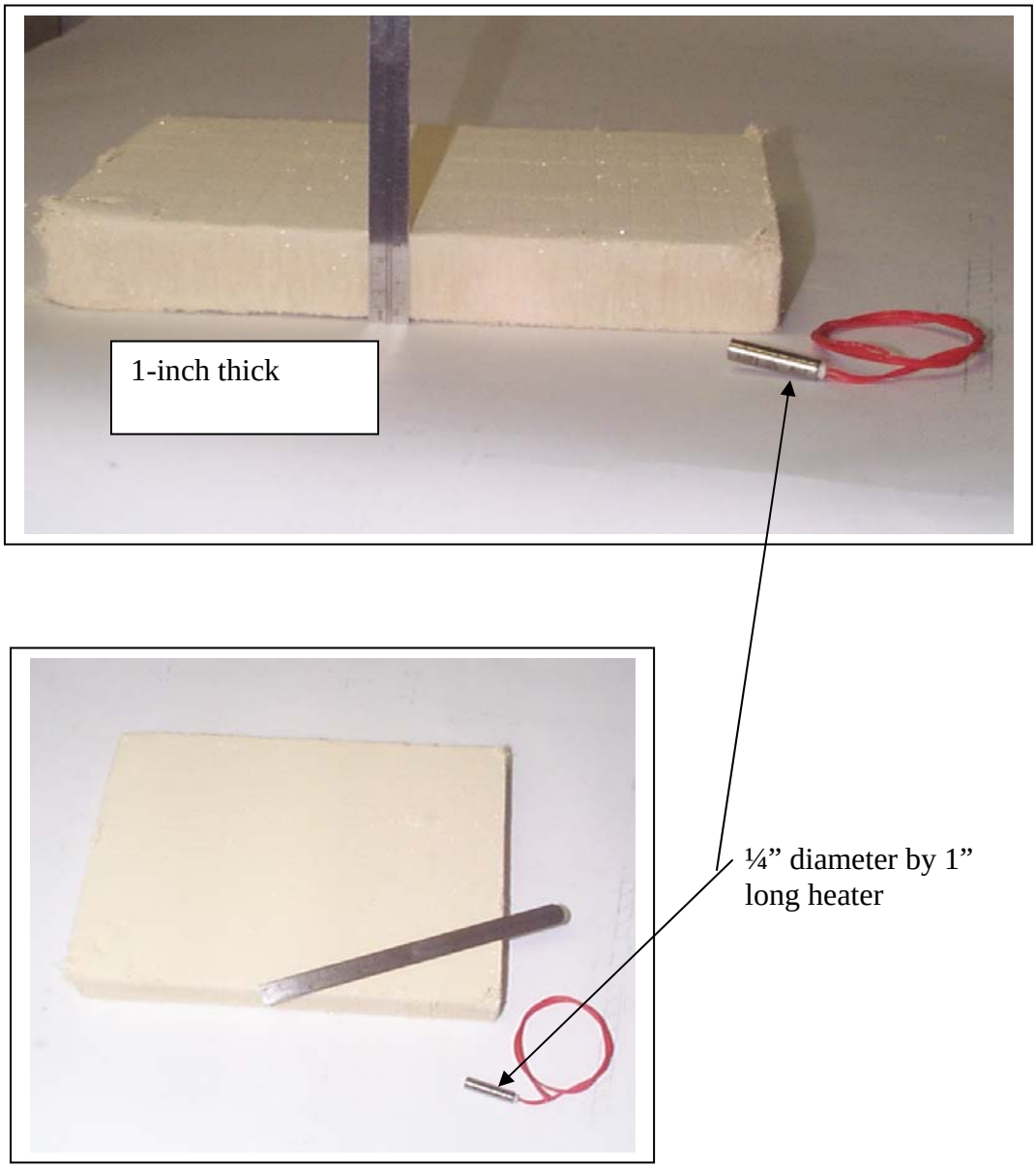

Thermal Ceramics Min-K 2000 Sample, 20 lb/ft^3

Thermal Ceramic Min-K 2000 is used to protect airline flight data and cockpit voice recorders. The material is non-endothermic and is unaffected by temperatures up to1,800°F. It is a light weight and has good compression strength.

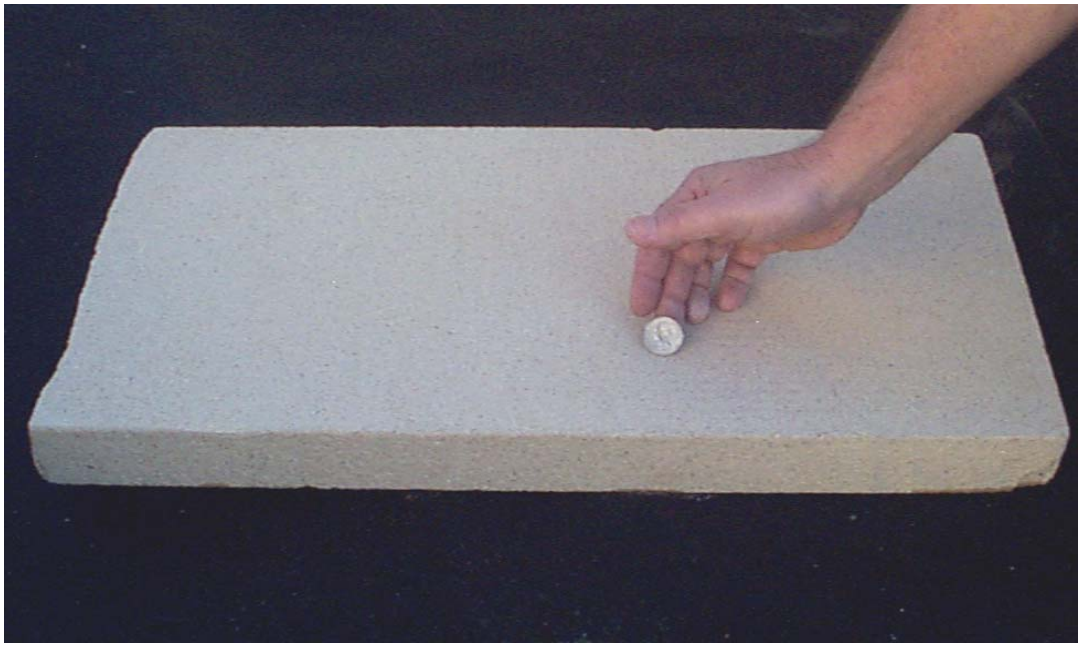

Thermal Ceramics TR-19 Sample, 23 lb/ft^3

Thermal Ceramics TR-19 Block insulation shown is composed of vermiculite granules mixed with high temperature bonding materials. TR-19 has good high temperature strength with minimal shrinkage up to 1,900°F even when exposed to direct flame. It has a nominal density of 23 lb/ft^3. It is manufactured in 36" x 12" blocks up to 7 inches thick.

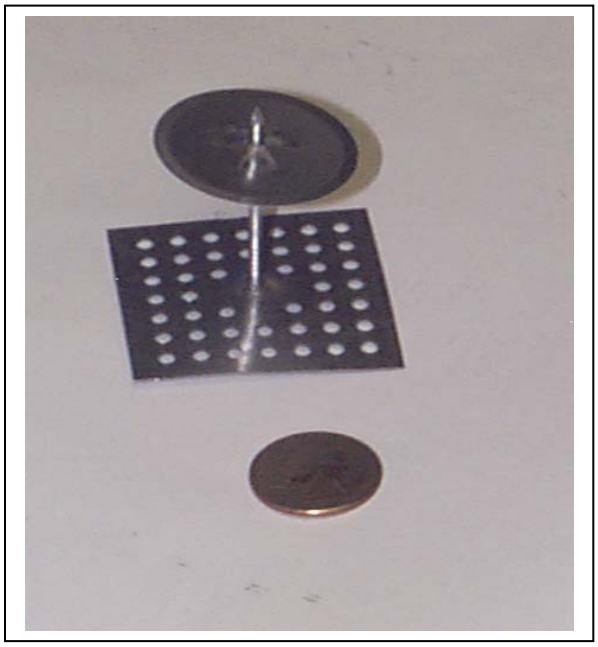

Stud and Washer for Fiberfrax Insulation Blanket Installation on Overpack Liner

The stud is a 4d nail attached to a 2-inch square perforated 30 gauge (.012-inch) sheet metal stock frame. The stud is1½ Long, made of 316 SS, and is procured through McMaster-Carr; Part Number 97990A102. The lock washer disk is 1½-inch diameter, 30 gauge (.012-inch) SS and is procured through McMaster-Carr; Part Number 93610A410.

The stud is installed to the drum liner by spot welding. The precut Fiberfrax blankets are wrapped around the liner and impaled on the studs. The washers are then pressed onto the studs capturing the Fiberfrax against the liner.

This Page is Intentionally Left Blank.

APPENDIX 2.4

9965 CONE-SEAL CLOSURE PERFORMANCE AT -40°F

This Page Intentionally Left Blank

9965 Cone Seal Closure Performance at –40°F

April 2, 1990 SRL-PTG-90-0047

To: E. K. Opperman, 730-A
Manager, Packaging and Transportation (P&T) Group

From: J. E. Cox, 730-A
Associate Engineer, P&T Group

9965 Cone Seal Closure Performance at -40°F

Ref: U. S. DOE Memo to G. W. May, from J. G. Leonard, Acting Chief-Packaging Certification Staff-Office of Security Evaluations-Defense Programs, "Questions from Q0 Review of 9965, 9966, 9967, and 9968 Packages, Docket 88-4-9965", 4/7/89.

A question from the Central Certification Office (3.1 of Reference) concerning the Viton seal low temperature performance of the 9965-9968 shipping packages initiated a P&T investigation.

P&T evaluated the information in the SARP (DPSPU 83-124-1, Sec 2.6.2) and determined that additional information was necessary to qualify the Viton "GLT" O-rings at -40°F. The P&T Group and Equipment Engineering Section (EES) of SRL developed hardware and wrote a test procedure, EES Special Procedure No. 407, Rev. 0, to perform helium leak testing on the 9965 Cone Seal Closure at -40°F.

EES performed an initial helium leak test (EES-900055, Record No. 465) at room temperature according to DPSOL 324-3-3404. P&T and EES then cooled the 9965 primary containment vessel (PCV) to -40°F and repeated the leak test. The results (EES-900055, Record No. 458) document that the PCV was leak tight (less than 1×10^{-7} atm cc/sec air per ANSI N 14.5-1987) for 10 minutes with an internal pressure of 15 psig. P&T and EES warmed the PCV to room temperature and installed a new set of O-rings. EES performed an initial leak test (EES-900055, Record No. 463) on the reassembled 9965 at room temperature. After cooling the PCV, EES and P&T repeated the -40°F leak test (EES-900055, Record No. 462) with leak tight results.

P&T documented the tests in the 9965-9968 QA file 810000574 located in SRL and revised Section 2.6.2 of the SARP. DOE/Savannah River will transmit the revised SARP to the Central Certification Office for review after P&T addresses all of the QOs and incorporates the changes into the SARP. All "scoping" work leading up to the final tests will be on file in the P&T Group files.

If you have any questions, please contact me, extension 5-1713.

CC G. Cadelli

APPENDIX 2.3

9977 GENERAL PURPOSE FISSILE PACKAGING WEIGHTS

This Page is Intentionally Left Blank

Calculation Cover Sheet

Project	Calculation No.	Project No.
N/A	M-CLC-G-00261	N/A
Title 9977 General Purpose Fissile Packaging Weights (U)	**Functional Classification** SS	Sheet 1 of 14
	Discipline Mechanical	
Calc Level ☒ Type 1 ☐ Type 2	**Type 1 Calc Status** ☐ Preliminary ☒ Confirmed	
Computer Program No. NA ☒ MicroStation, ProE, Solid Edge	**Version/Release No.** Version 07.01.04.07, Wildfire 2.0 M080, 18.00.00.69	

Purpose and Objective

The purpose of this calculation is to estimate the minimum, nominal and maximum weights for the components of the Model 9977 series General Purpose Fissile Package (GPFP). This data is used in the 9977 Safety Analysis Report for Packaging. The weights reported here do not include the weight of the package contents.

Summary of Conclusion

The nominal and the bounding maximum and minimum weights of the Model 9977 Packaging with the Five Inch Diameter Containment Vessel are 218.8 pounds, 237.5 pounds and 201.6 pounds, respectively.

The nominal and the bounding maximum and minimum weights of the Model 9977 Packaging with the Six Inch Diameter Containment Vessel are 235.0 pounds, 254.8 pounds and 216.7 pounds, respectively.

Revisions

Rev. No.	Revision Description
0	Original Issue

Sign Off

Rev. No.	Originator (Print) Sign/Date	Verification/ Checking Method	Verifier/Checker (Print) Sign/Date	Manager (Print) Sign/Date
0	K. R. Eberl 5/17/06	Document Review	G. A. Abramczyk 5-17-06	J. S. Bellamy 5/17/06

Design Authority -- (Print)	Signature	Date
Release to Outside Agency -- (Print) N/A	**Signature** N/A	**Date** N/A

Security Classification of the Calculation

(U)

Calculation Continuation Sheet

Calculation No.	Sheet No.	Rev.
M-CLC-A-00261	2	**0**

OPEN ITEMS

None

Calculation Continuation Sheet

Calculation No.	Sheet No.	Rev.
M-CLC-A-00261	3	**0**

RECORD OF REVISION					
REV. NO.	PAGES SUPERSEDED	PAGES ADDED	PAGES DELETED	PAGES REVISED	DESCRIPTION OF REVISIONS
0					Original Issue

Calculation Continuation Sheet

Calculation No.	Sheet No.	Rev.
M-CLC-A-00261	4	0

Table of Contents

Calculation Continuation Sheet

Calculation No.	Sheet No.	Rev.
M-CLC-A-00261	5	**0**

1.0 Purpose

The purpose of this calculation is to document the minimum, nominal, and maximum weights for the components of the Model 9977 series General Purpose Fissile Package (GPFP) to support generation of its Safety Analysis Report for Packaging (SARP). The 9977 shipping packaging is composed of a stainless steel containment vessel (CV) housed within the liner of an insulated stainless steel drum. Two shipping configurations exist for the 9977 package: (1) contents contained within a five-inch diameter CV (5CV), and (2) contents contained within a six-inch diameter CV (6CV). The differences between the two shipping configurations that affect the package weight are described in the calculation below.

The calculation of the weights of the package configurations are based on the Revision 0 drawings included in Appendix1.1 of the Model 9977 SARP, S-SARP-G-00001.

Assumptions incorporated in this calculation are listed in the Footnotes of Table 3 and Table 4, and elsewhere in this document.

2.0 Input

The following Revision 0 drawings were used as input for the analyses contained herein:

R-R1-G-00020	R-R2-G-00017	R-R2-G-00019	R-R2-G-00033	R-R2-G-00043
R-R1-G-00021	R-R2-G-00018	R-R2-G-00032	R-R2-G-00042	

3.0 Conclusions

Weights shown in Table 3 and Table 4 represent the nominal, minimum and maximum weights of the Model 9977 series General Purpose Fissile Package (GPFP). The calculated values are consistent with measured weights of similar Containment Vessels and the GPFP prototypes.

4.0 Weight Calculations and Measurements

The numerical data for the volumes listed in Table 1 and Table 2 were generated using three-dimensional (3D) computer aided design (CAD) models generated with Pro/ENGINEER and Solid Edge software. The 3D models were generated using information from the Revision 0 drawings included in Appendix 1.1 of the Model 9977 SARP, S-SARP-G-00001 which were created using MicroStation CAD software. The methodology for determining the minimum and maximum values are summarized in the Footnotes of Table 1 and Table 2 and in Section 4.1. These calculated values are compared to actual measured weights of containment vessels and drum assemblies documented elsewhere. A summary of the compared values follows.

4.1 Calculated Weights

The nominal weights for the components of the 9977 series General Purpose Fissile Package (GPFP) were calculated by using volume information generated by Pro/ENGINEER and Solid Edge 3D CAD models which were created using the dimensions on the design drawings include in S-SARP-A-00001, Rev. 0.

The maximum and minimum weights of the Drum Assembly (excluding the insulation) and the Drum Lid (excluding the insulation) were calculated using maximum and minimum volumes generated by the 3D CAD models by changing the nominal dimensions to reflect the variations defined by the minimum and maximum tolerances on the drawings.

The maximum and minimum weights of the Containment Vessels (5CV and 6CV), Load Distribution Fixtures (Top and Bottom), Bolts and Washers, PPI Parts (Gland Nut and Plug), Honeycomb Parts (Lower Spacer, Annular Spacer and Upper Spacer), the Caplugs and Drum and Lid Welds were calculated using volume variations which incorporate expected fabrication and material variations. The percent variations used to generate the maximum and minimum volumes of these parts is as follows:

Insulating Blankets	Volume variation from nominal volume is +/- 25% (Assumes uncompressed insulation)
Last-A-Foam	Volume variation from nominal volume is +/- 5%
Welds	Volume variation from nominal volume is +/- 15%
TR-19 Block	Volume variation from nominal volume is +/- 10%
Min-K 2000	Volume variation from nominal volume is +/- 15%
Bolts and Washers	Volume variation from nominal volume is +/- 5%
PPI Nut and Plug	Volume variation from nominal volume is +/- 5%
CV Weldment	Volume variation from nominal volume is +/- 10%
CV Nut and Plug	Volume variation from nominal volume is +/- 2%
Honeycomb Spacers	Volume variation from nominal volume is +/- 15%
Load Dist. Fixtures	Volume variation from nominal volume is +/- 5%
Caplugs	Volume variation from nominal volume is +/- 5%

The weights of the other miscellaneous material (RTV, O-rings, Retaining Ring, Krytox and Tape) used in the calculations for the nominal, minimum and maximum weights was estimated to be .5 lb., 0 lb. and 1 lbs., respectively.

The calculated volumes (nominal, minimum, maximum) were multiplied by the material densities to obtain the weights. The densities used are as follows:

Stainless Steel (304/304L)	0.286 lbm/in^3	ASME B&PVC Sec II Part A and D
Nitronic-60	0.2756 lbm/in^3	ASME B&PVC Sec II Part A and D
Aluminum (6061-T6)	0.098 lbm/in^3	ASME B&PVC Sec II Part D, Table NF-2

Last-A-Foam	18.317 lbm/ft^3	Reference GPFP prototype; not free rise density
TR-19 Block	23 lbm/ft^3	Thermal Ceramics data sheet
Min-K 2000	20 lbm/ft^3	Thermal Ceramics data sheet
Fiberfrax	8.5 lbm/ft^3	Reference KCP SS-R51507, 7-10 lbm/ft^3 quilted

The calculated weights for the Model 9977 series General Purpose Fissile Package are given in Table 1 and Table 2.

4.2 Measured Weights

Weights of five 9975 Shipping Package containments vessels (referred to as Primary and Secondary Containment Vessels) are documented in correspondence from the fabricator (Accurate Machine Products Corporation - Reference 1). The 9975 Primary and Secondary Containment Vessels are identical to the 9977 5CV and 6CV, respectively. A comparison of the data in that correspondence is made with the calculated values in Table 3.

Weights of the 9975 Shipping Package Secondary Containment Vessel used in 9977 Thermal Benchmark Testing (Ref. 6.5) are documented in Reference 6.4. A comparison of the data in that correspondence is made with the calculated values in Table 3.

Weights of the 9975 Shipping Package Load Distribution Fixtures used in 9977 Thermal Benchmark Testing (Ref. 6.5) are documented in Reference 6.4. A comparison of the data in that correspondence is made with the calculated values in Table 4.

Weights of components of four 9977/GPFP prototypes are documented in SRNL-EDS-2006-00010 (February 14, 2006) (Reference 2). A comparison of the data in that report is made with the calculated values in Table 4.

4.3 Calculated Volume of the Region Between the Outside of the 6CV and the Drum Liner

To document the volume occupied by air between the outside of the 6CV and the inside of the Drum (within the Drum Liner and below the Drum Lid), a calculation was performed. The Revision 0 drawings included in Appendix 1.1 of the Model 9977 SARP, S-SARP-G-00001 were used to create a two-dimensional section that was rotated to create an axi-symmetric volumetric region.

The following assumptions were made:

- Nominal dimensions were used,
- The 2.5-in square boss on the Cone-Seal Nut was modeled as a circle of the same area,
- The Cone-Seal Nut protruded above the vessel weldment top by 0.0342-inches, and
- The key way in bottom of the skirt was not modeled.

The calculated volumetric region between the 6CV and the drum is 792.57-in^3.

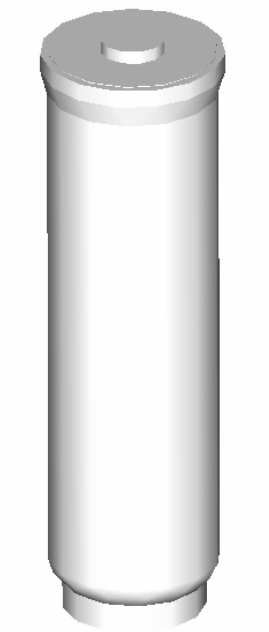

5.0 Results

The calculated nominal, minimum and maximum weights for the 9977 Series GPFP components are documented in Tables 1 and 2 for the 5CV and 6CV configurations, respectively.

Comparisons of the calculated weights to actual measured weights are documented in Tables 3 and 4. The maximum and minimum calculated values bound the measured weights of the 9977 Series GPFP.

Calculation Continuation Sheet

Calculation No.	Sheet No.	Rev.
M-CLC-A-00261	9	**0**

Table 1: Weight Calculations of the 9977 with 5 Inch CV

Item Description	Drawing Reference	Density (lbm/in3)	Vol. (in3)	Item Wt. (lbm)	Qty	Weights Nom. (lbm)	Weights Min. (lbm)	Weights Max. (lbm)	Notes
DRUM SIDE/BOTTOM WELDMENT	R-R2-G-00017-B,C	0.286	106.24	30.38	1	30.4	27.6	33.8	1
DRUM WEAR RING	R-R2-G-00017-K	0.286	9.96	2.85	1	2.8	2.4	3.1	1
DRUM RIM	R-R2-G-00017-H	0.286	31.50	9.01	1	9.0	8.0	10.1	1
DRUM TOP PLATE	R-R2-G-00017-F	0.286	38.67	11.06	1	11.1	9.9	12.3	1
DRUM LINER RING	R-R2-G-00017-G	0.286	5.61	1.60	1	1.6	1.4	1.8	1
THREADED FITTING (DRUM)	R-R2-G-00017-I	0.286	1.13	0.32	8	2.6	2.5	2.6	1
DRUM LINER SIDE/BOTTOM	R-R2-G-00017-D,E	0.286	39.96	11.43	1	11.4	10.5	12.6	1
INSULATING BLANKET (DRUM)	R-R2-G-00019-B,C,D	0.005	1037.06	5.10	1	5.1	3.8	6.4	2
LAST-A-FOAM (DRUM)	R-R2-G-00020,21	0.011	6778.21	71.85	1	71.8	68.3	75.4	3
DRUM Welds	R-R2-G-00017	0.286	1.93	0.56		0.6	0.5	0.6	5
DRUM TOTAL						**146.4**	**134.9**	**158.7**	
DRUM LID	R-R2-G-00018-B,C,D	0.286	52.59	15.04	1	15.0	14.4	16.5	1
INSULATING BLANKET (LID)	R-R2-G-00018	0.005	53.46	0.26	1	0.3	0.2	0.3	2
VERMICULITE TR-19 (LID)	R-R2-G-00018	0.013	195.29	2.60	1	2.6	2.3	2.9	6
MIN-K 2000 (LID)	R-R2-G-00018	0.012	144.31	1.67	1	1.7	1.4	1.9	6
DRUM LID Welds	R-R2-G-00018	0.286	0.14	0.04		0.0	0.0	0.0	5
DRUM LID TOTAL						**19.6**	**18.4**	**21.6**	
5/8" WASHER, PL, NARROW, TP B	R-R1-G-00020,21	0.286	0.09	0.03	8	0.2	0.2	0.2	6
5/8" SCREW, HEAVY HEX	R-R1-G-00020,21	0.286	0.79	0.23	8	1.8	1.7	1.9	6
BOLTS/WASHERS WEIGHT TOTAL						**2.0**	**1.9**	**2.1**	
GLAND NUT (PPI) (CV Fitting)	R-R2-G-00042,43	0.286	0.14	0.04	1	0.0	0.0	0.0	7
PLUG (PPI) (CV Fitting)	R-R2-G-00042,43	0.286	0.06	0.02	1	0.0	0.0	0.0	7
PPI PARTS WEIGHT TOTAL						**0.1**	**0.1**	**0.1**	
5" DIA CV WELDMENT	R-R2-G-00043-B	0.286	80.94	23.15	1	23.1	20.8	25.5	8
5" DIA CV CONE SEAL NUT	R-R2-G-00043-D	0.275	16.13	4.44	1	4.4	4.3	4.5	9
5" DIA CV CONE SEAL PLUG	R-R2-G-00043-C	0.286	16.21	4.64	1	4.6	4.5	4.7	9
5" CV WEIGHT TOTAL						**32.2**	**29.7**	**34.7**	
BOTTOM LOAD DIST FIXTURE	R-R4-G-00032-A	0.098	105.27	10.32	1	10.3	9.8	10.8	9
TOP LOAD DIST FIXTURE	R-R4-G-00032-B	0.098	39.42	3.86	1	3.9	3.7	4.1	9
LOAD DISTRIBUTION FIXTURES TOTAL						**14.2**	**13.5**	**14.9**	
LOWER SPACER FOR 5" CV	R-R4-G-00033-A	0.007	95.47	0.67	1	0.7	0.6	0.8	6
ANNULAR SPACER FOR 5" CV	R-R4-G-00033-B	0.007	338.22	2.37	1	2.4	2.0	2.7	6
UPPER SPACER FOR 5" CV	R-R4-G-00033-C	0.007	103.05	0.72	1	0.7	0.6	0.8	6
HONEYCOMB PARTS WEIGHT TOTAL						**3.8**	**3.2**	**4.3**	
MISC WEIGHT (RTV, CAPLUGS,O-RINGS, RETAINING RING, KRYTOX, TAPE)						**0.5**	**0.0**	**1.0**	
9977 WITH 5 INCH DRUM ASSEMBLY TOTAL						**218.8**	**201.6**	**237.5**	

Calculation Continuation Sheet

Calculation No.	Sheet No.	Rev.
M-CLC-A-00261	10	**0**

Table 2: Weight Calculations of the 9977 with 6 Inch CV

Item Description	Drawing Reference	Density (lbm/in3)	Item Vol. (in3)	Item Wt. (lbm)	Qty	Weights Nom. (lbm)	Weights Min. (lbm)	Weights Max. (lbm)	Notes
DRUM SIDE/BOTTOM WELDMENT	R-R2-G-00017-B,C	0.286	106.24	30.38	1	30.4	27.6	33.8	1
DRUM WEAR RING	R-R2-G-00017-K	0.286	9.96	2.85	1	2.8	2.4	3.1	1
DRUM RIM	R-R2-G-00017-H	0.286	31.50	9.01	1	9.0	8.0	10.1	1
DRUM TOP PLATE	R-R2-G-00017-F	0.286	38.67	11.06	1	11.1	9.9	12.3	1
DRUM LINER RING	R-R2-G-00017-G	0.286	5.61	1.60	1	1.6	1.4	1.8	1
THREADED FITTING (DRUM)	R-R2-G-00017-I	0.286	1.13	0.32	8	2.6	2.5	2.6	1
DRUM LINER SIDE/BOTTOM	R-R2-G-00017-D,E	0.286	39.96	11.43	1	11.4	10.5	12.6	1
INSULATING BLANKET (DRUM)	R-R2-G-00019-B,C,D	0.005	1037.06	5.10	1	5.1	3.8	6.4	2
LAST-A-FOAM (DRUM)	R-R2-G-00020,21	0.011	6778.21	71.85	1	71.8	68.3	75.4	3
DRUM Welds	R-R2-G-00017	0.286	1.93	0.56		0.6	0.5	0.6	5
DRUM TOTAL						**146.4**	**134.9**	**158.7**	
DRUM LID	R-R2-G-00018-B,C,D	0.286	52.59	15.04	1	15.0	14.4	16.5	1
INSULATING BLANKET (LID)	R-R2-G-00018	0.005	53.46	0.26	1	0.3	0.2	0.3	2
VERMICULITE TR-19 (LID)	R-R2-G-00018	0.013	195.29	2.60	1	2.6	2.3	2.9	6
MIN-K 2000 (LID)	R-R2-G-00018	0.012	144.31	1.67	1	1.7	1.4	1.9	6
DRUM LID Welds	R-R2-G-00018	0.286	0.14	0.04		0.0	0.0	0.0	5
DRUM LID TOTAL						**19.6**	**18.4**	**21.6**	
5/8" WASHER, PL, NARROW, TP B	R-R1-G-00020,21	0.286	0.09	0.03	8	0.2	0.2	0.2	6
5/8" SCREW, HEAVY HEX	R-R1-G-00020,21	0.286	0.79	0.23	8	1.8	1.7	1.9	6
BOLTS/WASHERS WEIGHT TOTAL						**2.0**	**1.9**	**2.1**	
GLAND NUT (PPI) (CV Fitting)	R-R2-G-00042,43	0.286	0.14	0.04	1	0.0	0.0	0.0	7
PLUG (PPI) (CV Fitting)	R-R2-G-00042,43	0.286	0.06	0.02	1	0.0	0.0	0.0	7
PPI PARTS WEIGHT TOTAL						**0.1**	**0.1**	**0.1**	
BOTTOM LOAD DIST FIXTURE	R-R4-G-00032-A	0.098	105.27	10.32	1	10.3	9.8	10.8	9
TOP LOAD DIST FIXTURE	R-R4-G-00032-B	0.098	39.42	3.86	1	3.9	3.7	4.1	9
LOAD DISTRIBUTION FIXTURES TOTAL						**14.2**	**13.5**	**14.9**	
6" DIA CV WELDMENT	R-R2-G-00042-B	0.286	138.16	39.51	1	39.5	35.6	43.5	8
6" DIA CV CONE SEAL NUT	R-R2-G-00042-D	0.275	22.02	6.06	1	6.1	5.9	6.2	9
6" DIA CV CONE SEAL PLUG	R-R2-G-00042-C	0.286	23.10	6.61	1	6.6	6.5	6.7	9
6" CV WEIGHT TOTAL						**52.2**	**48.0**	**56.4**	
MISC WEIGHT (RTV, CAPLUGS,O-RINGS, RETAINING RING, KRYTOX, TAPE)						**0.5**	**0.0**	**1.0**	
9977 WITH 6 INCH DRUM ASSEMBLY TOTAL						**235.0**	**216.7**	**254.8**	

Table 3: Actual Weights of the 9975 CVs and Calculated Weights of the 9977 CVs

	9977 Calculated Minimum (lbm)	9975 Measured Minimum (lbm)	9975 Measured Maximum (lbm)	9977 Calculated Maximum (lbm)	Ref.erence for Measured Weights
5” CV Weldment	20.8	24.5	25.25	25.5	Ref. 6.1
5” CV Cone Seal Plug	4.5	4.59	4.61	4.7	Ref. 6.1
5” CV Cone Seal Nut	4.3	4.31	4.37	4.5	Ref. 6.1
6” CV Weldment	35.6	40.00	42.00	43.5	Ref. 6.1, 6.4
6” CV Cone Seal Plug	6.5	6.69	6.7	6.7	Ref. 6.4
6” CV Cone Seal Nut	5.9	5.90	5.96	6.2	Ref. 6.1, 6.4

Note: The actual variation in the weight of the CV weldment varies more than the other stainless steel parts due to the larger variation in tolerances of stock pipe and pipe caps than that of machined parts.

Table 4: Actual and Calculated Weights of 9977 Drum and Components

	9977 Calculated Minimum (lbm)	9977 Prototype Measured Minimum (lbm)	9975 Prototype Measured Maximum (lbm)	9977 Calculated Maximum (lbm)	Ref.erence for Measured Weights
Drum Body	134.9	150.0	151.7	158.7	Ref. 6.2
Drum Lid	18.4	19.0	19.3	21.9	Ref. 6.2
Bolts/Washers	1.9	1.6	1.6	2.1	Ref. 6.2
Top Load Distribution Fixture	3.7	3.899	3.9	4.1	Ref. 6.2, 6.4
Bottom Load Distribution Fixture	9.8	10	10.1	10.8	Ref. 6.2, 6.4
Last-A-Foam, FR 3716	68.3	75	75	75.4	Ref. 6.2

Note: Bolts/Washers are larger on the 9977 than on the Prototypes. The configuration of the Prototypes differs slightly from the 9977 design which is shown in the referenced drawings. (See Reference 6.3).

Footnotes for Table 1 and Table 2:

1. Maximum and minimum volume was generated using the tolerances defined on the Rev 0 drawings referenced in Appendix 1.1 of S-SARP-A-00001, Rev.0.
2. Volume based on uncompressed insulation; Volume tolerance used is +/- 25%
3. Volume tolerance used is +/- 5%.
4. Volume tolerance used is +/- 5% (Caplugs not listed separately).
5. Volume tolerance used is +/- 15%.
6. Volume tolerance used is +/- 15%.
7. Volume tolerance used is +/- 5%.
8. Volume tolerance used is +/- 10%; O-ring volume/weight not included.
9. Volume tolerance used is +/- 2%.

6.0 References

6.1 Correspondence from Accurate Machine Products Corporation, P. S. Blanton.

6.2 SRNL-EDS-2006-00010, dated 2/14/06, “GPFP Packaging Weight Compilation”, L. F. Gelder.

6.3 9977 Production Packaging Comparisons with the Development GPFP Prototypes, S-SARP-A-00001, Rev. 0, Appendix 2.8.

6.4 SRNL-EES-2006-00003, Documentation of 9975 and 9977 Shipping Package Components Weights.

6.5 S-TSM-A-00001, Thermal Benchmark Test, K. R. Eberl.

Calculation Continuation Sheet

Calculation No.	Sheet No.	Rev.
M-CLC-A-00261	14	**0**

This Page is Intentionally Left Blank

APPENDIX 2.2

GENERAL DESIGN AND ASME CALCULATIONS

FOR THE

9977 CONTAINMENT VESSELS

This Page is Intentionally Left Blank

Calculation Cover Sheet

Project	Calculation No.	Project No.
N/A	M-CLC-A-00258	N/A
Title General Design and ASME Calculations for the 9977 Containment Vessels (U)	**Functional Classification** SS	Sheet 1 of ~~105~~ 98 4A
	Discipline Mechanical	
Calc Level ☒ Type 1 ☐ Type 2	**Type 1 Calc Status** ☐ Preliminary ☒ Confirmed	
Computer Program No. Abaqus NA ☐	**Version/Release No.** 6.5.3 / 2005_03_03-17.29.04 57675	

Purpose and Objective

The purpose of this calculation is to document structural analysis of the 5-inch diameter containment vessel and 6-inch diameter containment vessel for use in the Model 9977 package to support generation of the Safety Analysis Report for Packaging, S-SARP-G-00001.

Summary of Conclusion

Analysis presented in this calculation meets the design criteria required by 10 CFR 71in the evaluation of the Model 9977.

Revisions

Rev. No.	Revision Description
0	Original Issue

Sign Off

Rev. No.	Originator (Print) Sign/Date	Verification/ Checking Method	Verifier/Checker (Print) Sign/Date	Manager (Print) Sign/Date
0	Tsu-Te Wu Tsu-Te Wu 5/17/06	Document Review	N. K. Gupta N. K. Gupta 5/17/06	J. S. Bellamy J S Bellamy 5/17/06

Design Authority -- (Print)	Signature	Date
Release to Outside Agency -- (Print) N/A	**Signature** N/A	**Date** N/A

Security Classification of the Calculation

(U)

OPEN ITEMS

None

RECORD OF REVISION					
Revision No.	Pages Deleted	Pages Added	Pages Superseded	Pages Revised	Description of Revisions
0					Original Issue

OPEN ITEMS

NONE

TABLE OF CONTENTS

1.0 INTRODUCTION

The purpose of this calculation is to document structural analysis of the 5-inch diameter containment vessel and 6-inch diameter containment vessel for use in the Model 9977 package to support generation of the Safety Analysis Report for Packaging, S-SARP-G-00001. In this report the use of 5CV and 6V are synonymous with the 5-inch diameter containment vessel and 6-inch diameter containment vessel, respectively.

A baseline stress analysis was performed to determine the resulting stresses in the 9977 5CV and 6CV subject to the unit load of 150 psi internal pressure at 300 °F.

With this baseline and a given normal operating or test condition, the following was performed:

- Determine the actual stresses at other pressures by multiplying the baseline stresses by the ratio of the actual operating pressure to the unit loading pressure of 150 psi.
- Determine the allowable maximum normal operating pressure for a given operating temperature.
- Determine the allowable maximum normal operating temperature for a given normal operating pressure.

Based on the analytical results for the unit load, the stresses in the 5CV and 6CV for the following loading conditions were also determined:

- Internal pressure of 900 psi in the 5CV and 800 psi in the 6CV, which are the design pressures (see Table 1.a).
- Internal pressures of 1365+/-10 psi in the 5CV and 1235+/-10 psi in the 6CV, which are the hydrostatic test conditions [NOTE: These pressures are a SRS design criteria and are 1.5 times the design pressures] (see Table 1.b).

All resulting stresses are within the allowable limits defined in the ASME code, Section III, Subsection NB. The results for the load cases of 800 and 900 psi and the corresponding hydrostatic test cases of 1235 and 1365 psi are listed with the detailed analysis in Tables 5a and 5b, respectively.

A closure analysis is performed to determine if the installation torque is sufficient to maintain metal-to-metal contact between the male cone seal plug and the containment vessel female conical surface during pressurization. The analysis (Table 2) shows that, for the coefficient of friction expected at the lubricated surfaces, the installation torque is sufficient to maintain metal-to-metal contact with the containment vessel for pressures up to about 500 psig.

Of greater importance than whether the conical lid/body joint remains seated is the pressure capacity of the O-rings in the joint. In Figure 1, reproduced from the *Parker O-Ring Handbook*,[1] the pressure capacity of O-rings versus the clearance gap between surfaces is shown. The largest gaps correspond to a coefficient of friction of 0.15. The gap width decreases with decreasing coefficients of friction. The largest gaps for the 5CV and 6CV are calculated and are added to Figure 1. The intersection of the 5CV and 6CV gap curve with the O-ring capacity curve shows that (1) loss of pressure capacity due to unseating is minimal and (2) the capacity of the joint far exceeds the design pressure of the 5CV and 6CV.

Buckling analysis (using Code Case N-284) and fatigue analysis are given at the end of the computation section.

2.0 INPUT

The following drawings were used as input for the analyses contained herein:

R-R2-G-00042	Rev 0	Six Inch Diameter Containment Vessel Subassembly
R-R2-G-00043	Rev 0	Five Inch Diameter Containment Vessel Subassembly

3.0 RESULTS

The following tables summarize the stress results of the analyses performed in the next section. Table 1a includes stresses obtained using the design pressures. Table 1b includes stresses for the hydrostatic test pressure case, and Table 2 includes the unseating pressures.

Table1.a Stress Analysis Results with 900 psi (5CV) and 800 psi (6CV) Internal Pressures and ASME Evaluation for NCT

	P_m (psi)	P_m+P_b (psi)	P_m+P_b+Q (psi)	P_m+P_b+Q+F (psi)	$P_{m,pure-shear}$ (psi)	Minimum Code Margin[d]
Stress Limit	S_m=16700	1.5S_m=25050	3S_m=50100	2S_a=338000[a]	1.2S_m=20040	
5CV Body						
Section AA (pipe wall)	9264	10092				0.45
Section BB (CV head transition)	4667		12680 [b]	15576 [c]		0.72
Section CC (pipe cap radius)	6116		12260 [b]	13311 [c]		0.63
Section DD (pipe cap bottom)	9005	13938				0.44
5CV Cone-Seal Plug (preload only)	53.18	1575				0.94
5CV Cone-Seal Nut					3636	0.82
5CV Tapered Wall Thread					7868	0.61
5CV Tapered Wall Minimum Section	6022		29706 [b]	118824[c]		0.41
6CV Body						
Section AA (pipe wall)	9066	9808				0.46
Section BB (CV head transition)	4687		12899 [b]	15659 [c]		0.72
Section CC (pipe cap radius)	6456		12070 [b]	12807 [c]		0.61
Section DD (pipe cap bottom)	9004	13210				0.46
6CV Cone-Seal Plug (preload only)	63.86	2716				0.89
6CV Cone-Seal Nut					3927	0.80
6CV Tapered Wall Thread					8485	0.58
6CV Tapered Wall Minimum Section	3831		17738 [b]	70963 [c]		0.65

a) S_a =169KSI from ASME III, Fig. I-9.2.1 Allowable for 1000 load cycles (100 year design life at 10 shipments per year)
b) Includes through wall bending stresses, but not thermal stress.
c) Includes maximum surface stresses, but not thermal stress or stress concentrations where finite element analysis has been performed except at threaded portion of tapered wall.
d) Minimum value from those calculated in row using Margin=1-(Stress/Stress Limit)

Table 1.b Stress Analysis Results for Hydrostatic Test Conditions

Based on Internal Design Pressure of 900 psi for 5CV and 800 psi for 6CV (Test Pressure = 1375 psi for 5CV and 1245 psi for 6CV)

	P_m (psi)	$P_m + P_b$ (psi)	Minimum
Test Limits	**$0.9S_y$=22500 psi**	**$1.35S_y$=33750 psi**	**Margin**
5CV Body:			
Section AA	14153	15418	0.37
Section BB	7132		0.68
Section CC	9344		0.58
Section DD	13758	21294	0.37
5CV Plug (preload only)	53.18	1575	0.95
5CV Nut	5555		0.75
5CV Tapered wall thread	12021		0.47
5CV Tapered wall minimum section	9200		0.59
6CV Body:			
Section AA	14109	15264	0.37
Section BB	7294		0.68
Section CC	10047		0.55
Section DD	14012	20558	0.38
6CV Plug (preload only)	63.86	2716	0.92
6CV Nut	6111		0.73
6CV Tapered wall thread	13205		0.41
6CV Tapered wall minimum section	5747		0.73

Table 0.2 Unseating Pressure (psig)

Condition	5CV	6CV
Installation torque (ft-lb)	50	100
Threads and cone seal surface ungreased Unseating pressure, $\mu = 0.15$, $\mu_t = 0.15$	137	161
Threads greased and cone seal surface clean* Unseating pressure, $\mu_t = 0.05$, $\mu = 0.15$	515	563
Threads greased and cone seal surface lubricated with grease $\mu = \mu_t = 0.05$	771	833

*Design condition where threads are greased with KRYTOX lubricant and the cone seal contact surface is clean.

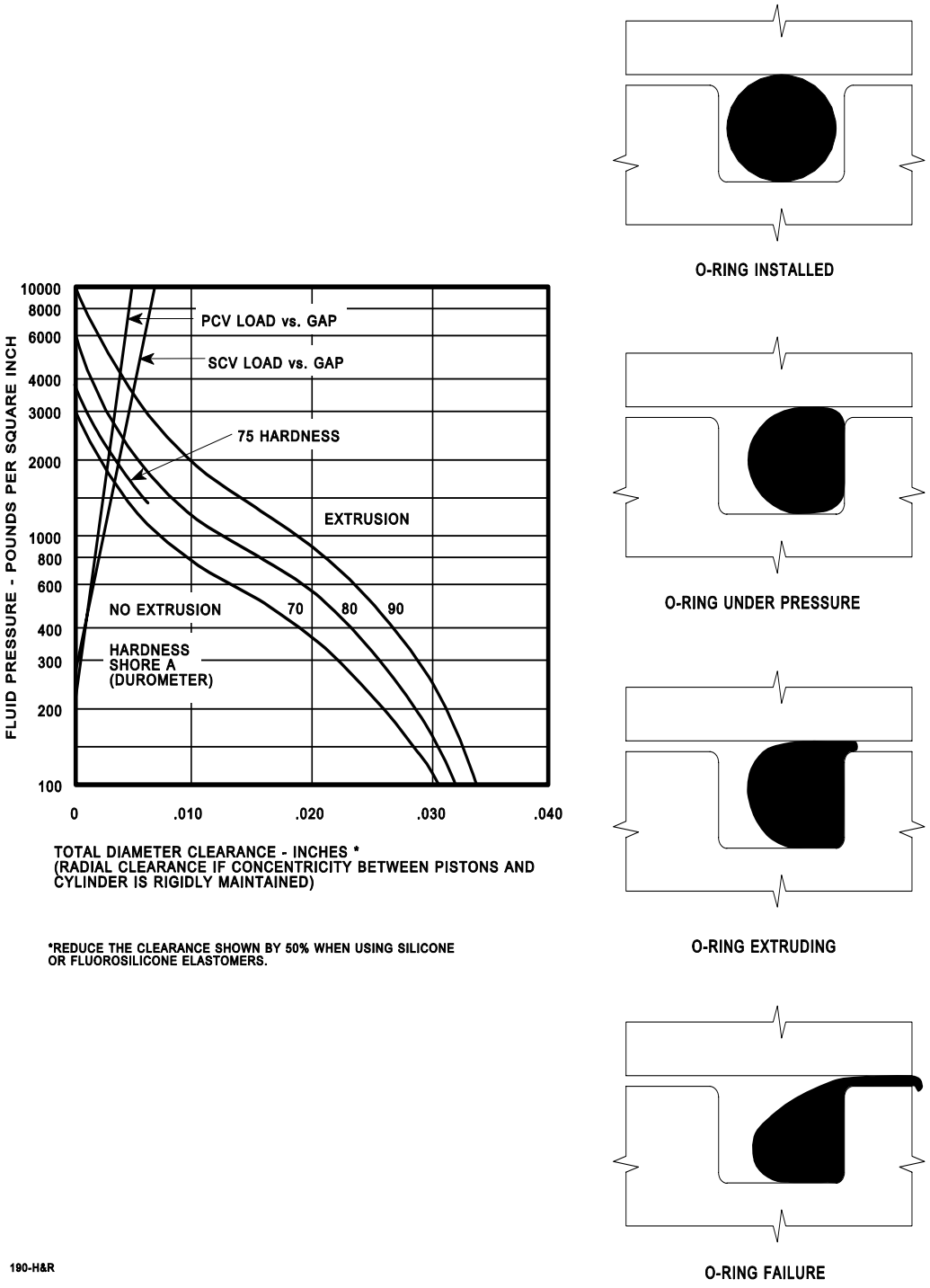

Figure 1 Clearance Gap Versus O-Ring Pressure Capacity

Source: Parker O-Ring Handbook. ORD 5700, The Parker Seal Group, Parker Hannifin Corporation, Lexington, KY (1991).

4.0 COMPUTATIONS

The following computations were performed to establish structural adequacy of the 9977 packaging.

4.1 Methodology

A unit load of 150 psi internal pressure was used in the stress analysis for the 5CV and 6CV. In addition, a unit load of 20 psi external pressure was used in the buckling analysis for the 5CV and 6CV. The unit loads used in the analyses are summarized in Table 3. The stresses obtained from the unit load analysis were factored to obtain the stresses for the 900psig 5CV and 800psig 6CV design pressures. Calculated stresses were compared to Allowable stress intensity values from ASME Section II, Part D[5], which are summarized in Table 4.

Table 3. Unit Loads

Operating Conditions	Internal Pressure	External Pressure
Pressure (psig)	150	-20

Table 4. Allowable Tensile Stress Intensities

Component	Material	Sm[a] (psi) (at temperature ≤ 300°F)
Seamless pipe	ASME SA-312 Grade TP-304L	16700
Ellipsoidal cap	ASME SA-403 Grade WP 304L	16700
Male cone seal, cone seal nut and female cone seal and threads (machined from bar stock)	ASME SA-479 Grade 304L	16700
Cone seal nut and nut threads	ASME SA-479 UNS-S21800	22100

a) Design Stress Intensity values Sm extracted from Table 2A of ASME Section II, Part D, for Class 1 Ferrous material. Calculated stresses in the containment vessel are compared to the lower bound value for Sm of the seamless pipe, 14,700 psi.

4.2 ASME Section III, Subsection NB, Stress Analysis for the 5CV and 6CV

The 5CV and 6CV consist of a section of 5-in. or 6-in. Schedule 40 pipe with a schedule 40 pipe cap on one end and an unstayed flat head and a male cone seal plug on the opposite end, as shown in Figure 2. The unstayed flat head is attached to the containment vessel (CV) by a threaded ring. The unstayed flat head and threaded ring are referred to as the cone seal plug and cone seal nut, respectively.

The finite-element analysis[14] was performed for the 5CV and 6CV subject to the unit load of internal pressure 150 psi. The analytical results serve as the baseline stress state. As discussed in Section 1, the resulting stresses in the 5CV and 6CV under the selected design pressures can be calculated from this baseline. The unit load (150 psi) stress analysis results for the 5CV and 6CV follow are summarized in Tables 5.a and 5.b.

Table 5.a Stress Analysis Results for 150 psi Internal Pressure and ASME Evaluation for NCT

	P_m (psi)	P_m+P_b (psi)	P_m+P_b+Q (psi)	P_m+P_b+Q+F (psi)	$P_{m,pure\text{-}shear}$ (psi)
Stress Limit	**S_m =16700**	**1.5S_m=25050**	**3S_m=50100**	**2S_a=338000***	**1.2S_m=20040**
5CV Body					
Section AA	1544	1682.0			
Section BB	777.82		2113.0	2596.0	
Section CC	1019.27		2042.63	2218.5	
Section DD	1500.8	2323.0			
5CV Plug (preload only)	53.18	1575.0			
5CV Nut (e)	605.96				605.96
5CV Tapered wall thread (f)	1311.39				1311.39
5CV Tapered wall minimum section (g-g)	1003.7		4951	19804	
6CV Body					
Section AA	1699.86	1839.0			
Section BB	878.85		2418.52	2936	
Section CC	1210.57		2263.01	2401.29	
Section DD	1688.25	2477.0			
6CV Plug (preload only)	63.86	2716.0			
6CV Nut (e)	735.06				736.23
6CV Tapered wall thread (f)	1588.46				1590.98
6CV Tapered wall minimum section (g-g)	718.4		3326	13305	

*S_a =169KSI from ASME III, Fig. I-9.2.1 Allowable value for 1000 load cycles (=100 year design life at 10 shipments per year)

Table 5.b Stress Analysis Results for Hydrostatic Test Conditions

Based on 150 psi Internal Pressure (Test Pressure = 1.5 x 150)

	P_m (psi)	P_m+P_b (psi)
Test Limits	**$0.9S_y$=22500 psi**	**$1.35S_y$=33750 psi**
5CV Body:		
Section AA	2316	2523.0
Section BB	1167	
Section CC	1528.9	
Section DD	2251.2	3484.5
5CV Plug (preload only)	53.18	1575.0
5CV Nut (e)	908.94	
5CV Tapered wall thread (f)	1967.1	
5CV Tapered wall minimum section (g-g)	1505.6	
6CV Body:		
Section AA	2549.8	2758.5
Section BB	1318.3	
Section CC	1815.9	
Section DD	2532.4	3715.5
6CV Plug (preload only)	63.86	2716.0
6CV Nut (e)	1102.6	
6CV Tapered wall thread (f)	2382.7	
6CV Tapered wall minimum section (g-g)	1077.5	

4.2.1 Geometry

Dimensions for the geometry are given in Table 6. Refer to Figure 2 for nomenclature. All units are in inches, kilopounds, and degrees Fahrenheit, unless otherwise noted. The containment vessel body and ellipsoidal head are made of Schedule 40 piping and products.

4.2.2 Stress Analysis of 5CV Subject to Unit Load of 150 psi:

A finite-element analysis[14] was performed for the 5CV subject to the unit load of 150 psi by using the ABAQUS computer code[13]. The axisymmetric 4-node bilinear solid elements were used to model the 5CV components, including the cylindrical body, ellipsoidal head, female cone seal, male cone seal plug and cone seal nut. Figures 3 through 6 show the finite-element model for the 5CV components.

Based on the results of this finite-element analysis, the stress intensities at the critical locations of the 5CV are calculated in accordance with the ASME Code, Section III, Subsection NB[7] as follows. Figure 6 shows the critical locations (Sections A-A, B-B, C-C and D-D) where the stress intensities were calculated.

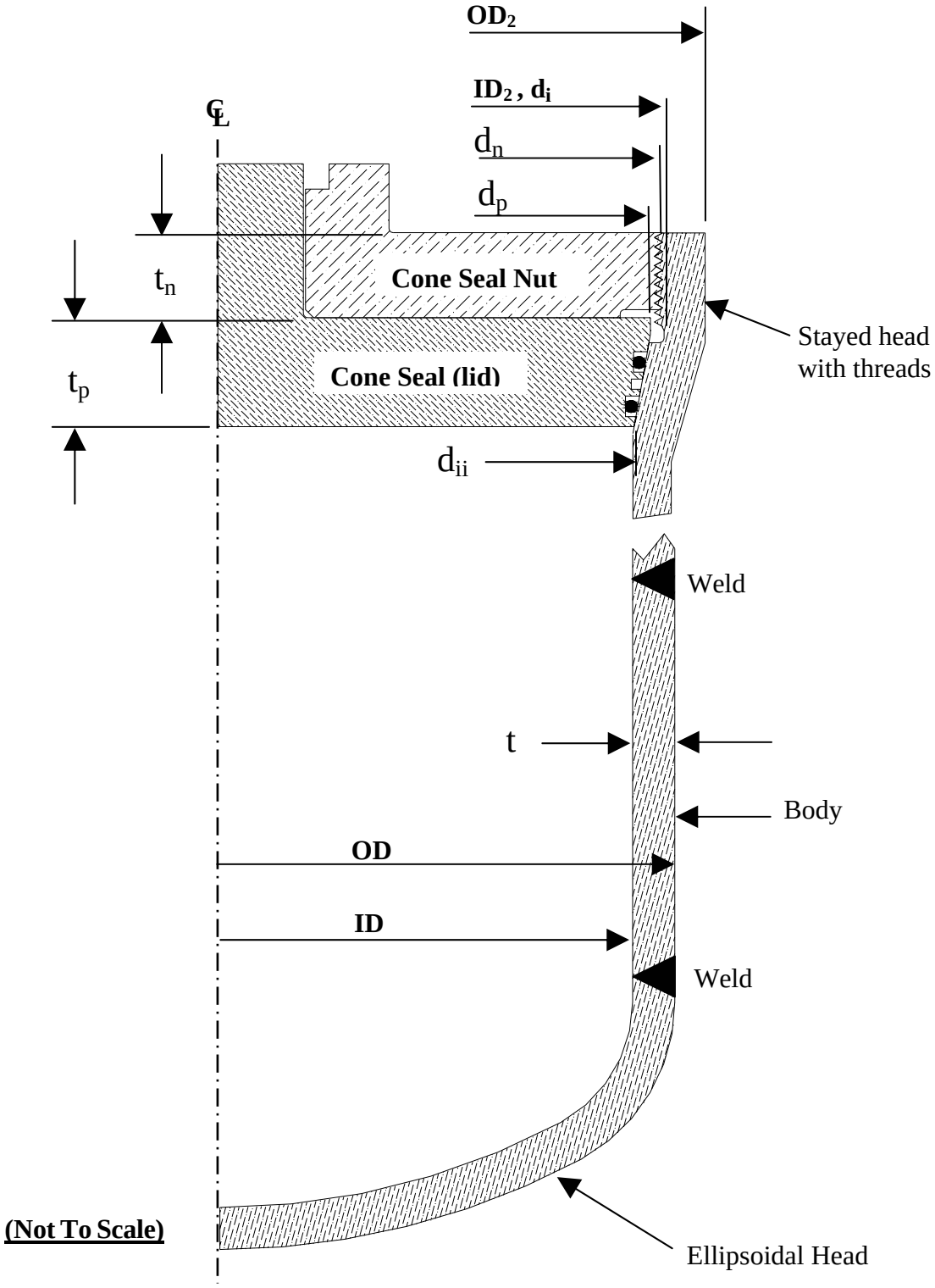

Figure 2 Typical Vessel Cross Section

Table 6. Vessel Dimensions

Dimension	5CV (in.)	6CV (in.)
Body ID	5.047 (5.111)	6.065 (6.135)
Body OD	5.563	6.625
Nominal body thickness, t_m	0.258 (0.226)	0.28 (0.245)
Mean body radius, R	2.6525 (2.6685)	3.1725 (3.19)
Inside body radius, R_i	2.5235 (2.556)	3.0325 (3.0675)
Cone seal plug diameter, d_p	5.27	6.31
Cone seal plug thickness, t_p	0.75	0.75
Cone seal (lid) nut diameter, d_n	5.5	6.5
Cone seal (lid) nut thickness, t_n	0.625	0.625
Female cone seal, OD2 or d_o	5.87	7.12
Female cone seal, ID2 or d_i (thread relief)	5.505	6.51

Note: Dimensions taken from Drawings in Section 2.0, with values in parentheses based on 12.5% wall thickness reduction per ASTM 312[20]

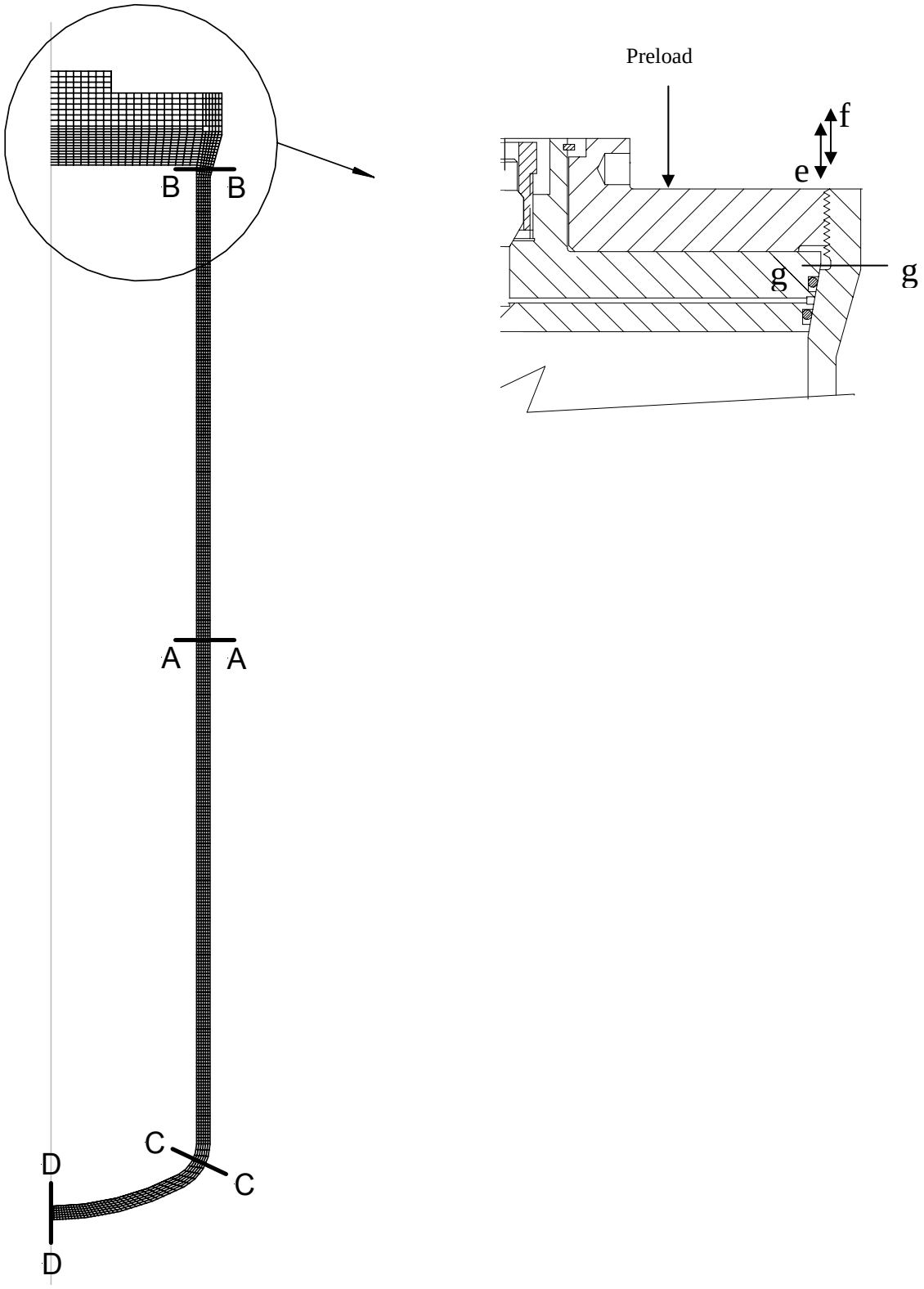

Figure 3 Overall Finite-Element Model of 5CV

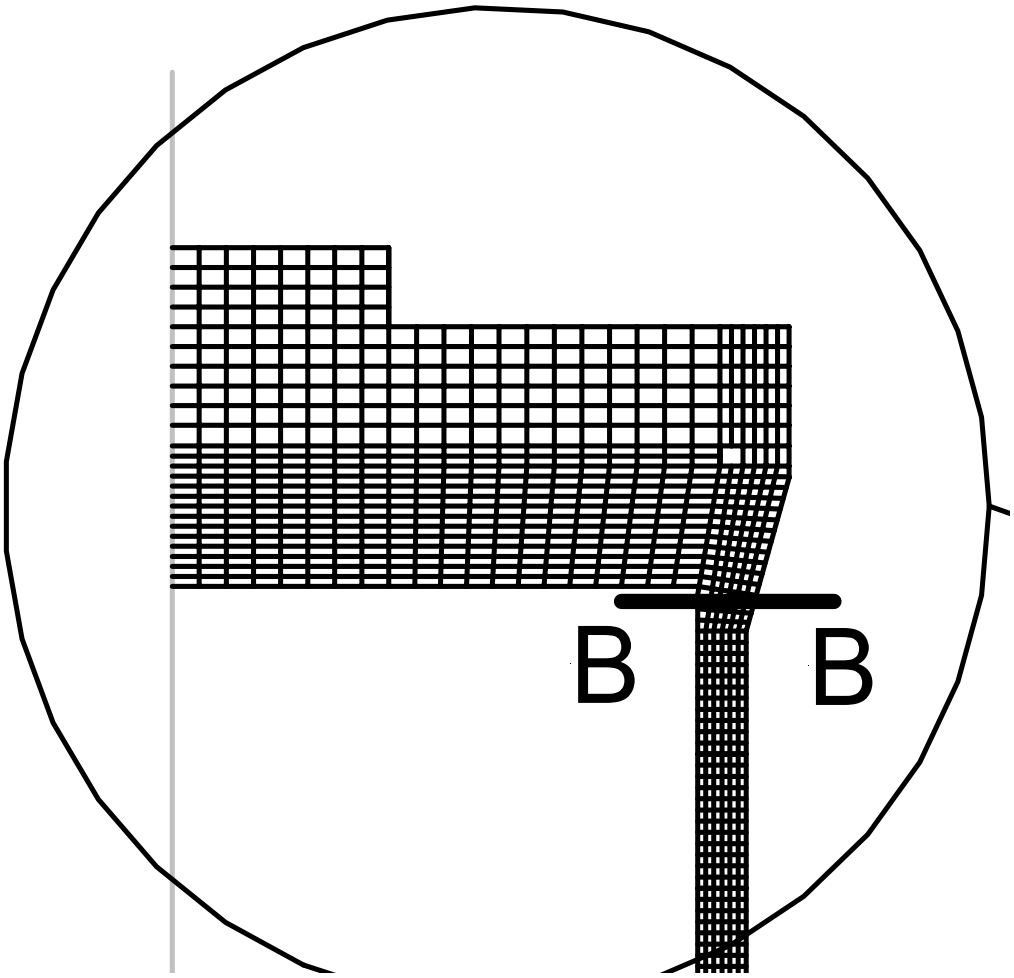

Figure 4 Upper Region of 5CV Finite-Element Model

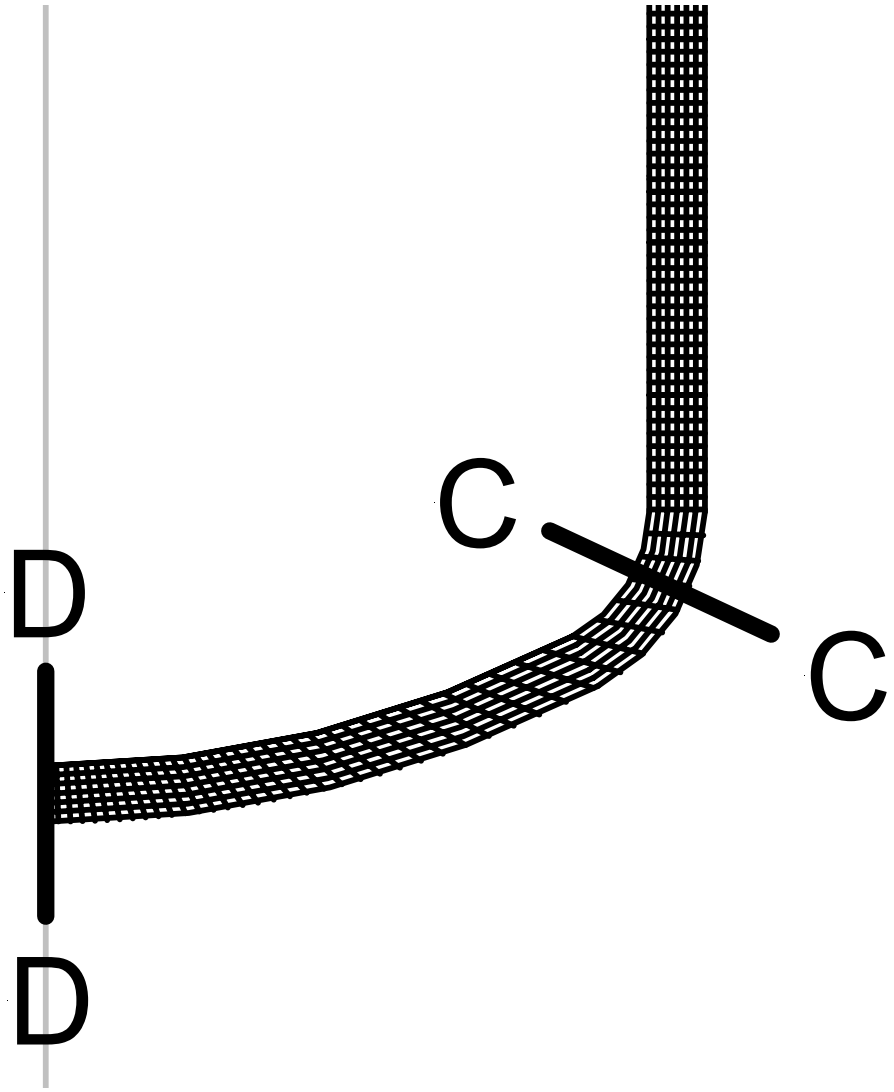

Figure 5 Ellipsoidal Head Region of 5CV Finite-Element Model

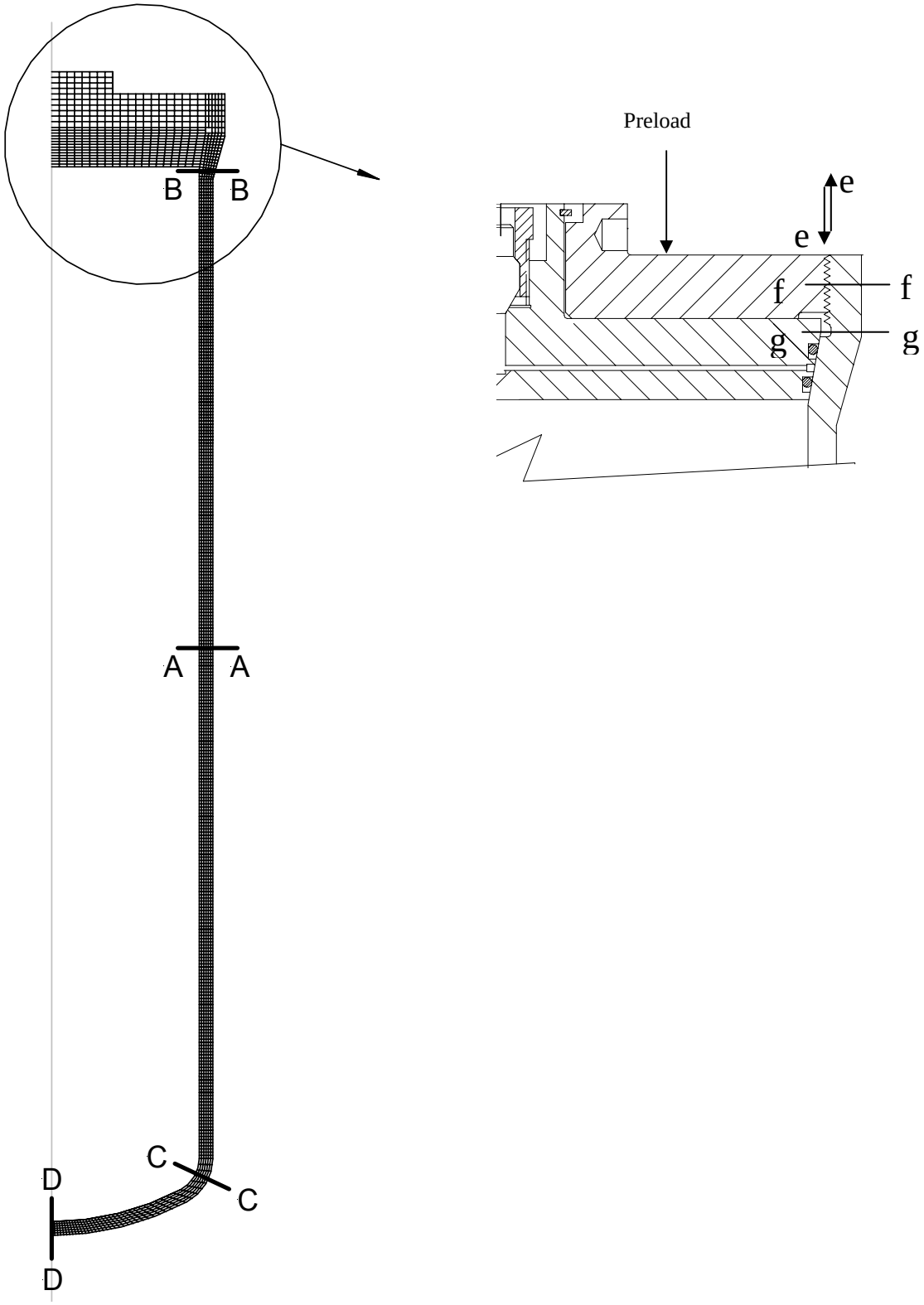

Figure 6 Critical Locations of Stress Distributions in 5CV

4.2.2.1 Section A – A

The stress components across Section A-A, Figure 6, are classified in accordance with the ASME Code, Section III as follows.

(a) Primary Membrane Stress Intensity:

The average values of the normal stress components in the radial, axial, and circumferential directions as well as the shear stress are:

$$\sigma_r = \frac{1}{2}(-150.0 + 0) = -75.0\,psi$$

$$\sigma_a = 698.0\,psi$$

$$\sigma_t = (1532.0 + 1518.0 + 1491.0 + 1466.0 + 1441.0 + 1418.0 + 1417.0)/7 = 1469.0\,psi$$

$$\tau_{ra} = 0.0$$

where σ_r = normal stress in radial direction
σ_a = normal stress in axial direction
τ_{ra} = shear stress on the planes normal to the radial and axial directions

The principal stresses of the above stress components are:

$$\sigma_1 = \sigma_t = 1468.0 \text{ psi}$$

$$\sigma_2 = \sigma_a = 698.0 \text{ psi}$$

$$\sigma_3 = \sigma_r = -75.0 \text{ psi}$$

Consequently, the maximum primary membrane stress intensity is:

$$P_m = \sigma_1 - \sigma_3 = 1469.0 + 75.0 = 1544.0 \text{ psi}$$

(b) Primary Membrane Plus Primary Bending Stress Intensity:

On the inner surface of the cylindrical shell, the stress components are:

$$\sigma_r = -150.0 \text{ psi}$$

$$\sigma_a = 698.0 \text{ psi}$$

$$\sigma_t = 1532 \text{ psi}$$

$$\tau_{ra} = 0.0$$

The principal stresses are:

$$\sigma_1 = \sigma_t = 1532 \text{ psi}$$

$$\sigma_2 = \sigma_a = 698 \text{ psi}$$

$$\sigma_3 = \sigma_r = -150 \text{ psi}$$

Thus, the maximum Primary Membrane Plus Primary Bending Stress Intensity is:

$$P_m + P_b = \sigma_1 - \sigma_3 = 1532 + 150 = 1682.0 \text{ psi}$$

4.2.2.2 Section B – B

The axial and hoop stress components on Section B-B, Figure 6, obtained from the finite-element analysis are not linearly distributed across the vessel wall. The linearized bending and membrane stresses equivalent to these components are calculated and displayed in Figure 7. These equivalent stresses are then classified in accordance with the ASME Code, Section III as follows.

The terms of some stress components used in Figure 7. are defined as follows.

$\sigma_{a,e} =$ equivalent membrane plus bending stress in axial direction
$(\sigma_{a,m})_e, (\sigma_{t,m})_e =$ equivalent membrane stresses in the axial and circumferential directions, respectively.

(a) Primary Membrane Stress Intensity

The stress components are as follows:

$$\sigma_r = (-279.8 + 116.4 + 158.5 + 95.94 + 31.45 - 12.57 + 60.34)/7 = 24.32 \text{ psi}$$

$$\sigma_a = 711.617 \text{ psi}$$

$$\sigma_t = 279.75 \text{ psi}$$

$$\tau_{ra} = (-158.4 - 248.0 - 36.1 - 229.5 - 189.4 - 128.3 - 176.6)/7 = -166.61 \text{ psi}$$

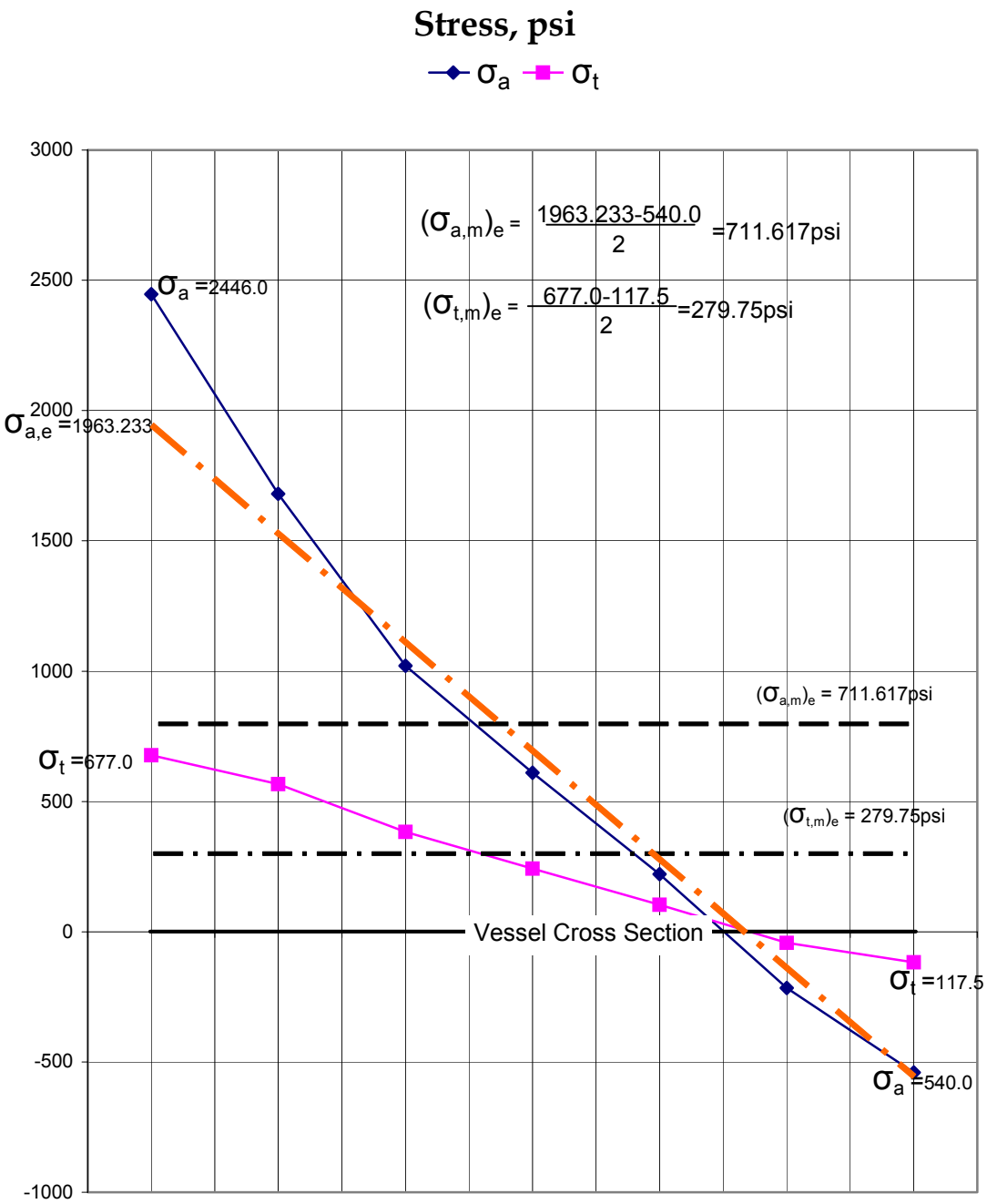

Figure 7 Equivalent Membrane and Bending Stresses on Section BB

The principal stresses in the planes perpendicular to the radial and axial directions are:

$$\sigma_1, \sigma_2 = \frac{\sigma_r + \sigma_a}{2} \pm \sqrt{\left(\frac{\sigma_r - \sigma_a}{2}\right)^2 + \tau_{ra}^2}$$

$$= \frac{24.32 + 711.617}{2} \pm \sqrt{\left(\frac{24.32 - 711.617}{2}\right)^2 + (-166.61)^2}$$

$$= 367.969 \pm 381.93$$

or,

$$\sigma_1 = 749.90 \text{ psi}$$

$$\sigma_2 = -13.96 \text{ psi}$$

The principal stresses in the three dimensional space then become:

$$\sigma_I = 763.86 \text{ psi}$$

$$\sigma_{II} = 279.75 \text{ psi}$$

$$\sigma_{III} = -13.96 \text{ psi}$$

Consequently, the primary membrane stress intensity is:

$$P_m = \sigma_I - \sigma_{III} = 763.86 + 13.96 = 777.82 \text{ psi}$$

(b) Primary Membrane Plus Primary Bending Plus Secondary Stress Intensity

The stress components are:

$$\sigma_r = -150 \text{ psi}$$

$$\sigma_a = \sigma_{a,e} = 1963 \text{ psi}$$

$$\sigma_t = 677 \text{ psi}$$

$$\tau_{ra} = 0$$

Then, the principal stresses are:

$$\sigma_1 = \sigma_a = 1963 \text{ psi}$$

$$\sigma_2 = \sigma_t = 677 \text{ psi}$$

$$\sigma_3 = \sigma_r = -150 \text{ psi}$$

Thus, the Primary Membrane Plus Primary Bending Plus Secondary Stress Intensity is:

$$P_m + P_b + Q = \sigma_1 - \sigma_3 = 1963 + 150 = 2113 \text{ psi}$$

(c) Primary Membrane Plus Primary Bending Plus Secondary Plus Peak Stress Intensity

The stress components are as follow:

$$\sigma_r = -150.0 \text{ psi}$$

$$\sigma_a = 2446.0 \text{ psi}$$

$$\sigma_t = 677.0 \text{ psi}$$

$$\tau_{ra} = 0.0 \text{ psi}$$

Then, the principal stresses are:

$$\sigma_1 = \sigma_a = 2446.0 \text{ psi}$$

$$\sigma_2 = \sigma_t = 677.0 \text{ psi}$$

$$\sigma_3 = \sigma_r = -150.0 \text{ psi}$$

Thus, the Primary Membrane Plus Primary Bending Plus Secondary Plus Peak Stress Intensity is:

$$P_m + P_b + Q + F = \sigma_1 - \sigma_3 = 2446.0 + 150.0 = 2596.0 \text{ psi}$$

4.2.2.3 Section C – C

The normal and shear stress components in the vessel axial and radial directions across Section C-C, Figure 6, obtained from the finite-element analysis are not the normal and shear stresses with respect to the Cross Section C-C. The normal and shear stresses on the surface of Section C-C can be calculated in terms of the finite-element results by using the following equations:

$$\sigma_n = \sigma_r \cos^2\alpha + \sigma_a \sin^2\alpha + 2\tau_{ra} \sin\alpha \cos\alpha$$

$$\tau_{nR} = \tau_{ar}(\cos^2\alpha - \sin^2\alpha) + (\sigma_a - \sigma_r)\sin\alpha\cos\alpha$$

where σ_n = normal stress component on Section C-C

τ_{nR} = shear stress component on Section C-C

α = inclination angle between the normal vector of Section C-C surface and vessel radial direction

The linearized equivalent stresses of the stress components σ_n and σ_t are then generated in the same manner as discussed for Section B-B. Figure 8 shows the equivalent stress components. The resulting stresses are classified in accordance with the ASME Code, Section III as follows.

The terms of some stress components shown in Figure 8 are defined as follows.

$\sigma_{n,e}$ = equivalent membrane plus bending stress in the normal direction

$(\sigma_{n,m})_e, (\sigma_{t,m})_e$ = equivalent membrane stresses in the normal and circumferential directions, respectively

$(\sigma_{n,b})_e, (\sigma_{t,b})_e$ = equivalent bending stresses in the normal and circumferential directions, respectively

(a) Primary Membrane Stress Intensity

The stress components perpendicular to the cross section of the vessel wall, in the hoop direction and perpendicular to the vessel wall are respectively given as follows:

$$\sigma_n = 755.376 \text{ psi}$$

$$\sigma_t = -163.65 \text{ psi}$$

$$\sigma_R = \frac{-150+0}{2} = -75 \text{ psi}$$

The shear stress across the section is approximately:

$$\tau_{nR} = (-844.1472 - 668.7936 - 419.0789 - 228.5179 - 76.32464 + 54.58398 + 113.4907)/7$$

= -295.541 psi

The principal stresses on the meridian plane are calculated as follows:

$$\sigma_1, \sigma_2 = \frac{\sigma_R + \sigma_n}{2} \pm \sqrt{\left(\frac{\sigma_R - \sigma_n}{2}\right)^2 + \tau_{nR}^2}$$

$$= \frac{-75 + 755.376}{2} \pm \sqrt{\left(\frac{-75 - 755.376}{2}\right)^2 + (-295.54)^2}$$

$$= 340.188 \pm 509.633$$

or, $\sigma_1 = 849.821\,\text{psi}$

$\sigma_2 = -169.445\,\text{psi}$

Then, the principal stresses are:

$\sigma_I = \sigma_1 = 849.821\,\text{psi}$

$\sigma_{II} = \sigma_t = -163.65\,\text{psi}$

$\sigma_{III} = \sigma_2 = -169.445\ \text{psi}$

Thus, the Primary Membrane Stress Intensity is:

$P_m = \sigma_I - \sigma_{III} = 849.821 + 169.445 = 1019.266\,\text{psi}$

(b) Primary Membrane Plus Primary Bending Plus Secondary Stress Intensity

The linearized stress components on the inner surface of the vessel are:

$\sigma_n = 1892.632\ \text{psi}$

$\sigma_t = 192.9\ \text{psi}$

$\sigma_R = -150.0\ \text{psi}$

Then the principal stresses are:

$\sigma_1 = \sigma_n = 1892.63\,\text{psi}$

$\sigma_2 = \sigma_t = 192.9\,\text{psi}$

$\sigma_3 = \sigma_R = -150.0\,\text{psi}$

Thus, the Primary Membrane Plus Primary Bending Plus Secondary Stress Intensity is:

$$P_L + P_b + Q = \sigma_1 - \sigma_3 = 1892.632 + 150.0 = 2042.632\ \text{psi}$$

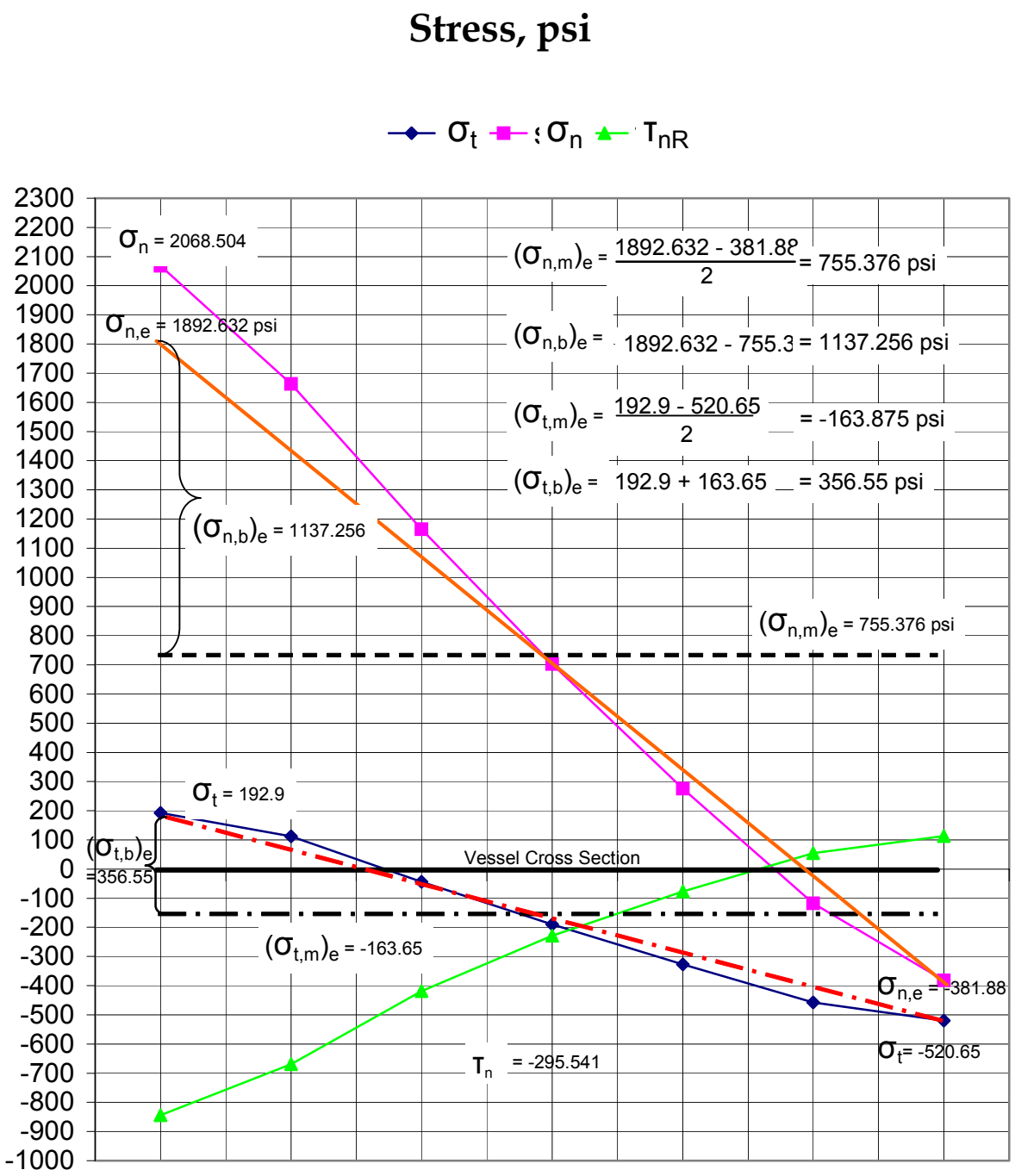

Figure 8 Equivalent Membrane and Bending Stresses in Section CC

(c) Primary Membrane Plus Primary Bending Plus Secondary Plus Peak Stress Intensity

The stress components on the inner surface of the vessel are:

$$\sigma_n = 2068.504 \text{ psi}$$

$$\sigma_t = 192.9 \text{ psi}$$

$$\sigma_r = -150.0 \text{ psi}$$

Then, the principal stresses are:

$$\sigma_1 = \sigma_n = 2068.504 \text{ psi}$$

$$\sigma_2 = \sigma_t = 192.9 \text{ psi}$$

$$\sigma_3 = \sigma_R = -150.0 \text{ psi}$$

Thus, the Primary Membrane Plus Primary Bending Plus Secondary Plus Peak Stress Intensity is:

$$P_L + P_b + Q + F = \sigma_1 - \sigma_3 = 2068.504 + 150.0 = 2218.504 \text{ psi}$$

4.2.2.4 Section D – D

(a) Primary Membrane Stress Intensity

$$\sigma_r = \sigma_t = \frac{1}{2}\left(528.6 + 2323.0\right) = 1425.8 \text{ psi}$$

$$\sigma_a = \frac{1}{2}\left(-150.0 + 0\right) = \text{-}75.0 \text{ psi}$$

$$\tau_{ra} = 0 \text{ psi}$$

Then, the principal stresses are:

$$\sigma_1 = \sigma_2 = \sigma_r = \sigma_t = 1425.8 \text{ psi}$$

$$\sigma_3 = \sigma_a = -75 \text{ psi}$$

Thus, the Maximum Primary Membrane Stress Intensity is:

$$P_m = \sigma_1 - \sigma_3 = 1425.8 + 75.0 = 1500.8 \text{ psi}$$

(b) Primary Membrane Plus Primary Bending Stress Intensity

On the outer surface of the elliptical head, the stress components are:

$$\sigma_r = \sigma_t = 2323\,\text{psi}$$

$$\sigma_a = 0\,\text{psi}$$

Then, the principal stresses are:

$$\sigma_1 = \sigma_2 = \sigma_r = \sigma_t = 2323\ \text{psi}$$

$$\sigma_3 = \sigma_a = 0$$

Thus, the Primary Membrane Plus Primary Bending Stress Intensity is:

$$P_m + P_b = \sigma_1 - \sigma_3 = 2323\,\text{psi}$$

4.2.3 Stress Analysis of 6CV Subject to Unit Load of 150 psi

A finite-element analysis[14] was performed for the 6CV subject to the unit load of 150 psi by using the ABAQUS computer code[13]. The axisymmetric 4-node bilinear solid elements were used to model the 5CV components, including the cylindrical body, ellipsoidal head, female cone seal, male cone seal plug and cone seat nut. Figures 9 through 11 show the finite-element model for the 6CV components.

Based on the results of this finite-element analysis, the stress intensities at the critical locations of the 6CV are calculated in accordance with the ASME Code, Section III as follows. Figure 12 shows the critical locations where the stress intensities were calculated.

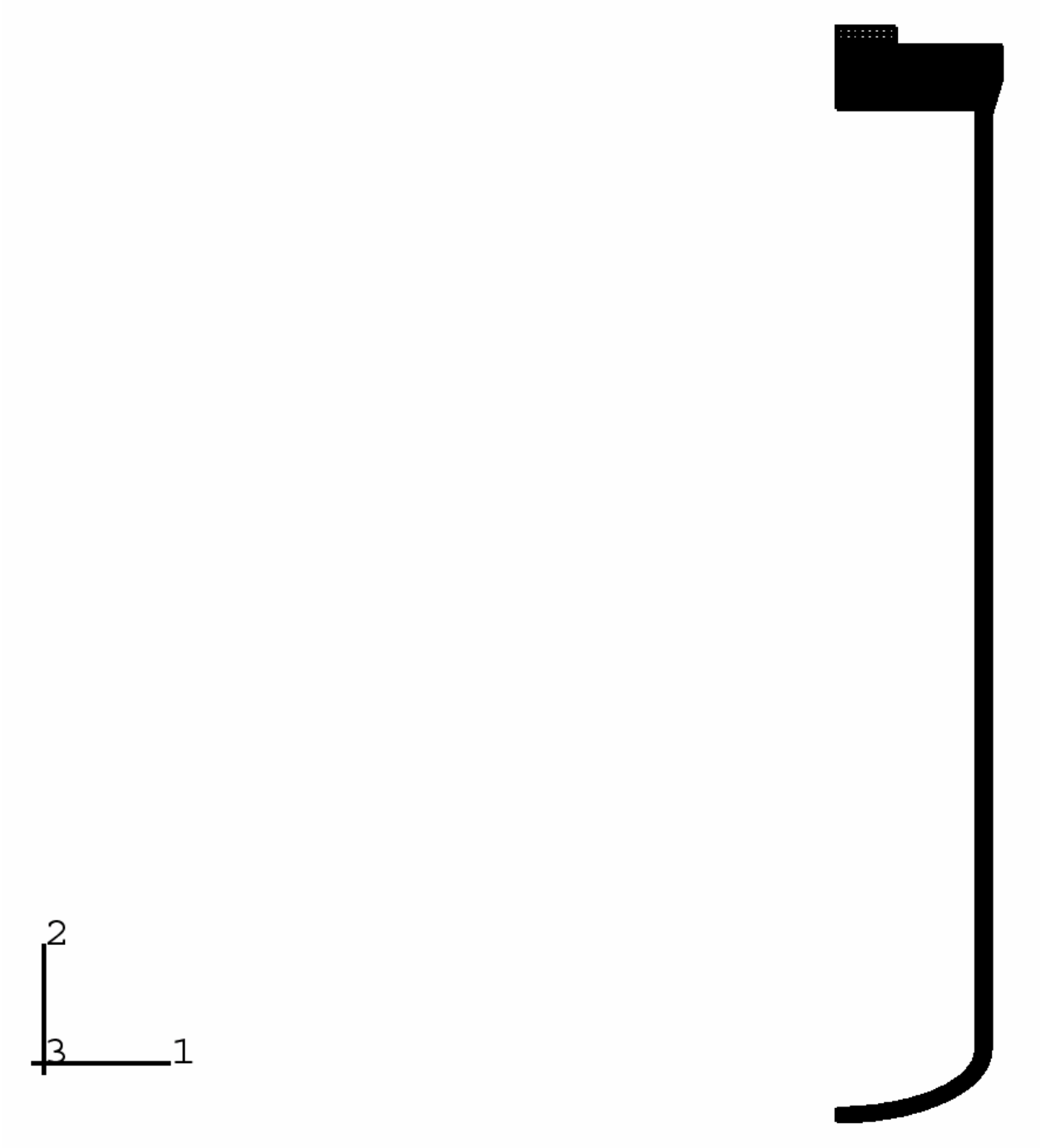

Figure 9 Overall Finite-Element Model of 6CV

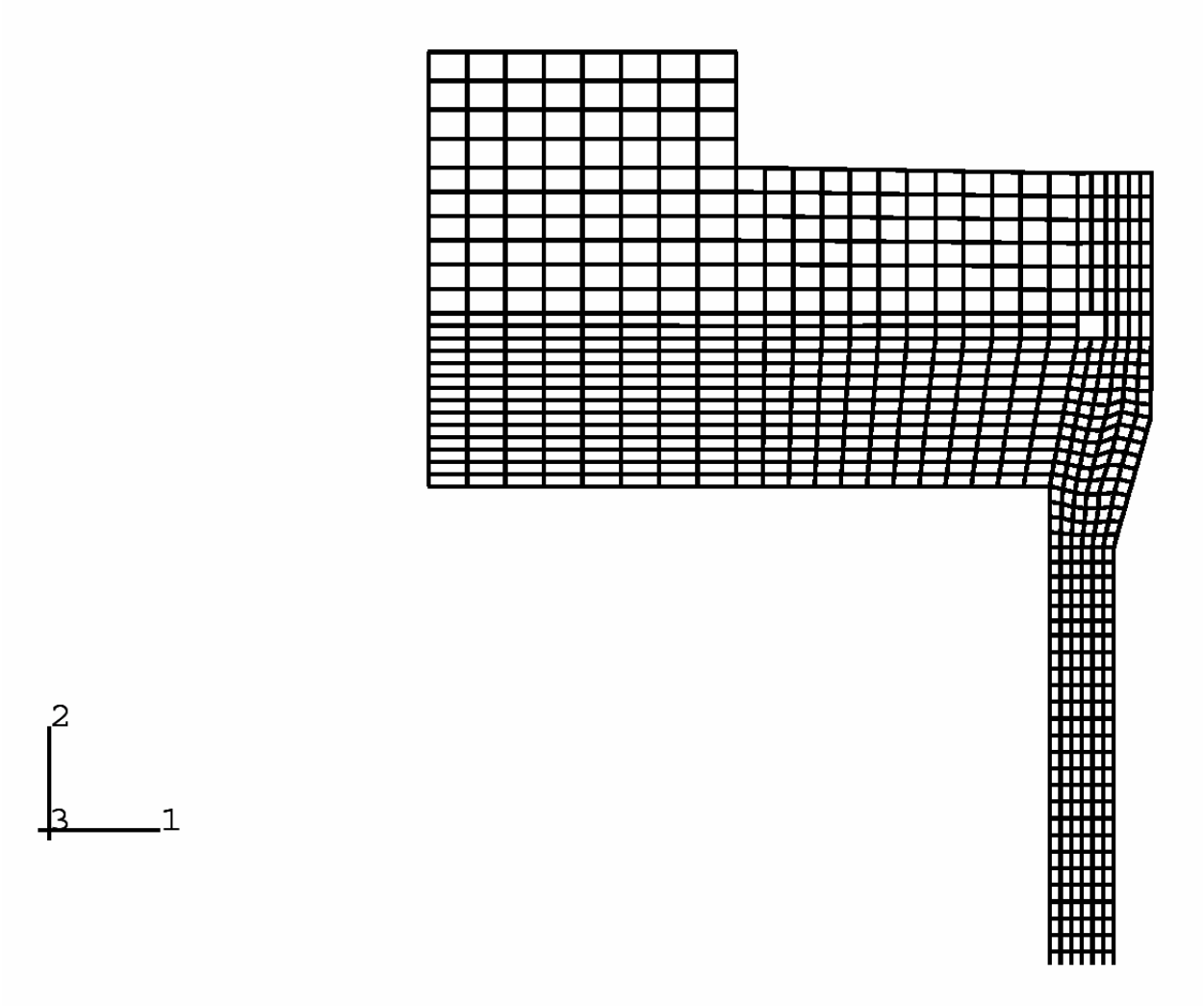

Figure 10 Upper Region of 6CV Finite-Element Model

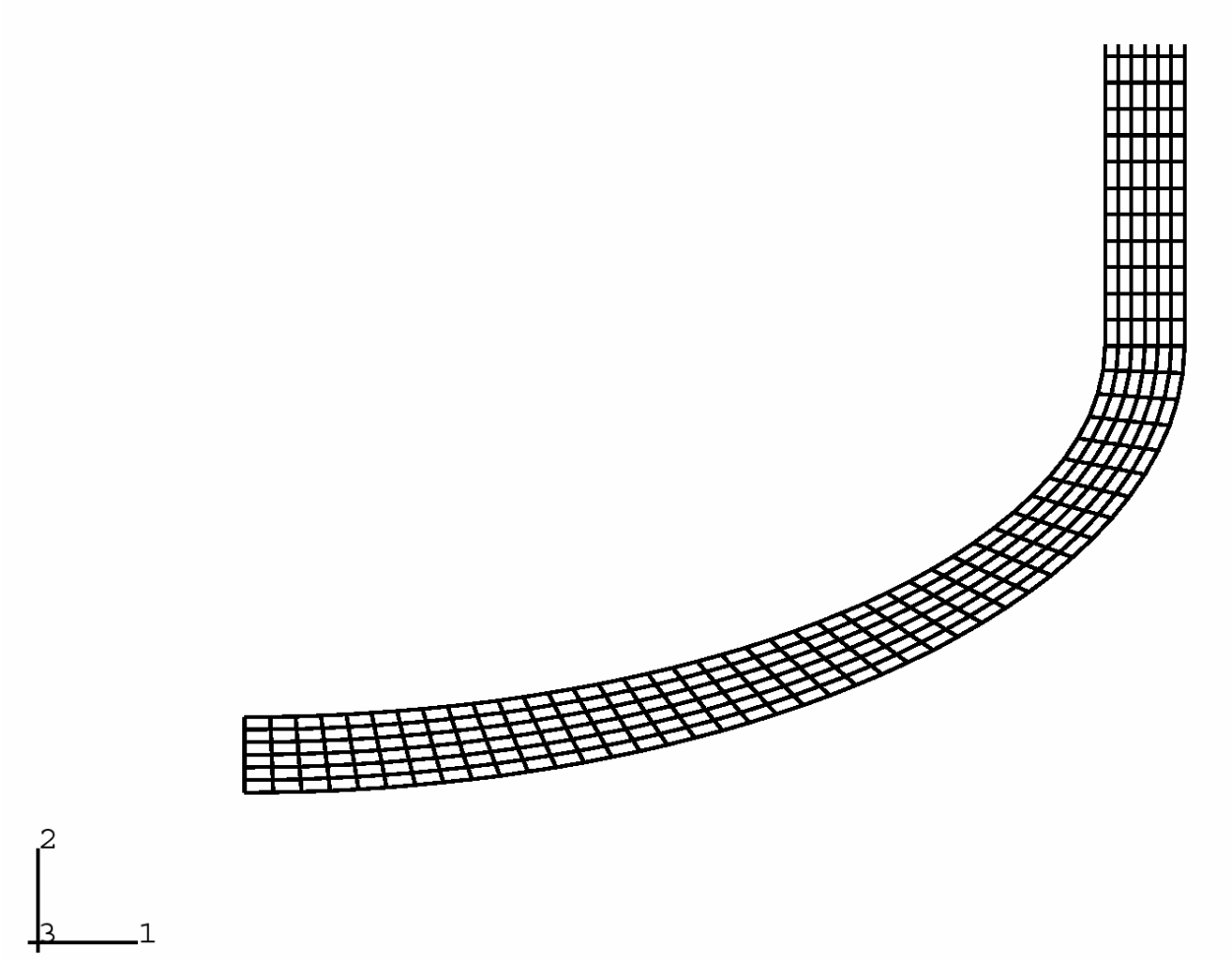

Figure 11 Ellipsoidal Head Region of 6CV Finite-Element Model

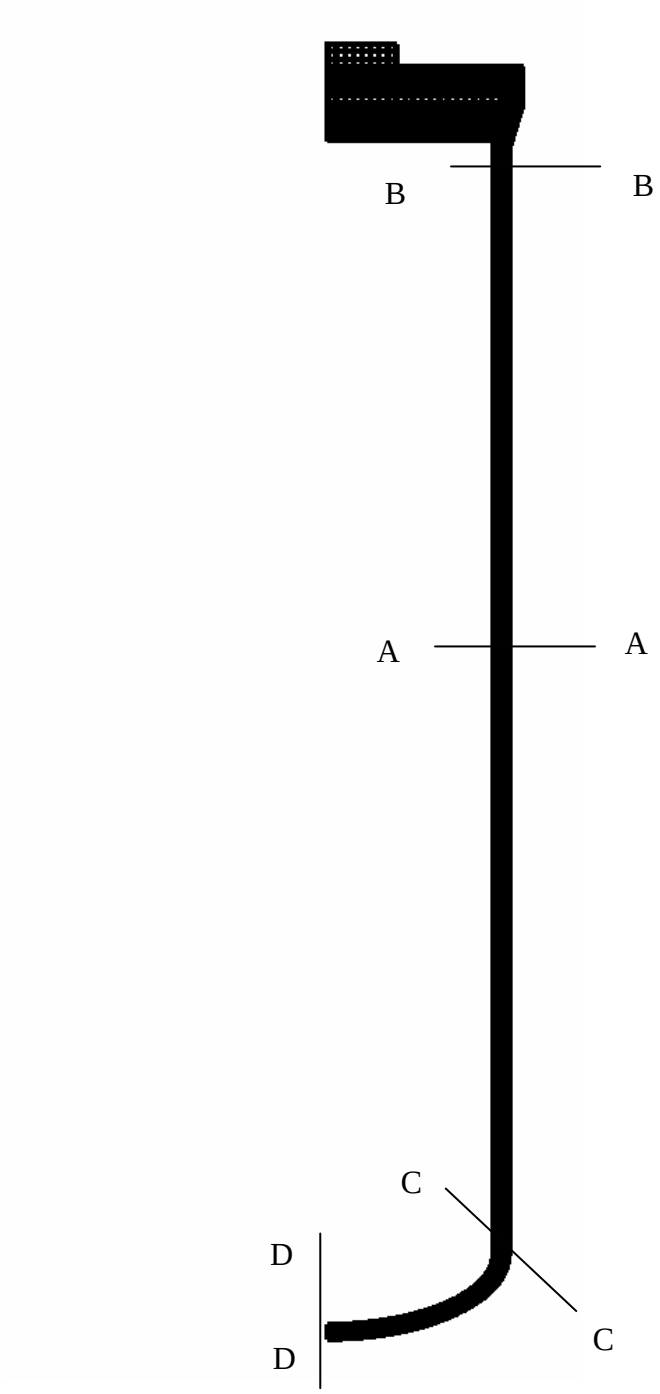

Figure 12 Critical Locations of Stress Distributions in 5CV

4.2.3.1 Section A – A (Figure 12)

(a) Primary Membrane Stress Intensity

The stress components are:

$$\sigma_r = \frac{1}{2}(-150 + 0) = -75 \text{ psi}$$

$$\sigma_a = 776.4 \text{ psi}$$

$$\sigma_t = (1689.0 + 1675.0 + 1649.0 + 1623.0 + 1599.0 + 1575.0 + 1564.0)/7 = 1624.86 \text{ psi}$$

$$\tau_{ra} = 0.0 \text{ psi}$$

Then, the principal stresses are:

$$\sigma_1 = \sigma_t = 1624.86 \text{ psi}$$

$$\sigma_2 = \sigma_a = 776.4 \text{ psi}$$

$$\sigma_3 = \sigma_r = -75.0 \text{ psi}$$

Thus, the maximum Primary Membrane Stress Intensity is:

$$P_m = \sigma_1 - \sigma_3 = 1624.86 + 75.0 = 1699.86 \text{ psi}$$

(b) Primary Membrane Plus Primary Bending Stress Intensity

On the inner surface of the cylindrical body, the stress components are:

$$\sigma_r = -150.0 \text{ psi}$$

$$\sigma_a = 776.4 \text{ psi}$$

$$\sigma_t = 1689.0 \text{ psi}$$

$$\tau_{ra} = 0.0 \text{ psi}$$

The principal stresses are:

$$\sigma_1 = \sigma_t = 1689.0 \text{ psi}$$

$$\sigma_2 = \sigma_a = 776.4\,\text{psi}$$

$$\sigma_3 = \sigma_r = -150.0\ \text{psi}$$

Thus, the maximum Primary Membrane Plus Primary Bending Stress Intensity is:

$$P_m + P_b = \sigma_1 - \sigma_3 = 1689.0 + 150.0 = 1839.0\ \text{psi}$$

4.2.3.2 Section B – B

The linearized equivalent stress components shown in Figure 13 are generated in the same manner as discussed for the 5CV. The resulting stresses are classified in accordance with the ASME Code, Section III as follows.

The terms of some stress components shown in Figure 13 are defined as follows.

$\sigma_{a,e}$ = equivalent membrane plus bending stresses in the axial direction.
$(\sigma_{a,m})_e, (\sigma_{t,m})_e$ = equivalent membrane stresses in the axial and circumferential directions, respectively

(a) Primary Membrane Stress Intensity

The stress components are:

$$\sigma_r = (-308.0 + 108.6 + 210.6 + 144.8 + 50.88 - 29.15 + 61.38)/7 = 34.16\ \text{psi}$$

$$\sigma_a = (\sigma_{a,m})e = 788.209\,\text{psi}$$

$$\sigma_t = (\sigma_{t,m})e = 255.25\ \text{psi}$$

$$\tau_{ra} = (-153.1 - 250.3 - 340.8 - 244.8 - 190.3 - 188.1 - 212.6)/7 = -225.71\,\text{psi}$$

The principal stresses on the planes perpendicular to the radial and axial directions are calculated as follows:

$$\sigma_1, \sigma_2 = \frac{\sigma_r + \sigma_a}{2} \pm \sqrt{\left(\frac{\sigma_r - \sigma_a}{2}\right)^2 + \tau_{ra}^2}$$

$$= \frac{34.16 + 788.209}{2} \pm \sqrt{\left(\frac{34.16 - 788.209}{2}\right)^2 + (-225.71)^2}$$

$$= 411.185 \pm 439.423$$

$\sigma_1 = 850.608$ psi

$\sigma_2 = -28.238$ psi

Then, the principal stresses are:

$\sigma_I = \sigma_1 = 850.608$ psi

$\sigma_{II} = \sigma_t = 255.25$ psi

$\sigma_{III} = \sigma_2 = -28.238$ psi

The Membrane Stress Intensity is:

$P_m = \sigma_I - \sigma_{III} = 850.608 + 28.238 = 878.846$ psi

(b) Primary Membrane Plus Primary Bending Plus Secondary Stress Intensity

The stress components are:

$\sigma_r = -150.0$ psi

$\sigma_a = \sigma_{a,e} = 2268.517$ psi

$\sigma_t = 725.1$ psi

$\tau_{ra} = 0.0$ psi

Then, the principal stresses are:

$\sigma_1 = \sigma_a = 2268.517$ psi

$\sigma_2 = \sigma_t = 725.1$ psi

$\sigma_3 = \sigma_r = -150.0$ psi

Thus, the Primary Membrane Plus Primary Bending Plus Secondary Stress Intensity is:

$P_m + P_b + Q = \sigma_1 - \sigma_3 = 2268.517 + 150.0 = 2418.517$ psi

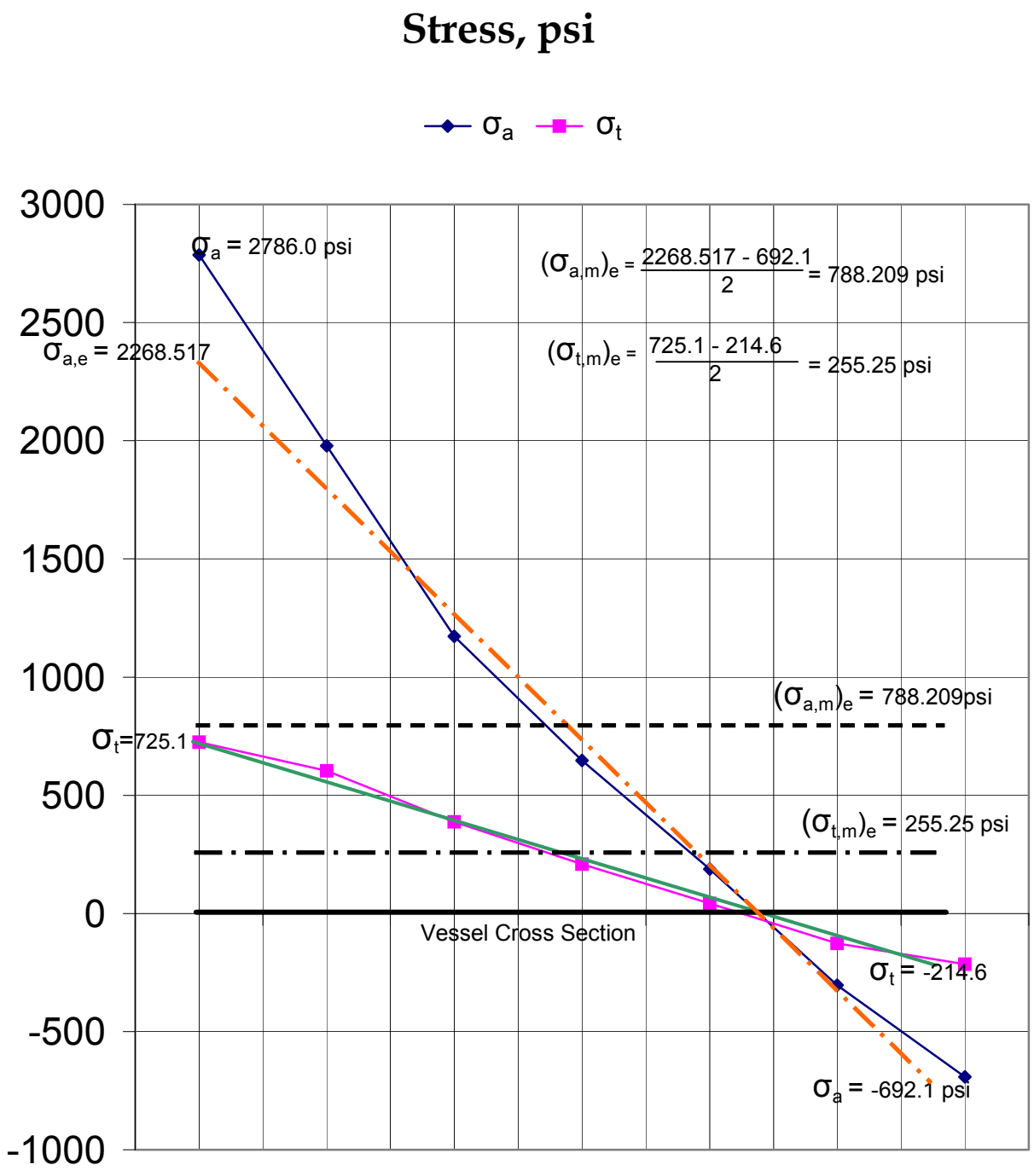

Figure 13 Equivalent Membrane and Bending Stresses on Section BB

(c) Primary Membrane Plus Primary Bending Plus Secondary Plus Peak Stress Intensity

The stress components on the inner surface of the vessel body are:

$\sigma_r = -150.0$ psi

$\sigma_a = 2786.0$ psi

$\sigma_t = 725.1$ psi

$\tau_{ra} = 0.0$

The principal stresses are:

$\sigma_1 = \sigma_a = 2786.0$ psi

$\sigma_2 = \sigma_t = 725.1$ psi

$\sigma_3 = \sigma_r = -150.0$ psi

The Primary Membrane Plus Primary Bending Plus Secondary Plus Peak Stress Intensity is:

$P_m + P_b + Q + F = \sigma_1 - \sigma_3 = 2786.0 + 150.0 = 2936.0$ psi

4.2.3.3 Section C – C

The stress components obtained from the finite-element analysis are rotated with respected to the surface of Section C-C and the linearized equivalent stresses are generated in the same manner as discussed in for the 5CV. Figure 14 shows the linearized equivalent stress components. The resulting stresses are classified in accordance with the ASME Code, Section III as follows.

The terms of some stress components shown in Figure 14 are defined below.

$\sigma_{n,e}$ = equivalent membrane plus bending stress in the normal direction.
$(\sigma_{n,m})_e, (\sigma_{t,m})_e$ = equivalent membrane stresses in the normal and circumferential directions, respectively
$(\sigma_{n,b})_e, (\sigma_{t,b})_e$ = equivalent bending stresses in the normal and circumferential directions, respectively

(a) Primary Membrane Stress Intensity

The membrane stress components after the stress results are linearized are:

$\sigma_n = (\sigma_{n,m})e = 824.202$ psi

$$\sigma_t = (\sigma_{,mt})e = -278.75\,\text{psi}$$

$$\sigma_R = \frac{-150+0}{2} = -75\ \text{psi}$$

The average shear stress across the cross section of the vessel is:

$$\tau_{nR} = (-944.545 - 755.769 - 478.148 - 259.133 - 80.159 + 73.089 + 140.475)/7$$

$$= \text{-329.17 psi}$$

The principal stresses on the planes perpendicular to R and n directions are:

$$\sigma_{1,}\sigma_2 = \frac{\sigma_R + \sigma_n}{2} \pm \sqrt{\left(\frac{\sigma_R - \sigma_n}{2}\right)^2 + \tau_{nR}^2}$$

$$= \frac{-75 + 824.202}{2} \pm \sqrt{\left(\frac{-75 - 824.202}{2}\right)^2 + (-329.17)^2}$$

$$= 374.601 \pm 557.22$$

or,

$$\sigma_1 = 931.821\,\text{psi}$$

$$\sigma_2 = -182.619\,\text{psi}$$

Then, the principal stresses are:

$$\sigma_I = \sigma_1 = 931.821\,\text{psi}$$

$$\sigma_{II} = \sigma_2 = -182.619\,\text{psi}$$

$$\sigma_{III} = \sigma_t = (\sigma_{t,m})e = -278.75\,\text{psi}$$

Thus, the Primary Membrane Stress Intensity is:

$$P_m = \sigma_I - \sigma_{III} = 931.821 + 278.75 = 1210.571\,\text{psi}$$

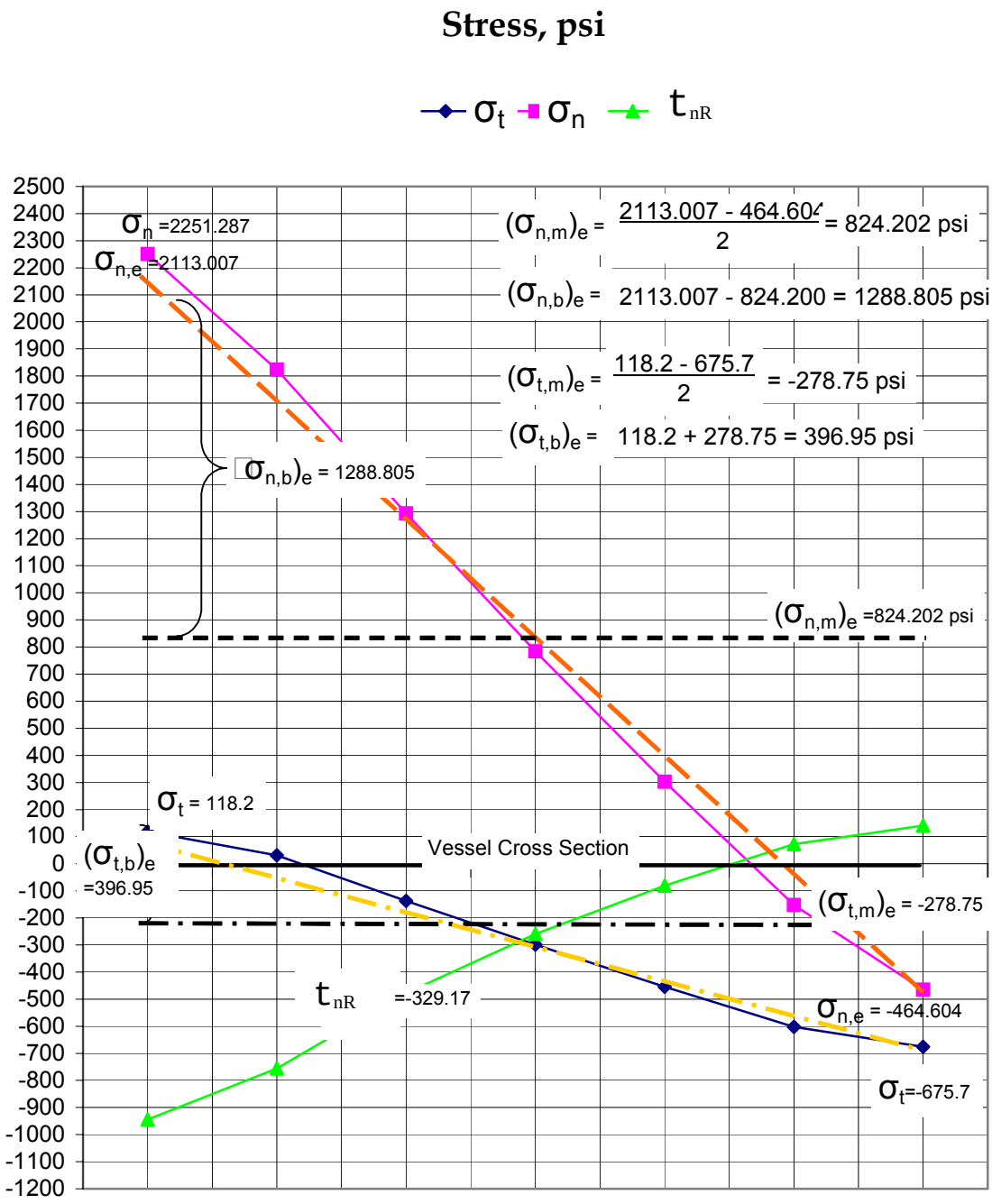

Figure 14 Equivalent Membrane and Bending Stresses in Section CC

(b) Primary Membrane Plus Primary Bending Plus Secondary Stress Intensity

The stress components on the inner surface of the vessel after the calculated stresses are linearized are as follows:

$$\sigma_n = \sigma_{n,e} = 2113.007 \text{ psi}$$

$$\sigma_t = 118.2 \text{ psi}$$

$$\sigma_R = -150.0 \text{ psi}$$

Then, the principal stresses are:

$$\sigma_1 = \sigma_n = 2113.007 \text{ psi}$$

$$\sigma_2 = \sigma_t = 118.2 \text{ psi}$$

$$\sigma_3 = \sigma_R = -150.0 \text{ psi}$$

Thus, the Primary Membrane Plus Primary Bending Plus Secondary Stress Intensity is:

$$P_m + P_b + Q = \sigma_1 - \sigma_3 = 2113.007 + 150.0 = 2263.007 \text{ psi}$$

(c) Primary Membrane Plus Primary Bending Plus Secondary Plus Peak Stress Intensity

The stress components on the inner surface of the vessel wall are:

$$\sigma_n = 2251.287 \text{ psi}$$

$$\sigma_t = 118.2 \, psi$$

Then, the principal stresses are:

$$\sigma_1 = \sigma_n = 2251.287 \text{ psi}$$

$$\sigma_2 = \sigma_t = 118.2 \text{ psi}$$

$$\sigma_3 = \sigma_R = -150.0 \text{ psi}$$

Thus, the Primary Membrane Plus Primary Bending Plus Secondary Plus Peak Stress Intensity is:

$$P_m + P_b + Q + F = \sigma_1 - \sigma_3 = 225.287 + 150.0 = 2401.287 \text{ psi}$$

4.2.3.4 Section D – D

(a) Primary Membrane Stress Intensity

The average stresses across the section are:

$$\sigma_r = \sigma_t = \frac{1}{2}(749.5 + 2477.0) = 1613.25 \text{ psi}$$

$$\sigma_a = \frac{1}{2}(-150 + 0)) = -75 \text{ psi}$$

$$\tau_{ar} = 0$$

The principal stresses are:

$$\sigma_1 = \sigma_2 = \sigma_r = \sigma_t = 1613.25 \text{ psi}$$

$$\sigma_3 = \sigma_a = -75 \text{ psi}$$

The maximum Primary Membrane Stress Intensity is:

$$P_m = \sigma_1 - \sigma_3 = 1613.25 + 75.0 = 1688.25 \text{ psi}$$

(b) Primary Membrane Plus Primary Bending Stress Intensity

On the outer surface of the elliptical head, the stress components are:

$$\sigma_r = \sigma_t = 2477.0 \text{ psi}$$

$$\sigma_a = 0$$

The principal stresses are:

$$\sigma_1 = \sigma_2 = \sigma_r = \sigma_t = 2477.0 \text{ psi}$$
$$\sigma_3 = \sigma_a = 0$$

Thus, the Primary Membrane Plus Primary Bending Stress Intensity is:

$$P_m + P_b = \sigma_1 - \sigma_3 = 2477.0 \text{ psi}$$

4.2.4 Calculation of Stresses in Male Cone Seal Plug Subject to 150 psi

The maximum stresses in the male cone seal plug are caused by the preload. The internal pressure will reduce the stresses caused by the preload. When the internal pressure is high enough to balance the preload, the lid will be pushed against the cone seal nut and lose contact with the conical seat. When this happens, the lid merely transfers all the pressure load to the cone seal nut and will not deflect due to the pressure load.

(a) Primary Membrane Stress Intensity

The cone seal nut preload during tightening is developed in Section 4.3.2.4.1. The preloads for the 5CV and 6CV are:

$F_p = 2320$ lbs. (for 5CV)

$F_p = 4000$ lbs. (for 6CV)

The equivalent pressure applied to the lid by the preload can be calculated from the following equation:

$$\frac{1}{4}\pi d_p^2 P_p = F_p$$

Then, the equivalent pressure due to preload is:

$P_p = 106.36$ psi (for 5CV)

$P_p = 127.71$ psi (for 6CV)

The stresses across the thickness of the flat head under a pressure load are pure bending stresses and the membrane stresses are equal to zero for the case of small deflection. Therefore, the maximum membrane stress components are as follows:

$\sigma_r = 0$; $\sigma_t = 0$

$$\sigma_a = -\frac{106.36}{2} = -53.18 \text{ psi} \quad \text{(for 5CV)}$$

$$= -\frac{127.71}{2} = -63.86 \text{ psi} \quad \text{(for 6CV)}$$

where the subscripts a, r and t denote the axial, radial and tangential direction, respectively. Thus, the primary membrane stress intensities for the 5CV and 6CV are:

$P_m = \sigma_r - \sigma_a = 0 + 53.18 = 53.18$ psi (for 5CV)

$$P_m = \sigma_r - \sigma_a = 0 + 63.86 = 63.86 \text{ psi} \qquad \text{(for 6CV)}$$

(b) Primary Membrane Plus Primary Bending Stress Intensity

To calculate the maximum stress, UG-34, for a flat head, set the weld efficiency factor, E, to 1 because no welds are present in the conical lid. The head attachment factor for a threaded ring is

C = 0.3

$$\sigma_r = \sigma_t = \frac{CP_p\left(\frac{d_p}{t_p}\right)^2}{E}$$

$$= 0.3 \times 106.36\left(\frac{5.27}{0.75}\right)^2 = 1575 \text{ psi} \qquad \text{(for 5CV)}$$

$$= 0.3 \times 127.71\left(\frac{6.315}{0.75}\right)^2 = 2716 \text{ psi} \qquad \text{(for 6CV)}$$

The axial stress on the inner surface of the flat head is:

$$\sigma_a = 0$$

Then, the principal stresses for the are:

$$\sigma_1 = \sigma_2 = \sigma_r = \sigma_t = 1575 \text{ psi} \qquad \text{(for 5CV)}$$

$$= 2716 \text{ psi} \qquad \text{(for 6CV)}$$

$$\sigma_3 = \sigma_a = 0 \qquad \text{(for 5CV and 6CV)}$$

Thus, the Primary Membrane Plus Primary Bending Stress Intensities are:

$$P_m + P_b = \sigma_1 - \sigma_3 = 1575 \text{ psi} \qquad \text{(for 5CV)}$$

$$= 2716 \text{ psi} \qquad \text{(for 6CV)}$$

4.2.5 Calculation of Shear Stress in Cone Seal Nut Subject to 150 psi

(a) Condition of Zero Contact Force on Conical Seat

The equilibrium equation of the forces acting at the conical seal nut is:

$$\frac{1}{4}\pi d_{ii}^{2} p - F_p + F_n \cos\alpha = 0$$

where d_i = diameter of bottom surface of seal nut
p = internal pressure of vessel
F_p = preload
F_n = contact force on conical seat
α = inclination angle of conical seat

The preload for the 5CV and 6CV are the same as given in Section 4.2.4:

$F_p = 2320$ lbs. (for 5CV)

$F_p = 4000$ lbs. (for 6CV)

The diameters of the bottom surfaces of the seal nuts are:

$d_{ii} = 5.0$ inches (for 5CV)

$d_{ii} = 6.0$ inches (for 6CV)

Substituting the above values into the equation above, we have

$p = 118.16$ psi (for 5CV)

$p = 141.47$ psi (for 6CV)

This implies that, when the internal pressure is equal to or greater than 118.16 psi for the 5CV and 141.47 psi for the 6CV, most of the preload is balanced by the internal pressure and the only remaining preload is the load that keeps the O-rings in place. Thus, when the internal pressure is equal to or greater than 150 psi, the preloads should not be accounted for in the calculations of the stresses in the vessel components.

Rigid body analysis of the closure would result in this conclusion. The detailed closure analysis included later in the computations, however, considers the radial elastic deformations of the conical seat in the CV as the cone seal plug is preloaded and locked in place by the nut. That analysis concludes that the unseating pressure ranges from 137 to 833 psi depending on the coefficient of friction and other parameters.

In the closure analysis presented in Section 4.3, the axial movement of the male cone seal plug is assumed to be constrained only by the nut preload. In reality, the male cone seal plug is mainly constrained by the cone seal nut. Even if the preload becomes zero, the vertical deflection of the male cone seal plug is limited by the cone seal nut. Since the closure analysis does not accounted for the effect of the stiffness of the cone seal nut, the analysis is very conservative.

In any event, the 9977 design pressures are 900 psi and 800 psi, which are above the unseating pressures, so this unit load analysis can be ratioed up to the actual design pressures.

(b) Shear Stresses in Seal Nuts

The axial forces acting on the conical plug due to the internal pressure are:

$$F_i = \frac{P\pi d_p^2}{4}$$

$$= \frac{150 \times \pi \times (5.27)^2}{4} = 3271.918 \text{ lbs.} \qquad \text{(for 5CV)}$$

$$= \frac{150 \times \pi \times (6.31)^2}{4} = 4690.724 \text{ lbs.} \qquad \text{(for 6CV)}$$

The shear stresses in the cone seal units of the 5CV and 6CV are

$$\tau = \frac{F_1}{\pi d_n t_n}$$

$$= \frac{3271.918}{\pi \times 5.5 \times 0.625} = 302.98 \text{ psi} \qquad \text{(for 5CV)}$$

$$= \frac{4690.724}{\pi \times 6.5 \times 0.625} = 367.533 \text{ psi} \qquad \text{(for 6CV)}$$

The stress intensities are 2 times the maximum shear stresses:

$$P_{m,shear} = 2 \times \tau = 2 \times 302.98 = 605.96 \text{ psi} \qquad \text{(for 5CV)}$$

$$P_{m,shear} = 2 \times \tau = 2 \times 367.533 = 735.06 \text{ psi} \qquad \text{(for 6CV)}$$

The stress limits for pure shear stress are $1.2S_m$.

4.2.6 Stresses in Region of Tapered Wall Seal Threads Subject to 150 psi

(a) Shear Stresses in Threads

Assume 7 out of 7.5 threads are engaged (see Figure 15).

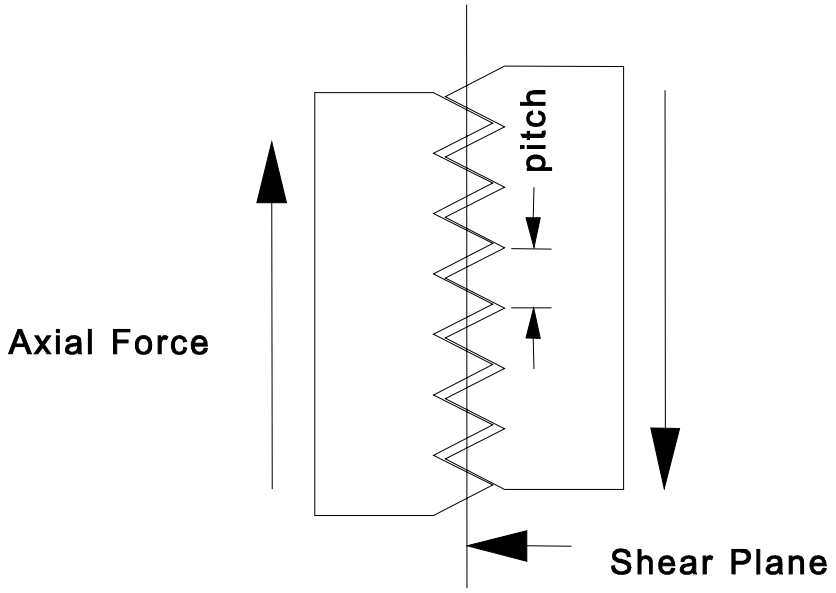

Figure 15. Thread Cross Section

$$pitch = \frac{1}{12} \text{ in.}$$

$$\text{thread area } = A_t = \frac{7\, pitch\, \pi d_{pitch}}{2}$$

where $d_{pitch} =$ pitch diameter of thread

$$A_t = \frac{7 \times 1 \times \pi \times 5.4459}{12 \times 2} = 4.99 \text{ in}^2$$

$$A_t = \frac{7 \times 1 \times \pi \times 6.4459}{12 \times 2} = 5.906 \text{ in}^2$$

The shear stresses in the tapered wall seal threads of the 5CV and 6CV are:

$$\tau = \frac{F_1}{A_t}$$

$$= \frac{3271.918}{4.99} = 655.695 \text{ psi} \qquad \text{(for 5CV)}$$

$$= \frac{4690.724}{5.906} = 794.23 \text{ psi} \qquad \text{(for 6CV)}$$

The stress intensities are 2 times the maximum shear stresses:

$$P_{m,shear} = 2 \times \tau = 2 \times 655.695 = 1311.39 \text{ psi} \quad \text{(for 5CV)}$$

$$P_{m,shear} = 2 \times \tau = 2 \times 794.23 = 1588.46 \text{ psi} \quad \text{(for 6CV)}$$

(b) Stresses in Minimum Cross Section Area

The minimum cross section area in the tapered wall at the thread relief below the threads is:

$$A_{\min} = \frac{\pi}{4}\left(d_0^2 - d_i^2\right)$$

where d_0 and d_i designate the outer and inner diameters of the cross section. Thus,

$A_{\min} = 3.26 \text{ in}^2$ (for 5CV)

$= 6.53 \text{ in}^2$ (for 6CV)

The average tensile stress, P_m, on this vessel section due to the outward 150 psi pressure load is calculated using the lid forces calculated in Section 3.5, (b); namely,

$F_i = 3272$ lbs. (for 5CV)

$F_i = 4691$ lbs. (for 6CV)

The values of P_m are then:

$$P_m = \frac{F_i}{A_{\min}}$$

$P_m = 1003.7$ psi (for 5CV)

$P_m = 718.4$ psi (for 6CV)

The stress limit for P_m is S_m.

In addition, an end moment is applied to the vessel section, since the thread shear force is offset from the wall centerline. The offset distance is the distance from the thread pitch diameter to the centerline.

Offset = Mean Vessel Radius – (Pitch Diameter)/2

Since,

Mean Radius (5CV) = (5.87 + 5.50)/4 = 2.8425 in.

Mean Radius (6CV) = (7.12 + 6.51)/4 = 3.4075 in.

Pitch Radius (5CV) = 5.4459/2 = 2.7229 in.

Pitch Radius (6CV) = 6.4459/2 = 3.2229 in.

the values of the offsets are:

Offset (5CV) = 2.8425 – 2.7229 = 0.1196 in.

Offset (6CV) = 3.4050 – 3.2229 = 0.1846 in.

The moment applied by the thread shear force about the wall centerline can be calculated by the following equation:

$$\text{Applied Moment} = F_i \times \text{Offset} \times \frac{1}{2\pi \times MeanRadius}$$

Then,

Applied Moment (5CV) = 21.91 in-lb/in

Applied Moment (6CV) = 40.44 in-lb/in

Roark[3] considers this case as case 15 in Table XIII. The maximum longitudinal bending stress is $6M/t^2$ and the maximum hoop bending stress is:

$$\sigma_t = \frac{2M}{t^2}\sqrt{3(1-\upsilon^2)}$$

Thus, for wall thickness, t, equal 0.1825 inches for the 5CV and 0.305 inches for the 6CV, and ν=0.3:

Longitudinal Bending Stress (5CV) = 3947 psi

Longitudinal Bending Stress (6CV) = 2608 psi

Hoop Bending Stress (5CV) = 2174 psi

Hoop Bending Stress (6CV) = 1436 psi

On the inside surface of the vessel, both longitudinal and hoop bending stresses are tensile. For the 5CV, the principal stresses are:

$$\sigma_1 = 1003.7 + 3947 = 4951 \text{ psi}$$

$$\sigma_2 = 2174.0 \text{ psi}$$

$$\sigma_3(radial) = 0$$

Thus, the Membrane Plus Bending Stress Intensity is:

$$P_m + P_b = 4951\,\text{psi}$$

which, because it is a secondary stress, has a limit of $3S_m$.

On the inside surface of the 6CV, the principal stresses are:

$$\sigma_1 = 718.4 + 2608 = 3310\,\text{psi}$$

$$\sigma_2 = 1436\ \text{psi}$$

$$\sigma_3(radial) = 0$$

Thus, the Membrane Plus Bending Stress Intensity is:

$$P_m + P_b = 3326\,\text{psi}$$

which, because it is a secondary stress, has a limit of $3S_m$.

These stresses occur in the inside surface of the threaded wall. Accordingly, a stress concentration factor must be applied to obtain the peak stress. Then, the Primary Membrane Plus Primary Bending Plus Peak Stress Intensity becomes:

$$P_m + P_b + F = K(P_m + P_b)$$

Using a K of 4 as specified in Reg. Guide 7.6, we have:

$$P_m + P_b + F = 4 \times 4951 = 19804\ \text{psi} \qquad \text{(for 5CV)}$$

$$= 4 \times 3326 = 13305\ \text{psi} \qquad \text{(for 6CV)}$$

4.2.7 Internal Pressure Stress Summary

4.2.7.1 Stresses for Internal Pressure of 150 psi in 5CV and 6CV

The stress results obtained from the analysis for the internal pressure of 150 psi as calculated in the previous sections are summarized in Table 5.a.

4.2.7.2 Stresses for Hydrostatic Tests Based on 150 psi Pressure in 5CV and 6CV

The stress results for the hydrostatic test pressure of (1.5x150) psi in the 5CV and 6CV can be obtained from the results given in Table 5.a by multiplying a factor of 1.5. The stress results are presented in Table 5.b.

4.2.7.3 Stresses for Internal Pressure of 900 psi in 5CV and 800 psi in 6CV

The stresses for the internal pressure of 900 psi in the 5CV and 800 psi in the 6CV can be obtained from the analytical results presented in Table 5.a by multiplying the 5CV stresses by a factor of (900/150=6) and by multiplying the 6CV stresses by a factor of (800/150=5.3333). The stress results are presented in Table 1.a.

4.2.7.4 Stresses for Hydrostatic Tests Based on Design Pressure of 900 psi in 5CV and 800 psi in 6CV

The stresses for the hydrostatic test pressures of (1.5x900) psi in the 5CV and of (1.5x800) psi in the 6CV can be obtained from the results given in Table 5.b by multiplying a factor of 1.5. The results are presented in Table 1.b. Note that the ASME limits for test conditions differ from those for design conditions and that both must be satisfied.

4.2.8 External Pressure

The stress analysis was performed for the 5CV and 6CV in accordance with the ASME Code, Section III for the internal pressure of 150 psi. The results are documented in Section 4.2. The values of the stress intensities in the vessels subjected to the external pressure of 20 psi can be obtained from the results given in Section 4.2 by multiplying the factor of (20/150). The results are summarized in Table 6.b.

Table 6.b Stress Analysis Results for 20 psi External Pressure and ASME Evaluation for NCT

	P_m (psi)	P_m+P_b (psi)	P_m+P_b+Q (psi)	P_m+P_b+Q+F (psi)
Stress Limit	S_m =16700	$1.5S_m$=25050	$3S_m$=50100	$2S_a$=338000*
5CV Body				
Section AA	206	224		
Section BB	104		282	346
Section CC	136		272	296
Section DD	200	310		
6CV Body				
Section AA	227	245		
Section BB	117		322	391
Section CC	161		302	320
Section DD	225	330		

As shown in the above table, the values of the stress intensities resulting from the external pressure of 20 psig are within the allowable limits.

The buckling analyses for the 5CV and 6CV are reported in Section 4.4.

4.3 Primary and Secondary Containment Vessel Closure Analysis

The 5CV and 6CV are closed by a male cone seal plug and cone seal nut as shown in Figure 16.

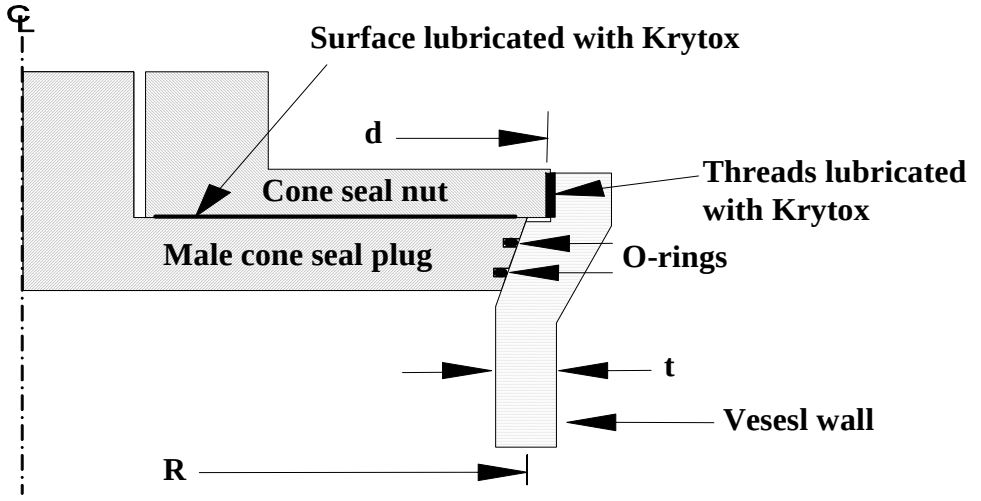

Note: Taps and attachments omitted for clarity

(NOT TO SCALE)

Figure 16 Containment Vessel Closure Simplified Cross Section

The purpose of this calculation is to determine if the conical plug remains seated against the female seal surface when the containment vessel is pressurized. This is determined by calculating the forces perpendicular to the tapered containment vessel wall before and after pressurization. Compressive forces on the tapered containment vessel wall indicate that the plug remains seated.

4.3.1 Methodology

Tightening the cone seal nut forces the outer rim of the conical plug down against the tapered wall of the containment vessel and causes the vessel wall to expand. This mechanism is represented by the simple structural model in Figure 17, where

W = nut preload force,
H = radial clamping force, resisting expansion of the containment vessel wall,
K = radial stiffness of the containment vessel wall due to a ring load, H,
Y = vertical displacement of the plug,
X = radial displacement of the containment vessel wall,
α = taper angle of the containment vessel wall.

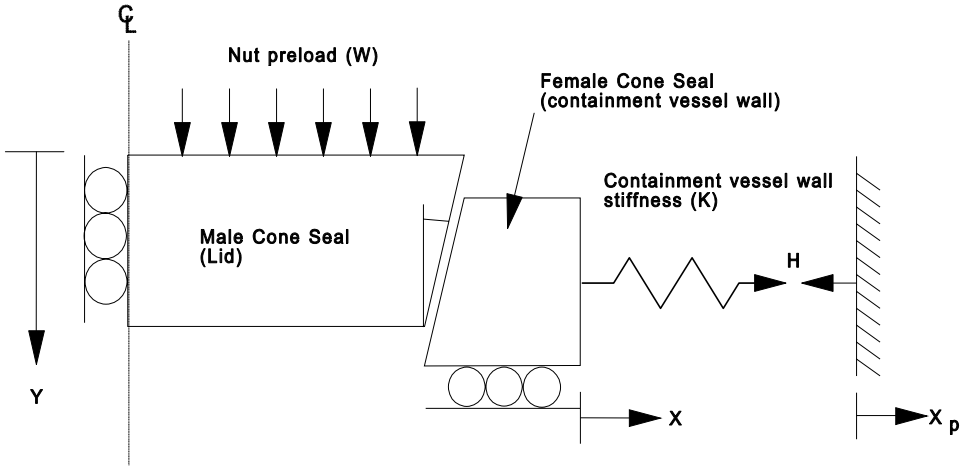

Figure 17 Simplified Structural Model

As the containment vessel is pressurized, its wall displaces radially and the radial clamping force, *H*, is reduced. This mechanism is represented in the simple structural model by setting the right support displacement equal to the internal pressure radial displacement, *Xp*.

Compatibility of displacements, shown in Figure 18, is used to relate the vertical displacement of the plug to the radial expansion of the containment vessel wall. The components of the forces acting on the tapered containment vessel wall are also shown in Figure 18.

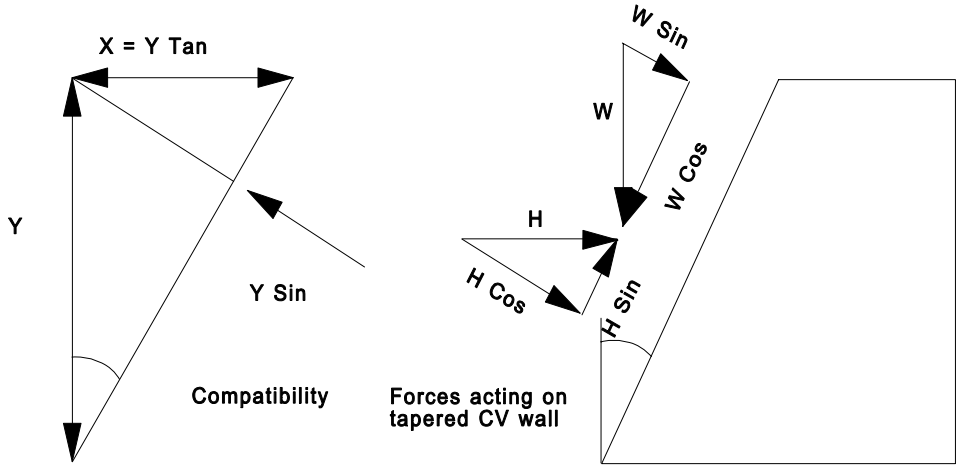

Figure 18 Compatibility of Deformation and Forces Acting on Tapered Containment Vessel Wall

When the sum of forces parallel to the taper is greater than 0, sliding occurs, and when the sum of forces parallel to the taper is equal to zero, sliding arrests. The forces perpendicular to the taper are

$$\sum F_{\perp} = W \sin\alpha + H \cos\alpha .$$

Summing forces parallel to the taper, including frictional forces with a coefficient of friction, μ, yields

$$\sum F_{||} = W \cos\alpha - H \sin\alpha - \mu\ (\ W \sin\alpha + H \cos\alpha\ )$$

Setting $\Sigma F_{||} = 0$ and solving for H yields

$$H = \frac{-W\ (\ \cos\alpha - \mu \sin\alpha\ )}{-\mu \cos\alpha - \sin\alpha}$$

4.3.2 Solution

4.3.2.1 Geometry and Material Constants

5CV and 6CV dimensions and material constants are as follows:

d = thread diameter of the cone seal nut,
R = mean radius of containment vessel wall,
t = nominal thickness of containment vessel wall,
D_{eo} = outside diameter of the female cone seal,
D_{ei} = thread root diameter of the female cone seal,
α = the taper angle = 10.0 degrees,
v = Poisson's ratio and = 0.3,
E = Young's modulus at 500°F = 25,800 ksi.

Dimensions	5CV	6CV
d	5.5	6.5
R	2.6525	3.1725
t	0.258	0.28
D_{eo}	5.87	7.12
D_{ei}	5.505	6.52
r_e	2.84375	3.41
t_e	0.1825	0.3

Source: Drawings in Appendix 1.1.

where

$$r_e = \frac{(D_{eo} + D_{ei})}{4}, \text{ and}$$

$$t_e = \frac{(D_{eo} - D_{ei})}{2}.$$

M_t is the cone seal nut installation torque in kilopounds-inch and W is the total nut preload in kilopounds

$$M_t\ (\text{PCV}) = 50 \text{ lb-ft} = 0.6 \text{ kip-in}.$$

$$M_t\ (\text{SCV}) = 100 \text{ lb-ft} = 1.2 \text{ kip-in}.$$

4.3.2.2 Development of Displacement and Force Relationships

As shown in Figure 17, the containment vessel shell consists of two cylinders connected by a tapered, cone-shaped transition piece. In this analysis, the geometry of the containment vessel shell is represented by two cylinders, as shown in Figure 19. The deformation of the containment vessel shells are adapted from R. J. Roark and W. C. Young, *Formulas for Stress and Strain*[3] Table 29, Case 1, and Table 30, Cases 1, 3, 8, and 10. The nomenclature from Roark and Young is used in this section when practical.

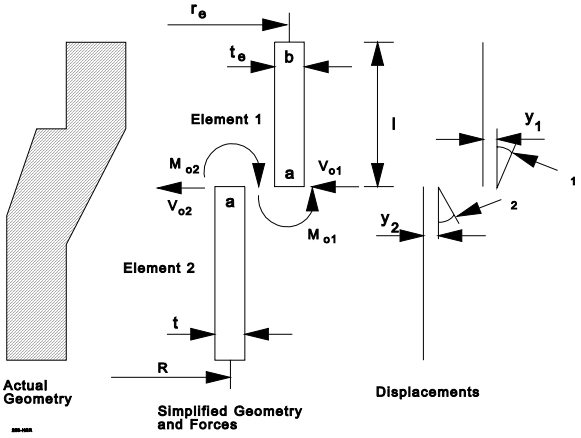

Figure 19 Containment Vessel Shell Structural Model—Forces and Displacements

The cone seal nut and cone seal plug are in contact with the containment vessel over a finite length. This contact imparts a rotational restraint on the bending of the containment vessel shell. Rotational restraint stiffens the containment vessel shell, thereby reducing deformations due to installation loads and internal pressure. Reduced deformation translates into larger contact stresses and a seal that remains closed at higher pressures. Rotational restraint is conservatively neglected in this analysis.

Define constants, where

λ_1, λ_2	=	shell stiffness parameter for elements 1 and 2 (1/in.),
D_1, D_2	=	plate bending stiffness parameter for elements 1 and 2 (in. kip),
V_{o1}, V_{o2}	=	ring load for elements 1 and 2 (kip/in.),
M_{o1}, M_{o2}	=	ring moment for elements 1 and 2 (in. kip/in.),
$C_{11}, C_{12}, C_{13}, C_{14}$	=	intermediate terms in the short-shell solution for element 1.

$$l = \left(0.75 + \frac{0.75}{2} \right) \text{in.}$$

$$\lambda_1 = \left[\frac{3\,(1-\nu^2)}{(r_e\ t_e)^2} \right]^{\frac{1}{4}}$$

$$\lambda_2 = \left[\frac{3\,(1-\nu^2)}{(R\ t)^2} \right]^{\frac{1}{4}}$$

$$D_1 = \frac{E\ t_e^3}{12\,(1-\nu^2)}$$

$$D_2 = \frac{E\ t^3}{12\,(1-\nu^2)}$$

$$C_{11} = \sinh^2(\lambda_1 l) - \sin^2(\lambda_1 l)$$

$$C_{12} = \cosh(\lambda_1 l)\sinh(\lambda_1 l) + \cos(\lambda_1 l)\sin(\lambda_1 l)$$

$$C_{13} = \cosh(\lambda_1 l)\sinh(\lambda_1 l) - \cos(\lambda_1 l)\sin(\lambda_1 l)$$

$$C_{14} = \sinh^2(\lambda_1 l) + \sin^2(\lambda_1 l).$$

4.3.2.2.1 Unit Radial Load

Determine the radial stiffness by applying a radial ring load (kilopounds per inch) at the junction between the two shells, solving for the displacements and letting the stiffness equal load/displacement.

Determine the displacements at the end of each of the two shells:

$$\psi_1 = \frac{V_{o1} C_{14}}{2 D_1 \lambda_1^2 C_{11}} - \frac{M_{o1} C_{12}}{D_1 \lambda_1 C_{11}}$$

$$y_1 = \frac{-V_{o1} C_{13}}{2 D_1 \lambda_1^3 C_{11}} + \frac{M_{o1} C_{14}}{2 D_1 \lambda_1^2 C_{11}}$$

$$\psi_2 = \frac{V_{o2}}{2 D_2 \lambda_2^2} - \frac{M_{o2}}{D_2 \lambda_2}$$

$$y_2 = \frac{-V_{o2}}{2 D_2 \lambda_2^3} + \frac{M_{o2}}{2 D_2 \lambda_2^2}$$

where ψ represents shell rotations and the *y* represents deformations (see Figure 19). Compatibility of displacements requires that

$$y_1 = y_2$$

$$\psi_1 = -\psi_2.$$

Equilibrium of forces requires that

Applied force = $V_{o1} 2\pi r_e + V_{o2} 2\pi R = F_R * 2\pi R$

Applied moment = $M_{o1} 2\pi r_e - M_{o2} 2\pi R = 0$

Solve the compatibility and equilibrium equations for V_{o1}, V_{o2}, M_{o1}, and M_{o2}. Calculate deformations and stiffness. F_R is the applied ring load in kilopounds per inch.

$K = 2\pi R F_R / y$

The results are provided in Table 7. *K* is the stiffness of the containment vessel shell. *K* can also be interpreted as the radial force required to get 1 in. of radial displacement. *M* is the longitudinal moment in the shell wall due to a radial force. The units of *M* are inch-kilopounds/inch. The units for radial force are kilopounds per inch.

Table 7 Results for Unit Radial Load (1 kip/in.)

	5CV	6CV
V_{o1} (kip/in.)	0.401	0.444
V_{o2} (kip/in.)	0.570	0.523
$M_{o1}\left(\frac{\text{in.-kip}}{\text{in.}}\right)$	0.134	0.184
$M_{o2}\left(\frac{\text{in.-kip}}{\text{in.}}\right)$	0.143	0.198
$\psi_1\left(\frac{\text{in.-}F_R}{\text{kip}}\right)$	-0.000636	0.00008836
$\psi_2\left(\frac{\text{in.-}F_R}{\text{kip}}\right)$	0.000636	-0.00008836
$y_1\left(\frac{\text{in.}^2\text{-}F_R}{\text{kip}}\right)$	-0.0011402	-0.0009618
$y_2\left(\frac{\text{in}^2\text{-}F_R}{\text{kip}}\right)$	-0.0011402	-0.0009618
K (kip/in.)	14616	20726
M (in.-F_R)	0.143	0.198

4.3.2.2.2 Unit Internal Pressure

Determine the displacement due to internal pressure.

The displacements at the end of each of the two shells are

$$\psi_1 = \frac{V_{o1} C_{14}}{2 D_1 \lambda_1^2 C_{11}} - \frac{M_{o1} C_{12}}{D_1 \lambda_1 C_{11}}$$

$$y_1 = - \left(\frac{V_{o1} C_{13}}{2 D_1 \lambda_1^3 C_{11}} \right) + \frac{M_{o1} C_{14}}{2 D_1 \lambda_1^2 C_{11}}$$

$$\psi_2 = \frac{V_{o2}}{2 D_2 \lambda_2^2} - \frac{M_{o2}}{D_2 \lambda_2}$$

$$y_2 = \frac{-V_{o2}}{2 D_2 \lambda_2^3} + \frac{M_{o2}}{2 D_2 \lambda_2^2} + \frac{P R^2}{E t}.$$

Note that displacement due to internal pressure is the last term of y_2. Because a similar term is omitted from y_1, pressure is applied only to Element 2, shown in Figure 19. The junction between Elements 1 and 2 is halfway between the two O-rings on the cone lid. If the bottom O-ring is ineffective and the top O-ring marks the pressure boundary, then a small pressure term could be added to y_1. However, the distance between O-rings is small (≈3/16 in.) and the magnitude of this pressure term is negligible.

Compatibility of displacements requires that

$$y_1 = y_2$$
$$\psi_1 = -\psi_2 .$$

Put the forces in equilibrium:

$$\sum F = 0 = V_{o1} 2 \pi r_e + V_{o2} 2 \pi R$$
$$\sum M = 0 = M_{o1} 2 \pi r_e - M_{o2} 2 \pi R .$$

Solve the compatibility and equilibrium equations for V_{o1}, V_{o2}, $M_{o1,}$ and M_{o2}. Calculate the radial deformation due to internal pressure, D_r. The results are provided in Table 8. D_r (=y_1=y_2) is the radial displacement of the junction of Elements 1 and 2 due to internal pressure on element 2. M_p is the longitudinal moment in the shell wall due to the internal pressure. The units of M are inch-kilopounds/inch. Pressure is in kilopounds/inch^2 (ksi).

4.3.2.2.3 Installation

4.3.2.2.3.1 Bolt Preload Calculation (Simplified Handbook Solution).

M_t is the cone seal nut installation torque in kilopounds-inch and W is the total nut preload in kilopounds

$$M_t \text{ (PCV)} = 50 \text{ lb-ft.} = 0.6 \text{ kip-in.}$$
$$M_t \text{ (SCV)} = 100 \text{ lb-ft.} = 1.2 \text{ kip-in.}$$

Table 8. Results for Unit Pressure (1 ksi)

	5CV	6CV
V_{o1} (in . pressure)	-0.109	-0.148
V_{o2} (in . pressure)	0.117	0.159
M_{o1} (in .^{2} pressure)	-0.0127913	-0.01104
M_{o2} (in .^{2} pressure)	-0.0137136	-0.01186
$\psi_1 \left(\frac{\text{in .}^2 \text{ pressure}}{\text{kip}} \right)$	-0.00081549	-0.00099
$\psi_2 \left(\frac{\text{in .}^2 \text{ pressure}}{\text{kip}} \right)$	0.00081549	0.00099
$y_1 \left(\frac{\text{in .}^3 \text{ pressure}}{\text{kip}} \right)$	0.000602	0.000729
$y_2 \left(\frac{\text{in .}^3 \text{ pressure}}{\text{kip}} \right)$	0.000602	0.000729
$D_r \left(\frac{\text{in .}^3 \text{ pressure}}{\text{kip}} \right)$	0.000602	0.000729
M_p (in .^{2} pressure)	-0.0013714	-0.01186

The solution is based on nominal bolt dimensions and a coefficient of friction of 0.15:[2]

$$W\ (PCV\ ) = \frac{5 M_t}{d} = 0.545 \text{ kip}$$

$$\text{W (SCV) } = 0.923 \text{ kip .}$$

Because the bearing area between the male cone seal lid and cone seal nut is not typical of common bolt dimensions, an alternate solution is used in the next section. This solution is included for reference only.

4.3.2.2.3.2 Bolt Preload Calculation (Alternate Handbook Solution).

M_t is the cone seal nut installation torque in kilopounds-inch and W is the total nut preload in kilopounds:

M_t (PCV) = 50 lb-ft. = 0.6 kip-in.

M_t (SCV) = 100 lb-ft. = 1.2 kip-in.

Blake[2] also gives another formula to calculate the preload on a bolt,

$$W = \frac{M_t}{r_t\left(\frac{\cos\theta_n \tan\alpha_t + \mu_t}{\cos\theta_n - \mu_t \tan\alpha_t} + \frac{r_c\,\mu_t}{r_t}\right)}$$

where

μ_t = coefficient of friction,
r_t = radius at nut thread,
r_i = inside radius of cone seal nut,
r_c = average radius of head contact area,
θ_t = thread half angle,
θ_n = f(θ_t) defined below,
α_t = thread pitch angle.

$$r_t = \frac{d}{2}$$

r_t (PCV) = 2.75 in.

r_t (SCV) = 3.250 in.

$$r_i = \left(\frac{1.28}{2} + 0.06\right)\text{in.}$$

r_i = 0.7 in.

$$r_c = \frac{r_i + r_t}{2}$$

r_c (PCV) = 1.725 in.

r_c (SCV) = 1.975 in.

$L = \frac{1\text{ in.}}{12}$; (L is the lead of the thread)

$$\alpha_t = \tan^{-1}\left(\frac{L}{2\,\pi\,r_t}\right)$$

α_t (PCV) = 0.004823 radians

α_t (SCV) = 0.004081 radians

θ_t = 30 degrees = 0.5236 radians

$\theta_n = \tan^{-1}\left[\tan\theta_t \cos\alpha_t\right]$

θ_n (PCV) = 0.5236 radians

θ_n (SCV) = 0.5236 radians

Conservatively, assume a thread coefficient of friction of 0.15 (Page 585 of Reference 2):

$\mu_t = 0.15$

and *W*, the preload on the cone seal plug, is[2]

$$W\ (\ \mathrm{PCV}) = 0.801\,\mathrm{kip}$$
$$W\ (\mathrm{SCV}) = 1.375\,\mathrm{kip}.$$

The actual coefficient of friction for machined and lubricated surfaces is approximately 1/3 of the assumed value[2]. Recalculate the preload on the basis of a realistic coefficient of friction:

$$\mu_t = 0.05$$

and the preload on the cone seal plug is

$$W\ (\ \mathrm{PCV}) = 2.32\,\mathrm{kip}$$
$$W\ (\mathrm{SCV}) = 4.00\,\mathrm{kip}.$$

Note that the stress analysis in Section 4.2.3 is based on the larger of these two preloads.

4.3.2.2.3.3 Calculation of Installation Loads. Assume a coefficient of friction between the cone seal lid and the tapered wall of the containment vessel. Note that this surface is not lubricated and the traditional coefficient of friction for a threaded fastener is appropriate[2]:

$$\mu = 0.15.$$

Grease from the O-rings or other sources may contaminate the sealing surface, thereby causing the coefficient of friction to be lower. The installation calculations are repeated in Section 4.3.2.4 with a "greased" coefficient of friction.

Solve for the total radial force, *H*, between the male cone seal plug and the tapered containment vessel wall due to torquing the cone seal nut:

$$H = \frac{W\cos\alpha - \mu W\sin\alpha}{\mu\cos\alpha + \sin\alpha}$$
$$H\ (\ \mathrm{PCV}) = 2.39\,\mathrm{kip}$$
$$H\ (\mathrm{SCV}) = 4.10\,\mathrm{kip}$$

where *W* is the cone seal nut preload (0.801Kip 5CV, 1.375Kip 6CV) based on a thread coefficient of friction μ_t = 0.15 and the installation torques are 50 and 100 ft-lb.

The radial displacement of the tapered containment vessel wall during installation is

$$dx = \frac{H}{K}$$

where *dx* is radial displacement (See Table 7 for K). Therefore,

$$dx\ (\text{PCV}) = 0.0001635\,\text{in}$$
$$dx\ (\text{SCV}) = 0.000198\,\text{in.}$$

and the vertical displacement (down) of the male cone seal lid during installation is (See Figure 18):

$$dy = \frac{dx}{\tan\alpha}$$
$$dy\ (\text{PCV}) = 0.000927\,\text{in}$$
$$dy\ (\text{SCV}) = 0.00112\,\text{in.}$$

where *dy* is the vertical displacement.

The radial force and longitudinal bending moment in the wall of Element 2, due to the installation load, *H,* are

$$F_R = \frac{H}{2\pi R}$$
$$F_R\ (\text{PCV}) = 0.1434\,\text{kip/in.}$$
$$F_R\ (\text{SCV}) = 0.2058\,\text{kip/in.}$$
$$M_b = M * F_R$$
$$M_b\ (\text{PCV}) = 0.0205\,\text{in.-kip/in.}$$
$$M_b\ (\text{SCV}) = 0.0408\,\text{in.-kip/in.}$$

where F_R is radial force and M_b is longitudinal bending moment.

Because the total bending moment between Elements 1 and 2 is in equilibrium, and Element 1 has a larger radius than Element 2, the distributed bending moment (inch-kilopounds/inch) on Element 1 is smaller than the distributed bending moment on Element 2.

4.3.2.3 Displacement and Force Calculations

4.3.2.3.1 150 psig

Given internal pressure of 150 psig (0.15 ksi), the radial expansion of the tapered containment vessel wall is

$$P = 0.150\ \text{ksi}$$
$$X_p = D_r\ x\ P$$

where X_p is radial expansion, and D_r is given in Table 8.

$$X_p\ (\text{PCV}) = 0.0000903\,\text{in.}$$
$$X_p\ (\text{SCV}) = 0.000109\,\text{in.}$$

H_2 is the total radial force between the conical plug and the tapered containment vessel wall after torquing the cone seal nut and applying 150 psig internal pressure. The radial force for $\mu_t = 0.15$ is

$$H_2 = H - K X_p$$
$$H_2 (\text{PCV}) = 1.071 \text{ kip}$$
$$H_2 (\text{SCV}) = 1.835 \text{ kip}.$$

The contact force, normal to the tapered containment wall, is

$$F_c = (W - P \pi R^2) \sin\alpha + H_2 \cos\alpha$$

where F_c is the contact force.

$$F_c (\text{PCV}) = 0.618 \text{ kip}$$
$$F_c (\text{SCV}) = 1.223 \text{ kip}$$

Because the contact force is compression, the lid remains in contact with the tapered containment vessel wall at 150 psig.

The longitudinal bending moment in the wall of Element 2, due to the installation load, *H*, and an internal pressure of 150 psig is:

$$F_R = \frac{H}{2\pi R}$$
$$F_R (\text{PCV}) = 0.1434 \text{ kip/in}.$$
$$F_R (\text{SCV}) = 0.2058 \text{ kip/in}.$$

Combining M and M_p from Tables 6 and 7, we get

$$M_b = M * F_R + M_p * P$$
$$M_b (\text{PCV}) = 0.0204 \text{ in.-kip/in}.$$
$$M_b (\text{SCV}) = 0.0390 \text{ in.-kip/in}.$$

Note: The addition of internal pressure reduces the longitudinal bending moment in the wall.

4.3.2.3.2 Varying Pressure

The total radial force between the conical plug and the tapered containment vessel wall after torquing the lid nut and applying pressure is

$$H_2 = H - K D_r P$$
$$H_2 (\text{PCV}) = 2.391 \text{ kip} - 8.799 \text{ in.}^2 \text{ x P}$$
$$H_2 (\text{SCV}) = 4.102 \text{ kip} - 15.108 \text{ in.}^2 \text{ x P}.$$

and the contact force, normal to the tapered containment vessel wall, is

$F_c = (W - P \pi R^2) \sin\alpha + H_2 \cos\alpha$

$F_c\ (PCV) = 2.494\,kip - 12.637\,in.^2\ x\ P$

$F_c\ (SCV) = 4.278\,kip - 20.37\,in.^2\ x\ P$.

Solve for the maximum pressure corresponding to zero contact force:

$P_o\ (PCV) = 0.197\,ksi$

$P_o\ (SCV) = 0.210\,ksi$.

The plot of the relationship between contact force and internal pressure is shown in Figure 20.

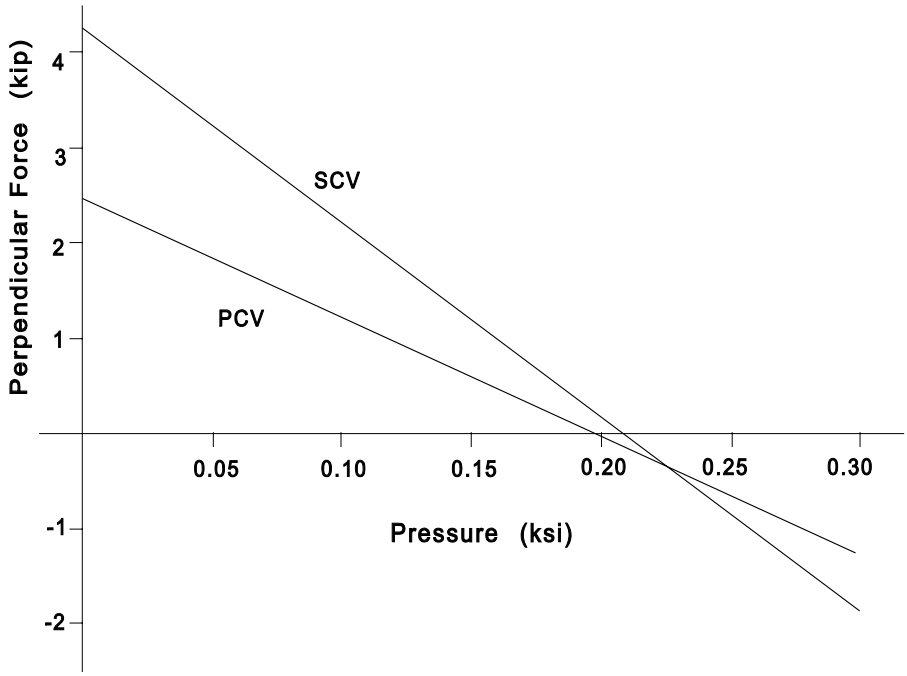

Figure 20 Contact vs. Internal Pressure, μ_{thread} = 0.15, μ = 0.15

On the basis of the current assumptions, the plug is in contact with the tapered wall at internal pressures up to 197 psig and 210 psig for the 5CV and 6CV, respectively.

The plot of the gap between the plug and the tapered CV wall at pressures beyond the design pressure is shown in Figure 21.

$Gap = -\cos\alpha\ (d\,x - X_p)$

$Gap\ (PCV) = -0.000161 + 0.000593 \dfrac{in.^3\ x\ P}{kip}$

$Gap\ (SCV) = -0.0001949 + 0.0007179 \dfrac{in^3\ x\ P}{kip}$

A common failure mode for O-rings is extrusion through the gap between two mating surfaces, and the pressure capacity of an O-ring is highly dependent on the gap width.[1] The O-ring pressure capacity, given the gap sizes calculated previously, is computed later in this section to be more than an order of magnitude larger than the design pressure.

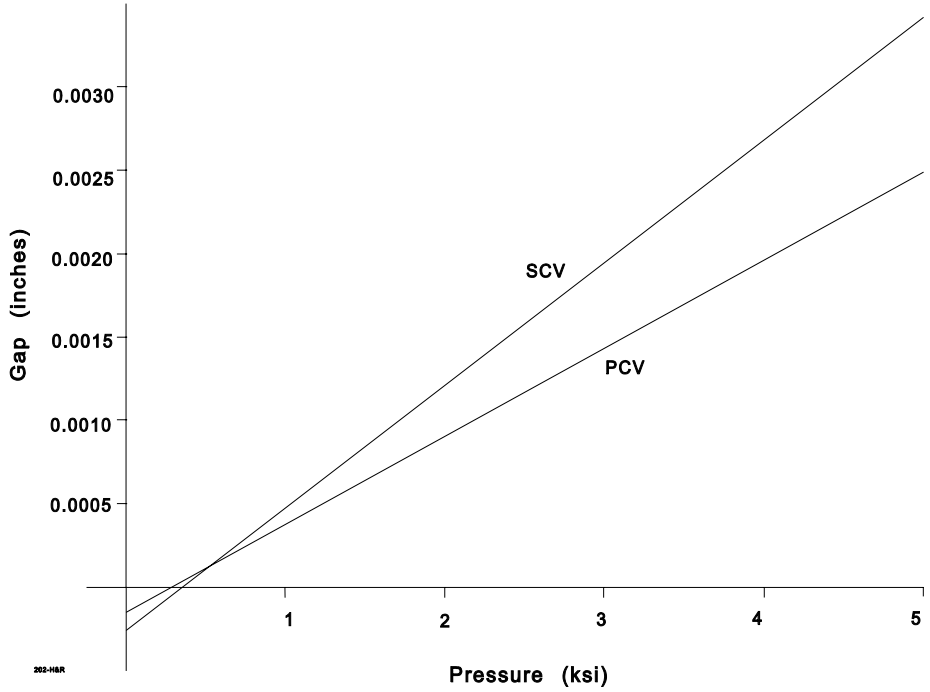

Figure 21 Gap vs. Internal Pressure, μ_{thread} = 0.15, μ = 0.15

4.3.2.4 Solution Sensitivity to the Lubricated Coefficient of Friction

4.3.2.4.1 Nut preload

Grease from the O-rings or other sources may contaminate the sealing surface, thereby causing the coefficient of friction to be lower than previously considered. Thus, the closure analysis is repeated with a realistic "greased" coefficient of friction of μ = 0.05 between sealing surfaces.

The corresponding nut preload *W* for μ_t = .05 is

$$W = \frac{M_t}{r_t \left(\frac{\cos\theta_n \tan\alpha_t + \mu_t}{\cos\theta_n - \mu_t \tan\alpha_t} + \frac{r_c \mu_t}{r_t} \right)}$$

$$W\ (\text{PCV}) = 2.32 \text{ kip}$$

$$W\ (\text{SCV}) = 4.00 \text{ kip}.$$

where *W* is the cone seal nut preload based on a thread coefficient of friction μ_t = 0.05 and the installation torques of 50 and 100 lb-ft are as calculated previously.

4.3.2.4.2 Installation

Solve for the total radial force between the seal cone lid and the tapered containment vessel wall due to torquing of the cone seal nut and coefficient of friction at the sealing surfaces, $\mu = 0.05$.

$$H = \frac{W \cos\alpha - \mu W \sin\alpha}{\mu \cos\alpha + \sin\alpha}$$

$$H\ (\text{PCV}) = 10.1716\ \text{kip}$$

$$H\ (\text{SCV}) = 17.5353\ \text{kip}.$$

The radial displacement of the tapered containment vessel wall during installation is

$$dx = \frac{H}{K}$$

$$dx\ (\text{PCV}) = 0.000696\ \text{in}.$$

$$dx\ (\text{SCV}) = 0.000846\ \text{in}.$$

and the vertical displacement (down) of the lid during installation is

$$dy = \frac{dx}{\tan\alpha}$$

$$dy\ (\text{PCV}) = 0.00395\ \text{in}.$$

$$dy\ (\text{SCV}) = 0.00480\ \text{in}.$$

The longitudinal bending moment in the wall of element 2, due to the installation load, *H*, is

$$F_R = \frac{H}{2\pi R}$$

$$F_R\ (\text{PCV}) = 0.610\ \text{kip/in}.$$

$$F_R\ (\text{SCV}) = 0.880\ \text{kip/in}.$$

$$M_b\ (\text{PCV}) = 0.0872\ \text{in}.\text{-kip/in}.$$

$$M_b\ (\text{SCV}) = 0.1742\ \text{in}.\text{-kip/in}.$$

Because the total bending moment between elements 1 and 2 is in equilibrium and element 1 has a larger radius than element 2, the distributed bending moment (inch-kilopounds) on element 1 is smaller than the distributed bending moment on element 2.

4.3.2.4.3 Varying Pressure

The total radial force between the conical plug and the tapered containment vessel wall after torquing the lid nut and applying pressure is

$$H_2 = H - K\ D_r\ P$$
$$H_2\ (\text{PCV}) = 10.1716\ \text{kip} - 8.799\ \text{in}^2 \text{ x P}$$
$$H_2\ (\text{SCV}) = 17.5353\ \text{kip} - 15.11\ \text{in}^2 \text{ x P}$$

and the contact force, normal to the tapered containment vessel wall, is

$$F_c = (\text{W} - \text{P}\ \pi\ \text{R}^2)\ \sin\alpha + \text{H}_2 \cos\alpha$$
$$F_c\ (\text{PCV}) = 10.4199\ \text{kip} - 12.5036\ \text{in}^2 \text{ x P}$$
$$F_c\ (\text{SCV}) = 17.9642\ \text{kip} - 20.37\ \text{in}^2 \text{ x P}.$$

Solve for the maximum pressure corresponding to zero contact force:

$$P_o\ (\text{PCV}) = 0.833\ \text{ksi}$$
$$P_o\ (\text{SCV}) = 0.882\ \text{ksi}.$$

The plot of the relationship between contact force and internal pressure is shown in Figure 22.

Lubricating the tapered containment vessel wall increases the liftoff pressure from 197 and 210 psig to 833 and 882 psig for the 5CV and 6CV, respectively.

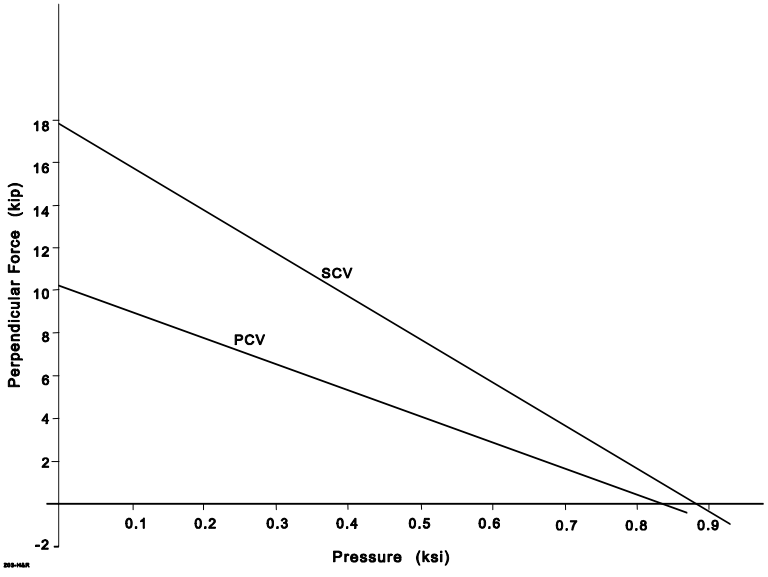

Figure 22 Contact vs. Internal Pressure, μ_{thread} = 0.05, μ = 0.05

The plot of the gap between the conical lid and the tapered containment vessel wall at pressures beyond the design pressure is shown in Figure 23.

$$Gap = -\cos\alpha\ (d\,x - X_p)$$

$$Gap\ (PCV) = -0.000685\,in. + 0.000593\,\frac{in.^3\ x\ P}{kip}$$

$$Gap\ (SCV) = -0.000833\,in. + 0.0007179\,\frac{in^3\ x\ P}{kip}.$$

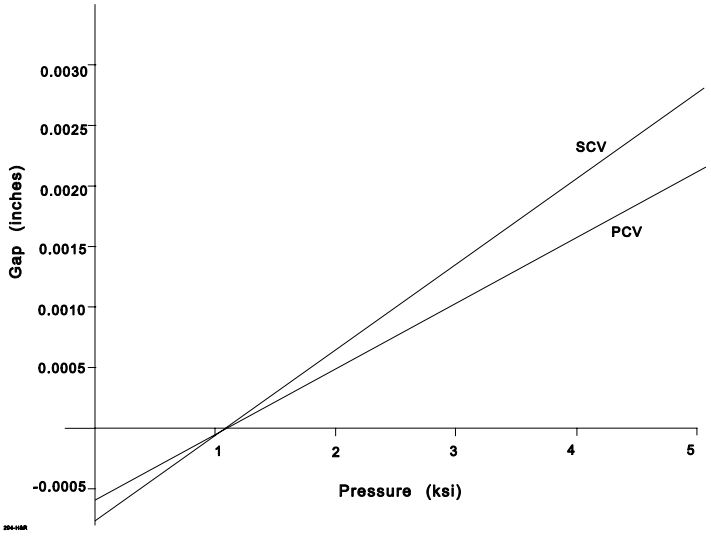

Figure 23 Gap vs. Internal Pressure, μ_{thread} = 0.05, μ = 0.05

Note that the gap size based on a "greased" coefficient of friction is less (more negative) than the gap size originally calculated (Figure 21). Because the pressure capacity of the O-ring is increased with reduced gap size, lubricating the tapered containment vessel wall increases the pressure capacity of the O-ring.

4.3.2.5 Consideration of O-Ring Compression Force

The closure analysis thus far has not considered the force required to compress the O-rings in the cone seal plug. The compression force will tend to reduce the contact force between sealing surfaces for certain installation torque values; however, the impact of this force is very small. The following analysis will evaluate this impact by introducing the O-ring force in the various equations.

4.3.2.5.1 Analysis with Zero Gap

The forces required to compress the O-rings in the glands in the 5CV and 6CV are calculated here. The O-ring type is V835-75. The O-ring cross-sectional diameter is 0.139 in. and the mean depth of the O-ring gland is 0.0995 in. (see Drawing in Appendix 1.1).

Therefore,

$$\%\ compression = \frac{0.139 - 0.0995}{0.139} = 0.28\ or\ 28\%$$

The O-ring Shore A hardness is 75; therefore, the compression force per linear inch of O-ring is

calculated from Table A4-4 and Figure A4-14 of the *O-Ring Handbook*.[1] This force is about 25 lb/in. Therefore, the forces required to compress two rings in each vessel are

$$\text{force for 5CV} = 2 \times \pi \times d \times 25 = 2 \times \pi \times 5 \times 25 = 785 \text{ lb}$$

$$\text{force for 6CV} = 2 \times \pi \times d \times 25 = 2 \times \pi \times 6.25 \times 25 = 982 \text{ lb}$$

where d is the mean diameter of each of the two O-rings in the 5CV and 6CV.

This compression force reduces the contact force between the cone seal plug and the cone seal nut, thereby reducing the maximum internal pressure to ensure metal-to-metal contact. Table 9 gives the unseating vessel pressures considering the normal force exerted by the O-rings.

Table 9 shows that the unseating pressures are less than the design pressures of 900 psi and 800 psi; therefore, the contact force between the cone seal plug and cone seal nut may be lost. However any resulting gap will be small.

Table 9. Unseating Pressures

	5CV	6CV
Installation torque (ft-lb) μ_t=μ=0.15 - threads and sealing surfaces dry Internal pressure (psig) Contact force due to installation torque and pressure (lb) O-ring compression force at zero gap (lb) Resultant contact force (lb)	50 137 ~ 785 -785 0	100 161 ~ 982 -982 0
Installation torque (ft-lb) μ_t=0.05—threads greased μ=0.15—cone seal contact surfaces dry Internal pressure (psig) Contact force due to installation torque and pressure (lb) O-ring compression force at zero gap (lb) Resultant contact force (lb)	50 515 ~ 785 -785 0	100 563 ~ 982 -982 0
Installation torque (ft-lb) μ_t=μ=0.05—threads and cone seal contact surfaces greased Internal pressure (psig) Contact force due to installation torque and pressure (lb) O-ring compression force at zero gap (lb) Resultant contact force (lb)	50 771 ~ 785 -785 0	100 833 ~ 982 -982 0

4.3.2.5.2 Analysis with Gap

A review of the O-ring sealing pressure curves shows that O-rings with a Shore A hardness of 75 are capable of containing a pressure of 1000 psig with a uniform gap of 0.01 in.[1] In the following analysis, the internal containment pressure required to produce a gap of 0.01 in. is calculated. If this pressure is greater than the 1000 psig, the containment vessel O-rings will be able to hold 1000 psig.

Approximate O-ring compression force for a gap of 0.01 in. is calculated by estimating the percent compression of the O-ring. The compressed O-ring geometry is shown in Figure 24.

$$\%\ \text{compression} = \frac{0.139 - 0.1095}{0.139} = 21.2\%$$

Approximate compression force per linear inch from Figure A4-14 of the *O-Ring Handbook*[1] is about 10 lb/linear-inch for a compression of 21.2%. This is equivalent to a compression force of 314 lb for the two 5CV O-rings. The gap analysis given earlier gives a gap equation in which the O-ring force is not considered. The modified equation for 5CV (Section 4.2.3.2) with the O-ring force is given here.

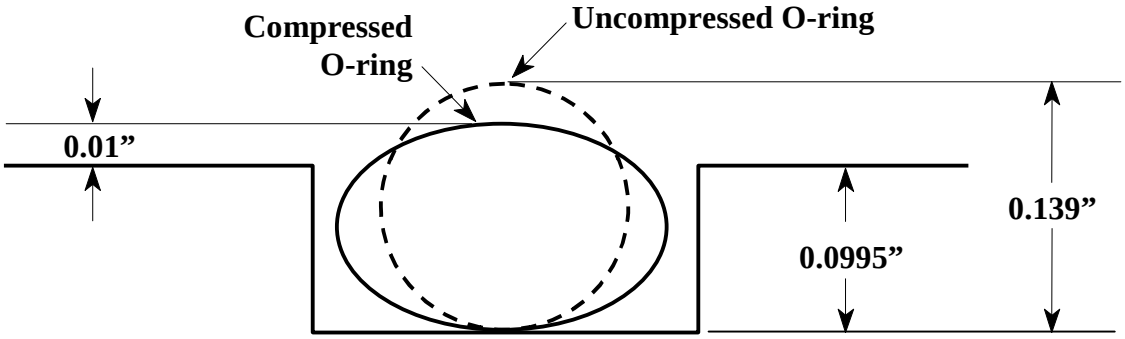

Figure 24 Compressed O-ring Geometry

$$\text{Gap} = -\cos^2\alpha \frac{\text{O-ring force}}{\text{PCV wall stiffness}} - 1.161 \times 10^{-4} + 5.93 \times 10^{-4}\, p$$

where

α = cone lid angle = 10°
p = 5CV internal pressure
5CV wall stiffness = 14616 kip/in. (Table 7)

For a gap of 0.01 in., *p* can be calculated from the preceding equation. Substituting various values yields

$$0.01 = -\cos^2(10°)\frac{0.314}{14616} - 1.161 \times 10^{-4} + 5.93 \times 10^{-4}\, p$$

$$p = 17{,}094 \text{ psi}.$$

This calculation shows that for a pressure of 1000 psig the gap will remain well below 0.01 in. and, therefore, the O-ring will provide a leak tight seal. By inspection, the conclusion can be drawn that the 6CV will also remain leaktight for 1000 psig.

4.3.2.6 Conclusions

The conical plug may or may not remain seated against the tapered containment vessel wall at the design pressures of 900 and 800 psi with lubricated threads. Depending on the coefficient of friction (lubrication) and which containment vessel is being examined, the plug separates from the tapered containment vessel wall at a pressure between 137 and 833 psig. After separation, the gap between the lid and tapered containment vessel wall remains less than 0.0028 in. for internal pressures up to 5000 psig, as shown in Figure 23.

Cases with and without lubrication have been examined. Lubricating the threads, surface between the cone seal nut and conical plug, and tapered containment vessel wall will (1) increase the preload force; (2) increase the internal pressure at separation; (3) reduce the gap width after separation; and (4) increase the pressure capacity of the seal.

4.4 BUCKLING ANALYSIS FOR EXTERNAL PRESSURE

Buckling analyses on the long primary and secondary containment vessels of the 9977 package bound any shorter, similar vessel designs. Buckling modes due to external pressure and axial loading are considered.] The analysis will be performed for the enveloping condition of 20 psig external pressure. Per R. G. 7.8, thermal considerations are not required in conjunction with increased external pressure for Normal Conditions of Transport (NCT). An ambient temperature of -20°F in conjunction with no insolation and no decay heat is assumed per R. G. 7.8.

4.4.1 Buckling Analysis of Cylindrical Body under External Pressure

Buckling analysis for external pressure is performed in accordance with ASME Code Case N-284-1[4].

The theoretical buckling values are calculated per paragraph 1712.1.1(b) of Code Case N-284. These values are compared with the applied compressive stresses, which are corrected for the safety factors and correction factors defined in paragraphs 1400 through 1600 of the Code Case. The terminology is from Code Case N-284-1.

4.4.1.1 Primary Containment Vessel

4.4.1.1.1 Applied Stresses

All stresses are compressive.

$$\text{Axial pressure stress, } \sigma_\phi = \frac{PR}{2t}$$

where

σ_ϕ = longitudinal stress,

P = 20 psig,

R = mean radius = $\frac{5.047 + 5.563}{4} = 2.6525$ in.,

t = wall thickness = 0.258 in.

Therefore,

$$\sigma_\phi = \frac{20 \text{ x } 2.6525}{2 \text{ x } 0.258} = 103 \text{ psi}.$$

Circumferential pressure stress, $\sigma_\theta = 2 \times \sigma_\phi = 206$ psi .

4.4.1.1.2 Capacity Reduction Factor, $\alpha_{\phi L}$

$$M = \text{smaller of } M_\theta \text{ or } M_\phi = \frac{l_i}{\sqrt{Rt}}$$

where

$l_i = l_\phi$ length of the vessel = 17.75 in. or
$= l_\theta$ length in the circumference direction = 16.67 in.

Therefore,

$$M_\theta = \frac{16.67}{\sqrt{2.6525 \, x \, 0.258}} = 20.15 .$$
$$M_\phi = 21.47 \quad Take \, M = 20.15$$

• Evaluate the effect of R/t per paragraph 1511(a)(2) of the Code Case.[4]

$$\frac{R}{t} = \frac{2.6525}{0.258} = 10.28 < 600$$

$\alpha_{\phi L} = 1.0 \text{ x } 10^{-5} \times \sigma_y - 0.033 = 1.0 \text{ x } 10^{-5} \times 25000 - 0.033 = 0.217$

where

$\sigma_y = 25$ 000 psi at -20°F for SA312 TP304L[5] .

• Evaluate the effect of length.

Since M ≥ 10, from paragraph 1511(a)(2) of the code case,[4] we get

$\alpha_{\phi L} = 0.207$

Per paragraph 1511(a) use the larger of $\alpha_{\phi L}$ calculated above.

$\alpha_{\phi L} = 0.217$

For hoop compression:

$\alpha_{\theta L} = 0.8$ paragraph 1511(b) of the Code Case[4]

Elastic stress component,

$$\sigma_{\phi s} = \frac{\sigma_\phi \text{ x FS}}{\alpha_{\phi L}} = \frac{103 \text{ x } 2}{0.217} = 949 \text{ psi}$$
$$\sigma_{\theta s} = \frac{\sigma_\theta \text{ x FS}}{\alpha_{\theta L}} = \frac{206 \text{ x } 2}{0.8} = 515 \text{ psi}$$

where

FS = safety factor = 2 for NCT[4]

4.4.1.1.3 Plasticity Reduction Factor, η_ϕ

Axial compression:

$$\eta_\phi = 1.0 \text{ if } \frac{\sigma_\phi \text{ x FS}}{\sigma_y} < 0.55 \quad \text{paragraph 1610(a) of the Code Case}$$

where

σ_ϕ = 103 psi,
σ_y = yield stress of the vessel material (SA312 TP 304L) at -20°F; = 25,000 psi.[5]

Therefore,

$$\frac{\sigma_\phi \text{ x FS}}{\sigma_y} = \frac{103 \text{ x } 2}{25{,}000} = 0.008 < 0.55.$$

$$\eta_\phi = 1.0$$

Inelastic stress component,

$$\sigma_{\phi p} = \frac{\sigma_{\phi s}}{\eta_\phi} = 949 \text{ psi}$$

Hoop compression:

$$\eta_\theta = 1.0 \text{ if } \frac{\sigma_\theta \text{ x FS}}{\sigma_y} < 0.67 \quad \text{paragraph 1610(a) of the Code Case}$$

where,

σ_θ = 206 psi,

Therefore,

$$\frac{\sigma_\theta \text{ x FS}}{\sigma_y} = \frac{206 \text{ x } 2}{25{,}000} = 0.016 < 0.67.$$

Therefore,

$$\eta_\phi = 1.0$$

Inelastic stress component,

$$\sigma_{\theta p} = \frac{\sigma_{\theta s}}{\eta_\theta} = 515 \text{ psi}$$

4.4.1.1.4 Theoretical Buckling Value (per 1712.1.1(b) of the Code Case[4])

$$\sigma_{\theta eL} = \sigma_{heL} = \frac{C_{\theta h} E_t}{R}$$

where,

$\sigma_{\theta eL} = \sigma_{heL}$ = buckling value in the hoop direction,

E = modulus of elasticity at -20°F = 28.3×10^6 psi.[5]

$$\frac{1.65 \, x \, R}{t} = \frac{1.65 \text{ x } 2.6525}{0.258} = 16.96$$

$$M_\phi = 20.15 > 16.96 .$$

Therefore,

$$C_{\theta h} = 0.275 \frac{t}{R} + \frac{2.1}{M_\phi^4} \frac{R^3}{t^3} = 0.0375$$

$$\sigma_{heL} = \frac{.0375 \times 28.3 \times 10^6 \times 0.258}{2.6525} = 103192 \text{ psi} .$$

The local stresses $\sigma_{\theta s}$ and $\sigma_{\phi s}$ are in the elastic range. A review of the interaction equations in paragraph 1713[4] shows that paragraph 1713.1.1(a) is not applicable and per paragraph 1713.1.1(b), no interaction check is required since $\sigma_{\theta s} < 0.5 \, \sigma_{heL}$.

Since η_ϕ and η_θ are each equal to 1, interaction equations for inelastic buckling are not applicable per paragraph 1713.2[4].

This analysis shows that the stresses due to external pressure are small and will not cause local buckling.

4.4.1.2 Six-inch Diameter Containment Vessel

4.4.1.2.1 Applied Stresses

All stresses are compressive.

$$\text{Axial pressure stress, } \sigma_\phi = \frac{PR}{2t}$$

where,

$P = 20$ psig

$$R = \text{mean radius} = \frac{6.065 + 6.625}{4} = 3.1725 \text{ in.}$$

$$t = \text{wall thickness} = 0.28 \text{ in.}$$

Therefore,

$$\sigma_\phi = \frac{20 \text{ x } 3.1725}{2 \text{ x } 0.28} = 113 \text{ psi}$$

Circumferential pressure stress, $\sigma_\theta = 2 \times \sigma_\phi = 226$ psi

4.4.1.2.2 Capacity Reduction Factor, $\alpha_{\phi L}$

$$M = \text{smaller of } M_\theta \text{ or } M_\phi = \frac{l_i}{\sqrt{Rt}}$$

where

$l_i = l_\phi$ length of the vessel = 23.12 in. or
$= l_\theta$ length in the circumferential direction = 19.93 in.

Therefore,

$$M_\theta = \frac{19.93}{\sqrt{3.1725 \text{ x } 0.28}} = 21.15$$

$M_\phi = 24.54$, Take M = 21.15

• Evaluate the effect of R/t per paragraph 1511(a)(1) of the Code Case.[4]

$$\frac{R}{t} = \frac{3.1725}{0.28} = 11.33 < 600$$

$\alpha_{\phi L} = 1.0 \text{ x } 10^{-5} \text{ x } \sigma_y - 0.033 = 1.0 \text{ x } 10^{-5} \text{ x } 25000 - 0.033 = 0.217$

where

σ_y = 25000 psi at -20°F for SA312 TP304L[5]

• Evaluate the effect of length

Since M ≥ 10, from paragraph 1511(a)(2) of the Code Case,[4] we get

$\alpha_{\phi L}$ = 0.207 .

Per paragraph 1511(a) use the larger of $\alpha_{\phi L}$ calculated above, therefore

$\alpha_{\phi L}$ = 0.217 .

For hoop compression:

$\alpha_{\theta L}$ = 0.8 paragraph 1511(b) of the Code Case.

Elastic stress component,

$$\sigma_{\phi s} = \frac{\sigma_\phi \text{ x FS}}{\alpha_{\phi L}} = \frac{113 \text{ x } 2}{0.217} = 1041 \text{ psi}$$

$$\sigma_{\theta s} = \frac{\sigma_\theta \text{ x FS}}{\alpha_{\theta L}} = \frac{226 \text{ x } 2}{0.8} = 565 \text{ psi}$$

4.4.1.2.3 Plasticity Reduction Factor, η_ϕ

$$\eta_\phi = 1.0 \text{ if } \frac{\sigma_\phi \text{ x FS}}{\sigma_y} < 0.55 \quad \text{paragraph 1610(a) of the Code Case}$$

where

σ_ϕ = 113 psi,
FS = safety factor = 2 for NCT ,
σ_y = yield stress of TP 304L at -20°F = 25,000 psi .

Therefore,

$$\frac{\sigma_\phi \text{ x FS}}{\sigma_y} = \frac{113 \text{ x } 2}{25000} = 0.009 < 0.55.$$

Therefore,

$$\eta_\phi = 1.0$$

Inelastic stress component,

$$\sigma_{\phi p} = \frac{\sigma_{\phi s}}{\eta_{\phi}} = 1041 \text{ psi}.$$

Hoop compression:

$$\eta_{\theta} = 1.0 \text{ if } \frac{\sigma_{\theta} x \text{ FS}}{\sigma_y} < 0.67 \text{ paragraph 1610(a) of the Code Case}$$

where

σ_{θ}= 226 psi

therefore,

$$\frac{\sigma_{\theta} \text{ x FS}}{\sigma_y} = \frac{226 \text{ x } 2}{25{,}000} = 0.018 < 0.67.$$

Therefore,

$$\eta_{\phi} = 1.0$$

Inelastic stress component,

$$\sigma_{\phi p} = \frac{\sigma_{\phi s}}{\eta_{\phi}} = 565 \text{ psi}.$$

4.4.1.2.4 Theoretical Buckling Value (per 1712.1.1(b) of the Code Case[4])

$$\sigma_{\theta eL} = \sigma_{heL} = \frac{C_{\theta h} E_t}{R}$$

where

$\sigma_{\theta eL}$ = σ_{heL} = buckling value in the hoop direction,
E = modulus of elasticity at -20°F = 28.3×10^6 psi.

$$\frac{1.65 \text{ x R}}{\text{t}} = \frac{1.65 \text{ x } 3.1725}{0.28} = 18.7$$

M_{ϕ} = 24.54 > 18.70.

Therefore,

$$C_{\theta h} = 0.275\frac{t}{R} + \frac{2.1}{M_\phi^4}\frac{R^3}{t^3} = .033$$

$$\sigma_{heL} = \frac{0.033 \times 28.3 \times 10^6 \times 0.28}{3.1725} = 81660 \text{ psi}.$$

The local stresses $\sigma_{\theta s}$ and $\sigma_{\phi s}$ are in the elastic range. A review of the interaction equations in paragraph 1713[4] shows that paragraph 1713.1.1(a) is not applicable and per paragraph 1713.1.1(b), no interaction check is required since $\sigma_{\theta s} < 0.5\ \sigma_{heL}$.

Since η_ϕ and η_θ are each equal to 1, interaction equations for inelastic buckling are not applicable per paragraph 1713.2[4].

This analysis shows that the stresses due to external pressure are small and will not cause local buckling.

4.4.2 Buckling Analysis of Cylindrical Body under Axial Loading

This mode of buckling could occur due to impact loading during NCT or HAC. Because HAC requires a 30-foot drop, this loading envelopes the impact loading during NCT. A design temperature = 500°F is assumed for conservatism.

The buckling analysis will be performed in accordance with Code Case N-284.

4.4.2.1 Five-inch Containment Vessel

A review of the capacity reduction factor calculations above shows that if the yield stress at 500°F is used, capacity reduction factor is 0.207. Assuming a safety factor FS = 2, the amplified stress is

$$\sigma_{\phi s} = \frac{\sigma_\phi \, x \, 2}{0.207} < \sigma_{\phi eL} \text{ per paragraph } 1712.1.1(a) \text{ of the Code Case}^{[6]}$$

$$\sigma_{\phi eL} = \frac{C_\phi E\, t}{R} \text{ where, } C_\phi \text{ is } 0.605 \text{ for } M_\phi = 21.47 \geq 1.73 \text{ and,}$$

$$E = \text{Modulus of Elasticity} = 25.8 \times 10^6 \text{ psi at } 500°F^{[7]}$$

$$\sigma_{\phi eL} = \frac{C_\phi E\, t}{R} = \frac{0.605 \times 25.8 \times 10^6 \times 0.258}{2.6525} = 1.5 \times 10^6 \text{ psi}$$

Therefore,

$$\sigma_\phi = \frac{1.5 \times 10^6 \times 0.207}{2} = 157137 \text{ psi}.$$

However,

σ_ϕ x FS < σ_y per paragraph 1600 of the Code Case[4]

Where

$$\sigma_y = 16300 \text{ psi at } 500^\circ \text{F for SA 312, GR 304L}$$

Therefore,

$$\sigma_\phi = \frac{16300}{2} = 8150 \text{ psi.}$$

Take σ_ϕ =8150 psi. This gives an axial load of 35,045 lb for the 5CV having cross sectional metal area = 4.3 in^2. The 5CV weighs 33.9 lb (see Table 2.3 of the main text). This gives an equivalent G (deceleration in multiples of gravitational acceleration, g) loading of 1034 g.

A number of nonlinear dynamic analyses of the 9977 package were performed to simulate the 30-foot drops. The results show that the 5CV and 6CV will not experience any buckling due to impact loads. Therefore, the analysis presented herein is very conservative.

4.4.2.2 Six-inch Containment Vessel

A review of the capacity reduction factor calculations above shows that if the yield stress at 500°F is used, capacity reduction factor is 0.207. Assuming a safety factor FS = 2, the amplified stress is

$$\sigma_{\phi s} = \frac{\sigma_\phi \, x \, 2}{0.207} < \sigma_{\phi eL} \text{ per paragraph 1712.1.1(a) of the Code Case}^{[4]}$$

$$\sigma_{\phi eL} = \frac{C_\phi E \, t}{R} \text{ where } C_\phi \text{ is 0.605 for } M_\phi = 24.54 \geq 1.73$$

$$\sigma_{\phi eL} = \frac{C_\phi E \, t}{R} = \frac{0.605 \times 25.8 \times 10^6 \times 0.28}{3.1725} = 1.38 \times 10^6 \text{ psi}$$

Therefore,

$$\sigma_\phi = \frac{1.38 \times 10^6 \times 0.207}{2} = 142584 \text{ psi.}$$

However,

σ_ϕ x FS < σ_y per paragraph 1600 of the Code Case[4]

Where

$$\sigma_y = 16300 \text{ psi at } 500^\circ \text{F for SA 312, GR 304L}$$

Therefore,

$$\sigma_\phi = \frac{16300}{2} = 8150 \text{ psi.}$$

Take σ_ϕ = 8150 psi. This gives an axial load of 45,477 lb for 6CV having cross section metal area = 5.58 in^2. The 6CV weighs 54.1 lb (see Table 2.3 of the main text). This gives an equivalent G loading of 841 g.

A number of nonlinear dynamic analyses of the 9977 package were performed to simulate the 30-foot drops. The results show that the 5CV and 6CV will not experience any buckling due to impact loads. Therefore, the analysis presented herein is very conservative.

4.4.3 Buckling Analysis of Ellipsoidal Head under External Pressure

In accordance with the ASME Code, Section III, Division 1, Subsection NB, Paragraph NB-3200, Design by Analysis, the provisions of NB-3133 are applicable for the analysis for external pressure. Consequently, the allowable external pressures for the ellipsoidal heads of the 5CV and 6CV are determined as follows following the procedures discussed in NB-3133.

The ellipsoidal head is analyzed as an equivalent spherical shell. The factor A is defined as follows.

$$A = \frac{0.125}{R/T}$$

where R = inside radius of equivalent spherical shell, in.
T = thickness of equivalent spherical shell, in.

The values of R and T are are:

R = 5.01 – 0.258 = 4.752 in. for 5CV
R = 5.96 – 0.28 = 5.68 in for 6CV

and T = 2.258 in for 5CV
T = 0.28 in for 6CV

Then the values of the factor are calculated:

$$A = \frac{0.125}{(4.752/0.258)} = 0.00679 \text{ for 5CV}$$

and $$A = \frac{0.125}{(5.68/0.28)} = 0.00616 \text{ for 6CV}$$

Using the values of the factor A given above, the following values of the factor B are determined from the chart given in Figure CS-1, the ASME Code, Section II, Part D, Subpart 3

B = 13,000.0 for 5CV

and B = 12,500.0 for 6CV

The maximum allowable external pressures for the 5CV and 6CV are calculated as follows.

$$P_a = \frac{B}{(R/T)} = \frac{13{,}000.0}{(4.752/0.258)} = 706 \text{ psi} \qquad \text{for 5CV}$$

$$P_a = \frac{B}{(R/T)} = \frac{12{,}500.0}{(5.68/0.28)} = 616 \text{ psi} \qquad \text{for 6CV}$$

Since the design value of the 5CV and 6CV external pressure of 20 psi is less than the allowable pressures of 706 psi for the 5CV and 616 psi for the 6CV, buckling will not occur in the ellipsoidal heads of the 5CV and 6CV.

4.5 Thermal Stresses in Containment Vessels

Expansion of the various components of the 9977 package as a result of temperature changes during NCT/ HAC require investigation and are reported in Appendix 2.1. The thermal stresses within the containment vessels due to through wall temperature gradient are investigated below.

Differential Thermal Expansion within the Containment Vessels

From the NCT temperature data, the maximum temperature differential through the containment vessel thickness is less than 2°F, (SARP Chapter 3, Section, 2.2). Even though this temperature differential is small, thermal stresses due to thermal expansion are produced in the containment vessel. For conservatism a 10°F through wall temperature gradient was used for this evaluation. For a long cylinder (i.e., the containment vessel) with a hot inner surface, the tangential stress

Inner surface

$$\sigma_{li} = \sigma_{ti} = \frac{\alpha \Delta T E}{2(1 - \nu) \ln \frac{r_o}{r_i}} \left[1 - \frac{2 r_o^2 \ln \frac{r_o}{r_i}}{r_o^2 - r_i^2} \right]$$

(σ_t) and longitudinal stress (σ_l) are determined from the following equations [17].

where

σ_{li} and σ_{lo} = inner and outer longitudinal stresses, respectively (psi),
σ_{ti} and σ_{to} = inner and outer tangential stresses, respectively (psi),
α = coefficient of thermal expansion $\leq 9.37 \times 10^{-6}$ in./in./°F for temperatures below 500°F,
ΔT = temperature difference = 10°F (NCT),

Outer surface

$$\sigma_{lo} = \sigma_{to} = \frac{\alpha \Delta T E}{2(1 - \nu) \ln \frac{r_o}{r_i}} \left[1 - \frac{2 r_i^2 \ln \frac{r_o}{r_i}}{r_o^2 - r_i^2} \right]$$

E = modulus of elasticity = 28.3×10^6 psi at 70°F,
ν = Poisson's ratio = 0.3,

r_o = outer radius = 2.782 in. for the 5CV and 3.313 in. for the 6CV,
r_i = inner radius = 2.523 in. for the 5CV and 3.033 in. for the 6CV.

The maximum thermal bending stress, σ_b, for a plate (conical lid) or ellipsoidal shell (end cap) with end constraints is determined by [3]:

$$\sigma_b = \frac{\alpha \Delta T E}{2(1-\nu)}$$

The maximum thermal stresses within the containment vessel during NCT (and HAC) are presented in Table 12. For $\Delta T = 10°F$ the thermal stress is as follows:

Table 12 - Maximum Containment Vessel Secondary (Thermal) Stresses

Component	Thermal Stress (psi)		Maximum Temperature Difference (ΔT)
	5CV	6CV	
Body inside	1,830	1,720	10°F
Body outside	1,960	2,070	
Ellipsoidal head	1,900	1,900	
Conical lid	1,900	1,900	

Note: The signs for the stresses are ignored.

Thermal stresses may also develop at the junction between the cylinder walls and lid or at the junction between the cylinder walls and ellipsoidal head when each expands differently as a result of non-uniform temperature distributions or dissimilar materials. However, because the containment vessel lid (cone seal), body, and end cap are constructed of the same material, and are all exposed to similar boundary conditions, temperatures at these junctions are relatively even due to slow heating conditions. Because the lid and end cap will expand approximately the same as the containment vessel walls at the junction, any induced thermal stresses will be insignificant.

The cone seal plug is made of SA-479 Grade 304L stainless steel, and the cone seal nut is made of Nitronic-60. However, these are both austenitic stainless steels and, therefore, no thermal stresses due to dissimilar coefficients of thermal expansion are expected.

4.6 Allowable Stress Comparison

Table 13 is a summary of the primary membrane stresses (due to internal pressure) plus the primary bending stresses (bending due to pressure on the lid) plus secondary stress (thermal stress) in the containment vessel. For conservatism, all stresses are added directly, ignoring the sign and direction of application. The maximum stresses (primary plus secondary) listed in Table 13 are less than the allowable stress limits defined by Section III, Subsection NB of the ASME Code; therefore, as indicated by a minimum code margin of 0.41,the integrity of the containment vessel is assured for the evaluated conditions

Table 13-Containment Vessel Maximum Stress Summary

	Primary Pressure Stresses					Thermal Stress	Total Primary + Secondary	Total Stress Range	Stress Margin % [d]
	P_m	P_m+P_b	$P_m+P_b+Q_{pr}$	$P_m+P_b+Q_{pr}+F_{pr}$	$P_{m,pure-shear}$	Q_{th}	$P_m+P_b+Q_{total}$	$P_m+P_b+Q_{total}+F_{total}$	
Stress Limit	S_m=16700	1.5S_m=25050	3S_m=50100	2S_a=338000 [a]	1.2S_m=20040	–	3S_m=50100	2S_a=338000 [a]	
5CV Body									
Section AA	9264	10092				1960	12052	12052	45
Section BB	4667		12680 [b]	15576 [c]		1960	14640	17540	71
Section CC	6116		12260 [b]	13311 [c]		1900	14160	15210	63
Section DD	9005	13938				1900	15838	15838	44
5CV Cone-Seal Plug (preload only)	53.18	1575				1900	3475	3475	93
5CV Cone-Seal Nut (e)					3636		3636	3636	82
5CV Tapered Wall Thread (f)					7868		7868		61
5CV Tapered Wall Minimum Section (gg)	6022		29,706	118824 [c]			29706	118824	41
6CV Body									
Section AA	9066	9808				2070	11878	11878	46
Section BB	4687		12899 [b]	15659 [c]		2070	14969	17729	70
Section CC	6456		12070 [b]	12807 [c]		1900	13970	14707	61
Section DD	9004	13210				1900	15110	15110	46
6CV Cone-Seal Plug (preload only)	63.86	2716				1900	4616	4616	89
6CV Cone-Seal Nut (e)					3927		3927	3927	80
6CV Tapered Wall Thread (f)					8485		8485	8485	57
6CV Tapered Wall Minimum Section (gg)	3897		17653	70613			17650	70613	65

a) S_a =169KSI from ASME III, Fig. I-9.2.1 Allowable for 1000 load cycles (=100 year design life at 10 shipments per year)

b) Includes through wall bending stresses, but not thermal stress.

c) Includes maximum surface stresses, but not thermal stress or stress concentrations where finite element analysis has been performed except at threaded portion of tapered wall. Thermal stresses are calculated separately and reported in column 7. The total primary plus secondary stress intensities, which include both bending and thermal stresses, as the secondary stresses are included in column 8. The primary plus secondary stress intensities are derived by linealizing the stress components across the vessel wall to exclude the peak stresses. The primary plus secondary stress intensities may cause structure deformation, whereas the peak stresses only cause fatigue failure. Therefore, the stress criteria defined in the ASME Code are different for these two stress categories.

d) Minimum calculated value from columns using Margin of Safety = Stress Allowable/Stress

4.7 Minimum Wall Thickness Consideration

Previous calculations were performed using the nominal dimensions as given on the design drawings. Since the 5CV/6CV main bodies are fabricated from standard schedule pipe, it is possible that wall thickness may be smaller than the nominal values (5CV=0.258", 6CV=O.28"). Per ASTM 312[5], the wall thickness variation may be up to 12.5% under the nominal value (5CV=0.226", 6CV=O.245"). The dimensional variations, caused by the minimum thickness are shown in Table 6, and are now considered here.

Based on all the code margins listed in Table 13 for the 5CV and 6CV bodies, the code margins are roughly equivalent for the both vessels, but the two lowest code margins listed are for the 5CV. Since the vessels are similar in construction, and the 5CV has lower code margins, it will be analyzed rigorously using the minimum thickness. Adequate margins for the 5CV with reduced thickness demonstrate adequacy of the 6CV with minimum wall thickness.

Reducing the thickness of the 5CV wall affects calculations in the following Sections (Underlined Sections require the additional computations included in Section 4.7 that follows):

4.2.1 Geometry-Data already included in Table 6.
4.2.2 Stress Analysis of 5CV Subject to Unit Load of 150 psi.
4.2.3 Stress Analysis of 6CV Subject to Unit Load of 150 psi-6CV evaluation enveloped by 5CV reanalysis.
4.2.4 Calculation of Stresses in Male Cone Seal Plug Subject to 150 psi- No change required since the location of stress evaluation is machined from bar stock, and not standard pipe.
4.2.5 Calculation of Shear Stress in Cone Seal Nut Subject to 150psi-No change required since the location of stress evaluation is machined from bar stock, and not standard pipe.
4.2.6 Stresses in Region of Tapered Wall Seal Threads Subject to 150psi- No change required since the location of stress evaluation is machined from bar stock, and not standard pipe.
4.2.7 Internal Pressure Stress Summary-5CV portion requires scaling of the stresses calculated to address thickness change effects for Section 4.2.2.
4.2.8 External Pressure- 5CV portion requires scaling of the stresses calculated to address thickness change effects for Section 4.2.2.
4.3 Primary and Secondary Containment Vessel Closure Analysis- No change required since the location of stress evaluation is machined from bar stock, and not standard pipe.
4.4 Buckling Analysis for External Pressure-By inspection, the stresses for the 5CV evaluated with nominal thickness are orders of magnitude less than the critical values. For this reason, no additional consideration is included, but a FEM buckling analysis is presented to further demonstrate that the critical stress values greatly exceed the actual vessel stresses.
4.5 Fatigue Analysis-No change required due to low stresses, and minimal changes in expected response due to both mass and stiffness reduction from reduced thickness.
4.6 Differential Thermal Expansion-No changes required
4.7 Allowable Stress Comparison-Changes required to reflect new results.
4.8 Hypothetical Accident Condition (HAC)-No changes required because conservative analysis performed without over-pack, and higher than required drop height (55 feet).

To address required changes, the 5CV "nominal" FEM model was modified to include the thickness change from 0.258" to 0.226". The input file, and selected output file results for the unit load of 150psi, are included in Attachment 1 (WSRC-SA-2002-00008, 9975 Rev 0, Appendix 2.2, Attachment 1). The input file, and selected output file results for the model used in the external

pressure buckling analysis, are included in Attachment 2 (WSRC-SA-2002-00008, 9975 Rev 0, Appendix 2.2, Attachment 2). The following sections quantify the stress changes due to the reduced thickness.

4.7.1 5CV Pressure Stresses due to Reduced Thickness

As stated in the previous section, the original FEM model was modified to reflect the 0.226" body thickness. The model was subjected to the 150psi internal pressure load case, and the stresses extracted. The stresses for the various critical sections in 4.2.2 were extracted, and transformed into stresses for code comparison. The following sections include the critical section stress calculations as performed in 4.2.2.1 through 4.2.2.4, and also include scaling of the final unit load stresses to obtain the stresses for Hydrostatic test (Scale factor=1.5), 20psig External Pressure (Scale factor=0.133, 900psig Design pressure (Scale factor=6)), and 1375psig Test pressure (Scale factor=9.17 for primary membrane and primary membrane+bending only). After the critical location stresses are calculated, the results of the external pressure buckling analysis are given. In the next section, comparison of calculated stresses to allowable stresses is given with code margins tabularized with the stresses.

4.7.1.1 Section A – A

The stress components across Section A-A, Figure 6, are classified in accordance with the ASME Code, Section III as follows.

a) Primary Membrane Stress Intensity:

The average values of the normal stress components in the radial, axial, and circumferential directions as well as the shear stress are:

$$\sigma_r = \frac{1}{2}(-150.0 + 0) = -75.0\,psi$$

$$\sigma_a = 812.0\,psi$$

$$\sigma_t = (1775 + 1747.0 + 1720.0 + 1695.0 + 1670.0 + 1647.0 + 1625)/7 = 1697.0\,psi$$

[Note: ABAQUS output at surface nodes corrected to obtain, 1775 and 1625psi from regression equation y = 402.9x2 - 754.79x + 1774.8]

$$\tau_{ra} = 0.0$$

where σ_r = normal stress in radial direction

σ_a = normal stress in axial direction

τ_{ra} = shear stress on the planes normal to the radial and axial directions

The principal stresses of the above stress components are:

$$\sigma_1 = \sigma_t = 1697.0 \text{ psi}$$

$\sigma_2 = \sigma_a = 812.0$ psi

$\sigma_3 = \sigma_r = -75.0$ psi

Consequently, the maximum primary membrane stress intensity is:

$P_m = \sigma_1 - \sigma_3 = 1697.0 + 75.0 = 1772.0$ psi
$P_m(Hydro) = 1.5(1772.0) = 2658$ psi
$P_m(External) = 0.133(1772.0) = 236$ psi
$P_m(Design) = 6(1772.0) = 10632$ psi
$P_m(Test) = 9.17(1772.0) = 16243$ psi

b) Primary Membrane Plus Primary Bending Stress Intensity:

On the inner surface of the cylindrical shell, the stress components are:

$\sigma_r = -150.0$ psi

$\sigma_a = 812.0$ psi

$\sigma_t = 1775.0$ psi

$\tau_{ra} = 0.0$

The principal stresses are:

$\sigma_1 = \sigma_t = 1775.0$ psi

$\sigma_2 = \sigma_a = 812.0$ psi

$\sigma_3 = \sigma_r = -150$ psi

Thus, the maximum Primary Membrane Plus Primary Bending Stress Intensity is:

$P_m + P_b = \sigma_1 - \sigma_3 = 1775.0 + 150 = 1925.0$ psi
$P_m + P_b(Hydro) = 1.5(1925.0) = 2888$ psi
$P_m + P_b(External) = 0.133(1925) = 256$ psi
$P_m + P_b(Design) = 6(1925) = 11550$ psi
$P_m + P_b(Test) = 9.17(1925) = 17652$ psi

4.7.1.2 Section B – B

a) Primary Membrane Stress Intensity

The stress components, extracted directly from the output in Attachment 1 (WSRC-DA-2002-00008, 9975 Rev 0, Appendix 2.2, Attachment 1), are as follows:

*Values of -150 and 0 imposed on inner and outer surfaces respectively

$$\sigma_r = (-150.0 - 138.4 - 105.6 - 66.6 - 26.3 + 16.78 + 0.0)/7 = -67.16 \text{ psi}$$

$$\sigma_a = (825.1 + 827.6 + 816.9 + 797.6 + 780.7 + 780.1 + 802.9)/7 = 804.414 \text{ psi}$$

$$\sigma_t = (794.7 + 789.2 + 778.9 + 768.8 + 760.8 + 759.4 + 760.7)/7 = 773.214 \text{ psi}$$

$$\tau_{ra} = (-45.28 - 87.78 - 147.8 - 164.9 - 141.2 - 64.59 + 0.1917)/7 = -93.051 \text{ psi}$$

The principal stresses in the planes perpendicular to the radial and axial directions are:

$$\sigma_1, \sigma_2 = \frac{\sigma_r + \sigma_a}{2} \pm \sqrt{\left(\frac{\sigma_r - \sigma_a}{2}\right)^2 + \tau_{ra}^2}$$

$$= \frac{-67.16 + 804.414}{2} \pm \sqrt{\left(\frac{-67.16 - 804.414}{2}\right)^2 + (-93.051)^2}$$

$$= 368.627 \pm 445.611$$

or,

$$\sigma_1 = 814.24 \text{ psi}$$

$$\sigma_2 = -76.984 \text{ psi}$$

The principal stresses in the three dimensional space then become:

$$\sigma_I = 814.24 \text{ psi}$$

$$\sigma_{II} = 773.21 \text{ psi}$$

$$\sigma_{III} = -76.98 \text{ psi}$$

Consequently, the primary membrane stress intensity is:

$$P_m = \sigma_I - \sigma_{III} = 814.24 + 76.98 = 891.22 \text{ psi}$$
$$P_m(Hydro) = 1.5(891.22) = 1337 \text{ psi}$$
$$P_m(External) = 0.133(891.22) = 119 \text{ psi}$$
$$P_m(Design) = 6(891.22) = 5347 \text{ psi}$$
$$P_m(Test) = 9.17(891.22) = 8172 \text{ psi}$$

For the secondary and secondary plus peak stresses, the axial and hoop stress components on Section B-B, Figure 6, obtained from the finite-element analysis are not linearly distributed across the vessel wall. The linearized bending and membrane stresses equivalent to these components are calculated and displayed as shown progressively in the tables below. These equivalent stresses are then classified in accordance with the ASME Code, Section III as follows.

Table 4.9.1a: Inner Surface FEM Results for Section B-B

Radial Distance	S11	S22	S33
0	-150		
0.03767	-138.4	827.6	789.2
0.07533	-105.6	816.9	778.9
0.113	-66.6	797.6	768.8
0.150667	-26.3	780.7	760.8
0.18833	16.78	780.1	759.4
0.226	0		

Table 4.9.1b: Stresses Extrapolated from FEM Results for Section B-B

Radial Distance	Extrapolated S22 (Sigma_axial)	Extrapolated S33 (Sigma_cicumferential)
0	851.0	804.5
0.03767	830.0	789.5
0.07533	812.0	778.0
0.1136	797.5	769.0
0.150667	786.0	762.5
0.18833	777.5	759.0
0.226	772.5	758.0

The linearized stresses are then calculated from the extrapolated values as follows:
S22(membrane)=(851+2*(830+812+797.5+786+777.5)+772.5)/12=802.5
S22(bending)= =(2.5*(772.5-851)+4*(777.5-830)+2*(786-797.5))/12=-38.2
S33(membrane)=(804.5+2*(789.5+778+769+762.5+759)+758)/12=773.2
S33(bending)= =(2.5*(758-804.5)+4*(759-789.5)+2*(762.5-769))/12=-22.4

b) Primary Membrane Plus Primary Bending Plus Secondary Stress Intensity

The stress components are:

$$\sigma_r = -150 \text{ psi}$$

$$\sigma_a = \sigma_{a,e} = \sigma_{a,m} + \sigma_{a,b} = 802.5 + 38.2 = 840.7 \text{ psi}$$

$$\sigma_t = \sigma_{t,m} + \sigma_{t,b} = 773.2 + 22.4 = 795.6 \text{ psi}$$

$$\tau_{ra} = 0$$

Then, the principal stresses are:

$$\sigma_1 = \sigma_a = 840.7 \text{ psi}$$
$$\sigma_2 = \sigma_t = 795.6 \text{ psi}$$
$$\sigma_3 = \sigma_r = -150 \text{ psi}$$

Thus, the Primary Membrane Plus Primary Bending Plus Secondary Stress Intensity is:

$$P_m + P_b + Q = \sigma_1 - \sigma_3 = 840.7 + 150 = 990.7 \text{ psi}$$
$$P_m + P_b + Q(Hydro) = 1.5(990.7) = 1486 \text{ psi}$$
$$P_m + P_b + Q(External) = 0.133(990.7) = 132 \text{ psi}$$
$$P_m + P_b + Q(Design) = 6(990.7) = 5944 \text{ psi}$$

c) Primary Membrane Plus Primary Bending Plus Secondary Plus Peak Stress Intensity

The stress components are as follow:

$$\sigma_r = -150.0 \text{ psi}$$
$$\sigma_a = 851.0 \text{ psi}$$
$$\sigma_t = 804.5 \text{ psi}$$
$$\tau_{ra} = 0.0 \text{ psi}$$

Then, the principal stresses are:

$$\sigma_1 = \sigma_a = 851.0 \text{ psi}$$
$$\sigma_2 = \sigma_t = 804.5 \text{ psi}$$
$$\sigma_3 = \sigma_r = -150.0 \text{ psi}$$

Thus, the Primary Membrane Plus Primary Bending Plus Secondary Plus Peak Stress Intensity is:

$$P_m + P_b + Q + F = \sigma_1 - \sigma_3 = 851.0 + 150.0 = 1001.0 \text{ psi}$$
$$P_m + P_b + Q + F(Hydro) = 1.5(1001) = 1502 \text{ psi}$$
$$P_m + P_b + Q + F(External) = 0.133(1001) = 133 \text{ psi}$$
$$P_m + P_b + Q + F(Design) = 6(1001) = 6006 \text{ psi}$$

4.7.1.3 Section C – C

The normal and shear stress components in the vessel axial and radial directions across Section C-C, Figure 6, obtained from the finite-element analysis are not the normal and shear stresses with respect to the Cross Section C-C. The normal and shear stresses on the surface of Section C-C can be calculated in terms of the finite-element results by using the following equations:

$$\sigma_n = \sigma_r \cos^2\alpha + \sigma_a \sin^2\alpha + 2\tau_{ra}\sin\alpha\cos\alpha$$

$$\tau_{nR} = \tau_{ar}(\cos^2\alpha - \sin^2\alpha) + (\sigma_a - \sigma_r)\sin\alpha\cos\alpha$$

where σ_n = normal stress component on Section C-C

τ_{nR} = shear stress component on Section C-C

α = inclination angle between the normal vector of Section C-C surface and vessel radial direction, 1.330552 radians.

The linearized equivalent stresses of the stress components σ_n and σ_t are then generated in the same manner as discussed for Section B-B. Figure 8 shows the equivalent stress components. The resulting stresses are classified in accordance with the ASME Code, Section III as follows.

The terms of some stress components shown in Figure 8 are defined as follows.

$\sigma_{n,e}$ = equivalent membrane plus bending stress in the normal direction

$(\sigma_{n,m})_e, (\sigma_{t,m})_e$ = equivalent membrane stresses in the normal and circumferential directions, respectively

$(\sigma_{n,b})_e, (\sigma_{t,b})_e$ = equivalent bending stresses in the normal and circumferential directions, respectively

Where stresses were extracted directly from the FEM output in Attachment 1 (WSRC-SA-2002-00008, 9975 Rev 0, Appendix 2.2, Attachment 1), the following calculated values apply:

Table 4.9.1c: Inner Surface FEM Results for Section C-C

Radial Distance	S11	S22	S33	S12	Sn
0	-89.74	1907	338.3	484.4	2017.8
0.03767	28.32	1583	267.3	397.2	1678.6
0.07533	60.75	1150	130.6	310	1231.6
0.1136	57.16	772.4	3.364	211.5	829.7
0.150667	27.87	435.5	-116.7	102.4	459.8
0.18833	-19.44	127	-231.6	-16.3	111.2
0.226	-0.4373	-67.67	-287.9	-111.3	-115.3

Table 4.9.1d: Stresses Extrapolated from FEM Results for Section C-C

Radial Distance	S_nn	S_nr	Extrapolated S_nn (Normal Stress)	Extrapolated S33 (Circumferential Stress)
0	2017.8	31.9	2050.0	338.3
0.03767	1678.6	7.1	1640.0	260.0
0.07533	1231.6	-23.2	1240.0	140.0
0.1136	829.7	-22.3	830.0	3.4
0.150667	459.8	3.4	480.0	-120.0
0.18833	111.2	48.3	160.0	-231.0
0.226	-115.3	83.2	-1560.0	-288.0

The linearized stresses are then calculated from the extrapolated values as follows:
Snn(membrane)=(2050+2*(1640+1240+830+480+160)-1560)/12=765.8
Snn(bending)= =(2.5*(-1560-2050)+4*(160-1640)+2*(480-1240))/12=1372.1
S33(membrane)=(338.3+2*(260+140+3.4-120-231)-288)/12=12.9
S33(bending)= =(2.5*(-288-338.3)+4*(-231-260)+2*(-120-140))/12=337.5

a) Primary Membrane Stress Intensity

The stress components perpendicular to the cross section of the vessel wall, in the hoop direction and perpendicular to the vessel wall are respectively given as follows:

$$\sigma_n = 765.83 \text{ psi}$$
$$\sigma_t = 12.9 \text{ psi}$$
$$\sigma_R = \frac{-150+0}{2} = -75 \text{ psi}$$

The shear stress across the section is approximately:

$$\tau_{nR} = (31.91 + 7.07 - 23.17 - 22.26 + 3.4 + 48.3 + 83.16)/7 = 18.34 \text{ psi}$$

The principal stresses on the meridian plane are calculated as follows:

$$\sigma_1, \sigma_2 = \frac{\sigma_R + \sigma_n}{2} \pm \sqrt{\left(\frac{\sigma_R - \sigma_n}{2}\right)^2 + \tau_{nR}^2}$$
$$= \frac{-75 + 765.83}{2} \pm \sqrt{\left(\frac{-75 - 765.83}{2}\right)^2 + (18.34)^2}$$
$$= 345.42 \pm 420.81$$

or, $\sigma_1 = 766.23 \text{ psi}$
$\sigma_2 = -75.39 \text{ psi}$

Then, the principal stresses are:

$$\sigma_I = \sigma_1 = 766.23 \text{ psi}$$
$$\sigma_{II} = \sigma_t = -12.9 \text{ psi}$$
$$\sigma_{III} = \sigma_2 = -75.39 \text{ psi}$$

Thus, the Primary Membrane Stress Intensity is:

$$P_m = \sigma_I - \sigma_{III} = 766.23 + 75.39 = 841.62 \text{ psi}$$
$$P_m(Hydro) = 1.5(841.62) = 1262 \text{ psi}$$
$$P_m(External) = 0.133(841.62) = 112 \text{ psi}$$

$P_m(Design) = 6(841.62) = 5050$ psi
$P_m(Test) = 9.17(841.62) = 7718$ psi

b) Primary Membrane Plus Primary Bending Plus Secondary Stress Intensity

The linearized stress components on the inner surface of the vessel are:

$\sigma_n = \sigma_{n,m} + \sigma_{n,b} = 765.83 + 1372.08 = 2137.91$ psi
$\sigma_t = \sigma_{t,m} + \sigma_{t,b} = 12.9 + 337.5 = 350.4$ psi
$\sigma_R = -150.0$ psi

Then the principal stresses are:

$\sigma_1 = \sigma_n = 2137.91$ psi
$\sigma_2 = \sigma_t = 350.4$ psi
$\sigma_3 = \sigma_R = -150.0$ psi

Thus, the Primary Membrane Plus Primary Bending Plus Secondary Stress Intensity is:

$P_m + P_b + Q = \sigma_1 - \sigma_3 = 2137.91 + 150.0 = 2287.91$ psi
$P_m + P_b + Q(Hydro) = 1.5(2287.91) = 3432$ psi
$P_m + P_b + Q(External) = 0.133(2287.91) = 304$ psi
$P_m + P_b + Q(Design) = 6(2287.91) = 13727$ psi

4.7.1.4 Section D – D

a) Primary Membrane Stress Intensity

$\sigma_r = \sigma_t = \frac{1}{2}(875.3 + 2208.0) = 1541.7$ psi
$\sigma_a = \frac{1}{2}(-150.0 + 0) = -75.0$ psi
$\tau_{ra} = 0$ psi

Then, the principal stresses are:

$\sigma_1 = \sigma_2 = \sigma_r = \sigma_t = 1541.7$ psi
$\sigma_3 = \sigma_a = -75$ psi

Thus, the Maximum Primary Membrane Stress Intensity is:
$P_m = \sigma_1 - \sigma_3 = 1541.7 + 75.0 = 1616.7$ psi

$P_m(Hydro) = 1.5(1616.7) = 2425$ psi

$P_m(External) = 0.133(1616.7) = 215$ psi

$P_m(Design) = 6(1616.7) = 9700$ psi

$P_m(Test) = 9.17(1616.7) = 14825$ psi

b) Primary Membrane Plus Primary Bending Stress Intensity

On the outer surface of the head, the stress components are:

$\sigma_r = \sigma_t = 2208.0$ psi

$\sigma_a = 0$ psi

Then, the principal stresses are:

$\sigma_1 = \sigma_2 = \sigma_r = \sigma_t = 2208.0$ psi

$\sigma_3 = \sigma_a = 0$

Thus, the Primary Membrane Plus Primary Bending Stress Intensity is:

$P_m + P_b = \sigma_1 - \sigma_3 = 2208.0$ psi

$P_m + P_b(Hydro) = 1.5(2208) = 3312$ psi

$P_m + P_b(External) = 0.133(2208) = 294$ psi

$P_m + P_b(Design) = 6(2208) = 13248$ psi

$P_m + P_b(Test) = 9.17(2208) = 20247$ psi

4.7.1.5 Allowable Stress Comparison

The following tables summarize the stress results of the analyses performed in the previous sections. Review of Tables 13, 15 and 16 shows that the minimum margins for the 5CV body occur for the pressure only cases. For this reason, the results for the design pressure of 900psig and 1375psig test pressure are tabularized and listed below to assess the affects of minimum thickness.

Table 4.9.1e: Stress Analysis Results for 5CV with Internal Pressures 900 psi (ASME Evaluation for NCT)

	P_m (psi)	P_m+P_b (psi)	P_m+P_b+Q (psi)	P_m+P_b+Q+F (psi)	Minimum Code Margin [d]
Stress Limit	S_m=16700	$1.5S_m$=25050	$3S_m$=50100	$2S_a$=338000[a]	
Section AA (pipe wall)	10632	11550			0.36
Section BB (CV head transition)	5437		5944 [b]	6006 [c]	0.67
Section CC (pipe cap radius)	5050		13727 [b]		0.70
Section DD (pipe cap bottom)	9700	13248			0.42

a) S_a =169KSI from ASME III, Fig. I-9.2.1 Allowable for 1000 load cycles (100 year design life at 10 shipments per year)
b) Includes through wall bending stresses, but not thermal stress.
c) Includes maximum surface stresses, but not thermal stress or stress concentrations.
d) Minimum value from those calculated using Margin=1-(Stress/Stress Limit)

Table 4.9.1f Stress Analysis Results for 5CV for 1375 psi Test Pressure

	P_m (psi)	P_m+P_b (psi)	Minimum Code Margin [a]
Test Limit	0.9Sy=22500	1.35Sy=33750	
Section AA (pipe wall)	16243	17652	0.28
Section BB (CV head transition)	8172		0.64
Section CC (pipe cap radius)	7718		0.66
Section DD (pipe cap bottom)	14825	20247	0.34

a) Minimum value from those calculated using Margin=1-(Stress/Stress Limit)

4.7.2 Buckling Analysis of 5CV under External Pressure

The finite-element buckling analysis was performed by using the same finite-element model used for the pressure stress evaluation. The input file, and selected output are given in Attachment 2 (WSRC-SA-2002-00008, 9975 Rev 0, Appendix 2.2, Attachment 2).

The top surface of the closure is assumed to be constrained in the axial direction. The external pressure of 20 psi is used as the incremental load ("live load") in the buckling analysis. The calculated eigen-values for the first five buckling modes are:

Table 4.9.2 First Five Buckling Modes

Mode Number	Eigen Value
1	4918.3
2	6684.3
3	10023.0
4	10986.0
5	11056.0

The critical external pressure is calculated as follows.

$$P_{critical} = 4918.3 \times 20.0 = 98{,}366.0 \text{ psi}$$

The value given above is orders of magnitude greater than the stresses caused by external pressure (i.e., stress<1000psi), and it implies that the 5CV will not experience buckling.

4.7.3 Minimum Thickness Effects Summary

Though reduced slightly from the margins obtained using nominal wall thickness, the margins calculated for the 5CV with minimum (0.226") body wall thickness still show excessive capacity above what is required to withstand design loads. For buckling in response to external pressure, the minimum body wall thickness 5CV critical buckling pressure was shown to be orders of magnitude greater than the 20psig design value. Based on 6CV design similarities, and higher code margins at critical locations for nominal thickness, it is concluded that the 6CV also has adequate capacity in the minimum thickness condition to withstand design loads, and not buckle in response to the 20psig external design pressure

5.0 CONCLUSION

The 9977 package has sufficient structural capacity to withstand all postulated loads as shown by the results given in Table 13.

6.0 REFERENCES

1. *Parker O-Ring Handbook*. ORD 5700, The Parker Seal Group, Parker Hannifin Corporation, Lexington, KY (1991).

2. A. Blake. *Practical Stress Analysis in Engineering Design*. Marcel Dekker, Inc., New York, NY (1982).

3. R. J. Roark and W. C. Young. *Formulas for Stress and Strain*. 5th ed., McGraw-Hill, New York, NY (1975).

4. *ASME Boiler and Pressure Vessel Code*. Section III, Rules for Construction of Nuclear Power Plant Components," Code Case N-284-1, "Metal Containment Shell Buckling Design Methods" (July 1, 1995).

5. *ASME Boiler and Pressure Vessel Code*. Section II, "Materials," Part D, "Properties," American Society of Mechanical Engineers, New York NY (1992).

6. *NRC Regulatory Guide 7.6*. Rev. 1, U.S. Nuclear Regulatory Commission, Washington, D.C. (March 1976).

7. *ASME Boiler and Pressure Vessel Code*. Section III, "Rules for Construction of Nuclear Power Plant Components," Subsection NB and Appendix I, American Society of Mechanical Engineers, New York, NY (1992).

8. C. M. Harris. *Shock and Vibration Handbook*. 3rd ed., pp 34–26 and 41–12, McGraw Hill, New York, NY, (1988).

9. C. F. Magnuson. *Manufacture-to-Stockpile Sequence*. SAND83-0480, Sandia National Laboratory, Albuquerque, NM 87115 (June 1983).

10. J. M. Biggs. *Introduction to Structural Dynamics*. p 43, McGraw Hill, New York, NY, (1964).

11. D. S. Steinburg. *Vibration Analysis for Electronic Equipment*. 2nd ed., Wiley Interscience, New York, NY.

12. *Design Basis for Resistance to Shock and Vibration of Radioactive Material Packages Greater than One Ton in Truck Transport*. Draft, American National Standard N14.23, American National Standards Institute, New York, NY (May 1980).

13. ABAQUS Structural Analysis Code, Version 5.3, Hibbitt, Karlsson, and Sorensen, Inc., Pawtucket, Rhode Island

14. T. T. Wu, *Structural Analysis of 9975 PCV and SCV(U)*, M-CLC-F-00500, Westinghouse Savannah River Company, Aiken, SC 29802 (Oct. 1998).

15. D. R. Leader, *Packaging Material Compression Tests*, SRT-MTS-93-3119, Westinghouse Savannah River Company, Aiken, SC 29802 (November 1993).

16. T. T. Wu, Thermal Stress Analysis for 9975 5CV with 3013 Content Configuration, M-CLC-F-00831, Rev 0, (December 2002).

17. W. C. Young, *Roark's Formulas for Stress and Strain*, 6th ed., P. 723, McGraw-Hill, New York (1989).

18. N. K. Gupta, *Thermal Analysis of the 9975 Package for Normal Conditions of Transport and Accident Conditions*, M-CLC-F-00590, Rev. 6, (September 11, 2002).

19. ASTM 312/A 312M-02, *Standard Specification for Seamless and Welded Austenitic Stainless Steel Pipes*, ASTM International, 2003.

APPENDIX 2.9

Structural Evaluation of Model 9977 Package For HAC 40-inch Puncture Bar

This Page is Intentionally Left Blank

Calculation Cover Sheet

OSR 45-24 (Rev 11-15-2004)

Project	Calculation No.	Project No.
N/A	M-CLC-A-00276	N/A
Title Structural Evaluation of Model 9977 Package for HAC 40-inch Puncture Bar (U)	**Functional Classification** SS	Sheet 1 of 52
	Discipline Mechanical	
Calc Level ☒ Type 1 ☐ Type 2	**Type 1 Calc Status** ☐ Preliminary ☒ Confirmed	
Computer Program No. Abaqus NA ☐	**Version/Release No.** 6.5.3	

Purpose and Objective

The purpose of this calculation is to document the finite element analyses performed as part of the structural design of the Model 9977 series General Purpose Fissile Package (GPFP) to support generation of its Safety Analysis Report for Packaging

Summary of Conclusion

Analysis presented in this calculation meets the design criteria required by 10 CFR 71in the evaluation of the Model 9977.

Revisions

Rev. No.	Revision Description
0	Original Issue

Sign Off

Rev. No.	Originator (Print) Sign/Date	Verification/ Checking Method	Verifier/Checker (Print) Sign/Date	Manager (Print) Sign/Date
0	Tsu-Te Wu 5/17/06	Document Review	N. K. Gupta N. K. Gupta 5/17/06	J. S. Bellamy J S Bellamy 5/17/06

Design Authority -- (Print)	Signature	Date
Release to Outside Agency -- (Print) N/A	**Signature** N/A	**Date** N/A

Security Classification of the Calculation

(U)

OPEN ITEMS

None

RECORD OF REVISION					
REV. NO.	PAGES SUPERSEDED	PAGES ADDED	PAGES DELETED	PAGES REVISED	DESCRIPTION OF REVISIONS
0					Original Issue

Table of Contents

1 Purpose

The purpose of this calculation is to evaluate the structural response of a 9977 shipping package drum and containment vessel when subjected to a 40 inch free fall onto a vertically oriented 6-inch steel bar.

2 Scope

The equipment evaluated is the 9977 shipping package. A sketch of the package cross section is shown in Figure 1 (Reference 1). The following scenario was analyzed.

The analysis is to simulate a free drop of 40 inches onto a stationary and vertical mild steel bar of 6 inches diameter with its top edge rounded to a radius of not more than 0.25 inch. The bar should be of such a length as to cause maximum damage to the package; however, it should not be less than 8 inches long.

The package containment vessel is required to meet the stress criteria specified in the ASME Code, Section III, Appendix F (Reference 2) under this hypothetical accident condition. Damage to the overpack must be demonstrated to not affect the performance of the package when subjected to the subsequent HAC fire event.

This calculation evaluates the structural response of a 9977 shipping package oriented horizontally and vertically both perpendicular and at an angle of 45-degrees over the puncture bar. For the side drops the package temperatures were varied from -20 to 300 ºF. For the vertical top down drop the package was evaluated at 75 ºF.

3 Conclusion

Nonlinear dynamic analyses were performed for the 9977 shipping package to evaluate the structural responses of the containment vessel and overpack to the Hypothetical Accident Condition (HAC) of 40-inch drop onto a steel bar as defined in 10 CFR 71 (Reference 3).

The analytical results and the allowable maximum values of the primary membrane stress intensities are summarized in Table 1 for the containment vessel. The maximum value of primary membrane stress intensities in the containment vessel is 46.6 ksi and is well within the Level D service load allowable limits specified in the ASME Code, Section III, Appendix F, 57.8 ksi. The analytical results found no plastic deformation in the containment vessel during the impact condition.

The analytical results and the allowable strain values are summarized in Table 2 for the drum. The maximum calculated value of the effective plastic strain in the drum is 16% for the top down 45-degree drop. This value is less than the allowable strain of 35% for the 304L material. Therefore, the drum will not be ruptured by the 40-Inch drop of the

package onto the bar. Strain reported are maximum peak values and not averaged across the material thickness.

The analysis verifies that the containment vessel and overpack of the 9977 shipping package will be structurally adequate when subjected to the hypothetical accident condition of puncture impact.

Table 1 - Summary of Calculated Stress and Strain in the Containment Vessel and Overpack as a Function of Overpack Foam Temperature

Drop Orientation	**Maximum Stress Intensities for the Containment Vessel True Stress, P_L** (ksi)				**Allowable True Stress Intensity Limts** (ksi)[a]
Foam Temp	**-20 ºF**	**75 ºF**	**140 ºF**	**300 ºF**	
Side - Drum	46.55	45.41	40.89	46.48	Pm = 57.8 PL = 74.3
Side 45º - Drum	43.93	42.09	42.85	40.91	
Top - Lid	-	12.81	-	-	
Top 45º - Lid	-	9.54	-	-	

a) Criteria at 300 ºF

Drop Orientation	**Maximum Strains in Containment Vessel**				**Allowable Strain**
Foam Temp	**-20 ºF**	**75 ºF**	**140 ºF**	**300 ºF**	
Side (Drum)	.027	.024	.023	.016	0.35
Side 45º(Drum)	.019	.015	.014	.005	
Top (Lid)	-	0	-	-	
Top 45º(Lid)	-	0	-	-	

Drop Orientation	**Maximum Strain In Overpack Drum**				**Allowable Strain**
Foam Temp	**-20 ºF**	**75 ºF**	**140 ºF**	**260/300 ºF**	
Side (Drum)	.155	.154	.065	.057	0.35
Side 45º(Drum)	.147	.133	.073	.082	
Top (Lid)	-	.031	-	-	
Top 45º(Lid)	-	.158	-	-	

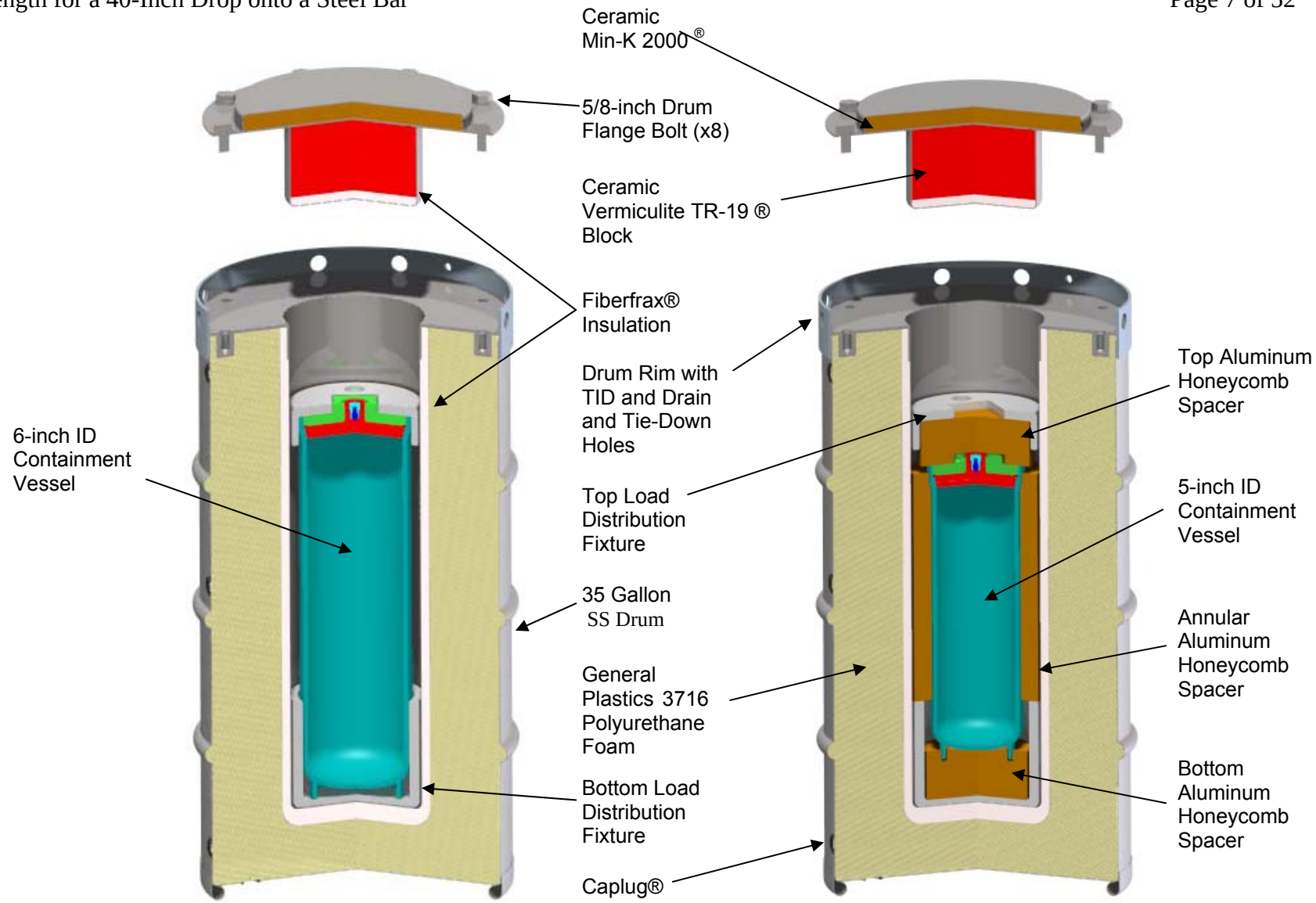

Figure 1 - Configurations of the 9977 Shipping Package

4 Input Data and Assumptions

Input Data

The components, weight and geometric configuration of the 9977 shipping package are given in Reference 1. The material specifications of the components are also given in Reference 1.

The stress versus strain curve of stainless steel 304L is shown in Appendix A. The strain curve used represents median centered properties, rather than code minimum properties. The effect of this modeling is to conservatively overestimate the stress response level during the impact condition. The generation of the stress-strain curves of aluminum alloy 6061-T6 and polyurethane foam materials are discussed in Appendix A.

Assumptions

a) The drum closure is modeled as an integral part of the drum; namely the bolt preload and corresponding flange pre-load is not modeled.
b) The heavier 6CV configuration with a 100 lb payload is dropped.
c) It's assumed the stresses and strains in the larger diameter 6CV configuration are bounding for the smaller diameter 5CV configuration.
d) Side drops were modeled with the 6CV 100 lb payload positioned at the top of the CV. (See Figure 2)
e) The stainless steel drum and insulation material properties in the drum lid are temperature insensitive between -40 to 300 ºF and therefore properties at room temperature are used for these components.
f) Side drop will bound results from a bottom drop orientation.

5 Computations and Analytical Methods

5.1 Description of Methodology

The structural responses of the 9977 shipping package to the hypothetical accident conditions were determined by performing nonlinear dynamic finite-element analysis with explicit time integration.

The ABAQUS/Explicit Computer Code, (Reference 6) was used to perform the computations. The finite-element meshes were generated using the ABAQUS Preprocessor CAE computer program (Reference 4). Modeling results were analyzed with MSC/PATRAN (Reference 5) and ABAQUS.

5.2 Description of Finite-Element Model

The basic geometry of the 9977 is shown in Figure 1. The principal components are shown in Table 2. The material properties of the package components are summarized in Table 3. Table 4 contains the weights of the package components. (Reference 1)

Table 2. 9977 Package Components

Item Number	Description	Material
1	Containment Vessel	Stainless Steel 304L
2	LDF Spacer	Aluminum 6061-T6
3	5CV Honeycomb Spacer	Aluminum 1100
4	Lid Upper Insulator	Min-K 2000
5	Lid Lower Insulator	TR-19
6	Fiberfrax Blanket	Fiberfrax
7	Drum / Liner / Lid	Stainless Steel 304L
8	Polyurethane Foam	FR-3716 Foam

Table 3. Material Properties of 9977 Package Components (Elastic Properties – See App A for Plastic Regime Properties used in the Model)

Component	Material	Modulus of Elasticity (psi)	Poisson's Ratio	Density ($lb\text{-}sec^2/in^4$)
Vessel, drum, lid, liner	Stainless steel 304L	28.3E6	0.3	7.324E-4
LDF Spacer	Aluminum 6061-T6	10.0E6	0.33	2.536E-4
5CV Honeycomb Spacer	Aluminum 1100	1.0E6	0.10	4.622E-5
Lid Upper Insulator	Min-K 2000	3.0E4	0.0	2.9953E-5
Lid Lower Insulator	TR-19	1.0E7	0.3	3.4447E-5
Polyurethane	Foam	2.7290E4	0.0	2.3963E-5

Since the arrangement of the package components is symmetric with respect to a plane containing the axis of the package, only one half of the package components are included in the finite-element model. The (unmodeled) symmetric portion is represented by an appropriate set of boundary conditions.

The finite-element model representation of the containment vessel, drum body, lid and liner consists of three dimensional shell elements (Type S4R elements in the ABAQUS Computer Code). The containment vessel flange, plug and nut, drum foam, and the puncture pin, are modeled using 3D brick elements (Type C3D8R).

Figure 2 shows the finite element model of the package. Figure 3 shows the finite-element model for the simulated scenarios described in Section 2.0.

Table 4 Weights of Package Components

Components	Weight (lb)
Overpack	167
Containment Vessel 6CV	52
Containment Vessel 5CV	32
Contents 6CV	100
Contents 5CV	50

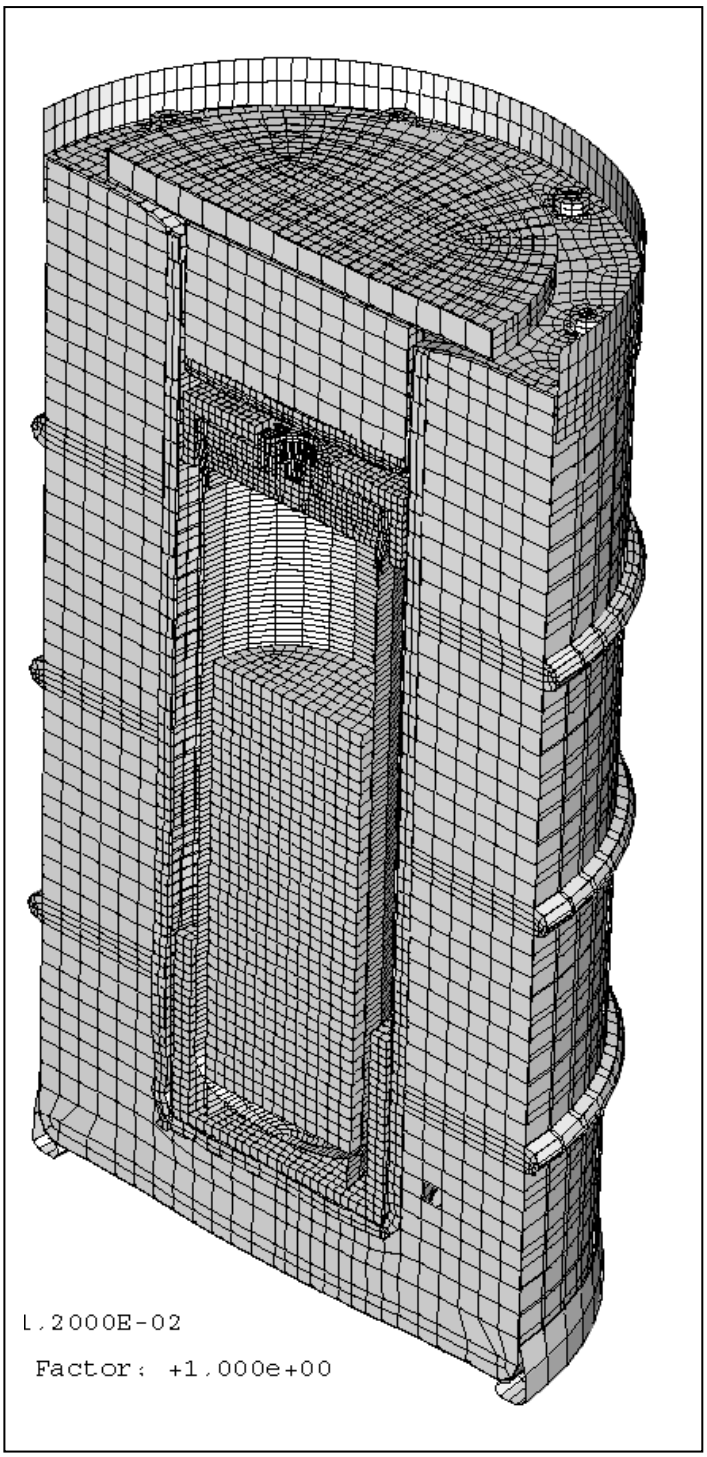

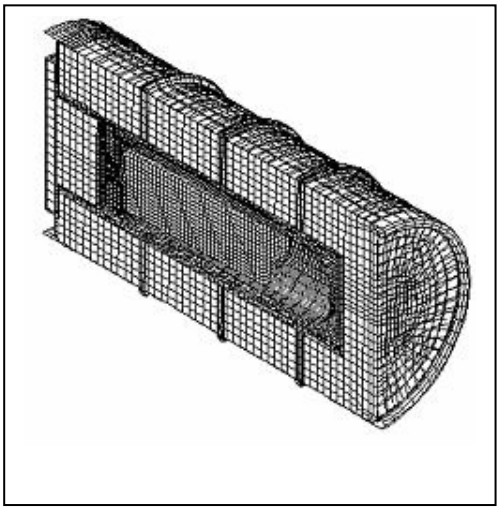

Side Drop 6CV Payload Position

Figure 2 - Shaded View of Finite-Element Model for 9977 Package

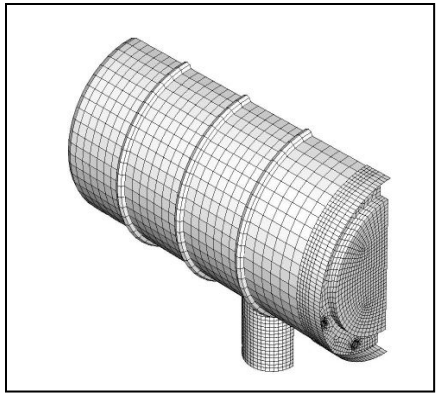

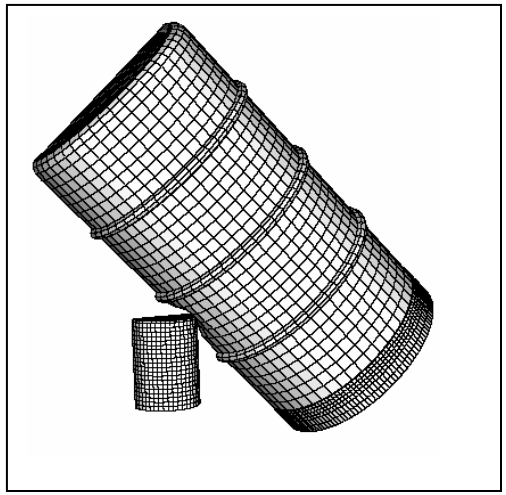

Horizontal Side Drop and at 45°

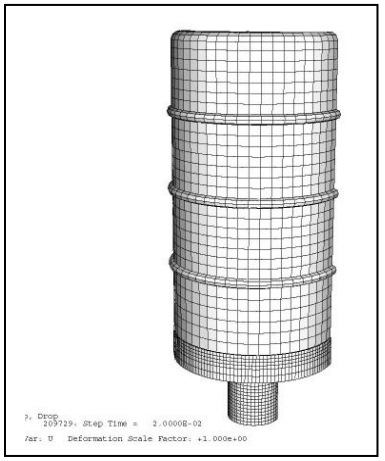

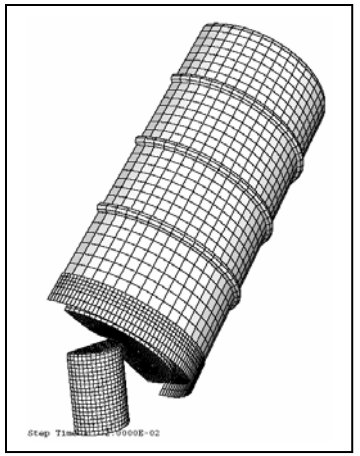

Vertical Top Drop and at 45°

Figure 3 - Puncture Test Simulations for 40-Inch Free Fall on to a Steel Bar

5.3 Applied Loads and Initial Conditions

The applied loads and initial conditions are the same for all the three cases analyzed.

Gravitational Load

The downward gravitational force of the falling package is represented by the gravitational load of 386.4 in/sec^2 in the negative "Z' direction of the model.

Initial Condition for 40-Inch Free Drop

The model of the package is initially located near the target floor so that the initial velocity is equal to the velocity of the package after a 40-inch free fall in the negative "Z" direction of the model. Therefore, the initial velocity can be calculated as follows.

$$V_0 = \sqrt{2gh} = \sqrt{2 \times 386.4 \frac{\text{in}}{\text{sec}^2} \times 40.0\,\text{in}} = 175.818 \frac{\text{in}}{\text{sec}}$$

5.4 Boundary Conditions

Due to the symmetrical conditions of the geometry and loading, the following boundary conditions are applied at the nodes of the shell elements:

$$UY = 0 \qquad RX = 0 \qquad RZ = 0\,;$$

and the following boundary condition is applied at the nodes of the brick elements:

$$UY = 0$$

The target bar is fixed and thus its boundary conditions of its reference node are as follows.

$$UX = UY = UZ = RX = RY = RZ = 0$$

5.5 Contact Conditions

The contact conditions between two surfaces are simulated by using the general contact options available in ABAQUS code (Reference 6).

6 Stress Criteria in Accordance with ASME Code

The dynamic load associated with the 40-inch drop of a 9977 package is classified as a Level D Service Load defined in the ASME Code, Section III, Appendix F and the stress limits are specified as follows (Reference 2):

$$P_m \le 0.7S_u$$

$$P_L \le 0.9S_u$$

where P_m = General primary membrane stress intensity
P_L = Local primary membrane stress intensity
S_u = Ultimate strength of material

The maximum temperature of the containment vessel under Normal Conditions of Transport with insolation and 19 Watt heat load is 321 ºF (see Section 3.3 of the 9977 SARP). The ultimate strength of 304L stainless steel is 61.2 ksi at 300 ºF and is used in this evaluation (Reference 7). The results of the finite-element analysis are expressed in terms of true stresses. Using the minimum required engineering elongation value of 35%, (Ref. 8), the true ultimate stress of the material is:

$$S_{tu} = S_u(\varepsilon + 1) = 61.2(0.35 + 1) = 82.62 \text{ ksi} \quad \text{for temperature = 300 ºF}$$

where,

S_{tu} = True ultimate stress of stainless steel 304L at 300 ºF
ε = Engineering strain corresponding to ultimate strength

Consequently, the stress limits in terms of true stresses are:

$$P_m \le 0.7S_{tu} = 0.7 \times 82.62 = 57.8 \text{ ksi} \quad \text{for temperature = } 300^{o}\text{F}$$

$$P_L \le 0.9S_{tu} = 0.9 \times 82.62 = 74.3 \text{ ksi} \quad \text{for temperature = } 300^{o}\text{F}$$

7 Strain Criterion for Components other than Containment Vessel

The components other than the containment vessel are not pressure boundaries and thus the stress values in those components may or may be not required to be evaluated in accordance with the ASME Code. For the puncture analysis the drum shell is not evaluated to the ASME Code.

Minimum engineering elongation of 35% for the drum material 304L SS is the acceptance criteria for drum shell.

8 Analytical Results Evaluation

Evaluations of Maximum Local Primary Membrane Stress Intensities and Maximum Equivalent Plastic Strains in Containment Vessel

For simplicity and conservatism, the maximum von Mises stress across the containment vessel walls (approximately equal to the Local Primary Membrane stress intensities, P_L) instead of the General and Local Membrane stress intensities are used for comparison with the allowable General (P_m) and Local (P_L) Primary Membrane stress intensities specified in the ASME Code, Section III, Appendix F.

The maximum value of von-Mises stress is higher than the actual local primary membrane stress intensity because the latter is calculated by averaging the stress components across the component thickness. This bounds the membrane stress and precludes potential local material damage due to local discontinuities.

The value for the minimum engineering elongation of 35% is used to evaluate the drum against rupture due to the puncture impacts

9 Discussion of Analytical Results

9.1 Side Drop and Side Drop at 45º (-20 ºF)

Energy History

The time-history plots of energy components for the two side puncture simulations shown in Figure 4 indicate that the kinetic energy approaches to zero at the end of the analysis. Therefore, we know that the analysis covers the entire impact duration.

9.1.1 Containment Vessel Stress-Strain Evaluation

The maximum value of the local primary membrane stress intensity in the containment vessel for the side drop is 46.55 ksi and 43.93 ksi for the side drop at an angle of 45º as shown in Figure 5. The maximum value of the equivalent plastic strains in the containment vessel is 0.027 and 0.019 for the side and 45º angled drop, respectively, are shown in Figure 6.

The calculated stresses in the containment vessel are significantly less than the allowable value of 57.8 ksi for the general primary membrane stress intensity, P_m and of 74.3 ksi for the local primary membrane stress intensity, P_L (as given in Section 6.0). The containment vessel equivalent plastic strains are negligible when compared to the Code allowable strain of 0.35 for each of the cases.

9.1.2 Drum Strain Evaluation

Strain contour deformation plots of the drum for the side drop and the side drop at an angle of 45º are shown in Figures 7 and 8, respectively. The maximum value of the equivalent plastic strains in the drum is 0.155 for the side and 0.147 for the 45º angled drop. These are less than the allowable strain of 0.35. Therefore, the drum will not be ruptured during the hypothetical accident condition of 40-inch drop on at 6 inch steel bar.

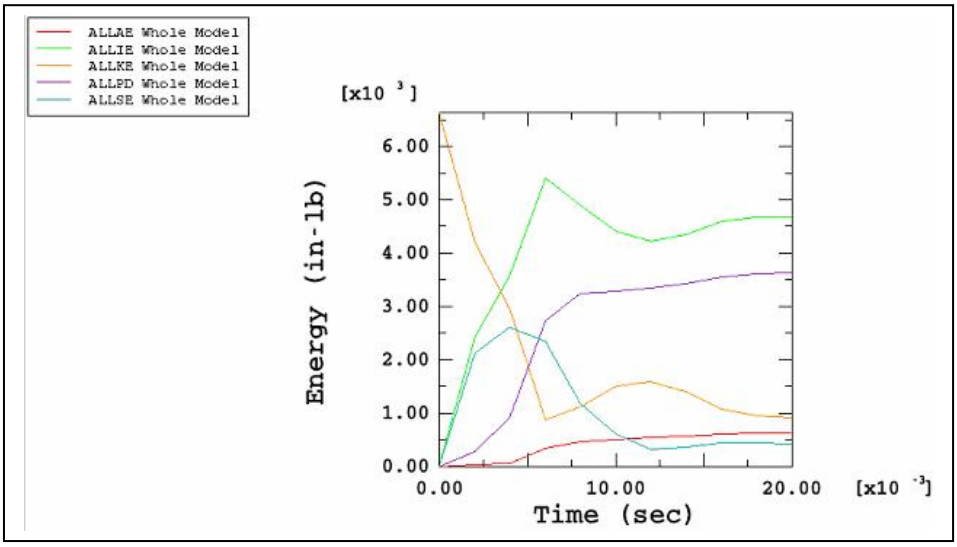

Side Drop (-20 ºF)

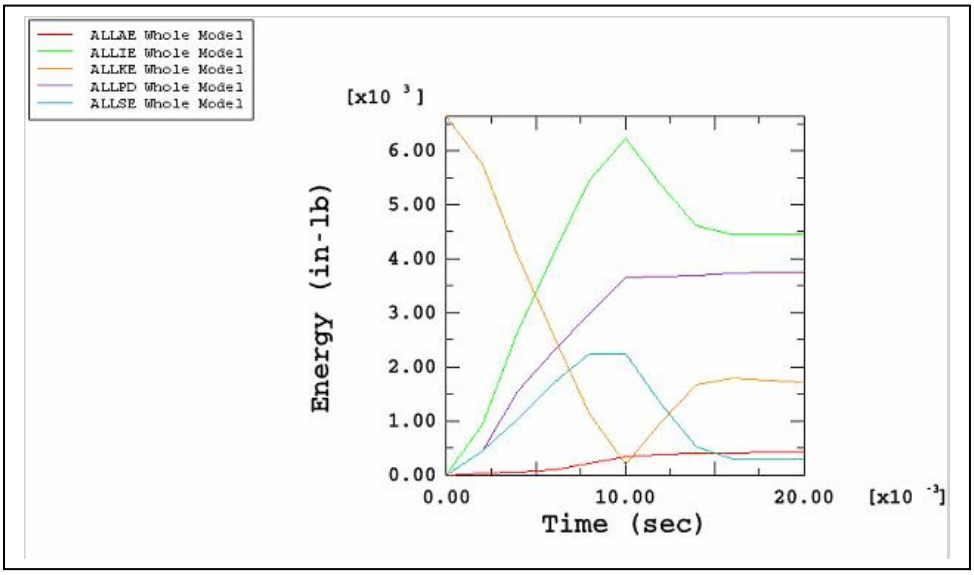

Side Drop 45º (-20 ºF)

(ALLKE = kinetic energy; ALLIE = total strain energy; ALLSE = elastic strain energy; ALLPD = plastic strain energy; ALLAE = artificial energy)

Figure 4 - Time-History of Energy Components (-20 ºF)

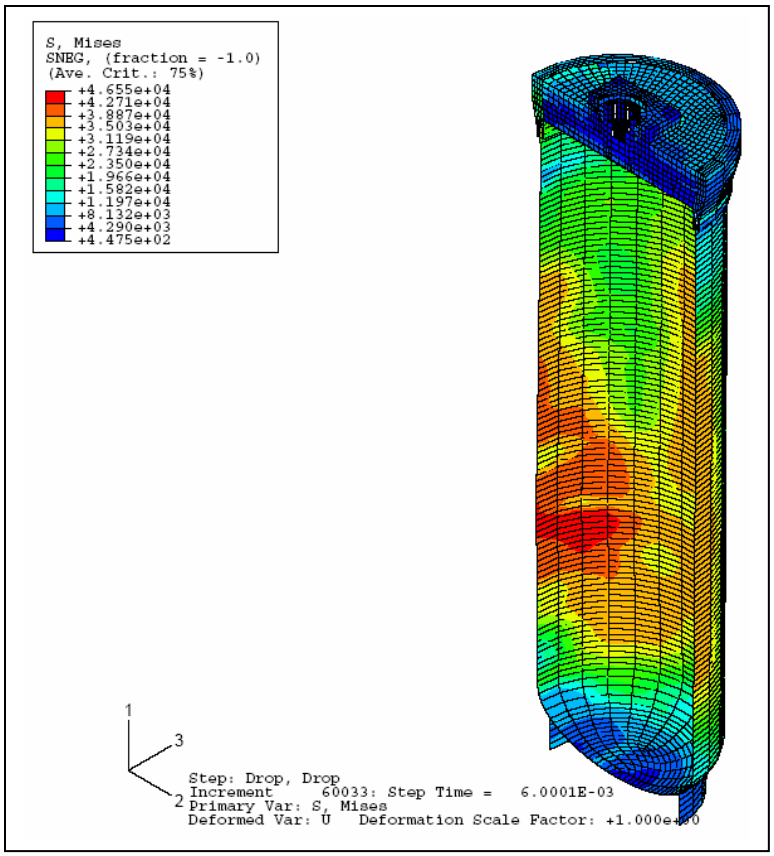

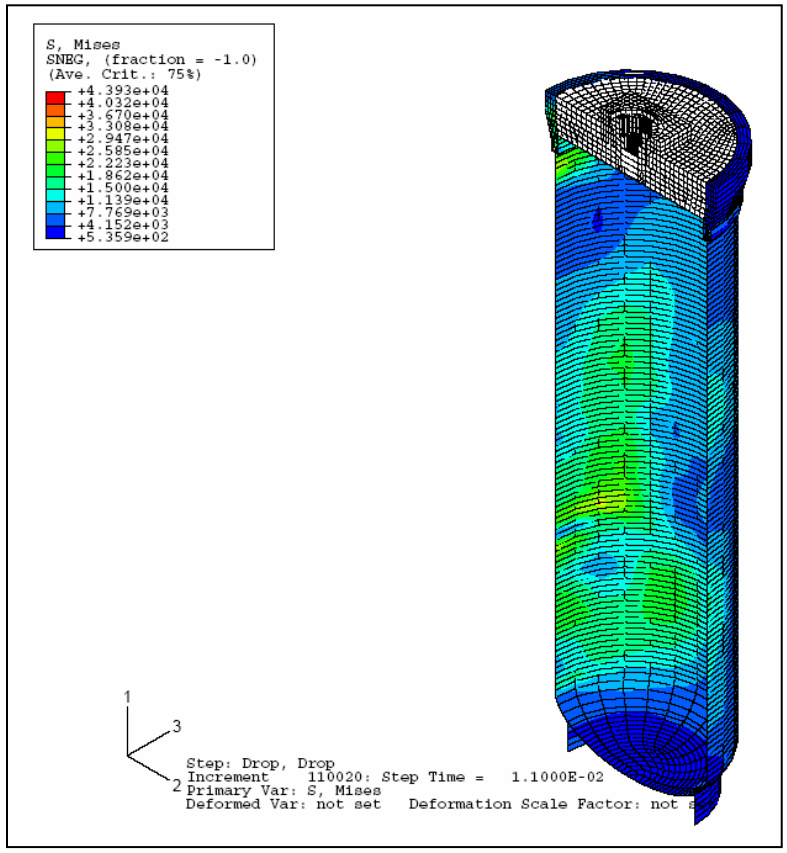

Side Drop **45º Side Drop**

Figure 5 - Stress Distribution in Containment Vessel Side Drop and Side Angle Drop at 45º(-20 ºF)

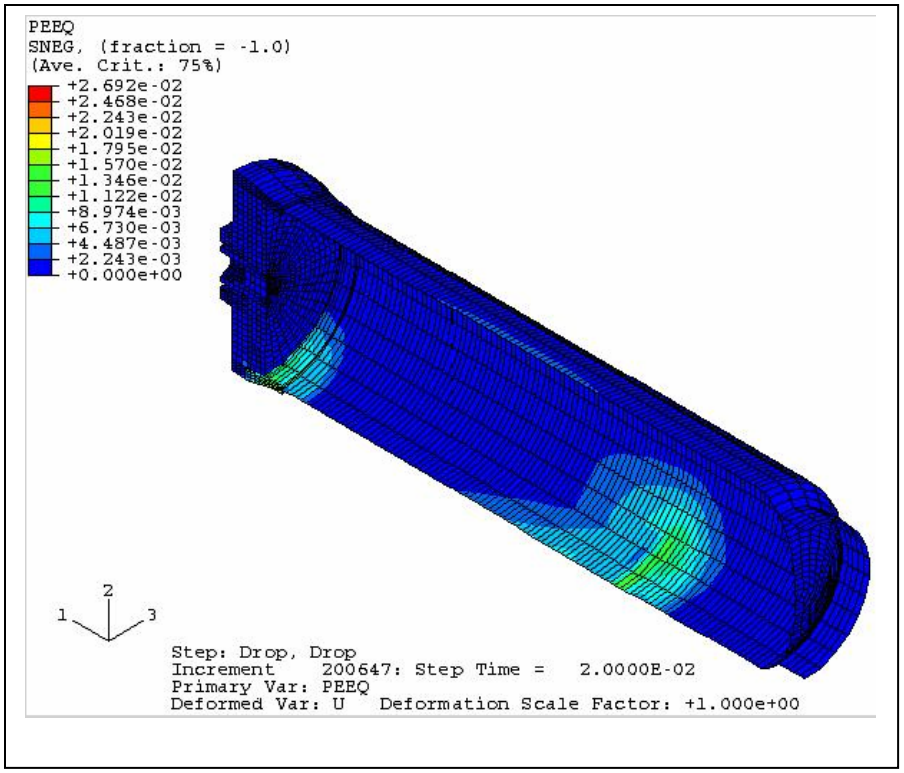

Side Drop

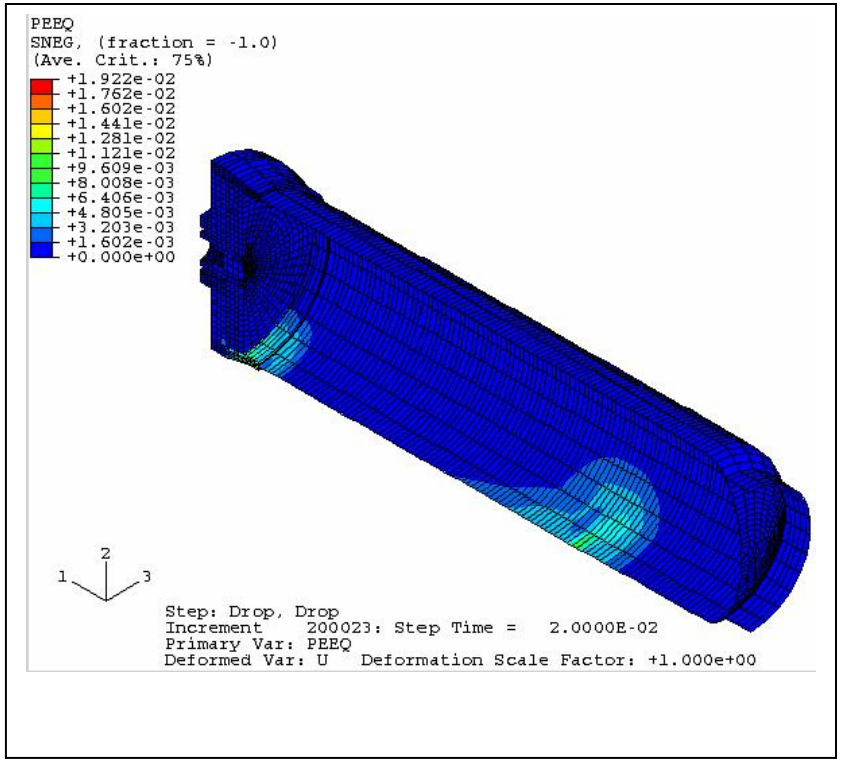

45º Side Drop

Figure 6 - Strain Distribution in Containment Vessel Side Drop and Side Angle Drop at 45º (-20 ºF)

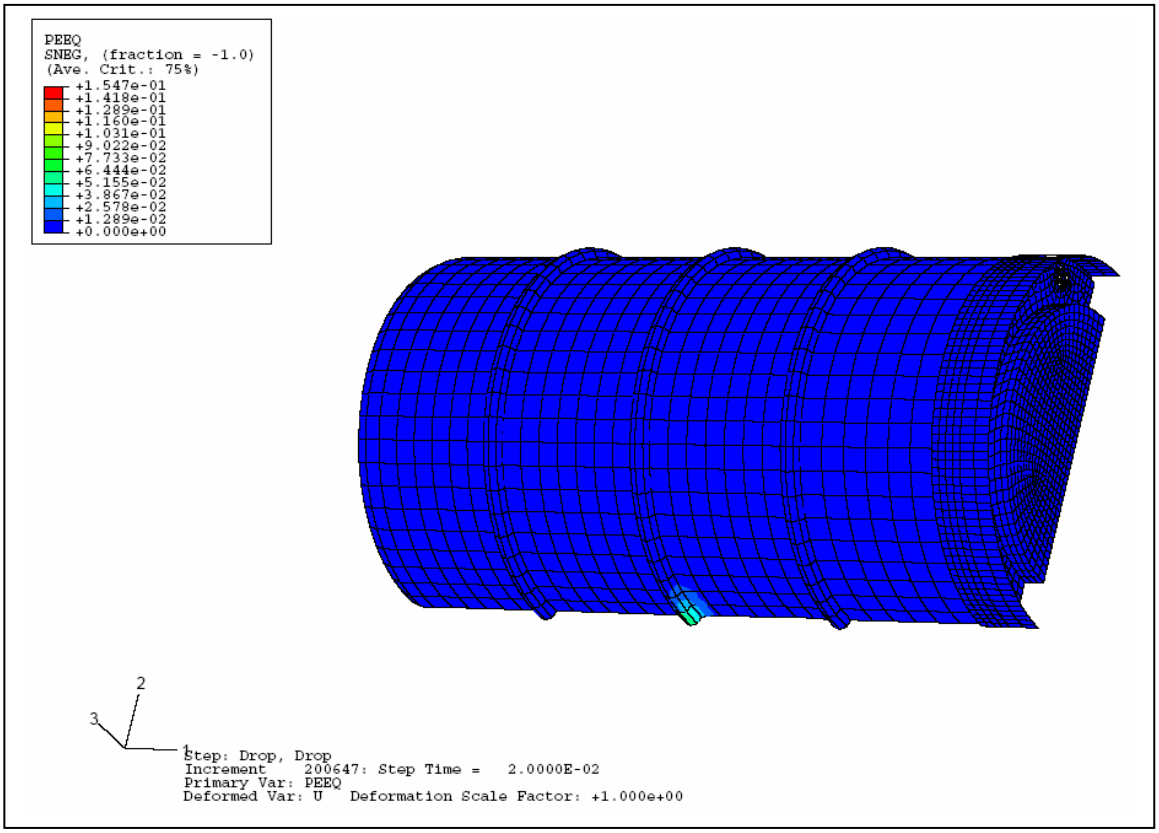

Figure 7 - Strain Contour Plot for Drum at Side Drop (-20ºF)

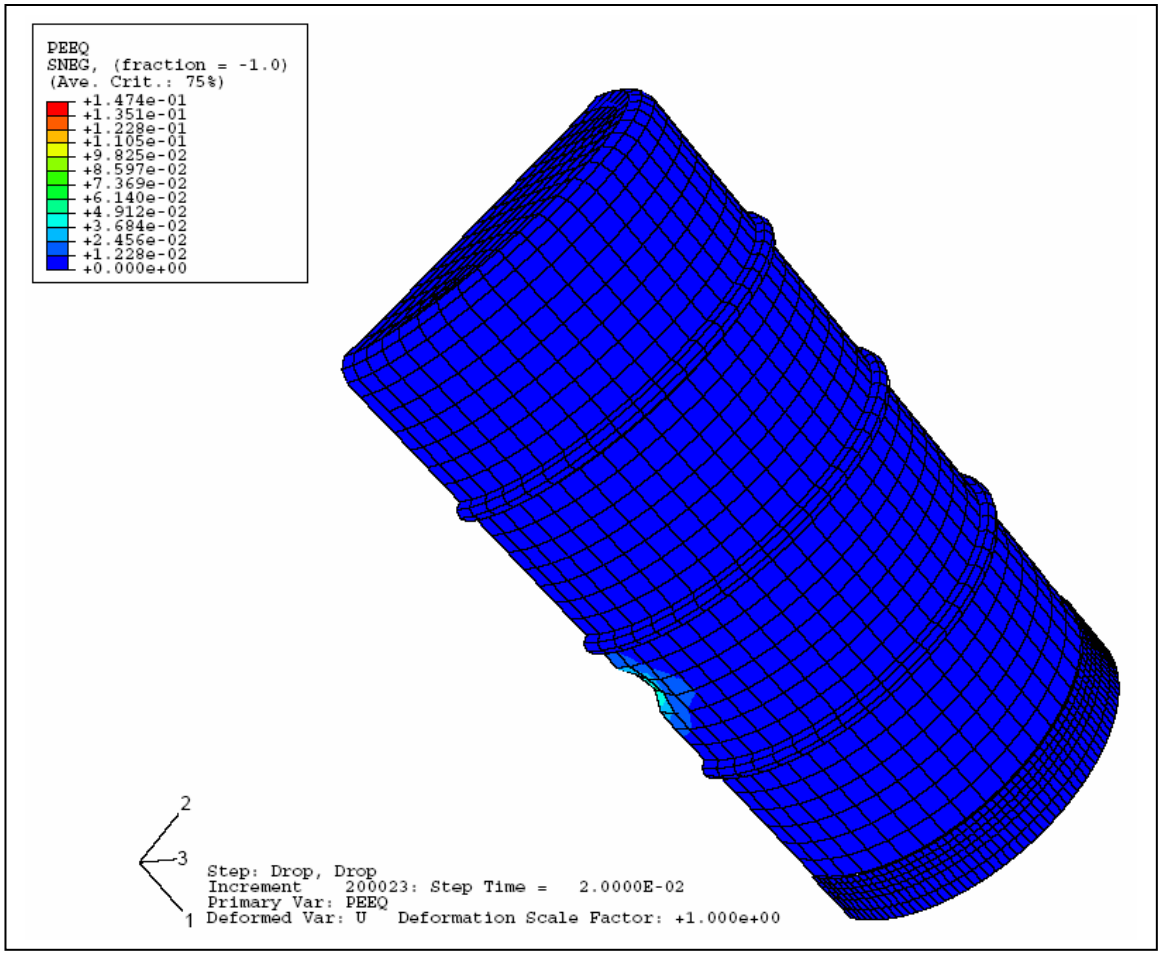

Figure 8 - Strain Contour Plot for Drum Side Angle Drop at 45º (-20ºF)

9.2 Side Drop and Side Drop at 45º (75 ºF)

Energy History

The time-history plots of energy components for the two side puncture simulations shown in Figure 9 indicate that the kinetic energy approaches to zero at the end of the analysis. Therefore, we know that the analysis covers the entire impact duration.

9.2.1 Containment Vessel Stress-Strain Evaluation

The maximum value of the local primary membrane stress intensity in the containment vessel for the side drop is 45.41 ksi and 42.09 ksi for the side drop at an angle of 45º as shown in Figure 10. The maximum value of the equivalent plastic strains in the containment vessel is 0.024 and 0.015 for the side and 45º angled drop, respectively, are shown in Figure 11.

The calculated stresses in the containment vessel are significantly less than the allowable value of 57.8 ksi for the general primary membrane stress intensity, P_m and of 74.3 ksi for the local primary membrane stress intensity, P_L (as given in Section 6.0). The containment vessel equivalent plastic strains are negligible when compared to the Code allowable of 0.35 for each of the cases.

9.2.2 Drum Strain Evaluation

Strain contour deformation plots of the drum for the side drop and the side drop at an angle of 45º are shown in Figures 12 and 13, respectively. The maximum value of the equivalent plastic strains in the drum is 0.154 for the side and 0.133 for the 45º angled drop. These are less than the Code minimum required elongation strain of 0.35. Therefore, the drum will not be ruptured during the hypothetical accident condition of 40-inch drop on at 6 inch steel pipe.

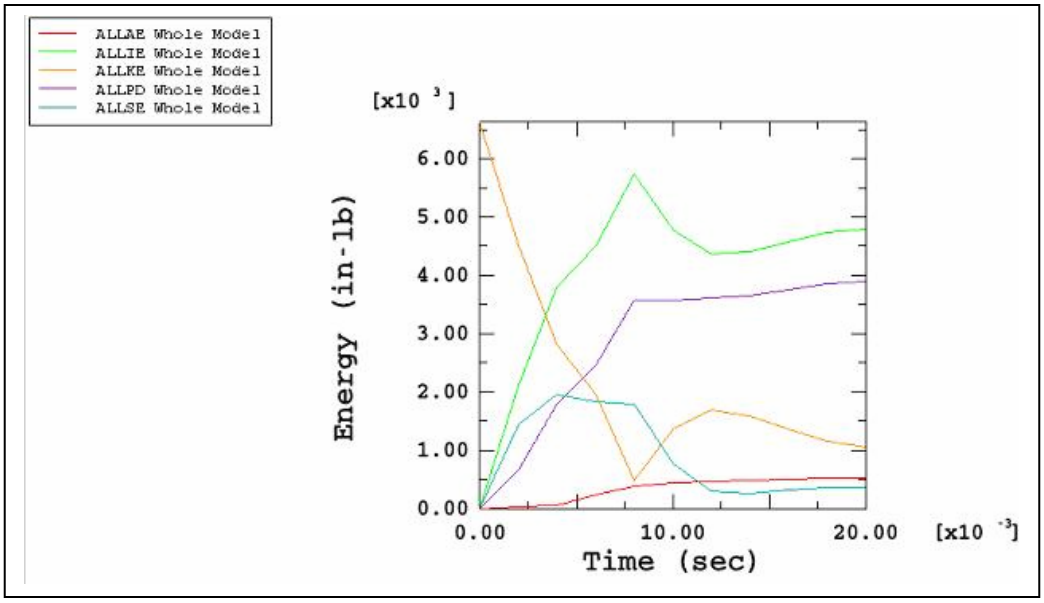

Side Drop (75 ºF)

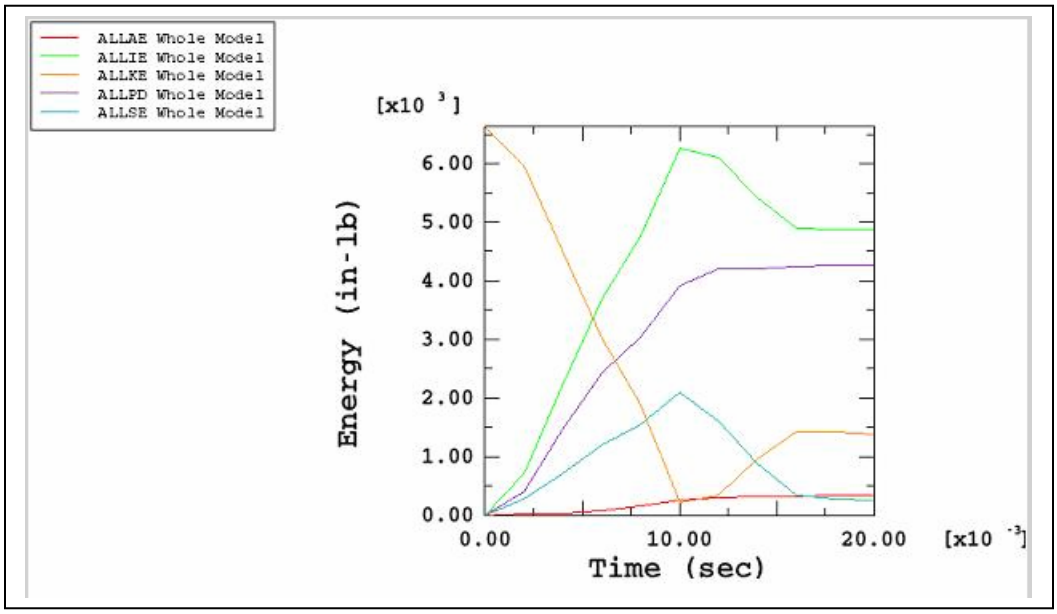

Side Drop 45º (75 ºF)

(ALLKE = kinetic energy; ALLIE = total strain energy; ALLSE = elastic strain energy; ALLPD = plastic strain energy; ALLAE = artificial energy)

Figure 9 - Time-History of Energy Components (75 ºF)

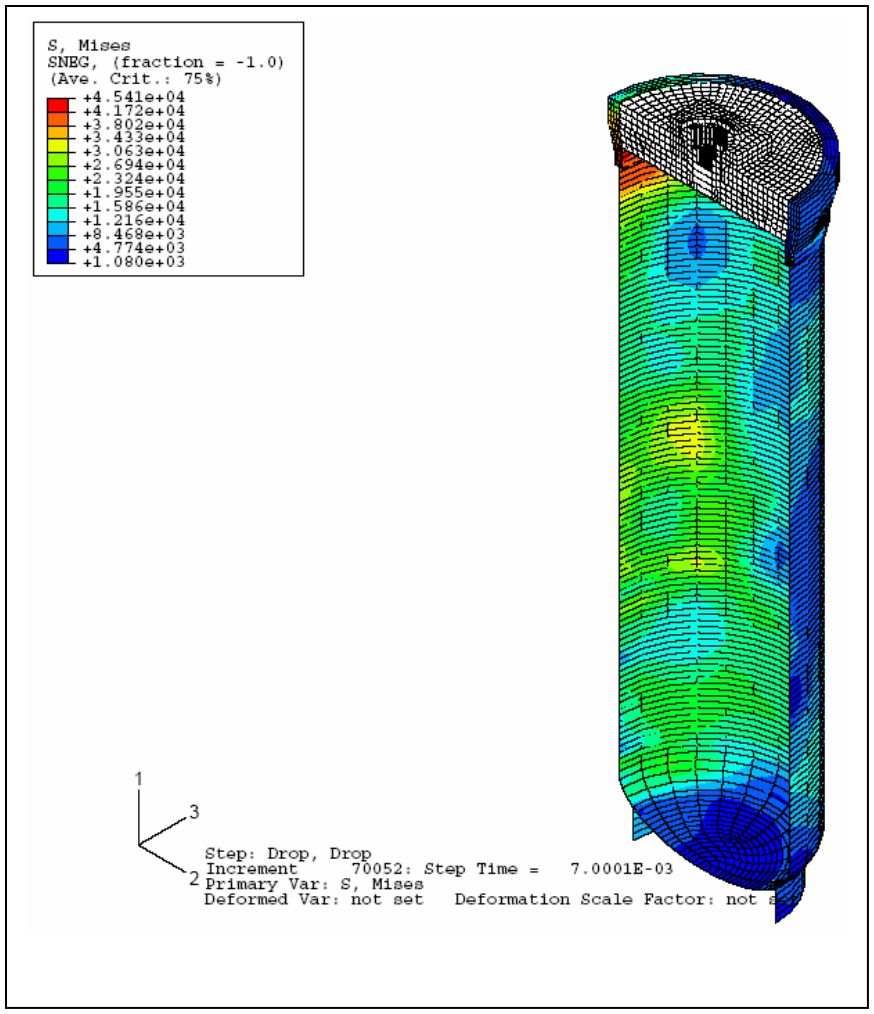

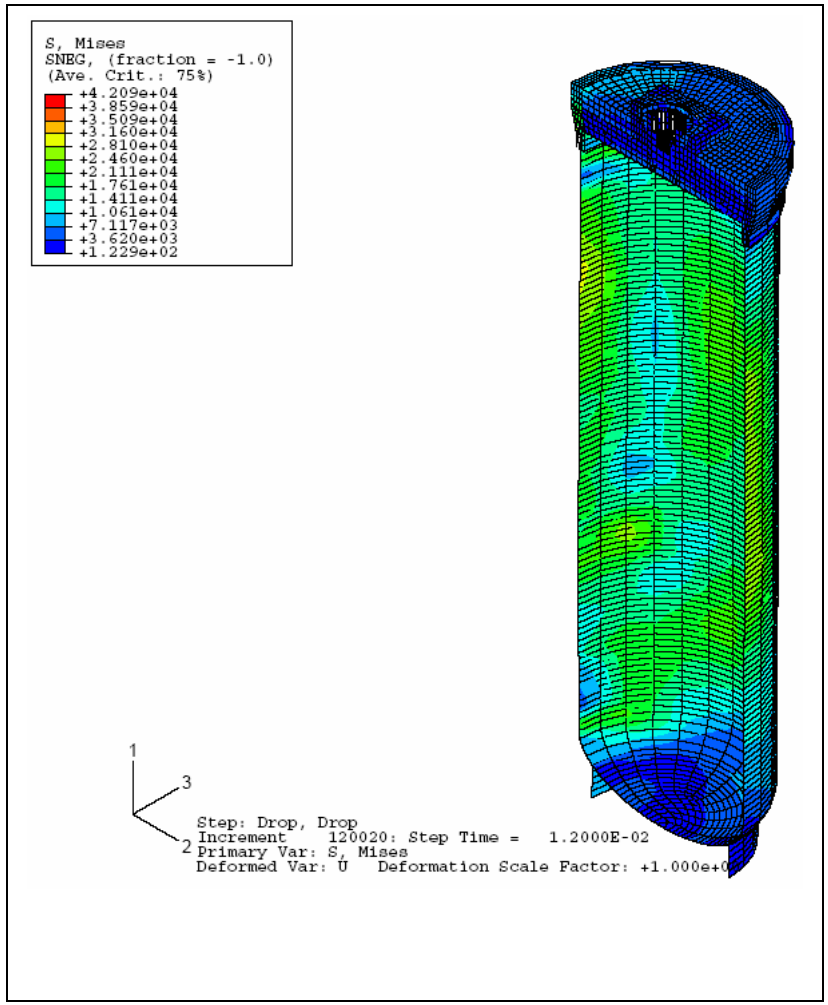

Side Drop **45° Side Drop**

Figure 10 - Stress Distribution in Containment Vessel Side Drop and Side Angle Drop at 45º(75ºF)

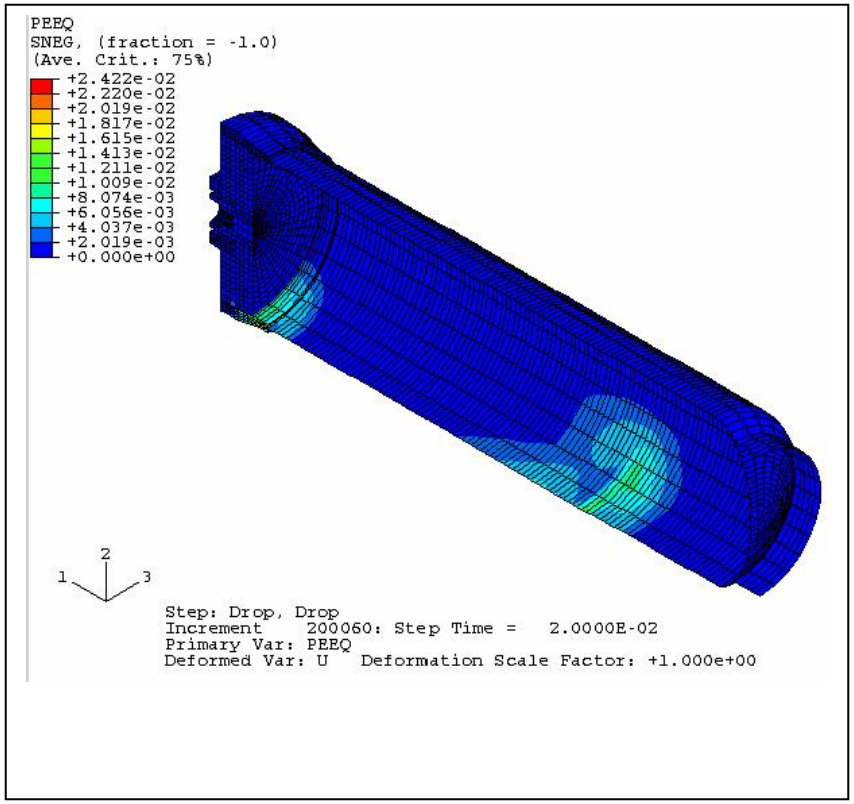

Side Drop

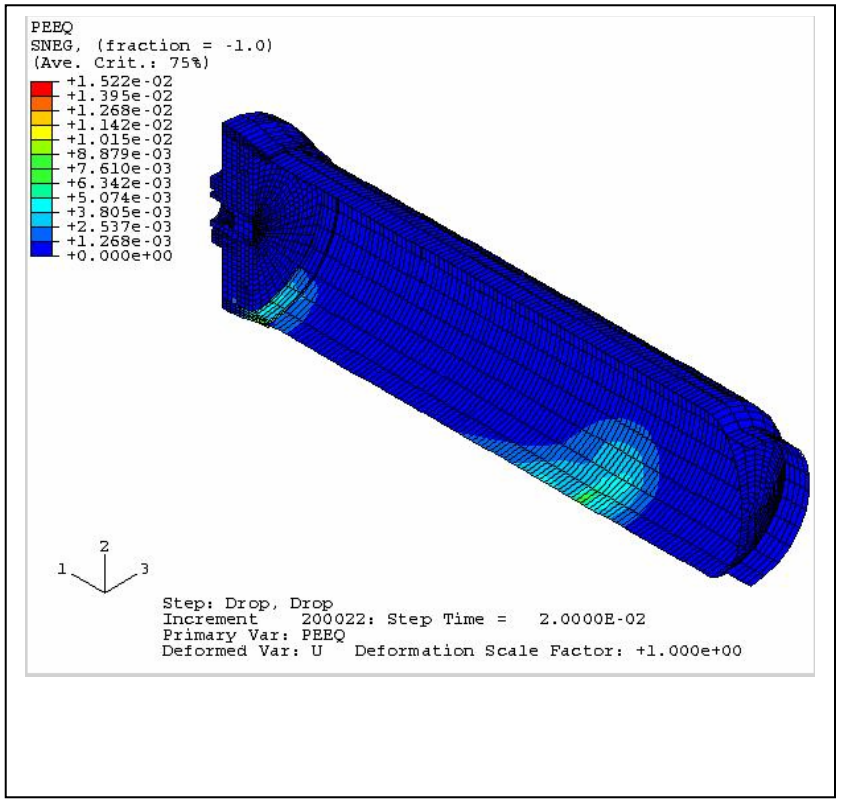

45º Side Drop

Figure 11 - Strain Distribution in Containment Vessel Side Drop and Side Angle Drop at 45º (75 ºF)

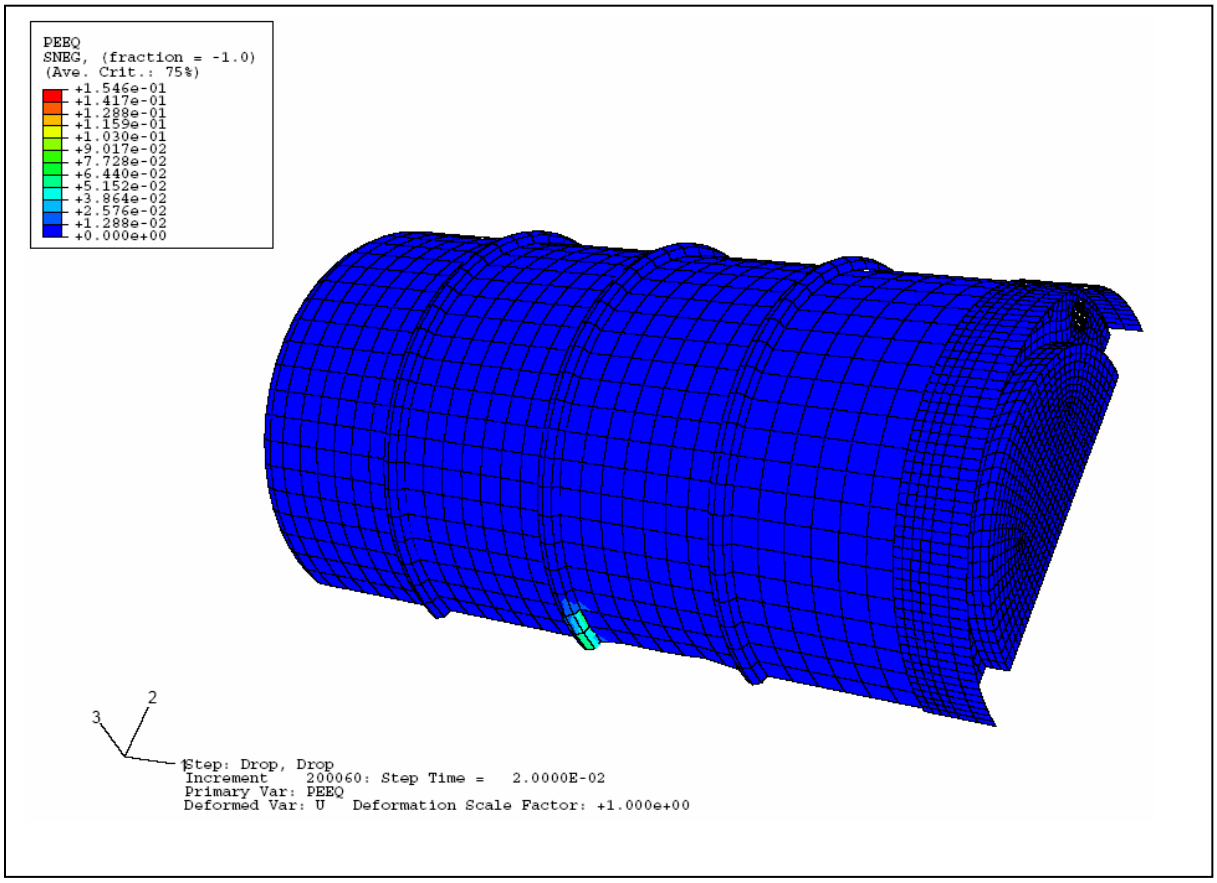

Figure 12 - Strain Contour Plot for Drum at Side Drop (75ºF)

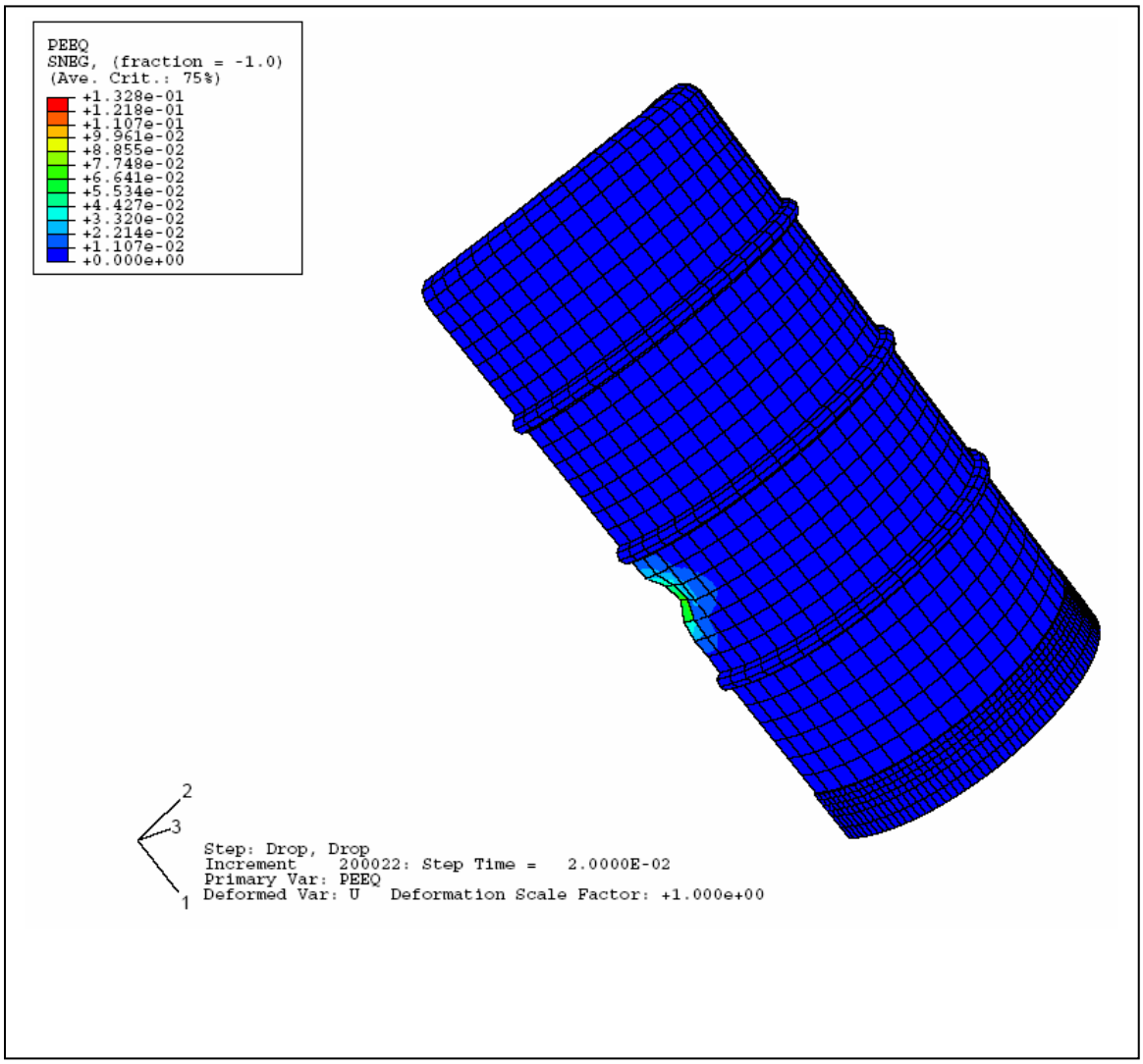

Figure 13 - Strain Contour Plot for Drum Side Angle Drop at 45º (75ºF)

9.3 Side Drop and Side Drop at 45º (140 ºF)

Energy History

The time-history plots of energy components for the two side puncture simulations shown in Figure 14 indicate that the kinetic energy approaches to zero at the end of the analysis. Therefore, we know that the analysis covers the entire impact duration.

9.3.1 Containment Vessel Stress-Strain Evaluation

The maximum value of the local primary membrane stress intensity in the containment vessel for the side drop is 40.89 ksi and 42.85 ksi for the side drop at an angle of 45º as shown in Figure 15. The maximum value of the equivalent plastic strains in the containment vessel is 0.023 and 0.014 for the side and 45º angled drop, respectively, are shown in Figure 16.

The calculated stresses in the containment vessel are significantly less than the allowable value of 57.8 ksi for the general primary membrane stress intensity, P_m and of 74.3 ksi for the local primary membrane stress intensity, P_L (as given in Section 6.0). The containment vessel equivalent plastic strains are negligible when compared to the allowable strain of 0.35 for each of the cases.

9.3.2 Drum Strain Evaluation

Strain contour deformation plots of the drum for the side drop and the side drop at an angle of 45º are shown in Figures 17 and 18, respectively. The maximum value of the equivalent plastic strains in the drum are 0.065 for the side and 0.073 for the 45º angled drop. These are less than the allowable strain of 0.35. Therefore, the drum will not be ruptured during the hypothetical accident condition of 40-inch drop on at 6 inch steel bar.

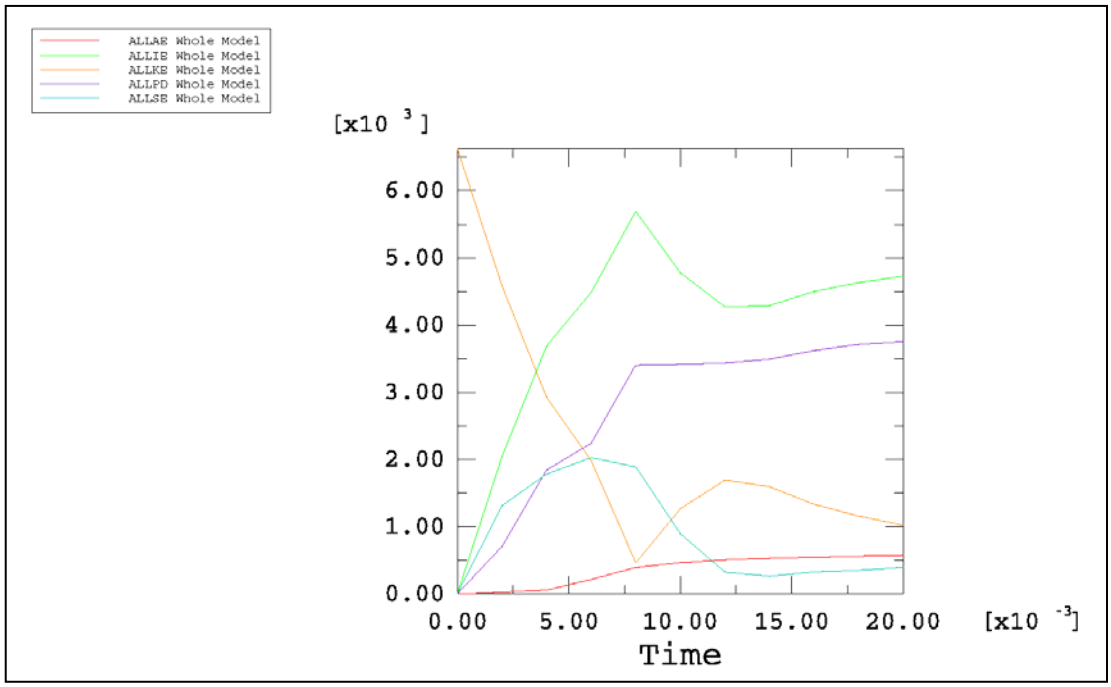

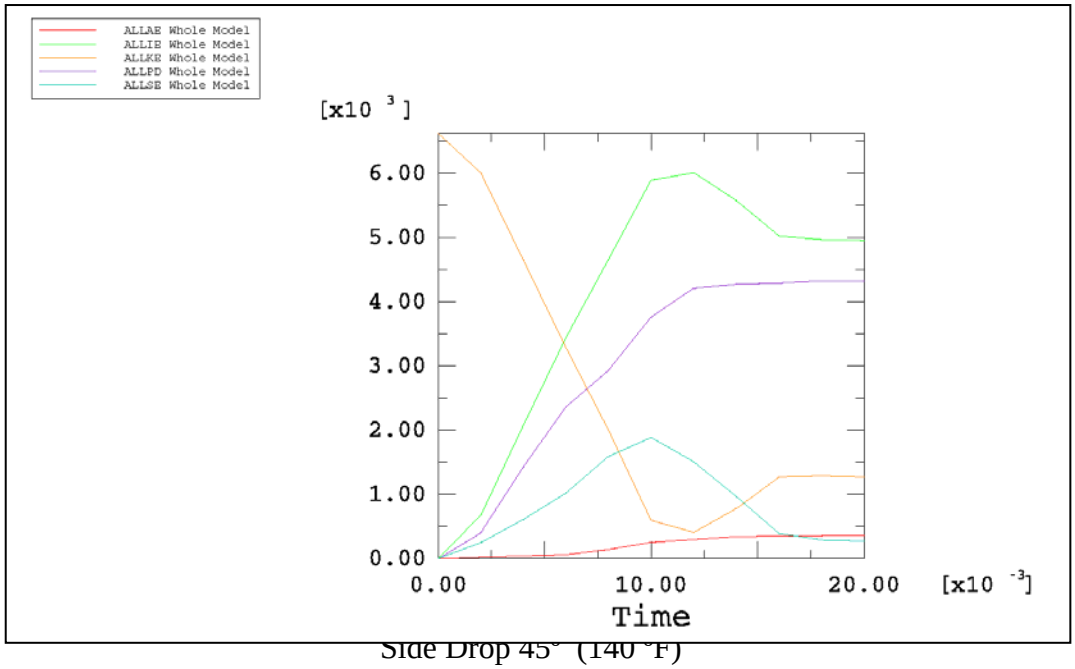

Side Drop 45° (140 °F)

(ALLKE = kinetic energy; ALLIE = total strain energy; ALLSE = elastic strain energy; ALLPD = plastic strain energy; ALLAE = artificial energy)

Figure 14 - Time-History of Energy Components (140 ºF)

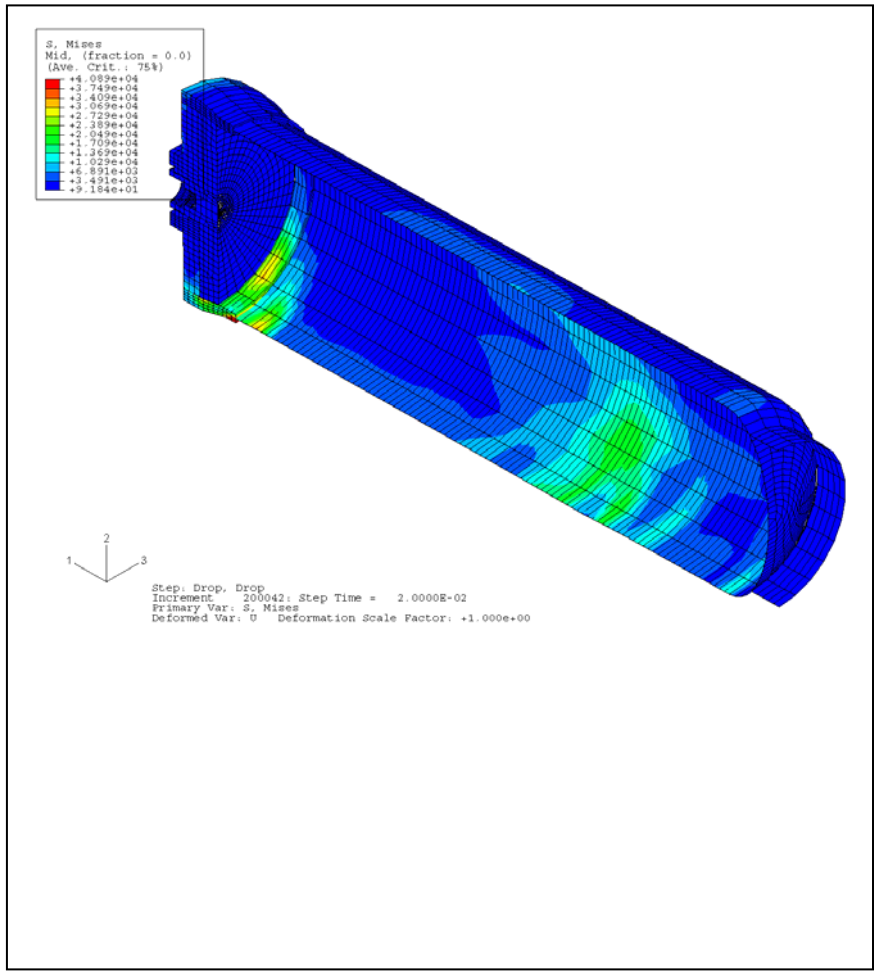

Side Drop

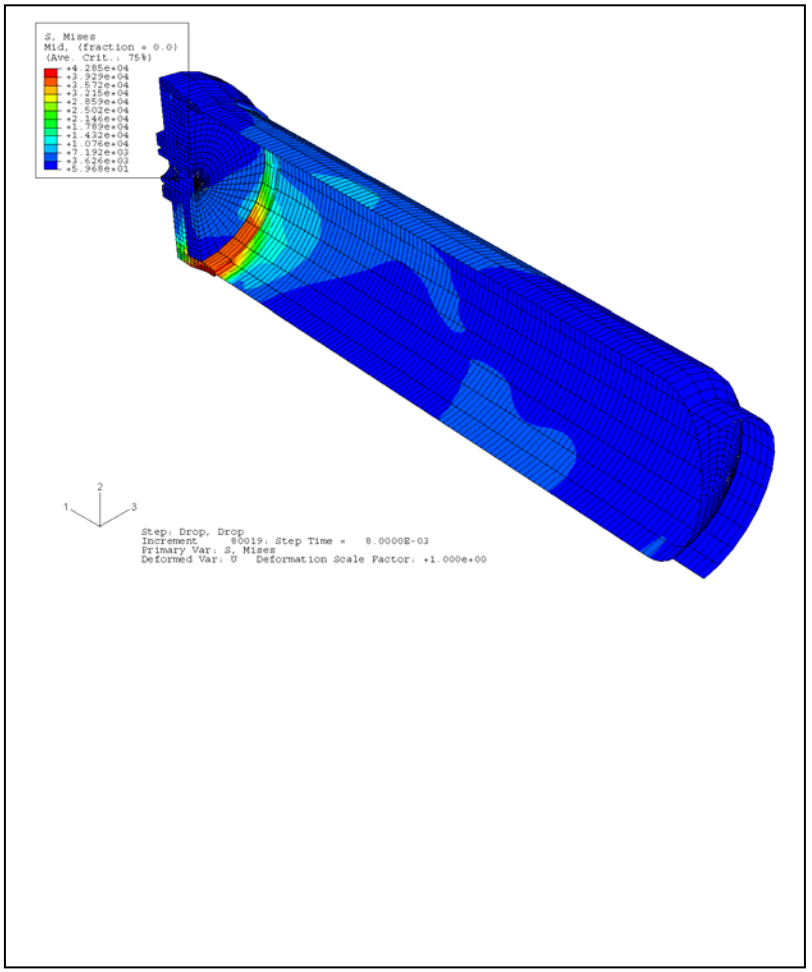

45º Side Drop

Figure 15 - Stress Distribution in Containment Vessel Side Drop and Side Angle Drop at 45º(140ºF)

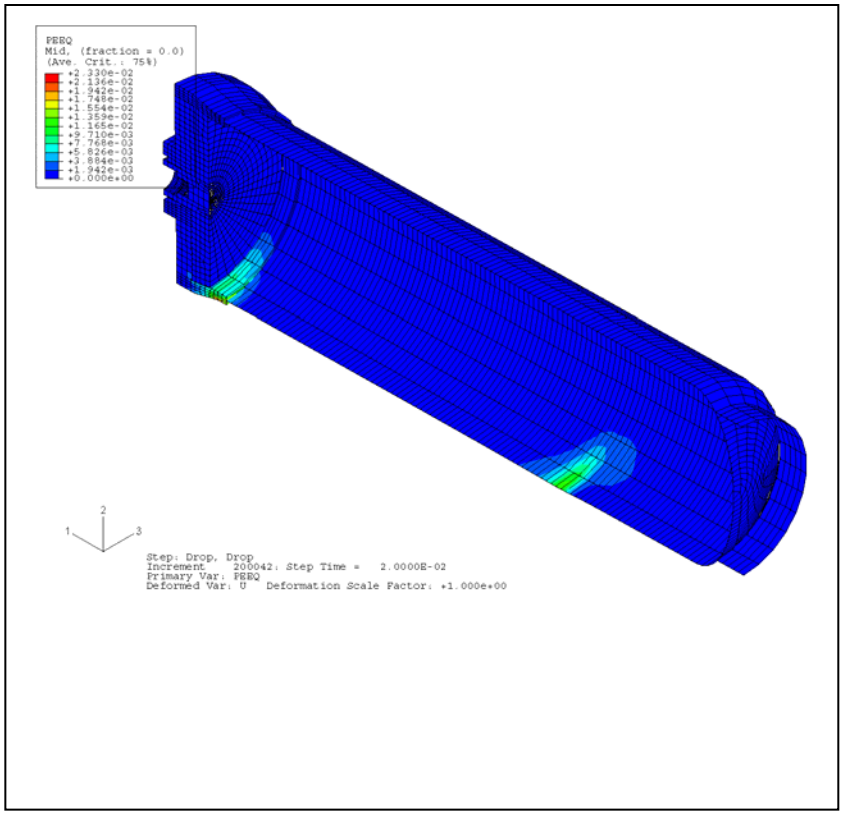

Side Drop

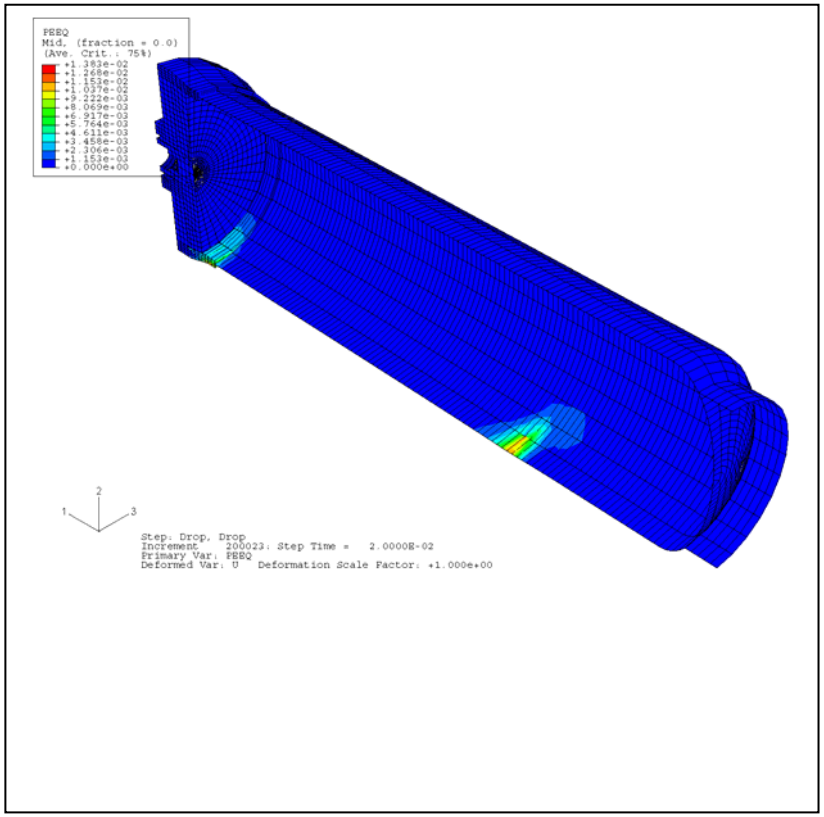

45º Side Drop

Figure 16 - Strain Distribution in Containment Vessel Side Drop and Side Angle Drop at 45º (140 ºF)

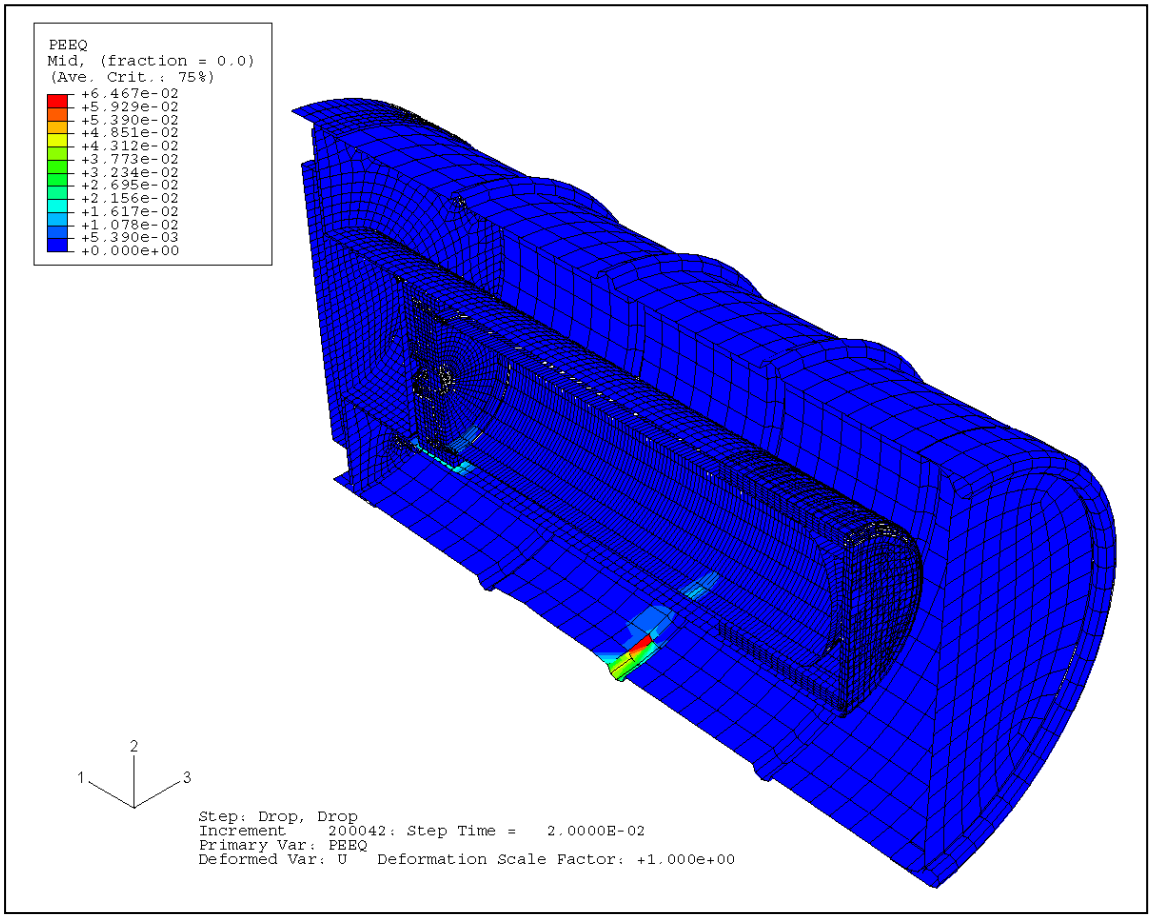

Figure 17 - Strain Contour Plot for Drum at Side Drop (140ºF)

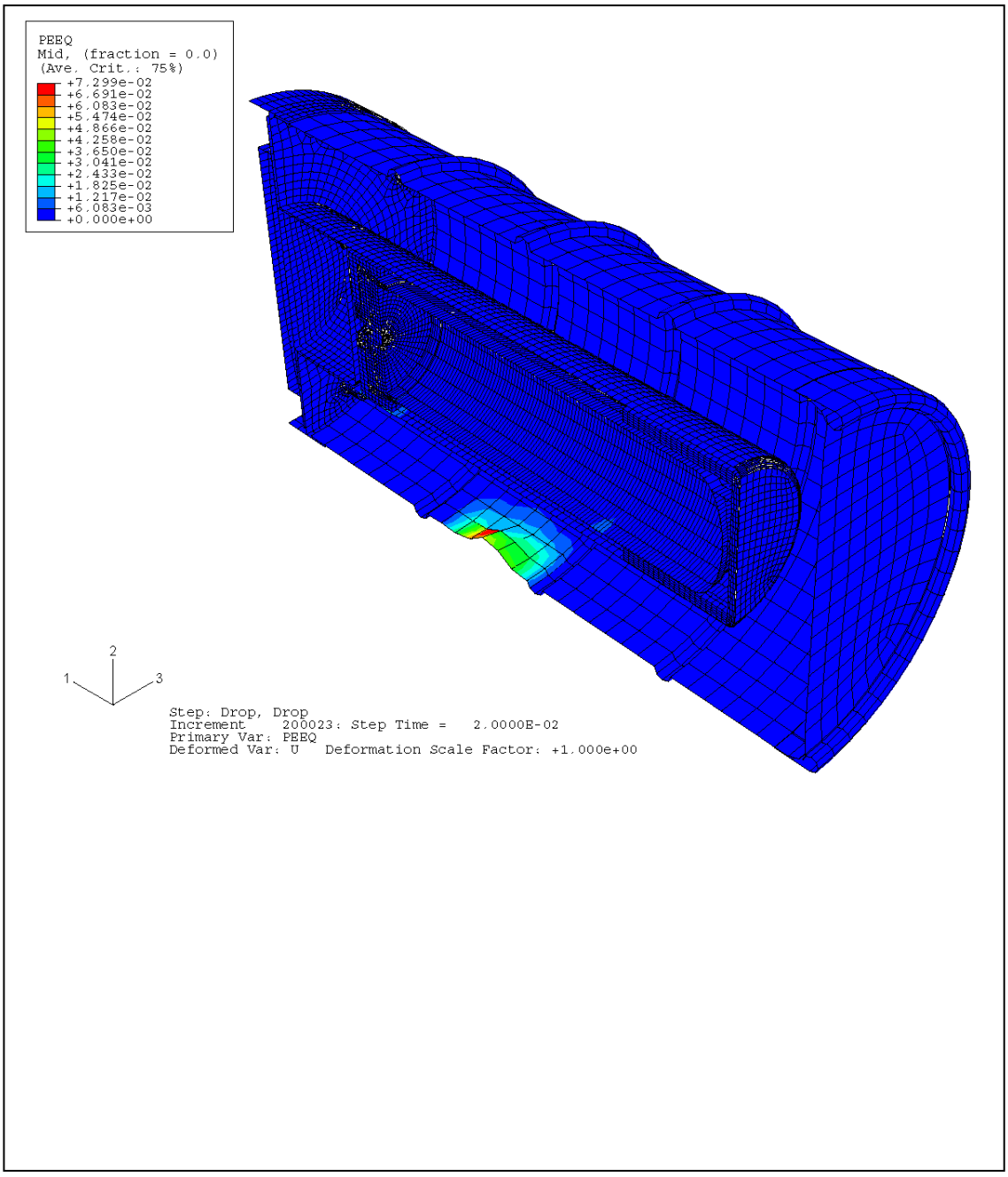

Figure 18 - Strain Contour Plot for Drum Side Angle Drop at 45º (140ºF)

9.4 Side Drop and Side Drop at 45º (300 ºF)

Energy History

The time-history plots of energy components for the two side puncture simulations shown in Figure 19 indicate that the kinetic energy approaches to zero at the end of the analysis. Therefore, we know that the analysis covers the entire impact duration.

9.4.1 Containment Vessel Stress-Strain Evaluation

The maximum value of the local primary membrane stress intensity in the containment vessel for the side drop is 46.48 ksi and 40.91 ksi for the side drop at an angle of 45º as shown in Figure 20. The maximum value of the equivalent plastic strains in the containment vessel is 0.016 and 0.005 for the side and 45º angled drop, respectively, are shown in Figure 21.

The calculated stresses in the containment vessel are significantly less than the allowable value of 57.8 ksi for the general primary membrane stress intensity, P_m and of 74.3 ksi for the local primary membrane stress intensity, P_L (as given in Section 6.0). The containment vessel equivalent plastic strains are negligible when compared to the allowable strain of 0.35 for each of the cases.

9.4.2 Drum Strain Evaluation

Strain contour deformation plots of the drum for the side drop and the side drop at an angle of 45º are shown in Figures 22 and 23, respectively. The maximum value of the equivalent plastic strain in the drum is 0.057 for the side and 0.082 for the 45º angled drop. These are less than the allowable strain of 0.35. Therefore, the drum will not be ruptured during the hypothetical accident condition of 40-inch drop on at 6 inch steel bar.

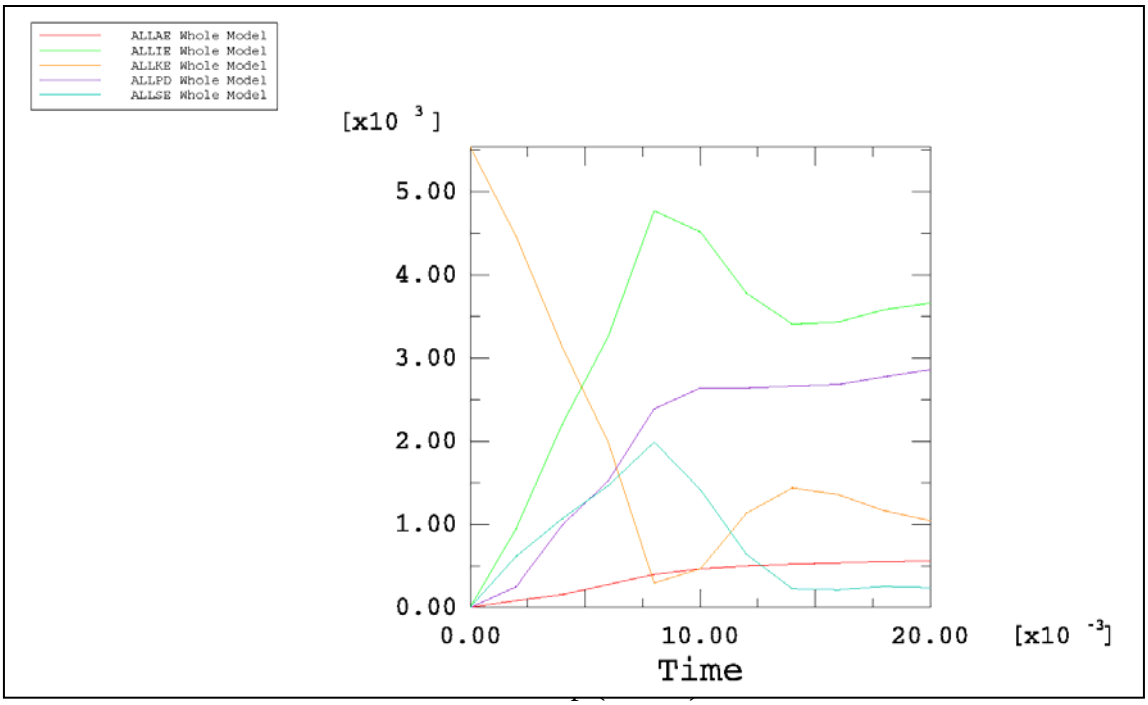

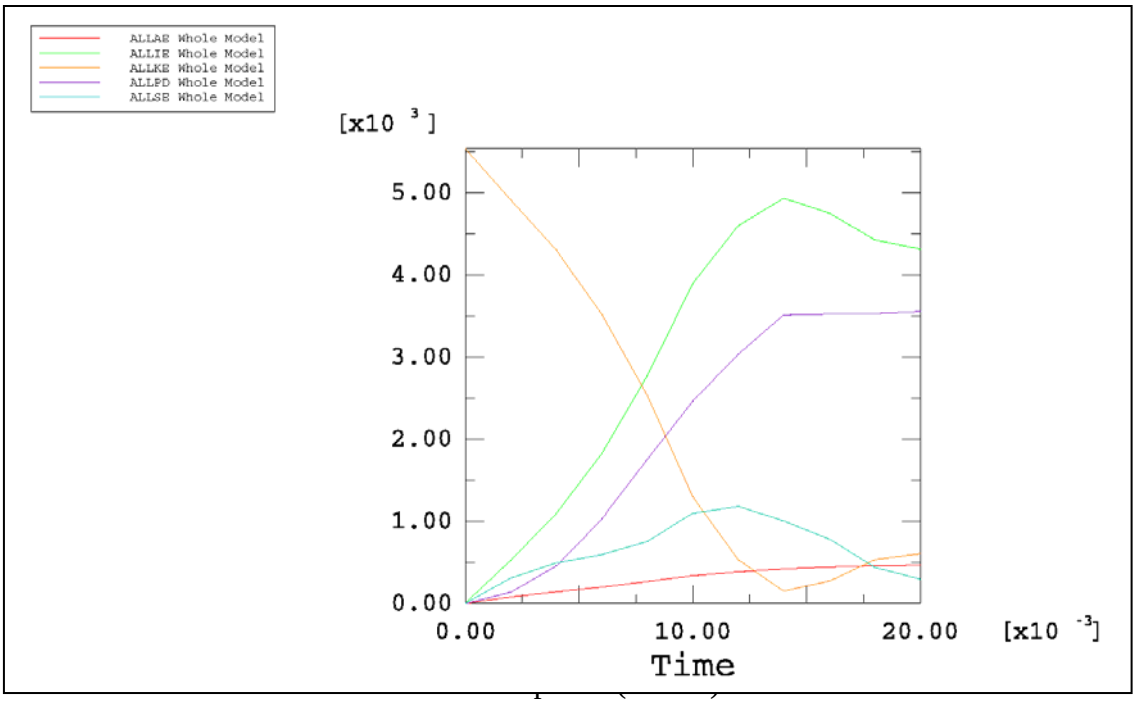

(ALLKE = kinetic energy; ALLIE = total strain energy; ALLSE = elastic strain energy; ALLPD = plastic strain energy; ALLAE = artificial energy)

Figure 19 - Time-History of Energy Components (300 ºF)

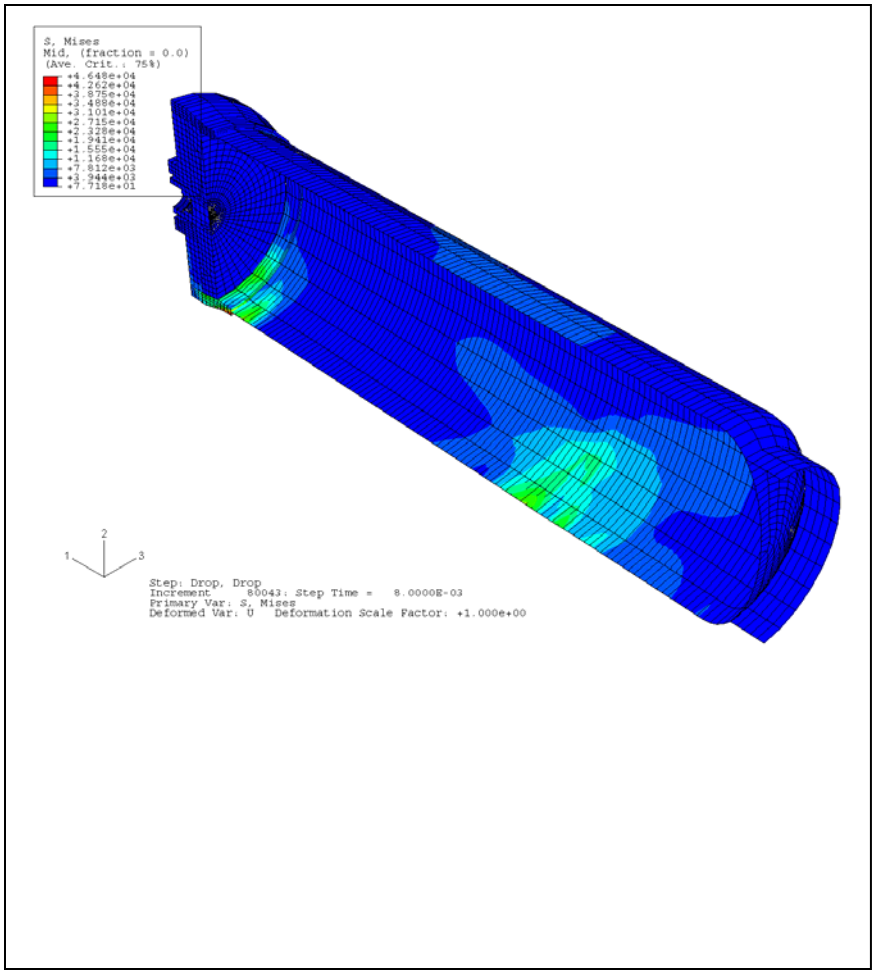

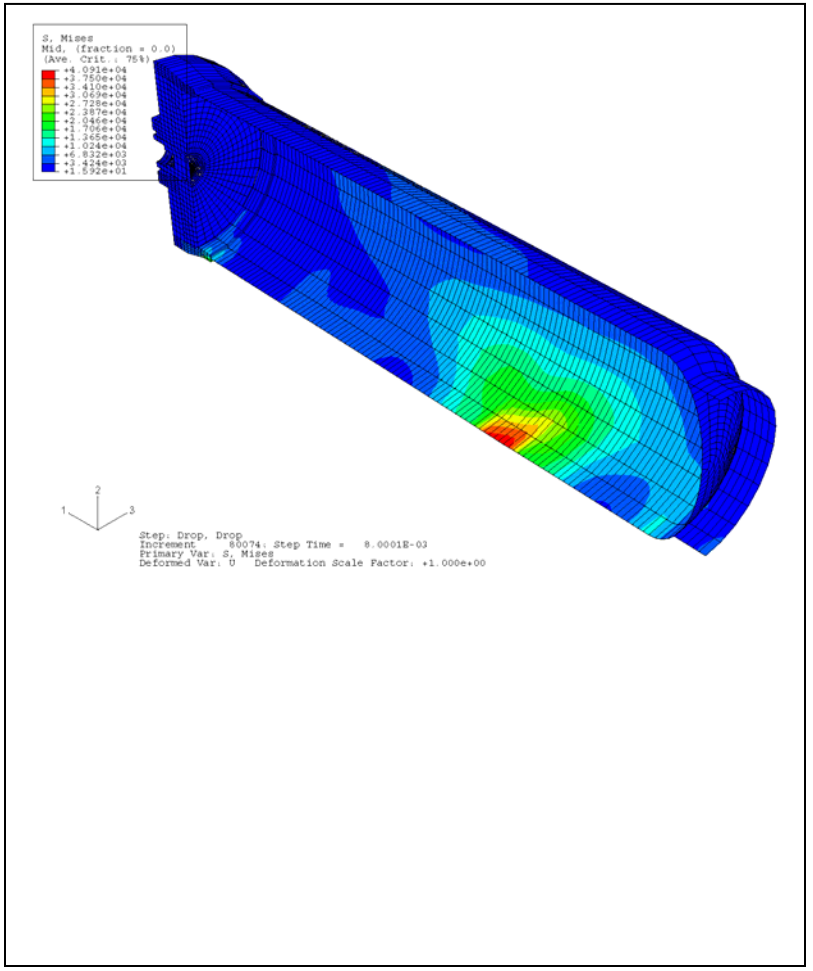

Side Drop **45º Side Drop**

Figure 20 - Stress Distribution in Containment Vessel Side Drop and Side Angle Drop at 45º(300ºF)

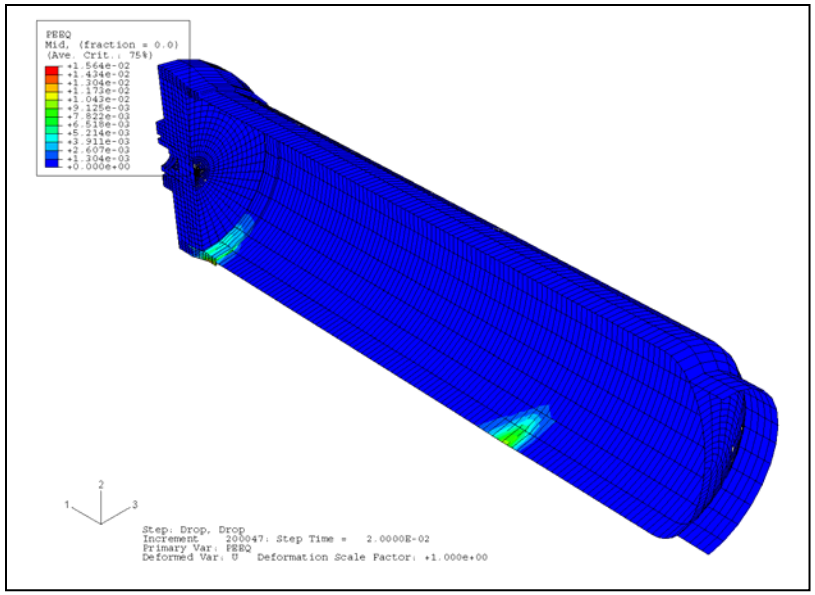

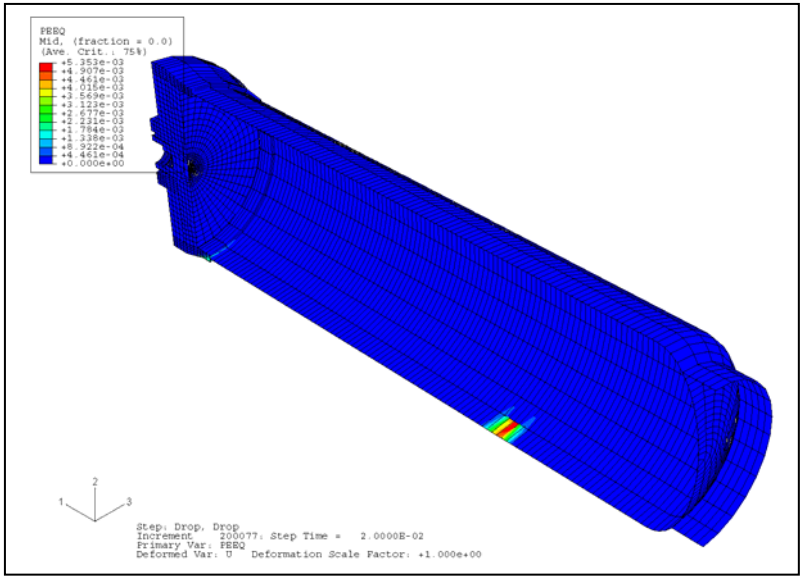

Side Drop **45º Side Drop**

Figure 21 - Strain Distribution in Containment Vessel Side Drop and Side Angle Drop at 45º (300 ºF)

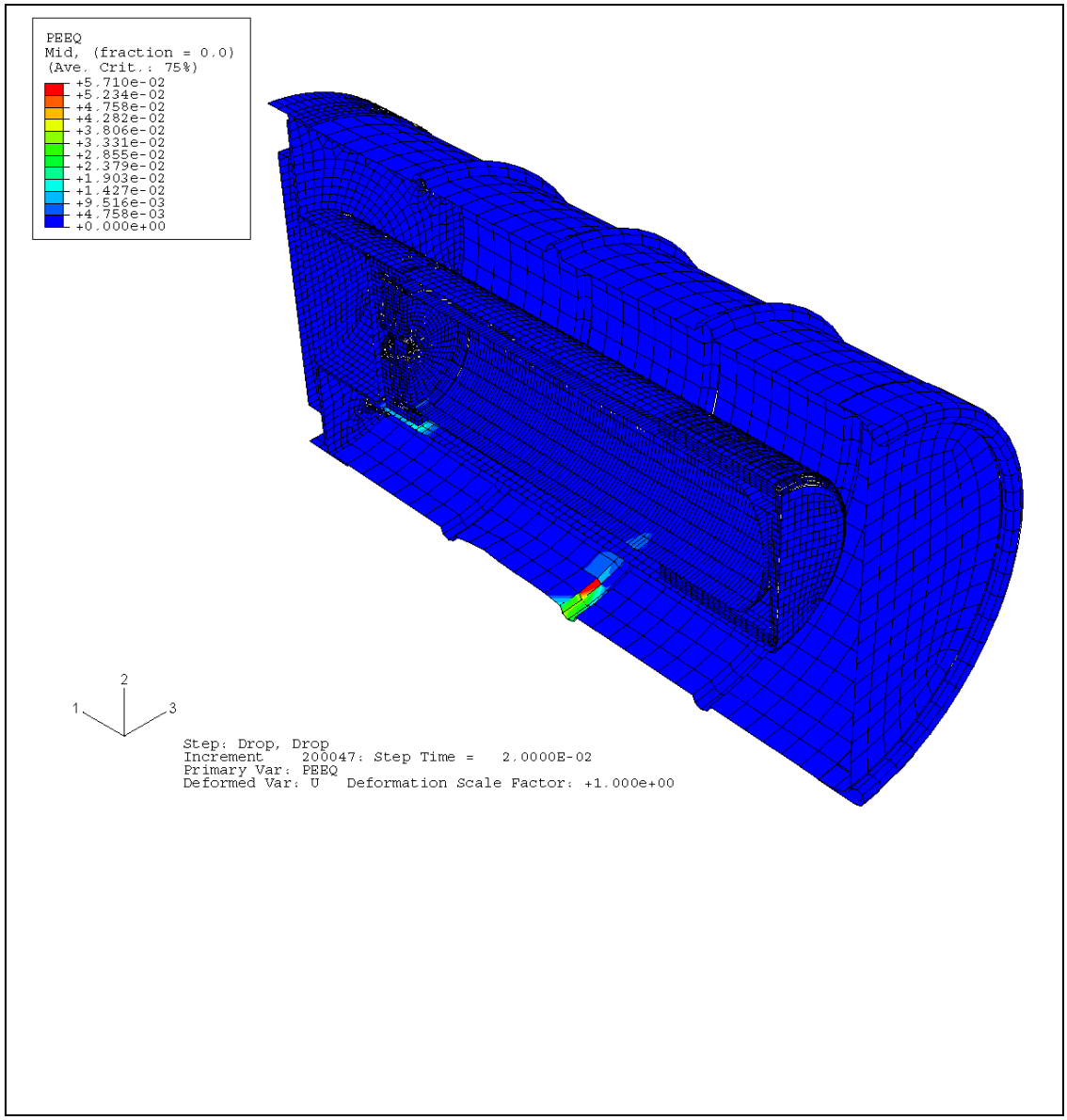

Figure 22 - Strain Contour Plot for Drum at Side Drop (300ºF)

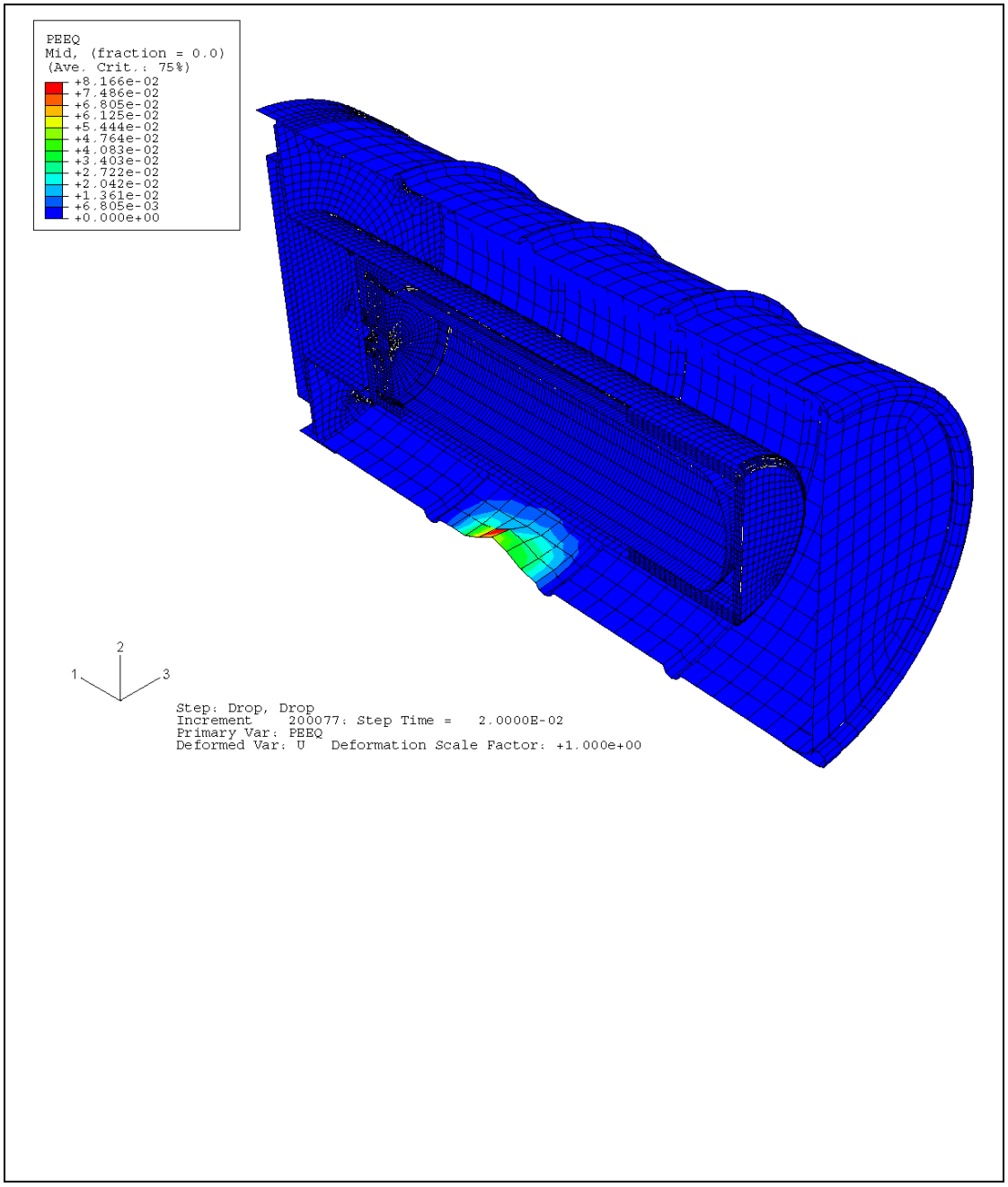

Figure 23 - Strain Contour Plot for Drum Side Angle Drop at 45º (300ºF)

9.5 Top Drop and Top Drop at 45º (75ºF)

Energy History

The time-history plots of energy components for the two side puncture simulations shown in Figure 24 indicate that the kinetic energy approaches to zero at the end of the analysis. Therefore, we know that the analysis covers the entire impact duration.

9.5.1 Containment Vessel Stress-Strain Evaluation

The maximum value of the local primary membrane stress intensity in the containment vessel for the side drop is 12.81 ksi and 9.54 ksi for the side drop at an angle of 45º as shown in Figure 25. The maximum value of the equivalent plastic strains in the containment vessel is 0 for both the side and 45º angled drops, are shown in Figure 26.

The calculated stresses in the containment vessel are significantly less than the allowable value of 57.8 ksi for the general primary membrane stress intensity, P_m and of 74.3 ksi for the local primary membrane stress intensity, P_L (as given in Section 6.0). The containment vessel equivalent plastic strains are negligible when compared to the allowable strain of 0.35 for each of the cases.

9.5.2 Drum Strain Evaluation

Strain contour deformation plots of the drum for the side drop and the side drop at an angle of 45º are shown in Figures 27 and 28, respectively. The maximum value of the equivalent plastic strain in the drum is 0.031 for the side and 0.158 for the 45º angled drop. These are less than the allowable strain of 0.35. Therefore, the drum will not be ruptured during the hypothetical accident condition of 40-inch drop on at 6 inch steel bar

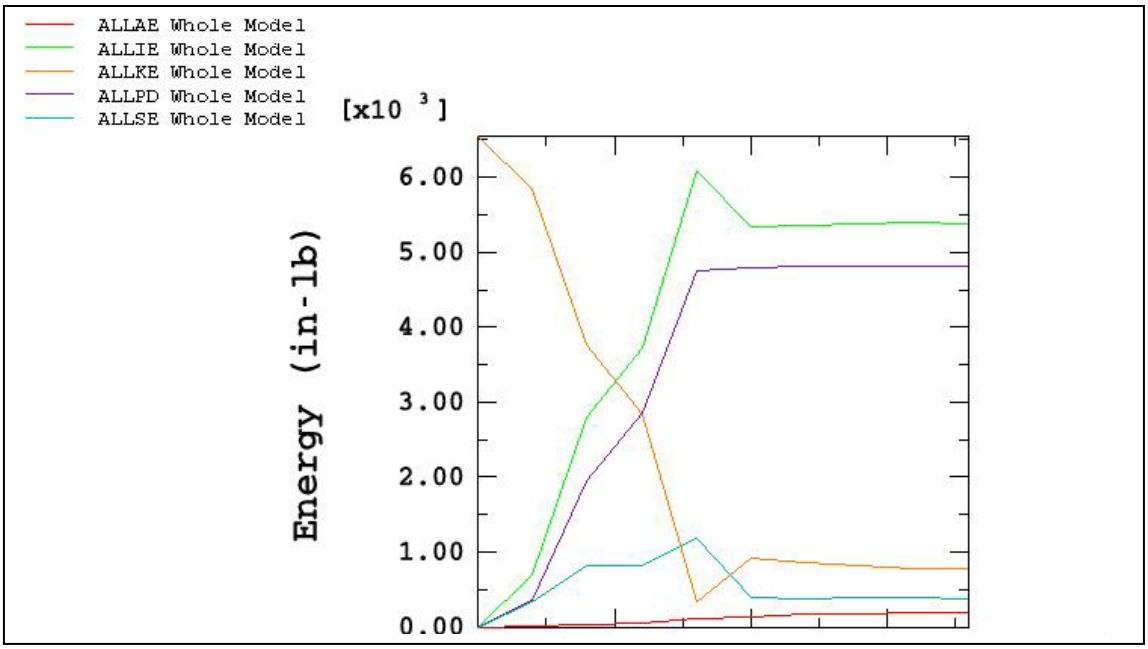

Top Drop (75 ºF)

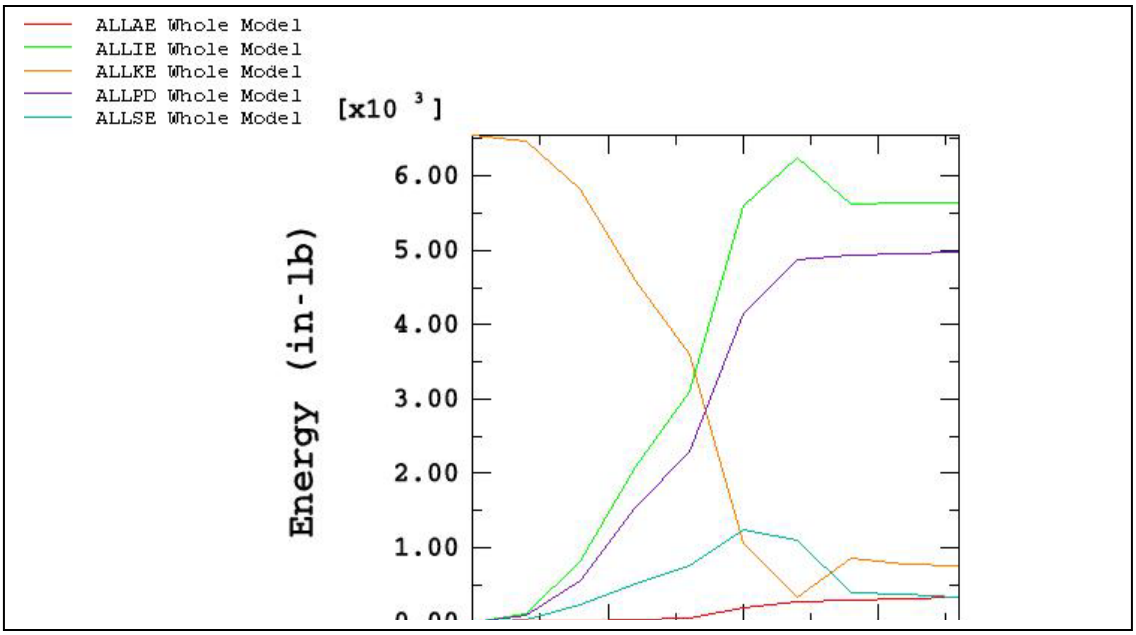

Top Drop 45º (75 ºF)

(ALLKE = kinetic energy; ALLIE = total strain energy; ALLSE = elastic strain energy; ALLPD = plastic strain energy; ALLAE = artificial energy)

Figure 24 - Time-History of Energy Components Top Drops (75 ºF)

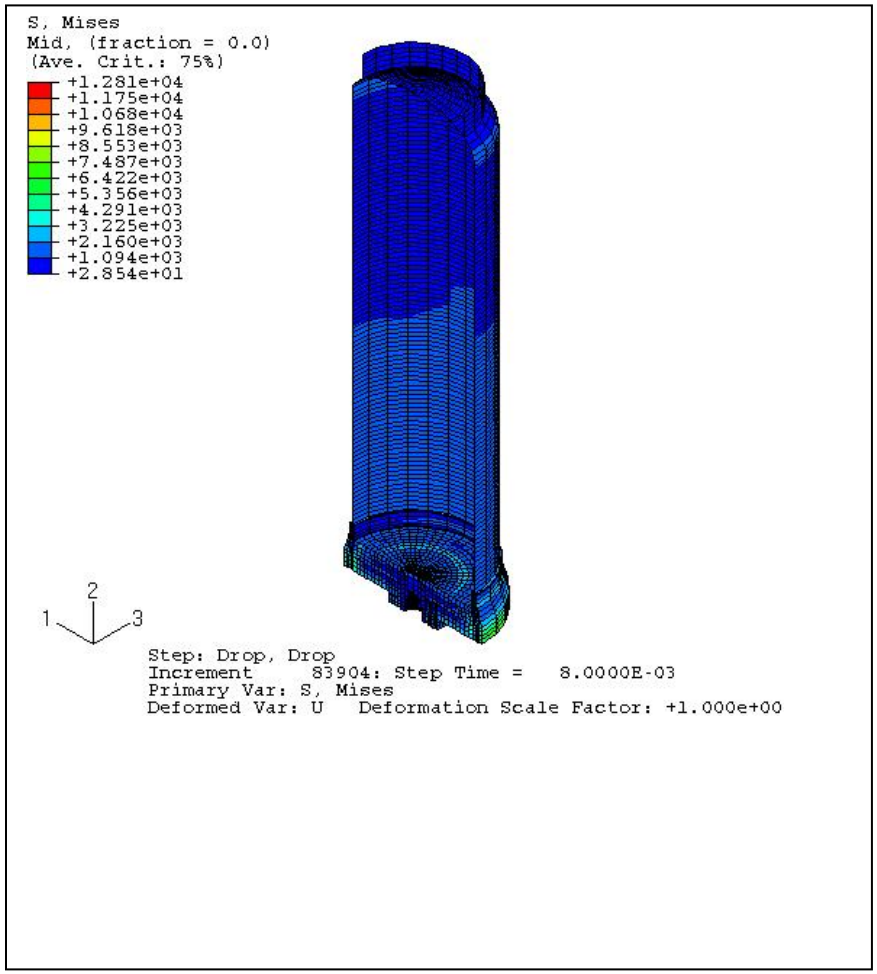

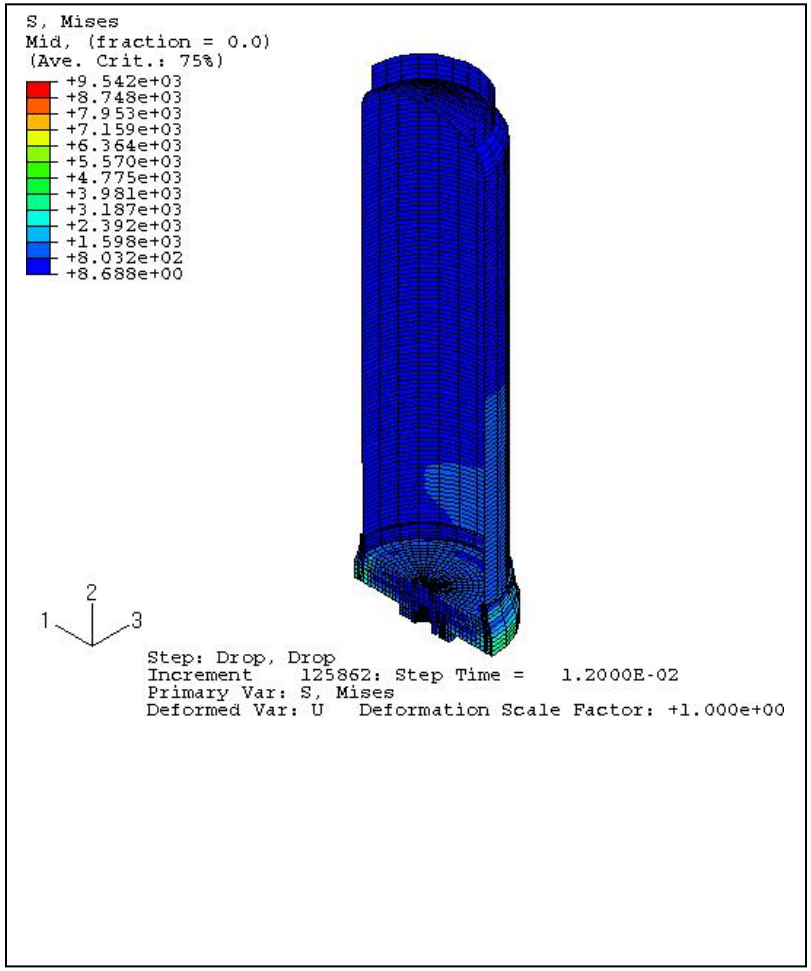

Side Drop **45º Side Drop**

Figure 25 - Stress Distribution in Containment Vessel Top Drop and Top Angle Drop at 45º(300ºF)

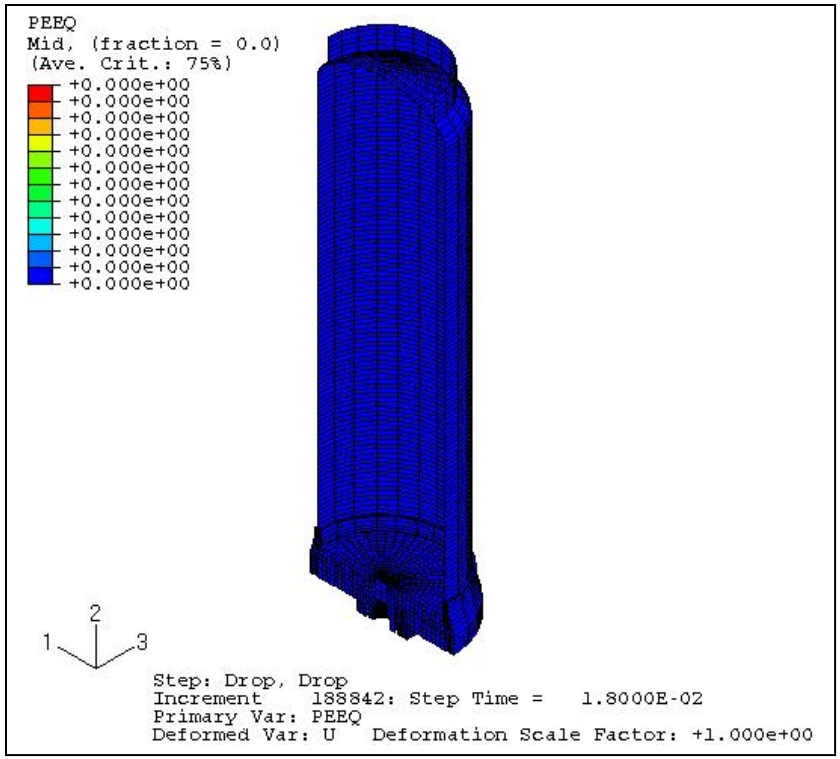

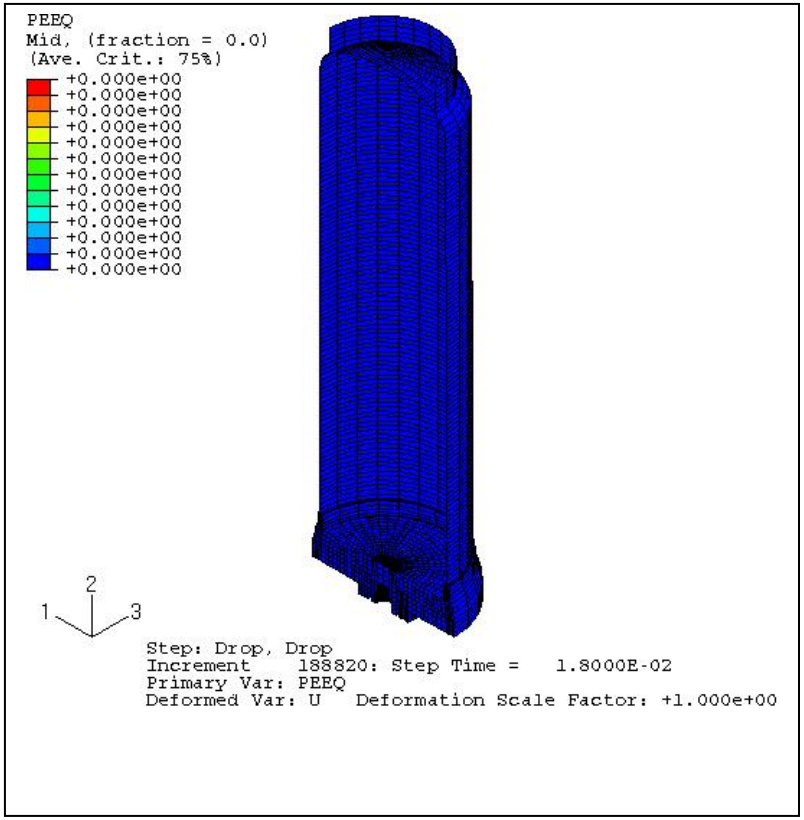

Top Drop **45º Top Drop**

Figure 26 - Strain Distribution in Containment Vessel Top Drop and Top Angle Drop at 45º (300 ºF)

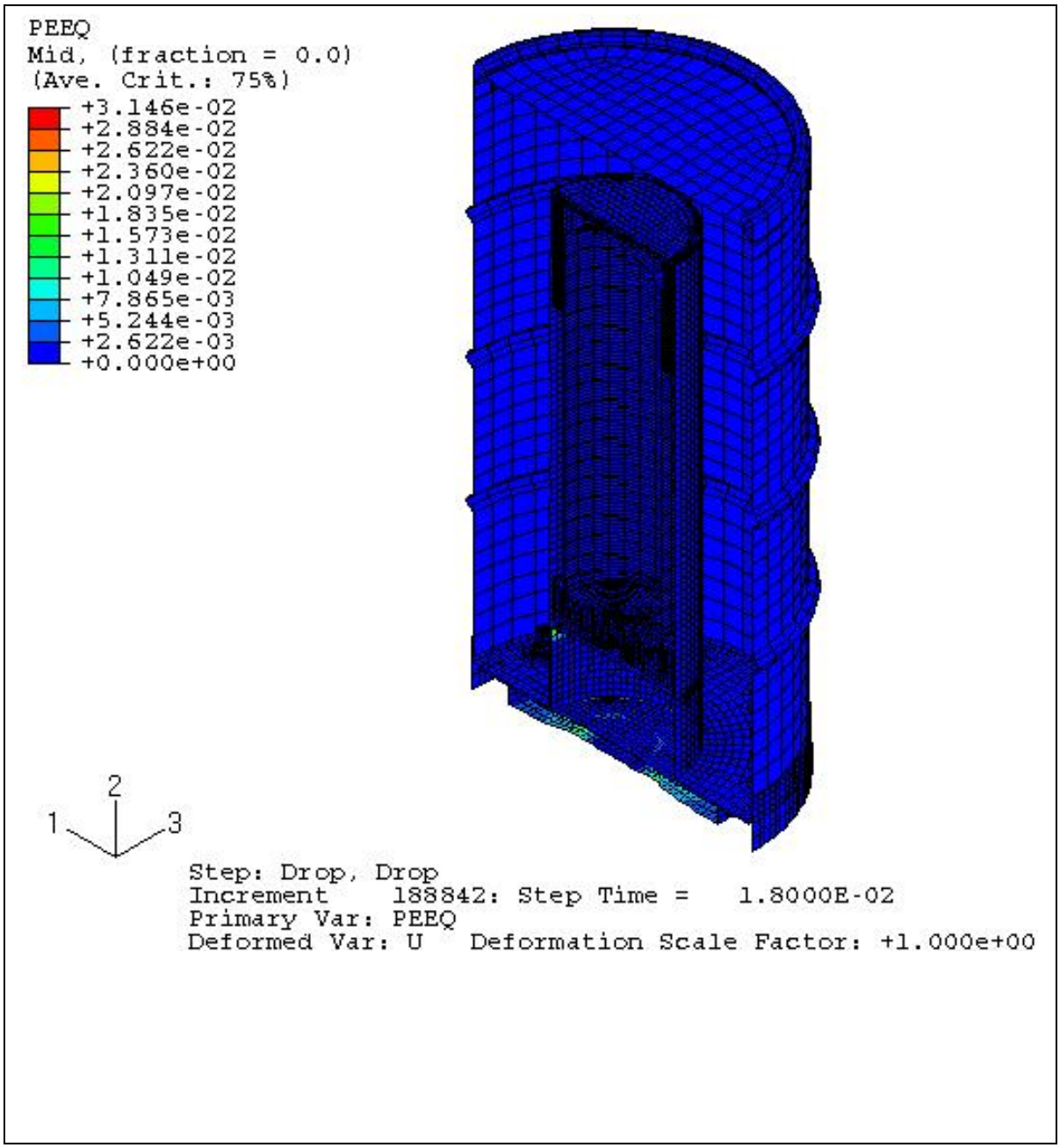

Figure 27 - Strain Contour Plot for Drum Top Drop (75ºF)

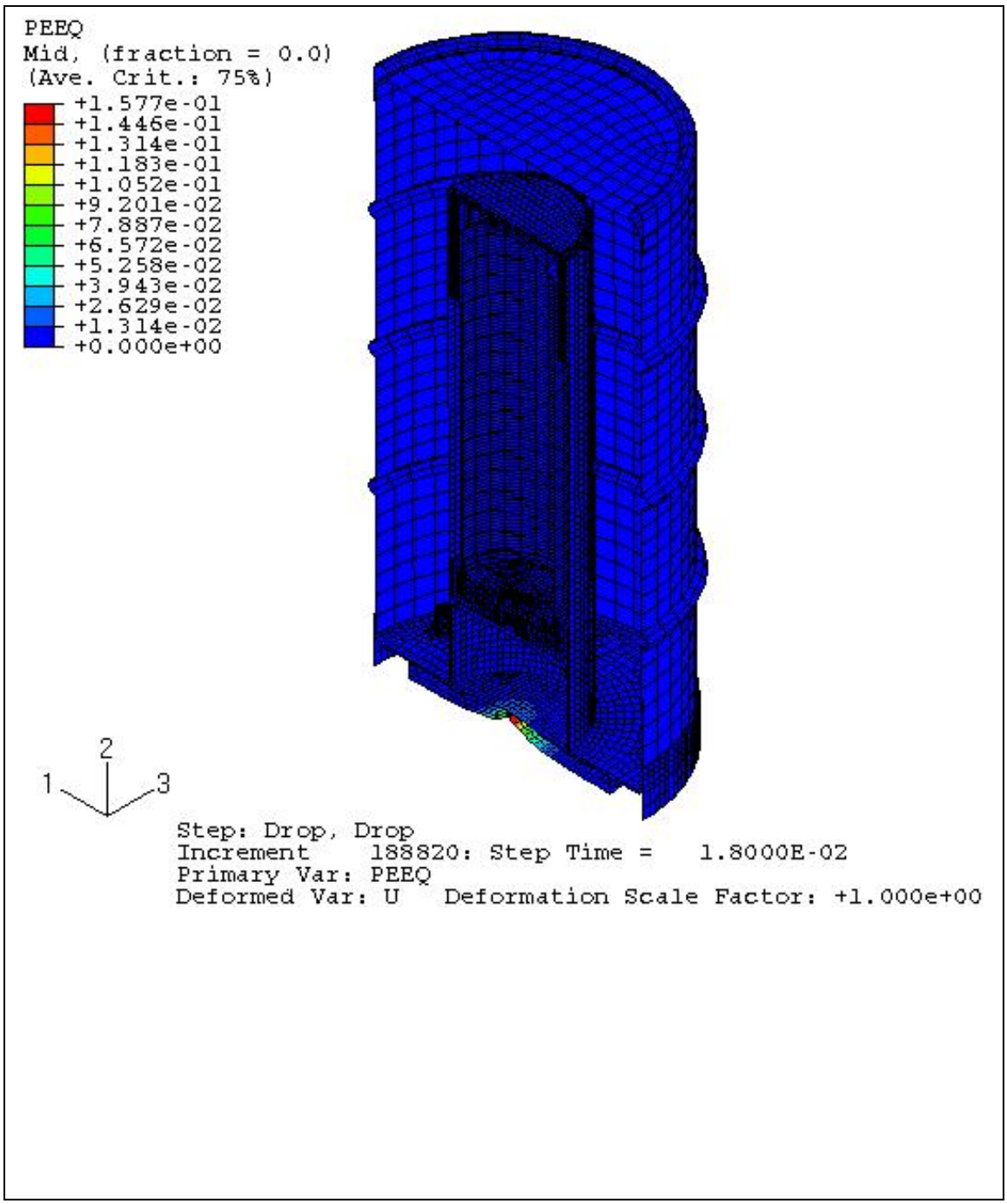

Figure 28 - Strain Contour Plot for Drum Top Drop Angle at 45º (75ºF)

10 References

1 S-SARP-2006-00001. Safety Analysis Report for Packaging Model 9977 (U) (April 2006).

2 ASME Boiler and Pressure Vessel Code, Section III, Appendix F, January 2004.

3 Code of Federal Regulations, 10CFR 71, January 2006.

4 ABAQUS/CAE, Version 6.5-3, ABAQUS, Inc. Build ID:2005:03_03-17.29.04 57675, Providence, RI.

5 MSC/PATRAN, Version 2003r2, MacNeal-Schwendler Corporation.

6 ABAQUS/Explicit Code, Version 6.5.3, ABAQUS, Inc., Providence, RI.

7 ASME Boiler and Pressure Vessel Code, Section II, Part D, “Properties”, (2004).

8 Sindelar, R. L., “Tensile Properties of Type 304/304L Stainless Steel for Impact Deformation Analysis of Nuclear Containers,” SRT-MTS-93-3113, November 10, 1993.

11 Appendix A - Material Property Data

A.1 Stress-Strain Relationship of Stainless Steel 304L

Figure A1 shows the stress-strain curve of stainless steel 304L (Reference 8).

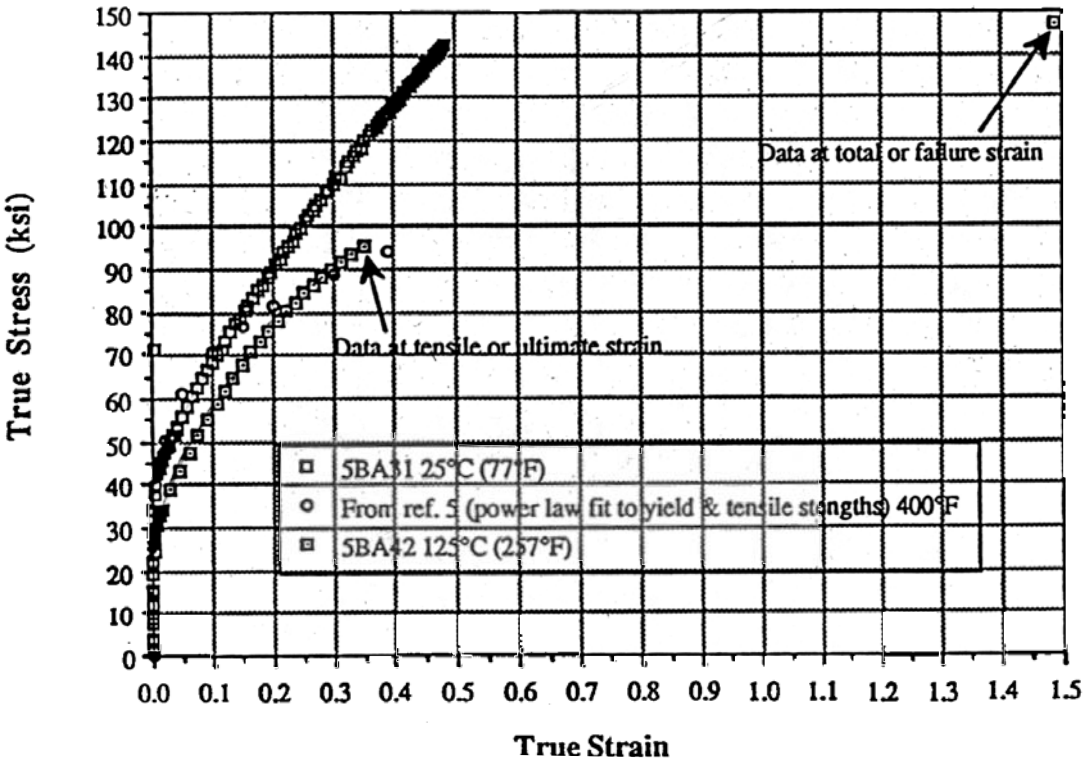

Figure A-1. Stress vs. Strain Curve of Stainless Steel 304L

A.2 Stress-Strain Relationship of Aluminum 6061-T6.

The material properties for aluminum are given as follows.

Nominal yield Stress, σ_y = 32,000.0 psi
Nominal ultimate strength, σ_u = 38,000.0 psi
Uniform elongation to maximum load, $\varepsilon_u = 0.17$
Young's modulus, E = 10.0E6 psi
Poisson ration, ν = 0.33
Density, ρ = 0.098 lb/in^3

From the values given above, we can calculate the following values.

Yield strain, $\varepsilon_y = \dfrac{\sigma_y}{E} = \dfrac{32000.0}{10\times10^6} = 0.0032$

True ultimate strain, $\varepsilon_{u,t} = \ln(1+\varepsilon_u) = \ln(1+0.17) = 0.157$

True ultimate stress, $\sigma_{u,t} = \sigma_u(\varepsilon_u + 1) = 38000.0(0.17+1) = 44{,}460.0$ psi

Density, $\rho = \dfrac{0.098\dfrac{lb}{in^3}}{386.4\dfrac{in}{\sec^2}} = 2.536\times10^{-4}\dfrac{lb-\sec^2}{in^4}$

The flow curve of aluminum 6061-T6 in the region of uniform plastic deformation can be expressed by the following power curve relation.

$$\sigma_t = K\varepsilon_t^{\,n} \qquad \text{(A-1)}$$

where η is the strain-hardening exponent and K is the strength coefficient; σ_t and ε_t are true stress and true strain, respectively.

At the ultimate strain where metal necking occurs, the following relationship is valid.

$$\varepsilon_{u,t} = \eta \qquad \text{(A-2)}$$

The strength coefficient, K, can be calculated from Equations (A-1) and (A-2) as follows.

$$\sigma_{u,t} = K\varepsilon_{u,t}^{n}$$

$$44{,}460.0 = K(0.157)^{0.157} = 0.74775K$$

Then,

$$K = 59{,}458.0$$

Substituting the values of K and η into Equation (A-1), we obtain the flow curve equation of aluminum 6061-T6 as follows.

$$\sigma_t = 59458\varepsilon_t^{0.157} \qquad \text{(A-3)}$$

Based on the above equation together with the values of Young's modulus and the yield stress, we are able to generate the stress-strain curve of aluminum 6061-T6 as shown in Figure A-2.

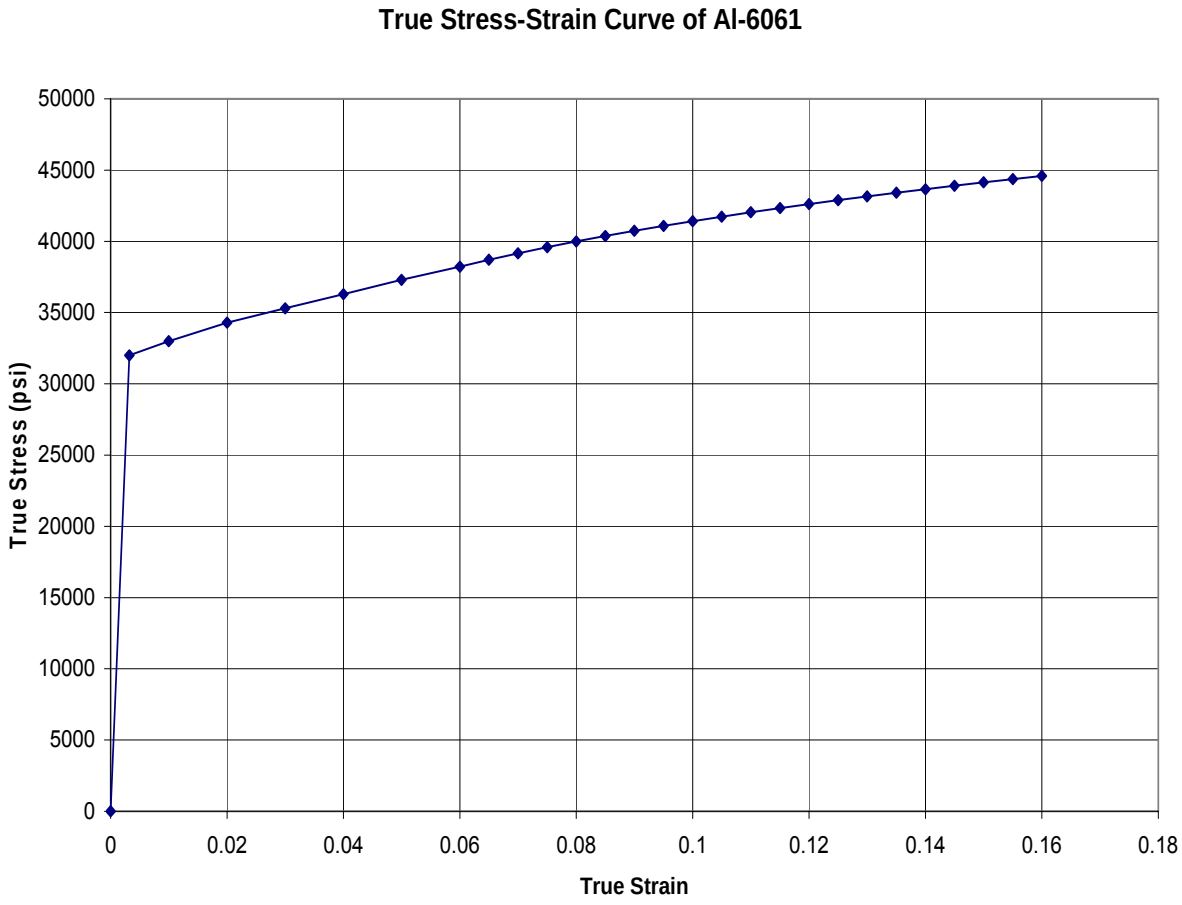

Figure A-2. Stress vs. Strain Curve of Aluminum 6061-T6

A.3 Stress-Strain Relationship of FR-3716 Polyurethane Foam

The stress-strain curve of FR-3716 polyurethane foam parallel and perpendicular to rise for dynamic compression is shown below in Figure A-3.

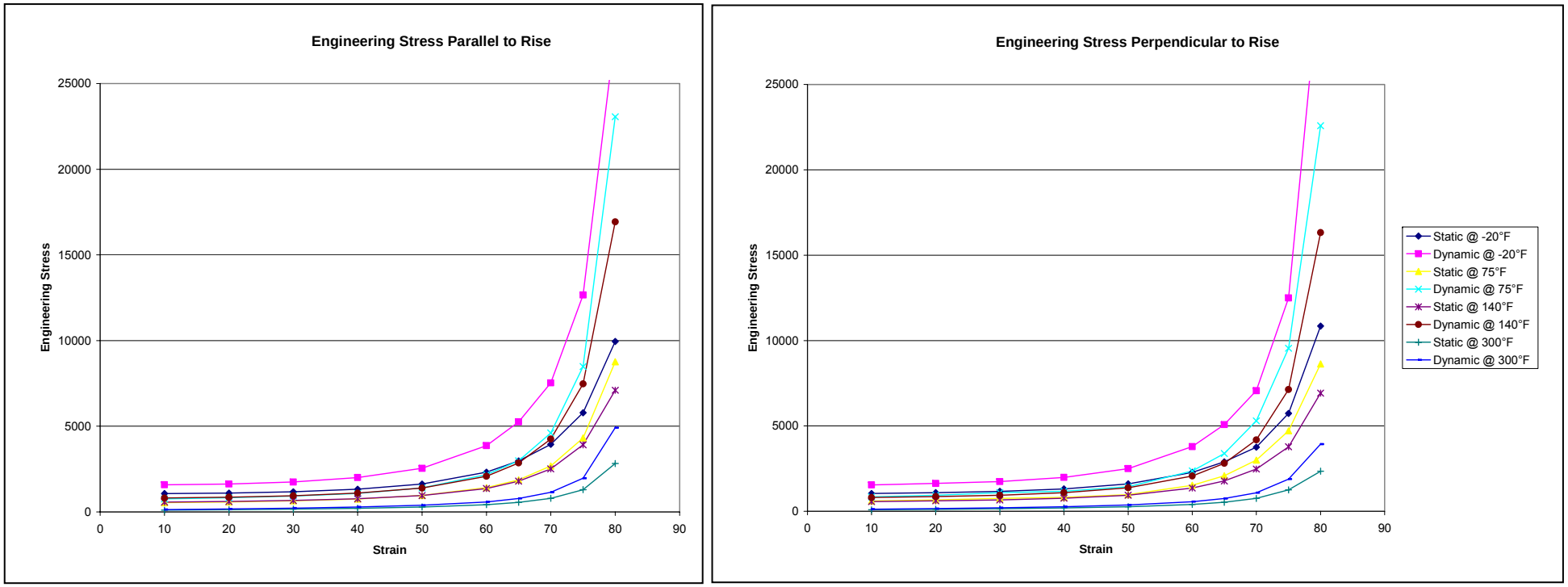

Figure A-3 Engineering Stress vs. Engineering Strain Curve for FR-3716 Foam – Parallel and Perpendicular to Rise

This Page is Intentionally Left Blank

APPENDIX 2.10

9977 GENERAL PURPOSE FISSILE PACKAGING PROTOTYPE TESTING

M-TRT-A-00007

This Page Intentionally Left Blank

9977 General Purpose Fissile Packaging Prototype Testing

May 2006

Keywords: GPFP, Prototype, Packaging

Prepared by: L.F. Gelder, C.M. May

Washington Savannah River Company
Savannah River Site
Aiken, SC 29808

SAFETY • RESPONSIBILITY • SECURITY
SRS
SAVANNAH RIVER SITE

Prepared for the U.S. Department of Energy Under Contract NO. DE-AC09-96SR18500

Disclaimer

General Purpose Fissile Packaging Prototype Testing

FINAL REPORT

PREPARED BY

L. F. Gelder, Test Engineer, SRPT — Date 5/9/06

C. M. May, Test Engineer, SRPT — Date 5/8/06

REVIEWED BY

A. C. Smith, Fellow Engineer, SRPT — Date 5/8/06

APPROVED BY:

J. S. Bellamy, Manager, SRPT — Date 5/8/06

S. L. Tibrea, Manager, SRNL/EE&S — Date 5/9/06

Table of Contents

List of Tables

List of Figures

Summary

The General Purpose Fissile Packaging (GPFP) prototype design was subjected to the *Normal Conditions of Transport* (NCT), 10CFR71.71, vibration, water-spray, free-drop, penetration, and compression tests, and the *Hypothetical Accident Conditions* (HAC), 10CFR71.73, free-drop, crush, puncture, and thermal performance tests for Type B packagings.

Prior to the regulatory performance tests, except for the vibration test, each package containment vessel (CV) was leak tested and found to be helium leak tight, that is, $< 2.0 \times 10^{-7}$ cc/s per ANSI 14.5.

A single test specimen, SN-2, was subjected to each of the NCT performance tests, and then subjected to the HAC performance tests. Three test specimens, SN-3 through SN-5, were subjected to the HAC performance tests only.

A single test specimen, SN-3, was stored in a ≤ -20F environment prior to the HAC drop, crush, and puncture tests. All other packages were tested at seasonal ambient conditions.

A reverse-strain induced tear, approximately 11-in long by ¼ in tall, developed on the bottom of SN-3 from the crush test. This tear increased the overall vent area of the drum and the vulnerability of the bottom of the package to the subsequent puncture and thermal tests. The test engineers were marginally successful exploiting the tear damage during the puncture test, increasing the tear-gap height by ¼-in. During the thermal test, the tear allowed greater than normal foam loss. Despite the tear and foam loss, there was no loss of containment.

All packages were nondestructively examined, using digital radiography after fabrication and following the drop, crush, and thermal tests. SN-2 was radiographed before and after the vibration test. All drums were destructively examined following post-thermal test radiography.

Following the HAC tests, the containment vessels were removed from the packages and helium leak tested per ANSI 14.5. All CVs remained leak-tight following the HAC tests.

Therefore, the performance tests demonstrated that the GPFP design provides adequate containment of the contents for NCT and HAC.

1.0 Background

The Department of Transportation (DOT) 6M specification packagings have been widely used for transportation of radioactive materials since the 1960's. However, since the 6M specification was issued, there have been major advances in the state of the art of radioactive materials packaging as well as changes in the regulatory requirements.

The existing fleet of 6M packagings is aging and is marked by significant variability in quality. In addressing these issues, the DOT has instituted the phased elimination of the 6M specification packaging (and others) in favor of performance-based certified packagings. As a result of this action, a 6M replacement has become an important need for the DOE Complex. The "General Purpose Fissile Packaging" (GPFP-1), developed by the Savannah River National Laboratory Packaging Technology Group (SRPT) is one candidate for replacement of the 6M. A 1st generation GPFP prototype design was developed by SRPT and tested in the summer of 2004.[1]

Although the 1st generation prototype provided containment of the contents from the HAC tests, the extent of thermal degradation of the foam insulation in the upper drum and top was considered undesirable. Consequently, the package was redesigned to improve the margin of safety. The enhanced 2nd generation GPFP prototype is the subject of this test report.

The 2nd generation GPFP prototypes were designed, developed, and procured by SRPT and Honeywell Federal Manufacturing & Technologies, LLC; also known as the Kansas City Plant (KCP).

2.0 Test Program

The objective of this testing was to provide performance data to analysts to evaluate the adequacy of the GPFP design with respect to the applicable package performance requirements of 10CFR71.71 (NCT) and 10CFR71.73 (HAC).[2]

2.1 Test Plans

A test plan was prepared by SRPT, and presented and discussed on 10/17/05 with the Lawrence Livermore National Laboratory's SARP Review Team.[3]

The vibration test of SN-2 was performed offsite at the Sandia National Laboratory by Sandia personnel per a Memorandum Purchase Order, which includes a scope of work and test plan.[4]

The HAC thermal tests were performed offsite at the South Carolina Fire Academy and performed by a subcontractor per a Purchase Order, and performed the work under the direction of the SRNL Test Team. The subcontractor submitted a test plan and procedures, which were reviewed and accepted by SRNL.[5, 6, 7, and 8]

2.2. Failure Modes of Interest

The failure modes of interest are any damage to the packaging that:

- Results in the containment vessel failing the post-test leak test, or
- Significantly reduces the effectiveness of the packaging.

2.3 Performance Requirement

The Type B packaging regulations require that the selection of the initial test conditions for both NCT and HAC is most unfavorable for the packaging feature under consideration: ambient air temperature between -20F and 100F, and CV pressure at its maximum normal operating pressure (MNOP) or lower.

Specifically, the package must meet the applicable requirements of 10CFR71.51 listed below:

> (a) A Type B package, in addition to satisfying the requirements of 10CFR71.41 through 71.47, must be designed, constructed, and prepared for shipment so that under the tests specified in:
>
> (1) Section 71.71 ("Normal conditions of transport"), there would be no loss or dispersal of radioactive contents--as demonstrated to a sensitivity of 10^{-6} A_2 per hour, no significant increase in external surface radiation levels, and no substantial reduction in the effectiveness of the packaging; and
>
> (2) Section 71.73 ("Hypothetical accident conditions"), there would be no escape of krypton-85 exceeding 10 A_2 in 1 week, no escape of other radioactive material exceeding a total amount A_2 in 1 week, and no external radiation dose rate exceeding 10 mSv/h (1 rem/h) at 1 m (40 in) from the external surface of the package.

The packages were leak-tested prior to and following the NCT (except the vibration test) and HAC performance tests. This data is provided to the containment analysis to demonstrate compliance with applicable requirements.

The physical measurement and radiograph data and information from the performance tests is provided to the structural, thermal, nuclear criticality, and shielding analysts to demonstrate compliance with applicable requirements.

3.0 Packaging Test Specimens

Test specimens were procured and provided to SRPT by the KCP. The fabrication drawings (as-builts), and material certifications of the GPFP are available in the project Job Folder.[9, 10, 11] A brief description packaging and components is provided below, and photograph of the packaging in Figure 1.

Figure 1 - Packaging Components

The GPFP drum design uses a standard 18-gauge, 304L stainless-steel, open-head, 35-gallon drum, which is modified to add an upper flange, a bolted-lid closure system, and containment vessel liner. The final overall dimensions of the GPFP are approximately 36-in by 18-3/4 inches in diameter.

The drum lid interior is insulated with a 1-in layer of 7 to 10 lb/ft^3 ceramic fiber insulation and approximately a 4.3-in layer of refractory block. The block is connected to the lid interior side and top with a multi-purpose silicon sealant. The lid exterior flange is capped and insulated with a 1-in disk of ceramic insulation. The lid is closed using a total of eight, 5/8-11UNC-2A x 1-1/4 in bolts, torqued to 40-45 ft-lb.

The exterior of the Drum liner is enveloped in a 1-in layer of 7 to 10 lb/ft^3 ceramic fiber insulation. The insulation is held in place with filament tape.

The space between the drum interior and Drum liner is filled with closed-cell rigid polyurethane foam. The foam density is approximately 16 lb/ft^3.

The GPFP test packages used a 6-in diameter (ID) Chalfant containment vessel (CV), which is used in the DOE certified Model USA/9975/B(M)F-85 packaging.[12] The CV was modified for

the performance tests by the addition of a leak test port on the bottom of the CV to support a post-test helium leak test. The CV uses a threaded cone seal nut closure torqued to 95-105 ft-lb.

For this test program, each CV was loaded with approximately 100-lb of stainless-steel round to simulate the maximum weight of the proposed contents. The steel rounds are approximately 5 ½ -in diameter by 13-in long. The overall usable internal length of the CV is approximately 21-in; consequently, 8-in of head space exists within the CV. No dunnage or spacers were used in the CV to restrain axial movement of the steel round during the tests; however, the unintended consequence of not restraining the simulated contents was the physical damage of the majority of the temperature indicating labels internal to the CV.

Top and bottom aluminum load distribution fixtures position the CV within the liner.

The removable components of the packaging are:

- Lid,
- Lid bolts,
- Top and Bottom load distribution fixtures, and
- CV

A cross-section of the packaging is illustrated in Figure 2.

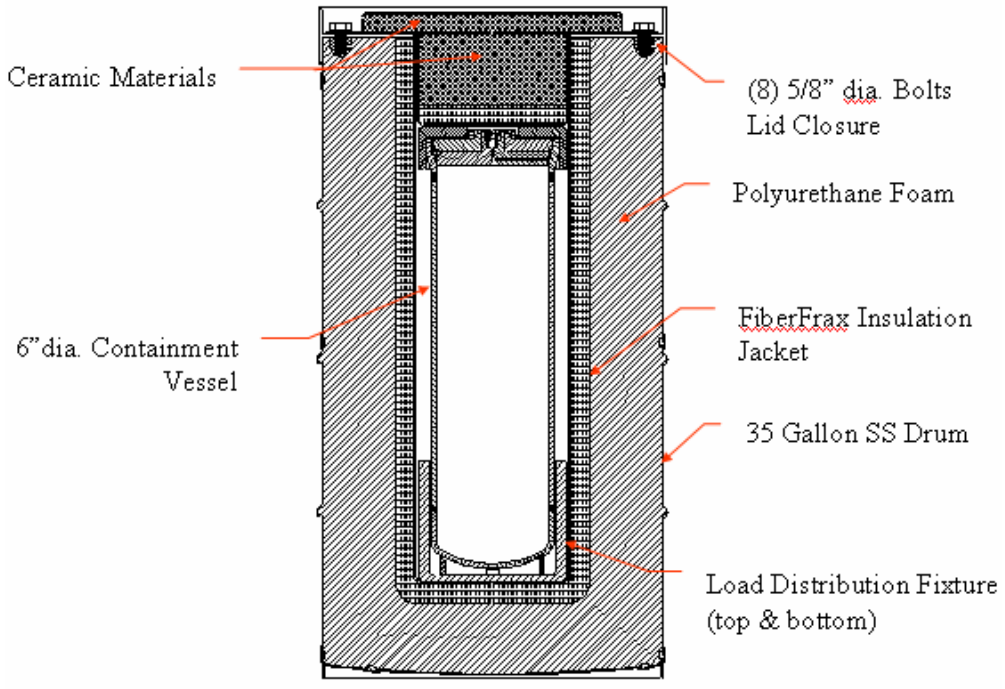

Figure 2 - Cross-section of the GPFP

3.1 Packaging Identification Numbers

The test packagings were assigned serial numbers: SN-2 through SN-5.

3.2 Packaging Component Weights

Table 1 below lists the pre-test component weights per procedure FP-1023. Data sheets are available in the EES Job Folder.[9]

Table 1 - Pre-test Packaging Weights

GPFP Test Package Number	Empty drum (lb)	Foamed drum (lb)	CV (lb)	Slugs (lb)	Aluminum Distribution Fixtures (top and bottom) (lb)	Lid (lb)	Hardware (lb)
SN-2	68	143	54	101	13.9	19.5	1.6
SN-3	68	143	54	101	13.9	19.0	1.6
SN-4	70	145	54	101	13.9	19.5	1.6
SN-5	70	145	54	101	13.9	19.3	1.6

3.3 Initial Test Conditions

The following initial test conditions for the performance tests were provided by the GPFP project manager and technical lead.

3.3.1 Internal Pressure

The initial internal pressure of the containment system for SN-2 through SN-5 was ambient (i.e., the CV was not pressurized). The internal pressure during the HAC thermal test was not measured or monitored.

3.3.2 Internal Temperatures

The initial temperature of SN-2 for all NCT tests was ambient. The initial temperature for the HAC drop, crush, and puncture test for SN-2, SN-4, and SN-5 was ambient. SN-3 was chilled to <-20F prior to and after the HAC drop, crush and puncture tests.

3.3.2 Thermal Test Preheat Temperature

Each package was preheated for 4 days (min) in an SRNL environmental chamber to simulate the thermal conditions generated by the proposed contents, then transported to the HAC thermal test site. At the test site, each test package was fitted with two electrical band heaters, set to 200F and covered with an insulated box. The surface temperature of the drum was measured and monitored with the same thermocouples/data logger system used for the actual HAC test.

The drum lid pan was modified prior to the thermal test to provide pressure relief, by drilling 4 holes in the pan : 4, 1/8-in holes were drilled into SN-2, and 4, ¼-in holes into SN-3 thru SN-5.

3.4 Pretest Preparations

3.4.1 Job Hazards Analysis

A Job Hazards Analysis (JHA) [13] of all the applicable test activities conducted at the Savannah River Site was led and prepared by SRPT personnel with a team comprised of test personnel and the SRNL Safety Engineer. The JHA identifies key job steps, identifies the hazard, and recommends hazard mitigation options. The results of the JHA were implemented into the test procedures.

3.4.2 Package Preparation and Test Procedures

The procedures listed in Table 2 were used to prepare the packaging and execute the performance tests.[9]

Table 2 - Package Preparation and Test Procedures

Procedure Number	Title	Rev	Approval Date
FP-1023	GPFP Drum Inspection	0	7/13//05
FP-1025	Helium Leak Test of GPFP Containment Vessel for NCT/HAC Testing	1	10/6/05
FP-1026	GPFP Package Assembly Prior to Performance Testing	0	9/21/05
FP-1027	Low Temperature Testing of General Purpose Fissile Packages	0	10/18/05
FP-1028	Digital Radiography of General Purpose Fissile Package	0	7/18/05
FP-1031	GPFP NCT Free Drop	0	10/10/05
FP-1032	General Purpose Fissile Package (GPFP) Water Spray Test	0	10/10/05
FP-1036	General Purpose Fissile Package (GPFP) Penetration Test	0	10/10/05
FP-1035	General Purpose Fissile Package (GPFP) Compression Test	0	10/10/05
FP-1039	GPFP Disassembly & Examination Procedure	0	12/19/05
L9.5-9150	Drop Testing of Radioactive Material Packages (*covers HAC, 30-ft drop, and puncture tests*)	1	10/22/03
FP-988	Crush Test of GPFP Prototype Units	1	6/28/04
NT-TDR-05-107	SRNL Package Burn Test Procedures (*HAC Thermal Test*)	0	12/1/05

3.4.3 Drum and Component Inspection

The purchased components were inspected per Field Procedure FP-1023. The scope of this procedure is to identify and record defects, measure and record drum dimensions to baseline subsequent measurement data, and weigh package components. The drums and components were found in satisfactory condition; with no significant defects. Data sheets are available in the EES Job Folder.[9]

3.4.4 Temperature Indicating Labels

Non-reversible temperature indicating labels (TIL), ranging from 170-500 degrees-F, were placed on the exterior and interior of each CV, the Drum liner, and bottom of the drum lid. The TILs were applied per procedure FP-1026 and instructions provided by the test engineer.[14] A sketch of the locations is provided in Figure 3.

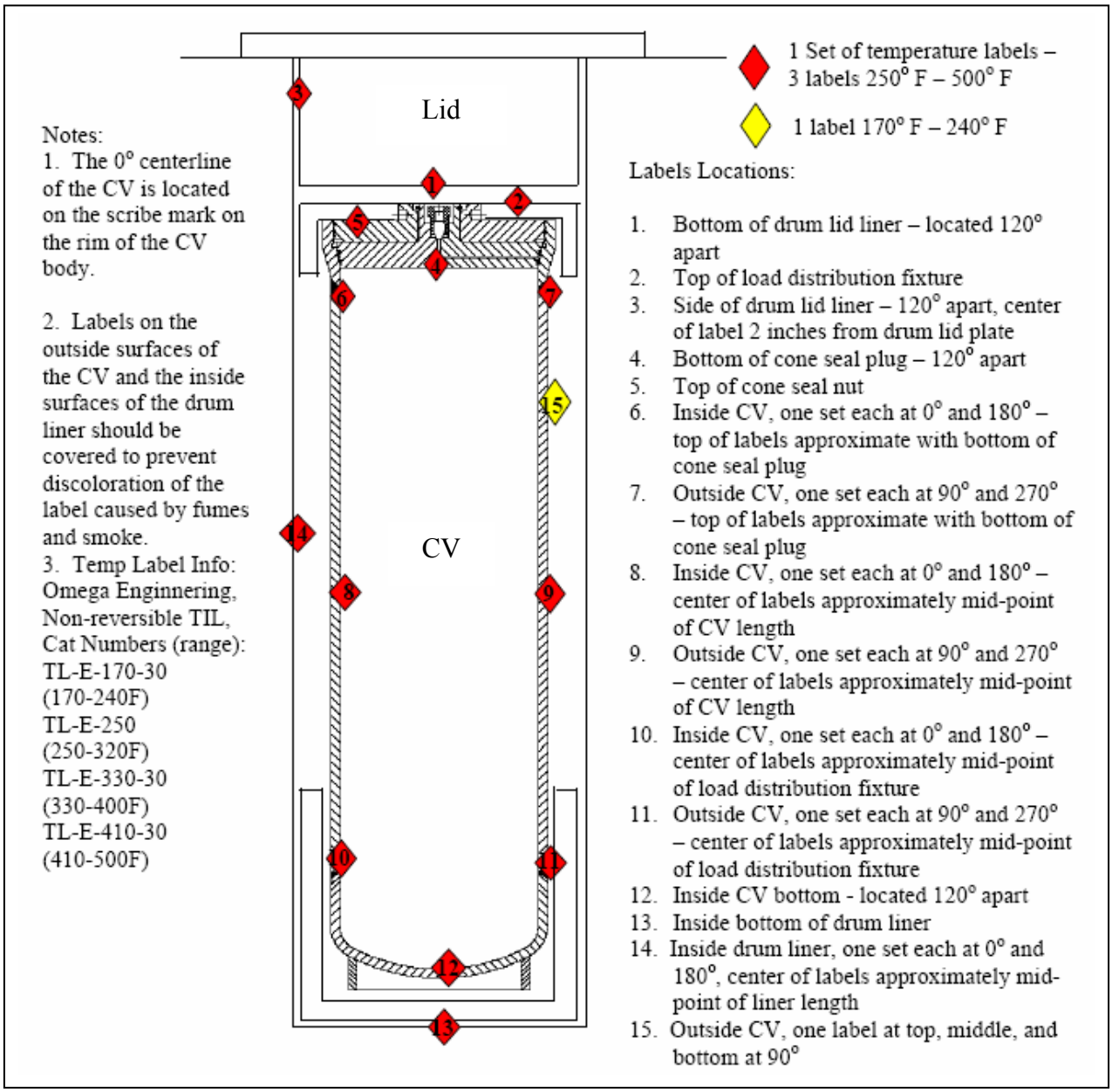

Figure 3 - Temperature Indicating Label Ranges and Locations

3.4.5 Containment Vessel Modification and Helium Leak Test

A leak-test port plug was added to the bottom of CV in order to perform a post HAC helium leak test, without the disturbing the CV lid and o-rings. The containment vessels were loaded with 100-lb steel rounds and closed. The lid torque is 100 ± 5 ft-lb. The CVs were helium leak tested, using the bell jar method, then backfilled to atmospheric pressure with nitrogen gas per procedure FP-1025. The bottom leak test port was plugged with a ¼-in threaded pipe plug torqued to 30±5 ft-lb.

The maximum acceptable helium leak rate for a leak-tight container is $2E^{-07}$ cc/s.[15] Each CV passed the leak test; the results are recorded in Table 3.[16] Leak test data sheets are available in the EES Job Folder.[9]

Table 3 - Pre-test Helium Leak Test Results

Package	Vessel SN	Measured Leak Rate (std cc He/sec)	Max Allowable Helium Leak Rate for leak-tight (cc/sec)	Results (pass/fail)
SN-2	03084	$< 1.0E^{-09}$	2×10^{-07}	Pass
SN-3	03967	$2.0E^{-09}$		Pass
SN-4	03999	$< 9.7E^{-10}$		Pass
SN-5	03224	$< 1.0E^{-09}$		Pass

3.4.6 Package Assembly

The packages were assembled per procedure FP-1026. The leak-tested CVs were loaded into their respective drums, the drum lids were installed and bolts torqued between 40-45 ft-lb, and the fully assembled packages were weighed. The data is presented in Table 4 below.[17] Final assembly data sheets are available in the EES Job Folder.[9]

Table 4 - Final Assembly Data

Package SN	Vessel SN	CV Lid-Nut Torque (ft-lb)	Drum Lid-Bolt Torque (ft-lb)	Final Pretest Weight (lb)
SN-2	03084	101.7	42.5	341.4
SN-3	03967	100.0	42.5	340.6
SN-4	03999	100.2	42.5	339
SN-5	03224	100.7	42.5	341.6

3.4.7 Drum Reference Marking

The drums were marked per procedure FP-1023, as shown in Figure 4. The drum was labeled with the reference markings in order to measure the deformation caused by the performance tests. These marks coincide with the drum vent holes. The vent holes are spaced at 90-degrees intervals along the drum circumference. In addition, the drum was also marked, with a felt-tip marker, in degrees at the top with 0º coincident with Ref Mark 5 and increasing clockwise to 270º at Ref Mark 8. The degree marking is used as the datum for radiography.

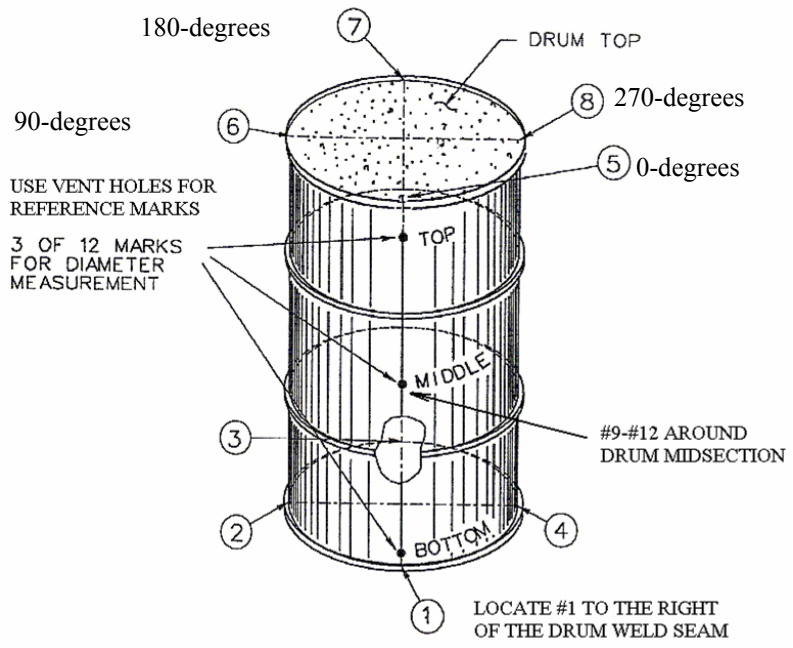

Figure 4 - GPFP Drum Reference Marking

3.4.8 Low Temperature Test Preparations

Package SN-3 was prepared for HAC drop, crush, and puncture testing at ambient air temperature of -20F per procedure FP-1027. This package was cooled at -40F for 96 hours in a SRNL Environmental Chamber. The package was removed the chamber and placed into an insulated box packed with dry-ice to maintain a -20F ambient air temperature before and after the HAC tests and while in transit to radiography. The air temperature in the box was monitored with a single thermocouple and hand held instrument.

3.4.9 Baseline Digital Radiographs

The packages were radiographed per procedure FP-1028 and the analysis reported to SRPT.[18] Digital radiographs (DR) of the empty and fully loaded drums were performed at SRNL. The purpose of the baseline DR was to provide a reference point to assess the progressive cumulative damage to the package from the performance tests.

With the exception of SN-2, the baseline radiographs for establishing initial internal conditions of all the packages were made before testing began. The baseline radiographs of SN-2 were made after the vibration test, but before the remaining NCT tests. The sequence of the NCT tests was vibration, water spray, free drop (4 ft) drop, penetration, and compression. Additional radiographs of SN-2 were made after the series of NCT tests and after each HAC test.

All other packages were radiographed after each HAC test (except the puncture test) for comparison to the baseline radiographs. The HAC testing sequence was free drop (30 ft), crush, puncture, and thermal.

The radiographs show damage to the internal and external components of the packages; however, none of the radiographs show damage to any of the CVs or contents.

The image in Figure 5 identifies the nomenclature and components of the GPFP.

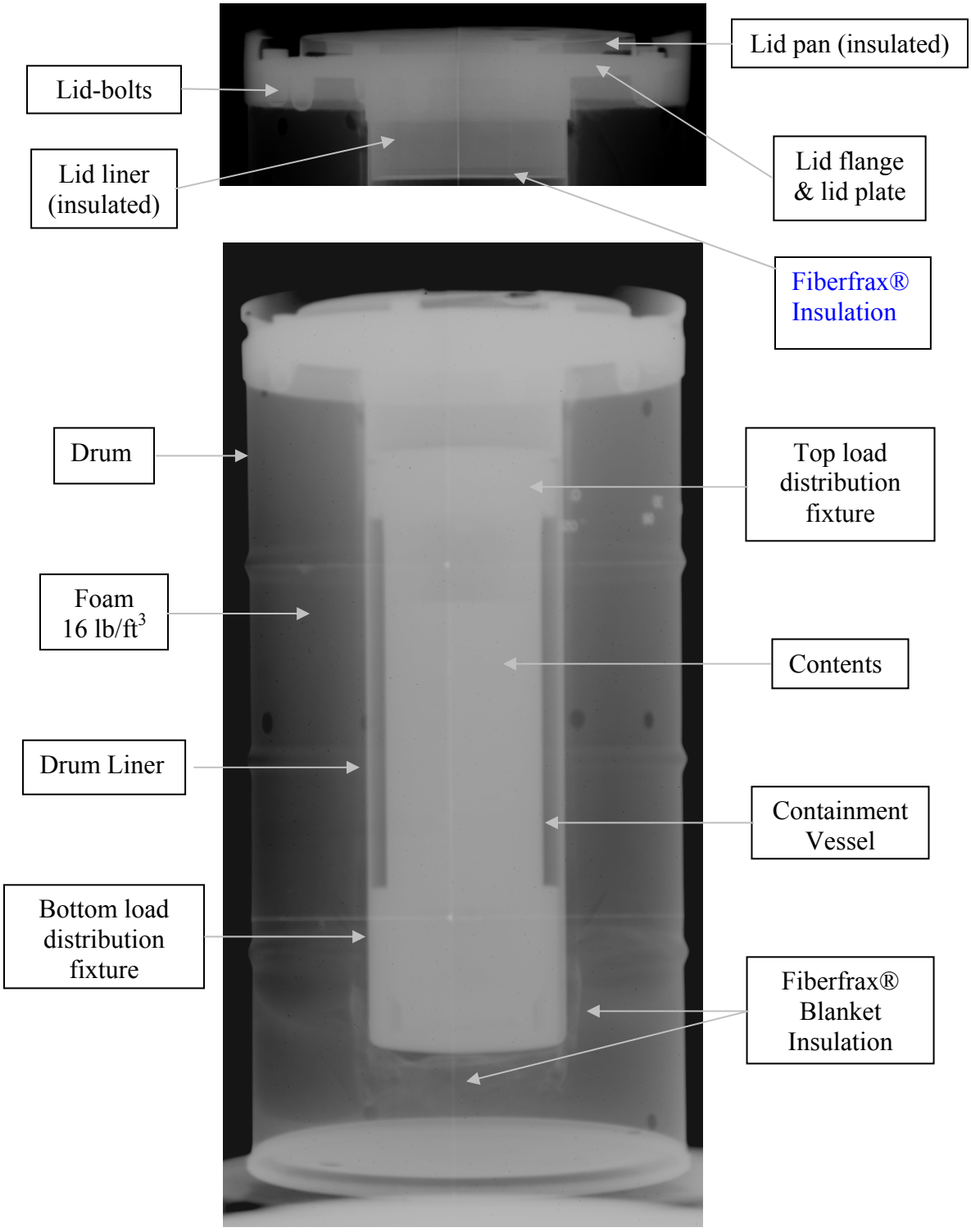

Figure 5 - Baseline Radiograph, Packaging Components Identified

3.4.10 Vibration Test Preparations

Package SN-2 was selected for vibration testing at the Sandia National Laboratory and subsequent NCT and HAC performance tests at SRS.

SN-2 was prepared by centering the 100-lb test weight into a CV, using aluminum honeycomb for the spacing material, as shown in Figure 6. The CV was not leak-tested. After the package was returned to SRS, it was radiographed to evaluate the performance of the package with respect to the vibration test. The package was then disassembled, components inspected, labeled with temperature indicating labels, then reassembled with a leak tested CV: serial number 03084.

The vibration testing at Sandia was conducted in August 2005.[19] The vibration test data will be evaluated and discussed in the GPFP Safety Analysis Report, and therefore is not included in this report.

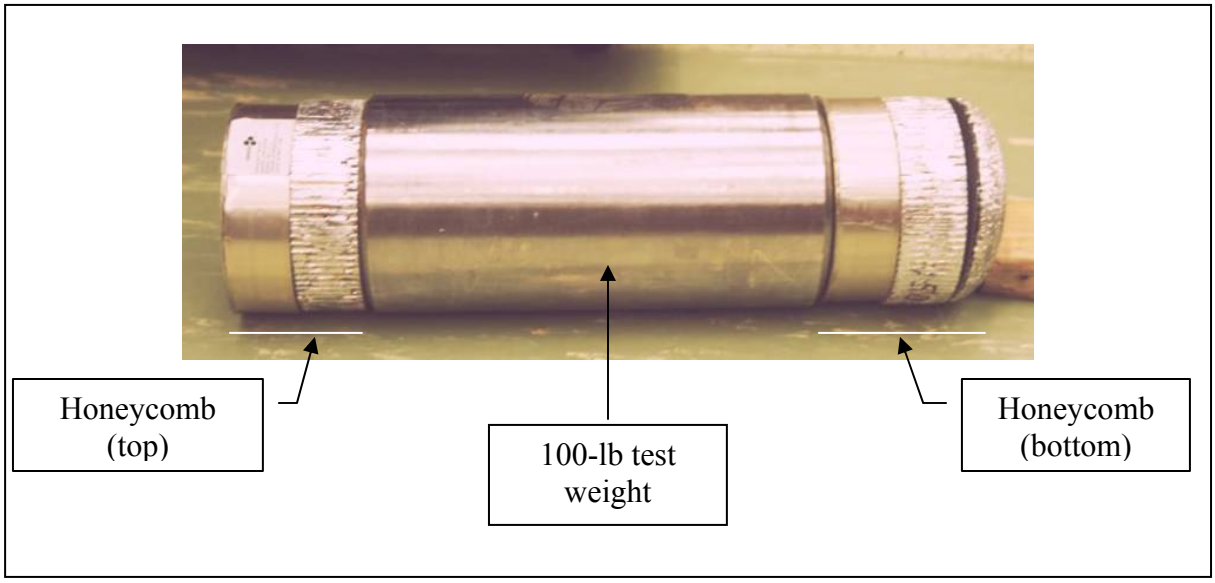

Figure 6 - CV Contents for Vibration Test

4.0 Packaging Testing

4.1 Procedures and Facilities

A list of the applicable test procedures was presented earlier in Table 2 of this report. A list of the test facilities is provided below in Table 5.

Table 5 - Test Facilities

Test		Facility
NCT	Vibration	Sandia National Lab
	Water Spray	SRNL, 723-A
	4-ft Free Drop	SRNL, 723-A
	Penetration	SRNL, 723-A
	Compression	SRNL, 723-A
HAC	Free Drop	SRNL, 723-A
	Crush	SRS, Central Shops
	Puncture	SRNL, 723-A
	Thermal	South Carolina Fire Academy
Other	Leak Test	SRNL, 723-A
	Radiography	SRS, Central Shops

The NCT Tests, except for the vibration test, as well as the HAC Drop and Puncture Tests were conducted at SRNL in the 723-A facility. The drop test surface in 723-A is constructed from 6.25-in thick steel armor plate, approximately 5-ft squared, anchored in a 30-in thick reinforced concrete slab.[20] The target slab is isolated from the concrete floor of the building. The target slab weighs approximately 15,600 lb, which is greater than 40 times the weight of the heaviest test unit (i.e., 342 lb.). The puncture test pin is welded to the drop test surface for the puncture tests and removed at the completion of the tests. The carbon-steel puncture test pin is 6-in diameter x 40-in length, welded to a 2-in thick x 18-in base and 3, 5 ½-in x ½-in thick angle braces.

The crush tests were performed at Central Shops on an abandoned building foundation (Building 8453) that was modified for the crush test. The crush test base plate was fabricated from carbon steel, is approximately 48-in squared by 3-in thick, and was installed over existing 48-in squared reinforced concrete footer. The plate was set into a grout-bed and is secured to the footer using 5/8-in x 7-in anchor bolts. This footer is not isolated from the building foundation. The rigidity of the base plate was tested and evaluated by SRNL structural engineering using a fixed response modal test method, and concluded that the base plate is essentially an unyielding surface relative to the response of the drop test surface in 723-A.[21] The crush test plate was fabricated from carbon steel, is approximately 40-in squared by 2-½ in thick, and weighs approximately 1,170 lb (531 kg). The crush test plate was hoisted using a crane and dropped from a circular electromagnet.

Thermal testing was performed at the South Carolina Fire Academy in Columbia, SC. An insulated, water-cooled wind fence and test stand were erected on a walled pool to establish the

appropriate sized pool fire. A thorough description of the facility and equipment is provided in vendor test report.[22]

Digital radiography was performed at the Radiograph Facility in Central Shops, 711-6N. A thorough description of the radiography facility and imaging methodology is provided in the radiography report.[18]

Leak-testing of the CVs was performed at the High Pressure Laboratory, in 723-A.

The HAC Tests performed at SRS were videotaped using a high speed camera and camcorder.

4.2 Test Chronology

All NCT and HAC tests were conducted per the test schedule in Table 6 below.

Table 6 - Test Schedule

Item	Test/Activity	Start Date	End Date	GPFP SN	Video	Comment
1	Vibration	Aug 9	Sept 16	2	None	Package tested at SNL.
2	Radiograph (DR)	Oct 3	Oct 4	2	None	None
3	Water Spray	Oct 10	Oct 10	2	None	None
4	Free Drop (4')					None
5	Penetration					None
6	Compression	Oct 10	Oct 11			Transfer package to DR at the completion of this test.
7	Radiograph (DR)	Oct 12	Oct 13			None
8	Free Drop (30')	Oct 17	Oct 18	2-5	HS & VHS	Transfer packages to Central Shop for DR at the completion the test
9	DR	Oct 19	Oct 20	2-5	None	DR SN3 first and return to chill in Environmental Chamber
10	Crush	Oct 25	Oct 27	2-5	HS & VHS	Set-up and practice on Oct 24th. Small tear in the bottom of SN-3
11	DR	Oct 26	Oct 28	2-5	None	DR SN3 first and return to chill in Environmental Chamber.
12	Puncture	Oct 31	Nov 1	2, 4,5	HS & VHS	Test SNs 2, 4, & 5. Test hold on SN-3 for consultation with SARP Team. Skip DR. Transfer packages to Environmental Chamber to pre-heat for fire test. Transfer to Fire Academy when notified by the subcontractor.
13	Puncture	Nov 7	Nov 7	3	HS & VHS	Test in two orientations per Program Manager: horizontal and CGOC to exploit damage from the crush test.
14	Thermal	Dec 2	Dec 14	2-5	VHS	Pool Fire tests performed at the South Carolina Fire Academy by subcontractor.
15	DR	Dec 19	Dec 20	2-5	None	None
16	Post test insp.	Dec	Jan 21	2-5	None	Destructive inspection in SRS Machine Shop.

4.3 Test Matrix

The package test orientations and input conditions, the test matrix, is listed Table 7. The basis for these conditions and test orientations will be discussed in the GPFP Safety Analysis Report.

Table 7 - Test Matrix

Package SN	Initial Conditions		Normal Conditions of Transport					Hypothetical Accident Conditions			
	Pressure (MNOP/Ambient)	-20°F to 100°F	Vibrations 10CFR71.71(c)(5)	Water Spray 10CFR71.71(c)(6)	4-ft Free Drop 10CFR71.71(c)(7)	Compression 10CFR71.71(c)(9)	Penetration 10CFR71.71(c)(10)	30-ft Drop 10CFR71.73(c)(1)	Crush 10CFR71.73(c)(2)	Puncture 10CFR71.73(c)(3)	Thermal 10CFR71.73(c)(4)
2	Amb.	Amb.	H/VT	X	VB	X	X	CGT	CGT	H	VB
3	Amb.	-20	-	-	-	-	-	H	H	H& CGT	H
4	Amb.	Amb.	-	-	-	-	-	VB	VT	H	VT
5	Amb.	Amb.	-	-	-	-	-	VT	CGT	H	VT

Abbreviations:
Amb. - Ambient
H – Horizontal
VB – Vertical, Bottom Up
CGT - Center of Gravity over Top Corner
VT - Vertical, Top Up
X - Will be performed

4.4 Post-Test Leak Testing and Package Disassembly & Examination

The CVs were removed from the drums of SN2, SN4, and SN5 by making a circumferential cut near the bottom of the drum, just above the lower rolling hoop. The vessel liner was then cut circumferentially to remove the bottom of the liner and access the bottom load fixture and CV. The load fixture and CV were pulled out from the opening in the liner. For SN3, the drum was sectioned by cutting down its full length, after the lid had been removed and CV extracted. The external temperature indicating label data was recorded, then the CVs were leak tested at Building 723-A. After leak-testing, the CVs were opened to record the internal temperature indicating label data.

Upon completion of the CV removal, the packagings were examined by destructively dissecting the drum and other components, as directed by the test engineer. Each drum was cut into sections, primarily to inspect the foam insulation. In some cases the drum lids were bisected to inspect the insulation within the lid pan and lid.

The results of the drop, crush, puncture, thermal, and post test inspections for each packaging are described in detail in the following Sections 5.1 through 5.4 of this report.

5.0 Test Results

The sketch of the temperature indicating label locations was shown in Figure 3. The temperature indicating label data was consolidated from the FP-1039 data sheets and is shown in Table 8.[23]

Table 8 - Temperature Indicating Label Data

Label Locations	Temp. Range (ºF)	Package Temp Max (ºF)				Comments
		SN-2	SN-3	SN-4	SN-5	
1. Bottom of drum lid liner – located 120 degrees apart	250-500	280-290	370-380	420-435	420-435	
2. Top of load distribution fixture	250-500	2a	290-320 & 2b	280-290	250-260	2a. Labels missing 2b. 300 & 310F dots questionable
3. Side of drum lid liner – 120 degrees apart, center of label 2 inches from drum lid plate	250-500	3a	>500 & 3b	3c	3d	3a. Labels not accessible 3b. All labels burned away 3c. Labels not accessible 3d. Labels not accessible
4. Bottom of cone seal plug – 120 degrees apart	250-500	<250 & 4a.	260-270	260-270 & 4b	4c	4a. Labels damaged, but low end of 250F label is not discolored 4b. 330 & 410F labels damaged 4c. Labels damaged
5. Top of cone seal nut	250-500	5a	5b	270-280	250-260	5a. Labels damaged & illegible 5b. 250F label illegible, 330 & 410F labels damaged, but not discolored.
6. Inside CV, one set each at 0 and 180 degrees – top of labels approximately even with bottom of cone seal plug						
0-degrees set	250-500	<250 & 6a	260-270 & 6c	250-260	<250 & 6f	6a. Labels damaged, but low end of 250F label is not discolored 6b. Labels missing & damaged 6c. 330 & 410F labels missing 6d. Labels missing 6e. Labels missing 6f. 250F label found in bottom of the CV, bottom 3 dots not discolored 6g. Labels damaged, but legible
180-degrees set	250-500	6b	6d	6e	<250 & 6g	
7. Outside CV, one set each at 90 and 270 degrees – top of labels						

Label Locations	Temp. Range (ºF)	Package Temp Max (ºF)				Comments
		SN-2	SN-3	SN-4	SN-5	
approximately even with bottom of cone seal plug						
90-degrees set	250-500	<250	260-270	250-260	<250	
270-degrees set	250-500	<250	260-270	250-260	<250	
8. Inside CV, one set each at 0 and 180 degrees – center of labels at mid-point of CV length						
0-degrees set	250-500	<330 & 8a	<250 & 8c	8e	<250	8a. 250 & 410F labels damaged, 330F label is not discolored 8b. Labels damaged 8c. 330 & 410F labels missing 8d. 410F label missing 8e. Labels damaged 8f. Labels damaged, 360F dot is not discolored
180-degrees set	250-500	8b	<250 & 8d	8f	<250	
9. Outside CV, one set each at 90 and 270 degrees – center of labels at mid-point of CV length						
90-degrees set	250-500	<250	<250	<250	<250	
270-degrees set	250-500	<250	<250	<250	<250	
10. Inside CV, one set each at 0 and 180 degrees – center of labels at mid-point of load distribution fixture						
0-degrees set	250-500	10a	10c.	10e	<250 & 10f	10a. Labels damaged 10b. Labels damaged 10c. 250 & 330F labels damaged, 410F labels is not discolored 10d All labels damaged, but low end of 250F label is not discolored 10e. Labels damaged, 330F dot is not discolored 10f. Labels damaged, but legible 10g. Labels damaged, but 250 & 260F dot are not discolored
180-degrees set	250-500	10b	<250 & 10d	<250	<250	
11. Outside CV, one set each at 90 and 270 degrees – center of labels at mid-point of						

Label Locations	Temp. Range (ºF)	Package Temp Max (ºF)				Comments
		SN-2	SN-3	SN-4	SN-5	
load distribution fixture						
90-degrees set	250-500	11a	<250	<250	<250	11a. Labels damaged 11b. Labels damaged, but low end of 250F label is not discolored
270-degrees set	250-500	<250 & 11b	<250	<250	<250	
12. Inside CV bottom - located 120 degrees apart	250-500	<250	250-260	<250	<250	
13. Inside bottom of drum liner	250-500	250-260 & 13a.	330-340	<250	<250	13a. Readings questionable
14. Inside drum liner, one set each at 0 and 180 degrees, center of labels at midpoint of liner length						
0-degrees set	250-500	<250 & 14a	260-270 & 14c	<250	<250	14a. Labels damaged 14b. Labels damaged 14c. 250F labels slightly damaged
180-degrees set	250-500	<250 & 14b	260-270	<250	<250	
15. Outside CV, one label at top, middle, and bottom at 90 degrees						
Top	170-240	210-220 & 15a	>240	>240	>240	15a. 200F dot questionnable 15b. 200F dot questionnable 15c. Labels missing
Middle	170-240	210-220 & 15b	>240	220-230	220-230	
Bottom	170-240	15c	>240	210-220	220-230	

The post-test leak test results for all packages are shown in Table 9 below.[16]

Table 9 - Initial and Final Helium Leak Test Results

Package SN	Vessel SN	Initial Leak Rate (std cc He/sec)	Final Leak Rate (std cc He/sec)	Max Allowable Helium Leak Rate for leak tightness (cc/sec)	Final Results (pass/fail)
SN-2	03084	$< 1.0E^{-09}$	$<8.8E^{-10}$	2×10^{-07}	Pass
SN-3	03967	$2.0E^{-09}$	$<1.8E^{-09}$		Pass
SN-4	03999	$< 9.7E^{-10}$	$2.1E^{-09}$		Pass
SN-5	03224	$< 1.0E^{-09}$	$<8.8E^{-10}$		Pass

The packaging weights before and after the HAC thermal test are shown in Table 10 below.[17] The weight difference is due to the loss of foam insulation during the thermal test.

Table 10 - Pre and Post Test Packaging Weights

Package SN	Before Weight (lb)	After Weight (lb)	Change (%)
SN-2	342.3	293.1	66
SN-3	339.8	286.3	71
SN-4	343.4	291.6	69
SN-5	341.0	291.4	66

5.1 Prototype SN-2

5.1.1 Baseline Radiograph

The radiography report noted two anomalies, as shown in Figure 7:

- Linear voids in the polyurethane foam, that do not appear to span the full length of the drum, and
- Excess Fiberfrax® insulation unfurled beneath the drum liner (which was confirmed during subsequent destructive examination).

Two linear indications running in the vertical direction in the polyurethane foam were visible in the 30, 60, and 90 degree views of the upper section of the package in the baseline radiographs and were most prominent in the 60-degree view (Figure 7). These indications were interpreted as voids caused during the foam installation. The outline of the Fiberfrax® blanket insulation between the foam and drum liner can be seen as a lightly shaded area surrounding the drum liner. It appears that the Fiberfrax® began to unfurl below the bottom of the drum liner, which is indicated by light wavy lines immediately below the drum liner bottom (Figure 7).

The linear voids and unfurled Fiberfrax® were confirmed during disassembly and inspection (see 5.1.3.5.1).

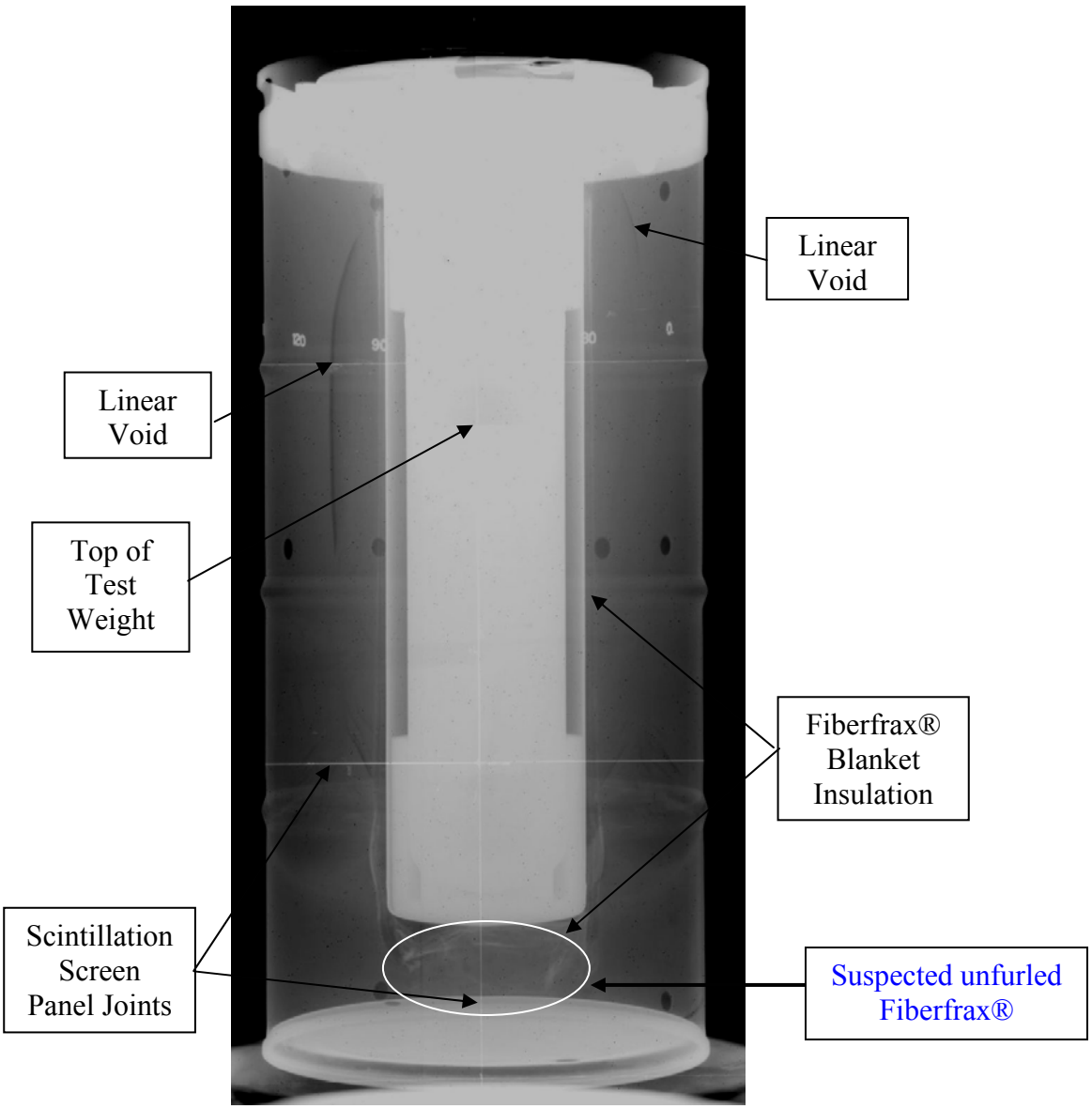

Figure 7 – Sixty-Degree Baseline Radiograph of SN-2 with CV Installed

5.1.2 NCT Tests

This package was subjected to the 10CFR71.71 vibration, water spray, 4-ft free drop, penetration, and compression test in sequence.

The package was prepared with a non-leak-tested CV for vibration testing at the Sandia National Laboratory. The CV was loaded with a test weight that was centered in the CV using aluminum honeycomb pieces as shims. After vibration testing, this CV was replaced with a leak tested CV, loaded with a test weight and no shims.

The SRS test start and stop times, and dates are listed below in Table 11 below. The ambient temperature during these tests was approximately 70F.

Table 11 - NCT Test Start/Stop Times

NCT Test	Test Start Time	Test Stop Time	Date Started - Stopped
Water Spray	2:12 pm	3:12 pm	10/10/05
4-ft Free Drop	4:56 pm	4:56 pm	10/10/05
Penetration	5:18 pm	5:18 pm	10/10/05
Compression	5:46 pm	5:52 pm	10/10/05-10/11/05

5.1.2.1 Vibration Incident to Transport

A discussion of the vibration test and results are not provided in this report, but will be presented in the Safety Analysis Report.

5.1.2.2 Water Spray

A four-shower head device was fabricated at SRS and used for the water spray test to simulate rainfall of approximately 2-in/hr for 1 hour. See Figure 8. The water spray rate exceeded 2-in per hour for the entire 1 hour duration of the test.

The package was weighed before and after the water spray test per procedure FP-1032. The weight increased from approximately 340 lb to 355 lb as water leaked into and accumulated in the drum liner through the small gaps between the drum lid and seating surface.

Figure 8 - Water Spray Setup (right) and Test In-Progress (left)

5.1.2.3 4-ft Free Drop

The package was oriented vertically, drum-bottom up so that the top (lid) impacted the drop test surface. See Figure 9 for test setup. As the package was being rigged for the test, water, which had accumulated in the Drum liner during the water-spray test, discharged from the liner.

This package was dropped from 4-ft and performed 1-hour and 42 minutes after the water-spray test, which meets the CFR criteria for free drop test weight/distance, and performed 1.5 – 2.5 hours at the conclusion of the water-spray test.

The drop impact produced minor crowning on the lid pan. See Figure 10.

Figure 9 - NCT Drop Test Setup of SN-2

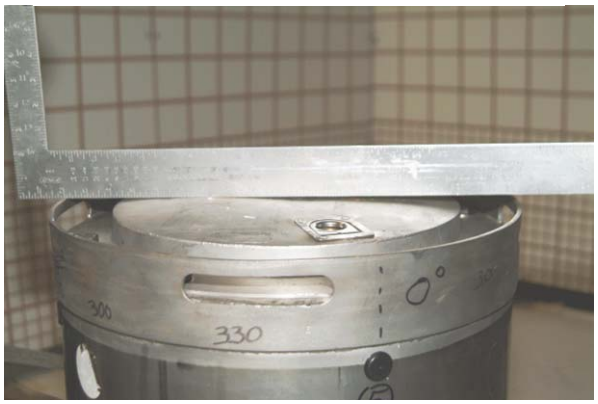

Figure 10 - Lid Pan Crown

5.1.2.4 Penetration

A 13-lb steel cylindrical bar, with one hemispherical end was dropped onto the drum lid from a distance of 40-in. See Figure 11 for test setup. The bar rebounded 2-3 times on the lid. The primary impact caused a small dent (dimple); the secondary impact caused an even smaller dent.

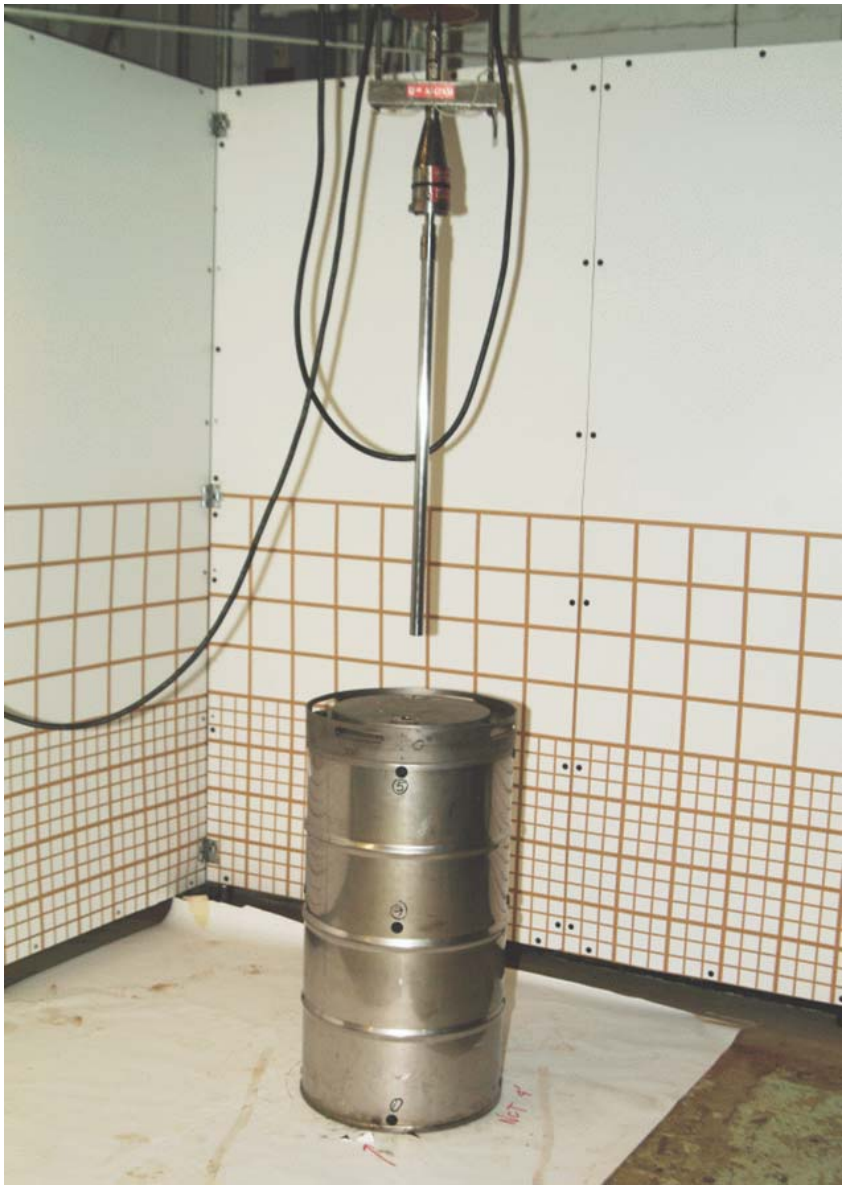

Figure 11 - NCT Penetration Test Setup

5.1.2.5 Compression

The compressive load for this test is required to be the greater of 2-lbf/in^2 multiplied by the vertical projected area of the package, or 5-times the weight of the package. The vertical projected area of the package is 675 in^2 (36-in x 18.75-in), which results in a force of 1,350 lb. The package weighed 342 lb, which results in for of 1,710 lb. Therefore, the latter option was chosen for the test.

The package was placed under 1750 lb of test weights, as shown in Figure 12, and remained under load for 24 hours and 6 minutes. No external damage was observed from this test.

Figure 12 - NCT Compression Test

5.1.2.6 Post NCT Radiographs

The radiographs after NCT tests showed no detectable changes to the containment vessel or the polyurethane foam.

5.1.3 HAC Tests

The package was subjected to the drop, crush, puncture, and thermal test in sequence. The package was radiographed following the drop, crush, and thermal tests.

5.1.3.1 30-ft Drop Test

The 30-ft drop was performed with the packaging oriented so that its axis was approximately 66°, top down (CGOC), at release, to strike the target pad near reference mark 7. The test setup is shown in Figure 13.

The package struck the target pad, rebounded, and struck the opposite lid corner at nearly the primary impact angle (66º). The test was videotaped with a high speed camera and camcorder.

The primary impact resulted in:

- Crushed region at the top of drum along its circumference, beneath the weld of the drum to drum-flange connection. The crush region is approximately 18-in. long and resembles the shape of a drum rolling hoop. See Figure 14.
- Reduction in the overall height of the drum at the point of impact by 1-½ inches (i.e., from 36 to 34-½ in). The drum flange was bent inward toward the lid approximately 90 degrees. See Figure 14.
- Lid cap was flattened at the point of impact and radial crease formed on the lid cap. See Figure 14.
- The lid assembly heaved and scalloping (humps) of the lid between the bolts. See Figure 15 and Figure 16.

The secondary impact resulted in a slight inward bend of the drum-flange.

The radiograph images after the 30-drop show internal damage to the package. Figure 17 shows a before and after 30-ft drop test for comparison. There was no discernable damage to the polyurethane foam and no changes in the general position of drum liner and contents. However, the right image in Figure 18 shows the deformation of the drum lid liner bottom, caused by the impact of the CV and contents during the drop. The drum lid liner bottom is bulged causing a dent in the drum liner. Also noted, is the increased gap between the lid liner bottom and top load distribution fixture before and after the drop.

Figure 13 - HAC Drop Test Setup of SN-2

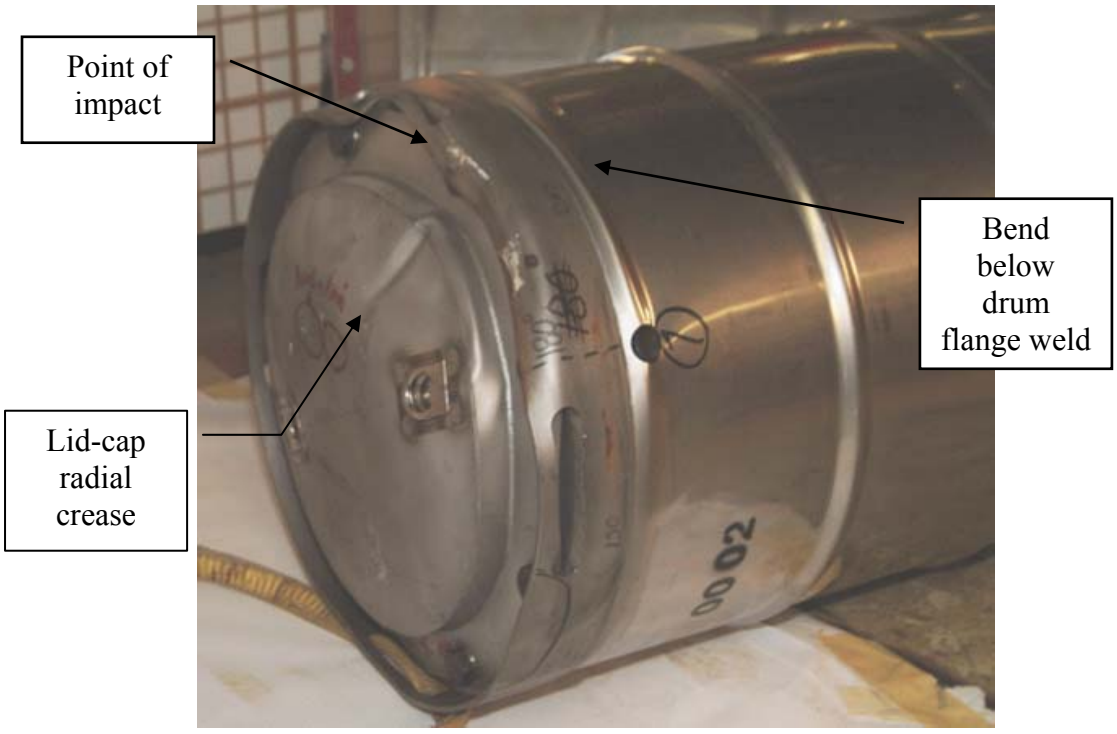

Figure 14 - HAC Drop Test Impact Damage

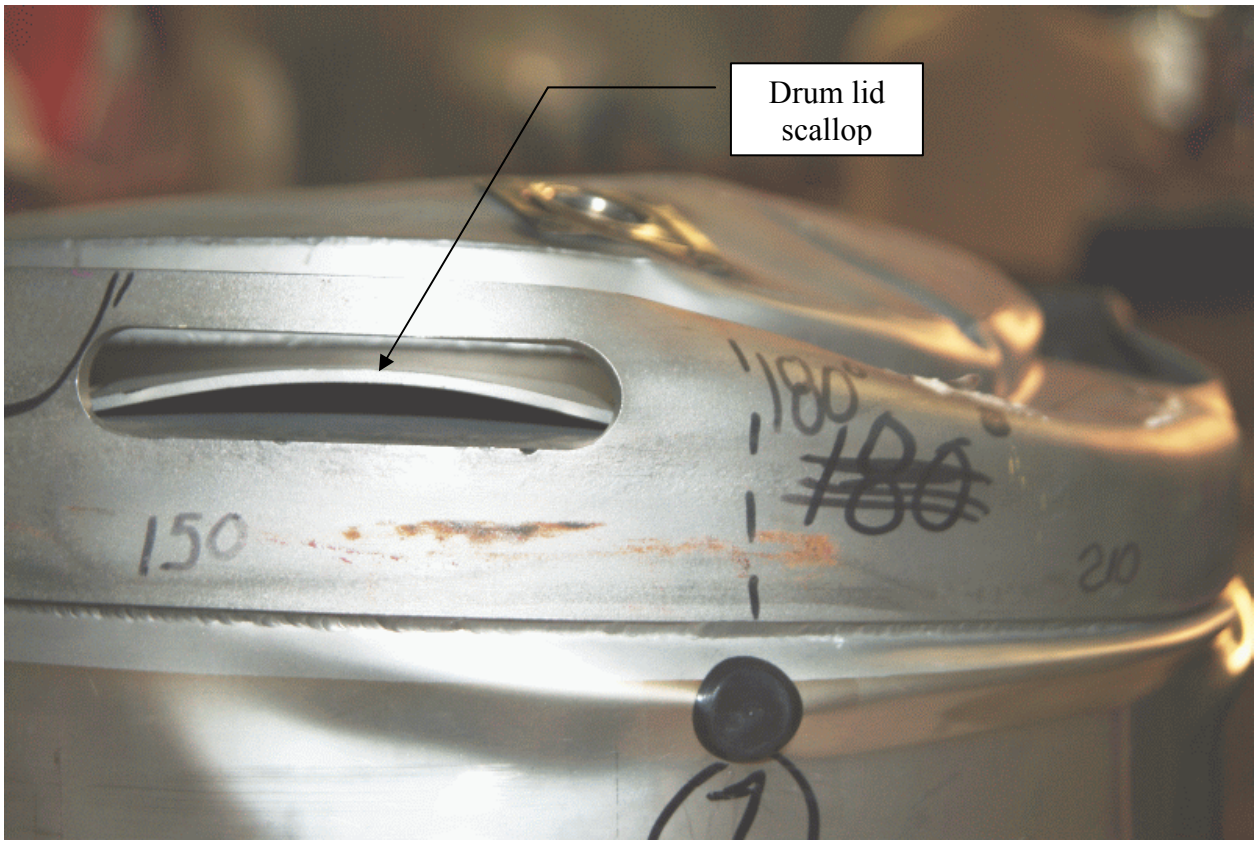

Figure 15 - Drum Lid Scallop

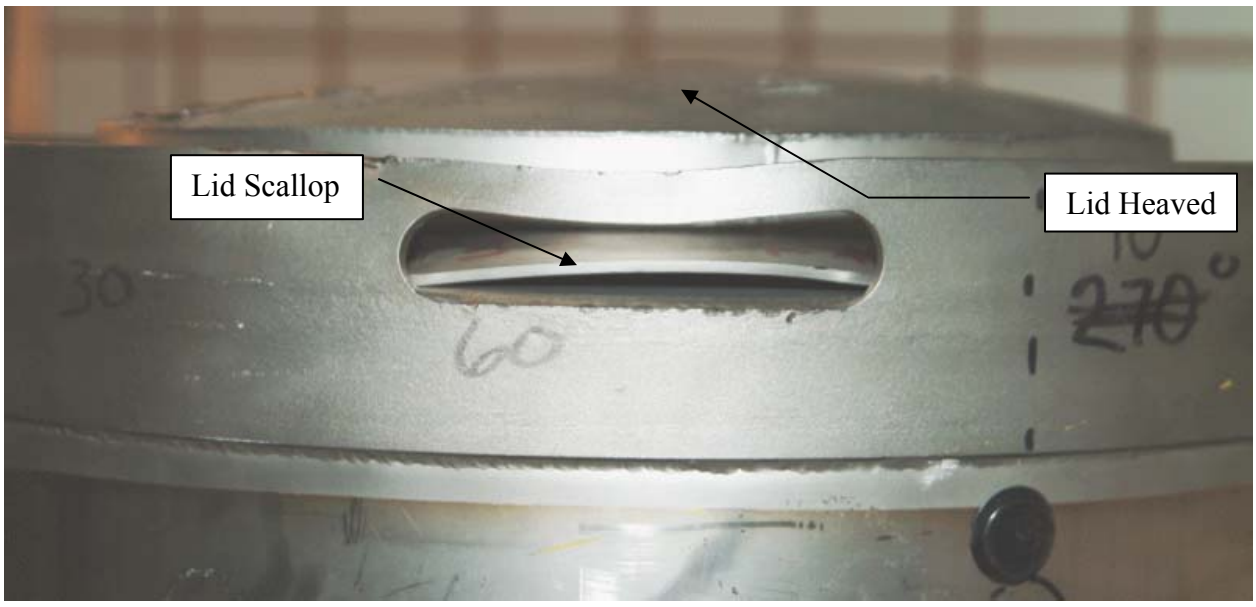

Figure 16 - Drum Lid Scallop and Lid Heaving

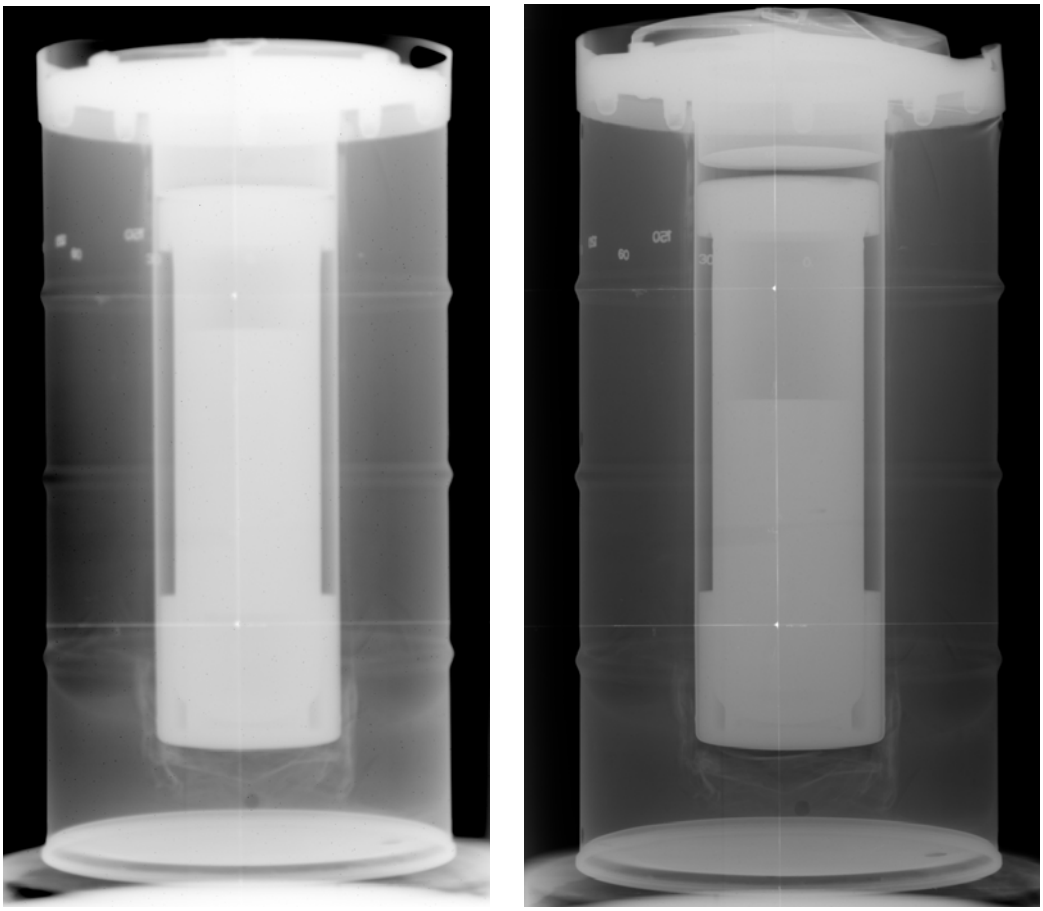

Figure 17 - Before and After 30-ft Drop

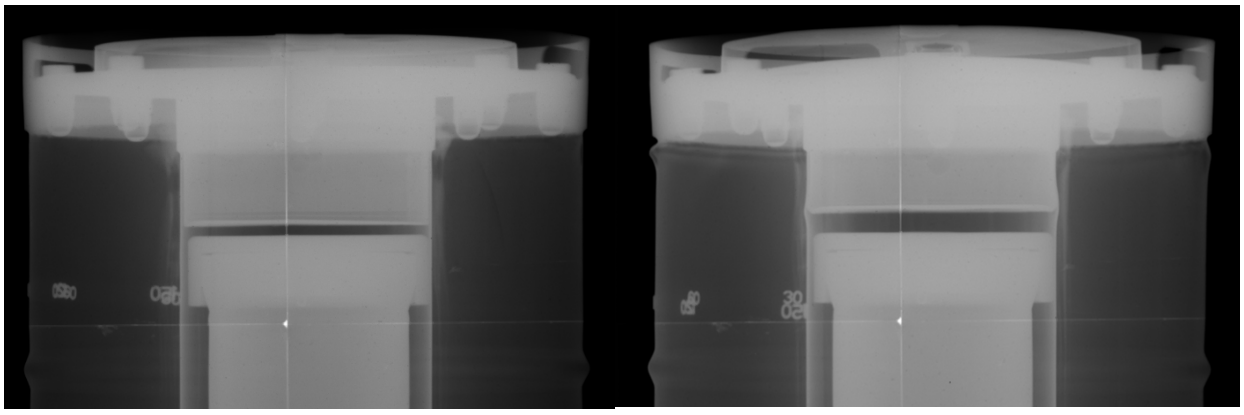

Figure 18 - Lid Gap Before and After 30-ft Drop

5.1.3.2 Crush Test

The 30-ft crush test was performed with the packaging oriented so that its axis was approximately 64°, top up (CGOC), for the crush plate to strike the packaging between Reference marks 6 and 7. The packaging was balanced at this angle by a rubber tire-chock at the base of the package and a rope tied off from the package to a fixed support. A setup of the test is shown in Figure 19.

The crush test plate struck the packaging at compound angle near reference mark 7. A still photo of the plate angle of impact is shown in Figure 20. After the initial hit, the plate and package rebounded and became airborne. The plate hit the package as a second time between reference marks 11 and 12, while they were both still airborne. The package landed top down near reference mark 7 at approximately a 45-degree angle on the crush test base, pirouetted, and landed bottom down near reference mark 1 onto the adjacent concrete foundation. The test was videotaped with a high speed camera and camcorder.

The primary impact resulted in:

- Extenuation of deformation at the top of the drum initiated by the HAC drop test
- The crushed region at the top of drum increased along its circumference, beneath the weld connecting the drum to drum-flange, from approximately 18-in. to 34 inches in length. See Figure 21.
- The bottom corner of the drum, opposite the point of plate impact, is now crushed approximately 2-¾-in between reference marks 1 & 4. See Figure 22.
- The top corner of the drum, at the point of impact, is dented such that the top of the drum is approximately 27 degrees below horizontal. See Figure 23.
- Further reduction in the overall height of the drum at the point of impact from 34-½ to 34-3/8 inches. The overall height of the side opposite the impact decreased from 36 to 34-¼ inches.
- Lid heave (flat to convex) is now approximately 2-in above the drum flange. Some scallops (humps) of the lid flange between the bolts were flattened from the crush plate.
- The lid pan developed a crack along its perimeter from the plate impact. See Figure 24.

The second impact impressed the corner of the plate into the drum between reference marks 11 and 12. The subsequent contact with the base plate and foundation did negligible damage to the drum.

The effects of the crush test are shown in radiograph Figure 25, Figure 26, and Figure 27 . The unevenness of the gap between the drum lid liner bottom and the top load distribution fixture increased, and a gap developed between the top of the CV and top load distribution fixture. The fixture also appears wedged against the rectangular section of the CV cone seal nut. Creases on the drum exterior are also visible on the radiographs in Figure 25 and Figure 26. Additionally, the drum liner directly above the bottom load distribution fixture was deformed by the crush test as shown in Figure 27.

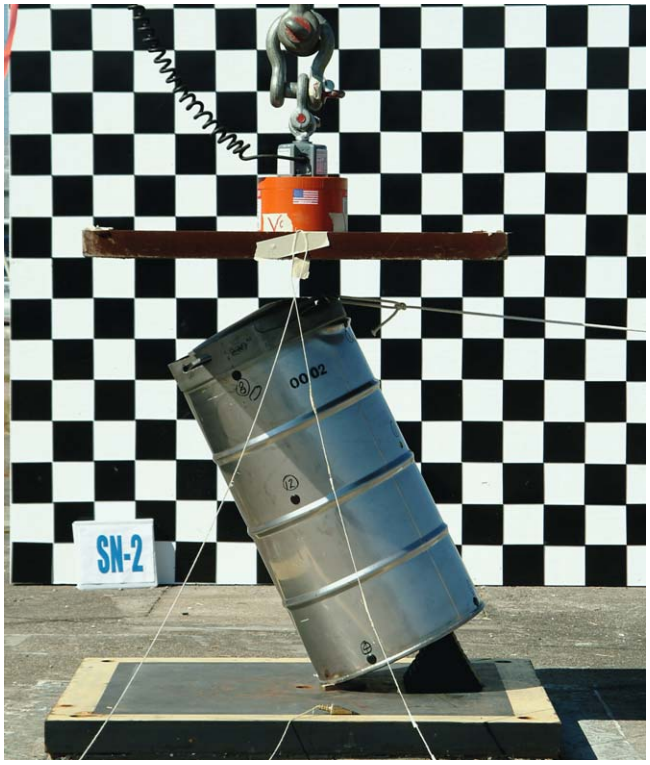

Figure 19 - HAC Crush Test Setup of SN-2

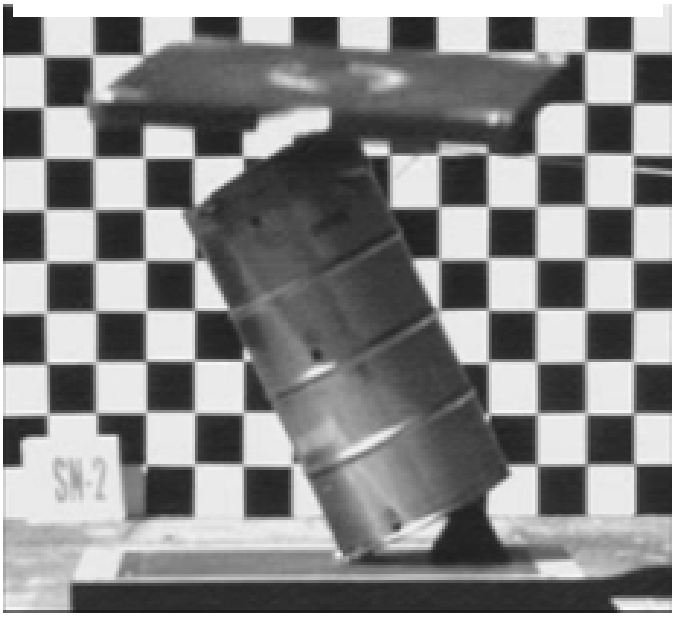

Figure 20 - Crush Plate Angle of Impact

Figure 21 - Pre and Post Crush Test Drum Point of Plate Impact, Top Corner

Figure 22 - Pre and Post Crush Test, Opposite Corner of Plate Impact

Figure 23 - SN-2 Lid and Drum Crush Deformation, Approx. 27 Degrees

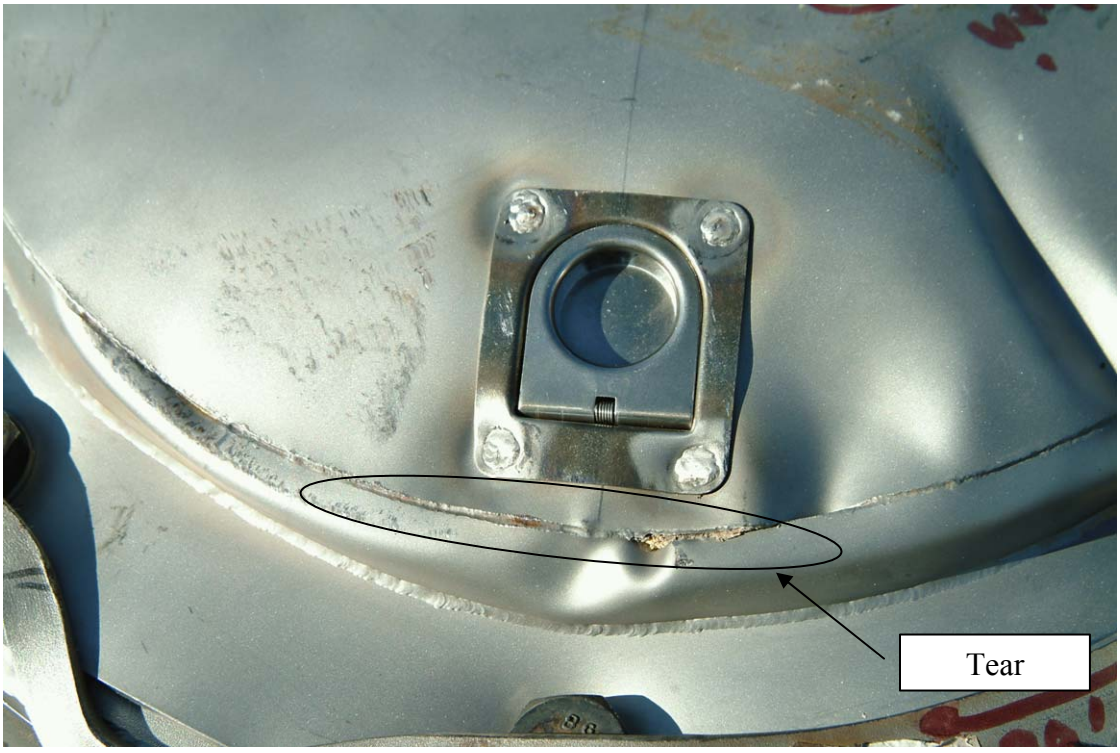

Figure 24 - SN-2 Lid Pan Opening along its Perimeter

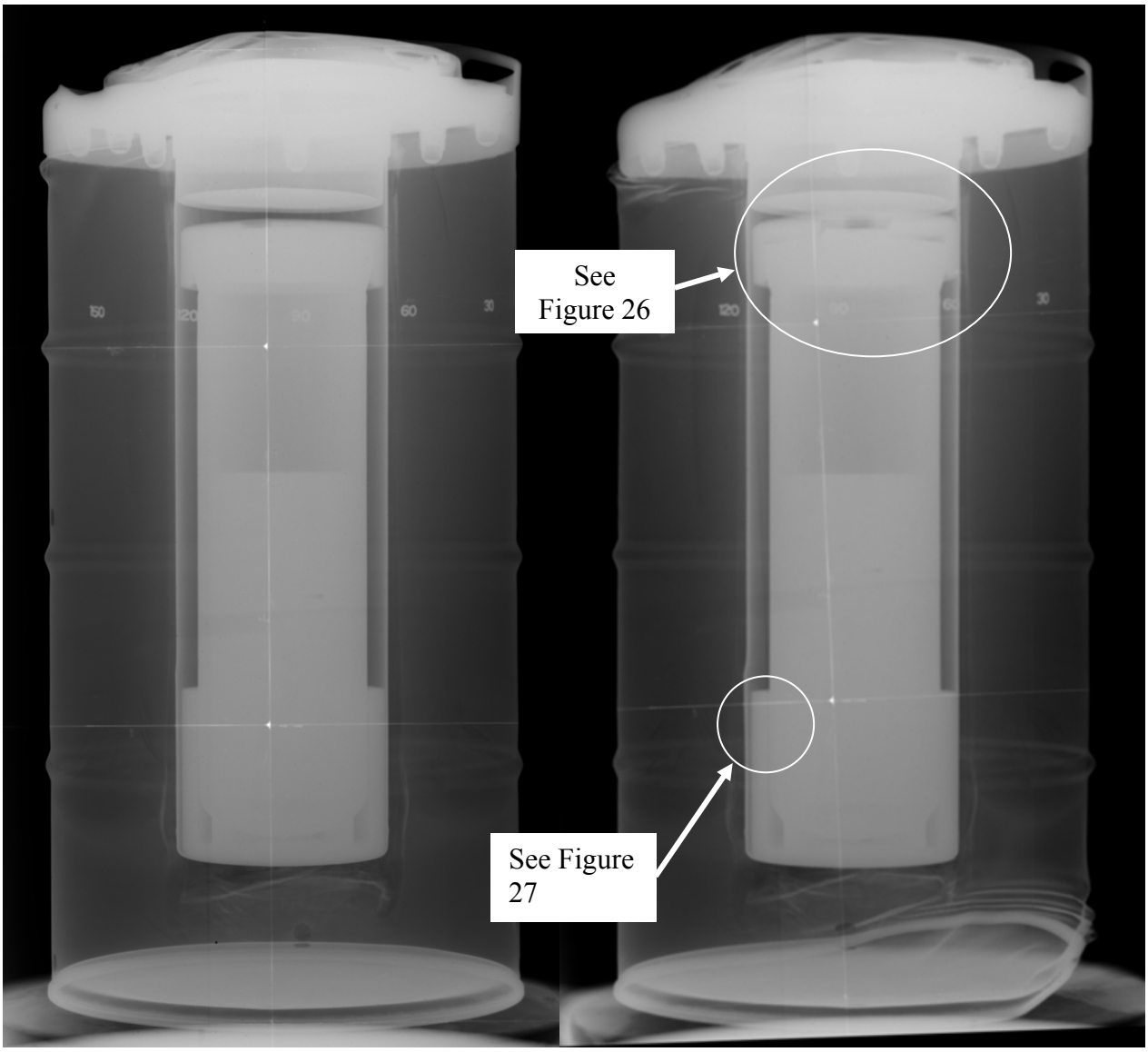

Figure 25 – SN-2 before (left) and after (right) Crush Test. Damage noted

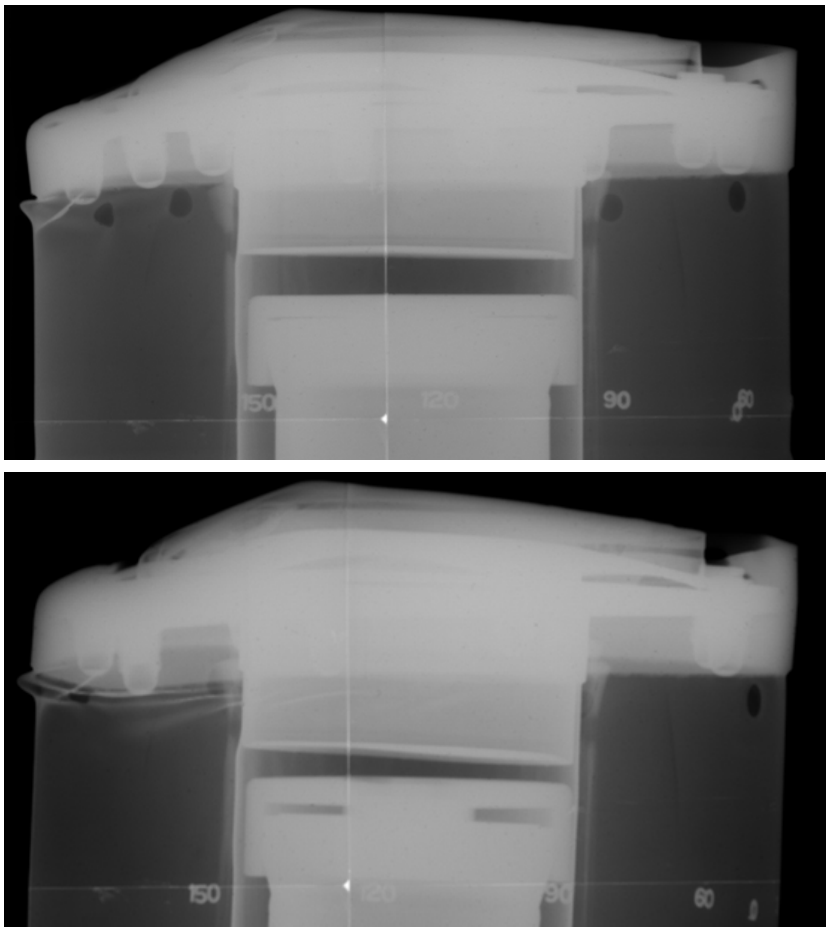

Figure 26 – Upper Load Distribution Fixture Position, before (top) and after (bottom) Crush Test

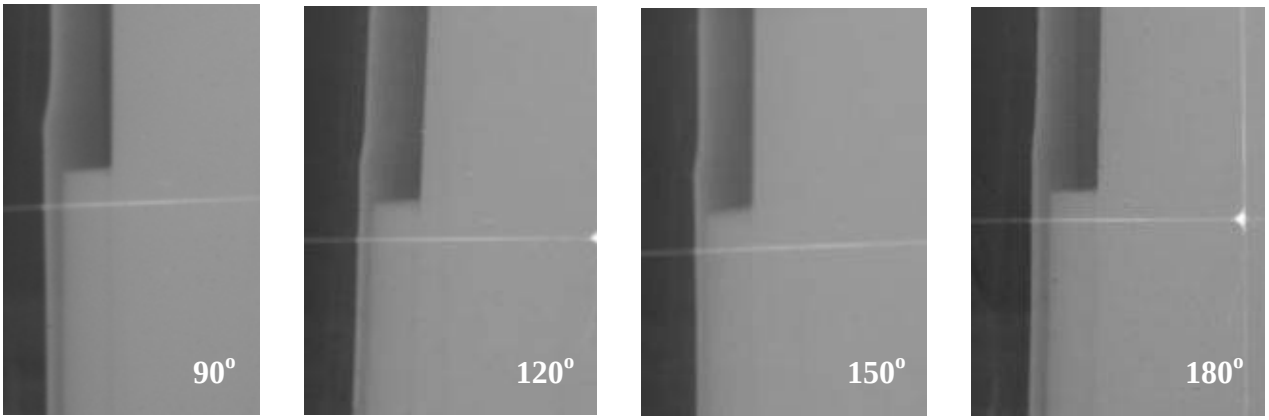

Figure 27 - SN-2 Drum Liner Deformation above Bottom Load Distribution Fixture, 90-180 degrees

5.1.3.3 40-in Puncture Test

The 40-in puncture test was performed with the packaging oriented horizontally, to strike the puncture pin on reference mark 11. The test setup is shown in Figure 28.

The packaging struck the pin on reference mark 11, rebounded, and landed top down at a steep angle, approximately 80-degrees. The test was videotaped with a high speed camera and camcorder.

The primary impact resulted in an impression of the puncture pin top about reference mark 11. See Figure 29. No additional damage was noted.

The package was not radiographed after the puncture test.

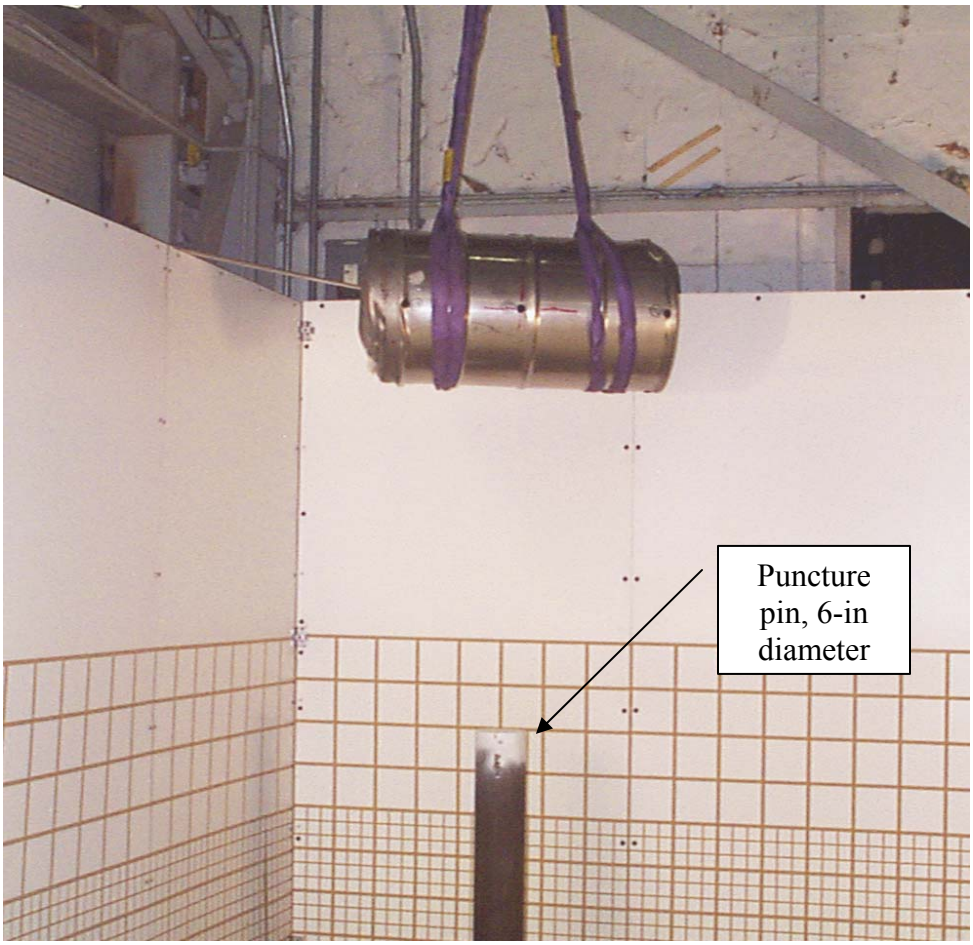

Figure 28 - Puncture Test Setup of SN-2

Figure 29 - Puncture Pin Impression

5.1.3.4 Thermal Test

The thermal test report [22] describes the packaging tests and regulatory compliance in great detail. Therefore, this section of the report will only summarize the thermal test and provide supplemental information to the thermal test report.

None of the packagings contained an internal heater due to unlikelihood of the heater system surviving the preceding HAC tests. However, each packaging was individually preheated at SRS for a minimum of 96 hours in an environmental chamber set to 200ºF ambient to approximate the effect of an internal heat source.

The internal pressure of the containment system was not measured or monitored during the thermal test.

When the weather forecasts were conducive to pool fire testing, the packaging was removed from the chamber, wrapped in insulation, loaded in a van, and transported to the South Carolina Fire Academy (SCFA) to prepare it for the thermal test. The vendor at SCFA installed band heaters on the packaging, wrapped it in insulation, and covered it with an insulated box to maintain the heat soaked condition, until approximately 1-hr before the start of the test.

Flame and packaging temperatures were measured by a network of 14, Type K thermocouples (TC) and a hand-held infrared thermometer (IRT). Four TC were configured as directional flame thermometers (DFT), eight TC were suspended 30 to 56-in above the pool in a grid configuration, one TC was attached to the top of the packaging, and one TC was attached to steel grating in contact with the bottom of the packaging. The TC measurements were recorded on a pair of data-loggers at 5-second intervals; each data-logger was connected to 7 of the 14 TC. The flame temperatures in the vicinity of the packaging were measured using the IRT every 3-minutes. The IRT was also used to measure the surface temperature of the packaging after the pool fire died out.

SN-2 was placed in the test fixture in the top down position as shown in Figure 30.

The pool fire was filled with approximately 50 gallons of fuel then ignited by SCFA personnel at 0815 hours. The packaging was fully engulfed in flames within 1 minute and is shown in Figure 31. The fire was fed with fuel until 0846 hours. The flames died out such that at 0849 hours, the packaging was no longer fully engulfed. The pool fire consumed 509 gallons of fuel.

A photo of SN-2 after the test is shown in Figure 32.

The 30-minute average temperatures and environmental conditions during the test for SN-2 are listed below in Table 12.[22] All TC were calibrated prior to the test, except as noted.

Table 12 - Thirty Minute Average Thermal Test Temperatures and Conditions for SN-2

SN-2	Fire (8 TC)	DFT (4 TC)	Package Surface (2 TC)	IRT (range)
Temperature Average(ºC)	1,023	1,109	968[a]	885-996[b]
Range and Average Wind Speed (knots (mph))	Range: 0 – 3.1 (0 – 3.6), Average: 1.6 (1.8)			
Range and Average Ambient Temperature (ºC)	Range: 4.5 – 6.1, Average: 5.0			

Table 12 Notes

a. These TC were not calibrated; consequently, the results reported are for information only: TC averages 1051C (top of packaging) and 885C (bottom of packaging).
b. The IRT reading at the 30 minute mark was 278C, and was excluded from this range because the measurement was taken after the fuel supply was cut off.

SN-2 lost approximately 66% of its foam mass during the thermal test (Refer to Table 10).

The post thermal test radiograph, Figure 33, indicates a clearly delineated region of deteriorated foam (a.k.a. charfoam) between the drum and drum liner. However, an undamaged layer of foam still envelops the drum liner, except for a slight gap between the drum top plate and undamaged foam. The depth of foam deterioration did not exceed the linear void first presented in the baseline image (Figure 7) is noted in Figure 33 below. Additionally, the position of the top load distribution, which was askew after the crush test (Figure 26), is now shown seated normally on the CV.

Figure 30 - SN-2, Pre Thermal Test

Figure 31 - SN-2 Thermal Test in Progress

Figure 32 - SN-2, Post Thermal Test

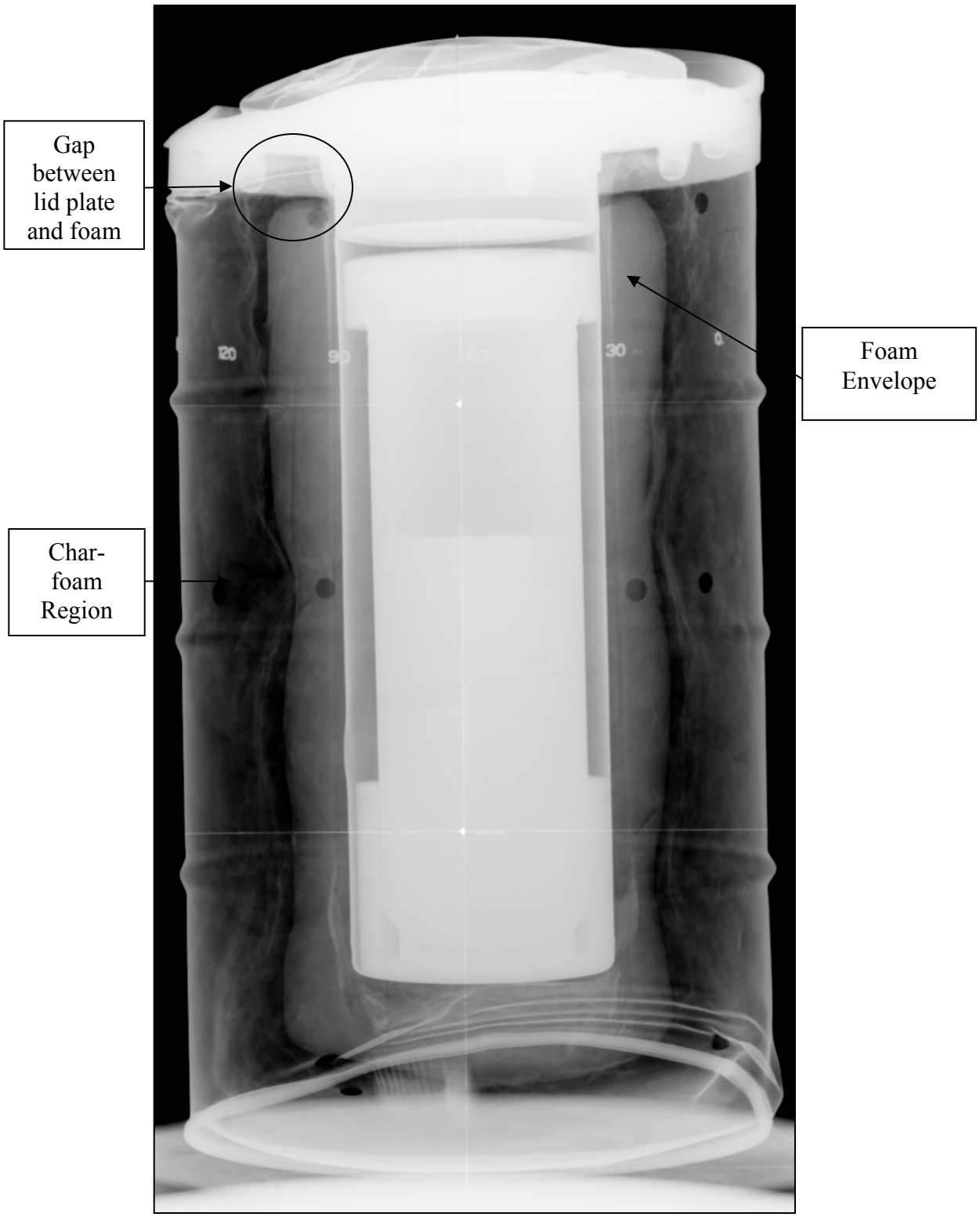

Figure 33 - Post Thermal Test Image of SN-2

5.1.4 Post-Test Packaging Disassembly and Examination

Packaging disassembly and examination was performed per FP-1039. Each package was opened to remove its CV for leak testing, inspect and record temperature label data, and inspect the accumulated damage to the internals if the package from the HAC tests. Following the leak test, the CVs were opened to inspect and record the data from the internal temperature indicating labels. The continuous service temperature for the CV o-rings is approximately 600F for 40 minutes; however, previous testing at SRS demonstrated that these o-rings are able to pass the helium leak test (10^{-7} std-cc/He/s), after exposing the CV to 600F, for 16 hours, at 1000 psig.[24]

5.1.4.1 Disassembly

Prior to disassembly, the condition of the drum observed to have an overall oxidized surface, with some charred foam residue around the vent holes. See Figure 34.

The drum was cut into 4 sections as illustrated in the Figure 35 sketch.

The package was turned upside down (i.e., top-down) to make the 1st sectional cut, which was a circumferential cut of the drum wall, approximately 1l-in above the bottom chime, as shown in Figure 34. Removal of the bottom drum section revealed mostly friable combusted foam (a.k.a., charfoam) as shown in Figure 36. The density of the foam increased towards the drum liner, with solid foam enveloping the bottom of the drum liner.

After the drum bottom section was separated and the loose foam removed, a circumferential cut was made below the estimated base of the drum liner, through the solid layer of foam and Fiberfrax, to expose the drum liner. The solid foam thickness ranged from 1-¼ (sides) to 2-¼ inches (top). The drum liner bottom was cut off, and the LDF removed and inspected. The CV was pulled out and inspected for deformation, discoloration, and temperature label data. The top load distribution fixture was wedged into the drum liner due to a small buckle that caused a restriction in the liner wall.

The 2nd and 3rd sections of the drum were made by 2-cuts along the long axis of the drum, 180 degrees apart, followed by a single circumferential cut below the drum top flange. These cuts completely separated the drum body from the package, exposing the remaining foam and drum liner. Some very thin, large flakes of foam material were observed on the outer charfoam surface. The inspector surmised that the combusted foam flakes appeared to have delaminated from the inside surface of the drum. During removal of these drum sections, loose charfoam separated and fell away from the less combusted foam.

The lid assembly was cut away from the drum body to observe the temperature indicating labels on the lid bottom. The lid assembly was not destructively inspected.

5.1.4.2 Examination of Component Condition

The as found condition of the package components are as follows:

- The outside bottom of the LDF was noticeable abraded, which was attributed to the regulatory vibration test
- No damage or anomalies to the CV were observed by the inspector.
- The temperature indicating labels were inspected and their indications recorded. See Table 8. The maximum temperature seen by the CV exterior was <250F. The temperature seen by the lid underside was <290F. Nearly all of the external temperatures indicating labels were damaged from the vibration, NCT, and HAC tests.
- The condition of the foam composition ranged from mostly friable on the outermost regions near the drum interior walls to a progressively solid layer enveloping the drum liner, as shown in Figure 37.
- The inspector observed an opening in the foam extending from the top edge of the foam envelop at the drum flange that ran longitudinally along the entire length of the envelope. The foam opening coincided with the 180 degrees mark (at the top of the drum), near Ref. Mark 7. The maximum width of the opening is approximately 1/8-in, which occurs in the first 8 inches. The opening then closes and appears as a crack for the remainder of its length. The baseline radiographs show a longitudinal void with similar characteristics in the same area prior to the drop tests and thermal test. A comparison of the baseline image and the disassembled package showing the foam anomaly is shown if Figure 38.
- The Fiberfrax lining appeared unaffected by the heat from the thermal test. The drum liner surface showed no indication of heat effects.

Figure 34 - SN-2 Drum Oxidation/Discoloration from Thermal Tests

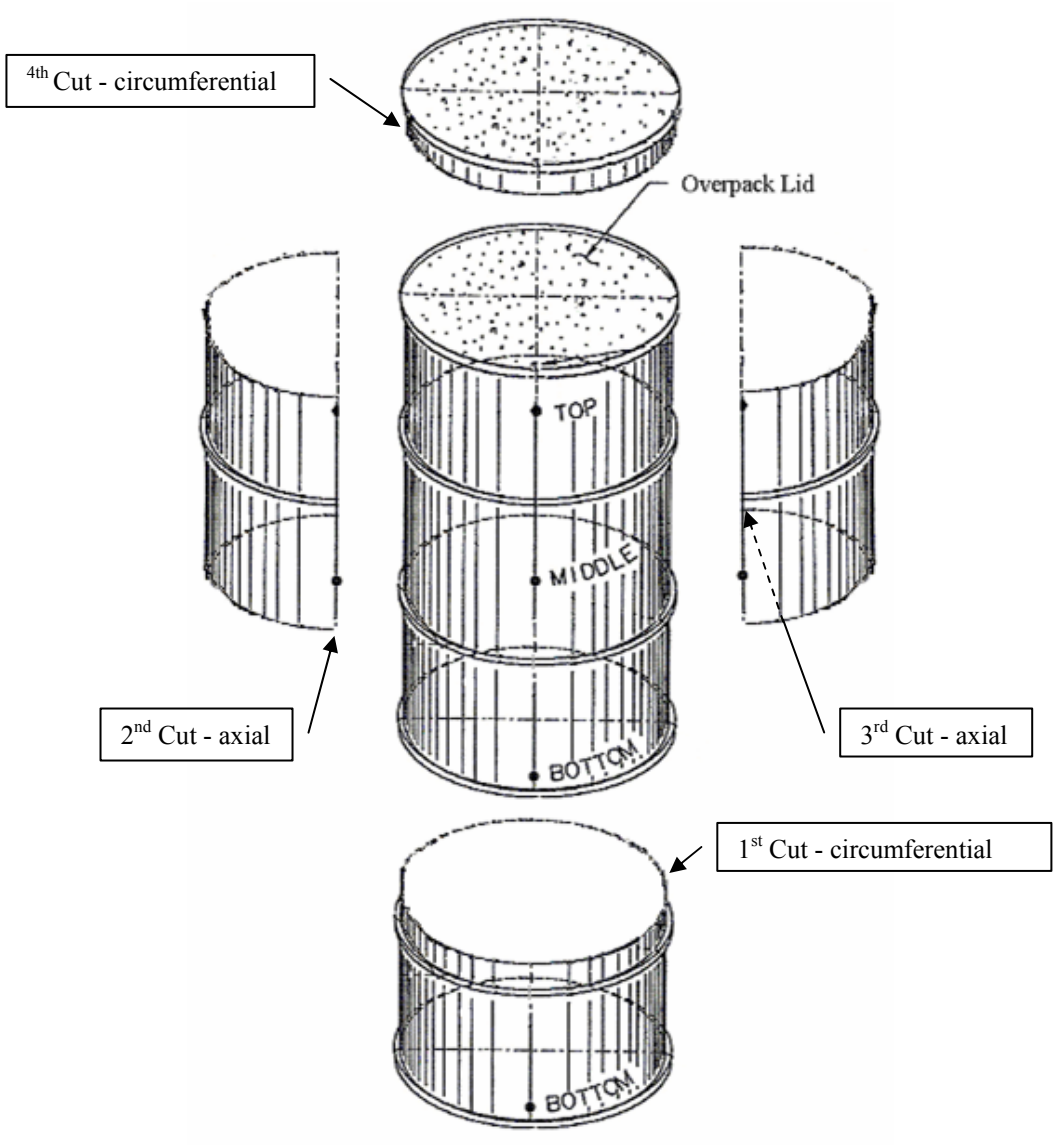

Figure 35 - Sectional cuts of SN-2

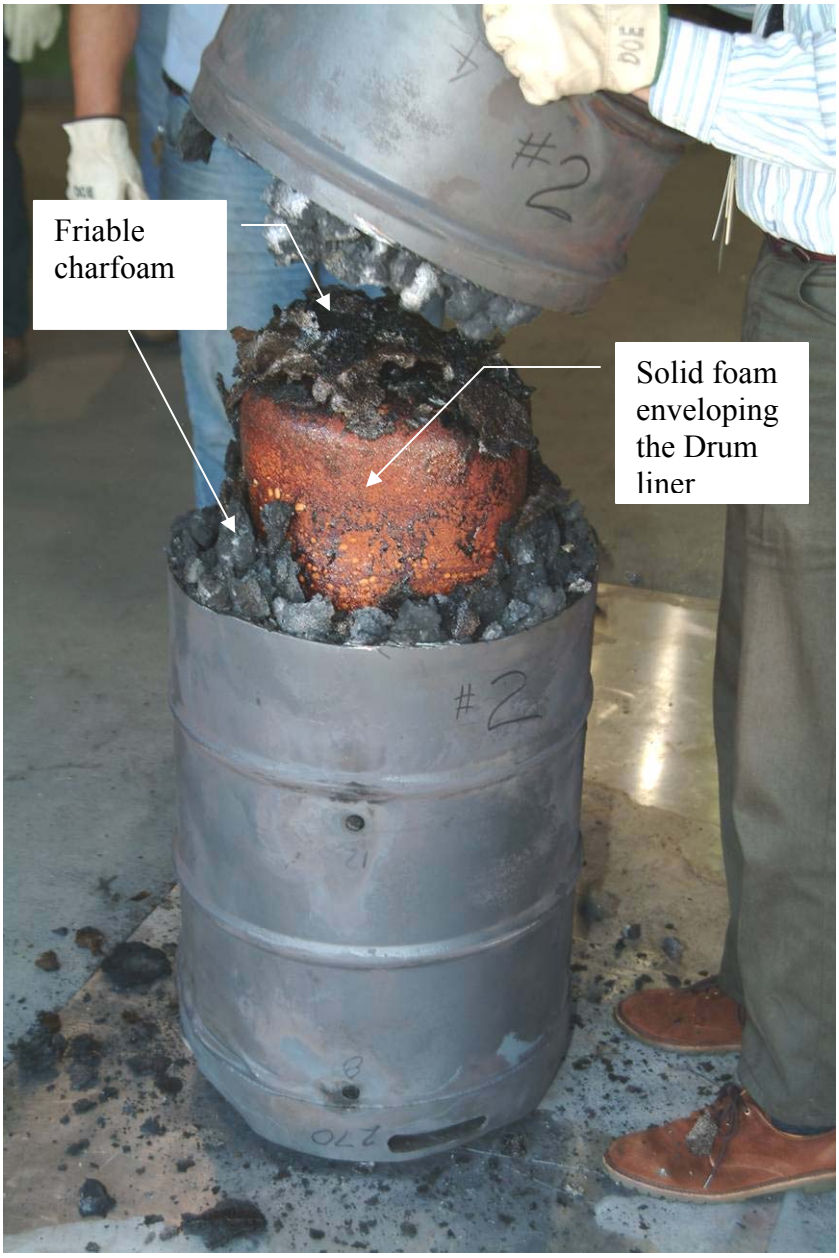

Figure 36 - 1st Sectional Cut and Bottom Removal of SN-2

Figure 37 - SN-2 Foam Enveloping the Drum liner

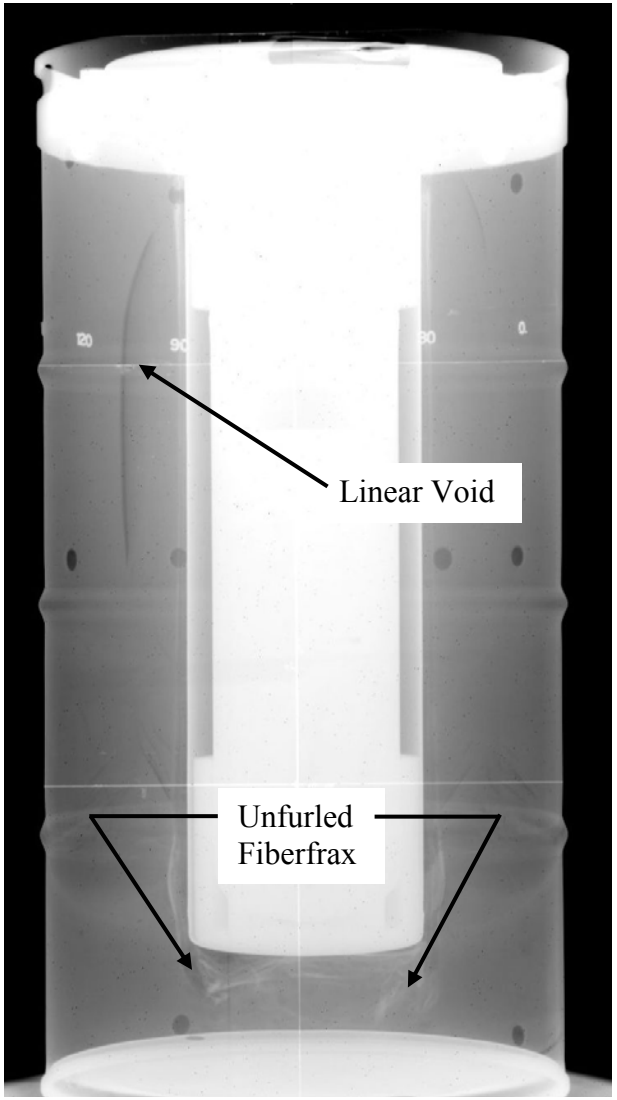

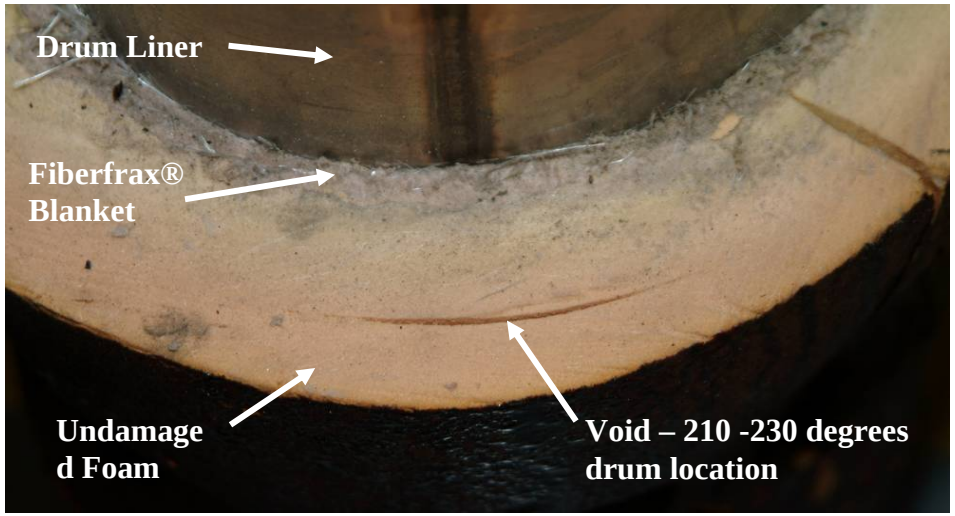

Foam cross-section showing unfurled Fiberfrax

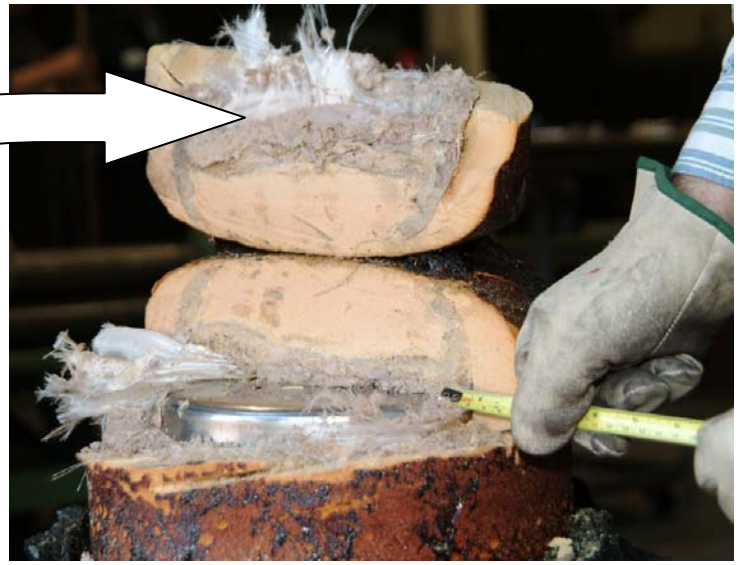

Figure 38 – Foam Anomalies Confirmed During Disassembly and Examination of SN-2

5.1.5 CV Leak Test and Disassembly

After the CV was removed from the SN-2 packaging and visually inspected, a helium leak test was performed to determine if the packaging had provided adequate containment of the contents. The measured leak rate CV was $<8.8^{E-10}$ std-cc He/s, (Ref Table 9) which demonstrates the packaging design provided adequate containment of the contents following the regulatory performance tests.

Following the leak test, the CV was opened to inspect and record the data from the internal temperature indication labels. The data is reported in Table 8; however, nearly all of the labels were damaged due to abrasion by the unrestrained surrogate contents. The internal temperature recorded was consistently <250F near the top middle and bottom of the CV body; the maximum temperature recorded was <330F, located on the underside of the CV lid.

5.2 Prototype SN-3

5.2.1 Baseline Radiograph

The radiography report [18] noted two pretest anomalies, as shown in Figure 39 and Figure 40.

- Lower density (voids) in the foam just beneath the drum liner
- Excess Fiberfrax® insulation unfurled beneath the drum liner.

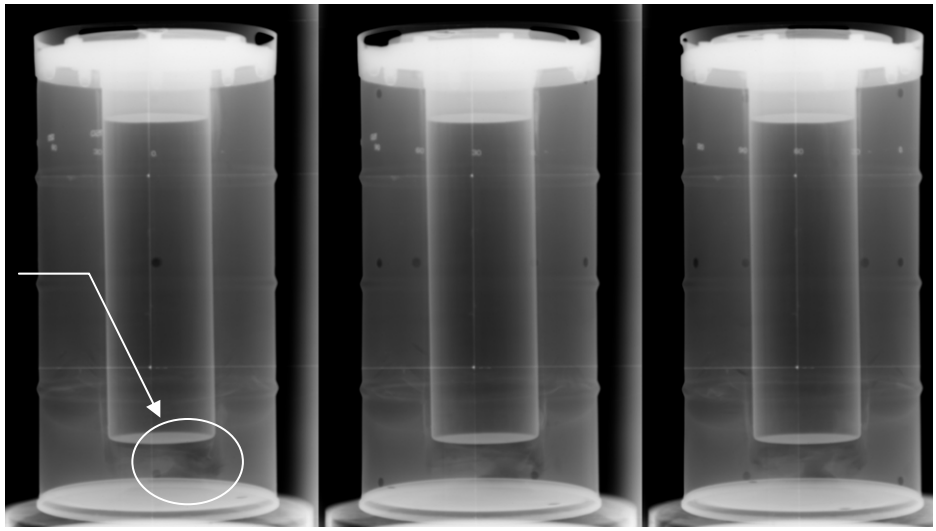

Figure 39 - SN-3 Baseline Images: 0, 30, and 60 degrees (left to right)

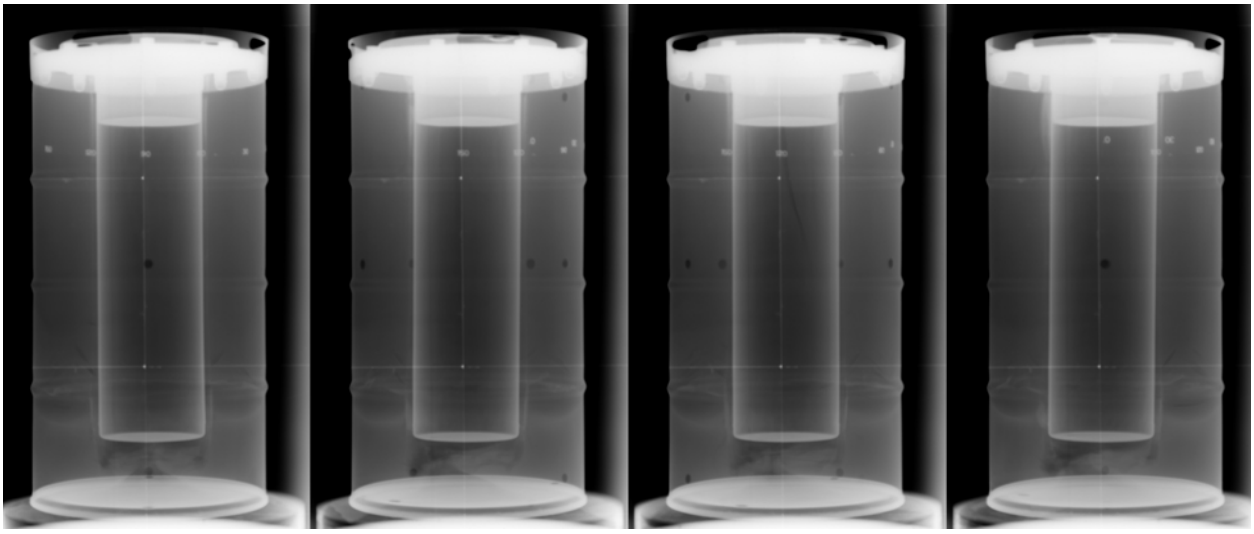

Figure 40 - SN-3 Baseline Images: 90, 120, 150, & 180 degrees (left to right)

5.2.2 NCT Tests

The NCT tests were not performed on this package.

5.2.3 HAC Tests

Package SN-3 was prepared for HAC drop, crush, and puncture testing at ambient air temperature of -20F per procedure FP-1027. This package was cooled at -40F for 96 hours in a SRNL Environmental Chamber. The package was removed from the chamber and placed into an insulated transportation and storage box packed with dry-ice to maintain a -20F ambient air temperature before and after the HAC tests and while in transit to radiography. The air temperature in the box was monitored with a single thermocouple and hand held instrument. A photo of the package prior to exiting the environmental chamber at -40F is shown below in Figure 41.

Figure 41 - SN-3 Prior to Removal from Chamber at -40F

5.2.3.1 30-ft Drop Test

The package was removed from the chamber at 0925 hours and transported directly to the test area. The ambient air temperature in the test area was approximately 63F. The actual drop test occurred at 0959 hours. The package was placed back into the chamber at 1048 hours.

The 30-ft drop was performed with the packaging oriented horizontally, to strike the target pad at the mid point between Ref Marks 1-4, 9-12, and 5-8. The test setup is shown in Figure 42.

The package struck the target pad, rebounded, rotated approximately 270 degrees, struck bottom corner of the drum near Ref Mark 1, bounced a second and third time, and then tipped over on its side to complete the 360 degree rotation. The actual impact angle is approximately 3-degrees from horizontal and is shown in Figure 43.

The test was videotaped with a high speed camera and camcorder.

The primary impact resulted in:

- Flattened region along the point of impact, as shown in Figure 44 and Figure 45.
- Reduction in the overall drum diameter along the point of impact: by 3/8-in at the top, ¼-in at the rolling hoops and ¼ in at the bottom chime.

The secondary impact resulted in a buckled region at the bottom of the drum near Ref Mark 1 as shown in Figure 46. Three minor dents on the side of the drum were caused by the impact of the rigging hardware.

The radiographs indicate that the 30-ft drop caused two radial foam cracks at and opposite the point of impact, and deformation of the drum liner at several locations. See Figure 47 and Figure 48 respectively.

Although the radial cracks are clearly visible in Figure 47, there is no evidence at this point to indicate the length in the axial direction.

The deformation of the drum liner is in close proximity to the upper and lower load distribution fixtures as seen in Figure 48. In addition, the buckled region at the bottom chime is noted.

Figure 42 – HAC Drop Test Setup of SN-3

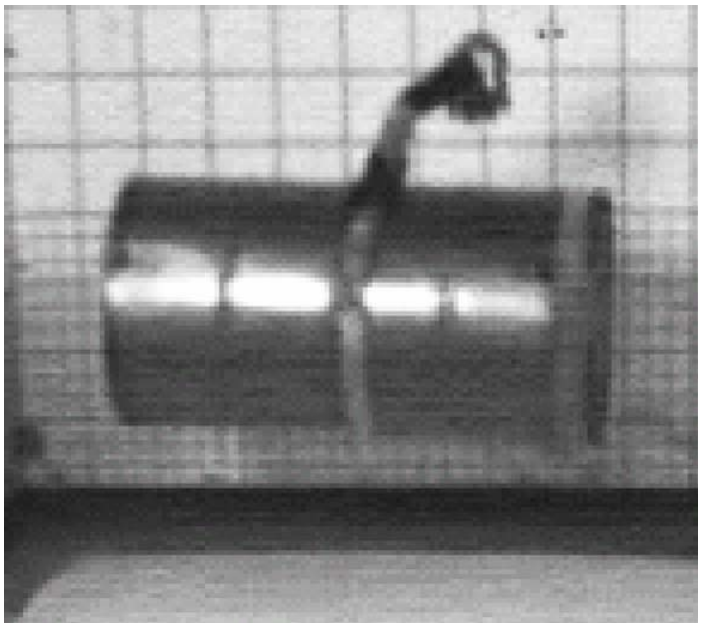

Figure 43 - Angle of Impact

Figure 44 - SN-3 Bottom Chime Flattened

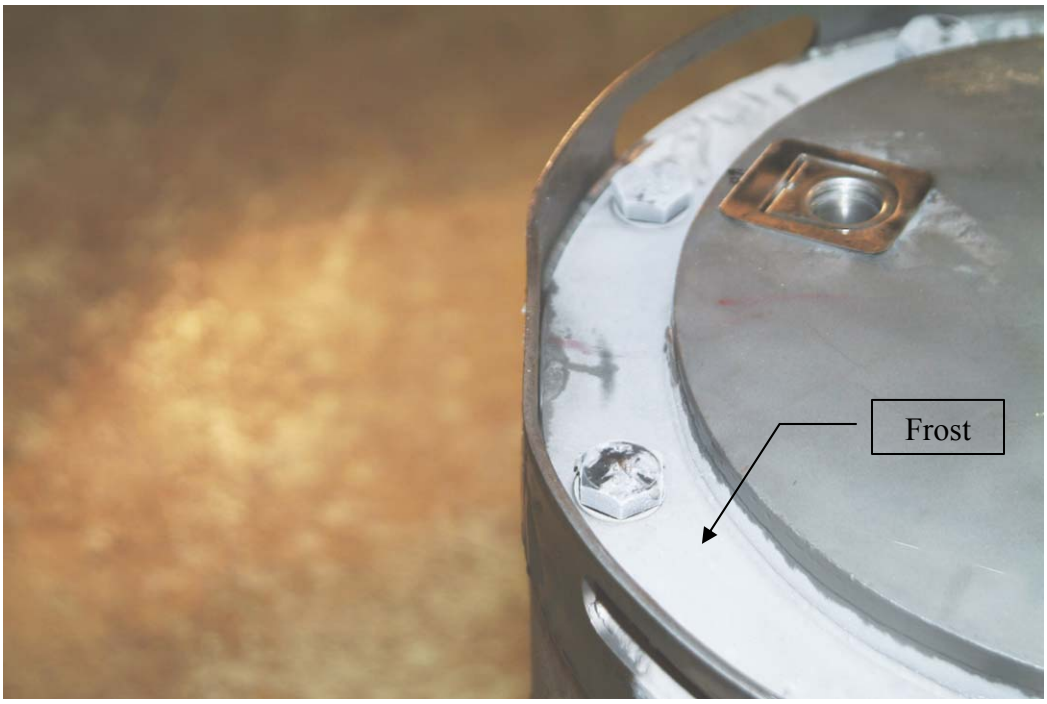

Figure 45 - 3/16th Inch Thick Drum Flange Flattened

Figure 46 - Drum Buckled from Secondary Impact

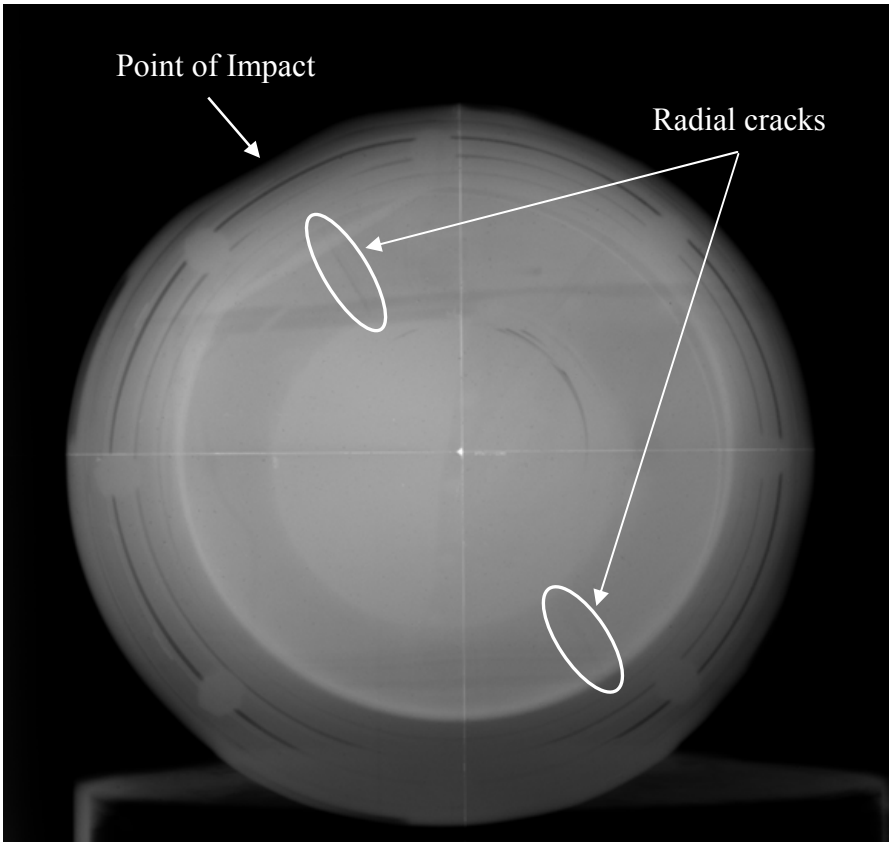

Figure 47 - Radial Cracks from HAC Drop Test

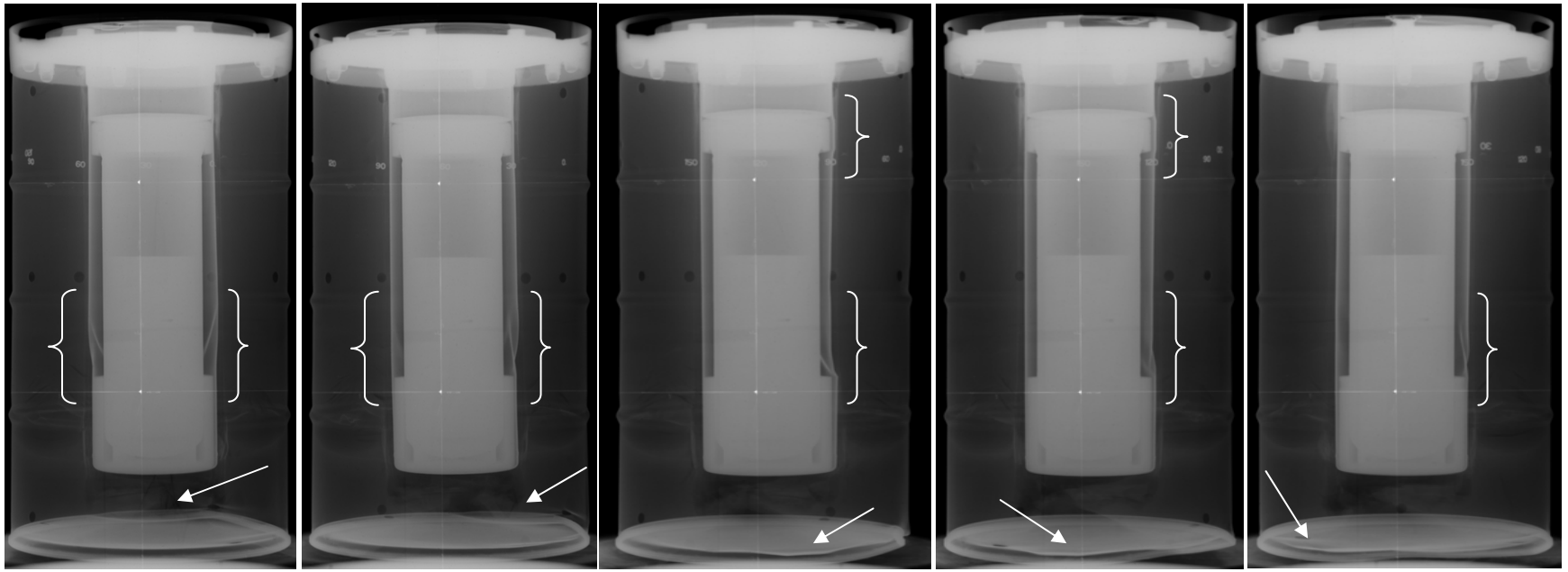

30º 60º 120º 150º 180º

Figure 48 - Post Drop Test Image of SN-3, 30-180 degree rotations as shown. Deformation to the Upper and Lower Load Distribution Fixtures Noted. The damage to the bottom chime is indicated by the arrow, and also shown in the Figure 46 photograph.

5.2.3.2 Crush Test

The package was stored in the insulated box filled with CO2 pellets prior to the test,. The box air temperature at time the package was removed for the test was -21F. The weather conditions on the day of the test, 10/26/05, at the crush test location (outdoors) at 1130 hours, reported by SRNL Atmospheric Technologies, was: ground level air temperature 57.3F, wind speed 4.3 mph (15 average), with max 9.1 mph (gust).

The 30-ft crush test was performed with the packaging oriented horizontally, so that the plate struck the package along the Ref Mark 1-9-5 axis. A setup of the test is shown in Figure 49.

The crush test plate struck the packaging at compound angle along the targeted axis: the crush plate slapped-down onto the package, striking the lid end first, then the bottom chime. The plate and package rebounded and went airborne in opposite directions before coming to rest. A photo of the plate just prior to release is shown in Figure 50. The impact angle and bottoming sequence are shown in Figure 51. Pre and post test photos are shown Figure 52 and Figure 53, and annotated where applicable.

The test was videotaped with a high speed camera and camcorder.

The primary impact resulted in:

- A reverse-strain induced tear, approximately 11-in long by ¼ in tall, developed on the bottom of SN-3 about Ref Mark 2 as shown in Figure 54.
- The crush caused ripples across the bottom of the drum, as shown in Figure 55.
- The drum assumed an oval shape across its diameter on both ends, as shown in Figure 56. The oval is more pronounced at the bottom end. The dimensional changes through the crush test are listed in Table 13 below.

Table 13 - Dimensional Changes of SN-3 at the Drum Top and Bottom

	Drum Diameter	Pretest (in)	HAC Drop (in)	HAC Crush (in)
Min	Top	18-1/8	18-1/4	18-1/4
	Bottom	18-1/4	17-7/8	14-1/2
Max	Top	18-1/4	18-3/8	18-7/16
	Bottom	18-1/4	18-7/16	19-3/16

- The bottom of the drum is now displaced approximately 2-in below the bottom chime, such that the maximum overall height of the drum changed from 36 to 38 inches. See Figure 53.

The second impact from rebounding onto the base plate then rolled off onto the concrete foundation, producing minor dents and scuff marks on the drum.

End view radiographs of the drum, shown in Figure 57, indicate that the radial cracks were essentially unchanged by the crush test. The negative images in Figure 58 show the progression of additional deformation to the drum liner and foam density change in the drum bottom.

Figure 49 - Crush Test Setup of SN-3

Figure 50 - Crush Plate at Test Height

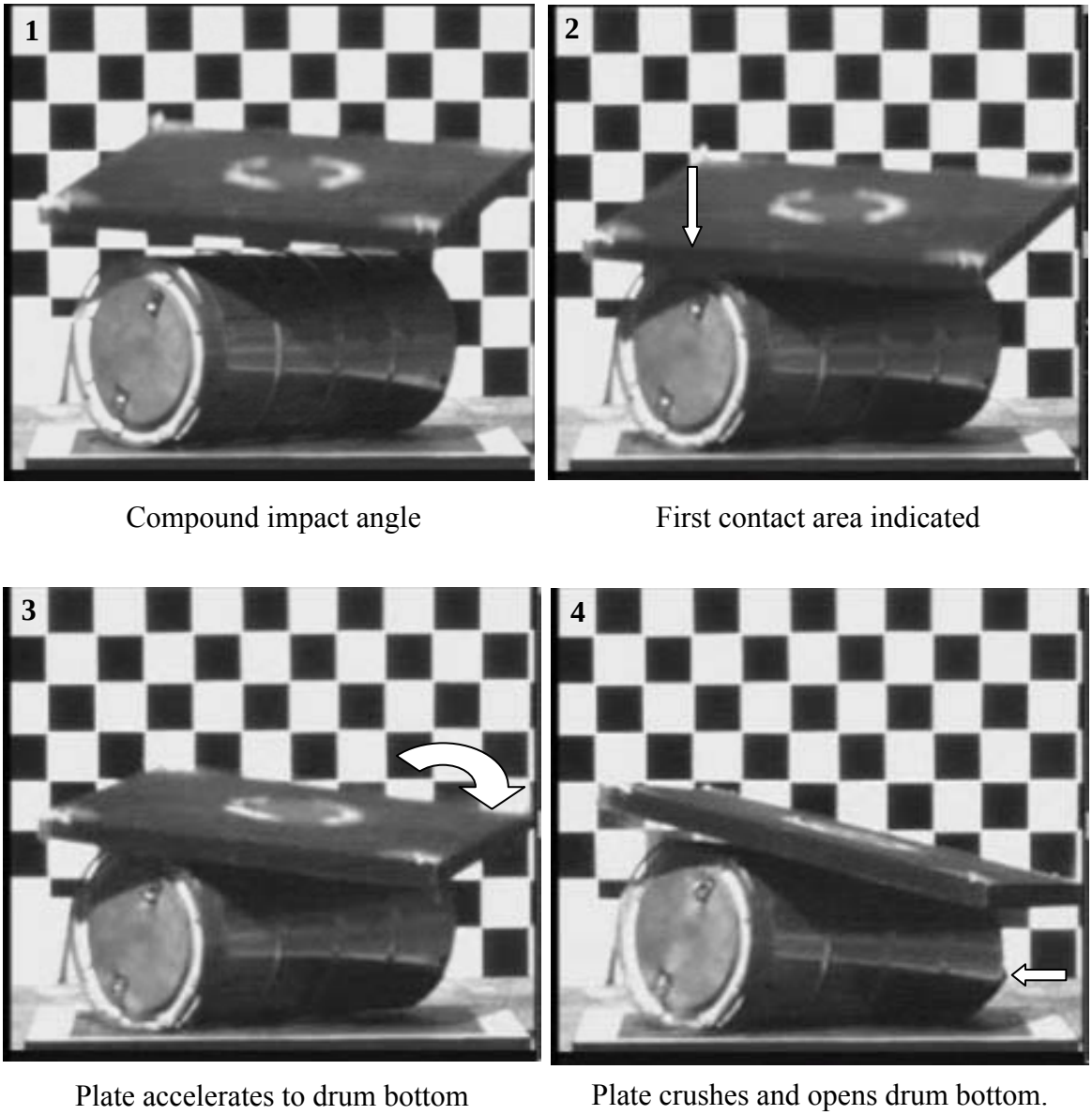

Compound impact angle

First contact area indicated

Plate accelerates to drum bottom

Plate crushes and opens drum bottom. Opening indicated.

Figure 51 - Crush Test Plate Angle of Impact and Bottom Opening Sequence of SN-3

Figure 52 - Pre Crush Drum Condition 360 Degree View, Top Up

Plate impact to left of 3 vents holes	Drum bottom opening indicated	Side opposite plate impact to left of vent holes	Drum bottom domed approx. 2 inches

Figure 53 - Post Crush Drum Condition 360 Degree View, Top Down

Figure 54 - Reverse Strain Induced Tear on Drum Bottom

Figure 55 - Drum Bottom Damage SN-3

Figure 56 - Bottom (left) and Top (right) Ovalized from Crush

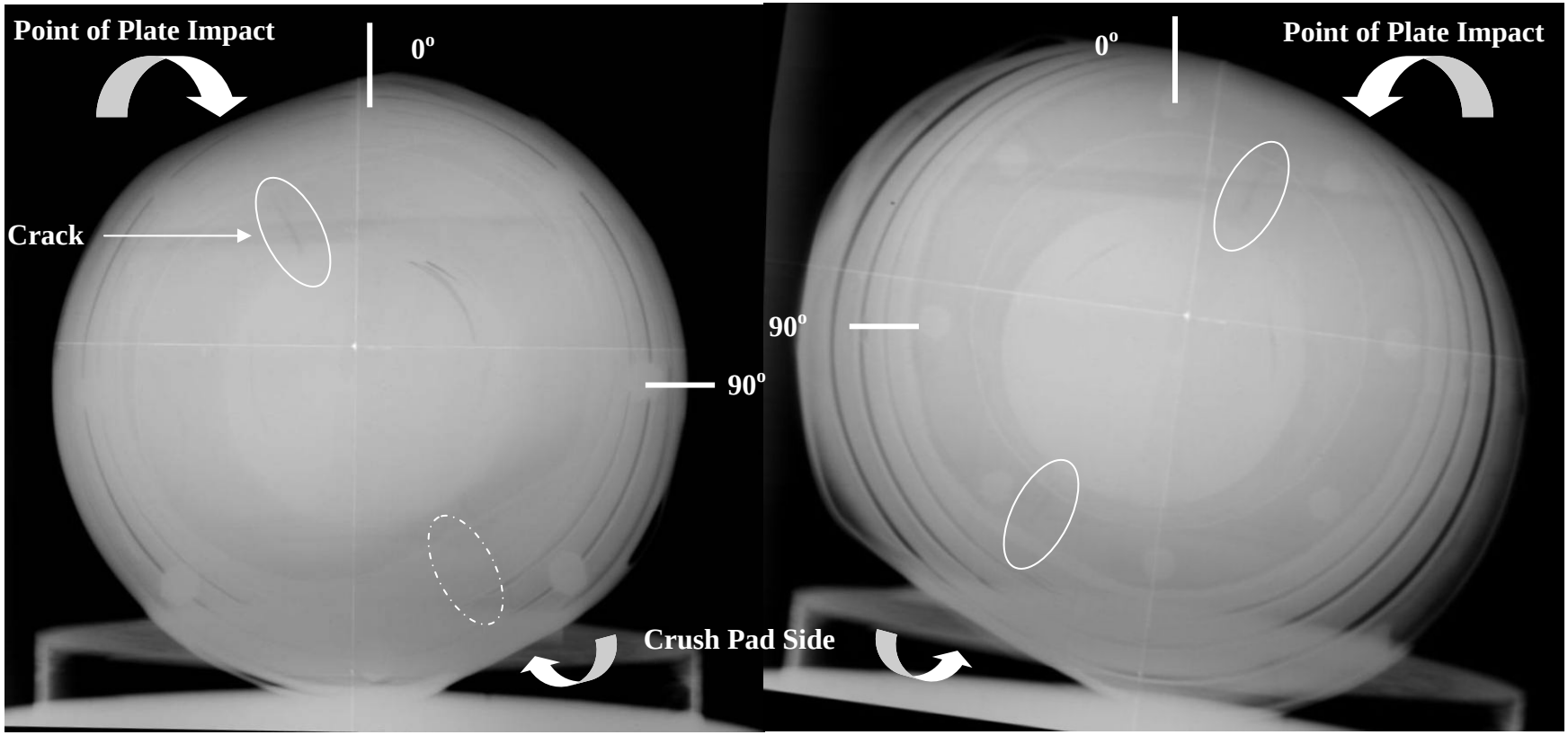

Bottom View - Crack near zero-degree mark visible, the dotted line indicates the likely location of a crack that is not visible in this image.

Top View – Both cracks are visible and nearly perpendicular to the plane of impact. Both cracks visible in this image

Figure 57 - End-to-End Post Crush Test Image of SN-3

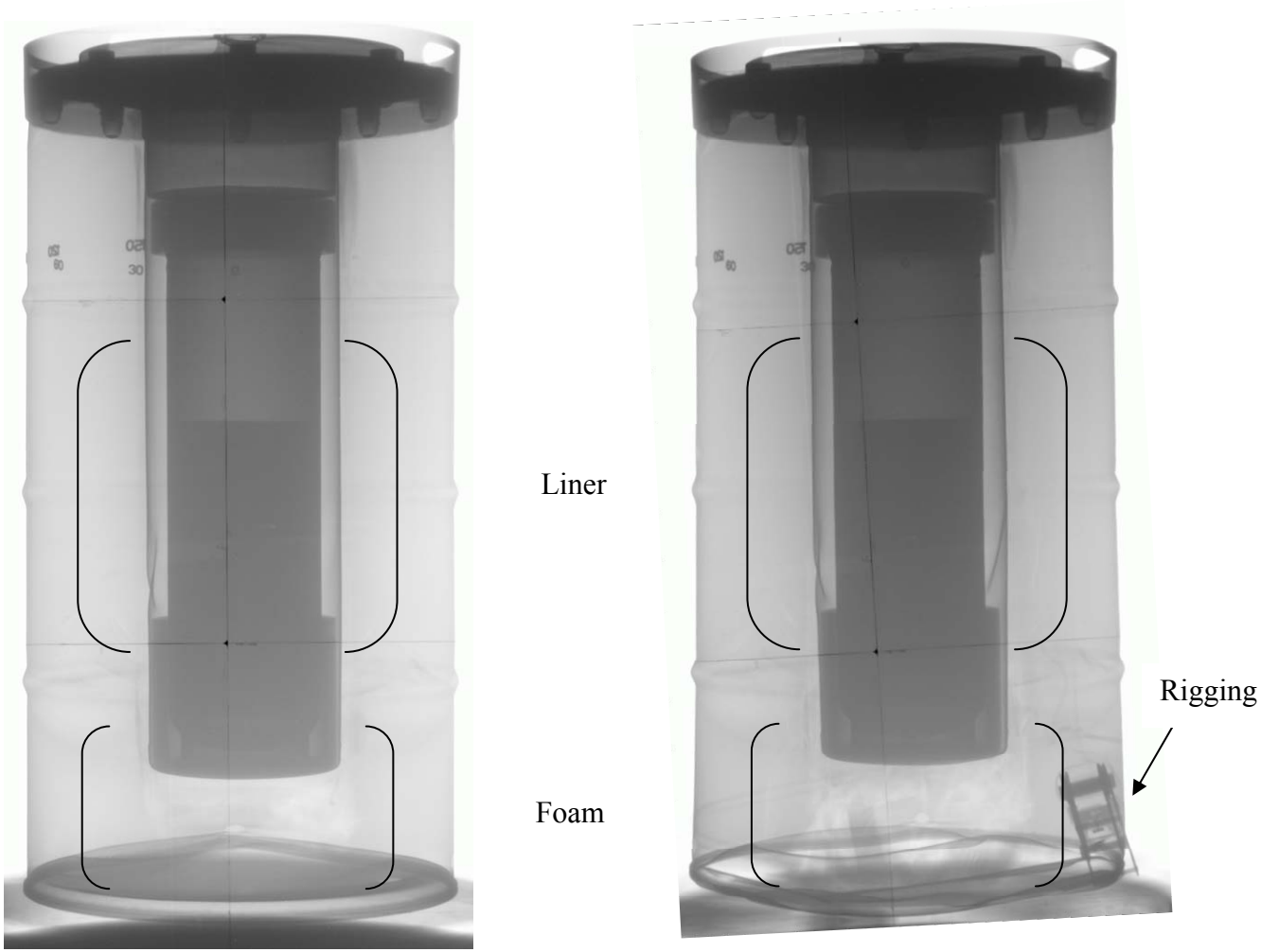

Post HAC Drop

Post HAC Crush – Additional drum liner deformation.
Foam density decrease at the drum bottom

Figure 58 – Negative Image of Drum Liner Deformation and Foam Density Decrease from HAC Drop to Crush Tests

5.2.3.3 40-in Puncture Test

The packaging was removed from the insulated box at 0845 hours. The air temperature inside the box was -93F, and ambient air temperature in the test area (indoors) was 73F. The first puncture test was executed at approximately 0930 hours, and the second test at approximately 1028 hours.

SN-3 was puncture tested in two different orientations. The first puncture test was conducted to exploit the tear in the bottom of the packaging caused by the crush test. The package was oriented top-up, 60 degrees from horizontal, aligned to strike the puncture pin on the bottom of the drum near Ref Mark 2. The second test was performed with the packaging oriented horizontally, to strike the puncture pin on reference mark 11. Both test setups are shown in Figure 59.

Both tests were videotaped with a high speed camera and camcorder.

During the first test, the packaging struck the puncture pin, rebounded and lightly struck the pin a second time. The initial impact sequence is shown in Figure 60. The impact caused the drum bottom gap to increase from ¼- to ½-in maximum, but did not change the overall length of the tear, and caused the foam at the drum opening to crumble. See Figure 62.

During the second test, the packaging struck the puncture pin on reference mark 11, rebounded, rotated approximately 30 degrees, and struck the pin a second time near reference mark 11. The primary impact resulted in an impression of the puncture pin top about reference mark 11, and the secondary impact made a similar, but smaller indentation. See Figure 63.

The package was not radiographed after the puncture test.

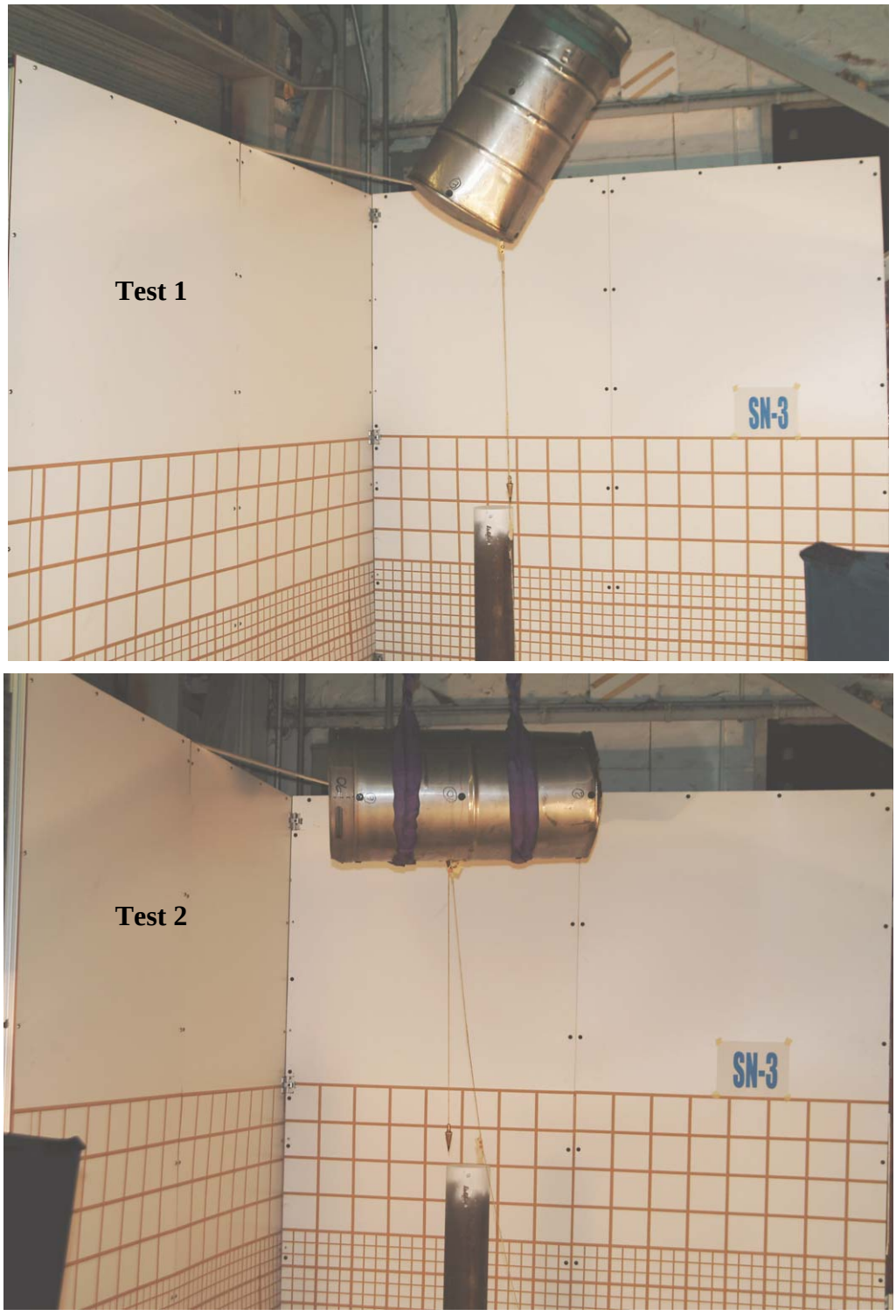

Figure 59 - HAC Puncture Test Setups for SN-3

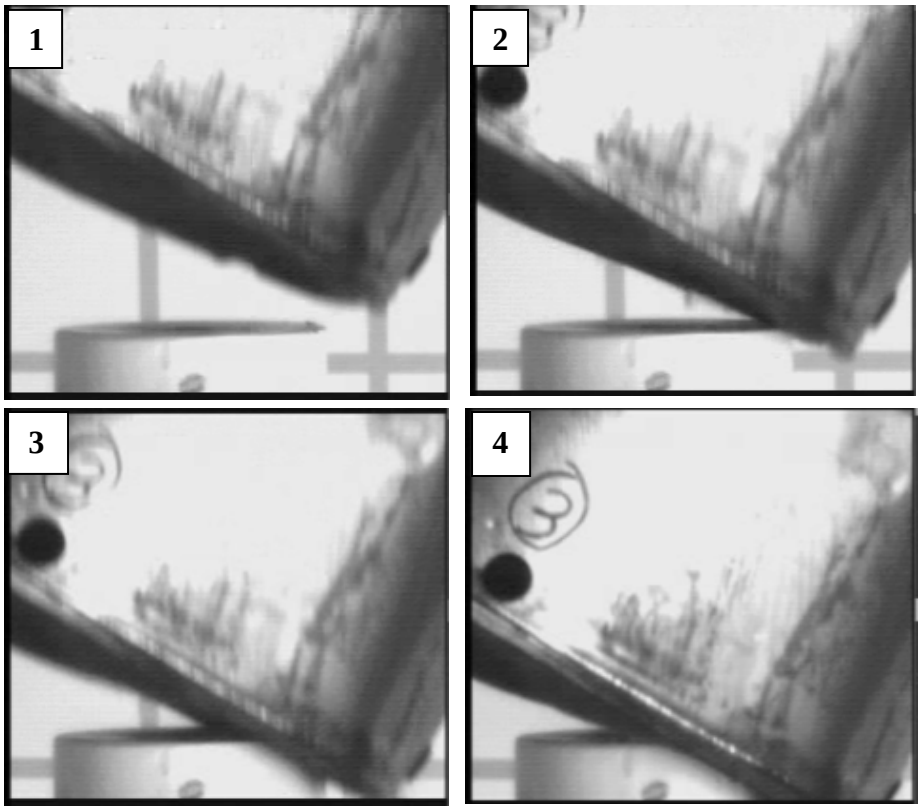

Figure 60 - Puncture Test 1 Initial Impact Sequence

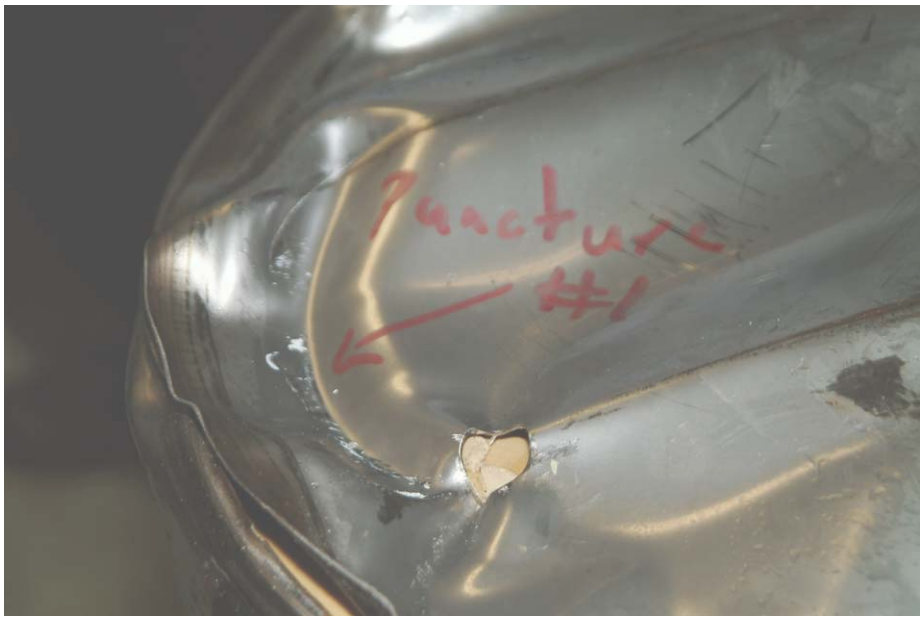

Figure 61 - Puncture Test 1 Pin Impression

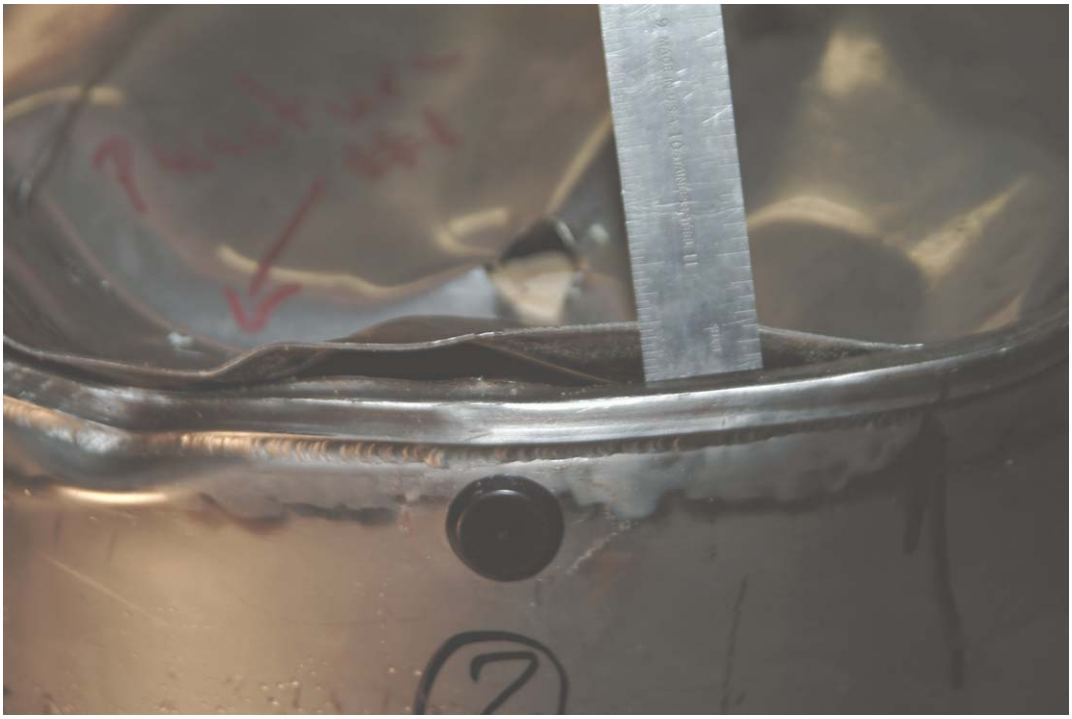

Figure 62 - Puncture Test 1: Drum Bottom Gap Opening 1/2 Inch Maximum

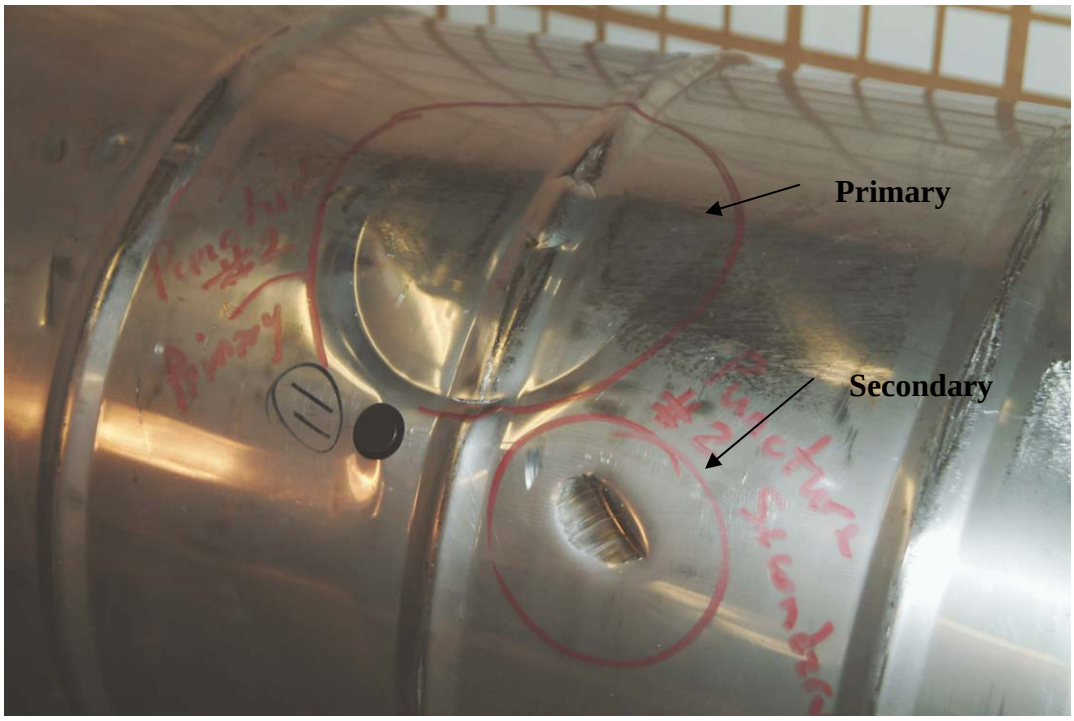

Figure 63 - Puncture Test 2 of SN-3: Primary and Secondary Dents Noted

5.2.3.4 Thermal Test

SN-3 was placed in the test fixture in the horizontal position as shown in Figure 64. It was observed by test personnel, while removing the band heaters, that the foam at the bottom of the drum where the tear occurred was melted and discolored: see Figure 65

The pool was filled with approximately 75 gallons (189 liters) of fuel then ignited at approximately 0819 hours by an SCFA employee. Within less than a minute the package was fully engulfed and the test was officially started. A photo of the fire engulfment is shown in Figure 66. The fire was fed with fuel until 0849 hours. The flames died out such that at 0853 hours, the packaging was no longer fully engulfed. The pool fire consumed 605 gallons of fuel.

A post test photo of SN-3 is shown in Figure 67.

The 30-minute average temperatures and environmental conditions during the test for SN-3 are listed below in Table 14.[22] All TC were calibrated prior to the test.

Table 14 - Thirty Minute Average Thermal Test Temperatures and Conditions for SN-3

SN-3	Fire (8 TC)	DFT (4 TC)	Package Surface (2 TC)	IRT (range)
Temperature Average(ºC)	800	972	963	888-1099[a]
Range and Average Wind Speed (knots/(mph))	Range: 2.4 – 7.3 (2.8 – 8.5), Average: 4.3 (5.0)			
Range and Average Ambient Temperature (ºC)	Range: 1.3 – 2.1, Average: 1.6			

Table 14 Notes

a. The IRT minimum reading of 888C was taken at the 30 minute mark as the fuel supply was cut off.

SN-3 lost approximately 71% of its foam mass during the thermal test (Refer to Table 10).

The heat from the thermal tests drastically degraded the polyurethane foam as seen in the radiograph Figure 68. The foam in the bottom portion of the drum was completely charred leaving only the Fiberfrax® blanket covering the bottom portion of the drum liner. The opening caused by the crush test in the bottom of the drum contributed to this condition.

The undamaged foam is separated into two lobes around the drum liner. The foam deteriorated longitudinally along the drum liner in the same locations as the two cracks seen in previous radiographs. Before and after thermal test radiographs are shown in Figure 69 and a negative image of the post thermal condition in Figure 70. The radial cracks provided a thermal pathway for the thermally driven degradation mechanism to exploit, causing increased degradation of the polyurethane foam in those locations.

Figure 64 - HAC Thermal Test Orientation of SN-3

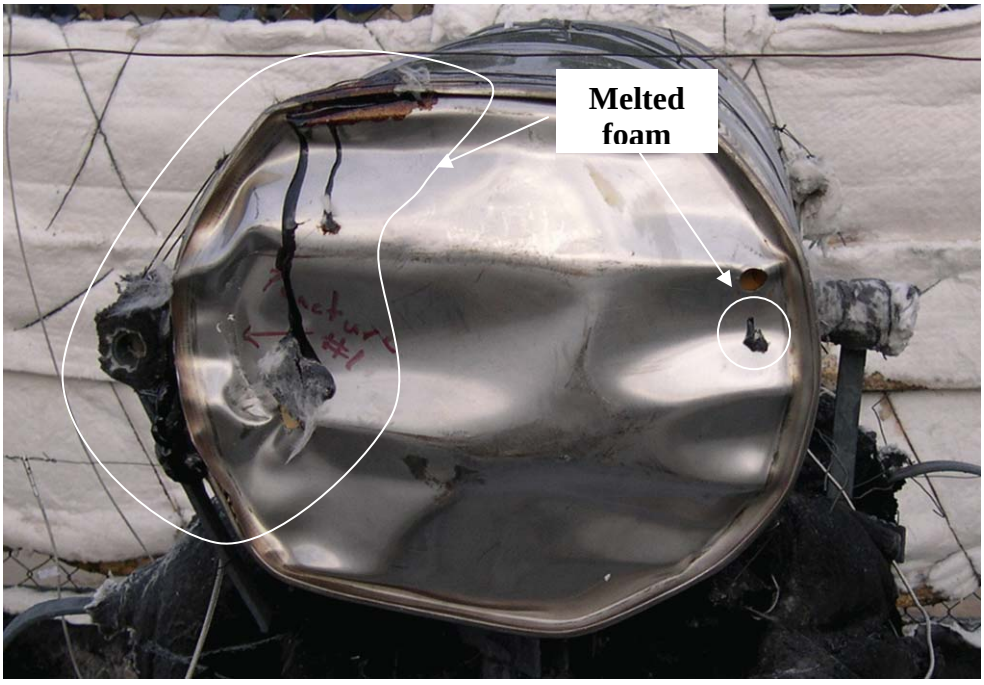

Figure 65 - Foam Melted at SN-3 Drum Bottom from Band Heaters

Figure 66 - HAC Thermal Test in Progress of SN-3

Figure 67 - Post HAC Thermal Test of SN-3

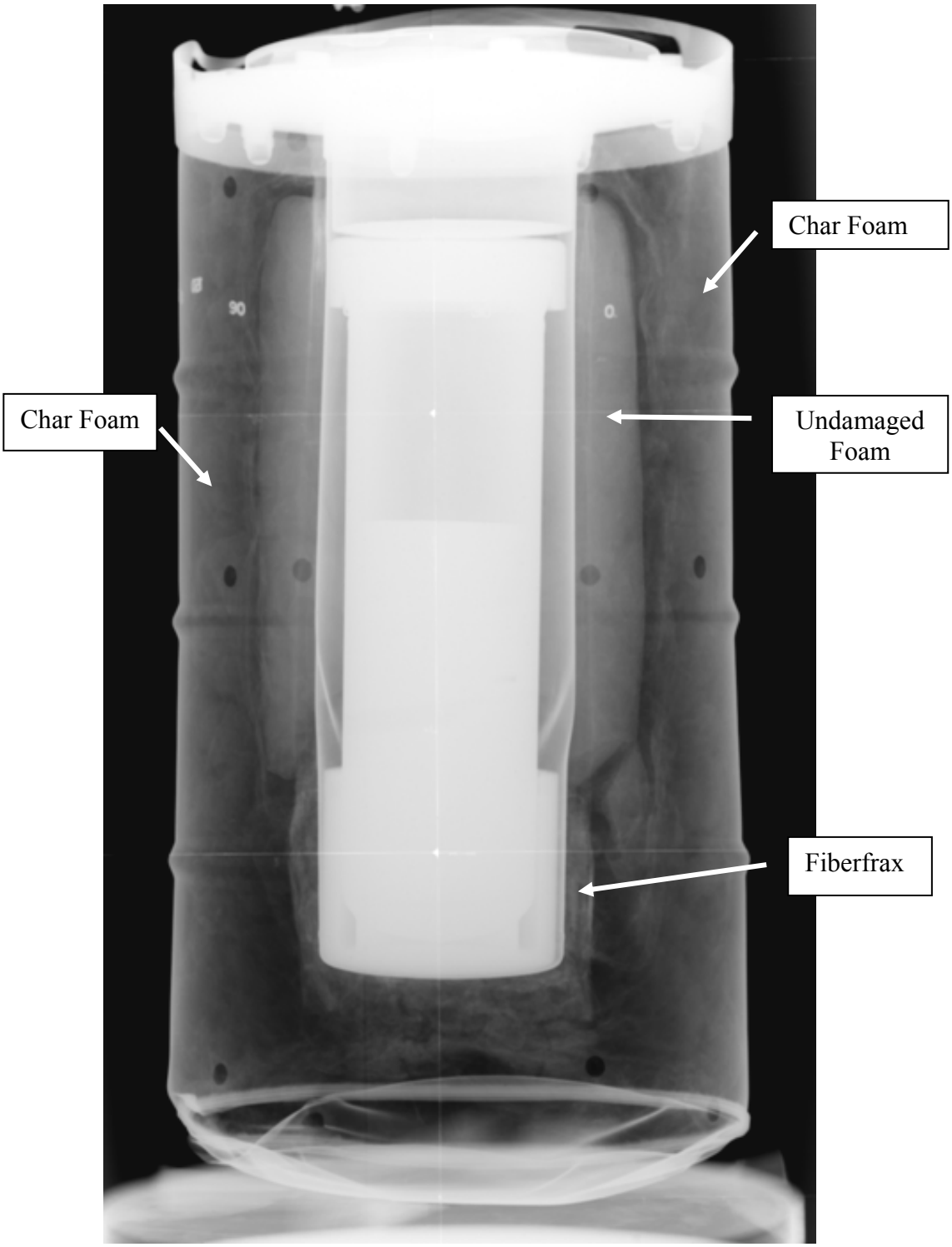

Figure 68 - Post Thermal Test Image of SN-3

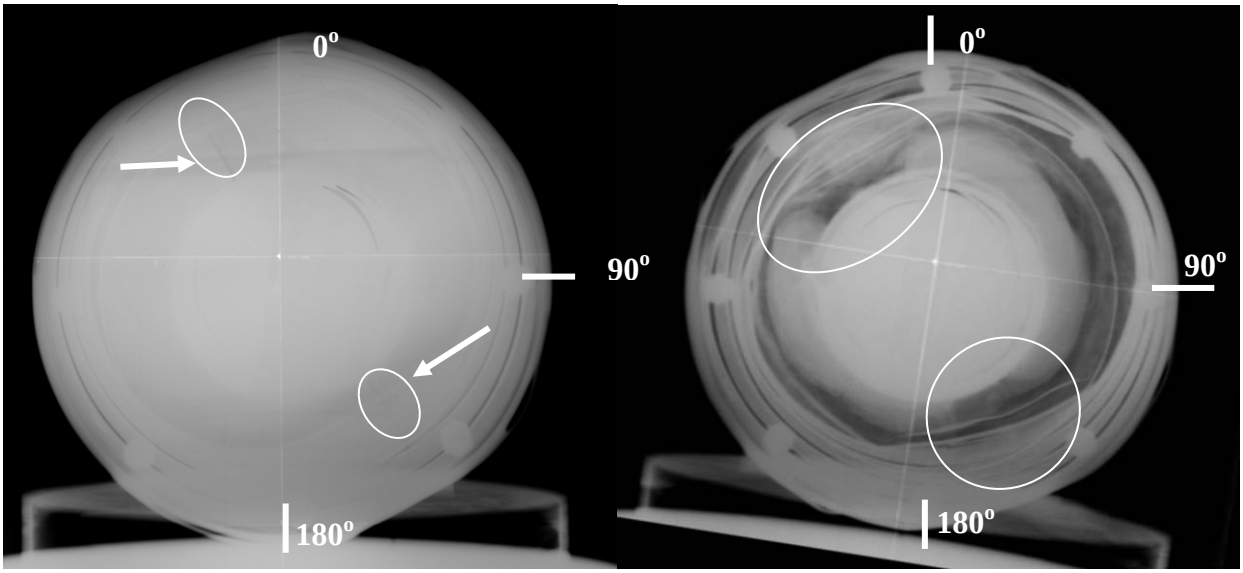

Figure 69 – Left: Radial cracks regions indicted in insulation at 330 degrees and 150 degrees prior to thermal test. Right: Deterioration of foam indicated at 330 degrees and 150 degrees after the thermal test.

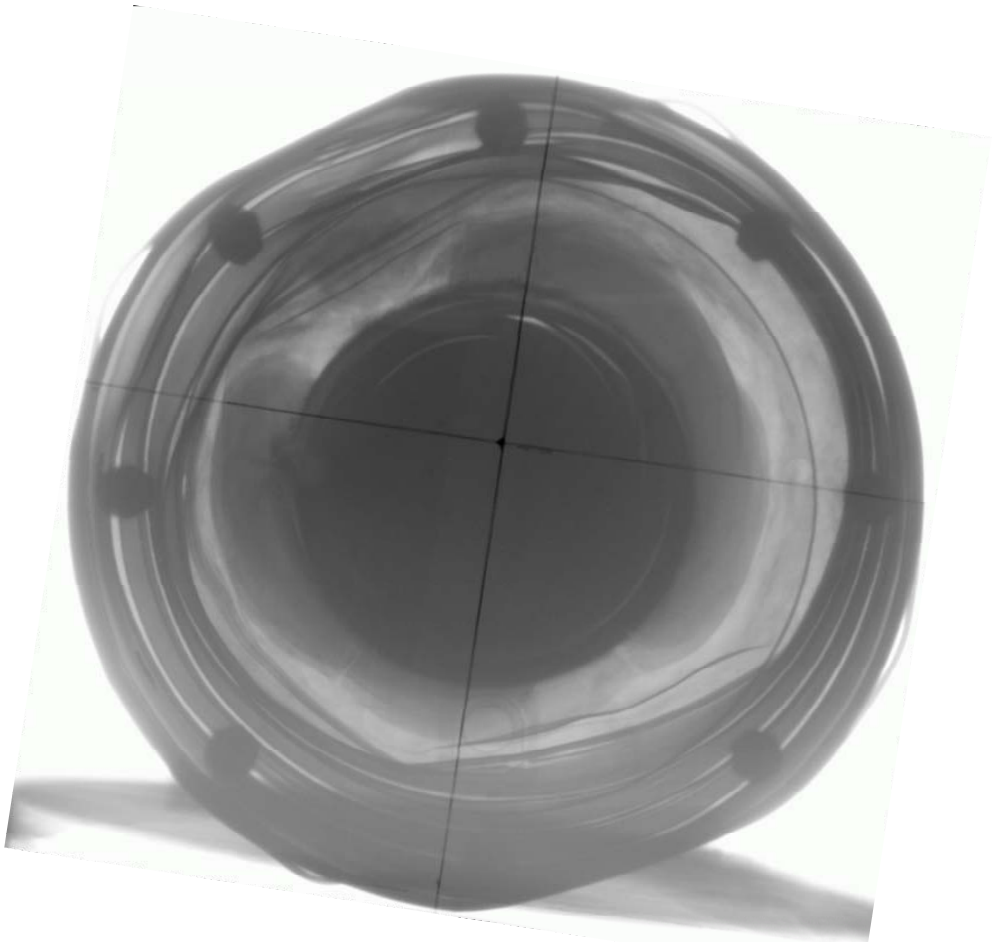

Figure 70 - Negative Image of SN-3 to Emphasize Foam Loss

5.2.4 Post-Test Packaging Disassembly and Examination

Packaging disassembly and examination was performed per FP-1039, as described previously in Section 5.2.1 of this report.

5.2.4.1 Disassembly

Prior to disassembly, the condition of the drum observed to have an overall oxidized surface, with some charred foam residue around the vent holes. This condition is typical of all the prototypes (e.g., Figure 34). The drum bottom opening increased one full inch, from ½ in to 1 ½ in, due to the combination of heat from the pool fire and pressure from the foam expansion and migration out of the packaging.

The drum lid cap was slightly bulged from the thermal test. Two of eight lid bolts had to be cut off, but the remaining bolts were loosened with a torque wrench to remove the lid. The bolt breaking torques ranged from 20 - 240 in-lbs (1.6 – 20 ft-lb). The top load distribution fixture was removed, then the CV. The CV was inspected for deformation, discoloration, and exterior temperature label data.

The drum was cut into sections as illustrated in the Figure 71 sketch.

The 1st sectional cutting of the drum was made parallel to the crushed sides of the drum, at approximately 60 and 240 degrees, to expose a cross section of insulation in the region of the packaging that sustained the most damage from the HAC testing. The cut revealed a surface of mostly small pieces of loose, friable, lumps of charfoam. See Figure 72. Beneath the surface, the charfoam composition changed to a more plastic, layered form that was more rigid and stronger than the lumps. The loose charfoam was dug out and removed from the drum cavity to examine the condition of the remaining solid foam, Fiberfrax, and drum liner. See Figure 73. The excavated cavity revealed a layer of foam that had not been damaged by the heat. The solid foam consisted of 2 distinct pieces, separated at approximately 150 and 330 degrees, approximately 20-in long and 1 ½ to 2-in thick, with a 1 to 2-in gap between the lobes as shown in Figure 73. The remainder of the drum body was cut from the drum flange to expose the opposite side. The gap between the lobes on this side of the packaging tapered from 4 to 9-in, towards the bottom of the drum liner as shown in Figure 74. The Fiberfrax lining and undamaged foam was cut down the middle of the larger gap between the lobes. The lining and undamaged foam was slid off the drum liner to examine the insulation and drum liner, see Figure 75. Finally, the drum lid was cut in half (cross-sectioned) to expose the interior insulation for examination as shown in Figure 76.

5.2.4.2 Examination of Component Condition

The as found condition of the package components are as follows:

- No damage or anomalies to the CV were observed by the inspector, see Figure 77.

- The CV exterior temperature indicating labels were inspected and their indications recorded. See Table 8. The maximum temperature seen by the CV exterior walls was <270F, the labels on the CV lid were illegible or damaged. The maximum temperatures recorded on the other components are as follow: <370F on the lid underside, <320F on the top of the top load distribution fixture, <270F on the drum liner walls, and <340F on the drum liner interior bottom. The higher temperatures at the top and bottom of the drum liner cavity correlate to the greater foam loss at these regions.
- The condition of the foam composition ranged from mostly friable on the outermost regions near the drum interior walls, top, and bottom, to a pair of the 1 ½ to 2-in thick solid lobes on opposite sides of the drum liner midsection.
- The inspector observed an absence of solid foam (i.e., foam gap) 4-in down from the underside of the drum lid plate, and 8-in up from the drum bottom, as shown in Figure 73. The undamaged foam formed two lobes around the drum liner. The lobes were separated at 150 and 330 degrees.
- There was a 5/8 inch air gap around the drum liner top between the top edge of the Fiberfrax liner and drum lid plate; however, the baseline and other radiographs prior to the thermal test indicate that gap was present before the thermal test. The section of Fiberfrax insulation covering the bottom of the drum liner was exposed (i.e., not enveloped with solid foam) for about 8 inches. At 330 degrees, a strip of Fiberfrax approximately 1 inch wide x 16 inches long was exposed (starting at the bottom of the foam), and at 150 degrees, a section of Fiberfrax approximately 4 inches wide for the entire length of the foam was exposed. Except for the narrow strip at 330 degrees, the fiberglass fabric liner, sheathing the Fiberfrax, was blackened, but was still solid and resistant to puncture. At 330 degrees, the fabric was torn along the center of the length. The Fiberfrax liner and undamaged foam were cut down the middle of the 4-in gaps between the foam lobes to examine the area in contact with the drum liner. The Fiberfrax cross-section exposed by the cut was light brown in color. Although degradation had started, the Fiberfrax retained its strength and form. The fiberglass fabric liner in contact with the drum liner was also discolored ranging from black to light brown; however, the colors lightened towards the areas protected by the remaining foam, where at the maximum foam thickness, the fabric liner retained its original white color as shown in Figure 75.
- The drum liner was distorted around the circumference just above the bottom load distribution fixture and at the top load distribution fixture. The major damage was just above the bottom load distribution fixture where “wrinkles” were formed by the drop and crush tests, see Figure 75 and Figure 78. Previous radiographs (Ref Figure 58) from HAC tests showed this distortion. The drum liner exterior surface was discolored in areas where hot gasses penetrated under the Fiberfrax fabric liner. The bottom of the drum liner was discolored with a tacky brown residue of melted fabric liner.
- The lid cross section revealed that the insulation in the lid pan was discolored along its circumference, but not in the area above the lid liner. The discoloration was most likely caused by the heat ingress through the ¼ in holes in the side wall of the pan. The insulation in the lid liner was discolored on the bottom facing the load distribution fixture, as shown in Figure 76.

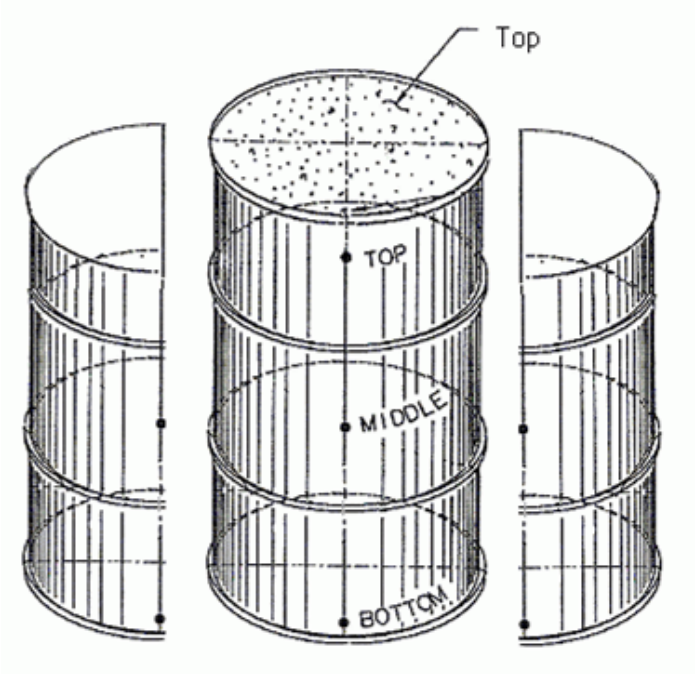

Figure 71 - SN-3 Sectional Cuts

Figure 72 - 1st Cross Section Cut of SN-3 Exposing Charfoam Layer

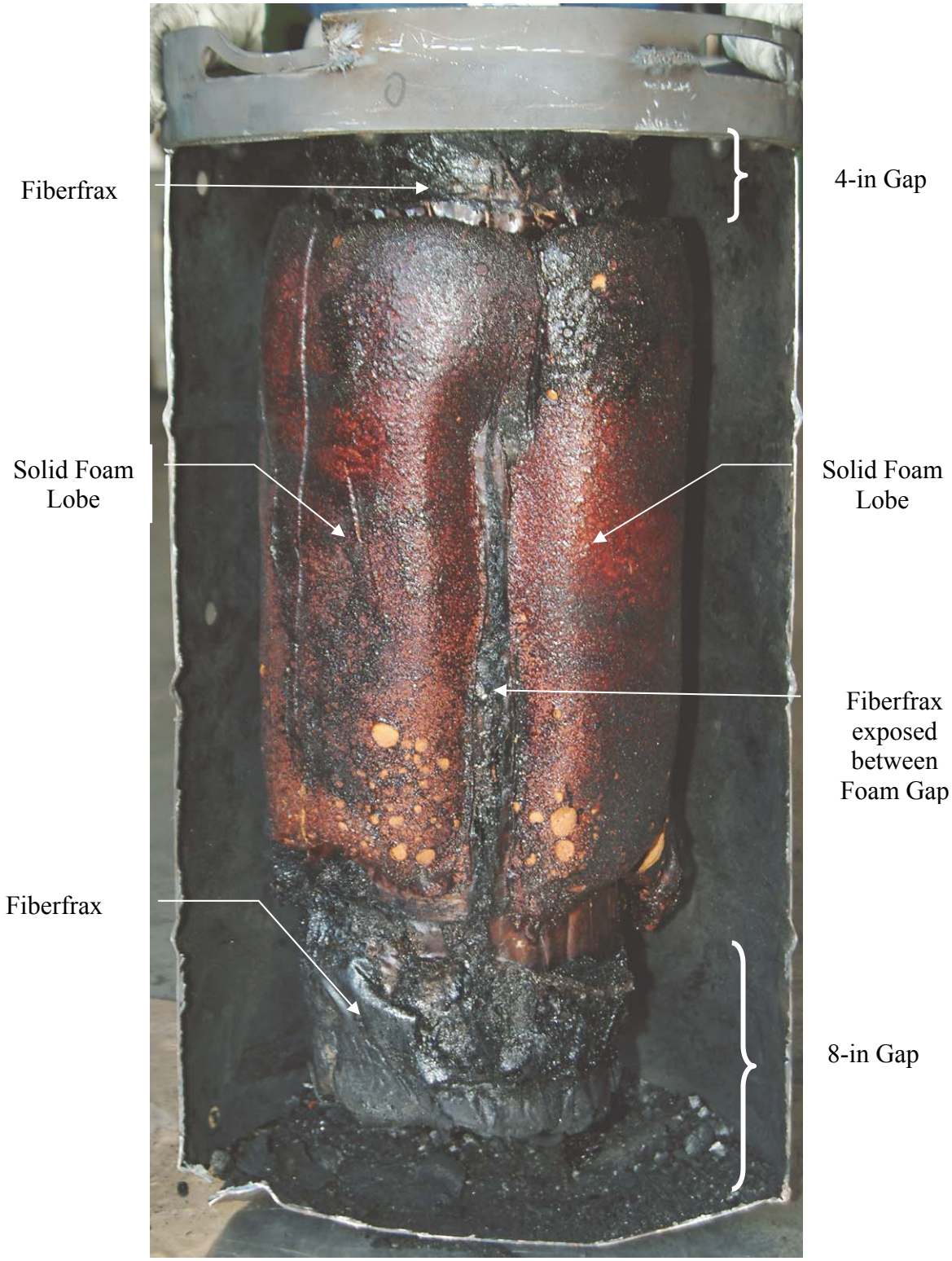

Figure 73 - Cross Section of SN-3 with Charfoam Removed

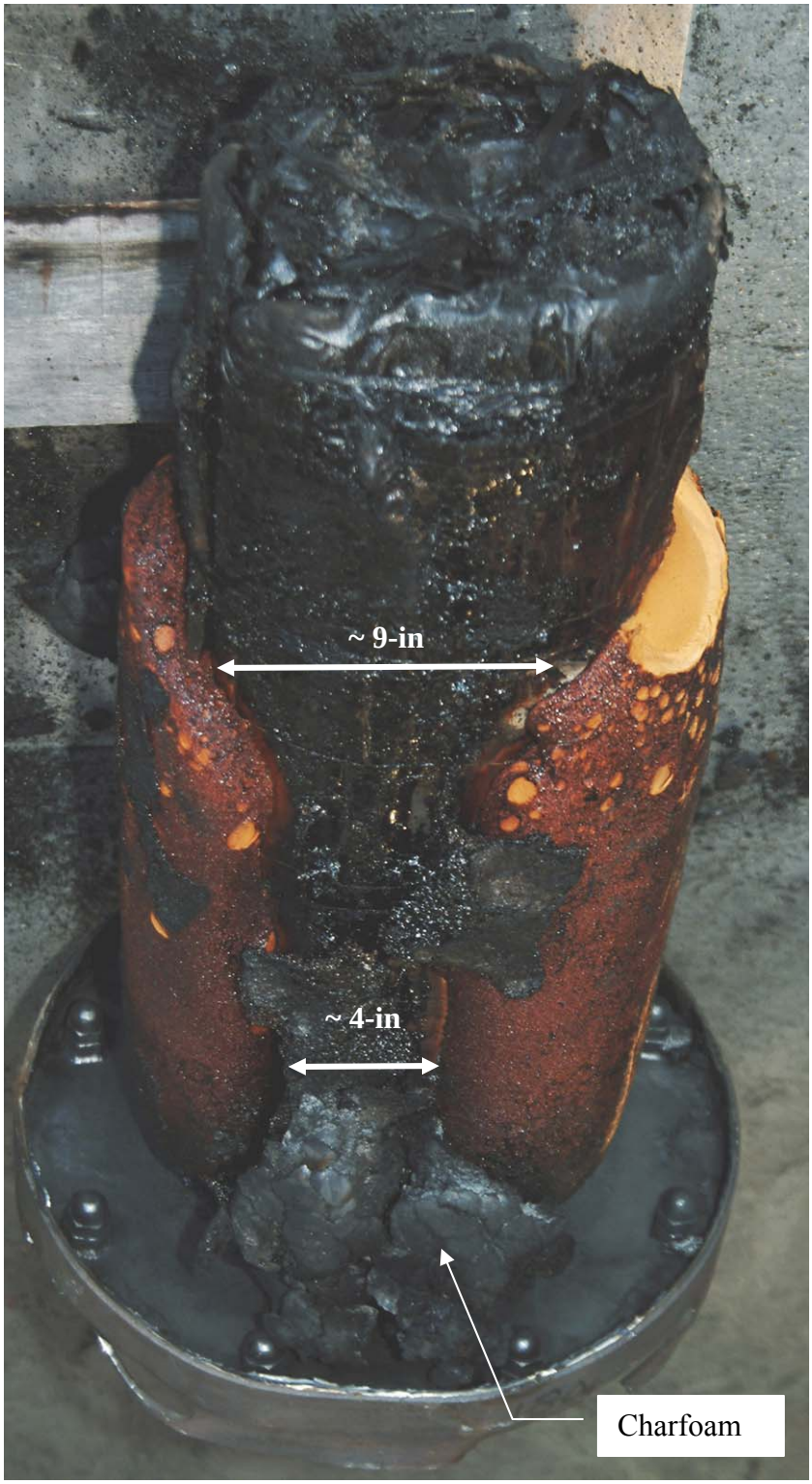

Figure 74 - Opposite Side View of Figure 73

Figure 75 - Insulation and Drum Liner of SN-3

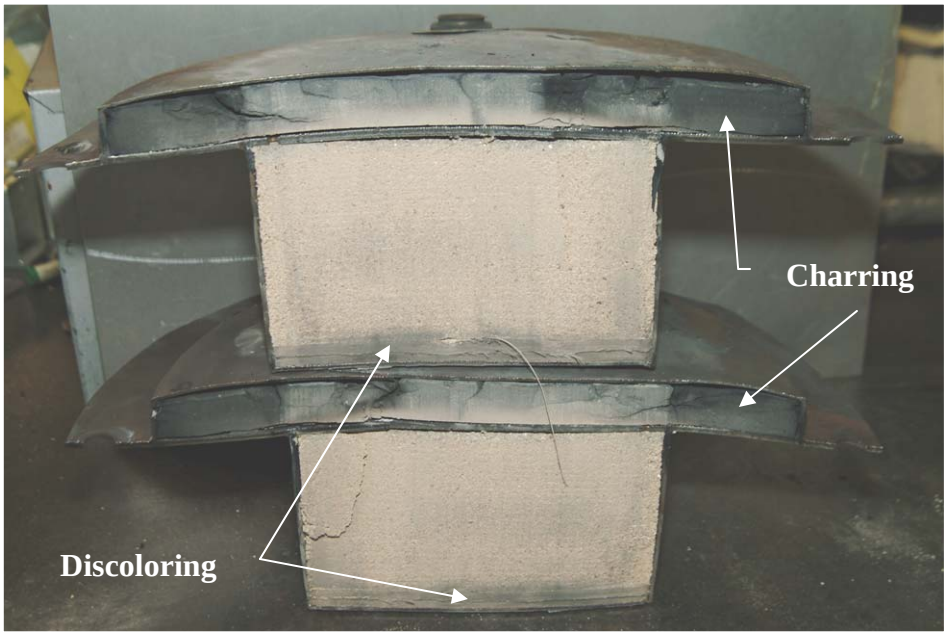

Figure 76 - Lid Cross Sections

Figure 77 - CV from SN-3

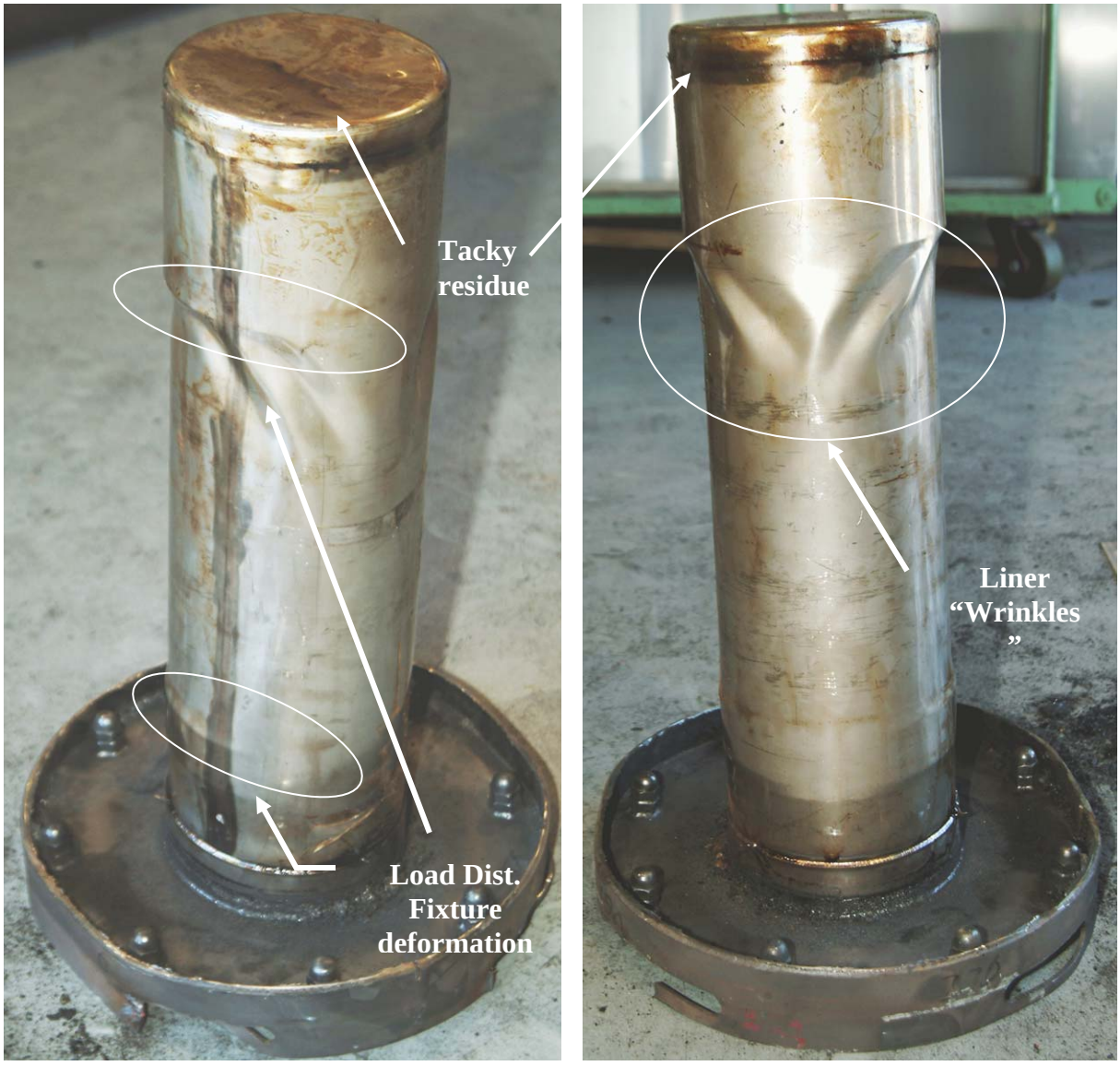

Figure 78 - Drum Liner Deformation

5.2.5 CV Leak Test and Disassembly

After the CV was removed from the SN-3 packaging and visually inspected, a helium leak test was performed to determine if the packaging had provided adequate containment of the contents. The measured leak rate of the CV was <1.8E-09 std-cc He/s (Ref Table 9), which demonstrates the packaging design provided adequate containment of the contents following the regulatory performance tests.

Following the leak test, the CV was opened to inspect and record the data from the internal temperature indication labels. The data is reported in Table 8; however, nearly all of the labels were damaged due to abrasion by the unrestrained surrogate contents. The internal temperatures along the CV body were: <270F at the top, <250F at the middle, and <250F at the bottom. The temperatures on the underside of the CV lid and inside bottom were <270F and <250F respectively. Despite the foam loss at the bottom and sides of the drum liner, the CV was well insulated by the charfoam and Fiberfrax insulation.

5.3 Prototype SN-4

5.3.1 Baseline Radiograph

The baseline radiographs of SN-4 show unfurled Fiberfrax at the base of the drum liner, which is typical of all units, and single foam void extending approximately 1/3 the length of the drum liner. In the end-to-end radiographs, it is a radial indication located at approximately the 75 degree radial line, as shown in Figure 79.

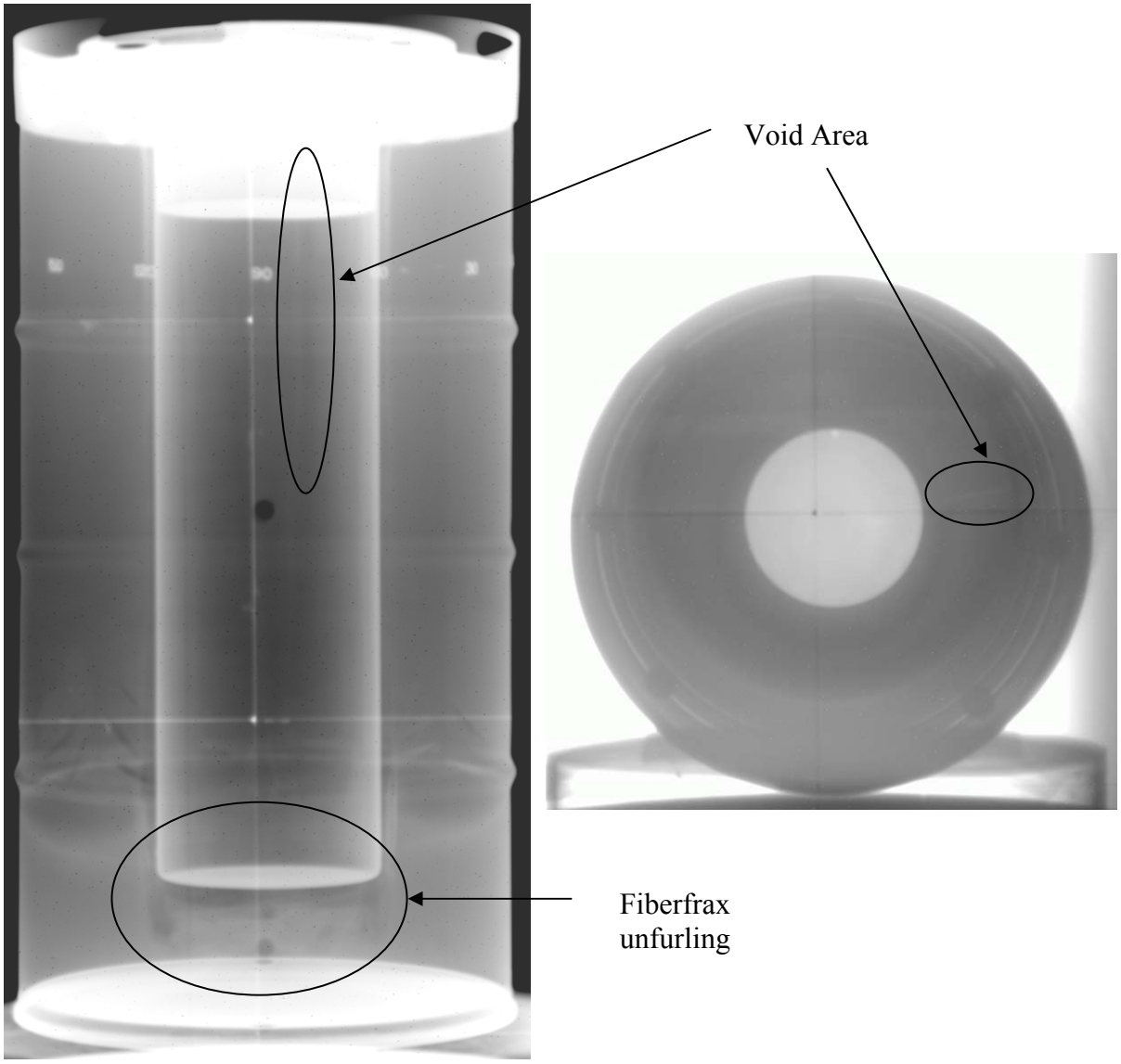

Figure 79 - Baseline Images of SN-4

5.3.2 NCT Tests

The NCT tests were not performed on this package.

5.3.3 HAC Tests

SN-4 was tested in ambient air conditions for the drop, crush, and puncture tests.

5.3.3.1 30-ft Drop Test

The 30-ft drop was performed with the packaging oriented top-down in the vertical position. The test setup is shown in Figure 80.

The package struck the target pad, rebounded approximately 2-in vertically, and landed within 10-in of the primary impact area. The rebound of the surrogate contents within the CV during the initial impact could have dampened the overall rebound response of the packaging. The test was videotaped with a high speed camera and camcorder.

The primary impact resulted in:

- Formation of a buckle, much like a rolling hoop, along the circumference of the drum, directly beneath the drum flange weld. The hoop was more pronounced on the side of the drum from Ref Marks 5-8: see Figure 81.
- Reduction in the overall height of the drum at the point of impact by ¼-in from Ref Marks 1-5 and 4-8. The height of the opposite side (Ref Marks 2-6 and 3-7) was unchanged. The "rolling hoop" formation correlates to the change in height of the drum. The dimensional shift was in the direction of the drop top, where the impact occurred.
- Lid cap form changed from a flat to dome shape. The dome extended ½ inch above the drum flange, as shown in Figure 82.
- The lid assembly heaved with series of mostly uniform scallops (humps) on the lid between the bolts. The gap sizes were approximately 1/8 inch tall. See Figure 83.

There was no damaged caused from the secondary impact.

The radiograph images after the 30-drop in Figure 84 show a mushrooming of the bottom of the drum lid liner, which was pinched between CV and top load distribution fixture and the drop test pad, and a large gap between the top load distribution fixture and the drum lid. . There was no discernable damage to the polyurethane foam and no changes in the general position of drum liner and contents.

Figure 80 - HAC Drop Test Setup SN-4

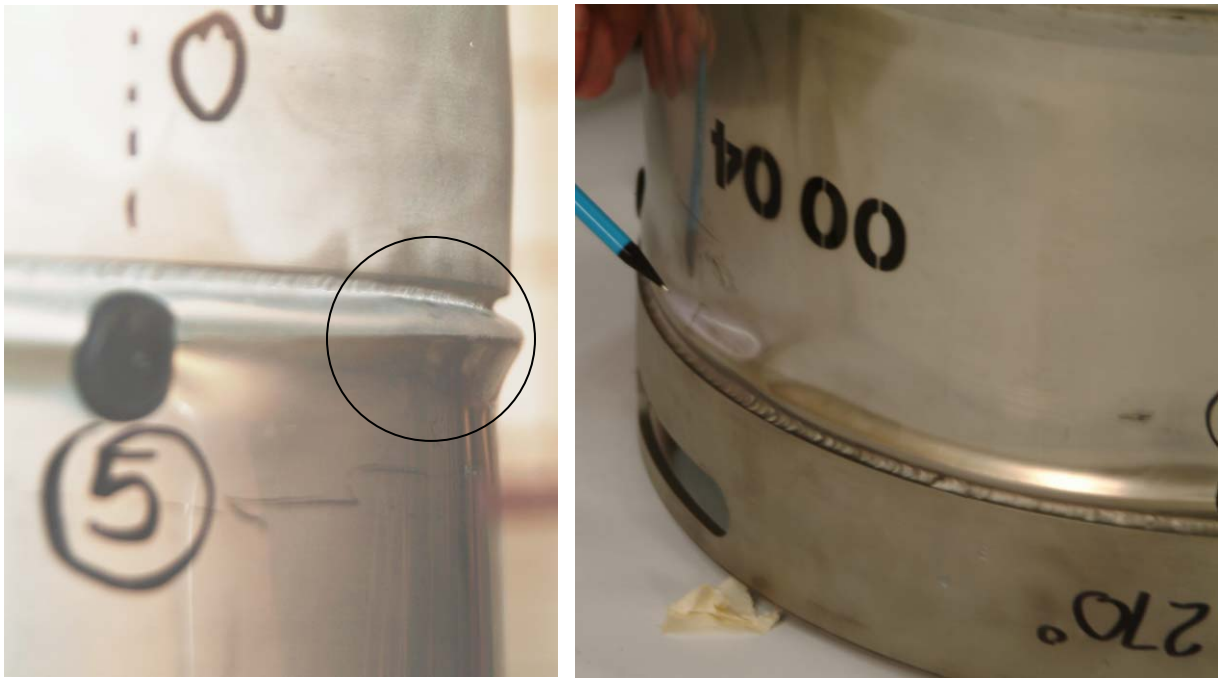

Figure 81 - Formation of New Rolling Hoop below Drum Flange Weld Indicated

Figure 82 - Drum Lid Cap Dome, Approximately ½ in Tall on SN-4

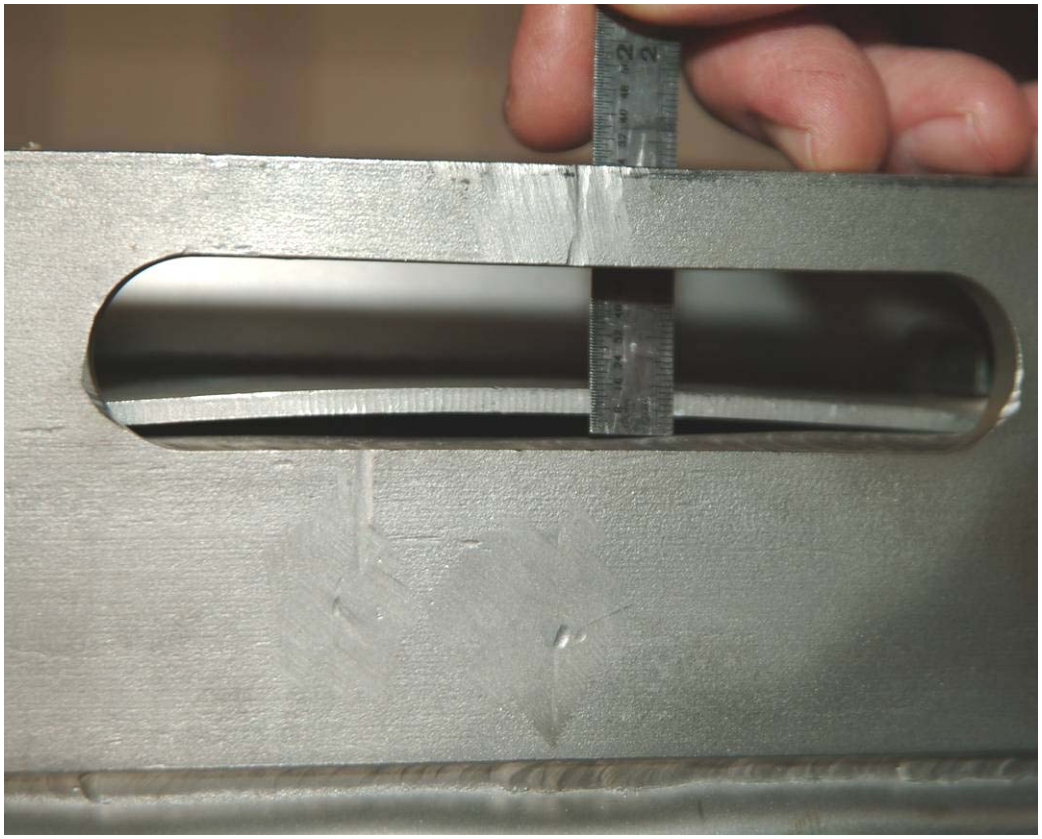

Figure 83 - Drum Lid Flange Gap 1/8 in Tall between Bolts

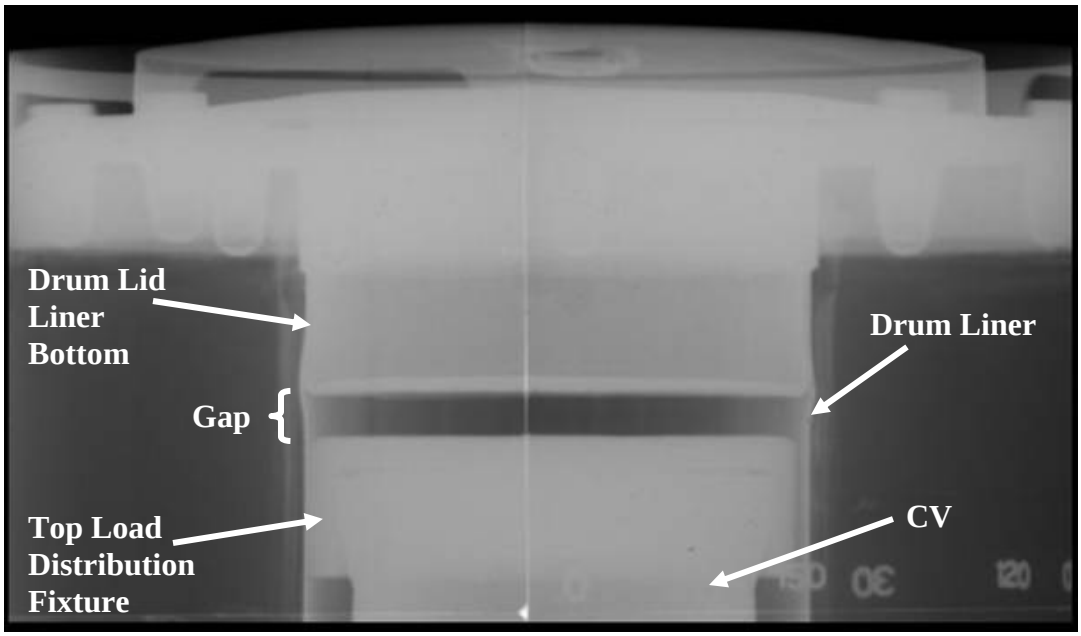

Figure 84 - Mushrooming of the SN-4 Drum Lid and Formation of Gap

5.3.3.2 Crush Test

The 30-ft crush test was performed with the packaging oriented top-up in the vertical position. A setup of the test is shown in Figure 85.

The crush test plate struck the packaging at a 9-degree, leftward tilt as seen in the Figure 86, striking over reference Ref Marks 2-10-6, or the 90-degree packaging view (Figure 4). The package and plate rebounded energetically in the direction of the tilt angle. The package hit the ground and was then hit again by the plate near Reference Marks 11-7. Pre and post test photos are shown Figure 87 and annotated where applicable.

The test was videotaped with a high speed camera and camcorder.

The primary impact resulted in:

- Increase of the "rolling hoop" under the drum flange initiated by the drop test now spans the entire circumference.
- Bottom rolling hoop on the drum body was compressed. Maximum drum diameter is now 19 ½ in, originally 18 3/8 inches. See Figure 88 for a profile view.
- An imprint of the drum liner was transferred to the bottom of the drum. See Figure 89.
- The overall minimum and maximum height of the drum is now 34-13/16 and 35-3/8 in at Ref Marks 2-6 and 4-8 respectively. The original height at these locations was 36-1/16 and 36-1/8 respectively.
- The lid cap dome initiated by the HAC Drop, was flattened such that it no longer extends above the drum flange rim.

The second plate hit occurred near the top half of the drum nearest Ref Marks 11-7. See Figure 90. The plate corner created a dimple near Ref Mark 11, minor flattening of the rolling hoops (including the one formed under the drum flange), and inward bend of the drum flange. See Figure 91.

The radiographs indicate that the CV and foam were not damaged from the crush; however, the lid and drum liner are severely deformed. The lid is firmly crimped in the drum liner cavity. The top of the drum liner bucked from the compressing effect of the plate impact. See Figure 92 for a Post Drop and Crush comparison in the lid region.

Figure 85 - HAC Crush Test Setup of SN-4

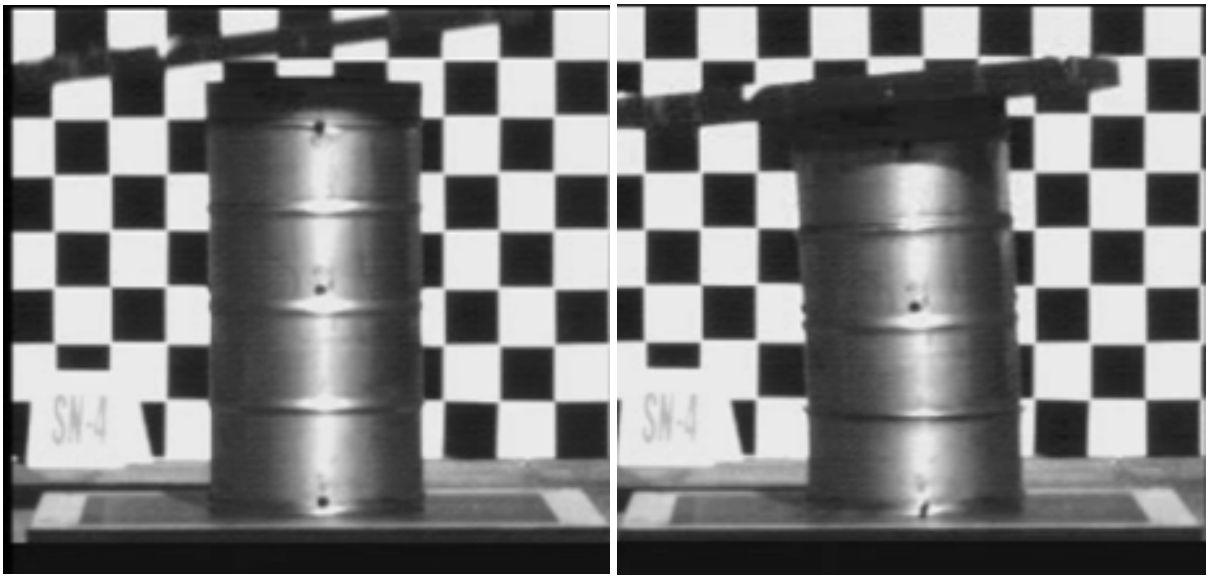

Figure 86 - Angle of Plate Impact (9 degrees) and Initial Crushing. Ref Marks 1-9-5 are facing Camera. Ref Marks 2-10-6 take Initial Impact.

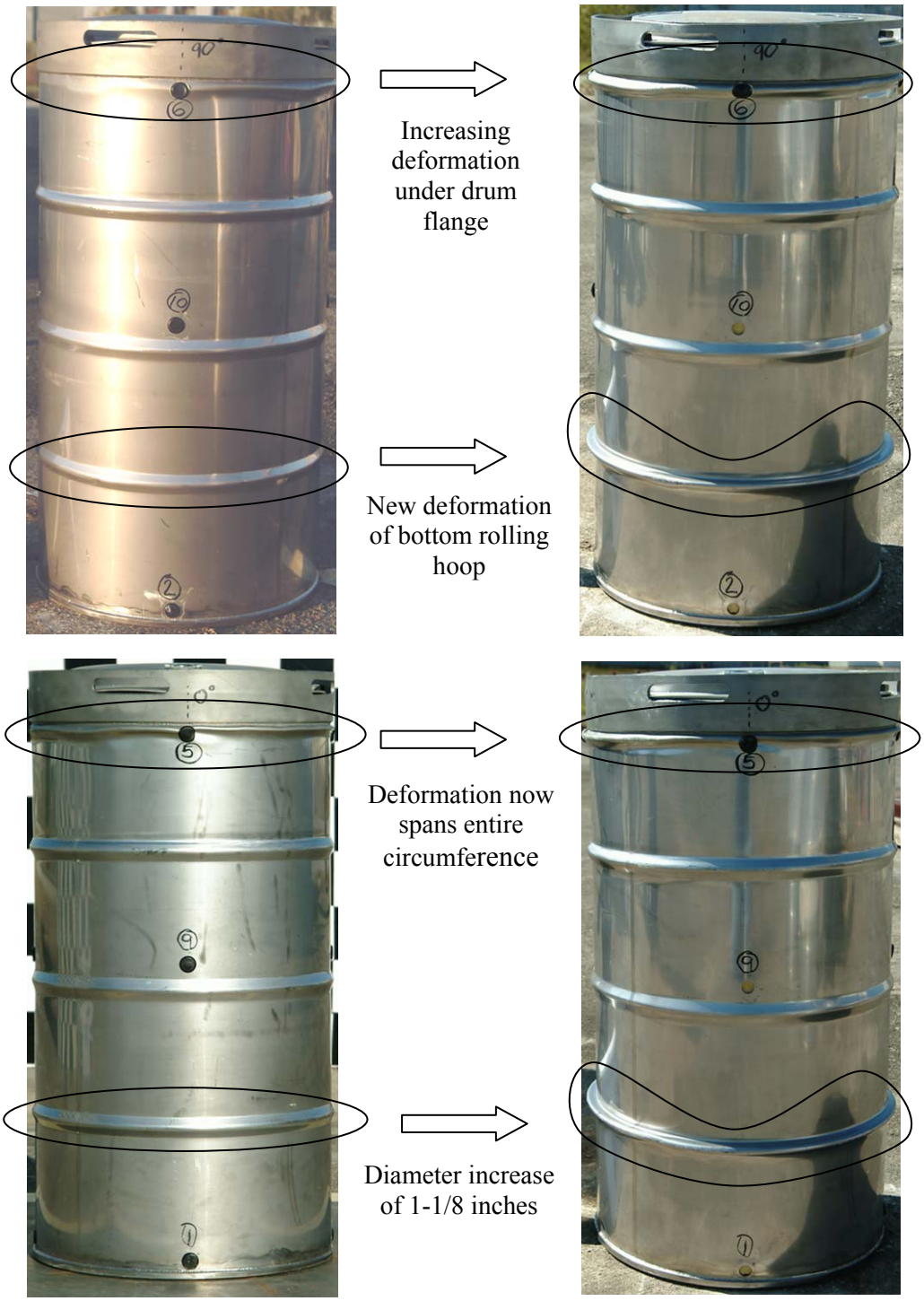

Figure 87 - Pre and Post Crush Test Views of SN-4. Top Photos Show the 2-10-6 Plane (90-degree View) where the Plate Hit Directly and Caused Most Deformation. The Bottom Photos Represent the Deformation on the Adjacent Plane (1-9-5)

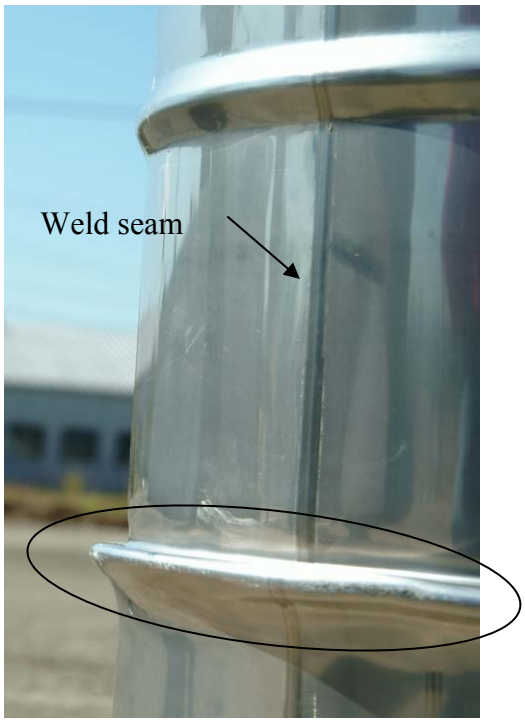

Figure 88 - Bottom Rolling Hoop Deformation Profile

Figure 89 - Drum Liner Imprint Stamped on Drum Bottom

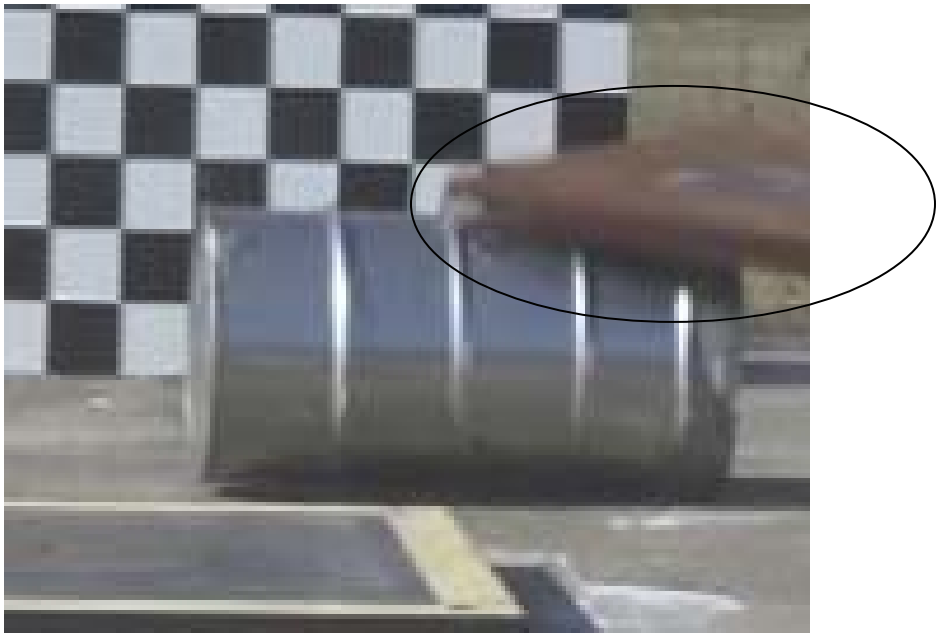

Figure 90 - Second Plate Hit on SN-4

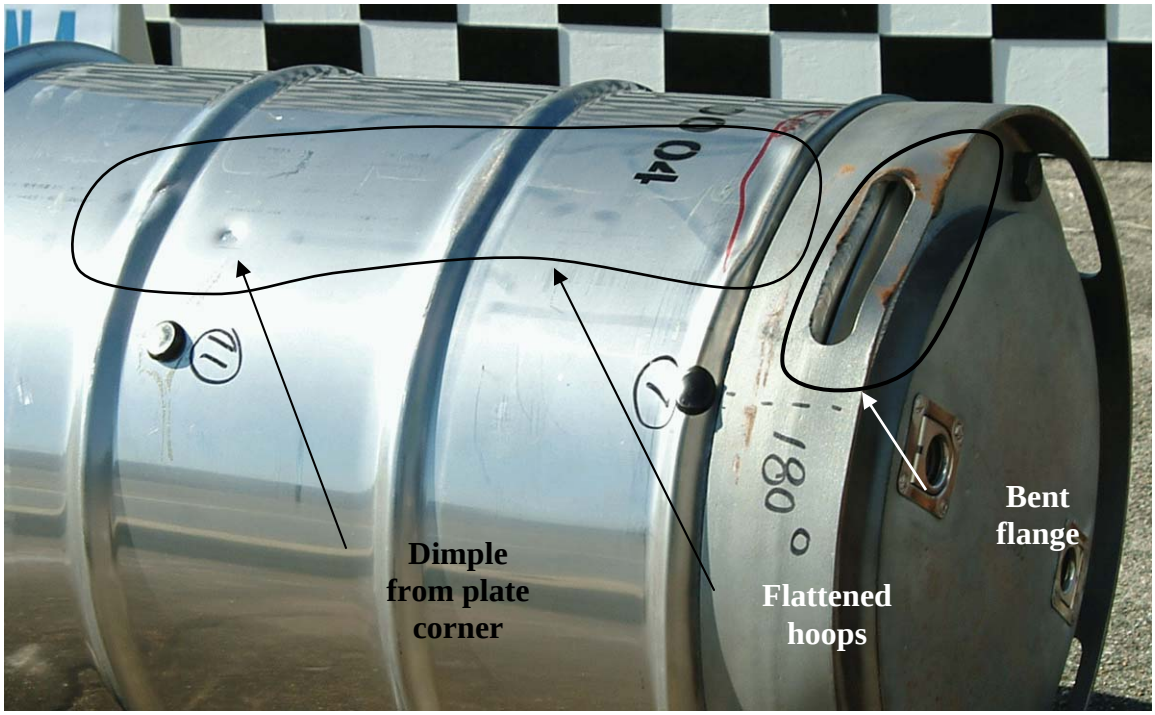

Figure 91 - Damage from Second Plate Hit Contact Points Indicated

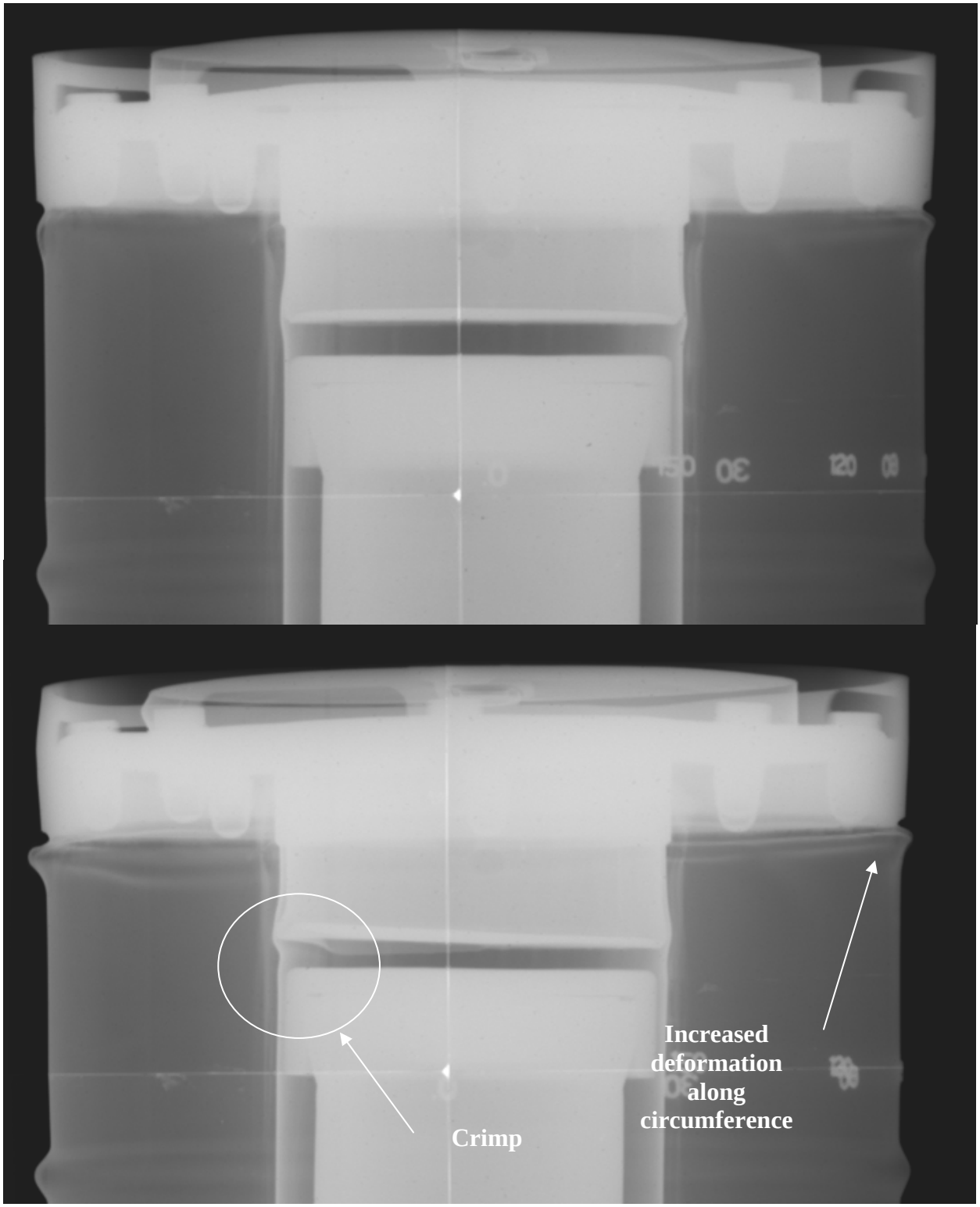

Figure 92 - Lid Damage Region Post Drop (top) and Crush (bottom)

5.3.3.3 40-in Puncture Test

The 40-in puncture test was performed with the packaging oriented horizontally, to strike the puncture pin on reference mark 11. The test setup for SN-4 is identical to SN-2, Figure 28.

The packaging struck the pin on reference mark 11, rebounded, rotated, and struck the pin a second time at approximately 45 degrees from horizontal, just below the middle rolling hoop, then struck the pin a third time with glancing blow on the upper rolling hoop. The test was videotaped with a high speed camera and camcorder.

The primary impact resulted in an impression of the puncture pin top about reference mark 11. This damage was essentially identical to the previous horizontal puncture test (see Figure 29). The secondary hit produced a half-moon shaped dent about 4-in from Ref Mark 11. The dent was approximately ¼ deep, 2-in long, and 1-in tall. The third hit dented the upper rolling hoop. Figure 93 shows the damage to SN-4 from all three hits.

The package was not radiographed after the puncture test.

Figure 93 - Puncture Test Damage to SN-4

5.3.3.4 Thermal Test

SN-4 was placed in the test fixture in the vertical top-up position as shown in Figure 94.

The pool was filled with approximately 56 gallons (212 liters) of fuel then ignited at approximately 0854 hours by an SCFA employee. Within less than a minute the package was fully engulfed and the test was officially started. A photo of the fire engulfment is shown in Figure 95. The test was extended to 35 minutes due to observations that there were short intervals that the packaging was not fully engulfed. The fire was fed with fuel until 0929 hours, and within 1 ½ minutes the fire began to die out. The fire consumed an estimated 600 gallons of fuel.

A post test photo of SN-4 is shown in Figure 96.

The 30-minute average temperatures and environmental conditions during the test for SN-4 are listed below in Table 15.[22] All TC were calibrated prior to the test, except as noted.

Table 15 - Thirty Minute Average Thermal Test Temperatures and Conditions for SN-4

SN-4	Fire (8 TC)	DFT (4 TC)	Package Surface (2 TC)	IRT (range)
Temperature Average(ºC)	848	888	791[a]	962-1068
Range and Average Wind Speed (knots/(mph))	Range: 0.0 – 3.0 (0.0 – 3.5), Average: 1.6 (1.8)			
Range and Average Ambient Temperature (ºC)	Range: 1.9 – 3.2, Average: 1.5			

Table 15 Notes

a. These TC were not calibrated; consequently, the results reported are for information only: TC averages 860C (top of packaging) and 723C (bottom of packaging).

SN-4 lost approximately 69% of its foam mass during the thermal test (Refer to Table 10).

The radiograph of SN-4 is very similar to SN-2 (Ref Figure 33). The post thermal test radiograph, Figure 97, indicates a clearly delineated region of deteriorated foam (a.k.a. charfoam) between the drum and drum liner. However, an undamaged layer of foam still envelops the drum liner, except for a slight gap between the drum top plate and undamaged foam. The image also indicates that most of the foam at the bottom of the drum deteriorated.

Figure 94 - HAC Thermal Test Setup for SN-4

Figure 95 - Full Engulfment of SN-4

Figure 96 - Post Thermal Test View of SN-4

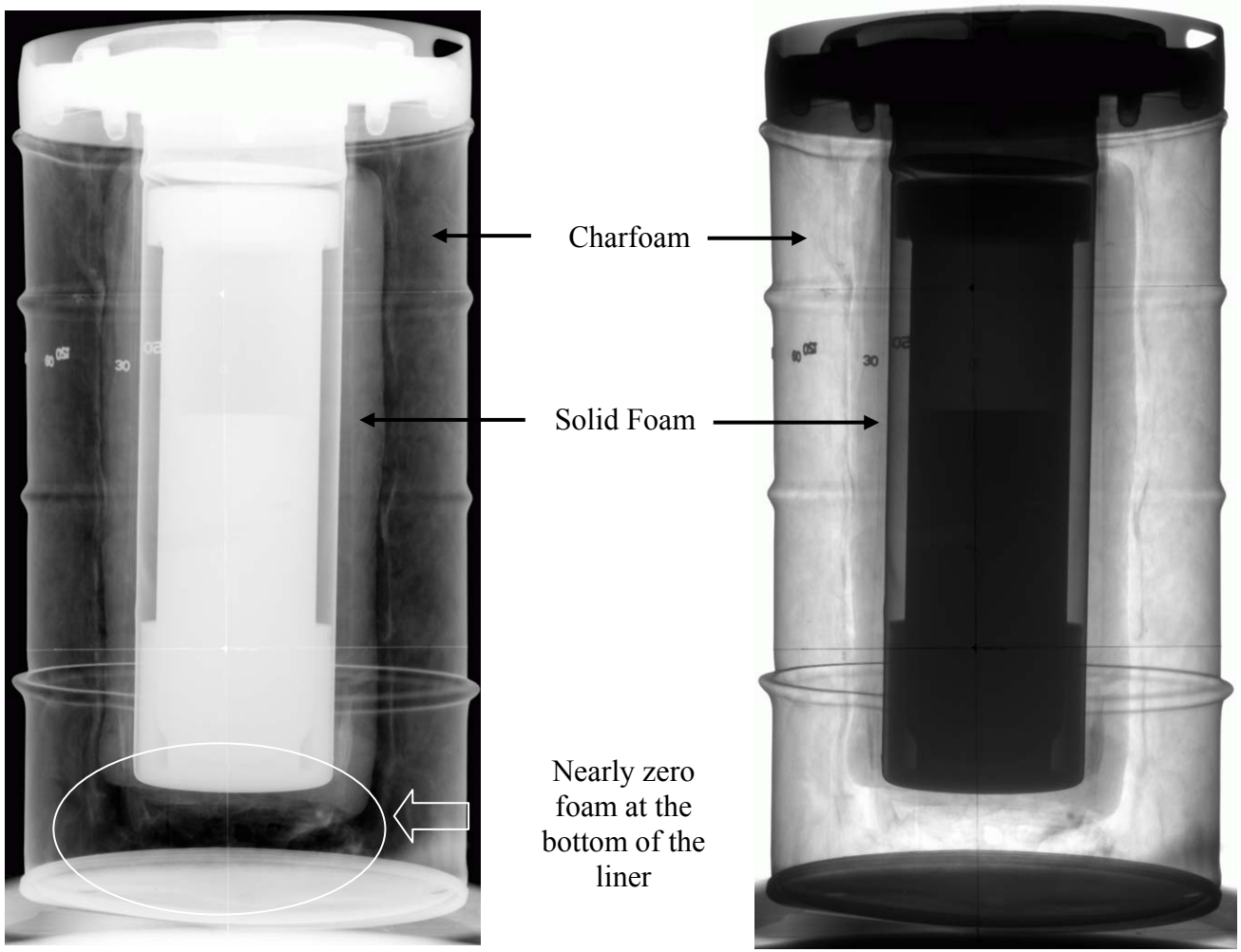

Figure 97 - Post Thermal Test Positive (left) and Negative (right) Image of SN-4

5.3.4 Post-Test Packaging Disassembly and Examination

Packaging disassembly and examination was performed per FP-1039, as described previously in Section 5.2.1 of this report.

5.3.4.1 Disassembly

Prior to disassembly, the condition of the drum was observed to have an overall oxidized surface, with some charred foam residue around the vent holes. This condition is typical of all the prototypes (e.g., Figure 34).

The drum was cut into 4 sections in the same steps as SN-2 (Ref Figure 35 sketch).

The package was turned upside down (i.e., top-down) to make the 1st sectional cut, which was a circumferential cut of the drum wall, approximately 1l-in above the bottom chime. Removal of the bottom drum section revealed mostly friable combusted foam (a.k.a., charfoam). The inspector observed that the foam was completely burned away from the bottom of the drum liner for 2 ½-in leaving a partial shell of the plastic-like charfoam. This condition is consistent with the radiograph. The bottom of the drum liner was covered with two ½-inch thick Fiberfrax discs. The Fiberfrax on the sides were wrapped over the edges of the discs and held with tape. The foam covering the bottom was completely burned away leaving only the Fiberfrax and tape. The Fiberfrax was discolored but was pliable and held its shape. See Figure 98 and Figure 99.

After the drum bottom section was separated and the loose foam removed, a circumferential cut was made below the estimated base of the drum liner, through the solid layer of foam and Fiberfrax, to expose the drum liner. The solid foam thickness enveloping the drum liner ranged from 1-1 ½ inches. The drum liner bottom was cut off, and the LDF removed and inspected. The CV was pulled out and inspected for deformation, discoloration, and temperature label data. The top load distribution fixture came out with the CV and was inspected. The drum lid was firmly crimped into the drum liner cavity, and not removed.

The 2nd and 3rd sections of the drum were made by 2-cuts along the long axis of the drum, 180 degrees apart, followed by a single circumferential cut below the drum top flange. These cuts completely separated the drum body from the package, exposing the remaining foam and drum liner. Some very thin, large flakes of foam material were observed on the outer charfoam surface. The inspector surmised that the combusted foam flakes appeared to have delaminated from the inside surface of the drum. During removal of these drum sections, loose charfoam separated and fell away from the less combusted foam.

The lid assembly was cut away from the drum body, but not destructively inspected; therefore the temperature indicating label on the side of the lid was not accessible.

5.3.4.2 Examination of Component Condition

The as found condition of the package components are as follows:

- No damage or anomalies to the CV were observed by the inspector.
- The temperature indicating labels were inspected and their indications recorded. See Table 8. The maximum temperature seen by the CV exterior was <250F, which was located at the top of the CV plug. The temperatures along the CV walls ranged from 210-260F. The temperature seen by the drum lid underside, which was also the highest temperature recorded, was 420-435F; however the temperature on the top load distribution fixture was only 280-290F.
- The condition of the foam composition ranged from mostly friable on the outermost regions near the drum interior walls to a progressively solid layer enveloping the drum liner.
- The undamaged foam extended from the bottom of the drum liner to within 3-in of the drum flange plate underside. At 75 degrees a gap starts at the top edge of the foam envelop and extends toward the bottom of the drum liner. The maximum gap opening is 3/16-in and the length is 8-inches. The gap narrows to a crack, which extends to the bottom end of the foam envelop. See Figure 100. This crack was identified on the pre-test radiograph.
- The upper 2-in of Fiberfrax lining near the drum flange plate underside, where the foam had burn away, was discolored by the heat, but not deteriorated. The lining at the bottom of the drum liner was also discolored, but not deteriorated.

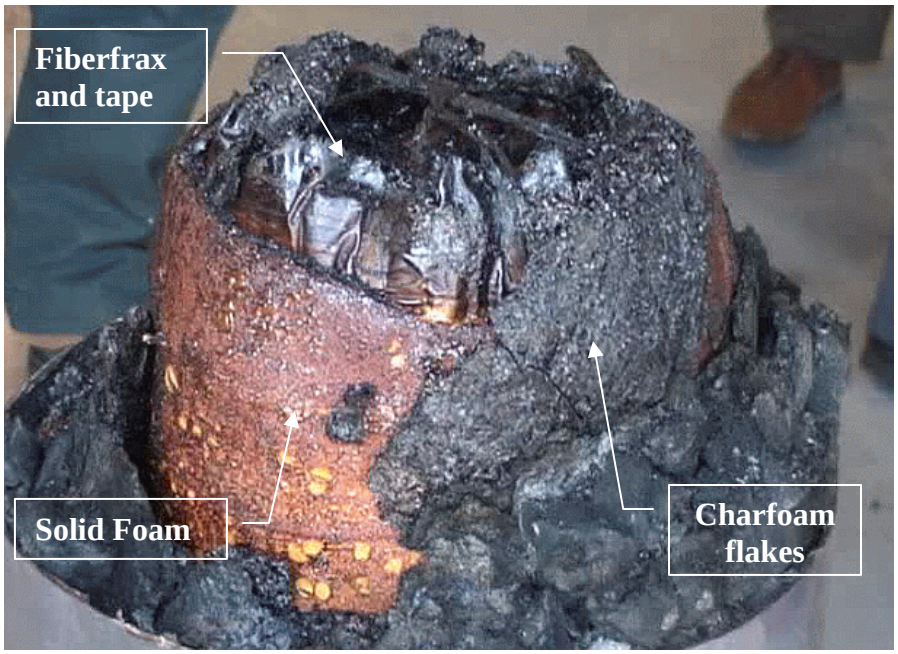

Figure 98 - Drum Liner Bottom of SN-4

Foam Section from Drum Liner Bottom

Fiberfrax Discs (2) under the Foam Section

Figure 99 - Foam and Fiberfrax Discs on the Drum Liner Bottom

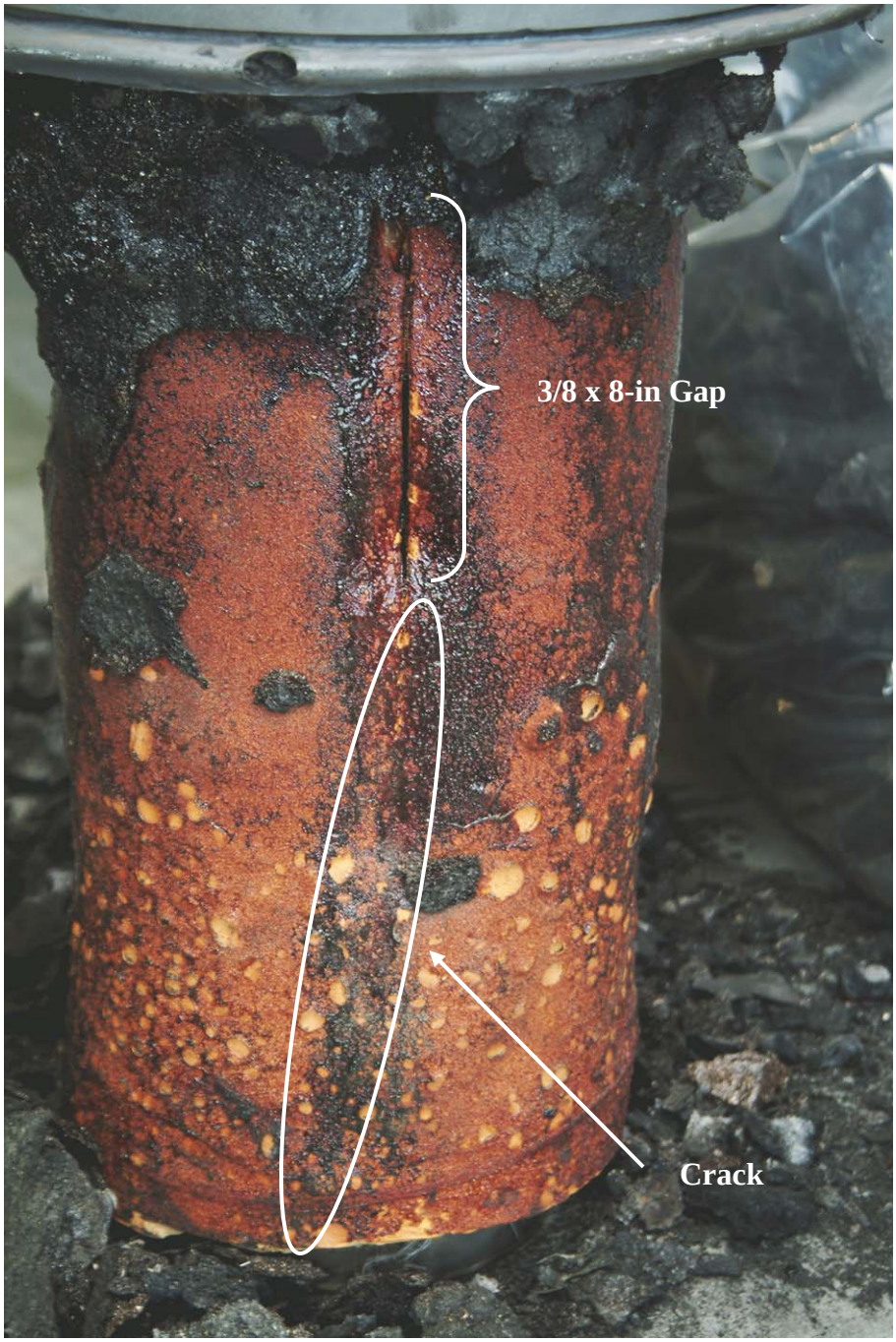

Figure 100 - Foam Gap and Crack on SN-4

5.3.5 CV Leak Test and Disassembly

After the CV was removed from the SN-4 packaging and visually inspected, a helium leak test was performed to determine if the packaging had provided adequate containment of the contents. The measured leak rate of the CV was <2.1E-09 std-cc He/s (Ref Table 9), which demonstrates the packaging design provided adequate containment of the contents following the regulatory performance tests.

Following the leak test, the CV was opened to inspect and record the data from the internal temperature indication labels. The data is reported in Table 8; however, nearly all of the labels were damaged due to abrasion by the unrestrained surrogate contents. The internal temperatures along the CV body were: 250-260F at the top, indeterminate at the middle, and <250F at the bottom. The temperature on the underside of the CV lid and inside bottom ranged from 260-270F and <250F respectively. Despite the foam loss at the bottom and top of the drum liner, the CV was well insulated by the charfoam and Fiberfrax insulation.

5.4 Prototype SN-5

5.4.1 Baseline Radiograph

The baseline radiographs of SN-5, without the CV and load distribution fixtures, show unfurled Fiberfrax at the base of the drum liner, which is typical of all units, and single foam void extending approximately ½ the length of the drum liner. In the end-to-end radiographs, it is a radial indication located at approximately the 375 degree radial line, as shown in Figure 101.

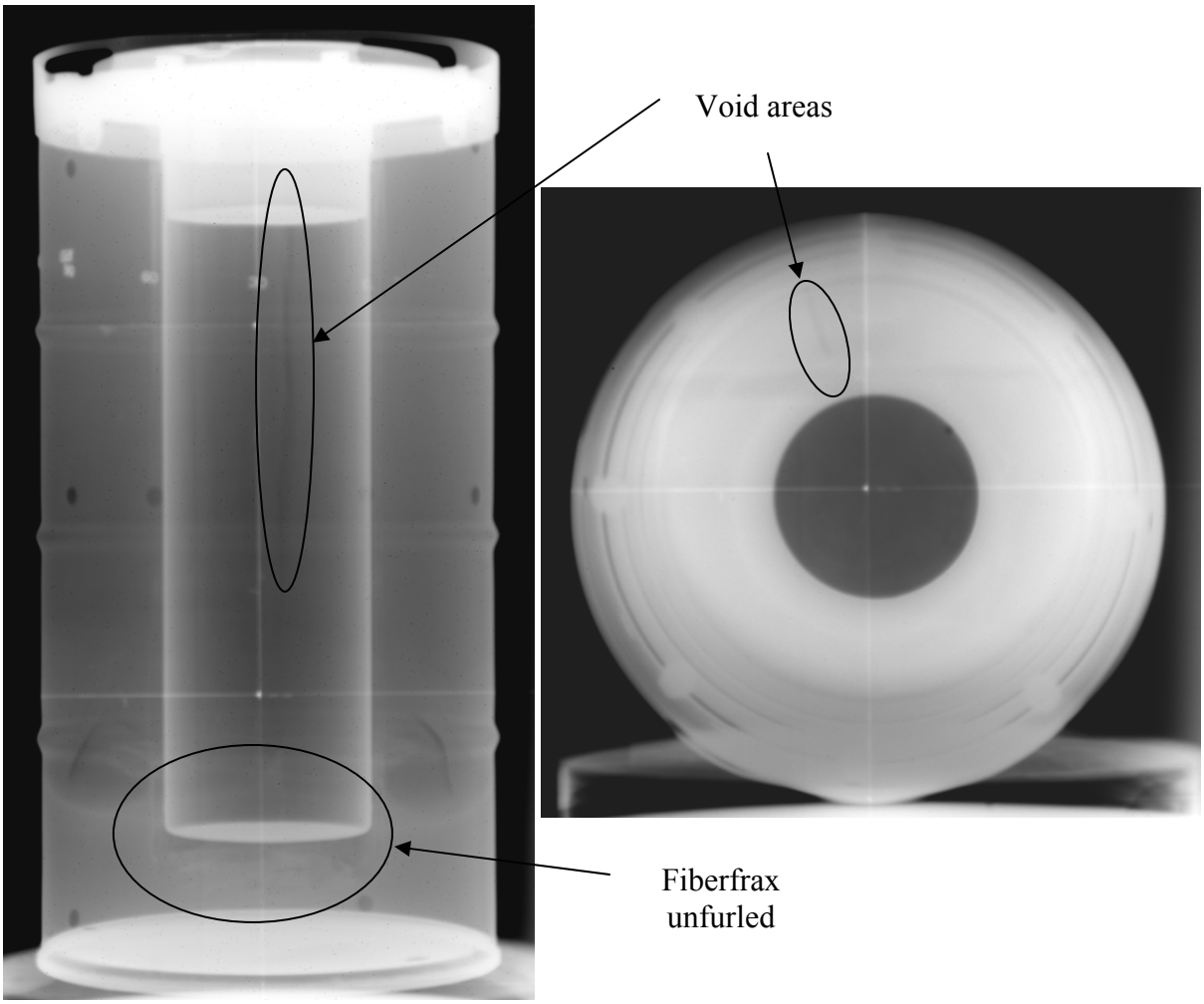

Figure 101 - Baseline Images of SN-5

5.4.2 NCT Tests

The NCT tests were not performed on this package.

5.4.3 HAC Tests

SN-5 was tested in ambient air conditions for the drop, crush, and puncture tests.

5.4.3.1 30-ft Drop Test

The 30-ft drop was performed with the packaging oriented bottom-down in the vertical position. The test setup is shown in Figure 102.

The package struck the target pad, rebounded very energetically approximately 5 ½ ft, rotated, and landed bottom first at a 45-50 degree angles. Photos prior to impact and at full impact are shown in Figure 103 .The test was videotaped with a high speed camera and camcorder.

The primary impact resulted in:

- Formation of a buckle resembling a new "rolling hoop" along the ¾ of the drum bottom chime circumference along Ref Marks 3-4-1, which increased the overall diameter from 18-3/8 to 19-3/8-in. The hoop was more pronounced on the side of the drum near Ref Mark 4. See Figure 104.
- Reduction in the overall height of the drum on 3 sides: Ref Marks 1-5, 3-7, and 4-8 changed by 3/8, ½, and 11/16 respectively. The lowest height is now 35 ¼ at Ref Marks 1-4. The height on the 2-6 side was unchanged from Marks 1-5 and 4-8. The height of the opposite side (Ref Marks 2-6 and 3-7) was unchanged.
- The bottom of the drum is essentially flush with the bottom chime. Typically the bottom is inset from the chime by ¼ inch.
- The drum leans away from the 2-10-6 side.

The secondary impact curled over a small section of the bottom chime, and then slightly bent the drum flange.

The radiograph images after the 30-drop show a slight deformation of the drum liner in the area of the drum liner near the lid bottom and the top load distribution fixture. See Figure 105. There was no other discernable damage observed.

Figure 102 - HAC Drop Test Setup of SN-5

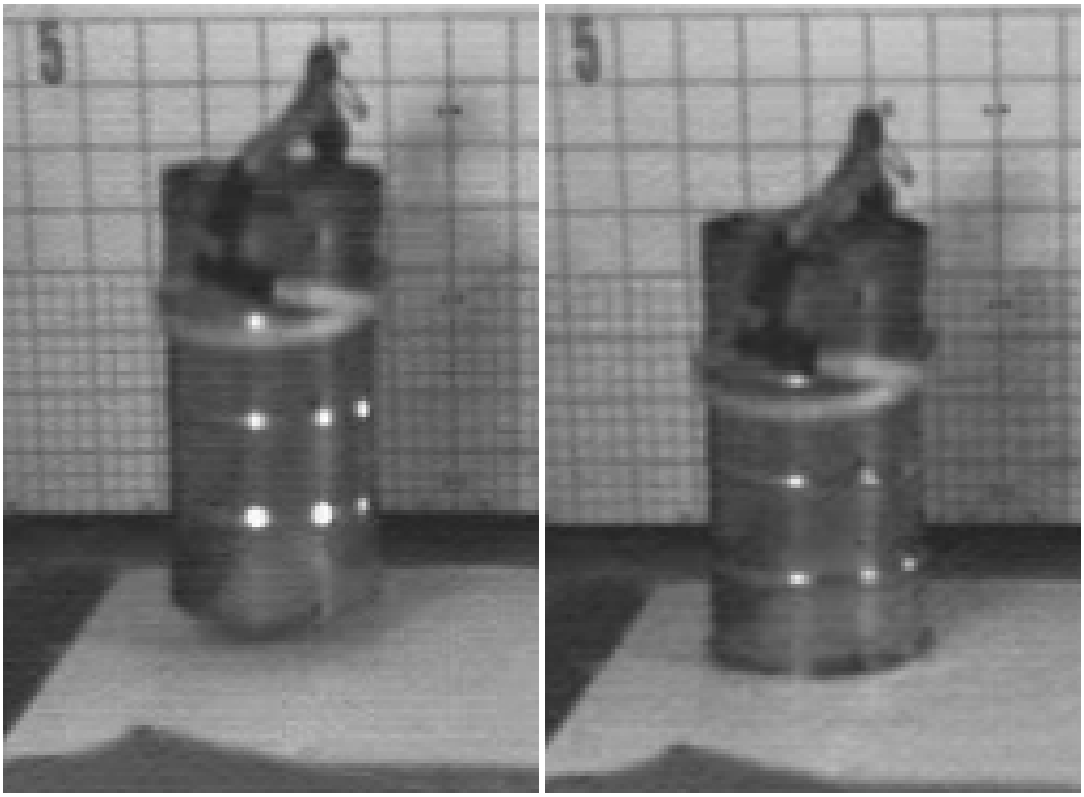

Figure 103 - Prior to Impact (left) and Full Impact (right)

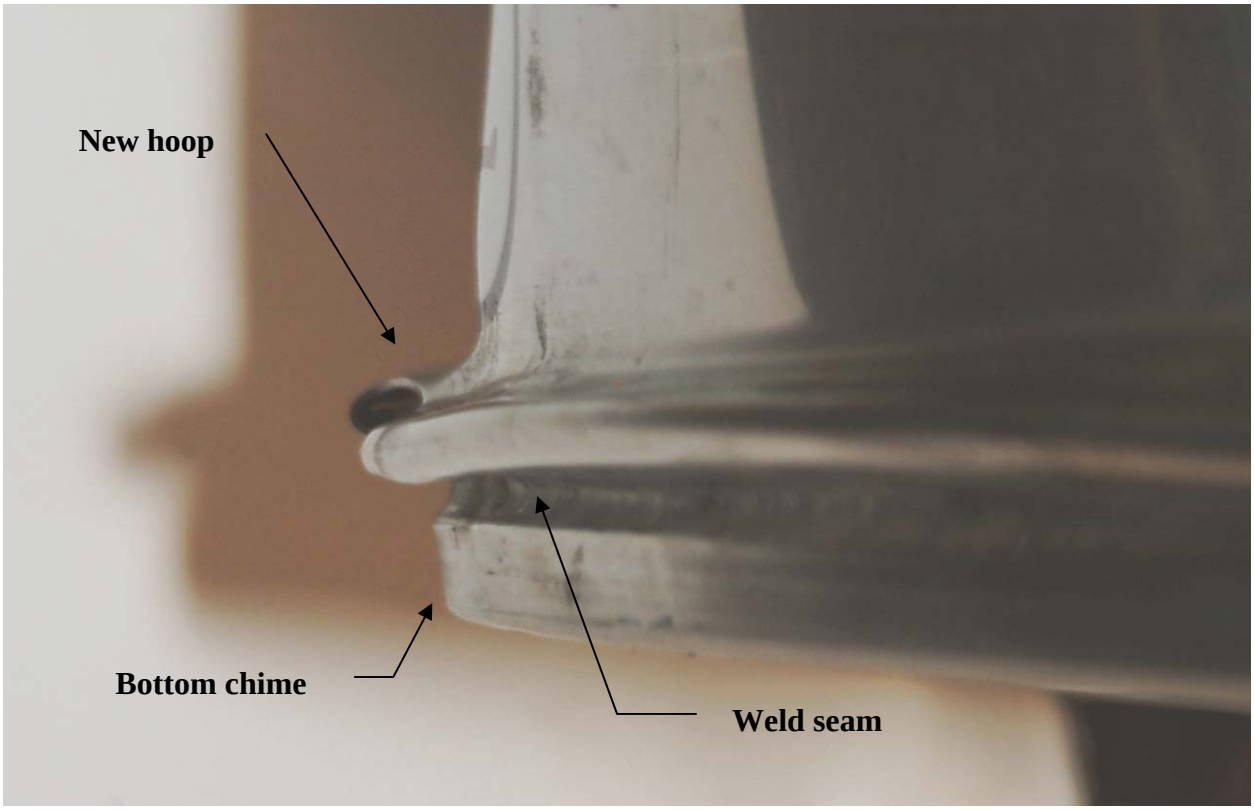

Figure 104 - New Rolling Hoop Formed Above Bottom Chime

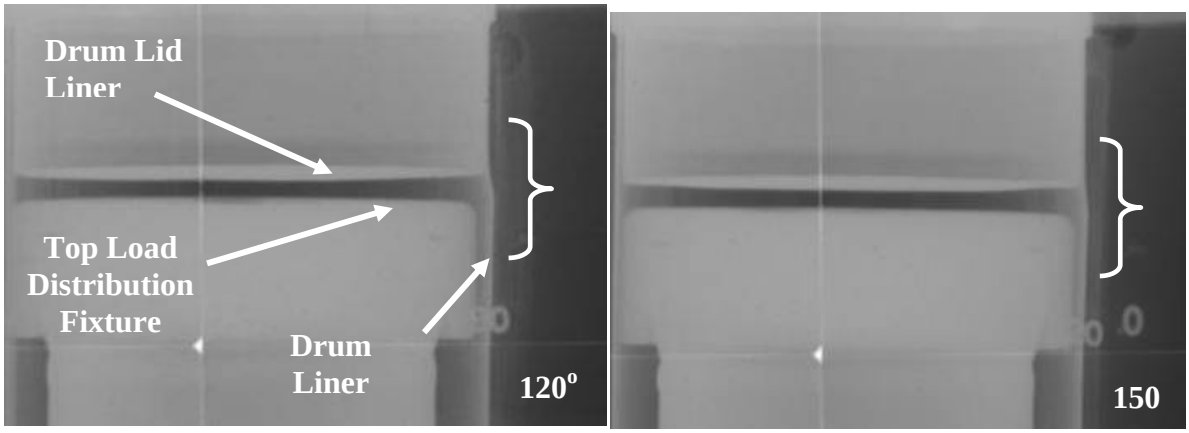

Figure 105 - Image of Drum Liner Deformation from HAC Drop Test

5.4.3.2 Crush Test

The 30-ft crush test was performed with the packaging oriented top-up at a 64-degree angle (i.e., center of gravity over corner), with plate targeted to strike between Ref. Marks 5-6, above the drum weld seam. The packaging was balanced on edge, with guy-lines and a rubber tire chock to maintain the angle. A setup of the test is shown in Figure 106.

The crush test plate struck the packaging at a compound angle as shown in Figure 107 and Figure 108. Due to the impact angle, the plate hit closer to Ref Mark 6, which is the 2-10-6 side of the packaging. The package and plate rebounded energetically in opposite directions: the plate traveled in the direction of the impact angle and the packaging in the direction of the orientation angle. Pre- and post-test photos are shown Figure 109 and Figure 110, and annotated where applicable.

The test was videotaped with a high speed camera and camcorder.

The primary impact resulted in:

- Major compression on both ends of the packaging in the center of gravity axis: the impact corner and corner that the packaging was balanced on (i.e., Ref Marks 6 & 2 respectively). The impact corner is approximately 26-degrees from horizontal. See Figure 111.
- Dimension change from Ref Marks 2-6 and 4-8: 36 to 34-¾ and 35-¼ to 34-¼ inches.
- Bottom rolling hoop formed by the drop test now spans the entire circumference of the drum. See Figure 110
- New rolling hoop formed directly beneath the drum flange weld, spanning from Ref Marks 6-7. See Figure 110, 0, 90, and 180 degree views.
- Slight doming of the lid cap. See Figure 110, 90-degree view. The lid cap shape in now convex.

The radiographs indicate that the CV and foam were not damaged from the crush. See Figure 112. The damage at the top load distribution fixture initiated by the drop test marginally changed.

Figure 106 - HAC Crush Test Setup of SN-5

Figure 107 - Prior to Crush Plate Impact: Cameras approximately 90-degree to Each Other

Figure 108 - Crush Plate at Full Impact

Figure 109 - Pre Crush Test: 0, 90, 180, and 270 Degree Views of SN-5

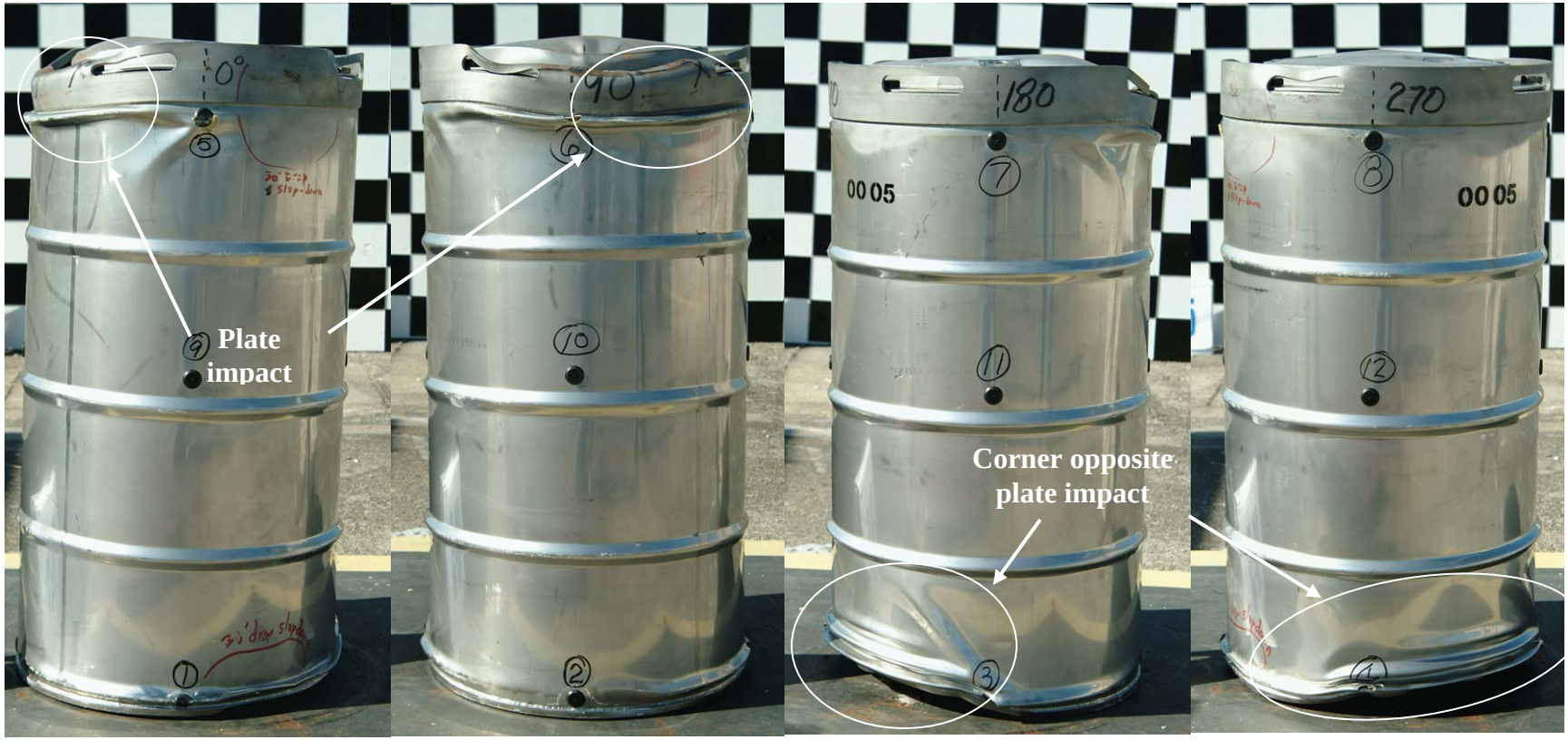

Figure 110 - Post Crush Test: 0, 90, 180, and 270 Degree Views of SN-5

Figure 111 - Point of Impact and Drum Top Deformation Angle of SN-5

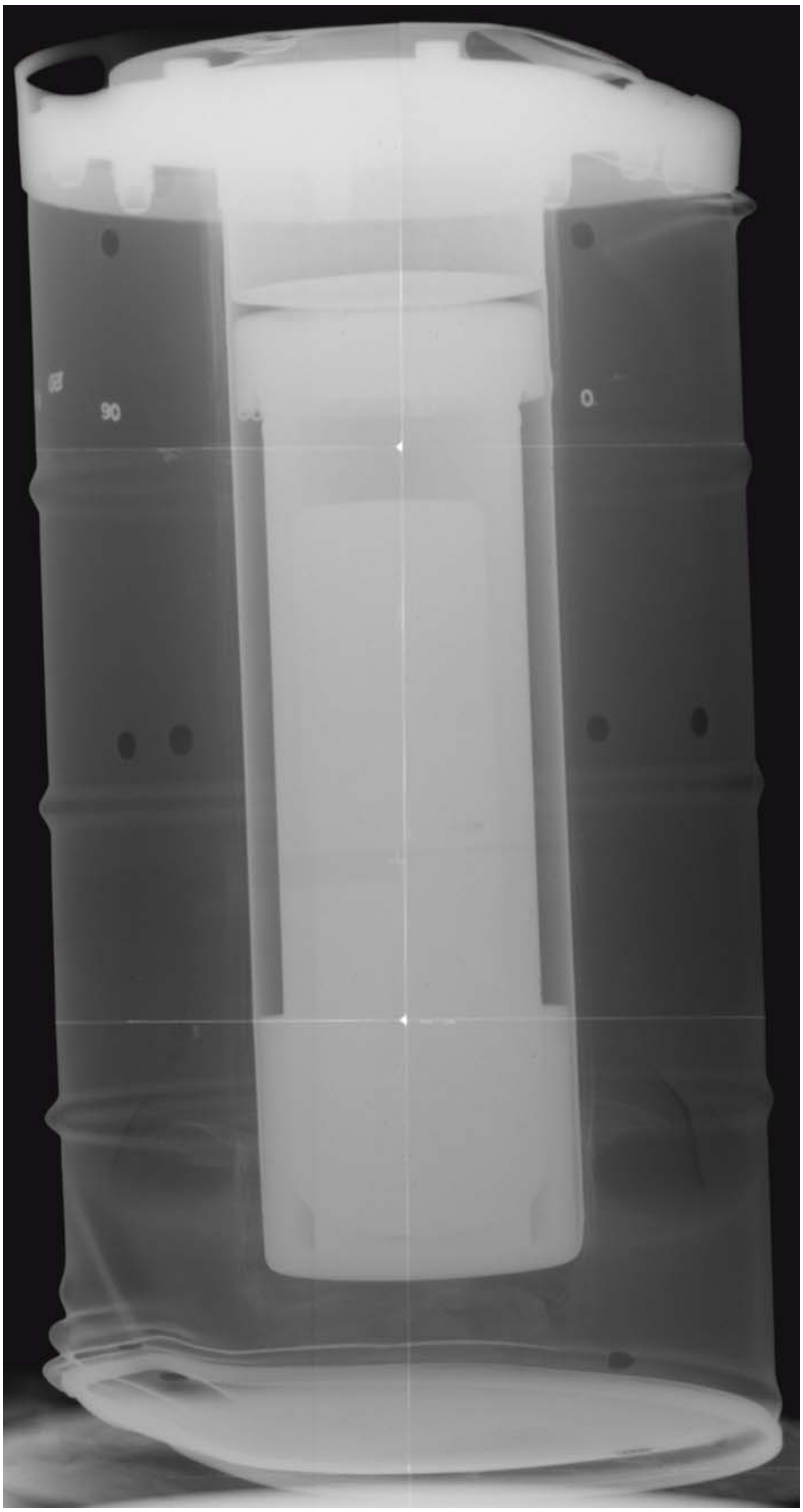

Figure 112 - Post Crush Test Image of SN-5

5.4.3.3 40-in Puncture Test

The 40-in puncture test was performed with the packaging oriented horizontally, to strike the puncture pin on reference mark 11. The test setup for SN-5 is identical to the previous packages.

The packaging struck the pin on reference mark 11, rebounded, rotated, and struck the pin a second time at approximately 45 degrees from horizontal, just below the middle rolling hoop. The test was videotaped with a high speed camera and camcorder.

The primary impact resulted in an impression of the puncture pin top about reference mark 11. This damage was essentially identical to the previous horizontal puncture tests. The secondary hit produced a half-moon shaped dent about 4-in from Ref Mark 11. The dent was approximately ¼ deep, 2 ½ -in long, and 1-1/8 in tall. Figure 113 shows the deformation to SN-5 from the puncture test.

The package was not radiographed after the puncture test.

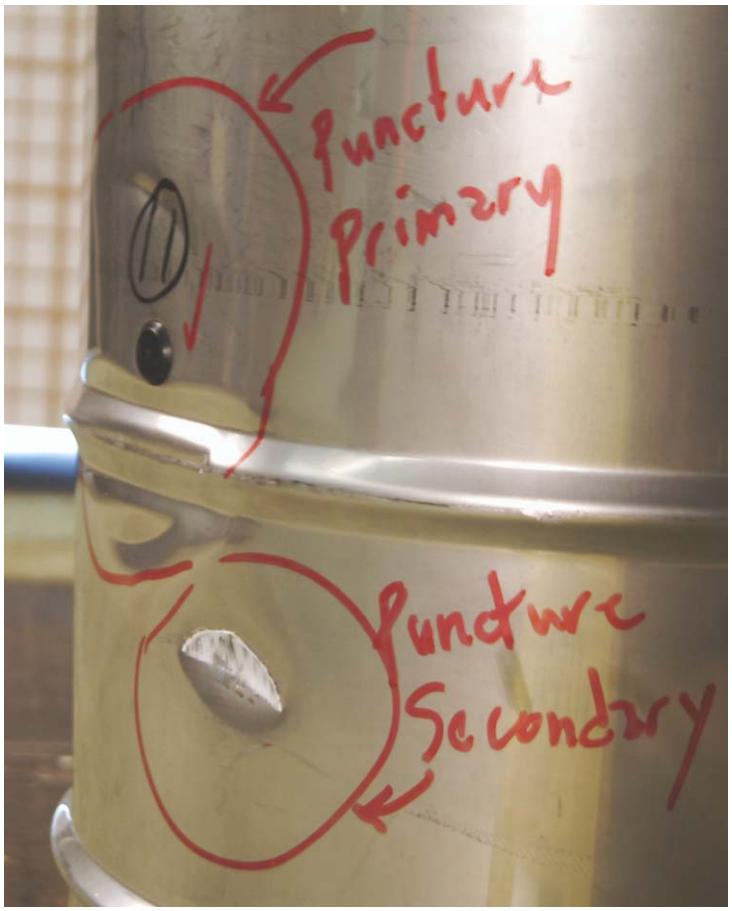

Figure 113 - HAC Puncture Test Deformation to SN-5

5.4.3.4 Thermal Test

SN-5 was placed in the test fixture in the vertical top-up position as shown in Figure 114.

The pool was filled with approximately 75 gallons (284 liters) of fuel then ignited at approximately 0804 hours by an SCFA employee. Within less than a minute the package was fully engulfed and the test was officially started. A photo of the fire engulfment is shown in Figure 115. The fire was fed with fuel until 0835 hours, and within 5-minutes the packaging was no loner engulfed. The fire consumed 627 gallons of fuel.

A post test photo of SN-5 is shown in Figure 116.

The 30-minute average temperatures and environmental conditions during the test for SN-5 are listed below in Table 16.[22] All TC were calibrated prior to the test, except as noted.

Table 16 - Thirty Minute Average Thermal Test Temperatures and Conditions for SN-5

SN-5	Fire (8 TC)	DFT (4 TC)	Package Surface (2 TC)	IRT (range)
Temperature Average(ºC)	883	892	691[a]	1032-1100
Range and Average Wind Speed (knots/(mph))	Range: 0.0 – 4.4 (0.0 – 5.1), Average: 1.5 (1.8)			
Range and Average Ambient Temperature (ºC)	Range: 1.5 – 2.4, Average: 2.1			

Table 16 Notes

a. The bottom TC failed within the first 5 minutes of the test. The TCs averaged 995C (top of packaging) and 387C (bottom of packaging) for the test duration.

SN-5 lost approximately 66% of its foam mass during the thermal test (Refer to Table 10).

The radiograph of SN-5 is very similar to SN-2 and SN-4. The post thermal test radiograph shown in Figure 117 indicates a clearly delineated region of deteriorated foam (a.k.a. charfoam) between the drum and drum liner. However, a fairly uniform undamaged layer of foam still envelops the drum liner, except for a slight gap between the drum top plate and undamaged foam.

Figure 114 - HAC Thermal Test Setup of SN-5

Figure 115 - Full Engulfment of SN-5

Figure 116 - Post Thermal Test Photo of SN-5

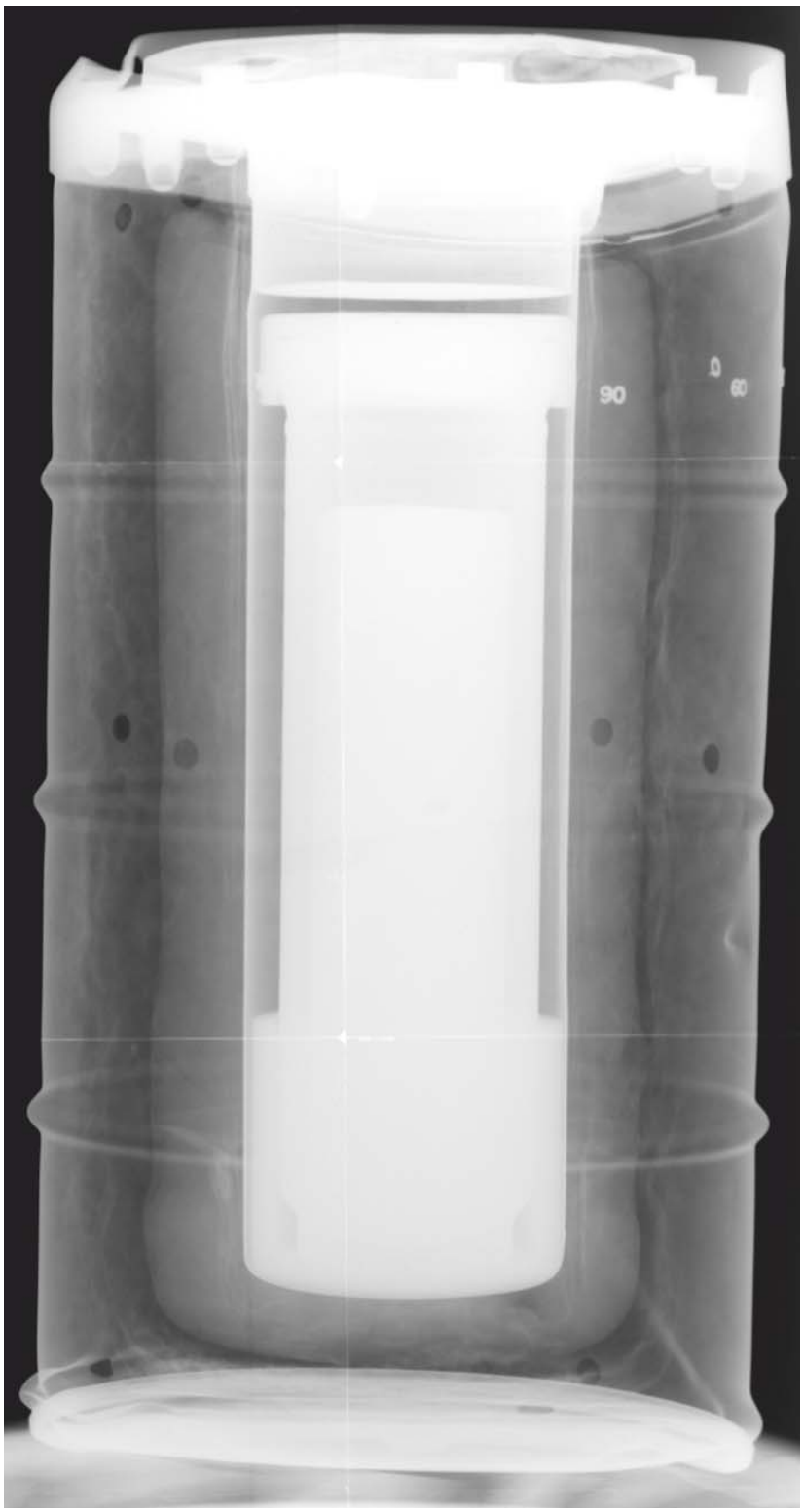

Figure 117 - Post Thermal Test Image of SN-5

5.4.4 Post-Test Packaging Disassembly and Examination

Packaging disassembly and examination was performed per FP-1039, as described previously in Section 5.2.1 of this report.

5.4.4.1 Disassembly

Prior to disassembly, the condition of the drum was observed to have an overall oxidized surface, with some charred foam residue around the vent holes. This condition is typical of all the prototypes (e.g., Figure 34).

The drum was cut into 4 sections in the same steps as SN-2 (Ref Figure 35 sketch).

The package was turned upside down (i.e., top-down) to make the 1st sectional cut, which was a circumferential cut of the drum wall, approximately 1l-in above the bottom chime. Removal of the bottom drum section revealed mostly friable combusted foam (a.k.a., charfoam) as shown in Figure 118. The density of the foam increased towards the drum liner, with solid foam enveloping the bottom of the drum liner.

After the drum bottom section was separated and the loose foam removed, a circumferential cut was made below the estimated base of the drum liner, through the solid layer of foam and Fiberfrax, to expose the drum liner. The solid foam thickness ranged from 1-2 inches. The drum liner bottom was cut off, and the LDF removed and inspected. The CV was pulled out and inspected for deformation, discoloration, and temperature label data. The top load distribution fixture was removed and inspected.

The 2nd and 3rd sections of the drum were made by two cuts along the long axis of the drum, 180 degrees apart, followed by a single circumferential cut below the drum top flange. These cuts completely separated the drum body from the package, exposing the remaining foam and drum liner. Some very thin, large flakes of foam material were observed on the outer charfoam surface. The inspector surmised that the combusted foam flakes appeared to have delaminated from the inside surface of the drum. During removal of these drum sections, loose charfoam separated and fell away from the less combusted foam.

The lid assembly was cut away from the drum body to observe the temperature indicating labels on the lid bottom. The lid assembly was not destructively inspected

5.4.4.2 Examination of Component Condition

The as found condition of the package components are as follows:

- No damage or anomalies to the CV were observed by the inspector.
- The temperature indicating labels were inspected and their indications recorded. See Table 8. The maximum temperature seen by the CV exterior was <250F. The temperature seen by the lid underside was <290F. Nearly all of the external temperatures indicating labels were damaged from the vibration, NCT, and HAC tests.
- The condition of the foam composition ranged from mostly friable on the outermost regions near the drum interior walls to a progressively solid layer enveloping the drum liner.
- The inspector observed a small crack in the foam extending from the top edge of the foam envelop at the drum flange that ran approximately 17-in longitudinally along the length of the envelope. The foam opening coincided with the 335 degrees mark (at the top of the drum), near Ref. Mark 5. See Figure 119. The baseline radiograph (Ref Figure 101) shows a longitudinal void with similar characteristics in the same area prior to the drop tests and thermal test.
- The Fiberfrax lining appeared unaffected by the heat from the thermal test. The drum liner surface showed no indication of heat effects

Figure 118 - Drum Bottom Removed from SN-5

Figure 119 - Foam Crack on SN-5 Indicated

5.4.5 CV Leak Test and Disassembly

After the CV was removed from the SN-5 packaging and visually inspected, a helium leak test was performed to determine if the packaging had provided adequate containment of the contents. The measured leak rate of the CV was <8.8E-10 std-cc He/s (Ref Table 9), which demonstrates the packaging design provided adequate containment of the contents following the regulatory performance tests.

Following the leak test, the CV was opened to inspect and record the data from the internal temperature indication labels. The data is reported in Table 8; however, nearly all of the labels were damaged due to abrasion by the unrestrained surrogate contents. The internal temperatures along the CV body were: <250F at the top, <250F at the middle, and <250F at the bottom. The temperature on the underside of the CV lid was indeterminate due to label damage. Despite the foam loss, the CV was well insulated by the charfoam and Fiberfrax insulation.

6.0 Test Observations

The objective of these tests was to evaluate the GPFP design to provide containment of the contents when subjected to the performance requirements of 10CFR71.71 and 10CFR71.73. The post test leak test results confirm that this design meets these performance requirements.

The greatest foam thermal decomposition typically occurred at the very top and bottom of the drum liner, and along foam cracks and voids. The baseline radiographs showing foam voids consistently and accurately predicated foam loss, and were confirmed correct during packaging disassembly and examination.

The packaging foam loss average was 68%.

The highest reading from the temperature indicating labels was >500F, which was read from the drum liner of SN-3. This package was the most severely damaged by the HAC tests.

As was case with the 1st generation prototype packagings, the horizontal orientation of the packaging for the crush test causes the most damage to the foam, and thus the greatest foam loss by weight. This test orientation was the only case that caused a drum breech (e.g., SN-3); however, the breech in the drum bottom was not severe enough to compromise the ability of the packaging to protect the CV from the subsequent thermal test.

The crush test was the most difficult test conducted at SRS, due to the equipment configuration and environmental conditions. This test was the only HAC test conducted outdoors at SRS. The plate release from the crane and electromagnet proved hard to keep horizontal during the free fall. Most of the impacts were at compound angles. However, one unintended result was a shallow angle crush of SN-3, which arguably, was a more favorable test condition for this packaging orientation.

7.0 Conclusions

The results of the prototype testing demonstrate that the GPFP design adequately provides containment of the contents when subjected to the packaging performance requirements of 10CFR71.71 and 10CFR71.73.

8.0 References

1. Gelder, L.F., Smith, A.C., Blanton, P.S., "***General Purpose Fissile Packaging Prototype Tests"***, M-TRT-G-A-00006, Rev. 0, May 2005
2. ***Packaging and Transportation of Radioactive Materials***, Code of Federal Regulations, Energy, Part 71, latest issue
3. Abramczyk, G.A., "***General Purpose Fissile Package Version 1, Packaging Design Presentation to EM-12"*** SRNL-IES-2006-000016, April 17, 2006. Note: Presentation was made in October 2005 via teleconference.
4. Gelder, L.F., "***Washington Savannah River Company Purchase Requisition"***, Req. No. 6L5423, August 4, 2005. Note: The Scope of Work and Test Requirements are included with the requisition.
5. Lutz, R.N., "***Washington Savannah River Company Purchase Requisition"***, Req. No. 5L5644, July 12, 2005. Note: The Scope of Work is included with the requisition.
6. Gelder, L.F., "***Westinghouse Savannah River Company Purchase Requisition Change Notice"***, Req. No. 69444P, September 12, 2005. Note: The Revised Scope of Work is included with the requisition.
7. Malloy, J., ***"SRNL Package Burn Test Plan"***, NT-TDR-05-105, Rev. 00, December 1, 2005, Contract No. AC450707N.
8. Malloy, J., ***"SRNL Package Burn Test Procedures"***, NT-TDR-05-107, Rev. 00, December 1, 2005, Contract No. AC450707N.
9. "***EES Job Folder 23047"***, Savannah River National Laboratory, (*Note: Job Folders consist of the record copy of design documents, development drawings, and other record documents that the responsible engineer deems vital for the successful completion and possible reconstruction of the task. The Job Folder also contains copies of all Field Procedures (blank and completed referenced in this report.)*
10. Gelder, L.F., ***"General Purpose Fissile Packaging Asbuilts from Accurate Machine Products"***, SRNL-EDS-2005-00025, June 28, 2005
11. Gelder, L.F., ***"General Purpose Fissile Packaging Data Package from Honeywell"***, SRNL-EDS-2005-00026, June 28, 2005
12. DOE Certificate No. 9975, http://www.rampac.com/
13. Prather, M.C., "***Job Hazards Analysis – Packaging Performance Testing at SRS*** ", EES-JHA-2005-001, October 6, 2005
14 Gelder, L.F., "Temperature Indicating Label Information", SRNL-EDS-2005-00052, November 14, 2005
15. "***American National Standard for Radioactive Materials - Leakage Tests on Packages for Shipment"***, ANSI N14.5-1997
16. Gelder, L.F., ***"GPFP Leak Test Results"***, SRNL-EDS-2006-00016, March 24, 2006
17. Gelder, L.F., ***"GPFP Packaging Weight Compilation"***, SRNL-EDS-2006-00010, February 14, 2006
18. Howard, B., ***"Digital Radiography of Special Nuclear Material Test Packages"***, WSRC-TR-2006-00060, February 2, 2006

19. Gelder, L.F.,***"GPFP Vibration Test Results from Sandia"***, SRNL-EDS-2006-00020, April 17, 2006
20. Procedure, ***"EES Drop Test Facility 723-A"***, L9.2-3602, Revision 3, October 6, 2000
21. Estochen, E.G, ***"Removable Crush Test Pad Evaluation"***, SRT-MTS-2004-20045, October 2004
22 Malloy, J., ***"SRNL Package Burn Test Report"***, NT-TDR-06-101, Rev. 01, March 27, 2006, Contract No. AC450707N.
23. Gelder, L.F., ***"Temperature Indicating Label Data"***, SRNL-EDS-2006-00014, March 22, 2006
24. Abramczyk, G.A., ***"Safety Analysis Report – Packages 9972-9975"***, WSRC-SA-7, Revision 15, See "Section 2.6.1 Heat"

This Page Intentionally Left Blank

This Page Intentionally Left Blank

Safety Analysis Report - 9977 Packaging

CHAPTER 3

THERMAL EVALUATION

Preface

This chapter presents the thermal analysis and package test results for Normal Conditions of Transport (NCT) and for Hypothetical Accident Conditions (HAC) required by 10 CFR 71.[1] Specifically, the analysis and test results demonstrate that the package meets the requirements specified in the general package standards of 10 CFR 71.33, 71.35, 71.43, and 71.87 and the additional requirements for Type B packages of 10 CFR 71.51.

This Page Intentionally Left Blank.

TABLE OF CONTENTS

LIST OF TABLES

Page

LIST OF FIGURES

NOMENCLATURE

h = Convection Heat Transfer Coefficient (Btu/hr-ft^2-°F)

k = Thermal Conductivity (Btu/hr-ft-°F)

k_i = Thermal conductivity of material in cylinder i (Btu/ft hr °F)

L = Characteristic Length (ft)

n = Total number of concentric cylinders

Pr = Prandtl Number

q = Heat Flow (Btu/hr).

r = Radial Location (ft).

r_i = Inner radius of cylinder i (ft)

Ra = Rayleigh Number

T = Temperature (°F).

T_{i+1} = Temperature at outer edge of cylinder i (°F)

ACRONYMS AND ABBREVIATIONS

CV	Containment Vessel
9977	General Purpose Fissile Package
HAC	Hypothetical Accident Conditions
LDF	Load Distribution Fixtures
NCT	Normal Conditions of Transport
SARP	Safety Analysis Report for Packaging
SS	Stainless Steel

3 THERMAL EVALUATION

This chapter provides the thermal design evaluation of the 9977 packaging as to its performance under NCT and HAC events. Detailed discussions of the packages thermal protective attributes important to the safety performance of the 9977 are provided. The 9977 package consists of two possible containment vessel (CV) configurations held within a drum assembly which provides physical and thermal protection. The drum assembly is comprised of a foam filled drum, closed with a bolt-on lid. The drum assembly and the lid both have multiple layers of insulating materials providing the principal thermal protection for the 9977. Geometric thermal protection, equally as important as the material insulating properties, is provided by the interior liner and bolt-on lid that confine the CV to the center of the drum under NCT and HAC events. Figure 3.1 shows the general arrangement of the 9977 and key dimensions. Figure 3.2 is a schematic of the package thermal features.

It is demonstrated that the combination of the 9977s materials of construction and geometric features comply with the thermal performance requirements of 10 CFR Part 71.[1]

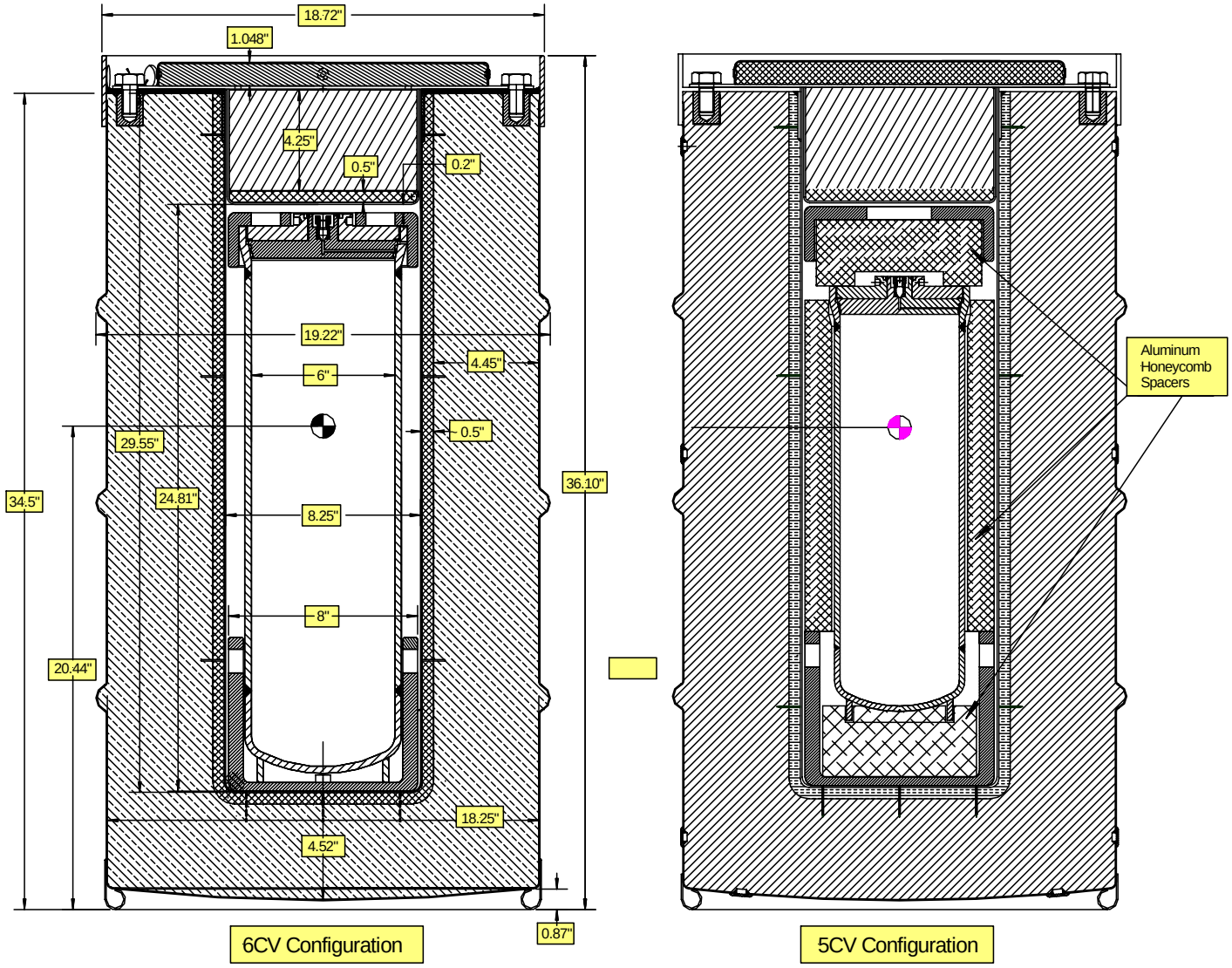

Figure 3.1 - Schematic of the 9977 containing the 6CV

3.1 Description of Thermal Design

The 9977 package is designed to reject heat passively. Thermal protection for the 9977 is provided by a insulation filled drum and its bolt-on lid, each having multiple layers of insulating materials. Figure 3.2 is a schematic of the principal thermal features of the 9977. The drum consists of a 35-gallon shell with an inner liner weldment. The liner weldment is wrapped with Fiberfrax® and the remaining drum volume is filled with polyurethane foam. The lid weldment consists of upper and lower shells filled with Fiberfrax, Min-K 2000, and TR-19 Block insulating materials. These materials are discussed in detail below. A detailed description of the packaging components and assembly details is provided in Section 1.2.1, and the package drawings are provided in Appendix 1.1. The maximum allowed content decay-heat rate is 19 watts.

As important as the material insulating properties, is the physical protection provided by the interior liner and bolt-on lid that confine the CV to the center of the drum under NCT and HAC events. The drum and lid include holes that allow venting of thermal decomposition gases during the HAC Thermal event and assure confinement is maintained. The package's ability to provide confinement under NCT and HAC events is discussed in Chapter 2.

The package design ensures that all package components operate below their thermal design limits. The components of interest include the containment vessels and their O-ring seals and the package insulating materials. The design temperature and pressure limits for these components are presented in Table 3.1 and discussed in detail in Sections 3.1.3 and 3.1.4, respectively.

Table 3.1 – Package Component Design Limits for NCT and HAC

Component (Material)	**Temperature**		**Pressure** (psig)
	Minimum (°F)	**Maximum** (°F)	
O-rings (Viton GLT)	-40 [a]	400 [NCT] 700 [HAC short term]	-
5CV (304L SS)		~~5~~300 (NCT)	800
6CV (304L SS)		3~~5~~00 (HAC)	900
LDFs (6061-T6 Aluminum)		400 [NCT] 800 [HAC]	-
Lid Bolts (SS)		300 [NCT] NA [HAC]	-
Last-A-Foam (Polyurethane) [b]		300 [NCT] NA [HAC]	-

a Regulatory Limit

b The remaining insulating materials are discussed in Section 3.1.1 but are not listed as their maximum operating temperatures exceed the Regulatory Test temperature (1475°F).

The containment vessel O-ring temperature limits are specified by the vendor.[2] The containment vessels temperature limits are based on the ASME Code.[3] These limits are significantly less than the capability of 304L stainless steel and were selected to maximize structural strength while accommodating the heat from a 19-watt content. Containment vessels pressure limits are taken from Chapter 2 and based on ASME Code allowable stresses. The aluminum Load Distribution Fixtures [LDFs] temperature limit is based on the ASME Code. The LDFs are not subjected to any tensile loads. The stainless steel lid bolt temperature limits are based on the ASME Code.[4] The Last-A-Foam temperature limits under NCT are based on material testing by the Vendor.[5] Under HAC, no temperature limit is specified for Last-A-Foam, because the material is permitted to decompose during the Thermal event.

Thermal performance of the package under NCT and HAC was verified by testing and quantified by analysis. The NCT and HAC test results are documented in Appendices 3.1 and 3.2. The NCT and HAC analyses are documented in Appendices 3.3 and 3.4 and summarized in Table 3.2. The calculated temperatures compare closely with the measured temperatures and are bounding for all contents and configurations identified in Section 1.2.3.

Table 3.2 – Maximum Temperatures under NCT and HAC Thermal (Fire and Cool-down)

Condition	**Method**	**Drum**[a] (°F)	**Poly Foam**[a] (°F)	**5 Inch CV** (°F)			**6 Inch CV** (°F)		
				Body	O-rings	Contents	Body	O-rings	Contents
NCT in Shade	Calculated {Measured}	105 {107}	185 {164}	n/c {n/t}	n/c {n/t}	n/c {n/t}	220 {190}	198 {165}	347 {n/m}
NCT w/ Insolation	Calculated	203	295 ~~304~~[b]	260	240	280	~~483~~21[ce] 3~~18~~02 [c]	~~5~~350 [b]	
HAC Thermal	Calculated {Measured}[d]	1,475 {1,704}	n/a {n/m}	n/c {n/t}	n/c {n/t}	n/c {n/t}	307 {250}	307 {270}	~~307~~347 {270}
Post-Fire Cool-down w/ Insolation	Calculated	202	n/a	n/c	n/c	n/c	400	381	425

n/a = Not Applicable; n/m = Temperature Not Measured; n/t = Configuration Not Tested; n/c = not calculated

a - Reported temperatures are for the 6 CV configuration and bound the 5 CV configuration

b - Based on a~~6CV with~~ distributed ~~point~~ source located ~~in a~~direct ~~contact~~ with bottom of the 6CV.

c - Based on a distributed source located at with top of the 6CV~~The 482 °F reading is a localized point on the bottom of the CV due to a postulated point source. The CV temperature profile for the CV quickly drops off to less than 300 °F considered to be the CV design temperature. As this is a point localized thermal effect, it is not considered in evaluating CV stresses and not mentioned further. However, the point source temperature is used for calculating the CV pressure~~.

d - Measured with a “temperature indicating label”, actual temperature value less than the value listed.

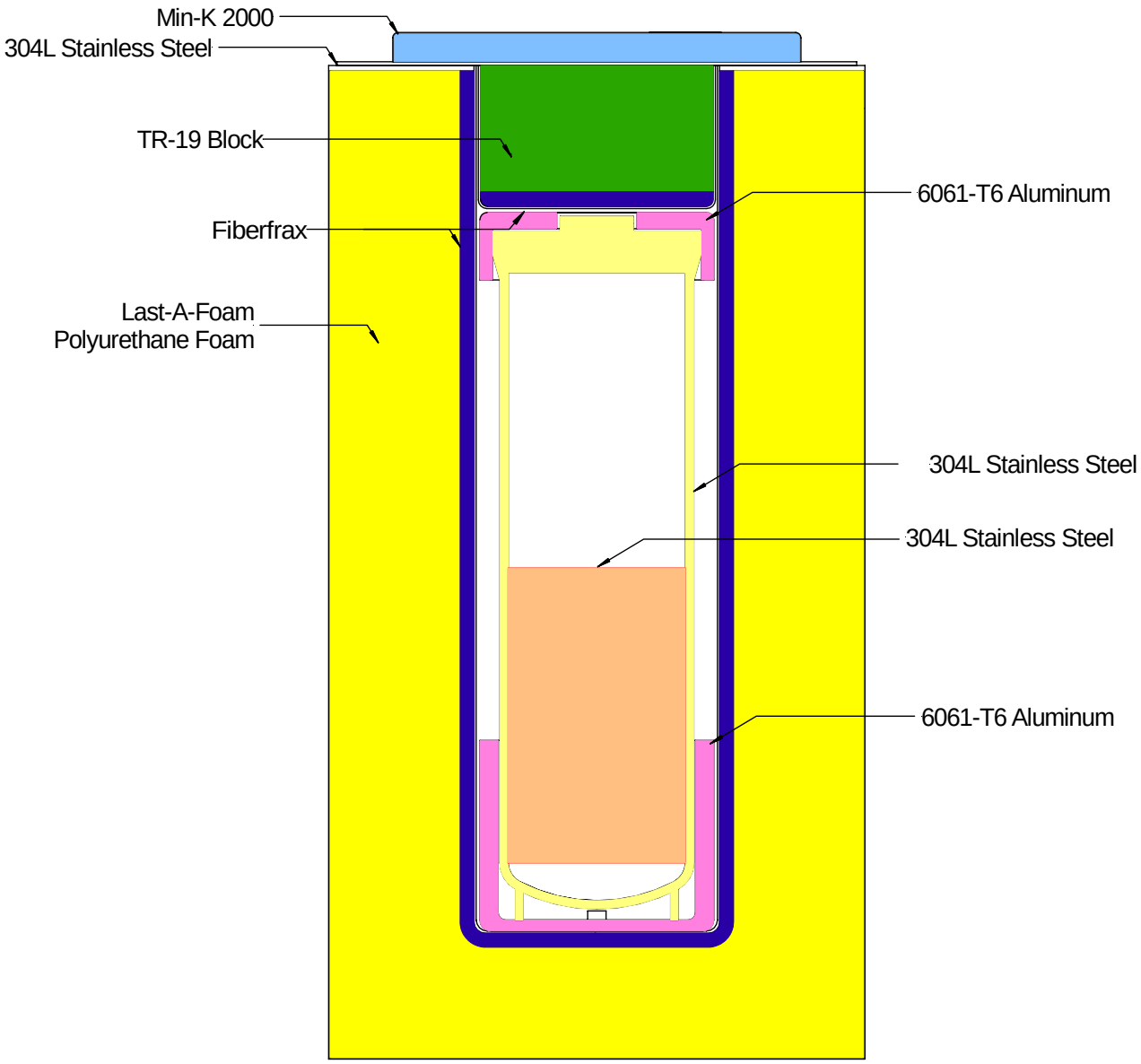

Figure 3.2 - Schematic of Thermal Features for the 9977*.

* - Figure 3.2 represents the basic thermal model for the 9977. Specific features such as the drum flange bolts, drum rim, drum hoops, and wear ring do not significantly affect heat transfer and are not detailed in the thermal model.

The regulatory Maximum Normal Operating Pressures (MNOP) are developed in Section 3.3.2 for NCT, the containment vessel pressures during HAC-fire event are developed in Section 3.4.3 and both are summarized in Table 3.3. The 5CV pressure corresponds to content envelope C.2 in food-pack cans. The 6CV pressure corresponds to content envelope C.1 with the RTG configuration. The respective CV pressures bound all other content configurations evaluated.

Table 3.3 – Maximum Pressures under NCT and HAC

Condition	6CV (psig)	6CV (Margin)	5CV (psig)	5CV (Margin)
NCT	41.2	95%	56.3	94%
HAC	35.0	96%	48.5	95%
Design Limit	800		900	

Note: Margin is defined as [1-(actual/allowable)]×100%.

During the HAC thermal event, the properties of polyurethane foam and Fiberfrax minimize heat transfer to the containment vessel. When the foam is exposed to temperatures greater than 532 °F it decomposes to form an intumescent char. This ablative process removes heat from the package during the HAC thermal event. Note: A bounding HAC test was performed that demonstrated, and analysis has confirmed that even with no foam the CV and its contents where maintained within design limits for the HAC. Package testing has shown that during the HAC fire the materials of construction and package geometry provide thermal protection for the containment vessel and its contents.

3.1.1 Design Features

A detailed description of the packaging components and their design functions is provided in Section 1.2.1 and Section 2.1.1, while fabrication details are provided in Section 2.3.1. Thermal properties of the component materials are provided in Section 3.2, and component technical specifications for the package are on the drawings included in Appendix 1.1. The drawing specifications include the applicable ASME Code requirements for the components and materials. Package design features important to the thermal analysis are summarized below and are shown in Figure 3.2.

3.1.1.1 Drum, Drum Liner, and Lid

The drum is fabricated from 18-gauge 304L stainless steel (SS) that is 36.10 inches tall and has a diameter of 18.72 inches, as measured across the rim. At three (3) axial elevations there are sets of four (4) vent holes in the side of the drum, 90° apart. Two additional vent holes are located in the bottom of the drum. All vent holes are closed with plastic Caplugs® to prevent the entry of moisture. In the HAC-fire event, the Caplugs® melt or burn and allow the drum to vent gases generated from thermal decomposition of the polyurethane foam.

A cylindrical drum liner having an inside length and diameter of 29.5 and 8.25 inches, respectively, is concentrically located within the drum. The drum liner is constructed of

18-gauge 304L SS. The drum liner is welded to the drum Top Plate. The liner well is closed by securing the drum lid to the Top Plate with eight bolts.

The lid is constructed in three sections. The Lid flange plate, top liner and bottom liner are fabricated from $^{1}/_{8}$-inch, 18-gauge and 14-gauge 304L SS, respectively. The bottom liner contains two layers of insulating material, ½-inch compressed Fiberfrax® blanket and a 4.3-inch thick piece of TR-19 Block vermiculite insulation. The lid top liner is filled with a 1-inch thick piece of Min-K-2000 insulation.

3.1.1.2 Fiberfrax®, Last-A-Foam®, TR-19 Block, and Min-K 2000

Two ½-inch thick Fiberfrax® insulation blankets are wrapped around the sides and bottom of the drum liner. The layered blankets are initially 1-inch thick, however, during the fabrication process the region between the outer surface of the Fiberfrax® and the inner surface of the drum wall is filled with polyurethane foam. The foam is emplaced as a liquid that expands as it cures, compressing the layer of Fiberfrax® against the drum liner. The compressed thickness of the Fiberfrax, as determined from examination of the tested packages, is approximately ½-inch. This thickness was used in the thermal analysis models. Because the Fiberfrax® thickness was halved, its density and thermal conductivity were doubled. Table 3.8 lists properties of compressed and uncompressed Fiberfrax®.

Two ½-inch thick Fiberfrax® insulation blankets are placed in the bottom of the Lid bottom liner. The layered blankets are initially 1-inch thick; however, during the fabrication process the layer is mechanically compressed to a total of ½-inch thick with TR-19 Block vermiculite insulation material. Welding the bottom liner to the lid flange plate maintains this compression.

Last-A-Foam polyurethane foam is used for both its thermal insulating and mechanical shock absorbing properties. During the HAC Thermal testing, a "Practice Package" was burned in order to validate the test facility, test procedures and for operator training. The Practice Package was a mock-up of the 9977 but excluded the polyurethane foam. The test burn was performed in compliance with 10 CFR 71.73 and was fully instrumented. This test showed that the limiting temperatures within the 9977 can be maintained in the HAC Thermal test with just the Fiberfrax® insulation in the drum body.

TR-19 Block vermiculite insulation is used in the lower liner of the lid. The material is cut to form and is used for insulation and impact resistance. Min-K 2000 insulation is used in the upper liner of the lid and is also used for insulation and impact resistance. Fiberfrax®, TR-19, and Min-K insulations are thermally stable from -40°F up to 1,800°F, which is well above the regulatory HAC fire temperature of 1,475°F.

3.1.1.3 Containment Vessel and O-Rings

Each CV is constructed from 304L SS pipe that is closed on one end by a pipe cap and the other by a ¾-inch thick cone-seal plug held in place by a 0.63-inch thick threaded cone-seal nut. The cone-seal plug incorporates machined grooves to receive two O-ring seals. The design temperature for both CVs is 300°F, for NCT and HAC respectively. The O-ring material is

Viton® GLT, a fluorocarbon elastomer with a service temperature range between -40 °F and 400 °F.[2]

3.1.2 Content's Decay Heat

The thermal analyses are based on a maximum heat load of 19 Watts. The decay heat rate of the authorized contents at the mass and radioactivity limits specified in Table 1.2 may exceed the 19W power limit. Therefore, the 19W heat load limits the activity, decay energy and mass of radioisotopes carried by the package which are summarized in Table 3.43.43.4, below.

Table 3.4 - Contents Parameters

Content Envelope	Calculated [a] Decay Heat (watts)	Maximum Weight (kg)
C.1 (Heat Sources)	56.5 [b]	0.1
C.2 (Pu/U Metals)	68.9 [b]	4.4
C.3 (Reserved)	-	-
C.4 (U Metals/Alloys)	0.001	13.5
C.5 (U Compounds)	0.001	13.5

a Maximum decay heat calculated from highest-heat selection of isotopes available from contents specifications given in Table 1.2

b The actual contents must be controlled and not allowed to exceed the package maximum of 19 watts.

3.1.3 Summary Tables of Temperatures

The summary of temperatures listed in Sections 3.1.3.1 for NCT and 3.1.3.2 for HAC, are derived from thermal models and physical testing. The 9977 thermal models are discussed in detail in Sections 3.3 (NCT) and 3.4 (HAC). The thermal testing is reported in Appendices 3.1 and 3.2.

The 9977 thermal analyses modeled a 19 Watt heat source located at the top, middle, and bottom of the CV. The calculated data reported in Sections 3.1.3.1 and 3.1.3.2 are conservatively based upon the maximum temperature for each component taken from the highest of these three cases.

3.1.3.1 NCT Summary Temperatures

For the NCT thermal analysis, the limiting component temperatures that would affect the structural, containment, shielding, and criticality integrity of the 9977 package are the O-rings of the CV, the CV and the foam. Maximum component temperatures during NCT were calculated using the models described in Section 3.3 and are listed in Table 3.5. They are compared against component limiting temperatures listed in Table 3.1.

The containment vessels' limiting temperature was selected at 5300 °F to maximize their allowed ASME BV&PC design pressures.[6] The CV local maximum temperature is 48321 °F. This is a highly localized temperature and is well below the limiting temperature for SS at the MNOP of

56.3 psig. The O-ring limiting temperatures for continuous service are -40 °F to 400 °F, as specified by the manufacturer.

The polyurethane foam limiting temperature is based on its mechanical performance, so to ensure that the 9977, during NCT and subsequent HAC testing, maintains structural integrity, containment, shielding and subcriticality. The foam limiting temperature was selected at 300 °F based on its mechanical properties and use in other packages. [5, 7]

Table 3.5 – NCT Package Component Temperatures

Insolation	**Drum** (°F) [n/s]	**Poly Foam** (°F) [300]	**5 Inch CV** (°F)			**6 Inch CV** (°F)		
			Body [3~~5~~00]	O-rings [400]	Contents [n/s]	Body [~~5~~300]	O-rings [400]	Contents [n/s]
no	105 {122}[a]	185	n/c	n/c	n/c	220	198	347
yes	203	304	260	240	280	~~482~~321 [b]	3~~1~~802~~-~~[~~c~~]	350

[limit] designates limiting temperature of the component; n/s – not specified ; n/c = not calculated

a - Regulatory Limit specified in 10CFR71.43(g) b – Heat source at top of CV~~Heat source at bottom of CV~~ ~~c – Heat source at top of CV~~

3.1.3.2 HAC Summary Temperatures

The limiting components of the HAC thermal analysis of the 9977 are the O-rings and the CV. Maximum component temperatures during HAC were calculated using the models described in Section 3.4 and are listed in Table 3.6. They are compared against component limiting temperatures listed in Table 3.1.

The package HAC analysis consists of three phases; the pre-fire conditioning, the HAC fire, and the post-fire cool-down period. The pre-fire component temperature distribution was determined from the NCT steady state (19 Watts without insolation). The fire phase was not explicitly modeled due to the complexity of the foam intumesces phenomenon; the increase in temperature of the package components was determined from physical testing. The post-fire cool-down phase temperatures were determined from evaluating the effects of variations in the remaining un-degraded foam and char-foam within the drum.

Note, for conservatism any individual temperature reported in the following table is the maximum from the five packages tested and all the maximum temperatures may not be from the same package.

Table 3.6 – HAC 6CV Component Temperatures

Condition and Package	**Method**	**Drum** (°F) [n/s]	**Body** (°F) [~~5~~300]	**O-rings** (°F) [400]	**Contents** (°F) [n/s]
Fire -Prototype Mock-up (w/o Foam)	Calculated @ 30 min {Measured}	1,475 {1,853}	426 {435}*	432 [a] {n/m}*	212 {n/m}*
Fire -Prototype	Calculated @ 30 min {Measured}	1,475 {1,873}	307 {250}*	307 {270}*	3~~07~~50 {270}*
Post-Fire - Prototype w/ Insolation	Calculated Steady State	202	400	381	425

n/m = Temperature Not Measured n/s = Not Specified
* Measured with a "temperature indicating label", value reported bounds the actual temperature
[limit] designates limiting temperature of the component

3.1.4 Summary Table of Maximum Pressures

The Maximum Normal Operating Pressure (MNOP) was calculated by the maximum content temperature in the CV and assuming an initial pressure of 14.7 psia at an initial temperature of 70°F. Off-gassing of 100 grams plastic was assumed to calculate the maximum pressures.

The maximum operating pressure under HAC is also based on the maximum content temperature during the HAC fire and the post-fire cool-down periods and assuming an initial pressure of 14.7 psia at an initial temperature of 70°F. The maximum pressure under HAC conditions occurs about 6.5 hours into the post-HAC cool down. The maximum HAC pressure also includes the off-gassing of the plastic bags.

Table 3.7 – Containment Vessel Pressures

Package Configuration	**Case**	**Pressure (psig)**	**Content Configuration**
5CV	NCT	56.3	Food-Pack Can
	HAC	48.5	
6CV	NCT	41.2	RTG
	HAC	35.0	

3.2 Material Properties and Component Specifications

3.2.1 Material Properties

The constitutive properties of the packaging materials used in the NCT and HAC thermal analyses are provided in Tables 3.8 to 3.10. The emissivities used in the analyses are presented in Table 3.11 and were adjusted from the theoretical values to provide conservative temperature predictions for each of the regulatory accident scenarios. Table 3.12 presents the surface natural convection coefficients that were used for modeling.

The constitutive properties of the polyurethane foam insulation (FR-3716) are provided in Table 3.8. The foam has a glass transition temperature (Tg) of 279°F.[7] The foam is limited to a bulk temperature of 300 °F. If the polyurethane foam is confined and no mechanical loads are applied, it can be held at up to 300°F for an extended period and retain its form.[7] At temperatures greater than Tg the foam slowly softens. Off-gassing and melting/oxidation is not observed below about 500°F. Thermal decomposition of FR-3716 occurs at 534°F. First the melted foam undergoes an endothermic chemical reaction to form oligomers and char. The oligomers later recombine in a non self-sustaining exothermic reaction that ceases when heat is no longer supplied by an external source. The endothermic phase of the reaction utilizes heat that would otherwise be used to raise the temperature of surrounding materials. The foam becomes a flowing liquid just below the ignition temperature, which is greater than 600 °F.

The constitutive properties of the remaining package insulating materials, TR-19 Block, Min-K, and Fiberfrax are provided in Table 3.8. The thermal properties of the package metal materials are provided in Table 3.9. All these materials are thermally stable from -20°F to well above the regulatory HAC fire temperature of 1,475°F.

Table 3.8 – Thermal Properties of Fiberfrax under Varied Conditions

Material	Thermal Conductivity (Btu/hr ft °F)	Density (lbm/ft^3)	Specific Heat (Btu/lbm °F)
Fiberfrax (uncompressed) Values are for Lo-Con Blanket®[8]	0.0228 @ 200.0°F 0.030 @ 400.0°F 0.0399 @ 600.0°F	10	0.27
Fiberfrax (compressed) Values are for Lo-Con Blanket® thermal conductivity assumed 2 × the value of uncompressed material	0.0455 @ 200.0°F 0.060 @ 400.0°F 0.0798 @ 600.0°F	20	0.27
TR-19 [9]	6.33E-02 @ 400.0°F 6.67E-02 @ 600.0°F 7.00E-02 @ 800.0°F 7.33E-02 @ 1000.0°F 7.75E-02 @ 1200.0°F 8.17E-02 @ 1400.0°F 1.08E-01 @ 1600.0°F	23.0	0.20
MIN-K 2000 [10] Tabulated thermal conductivities for Min-K-2000 are less than those for air, hence, values for TR-19 were used in the analysis.	1.58E-02 @ 300.0°F 1.67E-02 @ 400.0°F 1.83E-02 @ 600.0°F 2.08E-02 @ 800.0°F 2.50E-02 @ 1000.0°F 3.33E-02 @ 1200.0°F 4.17E-02 @ 1500.0°F 4.50E-02 @ 1600.0°F	20.0	0.23 @ 400.0°F 0.25 @ 800.0°F 0.27 @ 1200.0°F 0.27 @ 1600.0°F
LAST-A-FOAM® FR-3716	2.75E-02 @ 76.5°F 3.12E-02 @ 140.7°F 3.71E-02 @ 248.4°F 4.33E-02 @ 348.6°F	14-17	0.353

- Polyurethane foam properties are isotropic.

Table 3.9 – Thermal Properties of Package Metals

Material	Thermal Conductivity (Btu/hr ft °F)	Density (lbm/ft^3)	Specific Heat (Btu/lbm °F)
Aluminum [12] (Alloy 6061-T6)	96.1 @ 70°F 96.9 @ 100°F 98.0 @ 150°F 99.0 @ 200°F 99.8 @ 250°F 100.6 @ 300°F 101.3 @ 350°F 101.9 @ 400°F	169.3	0.23 @ 212°F
304L Stainless Steel[11]	7.74108 @ 32.0°F 9.43444 @ 212.0°F 12.5793 @ 932.0°F 14.9983 @ 1292.0°F	494.429	1.200E-01 @ 32.0°F 1.350E-01 @ 752.0°F
Mock Load (note 1)	126.0	0.05	0.10

Note 1 – Mock load is the high thermal conductivity, high diffusivity, and low thermal inertia dummy material to maximize heat transfer from the source to CV.

Table 3.10 – Thermal Properties of Air (1 atm)

Thermal Conductivity (Btu/hr ft °F)	Density (lbm/ft^3)	Specific Heat (Btu/lbm °F)	Coeff. Thermal Expansion (1/°F)	Viscosity (lbm/hr-ft)
1.5161E-02 @ 80.33°F 1.9443E-02 @ 260.33°F	$\rho = \frac{1}{2.5203 \times 10^{-2}(T + 459.67)}$	0.24044	$\beta = \frac{1}{(T + 459.67)}$	4.8E-02 @ 80.33°F 5.1E-02 @ 170.33°F 5.58E-02 @ 260.33°F 6.08E-02 @ 350.33°F

Table 3.11 – Package Component Surface Emissivities

Component	Material	Model Emissivity	
		NCT	HAC
CV	SS	0.30	0.30
Drum Liner	SS	0.30	0.30
Bottom of Drum Lid	SS	0.30	0.30
Heater Billet	SS	0.30	0.60
Drum Exterior	SS	0.21	0.8
RTG Component	Al	0.20	0.20
Food Pack Cans	SS	0.2	0.20
3013 Outer	SS	0.30	0.30
Load Distributors	Al	0.20	0.20

Table 3.12 – Natural Convection Heat Transfer Coefficients

Convective Surface Orientation	9977 Boundary Condition	Surface	Correlation [11] (Btu/hr-ft^2-°F)
Vertical	Drum wall	Isothermal Plate With $Ra < 1.0\times10^9$	$h = \left(\frac{k}{L}\right)\left(0.68 + \frac{0.670\times Ra^{0.25}}{\left[1.0+\left(\frac{0.492}{Pr}\right)^{9/16}\right]^{4/9}}\right)$
Vertical	Drum wall	Isothermal Plate With $1.0\times10^9 < Ra$	$h = \left(\frac{k}{L}\right)\left(0.825 + \frac{0.387\times Ra^{1/6}}{\left[1.0+\left(\frac{0.492}{Pr}\right)^{9/16}\right]^{8/27}}\right)^2$
Horizontal	Drum Top	Hot Isothermal Plate Facing Upward With $1.0\times10^7 < Ra < 3.0\times10^{10}$	$h = \left(\frac{k}{L}\right)0.15\times Ra^{1/3}$
Horizontal	Drum bottom	hot isothermal plate facing downward with $3.0\times10^5 < Ra < 3.0\times10^{10}$	$h = \left(\frac{k}{L}\right)0.27\times Ra^{1/4}$

3.2.2 Component Specifications

Technical specifications for the package components are provided on the package drawings included in Appendix 1.1. The drawing specifications include the applicable ASME Code requirements for the components and materials. Technical specifications relevant to the thermal analysis are summarized in this section.

3.2.2.1 Drum, Drum Liner and Lid

The confinement for the package is a 35-gallon stainless steel drum with a removable closure lid, both constructed from 304L stainless steel (SS). The drum incorporates a 304L SS liner in which the Contents/CV and Load Distribution fixtures are confined. The drum incorporates twelve vent holes located on the side of the drum. Two additional vent holes are located on the bottom of the drum. The vent holes are closed with plastic Caplugs to prevent entry of water during NCT. In the HAC-fire event, the fusible Caplugs are consumed and allow the drum to vent gases generated from thermal decomposition of the polyurethane foam insulation. The closure lid flange is attached to the mating drum flange with eight $^{5}/_{8}$-inch steel bolts.

3.2.2.2 Fiberfrax, Polyurethane, TR-19 and Min-K Insulation

Fiberfrax is manufactured by Unifrax Corporation of Niagara Falls, NY and is a lightweight batting, comprised of bulk ceramic fibers sandwiched between strong, high temperature fiberglass-cloth. The ceramic fibers i.e., the core insulation, has an operating temperature of up to 2,300°F. The core insulation is quilted front and back with a non-combustible E-Grade Fiberglass Fabric (EG) covering that can be used continuously up to 1,200°F. Two (2) ½-inch thick blankets of Fiberfrax® Insulation material (Lo-Con Blanket) with a density of 7 - 10 lb/ft^3, surround the drum liner. The blankets' thermal properties are unaffected by water immersion or exposure to humidity.

The polyurethane foam used in the 9977 is manufactured by General Plastics under the registered sign Last-A-Foam® FR-3716. It is a closed-cell, intumescing, polyurethane foam emplaced in the drum as a liquid through a hole in the bottom that expands to fill the free volume. It cures to solid density of 15-17 lb/ft3. When cured, the foam is not soluble in water and has a flashpoint greater than 600°F. The material is flame resistant and self extinguishing. A minimum of 4.04-inches of polyurethane foam is located between the bottom of the drum and Fiberfrax attached to the bottom of the drum liner and 4.46-inches radially between the drum and the Fiberfrax wrapped liner. The foam protects the containment vessels during NCT and HAC events.

TR-19 insulation block is used in the lower liner of the lid for its impact and thermal insulation properties. TR-19 is manufactured by Thermal Ceramics, Inc. and is composed of vermiculite granules and high temperature bonding materials. TR-19 has good high temperature strength with minimal shrinkage up to 1,900°F even when exposed to direct flame. The material density is nominally, 23 lb/ft^3.

Thermal Ceramic Min-K 2000 is used to protect airline flight data and cockpit voice recorders. The material is non-endothermic and is unaffected by NCT and HAC temperatures. It is a light weight compression resistant material with a maximum service temperature of 1,800°F. The

material density is nominally, 20 lb/ft^3. A one (1) inch thick block of Min-K 2000 insulation fills the volume of the lid top liner. Min-K 2000 is manufactured by Thermal Ceramics of Elkhart, IN.

3.2.2.3 5-Inch and 6-Inch Inside Diameter Containment Vessels

Together, the 5CV and 6CV provide containment of the package contents and are designed, fabricated and examined in accordance with the ASME Code. The materials of construction are as specified in ASME Section II, Subpart D.[6]

3.2.2.4 Containment O-Rings

A containment boundary is provided in part by the containment vessel body and closure but is completed by the inner O-ring mounted on the cone-seal plug. The O-ring material is Viton® GLT, a fluorocarbon elastomer with a service temperature range between -40°F and 400°F. When not in service and stored in accordance with Society of Automotive Engineers, Aerospace Recommended Practice, 5316, Revision B, the O-rings have an unlimited shelf life. [13]

The containment vessel O-ring temperature limit is specified by the vendor.[2] The containment vessels temperature limits are based on the ASME Code.[6] These limits are chosen significantly less than the capability of 304L stainless steel and were selected to maximize structural strength while accommodating the heat from a 19-watt content. The polyurethane foam temperature limit under NCT is based on Vendor material testing.[5] Under HAC, no temperature limit is specified for polyurethane foam, because the material is permitted to decompose during the thermal event. Containment vessels pressure limits are taken from Table 2.1 and based on ASME Code allowable stresses. The limiting temperatures for Fiberfrax, TR-19, and Min-k 2000, which comprise the remainder of the package insulating material, are above the regulatory HAC Thermal test temperature (1475 °F).[8, 9, 10]

Table 3.13 lists the temperature limits for those package components that are both subjected to elevated temperatures during NCT and HAC, and are most likely to incur damage during a thermal excursion.

Table 3.13 – Package Component Design Limits

Component	**Temperature** (°F)	
	NCT	HAC
O-rings	400	
CV	~~53~~00	
Last-A-Foam FR-3716	300	N/A

3.3 Thermal Evaluation under Normal Conditions of Transport

The thermal evaluations presented in this section provide the temperatures throughout the package and summarizes the components of interest; the CV atmospheres, the CV, O-rings, the insulation, and the external surface of the package. Results of prototype package testing and analyses show that temperatures within the package do not exceed applicable material limits, do not result in thermal degradation of materials with functions important to safety, nor cause the containment vessels internal pressures to exceed their respective limits. The analyses also show that the maximum temperature of accessible surfaces of the shaded package subjected to 100°F ambient temperature remains below 122°F.

Note: The details of the thermal analyses in this section are documented in Appendix 3.3. Fiberfrax thermal conductivity values used in the analyses in Appendix 3.3 are 12% to 37% lower than the values listed in Table 3.8. Therefore, the CV, O-ring, and contents temperatures reported in this section are conservative (higher). However, since the compressed Fiberfrax thickness is only ½ inch, the effect on the actual values will be small.

3.3.1 Heat and Cold

The following sections present the analysis and testing that show that there is no significant reduction in the 9977 effectiveness when subjected to the initial conditions and tests as specified in 10 CFR 71.43(f). Additionally, analyses demonstrate that all accessible surfaces of the package meets the maximum surface temperature requirements specified in 10 CFR 71.43(g).

3.3.1.1 Thermal Analyses

The thermal models presented in Appendices 3.3 and 3.4 were developed from the 9977 package design drawings given in Appendix 1.1 and from the contents configurations presented in Section 1.2.3. A number of different package configurations and heat-source locations were analyzed as depicted in Section 1.2.3. The analyzed configurations incorporate some simplifying assumptions that do not significantly affect temperature distributions within the packaging. The analyses demonstrate that packaging temperature distributions are not significantly influenced by the small variations within specific payload configurations, i.e., 3013 and food pack configurations. These configurations do result in different temperature profiles within the source material and their immediate surroundings. The addition of product can mass or division of source material among product cans results in lower maximum temperatures in the packaging components. Physical properties of the constitutive materials employed in the thermal models are summarized in Section 3.2.1. Parameters affecting internal and external heat transfer that include natural convection and radiation as mechanisms for heat transfer are also summarized in Section 3.2.1.

Table 3.14~~3.14~~~~3~~.14 lists the configurations of containment vessels and contents that were evaluated in the thermal models and illustrates the bounding configurations for establishing the package MNOP and material temperature limits. The "point" source is a heat source having 19-watts of power with the dimensions of 1-inch length × ¼-inch diameter. (This matches the dimensions of the actual heater used in NCT testing.) The point source simulates a highly concentrated content configuration. A "distributed" heat source is this "point" source

surrounded by high thermal conductivity material to maximize heat transfer to the CV walls. A distributed source simulates a more practical content configuration. These models are discussed in detail in the following sections.

Table 3.14 – Thermal Model Content Configurations

Sources	Content Configuration	5CV	6CV	MNOP (psig)	Material Limit Basis
Sensitivity Studies	Point Source at top	a →	X →		O-rings
	Distributed Source located at Top		↑ d		
	Distributed Source located at Middle		↓↑		
	Distributed Source located at Bottom		↓ e		
	Point Source at Bottom	a →	X →	56.3 (5CV) 41.2 (6CV)	Containment Vessel Last-A-Foam
Content	Food Pack Cans	↑ c			
	3013	↑ b			
	RTG Configuration		↑		

Notes a: Bounded by the equivalent configuration in the 6CV
b: Bounded by the Food Pack Can configuration
c: Bounded by the Point Source at Bottom
d: Bounded by the Point Source at Top
e: Bounded by the Point Source at Bottom

Configuration not Analyzed

3.3.1.1.1 Modeling Software

Models for the Normal Conditions of Transport (NCT) and the Hypothetical Accident Conditions (HAC) were developed using the MSC/PATRAN-THERMAL® (M/PT)[11] general purpose heat transfer software. The PATRAN module of M/PT is used as the pre processor for creating the finite element model of the package and the post processor for evaluating the modeling output. The P/Thermal module of M/PT performed the computations, including determination of radiation view factors between adjacent package components. The Quality Assurance benchmarking of the P/Thermal code is described in Appendix 3.5. A detailed description of PATRAN and P/Thermal which provide the justification for their use in evaluating the 9977 is provided in Appendix 3.6.

3.3.1.1.2 Modeling Assumptions and Justifications

For all models the following simplifying assumptions were made. These assumptions do not significantly effect the temperature distributions to the package. Justification for each assumption is given when appropriate.

- The drum is in an upright position. This is the transportation and storage configuration.
- The drum wear ring and rim are not modeled as their metal mass is small.
- The bottom surface is adiabatic. This is conservative and gives higher temperatures.
- There is radiative heat transfer from the sides and top of the drum to the ambient.
- There is natural convection heat transfer from the sides and top of the drum to the ambient.
- The NCT and the pre-HAC (except for the HAC Thermal) ambient temperature is 100^{o}F.
- Heat transfer across gas-filled volumes was assumed to occur via conduction and thermal radiation, convection in these spaces was neglected.
- Compositions of the contents were not modeled. Contents were modeled as 1-inch long, ¼-inch diameter, source at the 19W maximum decay heat rate for the package.
- Specific geometries of the content configurations were not modeled. A configuration with 19W and maximum heat conduction was modeled located at the top, middle and bottom of the CV to maximize package component temperatures. The source was embedded in a cylindrical slug of material that was in direct contact at the top and bottom of the CV, and is not in contact when modeled in the middle of the CV.
- Content containers and fixtures (with the exception of the RTG Assembly) within the containment vessel are ignored in the model. This is conservative since the inclusion of convenience cans will increase the overall conductance of the model.
- The Fiberfrax® blanket surrounding the drum liner was estimated to be ½-inch thick after placement of the foam.
- The containment vessel is concentric with the drum assembly. Slight eccentricity will only have higher order effects on the temperatures.
- Convection is not modeled inside the containment vessel or in the gap between the containment vessel and the drum assembly liner. Radiation heat transfer is considered in air spaces.
- Contact resistance is not modeled between different contacting surfaces with the containment vessel. This is higher order effect and will have only minor influence on the temperature distributions within containment vessel components.
- For cases with insolation, there is a total insolation of 800 cal/cm^2 applied over a period of 12 hours on top of the drum and 400 cal/cm^2 over a period of 12 hours on the side of the drum and the absorptivity of the drum is assumed unity for solar radiation. For

conservatism, the insolation is applied continuously, rather than as a step function with a period of 12 hours, as prescribed by 10 CFR 71.71. The corresponding time averaged heat fluxes are 245.77 Btu/ft^2 hr on the top of the package and 122.88 Btu/ft^2 hr on the side of the package.

- All models are steady-state for NCT and pre-HAC conditions.

3.3.1.1.3 Benchmarking the Thermal Model

To validate the NCT thermal model, a transient thermal test was performed on a prototype of the 9977 package (prototype SN-6) with the 6 inch diameter CV (6CV) configuration.[14] Figure 3.3 is a schematic of the 9977 with a mock source installed in a 6CV and the thermocouple locations for the thermal benchmark tests. SN-6, at a uniform temperature of 73°F and containing a 19 Watt heat source, was subjected to a fixed ambient temperature of 100°F in an environmental chamber. The 100°F ambient condition in the environmental chamber simulates NCT without insolation. The base of the package was elevated above the environmental chamber floor, and thus, natural convection and thermal radiation boundary conditions were applied to the entire exterior of the package. Figure 3.4 shows the prototype in the environmental chamber prior to the test. The power supplied to the heater was monitored and manually controlled. For these tests, the contents were mocked-up with a heater embedded in a 304L stainless steel billet. The duration of the heating test was approximately 140 hours and was based on preliminary thermal analysis. In the experiment, temperatures were recorded every minute for the first four minutes, then the next measurement was taken at 18 minutes, and then temperatures were recorded at intervals of 6 minutes until 1,600 minutes. From 1,600 minutes to the end of the test, temperatures were recorded every 3 minutes until the end of the test at approximately 142.7 hours. Reference 15 describes the transient thermal test in detail and Appendix 3.3 details the transient thermal benchmarking analysis for the prototype. Although it was planed to hold the environmental chamber at a constant temperature of 100 °F, due to a failed cooling unit the environmental chamber temperature gradually increased over the test. The average chamber ambient temperature was approximately 103 °F.

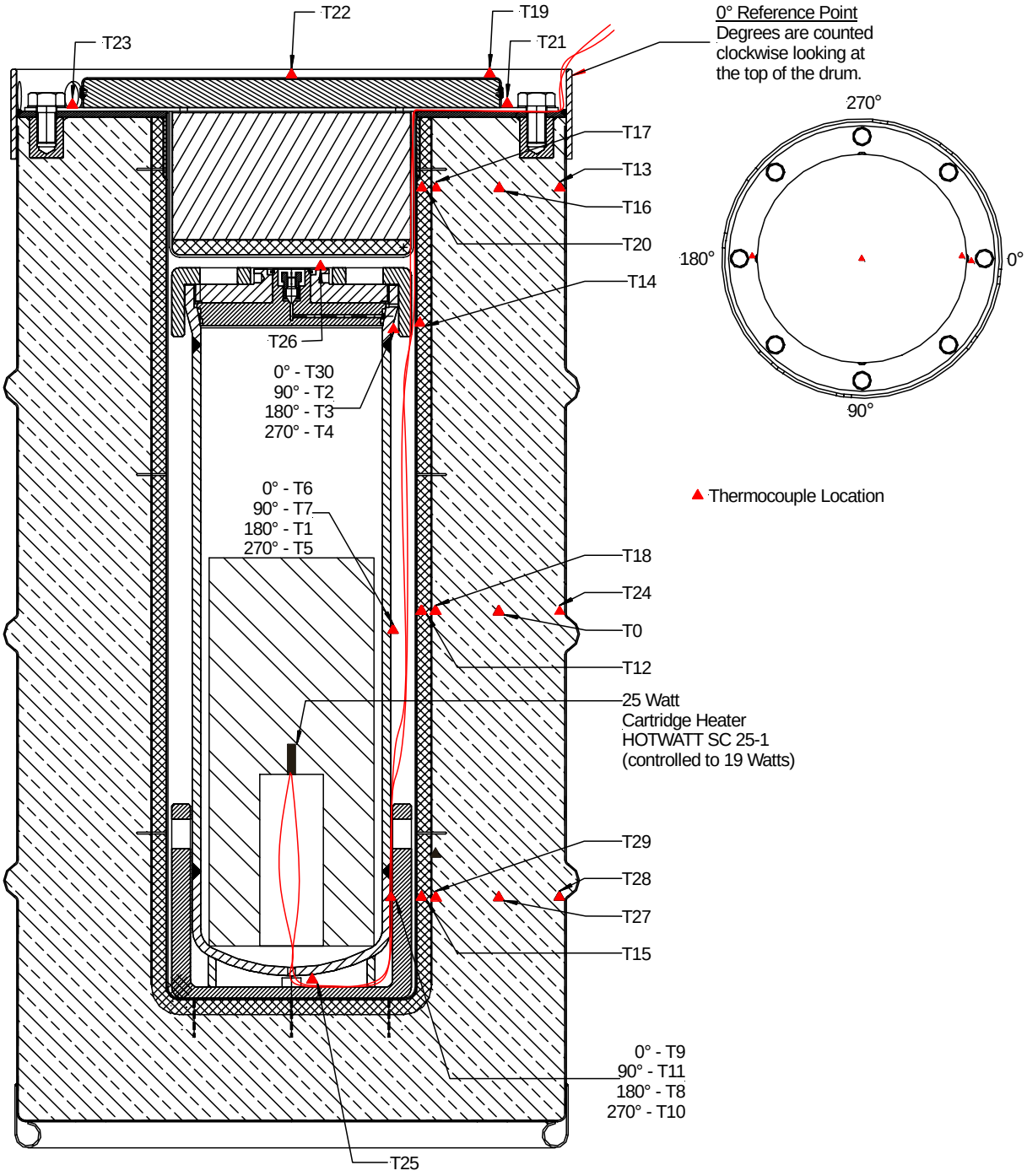

Figure 3.3 – NCT Baseline Test Package Schematic

Figure 3.4 – Test Package SN-6 Positioned in Environmental Thermal Chamber

The transient benchmark analysis model used the material configurations and source location shown in Figure 3.5. The model was axisymmetric. All exposed internal package surfaces were modeled as radiation boundaries. All exposed external package surfaces are modeled with natural convection and radiation boundary conditions. Initial benchmark analyses over predicted the prototype package temperatures by roughly 25% using vendor property data for the foam. By increasing the thermal conductivity property data for the foam, the benchmark analysis better approximated the measured temperature results. For all cases the emissivity of exterior surface of the drum, 0.21, was maintained. The temperature profile predicted by the analyses showed less sensitivity to internal surface emissivity changes than changes to foam material conductivity. Figure 3.6 compares the measured data from the environmental chamber; to the temperatures calculated using the Vendor property data for foam conductivity and to temperatures calculated with the modified foam thermal conductivity. The Vendor foam conductivity had to be approximately doubled to reach 95% correlation with measured data.

Because the use of the Vendor foam thermal conductivity is more conservative, producing higher temperatures in the package, the Vendor data was used for evaluation in the NCT and HAC models.

Table 3.15 gives a detailed listing of the measured and predicted temperatures.

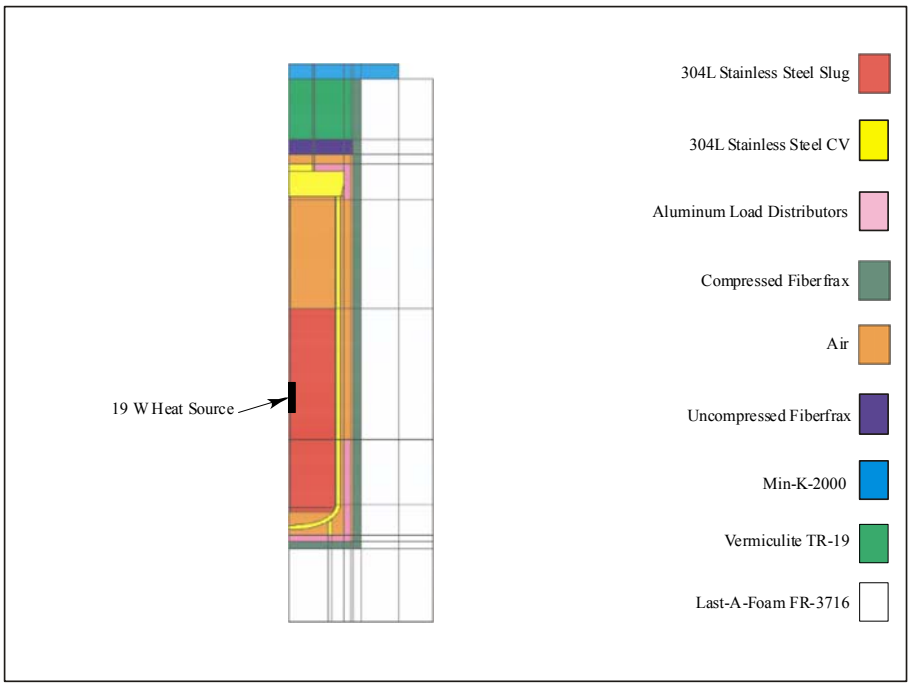

Figure 3.5 – Material configuration for Benchmark Analysis.

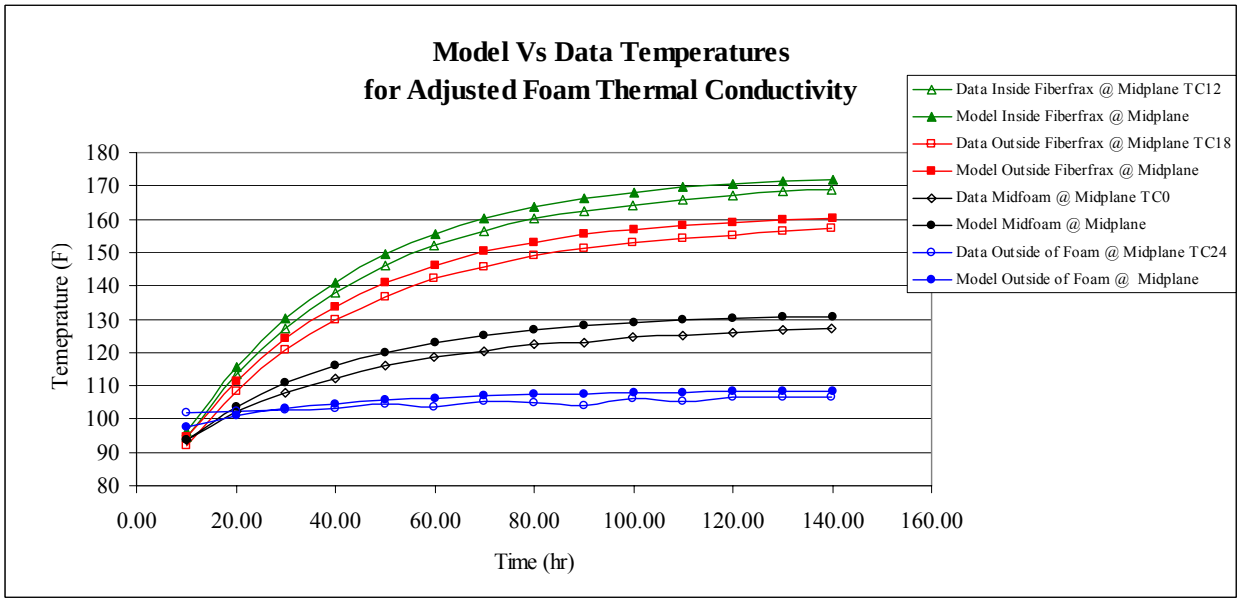

Figure 3.6 – Temperatures Measured vs. Calculated with Adjusted Foam Thermal Conductivity.

Table 3.15 – Correlation Between Measured and Predictions Temperatures

		Foam Thermal Conductivity Tabulated			Foam Thermal Conductivity Modified		
Thermocouple	**Measured (°F) ***	**Model (°F)**	**Model minus Measured (°F)**	**% Correlation**	**Model (°F)**	**Model minus Measured (°F)**	**% Correlation**
T0	125.03	142.68	17.65	14.12	129.65	4.62	3.70
T12	166.04	204.82	38.78	23.36	169.56	3.51	2.12
T13	106.01	102.40	-3.60	-3.40	102.96	-3.04	-2.87
T14	150.94	189.44	38.50	25.51	157.02	6.08	4.03
T15	177.37	210.66	33.29	18.77	176.11	-1.26	-0.71
T16	110.54	115.13	4.59	4.16	110.44	-0.10	-0.09
T17	117.95	126.93	8.97	7.61	116.73	-1.23	-1.04
T18	154.36	192.10	37.74	24.45	158.22	3.85	2.50
T19	105.96	115.13	9.17	8.65	100.46	-5.50	-5.19
T20	118.99	129.63	10.65	8.95	118.54	-0.45	-0.38
T22	104.89	103.65	-1.24	-1.18	102.56	-2.33	-2.22
T24	105.12	103.65	-1.47	-1.40	108.08	2.96	2.82
T25	184.39	221.55	37.16	20.15	190.19	5.80	3.15
T26	158.75	194.85	36.10	22.74	163.90	5.15	3.25
T27	127.57	139.91	12.33	9.67	128.76	1.19	0.93
T28	104.91	106.57	1.66	1.58	108.27	3.35	3.20
T29	160.47	196.90	36.43	22.71	163.13	2.67	1.66
T31	103.25	100.00	-3.25	-3.15	100.00	-3.25	-3.15
T1, 5, 6, 7 (ave)	185.81	220.44	34.63	18.64	189.71	3.90	2.10
T8, 9, 10, 11 (ave)	187.16	223.69	36.52	19.51	192.86	5.70	3.04
T2, 3, 4, 30 (ave)	161.56	195.70	34.14	21.13	164.68	3.11	1.93
T21, 23 (ave)	107.05	101.21	-5.85	-5.46	101.70	-5.36	-5.01

* Temperatures measured at test time of 110 hours

3.3.1.1.4 Thermal Model Source Sensitivity

Analyses have shown that the location of the radioactive material contents within the containment vessel affects component temperatures in a package. A source in intimate contact with the inside of the CV will maximize the temperature at that location, with the local temperature gradient dependent upon the configuration (materials and volume) of the adjacent materials. A source located at the top of the CV will maximize the temperature at the O-Rings. A source located at the bottom of the CV will maximize the heat transfer to and the temperatures of the packaging components (e.g. liner, foam) immediately adjacent to it.

A total of eight (8) content configurations were considered for evaluating the 9977 component temperatures to the Normal Conditions of Transport. Five (5) consisted of the distributed source configurations. In the distributed source configurations, the content was modeled as a 19 Watt source embedded along the centerline of a 6.75-in high cylinder with high thermal conductivity, which touches the wall of the CV. The contents were positioned at the top, middle and bottom of the 6CV (shown in Figure 3.7) and the top and bottom of the 5CV (Figure 3.8) to maximize the heat transfer to the CV and the drum assembly.

These locations are representative of the possible content configurations as specified in Section 1.2.3.2. The case with the distributed source located at the top of the CV maximizes the heat input and temperatures of the Cone-Seal Assembly, upper CV body and the O-rings. The case with the distributed source located at the bottom of the CV maximizes the temperatures in the bottom of the package. The case with the distributed source located at the mid-height of the CV investigates the effects when the source is between the extreme cases and verifies that the temperatures from this configuration are also bounded by the extremes.

Two (2) content configurations consisted of point sources. The case with the point source in intimate contact with the bottom of the Cone-Seal Plug maximizes the temperature at the point of contact. The case with the point source in intimate contact with the bottom of the CV maximizes the temperature at the inside of the Pipe Cap. The "distributed" and "point source" models determined the effect of concentrating the heat flux on the temperature distributions of the package components. Figure 3.9 shows the two point source configurations.

Finally, a detailed content configuration for the RTG assembly was also analyzed and is shown in Figure 3.10.

Table 3.163~~.163.16~~ summarizes the analyses results and highlights the maximum component temperatures for each case. It can be seen that for similar content configurations the 6CV configuration bounds the 5CV and concentrated sources bound the distributed ones. Table 3.143~~.143.14~~ illustrates the relationships between the various configurations. The extreme nature of the point source configuration produces high localized CV temperatures ~~that are still within the allowable limits.~~ . Since ~~T~~the point source is not representative of any actual content shipping conditions~~.~~ is not considered in evaluating CV stresses and not mentioned further. However, the point source temperature is used for calculating the CV Maximum Normal Operating pressure. The temperatures for the RTG case are all well below the limiting temperatures.

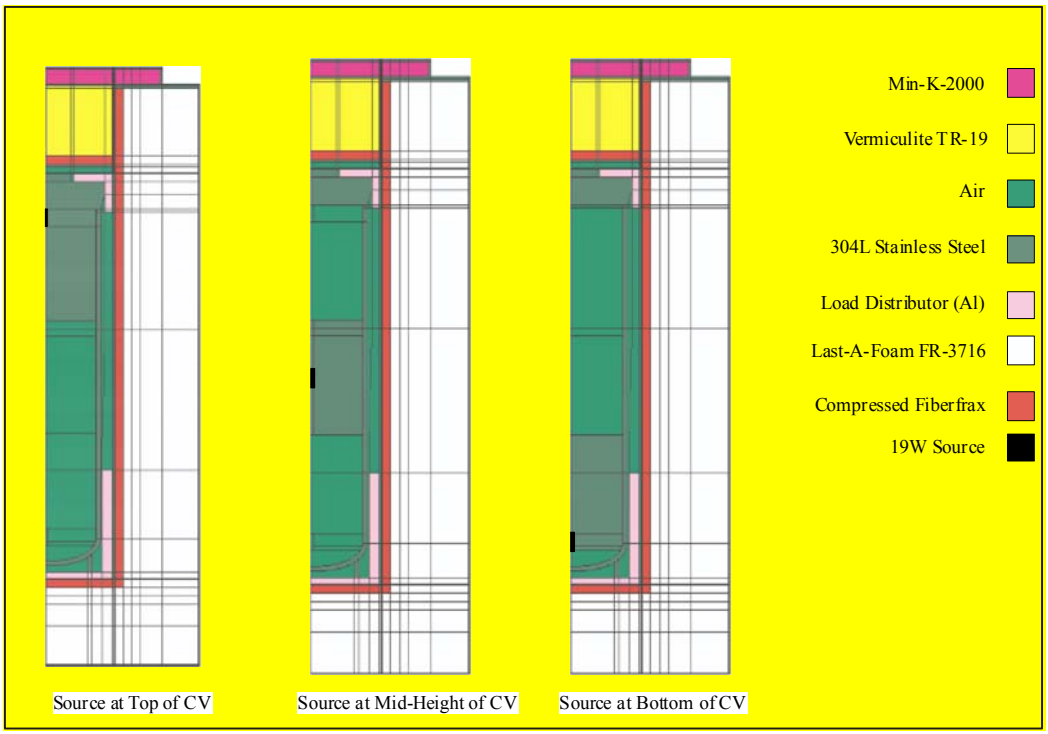

Figure 3.7 – 6CV Distributed Source Configurations

(Note that the foam is replaced with air when modeling the HAC fire transient.)

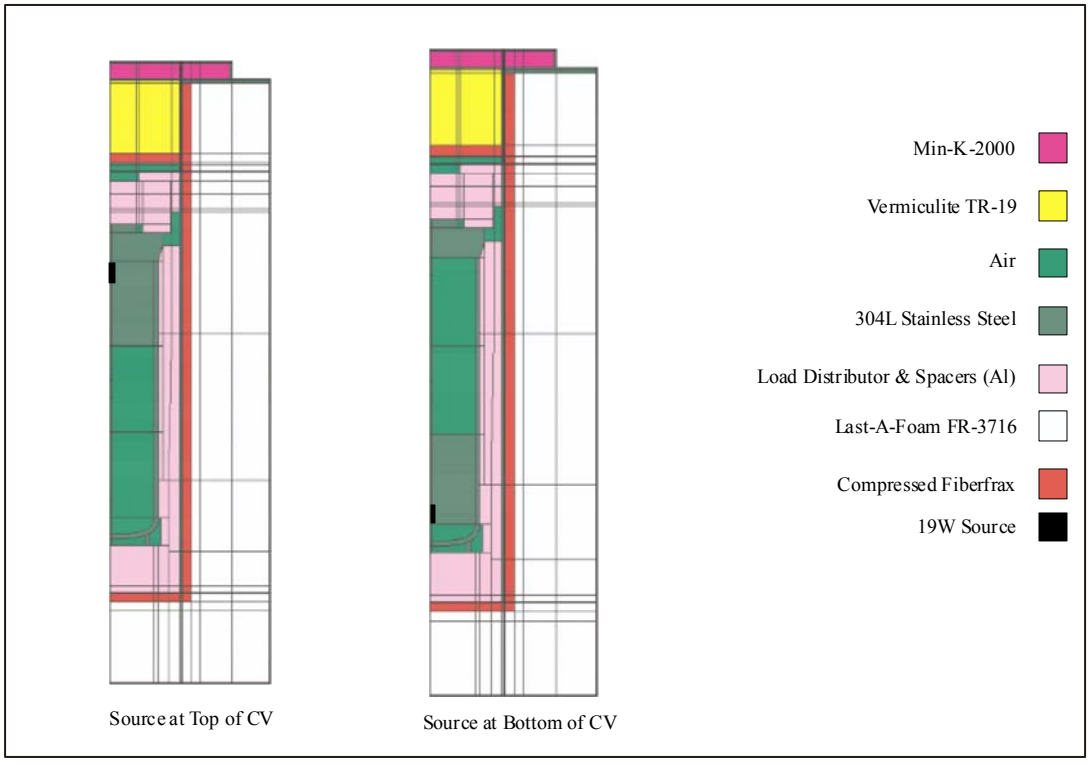

Figure 3.8 – 5CV Distributed Source Configurations

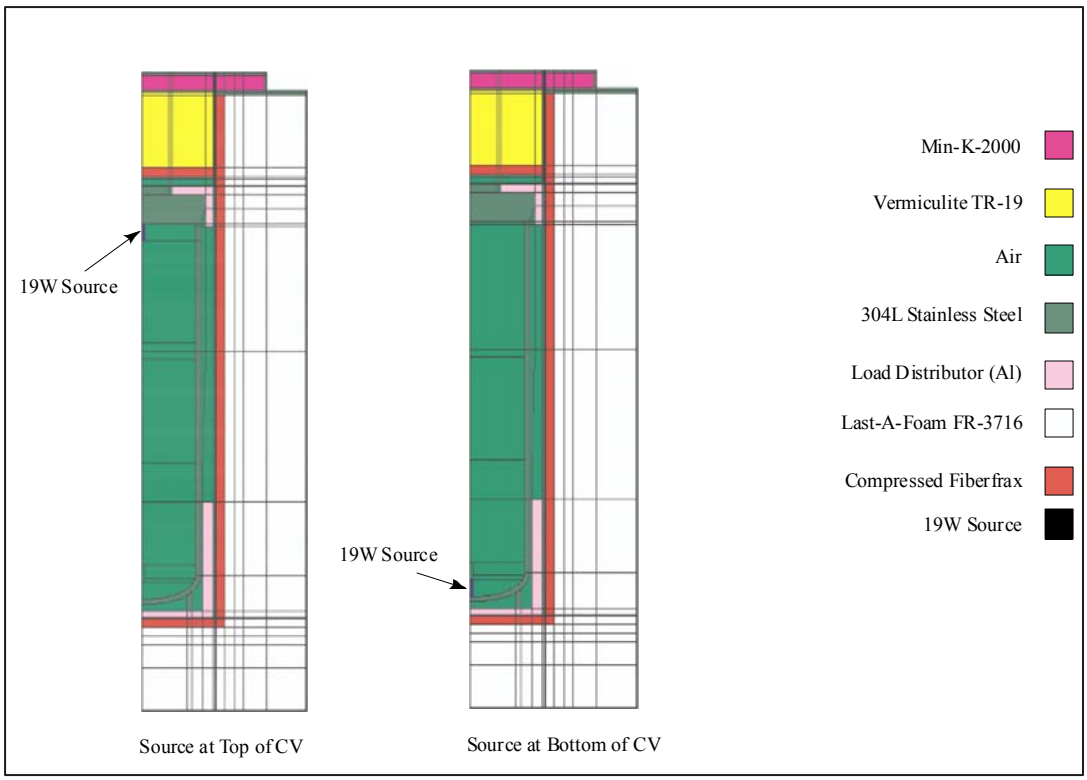

Figure 3.9 – 6CV Point Source Configurations

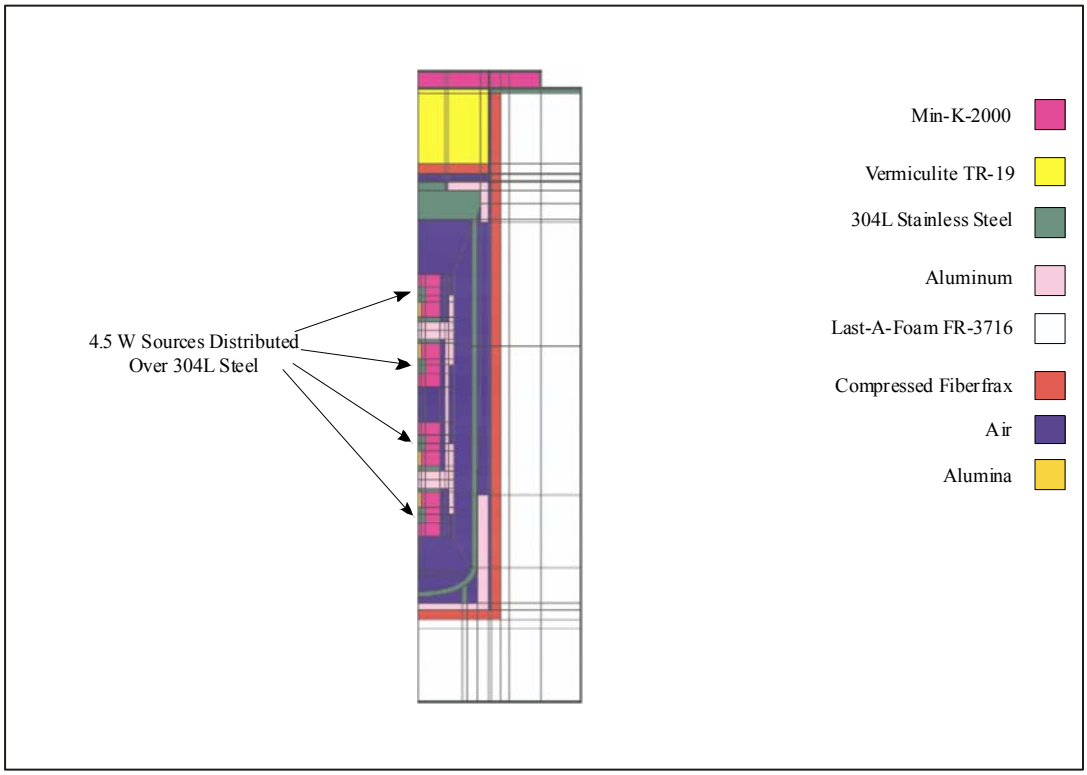

Figure 3.10 – 6CV with RTG Configuration

Table 3.16 - Calculated Temperatures under NCT with Insolation

Source Condition	Source Location	Drum (°F)	Poly Foam (°F)	5 Inch CV (°F)			6 Inch CV (°F)		
				Body	O-rings	Contents	Body	O-rings	Contents
Point	Top	202	278	n/c	n/c	n/c	417	318	473
	Bottom	203	304	n/c	n/c	n/c	482	265	535
Distributed	Top	202	275	260	240	272	321	302	333
	Mid-Height	203	274	n/c	n/c	n/c	303	278	333
	Bottom	203	295	241	240	280	312	265	350

n/c = Not Calculated

3.3.1.1.5 Thermal Model - Contents

The contents specified in Table 1.2 are evaluated against the source sensitivity analysis, presented in Section 3.3.1.1.4, to first to verify that the source location analysis bounds the specified content packing configurations, and second to determine the maximum temperature for the content configurations.

3.3.1.1.5.1 Content C.1 Heat Sources

Content C1 bounds the isotopes used in the Radioisotope Thermoelectric Generators (RTGs)[15] that will be shipped in the configuration shown in Section 1.2.3.2. Thermal analysis for the RTG configuration is presented in Appendix 3.3. The thermal model is shown in Figure 3.10.

RTGs are shipped within the 6CV secured in an assembly designed to withstand road, air, and routine handling shocks and vibrations that could affect their operating performance, as shown in Figure 1.6. The assembly incorporates axially opposing compression springs located at the top and bottom of the fixture used for dampening axial loads. The springs roughly center the housing in the middle of the CV. The housing also incorporates four (4) aluminum Cups with spiraling fins that are designed to contact the walls of the CV to dissipate heat from the RTGs to the packaging and for dampening radial loads. Two (2) polyurethane energy absorbers are included at the top and bottom of the assembly to limit total travel of the RTGs under extreme shocks.

For thermal analysis modeling, the housing is simplified, the housing is assumed to be suspended in the middle of the CV with no contact axially or radially with side walls. The polyurethane shock absorbers and the compression springs are not modeled. For simplicity the spiraling aluminum fins were also were not modeled. Thermal modeling and testing performed at Sandia with RTG prototype fixtures has shown that the aluminum fins have minimal effect on heat transfer between the fixture and the CV.[16] In addition to the simplification of the assembly components, detailed features of the RTG components were not modeled. However, the simplification of the RTGs is conservative, in that it raises the RTG temperatures and maximizes the temperature profile of the assembly and bounds the true component temperatures.

Results of the RTG analysis are summarized in Table 3.17 and shown in Figure 3.11 below. The RTGs, the RTG assembly, and the packaging components do not exceed their individual temperature limits for packaging requirements.

Table 3.17 - Component Temperatures for NCT with RTG Contents

Component	**Maximum Calculated Temperature** (°F)	**NCT w/ Insolation Temperature Limit** (°F)
O-rings	274	400
CV	288	3500
Last-A-Foam® FR-3716	272	279
RTG – ^{238}Pu	635	2000
RTG – Min-K insulation	<260	1800
RTG Assembly – Al components	<600	1100
RTG Assembly – Polyurethane Shock Absorbers	<300 [a]	350

a - not modeled, temperature is average between RTG shell and CV

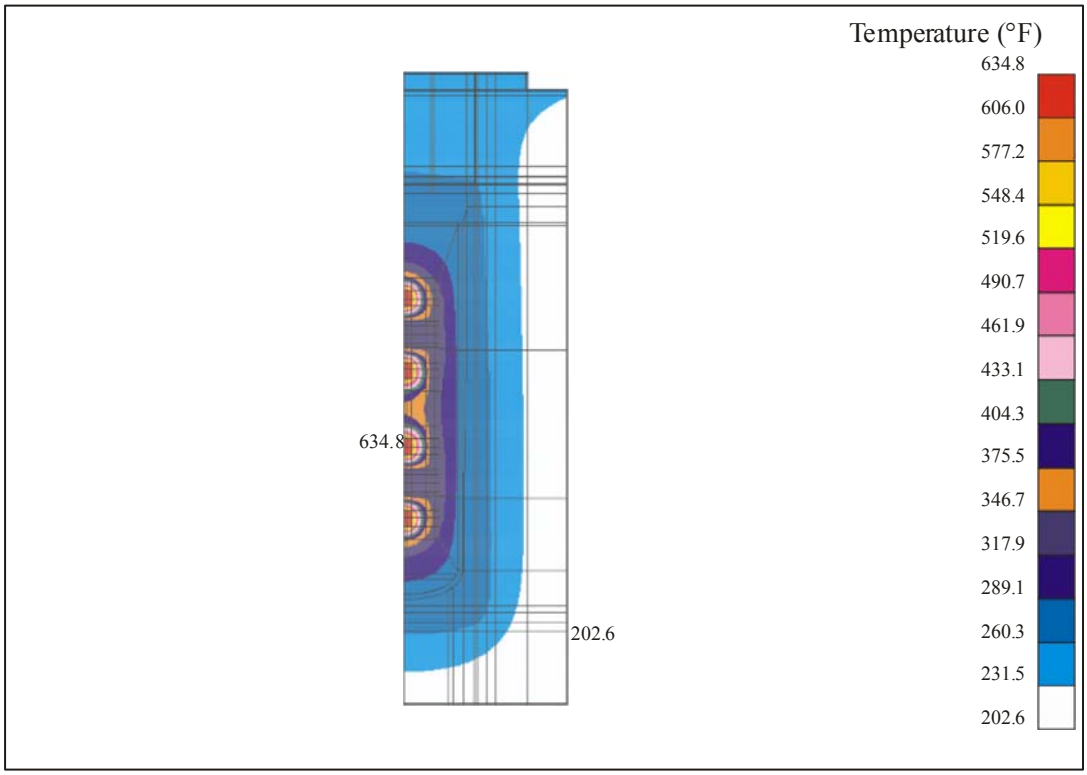

Figure 3.11 – NCT temperature profile for RTG contents.

3.3.1.1.5.2 Content C.2 Uranium/Plutonium Metals

Thermal analysis for the C.2 content configuration is presented in Appendix 3.3. Per Section 1.2.3.3.2, Content C.2 may be shipped in either the DOE-3013-STD storage containers or Food Pack Can (FPC) configurations. Analyses[17] done for the 9975 Primary Containment Vessel, which is identical to the 9977 5CV, has shown that the FPC configuration thermally bounds the 3013 configuration with similar contents for the O-ring and the average CV gas temperatures. Therefore, the 3013 configuration is not modeled in the NCT calculation.

For thermal analysis modeling, the FPC configuration is simplified and it is assumed that a cylindrical 19 Watt source that was approximately 1 inch long with a diameter of 0.25-in. was embedded in a cylindrical slug of 304L stainless steel, in direct contact with adjacent inner surfaces of the CV located at either the top or the bottom of the 5CV, as shown in Figure 3.12. By embedding the source in the cylinder, the distribution of heat generated by the source was more realistic than if the cylinder had been surrounded by air. ~~FPC is gone and the contents are placed directly in contact with the inside bottom surface of the 5CV as shown in Figure 3.12. This simplification of the FPC configuration is conservative in that it maximizes the surface temperatures of the 5CV in which it is in contact and the temperature of the adjacent polyurethane foam.~~ Results of the C.2 analysis are summarized in Table 3.18. The CV and the packaging do not exceed their individual temperature limits for packaging requirements.

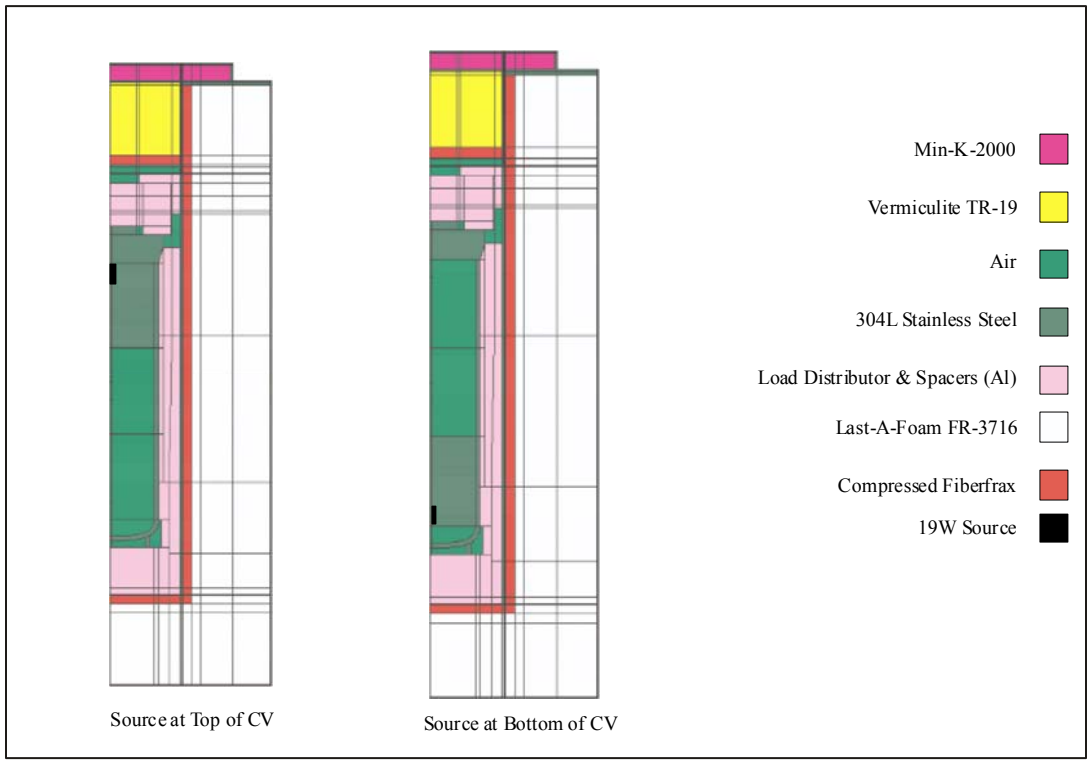

Figure 3.12 – NCT Model for Bounding C.2 Content Configuration in the 5CV.

Table 3.18 - Component Temperatures for NCT with Contents C.2

Component	**Maximum Calculated Temperature** (°F)	**NCT w/ Insolation Temperature Limit** (°F)
O-rings	240	400
CV	260	~~5~~300
Last-A-Foam® FR-3716	275	300
Contents	280	2000

3.3.1.1.5.3 Content C.4 Uranium Metals/Alloys

The decay heat rate for 13,500 grams of 235U, and permitted impurities, is less than $^{1}/_{100}^{th}$ of a Watt. This negligible heat loading will not affect the package and was not explicitly analyzed.

3.3.1.1.5.4 Content C.5 Uranium Oxides

The decay heat rate for 13,500 grams of 235U, and permitted impurities, is less than $^{1}/_{100}^{th}$ of a Watt. This negligible heat loading will not affect the package and was not explicitly analyzed.

3.3.1.2 Description of NCT Model with Limiting Contents

For the thermal analysis, the limiting components include the containment vessel, the O-ring seals and the Last-A-Foam® insulation. Temperature limits for components of the 9977 for the NCT and HAC are listed in Table 3.1.

3.3.1.3 Results for the NCT Model with Limiting Contents

The maximum NCT temperatures occur for the configuration of a distributed~~highly concentrated~~ point source located at the end of the CV closest to the component of interest~~configuration~~. The two cases modeled for NCT consisted of a 19 Watt heat source embedded in a high conductivity cylinder located at the top and at the bottom of the CV. The maximum predicted temperatures of the limiting components for the two cases are listed in Table 3.19.

Table 3.19 - Component Temperatures for NCT with Distributed~~Point~~ Sources

Component	**Temperature** (°F)	
	Maximum Predicted	**NCT Limit**
O-rings	3~~18~~02 [a]	400
CV	34~~8~~21 [~~b~~a]	~~5~~300
Last-A-Foam® FR-3716	295~~304~~ [b]	300

a Source at top of CV

b Source at bottom of CV

Temperature profiles for each of the three cases are shown in Appendix 3.3.

The constitutive properties of the polyurethane foam insulation are provided in Table 3.8. The foam is limited to a bulk temperature of 300 °F [7] and, if the polyurethane foam is confined and no mechanical loads are applied, it can be held at this temperature for an extended period and retain its form.[7] Thermal decomposition of FR-3716 occurs at 534 °F. Off-gassing and melting/oxidation is not observed below about 500 °F. Therefore, the localized high temperature for a highly concentrated heat source configuration is acceptable.

3.3.1.4 NCT Model with RTG Contents

To investigate the bounding NCT temperature profile with more realistic contents a model was developed for a set of RTG's, the baseline NCT model was modified as follows:

1. Insolation is applied.

2. As shown in Figure 3.11, the RTG contains 4 heat sources, each outputting 4.5 Watts of decay power. Each of the heat sources was distributed over a cylinder approximately $^{7}/_{8}$-inch long with a diameter of $^{7}/_{16}$-inch.

Emissivities used in the model are summarized in Table 3.11. The NCT temperature profiles calculated for the package and its contents are shown in Figure 3.11. Table 3.17 lists the predicted NCT temperatures of the limiting components for RTG contents.

3.3.2 Maximum Normal Operating Pressures

The Maximum Normal Operating Pressure (MNOP) for the CV was calculated by using the maximum content temperature, T_f, and using the relation

$$P_f = \left(\frac{14.7 T_f}{529.67} + \delta P_a \right) \qquad 3.3.2.\text{-}1$$

where: δP_a = Actual increase in pressure due to degradation of the plastic (psia).

$$\delta P_a = \frac{T_f \rho_a}{T_{test} \rho_{test}} \delta P_{test}$$

T_f = Actual gas temperature in the CV (R).

ρ_a = Actual mass of plastic per free volume of the CV.

ρ_{test} = Test mass of plastic per free volume during the plastic degradation test.

T_{test} = Test temperature for the plastic test (R).

δP_{test} = Change in pressure due to plastic degradation during the plastic test at temperature T_{test} (psia).

The reference temperature and pressure are representative of the state of the gas when the CV was sealed. The pressure calculation includes off-gassing of 100-grams of plastic bags. Appendix 3.7 gives the methodology to calculate the pressure contribution due to off-gassing of plastic bags. Since 6CV temperatures bound 5CV results, 6CV temperatures are used for all calculations. Furthermore, bare source temperatures are used as the final air temperatures inside the CV for conservatisms. Appendix 3.8 gives the MNOP calculations.

As shown in Table 3.16, bare source models give higher content temperatures than the mock-up content models. Although the point sources are not represent credible content configurations, these configurations resulted in the highest content temperatures an so were used to calculate the bounding pressures within the CVs under normal operating conditions. As added conservatism, the average air temperature within the CV was set equal to the content temperature. The MNOPs for the two source locations are listed in Table 3.20.

Table 3.20 - Normal Operating Pressures

Source Location	**Pressure (psig)**	
	5CV	**6CV**
Bottom of CV	56.32	41.17
Top of CV	51.89	37.69

3.4 Thermal Evaluation under Hypothetical Accident Conditions

The 9977 package was evaluated under HAC by tests and analyses. The tests included a practice burn and a series of pool fire tests. Prior to the pool fire, the packages had undergone the sequence of free drop, crush, and puncture tests required by 10 CFR 71.73 for HAC. The data from the tests were used to validate the thermal models. The HAC thermal models consist of three sequential phases, corresponding respectively to the pre-fire, fire and post-fire conditions. The pre-fire model, which is identical to the model for NCT except that insolation is neglected, determines the temperature profile in the package prior to the HAC fire transient. The fire transient determines the bounding package temperature, with respect to 10 CFR 71.73, during a hypothetical fire. Finally, the post fire transient is used to predict the bounding temperature of the components of the 9977 after the fire has been extinguished.

The maximum temperatures of the limiting components are compared against their limit temperatures in Table 3.21.

Table 3.21 – 6CV Component Temperatures under HAC

Condition and Package	**Method**	**Drum** (°F)	**Body** (°F) [~~5~~300]	**O-rings** (°F) [400]
Fire - Prototype Mock-up (w/o Foam)	Calculated @ 30 min {Measured}	1,475 {1,853}	426 {435}[b]	432 [a] {n/m}
Fire - Prototype	Calculated @ 30 min {Measured}	1,475 {1,873}	307 {250}[b]	307 {270}[b]
Post-Fire - Prototype w/ Insolation	Calculated Steady State	202	400	381

n/m = Temperature Not Measured

a – Package modeled without foam

b - Measured with a "temperature indicating label", value reported bounds the actual temperature

[limit] designates limiting temperature of the component

Table 3.21 shows that the maximum temperatures of the components are below their limit temperatures. The exceedance for O-rings is for the hypothetical case where no foam was present. The CV passed the leak test for this fire test. The test preparation, post-fire evaluation, and results are described in Appendix 3.2.

Note: The details of the HAC thermal analyses in this section are documented in Appendix 3.4. Fiberfrax thermal conductivity values used in the analyses in Appendix 3.4 are 12% to 37% lower and the density values are 80% higher than the values listed in Table 3.8. This is equivalent to actual thermal diffusivity ($\alpha = \frac{k}{\rho C_p}$) of the Fiberfrax being higher than used in the analyses in Appendix 3.4. Since the compressed Fiberfrax thickness is only ½ inch, the effect on the actual values will be small. There is no impact on the 30 minutes fire phase of the transient because the values in Table 3.21 are based on the measured temperatures in actual fire tests. The impact on the post-fire period will only be that the actual highest temperatures will reach a little sooner than reported in Appendix 3.4.

3.4.1 Initial Conditions

A series of pool fire tests were conducted on 9977 packages. Prior to the pool fire the packages had undergone the sequence of free drop, crush and puncture tests required by 10 CFR 71.73 for Hypothetical Accident Conditions. As specified in 10 CFR 71.73 the package must be "engulfed, except for a simple support system, in a hydrocarbon fuel/air fire of sufficient extent, and in sufficiently quiescent conditions, to provide an average emissivity coefficient of 0.9, with an average flame temperature of at least 800°C (1475°F) for at least 30 minutes." Further, "the fuel source must extend horizontally at least 1m (40 in), but may not extend more than 3 m (10

ft), beyond any external surface of the specimen, and the specimen must be positioned 1 m (40 in) above the surface of the fuel source."

Pool fire tests that met or exceeded the requirements listed above were conducted by NovaTech Innovative Technologies International, using 9977 mockups, at the South Carolina Fire Academy. Initial conditions such as ambient temperature, wind speed and direction were also judged favorable at the time of the tests.

3.4.1.1 Description of Pre-Fire HAC Model

The model for the pre-fire HAC was the same as that for the NCT except that the insolation heat flux was omitted. Convection boundary conditions are listed in Table 3-11 and material property data is listed in Tables 3.8 to 3.10. Specific application of correlations and parameters are described in the summary below. Appendix 3.4 gives the details of the model and the results.

1. The drum is in an upright position.
2. The bottom surface is adiabatic.
3. There is radiative heat transfer from the sides and top of the drum to the ambient.
4. There is natural convection heat transfer from the sides and top of the drum to the ambient, see Table 3.11.
5. The ambient temperature is 100^{o}F.
6. There is no insolation heat flux.
7. The foam thermal conductivity tabulated in the General Plastics Company data is used, see Table 3.8.
8. Material properties for compressed Fiberfrax® were applied to the blanket surrounding the drum liner. The blanket was assumed to be ½ inch thick.
9. The contents contain a heat source outputting 19 Watts of total decay power, distributed over a cylinder approximately 1 inch long with a diameter of 0.25 inches. The cylinder was embedded in a material with a high thermal conductivity.
10. Three source locations were considered, see Figure 3.7:
    i. Source at the top of the CV.
    ii. Source at the middle of the CV.
    iii. Source at the bottom of the CV.
11. The model was steady-state.
12. Emissivities for the pre-fire HAC analysis are listed in Table 3.22.

Table 3.22 - Surface Emissivities for Pre-Fire HAC

Surface	Emissivity
CV	0.30
Drum Liner	0.30
Bottom of Lid	0.30
Load Distributor	0.20
Slug	0.30
Exterior of Drum	0.21

Pre-fire HAC temperature profiles for all three source locations are shown in Figures 3.13 and 3.14. Figure 3.13 shows the overall temperature profiles in the package, while Figure 3.14 shows the temperature profiles in the CV. Table 3.23 lists the maximum content and CV temperatures for all three source locations.

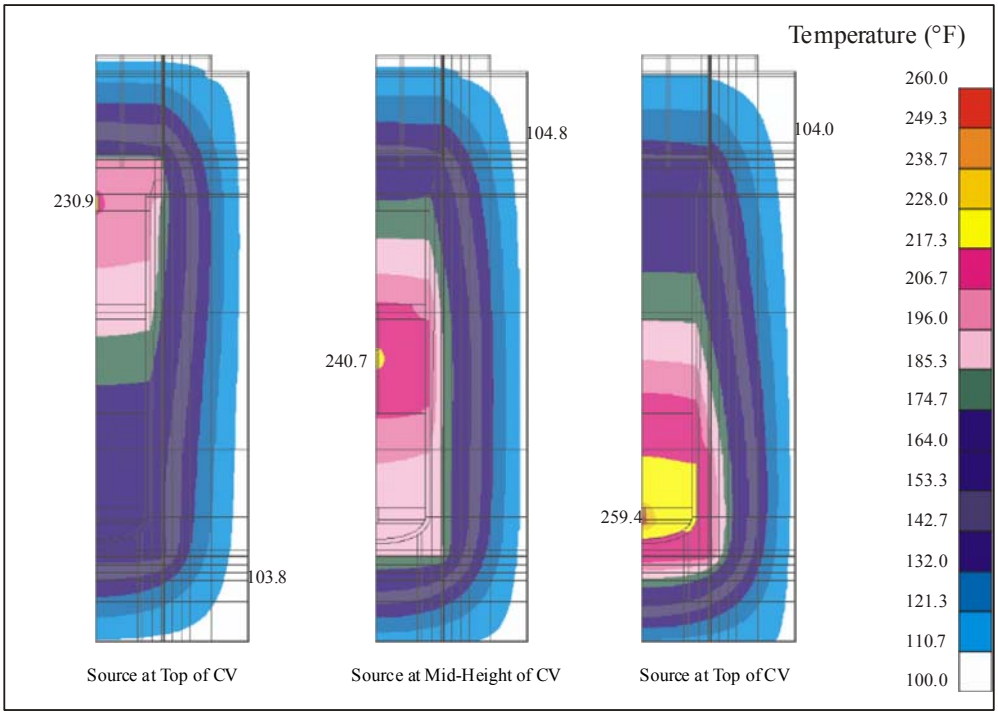

Figure 3.13 - Overall pre-fire HAC temperature profile for 3 different source locations.

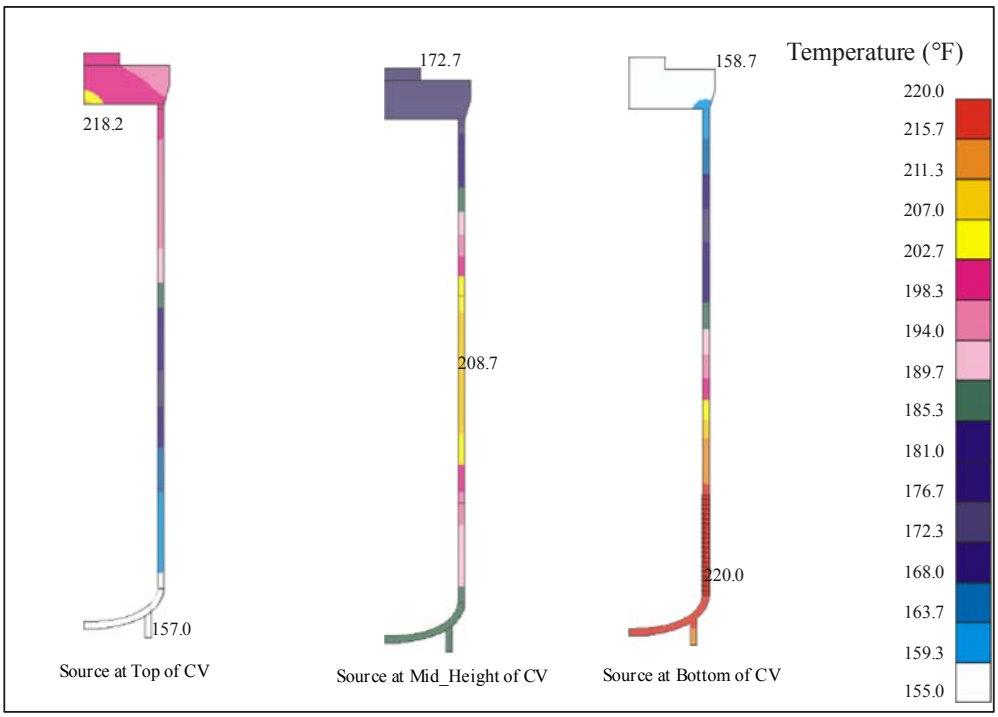

Figure 3.14 - Pre-Fire HAC Temperature Profile of CV for 3 Source Locations.

Table 3.23 - Content and CV Temperatures for the Pre-Fire HAC Model

Component	Temperature (°F)		
	Source Location in CV		
	Top	Mid-Height	Bottom
Contents & Internal Air	231	241	259
CV	218	209	220

3.4.1.1.1 Actual Test Package Contents

Prior to the burn test, the packages had been subjected to the sequence of impacts required by 10 CFR 71.73. Although actual packages would have an internal heat source, for practical considerations **the test packages did not** have heat sources. In the actual packages the heat source would raise the initial temperature of the package at the start of the fire, thus resulting in higher final temperatures at the end of the 30 minute fire. To simulate the initial temperature of the packages at the onset of the fire, each of the test packages was heated in an environmental chamber prior to the burn tests. Details of the preheating process included heating in an environmental chamber at 200ºF and subsequent transport of the heated package to the test site. For the transport to the burn site, the package was wrapped in a 4 inch thick Kaowool blanket.

At the test site, the package was surrounded with insulation and drum heaters were used to mitigate heat loss from the package. These details and subsequent steps leading to the estimate of pre-fire temperatures are described in Appendix 3.2. Material configurations for the package mock-up during preparation for the pre-fire conditions are shown in Figure 3.15.

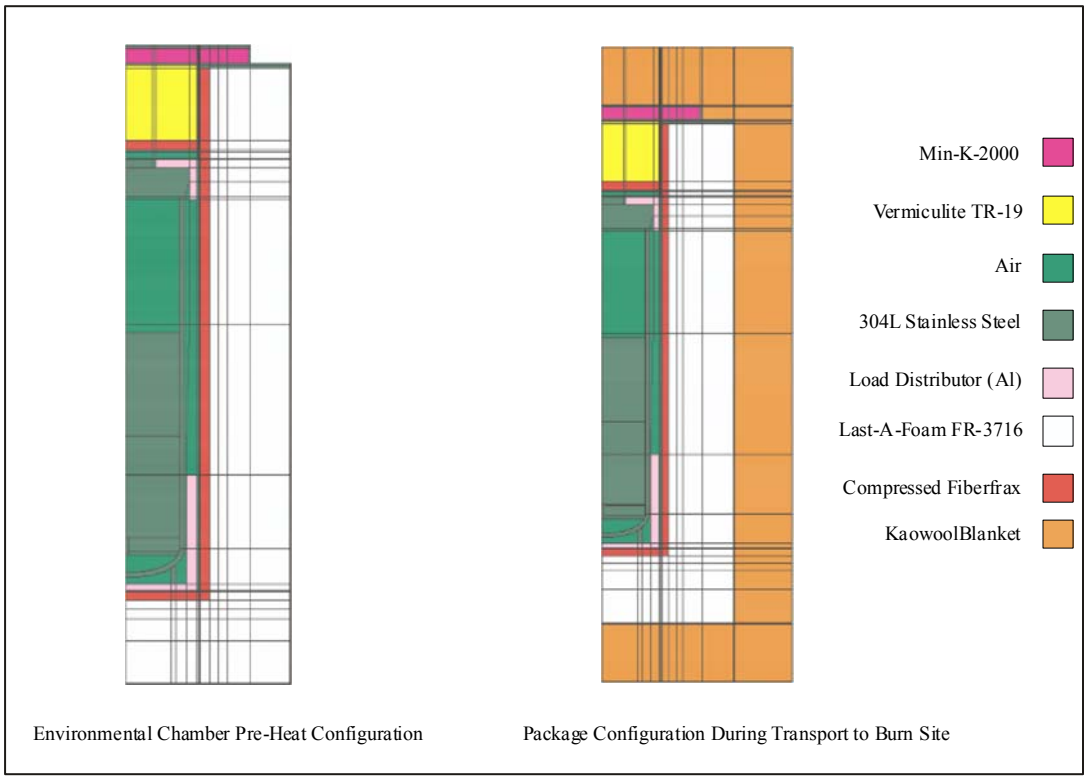

Figure 3.15 - Material Configuration for Prototype Package in the Environmental Chamber and During Transport

3.4.1.1.2 Actual Test Package Thermal Model

The test package pre-heat, transport, and pre-test conditions were modeled and analyzed to predict the actual component temperatures immediately preceding the HAC thermal test. Predicted temperature profiles at the end of the pre-heating of the 9977 test package and at the end of the shipping process are shown in Figure 3.16. The calculated temperature of the CV after heating in the environmental chamber at 200°F for 96 hrs and after transit to burn site while wrapped in 4 in of Kaowool for 2 hours at an ambient temperature of 32°F was ~183°F, rounded down, at the location of the temperature label that gave the maximum post-HAC reading. This was the true pre-fire condition prior to the beginning of the fire test. Since the package did not include the heat source, adjustments had to be made to the temperature distribution within the package to account for the absent heat load. These adjustments are explained in the HAC fire thermal model Section 3.4.2.3.

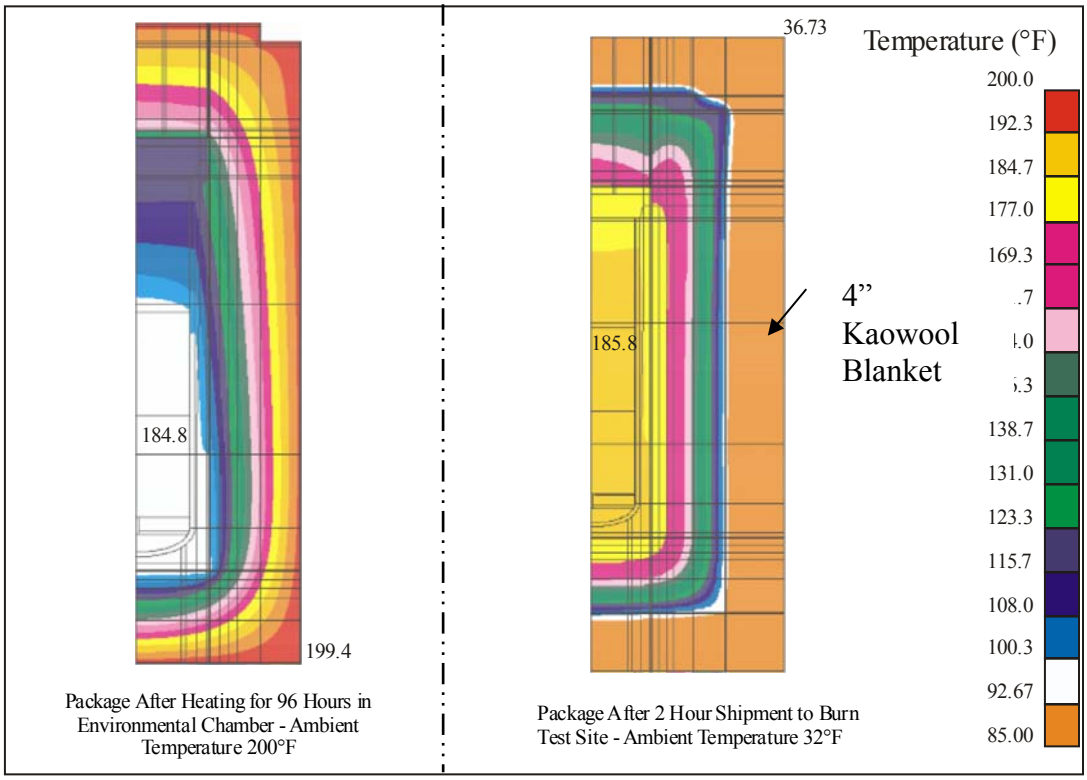

Figure 3.16 - Temperature Profiles in the Prototype Package, after Pre-Soak and after Shipment (Note: Temperature scale in Figure 3.16 applies only to after Shipment Profile)

3.4.2 Fire Test Conditions

As discussed in Chapter 2, a series of five thermal (i.e. fire) tests were performed. The first, and most relevant to the HAC fire model, was a practice burn in which a 9977 prototype without the LAST-A-FOAM® which had not been impact tested was exposed to a 30 minute pool fire. The remaining four tests were for prototype 9977's that both had foam and had been subjected to the required sequence of impact tests. In the drop tests for each of these four packages, initial contact with the ground occurred at a different location on the outer drum;

- top corner (SN-2),
- drum top (SN-4),
- bottom (SN-5), and
- side (SN-3).

The data monitored for all tests included:

1. The ambient temperature.
2. The wind speed and direction.
3. The fire temperature, via an array of 8 thermocouples suspended within the enclosure for the package, see Figure 3.17.
4. The radiant fire temperature via four directional flame thermocouples (DFT's), see Figure 3.17.

A detailed description of the fire tests, the data collection systems, and the results obtained from them is given in Appendix 3.2.

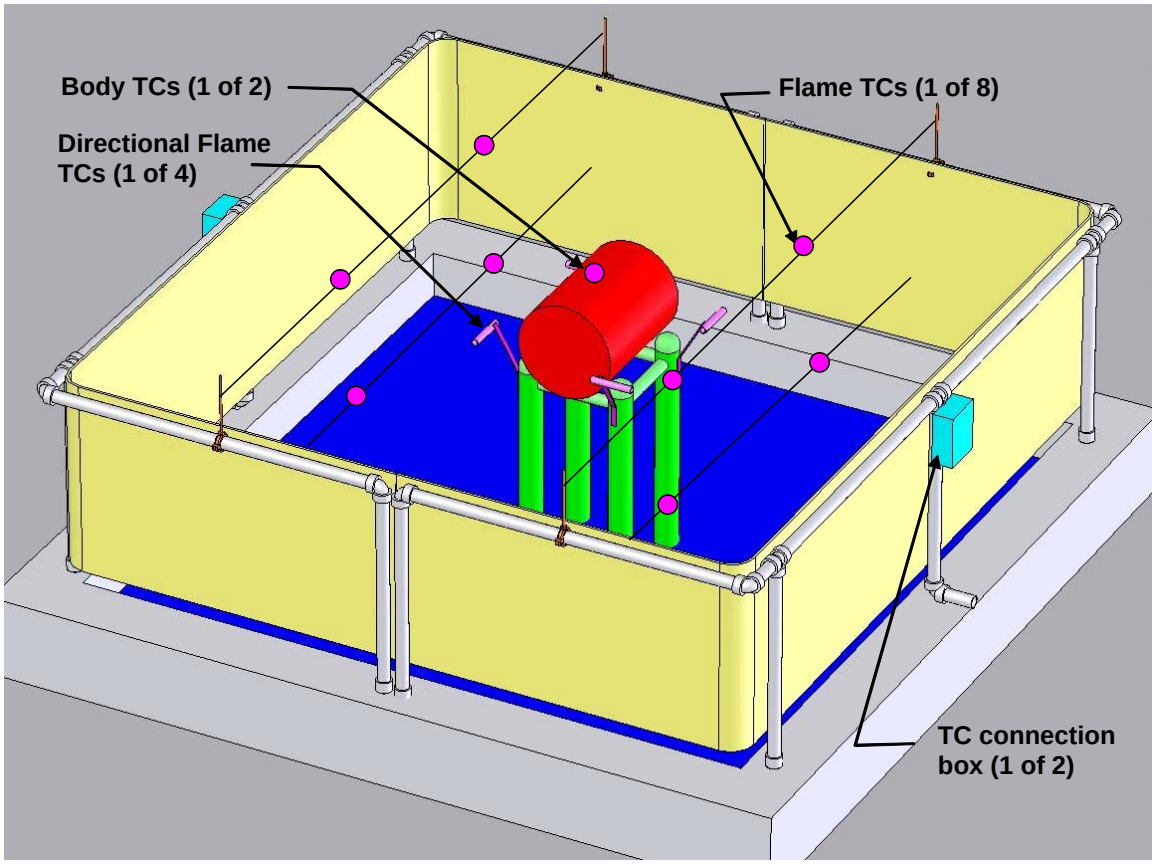

Figure 3.17 - Locations of DFT's and Thermocouples Measuring HAC Flame Temperature.

3.4.2.1 Practice Burn Test

The analytical model for this test assumes that the foam instantaneously vanishes at the onset of the fire. Since the prototype used for this burn test did not have any foam, leak test results from the practice burn test established the integrity of the 9977 under HAC thermal conditions without the benefit of the foam insulation in the drum. Internal component temperatures were measured with thermocouples and temperature labels. The external fire temperature was measured with

thermocouples suspended in the fire. The radiant emissivity of the fire was measured with directional thermocouples and an attempt was made to measure the outer surface temperature of the package with an optical pyrometer. The ambient temperature and wind data was also monitored during the test. Test procedures are described in the test plan in Appendix 3.2.

Figure 3.18 is a photograph of the prototype 9977 on the test stand prior to the burn, Figure 3.19 shows the engulfment of the package by the fire and Figure 3.20 shows the package after the 30 minute burn.

In the practice burn test, temperature data for the CV was obtained from temperature labels affixed to its top, bottom and sides. CV temperatures along with the mean temperature of the fire are listed in Table 3.24.

Figure 3.18 - Practice Burn 9977 on Stand Prior to Test.

(Note: Thermocouples used to measure the fire temperature and their support wires can also be seen in the photograph.)

Figure 3.19 - Extent of Engulfment of the Practice Burn 9977

Figure 3.20 - Practice Burn 9977 after the Fire Self Extinguished.

3.4.2.2 Thermal Model for the Practice Burn

A thermal model was prepared to calculate package temperatures for comparison with the measured test temperatures. The model included radiation and conduction effects inside the drum but required some correction to the Fiberfrax thermal properties to account for the convection effects inside the drum and the flow of hot gases thru the vent holes. The analysis demonstrated the adequacy of the model to simulate the measured temperatures. The model, however, was not used for HAC fire analyses because of the presence of foam in the regulatory burn tests. Figure 3.21 gives the material configuration of the model. Table 3.24 compares measured CV temperatures to those predicted at the location of the temperature labels following a 30 minute engulfment by fire having an average flame temperature of 1853°F. The 9977 initial temperature was assumed to be uniformly 50°F. The temperature profile after the 30 minute fire is shown in Figure 3.22.

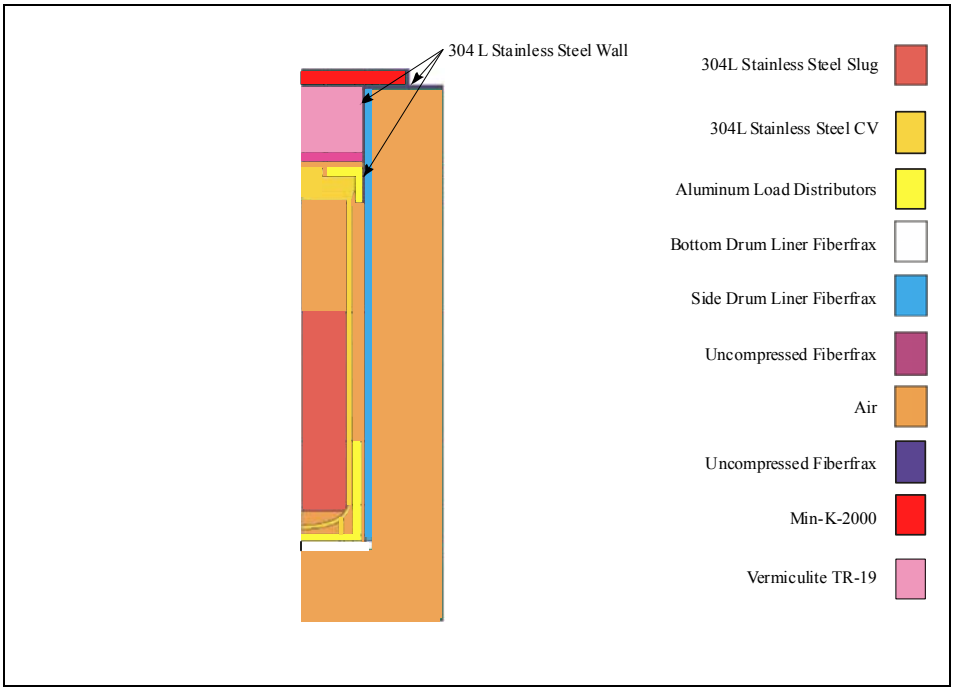

Figure 3.21 - Material Configuration for the 9977 model of the Practice Burn.

Table 3.24 – Practice Burn Measured vs. "Tuned Model" Predicted Temperatures

	Temperature at Location (°F)			
	Mean Fire	**Top of CV**	**Bottom of CV**	**Side of CV**
Measured	1853	420-435	330-340	330-340
Predicted	NA	426 (Node 8660)	331 (Node 2246)	334 (Node 3585)

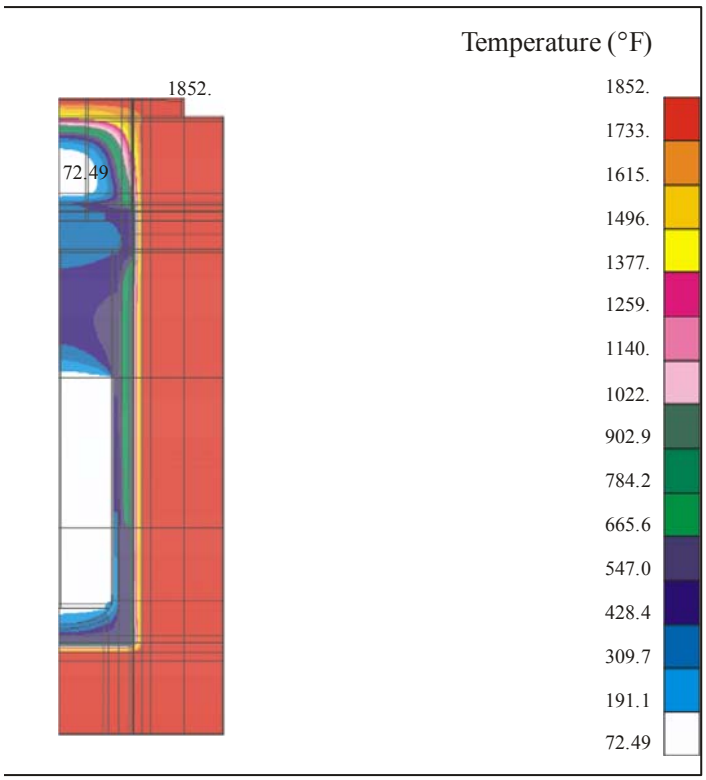

Figure 3.22 - Predicted Temperature Profile in 9977 without Foam after 30-min 1853°F Fire.

(Note: There was no internal heat source for this model.)

3.4.2.3 HAC Fire Thermal Model

The full HAC thermal model consists of three sequential phases, corresponding respectively to the pre-fire, fire and post-fire conditions. The pre-fire model, which is identical to the model for NCT except that insolation is not included, determines the temperature profile in the package prior to the HAC fire transient. This is described in Section 3.4.1.

When the foam is exposed to the high temperatures during the fire portion of the HAC, it decomposes to form an intumescent (expanding) char that fills voided spaces within and expands out of the drum. Foam properties vary widely as it is heated. At a temperature of about 279°F the foam reaches its glass transition temperature and at temperatures above 480°F the molten foam undergoes an endothermic chemical reaction to form oligomers and char.[5] The oligomers later undergo a non self-sustaining exothermic reaction that eventually ceases when heat is no longer supplied by an external source. The endothermic phase of the reaction utilizes heat that would otherwise be used to raise the temperature of surrounding materials. For this reason, the degradation of the foam during the fire transient serves to thermally protect the package contents, the CV and its O-rings.

The parameters governing heat transfer during the heating, phase change and thermally driven chemical reactions of the foam are not known. Further, the complexity of foam degradation, heat transfer and flow of hot gasses preclude a direct analysis of the 9977 package during the fire. For this reason, the heating of the contents of the 9977 during the fire phase of the HAC

was not modeled numerically. Rather, data from the HAC burn tests, see Appendix 3.2, was used to estimate the temperatures within the package after the fire. This process involved using the temperature-indicating label data to estimate the increase in the component temperatures during the fire and then superposing this temperature change onto component temperatures predicted for the pre-fire HAC. These estimates would give the upper bound of the temperatures during the fire phase. They will then be used as initial values for the post-fire HAC.

Since there was no heater in the test packages during the fire tests, adjustments were made to the observed temperatures during fire test to conservatively estimate the impact of the missing heater on internal package temperatures. As pointed out in Section 3.4.1.1.2, just before the fire, the temperature at the CV location with the highest post-fire temperature was approximately 183ºF. However, after the burn test, including the cool down, the temperature label reading at this location on the CV was ≤ 270°F, see Appendix 3.2. This implies a CV temperature increase of 87°F (270ºF – 183ºF) during the fire. This increase was superposed onto the maximum temperatures of all regions within the drum liner in Table 3-23. Table 3-25 lists the package component temperatures that are obtained after superposition and they will be treated as representative of the temperatures following the 30 minutes fire test. These temperatures become the initial conditions for the post-fire thermal model.

Table 3.25 - Temperatures at End of 30-Minute HAC Fire (Initial Post-HAC)

Component	Temperature (°F)		
	Source Location in CV		
	Top	Mid-Height	Bottom
Contents & CV Gases	318	328	347
CV	305	296	307
Foam to CV	400	400	400
Min-K-2000®	1000	1000	1000
TR-19®Block	400	400	400
Char and External Metal	1475	1475	1475

The fire transient was approximated as described above and determines the bounding package temperature, with respect to 10 CFR 71.73, during a 30 minute hypothetical fire. The temperatures within the 9977 package at the end of the fire are the initial temperatures for the post-fire HAC thermal analysis. Finally, the post fire transient is used to predict the bounding temperature of the components of the 9977 after the fire has self extinguished.

All models for the 9977 under HAC were developed with the MSC/PATRAN-THERMAL® general purpose heat transfer software. As for the NCT, the contents of the package were not explicitly defined, except that the total source was 19 Watts. Hence, as noted in Section 3.1, the power density and location of the source were conservatively modeled at three different locations to produce the highest temperatures for the limiting components of the 9977. The

highest predicted temperatures for any source location were compared to the component temperature limits.

3.4.2.4 Description of the Post-Fire HAC Model

In the HAC thermal tests, the hot 9977 package continued to off-gas combustible vapors through openings in the shell of the drum after the pool fire fuel burned off. Openings in the outer drum were either holes formerly covered by Caplugs® or gaps resulting from impact damage. It was observed that the gas burned for approximately 45 minutes after cessation of the 30 minute fire. Off-gas combustion, which is more or less a surface phenomenon, is not believed to significantly heat the 9977.

In the tested 9977's, a layer of foam remained around the drum liner following the fire. By virtue of its presence, the foam and, thus, the internal components it surrounds, could not have exceeded the foam melting temperature, which is less than 500°F.

Following the fire the cooling rate of the package is controlled by heat generation from the internal 19W source, insolation and the amount of insulation about the internal components. Disassembly of the test packages following the pool fire tests revealed that the remaining amount of foam was equivalent to a layer between 1 and 2.3 inches thick surrounding the drum liner, see Appendices 3.2 and 3.9. Analyses were performed for three cases.

1. A 1 inch thick layer of foam surrounding the drum liner. The remainder of the foam volume was filled with char.
2. A 2.3 inch thick layer of foam surrounding the drum liner. The remainder of the foam volume was filled with char.
3. All foam replaced with char.

The char was assumed to have the thermal properties of air, see Table 3.10, and to completely fill the available space. Therefore, since char fills the voided space between the unburned foam and the drum, no radiation heat transfer was modeled in this space. Material compositions assumed for the 9977 package during the post-fire transient are shown in Figure 3.23. Figure 3.23 should be interpreted with the three configurations described above.

Three source locations were considered, see Figure 3.23:

1. Source at the top of the CV.
2. Source at the middle of the CV.
3. Source at the bottom of the CV.

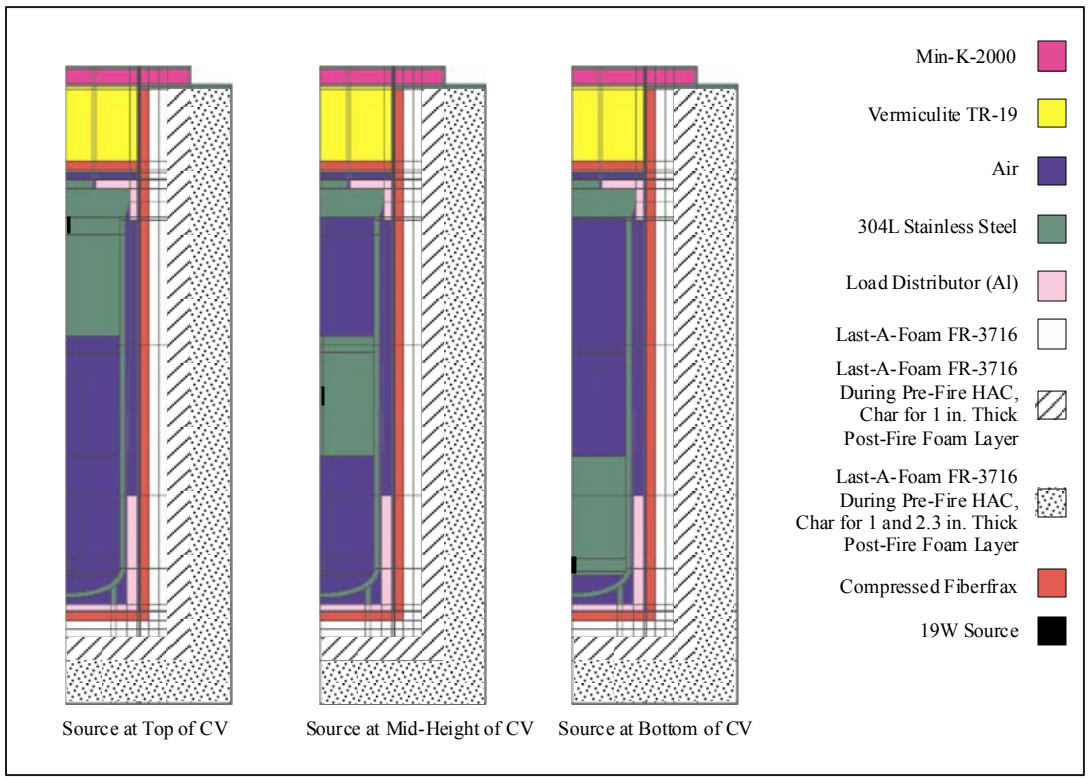

Figure 3.23 – Material representation for the Post-Fire Thermal Models

Emissivities for the post-fire HAC analysis are listed in Table 3.26.

Table 3.26 - Surface Emissivities for Post-Fire HAC

Surface	Emissivity
CV	0.30
Drum Liner	0.30
Bottom of Lid	0.30
Load Distributor (interior)	0.20
Slug	0.30
Exterior of Drum	0.80

Initial component temperatures for the post-fire phase of the HAC are as follows:

1. The initial temperature of the contents of the CV, including the air, are determined by superposing the 87°F CV temperature increase measured during the fire tests onto the maximum content temperature from the pre-fire HAC model. The subsequent temperature is uniformly applied to the contents.
2. The initial temperature of the CV is determined by superposing the 87°F CV temperature increase measured during the fire tests onto the maximum temperature of the CV. The subsequent temperature is uniformly applied to the CV.
3. The temperature of intact foam, remaining after the fire was uniformly set to 400°F (Table 3.25).
4. The temperature of char and exterior metal surfaces of the package were uniformly set to 1475°F.
5. The temperature of the Min-K-2000® and adjacent interior metal surfaces was uniformly set to1000°F.
6. The temperature of the TR-19® insulation was uniformly set to 400°F.

Temperatures in items 1 and 2 above are obtained by adding 87°F to the temperatures in Table 3.23. Table 3.24 lists the 9977 package component temperatures assumed at the beginning of the post-fire HAC transient.

The post-fire transient analysis was monitored and run until after the temperatures in the package began to decrease.

3.4.2.5 Results for the Post-Fire Phase of the HAC Model

The results from the post-fire HAC Model are shown in Table 3.27. The table shows the transient O-ring and maximum CV temperatures in terms of the minutes following the end of the fire. The detailed analyses are documented in Appendix 3.4.

Table 3.27 - O-Ring & CV Temperatures in the Post-HAC Fire Phase

Time After End of Fire (Min)	O-Ring/CV Temperatures (°F)			
	Source Location			
	Bottom	Mid-Height	Top	Limit
(Initial Condition) 0	307/307	296/296	305/305	400/~~5~~300
30	360/394	353/400	338/392	400/3~~5~~00
60	375/382	368/393	346/387	400/3~~5~~00
90	381/381	373/385	351/382	400/3~~5~~00
≥180	374/388	367/372	363/382	400/3~~5~~00

The maximum contents temperature is 425ºF and occurs about 6.5 hours into the post-HAC cool down.

3.4.3 Maximum Temperatures and Pressures

Fourteen ventilation holes are located in the drum shell and bottom to prevent it from becoming pressurized due to the temperature increase and the decomposition of the polyurethane foam. Likewise, the lid has four ventilation holes that release heated air and the gases from decomposing RTV sealant. However, the CV is pressurized by heated air, and thermal decomposition of plastic bagging.

For the purpose of calculating regulatory MNOPs, material containers are assumed to leak freely into the CV. Component volumes that support the pressure evaluations are given in Appendix 3.8. The pressurization of CV is described in Section 3.4.3.2.

3.4.3.1 Maximum Temperature

The maximum temperature for the 6CV bound the temperatures for the 5CV. Therefore, 6CV maximum temperatures are used for the pressure calculations for both CVs. The maximum CV temperature is the content temperature during the fire transient. This temperature is 425ºF and occurs about 6.5 hours into the post-HAC cool down. This temperature is used as the gas temperature inside the CV for pressure calculations.

3.4.3.2 CV Internal Pressure

The free volume within the CV is the volume remaining after subtracting the volumes occupied by radioactive contents, material containers, plastics (if present) and aluminum spacers. For the 5CV internal pressure, the Food Can configuration gives the minimum free volume inside the CV. The minimum volume is found to be 0.1145 ft^3. The pressure contribution from thermal decomposition of plastic bagging is evaluated in Appendix 3.7.

The free volume of 6CV is calculated by subtracting the volume of RTG configuration. From their respective drawings, the internal volume of 6CV is 608 in^3 and that of RTG is 97 in^3. For pressure calculations, the free volume of the 6CV is conservatively taken as 304 in^3.

The gas temperature inside the inner can is conservatively taken as the maximum temperature of the content. The maximum pressure calculations are given in Appendix 3.8. The maximum pressures are listed in Table 3.28.

Table 3.28 – Pressures under HAC

Condition	**5CV (psig)**	6CV **(psig)**
HAC	48.5	35.0

3.4.4 Maximum Thermal Stress

The contents are shipped in material containers (food-pack cans or 3013 containers) inside the CV. Radially, the cans are loose fitting. The heat source does not directly contact the CV, and the CV fits loosely within the Load Distribution Fixtures, which fit loosely into drum inner liner. The CV is free to expand axially and circumferentially, thereby precluding formation of significant thermal stresses. The liner is in contact with the Fiberfrax, but the Fiberfrax material offers no resistance to thermal expansion.

Regulatory Guide 7.8 requires that the package be evaluated for NCT at -40ºF, no heat source, and no insolation. If the package is assembled at room temperature (70ºF), the worst case for development of thermal stresses occurs at -40ºF between the aluminum LDF's and the SS304L containment vessel due to the larger coefficient of thermal expansion for aluminum. It is found that there is sufficient radial clearance between the two components to preclude any mechanical interference. Thermal stresses are evaluated in Section 2.6.1.2.

~~The worst case for development of thermal stresses is simply the hottest content inside the coldest CV. However, the loose fit between the heat sources and the CV accommodates large differential thermal expansion and thereby precludes mechanical interference, even at an ambient temperature of -40°F and maximum allowable internal heating. In addition, differential thermal expansion during NCT is insignificant, as are the thermal stresses imposed on package components (Section 2.6.1.2).~~

The 304L stainless steel of the cone-seal plug and containment vessel body are compatible with the Nitronic-60 stainless steel of the cone-seal nut. The thermal expansion characteristics of these alloys are similar. Specifically, Appendix 2.1 lists the thermal coefficients of expansion for 18Cr-8Ni material (which includes both 304 and Nitronic-60 stainless steels) reported in Table TE-1 of the 1992 ASME Code, Section II, Part D. Therefore, no significant thermal stresses are sustained by any package components.

3.4.5 Accident Conditions for Fissile Material Packages for Air Transport

The 9977 has not been evaluated for transport by air.

3.5 References

1 *Packaging and Transportation of Radioactive Material*, Code of Federal Regulations, Title 10, Part 71, Washington, DC (January 2006).

2 Parker O-ring Handbook, ORD-5700A, The Parker Seal Group, Parker Hannifin Corporation, Cleveland, OH, (2001), http://www.parker.com/o-ring

3 *Rules for Construction of Nuclear Power Plant Components, ASME Boiler and Pressure Code*, Section III, Subsection NB, American Society of Mechanical Engineers, New York, NY (2004).

4 *Rules for Construction of Nuclear Power Plant Components, ASME Boiler and Pressure Code*, Section III, Subsection NF, American Society of Mechanical Engineers, New York, NY (2004).

5 *Last-A-Foam® FR-3700 for Crash and Fire Protection of Nuclear Material Shipping Containers*, Manual, General Plastics Manufacturing Company, Tacoma WA (March 2001)

6 *Rules for Construction of Nuclear Power Plant Components, ASME Boiler and Pressure Code*, Section II, Materials, Part D, American Society of Mechanical Engineers, New York, NY (1992).

7 General Plastics Memo, J. Nichols to KR Eberl, (February 2006)

8 Fiberfrax® Lo-Con Blanket, Manufactured by Unifrax Corporation, Niagara Falls, NY

9 TR-19 Insulating Block, http://www.thermalceramics.com/upload/pdf/1014-100.pdf

10 Min-K 2000, http://www.thermalceramics.com/literature/MK201.pdf,

11 MSC.PATRAN THERMAL 2003 r2, Online Manual, MSC Software Company, Santa Ana, California.

12 ASME Section II, Part D; Thermal Conductivity, Table TCD, pg. 693; Specific Heat and Density, Table NF-2, pg. 703.

13 Society of Automotive Engineers, Aerospace Recommended Practice 5316

14 *9977 General Purpose Fissile Packaging Thermal Benchmark Test*, S-TSM-A-00001, K.R. Eberl, et. al., (April 2006)

15 G. Abramczyk, Letter Re: Sandia National Laboratory RTG Information, SRNL-IES-2006-00005, (February 2006)

16 Sandia Testing Report on the vibrations and thermal testing – Phillip Toone

17 Thermal Analysis of the 9975 Package for Normal Conditions of Transport and Accident Conditions, M-CLC-F-00590, Revision 8, N.K. Gupta (October 2003)

This Page Intentionally Left Blank

3.6 Appendices

Appendix	Description
3.1	9977 Thermal Benchmark Test, S-TSM-A-00001
3.2	SRNL Package Burn Test Report, NT-TDR-06-101
3.3	NCT Thermal Model for the 9977 Package, M-CLC-A-00255
3.4	HAC Thermal Model for the 9977 Package, M-CLC-A-00256
3.5	MSC/PATRAN/THERMAL Version 2003 Software Test Documentation
3.6	PATRAN-PLUS and P/Thermal Code Descriptions
3.7	Pressure Contribution Due to Plastic Bags
3.8	MNOP and Maximum Operating Pressure in 9977 Package GPFP, M-CLC-A-00257
3.9	Determination of the Volume of Last-A-Foam remaining in the 9977 Packaging after the HAC Thermal Test

This Page Intentionally Left Blank

APPENDIX 3.1

NCT THERMAL ANALYSIS BENCHMARKING

This Page Intentionally Left Blank

9977 Thermal Benchmark Test

March 2006

Keywords: GPFP, Prototype, Packaging

Prepared by: K.R. Eberl, G.A. Abramczyk

Washington Savannah River Company

Savannah River Site

Aiken, SC 29808

Prepared for the U.S. Department of Energy Under Contract NO. DE-AC09-96SR18500

Disclaimer

This report was prepared by Washington Savannah River Company (WSRC) for the United States Department of Energy under contract DE-AC09-96SE18500 and is an account of work performed under that contract. The United States, the United States Department of Energy nor WSRC, nor any of their employees, makes any warranty, express or implied, or assumes any legal liability or responsibility for the accuracy, completeness, or usefulness of any information, apparatus, product or process disclosed herein, or represents that its use will not infringe privately owned rights. Reference herein to any specific commercial product, process or service by trade name, mark, manufacturer, or otherwise does not necessarily constitute or imply endorsement, recommendation, or favoring or same by WSRC or by the United States Government or any agency thereof. The views and opinions of authors expressed herein do not necessarily state or reflect those of the United States Government or any agency thereof.

9977 Thermal Benchmark Test

FINAL REPORT

PREPARED BY

K. R. Eberl, Principal Engineer, SRPT — 5/16/06 — Date

G. A. Abramczyk, Senior Technical Advisor, SRPT — 5-16-2006 — Date

REVIEWED BY

P. B. Blanton, Program Manager, SRPT — 5-16-2006 — Date

APPROVED BY:

J. S. Bellamy, Manager, SRPT — 5-16-06 — Date

This Page Intentionally Left Blank

Table of Contents

List of Figures

List of Tables

1 Summary

In order to validate the finite element thermal model, a prototype 9977 package was instrumented and tested at conditions best reproducible for simulating the "Initial Conditions" described in 10 CFR 71.71 Normal Conditions of Transport, which for this test are defined as:

- 100 °F ambient air temperature,
- no insolation, and
- the maximum Content of 19 Watts of decay heat.

The test was run for over 140 hours with temperatures being recorded at 31 locations in and on the package. The results from this test are summarized below.

1.1 Discussion

1.1.1 Requirements

10 CFR 71.71 Normal Conditions of Transport (NCT) requires that the package be evaluated for specified tests and conditions and that the package being tested first be prepared as defined in 71.71(b) as:

> Initial conditions. With respect to the initial conditions for the tests in this section, the demonstration of compliance with the requirements of this part must be based on the ambient temperature preceding and following the tests remaining constant at that value between -29 °C (-20 °F) and +38 °C (+100 °F) which is most unfavorable for the feature under consideration. The initial internal pressure within the containment system must be considered to be the Maximum Normal Operating Pressure, unless a lower internal pressure consistent with the ambient temperature considered to precede and follow the tests is more unfavorable.

In considering the most unfavorable initial condition, the lower ambient temperature specified (-20 °F) was determined to be less challenging for the materials of construction of the 9977 than the higher temperature condition. The Maximum Normal Operating Pressure (MNOP) is achieved with the containment vessel at its greatest temperature. The package maximum temperatures occur when the contents are at the maximum allowed decay heat, the exterior of the package is at the highest ambient temperature (100 °F), and with insolation. So the MNOP requirement is incompatible with the -20 °F ambient temperature condition. In conjunction with the most "unfavorable initial conditions," the low temperature performance of the 9977 under the HAC was investigated with a series of tests performed with a package cooled to -20 °F.

A finite element thermal model was developed to calculate steady-state and transient package temperature distributions under the NCT initial and the HAC conditions. This model is discussed in Chapter 3 of the 9977 Safety Analysis Report for Packaging (SARP). To validate

the calculated temperatures, a transient thermal test was performed on a prototype 9977 package in the 6-inch diameter CV (6CV) configuration with a mock content mass containing a small cartridge heater to simulate content with 19-Watts of decay heat. The package was instrumented and placed in a temperature controlled chamber. The test simulated the "Initial Conditions" of 10 CFR 71.71 requirements: an ambient chamber temperature of 100°F, "no isolation" (due to the closed chamber environment), and a package heat load of 19 Watts.

1.1.2 Test Setup

1.1.2.1 Prototype Package

The prototype General Purpose Fissile Package (GPFP)/Model 9977 unit SN-6, shown in Figure 1, was selected for this test. Figure 2 is a general arrangement sketch of the 9977 prototype package with the heater and the thermocouple instrumentation. SN-6 was an untested prototype which was reserved for additional testing. SN-6 was not significantly altered for or by the "benchmark" NCT test and is available for additional testing. The Secondary Containment Vessel (SCV) from the 9975 packaging is identical in design to the 9977 6CV. A spare SCV, identified as "9975-KAMS TEST-2", was used for this test. The 9975-KAMS-TEST-2 SCV had previously been modified with a ¼-20 UNC hole drilled and tapped in the center of the Pipe Cap end for leak-rate testing.

1.1.2.2 Contents/Heater

The mock "contents" consisted of a 102-lb stainless steel billet with an internal 19-Watt heat source. The heat source, a cartridge heater (HOTWATT® SC25-1 10 to 25-Watt cartridge heater, 1" long × ¼" diameter), was installed in a central well in the billet with thermally conductive epoxy (Cotronics Corp. #918 High Temperature Adhesive). The heater was controlled to output 19-Watts by manually adjusting the power with a variable Autotransformer (Type 3PN1010) read on a calibrated display (VECTOR-VID). Figure 3 is a photograph of the "contents" (i.e. the heater in the SS billet) and Figure 4 is a schematic. The major package components are seen prior to assembly in Figure 5. The "contents" were placed into the 6CV/SCV with the heater wires run out of the CV through the hole in the pipe cap, see Figure 6. The heater wires were run between the 6CV and the inside of the drum liner and out between the lid and drum top plate. A spare heater is shown for scale in Figure 6 and various other photographs.

1.1.2.3 Environmental Chamber

The environmental chamber used for the transient thermal test is a Tenney Environmental Test Chamber (Model T405-2, Serial # 30253-01) with a Watlow 942 Controller. The environmental chamber is shown in Figures 7 and 8.

1.1.2.4 Temperature Recording System

The thermocouples were connected to a data collector (National Instruments SCXI-1001) controlled by a personal computer (Dell OptiPlex GX300) to continuously record

time/temperature data. Confirmatory manual readings were also taken at the beginning and end of each work shift, and periodically.

The temperature data was recorded at the rates listed in Table 1.

Table 1 – Temperature Measurement Recording Frequency

Start Time		End Time		Recording Period	Note
Minutes	Hours	Minutes	Hours	(minutes between readings)	
0	0	85	1.4	1	No data recorded from minute 4 until 18.
85	1.4	1,600	26.6	6	
1,600	26.6	8,564	143	3	4 readings missed: ~ at hours 49, 65, 90, & 114

1.1.2.5 Thermocouples

Thirty-one (31) calibrated, Type E, thermocouples were installed onto the 6CV and into SN-6 at the locations identified in Figure 2. The thermocouples were labeled starting with "0" to match the data input number of the temperature recording system.

Figures 9 through 22 depict the locations of the fourteen (14) thermocouples attached to the CV. The thermocouple wires were run along the inside of the drum liner and out between the lid and drum top plate.

Thirteen (13) thermocouples were installed in and on the drum as indicated in Figure 2 including four (4) attached to the inside of the liner and nine (9) positioned at different radial depths and at three different heights within the foam insulation region. The wires of the thermocouples attached to the liner were run along the inside of the liner and out between the lid and the drum top plate. The wires from the thermocouples located within the insulation exited the drum through the outside wall of the drum.

A short section of wire cord was tack-welded to the top edge of the drum liner to prevent the thermocouple wires and the heater power cord from getting pinched between it and the drum lid, see Figure 23. A length of O-ring stock (approximately 0.1-inch diameter) was also laid around the drum top plate within the bolt circle to prevent the thermocouple wires and the heater power cord from getting pinched and shorting when the lid was emplaced, see Figure 24.

The last four (4) thermocouples were attached to the package lid as indicated in Figures 25, 26, and 27. In addition to the thermocouples attached to the package, a single thermocouple, T31, monitored the ambient temperature within the environmental chamber. The thermocouple was mounted to a thin metal plate that was free standing, orientated vertically, and had been painted black. The stand for this plate was set on the left Uni-strut drum support. T31 is indicated in Figure 8.

Figure 1 – 9977 Prototype SN-6

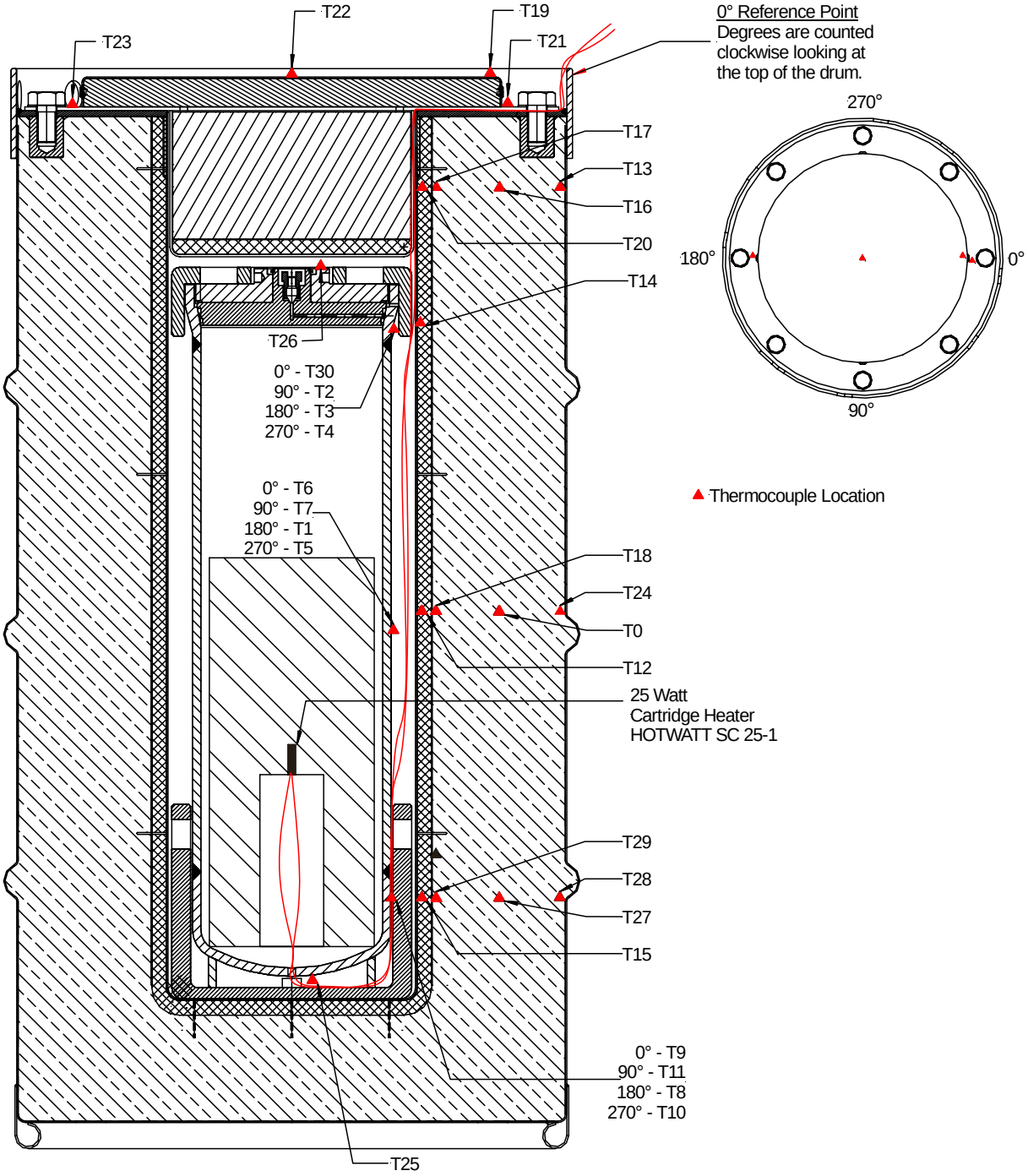

Figure 2 – 9977 Heater Test Package Schematic and Thermocouple Map

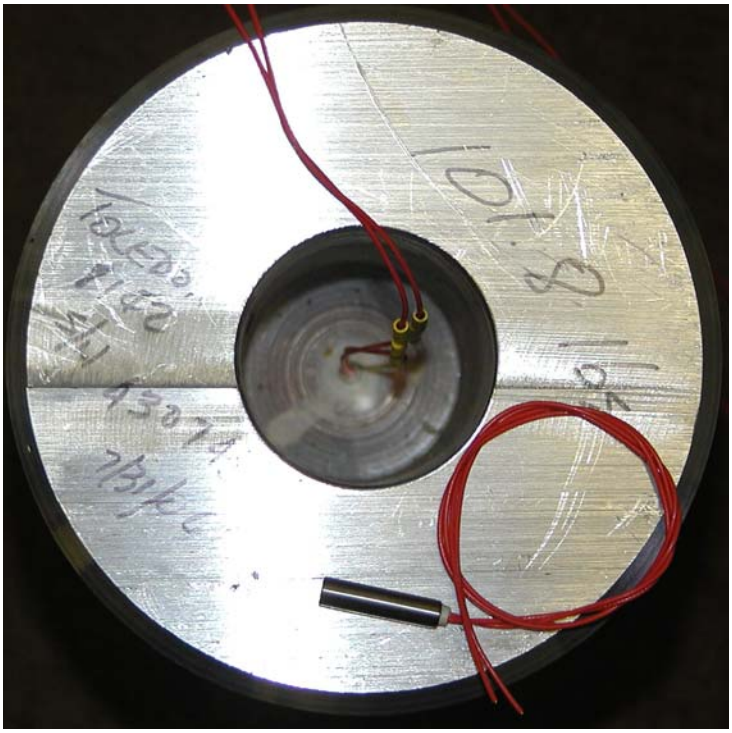

Figure 3 – Stainless Steel Billet "Contents" with Heater

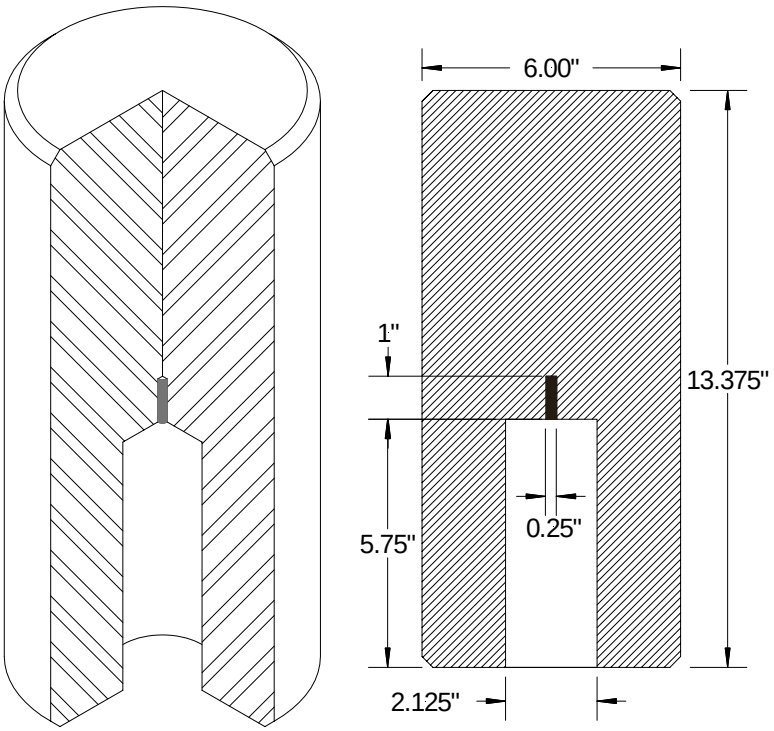

Figure 4 – Mock Content – Steel Billet with 25 Watt Heater (Controlled to 19 Watts)

Figure 5 – 9977 Prototype SN-6 Disassembled

Figure 6 – Stainless Steel Billet, 6CV, and Heater

Figure 7 – SN-6 with Thermocouple Leads

Figure 8 – SN-6 in Environmental Thermal Chamber

1.1.3 Test Procedure

The field procedure for this test, *Experimental Validation of GPFP Thermal Model*, FP-1034, 10/07/05, is attached as Appendix 1.

SN-6, containing the 19 Watt heat source, was placed into the environmental chamber (EC). The thermocouples were then connected to the data recording instrument, insulation was applied to the hole from which the thermocouples exited the chamber and the EC door was closed. SN-6 had a uniform internal temperature of 73°F (as measured by the thermocouples) and the EC was at 78°F. The EC ambient temperature was set to be controlled to 100°F and the heater was energized and set to 19-Watts using the Variable Autotransformer. The package orientation and position within the environmental chamber is shown in Figures 7 and 8. The package was elevated above the chamber floor to provide a more uniform natural convection and radiation environment. The power supplied to the heater was monitored and manually controlled. The duration of the heating test was greater than 140 hours which was based on preliminary thermal analysis as well as test data trend analysis. The length of the test was determined by the Test Engineer and Thermal modeler. Temperatures were recorded at intervals as indicated in Table 1. Since the purpose of the test was to obtain temperature data for comparison with the calculated results, it was not necessary to run the test until the package reached steady state. The heat to the environmental chamber was turned off at 8,563 minutes (142.7 hours).

1.2 Results

All the data recorded during this test is attached to this report as an Appendix on a CD. The measurements have been summarized and sorted by area of the package or by component and graphed. Table 2 lists the thermocouples by number, shows their location and the temperature they were reading at the end of the test run (approximately 143 hours). Table 3 has the same information but the data is sorted to list temperatures by area of the package. These graphs are listed below:

Figure	Area illustrated
28	The environmental chamber ambient temperature
29	The top of the CV body – 22" above the bottom of the skirt
30	The middle of the CV body – 12" above the bottom of the skirt
31	The bottom of the CV body – 3" above the bottom of the skirt
32	The top of the Drum overpack – adjacent to the top of the CV body
33	The middle of the Drum overpack – adjacent to the middle of the CV body
34	The bottom of the Drum overpack – adjacent to the bottom of the CV body
35	The top of the Drum Lid
36	The Drum Liner – at the Fiberfrax interface
37	The top of the Drum Lid

As can be seen in Figure 28, although the test plan was to hold the environmental chamber (EC) at a constant temperature of 100 °F, the EC's temperature was neither constant nor 100 °F. The EC temperature averaged around 102.5 °F until 2,630 minutes when the temperature began drifting upward. It was discovered that the EC cooling unit had failed and there was no way to cool the chamber. By 3,224 minutes the chamber temperature had drifted to above 103 °F and was manually adjusted lower. The EC ambient was lowered to 102 °F where it held for approximately 6 hours before it started drifting upward again. This cycle was repeated three more times before the test ended each time reaching a greater temperature before the controller was turned down and not decreasing to as low a temperature before leveling out. The average EC chamber ambient temperature was approximately 103.3 °F.

Table 2 – Component Temperatures at 140 Hours – listed Sequentially

Thermocouple	Location					Temperature
	Component	Area	Elevation	Radial	Angle	(°F)
T0	Foam	side	mid-height	mid-thickness	0°	127
T1	CV	body	mid-height	outside	180°	191
T2	CV	body	top	outside	90°	164
T3	CV	body	top	outside	180°	165
T4	CV	body	top	outside	270°	165
T5	CV	body	mid-height	outside	270°	Bad data
T6	CV	body	mid-height	outside	0°	Bad data
T7	CV	body	mid-height	outside	90°	189
T8	CV	body	bottom	outside	180°	191
T9	CV	body	bottom	outside	0°	191
T10	CV	body	bottom	outside	270°	190
T11	CV	body	bottom	outside	90°	191
T12	Liner	outside	mid-height	outside	0°	169
T13	Foam	side	top	at drum	0°	108
T14	Liner	outside	O-ring	outside	0°	154
T15	Liner	outside	bottom	outside	0°	181
T16	Foam	side	top	mid-thickness	0°	112
T17	Foam	side	top	at Fiberfrax	0°	120
T18	Foam	side	mid-height	at Fiberfrax	0°	157
T19	Lid	top plate	edge	--	0°	108
T20	Liner	outside	top	outside	0°	121
T21	Lid	deck plate	top	--	0°	109
T22	Lid	top plate	top	--	-	107
T23	Lid	deck plate	top	--	180°	108
T24	Foam	side	mid-height	at drum	0°	107
T25	CV	end cap	bottom	--	--	188
T26	CV	closure nut	top	--	--	162
T27	Foam	side	bottom	mid-thickness	0°	130
T28	Foam	side	bottom	at drum	0°	107
T29	Foam	side	bottom	at Fiberfrax	0°	164
T30	CV	body	top	outside	0°	165
T31	Chamber Ambient	--	--	--	--	105

Table 3 – Component Temperatures at 140 Hours – Grouped by Area

Thermocouple	Location					Temperature
	Component	Area	Elevation	Radial	Angle	(°F)
T14	Liner	outside	O-ring	outside	0°	154
T2	CV	body	top	outside	90°	164
T3	CV	body	top	outside	180°	165
T4	CV	body	top	outside	270°	165
T30	CV	body	top	outside	0°	165
T1	CV	body	mid-height	outside	180°	191
T5	CV	body	mid-height	outside	270°	Bad data
T6	CV	body	mid-height	outside	0°	Bad data
T7	CV	body	mid-height	outside	90°	189
T8	CV	body	bottom	outside	180°	191
T9	CV	body	bottom	outside	0°	191
T10	CV	body	bottom	outside	270°	190
T11	CV	body	bottom	outside	90°	191
T20	Liner	outside	top	outside	0°	121
T17	Foam	side	top	at Fiberfrax	0°	120
T16	Foam	side	top	mid-thickness	0°	112
T13	Foam	side	top	at drum	0°	108
T12	Liner	outside	mid-height	outside	0°	169
T24	Foam	side	mid-height	at drum	0°	107
T0	Foam	side	mid-height	mid-thickness	0°	127
T18	Foam	side	mid-height	at Fiberfrax	0°	157
T15	Liner	outside	bottom	outside	0°	181
T28	Foam	side	bottom	at drum	0°	107
T27	Foam	side	bottom	mid-thickness	0°	130
T29	Foam	side	bottom	at Fiberfrax	0°	164
T22	Lid	top plate	center	--	-	107
T19	Lid	top plate	edge	--	0°	108
T21	Lid	deck plate	top	--	0°	109
T23	Lid	deck plate	top	--	180°	108
T25	CV	end cap	bottom	--	--	188
T26	CV	closure nut	top	--	--	162
T31	Chamber Ambient	--	--	--	--	105

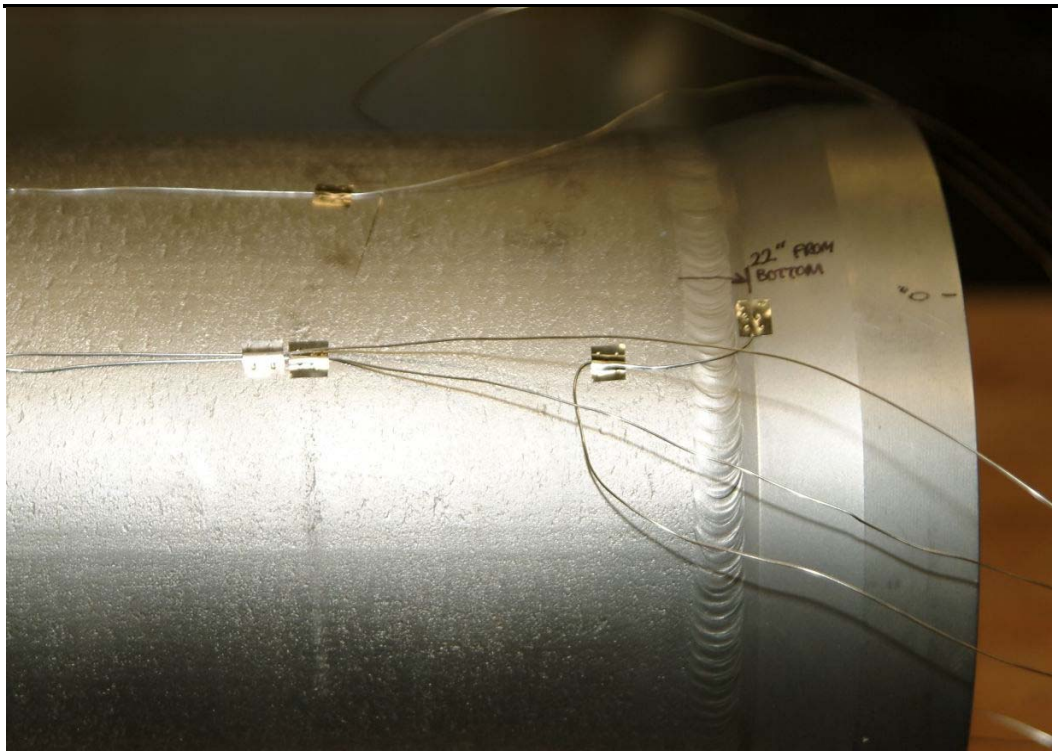

Figure 9 – CV at 0° Orientation – Thermocouple T30 at Top Location

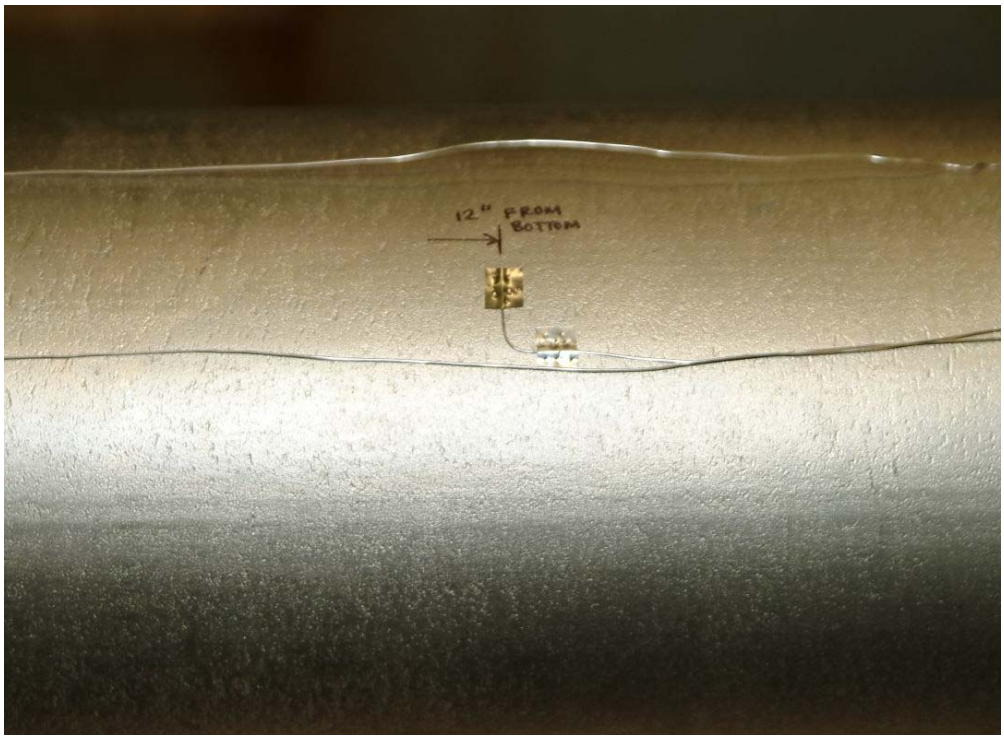

Figure 10 – CV at 0° Orientation – Thermocouple T6 at Middle Location

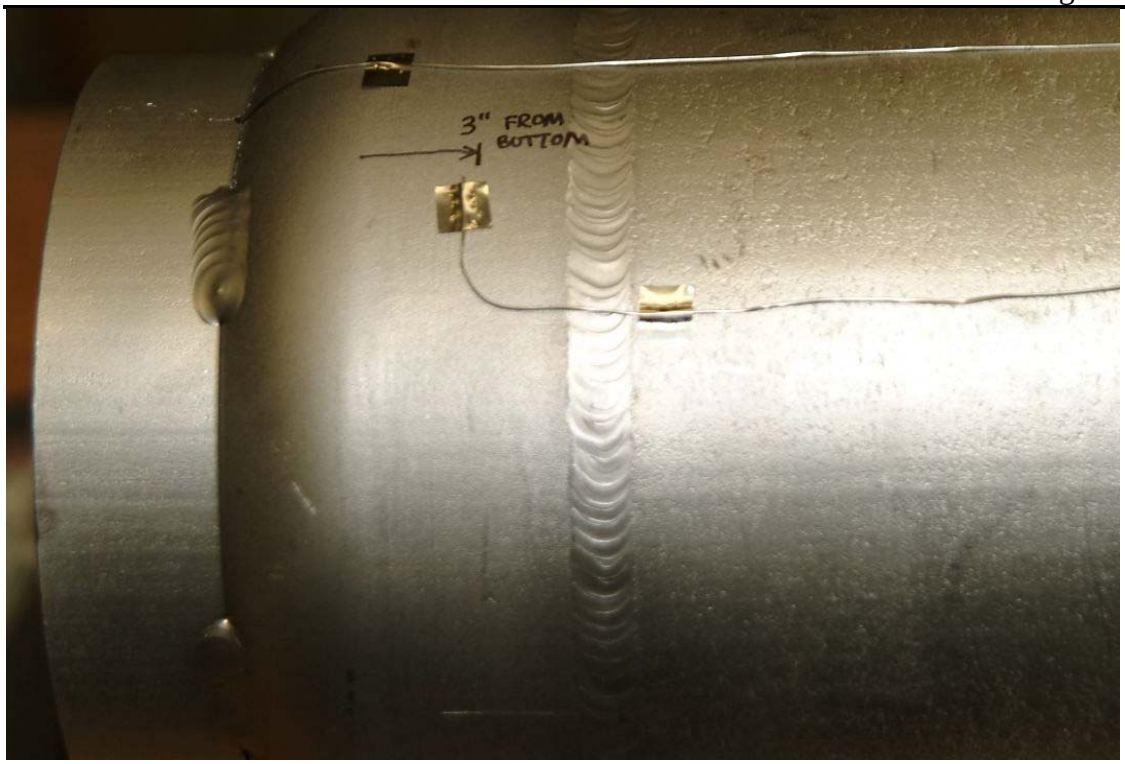

Figure 11 – CV at 0° Orientation – Thermocouple T9 at Bottom Location

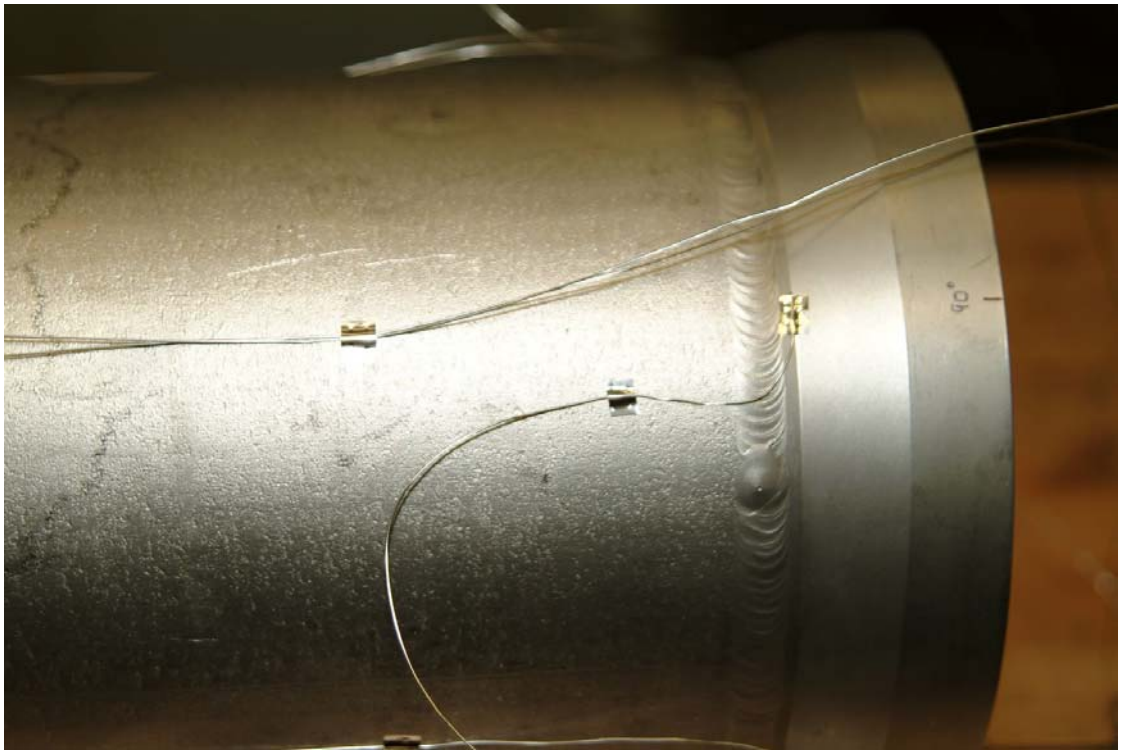

Figure 12 – CV at 90° Orientation – Thermocouple T2 at Top Location

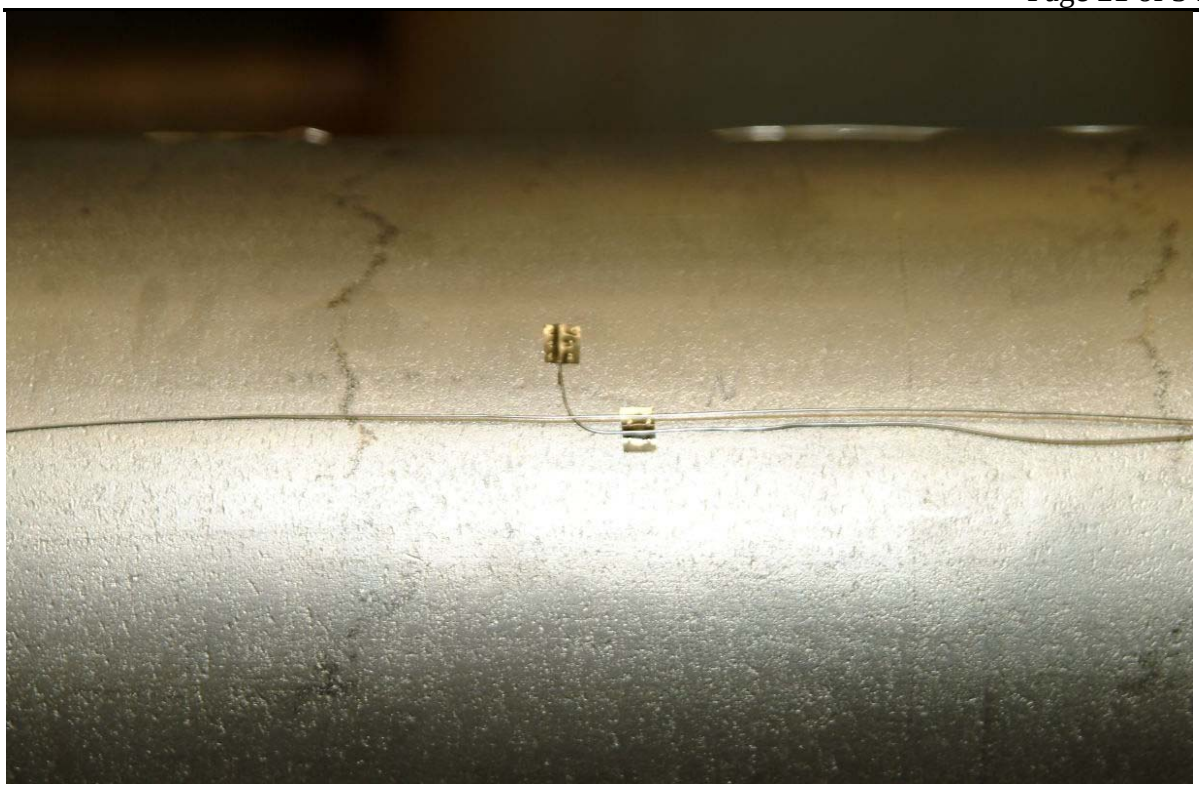

Figure 13 – CV at 90° Orientation – Thermocouple T7 at Middle Location

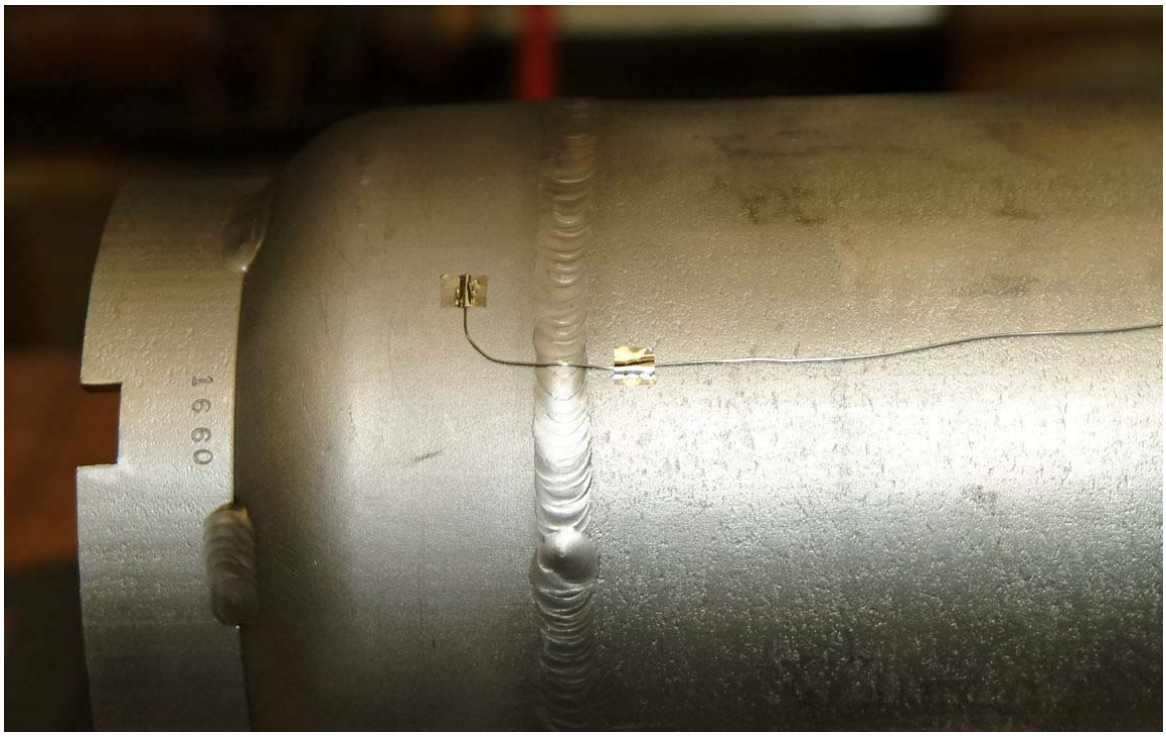

Figure 14 – CV at 90° Orientation – Thermocouple T11 at Bottom Location

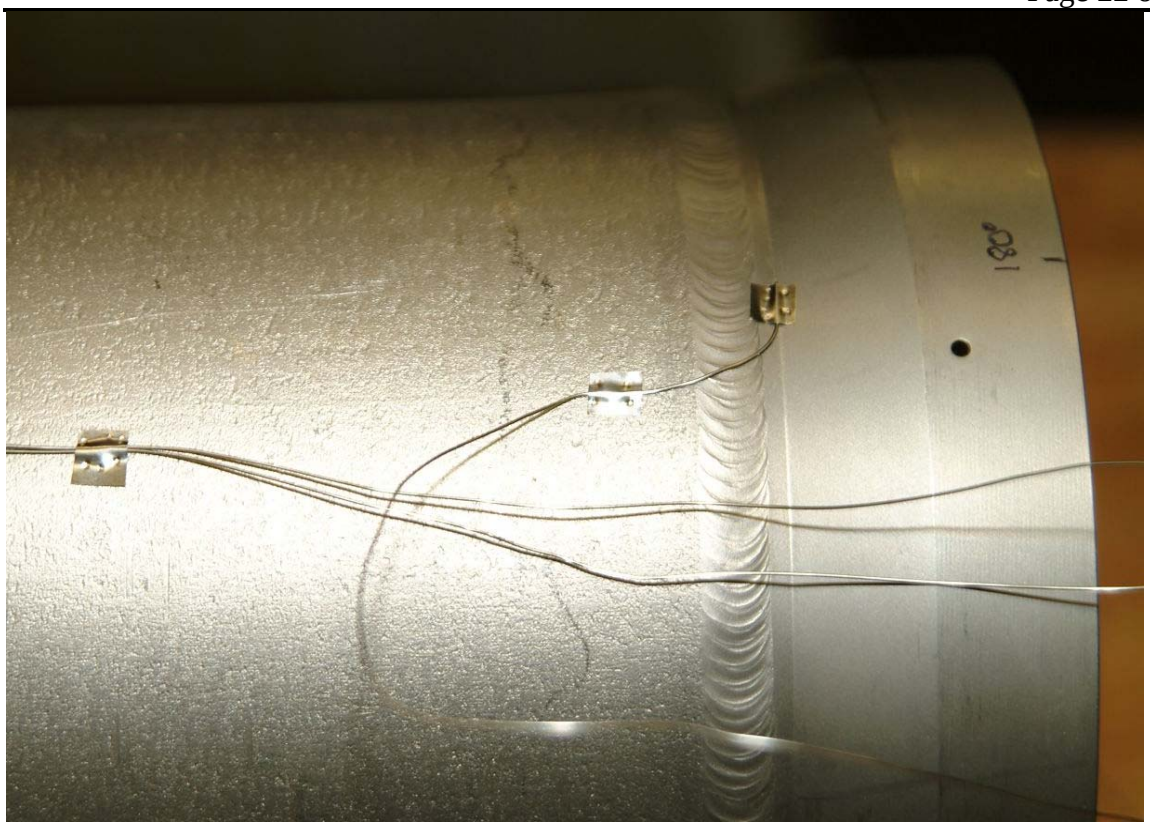

Figure 15 – CV at 180° Orientation – Thermocouple T3 at Top Location

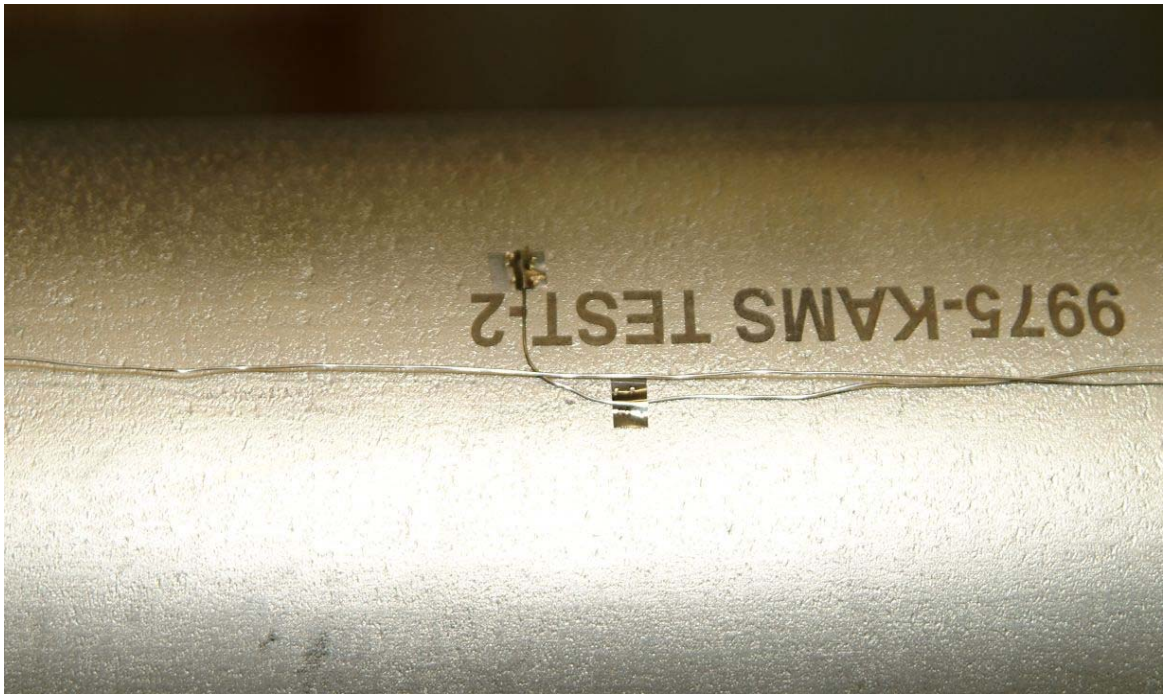

Figure 16 – CV at 180° Orientation – Thermocouple T1 at Top Location

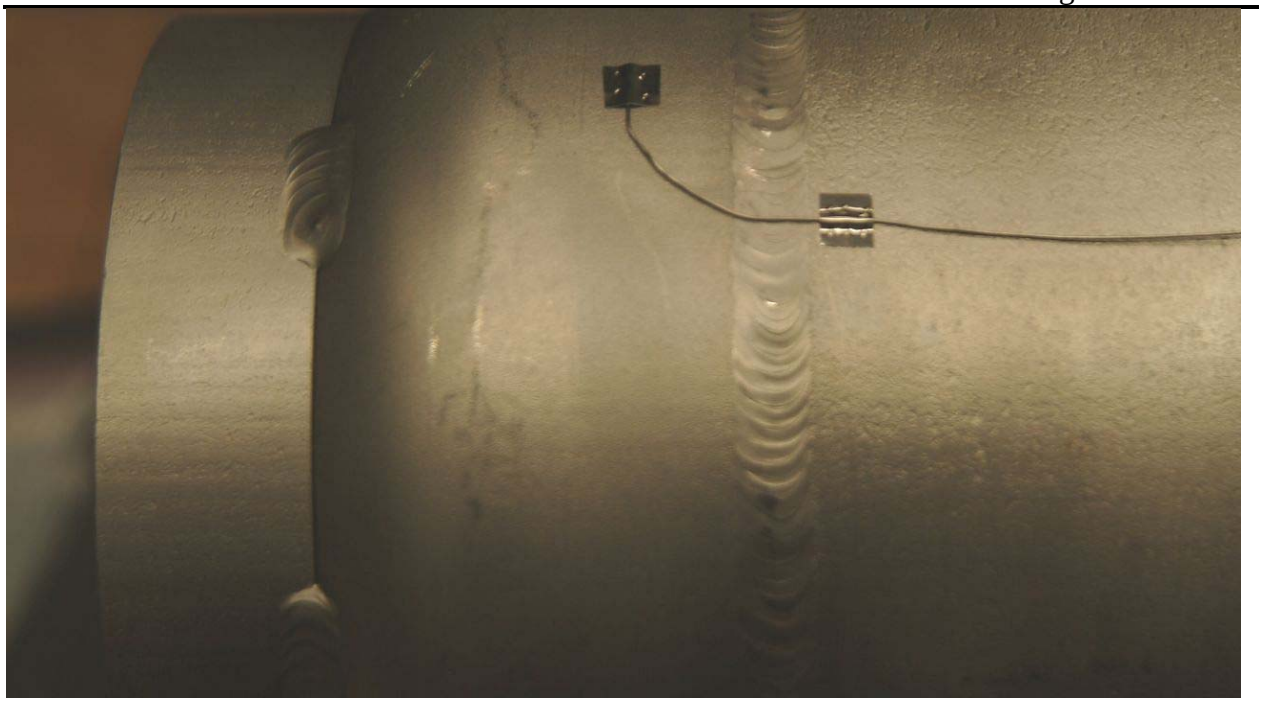

Figure 17 – CV at 180° Orientation – Thermocouple T8 at Bottle Location

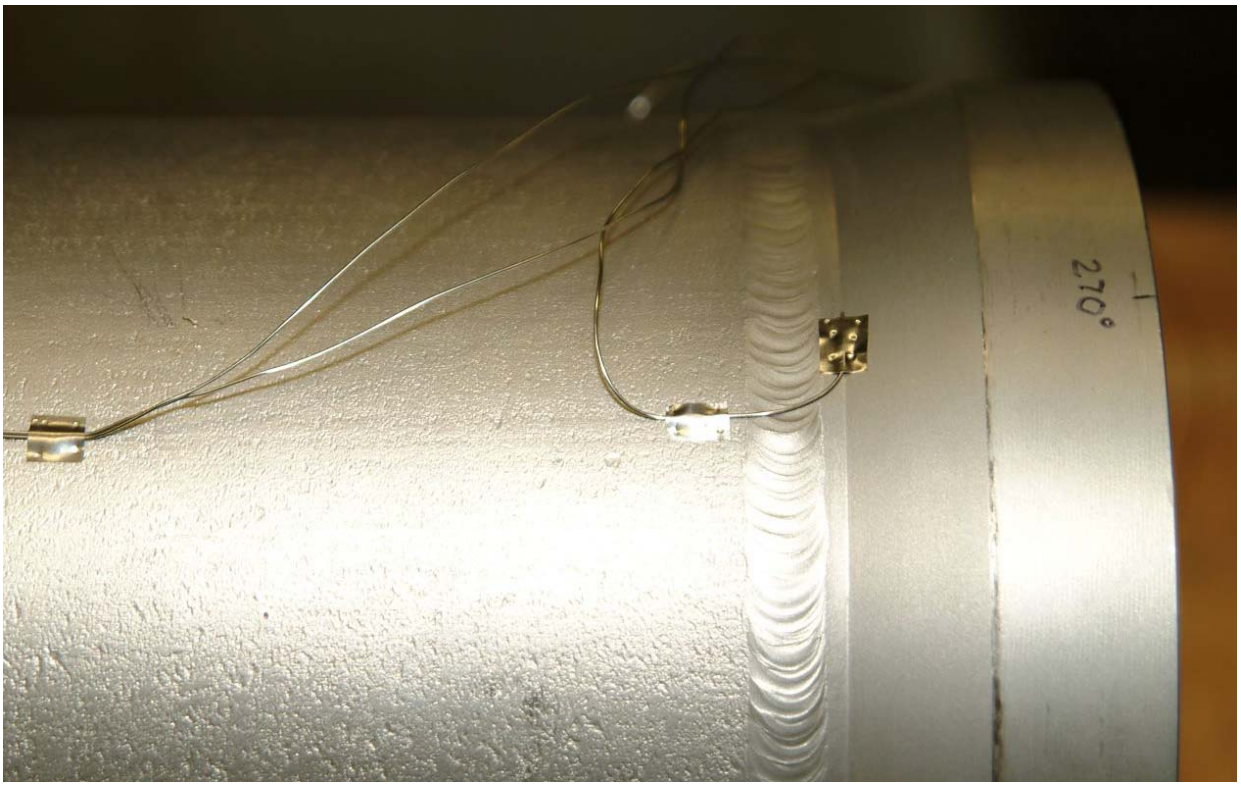

Figure 18 – CV at 270° Orientation – Thermocouple T4 at Top Location

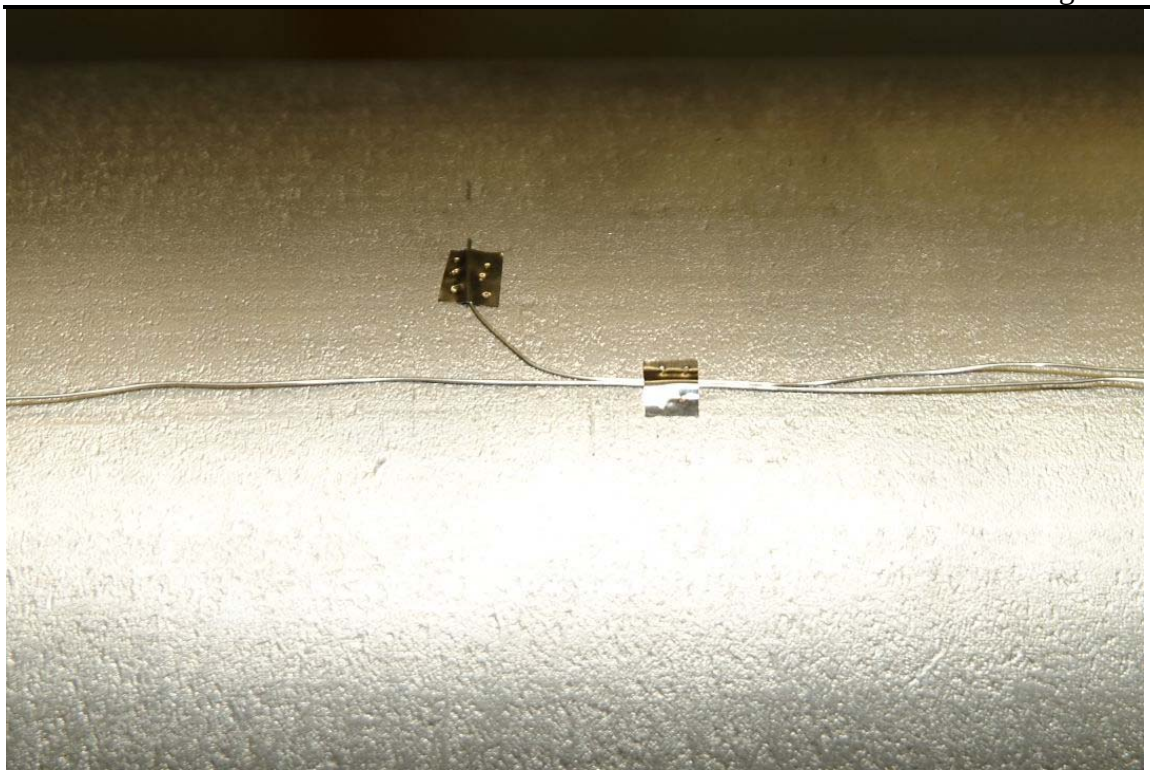

Figure 19 – CV at 270° Orientation – Thermocouple T5 at Middle Location

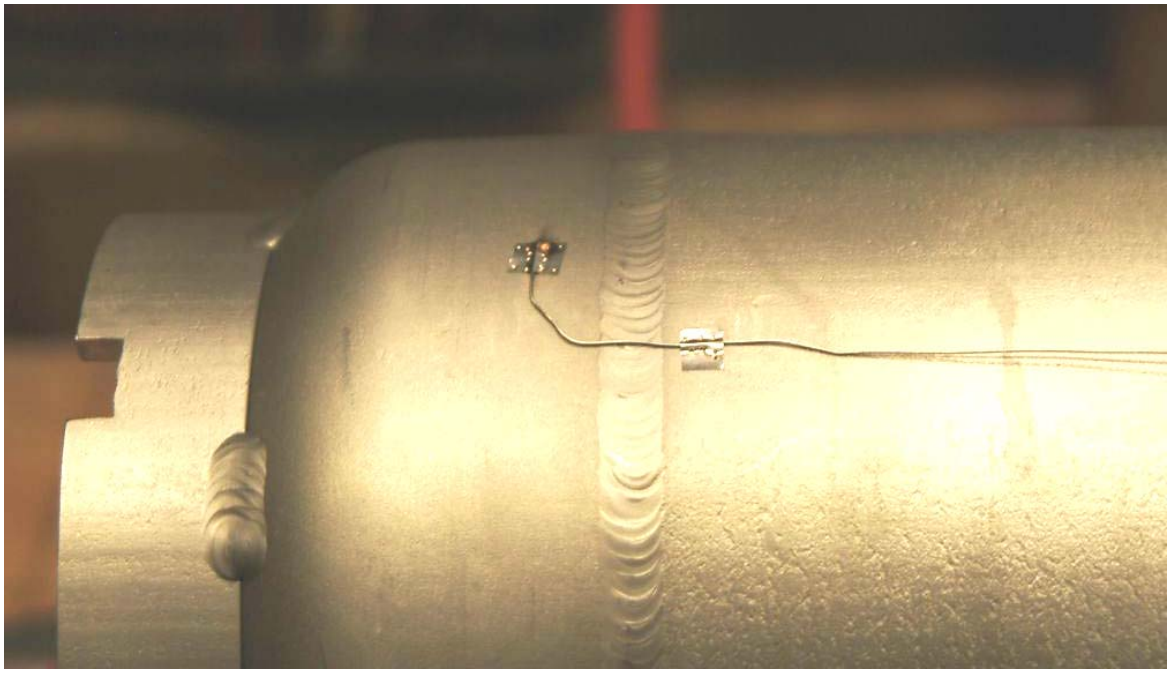

Figure 20 – CV at 270° Orientations – Thermocouple T10 at Bottom Location

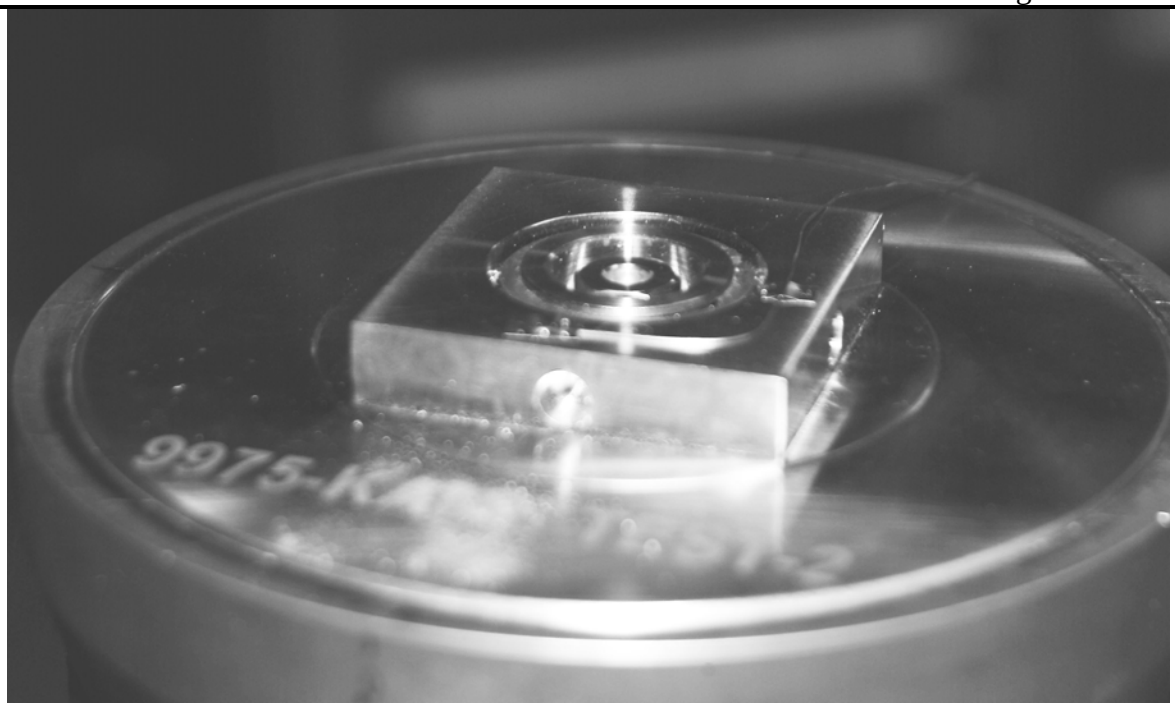

Figure 21 – CV Closure – Thermocouple T26 on Cone Seal Nut

Figure 22 – CV Closure – Thermocouple T25 on CV Pipe Cap

Figure 23 – Shim Stock for Holding and Wire Cord Used to Protect TC Wires

Figure 24 – Drum Top Showing TC wires and the gasket used to protect them

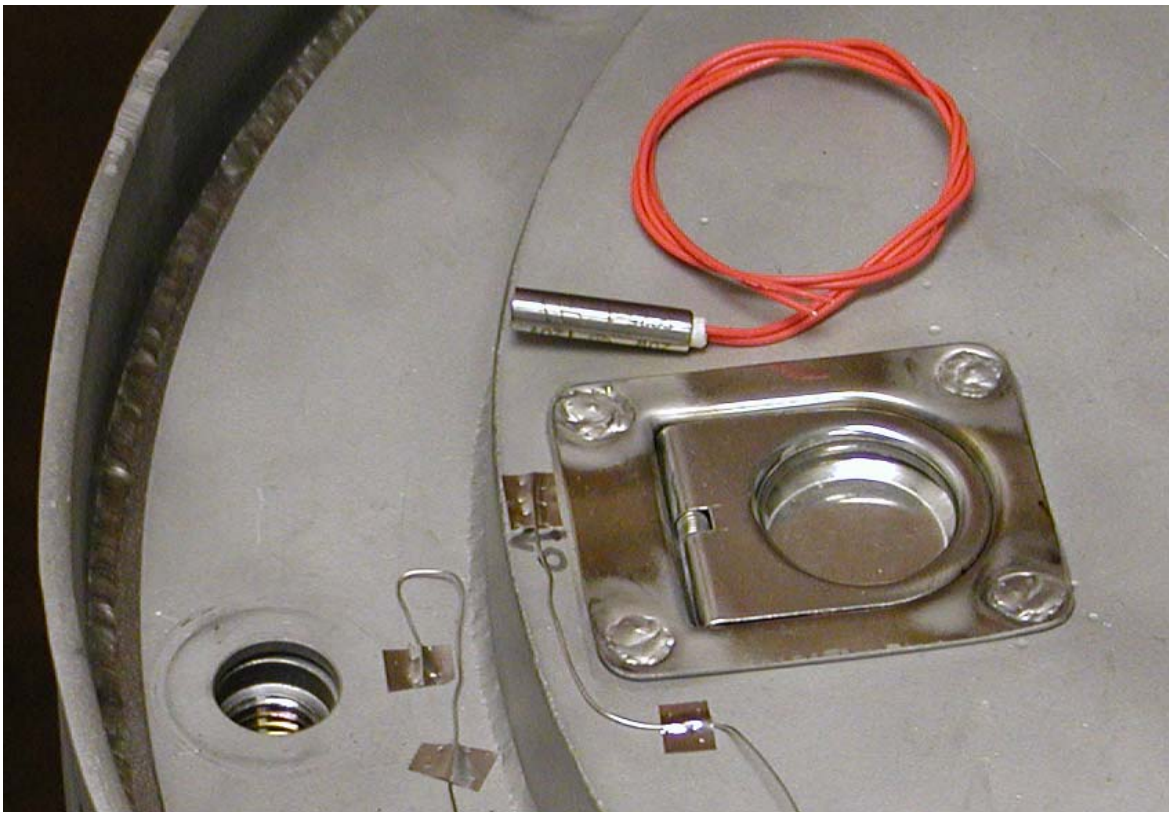

Figure 25 – Drum Lid – Thermocouples T19 (by handle) and T21 (by bolt hole)

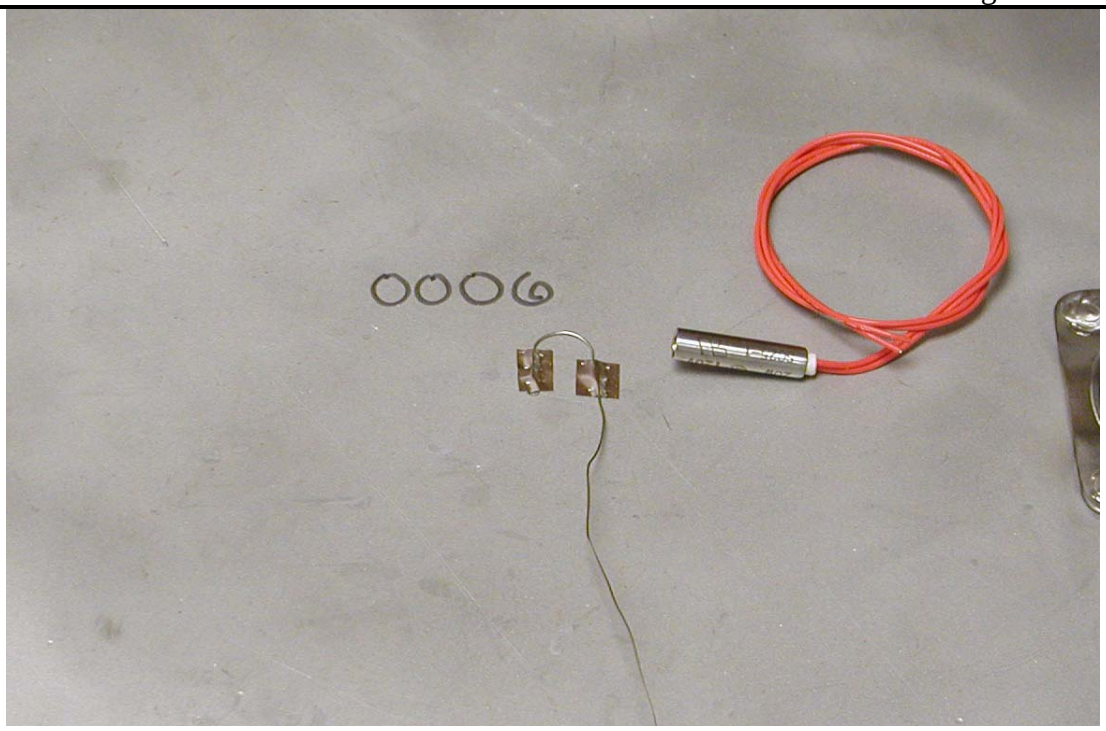

Figure 26 – Thermocouple T22 at Center of Lid

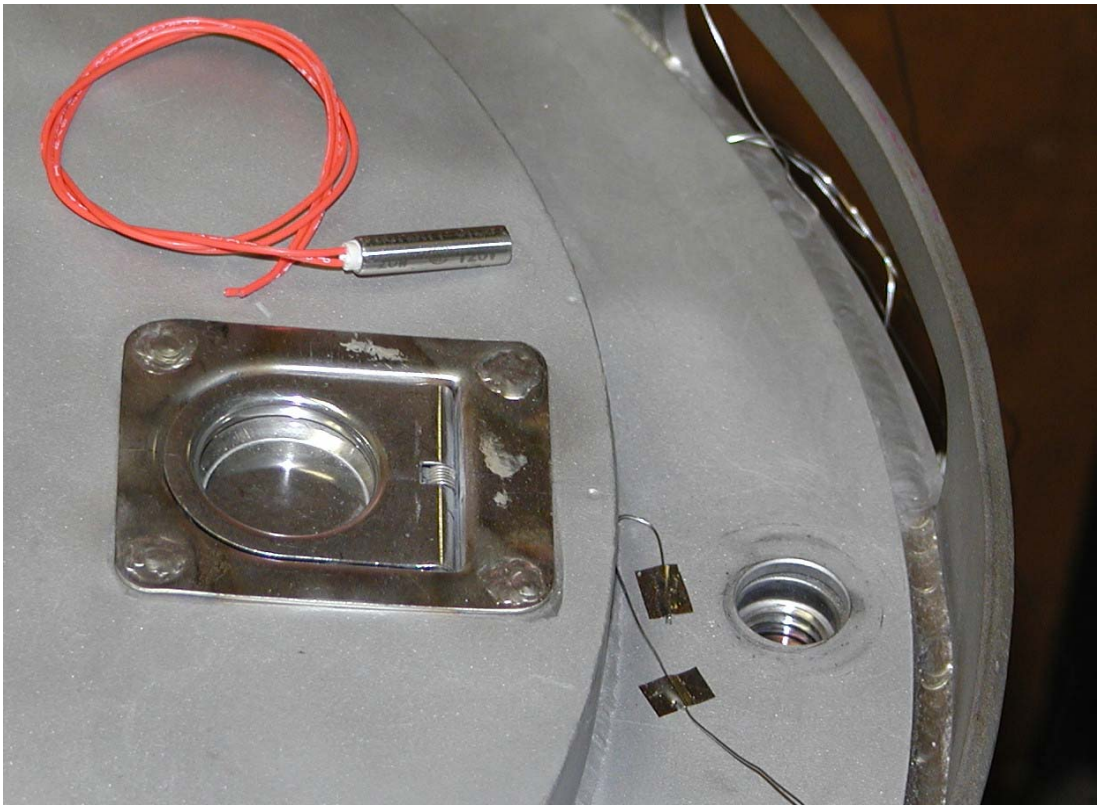

Figure 27 – Drum Lid - Thermocouple T23 by bolt hole

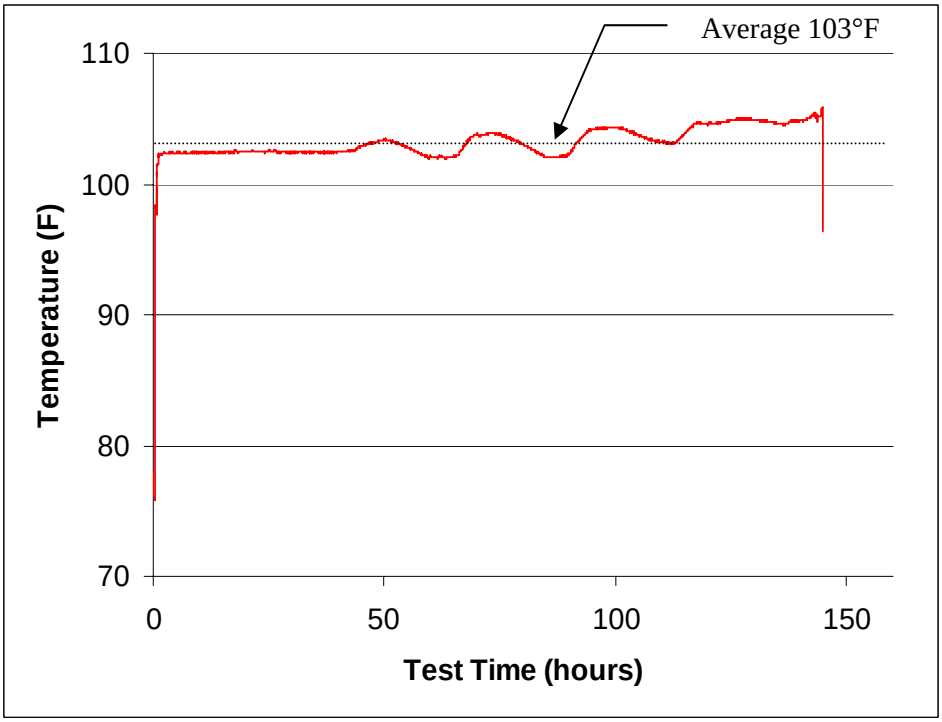

Figure 28 – Environmental Chamber Ambient Temperature

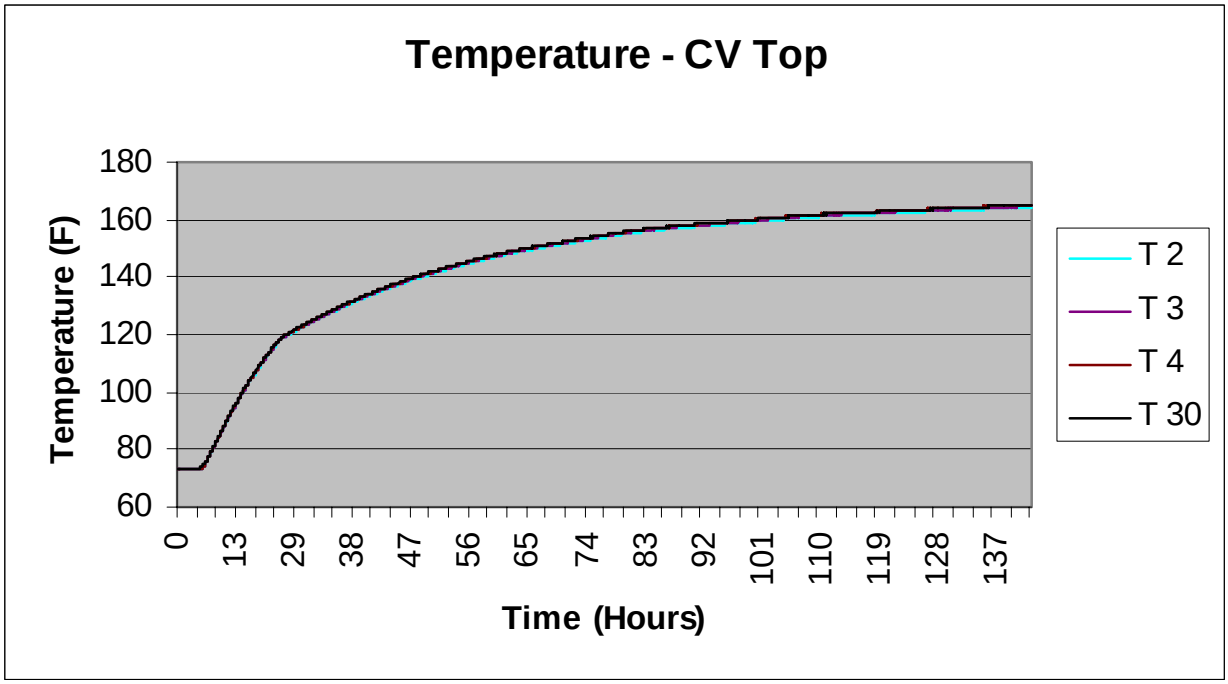

Figure 29 – CV Body – Top (4 Locations)

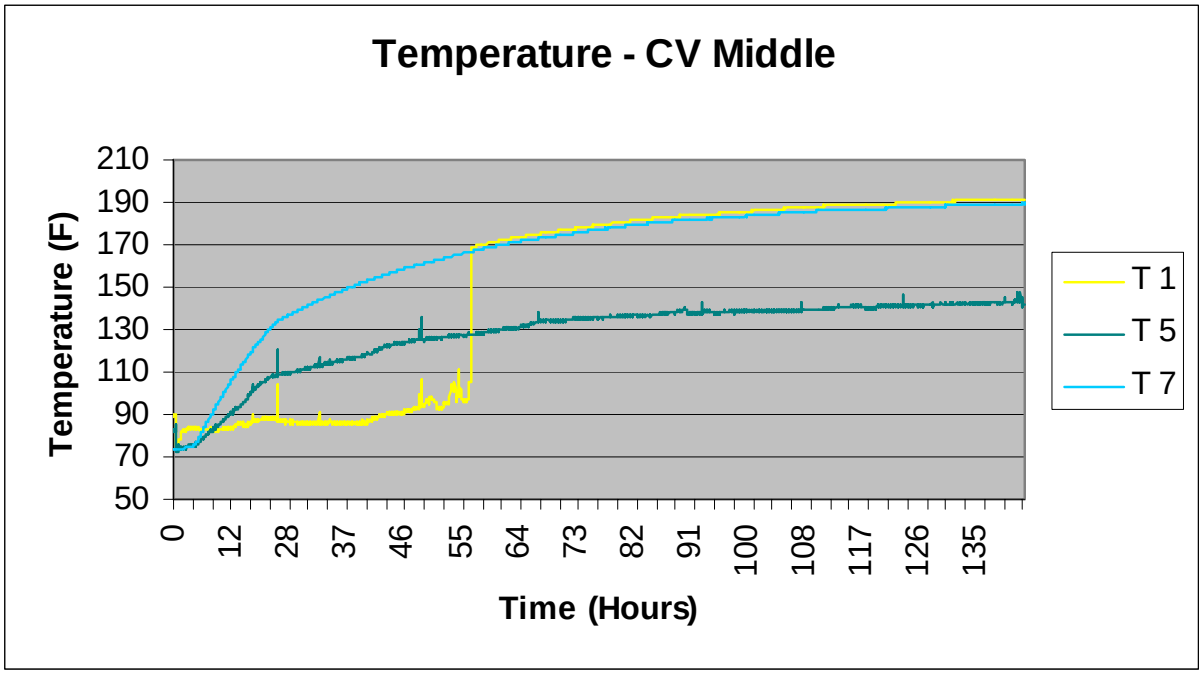

Figure 30 – CV Body – Middle (2 Locations – T5 and T6 gave bad data)

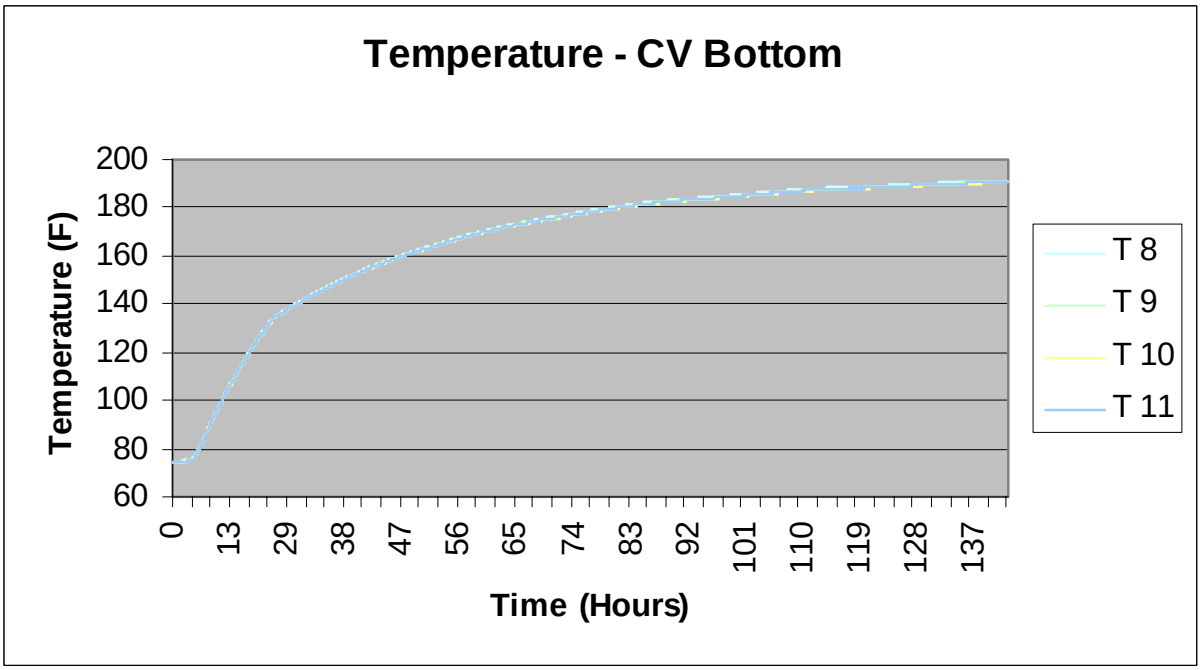

Figure 31 – CV Body – Bottom (4 Locations)

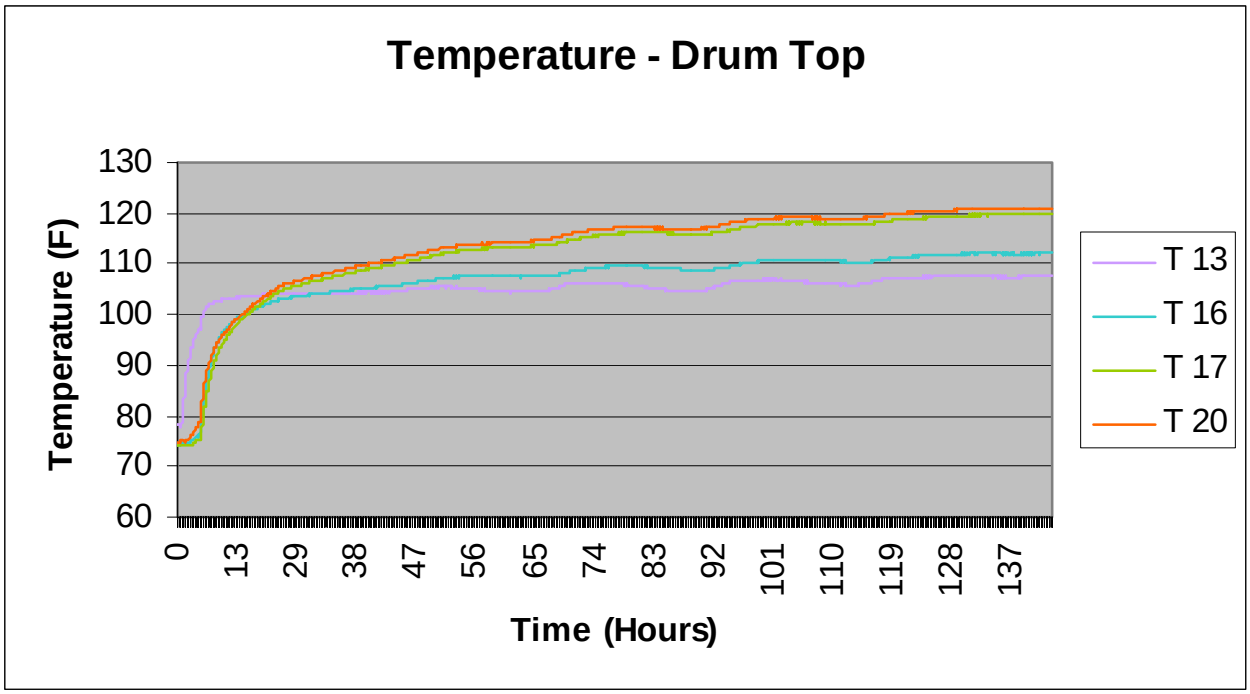

Figure 32 – Drum Liner and Foam – Top Cross section

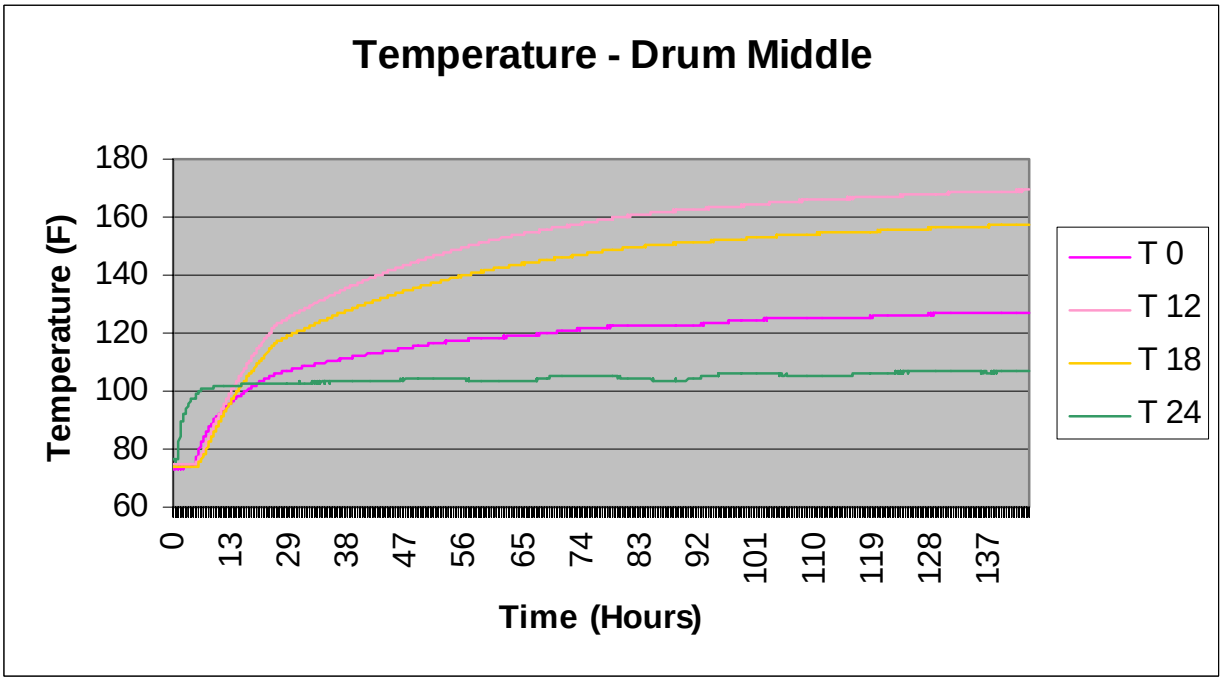

Figure 33 – Drum Liner and Foam – Middle Cross section

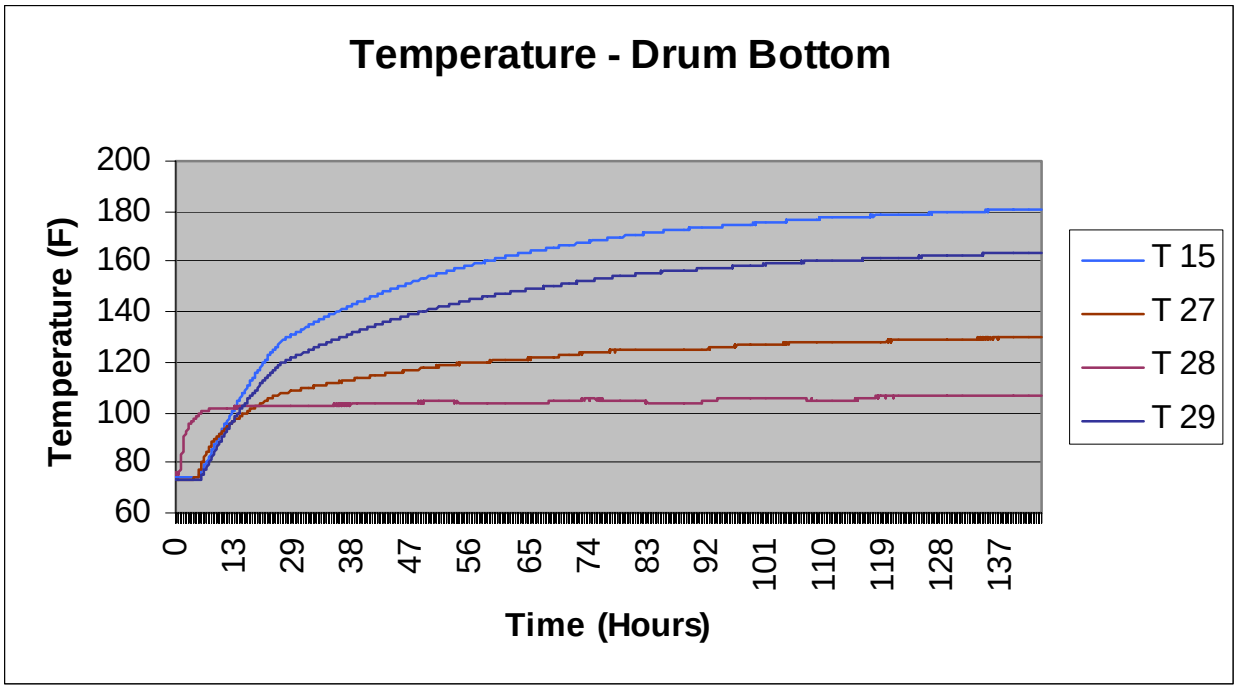

Figure 34 – Drum Liner and Foam – Bottom Cross section

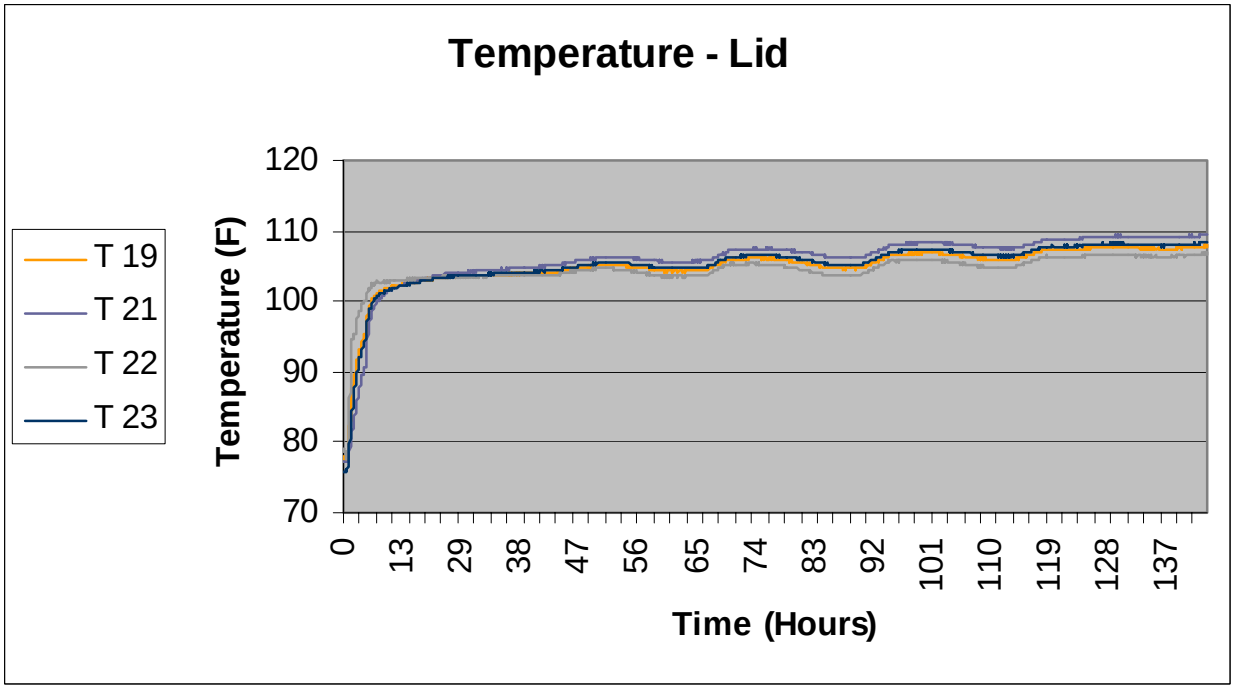

Figure 35 – Drum Lid

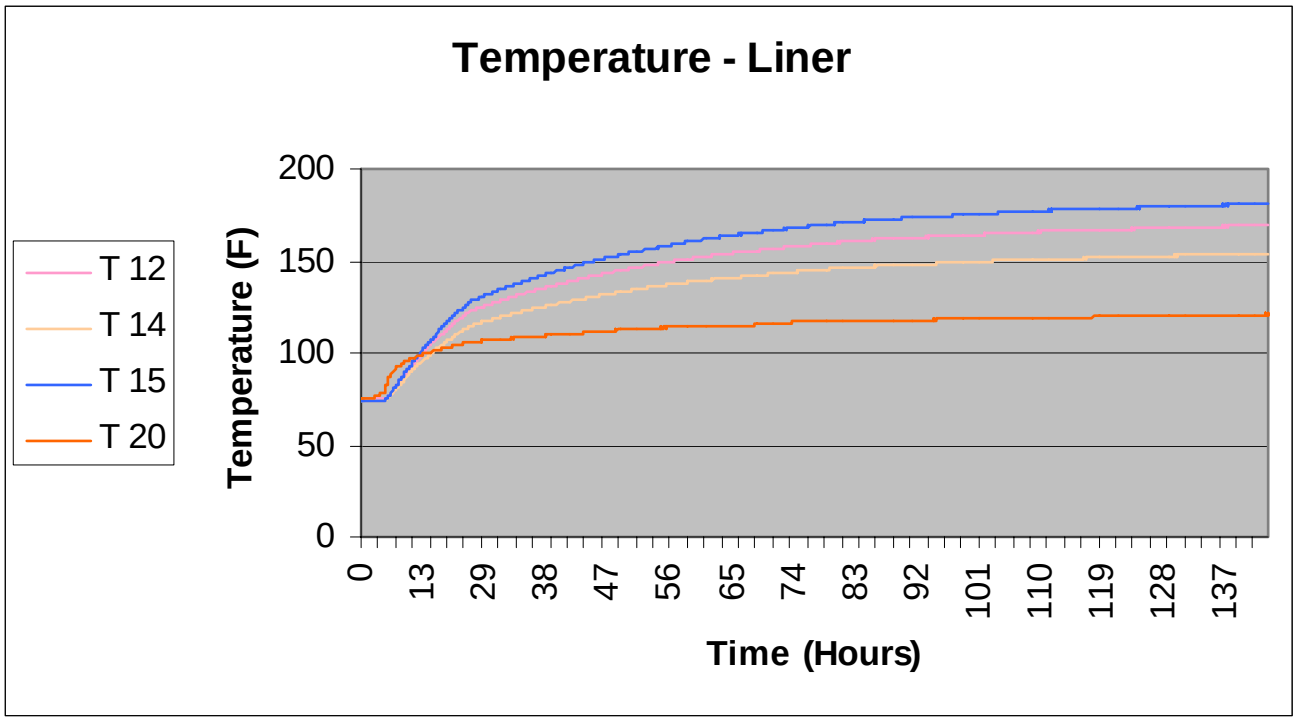

Figure 36 – Drum Liner – Four Elevations

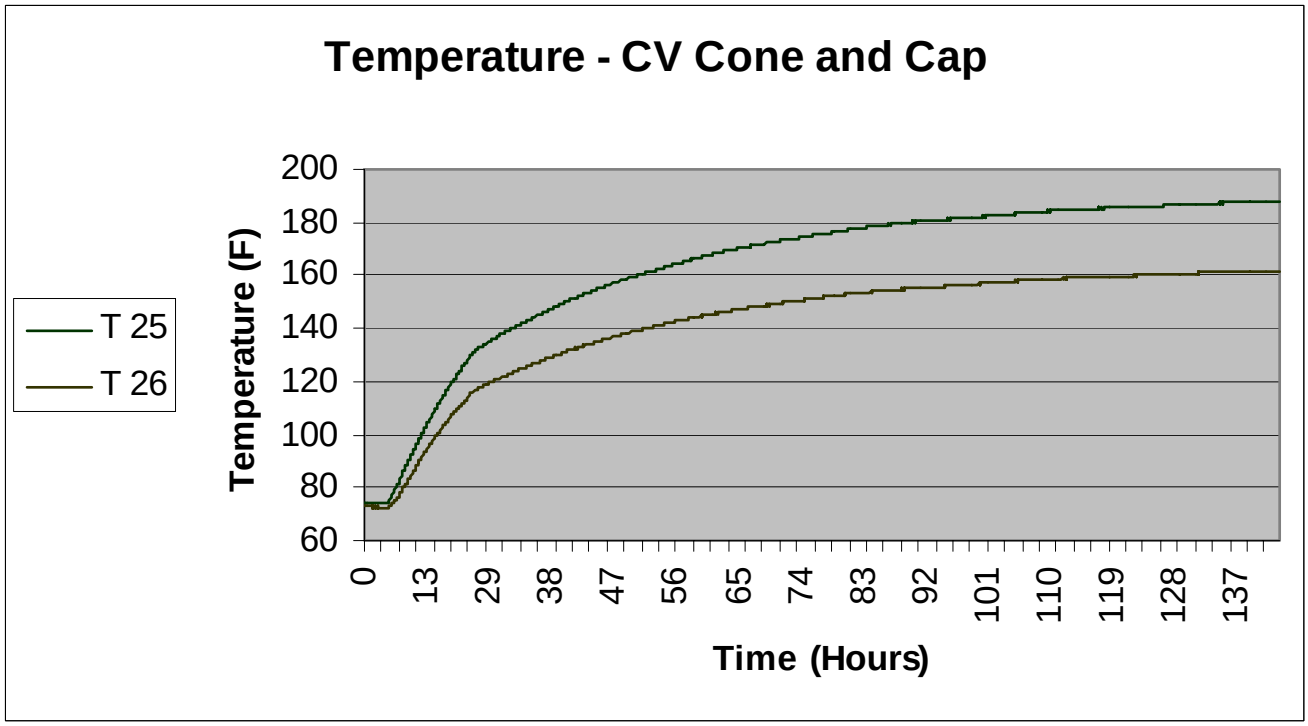

Figure 37 – CV Top and Bottom – T26 on Cone Seal Nut T25 on Pipe Cap

This Page Intentionally Left Blank

APPENDIX 3.8

MNOP AND MAXIMUM OPERATING PRESSURE FOR THE 9977 PACKAGE

This Page Intentionally Left Blank

OSR 45-24 (Rev 11-15-2004)

Calculation Cover Sheet

Project 9977 SARP	Calculation No. M-CLC-A-00256	Project No. NA
Title MNOP and Maximum Operating Pressure for the 9977 Package	Functional Classification SC	Sheet 1 of 7
	Discipline Mechanical	
Calc Level ☒ Type 1 ☐ Type 2	Type 1 Calc Status ☐ Preliminary ☒ Confirmed	
Computer Program No. ☒ N/A	Version/Release No.	

Purpose and Objective

The purpose of the calculation was to calculate the Maximum Normal Operating Pressure (MNOP) during Normal Conditions of Transport (NCT) specified by 10 CFR 71.71 and operating pressures during Hypothetical Accident Conditions (HAC) specified by 10 CFR 71.73. The calculations were extremely conservative and utilized the maximum temperatures over the Containment Vessel (CV), rather than the lower maximum gas temperatures, to calculate the gas pressures. Further, the pressure contribution due to the degradation of 100 grams of plastic within the CV was included in the pressure calculations. Pressure calculations were performed for both the 6 and 5-inch CV's.

Summary of Conclusion

Under NCT, the maximum pressures for the 5 and 6-inch CVs were found to be 71.02 and 55.87 psia, respectively. Under HAC, the maximum pressures for the 5 and 6-inch CVs were found to be 63.16 and 49.69 psia, respectively.

Revisions

Rev No.	Revision Description
0	Original Issue

Sign Off

Rev No.	Originator (Print) Sign/Date	Verification/ Checking Method	Verifier/Checker (Print) Sign/Date	Manager (Print) Sign//Date
0	Bruce Hardy Bruce Hardy 4/24/06	Individual Review	N. K. GUPTA N. K. Gupta 4/24/06	G. P. HOLDING SMITH G P Holding Smith 4/25/06

Design Authority — (Print)	Signature	Date
Release to Outside Agency – (Print)	Signature	Date

Security Classification of the Calculation

Unclassified

Revisions

Revision	Description
0	Original Issue

Acronyms and Abbreviations

CV	Containment Vessel
DOT	Department of Transportation
GPFP	General Purpose Fissile Package
HAC	Hypothetical Accident Conditions
MNOP	Maximum Normal Operating Pressure
NCT	Normal Conditions of Transport
SARP	Safety Analysis Report for Packaging
SS	Stainless Steel

Containment Vessel Pressure for the 9977 Package

The Department of Transportation (DOT) Fissile Specification 6M package is being removed from service. As a result, a new general purpose fissile package, designated as the Model 9977 Shipping Package, has been designed as a replacement. The 9977 package consists of a Containment Vessel (CV), a drum overpack filled with foam and a bolt-on lid that has several layers of insulation. This package is described in References 1 and 2.

Maximum pressures occurring in the CV for both the NCT and HAC are calculated in this document. The calculated pressures are a combination of both the rise in air pressure due to temperature and the pressure resulting from gasses produced during degradation of 100 grams of plastic within the CV. Calculations in this document are extremely conservative and are based on the maximum temperature occurring in the CV for References 1 and 2.

In Reference 3 a formula was prescribed for calculating the contribution to CV pressure due to degradation of the plastic

$$\delta P_a = \frac{T_f \rho_a}{T_{test} \rho_{test}} \delta P_{test} \qquad 1$$

where: δP_a = Actual increase in pressure due to degradation of the plastic (psia).
T_f = Actual gas temperature in the CV (R).
ρ_a = Actual mass of plastic per free volume of the CV (100g).
ρ_{test} = Test mass of plastic per free volume during the plastic degradation test.
T_{test} = Test temperature for the plastic degradation test (R).
δP_{test} = Change in pressure due to plastic degradation during the test at temperature T_{test} (psia).

For a CV sealed at 70°F (529.67R) and 1 atm (14.7psi), then raised to a temperature T_f, the resulting pressure P_f (psia) is given by

$$P_f = \left(\frac{14.7}{529.67} + \frac{\delta P_{test} \rho_a}{T_{test} \rho_{test}} \right) T_f . \qquad 2$$

5-Inch CV Calculations

If the 9977 package with a 5-inch CV (5CV) contains the same amount of plastic as the 9975 package, then ρ_a is obtained from Reference 3. The test parameters are also obtained from Reference 3. These values are listed in Table 1.

Table 1 Parameter Values for Different Plastics

	Polyethylene	RFETS Nylon_1	RFETS Nylon_2	FB-Line Nylon
$\delta P_{test\ plastic}$	2.50 psia	9.50 psia	17.00 psia	32.10 psia
$\rho_{test\ plastic}$	595 g/ft^3	600 g/ft^3	600 g/ft^3	793 g/ft^3
$T_{test\ plastic}$	1011.67 R	684.67 R	809.67 R	809.67 R
ρ_a	873 g/ft^3	829 g/ft^3	873 g/ft^3	873 g/ft^3
$\frac{\delta P_{test}\rho_a}{T_{test}\rho_{test}}$	0.00362575	0.019171036	0.030549483	0.04364536

From Equation 2, it can be seen that the maximum value of $\frac{\delta P_{test}\rho_a}{T_{test}\rho_{test}}$ determines the maximum value of P_f for the 5CV. Hence taking $\frac{\delta P_{test}\rho_a}{T_{test}\rho_{test}} = 0.04364536$ will give the maximum pressure.

Bare source NCT temperatures within the CV bound those for sources embedded in a media. Hence, they are used to calculate the maximum pressure under NCT, see References 1 and 2. As a further conservatism, the highest temperature of any component within the CV, including the CV itself, not just the maximum gas temperature, is used in the pressure calculations. Although bare source thermal calculations were performed for the 6CV but not the 5CV, it was found that under NCT the 6CV temperatures bound those for the 5CV. Therefore, 6CV bare source temperatures were used to calculate the 5CV maximum pressure under NCT. From Reference 1 the maximum NCT component temperature within the 9977 6-inch CV is 535°F for the bare source at the bottom of the CV. In this case Equation 2 yields a CV pressure of 71.02 psia or 56.32 psig for NCT in the 9977 5CV.

HAC thermal calculations were not performed for the 5CV, hence, 6CV HAC temperatures were used to calculate the operating pressure during HAC. As a conservatism, the highest temperature of any component within the CV, including the CV itself, not just the maximum gas temperature, was used in the pressure calculations. From Reference 2 the maximum HAC temperature within the 9977 6-inch CV is 425°F and occurs 6.5 hours into the post-fire transient for the source at the bottom of the CV with a 2.3 inch thick layer of foam remaining after the fire. In this case Equation 2 yields a CV pressure of 63.16 psia or 48.46 psig for HAC in the 9977 5CV.

6-Inch CV Calculations

If the 9977 package with a 6-inch CV (6CV) contains 100 grams of plastic and the free volume of the CV is half that of the total volume, then ρ_a is given by

$$\rho_a = \frac{m_{plastic}}{V_{6CV\ Free}} \qquad 3$$

where: $m_{plastic}$ = 100 grams

$V_{6CV\ Free} = 0.5\,V_{6CV} = 0.017593\ ft^3$

$V_{6CV} = 608\ in^3 = 0.035185\ ft^3$ [See Reference 4]

The parameters $\delta P_{test\ plastic}$, $\rho_{test\ plastic}$ and $T_{test\ plastic}$ remain the same as in Table 1. The test parameters are also obtained from Reference 3. Values for the parameters are listed in Table 2.

Table 2 Parameter Values for Different Plastics

	Polyethylene	**RFETS Nylon_1**	**RFETS Nylon_2**	**FB-Line Nylon**
$\delta P_{test\ plastic}$	2.50 psia	9.50 psia	17.00 psia	32.10 psia
$\rho_{test\ plastic}$	595 g/ft^3	600 g/ft^3	600 g/ft^3	793 g/ft^3
$T_{test\ plastic}$	1011.67 R	684.67 R	809.67 R	809.67 R
ρ_a	568 g/ft^3	568 g/ft^3	568 g/ft^3	568 g/ft^3
$\frac{\delta P_{test}\rho_a}{T_{test}\rho_{test}}$	0.00236077	0.013145019	0.019891145	0.02841803

As for the 5CV, the maximum value of $\frac{\delta P_{test}\rho_a}{T_{test}\rho_{test}}$ determines the maximum value of P_f for the 6CV. Hence taking $\frac{\delta P_{test}\rho_a}{T_{test}\rho_{test}}$ =0.05683606 will give the maximum pressure.

As a conservatism, the highest temperature of any component within the CV, including the CV itself, not just the maximum gas temperature, was used in the pressure calculations. From Reference 1 the maximum NCT temperature within the 9977 6-inch CV is 535°F and occurs for a bare source at the bottom of the CV. In this case Equation 2 yields a CV pressure of 55.87 psia or 41.17 psig for NCT in the 9977 6CV.

From Reference 2 the maximum HAC temperature within the 9977 6-inch CV is 425°F and occurs 6.5 hours into the post-fire transient for the source at the bottom of the CV with a 2.3 inch thick layer of foam remaining after the fire. As for the NCT pressure calculation, the highest temperature of any component within the CV, including the CV itself, not just the maximum gas temperature, was used in the pressure calculations. In this case Equation 2 yields a CV pressure of 49.69 psia or 34.99 psig for HAC in the 9977 6CV.

References

1. M-CLC-A-00255, Rev. 0. NCT Thermal Model for the 9977 Package. WSRC Document (2006).
2. M-CLC-A-00257, Rev. 0. HAC Thermal Model for the 9977 Package. WSRC Document (2006).
3. WSRC-SA-2002-00008, Appendix 3.14. Pressure Contribution Due to Plastic Bags. WSRC Document (2002).
4. Drawing
   - R-R2-G-00042, Rev.0.

This Page Intentionally Left Blank

APPENDIX 3.7

PRESSURE CONTRIBUTION DUE TO PLASTIC BAGS

This Page Intentionally Left Blank.

PRESSURE CONTRIBUTION DUE TO PLASTIC BAGS

The content food pack cans are to be packed in no more than 100 g of low density polyethylene,[1] RFETS nylon, or FB-Line nylon. The plastic melts at temperatures less than those calculated during NCT for each of the packages. Off-gas tests of low-density polyethylene[2],RFETS nylon[3] and FB-Line nylon[4] were conducted over a range of temperatures. The Tables below summarize the contributions to PCV and SCV pressures from the thermal degradation of the plastic using the following equation.[2]

$$\delta P_a = \frac{\delta P T_a \rho_a}{T \rho} \qquad 1$$

where: δP_a is the increase in pressure due to the thermal degradation
T_a is the average air temperature (R) in the package vessel
ρ_a is the plastic mass (100 g) per free volume in the package vessel
ρ is the mass of plastic per free volume during the plastic test
T is the plastic test temperature (R)
δP is the change in pressure during the plastic test at the test temperature T

Table 1: Primary Containment Vessel NCT – Low Density Polyethylene[2]

Package	T_a (°F)	T (°F)	δP (psia)	ρ_a (g/ft.^{3})	ρ (g/ft.^{3})	δP_a (psia)
9965	276	552	2.5	941	595	2.9
9968	310	552	2.5	641	595	2.0
9972	289	552	2.5	941	595	2.9
9973	311	552	2.5	941	595	3.0
9974	308	552	2.5	941	595	3.0
9975	313	552	2.5	873	595	2.8

Table 2: Primary Containment Vessel NCT– RFETS Nylon[3]

Package	T_a (°F)	T (°F)	δP (psia)	ρ_a ($g/ft.^3$)	ρ ($g/ft.^3$)	δP_a (psia)
9975	194	225	9.5	829	600	12.5
9975	313	350	17.0	873	600	23.6

Table 3: Primary Containment Vessel/NCT—FB-Line Nylon[4]

Package	T_a (°F)	T (°F)	δP (psia)	ρ_a ($g/ft.^3$)	ρ ($g/ft.^3$)	δP_a (psia)
9975	313	350	32.1	873	793	33.7

References:

[1] ASTM-4635.

[2] Vormelker, P.R., *Polymer Film Out-Gassing Tests for Shipping Containers*, SRT-MTS-945190, February 1995.

[3] Skidmore, T. E., O*ff-Gas Pressure Evaluation of RFETS Nylon Bagging Material, Rev. 1 (U)*, SRT-MTS-98-4112, August 1998.

[4] Skidmore, T.E., *Off-Gas Pressure Evaluation of FB-Line Material (U)*, SRT-MTS-99-4031, April 1999.

APPENDIX 3.6

PATRAN-PLUS AND P/THERMAL CODE DESCRIPTIONS

This page intentionally left blank.

PATRAN-PLUS AND P/THERMAL CODE DESCRIPTIONS

1. INTRODUCTION

PATRAN (version 2.5) is the pre- and post-processing software package for the finite element modeling of the 9965, 9968, 9972, 9973, 9974, and 9975 shipping packages. The P/Thermal (version 2.6) software package is used to solve for temperatures. PATRAN and P/Thermal, both developed by PDA Engineering[1] of Costa Mesa, California, are tightly coupled. Because P/Thermal performs the calculations for temperatures, the majority of this discussion will focus upon the use of P/Thermal.

PATRAN was used for all aspects of model development. Dimensions from the package drawings were input to create the axisymmetric model for each package. The model geometry was then meshed, and loads and boundary conditions, including internal heat generation, heat flux, radiation, and convection, were applied. The model is output in a neutral file and analysis is completed with P/Thermal.

P/Thermal is a thermal modeling and analysis software package optimized for large, highly nonlinear models. The code supports a wide range of complex boundary conditions and includes a library of 37 convection correlations as well as an extensive material database. P/Thermal solves for temperature distributions using any combination of the five primary heat transfer modes; namely, conduction, convection, radiation, phase change, and advection. Radiation viewfactors between element surfaces are calculated with a companion program to P/Thermal, P/Viewfactor. Radiation properties may be a function of both wavelength and direction. P/Viewfactor is integrated into P/Thermal in such a way as to make its operation transparent to the user.

2. JUSTIFICATION

Numerous thermal analysis programs exist to calculate the temperature profiles within the shipping packages. The most common software appears in a guide from Lawrence Livermore National Laboratory.[2] P/Thermal meets or exceeds the capabilities of each of these programs based upon the description of the programs' advertised capabilities.

P/Thermal is relatively new and is gaining acceptance as a reliable thermal analysis code. Numerous benchmark problems have been correctly solved by P/Thermal, such as the UK-1 problem posed by the Nuclear Committee on Reactor Physics, which has defined a standard problem set for benchmarking thermal codes.

P/Thermal agrees closely with the analytical solution for the Kershaw problem. The Kershaw problem is a standard benchmark designed to test for errors introduced by skewed meshes. Many available thermal analysis codes fail this test.

3. CAPABILITIES

P/Thermal supports a wide range of boundary conditions such as nodal, surface, and volumetric heat sources, nodal temperatures, and convective and radiative surfaces. All boundary conditions may be input as constant, time-dependent, or temperature-dependent, and can be defined by any combination of microfunctions or user-subroutines.

P/Thermal creates a resistor-capacitor network using all finite element cross-derivative terms. This allows an exact mathematical representation of the model. The element library includes two-dimensional and three-dimensional elements as well as axisymmetric bar, triangle, quadrilateral, tetrahedral, wedge, and hexahedral elements.

The solution scheme offers several explicit and implicit algorithms. Automatic selection of implicit or explicit solution techniques can be specified on a node or time step basis. Convergence is based partially on an estimated maximum error that protects against false convergence in stiff thermal problems. Convergence is also based upon the maximum iterative relaxation and system energy balance.

4. INPUT AND OUTPUT

The PATRAN neutral file is output by PATRAN after the model has been completed. The neutral file contains all node and element data, boundary condition assignments, and material property definitions. The neutral file is named PATRANOUT.

A total of five files are required for the P/Thermal analyses of the shipping packages: MATDAT, TEMPLATEDAT, QINDAT, MICRODAT, and VFCTL. Several other files are created during execution of the program, but may be ignored for the purpose of this discussion because they are used only for internal record keeping. A brief description of the six necessary input files follows:

PATRANOUT:	neutral file of model data
MATDAT:	material properties
TEMPLATEDAT:	convection correlations, radiative surface properties
QINDAT:	all P/Thermal run control parameters
MICRODAT:	internal and solar heat source data
VFCTL:	radiation viewfactor convergence criteria and options

The files MATDAT, TEMPLATEDAT, and MICRODAT for the 9975 NCT thermal analyses are attached as representative input.

The first step in running P/Thermal is to invoke the script PATQ and select menu option 2 (PATQ-2) to translate the neutral file (PATRANOUT) into a resistor-capacitor network. PATQ-3 also reads in the TEMPLATEDAT file and produces eleven output files containing resistor and capacitor data. After successful completion of PATQ-2, PATQ menu option 3 (PATQ-3) is selected to generate radiation viewfactors. After the viewfactors have been created, PATQ menu option 4 (PATQ-4) is picked to create a new FORTRAN main program source file, Q/TRAN, from existing files. The executable file produced from Q/TRAN (QTRANEXE) is normally submitted to a batch queue and iterates until convergence is achieved.

Output from P/Thermal is in the form of nodal results files. Nodal results files contain all nodes in the model and the temperatures at the nodes. These files are read into PATRAN when the model is post-processed to view the results, normally as fringe or contour plots.

5. REFERENCES

1. PDA Engineering. 1975 Redhill Avenue, Costa Mesa, CA 92626.

2. L. E. Fischer, et al. Packaging Review Guide for Reviewing Safety Analysis Reports for Packaging. UCID-21218, Lawrence Livermore Laboratory, pp 5-4 to 5-6, (October 1988).

Jul 16 1994 13:49:48 **mat.dat** Page 1

```
*
*     The material properties in this sample MAT.DAT file are in SI units
*     The table entries use the index independent variable option
*     All tables have been bounded - this is good practice for all tables
*
MPID 100301 CONSTANT F 1.0
ENERGY ABSORBER --> Thermal Conductivity (Btu/hr-ft-F)
MDATA 3.82
/
MPID 100303 CONSTANT F 1.0
ENERGY ABSORBER --> Thermal Conductivity (Btu/hr-ft-F)
MDATA 7.62
/
MPID 100304 CONSTANT F 1.0
ENERGY ABSORBER --> Density (lbm/ft**3)
MDATA 16.2
/
MPID 100305 CONSTANT F 1.0
ENERGY ABSORBER --> Specific heat (Btu/lbm)
MDATA 0.22
/
MPID 100601 ITABLE  F 1.0
CELOTEX --> Thermal Conductivity
MDATA 76.0  0.031
MDATA 77.0  0.031
MDATA 187.0 0.034
MDATA 295.0 0.036
MDATA 439.0 0.038
MDATA 532.0 0.029
MDATA 533.0 0.029
/
MPID 100604 ITABLE  F 1.0
CELOTEX --> Density
MDATA 76.5  16.86
MDATA 77.0  16.86
MDATA 187.0 17.36
MDATA 295.0 17.86
MDATA 439.0 18.54
MDATA 532.0 19.54
/
MPID 100605 ITABLE F 1.0
CELOTEX --> Specific Heat
MDATA 76.0  0.306
MDATA 77.0  0.306
MDATA 187.0 0.360
MDATA 295.0 0.417
MDATA 439.0 0.489
MDATA 532.0 0.493
MDATA 533.0 0.493
/
MPID 100701 CONSTANT  F  1.0
UPPER PLATE (ALUMINUM) --> Thermal Conductivity
MDATA 126.0
/
MPID 100704 CONSTANT F 1.0
UPPER PLATE (ALUMINUM) --> Density
MDATA 169.3
/
MPID 100705 CONSTANT F 1.0
UPPER PLATE (ALUMINUM) --> Specific Heat
MDATA 0.216
/
MPID  35701  TABLE  FAHRENHEIT  1.0
STEEL, STAINLESS 304 --> Thermal Conductivity (Btu/(hr*ft*F))
References:  1,4,37
Data Quality:  EXCELLENT
MDATA -3.28000E+02  3.99150E+00
MDATA -1.48000E+02  6.28963E+00
MDATA  3.20000E+01  7.74108E+00
MDATA  2.12000E+02  9.43444E+00
MDATA  9.32000E+02  1.25793E+01
MDATA  1.29200E+03  1.49983E+01
MDATA  1.29300E+03  1.49983E+01
/
MPID  81201  TABLE  FAHRENHEIT  1.0
AIR --> Thermal Conductivity (Btu/(hr*ft*F))
```

Jul 16 1994 13:49:48 **mat.dat** Page 2

```
References:  1,2,46
Data Quality:  EXCELLENT
MDATA -3.17830E+02  3.99150E-03
MDATA -1.48000E+02  9.09577E-03
MDATA  3.20000E+01  1.39581E-02
MDATA  2.12000E+02  1.83851E-02
MDATA  3.92000E+02  2.23766E-02
MDATA  5.72000E+02  2.59326E-02
MDATA  7.52000E+02  2.92710E-02
MDATA  7.53000E+02  2.92710E-02
/
MPID  35704  CONSTANT  FAHRENHEIT  1.0
STEEL, STAINLESS 304 --> Density (lbm/ft**3)
References:  1,4,37
Data Quality:  EXCELLENT
MDATA  4.94429E+02
/
MPID  35705  TABLE  FAHRENHEIT  1.0
STEEL, STAINLESS 304 --> Specific Heat (Btu/(lbm*F))
References:  1,4,37
Data Quality:  EXCELLENT
MDATA  3.20000E+01  1.20000E-01
MDATA  7.52000E+02  1.35000E-01
MDATA  7.53000E+02  1.35000E-01
/
MPID  81204  CONSTANT  FAHRENHEIT  1.0
AIR --> Density (lbm/ft**3)
References:  1,2,46
Data Quality:  EXCELLENT
MDATA  8.05321E-02
/
MPID  81205  TABLE  FAHRENHEIT  1.0
AIR --> Specific Heat (Btu/(lbm*F))
References:  1,2,46
Data Quality:  EXCELLENT
MDATA -2.38000E+02  2.40000E-01
MDATA  2.12000E+02  2.37000E-01
MDATA  2.13000E+02  2.37000E-01
/
MPID  81207 ITABLE FAHRENHEIT  1.0
AIR --> Absolute Viscosity
MDATA  80.0   4.482E-02
MDATA  80.6   4.482E-02
MDATA 170.6   5.033E-02
MDATA 261.0   5.551E-02
MDATA 351.0   6.030E-02
MDATA 441.0   6.487E-02
MDATA 531.0   6.919E-02
MDATA 532.0   6.919E-02
/
MPID  81208 CONSTANT FAHRENHEIT 1.0
AIR --> Coefficient of thermal expansion
MDATA  1.642E-03
/
MPID   2101  TABLE  FAHRENHEIT  1.0
LEAD --> Thermal Conductivity (Btu/(hr*ft*F))
References:  2,1,32,27,37,42
Data Quality:  EXCELLENT
MDATA  6.80000E+01  1.99817E+01
MDATA  2.08940E+02  1.95704E+01
MDATA  4.00100E+02  1.83125E+01
MDATA  4.98920E+02  1.69336E+01
MDATA  5.81000E+02  1.45145E+01
MDATA  6.29960E+02  1.20954E+01
MDATA  7.17080E+02  9.67635E+00
MDATA  7.99880E+02  9.02320E+00
MDATA  9.80060E+02  8.70872E+00
MDATA  1.27598E+03  8.66033E+00
/
MPID   2104  CONSTANT  FAHRENHEIT  1.0
LEAD --> Density (lbm/ft**3)
References:  2,1,32,27,37,42
Data Quality:  EXCELLENT
MDATA  7.08557E+02
/
MPID   2105  TABLE  FAHRENHEIT  1.0
```

Jul 16 1994 13:49:48 **mat.dat** Page 3

```
LEAD --> Specific Heat (Btu/(lbm*F))
References:  2,1,32,27,37,42
Data Quality:  EXCELLENT
MDATA  3.20000E+01  3.05000E-02
MDATA  2.12000E+02  3.15000E-02
MDATA  6.21500E+02  3.38000E-02
MDATA  6.21680E+02  3.40000E-02
MDATA  1.83200E+03  3.28000E-02
MDATA  3.17120E+03  3.03000E-02
/
MPID  35301  TABLE  FAHRENHEIT  1.0
STEEL, CARBON, TYPE 1020 (0.2 - 0.6 C) --> Thermal Conductivity (Btu/(hr*ft*F))
References:  1,20,37
Data Quality:  EXCELLENT
MDATA -9.94000E+01  4.71722E+01
MDATA  7.70000E+01  4.11245E+01
MDATA  1.47200E+03  1.69336E+01
MDATA  2.37200E+03  1.81432E+01
/
MPID  35304  CONSTANT  FAHRENHEIT  1.0
STEEL, CARBON, TYPE 1020 (0.2 - 0.6 C) --> Density (lbm/ft**3)
References:  1,20,37
Data Quality:  EXCELLENT
MDATA  4.90684E+02
/
MPID  35305  TABLE  FAHRENHEIT  1.0
STEEL, CARBON, TYPE 1020 (0.2 - 0.6 C) --> Specific Heat (Btu/(lbm*F))
References:  1,20,37
Data Quality:  EXCELLENT
MDATA  3.20000E+01  1.05000E-01
MDATA  1.67000E+02  1.20000E-01
MDATA  3.92000E+02  1.35000E-01
MDATA  7.52000E+02  1.50000E-01
MDATA  1.11200E+03  1.70000E-01
MDATA  1.29200E+03  2.00000E-01
MDATA  1.40540E+03  2.00000E-01
MDATA  1.41440E+03  1.64800E+00
MDATA  1.42340E+03  1.68000E-01
MDATA  1.74200E+03  1.60000E-01
/
MPID   3001  TABLE  FAHRENHEIT  1.0
PLUTONIUM --> Thermal Conductivity (Btu/(hr*ft*F))
References:  20,31,3,27,43,42,41,36,44
Data Quality:  EXCELLENT
MDATA -1.89400E+02  9.67635E-01
MDATA -8.14000E+01  1.93527E+00
MDATA -4.54000E+01  2.66100E+00
MDATA  6.26000E+01  4.59627E+00
MDATA  1.34600E+02  5.80581E+00
MDATA  2.06600E+02  7.25726E+00
MDATA  2.42600E+02  7.74108E+00
MDATA  2.66000E+02  9.19253E+00
MDATA  1.11200E+03  1.83851E+01
/
MPID   3004  CONSTANT  FAHRENHEIT  1.0
PLUTONIUM --> Density (lbm/ft**3)
References:  20,31,3,27,43,42,41,36,44
Data Quality:  EXCELLENT
MDATA  1.19862E+03
/
MPID   3005  TABLE  FAHRENHEIT  1.0
PLUTONIUM --> Specific Heat (Btu/(lbm*F))
References:  20,31,3,27,43,42,41,36,44
Data Quality:  EXCELLENT
MDATA  3.20000E+01  3.20000E-02
MDATA  2.12000E+02  3.28000E-02
MDATA  2.57000E+02  1.74400E-01
MDATA  3.02000E+02  2.94000E-02
MDATA  3.47000E+02  2.94000E-02
MDATA  3.92000E+02  7.24000E-02
MDATA  4.37000E+02  3.99000E-02
MDATA  8.42000E+02  3.99000E-02
MDATA  8.87000E+02  1.12000E-01
MDATA  9.32000E+02  3.43000E-02
MDATA  1.18040E+03  3.43000E-02
/
```

Jul 18 1994 13:58:59 **template.dat** Page 1

```
*************************************************************************
*  P/THERMAL EXAMPLE TEMPLATE FILE
*
*  Note:  All lines beginning with an "*" are comment lines.
*
*************************************************************************
*
*  MID Template
*  Format:  "MID  Tid  Kx  Ky  Kz  Rho  Cp  PHID"
*
*-----------------------------------------------------------------------
*
* MID's
* 1001 --> air gaps
* 1002 --> SECN
* 1003 --> ENS(A-C)
* 1004 --> PRIM
* 1005 --> PUO2
* 1006 --> CELOTEX
* 1007 --> PLATEA (1100 AL)
* 1008 --> PLATEB ( LEAD )
* 1009 --> FOOD
* 1011 --> SHELL (DRUM)
* 1012 --> AIR UNDER DRUM LID
* 1013 --> LEAD SHLD (9968 ONLY)
* 1014 --> CHARRED CELOTEX REGION (1.4")
*
*     Tid     Kx     Ky     Kz     Rho     Cp     PHID
*     ---     ---    ---    ---    ---     ---    ----
MID  1001  81201  81201  81201   81204  81205      0
MID  1002  35701  35701  35701   35704  35705      0
MID  1003 100301 100303 100301  100304 100305      0
MID  1004  35701  35701  35701   35704  35705      0
MID  1005   3001   3001   3001    3004   3005      0
MID  1006 100601 100601 100601  100604 100605      0
MID  1007 100701 100701 100701  100704 100705      0
MID  1008   2101   2101   2101    2104   2105      0
MID  1009  35301  35301  35301   35304  35305      0
MID  1011  35701  35701  35701   35704  35705      0
MID  1012  81201  81201  81201   81204  81205      0
MID  1013   2101   2101   2101    2104   2105      0
MID  1014 100601 100601 100601  100604 100605      0
*
*************************************************************************
*
*  MACRO Templates
*  Format:  "MACRO Tid  Microfunction_Count Node_1 Node_2  Scale_Factor"
*           "Micro_id_1  Micro_id_2  ...  Micro_Id_n"
*
*-----------------------------------------------------------------------
*
*  TMACROfunction Template 17
* Solar flux to side of drum
MACRO  20  1  0  0 0.65
120
*
* Solar flux to top of drum
MACRO  22  1  0  0  0.65
122
*
* Volumetric heat generation for top tuna can
MACRO  13  1  0  0  1.0
113
*
* Volumetric heat generation for bottom tuna can
MACRO  15  1  0  0  1.0
115
*
* Heat flux rejection to ambient by radiation.
MACRO  16  1 9999 0 0.21
116
*
*************************************************************************
*
*  CONV Templates
*  Format:  "CONV  uid  cfig  #gp  #mpid"
```

Jul 18 1994 13:58:59 **template.dat** Page 2

```
*           "gp_1  gp_2  ...  gp_n"
*           "mpid_1  mpid_2  ...  mpid_n"
*
*----------------------------CONVECTION FROM HORIZONTAL-------------------------
* CONVECTION FROM TOP/BOTTOM OF FLAT PLATES
*CONV  10  26  2  0
*0.19 0.33
*
* CONVECTION FROM CYLINDRICAL SIDE OF CASK
*CONV  8  26  2  0
*0.18  0.33
*-------------------------CONVECTION FROM VERTICAL---------------------------
* NATURAL CONVECTION FROM TOP OF CASK
CONV  10  26  2  0
0.22 0.33
*
* NATURAL CONVECTION FROM SIDE OF CASK
* 0.19 0.33 - from 5320 work
*0.234 0.25 - from original SARP.
CONV  8  26  2  0
0.19 0.33
*
*-------------------------------FOR RAL CONSIDERATION-------------------------
* NATURAL CONVECTION FROM TOP OF CASK
*CONV  10  13  4  5
* 0.375 0.375 90.0 4.17e+08
* rho Mu  Beta  Cp  k
*81204  81207  81208 81205  81201
*
* NATURAL CONVECTION FROM SIDE OF CASK
*CONV  8   13  2  5
* 0 4.17E+08
* rho  Mu  Beta  Cp k
*81204 81207 81208 81205 81201
*#############################################################################
*
*  Radiation Templates
*
*  Format:  "VFAC           uid      [nbands]"
*           "Ec [Tc [Empid [Tmpid [L1 L2 [Kflag [Collapse] ] ] ] ] ]
*
*-----------------------------------------------------------------------------
*
*** ENCLOSURE 1
* FOOD CAN INSIDE
VFAC 111 0
0.14 1.0 0 0 0 0 0 1
VFAC 112 0
0.14 1.0 0 0 0 0 0 2
VFAC 113 0
0.14 1.0 0 0 0 0 0 3
* TUNA CAN OUTSIDE
VFAC 121 0
0.14 1.0 0 0 0 0 0 7
VFAC 122 0
0.14 1.0 0 0 0 0 0 8
***
*** ENCLOSURE 2
VFAC 114 0
0.14 1.0 0 0 0 0 0 4
VFAC 115 0
0.14 1.0 0 0 0 0 0 5
VFAC 116 0
0.14 1.0 0 0 0 0 0 6
VFAC 126 0
0.14 1.0 0 0 0 0 0 9
VFAC 127 0
0.14 1.0 0 0 0 0 0 10
***
** ENCLOSURE 3
* FOOD
VFAC 131 0
0.14 1.0 0 0 0 0 0 11
* PRIMARY
VFAC 141 0
0.6 1.0 0 0 0 0 0 12
```

Jul 18 1994 13:58:59 **template.dat** Page 3

```
VFAC 142 0
0.6 1.0 0 0 0 0 0 13
VFAC 143 0
0.6 1.0 0 0 0 0 0 14
* ENERGY ABSORBER C
VFAC 151 0
0.2 1.0 0 0 0 0 0 29
***
*** ENCLOSURE 4
* PRIMARY
VFAC 171 0
0.6 1.0 0 0 0 0 0 15
VFAC 172 0
0.6 1.0 0 0 0 0 0 16
* ENERGY ABSORBER B
VFAC 201 0
0.2 1.0 0 0 0 0 0 26
***
*** ENCLOSURE 5
* PRIMARY
VFAC 173 0
0.6 1.0 0 0 0 0 0 17
VFAC 174 0
0.6 1.0 0 0 0 0 0 18
VFAC 175 0
0.6 1.0 0 0 0 0 0 19
VFAC 176 0
0.6 1.0 0 0 0 0 0 20
VFAC 177 0
0.6 1.0 0 0 0 0 0 21
VFAC 178 0
0.6 1.0 0 0 0 0 0 22
* ENERGY ABSORBER C
VFAC 168  0
0.2 1.0 0 0 0 0 0 36
* SECONDARY
VFAC 181 0
0.6 1.0 0 0 0 0 0 23
VFAC 182 0
0.6 1.0 0 0 0 0 0 24
VFAC 183 0
0.6 1.0 0 0 0 0 0 25
* AL BOTTOM PLATE(0.2)  OR LEAD (9967,68) (.28)
VFAC 202 0
0.28 1.0 0 0 0 0 0 50
***
*** ENCLOSURE 6
* PUO2 BUTTON
VFAC 91 0
1.0
* TUNA CAN INSIDE
VFAC 117 0
0.14 1.0 0 0 0 0 0 30
VFAC 118 0
0.14 1.0 0 0 0 0 0 31
VFAC 119
0.14 1.0 0 0 0 0 0 32
***
*** ENCLOSURE 7
* PUO2 BUTTON
VFAC 911 0
1.0
* TUNA CAN
VFAC 1171
0.14 1.0 0 0 0 0 0 33
VFAC 1181
0.14 1.0 0 0 0 0 0 34
VFAC 1191
0.14 1.0 0 0 0 0 0 35
***
*** ENCLOSURE 8
* LEAD SHIELD(0.28) or CELOTEX(0.5)
VFAC 2201 0
0.28 1.0 0 0 0 0 0 37
VFAC 2202 0
0.28 1.0 0 0 0 0 0 38
```

Jul 18 1994 13:58:59 **template.dat** Page 4

```
VFAC 2203 0
0.28 1.0 0 0 0 0 0 39
* SECONDARY
VFAC 2104 0
0.6 1.0 0 0 0 0 0 40
VFAC 2105 0
0.6 1.0 0 0 0 0 0 41
VFAC 2106 0
0.6 1.0 0 0 0 0 0 42
VFAC 2107 0
0.6 1.0 0 0 0 0 0 43
VFAC 2108 0
0.6 1.0 0 0 0 0 0 44
VFAC 2109 0
0.6 1.0 0 0 0 0 0 45
VFAC 2110 0
0.6 1.0 0 0 0 0 0 46
VFAC 2111 0
0.6 1.0 0 0 0 0 0 47
VFAC 2103 0
0.6 1.0 0 0 0 0 0 51
* AL BOTTOM PLATE (0.2) OR LEAD (9967,68)
VFAC 2002 0
0.28 1.0 0 0 0 0 0 27
* AL TOP PLATE (0.2) OR LEAD (0.28) (9967)
VFAC 2003 0
0.20 1.0 0 0 0 0 0 28
***
*** ENCLOSURE 9
* FOOD CAN INSIDE
VFAC 1110 0
0.14 1.0 0 0 0 0 0 60
VFAC 1111 0
0.14 1.0 0 0 0 0 0 61
VFAC 1112 0
0.14 1.0 0 0 0 0 0 62
***
*** ENCLOSURE 10
* PRIMARY
VFAC 1701 0
0.6 1.0 0 0 0 0 0 52
VFAC 1702 0
0.6 1.0 0 0 0 0 0 53
VFAC 1703 0
0.6 1.0 0 0 0 0 0 54
* ENERGY ABSORBER C
VFAC 1901 0
0.2 1.0 0 0 0 0 0 55
* SECONDARY
VFAC 1801 0
0.6 1.0 0 0 0 0 0 56
***
*** ENCLOSURE 11
* SECONDARY
VFAC 2101 0
0.6 1.0 0 0 0 0 0 49
VFAC 2102 0
0.6 1.0 0 0 0 0 0 50
* BOTTOM PLATE (0.2) OR LEAD (0.28)
VFAC 2001 0
0.28 1.0 0 0 0 0 0 48
***
*  Gray Radiation Template 7:  Emissivity from MPID 4000, Transmissivity = 0.8
*
VFAC  7  0
0.0 0.8 4000
*
*-------------------------------------------------------------------------------
*
*  Gray Radiation Template 6:  Emissivity (Time Dependent) from MPID 3000,
*                              Transmissivity = 0.8
*
VFAC  6  0
0.0 0.8  -3000
*
*-------------------------------------------------------------------------------
```

```
*
*  Spectral Radiation Template 99:  2 Wave Bands (0.0-5.0 and 5.0-1.0E+10
*                                   microns), Transmissivity of both bands
*                                   = 1.0, Emissivity of 0.0-5.0 micron band
*                                   is time dependent from MPID 1000, while
*                                   the emissivity for the 5.0-1.0E+10 band
*                                   is temperature dependent and taken from
*                                   MPID 2000.
*
VFAC 99  2
0.0 1.0 -1000  0 0.0 5.0
0.0 1.0  2000  0 5.0 1.0E+10
*
*-------------------------------------------------------------------------------
*
*  Spectral Radiation Template 79:  2 Wave Bands (0.0-5.0 and 5.0-1.0E+10
*                                   microns), Transmissivity of both bands
*                                   = 1.0, Emissivity of 0.0-5.0 micron band
*                                   is time dependent from MPID 1000, while
*                                   the emissivity for the 5.0-1.0E+10 band
*                                   is temperature dependent and taken from
*                                   MPID 2000. Radiosity nodes are collapsed.
*
VFAC 79  2
0.0 1.0 -1000  0 0.0 5.0          0  2
0.0 1.0  2000  0 5.0 1.0E+10      0  2
*
*###############################################################################
```

Jul 16 1994 09:42:02 **micro.dat** Page 1

```
*  Solar flux on top of drum
*  Solar flux on top/bottom of drum
* 246.0 for top (vertical case)
* 61.4 for top/bottom (horizontal case)
*MICRO 122  0  1
*MICDAT 0.0
MICRO 122  0  18
MICDAT  0.0   0.0
MICDAT  0.01  246.0
MICDAT 12.0   246.0
MICDAT 12.01  0.0
MICDAT 24.00  0.0
MICDAT 24.01  246.0
MICDAT 36.0   246.0
MICDAT 36.01  0.0
MICDAT 48.0   0.0
MICDAT 48.01  246.0
MICDAT 60.0   246.0
MICDAT 60.01  0.0
MICDAT 72.0   0.0
MICDAT 72.01  246.0
MICDAT 84.0   246.0
MICDAT 84.01  0.0
MICDAT 96.0   0.0
MICDAT 96.01  246.0
MICDAT 108.0  246.0
MICDAT 108.01 0.0
MICDAT 120.0  0.0
MICDAT 120.01 246.0
MICDAT 132.0  246.0
MICDAT 132.01 0.0
MICDAT 144.0  0.0
MICDAT 144.01 246.0
MICDAT 156.0  246.0
MICDAT 156.01 0.0
MICDAT 168.0  0.0
MICDAT 168.01 246.0
MICDAT 180.0  246.0
/
*
*  Solar flux on side of drum
* 123.0 for curved surface (horizontal case or vertical case)
*MICRO 120  0  1
*MICDAT 0.0
MICRO 120  0  18
MICDAT  0.0   0.0
MICDAT  0.01  123.0
MICDAT 12.0   123.0
MICDAT 12.01  0.0
MICDAT 24.00  0.0
MICDAT 24.01  123.0
MICDAT 36.0   123.0
MICDAT 36.01  0.0
MICDAT 48.0   0.0
MICDAT 48.01  123.0
MICDAT 60.0   123.0
MICDAT 60.01  0.0
MICDAT 72.0   0.0
MICDAT 72.01  123.0
MICDAT 84.0   123.0
MICDAT 84.01  0.0
MICDAT 96.0   0.0
MICDAT 96.01  123.0
MICDAT 108.0  123.0
MICDAT 108.01 0.0
MICDAT 120.0  0.0
MICDAT 120.01 123.0
MICDAT 132.0  123.0
MICDAT 132.01 0.0
MICDAT 144.0  0.0
MICDAT 144.01 123.0
MICDAT 156.0  123.0
MICDAT 156.01 0.0
MICDAT 168.0  0.0
MICDAT 168.01 123.0
MICDAT 180.0  123.0
```

Jul 16 1994 09:42:02 **micro.dat** Page 2

```
/
*
*  Heat generation of top tuna can
* Use 39796.7 for 10 W.
* Use 75613.8 for 19 W.
* Use 119390.2 for 30 W.
* Use 83573.14 for 21 W.
MICRO 113  0  1
MICDAT 83573.14
/
*
*  Heat generation of bottom tuna can
* Use 3372.0 for completely full can of 15 W (9965 vertical).
* Use 3203.0 for completely full can of 15 W (9965 horizontal & 65v_a).
* Use 1067.7 for completely full can of 5 W (9965 horizontal).
* Use 272660.8 for high density (11 g/cc) of 13.5 W.
MICRO 115  0  1
MICDAT 462600.1
/
*
*  MFID 1:  Straight Line Function of sigma * (T1**4 - T2**4)
*  Radiation rejected to environment
*
MICRO  116  3  17
MICDAT 1.0  0.0
/
```

This Page Intentionally left Blank

APPENDIX 3.5

MSC/PATRAN/THERMAL VERSION 2003

SOFTWARE TEST DOCUMENTATION

This Page Intentionally Left Blank

MSC/PATRAN/THERMAL Version 2003
Software Test Documentation

Approvals:

N. K. Gupta, Author
Engineering Modeling & Simulation Group — Date: 9/19/05

S. J. Hensel, Independent Reviewer (IR-2)
Engineering Modeling & Simulation Group — Date: 9/21/2005

Julio Pardo, Cognizant Quality Function
Quality Engineering — Date: NA

N. K. Gupta, Design Agency
Engineering Modeling & Simulation Group — Date: 9/19/05

Cynthia Holding-Smith, Design Authority
Manager, Engineering Modeling & Simulation Group — Date: 9/29/05

Title: MSC/PATRAN/THERMAL Version 2003 Software Test Documentation

Software Revision Number: 2

Revision History Log

Revision #	Date	Description of Revision
0		Initial Issue

Table of Contents

1.0 SCOPE

The software MSC/PATRAN/THERMAL is a general purpose engineering analysis program. Here at SRS, the software is used for building finite element models and analyzing complex structural and thermal analyses problems. For structural analysis, the software creates an input file (model.inp) which is subsequently used by software ABAQUS for detailed stress analysis purposes. For thermal analysis, the software has an integral THERMAL analysis module that is used for analyzing conduction/radiation dominated problems.

The Software Test Plan (STP) delineated in this document will cover the software requirement's [3.1] testing, software acceptance, and software baseline of the MSC/PATRAN/THERMAL software.

2.0 SOFTWARE AND PRODUCT IDENTIFICATION

Project Name:	Not applicable
Software Product Name:	MSC/PATRAN/THERMAL
Operating Division:	Savannah River Technology Center
Facility:	Engineering Modeling & Simulation
Location of Target System:	703-44A
Software Lead Engineer:	Nick Gupta/Tommy Ensley 773-42A, Room 141 (803) 725-5300

3.0 REFERENCE DOCUMENTS

3.1 G-SQP-A-00004, Software Quality Assurance Plan for MSC/PATRAN/THERMAL, April 2004.
3.2 IEEE Std. 829-1998, IEEE Standard for Software Test Documentation.

4.0 RESOURCES

4.1 Test Lead Engineer

4.1.1 MSC/PATRAN/THERMAL – Nick Gupta

4.2 Special Equipment

SRTC computer IBM pSeries 630 Model 6C4.

4.3 System Configuration

IBM AIX Version 5.1.

5.0 TESTING ACTIVITIES

5.1 Software Operating Environment

The MSC/PATRAN/THERMAL will operate under the UNIX Operating Environment.

5.2 Existing Test Plans

The earlier versions of this software have been tested in the past [see Attachment 9.1]. These tests have been found to meet the structural and thermal analysis needs for services provided by Engineering Modeling & Simulation group. The Software Evaluation Package is attached in Attachment 9.3.

5.3 Test Problems

For computer software, one acceptable method of testing is technical evaluation by tests which demonstrate its capability to produce valid results for the test cases. The test plan for validating the software requirements requires matching the requirements with the test problems, making sure that the test problem is well defined, building the model using the software, inputting required data such as, material properties, loadings conditions, and boundary conditions, setting the model for run, and finally comparing the results. One test problem can validate more than one requirement in a test run. Fifteen problems have been selected to test the code analysis options that are frequently used in analyses at SRS. These test problems are described in Attachment 9.1. These problems have been used in the past for the dedication of this software. For each problem, written and graphical descriptions are provided to define the problem. The option tested is identified and the expected solution is given along with the methodology used in arriving at the solution. The expected solution is obtained from an analytical solution, experimental results, or results from other industry standard software codes.

Attachment 9.1 consists of a set of problems for which solutions have been published, or for which solutions are derived using standard analytical methods, or solution comparison with other software codes, or recommended benchmark problems. The problems were selected with the intent of testing a wide range of: 1) element types, and 2) analysis procedures. 2-D, 3-D, and axisymmetric problems with radiation boundary conditions, Dirichlet (T=constant), and Neumann (dT/dX=constant) boundary conditions have been solved. These test cases provide an excellent baseline for the analysis and development work which is performed in the SRTC at the SRS.

Note regarding units: Units are not important in the assessment of the test problems, and they are not used by MSC/THERMAL. The only stipulation is that

units must be consistent throughout the problem so that the answer will be easily evaluated.

5.4 Acceptance Criteria

The accuracy of solution should be within 0.5% for typical benchmark problems, and within 5% for non-standard problems in comparison with solutions from "industry accepted" codes or experiments.

5.5 Test Logs/Reports

The Test Engineer will create a test logbook for recording any errors or deficiencies encountered during testing, if necessary. The test cases and printed input/output files from the software shall also serve as test documentation. All result directories shall be preserved to verify the input parameters. Input/output files for the various test cases are listed in Attachment 9.4.

5.6 Special Plant/System Configuration

The computer system is IBM RS/6000 with the operating system is IBM AIX, version 5.1.

5.7 Training Requirements

The Test Engineer shall be trained in the use of the software. The Owner shall document the training and the background experience of the Test Engineer.

Testing Complete:

C D Holding-Smith — 9/29/05

Owner, Cynthia Holding-Smith — Date

N. K. GUPTA N. K. Gupta — 9/19/05

Test Engineer, N. K. Gupta — Date

5.8 Schedule

Not Applicable.

5.9 Limiting Conditions

Not Applicable

5.10 Initial Conditions

Software shall be installed on target machine. Material databases shall be installed along with the source file installation.

5.11 Error/Deficiencies Handling

If errors or deficiencies during testing are found, the Test Engineer shall take the following steps:

- immediately stop the testing
- contact the software Owner for error/deficiency resolution
- software Owner shall review the requirements, test method, or Test Engineer's steps to determine the source of error
- The software Owner may revise the requirement, revise the test method or revise the Test Engineer's steps to resolve the error/deficiency.

5.12 Regression Testing

If a requirement or test case is rewritten, all previously testing requirements shall be retested to ensure no adverse effects.

5.13 Recovery Plan

Not applicable.

6.0 ACCEPTANCE

Test results review and approval:

N.K. GUPTA	N.K. Gupta	9/19/05
DA, Printed Name	DA, Signature	Date
Steve Hensel	Steve Hensel	9/21/2005
IR-2, Printed Name	IR-2, Signature	Date

Owner Acceptance of Software:

C.P. HOLDING-SMITH	C.P. Holding-Smith	9/29/05
Printed Name	Signature	Date

7.0 BASELINE ESTABLISHED

Test Lead Engineer:

Printed Name	Signature	Date
N.K. GUPTA	N.K. Gupta	9/19/05

Design Agency:

Printed Name	Signature	Date
N.K. GUPTA	N.K. Gupta	9/19/05

Design Authority:

Printed Name	Signature	Date
C.P. HOLDING-SMITH	C.P. Holding-Smith	9/29/05

8.0 SUMMARY AND CONCLUSIONS

The MSC/PATRAN/THERMAL software is classified, tested, and maintained in accordance with the requirements set forth in QAP 20-1 of Manual 1Q. The test problems modeled and run on this software give results that meet the stated acceptance criteria. It is concluded that the MSC/PATRAN/THERMAL software will perform its intended safety function.

9.0 ATTACHMENTS

9.1 SRT-EMS-940084, Heat Transfer Software Test Plan, February 1995.
9.2 Test Results and Tester Comments.
9.3 Software Evaluation Package
9.4 Computer Input/Output Files

ATTACHMENT 9.1 – TEST PROBLEMS

Table of Contents

PROBLEM 1 :

Infinitely Long Hollow Cylinder with Applied Heat Flux

OPTION(S) TESTED:

Conduction with heat flux (Steady-state, British units)

DESCRIPTION:

A heat flux (q") is applied at the right wall (r_2) and temperature (T_o) is held constant at the left wall (r_1) . Steady-state temperatures are calculated assuming an axisymmetric geometry.

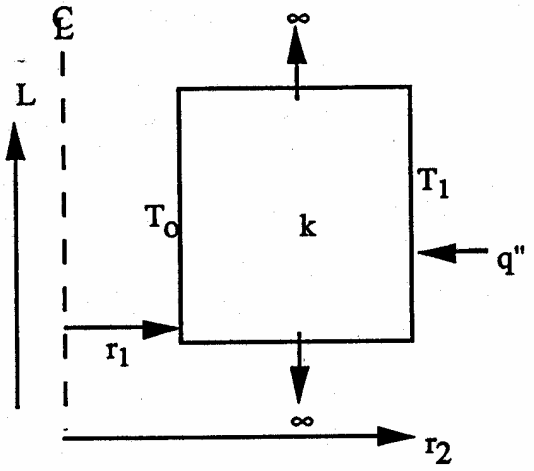

Parameters:

q" = 20 Btu/hr-ft^2	r_2= 3 ft.
T_o = 100° F	k = 1 Btu/hr-ft-°F
r_1 = 2 ft.	L = length (infinite)

EXPECTED SOLUTION:

The temperature at the right boundary (r_2) can be found from the expression:

$$q = \frac{2\pi Lk(T_1 - T_o)}{\ln(r_2/r_1)}$$

Rearranging,

$$T_1 = T_0 + \frac{\ln(r_2/r_1)q}{2\pi kL}$$

By definition the heat rate (q) in Btu/hr can be written as

$$q = 2\pi r_2 L q''.$$

Substituting into the previous equation yields

$$T_1 = T_0 + \frac{\ln(r_2/r_1)2\pi r_2 L q''}{2\pi k L}$$

Simplifying and substituting values gives

$$T_1 = T_0 + \frac{\ln(r_2/r_1) r_2 q''}{k}$$

$$T_1 = 100 + \frac{\ln(3/2)(3)(20)}{1}$$

$$T_1 = 100 + 24.328$$

$$T_1 = 124.328$$

The temperature at the right wall (r_2) is found analytically to be 124.328°F.

REFERENCE: Kreith, Frank, and Black, William Z. Basic Heat Transfer, Harper & Row, New York, 1980, pg 55.

PROBLEM 2 :

Infinitely Long Cylinder with Internal Heat Generation and Convection

OPTION(S) TESTED:

Internal heat generation and convection (Steady-state, British units)

DESCRIPTION:

Heat is generated internally (q''') throughout the solid and is conducted to the right wall at temperature T_s where it is transported by convection to the environment at temperature T_∞. The convective heat transfer coefficient is constant. Steady-state temperatures at the centerline (T(0))are calculated assuming an axisymmetric geometry.

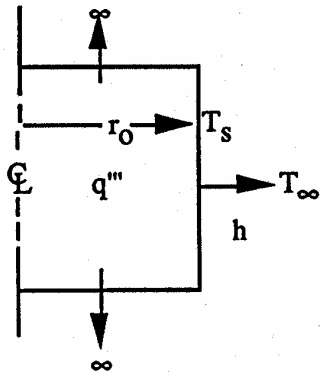

Parameters:

$q''' = 50$ Btu/hr-ft^3
$h = 1$ Btu/hr-ft-°F
$T_\infty = 100$ °F
$r_o = 1$ ft.
$k = 1$ Btu/hr-ft-°F

EXPECTED SOLUTION:

The temperature at the outside surface (r_o) can be found from Newton's law of cooling

$$q = hA(T_s - T_\infty)$$

where A is the surface area of the outside of the cylinder:

$$A = 2\pi r_o L.$$

The heat rate (q) in Btu/hr is found from the cylinder volume and volumetric heat generation (q'''):

$$q = q'''(\pi r_o^{\,2} L)$$

Rearranging Newton's law of cooling and substituting the volumetric heat source gives

$$T_s = T_\infty + \frac{q'''r_o}{2h}$$

$$T_s = 100 + \frac{50(1)}{2(1)}$$

$$T_s = 125$$

The centerline temperature (T(0)) can be found from:

$$T(r) = \frac{q'''r_o^2}{4k}\left(1 - \frac{r^2}{r_o^2}\right) + T_s$$

Substituting at r = 0

$$T(0) = \frac{50(1)}{4(1)} + 125$$

$$T(0) = 12.5 + 125$$

$$T(0) = 137.5$$

The temperature at the centerline(T(0)) is found analytically to be 137.5 °F.

REFERENCE:

Kreith, Frank, and Black, William Z. Basic Heat Transfer, Harper & Row, New York, 1980, pg 72.

PROBLEM 3 :

1D Slab with Internal Heat Generation

OPTION(S) TESTED:

Temperature dependent conductivity (Steady-state, British units)

DESCRIPTION:

Heat is generated internally (q''') in a slab with thickness 2L. The heat is conducted through the solid slab to a fixed wall temperature of T_o. The conductivity is linearly dependent on temperature. Steady-state temperatures at the centerline (x=0) are calculated assuming a slab geometry.

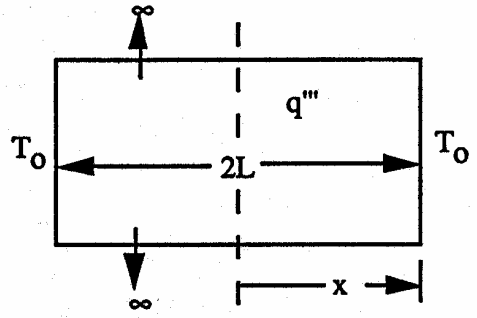

Parameters:	$T_o = 100^\circ F$	$L = 1$ ft
	$q''' = 500$ Btu/hr-ft^3	$k = k_0(1 + bT)$
	$k_0 = 1$ Btu/hr-ft-°F	$b = 0.1^\circ F^{-1}$

EXPECTED SOLUTION:

The thermal conductivity is expressed as $k = k_0(1 + bT)$.

The temperature at x=0 can be found from the expression:

$$\frac{(T(x) - T_0) + \frac{b}{2}(T^2(x) - T_0^2)}{q''' L^2/2k_0} = 1 - (x/L)^2$$

Substituting for x = 0 yields

$$\frac{(T(0) - T_0) + \frac{b}{2}(T^2(0) - T_0^2)}{q'''L^2/2k} = 1$$

$$T(0) - T_0 + \frac{b}{2}(T^2(0) - T_0^2) = \frac{q'''L^2}{2k}$$

$$T(0) - 100 + 0.05T^2(0) - 500 = 250$$

$$T(0) = \frac{-1 \pm \sqrt{1 + 4(0.05)(850)}}{0.1} = \frac{-1 \pm \sqrt{171}}{0.1} = 120.767, -140.770$$

Since −140.770 is a physically meaningless root for this problem, T(0) = 120.767.

The temperature at the centerline (x=0) is found analytically to be 120.767 °F.

REFERENCE: Arpaci, Vedat S. Conduction Heat Transfer, Addison-Wesley Publishing Company, Reading, MA., 1966, pg 131.

PROBLEM 4 :

Transient Conduction in a Semi-infinite Solid

OPTION(S) TESTED:

Transient solution (Transient, British units)

DESCRIPTION:

A heat flux (q") is conducted into a semi-infinite solid having an initial temperature (T_0) of 100°F. The temperature at the surface x=0 is calculated in 0.5 hr intervals from 0 to 2 hours.

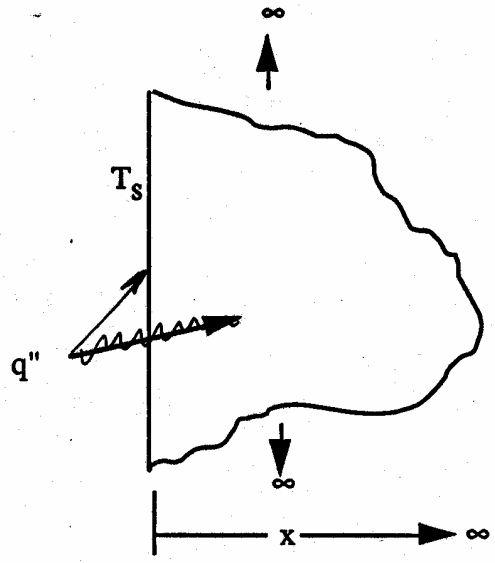

Parameters:

k = 1 Btu/ft-hr-°F	T_0 = 100°F
c_p = 1 Btu/lbm-°F	q" = 10 Btu/hr-ft^2
ρ = 1 lbm/ft^3	

EXPECTED SOLUTION:

The transient temperature at the left boundary can be found from the expression:

$$T_s = T_0 + \frac{2q''\left(\frac{\alpha t}{\pi}\right)^{1/2}}{k}$$

Substituting values gives

$$T_s = T_0 + 20\sqrt{t/\pi}$$

The temperatures at the surface in 0.5 hour intervals are found analytically:

time (minutes)	Temperature (°F) at x=0
0	100.000
0.5	107.979
1.0	111.284
1.5	113.820
2.0	115.958

REFERENCE:

Incropera, Frank P., and DeWitt, David.P. Fundamentals of Heat Transfer, John Wiley & Sons, New York, 1981. pg 205.

PROBLEM 5 :

Concentric Cylinders Modeled as 2-D Plates with Radiation

OPTION(S) TESTED:

Radiation (Transient, British units)

DESCRIPTION:

Radiative heat transfer occurs between concentric regions 2 and 4 (region 3 is void). All surface emmittances and absorptivites are 1. Region 2 radiates to region 4 and region 4 radiates to the ambient. Region 1 is a heat source of 3702.6 Btu/hr-ft.^{3}. The temperatures at locations T3, T8, and T4 are calculated for times of 0, 30, and 90 minutes.

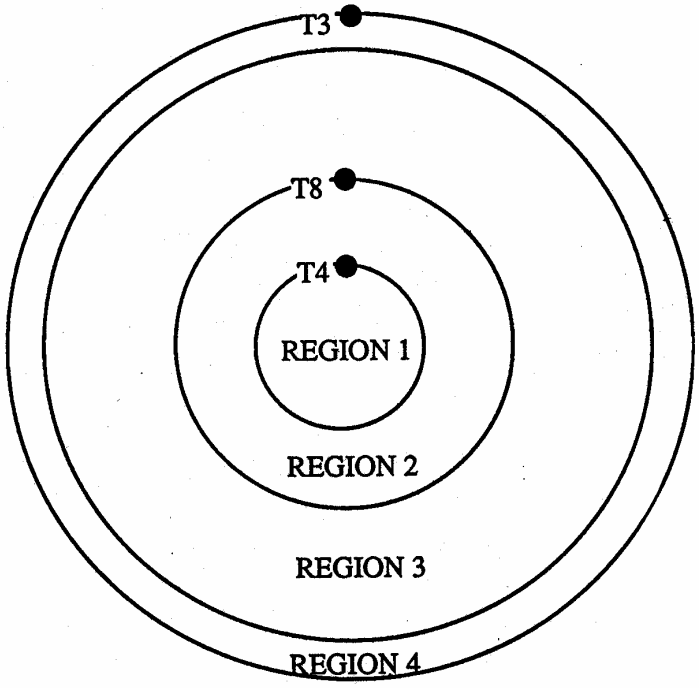

REGION	~~O.D.~~ RADIUS (inches)
1	~~6.9~~ ~~6.5~~
2	15.25
3	21.25
4	21.5

Material	Conductivity (Btu/hr-ft-°F)	Specific Heat (Btu/lb$_m$)	Density (lb$_m$/ft^3)
REGION 1	139.7	0.214	169
REGION 2	26	0.113	489
REGION 4	26	0.113	489

Table 1: Material Properties

Time (minutes)	Ambient Temperature (°F)
0	130°F
0 - 30	1475°F
30 - 90	130°F

Table 2: Ambient Temperature

EXPECTED SOLUTION:

The temperatures at locations T3, T8, and T4 are shown below for times of 0, 30, and 90 minutes.

Time (minutes)	Temperatures (°F)		
	T3	T8	T4
0	278.6	399.2	417.5
30	1272.2	708.8	505.4
90	397.4	568.4	595.4

REFERENCE:

Glass, Robert E., Sample Problem Manual For Benchmarking of Cask Analysis Codes (SAND88-0190 TTC-0780 UC-71), Sandia National Laboratories, Albuquerue, NM 87185, February 1988.

PROBLEM 6 :

Freezing of a Square Solid - The Two Dimensional Stefan Problem

OPTION(S) TESTED:

Phase change (Transient, SI units)

DESCRIPTION:

This problem is the two-dimensional Stefan problem: a square block of material is initially liquid, just above the freezing temperature. The temperature of its outside perimeter is reduced suddenly by -45°, so that the block starts to freeze from the outside towards the core. The latent heat of freezing (70.26 J/kg) occurs between the solidus and liquidus temperatures of -0.25° C and -0.15° C, respectively. The initial temperature of the material is 0° C.

The block is a square with a side length of 8 meters. Symmetry allows the mesh to be generated on only one quarter of the model. A graphical ABAQUS solution is presented for the first 5 seconds of the transient at the points 'A' and 'B' which are shown in the figure below. The ABAQUS element used is type DC2D4 (four-node, bilinear quadrilateral).

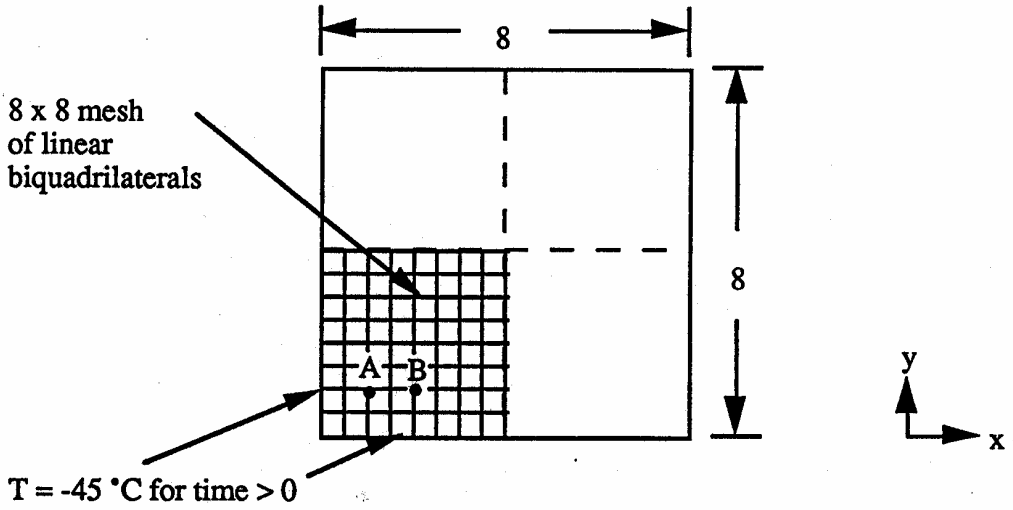

Parameters: $k = 1.08$ W/m-°C $\quad c_p = 1.0$ J/kg
$\rho = 1.0$ kg/m^3

EXPECTED SOLUTION:

Plots of the temperatures computed by P3/THERMAL should be similar to those computed by ABAQUS.

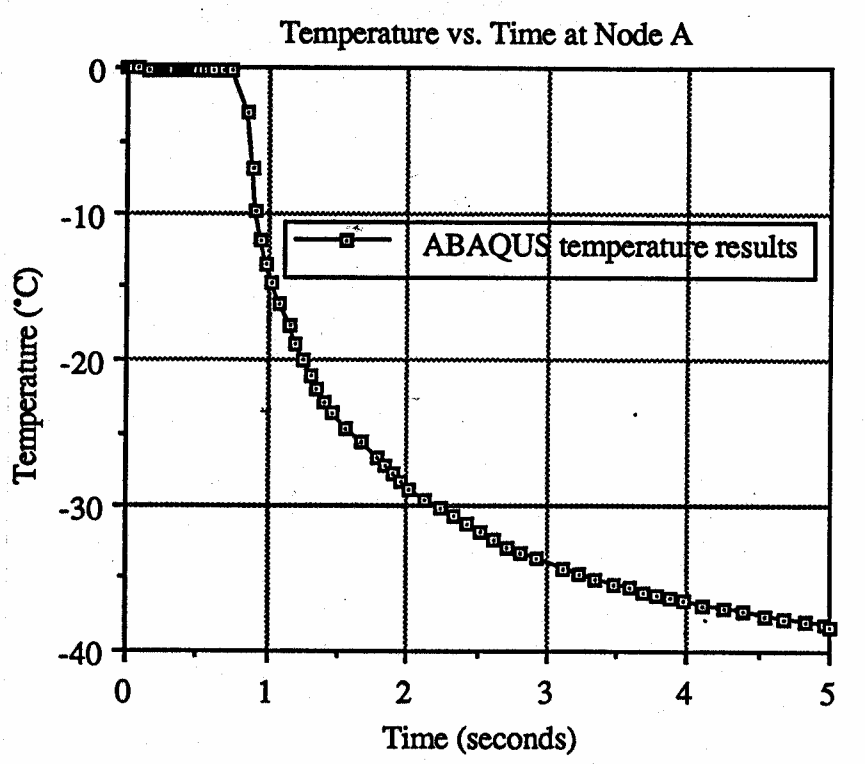
Temperature vs. Time at Node A
0
-10
-20
-30
-40
Temperature (°C)
ABAQUS temperature results
0
1
2
3
4
5
Time (seconds)

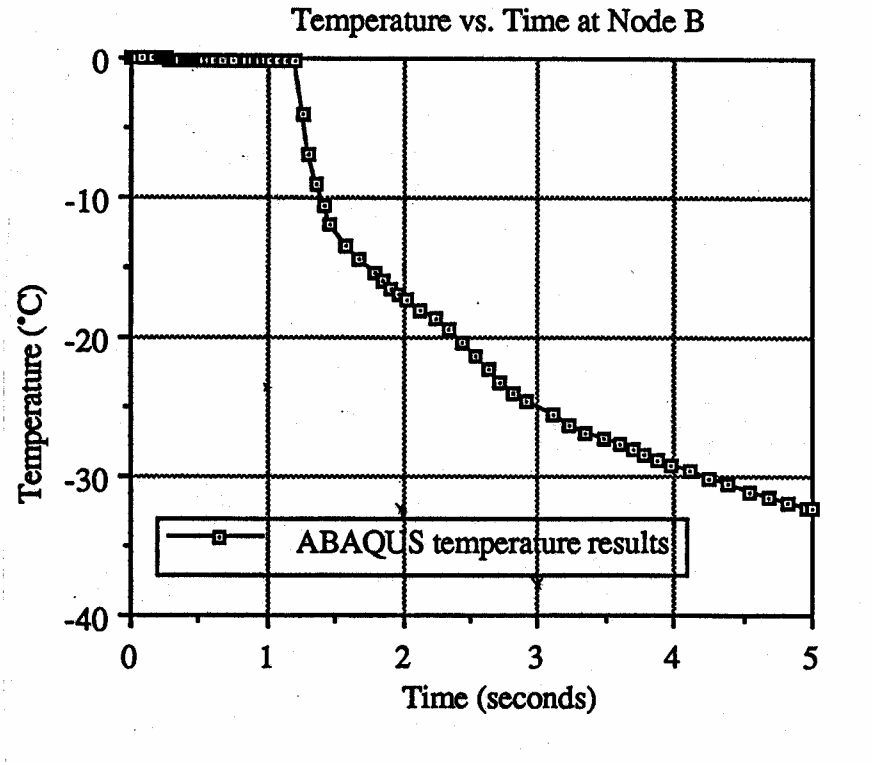
Temperature vs. Time at Node B
0
-10
-20
-30
-40
Temperature (°C)
ABAQUS temperature results
0
1
2
3
4
5
Time (seconds)

PROBLEM 7 :

Insulated Slab with Radiation

OPTION(S) TESTED:

Conduction and radiation (Steady-state, SI units)

DESCRIPTION:

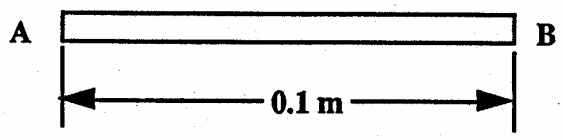

Parameters: $T_a = 1000$ K $\quad \varepsilon_b = 0.98$
$T_{ambient} = 300$ K $\quad k = 55.6$ W/m-° C

This problem is found in ABAQUS V5.2 Verification Manual, page 6.2.2. The ABAQUS element type tested is DC2D8 (8 noded quadrilateral elements). The model used a uniform mesh with 10 elements along the length.

Geometry consists of a rectangular region with zero heat flux along the top and bottom boundary, and fixed temperature (T_a) at the left end. Heat is conducted through the solid to the right end at temperature (T_b) which radiates to an environment at 300 K. The right end has an emissivity (ε_b). There is no internal heat generation.

This is a test recommended by the National Agency for Finite Element Methods and Standards (U.K.): Test T2 from NAFEMS publication TNSB, Rev. 3, "The Standard NAFEMS Benchmarks," October 1990. The temperature results are compared for point B.

EXPECTED SOLUTION:

The temperature at point B is computed by ABAQUS to be 653.80 °C.

PROBLEM 8 :

Insulated Slab with Variable Temperature Boundary Condition

OPTION(S) TESTED:

Transient analysis using a variable temperature boundary condition (Transient, SI units)

DESCRIPTION:

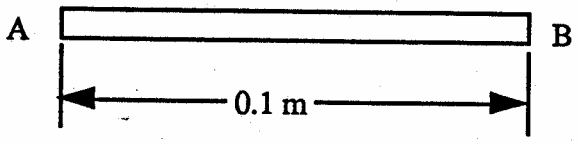

Parameters:

$T_a = 0°$ C
$T_b = 100\sin(\Pi t/40)°$ C where t is in seconds
$\rho = 7200$ kg/m^3
$k = 35.0$ W/m-°C
$c_p = 440.5$ J/kg°C

This problem is found in ABAQUS V5.2 Verification Manual, pg 6.2.3. The ABAQUS element type tested is DC1D3 (1-D with 3 nodes per bar element).

Geometry consists of a rectangular region with zero heat flux along the top and bottom boundary, and fixed temperature (T_a) at the left end and with a varying temperature (T_b) at the right end. There is no internal heat generation.

This is a test recommended by the National Agency for Finite Element Methods and Standards (U.K.): Test T3 from NAFEMS publication TNSB, Rev. 3, "The Standard NAFEMS Benchmarks," October 1990. The temperature results are compared for .

EXPECTED SOLUTION:

The target solution is 36.60° C at x = 0.08 m and 32 secs .

PROBLEM 9 :

2-D Slab with Convection

OPTION(S) TESTED:

2-D with convection (Steady-state, SI units)

DESCRIPTION:

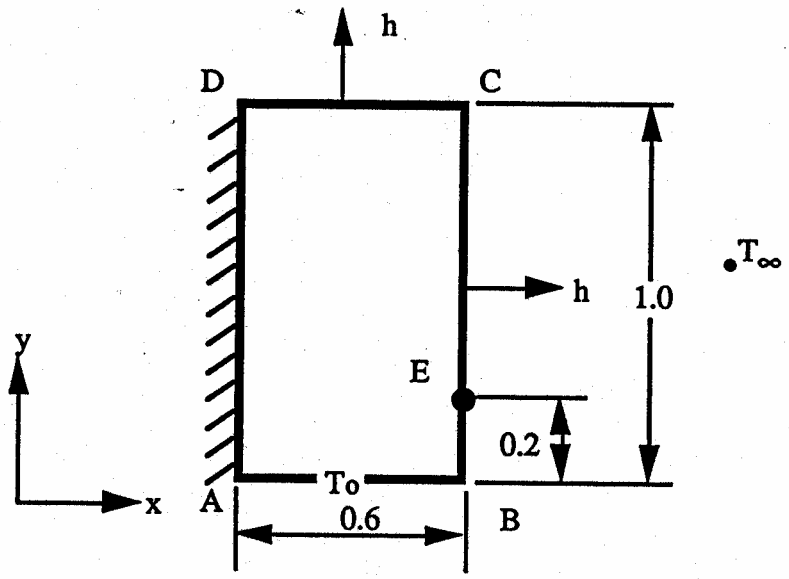

Parameters: $h = 750\ W/m^2 \cdot C$; $T_o = 100^\circ C$; $k = 52\ W/m^\circ C$, $T_\infty = 0^\circ C$

This problem is found in ABAQUS V5.2 Verification Manual, page 6.2.4. The ABAQUS element type tested is DC3D8 (3-D with 8 nodes per hexagonal element). The mesh is uniform and the width (Δx) and height (Δy) for each element is 0.1 m. There are four elements through the thickness (Δz) for the ABAQUS model.

Geometry consists of a rectangular region with zero heat flux along the left boundary, and convection to the ambient at T_∞ along right and top boundaries. The bottom is held at a constant temperature (T_o). There is no internal heat generation.

This is a test recommended by the National Agency for Finite Element Methods and Standards (U.K.): Test T4 from NAFEMS publication TNSB, Rev. 3, "The Standard NAFEMS Benchmarks," October 1990.

EXPECTED SOLUTION:

The temperature at point E as computed by ABAQUS is 18.26 °C.

PROBLEM 10 :

1M X 1M Square Aluminum Plate

OPTION(S) TESTED:

Nodal point heat source (Steady-state, SI units)

DESCRIPTION:

A square aluminum plate has a left boundary fixed at 100.0 K and a right boundary with a constant heat flux of 1000.0 W/m^2. At the bottom heat is lost to the environment at 300K through convection with a coefficient of 13.4 W/m^2-K. The top boundary is insulated. At the center of the plate (0.5, 0.5) is a nodal point heat source of 1000W. The plate is uniformly meshed (4x4) with sixteen 4-noded quadrilaterals. P3/THERMAL results are compared to ABAQUS results at the specified coordinates.

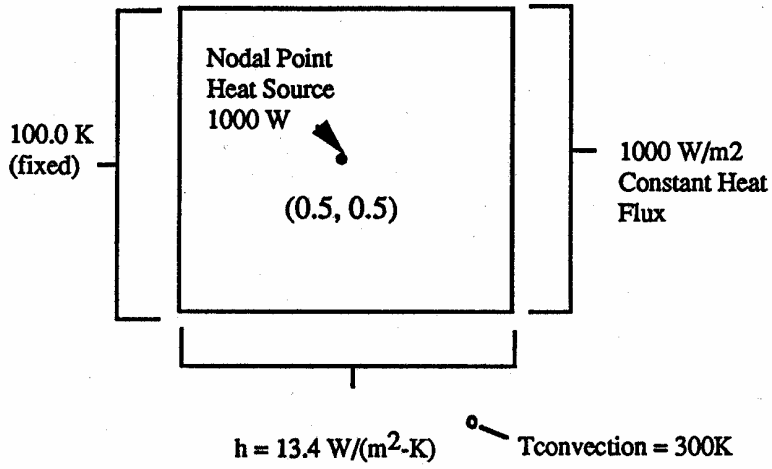

Parameters: $k_{aluminum}$ = 293.076 W/mK

EXPECTED SOLUTION:

The temperatures computed by ABAQUS at three coordinates are shown below:

Coordinates	Temperature (K)
(1, 1)	108.0906
(0.5, 0.5)	107.1976
(1, 0)	112.1438

PROBLEM 11 :

"Stiff" Thermal Problem with the Direct Solver

OPTION(S) TESTED:

Numerical convergence (Steady-state, SI units)

DESCRIPTION:

This problem has been designed to illustrate the thermally "stiff" problem. A material with a lower thermal conductivity and width of 0.5 m is sandwiched between two materials with a higher conductivity and width of 1 m. Temperature and heat flux boundary conditions are imposed on the surfaces as illustrated. QTRAN has Iterative (SOL = 0) and Direct (SOL=2) solution options. For "stiff" thermal problems iterative solvers tend to converge very slowly while direct solvers work very efficiently. This problem is solved using the direct solver. Temperature results are compared to ABAQUS V5.2 temperature results at the coordinates x = 1.0 and y = 9.0.

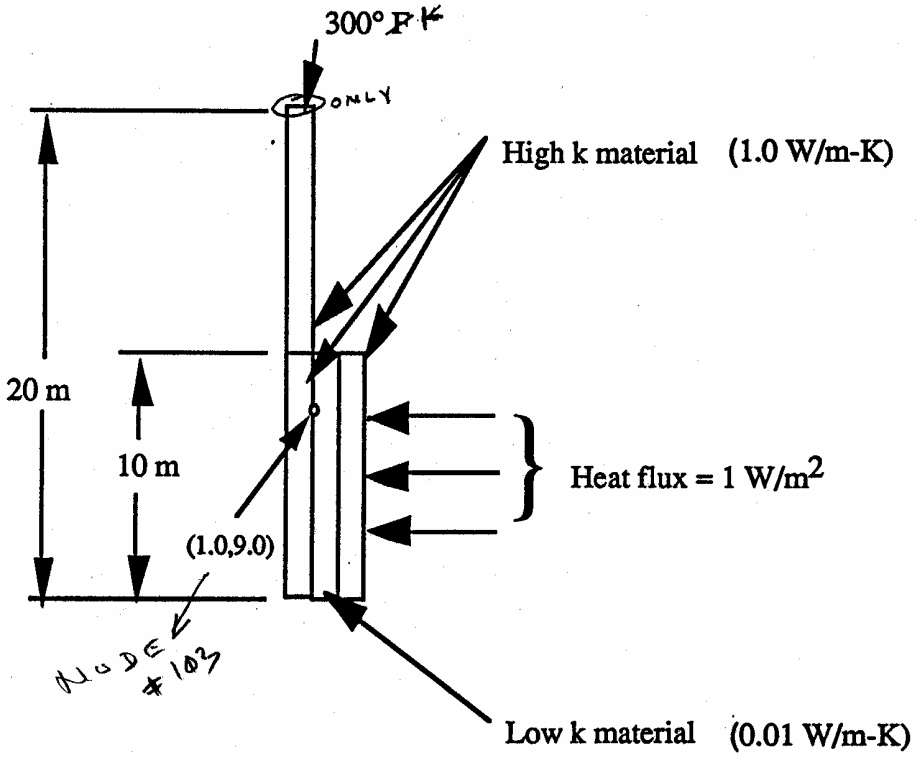

EXPECTED SOLUTION:

The temperature at coordinates (1.0,9.0) is computed by ABAQUS to be 409.690502 K.

PROBLEM 12 :

Infinitely Long Hollow Cylinder with Multiple Materials

OPTION(S) TESTED:

Conduction through multiple materials (Steady-state, British units)

DESCRIPTION:

An infinitely long hollow cylinder is composed of 9 concentric cylinders of various materials, some of which have temperature dependent thermal conductivities. There are constant temperature boundary conditions at the inner cylinder wall of 339° F and between the stainless steel/fiberglass interface of 190° F. The objective is find the temperature at the fiberfrax/stainless steel interface.

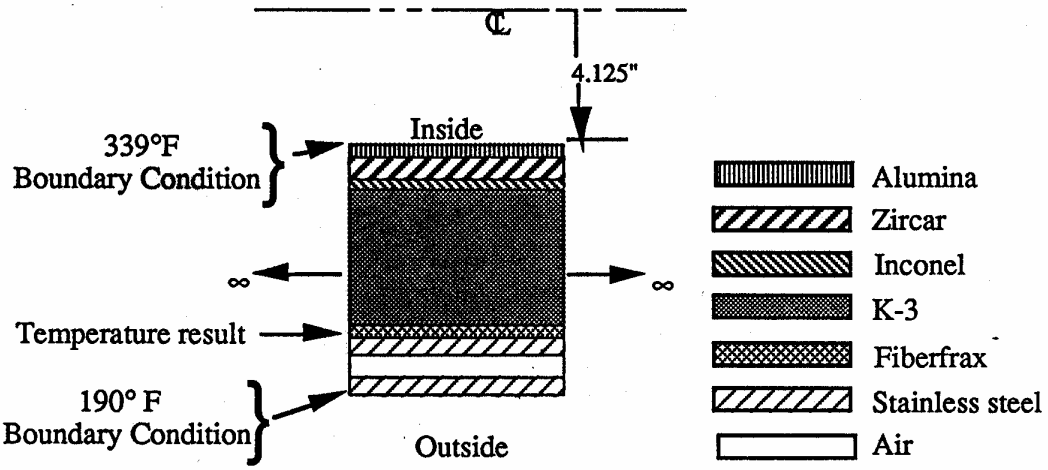

Parameters: $T_i = 339°$ F $\quad T_o = 190°$ F
$r_o = 14.275$ $\quad r_i = 4.125$
L = length (infinite)

Material	outer radius (r_o) (inches)	inner radius (r_i) (inches)	Conductivity (k) (Btu/hr-ft-°F)
Alumina	4.455	4.125	13.1 @ 339° F
Zircar	5.195	4.455	0.054 @ 305° F
Inconel	5.5	5.195	8.16 @ 271° F
K-3	11.25	5.5	2.5 @ 268° F
Fiberfrax	12.0	11.25	0.055 @ 251° F
Stainless steel	13.4	12.0	9.54 @ 237° F
Air	13.9	13.4	0.0184 @ 214° F
Stainless steel	14.275	13.9	9.23 @190° F

The rate of heat transfer by conduction across the materials (q) can be determined from

$$q = \frac{2\pi kL(T_i - T_o)}{\ln(r_o/r_i)} = \frac{(T_i - T_o)}{R_t}$$

The rate of heat transfer by conduction across the materials (q) can be determined from

$$q = \frac{2\pi kL(T_i - T_o)}{\ln(r_o/r_i)} = \frac{(T_i - T_o)}{R_t}$$

The total thermal resistance (R_t) is found by the summation of individual resistances:

$$R_t = \Sigma \frac{\ln(r_o/r_i)}{2\pi kL}$$

Substituting values between the 339° F boundary condition (T_i) and 190° F boundary condition (T_o) yields $R_t = 1.0064$. When $T_i = 339°$ F and $T_o = 190°$ F, q = 148.0451 Btu/hr.

The total thermal resistance (R_t) between the 190° F boundary condition and the stainless steel/fiberglass interface is calculated to be 0.3192. Substituting R_t = 0.3192, q = 148.0451, and $T_o = 190°$ F into the equation for heat transfer by conduction gives $T_i = 237.25°$ F.

EXPECTED SOLUTION:

The temperature at the stainless steel/fiberfrax interface is analytically found to be 237° F.

REFERENCE: Kreith, Frank, and Black, William Z. Basic Heat Transfer, Harper & Row, New York, 1980, pp 55, 56.

PROBLEM 13 :

2-D Plate with Two Isothermal Boundaries

OPTION(S) TESTED:

Spatially dependent temperature boundary condition (Steady-state, SI units)

DESCRIPTION:

A 2-D plate has a constant temperature of 0 K at the left and right boundaries. A spatially dependent temperature boundary condition is imposed at the top and bottom of the plate as shown below:

$$T(x, y) = x \qquad 0 \le x \le 1$$
$$T(x, y) = 2 - x \qquad 1 < x \le 2.$$

Temperatures are calculated analytically at three randomly selected nodal locations: (1.45, 1.1), (0.85, 1.5), and (0.15, 0.7).

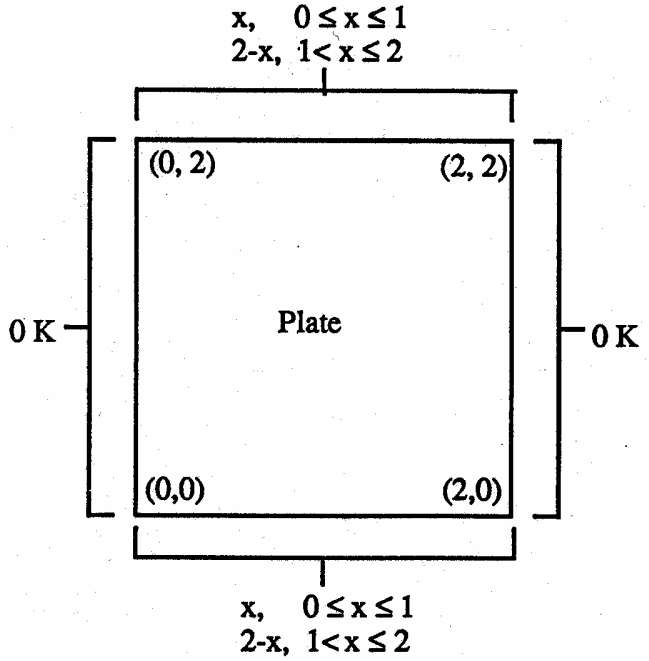

Parameters:

a = 2 m (plate length) b = 2 m (plate width)

EXPECTED SOLUTION:

The temperature at any (x,y) coordinate within the domain can be found from

$$T(x,y) = \frac{8}{\pi^2}\sum_{n=1}^{\infty}\frac{\sin(n\pi/2)}{n^2}\left\{\frac{\sinh\left(\frac{n\pi}{a}\right)y + \sinh\left[\frac{n\pi}{a}(b-y)\right]}{\sinh\left(\frac{n\pi}{a}\right)b}\right\}\sin\left(\frac{n\pi}{a}\right)x$$

The solution is found from the following FORTRAN program and output after substituting values for the plate length and width and summing the first 35 terms. Temperatures are calculated at the three arbitrarily selected points within the domain: (1.45, 1.1), (0.85, 1.5), and (0.15, 0.7).

PROGRAM

```
                program sum
c
      print*, 'Enter x : '
      read (*,*) x
      print*, 'Enter y : '
      read (*,*) y
c
      tsum = 0.0
      pi = 3.14159265
      do 10 n = 1, 35
       at = n*pi/2.0
       gin = (sinh(at*y) + sinh(at*(2-y)))/sinh(n*pi)
       sum = sin(at)/n**2 * gin * sin(at*x)
       tsum = tsum + sum
 10   continue
c
      write (*, *) 'sum = ', 8.0*tsum/pi**2
c
      stop
      end
```

OUTPUT

```
 f77 sum.f
% a.out
 Enter x :
1.45
 Enter y :
1.1
 sum =   0.2477080
% a.out
 Enter x :
0.85
 Enter y :
1.5
 sum =   0.4228634
% a.out
 Enter x :
0.15
 Enter y :
0.7
 sum =   8.1770860E-02
```

The temperatures calculated at the three points are shown below :

Node	Coordinates	Temperature (K)
472	(1.45, 1.1)	0.2477080
1479	(0.85, 1.5)	0.422863
1145	(0.15, 0.7)	0.081771

REFERENCE:

Powers, David L. Boundary Value Problems, Clarkson College of Technology, Academic Press, Inc., 1979. pp 182, 183.

PROBLEM 14 :

Radiation Exchange between Two Infinitely Long Cylinders and Space

OPTION(S) TESTED:

Radiation view factor calculations (Steady-state, SI units)

DESCRIPTION:

To test performance of P3/THERMAL's integrated viewfactor/radiation resistor generation program, a benchmark analysis was chosen that has an exact solution. This thermal radiation benchmark consists of two parallel cylinders, each 1-meter in radius, with the centerlines separated by 2.25 meters. A uniform heat flux of 1000 W/m^2 is applied on the outer surfaces. The cylinder material is assumed to be a near perfect conductor (thermal conductivity of 7920 W/m-K) to make the radial temperature gradient small so that the analytical solution can be easily shown. The surface emissivity is 1.0. The space temperature (T_∞) is taken as absolute zero. The relatively close proximity of the cylinders makes this benchmark a significant challenge to a radiation view factor code. This benchmark demonstrates P3/THERMAL's view factor program accuracy for a complicated view factor problem as well as the capability of the solver to model the radiation network.

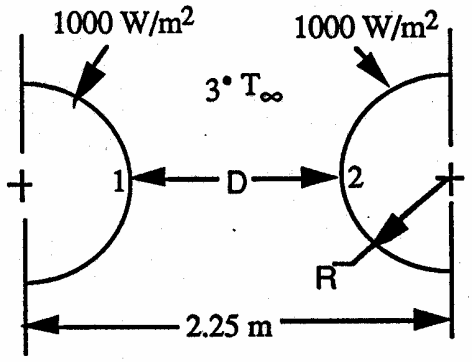

Parameters: D = 0.25 m, R = 1 m, q" = 1000 W/m^2, $\sigma = 5.7(10)^{-8}$ W/m^2-K^4

EXPECTED SOLUTION:

The net heat flux between surface 1 and the environment is

$$q''_{1-3} = \sigma F_{1-3}(T_1^4 - T_3^4)$$

The viewfactors (F) for this arrangement can be expressed as

$$F_{1-2} + F_{1-3} = 1.0.$$

with

with

$$F_{1-2} = \frac{2}{\pi}\left[(X^2 - 1)^{1/2} + \frac{\pi}{2} - \cos^{-1}\left(\frac{1}{X}\right) - X \right]$$

$$\text{where } X = 1 + \frac{D}{2R}$$

Evaluating, $F_{1-2} = 0.30895$ and $F_{1-3} = 0.69105$.

Substituting these values into the expression for the net heat flux q''_{1-3} yields $T_1 = 399.700$ K.

The temperature of the cylinder surface is analytically found to be 399.700 K.

REFERENCES:

Siegel, Robert and Howell, John. Thermal Radiation Heat Transfer, 2nd. ed., Hemisphere Publishing Co., 1981. pg 205.

PROBLEM 15 :

3-D Brick with Heat Flux, Convection, and Temperature Boundary Conditions

OPTION(S) TESTED:

3-D conduction (Steady-state, SI units)

DESCRIPTION:

A brick has a width of 1.0 m (Δz), length of 2.0 m (Δx), and height of 1.0 m (Δy). A heat flux (q''_f) of 245 W/m^2 is applied at the plane $z = 1$. Convection (q''_c) with a convective heat transfer coefficient of 180 W/m^{2}K occurs to an environment at 250 K at the plane $x = 2$. The boundary at $y = 0$ is held at a constant temperature of 300 K. The remaining boundaries are insulated. The thermal conductivity of the brick is 40 W/mK.

The brick is uniformly meshed with 250 8-noded hexahedrons, each having an element edge length of 0.2 m. Temperatures computed by ABAQUS are shown at three arbitrarily selected nodal locations within the brick.

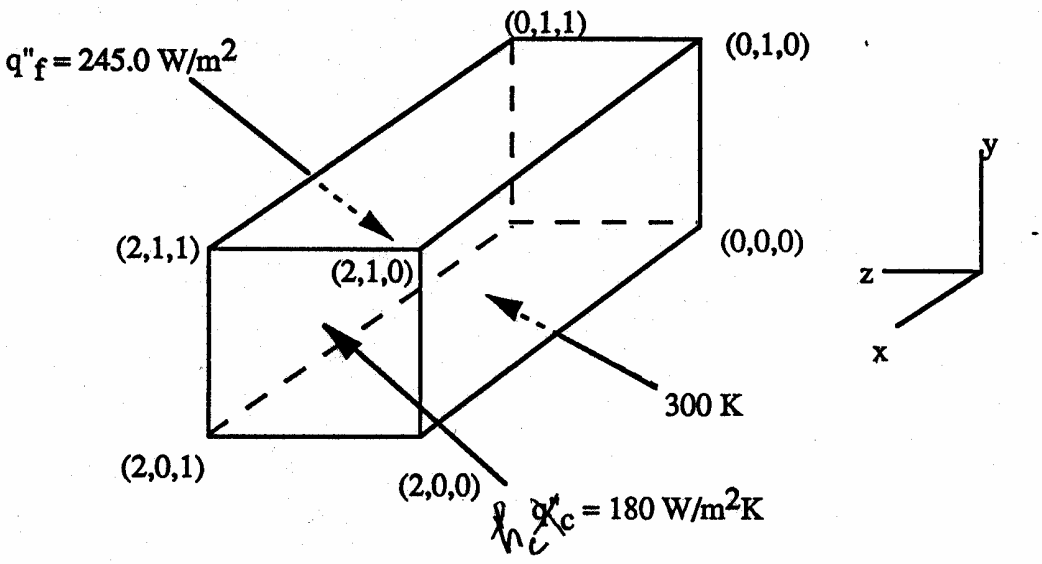

EXPECTED SOLUTION:

The temperatures at three nodes are found by ABAQUS as shown below:

Node	Coordinates (x,y,z)	Temperature (K)
305	(1.4, 0.6, 0.8)	287.566078
227	(1.2, 0.4, 0.6)	293.430702
82	(0.8, 0.2, 0.2)	298.230642

Intentionally left blank

Intentionally left blank

ATTACHMENT 9.2 – TEST RESULTS

The following results compare the MSC/THERMAL solutions to the theoretical or other solutions at the specified critical points. The test cases (Problem #s) identified in Attachment 9.1 were run on IBM AIX version 5.1 and therefore satisfy the RSS #1 [3.1]. Computer input and output files are listed in Attachment 9.4.

Test Problem 1: Infinitely Long Hollow Cylinder with Applied Heat Flux

Results: The temperature at the right boundary (r_2)

MSC/Thermal (°F)	Analytical (°F)	Error (%)
124.307	124.328	< 0.01

The temperature contours are shown in Figure 1.

Tester's Comments: This problem satisfies the RSS # 2a, 2b, 2d, 3, 4b, 4e, and 6. Software calculated result meets the acceptance criteria.

Test Problem 2: Infinitely Long Hollow Cylinder with Internal Heat Generation and Convection

Results: The temperature at the centerline (r_o)

MSC/Thermal (°F)	Analytical (°F)	Error (%)
137.481	137.5	< 0.01

The temperature contours are shown in Figure 2.

Tester's Comments: This problem satisfies the RSS # 2a, 2b, 2d, 3, 4a, 4b, 4g, and 6. Software calculated result meets the acceptance criteria.

Test Problem 3: 1-D Slab with Internal Heat Generation

Results: The temperature at the left boundary:

MSC/Thermal (°F)	Analytical (°F)	Error (%)
120.767	120.767	< 0.01

The temperature contours are shown in Figure 3.

Tester's Comments: This problem satisfies the RSS # 2a, 2b, 2d, 3, 4b, 4e, 4g, and 6. Software calculated result meets the acceptance criteria.

Test Problem 4: Transient Conduction in a Semi-infinite solid

Results: The temperatures at x = 0, Node #203 at 30 minute interval:

Time (Hours)	MSC/Thermal (°F)	Analytical (°F)	Error (%)
0	100.000	100.000	< 0.01
0.5	107.977	107.977	< 0.01
1.0	111.283	111.283	< 0.01
1.5	113.821	113.821	< 0.01
2.0	115.959	115.959	< 0.01

The temperature contours are shown in Figure 4.

Tester's Comments: This problem satisfies the RSS # 2a, 2b, 2d, 2f, 2g, 3, 4b, 4e, and 6. Software calculated results meet the acceptance criteria.

Test Problem 5: Concentric Cylinders Modeled as 2-D Plates with Radiation

Results: The temperatures at T3, T4, and T8 are:

Time (mts)	MSC/Thermal (°F)			Reference (°F)			Error (%)		
	T3	T8	T4	T3	T8	T4	T3	T8	T4
0	278.9	400.5	418.3	278.6	399.2	417.5	0.107	0.326	0.191
30	1270.5	708.2	505.3	1272.2	708.8	505.4	0.133	0.085	0.02
90	398.3	569.1	596.7	397.4	569.4	595.4	0.226	0.053	0.218

The temperature contours are shown in Figure 5.

Tester's Comments: This problem satisfies the RSS # 2a, 2b, 2d, 2e, 2f, 3, 4b, 4f, 4g, and 6. Software calculated results meet the acceptance criteria.

Problem 6: Freezing of a Square Solid – The 2-D Stefan Problem

Results: The temperatures at Points A and B are given in Figure 6:

Tester's Comments: This problem satisfies the RSS # 2a, 2b, 2c, 2d, 2f, 2h, 3, 4b, 4e, 5, and 6. The temperatures calculated by MSC/THERMAL are in excellent agreement with ABAQUS results except for a brief period during phase change. This is due to extreme nonlinearity during phase change. The discrepancy appears to be due to the limitation in MSC/THERMAL where it accepts only one freezing temperature for the liquid material as compared to ABAQUS code which uses solidus and liquidus temperatures to model phase change. A phase change temperature of -0.2ºC based on an average of solidus (-0.25ºC) and liquidus (-0.15ºC) temperatures was input in the MSC/THERMAL model. A trial run using ABAQUS where the solidus and liquidus temperatures are close to -0.2ºC brings the MSC/THERMAL and ABAQUS results closer during phase change. Based on these observations, the results obtained using MSC/THERMAL are quite acceptable.

Problem 7: Insulated Slab with radiation

Results: The temperature at point B is:

MSC/Thermal (°C)	ABAQUS (°C)	Error (%)
653.862	653.80	< 0.01

The temperature contours are shown in Figure 7.

Tester's Comments: This problem satisfies the RSS # 2a, 2b, 2d, 2e, 2f, 3, 4b, 4f, and 6. Software calculated result meets the acceptance criteria.

Problem 8: Insulated Slab with Variable Temperature Boundary Condition.

Results: The temperature at point B (x = 0.08 m and 32 secs) is:

MSC/Thermal (°C)	ABAQUS (°C)	Error (%)
36.564	36.60	0.098

The temperature contours are shown in Figure 8.

Tester's Comments: This problem satisfies the RSS # 2a, 2b, 2d, 2f, 3, 4b, 4c, 4e, 4h, and 6. Software calculated result meets the acceptance criteria.

Problem 9: 2-D Slab with Convection

Results: The temperature at point E is:

MSC/Thermal (°C)	ABAQUS (°C)	Error (%)
18.415	18.26	0.85

The temperature contours are shown in Figure 9.

Tester's Comments: This problem satisfies the RSS # 2a, 2b, 2d, 2f, 3, 4a, 4b, 4e, and 6. Software calculated result meets the acceptance criteria.

Problem 10: 1M X 1M Square Aluminum Plate

Results: The temperatures at three nodes are:

Node	Coordinates	MSC/Thermal (°K)	ABAQUS (K)	Error (%)
441	(1, 1)	108.1220	108.0906	0.03
221	(0.5, 0.5)	108.1371	107.1976	0.876
21	(1, 0)	112.1450	112.1438	< 0.01

The temperature contours are shown in Figure 10.

Tester's Comments: This problem satisfies the RSS # 2a, 2b, 2d, 2f, 3, 4a, 4b, 4e, 4g, and 6. Software calculated results meet the acceptance criteria.

Problem 11: "Stiff" Thermal Problem with Direct Solver

Results: The temperature at coordinate (1.0, 9.0) is:

MSC/Thermal (°K)	ABAQUS (°K)	Error (%)
409.687	409.690502	< 0.01

The temperature contours are shown in Figure 11.

Tester's Comments: This problem satisfies the RSS # 2a, 2b, 2d, 2f, 3, 4b, 4e, and 6. Software calculated result meets the acceptance criteria.

Problem 12: Infinitely Long Hollow Cylinder with Multiple Materials

Results: The temperature at the Fiberfrax/stainless steel interface is:

MSC/Thermal (°F)	Analytical (°F)	Error (%)
237.257	237	0.108

The temperature contours are shown in Figure 12.

Tester's Comments: This problem satisfies the RSS # 2a, 2b, 2d, 2f, 3, 4b, 4e, and 6. Software calculated result meets the acceptance criteria.

Problem 13: 2-D Plate with Two Isotherm Boundaries

Results: The temperatures at the selected nodal points are:

Node	Coordinates	MSC/Thermal (°K)	Analytical (K)	Error (%)
1212	(1.45, 1.1)	0.2477	0.2477080	< 0.01
728	(0.85, 1.5)	0.4229	0.422863	< 0.01
138	(0.15, 0.7)	0.0819	0.081973	< 0.01

The temperature contours are shown in Figure 13.

Tester's Comments: This problem satisfies the RSS # 2a, 2b, 2d, 2f, 3, 4b, 4d, 4e, and 6. Software calculated results meet the acceptance criteria.

Problem 14: Radiation Exchange between Two Infinitely Long Cylinders and Space
Results: The temperature at the cylindrical surface is:

MSC/Thermal (°K)	Analytical (°K)	Error (%)
398.597	399.700	0.276

The temperature contours are shown in Figure 14.

Tester's Comments: This problem satisfies the RSS # 2a, 2b, 2d, 2e, 2f, 3, 4b, 4e, 4f, and 6. Software calculated result meets the acceptance criteria.

Problem 15: 3-D Brick with Heat Flux, Convection, and Temperature Boundary Conditions

Results: The temperature at the cylindrical surface is:

Node	Coordinates	MSC/Thermal (°K)	ABAQUS (°K)	Error (%)
305	(1.4, 0.6, 0.8)	287.337	287.566078	0.08
227	(1.2, 0.4, 0.6)	293.189	293.430702	0.082
82	(0.8, 0.2, 0.2)	298.148	298.230642	0.028

The temperature contours are shown in Figure 15.

Tester's Comments: This problem satisfies the RSS # 2a, 2b, 2d, 2e, 2f, 3, 4a, 4b, 4e, and 6. Software calculated results meet the acceptance criteria.

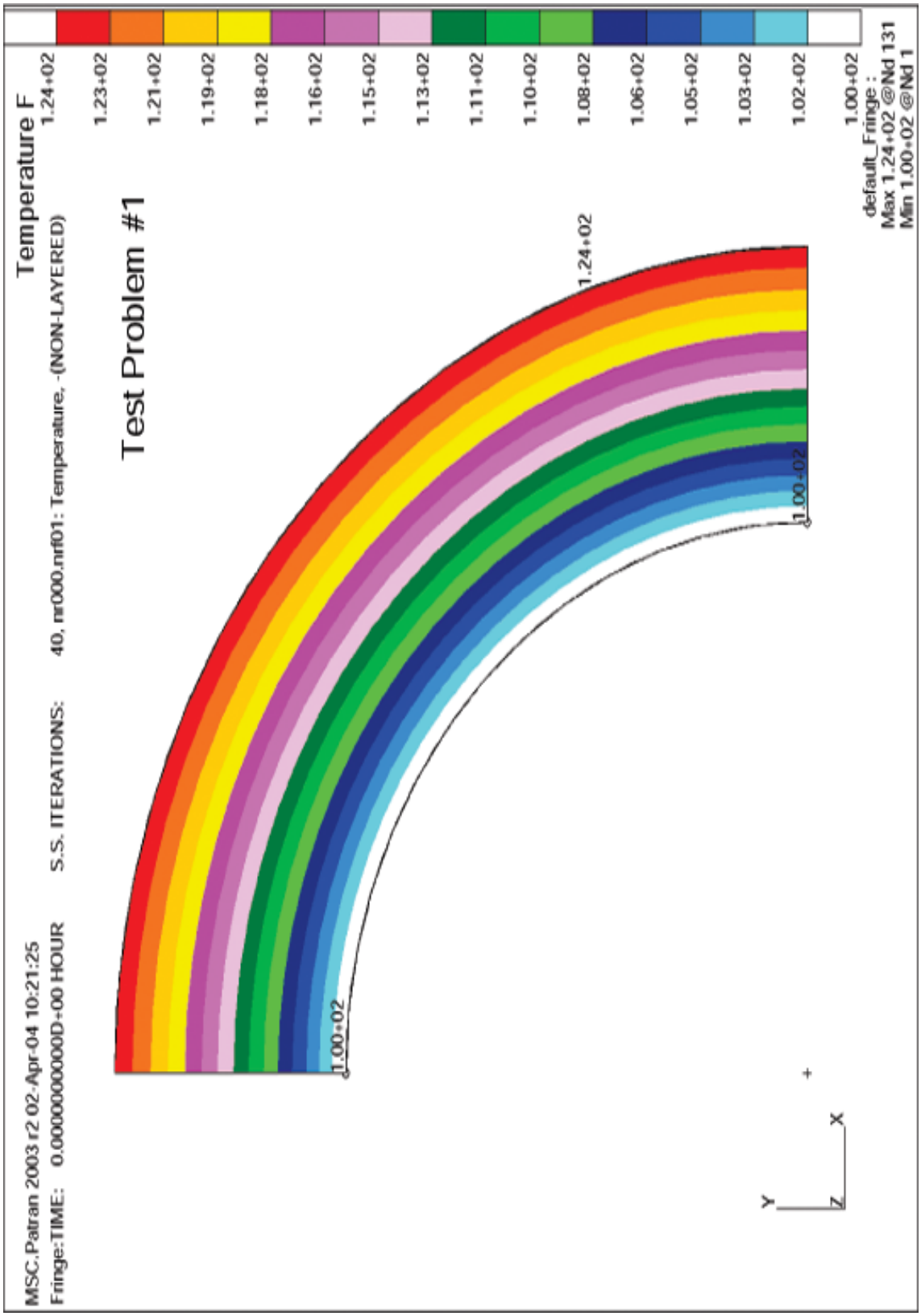

Figure 1 – Temperature Contours for Test Problem No. 1

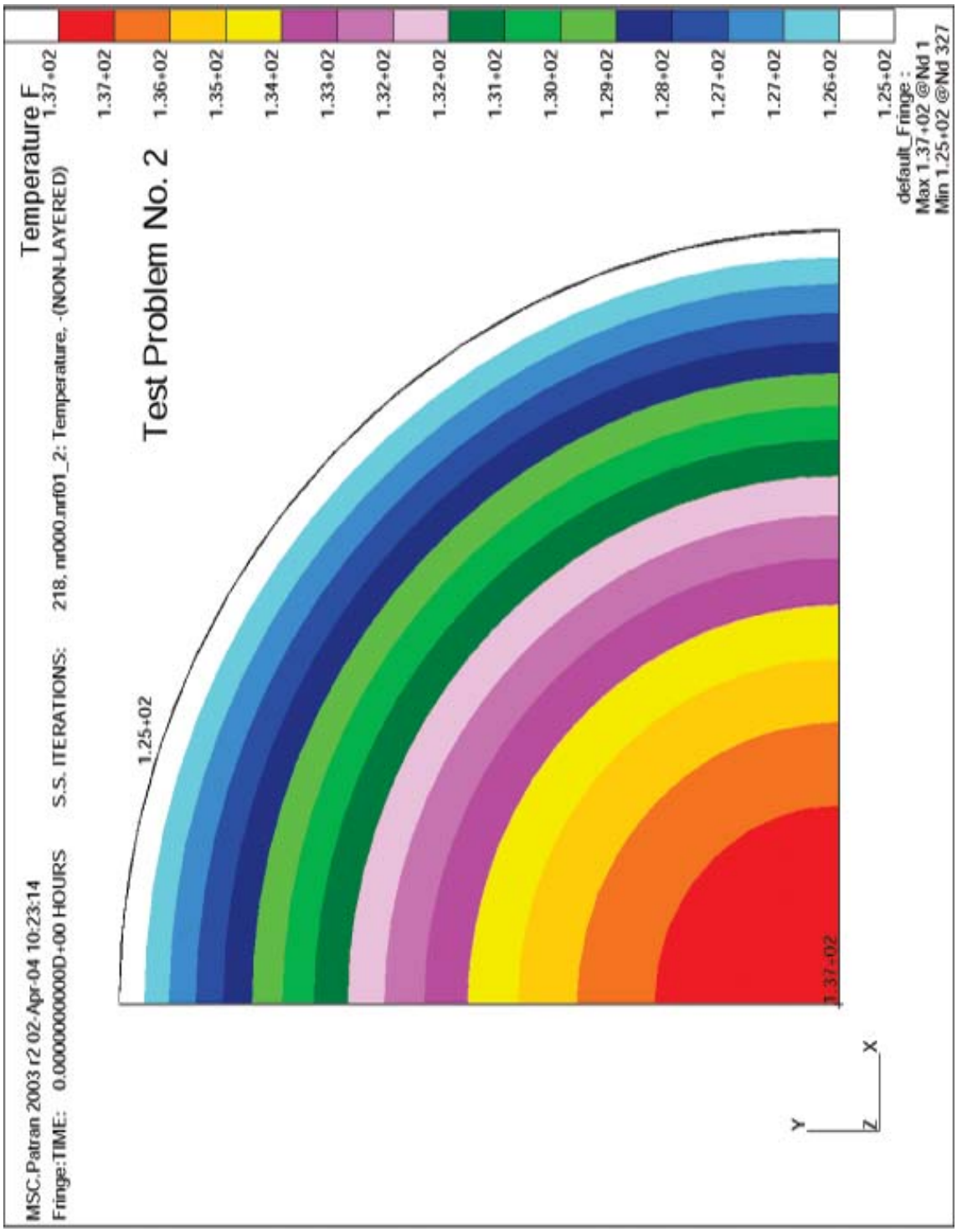

Figure 2 – Temperature Contours for Test Problem No. 2

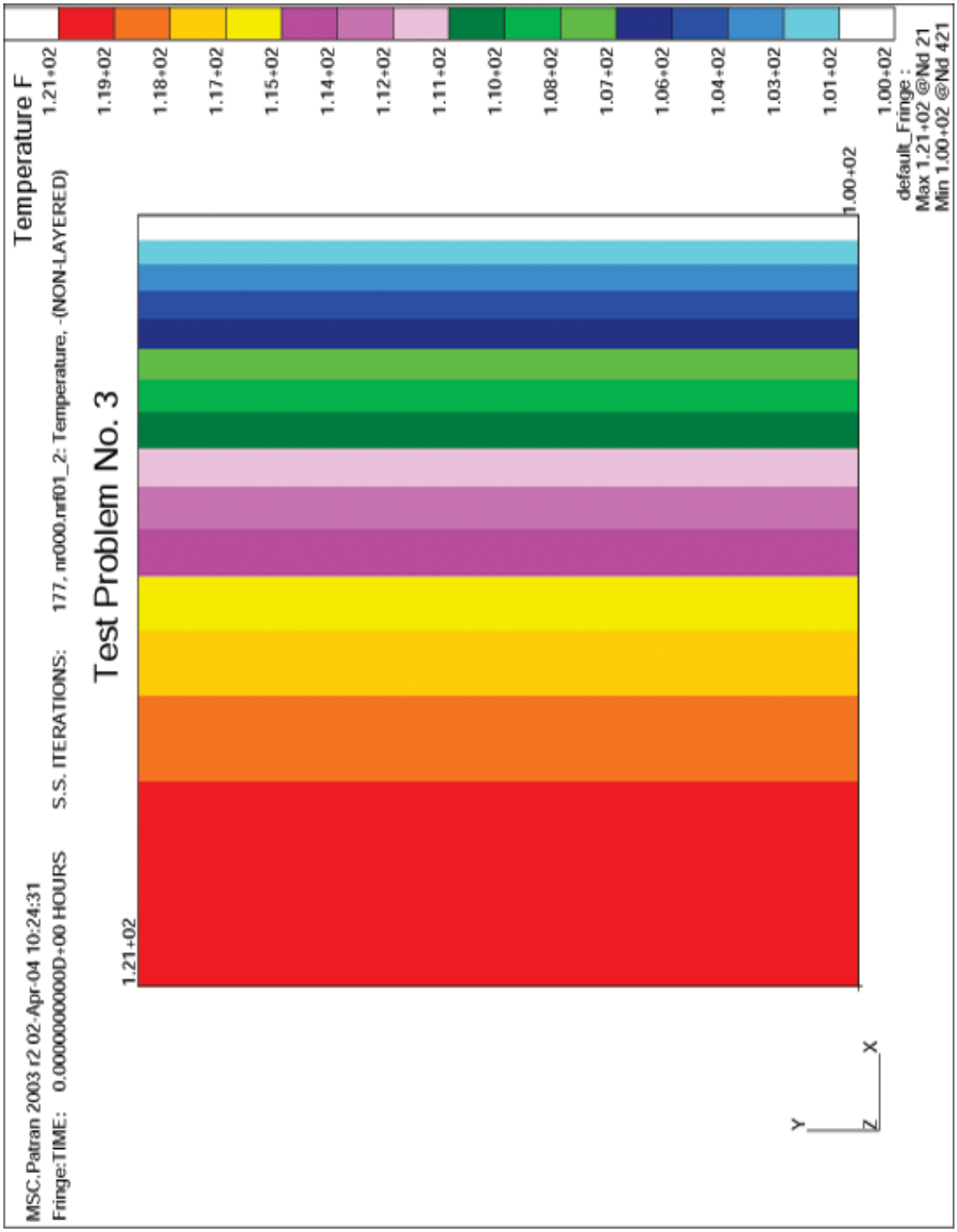

Figure 3 – Temperature Contours for Test Problem No. 3

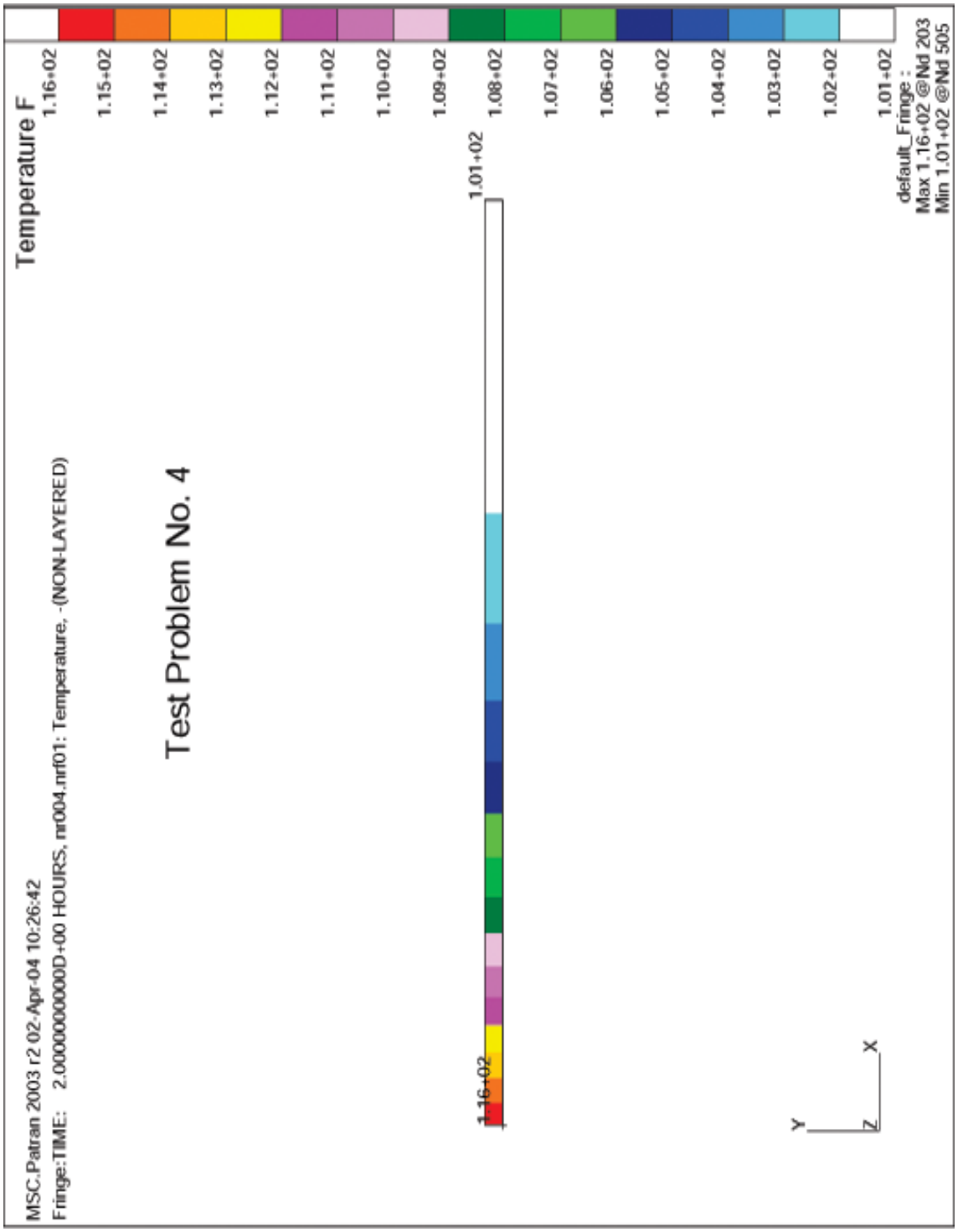

Figure 4 – Temperature Contours for Test Problem No. 4

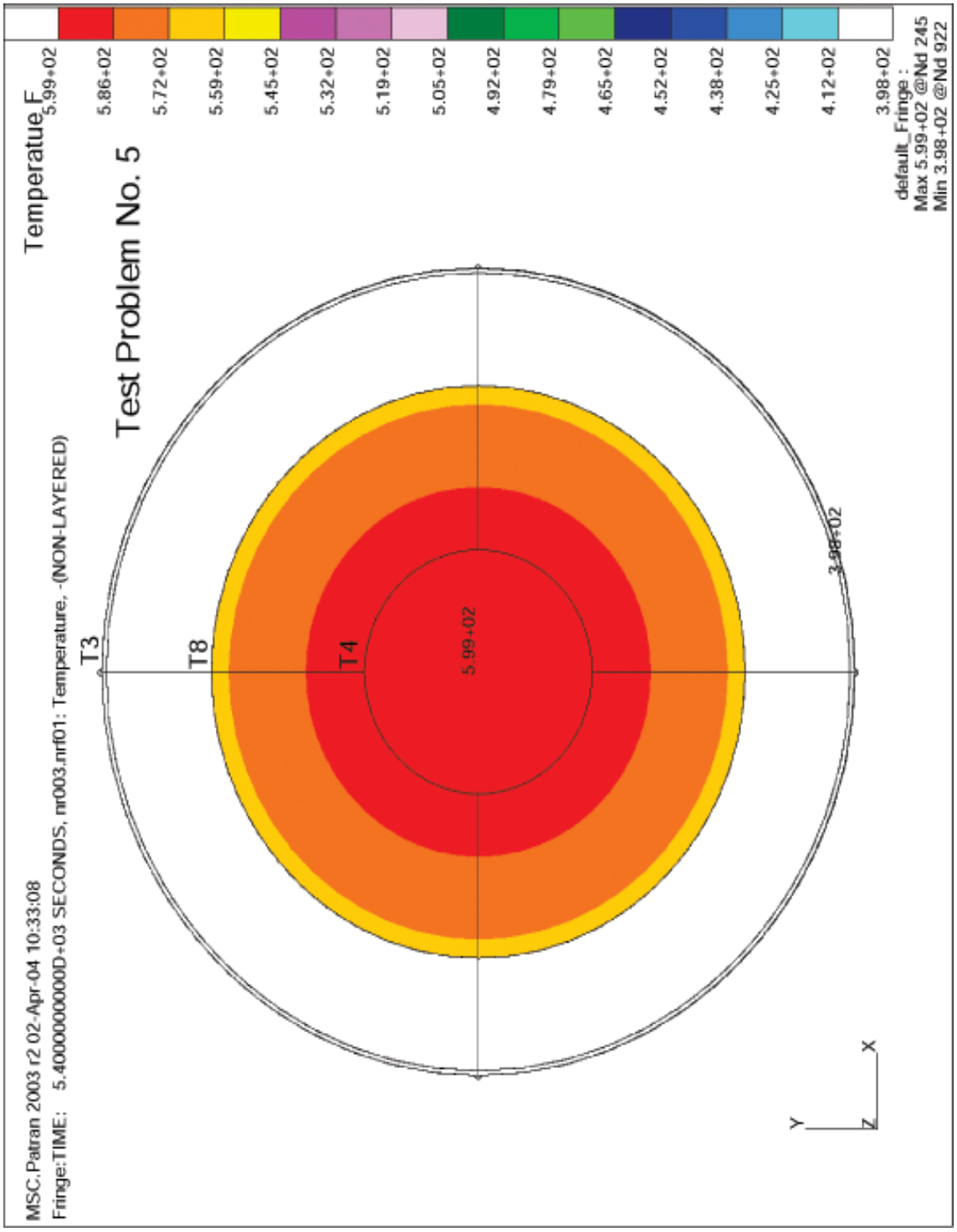

Figure 5 – Temperature Contours for Test Problem No. 5

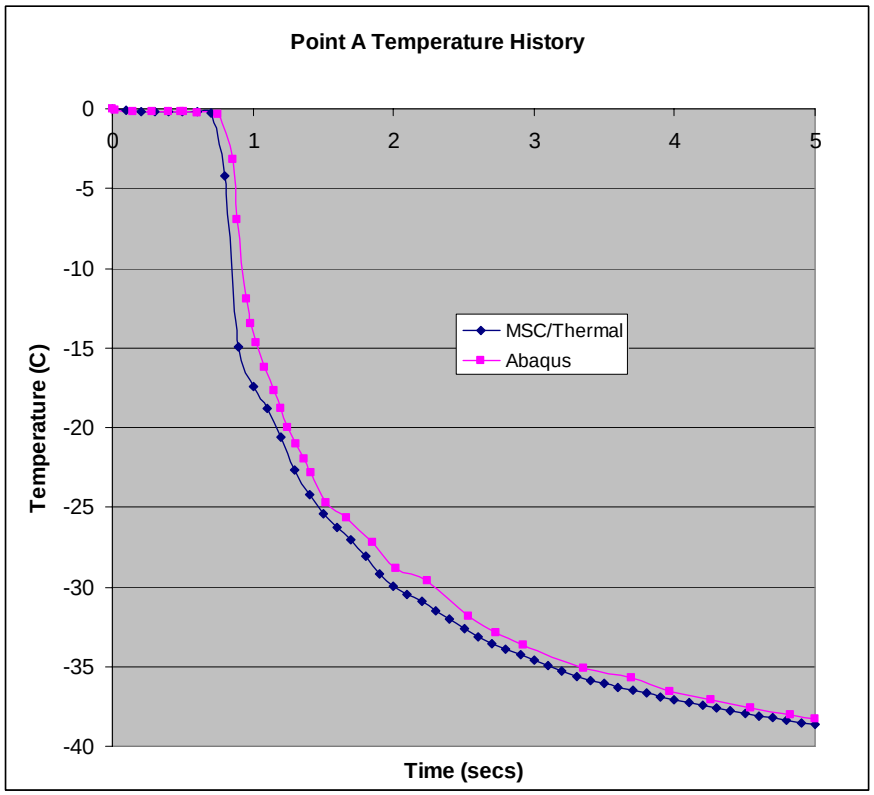

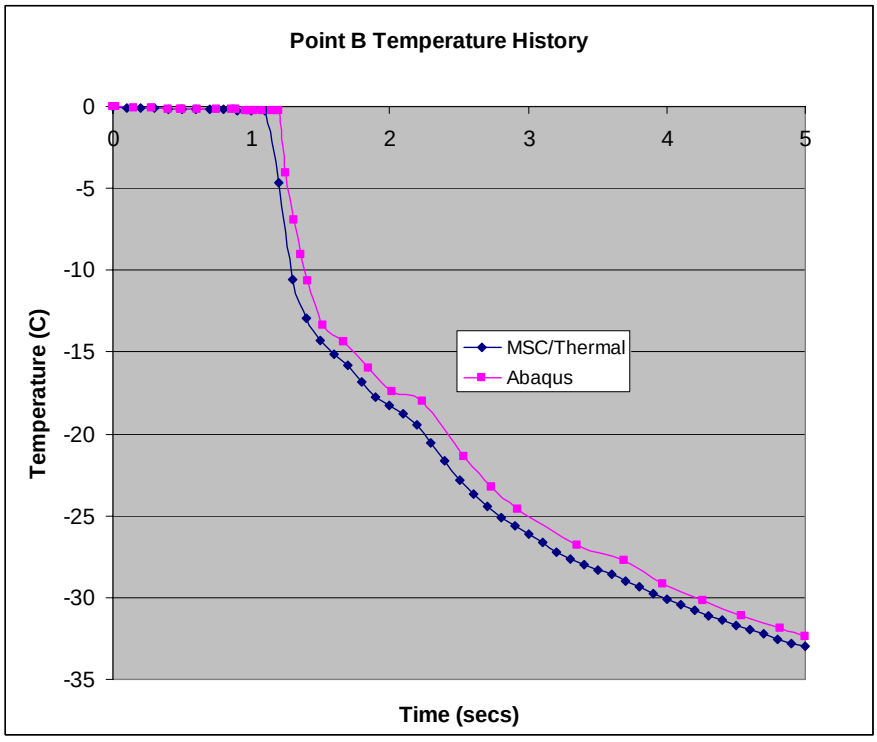

Figure 6 - Temperature Plots for Test Problem No. 6

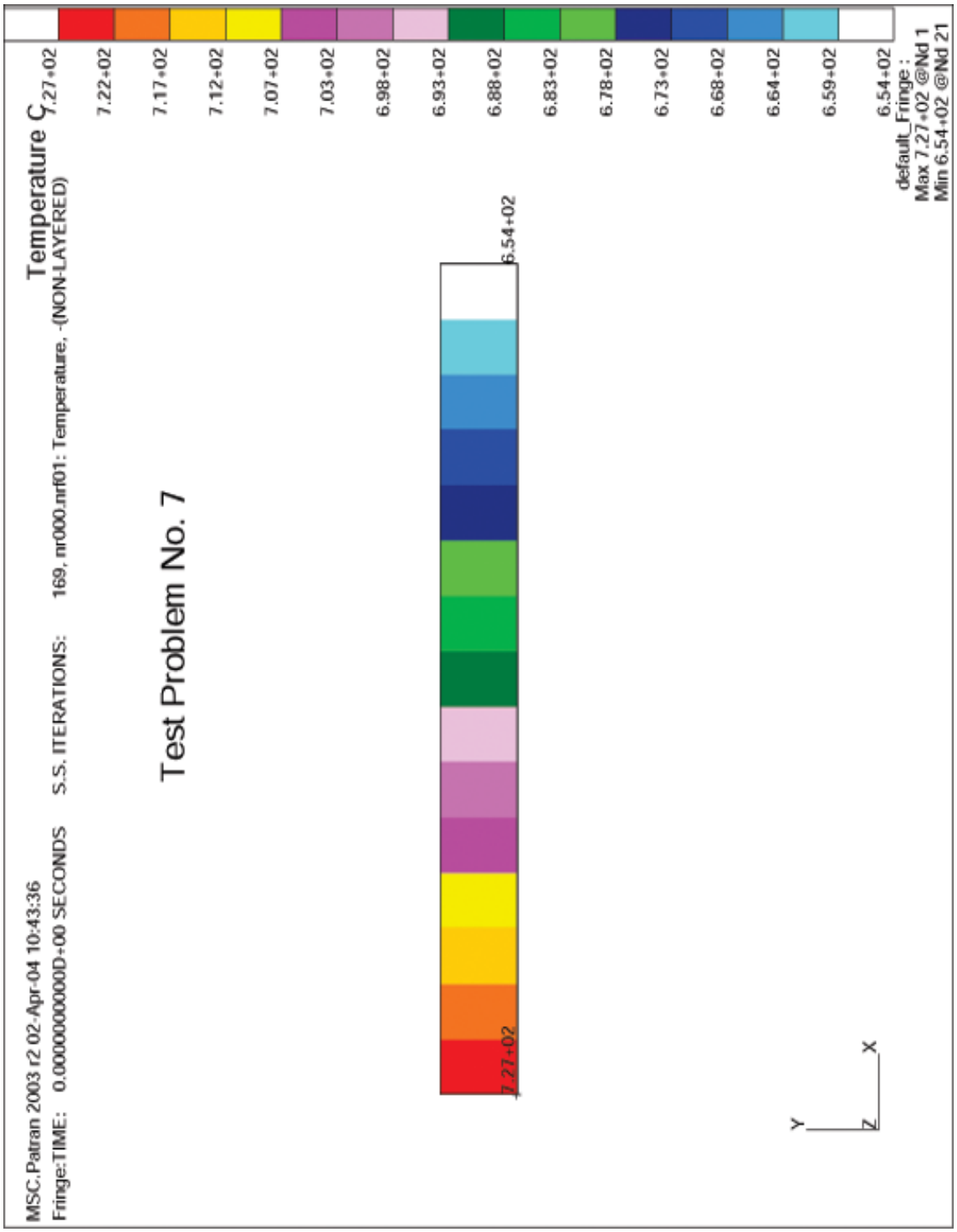

Figure 7– Temperature Contours for Test Problem No. 7

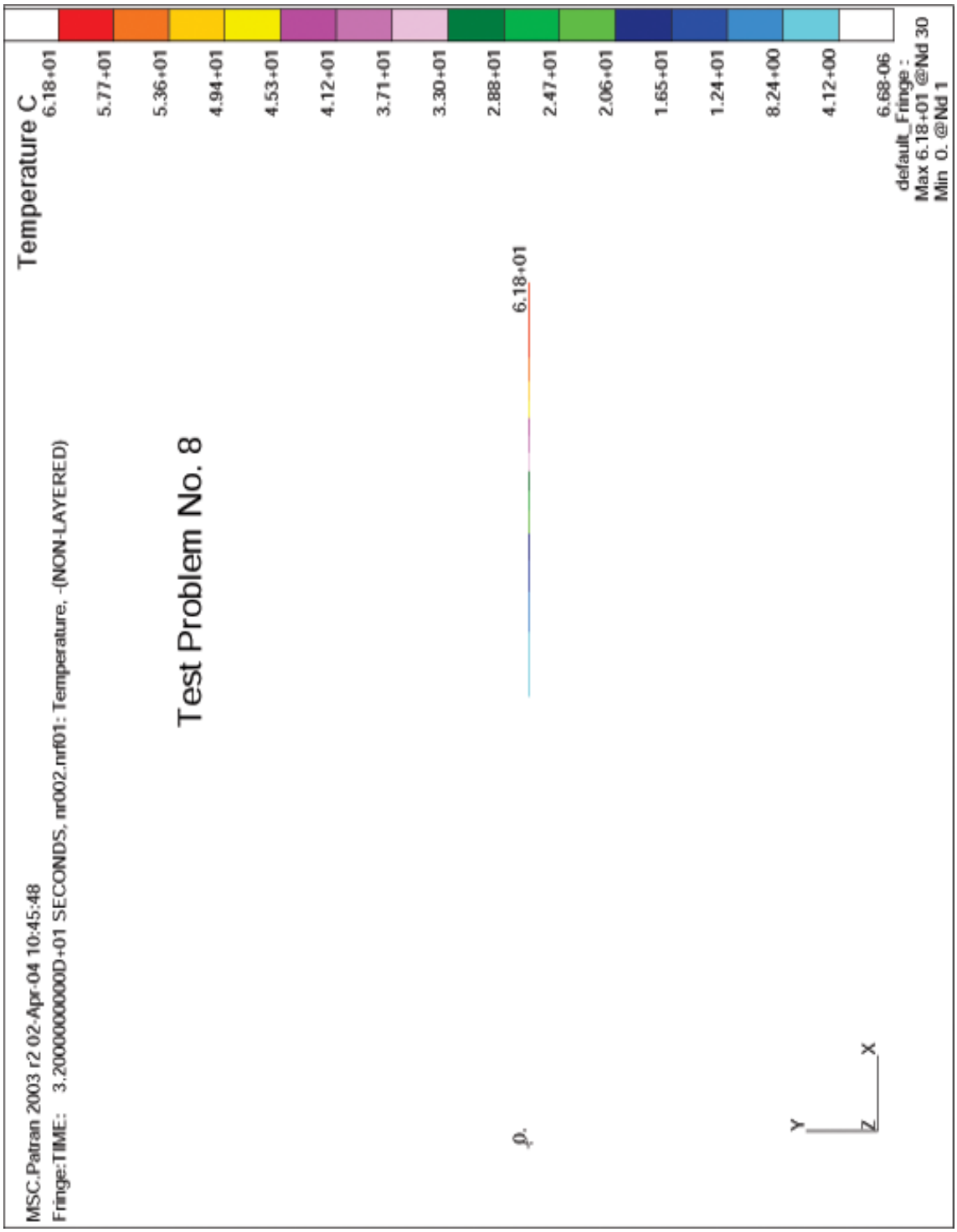

Figure 8– Temperature Contours for Test Problem No. 8

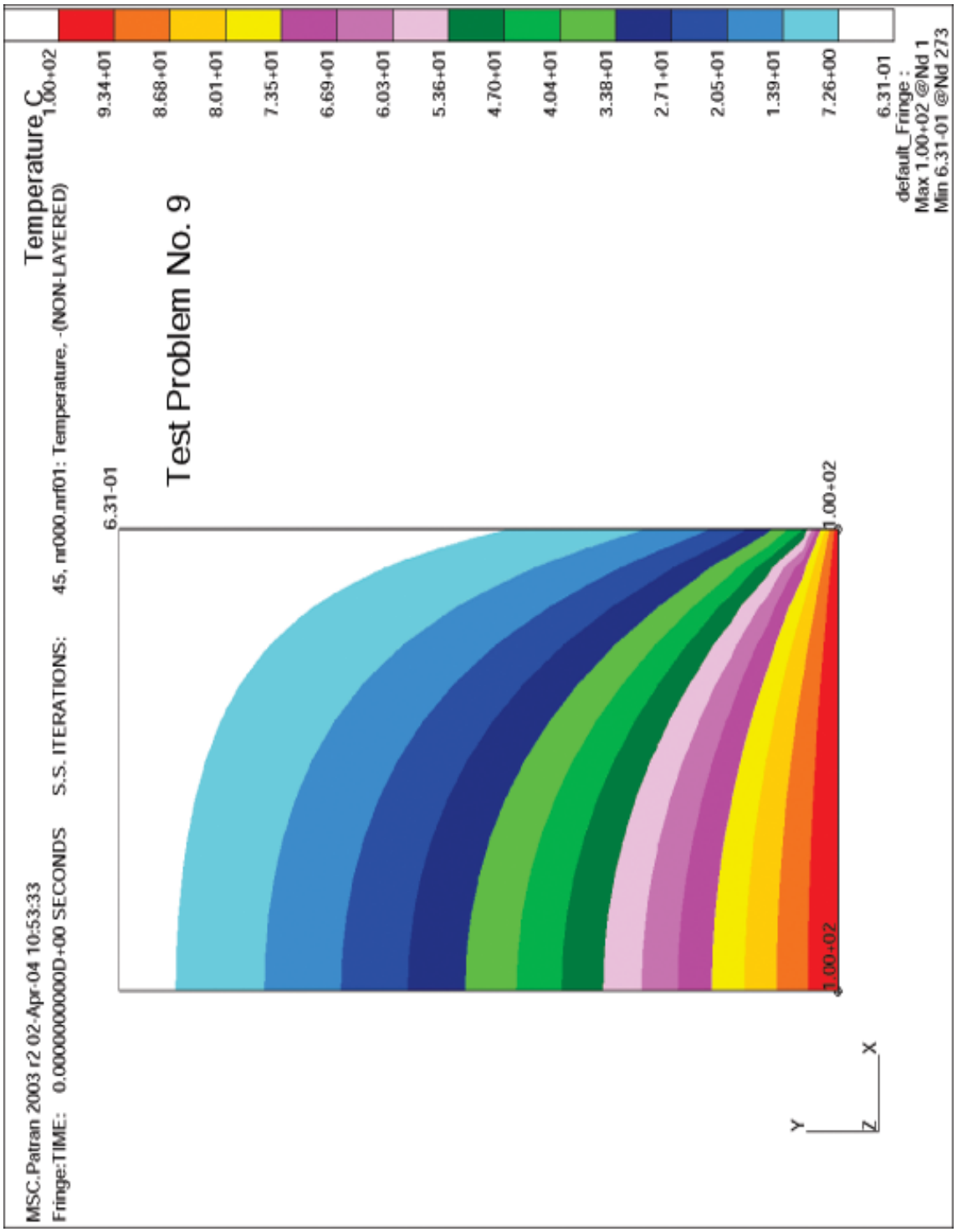

Figure 9– Temperature Contours for Test Problem No. 9

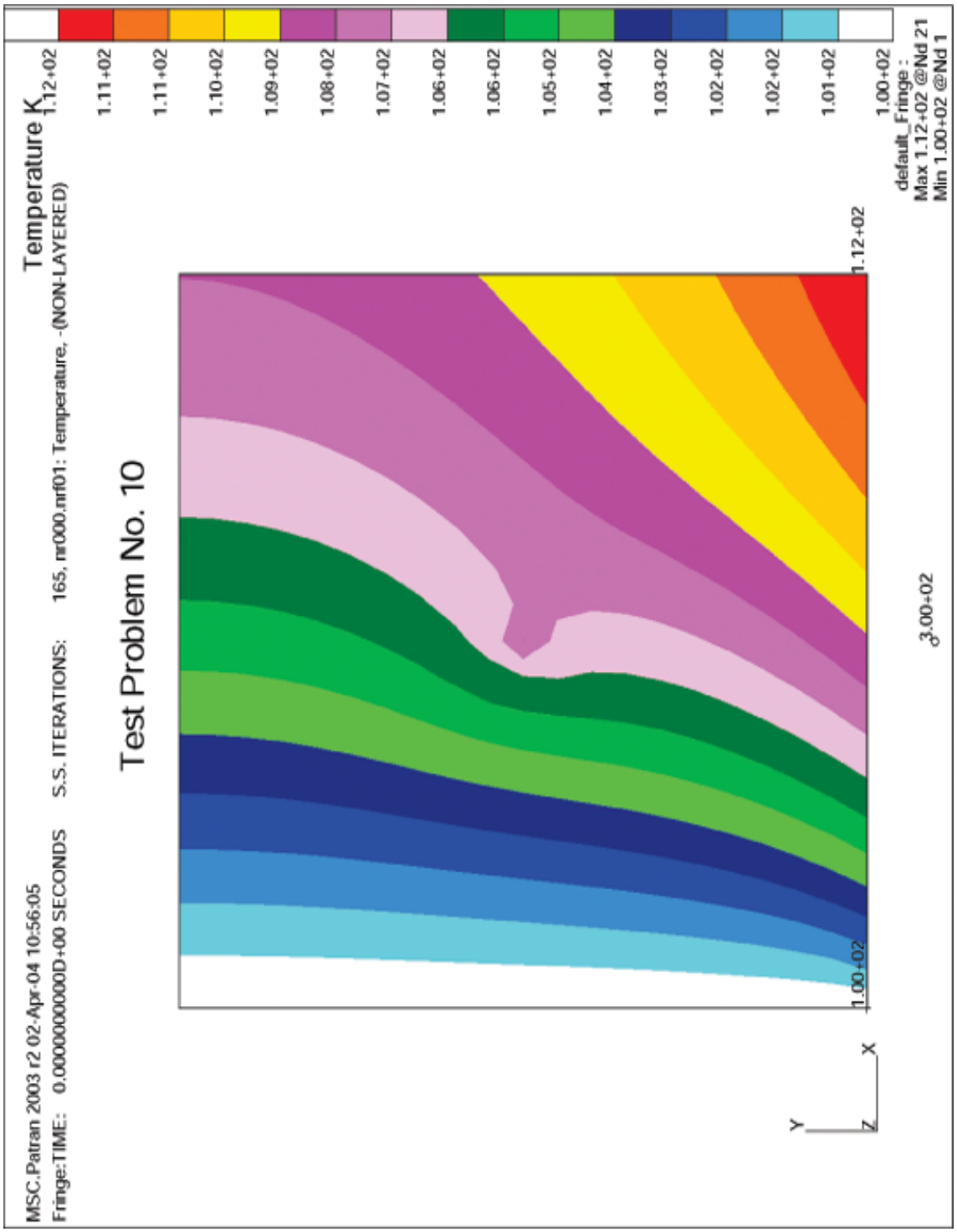

Figure 10– Temperature Contours for Test Problem No. 10

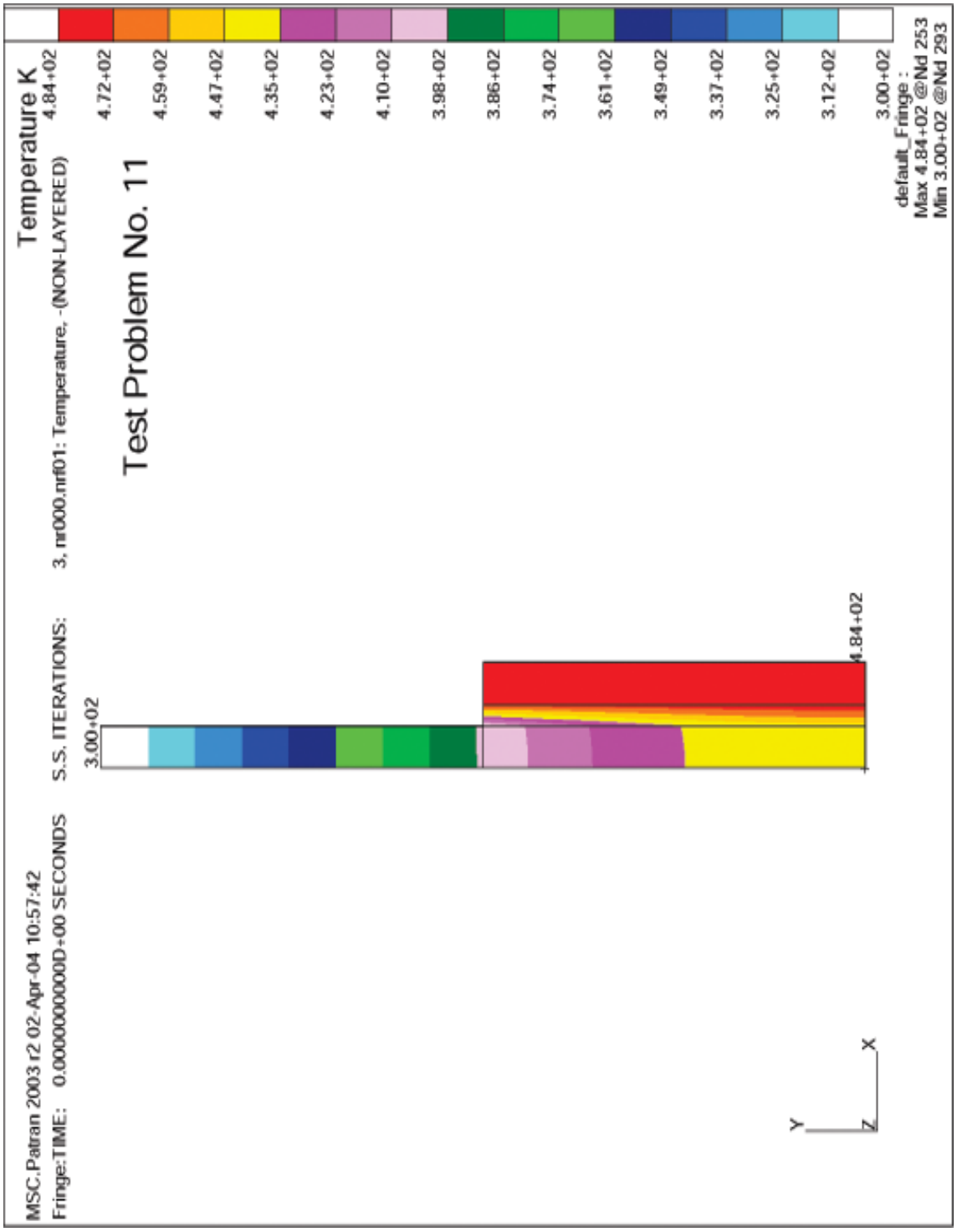

Figure 11– Temperature Contours for Test Problem No. 11

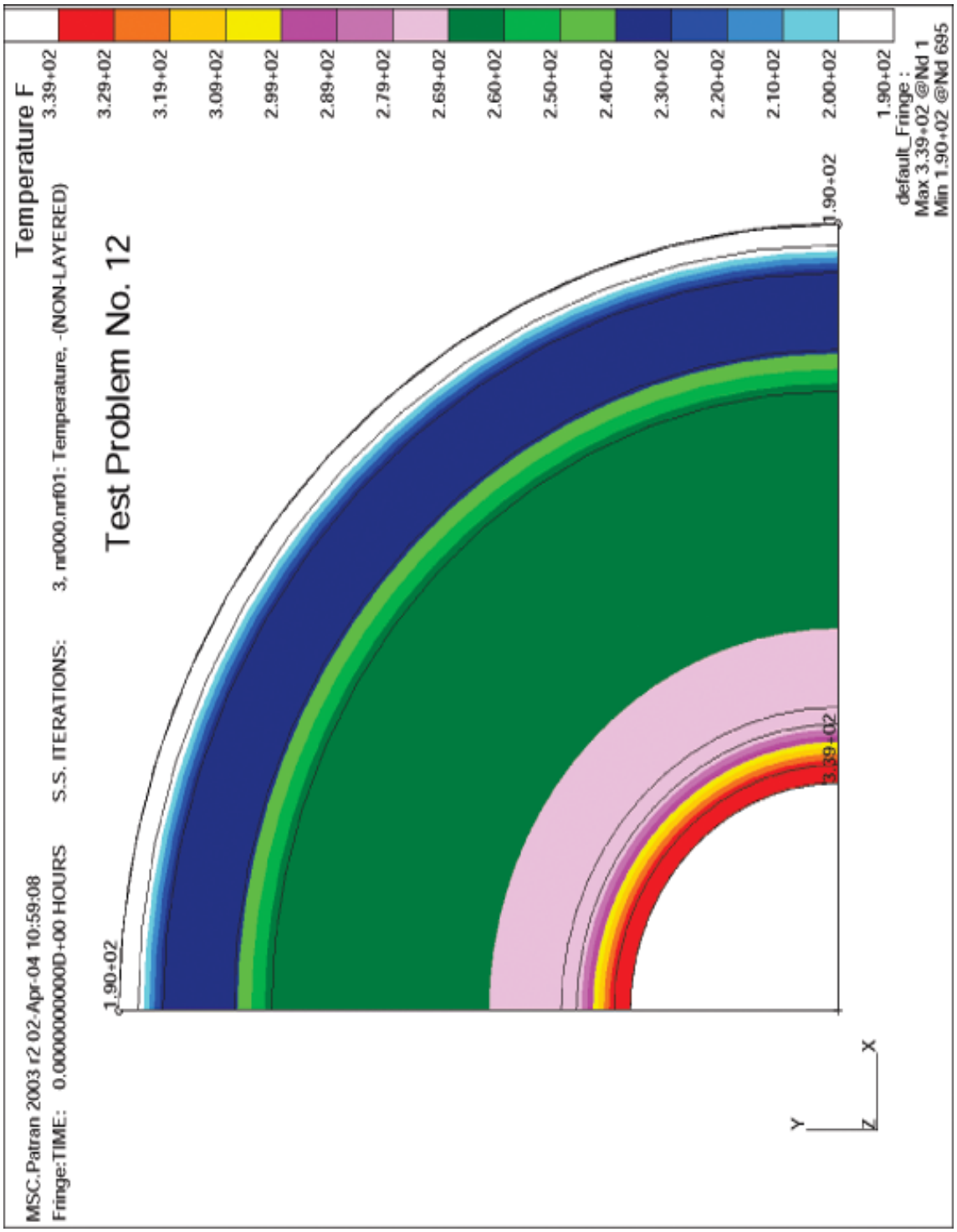

Figure 12– Temperature Contours for Test Problem No. 12

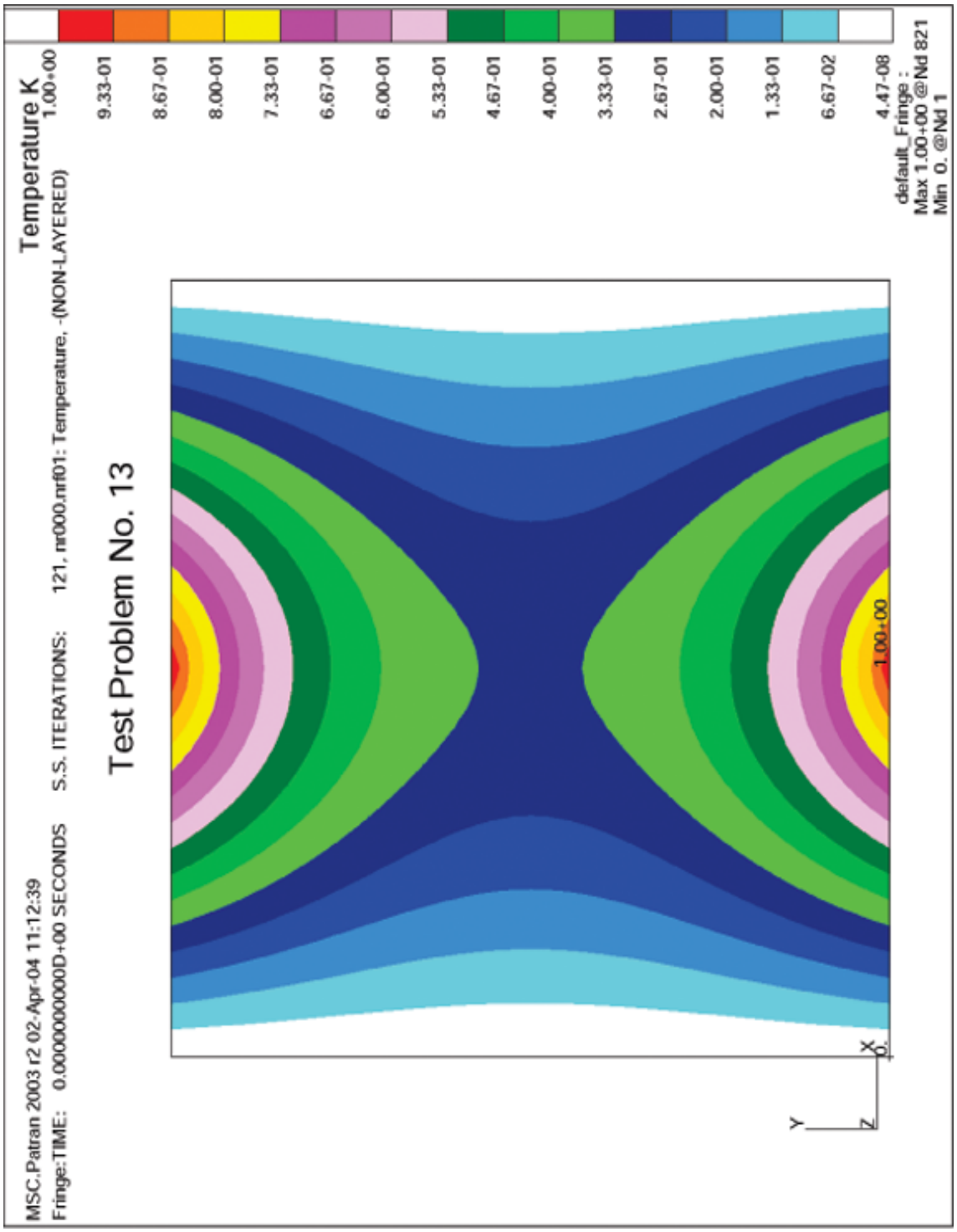

Figure 13– Temperature Contours for Test Problem No. 13

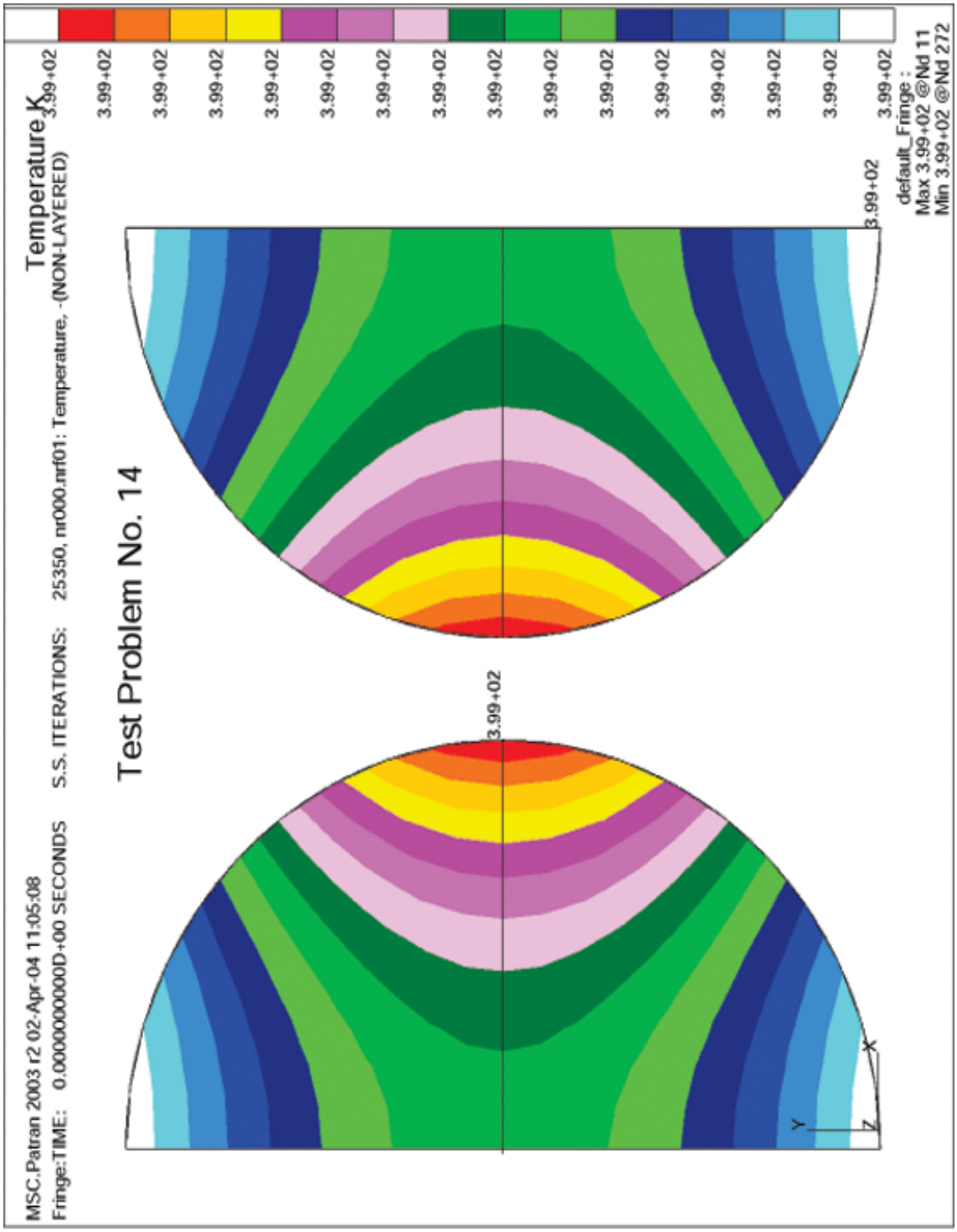

Figure 14– Temperature Contours for Test Problem No. 14

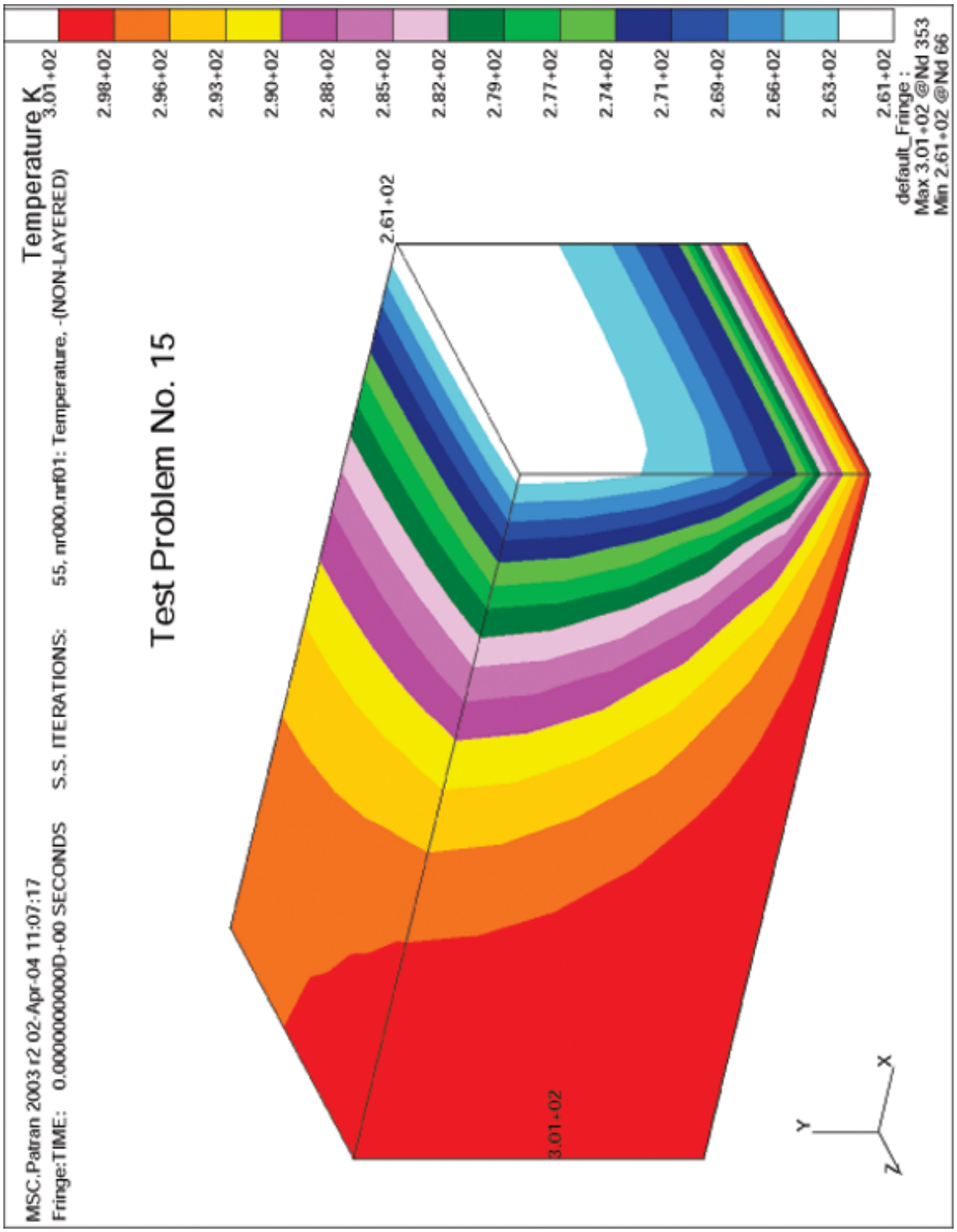

Figure 15– Temperature Contours for Test Problem No. 15

Attachment 9.3 - Software Evaluation Package (SEP)

Software Evaluation Package	**Rev. No.**
Software Evaluation Package No.	**Page ____of____**

Section 1 Prerequisites

1.1 Software classification adequate for intended end use?

___x___ Yes _____ No

If no, determine classification in accordance with E7, 5.05. Provide basis for new classification below or reference, as necessary.

1.2 Software Quality Assurance Plan (SQAP) exist and adequate?

___x___ Yes _____ No

If no, complete a SQAP in accordance with E7, 5.03. (Attach or reference as necessary).

Section 2 Identification of Requirements

2.0 Engineering process documentation per Section 5.1.2 adequate and complete in accordance with the SQAP?

___x___ Yes _____ No

If no, modify and obtain the DA/Owner approval for the inadequate documents. (Attach or reference as necessary).

2.1 Do the engineering technical/functional requirements of the Requirements Specification-Software (RSS) and Requirements Traceability Matrix (RTM) stated technical and/or functional requirements support the intended use?

___x___ Yes _____ No

If no, revise the RSS and RTM, as necessary. (Attach or reference as necessary).

NOTE: SQAP does not require RTM and DDS for this software. SEP will evaluate that the Requirements Specifications have been met.

Section 3 Failure Analysis

3.1 Identification of potential causes of system failures.

There are no known software failures due to specific system failures. On rare occasions, the software will crash but the automatic saving feature is able to save most of the new or changed data.

3.2 Assessment of the significance of identified failures.

The automatic save feature is able to save most of the data therefore, the significance of rare failures is negligible.

3.3 Identification of appropriate resolutions for identified failures.

If bugs are found, the vendor is called to investigate the failure and identify the course of action.

3.4 Based on failure analysis, do the software engineering technical/functional requirements require updating?

_____ Yes ___x__ No

If yes, modify in accordance with E7, 5.20. (Attached or reference as necessary).

Section 4 Existing Software Evaluation

4.1 Does existing software meets all requirements and deemed acceptable for end use?

___x___ Yes _____ No

If no, proceed to Section 6.0 for final acceptance testing, as necessary.

Section 5 Acquisition of Commercial Grade Software

5.1 Establish and document the acceptance criteria based on software classification necessary to qualify the software for use at SRS for its intended end use.

MSC/PATRAN/THERMAL software has been used at SRS for over ten years and has been found to meet the needs for services provided by EM&S Group. The acceptance criteria are documented in the Requirement Specifications documented in SQAP.

5.2 Determine method(s) in accordance with EPRI NP-5652 to be used to accept commercial grade software.

_____ Method 1 – Special Test Cases

___x__ Method 2 – Commercial Grade Survey of the Supplier

__ x___ Method 3 – Acceptable Supplier Performance Record
5.3 Prepare procurement specification per Manual E7, Procedure 2.14 and/or purchase order per Manual 7B. Specification No. _____. Purchase Order No. _____.
Section 6 Software Testing
6.1 Past testing, by either supplier or SRS, provide adequate assurance that software product/technical requirements were met? ___x___ Yes _____ No If yes, provide justification: *The tests are documented in the Test Plan SRT-EMS-940084. The same tests are being used for the new version of the software.* If no, develop and execute test plan/cases, as needed, including acceptance criteria in accordance with E7, 5.40 or the product SQAP. Test Plan/Cases No. _____ Developed/Approved on _____. Date Test Plan/Cases No. _____ Execution completed/approval on _____. Date
Section 7 New Baseline
Results of Sections 1 through 6 require correction of inadequacies in the documentation? _____ Yes __x___ No If yes, identify specifically which revised document constitutes a new baseline.
Section 8 References

National Codes/Standards	Safety Analysis Report	Drawings/Design
Supplier Information		

Other		
Section 9 Software Evaluation Package Approval		
Prepared by (Name/Signature) N.K. Gupta/ _____	Date	Reviewed by (Name/Signature) Date
Approved by (Name/Signature) Cynthia Holding-Smith, DA _____		Date

Revision Summary

Revision	Scope	Description
0	Initial Issue	

Attachment 9.4 - Computer Input/Output Files

Test Case	Model Input File	Results Directory	Files Location/Address
1	problem_1.db	problem_1	/project/ems/y6203/PATRAN_QA/p2003r2QA
2	problem_2.db	problem_2	/project/ems/y6203/PATRAN_QA/p2003r2QA
3	problem_3.db	problem_3	/project/ems/y6203/PATRAN_QA/p2003r2QA
4	problem_4.db	problem_4	/project/ems/y6203/PATRAN_QA/p2003r2QA
5	problem_5.db	problem_5	/project/ems/y6203/PATRAN_QA/p2003r2QA
6	problem_6.db problem_6.inp	problem_6 prob_6_ABQ	/project/ems/y6203/PATRAN_QA/p2003r2QA /project/ems/y6203/PATRAN_QA/ prob_6_ABQ
7	problem_7.db	problem_7	/project/ems/y6203/PATRAN_QA/p2003r2QA
8	problem_8.db	problem_8	/project/ems/y6203/PATRAN_QA/p2003r2QA
9	problem_9.db	problem_9	/project/ems/y6203/PATRAN_QA/p2003r2QA
10	problem_10.db	problem_10	/project/ems/y6203/PATRAN_QA/p2003r2QA
11	problem_11.db	problem_11	/project/ems/y6203/PATRAN_QA/p2003r2QA
12	problem_12.db	problem_12	/project/ems/y6203/PATRAN_QA/p2003r2QA
13	problem_13.db	problem_13	/project/ems/y6203/PATRAN_QA/p2003r2QA
14	problem_14.db	problem_14	/project/ems/y6203/PATRAN_QA/p2003r2QA
15	problem_15.db	problem_15	/project/ems/y6203/PATRAN_QA/p2003r2QA

Notes: 1. problem_*.db are the files for the thermal models while problem_* are the results' directories for the MSC/THERMAL results files.
2. problem_6.inp is the input file for the ABAQUS software and it is located, along with the results, in prob_6_ABQ directory.

This Page Intentionally Left Blank

APPENDIX 3.4

HAC THERMAL MODEL FOR THE 9977 PACKAGE

This Page Intentionally Left Blank

OSR 45-24 (Rev 11-15-2004)

Calculation Cover Sheet

Project	Calculation No.	Project No.
9977 SARP	M-CLC-A-00257	NA
Title	**Functional Classification**	**Sheet 1 of**
HAC Thermal Model for the 9977Package	SC	28
	Discipline	
	Mechanical	
Calc Level	**Type 1 Calc Status**	
☒ Type 1 ☐ Type 2	☐ Preliminary ☒ Confirmed	
Computer Program No.	**Version/Release No.**	
MSC.PATRAN.THERMAL ☐ N/A	2003 r2	

Purpose and Objective

The purpose of the calculation was to predict the temperatures of limiting components of the 9977 package under Hypothetical Accident Conditions (HAC) postulated in 10 CFR 71.73. The calculations included a 19W heat source, having limiting dimensions, located at 3 axial positions in the Containment Vessel (CV). The impact of thermal degradation of the foam layer incorporated in the 9977 package was examined by considering 3 post-fire conditions: complete replacement of the foam by char, a 1 in. thick residual foam layer with the remainder of the cavity filled with char, and a 2.3 in. thick residual foam layer with the remainder of the cavity filled with char.

Summary of Conclusion

Based on the superposition of component temperature increases measured during the burn tests onto calculated initial pre-fire HAC temperatures, component temperatures at the end of the 30 min 1475°F fire were below their respective temperature limits. Maximum component temperatures during the post-fire phase of the HAC were 381°F for the O-rings and 400°F for the CV.

Revisions

Rev No.	Revision Description
0	Original Issue

Sign Off

Rev No.	Originator (Print) Sign/Date	Verification/ Checking Method	Verifier/Checker (Print) Sign/Date	Manager (Print) Sign//Date
0	Bruce Hardy 4/24/06	Individual Review	N. K. GUPTA N. K. Gupta 4/24/06	C. P. HOLDING-SMITH C P Holding-Smith 4/25/06

Design Authority — (Print)	Signature	Date
Release to Outside Agency – (Print)	Signature	Date

Security Classification of the Calculation

Unclassified

Revisions

Revision	Description
0	Original Issue

Nomenclature

h = Convection Heat Transfer Coefficient (Btu/hr-ft^2-°F)
k = Thermal Conductivity (Btu/hr-ft-°F)
k_i = Thermal Conductivity of Material in Cylinder i (Btu/ft hr °F)
L = Characteristic Length (ft)
n = Total Number of Concentric Cylinders
Pr = Prandtl Number
q = Heat Flow (Btu/hr)
r = Radial Location (ft)
r_i = Inner Radius of Cylinder i (ft)
Ra = Rayleigh Number
T = Temperature (°F)
T_{i+1} = Temperature at outer edge of cylinder i (°F)

Acronyms and Abbreviations

CV	Containment Vessel
DOT	Department of Transportation
GPFP	General Purpose Fissile Package
HAC	Hypothetical Accident Conditions
MSC	McNeal Scwindler Corporation
NCT	Normal Conditions of Transport
SARP	Safety Analysis Report for Packaging
SS	Stainless Steel

1.0 Introduction and Background

The Department of Transportation (DOT) Fissile Specification 6M package is being removed from service. As a result, a new general purpose fissile package, designated as the Model 9977 Shipping Package, has been designed as a replacement. The 9977 package consists of a Containment Vessel (CV), a drum overpack filled with foam and a bolt-on lid that has several layers of insulation. Figures 1 and 2, respectively, show schematics of the 9977 and CV. Contents for the package will be placed within the CV, which is closed with a screw on cap that is sealed by a double set of O-rings. The CV is loaded into a cylindrical drum liner and held in place by upper and lower load distributors. The package is closed by bolting the lid in place.

This document describes the thermal model for the Hypothetical Accident Conditions (HAC) to be used for the 9977 SARP (Safety Analysis Report for Packaging)[1].

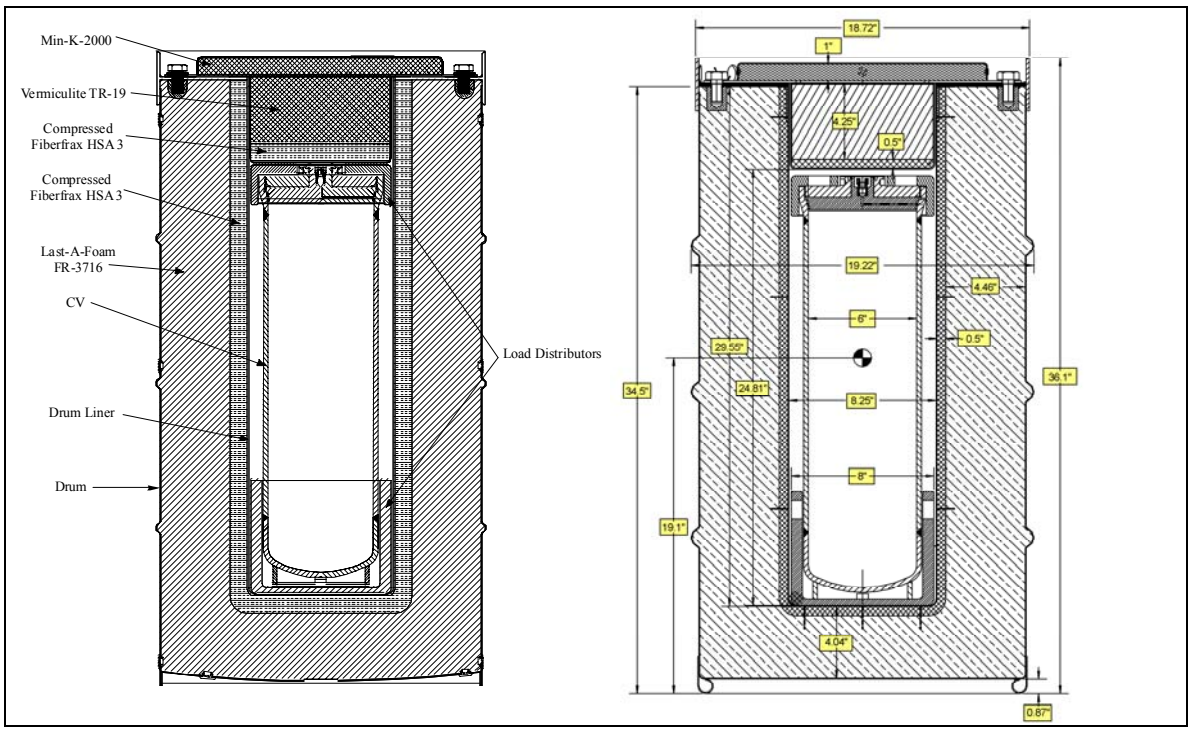

Figure 1 Schematic and dimensions of the 9977 containing the 6-inch CV.

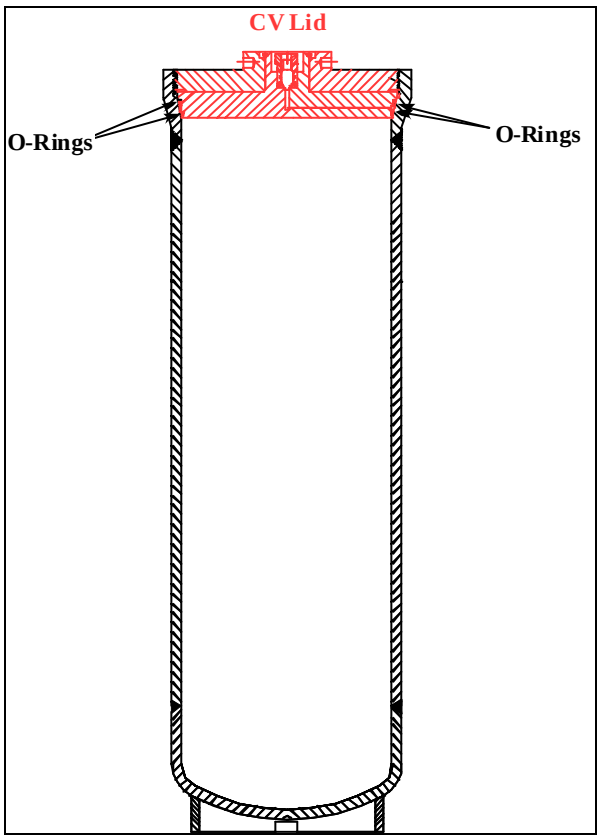

Figure 2 Schematic of the CV

Technical specifications for the package components are provided on the package drawings included in Reference 2. The drawing specifications include the applicable ASME Code requirements for the components and materials. Package design specifications relevant to the thermal analysis are summarized below.

Drum, Drum Liner and Lid

The outermost shell of the 9977 is an 18-gauge 304L stainless steel drum that is 36.10 inches tall, as measured from the lower edge to the top of the drum flange, and has a diameter of 18.72 in. to the outside of the drum flange, see Figure 1. At 3 axial elevations there are sets of 4 vent holes in the side of the drum, 90° apart. Two additional vent holes are located in the bottom of the drum. All vent holes have diameters of ¾ in. and are closed with plastic Caplugs® to prevent entry of rainwater during NCT. In the HAC-fire event, the fusible Caplugs® are consumed and allow the drum to vent gases generated from thermal decomposition of the Last-A-Foam® insulation[3]. A cylindrical drum liner having an inside length and diameter of 29.5 and 8.25 inches, respectively, is concentrically located within the drum. The drum liner is constructed of 18 gauge 304L stainless steel and has exterior studs to secure a Fiberfrax® insulating blanket.

The drum liner is closed by securing a lid to the drum flange with eight 5/8 inch bolts. The lid is constructed from 18-gauge 304L stainless steel and incorporates three layers of insulating material: uncompressed Fiberfrax® HSA System No. 3 blanket at 16 lbm/ft^3,

Min-K-2000 insulation manufactured by the Thermal Ceramics Company, and Vermiculite TR-19 insulation manufactured by the Thermal Ceramics Company.

Compressed Fiberfrax® and Last-A-Foam®

A layer of Fiberfrax® HSA System No. 3 blanket at 16 lbm/ft^3 is wrapped around the sides and bottom of the drum liner. Initially, the Fiberfrax® blanket is 1 in. thick, however, during the fabrication process the region between the outer surface of the Fiberfrax® and the inner surface of the drum wall is filled with Last-A-Foam® FR-3716 manufactured by the General Plastics Manufacturing Company. Last-A-Foam® FR-3716 is a rigid polyurethane foam that expands to a density of approximately 16 lbm/ft^3 as it cures. As it expands the foam compresses the layer of Fiberfrax® against the drum liner. The compressed thickness of the Fiberfrax® is unknown but was estimated to be approximately ½ in. for the model used in the thermal analysis. Because the thickness of the Fiberfrax® was halved, its density is doubled and it is assumed that its thermal conductivity is also doubled. Table 2 lists properties of compressed and uncompressed Fiberfrax®.

Containment Vessel and Containment O-Rings

The CV is constructed from either 6-inch diameter or 5-inch diameter, seamless Schedule 40S, Type 304L stainless steel (SS) pipe. One end of the pipe is closed by a Schedule 40S, Type 304L SS pipe cap. The CV is closed by ¾-inch thick 304L SS cone-seal plug held in place by a 0.63-inch thick male-threaded Nitronic-60 cone-seal nut. The cone-seal plug incorporates machined grooves to receive two O-ring seals. The design pressure for the 6-inch CV at 300°F is 800 psig and is 900 psig for the 5-inch CV.

A containment boundary is provided in part by the CV body and closure but is completed by the outer O-ring mounted on the cone-seal plug and by the SS leak-test port plug. The O-ring material is Viton® GLT, a fluorocarbon elastomer with a service temperature range between -40°F and 400°F.[4] When not in service and stored in accordance with Society of Automotive Engineers, Aerospace Recommended Practice, 5316, Revision B, the O-rings have an unlimited shelf life[5].

The CV is supported by aluminum load distribution fixtures. Unless otherwise specified their properties were assumed to be that of type 1100 aluminum. However, test cases were run with Type 6061 T-6 aluminum to investigate possible effects on the temperature profile.

2.0 HAC Thermal Model

The HAC thermal model consists of three sequential phases, corresponding respectively to the pre-fire, fire and post-fire conditions. The pre-fire model, which is identical to the model for NCT except that insolation is neglected, determines the temperature profile in the package prior to the HAC fire transient. The fire transient determines the bounding package temperature, with respect to a 10 CFR 71.73[6] fire. Finally, the post fire

transient is used to predict the bounding temperature of the components of the 9977 after the fire has been extinguished.

Thermal models for the 9977 pre-fire and post-fire HAC were developed with the MSC/Patran.Thermal®[7] general purpose heat transfer software. Temperature increases during the fire were based on the measured temperature rise during the fire tests[8]. As for the model of the NCT[9], the contents of the package were not explicitly defined. Rather, reasonable but bounding, content configurations were used to predict the maximum component temperatures experienced by limiting components of the package, which were compared to their individual maximum allowable temperatures. The limiting components for the HAC are the containment vessel and the O-ring seals. Temperature limits for components of the 9977 for the HAC are tabulated along with predicted maximum temperatures for each individual model. The 9977 model for all HAC analyses includes interior metal surfaces, namely the drum liner, liner around the inner lid, and the metal interface between the lid and the drum.

Because the location of the source affects component temperatures in the 9977, three configurations were considered. The three source configurations were for a source at the top, middle and bottom of the CV, see Figure 3. Each of these configurations consisted of a cylindrical 19 Watt source that was approximately 1 inch long and had a diameter of 0.25 inches. The source was embedded in a cylindrical slug of 304L stainless steel, which was in direct contact with adjacent inner surfaces of the CV. The slug served to distribute the heat generated by the source and resulted in more realistic temperatures within the CV than if the source were in contact with air.

The compositions used in the 9977 package for the HAC analyses are shown in Figure 3. Tables 1, 2, and 3 contain the convection boundary conditions and material properties used in the HAC analyses. The post-fire phase of the HAC was analyzed for three separate foam conditions; the foam replaced entirely with char, a 1 inch thick layer of foam surrounding the drum liner and a 2.3 inch thick layer of foam surrounding the drum liner, see Figure 3.

The fire and post-fire phase-HAC models are based on results and observations from the fire tests. An important observation was that there was no void space in the drum as the foam was transformed to char. Intumescence during thermal degradation of the foam causes the resultant char to fill the cavity previously occupied by the foam. Post test examination of the package revealed that the fiberfrax covered drum liner was surrounded by a layer of foam that did not differ significantly in appearance from its original state. This foam layer was surrounded by a layer of foam that had a degraded appearance, including some discoloration, texture changes, melting and charring. Finally, the layer of degraded foam was surrounded by char that extended to the outer wall of the package. It was estimated that the layer of foam appearing as the original state had an equivalent thickness of 1 to 2.3 inches[10] measured from the exterior of the fiberfrax, see Figure 3.

The complex behavior of the foam during the fire-phase of the HAC precluded the use of a model to determine component temperatures. Hence, measurements of maximum component temperatures were used to determine initial temperatures for the post-fire HAC transient.

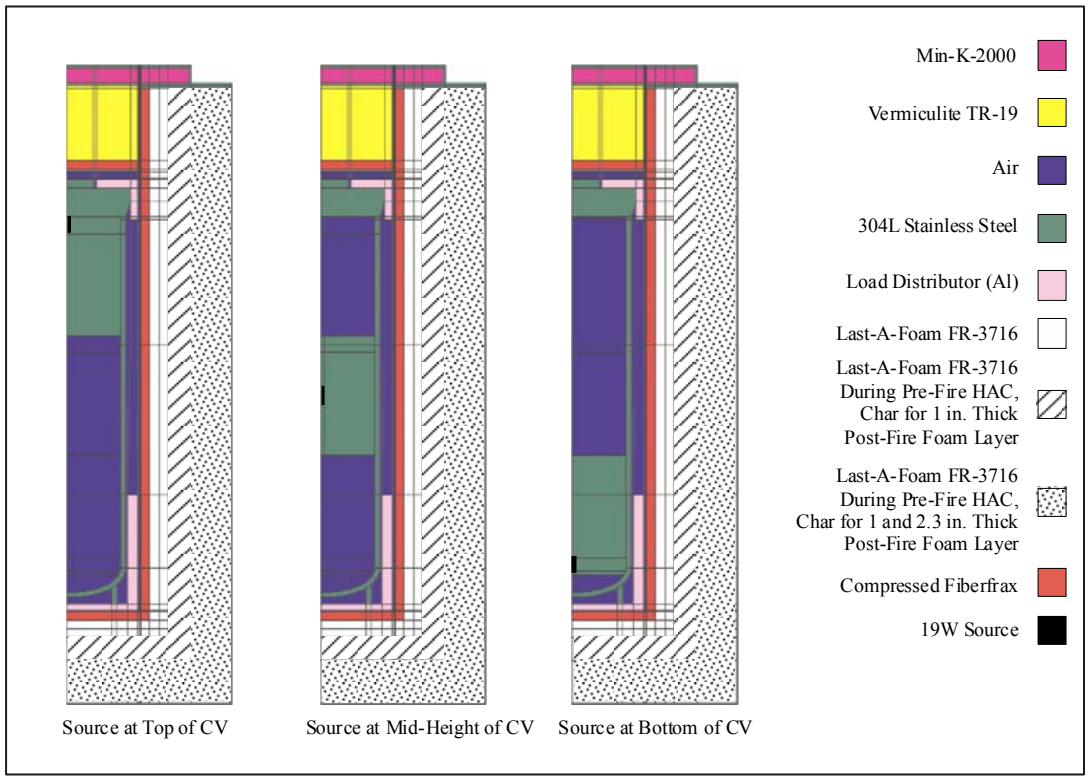

Figure 3 9977 material configurations used in the HAC models. Note that regions of the foam are replaced with layers of char for the post-fire analysis:

1. The dotted region with a white background is char for post-fire HAC models for 1 and 2.3 inch thick layers of foam around the drum liner.
2. The diagonally striped region is char for the post-fire HAC model for a 1 inch thick layer of foam around the drum liner.
3. The dotted, striped and white regions are all char for the post-fire HAC model that replaces all foam with char.
4. The white, striped and dotted regions are foam for the pre-fire HAC model.

Table 1 Natural Convection Heat Transfer Coefficients [Ref. 7]

Model Orientation	Surface	Correlation (Btu/hr-ft^2-°F)
Vertical	isothermal plate with $Ra < 1.0\times10^9$	$h = \left(\frac{k}{L}\right)\left(0.68 + \frac{0.670\times Ra^{0.25}}{\left[1.0+\left(\frac{0.492}{Pr}\right)^{9/16}\right]^{4/9}}\right)$
Vertical	isothermal plate with $1.0\times10^9 < Ra$	$h = \left(\frac{k}{L}\right)\left(0.825 + \frac{0.387\times Ra^{1/6}}{\left[1.0+\left(\frac{0.492}{Pr}\right)^{9/16}\right]^{8/27}}\right)^2$
Horizontal	hot isothermal plate facing upward with $1.0\times10^7 < Ra < 3.0\times10^{10}$	$h = \left(\frac{k}{L}\right)0.15\times Ra^{1/3}$
Horizontal	hot isothermal plate facing downward with $3.0\times10^5 < Ra < 3.0\times10^{10}$	$h = \left(\frac{k}{L}\right)0.27\times Ra^{0.25}$

Table 2 Thermal Properties of Solid Packaging Materials

Material	Thermal Conductivity (Btu/hr ft °F)	Density (lbm/ft^3)	Specific Heat (Btu/lbm °F)
Fiberfrax (uncompressed) Values are for HSA System 3®[1]	0.02 @ 400°F 0.03 @ 800.0°F 0.04 @ 1200.0°F 0.05 @ 1600.0°F	16.0	0.27
Fiberfrax (compressed) Values are for HSA System 3® thermal conductivity assumed 2* the value of uncompressed material	0.040 @ 400°F 0.060 @ 800.0°F 0.080@ 1200.0°F 0.100 @ 1600.0°F	32.0	0.27
Vermiculite TR-19[2]	6.33E-02 @ 400.0°F 6.67E-02 @ 600.0°F 7.00E-02 @ 800.0°F 7.33E-02 @ 1000.0°F 7.75E-02 @ 1200.0°F 8.17E-02 @ 1400.0°F 1.08E-01 @ 1600.0°F	23.0	0.20
MIN-K 2000[3] Tabulated thermal conductivities for Min-K-2000 are less than those for air, hence, values for Vermiculite TR-19 were used in the analysis.	1.58E-02 @ 300.0°F 1.67E-02 @ 400.0°F 1.83E-02 @ 600.0°F 2.08E-02 @ 800.0°F 2.50E-02 @ 1000.0°F 3.33E-02 @ 1200.0°F 4.17E-02 @ 1500.0°F 4.50E-02 @ 1600.0°F	20.0	0.23 @ 400.0°F 0.25 @ 800.0°F 0.27 @ 1200.0°F 0.27 @ 1600.0°F
Kaowool Blanket	3.92E-02 @ 500.0°F 8.42E-02 @ 1000.0°F 1.44E-01 @ 1500.0°F 1.83E-01 @ 1800.0°F	6.0	0.20
LAST-A-FOAM® FR-3716 @ 16 lb/ft^3[4]	2.75E-02 @ 76.5°F 3.12E-02 @ 140.7°F 3.71E-02 @ 248.4°F 4.33E-02 @ 348.6°F 4.33E-02 @1000.0°F **5.250E-2** Adjusted to match Environmental Chamber data	16.0	0.353
Aluminum (Type 1100)[5]	126.0	169.3	0.216
Aluminum (Type 6061 T-6)[5]	90.0	169.3	0.216
304L Stainless Steel[7]	7.74108 @ 32.0°F 9.43444 @ 212.0°F 12.5793 @ 932.0°F 14.9983 @ 1292.0°F	494.429	1.200E-01 @ 32.0°F 1.350E-01 @ 752.0°F

[1] Fiberfrax® HSA System No. 3 blanket manufactured by the Standard Oil Engineered Materials Company.
[2] Vermiculite TR-19® insulation manufactured by the Thermal Ceramics Company.
[3] Min-K-2000® insulation manufactured by the Thermal Ceramics Company.
[4] Last-A-Foam® FR-3716 manufactured by the General Plastics Manufacturing Company.
[5] Kaufman, J. Gilbert (2004). Aluminum Alloy Database. Knovel. Online version.

Table 3 Thermal Properties of Gaseous Components

Material	Thermal Conductivity (Btu/hr ft °F)	Density (lbm/ft^3)	Specific Heat (Btu/lbm °F)	Thermal Expansion Coeff. (1/°F)	Viscosity (lbm/hr-ft)
Air at 1 atm pressure	1.5E-02@80.33°F 1.9E-02@260.33°F	$\rho = \frac{1}{2.5203 \times 10^{-2}(T + 459.67)}$ T is in °F	0.24044	$\beta = \frac{1}{(T + 459.67)}$ T is in °F	4.8E-02@80.33°F 5.08E-02@170.33°F 5.58E-02@260.33°F 6.08E-02@350.33°F

2.1 Model of the Pre-Fire Phase of the HAC

The model for the pre-fire HAC was the same as that for the NCT[9] except that the insolation heat flux was omitted. Convection boundary conditions are listed in Table 1 and material property data are listed in Tables 2 and 3. Specific application of correlations and parameters are described in the summary below.

Description of the Pre-Fire HAC Model

1. The drum is in an upright position.
2. The bottom surface is adiabatic.
3. There is radiative heat transfer from the sides and top of the drum to the ambient.
4. There is natural convection heat transfer from the sides and top of the drum to the ambient, see Table 1.
5. The ambient temperature is 100°F.
6. There is no insolation heat flux.
7. The foam thermal conductivity tabulated in the General Plastics Company data is used, see Table 2
8. Material properties for compressed Fiberfrax® were applied to the blanket surrounding the drum liner. The blanket was assumed to be ½ inch thick.
9. The contents contain a heat source outputting 19 Watts of total decay power, distributed over a cylinder approximately 1 inch long with a diameter of 0.25 inches. The source was embedded in a 340L stainless steel slug, see Figure 3.
10. Three source locations were considered, see Figure 3:
    i. Source at the top of the CV.
    ii. Source at the middle of the CV.
    iii. Source at the bottom of the CV.
11. The model was steady-state.
12. Emissivities for the pre-fire HAC analysis are listed in Table 4.

Table 4 Surface Emissivities

Surface	Emissivity
CV	0.30
Drum Liner	0.30
Bottom of Lid	0.30
Load Distributor	0.20
Slug	0.30
Exterior of Drum	0.21

Results From the Pre-Fire HAC Model

Pre-fire HAC temperature profiles for all three source locations are shown in Figures 4 and 5. Figure 4 shows the overall temperature profiles in the package, while Figure 5 shows the temperature profiles in the CV. Table 5 lists the maximum content and CV temperatures for all three source locations.

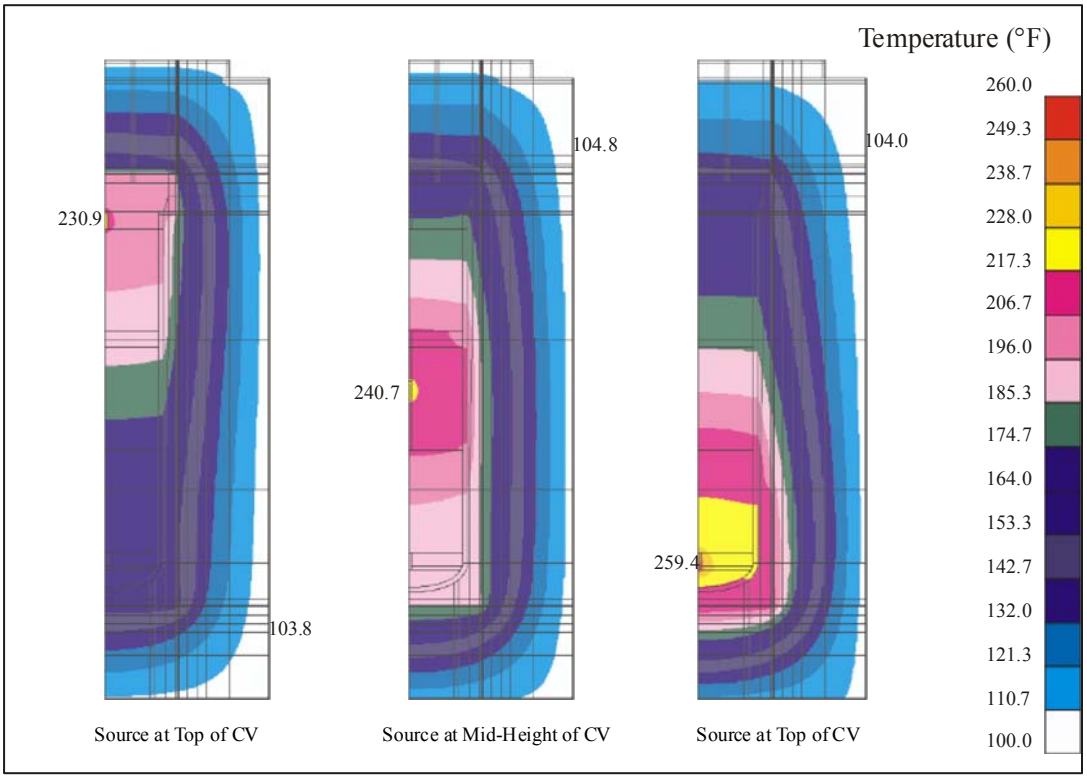

Figure 4 Overall pre-fire HAC temperature profile for 3 different source locations.

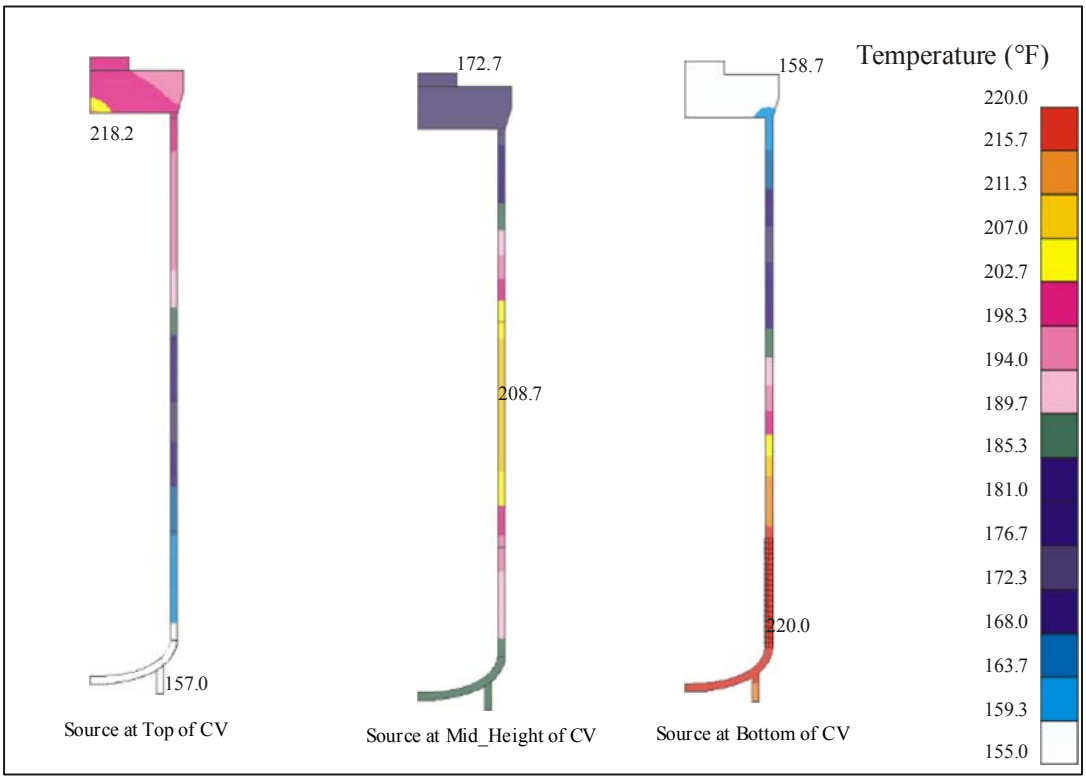

Figure 5 Pre-Fire HAC temperature profile in the CV for 3 different source locations.

Table 5 Maximum Content and CV Temperatures (°F) for the Pre-Fire HAC Model

	Source at Top of CV	Source at Mid-Height of CV	Source at Bottom of CV
Contents & Internal Air	231	241	259
CV	218	209	220

2.2 Model of the Fire Phase of the HAC

The temperatures within the 9977 package at the end of the fire are the initial temperatures for the post-fire HAC thermal analysis. When the foam is exposed to the high temperatures during the fire portion of the HAC, it decomposes to form an intumescent (expanding) char that fills voided spaces and expands out of the drum. Foam properties vary widely as it is heated. At a temperature of about 279°F the foam reaches its glass transition temperature and at temperatures above 480°F the molten foam undergoes an endothermic chemical reaction to form oligomers and char[3]. The oligomers later undergo a non self-sustaining exothermic reaction that eventually ceases when heat is no longer supplied by an external source. The endothermic phase of the reaction utilizes heat that would otherwise be used to raise the temperature of surrounding materials. For this reason, the degradation of the foam during the fire transient serves to thermally protect the CV and its O-rings.

The parameters governing heat transfer during the heating, phase change and thermally driven chemical reactions of the foam are not known. Further, the complexity of foam degradation, heat transfer and flow of hot gasses preclude a direct analysis of the 9977 package during the fire. For this reason, the heating of the contents of the 9977 during the fire phase of the HAC was not modeled numerically. Rather, data from the HAC burn tests[8] was used to estimate the temperatures of the components of the package after the fire. This process involved using the test data to estimate the temperature increase in the component temperatures during the fire and then superposing this temperature change onto component temperatures predicted for the pre-fire HAC. These estimates would then be used as initial values for the post-fire HAC. To more fully understand this methodology, it is necessary to digress to a discussion of the burn tests.

The 9977 packages used in the burn tests had the material configuration shown in Figure 3. Prior to the burn test the packages had been subjected to the sequence of impacts required by 10 CFR 71.73. Although actual packages would have an internal heat source, the test packages did not. In the actual packages the heat source would raise the initial temperature of the package at the start of the fire, thus resulting in higher final temperatures at the end of the 30 minute fire. To simulate the initial temperature of the packages at the onset of the fire, each of the test packages was heated in an environmental chamber before the start of the burn tests. Details of the preheating process are:

1. The package is exposed to an ambient temperature of 200°F
2. The package is heated for 96 hours.
3. The top, side and bottom external surfaces have natural convection boundary conditions, listed in Table 1.
4. There is thermal radiation applied to the top, side and bottom external surfaces.
5. Heat transfer across internal air-filled cavities occurs via thermal radiation and conduction, natural convection is neglected.
6. Emissivities are listed in Table 4.
7. Tabulated foam properties, rather than those fitted to the environmental chamber test[9], are used in the analysis.
8. The initial temperature of the package is conservatively assumed to be uniform at 70°F.
9. Material properties are listed in Tables 2 and 3.
10. Dimensions of the package are given in Reference 2.
11. The material configuration for the heating process is shown in Figure 6.

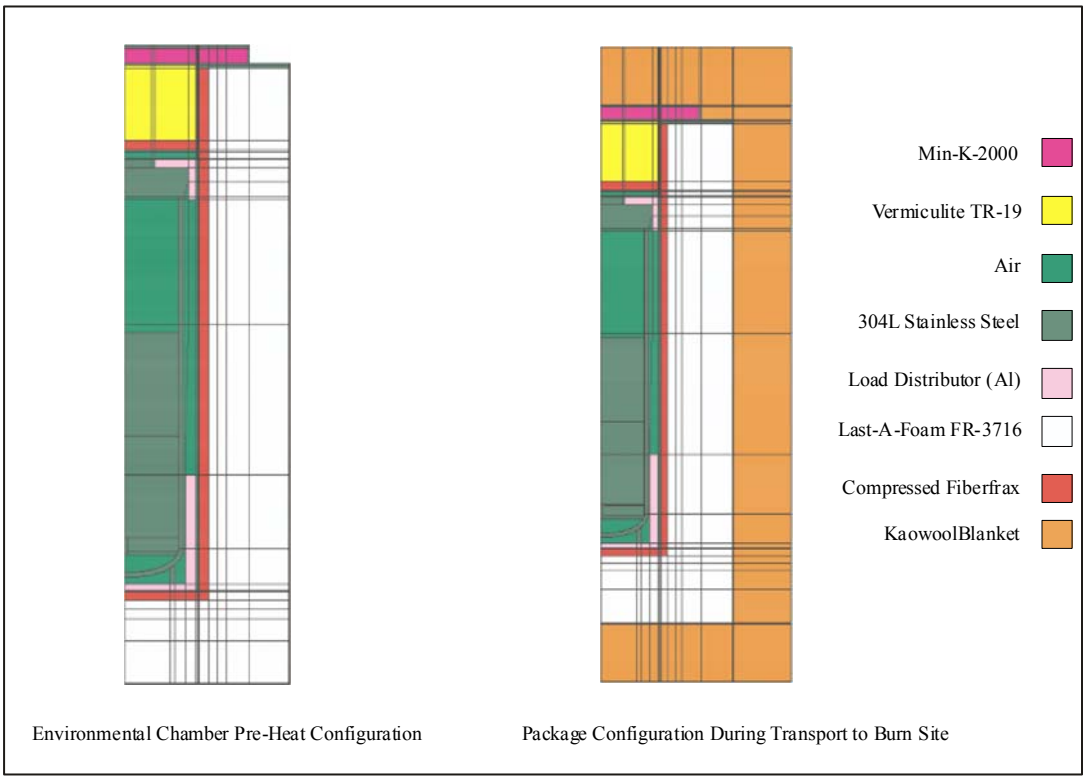

Figure 6 Material configuration for package mock-up during heating in the environmental chamber and during transport to the burn site.

Following the pre-heating process, the package was wrapped in a 4 inch thick Kaowool blanket and transported to the burn site. At the site, drum heaters were used to mitigate heat loss from the package. During this period of time heat transfer within the package, and exposure to the outside temperature, altered the temperature profile within the package. The model of the transport process is summarized as:

1 The initial temperature of the package is that after being heated for 96 hours in the environmental chamber.
2 The initial temperature of the Kaowool is assumed to be 60°F.
3 The package is wrapped in a 4 inch thick Kaowool insulating blanket.
4 The ambient temperature is 32°F.
5 The top and side external surfaces has natural convection boundary conditions, listed in Table 1.
6 There is thermal radiation applied to the top and side external surfaces.
7 Heat transfer across internal air-filled cavities is by thermal radiation and conduction, natural convection was neglected.
8 Emissivities are listed in Table 4.
9 Tabulated foam properties, rather than those fitted to the environmental chamber test[9], are used in the analysis.
10 Material properties are listed in Tables 2 and 3
11 Dimensions of the package are given in Figure 1.

12 The material configuration of the package during transport to the burn site is shown in Figure 6.
13 The transient lasts for 2 hours.

Predicted temperature profiles at the end of the pre-heating of the 9977 test package, and at the end of the shipping process are shown in Figure 7. After heating in the environmental chamber at 200°F for 96 hrs, and after transit to burn site while wrapped in 4 in of Kaowool for 2 hours at an ambient temperature of 32°F the calculated temperature of the CV, at the temperature label location that gave the maximum reading was 183°F, rounded down. This also happened to be the lowest calculated temperature of the CV. After the burn test the temperature label reading at this location was ≤ 270°F, see Table A-1 of the Appendix. The temperature, 270°F, also happens to be the highest measured temperature for the CV. This implies a maximum CV temperature increase of 87°F during the fire, which will be superposed onto the maximum temperatures of all regions within the drum liner.

It is recognized that the temperature of the internal components of the package continues to rise after the fire has been extinguished. This phenomenon is due to the transfer of heat from higher temperature components lying near the hot outer surface of the package to the cooler inner components, as well as toward the outside surface of the package as it cools. Because the temperature indicating label can only relay the maximum temperature achieved, the maximum temperature increase of 87°F used for the CV is conservative and really represents a temperature attained at some time after the fire was extinguished.

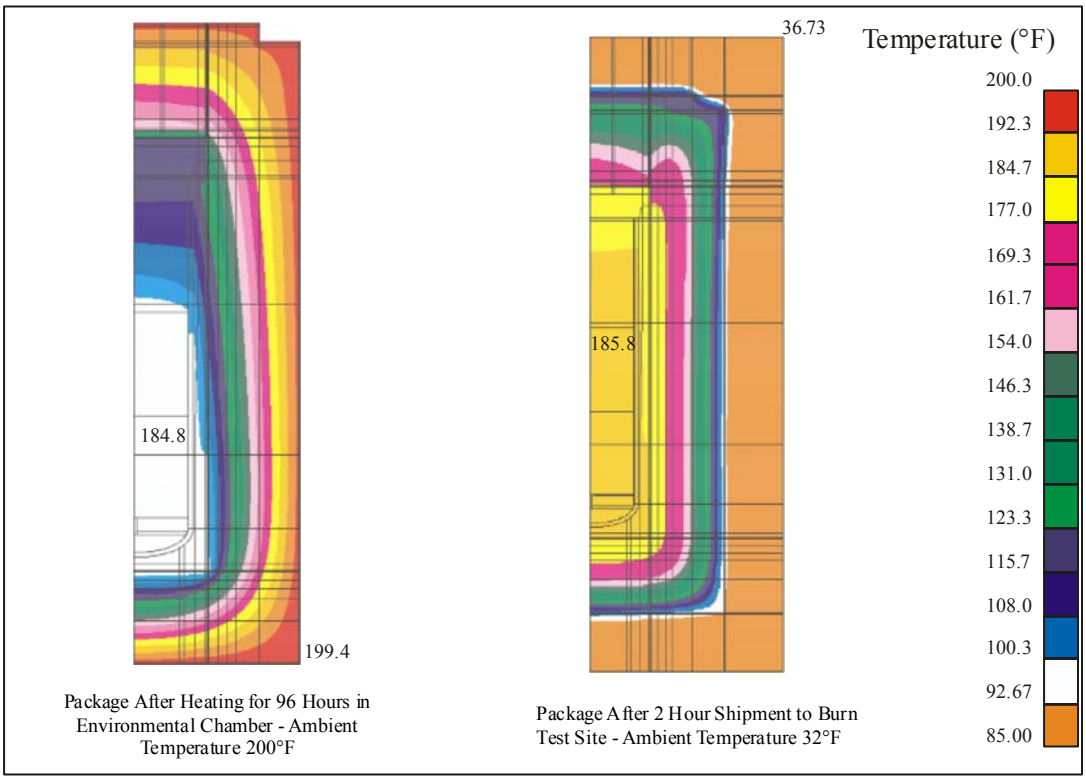

Figure 7 Temperature profiles in the test package after heating for 96 hours in the environmental chamber (left) and after wrapping in Kaowool and shipping for two additional hours.

2.3 Post-Fire Phase of the HAC

Description of the Post-Fire HAC Model

In the NovaTech® tests, the hot 9977 continued to offgas combustible vapors through openings in the outer shell of the drum after the pool fire was extinguished. Openings in the outer drum were either holes formerly covered by Caplugs® or gaps resulting from impact damage. It was observed that the gas burned for approximately 45 minutes after cessation of the 30 minute fire. Offgas combustion, which is more or less a surface phenomena, is not believed to significantly heat the 9977.

In the actual 9977's there was a layer of foam remaining about the drum liner following the fire transient. By virtue of its existence, the foam and, thus, the internal components it surrounds can not have exceeded the foam melting temperature, which is less than 400°F.

Following the fire the cooling rate of the package is controlled by heat generation from the internal 19W source, insolation and the amount of insulation surrounding the internal components. The volume bounded by the Fiberfrax® surrounding the drum liner and the drum wall, which was occupied by foam prior to the fire, is now filled with various thicknesses of foam surrounded by char.

For the post-fire phase of the HAC the model conditions are:

1. The drum is in an upright position.
2. There is thermal radiation from the external surfaces; the top, sides and bottom of the drum to the ambient.
3. There is natural convection from the external surfaces; the top and sides of the drum to the ambient. Convection coefficients were obtained from natural convection correlations in the MSC/Patran-Thermal database, see Table 1.
4. The ambient temperature is 100ºF.
5. Disassembly of the test packages following the pool fire tests revealed that the remaining amount of foam was equivalent to a layer between 1 and 2.3 inches thick surrounding the drum liner[10]. Analyses were performed for three cases.
   i. A 1 inch thick layer of foam surrounding the drum liner. The remainder of the foam volume was filled with char.
   ii. A 2.3 inch thick layer of foam surrounding the drum liner. The remainder of the foam volume was filled with char.
   iii All foam replaced with char.

   The char was assumed to have the thermal properties of air, see Table 3, and to completely fill the available space, precluding thermal radiation within the volume. Material compositions assumed for the 9977 package during the post-fire transient are shown in Figure 3
6. There is a total insolation heat fluence of 800 cal/cm^2 over a period of 12 hours on top of the drum and 400 cal/cm^2 over a period of 12 hours on the side of the drum (the absorptivity of the drum is assumed unity for solar radiation). As a conservatism, these heat fluences are applied continuously, rather than as a step function with a period of 12 hours, as prescribed by 10CFR 71.71. The corresponding time averaged heat fluxes are 245.77 Btu/ft^2 hr on the top of the package and 122.88 Btu/ft^2 hr on the side of the package.
7. The Fiberfrax® surrounding the drum liner is assigned its pre-fire thermal conductivity, which serves to resist heat transfer and is more conservative.
8. The contents contain a heat source outputting 19 Watts of total decay power, distributed over a cylinder approximately 1 inch long with a diameter of 0.25 inches. The cylinder is embedded in a slug of 304L stainless steel.
9. Three source locations were considered, see Figure 3:
   i Source at the top of the CV.
   ii Source at the middle of the CV.
   iii Source at the bottom of the CV.
10. The post-fire transient is monitored until after the temperatures in the package begin to decrease.
11. Emissivities for the post-fire HAC analysis are listed in Table 6.

Table 6 Surface Emissivities for Post-Fire HAC

Surface	Emissivity
CV	0.30
Drum Liner	0.30
Bottom of Lid	0.30
Load Distributor (interior)	0.20
Slug	0.30
Exterior of Drum	0.80

Initial component temperatures for the post-fire phase of the HAC are as follows:

1. The initial temperature of the contents of the CV, including the air, are determined by superposing the 87°F CV temperature increase measured during the fire tests onto the maximum content temperature from the pre-fire HAC model. The subsequent temperature is uniformly applied to the contents.
2. The initial temperature of the CV is determined by superposing the 87°F CV temperature increase measured during the fire tests onto the maximum temperature of the CV. The subsequent temperature is uniformly applied to the CV.
3. The temperature of intact foam, remaining after the fire was uniformly set to 400°F[3].
4. The temperature of char and exterior metal surfaces of the package were uniformly set to 1475°F.
5. The temperature of the Min-K-2000® and adjacent interior metal surfaces was uniformly set to1000°F.
6. The temperature of the Vermiculite TR-19® insulation was uniformly set to 400°F.

Temperatures in items 1 and 2 above are obtained by adding 87°F to the temperatures in Table 5. Table 7 lists the 9977 package component temperatures assumed at the beginning of the post-fire HAC transient.

Table 7 Initial Post-Fire HAC Temperatures

	Source at Top of CV	Source at Mid-Height of CV	Source at Bottom of CV
CV Contents & Internal Air	318°F	328°F	347°F
CV	305°F	296°F	307°F
Foam to CV	400°F	400°F	400°F
Min-K-2000®	1000°F	1000°F	1000°F
Vermiculite TR-19®	400°F	400°F	400°F
Char and External Metal	1475°F	1475°F	1475°F

Results From the Post-Fire HAC Model

The results from the post-fire HAC Model are shown in Table 8. The table shows the transient O-ring and maximum CV temperatures in terms of the hours following the end of the fire. Maximum temperatures occurring during the transient are highlighted in bold red. Steady-state O-ring and maximum CV temperatures, attained as the post-fire transient continues for an infinite period of time are listed at the bottom of Table 8.

The maximum temperature attained by the contents of the CV during the post-fire phase of the HAC was 425°F. This temperature occurred 6.5 hours after the end of the fire phase for the case in which the source was at the bottom of the CV and a 2.3 inches thick layer of foam remained outside the fiberfrax surrounding the drum liner. The location of the maximum temperature was within the source.

Table 8 Transient Post-Fire HAC Temperatures

	Source at Bottom of CV						Source at Mid-Height of CV						Source at Top of CV					
	2.3 in. Foam		1 in. Foam		Char		2.3 in. Foam		1 in. Foam		Char		2.3 in. Foam		1 in. Foam		Char	
Time (hr)	O-rings	CV	O-rings	CV	O-rings	CV	O-rings	CV	O-rings	CV	O-rings	CV	O-rings	CV	O-rings	CV	O-rings	CV
0.0	307	307	307	307	307	307	296	296	296	296	296	296	305	305	305	305	305	305
0.5	349	375	349	375	360	394	343	**377**	343	**377**	353	**400**	338	379	332	369	337	392
1.0	360	372	358	370	375	383	353	374	352	374	368	393	345	377	340	367	346	387
1.5	367	373	363	369	381	381	358	372	358	370	373	385	350	376	345	364	351	382
2.0	371	375	**365**	372	**381**	382	361	370	**359**	366	**373.33**	379	354	374	349	366	354	377
2.5	**372**	378	364	373	379	383	**360.70**	368	358	363	371	374	357	375	351	369	356	374
3.0	371	381	361	374	374	384	360	367	356	362	367	372	359	378	353	371	357	375
3.5	369	383	358	375	369	384	358	368	353	364	363	374	361	379	354	372	357	376
4.0	367	385	354	376	364	385	355	370	350	366	358	375	362	381	354	373	**357.1**	**375.9**
4.5	363	386	350	376	359	385	353	372	347	367	354	376	363	381	**353.98**	**372.7**	357	**375.9**
5.0	360	387	346	**376.3**	354	385	350	373	344	367	357	376	363	**381.6**	354	373	357	376
5.5	357	388	342	**376.3**	350	**385.4**	348	373	341	367	347	376	**362.9**	**381.6**	353	372	356	375
6.0	353	388	338	376	346	**385.4**	345	373	338	367	344	376	363	382	353	372	356	375
6.5	350	**388.2**	335	376	342	385	343	373	335	367	342	375	362	381	352	371	355	374
7.0	347	388	332	376	338	385	341	373	333	366	339	374	362	381	352	371	355	374
7.5			328	375	335	385			331	365			361	380	351	370		
8.0													360	379				
SS			254	313	263	325			263	297			278	297	288	307		

3.0 CONCLUSIONS

While it was not possible to calculate the temperature profile during the fire transient, data obtained from the NovaTech® pool fire tests were used to estimate temperatures in the 9977 package with a 19 Watt heat source. When input as initial temperatures for the post-fire HAC model, a conservative estimate of the temperatures of the limiting components was obtained.

4.0 References

1. S-SARP-2006-00001, Safety Analysis Report-9977 Packaging, Rev. 0, WSRC, (2006).
2. Drawings
   - R-R1-G-00020, Rev.0
   - R-R1-G-00021, Rev.0
   - R-R2-G-00017, Rev.0
   - R-R2-G-00018, Rev.0
   - R-R2-G-00019, Rev.0
   - R-R2-G-00042, Rev.0
   - R-R2-G-00043, Rev.0
   - R-R4-G-00032, Rev.0
   - R-R4-G-00033, Rev.0
3. General Properties Last-A-FoamFR-3700 for Crash and Fire Protection of Nuclear Material Shipping Containers, General Plastics Manufacturing Company, Tacoma WA.
4. Parker O-ring Handbook ORD-5700a, The Parker Seal Group, Parker Hannifin Corp., Cleveland OH (2001).
5. SAE, Aerospace Recommended Practice, 5316, Rev. B.
6. Packaging and Transportation of Radioactive Materials. Code of Federal Regulations Title 10, Part 71, Washington, DC (2006)..
7. MSC.PATRAN THERMAL 2003 r2, Online Manual, MSC Software Company, Santa Ana, California.
8. NT-TDR-06-101, SRNL Package Burn Test Report, NovaTech, March, 2006.
9. M-CLC-A-00255, Rev. 0, NCT Thermal Model for the 9975 Package, WSRC Document (2006).
10. M-CLC-A-00254, Determination of the Volume of Last-A-Foam Remaining in the 9977 Package after the Thermal Test. WSRC Document (2006).

APPENDIX

Pool Fire Tests

A series of pool fire tests were conducted on 9977 mockups by NovaTech Innovative Technologies International, [8]. Prior to the pool fire, the packages had undergone the sequence of free drop, crush and puncture tests required by 10 CFR 71.73 for Hypothetical Accident Conditions. As specified in 10 CFR 71.73 the package must be "engulfed, except for a simple support system, in a hydrocarbon fuel/air fire of sufficient extent, and in sufficiently quiescent conditions, to provide an average emissivity coefficient of 0.9, with an average flame temperature of at least 800°C (1475°F) for at least 30 minutes." Further, "the fuel source must extend horizontally at least 1m (40 in), but may not extend more than 3 m (10 ft), beyond any external surface of the specimen, and the specimen must be positioned 1 m (40 in) above the surface of the fuel source."

The pool fire tests met or exceeded the requirements listed above. A sequence of four tests were performed:

1 A preliminary burn test on a package that had no foam and was not subjected to impact tests.
2 A test for a package that was burned in an upright orientation and had been subjected to the sequence of impact tests prescribed by 10 CFR 71.73. In the drop test for this package initial contact with the ground occurred at the top.
3 A test for package that was burned upside down and had been subjected to the sequence of impact tests prescribed by 10 CFR 71.73. In the drop test for this package initial contact with the ground occurred at the bottom.
4 A test for a package that burned on its side and had been subjected to the sequence of impact tests prescribed by 10 CFR 71.73. In the drop test for this package initial contact with the ground occurred on the side.

Data monitored for the burn tests included:

1. The ambient temperature.
2. The wind speed and direction.
3. The fire temperature, via an array of 8 thermocouples suspended within the enclosure for the package, see Figure A.1[6].
4. The radiant fire temperature via four directional flame thermocouples (DFT's), see Figure A.1.
5. Temperature data within the package was obtained from temperature indicating labels, see Table A-1.

[6] All fire temperatures, including those for the DFT's , were monitored by recorders located at two separate stations

Figure A.2 is a photograph of the 9977 in an upright orientation on its test stand prior to the burn test. Figure A.3 shows the engulfment of the 9977 by the fire and Figure A.4 shows the package after the 30 minute burn.

A detailed description of the fire tests and the results obtained from them is given in Reference 8.

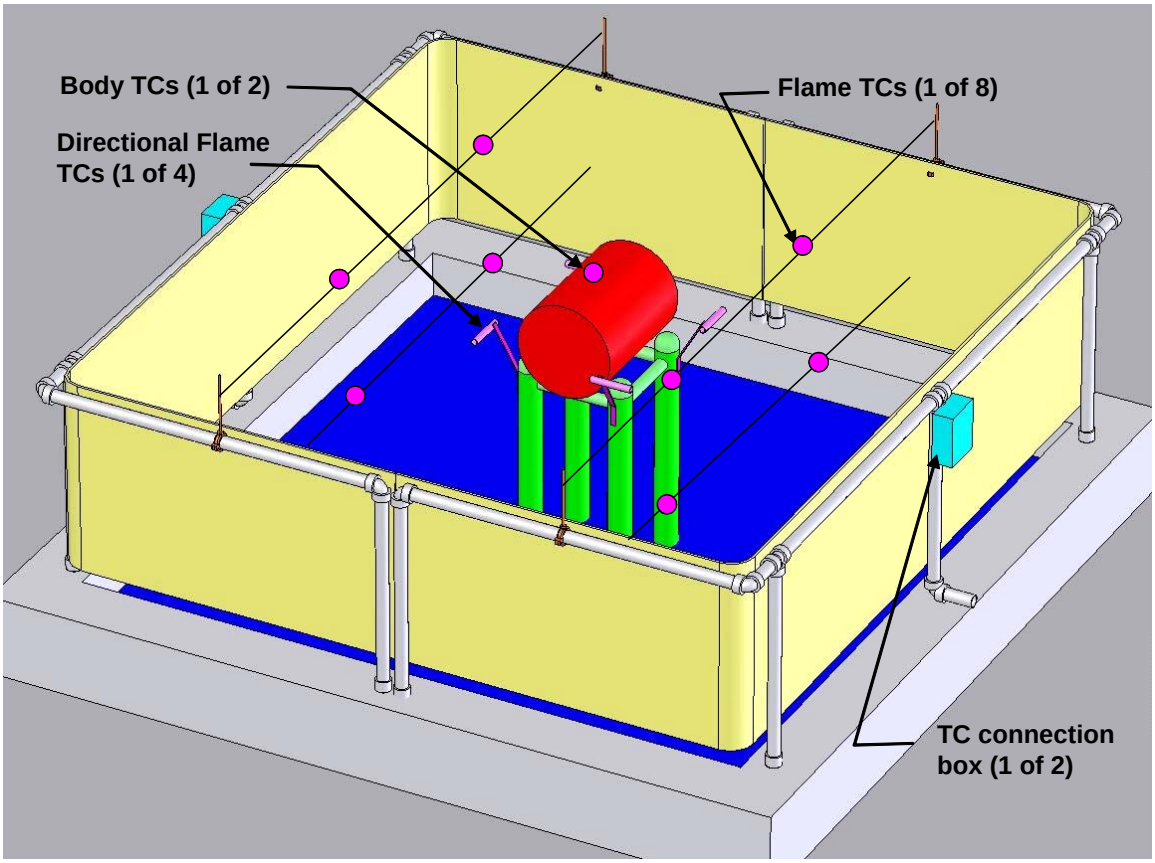

Figure A.1 Relative locations of DFT's and thermocouples used to measure the flame temperature.

Figure A.2 Practice burn 9977 on its test stand prior to burn test. Thermocouples used to measure the fire temperature and their support wires can be seen in the photograph.

Figure A.3 Extent of engulfment of the practice burn 9977 by the fire.

Figure A.4 Practice Burn 9977 after the fire was extinguished.

Table A-1 Measured CV Temperatures

Label Locations:	Overpack 2 Temperature Degrees F	Overpack 3 Temperature Degrees F	Overpack 4 Temperature Degrees F	Overpack 5 Temperature Degrees F	Comments
1. Bottom of drum lid liner – located 120 degrees apart	>280 <290	>370<380	>420<435	>420<435	
2. Top of load distribution fixture	Missing Label	>290<320	>280<290	>250<260	O'Pack 3 - 300 & 320 dots Questionable
3. Side of drum lid liner – 120 degrees apart, center of label 2 inches from drum lid plate	Not Available	>500	Not Available	Not Available	
4. Bottom of cone seal plug – 120 degrees apart	<250	>260<270	>260<270	Labels Damaged	
5. Top of cone seal nut	Damaged Labels	Damaged Labels	>270<280	>250<260	O'Pak 3 - 250 label abraded, all others not discolored
6. Inside CV, one set each at 0 and 180 degrees – top of labels approximately even with bottom of cone seal plug					
0-degrees set	<250	>260<270	>250<260	<250	
180-degrees set	Labels Missing	Labels Missing	Labels Damaged	<250	
7. Outside CV, one set each at 90 and 270 degrees – top of labels approximately even with bottom of cone seal plug					
90-degrees set	<250	>260<270	>250<260	<250	
270-degrees set	<250	>260<270	>250<260	<250	
8. Inside CV, one set each at 0 and 180 degrees – center of labels at mid-point of CV length					
0-degrees set	Damaged Labels	<250	Labels Damaged	<250	
180-degrees set	Damaged Labels	<250	<360	<250	O'Pak 4 - Labels abraded, 360 dot not discolored
9. Outside CV, one set each at 90 and 270 degrees – center of labels at mid-point of CV length					
90-degrees set	<250	<250	<250	<250	
270-degrees set	<250	<250	<250	<250	
10. Inside CV, one set each at 0 and 180 degrees – center of labels at mid-point of load distribution fixture					
0-degrees set	Damaged Labels	Damaged Labels	<330	<250	O'Pak 4 - 250 Labels damaged, 330 dot not discolored
180-degrees set	Damaged Labels	<250	<250	<250	

Table A-1 (contd) Measured CV Temperatures

Label Locations:	Overpack 2 Temperature Degrees F	Overpack 3 Temperature Degrees F	Overpack 4 Temperature Degrees F	Overpack 5 Temperature Degrees F	Comments
11. Outside CV, one set each at 90 and 270 degrees – center of labels at mid-point of load distribution fixture					
90-degrees set	Damaged Labels	<250	<250	<250	
270-degrees set	<250	<250	<250	<250	
12. Inside CV bottom - located 120 degrees apart	<250	>250<260	<250	<250	
13. Inside bottom of drum liner	>250<260	>330<340	<250	<250	
14. Inside drum liner, one set each at 0 and 180 degrees, center of labels at midpoint of liner length					
0-degrees set	<250	>260<270	<250	<250	
180-degrees set	<250	>260<270	<250	<250	
15. Outside CV, one label at top, middle, and bottom at 90 degrees					
Top	>210<220	>240	>240	>240	1 Label - 240 max temperature
Middle	>210<220	>240	>220<230	>220<230	1 Label - 240 max temperature
Bottom	Labels Missing	>240	>210<220	>220<230	1 Label - 240 max temperature

In Table A-1 the CV temperature indicator label highlighted in yellow was damaged and did not provide a credible temperature. The highest credible CV temperature is that highlighted in blue, namely a maximum value of 270°F.

This Page Intentionally Left Blank

This Page Intentionally Left Blank

APPENDIX 3.3

NCT THERMAL MODEL FOR THE 9977 PACKAGE

This Page Intentionally Left Blank

OSR 45-24 (Rev 11-15-2004)

Calculation Cover Sheet

Project	Calculation No.	Project No.
9977 SARP	M-CLC-A-00255	NA
Title	**Functional Classification**	**Sheet 1 of**
NCT Thermal Model for the 9977 Package	SC	34
	Discipline	
	Mechanical	
Calc Level	**Type 1 Calc Status**	
☒ Type 1 ☐ Type 2	☐ Preliminary ☒ Confirmed	
Computer Program No.	**Version/Release No.**	
MSC.PATRAN.THERMAL ☐ N/A	2003 r2	

Purpose and Objective

The purpose of the calculation was to predict the temperatures of limiting components of the 9977 package under Normal Conditions of Transport (NCT) postulated in 10 CFR 71.71. The base case calculations included a 19W heat source, having limiting dimensions, embedded in a stainless steel slug that was located at 3 axial positions in a 6-inch Containment Vessel (6CV). Additional calculations were performed for: bare 19W sources touching the top and bottom of the CV, a nominal RTG load configuration and 19W embedded source locations at the top and bottom of a 5-inch containment vessel (5CV).

Summary of Conclusion

For all configurations, except the bare sources, the temperatures of the bounding components were below their respective temperature limits. Temperatures for the 5CV source locations were bounded by the 6CV temperatures for source at equivalent locations.

Revisions

Rev No.	Revision Description
0	Original Issue

Sign Off

Rev No.	Originator (Print) Sign/Date	Verification/ Checking Method	Verifier/Checker (Print) Sign/Date	Manager (Print) Sign//Date
0	Bruce Hardy 4/20/06	Individual Review	N. K. GUPTA 4/20/06	C. R. HOLDING-SMITH 4/25/06

Design Authority — (Print)	Signature	Date
G Abramczyk	G Abramczyk	5-2-06
Release to Outside Agency – (Print)	**Signature**	**Date**

Security Classification of the Calculation

Unclassified

Revisions

Revision	Description
0	Original Issue

Nomenclature

h = Convection Heat Transfer Coefficient (Btu/hr-ft^2-°F)
k = Thermal Conductivity (Btu/hr-ft-°F)
k_i = Thermal Conductivity of Material in Cylinder i (Btu/ft hr °F)
L = Characteristic Length (ft)
n = Total Number of Concentric Cylinders
Pr = Prandtl Number
q = Heat Flow (Btu/hr)
r = Radial Location (ft)
r_i = Inner Radius of Cylinder i (ft)
Ra = Rayleigh Number
T = Temperature (°F)
T_{i+1} = Temperature at outer edge of cylinder i (°F)

Acronyms and Abbreviations

CV	Containment Vessel
DOT	Department of Transportation
GPFP	General Purpose Fissile Package
HAC	Hypothetical Accident Conditions
MSC	McNeal Schwendler Corporation
NCT	Normal Conditions of Transport
SARP	Safety Analysis Report for Packaging
SS	Stainless Steel

1.0 Introduction and Background

The Department of Transportation (DOT) Fissile Specification 6M package is being removed from service. As a result, a new general purpose fissile package, designated as the Model 9977 Shipping Package, has been designed as a replacement. The 9977 package consists of a Containment Vessel (CV), a drum overpack filled with foam and a bolt-on lid that has several layers of insulation. Figures 1 and 2, respectively, show schematics of the 9977 and CV. Contents for the package will be placed within the CV, which is closed with a screw on cap that is sealed by a double set of O-rings. The CV is loaded into a cylindrical drum liner and held in place by upper and lower load distributors. The package is closed by bolting the lid in place.

This document describes the thermal model for the Normal Conditions of Transport (NCT) to be used for the 9977 SARP (Safety Analysis Report for Packaging[1].

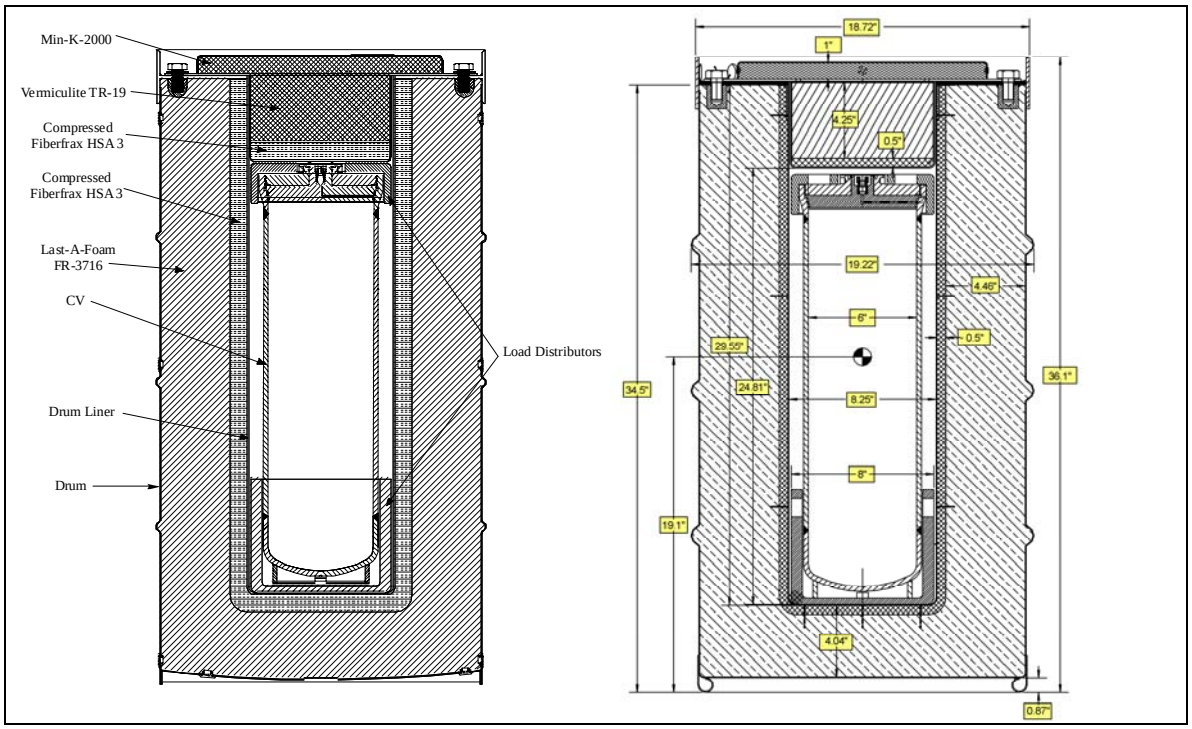

Figure 1 Schematic and dimensions of the 9977 containing the 6-inch CV.

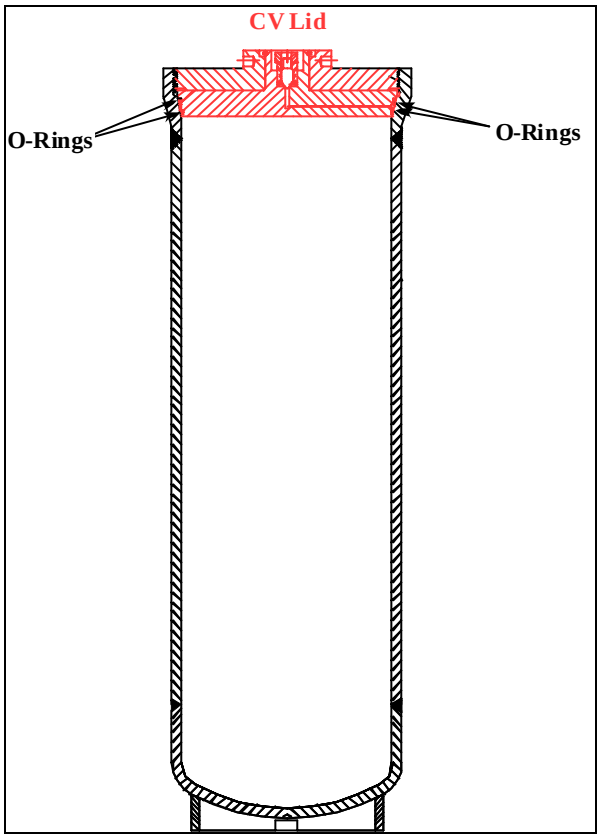

Figure 2 Schematic of the CV

Technical specifications for the package components are provided on the package drawings in Reference [2]. The drawing specifications include the applicable ASME Code requirements for the components and materials. Package design specifications relevant to the thermal analysis are summarized below

.

Drum, Drum Liner and Lid

The outermost shell of the 9977 is an 18-gauge 304L stainless steel drum that is 36.10 inches tall, as measured from the lower edge to the top of the drum flange, and has a diameter of 18.72 in. to the outside of the drum flange, see Figure 1. At 3 axial elevations there are sets of 4 vent holes in the side of the drum, 90° apart. Two additional vent holes are located in the bottom of the drum. All vent holes have diameters of ¾ in. and are closed with plastic Caplugs® to prevent entry of rainwater during NCT. In the HAC-fire event, the fusible Caplugs® are consumed and allow the drum to vent gases generated from thermal decomposition of the Last-A-Foam® insulation. A cylindrical drum liner having an inside length and diameter of 29.5 and 8.25 inches, respectively, is concentrically located within the drum. The drum liner is constructed of 18 gauge 304L stainless steel and has exterior studs to secure a Fiberfrax® insulating blanket.

The drum liner is closed by securing a lid to the drum flange with eight 5/8 inch bolts. The lid is constructed from 18-gauge 304L stainless steel and incorporates three layers of insulating material: uncompressed Fiberfrax® HSA System No. 3 blanket at 16 lbm/ft^3,

Min-K-2000 insulation manufactured by the Thermal Ceramics Company, and Vermiculite TR-19 insulation manufactured by the Thermal Ceramics Company.

Compressed Fiberfrax® and Last-A-Foam®

A layer of Fiberfrax® HSA System No. 3 blanket at 16 lbm/ft^3 is wrapped around the sides and bottom of the drum liner. Initially, the Fiberfrax® blanket is 1 in. thick, however, during the fabrication process the region between the outer surface of the Fiberfrax® and the inner surface of the drum wall is filled with Last-A-Foam® FR-3716 manufactured by the General Plastics Manufacturing Company. Last-A-Foam® FR-3716 is a rigid polyurethane foam that expands to a density of approximately 16 lbm/ft^3 as it cures. As it expands the foam compresses the layer of Fiberfrax® against the drum liner. The compressed thickness of the Fiberfrax® is unknown but was estimated to be approximately ½ in. for the model used in the thermal analysis. Because the thickness of the Fiberfrax® was halved, its density is doubled and it is assumed that its thermal conductivity is also doubled. Table 3 lists properties of compressed and uncompressed Fiberfrax®.

Containment Vessel and Containment O-Rings

The CV is constructed from either 6-inch diameter or 5-inch diameter, seamless Schedule 40S, Type 304L stainless steel (SS) pipe. One end of the pipe is closed by a Schedule 40S, Type 304L SS pipe cap. The CV is closed by ¾-inch thick 304L SS cone-seal plug held in place by a 0.63-inch thick male-threaded Nitronic-60 cone-seal nut. The cone-seal plug incorporates machined grooves to receive two O-ring seals.

A containment boundary is provided in part by the CV body and closure but is completed by the outer O-ring mounted on the cone-seal plug and by the leak-test port plug. The O-ring material is Viton® GLT, a fluorocarbon elastomer with a service temperature range between -40°F and 400°F.[3] When not in service and stored in accordance with Society of Automotive Engineers, Aerospace Recommended Practice, 5316, Revision B, the O-rings have an unlimited shelf life[4].

The CV is supported by aluminum load distribution fixtures. Unless otherwise specified their properties were assumed to be that of type 1100 aluminum.

2.0 Model Validation Test

2.1 Description of Experiment

To validate the NCT thermal model, a transient thermal test was performed on a prototype of the 9977. The prototype, designated as SN-6, contained a 20W cartridge heater, was initially at a uniform temperature of 73°F, and was placed in a fixed 100°F environmental chamber. Figure 3 is a schematic of the 9977 with a mock source installed in a 6-inch diameter CV (6CV) for the thermal benchmark tests. The mock source consisted of a cartridge heater embedded at the bottom of a 5.25-inch diameter by 5 inch deep hole that was center bored into a 6-inch diameter, 13.375 inch long 304L stainless steel slug. The center bore permits the cartridge heater to be approximately centered

within the steel slug. The cartridge heater is stainless steel clad and ¼-inch diameter by 1-inch long. The hole in the test weight that holds the heater was sized for a snug fit of the cartridge heater. Figure 4 is a photograph of the CV and heater assembly before it was installed into the CV. The mock source was placed in the bottom of the 6CV with no packing above it. The 6CV was then closed with a screw on cap that is sealed by a double set of O-rings. The 6CV was loaded into the drum liner and held in place by upper and lower load distribution fixtures. The package was closed by bolting the lid in place. The bottom pipe cap of the 6CV was drilled with a ¼ inch diameter hole that permitted the heater power wiring to exit. As shown in Figure 3, the wiring was routed along the inside of the liner and out between the lid and drum top. A full description of the test procedure is provided in Reference [5]. The thermal test report is provided in Reference [6].

The power supplied to the cartridge heater was monitored and manually controlled to produce 19 watts, the maximum heat load for the 9977. Figure 5 shows the 9977 positioned in the environmental chamber prior to testing. The 9977 test package was instrumented with 31 Type-K thermocouples. Their relative locations are shown in Figure 6.

The duration of the heating test was approximately 140 hours and was based on preliminary calculations with the thermal model. 9977 component temperatures were measured by thermocouples placed at the locations shown in Figure 6. In the experiment, temperatures were recorded at intervals of 1 minute after the first 19 minutes of the test. Up to the first 19 minutes of the test, temperatures were recorded at irregular intervals.

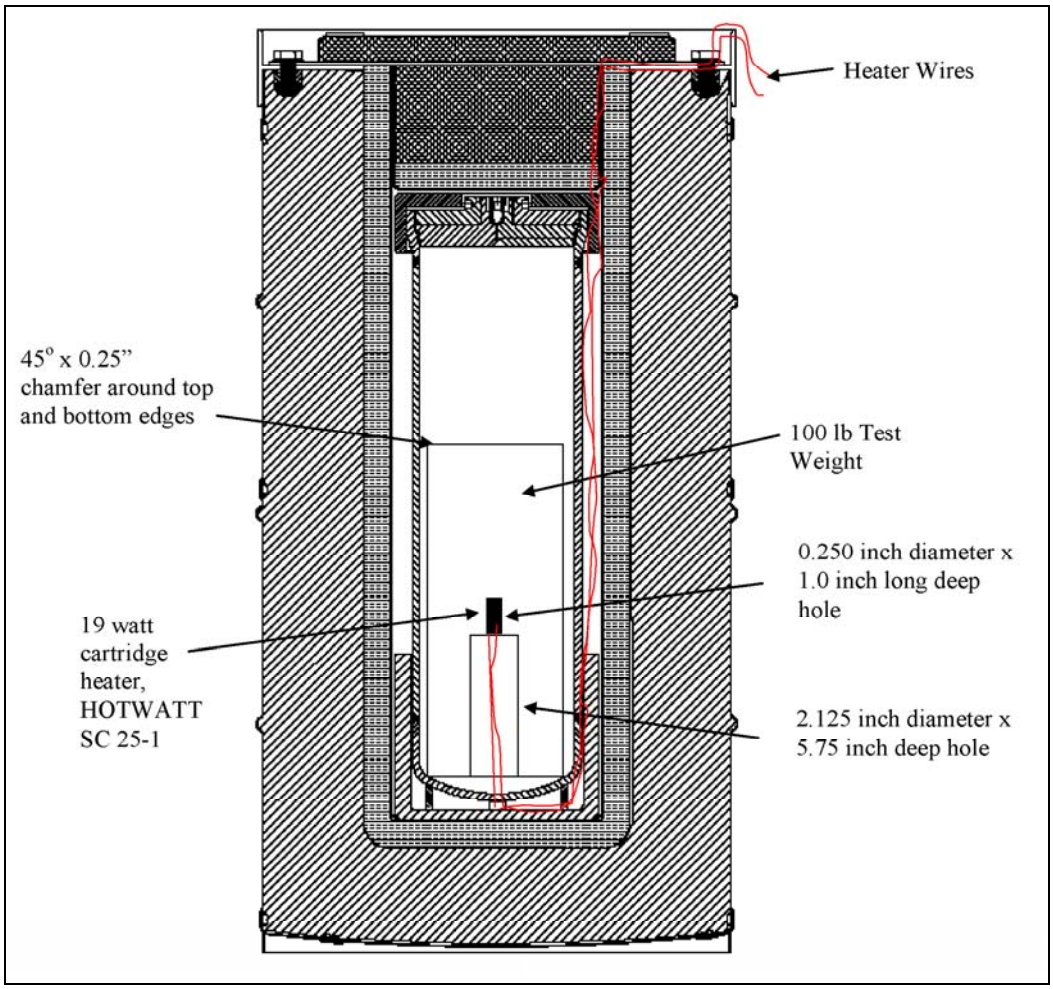

Figure 3 Schematic of 9977 test package.

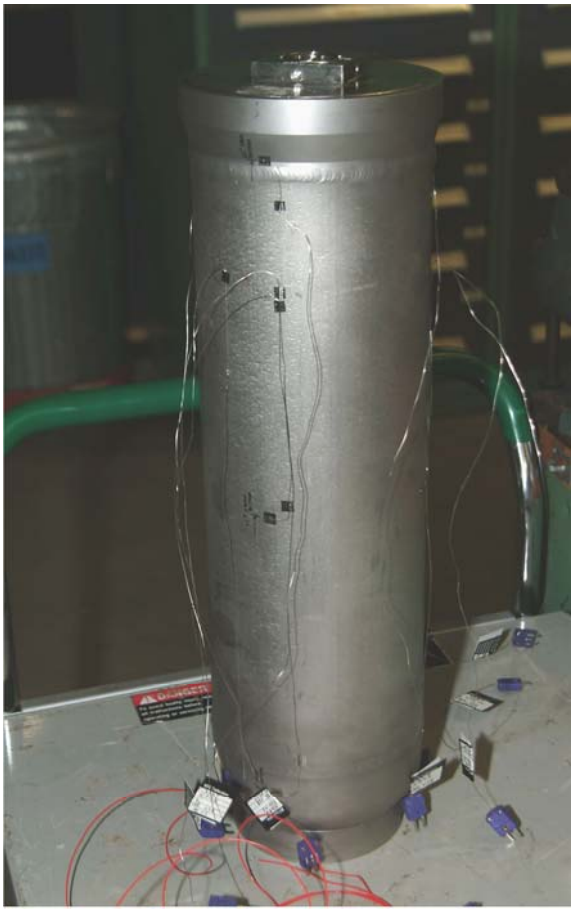

Figure 4 Photograph of 9977 6CV with thermocouples and heater assembly.

Figure 5 9977 test package SN-6 positioned in environmental thermal chamber.

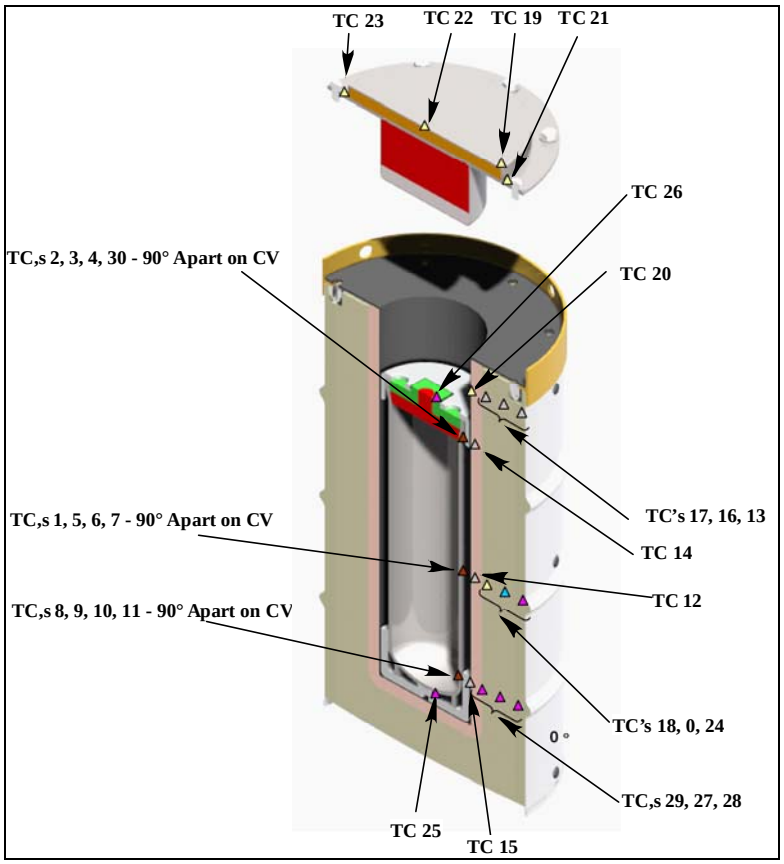

Figure 6 Location of thermocouples for SN-6 in the environmental chamber.

2.2 Description of Model

A thermal model of the test was developed with the MSC.Patran Thermal® [7] general purpose heat transfer software. The model replicated the boundary conditions within the chamber, as well as the material configuration of the test 9977 package. As for the test mockup, the model contained a 19 Watt source and was initially at a uniform temperature of 73°F prior to the start of the test. After the start of the test the model was subjected to a fixed ambient temperature of 100°F. Because the base of the package was not in contact with the floor of the environmental chamber, natural convection and thermal radiation boundary conditions were applied there. The material configuration and source location for the model are shown in Figure 7. Emissivities employed by the model are listed in Table 1. The emissivities were based on the type of material and an assessment of the surface characteristics. Later in this document it will be shown that the variation in predicted temperature due to variation in emissivities is small. Natural convection boundary conditions are listed in Table 2 and material property data are listed in Tables 3 and 4. Because the Fiberfrax® blanket that surrounds the drum liner was compressed from 1 inch to ½ inch by the expanding foam, its density was doubled and its thermal conductivity was assumed to be twice that of the uncompressed value. Properties for uncompressed and compressed Fiberfrax® are also listed in Table 3.

Because of the relatively low heat fluxes, the internal metal surfaces (such as the drum liner, liner around the inner lid and the metal interface between the lid and the drum) were omitted from the model. To show that the presence of these surfaces had little effect on the temperature profile, the metal surfaces were included in later model. Exclusion of the interior metal surfaces only replaced the thickness of the metal with the adjacent material properties, however, the appropriate emissivities were applied.

Table 1 Surface Emissivities

Surface		Emissivity
CV	304L Stainless Steel	0.30
Drum Liner	304L Stainless Steel	0.60
Bottom of Lid	304L Stainless Steel	0.60
Load Distributor	Aluminum	0.20
Slug	304L Stainless Steel	0.60
Exterior of Drum	304L Stainless Steel	0.21

Table2 Natural Convection Heat Transfer Coefficients [Ref. 7]

Model Orientation	Surface	Correlation (Btu/hr-ft^2-°F)
Vertical	isothermal plate with $Ra < 1.0\times10^9$	$h = \left(\frac{k}{L}\right)\left(0.68 + \frac{0.670\times Ra^{0.25}}{\left[1.0+\left(\frac{0.492}{Pr}\right)^{9/16}\right]^{4/9}}\right)$
Vertical	isothermal plate with $1.0\times10^9 < Ra$	$h = \left(\frac{k}{L}\right)\left(0.825 + \frac{0.387\times Ra^{1/6}}{\left[1.0+\left(\frac{0.492}{Pr}\right)^{9/16}\right]^{8/27}}\right)^2$
Horizontal	hot isothermal plate facing upward with $1.0\times10^7 < Ra < 3.0\times10^{10}$	$h = \left(\frac{k}{L}\right)0.15\times Ra^{1/3}$
Horizontal	hot isothermal plate facing downward with $3.0\times10^5 < Ra < 3.0\times10^{10}$	$h = \left(\frac{k}{L}\right)0.27\times Ra^{0.25}$

Table 3 Thermal Properties of Solid Packaging Materials

Material	Thermal Conductivity (Btu/hr ft °F)	Density (lbm/ft^3)	Specific Heat (Btu/lbm °F)
Fiberfrax (uncompressed) Values are for HSA System 3®[1]	0.02 @ 400°F 0.03 @ 800.0°F 0.04 @ 1200.0°F 0.05 @ 1600.0°F	16.0	0.27
Fiberfrax (compressed) Values are for HSA System 3® thermal conductivity assumed 2* the value of uncompressed material	0.040 @ 400°F 0.060 @ 800.0°F 0.080@ 1200.0°F 0.100 @ 1600.0°F	32.0	0.27
Vermiculite TR-19[2]	6.33E-02 @ 400.0°F 6.67E-02 @ 600.0°F 7.00E-02 @ 800.0°F 7.33E-02 @ 1000.0°F 7.75E-02 @ 1200.0°F 8.17E-02 @ 1400.0°F 1.08E-01 @ 1600.0°F	23.0	0.20
MIN-K 2000[3] Tabulated thermal conductivities for Min-K-2000 are less than those for air, hence, values for Vermiculite TR-19 were used in the analysis.	1.58E-02 @ 300.0°F 1.67E-02 @ 400.0°F 1.83E-02 @ 600.0°F 2.08E-02 @ 800.0°F 2.50E-02 @ 1000.0°F 3.33E-02 @ 1200.0°F 4.17E-02 @ 1500.0°F 4.50E-02 @ 1600.0°F	20.0	0.23 @ 400.0°F 0.25 @ 800.0°F 0.27 @ 1200.0°F 0.27 @ 1600.0°F
LAST-A-FOAM® FR-3716 @ 16 lb/ft³[4]	2.75E-02 @ 76.5°F 3.12E-02 @ 140.7°F 3.71E-02 @ 248.4°F 4.33E-02 @ 348.6°F 4.33E-02 @1000.0°F **5.250E-2** Adjusted to match Environmental Chamber data	16.0	0.353
Aluminum (Type 1100)[5]	126.0	169.3	0.216
Aluminum (Type 6061 T-6)[5]	90.0	169.3	0.216
304L Stainless Steel[7]	7.74108 @ 32.0°F 9.43444 @ 212.0°F 12.5793 @ 932.0°F 14.9983 @ 1292.0°F	494.429	1.200E-01 @ 32.0°F 1.350E-01 @ 752.0°F

[1] Fiberfrax® HSA System No. 3 blanket manufactured by the Standard Oil Engineered Materials Company.
[2] Vermiculite TR-19® insulation manufactured by the Thermal Ceramics Company.
[3] Min-K-2000® insulation manufactured by the Thermal Ceramics Company.
[4] Last-A-Foam® FR-3716 manufactured by the General Plastics Manufacturing Company.
[5] Kaufman, J. Gilbert (2004). Aluminum Alloy Database. Knovel. Online version.

Table 4 Thermal Properties of Gaseous Packaging Materials

Material	Thermal Conductivity (Btu/hr ft °F)	Density (lbm/ft^3)	Specific Heat (Btu/lbm °F)	Thermal Expansion Coeff. (1/°F)	Viscosity (lbm/hr-ft)
Air at 1 atm pressure	1.5161E-02@80.33°F 1.9443E-02@260.33°F	$\rho = \frac{1}{2.5203 \times 10^{-2}(T + 459.67)}$ T is in °F	0.24044	$\beta = \frac{1}{(T + 459.67)}$ T is in °F	4.797E-02@80.33°F 5.020E-02@170.33°F 5.530E-02@260.33°F 6.009E-02@350.33°F

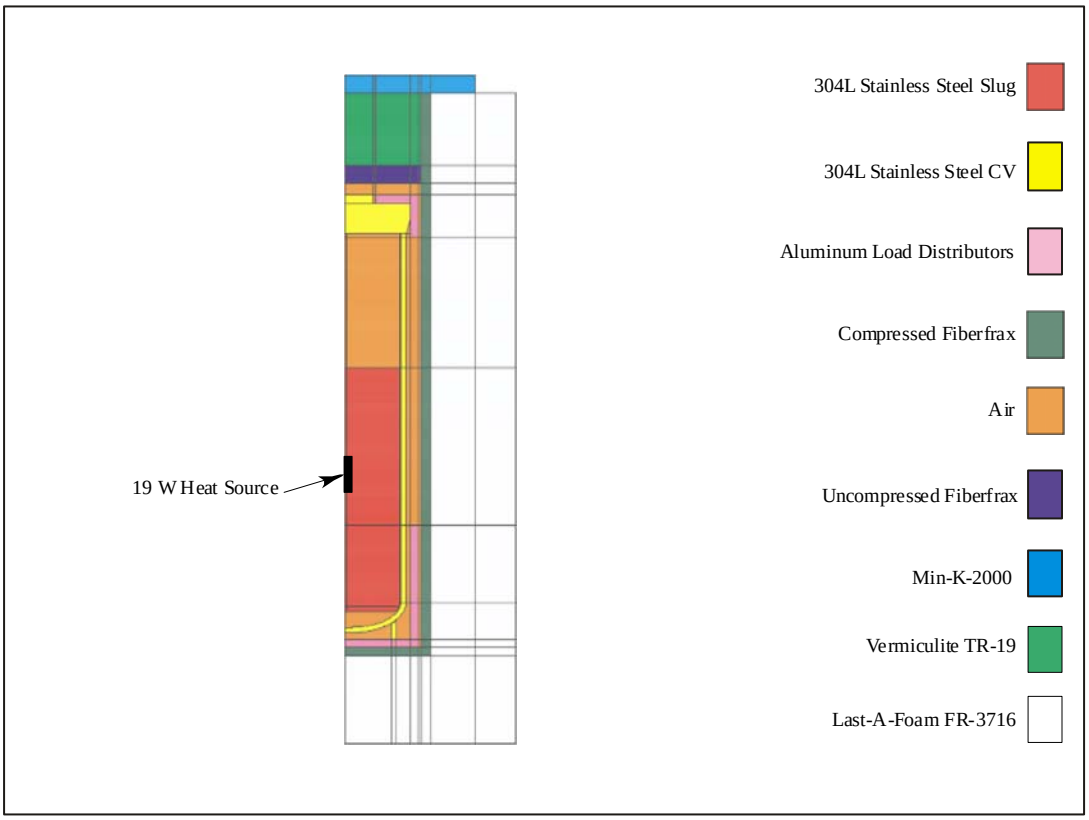

Figure 7 Material configuration for the model of SN-6.

2.3 Model to Data Comparison

A comparison between temperatures predicted by the model, using tabulated property data, and temperatures measured during the test is shown in Figure 8. From the figure, it can be seen that at a given instant in time the radial temperature difference across the Fiberfrax® is nearly the same for the model and the data. This suggests that the approximations made for the thickness and thermal conductivity compressed Fiberfrax® were reasonable. However, the predicted radial temperature difference across the foam is in significant disagreement with the measured values. Because the discrepancy in the temperature difference continues toward steady state, it is attributable to the thermal conductivity used to model the foam.

To evaluate the data used in the model, predicted temperatures were compared with test data along the mid-height of the 9977, where radial conduction is expected to predominate. In this case, the heat flow is approximated as that for a series of concentric cylinders

$$q = \frac{2\pi L\left(T_1 - T_{n+1}\right)}{\sum_{i=1}^{n} \frac{1}{k_i} \ln\left(\frac{r_{i+1}}{r_i}\right)} \qquad 1$$

where: q = Heat flow (Btu/hr)
L = Length of cylinder (ft)
k_i = Thermal conductivity of material in cylinder i (Btu/ft hr °F)
n = Total number of concentric cylinders
T_{i+1} = Temperature at outer edge of cylinder i (°F)
r_i = Inner radius of cylinder i (ft)

An iterative approach using Equation 1 in conjunction with the numerical model was used to adjust the thermal conductivity of the foam. The iterative scheme used the predicted radial temperature difference across the fiberfrax, which was approximately the same as that from the temperature data, to estimate the radial heat flux. Equation 1 was used to estimate the foam thermal conductivity based on the measured foam temperatures at the foam-fiberfrax interface and the outer surface of the package. The estimated foam thermal conductivity was input to the thermal model and the calculated temperatures were compared to the data. The process was repeated until temperatures predicted by the model were in reasonably close agreement to temperature data at corresponding locations. When used in the model, the adjusted foam thermal conductivity shown in Table 3, significantly reduced the difference between the predicted temperatures and those obtained from the experiments, as shown in Figure 9.

Table 5 compares data and model temperatures at all thermocouple locations, at 110 hours after the start of the test, for both the tabulated and adjusted foam thermal conductivities; and with adjusted foam properties with and without interior metal surfaces. Thermocouple locations referenced in Table 5 are shown in Figure 6. Averages were taken for those thermocouples that differ only in azimuthal position (i. e. with the same radial and axial coordinates). It can clearly be seen that temperatures predicted with the adjusted thermal conductivity are in much better agreement with the data than those based on the tabulated values. The improved agreement extends even to those locations for which the heat flux is not predominantly in the radial direction. Further, it can be seen that the interior metal surfaces have a relatively small effect on the temperatures for an NCT and pre-fire HAC conditions.

Values used for emissivities of interior surfaces have always been somewhat subjective. For this reason, calculations were performed to test the sensitivity of the model to uncertainty in these parameters. Figure 10 shows a comparison between temperatures predicted by the base case model, with emissivities listed in Table 1 and with models having the emissivities for all interior surfaces set to 0.3 and 0.6, see Tables 6 and 7, respectively. For all cases the emissivity of exterior surface of the drum was maintained

at 0.21. From Figure 10 it can be seen that changes in the internal surface emissivities result in a relatively small change in the predicted temperatures.

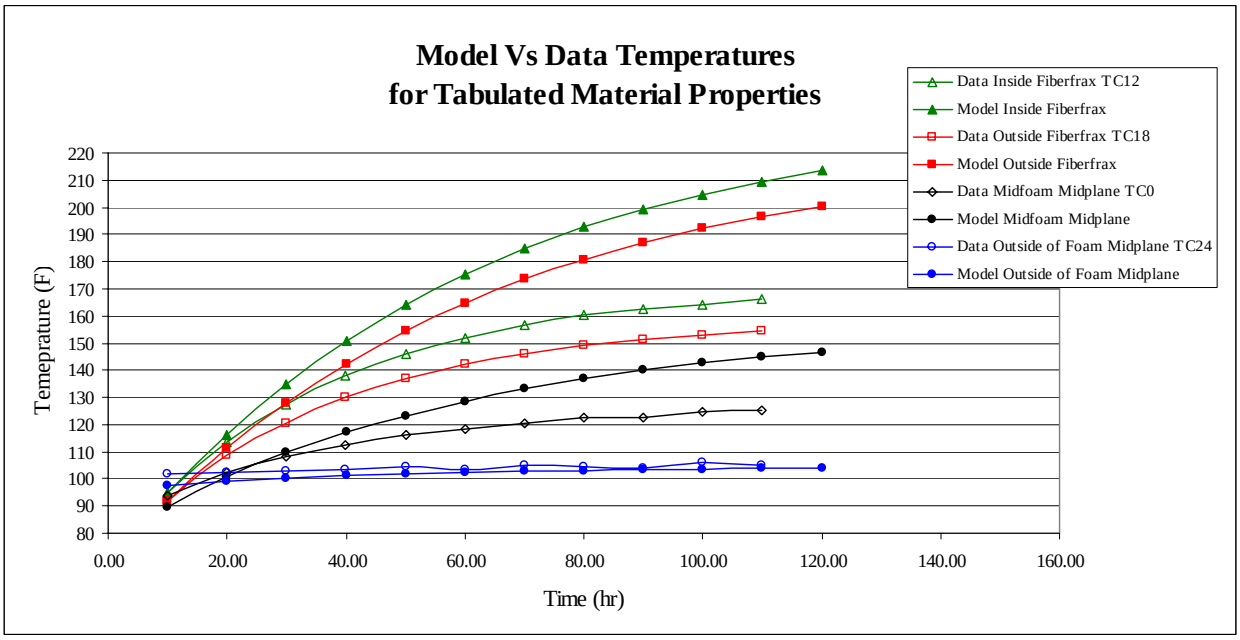

Figure 8 Comparison of test data with model predictions for tabulated data values. Thermocouple locations are shown in Figure 6.

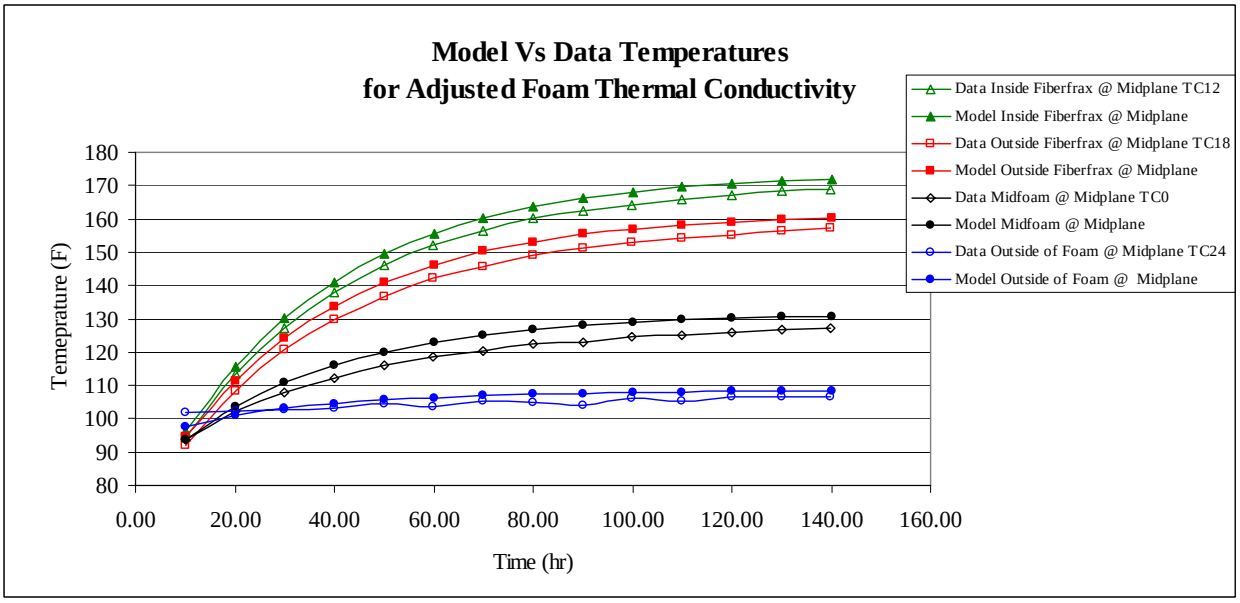

Figure 9 Comparison of test data with model predictions for adjusted foam thermal conductivity. Thermocouple locations are shown in Figure 6.

Table 5 Comparison Between Temperature Measurements and Predictions for the Tabulated and Adjusted Foam Thermal Conductivities With and Without Interior Metal Surfaces at 110 Hours

		Tabulated Foam Thermal Conductivity No Interior Metal Surfaces			Modified Foam Thermal Conductivity No Interior Metal Surfaces			Modified Foam Thermal Conductivity With Interior Metal Surfaces		
Thermocouple #	Data (°F)	Model (°F)	Difference Between Model and Data (°F)	%Error	Model (°F)	Difference Between Model and Data (°F)	%Error	Model (°F)	Difference Between Model and Data (°F)	%Error
T0	125.03	142.68	17.65	14.12	129.65	4.62	3.70	123.46	-1.57	-1.26
T12	166.04	204.82	38.78	23.36	169.56	3.51	2.12	158.07	-7.97	-4.80
T13	106.01	102.40	-3.60	-3.40	102.96	-3.04	-2.87	103.98	-2.03	-1.91
T14	150.94	189.44	38.50	25.51	157.02	6.08	4.03	139.79	-11.15	-7.39
T15	177.37	210.66	33.29	18.77	176.11	-1.26	-0.71	170.71	-6.66	-3.76
T16	110.54	115.13	4.59	4.16	110.44	-0.10	-0.09	108.70	-1.83	-1.66
T17	117.95	126.93	8.97	7.61	116.73	-1.23	-1.04	114.50	-3.46	-2.93
T18	154.36	192.10	37.74	24.45	158.22	3.85	2.50	148.67	-5.69	-3.68
T19	105.96	115.13	9.17	8.65	100.46	-5.50	-5.19	104.79	-1.18	-1.11
T20	118.99	129.63	10.65	8.95	118.54	-0.45	-0.38	116.62	-2.37	-1.99
T22	104.89	103.65	-1.24	-1.18	102.56	-2.33	-2.22	104.30	-0.59	-0.56
T24	105.12	103.65	-1.47	-1.40	108.08	2.96	2.82	106.86	1.74	1.66
T25	184.39	221.55	37.16	20.15	190.19	5.80	3.15	180.57	-3.82	-2.07
T26	158.75	194.85	36.10	22.74	163.90	5.15	3.25	147.99	-10.76	-6.78
T27	127.57	139.91	12.33	9.67	128.76	1.19	0.93	131.80	4.23	3.31
T28	104.91	106.57	1.66	1.58	108.27	3.35	3.20	107.19	2.28	2.17
T29	160.47	196.90	36.43	22.71	163.13	2.67	1.66	158.64	-1.83	-1.14
T31 (Ambient)	103.25	100.00	-3.25	-3.15	100.00	-3.25	-3.15	100.00	-3.25	-3.15
T1,5,6,7avg	185.81	220.44	34.63	18.64	189.71	3.90	2.10	179.97	-5.84	-3.14
T8,9,10,11avg	187.16	223.69	36.52	19.51	192.86	5.70	3.04	182.60	-4.56	-2.44
T2,3,4,30avg	161.56	195.70	34.14	21.13	164.68	3.11	1.93	148.87	-12.69	-7.86
T21,23avg	107.05	101.21	-5.85	-5.46	101.70	-5.36	-5.01	105.28	-1.78	-1.66

Table 6 Interior Surface Emissivities All at 0.3

Surface		Emissivity
CV	304L Stainless Steel	0.30
Drum Liner	304L Stainless Steel	0.30
Bottom of Lid	304L Stainless Steel	0.30
Load Distributor	Aluminum	0.30
Slug	304L Stainless Steel	0.30
Exterior of Drum	304L Stainless Steel	0.21

Table 7 Interior Surface Emissivities All at 0.6

Surface		Emissivity
CV	304L Stainless Steel	0.60
Drum Liner	304L Stainless Steel	0.60
Bottom of Lid	304L Stainless Steel	0.60
Load Distributor	Aluminum	0.60
Slug	304L Stainless Steel	0.60
Exterior of Drum	304L Stainless Steel	0.21

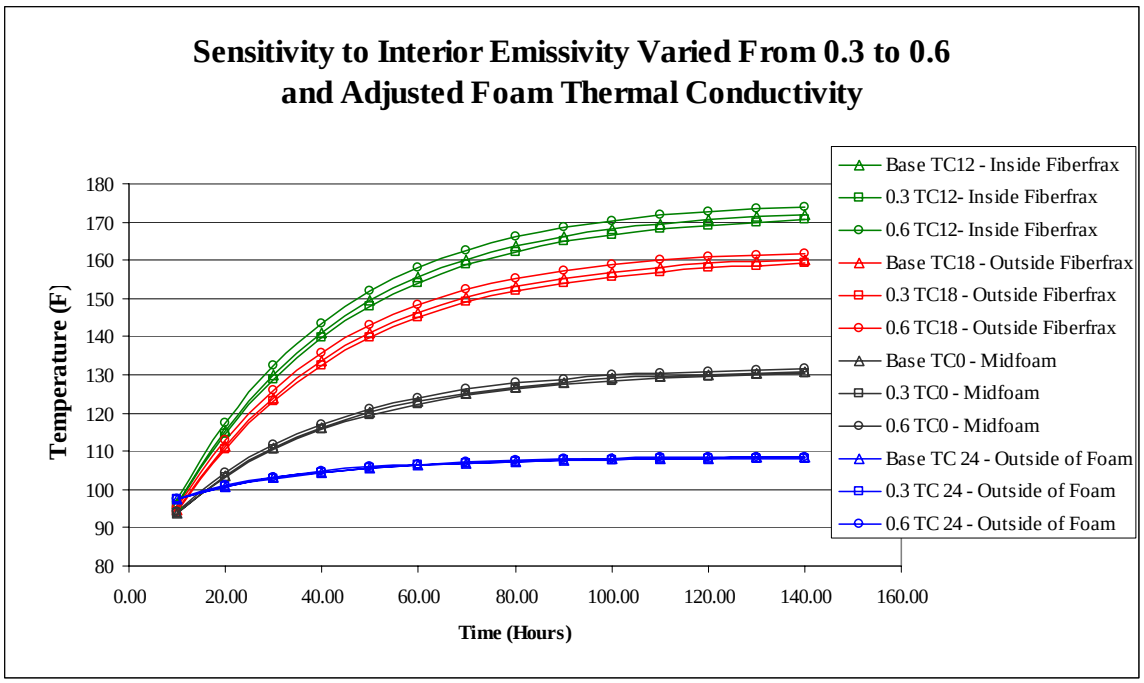

Figure10 Sensitivity of model to interior emissivities, the emissivity of the exterior surface of the package remained at 0.21. Thermocouple locations are shown in Figure 6.

3.0 Description of the NCT Thermal Model

The models for the Normal Conditions of Transport (NCT) were developed using the MSC/Patran-Thermal®[7] general purpose heat transfer software. Boundary conditions used in the models either satisfied or were more limiting than those specified for NCT in 10CFR 71.71[8]. In the thermal analysis, the limiting components are the containment vessel, its O-ring seals, and the Last-A-Foam® insulation. Temperature limits for components of the 9977 for the NCT are tabulated along with predicted maximum temperatures for each individual model. The 9977 model for all NCT analyses includes interior metal surfaces, namely the drum liner, liner around the inner lid and the metal interface between the lid and the lower part of the drum.

General material properties for the NCT analyses are listed in Tables 3 and 4, convection correlations are listed in Table 2 and the nominal emissivities are listed in Table 8. In comparisons between the thermal model and experimental data obtained in Section 2.0, it was found that the tabulated thermal conductivity of the Last-A-Foam® needed to be increased for the model to adequately predict temperatures measured in the test. However, using a lower value for the foam thermal conductivity in the model leads to conservative (higher) temperature predictions for internal components of the package. For this reason, the tabulated (lower) foam thermal conductivities were used in the NCT model. Also, because the Fiberfrax® blanket that surrounds the drum liner was compressed from 1 inch to ½ inch by the expanding foam, its density was assumed to be twice the tabulated value and its thermal conductivity was assumed to be twice that of the uncompressed value. Properties for uncompressed and compressed Fiberfrax® are listed in Table 3. Other specific applications of tabulated parameters are summarized in the description of the NCT model.

Table 8 Surface Emissivities for NCT

Surface	Emissivity
CV	0.30
Drum Liner	0.30
Bottom of Lid	0.30
Load Distributor	0.20
Slug	0.30
Exterior of Drum	0.21

Description of the NCT Model

All NCT calculations were performed under the following conditions:

1. The drum is in an upright position.
2. The bottom surface is adiabatic.
3. There is radiative heat transfer from the sides and top of the drum to the ambient.
4. There is natural convection heat transfer from the sides and top of the drum to the ambient. Natural convection correlations used in the model are listed in Table 2.

5. The ambient temperature is 100°F.
6. There is a total insolation heat fluence of 800 cal/cm^2 over a period of 12 hours on top of the drum and 400 cal/cm^2 over a period of 12 hours on the side of the drum (the absorptivity of the drum is assumed unity for solar radiation). As a conservatism, these heat fluences are applied continuously, rather than as a step function with a period of 12 hours, as prescribed by 10CFR 71.71. The corresponding time averaged heat fluxes are 245.77 Btu/ft^2 hr on the top of the package and 122.88 Btu/ft^2 hr on the side of the package; applied over an infinite amount of time.
7. The foam thermal conductivity is the tabulated value obtained from Reference [9], which is more conservative for the NCT model than thermal conductivity consistent with the experiments discussed in Section 2.0.
8. Material properties for compressed Fiberfrax® were applied to the blanket surrounding the drum liner.
9. The contents contain a heat source outputting 19 Watts of total decay power, distributed over a cylinder approximately 1 inch long with a diameter of 0.25 inches. The cylinder was embedded in a 340L stainless steel slug, see Figure 11.
10. Three source locations were considered, see Figure 11:
    i. Source at the top of the CV.
    ii. Source at the middle of the CV.
    iii. Source at the bottom of the CV.
11. The model was steady-state.

3.1 General NCT Model

Specific compositions and geometries of the contents of the 9977 were not considered in the general NCT thermal analysis. Rather, reasonable but bounding, content configurations were used to predict the maximum component temperatures experienced by limiting components of the package, which were compared to their individual maximum allowable temperatures. The limiting components for the NCT are the containment vessel, the O-ring seals, and the Last-A-Foam® insulation. The general 9977 NCT model focused on the 6CV, but comparisons were made to the 5CV to show that the temperatures of limiting components for the 6CV were bounding.

Because the location of the source affects component temperatures in the 9977, three configurations were considered. The three source configurations were for a source at the top, middle and bottom of the CV, see Figure 11. Each of these configurations consisted of a cylindrical 19 Watt source that was approximately 1 inch long and had a diameter of 0.25 inches. The source was embedded in a cylindrical slug of 304L stainless steel, which was in direct contact with adjacent inner surfaces of the CV. By embedding the source in the cylinder, the distribution of heat generated by the source was more realistic than if the cylinder had been surrounded by air.

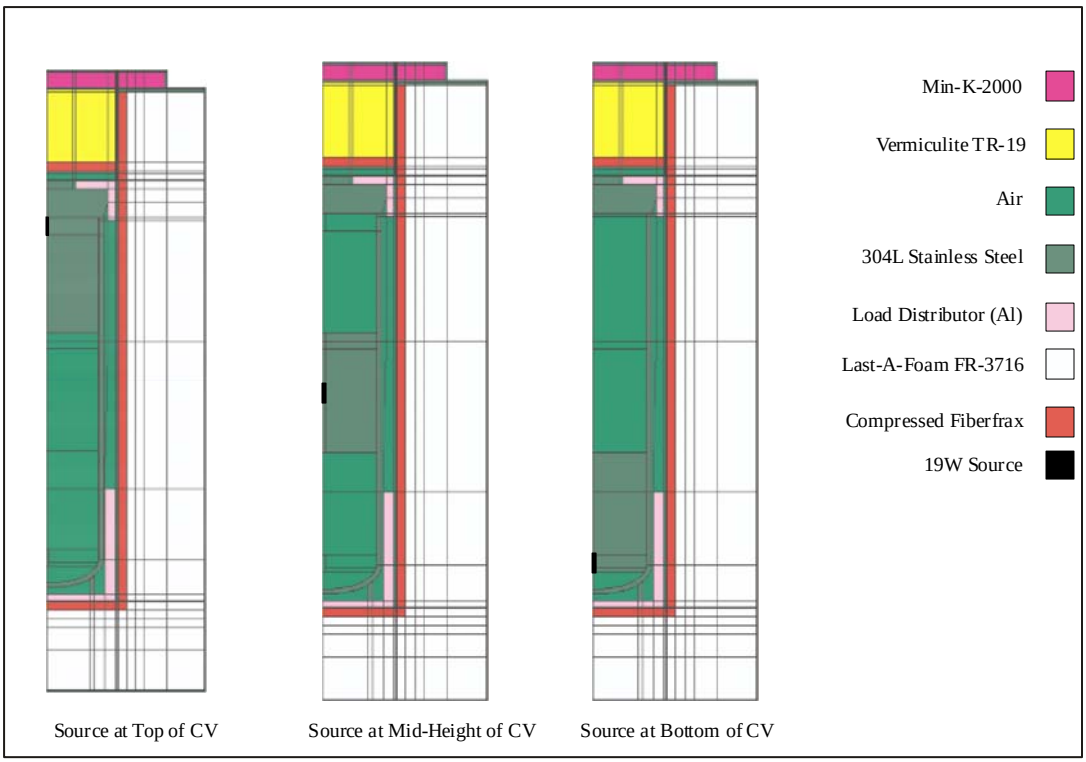

Figure 11 Material configurations for the 9977 6CV used in NCT models.

3.2 RTG NCT Model

A model was developed to evaluate the temperature profile for a representative RTG content configuration under NCT. The RTG was modeled as having 4 heat sources, each producing 4.5W of thermal power. The heat sources were distributed over solid blocks of 304L stainless steel that were embedded in Min-K-2000® insulation. An aluminum framework was used to support the heat thermal generators, see Figure 12. Support for the frame within the CV is effected by thin fin-like springs that do not transfer significant amounts of heat from the RTG's to the walls of the CV. Hence, as an approximation, the spring supports were omitted from the model.

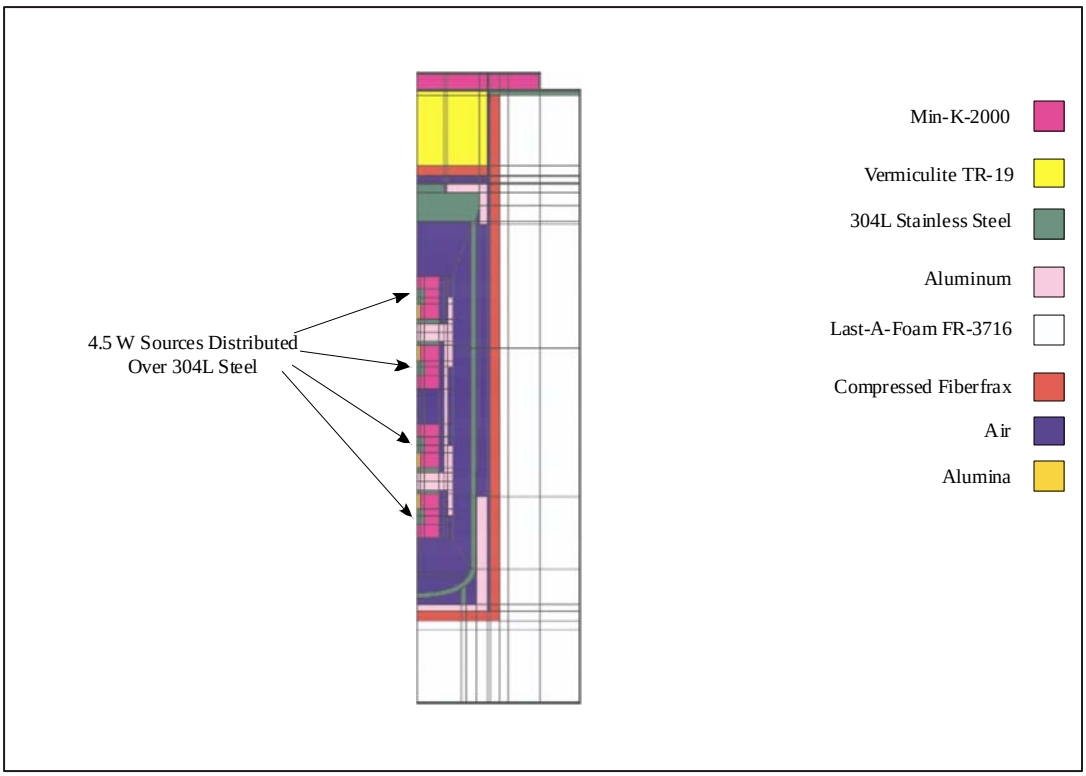

Figure 12 Material configuration for the 9977 6CV with a representative RTG geometry.

3.3 5CV NCT Model

An NCT model for the 5CV was developed to determine whether the temperatures calculated for limiting components of the 6CV were limiting. The material configuration for the 5CV, shown in Figure 13, is similar to that for the 6CV except for the presence of the aluminum spacers. Aside from the dimensional changes required for the 5 inch CV and the inclusion of spacers (modeled as type 1100 Al), the structure, sources and boundary conditions are identical to those for the general case 6CV NCT model.

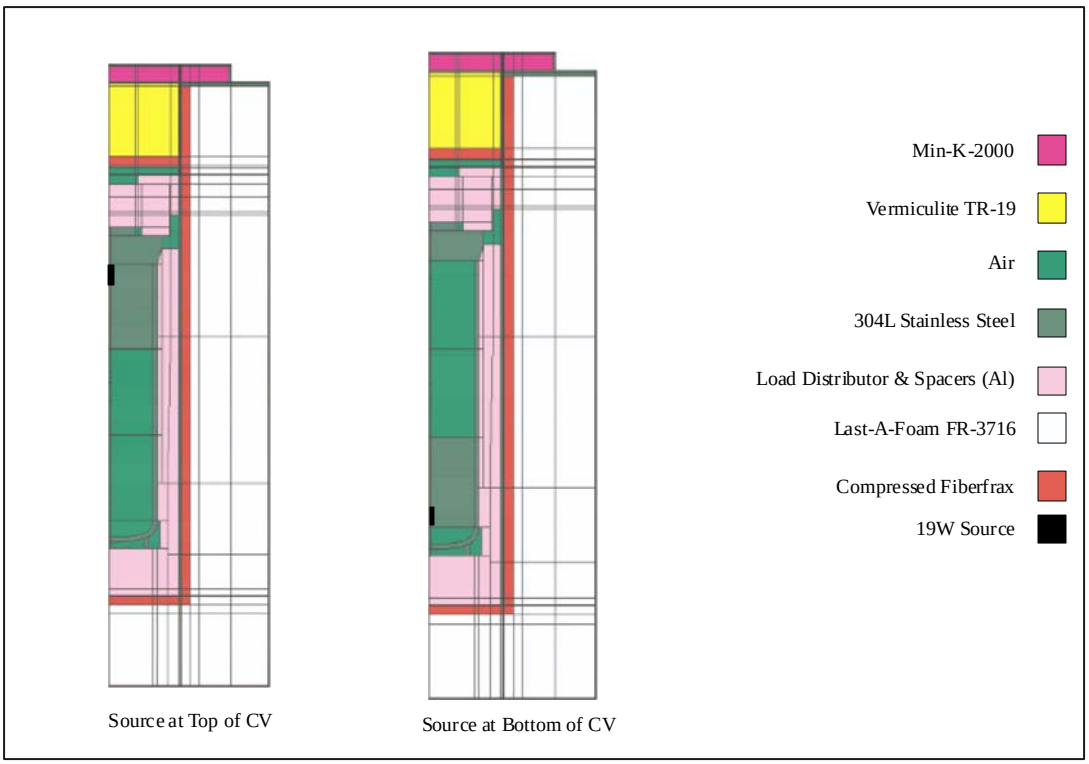

Figure 13 Material configurations for the 9977 5CV used in the NCT models.

3.4 Bare Source Models

As an extreme limiting case for CV temperatures models were developed for bare sources in direct contact with the top and bottom of the 6CV. The model had the same dimensions as used in the 6CV model. Aside from eliminating the 304L slug, in which the sources were embedded, all other material configurations and boundary conditions are the same as for the general case NCT model. The material configuration for the bare source models are shown in Figure 14.

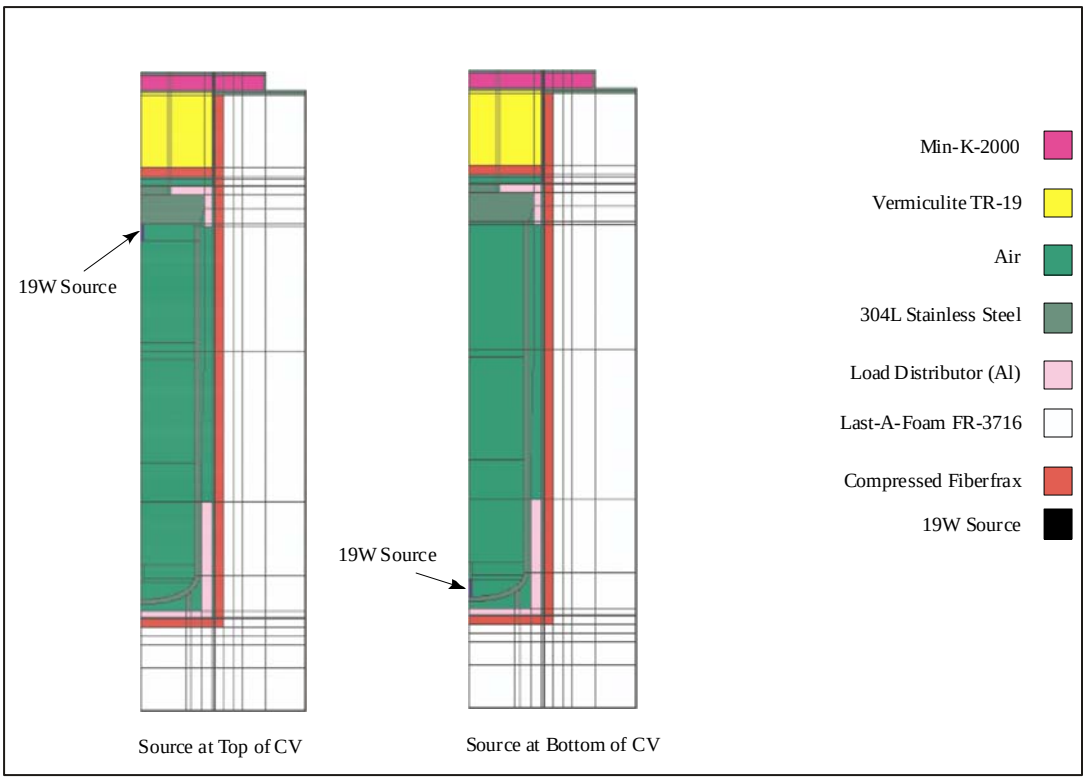

Figure 14 Material configurations for the 9977 6CV bare source NCT models.

3.5 Alternative Material Properties for the Load Distributors

The load distributors are fabricated form Type 6061 T-6 aluminum. However, models for both the 10 CFR 71 NCT and HAC, used type 1100 aluminum properties for the load distributors. To demonstrate that the choice of aluminum properties had little effect, models for the general NCT were re-run with Type 6061 T-6 aluminum properties for the load distributors. Material configurations for these models are those shown in Figure 11.

4.0 Results of the NCT Thermal Analyses

4.1 General NCT Model

The three cases for the general NCT model examined temperature profiles for a cylindrical 19 Watt heat source located at the top, the middle and the bottom of the 6CV. The heat source was 1 in. long and had a diameter of 0.25 in. The maximum predicted temperatures of the limiting components for all three cases are listed in Table 9.

Table 9 Maximum Package Component Temperatures of All Three Source Locations for the General NCT

Component	Maximum Predicted Temperature (°F)	NCT Temperature Limit (°F)
O-rings	302[a]	400
CV	320.5[a]	300
Last-A-Foam® FR-3716	295[b]	300

a Source at top of CV
b Source at bottom of CV

Overall 9977 temperature profiles for each of the three cases are shown in Figure 15, temperature profiles in the CV and foam are shown in Figures 16 and 17, respectively.

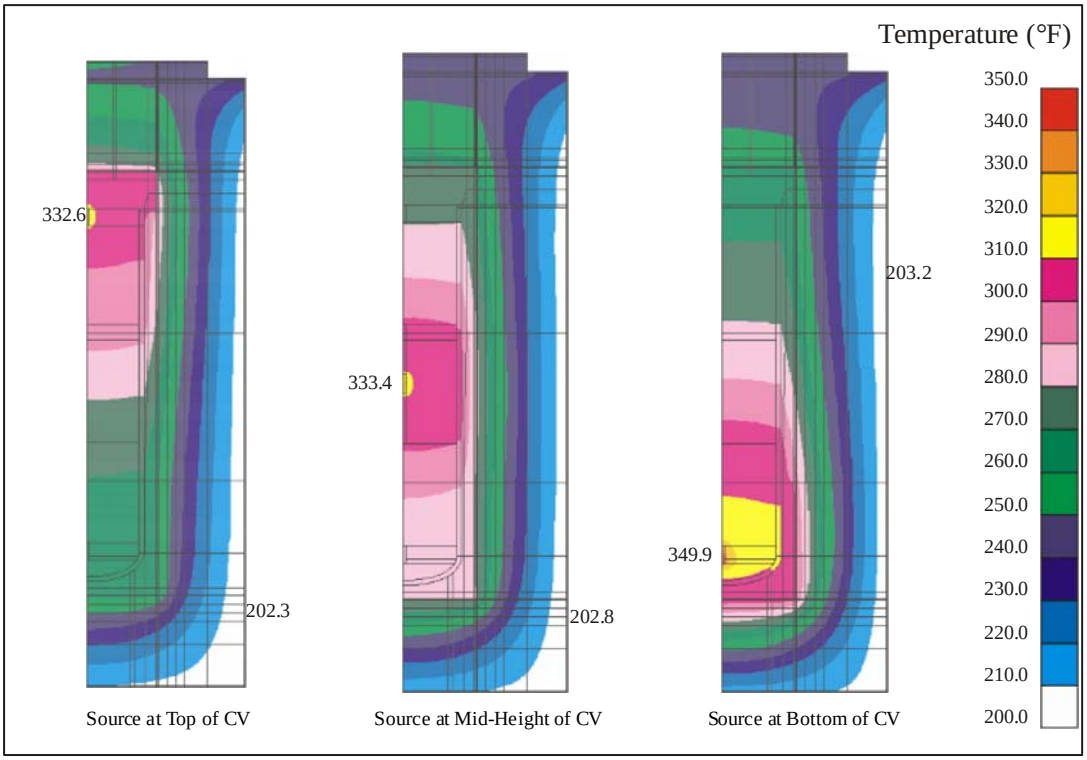

Figure 15 9977 6CV NCT temperature profiles for the three source locations. The centerline of the 9977 is on the left hand side of each figure.

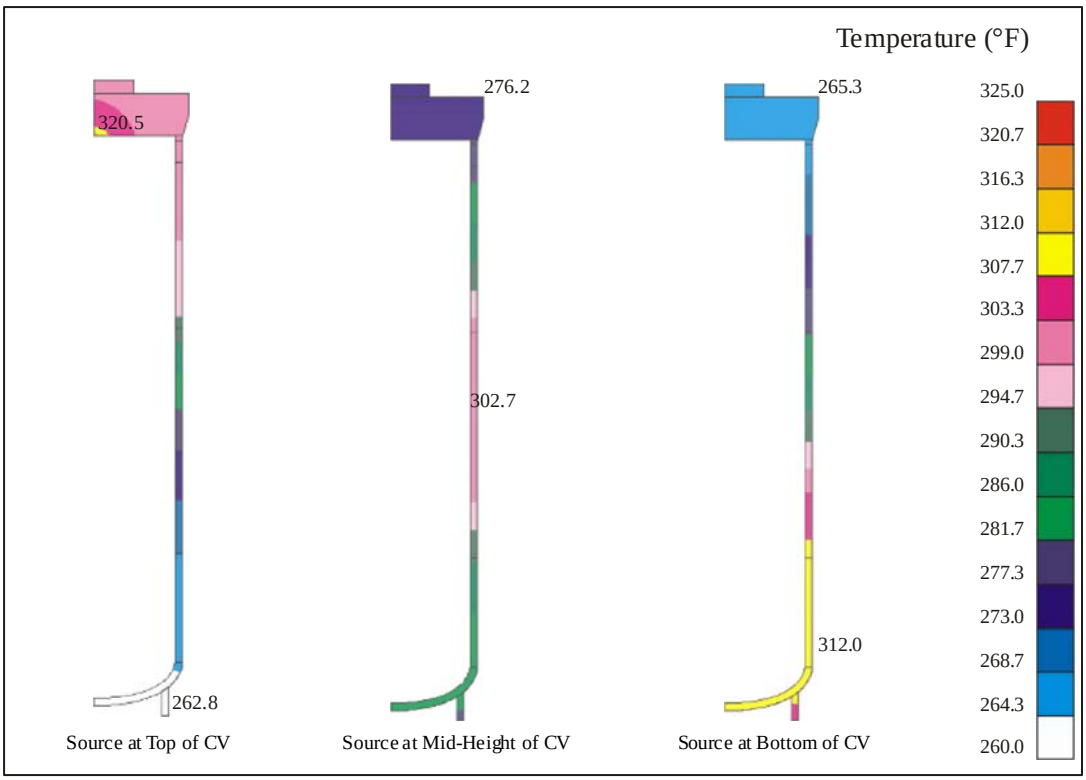

Figure 16 9977 NCT 6CV temperature profiles for the three source locations. The centerline of the 9977 is on the left hand side of each figure.

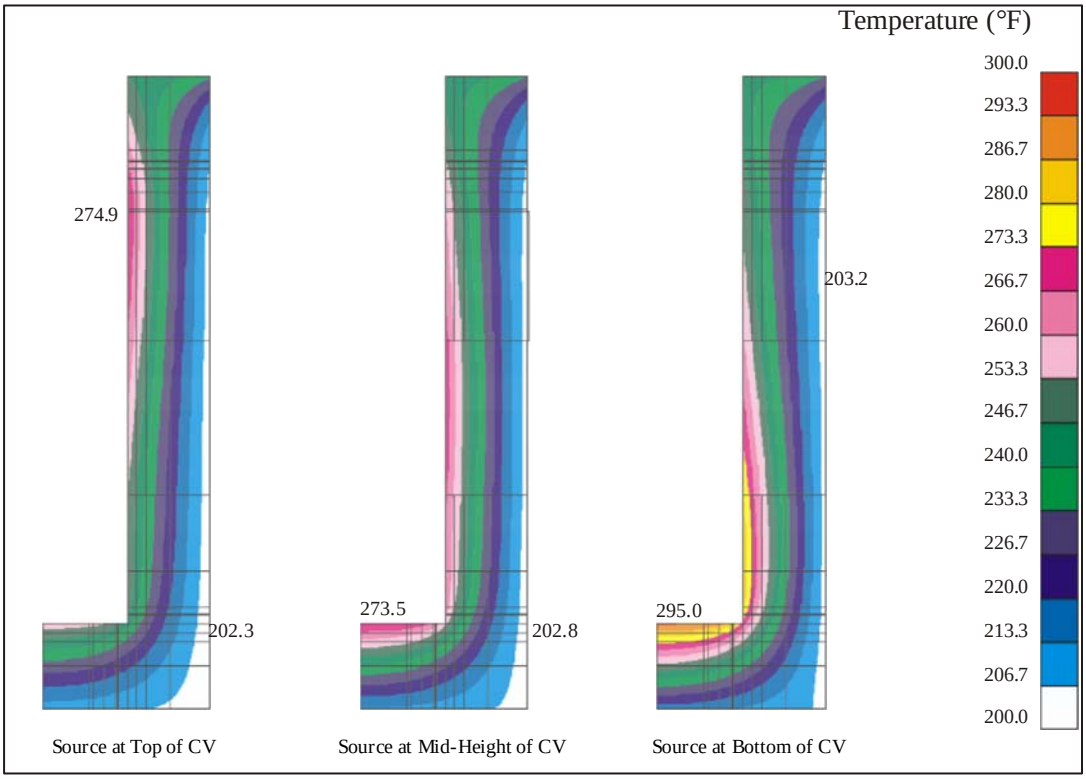

Figure 17 9977 NCT foam temperature profiles for the three source locations. The centerline of the 9977 is on the left hand side of each figure.

4.2 RTG NCT Model

The temperature profile for the RTG thermal model is shown in Figure 18 and the maximum predicted temperatures of the limiting components are listed in Table 10.

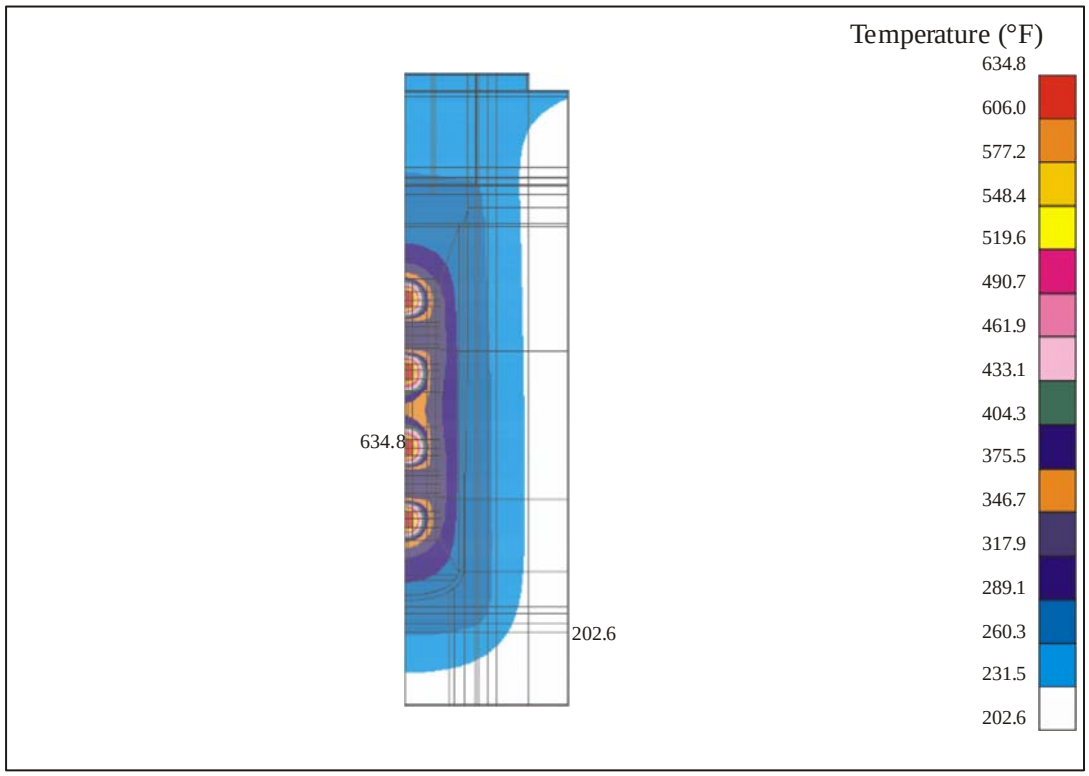

Figure 18 9977 temperature profiles for the RTG under NCT. The centerline of the 9977 is on the left hand side of the figure.

Table 10 Maximum Temperatures of Limiting Components for the RTG Model

Component	**Maximum Predicted Temperature** (°F)	**NCT Temperature Limit** (°F)
O-rings	274	400
CV	288	300
Last-A-Foam® FR-3716	272	300

4.3 5CV NCT Model

In the NCT thermal analyses for the 6CV it was found that bounding temperatures occurred for sources located at the top or bottom of the CV. Hence, to evaluate the NCT

thermal behavior of the 9977 package with a 5CV, cases with a source at the top and bottom of the CV were investigated. The results of these analyses are shown in Figures 19-21. Table 11 lists the maximum temperatures of limiting components.

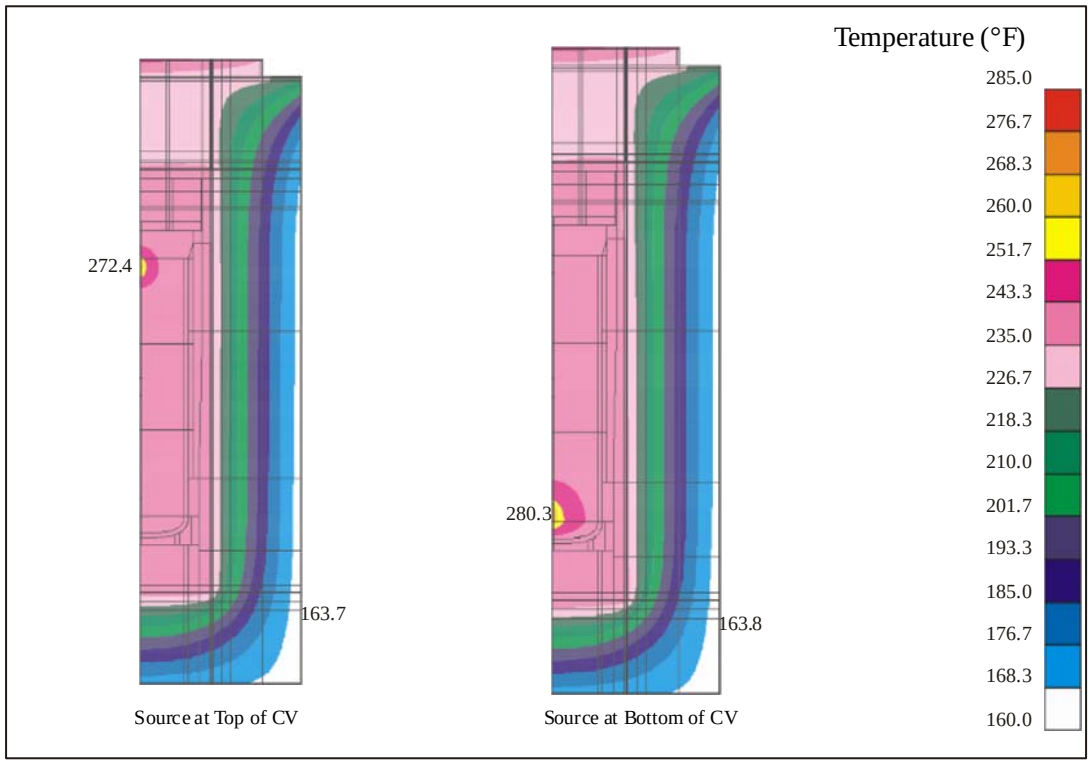

Figure 19 9977 temperature profiles under NCT for the 5CV with sources at the top and bottom of the CV. The centerline of the 9977 is on the left hand side of the figure.

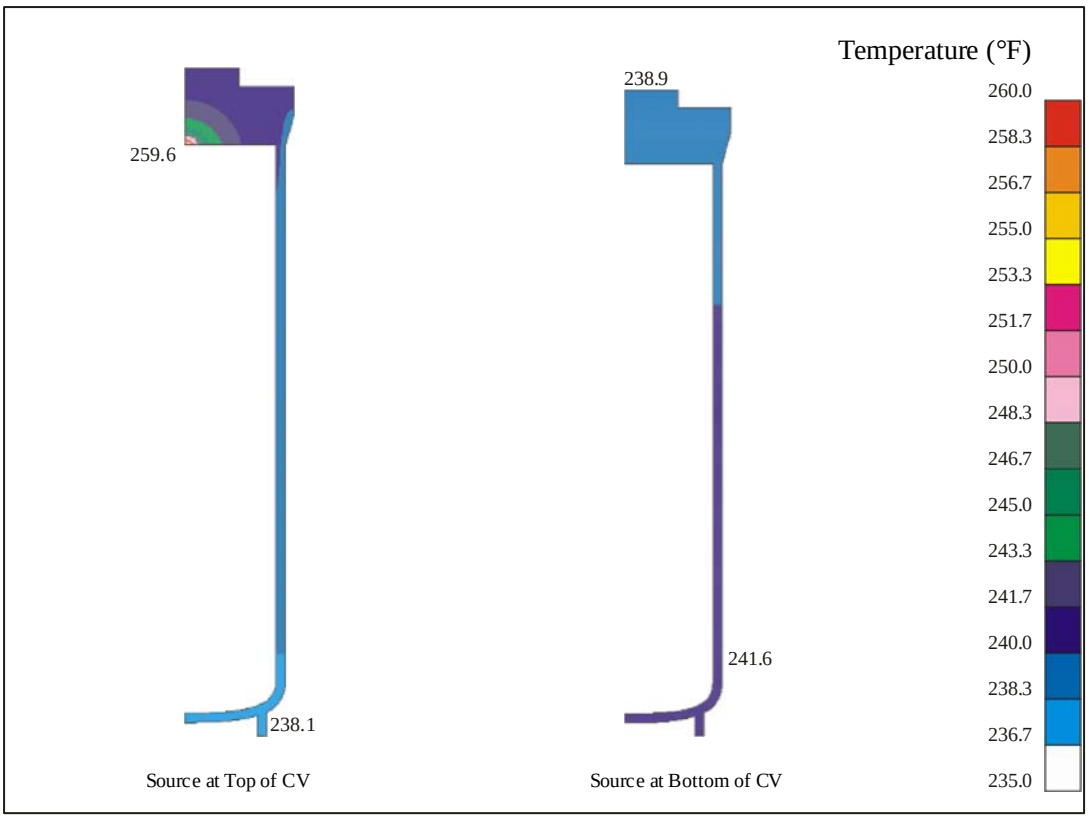

Figure 20 9977 CV temperature profiles under NCT for the 5CV with sources at the top and bottom of the CV. The centerline of the 9977 is on the left hand side of the figure.

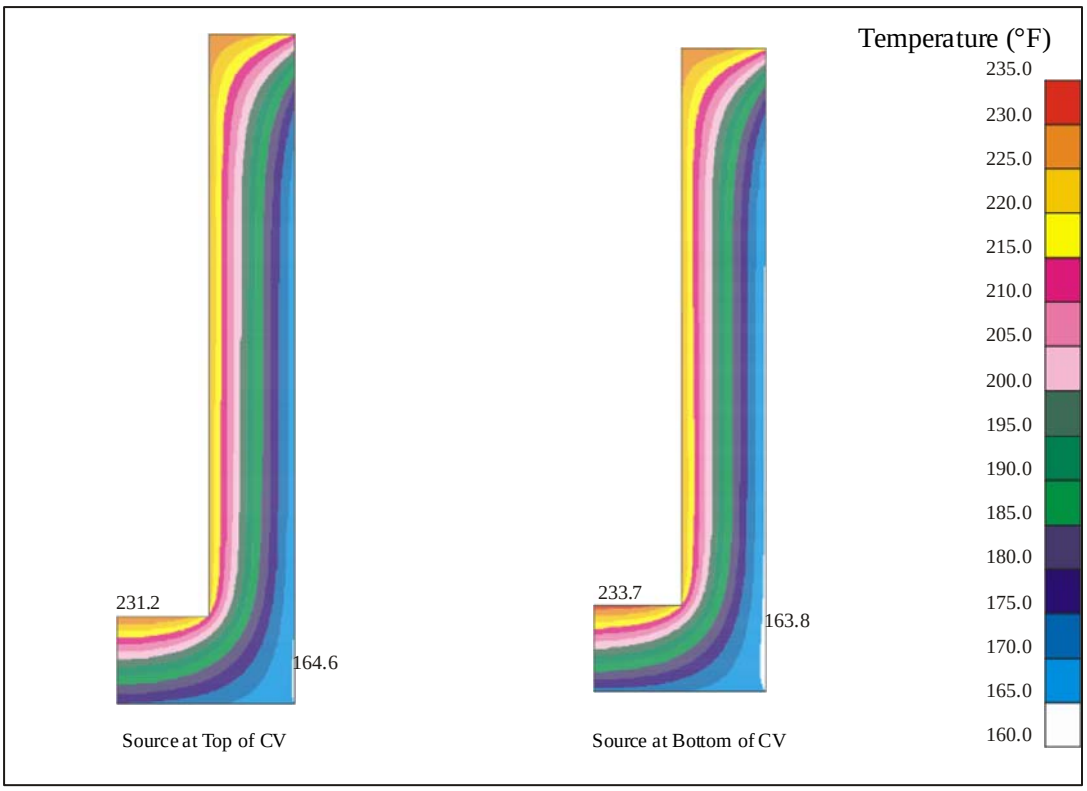

Figure 21 9977 foam temperature profiles under NCT for the 5CV with sources at the top and bottom of the CV. The centerline of the 9977 is on the left hand side of the figure.

Table 11 Maximum Temperatures of Limiting Components for the 5CV Model

Component	**Maximum Predicted Temperature** (°F)	**NCT Temperature Limit** (°F)
O-rings	240[a,b]	400
CV	260[a]	300
Last-A-Foam® FR-3716	234[b]	300

a Source at top of CV
b Source at bottom of CV

4.4 Bare Source Models

The temperature profiles for the bare source models for the 9977 6CV NCT are shown in Figures 22-24. Figure 22 shows the overall temperature profile, Figure 23 shows the temperature profiles in the CV and Figure 24 shows the temperature profiles in the foam. The maximum predicted temperatures of the limiting components for all three cases are listed in Table 12.

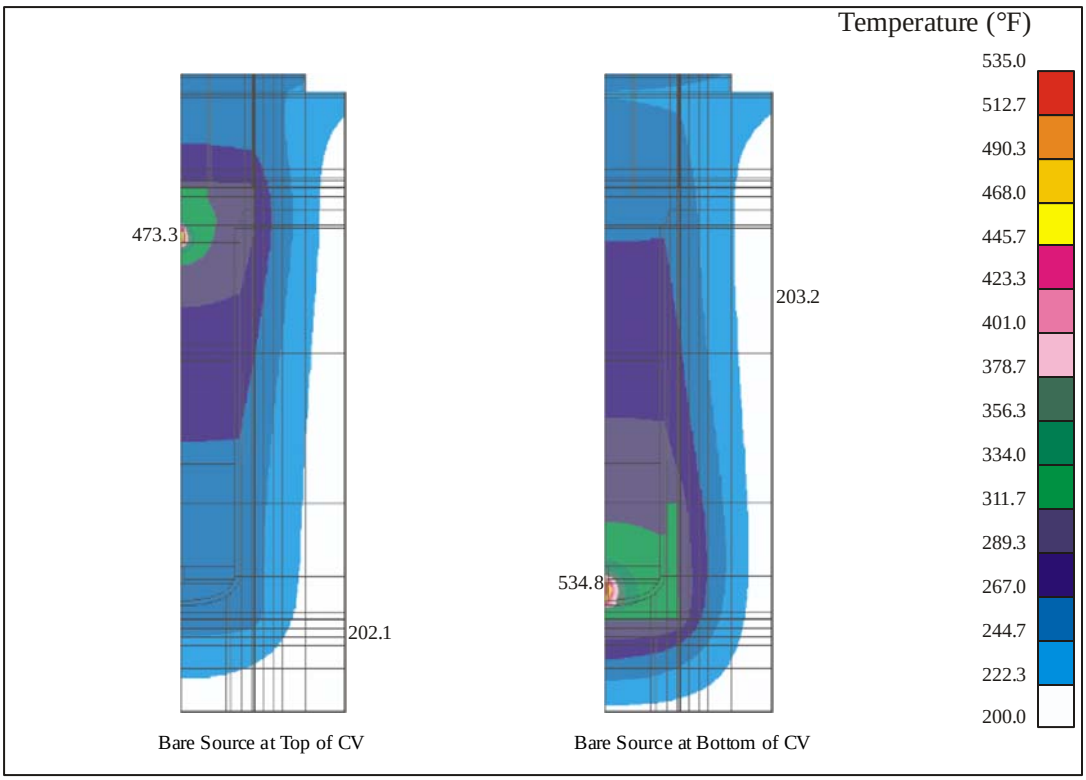

Figure 22 9977 NCT temperature profiles for the upper and lower bare source locations. The centerline of the 9977 is on the left hand side of each figure.

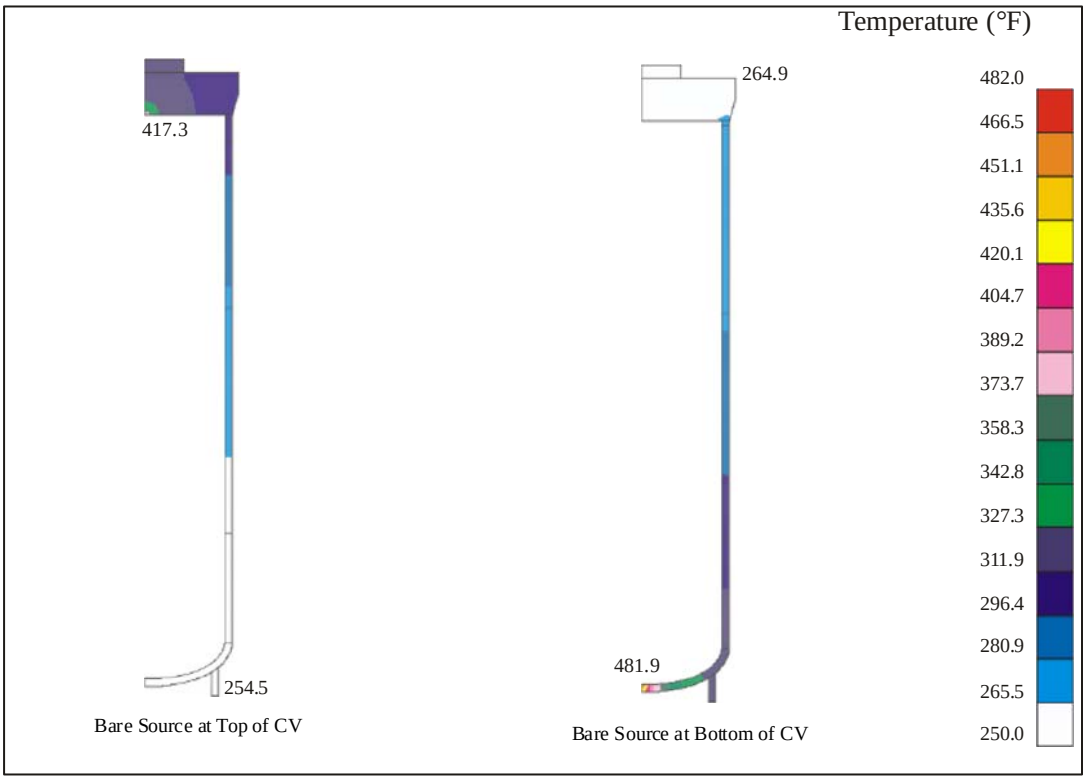

Figure 23 9977 NCT CV temperature profiles for the upper and lower bare source locations. The centerline of the 9977 is on the left hand side of each figure.

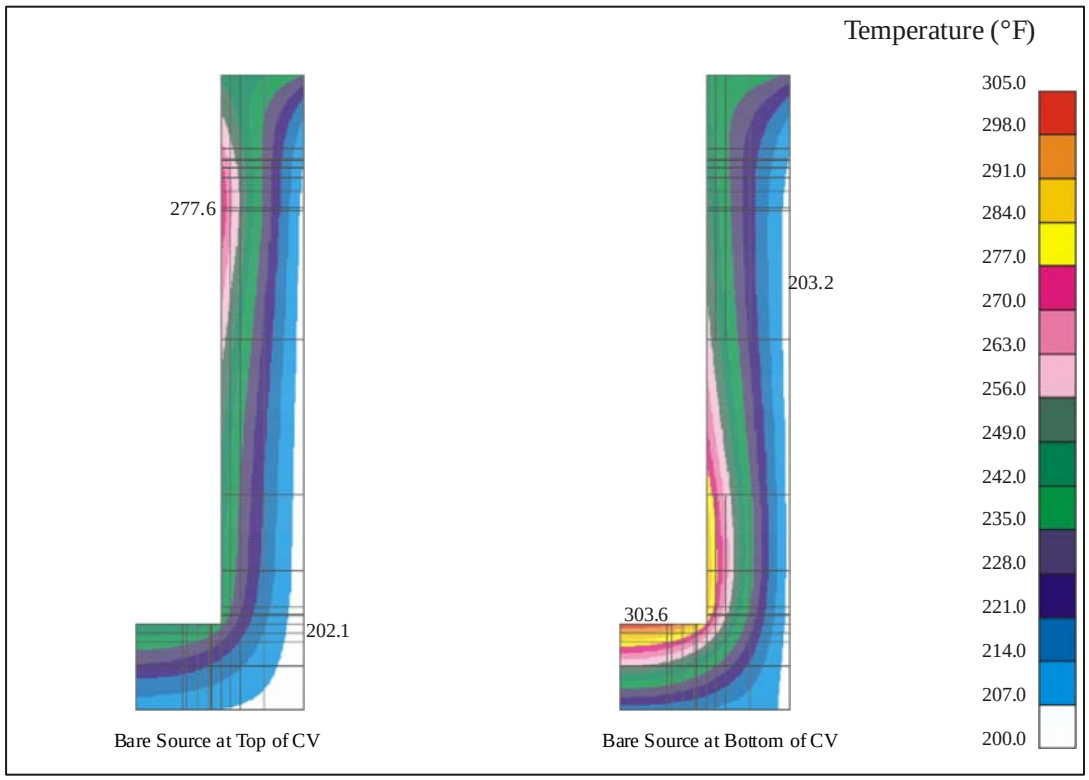

Figure 24 9977 NCT foam temperature profiles for the upper and lower bare source locations. The centerline of the 9977 is on the left hand side of each figure.

Table 12 Maximum Temperatures of Limiting Components for the Bare Source Model

Component	**Maximum Predicted Temperature** (°F)	**NCT Temperature Limit** (°F)
O-rings	310[a]	400
CV	482[b]	300
Last-A-Foam® FR-3716	304[b]	300

a Source at top of CV
b Source at bottom of CV

4.5 Alternative Material Properties for the Load Distributors

Changing the material properties for the load distributors from type 1100 aluminum to type 6061 T-6 aluminum resulted in very little difference in the temperature profiles. The maximum CV temperature increased by approximately 2.2°F, while in the foam the difference between the maximum temperatures increased by approximately 1.6°F.

5.0 Conclusions

5.1 Model Validation Test

Once the thermal conductivity of the Last-A-Foam® was increased relative to the value provided by the General Plastics Company, the temperatures predicted by the model were in good agreement with those measured in the environmental chamber tests. Because the use of a lower foam thermal conductivity is more conservative for NCT, producing higher temperatures in the CV and foam, the tabulated foam thermal conductivity was used in the NCT models for the SARP.

It was also found that the temperature profile predicted by the numerical model shows little sensitivity to emissivities of internal surfaces. Hence, changes in the emissivities of the internal surfaces of the package caused by oxidation or other effects, will not significantly affect the temperature profile.

5.2 NCT Models

For all NCT models the insolation heat flux on the top and sides of the package was assumed to be the total insolation fluence, specified in 10CFR 71.71, averaged over 12 hours and applied continuously. The ambient external temperature was held constant at 100°F. The NCT calculations were steady-state, thus implying the boundary conditions persist for an infinite period of time.

NCT thermal calculations performed for the 9977 6CV considered a 19 Watt internal source in the form of a 1 inch long cylinder with a 0.25 inch diameter, embedded in a 304L stainless steel slug, at three axial locations. These three cases represent bounds on contained 19 Watt sources transported in the 6CV 9977 package. For these configurations the predicted foam and O-ring temperatures did not exceed their respective limits. The CV exceeded its limit by 21°F, which will not affect its material properties.

As a more realistic model, the NCT calculations were repeated for the RTG configuration containing four 4.5 Watt sources. The predicted temperatures of the foam, O-rings and CV did not exceed their respective limits.

The 6CV NCT thermal model was applied to a 5CV configuration. Two cases were considered, a source at the top of the CV and a source at the bottom. Predicted foam, O-ring and CV temperatures for this model did not exceed the limits of these components.

NCT models were run for the 6CV with a bare 19 Watt source, in the form of a 1 inch long cylinder with a 0.25 inch diameter, either touching the top of the CV or touching the bottom of the CV. Predicted O-ring temperatures were within the temperature limits. The foam temperature limit was exceeded by approximately 4°F over a local region below the base of the CV when the source was located at the bottom of the CV, see Figure 24 and Table 12.

Changing the properties of the load distributors from Type 1100 to Type 6061 T-6 Al resulted in temperature differences less than or equal to 2.2°F.

6.0 References

1. S-SARP-2006-00001, Safety Analysis Report-9977 Packaging, Rev. 0, WSRC, (2006).
2. Drawings
   - R-R1-G-00020, Rev.0
   - R-R1-G-00021, Rev.0
   - R-R2-G-00017, Rev.0
   - R-R2-G-00018, Rev.0
   - R-R2-G-00019, Rev.0
   - R-R2-G-00042, Rev.0
   - R-R2-G-00043, Rev.0
   - R-R4-G-00032, Rev.0
   - R-R4-G-00033, Rev.0
3. Parker O-ring Handbook ORD-5700a, The Parker Seal Group, Parker Hannifin Corp., Cleveland OH (2001).
4. Society of Automotive Engineers, Aerospace Recommended Practice, 5316, Rev. B.
5. Experimental Validation of GPFP Thermal Model, FP-1034, Rev. 0, WSRC, (2005).
6. 9977 Thermal Benchmarking Test, S-TSM-A-00001, WSRC, (2005).
7. MSC.PATRAN THERMAL 2003 r2, Online Manual, MSC Software Company, Santa Ana, California.
8. Packaging and Transportation of Radioactive materials, Code of Federal Regulations, Title 10, Part 71, Washington, DC (2002).
9. General Properties Last-A-FoamFR-3700 for Crash and Fire Protection of Nuclear Material Shipping Containers, General Plastics Manufacturing Company, Tacoma WA.

This Page Intentionally Left Blank

APPENDIX 3.2

SRNL PACKAGING BURN TEST REPORT

NT-TDR-06-101

This Page Intentionally Left Blank

Document Control Number: NT-TDR-06-101
Revision Number: 01

SRNL PACKAGE BURN TEST REPORT

March 27, 2006

John Malloy
NOVATECH
Innovative Technologies International

Submitted to: WSRC
Contract No. AC45707N

REVIEWED: RF Rochow **Date:** MAR 27, 2006

APPROVED: MW Ade **Date:** 3/27/06

220 Jefferson Ridge Parkway Lynchburg, VA 24501 Tel: 434.239.1979 Fax: 434.239.6232

Table of Contents

Background:

NovaTech provided technical support to assist the Savannah River National Laboratory (SRNL) in the development of their General Purpose Fissile Package version 1 (GPFP), which for Certification has been designated the 9977. Record documents may still use the GPFP designation for the 9977 Packaging. With the support of the South Carolina Fire Academy (SCFA), one of their burn props was modified to support these burn tests. Five tests were performed between December 1 and December 14, 2005. These tests were performed according to the methodology described in NovaTech test plan NT-TDR-05-105 (Reference 1) and according to test procedure NT-TDR-05-106 (Reference 2), "SRNL Package Burn Test Procedures" (December 2005), which was reviewed and approved by WSRC before the testing. The procedures and the resulting tests were performed to satisfy 10 CFR 71.73 (Reference 3) and were performed in accordance with ASTM-E220-02 (Reference 4) except for the use of thick-walled calorimeters. As explained in the Test plan, these were replaced with directional flame thermometers (DFT's).

Evaluation by Test

In addition to thermal analysis, the 9977 was evaluated by full-scale thermal testing. This testing was performed using one of the training props at the South Carolina Fire Academy (SCFA) in Columbia, SC. This prop consists of a concrete walled pool, roughly 12 feet across the outside walls and 12 inches high (Figure 1). Water and fuel lines run from central pumping stations into the pool. A drain is provided to empty the pool when desired. A stand-pipe system maintained a constant water level during the testing even with constant water addition to the pool.

The pool inside the prop was approximately 11 feet square (3.4 m). For burns with the package in a vertical orientation, surface of the pool extended approximately 56 inches (1.4 m) beyond the sides of the package. When the package was horizontal, the pool extended approximately 48 inches (1.2 m) beyond two ends and 56 inches (1.4 m) beyond the sides. Fuel was continually pumped into the pool and distributed by a manifold under the surface of the water that surrounded the test package and stand to ensure that the pool surface was completely covered by fuel The prop had a flat floor allowing the use of a metal stand to place the test article the proscribed 1.0 meters above the surface of the pool.

The South Carolina Fire Academy provided the basic infrastructure needed to perform the fire tests. This included:

- Appropriately sized burn pool,
- Water distribution and drain system,
- Fuel storage and distribution system,
- Trained personnel to maintain the infrastructure and handle fire safety,
- Federal and state permits to allow extended burns with a kerosene like fuel.

The facility was modified, however, to perform the burn tests. These modifications included:

- A structure to mitigate the effects of wind so that the package remains fully engulfed by the fire and to support/protect instrumentation,

- A structure to hold the test article one meter above the surface of the pool,
- A structure to insulate the package during the preheat before the fire test.

Figure 1 – Test Site at South Carolina Fire Academy (Viewed from SW)

The high temperature wind fence was fabricated in two modular sections, each covering half of the pool perimeter. The support frame was fabricated from two-inch schedule 40 steel pipe and two inch pipe fittings. The frame was water-cooled with an inlet at the bottom of the center support leg, and exits at the bottom of the other four legs. An additional outlet was provided above each thermocouple junction box to provide cooling for the instrumentation wiring. Galvanized chain link fencing, 48 inches tall, was attached to the frame to support ½ inch thick alumina-silica blanket insulation on the inside face of the fence structure. The bottom of the fence was not covered with insulation to provide a flow path for combustion air to enter the pool fire. With the insulation in place, the inside dimensions of the fence structure were 135 x 140 inches, with the fence extending approximately 52 inches above the surface of the pool. The modified site with the wind fence is shown in Figure 2.

The 9977 test articles were held by a water-cooled, steel support structure. The water cooling feature was used to assure the support structure retained its mechanical strength and maintained the test article position and orientation throughout the thermal test. This structure consisted of four vertical four-inch schedule 40 pipes cross connected by two-inch schedule 40 pipe, one meter above the surface of the pool, all welded to a base constructed from welded steel channel. The support structure was wrapped with an inch of Kaowool insulation to:

- reduce the heat transfer to the structure,
- minimize the potential for cooling of the flames around the test article, and
- insulate the test article from the water-cooled stand.

An un-cooled steel grating with vertical supports was mounted on the stand to support the test articles and prevent tipping when they were mounted in a vertical orientation. The test stand is shown in Figure 3.

Figure 2 – Test Site With Wind Fence and Instrumentation Data Recorders

A cover, made from two-inch thick Styrofoam® aluminized on the outside side, was used to protect the test article and electrical heaters before the burn test. This cover was approximately 29 x 43 inches in cross section and 50 inches tall. After a heated test article was transported to the burn site, electrical heaters were installed, test article was mounted on the test stand, and the Styrofoam® cover was lowered over it. Sufficient fiberglass insulation was secured under the package to minimize heat loss below the test article. This is shown in Figure 4.

Figure 3 – Test Article Support Stand

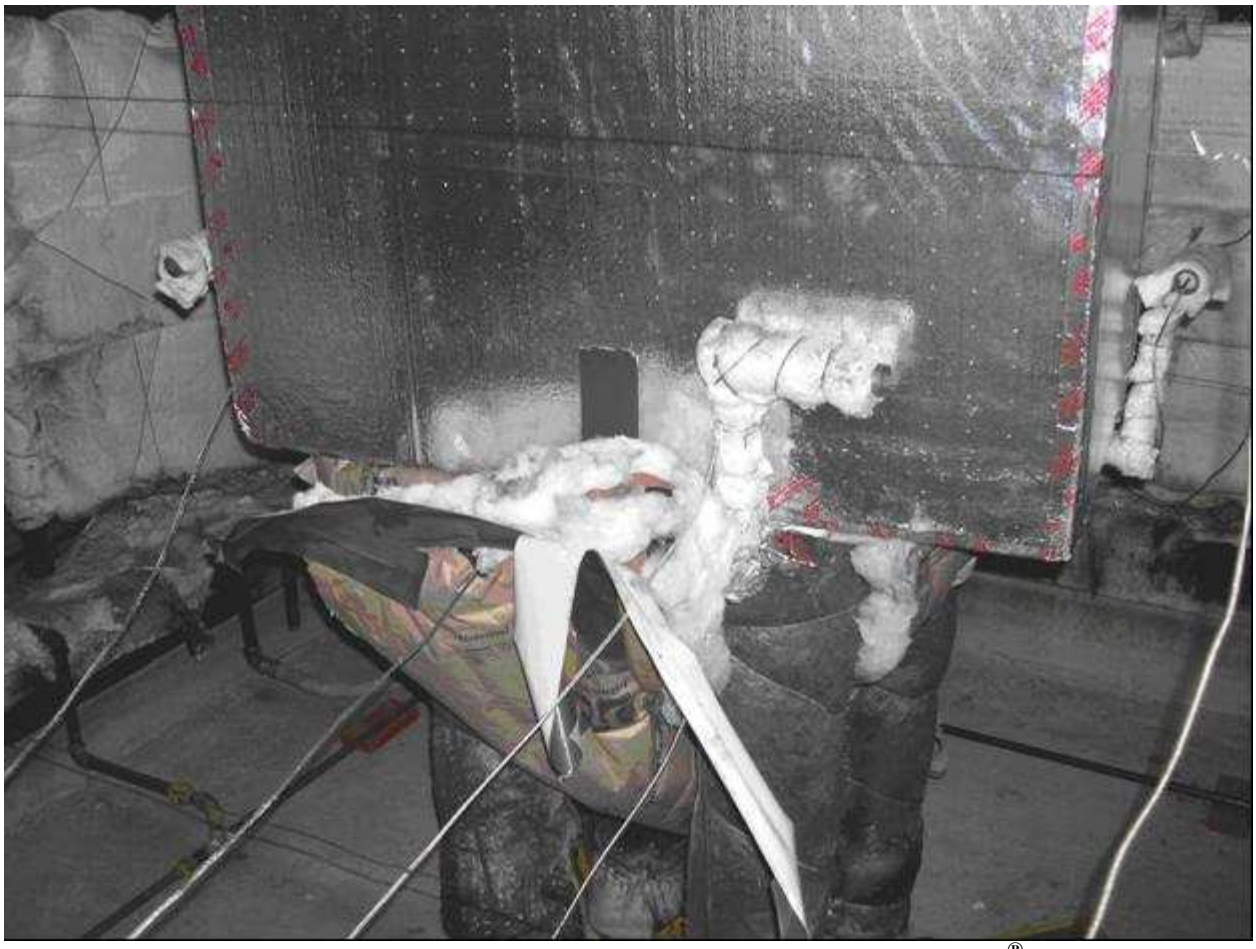

Figure 4 – Fiberglass Insulation at the Bottom of the Styrofoam® Cover

Five packages were subjected to burn tests. One was a semi-prototypical package with only Fiberfrax® insulation instead of having both polyurethane foam and Fiberfrax® insulation around the liner. This package was used for practice to verify all burn test equipment and procedures. Four packages were burn tested after they had been subjected to mechanical testing. The order and orientation of the packages in the burn tests are shown in Table 1. Figures 5 and 6 show the test articles in vertical and horizontal orientations respectively.

Table 1 – Package Orientations for Burn Test

Burn Test	Package	Orientation	End Facing Down
Practice	Practice Package	Vertical	Bottom
Regulatory Burn 1	SN-2	Vertical	Top
Regulatory Burn 2	SN-4	Vertical	Bottom
Regulatory Burn 3	SN-5	Vertical	Bottom
Regulatory Burn 4	SN-3	Horizontal	NA

Figure 5 – Test Article in Vertical Orientation

Figure 6 – Test Article in Horizontal Orientation

Fourteen thermocouples were used in each test. Four were mounted inside insulated enclosures with one side of the enclosures open to measure radiative flame temperatures. These are called directional flame thermometers (DFTs) and were mounted on the test stand facing away from the package. Eight thermocouples were mounted approximately 24 inches (0.61 m) away from the package at the corners of the pool. These thermocouples were suspended by metal wires. Four of these thermocouples were located approximately 30 inches (0.76 m) above the pool surface before the test and four were located approximately 56 inches (1.42 m) above the pool surface at the beginning of the test. Thermal expansion of the wires holding these thermocouples allow the thermocouples to sag between 6 and 8 inches (15 and 20 cm) below their pre-test height during the burn. One thermocouple was mounted on the top of the test article and a second was mounted on the un-cooled grating directly below the test article. The thermocouple locations are shown in Figure 7.

The male connectors of the thermocouples were attached via female connectors to 20 gage, Teflon coated, duplex insulated thermocouple wire in two connection boxes at the North and South ends of the fire enclosure. The boxes were mounted on the inlet water pipes and were wrapped with Kaowool insulation. The thermocouple wire was routed down the inlet water pipe, and also protected by Kaowool insulation. Two sets of 6 wires each were run to where they connected to two OM-CP-OCTTEMP data loggers, one each on the North and South sides of and a safe

distance away from the burn facility. The two package thermocouples were run from the connection box and were connected to an Omega instruNet Model 100 Analog/Digital Data Acquisition System and a notebook computer to allow real-time monitoring of the temperatures above and below the package during the burn tests.

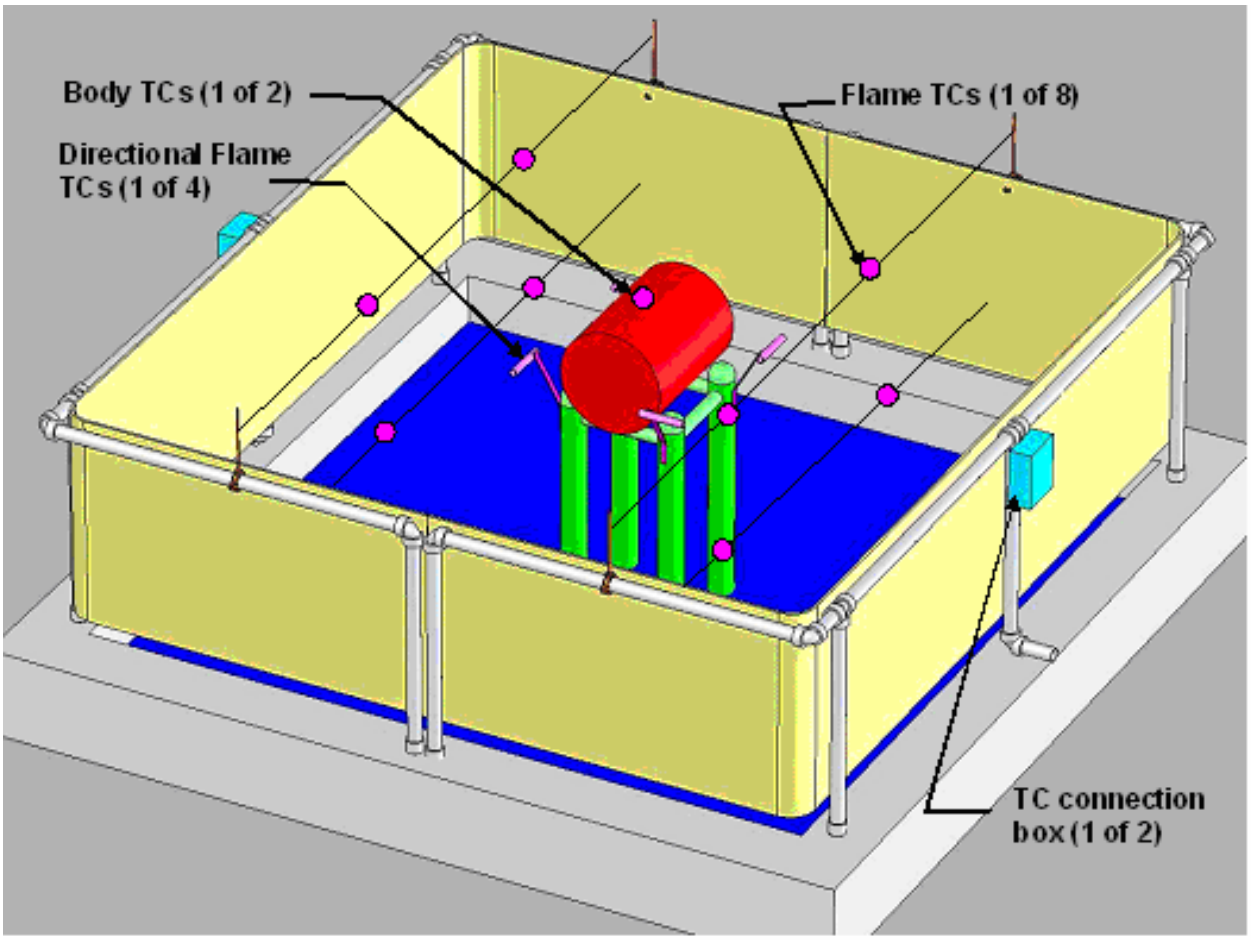

Figure 7 – Location of Thermocouples

Thermal Evaluation Under Hypothetical Accident Conditions

According to 10 CFR 71.73, the package is to be subjected to a thermal test. "Thermal exposure of the specimen fully engulfed, except for a simple support system, in a hydrocarbon fuel/air fire of sufficient extent, and in sufficiently quiescent ambient conditions, to provide an average emissivity coefficient of at least 0.9, with an average flame temperature of at least 800ºC (1475ºF) for a period of 30 minutes, or any other thermal test that provides the equivalent total heat input to the package and which provides a time averaged environmental temperature of 800ºC. The fuel source must extend horizontally at least 1 m (40 in), but may not extend more than 3 m (10 ft), beyond any external surface of the specimen, and the specimen must be positioned 1 m (40 in) above the surface of the fuel source. For purposes of calculation, the surface absorptivity

coefficient must be either that value which the package may be expected to possess if exposed to the fire specified or 0.8, whichever is greater; and the convective coefficient must be that value which may be demonstrated to exist if the package were exposed to the fire specified. Artificial cooling may not be applied after cessation of external heat input, and any combustion of materials of construction, must be allowed to proceed until it terminates naturally."

The 9977 certification process will rely on full-scale burn tests to demonstrate the acceptability of the design. In addition to one practice article, four test articles were burn tested. Each test article had been subjected to the entire suite of 10 CFR 71.73 regulatory testing before the burn tests were performed. Burns were conducted in a manner so as to ensure full engulfment of the package (except for transitory movement of flames) and exposure to flame temperatures greater than 800°C.

Initial conditions

The 9977 is a Type B package that contains radioactive materials during transport. The resulting decay heat rate can result in significant differential temperatures between the inside and outside of the package. To correctly model this characteristic, all of the test articles used in the regulatory tests were placed in a thermal chamber at SRNL for at least four days to heat them to a uniform 93°C. Approximately 20 hours before the burn test, a test article was removed from the chamber, wrapped in fiberglass and/or mineral wool insulation and transported to the SCFA site. There it was unwrapped and placed on the test stand. Thermocouples were attached by wire to the package and two, 750 W band heaters were installed. Each band heater was three inches (7.6 cm) wide and attached tightly to the drum using a spring connector. The test article was then rewrapped with fiberglass insulation, and the Styrofoam® cover was emplaced. Insulation was also wrapped under the support grate to minimize heat loss through the bottom of the package. This procedure was modified in the last test where the package was tested horizontally. The Styrofoam® cover was not used. Instead, insulation was placed completely around the test article and covered with a tarp that was secured under the test stand grate to serve as an additional wind and vapor barrier.

The ambient temperature before the first regulatory test was approximately 2°C. The thermocouple near the top of the test article read 18°C. In regulatory test 2, the settings on the band heaters were changed and, even though the air temperature before the burn was 0°C, the DFT thermocouples that were enclosed next to the test article were 60 to 75°C depending on the location. Before the third regulatory test, the air temperature was approximately -1°C. The DFT temperatures before the insulation was removed were 20°C. In this case, some of the insulation was placed between the DFTs and the package causing a lower reading. Before regulatory test four, the thermocouple on the top of the package read 52°C and the thermocouple on the test stand grate (below the package) read 16°C. The ambient temperature was approximately 0.5°C.

In all tests, the package was uncovered and the drum heaters removed approximately one hour before the beginning of the burn test. As a result, the package outer shell temperature dropped to near ambient temperature. Due to the insulating polyurethane, there would have been little change in the internal component temperatures.

Fire Test Conditions

By scheduling tests to minimize wind and through the use of the wind fence, burn conditions exceeded regulatory requirements. Full engulfment was achieved (Figure 8) except for limited periods of time during the second regulatory burn test (Figure 9). This test was extended to 35 minutes to ensure regulatory requirements were met.

Temperatures were measured by type K thermocouples in the flames around the package (8), in DFTs (4) and loosely attached to the top and bottom of the package. Temperatures were recorded every 5 seconds at these locations. In addition, a hand-held infrared thermometer was used to measure the temperature of the flames in the vicinity of the package, and to measure the external package temperature after the fire test was completed. These measurements were made every three minutes. Thirty minute averages of this data are summarized in Table 2.

Table 2 – 30 Minute Temperature Averages

Test	Package Number	Fire (°C)	DFT (°C)	Package (°C)	Optical Thermometer (°C)
Practice	Practice Package	1014	797 (978 [a])	889 [b]	1041
Regulatory Test 1	SN-2	1023	1109	968 [c]	883
Regulatory Test 2 [d]	SN-4	848	888	791 [c]	1009
Regulatory Test 3	SN-5	866	892	995 [e]	1065 [f]
Regulatory Test 4	SN-3	800	897	963	1009

a – Value corrected for ten minute offset from burn time due to thermocouple lag
b – TC on top of package only, lower TC moved inside package
c – These thermocouples were not calibrated for this test
d – 35 minute average used because of longer burn
e – TC at the bottom of the package is not included because of false readings
f – Only optical thermometer readings with 0.9 emissivity included in average

Two tests produced low temperature readings from one source of data. In regulatory test 2, the thermocouples above and below the package averaged below 800°C. The thermocouple above the package was above 800°C but the sensor mounted below the package averaged below 800°C. This is consistent with the limited fuel flow during that test. Unfortunately, due to difficulties in the instrumentation system, neither of these thermocouples was calibrated before the test. All other temperatures measured were significantly above 800°C. Based upon the thirteen temperature readings (8 fire TCs, the 4 DFTs and the optical thermometer), the engulfing fire exceeded the regulatory mandated fire temperature. Therefore, the test is not invalidated by the low temperature readings from the uncalibrated package thermocouples.

Regulatory test 4 resulted in an average fire temperature of 800°C. When the standard errors for type K thermocouples and the data loggers are taken into account (2.2°C or 0.75% of indicated reading for the thermocouple and ± 0.5°C for the OM-CP-OCTTEMP data loggers), actual average temperature may have been as low as 794°C. This is in contrast with the high

temperature readings from the DFTs, the thermocouples above and below the package (that were calibrated) and the optical thermometer. This contrast is even larger if the 30 minute average for the DFTs is shifted by four minutes to compensate for the thermal inertia of the DFT tubes. With this shift, the 30 minute average for the DFTs was 972°C. This difference between the readings from the 8 fire thermocouples and the shielded DFTs was probably due to the higher wind conditions experienced during the test. As shown in Figure 10, the wind disturbed the flame column. The eight thermocouples measuring the flame temperature were closer to the edge of the pool than the other sets of thermocouples and would have been affected more. It is therefore reasonable that the flame thermocouples would have measured lower temperatures than the effective temperature that the package experienced during the test. It should be noted that the test article remained fully engulfed during this test because it was mounted horizontally in the test stand. That was factored into the decision to perform the test on that day, in spite of the higher winds.

Figure 8 - Package Fully Engulfed in Flame (Regulatory Burn Test 1) (SN-2)

Figure 9 – Package Temporarily Exposed Due To Fuel Flow Problems (Regulatory Test 2) (SN-4)

Figure 10 - Flames During Wind Gust (Regulatory Test 4) (SN-3)

Regulatory requirements specify both flame temperature and flame emissivity. The test approach provides very little control over either. Based on fuel and pool geometry, flame temperatures and flame emissivity are essentially fixed. As shown in Table 2, the flame temperatures around the package were typically well above the 800°C required by 10 CFR 71.73. The combined temperature and emissivity requirement defines a heat flux dependent upon the temperature and emissivity of the test article. As shown in Figure 11, that heat flux varied from over 4.5 W/cm^2 when the package is at 400°C, to 1.0 W/cm^2 when the package is at 750°C.

The sensors that best measure the radiative heat flux from the fire were the thermocouples used in the directional flame thermometers (DFT's) and the hand held infrared thermometer. As shown in Table 2 above, the 30-minute average temperatures measured by the DFTs during the burn were all substantially above 800°C. This value is very conservative, however, because the thermal inertia of the DFT pipe resulted in a slow heatup of the DFT's during the test. If the temperature measurements during only the final 20 minutes of the tests are averaged, the values are significantly higher (Table 3). These values range between 925 and 1002°C. The higher fire

temperature will result in significantly higher heat fluxes, even if the emissivity is below 0.9. Figure 12 shows the calculated heat flux on a test article with a surface emissivity of 0.8 based on a fire temperature of 925°C. Even at very low package surface temperatures (400°C) and very low fire emissivities (0.5), the fire will meet regulatory requirements. As shown in the thermal analysis above, the package temperature would quickly reach equilibrium much greater than 400°C.

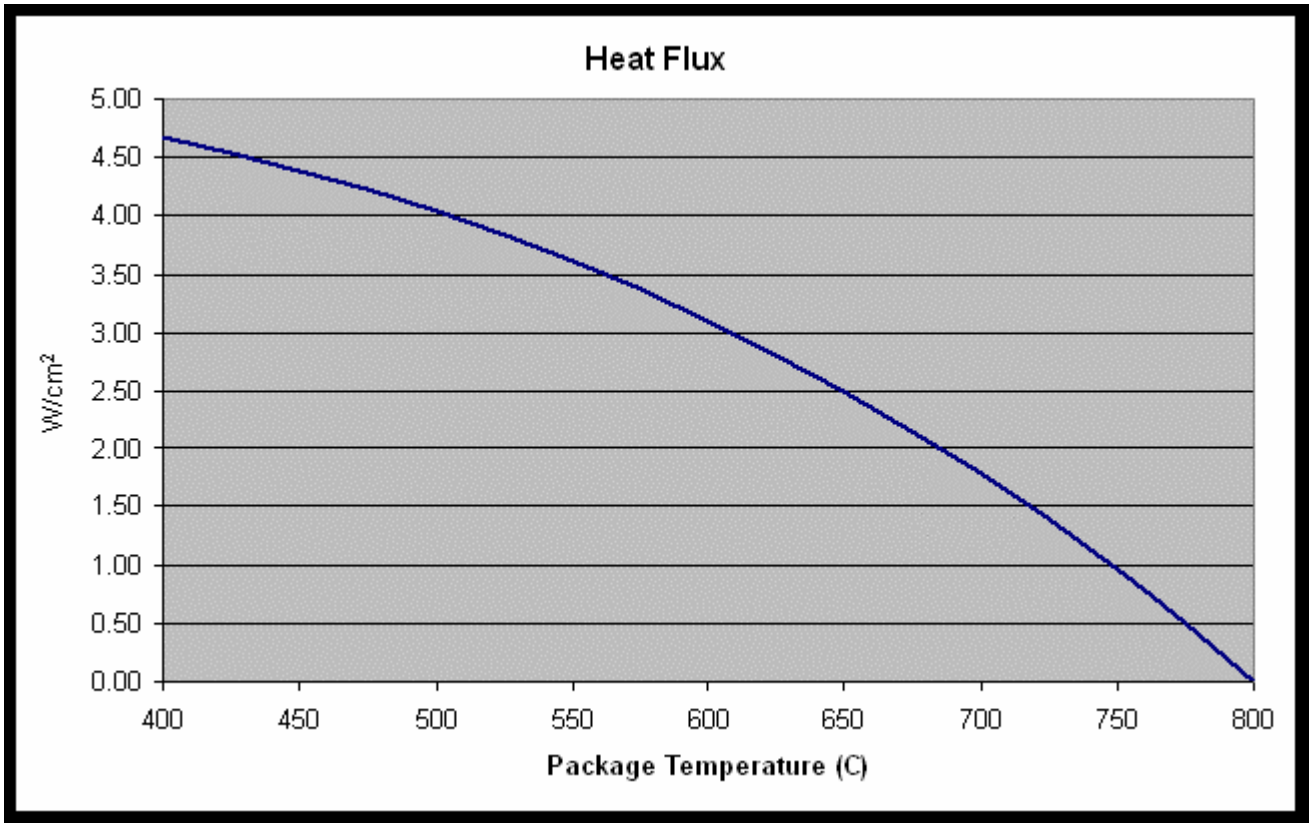

Figure 11 – Heat Flux on Test Article Based on Proscribed Flame Temperatures and Emissivities

Table 3 – Average DFT Temperatures

Test	20 Min. Ave.	30 Min. Ave.
Practice Package	983	797
Regulatory Test 1	1002	978
Regulatory Test 2	925	888
Regulatory Test 3	966	892
Regulatory Test 4	994	897

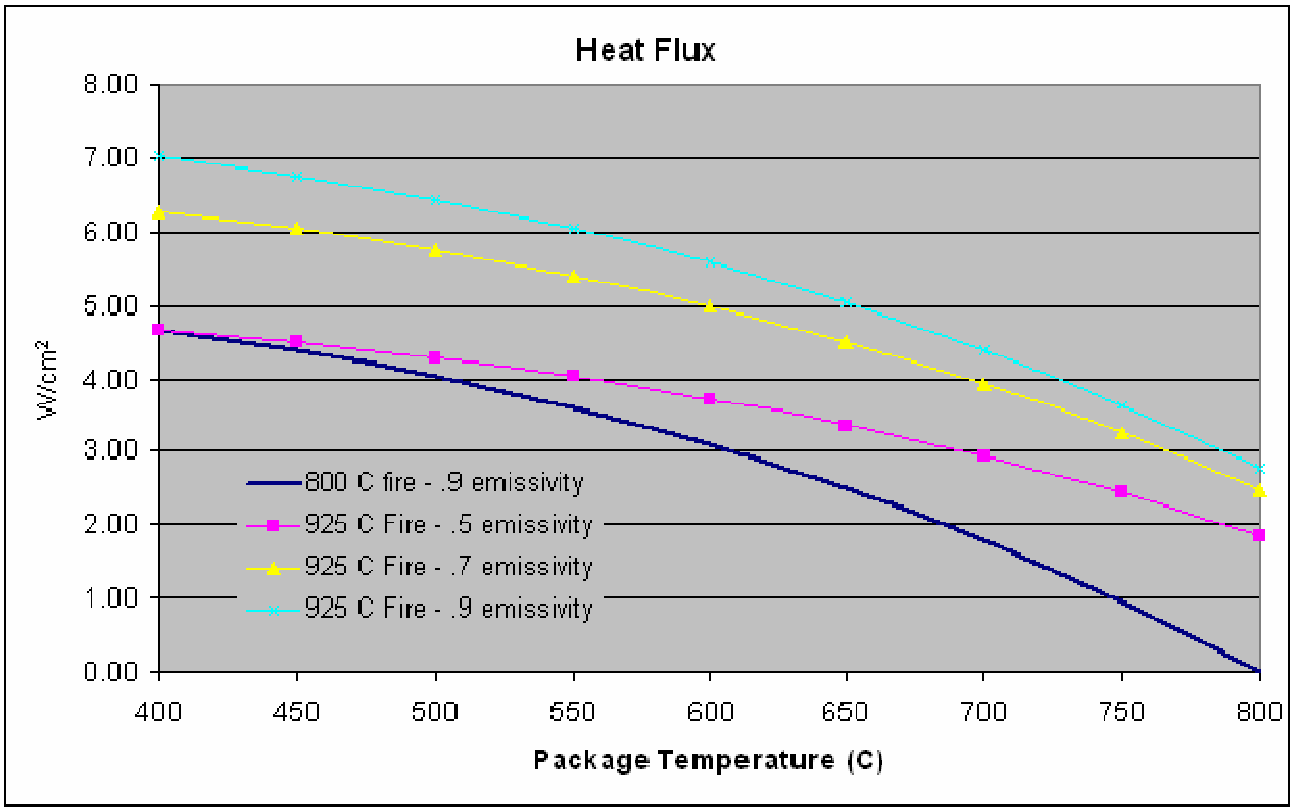

Figure 12 – Heat Flux Generated by 925°C Fires of Different Emissivities

The fire emissivity was also confirmed indirectly by the handheld infrared thermometer. This device measures radiation intensity and calculates a temperature based on an assumed emissivity. This assumed emissivity is input into the device. With the exception of a short period during regulatory burn test 3, the optical thermometer was always set to a 0.9 emissivity. The average optical thermometer readings were always slightly higher than the corresponding thermocouple readings, indicating that the actual fire emissivity was greater than 0.9. The valid temperature measurement data from the fourteen thermocouples negated the loss of data from the infrared thermometer during this period.

References

1. NT-TDR-05-105, SRNL Package Burn Test Plan, December 1, 2005
2. NT-TDR-05-107, SRNL Package Burn Test Procedures, December 1, 2005
3. United States Code of Federal Regulations (CFR) Title 10, part 71, section 73(c)(4).2003
4. ASTM E 2230-02, “Standard Practice for Thermal Qualification of Type B Packages for Radioactive Material”, Aug 2002, Annual Book of ASTM Standards, Vol. 04.07

Appendices

A detailed description of the tests performed is provided in the appendices. These appendices are:

Appendix A 9977 Practice Burn
Appendix B 9977 Regulatory Burn 1 (**SN**-2)
Appendix C 9977 Regulatory Burn 2 (**SN**-4)
Appendix D 9977 Regulatory Burn 3 (**SN**-5)
Appendix E 9977 Regulatory Burn 4 (**SN**-3)

Appendix A 9977 Practice Burn

A burn test was performed on a modified prototype test article with just Fiberfrax® insulation surrounding the package drum liner instead of both Fiberfrax® and polyurethane. The primary purposes of the test were:

- Confirm correct operation of the SCFA facilities and equipment added to support the burn tests
- Practice procedures needed to perform the burn test and provide participants with test experience
- Confirm fire conditions produced by the facility met regulatory requirements
- Determine modified prototype package response to burn test conditions

The prop fuel line was modified to incorporate a fuel flow meter to measure the total amount of fuel pumped into the pool and to estimate the fuel flow rate during the test. The fuel line was connected to a "C" shaped fuel header inside the pool with distribution holes along the length. The header surrounded the support stand to provide an even distribution of fuel around the package. The water lines to the prop were also modified to provide two separate lines; one for the support stand, and the second for the wind fence. This ensured sufficient water for cooling for both structures. The test stand was placed in the approximate center of the burn pool and connected to the water line. The sides of the concrete pool were covered with Kaowool insulation and two halves of the wind fence were mounted on top of the pool walls (Figure A1). Inconel sheathed, type K, thermocouples were then mounted in the pool. Eight thermocouples were mounted in the corners of the pool to measure flame temperatures around the test article and four were inserted into four one inch schedule 40 pipes. The 8 inch (20.3 cm) long pipes were insulated with Kaowool 0.50 inches (1.27 cm) thick and served as the body of the DFTs. The ends of the thermocouples were connected to the 20 gage, type K extension wire in two insulated and water-cooled junction boxes, one located on the North and the second on the South end of the wind fence.

A short test burn was performed on November 21, 2005, before loading the prototype test article onto the test stand. Water flow to the stand and wind fence was started and the pool was filled. When filled to the maximum height, the water depth was eight inches (20.3 cm) on the North-east end of the pool and 10 inches (25.4 cm) on the South-west end of the pool. The bottom of the pool slopes toward the drain located at the South-west end. 51 gallons (193 liters) of fuel were pumped into the pool then the fuel valve was closed and the fuel pump was secured. The fuel was ignited and allowed to burn until flame levels began to drop. The fuel valve was then opened and fuel from one of the site's two tanks (located approximately 400 yards away) flowed into the pool. Flames returned to their full height and test stand was fully engulfed (Figure A2). After approximately seven minutes (from ignition) the fuel valve was closed and the flame began to die almost immediately. A total of 63 gallons (238 liters) of fuel was used.

Figure A1 - Wind Fence Installed Before Practice Test

Figure A2 - Initial Burn to Checkout Hardware

The practice test article (Figure A3) was mounted on the test stand November 29. One inconel sheathed thermocouple was mounted to the top of the test article. (A similar thermocouple was inserted into the test article before transport to the SCFA.) The leads from these thermocouples were routed to the North junction box and connected with type K extension wire approximately 60 feet long. Two OM-CP-OCTTEMP 8 channel, battery powered, thermocouple data loggers were placed in steel boxes, one on the North side of the pool and one on the South side of the pool, each approximately 20 feet (6.1 m) from the wind fence. Thermocouples were connected to the data recorders as shown in Tables A1 and A2. The leads from the thermocouples mounted on the top of the package and inside the package were connected to notebook computer based data acquisition system using Instrunet hardware and software. The thermocouple located inside the package was connected to channel 1 and the thermocouple connected to the top of the package was connected to channel 4.

Figure A3 – Practice Test Article Before the Burn

Table A1 – North Data Recorder Channels (M21255)

Channel No	Thermocouple Location
1	NW DFT
2	WE DFT
3	NW Lower Fire
4	Empty
5	NE Upper Fire
6	NE Lower Fire
7	NW Upper Fire
8	Empty

Table A2 – South Data Recorder Channels (M20547)

Channel No	Thermocouple Location
1	SW DFT
2	SE DFT
3	SW Lower Fire
4	Empty
5	SE Upper Fire
6	SE Lower Fire
7	NSW Upper Fire
8	Empty

The practice burn test was performed on the morning of November 30, 2005. Approximately 50 gallons (189 liters) of fuel was pumped into the pool shortly after 0800. The fuel valve was closed but the fuel pump was left running. At approximately 0816, the fuel in the pool was lit by an SCFA employee. By 0817, the package was fully engulfed and the test was officially started. The fuel valve was then opened and adjusted to maintain full package engulfment until 0847. At that time, the fuel valve was closed, pumps were secured, and the fire was allowed to burn out. By 0849, the package was no longer engulfed.

Ambient temperatures and wind speeds were measured using a Skymate portable anemometer. The operator was standing approximately 100 yards (91 m) uphill from the test article. Data taken is provided in Table A3. Wind speeds were typically very low during the test allowing the test article to remain fully engulfed.

Flame temperatures measured around the test article remained high throughout the test (Figure A4). The average flame temperature over the 30 minutes of the test was 1014°C. Very little variation was noted between the different corners of the pool and between the upper and lower thermocouples.

Table A3 – Ambient Temperature and Wind Conditions

	Time	Ambient Temp (F)	Wind Speed (kts)	Wind Direction
Ignition	8:18	48.7	0	NA
Start of Test (SoT)	8:19	48.8	0	NA
SoT + 3min	8:22	48.4	0.2	292
SoT + 6min	8:25	44.8	1.7	310
SoT + 9min	8:28	46.1	3.4	38
SoT + 12min	8:31	47.6	0.7	0
SoT + 15min	8:34	45.6	0	NA
SoT + 18min	8:37	47.3	0	NA
SoT + 21min	8:40	48.1	1.3	312
SoT + 24min	8:43	48.9	1.1	340
SoT + 27min	8:46	48.6	1.7	272
SoT + 30 min	8:49	47.4	2.5	350
SoT + 33 min	8:52	46.6	1.9	300
SoT+45 min	9:04	50.4	1.3	346
SoT+ 60 min	9:19	50.2	2.3	26
SoT + 75 min	9:49	56.2	3.8	280
SoT + 90 min				
SoT + 105 min				
SoT + 120 min				

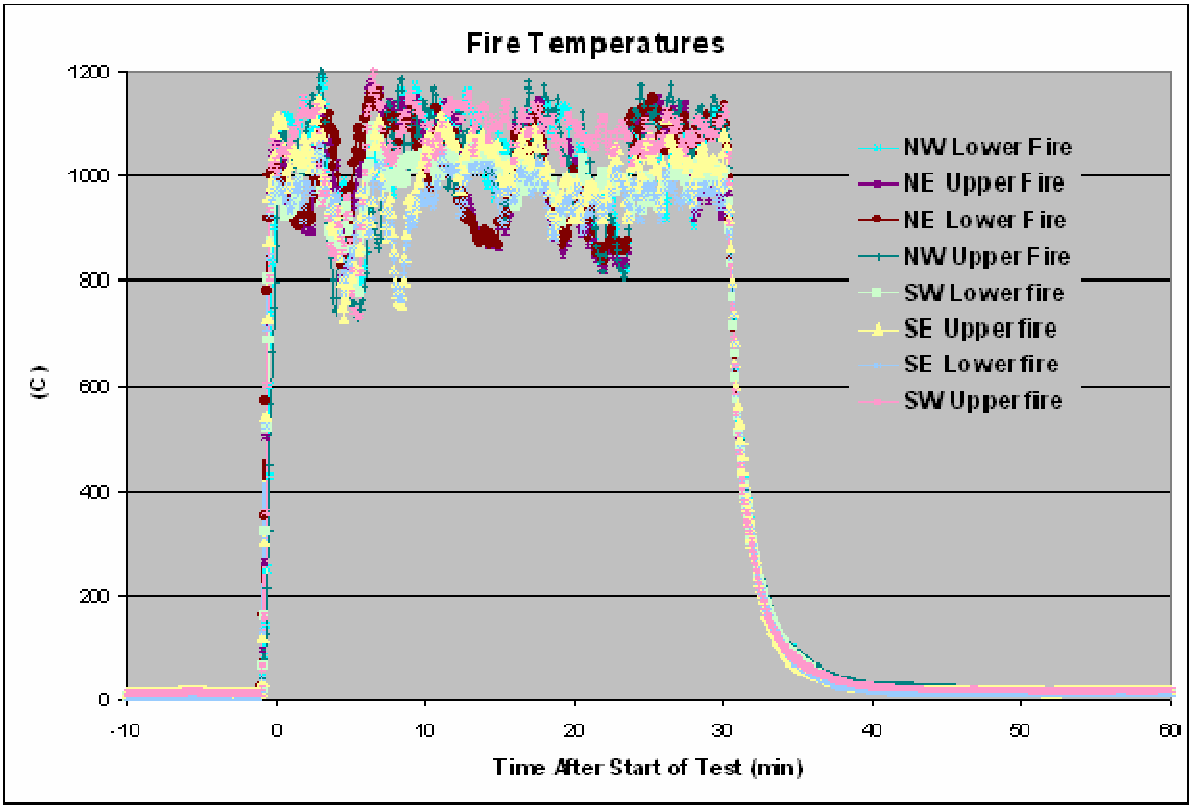

Figure A4 – Fire Temperatures Measured During Practice Burn

The thermocouples located in the four DFT's recorded a much lower average temperature of 797°C during the 30 minute burn. As shown in Figure A5, this is due to the long time lag in the DFT readings. When averaged for the 30 minutes beginning 10 minutes after the start of the test, the average temperature jumps to 978°C. Each DFT consists of an eight inch (20.3 cm) long one inch diameter schedule 40 pipe with a 1.32/1.05 inch (3.35/2.67 cm) outside and inside diameter respectively. The total pipe weight was approximately 1.2 lbs (0.53 kg) and with a heat capacity between 0.113 and 0.116 BTU/lb-F (0.448 and 0.481 J/g – C), the tubes required approximately 271 BTU (270 kJ) to reach 1100°C. This took over 20 minutes because of the 1 inch (2.5 cm) thick layer of Kaowool protecting the outer surface of the tube. Flame temperatures equal or greater than 1100°C were required to produce this response.

Temperature measurements were also made using an Omega OS523 handheld infrared thermometer. These measurements were made by standing at safe distance (approximately 20 yards or 18 m from the pool) and pointing the thermometer at the test article or the flame hiding the test article. Measurements were recorded every 3 minutes. As shown in Table A4, these measurements show flame temperatures between 1000 and 1100°C during the fire test.

Emissivity measurements were not taken of the fire. The regulatory requirement is for an 800°C fire with a flame emssivity of 0.9. Simplified heat flux calculations can be performed assuming equal surfaces using the formula:

$$Q = [1/(1/e_{fire} + 1/e_{package} - 1)] \sigma A (T_{fire}^4 - T_{package}^4)$$

Where:

Q is the heat flux (W)

e_{fire} and $e_{package}$ are the emissivities of the fire and the package respectively

σ is the Stefan-Boltzmann's constant = 5.67×10^{-12} $W/cm^2 - K^4$

and, A is the package area

For a room temperature package with an emissivity of 0.8, the heat flux is approximately 5.49 w/cm^2. If the package is 600°C, then the heat flux drops to 3.10 w/cm^2. If the fire temperature increases to 1000°C and the package emissivity remains the same, flame emissivity may drop to 0.41 (for the room temperature package) or 0.29 (for the 600°C package). This test clearly satisfied the heat flux requirements from the fire.

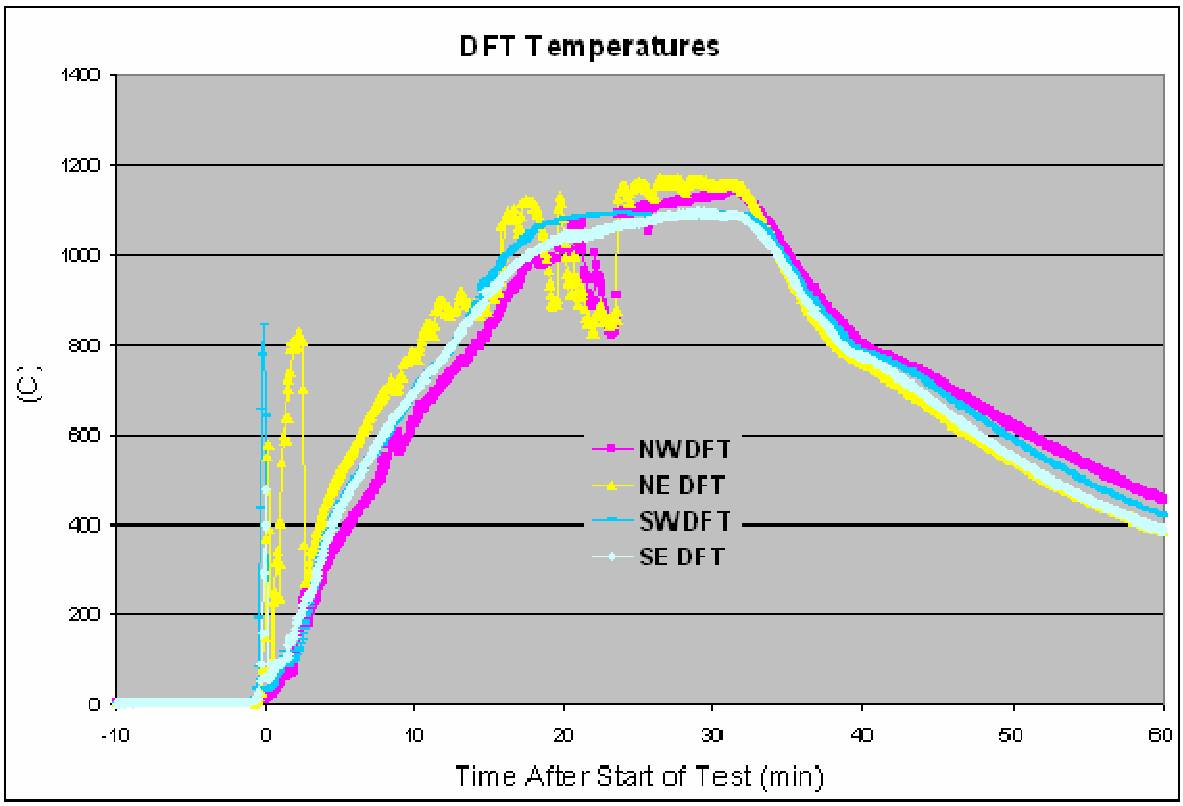

Figure A5 – DFT Measurements During Practice Burn

Temperature data was also taken from a thermocouple located inside the prototype package and from a thermocouple mounted above the top of the package. This data was monitored during the test using the notebook computer based instruNet data acquisition system. As shown in Figure A6, the temperatures measured at the top of the package were similar, but slightly lower, than those recorded around the package. The 30 minute average temperature, beginning at the start of the test, of 889°C was observed. The internal thermocouple provided erratic readings. The large spikes are probably due to a frayed section of the thermocouple lead found at the location where the thermocouple lead left the package. A transient short at this location could produce signals similar to those observed by the data acquisition system.

Table A4 – Optical Thermometer Data

	Time	Middle of Package (°F)	Comments
Ignition	8:17	1016	62 ft from target
Start of Test (SoT)	8:18	999	2 min offset to time keeper
SoT + 3min.	8:21	604	
SoT + 6min.	8:24	1049	
SoT + 9min.	8:27	1148	
SoT + 12min.	8:30	1214	
SoT + 15min.	8:33	1040	1 min average
SoT + 18min.	8:36	1102	1 min average
SoT + 21min.	8:39	1085	1 min average
SoT + 24min.	8:42	1062	1 min average
SoT + 27min.	8:45	1064	1 min average
SoT + 30min.	8:48	17[a]	15 sec average
SoT + 33min.	8:51	255	15 sec average
SoT + 36min.	8:54	230	15 sec average
SoT + 45min.	9:03	277	15 sec average
SoT + 60min.	9:18	49	18 sec average, 6 ft from target
SoT + 75min.	9:33	31	15 sec average, 6 ft from target
SoT + 90min.	9:48	27	15 sec average, 6 ft from target
SoT + 105min.	10:03	23	15 sec average, 6 ft from target
SoT + 120min.	10:18	11	15 sec average, 6 ft from target

[a] Optical thermometer incorrectly sighted resulting in temperature measurement of sky

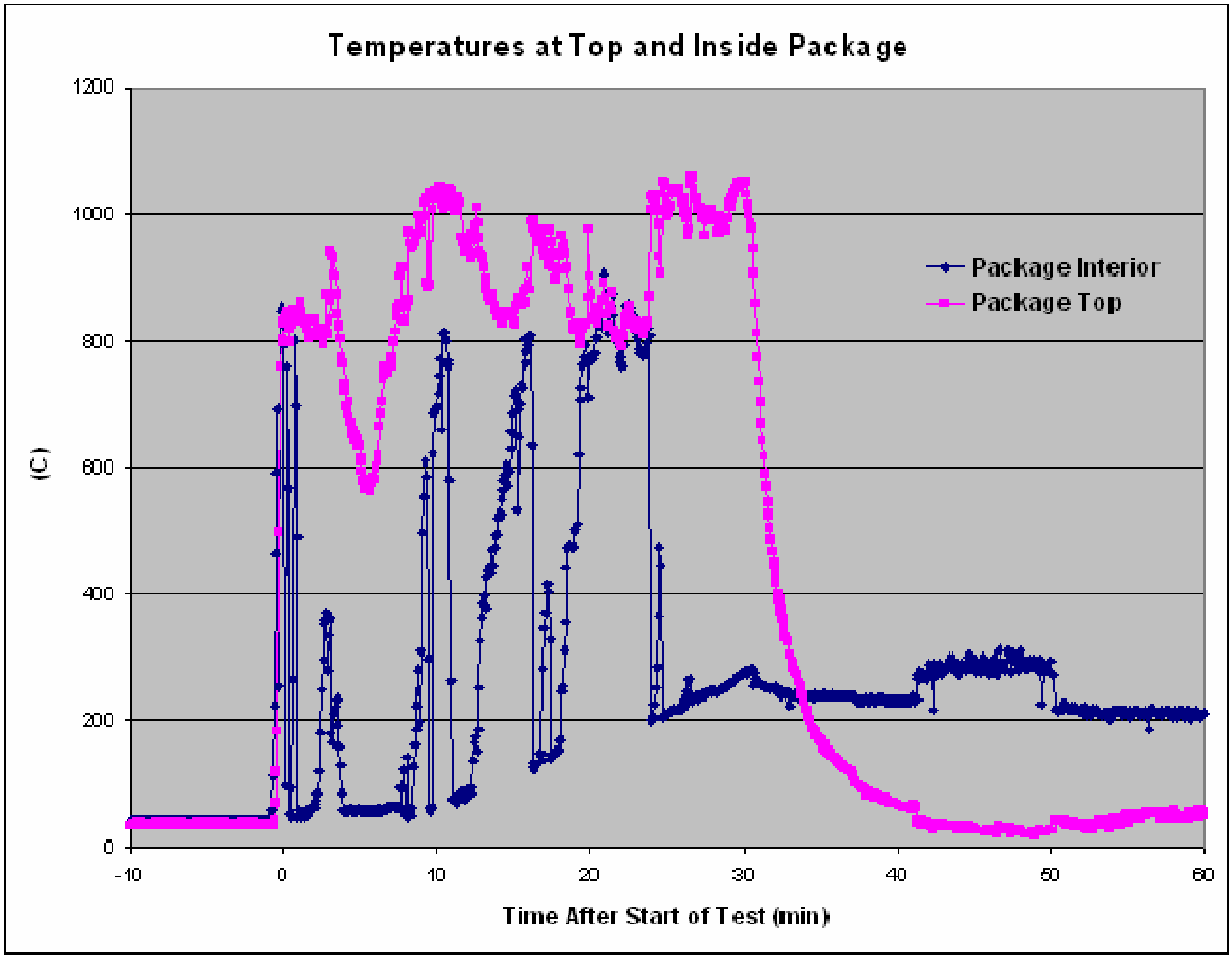

Figure A6 – Temperatures Inside and on the Top of the Practice Package

Appendix B 9977 Regulatory Burn 1 (SN-2)

The first regulatory burn was performed on December 2, 2005. Preparations for this burn began on November 30 with the replacement of all of the thermocouples used in the practice burn (described in Appendix A). Two DFT mounts that had sagged during the practice burn were adjusted to bring them to a height above the pool floor between 56.0 and 56.5 inches (142 to 144 cm). (The elevation of the DFTs had changed but the orientation the the DFTs had remained constant.) The lower flame thermocouples were mounted 42.0 to 43.5 inches (107 to 110 cm) above the pool floor. The upper flame thermocouples were mounted 66.5 to 68.1 inches (169 to 173 cm) above the pool floor. The thermocouples were connected at the junction boxes as described in Appendix A. The recorded measurements of these thermocouples were compared with simultaneous measurements made with a NIST traceable calibrated digital thermometer using a Type K thermocouple. All thermocouple readings were within the standard error band of the type K thermocouple at lower temperatures (2.2°C).

The first regulatory burn test article, SN-2, (Figure B1) was mounted on the test stand December 1 after being transported from the preheating furnace at SRNL where it was preheated to approximately 93°C. The base of the package was 47 inches (119 cm) above the base of the pool. The water depth, when the pool was filled was approximately 9 inches (23 cm), resulting in the base of the package being approximately 38 inches (97 cm) above the surface of the pool. The distance from the pool perimeter to the package was also measured (Table B1). Two thermocouples were mounted on the package, one at the top and the second on the bottom (attached to the grate below the package). Two 750W-30 gallon drum heaters were attached to the test article and then the package was covered with thermal insulation and the Styrofoam® cover.

The burn was performed essentially the same way as described in Appendix A. Approximately 50 gallons (189 liters) of fuel was pumped into the pool shortly after 0800. The fuel valve was closed but the fuel pump was left running. At approximately 0815, the fuel in the pool was lit by an SCFA employee. By 0816, the package was fully engulfed and the test was officially started. The fuel valve was then opened and adjusted to maintain full package engulfment until 0846 (Figures B2 and B3). At that time, the fuel valve was closed, pumps were secured, and the fire was allowed to burn out. By 0849, the package was no longer engulfed (Figure B4). A total of 509 gallons (1927 liters) of fuel was used in the test.

Ambient temperatures and wind speeds were measured using a Skymate portable anemometer. The operator was standing approximately 100 yards (91 m) uphill from the test article. Data taken is provided in Table B2. Wind speeds were typically very low during the test allowing the test article to remain fully engulfed.

Flame temperatures measured around the test article remained high throughout the test (Figure B5). The average flame temperature over the 30 minutes of the test was 1023°C. Little variation was noted between the different corners of the pool and between the upper and lower thermocouples.

Figure B1 – Test Article Before Regulatory Burn 1 (SN-2)

Table B1 – Package Position Inside Pool (SN-2)

Direction	Distance to Perimeter (in/m)
North	56 / 1.4
West	57 / 1.4
South	58 / 1.5
East	52 / 1.3

Table B2 – Ambient Temperature and Wind Conditions (SN-2)

	Time	Ambient Temp (F)	Wind Speed (kts)	Wind Direction
Ignition	8:03	43	0	NA
Start of Test (SoT)	8:03	43	0	NA
SoT + 3min	8:06	42.2	1.1	352
SoT + 6min	8:09	40.6	2.5	6
SoT + 9min	8:12	40.1	3.1	12
SoT + 12min	8:15	40.5	2.5	16
SoT + 15min	8:18	41.1	0.3	16
SoT + 18min	8:21	41.1	0	NA
SoT + 21min	8:24	40.3	3.1	276
SoT + 24min	8:27	41.1	2.9	306
SoT + 27min	8:30	40.7	1.1	10
SoT + 30 min	8:33	40.9	1.1	342
SoT + 33 min	8:36	41.8	5.2	330
SoT+45 min	8:48	44.2*	0	NA
SoT+ 60 min	9:03	46*	4.6	260
SoT + 75 min	9:33	50.9	2.5	236
SoT + 90 min				
SoT + 105 min				
SoT + 120 min				

* measurement from hand held anemometer

Figure B2 – First Regulatory Burn Test (SN-2)

Figure B3 – First Regulatory Burn Test (SN-2) – Close Up View

Figure B4 – End of First Regulatory Burn Test (SN-2)

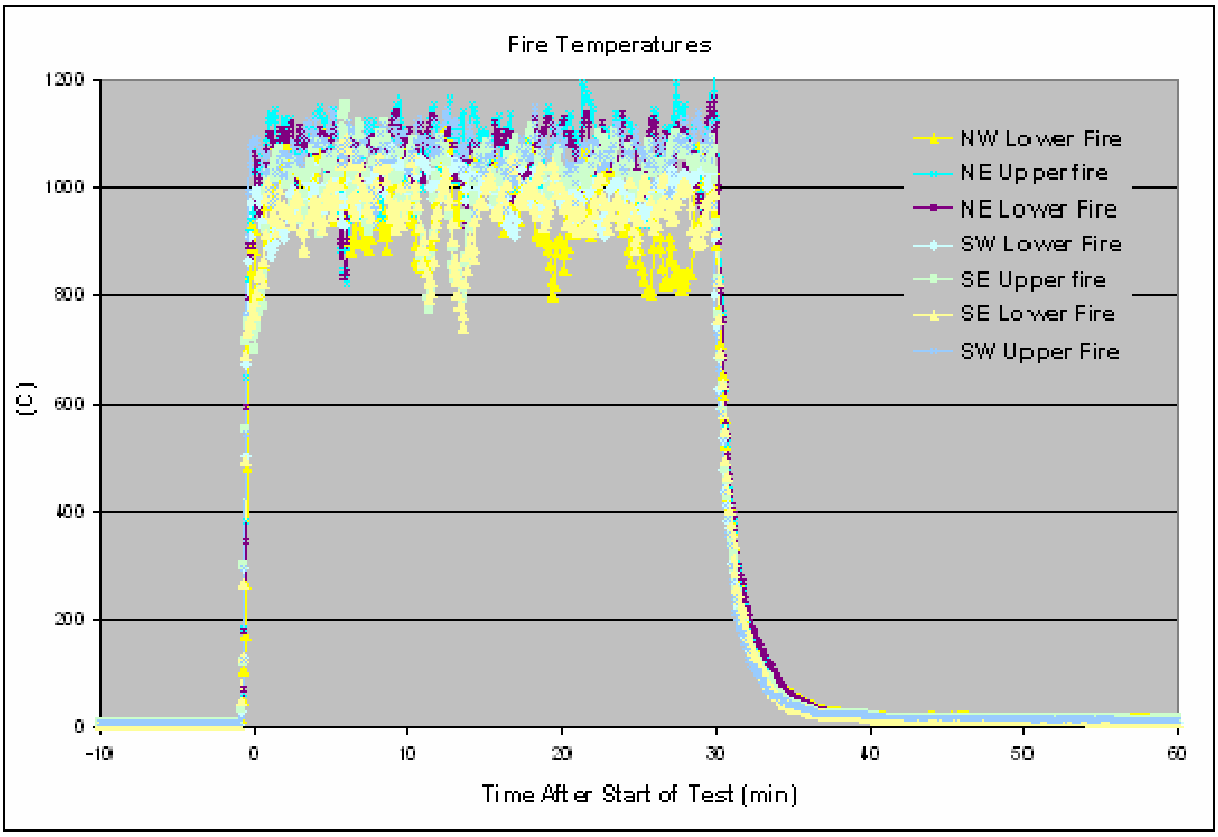

Figure B5 – Fire Temperatures Measured During First Regulatory Burn (SN-2)

The 30 minute average of the thermocouples readings in the four DFT's (10 minutes after start of test to 40 minutes after start of test) was 978°C. The average temperature recorded by the four DFTs at the end of the test was 1109°C (Figure B6).

Temperature measurements were also made using an Omega OS523 handheld infrared thermometer. These measurements were made by pointing the thermometer at the test article or the flame hiding the test article. Measurements were recorded every 3 minutes. As shown in Table B3, these measurements show flame temperatures between 885 and 996°C during the fire test.

Data from the two thermocouples attached to the top and bottom of the test article are shown in Figure B7. Because the thermocouples were not calibrated with the InstruNet system in operation, the results are provided for general information only.

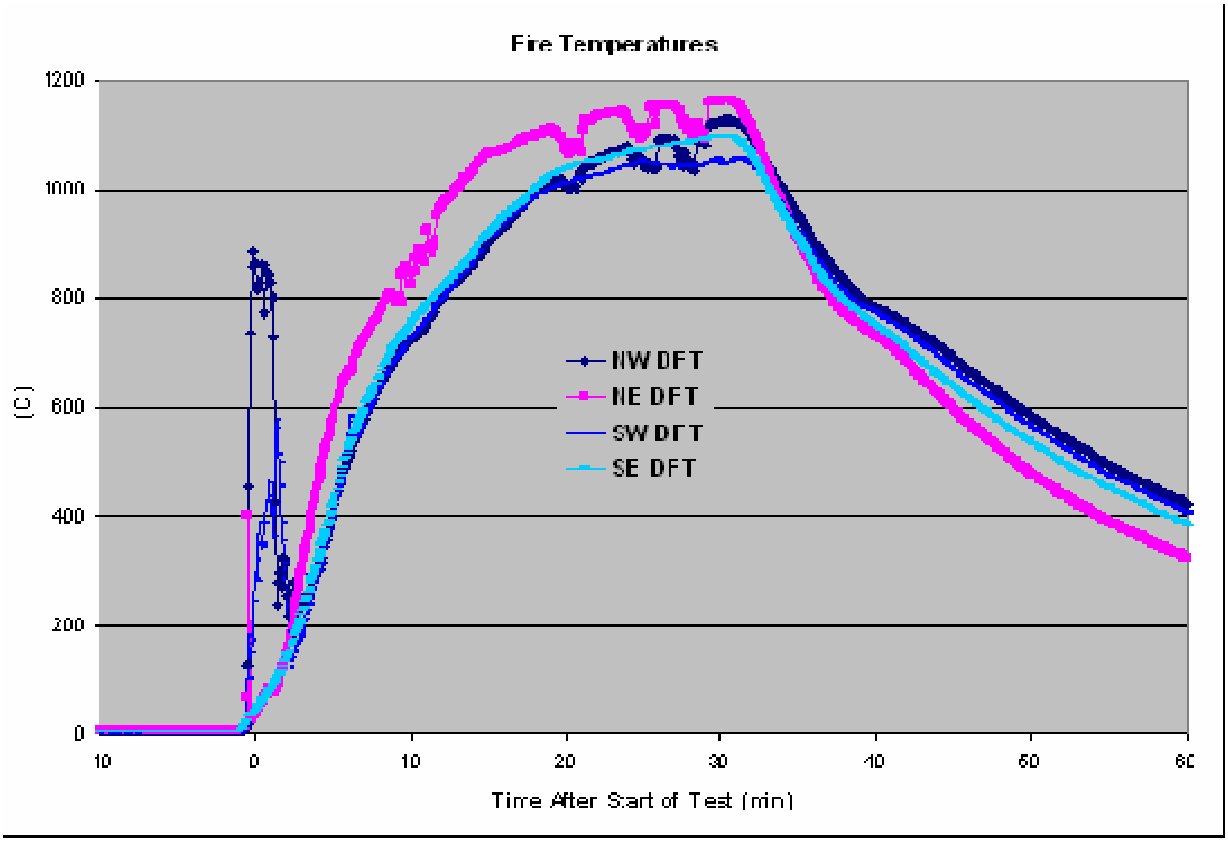

Figure B6 – DFT Measurements During First Regulatory Burn (SN-2)

Table B3 – Optical Thermometer Data (SN-2)

	Time	Middle of Package (°F)	Comments
Ignition	8:15	804	
Start of Test (SoT)	8:16	926	
SoT + 3min.	8:19	885	
SoT + 6min.	8:22	952	
SoT + 9min.	8:25	930	
SoT + 12min.	8:28	932	
SoT + 15min.	8:31	981	
SoT + 18min.	8:34	931	
SoT + 21min.	8:37	966	
SoT + 24min.	8:40	996	
SoT + 27min.	8:43	938	
SoT + 30min.	8:46	278	
SoT + 33min.	8:49	318	
SoT + 36min.	8:52	213	
SoT + 45min.	9:01	108	
SoT + 60min.	9:16	54	
SoT + 75min.	9:31	18	
SoT + 90min.	9:46	13	
SoT + 105min.	10:01	6	
SoT + 120min.	10:16	-	

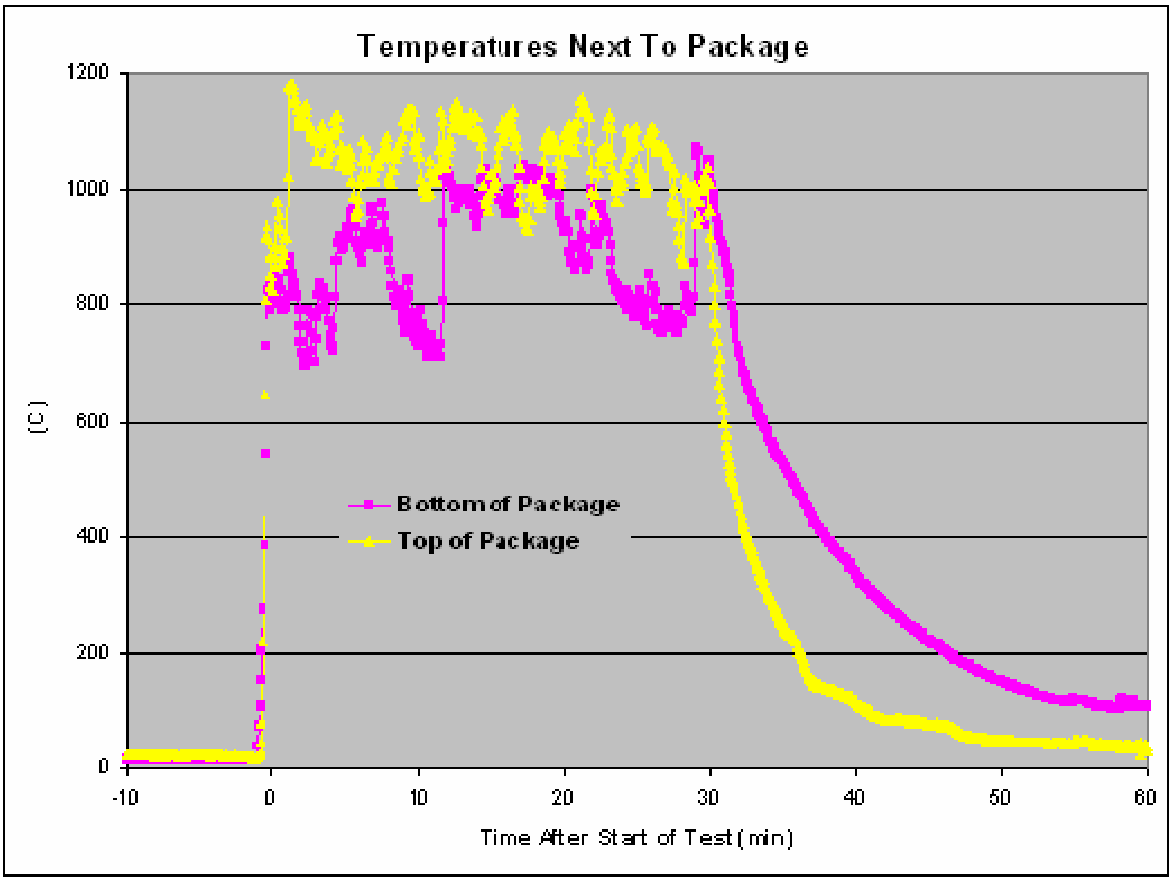

Figure B7 – Temperature Measurements at the Top and Bottom of the Test Article (SN-2)

Appendix C 9977 Regulatory Burn 2 (SN-4)

The second regulatory burn was performed on December 7, 2005. Preparations for this burn began on December 2, immediately after the first regulatory burn. All thermocouples except for the sensor mounted below the test article were replaced. Thermocouple leads were connected in the junction boxes to maintain the same datalogger channel identification described in Appendix A.

The DFT mounts that had sagged during the practice burn and the first regulatory burn were removed. The length was cut down to approximately 3 inches (7.6 cm) and attached to the uprights on the support grate. The four DFTs were mounted on the North, West, South and East sides of the support stand facing away from the package. The insulated pipe sections were approximately 12 inches (30 cm) above the base of the test article.

With the exception of the DFT locations, all of the new thermocouples were mounted in the same locations as the ones used in the first regulatory burn test (Appendix B) and the practice test (Appendix A). The recorded measurements from these thermocouples were compared with simultaneous measurements made with a NIST traceable calibrated digital thermometer using a Type K thermocouple. All thermocouple readings were within the standard error band of the type K thermocouple at lower temperatures (2.2°C).

The second regulatory burn test article (SN-4) was mounted on the test stand December 6 after being transported from the preheating furnace at SRNL where it was preheated to approximately 93°C. The test article was mounted in a vertical orientation with the package top facing up. The base of the package was 47 inches (119 cm) above the base of the pool. The water depth, when the pool if filled is approximately 9 inches (23 cm), resulting in the base of the package being approximately 38 inches (97 cm) above the surface of the pool. The distance from the pool perimeter to the package was also measured (Table C1). Using the same technique used in the first regulatory burn, two thermocouples were mounted on the package, one at the top and the second on the bottom (attached to the grate below the package). The two 750W, 30 gallon drum heaters were attached to the test article and then the package was covered with thermal insulation and the Styrofoam® cover.

The burn was performed essentially the same way as described in Appendix B. Approximately 56 gallons (212 liters) of fuel was pumped into the pool. This was done over an extended period because fuel flow rate was not as high as in earlier tests. SCFA personnel visually checked pump operation and valve positions to confirm correct system settings. Fuel flow did increase to approximately 0.37 gallons per second (1.4 liters per second). It was estimated that this flow would provide over 600 gallons (2271 liters) over the 30 minute test. It was therefore decided to perform the test. At approximately 0854, the fuel in the pool was lit by an SCFA employee. By 0855, the package was fully engulfed and the test was officially started (Figure C1). The fuel valve was then opened and valve was left in the full open position during most of the test. The fire was not as engulfing as the earlier tests (Figure C2), so the test was continued for an additional five minutes. At 0929 the fuel valve was closed, pumps were secured, and the fire was

allowed to burn out. Within a minute and a half, the fire began to die out. A total of 549 gallons (2078 liters) of fuel was used in the test. Figure C3 shows the test article after the test.

After the test, the fuel system was examined in detail. The fuel manifold inside the burn pool was removed and flushed and all valve positions were rechecked. It was subsequently learned that, during the test, the fuel tank being used was almost empty (3 inches or 7.6 cm of fuel left in the tank. A full fuel tank has a level over seven feet (2.1 m). This additional head allows significantly higher fuel flow, even with the tank's fuel pump running.

Ambient temperatures and wind speeds were measured using a Skymate portable anemometer. The operator was standing approximately 100 yards (91 m) uphill from the test article. Data taken is provided in Table C2. Wind speeds were low during the test.

Flame temperatures measured around the test article oscillated during the test depending upon location (Figure C4). The average flame temperature over the 35 minutes of the test was 848°C. There was a greater variation in the temperatures recorded by the upper thermocouples which was consistent with the smaller column of flame.

Figure C1 – Regulatory Burn Test 2 (SN-4)

Figure C2 – View of Regulatory Burn Test 2 Showing Period of Partial Package Engulfment (SN-4)

Table C1 – Package Position Inside Pool (SN-4)

Direction	Distance to Perimeter (in/m)
North	57 / 1.4
West	56 / 1.4
South	55 / 1.4
East	55 / 1.4

Table C2 – Ambient Temperature and Wind Conditions (SN-4)

	Time	Ambient Temp (F)	Wind Speed (kts)	Wind Direction
Ignition	8:49	36.7	0	-
Start of Test (SoT)	8:50	36.4	1.7	N
SoT + 3min	8:53	35.6	1.3	NW
SoT + 6min	8:56	36.3	0	-
SoT + 9min	8:59	37	1.5	NW
SoT + 12min	9:02	37.2	0	-
SoT + 15min	9:05	37.3	0	-
SoT + 18min	9:08	35.7	1.3	NNW
SoT + 21min	9:11	35.5	2.2	NW
SoT + 24min	9:14	36.5	2	NW
SoT + 27min	9:17	35.9	1.7	NW
SoT + 30 min	9:20	36.4	2.2	N
SoT + 33 min	9:23	36.3	2.2	NNW
	9:26	37.7	1.5	N
SoT+45 min	9:35	37.3	1.3	W
SoT+ 60 min	9:50	38.4	1.7	SW
SoT + 75 min				
SoT + 90 min	10:20	-	-	
SoT + 105 min				
SoT + 120 min	10:50	-	-	

Figure C3 – Test Article After Second Regulatory Burn Test (SN-4)

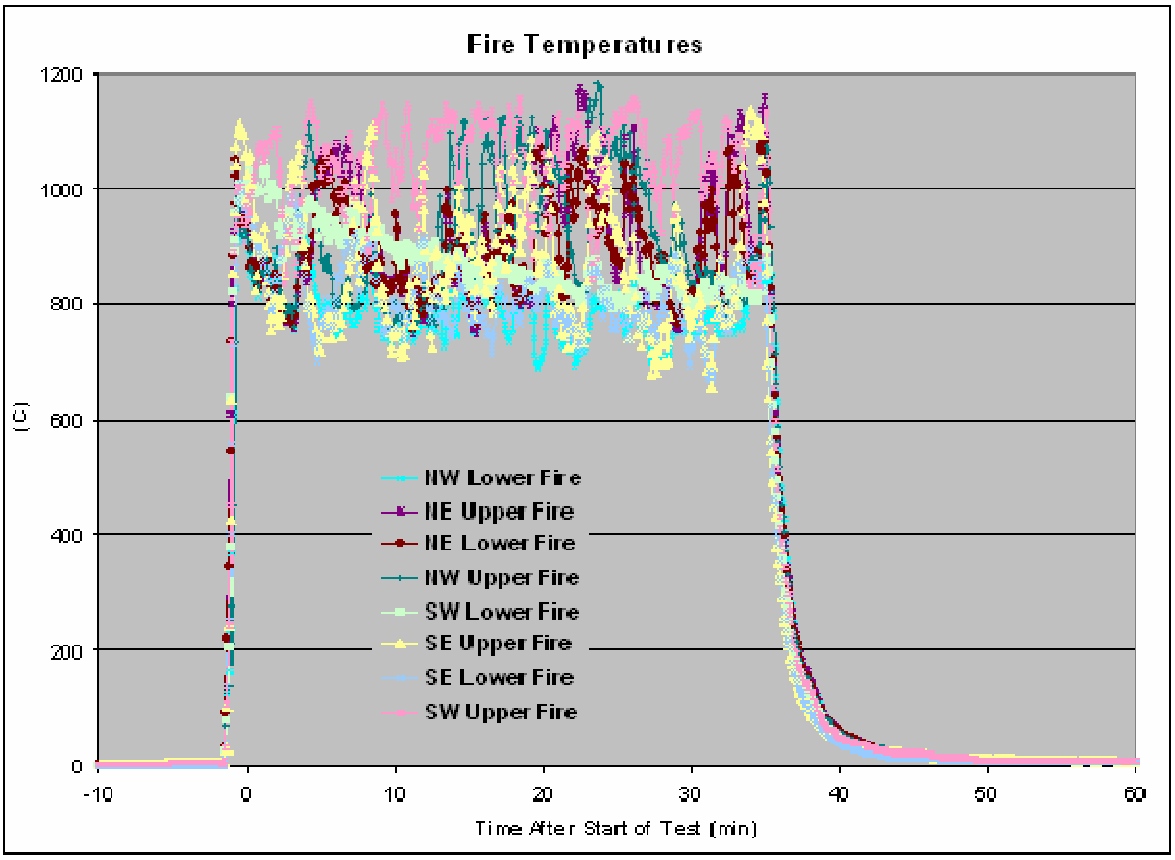

Figure C4 – Fire Temperatures Measured During Practice Burn (SN-4)

The 35 minute average of the thermocouples readings in the four DFT's was 888°C. The average temperature recorded by the four DFTs at the end of the test was 983°C (Figure C5).

Temperature measurements were also made using an Omega OS523 handheld infrared thermometer. These measurements were made by pointing the thermometer at the test article or the flame hiding the test article. Measurements were recorded every 3 minutes. As shown in Table C3, these measurements show high flame temperatures between 962 and 1068°C during the fire test. This data was taken from the North side which was fully engulfed. The data from the optical thermometer was time averaged over approximately 30 seconds minimizing the transient flame effects.

Data from the two thermocouples attached to the top and bottom of the test article are shown in Figure C6. Because the thermocouples were not calibrated with the InstruNet system in operation, the results are provided for general information only.

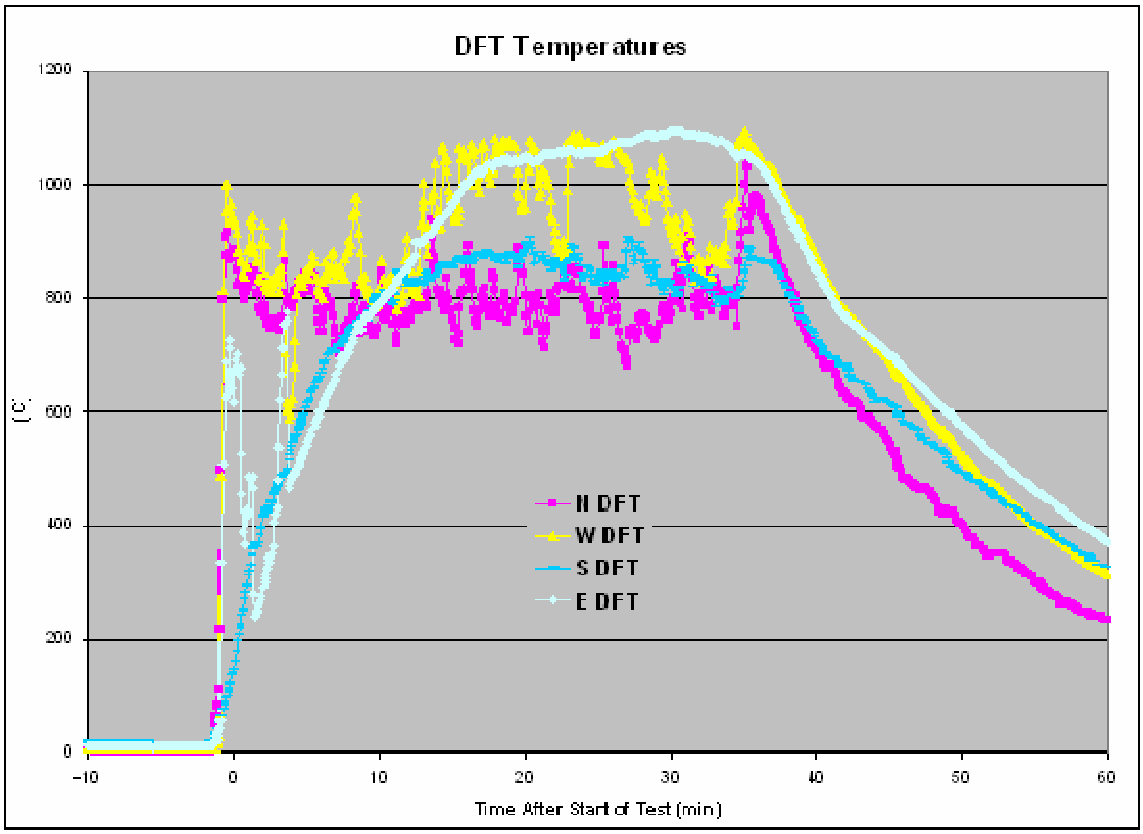

Figure C5 – DFT Measurements During Practice Burn (SN-4)

Table C3 – Optical Thermometer Data (SN-4)

	Time	Middle of Package (°F)	Comments
Ignition	8:52	502	
Start of Test (SoT)	8:53	1009	
SoT + 3min.	8:56	1016	
SoT + 6min.	8:59	1058	
SoT + 9min.	9:02	1014	
SoT + 12min.	9:05	1002	
SoT + 15min.	9:08	1016	
SoT + 18min.	9:11	982	
SoT + 21min.	9:14	962	
SoT + 24min.	9:17	973	
SoT + 27min.	9:20	1011	
SoT + 30min.	9:23	1052	
SoT + 33min.	9:26	1068	
SoT + 36min.	9:29	831	
SoT + 45min.	9:38	195	
SoT + 60min.	9:53	64	
SoT + 75min.	10:08	42	
SoT + 90min.	10:23	29	
SoT + 105min.	10:38	67	
SoT + 120min.	10:53	68	

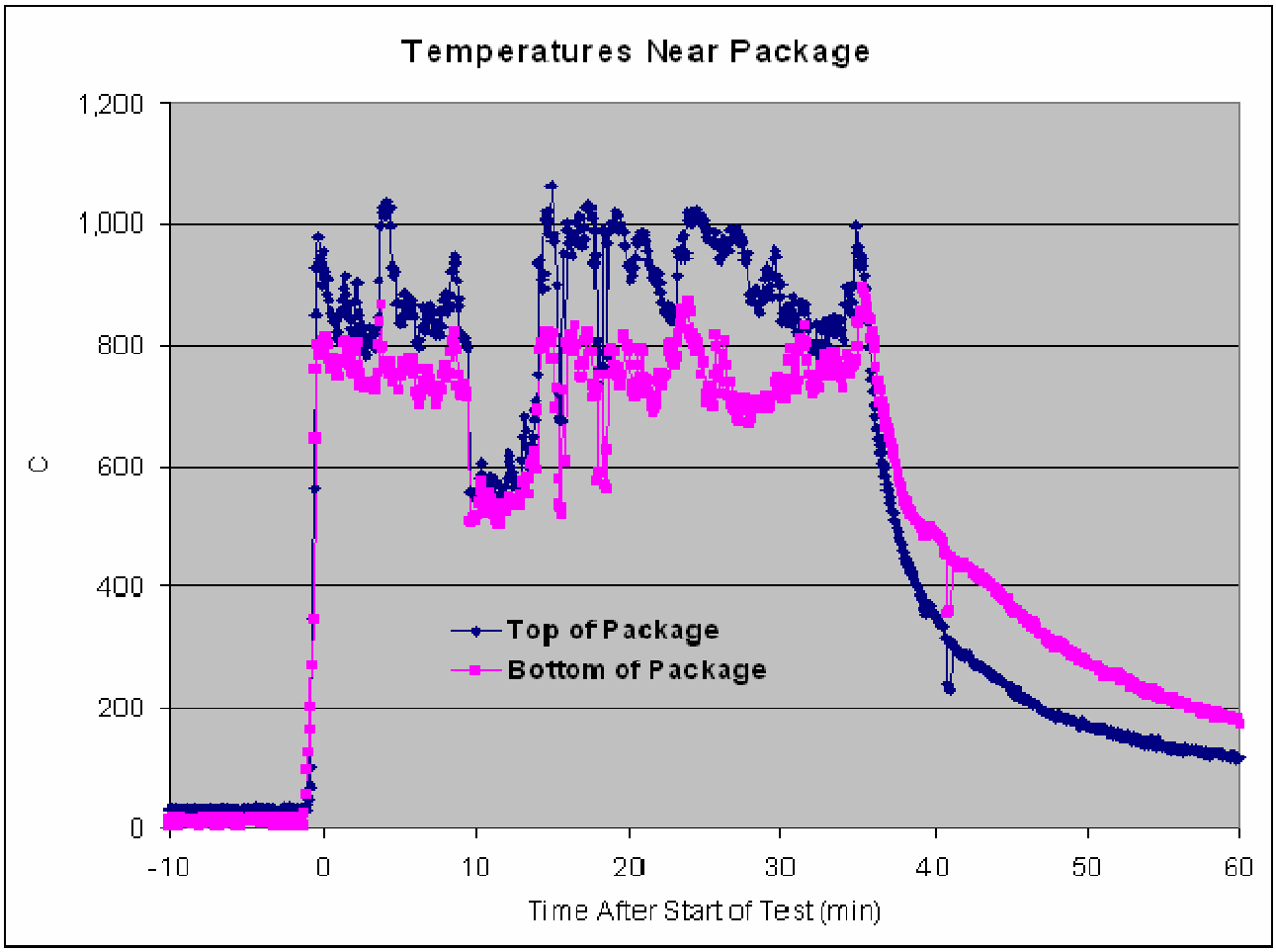

Figure C6 – Temperature Measurements at the Top an Bottom of the Test Article (SN-4)

Appendix D 9977 Regulatory Burn 3 (SN-5)

The third regulatory burn was performed on December 13, 2005. Preparations for this burn began on December 7 with the replacement of all of the thermocouples used in the second regulatory burn (described in Appendix C). All of the thermocouples were replaced at that time.

Due to fuel feed problems in the second regulatory burn, a subsequent test burn was performed on December 12 to verify the adequacy of the fuel flow. This test lasted approximately eight minutes and 83 gallons (313 liters) of fuel was pumped into the pool and burned. A fuel flow of approximately 0.3 gallons/sec (1.1 liter/s) was achieved. Full pool coverage was achieved allowing the third regulatory burn to proceed.

Before the burn test, measurements from all of the thermocouples were compared to measurements made with a NIST traceable calibrated digital thermometer. Three thermocouples were determined to be outside of normal error ranges (2.2°C for type K thermocouples near room temperature). The thermocouples at the top and bottom of the package were off by 9 and 12°C respectively. This was noted and the data collected during the test was corrected accordingly. The thermocouple in the west facing DFT was reading 4.1°C below the calibrated thermometer. Because this was conservative, no correction was made.

The third regulatory burn test article (SN-5) was mounted on the test stand December 12 after being transported from the preheating furnace at SRNL where it was preheated to approximately 93°C. The test article was mounted in a vertical orientation with the package top facing up. The base of the package was 47 inches (119 cm) above the base of the pool. The depth of the water in the pool at that location is approximately nine inches (23 cm). Therefore the base of the package was 38 inches (96 cm) above the surface of the pool. The distance from the pool perimeter to the package was also measured (Table D1). Two thermocouples were mounted on the package, one at the top and the second on the bottom (attached to the grate below the package). Two 750W, 30 gallon drum heaters were attached to the test article and then the package was covered with thermal insulation and the Styrofoam® cover.

The burn was performed essentially the same way as earlier burns except the pool was filled with approximately 75 gallons (189 liters) of fuel instead of 50 gallons (189 liters). At approximately 0804, the fuel in the pool was lit by an SCFA employee. By 0805 the package was fully engulfed and the test was officially started. The fuel valve was then opened and adjusted to maintain full package engulfment until 0835 (Figures D1 and D2). At that time, the fuel valve was closed, pumps were secured, and the fire was allowed to burn out. By 0840, the package was no longer engulfed (Figure D3). A total of 627 gallons (2373 liters) of fuel was used in the test.

As in previous tests, ambient temperatures and wind speeds were measured using a Skymate portable anemometer. The operator was standing approximately 100 yards (91 m) uphill from the test article. Data taken is provided in Table D2. Wind speeds were typically very low during the test allowing the test article to remain fully engulfed.

Flame temperatures measured around the test article remained high throughout most of the test (Figure D4). The average flame temperature over the 30 minutes of the test was 883°C. This average was reduced by the failure of the wires holding the upper and lower thermocouples on the North end of the pool. The upper wire failed approximately 24 minutes into the test and the lower wire failed approximately four minutes later. This allowed some of the thermocouples to fall into the pool, immediately cooling them.

Table D1 – Package Position Inside Pool (From Package Centerline) (SN-5)

Direction	Distance to Perimeter (in/m)
North	65 / 1.7
West	69 / 1.8
South	62 / 1.6
East	62 / 1.6

Table D2 – Ambient Temperature and Wind Conditions (SN-5)

	Time	**Ambient Temp (F)**	**Wind Speed (kts)***	**Wind Direction**
Ignition	8:04	33.5	0	-
Start of Test (SoT)	8:05	33.5	0	-
SoT + 3min	8:08	34	0	-
SoT + 6min	8:11	34.7	0	-
SoT + 9min	8:14	35.5	0	-
SoT + 12min	8:17	35.4	0	-
SoT + 15min	8:20	35.5	0.8	248
SoT + 18min	8:23	35.7	1.7	264
SoT + 21min	8:26	36.2	1.3	290
SoT + 24min	8:29	36.4	2.4	264
SoT + 27min	8:32	36.4	3.1	278
SoT + 30 min	8:35	36.1	4.4	266
SoT + 33 min	8:38	36.1	3.3	250
SoT+45 min	8:50	36.2	3.3	280
SoT+ 60 min	9:05	39.9	2.2	278
SoT + 75 min				
SoT + 90 min				
SoT + 105 min				
SoT + 120 min				

Figure D1 – Third Regulatory Burn Test (SN-5)

Figure D2 – Third Regulatory Burn Test (SN-5) – Close Up View

Figure D3 – Package at the End of Third Regulatory Burn Test (SN-5)

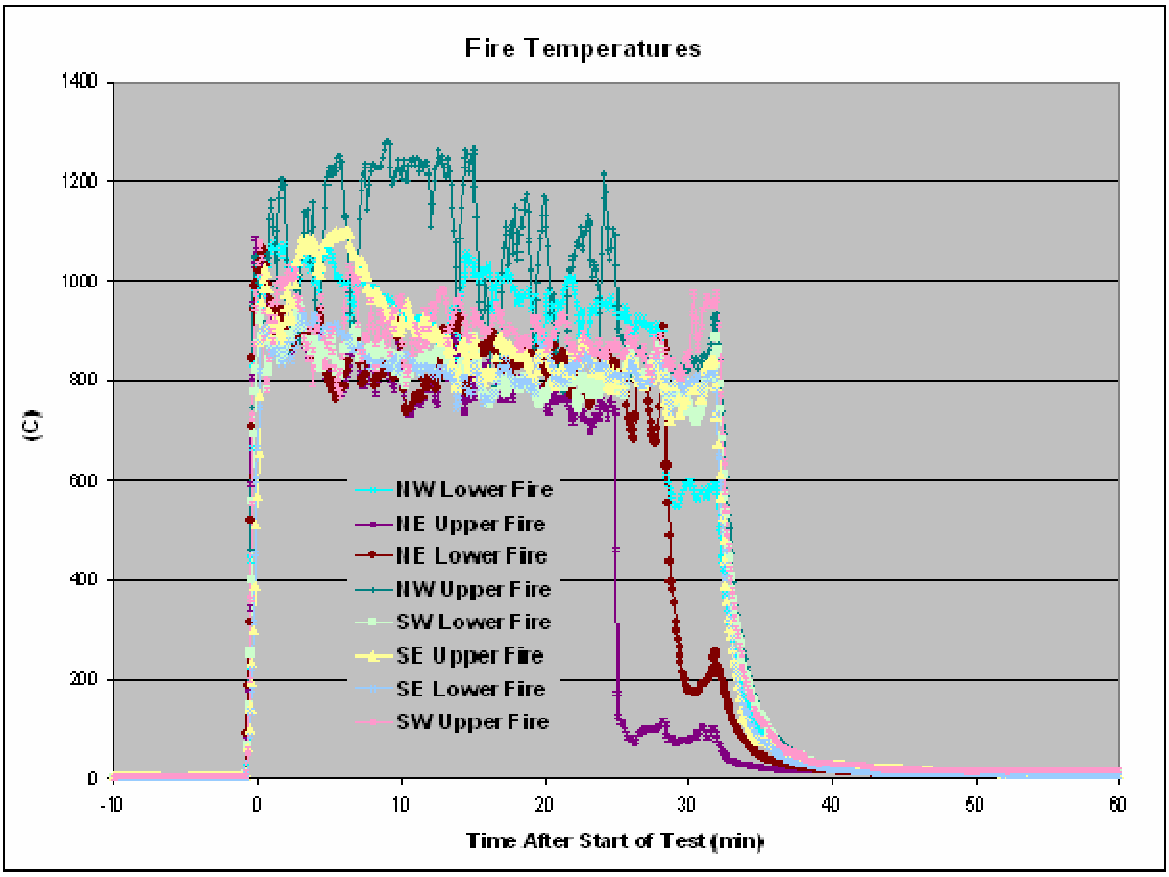

Figure D4 – Fire Temperatures Measured During the Third Regulatory Burn (SN-5)

The 30 minute average of the thermocouples readings in the four DFT's was 892°C. The average temperature recorded by the four DFTs at the end of the test was 1037°C (Figure D5).

Temperature measurements were also made using an Omega OS523 handheld infrared thermometer. Like the previous tests, these measurements were made by pointing the thermometer at the test article or the flame hiding the test article. Measurements were recorded every 3 minutes. Initially, the infrared thermometer was incorrectly set to a 0.1 emissivity. During the test, this was corrected. As shown in Table D3, after the emissivity setting was corrected these measurements show flame temperatures between 1032 and 1100°C during the fire test.

Data from the two thermocouples attached to the top and bottom of the test article are shown in Figure D6. These values have been corrected to match the room temperature readings of the calibrated digital thermometer as described above. The lower thermocouple appears to be faulty because the temperatures suddenly drop during the test, then rise to original values after the test is concluded.

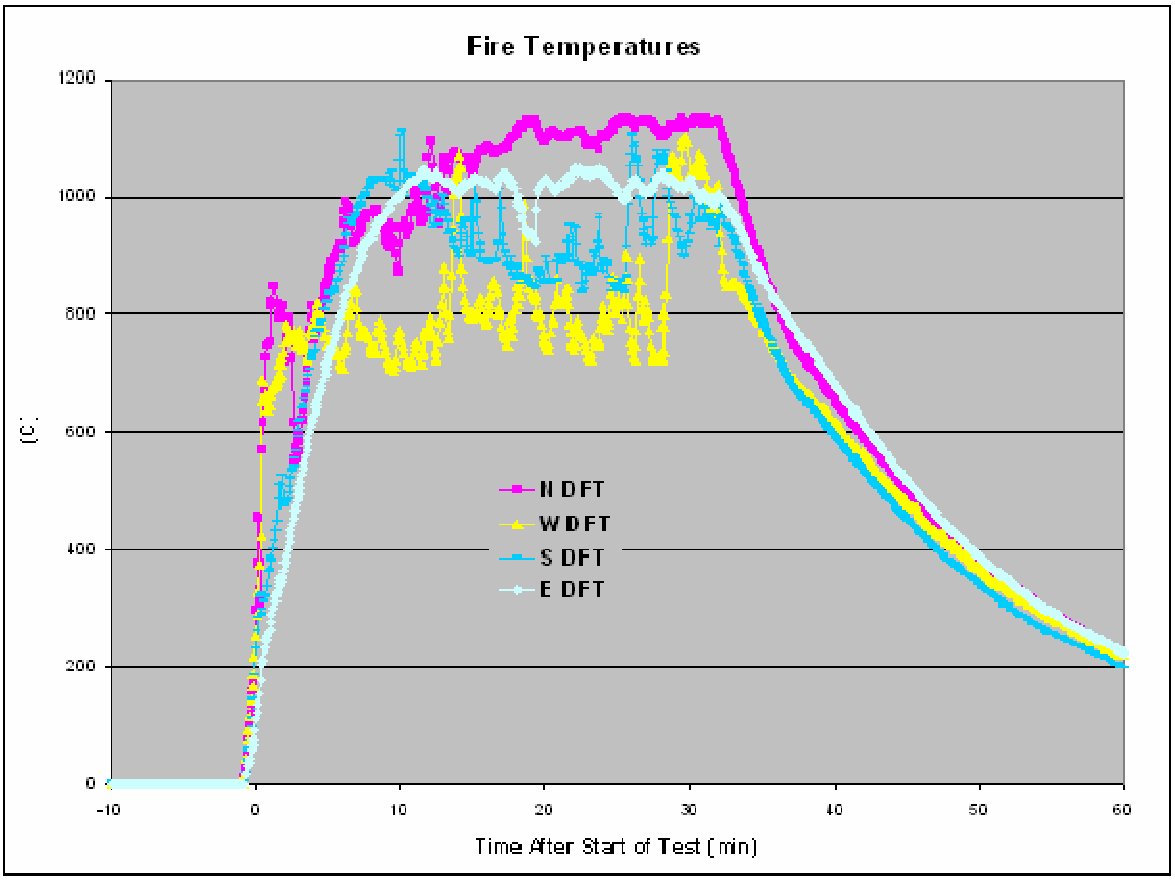

Figure D5 – DFT Measurements From the Third Regulatory Burn (SN-5)

Table D3 – Optical Thermometer Data (SN-5)

	Time	Middle of Package (°F)	Comments
Ignition	8:08	1371 *	emissivity set to 0.1
Start of Test (SoT)	8:09	1371 *	emissivity set to 0.1
SoT + 3min.	8:12	1371 *	emissivity set to 0.1
SoT + 6min.	8:15	1371 *	emissivity set to 0.1
SoT + 9min.	8:18	1371 *	emissivity set to 0.1
SoT + 12min.	8:21	1371 *	emissivity set to 0.1
SoT + 15min.	8:24	1371 *	emissivity set to 0.1
SoT + 18min.	8:27	1100	emissivity set to 0.9
SoT + 21min.	8:30	1100	emissivity set to 0.9
SoT + 24min.	8:33	1032	emissivity set to 0.9
SoT + 27min.	8:36	1039	emissivity set to 0.9
SoT + 30min.	8:39	1052	emissivity set to 0.9
SoT + 33min.	8:42	501	emissivity set to 0.9
SoT + 36min.	8:45	362	emissivity set to 0.9
SoT + 45min.	8:54	223	emissivity set to 0.9
SoT + 60min.	9:09	104	emissivity set to 0.9
SoT + 75min.	9:24	98	emissivity set to 0.9
SoT + 90min.	9:39	83	emissivity set to 0.9
SoT + 105min.			
SoT + 120min.			

* Optical thermometer was incorrectly set for an emissivity of 0.1 instead of 0.9. This was observed during the test and corrected.

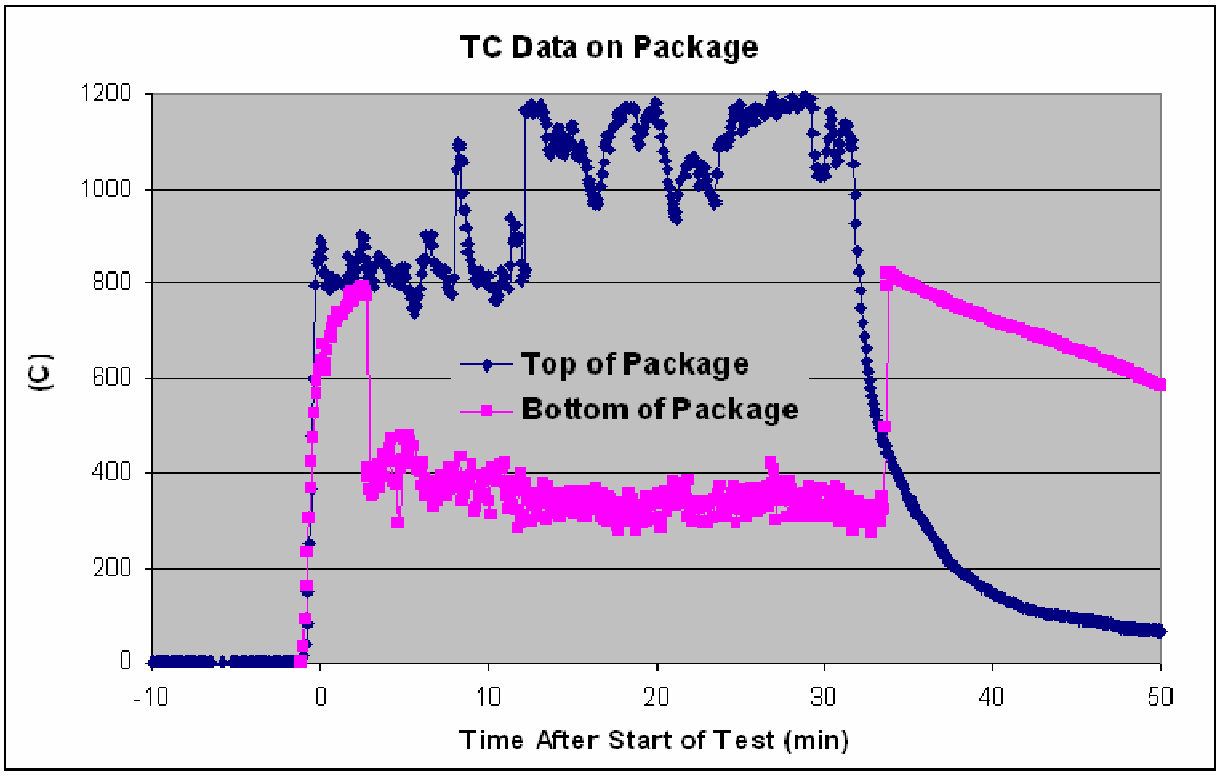

Figure D6 – Temperature Measurements at the Top and Bottom of the Test Article (SN-5)

Appendix E 9977 Regulatory Burn 4 (SN-3)

The fourth regulatory burn was performed on December 14, 2005. Preparations for this burn began on December 13 with the replacement of all of the thermocouples used in the third regulatory burn (described in Appendix D). The thermocouple locations remained the same.

Before the burn test, measurements from all of the thermocouples were compared to measurements made with a NIST traceable calibrated digital thermometer. Two thermocouples were determined to be outside of normal error ranges (2.2°C for type K thermocouples near room temperature). The thermocouples at the bottom of the package were off by 12°C. This was noted and the data collected during the test was corrected accordingly. The thermocouple in the South facing DFT was reading 4.3°C below the calibrated thermometer. Because this was conservative, no correction was made.

The fourth regulatory burn test article (SN-3) was mounted on the test stand December 13 after being transported from the preheating furnace at SRNL where it was preheated to approximately 93°C. Unlike the earlier test articles, this package was mounted horizontally with the package top end facing North (Figure E1). The lowest part of the package was 47 inches (119 cm) above the base of the pool. As in the earlier tests, this placed the lowest part of the package approximately 38 inches (97 cm) above the surface of the pool. The distance from the pool perimeter to the package was also measured (Table E1). Two thermocouples were mounted on circumference of the package, one at the top and the second on the bottom (attached to the grate below the package). Two 750W, 30 gallon drum heaters were attached to the test article and then the package was covered with thermal insulation. The package and insulation was covered with a tarp during the night.

The burn was performed essentially the same way as earlier burns except the pool was filled with approximately 75 gallons (189 liters) of fuel. At approximately 0819, the fuel in the pool was lit by an SCFA employee. Within less than a minute the package was fully engulfed and the test was officially started. The fuel valve was then opened and adjusted to maintain full package engulfment until 0849 (Figures E2 and E3). At that time, the fuel valve was closed, pumps were secured, and the fire was allowed to burn out. By 0853, the package was no longer engulfed (Figure E4). A total of 605 gallons (2291 liters) of fuel was used in the test.

As in previous tests, ambient temperatures and wind speeds were measured using a Skymate portable anemometer. The operator was standing approximately 100 yards (91 m) uphill from the test article. Weather data taken is provided in Table E2. Wind speeds were much higher than previous tests, sometimes exceeding 7 knots (13 Km/hr). The wind fence and the horizontal orientation of the test article allowed the burn to proceed on this moderately windy day without exposing the package.

Flame temperatures measured around the test article were higher at the beginning of the test and dropped as the test progressed (Figure E5). The average flame temperature over the 30 minutes of the test was 800°C. The drop in temperature corresponds with the rising wind speed that

increased the cool air flow into the pool. This effect is greater at the pool perimeter. In contrast, the 30 minute average of the thermocouples readings in the four DFT's was 897°C over the same time period (Figure E6). When the times used for the average readings are shifted by four minutes to compensate for the time delay in the DFTs, the 30 minute average increases to 972°C. The latter agrees with measurements made using the hand-held optical thermometer (Table E4) and the two thermocouples mounted on the package (Figure E7). The 30 minute average temperature for these thermocouples was 963°C.

Figure E1 – Final Burn Test Article on Test Stand

Table E1 – Package Position Inside Pool (From Package Centerline) (SN-3)

Direction	Distance to Perimeter (in/m)
North	66 / 1.7
West	70 / 1.8
South	67 / 1.7
East	62 / 1.6

Table E2 – Ambient Temperature and Wind Conditions (SN-3)

	Time	Ambient Temp (F)	Wind Speed (kts)*	Wind Direction
Ignition	8:16	33.8	2.4	118
Start of Test (SoT)	8:16	33.8	2.5	118
SoT + 3min	8:19	34.8	4.4	104
SoT + 6min	8:22	34.3	3.1	80
SoT + 9min	8:25	34.6	3.1	80
SoT + 12min	8:28	34.5	4.2	80
SoT + 15min	8:31	34.8	3.1	60
SoT + 18min	8:34	34.7	7.3	98
SoT + 21min	8:37	35.2	2.4	40
SoT + 24min	8:40	35.2	5.1	92
SoT + 27min	8:43	34.8	4.4	60
SoT + 30 min	8:46	35.7	4.9	60
SoT + 33 min	8:49	35.7	5.5	86
SoT+45 min	9:01	35.3	4.8	86
SoT+ 60 min	9:16	39.9	8	86
SoT + 75 min				
SoT + 90 min				
SoT + 105 min				
SoT + 120 min				

Figure E2 – Fourth Regulatory Burn Test (SN-3)

Figure E3 – Fourth Regulatory Burn Test (SN-3) – Close Up View

Figure E4 – Package at the End of Third Regulatory Burn Test (SN-3)

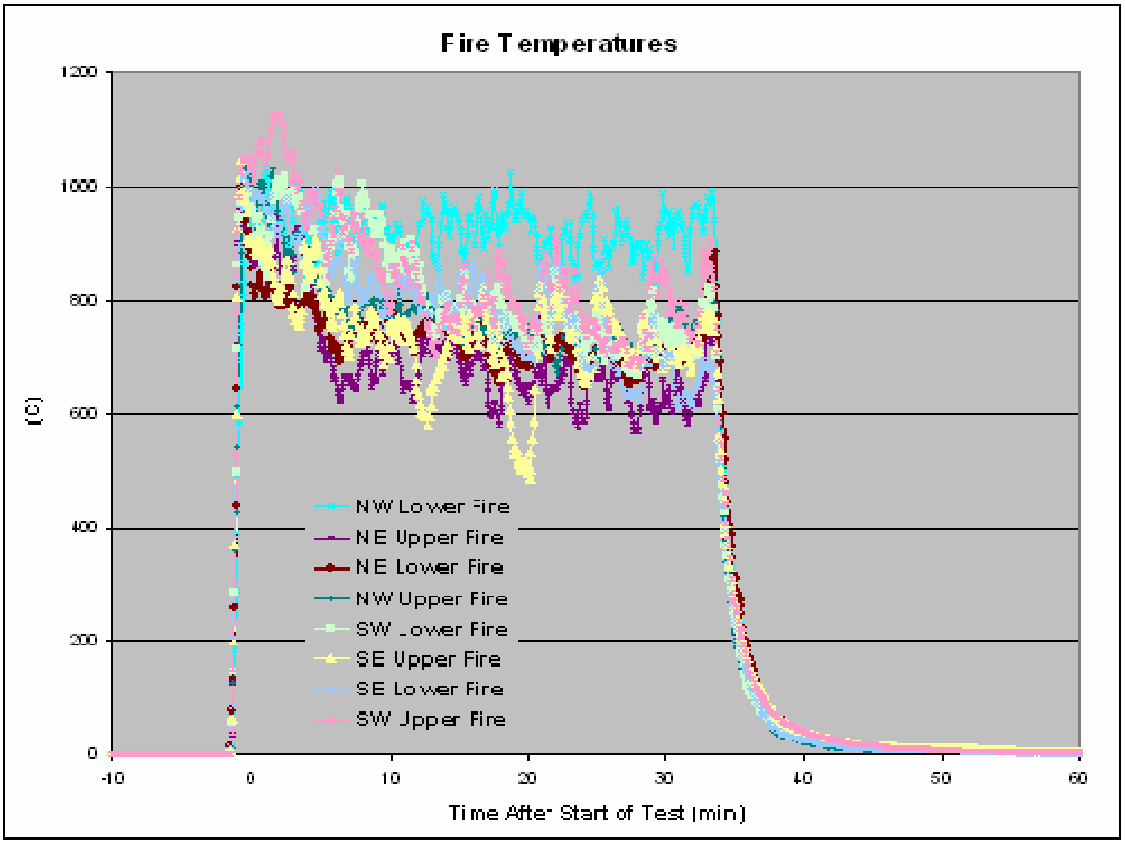

Figure E5 – Fire Temperatures Measured During the Third Regulatory Burn (SN-3)

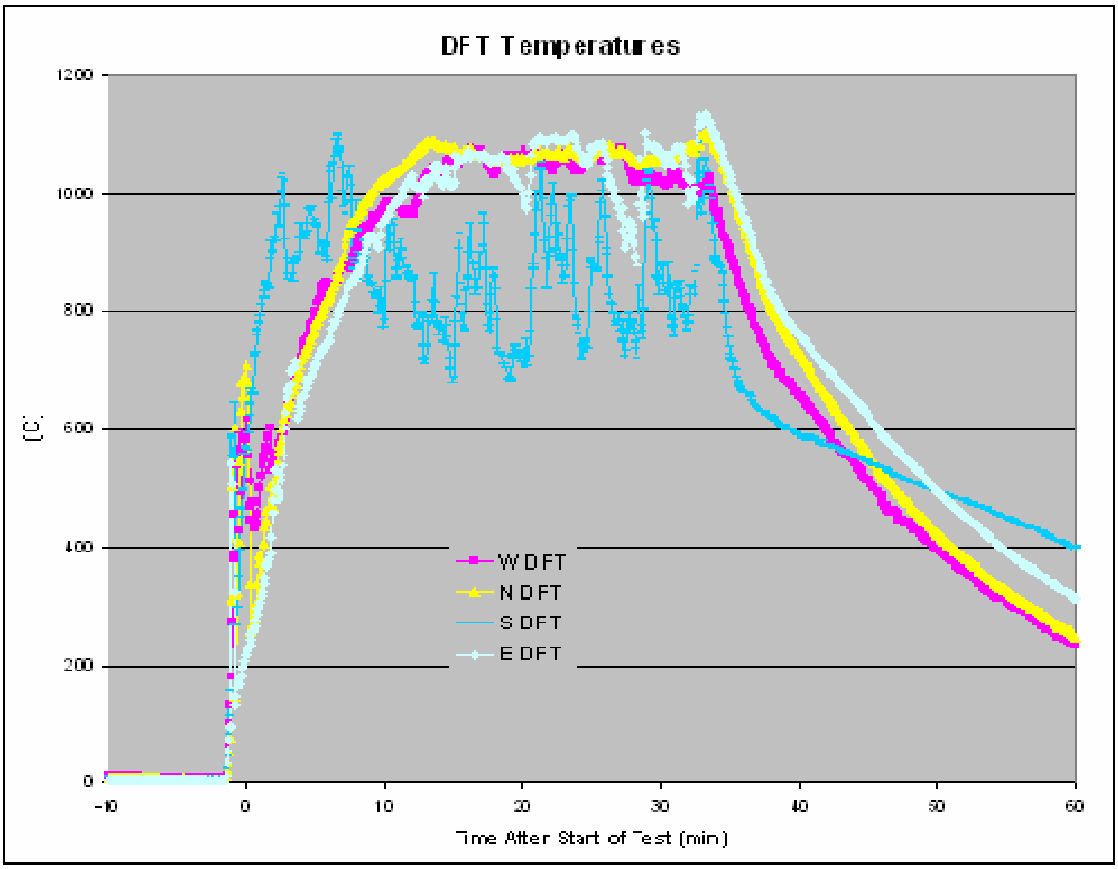

Figure E6 – DFT Measurements During Third Regulatory Burn (SN-3)

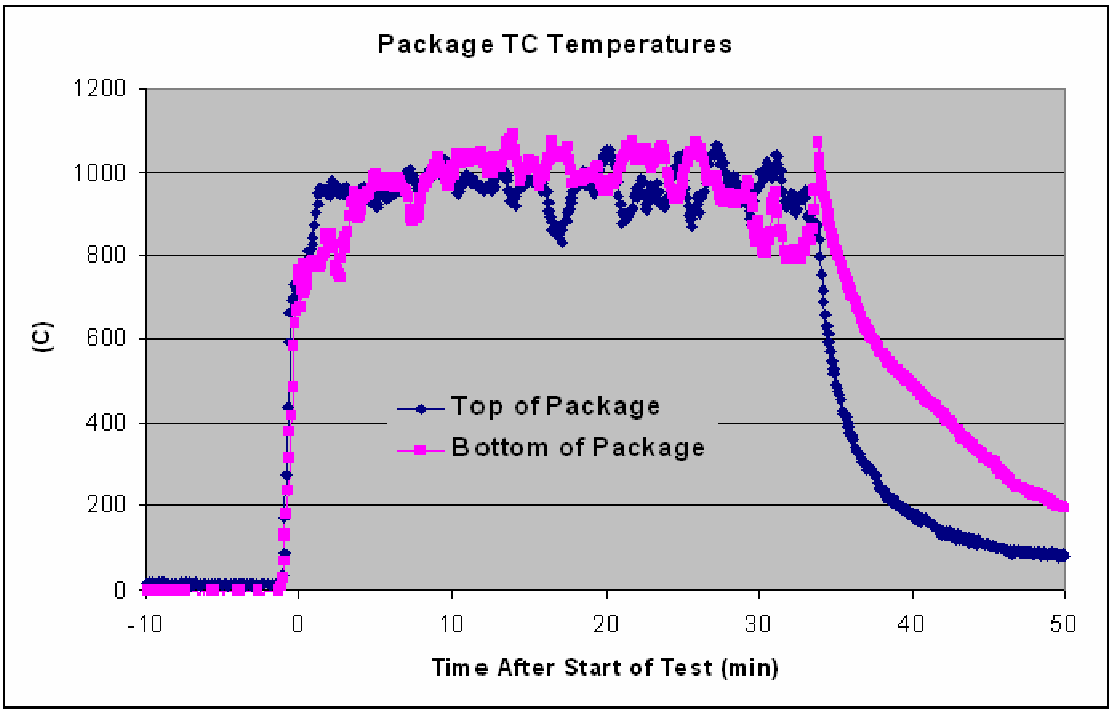

Figure E7– Temperature Measurements at the Top and Bottom of the Test Article (SN-3)

Table E3 – Optical Thermometer Data (SN-3)

	Time	Middle of Package	Comments
Ignition	8:19:00	900	
Start of Test (SoT)	8:19:30	950	
SoT + 3min	8:22:30	991	
SoT + 6min	8:25:30	1031	
SoT + 9min	8:28:30	1028	
SoT + 12min	8:31:30	961	
SoT + 15min	8:34:30	1099	
SoT + 18min	8:37:30	1002	
SoT + 21min	8:40:30	1059	
SoT + 24min	8:43:30	1006	
SoT + 27min	8:46:30	1087	
SoT + 30 min	8:49:30	888	fuel turned off mid reading
SoT + 33 min	8:52:30	930	
SoT + 36 min	8:55:30	58	flames mostly out, no good view of package
SoT+45 min	9:04:30	176	
SoT+ 60 min	9:19:30	57	
SoT + 75 min	9:34:30	no data	
SoT + 90 min	9:49:30	20	
SoT + 105 min			
SoT + 120 min			

This Page Intentionally Left Blank

This Page Intentionally Left Blank

APPENDIX 3.9

DETERMINATION OF THE VOLUME OF LAST-A-FOAMING REMAINING IN THE 9977 PACKAGE AFTER THE HYPOTHETICAL ACCIDENT CONDITIONS (HAC) THERMAL TEST

This Page Intentionally Left Blank

OSR 45-24# (Rev 1-10-2000)

Calculation Cover Sheet

Project	Calculation Number	Project Number
9977 Packaging	M-CLC-A-00254	
Title: Determination of the volume of Last-A-Foaming remaining in the 9977 Package after the Hypothetical Accident Conditions (HAC) thermal test.	Functional Classification: SC	Sheet 1 of 7
	Discipline: Mechanical	

☐ Preliminary ☒ Confirmed

Computer Program No.	Version/Release No.
☒ N/A	

Purpose and Objective

The purpose of this calculation is to estimate the uniform thickness of the Last-A-Foam left in the 9977 package after the HAC burn test. This information will be used to make a more realistic thermal model for estimating the post-HAC package temperatures.

Summary of Conclusion

Based upon the weight lost by the 9977 packages in the HAC fire and assuming a uniform thickness of Last-A-Foam remains, there is approximately 2.3-inches of foam remaining around the drum liner and Fiberfrax after the HAC fire.

Revisions

Rev No.	Revision Description
0	Original

Sign Off

Rev No.	Originator (Print) Sign/Date	Verification/ Checking Method	Verifier/Checker (Print) Sign/Date	Manager (Print) Sign//Date
0	G Abramazyk G Abramazyk 4/3/06		N.K. Gupta N.K. GUPTA 4/3/06	J.S. Bellamy 4/4/06

Release to Outside Agency – Design Authority (Print)	Signature	Date

Security Classification of the Calculation: (U)

UNCLASSIFIED
DOES NOT CONTAIN
UNCLASSIFIED CONTROLLED
NUCLEAR INFORMATION

ADC & Reviewing Official: S. Blanton 4/12/06
(Name and Title)

Date:

Introduction

Last-A-Foam polyurethane foam is used within the 9977 packaging for thermal protection and impact resistance. See Figure 1. The foam decomposes at 532°F to form an intumescent char. The thermal performance of the 9977 has been calculated for normal conditions of transportation. However, the intumescent properties of the foam are not understood well enough to permit modeling of the package during the Hypothetical Accident Condition (HAC) thermal test. If the average post-fire package conditions could be determined from measurements and examination, the post-HAC cool-down package performance could be modeled.

This calculation estimates the volume of foam remaining around the drum liner after the HAC-Thermal (fire) test.

Background

The Last-A-Foam polyurethane foam in the 9977 packaging is used for thermal protection and impact resistance. When the foam is exposed to temperatures greater than 532°F it decomposes to form an intumescent char. During the Hypothetical Accident Condition (HAC) thermal test, the package is exposed to a fire at a minimum of 1475°F and polyurethane foam intumesces, either remaining within the drum cavity as char or exiting through the drum vent holes and combusting when combined with free oxygen. The polyurethane foam that does not melt/intumesce continues to provide thermal protection to the radioactive material contents and the containment vessel. The foam that remains after the HAC fire retains some thermal energy and both adds heat to and insulates the contents/CV after the fire ends.

Input

Four (4) 9977s were subjected to the suite of HAC testing as required by 10 CFR 71.73. As manufactured, these packages each contained 75-lbs of foam, as reported by General Plastics Manufacturing Corporation, who foamed the drums. After the HAC 30-foot drop, Crush, and Puncture test, the packages were subjected to the proscribed “Thermal” conditions.

The drum skin on three (3) of the tested 9977s (SN-2, SN-4 and SN-5) had the fourteen (14) designed vent holes. The fourth (4th) 9977 (SN-3) had an additional tear in the drum bottom. (Reference 9977 Test Report.)

Packages SN-2, SN-4 and SN-5 lost an average of 48.2-lb. Package SN-3, because of its greater vent area, lost 54.3-lbs.

Discussion

Post testing examination of packaging SN-2 is seen in Figures 2 and 3. Note that the polyurethane foam and Fiberfrax covering the bottom end of the drum liner have been removed as well as the bottom of the liner. This was done to remove the CV for testing. Figure 2 illustrates the typical annular region of char foam between the drum skin and the polyurethane foam which did not melt. Figure 3 shows the packaging after the drum skin and all char have been removed. Since the remaining foam is not melted (except for a residual on the surface) the temperature of this foam did not exceed 532°F.

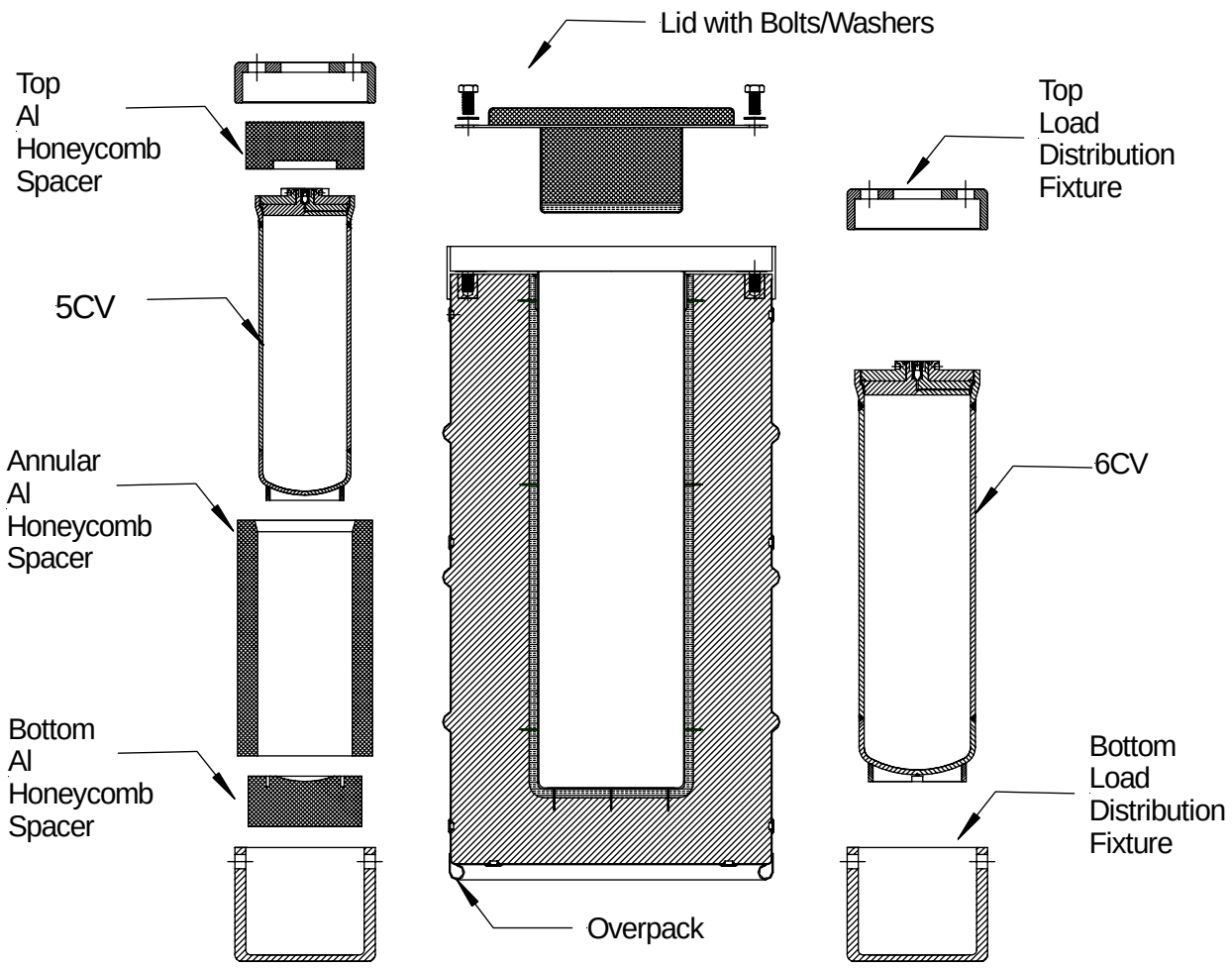

Figure 1 – Exploded view of 9977 showing key features and components.

The average Last-A-Foam remaining, from the pre- and post-HAC weights, 75lb – 48lb = 27lb.

This calculation estimates the depth of foam that will remain around the drum liner in this condition.

The evaluation demonstrates that this mass equates to approximately 2.32-inches of foam surrounding the Fiberfrax and the remaining drum volume filled with “char-foam” material.

Note: Although the HAC Thermal tests were performed on 9977s in the 6CV configuration, the differences between the 5CV and 6CV configurations are all internal to the liner and have no effect on the configuration or function of the overpack. Therefore, this calculation is equally applicable to both the 5CV and 6CV configurations.

Figure 2 – Sectioned 9977 SN-2 after HAC Fire, showing annulus of char and region of un-melted foam (Note: The drum top is to the left. The bottoms of the drum, liner, and Fiberfrax and the remaining foam and char have been removed.)

Figure 3 – Sectioned 9977 SN-3 after HAC Fire, all char removed, showing remaining un-melted foam. (Note: The drum lid is down. The drum below the rim, the char and the ends of the liner, foam, and the Fiberfrax have been removed.

Computational and Analytical Methods

It is assumed that the foam chars uniformly and leaving a layer of un-melted foam surrounding the Fiberfrax/liner. This assumption is reasonable for modeling the post-HAC cool-down process.

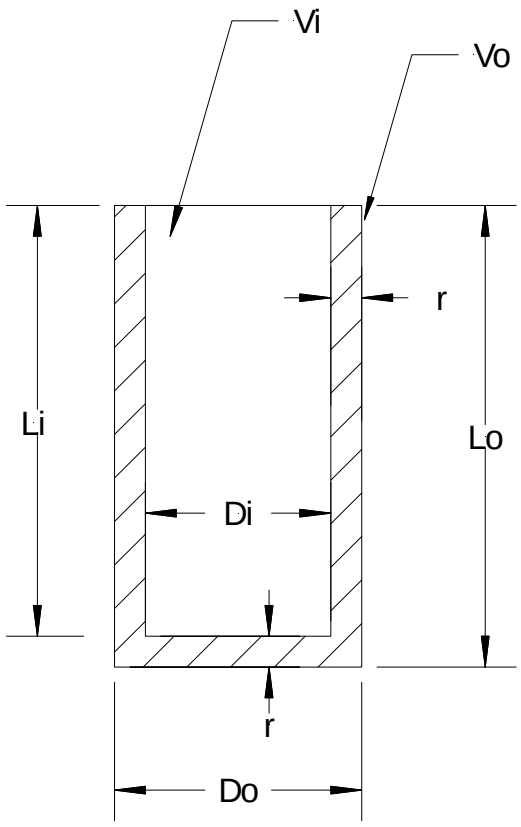

Figure 4 – Mathematical construction for calculating remaining polyurethane foam. The volume "Vi" represents the drum liner with Fiberfrax.

The volume of a cylinder is:

$$V = \pi \times R^2 \times L = \pi R^2 L \quad \text{(eq. 1)}$$

Where R and L are the cylinder's radius and length respectively.

Therefore, the volume of the remaining foam annulus is:

$$Vr = Vo - Vi$$

$$Vr = \pi Ro^2 Lo - \pi Ri^2 Li$$

$$Vr = \pi(Ro^2 Lo - Ri^2 Li)$$

Where:

$$Ro = Do/2 \text{ and } Ri = Ri/2$$

$$Vr = (\pi/4)(Do^2Lo - Di^2L) \quad \text{(eq. 2)}$$

If we assume the foam is at a uniform thickness on the sides and the bottom of the liner:

$$Do = Di + 2r \text{ and } Lo = Li + r$$

Substituting into equation 2:

$$Vr = (\pi/4)((Di + 2r)^2(Li + r) - Di^2Li) = (\pi/4)(4DiLir + 4r^2Li + Di^2r + 4Dir^2 + 4r^3)$$

Simplifying:

$$Vr = \pi(DiLir + r^2Li + (1/4)Di^2r + Dir^2 + r^3) \quad \text{(eq 3)}$$

From the foam installation and from weighing of the drums before and after the thermal test, we know the mass lost during the HAC fire:

$$\text{Mass lost (average)} = [\text{Pre-Fire Wt}](\text{ave}) - [\text{Post-Fire Wt}](\text{ave}) = 340.6 - 292.4 = 48.2\text{lb}$$

$$\text{Foam mass remaining} = 75 - 48 = 27\text{lb} = Mr$$

We know the foam density:

$$\rho = 16\text{lb/ft}^3$$

Therefore:

$$\text{Foam mass remaining} = Mr = \text{Volume remaining} \times \text{density} = Vr\rho = 27\text{lb} \quad \text{(eq 4)}$$

Solving equation 4 for "Vr"

$$Vr = (27\text{ lb})/(16\text{lb/ft}^3) = 1.6875\text{ft}^3$$

Combining with equation 3:

$$1.6875\text{ft}^3 = \pi(DiLir + r^2Li + (1/4)Di^2r + Dir^2 + r^3)$$

From the drawing R-R2-G-00016 we get:

$$Di = 8.25 \text{ (liner ID)} + 2 \times 0.048 \text{ (wall thickness)} + 2 \times 0.5 \text{ (compressed Fiberfrax)} = 9.346 \text{ inches}$$

$$Li = 30 \text{ inches}$$

$$1.6875 ft^3 = (\pi((9.346)(30)r + r^2(30) + (1/4)(9.346)^2 r + (9.346)r^2 + r^3))/12^3$$

If we solve this iteratively substituting values for "r" until we equal "1.6875" we find:

$$r \cong 2.32\text{-inches}$$

Conclusion:

Assuming that the Last-A-Foam remaining after the HAC Thermal fire is distributed to an equal depth on the sides and bottom of the Fiberfrax around the drum liner, the average thickness of the remaining Foam is:

$$r \cong 2.32\text{-inches}$$

Reference:

1) *9977 GENERAL PURPOSE FISSILE PACKAGING PROTOTYPE TESTING*, M-TRT-A-00007, Revision 0, L.F. Gelder, C.M. May, Washington Savannah River Company, (April, 2006)
2) *SRNL Package Burn Test Report*, NT-TDR-06-101, Revision 1, NovaTech Innovative Technologies International, Lynchburg VA, (March, 2006)

This Page Intentionally Left Blank

Safety Analysis Report - 9977 Packaging

CHAPTER 4

CONTAINMENT

Preface

The 9977 Package is a single containment packaging designed primarily to ship plutonium and uranium in solid form. The containment vessel is designed, fabricated, and shown by physical testing to meet the containment requirements of 10 CFR 71.[1] When transported in the package, the containment vessel (CV) meets the leaktight requirements of ANSI N14.5,[2] and applicable containment performance requirements for the *normal conditions of transport* (NCT) specified in 10 CFR 71.71 and for the *hypothetical accident conditions* (HAC) specified in 10 CFR 71.73.

Radioactive material is packaged in convenience containers and loaded into either a 5-inch or a 6-inch diameter containment vessel (5CV or 6CV). The convenience containers confine the material, minimize contamination, and simplify material handling and storage, but they are not credited with nor required to provide any measure of containment during transport.

This Page Intentionally Left Blank.

TABLE OF CONTENTS

Page

LIST OF FIGURES

Page

ACRONYMS AND ABBREVIATIONS

5CV	5-inch Diameter Containment Vessel
6CV	6-inch Diameter Containment Vessel
ANSI	American National Standards Institute
ASME	American Society of Mechanical Engineers
CFR	Code of Federal Regulations
HAC	Hypothetical Accident Conditions
MNOP	Maximum Normal Operating Pressure
NCT	Normal Conditions of Transport
NRC	Nuclear Regulatory Commission

4 CONTAINMENT

4.1 DESCRIPTION OF THE CONTAINMENT SYSTEM

The 9977 packaging is a single-containment design incorporating a leak-testable Containment Vessel (CV). The 9977 package utilizes either of two different size CVs, with an inside diameter of either 5 or 6-inches (5CV or 6CV).

The 5CV approximately 18.6 inches in length and fabricated from 5-inch diameter Schedule 40S pipe with an internal volume of approximately 313 cubic inches and an assembled weight of approximately 34 lb. In the closed condition, it has a cavity approximately 16½ inches (as measured from the bottom of the pipe cap to the closure plug) with a minimum diameter of 5 inches in the pipe section.

The 6CV is identical to the 5CV, except that the 6CV vessel is taller in height and larger in diameter. The 6CV approximately 24 inches in length and fabricated from 6-inch diameter Schedule 40S pipe with an internal volume of approximately 604 cubic inches and an assembled weighted of approximately 56 lb. In the closed condition, it has a cavity approximately 21½ inches (as measured from the bottom of the pipe cap to the closure plug) with a minimum diameter of 6 inches in the pipe section.

The containment boundary is formed by the containment vessel body, the Cone-Seal Plug, and the inner O-ring seal. The geometric relationship of these components and the containment boundary are illustrated in Figures 4.1 and 4.2.

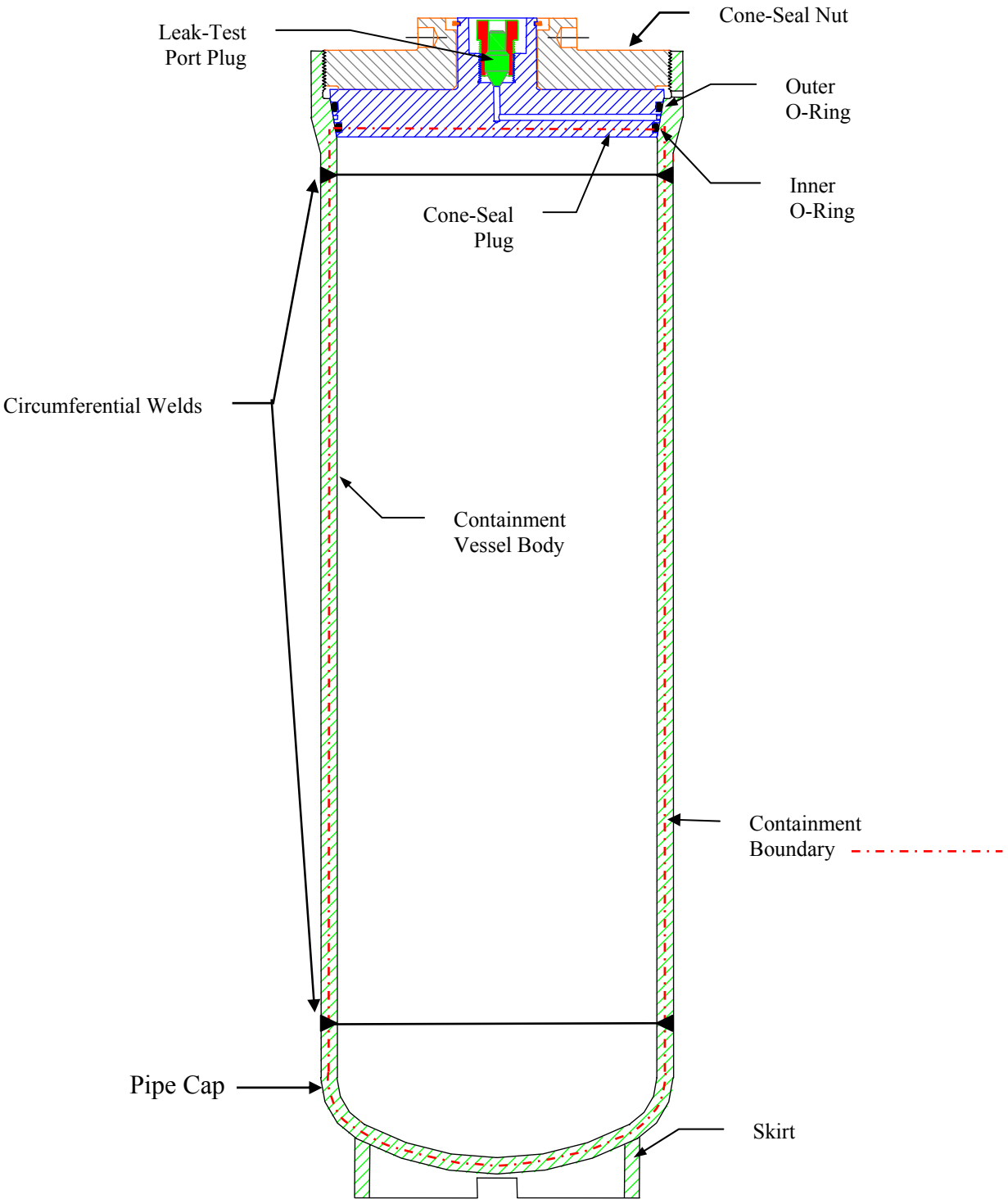

Figure 4.1 – Containment Boundary for Containment Vessel Assembly (typical)

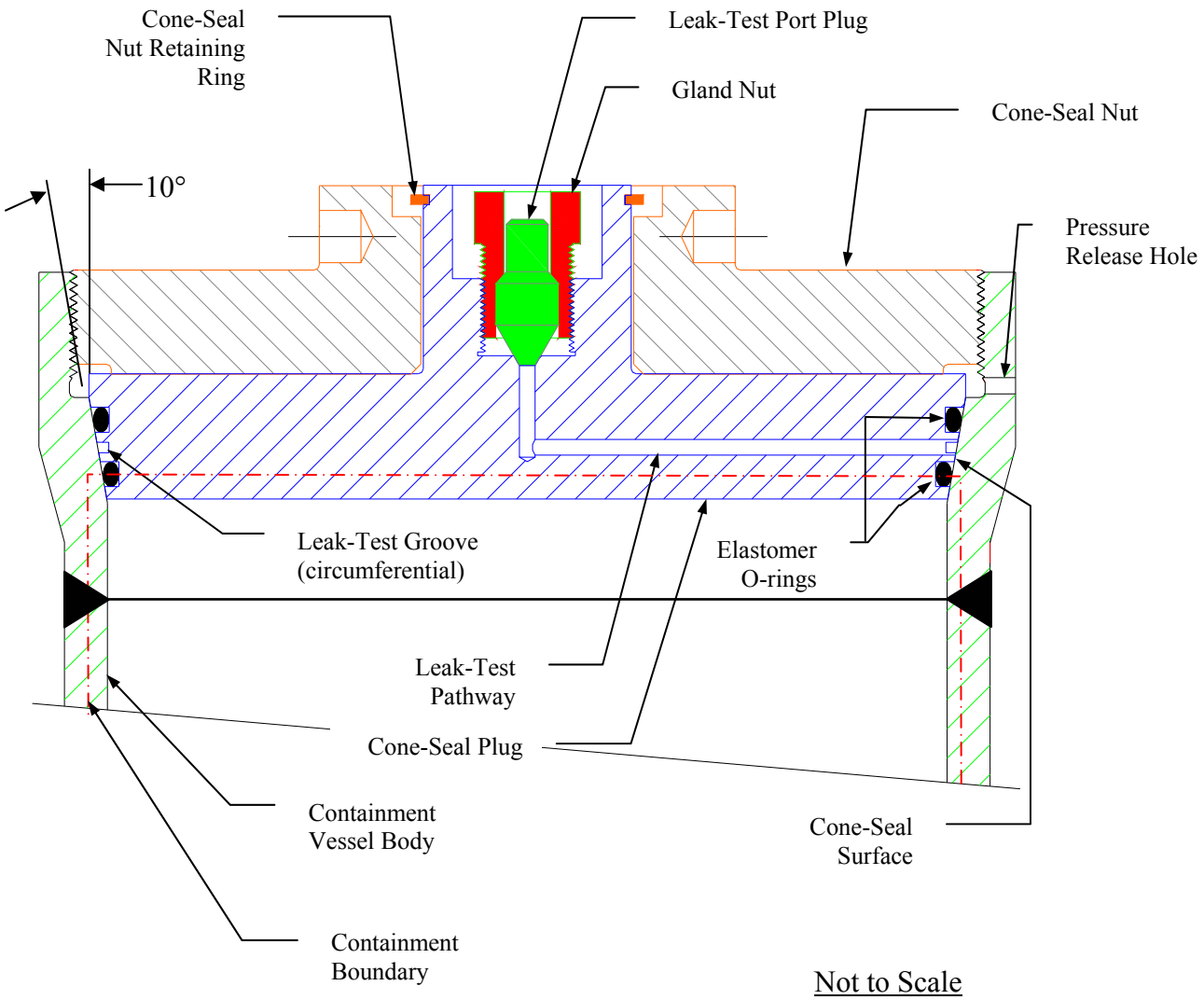

Figure 4.2 – Cross Section of the Containment Vessel Closure

4.1.1 Containment Vessel

The containment vessels (5CV or 6CV) are fabricated from stainless steel. Design drawings for the CVs are provided in Appendix 1.1. The containment vessels are designed, analyzed, fabricated, and examined in accordance with Section III, Subsection NB, of the ASME Boiler and Pressure Vessel Code, 2004 Edition. [3]

The 5CV is fabricated from 5-inch, Schedule 40S stainless steel (SS) pipe closed at one end by a Schedule 40S SS pipe cap. The open end of the vessel is formed by a stayed head machined from a 6½ inch diameter SS bar. The stayed head incorporates an internal cone O-ring seating surface having a 32 μin. finish. The threaded section of the weldment accepts a Cone-Seal Nut that secures the Cone-Seal Plug in place and compresses the O-rings. The radial welds joining the pipe cap to form the closed end of the pipe, and the stayed head at the open end, are full penetration welds examined by radiographic and liquid penetrant methods. The pipe end of the vessel incorporates a skirt to allow the vessel to stand vertically. Slots in the skirt engage keys in the support stand that prevents vessel rotation during opening and closing operations.

The CV is closed by a SS plug with an external cone that mates to the internal cone seating surface of the vessel body. The plug, referred to as the Cone-Seal Plug, incorporates two machined O-ring groves and a machined test port and groove for leak-rate testing. The Cone-Seal Plug is held in place by a Cone-Seal Nut that establishes the compression force for sealing the closure. The Cone-Seal Nut is fabricated from Nitronic-60® SS to reduce the potential for galling between it and the vessel body, which is fabricated from 304L SS. The leak-test port is closed by a ¼-inch 316 SS plug held by a gland nut fabricated from 410 SS. The plug and nut are manufactured by Pressure Products Industries and rated for high pressure service. Galling between the Cone-Seal Plug (304L SS) and gland nut (410SS) is mitigated by the difference in hardness of the materials. Chemical and galvanic reactions between the CV materials are discussed in Section 2.2.2. The 6CV closure design is identical to that used on the 5CV, except that the 6CV vessel is greater in height and diameter.

The CV, when sealed, does not include any feature that would permit venting. When the CV is being opened, any pressure differential will vent past the O-rings when the cone-seal nut has been unthreaded approximately 2¼ turns. The cone seal plug is protected by the cone seal nut. The cone seal nut is threaded into the stayed head so that the top of the nut is approximately flush with the top of the vessel.

The CVs satisfy the Nuclear Regulatory Commission (NRC) Regulatory Guide 7.6[4] stress requirements at the internal design pressures and temperature of 800 psig and 900 psig at 300°F, for the 6CV and 5CV, respectively. The design conditions exceed the NCT and HAC pressures, and the temperatures as shown in Tables 3.2 and 3.3. As discussed in Section 4.1.3.1, a -40°F cold test was performed on a prototype CV.

4.1.2 Containment Penetrations

The CV has no pressure relief devices, valves, nor penetrations through the containment boundary.

4.1.3 Seals and Welds

There is one seal (inner O-ring) and two welds in the containment boundary of each vessel. A second O-ring (the outer) is used to verify the assembly of the vessel prior to transport but it is not a part of the containment boundary.

4.1.3.1 Seals

The CV incorporates a static seal design using concentric elastomer O-rings fit within circumferential grooves machined into the Cone-Seal Plugs as illustrated in Figure 4.2 and in Drawings R-R2-F-00042 and R-R2-F-00043 (Appendix 1.1). The inner O-ring of the Cone-Seal Plug functions as the containment boundary seal. The outer O-ring forms a test volume to qualify the inner O-ring. The outer O-ring is not part of the containment boundary, but it does present a significant barrier to the release of material. The same size O-ring (i.e., major diameter and cross-sectional diameter) is used for the inner and outer seals.

The O-rings are made of Viton® GLT, manufactured by the Parker O-ring Company as specified on Drawings R-R2-F-00042 and R-R2-F-00043, and have a continuous service temperature range from -40 to 400°F.[5]

The CV was helium leak-rate tested per RG 7.4[6] and the bell jar method described in ANSI N14.5. The CV was fitted with two, Viton® GLT O-rings and cooled to -40°F. The bell jar was evacuated and the CV was pressurized to 15 psig helium internal pressure. The test showed that the CV remained leaktight to a sensitivity less than $1x10^{-7}$ ref cc/sec. Repeating the test confirmed the results; see Appendix 2.4.

Savannah River Site has tested the O-rings to heat-induced failure at 783°F in service within a containment vessel pressurized to 1000 psig. Following the test-to-failure, fresh O-rings were installed and the vessel was heated to 600°F at 1000 psig and held at these conditions for 16 hours. Following the 16-hour thermal test, the vessel was cooled to ambient temperature, and a helium leak-rate test demonstrated that it remained leaktight.[7] These tests demonstrate that the O-rings are adequate for use in the package containment boundary.

4.1.3.2 Welds

Fabrication of the containment vessel includes two circumferential, full-penetration welds as shown in Figure 4.1 and on Drawings R-R2-F-00042 and R-R2-F-00043 (Appendix 1.1). The upper circumferential weld joins the containment vessel stayed head to the Schedule 40S pipe section. The lower circumferential weld joins a standard weight pipe cap to the pipe section to close the lower end of the vessel. Containment vessel fabrication welds comply with Section III, Subsection NB, of the ASME Code. The welds are examined with liquid penetrant and are fully

radiographed. Details of the vessel weldment design, fabrication and examination are given in Section 9.3, Table 9.5.

4.1.4 Closure

The containment vessel closures consists of a male-female cone joint with surfaces that have been machined to matching 10-degree angles so that the Cone-Seal Plug mates with the containment vessel body with a nominal zero clearance (R-R2-F-00042 and R-R2-F-00043, Appendix 1.1). The sealing surfaces are machined to a 32 μin. finish. Two grooves are machined on the face of the Cone-Seal Plug for the O-rings. The male-closure is a two-piece assembly made up of a conically shaped plug (the Cone-Seal Plug) and a male-threaded ring (the Cone-Seal Nut). The two components are designed to be loosely joined using a snap-type retaining ring. The loose fit minimizes friction-induced rotation between the male-female cone surfaces as torque is applied. The retaining ring ensures removal of the Cone-Seal Plug as the Cone-Seal Nut is removed.

The Cone-Seal Nut is fabricated from Nitronic-60 stainless steel alloy and is cut with 6½-inch or 5½-inch 12UNS-2A external threads (6CV and 5CV respectively). The CV weldment is made from 304L stainless steel and is cut with 6½-inch inch or 5½-inch 12UNS-2B internal threads (6CV and 5CV respectively). The use of dissimilar metals between the Cone-Seal Nut and the vessel weldment reduces the potential for galling.

The Cone-Seal Nut is tightened to the prescribed torque value of 50 (+10/-0) ft-lb and 100 (+20/-0) ft-lb, for the 5CV and 6CV respectively. A maximum radial clearance of 0.0007 inch (Appendix 2.2) exists between the Cone-Seal Plug and vessel body. This close fit prevents the O-rings from extruding from the grooves under high pressure. The prescribed torque prevents the containment vessels from opening during NCT and HAC. The cone seal assembly has a non-standard size nut and must be opened with a special wrench; it cannot be opened inadvertently. The 5CV and 6CV assemblies are pressure tested to 1365 (± 10) psig and 1235 (± 10 psig), respectively, for acceptance, as described in 8.1.2, proving that the closures cannot be opened by internal pressure.

For transport, the containment boundary is leak-rate tested using an assembly verification leak test as provided for in Section 7.6 of ANSI N14.5 (Section 8.2.2.1). The entire containment boundary is tested to be leaktight (in accordance with ANSI N14.5) during acceptance testing, annually, or after any component in the containment boundary is repaired or replaced (Section 8.2.2.2).

4.2 CONTAINMENT UNDER NORMAL CONDITIONS OF TRANSPORT

The Code of Federal Regulations, 10 CFR 71.51(a)(1), requires that the containment vessel be designed, constructed, and prepared for shipment so that, under NCT test conditions, "there will be no loss or dispersal of radioactive contents, as demonstrated to a sensitivity of 10^{-6} A_2 per hour."

The 9977 contents are "Normal Form" per 10 CFR 71.4. For normal form material, the calculated hazard (in A_2 units) and total curies for the maximum 9977 content loading, shown in Table 1.2 of 4.4 kg of Pu/U, are 122,000 A_2 and >69,700 Ci, respectively; this calculation is documented in Appendix 4.1. Given this data, RG 7.11 specifies the radioactive material packaging design as "Category I". Based upon this value of A_2, the CVs would be required to be leaktight if an allowable leakage rate were to be calculated for NCT. Since the CVs are leaktight as defined by ANSI N14.5, there is no calculation of an allowable leak based on the A_2 value.

The results of the evaluation in Section 2.6.7 and analysis in Section 3.3 demonstrate that the containment system is not damaged and will remain leaktight during all of the NCT events. Consequently, the requirements of 10 CFR 71.51 are met and the system satisfies the containment requirement for NCT.

The 9977 is an unshielded package. There is no significant increase in 9977 external surface radiation levels during the NCT events, see Sections 2.6 and 5.1.

4.2.1 Containment of Radioactive Material

The contents of the CV include actinide metals and oxides limited to the quantities specified in Section 1.2.3. To ensure the containment of the radioactive material, a leaktight containment criterion is established for the CV. "Leaktight" is the most restrictive leak-rate requirement of ANSI N14.5.

The leak-test described in Section 8.1.4 is required for acceptance (first use), annually, and whenever a containment boundary component is repaired or replaced. During normal operations, the CV is tested in accordance with Section 7.6 of ANSI N14.5. The leak-test for normal operation is described in Section 8.2.2.1.

4.2.2 Pressurization of Containment Vessel

The containment boundary of the CV does not include any features which would permit continuous venting. Pressurization of the CV is due to:

- partial pressure from the formation of helium during radioactive decay,
- expansion of gas within the containment vessel from heating, and
- partial pressure from thermal degradation of plastic.

The partial pressures are calculated in Appendix 3.7. The MNOPs are 56.3 and 41.2 psig for the 5CV and 6CV respectively. These maximum pressures are much lower than the design pressures of 900 and 800 psig for the 5CV and 6CV as reported in Table 3.3.

When the CV is unloaded, any pressure differential will relieve past the Cone-Seal Plug O-rings when the cone-seal nut has been unscrewed approximately 2½ turns. The cone seal nut must be unscrewed approximately 5½ turns to completely disengage its threads from the CV.

4.2.3 Containment Criterion for NCT

The regulatory limit for the release of radioactive material during NCT (10^{-6} A_2/h) is met by measuring the CV leak rates relative to the leaktight criterion defined by ANSI N14.5. Prototypical CV's used in the NCT/HAC tests were modified to include a ¼-inch threaded pipe tap in the end cap. For the pre- and post-NCT/HAC leak-rate tests, each CV was evacuated and backfilled with helium to one atmosphere absolute pressure and then an "evacuated envelope – gas detector" leak test (described in ANSI N14.5 A.5.4) was performed. The ANSI N14.5 defined rate for leak-tight is $\leq 1x10^{-7}$ ref cm^3 air/sec ($2x10^{-7}$ ref cm^3 helium/sec). For these tests, the test port plug in the CV closure was removed to allow detection of helium leakage across just the inner O-ring seal.

4.2.3.1 6CV

Section 2.7 lists the leak-rates that were measured before the NCT and after the HAC testing of the prototype 6CVs. The leaktight performance of the CV after HAC demonstrates compliance with the containment criterion for NCT.

4.2.3.2 5CV

The 5CV was not physically tested as part of the 9977 testing program. The suitability of the 5CV design for NCT is demonstrated by:

- The 5CV closure design is identical to that used on the 6CV, except that the 5CV closure is smaller in diameter.
- The 5CV loading configuration has been analyzed for the NCT loading conditions and compared against the similar loadings for the 6CV loading configuration. The stress levels in the 5CV are equal to those calculated for the 6CV, within the resolution of the models.
- The 5CV is more robust, being designed, analyzed, and tested to withstand a greater maximum operating pressure (900 psig verses 800 psig).

4.3 CONTAINMENT UNDER HYPOTHETICAL ACCIDENT CONDITIONS

The Code of Federal Regulations, 10 CFR 71.51(a)(2), requires that the containment vessel be designed, constructed and prepared for shipment so that during the HAC, no escape of radioactive materials can occur in excess of A_2 in one week.

The maximum pressure generated during the HAC is 48.5 and 35.0 psig for the 5CV and the 6CV, respectively.

The CVs are tested as described in Section 8.2 to be leaktight per the ANSI N14.5 definition and, therefore, meet the requirement of 10 CFR 71.51 for containment of radioactive material. Since the containment vessels are leaktight there is no calculation of an allowable leak based on the A_2 value.

The results of the testing and analyses described in Sections 2.7 and 3.4 demonstrate that the containment system is not damaged and remains leaktight during and after the HAC. Consequently, requirements of 10 CFR 71.51 are met and the system satisfies the containment requirement for HAC.

The 9977 is an unshielded package. There is no significant increase in radiation dose levels for the 9977 following the HAC events. See Table 5.1

4.3.1 Fission Gas Products

The production of fission product gases from package contents identified in Section 1.2.3 is negligible. There is no increase in CV pressure due to fission gas products.

4.3.2 Containment of Radioactive Material

The CVs are designed and tested to leaktight conditions, as defined by ANSI N14.5. Since physical testing and analysis show that the containment boundary of the CV following HAC remain leaktight, the containment is maintained for the HAC events.

4.3.3 Containment Criterion for HAC

The regulatory limit for HAC is "no escape of radioactive material exceeding a total amount A_2 in one week." This condition is met by leak testing the CV to leaktight conditions as defined by ANSI N14.5. The leak test for acceptance, annual maintenance and for qualification after a component of the containment boundary is repaired or replaced is presented in Section 8.1.4. During normal or routine use, the containment boundary is tested in accordance with Section 7.6 of ANSI N14.5, as described in Section 8.2.2.1.

4.3.3.1 <u>6CV</u>

The leaktight performance of the 6CV under HAC (Section 2.7), demonstrates compliance with the containment criterion for HAC.

4.3.3.2 5CV

The 5CV was not physically tested as part of the 9977 testing program. The suitability of the 5CV design for HAC is demonstrated by:

- The 5CV closure design is identical to that used on the 6CV, except that the 5CV closure is smaller in diameter.
- The 5CV loading configuration has been analyzed for the NCT loading conditions and compared against the similar loadings for the 6CV loading configuration. The stress levels in the 5CV are equal to those calculated for the 6CV, within the resolution of the models.
- The 5CV is more robust, being designed, analyzed, and tested to withstand a greater maximum operating pressure (900 psig verses 800 psig).

4.4 LEAK RATE TESTS FOR TYPE B PACKAGES

4.4.1 Acceptance Test

The containment boundary is tested to be leaktight in accordance with ANSI N14.5 during acceptance testing or after any component in the containment boundary is repaired or replaced. Since there are no penetrations to permit the introduction of helium into the CV for leak testing, a helium filled cylinder is placed inside the containment vessel prior to closure. The cylinder is remotely opened, providing at final concentration of at least 50% helium. A peak-holding gauge records the pressure applied, confirming the concentration. The measured leak rate is adjusted for temperature and doubled to account for the helium concentration.

4.4.2 Annual Test

For annual testing, two new O-rings are installed and the containment vessel is tested to be leaktight in accordance with ANSI N14.5. Helium is introduced as described in 4.4.1.

4.4.3 Transport Test

For transport, the containment boundary is leak-rate tested using a gas pressure-drop leak test to verify the proper assembly of the CV. The leak-rate test procedure in Section 8.2.2.2 satisfies the requirements of ANSI N14.5

4.5 SPECIAL REQUIREMENTS

The contents of the package must be in solid form if the contents contain greater than 0.74 TBq (20 Ci) of plutonium in accordance with 10 CFR 71.63. The requirement is met by requiring all the contents to be solid form.

This Page Intentionally Left Blank

4.6 REFERENCES

1. *Packaging and Transportation of Radioactive Material*, Code of Federal Regulations, Title 10, Part 71, Washington, DC (January, 2005).

2. *American National Standard for Radioactive Material - Leakage Tests on Packages for Shipment*, ANSI N14.5, American National Standards Institute, Inc. (1997).

3. *ASME Boiler and Pressure Vessel Code, Section III, Rules for Construction of Nuclear Power Plant Components, Division 1*, *Subsection NB*, American Society of Mechanical Engineers, New York, NY (1992).

4. *Design Criteria for the Structural Analysis of Shipping Cask Containment Vessels*, Regulatory Guide 7.6, Rev. 1, U. S. Nuclear Regulatory Commission, Washington, DC (March, 1978).

5. *Parker O-ring Handbook*, ORD-5700A, The Parker Seal Group, Parker Hannifin Corporation, Cleveland, OH, (2001), http://www.parker.com/o-ring.

6. *Leakage Tests on Packages for Shipment of Radioactive Materials*, Regulatory Guide 7.4, U. S. NRC Office of Nuclear Regulatory Research (June 1975).

7. Chalfant, Gordon, *Test Summary Report - Specification 2R - Primary and Secondary Containment Vessel - High Temperature Leakage Test (U), Fall 1980,* M-TSM-A-00001, Revision 0, Westinghouse Savannah River Company, September 12, 2003.

This Page Intentionally Left Blank.

4.7 APPENDICES

Appendix	Description
4.1	Determination of A_2 for the 9977 Fissile Package with Contents

This Page Intentionally Left Blank

APPENDIX 4.1

DETERMINATION OF A_2 FOR THE 9977 FISSILE PACKAGE WITH CONTENTS

This Page Intentionally Left Blank.

DETERMINATION OF A_2 FOR THE GENERAL PURPOSE FISSILE PACKAGE (9977) WITH CONTENTS

Introduction

The containment criteria for radioactive, fissile material packages are given in 10 CFR 71.51(a)(1) for Normal Conditions of Transport (NCT) ($\leq 10^{-6}$ A_2/h) and in 71.51(a)(2) for Hypothetical Accident Conditions (HAC) ($\leq A_2$ in a week). The A_2 value for this mixture of radioisotopes must be determined to establish the content containment criteria and to determine the maximum release quantity that is allowed by the regulations. These values for a mixture of isotopes are determined by the methodology given in 10 CFR 71, Appendix A, "Determination of A_1 and A_2," Section IV. The results of these analyses are used to demonstrate compliance of the 9977 with the containment requirements of 10 CFR 71.

Scope

The A_2 value of the 9977 content is calculated using the highest, bounding isotopic masses and weight percents for Pu/U content shown in Table 1. The weight percents shown in Table 1 are the ones that generate the largest activity within the known weight percent ranges. By applying the maximum weight percents of Pu/U isotopes, the maximum activity, minimum A_2 value, and the minimum leakage requirements were determined.

Table 1. Isotopic mass and weight percent for the highest, bounding Pu/U content [a]

Nuclide	Weight Percent	Mass (g)
Pu-238	2.	1.0E-+2
Pu-239	100.	4.4E+03
Pu-240	40.	1.76E+03
Pu-241	15.	6.6E+02
Pu-242	5.	2.2E+02
U-232		0.0005
U-233	0.5	2.2E+01
U-234	100.	4.4E+03
U-235	100.	4.4E+03
U-236	40.	1.76E+03
U-238	100.	4.4E+03
Total	----	----

[a] Weight percents taken from SARP Table 1.2, C.2 or C.3 content.

According to 10 CFR 71, Appendix A, parent nuclides and their progeny (daughters) are considered to be a mixture of different nuclides. The radioactive of Pu (refer to the decay chains presented by Dr. David C. Kocher, *Radioactive Decay Data Tables* [Kocher 1981]) isotopes will accumulate enough activity to exceed their respective criteria for limited quantities (*Shippers—General Requirements for Shipments and Packagings* [49 CFR 173.423], Table A-7, *Activity Limits for Limited Quantities, Instruments, and Articles*) and for Type A quantities of radionuclides (10 CFR 71, Table A-1, *A_1 and A_2 Values for Radionuclides*).

Analysis

Decay History. The bounding mass and weight fractions for Pu/U isotopes in the 9977 are provided in Table 1. The radionuclide concentrations listed in Table 1 are taken from Table 1.2 in SARP.

A_2 Value for the Pu Mixture. The A_2 value for the mixture of radionuclides in the Pu/U mixture was calculated using the procedure described in Appendix A to Part 71, Section IV(d.). For a mixture of radionuclides in normal form, the following formula is used to calculate the A_2 value.

$$A_2(\text{mixture}) = \frac{1}{\sum_i \frac{f(i)}{A_2(i)}}$$

where f(i) is the fraction of activity for radionuclide "i" in the mixture, and $A_2(i)$ is the appropriate A_2 value for radionuclide "i".

The results of these intermediate parameters are provided in Table 2. A summary of the content activity for the A_2 value and the maximum number of A_2s per package is given in Table 3.

$$A_2(\text{mixture}) = \frac{1}{\sum_i \frac{f(i)}{A_2(i)}} = \frac{1}{4.7250 \times 10^{1}\ \text{Tbq}^{-1}} = 2.1164 \times 10^{-2}\ \text{Tbq}$$

Results

The A_2 value of 2.1164 x 10^{-2} TBq (5.7143×10^{-1} Ci) in conjunction with the maximum activity-to-A_2 value ratio of 1.22 x 10^5. These results indicate that 9977 contents must be shipped in a Type B material package. The content falls into the highest hazard category, Category I, for Type B quantities. Consequently, the highest level Type B containment design requirements apply.

Table 2. A_2 Value Calculation for The bounding GPFB Content

Isotope	**Mass** (g)	**Specific Activity** (TBq/g)	**Activity** (TBq)	**A_2** (TBq)	**f(i)** (TBq/TBq)	**f(i) / A_2** (1/TBq)
Pu-238	8.8000E+01	6.3000E-01	5.5440E+01	1.0000E-03	2.1410E-02	2.1410E+01
Pu-239	4.4000E+03	2.3000E-03	1.0120E+01	1.0000E-03	3.9082E-03	3.9082E+00
Pu-240	1.7600E+03	8.4000E-03	1.4784E+01	1.0000E-03	5.7094E-03	5.7094E+00
Pu-241	6.6000E+02	3.8000E+00	2.5080E+03	6.0000E-02	9.6856E-01	1.6143E+01
Pu-242	2.2000E+02	1.5000E-04	3.3000E-02	1.0000E-03	1.2744E-05	1.2744E-02
U-232	5.0000E-04	8.3000E-01	4.1500E-04	1.0000E-03	1.6027E-07	1.6027E-04
U-233	2.2000E+01	3.6000E-04	7.9200E-03	6.0000E-03	3.0586E-06	5.0977E-04
U-234	4.4000E+03	2.3000E-04	1.0120E+00	6.0000E-03	3.9082E-04	6.5137E-02
U-235	4.4000E+03	8.0000E-08	3.5200E-04	1.000E+307	1.3594E-07	0.0000E+00
U-236	1.7600E+03	2.4000E-06	4.2240E-03	6.0000E-03	1.6313E-06	2.7188E-04
U-238	4.4000E+03	1.2000E-08	5.2800E-05	1.000E+307	2.0391E-08	0.0000E+00
Total Mass =	2.2110E+04	Σ Act. =	2.5894E+03		Σ f(i) / A_2 =	4.7250E+01

$$A_2(\text{mixture}) = \frac{1}{\sum_i \frac{f(i)}{A_2(i)}} = \frac{1}{4.7250 \times 10^{1}\ \text{Tbq}^{-1}} = 2.1164 \times 10^{-2}\ \text{Tbq}$$

This Page Intentionally Left Blank.

Safety Analysis Report - 9977 Packaging

CHAPTER 5

SHIELDING EVALUATION

Preface

The shielding evaluation performed on the 9977 is described in this chapter. Chapter 1 describes five Content Envelopes (C.1 through C.5), with one (C.3) being reserved for future implementation. The objective of these evaluations is to demonstrate compliance with the performance requirements specified in 10 CFR 71.47[1], 10 CFR 71.51, 49 CFR 173.403[2], and 49 CFR 173.441 for each content envelope. These regulations specify that the dose rate limits for an undamaged package are 200 mrem/h at the accessible surface of the package, 10 mrem/h at 1-meter from the accessible surface of the package, and 1000 mrem/h at 1-meter from the surface of a damaged package after a hypothetical accident. Shielding analyses results based on the most radioactive contents indicate that the 9977 complies with the federal regulations for non-exclusive use. The overall results are shown in Table 5.1. It has been demonstrated that for the content envelopes the requirements of 10 CFR 71 for radiation dose rate limits are met under both normal and hypothetical accident conditions.

This Page Intentionally Left Blank

TABLE OF CONTENTS

LIST OF TABLES

LIST OF FIGURES

ACRONYMS AND ABBREVIATIONS

5CV	5-inch Diameter Containment Vessel
6CV	6-inch Diameter Containment Vessel
CV	Containment Vessel, applies to both 5CV and 6CV
HAC	Hypothetical Accident Conditions
MCNP	Monte Carlo N Particle Transport Code
NCT	Normal Conditions of Transport
RASTA	Radioactive Source Term Analysis
RTG	Radioisotope Thermoelectric Generator
SS	Stainless Steel

5 SHIELDING EVALUATION

5.1 DESCRIPTION OF SHIELDING DESIGN

5.1.1 Design Features

The 9977 Shipping Package, developed as the General Purpose Fissile Package, is a single containment drum type package with a bolted flange closure and a right circular cylinder containment vessel enclosed by Fiberfrax and Last-A-Foam insulation. Major materials of construction include a stainless steel (SS) overpack drum, Last-A-Foam polyurethane insulation, aluminum Load Distribution Fixtures, and a SS containment vessel (CV). The double O-ring sealed CV is removable for loading and unloading. The physical arrangement of the 9977 is described in Chapter 1. The 9977 is designed to ship radioactive contents in three basic configurations; assemblies of Radioisotope Thermoelectric Generators (RTGs), arrangements of nested food-pack cans, or DOE STD 3013 containers. These content configurations minimize contamination, simplify handling, and facilitate long-term storage.

The shielding evaluation for the package shows that the requirements of 10 CFR 71 for radiation dose rate limits are met for Normal Conditions of Transport (NCT) and Hypothetical Accident Conditions (HAC). The Transport Index for shielding to be placed on the package label is determined by measurement at the time of transport and must be less than 10 as required by 10 CFR 71.47(a).

There are no design features effecting shielding performance of the packaging with the Content Envelopes evaluated.

5.1.2 Summary Table of Maximum Radiation Levels

The dose rates from gamma and neutron radiation were calculated using the Monte Carlo N Particle Transport Code (MCNP)[3] with its continuous energy cross-section library. Table 5.1 summarizes the maximum calculated dose rates[15] for NCT and HAC and compares the results against the regulatory limits for shipment in commerce. The reported neutron and photon dose results are at the 99% upper confidence level (i.e., mean plus three standard deviations). The highest NCT dose rates are calculated on contact at the drum bottom for the case of the C.2 Content located at the bottom of the CV. This dose rate bounds the doses at all other measurement and source locations. While not listed in Table 5.1, a case was analyzed with the C.2 source located against the side wall of the CV which confirmed that the source at the bottom was bounding.

Table 5.1 - External Radiation Levels (Non-Exclusive Use)

Contents	C.1	C.2	C.3	C.4		C.5		10 CFR
Material	^{238}Pu	Pu/U		^{233}U	^{235}U	$^{233}UO_2$	$^{235}UO_2$	Limits
Fissile Mass Limits (g)	100	4500		5200	13500	5200	13500	—
NCT Surface Dose Rates (mrem/hr)								
SIDE			RESERVED					
Neutrons	51.19							—
Photons	4.56							—
Total	55.75	**		**	**	**	**	200
TOP								
Neutrons	13.33							—
Photons	0.32							—
Total	13.66	**		**	**	**	**	200
BOTTOM								
Neutrons	128.27	174.2		0.03	2.6E-4	1.41	5.9E-4	—
Photons	12.90	22.3		3.03	0.29	4.43	0.21	—
Total	141.18	198.3		3.06	0.29	5.83	0.21	200
NCT 1 m away Dose Rates (mrem/hr)								
SIDE			RESERVED					
Neutrons	1.77							—
Photons	0.15							—
Total	1.93	**		**	**	**	**	10*
TOP								
Neutrons	0.69							—
Photons	0.03							—
Total	0.72	**		**	**	**	**	10*
BOTTOM								
Neutrons	2.31	3.5		6.67E-4	1.47E-5	0.03	1.5E-5	—
Photons	0.25	0.5		0.08	7.74E-3	0.10	8.2E-3	—
Total	2.56	4.1		0.08	0.01	0.13	0.01	10*
HAC 1 m away Dose Rates (mrem/hr)								
SIDE			RESERVED					
Neutrons	2.06							—
Photons	0.26							—
Total	2.32	***		***	***	***	***	1000
TOP								
Neutrons	0.76							—
Photons	0.04							—
Total	0.80	***		***	***	***	***	1000
BOTTOM								
Neutrons	1.65							—
Photons	0.25							—
Total	1.89	***		***	***	***	***	1000

* Transport index may not exceed 10.

** The evaluation of Envelope C.1 showed the top and side were bounded by the bottom so those receptor locations were not analyzed for Envelopes C.2 – C.5

*** The evaluation of Envelope C.1 showed the HAC 1 m dose rate was bounded by the NCT surface dose rate so the HAC dose rates were not analyzed for Envelopes C.2 – C.5

5.2 SOURCE SPECIFICATION

Chapter 1 describes five Content Envelopes (C.1 through C.5), with one (C.3) being reserved for future implementation. Radiation sources were derived for these contents. The content selected for analyses is shown in Table 5.2.

The primary source term for Content Envelope C.1 is from (α,n) interactions. Modeling only Pu-238 and ignoring other isotopes maximizes the (α,n) interactions. In addition, 0.005 g of beryllium (Be) was included with the Pu-238 oxide to account for impurities in the RTG material. This is based on the maximum impurity content found in the Reference 4, which shows aluminum (Al) at a maximum of 120 ppm, with a 35 g limit for Pu-238. Using Be as the impurity target will bound all other (α,n) targets.

The C.2 analysis used a content distribution which summed to greater than 100%, a bounding scenario as (α,n) reactions are not a significant portion of the source term. A content mass of 4.5-kg was conservatively used in the analysis, verses the permitted mass of 4.4-kg. The maximum content for each isotope was included in the source term. The maximum was based on either the weight percent limit or the 19 Watt limit of the 9977. Pu-238 has a decay heat of 567 W/kg and Am-241 has a decay heat of 114.8 W/kg[5]. The C.4 and C.5 contents were 5.2 kg of U-233 or 13.5 kg of U-235 as either metal or compounds. Because of their greater mass, the C.4 and C.5 uranium dose analysis bounds the C.2 uranium dose.

Uranium-233 does not occur naturally and U-232 is a contaminant associated with its creation. U-232 has daughter products (specifically Tl-208) that emit high energy gammas. The maximum dose rate occurs after 10 years of decay. All U-232 contents used to obtain dose rates assume the optimally decayed composition.

Table 5.2 - Content Evaluated for Shielding Concerns

Isotope	Analyzed Composition (grams) [a]						
	C.1	C.2	C.3	C.4		C.5	
	238Pu Heat Sources	Pu/U Metals	Pu/U Oxides	U-233 Metal	U-235 Metal	U-233 Oxide	U-235 Oxide
233U				5200		5200	
235U					13500		13500
243Am			RESERVED				
244Cm							
237Np							
236Pu	1E-4	4.5E-6					
238Pu	100	33.51b					
239Pu		4500					
240Pu		1125					
241Pu		675					
242Pu		225					
241Am		165.5 [b]					
Total	100	6724		5200	13500	5200	13500

a) One gram of U-232 analyzed separately

b) Mass limits based on 19 Watt Limit; Pu-238 generates 567 W/kg and Am-241 generates 114.8 W/kg

5.2.1 Gamma Source

The contributing mechanisms for photon (gamma) production include: (1) nuclide decay, (2) decay of daughters, (3) fission product decay, (4) spontaneous fission, (5) bremsstrahlung, (6) neutron activation of the stainless steel containers, and (7) alpha interaction with light nuclides (α,n reactions). The source strengths (photons/sec) for contents evaluated are shown in Table 5.3.

The source term computations were performed using the industry standard ORIGEN-S code [6] and the Washington Safety Management Solutions RASTA code [7] and by incorporating the maximum activity source terms. These assumptions introduce a stronger source term to the shielding calculations than that of the actual source term from each envelope (Attachment 5-1).

The RASTA code was used to calculate the energy dependent decay source terms in a modified BUGLE-80 [8] twenty-group structure that better accounts for the low energy gammas from Am-241. The effect of subcritical multiplication is not included in the RASTA calculations, but is treated explicitly in MCNP. The source spectrum was input into MCNP

as a histogram and the total source was used as a multiplier to convert the dose rates from units of per source particle to total dose rate.

Among the isotopes of the content envelopes, the main contributors to the photon source are ^{241}Am, ^{236}Pu, ^{238}Pu, ^{240}Pu and ^{232}U.

Table 5.3 - Photon Source Strength

Upper Energy Limit (MeV)	Lower Energy Limit (MeV)	C.1 Normalized Spectrum	C.2 Normalized Spectrum	C.3 Normalized Spectrum	C.4 U-233 Normalized Spectrum	C.5 U-233 Normalized Spectrum	C.4 U-235 Normalized Spectrum	C.5 U-235 Normalized Spectrum
1.00E+01	8.00E+00	3.23E-11	5.18E-11	RESERVED	3.71E-14	3.71E-14	3.10E-12	3.10E-12
8.00E+00	7.00E+00	7.92E-09	6.52E-11		2.18E-10	1.54E-10	4.32E-12	3.50E-12
7.00E+00	6.00E+00	1.83E-10	2.93E-10		2.10E-13	2.10E-13	1.76E-11	1.76E-11
6.00E+00	5.00E+00	4.27E-10	6.85E-10		4.90E-13	4.90E-13	4.11E-11	4.11E-11
5.00E+00	4.00E+00	4.81E-08	2.19E-09		1.24E-09	8.74E-10	1.36E-10	1.30E-10
4.00E+00	3.00E+00	4.79E-09	7.33E-09		5.25E-12	5.25E-12	4.40E-10	4.40E-10
3.00E+00	2.00E+00	3.04E-08	2.43E-08		1.74E-11	8.57E-09	1.46E-09	1.54E-09
2.00E+00	1.50E+00	2.92E-08	2.59E-08		1.85E-11	1.18E-08	1.55E-09	2.02E-09
1.50E+00	1.00E+00	1.81E-07	6.71E-08		4.04E-11	1.35E-08	3.38E-09	3.75E-09
1.00E+00	8.00E-01	8.22E-07	1.60E-07		3.16E-11	3.16E-11	2.65E-09	2.65E-09
8.00E-01	7.00E-01	4.19E-06	2.06E-06		1.85E-11	1.85E-11	8.05E-06	8.05E-06
7.00E-01	6.00E-01	2.03E-08	1.29E-06		1.25E-05	1.25E-05	1.89E-09	1.89E-09
6.00E-01	4.00E-01	4.58E-08	7.03E-06		5.17E-11	5.17E-11	8.62E-05	8.62E-05
4.00E-01	2.00E-01	4.13E-07	3.89E-05		6.34E-03	6.34E-03	3.41E-02	3.41E-02
2.00E-01	1.00E-01	9.47E-05	6.20E-04		7.43E-03	7.43E-03	6.77E-01	6.77E-01
1.00E-01	8.00E-02	7.55E-04	1.09E-03		1.03E-02	1.03E-02	7.16E-02	7.16E-02
8.00E-02	6.00E-02	5.09E-09	2.10E-04		1.36E-03	1.36E-03	1.69E-03	1.69E-03
6.00E-02	5.90E-02	1.42E-10	2.61E-01		1.63E-13	1.63E-13	1.37E-11	1.37E-11
5.90E-02	5.00E-02	1.28E-09	2.30E-04		2.77E-03	2.77E-03	9.46E-04	9.46E-04
5.00E-02	4.00E-02	3.33E-03	9.48E-04		1.19E-02	1.19E-02	5.05E-04	5.05E-04
4.00E-02	3.00E-02	2.88E-09	9.72E-04		1.65E-04	1.65E-04	1.12E-04	1.12E-04
3.00E-02	2.00E-02	9.21E-02	7.60E-02		3.01E-03	3.01E-03	2.58E-10	2.58E-10
2.00E-02	1.00E-02	9.04E-01	5.62E-01		9.57E-01	9.57E-01	2.14E-01	2.14E-01
1.00E-02	1.00E-08	1.07E-09	9.73E-02		1.23E-12	1.23E-12	1.03E-10	1.03E-10
	Total (p/s)	**7.15E+12**	**2.88E+13**		**1.29E+11**	**1.29E+11**	**1.38E+09**	**1.38E+09**

5.2.2 Neutron Source

The contributing mechanisms for neutron sources are spontaneous fission and alpha interactions with oxygen and beryllium. The total neutron source strength is shown in Table 5.4.

The RASTA code was used to calculate the energy dependent decay source terms in the BUGLE-80 twenty-seven group structure. As with photons, the effect of subcritical multiplication is not included in the source strength, but accounted for during the radiation transport calculations. The source spectrum was input into MCNP as a histogram and the total source was used as a multiplier to convert the dose rates from units of per source particle to total dose rate.

Table 5.4 - Neutron Source Strength

Upper Energy Limit (MeV)	Lower Energy Limit (MeV)	C.1 Normalized Spectrum	C.2 Normalized Spectrum	C.3 Normalized Spectrum	C.4 U-233 Normalized Spectrum	C.5 U-233 Normalized Spectrum	C.4 U-235 Normalized Spectrum	C.5 U-235 Normalized Spectrum
1.73E+01	1.42E+01	2.03E-06	9.72E-06		2.64E-07	3.12E-09	6.08E-06	1.82E-06
1.42E+01	1.22E+01	1.11E-05	5.90E-05		1.43E-06	1.68E-08	4.04E-05	1.21E-05
1.22E+01	1.00E+01	2.43E-03	5.29E-04		2.68E-03	2.25E-05	3.52E-04	1.05E-04
1.00E+01	8.61E+00	2.11E-02	1.92E-03		6.72E-02	5.61E-04	1.81E-03	4.76E-04
8.61E+00	7.41E+00	2.83E-02	4.39E-03		1.09E-01	9.08E-04	4.42E-03	1.19E-03
7.41E+00	6.07E+00	3.51E-02	1.29E-02		1.38E-01	1.14E-03	1.23E-02	3.50E-03
6.07E+00	4.97E+00	3.75E-02	2.68E-02		7.03E-02	7.12E-04	2.40E-02	7.11E-03
4.97E+00	3.68E+00	1.08E-01	7.76E-02		2.01E-01	1.14E-02	7.32E-02	2.69E-02
3.68E+00	3.01E+00	1.61E-01	7.71E-02		1.44E-01	1.14E-01	7.50E-02	5.66E-02
3.01E+00	2.73E+00	9.03E-02	4.31E-02		6.42E-02	1.13E-01	4.27E-02	7.29E-02
2.73E+00	2.47E+00	8.68E-02	4.69E-02		3.92E-02	1.37E-01	4.65E-02	1.04E-01
2.47E+00	2.37E+00	3.31E-02	1.99E-02		1.23E-02	5.95E-02	1.98E-02	4.81E-02
2.37E+00	2.35E+00	6.53E-03	4.12E-03		2.34E-03	1.20E-02	4.10E-03	1.01E-02
2.35E+00	2.23E+00	3.84E-02	2.57E-02		1.33E-02	7.18E-02	2.56E-02	6.43E-02
2.23E+00	1.92E+00	8.80E-02	7.41E-02		2.78E-02	1.65E-01	7.40E-02	1.70E-01
1.92E+00	1.65E+00	6.05E-02	7.38E-02		1.57E-02	1.02E-01	7.41E-02	1.26E-01
1.65E+00	1.35E+00	5.31E-02	9.19E-02		1.68E-02	7.56E-02	9.28E-02	9.70E-02
1.35E+00	1.00E+00	4.97E-02	1.18E-01		2.72E-02	5.41E-02	1.20E-01	7.92E-02
1.00E+00	8.21E-01	2.26E-02	6.33E-02		1.44E-02	1.74E-02	6.47E-02	3.27E-02
8.21E-01	7.43E-01	9.48E-03	2.77E-02		6.28E-03	5.27E-03	2.84E-02	1.34E-02
7.43E-01	6.08E-01	1.57E-02	4.75E-02		1.09E-02	7.11E-03	4.88E-02	2.09E-02
6.08E-01	4.98E-01	1.24E-02	3.77E-02		7.73E-03	6.49E-03	3.87E-02	1.50E-02
4.98E-01	3.69E-01	1.32E-02	4.19E-02		6.15E-03	9.98E-03	4.31E-02	1.58E-02
3.69E-01	2.97E-01	6.38E-03	2.17E-02		1.62E-03	6.23E-03	2.23E-02	7.77E-03
2.97E-01	1.83E-01	9.39E-03	3.05E-02		8.51E-04	1.23E-02	3.15E-02	1.16E-02
1.83E-01	1.11E-01	5.33E-03	1.59E-02		3.29E-04	7.79E-03	1.63E-02	7.33E-03
1.11E-01	5.74E-02	3.10E-03	9.20E-03		1.86E-04	4.37E-03	9.49E-03	4.89E-03
5.74E-02	4.09E-02	7.84E-04	2.21E-03		4.27E-05	1.10E-03	2.28E-03	1.31E-03
4.09E-02	3.18E-02	3.89E-04	1.06E-03		1.98E-05	5.42E-04	1.09E-03	6.65E-04
3.18E-02	2.61E-02	2.20E-04	5.93E-04		1.09E-05	3.02E-04	6.11E-04	3.90E-04
2.61E-02	2.42E-02	6.89E-05	1.84E-04		3.35E-06	9.28E-05	1.90E-04	1.25E-04
2.42E-02	2.19E-02	7.98E-05	2.14E-04		3.86E-06	1.06E-04	2.21E-04	1.47E-04
2.19E-02	1.50E-02	2.11E-04	5.75E-04		1.02E-05	2.76E-04	5.93E-04	4.05E-04
1.50E-02	7.10E-03	1.80E-04	5.09E-04		8.65E-06	2.22E-04	5.25E-04	3.53E-04
7.10E-03	3.35E-03	5.60E-05	1.67E-04		2.64E-06	6.46E-05	1.72E-04	1.10E-04
3.35E-03	1.58E-03	1.76E-05	5.41E-05		8.00E-07	1.94E-05	5.58E-05	3.44E-05
1.58E-03	4.54E-04	6.99E-06	2.19E-05		3.11E-07	7.53E-06	2.26E-05	1.37E-05
4.54E-04	2.14E-04	8.52E-07	2.70E-06		3.79E-08	9.07E-07	2.79E-06	1.66E-06
2.14E-04	1.01E-04	2.75E-07	8.74E-07		1.23E-08	2.92E-07	9.01E-07	5.37E-07
1.01E-04	3.73E-05	1.02E-07	3.25E-07		4.56E-09	1.08E-07	3.35E-07	1.99E-07
3.73E-05	1.07E-05	2.51E-08	7.97E-08		1.12E-09	2.65E-08	8.22E-08	4.86E-08
1.07E-05	5.04E-06	3.10E-09	9.78E-09		1.37E-10	3.23E-09	1.01E-08	6.08E-09
5.04E-06	1.86E-06	1.13E-09	3.63E-09		5.10E-11	1.22E-09	3.74E-09	2.18E-09
1.86E-06	8.76E-07	2.44E-10	7.17E-10		1.00E-11	2.12E-10	7.40E-10	4.48E-10
8.76E-07	4.14E-07	6.58E-11	2.35E-10		3.23E-12	8.87E-11	2.41E-10	1.42E-10
4.14E-07	1.00E-07	3.31E-11	9.04E-11		1.38E-12	2.21E-11	9.89E-11	5.17E-11
1.00E-07	1.00E-11	2.44E-12	9.31E-12		1.99E-13	1.09E-13	1.17E-11	3.54E-12
	Total (n/s)	**2.24E+06**	**1.64E+06**		**2.94E+02**	**2.49E+04**	**4.09E+00**	**1.37E+01**

RESERVED

5.3 SHIELDING MODEL

The 9977 is a single containment drum type package with a bolted flange closure and a right circular cylinder containment vessel enclosed by Last-A-Foam and Fiberfrax insulation. Major materials of construction include stainless steel, polyurethane, and aluminum.

5.3.1 Configuration of Source and Shielding

The drum consists of a SS outer shell with a SS liner, aluminum load distribution fixtures and miscellaneous other hardware, as shown in Figure 5.1. The drum is modeled as a right circular cylinder, simplifying some of the components. This simplification is conservative since it places the source material closer to the surface of the drum being analyzed. These simplifications include:

- The bottom of the drum is modeled as flat rather than convex.
- The drum top rim and bottom wear ring are not modeled.
- The drum rolling hoops are not modeled.

There are two different size options for the CV. The 6-inch diameter CV (6CV) will only be used for content envelope C.1 and the 5-inch diameter CV (5CV) will be used for content envelopes C.2 through C.5. The 6CV configuration is analyzed for shielding purposes. It is modeled as a cylindrical main portion with a conical transition at the top, a short upper cylinder, a cone seal plate, and the cone seal nut. Some of the components of the CV that are easy to model (e. g., the conical transition at the top) are included exactly. Other components that are more complex are modeled as simpler shapes, these are discussed below.

- The gland nut is a complex set of cones and cylinders inside the gland plug. For simplicity the nut and plug are modeled together as a single cylinder of 304L stainless steel with a small cylindrical cavity at the top to account for the nut being shorter than the plug. This should not impact the radiation transport calculations.
- The End Cap of the CV is modeled as a 2/1 ellipse with the axis of rotation (the "z-axis") set to half the radius of the CV cylindrical portion and the minor axis set to the radius of the CV cylindrical portion. The bottom of the cylindrical portion of the CV is extended down to the point at which the ellipse intersects it.

For NCT, the package is considered to be intact and dose rates are calculated on contact and at 1-meter from the side, bottom, and top. The source is modeled as a sphere placed at the center of the CV for dose points at the side and top of the package, and on the bottom of the CV for dose points at the bottom of the package.

The use of the 6CV for NCT shielding calculations does not impact the calculated dose rates at the surface of the package or at 1-meter from the surface since the source is modeled as a

sphere centered in the CV or at the bottom of the CV. The slight difference in CV wall thickness is not significant since the dose rate is dominated by neutron dose.

For HAC, the drum, Fiberfrax, and Last-A-Foam are assumed to be lost leaving only the CV. This model (Figure 5.2) is obtained from the NCT model by setting the material outside the CV as void. Dose rates are calculated at 1-meter from the side, bottom, and top of the CV. The source is modeled as a sphere placed at the center of the CV for dose points at the side and top of the package, and on the bottom of the CV for dose points at the bottom of the package.

The use of the 6CV for HAC shielding calculations does not impact the calculated dose rates at 1-meter from the surface of the CV since the source is modeled as a sphere centered in the CV or at the bottom of the CV. The distance to the dose point would only vary by about 2% which would translate to less than 4% change in dose rate. The slight difference in CV wall thickness is not significant since the dose rate is dominated by neutron dose.

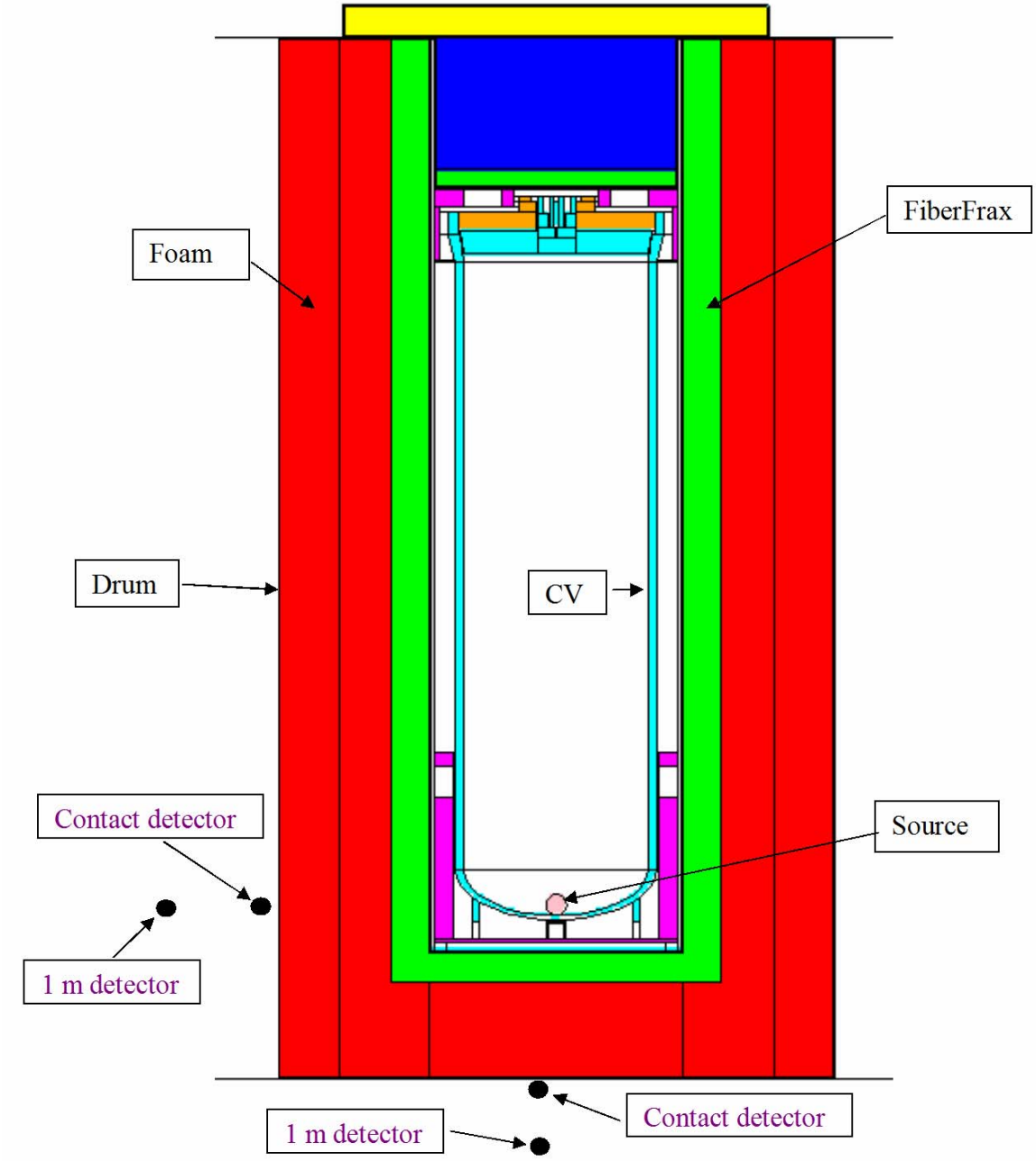

Figure 5.1 - Shielding Model of 9977 Under NCT

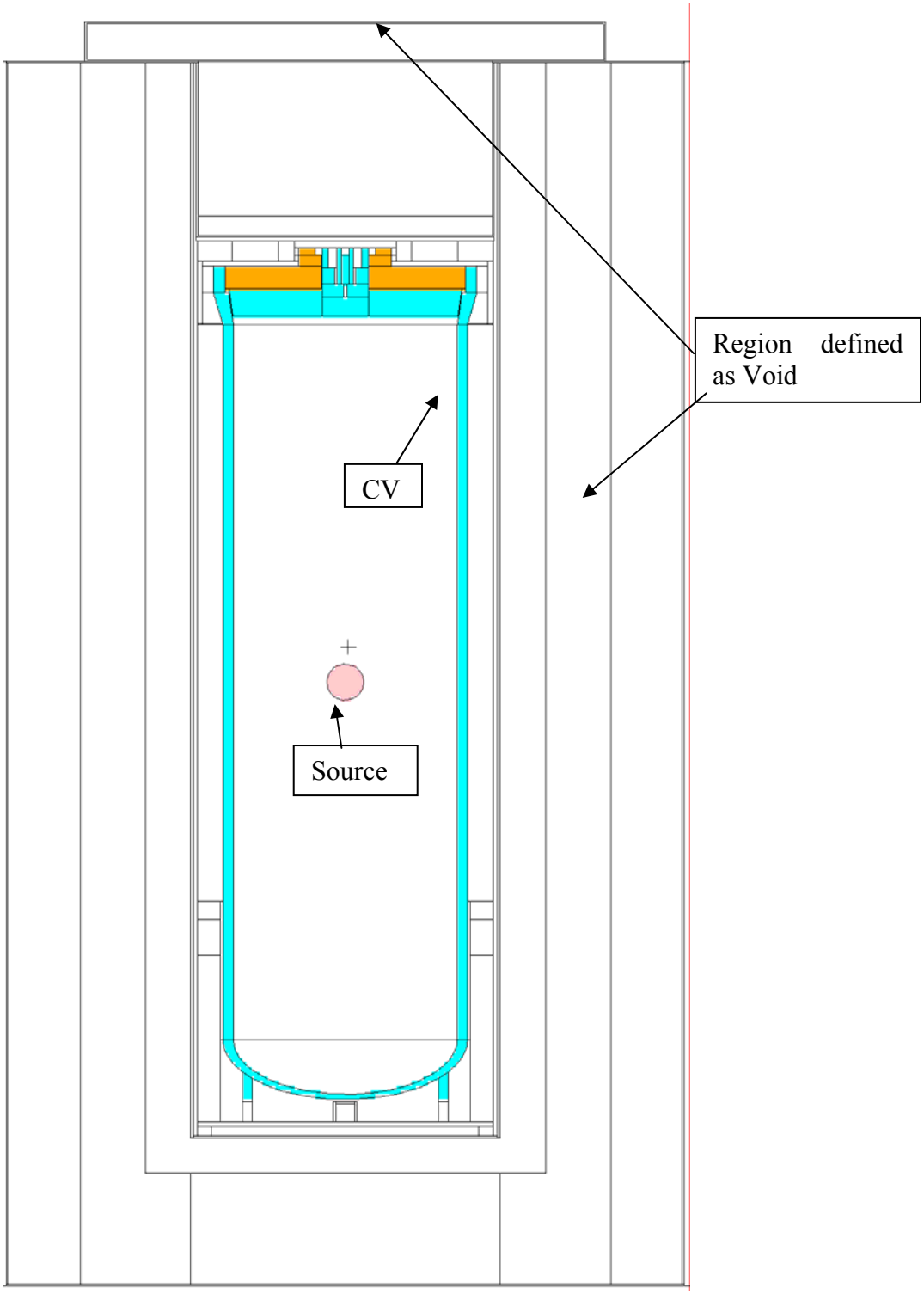

Figure 5.2 - Shielding Model of 9977 Under HAC

5.3.2 Material Properties

The 9977 shipping container consists of a stainless steel cylindrical containment vessel, a 35-gallon steel drum, Fiberfrax, Last-A-Foam insulation, aluminum load distribution fixtures, and a lid filled with TR-19 Block/Min-K2000. Neither the materials nor the geometry are specifically designed to provide significant shielding. Though some attenuation is provided by the materials, dose attenuation is primarily provided by the distance between the source and points external to the package.

Seven material compositions, other than the source region, (Table 5.5), are used to model the 9977 [4, 9, 10,].

Table 5.5 - Material Compositions

density (g/cc)	Nitronic 60	304L SS	6061-T6 Aluminum	Last-A-Foam	TR-19 Block	Min-K 2000	Fiberfrax
	7.584	7.9	2.7	0.256	0.3684	0.3204	0.2563
Element	Weight Percent						
H				4.1		0.84	
C		0.03		54.4		1.28	
O				29.4	45.53	48.01	50.03
N	0.14			12.1			
Si	4	1	0.6		21.22	37.71	23.14
Ni	8.5	10					
Cr	17	19	0.2				
Mn	8	2					
Fe	62.36	67.895			5.4		
P		0.045					
S							
Al			97.9		5.47	6.39	26.46
Cu			0.28				
Mg			1		8.9		
Ti					0.82	5.53	
Na					1.09		0.37
K					1.22		
Ga						0.15	
Sb						0.09	

5.4 SHIELDING EVALUATION

5.4.1 Methods

The radiation source terms were characterized using RASTA, and the MCNP code package was used for subsequent three dimensional Monte Carlo transport calculations to determine absorbed dose rates outside the 9977 shipping container. The ORIGEN-S Module of the SCALE Code system was used to decay U-232 to allow for in-growth of daughter isotopes.

The following are excerpts from the reference documentation for each of the codes that are used in the calculations. These excerpts are selected to provide general descriptions of the analytical methods employed.

> **ORIGEN-S** computes time-dependent concentrations and source terms of a large number of isotopes, which are simultaneously generated and depleted through neutronic transmutation, fission, radioactive decay, input feed rates, and physical or chemical removal rates. The matrix exponential model of the ORIGEN code is unaltered in ORIGEN-S. The version of ORIGEN applied in the SCALE system, ORIGEN-S, has several improvements over the original program. The code has been modified to include dynamic storage allocation, free-form input processing, and flexible dimensioning.
>
> **RASTA** (Radiation Source Term Analysis) is a code that computes neutron and photon source terms arising from (α, n) events, spontaneous fission, bremsstrahlung, and decay. The code was written to consolidate existing capabilities into a single, easy to use code with flexible, extensive output edits, while also adding new capabilities. Specifically, the gamma decay calculation from the GAMSRC code, bremsstrahlung production calculations from the BREMRAD code, and the (α, n) and spontaneous fission neutron calculations from the SOURCES code have been incorporated into RASTA. These three codes require different inputs and output their results on different bases. RASTA provides a single, easy to use input and output for these modules. In addition, RASTA provides calculational routines to find the photon source arising from decay of the product isotope resulting from an (α, n) calculation, and to find the photon source arising from both prompt and delayed spontaneous fission events. Finally, RASTA incorporates a methodology similar to that used in KMULT to account for subcritical neutron multiplication.
>
> **MCNP:** MCNP treats an arbitrary three - dimensional configuration of materials in geometric cells bounded by first- and second-degree surfaces and some special fourth-degree surfaces. Point-wise continuous-energy cross section data are used, although multi-group data may also be used. Fixed-source adjoint calculations may be made with the multi-group data option. For neutrons, all reactions in a particular cross-section evaluation are accounted for. Both free gas and S(alpha, beta) thermal treatments are used. Criticality sources as well as fixed and surface sources are available. For photons, the code takes account of incoherent and coherent scattering with and without electron binding effects, the possibility of fluorescent emission

following photoelectric absorption, and absorption in pair production with local emission of annihilation radiation. A very general source and tally structure is available. The tallies have extensive statistical analysis of convergence. Rapid convergence is enabled by a wide variety of variance reduction methods. Energy ranges are 0 - 60 MeV for neutrons (data generally only available up to 20 MeV) and 1 keV - 1 GeV for photons and electrons.

The RASTA, MCNP, and ORIGEN-S calculations were performed on the WSMS Linux Cluster computers, using code and libraries verified on that system [11, 12, 13, 14].

5.4.2 Input and Output Data

The input files of the computer codes are listed in Reference 15 (Attachment 5-1). Input and output files are available on CD.

5.4.3 Flux-to-Dose-Rate Conversion

Neutron and photon dose conversion factors were obtained from the American National Standards Institute, ANSI/ANS-6.1.1-1977 [16] and are given in Table 5.6. The 1977 values were used rather than those from the 1991 standard because the neutron dose conversion factors more closely reflect those provided in 49CFR173.403, and the photon dose conversion factors more closely correspond to the response measured by instrumentation.

Table 5.6 - Flux-to-Dose Conversion Factors

Neutron		Photon	
Energy (MeV)	Biological	Energy (MeV)	Biological
2.50E-08	3.67E-06	1.00E-02	3.96E-06
1.00E-07	3.67E-06	3.00E-02	5.82E-07
1.00E-06	4.46E-06	5.00E-02	2.90E-07
1.00E-05	4.54E-06	7.00E-02	2.58E-07
1.00E-04	4.18E-06	1.00E-01	2.83E-07
1.00E-03	3.76E-06	1.50E-01	3.79E-07
1.00E-02	3.56E-06	2.00E-01	5.01E-07
1.00E-01	2.17E-05	2.50E-01	6.31E-07
5.00E-01	9.26E-05	3.00E-01	7.59E-07
1.00E+00	1.32E-04	3.50E-01	8.78E-07
2.50E+00	1.25E-04	4.00E-01	9.85E-07
5.00E+00	1.56E-04	4.50E-01	1.08E-06
7.00E+00	1.47E-04	5.00E-01	1.17E-06
1.00E+01	1.47E-04	5.50E-01	1.27E-06
1.40E+01	2.08E-04	6.00E-01	1.36E-06
2.00E+01	2.27E-04	6.50E-01	1.44E-06
		7.00E-01	1.52E-06
		8.00E-01	1.68E-06
		1.00E+00	1.98E-06
		1.40E+00	2.51E-06
		1.80E+00	2.99E-06
		2.20E+00	3.42E-06
		2.60E+00	3.82E-06
		2.80E+00	4.01E-06
		3.25E+00	4.41E-06
		3.75E+00	4.83E-06
		4.25E+00	5.23E-06
		4.75E+00	5.60E-06
		5.00E+00	5.80E-06
		5.25E+00	6.01E-06
		5.75E+00	6.37E-06
		6.25E+00	6.74E-06
		6.75E+00	7.11E-06
		7.50E+00	7.66E-06
		9.00E+00	8.77E-06
		1.10E+01	1.03E-05
		1.30E+01	1.18E-05
		1.50E+01	1.33E-05

5.4.4 External Radiation Levels

The NCT and HAC dose rates associated with the contents are given in Table 5.1. The NCT dose rate calculations show that the maximum package dose rate is on the bottom of the drum.

The Content Envelopes meet the 10 CFR 71.47 Regulatory Limits to be shipped as non-exclusive use if the following content limits are followed.

Content	Additional Limit to Envelope
C.1	≤ 0.005 g of (α,n) impurities, and ≤ 0.14 mg U-232
C.2	≤ 0.005 g of (α,n) impurities, and ≤ 4.5 μg U-232, and ≤ 25% Pu-240 for C.2
C.4 and C.5	≤ 0.005 g of (α,n) impurities, and ≤ 0.49 mg U-232 in C.4, or ≤ 0.57 mg U-232 in C.5.

This Page Intentionally Left Blank

5.5 REFERENCES

1. *Packaging and Transportation of Radioactive Material*, Code of Federal Regulations, Title 10, Part 71, U.S.NRC, Washington, DC (January, 2002).

2. *Shippers-General Requirements for Shipments and Packagings*, Code of Federal Regulations, Title 49, Part 173, Washington, DC (October, 2003).

3. X-5 Monte Carlo Team, *MCNP — A General Monte Carlo N-Particle Transport Code, Version 5*, LA-UR-03-1987, Los Alamos National Laboratory, Los Alamos, NM (April, 2003).

4. Abramczyk, G. A., *Re: Sandia National Laboratory RTG Information*, SRNL-IES-2006-00005, Savannah River National Laboratory, Aiken, SC (February 2006).

5. *Stabilization, Packaging, and Storage of Plutonium-Bearing Materials*, DOE-STD-3013-2004, U. S. Department of Energy, Gaithersburg, MD (April 2004).

6. Hermann, O. W and Westfall, R. M., *ORIGEN-S: Scale System Module to Calculate Fuel Depletion, Actinide Transmutation, Fission Product Buildup and Decay, and Associated Radiation Source Terms*, NUREG/CR-0200, Revision 6, Volume 2, Section F7, Oak Ridge National Laboratory, Oak Ridge, TN (March 2000).

7. Nathan, S. J., Ed., *Radiation Source Term Analysis Code RASTA User Guide (U),* WSMS-CRT-97-0013, Rev.4, Washington Safety Management Solutions, Aiken, SC (February 2004).

8. Roussin, R. W., *BUGLE-80:Coupled47-Neutron, 20-Gamma-Ray, P3, Cross-Section Library for LWR Shielding Calculations*, Informal notes (June 1980).

9. Barnett, M. H., *Radiological Engineering Shielding Material Composition*, WSMS-CRT-02-0060, Revision 1, Westinghouse Safety Management Solutions, Aiken, SC (September 2003).

10. Harmon II, C. D., Busch, R. D., Briesmeister, J. F., and Forster, R.A., *Criticality Calculations with MCNP: A Primer*, LA-12827-M, Los Alamos National Laboratory, Los Alamos, NM (August 1994).

11. Nathan, S. J., *MCNP5 Test Report (U)*, WSMS-CRT-03-0117, Rev. 1, Washington Safety Management Solutions, Aiken, SC (March 2004).

12. Revolinski, S. M., Software *Configuration and Control Guidance for MCNP5 with Linux Workstation Cluster (U)*, WSMS-CRT-03-0116, Rev. 1, Washington Safety Management Solutions, Aiken, SC (March 2004).

13. Revolinski, S M., *SCALE5 Test Report (U)*, WSMS-CRT-04-0080, Rev. 0, Washington Safety Management Solutions, Aiken, SC (September 2004).

14. Gaul, J., Knecht, K., and Barnett, M. H., *Verification of Rasta Version 5.1*, WSMS-CRT-05-0044, Washington Safety Management Solutions, Aiken, SC, June 15, 2005.

15. Barnett, M. H., *9977 Shielding Analysis*, N-CLC-H-00119, Revision 0, Washington Safety Management Solutions, Aiken, SC (February 2006). [Attachment 5-1]

16. ANSI/ANS-6.1.1-1977, *Neutron and Gamma-Ray Flux-to-Dose Rate Factors*, American Nuclear Society, Le Grange Park, IL (March 1977).

5.6 APPENDIX

Appendix	Description
5.1	9977 Shielding Analysis

Note: The input and output files associated with this chapter are listed in Appendix 5.1 and are available on a CD.

This Page Intentionally Left Blank

APPENDIX 5.1

9977 SHIELDING ANALYSIS

This Page Intentionally Left Blank

Calculation Cover Sheet

Project	Calculation Number	Project Number
9977	N-CLC-G-00119	SR06.KM56564W.007.LTCDPSUBC
Title: 9977 Shielding Analysis	Functional Classification: SS	Page 1 of 51
	Discipline: Nuclear	

☐ Preliminary ☒ Confirmed

Computer Program No.	Version/Release No.
MCNP, RASTA, ORIGEN-S	5, 5, 5

Purpose and Objective

The purpose of this calculation is to document the shielding analysis of the 9977.

Summary of Conclusion

The C.1 contents with 0.005 g of (α,n) target impurities meet the regulatory limits to be shipped. The C.2 and C.3 contents with 0.005 g of (α,n) target impurities exceed the regulatory limit of 200 mrem/hr at contact and require: 1) no more than 25% Pu-240; 2) 50% Pu-240 and no more than 3375 g total Pu for C.2 or 3000 g total Pu for C.3; or 3) a distance of 6.32 in. from the content to the bottom of the drum. Envelope C.1 is restricted to 0.14 mg U-232, while Envelopes C.2 and C.3 are restricted to 4.5 μg U-232. Envelopes C.4 and C.5 meet the regulatory limit, with a restriction of 0.49 mg U-232 in C.4 and 0.57 mg U-232 in C.5. Plutonium fluorides exceed the regulatory dose rate limit for both exclusive and non-exclusive use shipments.

Revisions	
Rev No.	Revision Description
0	Original Issue

Sign Off (signatures of previous revision on file)

Rev No.	Originator (Print) Sign/Date	Verification/Checking Method	Verifier/Checker (Print) Sign/Date	Manager (Print) Sign/Date
0	M. H. Barnett M. H. Barnett 2/24/06	Complete document review per E7	R. L. Reed Raymond Reed 2-24-06	J. Brotherton J. Brotherton 2/28/06

Design Authority – (Print)	Signature	Date
G. Abramczyk		
Release to Outside Agency – (Print)	Signature	Date

Classification

UNCLASSIFIED
DOES NOT CONTAIN
UNCLASSIFIED CONTROLLED
NUCLEAR INFORMATION

DC & Reviewing Official: Steven J. Nathan

Date: February 24, 2006

IG-SR-3, 2/04

RECORD OF REVISION

Project: 9977					Calculation No: N-CLC-G-00119
Subject: 9977 Shielding Analysis					Sheet No: 2 of 51
Originator: M. H. Barnett MHB	Date: 2/24/06	Checker: R. L. Reed RLR	Date: 2/24/06	Rev. No: 0	

REV. NO.	PAGES REPLACED	PAGES ADDED	PAGES DELETED	PAGES REVISED	DESCRIPTION OF REVISIONS
0		All			Original Issue

Keywords:

9977

Shipping

Shielding

DISCLAIMER

TABLE OF CONTENTS

LIST OF TABLES

LIST OF FIGURES

COMPUTER PROGRAMS USED

NAME	Version	Configuration Control	If NO Description on page/in reference
MCNP	5	Yes	
RASTA	5	Yes	
ORIGEN-S	5	Yes	

Introduction

As the 6M containers are being removed from service, a new general purpose fissile package is needed. The new package is designated the 9977. This calculation documents the shielding analysis of the 9977 for contents consisting of Radioisotope Thermoelectric Generator (RTG) sources, plutonium isotopes, and other 6M contents.

Input

Tables 1 and 2 present the dimensions[1] of the 9977 and its components as generally analyzed in this document. Tables 1 and 2 were derived from preliminary versions of the final drawings listed in References 1 and 2. Thickness of pipe walls is taken from Reference 3. Gauge thickness is taken from Reference 4.

Compositions for materials other than the source material are shown in Table 3. Data for 304L Stainless Steel, Nitronic-60, Aluminum, and Air are taken from the standard materials library [Reference 5]. The composition and density for Fiberfrax, Vermiculite, and Min-K 2000 are taken from Reference 7.

The source isotopes considered for the 9977 are given in Reference 8 and are shown in Table 4. Envelope C.3 and U-233 in C.4 and C.5 have been reserved. Envelope C.3 had the same isotopic composition as Envelope C.2 and the U-233 component in Envelopes C.4 and C.5 was for 5.2 kg. The analysis for these compositions are still considered in this calculation. Source material density values are taken from Reference 9, 11.46 g/cc[2] for Pu and U oxides and 19.84 g/cc for Pu metals and 18.95 g/cc for U metals.

Regulatory Requirements

The Department of Transportation (DOT) grants the Department of Energy (DOE) the authority to evaluate, approve, and certify packages used for the transportation of radioactive materials against packaging standards equivalent to those specified in 10CFR71 (49CFR173.7(d)). The requirements applicable to shielding are detailed in 10CFR71.47 and 10CFR71.51. 10CFR71.4 is also applicable, as it defines two key terms: Exclusive Use and Transport Index. These definitions are paraphrased here:

> *Exclusive Use* (also referred to in other regulations as "sole use" or "full load") means the sole use by a single consignor of a conveyance for which all initial, intermediate, and final loading and unloading are carried out in accordance with the direction of the consignor or consignee. The consignor and the carrier must ensure that any loading or unloading is performed by personnel having radiological training and resources appropriate for safe handling of the consignment. The consignor must issue specific

[1] The final drawings had minor differences from the analyzed model dimensions given in Tables 1 and 2. The only change which impacted dose rate was the decreased distance from the content to the external bottom of the drum. As discussed in the section "Radiation Transport," several cases were re-analyzed to account for the decreased distance.

[2] A maximum density of 11.46 g/cc was used for shielding purposes. Lower densities would decrease the dose rate by decreasing the sub-critical multiplication and increasing the distance from source center to detector.

instructions, in writing, for maintenance of exclusive use shipment controls, and include them with the shipping paper information provided to the carrier by the consignor.

Transport Index (TI) means the dimensionless number (rounded up to the next tenth) placed on the label of a package, to designate the degree of control to be exercised by the carrier during transportation. The transport index is the number determined by multiplying the maximum radiation level in millisievert (mSv) per hour at 1 meter (3.3 ft) from the external surface of the package by 100 (equivalent to the maximum radiation level in millirem per hour at 1 meter (3.3 ft)).

10CFR71.47 requires that for each package of radioactive material offered for transportation that the radiation dose rate at any point on the external surface of a package cannot exceed 200 mrem/hr, and the Transport Index must not exceed 10. However, an exception is granted if the package is to be shipped "Exclusive Use." In this case, the limit at the accessible package external surface is 1000 mrem/hr, provided (1) the shipment is made in a closed transport vehicle, (2) the packages are secured such that they don't move during transport, and (3) there are no loading and unloading operations between the beginning and end of the transportation. In addition to the 1000 mrem/hr limit at the accessible surface, the following criteria must be met: (1) the radiation dose rate at any point on the external surface of the transport vehicle must not exceed 200 mrem/hr; (2) the dose rate at any point two meters from the outer lateral surfaces of the transport vehicle must not exceed 10 mrem/hr; and (3) the dose rate must not exceed 0.02 mSv/h (2 mrem/h) in any normally occupied space, except that this provision does not apply to private carriers, if exposed personnel under their control wear radiation dosimetry devices in conformance with 10 CFR 20.1502.

10CFR71.51 requires that the radiation dose rate not exceed 1000 mrem/hr at a distance of one meter from the external surface of the package under hypothetical accident conditions.

Radiation Dose Rate Limits for the 9977

Based on the regulatory requirements, the radiation dose rate limits that must be met for the 9977 are:

Under Normal Conditions of Transport (NCT):

1. The radiation dose rate at the accessible surface of the package must not exceed 200 mrem/hr;
2. The radiation dose rate at any point one meter from the accessible surface of the package must not exceed 10 mrem/hr.

Under Hypothetical Accident Conditions (HAC):

1. The radiation dose rate at a distance of one meter from the external surface of the package must not exceed 1000 mrem/hr.

Open Items

There are no open items.

Assumptions

- The Last-A-Foam in the 9977 is modeled as pure polyurethane [6] with a density of 16 lbm/cu-ft. Modeling the Last-A-Foam as polyurethane is appropriate since both are plastics. [7].
- Only the 6-inch Containment Vessel (CV) is modeled. The dose rates will not change for the 5-inch CV when the aluminum honeycombs are not credited. Crediting the honeycombs would increase the distance between the source surface and detector position, thereby reducing the dose rates. The 5-inch CV is 0.022 inch thinner than the 6-inch CV. This variation in thickness does not impact shielding and is important only in relationship to distances as discussed in the "Radiation Transport" Section.
- Specific modeling assumptions are addressed in the Analytical Methods section.

Analytical Methods

The radiation source terms were characterized using ORIGEN-S [10] and RASTA [11]. The MCNP [12] code package was used for three dimensional Monte Carlo transport calculations to determine absorbed dose rates outside the 9977. The calculations performed are grouped into two sets: Normal Conditions of Transport (NCT) and Hypothetical Accident Conditions (HAC).

ORIGEN-S computes time-dependent concentrations and source terms of a large number of isotopes, which are simultaneously generated and depleted through neutronic transmutation, fission, radioactive decay, input feed rates, and physical or chemical removal rates. The matrix exponential model of the ORIGEN code is unaltered in ORIGEN-S. The version of ORIGEN applied in the SCALE system, ORIGEN-S, has several improvements over the original program. The code has been modified to include dynamic storage allocation, free-form input processing, and flexible dimensioning.

RASTA (RAdiation Source Term Analysis) is a code that computes neutron and photon source terms arising from (α,n) events, spontaneous fission, bremsstrahlung, and decay. The code was written to consolidate existing capabilities into a single, easy to use code with flexible, extensive output edits, while also adding new capabilities. Specifically, the gamma decay calculation from the GAMSRC code, bremsstrahlung production calculations from the BREMRAD code, and the (α,n) and spontaneous fission neutron calculations from the SOURCES code have been incorporated into RASTA… In addition, RASTA provides calculational routines to find the photon source arising from decay of the product isotope resulting from an (α,n) calculation, and to find the photon source arising from both prompt and delayed spontaneous fission events… The RASTA methodology for all processes is generalized and applicable to any isotopes for which data is available.

MCNP is a general-purpose Monte Carlo N–Particle code that can be used for neutron, photon, electron, or coupled neutron/photon/electron transport, including the capability to calculate eigenvalues for critical systems. The code treats an arbitrary

three-dimensional configuration of materials in geometric cells bounded by first- and second-degree surfaces and fourth-degree elliptical tori. Pointwise cross-section data are used. For neutrons, all reactions given in a particular cross-section evaluation (such as ENDF/B-VI) are accounted for. Thermal neutrons are described by both the free gas and S(α,β) models. For photons, the code accounts for incoherent and coherent scattering, the possibility of fluorescent emission after photoelectric absorption, absorption in pair production with local emission of annihilation radiation, and bremsstrahlung. A continuous-slowing-down model is used for electron transport that includes positrons, k x-rays, and bremsstrahlung, but does not include external or self-induced fields.

The MCNP, RASTA, and ORIGEN-S calculations were performed on the WSMS Linux Cluster computers, using code and libraries verified on that system [13, 14, 15].

Geometric Models

Normal Conditions of Transport

The drum consists of a stainless steel outer shell with a stainless steel liner, aluminum load distribution fixtures and miscellaneous other hardware as shown in Figure 1. Some of the components of the drum are approximated to facilitate modeling:

- The bottom of the drum may be convex. The drum is modeled as a right circular cylinder with a flat bottom. This is slightly conservative since it places the source material closer to the bottom of the drum.

The containment vessel (CV) (Figure 2) is modeled as a cylindrical main portion with a conical transition at the top, a short upper cylinder, a cone seal plate, and the cone seal nut. Some of the components of the CV that are easy to model (e.g., the conical transition at the top) are included exactly, others that are more complex are modeled as simpler shapes as discussed below.

- The gland nut is a complex set of cones and cylinders inside the gland plug. For simplicity the nut and plug are modeled together as a single cylinder of 304L stainless steel with a small cylindrical cavity at the top to account for the nut being shorter than the plug.
- The End Cap of the CV is modeled as a 2/1 ellipsoid with the axis of rotation (the "z-axis") set to half the radius of the CV cylindrical portion and the minor axis set to the radius of the CV cylindrical portion. The bottom of the cylindrical portion of the CV is extended down to the point at which the ellipsoid intersects it.

The end cap model is described by the following equation:

$$\frac{x^2}{R^2}+\frac{y^2}{R^2}+\frac{z^2}{H^2}=1$$

Where R is the radius of the ellipsoid and H is its height. This is equivalent to the equation for a general ellipsoid in MCNP:

$$A(x-\bar{x})^2+B(y-\bar{y})^2+C(z-\bar{z})^2+2D(x-\bar{x})+2E(y-\bar{y})+2F(z-\bar{z})+G=0$$

With:

$A = 1$
$B = 1$
$C = R^2/H^2 = 4$
$D = 0$
$E = 0$
$F = 0$
$G = -R^2$

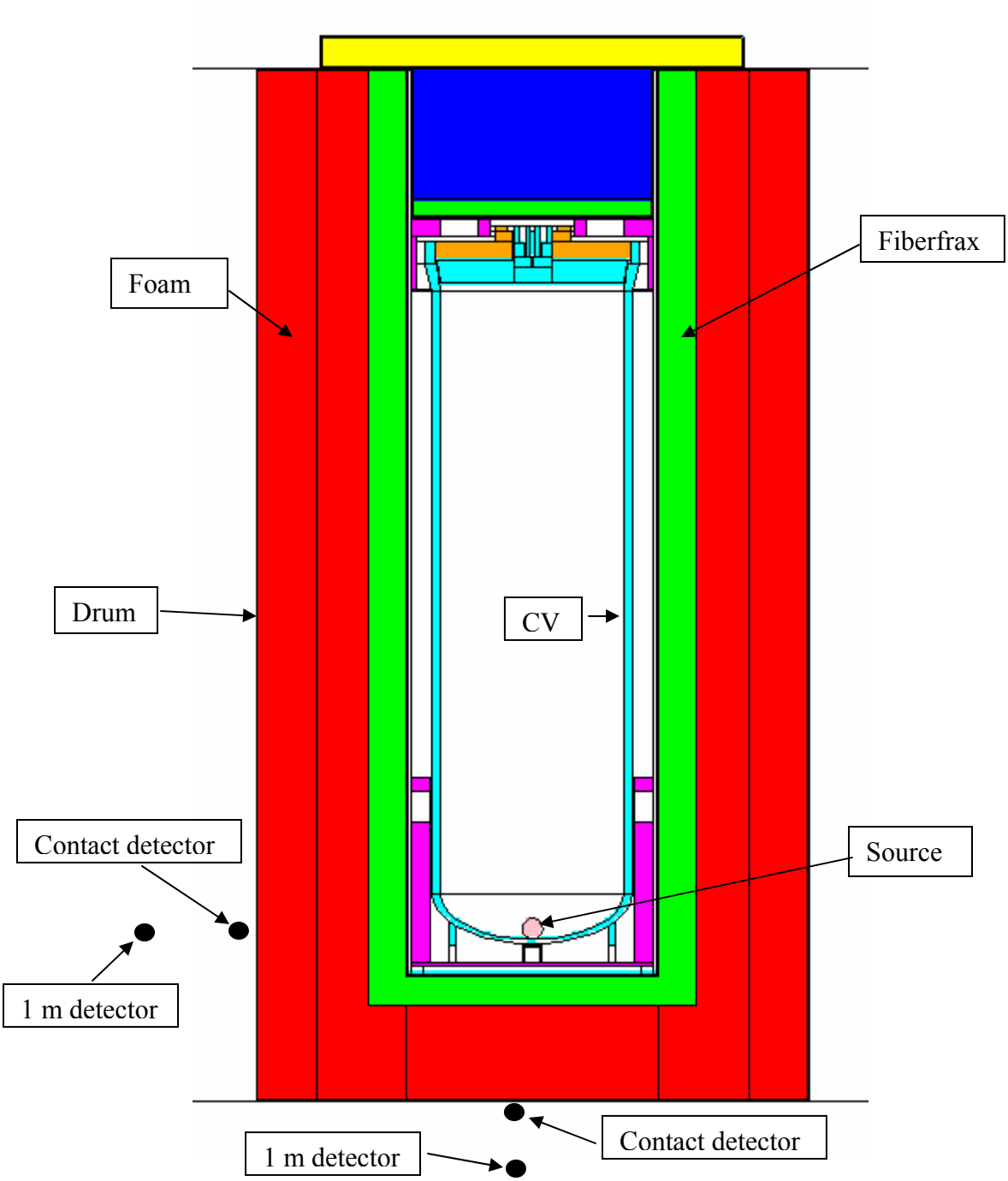

Figure 1. 9977 Model with Source at Bottom

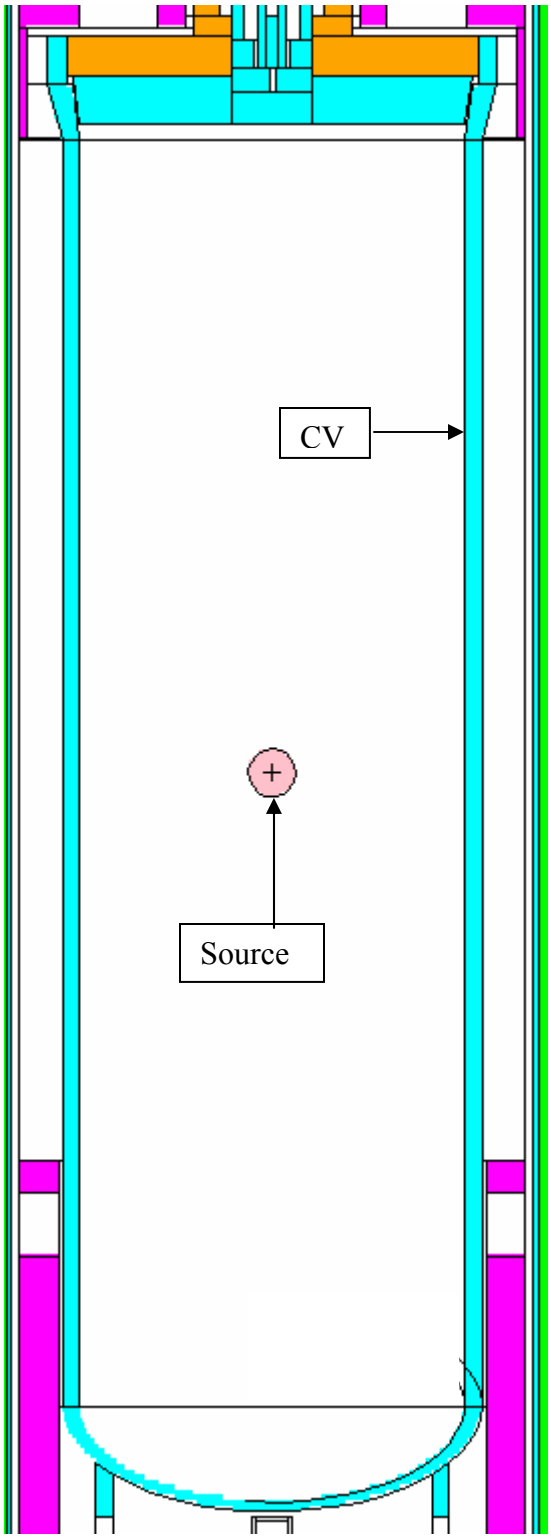

Figure 2. CV Model with Source in Center (zoomed in on the CV)

Hypothetical Accident Conditions

The HAC was analyzed assuming everything outside the containment vessel (CV) has been removed (Figure 3). This was done in the model by making everything outside the CV void.

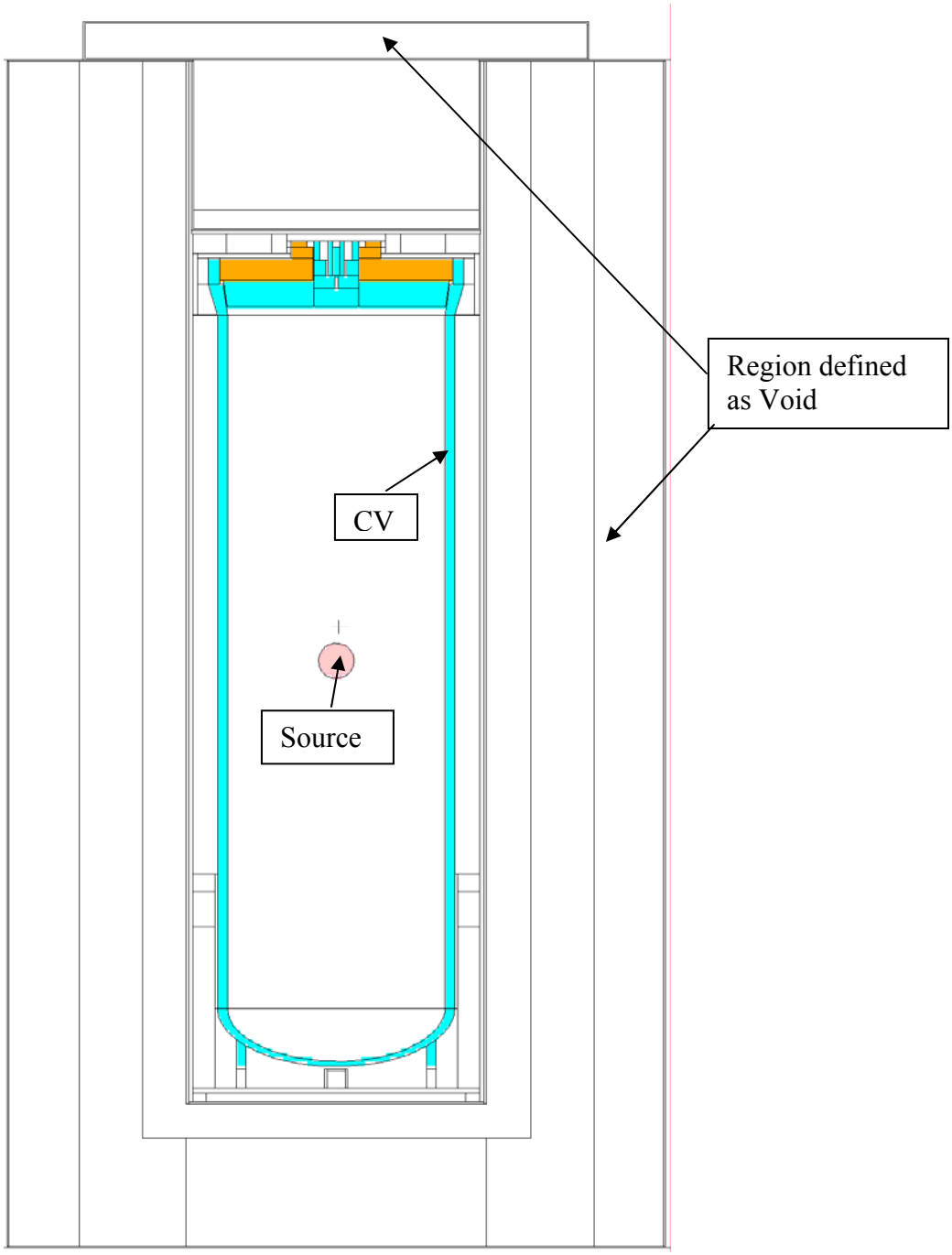

Figure 3. HAC Model

Material Compositions

The 9977 shipping container consists of a stainless steel cylindrical containment vessel, a 35-gallon steel drum, Fiberfrax, Last-A-Foam insulation, load bearing plates, and a Vermiculite/Min-K 2000/Fiberfrax lid. Neither the package materials nor the geometry is specifically designed to enhance shielding. Though some attenuation is provided by the materials, attenuation is primarily provided by the distance between the source and points external to the package.

Seven material compositions (Table 3), other than the source region, are used to model the 9977 and are taken from References 5, 6, and 7.

Radiation Sources

Radiation sources were derived using the RASTA computer code for each of the contents given in Table 5. The Radioisotope Thermoelectric Generator (RTG) source (C.1)was modeled as 100 g of Pu-238 as oxide and 0.1 mg Pu-236 (1 ppm of Pu-238). The primary dose source term is from (α,n) reactions. Modeling only the Pu-236 and Pu-238, and ignoring other plutonium isotopes, maximizes the (α,n) interactions. Other isotopes would compete with the (α,n) targets for alphas, reducing the fraction of alpha particles captured in (α,n) target material and therefore the (α,n) source.

The C.2 and C.3 analyses used a content distribution which summed to greater than 100%, a bounding scenario as (α,n) reactions are not a significant portion of the source term. The maximum content for each isotope was included in the source term. The maximum was based on either the weight percent limit given in Table 4 or the 19 Watt limit of the 9977. Pu-238 has a decay heat of 567 W/kg and Am-241 has a decay heat of 114.8 W/kg [16]. The C.4 and C.5 contents were 5.2 kg of U-233 or 13.5 kg of U-235 as either metal or compounds. The analyzed compositions are given in Table 5. The C.2 and C.3 plutonium analysis will bound the C.4 and C.5 plutonium, and the C.4 and C.5 uranium analysis will bound the C.2 and C.3 uranium.

Plutonium compounds involving fluorine were assumed to be PuF_4 as that will bound other plutonium fluoride compounds. Only uranium oxide was considered as a uranium compound.

Uranium-233 does not occur naturally and U-232 is a contaminant associated with its creation. U-232 has daughter products (specifically Tl-208) that emit high energy gammas. Therefore, ORIGEN-S was used to decay U-232 to build in the daughter products. The maximum dose rate occurs after 10 years of decay. All U-232 contents used to obtain dose rates assume the optimally decayed composition.

In addition, 0.005 g of beryllium (Be) was added to each composition to determine the impurity source term. This is based on the maximum (α,n) target impurity content specified in Reference 17 for C.1, which shows aluminum (Al) as the only (α,n) target measurable, at a maximum of 120 ppm; boron (B) and beryllium are listed but are below the sensitivity limit. With the Pu-238 limited to 35 g due to the 19 Watt limit, the maximum (α,n) target impurity would be 0.0042 g. Using Be as the impurity target will bound all other (α,n) targets. Since no impurity information was given for content envelopes other than C.1, 0.005 g of Be was

assumed for all content envelopes to account for small levels of impurities in all content envelopes. Table 4 gives impurity mass limits. Impurities which are an (α,n) target are the only impurities of concern for shielding and are limited as discussed above.

The neutron and photon source spectra are given in Tables 6 and 7, respectively.

The RASTA input decks used are listed in Appendix A.

Radiation Transport

Radiation transport calculations were performed using MCNP5. Two separate calculation sets were analyzed: Normal Conditions of Transport and Hypothetical Accident Conditions. Separate runs were made for neutron and photon sources. The neutron source runs included the contribution from secondary photons resulting from neutron interaction with the material in the 9977 shipping container. The source strengths used are listed in Tables 6 and 7. The flux-to-dose conversion factors used are those recommended by ANSI/ANS-6.1.1-1977 [18]. These are listed in Table 8.

In Content Envelopes C.4 and C.5, 5200 g of U-233 was analyzed with no U-232 present. U-232 was analyzed separately to determine the maximum allowed amount of U-232 in Envelopes C.1, C.4, and C.5. Envelopes C.2 and C.3 are assumed to have 1 ppb (4.5 μg U-232).

Subcritical multiplication in the source material was explicitly treated as part of the transport calculation. The MCNP runs for plutonium used a 50/50 mix of Pu-239 and Pu-240 for all analysis[3]. Assuming all Pu-239 for subcritical multiplication would be overly conservative as the majority of the source term is due to the spontaneous fission of Pu-240 (scoping calculations show that having no Pu-240 reduces the starting neutron/sec by a factor of 5 and only increases the subcritical multiplication by less than 2). The uranium dose rate calculation used 100% U-233 or U-235 depending on the isotope being analyzed.

The sources were placed in the middle of the containment vessel (CV) as well as at the bottom (Figures 1 and 2). Sources were not placed at the top of the containment vessel as the dose rate from the sources at the bottom will bound the dose rates from the sources at the top due to: 1) larger distance from the top of the CV to the top of the 9977 as compared to the bottom location; and 2) the packaging material at the top of the 9977.

Surface detectors were used for neutron and secondary photon cases, while point and ring detectors were used for primary photon cases.

After completion of some dose calculations, structural performance test results required the redesign of the bottom of the 9977. The new bottom reduced the distance from the inner container to the bottom of the drum to 5.057 inches (The 5.057 inch is actually for the 5-inch CV, however the MCNP model placed the 6-inch CV at that distance). As the distance is the primary driver for the dose, and several calculations were already at the regulatory limit, several cases were re-analyzed with the new distance.

[3] A few photon cases did not use the 50/50 split. However, for primary photons, there is no subcritical multiplication calculation and the isotopic composition are not significant, only the density and size for self shielding.

As Pu-240 is a significant neutron source due to spontaneous fissions, it greatly impacts the dose rate. Examinations on the effect of Pu-240 were made by either reducing the allowed percentage of Pu-240 or by reducing the total mass. For cases where the percent of Pu-240 was reduced, the ratio in the MCNP input was changed to match the reduced percentage to properly calculate sub-critical multiplication.

The MCNP input files are listed in Appendix A.

Results and Discussion

The NCT dose rates associated with the contents are given in Tables 9-14. The C.1 dose results show that the package bottom dose rate, with the source at the bottom of the CV, is the limiting case. Therefore, that was the case analyzed for the other contents. The HAC dose rates for C.1 are given in Table 17. The HAC dose rates are bounded by the NCT contact dose rates. As the HAC dose rates are not bounding, they were not determined for other source positions or the other contents. The total dose rates given in the tables are the mean values plus 3 times the Standard Deviation (SD) for the neutrons, secondary photons, and primary photons.

As seen in Tables 10 and 12, the dose rates for contents C.2 and C.3 exceed 200 mrem/hr on contact. Several options were explored to reduce the dose rate: 1) reduce the allowed percentage of Pu-240; 2) reduce the allowed total mass; and 3) increase the distance between the source and the bottom. The results are shown in Tables 10, 11, and 13. To meet the regulatory dose limit, Envelope C.2 is limited to either 25% Pu-240 or 3375 g Pu total. To meet the regulatory dose limit, Envelope C.3 is limited to either 24% Pu-240 or 3000 g Pu total. For both content envelopes, the dose rate falls below the regulatory limit if the source is placed 6.32 inches above the bottom of the drum.[4] Since the source location at the bottom was moved to reduce the dose rate at the bottom, a case was analyzed with the C.2 source located on the side of the CV to confirm that the source at the bottom was still the bounding case. As seen in Table 10, the contact dose rate for the source at the side is 155 mrem/hr, less than the dose rate at the package bottom. Tables 10-13 include the contribution from 1 ppb (4.5 μg) U-232.

Tables 14 and 15 show the dose rates for content envelopes C.4 and C.5. The U-233 dose rates given are only for pure U-233. As seen, 4500 g of PuF_4 is greater than 19 rem/hr on contact.

Table 16 gives the dose rates for 1 g of U-232. As seen, 1 g of U-232 metal gives 400 rem/hr at contact and 1 g of U-232 as oxide gives 340 rem/hr at contact. The maximum allowed U-232 can be determined by linearly scaling the dose rate to the regulatory limit of 200 mrem/hr (subtracting out 3.1 mrem/hr for U-233 metal and 5.8 mrem/hr for U-233 as oxide). To comply with the 200 mrem/hr at contact limit, only 0.49 mg of U-232 metal or 0.57 mg of U-232 as oxide can be present in the U-233. Using the same analysis for the C.1 content allows 0.14 mg of U-232.

[4] This case was analyzed as 1 inch above the CV with the original bottom. Since the new bottom doesn't impact shielding material, only distance to the CV, the total distance analyzed is still appropriate.

The above cases were analyzed for the 6-inch CV. The dose rates will not change for the 5-inch CV when the aluminum honeycombs are not credited. Crediting the honeycombs would increase the distance between the source and dose receptor location, thereby reducing the dose rates.

MCNP performs ten statistical checks. Not all calculations passed all ten checks. However, several passed all ten, the results trended well, and point detectors agreed with volume detectors. Therefore, the results were accepted.

Conclusions

The contents meet the regulatory limits if the following content limits are followed.

Content	Additional Limit to Envelope
C.1	≤ 0.005 g of (α,n) impurities, and ≤ 0.14 mg U-232
C.2 and C.3	≤ 0.005 g of (α,n) impurities and ≤ 4.5 μg U-232 and either: 1) ≤ 25% Pu-240 for C.2 or 24% Pu-240 for C.3, or 2) ≤ 50% Pu-240 and no more than 3,375 g total Pu for C.2 or 3,000 g total Pu for C.3; or 3) ≥ 6.32-inches from the bottom of the content to the exterior bottom of the drum.
C.4 and C.5	≤ 0.005 g of (α,n) impurities, and ≤ 0.49 mg U-232 in C.4, or ≤ 0.57 mg U-232 in C.5. Plutonium fluorides are prohibited.

References

1 Containment Vessel Drawings:

A. *9977 General Purpose Fissile Package – Spacer Part Details for 6-inch Containment Vessel*, R-R2-G-00042, Rev 0, SRNL, Aiken, SC.

B. *9977 General Purpose Fissile Package –6-inch Diameter Containment Vessel (CV) Subassembly*, R-R4-G-00032, Rev 0, SRNL, Aiken, SC.

2 35 Gallon Drum Drawings:

A. *9977 General Purpose Fissile Package – Assembly with 6-inch Containment Vessel*, R-R1-G-00020, Rev 0, SRNL, Aiken, SC.

B. *9977 General Purpose Fissile Package – Drum and Liner Subassembly*, R-R2-G-00017, Rev 0, SRNL, Aiken, SC.

C. *9977 General Purpose Fissile Package – Drum Lid Subassembly*, R-R2-G-00018, Rev 0, SRNL, Aiken, SC.

D. *9977 General Purpose Fissile Package – Insulating Blanket Subassembly*, R-R2-G-00019, Rev 0, SRNL, Aiken, SC.

3 *Stainless Steel Pipe*, ANSI/ASME B36.19, American Society of Mechanical Engineering, New York, 2004.

4 American Institute of Steel Construction, *AISC Manual of Steel Construction*, 7th ed. AISC, New York, 1970.

5 Barnett, M. H. *Radiological Engineering Shielding Material Composition*, WSMS-CRT-02-0060, Revision 1, Westinghouse Safety Management Solutions, Aiken, SC, September 2003.

6 Harmon II, C. D., Busch, R. D., Briesmeister, J. F., and Forster, R.A., *Criticality Calculations with MCNP: A Primer*, LA-12827-M, Los Alamos National Laboratory, Los Alamos, NM, August 1994.

7 Abramczyk, G. A., *Re: Material Properties for Components of the 9977*, SRNL-IES-2006-00007, February 2006.

8 Abramczyk, G. A., *Content Definition for the 9977*, SRNL-IES-2006-00009, February 2006.

9 Barnett, M. H., *9975 Shipping Container – Impurity Shielding Analysis*, N-CLC-G-00102, Rev. 0, November 12, 2002.

10 Hermann, O. W and Westfall, R. M., *ORIGEN-S: Scale System Module to Calculate Fuel Depletion, Actinide Transmutation, Fission Product Buildup and Decay, and Associated Radiation Source Terms*, NUREG/CR-0200, Revision 6, Volume 2, Section F7, Oak Ridge National Laboratory, Oak Ridge, TN (March 2000).

11 Nathan, S. J., Ed., *Radiation Source Term Analysis Code RASTA User Guide (U)*, WSMS-CRT-97-0013, Rev. 4, Washington Safety Management Solutions, Aiken, SC, February 2004.

12 X-5 Monte Carlo Team, *MCNP — A General Monte Carlo N-Particle Transport Code, Version 5*, LA-UR-03-1987, Los Alamos National Laboratory, Los Alamos, NM, April 24, 2003.

13 MCNP Verification

A. Nathan, S. J., *MCNP5 Test Report (U),* WSMS-CRT-03-0115, Rev. 2, Washington Safety Management Solutions, Aiken, SC, May 20, 2004.

B. Nathan, S. J., Monte Carlo N-Particle Transport Code System MCNP5 Shielding Validation Report (U), WSMS-CRT-03-127, Rev. 0, Westinghouse Safety Management Solutions, Aiken, SC, September 2003.

14 Gaul, J., Knecht, K., and Barnett, M. H., *Verification of Rasta Version 5.1*, WSMS-CRT-05-0044, Washington Safety Management Solutions, Aiken, SC, June 15, 2005.

15 Revolinski, S M., *SCALE5 Test Report (U)*, WSMS-CRT-04-0080, Rev. 0, Washington Safety Management Solutions, Aiken, SC, September 2004.

16 *Stabilization, Packaging, and Storage of Plutonium-Bearing Materials*, DOE-STD-3013-2004, April 2004.

17 Abramczyk, G. A., *Re: Sandia National Laboratory RTG Information*, SRNL-IES-2006-00005, February 2006.

18 *Neutron and Gamma-Ray Flux-to-Dose Rate Factors*, ANSI/ANS-6.1.1-1977, 1977.

Table 1 Containment Vessel Dimensions

Component	Part	Dimension		Material
		Description	(Inches)	
Cylindrical Body	Overall	Height	23.5	304L
		Height	19.84375	
		OD	6.625	
		Thickness	0.28	
End Cap		OR	3.3125	
		IR	3.0325	
Transition Section		Height	0.87	
		Base OR	3.3125	
		Top OD	7.12	
		Base IR	3.0325	
		Top ID	6.3	
Top Cylinder		Height	0.75	
		OR	3.56	
		ID	6.5	
Cone Seal Plug	Lower Section	Height	0.75	304L
		OD of Top	6.31	
		OD of Bottom	6.094	
	Upper Section	Height	1.13	304L
		OD	1.25	
		Top Cavity ID	0.9	
		Top Cavity H	0.56	
		Bottom Cavity ID	0.57	
		Bottom Cavity H	0.44	
		Vertical Tube D	0.94	
		Vertical Tube H	0.7	
Cone Seal Nut	Lower Section	OD	6.5	Nitronic-60
		ID	1.28	
		Height	0.63	
	Upper Section	Outside Square	2.5	
		Height	0.5	
		Top Cavity ID	1.63	
		Top Cavity H	0.18	
		Bottom Cavity ID	1.28	
		Bottom Cavity H	0.32	
Gland Nut/Plug		OR	0.225	304L
		Height	1	
		Cavity D	0.187	
		Cavity H	0.18	
Support	Ring	OD	5.563	
		Thickness	0.258	
		Base Elevation	-2.03625	
	Slot	Width	0.63	
		Height	0.31	

Table 2 Drum Dimensions

Component	Part	Dimension		Material
		Description	(inches)	
Drum	Overall	Height	36.1	304L
	Side	ID	18.25	
		IR	9.125	
		Thickness	0.0478	
		OR	9.1728	
		Height	33.874	
	Lid	Flange OD	18.72	
		Flange OR	9.36	
		Flange Thickness	0.1875	
		Lid OR	9.1725	
		Lid Thickness	0.0478	
	Bottom	OR	9.1728	
		Thickness	0.0478	
Last-A-Foam	Upper Region	OD	18.25	Polyurethane
		OR	9.125	
		IR	5.4189	
		H	30.8	
	Lower Region	D	18.25	
		R	9.125	
		H	3.07	
Bottom Load Distribution Assembly	Side	OD	8	AL 6061-T6
		OR	4	
		ID	6.75	
		IR	3.375	
		Height	6.13	
	Bottom	OR	4	
		Thickness	0.37	
	Slot	Width	8	
		Depth	0.6	
		Height	0.255	
	Penetration (cx)	ID	1	
		IR	0.5	
		C/L	1	
Top Load Distribution Fixture	Side	OD	8	AL 6061-T6
		OR	4	
		ID	7.15	
		IR	3.575	
		Height	1.75	
	Top	OR	4	
		Thickness	0.55	
	Penetration (cz)	ID	1.25	
		IR	0.625	
		C/L	2.43	
	Center Penetration	Sides	2.75	

Table 2 (cont.)

Component	Part	Dimension		Material
		Description	(inches)	
Fiberfrax				Fiberfrax
	Side	OD	10.8378	
		OR	5.4189	
		IR	2.8789	
		Height	32.04	
Lid	Top - Liner	ID	14	
		OD	14.0956	Min-K2000
		OR	7.0478	
		IH	1	
		OH	1.0956	
	Bottom - liner	ID	7.96	
		OD	8.0556	
		OH	4.88	
		IH	4.8322	
	Vermiculite	ID	7.96	Vermiculite
		IH	4.3	
	Fiberfrax	ID	7.96	Fiberfrax
		IH	0.5322	

Table 3 Material Compositions

	Nitronic 60	SS 304L	6061 Aluminum	Foam	Vermiculite	Min-K 2000	Fiberfrax
density (g/cc)	7.584	7.9	2.7	0.256	0.3684	0.3204	0.2563
Element	Weight Percent						
H				4.1		0.84	
C		0.03		54.4		1.28	
O				29.4	45.53	48.01	50.03
N	0.14			12.1			
Si	4	1	0.6		21.22	37.71	23.14
Ni	8.5	10					
Cr	17	19	0.2				
Mn	8	2					
Fe	62.36	67.895			5.4		
P		0.045					
S							
Al			97.9		5.47	6.39	26.46
Cu			0.28				
Mg			1		8.9		
Ti					0.82	5.53	
Na					1.09		0.37
K					1.22		
Ga						0.15	
Sb						0.09	

Table 4 Content Envelope Compositions

		Material [a, b]	C.1 Heat Sources	C.2 Pu/U Metals [c]	C.3 Pu/U Oxides
Fissile Materiel	Weight %	238Pu	100	2	
		239Pu	40	100	
		240Pu d	13	40	
		241Pu	1	15	
		242Pu	1.5	5	
		232U	1.4×10^{-4}	1×10^{-7}	
		233U	0.2	0.5	
		234U	40	100	Reserved
		235U	40	100	
		236U	16	40	
		238U	40	100	
Impurities [e]	(grams)	Ca	15		
		Fe	5		
		Cr	2		
Total Mass	(kilograms)	Radioactive Materials	0.1	4.4	
		Impurities	0.02	3.08 [f]	
		All Contents	0.1	4.4	

Notes

a All contents shall be dry.

b Pu/U content bulk density shall be no greater than 19.84 g/cc and no less than 2.0 g/cc.

c Contents shall be stabilized in accordance with DOE-STD-3013, Section 6.1.1.

d ^{240}Pu shall be greater than ^{241}Pu.

d Less than 5mg of total (α, n) impurities {aluminum, beryllium, boron, fluorine, lithium, magnesium, and sodium}are permitted.

e The impurity limit is based on the DOE-STD-3013 requirement that plutonium plus uranium mass shall not be less than 30 weight percent of the total content mass.

Table 4 cont.

	Material [a, b, c]	C.4 "6M" Metal or Alloy	C.5 "6M" Compounds	
		H/X=0 [c, d]	H/X=0 [c]	H/X≤3 [c]
Fissile Materiel Mass (kg)	^{233}U	Reserved		
	^{235}U	13.5	4.4	4.4

Notes

a Except as permitted for compounds, all contents shall be dry. The moisture content of the compounds shall be less than 0.5 weight percent of the total content mass.

b U content bulk density shall be no greater than 19.84 g/cc and no less than 2.0 g/cc.

c H/X is the ratio of hydrogen to fissile atoms that can be mixed with the fissile material contents. The moisture content of the materials shall be less than 0.5 weight percent of the total content mass.

d Pieces shall have a specific surface area less than 100 mm^2/g. This limit may be implemented by either restricting each piece mass to at least 50 g or by performing calculations and measurements.

Table 5 Analyzed Compositions

Isotope	Analyzed Composition (grams)[a]							
	C.1 ^{238}Pu Heat Sources	**C.2** Pu/U Metals	**C.3** Pu/U Oxides	**C.4** U-233 Metal	**C.4** U-235 Metal	**C.5** U-233 Oxide	**C.5** U-235 Oxide	**C.5** PuF_4
^{233}U				5200		5200		
^{235}U					13500		13500	
^{243}Am								0.0045
^{244}Cm								0.0045
^{237}Np								225
^{236}Pu	1E-4	4.5E-6	4.5E-6					4.5E-6
^{238}Pu	100	33.51[b]	33.51[b]					33.51[b]
^{239}Pu		4500	4500					4500
^{240}Pu		2250	2250					2250
^{241}Pu		675	675					495
^{242}Pu		225	225					225
^{241}Am		165.5[b]	165.5[b]					165.5[b]
Total	100	7849	7849	5200	13500	5200	13500	7894

a) One gram of U-232 analyzed separately

b) Mass limits based on 19 Watt Limit; Pu-238 generates 567 W/kg and Am-241 generates 114.8 W/kg

Table 6 Neutron Source Spectra

Neutron Energy									
Upper Limit (MeV)	Lower Limit (MeV)	C.1 Normalized Spectrum	C.2 Normalized Spectrum	C.3 Normalized Spectrum	C.4 U-233 Normalized Spectrum	C.4 U-235 Normalized Spectrum	C.5 U-233 Normalized Spectrum	C.5 U-235 Normalized Spectrum	C.5 PuF4 Normalized Spectrum
1.73E+01	1.42E+01	2.03E-06	9.26E-06	6.13E-06	2.64E-07	6.08E-06	3.12E-09	1.82E-06	8.64E-08
1.42E+01	1.22E+01	1.11E-05	5.69E-05	3.76E-05	1.43E-06	4.04E-05	1.68E-08	1.21E-05	5.24E-07
1.22E+01	1.00E+01	2.43E-03	4.91E-04	3.18E-04	2.68E-03	3.52E-04	2.25E-05	1.05E-04	4.18E-06
1.00E+01	8.61E+00	2.11E-02	1.65E-03	1.03E-03	6.72E-02	1.81E-03	5.61E-04	4.76E-04	1.22E-05
8.61E+00	7.41E+00	2.83E-02	4.01E-03	2.56E-03	1.09E-01	4.42E-03	9.08E-04	1.19E-03	3.23E-05
7.41E+00	6.07E+00	3.51E-02	1.24E-02	8.10E-03	1.38E-01	1.23E-02	1.14E-03	3.50E-03	1.07E-04
6.07E+00	4.97E+00	3.75E-02	2.63E-02	1.77E-02	7.03E-02	2.40E-02	7.12E-04	7.11E-03	2.32E-04
4.97E+00	3.68E+00	1.08E-01	7.67E-02	6.73E-02	2.01E-01	7.32E-02	1.14E-02	2.69E-02	6.79E-04
3.68E+00	3.01E+00	1.61E-01	7.67E-02	1.11E-01	1.44E-01	7.50E-02	1.14E-01	5.66E-02	1.89E-03
3.01E+00	2.73E+00	9.03E-02	4.31E-02	6.92E-02	6.42E-02	4.27E-02	1.13E-01	7.29E-02	1.09E-02
2.73E+00	2.47E+00	8.68E-02	4.69E-02	7.35E-02	3.92E-02	4.65E-02	1.37E-01	1.04E-01	2.39E-02
2.47E+00	2.37E+00	3.31E-02	2.00E-02	2.98E-02	1.23E-02	1.98E-02	5.95E-02	4.81E-02	1.39E-02
2.37E+00	2.35E+00	6.53E-03	4.13E-03	6.02E-03	2.34E-03	4.10E-03	1.20E-02	1.01E-02	3.23E-03
2.35E+00	2.23E+00	3.84E-02	2.57E-02	3.62E-02	1.33E-02	2.56E-02	7.18E-02	6.43E-02	2.27E-02
2.23E+00	1.92E+00	8.80E-02	7.43E-02	9.19E-02	2.78E-02	7.40E-02	1.65E-01	1.70E-01	9.18E-02
1.92E+00	1.65E+00	6.05E-02	7.41E-02	7.68E-02	1.57E-02	7.41E-02	1.02E-01	1.26E-01	1.19E-01
1.65E+00	1.35E+00	5.31E-02	9.23E-02	8.29E-02	1.68E-02	9.28E-02	7.56E-02	9.70E-02	1.63E-01
1.35E+00	1.00E+00	4.97E-02	1.19E-01	9.52E-02	2.72E-02	1.20E-01	5.41E-02	7.92E-02	1.98E-01
1.00E+00	8.21E-01	2.26E-02	6.36E-02	4.84E-02	1.44E-02	6.47E-02	1.74E-02	3.27E-02	8.85E-02
8.21E-01	7.43E-01	9.48E-03	2.78E-02	2.10E-02	6.28E-03	2.84E-02	5.27E-03	1.34E-02	3.56E-02
7.43E-01	6.08E-01	1.57E-02	4.78E-02	3.59E-02	1.09E-02	4.88E-02	7.11E-03	2.09E-02	5.64E-02
6.08E-01	4.98E-01	1.24E-02	3.79E-02	2.87E-02	7.73E-03	3.87E-02	6.49E-03	1.50E-02	4.26E-02
4.98E-01	3.69E-01	1.32E-02	4.21E-02	3.21E-02	6.15E-03	4.31E-02	9.98E-03	1.58E-02	4.76E-02
3.69E-01	2.97E-01	6.38E-03	2.18E-02	1.66E-02	1.62E-03	2.23E-02	6.23E-03	7.77E-03	2.45E-02
2.97E-01	1.83E-01	9.39E-03	3.07E-02	2.38E-02	8.51E-04	3.15E-02	1.23E-02	1.16E-02	3.17E-02
1.83E-01	1.11E-01	5.33E-03	1.59E-02	1.26E-02	3.29E-04	1.63E-02	7.79E-03	7.33E-03	1.46E-02
1.11E-01	5.74E-02	3.10E-03	9.25E-03	7.27E-03	1.86E-04	9.49E-03	4.37E-03	4.89E-03	6.75E-03
5.74E-02	4.09E-02	7.84E-04	2.22E-03	1.77E-03	4.27E-05	2.28E-03	1.10E-03	1.31E-03	1.34E-03
4.09E-02	3.18E-02	3.89E-04	1.06E-03	8.50E-04	1.98E-05	1.09E-03	5.42E-04	6.65E-04	5.97E-04
3.18E-02	2.61E-02	2.20E-04	5.95E-04	4.77E-04	1.09E-05	6.11E-04	3.02E-04	3.90E-04	3.21E-04
2.61E-02	2.42E-02	6.89E-05	1.85E-04	1.49E-04	3.35E-06	1.90E-04	9.28E-05	1.25E-04	9.80E-05
2.42E-02	2.19E-02	7.98E-05	2.15E-04	1.72E-04	3.86E-06	2.21E-04	1.06E-04	1.47E-04	1.12E-04
2.19E-02	1.50E-02	2.11E-04	5.78E-04	4.61E-04	1.02E-05	5.93E-04	2.76E-04	4.05E-04	2.95E-04
1.50E-02	7.10E-03	1.80E-04	5.12E-04	4.04E-04	8.65E-06	5.25E-04	2.22E-04	3.53E-04	2.51E-04
7.10E-03	3.35E-03	5.60E-05	1.67E-04	1.30E-04	2.64E-06	1.72E-04	6.46E-05	1.10E-04	7.92E-05
3.35E-03	1.58E-03	1.76E-05	5.44E-05	4.19E-05	8.00E-07	5.58E-05	1.94E-05	3.44E-05	2.52E-05
1.58E-03	4.54E-04	6.99E-06	2.20E-05	1.69E-05	3.11E-07	2.26E-05	7.53E-06	1.37E-05	1.01E-05
4.54E-04	2.14E-04	8.52E-07	2.72E-06	2.08E-06	3.79E-08	2.79E-06	9.07E-07	1.66E-06	1.24E-06
2.14E-04	1.01E-04	2.75E-07	8.78E-07	6.72E-07	1.23E-08	9.01E-07	2.92E-07	5.37E-07	4.00E-07
1.01E-04	3.73E-05	1.02E-07	3.27E-07	2.50E-07	4.56E-09	3.35E-07	1.08E-07	1.99E-07	1.49E-07
3.73E-05	1.07E-05	2.51E-08	8.01E-08	6.14E-08	1.12E-09	8.22E-08	2.65E-08	4.86E-08	3.64E-08
1.07E-05	5.04E-06	3.10E-09	9.83E-09	7.51E-09	1.37E-10	1.01E-08	3.23E-09	6.08E-09	4.51E-09
5.04E-06	1.86E-06	1.13E-09	3.64E-09	2.79E-09	5.10E-11	3.74E-09	1.22E-09	2.18E-09	1.61E-09
1.86E-06	8.76E-07	2.44E-10	7.21E-10	5.61E-10	1.00E-11	7.40E-10	2.12E-10	4.48E-10	3.50E-10
8.76E-07	4.14E-07	6.58E-11	2.37E-10	1.75E-10	3.23E-12	2.41E-10	8.87E-11	1.42E-10	1.09E-10
4.14E-07	1.00E-07	3.31E-11	9.05E-11	6.84E-11	1.38E-12	9.89E-11	2.21E-11	5.17E-11	3.40E-11
1.00E-07	1.00E-11	2.44E-12	8.92E-12	6.74E-12	1.99E-13	1.17E-11	1.09E-13	3.54E-12	4.53E-12
	Total (n/s)	**2.24E+06**	**2.79E+06**	**4.22E+06**	**2.94E+02**	**4.09E+00**	**2.49E+04**	**1.37E+01**	**3.18E+08**

Table 6 cont.

Neutron Energy											
Upper Limit (MeV)	Lower Limit (MeV)	C.2 30% Pu-240	C.2 25% Pu-240	C.2 3600 g	C.2 3375 g	C.3 25% Pu-240	C.3 24% Pu-240	C.3 3375 g	C.3 3000 g	1 g U-232 metal	1 g U-232 oxide
1.73E+01	1.42E+01	9.59E-06	9.72E-06	9.31E-06	9.33E-06	5.49E-06	5.45E-06	5.69E-06	5.62E-06	2.85E-05	4.56E-10
1.42E+01	1.22E+01	5.84E-05	5.90E-05	5.71E-05	5.72E-05	3.33E-05	3.31E-05	3.48E-05	3.44E-05	1.41E-04	2.26E-09
1.22E+01	1.00E+01	5.17E-04	5.29E-04	5.06E-04	5.11E-04	2.89E-04	2.87E-04	3.05E-04	3.03E-04	9.30E-04	1.49E-08
1.00E+01	8.61E+00	1.84E-03	1.92E-03	1.79E-03	1.84E-03	9.89E-04	9.87E-04	1.05E-03	1.06E-03	2.35E-03	3.76E-08
8.61E+00	7.41E+00	4.27E-03	4.39E-03	4.19E-03	4.26E-03	2.34E-03	2.33E-03	2.50E-03	2.50E-03	5.58E-03	8.92E-08
7.41E+00	6.07E+00	1.28E-02	1.29E-02	1.26E-02	1.27E-02	7.13E-03	7.07E-03	7.62E-03	7.55E-03	1.65E-02	1.13E-04
6.07E+00	4.97E+00	2.67E-02	2.68E-02	2.65E-02	2.66E-02	1.56E-02	1.55E-02	1.66E-02	1.64E-02	3.26E-02	2.99E-03
4.97E+00	3.68E+00	7.73E-02	7.76E-02	7.70E-02	7.71E-02	6.64E-02	6.64E-02	6.73E-02	6.73E-02	8.68E-02	1.00E-01
3.68E+00	3.01E+00	7.70E-02	7.71E-02	7.68E-02	7.69E-02	1.22E-01	1.22E-01	1.17E-01	1.18E-01	8.16E-02	1.93E-01
3.01E+00	2.73E+00	4.31E-02	4.31E-02	4.31E-02	4.31E-02	7.68E-02	7.72E-02	7.33E-02	7.39E-02	4.46E-02	1.13E-01
2.73E+00	2.47E+00	4.69E-02	4.69E-02	4.69E-02	4.68E-02	8.06E-02	8.11E-02	7.72E-02	7.78E-02	4.78E-02	1.10E-01
2.47E+00	2.37E+00	1.99E-02	1.99E-02	1.99E-02	1.99E-02	3.23E-02	3.25E-02	3.11E-02	3.13E-02	2.01E-02	4.21E-02
2.37E+00	2.35E+00	4.12E-03	4.12E-03	4.12E-03	4.12E-03	6.50E-03	6.52E-03	6.26E-03	6.29E-03	4.15E-03	8.29E-03
2.35E+00	2.23E+00	2.57E-02	2.57E-02	2.57E-02	2.57E-02	3.89E-02	3.90E-02	3.75E-02	3.77E-02	2.58E-02	4.85E-02
2.23E+00	1.92E+00	7.41E-02	7.41E-02	7.42E-02	7.41E-02	9.61E-02	9.64E-02	9.39E-02	9.42E-02	7.35E-02	1.10E-01
1.92E+00	1.65E+00	7.39E-02	7.38E-02	7.40E-02	7.40E-02	7.70E-02	7.70E-02	7.68E-02	7.68E-02	7.23E-02	7.38E-02
1.65E+00	1.35E+00	9.20E-02	9.19E-02	9.22E-02	9.21E-02	7.97E-02	7.95E-02	8.11E-02	8.08E-02	8.89E-02	5.97E-02
1.35E+00	1.00E+00	1.18E-01	1.18E-01	1.19E-01	1.19E-01	8.81E-02	8.77E-02	9.13E-02	9.07E-02	1.13E-01	4.86E-02
1.00E+00	8.21E-01	6.34E-02	6.33E-02	6.35E-02	6.34E-02	4.40E-02	4.37E-02	4.60E-02	4.57E-02	5.99E-02	2.00E-02
8.21E-01	7.43E-01	2.78E-02	2.77E-02	2.78E-02	2.78E-02	1.91E-02	1.89E-02	2.00E-02	1.98E-02	2.61E-02	8.17E-03
7.43E-01	6.08E-01	4.76E-02	4.75E-02	4.77E-02	4.76E-02	3.25E-02	3.23E-02	3.40E-02	3.38E-02	4.48E-02	1.31E-02
6.08E-01	4.98E-01	3.77E-02	3.77E-02	3.78E-02	3.78E-02	2.60E-02	2.58E-02	2.72E-02	2.70E-02	3.54E-02	1.05E-02
4.98E-01	3.69E-01	4.19E-02	4.19E-02	4.20E-02	4.20E-02	2.91E-02	2.90E-02	3.05E-02	3.02E-02	3.93E-02	1.21E-02
3.69E-01	2.97E-01	2.17E-02	2.17E-02	2.17E-02	2.17E-02	1.50E-02	1.49E-02	1.57E-02	1.56E-02	2.03E-02	6.10E-03
2.97E-01	1.83E-01	3.06E-02	3.05E-02	3.06E-02	3.06E-02	2.16E-02	2.15E-02	2.26E-02	2.24E-02	2.87E-02	9.32E-03
1.83E-01	1.11E-01	1.59E-02	1.59E-02	1.59E-02	1.59E-02	1.15E-02	1.15E-02	1.20E-02	1.19E-02	1.49E-02	5.35E-03
1.11E-01	5.74E-02	9.22E-03	9.20E-03	9.23E-03	9.22E-03	6.67E-03	6.64E-03	6.94E-03	6.89E-03	8.65E-03	3.02E-03
5.74E-02	4.09E-02	2.21E-03	2.21E-03	2.22E-03	2.22E-03	1.63E-03	1.62E-03	1.69E-03	1.68E-03	2.08E-03	7.52E-04
4.09E-02	3.18E-02	1.06E-03	1.06E-03	1.06E-03	1.06E-03	7.86E-04	7.82E-04	8.14E-04	8.09E-04	9.93E-04	3.69E-04
3.18E-02	2.61E-02	5.93E-04	5.93E-04	5.94E-04	5.94E-04	4.42E-04	4.40E-04	4.58E-04	4.55E-04	5.58E-04	2.06E-04
2.61E-02	2.42E-02	1.85E-04	1.84E-04	1.85E-04	1.85E-04	1.38E-04	1.37E-04	1.43E-04	1.42E-04	1.74E-04	6.36E-05
2.42E-02	2.19E-02	2.14E-04	2.14E-04	2.15E-04	2.14E-04	1.60E-04	1.59E-04	1.65E-04	1.64E-04	2.01E-04	7.31E-05
2.19E-02	1.50E-02	5.76E-04	5.75E-04	5.76E-04	5.76E-04	4.26E-04	4.24E-04	4.42E-04	4.39E-04	5.41E-04	1.91E-04
1.50E-02	7.10E-03	5.10E-04	5.09E-04	5.11E-04	5.10E-04	3.72E-04	3.70E-04	3.86E-04	3.84E-04	4.79E-04	1.58E-04
7.10E-03	3.35E-03	1.67E-04	1.67E-04	1.67E-04	1.67E-04	1.19E-04	1.19E-04	1.24E-04	1.23E-04	1.57E-04	4.78E-05
3.35E-03	1.58E-03	5.42E-05	5.41E-05	5.43E-05	5.42E-05	3.83E-05	3.81E-05	4.00E-05	3.97E-05	5.09E-05	1.47E-05
1.58E-03	4.54E-04	2.20E-05	2.19E-05	2.20E-05	2.20E-05	1.54E-05	1.54E-05	1.61E-05	1.60E-05	2.07E-05	5.75E-06
4.54E-04	2.14E-04	2.71E-06	2.70E-06	2.71E-06	2.71E-06	1.90E-06	1.89E-06	1.98E-06	1.97E-06	2.55E-06	6.96E-07
2.14E-04	1.01E-04	8.75E-07	8.74E-07	8.76E-07	8.76E-07	6.13E-07	6.09E-07	6.40E-07	6.35E-07	8.23E-07	2.24E-07
1.01E-04	3.73E-05	3.26E-07	3.25E-07	3.26E-07	3.26E-07	2.28E-07	2.27E-07	2.38E-07	2.36E-07	3.06E-07	8.33E-08
3.73E-05	1.07E-05	7.98E-08	7.97E-08	7.99E-08	7.99E-08	5.60E-08	5.56E-08	5.84E-08	5.80E-08	7.50E-08	2.04E-08
1.07E-05	5.04E-06	9.79E-09	9.78E-09	9.81E-09	9.80E-09	6.85E-09	6.81E-09	7.15E-09	7.10E-09	9.19E-09	2.46E-09
5.04E-06	1.86E-06	3.63E-09	3.63E-09	3.64E-09	3.63E-09	2.54E-09	2.53E-09	2.66E-09	2.64E-09	3.41E-09	1.01E-09
1.86E-06	8.76E-07	7.18E-10	7.17E-10	7.19E-10	7.19E-10	5.14E-10	5.11E-10	5.36E-10	5.32E-10	6.64E-10	1.72E-10
8.76E-07	4.14E-07	2.36E-10	2.35E-10	2.36E-10	2.36E-10	1.58E-10	1.58E-10	1.66E-10	1.64E-10	2.11E-10	5.53E-11
4.14E-07	1.00E-07	9.05E-11	9.04E-11	9.04E-11	9.04E-11	6.28E-11	6.25E-11	6.57E-11	6.53E-11	8.66E-11	1.29E-11
1.00E-07	1.00E-11	9.20E-12	9.31E-12	8.97E-12	8.99E-12	6.44E-12	6.42E-12	6.55E-12	6.52E-12	6.62E-12	9.27E-13
	Total (n/s)	**1.87E+06**	**1.64E+06**	**2.26E+06**	**2.12E+06**	**2.91E+06**	**2.85E+06**	**3.26E+06**	**3.16E+06**	**1.11E+00**	**6.93E+04**

Table 7 Photon Source Spectra

Photon Energy									
Upper Limit (MeV)	Lower Limit (MeV)	C.1 Normalized Spectrum	C.2 Normalized Spectrum	C.3 Normalized Spectrum	C.4 U-233 Normalized Spectrum	C.4 U-235 Normalized Spectrum	C.5 U-233 Normalized Spectrum	C.5 U-235 Normalized Spectrum	C.5 PuF4 Normalized Spectrum
1.00E+01	8.00E+00	3.23E-11	8.55E-11	9.05E-11	3.71E-14	3.10E-12	3.71E-14	3.10E-12	9.36E-11
8.00E+00	7.00E+00	7.92E-09	7.98E-11	7.26E-11	2.18E-10	4.32E-12	1.54E-10	3.50E-12	4.72E-11
7.00E+00	6.00E+00	1.83E-10	4.85E-10	5.13E-10	2.10E-13	1.76E-11	2.10E-13	1.76E-11	5.30E-10
6.00E+00	5.00E+00	4.27E-10	1.13E-09	1.20E-09	4.90E-13	4.11E-11	4.90E-13	4.11E-11	1.24E-09
5.00E+00	4.00E+00	4.81E-08	3.45E-09	3.58E-09	1.24E-09	1.36E-10	8.74E-10	1.30E-10	3.54E-09
4.00E+00	3.00E+00	4.79E-09	1.21E-08	1.29E-08	5.25E-12	4.40E-10	5.25E-12	4.40E-10	1.33E-08
3.00E+00	2.00E+00	3.04E-08	4.02E-08	4.62E-08	1.74E-11	1.46E-09	8.57E-09	1.54E-09	4.62E-08
2.00E+00	1.50E+00	2.92E-08	4.27E-08	4.86E-08	1.85E-11	1.55E-09	1.18E-08	2.02E-09	4.48E-07
1.50E+00	1.00E+00	1.81E-07	1.04E-07	1.14E-07	4.04E-11	3.38E-09	1.35E-08	3.75E-09	1.32E-06
1.00E+00	8.00E-01	8.22E-07	1.86E-07	1.97E-07	3.16E-11	2.65E-09	3.16E-11	2.65E-09	1.62E-06
8.00E-01	7.00E-01	4.19E-06	2.01E-06	2.12E-06	1.85E-11	8.05E-06	1.85E-11	8.05E-06	2.17E-06
7.00E-01	6.00E-01	2.03E-08	1.32E-06	1.40E-06	1.25E-05	1.89E-09	1.25E-05	1.89E-09	1.45E-06
6.00E-01	4.00E-01	4.58E-08	6.84E-06	7.24E-06	5.17E-11	8.62E-05	5.17E-11	8.62E-05	1.42E-05
4.00E-01	2.00E-01	4.13E-07	3.77E-05	4.00E-05	6.34E-03	3.41E-02	6.34E-03	3.41E-02	4.13E-05
2.00E-01	1.00E-01	9.47E-05	6.16E-04	6.52E-04	7.43E-03	6.77E-01	7.43E-03	6.77E-01	5.56E-04
1.00E-01	8.00E-02	7.55E-04	1.05E-03	1.11E-03	1.03E-02	7.16E-02	1.03E-02	7.16E-02	9.43E-04
8.00E-02	6.00E-02	5.09E-09	2.02E-04	2.14E-04	1.36E-03	1.69E-03	1.36E-03	1.69E-03	2.15E-04
6.00E-02	5.90E-02	1.42E-10	2.52E-01	2.66E-01	1.63E-13	1.37E-11	1.63E-13	1.37E-11	2.72E-01
5.90E-02	5.00E-02	1.28E-09	2.22E-04	2.35E-04	2.77E-03	9.46E-04	2.77E-03	9.46E-04	2.40E-04
5.00E-02	4.00E-02	3.33E-03	1.06E-03	1.12E-03	1.19E-02	5.05E-04	1.19E-02	5.05E-04	1.14E-03
4.00E-02	3.00E-02	2.88E-09	9.39E-04	9.94E-04	1.65E-04	1.12E-04	1.65E-04	1.12E-04	1.01E-03
3.00E-02	2.00E-02	9.21E-02	7.66E-02	8.10E-02	3.01E-03	2.58E-10	3.01E-03	2.58E-10	8.25E-02
2.00E-02	1.00E-02	9.04E-01	5.74E-01	6.07E-01	9.57E-01	2.14E-01	9.57E-01	2.14E-01	6.18E-01
1.00E-02	1.00E-08	1.07E-09	9.39E-02	4.14E-02	1.23E-12	1.03E-10	1.23E-12	1.03E-10	2.42E-02
	Total (p/s)	**7.15E+12**	**2.98E+13**	**2.82E+13**	**1.29E+11**	**1.38E+09**	**1.29E+11**	**1.38E+09**	**2.76E+13**

Table 7 cont.

Photon Energy											
Upper Limit (MeV)	Lower Limit (MeV)	C.2 30% Pu-240	C.2 25% Pu-240	C.2 3600 g	C.2 3375 g	C.3 25% Pu-240	C.3 24% Pu-240	C.3 3375 g	C.3 3000 g	1 g U-232 metal	1 g U-232 oxide
1.00E+01	8.00E+00	5.87E-11	5.18E-11	7.16E-11	6.79E-11	5.49E-11	5.34E-11	6.69E-11	6.42E-11	5.35E-16	7.69E-16
8.00E+00	7.00E+00	6.81E-11	6.52E-11	7.99E-11	8.04E-11	5.65E-11	5.58E-11	6.91E-11	6.91E-11	2.70E-16	3.88E-16
7.00E+00	6.00E+00	3.33E-10	2.93E-10	4.06E-10	3.85E-10	3.11E-10	3.03E-10	3.79E-10	3.64E-10	3.03E-15	4.36E-15
6.00E+00	5.00E+00	7.77E-10	6.85E-10	9.47E-10	8.98E-10	7.27E-10	7.07E-10	8.85E-10	8.49E-10	7.07E-15	1.02E-14
5.00E+00	4.00E+00	2.45E-09	2.19E-09	2.96E-09	2.84E-09	2.24E-09	2.19E-09	2.74E-09	2.64E-09	2.02E-14	2.87E-13
4.00E+00	3.00E+00	8.32E-09	7.33E-09	1.01E-08	9.62E-09	7.82E-09	7.61E-09	9.51E-09	9.13E-09	7.57E-14	1.96E-10
3.00E+00	2.00E+00	2.76E-08	2.43E-08	3.36E-08	3.19E-08	2.92E-08	2.85E-08	3.49E-08	3.36E-08	1.16E-01	1.66E-01
2.00E+00	1.50E+00	2.93E-08	2.59E-08	3.58E-08	3.39E-08	3.05E-08	2.98E-08	3.66E-08	3.52E-08	1.05E-02	3.20E-06
1.50E+00	1.00E+00	7.46E-08	6.71E-08	8.87E-08	8.48E-08	7.56E-08	7.40E-08	8.87E-08	8.57E-08	3.25E-03	6.65E-04
1.00E+00	8.00E-01	1.65E-07	1.60E-07	1.77E-07	1.75E-07	1.69E-07	1.68E-07	1.80E-07	1.78E-07	1.65E-02	1.89E-02
8.00E-01	7.00E-01	2.05E-06	2.06E-06	2.06E-06	2.07E-06	2.18E-06	2.19E-06	2.18E-06	2.18E-06	4.43E-02	3.10E-03
7.00E-01	6.00E-01	1.30E-06	1.29E-06	1.29E-06	1.29E-06	1.37E-06	1.37E-06	1.33E-06	1.32E-06	5.35E-04	1.49E-04
6.00E-01	4.00E-01	6.99E-06	7.03E-06	5.94E-06	5.70E-06	7.45E-06	7.46E-06	5.69E-06	5.51E-06	1.39E-01	1.96E-01
4.00E-01	2.00E-01	3.87E-05	3.89E-05	3.46E-05	3.38E-05	4.13E-05	4.14E-05	3.44E-05	3.38E-05	1.47E-01	2.00E-01
2.00E-01	1.00E-01	6.19E-04	6.20E-04	5.43E-04	5.24E-04	6.57E-04	6.58E-04	5.26E-04	5.12E-04	1.56E-02	6.07E-03
1.00E-01	8.00E-02	1.08E-03	1.09E-03	9.19E-04	8.85E-04	1.15E-03	1.15E-03	8.86E-04	8.60E-04	3.77E-02	4.63E-02
8.00E-02	6.00E-02	2.08E-04	2.10E-04	2.04E-04	2.05E-04	2.22E-04	2.23E-04	2.14E-04	2.14E-04	1.13E-01	1.50E-01
6.00E-02	5.90E-02	2.59E-01	2.61E-01	2.61E-01	2.64E-01	2.76E-01	2.77E-01	2.78E-01	2.79E-01	5.67E-04	1.29E-04
5.90E-02	5.00E-02	2.28E-04	2.30E-04	2.15E-04	2.13E-04	2.44E-04	2.44E-04	2.20E-04	2.18E-04	6.63E-03	2.36E-03
5.00E-02	4.00E-02	9.71E-04	9.48E-04	1.04E-03	1.03E-03	1.01E-03	1.00E-03	1.07E-03	1.07E-03	8.57E-03	2.01E-03
4.00E-02	3.00E-02	9.65E-04	9.72E-04	9.68E-04	9.76E-04	1.03E-03	1.03E-03	1.03E-03	1.03E-03	1.60E-02	2.91E-03
3.00E-02	2.00E-02	7.61E-02	7.60E-02	7.78E-02	7.81E-02	8.06E-02	8.06E-02	8.18E-02	8.19E-02	1.91E-02	4.68E-03
2.00E-02	1.00E-02	5.64E-01	5.62E-01	5.79E-01	5.80E-01	5.96E-01	5.95E-01	6.06E-01	6.06E-01	1.61E-01	1.61E-01
1.00E-02	1.00E-08	9.66E-02	9.73E-02	7.80E-02	7.39E-02	4.29E-02	4.30E-02	3.02E-02	2.89E-02	1.45E-01	3.95E-02
Total (p/s)		**2.90E+13**	**2.88E+13**	**2.87E+13**	**2.84E+13**	**2.72E+13**	**2.71E+13**	**2.70E+13**	**2.69E+13**	**2.40E+12**	**1.67E+12**

Table 8 Flux-to-Dose Conversion Factors

Neutron		Photon	
Energy (MeV)	Factor	Energy (MeV)	Factor
2.50E-08	3.67E-06	1.00E-02	3.96E-06
1.00E-07	3.67E-06	3.00E-02	5.82E-07
1.00E-06	4.46E-06	5.00E-02	2.90E-07
1.00E-05	4.54E-06	7.00E-02	2.58E-07
1.00E-04	4.18E-06	1.00E-01	2.83E-07
1.00E-03	3.76E-06	1.50E-01	3.79E-07
1.00E-02	3.56E-06	2.00E-01	5.01E-07
1.00E-01	2.17E-05	2.50E-01	6.31E-07
5.00E-01	9.26E-05	3.00E-01	7.59E-07
1.00E+00	1.32E-04	3.50E-01	8.78E-07
2.50E+00	1.25E-04	4.00E-01	9.85E-07
5.00E+00	1.56E-04	4.50E-01	1.08E-06
7.00E+00	1.47E-04	5.00E-01	1.17E-06
1.00E+01	1.47E-04	5.50E-01	1.27E-06
1.40E+01	2.08E-04	6.00E-01	1.36E-06
2.00E+01	2.27E-04	6.50E-01	1.44E-06
		7.00E-01	1.52E-06
		8.00E-01	1.68E-06
		1.00E+00	1.98E-06
		1.40E+00	2.51E-06
		1.80E+00	2.99E-06
		2.20E+00	3.42E-06
		2.60E+00	3.82E-06
		2.80E+00	4.01E-06
		3.25E+00	4.41E-06
		3.75E+00	4.83E-06
		4.25E+00	5.23E-06
		4.75E+00	5.60E-06
		5.00E+00	5.80E-06
		5.25E+00	6.01E-06
		5.75E+00	6.37E-06
		6.25E+00	6.74E-06
		6.75E+00	7.11E-06
		7.50E+00	7.66E-06
		9.00E+00	8.77E-06
		1.10E+01	1.03E-05
		1.30E+01	1.18E-05
		1.50E+01	1.33E-05

Table 9 C.1 NCT Dose Rates

Contact Dose Rates (rem/hr except as noted)								
		neutron		secondary photon		primary photon		**Total[+]**
source location	detector location	mean	FSD	mean	FSD	mean	FSD	**(mrem/hr)**
center	side	5.11E-02	0.0004	1.35E-04	0.0017	4.06E-03	0.0301	**55.7**
center	bottom	1.88E-02	0.0029	5.00E-05	0.0103	1.50E-03	0.0182	**20.6**
center	top	1.32E-02	0.0041	4.41E-05	0.0124	2.61E-04	0.0206	**13.7**
bottom	bottom	1.28E-01	0.0013	3.22E-04	0.0048	1.19E-02	0.0198	**141.2**
1 m Dose Rates (rem/hr except as noted)								
		neutron		secondary photon		primary photon		**Total[+]**
source location	detector location	mean	FSD	mean	FSD	mean	FSD	**(mrem/hr)**
center	side	1.77E-03	0.0007	4.53E-06	0.0022	1.47E-04	0.0052	**1.9**
center	bottom	1.13E-03	0.0093	1.53E-06	0.0379	1.10E-04	0.0053	**1.3**
center	top	6.69E-04	0.012	1.29E-06	0.0436	2.75E-05	0.0084	**0.7**
bottom	bottom	2.26E-03	0.0074	5.37E-06	0.0227	2.27E-04	0.0302	**2.6**

[+]The total is the sum of the means * (1 + 3 * FSD)

Table 10 C.2 NCT Dose Rates

Contact Dose Rates (rem/hr except as noted)								
		neutron		secondary photon		primary photon		**Total[+]**
source location*	detector location	mean	FSD	mean	FSD	mean	FSD	**(mrem/hr)**
bottom	bottom	2.26E-01	0.002	1.33E-03	0.0048	1.65E-02	0.0771	**250.7**
side	side	1.48E-01	0.0022	9.14E-04	0.0062	1.86E-03	0.2809	**155.1**
2 cm	bottom	2.03E-01	0.0018	1.18E-03	0.0044	1.51E-02	0.0655	**225.3**
1 in	bottom	1.76E-01	0.0023	1.02E-03	0.0055	1.20E-02	0.0465	**193.6**
1 m Dose Rates (rem/hr except as noted)								
		neutron		secondary photon		primary photon		**Total[+]**
source location	detector location	mean	FSD	mean	FSD	mean	FSD	**(mrem/hr)**
bottom	bottom	4.83E-03	0.0102	2.89E-05	0.0283	4.10E-04	0.0564	**5.5**
side	side	4.41E-03	0.0012	2.74E-05	0.0019	4.93E-04	0.3876	**5.6**
2 cm	bottom	4.70E-03	0.0088	2.70E-05	0.0246	4.03E-04	0.0663	**5.4**
1 in	bottom	4.46E-03	0.0104	2.68E-05	0.0291	3.54E-04	0.0433	**5.1**

* source location is the position of the source relative to the CV. The distances listed are the distance the source is placed above the bottom of the CV. For this table, the distance from the CV to the bottom of the package is 5.32"

[+]Total includes contribution from 1 ppb U-232 and is the sum of the means * (1 + 3 * FSD)

Table 11 C.2 with Reduced Pu-240

Contact Dose Rates (rem/hr except as noted)*							
source description	neutron		secondary photon		primary photon		**Total[+]**
	mean	FSD	mean	FSD	mean	FSD	**(mrem/hr)**
4500 g, 30% Pu-240	1.90E-01	0.002	1.16E-03	0.0046	1.76E-02	0.0598	**215.0**
4500 g, 25% Pu-240	1.73E-01	0.0018	1.07E-03	0.0039	1.75E-02	0.0702	**198.3**
3600 g, 50% Pu-240	1.79E-01	0.0019	1.04E-03	0.0045	1.74E-02	0.0664	**204.0**
3375 g, 50% Pu-240	1.66E-01	0.0016	9.68E-04	0.0039	1.74E-02	0.0539	**189.5**
1 m Dose Rates (rem/hr except as noted)*							
source description	neutron		secondary photon		primary photon		**Total[+]**
	mean	FSD	mean	FSD	mean	FSD	**(mrem/hr)**
4500 g, 25% Pu-240	3.46E-03	0.0086	2.16E-05	0.0235	4.03E-04	0.0559	**4.1**
3375 g, 50% Pu-240	3.24E-03	0.0084	1.93E-05	0.0236	3.86E-04	0.0338	**3.8**

*For this table, the distance from the CV to the bottom of the package is 5.057"

[+]Total includes contribution from 1 ppb U-232 and is the sum of the means * (1 + 3 * FSD)

Table 12 C.3 NCT Dose Rates

Contact Dose Rates (rem/hr except as noted)								
		neutron		secondary photon		primary photon		**Total[+]**
source location*	detector location	mean	FSD	mean	FSD	mean	FSD	**(mrem/hr)**
bottom	bottom	2.22E-01	0.0019	1.28E-03	0.0046	2.13E-02	0.1064	**254.1**
1 in	bottom	1.75E-01	0.0018	9.84E-04	0.0044	1.52E-02	0.0451	**195.9**
1 m Dose Rates (rem/hr except as noted)								
		neutron		secondary photon		primary photon		**Total[+]**
source location	detector location	mean	FSD	mean	FSD	mean	FSD	**(mrem/hr)**
bottom	bottom	4.96E-03	0.0096	2.79E-05	0.0267	5.05E-04	0.0303	**5.7**
1 in	bottom	4.66E-03	0.0084	2.57E-05	0.0239	4.74E-04	0.0393	**5.4**

* source location is the position of the source relative to the CV. The distances listed are the distance the source is placed above the bottom of the CV. For this table, the distance from the CV to the bottom of the package is 5.32"

[+]Total includes contribution from 1 ppb U-232 and is the sum of the means * (1 + 3 * FSD)

Table 13 C.3 with Reduced Pu-240

Contact Dose Rates (rem/hr except as noted)*							
source description	neutron		secondary photon		primary photon		**Total[+]**
	mean	FSD	mean	FSD	mean	FSD	**(mrem/hr)**
4500 g, 25% Pu-240	1.72E-01	0.002	1.03E-03	0.0048	2.34E-02	0.0383	**201.8**
4500 g, 24% Pu-240	1.69E-01	0.0017	1.01E-03	0.0041	2.32E-02	0.0295	**197.7**
3375 g, 50% Pu-240	1.72E-01	0.0015	9.64E-04	0.0038	2.36E-02	0.0317	**201.5**
3000 g, 50% Pu-240	1.68E-01	0.0015	9.28E-04	0.0037	2.35E-02	0.0302	**196.3**
1 m Dose Rates (rem/hr except as noted)*							
source description	neutron		secondary photon		primary photon		**Total[+]**
	mean	FSD	mean	FSD	mean	FSD	**(mrem/hr)**
4500 g, 24% Pu-240	3.70E-03	0.0102	2.24E-05	0.0284	5.44E-04	0.0157	**4.4**
3000 g, 50% Pu-240	3.45E-03	0.008	1.92E-05	0.0228	5.42E-04	0.016	**4.2**

*For this table, the distance from the CV to the bottom is 5.057"

[+]Total includes contribution from 1 ppb U-232 and is the sum of the means * (1 + 3 * FSD)

Table 14 C.4 NCT Dose Rates

Contact Dose Rates (rem/hr except as noted)							
source description	neutron		secondary photon		primary photon		**Total[+]**
	mean	FSD	mean	FSD	mean	FSD	**(mrem/hr)**
U-235	2.61E-07	0.0026	1.53E-09	0.0059	2.13E-04	0.1139	**0.3**
U-233	2.96E-05	0.0017	2.05E-07	0.0037	2.57E-03	0.0587	**3.1**
1 m Dose Rates (rem/hr except as noted)							
source description	neutron		secondary photon		primary photon		**Total[+]**
	mean	FSD	mean	FSD	mean	FSD	**(mrem/hr)**
U-235	1.43E-08	0.0097	8.39E-11	0.024	6.22E-06	0.0815	**0.008**
U-233	6.51E-07	0.0085	4.36E-09	0.0209	6.69E-05	0.0697	**0.08**

[+]The total is the sum of the means * (1 + 3 * FSD)

Table 15 C.5 NCT Dose Rates

Contact Dose Rates (rem/hr except as noted)							
source description	neutron		secondary photon		primary photon		**Total[+]**
	mean	FSD	mean	FSD	mean	FSD	**(mrem/hr)**
U-235	5.91E-07	0.0024	3.27E-09	0.0056	1.17E-04	0.2601	**0.2**
U-233	1.40E-03	0.0019	8.42E-06	0.0043	2.92E-03	0.1702	**5.8**
PuF4	1.90E+01	0.0024	1.22E-01	0.0052	3.48E-02	0.1621	**19299.5**
1 m Dose Rates (rem/hr except as noted)							
source description	neutron		secondary photon		primary photon		**Total[+]**
	mean	FSD	mean	FSD	mean	FSD	**(mrem/hr)**
U-235	1.49E-08	0.0114	8.64E-11	0.0285	7.04E-06	0.0528	**0.008**
U-233	3.20E-05	0.0094	1.92E-07	0.0245	8.69E-05	0.0402	**0.13**

[+]The total is the sum of the means * (1 + 3 * FSD)

Table 16 Dose Rate for 1 g of U-232

Contact Dose Rates (rem/hr except as noted)							
source description	neutron		secondary photon		primary photon		**Total[+]**
	mean	FSD	mean	FSD	mean	FSD	**(mrem/hr)**
Metal	3.74E-08	0.0015	6.86E-11	0.0067	3.93E+02	0.0049	**399204.3**
Oxide	2.37E-03	0.0008	4.69E-06	0.003	3.33E+02	0.0069	**339579.1**
1 m Dose Rates (rem/hr except as noted)							
source description	neutron		secondary photon		primary photon		**Total[+]**
	mean	FSD	mean	FSD	mean	FSD	**(mrem/hr)**
Metal	8.17E-10	0.0081	1.37E-12	0.0296	9.61E+00	0.0022	**9678.2**
Oxide	5.46E-05	0.0041	8.99E-08	0.0134	8.02E+00	0.0014	**8056.5**

[+]The total is the sum of the means * (1 + 3 * FSD)

Table 17 C.1 HAC Dose Rates

1 m Dose Rates (rem/hr except as noted)								
		neutron		secondary photon		primary photon		**Total[+]**
source location	detector location	mean	FSD	mean	FSD	mean	FSD	**(mrem/hr)**
center	side	2.05E-03	0.0005	3.55E-06	0.0017	2.53E-04	0.0093	**2.3**
center	bottom	1.62E-03	0.0054	9.65E-07	0.0329	2.17E-04	0.042	**1.9**
center	top	7.43E-04	0.008	8.02E-07	0.036	3.71E-05	0.0047	**0.8**

[+]The total is the sum of the means * (1 + 3 * FSD)

Appendix A Input Files

The following table lists the input files used in this calculation. Those files marked with an * are presented below.

File	Description
ORIGEN-S	
u232or*	ORIGEN-S input for U-232
RASTA	
RTG*	RASTA input for C.1
combm	RASTA input for C.2
combo	RASTA input for C.3
test	RASTA input for C.2 with no Pu-240
25pu240	RASTA input for C.2 with 25% Pu-240
30pu240	RASTA input for C.2 with 30% Pu-240
80pu	RASTA input for C.2 with 80% mass
75pu	RASTA input for C.2 with 75% mass
24puo	RASTA input for C.3 with 24% Pu-240
25puo	RASTA input for C.3 with 25% Pu-240
70puo	RASTA input for C.3 with 70% mass
67puo	RASTA input for C.3 with 2/3 mass
puf4	RASTA input for PuF4
u233be	RASTA input for C.4 with U-233
u233obe	RASTA input for C.5with U-233
u235be	RASTA input for C.4 with U-235
u235obe	RASTA input for C.5 with U-235
u232	RASTA input for 1 g U-232 metal
u232o	RASTA input for 1 g U-232 oxide
MCNP	
RTGn	C.1 content located in center of CV, neutron case, NCT
RTGp	C.1 content located in center of CV, photon case, NCT
hRTGn	C.1 content located in center of CV, neutron case, HAC
hRTGp	C.1 content located in center of CV, photon case, HAC
bRTGn*	C.1 content located at bottom of CV, neutron case, NCT
bRTGp	C.1 content located at bottom of CV, photon case, NCT
ncombm	C.2 content located at bottom of CV, neutron case, NCT

pcombm	C.2 content located at bottom of CV, photon case, NCT
ncombo	C.3 content located at bottom of CV, neutron case, NCT
pcombo	C.3 content located at bottom of CV, photon case, NCT
siden	C.2 content located at side of CV, neutron case, NCT
sidep	C.2 content located at side of CV, photon case, NCT
cm2n	C.2 content located 1 cm from bottom of CV, neutron case, NCT
cm2p	C.2 content located 1 cm from bottom of CV, photon case, NCT
inn	C.2 content located 1 in. from bottom of CV, neutron case, NCT
inp	C.2 content located 1 in. from bottom of CV, photon case, NCT
inno	C.3 content located 1 in. from bottom of CV, neutron case, NCT
inpo*	C.3 content located 1 in. from bottom of CV, photon case, NCT
n25puo	MCNP input for C.3 with 25% Pu-240, neutrons
n24puo	MCNP input for C.3 with 24% Pu-240, neutrons
n25pu240*	MCNP input for C.2 with 25% Pu-240, neutrons
n30pu240	MCNP input for C.2 with 30% Pu-240, neutrons
p25puo	MCNP input for C.3 with 25% Pu-240, photons
p24puo	MCNP input for C.3 with 24% Pu-240, photons
p25pu240	MCNP input for C.2 with 25% Pu-240, photons
p30pu240	MCNP input for C.2 with 30% Pu-240, photons
puf4n	MCNP input for C.5 with PuF4, neutrons
puf4p	MCNP input for C.5 with PuF4, neutrons
pun75	MCNP input for C.2 with 75% mass, neutrons
pun80	MCNP input for C.2 with 80% mass, neutrons
puon67	MCNP input for C.3 with 67% mass, neutrons
puon70	MCNP input for C.3 with 70% mass, neutrons
pup75	MCNP input for C.2 with 75% mass, photons
pup80	MCNP input for C.2 with 80% mass, photons
puop67	MCNP input for C.3 with 67% mass, photons
puop70	MCNP input for C.3 with 70% mass, photons
u232n	MCNP input for 1 g U-232 metal, neutrons
u232no	MCNP input for 1 g U-232 oxide, neutrons
u232p	MCNP input for 1 g U-232 metal, photons
u232po	MCNP input for 1 g U-232 oxide, photons
u233n	MCNP input for C.4, U-233, neutrons

u233no	MCNP input for C.5, U-233, neutrons
u233p	MCNP input for C.4, U-233, neutrons
u233po	MCNP input for C.5, U-233, photons
u235n	MCNP input for C.4, U-235, neutrons
u235no	MCNP input for C.5, U-235, neutrons
u235p	MCNP input for C.4, U-235, neutrons
u235po	MCNP input for C.5, U-235, photons

ORIGEN-S file *u232or*

```
'This SCALE input file was generated by
'OrigenArp Version  2.00   2-12-2002
#origens
0$$ a11 71 e t
Decay Case
3$$ 21 1 1 0 a16 2 a33 0 e t
35$$ 0 t
54$$ a8 1 a11 0 e
56$$ a2 10 a6 1 a10 0 a13 1 a14 5 a15 3 a17 4 e
57** 0 a3 1e-05 e  t
Case 1
1 gram U-232
60** 0.01 0.03 0.1 0.3 1 3 4 5 6 7
61** f1e-30
65$$
'Gram-Atoms   Grams   Curies   Watts-All   Watts-Gamma
 3z   1   0   0   3z   3z   3z   6z
 3z   1   0   0   3z   3z   3z   6z
 3z   1   0   0   3z   3z   3z   6z
73$$ 922320
74** 1
75$$ 2
t
56$$ 0 0 a10  1 e t
56$$ 0 0 a10  2 e t
56$$ 0 0 a10  3 e t
56$$ 0 0 a10  4 e t
56$$ 0 0 a10  5 e t
56$$ 0 0 a10  6 e t
56$$ 0 0 a10  7 e t
56$$ 0 0 a10  8 e t
56$$ 0 0 a10  9 e t
56$$ 0 0 a10  10 e t
54$$ a8 1 a11 0 e
56$$ a2 10 a6 1 a10 10 a14 5 a15 3 a17 4 e
57** 7 a3 1e-05 e  t
Case 2
1 gram U-232
60** 8 9 10 11 12 13 14 15 16 17
61** f1e-30
65$$
'Gram-Atoms   Grams   Curies   Watts-All   Watts-Gamma
 3z   1   0   0   3z   3z   3z   6z
 3z   1   0   0   3z   3z   3z   6z
 3z   1   0   0   3z   3z   3z   6z
t
56$$ 0 0 a10  1 e t
56$$ 0 0 a10  2 e t
56$$ 0 0 a10  3 e t
56$$ 0 0 a10  4 e t
56$$ 0 0 a10  5 e t
```

```
56$$ 0 0 a10  6 e t
56$$ 0 0 a10  7 e t
56$$ 0 0 a10  8 e t
56$$ 0 0 a10  9 e t
56$$ 0 0 a10  10 e t
54$$ a8 1 a11 0 e
56$$ a2 10 a6 1 a10 10 a14 5 a15 3 a17 4 e
57** 17 a3 1e-05 e  t
Case 3
1 gram U-232
60** 18 19 20 30 40 50 60 70 80 90
61** f1e-30
65$$
'Gram-Atoms   Grams   Curies   Watts-All   Watts-Gamma
 3z   1   0   0   3z   3z   3z   6z
 3z   1   0   0   3z   3z   3z   6z
 3z   1   0   0   3z   3z   3z   6z
t
56$$ 0 0 a10  1 e t
56$$ 0 0 a10  2 e t
56$$ 0 0 a10  3 e t
56$$ 0 0 a10  4 e t
56$$ 0 0 a10  5 e t
56$$ 0 0 a10  6 e t
56$$ 0 0 a10  7 e t
56$$ 0 0 a10  8 e t
56$$ 0 0 a10  9 e t
56$$ 0 0 a10  10 e t
56$$ f0 t
end
```

RASTA file *RTG*

```
C.3 PuMetals
100 gram of oxide
/nng  npg  cmf  wsbi  keff  sog  ebeam  idd
 -1   24    1     0     0    0     0     1
     2       2
942360   1E-4
942380   100
     /ni   iu
          4       2
     80160     1.331872E+01
     80170     5.675515E-03
     80180     3.004694E-02
     40090     0.005
/Photon Energy Groups
/Tailored to low energy photons (especially Am-241)
1.00E+01   8.00E+00   7.00E+00   6.00E+00   5.00E+00   4.00E+00
3.00E+00   2.00E+00   1.50E+00   1.00E+00   8.00E-01   7.00E-01
6.00E-01   4.00E-01   2.00E-01   1.00E-01   8.00E-02   6.00E-02
5.90E-02   5.00E-02   4.00E-02   3.00E-02   2.00E-02   1.00E-02
1.00E-08
```

MCNP file *bRTGn*

```
message:      runtpe=pu238n.r

pu238 m= 100 grams - Neutrons, source at bottom
c     drum bottom
    1   101  -7.9       1  -2  -6
c     drum side
    2   101  -7.9       5  -6  2  -3
c     drum lid
    3   101  -7.9       3  -4  -6 145
C   c    upper liner
```

```
C       4   101  -7.9       7  -3  9  -10
C   c    upper liner base
C       5   101  -7.9       7  -8  -9
C   c     upper foam
C       6     1  -0.256     8  -9  -3
c    lower liner
    7   101  -7.9       13  -3  11  -12   $  -MHB Change
c    lower liner base
    8   101  -7.9       -11  13  -14
c    Foam
    9     1  -0.256     -3  -5  10  2
c    Foam
   10     1  -0.256     12  -10  -3  2  (155:-150)   $  -MHB Change
c    Foam
   11     1  -0.256     2  -150  -12      $  -MHB Change
c     torque bar
   12   0       15  -16  24  -25  14  -26  $ MHB - remove torque bar
c    lower load distrib assy side
   13   151  -2.7       (22  -23  20  -21  )(27  )
   14   151  -2.7       (-23  14  -20  )(26  :-24  :25  )
   16     0  23  -11  14  -3 (140:-7)
   17     0  (24  -25  14  -26  -23  )(-24  :25  :-14  :19  :-15  :16  )
c    anti rotation bar
   18   0       20  -32  30  -31  28  -29   $ MHB - remove bar
c    upper load distr assy side
   19   151  -2.7       -23  34  37  -33
c    upper load distr assy
   20   151  -2.7       (((-23  33  -7  )(35  ))(36  ))(-38  :39  :-40  :41  )
c    upper load distr assy penet
   21     0  33  -7  -35
c    upper load distr assy penet
   22     0  33  -7  -36
c     vessel support skirt
   23   101  -7.9       -42  43  20  -49  44  47
c    cv end cap
   24   101  -7.9       -47  48  -49
   25     0  ((-43  -49  20  )(47  ))(44  :-45  :46  :-30  :31  )
   26     0  ((20  -49  42  -22  )(47  ))(44  :-45  :46  :-30  :31  )
   27     0  -27  22  -23
c   28     0  43  -42  32  -44  28  -29
c    CV cylindrical portion
   29   101  -7.9       49  -52  50  -51
   30     0  51  -22  49  -21
   31     0  21  -52  51  -23
c    cv transition portion
   32   101  -7.9       -54  53  -55
c    cv upper cylinder
   33   101  -7.9       55  -58  56  -57
   34     0  52  -37  -23  54
   35     0  37  54  -34  -55
   36     0  55  -58  -34  57
   37   106  -7.584     -58  59  -56  66
   38   106  -7.584     58  -64  60  -61  62  -63  66
   39   106  -7.584     -65  64  60  -61  62  -63  67
   40     0  58  -33  -34  66   #38
   41     0  -64  33  38  -39  40  -41  66   #38
   42     0  64  -65  38  -39  40  -41  69   #39
   43     0  -7  65  38  -39  40  -41
   44   101  -7.9       (-70  68  69  )
   45   101  -7.9       -69  68  -76
   46   101  -7.9       -69  -75  76  73
   47   101  -7.9       -69  75  -74  72
   48   101  -7.9       -69  74  -65  71
   49     0  59  -64  69  -66
   50     0  76  -75  -73
   51     0  -74  75  -72  77
   52     0  74  -65  -71  77
   53     0  80  -65  -78
   54   101  -7.9       -65  75  -77  78
```

```
   55   101  -7.9       -64  75  -78
   56     0  55  -59  -56  70
   57     0  68  -55  -53  70
   58     0  -53  -68
   59     0  -50  49  -52  88
   60     0  -48  -49  88
   62     0  4  -82  -84 (-4:100:130)
   63     0  1  -4  -84  6
   64     0  83  -1  -84
   65     0  20  -44  30  -31  45  -28
   66     0  20  -44  30  -31  29  -46
   67     0  32  -44  30  -31  28  -29
   68     0  (43  -42  20  -44  )(-45  :46  )
c
c  MHB
   100   4 -0.3204 -135 110 -105   $ Min-K 2000
   105   3 -0.3684 -145 115 -4     $ Vermiculite
   110   5 -0.2563 -145 120 -115   $ FiberFrax
   115   101 -7.9   4 -100 -130 (135:-110:105) $ steel liner
   120   101 -7.9 -140 125 -3   (145:-120:4)   $ steel liner
   125   5 -0.2563 -3 150 -155 (12:-13)         $ fiberfrax
   116   0         -140 7 -125     $void above top fixture
c    external void
  999     0  -83  :82  :84
c     source
1000     2  -11.46     -88

    1        pz      0.0
    2        pz      0.121
    3        pz     86.161 $drum lid bottom
    4        pz     86.283 $drum lid top
    5        cz     23.178 $drum IR
    6        cz     23.299 $drum OR
    7        pz     73.639
    8        pz     73.829 $base of upper liner
    9        cz     18.035
   10        cz     18.225 $upper liner
   11        cz     10.478
   12        cz     10.667 $lower liner
   13        pz     10.461 $lower liner base
   14        pz     10.583
   15        px     -9.208
   16        px      9.208
   19        pz     11.345
   20        pz     11.523 $top of lower load distrib assy - MHB change
   21        pz     27.093 $lower load dist assy top of sides - MHB change
   22        cz      8.573
   23        cz      10.16 $lower load distrib assy side
   24        py     -0.635
   25        py      0.635
   26        pz     11.231 $ - MHB change
   27       c/x          0     24.553    1.27   $lower load dist assy penetration - MHB
change
   28        px     -0.635
   29        px      0.635
   30        py     -7.976
   31        py      7.976
   32        pz     12.805
   33        pz     72.242
   34        cz      9.801
   35       c/z     -6.172          0      1.588
   36       c/z      6.172          0      1.588
   37        pz     67.797
   38        px     -3.493
   39        px      3.493
   40        py     -3.493
   41        py      3.493
   42        cz      7.065
   43        cz       6.41
```

```
   44        pz     12.958
   45        px       -0.8
   46        px        0.8
   47        sq          1          1          4          0          0
                0    -70.795          0          0     17.342
   48        sq          1          1          4          0          0
                0    -59.336          0          0     17.342
   49        pz     17.342
   50        cz      7.703
   51        cz      8.414
   52        pz     67.746
   53       trc          0          0     67.746          0          0
                2.2098      7.703      8.001
   54       trc          0          0     67.746          0          0
                2.2098      8.414      9.042
   55        pz     69.955
   56        cz      8.255
   57        cz      9.042
   58        pz      71.86
   59        pz      70.26
   60        px     -3.175
   61        px      3.175
   62        py     -3.175
   63        py      3.175
   64        pz     72.673
   65        pz      73.13
   66        cz      1.626
   67        cz       2.07
   68        pz     68.355
   69        cz      1.588
   70       trc          0          0      68.35          0          0
                1.91      7.739      8.014
   71        cz      1.143
   72        cz      0.724
   73        cz     0.1194
   74        pz     71.708
   75        pz      70.59
   76        pz     69.675
   77        cz      0.572
   78        cz      0.237
   80        pz     72.673
   81        so          0
   82        pz     189.065824 $top scoring plane
   83        pz       -100.
   84        cz      123.3
   85        cz          5 $segmenting surface for top and bottom planes
   86        pz     9.8  $segmenting plane for side scoring plane
   87        pz     19.8  $segmenting plane for side scoring plane
   88        sz    14.8  1.27715102918468
c
c  MHB add
c
c  lid
  100        pz 89.065824
  105        pz 88.944412
  110        pz 86.404412
  115        pz 75.361
  120        pz 74.009214
  125        pz 73.8878
  130        cz 17.901412
  135        cz 17.78
  140        cz 10.230612
  145        cz 10.1092
c
c fiberfrax
c
  150        pz 7.921
  155        cz 13.764006
```

```
mode  n p
m1    1001.60c         -0.041 $Polyurethane
      6000.60c         -0.544 8016.60c         -0.294 7014.60c         -0.121
m3    14000.60c            -21.22 $ Vermiculite
      13027.60c             -5.47
      20000.60c            -12.17
      26000.55c             -5.40
      22000.60c             -0.82
      12000.60c             -8.90
      11023.60c             -1.09
      19000.60c             -1.22
      16000.60c             -0.18
       8016.60c            -45.53
m4    14000.60c            -37.71 $ Min-K 2000
      22000.60c             -5.53
      13027.60c             -6.39
       6000.60c             -1.28
       1001.60c             -0.84
       8016.60c            -48.01
      51000.42c             -0.09
      31000.60c             -0.15
m5    13027.60c            -26.46 $FiberFlax
      14000.60c            -23.14
      11023.60c             -0.37
       8016.60c            -50.03
m101  6000.60c        -0.0003 $SS304L
      14000.60c         -0.01 15031.60c      -0.00045 16000.60c       -0.0003
      24000.50c         -0.19 25055.60c         -0.02 26000.55c      -0.67895
      28000.50c          -0.1
m151  13027.60c         -97.9 $6061 Al
      14000.60c          -0.6 29000.50c         -0.28 12000.60c            -1
      24000.50c          -0.2
m106  25055.60c            -8 $Nitronic 60
      14000.60c            -4 24000.50c           -17 7014.60c          -0.14
      28000.50c          -8.5 26000.55c        -62.36
m2    94238.60c        -1.0  $Pu Metal
imp:n  1           68r          0            1            $ 1, 1000
imp:p  1           68r          0            1            $ 1, 1000
sdef   erg d1   rad d2
       pos 0.0 0.0 14.8
si2   0.0  1.27715102918468
c  Neutron Groups
si1   1.00000E-11  1.00000E-07  4.14000E-07  8.76000E-07  1.86000E-06
      5.04000e-06  1.07000E-05  3.73000E-05  1.01000E-04  2.14000E-04
      4.54000e-04  1.58000E-03  3.35000E-03  7.10000E-03  1.50000E-02
      2.19000e-02  2.42000E-02  2.61000E-02  3.18000E-02  4.09000E-02
      5.74000e-02  1.11000E-01  1.83000E-01  2.97000E-01  3.69000E-01
      4.98000e-01  6.08000E-01  7.43000E-01  8.21000E-01  1.00000E+00
      1.35000e+00  1.65000E+00  1.92000E+00  2.23000E+00  2.35000E+00
      2.37000e+00  2.47000E+00  2.73000E+00  3.01000E+00  3.68000E+00
      4.97000e+00  6.07000E+00  7.41000E+00  8.61000E+00  1.00000E+01
      1.22000e+01  1.42000E+01  1.73000E+01
c  nct Neutron source strength
sp1  0.00000E+00  2.44196E-12  3.31109E-11  6.58288E-11  2.44246E-10
      1.13209E-09  3.10102E-09  2.50631E-08  1.02465E-07  2.74857E-07
      8.52137E-07  6.99352E-06  1.75649E-05  5.59558E-05  1.80225E-04
      2.11227E-04  7.98240E-05  6.88985E-05  2.20461E-04  3.88866E-04
      7.84008E-04  3.09556E-03  5.32795E-03  9.38978E-03  6.38202E-03
      1.32438E-02  1.23746E-02  1.56894E-02  9.47805E-03  2.25606E-02
      4.96617E-02  5.31152E-02  6.04907E-02  8.79830E-02  3.83893E-02
      6.53347E-03  3.31366E-02  8.68189E-02  9.03290E-02  1.61205E-01
      1.08260E-01  3.75303E-02  3.50887E-02  2.83268E-02  2.11299E-02
      2.43174E-03  1.11076E-05  2.03378E-06
ctme 150
f012:n 1  4  83  82
fs012  -85
sd012  78.5398 1.e40
       78.5398 1.e40
       78.5398 1.e40
```

```
       78.5398 1.e40
fm012 2.23685E+06   $  Pu Metal spherical source
tf012 4  2j  1
f022:n 6  84
fs022  -86  -87
sd022  1.e40 1463.9181 1.e40
       1.e40 7747.16094 1.e40
fm022 2.23685E+06   $  Pu Metal spherical source
tf022 2  2j  2
de0  2.5E-8 1.0E-7 1.0E-6 1.0E-5 1.0E-4 1.0E-3 1.0E-2 1.0E-1 5.0E-1 &
     1.0 2.5 5.0 7.0 10.0 14.0 20.0
df0  3.67E-6 3.67E-6 4.46E-6 4.54E-6 4.18E-6 3.76E-6 3.56E-6 2.17E-5 &
     9.26e-5 1.32E-4 1.25E-4 1.56E-4 1.47E-4 1.47E-4 2.08E-4 2.27E-4
f112:p 1  4  83  82
fs112  -85
sd112  78.5398 1.e40
       78.5398 1.e40
       78.5398 1.e40
       78.5398 1.e40
fm112 2.23685E+06   $  Pu Metal spherical source
tf112 4  2j  1
de112  .01 .03 .05 .07 .1 .15 .2 .25 .3 .35 .4 .45 .5 .55 .6 .65 &
       .7 .8 1. 1.4 1.8 2.2 2.6 2.8 3.25 3.75 4.25 4.75 5.0 5.25 &
      5.75 6.25 6.75 7.5 9. 11. 13. 15.
df112 3.96E-6 5.82E-7 2.9E-7 2.58E-7 2.83E-7 3.79E-7 5.01E-7 6.31E-7 &
      7.59e-7 8.78E-7 9.85E-7 1.08E-6 1.17E-6 1.27E-6 1.36E-6 1.44E-6 &
      1.52e-6 1.68E-6 1.98E-6 2.51E-6 2.99E-6 3.42E-6 3.82E-6 4.01E-6 &
      4.41e-6 4.83E-6 5.23E-6 5.6E-6 5.8E-6 6.01E-6 6.37E-6 6.74E-6 &
      7.11e-6 7.66E-6 8.77E-6 1.03E-5 1.18E-5 1.33E-5
f122:p 6  84
fs122  -86  -87
sd122  1.e40 1463.9181 1.e40
       1.e40 7747.16094 1.e40
fm122 2.23685E+06   $  Pu Metal spherical source
tf122 2  2j  2
de122  .01 .03 .05 .07 .1 .15 .2 .25 .3 .35 .4 .45 .5 .55 .6 .65 &
       .7 .8 1. 1.4 1.8 2.2 2.6 2.8 3.25 3.75 4.25 4.75 5.0 5.25 &
      5.75 6.25 6.75 7.5 9. 11. 13. 15.
df122 3.96E-6 5.82E-7 2.9E-7 2.58E-7 2.83E-7 3.79E-7 5.01E-7 6.31E-7 &
      7.59e-7 8.78E-7 9.85E-7 1.08E-6 1.17E-6 1.27E-6 1.36E-6 1.44E-6 &
      1.52e-6 1.68E-6 1.98E-6 2.51E-6 2.99E-6 3.42E-6 3.82E-6 4.01E-6 &
      4.41e-6 4.83E-6 5.23E-6 5.6E-6 5.8E-6 6.01E-6 6.37E-6 6.74E-6 &
      7.11e-6 7.66E-6 8.77E-6 1.03E-5 1.18E-5 1.33E-5
fq0  f  s
```

MCNP file *inpo*

```
message:      runtpe=pu239p.r

pu239 m= 4500 grams - Photons, source at bottom
c     drum bottom
    1   101  -7.9       1  -2  -6
c     drum side
    2   101  -7.9       5  -6  2  -3
c     drum lid
    3   101  -7.9       3  -4  -6 145
C   c    upper liner
C       4   101  -7.9       7  -3  9  -10
C   c    upper liner base
C       5   101  -7.9       7  -8  -9
C   c     upper foam
C       6     1  -0.256     8  -9  -3
c    lower liner
    7   101  -7.9       13  -3  11  -12   $  -MHB Change
c    lower liner base
    8   101  -7.9       -11  13  -14
c    Foam
    9     1  -0.256     -3  -5  10  2
c    Foam
```

```
   10     1  -0.256     12  -10  -3  2  (155:-150)   $  -MHB Change
c    Foam
   11     1  -0.256     2  -150  -12      $  -MHB Change
c     torque bar
   12   0       15  -16  24  -25  14  -26  $ MHB - remove torque bar
c    lower load distrib assy side
   13   151  -2.7       (22  -23  20  -21  )(27  )
   14   151  -2.7       (-23  14  -20  )(26  :-24  :25  )
   16     0  23  -11  14  -3 (140:-7)
   17     0  (24  -25  14  -26  -23  )(-24  :25  :-14  :19  :-15  :16  )
c    anti rotation bar
   18   0       20  -32  30  -31  28  -29   $ MHB - remove bar
c    upper load distr assy side
   19   151  -2.7       -23  34  37  -33
c    upper load distr assy
   20   151  -2.7       (((-23  33  -7  )(35  ))(36  ))(-38  :39  :-40  :41  )
c    upper load distr assy penet
   21     0  33  -7  -35
c    upper load distr assy penet
   22     0  33  -7  -36
c     vessel support skirt
   23   101  -7.9       -42  43  20  -49  44  47
c    cv end cap
   24   101  -7.9       -47  48  -49
   25     0  ((-43  -49  20  )(47  ))(44  :-45  :46  :-30  :31  )
   26     0  ((20  -49  42  -22  )(47  ))(44  :-45  :46  :-30  :31  )
   27     0  -27  22  -23
c   28     0  43  -42  32  -44  28  -29
c    CV cylindrical portion
   29   101  -7.9       49  -52  50  -51
   30     0  51  -22  49  -21
   31     0  21  -52  51  -23
c    cv transition portion
   32   101  -7.9       -54  53  -55
c    cv upper cylinder
   33   101  -7.9       55  -58  56  -57
   34     0  52  -37  -23  54
   35     0  37  54  -34  -55
   36     0  55  -58  -34  57
   37   106  -7.584     -58  59  -56  66
   38   106  -7.584     58  -64  60  -61  62  -63  66
   39   106  -7.584     -65  64  60  -61  62  -63  67
   40     0  58  -33  -34  66   #38
   41     0  -64  33  38  -39  40  -41  66   #38
   42     0  64  -65  38  -39  40  -41  69   #39
   43     0  -7  65  38  -39  40  -41
   44   101  -7.9       (-70  68  69  )
   45   101  -7.9       -69  68  -76
   46   101  -7.9       -69  -75  76  73
   47   101  -7.9       -69  75  -74  72
   48   101  -7.9       -69  74  -65  71
   49     0  59  -64  69  -66
   50     0  76  -75  -73
   51     0  -74  75  -72  77
   52     0  74  -65  -71  77
   53     0  80  -65  -78
   54   101  -7.9       -65  75  -77  78
   55   101  -7.9       -64  75  -78
   56     0  55  -59  -56  70
   57     0  68  -55  -53  70
   58     0  -53  -68
   59     0  -50  49  -52  88
   60     0  -48  -49  88
   62     0  4  -82  -84 (-4:100:130)
   63     0  1  -4  -84  6
   64     0  83  -1  -84
   65     0  20  -44  30  -31  45  -28
   66     0  20  -44  30  -31  29  -46
   67     0  32  -44  30  -31  28  -29
```

```
   68     0  (43  -42  20  -44  )(-45  :46  )
c
c  MHB
   100   4 -0.3204 -135 110 -105   $ Min-K 2000
   105   3 -0.3684 -145 115 -4     $ Vermiculite
   110   5 -0.2563 -145 120 -115   $ FiberFrax
   115   101 -7.9   4 -100 -130 (135:-110:105) $ steel liner
   120   101 -7.9 -140 125 -3   (145:-120:4)   $ steel liner
   125   5 -0.2563 -3 150 -155 (12:-13)         $ fiberfrax
   116   0         -140 7 -125     $void above top fixture
c    external void
  999     0  -83  :82  :84
c     source
1000     2  -11.46     -88

    1        pz      0.0
    2        pz      0.121
    3        pz     86.161 $drum lid bottom
    4        pz     86.283 $drum lid top
    5        cz     23.178 $drum IR
    6        cz     23.299 $drum OR
    7        pz     73.639
    8        pz     73.829 $base of upper liner
    9        cz     18.035
   10        cz     18.225 $upper liner
   11        cz     10.478
   12        cz     10.667 $lower liner
   13        pz     10.461 $lower liner base
   14        pz     10.583
   15        px     -9.208
   16        px      9.208
   19        pz     11.345
   20        pz     11.523 $top of lower load distrib assy - MHB change
   21        pz     27.093 $lower load dist assy top of sides - MHB change
   22        cz      8.573
   23        cz      10.16 $lower load distrib assy side
   24        py     -0.635
   25        py      0.635
   26        pz     11.231 $ - MHB change
   27       c/x          0     24.553    1.27   $lower load dist assy penetration - MHB
change
   28        px     -0.635
   29        px      0.635
   30        py     -7.976
   31        py      7.976
   32        pz     12.805
   33        pz     72.242
   34        cz      9.801
   35       c/z     -6.172          0      1.588
   36       c/z      6.172          0      1.588
   37        pz     67.797
   38        px     -3.493
   39        px      3.493
   40        py     -3.493
   41        py      3.493
   42        cz      7.065
   43        cz       6.41
   44        pz     12.958
   45        px       -0.8
   46        px        0.8
   47        sq          1          1          4          0          0
                0    -70.795          0          0     17.342
   48        sq          1          1          4          0          0
                0    -59.336          0          0     17.342
   49        pz     17.342
   50        cz      7.703
   51        cz      8.414
   52        pz     67.746
   53       trc          0          0     67.746          0          0
```

```
                2.2098      7.703      8.001
   54       trc          0          0     67.746          0          0
                2.2098      8.414      9.042
   55        pz     69.955
   56        cz      8.255
   57        cz      9.042
   58        pz      71.86
   59        pz      70.26
   60        px     -3.175
   61        px      3.175
   62        py     -3.175
   63        py      3.175
   64        pz     72.673
   65        pz      73.13
   66        cz      1.626
   67        cz       2.07
   68        pz     68.355
   69        cz      1.588
   70       trc          0          0      68.35          0          0
                1.91      7.739      8.014
   71        cz      1.143
   72        cz      0.724
   73        cz     0.1194
   74        pz     71.708
   75        pz      70.59
   76        pz     69.675
   77        cz      0.572
   78        cz      0.237
   80        pz     72.673
   81        so          0
   82        pz     189.065824 $top scoring plane
   83        pz       -100.
   84        cz      123.3
   85        cz          5 $segmenting surface for top and bottom planes
   86        pz     15.64  $segmenting plane for side scoring plane
   87        pz     25.64  $segmenting plane for side scoring plane
   88        sz    20.64  4.54268994452959
c
c  MHB add
c
c  lid
  100        pz 89.065824
  105        pz 88.944412
  110        pz 86.404412
  115        pz 75.361
  120        pz 74.009214
  125        pz 73.8878
  130        cz 17.901412
  135        cz 17.78
  140        cz 10.230612
  145        cz 10.1092
c
c fiberfrax
c
  150        pz 7.921
  155        cz 13.764006

mode  p
m1    1001.            -0.041 $Polyurethane
      6000.            -0.544 8016.            -0.294 7014.            -0.121
m3    14000            -21.22 $ Vermiculite
      13000             -5.47
      20000            -12.17
      26000             -5.40
      22000             -0.82
      12000             -8.90
      11000             -1.09
      19000             -1.22
      16000             -0.18
```

```
       8000            -45.53
m4    14000            -37.71 $ Min-K 2000
      22000             -5.53
      13000             -6.39
       6000             -1.28
       1001             -0.84
       8000            -48.01
      51000             -0.09
      31000             -0.15
m5    13000            -26.46 $FiberFlax
      14000            -23.14
      11000             -0.37
       8000            -50.03
m101  6000.           -0.0003 $SS304L
      14000.            -0.01 15000.         -0.00045 16000.          -0.0003
      24000.            -0.19 25000.            -0.02 26000.         -0.67895
      28000.             -0.1
m151  13000.            -97.9 $6061 Al
      14000.             -0.6 29000.            -0.28 12000.               -1
      24000.             -0.2
m106  25000.               -8 $Nitronic 60
      14000.               -4 24000.              -17 7000.             -0.14
      28000.             -8.5 26000.           -62.36
m2    94239        -1.0  $Pu Metal
imp:p  1            68r          0            1            $ 1, 1000
sdef   erg d1   rad d2
       pos 0.0 0.0 20.64
si2   0.0  4.54268994452959
c  Photon Groups
si1   1.00000E-08  1.00000E-02  2.00000E-02  3.00000E-02  4.00000E-02
      5.00000E-02  5.90000E-02  6.00000E-02  8.00000E-02  1.00000E-01
      2.00000E-01  4.00000E-01  6.00000E-01  7.00000E-01  8.00000E-01
      1.00000E+00  1.50000E+00  2.00000E+00  3.00000E+00  4.00000E+00
      5.00000E+00  6.00000E+00  7.00000E+00  8.00000E+00  1.00000E+01
c  Photon source strength
sp1   0.00000E+00  4.13599E-02  6.06894E-01  8.10465E-02  9.93846E-04
      1.12094E-03  2.34975E-04  2.66321E-01  2.14198E-04  1.11164E-03
      6.51615E-04  3.99543E-05  7.23687E-06  1.39646E-06  2.12439E-06
      1.97111E-07  1.14278E-07  4.85917E-08  4.61915E-08  1.28531E-08
      3.57719E-09  1.19729E-09  5.12832E-10  7.26436E-11  9.05031E-11
sb1   0            1.00000E-03           9r  1.00000E-03  0.002
      0.01         0.02         0.1          0.1          0.2
      7r
ctme 300
f112:p 1  4  83  82
fs112  -85
sd112  78.5398 1.e40
       78.5398 1.e40
       78.5398 1.e40
       78.5398 1.e40
fm112 2.81780E+13  $  Pu Metal spherical source
tf112 4  2j  1
de112  .01 .03 .05 .07 .1 .15 .2 .25 .3 .35 .4 .45 .5 .55 .6 .65 &
       .7 .8 1. 1.4 1.8 2.2 2.6 2.8 3.25 3.75 4.25 4.75 5.0 5.25 &
      5.75 6.25 6.75 7.5 9. 11. 13. 15.
df112 3.96E-6 5.82E-7 2.9E-7 2.58E-7 2.83E-7 3.79E-7 5.01E-7 6.31E-7 &
      7.59e-7 8.78E-7 9.85E-7 1.08E-6 1.17E-6 1.27E-6 1.36E-6 1.44E-6 &
      1.52e-6 1.68E-6 1.98E-6 2.51E-6 2.99E-6 3.42E-6 3.82E-6 4.01E-6 &
      4.41e-6 4.83E-6 5.23E-6 5.6E-6 5.8E-6 6.01E-6 6.37E-6 6.74E-6 &
      7.11e-6 7.66E-6 8.77E-6 1.03E-5 1.18E-5 1.33E-5
f122:p 6  84
fs122  -86  -87
sd122  1.e40 1463.9181 1.e40
       1.e40 7747.16094 1.e40
fm122 2.81780E+13   $  Pu Metal spherical source
tf122 2  2j  2
de122  .01 .03 .05 .07 .1 .15 .2 .25 .3 .35 .4 .45 .5 .55 .6 .65 &
       .7 .8 1. 1.4 1.8 2.2 2.6 2.8 3.25 3.75 4.25 4.75 5.0 5.25 &
      5.75 6.25 6.75 7.5 9. 11. 13. 15.
```

```
df122 3.96E-6 5.82E-7 2.9E-7 2.58E-7 2.83E-7 3.79E-7 5.01E-7 6.31E-7 &
      7.59e-7 8.78E-7 9.85E-7 1.08E-6 1.17E-6 1.27E-6 1.36E-6 1.44E-6 &
      1.52e-6 1.68E-6 1.98E-6 2.51E-6 2.99E-6 3.42E-6 3.82E-6 4.01E-6 &
      4.41e-6 4.83E-6 5.23E-6 5.6E-6 5.8E-6 6.01E-6 6.37E-6 6.74E-6 &
      7.11e-6 7.66E-6 8.77E-6 1.03E-5 1.18E-5 1.33E-5
fq0  f  s
f5:p   0 0 -1 1
        0 0 -99.9 1
        0 0 90.1 1
        0 0 189. 1
f15z:p  20.64 24.2994 1
           20.64 123.2994 1
fm5 2.81780E+13  $  Pu Metal spherical source
fm15 2.81780E+13  $  Pu Metal spherical source
de0  .01 .03 .05 .07 .1 .15 .2 .25 .3 .35 .4 .45 .5 .55 .6 .65 &
       .7 .8 1. 1.4 1.8 2.2 2.6 2.8 3.25 3.75 4.25 4.75 5.0 5.25 &
      5.75 6.25 6.75 7.5 9. 11. 13. 15.
df0 3.96E-6 5.82E-7 2.9E-7 2.58E-7 2.83E-7 3.79E-7 5.01E-7 6.31E-7 &
      7.59e-7 8.78E-7 9.85E-7 1.08E-6 1.17E-6 1.27E-6 1.36E-6 1.44E-6 &
      1.52e-6 1.68E-6 1.98E-6 2.51E-6 2.99E-6 3.42E-6 3.82E-6 4.01E-6 &
      4.41e-6 4.83E-6 5.23E-6 5.6E-6 5.8E-6 6.01E-6 6.37E-6 6.74E-6 &
      7.11e-6 7.66E-6 8.77E-6 1.03E-5 1.18E-5 1.33E-5
```

MCNP file *n25pu240*

```
message:      runtpe=pu239n.r

pu239 m= 4500 grams - Neutrons, source at bottom, 25% Pu-240, 5.057" distance
c     drum bottom
    1   101  -7.9       1  -2  -6
c     drum side
    2   101  -7.9       5  -6  2  -3
c     drum lid
    3   101  -7.9       3  -4  -6 145
C   c    upper liner
C       4   101  -7.9       7  -3  9  -10
C   c    upper liner base
C       5   101  -7.9       7  -8  -9
C   c     upper foam
C       6     1  -0.256     8  -9  -3
c    lower liner
    7   101  -7.9       13  -3  11  -12   $  -MHB Change
c    lower liner base
    8   101  -7.9       -11  13  -14
c    Foam
    9     1  -0.256     -3  -5  10  2
c    Foam
   10     1  -0.256     12  -10  -3  2  (155:-150)   $  -MHB Change
c    Foam
   11     1  -0.256     2  -150  -12      $  -MHB Change
c     torque bar
   12   0       15  -16  24  -25  14  -26  $ MHB - remove torque bar
c    lower load distrib assy side
   13   151  -2.7       (22  -23  20  -21  )(27  )
   14   151  -2.7       (-23  14  -20  )(26  :-24  :25  )
   16     0  23  -11  14  -3 (140:-7)
   17     0  (24  -25  14  -26  -23  )(-24  :25  :-14  :19  :-15  :16  )
c    anti rotation bar
   18   0       20  -32  30  -31  28  -29   $ MHB - remove bar
c    upper load distr assy side
   19   151  -2.7       -23  34  37  -33
c    upper load distr assy
   20   151  -2.7       (((-23  33  -7  )(35  ))(36  ))(-38  :39  :-40  :41  )
```

```
c    upper load distr assy penet
   21     0  33  -7  -35
c    upper load distr assy penet
   22     0  33  -7  -36
c     vessel support skirt
   23   101  -7.9       -42  43  20  -49  44  47
c    cv end cap
   24   101  -7.9       -47  48  -49
   25     0  ((-43  -49  20  )(47  ))(44  :-45  :46  :-30  :31  )
   26     0  ((20  -49  42  -22  )(47  ))(44  :-45  :46  :-30  :31  )
   27     0  -27  22  -23
c   28     0  43  -42  32  -44  28  -29
c    CV cylindrical portion
   29   101  -7.9       49  -52  50  -51
   30     0  51  -22  49  -21
   31     0  21  -52  51  -23
c    cv transition portion
   32   101  -7.9       -54  53  -55
c    cv upper cylinder
   33   101  -7.9       55  -58  56  -57
   34     0  52  -37  -23  54
   35     0  37  54  -34  -55
   36     0  55  -58  -34  57
   37   106  -7.584     -58  59  -56  66
   38   106  -7.584     58  -64  60  -61  62  -63  66
   39   106  -7.584     -65  64  60  -61  62  -63  67
   40     0  58  -33  -34  66   #38
   41     0  -64  33  38  -39  40  -41  66   #38
   42     0  64  -65  38  -39  40  -41  69   #39
   43     0  -7  65  38  -39  40  -41
   44   101  -7.9       (-70  68  69  )
   45   101  -7.9       -69  68  -76
   46   101  -7.9       -69  -75  76  73
   47   101  -7.9       -69  75  -74  72
   48   101  -7.9       -69  74  -65  71
   49     0  59  -64  69  -66
   50     0  76  -75  -73
   51     0  -74  75  -72  77
   52     0  74  -65  -71  77
   53     0  80  -65  -78
   54   101  -7.9       -65  75  -77  78
   55   101  -7.9       -64  75  -78
   56     0  55  -59  -56  70
   57     0  68  -55  -53  70
   58     0  -53  -68
   59     0  -50  49  -52  88
   60     0  -48  -49  88
   62     0  4  -82  -84 (-4:100:130)
   63     0  1  -4  -84  6
   64     0  83  -1  -84
   65     0  20  -44  30  -31  45  -28
   66     0  20  -44  30  -31  29  -46
   67     0  32  -44  30  -31  28  -29
   68     0  (43  -42  20  -44  )(-45  :46  )
c
c  MHB
   100   4 -0.3204 -135 110 -105   $ Min-K 2000
   105   3 -0.3684 -145 115 -4     $ Vermiculite
   110   5 -0.2563 -145 120 -115   $ FiberFrax
   115   101 -7.9   4 -100 -130 (135:-110:105) $ steel liner
   120   101 -7.9 -140 125 -3   (145:-120:4)   $ steel liner
   125   5 -0.2563 -3 150 -155 (12:-13)         $ fiberfrax
   116   0         -140 7 -125     $void above top fixture
c    external void
  999     0  -83  :82  :84
c     source
1000     2  -19.84     -88

    1        pz      0.6457  $ moved up 0.6457
```

```
    2        pz      0.7667  $ moved up 0.6457
    3        pz     86.161 $drum lid bottom
    4        pz     86.283 $drum lid top
    5        cz     23.178 $drum IR
    6        cz     23.299 $drum OR
    7        pz     73.639
    8        pz     73.829 $base of upper liner
    9        cz     18.035
   10        cz     18.225 $upper liner
   11        cz     10.478
   12        cz     10.667 $lower liner
   13        pz     10.461 $lower liner base
   14        pz     10.583
   15        px     -9.208
   16        px      9.208
   19        pz     11.345
   20        pz     11.523 $top of lower load distrib assy - MHB change
   21        pz     27.093 $lower load dist assy top of sides - MHB change
   22        cz      8.573
   23        cz      10.16 $lower load distrib assy side
   24        py     -0.635
   25        py      0.635
   26        pz     11.231 $ - MHB change
   27       c/x          0     24.553    1.27   $lower load dist assy penetration - MHB
change
   28        px     -0.635
   29        px      0.635
   30        py     -7.976
   31        py      7.976
   32        pz     12.805
   33        pz     72.242
   34        cz      9.801
   35       c/z     -6.172          0      1.588
   36       c/z      6.172          0      1.588
   37        pz     67.797
   38        px     -3.493
   39        px      3.493
   40        py     -3.493
   41        py      3.493
   42        cz      7.065
   43        cz       6.41
   44        pz     12.958
   45        px       -0.8
   46        px        0.8
   47        sq          1          1          4          0          0
                0    -70.795          0          0     17.342
   48        sq          1          1          4          0          0
                0    -59.336          0          0     17.342
   49        pz     17.342
   50        cz      7.703
   51        cz      8.414
   52        pz     67.746
   53       trc          0          0     67.746          0          0
                2.2098      7.703      8.001
   54       trc          0          0     67.746          0          0
                2.2098      8.414      9.042
   55        pz     69.955
   56        cz      8.255
   57        cz      9.042
   58        pz      71.86
   59        pz      70.26
   60        px     -3.175
   61        px      3.175
   62        py     -3.175
   63        py      3.175
   64        pz     72.673
   65        pz      73.13
   66        cz      1.626
   67        cz       2.07
```

```
   68         pz     68.355
   69         cz      1.588
   70        trc          0           0      68.35          0          0
                 1.91      7.739      8.014
   71         cz      1.143
   72         cz      0.724
   73         cz     0.1194
   74         pz     71.708
   75         pz      70.59
   76         pz     69.675
   77         cz      0.572
   78         cz      0.237
   80         pz     72.673
   81         so          0
   82         pz     189.065824 $top scoring plane
   83         pz       -100.
   84         cz      123.3
   85         cz          5 $segmenting surface for top and bottom planes
   86         pz     12.3  $segmenting plane for side scoring plane
   87         pz     22.3  $segmenting plane for side scoring plane
   88         sz    17.3  3.7832125836477
c
c  MHB add
c
c  lid
  100         pz 89.065824
  105         pz 88.944412
  110         pz 86.404412
  115         pz 75.361
  120         pz 74.009214
  125         pz 73.8878
  130         cz 17.901412
  135         cz 17.78
  140         cz 10.230612
  145         cz 10.1092
c
c fiberfrax
c
  150         pz 7.921
  155         cz 13.764006

mode  n p
m1    1001.60c         -0.041 $Polyurethane
      6000.60c         -0.544 8016.60c         -0.294 7014.60c         -0.121
m3    14000.60c            -21.22 $ Vermiculite
      13027.60c             -5.47
      20000.60c            -12.17
      26000.55c             -5.40
      22000.60c             -0.82
      12000.60c             -8.90
      11023.60c             -1.09
      19000.60c             -1.22
      16000.60c             -0.18
       8016.60c            -45.53
m4    14000.60c            -37.71 $ Min-K 2000
      22000.60c             -5.53
      13027.60c             -6.39
       6000.60c             -1.28
       1001.60c             -0.84
       8016.60c            -48.01
      51000.42c             -0.09
      31000.60c             -0.15
m5    13027.60c            -26.46 $FiberFlax
      14000.60c            -23.14
      11023.60c             -0.37
       8016.60c            -50.03
m101  6000.60c        -0.0003 $SS304L
      14000.60c         -0.01 15031.60c      -0.00045 16000.60c       -0.0003
      24000.50c         -0.19 25055.60c         -0.02 26000.55c      -0.67895
```

```
      28000.50c          -0.1
m151  13027.60c         -97.9 $6061 Al
      14000.60c          -0.6 29000.50c         -0.28 12000.60c            -1
      24000.50c          -0.2
m106  25055.60c            -8 $Nitronic 60
      14000.60c            -4 24000.50c           -17 7014.60c          -0.14
      28000.50c          -8.5 26000.55c        -62.36
m2    94240.60c        -0.25  $Pu Metal
      94239.60c        -0.75
imp:n  1            68r          0            1            $ 1, 1000
imp:p  1            68r          0            1            $ 1, 1000
sdef   erg d1   rad d2
       pos 0.0 0.0 17.3
si2   0.0  3.7832125836477
c  Neutron Groups
si1   1.00000E-11  1.00000E-07  4.14000E-07  8.76000E-07  1.86000E-06
      5.04000e-06  1.07000E-05  3.73000E-05  1.01000E-04  2.14000E-04
      4.54000e-04  1.58000E-03  3.35000E-03  7.10000E-03  1.50000E-02
      2.19000e-02  2.42000E-02  2.61000E-02  3.18000E-02  4.09000E-02
      5.74000e-02  1.11000E-01  1.83000E-01  2.97000E-01  3.69000E-01
      4.98000e-01  6.08000E-01  7.43000E-01  8.21000E-01  1.00000E+00
      1.35000e+00  1.65000E+00  1.92000E+00  2.23000E+00  2.35000E+00
      2.37000e+00  2.47000E+00  2.73000E+00  3.01000E+00  3.68000E+00
      4.97000e+00  6.07000E+00  7.41000E+00  8.61000E+00  1.00000E+01
      1.22000e+01  1.42000E+01  1.73000E+01
c  nct Neutron source strength
sp1   0.00000E+00  9.31150E-12  9.04471E-11  2.35295E-10  7.16679E-10
      3.62630E-09  9.78101E-09  7.97039E-08  3.25280E-07  8.74078E-07
      2.70316E-06  2.19425E-05  5.41032E-05  1.66661E-04  5.09149E-04
      5.74899E-04  2.14019E-04  1.84497E-04  5.92521E-04  1.05584E-03
      2.21097E-03  9.20435E-03  1.58525E-02  3.05440E-02  2.16732E-02
      4.18674E-02  3.76850E-02  4.75336E-02  2.77124E-02  6.32816E-02
      1.18252E-01  9.19361E-02  7.38417E-02  7.40742E-02  2.56644E-02
      4.11899E-03  1.99302E-02  4.68545E-02  4.31025E-02  7.70740E-02
      7.75534E-02  2.68423E-02  1.29097E-02  4.38579E-03  1.91935E-03
      5.28809E-04  5.90486E-05  9.72344E-06
ctme 150
f012:n 1  4  83  82
fs012  -85
sd012  78.5398 1.e40
       78.5398 1.e40
       78.5398 1.e40
       78.5398 1.e40
fm012 1.63934E+06   $  Pu Metal spherical source
tf012 4  2j  1
f022:n 6  84
fs022  -86  -87
sd022  1.e40 1463.9181 1.e40
       1.e40 7747.16094 1.e40
fm022 1.63934E+06   $  Pu Metal spherical source
tf022 2  2j  2
de0  2.5E-8 1.0E-7 1.0E-6 1.0E-5 1.0E-4 1.0E-3 1.0E-2 1.0E-1 5.0E-1 &
     1.0 2.5 5.0 7.0 10.0 14.0 20.0
df0  3.67E-6 3.67E-6 4.46E-6 4.54E-6 4.18E-6 3.76E-6 3.56E-6 2.17E-5 &
     9.26e-5 1.32E-4 1.25E-4 1.56E-4 1.47E-4 1.47E-4 2.08E-4 2.27E-4
f112:p 1  4  83  82
fs112  -85
sd112  78.5398 1.e40
       78.5398 1.e40
       78.5398 1.e40
       78.5398 1.e40
fm112 1.63934E+06   $  Pu Metal spherical source
tf112 4  2j  1
de112  .01 .03 .05 .07 .1 .15 .2 .25 .3 .35 .4 .45 .5 .55 .6 .65 &
       .7 .8 1. 1.4 1.8 2.2 2.6 2.8 3.25 3.75 4.25 4.75 5.0 5.25 &
      5.75 6.25 6.75 7.5 9. 11. 13. 15.
df112 3.96E-6 5.82E-7 2.9E-7 2.58E-7 2.83E-7 3.79E-7 5.01E-7 6.31E-7 &
      7.59e-7 8.78E-7 9.85E-7 1.08E-6 1.17E-6 1.27E-6 1.36E-6 1.44E-6 &
      1.52e-6 1.68E-6 1.98E-6 2.51E-6 2.99E-6 3.42E-6 3.82E-6 4.01E-6 &
```

```
      4.41e-6 4.83E-6 5.23E-6 5.6E-6 5.8E-6 6.01E-6 6.37E-6 6.74E-6 &
      7.11e-6 7.66E-6 8.77E-6 1.03E-5 1.18E-5 1.33E-5
f122:p 6  84
fs122  -86  -87
sd122  1.e40 1463.9181 1.e40
       1.e40 7747.16094 1.e40
fm122 1.63934E+06   $  Pu Metal spherical source
tf122 2  2j  2
de122  .01 .03 .05 .07 .1 .15 .2 .25 .3 .35 .4 .45 .5 .55 .6 .65 &
       .7 .8 1. 1.4 1.8 2.2 2.6 2.8 3.25 3.75 4.25 4.75 5.0 5.25 &
      5.75 6.25 6.75 7.5 9. 11. 13. 15.
df122 3.96E-6 5.82E-7 2.9E-7 2.58E-7 2.83E-7 3.79E-7 5.01E-7 6.31E-7 &
      7.59e-7 8.78E-7 9.85E-7 1.08E-6 1.17E-6 1.27E-6 1.36E-6 1.44E-6 &
      1.52e-6 1.68E-6 1.98E-6 2.51E-6 2.99E-6 3.42E-6 3.82E-6 4.01E-6 &
      4.41e-6 4.83E-6 5.23E-6 5.6E-6 5.8E-6 6.01E-6 6.37E-6 6.74E-6 &
      7.11e-6 7.66E-6 8.77E-6 1.03E-5 1.18E-5 1.33E-5
fq0  f  s
```

This Page Intentionally Left Blank

Safety Analysis Report - 9977 Packaging

CHAPTER 6

CRITICALITY EVALUATION

Preface

The criticality safety evaluation performed for the 9977 package is described in this chapter. The contents are specified in five content envelopes (C.1 through C.5) as described in Section 1.2.3 and in Table 1.2. Revision 0 of the 9977 SARP evaluates shipment of contents C.1 (Heat Sources), C.2 (Pu/U Metals), C.4 (U Alloys) and C.5 (U Compounds). This evaluation demonstrates compliance with the performance requirements of Title 10 of the Code of Federal Regulations (CFR), 10 CFR 71.55 and 71.59[1] for criticality safety. The information presented in this Chapter is in the format specified in the US NRC Regulatory Guide 7.9 (Revision 2).[2]

The analysis demonstrates that the package is subcritical for all single package and array configurations. The package Criticality Safety Index is 1.0.

This Page Intentionally Left Blank

TABLE OF CONTENTS

LIST OF TABLES

Page

LIST OF FIGURES

Page

ACRONYMS AND ABBREVIATIONS

5CV	5-inch Inside Diameter Containment Vessel
6CV	6-inch Inside Diameter Containment Vessel
ANS	American Nuclear Society
ANSI	American National Standards Institute
CFR	Code of Federal Regulations
CSI	Criticality Safety Index
CV	Containment Vessel
HAC	Hypothetical Accident Conditions
ID	Inside Diameter
LAW	Library to Analyze Waste
NCSE	Nuclear Criticality Safety Evaluation
NCT	Normal Conditions of Transport
SP	Single Package
SS	Stainless Steel
WSMS	Washington Safety Management Solutions LLC

This Page Intentionally Left Blank

6 CRITICALITY EVALUATION

6.1 DESCRIPTION OF CRITICALITY DESIGN

6.1.1 Design Features

The 9977 Shipping Package, referred to during its development as the General Purpose Fissile Package (GPFP), is a single containment drum type package with a bolted flange closure and a right circular cylindrical containment vessel enclosed by stainless steel (SS), Fiberfrax and Last-A-Foam insulation. Major component materials of construction include a SS overpack drum, Last-A-Foam insulation impact absorbers, and a SS containment vessel (CV). The CV is removed from the drum for loading and unloading. Two configurations are used in the 9977 packaging, a 5-inch inside diameter (5CV) and a 6-inch inside diameter (6CV) containment vessel. The physical configuration of the 9977 is described in Chapter 1. The package is designed for fissile material transport and is evaluated in Chapter 6 for solid forms of uranium and plutonium as either metal or oxide. The design features of the 9977 that are important to criticality control are the loading of fissile material contents into the CV, which prevents their release, and the drum, which remains intact maintaining spacing between contents.

There are no other design features, (e.g. neutron absorbing, flux traps, spacers, etc.) that provide criticality control in the 9977.

6.1.2 Summary Table of Criticality Evaluation

The criticality safety evaluation includes the single package analyses required by 10 CFR 71.55 and array analyses for Normal Conditions of Transport (NCT) and Hypothetical Accident Conditions (HAC) required by 10 CFR 71.59. The 9977 is analyzed for the transport of four content envelopes. The content envelopes are identified as C.1 through C.5 and are described in Section 1.2.3. Content C.3 (Pu/U Oxides) is reserved for a later SARP revision. Revision 0 of the 9977 SARP evaluates shipment of contents C.1 (Heat Sources), C.2 (Pu/U Metals), C.4 (U Metal Alloys) and C.5 (U Compounds). The criticality analysis results for these contents are summarized in Table 6.1.

Table 6.2 provides a summary of the parameters used in the package array analysis. As required by 10 CFR 71.59, an array of 5N (N = 50) (250) undamaged packages remains subcritical. This NCT condition is demonstrated by calculations performed with an infinite array of undamaged containers with 100% 239Pu, the most reactive fissile contents. The HAC analyses show that an array of 100 damaged packages, loaded with any of content envelopes C.1 (6CV configuration) and C.2, C.3, or C.5 (5CV configuration), is subcritical. This complies with 10 CFR 71.59, which requires that an array of 2N containers remain subcritical when subjected to the HAC with optimum moderation and water reflection.

The analysis is performed using the Monte Carlo method as implemented by the CSAS26 sequence of SCALE 5.[3] Parametric analyses show that a spherical shape is the most reactive configuration possible for the contents for the single package and array cases.[4] Although a spherical shape is not a credible configuration for the metal and oxide in the content envelopes, a spherical shape is conservatively assumed in the analyses. The HAC model includes radial and axial reduction of drum dimensions and loss of insulation due to the accident events. The

amount of damage modeled is based on the results of full-scale drop and fire-event testing of the package.[5, 6] Flooding of the CV is considered in the single package analysis. One hundred grams of plastic material (polyethylene or equivalent), typically used for contamination control, is assumed to be closely wrapped around the fissile contents.

The analysis demonstrates that the 9977 package, loaded with content envelope C.1 in the 6CV configuration or any of envelopes C.2, C.3, or C.5 in the 5CV configuration, is subcritical for all single package NCT and HAC cases.

6.1.3 Criticality Safety Index

The criticality safety index (CSI) of the 9977 package is 1.0 (N = 50) as calculated in accordance with 10 CFR 71.59(b). The calculation of the CSI for the NCT is conservatively based on the 6x6x7 array size (252 packages) and for the HAC is based on the 6x6x3 array size (108 packages).

Table 6.1 Summary of Criticality Safety Analysis Results

Content Envelope [a, b]	C.2	C.4	C.5
Single Package Results			
Package calculated to be subcritical under conditions for maximum reactivity (for flooded conditions)	Maximum k_{eff} = 0.908 k-safe=0.931	Maximum k_{ef} = 0.740 k-safe=0.931	Maximum keff = 0.755 k-safe=0.931
Most reactive configuration	^{239}Pu metal (sphere), 19.84 g/cc	^{235}U metal (sphere), 19.05 g/cc	^{235}U solution, 2.66 g/cc
Moderation for most reactive configuration	Flooded CV	Flooded CV	Flooded CV
Reflection for most reactive configuration (package materials and/or 30 cm water)	30 cm water	30 cm water	30 cm water
Array Results			
NCT Array	Maximum k_{eff} = 0.874 k-safe=0.931	Maximum k_{eff} = 0.798 k-safe=0.931	Bounded by C.4
Number of packages	Required: 250 Analyzed: infinite	Required: 250 Analyzed: infinite	
Most reactive fissile content	^{239}Pu metal, 19.84 g/cc	^{235}U metal, 19.05 g/cc	
Reflection surrounding array	Not applicable for infinite array	Not applicable for infinite array	
HAC Array	Maximum k_{eff} = 0.890 k-safe = 0.931	Bounded by C.2	Bounded by C.2
Number of packages	Required: 100 Analyzed 108 (6 x 6 x 3)		
Most reactive fissile content:	^{239}Pu metal, 19.84 g/cc		
Moderation to credible extent	None		
Reflection Surrounding Array	30 cm water		

a. The fissionable material mass limits for content envelopes C.2, C.4, and C.5 are shown in Table 6.3 and Table 6.4.

b. For content envelopes C.1, the ^{238}Pu mass limit is 100 grams and criticality is not a credible event.

Table 6.2 Criticality Evaluation Parameters for Package Arrays

Normal Conditions of Transport (N = 50)	
Number of undamaged packages that remain subcritical in array	Required: 5×N=250 Analyzed: Infinite
Most reactive credible physical and chemical form of fissile material	^{239}Pu metal
Most reactive interspersed hydrogenous moderation	Flooded Package Water between drums
Most reactive reflecting material	Not applicable for infinite array
Reflection surrounding the array	Not applicable for infinite array
Hypothetical Accident Conditions (N = 50)	
Number of damaged packages to remain subcritical	Required: 2 × N=100 Analyzed: 108 (6 x 6 x 3)
Most reactive credible physical and chemical form of fissile material	^{239}Pu metal
Most reactive interspersed hydrogenous moderation	Dry* Last-A-Foam insulation No moderating material between drums
Most reactive reflecting material	water
Reflection surrounding the array	30 cm water

* Dry means zero water content.

Table 6.3: Requested Content Envelopes C.1 - C.3

	Material	C.1 Heat Sources	C.2 Pu/U Metals	C.3 Pu/U Oxides
Fissile Material Maximum Weight %	^{238}Pu	100	2	Reserved For Future Use
	^{239}Pu	40	100	
	^{240}Pu	13	40	
	^{241}Pu	1	15	
	^{242}Pu	1.5	5	
	^{232}U	1.4×10^{-4}	1×10^{-7}	
	^{233}U	0.2	0.5	
	^{234}U	40	100	
	^{235}U	40	100	
	^{236}U	16	40	
	^{238}U	40	100	
Impurities (grams)	Ca	15	--	
	Fe	5	--	
	Cr	2	--	
Maximum Total Mass (kilograms)	Radioactive Materials	0.1	4.4	
	Impurities	0.02	3.08	
	All Contents	0.1	4.4	

Table 6.4: Requested Content Envelopes C.4 - C.5

	Material	C.4 Metal or Alloy H/X=0	C.5 Compounds H/X=0	C.5 Compounds H/X≤3
Fissile Material Mass (kg)	^{233}U	Reserved For Future Use		
	^{235}U	13.5	4.4	4.4

6.2 FISSILE MATERIAL CONTENTS

The package content loading limits are given in Table 1.2 of Chapter 1 and are defined as content envelopes C.1 through C.5. The limits on fissile, non-fissile and non-fissionable materials include consideration of typical packing materials, product impurities, moisture content and fissile and non-fissile contents of alloy metals. The limits presented for radionuclides and impurities apply for both the single package and array analyses. Contents are solid form (metal or oxide) and have fissionable components as shown in Table 6.3 and Table 6.4. This Criticality chapter only evaluates shipment of contents C.1 (Heat Sources), C.2 (Pu/U Metals), C.4 (U Metal Alloys) and C.5 (U Compounds).

The following limits/controls apply to the 9977 shipping packages evaluated in this analysis:

1. The 6CV configuration is only authorized to ship content envelope C.1.
2. Only the 5CV configuration shall be used to contain fissile material (content envelopes C.2 through C.5).
3. Only the material within the bounds of the content envelopes identified in Table 6.3 shall be shipped.
4. Each package shall be assigned a CSI=1.0 for material within the bounds of the content envelopes identified in Table 6.3.
5. Each package shall be assigned a CSI=0 for material within the bounds of content envelope C.1 identified in Table 6.3.
6. If a package contains greater than or equal to (≥) 3.0 kg of fissile material:
    a. The sum of the radial wall thicknesses of all cans (convenience can, inner can, and outer can) constituting a 3013 shall not exceed 0.26 inch,
    b. The sum of the axial thicknesses (top and bottom) of all can constituting a 3013 shall not exceed 1.77 inches,
    c. The volume of the convenience can shall not be less than 50.3 in^3. If multiple convenience cans are use, the volume limit shall be applied to the sum of the internal volumes of all convenience cans in a 3013,
    d. If a nested two-can configuration is used (e.g., an inner can and an outer can) instead of a three nested-can configuration, the volume limit shall be applied to the inner can(s).

The content envelopes, along with brief discussion of their modeling, are summarized below.

- Content Envelope C.1 – Plutonium-238 Oxide Heat Sources

  Content envelope C.1 was not modeled for criticality safety because 100 grams or less of heat source material is not a criticality concern. Envelope C.1 is dominated by ^{238}Pu, with small amounts of other plutonium isotopes, americium, neptunium, thorium and uranium. Due to the package decay heat rate limit, the contents are limited to a maximum fissile plutonium mass of 41 grams (40 grams of ^{239}Pu and 1 gram of ^{241}Pu). The critical mass of ^{238}Pu oxide is 10.4 kg with steel reflection and 16.6 kg with water reflection.[7] The heat generation of 0.57 watts/gram from alpha-particle decay and the resulting high temperature would preclude the assembly of large quantities of ^{238}Pu.

Therefore, for content envelope C.1 with a maximum of 100 grams of heat source material, criticality is not credible.

- Content Envelope C.2 – Plutonium and/or Uranium Metal (4.4 kg of Pu/U)

  This envelope does not permit the presence of more than 1 gram of reflecting material that is a better reflector than water (e.g., carbon or beryllium).[8] The total fissile material (i.e., ^{239}Pu or ^{235}U) mass in content envelope C.2 is limited to 4.4 kg.

- Content Envelope C.3 – Plutonium and/or Uranium Oxides (5.0 kg Pu/U Oxide)

  Content Envelope C.3 is not being requested in Revision 0 of the SARP.

- Content Envelope C.4 – Uranium Metal or Alloy

  Content envelope C.4 specifies a maximum of 13.5 kg of ^{235}U. ^{233}U which is also specified as a component of this content envelope was not analyzed during Revision 0 of the SARP.

- Content Envelope C.5 – Uranium Compounds

  Content envelope C.5 specifies uranium compounds with varying hydrogen to fissile ratios. ^{233}U which is also specified as a component of this content envelope was not analyzed during Revision 0 of the SARP.

6.3 GENERAL CONSIDERATIONS

The computational models used in the criticality analysis for single package and NCT and HAC arrays are presented in this section.

Some models include 100 grams of polyethylene material (density 0.95 g/cc) to account for the presence of nylon/plastic/PVC or equivalent hydrogenous materials used for contamination control and for moisture inside the CV. The polyethylene is conservatively assumed to be a shell of uniform thickness on the outer surface of the fissile material.

6.3.1 Model Configuration

The 9977 shipping package consists of a 35-gallon stainless steel drum with an external diameter and height of 18.72" and 36.1", respectively. Each 9977 has a single containment vessel. There are two size options for the CV. The 6CV will be used only for content envelope C.1 and the 5CV will be used for content envelopes C.2, C.4, and C.5. The need for the 6CV is based on the physical size of the Radioisotope Thermoelectric Generators (RTGs).

The 5CV for fissile material transport is a stainless steel pressure vessel with a nominal 5.047" inside diameter (ID) and is 18.6" high.[9] Nuclear fuel material contained in a product can is loaded into the CV. The CV is sealed with a stainless steel (SS) Cone-Seal Plug and locking Cone-Seal Nut. The Cone-Seal Plug is pressed into the CV body by the Cone-Seal Nut and has two O-rings that provide a leak tight seal. The containment boundary is defined as the CV body, the inner O-ring and the CV plug. An aluminum Bottom Load Distribution Fixture (LDF) is placed into the bottom of the drum liner followed by an aluminum honeycomb Bottom Spacer. The 5CV is placed on the Bottom Spacer. Aluminum Annular and Top Spacers go around the 5CV. A Top LDF goes above the Top Spacer inside the steel liner. The liner is welded to the drum top plate. Last-A-Foam and Fiberfrax surround the liner to fill the remainder of the 35-

gallon drum. The package lid has a bottom filled with Vermiculite and Fiberfrax insulation and a Top filled with Min-K 2000 insulation. The confinement boundary is the flanged stainless steel 35-gallon drum and Lid assembly.

Figure 6.1 shows a schematic of the 9977 shipping package with a 6CV. Figure 6.2 depicts the 9977 package with a 5CV. The differences in the two figures are all within the drum liner where the CV and supporting spacers are placed. Inside the liner, the 5CV requires additional spacing material to maintain its horizontal and vertical position. These spacers are aluminum honeycomb (see Table 6.9 for material details) and the dimensional details of these three spacers are also provided in Figure 6.2.

The 5CV will contain product cans with fissile material. Product cans that comply with DOE-STD-3013[10] are thick walled welded stainless steel cans. The 3013 container is comprised of nested welded inner and outer containers. The material being shipped which may be in a convenience can or directly loaded into the inner container. Product cans that do not comply with DOE-STD-3013 are commonly thin walled food-pack cans with a screw top, crimp seal, or slip-lid top. The non-3013 product cans vary widely in height and diameter.

Table 6.5 lists the specification dimensions of various components of the 9977 shipping package, the as-modeled dimensions of each component, and the reference drawings providing the specifications for each component. The specification column of Table 6.5 indicates the nominal (reference) dimensions of each component that were used for the base KENO[11] models (see the descriptions of the KENO models in Sections 6.3.1.2 through 6.3.1.4).

The 6” CV was modeled for the NCT and HAC configurations. However, the 5” CV was modeled for the single package (SP) configurations. During the course of this analysis it became apparent that the 6” CV volume was too large for the SP configurations required by 10 CFR 71 to remain subcritical over the desired fissile mass range. Thus, the SP configurations dictated the need for the 5” CV. The 6” CV for the NCT and HAC analyses is equivalent to the 5” CV since the distances between interacting fissile masses would not be affected by the CV dimensions. The 5” CV has aluminum honeycomb spacers holding it farther from the liner than the 6” CV. Thus a more realistic model for the 5” CV could result in modeling greater separation distance between fissile units in adjacent packages for the HAC analysis (2-cluster and 4-cluster configurations). Since modeling greater separation distance between fissile units in adjacent packages reduces the system reactivity, the 6” CV model is equivalent to the 5” CV model.

The 6” CV was modeled with a wall thickness of 0.28” [15] and the 5” CV was modeled with a wall thickness of 0.258” [9] for a difference of 0.022”. It has been demonstrated that k_{eff} varied by approximately 1% as the steel thickness of 3013 cans ranged from 0” to 0.16”. [17 - App 3] Since the steel 3013 can studied was closer to the fissile material than are the walls of the CV, the 0.022” difference in wall thickness between the 5” CV and the 6” CV has a negligible effect on calculated reactivity.

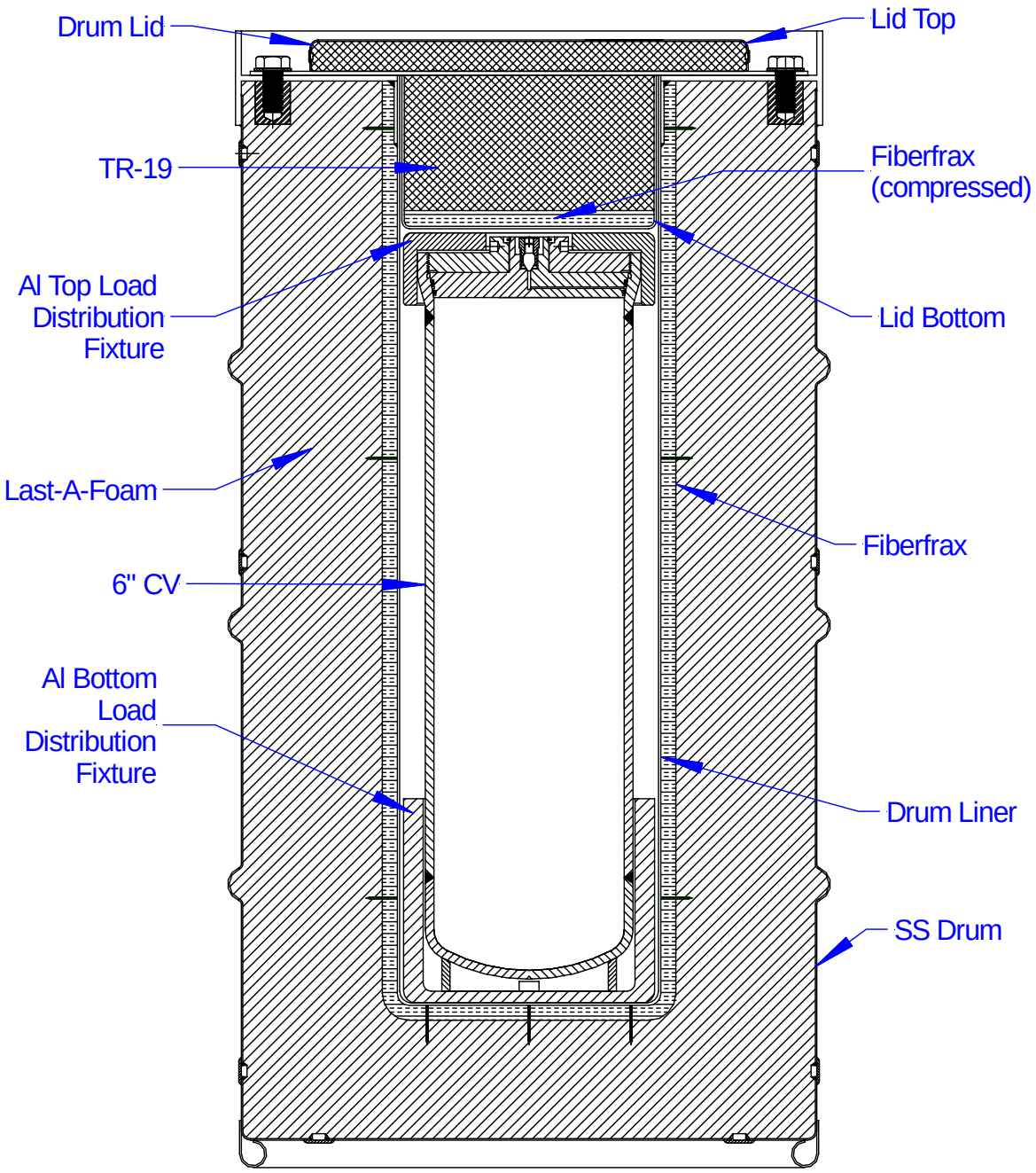

Figure 6.1 9977 Shipping Package with 6CV

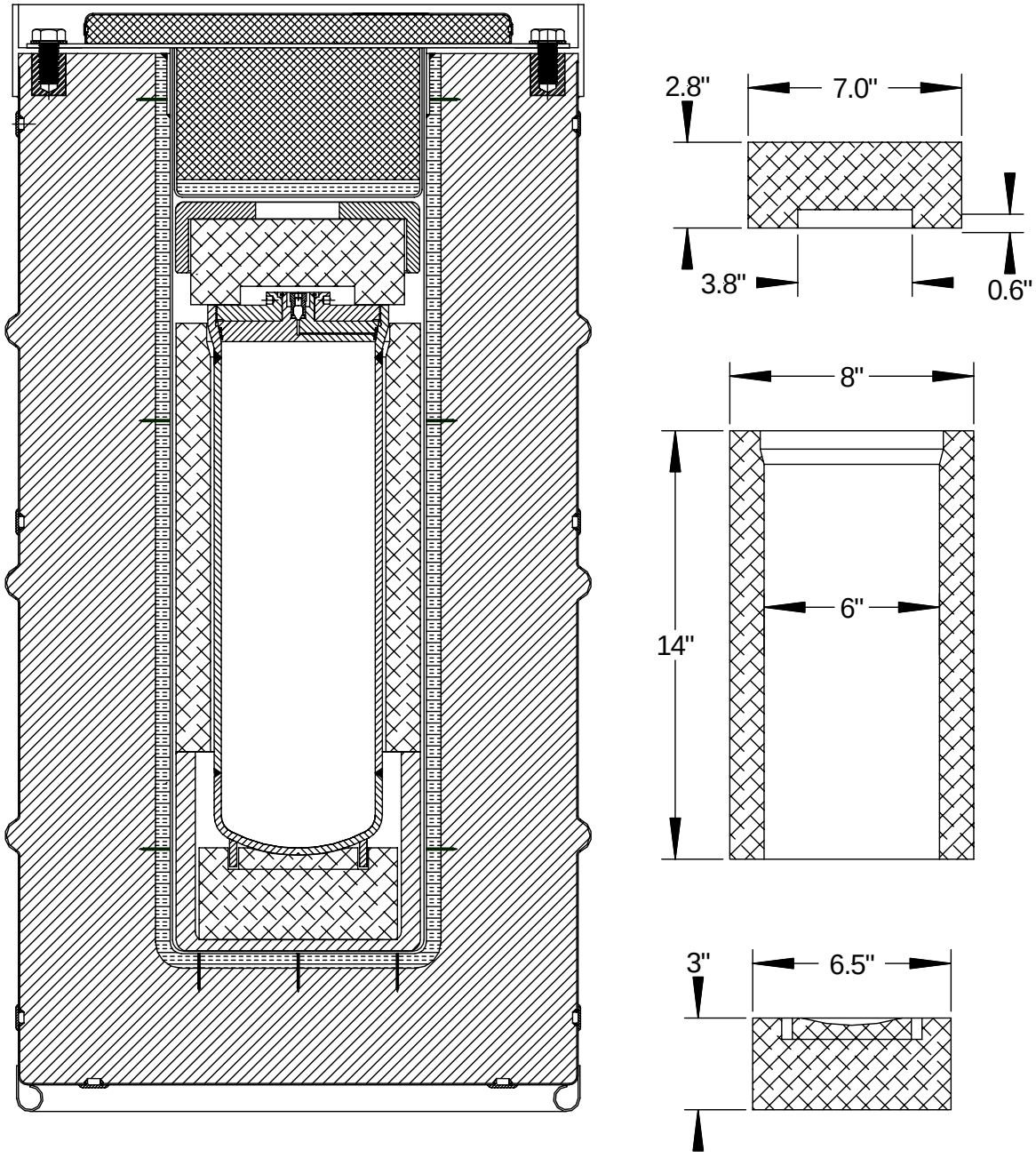

Figure 6.2 9977 Shipping Package with 5CV

Table 6.5 Geometric Specifications for the 9977 Shipping Packages

Sheet 1 of 4				
Component	**Parameter**	**Specification (inch)**	**KENO Model (cm)**	**Reference**
Drum Lid Plate	OD	17.8	--	R-R2-G-00018[12]
	OR	8.9	22.606	
	Thickness	0.125	0.3175	
Drum Liner	OD	8.346	--	R-R2-G-00017[13]
	OR	4.173	10.5994	
	ID	8.25	--	
	IR	4.125	10.4775	
	Internal Height	29.5	74.930	
	Thickness	18 gauge (0.048)	0.1219	
Drum	ID	18.25	--	R-R2-G-00017
	IR	9.125	23.1775	
	OR	9.125 + 0.048 (18 GA) = 9.173	23.2994	
	External Height	36.1	86.868 †	
	Inner Height	33.1	86.7461 †	
	Thickness	18 gauge (0.048)	0.1219	
† It is noted that the KENO model values (in centimeters) differ from the specification value (in inches). These differences are conservative for this analysis.				

Table 6.5 Geometric Specifications for the 9977 Shipping Packages

Sheet 2 of 4				
Component	**Parameter**	**Specification (inch)**	**KENO Model (cm)**	**Reference**
Aluminum Bottom Support	ID	6.75	--	R-R4-G-00032[14]
	IR	3.375	8.573	
	OD	8.00		
	OR	4.00	10.160	
	Internal Height	6.13	15.5702	
	External Height	6.50	16.51	
	Side Thickness	0.625	1.5875	
	Bottom Thickness	0.370	0.9398	
Aluminum Top Support	ID	7.15	--	R-R4-G-00032
	IR	3.575	9.081	
	OD	8.0		
	OR	4.0	10.160	
	Internal Height	1.75	4.445	
	External Height	2.30	5.842	
	Side Thickness	0.425	1.0795	
	Top Thickness	0.550	1.397	
	Central Hole	2.75x2.75	6.985x6.985	

Table 6.5 Geometric Specifications for the 9977 Shipping Packages

Sheet 3 of 4				
Component	**Parameter**	**Specification (inch)**	**KENO Model (cm)**	**Reference**
6CV	Upper OD	7.12	--	R-R2-G-00042[15]
	Upper OR	3.56	9.042	
	Upper ID	6.31	16.028	
	Cylinder OD	6.625		
	Cylinder OR	3.313	8.414	
	Cylinder ID	6.065		
	Cylinder IR	3.033	7.703	
	External Height	23.12	58.725	
	Max. Internal Solution Height	21.22	53.57 †	
	Side Thickness	0.28	0.7112	
	Top Steel portion Height	0.75	1.905	
	Tapered Portion Height	0.82	2.21 †	
	Height up to Leg	23.5	59.69	
	Leg OD	5.563	14.13	
	Leg ID	5.047	12.82	
† It is noted that the KENO model values (in centimeters) differ from the specification value (in inches). These differences are conservative for this analysis.				

Table 6.5 Geometric Specifications for the 9977 Shipping Packages

Sheet 4 of 4				
Component	**Parameter**	**Specification (inch)**	**KENO Model (cm)**	**Reference**
5CV	Upper OD	5.87	15.498 †	R-R3-F-0016[16]
	Upper ID	5.27	14.13 †	
	Cylinder OD	5.563	14.13	
	Cylinder ID	5.047	12.82	
	External Height	17.75	46.16 †	
	Max. Internal Solution Height	15.87	41 †	
	Side Thickness	0.258	0.655	
	Tapered Portion Height	1.62	4.445 †	
	Bottom of leg up to bottom of CV	0.31	Not specified	
	Leg OD	4.5	11.43	
	Leg ID	4.026	10.226	
Lid Liner Bottom	ID	7.98	--	R-R2-G-00018
	IR	3.995	10.147	
	OD	8.13		
	OR	4.065	10.325	
	Internal Height	4.81	12.207 †	
	External Height	4.88	12.395	
	Thickness	0.07	0.178	
Lid Liner Top	ID	13.904		R-R2-G-00018
	IR	6.952	17.658	
	OD	14.0	--	
	OR	7.00	17.780	
	Internal Height	0.952	2.418	
	External Height	1.00	2.54	
	Thickness	0.048 (18 gauge)	0.122	
DRUM Flange	Thickness	3/16	0.4763	R-R2-G-00017
† It is noted that the KENO model values (in centimeters) differ from the specification value (in inches). These differences are conservative for this analysis.				

Table 6.5 shows the package dimensions that are modeled in the base case for the single package, NCT and HAC models. The drum and Last-A-Foam radial dimensions used in the NCT and HAC cases for KENO Model are shown in Table 6.6.

The base KENO model was developed from the set of drawings referenced in Table 6.4. Table 6.4 includes specifications and as-modeled dimensions for various components of the 9977 shipping package.

Nominal 9977 component dimensions were used, since the dimensional tolerances are tight and the effect on reactivity of slight variations in material thicknesses was judged to be insignificant. In this analysis, the three rolling hoops of the 9977 containers were neglected. Neglecting these geometric details reduces the effective drum diameter, which in turn conservatively models the array pitch.

Simplifications made to the 9977 SCALE/KENO model include:

- Overpack Drum is approximated as a right circular cylinder with a flat bottom,
- Rolling hoops are ignored,

Table 6.6 shows the 9977 drum dimensions used for the single package, NCT and HAC model.

Table 6.6 Drum Dimensions for Various Models

Dimension	Specification	Single Package Model	NCT Model (cm)	HAC Model (cm)
Drum Inner Radius	23.1775 cm	23.1775 cm	Same as SP	19.3063 - 0.1684 = 19.1379
Drum Wall Thickness	(0.048 inch) 0.1219 cm	0.1219 cm		0.1684 (thickness is increased to conserve the drum mass)
Drum Outer Radius	23.2994 cm	23.2994 cm		(23.2994-1*2.54) *0.93 = 19.3063 Note: 1.0" (2.54 cm) is the drum radial reduction due to impact (see Table 6.7)

The following conservative assumptions are made in developing the criticality models:

1. *Geometric shape of fissile content*. The fissile content is assumed to be spherical. This is found to be the most reactive configuration in the single package and array analyses.[8]
2. *Plastics*. It was assumed in this analysis that 100 grams of plastic, modeled as a

C_2H_4 polymer (polyethylene), at a density of 0.95 g/cc, is present as a shell surrounding the fissile content.

3. *Fissile density*. The maximum theoretical densities, plutonium metal and uranium metal and oxides are assumed. The theoretical densities are higher than the actual densities that are commonly achieved.
4. *Fissile composition*. The content envelopes permit a wide range of isotopic compositions. The most reactive composition is assumed in the criticality analyses.
5. *Drum dimensions.* The rolling hoops and the drum lid closure hardware are ignored.
6. *Moderation*. Any amount of interstitial water in any form (ice, mist, etc.) between adjacent drums in an array reduces reactivity, since this increases isolation between units. Therefore, the absence of moderating material between drums is the most reactive condition.[17]

6.3.1.1 3013 Containers

Two basic packaging configurations are permitted within the 5CV: food-pack cans and 3013s. The evaluation model is a 3013 container configuration.

The 3013 container model is comprised of a convenience can inside two nested (an inner and an outer) welded closure containers. The size of the 3013 cans is important, the smaller the can, the closer the reflection. A sensitivity study of the 3013 can wall thickness was performed. [17 - App 3] Two different 3013 can volumes were used and the wall thickness was varied from minimum to maximum values. The $k_{eff}+2\sigma$ value results ranged from 0.8764 without any steel reflection from a 3013 can to 0.8875 for the minimum size (volume) 3013 can with maximum wall thickness. Based upon this analysis,[17 - App 3] the following restrictions are necessary when a 3013 can in a 9975 shipping package contains greater than or equal to (≥) 3.0 kg of fissile material:

a) The sum of the radial wall thicknesses of all cans (convenience can, inner can, and outer can) constituting a 3013 shall not exceed 0.67 cm,
b) The sum of the axial thicknesses (top and bottom) of all cans constituting a 3013 shall not exceed 4.5 cm,
c) The volume of the convenience can shall not be less than 825 cm^3. If multiple convenience cans are used, the volume limit shall be applied to the sum of the internal volumes of all convenience cans in a 3013,
d) If a two-can configuration is used (e.g., an inner can and an outer can) instead of a three nested-can configuration, the convenience can volume limit shall be applied to the inner can(s).

When less than 3.0 kg of fissile material is present, the restriction on the wall thicknesses and the restriction on the convenience can volume does not apply.[17 - App 3]

The study [17 - App 3] focused on the effect of varying the 3013 can size and volume while holding all other parameters constant. The 9975 shipping package contained two containment vessels (a

primary and secondary) whereas the 9977 has only one CV in the package. Thus, the steel reflection present in the study for the 9975 bounds the amount of steel reflection in the 9977 package.[17] Therefore, these results and restrictions are applied to the 9977 shipping package without further analyses.

Non-3013 product cans commonly used for packaging fissile material are thin wall containers (soup cans). Most of these cans have a slip-lid, screw top, or crimp seal lid. Most of the slip-lid and screw top product cans have some amount of tape on the can to help ensure the lid remains on the can body. Furthermore, it is expected that non-3013 product cans will be wrapped in some amount of plastic during a glove-box bag-out process.

To account for the tape and plastic for non-3013 product cans, 100 g of polyethylene was modeled around the fissile material as a reflector in some cases. Thin walled cans were not considered as part of this analysis since the thick steel reflection of a 3013 container is considered bounding for the reflection due to the product can.

6.3.1.2 Single Package Model

A single 9977 package was modeled as surrounded by 30 cm of water on all sides. All SP models analyzed the 5" CV. The contents of the package were varied to include metal, oxides and solutions. The analysis of the metal and oxide material forms represents the desired fissile mass. The solution analysis meets a 10 CFR 71 requirement to demonstrate that a single package fully flooded under worst case conditions remains subcritical.

For the metal and oxide cases, a sphere of the fissile material and form selected was placed in the radial center of the CV near the bottom to maximize reflection from the CV steel. The radius of the fissile sphere and its vertical center was varied based on the selection of Pu or U, and metal or oxide. Some cases modeled Pu and U oxide with H/X equal to 0 and 3. Some metal and oxide cases considered the presence of 100 g polyethylene as a spherical shell around the fissile material.

A series of calculations was performed by varying the concentration of fissile material in an aqueous mixture. The solution was assumed to be the only material present in the CV. This is conservative since the presence of product cans would add interstitial void and/or absorbers in the fissile solution. For most solution concentrations, the CV was filled with solution to a cylindrical solution to a height corresponding to fissile mass and concentration selected.

6.3.1.3 NCT Model

Most NCT models in this evaluation are infinite in the x, y, and z direction. In the infinite models, there is no leakage from the system and drum spacing is irrelevant. A single 9977 package was modeled inside a tight fitting cuboid and mirror boundary conditions were defined for the four x & y faces and periodic boundary conditions were defined for the z faces of the cuboid using standard KENO options. These boundary conditions reflected all escaping neutrons back into the system thus simulating an infinite square pitch array of packages.

In the NCT model, an infinite array of undamaged stacked drums was analyzed with and without the 3013 container in the dry condition. Since the drum does not have a gasket, there is a possibility for water to enter the drum and fill the liner (outside the CV). Several additional

cases were analyzed where water is present in the interstitial spaces between drums and inside the drums to account for the potential presence of water. It is assumed in the NCT array study that no water would enter the CV.

6.3.1.4 HAC Model

For the HAC array model, the drum radius was uniformly decreased corresponding to drop and crush test damage in the amount specified in Table 6.7, and then the radial component was further reduced by 7% to simulate a triangular pitch array. The values listed in Table 6.7 are bounding of the maximum dents and bulges observed in localized areas on the packages following the completion of all accident testing. The HAC models in this Nuclear Criticality Safety Evaluation (NCSE) uniformly reduce the radial and axial dimensions based on these maximum damage values. Therefore, the uniform dimension reductions modeled are very conservative, representing a closer spacing than actually possible with the observed drum damage.

A triangular pitch array model places fissile material units (drums) as close as possible, maximizing the real density of fissile units, and thereby increasing the reactivity effect due to interaction. It was shown [27] that if the drum radius in the rectangular array is reduced by 7%, it is equivalent to a triangular pitch drum array in terms of resulting k_{eff} values. In order to preserve the drum wall mass, the drum wall thickness was adjusted (See Table 6.6).

Conservative assumptions regarding the radial and axial reduction of drum dimensions due to drop and the amount of insulation charred due to fire were used in the damaged array model as shown in Table 6.7 (see Figure 6.3). Charred insulation is assumed to be completely vaporized. Additional reduction factors were added to the burn and drop test data for conservatism. The effect of the amount of insulation was also studied. Figure 6.3 is a sketch of the 9977 package that indicates the dimensions reduced for HAC analysis. Figure 6.3 contains more detail than present in the model.

The HAC model used a 6x6x3 array of damaged 9977 containers, reflected by 30 cm of water along all sides of the array. The damaged 9977 container was dry. The analysis was performed with and without the 3013 container.

Table 6.7 Fire and Drop Test Data for the HAC Model

Dimension	Insulation Burn Test Data	HAC Model	Drop Test Data (inch)	HAC Model (inch)
Radial	All foam	All foam and Fiberfrax replaced with void or water	0.5	1.0
Axial (top/bottom)	All Vermiculite	All Vermiculite, Fiberfrax and Min-K 2000 replaced with void or water	1 ⅛ (total)	2.0/1.0
Reference	Reference 6		Reference 5	

The basic HAC model is described in this section. The variations of the basic model are discussed in Section 6.6.

A conservative HAC model is constructed by assuming maximum movement of the CV. Fissile origin (coordinates) varies depending on whether it is inside the 3013 or in a food pack can. This movement gets the fissile mass to the side of the CV or the side of the 3013 container. Figure 6.4 depicts the package contents shifted to the left for maximum interaction with another package for a two-cluster configuration. The two-cluster configuration is discussed further in Section.6.6.

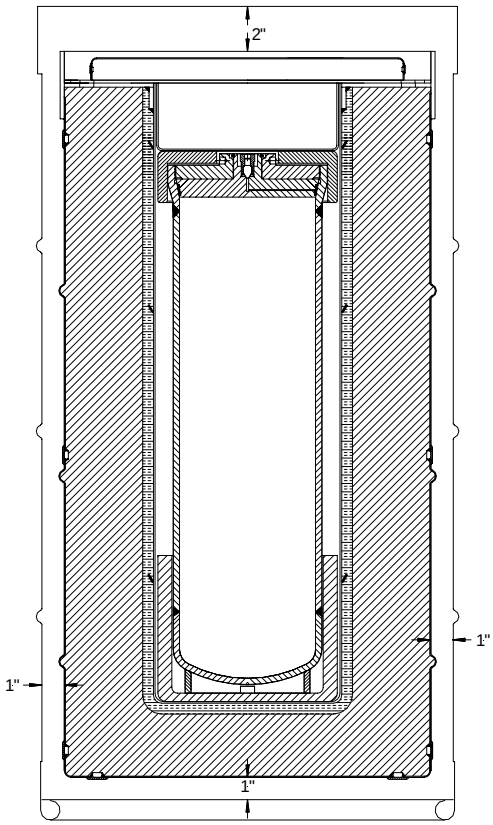

Figure 6.3 Outer Dimension Reductions for HAC

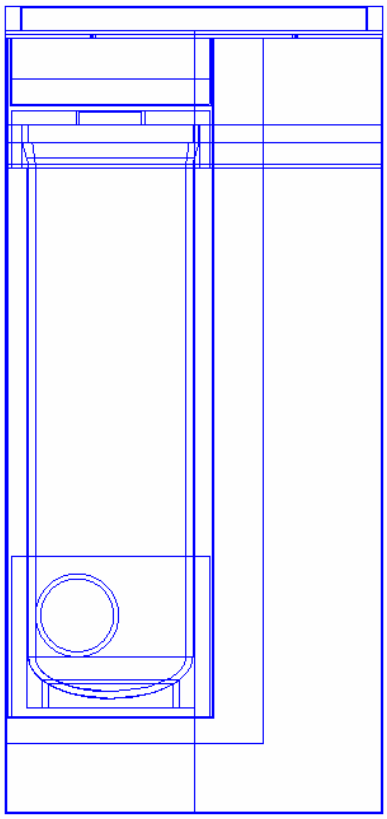

Figure 6.4 Radial Offset for HAC

6.3.1.5 Content Envelope Analysis

The following subsections discuss the justification for modeling choices related to the content envelopes and provide the basis for some of the content envelope limitations.

ANSI/ANS-8.1[18] ^{239}Pu limits apply to isotopic mixtures of plutonium provided that the concentration of ^{240}Pu exceeds that of ^{241}Pu and all isotopes are considered to be ^{239}Pu. The package contents meet this restriction. Therefore, plutonium in content envelope C.2 is conservatively modeled as 100% ^{239}Pu.

Uranium can also be transported in accordance with content envelopes C.2, C.4 and C.5. ANSI/ANS-8.1 subcritical mass limits demonstrate that ^{235}U metal can conservatively be treated as ^{239}Pu metal. Therefore, content envelope C.2, with uranium metal, is less reactive than content envelope C.2 with plutonium metal. Plutonium and uranium oxides have lower densities and significantly higher subcritical mass limits than the metal form. The criticality analyses show that the reactivity of content envelope C.2 (metal) bounds the reactivity of content envelope C.5 (oxide).

Envelope C.1

Content envelope C.1 as 100 grams or less of heat source oxide material has no criticality concern. Envelope C.1 is dominated by ^{238}Pu, with small amounts of other plutonium isotopes, and uranium isotopes. The content can have a maximum gross mass of 100 grams. Table 6.8 compares the maximum mass of each isotope allowed by content envelope C.1 against the minimum subcritical mass reported for each isotope.

Table 6.8 Content Envelope C.1 Mass Analysis

Isotope	C.1 Maximum Mass (g)	Subcritical Mass Limit (g)	Reference
^{238}Pu	100	3,000	Reference 7
^{239}Pu	40	450	Reference 7
^{240}Pu	13	15,000	Reference 7
^{241}Pu	1	200	Reference 7
^{242}Pu	1.5	40,000	Reference 7
^{232}U	1.4e-4	†	Reference 7
^{233}U	0.2	500	Reference 18
^{234}U	40	†	Reference 7
^{235}U	40	700	Reference 18
^{236}U	16	†	Reference 7
^{238}U	40	†	Reference 7
† Appendix A of Reference 7 predicts a k_∞ >1.0 but no critical or subcritical mass values are indicated for these isotopes. Thus it is understood that the subcritical mass limit values for these isotopes are larger than kilogram quantities.			

Based on Table 6.8, the content envelope C.1 gross mass limit of 100 grams is significantly less than the subcritical mass limit for any isotope. Therefore, for the C.1 content envelope with a

maximum of 100 grams of the heat source isotopes specified in Table 6.8, a criticality is not possible and no further analysis is necessary.

Envelope C.2

C.2 allows for a maximum metal mass of 4.4 kg Pu/U. The weight percent of various isotopes of Pu and U are specified in Table 6.3. The models in this evaluation are based on 4.4 kg ^{239}Pu or 13.5 kg ^{235}U. Thus, the analysis of 13.5 kg ^{235}U metal bounds the requested C.2 envelope mass of 4.4 kg of ^{235}U.

The analysis only considered the specific isotopes ^{239}Pu and ^{235}U. Based on the subcritical mass limits in Table 6.8, the analysis of the two fissile isotopes specified (^{239}Pu and ^{235}U) bound any mass of the following isotopes: ^{238}Pu, ^{240}Pu, ^{242}Pu, ^{232}U, ^{234}U, ^{236}U, ^{238}U.

This NCSE does not model the presence of Pu and U in the same package. Instead, this NCSE relies on Standards information to justify the combined presence of Pu and U in the same package. Given that all fissile material is processed in accordance with DOE-STD-3013 prior to placing it in a 9977 shipping package, the fissile material is credited for having the following characteristics important to this NCSE:

- the gross weight of the material in a 3013 can is less than or equal to 5.0 kg,
- the maximum water content in the oxide material is 0.5 wt%,
- the ^{233}U content is limited to a maximum of 0.5 wt%, and
- plutonium-bearing metals and oxides contain at least 30 wt% plutonium plus uranium.

Based on this material characteristic information, it is concluded[10 - Section A.6.3.2.1] that the 4.4 kg fissile mass limit for the 3013 can applies to all fissile species (i.e., ^{233}U, ^{235}U, ^{237}Np, or higher plutonium isotopes), because the critical masses of these fissile radioisotopes are greater than that of ^{239}Pu. This conclusion is consistent with the conservative approach outlined in ANSI/ANS-8.1. [18 - Section 5] Thus it is conservative to account for each gram of a fissile isotope as one gram of ^{239}Pu (i.e., gram for gram substitution) up to the fissile mass limit of 4.4 kg for a 3013 can. [10] Since these arguments are based on mass and material composition, the gram for gram substitution previously discussed is acceptable for fissile material inside a non-3013 can.

The analysis basis for this content envelope does not allow for the presence of unrestricted quantities of fissile isotopes other than ^{239}Pu (e.g., ^{241}Pu) in the same 9977 package. Quantities of ^{241}Pu are acceptable provided the mass of ^{240}Pu is greater than or equal to the mass of ^{241}Pu when ^{239}Pu is the predominant isotope.[19]

This content envelope does not account for the presence of more than 1 gram of reflecting material that is considered better than water (e.g., polyethylene, carbon, beryllium, etc.).[20] The analysis models fissile metal content in C.2 as 100% ^{239}Pu or 100% ^{235}U. Modeling 4.4 kg Pu as 100% ^{239}Pu generally bounds the 13.5 kg ^{235}U content cases. A few cases with 100% ^{235}U were run for comparison and verification. In addition to the fissile mass allowed, a maximum of 100 g of polyethylene was considered present with the fissile material as a reflector. It is expected that the 100 g polyethylene mass would bound the plastic that may be present around slip-lid and screw-top type product cans due to the bag-out process from a glovebox.

Envelope C.3

Table 6.3 indicates that an analysis of Pu/U oxides is not requested at this time.

Envelope C.4

Table 6.3 requests a metal or alloy fissile mass of 13.5 kg ^{235}U be analyzed. As noted in the discussion of content envelope C.2 the analysis of 4.4 kg ^{239}Pu metal bounds the analysis of 13.5 kg ^{235}U. Therefore, content envelope C.4 is considered by this evaluation as a subset of content envelope C.2.

Envelope C.5

Table 6.3 requests that ^{235}U compounds be analyzed up to a maximum of 4.4 kg. The analysis for Pu and U metal under content envelope C.2 is considered to bound the request for UO_2 in content envelope C.5.

6.3.2 Material Properties

The CV and the drum are made of 304L stainless steel. The liner, lid plate, top and bottom lid liner shells are also made of 304L stainless steel.

There are four types of insulating materials used in the 9977. The foam used in the drum is General Plastics Last-A-Foam FR-3716. The foam density was specified as 16 lb/ft^3 (0.2563 g/cc). [21] Fiberfrax insulation surrounds the liner in the drum and is also placed on the bottom of the bottom lid liner. It consists of Fiberfrax HSA, Grade E and is 1 inch thick and has a nominal density of 16 lb/ft^3 (0.2563 g/cc). The Fiberfrax insulation is sheathed with Fiberglass, Grade E on both sides. Vermiculite insulation in the bottom lid liner is a type of thermal ceramic, TR-19, and is made of Vermiculite granules and high temperature bonding material and has a density of 23 lb/ft^3 (0.3684 g/cc). This material exhibits minimal shrinkage at high temperature and will not decompose even when exposed directly to flame. The top lid liner contains a thermal ceramics material called Min-K 2000. It is made of silica and glass wool products and the nominal density is 20 lb/ft^3 (0.3204 g/cc).

The top and bottom LDF are solid. The standard material density of aluminum is 2.7 g/cc. Aluminum honeycomb is used as a spacer around the CV. The honeycomb bulk density is 12 lbs/ft^3 (0.1922 g/cc).[22]

The 9977 shipping package material data are shown in Table 6.9 through Table 6.13. Table 6.9 also lists other materials (e.g., water) in addition to the 9977 package construction materials and the densities used in the Sections 6.4 – 6.6 analyses.

Table 6.9 provides a summary of materials used in this analysis, the density of the material based on reference information, and the material density as modeled. The following is a brief discussion of the modeling choices made for this analysis.

Plutonium metal was modeled with a density of 19.84 g/cc. Plutonium was conservatively modeled as 100% by weight ^{239}Pu. Uranium metal was modeled with a density of 19.05 g/cc. The isotopic distribution for uranium was 100% ^{235}U. Lower densities were not studied since these maximum theoretical densities provide bounding results.

Plutonium was also modeled as PuO_2 with 100% by weight ^{239}Pu and a density of 11.46 g/cc. Uranium was also modeled as UO_2 with 100% by weight ^{235}U and a density of 10.96 g/cc. Lower densities were not studied since these maximum theoretical densities provide bounding results.

The "Standard Composition Library" in SCALE was used for the compositions of polyethylene, ^{239}Pu, ^{235}U, PuO_2, UO_2, SS 304, aluminum, and water.

Water density is conservatively taken as 1.0 g/cc instead of a nominal value of 0.9982 g/cc at 20ºC to cover temperatures as low as 0º C.

Polyethylene (C_2H_4) is conservatively used to represent plastic materials, as it has the highest hydrogen density among common types of plastic materials. The nominal polyethylene density is about 0.92 g/cc; however, a slightly higher density of 0.95 g/cc is used for conservatism.

Stainless Steel 304 with a density of 7.94 g/cc was modeled in the analysis although SS 304L was used to construct many of the package components. The small difference in composition between SS 304 and SS 304L will have a negligible effect on reactivity. [25 - App 2]

Table 6.9 Material Specifications for the 9977 Package Models

Components	Material	Density (g/cc) (as-modeled)	Reference
Water	H_2O	0.9982 at 20°C 0.99998 at 4°C (used 1.0 g/cc)	References 23 and 24
CV & Liner	304L-Stainless Steel (used SS 304)	7.94	Reference 23
Aluminum Top and Bottom Support Plates	Aluminum	2.7	Reference 23
Aluminum Honeycomb	Aluminum	0.1922 g/cc	Reference 22
Polyethylene	C_2H_4	0.92 (used 0.95 g/cc)	Reference 23
Foam See Table 6.10	General Plastics Last-A-Foam, FR-3716	16 lb/ft^3 (0.2563 g/cc)	Reference 21
Fiberfrax See Table 6.11	Fiberfrax HSA, Grade E	16 lb/ft^3 (0.2563 g/cc)	Reference 21
Vermiculite See Table 6.12	Thermal Ceramics, TR-19	23 lb/ft^3 (0.3684 g/cc)	Reference 21
Min-K 2000 See Table 6.13	Thermal Ceramics	20 lb/ft^3 (0.3204 g/cc)	Reference 21
Fissile Content	Pu Metal	19.84	Reference 23
	U Metal	19.05	
	Pu Oxide	11.46	
	U Oxide	10.96	

Table 6.10 Foam Composition

Element	Wt %, Sample A	Wt %, Sample B	Normalized for KENO input
Cl	0.1	0.2	0.15
Si	*	*	0.82
P	*	*	0.82
O	22.42	22.78	22.60
C	62.85	62.9	62.88
H	6.84	6.84	6.84
N	5.9	5.88	5.89
Total	98.11	98.6	100.00
* Si and P are known to be present, but were not measured.			

Table 6.11 Fiberfrax Composition

Compound	Wt %	Wt %, (average) For KENO
Al_2O_3	46-54	50
SiO_2	46-54	49.5
Na_2O	0.5	0.5
Total		100
Element		**Calculated**
Al		26.462
Si		23.138
Na		0.3709
O		50.029
Total		100

Table 6.12 Vermiculite Composition

Compound	Wt % (after fire)	Wt % (normalized) before fire	Element	Wt% For KENO
SiO_2	40	45.403	Si	21.223
Al_2O_3	9.1	10.3292	Al	5.4667
CaO	15	17.0261	Ca	12.168
Fe_2O_3	6.8	7.7185	Fe	5.3985
TiO_2	1.2	1.36209	Ti	0.8164
MgO	13	14.756	Mg	8.8984
Na_2O	1.3	1.4756	Na	1.0947
K_2O	1.3	1.4756	K	1.225
SO_3	0.4	0.45403	S	0.1818
Total	88.1	100.000	O	43.527

			Total	100

Table 6.13 MIN-K 2000 Composition

Compound Name	Compound	Minimum Wt%	Maximum Wt%	Average Wt%	Normalized Wt%
Amorphous Silica	SiO_2	35	95	65	48.01
Fibrous Silica	SiO_2	5	30	17.5	12.92
Micronized Silicon	Si	0	25	12.5	9.23
Titanium Dioxide	TiO_2	0	25	12.5	9.23
Hydrated Alumina	$Al(OH)_3$	0	50	25	18.46
Decabromodiphenyl Oxide	C_7H8O_2	0	5	2.5	1.85
Antimony Trioxide	Sb_2O_3	0	0.3	0.15	0.11
Phenol Formaldehyde Resin	$C_{12}Br_{10}O$	0	0.5	0.25	0.18
Total				135.4	100
	Element	Calculated wt%			
	Si	37.71			
	Ti	5.53			
	Al	6.39			
	C	1.28			
	H	0.84			
	O	48.01			
	Sb	0.09			
	Br	0.15			
	Total	100			

6.3.3 Computer Codes and Cross-Section Libraries

The CSAS26 driver of the SCALE 5 Computer Code System was used. It calls the BONAMI and CENTRM modules for the generation of problem-dependent cross sections library (accounting for resonance self-shielding) and then calls the KENO VI module to perform the Monte Carlo keff calculations. SCALE 5 is an industry recognized computational tool for criticality analysis.

Criticality calculations were made using the Library to Analyze Waste (LAW) 238-group cross-section library.[25] All calculations employed a P_3 Legendry expansion. Calculations were performed using numbers of generations and neutrons per generation to achieve a calculated statistical uncertainty (σ) less than 0.002. In all cases, convergence on k_{eff} is checked by viewing the graph of average k_{eff} by generation and by checking the k_{eff} histogram to verify that a normal distribution has been produced. KENO VI provides plots showing the geometry of the system and the distribution of materials. In all cases, these plots are examined to ensure the model is performing as intended. Example input files are provided on a CD included with the SARP. Validation of KENO VI for transport package criticality calculations is discussed in Section 6.5.

The calculated value of k_{eff} must be less than the value of k-safe, where k-safe includes a subcritical margin, the system bias, and uncertainties in that bias.[18] The reported values of k_{eff} are the calculated values plus 2 standard deviations. SCALE 5 has been certified on the Washington Safety Management Solutions (WSMS) computing system in accordance with approved quality assurance procedures.

6.3.4 Demonstration of Maximum Reactivity

The contingencies that are considered for the 9977 shipping package criticality analysis are specified in 10 CFR 71. Specifically, the objective of this evaluation is to demonstrate compliance with the performance requirements for each content envelope as specified in

- 10 CFR 71.55 – General requirements for fissile material packages,
- 10 CFR 71.59 – Standards for arrays of fissile material packages.

The requirements of 10 CFR 71 are thorough and ensure that the maximum value of k_{eff} is found in the analysis based on credible scenarios. The following specific scenarios are analyzed based on the 10 CFR 71 requirements:

Single Package – dry and flooded

Normal Conditions of Transport (NCT) array – dry and flooded

Hypothetical Accident Conditions (HAC) array – dry and flooded

The following conservative modeling assumptions are used in the criticality analysis for the 9977 shipping package:

i) Water is assumed to leak into the CV as well as the overpack package container for the single package analysis.
ii) A very conservative HAC model was analyzed. The HAC model included reduction of package diameter and height due to drop and crush as well as loss of foam insulation during fire and extreme movement of the CV within the drum. The 9977 shipping package drop test data and the foam burn data were taken from the actual test reports for the HAC calculations.
iii) A mass of 100 grams of plastic material (polyethylene or equivalent) was conservatively assumed to be closely wrapped around the plutonium/uranium metal. Polyethylene $(C_2H_4)_n$ with a density not exceeding 0.95 g/cc is used as the plastic material, as it contains the highest hydrogen density among the common form of plastic materials and has the highest reactivity effect.
iv) The plutonium isotopic composition is conservatively chosen as 100% ^{239}Pu. The uranium isotopic composition is conservatively chosen as 100% ^{235}U.

6.4 SINGLE PACKAGE ANALYSES

The single package (SP) analysis consists of two sets of moderation conditions, one for dry material and one for solution. The dry analysis places fissile metal or oxide as a sphere in the CV. The solution portion places a fissile solution in the CV at various concentrations to account for the dispersion of fissile material due to water in the CV.

6.4.1 Configuration

6.4.1.1 Dry

The single package base case model was developed without the 3013 containers. Fissile contents of plutonium metal, uranium metal, plutonium oxide and uranium oxide were used. The fissile material, in the form of a sphere, was located at the bottom of the CV in the base model. Several variations of the base case with plutonium metal were modeled to examine the effects of the 3013 container, location of fissile material within the CV, and the effect of polyethylene material. Some of the cases examined the effect of surrounding the fissile sphere with 100 grams of polyethylene to bound the presence of plastic commonly associated with a non-3013 (food pack) can.

Figure 6.5 depicts an x-ray view of the SP model with a single Pu sphere at the bottom center of the CV. Figure 6.6 provides a color coded guide to the materials used in modeling a fissile solution in the CV. Table 6.14 provides a description of the material for each material number in the legend of Figure 6.6. A discussion of materials used in this analysis is provided in Section 6.3.2.

Table 6.14 Material Description for Figure 6.6 and Figure 6.7

Material #	Description
1	Fissile solution
2	Fiberfrax
3	Foam
4	Vermiculite
5	Min-K 2000
6	SS304
7	Aluminum
8	Water
9	Low density Aluminum to simulate Aluminum
10	Polyethylene

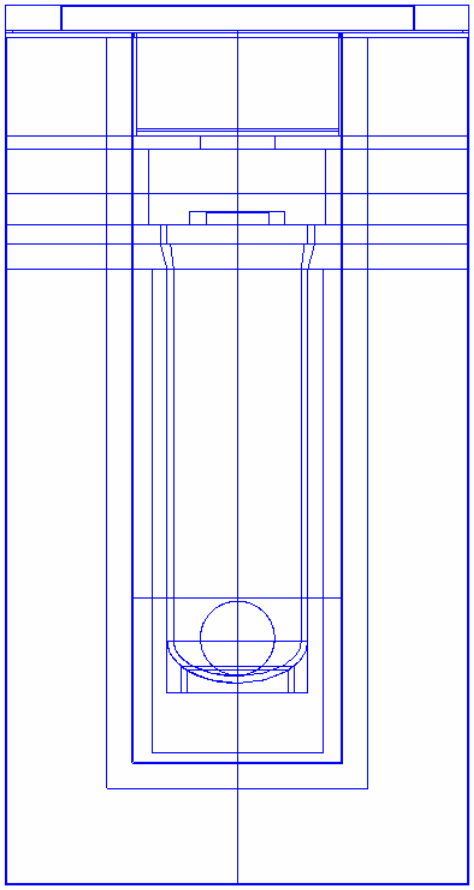

Figure 6.5 SP with Metal in 5CV

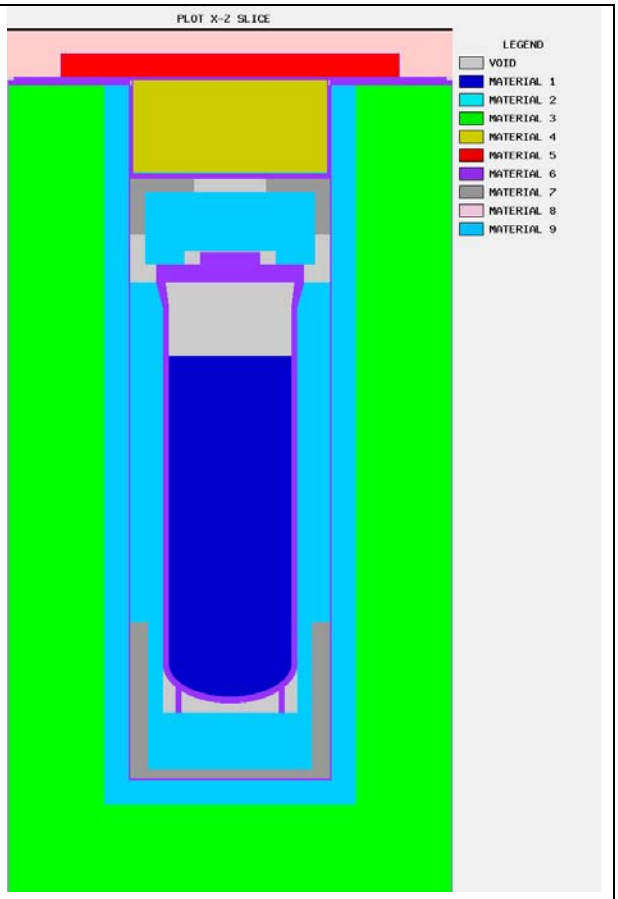

Figure 6.6 SP with Solution in 5CV

Figure 6.7 has two different depictions of a single 9977 with a 3013 can. The 3013 can was elevated in the CV for ease of modeling. This position has a negligible impact on the system reactivity. Table 6.14 provides a description of the material for each material number in the legend of Figure 6.7. Not shown in Figure 6.7 is the 30 cm of water reflection on all six sides of the single package as required by 10 CFR 71.55(e). This reflection condition was consistent for all single package cases reported for dry and solution conditions.

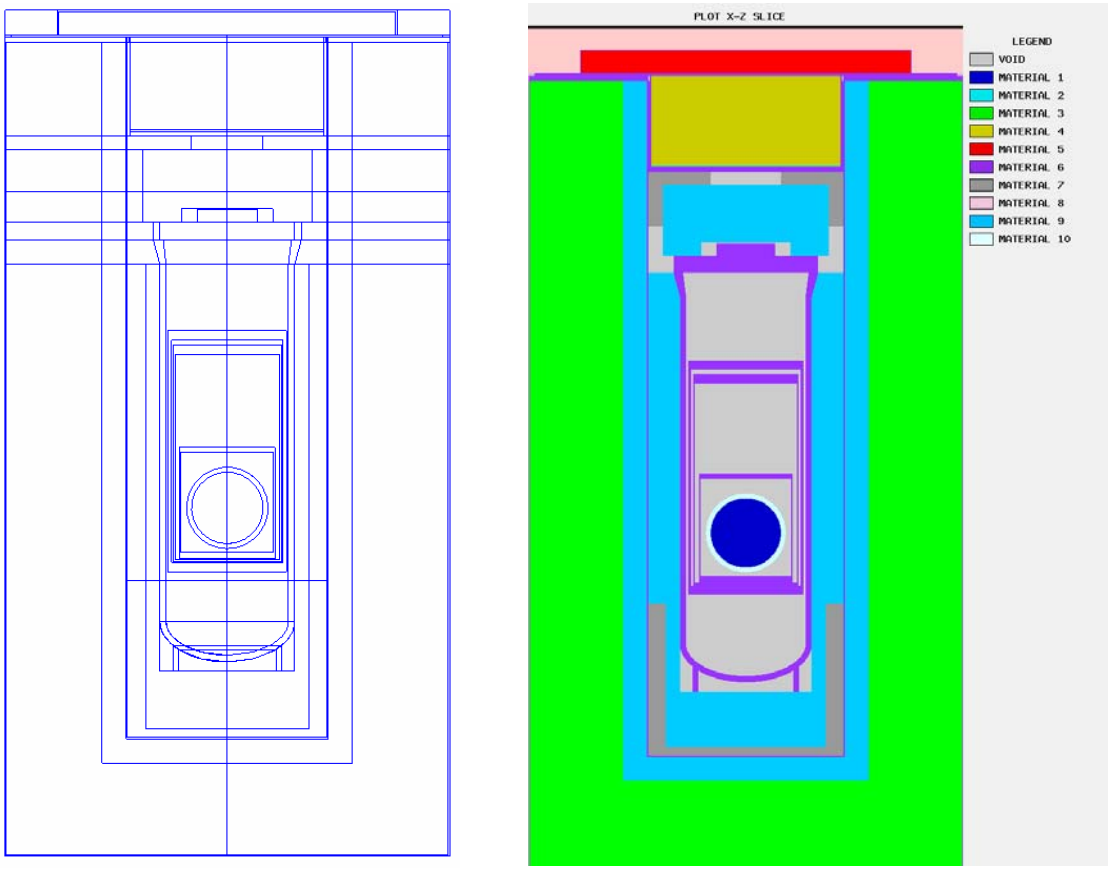

Figure 6.7 SP With 3013 in 5CV

Table 6.15 Single Package – Dry Cases

Case No.	File ID	Description	$k_{eff} \pm \sigma$	$k_{eff} + 2\sigma$
1	su_pu_mtl_01	Bare 4.4 kg ^{239}Pu metal sphere centered in bottom of CV. See Figure 6.5.	0.8054 ±0.0013	0.8080
2	su_pu_mtl_02	Bare 3.0 kg ^{239}Pu metal sphere centered in bottom of CV.	0.7452 ±0.0011	0.7474
3	su_u35_mtl_01	Bare 13.5 kg ^{235}U metal sphere centered in bottom of CV.	0.7377 ±0.0010	0.7397
4	su_u35_mtl_02	Bare 10 kg ^{235}U metal sphere centered in bottom of CV.	0.6668 ±0.0010	0.6687
5	su_PuO2_01_in	4.4 kg ^{239}Pu as PuO_2 with H/X=3 as a bare sphere centered in bottom of CV.	0.5354 ±0.0012	0.5378
6	su_UO2_01_in	4.4 kg ^{235}U as UO_2 with H/X=3 as a bare sphere centered in bottom of CV.	0.4237 ±0.0010	0.4257
7	su_pu_mtl_03_in	4.4 kg ^{239}Pu metal sphere centered in bottom of CV; 100 g poly surrounding fissile sphere. See Figure 6.5.	0.8289 ±0.0013	0.8315
8	su_pu_mtl_04_in	4.4 kg ^{239}Pu metal sphere centered in bottom of CV; 100 g poly surrounding fissile sphere inside 3013 can (poly is not allowed in a 3013 per DOE-STD-3013). See Figure 6.7.	0.8360 ±0.0015	0.8390
9	su_pu_mtl_05_in	4.4 kg ^{239}Pu metal sphere centered in bottom of CV; no poly surrounding fissile sphere; 3013 can present. See Figure 6.7.	0.8094 ±0.0013	0.8120
10	su_pu_mtl_06_in	4.4 kg ^{239}Pu metal sphere centered in bottom of CV; water fills CV, poly surrounding fissile sphere.	0.9056 ±0.0013	0.9082
11	su_PuO2_02_in	4.4 kg ^{239}Pu as PuO_2 with H/X=0 as a bare sphere centered in bottom of CV.	0.6015 ±0.0010	0.6035
12	su_UO2_02_in	4.4 kg ^{235}U as UO_2 with H/X=0 as a bare sphere centered in bottom of CV.	0.3763 ±0.0007	0.3778

Cases 1 through 6 compare the k_{eff} values for different types of fissile materials and material forms. The fissile material was located near the bottom of the CV in these cases (see Figure 6.5). These cases show that the 9977 with plutonium metal results in the highest k_{eff} values compared to cases with uranium metal and plutonium/uranium oxides. Therefore, the analysis of plutonium metal for the dry configurations is bounding of the other materials and material forms in content envelopes C.2 and C.5.

Cases 7 – 9 investigate the significance of 100 g of polyethylene surrounding the Pu metal sphere and the presence of the material in a 3013 container. These investigations address the issue of reflection provided by items or material that may be present. Case 7 has a $k_{eff}+2\sigma$ value that is approximately 2.3% higher than for case 1. The only difference between these two cases was the presence of 100 g of polyethylene. Case 9 has a $k_{eff}+2\sigma$ value that is only 0.4% higher than case 1. The only difference between case 1 and 9 was the presence of the 3013 container. Case 8 demonstrates that the combined effect of polyethylene and the 3013 container is an increase of approximately 3.1% in $k_{eff}+2\sigma$ value. Thus, the presence of the 3013 container does provide a positive, non-zero contribution to the system reactivity in the SP analysis.

The 3013 container is comprised of a convenience can located inside two nested sealed inner and outer containers. The addition of these three stainless steel cans adds a small amount of stainless steel inside the CV, which provides the competing effects of increasing neutron absorption and reflection by a small amount. Therefore, there are competing effects with the addition of 3013 containers inside the CV, but the reflection effect dominates for the single package and the reactivity increases as a result.

Case 10 filled the CV with water and bounds the requirements for analysis per 10 CFR Part 71, §71.55 (b). The fissile sphere was reflected by a 100 gram polyethylene shell in addition to the CV full of water. Case 10 produced the highest $k_{eff}+2\sigma$ value by approximately 7%.

6.4.1.2 Solution

Figure 6.6 provides a color coded guide to the materials used in modeling a fissile solution in the CV. Table 6.14 provides a description of the material for each material number in the legend of Figure 6.6.

The SP solution cases explicitly modeled a 5CV with a specified fissile mass and varied the fissile concentration. Fissile mass values less than the maximum specified by the content envelopes were modeled to achieve lower fissile concentrations. The maximum fissile concentration was limited to a value slightly less than the maximum theoretical density for the fissile metal. The minimum fissile concentration was limited by the maximum volume of the CV. This volume was calculated as 5.068 liters. The CV model was composed of a cylinder with an elliptical bottom. The calculated volume of the elliptical bottom was 0.2256 liters. Once the elliptical bottom was filled with solution, the cylinder was filled until the desired total volume (elliptical bottom plus cylinder) was achieved. Fissile concentrations resulting in a solution volume larger than the CV volume were not allowed due to the physical limitations of the CV. The maximum solution height in the cylinder portion of the CV was 37.51 cm. Various fissile mass values were selected for Pu and U thus allowing for a wide range of fissile concentrations in the CV solution study. Table 6.16 and Table 6.17 specify the fissile mass, fissile concentration, and solution height in the cylindrical portion of the CV.

It should be noted that immersion will not result in water in-leakage into the CV of a 9977 package. This was demonstrated by the fact that the HAC test with the 30 foot drop, puncture, impact and fire resulted in no observable containment vessel deformation, which otherwise could result in in-leakage. In-leakage, if it were to occur, would likely be through the seal region of the CV. Testing has shown that the seal region is helium leak tight following the sequential drop, puncture, and fire tests. [5] However, flooding in a single package was considered in order to examine the most adverse condition and to comply with 10 CFR 71.

All cases reported in this section were reflected on all six sides by 30 cm of water per the requirements of 10 CFR Part §71.55 (e).

6.4.2 Results

Table 6.15 provides the results for the dry cases in the SP study. The flooded case results are presented in Tables 6.16 and 6.17.

The dry unit results presented in Table 6.15 provide the opportunity for a few observations and conclusions. All the cases resulted in a $k_{eff}+2\sigma$ values less than k_{safe}. Thus, a maximum of 4.4 kg ^{239}Pu or 13.5 kg ^{235}U will remain subcritical inside the CV during dry (normal) conditions.

Table 6.16 Single Package – Flooded Cases – Plutonium

Case No.	File ID	Mass ^{239}Pu (kg)	Conc. (kg/L)	Sol. Height (cm)	k_{eff}	$\pm\sigma$	$k_{eff} + 2\sigma$
1	su_pu_sol_07	4.4	0.86823	37.51	0.7088	0.0013	0.7114
2	su_pu_sol_08	4.4	1	32.339	0.7057	0.0017	0.7091
3	su_pu_sol_09	4.4	1.5	20.977	0.6910	0.0016	0.6942
4	su_pu_sol_10	4.4	5	5.069	0.6085	0.0013	0.6111
5	su_pu_sol_11	4.4	10	1.661	0.6170	0.0011	0.6192
6	su_pu_sol_12	4.4	15	0.524	0.6856	0.0014	0.6884
7	su_pu_sol_13	4.4	18	0.146	0.7369	0.0011	0.7391
8	su_pu_sol_20	3.5	0.69063	37.51	0.6935	0.0016	0.6967
9	su_pu_sol_21	3.5	0.7	36.987	0.6974	0.0015	0.7004
10	su_pu_sol_22	3.5	1	25.367	0.6751	0.0014	0.6779
11	su_pu_sol_23	3.5	1.5	16.328	0.6500	0.0013	0.6526
12	su_pu_sol_24	3.5	5	3.675	0.5412	0.0011	0.5434
13	su_pu_sol_25	3.5	10	0.963	0.5580	0.0011	0.5602
14	su_pu_sol_26	3.5	15	0.060	0.6289	0.0011	0.6311
15	su_pu_sol_32	2.5	0.49330	37.51	0.6750	0.0014	0.6778
16	su_pu_sol_33	2.5	0.5	36.987	0.6736	0.0014	0.6764
17	su_pu_sol_34	2.5	0.6	30.531	0.6620	0.0014	0.6648
18	su_pu_sol_35	2.5	0.7	25.920	0.6543	0.0016	0.6575
19	su_pu_sol_36	2.5	1	17.620	0.6220	0.0013	0.6246
20	su_pu_sol_37	2.5	1.5	11.164	0.5825	0.0013	0.5851
21	su_pu_sol_38	2.5	5	2.126	0.4548	0.0010	0.4567
22	su_pu_sol_39	2.5	10	0.189	0.4844	0.0010	0.4864
23	su_pu_sol_40	2.5	15	2.582 †	0.5137	0.0010	0.5156
24	su_pu_sol_41	2.5	18	2.152 †	0.5311	0.0010	0.5331

† These values are the solution height in the elliptical bottom of the CV. In these cases, the solution level is below the cylindrical portion of the CV.

A comparison between case 7 of Table 6.16 and case 1 of Table 6.15 indicates that the bare metal sphere configuration bounds the same fissile mass in solution in a 5CV since the metal sphere produces a higher reactivity than the solution in the 5CV. Table 6.16 indicates that the system reactivity tends to increase as the mixture density approaches that of metal. Note that Table 6.16 also indicates that reactivity increases as the fissile concentration decreases and solution height in the 5CV increases up to the maximum allowed volume. Scoping calculations indicated that a 6CV provided sufficient volume that the system maximum $k_{eff}+2\sigma$ values occurred at lower fissile concentration and these maximum values occasionally exceeded 1.0. The maximum $k_{eff}+2\sigma$ value for cases in Table 6.16 occur at the maximum mixture density studied (see case 7) indicates that the fissile material in the 5CV is under moderated due to the restricted volume of the 5CV.

Table 6.17 Single Package – Flooded Cases – Uranium

Case No.	File ID	Mass ^{235}U (kg)	Conc. (kg/L)	Sol. Height (cm)	k_{eff}	$\pm\sigma$	$k_{eff} + 2\sigma$
1	su_u235_sol_09	13.5	2.66386	37.51	0.7516	0.0017	0.7550
2	su_u235_sol_10	13.5	5	19.169	0.7366	0.0014	0.7394
3	su_u235_sol_11	13.5	10	8.710	0.7167	0.0013	0.7193
4	su_u235_sol_12	13.5	15	5.224	0.7206	0.0011	0.7228
5	su_u235_sol_13	13.5	18	4.062	0.7348	0.0010	0.7368
6	su_u235_sol_23	10	1.97323	37.51	0.7350	0.0016	0.7382
7	su_u235_sol_24	10	5	13.746	0.6849	0.0013	0.6875
8	su_u235_sol_25	10	10	5.999	0.6440	0.0011	0.6462
9	su_u235_sol_26	10	15	3.417	0.6413	0.0010	0.6433
10	su_u235_sol_27	10	18	2.556	0.6522	0.0011	0.6544
11	su_u235_sol_36	7	1.38125	37.51	0.7206	0.0014	0.7234
12	su_u235_sol_37	7	1.5	34.405	0.7165	0.0017	0.7199
13	su_u235_sol_38	7	5	9.098	0.6081	0.0011	0.6103
14	su_u235_sol_39	7	10	3.675	0.5505	0.0011	0.5527
15	su_u235_sol_40	7	15	1.867	0.5503	0.0010	0.5522
16	su_u235_sol_41	7	18	1.265	0.5679	0.0010	0.5699
17	su_u235_sol_49	4.4	0.86822	37.51	0.7031	0.0016	0.7063
18	su_u235_sol_50	4.4	1	32.339	0.6890	0.0015	0.6920
19	su_u235_sol_51	4.4	1.5	20.977	0.6536	0.0015	0.6566
20	su_u235_sol_52	4.4	5	5.069	0.4960	0.0012	0.4984
21	su_u235_sol_53	4.4	10	1.661	0.4418	0.0009	0.4435
22	su_u235_sol_54	4.4	15	0.524	0.4537	0.0008	0.4553
23	su_u235_sol_55	4.4	18	0.146	0.4734	0.0010	0.4754

All of the cases in Table 6.16 and Table 6.17 resulted in $k_{eff}+2\sigma$ values significantly less than k_{safe}. Thus, a maximum of 4.4 kg ^{239}Pu or 13.5 kg ^{235}U will remain subcritical inside the 5" CV even if water leaks into the 5" CV. The primary basis of this condition is the volume limitation provided by the CV. Scoping calculations indicate that significantly lower mass limits would be required for the package if fissile material were to be shipped in the 6" CV.

All the $k_{eff}+2\sigma$ values in Table 6.16 and Table 6.17 were less than those for the dry analysis reported in Table 6.15. Thus, for a single package with the 5" CV (see Table 6.5), the results of a bare Pu metal sphere (case 1 in Table 6.15) bound the fissile solution results.

All SP cases in Table 6.15, Table 6.16, and Table 6.17 are below the k_{safe} value of 0.931. Therefore, the 10 CFR § 71.55(b) requirements related to a flooded single package are satisfied.

6.5 EVALUATION OF PACKAGE ARRAYS UNDER NORMAL CONDITIONS OF TRANSPORT

6.5.1 Configuration

In the NCT undamaged package array model, the package was modeled with the dimensions specified in Table 6.5. Cases modeled an infinite square pitch array of stacked packages with dry and partially flooded conditions unless specified otherwise. The flooded conditions studied for the NCT analysis modeled water in the liner and insulation regions. One case (Table 6.18

case 2) modeled water filling the volume inside the CV even though the test results indicate that the CV remained helium leak tight.[5] Since the CV remained leak tight following the prescribed accident tests, case 2 exceeds the analysis requirements for NCT conditions.

The 9977 was modeled with water in the liner and insulation regions. This is conservative since tests per 10 CFR § 71.71(c)(6) indicate that only the liner region can retain water. The infinite square pitch array was simulated by modeling a single package in a cuboid. This outer region was assigned mirror reflection boundaries in the x and y directions, and periodic boundary conditions in the z direction. Some cases specifically modeled a 6x6x7 array of 9977 packages with 30 cm of full density water reflection surrounding the array. Table 6.18 specifies which cases specifically modeled a defined array size. Most cases reported in Table 6.18 modeled the packages in an infinite square pitch array configuration. Table 6.18 shows the k_{eff} results and provides a brief description of each case.

6.5.2 Results

Table 6.18 shows the k_{eff} results and provides a brief description of each case.

Table 6.18 indicates that any analysis for 4.4 kg Pu metal results in higher $k_{eff}+2\sigma$ values than an analysis for 13.5 kg ^{235}U metal (see cases 1-5). Thus, the plutonium metal analysis in the NCT cases bounded the uranium analysis.

The two cases that modeled a defined array size surrounded by 30 cm of water reflection (cases 1a and 5a) resulted in $k_{eff}+2\sigma$ values approximately 1% lower than when the infinite array was modeled (cases 1 and 5). This difference in $k_{eff}+2\sigma$ values is statistically significant and indicates the infinite array models are conservative compared to the 6x6x7 limited array with full water reflection.

Cases 1, 5, 7 and 9 in Table 6.18 show that the uranium metal and oxide configurations and the plutonium oxide configurations are much less reactive than the corresponding configuration of plutonium metal in an infinite array of 9977 containers. Therefore the other cases in Table 6.18 were evaluated with plutonium metal (assumed as 100% ^{239}Pu). A similar trend was also observed in the single package cases.

Table 6.18 NCT Array Configuration Results

Case No.	File ID	Description	k_{eff}	σ	$k_{eff}+2\sigma$
1	nct_135kgu.out	13.5 kg ^{235}U metal sphere surrounded by a 100 g poly shell	0.7959	0.0011	0.7981
1a	nct_135kgu_in.out	Same as case 1 but specifically modeled in a 6x6x7 array with 30 cm water reflection on the array boundary	0.7777	0.0011	0.7799
2	nct_cvfl.out	4.4 kg ^{239}Pu metal sphere surrounded by a 100 g poly shell in a 3013, CV and package flooded with water, water between the packages	0.8715	0.0013	0.8741
3	nct_drumfl.out	4.4 kg ^{239}Pu metal sphere surrounded by a 100 g poly shell in a 3013, water between the packages and each package flooded with water	0.8510	0.0013	0.8536
4	nct_interfl.out	4.4 kg ^{239}Pu metal sphere surrounded by a 100 g poly shell in a 3013, water only between the packages	0.8491	0.0012	0.8515
5	nct_pu1.out	4.4 kg ^{239}Pu metal sphere surrounded by a 100 g poly shell	0.8500	0.0013	0.8526
5a	nct_pu1_in.out	Same as case 5 but specifically modeled in a 6x6x7 array with 30 cm water reflection on the array boundary	0.8410	0.0013	0.8436
6	nct_pu_3013.out	4.4 kg ^{239}Pu metal sphere surrounded by a 100 g poly shell in a 3013	0.8618	0.0014	0.8646
7	nct_puox1.out	4.4 kg ^{239}Pu as PuO_2 in a sphere with H/X=0 surrounded by a 100 g poly shell	0.6517	0.0011	0.6539
8	nct_u1.out	4.4 kg ^{235}U metal sphere surrounded by a 100 g poly shell	0.5507	0.0009	0.5525
9	nct_uox1.out	4.4 kg ^{235}U as UO_2 in a sphere with H/X=0 surrounded by a 100 g poly shell	0.4280	0.0008	0.4295

The presence of water inside the 9977 package but outside the CV lowers the $k_{eff}+2\sigma$ value of the system. Cases 2, 3 and 4 analyze various flooded conditions. Cases 2 and 3 filled the liner, foam and Fiberfrax regions with water (referred to as "package flooded with water"). In addition, Case 2 filled the CV with water. Case 4 placed water in the array only between the packages. Comparing case 4 and case 6 demonstrates that k_{eff} is reduced by water between the packages even if there is not water inside the packages. Together, these cases demonstrate that the optimum water conditions were analyzed.

All NCT cases in Table 6.18 were below the k_{safe} value of 0.931. Therefore, the 10 CFR § 71.55(d) and § 71.59(a)(1) requirements related to NCT analyses are satisfied.

6.6 PACKAGE ARRAYS UNDER HYPOTHETICAL ACCIDENT CONDITIONS

6.6.1 Configuration

Models were developed to satisfy the prescribed requirements of 10 CFR 71.55. The models developed assumed that no water would enter the CV. This assumption was based on test results that indicate no damage occurred to the CV as a result of the required test conditions.[5] This modeling selection is consistent with 10 CFR § 71.55(e)(1).

To study k_{eff} for HAC, a 6x6x3 square pitch array of 9977 packages was reflected by 30 cm of water in all six directions. The 9977 packages were modeled under the prescribed accident conditions. Each 9977 package contained a 4.4 kg ^{239}Pu sphere that was surrounded by 100 g polyethylene. The 6CV was used in the HAC models as discussed in Section 6.3.1.

Array analyses were performed using a 7% reduced drum radius to approximate an equivalent triangular pitch array configuration.[27] This 7% radius reduction was in addition to the damage values demonstrated by the test results (see Table 6.7). Test results indicate that a 2" (5.08 cm) reduction in the package diameter and a 2" (5.08 cm) reduction in the package height bound the HAC (see Table 6.7). Some cases modeled a 3" (7.62 cm) reduction in the package height for additional conservatism. In all models, the reduction in package diameter and height were uniform. The test results reported for package damage were for maximum dents and bulges localized on the package (see Table 6.7). Therefore, the uniform dimension reductions modeled are very conservative, representing a closer spacing than actually possible with the observed drum damage. The dimension reductions were taken in the foam region of the package. Thus, for all the cases in Table 6.19 that indicate a reduced dimension, the radial and/or axial foam thickness was reduced to produce the outer package dimensions desired.

Some of the cases presented in Table 6.19 studied the absence of some/all of the insulating material. Each of the cases in Table 6.19 that reduced the diameter, the height, or both, resulted in a smaller volume for the foam region. The foam density was not increased to conserve mass in the foam region due to the reduced volume of the foam region. Some cases studied the absence of the foam, thus eliminating the need for a parametric study of the system reactivity versus foam density. In the 2-cluster and 4-cluster models, the mass of the insulation was conserved when compared to the centered configuration, since the models simply shifted the container contents.

Figure 6.8 depicts a top view of the normal 6x6x3 square pitch array used in the HAC analysis. The normal configuration reduced the outer package dimensions but did not shift the interior contents. Figure 6.9 depicts a systematic shift in the interior contents where the distance between the fissile content in every pair of packages was minimized. Figure 6.10 extended the concept shown in Figure 6.9 to groups of four packages. The primary purpose of the two-group and four-group cluster models was to analyze the need for relying on the construction materials and design to maintain the CV integrity and location inside the package. The shift of contents in one direction allowed for mass and volume of the insulating material to be conserved because it was simply displaced in the opposite direction of the shift.

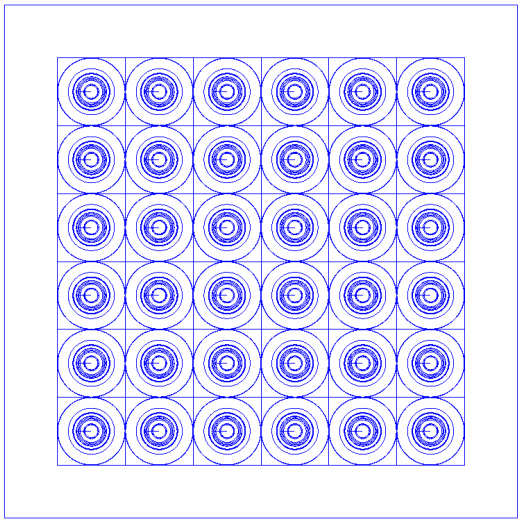

Figure 6.8 Centered Array

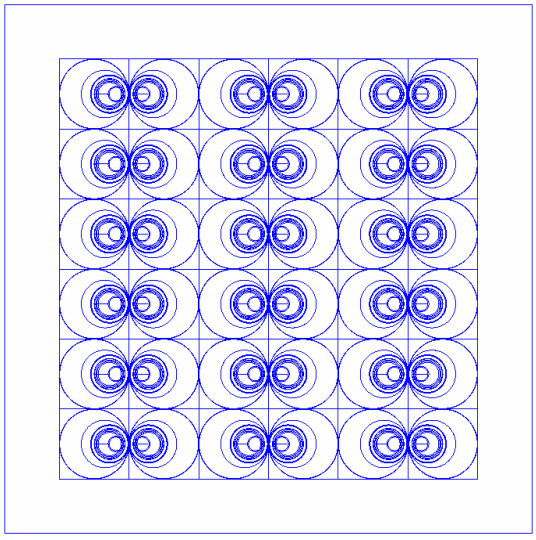

Figure 6.9 Two Cluster HAC Model

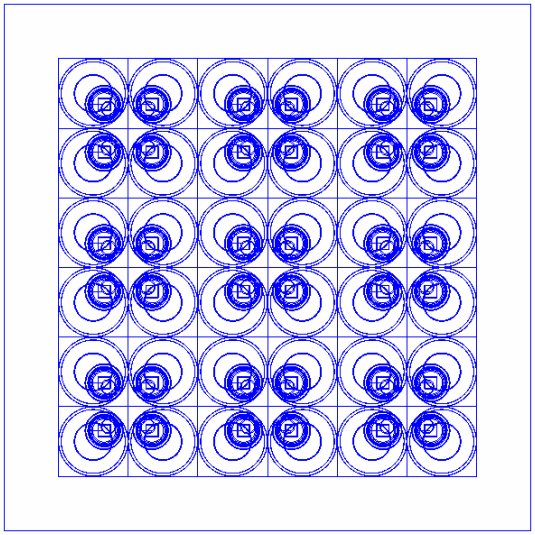

Figure 6.10 Four Cluster HAC Model

6.6.2 Results

The HAC series of calculations reported in Table 6.19 begin with a NCT package in a 6x6x3 array. The study removed insulation, reduced radius and height corresponding to damage, further reduced the radius to approximate a triangular pitch array, and the contents of the packages were studied in two positions that maximize the interaction of the fissile material in the package.

Table 6.19 HAC Analysis Results

Case No.	File ID	Description	k_{eff}	σ	$k_{eff}+2\sigma$
1	hac1_663	6x6x3 square pitch array of drums in contact, array reflected with 30 cm of water in all 6 directions, each drum with 4.4 kg ^{239}Pu sphere surrounded by 100 g polyethylene, no 3013, nominal container dimensions; normal presence of foam, Fiberfrax, Vermiculite and Min-K 2000, fissile sphere radially centered in drum. See Figure 6.1 and Figure 6.8.	0.8371	0.0013	0.8397
2	hac_663_foam	Identical to case 1 but reduced container OD by 2" and the outer height was reduced 2" (1" top and bottom) corresponding to HAC conditions. See Figure 6.3 and Figure 6.8.	0.8474	0.0014	0.8502
3	hac_663	Identical to case 2 but no foam present (all other insulators were present). See Figure 6.3 and Figure 6.8.	0.8604	0.0013	0.8630
4	hac_sym	6x6x3 square pitch array of drums, array reflected by 30 cm water in –x, –y, +z, and –z direction, each drum with 4.4 kg ^{239}Pu sphere radially centered in drum surrounded by 100 g polyethylene, no 3013; no foam, Fiberfrax, Vermiculite or Min-K 2000 present; HAC diameter from case 2 was reduced by 7% to approximate triangular pitch array; HAC top height was reduced by 1". See Figure 6.3 and Figure 6.8.	0.8544	0.0014	0.8572
5	bk_hac_r1_in	Same as case 4 with array reflected by 30 cm of water in all 6 directions.	0.8631	0.0014	0.8659
6	hac_2clus	Same as case 5 but created pairs (2-cluster model) of drums with fissile material, CV, insulation region, etc., displaced to allow closer interaction with fissile material from one other drum. See Figure 6.3 and Figure 6.9.	0.8867	0.0014	0.8895
7	hac_4clus	Same as case 5 but created groups of four drums (4-cluster model) with fissile material, CV, insulation region, etc., displaced to allow fissile material from all four drums to move towards a common center. See Figure 6.3 and Figure 6.10.	0.8818	0.0014	0.8846
8	hac_2clus_water_2_in	Same as case 6 but water fills the liner, and foam regions in the 9977, and between packages in the array.	0.8628	0.0016	0.8660
9	hac_2clus_al_1_in.out	Same as case 6 but replaced Al in LDF with void.	0.8753	0.0014	0.8781
10	hac_2clus_al_2_in.out	Removed void space occupied by LDF in case 9 by shifting CV an additional 1.57 cm closer to edge of package.	0.8875	0.0017	0.8909

All of the cases in Table 6.19 resulted in $k_{eff}+2\sigma$ values significantly less than k_{safe}. This directly demonstrates that a maximum of 4.4 kg ^{239}Pu as metal will remain subcritical inside the 9977 package under HAC conditions. Section 6.5 demonstrated that an analysis with 4.4 kg ^{239}Pu as metal provides a bounding analysis for 13.5 kg ^{235}U as metal. Section 6.5 also demonstrated that an analysis with 4.4 kg ^{239}Pu as metal provides a bounding analysis for 4.4 kg of fissile material in oxide form (PuO_2 or UO_2) with $H/X \leq 3$. Therefore, the HAC analysis results in Table 6.19 bound that of 13.5 kg ^{235}U as metal and 4.4 kg of dry fissile material in oxide form (PuO_2 or UO_2).

Per the requirements of 10 CFR §71.59(a)(2), the optimum interspersed hydrogenous moderation must be considered. The model developed in case 8 exceed the requirement for interspersed moderation in that water was modeled inside the foam and liner regions of each package in the model. Water was not modeled inside the CV since this is not a requirement based on the test results indicating the CV remains helium leak tight.[5] Case 6 was selected as the base case for the moderation study since it had the highest $k_{eff}+2\sigma$ value without moderation. The Table 6.19 result for case 8 indicates that the system reactivity decreases due to the presence of water in the model.

All HAC cases in Table 6.19 were below the k_{safe} value of 0.931. Therefore, the 10 CFR § 71.55(e) and § 71.59(a)(2) requirements related to HAC analyses are satisfied.

6.7 FISSILE MATERIAL PACKAGES FOR AIR TRANSPORT

This section is not applicable since the 9977 Shipping Package will not be used for Air Transport.

6.8 BENCHMARK EVALUATIONS

This section provides the validation of the CSAS26 criticality analysis sequence contained in Version 5 of the SCALE package. Validation is required by the criticality safety standard ANSI/ANS-8.1. The section describes the method, computer program and cross-section libraries used, experimental data, areas of applicability, and bias and uncertainty. A complete description of the benchmarks, and calculation of k-safe, is provided. [25 & 26]

The criticality safety method is CSAS26 embedded in SCALE version 5. CSAS26 includes the SCALE Material Information Processor, BONAMI, CENTRM and KENO VI. The Material Information Processor generates number densities for standard compositions, prepares geometry data for resonance self-shielding, and creates data input files for the cross-section processing codes. The BONAMI and CENTRM codes are used to prepare a resonance-corrected cross-section library in AMPX working format. The KENO VI code uses Monte Carlo techniques to calculate the model k_{eff}. The ENDF/B-V neutron cross-section library was used in the validation.

6.8.1 Code Validation and Bias for Pu and U Metal and Oxide Contents

SCALE 5 has been validated for Pu metal and oxide, Pu solution, highly enriched uranium (HEU) metal, HEU oxide, and HEU solution systems on the WSMS Linux system.[26] The values reported for σ_B in Table 6.20 were taken from the respective reference document indicated. No critical experiments similar to the 9977 shipping package systems with Pu/U metal are available. Therefore, a wide set of validation experiments were chosen for this study. Table 6.20 shows the biased k_{eff} and k_{safe} values for different systems. The NUREG document[27] specifies a minimum required margin of subcriticality of 0.05 for packaging applications. Based on the fact that a large Minimum Subcritical Margin (MSM) has been used for the 9977 analysis using common fissile material (i.e., ^{239}Pu and ^{235}U) and drum components, no additional margin due to 'areas of applicability' is necessary.

The results of the indicated validation reports were evaluated to determine the k_{safe} value applicable to this analysis. It is seen from Table 6.20 that the lowest k_{safe} value derived from the WSMS validations is 0.931. Therefore, a k_{safe} value of 0.931 is used in this evaluation.

Table 6.20 Validation K_{safe} Values

System	Biased k_{eff} Value k_B	Minimum Subcritical Margin (MSM) $- \sigma_M$	k-safe SCALE 5, 238-group $= k_{safe}$
Plutonium Metal	0.981	0.05	0.931
Uranium Metal	0.981^+	0.05	0.931
Plutonium Solution	0.997	0.05	0.947
Uranium Solution	0.991	0.05	0.941
Plutonium Oxide, dry	0.996	0.05	0.946
Uranium Oxide, dry	0.988	0.05	0.938
+ 0.981 is the value at the lowest point on the lower tolerance band curve.			

6.9 REFERENCES

1. *Packaging and Transportation of Radioactive Material*. Code of Federal Regulations, Title 10, Part 71, Washington, DC (January 2002).
2. *Standard Format and Content of Part 71 Applications for Approval of Packages for Radioactive Material*, Regulatory Guide 7.9, Revision 2, U.S. Nuclear Regulatory Commission, Washington, DC (March 2005).
3. *RISC Computer Code Collection, SCALE 5, Modular Code System for Performing Standardized Computer Analyses for Licensing Evaluation,* CCC-725, Oak Ridge National Laboratory, Oak Ridge, Tennessee (April 2005).
4. B. R. Kerr, *NCSE 9977 Shipping Package Analysis for SARP (U)*, N-NCS-A-00014, Rev. 0, Washington Safety Management Solutions, LLC, Aiken, SC (February 2006).
5. L.F. Gelder, C.M. May, *9977 General Purpose Fissile Packaging Prototype Testing*, M-TRT-A-00007, Rev. 0, Washington Savannah River Company, Aiken, SC (February 2006).
6. J. Malloy, *SRNL Package Burn Test Report*, NT-TDR-06-101, Rev. 0, NovaTech Innovative Technologies International, Lynchburg, VA (February 2006).
7. *Nuclear Criticality Control of Special Actinide Elements,* ANSI/ANS-8.15-1981.
8. B. R. Kerr, *NCSE: Minimum Mass of Concern for Carbon and Beryllium in Solid Waste*, N-NCS-E-00028, Rev. 0, Washington Safety Management Solutions, LLC, Aiken, SC (July 2005).
9. R-R3-F-0016, Rev. 10, *9975 Shipping Package – Containment Vessel Weldments*, Westinghouse Savannah River Company, Aiken, SC (June 2004).
10. *Stabilization, Packaging, and Storage of Plutonium-Bearing Materials*, DOE-STD-3013-2000, United States Department of Energy, Washington, D.C., (September, 2000).
11. D. F. Hollenbach, L. M. Petrie, and N. F. Landers, *KENO-VI: A General Quadratic Version of the KENO Program*, ORNL/TM-2005/39, Version 5, Vol. II, Book 3, Sect. F17, Oak Ridge National Laboratory (April 2005).
12. R-R2-G-00018, Rev. 0, *9977 General Purpose Fissile Package - Drum Lid Subassembly,* Washington Savannah River Company, Aiken, SC (February 2006).
13. R-R2-G-00017, Rev. 0, *9977 General Purpose Fissile Package - Drum and Liner Subassembly*, Washington Savannah River Company, Aiken, SC (February 2006).
14. R-R4-G-00032, Rev. 0, *9977 General Purpose Fissile Package - Spacer Part Details for 6-inch Containment Vessel*, Washington Savannah River Company, Aiken, SC (February 2006).
15. R-R2-G-00042, Rev. 0, *9977 General Purpose Fissile Package - 6-inch Diameter Containment Vessel (CV) Subassembly*, Washington Savannah River Company, Aiken, SC (February 2006).
16. R-R3-F-0016, Rev. 10, *9975 Shipping Package – Containment Vessel Weldments*, Westinghouse Savannah River Company, Aiken, SC (June 2004).
17. Biswas, D., *NCSE: 9975 Shipping Container Analysis with Revised Contents for SARP, Rev. 0*, Rev. 2, October 2003.

18. *Nuclear Criticality Safety in Operations with Fissionable Materials Outside Reactors*, ANSI/ANS-8.1-1998.

19. NUREG/CR-0095, ORNL/NUREG/CSD-6, *Nuclear Safety Guide TID-7016 Revision 2* (May 1978).

20. Kerr, B. R., *NCSE: Minimum Mass of Concern for Carbon and Beryllium in Solid Waste*, N-NCS-E-00028, Rev. 0, Washington Safety Management Solutions, LLC, Aiken, SC (July 2005).

21. Abramczyk, G. A., *RE: Material Properties for Components of the 9977*, SRNL-IES-2006-00007, Washington Savannah River Company, Aiken, SC (February 2006).

22. R-R4-G-00033, Rev. 0, *9977 General Purpose Fissile Package – Spacer Part Details for Five Inch Containment Vessel*, Washington Savannah River Company, Aiken, SC (February 2006).

23. L.M. Petrie, P.B. Fox, and K. Lucius, *Standard Composition Library*, ORNL/TM-2005/39, Version 5, Vol. III, Sect. M8, Oak Ridge National Laboratory, (April 2005).

24. *CRC Handbook of Chemistry & Physics*, 77th Ed., 1996.

25. N.M. Green, et. al., *The LAW-238 Library – A Multigroup Cross-Section Library for Use in Radioactive Waste Analysis Calculations*, ORNL/TM-12370, Oak Ridge National Laboratory, Oak Ridge, TN, (August, 1994).

26a. S. M. Revolinski, *WSMS SCALE Version 5: Plutonium Metal and Oxide Validation for LINUX-5 Workstation Cluster*, WSMS-CRT-05-0007, Rev. 0, (February 2005).

26b. S. M. Revolinski, *WSMS SCALE Version 5: Highly Enriched Uranium Metal Validation for Linux 5 Workstation Cluster*, WSMS-CRT-05-0026, Rev. 0, Washington Safety Management Solutions, LLC, Aiken, SC (May 2005).

26c. S. M. Revolinski, *WSMS SCALE Version 5: Highly Enriched Uranium Solution Validation for LINUX-5 Workstation Cluster*, WSMS-CRT-05-0056, Rev. 0, Washington Safety Management Solutions, LLC, Aiken, SC (August 2005).

26d. S. M. Revolinski, *WSMS SCALE Version 5: Plutonium Solution Validation for Linux 5 Workstation Cluster*, WSMS-CRT-05-0067, Rev. 0, Washington Safety Management Solutions, LLC, Aiken, SC (September 2005).

26e. S. M. Revolinski, *WSMS SCALE Version 5: HEU Oxide Validation for Linux 5 Workstation Cluster*, WSMS-CRT-05-0091, Rev. 0, Washington Safety Management Solutions, LLC, Aiken, SC (October 2005).

27. NUREG/CR-5661, ORNL/TM-11936, *Recommendations for Preparing the Criticality Safety Evaluation of Transportation Packages* (April 1997).

6.10 APPENDICES

Appendix	Description
6.1	Nuclear Criticality Safety Evaluation: 9977 Shipping Package Analysis for SARP

Input Files

Input and output Files are provided on a CD included with the SARP

This Page Intentionally Left Blank

APPENDIX 6.1

NUCLEAR CRITICALITY SAFETY EVALUATION

This Page Intentionally Left Blank

WASHINGTON SAFETY MANAGEMENT SOLUTIONS
Criticality And Radiation Transport Services

March 2006

Classification
UNCLASSIFIED
DOES NOT CONTAIN
UNCLASSIFIED CONTROLLED
NUCLEAR INFORMATION

DC and Reviewing Official:

Steven J. Nathan, WSMS
Date: March 2, 2006
IG-SR-3, 2/04

KEYWORDS:
SARP
9977
Shipping Package
Plutonium
Uranium

Retention:
Lifetime

Nuclear Criticality Safety Evaluation: 9977 Shipping Package Analysis for SARP

APPROVALS

Author Criticality Safety Support	B. R. Kerr	3/2/2006 Date
Technical Review Radiological Engineering	R. L. Reed	3/2/06 Date
Manager Radiological Engineering	J. Brotherton	3/2/06 Date
Facility Reviewer: SRNL Packaging Technology	P. S. Blanton	5/17/06 Date

Distribution

E. F. Trumble	CCC-3	R. L. Reed	CCC-3
J. Brotherton	CCC-3	S. J. Nathan	CCC-3
P. S. Blanton	773-41A		
G. A. Abramczyk	773-42A	WSMS CRT Files c/o Lori Korth	CCC-3
J. S. Bellamy	773-41A	WSMS Files c/o Debbie Strautmann	CCC-3
B. R. Kerr	CCC-3	Records Management	730-B

DISCLAIMER

Revision Summary

Rev. #	Author	Changes	Date
0	B. R. Kerr	Initial issuance.	March 2006

Table of Contents

List of Tables

List of Figures

1 Introduction

A new general purpose fissile material shipping package, assigned the model number 9977, has been designed to ship plutonium and highly enriched uranium metal and oxide in the DOE complex. This Nuclear Criticality Safety Evaluation (NCSE) demonstrates the safe configurations of the new shipping package for plutonium and uranium metal/oxide loading under various conditions for the Safety Analysis Report for Packaging (SARP). This evaluation is in compliance with the performance requirements of Title 10 of the Code of Federal Regulation (CFR), specifically 10 CFR 71.55 and 71.59 for criticality safety.

The evaluation in this NCSE demonstrates that the 9977 shipping package is subcritical with adherence to design features, limits and controls specified in Section 7.

1.1 Overview and Scope

This NCSE has specifically addressed and/or assessed the following features:

i) The criticality safety index (CSI) should be as low as achievable, preferably 1.0 or less, to maximize flexibility during transportation.
ii) Water is assumed to leak into the Containment Vessel (CV) as well as the overpack package container for the single package (SP) analysis.
iii) The CV remains dry during the normal conditions of transport (NCT) and the hypothetical accident conditions (HAC).
iv) A very conservative HAC model was analyzed. The HAC model included reduction of package diameter and height based on drop and crush test results, as well as loss of foam insulation during a fire and extreme movement of the CV within the drum. The 9977 shipping package drop test data and the foam burn data taken from the test reports form the basis of the HAC calculations.
v) The models were developed from the drawings provided (see Table 3).
vi) Nominal dimensions of the 9977 components were used in this analysis.
vii) A mass of 100 grams of plastic material (polyethylene or equivalent) was conservatively assumed to be closely wrapped around the plutonium/uranium metal. Polyethylene $(C_2H_4)_n$ with a density not exceeding 0.95 g/cc is used as the plastic material, as it has the highest hydrogen density among the common forms of plastic materials and has the highest reactivity effect.
viii) All fissile material placed in a 9977 shipping package will have been processed in accordance with DOE-STD-3013. The material may be in a 3013 can or a non-3013 can inside the CV.

2 Description

The information provided in this section is intended only as descriptive information and is not intended to specify any controls or limits on the 9977 shipping package. Nuclear Criticality Safety controls and limits are specified in Section 7 of this NCSE.

The content envelopes, geometry, and materials of construction for the 9977 shipping package are described in the following subsections.

2.1 Content Envelopes

The content envelopes requested for evaluation, as specified in Reference 1, are presented in Table 1 and Table 2. See Section 6.2 for a discussion of each content envelope related to this NCSE.

Table 1: Requested Content Envelopes C.1 - C.3

	Material	C.1 Heat Sources	C.2 Pu/U Metals	C.3 Pu/U Oxides
Fissile Material Maximum Weight %	^{238}Pu	100	2	Reserved For Future Use
	^{239}Pu	40	100	
	^{240}Pu	13	40	
	^{241}Pu	1	15	
	^{242}Pu	1.5	5	
	^{232}U	1.4×10^{-4}	1×10^{-7}	
	^{233}U	0.2	0.5	
	^{234}U	40	100	
	^{235}U	40	100	
	^{236}U	16	40	
	^{238}U	40	100	
Impurities (grams)	Ca	15	--	
	Fe	5	--	
	Cr	2	--	
Maximum Total Mass (kilograms)	Radioactive Materials	0.1	4.4	
	Impurities	0.02	3.08	
	All Contents	0.1	4.4	

Table 2: Requested Content Envelopes C.4 - C.5

	Material	C.4 Metal or Alloy H/X=0	C.5 Compounds H/X=0	C.5 Compounds H/X≤ 3
Fissile Material Mass (kg)	^{233}U	Reserved For Future Use		
	^{235}U	13.5	4.4	4.4

2.2 9977 Shipping Package – Geometry

The 9977 shipping package consists of a 35-gallon stainless steel drum with an external (nominal) diameter and height of 18.72" and 36.1", respectively. Each 9977 has one containment vessel (CV). There are two size options for the CV. The 6" CV will be used only for content envelope C.1 and the 5" CV will be used for content envelopes C.2, C.3, C.4 and C.5. The need for the 6" CV is based on the size of the heat sources.

The 5" CV for fissile material transport is a stainless steel pressure vessel with a nominal 5.047" inner diameter (ID) and is 17.75" high[2]. Nuclear material contained in a product can is loaded into the CV. The CV is sealed with a stainless steel plug and locking nut. The steel plug (attached to the locking nut) that screws into the CV body has two O-rings that provide a leak tight seal. The confinement boundary is the flanged stainless steel 35-gallon drum. The containment boundary is defined as the CV body, the inner O-ring and the CV plug. This containment boundary applies to both the 5" and 6" CV.

The CV body is placed on an aluminum bottom load distribution fixture (LDF). There is also an aluminum top LDF to cover the CV head. The CV and the CV load distribution fixtures are placed inside the steel liner. The liner is welded to the top lid flange. Foam and Fiberfrax surround the liner to fill the remainder of the 35-gallon package. The package lid has a bottom liner filled with Vermiculite and Fiberfrax insulation and a top liner filled with Min-K 2000 insulation.

Figure 1 shows a schematic of the 9977 shipping package with a 6" CV. Figure 2 depicts the 9977 package with a 5" CV. Table 3 provides the dimensions of the 9977 package including the 6" CV and the 5" CV. The differences in the two figures are all within the liner where the CV and supporting spacers are placed. Inside the liner, the 5" CV requires additional spacing material to maintain its horizontal and vertical position. These spacers are aluminum honeycomb (see Table 4 for material details) and the dimensional details of these three spacers are also provided in Figure 2.

The 5" CV will contain product cans with fissile material. Product cans that comply with DOE-STD-3013[3] are thick walled welded stainless steel cans. The 3013 container is comprised of a convenience can located inside two nested welded inner and outer containers. Product cans that do not comply with DOE-STD-3013 are commonly thin walled (soup can) with a screw top, crimp seal, or slip-lid top. The non-3013 product cans vary widely in height and diameter.

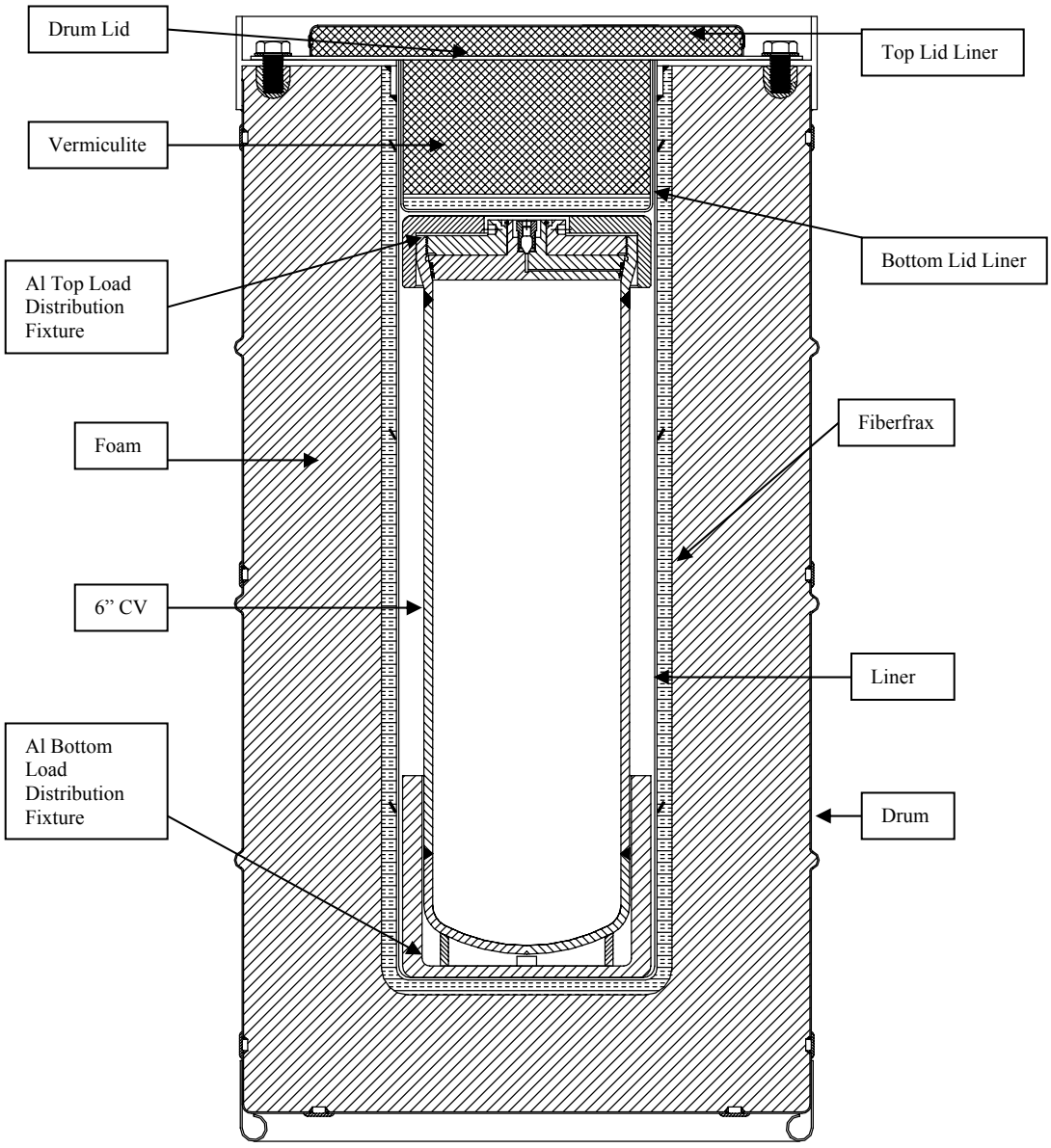

Figure 1: 9977 Shipping Package with 6" CV

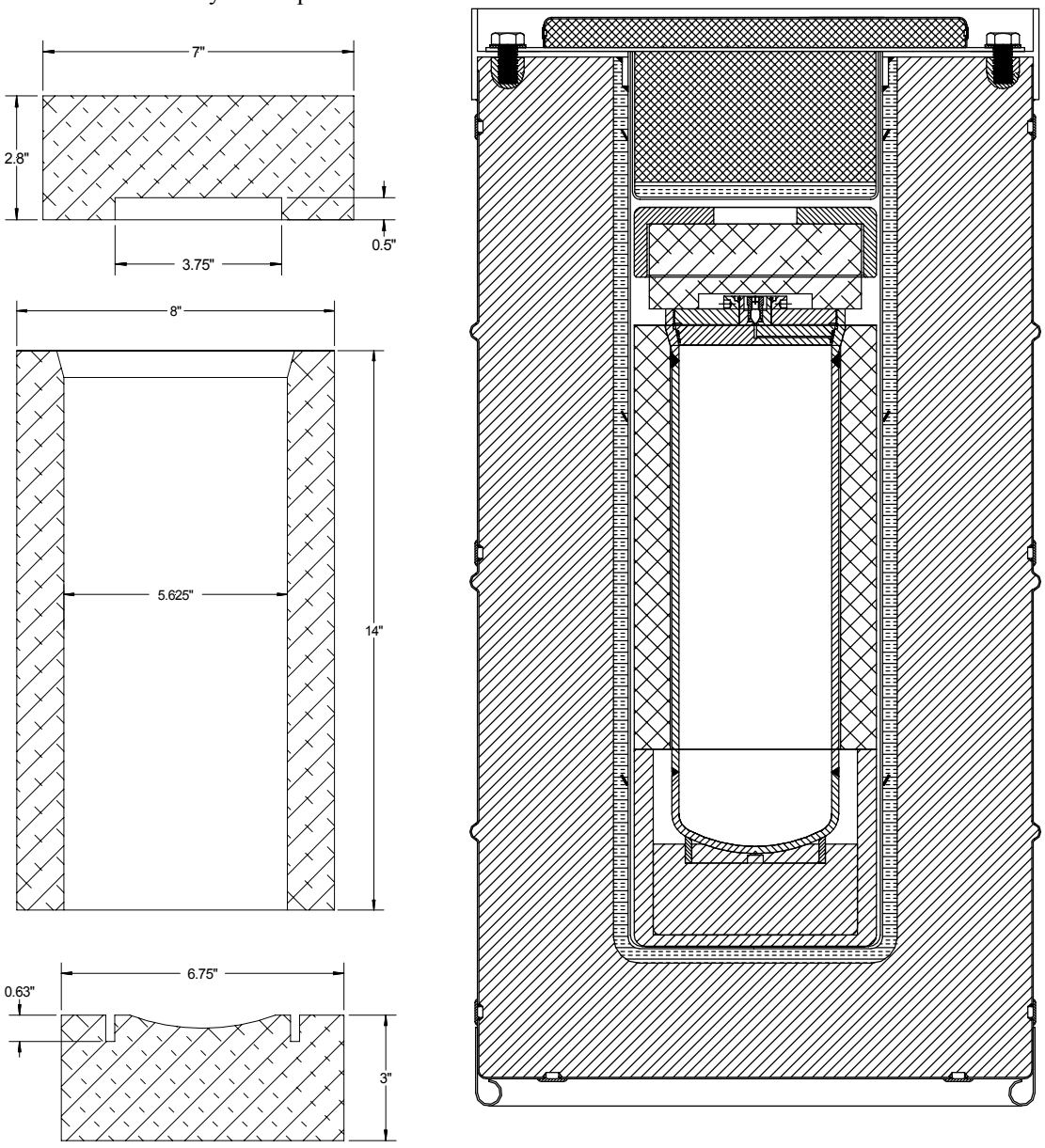

Figure 2: 9977 Shipping Package with 5" CV

Table 3: Geometric Specifications for the 9977 Shipping Packages

Sheet 1 of 4

Component	Parameter	Specification (inch)	KENO Model (cm)	Reference
Drum Lid Plate	OD	17.8	--	R-R2-G-00018[4]
	OR	8.9	22.606	
	Thickness	0.125	0.3175	
Drum Liner	OD	8.346	--	R-R2-G-00017[5]
	OR	4.173	10.5994	
	ID	8.25	--	
	IR	4.125	10.4775	
	Internal Height	29.5	74.930	
	Thickness	18 gauge (0.048)	0.1219	
Drum	ID	18.25	--	R-R2-G-00017
	IR	9.125	23.1775	
	OR	9.125 + 0.048 (18 GA) = 9.173	23.2994	
	External Height	36.1	86.868 †	
	Inner Height	33.1	86.7461 †	
	Thickness	18 gauge (0.048)	0.1219	

† It is noted that the KENO model values (in centimeters) are not equivalent to the specification values (in inches). These differences are conservative for this analysis.

Table 3: Geometric Specifications for the 9977 Shipping Packages

Sheet 2 of 4				
Component	**Parameter**	**Specification (inch)**	**KENO Model (cm)**	**Reference**
Aluminum Bottom Support	ID	6.75		R-R4-G-00032[6]
	IR	3.375	8.573	
	OD	8.00		
	OR	4.00	10.160	
	Internal Height	6.13	15.5702	
	External Height	6.50	16.51	
	Side Thickness	0.625	1.5875	
	Bottom Thickness	0.370	0.9398	
Aluminum Top Support	ID	7.15		R-R4-G-00032
	IR	3.575	9.081	
	OD	8.0		
	OR	4.0	10.160	
	Internal Height	1.75	4.445	
	External Height	2.30	5.842	
	Side Thickness	0.425	1.0795	
	Top Thickness	0.550	1.397	
	Central Hole	2.75x2.75	6.985x6.985	

Table 3: Geometric Specifications for the 9977 Shipping Packages

Sheet 3 of 4

Component	Parameter	Specification (inch)	KENO Model (cm)	Reference
6" CV	Upper OD	7.12		R-R2-G-00042[7]
	Upper OR	3.56	9.042	
	Upper ID	6.31	16.028	
	Cylinder OD	6.625		
	Cylinder OR	3.313	8.414	
	Cylinder ID	6.065		
	Cylinder IR	3.033	7.703	
	External Height	23.12	58.725	
	Max. Internal Solution Height	21.22	53.57 †	
	Side Thickness	0.28	0.7112	
	Top Steel portion Height	0.75	1.905	
	Tapered Portion Height	0.82	2.21 †	
	Height up to Leg	23.5	59.69	
	Leg OD	5.563	14.13	
	Leg ID	5.047	12.82	

† It is noted that the KENO model values (in centimeters) are not equivalent to the specification values (in inches). These differences are conservative for this analysis.

Table 3: Geometric Specifications for the 9977 Shipping Packages

Sheet 4 of 4				
Component	**Parameter**	**Specification (inch)**	**KENO Model (cm)**	**Reference**
5" CV	Upper OD	5.87	15.498 †	R-R3-F-0016[2]
	Upper ID	5.27	14.13 †	
	Cylinder OD	5.563	14.13	
	Cylinder ID	5.047	12.82	
	External Height	17.75	46.16 †	
	Max. Internal Solution Height	15.87	41 †	
	Side Thickness	0.258	0.655	
	Tapered Portion Height	1.62	4.445 †	
	Bottom of leg up to bottom of CV	0.31	Not specified	
	Leg OD	4.5	11.43	
	Leg ID	4.026	10.226	
Lid Liner Bottom	ID	7.98		R-R2-G-00018
	IR	3.99	10.147 †	
	OD	8.13		
	OR	4.065	10.325	
	Internal Height	4.81	12.207 †	
	External Height	4.88	12.395	
	Thickness	0.075	0.178 †	
Lid Liner Top	ID	13.904		R-R2-G-00018
	IR	6.952	17.658	
	OD	14.0		
	OR	7.00	17.780	
	Internal Height	0.952	2.418	
	External Height	1.00	2.54	
	Thickness	0.048 (18 gauge)	0.122	
DRUM Flange	Thickness	3/16	0.4763	R-R2-G-00017
† It is noted that the KENO model values (in centimeters) are not equivalent to the specification values (in inches). These differences are conservative for this analysis.				

2.3 9977 Shipping Package - Materials of Construction

The CV and the drum are made of 304L stainless steel. The liner, lid plate, top and bottom lid liner shells are also made of 304L stainless steel.

Reference 8 provides material specifications for the 9977 components modeled in this NCSE.

There are four types of insulating materials used in the 9977. The foam used in the drum is General Plastics Last-A-Foam FR-3716. The foam density was specified as 16 lb/ft^3 (0.2563 g/cc) in Reference 8. Fiberfrax insulation surrounds the liner in the drum and is also placed on the bottom of the bottom lid liner. It consists of Fiberfrax HSA, Grade E and is 1 inch thick and has a nominal density of 16 lb/ft^3 (0.2563 g/cc) [8]. The Fiberfrax insulation is sheathed with Fiberglass, Grade E on both sides. Vermiculite insulation in the bottom lid liner is a type of thermal ceramic, TR-19, and is made of Vermiculite granules and high temperature bonding material and has a density of 23 lb/ft^3 (0.3684 g/cc) [8]. This material exhibits minimal shrinkage at high temperature and will not decompose even when exposed directly to flame. The top lid liner contains a thermal ceramics material called Min-K 2000. It is made of silica and glass wool products and the nominal density is 20 lb/ft^3 (0.3204 g/cc) [8].

The top and bottom aluminum LDF are solid. The standard material density of aluminum is 2.7 g/cc. Aluminum honeycomb is used as a spacer around the 5" CV. The honeycomb bulk density is reported as 12 lbs/ft^3 (0.1922 g/cc)[9].

The 9977 shipping package material data are shown in Table 4 through Table 8. Table 4 also lists other materials (e.g., water) and densities used in the Section 6 analysis in addition to the 9977 package construction materials.

Table 4: Material Specifications for the 9977 Package

Components	Material	Density (g/cc) (as-modeled)	Reference
Water	H_2O	0.9982 at 20°C 0.99998 at 4°C (used 1.0 g/cc)	References 10 and 11
CV & Liner	304L-Stainless Steel (used SS 304)	7.94	Reference 10
Aluminum Top and Bottom Support Plates	Aluminum	2.7	Reference 10
Aluminum Honeycomb	Aluminum	0.1922 g/cc	Reference 9
Polyethylene	C_2H_4	0.92 (used 0.95 g/cc)	Reference 10
Foam See Table 5	General Plastics Last-A-Foam, FR-3716	16 lb/ft^3 (0.2563 g/cc)	Reference 8
Fiberfrax See Table 6	Fiberfrax HSA, Grade E	16 lb/ft^3 (0.2563 g/cc)	Reference 8
Vermiculite See Table 7	Thermal Ceramics, TR-19	23 lb/ft^3 (0.3684 g/cc)	Reference 8
Min-K 2000 See Table 8	Thermal Ceramics	20 lb/ft^3 (0.3204 g/cc)	Reference 8
Fissile Content	Pu Metal	19.84	Reference 10
	U Metal	19.05	
	Pu Oxide	11.46	
	U Oxide	10.96	

Table 5: Foam Composition

Elements	Wt %, Sample A	Wt %, Sample B	Normalized for KENO input
Cl	0.1	0.2	0.15
Si	*	*	0.82
P	*	*	0.82
O	22.42	22.78	22.60
C	62.85	62.9	62.88
H	6.84	6.84	6.84
N	5.9	5.88	5.89
Total	98.11	98.6	100.00
* Si and P are known to be present, but were not measured.			

Table 6: Fiberfrax Composition

Compound	Wt %	Wt %, (average) For KENO
Al_2O_3	46-54	50
SiO_2	46-54	49.5
Na_2O	0.5	0.5
Total		100
Elements		**Calculated**
Al		26.462
Si		23.138
Na		0.3709
O		50.029
Total		100

Table 7: Vermiculite Composition

Compound	Wt % (after fire)	Wt % (normalized) before fire	Elements	Wt% For KENO
SiO_2	40	45.403	Si	21.223
Al_2O_3	9.1	10.3292	Al	5.4667
CaO	15	17.0261	Ca	12.168
Fe_2O_3	6.8	7.7185	Fe	5.3985
TiO_2	1.2	1.36209	Ti	0.8164
MgO	13	14.756	Mg	8.8984
Na_2O	1.3	1.4756	Na	1.0947
K_2O	1.3	1.4756	K	1.225
SO_3	0.4	0.45403	S	0.1818
Total	88.1	100.000	O	43.527
			Total	100

Table 8: Min-K 2000 Composition

Compound Name	Compound	Minimum Wt%	Maximum Wt%	Average Wt%	Normalized Wt%
Amorphous Silica	SiO_2	35	95	65	48.01
Fibrous Silica	SiO_2	5	30	17.5	12.92
Micronized Silicon	Si	0	25	12.5	9.23
Titanium Dioxide	TiO_2	0	25	12.5	9.23
Hydrated Alumina	$Al(OH)_3$	0	50	25	18.46
Decabromodiphenyl Oxide	C_7H8O_2	0	5	2.5	1.85
Antimony Trioxide	Sb_2O_3	0	0.3	0.15	0.11
Phenol Formaldehyde Resin	$C_{12}Br_{10}O$	0	0.5	0.25	0.18
Total				135.4	100
	Element	**Calculated wt%**			
	Si	37.71			
	Ti	5.53			
	Al	6.39			
	C	1.28			
	H	0.84			
	O	48.01			
	Sb	0.09			
	Br	0.15			
	Total	100			

3 Requirements Documentation

This NCSE is prepared in accordance with the Savannah River Site Nuclear Criticality Safety Manual[12], the Nuclear Criticality Safety Methods Manual[13] and 10 CFR 71, 'Packaging and Transportation of Radioactive Materials' [14].

The NUREG guidance document[15] prepared by the Oak Ridge National Laboratory (ORNL) for criticality safety evaluation of transportation packages was also followed.

4 Methodology

The following sections provide a high level overview of the criticality safety computer codes used in this analysis, justify the biased k_{eff} value (k_b) and the minimum subcritical margin, define the area of applicability, and justify a value for k_{safe} for this analysis. Other sections address material compositions and various analysis methods utilized in this analysis.

4.1 Computer Codes

The SCALE 5 / KENO VI code system[16] operating on the WSMS Linux Workstation Cluster was used to calculate k_{eff} values for this study. The SCALE system is under configuration control[17, 18]. The CSAS26 driver was used. It calls the BONAMI and CENTRUM modules for the generation of a problem-dependent cross sections library (accounting for resonance self-shielding) and then calls the KENO VI module to perform the Monte Carlo k_{eff} calculations. The 238-group ENDF/B-V cross section set[19] was used for all calculations. Calculations were performed using numbers of generations and neutrons per generation to achieve a calculated statistical uncertainty (σ) less than 0.002.

4.2 Code Validation and Bias

SCALE 5 has been validated for Pu metal and oxide[20], Pu solution[21], highly enriched uranium (HEU) metal[22], HEU oxide[23], and HEU solution[24] systems on the WSMS Linux system. The values reported for k_B in Table 9 were taken from the respective reference document indicated. No critical experiments directly similar to the 9977 shipping package systems with Pu/U metal are available. Table 9 shows the biased k_{eff} and k_{safe} values for various systems. The NUREG document[15] specifies a minimum required margin of subcriticality of 0.05 for packaging applications. Based on the fact that a large Minimum Subcritical Margin (MSM) has been used for the 9977 analysis using common fissile material (i.e., ^{239}Pu and ^{235}U) and drum components, no additional margin due to 'areas of applicability' is necessary.

Table 9: Validation K_{safe} Values

System	Biased k_{eff} Value k_B	Minimum Subcritical Margin (MSM) $-\sigma_M$	$= k_{safe}$
Plutonium Metal	0.981	0.05	0.931
Uranium Metal	0.981[+]	0.05	0.931
Plutonium Solution	0.997	0.05	0.947
Uranium Solution	0.991	0.05	0.941
Plutonium Oxide, dry	0.996	0.05	0.946
Uranium Oxide, dry	0.988	0.05	0.938
+ 0.981 is the value at the lowest point on the lower tolerance band curve.			

The results of the indicated validation reports were evaluated to determine the k_{safe} value applicable to this analysis. It is seen from Table 9 that the lowest k_{safe} value derived from the WSMS validations is 0.931. Therefore, a k_{safe} value of 0.931 is used in this evaluation.

4.3 Material Compositions

Table 4 provides a summary of materials used in this analysis, the density of the material based on reference information, and the material density as modeled. The following is a brief discussion of the modeling choices made for this analysis.

Plutonium metal was modeled with a density of 19.84 g/cc. Plutonium was conservatively modeled as 100% by weight ^{239}Pu. Uranium metal was modeled with a density of 19.05 g/cc. The isotopic distribution for uranium was 100% ^{235}U. Lower densities were not studied since these maximum theoretical densities provide bounding results.

Plutonium was also modeled as PuO_2 with 100% by weight ^{239}Pu and a density of 11.46 g/cc. Uranium was also modeled as UO_2 with 100% by weight ^{235}U and a density of 10.96 g/cc. Lower densities were not studied since these maximum theoretical densities provide bounding results.

The "Standard Composition Library" in SCALE was used for the compositions of polyethylene, ^{239}Pu, ^{235}U, PuO_2, UO_2, SS 304, aluminum, and water.

Water density is conservatively taken as 1.0 g/cc instead of a nominal value of 0.9982 g/cc at 20ºC to cover temperatures as low as 0º C.

Polyethylene (C_2H_4) is conservatively used to represent plastic materials, as it has the highest hydrogen density among common types of plastic materials. The nominal polyethylene density is about 0.92 g/cc; however, a slightly higher density of 0.95 g/cc is used for conservatism.

Stainless Steel 304 with a density of 7.94 g/cc was modeled in the analysis although SS 304L was used to construct many of the package components. Based on the study in Appendix 2 of Reference 25, the small difference in composition between SS 304 and SS 304L will have a negligible effect on reactivity.

4.4 Analysis Methods

The following subsections contain some additional discussion on particular components or contents pertinent to the methods employed by this analysis.

4.4.1 Containment Vessel

The 6" CV was modeled for the NCT and HAC configurations. However, the 5" CV was modeled for the SP configurations. During the course of this analysis it became apparent that the 6" CV volume was too large for the SP configurations required by 10 CFR 71 to remain subcritical over the desired fissile mass range. Thus, the SP configurations dictated the need for the 5" CV. The 6" CV for the NCT and HAC analyses is equivalent to the 5" CV since the distances between interacting fissile masses would not be affected by the CV dimensions. The 5" CV has aluminum honeycomb spacers holding it farther from the liner than the 6" CV. Thus a more realistic model for the 5" CV could result in modeling greater separation distance between fissile units in adjacent packages for the HAC analysis (2-cluster and 4-cluster configurations). Since modeling greater separation distance between fissile units in adjacent packages reduces the system reactivity, the 6" CV model is equivalent to the 5" CV model.

The 6" CV was modeled with a wall thickness of 0.28" (Reference 7) and the 5" CV was modeled with a wall thickness of 0.258" (Reference 2) for a difference of 0.022". Appendix 3 of Reference 25 demonstrated that k_{eff} varied by approximately 1% as the steel thickness of 3013 cans ranged from 0" to 0.16". Since Appendix 3 of Reference 25 studied the steel 3013 can which is closer to the fissile material than the walls of the CV, the 0.022" difference in wall thickness between the 5" CV and the 6" CV has a negligible effect on calculated reactivity.

4.4.2 Compounds or Oxides

This NCSE only considers the presence of PuO_2 and UO_2 in the content envelopes C.3 and C.5. This excludes other fissile compounds until further analyses demonstrate their compliance to the 10 CFR 71 requirements.

4.4.3 Geometry Modeling

Table 3 lists the specification dimensions of various components of the 9977 shipping package, the as-modeled dimensions of each component, and the reference drawings providing the specifications for each component. The specification column of Table 3 indicates the nominal (reference) dimensions of each component. The KENO model column indicates the values that were used for the base KENO models (see the Section 6 descriptions of the KENO models).

5 Discussion of Contingencies

The contingencies that are to be considered for the 9977 shipping package criticality analysis are specified in 10 CFR 71[14]. Specifically, the objective of this evaluation is to demonstrate compliance with the performance requirements for each content envelope as specified in

- 10 CFR 71.55 – General requirements for fissile material packages,
- 10 CFR 71.59 – Standards for arrays of fissile material packages.

The requirements of 10 CFR 71 are thorough and ensure that the maximum value of k_{eff} is found in the analysis based on prescribed configurations. These configurations are related to and bounding of the conditions (including accident scenarios) a shipping package may be subjected to during its service life. 10 CFR 71 requires that the system k_{eff} remain less than k_{safe} for each of the prescribed configurations. Thus, 10 CFR 71 does not require a contingency analysis.

6 Evaluation of Results

Calculations and evaluations were performed to demonstrate that the 9977 shipping packages with approved contents could be safely transported.

6.1 Model Descriptions

The base KENO model was developed from the set of drawings referenced in Table 3. Table 3 includes specifications and as-modeled dimensions for various components of the 9977 shipping package.

6.1.1 Modeling Approximations

Reference 5 indicates that the bottom of the 9977 package may be convex with a tolerance range from 0.5-0.9 inches. However, the use of a right circular cylinder to approximate this portion of the package does not adversely impact the analysis.

Nominal 9977 component dimensions were used, since the dimensional tolerances are small and their effects on reactivity are insignificant (see Section 6.6). In this analysis, the three rolling hoops of the 9977 containers were neglected. Neglecting these geometric details reduces the effective drum diameter, which in turn conservatively models the array pitch.

In summary, approximations made to the 9977 SCALE/KENO model are:

- Drum is approximated as a right circular cylinder at the bottom,
- Rolling hoops are ignored.

6.1.2 NCT and HAC Dimensions

Table 10 shows the 9977 drum dimensions used for the single package, NCT and HAC models. These are the primary dimensions modified from Table 3.

Table 10: Drum Dimensions for SP, NCT & HAC Models

Dimension	Specification	Single Package Model	NCT Model (cm)	HAC Model (cm)
Drum Inner Radius	23.1775 cm	23.1775 cm	Same as SP	19.3063 - 0.1684 = 19.1379
Drum Wall Thickness	(0.048 inch) 0.1219 cm	0.1219 cm	Same as SP	0.1684 (thickness is increased to conserve mass of the drum material)
Drum Outer Radius	23.2994 cm	23.2994 cm	Same as SP	(23.2994-1*2.54) *0.93 = 19.3063 Note: 1.0” (2.54 cm) is the drum radial reduction due to impact (see Table 11)

6.1.3 3013 Containers

The 3013 container is typically comprised of a convenience can inside two nested welded inner and outer containers. The size of the 3013 cans is important in the sense that the smaller the can, the closer the reflection. A sensitivity analysis (Appendix 3 of Reference 25) showed that small 3013 cans with thick walls bound large 3013 cans with thin walls from the point of view of reactivity effects. Appendix 3 of Reference 25 developed the bounding dimensions of the three cans of a 3013 container for the KENO model. The reference 3013 container used in this NCSE is identical to that from Appendix 3 of Reference 25.

6.1.4 Non-3013 Product Cans

Non-3013 product cans commonly used for packaging fissile material are thin wall containers (soup cans). Most of these cans have a slip-lid, screw top, or crimp seal lid. Most of the slip-lid and screw top product cans have some amount of tape on the can to help ensure the lid remains on the can body. Furthermore, it is expected that non-3013 product cans will be wrapped in some amount of plastic during a glovebox bag-out process.

To account for the tape and plastic for non-3013 product cans, 100 g of polyethylene was modeled around the fissile material as a reflector. Thin walled cans were not considered as part of this analysis since the thick steel reflection of a 3013 container is considered bounding for the reflection due to the product can.

6.1.5 Single Package Model

A single 9977 package was modeled and surrounded by 30 cm of water on all sides. All SP models analyzed the 5" CV. The contents of the package were varied to include metal, oxides and solutions. The analysis of the metal and oxide material forms represents the desired fissile mass. The solution analysis meets a 10 CFR 71 requirement to demonstrate that a single package fully flooded under worst case conditions remains subcritical.

For the metal and oxide cases, a sphere of the fissile material and form selected was placed in the radial center of the CV near the bottom to maximize reflection from the CV steel. The radius of the fissile sphere and its vertical center was varied based on the selection of Pu or U, and metal or oxide. Some cases modeled Pu and U oxide with H/X equal to 0 and 3. Some metal and oxide cases considered the presence of 100 g polyethylene as a spherical shell around the fissile material.

A series of calculations was performed by varying the concentration of fissile material in an aqueous mixture. The solution was assumed to be the only material present in the CV. This is conservative since the presence of product cans would add interstitial void and/or absorbers in the fissile solution. For most solution concentrations, the CV was filled with solution to a solution height corresponding to fissile mass and concentration selected.

6.1.6 NCT Model

Most NCT models in this NCSE are infinite in the x, y, and z direction. In the infinite models, there is no leakage from the system and drum spacing is irrelevant. A single 9977 package was modeled inside a tight fitting cuboid and mirror boundary conditions were defined for the four x & y faces and periodic boundary conditions were defined for the z faces of the cuboid using standard KENO options. These boundary conditions reflected all incident neutrons back into the system thus simulating an infinite square pitch array of packages.

In the NCT model, an infinite array of undamaged stacked drums was analyzed with and without the 3013 container in the dry condition. Since the drum does not have a gasket, there is a possibility for water to enter the drum and fill the liner (outside the CV). Several additional cases were analyzed where water is

present in the interstitial spaces between drums and inside the drums to account for the potential presence of water. It is assumed in the NCT array study that no water would enter the CV.

6.1.7 HAC Model

The basic HAC model is described in this section. The variations of the basic model are discussed in Section 6.5.

For the HAC array model, the drum radius was uniformly decreased corresponding to drop and crush test damage in the amount specified in Table 11, and then the radial component was further reduced by 7% to simulate a triangular pitch array. The values listed in Table 11 are bounding of the maximum dents and bulges observed in localized areas on the packages following the completion of all accident testing. The HAC models in this NCSE uniformly reduce the radial and axial dimensions based on these maximum damage values. Therefore, the uniform dimension reductions modeled are very conservative, representing a closer spacing than actually possible with the observed drum damage.

A triangular pitch array model places fissile material units (drums) as close as possible, maximizing the areal density of fissile units, and thereby increasing the reactivity effect due to interaction. It was shown in Reference 15 that if the drum radius in the rectangular array is reduced by 7%, it is equivalent to a triangular pitch drum array in terms of resulting k_{eff} values. In order to preserve the drum wall mass, the drum wall thickness was adjusted (See Table 10).

Conservative assumptions regarding the radial and axial reduction of drum dimensions due to drop and the amount of insulation charred due to fire were used in the damaged array model as shown in Table 11 (see Figure 3). Charred insulation is assumed to be completely vaporized. Additional reduction factors were added to the burn and drop test data for conservatism. The effect of the amount of insulation was also studied. Figure 3 is a sketch of the 9977 package that indicates the dimensions reduced for HAC analysis. Figure 3 contains more detail than present in the model.

The HAC model used a 6x6x3 array of damaged 9977 containers, reflected by 30 cm of water along all sides of the array. The damaged 9977 container was dry. The analysis was performed with and without the 3013 container.

Table 11: Fire and Drop Test Data for the HAC Model

Dimension	Insulation Burn Test Data	HAC Model	Drop Test Data (inch)	HAC Model (inch)
Radial	All foam	All foam and Fiberfrax replaced with void or water	0.5	1.0
Axial (top/bottom)	All Vermiculite	All Vermiculite, Fiberfrax and Min-K 2000 replaced with void or water	1 ⅛ (total)	2.0/1.0
Reference	Reference 26		Reference 27	

A conservative HAC model is constructed by assuming maximum movement of the CV. Fissile origin (coordinates) varies depending on whether it is inside the 3013 or in a food pack can. This movement gets the fissile mass to the side of the CV or the side of the 3013 container. Figure 4 depicts the package contents shifted to the left for maximum interaction with another package for a two-cluster configuration. The two-cluster configuration is discussed further in Section 6.5.

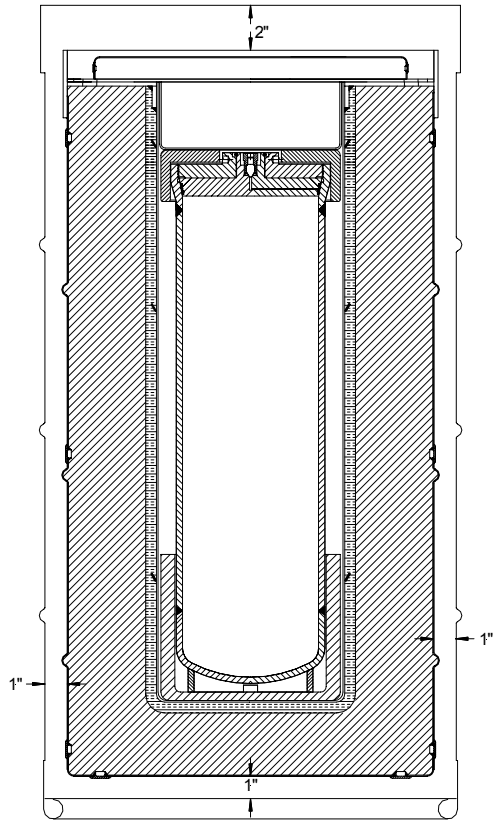

Figure 3: Outer Dimension Reductions for HAC

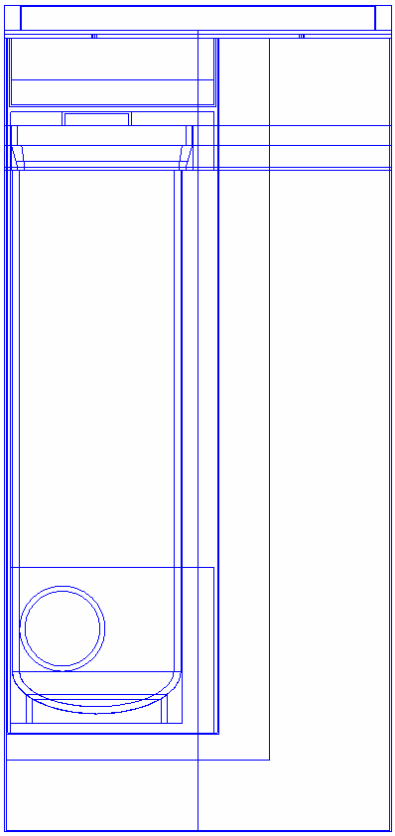

Figure 4: Radial Offset for HAC

6.2 Content Envelope Analysis

The following subsections discuss the justification for modeling choices related to the content envelopes and provide the basis for some of the content envelope limitations.

6.2.1 Envelope C.1

Content envelope C.1 as 100 grams or less of heat source oxide material has no criticality concern. Envelope C.1 is dominated by ^{238}Pu, with small amounts of other plutonium isotopes, and uranium isotopes. The content can have a maximum gross mass of 100 grams. Table 12 compares the maximum mass of each isotope allowed by content envelope C.1 against the minimum subcritical mass reported for each isotope.

Table 12: Content Envelope C.1 Mass Analysis

Isotope	C.1 Maximum Mass (g)	Subcritical Mass Limit (g)	Reference
^{238}Pu	100	3,000	Reference 28
^{239}Pu	40	450	Reference 29
^{240}Pu	13	15,000	Reference 28
^{241}Pu	1	200	Reference 28
^{242}Pu	1.5	40,000	Reference 28
^{232}U	1.4e-4	†	Reference 28
^{233}U	0.2	500	Reference 29
^{234}U	40	†	Reference 28
^{235}U	40	700	Reference 29
^{236}U	16	†	Reference 28
^{238}U	40	†	Reference 28
† Appendix A of Reference 28 predicts a k_∞ >1.0 but no critical or subcritical mass values are indicated for these isotopes. Thus it is understood that the subcritical mass limit values for these isotopes are larger than kilogram quantities.			

Based on Table 12, the content envelope C.1 gross mass limit of 100 grams is significantly less than the subcritical mass limit for any isotope. Therefore, for the C.1 content envelope with a maximum of 100 grams of the heat source isotopes specified in Table 12, a criticality is not possible and no further analysis is necessary.

6.2.2 Envelope C.2

C.2 allows for a maximum metal mass of 4.4 kg Pu/U. The weight percent of various isotopes of Pu and U are specified in Table 1. The models in this NCSE are based on 4.4 kg ^{239}Pu or 13.5 kg ^{235}U. Thus, the analysis of 13.5 kg ^{235}U metal bounds the requested C.2 envelope mass of 4.4 kg of ^{235}U. The analysis only considered the specific isotopes ^{239}Pu and ^{235}U. Based on the subcritical mass limits in Table 12 above, the analysis of the two fissile isotopes specified (^{239}Pu and ^{235}U) bound any mass of the following isotopes: ^{238}Pu, ^{240}Pu, ^{242}Pu, ^{232}U, ^{234}U, ^{236}U, ^{238}U.

The analysis basis for this content envelope does not allow for the presence of unrestricted quantities of fissile isotopes other than ^{239}Pu (e.g., ^{241}Pu) in the same 9977 package. Quantities of ^{241}Pu are acceptable provided the mass of ^{240}Pu is greater than or equal to the mass of ^{241}Pu when ^{239}Pu is the predominant isotope[30]. Reference 29 supports this analysis approach.

This NCSE does not model the presence of Pu and U in the same package. Instead, this NCSE relies on Standards information to justify the combined presence of Pu and U in the same package. Given that all fissile material is processed in accordance with DOE-STD-3013[3] prior to placing it in a 9977 shipping package, the fissile material is credited for having the following characteristics important to this NCSE:

- the gross weight of the material in a 3013 can is less than or equal to 5.0 kg,
- the maximum water content in the oxide material is 0.5 wt%,
- the ^{233}U content is limited to a maximum of 0.5 wt%, and
- plutonium-bearing metals and oxides contain at least 30 wt% plutonium plus uranium.

Based on this material characteristic information, Section A.6.3.2.1 of Reference 3 concluded that the 4.4 kg fissile mass limit for the 3013 can applies to all fissile species (i.e., ^{233}U, ^{235}U, ^{237}Np, or higher plutonium isotopes) because the critical masses of these fissile radioisotopes are greater than that of ^{239}Pu. This conclusion is consistent with the conservative approach outlined in Section 5 of Reference 29. Thus, based on this conclusion in Reference 3, it is conservative to account for each gram of a fissile isotope as one gram of ^{239}Pu (i.e., gram for gram substitution) up to the fissile mass limit of 4.4 kg for a 3013 can. Since these arguments are based on mass and material composition, the gram for gram substitution previously discussed is acceptable for fissile material inside a non-3013 can.

This envelope does not account for the presence of more than 1 gram of reflecting material that is considered a better reflector than water (e.g., polyethylene, carbon, beryllium, etc.)[31]. The analysis models fissile metal content in C.2 as 100% ^{239}Pu or ^{235}U. Results in this NCSE indicate that modeling 4.4 kg Pu as 100% ^{239}Pu bounds the 13.5 kg ^{235}U content cases. A few cases with 100% ^{235}U were run for comparison and verification. In addition to the fissile mass allowed, a maximum of 100 g of polyethylene was considered present with the fissile material as a reflector. It is expected that the 100 g polyethylene mass would bound the plastic that may be present around slip-lid and screw-top type product cans due to the bag-out process from a glovebox.

6.2.3 Envelope C.3

Table 1 indicates that an analysis of Pu/U oxides is not requested at this time. Since the analysis was complete prior to this change in the content envelope table, the analysis for content envelope C.3 is presented in this NCSE.

Content envelope C.3 has similar composition (radionuclides and impurities) limits as those for C.2, except that the C.3 content envelope is in oxide form and thus has a higher total mass limit of 5.0 kg. The analysis basis is 4.4 kg of fissile material in the oxide form which results in 4988 g PuO_2 and 4999 g UO_2 when 100% of the Pu is ^{239}Pu and 100% of the U is ^{235}U. A constant fissile mass of 4.4 kg implies the oxide mass decreases slightly (<9 grams) as the weight percent of ^{240}Pu or ^{238}U increases over the enrichment ranges for the respective oxides. Since the fissile mass is the limiting parameter, the presence of non-fissile material/isotopes to achieve a bulk mass of 5 kg is conservative, provided the non-fissile material is not a better moderator than water (e.g., polyethylene, carbon, beryllium, etc.).

Dry plutonium/uranium oxides have lower densities and significantly higher subcritical mass limits than the corresponding elements in metal form. For example the subcritical mass of ^{239}Pu is 10.2 kg for oxide and 5.0 kg for metal[29]. Therefore the criticality analyses for content envelope C.2 will bound the C.3 content envelope provided the 4.4 kg fissile mass limit is maintained. Only a few calculations were performed to obtain the k_{eff} values for comparison.

The moderation content of the oxide material (PuO_2 or UO_2) is defined by an H/X ratio. The H/X ratio is the ratio of the number of hydrogen atoms divided by the number of fissile atoms (^{239}Pu or ^{235}U). The maximum ratio studied in this analysis was H/X=3. Thus, the C.3 content envelope is required to reflect this limitation of the analysis.

6.2.4 Envelope C.4

Table 2 requests a metal or alloy fissile mass of 13.5 kg ^{235}U be analyzed. As noted in Section 6.2.2, the analysis of 4.4 kg ^{239}Pu metal bounds the analysis of 13.5 kg ^{235}U. Therefore, content envelope C.4 is considered by this NCSE as a subset of content envelope C.2.

6.2.5 Envelope C.5

Table 2 requests that ^{235}U compounds be analyzed up to a maximum of 4.4 kg. As noted in Section 6.2.3 for content envelope C.3, only two compounds are considered by this NCSE: PuO_2 and UO_2. Plutonium oxide is not a requested compound in Table 2. The analysis for PuO_2 and UO_2 under content envelope C.3 is considered to bound the request for UO_2 in content envelope C.5.

6.3 Single Package Analyses

10 CFR 71.55 contains the following requirements for SP analyses:

> (b) Except as provided in paragraph (c) or (g) of this section, a package used for the shipment of fissile material must be so designed and constructed and its contents so limited that it would be subcritical if water were to leak into the containment system, or liquid contents were to leak out of the containment system so that, under the following conditions, maximum reactivity of the fissile material would be attained:
>
> (1) The most reactive credible configuration consistent with the chemical and physical form of the material;
>
> (2) Moderation by water to the most reactive credible extent; and
>
> (3) Close full reflection of the containment system by water on all sides, or such greater reflection of the containment system as may additionally be provided by the surrounding material of the packaging.

The SP analysis consists of two sets of moderation conditions, one for dry material and one for solution. The dry analysis places fissile metal or oxide as a sphere in the CV. The solution portion places a fissile solution in the CV at various concentrations to account for the dispersion of fissile material due to water in the CV.

6.3.1 Dry

The single package base case model was developed without the 3013 containers. Fissile contents of plutonium metal, uranium metal, plutonium oxide and uranium oxide were used. The fissile material, in the form of a sphere, was located at the bottom of the CV in the base model. Several variations of the base case with plutonium metal were modeled to examine the effects of the 3013 container, location of fissile material within the CV, and the effect of polyethylene material. Some of the cases examined the effect of surrounding the fissile sphere with 100 grams of polyethylene to bound the presence of plastic commonly associated with a non-3013 (food pack) can.

Figure 5 depicts an x-ray view of the SP model with a single Pu sphere at the bottom center of the CV. Figure 6 provides a color coded guide to the materials used in modeling a fissile solution in the CV. Table 13 provides a description of the material for each material number in the legend of Figure 6. A discussion of materials used in this analysis is provided in Section 4.3.

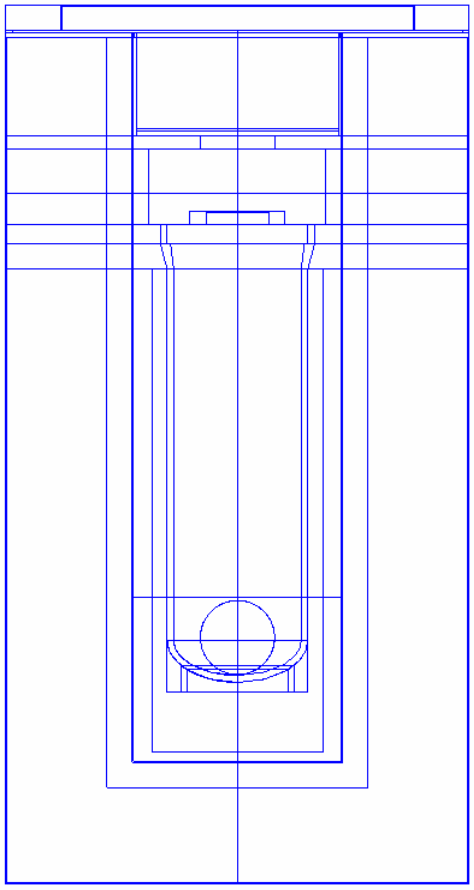

Figure 5: SP With Metal In 5" CV

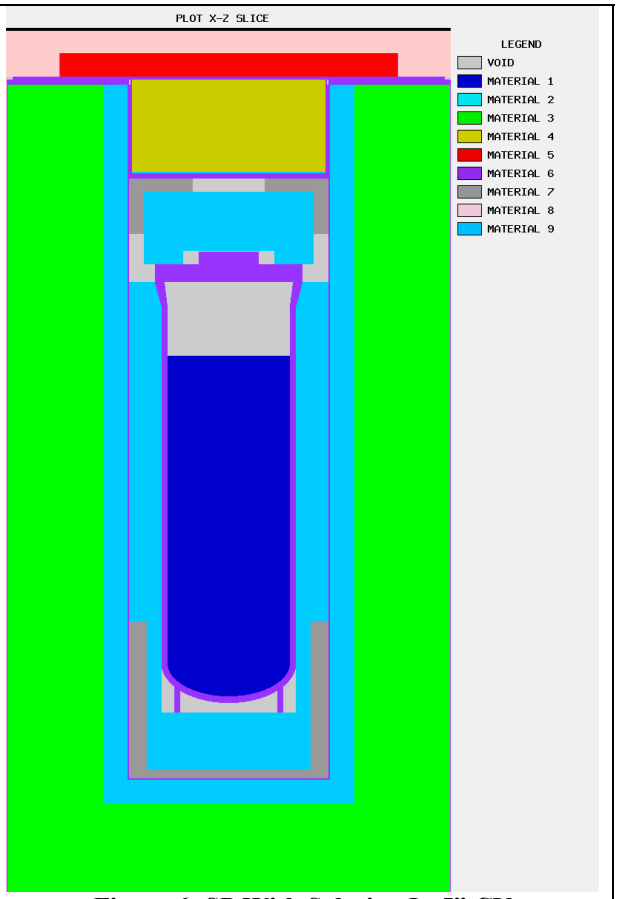

Figure 6: SP With Solution In 5" CV

Table 13: Material Description for Figure 6 and Figure 7

Material #	Description
1	Fissile solution
2	Fiberfrax
3	Foam
4	Vermiculite
5	Min-K 2000
6	SS304
7	Aluminum
8	Water
9	Low density Aluminum to simulate Aluminum honeycomb
10	Polyethylene

Figure 7 has two different depictions of a single 9977 with a 3013 can. The 3013 can was elevated in the CV for ease of modeling. This position has a negligible impact on the system reactivity. Table 13 provides a description of the material for each material number in the legend of Figure 7. Not shown in Figure 7 is the 30 cm of water reflection on all six sides of the single package as required by 10 CFR 71.55(b). This reflection condition was consistent for all single package cases reported for dry and solution conditions.

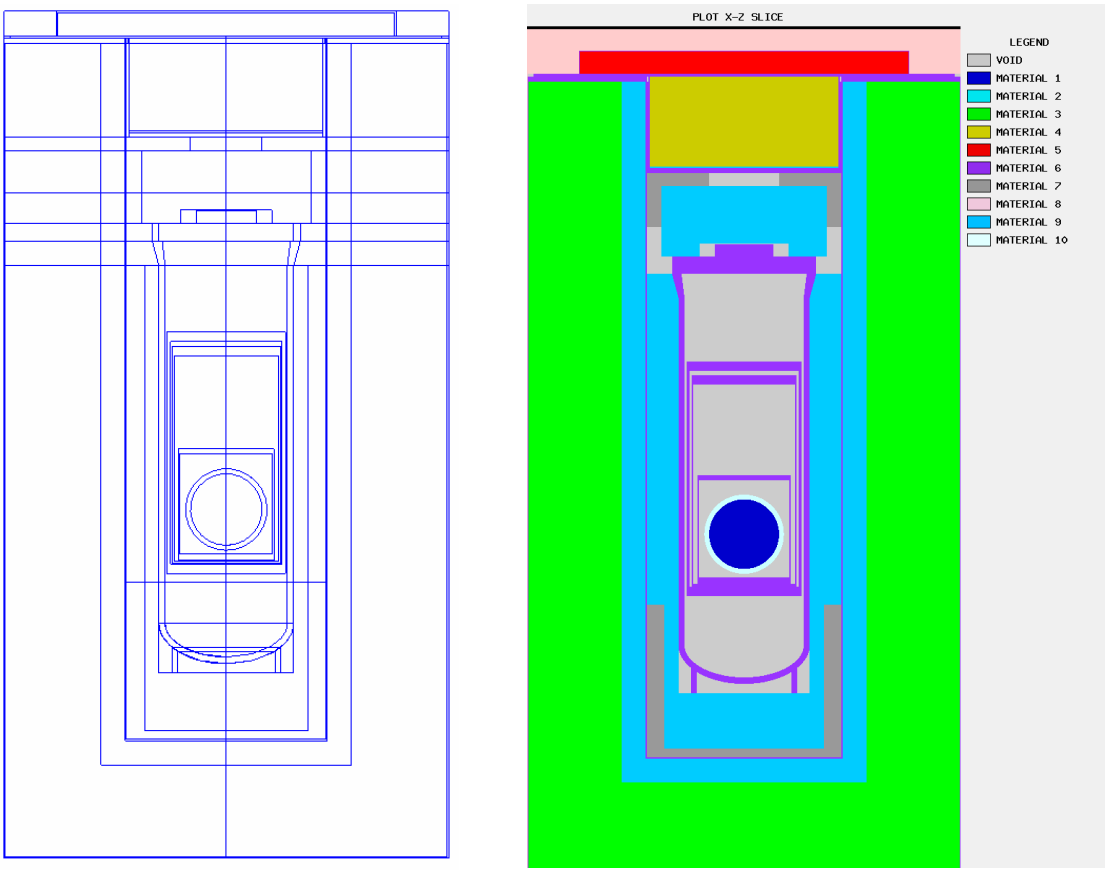

Figure 7: SP With 3013 In 5” CV

Table 14: Single Package – Dry Cases

Case No.	File ID	Description	$k_{eff} \pm \sigma$	$k_{eff} + 2\sigma$
1	su_pu_mtl_01	Bare 4.4 kg ^{239}Pu metal sphere centered in bottom of CV. See Figure 5.	0.8054 ±0.0013	0.8080
2	su_pu_mtl_02	Bare 3.0 kg ^{239}Pu metal sphere centered in bottom of CV.	0.7452 ±0.0011	0.7474
3	su_u35_mtl_01	Bare 13.5 kg ^{235}U metal sphere centered in bottom of CV.	0.7377 ±0.0010	0.7397
4	su_u35_mtl_02	Bare 10 kg ^{235}U metal sphere centered in bottom of CV.	0.6668 ±0.0010	0.6687
5	su_PuO2_01_in	4.4 kg ^{239}Pu as PuO_2 with H/X=3 as a bare sphere centered in bottom of CV.	0.5354 ±0.0012	0.5378
6	su_UO2_01_in	4.4 kg ^{235}U as UO_2 with H/X=3 as a bare sphere centered in bottom of CV.	0.4237 ±0.0010	0.4257
7	su_pu_mtl_03_in	4.4 kg ^{239}Pu metal sphere centered in bottom of CV; 100 g poly surrounding fissile sphere. See Figure 5.	0.8289 ±0.0013	0.8315
8	su_pu_mtl_04_in	4.4 kg ^{239}Pu metal sphere centered in bottom of CV; 100 g poly surrounding fissile sphere inside 3013 can (poly is not allowed in a 3013 per DOE-STD-3013). See Figure 7.	0.8360 ±0.0015	0.8390
9	su_pu_mtl_05_in	4.4 kg ^{239}Pu metal sphere centered in bottom of CV; no poly surrounding fissile sphere; 3013 can present. See Figure 7.	0.8094 ±0.0013	0.8120
10	su_pu_mtl_06_in	4.4 kg ^{239}Pu metal sphere centered in bottom of CV; water fills CV, poly surrounding fissile sphere.	0.9056 ±0.0013	0.9082
11	su_PuO2_02_in	4.4 kg ^{239}Pu as PuO_2 with H/X=0 as a bare sphere centered in bottom of CV.	0.6015 ±0.0010	0.6035
12	su_UO2_02_in	4.4 kg ^{235}U as UO_2 with H/X=0 as a bare sphere centered in bottom of CV.	0.3763 ±0.0007	0.3778

Table 14 presents the results for the dry cases in the SP study. All the cases resulted in a $k_{eff}+2\sigma$ values less than k_{safe}. Thus, a maximum of 4.4 kg ^{239}Pu or 13.5 kg ^{235}U will remain subcritical inside the CV during dry (normal) conditions.

Cases 1 through 6 compare the k_{eff} values for different types of fissile materials and material forms. The fissile material was located near the bottom of the CV in these cases (see Figure 5). These cases show that the 9977 with plutonium metal results in the highest k_{eff} values compared to cases with uranium metal and plutonium/uranium oxides. Therefore, the analysis of plutonium metal for the dry configurations is bounding of the other materials and material forms in content envelopes C.2 – C.5.

Cases 7 – 9 investigate the significance of 100 g of polyethylene surrounding the Pu metal sphere and the presence of the material in a 3013 container. These investigations address the issue of reflection provided by items or material that may be present. Case 7 has a $k_{eff}+2\sigma$ value that is approximately 2.3% higher than for case 1. The only difference between these two cases was the presence of 100 g of polyethylene. Case 9 has a $k_{eff}+2\sigma$ value that is only 0.4% higher than case 1. The only difference between case 1 and 9 was the presence of the 3013 container. Case 8 demonstrates that the combined effect of polyethylene and the 3013 container is an increase of approximately 3.1% in $k_{eff}+2\sigma$ value. Thus, the presence of the 3013 container does provide a positive, non-zero contribution to the system reactivity in the SP analysis.

The 3013 container is comprised of a convenience can located inside two nested sealed inner and outer containers. The addition of these three stainless steel cans adds a small amount of stainless steel inside the CV, which provides the competing effects of increasing neutron absorption and reflection by a small

amount. Therefore, there are competing effects with the addition of 3013 containers inside the CV, but the reflection effect dominates for the single package and the reactivity increases as a result.

Case 10 filled the CV with water and bounds the requirements for analysis per 10 CFR Part 71, §71.55 (b). The fissile sphere was reflected by a 100 gram polyethylene shell in addition to the CV full of water. Case 10 produced the highest $k_{eff}+2\sigma$ value by approximately 7%.

6.3.2 Solution

The SP solution cases explicitly modeled a 5" CV with a specified fissile mass and varied the fissile concentration. Fissile mass values less than the maximum specified by the content envelopes were modeled to achieve lower fissile concentrations. The maximum fissile concentration was limited to a value slightly less than the maximum theoretical density for the fissile metal. The minimum fissile concentration was limited by the maximum volume of the CV. This volume was calculated as 5.068 liters. The CV model was composed of a cylinder with an elliptical bottom. The calculated volume of the elliptical bottom was 0.2256 liters. Once the elliptical bottom was filled with solution, the cylinder was filled until the desired total volume (elliptical bottom plus cylinder) was achieved. Fissile concentrations resulting in a solution volume larger than the CV volume were not allowed due to the physical limitations of the CV. The maximum solution height in the cylinder portion of the CV was 37.51 cm. The maximum solution height in the elliptical bottom was 3.496 cm. Various fissile mass values were selected for Pu and U thus allowing for a wide range of fissile concentrations in the CV solution study. Table 15 and Table 16 specify the fissile mass, fissile concentration, and solution height in the cylindrical portion of the CV.

It should be noted that immersion will not result in water in-leakage into the CV of a 9977 package. This was demonstrated by the fact that the HAC test with the 30 foot drop, puncture, impact and fire resulted in no observable containment vessel deformation, which otherwise could result in in-leakage. In-leakage, if it were to occur, would likely be through the seal region of the CV. Testing has shown that the seal region is helium leak tight following the sequential drop, puncture, and fire tests [27]. However, flooding in a single package was considered in order to examine the most adverse condition and to comply with 10 CFR 71.

All cases reported in this section were reflected on all six sides by 30 cm of water per the requirements of 10 CFR Part §71.55 (e).

Table 15: Single Package – Solution Cases – Plutonium

Case No.	File ID	Mass ^{239}Pu (kg)	Conc. (kg/L)	Sol. Height (cm)	k_{eff}	$\pm\sigma$	$k_{eff} + 2\sigma$
1	su_pu_sol_07	4.4	0.86823	37.51	0.7088	0.0013	0.7114
2	su_pu_sol_08	4.4	1	32.339	0.7057	0.0017	0.7091
3	su_pu_sol_09	4.4	1.5	20.977	0.6910	0.0016	0.6942
4	su_pu_sol_10	4.4	5	5.069	0.6085	0.0013	0.6111
5	su_pu_sol_11	4.4	10	1.661	0.6170	0.0011	0.6192
6	su_pu_sol_12	4.4	15	0.524	0.6856	0.0014	0.6884
7	su_pu_sol_13	4.4	18	0.146	0.7369	0.0011	0.7391
8	su_pu_sol_20	3.5	0.69063	37.51	0.6935	0.0016	0.6967
9	su_pu_sol_21	3.5	0.7	36.987	0.6974	0.0015	0.7004
10	su_pu_sol_22	3.5	1	25.367	0.6751	0.0014	0.6779
11	su_pu_sol_23	3.5	1.5	16.328	0.6500	0.0013	0.6526
12	su_pu_sol_24	3.5	5	3.675	0.5412	0.0011	0.5434
13	su_pu_sol_25	3.5	10	0.963	0.5580	0.0011	0.5602
14	su_pu_sol_26	3.5	15	0.060	0.6289	0.0011	0.6311
15	su_pu_sol_32	2.5	0.49330	37.51	0.6750	0.0014	0.6778
16	su_pu_sol_33	2.5	0.5	36.987	0.6736	0.0014	0.6764
17	su_pu_sol_34	2.5	0.6	30.531	0.6620	0.0014	0.6648
18	su_pu_sol_35	2.5	0.7	25.920	0.6543	0.0016	0.6575
19	su_pu_sol_36	2.5	1	17.620	0.6220	0.0013	0.6246
20	su_pu_sol_37	2.5	1.5	11.164	0.5825	0.0013	0.5851
21	su_pu_sol_38	2.5	5	2.126	0.4548	0.0010	0.4567
22	su_pu_sol_39	2.5	10	0.189	0.4844	0.0010	0.4864
23	su_pu_sol_40	2.5	15	2.582 †	0.5137	0.0010	0.5156
24	su_pu_sol_41	2.5	18	2.152 †	0.5311	0.0010	0.5331

† These values are the solution height in the elliptical bottom of the CV. In these cases, the solution level is below the cylindrical portion of the CV.

A comparison between case 7 of Table 15 and case 1 of Table 14 indicates that the bare metal sphere configuration bounds the same fissile mass in solution in a 5" CV since the metal sphere produces a higher reactivity than the solution in the 5" CV. Table 15 indicates that the system reactivity tends to increase as the mixture density approaches that of metal. Note that Table 15 also indicates that reactivity increases as the fissile concentration decreases and solution height in the 5" CV increases up to the maximum allowed volume. Scoping calculations indicated that a 6" CV provided sufficient volume that the system maximum $k_{eff}+2\sigma$ values occurred at lower fissile concentration and these maximum values occasionally exceeded 1.0. That the maximum $k_{eff}+2\sigma$ value for cases in Table 15 occur at the maximum mixture density studied (see case 7) indicates that the fissile material in the 5" CV is under moderated due to the restricted volume of the 5" CV.

Table 16: Single Package – Solution Cases – Uranium

Case No.	File ID	Mass ^{235}U (kg)	Conc. (kg/L)	Sol. Height (cm)	k_{eff}	$\pm\sigma$	$k_{eff} + 2\sigma$
1	su_u235_sol_09	13.5	2.66386	37.51	0.7516	0.0017	0.7550
2	su_u235_sol_10	13.5	5	19.169	0.7366	0.0014	0.7394
3	su_u235_sol_11	13.5	10	8.710	0.7167	0.0013	0.7193
4	su_u235_sol_12	13.5	15	5.224	0.7206	0.0011	0.7228
5	su_u235_sol_13	13.5	18	4.062	0.7348	0.0010	0.7368
6	su_u235_sol_23	10	1.97323	37.51	0.7350	0.0016	0.7382
7	su_u235_sol_24	10	5	13.746	0.6849	0.0013	0.6875
8	su_u235_sol_25	10	10	5.999	0.6440	0.0011	0.6462
9	su_u235_sol_26	10	15	3.417	0.6413	0.0010	0.6433
10	su_u235_sol_27	10	18	2.556	0.6522	0.0011	0.6544
11	su_u235_sol_36	7	1.38125	37.51	0.7206	0.0014	0.7234
12	su_u235_sol_37	7	1.5	34.405	0.7165	0.0017	0.7199
13	su_u235_sol_38	7	5	9.098	0.6081	0.0011	0.6103
14	su_u235_sol_39	7	10	3.675	0.5505	0.0011	0.5527
15	su_u235_sol_40	7	15	1.867	0.5503	0.0010	0.5522
16	su_u235_sol_41	7	18	1.265	0.5679	0.0010	0.5699
17	su_u235_sol_49	4.4	0.86822	37.51	0.7031	0.0016	0.7063
18	su_u235_sol_50	4.4	1	32.339	0.6890	0.0015	0.6920
19	su_u235_sol_51	4.4	1.5	20.977	0.6536	0.0015	0.6566
20	su_u235_sol_52	4.4	5	5.069	0.4960	0.0012	0.4984
21	su_u235_sol_53	4.4	10	1.661	0.4418	0.0009	0.4435
22	su_u235_sol_54	4.4	15	0.524	0.4537	0.0008	0.4553
23	su_u235_sol_55	4.4	18	0.146	0.4734	0.0010	0.4754

All of the cases in Table 15 and Table 16 resulted in $k_{eff}+2\sigma$ values significantly less than k_{safe}. Thus, a maximum of 4.4 kg ^{239}Pu or 13.5 kg ^{235}U will remain subcritical inside the 5" CV even if water leaks into the 5" CV. The primary basis of this condition is the volume limitation provided by the CV. Scoping calculations indicate that significantly lower mass limits would be required for the package if fissile material were to be shipped in the 6" CV.

All the $k_{eff}+2\sigma$ values in Table 15 and Table 16 were less than those for the dry analysis reported in Table 14. Thus, for a single package with the 5" CV (see Table 3), the results of a bare Pu metal sphere (case 1 in Table 14) bound the fissile solution results.

All SP cases in Table 14, Table 15, and Table 16 are below the k_{safe} value of 0.931. Therefore, the 10 CFR § 71.55(b) requirements related to a flooded single package are satisfied.

6.4 Normal Conditions of Transport Array Analyses

10 CFR § 71.55 contains the following requirements for NCT criticality safety analyses:

> (d) A package used for the shipment of fissile material must be so designed and constructed and its contents so limited that under the tests specified in § 71.71 ("Normal conditions of transport") --
> (1) The contents would be subcritical;
> (2) The geometric form of the package contents would not be substantially altered;
> (3) There would be no leakage of water into the containment system unless, in the evaluation of undamaged packages under § 71.59(a)(1), it has been assumed that moderation is present to such an extent as to cause maximum reactivity consistent with the chemical and physical form of the material; and
> (4) There will be no substantial reduction in the effectiveness of the packaging, including:
> (i) No more than 5 percent reduction in the total effective volume of the packaging on which nuclear safety is assessed;
> (ii) No more than 5 percent reduction in the effective spacing between the fissile contents and the outer surface of the packaging;

In the NCT undamaged package array model, the package was modeled with the dimensions specified in Table 3. Cases modeled an infinite square pitch array of stacked packages with dry and partially flooded conditions unless specified otherwise. The flooded conditions studied for the NCT analysis modeled water in the liner and insulation regions. One case (Table 17 case 2) modeled water filling the volume inside the CV even though the test results indicate that the CV remained helium leak tight[27]. Since the CV remained leak tight following the prescribed accident tests, case 2 exceeds the analysis requirements for NCT conditions.

The 9977 was modeled with water in the liner and insulation regions. This is conservative since tests per 10 CFR § 71.71(c)(6) indicate that only the liner region can retain water. The infinite square pitch array was simulated by modeling a single package in a cuboid. This outer region was assigned mirror reflection boundaries in the x and y directions, and periodic boundary conditions in the z direction. Some cases specifically modeled a 6x6x7 array of 9977 packages with 30 cm of full density water reflection surrounding the array. Table 17 specifies which cases specifically modeled a defined array size. Most cases reported in Table 17 modeled the packages in an infinite square pitch array configuration. Table 17 shows the k_{eff} results and provides a brief description of each case.

Table 17: NCT Array Configuration Results

Case No.	File ID	Description	k_{eff}	σ	$k_{eff}+2\sigma$
1	nct_135kgu.out	13.5 kg ^{235}U metal sphere surrounded by a 100 g poly shell	0.7959	0.0011	0.7981
1a	nct_135kgu_in.out	Same as case 1 but specifically modeled in a 6x6x7 array with 30 cm water reflection on the array boundary	0.7777	0.0011	0.7799
2	nct_cvfl.out	4.4 kg ^{239}Pu metal sphere surrounded by a 100 g poly shell in a 3013, CV and package flooded with water, water between the packages	0.8715	0.0013	0.8741
3	nct_drumfl.out	4.4 kg ^{239}Pu metal sphere surrounded by a 100 g poly shell in a 3013, water between the packages and each package flooded with water	0.8510	0.0013	0.8536
4	nct_interfl.out	4.4 kg ^{239}Pu metal sphere surrounded by a 100 g poly shell in a 3013, water only between the packages	0.8491	0.0012	0.8515
5	nct_pu1.out	4.4 kg ^{239}Pu metal sphere surrounded by a 100 g poly shell	0.8500	0.0013	0.8526
5a	nct_pu1_in.out	Same as case 5 but specifically modeled in a 6x6x7 array with 30 cm water reflection on the array boundary	0.8410	0.0013	0.8436
6	nct_pu_3013.out	4.4 kg ^{239}Pu metal sphere surrounded by a 100 g poly shell in a 3013	0.8618	0.0014	0.8646
7	nct_puox1.out	4.4 kg ^{239}Pu as PuO_2 in a sphere with H/X=0 surrounded by a 100 g poly shell	0.6517	0.0011	0.6539
8	nct_u1.out	4.4 kg ^{235}U metal sphere surrounded by a 100 g poly shell	0.5507	0.0009	0.5525
9	nct_uox1.out	4.4 kg ^{235}U as UO_2 in a sphere with H/X=0 surrounded by a 100 g poly shell	0.4280	0.0008	0.4295

Table 17 indicates that any analysis for 4.4 kg Pu metal results in higher $k_{eff}+2\sigma$ values than an analysis for 13.5 kg ^{235}U metal (see cases 1-5). Thus, the plutonium metal analysis in the NCT cases bounded the uranium analysis.

The two cases that modeled a defined array size surrounded by 30 cm of water reflection (cases 1a and 5a) resulted in $k_{eff}+2\sigma$ values approximately 1% lower than when the infinite array was modeled (cases 1 and 5). This difference in $k_{eff}+2\sigma$ values is statistically significant and indicates the infinite array models are conservative compared to the 6x6x7 limited array with full water reflection.

Cases 1, 5, 7 and 9 in Table 17 show that the uranium metal and oxide configurations and the plutonium oxide configurations are much less reactive than the corresponding configuration of plutonium metal in an infinite array of 9977 containers. Therefore the other cases in Table 17 were evaluated with plutonium metal (assumed as 100% ^{239}Pu). A similar trend was also observed in the single package cases.

The presence of water inside the 9977 package but outside the CV lowers the $k_{eff}+2\sigma$ value of the system. Cases 2, 3 and 4 analyze various flooded conditions. Cases 2 and 3 filled the liner, foam and Fiberfrax regions with water (referred to as "package flooded with water"). In addition, Case 2 filled the CV with water. Case 4 placed water in the array only between the packages. Comparing case 4 and case 6 demonstrates that k_{eff} is reduced by water between the packages even if there is not water inside the packages. Together, these cases demonstrate that the optimum water conditions were analyzed.

All NCT cases in Table 17 were below the k_{safe} value of 0.931. Therefore, the 10 CFR § 71.55(d) and § 71.59(a)(1) requirements related to NCT analyses are satisfied.

6.5 Hypothetical Accident Conditions Analyses

10 CFR 71.55 contains the following requirements for HAC criticality safety analyses:

> (e) A package used for the shipment of fissile material must be so designed and constructed and its contents so limited that under the tests specified in § 71.73 ("Hypothetical accident conditions"), the package would be subcritical. For this determination, it must be assumed that:
> (1) The fissile material is in the most reactive credible configuration consistent with the damaged condition of the package and the chemical and physical form of the contents;
> (2) Water moderation occurs to the most reactive credible extent consistent with the damaged condition of the package and the chemical and physical form of the contents; and
> (3) There is full reflection by water on all sides, as close as is consistent with the damaged condition of the package.

Models were developed to satisfy these prescribed requirements of 10 CFR 71.55. The models developed assumed that no water would enter the CV. This assumption was based on test results that indicate no damage occurred to the CV as a result of the required test conditions[27]. This modeling selection is consistent with 10 CFR § 71.55(e)(1).

To study k_{eff} for HAC, a 6x6x3 square pitch array of 9977 packages was reflected by 30 cm of water in all six directions. The 9977 packages were modeled under the prescribed accident conditions. Each 9977 package contained a 4.4 kg ^{239}Pu sphere that was surrounded by 100 g polyethylene. The 6" CV was used in the HAC models as discussed in Section 4.4.1.

Array analyses were performed using a 7% reduced drum radius to approximate an equivalent triangular pitch array configuration[15]. This 7% radius reduction was in addition to the damage values demonstrated by the test results (see Table 11). Test results indicate that a 2" (5.08 cm) reduction in the package diameter and a 2" (5.08 cm) reduction in the package height bound the HAC (see Table 11). Some cases modeled a 3" (7.62 cm) reduction in the package height for additional conservatism. In all models, the reduction in package diameter and height were uniform. The test results reported for package damage were for maximum dents and bulges localized on the package (see Table 11). Therefore, the uniform dimension reductions modeled are very conservative, representing a closer spacing than actually possible with the observed drum damage. The dimension reductions were taken in the foam region of the package. Thus, for all the cases in Table 18 that indicate a reduced dimension, the radial and/or axial foam thickness was reduced to produce the outer package dimensions desired.

Some of the cases presented in Table 18 studied the absence of some/all of the insulating material. Each of the cases in Table 18 that reduced the diameter, the height, or both, resulted in a smaller volume for the foam region. The foam density was not increased to conserve mass in the foam region due to the reduced volume of the foam region. Some cases studied the absence of the foam, thus eliminating the need for a parametric study of the system reactivity versus foam density. In the 2-cluster and 4-cluster models, the mass of the insulation was conserved when compared to the centered configuration, since the models simply shifted the container contents.

Figure 8 depicts a top view of the normal 6x6x3 square pitch array used in the HAC analysis. The normal configuration reduced the outer package dimensions but did not shift the interior contents. Figure 9 depicts a systematic shift in the interior contents where the distance between the fissile content in every pair of packages was minimized. Figure 10 extended the concept shown in Figure 9 to groups of four packages. The primary purpose of the two-group and four-group cluster models was to analyze the need for relying on the construction materials and design to maintain the CV integrity and location inside the package. The shift of contents in one direction allowed for mass and volume of the insulating material to be conserved because it was simply displaced in the opposite direction of the shift.

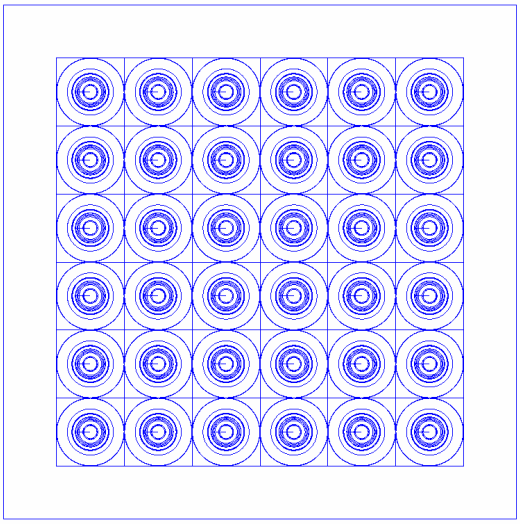

Figure 8: Centered Array

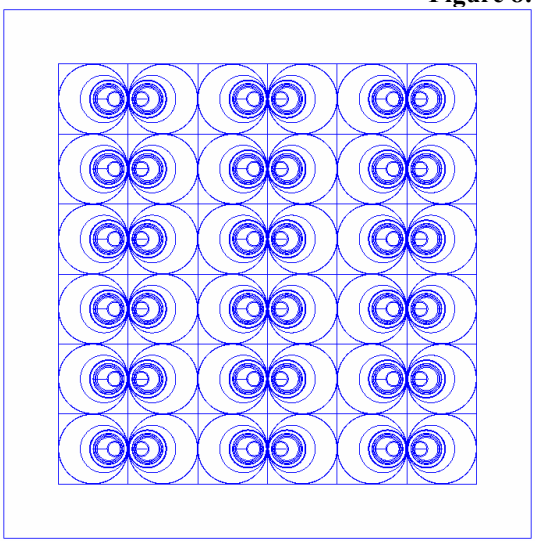

Figure 9: Two Cluster HAC Model

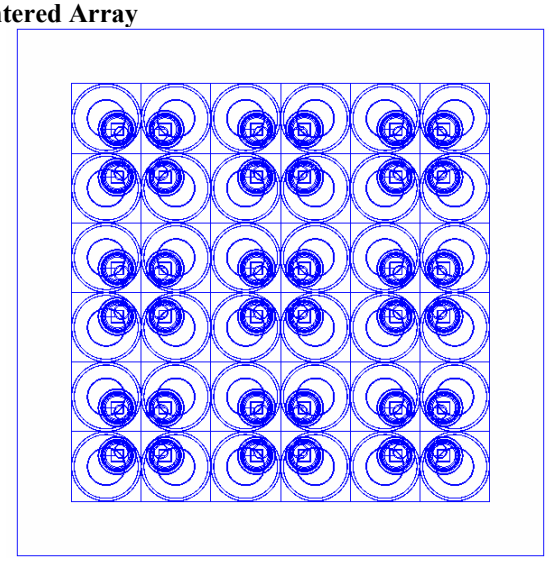

Figure 10: Four Cluster HAC Model

The HAC series of calculations reported in Table 18 begin with a NCT package in a 6x6x3 array. The study removed insulation, reduced radius and height corresponding to damage, further reduced the radius to approximate a triangular pitch array, and the contents of the packages were studied in two positions that maximize the interaction of the fissile material in the package.

Table 18: HAC Analysis Results

Case No.	File ID	Description	k_{eff}	σ	k_{eff} +2σ
1	hac1_663	6x6x3 square pitch array of drums in contact, array reflected with 30 cm of water in all 6 directions, each drum with 4.4 kg ^{239}Pu sphere surrounded by 100 g polyethylene, no 3013, nominal container dimensions; normal presence of foam, Fiberfrax, Vermiculite and Min-K 2000, fissile sphere radially centered in drum. See Figure 1 and Figure 8.	0.8371	0.0013	0.8397
2	hac_663_foam	Identical to case 1 but reduced container OD by 2" and the outer height was reduced 2" (1" top and bottom) corresponding to HAC conditions. See Figure 3 and Figure 8.	0.8474	0.0014	0.8502
3	hac_663	Identical to case 2 but no foam present (all other insulators were present). See Figure 3 and Figure 8.	0.8604	0.0013	0.8630
4	hac_sym	6x6x3 square pitch array of drums, array reflected by 30 cm water in –x, –y, +z, and –z direction, each drum with 4.4 kg ^{239}Pu sphere radially centered in drum surrounded by 100 g polyethylene, no 3013; no foam, Fiberfrax, Vermiculite or Min-K 2000 present; HAC diameter from case 2 was reduced by 7% to approximate triangular pitch array; HAC top height was reduced by 1". See Figure 3 and Figure 8.	0.8544	0.0014	0.8572
5	bk_hac_r1_in	Same as case 4 with array reflected by 30 cm of water in all 6 directions.	0.8631	0.0014	0.8659
6	hac_2clus	Same as case 5 but created pairs (2-cluster model) of drums with fissile material, CV, insulation region, etc., displaced to allow closer interaction with fissile material from one other drum. See Figure 3 and Figure 9.	0.8867	0.0014	0.8895
7	hac_4clus	Same as case 5 but created groups of four drums (4-cluster model) with fissile material, CV, insulation region, etc., displaced to allow fissile material from all four drums to move towards a common center. See Figure 3 and Figure 10.	0.8818	0.0014	0.8846
8	hac_2clus_water_2_in	Same as case 6 but water fills the liner, and foam regions in the 9977, and between packages in the array.	0.8628	0.0016	0.8660
9	hac_2clus_al_1_in.out	Same as case 6 but replaced Al in LDF with void.	0.8753	0.0014	0.8781
10	hac_2clus_al_2_in.out	Removed void space occupied by LDF in case 9 by shifting CV an additional 1.57 cm closer to edge of package.	0.8875	0.0017	0.8909

All of the cases in Table 18 resulted in $k_{eff}+2\sigma$ values significantly less than k_{safe}. This directly demonstrates that a maximum of 4.4 kg ^{239}Pu as metal will remain subcritical inside the 9977 package under HAC conditions. Section 6.4 demonstrated that an analysis with 4.4 kg ^{239}Pu as metal provides a bounding analysis for 13.5 kg ^{235}U as metal. Section 6.4 also demonstrated that an analysis with 4.4 kg ^{239}Pu as metal provides a bounding analysis for 4.4 kg of fissile material in oxide form (PuO_2 or UO_2) with $H/X \leq 3$. Therefore, the HAC analysis results in Table 18 bound that of 13.5 kg ^{235}U as metal and 4.4 kg of dry fissile material in oxide form (PuO_2 or UO_2).

Per the requirements of 10 CFR §71.59(a)(2), the optimum interspersed hydrogenous moderation must be considered. The model developed in case 8 exceeds the requirement for interspersed moderation in that water was modeled inside the foam and liner regions of each package in the model. Water was not modeled inside the CV since this is not a requirement based on the test results indicating the CV remains

helium leak tight[27]. Case 6 was selected as the base case for the moderation study since it had the highest $k_{eff}+2\sigma$ value without moderation. The Table 18 result for case 8 indicates that the system reactivity decreases due to the presence of water in the model.

All HAC cases in Table 18 were below the k_{safe} value of 0.931. Therefore, the 10 CFR § 71.55(e) and § 71.59(a)(2) requirements related to HAC analyses are satisfied.

6.6 Sensitivity Analyses

Consideration was given to reactivity changes due to tolerances in package dimensions, insulation material composition, and the thickness of steel present.

6.6.1 Package Dimensions

The drawing references identified in Table 3 specify tolerance values for each specification value. These tolerance values are +/- 0.03" or less based on the number of decimal places used on the drawing. The HAC analysis shifted the package contents for the 2-cluster and 4-cluster models in the directions to maximize system reactivity. Thus, the package contents were displaced several inches. Hence the system reactivity changes due to the small tolerance values for dimension specifications are bound by the large displacement of package contents in the HAC models.

6.6.2 Insulation Material

Table 4 through Table 8 indicate that "normalized" or "average" weight percent values were used to define the material compositions. This NCSE did not model specific variations in these compositions to study the change in system reactivity. Instead, the material presence, absence, or replacement with water was modeled to study the change in system reactivity.

Cases 3, 4, and 5 in Table 17 demonstrate that k_{eff} varies less than 1σ when all the insulation material is replaced with water. The increase in k_{eff} between case 2 and case 3 in Table 18 is approximately 1.2% and is strictly due to replacing the foam with void. Case 6 and case 8 in Table 18 differed by less than 1σ in k_{eff} value when the void regions normally occupied by insulation (case 6) was modeled filled with water (case 8). Since the gross changes in material presence, absence, or replacement with water resulted in the reactivity changes identified above, reactivity changes due to insulating material composition variation is negligible.

6.6.3 Steel Reflection

Appendix 3 of Reference 25 documents a sensitivity study of the 3013 can wall thickness. Two different 3013 can volumes were used and the wall thickness was varied from minimum to maximum values. The $k_{eff}+2\sigma$ value results ranged from 0.8764 without any steel reflection from a 3013 can to 0.8875 for the minimum size (volume) 3013 can with maximum wall thickness. Appendix 3 of Reference 25 concluded that the following restrictions are necessary when a 3013 can in a 9975 shipping package contains greater than or equal to (≥) 3.0 kg of fissile material:

a) The sum of the radial wall thicknesses of all cans (convenience can, inner can, and outer can) constituting a 3013 shall not exceed 0.67 cm,
b) The sum of the axial thicknesses (top and bottom) of all cans constituting a 3013 shall not exceed 4.5 cm,
c) The volume of the convenience can shall not be less than 825 cm^3. If multiple convenience cans are used, the volume limit shall be applied to the sum of the internal volumes of all convenience cans in a 3013,
d) If a two-can configuration is used (e.g., an inner can and an outer can) instead of a three nested-can configuration, the convenience can volume limit shall be applied to the inner can(s).

Appendix 3 of Reference 25 concluded that when less than 3.0 kg of fissile material is present, the restriction on the wall thicknesses and the restriction on the convenience can volume does not apply.

The study in Appendix 3 of Reference 25 focused on the 3013 can size and volume while holding all other parameters constant. The 9975 shipping package contained two containment vessels (a primary and secondary) whereas the 9977 has only one CV in the package. Thus, the steel reflection present in the Reference 25 study for the 9975 bounds the amount of steel reflection in the 9977 package. Therefore, the results and restrictions from Appendix 3 of Reference 25 are applied to the 9977 shipping package without further calculations.

6.7 Criticality Safety Index

The calculation of the Criticality Safety Index (CSI) for the 9977 shipping package is required to follow the explicit equations specified in 10 CFR Part §71.59. Those requirements are as follows:

> (a) A fissile material package must be controlled by either the shipper or the carrier during transport to assure that an array of such packages remains subcritical. To enable this control, the designer of a fissile material package shall derive a number "N" based on all the following conditions being satisfied, assuming packages are stacked together in any arrangement and with close full reflection on all sides of the stack by water:
>
> (1) Five times "N" undamaged packages with nothing between the packages would be subcritical;
>
> (2) Two times "N" damaged packages, if each package were subjected to the tests specified in § 71.73 ("Hypothetical accident conditions") would be subcritical with optimum interspersed hydrogenous moderation; and
>
> (3) The value of "N" cannot be less than 0.5.
>
> (b) The CSI must be determined by dividing the number 50 by the value of "N" derived using the procedures specified in paragraph (a) of this section. The value of the CSI may be zero provided that an unlimited number of packages are subcritical, such that the value of "N" is effectively equal to infinity under the procedures specified in paragraph (a) of this section. Any CSI greater than zero must be rounded up to the first decimal place.
>
> (c) For a fissile material package which is assigned a CSI value--
>
> (1) Less than or equal to 50, that package may be shipped by a carrier in a nonexclusive use conveyance, provided the sum of the CSIs is limited to less than or equal to 50.
>
> (2) Less than or equal to 50, that package may be shipped by a carrier in an exclusive use conveyance, provided the sum of the CSIs is limited to less than or equal to 100.
>
> (3) Greater than 50, that package must be shipped by a carrier in an exclusive use conveyance, provided the sum of the CSIs is limited to less than or equal to 100.

The calculation of the CSI for the NCT is conservatively based on the 6x6x7 array size and for the HAC is based on the 6x6x3 array size. The CSI calculations for NCT and HAC are shown in parallel in Table 19.

Table 19: CSI Calculation

Calculate the value of N for NCT:	Calculate the value of N for HAC:
5*N = 6x6x7 = 252 so N = 252/5 = 50.4	2*N = 6x6x3 = 108 so N = 108/2 = 54
The CSI is defined by 10 CFR §71.59 as,	The CSI is defined by 10 CFR §71.59 as,
CSI ≡ 50/N = 50/50.4 = 0.992	CSI ≡ 50/N = 50/54 = 0.926
Rounding up to the first decimal we get,	Rounding up to the first decimal we get,
CSI = 1.0	CSI = 1.0

Since the CSI calculations in Table 19 derive the same CSI value for NCT and HAC configurations, the CSI is equal to 1.0 for the 9977 package for content envelopes C.2 – C.5.

Based on the analysis in Section 6.2.1, a criticality is not possible for content envelope C.1. Thus, an infinite array of 9977 packages with content envelope C.1 in the NCT and HAC configurations are subcritical. Following the calculation methodology in Table 19, the CSI value for content envelope C.1 is zero (0) since N=∞ for an infinite array.

7 Design Features and Administrative Controlled Limits and Requirements

The following limits/controls apply to the 9977 shipping packages evaluated in this analysis:

1. Only the 5" CV shall be used to contain fissile material (content envelopes C.2, C.3, C.4, and C.5) in the 9977 package.

2. Only the material within the bounds of content envelopes C.1, C.2, C.3, C.4 and C.5 identified in Table 20 shall be placed in a 9977 package.

3. Each 9977 shipping package shall be assigned a CSI=1.0 for material within the bounds of content envelopes C.2, C.3, C.4 and C.5 identified in Table 20.

4. Each 9977 shipping package shall be assigned a CSI=0 for material within the bounds of content envelope C.1 identified in Table 20.

5. If a 9977 shipping package contains greater than or equal to (≥) 3.0 kg of fissile material:
    a. The sum of the radial wall thicknesses of all cans (convenience can, inner can, and outer can) constituting a 3013 shall not exceed 0.67 cm,
    b. The sum of the axial thicknesses (top and bottom) of all cans constituting a 3013 shall not exceed 4.5 cm,
    c. The volume of the convenience can shall not be less than 825 cm^3. If multiple convenience cans are used, the volume limit shall be applied to the sum of the internal volumes of all convenience cans in a 3013,
    d. If a two-can configuration is used (e.g., an inner can and an outer can) instead of a three nested-can configuration, the convenience can volume limit shall be applied to the inner can(s).

Table 20: Analyzed Content Envelopes

Content	Maximum Values Allowed				
	C.1 Heat Sources (g)	**C.2 Pu/U Metal [a] (kg)**	**C.3 Pu/U Oxide [a] (kg)**	**C.4 Pu/U Metal or Alloy [a] (kg)**	**C.5 Compounds (PuO_2 or UO_2) [a, c] (kg)**
H/X	n/a	n/a	H/X≤ 3	H/X=0	H/X≤ 3
^{238}Pu	100	0.088	0.088	0.088	0.088
^{239}Pu	40	4.4	4.4	4.4	4.4
^{240}Pu	13	1.76	1.76	1.76	1.76
^{241}Pu	1	0.66 [b]	0.66 [b]	0.66 [b]	0.66 [b]
^{242}Pu	1.5	0.22	0.22	0.22	0.22
Total Pu	100	4.4	4.4	4.4	4.4
^{232}U	1.4×10^{-4}	$1x10^{-7}$	$5x10^{-7}$	$5x10^{-7}$	$5x10^{-7}$
^{233}U	0.2	0.022	0.022	0.022	0.022
^{234}U	40	4.4	4.4	13.5	4.4
^{235}U	40	4.4	4.4	13.5	4.4
^{236}U	16	1.76	1.76	5.4	1.76
^{238}U	40	4.4	4.4	13.5	4.4
Total U	100	4.4	4.4	13.5	4.4
CSI	0	1.0	1.0	1.0	1.0

Notes
a) A mixture of Pu isotopes and U isotopes in the same 9977 package is allowed provided the total fissile mass remains ≤ 4.4 kg (see Section 6.2.2).
b) The mass of ^{241}Pu is required to be less than the mass of ^{240}Pu, and ^{239}Pu shall be the predominant isotope.
c) The only compounds analyzed and approved by this NCSE are PuO_2 and UO_2.

8 Summary and Conclusions

An evaluation of the 9977 shipping package was performed per the requirements of 10 CFR 71. The SCALE 5/KENO VI code system with the 238-group cross section set was used to assess the nuclear criticality safety of the storage and transportation of fissile material in the 9977 shipping packages. The analysis considered only the content envelopes specified in Table 20.

The 6x6x7 array analyzed for NCT and the 6x6x3 array size analyzed for the HAC resulted in a CSI value of 1.0 for content envelopes C.2 through C.5. Content envelope C.1 has a CSI value of 0.

9 References

1 Abramczyk, G. A., "GPFP Contents," SRNL-EDS-2005-00031, Rev. 1, February 2006.
2 R-R3-F-0016, Rev. 10, "9975 Shipping Package – Containment Vessel Weldments."
3 DOE-STD-3013-2004, "Stabilization, Packaging, and Storage of Plutonium-Bearing Materials," April, 2004
4 R-R2-G-00018, Rev. 0, "9977 General Purpose Fissile Package - Drum Lid Subassembly."
5 R-R2-G-00017, Rev. 0, "9977 General Purpose Fissile Package - Drum and Liner Subassembly."
6 R-R4-G-00032, Rev. 0, "9977 General Purpose Fissile Package - Spacer Part Details for 6-inch Containment Vessel."
7 R-R2-G-00042, Rev. 0, "9977 General Purpose Fissile Package - 6-inch Diameter Containment Vessel (CV) Subassembly."
8 Abramczyk, G. A., "RE: Material Properties for Components of the 9977," SRNL-IES-2006-00007, February 10, 2006.
9 R-R4-G-00033, Rev. 0, "9977 General Purpose Fissile Package – Spacer Part Details for Five Inch Containment Vessel."
10 Petrie, L. M., Fox, P. B., and Lucius, K., "Standard Composition Library," NUREG/CR-0200, Revision 6, SCALE Computer System, Volume 3, Section M8, Oak Ridge National Laboratory, Oak Ridge, TN, September 1998.
11 CRC Handbook of Chemistry & Physics 77th Edition, 1996.
12 "Westinghouse Savannah River Company Nuclear Criticality Safety Manual," WSRC-SCD-3, Rev. 19, June 2005.
13 "WSMS Nuclear Criticality Safety Methods Manual (U)," WSMS-CRT-01-0116, Rev. 4, October 2005.
14 10 CFR Part 71, U.S Nuclear Regulatory Commission, Washington, DC, January 2005.
15 NUREG/CR-5661, ORNL/TM-11936, "Recommendations for Preparing the Criticality Safety Evaluation of Transportation Packages," April 1997.
16 CCC-725, RISC Computer Code Collection, SCALE 5, Modular Code System for Performing Standardized Computer Analyses for Licensing Evaluation, Oak Ridge National Laboratory, Oak Ridge, Tennessee, May 2004.
17 Revolinski, S. M., "Software Configuration and Control Guidance for SCALE 5 with Linux Workstation Cluster (U)," WSMS-CRT-04-0079, September 2004.
18 Revolinski, S. M., "SCALE 5 Test Report," WSMS-CRT-04-0080, Rev. 1, May 2005.
19 Greene, N. M., *et. al.*, "The LAW-238 Library -- A Multigroup Cross-Section Library for Use in Radioactive Waste Analysis Calculations," ORNL/TM-12370, Oak Ridge National Laboratory, Oak Ridge, Tennessee, August, 1994.
20 Revolinski, S. M., "WSMS SCALE Version 5: Plutonium Metal and Oxide Validation for Linux-5 Workstation Cluster (U)," WSMS-CRT-05-0007, Rev. 0, February 2005.
21 Revolinski, S. M., "WSMS SCALE Version 5: Plutonium Solution Validation for Linux-5 Workstation Cluster (U)," WSMS-CRT-05-0067, Rev. 0, September 2005.
22 Revolinski, S. M., "WSMS SCALE Version 5: Highly Enriched Uranium Metal Validation for Linux-5 Workstation Cluster (U)," WSMS-CRT-05-0026, Rev. 0, May 2005.
23 Revolinski, S. M., "WSMS SCALE Version 5: HEU Oxide Validation for Linux-5 Workstation Cluster (U)," WSMS-CRT-05-0091, Rev. 0, October 2005.
24 Revolinski, S. M., "WSMS SCALE Version 5: Highly Enriched Uranium Solution Validation for Linux-5 Workstation Cluster (U)," WSMS-CRT-05-0056, Rev. 0, August 2005.
25 Biswas, D., "NCSE: 9975 Shipping Container Analysis with Revised Contents for SARP, Rev. 0," Rev. 2, October 2003.
26 Malloy, J., "SRNL Package Burn Test Report," NT-TDR-06-101, Rev. 0, NovaTech Innovative Technologies International, Lynchburg, VA, February 2006.
27 Gelder, L.F., May, C.M., "9977 General Purpose Fissile Packaging Prototype Testing," M-TRT-A-00007, Rev. 0, Washington Savannah River Company, February 2006.
28 ANSI/ANS-8.15-1981, "Nuclear Criticality Control of Special Actinide Elements," 1981.

29 ANSI/ANS-8.1-1998, “Nuclear Criticality Safety In Operations With Fissionable Material Outside Reactors,” 1998.

30 NUREG/CR-0095, ORNL/NUREG/CSD-6, “Nuclear Safety Guide TID-7016 Revision 2,” May 1978.

31 Kerr, B. R., “NCSE: Minimum Mass of Concern for Carbon and Beryllium in Solid Waste,” N-NCS-E-00028, Rev. 0, July 2005.

Appendix A

Example Input Files

Below are the selected SCALE input files on the referenced page numbers. These input files are provided in a landscape two column format that minimizes the space required. Sometimes the two column format forces the text of a long line to wrap to the next line.

Case su_Pu_mtl_06_in

```
=csas26    parm=Centrm
su_Pu_mtl_06_in: SU, dry,  4.4 kg pu sphere, no 3013, 100 g poly, pu bottom
' water fills CV
238group
read comp
pu-239       1  den=19.84  1.0 293 end
arbm-fiber 0.256 4 0 0 1 13027 26.46 14000 23.14 11000 0.37 8016 50.03 2 1.0 293
end
arbm-foam  0.256  7 0 0 1  17000 0.15  14000 0.82 15000 0.82 8016 22.6 6012
62.88
                    1001  6.84   7000  5.89  3 1.0 293 end
arbm-vermi 0.368 10 0 0 1  14000 21.22  13027 5.47 20000 12.17 26000 5.4 22000
0.82
                    12000 8.90   11000 1.09 19000 1.22 16000 0.18 8016 43.53
                    4 1.0 293 end
arbm-mink 0.320 8 0 0 1    14000 37.71  22000 5.53  13027 6.39 6012 1.28  1001
0.84
                    8016  48.01  51000 0.09  35000 0.15   5 1.0 293 end
ss304       6  den=7.94  1.0 293  end
al          7  den=2.70  1.0 293  end
h2o         8  den=1.00 1.0 293  end
al          9  den=0.1922 1.0 293 end
poly(h2o)  10  den=0.95 end
end comp
read parm
  tme=500 gen=425 npg=1000  nsk=25 run=yes plt=no nub=yes
end parm

read geom

unit 1
'upto bot of top al support
'Ellosoidal bottom and cv leg support'
sphere    12   3.755  origin z=11.1
sphere    20   4.2741 origin z=11.1
ellipsoid 1   6.41   6.41   3.496 origin z=10.2395 chord -z=0.0
ellipsoid 2   7.065  7.065  4.207 origin z=10.2395 chord -z=0.0
cylinder  3   5.113    8.532   5.0673
cylinder  4   5.715    8.533   5.0673
'bottom load support
cylinder  6   10.4775   14.605  -1.905
' Al honeycomb
cylinder  15   7.066    10.2395  5.0673
cylinder  16   8.5725   47.752  -0.9652
cylinder  17   10.4775  47.752  14.605
'cv
cylinder  13   6.41     47.752   10.2395
cylinder  14   7.065    47.752   10.2395
'liner
cylinder  8   10.5994    47.752  -2.027
cylinder  9   13.1394    47.752  -4.567
cylinder  10  23.1775    47.752  -14.197
cylinder  11  23.2994    47.752  -14.319

cuboid   100  4p23.2994  47.752  -14.319

media   1  1  12
media  10  1  20 -12
media   8  1  1 -20
media   6  1  2  -1
media   0  1  3  -2
media   6  1  4  -3 -2

'media   0  1  5 -4
media   7  1  6 -16

media   0  1  15 -20 -2 -4
media   9  1  16 -15 -14
media   9  1  17 -16

media   8  1  13 -20
media   6  1  14 -13

media   6  1  8  -17 -6
media   2  1  9  -8
media   3  1  10 -9
media   6  1  11 -10
media   8  1  100 -11
boundary 100

unit 2
'CV flared near top
cone     1  6.721 50.292  6.41   47.752
cone     2  7.749 50.292  7.065  47.752
plane    3  zpl=1 con= -55.220

'Al honeycomb
cylinder 5  10.4775      50.292  47.752
```

```
cylinder  6   10.4775    50.292   47.752
cylinder  7   10.5994    50.292   47.752
cylinder  8   13.1394    50.292   47.752
cylinder  9   23.1775    50.292   47.752
cylinder  10  23.2994    50.292   47.752
cuboid   100  4p23.2994  50.292   47.752

media   0  1  1 -3
media   6  1  1  3
media   6  1  2 -1 -3
media   6  1  2 -1  3

media   9  1  5  -2
media   0  1  6  -5
media   6  1  7  -6
media   2  1  8  -7
media   3  1  9  -8
media   6  1  10  -9
media   8  1  100 -10
boundary 100

unit 3
'CV  top
cylinder  13  7.065      52.197  50.292
cylinder  14  7.749      52.197  50.292

cylinder  6   10.4775    52.197   50.292
cylinder  7   10.5994    52.197   50.292
cylinder  8   13.1394    52.197   50.292
cylinder  9   23.1775    52.197   50.292
cylinder  10  23.2994    52.197   50.292
cuboid   100  4p23.2994  52.197   50.292

media   6  1  13
media   6  1  14 -13

media   0  1  6  -14
media   6  1  7  -6
media   2  1  8  -7
media   3  1  9  -8
media   6  1  10  -9
media   8  1  100 -10
boundary 100

unit 4
'Top support and lid liner-bottom
cuboid    1    4p3.175  53.467  52.197
cuboid    2    4p4.7625 53.594  52.197
cylinder  3      8.89   55.372  52.197

cylinder  4   10.4775    55.372  52.197
cylinder  5   10.5994    55.372  52.197
cylinder  6   13.1394    55.372  52.197
cylinder  7   23.1775    55.372  52.197
cylinder  8   23.2994    55.372  52.197
cuboid   100  4p23.2994  55.372  52.197

media   6  1  1
media   0  1  2 -1
media   9  1  3 -2

media   0  1  4  -3
media   6  1  5  -4
media   2  1  6  -5
media   3  1  7  -6
media   6  1  8  -7
media   8  1  100 -8
boundary 100

unit 5
'Top portion of top honeycomb
cylinder  10     8.89     59.817  55.372
cylinder  11    10.4775   59.817  55.372

cylinder  5   10.5994    59.817  55.372
cylinder  6   13.1394    59.817  55.372
cylinder  7   23.1775    59.817  55.372
cylinder  8   23.2994    59.817  55.372
cuboid   100  4p23.2994  59.817  55.372

media   9  1  10
media   7  1  11  -10

media   6  1  5  -11
media   2  1  6  -5
media   3  1  7  -6
media   6  1  8  -7
media   8  1  100 -8
boundary 100
```

```
unit 6
'Top support above honeycomb
cylinder  12     3.75     61.214  59.817
cylinder  13    10.4775   61.214  59.817

cylinder  5   10.5994    61.214  59.817
cylinder  6   13.1394    61.214  59.817
cylinder  7   23.1775    61.214  59.817
cylinder  8   23.2994    61.214  59.817
cuboid   100  4p23.2994  61.214  59.817

media   0  1  12
media   7  1  13  -12

media   6  1  5  -13
media   2  1  6  -5
media   3  1  7  -6
media   6  1  8  -7
media   8  1  100 -8
boundary 100

unit 7
'Lid liner bottom
cylinder   1   10.147   61.708   61.214
cylinder   2   10.147   61.886   61.214
cylinder   3   10.147   71.087   61.214
cylinder   4   10.4775  71.087   61.214

cylinder  5   10.5994    71.087  61.214
cylinder  6   13.1394    71.087  61.214
cylinder  7   23.1775    71.087  61.214
cylinder  8   23.2994    71.087  61.214
cuboid   100  4p23.2994  71.087  61.214

media  6  1  1
media  2  1  2 -1
media  4  1  3 -2
media  6  1  4 -3

media   6  1  5  -4
media   2  1  6  -5
media   3  1  7  -6
media   6  1  8  -7
media   8  1  100 -8
boundary 100

unit 8
'flange
cylinder 1  10.147 71.563  71.087
cylinder 2  10.325 71.563  71.087
'lid liner
cylinder  3   10.4775    71.563  71.087
cylinder  4   10.5994    71.563  71.087
'flange
cylinder 5    23.2994    71.563  71.087
cuboid   100  4p23.2994  71.563  71.087

media   4  1  1
media   6  1  2 -1
media   0  1  3 -2
media   6  1  4 -3
media   6  1  5 -4
media   8  1  100 -5
boundary 100

unit 9
'Drum LID  only
cylinder  1  22.606      71.881  71.563
cylinder  2  23.2994     71.881  71.563
cuboid   100  4p23.2994  71.881  71.563
media   6  1  1
media   0  1  2  -1
media   8  1  100 -2
boundary 100

unit 10
' Liner top
cylinder  1  17.658      74.299  71.881
cylinder  2  17.780      74.421  71.881
cuboid   100  4p23.2994  74.421  71.881
media   5  1  1
media   6  1  2 -1
media   8  1  100 -2
boundary 100

global
unit 20
cuboid   1  46.5988   0    46.5988   0   88.74  0
array  1  1   place  1  1  1   23.2994  23.2994  14.319
```

```
cuboid   2  76.5988   -30.0    76.5988   -30.0   118.74  -30.0
media  8  1  2  -1
boundary 2

end geom

read array
ara=1 nux=1 nuy=1 nuz=10 fill 1 2 3 4 5 6 7 8 9 10  end fill
end array

end data
end
```

Case su_Pu_mtl_04_in

```
=csas26    parm=Centrm
su_Pu_metal_04: SU, dry,  4.4 kg pu sphere, no 3013, 100 g poly, pu bottom
238group
read comp
pu-239       1  den=19.84  1.0 293 end
arbm-fiber 0.256 4 0 0 1 13027 26.46 14000 23.14 11000 0.37 8016 50.03 2 1.0 293
end
arbm-foam  0.256  7 0 0 1  17000 0.15  14000 0.82 15000 0.82 8016 22.6 6012
62.88
                    1001  6.84   7000  5.89  3 1.0 293 end
arbm-vermi 0.368 10 0 0 1  14000 21.22  13027 5.47 20000 12.17 26000 5.4 22000
0.82
                    12000 8.90   11000 1.09 19000 1.22 16000 0.18 8016 43.53
                    4 1.0 293 end
arbm-mink 0.320 8 0 0 1    14000 37.71  22000 5.53  13027 6.39 6012 1.28  1001
0.84
                    8016  48.01  51000 0.09  35000 0.15   5 1.0 293 end
ss304       6  den=7.94  1.0 293  end
al          7  den=2.70  1.0 293  end
h2o         8  den=1.00 1.0 293  end
al          9  den=0.1922 1.0 293 end
poly(h2o)  10  den=0.95 end
end comp
read parm
  tme=500 gen=425 npg=1000  nsk=25 run=yes plt=no nub=yes
end parm

read geom
unit 1
'upto bot of top al support
'Ellosoidal bottom and cv leg support'
sphere    12   3.755  origin z=22.2
sphere    20   4.2741 origin z=22.2
'3013 dry
cylinder  31   4.84    17.045  6.545 origin z=11
cylinder  32   5.00    17.545  5.845 origin z=11
cylinder  33   5.49    27.34   5.84  origin z=11
cylinder  34   5.65    28.34   5.54  origin z=11
cylinder  35   5.85    28.80   5.50  origin z=11
cylinder  36   6.20    29.80   4.50  origin z=11
' bottom support
ellipsoid 1   6.41   6.41   3.496 origin z=10.2395 chord -z=0.0
ellipsoid 2   7.065  7.065  4.207 origin z=10.2395 chord -z=0.0
cylinder  3   5.113    8.532   5.0673
cylinder  4   5.715    8.533   5.0673
cylinder  6   10.4775   14.605  -1.905
' Al honeycomb
cylinder  15   7.066    10.2395  5.0673
cylinder  16   8.5725   47.752  -0.9652
cylinder  17   10.4775  47.752  14.605
'cv
cylinder  13   6.41     47.752   10.2395
cylinder  14   7.065    47.752   10.2395
'liner
cylinder  8   10.5994    47.752  -2.027
cylinder  9   13.1394    47.752  -4.567
cylinder  10  23.1775    47.752  -14.197
cylinder  11  23.2994    47.752  -14.319

cuboid   100  4p23.2994  47.752  -14.319
' spheres
media   1  1  12
media  10  1  20 -12
' bottom support
media   0  1  1
media   6  1  2  -1
media   0  1  3  -2
media   6  1  4  -3 -2
' 3013 can
media   0  1  31 -20
media   6  1  32 -31
media   0  1  33 -32
media   6  1  34 -33
```

```
media   0  1  35 -34
media   6  1  36 -35

media   7  1  6 -16
' Al honeycomb
media   0  1  15 -20 -2 -4
media   9  1  16 -15 -14
media   9  1  17 -16
' CV
media   0  1  13 -36
media   6  1  14 -13
' liner
media   6  1  8  -17 -6
media   2  1  9  -8
media   3  1  10 -9
media   6  1  11 -10
media   8  1  100 -11
boundary 100

unit 2
'CV flared near top
cone     1  6.721 50.292  6.41   47.752
cone     2  7.749 50.292  7.065  47.752
plane    3  zpl=1 con= -55.220

'Al honeycomb
cylinder 5  10.4775      50.292  47.752

cylinder  6   10.4775    50.292   47.752
cylinder  7   10.5994    50.292   47.752
cylinder  8   13.1394    50.292   47.752
cylinder  9   23.1775    50.292   47.752
cylinder  10  23.2994    50.292   47.752
cuboid   100  4p23.2994  50.292   47.752

media   0  1  1 -3
media   6  1  1  3
media   6  1  2 -1 -3
media   6  1  2 -1  3

media   9  1  5  -2
media   0  1  6  -5
media   6  1  7  -6
media   2  1  8  -7
media   3  1  9  -8
media   6  1  10  -9
media   8  1  100 -10
boundary 100

unit 3
'CV  top
cylinder  13  7.065      52.197  50.292
cylinder  14  7.749      52.197  50.292

cylinder  6   10.4775    52.197   50.292
cylinder  7   10.5994    52.197   50.292
cylinder  8   13.1394    52.197   50.292
cylinder  9   23.1775    52.197   50.292
cylinder  10  23.2994    52.197   50.292
cuboid   100  4p23.2994  52.197   50.292

media   6  1  13
media   6  1  14 -13

media   0  1  6  -14
media   6  1  7  -6
media   2  1  8  -7
media   3  1  9  -8
media   6  1  10  -9
media   8  1  100 -10
boundary 100

unit 4
'Top support and lid liner-bottom
cuboid    1    4p3.175  53.467  52.197
cuboid    2    4p4.7625 53.594  52.197
cylinder  3      8.89   55.372  52.197

cylinder  4   10.4775    55.372  52.197
cylinder  5   10.5994    55.372  52.197
cylinder  6   13.1394    55.372  52.197
cylinder  7   23.1775    55.372  52.197
cylinder  8   23.2994    55.372  52.197
cuboid   100  4p23.2994  55.372  52.197

media   6  1  1
media   0  1  2 -1
media   9  1  3 -2

media   0  1  4  -3
```

```
media   6  1  5  -4
media   2  1  6  -5
media   3  1  7  -6
media   6  1  8  -7
media   8  1  100 -8
boundary 100

unit 5
'Top portion of top honeycomb
cylinder  10     8.89     59.817  55.372
cylinder  11     10.4775   59.817  55.372

cylinder  5   10.5994    59.817  55.372
cylinder  6   13.1394    59.817  55.372
cylinder  7   23.1775    59.817  55.372
cylinder  8   23.2994    59.817  55.372
cuboid   100  4p23.2994  59.817  55.372

media   9  1  10
media   7  1  11  -10

media   6  1  5  -11
media   2  1  6  -5
media   3  1  7  -6
media   6  1  8  -7
media   8  1  100 -8
boundary 100

unit 6
'Top support above honeycomb
cylinder  12     3.75     61.214  59.817
cylinder  13     10.4775   61.214  59.817

cylinder  5   10.5994    61.214  59.817
cylinder  6   13.1394    61.214  59.817
cylinder  7   23.1775    61.214  59.817
cylinder  8   23.2994    61.214  59.817
cuboid   100  4p23.2994  61.214  59.817

media   0  1  12
media   7  1  13  -12

media   6  1  5  -13
media   2  1  6  -5
media   3  1  7  -6
media   6  1  8  -7
media   8  1  100 -8
boundary 100

unit 7
'Lid liner bottom
cylinder   1   10.147   61.708   61.214
cylinder   2   10.147   61.886   61.214
cylinder   3   10.147   71.087   61.214
cylinder   4   10.4775  71.087   61.214

cylinder  5   10.5994    71.087  61.214
cylinder  6   13.1394    71.087  61.214
cylinder  7   23.1775    71.087  61.214
cylinder  8   23.2994    71.087  61.214
cuboid   100  4p23.2994  71.087  61.214

media  6  1  1
media  2  1  2 -1
media  4  1  3 -2
media  6  1  4 -3

media   6  1  5  -4
media   2  1  6  -5
media   3  1  7  -6
media   6  1  8  -7
media   8  1  100 -8
boundary 100

unit 8
'flange
cylinder 1  10.147 71.563  71.087
cylinder 2  10.325 71.563  71.087
'lid liner
cylinder  3   10.4775    71.563  71.087
cylinder  4   10.5994    71.563  71.087
'flange
cylinder 5    23.2994    71.563  71.087
cuboid   100  4p23.2994  71.563  71.087

media   4  1  1
media   6  1  2 -1
media   0  1  3 -2
media   6  1  4 -3
media   6  1  5 -4
```

```
media   8  1  100 -5
boundary 100

unit 9
'Drum LID  only
cylinder  1  22.606      71.881  71.563
cylinder  2  23.2994     71.881  71.563
cuboid   100  4p23.2994  71.881  71.563
media   6  1  1
media   0  1  2  -1
media   8  1  100 -2
boundary 100

unit 10
' Liner top
cylinder  1  17.658      74.299  71.881
cylinder  2  17.780      74.421  71.881
cuboid   100  4p23.2994  74.421  71.881
media   5  1  1
media   6  1  2 -1
media   8  1  100 -2
boundary 100

global
unit 20
cuboid   1  46.5988   0    46.5988   0   88.74  0
array  1  1   place  1  1  1   23.2994  23.2994  14.319
cuboid   2  76.5988   -30.0    76.5988   -30.0   118.74  -30.0
media  8  1  2  -1
boundary 2

end geom

read array
ara=1 nux=1 nuy=1 nuz=10 fill 1 2 3 4 5 6 7 8 9 10  end fill
end array

end data
end
```

Case su_PuO2_01_in

```
=csas26    parm=Centrm
su_PuO2_01_in: SU, dry,  4.4 kg pu sphere, no 3013, no poly, pu bottom
238group
read comp
' H/X=3 PuO2
puo2       1  den=11.46   0.466290489  293 94239 100 end
h2o        1  den=0.9982  0.533709511  end
arbm-fiber 0.256 4 0 0 1 13027 26.46 14000 23.14 11000 0.37 8016 50.03 2 1.0 293
end
arbm-foam  0.256  7 0 0 1  17000 0.15  14000 0.82 15000 0.82 8016 22.6 6012
62.88
                   1001  6.84   7000  5.89  3 1.0 293 end
arbm-vermi 0.368 10 0 0 1  14000 21.22  13027 5.47 20000 12.17 26000 5.4 22000
0.82
                   12000 8.90   11000 1.09 19000 1.22 16000 0.18 8016 43.53
                   4 1.0 293 end
arbm-mink 0.320 8 0 0 1    14000 37.71  22000 5.53  13027 6.39 6012 1.28  1001
0.84
                   8016  48.01  51000 0.09  35000 0.15   5 1.0 293 end
ss304      6  den=7.94  1.0 293  end
al         7  den=2.70  1.0 293  end
h2o        8  den=1.00 1.0 293  end
al         9  den=0.1922 1.0 293 end
end comp
read parm
  tme=500 gen=425 npg=1000  nsk=25 run=yes plt=no nub=yes
end parm

read geom

unit 1
'upto bot of top al support
'Ellosoidal bottom and cv leg support'
sphere    12   6.0631  origin z=13
ellipsoid 1   6.41   6.41   3.496 origin z=10.2395 chord -z=0.0
ellipsoid 2   7.065  7.065  4.207 origin z=10.2395 chord -z=0.0
cylinder  3   5.113    8.532   5.0673
cylinder  4   5.715    8.533   5.0673
'bottom load support
cylinder  6   10.4775   14.605  -1.905
' Al honeycomb
cylinder  15   7.066    10.2395  5.0673
```

```
cylinder  16   8.5725   47.752  -0.9652
cylinder  17   10.4775  47.752  14.605
'cv
cylinder  13   6.41     47.752   10.2395
cylinder  14   7.065    47.752   10.2395
'liner
cylinder  8   10.5994    47.752  -2.027
cylinder  9   13.1394    47.752  -4.567
cylinder  10  23.1775    47.752  -14.197
cylinder  11  23.2994    47.752  -14.319

cuboid   100  4p23.2994  47.752  -14.319

media   1  1  12
media   0  1  1 -12
media   6  1  2  -1
media   0  1  3  -2
media   6  1  4  -3 -2

'media   0  1  5 -4
media   7  1  6 -16

media   0  1  15 -12 -2 -4
media   9  1  16 -15 -14
media   9  1  17 -16

media   0  1  13 -12
media   6  1  14 -13

media   6  1  8  -17 -6
media   2  1  9  -8
media   3  1  10 -9
media   6  1  11 -10
media   8  1  100 -11
boundary 100

unit 2
'CV flared near top
cone     1  6.721 50.292  6.41   47.752
cone     2  7.749 50.292  7.065  47.752
plane    3  zpl=1 con= -55.220

'Al honeycomb
cylinder 5  10.4775      50.292  47.752
cylinder  6   10.4775    50.292   47.752
cylinder  7   10.5994    50.292   47.752
cylinder  8   13.1394    50.292   47.752
cylinder  9   23.1775    50.292   47.752
cylinder  10  23.2994    50.292   47.752
cuboid   100  4p23.2994  50.292   47.752

media   0  1  1 -3
media   6  1  1  3
media   6  1  2 -1 -3
media   6  1  2 -1  3

media   9  1  5  -2
media   0  1  6  -5
media   6  1  7  -6
media   2  1  8  -7
media   3  1  9  -8
media   6  1  10  -9
media   8  1  100 -10
boundary 100

unit 3
'CV  top
cylinder  13  7.065      52.197  50.292
cylinder  14  7.749      52.197  50.292

cylinder  6   10.4775    52.197   50.292
cylinder  7   10.5994    52.197   50.292
cylinder  8   13.1394    52.197   50.292
cylinder  9   23.1775    52.197   50.292
cylinder  10  23.2994    52.197   50.292
cuboid   100  4p23.2994  52.197   50.292

media   6  1  13
media   6  1  14 -13

media   0  1  6  -14
media   6  1  7  -6
media   2  1  8  -7
media   3  1  9  -8
media   6  1  10  -9
media   8  1  100 -10
boundary 100

unit 4
```

```
'Top support and lid liner-bottom
cuboid    1    4p3.175  53.467  52.197
cuboid    2    4p4.7625 53.594  52.197
cylinder  3     8.89   55.372  52.197

cylinder  4   10.4775    55.372  52.197
cylinder  5   10.5994    55.372  52.197
cylinder  6   13.1394    55.372  52.197
cylinder  7   23.1775    55.372  52.197
cylinder  8   23.2994    55.372  52.197
cuboid   100  4p23.2994  55.372  52.197

media   6  1  1
media   0  1  2 -1
media   9  1  3 -2

media   0  1  4  -3
media   6  1  5  -4
media   2  1  6  -5
media   3  1  7  -6
media   6  1  8  -7
media   8  1  100 -8
boundary 100

unit 5
'Top portion of top honeycomb
cylinder  10     8.89     59.817  55.372
cylinder  11    10.4775   59.817  55.372

cylinder  5   10.5994    59.817  55.372
cylinder  6   13.1394    59.817  55.372
cylinder  7   23.1775    59.817  55.372
cylinder  8   23.2994    59.817  55.372
cuboid   100  4p23.2994  59.817  55.372

media   9  1  10
media   7  1  11  -10

media   6  1  5  -11
media   2  1  6  -5
media   3  1  7  -6
media   6  1  8  -7
media   8  1  100 -8
boundary 100

unit 6
'Top support above honeycomb
cylinder  12     3.75     61.214  59.817
cylinder  13    10.4775   61.214  59.817

cylinder  5   10.5994    61.214  59.817
cylinder  6   13.1394    61.214  59.817
cylinder  7   23.1775    61.214  59.817
cylinder  8   23.2994    61.214  59.817
cuboid   100  4p23.2994  61.214  59.817

media   0  1  12
media   7  1  13  -12

media   6  1  5  -13
media   2  1  6  -5
media   3  1  7  -6
media   6  1  8  -7
media   8  1  100 -8
boundary 100

unit 7
'Lid liner bottom
cylinder   1   10.147   61.708   61.214
cylinder   2   10.147   61.886   61.214
cylinder   3   10.147   71.087   61.214
cylinder   4   10.4775  71.087   61.214

cylinder  5   10.5994    71.087  61.214
cylinder  6   13.1394    71.087  61.214
cylinder  7   23.1775    71.087  61.214
cylinder  8   23.2994    71.087  61.214
cuboid   100  4p23.2994  71.087  61.214

media  6  1  1
media  2  1  2 -1
media  4  1  3 -2
media  6  1  4 -3

media   6  1  5  -4
media   2  1  6  -5
media   3  1  7  -6
media   6  1  8  -7
media   8  1  100 -8
boundary 100
```

```
unit 8
'flange
cylinder 1  10.147 71.563  71.087
cylinder 2  10.325 71.563  71.087
'lid liner
cylinder  3   10.4775    71.563  71.087
cylinder  4   10.5994    71.563  71.087
'flange
cylinder 5    23.2994    71.563  71.087
cuboid   100  4p23.2994  71.563  71.087

media   4  1  1
media   6  1  2 -1
media   0  1  3 -2
media   6  1  4 -3
media   6  1  5 -4
media   8  1  100 -5
boundary 100

unit 9
'Drum LID  only
cylinder  1  22.606      71.881  71.563
cylinder  2  23.2994     71.881  71.563
cuboid   100  4p23.2994  71.881  71.563
media   6  1  1
media   0  1  2  -1
media   8  1  100 -2
boundary 100

unit 10
' Liner top
cylinder  1  17.658      74.299  71.881
cylinder  2  17.780      74.421  71.881
cuboid   100  4p23.2994  74.421  71.881
media   5  1  1
media   6  1  2 -1
media   8  1  100 -2
boundary 100

global
unit 20
cuboid   1  46.5988   0    46.5988   0   88.74  0
array  1  1   place  1  1  1   23.2994  23.2994  14.319
cuboid   2  76.5988   -30.0    76.5988   -30.0   118.74  -30.0
media  8  1  2  -1
boundary 2

end geom

read array
ara=1 nux=1 nuy=1 nuz=10 fill 1 2 3 4 5 6 7 8 9 10  end fill
end array

end data
end
```

Case su_Pu_sol_13_in

```
=csas26    parm=Centrm
su_Pu_sol_13: SU, dry,  4.4 kg pu , no 3013, no poly, pu bottom
238group
read comp
pu-239       1  den=19.84  .907 293 end
h2o          1  den=0.9982 .093 293 end
arbm-fiber 0.256 4 0 0 1 13027 26.46 14000 23.14 11000 0.37 8016 50.03 2 1.0 293
end
arbm-foam  0.256  7 0 0 1  17000 0.15  14000 0.82 15000 0.82 8016 22.6 6012
62.88
                    1001  6.84   7000  5.89  3 1.0 293 end
arbm-vermi 0.368 10 0 0 1  14000 21.22  13027 5.47 20000 12.17 26000 5.4 22000
0.82
                    12000 8.90   11000 1.09 19000 1.22 16000 0.18 8016 43.53
                    4 1.0 293 end
arbm-mink 0.320 8 0 0 1    14000 37.71  22000 5.53  13027 6.39 6012 1.28  1001
0.84
                    8016  48.01  51000 0.09  35000 0.15   5 1.0 293 end
ss304      6  den=7.94  1.0 293  end
al         7  den=2.70  1.0 293  end
h2o        8  den=1.00 1.0 293  end
al         9  den=0.1922 1.0 293 end
end comp
read parm
  tme=500 gen=425 npg=1000  nsk=25 run=yes plt=no nub=yes
end parm

read geom
```

```
unit 1
'upto bot of top al support
'Ellosoidal bottom and cv leg support'
ellipsoid 1   6.41   6.41   3.496 origin z=10.2395 chord -z=0.0
ellipsoid 2   7.065  7.065  4.207 origin z=10.2395 chord -z=0.0
cylinder  3   5.113    8.532   5.0673
cylinder  4   5.715    8.533   5.0673
'bottom load support
cylinder  6   10.4775   14.605  -1.905
' Al honeycomb
cylinder  15   7.066    10.2395  5.0673
cylinder  16   8.5725   47.752  -0.9652
cylinder  17   10.4775  47.752  14.605
'cv
cylinder  13   6.41     47.752   10.2395
cylinder  14   7.065    47.752   10.2395
'solution
cylinder  20   6.41     10.385   10.2395
ellipsoid 21   6.41   6.41   3.496 origin z=10.2395 chord -z=0.0
'liner
cylinder  8   10.5994    47.752  -2.027
cylinder  9   13.1394    47.752  -4.567
cylinder  10  23.1775    47.752  -14.197
cylinder  11  23.2994    47.752  -14.319

cuboid   100  4p23.2994  47.752  -14.319

media   1  1  20
media   1  1  21
media   6  1  2  -21
media   0  1  3  -2
media   6  1  4  -3 -2

media   7  1  6 -16

media   0  1  15 -2 -4
media   9  1  16 -15 -14
media   9  1  17 -16

media   0  1  13 -20
media   6  1  14 -13 -20

media   6  1  8  -17 -6
media   2  1  9  -8
media   3  1  10 -9
media   6  1  11 -10
media   8  1  100 -11
boundary 100

unit 2
'CV flared near top
cone     1  6.721 50.292  6.41   47.752
cone     2  7.749 50.292  7.065  47.752
plane    3  zpl=1 con= -55.220

'Al honeycomb
cylinder 5  10.4775      50.292  47.752

cylinder  6   10.4775    50.292   47.752
cylinder  7   10.5994    50.292   47.752
cylinder  8   13.1394    50.292   47.752
cylinder  9   23.1775    50.292   47.752
cylinder  10  23.2994    50.292   47.752
cuboid   100  4p23.2994  50.292   47.752

media   0  1  1 -3
media   6  1  1  3
media   6  1  2 -1 -3
media   6  1  2 -1  3

media   9  1  5  -2
media   0  1  6  -5
media   6  1  7  -6
media   2  1  8  -7
media   3  1  9  -8
media   6  1  10  -9
media   8  1  100 -10
boundary 100

unit 3
'CV  top
cylinder  13  7.065      52.197  50.292
cylinder  14  7.749      52.197  50.292

cylinder  6   10.4775    52.197   50.292
cylinder  7   10.5994    52.197   50.292
cylinder  8   13.1394    52.197   50.292
cylinder  9   23.1775    52.197   50.292
cylinder  10  23.2994    52.197   50.292
cuboid   100  4p23.2994  52.197   50.292
```

```
media   6  1  13
media   6  1  14 -13

media   0  1  6  -14
media   6  1  7  -6
media   2  1  8  -7
media   3  1  9  -8
media   6  1  10  -9
media   8  1  100 -10
boundary 100

unit 4
'Top support and lid liner-bottom
cuboid    1    4p3.175  53.467  52.197
cuboid    2    4p4.7625 53.594  52.197
cylinder  3      8.89   55.372  52.197

cylinder  4   10.4775    55.372  52.197
cylinder  5   10.5994    55.372  52.197
cylinder  6   13.1394    55.372  52.197
cylinder  7   23.1775    55.372  52.197
cylinder  8   23.2994    55.372  52.197
cuboid   100  4p23.2994  55.372  52.197

media   6  1  1
media   0  1  2 -1
media   9  1  3 -2

media   0  1  4  -3
media   6  1  5  -4
media   2  1  6  -5
media   3  1  7  -6
media   6  1  8  -7
media   8  1  100 -8
boundary 100

unit 5
'Top portion of top honeycomb
cylinder  10     8.89     59.817  55.372
cylinder  11    10.4775   59.817  55.372

cylinder  5   10.5994    59.817  55.372
cylinder  6   13.1394    59.817  55.372
cylinder  7   23.1775    59.817  55.372
cylinder  8   23.2994    59.817  55.372
cuboid   100  4p23.2994  59.817  55.372

media   9  1  10
media   7  1  11  -10

media   6  1  5  -11
media   2  1  6  -5
media   3  1  7  -6
media   6  1  8  -7
media   8  1  100 -8
boundary 100

unit 6
'Top support above honeycomb
cylinder  12     3.75     61.214  59.817
cylinder  13    10.4775   61.214  59.817

cylinder  5   10.5994    61.214  59.817
cylinder  6   13.1394    61.214  59.817
cylinder  7   23.1775    61.214  59.817
cylinder  8   23.2994    61.214  59.817
cuboid   100  4p23.2994  61.214  59.817

media   0  1  12
media   7  1  13  -12

media   6  1  5  -13
media   2  1  6  -5
media   3  1  7  -6
media   6  1  8  -7
media   8  1  100 -8
boundary 100

unit 7
'Lid liner bottom
cylinder   1   10.147   61.708   61.214
cylinder   2   10.147   61.886   61.214
cylinder   3   10.147   71.087   61.214
cylinder   4   10.4775  71.087   61.214

cylinder  5   10.5994    71.087  61.214
cylinder  6   13.1394    71.087  61.214
cylinder  7   23.1775    71.087  61.214
cylinder  8   23.2994    71.087  61.214
```

```
cuboid   100  4p23.2994  71.087  61.214

media  6  1  1
media  2  1  2 -1
media  4  1  3 -2
media  6  1  4 -3

media   6  1  5  -4
media   2  1  6  -5
media   3  1  7  -6
media   6  1  8  -7
media   8  1  100 -8
boundary 100

unit 8
'flange
cylinder 1  10.147 71.563  71.087
cylinder 2  10.325 71.563  71.087
'lid liner
cylinder  3   10.4775    71.563  71.087
cylinder  4   10.5994    71.563  71.087
'flange
cylinder 5    23.2994    71.563  71.087
cuboid   100  4p23.2994  71.563  71.087

media   4  1  1
media   6  1  2 -1
media   0  1  3 -2
media   6  1  4 -3
media   6  1  5 -4
media   8  1  100 -5
boundary 100

unit 9
'Drum LID  only
cylinder  1  22.606      71.881  71.563
cylinder  2  23.2994     71.881  71.563
cuboid   100  4p23.2994  71.881  71.563
media   6  1  1
media   0  1  2  -1
media   8  1  100 -2
boundary 100

unit 10
' Liner top
cylinder  1  17.658      74.299  71.881
cylinder  2  17.780      74.421  71.881
cuboid   100  4p23.2994  74.421  71.881
media   5  1  1
media   6  1  2 -1
media   8  1  100 -2
boundary 100

global
unit 20
cuboid   1  46.5988   0    46.5988   0   88.74  0
array  1  1   place  1  1  1   23.2994  23.2994  14.319
cuboid   2  76.5988   -30.0    76.5988   -30.0   118.74  -30.0
media  8  1  2  -1
boundary 2

end geom

read array
ara=1 nux=1 nuy=1 nuz=10 fill 1 2 3 4 5 6 7 8 9 10  end fill
end array

end data
end
```

Case su_U235_sol_09_in

```
=csas26    parm=Centrm
su_u235_sol_09: SU, dry,   kg u235 , no 3013, no poly, pu bottom
238group
read comp
u-235        1  den=19.05  0.140 293 end
h2o          1  den=0.9982 0.860 293 end
arbm-fiber 0.256 4 0 0 1 13027 26.46 14000 23.14 11000 0.37 8016 50.03 2 1.0 293
end
arbm-foam  0.256  7 0 0 1  17000 0.15  14000 0.82 15000 0.82 8016 22.6 6012
62.88
                    1001  6.84   7000  5.89  3 1.0 293 end
arbm-vermi 0.368 10 0 0 1  14000 21.22  13027 5.47 20000 12.17 26000 5.4 22000
0.82
                    12000 8.90   11000 1.09 19000 1.22 16000 0.18 8016 43.53
                    4 1.0 293 end
arbm-mink 0.320 8 0 0 1    14000 37.71  22000 5.53  13027 6.39 6012 1.28  1001
0.84
                    8016  48.01  51000 0.09  35000 0.15   5 1.0 293 end
ss304       6  den=7.94  1.0 293  end
al          7  den=2.70  1.0 293  end
h2o         8  den=1.00 1.0 293  end
al          9  den=0.1922 1.0 293 end
end comp
read parm
  tme=500 gen=425 npg=1000  nsk=25 run=yes plt=no nub=yes
end parm

read geom

unit 1
'upto bot of top al support
'Ellosoidal bottom and cv leg support'
ellipsoid 1   6.41   6.41   3.496 origin z=10.2395 chord -z=0.0
ellipsoid 2   7.065  7.065  4.207 origin z=10.2395 chord -z=0.0
cylinder  3   5.113    8.532   5.0673
cylinder  4   5.715    8.533   5.0673
'bottom load support
cylinder  6   10.4775   14.605  -1.905
' Al honeycomb
cylinder  15   7.066    10.2395  5.0673
cylinder  16   8.5725   47.752  -0.9652
cylinder  17   10.4775  47.752  14.605
'cv
cylinder  13   6.41     47.752   10.2395
cylinder  14   7.065    47.752   10.2395
'solution
cylinder  20   6.41     47.752   10.2395
ellipsoid 21   6.41   6.41   3.496 origin z=10.2395 chord -z=0.0
'liner
cylinder  8   10.5994    47.752  -2.027
cylinder  9   13.1394    47.752  -4.567
cylinder  10  23.1775    47.752  -14.197
cylinder  11  23.2994    47.752  -14.319

cuboid   100  4p23.2994  47.752  -14.319

media   1  1  20
media   1  1  21
media   6  1  2  -21
media   0  1  3  -2
media   6  1  4  -3 -2

media   7  1  6 -16

media   0  1  15 -2 -4
media   9  1  16 -15 -14
media   9  1  17 -16

media   0  1  13 -20
media   6  1  14 -13 -20

media   6  1  8  -17 -6
media   2  1  9  -8
media   3  1  10 -9
media   6  1  11 -10
media   8  1  100 -11
boundary 100

unit 2
'CV flared near top
cone     1  6.721 50.292  6.41   47.752
cone     2  7.749 50.292  7.065  47.752
plane    3  zpl=1 con= -55.220

'Al honeycomb
cylinder 5  10.4775      50.292  47.752
```

```
cylinder  6   10.4775    50.292   47.752
cylinder  7   10.5994    50.292   47.752
cylinder  8   13.1394    50.292   47.752
cylinder  9   23.1775    50.292   47.752
cylinder  10  23.2994    50.292   47.752
cuboid   100  4p23.2994  50.292   47.752

media   0  1  1 -3
media   6  1  1  3
media   6  1  2 -1 -3
media   6  1  2 -1  3

media   9  1  5  -2
media   0  1  6  -5
media   6  1  7  -6
media   2  1  8  -7
media   3  1  9  -8
media   6  1  10  -9
media   8  1  100 -10
boundary 100

unit 3
'CV  top
cylinder  13  7.065      52.197  50.292
cylinder  14  7.749      52.197  50.292

cylinder  6   10.4775    52.197   50.292
cylinder  7   10.5994    52.197   50.292
cylinder  8   13.1394    52.197   50.292
cylinder  9   23.1775    52.197   50.292
cylinder  10  23.2994    52.197   50.292
cuboid   100  4p23.2994  52.197   50.292

media   6  1  13
media   6  1  14 -13

media   0  1  6  -14
media   6  1  7  -6
media   2  1  8  -7
media   3  1  9  -8
media   6  1  10  -9
media   8  1  100 -10
boundary 100

unit 4
'Top support and lid liner-bottom
cuboid    1    4p3.175  53.467  52.197
cuboid    2    4p4.7625 53.594  52.197
cylinder  3      8.89   55.372  52.197

cylinder  4   10.4775    55.372  52.197
cylinder  5   10.5994    55.372  52.197
cylinder  6   13.1394    55.372  52.197
cylinder  7   23.1775    55.372  52.197
cylinder  8   23.2994    55.372  52.197
cuboid   100  4p23.2994  55.372  52.197

media   6  1  1
media   0  1  2 -1
media   9  1  3 -2

media   0  1  4  -3
media   6  1  5  -4
media   2  1  6  -5
media   3  1  7  -6
media   6  1  8  -7
media   8  1  100 -8
boundary 100

unit 5
'Top portion of top honeycomb
cylinder  10     8.89     59.817  55.372
cylinder  11    10.4775   59.817  55.372

cylinder  5   10.5994    59.817  55.372
cylinder  6   13.1394    59.817  55.372
cylinder  7   23.1775    59.817  55.372
cylinder  8   23.2994    59.817  55.372
cuboid   100  4p23.2994  59.817  55.372

media   9  1  10
media   7  1  11  -10

media   6  1  5  -11
media   2  1  6  -5
media   3  1  7  -6
media   6  1  8  -7
media   8  1  100 -8
boundary 100
```

```
unit 6
'Top support above honeycomb
cylinder  12     3.75     61.214  59.817
cylinder  13    10.4775   61.214  59.817

cylinder  5   10.5994    61.214  59.817
cylinder  6   13.1394    61.214  59.817
cylinder  7   23.1775    61.214  59.817
cylinder  8   23.2994    61.214  59.817
cuboid   100  4p23.2994  61.214  59.817

media   0  1  12
media   7  1  13  -12

media   6  1  5  -13
media   2  1  6  -5
media   3  1  7  -6
media   6  1  8  -7
media   8  1  100 -8
boundary 100

unit 7
'Lid liner bottom
cylinder   1   10.147   61.708   61.214
cylinder   2   10.147   61.886   61.214
cylinder   3   10.147   71.087   61.214
cylinder   4   10.4775  71.087   61.214

cylinder  5   10.5994    71.087  61.214
cylinder  6   13.1394    71.087  61.214
cylinder  7   23.1775    71.087  61.214
cylinder  8   23.2994    71.087  61.214
cuboid   100  4p23.2994  71.087  61.214

media  6  1  1
media  2  1  2 -1
media  4  1  3 -2
media  6  1  4 -3

media   6  1  5  -4
media   2  1  6  -5
media   3  1  7  -6
media   6  1  8  -7
media   8  1  100 -8
boundary 100

unit 8
'flange
cylinder 1  10.147 71.563  71.087
cylinder 2  10.325 71.563  71.087
'lid liner
cylinder  3   10.4775    71.563  71.087
cylinder  4   10.5994    71.563  71.087
'flange
cylinder 5    23.2994    71.563  71.087
cuboid   100  4p23.2994  71.563  71.087

media   4  1  1
media   6  1  2 -1
media   0  1  3 -2
media   6  1  4 -3
media   6  1  5 -4
media   8  1  100 -5
boundary 100

unit 9
'Drum LID  only
cylinder  1  22.606      71.881  71.563
cylinder  2  23.2994     71.881  71.563
cuboid   100  4p23.2994  71.881  71.563
media   6  1  1
media   0  1  2  -1
media   8  1  100 -2
boundary 100

unit 10
' Liner top
cylinder  1  17.658      74.299  71.881
cylinder  2  17.780      74.421  71.881
cuboid   100  4p23.2994  74.421  71.881
media   5  1  1
media   6  1  2 -1
media   8  1  100 -2
boundary 100

global
unit 20
cuboid   1  46.5988   0    46.5988   0   88.74  0
array  1  1   place  1  1  1   23.2994  23.2994  14.319
cuboid   2  76.5988   -30.0    76.5988   -30.0   118.74  -30.0
```

```
media  8  1  2  -1
boundary 2

end geom

read array
ara=1 nux=1 nuy=1 nuz=10 fill 1 2 3 4 5 6 7 8 9 10  end fill
end array

end data
end
```

Case nct_cvfl

```
=csas26    parm=Centrm
nct_cvfl  gpfp, NCT, dry,  4.4 kg pu , 3013,100g poly, CV flooded
'infinite array, all flooded cv flooded 3013 dry
238group
read comp
pu-239       1  den=19.84  1.0 293 end
arbm-fiber 0.256 4 0 0 1 13027 26.46 14000 23.14 11000 0.37 8016 50.03 2 1.0 293
end
arbm-foam  0.256  7 0 0 1  17000 0.15  14000 0.82 15000 0.82 8016 22.6 6012
62.88
                    1001  6.84   7000  5.89  3 1.0 293 end
arbm-vermi 0.368 10 0 0 1  14000 21.22  13027 5.47 20000 12.17 26000 5.4 22000
0.82
                    12000 8.90   11000 1.09 19000 1.22 16000 0.18 8016 43.53
                    4 1.0 293 end
arbm-mink 0.320 8 0 0 1    14000 37.71  22000 5.53  13027 6.39 6012 1.28  1001
0.84
                    8016  48.01  51000 0.09  35000 0.15   5 1.0 293 end
ss304       6  den=7.94  1.0 293  end
al          7  den=2.70  1.0 293  end
h2o         8  den=1.00  1.0 293  end
poly(h2o) 9  den=0.95  1.0 293 end
end comp
read parm tme=500 gen=425 npg=1000  nsk=25 run=yes plt=no nub=yes end parm
read geom

unit 1
'upto bot of top al support
'Ellosoidal bottom and cv leg support'
sphere    12   3.755 origin z=10.819
sphere    15   4.274 origin z=10.819
'3013 dry
cylinder  31   4.84    17.045  6.545
cylinder  32   5.00    17.545  5.845
cylinder  33   5.49    27.34   5.84
cylinder  34   5.65    28.34   5.54
cylinder  35   5.85    28.80   5.50
cylinder  36   6.20    29.80   4.50
ellipsoid 1   7.703  7.703  3.496 origin z=4.207 chord -z=0.0
ellipsoid 2   8.414  8.414  4.207 origin z=4.207 chord -z=0.0
cylinder  3   6.410   2.5   -0.9652
cylinder  4   7.075   2.5   -0.9652
'bot support
cylinder  5   8.5725     54.28  -0.9652
cylinder  6   10.16      14.605 -1.905
'cv
cylinder  13   7.703    54.28   4.207
cylinder  14   8.414    54.28   4.207
'liner
cylinder  7   10.4775    54.28  -1.905
cylinder  8   10.5994    54.28  -2.027
cylinder  9   13.1394    54.28  -4.567
cylinder  10  23.1775    54.28  -14.197
cylinder  11  23.2994    54.28  -14.319

cuboid   100  4p23.2994  54.28  -14.319

media   1  1  12
media   9  1  15 -12

media   0  1  31 -15
media   6  1  32 -31
media   0  1  33 -32
media   6  1  34 -33
media   0  1  35 -34
media   6  1  36 -35

media   8  1  1
media   6  1  2  -1
media   8  1  3  -2
media   6  1  4 -3 -2

media   8  1  5 -4 -2 -14
media   7  1  6 -5
```

```
media   8  1  13 -36
media   6  1  14 -13

media   8  1  7  -6 -5
media   6  1  8  -7
media   8  1  9  -8
media   8  1  10 -9
media   6  1  11 -10
media   8  1  100 -11
boundary 100

unit 2
'CV portion before the flare
cylinder  1   7.703    54.61  54.28
cylinder  2   8.414    54.61  54.28

'bottom portion of top support
cylinder 3  9.0805     54.61  54.28
cylinder 4  10.16      54.61  54.28

cylinder  6   10.4775    54.61   54.28
cylinder  7   10.5994    54.61   54.28
cylinder  8   13.1394    54.61   54.28
cylinder  9   23.1775    54.61   54.28
cylinder  10  23.2994    54.61   54.28
cuboid   100  4p23.2994  54.61  54.28

media   8  1  1
media   6  1  2  -1

media   8  1  3  -2
media   7  1  4  -3

media   8  1  6  -4
media   6  1  7  -6
media   8  1  8  -7
media   8  1  9  -8
media   6  1  10  -9
media   8  1  100 -10
boundary 100

unit 3
'CV flared near top
cone     1  8.014 56.82  7.703  54.61
cone     2  9.042 56.82  8.414  54.61
plane    3  zpl=1 con= -55.220

'top support
cylinder 4  9.0805       56.82  54.61
cylinder 5  10.16        56.82  54.61

cylinder  6   10.4775    56.82   54.61
cylinder  7   10.5994    56.82   54.61
cylinder  8   13.1394    56.82   54.61
cylinder  9   23.1775    56.82   54.61
cylinder  10  23.2994    56.82   54.61
cuboid   100  4p23.2994  56.82   54.61

media   8  1  1 -3
media   6  1  1  3
media   6  1  2 -1 -3
media   6  1  2 -1  3

media   8  1  4  -2
media   7  1  5  -4
media   8  1  6  -5
media   6  1  7  -6
media   8  1  8  -7
media   8  1  9  -8
media   6  1  10  -9
media   8  1  100 -10
boundary 100

unit 4
'CV  top
 cylinder  13  8.414      58.725  56.82
cylinder  14  9.042      58.725  56.82
'top support
cylinder 4  9.0805       58.725  56.82
cylinder 5  10.16        58.725  56.82

cylinder  6   10.4775    58.725   56.82
cylinder  7   10.5994    58.725   56.82
cylinder  8   13.1394    58.725   56.82
cylinder  9   23.1775    58.725   56.82
cylinder  10  23.2994    58.725   56.82
cuboid   100  4p23.2994  58.725   56.82

media   6  1  13
```

```
media   6  1  14 -13

media   8  1  4 -14
media   7  1  5  -4
media   8  1  6  -5
media   6  1  7  -6
media   8  1  8  -7
media   8  1  9  -8
media   6  1  10  -9
media   8  1  100 -10
boundary 100

unit 5
'Top support and lid liner-bottom
cuboid    1    4p3.175  59.995  58.725
cuboid    2    4p3.4925 60.122  58.725
cylinder  3     10.160   60.122  58.725

cylinder 11  10.147 72.549  63.348
cylinder 12  10.147 72.549  60.808
cylinder 13  10.325 72.549  60.630

cylinder  4   10.4775    72.549  58.725
cylinder  5   10.5994    72.549  58.725
cylinder  6   13.1394    72.549  58.725
cylinder  7   23.1775    72.549  58.725
cylinder  8   23.2994    72.549  58.725
cuboid   100  4p23.2994  72.549  58.725

media   6  1  1
media   8  1  2 -1
media   7  1  3 -2

media   8  1  11
media   8  1  12 -11
media   6  1  13 -12 -11

media   8  1  4 -3 -13
media   6  1  5  -4
media   8  1  6  -5
media   8  1  7  -6
media   6  1  8  -7
media   8  1  100 -8
boundary 100

unit 6
'flange
cylinder 1  10.147 73.025  72.549
cylinder 2  10.325 73.025  72.549
'lid liner
cylinder  3   10.4775    73.025  72.549
cylinder  4   10.5994    73.025  72.549
'flange
cylinder 5    23.2994    73.025  72.549
cuboid   100  4p23.2994  73.025  72.549

media   8  1  1
media   6  1  2 -1
media   8  1  3 -2
media   6  1  4 -3
media   6  1  5 -4
media   8  1  100 -5
boundary 100

unit 7
'Drum LID  only
cylinder  1  22.606     73.343  73.025
cylinder  2  23.2994    73.343  73.025
cuboid   100  4p23.2994 73.343  73.025
media   6  1  1
media   8  1  2  -1
media   8  1  100 -2
boundary 100

unit 8
' LIner top
cylinder  1  17.658   75.761  73.343
cylinder  2  17.780   75.883  73.343
cuboid   100  4p23.2994 75.883  73.343
media   5  1  1
media   6  1  2 -1
media   8  1  100 -2
boundary 100

global unit 10
cuboid   1  46.5988   0    46.5988   0   90.202  0
array  1  1   place  1  1  1   23.2994  23.2994  14.319
boundary 1
end geom
```

```
read array
ara=1 nux=1 nuy=1 nuz=8 fill 1 2 3  4 5 6  7 8  end fill
end array

read bound xyf=mirror zfc=periodic end bound

end data
end
```

Case nct_pu1

```
=csas26    parm=Centrm
nct_pu1  gpfp, NCT, dry,  4.4 kg pu , no 3013, 100g poly, infinite array
238group
read comp
pu-239       1  den=19.84  1.0 293 end
arbm-fiber 0.256 4 0 0 1 13027 26.46 14000 23.14 11000 0.37 8016 50.03 2 1.0 293
end
arbm-foam  0.256  7 0 0 1  17000 0.15  14000 0.82 15000 0.82 8016 22.6 6012
62.88
                    1001  6.84   7000  5.89  3 1.0 293 end
arbm-vermi 0.368 10 0 0 1  14000 21.22  13027 5.47 20000 12.17 26000 5.4 22000
0.82
                    12000 8.90   11000 1.09 19000 1.22 16000 0.18 8016 43.53
                    4 1.0 293 end
arbm-mink 0.320 8 0 0 1    14000 37.71  22000 5.53  13027 6.39 6012 1.28  1001
0.84
                    8016  48.01  51000 0.09  35000 0.15   5 1.0 293 end
ss304       6  den=7.94  1.0 293  end
al          7  den=2.70  1.0 293  end
h2o         8  den=1.00  1.0 293  end
poly(h2o) 9  den=0.95  1.0 293 end
end comp
read parm tme=500 gen=425 npg=1000  nsk=25 run=yes plt=no nub=yes end parm
read geom

unit 1
'upto bot of top al support
'Ellosoidal bottom and cv leg support'
sphere    12   3.755 origin z=8.519
sphere    15   4.274 origin z=8.519
ellipsoid 1   7.703  7.703  3.496 origin z=4.207 chord -z=0.0
ellipsoid 2   8.414  8.414  4.207 origin z=4.207 chord -z=0.0
cylinder  3   6.410   2.5   -0.9652
cylinder  4   7.075   2.5   -0.9652
'bot support
cylinder  5   8.5725     54.28  -0.9652
cylinder  6   10.16      14.605 -1.905
'cv
cylinder  13   7.703    54.28   4.207
cylinder  14   8.414    54.28   4.207
'liner
cylinder  7   10.4775    54.28  -1.905
cylinder  8   10.5994    54.28  -2.027
cylinder  9   13.1394    54.28  -4.567
cylinder  10  23.1775    54.28  -14.197
cylinder  11  23.2994    54.28  -14.319

cuboid   100  4p23.2994  54.28  -14.319

media   1  1  12
media   9  1  15 -12
media   0  1  1
media   6  1  2  -1
media   0  1  3  -2
media   6  1  4 -3 -2

media   0  1  5 -4 -2 -14
media   7  1  6 -5

media   0  1  13 -15
media   6  1  14 -13

media   0  1  7  -6 -5
media   6  1  8  -7
media   2  1  9  -8
media   3  1  10 -9
media   6  1  11 -10
media   0  1  100 -11
boundary 100

unit 2
'CV portion before the flare
cylinder  1   7.703    54.61  54.28
cylinder  2   8.414    54.61  54.28

'bottom portion of top support
cylinder 3  9.0805     54.61  54.28
```

```
cylinder 4  10.16      54.61  54.28

cylinder  6   10.4775    54.61   54.28
cylinder  7   10.5994    54.61   54.28
cylinder  8   13.1394    54.61   54.28
cylinder  9   23.1775    54.61   54.28
cylinder  10  23.2994    54.61   54.28
cuboid   100  4p23.2994  54.61  54.28

media   0  1  1
media   6  1  2  -1

media   0  1  3  -2
media   7  1  4  -3

media   0  1  6  -4
media   6  1  7  -6
media   2  1  8  -7
media   3  1  9  -8
media   6  1  10  -9
media   0  1  100 -10
boundary 100

unit 3
'CV flared near top
cone     1  8.014 56.82  7.703  54.61
cone     2  9.042 56.82  8.414  54.61
plane    3  zpl=1 con= -55.220

'top support
cylinder 4  9.0805       56.82  54.61
cylinder 5  10.16        56.82  54.61

cylinder  6   10.4775    56.82   54.61
cylinder  7   10.5994    56.82   54.61
cylinder  8   13.1394    56.82   54.61
cylinder  9   23.1775    56.82   54.61
cylinder  10  23.2994    56.82   54.61
cuboid   100  4p23.2994  56.82   54.61

media   0  1  1 -3
media   6  1  1  3
media   6  1  2 -1 -3
media   6  1  2 -1  3
media   0  1  4  -2
media   7  1  5  -4
media   0  1  6  -5
media   6  1  7  -6
media   2  1  8  -7
media   3  1  9  -8
media   6  1  10  -9
media   0  1  100 -10
boundary 100

unit 4
'CV  top
 cylinder  13  8.414      58.725  56.82
cylinder  14  9.042      58.725  56.82
'top support
cylinder 4  9.0805       58.725  56.82
cylinder 5  10.16        58.725  56.82

cylinder  6   10.4775    58.725   56.82
cylinder  7   10.5994    58.725   56.82
cylinder  8   13.1394    58.725   56.82
cylinder  9   23.1775    58.725   56.82
cylinder  10  23.2994    58.725   56.82
cuboid   100  4p23.2994  58.725   56.82

media   6  1  13
media   6  1  14 -13

media   0  1  4 -14
media   7  1  5  -4
media   0  1  6  -5
media   6  1  7  -6
media   2  1  8  -7
media   3  1  9  -8
media   6  1  10  -9
media   0  1  100 -10
boundary 100

unit 5
'Top support and lid liner-bottom
cuboid    1    4p3.175  59.995  58.725
cuboid    2    4p3.4925 60.122  58.725
cylinder  3     10.160   60.122  58.725

cylinder 11  10.147 72.549  63.348
```

```
cylinder 12  10.147 72.549  60.808
cylinder 13  10.325 72.549  60.630

cylinder  4   10.4775    72.549  58.725
cylinder  5   10.5994    72.549  58.725
cylinder  6   13.1394    72.549  58.725
cylinder  7   23.1775    72.549  58.725
cylinder  8   23.2994    72.549  58.725
cuboid   100  4p23.2994  72.549  58.725

media   6  1  1
media   0  1  2 -1
media   7  1  3 -2

media   4  1  11
media   2  1  12 -11
media   6  1  13 -12 -11

media   0  1  4 -3 -13
media   6  1  5  -4
media   2  1  6  -5
media   3  1  7  -6
media   6  1  8  -7
media   0  1  100 -8
boundary 100

unit 6
'flange
cylinder 1  10.147 73.025  72.549
cylinder 2  10.325 73.025  72.549
'lid liner
cylinder  3   10.4775    73.025  72.549
cylinder  4   10.5994    73.025  72.549
'flange
cylinder 5    23.2994    73.025  72.549
cuboid   100  4p23.2994  73.025  72.549

media   4  1  1
media   6  1  2 -1
media   0  1  3 -2
media   6  1  4 -3
media   6  1  5 -4
media   0  1  100 -5
boundary 100

unit 7
'Drum LID  only
cylinder  1  22.606     73.343  73.025
cylinder  2  23.2994    73.343  73.025
cuboid   100  4p23.2994 73.343  73.025
media   6  1  1
media   0  1  2  -1
media   0  1  100 -2
boundary 100

unit 8
' LIner top
cylinder  1  17.658   75.761  73.343
cylinder  2  17.780   75.883  73.343
cuboid   100  4p23.2994 75.883  73.343
media   5  1  1
media   6  1  2 -1
media   0  1  100 -2
boundary 100

global unit 10
cuboid   1  46.5988   0    46.5988   0   90.202  0
array  1  1   place  1  1  1   23.2994  23.2994  14.319
boundary 1
end geom

read array
ara=1 nux=1 nuy=1 nuz=8 fill 1 2 3  4 5 6  7 8  end fill
end array

read bound xyf=mirror zfc=periodic end bound

end data
end
```

Case hac_2clus

```
=csas26    parm=Centrm
hac_2clus.in gpfp, HAC, dry,4.4 kg pu, no 3013, 100g poly, 6x6x3, 30 cm refl
'damaged drum, dia reduced by 2", ht by 3" (2" top and 1" bot), no  foam, no
fiberfrax
'no vermiculite, no min-k-2000, dia reduced bt 7% for tri pitch REVISED cuboid
'cv and liner moved left and rigft for 2-cluster model, B-a B-a B-a
238group
read comp
pu-239       1  den=19.84  1.0 293 end
arbm-fiber 0.256 4 0 0 1 13027 26.46 14000 23.14 11000 0.37 8016 50.03 2 1.0 293
end
arbm-foam  0.256  7 0 0 1  17000 0.15  14000 0.82 15000 0.82 8016 22.6 6012
62.88
                    1001  6.84   7000  5.89  3 1.0 293 end
arbm-vermi 0.368 10 0 0 1  14000 21.22  13027 5.47 20000 12.17 26000 5.4 22000
0.82
                    12000 8.90   11000 1.09 19000 1.22 16000 0.18 8016 43.53
                    4 1.0 293 end
arbm-mink 0.320 8 0 0 1    14000 37.71  22000 5.53  13027 6.39 6012 1.28  1001
0.84
                    8016  48.01  51000 0.09  35000 0.15   5 1.0 293 end
ss304       6  den=7.94  1.0 293  end
al          7  den=2.70  1.0 293  end
h2o         8  den=1.00  1.0 293  end
poly(h2o) 9  den=0.95  1.0 293 end
end comp
read parm tme=500 gen=425 npg=1000  nsk=25 run=yes plt=no nub=yes end parm
read geom

unit 1
'B-right Pu - upto bot of top al support
'Ellosoidal bottom and cv leg support'
sphere    12   3.755 origin x=3.428 z=8.519
sphere    15   4.274 origin x=3.428 z=8.519
ellipsoid 1   7.703  7.703  3.496 origin z=4.207 chord -z=0.0
ellipsoid 2   8.414  8.414  4.207 origin z=4.207 chord -z=0.0
cylinder  3   6.410   2.5   -0.9652
cylinder  4   7.065   2.5   -0.9652
'bot support
cylinder  5   8.5725     54.28  -0.9652
cylinder  6   10.16      14.605 -1.905
'cv
cylinder  13   7.703    54.28   4.207
cylinder  14   8.414    54.28   4.207
'liner
cylinder  7   10.4775    54.28  -1.905
cylinder  8   10.5994    54.28  -2.027
cylinder  9   13.1394    54.28  -4.567  origin x=-2.54
cylinder  10  19.1379    54.28  -11.657 origin x= -8.5385
cylinder  11  19.3063    54.28  -11.779 origin x= -8.5385

cuboid   100  10.7678 -27.8448  2p19.3063  54.28  -11.779

media   1  1  12
media   9  1  15 -12
media   0  1  1
media   6  1  2  -1
media   0  1  3  -2
media   6  1  4 -3 -2

media   0  1  5 -4 -2 -14
media   7  1  6 -5

media   0  1  13 -15
media   6  1  14 -13

media   0  1  7  -6 -5
media   6  1  8  -7
media   0  1  9  -8
media   0  1  10 -9
media   6  1  11 -10
media   0  1  100 -11
boundary 100

unit 2
'CV portion before the flare
cylinder  1   7.703    54.61  54.28
cylinder  2   8.414    54.61  54.28

'bottom portion of top support
cylinder 3  9.0805     54.61  54.28
cylinder 4  10.16      54.61  54.28

cylinder  6   10.4775    54.61   54.28
cylinder  7   10.5994    54.61   54.28
cylinder  8   13.1394    54.61   54.28 origin x=-2.54
cylinder  9   19.1379    54.61   54.28 origin x= -8.5385
```

```
cylinder  10  19.3063    54.61   54.28 origin x= -8.5385
'cuboid   100  4p19.3063  54.61  54.28  origin x= -8.5385
cuboid   100  10.7678 -27.8448 2p19.3063  54.61  54.28
media   0  1  1
media   6  1  2  -1

media   0  1  3  -2
media   7  1  4  -3

media   0  1  6  -4
media   6  1  7  -6
media   0  1  8  -7
media   0  1  9  -8
media   6  1  10  -9
media   0  1  100 -10
boundary 100

unit 3
'CV flared near top
cone     1  8.014 56.82  7.703  54.61
cone     2  9.042 56.82  8.414  54.61
plane    3  zpl=1 con= -55.220

'top support
cylinder 4  9.0805       56.82  54.61
cylinder 5  10.16        56.82  54.61

cylinder  6   10.4775    56.82   54.61
cylinder  7   10.5994    56.82   54.61
cylinder  8   13.1394    56.82   54.61 origin x=-2.54
cylinder  9   19.1379    56.82   54.61 origin x= -8.5385
cylinder  10  19.3063    56.82   54.61 origin x= -8.5385
'cuboid   100  4p19.3063  56.82   54.61 origin x= -8.5385
cuboid   100  10.7678 -27.8448 2p19.3063  56.82   54.61
media   0  1  1 -3
media   6  1  1  3
media   6  1  2 -1 -3
media   6  1  2 -1  3

media   0  1  4  -2
media   7  1  5  -4
media   0  1  6  -5
media   6  1  7  -6
media   0  1  8  -7
media   0  1  9  -8
media   6  1  10  -9
media   0  1  100 -10
boundary 100

unit 4
'CV  top
 cylinder  13  8.414      58.725  56.82
cylinder  14  9.042      58.725  56.82
'top support
cylinder 4  9.0805       58.725  56.82
cylinder 5  10.16        58.725  56.82

cylinder  6   10.4775    58.725   56.82
cylinder  7   10.5994    58.725   56.82
cylinder  8   13.1394    58.725   56.82 origin x=-2.54
cylinder  9   19.1379    58.725   56.82 origin x= -8.5385
cylinder  10  19.3063    58.725   56.82 origin x= -8.5385
'cuboid   100  4p19.3063  58.725   56.82 origin x= -8.5385
cuboid   100  10.7678 -27.8448 2p19.3063  58.725   56.82
media   6  1  13
media   6  1  14 -13

media   0  1  4 -14
media   7  1  5  -4
media   0  1  6  -5
media   6  1  7  -6
media   0  1  8  -7
media   0  1  9  -8
media   6  1  10  -9
media   0  1  100 -10
boundary 100

unit 5
'Top support and lid liner-bottom
cuboid    1    4p3.175  59.995  58.725
cuboid    2    4p3.4925 60.122  58.725
cylinder  3    10.160   60.122  58.725

cylinder 11  10.147 67.4688  63.348
cylinder 12  10.147 67.4688  60.808
cylinder 13  10.325 67.4688  60.630

cylinder  4   10.4775    67.4688  58.725
cylinder  5   10.5994    67.4688  58.725
cylinder  6   13.1394    67.4688  58.725 origin x=-2.54
```

```
cylinder  7   19.1379    67.4688  58.725 origin x= -8.5385
cylinder  8   19.3063    67.4688  58.725 origin x= -8.5385
'cuboid   100  4p19.3063  67.4688  58.725 origin x= -8.5385
cuboid   100  10.7678 -27.8448 2p19.3063  67.4688  58.725
media   6  1  1
media   0  1  2 -1
media   7  1  3 -2

media   0  1  11
media   0  1  12 -11
media   6  1  13 -12 -11

media   0  1  4 -3 -13
media   6  1  5  -4
media   0  1  6  -5
media   0  1  7  -6
media   6  1  8  -7
media   0  1  100 -8
boundary 100

unit 6
'flange
cylinder 1  10.147 67.945  67.4688    origin x= -8.5385
cylinder 2  10.325 67.945  67.4688    origin x= -8.5385
'lid liner
cylinder  3   10.4775    67.945  67.4688  origin x= -8.5385
cylinder  4   10.5994    67.945  67.4688  origin x= -8.5385
'flange
cylinder 5    19.3063    67.945  67.4688  origin x= -8.5385
'cuboid   100  4p19.3063  67.945  67.4688  origin x= -8.5385
cuboid   100  10.7678 -27.8448 2p19.3063  67.945  67.4688
media   0  1  1
media   6  1  2 -1
media   0  1  3 -2
media   6  1  4 -3
media   6  1  5 -4
media   0  1  100 -5
boundary 100

unit 7
'Drum LID  only
cylinder  1  19.3063     68.263  67.945  origin x= -8.5385
'cylinder  2  19.3063     68.263  67.945 origin x= -8.5385
'cuboid   100  4p19.3063 68.263  67.945   origin x= -8.5385
cuboid   100  10.7678 -27.8448 2p19.3063  68.263  67.945
media   6  1  1
'media   0  1  2  -1
media   0  1  100 -1
boundary 100

unit 8
' LIner top
cylinder  1  17.658   70.6806  68.263   origin x= -8.5385
cylinder  2  17.780   70.8025  68.263   origin x= -8.5385
'cuboid   100  4p19.3063 70.8025  68.263 origin x= -8.5385
cuboid   100  10.7678 -27.8448 2p19.3063  70.8025  68.263
media   0  1  1
media   6  1  2 -1
media   0  1  100 -2
boundary 100

unit 11
'A-left Pu - upto bot of top al support
'Ellosoidal bottom and cv leg support'
sphere    12   3.755 origin x=-3.428 z=8.519
sphere    15   4.274 origin x=-3.428 z=8.519
ellipsoid 1   7.703  7.703  3.496 origin z=4.207 chord -z=0.0
ellipsoid 2   8.414  8.414  4.207 origin z=4.207 chord -z=0.0
cylinder  3   6.410   2.5   -0.9652
cylinder  4   7.065   2.5   -0.9652
'bot support
cylinder  5   8.5725     54.28  -0.9652
cylinder  6   10.16      14.605 -1.905
'cv
cylinder  13   7.703    54.28   4.207
cylinder  14   8.414    54.28   4.207
'liner
cylinder  7   10.4775    54.28  -1.905
cylinder  8   10.5994    54.28  -2.027
cylinder  9   13.1394    54.28  -4.567  origin x=2.54
cylinder  10  19.1379    54.28  -11.657 origin x=8.5385
cylinder  11  19.3063    54.28  -11.779 origin x=8.5385

cuboid   100  27.8448  -10.7678 2p19.3063  54.28  -11.779

media   1  1  12
media   9  1  15 -12
media   0  1  1
media   6  1  2  -1
media   0  1  3  -2
```

```
media   6  1  4 -3 -2

media   0  1  5 -4 -2 -14
media   7  1  6 -5

media   0  1  13 -15
media   6  1  14 -13

media   0  1  7  -6 -5
media   6  1  8  -7
media   0  1  9  -8
media   0  1  10 -9
media   6  1  11 -10
media   0  1  100 -11
boundary 100

unit 12
'CV portion before the flare
cylinder  1   7.703    54.61  54.28
cylinder  2   8.414    54.61  54.28

'bottom portion of top support
cylinder 3  9.0805     54.61  54.28
cylinder 4  10.16      54.61  54.28

cylinder  6   10.4775    54.61   54.28
cylinder  7   10.5994    54.61   54.28
cylinder  8   13.1394    54.61   54.28 origin x=2.54
cylinder  9   19.1379    54.61   54.28 origin x=8.5385
cylinder  10  19.3063    54.61   54.28 origin x=8.5385
'cuboid   100  4p19.3063  54.61  54.28  origin x=8.5385
cuboid   100  27.8448  -10.7678 2p19.3063  54.61  54.28
media   0  1  1
media   6  1  2  -1

media   0  1  3  -2
media   7  1  4  -3

media   0  1  6  -4
media   6  1  7  -6
media   0  1  8  -7
media   0  1  9  -8
media   6  1  10  -9
media   0  1  100 -10
boundary 100

unit 13
'CV flared near top
cone     1  8.014 56.82  7.703  54.61
cone     2  9.042 56.82  8.414  54.61
plane    3  zpl=1 con= -55.220

'top support
cylinder 4  9.0805       56.82  54.61
cylinder 5  10.16        56.82  54.61

cylinder  6   10.4775    56.82   54.61
cylinder  7   10.5994    56.82   54.61
cylinder  8   13.1394    56.82   54.61 origin x=2.54
cylinder  9   19.1379    56.82   54.61 origin x=8.5385
cylinder  10  19.3063    56.82   54.61 origin x=8.5385
'cuboid   100  4p19.3063  56.82   54.61 origin x=8.5385
cuboid   100  27.8448  -10.7678 2p19.3063  56.82   54.61
media   0  1  1 -3
media   6  1  1  3
media   6  1  2 -1 -3
media   6  1  2 -1  3

media   0  1  4  -2
media   7  1  5  -4
media   0  1  6  -5
media   6  1  7  -6
media   0  1  8  -7
media   0  1  9  -8
media   6  1  10  -9
media   0  1  100 -10
boundary 100

unit 14
'CV  top
 cylinder  13  8.414      58.725  56.82
cylinder  14  9.042      58.725  56.82
'top support
cylinder 4  9.0805       58.725  56.82
cylinder 5  10.16        58.725  56.82

cylinder  6   10.4775    58.725   56.82
cylinder  7   10.5994    58.725   56.82
cylinder  8   13.1394    58.725   56.82 origin x=2.54
cylinder  9   19.1379    58.725   56.82 origin x=8.5385
```

```
cylinder  10  19.3063    58.725   56.82 origin x=8.5385
'cuboid   100  4p19.3063  58.725   56.82 origin x=8.5385
cuboid   100  27.8448  -10.7678 2p19.3063  58.725   56.82
media   6  1  13
media   6  1  14 -13

media   0  1  4 -14
media   7  1  5  -4
media   0  1  6  -5
media   6  1  7  -6
media   0  1  8  -7
media   0  1  9  -8
media   6  1  10  -9
media   0  1  100 -10
boundary 100

unit 15
'Top support and lid liner-bottom
cuboid    1    4p3.175  59.995  58.725
cuboid    2    4p3.4925 60.122  58.725
cylinder  3    10.160   60.122  58.725

cylinder 11  10.147 67.4688  63.348
cylinder 12  10.147 67.4688  60.808
cylinder 13  10.325 67.4688  60.630

cylinder  4   10.4775    67.4688  58.725
cylinder  5   10.5994    67.4688  58.725
cylinder  6   13.1394    67.4688  58.725 origin x=2.54
cylinder  7   19.1379    67.4688  58.725 origin x=8.5385
cylinder  8   19.3063    67.4688  58.725 origin x=8.5385
'cuboid   100  4p19.3063  67.4688  58.725 origin x=8.5385
cuboid   100  27.8448  -10.7678 2p19.3063  67.4688  58.725
media   6  1  1
media   0  1  2 -1
media   7  1  3 -2

media   0  1  11
media   0  1  12 -11
media   6  1  13 -12 -11

media   0  1  4 -3 -13
media   6  1  5  -4
media   0  1  6  -5
media   0  1  7  -6
media   6  1  8  -7
media   0  1  100 -8
boundary 100

unit 16
'flange
cylinder 1  10.147 67.945  67.4688    origin x=8.5385
cylinder 2  10.325 67.945  67.4688    origin x=8.5385
'lid liner
cylinder  3   10.4775    67.945  67.4688  origin x=8.5385
cylinder  4   10.5994    67.945  67.4688  origin x=8.5385
'flange
cylinder 5    19.3063    67.945  67.4688  origin x=8.5385
'cuboid   100  4p19.3063  67.945  67.4688  origin x=8.5385
cuboid   100  27.8448  -10.7678 2p19.3063  67.945  67.4688
media   0  1  1
media   6  1  2 -1
media   0  1  3 -2
media   6  1  4 -3
media   6  1  5 -4
media   0  1  100 -5
boundary 100

unit 17
'Drum LID  only
cylinder  1  19.3063     68.263  67.945  origin x=8.5385
'cylinder  2  19.3063     68.263  67.945 origin x=8.5385
'cuboid   100  4p19.3063 68.263  67.945   origin x=8.5385
cuboid   100  27.8448  -10.7678 2p19.3063  68.263  67.945
media   6  1  1
'media   0  1  2  -1
media   0  1  100 -1
boundary 100

unit 18
' LIner top
cylinder  1  17.658   70.6806  68.263   origin x=8.5385
cylinder  2  17.780   70.8025  68.263   origin x=8.5385
'cuboid   100  4p19.3063 70.8025  68.263 origin x=8.5385
cuboid   100  27.8448  -10.7678 2p19.3063  70.8025  68.263
media   0  1  1
media   6  1  2 -1
media   0  1  100 -2
boundary 100
```

```
unit 50
cuboid   1  10.7678 -27.8448 2p19.3063  82.5815  0
array  1  1   place  1  1  1  0 0   11.779
boundary 1

unit 51
cuboid   1  27.8448  -10.7678 2p19.3063  82.5815  0
array  2  1   place  1  1  1    0  0  11.779
boundary 1

global unit 52
'com='6x6x3 array'
cuboid  200  231.6756  0  231.6756  0  247.7445  0
array 3 200 place 1 1 1  27.8448 19.3063  0
cuboid  201  261.6756  -30.0  261.6756  -30.0  277.7445  -30.0
media   8  1  201 -200
boundary 201

end geom
read array
ara=1 nux=1 nuy=1 nuz=8 fill 1 2 3  4 5 6  7 8  end fill
ara=2 nux=1 nuy=1 nuz=8 fill 11 12 13  14 15 16  17 18  end fill
ara=3 nux=6 nuy=6 nuz=3 fill   50  51  53Q2 end fill
end array
end data
end
```

Case bk_hac_r1_in

```
=csas26    parm=Centrm
bk_hac_r1 gpfp, HAC, dry,4.4 kg pu, no 3013, 100g poly, 6x6x3, 30 cm refl
'damaged drum, dia reduced by 2", ht by 3" (2" top and 1" bot), no  foam, no
fiberfrax
'no vermiculite, no min-k-2000, dia reduced bt 7% for tri pitch
238group
read comp
pu-239       1  den=19.84  1.0 293 end
arbm-fiber 0.256 4 0 0 1 13027 26.46 14000 23.14 11000 0.37 8016 50.03 2 1.0 293
end
arbm-foam  0.256  7 0 0 1  17000 0.15  14000 0.82 15000 0.82 8016 22.6 6012
62.88
                    1001  6.84   7000  5.89  3 1.0 293 end
arbm-vermi 0.368 10 0 0 1  14000 21.22  13027 5.47 20000 12.17 26000 5.4 22000
0.82
                    12000 8.90   11000 1.09 19000 1.22 16000 0.18 8016 43.53
                    4 1.0 293 end
arbm-mink 0.320 8 0 0 1    14000 37.71  22000 5.53  13027 6.39 6012 1.28  1001
0.84
                    8016  48.01  51000 0.09  35000 0.15   5 1.0 293 end
ss304       6  den=7.94  1.0 293  end
al          7  den=2.70  1.0 293  end
h2o         8  den=1.00  1.0 293  end
poly(h2o) 9  den=0.95  1.0 293 end
end comp
read parm tme=500 gen=425 npg=1000  nsk=25 run=yes plt=no nub=yes end parm
read geom

unit 1
'upto bot of top al support
'Ellosoidal bottom and cv leg support'
sphere    12   3.755 origin z=8.519
sphere    15   4.274 origin z=8.519
ellipsoid 1   7.703  7.703  3.496 origin z=4.207 chord -z=0.0
ellipsoid 2   8.414  8.414  4.207 origin z=4.207 chord -z=0.0
cylinder  3   6.410   2.5   -0.9652
cylinder  4   7.065   2.5   -0.9652
'bot support
cylinder  5   8.5725     54.28  -0.9652
cylinder  6   10.16      14.605 -1.905
'cv
cylinder  13   7.703    54.28   4.207
cylinder  14   8.414    54.28   4.207
'liner
cylinder  7   10.4775    54.28  -1.905
cylinder  8   10.5994    54.28  -2.027
cylinder  9   13.1394    54.28  -4.567
cylinder  10  19.1379    54.28  -11.657
cylinder  11  19.3063    54.28  -11.779

cuboid   100  4p19.3063  54.28  -11.779

media   1  1  12
media   9  1  15 -12
media   0  1  1
media   6  1  2  -1
media   0  1  3  -2
```

```
media   6  1  4 -3 -2

media   0  1  5 -4 -2 -14
media   7  1  6 -5

media   0  1  13 -15
media   6  1  14 -13

media   0  1  7  -6 -5
media   6  1  8  -7
media   0  1  9  -8
media   0  1  10 -9
media   6  1  11 -10
media   0  1  100 -11
boundary 100

unit 2
'CV portion before the flare
cylinder  1   7.703    54.61  54.28
cylinder  2   8.414    54.61  54.28

'bottom portion of top support
cylinder 3  9.0805     54.61  54.28
cylinder 4  10.16      54.61  54.28

cylinder  6   10.4775    54.61   54.28
cylinder  7   10.5994    54.61   54.28
cylinder  8   13.1394    54.61   54.28
cylinder  9   19.1379    54.61   54.28
cylinder  10  19.3063    54.61   54.28
cuboid   100  4p19.3063  54.61  54.28

media   0  1  1
media   6  1  2  -1

media   0  1  3  -2
media   7  1  4  -3

media   0  1  6  -4
media   6  1  7  -6
media   0  1  8  -7
media   0  1  9  -8
media   6  1  10  -9
media   0  1  100 -10
boundary 100

unit 3
'CV flared near top
cone     1  8.014 56.82  7.703  54.61
cone     2  9.042 56.82  8.414  54.61
plane    3  zpl=1 con= -55.220

'top support
cylinder 4  9.0805       56.82  54.61
cylinder 5  10.16        56.82  54.61

cylinder  6   10.4775    56.82   54.61
cylinder  7   10.5994    56.82   54.61
cylinder  8   13.1394    56.82   54.61
cylinder  9   19.1379    56.82   54.61
cylinder  10  19.3063    56.82   54.61
cuboid   100  4p19.3063  56.82   54.61

media   0  1  1 -3
media   6  1  1  3
media   6  1  2 -1 -3
media   6  1  2 -1  3

media   0  1  4  -2
media   7  1  5  -4
media   0  1  6  -5
media   6  1  7  -6
media   0  1  8  -7
media   0  1  9  -8
media   6  1  10  -9
media   0  1  100 -10
boundary 100

unit 4
'CV  top
 cylinder  13  8.414      58.725  56.82
cylinder  14  9.042      58.725  56.82
'top support
cylinder 4  9.0805       58.725  56.82
cylinder 5  10.16        58.725  56.82

cylinder  6   10.4775    58.725   56.82
cylinder  7   10.5994    58.725   56.82
cylinder  8   13.1394    58.725   56.82
cylinder  9   19.1379    58.725   56.82
```

```
cylinder  10  19.3063    58.725   56.82
cuboid   100  4p19.3063  58.725   56.82

media   6  1  13
media   6  1  14 -13

media   0  1  4 -14
media   7  1  5  -4
media   0  1  6  -5
media   6  1  7  -6
media   0  1  8  -7
media   0  1  9  -8
media   6  1  10  -9
media   0  1  100 -10
boundary 100

unit 5
'Top support and lid liner-bottom
cuboid    1    4p3.175  59.995  58.725
cuboid    2    4p3.4925 60.122  58.725
cylinder  3    10.160   60.122  58.725

cylinder 11  10.147 67.4688  63.348
cylinder 12  10.147 67.4688  60.808
cylinder 13  10.325 67.4688  60.630

cylinder  4   10.4775    67.4688  58.725
cylinder  5   10.5994    67.4688  58.725
cylinder  6   13.1394    67.4688  58.725
cylinder  7   19.1379    67.4688  58.725
cylinder  8   19.3063    67.4688  58.725
cuboid   100  4p19.3063  67.4688  58.725

media   6  1  1
media   0  1  2 -1
media   7  1  3 -2

media   0  1  11
media   0  1  12 -11
media   6  1  13 -12 -11

media   0  1  4 -3 -13
media   6  1  5  -4
media   0  1  6  -5
media   0  1  7  -6
media   6  1  8  -7
media   0  1  100 -8
boundary 100

unit 6
'flange
cylinder 1  10.147 67.945  67.4688
cylinder 2  10.325 67.945  67.4688
'lid liner
cylinder  3   10.4775    67.945  67.4688
cylinder  4   10.5994    67.945  67.4688
'flange
cylinder 5    19.3063    67.945  67.4688
cuboid   100  4p19.3063  67.945  67.4688

media   0  1  1
media   6  1  2 -1
media   0  1  3 -2
media   6  1  4 -3
media   6  1  5 -4
media   0  1  100 -5
boundary 100

unit 7
'Drum LID  only
cylinder  1  19.3063     68.263  67.945
'cylinder  2  19.3063     68.263  67.945
cuboid   100  4p19.3063 68.263  67.945
media   6  1  1
'media   0  1  2  -1
media   0  1  100 -1
boundary 100

unit 8
' LIner top
cylinder  1  17.658   70.6806  68.263
cylinder  2  17.780   70.8025  68.263
cuboid   100  4p19.3063 70.8025  68.263
media   0  1  1
media   6  1  2 -1
media   0  1  100 -2
boundary 100

unit 10
cuboid   1  38.6126   0    38.6126   0   82.5815  0
```

```
array  1  1   place  1  1  1   19.3063  19.3063  11.779
boundary 1

global unit 20

com='6x6x3 array'
cuboid  200  231.6756  0  231.6756  0  247.7445  0
array 2 200 place 1 1 1  0 0  0
cuboid  201  261.6756  -30.0  261.6756  -30.0  277.7445  -30.0
media   8  1  201 -200
boundary 201
end geom

read array
ara=1 nux=1 nuy=1 nuz=8 fill 1 2 3  4 5 6  7 8  end fill

ara=2 nux=6 nuy=6 nuz=3 fill 108*10 end fill
end array
end data
end
```

The End

This Page Intentionally Left Blank

This Page Intentionally Left Blank

Safety Analysis Report - 9977 Packaging

CHAPTER 7

PACKAGE OPERATIONS

Preface

This Chapter provides the minimum procedural elements that ensure the 9977 package is operated in accordance with its design. The implementation of these elements ensures safe performance of the 9977 package under Normal Conditions of Transport (NCT) and Hypothetical Accident Conditions (HAC). In addition to Safety Analysis Report for Packaging (SARP) requirements, facility-specific operating procedures shall also comply with all requirements provided in the Certificate of Compliance (CoC).

The procedural elements described in this chapter meet the requirements of:

- DOE Order 460.2A,[1]
- DOE Order 460.1B,[2]
- Title 10 CFR 20.1101(b) and 20.1906,[3]
- 10 CFR 71[4] and Subparts G and H, and
- 49 CFR 173[5]

The procedural elements cover packaging inspection, loading the radioactive contents, and package handling, receipt, and unloading. Also included are requirements for preparation of an empty packaging for shipment and for packaging storage.

The procedural elements of this Section comply with NRC Regulatory Guide 7.9.[6]

This Page Intentionally Left Blank

TABLE OF CONTENTS

LIST OF FIGURES

ACRONYMS AND ABBREVIATIONS

5CV	5-inch Diameter Containment Vessel
6CV	6-inch Diameter Containment Vessel
ALARA	As Low As Reasonably Achievable
CFR	Code of Federal Regulations
CoC	Certificate of Compliance
CV	generic Containment Vessel
DOE	Department of Energy
EM	office of Environmental Management
HAC	Hypothetical Accident Conditions
NCT	Normal Conditions of Transport
NRC	Nuclear Regulatory Commission
QA	Quality Assurance
RTG	Radioisotope Thermoelectric Generators
SARP	Safety Analysis Report for Packaging
TID	Tamper Indicating Device

This Page Intentionally Left Blank

7 PACKAGE OPERATIONS

7.0 GENERAL INFORMATION

All Users of the 9977 shall register with DOE's Assistant Secretary for Environmental Management (EM) prior to first use of the package. A written registration form shall be submitted to the Manager of the Packaging Certification Program and the User must have received a verification of registration prior to shipping. The protocol for registration of users of EM-approved packagings is located at http://www.rampac.com. A copy of the registration form is provided in Appendix 7.2.

7.0.1 Planning

Users shall prepare written site-specific operating procedures for inspections, tests and activities that meet the requirements of this Chapter, and comply with their facility's operational requirements. This SARP, the Certificate of Compliance (CoC), packaging hardware, engineering drawings and technical specifications should all be considered when preparing procedures.

The exact sequence of operational steps specified in this chapter may be altered to reflect site-specific needs. Implementation of SARP, CoC, and site radiological requirements shall reflect the principles of As Low As Reasonably Achievable (ALARA) as required by the *Standards for Protection Against Radiation* in 10 CFR 20.1101(b).[3].

7.0.2 Personnel Qualifications

All personnel who perform duties associated with package operations shall be qualified as described in Section 9.2.1.

7.0.3 Equipment

A complete list of equipment (devices, fixtures, tools, hoists, etc.), materials and material specifications necessary for packaging operations shall be provided in each site-specific operating procedure. The procedural activities outlined in the major section of this Chapter also list the equipment necessary for the tasks and where applicable, cite drawings of the special tools given in Appendix 7.1. All equipment, gages, instruments, and other measuring and testing devices used in activities affecting package quality shall be properly calibrated and controlled, as specified in the User's Quality Assurance (QA) Program.

7.0.4 Quality Assurance

Each site-specific procedure shall document the revision numbers of the CoC and SARP that are in effect at the time of that package operation. By doing so, the Shipper verifies that the operating procedures comply with the conditions of approval specified in the CoC and SARP.

The package User shall document compliance with all procedural elements required by this chapter.

Each site-specific procedure shall include instructions for the operator to follow in the event that a requirement cannot be met during implementation of the procedure. At a minimum, the operator shall document the event, then notify the appropriate level of Supervision and await further instruction.

7.0.5 Nomenclature

Figures 7.1 through 7.3 show cross-sections of the 9977 packaging assembly, including the two alternate containment vessels (5-inch diameter 5CV and 6-inch diameter 6CV), cone-seal closure assemblies, and call-outs for the nomenclature that is used in the following procedures.

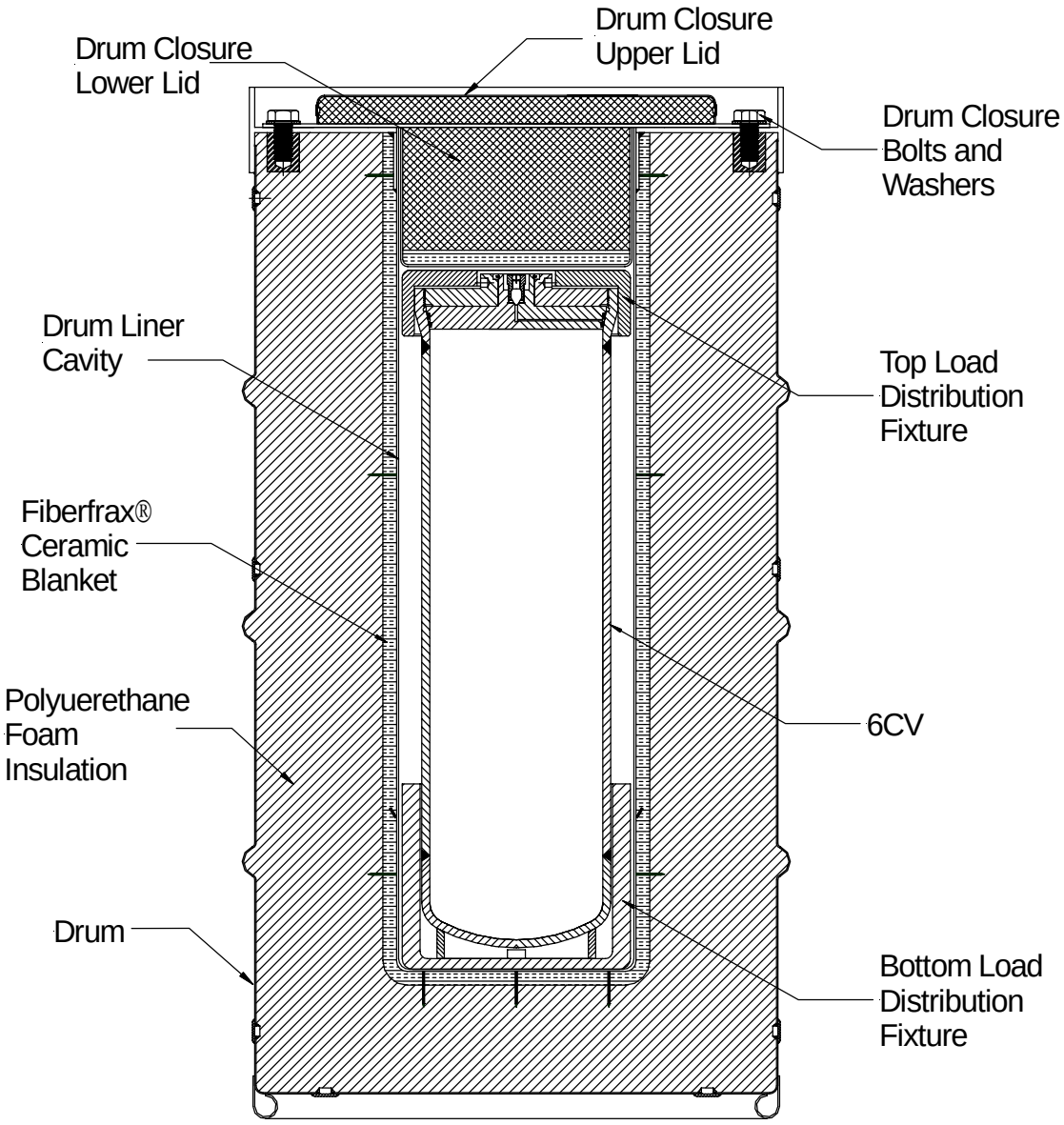

Figure 7.1 – Assembly Cross-Section of 9977 Packaging with 6CV

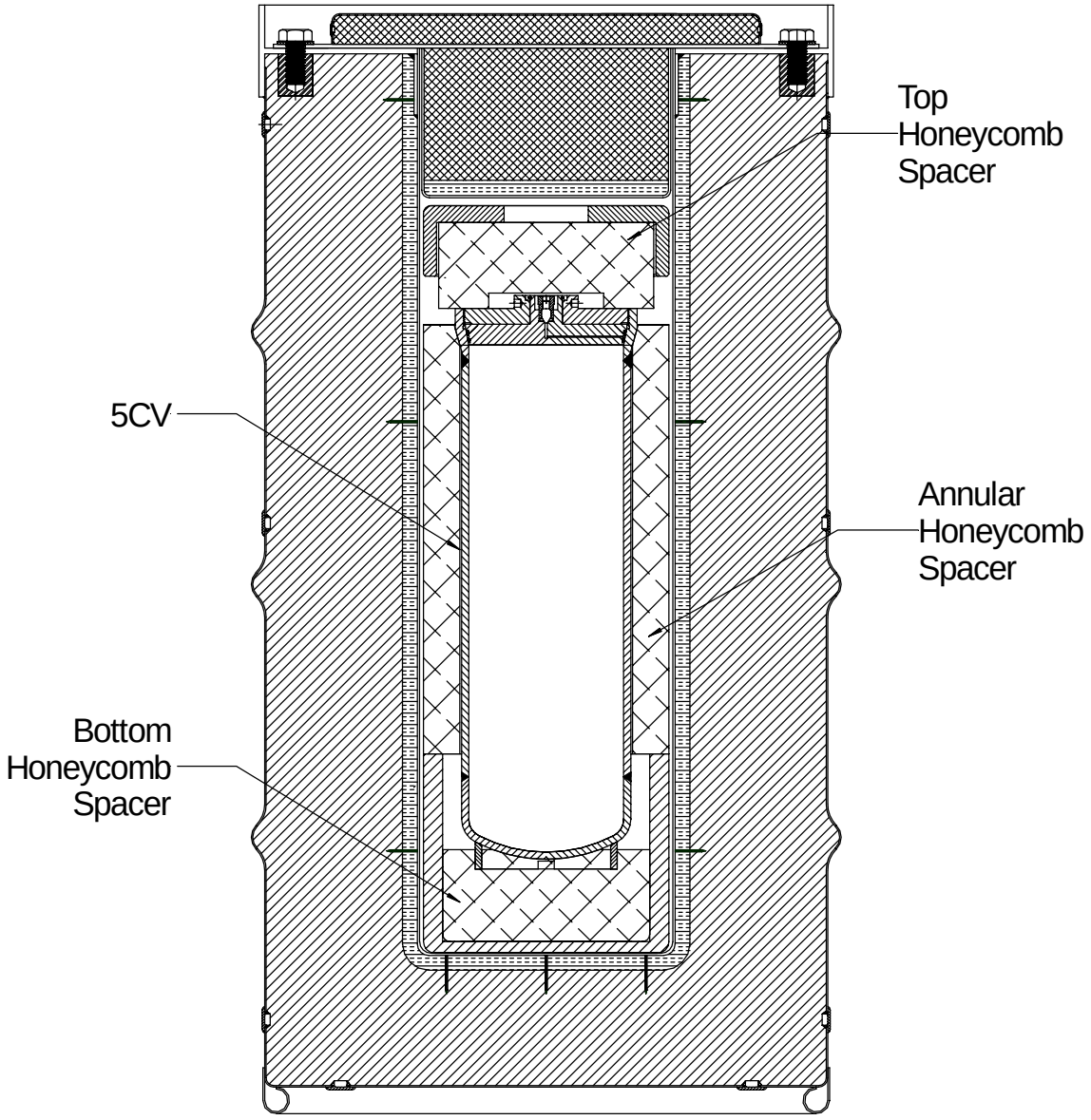

Figure 7.2 – Assembly Cross-Section of 9977 Packaging with 5CV

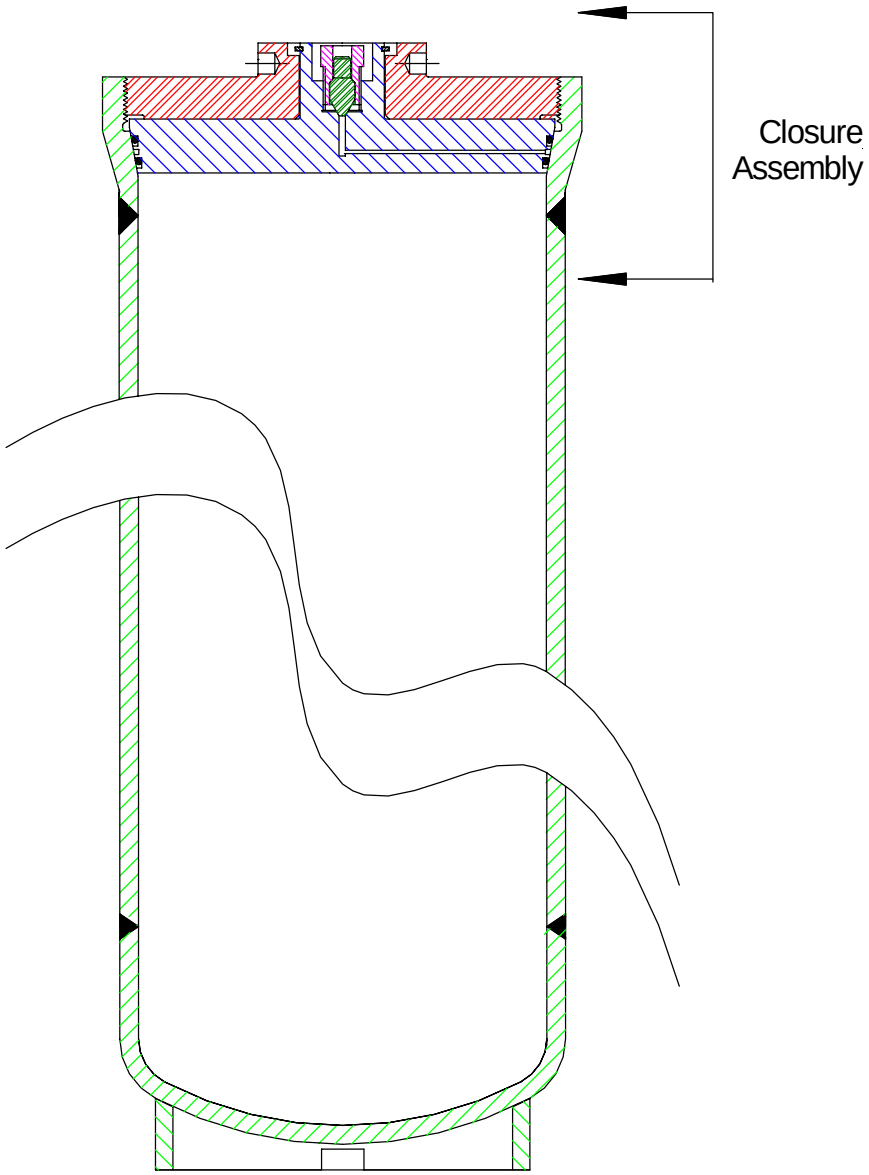

Figure 7.3 – Cross-Section of a Typical 9977 Containment Vessel

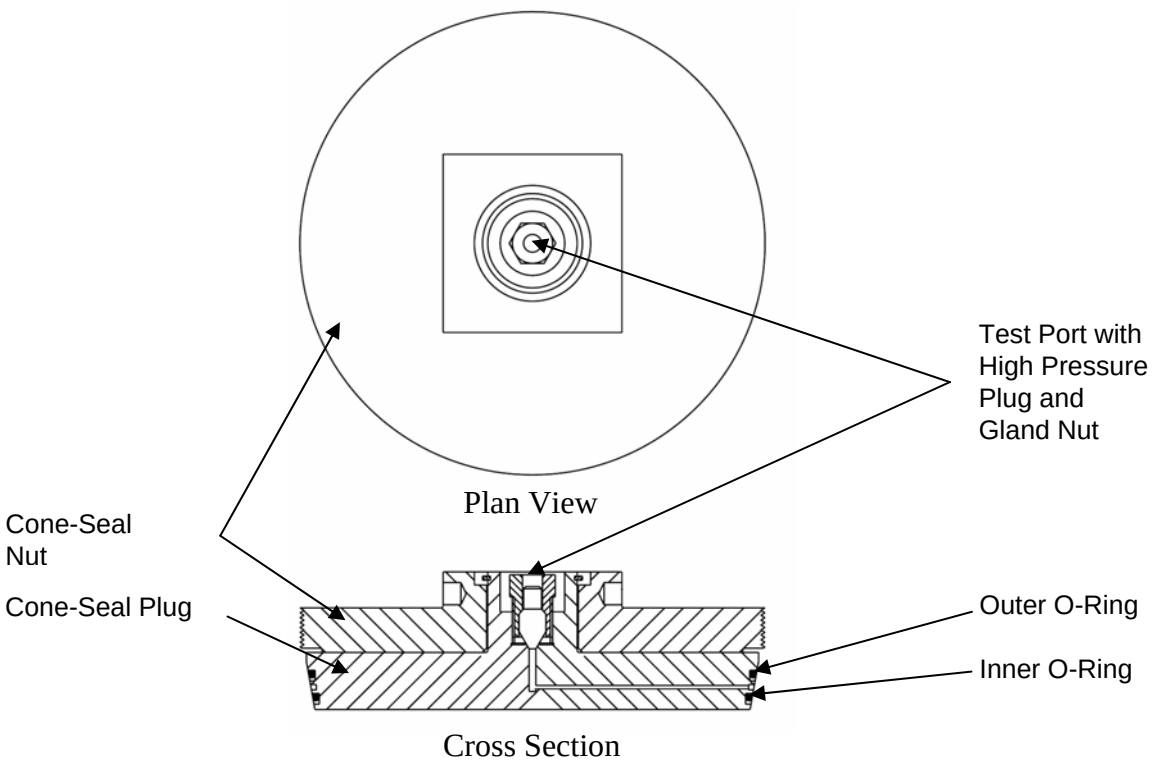

Figure 7.4 – Views of a Typical Cone-Seal Closure Assembly

CV: Used in this chapter where the discussion applies to either 5CV or 6CV. Otherwise, the specific abbreviation will be used.

Payload: Everything that is contained within the CV (e.g., radioactive material, containers, associated handling conveniences, materials used for contamination control, dunnage or packing components that secure the radioactive material within the CV, etc.).

Contents: Radioactive materials.

7.1 PACKAGE LOADING

Packages shall be loaded and closed in accordance with written operating procedures. Detailed operating procedures shall include, at a minimum, the procedural elements of this section and the completion of the Quality Assurance documentation as required in Section 9.17, *Quality Assurance Records*. Implementation of the procedural elements of this section ensures that:

- the condition of the packaging is unimpaired prior to loading,
- contents are authorized, and the package is loaded and closed correctly, and
- the package properly prepared for transport.

7.1.1 Preparation for Loading

Sections 7.1.1.1 and 7.1.1.2 do not need to be performed sequentially. This provision permits contents/payload preparation operations to be performed separately from the initial packaging preparation.

7.1.1.1 Packaging Preparation

1. Verify that the Identification Plate, as shown in Figure 7.5, is firmly welded to the drum and is legible.

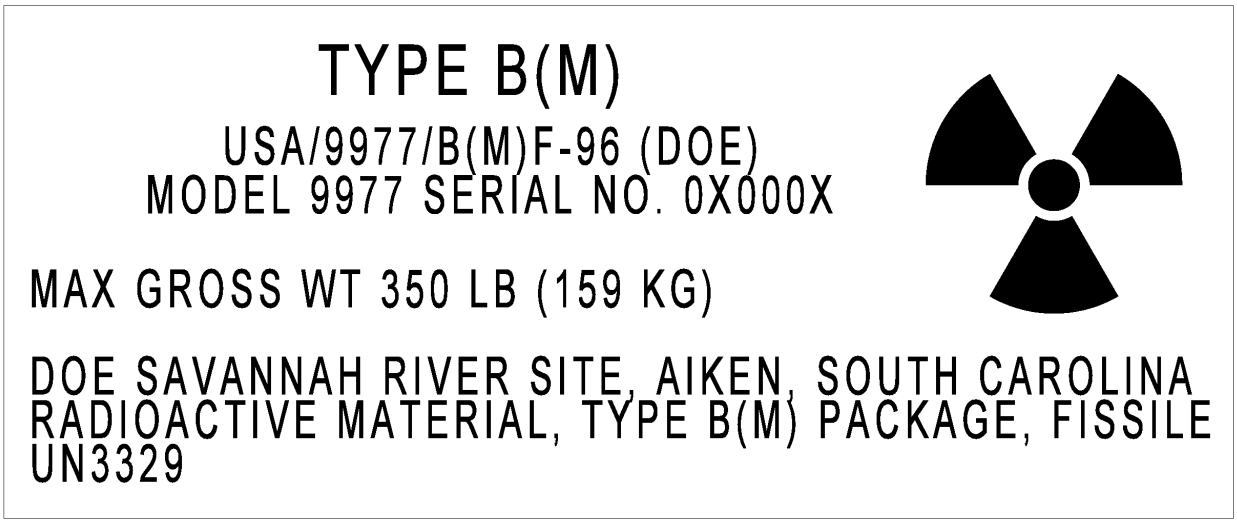

Figure 7.5 – Sample Packaging Identification Plate

2. Record the packaging model number and the serial number on the Loading Record.

3. Verify that the exterior surfaces of the drum and the accessible internal components (e.g., exposed surfaces of the drum closure lid, drum cavity, the Top and Bottom Load Distribution Fixtures, and the CV), do not exceed the applicable radioactive contamination limits specified in 10 CFR 835, Appendix D and 10 CFR 835.405.[7] Health Protection personnel shall document the results of the survey.

4. Verify that the Caplugs® are installed in all drum vent holes. Replace if damaged or missing.

5. Verify that the bolt holes in the drum closure lid align with the drum's threaded inserts and that the lid installs freely.

6. Verify that the drum closure bolts match those specified on the package drawings.

7. Verify that the drum closure bolts and mating threaded inserts (welded into the drum body) are clean (free of dirt and debris) and in proper working order.

8. Verify that the drum (top, bottom, and side) is not damaged in any way that would affect packaging or transportation operations. Small surface scratches and dents that would not affect packaging or transportation operations are acceptable.

9. Remove the CV from the drum and place it within a CV holder.

10. Verify the following on the leak-test label affixed to the outside of the drum (see Figure 8.1):

    a. CV annual leak-rate test was performed within the last year, and

    b. CV and overpack serial numbers match those noted.

11. Empty the drum liner.

12. Clean the drum liner surfaces to remove any dirt, debris, and/or moisture.

13. Ensure that a Bottom Load Distribution Fixture is installed topside-up in the drum liner.

14. If a 5CV will be loaded into the drum, ensure that a bottom honeycomb spacer and an annular honeycomb spacer are also installed in the drum liner as shown in Figure 7.6.

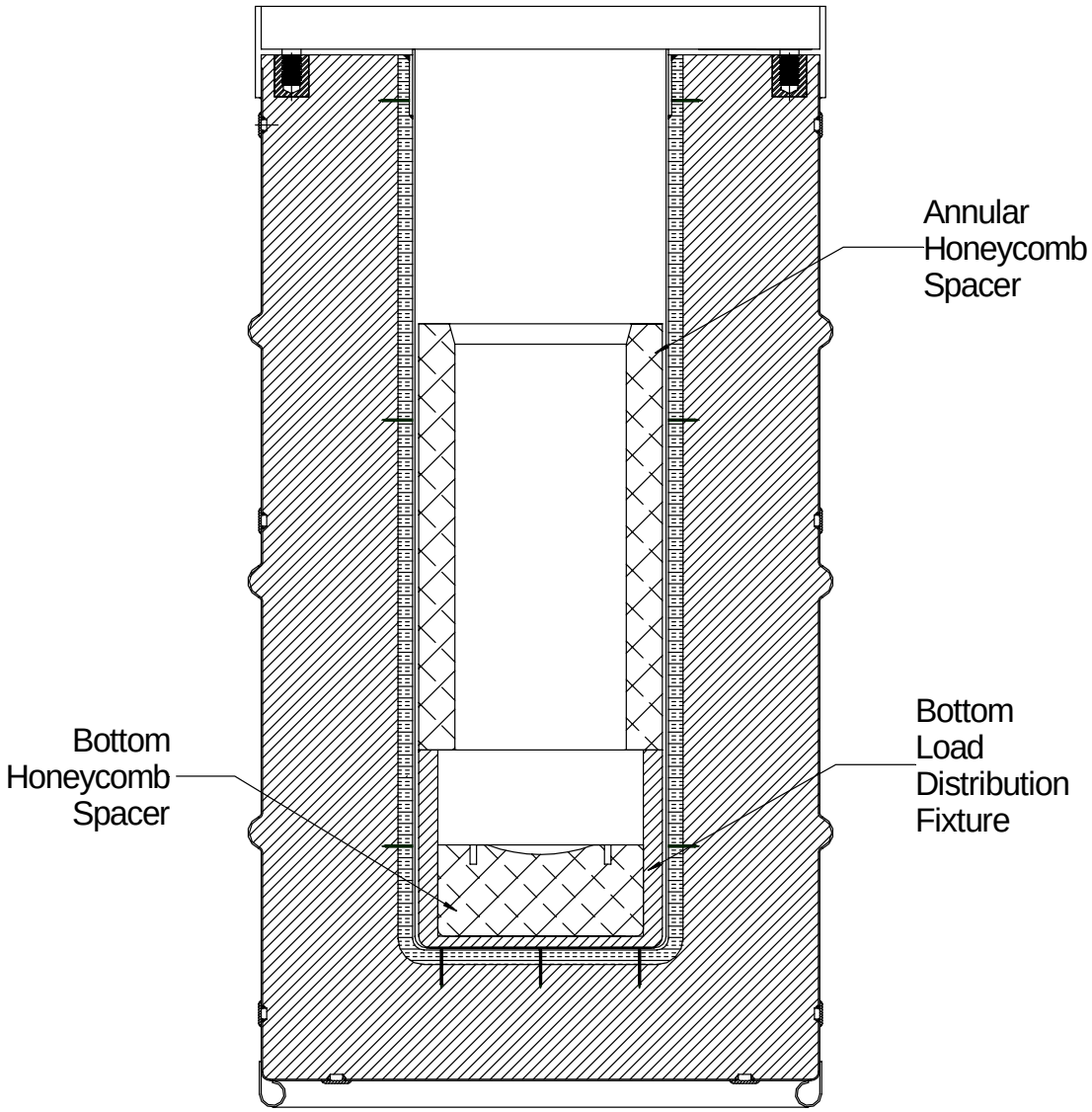

Figure 7.6 – Drum with 5CV Annular and Bottom Spacers

15. Verify that the aluminum Top Load Distribution Fixture and, if a 5CV will be loaded into the drum, the Top Honeycomb Spacer are available.

16. Verify that the serial numbers for the CV body and cone-seal plug/cone-seal nut (the closure assembly) all match.

17. Verify that the CV cone-seal nut and body scribe marks are visible (see Figure 7.7).

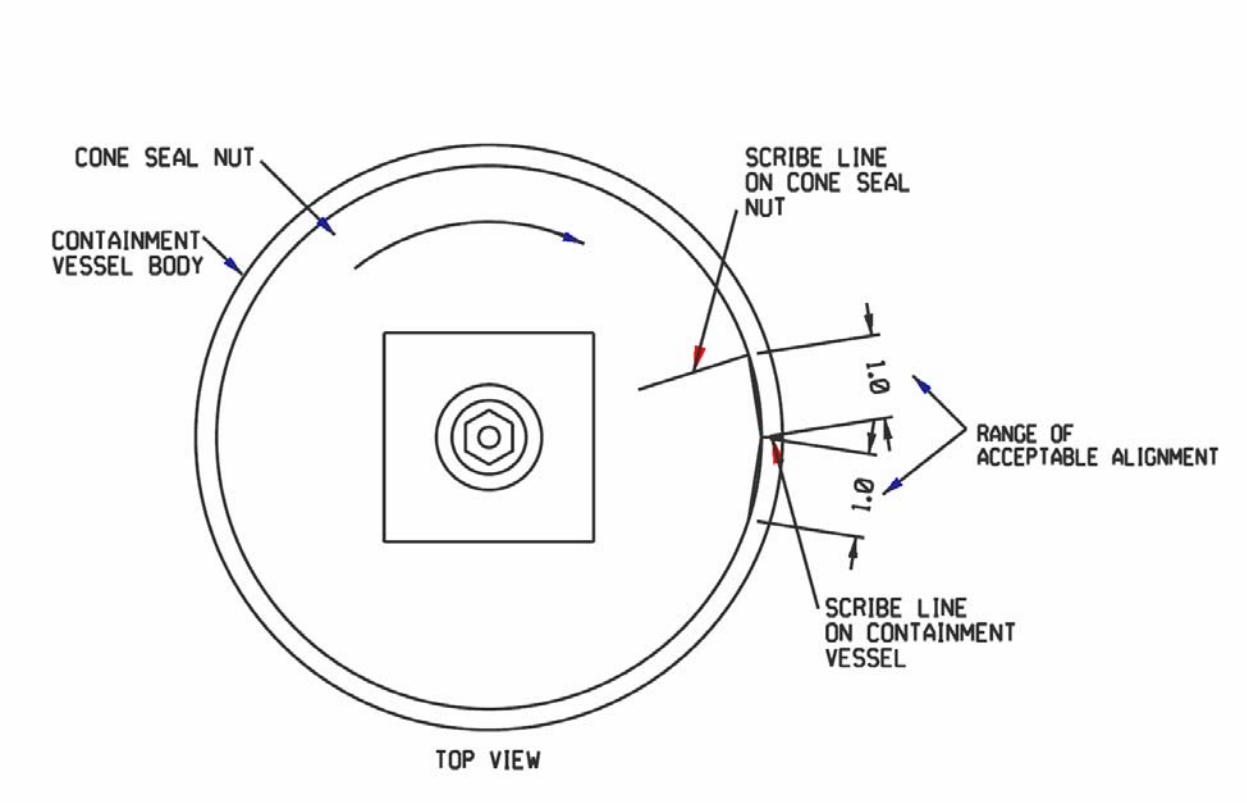

Figure 7.7 – Closure Assembly Scribe Marks

18. Remove the Closure Assembly from the CV by turning it counterclockwise with the Closure Assembly wrench and ratchet.

19. Verify that the CV is empty.

20. Remove the O-rings.

CAUTION: If a tool is used to perform this operation, it shall be fabricated from a material that will not damage the O-rings or the sealing surfaces of the O-ring grooves and the Cone-Seal Plug.

CAUTION: Positively identify each O-ring, as later it must be returned to the same groove it was removed from. (This is required because only the inner O-ring was verified as providing containment.)

21. Clean all sealing surfaces of the CV body and cone-seal plug and clean the O-rings with isopropyl or ethyl alcohol, as needed.

22. With a bright light, visually inspect the cleaned sealing surfaces and O-rings for gouges, nicks, cuts, cracks or scratches that could affect containment performance.

23. Verify the acceptable condition of the O-ring, if damaged, destroy it, and replace it with a new O-ring per Section 8.2.5.1.2.

24. Verify the acceptable condition of the containment vessel sealing surface, if it's damaged, the vessel assembly shall be removed from service and not used until its performance is proven acceptable as outlined in Section 8.1.3.

25. Lubricate the O-rings with a thin film of silicone high-vacuum grease.

26. Reinstall the O-rings, returning each to its original groove.

27. Lubricate the threads of the cone-seal nut with Krytox® vacuum grease.

28. Verify that the CV closure assembles and installs correctly as demonstrated by:

    a. Free threading of the cone-seal nut into the vessel body.

    b. Free turning, but not loose free-wheeling, between the cone-seal nut and cone-seal plug. A moderate but steady drag against rotation indicates the presence of lubricant between the nut and plug.

    c. Free threading of the gland nut into the cone-seal plug.

29. Verify that the correct spacer materials for the payload (Section 1.2.3) are available for service.

7.1.1.2 Contents/Payload Preparation

1. Verify that the radioactive contents and the total decay heat load are both in compliance with the CoC.

2. Verify that the contents are from a single Content Envelope as presented in Table 1.2.

3. Prior to placement inside the CV, verify that the radioactive material handling convenience(s) do not show signs of degradation (e.g., bulging, buckling or corrosion).

4. Assemble the contents into a payload configuration as described in Section 1.2.3.

7.1.2 Loading of Contents

The operating procedures for loading the radioactive material into the CV and for closing the CV shall include, as a minimum, the operational elements listed below. Integration of these procedural elements with facility-specific requirements shall be completed in a manner specified by ALARA principles.

In preparation for loading the CV, all of the steps identified in Section 7.1.1 shall have been completed, and all packaging hardware, lifting equipment, and other apparatus required shall be staged and ready.

1. Verify that the weight of the payload:

    a. everything to be placed into the 6CV shall not exceed 100 lb.

    b. everything to be placed into the 5CV shall not exceed 50 lb.

2. Place the payload within the CV using payload lifting equipment, as required. The configurations for the contents are described in Section 1.2.3 and are illustrated in Section 1.2.3.1.

    NOTE: For the protection of the CV sealing surface, it is recommended that a loading funnel be used. A typical funnel design is shown in Appendix 7.1.

3. Verify that both O-rings are in place on the cone-seal assembly.

4. Thread the cone-seal assembly into the CV body and tighten it to a torque of:

    a. 5CV: 50 (+10/-0) ft-lb.

    b. 6CV: 100 (+20/-0) ft-lb.

5. Verify that the scribe mark on the cone-seal assembly is aligned to within one inch either side of the scribe mark on the CV body as shown in Figure 7.7). If the scribe marks do not align correctly, then perform the following steps <u>once</u>:

    a. Remove the cone-seal closure assembly and inspect the threads of the assembly and the threads of the CV body for obstructions.

    b. Repeat Steps 4 and 5.

6. Verify the integrity of the CV inner O-ring seal by performing the O-ring seal test in accordance with Section 8.2.2.1.

7. Install the leak-test port plug and gland nut. Torque the gland nut to 15 (±5) ft-lb.

7.1.3 Preparation for Transport

Package closure shall be performed in accordance with a written procedure that includes the following elements:

1. Health Protection personnel shall survey the outer surfaces of the CV in accordance with 10 CFR 835.405 and 10 CFR 835, Appendix D. Health Protection personnel shall document the results of the survey. If the surface contamination measurements exceed the allowable limits, Stop Work and implement the appropriate contamination control procedures.

2. Load the CV into the drum.

   ***WARNING*:** *The loaded 6CV and 5CV assemblies have a high center of mass and weigh approximately 156-lbs and 134-lbs, respectively. Perform lift in accordance with site/facility heavy lifting procedures.*

3. If a 5CV is loaded into the drum, then place the Top Honeycomb Spacer on top of the 5CV.

4. Place the Top Load Distribution Fixture on top of the 6CV or 5CV's Top Honeycomb Spacer.

5. Close the drum as follows:

   a. Place the closure lid on the drum, aligning the bolt holes with the threaded inserts in the top plate of the drum body.

   b. Install the eight (8) sets of bolts and washers.

   c. Torque each bolt to 45 ± 5 ft-lb. No specific tightening sequence is required.

   d. Make two torque passes to confirm that all of the bolts are properly tightened.

6. Install a TID through two or more bolt heads as shown in Figure 7.9.

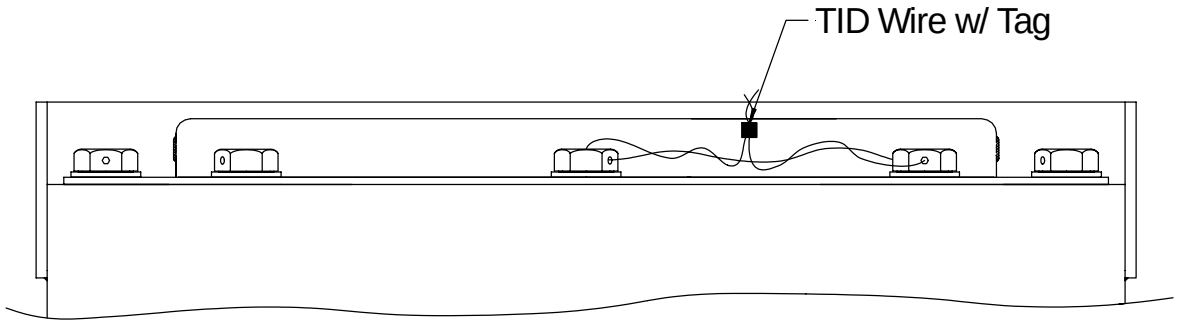

Figure 7.8 – Side View of the Top Portion of the Drum, Showing the TID Installation

7. Health Protection personnel shall survey the outer surfaces of the drum for surface contamination in accordance with 10 CFR 835.405 and 10 CFR 835, Appendix D. Health Protection personnel shall document the results of the survey.

8. Health Protection personnel shall perform and document a radiological survey of the closed drum. The survey measurements shall be used to perform the following:

    a. Determine the maximum radiation level at 1 meter from the drum top, side and bottom surfaces, in mrem/hr. This is defined as the Transport Index.

    b. Record the Transport Index on the Transport Record and on the drum's shipping label.

    c. If the Transport Index is greater than 10, the drum must be transported by exclusive shipment.

9. Verify that the gross package weight is 350 lb or less.

10. Attach radiation tags and labels to the drum, as specified in 49 CFR 172,[8] Subparts D and E.

11. When shipments of non-fissile materials are made, cover the word "fissile" on the nameplate with a durable opaque tape. Mark the proper shipping name and UN number using waterproof markings on the tape according to 49 CFR 172, Subpart E.

12. Ensure that any special instructions necessary for opening of the package, per 10 CFR 71.89,[4] are provided to the consignee prior to shipment of the package.

13. The 1-inch diameter holes located in the drum flange can be used as lifting or tie down devices. Standard industry practice and equipment may be used.

7.2 PACKAGE UNLOADING

Implementation of the following procedures shall incorporate ALARA principles. Package receipt shall be performed in accordance with written procedures that include the following elements.

7.2.1 Receipt of Package from Carrier

1. Make arrangements to receive the package in accordance with 10 CFR 20.1906.

2. Health Protection personnel shall survey the conveyance surfaces and package exterior surfaces for radiation levels in accordance with 10 CFR 71.47 and survey the package conveyance and package surfaces for surface contamination in accordance with 49 CFR 173.443 and/or 10 CFR 835.405 and 10 CFR 835, Appendix D as applicable. Health Protection personnel shall document the results of the survey.

3. Verify that the TID unbroken on receipt.

> **NOTE:** *If the TID is missing or broken, Stop Work, isolate the package and notify Nuclear Material Control personnel to implement the appropriate material accountability procedures. Additionally, contact supervision to evaluate the situation for occurrence reporting requirements per the Title 49CFR171.15, Immediate Notice of Certain Hazardous Materials Incidents.*

4. Verify that the package does not have any damage that may significantly reduce the package performance; if it does, segregate the package, notify Supervision, and report to the Certifying Authority in accordance with 10 CFR 71.95.

7.2.2 Removal of Contents

Package unloading procedures shall include the following elements:

1. Document the removal of the TID per the receiving site procedures.

2. Open the drum by removing the eight (8) closure bolts and removing the closure lid.

3. Perform a contamination survey on bottom surface of the closure lid.

> **NOTE:** *If the surface contamination measurements taken here or in the Steps below exceed the allowable limits, Stop Work and implement the appropriate contamination control procedures. Additionally, contact supervision to evaluate the situation for occurrence reporting requirements per the DOE Order, DOE Order 231.1A, Environmental, Safety, and Health Reporting.*[11]

> **WARNING:** *All interior components may be thermally hot. If manually removing the payload insulated gloves should be worn for the removal and disassembly steps.*

4. Remove the Top Load Distribution Fixture and, if present, the Top Honeycomb Spacer.

5. Perform a contamination survey on the Top Load Distribution Fixture, the Top Honeycomb Spacer if present, and the top surface of the CV.

6. Remove the CV from the drum.

> **WARNING:** *The loaded CV assemblies weigh approximately 156 pounds. Perform lift in accordance with site/facility lifting procedures.*

7. Perform a contamination survey of the exterior surface of the CV.

> **WARNING:** *Internal pressurization of a CV may occur due to increased temperature and gas generation. The CV has a pressure release hole in the vessel wall located adjacent to the top of the seated cone-seal plug. This pressure release hole will allow any trapped gas from the containment vessel cavity to vent after the seal is broken but before the closure threads are completely disengaged.*

8. Place the CV in a CV holder and rotate so that the pressure release hole is pointed away from personnel.

> **NOTE:** *Unless surface contamination was detected the Bottom Load Distribution Fixture and the Annular and Bottom Honeycomb Spacers (for the 5CV) should remain in the drum. If contamination is found remove all remaining hardware and perform a contamination survey on the hardware and the interior surface of the drum liner to verify that surfaces do not exceed radioactive contamination limits specified in 10 CFR 835, Appendix D.*

9. Inspect the containment vessel closure assembly scribe marks for alignment with the vessel body scribe mark. Verify that the scribe mark on the cone-seal assembly is aligned to within one inch either side of the scribe mark on the CV body as shown in Figure 7.7). If the scribe marks do not align correctly, then document and notify Supervision.

10. Loosen and remove the CV cone-seal nut.

11. Remove the packing and contents from the CV.

12. Compare the package contents and configuration with the shipping papers and the Certificate of Compliance and note any discrepancies. These discrepancies shall be reported to the Certifying Authority in accordance with 10 CFR 71.95.

13. Inspect and perform a contamination survey on radioactive material product containers upon removal from the CV. Any visible bulging, buckling, or evidence of corrosion shall be reported to the Certifying Official.

14. Inspect the containment vessel and other packaging components for damage. If the inspection identifies damage to a packaging component, the damaged component shall be handled in accordance with the site Packaging QA requirements.

7.3 PREPARATION OF EMPTY PACKAGE FOR TRANSPORT

An empty packaging shall be shipped per 49 CFR 173.428,[9] *Empty Class 7 (radioactive) Materials Packaging*. A non-empty packaging is a package that is internally contaminated as specified in 49 CFR 173.421,[10] *Limited Quantities of Radioactive Materials*, and shall be prepared for transport as specified in 49 CFR 173.421.

Packaging shall be prepared for transport per written procedures that include the following elements:

7.3.1 Shipping an Empty Packaging

1. The packaging shall be verified to be empty per 49 CFR 173.421.

2. The packaging shall be prepared for shipment as directed by Section 7.1.1.1 Steps 3 through 8 and 11 through 16.

   NOTE: *The O-rings are not removed and cleaned as part of the preparation for shipping an empty package. Not removing the O-rings obviates the need to institute controls assuring they are returned to their original groove.*

3. The packaging shall be closed as directed by Section 7.1.3 Steps 2 through 7 and 9, with the exception:

   Close the CV using a torque of 25 (+10/-0) ft-lb.

4. If required for verification that the CV and/or the drum overpack is empty, install a TID through two or more of the drum closure bolts as shown in Figure 7.8.

7.3.2 Shipping a Non-Empty Package

1. The packaging shall be prepared for shipment per Section 7.1.1.1, *Packaging Preparation*

2. The packaging shall be closed per Section 7.1.3, *Preparation for Transport.*

7.4 OTHER OPERATIONS

7.4.1 Packaging Storage

Packaging should be stored in a storage facility that provides protection from:

- the effects of temperature extremes and humidity (to prevent condensation),
- chemical vapors,
- accelerating forces,
- physical damages and airborne contamination (e.g., rain, snow, dust accumulation, dirt, salt spray, and fumes).

Drums are to be stored with the vent hole Caplugs in place and the drum lid installed (lid bolts may be hand tight).

7.4.2 Records and Reporting

The Package Loading Record shall be prepared in accordance with the requirements of 10 CFR 71.91, maintained in accordance with Section 9.17, and shall include as a minimum:

1) identification of the packaging by model number and serial number;
2) verification that there are no significant defects in the packaging, as shipped;
3) type and quantity of licensed material in each package, and the total quantity of each shipment;
4) date of the shipment;
5) any special controls exercised;
6) name and address of the transferee;
7) address to which the shipment was made; and
8) results of the determinations required by §71.87 and by the conditions of the package approval.

Records are only valid if stamped, initialed or signed, and dated by authorized personnel or otherwise authenticated.

References

1. *Departmental Materials Transportation and Packaging Management*, U.S. DOE Order 460.2A, U. S. Department of Energy, Washington, DC (December 22, 2004).

2. *Packaging and Transportation Safety*, U. S. DOE Order 460.1B, U.S. Department of Energy, Washington, DC (April 2003).

3. *Standards for Protection Against Radiation*, Code of Federal Regulations, Title 10, Part 20, Washington, DC (June 2003).

4. *Packaging and Transportation of Radioactive Material*, Code of Federal Regulations, Title 10, Part 71, Washington, DC (October 2004).

5. *Shippers - General Requirements for Shipments and Packagings*, Code of Federal Regulations, Title 49, Part 173, Washington, DC. (October 2003).

6. *Standard Format and Content Guide of Part 71 Applications for Approval of Packaging for Radioactive Material*, Regulatory Guide 7.9, Revision 2, Nuclear Regulatory Commission, Washington, DC (March 2005).

7. *Occupational Radiation Protection*, Code of Federal Regulations, Title 10, Part 835, Washington, DC (January 2001).

8. *Hazardous Materials Table, Special Provisions, Hazardous Materials Communications, Emergency Response Information, and Training Requirements*, Code of Federal Regulations, Title 49, Part 172, Washington, DC (October 2003).

9. *Empty Class 7 (Radioactive) Materials Packaging*, Code of Federal Regulations, Title 49, Part 173.428, Washington, DC (October, 2003).

10. *Excepted Packages for Limited Quantities of Class 7 (Radioactive) Materials*, Code of Federal Regulations, Title 49, Part 173.421, Washington DC (October 2003).

11. *Environment, Safety and Health Reporting*, DOE Order 231.1A-Change 1, Washington DC (June 2004).

This Page Intentionally Left Blank

7.5 APPENDICES

1. Special Tools
2. EM-24 Radioactive Material Package User-Registration Form

This Page Intentionally Left Blank

APPENDIX 7.1

SPECIAL TOOLS

This Page Intentionally Left Blank.

SPECIAL TOOLS

The following equipment is needed for operating the 9977. Where special tooling is required, design options are illustrated and drawings are available.

CV Lifting Device - Drawing EES-22498-R1-001.
Used for lifting a CV with a hoist.

CV Holder - Drawing XXX
Holds the CV securely in a vertical position and prevents it from rotating when the cone-seal closure is to be opened or closed.

CV Cart and Torquing Station – Drawings R-R3-0043-A and R-R1-F-0126.
The CV Cart is a mobile platform for the CV holder(s). The weighted Torquing Station locks the CV Cart down, resists opening and closing torques without being anchored to the floor, and provides a convenient place for performing Post-Load Leak Testing.

Lid Wrench - Drawing S5-2-11040-G.
Used for applying torque to the cone-seal nut.

Calibrated torque wrenches.

- 100 foot pounds, accuracy of 4% of reading or better. For closing the 6CV cone-seal nut.
- 50 foot pounds, accuracy of 4% of reading or better. For closing the 5CV cone-seal nut.
- 30 foot pounds, accuracy of 4% of reading or better. For closing the Leak-Test Port Gland Nut.

O-ring tool - MSC #09270059 (or equal).
Used for removing O-rings without scratching the O-ring groove.

KRYTOX® grade 240AC fluorinated vacuum grease.

Silicone high-vacuum grease, Dow Corning Part No. 976V.

Loading shield - Drawings XXXX & ZZZZ.
Used to protect the interior threads and sealing surfaces at the top of the CV body when loading the contents.

.

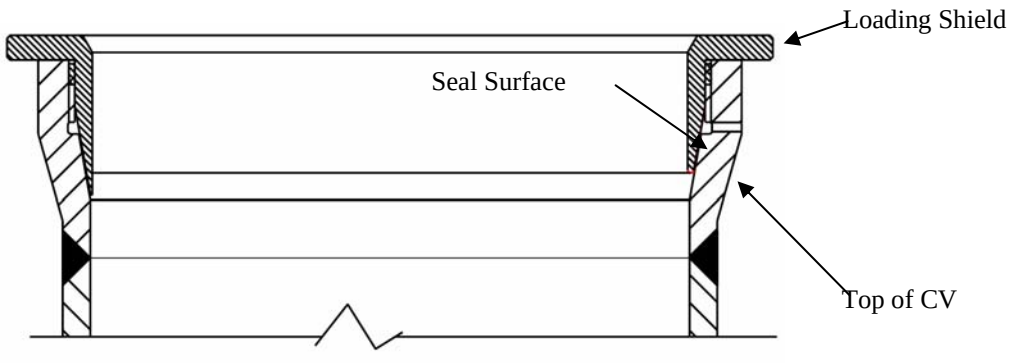

Loading Funnel

Long-reach vacuum lifter - McMaster Model No. 5795 A4
Lightweight vacuum lifter - McMaster Model No. 6971 A11
Used for removing the product cans from the Containment Vessel. The lifting tools were modified slightly (handles swapped) to fit the product cans and containment vessel cavities

3013 Lifter
Used for removing the 3013 cans from the Containment Vessel.

Containment Vessels Lifter - Drawings S5-2-11040 and M-FFD-F-00028.
Used for removing containment vessels from the drum by lifting by the recessed holes in the Cone-Seal Nut.

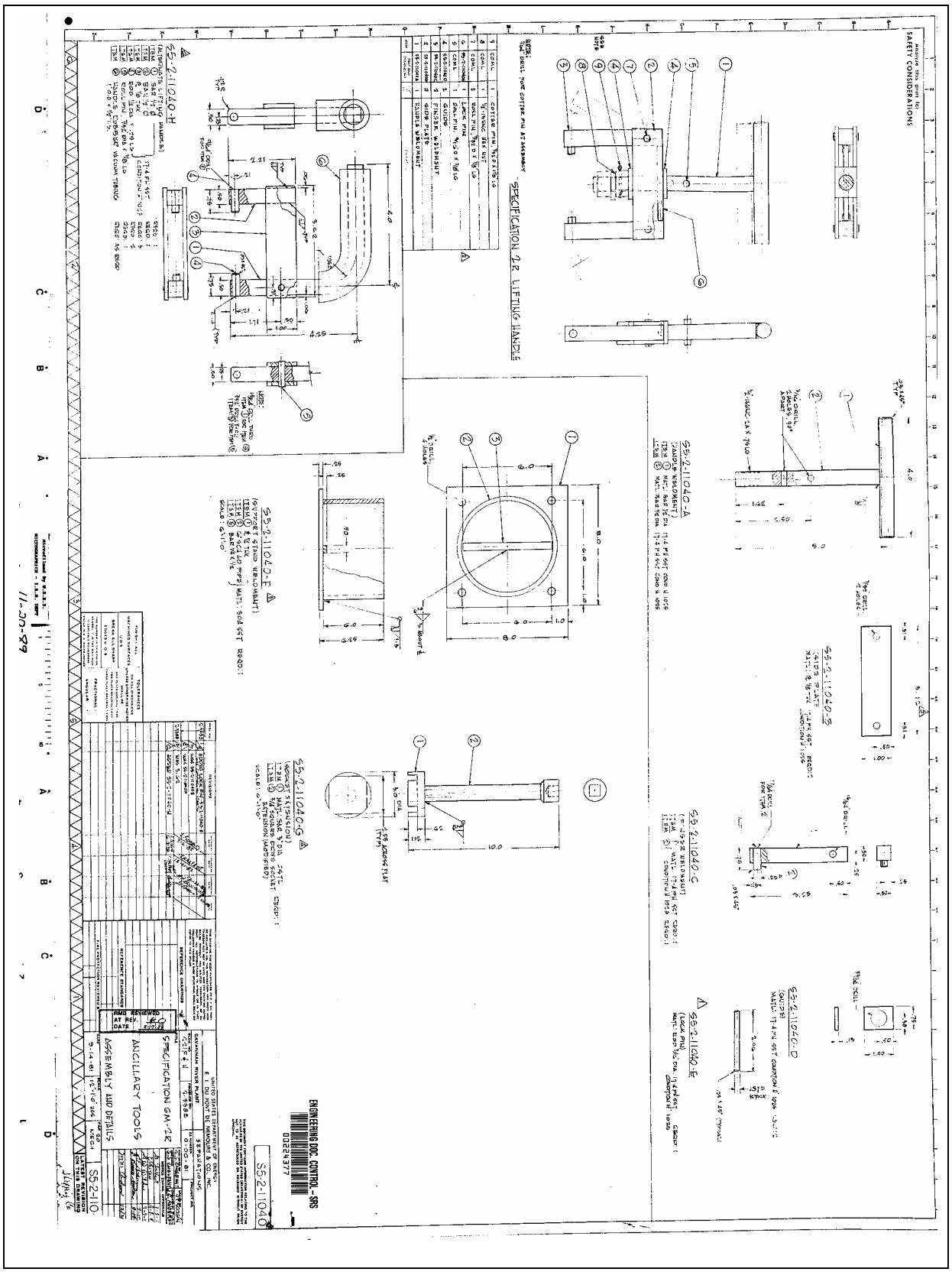

Specification 6M-2R Ancillary Tools Assembly and Details, SRS Drawing No. S5-2-11040

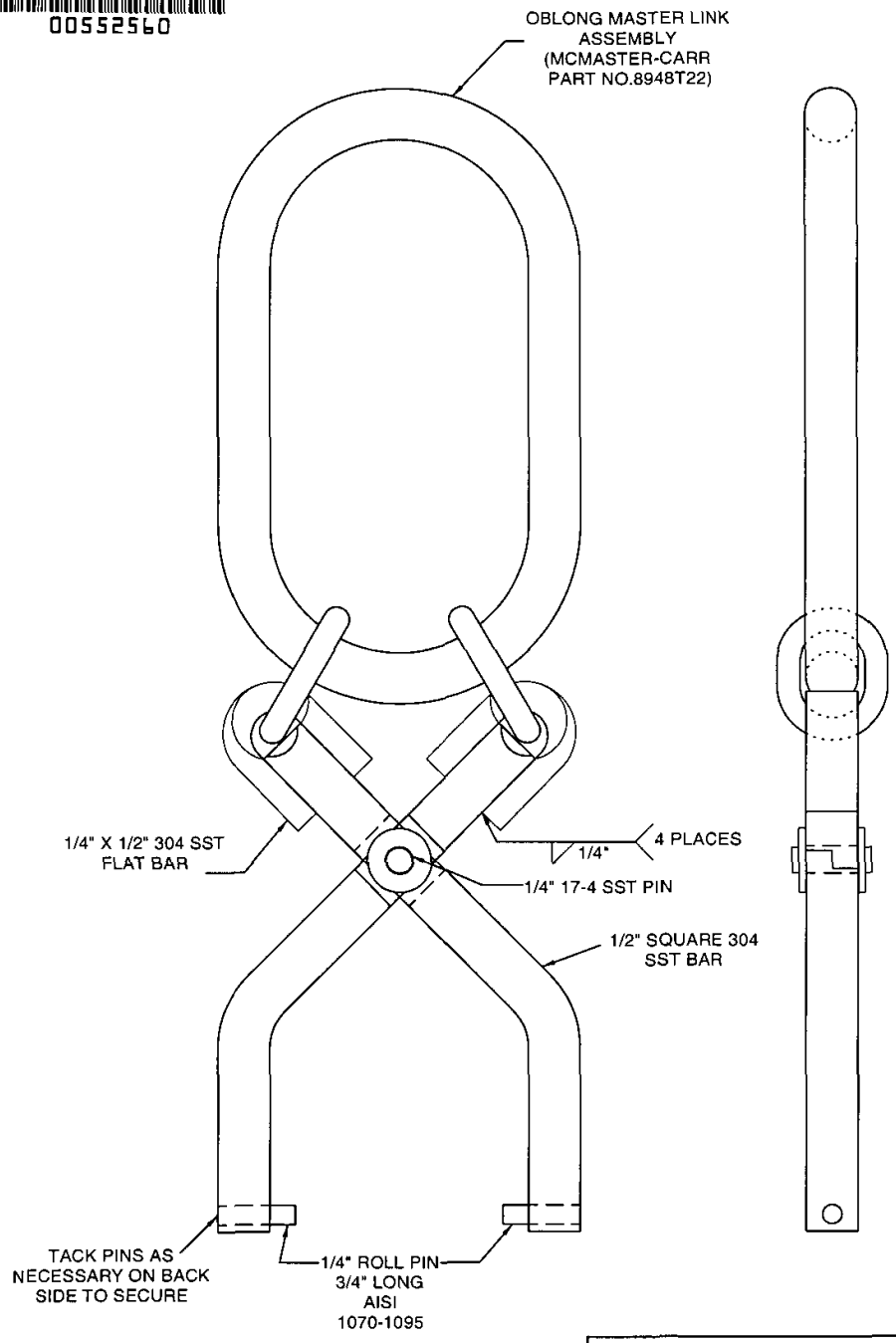

M-FFD-F-00028, REV. 1 PAGE 1 OF 2
2R LIFTING TOOL

APPROVAL Elizabeth R Hackney

DATE Nov. 30 '2000

NOTES:
1. ALL WELDING PER Y-12, 1.10
2. ALL WELDS ARE CONSIDERED STRUCTURAL WELDS.
3. LOAD TEST TOOL AT 125 LBS IN FIELD BEFORE USE

REMOVE ALL BURRS & ROUND ALL SHARP EDGES. SURFACE FINISH: 125 TOLERANCES ON ALL DIMENSIONS TO BE +/- 1/16" EXCEPT AS NOTED: DECIMALS: ONE PLACE: +/- 0.05" TWO PLACE: +/- 0.01"

2R Lifting Tool, SRS Drawing No. M-FFD-F-00028 Sheet 1 of 2

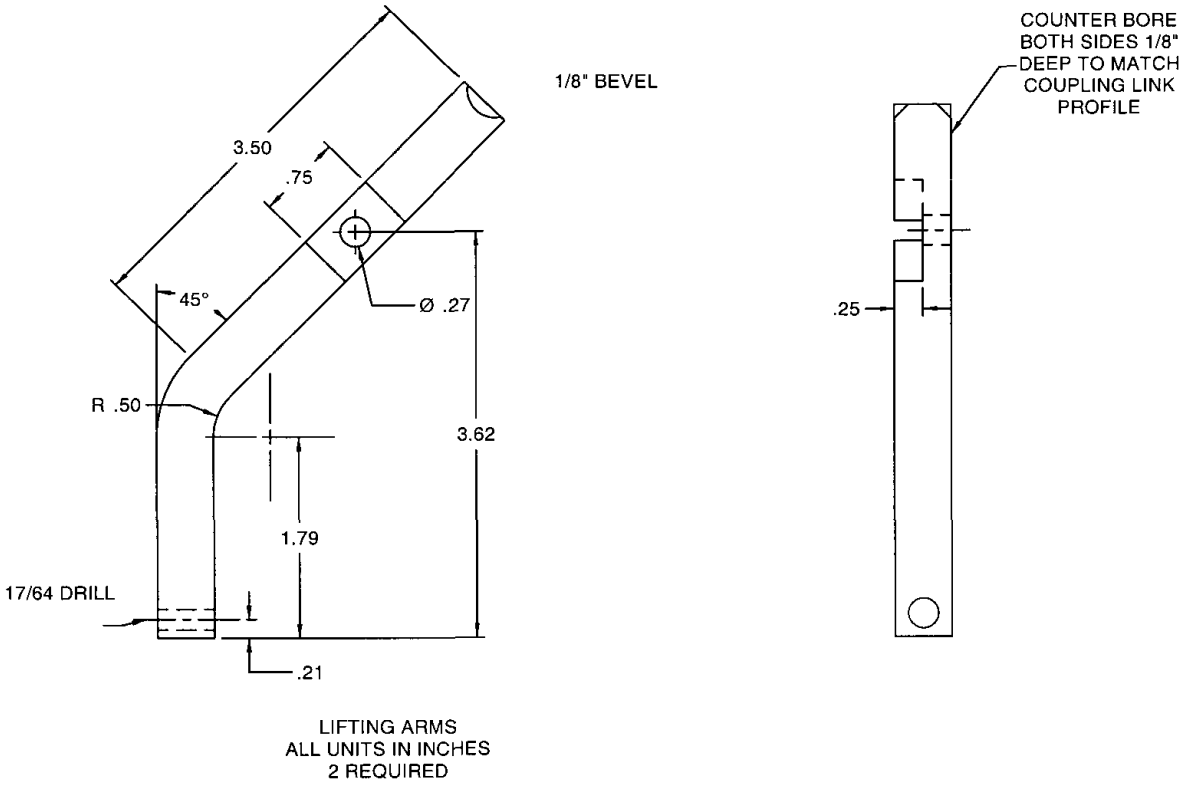

LIFTING ARMS
ALL UNITS IN INCHES
2 REQUIRED

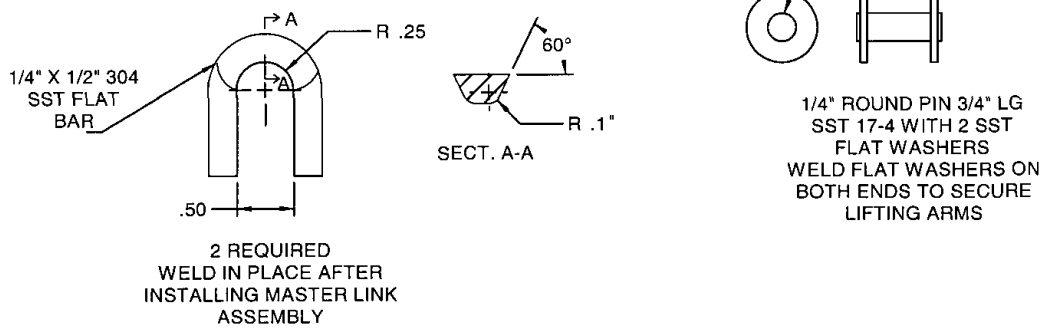

2 REQUIRED
WELD IN PLACE AFTER
INSTALLING MASTER LINK
ASSEMBLY

1/4" ROUND PIN 3/4" LG
SST 17-4 WITH 2 SST
FLAT WASHERS
WELD FLAT WASHERS ON
BOTH ENDS TO SECURE
LIFTING ARMS

M-FFD-F-00028, REV. 1 PAGE 2 OF 2
2R LIFTING TOOL

2R Lifting Tool, SRS Drawing No. M-FFD-F-00028 Sheet 2 of 2

This Page Intentionally Left Blank.

APPENDIX 7.2

EM-24 RADIOACTIVE MATERIAL PACKAGE USER-REGISTRATION FORM

This Page Intentionally Left Blank.

INSTRUCTIONS - Fill-in form electronically, print it, sign it, and mail it to:

ATTN: Manager, Packaging Certification Program
Office of Safety Management & Operations
Environment Management
Department of Energy
CLV-1081
1000 Independence Avenue, SW
Washington, D.C. 20585

DOE Order 460.1B requires that:

> *Each person who offers for transportation quantities of radioactive materials exceeding A_1 or A_2 or fissile quantity of radioactive material in a package certified by the Assistant Secretary for Environmental Management or another Secretarial Officer/Deputy Administrator, NNSA, shall:*
>
> *a. Meet the conditions specified in the certificate for the package issued by the Assistant Secretary for Environmental Management or a Secretarial Officer/Deputy Administrator, NNSA or NRC, and*
>
> *b. Register in writing with the Assistant Secretary for Environmental Management or the responsible Secretarial Officer/Deputy Administrator, NNSA prior to using the certificate.*

I certify that I have met the conditions specified in the package certificate and am submitting this letter to register with DOE-EM prior to first time use of the certificate.

Signature:_____ Date:_____

Name (Print):_____

Title:_____

Registrant status (i.e., certificate holder or user):_ _____

Affiliation:_____

Company address:_____

Telephone and fax numbers:_____Phone: Fax:_____

E-mail address (if available):_____

DOE Certificate of Compliance Number:_____ Revision No.:_____

Package Identification Number Specified in the CoC: _____

Reset Form Data

This Page Intentionally Left Blank

Safety Analysis Report 9977 Packaging

CHAPTER 8

ACCEPTANCE TESTS AND MAINTENANCE PROGRAM

Preface

The acceptance tests and the maintenance program for the package described in this chapter ensure compliance with the requirements of Subpart G of 10 CFR 71[1]. The acceptance tests and the maintenance program shall be conducted in accordance with the Quality Assurance (QA) program described in Chapter 9. The information presented is in the format specified in U.S. Nuclear Regulatory Commission Regulatory Guide 7.9.[2]

This Page Intentionally Left Blank.

TABLE OF CONTENTS

LIST OF FIGURES

ACRONYMS AND ABBREVIATIONS

5CV	5-inch diameter Containment Vessel
6CV	6-inch diameter Containment Vessel
ANSI	American National Standards Institute
CFR	Code of Federal Regulations
CV	Containment Vessel (used in common reference to both 5CV & 6CV)
NCR	Nonconformance Report
QA	Quality Assurance

8 ACCEPTANCE TESTS AND MAINTENANCE PROGRAM

8.1 ACCEPTANCE TESTS

Owner acceptance inspections and tests are performed (or verified through supplier document confirmation) prior to first use of the packaging to ensure compliance with applicable requirements of Subpart G of 10 CFR 71.[1] The Owner (through the Purchasing Organization) shall require the Supplier (through a procurement specification) to satisfy the inspection and testing requirements of this section and as detailed in Appendix 8.1. The Owner shall verify that all fabrication records and applicable rework records required by Chapter 9, Table 9.7, are controlled and retrievable by packaging serial number.

The inspections described in this section provide the Owner with verification that the Inspection Criteria have been met and that the packaging has been fabricated in accordance with the engineering drawings as referenced in the Certificate of Compliance.

The Owner shall prepare and issue a Nonconformance Report (NCR) per the requirements of Section 9.15, as needed. Disposition of the NCR shall be approved by the Design Authority, see Section 9.1.2.

8.1.1 Visual Inspection and Measurements

Visual inspections and dimensional measurements are performed throughout the fabrication process to assess and verify compliance with all materials and component dimensional requirements given in the drawings. The inspections detailed in Appendix 8.1, *Visual Inspection and Fabrication Verification Requirements* and Appendix 8.2 *Independent Verification and Documentation Requirements* ensure that newly fabricated 9977 packagings are complete and operable upon receipt.

8.1.2 Weld Examinations

A weld examiner shall be certified to examine specific welds in accordance with an employers written practice as defined in SNT-TC-1A. [3] Inspection methods, weld procedures, personnel qualifications, and weld reports shall meet ASME Code Section V.

8.1.3 Structural and Pressure Tests

Each CV shall be proof tested in accordance with procedure and acceptance criteria specified in Appendix 8.3, *Hydrostatic Pressure Test Procedures and Acceptance Criteria for the 9977 Packaging*. Verify that the 5-inch diameter CV (5CV) has been proof tested at an internal pressure of 1365 (± 10) psig or the 6-inch diameter (6CV) at an internal pressure of 1235 (± 10) psig. CVs not in compliance with the acceptance criteria shall be dispositioned in accordance with Section 9.15.

The test pressures are based on the design conditions specified in Chapter 2 and meet the criteria specified in ASME Section III, Subsection NB-6200[4] and 10 CFR 71.85(b).

Verify that the containment vessel assembly has been pressure tested as specified on the Containment Vessel Assembly (Drawings R-R2-G-00042 and R-R2-G-00043).

Verify that the drum and drum liner have been pressure tested as specified on the Drum and Liner Subassembly drawing (R-R2-G-00017).

8.1.4 Leakage Tests

Verify that the containment boundary of the CV has been leak-rate tested with helium in accordance with the evacuated envelope method (A.5.4) of ANSI N14.5.[5] This requires testing the entire containment vessel and its closure. The CV design does not incorporate a port for introduction of helium into the vessel from outside. Therefore, a device that releases helium inside the container must be sealed inside the CV prior to the leak-rate test. The CV is closed as given in Section 7.1.2, Steps 3 through 5, then tested for helium leak rate.

Test results must demonstrate that the leak-rate is less than 1×10^{-7} ref cm^3 air/sec (2×10^{-7} ref cm^3 helium/sec) with a sensitivity of 5×10^{-8} ref cm^3/sec (1×10^{-7} ref cm^3 helium/sec) or less, in accordance with the ANSI N14.5 definition of "leaktight."

Note that at the beginning of the test, a prescribed amount of helium, based upon He percentage and pressure within the enclosed device, is released and added to the air contained inside the CV. The final concentration of helium in the CV must be calculated, and the measured leak rate adjusted accordingly. For example, if the helium concentration is 50% (one atmosphere of "air" and one atmosphere of helium), then the measured leak rate must be multiplied by 2 to represent the leak rate of 100% helium required by the ANSI standard. Helium concentration must be greater than 10%, in accordance with ANSI N14.5, A.5.4.4.

An example of a procedure for helium leak-rate testing a 9977 CV is provided in Appendix 8.4 and includes description of the helium storage/release device used by the SRS.

Upon completion of the helium leak-rate test, the old data label shall be removed from the drum, the applicable data shall be written onto a new label as shown in Figure 8.1 and the label affixed to the drum adjacent to the bar-code label. The drum shall display only a single label that contains all the current data.

Annual Helium Leak-Rate Test

CV	Serial No.	Test Date	Record No.
____	_____	_____	_____

Packaging Serial No._____

Figure 8.1 - Leak-Rate Test Data Label

8.1.5 Component Tests

8.1.5.1 Valves, Rupture Discs, and Fluid Transport Devices

The 9977 packaging does not incorporate valves, rupture discs or fluid transport devices.

8.1.5.2 Gaskets

The CV O-ring seals are the only gaskets in the 9977 package. Performance testing of these O-rings is described in Section 8.1.3.

8.1.5.3 Miscellaneous

Acceptance of fabricated packagings does not require additional testing.

8.1.6 Shielding Integrity

Acceptance of fabricated packagings does not require shielding integrity testing. The packaging design does not include any features specifically credited with shielding.

8.1.7 Thermal Tests

Performance of thermal testing is not required for acceptance of fabricated packagings. The packaging design does not incorporate active heat transfer features nor are passive heat transfer mechanisms particularly sensitive to normal variations in the materials of construction or fabrication methods.

8.2 MAINTENANCE PROGRAM

The 9977 packaging shall be subjected to inspections and tests annually or prior to use. Note that annual maintenance need not be performed if the packaging is not to be placed in service within the next year. These annual activities ensure the continued and proper functioning of the packaging. The User shall verify by direct inspection, or confirm through QA records, that the inspection and testing requirements presented in this Section are satisfied prior to submitting a loaded package for shipment.

Packaging subassemblies may be repaired, refurbished, or replaced using procedures prepared and approved in accordance with the QA requirements given in Section 9.15. All such repairs shall be documented in accordance with the requirements of Section 9.6.

8.2.1 Structural and Pressure Tests

The 9977 maintenance program does not require recurring structural or pressure tests. However, pressure testing of the containment vessel as specified in Section 8.1.3 shall be repeated after any structural modifications to, or rebuilding of, the vessel weldments, cone-seal nut or cone-seal plug.

Replacement of the cone-seal gland nut, leak-test port plug or O-rings with equivalent items does not constitute a structural modification and hence, does not require pressure testing of the containment vessel.

8.2.2 Leakage Tests

The following tests are required after containment vessel loading and for routine maintenance.

8.2.2.1 Pre-shipment (Post-Load) Leak-Rate Test

After the containment vessel is loaded, a leak-rate test of the inner O-ring seal is required to verify that the cone-seal assembly has been installed properly. The acceptance criterion is a measured leak rate less than 1×10^{-3} ref·cm^3 air/sec, and the leak test shall be capable of indicating a leak rate of 5×10^{-4} ref·cm^3 air/sec or less. The leak-rate test shall implement the pressure-rise method (A.5.2) in accordance with Section 7.6 of ANSI N14.5.

8.2.2.2 Maintenance Leak-Rate Test

The containment vessel shall be leak-rate tested as specified in Section 8.1.4 after any of the following events.

- Structural modifications described in Section 8.2.1
- Replacement of containment vessel components, including:
  - Cone-seal plug
  - Cone-seal nut
  - Containment vessel weldment
  - Inner O-ring seal

An annual leak-rate test is also required within the 12 months prior to presenting a loaded package for shipment. As described in Section 8.1.4, the annual leak-rate test measures the rate that helium leaks through the inner O-ring closure seal of the CV via the evacuated-envelope method (A.5.4) of ANSI N14.5.[5]

Upon completion of the helium leak-rate test, applicable data shall be written onto a label as shown in Figure 8.1 and affixed to the drum as described in Section 8.1.4.

The annual leak-test report shall include the following data for each replacement O-ring:

- Material
- Size
- Date of manufacture

8.2.3 Component and Material Tests

The 9977 drum, drum liner and drum closure lid are stainless steel weldments that do not require annual maintenance. The drum closure bolts are not susceptible to fatigue and do not require periodic replacement. Pre-loading inspection requirements described in Section 7.1.1 will segregate out units that need repair.

8.2.4 Thermal Tests

Annual thermal performance testing is not required. See Section 8.1.7.

8.2.5 Miscellaneous Tests

8.2.5.1 Visual Inspection

All visual inspections shall be performed with at least five (5) power magnification and bright light.

8.2.5.1.1. Sealing Surfaces

Prior to CV closure, the sealing surfaces (Figure 8.2) shall be visually inspected for gouges, nicks, cuts, cracks, or scratches that could affect containment performance. If surface damage is found, the vessel shall be set aside and the condition documented via NCR in accordance with Section 9.15. The CV shall not be returned to service until the NCR has been dispositioned ("reworked", "repaired", or "used as is") and its closure performance has been proven acceptable by leak-rate testing described in Section 8.1.4.

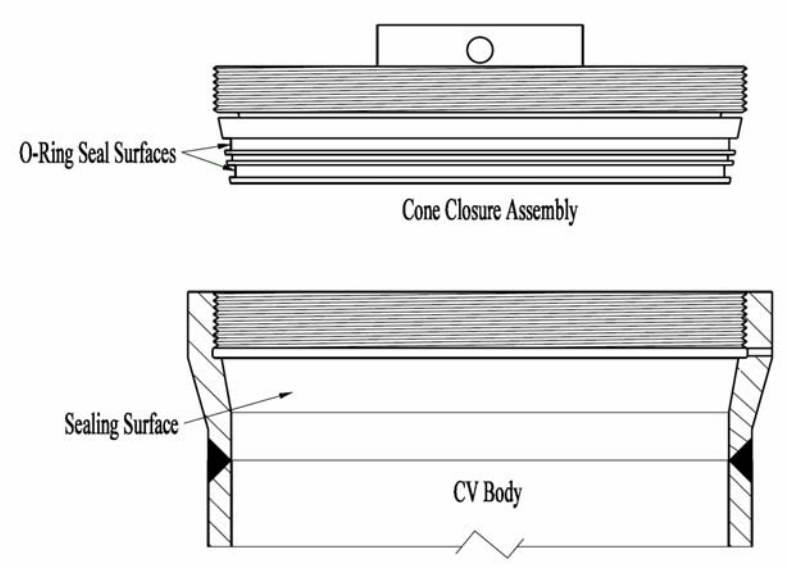

Figure 8.2 – CV Sealing Surfaces

8.2.5.1.2. O-Rings

Prior to closure of the CV, the two CV O-ring seals shall be inspected visually for gouges, nicks, cuts, cracks, or scratches that could affect containment performance. The O-rings shall then be cleaned with ethyl or isopropyl alcohol and lubricated with a thin film of silicone high-vacuum grease as described in Step 25 of Section 7.1.1.1.

Prior to the annual leak-rate test, new O-rings shall be installed in the O-ring grooves of the cone-seal plug. New O-rings shall also be installed when visual inspection or the post-load leak-rate tests indicate that replacement is needed. O-rings shall be as specified on drawings:

R-R2-G-00043, *5-Inch Diameter Containment Vessel Subassembly*, Item 8.

R-R2-G-00042, 6-*Inch Diameter Containment Vessel Subassembly*, Item 8.

Certification of O-ring material, size and date of manufacture shall be furnished by the vendor with each new O-ring. O-rings shall be individually wrapped to prevent damage in shipment and shall be labeled to ensure traceability. Spare part Viton GLT O-rings shall be received and stored by the shipper in accordance with the SAE ARP5316[6] and Parker O-ring Handbook.[7] O-rings shall be no more than 30 years past their cure date when installed. The shipper shall be responsible for traceability of each O-ring.

The Inner O-ring is part of the CV containment boundary. If the Inner O-ring is replaced, a Maintenance Leak Test must be performed per 8.2.2.2 with the new O-ring installed before the CV can be used for shipping.

The Outer O-ring is for assembly verification testing only. The Outer O-ring may be replaced whenever it is found to be damaged because it is not part of the CV containment boundary.

8.2.5.2 Shielding

The 9977 design does not incorporate shielding. Therefore, no annual maintenance of shielding integrity is required.

8.2.5.3 Cone-Seal Assembly Maintenance

Prior to the annual leak-rate test described in 8.2.2.2, the threaded surfaces of the cone-seal nut shall be cleaned with a suitable solvent (e.g., ethyl alcohol or Vortex®, Organic, Semi-Aqueous Solvent or other solvent approved by the Design Agency), dried and lubricated with a thin film of KRYTOX® or equivalent fluorinated grease as approved by the Design Agency (see Section 9.1.2).

In addition, the contacting surfaces between the cone-seal nut and the cone-seal plug shall be cleaned with a suitable solvent (e.g., ethyl alcohol or Vortex®, Organic, Semi-Aqueous Solvent or other solvent approved by the Design Agency), dried and lubricated with a thin film of KRYTOX or equivalent fluorinated grease as approved by the Design Agency.

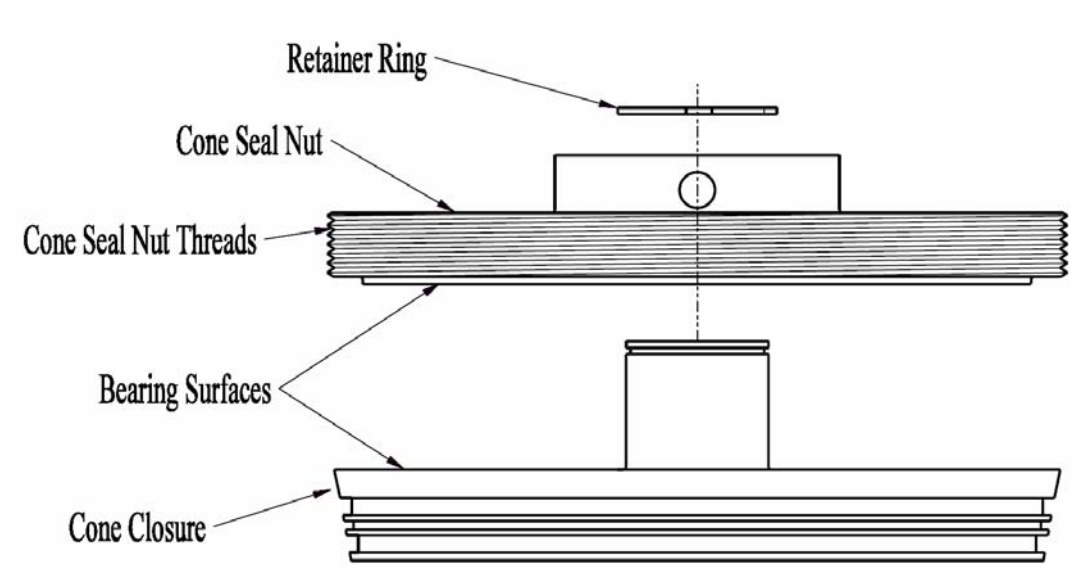

Figure 8.3 – Exploded View of the Cone Closure Assembly

This Page Intentionally Left Blank

8.3 REFERENCES

1. *Operating Controls and Procedures*, Subpart G - Code of Federal Regulations, Title 10, Part 71, Washington, DC (October 2004).

2. *Standard Format and Content Guide of Part 71 Applications for Approval of Packaging for Radioactive Material*, Regulatory Guide 7.9, Revision 2, Nuclear Regulatory Commission, Washington, DC (March 2005).

3. ASNT SNT-TC-1A-2001, *Recommended Practice No. SNT-TC-1A - Non-Destructive Testing* , American Society for Nondestructive Testing , (January 2001)

4. *ASME Boiler and Pressure Vessel Code Section III*, "Rules for Construction of Nuclear Power Plant Components," Division 1, American Society of Mechanical Engineers, New York, NY (2004).

5. *American National Standard for Radioactive Materials - Leakage Tests on Packages for Shipment*, ANSI N14.5, American National Standards Institute, Inc., New York, NY (1997).

6. *Society of Automotive Engineers (SAE) – Storage of Elastomer Seals and Seal Assemblies Which Include an Elastomer Element Prior to Hardware Assembly*, SAE ARP5316, Rev. A, SAE International, Warrendale, PA, http://www.sae.org. (2002).

7. *Parker O-ring Handbook*, ORD-5700A, The Parker Seal Group, Parker Hannifin Corporation, Cleveland, OH, http://www.parker.com/o-ring. (2001).

This Page Intentionally Left Blank

8.4 APPENDICES

8.1 Visual Inspection Criteria for the 9975 Packaging

8.2 Packaging Independent Verification Items

8.3 Example Pre-Shipment (Post-Load) Leak-Rate Test Procedures for the 9977 Packaging

8.4 Example Annual Leak Test Procedure for the 9977 Packaging

8.5 Example Hydrostatic Pressure Test Procedure for the 9977 Packaging

This Page Intentionally Left Blank

APPENDIX 8.1

Visual Inspection and Fabrication Verification Requirements for the 9977 Packaging

This Page Intentionally Left Blank

TABLE OF CONTENTS

PAGE

LIST OF FIGURES

PAGE

INSPECTION CRITERIA FOR THE 9977 PACKAGING

8.1.1 GENERAL INFORMATION

Inspections shall be based solely on those drawings and revisions thereof associated with the currently certified package. These drawings and revisions are given in Appendix 1.1. Full-size controlled copies of these drawings are available from Savannah River Site Document Control.

Prior to delivery to the Owner, the Supplier shall ensure by inspection and documentation that the following criteria are satisfied. The degree of inspection and documentation shall be detailed in the Supplier's Manufacturing and Inspection Plan as agreed upon between the Design Authority and Supplier. Deviations from the engineering drawings shall be resolved as specified in the procurement agreements; these shall be in agreement with the requirements of Sections 9.3 and 9.7.

8.1.2 DRUM ASSEMBLY

The following checks need to be made during fabrication because the inspection areas will not be accessible when the drum is completely fabricated.

8.1.3 Lid Weldment Assembly (R-R2-G-00018)

1. Verify that the materials for the lid are as required.
2. Before the two drum lid liners are welded to the drum lid plate, verify that the Fiberfrax insulating blanket and the Vermiculite and Min-K 2000 thermal ceramic blocks have been installed in the lid weldment as required, to ensure that the lid has the required thermal insulation.

   If the drum lid insulation is not installed as required, lid welding cannot proceed.
3. Inspect the welds in the drum lid as required to ensure good workmanship.

   If weld defects are found, they must be repaired and the repairs must be re-inspected.

8.1.4 Drum Liner (R-R2-G-00017)

Before the drum liner is welded to the drum:

1. Verify that the materials for the liner and insulation are as required.
2. Inspect the drum liner welds and hydrostatically test the drum liner welds as required to ensure good workmanship.

   If weld defects are found, they must be repaired and the repairs must be re-inspected.
3. Verify that the Fiberfrax insulating blanket has been installed on the drum liner as required to ensure that the drum will have the required thermal insulation.

If the drum lid insulation is not installed as required, the drum liner cannot be welded to the drum. Verify that the drum liner is perpendicular to the drum top plate as required, to ensure that the polyurethane foam will evenly protect the CVs.

8.1.5 Drum Weldment (R-R2-G-00017)

1. Verify that the materials for the drum weldment are as required.
2. Verify that the vent holes are sized, positioned, and plugged as required. Verify that plugs are BP ¾-in. Caplugs™ as required.
3. Verify that the convexity of the drum's bottom is as required, to ensure proper operation.
4. Verify that the drum has three expanded rolling hoops positioned as shown.
5. After the drum rim (Item 7) has been tack welded onto the drum, verify and document the drum's overall height to ensure proper operation.

   If the drum's overall height is not 36.1 ± 0.01", then the drum rim must be repositioned so the overall height is 36.1 ± 0.01".
6. Verify that the drum closure is as specified, including lid and flange welded as required.
7. Verify that the identification plate is lettered, positioned, and attached as required.
8. Verify that the drum's ID is as required.
9. Verify that the drum's closure nuts and bolts are as required.
10. Verify that the drum satisfies UN 1A2/350/S/yy/USA/*, Note 3. Where the "yy" will be the year the drum was manufactured and the * is the manufacturer's symbol. (Note: Drum Manufacturer shall provide test documentation to verify that the drum design meets the above UN specification).

8.1.6 Drum and Liner Weldment (R-R2-G-00017)

1. Inspect the welds as required to ensure good workmanship.
2. Verify that the welds have been hydrostatically tested as required to ensure that the welds are free of water leaks.
3. To ensure good workmanship verify by visual inspection that the drum top, bottom, and side are not breached by holes or by cracks. Surface scratches are acceptable. Sharp edged or pointed dents that may breach the drum are not acceptable. Drum damage that would affect packaging or transportation operations is not acceptable.
4. Verify that no sharp edges or burrs exist which may pose a personnel hazard or which may degrade any aspect of the packaging. This verification ensures operator safety and proper operation of the packaging.

5. Verify that the drum lid weldment fits (Drawing R-R2-G-00018) into the drum liner and rotates 360º without binding, to ensure proper operation.

8.1.7 Drum Foam Installation Subassembly (R-R2-G-00017)

Before the foam is stalled into the drum, check the following:

1. Check the perpendicularity of the drum liner
2. Verify that an 8” diameter x 25.5”long cylindrical blank (with ½” chamfers on each end) can seat can be inserted into the drum liner without binding, and verify that top of the blank is 5” below the drum top plate (Dimension “A” in Figure 8.1.1). This will ensure that the drum liner will hold its contents without interferences.

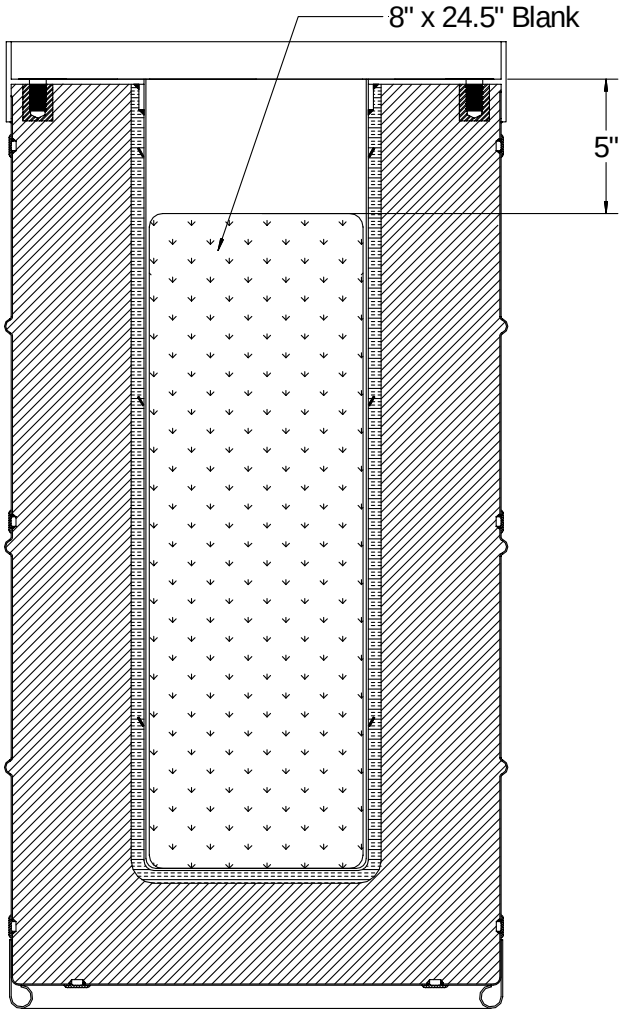

Figure 8.1.1 – Cross-Section of Drum with 8” Diameter x 24.5” Blank

3. Verify that the Fiberfrax® insulating blanket assembly has been installed with star washers and three tie wraps as required per Note 10.

4. Verify that the polyurethane foam has satisfied the inspection requirements, to ensure there are no significant voids in the polyurethane foam.
5. Verify that the drum bottom fill and vent holes are sized, positioned, and plugged as required. Verify that plugs are BP 1-in. Caplugs™ as required.

8.1.8 CONTAINMENT VESSEL ASSEMBLY (R-R2-G-00042 AND R-R2-G-00043)

8.1.8.1 Containment Vessel Weldments

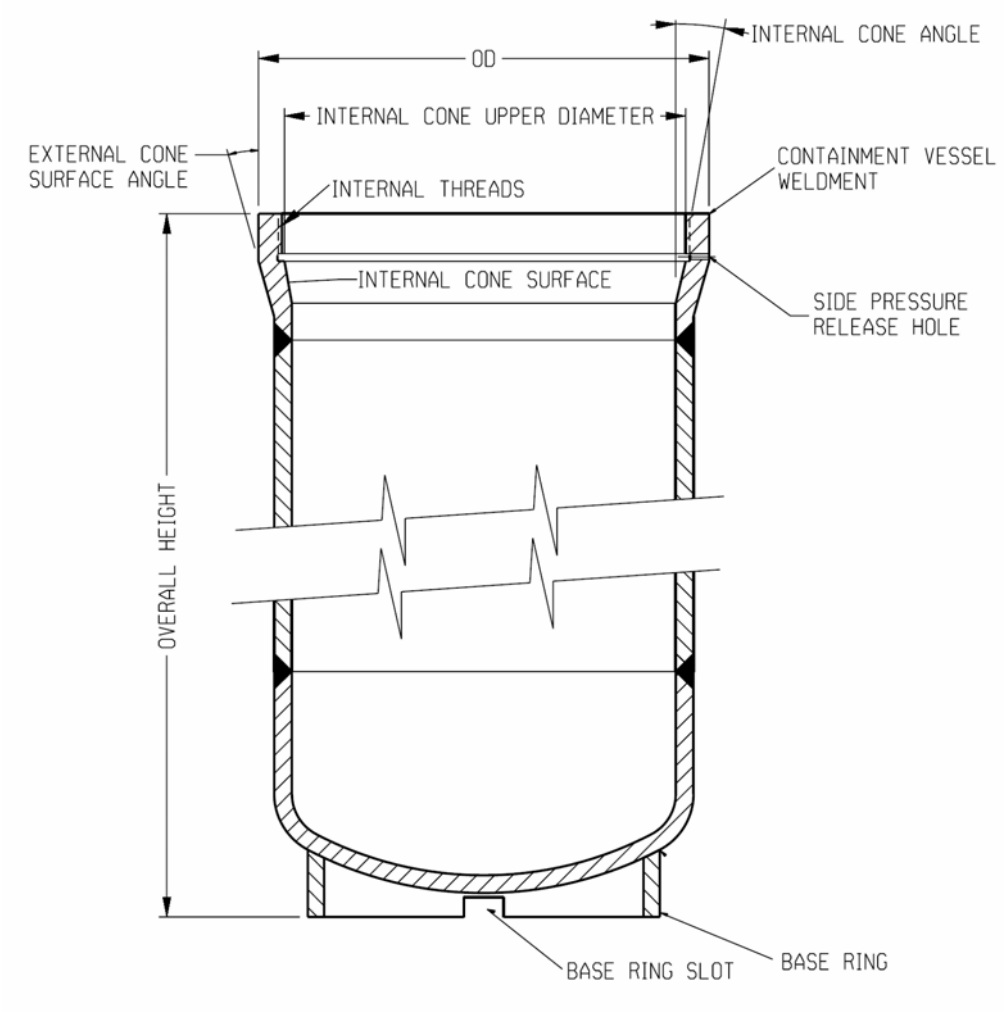

Figure 8.1.2.-.Inspection Diagram for 6CV Weldment

1. Verify that the materials for the drum weldment are as required.
2. Verify that the overall height and OD are as required.
3. Verify that the base ring slots are positioned and dimensioned as required.
4. Verify that the markings and serial numbers are as required.

5. Verify that the threading and thread relief are as required and the threading passes gage verification.
6. Verify that the side pressure-release hole is positioned and sized as required.
7. Verify that the internal cone surface upper diameter is as required.
8. Verify that the internal and external cone surfaces are angled as required.
9. Verify that the internal cone surface finish is as required.
10. Verify that the pipe surface finish is as required.
11. Verify that the welds have been inspected as required.
12. Verify that the 6CV and 5CV will accept the gauge blocks shown on R-R2-G-00042, Note 11 and R-R2-G-00043, Note 11 as required.

8.1.9 Cone Seal Nut (Drawings R-R2-G-00042 and R-R2-G-00043)

Verify the following to ensure proper operation:

1. The materials for the cone seal nut are as required.
2. The cone-seal nut is marked as required and the serial number is as required to ensure the cone seal closure assembly and the containment vessel weldment remain a matched set.
3. The cone-seal nut's thread diameter passes the test gage and is perpendicular to the base surface as required.
4. The cone-seal nut's ID and top ID and depth are as required.
5. The cone-seal nut's bottom inside perimeter is chamfered as required.
6. The cone-seal nut's bottom step is dimensioned as required.
7. The cone-seal nut's total height and nut height are as required.
8. The cone-seal nut's square flat widths are as required.
9. The cone-seal nut's square flat faces have holes positioned and dimensioned as required.

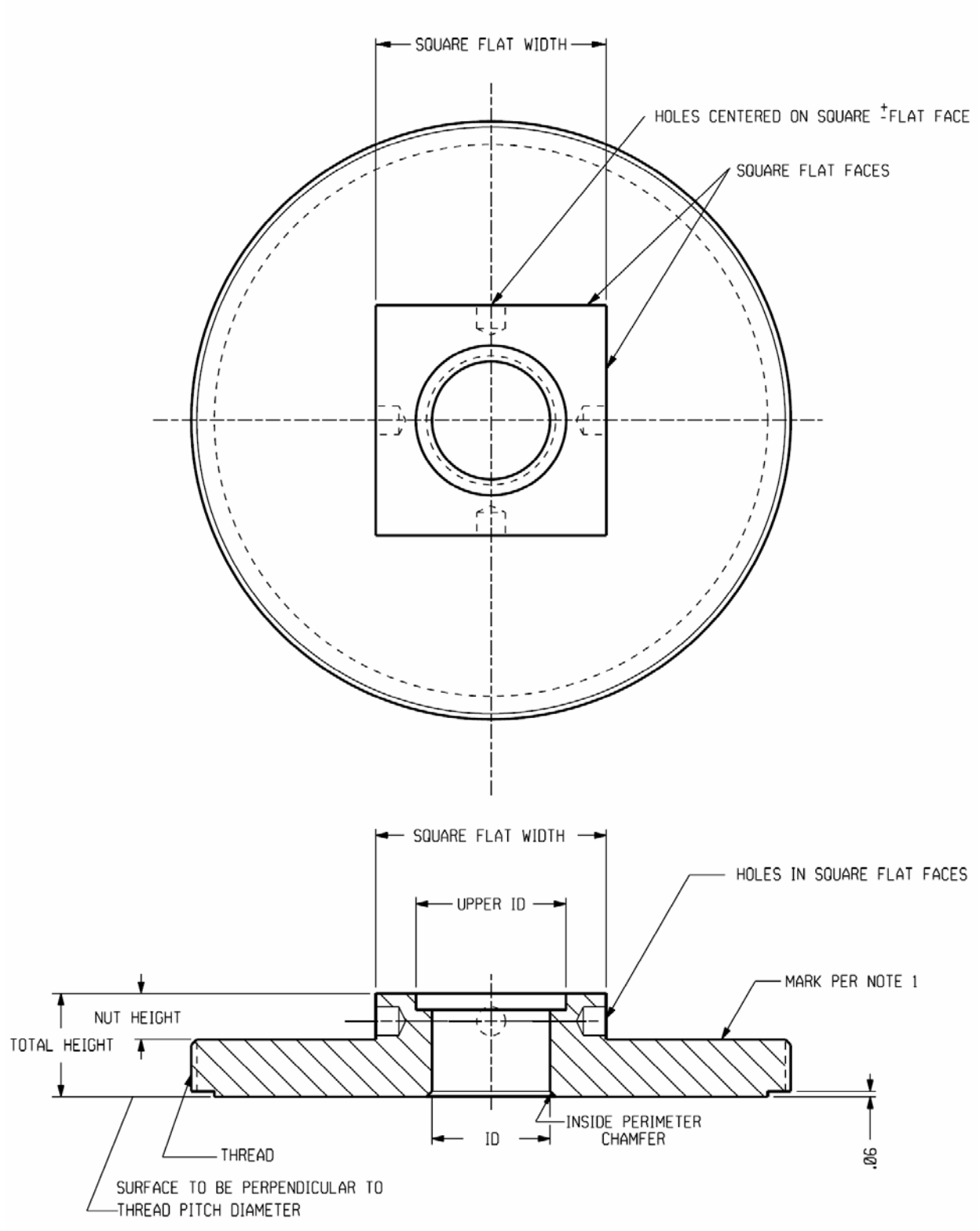

Figure 8.1.3 – Cone Seal Nut Inspection Diagram

8.1.10 Cone Seal Plug (Drawings R-R2-G-00042 and R-R2-G-00043)

Verify the following to ensure proper operation:

1. The materials for the cone seal plug are as required.
2. The "Q" dimensions are as required to ensure proper fit up and sealing.
3. The surface finish of the O-ring grooves is as required to ensure sealing.
4. The cone-seal plug's ODs are as required.
5. The cone-seal plug's total height and base heights are as required.
6. The upper and lower O-ring grooves and leak test groove are positioned and to the depths required and with the corner radii required.
7. The cone-seal plug's face finish and O-ring groove finishes are as required.
8. The cone-seal plug's leak-test port upper cavity is the diameter and depth required.
9. The cone-seal plug's leak-test port is threaded to the depth required, and with the bottom finish and thread relief required.
10. The cone-seal plug's leak-test port threading passes the gage test required.
11. The cone-seal plug's leak-test port radial hole is positioned and dimensioned as required and allows free gas passage form the port to the leak test groove.
12. The cone-seal plug's upper cylinder external groove is positioned and has the width and depth specified.

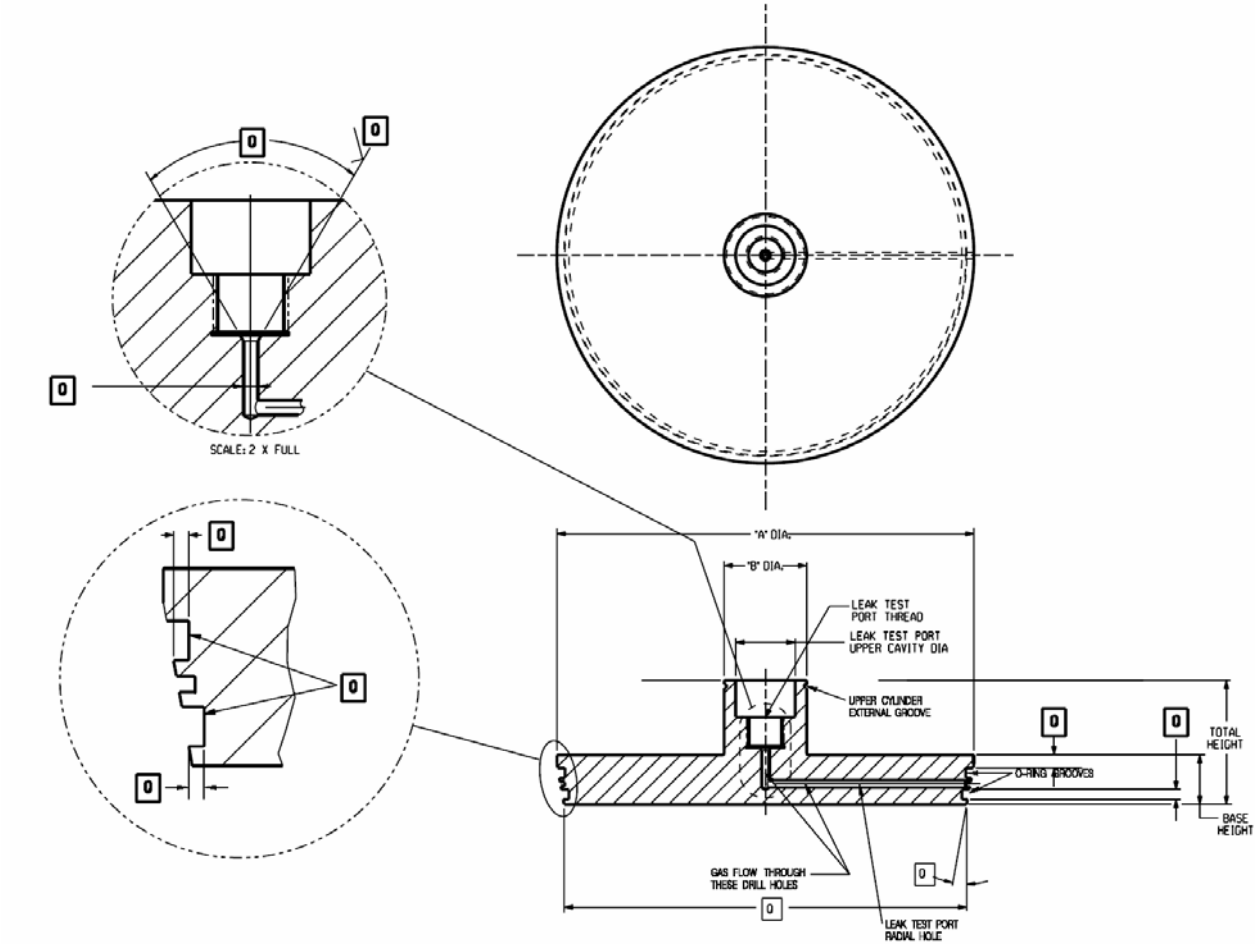

Figure 8.1.4 – Inspection Diagram for Cone Seal Plug

8.1.11 Containment Vessel Subassembly (Drawings R-R2-G-00042 and R-R2-G-00043)

1. Verify that the overall height and diameter are as required.
2. Verify that the surfaces indicated on the drawing are lubricated with Krytox vacuum grease, to ensure free movement between the cone seal plug and the cone seal nut, and between the screw threads on the cone seal nut and the 6CV vessel.
3 Verify that all threaded components assemble freely (gland nut, cone-seal nut) to ensure proper operability.
4. Verify that the cure dates for all of the O-rings installed are less then 3 years earlier than the date of installation on the 6CV, to ensure proper operability.
5. Verify that spare O-rings are packaged individually with the O-ring size, material certification (Viton GLT), cure date, and shelf life specified and labeled on the exterior of the package, to ensure proper operability. Verify that installed O-rings have no nicks, cracks, pits, or flat spots on the O-rings as specified by the O-ring vendor.

6. Verify that the gland nut and leak-test port plug are as required to ensure proper operability.
7. Verify that the retaining ring is installed and cone-seal plug and cone-seal nut have free relative rotational movement and limited relative axial movement, to ensure proper operability.
8. Verify that the containment vessel is cleaned as required to ensure proper operability and to prepare for the helium leak test.

8.1.12 OVERALL ASSEMBLY

8.1.12.1 Spacer Parts (R-R4-G-00032 and R-R4-G-00033)

1. Load Distribution Fixtures (R-R4-G-00032)

   Verify that the Top Load Distribution Fixture and the Bottom Load Distribution Fixture are present, are the proper materials, and that they have been machined to the required dimensions, to ensure the two Load Distribution Fixtures fit in the drum liner, and to ensure the two Load Distribution Fixtures fit on the 6CV.

2. Top, Annular and Bottom Spacers (R-R4-G-00033)

   Verify that the Top, Annular, and Bottom aluminum honeycomb spacers are present, are the proper materials, and that they have been machined to the required dimensions, to ensure the two Spacers fit with the Top and Bottom Load Distribution Fixtures, and to ensure the three spacers fit on the 5CV.

8.1.12.2 Assembly (R-R1-G-00020 and R-R1-G-00021)

1. Verify that all of the components fit into the drum without binding, as shown in the Assembly Drawing, to ensure proper operation.
2. Verify that all of the drum lid bolts and washers are present to ensure proper operation.
3. Verify that the drum lid bolts can be threaded through the drum lid and into the drum hand-tight until they reach the point of engagement with the drum lid, to ensure proper operation.
4. Verify that all drum vent hole Caplugs are in place, to ensure proper operation.
5. Verify that a security seal can be installed freely through the Tamper Indicating Device holes in the closure nuts, to ensure proper operation.
6. Verify that the packaging nameplate and barcode plate are lettered and installed to ensure package traceability and proper operation.

7. Verify that insertion of the two load distribution fixtures, the 6CV, and the drum lid assembly fit into the drum unhindered, to ensure proper operation.

8. Verify that insertion of the two load distribution fixtures and the aluminum honeycomb spacers, the 6CV, and the drum lid assembly fit into the drum unhindered, to ensure proper operation.

9. Verify and document that the net packaging weight is not greater than 350 pounds, to ensure that the packaging will not exceed shipping weight limits.

This Page Intentionally Left Blank

APPENDIX 8.4

Example Annual
Leak Test Procedure for the 9977 Packaging

This Page Intentionally Left Blank

1.0 PURPOSE

To give step-by-step instructions for the annual helium leak test certification of 9977 5-inch and 6-inch diameter Containment Vessels (CVs). The procedure is the same for both CVs.

1.0 SCOPE

1.1 This procedure applies to the annual helium leak test performed on 9977 CV's, see Figure 1, which must pass a leak test at 1-year intervals.

1.2 This procedure provides instructions for performing annual leak tests to the inner O-Ring seal of a 9977 CV after the CV has been removed from its drum and after its annual maintenance has been completed.

1.3 Acceptance Criteria

1.3.1 Per ANSI N 14.5, the Maximum Allowable Leak Rate is ≤1 X 10-7 ref cm3 air/sec at 1 atmosphere differential pressure (2.0 x 10-7 ref cm3 helium/sec under the same conditions). This procedure uses 50% helium concentration. ANSI N-14.5, Equation B.15 is used to calculate an adjusted acceptance criterion:

$$L = L_m \frac{P_m}{P_t} \text{ cm}^3\text{/sec}$$ where L = volumetric leak rate, cm^3/sec

L_m = measured leak rate, cm^3/sec
P_m = total pressure of the gas mixture, atm abs.
P_t = partial pressure of the tracer gas, atm abs.

This equation can be rearranged to solve for L_m:

$$L_m = L \frac{P_t}{P_m}$$ For 50% helium concentration, $\frac{P_t}{P_m}$ = 0.5

Therefore, the adjusted acceptance criterion for this procedure is:

$$L_m = L \frac{P_t}{P_m} = 2x10^{-7} * 0.5 = 1x10^{-7} \text{ ref cm}^3 \text{ helium/sec}$$

1.3.2 If a CV does not pass the annual leak test or is found to be damaged or defective, contact the 9977 Design Authority and the 9977 Design Agency. All repairs of a shipping containment vessel shall be documented with a Non-Conformance Report (NCR) being issued and dispositioned by the 9977 Design Authority and by the 9977 Design Agency before the repairs are performed. O-Ring replacement is authorized in this procedure without an NCR.

2.0 Terms and Definitions

2.1.1 CV: The Containment Vessel for the 9977.

2.1.2 Evacuated Envelope – Gas Detector Test: A helium leak test method where the inside of a test item is pressurized with helium tracer gas while the outside of the item is under a vacuum. A helium leak detector is connected to the vacuum chamber, and tracer gas that passes from the inside of the test item to the outside is detected as leakage. This method gives an overall leak rate for the test item, but it does not identify the leak location, if there is any.

3.0 Precautions and Limitations

3.1 This test shall be performed by certified Level II or Level III Leak Test Personnel or by Leak Test Trainees or Level I Personnel under the direct supervision of a Level II or Level III Leak Tester.

3.2 Only personnel certified to Level II or Level III may interpret test results or sign data sheets or test reports as the leak tester.

3.3 For CV's with a radiological history, this test must be performed per the Radiation Control Requirements of the test facility.

3.4 Wear steel-toed safety shoes while handling vessels.

3.5 Use proper lifting technique when lifting containment vessels.

4.0 PREREQUISITE ACTIONS

4.1 The annual maintenance of the CV shall be completed before starting this procedure.

4.2 Required Instrumentation & Equipment

4.2.1 M&TE calibrated standard helium leak with a leakage rate between 3 x 10^{-8} and 9 X 10^{-7} std cc/sec.

4.2.2 Helium mass spectrometer leak detector with sensitivity of 1 X 10 -9 atm cc/sec/division of helium or better.

4.2.3 M&TE Calibrated thermometer graduated in oC, capable of reading room temperature to $\pm$ 0.5oC.

4.2.4 M&TE calibrated absolute pressure transducer, ±.25 psi accuracy or better for pressures ranging from 0 to 100 psia.

4.2.5 M&TE calibrated Digital Manometer, 3 Bar range, with min/max function, 0.1% accuracy, Omni Instruments P/N LEO2-1-3BAR, Omni Instruments Inc, Tel: 1-800-308-6037. This gauge will be mounted on the sample cylinder assembly shown in Figure 2. Omni Instruments Inc

4.2.6 Helium gas cylinder, welding grade, 99.9% minimum purity.

4.2.7 Straps, clamps, etc needed to tie down the helium gas cylinder.

4.2.8 Regulator/Relief Valve with 100 psig set pressure, for helium cylinder.

4.2.9 Helium charging piping (See Figure 2 for piping schematic).

4.2.10 Testing apparatus piping (See Figure 3 for piping schematic)

4.2.11 Calibrated torque wrench (digital or dial readout), capable of reading 50 or 100 foot pounds of torque, for the 5CV and 6CV respectively, with ± 4% of reading uncertainty, or better (for applying closure torque to the CV cone-seal nut).

4.2.12 Calibrated torque wrench (digital or dial readout), capable of reading 30 foot pounds of torque with ± 4% of reading uncertainty, or better (for applying closure torque to the high pressure plug).

4.2.13 Lid wrench (See Figure 4).

4.2.14 Ratchet wrench with 9/16-inch socket (for removing/installing high pressure plug in the test port).

4.2.15 Torque wrench adapter, if needed to connect torque wrench to the lid wrench.

4.2.16 CV Lifting Device, for lifting the containment vessel with a hoist. See Figure 5 for design information.

4.2.17 Lid lifting handle (See Figure 6).

4.2.18 Anti-rotation Stand (See Figure 7).

4.2.19 Stopwatch, wall clock or watch.

4.2.20 6 inch steel ruler with 1/32" graduations for measuring the distance between scribe lines on the cone seal.

4.2.21 Sample Cylinder and associated equipment, for pressurizing the inside of the CV with helium (see Figure 8 for design information).

4.2.22 Loading shield for the CV (See Figure 9) (Optional). The shield protects the CV threaded opening and sealing surface when the Sample Cylinder is moved in and out of the CV.

4.2.23 DC Volt meter, capable of reading 12 to 14 volts DC. M&TE calibration is not required because the meter is used for an in-process check of batteries.

5.0 PERFORMANCE SECTIONS

5.1 Preliminary Actions

5.1.1 **ENSURE** the Pressure Transducer Readout is on.

5.1.2 **ENSURE** the helium leak detector is on.

5.1.3 **ENSURE** the electronic thermometer is ON.

5.2 Helium Leak Detector Preliminary Calibration

5.2.1 **RECORD** the containment vessel Serial Number, Test Date, M&TE data, and Leak Tester's Name on the Helium Leak Test Data Sheet, Attachment 1.

5.2.2 **RECORD** the Room Temperature (TR) on Attachment 1.

5.2.3 **CALCULATE AND RECORD** the temperature-corrected value (LTC) of the helium leak standard using the formula on Attachment 1.

5.2.4 **PERFORM** an instrument calibration on the helium leak detector per manufacturer's instructions.

5.2.5 **ADJUST** the leak detector to read the temperature-corrected value of the helium leak standard.

5.2.6 **RECORD** the Preliminary Helium Standard Reading and the Preliminary Background Reading on Attachment 1.

5.2.7 **CALCULATE** the First Standard Response per Attachment 1 AND RECORD on Attachment 1.

5.3 Sample Cylinder Charging

5.3.1 **PLACE** the CV in an anti-rotation stand.

5.3.2 **REMOVE** the cone seal from the CV.

5.3.3 **INSTALL** a loading shield in the opening of the CV (optional).

5.3.4 **PLACE** the Sample Cylinder in the CV with the magnetically actuated switch aligned with the scribe line on the top lip of the CV.

5.3.5 **CHARGE** the Sample Cylinder with helium by performing the following steps:

A. **CONNECT** the Sample Cylinder to the helium charging piping, as shown in Figure **2**

B. **ENSURE** the DC voltage across the battery pack is greater that 12 Volts DC by checking across the electrical terminals with a DC Voltmeter. **REPLACE** or **RECHARGE** the batteries if needed.

C. **ENSURE** the pressure transducer/readout is turned on.

D. **TURN** the Bypass Switch to "BYPASS". This will keep the horn from sounding during helium charging steps.

E. **OPEN** the solenoid valve by placing a magnet on the outside of CV as close to the magnetically activated switch as possible. (The magnet may be held in place with tape, large rubber band, etc.)

F. **ENSURE** the solenoid valve is open by briefly turning the Bypass Switch briefly to "ON". The horn will sound if the valve is open.

G. **TURN** the 3-way ball valve to "VAC".

H. **TURN ON** the vacuum pump and **PUMP DOWN** the Sample Cylinder to less than 0.1 psig.

I. **ENSURE** the helium cylinder valve is open.

J. **ENSURE** the helium regulator is adjusted to between 60 and 65 psig.

K. **TURN** the 3-way ball valve to "HE" and pressurize the Sample Cylinder to between 60 and 65 psig, as read on the pressure transducer/readout.

L. **TURN OFF** the vacuum pump.

M. **TURN** the 3-Way Valve to the "CLOSED" position (midway between "VAC" and "HE").

N. **ENSURE** the pressure transducer/readout still reads between 60 and 65 psig.

- **IF** the pressure is less than 60 psig, **TURN** the 3-Way Valve to the "HE" position and **ADJUST** the pressure regulator to between 60 and 65 psig. **THEN REPEAT** Steps M and N.
- **IF** the pressure is greater than 65 psig, **THEN DECREASE** the pressure by slowly venting off helium gas through the Vent Valve until the pressure is between 60 and 65 psig

O. **REMOVE** the magnet from the CV to close the solenoid valve.

P. **TURN** the Bypass Switch to "ON" to activate the horn.

Q. **DISCONNECT** the sample cylinder from the charging manifold.

5.3.6 If used, **REMOVE** the loading shield from the CV.

5.3.7 **CAREFULLY PLACE** the cone seal on the CV using care to ensure the male and female threads are not cross-threaded and hand tighten.

5.3.8 **TORQUE** the CV cone seal nut to between 50 and 60 ft-lbs or 100 and 120 ft-lbs, for the 5CV and 6CV respectively.

5.3.9 **DETERMINE** if the distance between the radial line scribed across the top of the cone seal nut and the radial line scribed on the top of the containment vessel body is equal to or less than 1 inch.

A. **IF** this distance is greater than 1 inch, **THEN CONTACT** the 9977 Design Authority for guidance.

B. **IF** the distance is less than or equal to 1 inch, **THEN CONTINUE** with this procedure.

5.3.10 **REMOVE** the 1/4" high pressure plug from the top of the cone seal.

5.4 Leak Test

5.4.1 **CONNECT** the leak detector to the CV test port using the special vacuum fitting.

5.4.2 **OPERATE** the helium leak detector per manufacturer's instructions to get a steady background reading.

5.4.3 **RECORD** the background reading on Attachment 1.

5.4.4 **PLACE** the magnet on the outer wall of the CV at the location of the magnetically activated switch to introduce helium into the CV.

5.4.4.1 **LISTEN** for the horn that is mounted on the sample cylinder to sound, indicating that the solenoid valve is activated.

5.4.4.2 **KEEP** the horn sounding for at least 20 seconds to ensure all the helium is introduced to the CV.

5.4.5 **WAIT** one minute, AND THEN RECORD the helium leak detector reading on Attachment 1.

5.4.6 **CALCULATE** the Leak Response per Attachment 1 **AND RECORD** on Attachment 1.

5.4.7 **ACTIVATE** the "VENT" mode on the helium leak detector.

5.4.8 **DISCONNECT** the leak detector from the CV.

5.5 Helium Leak Detector Post-Test Calibration

5.5.1 **PERFORM** a calibration check on the helium leak detector per manufacturer's instructions.

5.5.2 **RECORD** the Post-Test Helium Standard Reading and the Post-Test Background Reading on Attachment 1.

5.5.3 **CALCULATE** the Final Standard Response as shown on Attachment 1 AND RECORD on Attachment 1.

5.5.4 **CALCULATE** the Response Ratio as shown on Attachment 1 AND RECORD on Attachment 1.

5.6 Sample Cylinder Removal

5.6.1 **TURN** the CV so that the pressure release hole is pointed away from personnel.

WARNING: *At this point, the CV has ~ 15 psig internal gas pressure. The following steps includes a verification that the CV is not pressurized before the lid is completely removed.*

5.6.2 **UNSCREW** the cone seal nut two complete turns with the lid wrench.

5.6.3 **LISTEN** for helium escaping through the pressure release hole**, THEN UNSCREW** the cone seal and remove it from the CV.

WARNING: *If the helium does not escape through the pressure release hole the CV may be pressurized. Suspend this procedure and contact supervision for further instruction.*

5.6.4 **RECORD** the Sample Cylinder's maximum pressure reading on Attachment 1.

- **IF** the pressure reading is > 15 psig, **THEN** the leak test is valid.
- **IF** the pressure reading is ≤ 15 psig, **THEN** the leak test must be repeated. **TROUBLE SHOOT** the Sample Cylinder Assembly to determine the cause of the under-pressurization.

5.6.5 **PLACE** a loading shield into the top of the CV (optional)

5.6.6 **REMOVE** the sample cylinder from the CV.

5.6.7 If used, **REMOVE** the loading shield from the CV.

5.6.8 **CAREFULLY PLACE** the cone seal on the CV using care to ensure the male and female threads are not cross-threaded and hand tighten.

5.6.9 **TORQUE** the CV cone seal nut to between 25 and 35 ft.lbs.

5.7 Accept/Reject

5.7.1 **DETERMINE** the acceptability of the CV **AND RECORD** on Attachment 1. To be acceptable, the following must be TRUE:

- Leak Test Response < 1 x 10-7ref cm3 helium/sec
- Sample Cylinder's maximum pressure reading 15 psig.
- Response Ratio > 65%.
- **IF** the Response Ratio is ≤ 65%, **THEN NOTIFY** supervision that the leak detector requires maintenance. The CV that was being tested may be retested with a properly functioning leak detector.

5.7.2 **SIGN AND DATE** Attachment 1.

5.7.3 **PEER REVIEWER**: **REVIEW** Attachment 1 for completeness and accuracy of calculation **AND SIGN AND DATE** Attachment 1.

6.0 RECORDS

6.1 **SUBMIT** the completed Attachment 1to the appropriate Facility Manager.

7.0 REFERENCES

7.1 WSRC-SA-2002-00008, Revision 0, "Safety Analysis Report for Packaging Model 9977, Chapter 8, December 2003.

7.2 EESD Procedure L9.4-8303, "Proof/Leak Test Procedure".

7.3 ANSI N 14.5-1997, "American National Standard for Radioactive Materials - Leakage Tests on Packages for Shipment".

7.4 ASME Section V, Article 10.

8.0 ATTACHMENTS

8.1 Attachment 1, Helium Leak Test Data Sheet for 9977 Shipping Containment vessels.

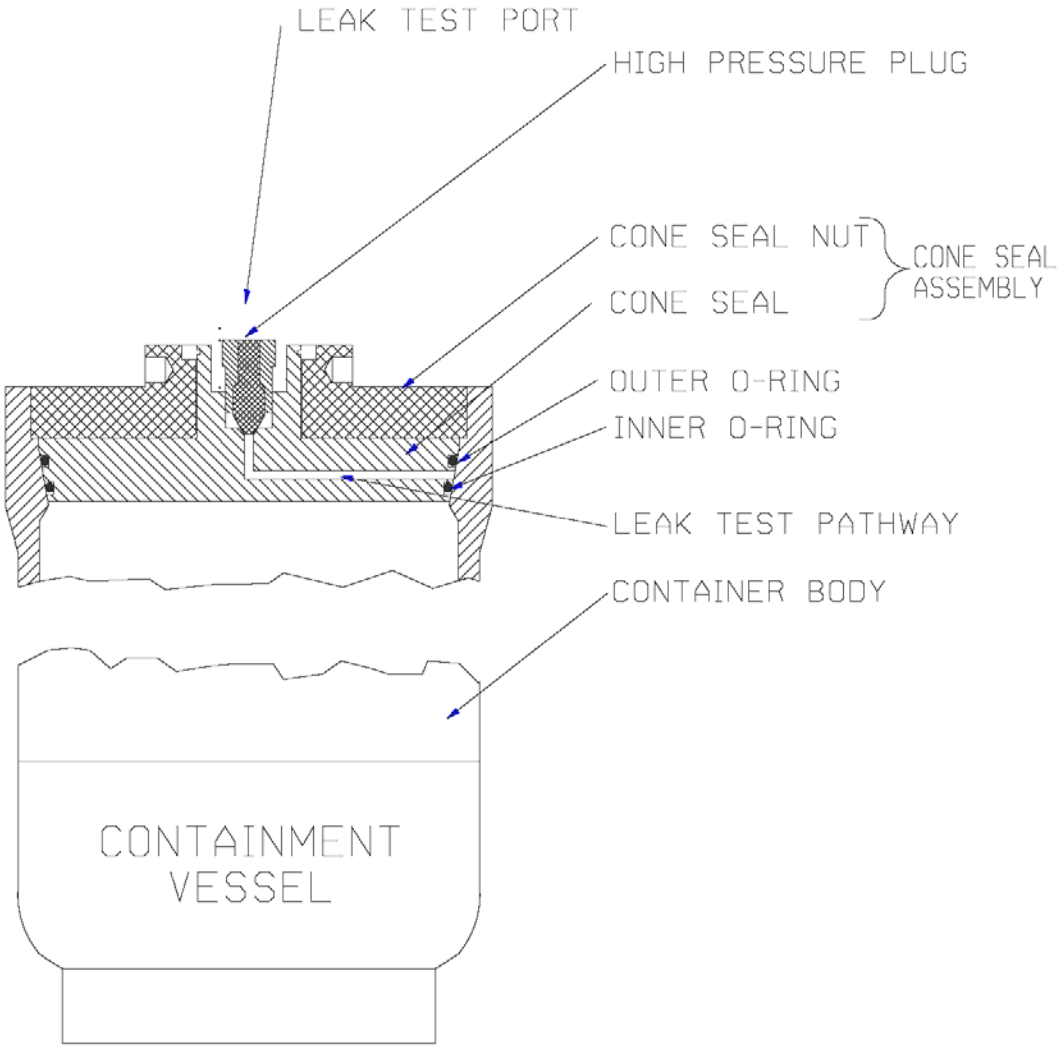

Figure 1 – CV Cross-Section

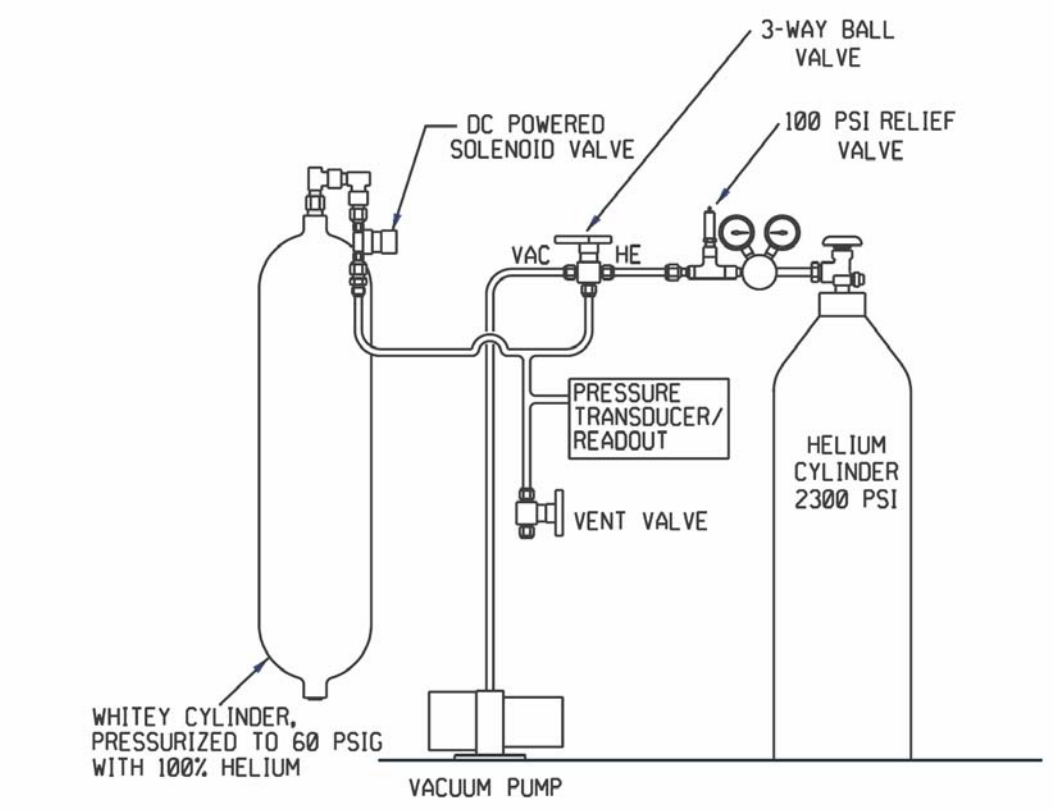

Figure 2 – Schematic for Filling Sample Cylinder

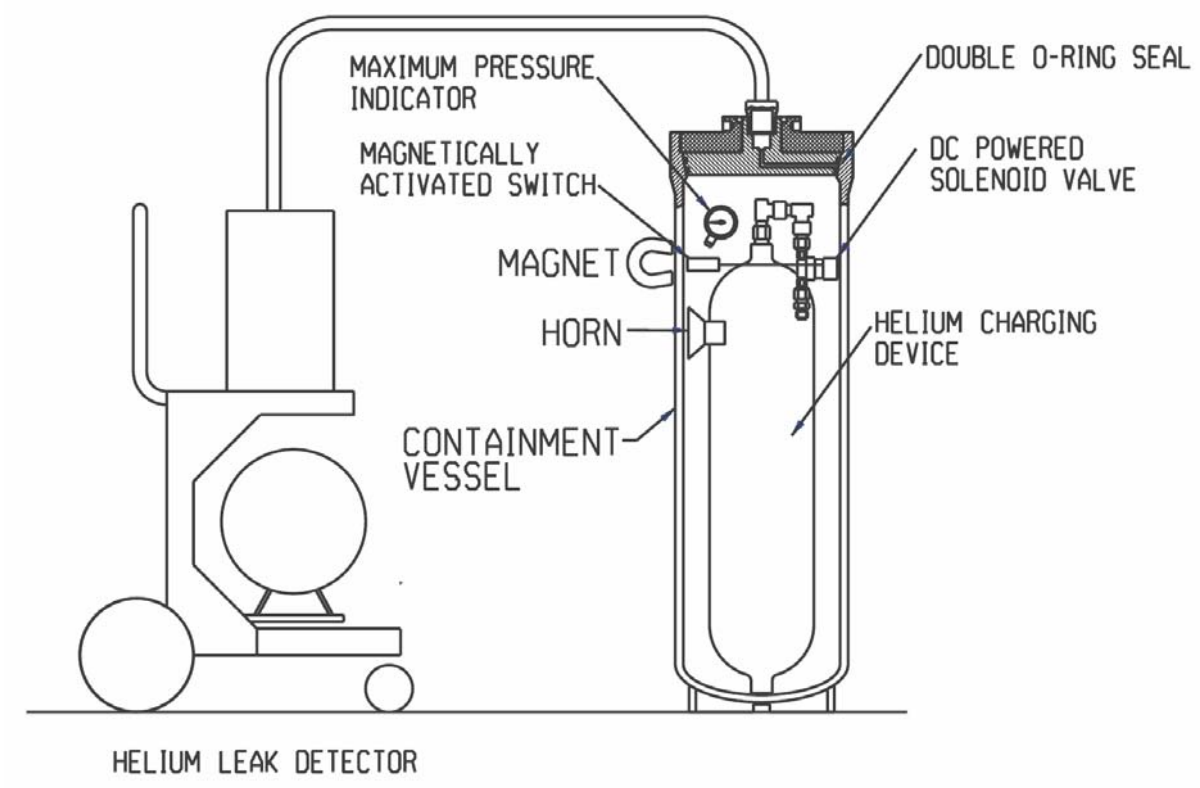

Figure 3 – CV Testing Apparatus

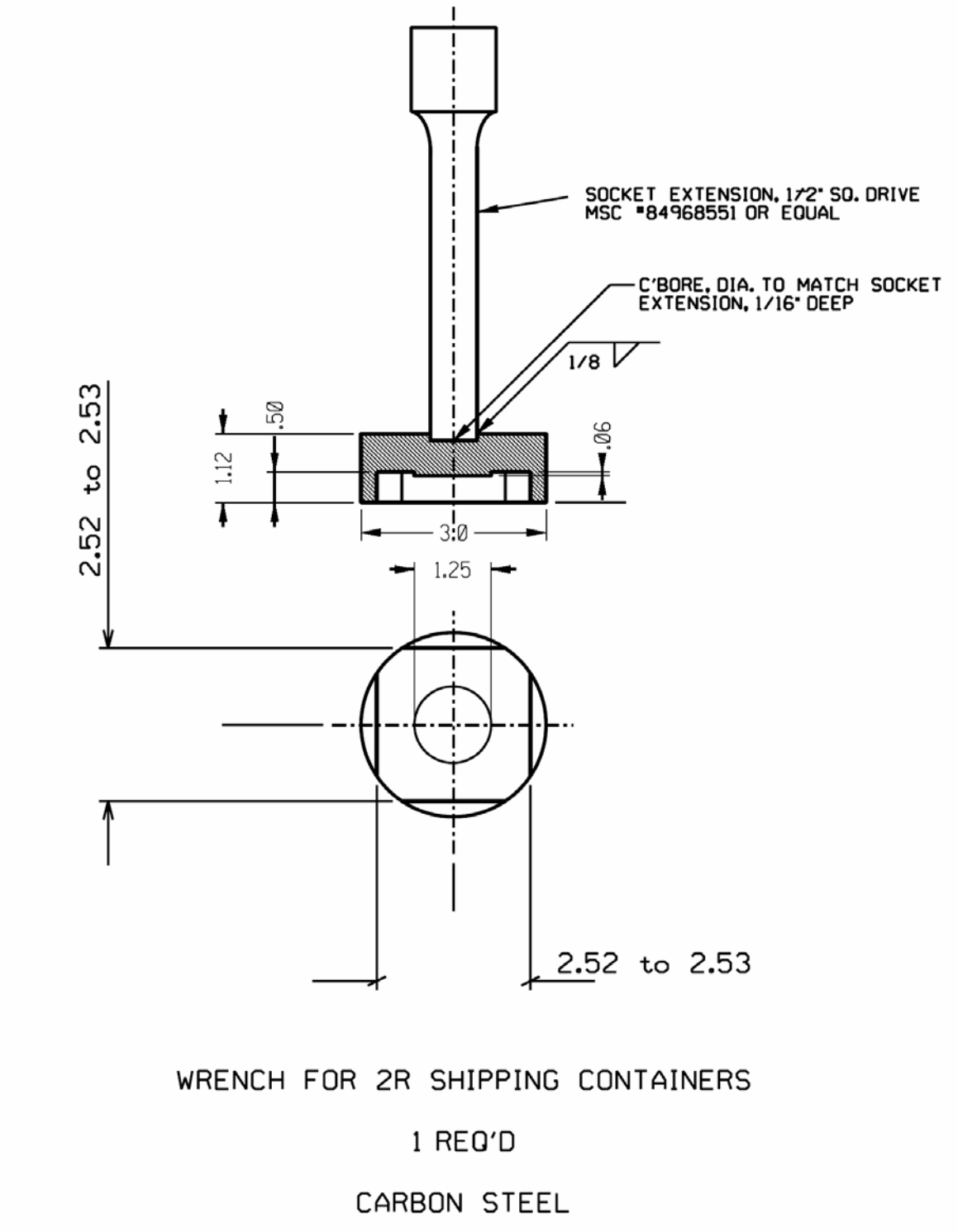

Figure 4 – Lid Wrench

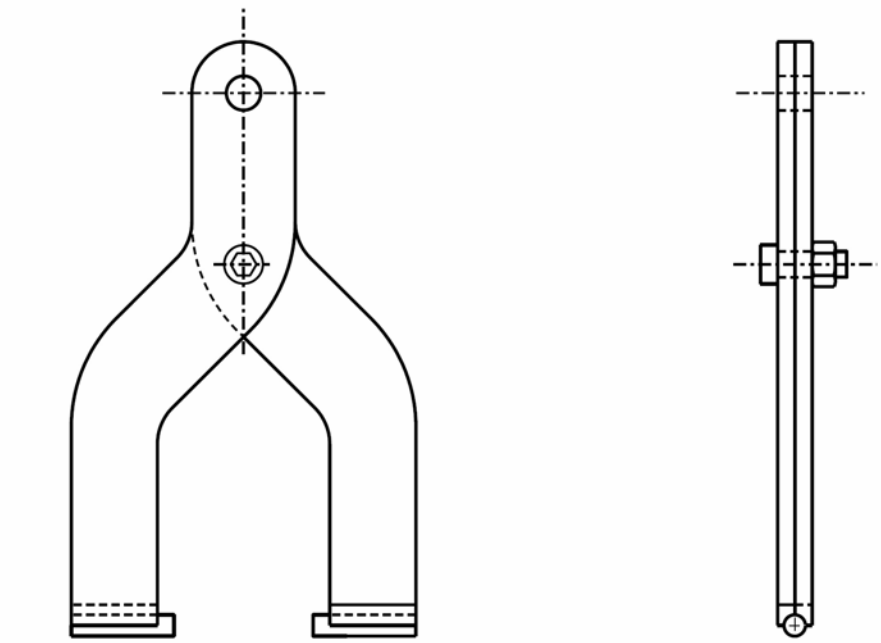

Figure 5 – CV Lifting Device

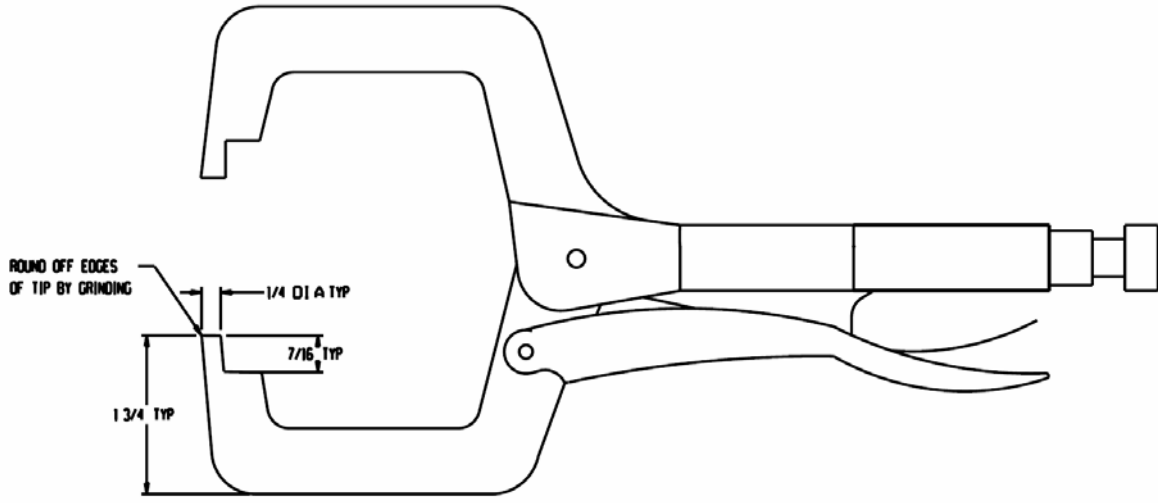

VISE GRIP MODIFIED

MATERIAL: MAKE FROM COML VISEGRIP IRWIN #11R REQ'D: 1 PER ASSY

EES-23047-R4-010-A

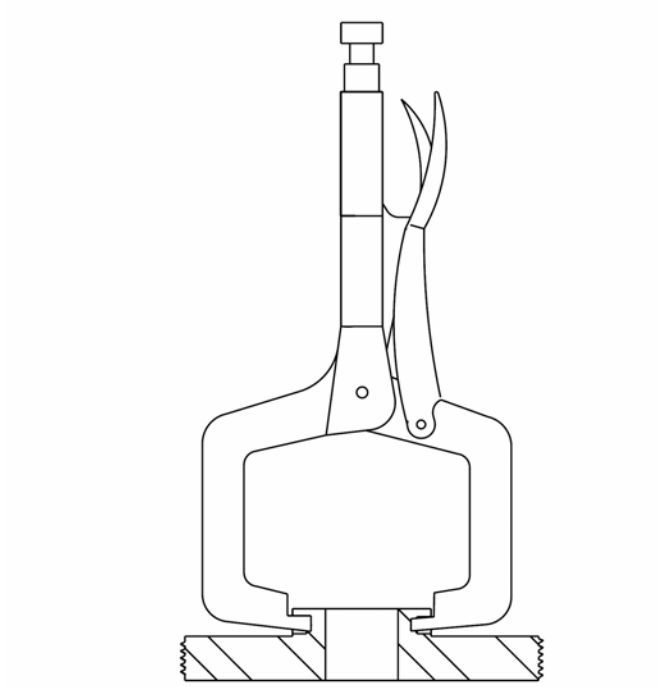

VISE GRIPS ARE USED TO CARRY LID

Figure 6 – Lid Lifting Handle

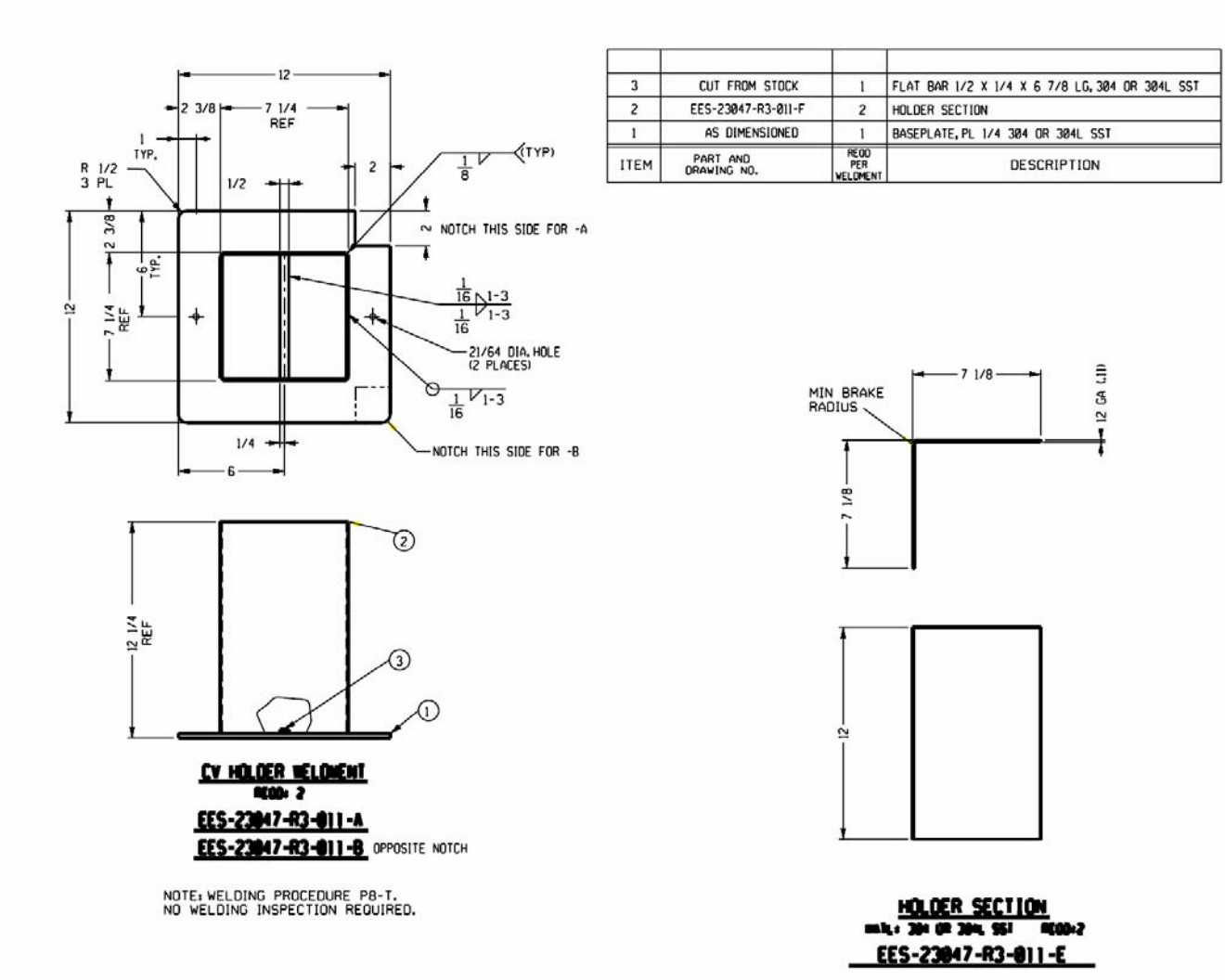

3	CUT FROM STOCK	1	FLAT BAR 1/2 X 1/4 X 6 7/8 LG, 304 OR 304L SST
2	EES-23047-R3-011-F	2	HOLDER SECTION
1	AS DIMENSIONED	1	BASEPLATE, PL 1/4 304 OR 304L SST
ITEM	PART AND DRAWING NO.	REQD PER WELDMENT	DESCRIPTION

Figure 7 – CV Support Stand

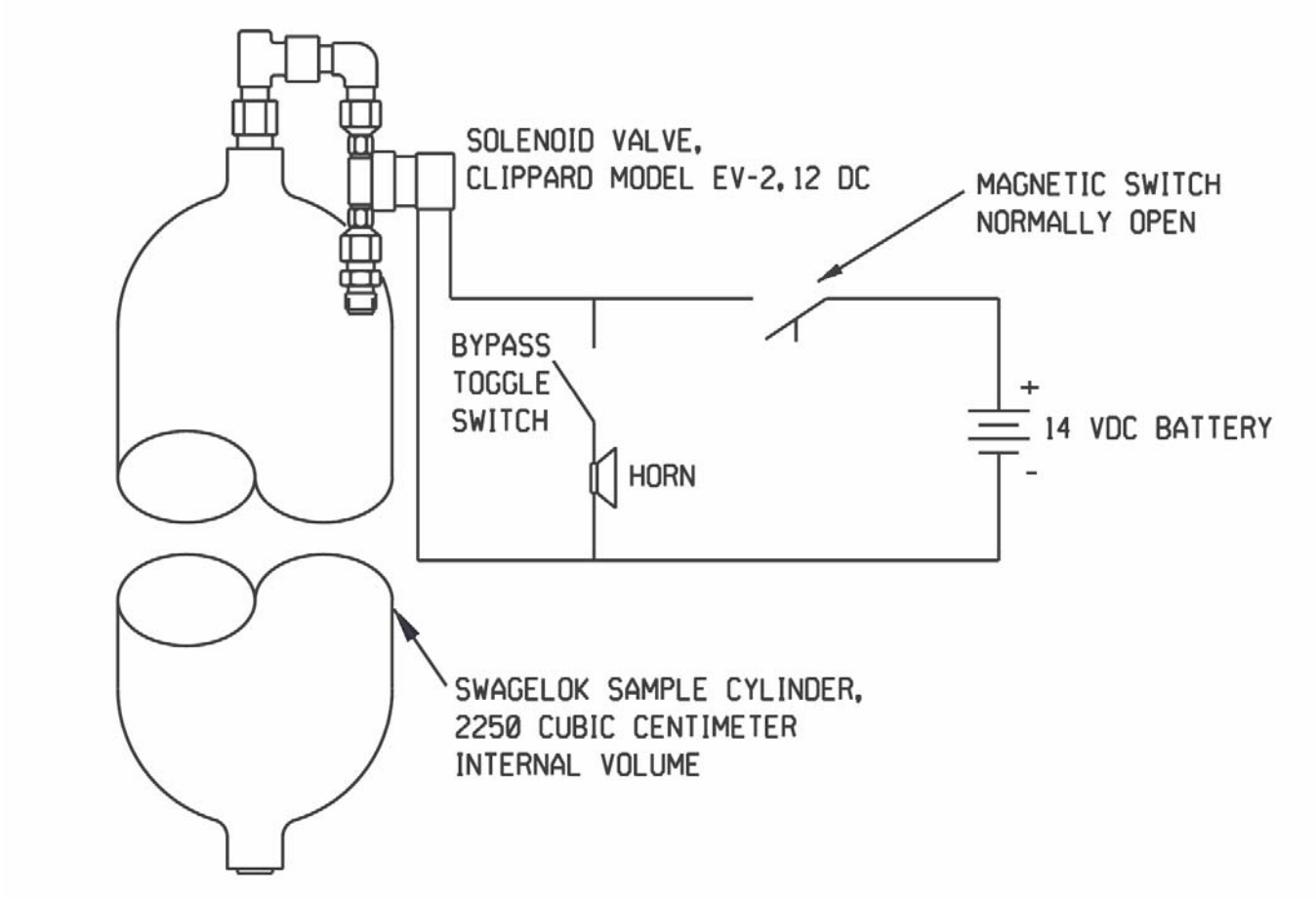

Figure 8 – Sample Cylinder Assembly

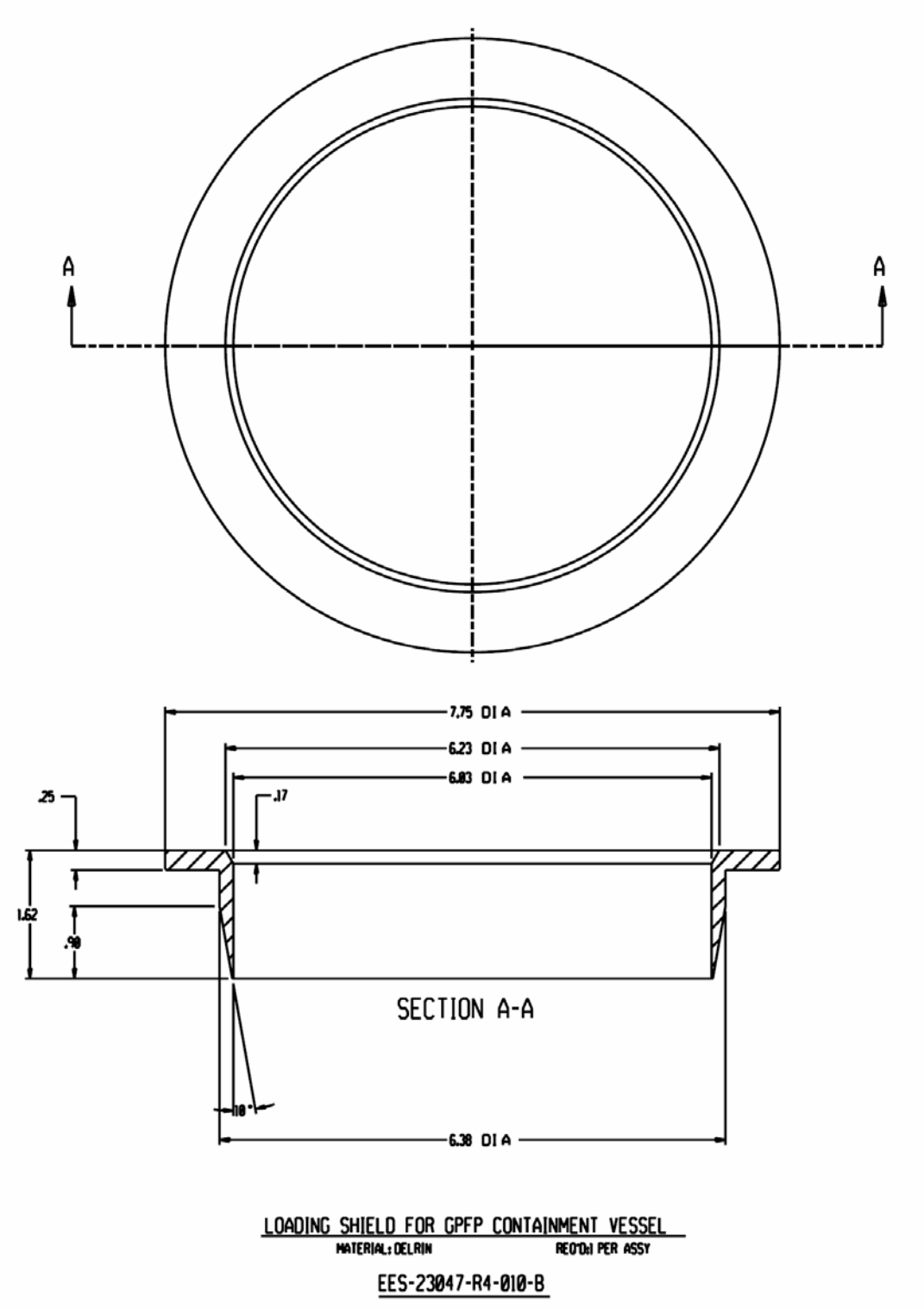

Figure 9 – Loading Shield (Optional)

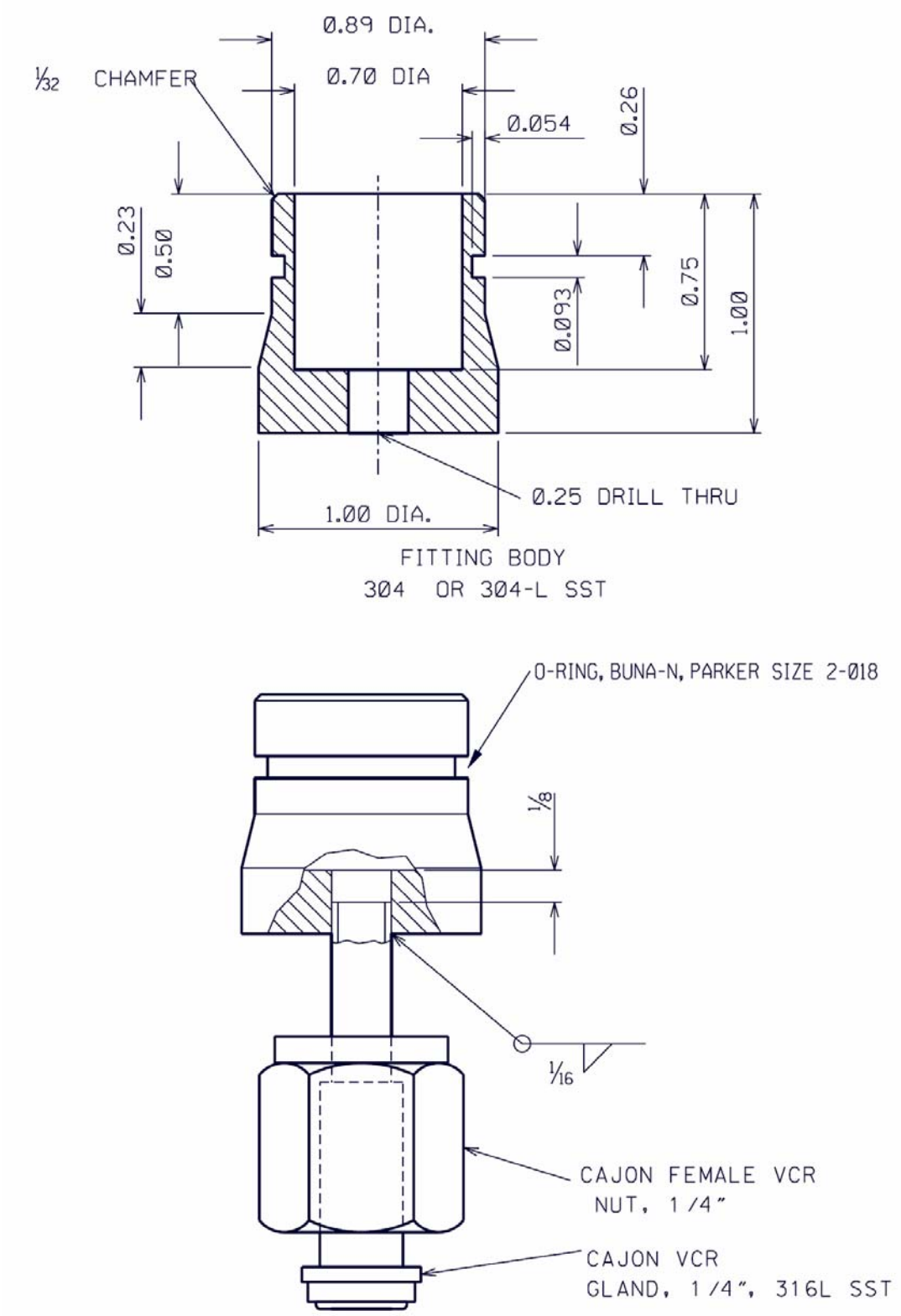

Figure 10 – Special Vacuum Fitting

Attachment 1

Helium Leak Test Data Sheet for 9977 Shipping Containment vessels

(5.2.1) Leak Test Date: _____ Leak Test Specialist's Name _____

((5.2.1) **M&TE No.**	**Description**	**Expires**
	Thermometer	
	Helium Leak Standard Calibrated Leak Rate, L_{CL}, ref cm^3 he/sec :_____ Calibration Temperature, T_{CL}, ºC: _____	
	Pressure Transducer	
	Torque Wrench	
	Torque Wrench	

	Step No.	DATA
Containment vessel SN	5.2.1	
Room Temperature, T_R, ºC	5.2.2	
Temperature Corrected Standard Leak Rate, ref cm^3 he/sec: $L_{TC} = L_{CL} * (1 + (T_R - T_{CL}) * .03)$	5.2.3	
A First Standard Reading, ref cm^3 he/sec:	5.2.6	
B First Standard Background, ref cm^3 he/sec:	5.2.6	
C First Standard Response (**A** – **B**)	5.2.7	
D Background, ref cm^3 he/sec:	5.4.3	
E Leak Reading, ref cm^3 he/sec:	5.4.5	
F Leak Response, ref cm^3 he/sec: (**E** – **D**)	5.4.6	
G Final Standard Reading, ref cm^3 he/sec.:	5.5.2	
H Final Standard Background, ref cm^3 he/sec:	5.5.2	
I Final Standard Response, ref cm^3 he/sec.: (**G** – **H**)	5.5.3	
J Response Ratio $\left(\frac{I}{C} * 100\%\right)$ (Must be > 65%)	5.5.4	
Sample Cylinder Maximum Pressure, psig	5.6.4	
ACCEPTABLE? (Is "F" less than 1s10^{-7} ref cm^3 he/sec?)	5.7.1	**(Yes/No)** *Circle One*

(5.6.5)_____

Leak Test Specialist's Printed Name/Certification/Signature/Date

(5.7.3)_____

Peer Reviewer's Printed Name/Signature/Date

This Page Intentionally Left Blank

APPENDIX 8.3

Example Pre-Shipment (Post Load) Leak Test Procedures For the 9977 Packaging

This Page Intentionally Left Blank

1.0 PURPOSE

This procedure provides step-by-step instructions for performing a post-load leak test on both 9977 5CV and 6CV containment vessels (from here on simply referred to as the CV). The 9977 SARP Section 8.1.4 requires a leak test of the inner O-ring seal each time that the container is loaded with nuclear materials and assembled.

2.0 SCOPE

A. This procedure includes steps for performing a gas pressure rise leak test on 9977 containment vessels. This procedure is done after Operations has loaded and assembled the shipping package per an approved procedure.

- O-Ring Seal Test: a gas pressure rise leak test with a full vacuum isolated in the annulus between the two cone seal O-rings. This tests the integrity of both the inner and outer O-ring seals. The inner O-ring seal is part of the containment boundary.

B. Acceptance Criteria

The O-Ring Seal Test is acceptable **if** after evacuating the annulus between the O-rings on the cone seal to less than 10 Torr, the pressure rise is less than or equal to 20 Torr over a 5 minute hold time. This is equivalent to a leak rate of less than 1×10^{-3} atm cc air/sec. (see Attachment 2 for calculations)

2.1 Terms and Definitions

2.1.1 Post-load Leak Test: A test that is performed on a shipping package after the package has been loaded and assembled. The post-load leak test assures the shipper that the package has been properly assembled and the inner seal is not leaking.

2.1.2 Gas Pressure Rise Test: A leak test in which the inside of the test item is evacuated with a vacuum pump and then it is isolated from the pump. The pressure and temperature are monitored over time. A leakage rate can be calculated using the ideal gas law.

2.1 Responsibilities

2.1.1 Leak Test Personnel:

This test shall be performed by certified Level II or Level III Leak Test Personnel or by Leak Test Trainees or Level I Personnel under the direct supervision of a Level II or Level III Leak Tester.

2.1.2 Operations personnel will be responsible for assembling and disassembling the shipping container.

3.0 PRECAUTIONS/LIMITATIONS:

3.1 Per Ref 7.2, the post load leak test must be done with the same CV weldment, cone seal and inner O-ring seal used in the annual leak test. If these components are replaced, the package must be given an annual leak test before the 9977 can be loaded.

3.2 The leak test described in this procedure uses a Go/No Go acceptance criterion which is set conservatively to ensure the leak rate below the 1×10^{-3} ref cm^3 air acceptance limit. If a leak rate is needed, it can be calculated using Equation 10 of Appendix 2.

3.3 When the CV test port is being evacuated during the O-ring Seal Test, it is possible to evacuate the inside of the CV as well if there is a large leak past the inner O-ring and if the vacuum pump is allowed to pump on the CV for a long time. The procedure includes steps to do a quick check for large leaks by isolating the test port from the vacuum pump 30 seconds after the start of evacuation. If the test manifold pressure rises quickly, it

indicates a large leak in the system, which requires troubleshooting before full vacuum can be applied to the test port

3.4 Safety

- Safety glasses are required when performing this test.
- Safety shoes are required.
- Only Operations shall open or move a loaded container.

3.5 This procedure shall be performed indoors in a temperature controlled area.

4.0 PREREQUISITE ACTIONS:

4.1 **ENSURE** that M&TE instruments are calibrated.

4.2 Instrumentation & Equipment Required

4.2.1 M&TE Calibrated Pressure Transducer and readout, capable of reading from 0 to atmospheric pressure +/- 5 Torr in 1 Torr increments or smaller, with accuracy +/- 0.5% of full scale. The internal volume of this transducer must be 5.1 cm^3 or less to maintain consistency with leak rate calculations in Appendix 3.

4.2.2 Timepiece for measuring test time.

4.2.3 1/4" high pressure cap

4.2.4 Rate-of-Rise test manifold, as shown in Figure 3.

4.2.5 Mechanical Vacuum Pump. An Edwards E2M1.5 is a small, light weight pump that works well for this test if portability is a concern.

4.2.6 Anti-rotation Stand (See Figure 5 for an example stand)

4.3 **ENSURE** the CV Serial Number, Post-Load Test Date, Test Time, Leak Tester's Name, and M&TE data have been recorded on the Post-Load Leak Test Data Sheet (Attachment 1).

5.0 PERFORMANCE SECTIONS:

5.1 System Checkout for Rate-of-Rise Manifold (Refer to Figure 3)

NOTE: The following steps are performed prior to post-load testing to make sure the Rate-of-Rise Manifold is working properly.

5.1.1 **ENSURE** that the pressure transducer is ON.

5.1.2 **ENSURE** the Vacuum/Vent Valve to turned to “VENT”.

5.1.3 **ENSURE** that the Isolation Valve is OPEN.

5.1.4 **ENSURE** the high pressure cap is REMOVED from the Rate-of-Rise Manifold.

5.1.5 **TURN** the Vacuum/Vent Valve to "VACUUM".

5.4.1 **TURN** the Vacuum Pump ON, **AND CHECK** for air flow being pulled into the manifold through the high pressure fitting.

A. **IF** there **is** flow, **THEN** proceed with the checkout.

B. **IF** there is **no** flow, **THEN TROUBLESHOOT** the system. Do not proceed with the manifold checkout test until flow is detected.

5.1.6 **INSTALL** a high pressure cap over the high pressure fitting on the manifold.

5.1.7 **EVACUATE** the manifold to below 10 Torr.

5.1.8 **CLOSE** the Isolation Valve

5.1.9 **TURN** the Vacuum/Vent Valve to "VENT".

5.1.10 **WAIT** at least 1 minute to allow system pressure and temperature to stabilize.

5.1.11 **NOTE** the pressure.

5.1.12 **NOTE** the pressure again after waiting at least 5 minutes.

1. **IF** the pressure has increased by more than 2 Torr in 5 minutes, **THEN TROUBLESHOOT** the system for leakage, repair the leaks, **AND THEN REPEAT** the system checkout.

2. **IF** the pressure has not increased by more than 2 Torr in 5 minutes, **THEN** the system is ready for post load testing.

5.1.13 **OPEN** the Isolation Valve.

5.1.14 **REMOVE** the high pressure cap from the manifold.

5.2 O-Ring Seal Test (refer to Figure 1):

5.2.1 **ENSURE** the high pressure plug is removed from the top of the container.

5.2.2 **THREAD** the Gas Pressure Rise Manifold into the CV Cone-Seal Assembly test port, **AND TIGHTEN** the high pressure nut to 30 ± 5 ft lb torque.

5.2.3 **ENSURE** that the Isolation Valve is OPEN.

5.2.4 **TURN** the Vacuum/Vent Valve to "VACUUM".

5.2.5 **TURN ON** the vacuum pump **AND EVACUATE** the test apparatus for 30 seconds.

5.2.6 **CLOSE** the Isolation Valve.

5.2.7 **OBSERVE** the pressure reading for 30 seconds.

A. **IF** the pressure reading is steady, **THEN PROCEED** to Step 5.2.8.

B. **IF** the pressure reading rises toward to atmospheric pressure, **THEN** there is a large leak in the test system.

1. **NOTIFY** Operations personnel responsible for assembling the package that the leak test of the inner O-ring seal has failed.

2. **GO** to Step 5.2.17

5.2.8 **OPEN** the Isolation Valve and continue pumping down the test manifold until the pressure reading is less than 10 Torr.

5.2.9 **TURN** the Vacuum/Vent Valve to "Vent".

5.2.10 **WAIT** one minute to allow the gas temperature to level out.

5.2.11 **IF** the pressure reading is greater than 10 Torr, **THEN REPEAT** Steps 5.2.8 through 5.2.10 one time, OR perform Section 5.1 to check out the test manifold.

5.2.12 **VERIFY** the pressure reading is less than 10 Torr, **THEN START** the stopwatch **AND RECORD** the initial pressure reading in the appropriate block of Attachment 1.

5.2.13 **TURN** the vacuum pump off.

5.2.14 **WHEN** at least 5 minutes has elapsed as indicated by the stopwatch, **THEN RECORD** the final pressure reading in the appropriate block of Attachment 1.

5.2.15 **CALCULATE AND RECORD** the pressure rise in the appropriate block of Attachment 1.

5.2.16 **DETERMINE** whether the test is Acceptable **OR** is a Reject, using the following acceptance criterion **AND RECORD** results on Attachment 1.

- Acceptable if pressure rise is less than or equal to + 20 Torr.

A. IF the package is a Reject, **THEN NOTIFY** Operations personnel responsible for assembling the package that the leak test of the inner O-ring seal has failed.

5.2.17 **OPEN** the Isolation Valve to vent the test setup.

5.2.18 **DISCONNECT** the Gas Pressure Rise Manifold from the CV.

5.2.19 **SIGN AND DATE** Attachment 1.

6.0 RECORDS

6.1 **SUBMIT** the completed Attachment 1 to the customer.

7.0 REFERENCES:

7.1 ANSI N 14.5-1997, "American National Standard for Radioactive Materials - Leakage Tests on Packages for Shipment"

7.2 SRT-SPS-95-0087, "Qualification Testing of Postload Leak Test Procedure for 2R Containers."

7.3 SRS Calculation M-CLC-F-00936, “Test Volume of O-ring Seal Test for Post-Load Leak Test of 2R Shipping Containers, 5/11/04

8.0 ATTACHMENTS:

8.1 Figure 1, Schematic Diagram of the Post-Load Leak Test.

8.2 Figure 2, Gas Pressure Rise Test Manifold

8.3 Table 1 - Parts for Pressure Rise Test Manifold

8.4 Figure 3, CV Anti-Rotation Stand

8.5 Attachment 1, Post-Load Leak Test Data Sheet

8.6 Attachment 2, Leak Rate Calculations for O-Ring Seal Test, Gas Pressure Rise

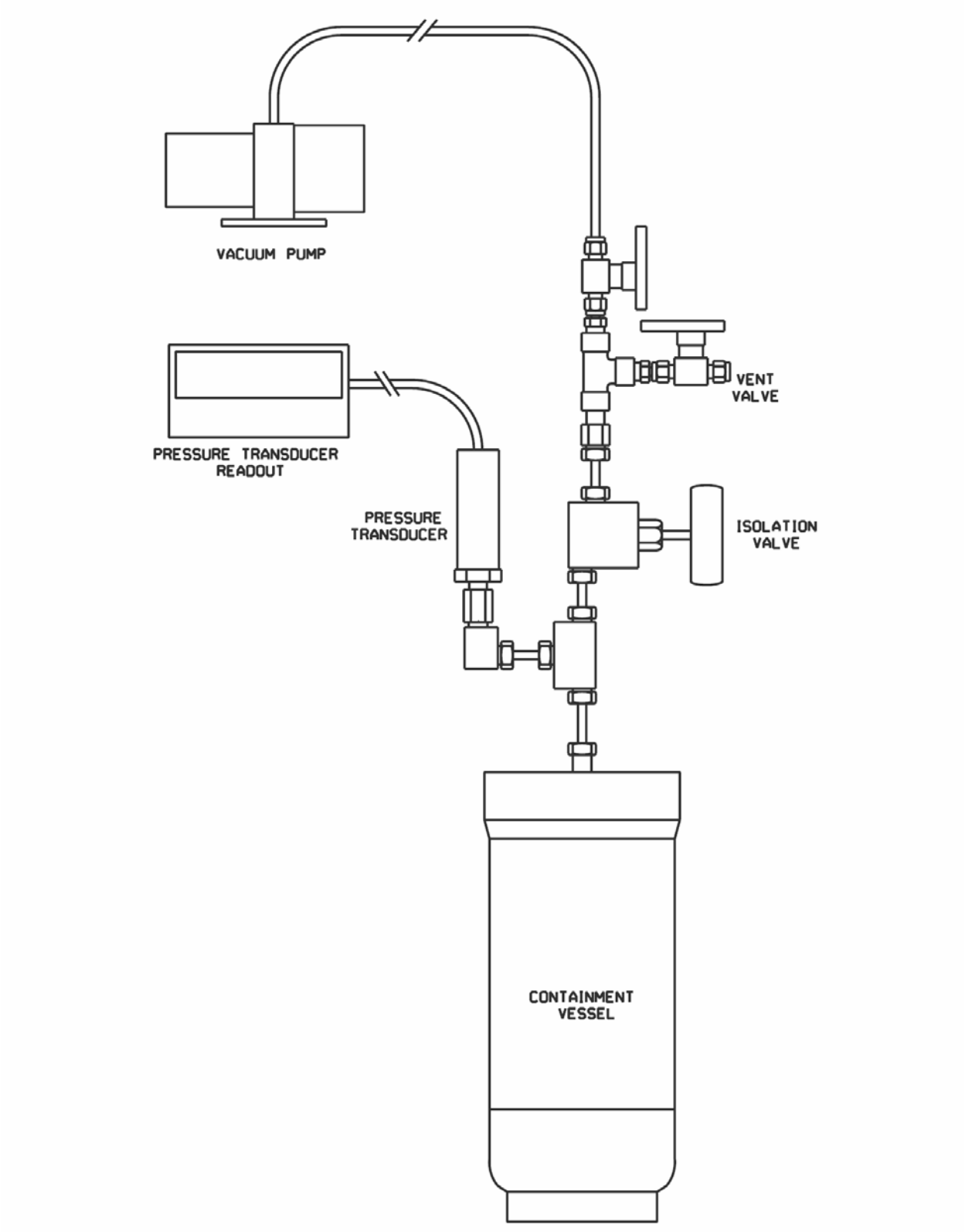

Figure 1 - Schematic Diagram of the Post-Load Leak Test

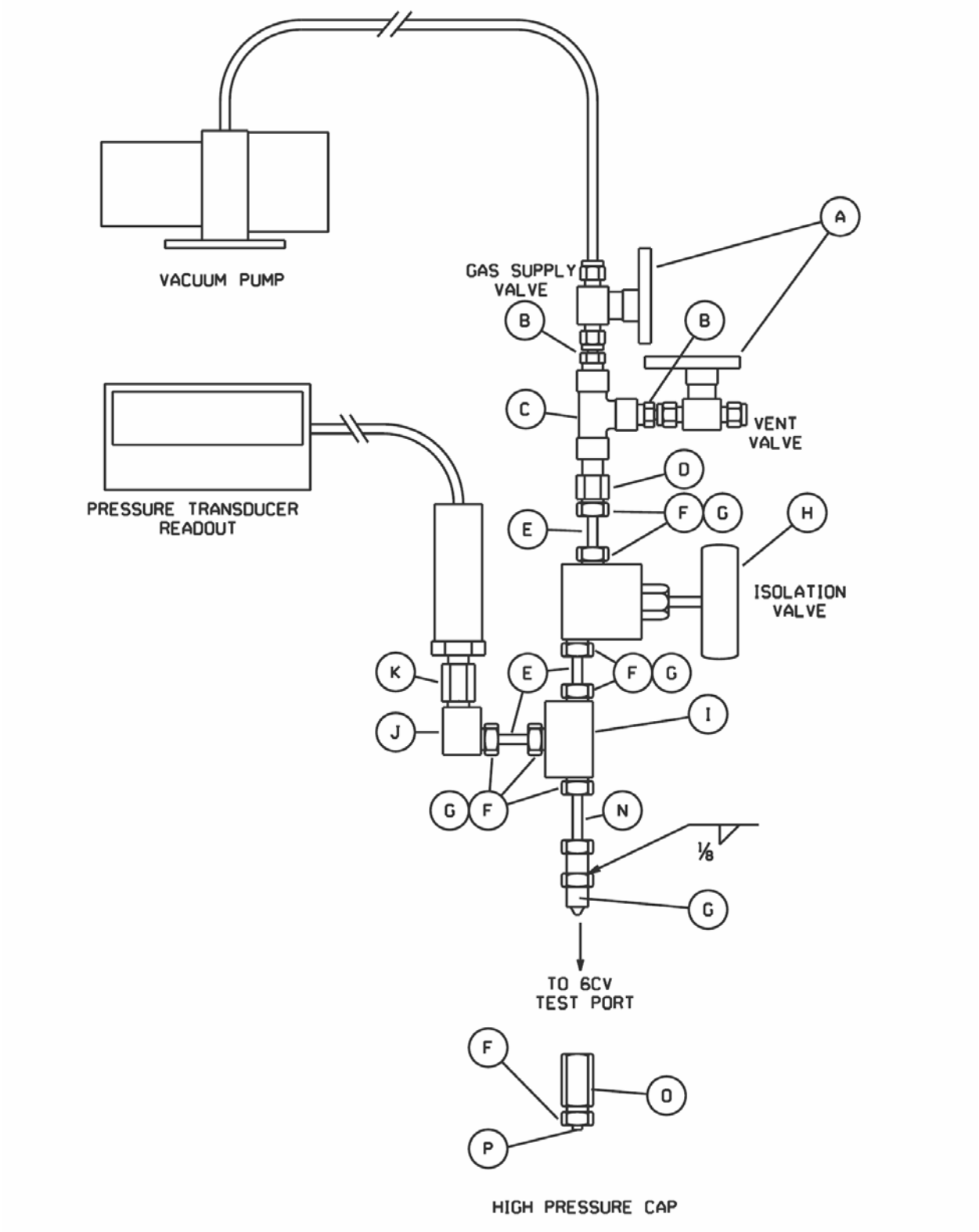

Figure 2 - Gas Pressure Rise Test Manifold

NOTE: It is important to use the parts specified in Table 1, to keep manifold volume consistent.

Table 1 - Parts for Pressure Rise Test Manifold

Item No.	Quantity	Description
A	2	Ball Valve, Whitey SS-43S4 or equivalent
B	2	Male Adapter, Swagelok SS-4-TA-1-4, or equivalent
C	1	Pipe Tee, 1” FPT, Swagelok SS-4-T, or equivalent
D	1	Adapter, 60 ksi high pressure to ¼” MPT, Autoclave Engineers 6M44N3
E	3	High Pressure Nipple, 2.75” long, Autoclave Engineers #CN4402-316
F	10	Gland Nut, Autoclave Engineers #AGL (40)
G	8	Collar, Autoclave Engineers #ACL (40)
H	1	Valve, Autoclave Engineers #60VM4081
I	1	Tee, Autoclave Engineers #CT4440
J	1	Elbow, Autoclave Engineers #CL-4400
K	1	Adapter, 60 ksi high pressure to ¼” FPT, Autoclave Engineers #6M44B8
L	1	Pressure Transducer, 0-30 psia range, Lucas #PS 10083-0005-030PA or equivalent.
M	1	Strain Gauge Meter, 115 VAC, Newport #INFCS-000 or equivalent
N	1	High Pressure Nipple, 4” long, Autoclave Engineers # CN4402-316
O	1	High Pressure Straight Coupling, Autoclave Engineers # F250C
P	1	High Pressure Plug, Autoclave Engineers # AP-40

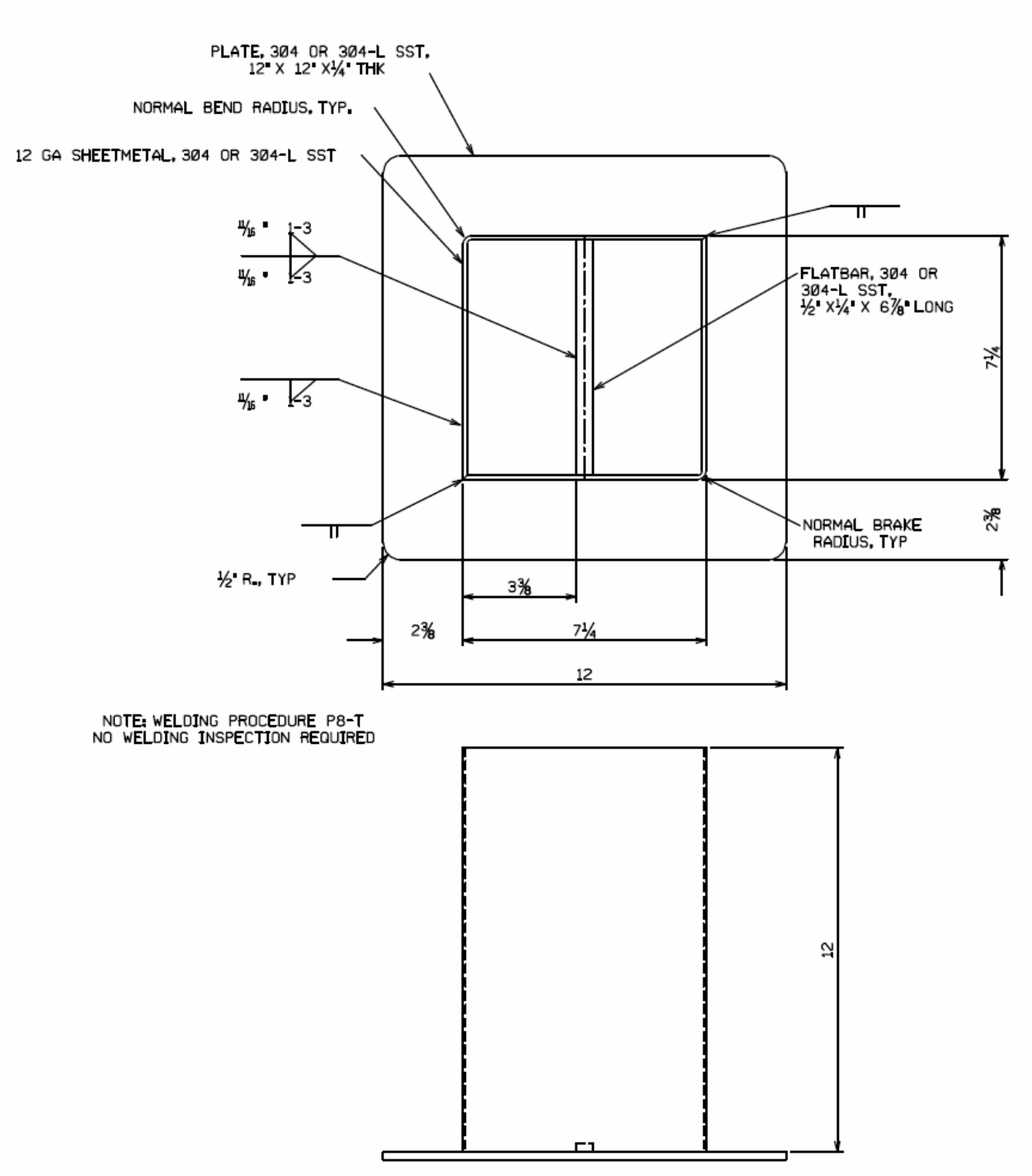

Figure 3 - CV Anti-Rotation Stand

Attachment 1, Post-Load Leak Test Data Sheet

9977 Serial No. :: _____ CV Serial No. _____

Post-Load Leak Test Date: _____ Test Start Time: _____

Leak Test Specialist's Name_____

(4.3)

M&TE No.	Description	Expires
	Pressure Transducer	
	Thermometer	
	Pressure Transducer	

O-Ring Seal Test

Gas Pressure Rise Method

	Pressure (Torr)	Temperature (^{O}C)	Elapsed Time (minutes)
Initial (5.1.13)			
Final (5.1.14)			$\geq$ 20
Difference: (5.1.15)			

Acceptance Criteria:

Maximum allowable Pressure Drop: 1 Torr

Maximum allowable Temperature Change: +/- 1^{O}C

Circle One: (5.1.16)

Acceptable	**Reject**

Comments: _____

(5.2.17)_____

Leak Test Specialist's Printed Name/Certification/Signature/Date

Attachment 2, Leak Rate Calculations for O-Ring Seal Test, Pressure

The acceptance criterion for the post-load test for the cone seal is 1 x 10^{-3} std cc air/sec with 150 psig internal air pressure. The pressure decay leak test uses the Ideal Gas Law to calculate in-leakage:

Ideal Gas Law:

$$PV = nRT \qquad \text{Equation 1}$$

where P= Absolute Pressure

V= Volume

n= moles of gas

R= Ideal Gas Constant

T= Absolute Temperature

$$n = \frac{PV}{RT} \qquad \text{Equation 2}$$

Leakage rate is the decrease in the amount of gas in the test volume during the leak test divided by the leak test time:

$$LeakageRate = \frac{n_2 - n_1}{\Delta t} \qquad \text{Equation 3}$$

where n_2 = moles of gas at the end of the leak test

n_1 = moles of gas at the start of the leak test

Δt = test time

$$LeakageRate = \frac{\frac{P_2 V}{RT_2} - \frac{P_1 V}{RT_1}}{\Delta t} \qquad \text{Equation 4}$$

To convert the leakage rate from moles to standard conditions:

$$LeakageRate = \frac{\frac{P_2 V}{RT_2} - \frac{P_1 V}{RT_1}}{\Delta t}\left[\frac{RT_{std}}{P_{std}}\right] = \frac{V}{\Delta t}\frac{T_{std}}{P_{std}}\left(\frac{P_2}{T_2} - \frac{P_1}{T_1}\right) \qquad \text{Equation 5}$$

Test Time Determination

For a CV, the volume of the space between the two O-ring seals was calculated to be 1.9 cc's. The volume of the test manifold shown in Figure 2 was measured to be 6.2 cc's which was measured dimensionally. Total volume = 8.1 cc's, round off to 10 cc's, which is conservative. (Ref. 7.3)

The acceptance criterion for this test is 1 x 10^{-3} ref cm^3 air/sec, but the test needs to be able to detect a leak that is half this size, or 5 x 10^{-4} ref cm^{-3} air/sec. Therefore, the leak rate in Equation 5 will be set to 5 x 10^{-3} ref cm^{-4} air/sec.

For rate-of-rise leak tests under vacuum over short periods of time, the effects of changes in ambient temperature will be negligible. Therefore, assume that $T_2 = T_1 = 298°K$ in Equation 5.

Standard Temperature, T_s, is 298ºK, and Standard Pressure, P_s, is one atmosphere, or 760 Torr.

$$5x10^{-4} = \frac{10cc}{\Delta t}\frac{298°K}{760Torr}\left(\frac{\Delta P}{298°K}\right) \qquad \text{Equation 6}$$

$$\Delta t = \frac{10cc}{5x10^{-4}} \frac{\Delta P}{760Torr} = 26.3\sec * \frac{1\min}{60\sec} * \Delta P \qquad \Delta t = 0.44 * \Delta P$$ Equation 7

For a test time of 5 minutes, the pressure rise is $\Delta P = \frac{5}{0.44} = 11.3$ Torr Equation 8

The pressure transducer is capable of measuring a 1 Torr change in pressure. Therefore, the test is sensitive enough to detect a leak that is well below 5 x 10^{-4} ref cm^{-3} air/sec.

For the 1 x 10^{-3} ref cm^{-3} air/sec acceptance criterion, the pressure rise limit is:

$$\Delta P = \frac{(5*60)*1x10^{-3}*760}{10} = 22.8$$ Torr for a 5 minute test. Equation 9

Reduce to 20 Torr allowable to be conservative.

A pressure rise of 20 Torr should be enough change to eliminate false rejects caused by outgassing in the test system.

Equation 5 can be rewritten with a 5 minute test time and with T = room temperature, ºC:

$$Leakrate = \frac{10cc}{\left(5\min * \frac{60\sec}{\min}\right)} \frac{298°K}{760Torr}\left(\frac{P_2 - P_1}{T + 278}\right) = .013 * \left(\frac{P_2 - P_1}{T + 278}\right)$$ Equation 10

Example:

A leak test was performed at 20ºC room temperature for 5 minutes. The initial pressure was 9 Torr and the final pressure was 32 Torr.

$$LeakRate = .013 * \left(\frac{32 - 9}{20 + 278}\right) = 1x10^{-3}$$ ref cm^3 air/sec Equation 11

With an acceptance criterion of 20 Torr maximum allowable pressure rise in five minutes, this test would have been a reject, even though it calculates to be right at the acceptable leak rate, which shows that the 20 Torr limit is slightly conservative.

Effects of Room Temperature

To study the effects of room temperature on the leak rate, use the test parameters for the above example to calculate the leak rate, but vary the room temperature.

15ºC Room Temperature:

$$LeakRate = .013 * \left(\frac{32 - 9}{15 + 278}\right) = 1.02x10^{-3}$$ Equation 12

20ºC Room Temperature:

$$LeakRate = .013 * \left(\frac{32 - 9}{20 + 278}\right) = 1.003x10^{-3}$$ Equation 13

25ºC Room Temperature:

$$LeakRate = .013 * \left(\frac{32-9}{25+278} \right) = 0.987x10^{-3}$$ Equation 13

30ºC Room Temperature:

$$LeakRate = .013 * \left(\frac{32-9}{25+278} \right) = 0.97x10^{-3}$$ Equation 14

Room temperature has negligible effect on the leak rate. Therefore, the room temperature does not need to be measured and recorded for this procedure. The “Precautions and Limitations” of this procedure requires the test to be done indoors in a temperature controlled area, so changes in room temperature during a 5 minute long test will also be negligible.

APPENDIX 8.2

PACKAGING INDEPENDENT VERIFICATION ITEMS

This Page Intentionally Left Blank

PACKAGING INDEPENDENT VERIFICATION ITEMS

Certain components and features of the 9977 packaging are defined as category A "Q" items (safety-related) in accordance with Chapter 9, Section 9.2.3. These components and or features require documented evidence that the attributes have been satisfied during packaging fabrication. Table 8.2.1 lists the "Q" items that require independent verification and the basis for designation of the items. The numbered items specifying dimensional, surface feature and material requirements are identified on the engineering drawings given in Chapter 1, Appendix 1.1.

Table 8.2.1 Dimensions/Materials Requiring Independent Verification Records

Number	Quality Item	Basis for Designation	Drawing Number
1	Cone seal face major diameter	Containment	R-R2-F-00042 and -00043
2	Cone seal face angle	Containment	R-R2-F-00042 and -00043
3	Cone seal face finish	Containment	R-R2-F-00042 and -00043
4	Cone seal plug angle	Containment	R-R2-F-00042 and -00043
5	Test port seat angle	Containment	R-R2-F-00042 and -00043
6	Test port seat finish	Containment	R-R2-F-00042 and -00043
7	Test port minor hole diameter	Containment	R-R2-F-00042 and -00043
8	Lower O-ring gland depth	Containment	R-R2-F-00042 and -00043
9	Upper O-ring gland depth	Containment	R-R2-F-00042 and -00043
10	O-ring gland finish	Containment	R-R2-F-00042 and -00043
11	Upper O-ring gland width	Containment	R-R2-F-00042 and -00043
12	Lower O-ring gland width	Containment	R-R2-F-00042 and -00043
13	Cone seal plug minor diameter	Containment	R-R2-F-00042 and -00043
14	O-ring size and material	Containment	R-R2-F-00042 and -00043

This Page Intentionally Left Blank

APPENDIX 8.5

Example Hydrostatic Pressure Test Procedure for the 9977 Packaging

This Page Intentionally Left Blank

TABLE OF CONTENTS

PAGE

LIST OF FIGURES

PAGE

HYDROSTATIC PRESSURE TEST FOR THE 9977 PACKAGING

8.4.1 GENERAL INFORMATION

The 9977 is a Type B Shipping Package designed and manufactured to meet the standards and requirements listed in the Code of Federal Regulations, 10CFR71 for Shipment of Radioactive Materials. The 9977 provides containment through a high strength pressure vessel. Each of the containment vessels (CVs) has a double O-ring design that allows post-load leak testing of the CV closure; Figures 8.4.1 and 8.4.2. These vessels are extensively tested by various methods and at various times during the fabrication process, and are extensively tested when the fabrication is complete.

All packagings, prior to their first use, must comply with the requirements listed in Subpart G of 10CFR71. More specifically, 10CFR71.85(b), "Preliminary determinations", states that, "before the first use of any packaging for the shipment of licensed material—where the maximum normal operating pressure will exceed 5-lbf/in^2 gauge, the licensee shall test the containment system at an internal pressure at least 50 percent higher than the maximum normal operating pressure, to verify the capability of that system to maintain its structural integrity at that pressure." Article NB-6221(a) of the ASME Boiler and Pressure Vessel Code, Section III Subsection NB, requires hydrostatic testing of the installed system to a pressure at least 1.25 times the design pressure.

Because of the high precision fit of the CV cone-seal to the stayed head, it is theoretically possible to obtain a metal-to-metal seal in the CV. Typically, CVs of this type have been hydrostatically tested by filling with water and applying pressure through the post-load leak test port. The test method described below eliminates the possibility of the theoretical metal-to-metal seal by substituting a pressure test plug in the place of the cone-seal plug used in package operation.

The Hydrostatic Test procedure shall clearly instruct the operator that if a requirement cannot be met during the procedure implementation, the operator shall document the event and then notify the appropriate level of Supervision and await further instruction prior to proceeding.

8.4.2 TEST PREPARATIONS:

The following steps need to be performed to prepare the CV for pressure testing.

1. Verify that the CV cone-seal nut and body scribe marks are visible (see Figure 8.4.1).
2. Remove the cone-seal assembly from the CV by turning it counterclockwise with the lid wrench and ratchet.
3. Verify that the CV is empty.
4. Read and note the Cone-Seal Nut and Cone-Seal Plug serial numbers.
5. Remove the Cone-Seal Plug retaining ring and separate the Cone-Seal Plug from the Cone-Seal Nut.

NOTE: *The hydrostatic test of the CV is conducted with the CV weldment, Cone-Seal Nut and a special Test-Plug (see Figure 8.4.2). The same Cone-Seal Nut and Cone-Seal Plug shall be reassembled following the hydrostatic pressure test.*

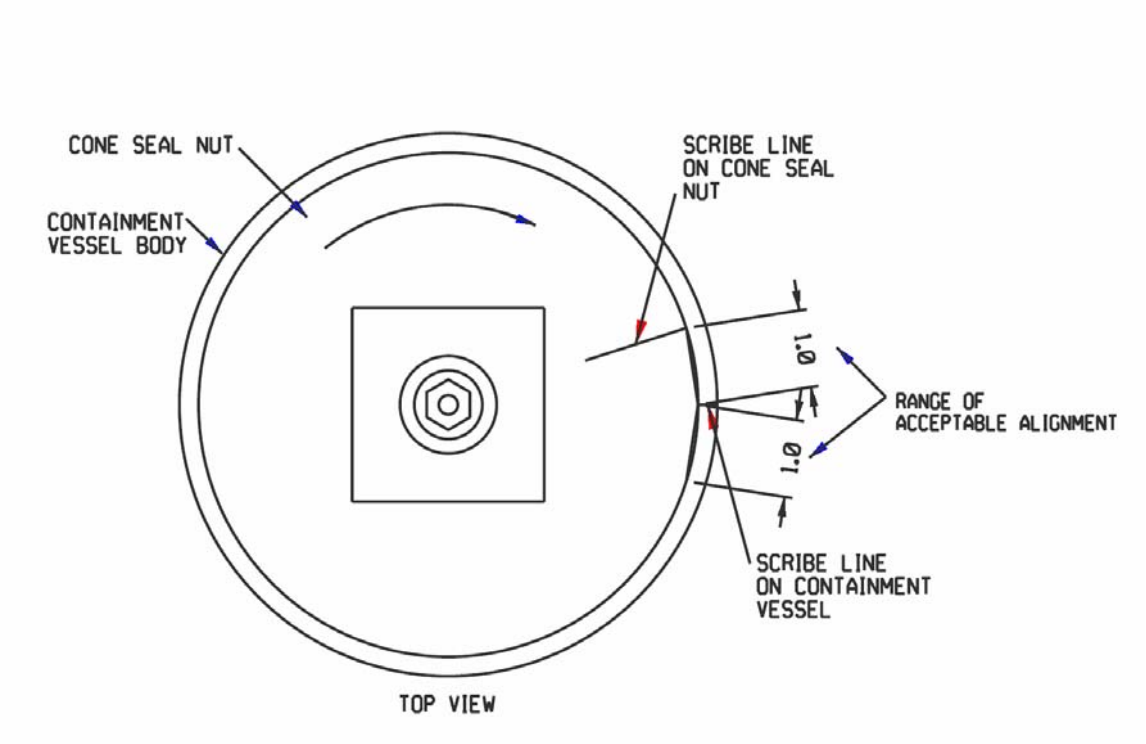

Figure 8.4.1– Closure Scribe Marks

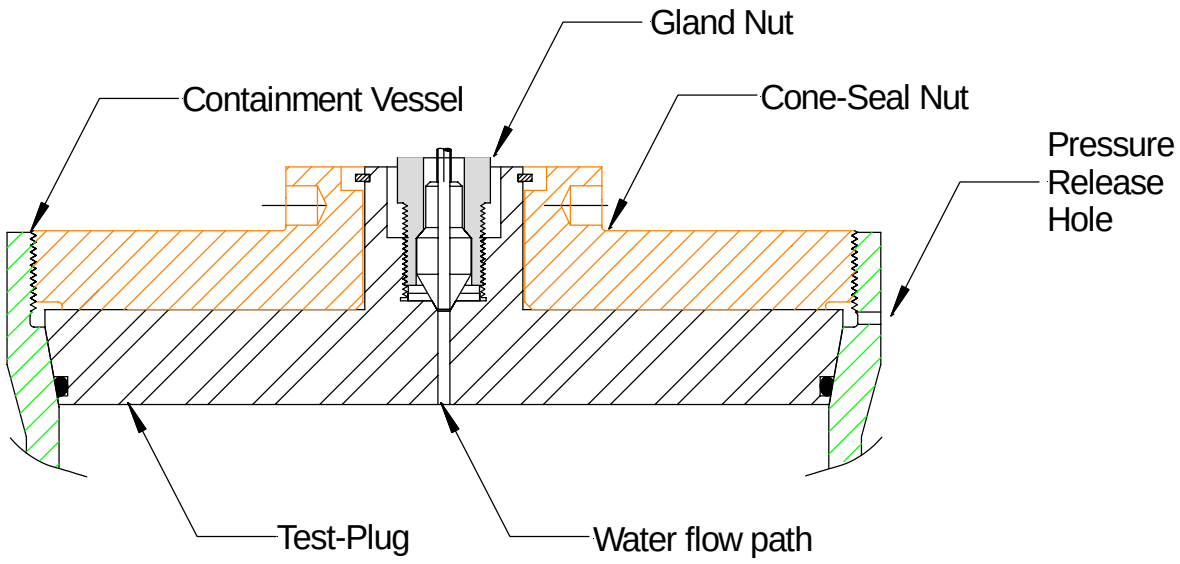

Figure 8.4.2– Hydrostatic Test Assembly

6. Inspect and clean all CV vessel and Test-Plug sealing surfaces with isopropyl or ethyl alcohol, as needed.
7. Inspect and clean the Test-Plug O-ring with isopropyl or ethyl alcohol, as needed.

NOTE: *The Test-Plug and its O-ring are components of the hydrostatic test assembly and not a package component being tested. Damage to or failure of the Test-Plug and the O-ring does not constitute failure of the CV but shall be avoided to prevent invalidating the hydrostatic test and possibly damaging the CV. A damaged Test-Plug shall be taken out of service until returned to acceptable condition. All such repairs shall be documented in accordance with the requirements of Section 9.6. A damaged O-ring shall be destroyed and replaced with a new O-ring that meets the specifications listed on the following drawings:*

- 5CV: Drawing R-R2-G-00043, *Containment Vessel Assembly*, Item 8.
- 6CV: Drawing R-R2-G-00042, *Containment Vessel Assembly*, Item 8.

8. Visually inspect the cleaned sealing surfaces with a bright light for gouges, nicks, cuts, cracks, or scratches that could affect containment performance.

NOTE: *If a containment vessel sealing surface is determined to be damaged, the vessel assembly shall be removed from service and not used until its performance is proven acceptable as outlined in Section 8.1.3. Subassemblies may be repaired, refurbished, or replaced using procedures prepared and approved in accordance with the QA requirements given in Section 9.15. All such repairs shall be documented in accordance with the requirements of Section 9.6.*

9. Lubricate the cone-seal nut thread surfaces with KRYTOX® fluorinated grease, or equivalent, as approved by the Design Agency.

NOTE: *The Design Agency is the Technical Agency assigned by the Design Authority to perform the detailed design and analysis activities of a package modification, see Section 9.1.3*).

10. Verify that the Cone-Seal Nut freely threads into the vessel body.
11. Remove the Cone-Seal Nut.
12. Install the Test-Plug into the vessel body.
13. Verify that the Test-Plug is fully seated and level within the female cone on the vessel body.
14. Lubricate the surface between the cone-seal nut and cone-seal plug with KRYTOX® fluorinated grease, or equivalent.
15. Install the Cone-Seal Nut into the vessel, verifying free turning between the cone-seal nut and test plug (a moderate but steady drag against rotation indicates the presence of viscous lubricant).

NOTE: *When installing the Cone-Seal Nut it is not necessary to install the retaining ring*.

CAUTION: *If the Cone-Seal Nut and Test-Plug are assembled without the retaining ring they will be held together via the KRYTOX® grease only. Care shall be taken not to drop the Test-Plug and damage the Plug or the CV.*

8.4.3 HYDROSTATIC PRESSURE TEST

1. Place the CV in a CV holder.
2. If installed, remove the Cone-Seal Nut and Test-Plug from the CV.

CAUTION: *If the Cone-Seal Nut and Test-Plug are assembled without the retaining ring they will be held together via the KRYTOX® grease only. Care shall be taken not to drop the Test-Plug and damage the Plug or the CV.*

3. Fill the CV weldment with demineralized (deionized) water to the level of the weep hole.
4. Verify that the O-ring is in place on the Test-Plug assembly.

NOTE: *A missing O-ring shall be replaced with a new O-ring that meets the specifications listed on the following drawings:*

- 5CV: Drawing R-R2-G-00043, *Containment Vessel Assembly*, Item 8.
- 6CV: Drawing R-R2-G-00042, *Containment Vessel Assembly*, Item 8.

5. Thread the cone-seal assembly into the CV body and tighten it to a torque of:
   - 5CV: 50 (+10/-0) ft-lb.
   - 6CV: 100 (+20/-0) ft-lb.

NOTE: *Screwing the Cone-Seal Assembly into the CV body will cause water to overflow out the CV pressure release hole and up through the test port hole indicating that the CV is filled.*

6. Dry the water overflow with air or an absorbent cloth.
7. Verify that the scribe mark on the cone-seal closure assembly is aligned to within 1 inch of either side of the scribe mark on the CV body (Figure 8.4.1).
   a. If the scribe marks do not align correctly, then perform the following steps once:
      - Remove the cone-seal closure assembly and inspect for obstructions in the threads on the assembly and in the CV body threads.
      - Repeat Steps 5 and 6.

8. Connect the hydrostatic test assembly to the gland nut connection on the Test-Plug.

NOTE: *The gland nut connection is part of the hydrostatic test assembly and not a package component being tested. Sufficient torque shall be applied to prevent the connection from leaking while minimizing wear of the nut-to-plug seal connection. Since the connection is a modified gland nut/plug, a torque of 30 (±5) ft-lb is recommended for the gland nut.*

9. Examine the hydro test system before pressure is applied to ensure that it is leak tight.
10. Ensure that all low-pressure connections and appurtenances that should not be connected to high pressure have been disconnected or isolated.
11. Pressurize the CV to:
    - 5CV: 1235 ±10 psig.
    - 6CV: 1365 ±10 psig.
12. Maintain the hydrostatic pressure for a minimum of 10 minutes.

NOTE: *Leakage of water at temporary gaskets and seals of the test fixture components may be permitted unless the leakage exceeds the capacity of the system to maintain the test pressure for the required period of time.*

13. Drop the hydrostatic pressure to:
    - 5CV: 900 ±10 psig.
    - 6CV: 1012 ±10 psig.
14. Examine the joints, connections, and external areas of the CV.
15. No leaks are permitted on the vessel being tested. Areas of leakage shall be marked for repair
16. No permanent deformation of any CV parts is permitted.

NOTE: *After the CV has been repaired, the unit shall be retested in accordance with this procedure.*

17. Vent the hydrostatic pressure to drain and allow the CV to depressurize.

8.4.4 POST HYDROSTATIC TEST

1. Disconnect the hydrostatic test assembly from the gland nut connection on the Test-Plug.
2. Remove the Cone-Seal Nut from the CV.
3. Remove the Test-Plug from the CV.

4. Dry and clean the Cone-Seal Nut and the Test-Plug per an approved cleaning procedure.

NOTE: *The O-ring used for the hydrostatic test may be reused.*

5. Empty the CV body of water and dry and clean the vessel per an approved cleaning procedure.
6. Retrieve the Cone-Seal Plug matched to the Cone-Seal Nut (plug was separated in Section 8.4.2.1 step 4.
7. Inspect and clean the Cone-Seal Plug sealing surfaces and O-rings with isopropyl or ethyl alcohol, as needed.
8. Visually inspect the cleaned sealing surfaces with a bright light for gouges, nicks, cuts, cracks, or scratches that could affect containment performance.
    - Damaged O-rings shall be replaced as required by Section 8.2.4 and the affected containment vessels leak-tested in accordance with 8.1.3.
    - If a containment vessel sealing surface is determined to be damaged, the vessel assembly shall be removed from service and not used until its performance is proven acceptable as outlined in Section 8.1.3.
9. Lubricate the O-rings with silicone high vacuum grease, as needed.
10. If removed, reinstall the O-rings, returning each to its original groove.
11. Verify that the Gland Nut and Plug are installed in the Cone-Seal Plug. If missing, obtain replacement parts meeting the description on Drawings R-R2-G-00042 or R-R2-G-00043 and install hand-tight.
12. Lubricate the surface between the Cone-Seal Nut and Cone-Seal Plug with KRYTOX® fluorinated grease, or equivalent.
13. Assemble the Cone-Seal Nut to the Cone-Seal Plug and reinstall the retaining ring.
14. Verify that the containment vessel closure assembles correctly and operates as intended. Correct assembly is evidenced by:
    - Free threading of the closure assembly into the vessel body.
    - Free turning between the Cone-Seal Nut and Cone-Seal Plug.
    - Free turning of the gland nut into the Cone-Seal Plug.

Safety Analysis Report - 9977 Packaging

CHAPTER 9

QUALITY ASSURANCE REQUIREMENTS

Preface

The Quality Assurance (QA) requirements for ensuring the safety of the package, as applied by Washington Savannah River Company (WSRC) at the Savannah River Site (SRS) are provided in this chapter. Requirements provided include the QA methodology and applicable areas of package design, purchasing, fabrication, handling, shipping, storage, cleaning, assembly, inspection, testing, operation, maintenance, repair and component modification.

Non-WSRC users of the package are responsible for setting up comparable QA programs. This chapter meets the requirements of, and is organized in accordance with the 18 criteria of Subpart H of 10 CFR 71[1], as presented in Sections 9.1 through 9.18.

This Page Intentionally Left Blank.

TABLE OF CONTENTS

LIST OF TABLES

LIST OF FIGURES

ACRONYMS AND ABBREVIATIONS

5CV	5-inch Inside-Diameter Containment Vessel
6CV	6-inch Inside-Diameter Containment Vessel
ASME	American Society of Mechanical Engineers
CFR	Code of Federal Regulations
CoC	Certificate of Compliance
CMTR	Certified Material Test Report
DOE	Department of Energy
EES	Engineering Equipment and Systems
FSS	Field Support Services Business Group
MIP	Manufacturing and Inspection Plan
M&TE	Measuring and Test Equipment
NCR	Nonconformance Report
NDE	Nondestructive Examination
PM	Procurement Management
QA	Quality Assurance
RG	Regulatory Guide
SRPT	Savannah River Packaging Technology
SARP	Safety Analysis Report for Packaging
SRS	Savannah River Site
SRNL	Savannah River National Laboratory
WSRC	Washington Savannah River Company

This Page Intentionally Left Blank.

9 QUALITY ASSURANCE

Purpose

Quality Assurance (QA) comprises those planned and systematic actions necessary to provide adequate confidence that a system or component will perform satisfactorily in service.

The QA requirements established in this chapter shall be applied to all activities related to the 9977 packaging that are important to safety. All personnel including users, subcontractors, and vendors who perform quality-affecting activities relative to the packaging shall be subject to the requirements of this chapter in accordance with their degree of involvement in the packaging activities.

Scope

Chapter 9.0 establishes QA requirements that apply to the design, procurement, fabrication, handling, shipping, storage, cleaning, assembly, use, periodic inspection, acceptance testing, maintenance, repair and modification of the packages in accordance with the requirements specified in the regulations of the U.S. Department of Energy (DOE) and the U.S. Department of Transportation (DOT). The chapter describes the package Owner's QA Program that meets the requirements of Title 10 of the Code of Federal Regulations (CFR), Part 71, Subpart H and is presented in the format of the Nuclear Regulatory Commission (NRC) Regulatory Guide 7.10[2] and ASME-NQA-1.[3]

9.1 ORGANIZATION

This section introduces the package Owner, Design Authority, Design Agency, package User and QA organizations. Figure 9.1 shows a WSRC organizational chart depicting the three responsible QA groups: Design Agency, User organization and Procurement Management (PM). The QA organization is within each of these main organizations and will be referred throughout this chapter are:

- Design Agency QA,
- User QA,
- Procurement Agency QA, or
- Supplier QA.

9.1.1 Package Owner -- Washington Savannah River Company

Westinghouse Savannah River Company (WSRC) is the SRS Management Contractor acting for the DOE, and as such has accepted the responsibilities of Owner for DOE 9977 packagings, until otherwise directed by the DOE. WSRC conducts its business consistent with the requirements of its DOE-approved QA Program as presented in the WSRC *Quality Assurance Manual*.[4] In those instances where DOE designates another organization as the owner, that organization shall have comparable QA controls. All organizational elements of WSRC are required to implement the applicable QA program elements consistent with the appropriate sections of American

Society of Mechanical Engineers (ASME), Nuclear Quality Assurance NQA-1 and Subpart H of 10 CFR 71.[1] A comparison of the WSRC QA Program to the 10 CFR 71, Subpart H program elements is provided in Table 9.1.

9.1.2 Design Authority and Design Agency -- Savannah River Packaging Technology

The Savannah River Packaging Technology (SRPT) organization of the Savannah River National Laboratory (SRNL) is the designated Design Authority and is responsible for the changes to, and final acceptance of, the design of the package.

The SRPT organization is the WSRC-designated Design Agency for all certified packaging designs at the SRS and hence, is also the Design Agency for the 9977.

9.1.3 Package User – WSRC and Others

A package User ships and receives materials in that specific package. SRS and DOE Complex-Wide shippers are responsible for the QA controls necessary to ensure that the certified packages and their use, maintenance, and testing meet the requirements of this Safety Analysis Report for Packaging (SARP) and the Certificate of Compliance.

WSRC is a package User. Any organization outside of WSRC that intends to maintain, ship or receive loaded or empty 9977 packages is a non-WSRC User. The User is responsible for preparation and implementation of facility-specific, detailed compliance procedures. All users of the 9977 package shall have in place a QA program that is compliant with Subpart H of 10 CFR 71.

9.1.4 Quality Assurance

Several organizational elements provide SRS QA support for the package. The SRNL QA Department is the Design Agency QA and responsible for performing QA audits and carrying out surveillance and inspection functions for the activities performed by the Design Agency. The Design Agency QA is also responsible for reviewing and approving the procurement documents for prototype and/or production units.

Table 9.1 - WSRC Quality Assurance Program and Corresponding Regulatory Criteria

10 CFR 71 Subpart H Criterion	WSRC 1Q Manual Section	1Q Section Title	Description
1	1.0	Organization	Establishes and describes the responsibilities and requirements for WSRC organizations that provide for the achievement and verification of quality in the items produced and activities performed under the direction of WSRC. Additionally, it establishes the responsibilities and defines the requirements for the initiation and resolution of formal Stop Work Orders issued to WSRC organizations.
2	2.0	QA Program	Provides requirements for the WSRC QA Program. This documented QA Program includes policy, plans, manuals and implementing procedures or instructions required to define and control activities affecting quality.
3	3.0 20.0	Design Control Software QA	The WSRC QA Manual uses two sections to describe the responsibilities and requirements necessary to meet Regulatory Element 3. Section 3 defines the responsibilities and requirements for WSRC's design control activities. Section 20, "Software Quality Assurance," is an extension of Design Control.
4	4.0	Procurement Document Control	Defines responsibilities and requirements for processing and control of documents associated with the WSRC procurement cycle.
5	5.0	Instructions, Procedures, and Drawings	Establishes the WSRC responsibilities and requirements for the systematic control of written management direction in the form of instructions, procedures and drawings.
6	6.0	Document Control	Describes the requirements to assure that information is controlled and provided to the user as needed to perform quality-related activities
7	7.0	Control of Purchased Items and Services	Defines the requirements and responsibilities for establishing procurement levels at WSRC, the QA controls associated with those levels and the control of purchased items and services.
8	8.0	Identification and Control of Items	Defines the requirements and responsibilities for the identification and control of items.
9	9.0	Control of Processes	Defines the responsibilities and requirements for performing processes for product acceptance or continued service. Special processes such as welding, heat treating, brazing, chemical cleaning, soldering, bonding, and nondestructive examination (NDE) are included within this section.

Table 9.1 (continued)

10 CFR 71 Subpart H Criterion	WSRC 1Q Manual Section	1Q Section Title	Description
10	10.0	Inspection	Establishes the requirements and responsibilities for specifying, planning, performing and documenting independent inspection and peer verification.
11	11.0	Test Control	Provides the requirements and responsibilities for planning, performing and documenting tests.
12	12.0	Control of Measuring and Test Equipment	Defines the requirements and responsibilities for the control of Standards and Measuring and Test Equipment.
13	13.0	Packaging, Handling, Shipping, and Storage	Defines the requirements and specify the responsibilities for the handling, shipping, packaging and storage of items to prevent damage, deterioration or loss.
14	14.0	Inspection, Test, and Operating Status	Establishes the methods and requirements associated with status indicators used to prevent inadvertent use or installation of unacceptable or unqualified items.
15	15.0 19.0	Control of Non-conforming Items Quality Improvement	Describes a system for identifying and resolving nonconforming items. WSRC Quality Assurance Manual 1Q, Section 19, "Quality Improvement," is an extension of Control of Non-conforming Items.
16	16.0	Corrective Action System	Establishes responsibilities and requirements for the WSRC corrective action system to assure that Significant Conditions Adverse to Quality are identified, reported and corrected to preclude recurrence.
17	17.0	Quality Assurance Records	Establishes requirements for the preparation, indexing, validation, receipt, storage and correction of documents designated as QA records.
18	18.0	Audits	Defines the WSRC QA requirements for the Audit Program.

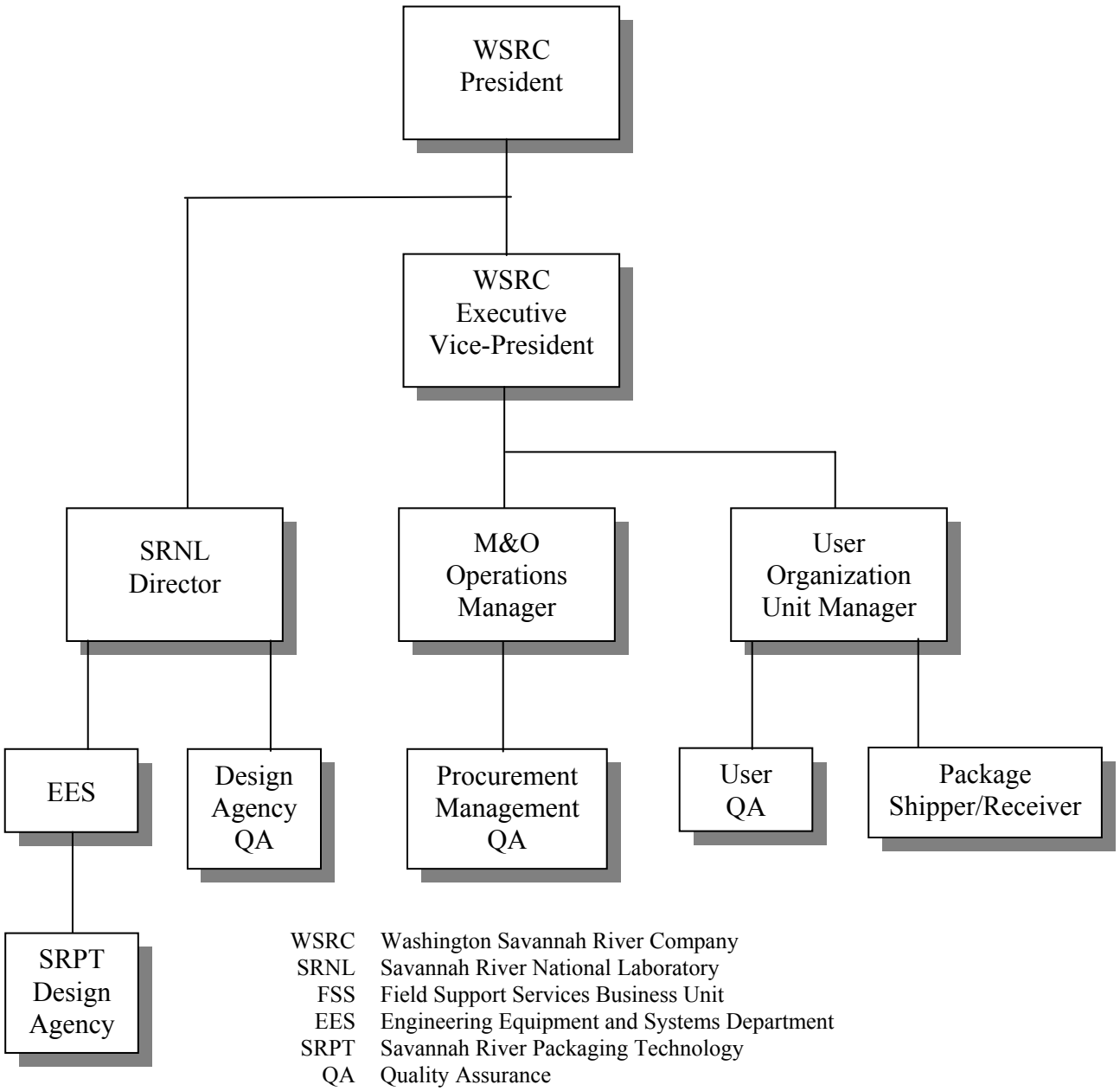

Figure 9.1 - SRS Quality Assurance Functional Organization Chart

The User QA organization monitors the activities by performing QA audits, surveillance and inspections. In addition, these organizations are responsible for reviewing and approving procedures and procurement documents for certified packages.

The WSRC QA Program contains provisions for maintenance of the WSRC *Quality Assurance Manual* as well as for providing training and certification of QA personnel at the SRS. In addition, the QA Program contains provisions for supplier evaluations, surveillance and receiving inspection.

The duties and responsibilities of the User QA organization include, but are not limited to, the following:

- Reviewing and approving the administrative procedures of their respective organizations that implement the requirements of the User's QA program
- Reviewing and approving selected operating procedures prepared within the performing organization for quality-related activities
- Assisting the line organization in problem identification and problem solving
- Reviewing nonconformance documentation
- Performing and documenting independent inspections and tests where applicable
- Evaluating selected QA data and reporting results to appropriate levels of management
- Identifying and documenting, through inspection planning and/or procedure review, necessary witness and hold points
- Issuing Stop-Work Orders when conditions adverse to quality require immediate corrective action
- Assessing the adequacy of the User organization's QA Program.

The User QA organization shall monitor the activities of its users by performing QA audits, surveillance and inspections. In addition, the User QA organization is responsible for reviewing and approving procedures that implement the requirements of this SARP.

9.2 QUALITY ASSURANCE PROGRAM

9.2.1 General

The WSRC *Quality Assurance Management Plan*[5] is based on the requirements provided in DOE Order 414.1A.[6] The WSRC *Quality Assurance Manual* describes the procedures to be followed in implementing the QA Plan. The WSRC *Quality Assurance Manual* QA Program complies with DOE Order 460.1B[7] and 10 CFR 830.120.[8] The QA program contains supplemental controls that maintain compliance with Subpart H of 10 CFR 71 and with NQA-1. The interrelationship among the WSRC QA Program documents, including implementing procedures, is depicted in Figure 9.2.

At the SRS, the Design Agency, in combination with the QA organizations, the Users, and Procurement organizations, controls activities related to the design, procurement, fabrication, handling, shipping, storage, cleaning, assembly, periodic inspection, acceptance testing, maintenance, repair and modification of the packages. Control of fabrication, examination and inspection is ensured by including appropriate sections of NQA-1 requirements in the procurement specifications. The performing organization and the respective QA organizations implement the requirements of the WSRC QA Program by using the QA procedures contained in the WSRC *Quality Assurance Manual* or through the use of implementing procedures and instructions provided in derivative procedures (see Figure 9.2 for depiction of the WSRC QA Program document relationships).

All WSRC employees are responsible for implementing the requirements of the WSRC *Quality Assurance Manual* within the limits of their job assignments. WSRC management assesses the proper implementation, adequacy and effectiveness of the QA Program at least annually. Documentary evidence and independent verification, where appropriate, are used to demonstrate that specific objectives are achieved.

Personnel who perform inspections, tests and examinations are qualified in accordance with applicable requirements, including specific provisions for education and/or experience. Qualification programs include documentation of capability, through either written testing or physical demonstrations of skill, as well as evidence of maintenance of proficiency based on retraining or continued satisfactory performance. Certificates of qualification, or other similar documentation, specify activities for which the individual is qualified and the basis for their certification.

The initial and continuing employee indoctrination program consists of:

- General employee indoctrination managed by Training Integration.
- Area/division indoctrination as established by the Business Units.
- Radiation Worker Training managed by the Environmental, Safety and Health Department.

General QA program indoctrination shall be a part of employee indoctrination and provide familiarization with the QA Program administered at WSRC. The Design Agency QA shall develop and implement the QA indoctrination program and the training for the applicable site QA Program elements as defined in the WSRC *Quality Assurance Manual*.

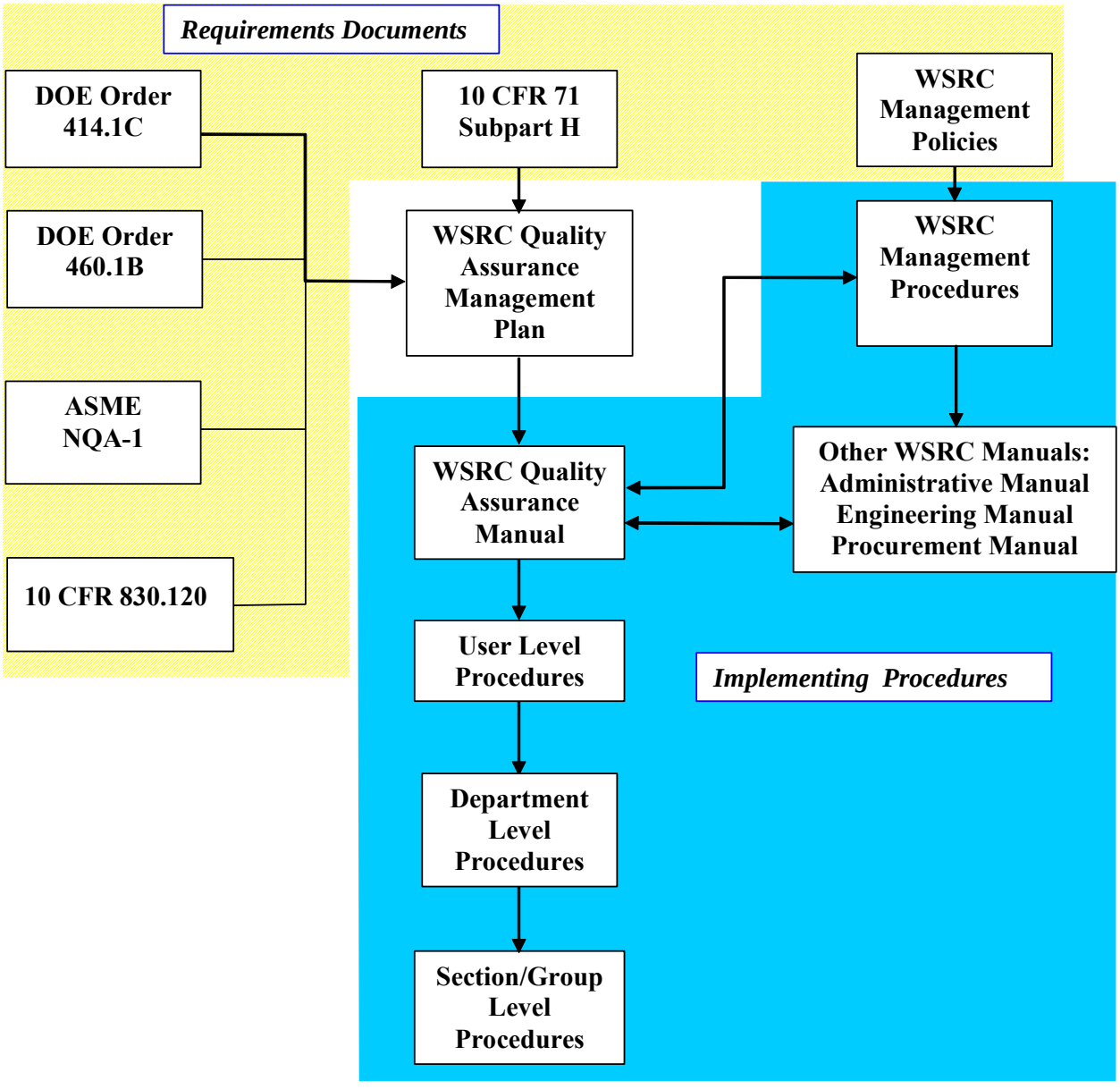

Figure 9.2 - WSRC Quality Assurance Program Description Documents

At a minimum, indoctrination shall include familiarization with requirements associated with the applicable aspects of the following as related to the job function:

- General criteria including codes and standards and their technical objectives
- Administrative and implementing procedures
- Applicable QA Program elements
- Job responsibilities and authorities

9.2.2 Package Program

The package was designed and tested as described in Chapters 1 through 8 of this document. QA requirements are invoked in the design, procurement, fabrication, assembly, testing, maintenance, and use of the package to ensure that established standards are maintained. Items and activities to be controlled and documented are described in this chapter.

At SRS, the requirements of the WSRC *Quality Assurance Manual*, in conjunction with procedures written to address specific shipping activities, are implemented by the appropriate WSRC user.

Training in the use of the package is documented and maintained in the Operators' training files. Personnel from the User QA shall monitor and review operations at least annually and report to management independent of the operation being monitored.

9.2.3 Safety-Related Items

Safety-related or "Q" items have been determined for the packages on the basis of the following definitions:

- **"Q" item** — Safety-related item, judged to have a significant impact on nuclear criticality control, off-site contamination release, or operations personnel exposure. "Q" items require a formal QA program.
- **Non-"Q" item** — Not related to safety and requires no formal QA program.

"Q" items were subcategorized as A, B, or C according to Nuclear Regulatory Commission Regulatory Guide (RG) 7.10[2] by the Design Agency. Category A items are critical to safe operation; Category B items have a major impact on safety; Category C items have a minor impact on safety; and Non-Q items are not important to safety.

QA Categories and functions of the package components are listed in Table 9.3. The level of QA effort for each QA category is indicated in Table 9.4. This graded QA effort is implemented by the WSRC *Quality Assurance Manual* 1Q.[4]

The package has undergone an assessment to determine which components are critical to safety ("Q" items) and what steps or procedures are required to verify their adequacy. The results of the assessment to determine safety and category are provided in Chapter 8 (Appendix 8.2, Table 8.2.1) and are shown in Table 9.3.

Table 9.2 - Safety Assessment of Packaging Features

Feature	Q Category	Function (Drawing Number)
Containment Vessel (5CV and 6CV)	A	Provides containment (R-R2-G-00042 and R-R2-G-00043)
Cone-Seal Plug (5CV and 6CV)	A	Provides containment (R-R2-G-00042 and R-R2-G-00043)
Cone-Seal Nut (5CV and 6CV)	A	Provides containment (R-R2-G-00042 and R-R2-G-00043)
Cone-Seal Nut C-ring (5CV and 6CV)	C	Joins cone-seal plug to cone-seal nut (R-R2-G-00042 and R-R2-G-00043)
Leak Test Port Plug (5CV and 6CV)	A	Protects the test port from debris and redundancy for Inner O-ring (R-R2-G-00042 and R-R2-G-00043)
Leak Test Port Gland Nut (5CV and 6CV)	A	Protects the test port from debris and redundancy for Inner O-ring (R-R2-G-00042 and R-R2-G-00043)
Outer O-ring (5CV and 6CV)(1)	A	Provides means for post-load leak rate test and redundancy for Inner O-ring (R-R2-G-00042 and R-R2-G-00043)
Inner O-ring (5CV and 6CV)	A	Provides containment (R-R2-G-00042 and R-R2-G-00043)
Drum Weldment	B	Protects insulation and package components (R-R2-G-00017)
Drum Lid	B	Provides insulation, protects package components (R-R2-G-00018)
Drum Liner	B	Protects insulation and package components (R-R-G-00017)
Drum Bolts	B	Maintains drum lid in place. (R-R1-F-00020 and R-R1-G-00021)
Drum Washers	C	Provides additional load bearing surface for bolt heads (R-R1-F-00020 and R-R1-G-00021)
Polyurethane Foam	B	Provides impact and thermal protection during accident (R-R1-F-00020 and R-R1-G-00021)
Fiberfrax Insulation	B	Provides impact and thermal protection during accident (R-R1-F-00020 and R-R1-G-00021)
Identification plate	C	Provides package identification. (R-R2-G-00017)
Drum vent plugs, Caplugs	C	Prevents moisture or rainwater from entering drum through vent holes. (R-R2-G-00017)
Load Distribution Fixtures, Top and Bottom (for 6CV and 5CV)	C	Provides additional load bearing surface against the drum liner for 6CV (R-R4-G-00032)
Aluminum Honeycomb Spacers, Top, Bottom and Annular (for 5CV)	C	Provides additional load bearing surface against the drum liner for 5CV (R-R4-G-00033)

Note: Weld material category shall be the same as the Q category of the base component.

(1) The outer O-ring is not needed for containment, but it is classified Category A because it has the same specifications as the inner O-ring. This will simplify O-ring procurement and will prevent mixing up replacement inner and outer O-rings.

Table 9.3 - Level of Quality Assurance Effort for Q Categories

QA Element	Level of Effort	Q Category		
		A	B	C
1	Quality Assurance Organization			
	• Structure and authority	X	X	X
	• Responsibilities defined	X	X	X
	• Reporting levels established	X	X	X
	• Management endorsement	X	X	X
2	Quality Assurance Program			
	• Procedures written	X	X	X
	• Trained personnel	X	X	X
	• Activities controlled	X	X	X
3	Package Design Control			
	• Control of design process	X		
	• Codes and Standards	X		
	• Control of design input	X	X	
	• Control of design verification (prototype tests/ analysis)	X	X	
	• Commercial item (off-the-shelf)			X
4	Procurement Document Control			
	• Complete traceability	X		
	• Qualified suppliers list	X		
	• Non-Qualified Supplier List supplier acceptable		X	
	• Traceability not required		X	
	• Off-the-shelf item			X
5	Instructions, Procedures and Drawings			
	• Must be written and controlled	X		
	• Qualitative or quantitative acceptance criteria	X		
	• Standard work practices are acceptable		X	X
6	Document Control			
	• Issue must be controlled	X		
	• Changes must be controlled	X		
	• Only on safety items	X	X	
	• Minor changes acceptable without formal trace		X	
	• Procurement documents	X	X	X
7	Control of Purchased Material , Equipment, and Services			
	• Source evaluation and selection plans	X		
	• Evidence of QA at supplier	X	X	
	• Inspections at supplier	X		
	• Formal receiving inspection	X	X	X
	• Objective proof that all specifications are met	X	X	X
	• Audits or surveillance at supplier facility	X		

(Continued)

Table 9.3 (continued)

QA Element	Level of Effort	Q Category		
		A	B	C
8	Identification and Control of Material, Parts, and Components			
	• Positive identification and traceability of each item	X		
	• Identification and traceable to heats, lots or other groupings	X	X	
	• Identification to end use drawings, etc.	X	X	X
9	Control of Special Processes			
	• All welding, heat treating, and nondestructive testing done by qualified personnel	X	X	
	• Qualification records and training of personnel	X	X	
	• No special processes			X
10	Inspection			
	• Documented inspection of all specifications required	X		
	• Examination, measurement, or test of material or processed product to assure quality	X		
	• Process monitoring if quality requires it	X		
	• Inspectors must be independent of those performing operations	X		
	• Qualified inspectors only	X	X	
	• Receiving inspection	X	X	X
11	Test Control			
	• Written test program	X		
	• Written test procedures for all requirements in the package approval	X		
	• Documentation of all testing and evaluation	X	X	
	• Buyer's representative of observes all supplier acceptance tests	X		
	• No physical tests required			X
12	Control of Measuring and Test Equipment			
	• Tools, gauges, and instruments must be in a formal calibration program	X	X	
	• Only qualified inspectors	X	X	
	• No test required			X
13	Handling, Storage, and Shipping Control			
	• Written plans and procedures required	X	X	
	• Routine handling			X
14	Inspection, Test, and Operating Status			
	• Individual items identified as to status or condition	X	X	
	• Stamps, tags, labels , etc., must clearly show status	X	X	
	• Visual examination only			X

(Continued)

Table 9.3 (continued)

QA Element	Level of Effort	Q Category		
		A	**B**	**C**
15	Nonconforming Materials, Parts or Components • Written program to prevent inadvertent use • Nonconformance must be documented and closed • Disposal without records	 X X 	 X X 	 X
16	Corrective Action • Written plan to correct all conditions adverse to quality • No written documents	X	X	 X
17	Quality Assurance Records • Design and use records • Results of reviews, inspections, test, audits, surveillance, and materials analysis • Personnel qualifications • Records of fabrication retained throughout the life of package • Record of package use kept for 3 years after shipment • All records managed by written plans for retention and disposal • Procurement records	 X X X X X X	 X X X X X X	 X
18	Audits • Written plan of periodic audits • All certified auditors • Lead auditor certified	 X X X	 X X	 X

9.3 DESIGN CONTROL

9.3.1 Design Control

Design control for the package is the responsibility of the Design Agency at SRS. The design, materials, fabrication requirements, and examination requirements for the 5CV and the 6CV, except as otherwise specified, conform to Section III, Subsection NB of the ASME Code, 2004 edition[9] with 2005 Addenda. The application and any exceptions are described in Table 9.4. The table presents details of the design, fabrication and testing criteria that are specified for the 5CV and the 6CV. Regulatory Guide 7.6[10] is the basis for application of ASME Section III design requirements for the containment vessel design. NUREG/CR-3854[11] provides guidance on acceptable criteria for shipping container design materials, fabrication and testing. NUREG/CR-3019[12] is the basis for the containment vessel welding requirements.

Table 9.5 presents details of the design, fabrication and testing criteria that are specified for the bolted-flange drum closure. The design configuration, materials, fabrication requirements, and examination requirements conform to Section III, Subsection NF of the ASME Code.

The Design Agency shall establish measures for the identification and control of design interfaces and for coordination among participating design organizations. These measures must include the establishment of written procedures, among participating design organizations, for the review, approval, release, distribution, and revision of documents involving design interfaces. The design control measures must provide for verifying or checking the adequacy of design, by methods such as design reviews, alternate or simplified calculational methods, or by a suitable testing program. For the verifying or checking process, the licensee shall designate individuals or groups other than those who were responsible for the original design, but who may be from the same organization. Where a test program is used to verify the adequacy of a specific design feature in lieu of other verifying or checking processes, the licensee shall include suitable qualification testing of a prototype or sample unit under the most adverse design conditions. The licensee shall apply design control measures to items such as the following:

1) Criticality physics, radiation shielding, stress, thermal, hydraulic, and accident analyses;
2) Compatibility of materials;
3) Accessibility for in-service inspection, maintenance, and repair;
4) Features to facilitate decontamination; and
5) Delineation of acceptance criteria for inspections and tests.

The Design Agency shall submit all package design changes, including field changes, to design-control measures commensurate with those applied to the original design. Changes in the parameters specified in the Certificate of Compliance (CoC) require DOE approval.

The Design Authority shall review and approve all changes to this design. The design includes the physical dimensions for the package, dimensional tolerances and necessary material and testing specifications.

All design changes affecting the safety, configuration and functional design of the package that are not addressed in this SARP must be reviewed and approved by the SRS Design Agency before requesting approval from the DOE Certifying Authority.

After the package design and the SARP is finalized and approved by DOE Certifying Authority, a Certificate of Compliance is issued. Revisions to the package shall be made in accordance with the following requirements:

(1) Requests for design modifications shall be routed to the Design Agency. Modifications include any deviation from the evaluated contents or their configuration within the package or from the specified packaging design and drawings or any revision to the specified design. The Design Agency shall determine if the modification affects the safety performance of the packaging or the conditions of approval as cited in the certificate of compliance.

(2) The Design Agency shall perform all design modifications. The Design Agency and the Design Authority shall approve all modifications. The DOE Certifying Authority is the final approver.

(3) The Design Agency shall submit modifications affecting safety performance or the certification conditions of approval to the certifying official for approval prior to implementation. Modifications that do not affect the safety performance or the certification conditions shall be accumulated and included no later than the next SARP revision and or certificate extension, whichever occurs first.

(4) Approved SARP revisions shall be distributed on a timely basis to all holders of controlled copies of the SARP.

Table 9.4 - Package Containment Vessels:
Application of ASME Code Section III, Division 1, Subsection NB, Class 1 Components

	Bottom Head	Shell	Upper Shell	Cone-seal	Cone-seal Nut	Skirt
MATERIALS	SA403, 304L fitting ☑	SA312, 304L pipe ☑	SA479, 304L bar ☑	SA479, 304L bar ☑	SA479, S21800 bar ☑	SA312, 304L pipe ☑
	LP (NB-2556, NB-2551(b)) ☑	UT (NB-2551(a)(2)) ☑	LP, UT bar (NB-2540) ☑	LP, UT bar (NB-2541(a)) ☑	LP, UT bar (NB-2541(a)) ☑	SA materials (NB-1132.1(b)(2)(c), NB-2190(a)) ☑
	Weld metal Chemistry and delta-ferrite (NB-2410,NB-2420, NB-2430) ☑					Chemical analysis (NB-2433) ☑
DESIGN	Full penetration welds (NB-3352, NB-4241, NB-2430) ☑			O-rings ☒ (1)	Threaded head ☒ (2)	Intermittent weld (NB-4435) ☑
	Design analysis (NB-3100, NB3200) ☑ (9)			Design analysis (NB-3100, NB-3200) ☒ (3)	Design analysis (NB-3100, NB-3200) ☒ (4)	NB-3000 ☒ (5)
	Contain or relieve the design pressure (NB-7000) ☑					
FABRICATION & EXAMINATION	Forming, Fitting and Aligning (NB-4212) Welder and weld qualifications (NB-4320) ☑					Welder and weld qualifications (NB-4320) ☑
		LP after machining (NB-4121.3, NB-2547 (c), NB-5100, NB-5350) ☑				LP skirt-vessel weld (NB-5262) ☒ (6)
	100% RT welds, LP final pass (NB-5100, NB-5210, NB-5220, NB-5300) ☑					
PRESSURE TEST	Hydrostatic pressure test at 125% design pressure (NB-6200) ☑					
QUALITY PROGRAM	Certified Material Test Reports (CMTRs), Material Identification, NB-2130, NB-2140, NB-2150 ☑ Design specification, Design report, Code NQA-1 quality system program ☒ (8) Overpressure protection report, N stamp certificate, vessel stamp, ANI review ☐					

☐ = not applicable or not required
☑ = required
☒ = exception (qualified)

Table 9.4 (Continued)

Table 9.4 Notes:

1 The use of elastomer O-rings is not addressed in ASME Section III NB and is not a practice in the design of ASME Section III NB vessels. The use of O-rings as a component of the containment vessels is evaluated and supported in SARP Chapters 2, 3, and 4 and their containment performance proven through packaging testing.

2 The use of threaded heads is not addressed in ASME III NB and is not a practice in the design of ASME Section III NB vessels. The use of threaded heads as a component of the containment vessels is evaluated and supported in SARP Chapters 2 and 4 and their containment performance is proven through packaging testing.

3 Design analysis of the cone seal (a flat head) is done to ASME Section VIII Division1 rather than ASME Section III Division1. The structural evaluation performed in accordance with ASME Section VIII practice, as presented in Chapter 2, is technically acceptable for flat head design.

4 The flat head design (cone-seal nut) is excepted from the Section III stress criteria. The design analysis presented in Chapter 2 is technically acceptable for the packaging.

5 The vessel skirt is not analyzed to the ASME Code rules for vessel support structures. Analysis verifies that the design is adequate for the application.

6 ASME Section III Subsection NB requires the skirt to vessel weld to be PT examined. Visual and dimensional examinations in lieu of PT are considered sufficient for this application, based on design calculations.

7 The SARP fulfills the ASME Section III requirement for a Design Specification and Design Report. The vessel materials are procured with Certified Material Test Reports (CMTRs). The supplier is required to implement a Quality Assurance Program in compliance with ASME NQA-1 with the exception of Criteria 3, Design Control. However, the supplier is not required to possess an ASME Section III Code Stamp, and Code Stamping of the vessel is not required.

8 The ellipsoidal head for external pressure is evaluated by the provisions of NB-3133, ASME Code, Section III.

Table 9.5 - Drum Bolted Closure:
Application of ASME Code, Section III, Division 1, Subsection NF – Class 3 Plate and Shell Type Support for Component

<table>
<tr><td rowspan="2"></td><td rowspan="2">Drum
(Drum Top Plate)</td><td rowspan="2">Drum Lid
(Lid Plate)</td><td colspan="2">Fasteners
(Bolting)</td></tr>
<tr><td>Closure Nut
(Threaded Fitting)</td><td>Closure Bolt
(Heavy Hex Screw)</td></tr>
<tr><td rowspan="3">MATERIALS</td><td>SA-240, 304L
[Table NF-2121(a)-1] ☑</td><td>SA-240, 304L
[Table NF-2121(a)-1] ☑</td><td>SA-194 and SA-320, Grade 8
☑</td><td>SA-193 and SA-320, Grade B8, Class 2</td></tr>
<tr><td colspan="2">Examined in accordance with Material Specification
(NF-2510) ☑</td><td>Visually Examined
(NF-2581.2) ☑</td><td>Visually Examined
(NF-2581.2) ☑</td></tr>
<tr><td colspan="3">Weld metal
Chemistry and delta-ferrite (NF-2400) ☑</td><td></td></tr>
<tr><td rowspan="2">DESIGN</td><td>Design by Analysis</td><td>Bolting</td><td colspan="2">Weld Joint</td></tr>
<tr><td>(Appendix F-1335)
☒</td><td>(NF3555)
☑</td><td colspan="2">(NF-3266, NF-3556)
☑</td></tr>
<tr><td rowspan="2">FABRICATION & EXAMINATION</td><td colspan="2" rowspan="2">Weld Qualifications (NF4300) ☑</td><td>Per Material Specification</td><td>Weld Qualifications (NF4300) ☑</td></tr>
<tr><td colspan="2">Visually examined (NF-5231, NF-5232) ☑ (1)</td></tr>
<tr><td>QUALITY PROGRAM</td><td colspan="4">Overpressure protection report, N stamp certificate, vessel stamp, ANI review ☐
Certified Material Test Reports (CMTRs), ☑
Design specification, Design report, Code NQA-1 quality system program ☒ (2)</td></tr>
</table>

☐ = not applicable or not required

☑ = required

☒ = exception (qualified)

Table 9.5 (Continued)

Table 9.5 Notes

1 Visual inspection acceptance standards shall be per NF-5360 or AWS D1.6.

2 The SARP fulfills the ASME Section III requirement for a Design Specification and Design Report. The vessel materials are procured with CMTRs. The supplier is required to implement a QA Program in compliance with ASME NQA-1 with the exception of Criteria 3, Design Control. However, the supplier is not required to possess an ASME Section III Code Stamp, and Code Stamping of the vessel is not required.

9.3.2 Software Control

The Code of Federal Regulation 10 CFR 71 Subpart H includes the Control of Software in Criterion 3.0. However, WSRC Manual 1Q Section 20.0 defines the QA requirements for software control. Section 20.0 defines design, testing, validation, operation, maintenance, and configuration control requirements for software. Also, defined and specified are requirements for the purchase of software using the procurement process controlled per WSRC Quality Assurance Manual Sections 4.0 and 7.0. Levels A, B, and C software are purchased as WSRC Procurement Levels 1, 2, and 3 respectively. In addition, Section 20.0 specifies that existing or acquired software which was not developed in accordance with Section 20.0 be classified, evaluated, placed under configuration control, and controlled in accordance with the remaining life cycle requirements of the program.

Software is controlled throughout its life cycle, using a graded approach based upon its software classification level. Additive controls are defined at each higher level. The three software classification levels important to the 9977 are Levels A, B, and C that correspond to the A, B, and C Level defined in Table 9.2 above.

This section applies to software used in the design, procurement, fabrication, handling, shipping, storing, cleaning, assembly, inspection, test, operation, maintenance, repair, modification, and use of the 9977 packaging.

9.4 PROCUREMENT DOCUMENT CONTROL

Purchasers of packages and replacement items shall use a graded QA approach. As noted in Section 9.2.3 and Table 9.3, the "A" items are critical to safe operation and are subject to the most stringent quality controls.

Procurement Agency QA Procurement documentation specifications shall contain the applicable requirements including, as appropriate, standards, specifications, codes, documentation and any other special conditions. Specifications prescribe the necessary inspections, tests and other pertinent QA considerations as well as packaging, shipping and handling requirements.

The initiator of the purchase requisition or order is responsible for including the applicable QA requirements on the requisition and for obtaining proper approval signatures. Suppliers are evaluated to assess the supplier's capability to meet the QA program requirements specified in the procurement documents. Also, where sub-tier suppliers are involved, the QA provisions appropriate to these procurements are specified. The extent of the supplier's or sub-tier supplier's QA program depends on the particular item or service being procured.

The Design Agency is responsible for package design and shall approve the procurement specifications issued for all new packages. A new package shall be fabricated by a supplier that has been evaluated and approved in accordance with a DOE-approved QA Program. Before fabrication begins, the supplier shall have a QA program in place that includes those elements of NQA-1 that have been specified by the Design Agency QA, the User QA, and the Receiver's QA organizations.

At the SRS, changes to the procurement documents must be approved by the organizations that approved the original documents.

9.5 INSTRUCTIONS, PROCEDURES AND DRAWINGS

Activities concerning loading, leak-rate testing and shipping are performed in accordance with operating procedures developed by the package user. Requirements, including sequential setups, technical constraints, acceptance criteria and references, will be specified in the written operating procedures. Procedures are issued as controlled documents.

Personnel must receive appropriate training in the procedural requirements on the basis of the particular aspects of the procedure in which they are involved. Chapter 7, Operating Procedures, of this SARP provides specific information governing loading and unloading procedures for these packages. Chapter 8 of this SARP provides specific information governing acceptance tests, inspections and maintenance activities associated with these packages. Changes in the approved procedures require the same level of approval as the initial issue.

The user organization must prepare written procedures or instructions for repair, rework, modification and maintenance of packages and components and obtain approval of these procedures or instructions prior to their use. Inspection, testing and independent verification, if required, will be included in the procedures.

The Design Agency is responsible for the preparation of package design drawings and subsequent drawing revisions. The drawings are issued as controlled documents.

9.6 DOCUMENT CONTROL

Each department within WSRC is responsible for the establishment, development, review, approval, distribution, revision and retention of its own documents. A document is a publication that prescribes requirements for items or activities affecting quality. Documents are controlled to ensure that correct versions (e.g. current revision) are being used and to provide assurance that record requirements are met. Documents requiring control, the level of control and personnel responsibilities (including training requirements) are defined in WSRC departmental procedures. Upon completion, many of these documents become QA Records.

Documents to be controlled include the following as a minimum:

- Design documents
- Prototype test plan and procedures
- Procurement documents
- QA manuals
- Maintenance and modification procedures and log
- Inspection and test procedures
- Nonconformance reports
- Design change requests
- Shipment documentation
- Repair procedures
- Certificate of Compliance and the SARP and its amendments
- Loading and unloading procedures
- Packaging for transport procedures
- Fabrication records
- Drawings of packages and components
- Test reports/records (Prototype, fabrication, periodic, post-load, and post-maintenance or modification)

Section 9.3 defines controls for modification of design basis documents. Revisions to documents are handled in a manner similar to the original issue via review and approvals from the original departments. Document control measures ensure that only the currently approved version is available for use at the work facility.

9.7 CONTROL OF PURCHASED MATERIAL, EQUIPMENT AND SERVICES

Established procedures ensure that purchased materials, equipment and services conform to procurement document requirements. The procurement process for the package incorporates the graded approach defined in Appendix A of Regulatory Guide 7.10.

The procurement of replacement parts shall be done under a QA program that meets the requirements of 10 CFR 71, Subpart H. Procurement documentation specifications shall contain the applicable requirements including (as appropriate) standards, specifications, codes, documentation, and any other special conditions. Specifications prescribe the necessary inspections, tests and other pertinent QA considerations as well as packaging, shipping, and handling requirements.

Only evaluated and approved manufacturers may supply packages. The suppliers must submit a copy of their administrative procedural controls and a Manufacturing and Inspection Plan (MIP) for the Design Agency review and approval prior to the start of fabrication. The Design Agency and the purchaser use the MIP to establish witness and hold points to be observed during the manufacture of the packages. The supplier's QA program must address the requirements of ASME NQA-1, with the exception of Design Control.

The supplier's MIP shall address the following items as required in the procurement specifications:

- material identification and material certifications including traceability of materials
- welding procedure specifications and welding procedure qualification records
- welder qualification records and process qualification
- types of inspections and tests to be performed and by whom
- nondestructive examination (NDE) procedures
- NDE personnel qualification records
- weld inspection records
- NDE reports
- dimensional inspection reports
- cleaning procedures
- procedures for controlling nonconformance
- manufacturing and test procedures
- qualifications of individuals involved in the QA support for these packagings

9.8 IDENTIFICATION AND CONTROL OF MATERIALS, PARTS AND COMPONENTS

Items that require protection to ensure their intended use or that have unique characteristics must be identified and controlled throughout fabrication, assembly and storage. Traceability of these controlled items must be ensured. Each user is responsible for identifying these items and the level of control to be maintained.

Each 9977 containment vessel is identified with a drawing number, revision number and individual serial number. The serial number is electro-etched onto the exterior surface of the vessel body and onto the visible surfaces of cone-seal closure components.

Any packaging component not meeting all specifications shall have an NCR issued against it and shall be tagged and segregated until the disposition of the NCR has been approved and implemented.

Equivalent to the original parts, replacement parts must be identified clearly to ensure correct usage. Elastomer seals shall be individually packaged and marked with material certification, size, cure date and purchase order number.

9.9 CONTROL OF SPECIAL PROCESSES

During fabrication, the containment vessels are welded in accordance with Section III, Subsection NB-4000, of the ASME Code. Welds are radiographed and examined with liquid penetrant in accordance with Section III, Subsection NB-5000 of the Code (See Table 9.4).

Also during fabrication, independent inspectors shall verify the dimensions specified in Chapter 8, Appendix 8.2, the welding process (i.e., welder qualification records, weld procedure qualifications, inspection of the welds and review of the weld records, including any repairs) and carry out other inspections as required by the procurement documents.

9.10 INSPECTION

The packaging is required to undergo fabrication inspections by the supplier and independent inspections performed by the purchaser.

Supplier inspections (as defined in the MIP) are designed to ensure that an accepted packaging or item conforms to the tested and certified design criteria. The supplier is required to submit an MIP for approval prior to the start of fabrication. Approvers of the MIP include Design Agency, and QA (e.g. User QA). The MIP is a tool for establishing witness and hold points. The MIP details how fabrications and inspections are to be performed and describes the qualifications of the suppliers and inspectors. Inspections shall be documented and the results shall be delivered to the purchaser along with the packaging.

Independent inspections shall be performed by qualified inspectors. The activities shall include verifications of conformance with accept/reject criteria, completion of prerequisites, personnel qualifications and equipment calibrations.

Inspections shall be performed upon receipt of the packaging; prior to first usage (implemented by User procedures) and annually. Post-loading inspections shall be performed prior to shipment in all cases.

Procedures shall be established by the Supplier and approved by the Purchaser and the SRS Design Agency to ensure that inspectors are qualified in accordance with applicable codes and standards, as well as with the User's training program. The procedures require that the inspection personnel certifications are kept current and that inspection personnel are independent from individuals performing the activity being inspected.

The inspections to be performed by qualified personnel shall include the inspections or examinations included in Chapter 7, *Operating Procedures*, and in Chapter 8, *Acceptance Testing and Maintenance Program*. Required inspections and examinations are reported as part of the package documentation record.

9.11 TEST CONTROL

Personnel conducting tests, the test equipment and the test procedures must be qualified with appropriate documentation as listed in the WSRC *Quality Assurance Manual*. The test control procedures shall provide for a written test program supported by approved procedures. The test program shall require documentation of the test objectives, conditions and results. Acceptance tests performed by the supplier shall be observed by the owner or owner representative. The requirements for testing the package and its components are provided in Chapter 8.

Acceptance testing of the package is in accordance with the requirements of Section 8.1 of Chapter 8. Maintenance testing of the accepted package is performed in accordance with the requirements of Section 8.2.

9.12 CONTROL OF MEASURING AND TEST EQUIPMENT

Measuring and Test Equipment (M&TE) is defined as devices or systems used to calibrate, measure, gage, test or inspect, in order to control and validate acquired data and to verify conformance to specified requirements. M&TE used for acceptance and verification is maintained under control systems that identify the status of all M&TE. Calibration procedures, as well as vendor manuals, detail the requirements for M&TE calibration (including frequency and maintenance), the use of appropriate standards and organizational responsibilities for establishing, implementing and ensuring effectiveness of the calibration program. Measuring and test instruments are calibrated with standards traceable to the U.S. National Institute of Standards and Technology.

Procedures are designed to ensure accuracy within established standards and include disposition and/or corrective measures when discrepancies are noted. Damaged or inaccurate M&TE is immediately removed from service until repaired, recalibrated or replaced. If M&TE is found to be out of calibration, the validity of previously performed inspections is determined and documented. If previously performed inspections are determined to be invalid, a nonconformance report shall be completed and dispositioned in accordance with the requirements of this chapter. If any M&TE is consistently out of calibration, it shall be repaired or replaced.

9.13 HANDLING, STORAGE AND SHIPPING

The User shall develop written operating procedures from the procedural requirements presented in Chapter 7 to address handling and storage of the package components. Limited-life components must be addressed in these procedures to assure replacement within the required period of time. Limited-life components include both outer and inner O-rings for the CV closure.

The User is responsible for shipment of both loaded packages and empty packagings and is responsible for verifying compliance with the requirements listed in Chapter 7. Upon delivery, all packages shall be visually inspected by the receiving organization for obvious damage.

9.14 INSPECTION, TEST AND OPERATING STATUS

Each user shall perform maintenance on each package and it's CV in accordance with a procedure that outlines and records each step in preparation of the package for shipment. Details are provided in Chapter 7. The inspection, test and operating status of any package shall be identified clearly by using status indicators (i.e., tags) or records traceable to the individual units.

9.15 NONCONFORMING MATERIAL, PARTS OR COMPONENTS

9.15.1 Identification

Procedures shall be established to identify and document any nonconforming item or activity. If the inspection identifies an out of conformance item or activity, the purchaser/user documents the nonconformance and recommends one of several disposition options: "repair," "rework," "reject" or "use-as-is." The Purchaser/User is responsible for obtaining approval of the nonconformance disposition from the SRS Design Authority and Design Agency (See Section 9.1.2).

Defects in the packaging or packaging components, or departure from CoC requirements, that significantly reduce the safety performance of the packaging shall be reported to the DOE Certifying Authority within 30 days of the discovery in accordance with 10 CFR 71.95.[1]

9.15.2 Segregation

Nonconforming items are marked, tagged, segregated and placed in controlled areas until disposition is complete.

9.15.3 Disposition

The evaluation for disposition of the nonconformance may include the following:

- **Rework**: The process by which an item is made to conform to original requirements by completion or correction.
- **Repair**: The process of restoring a nonconforming characteristic to a condition such that the capability of an item to function reliably and safely is unimpaired, even though that item still does not conform to the original requirements (technical justification required).
- **Use-as-is**: A disposition permitted for a nonconforming item when it can be established that the item is satisfactory for its intended use (technical justification required).
- **Reject**: Action taken to eliminate a nonconforming item from its specified use (scrap, return to supplier, etc.). Specific action shall be identified in Disposition Details.

In all cases of action, final disposition of nonconformance must be identified and documented, and the documentation must be maintained as a QA record.

9.16 CORRECTIVE ACTION

Nonconforming "Q" items shall be promptly identified and the causes of these conditions corrected in accordance with the WSRC *Quality Assurance Manual*, QAP 16-1, to prevent recurrence.

9.17 QUALITY ASSURANCE RECORDS

9.17.1 General

A record is a completed document that furnishes evidence of the quality of items and/or activities affecting quality. Individual packaging QA records shall be maintained for each package by model number and serial number (i.e. 9977-SN010001). The retention periods for various types of QA records are presented in Table 9.7. Record retention periods, at a minimum, shall comply with 10 CFR 71.91 and 10 CFR 71, Subpart H. The procurement specification defines the documents that suppliers are to generate and when the records are to be submitted.

9.17.2 Storage, Preservation, and Safekeeping

To minimize the risk of damage or destruction to the QA records from natural causes, such as extreme temperatures; moisture from rain, snow, or high humidity; insects; mold; or fire, designated records-storage facilities (e.g., a vault with fire protection) are strongly recommended. However, in the event that such facilities are not available, Underwriters Laboratory®-listed one-hour rated fire cabinets are recommended. Security systems and facility activity classifications shall be established to prevent access to records by unauthorized personnel.

Table 9.6 - Quality Assurance Records

Name of record	Retention Period [a, b, c]	Produced By
Prototype test plan and procedures	LOP	Design Authority
Prototype test reports	LOP	Design Authority
SARP	LOP	Design Authority
Design drawings	LOP	Design Authority
Package modification records	LOP	Design Authority
Instrument calibration records	3 years	Supplier
Supplier manufacturing and inspection plan	LOP	Supplier
Material test report or certification required on all material used	LOP	Supplier
Packaging Independent Verification Items (Appendix 8.2, Table 8.2.1)	LOP	Supplier
Welding procedure specification	LOP	Supplier
Procedure qualification record	LOP	Supplier
Welder or welding operator qualification tests	LOP	Supplier
Record of qualification of personnel performing radiographic and liquid penetrant inspection	LOP	Supplier
Containment vessel cleaning procedure	LOP	Supplier
Weld radiographs	LOP	Supplier
Liquid penetrant reports	LOP	Supplier
Structural test (hydrostatic) report	LOP	Supplier
Leak-rate test report (fabrication)	LOP	Supplier
Leak-rate testing personnel qualification records	S	Supplier
Leak-rate test report (periodic)	S	Owner
Inspection Documentation (Appendix 8.1)	LOP	Supplier/Owner
Package loading procedure	S	Owner
Leakrate test results (post-loading)	S	Owner
Procedures for preparing a package for transport (empty or loaded)	S	Owner
Maintenance procedures	S	Owner
Repair procedures	LOP	Owner
Procurement documentation	LOP	Owner
Audit reports	LOP	Owner
Maintenance log	LOP	Owner
Corrective action reports	LOP	Owner
Shipment records per 10 CFR 71.91(a)	S	Owner
Nonconformance reports	LOP	Owner
Package unloading procedure	S	Receiver

a LOP – Retention by Design Authority for Lifetime of the Packaging plus 3 years.

b S - Retention by Design Authority for shipping date plus 3 years (Records for packages to be used as storage containers shall be kept for the lifetime of the package plus 3 years.)

c Copies of all QA Records generated by Supplier are to be retained by the Supplier for a period of 3 years after delivery of packaging and. by the Design Authority for either LOP or S, as appropriate.

9.18 AUDITS

The User or Design Agency QA are responsible for scheduling, planning and conducting audits at SRS. The schedule may be updated during the year on the basis of reports of surveillance, inspections and audits by outside agencies/customers. The program provides for re-audits, as necessary, to verify corrective action and implementation.

Audits are planned activities performed by qualified personnel, independent of the group or function being audited, using written procedures and/or checklists. A written report documenting the audit results is prepared within 30 days and distributed to appropriate management personnel. When corrective action is required, the report requires the audited organization to reply within a specified time and to identify planned corrective actions and a schedule for implementation.

Regularly scheduled audits are occasionally supplemented by additional audits of specific subjects when necessary to provide adequate coverage. Supplemental audits are performed under the following circumstances:

- The quality of an item, product, process, or structure is suspected to not conform with the agreed-upon requirements or commitments.
- A systematic, independent assessment of program effectiveness is considered desirable.
- Implementation of a required corrective action must be verified.

Unscheduled audits are performed under the following circumstances:

- Situations, circumstances, or occurrences dictate the need for current status.
- Information of a critical nature is required.
- The audit is considered necessary by the manager of the User QA.

The User or Design Agency QA are responsible for verifying that corrective action has been implemented and is acceptable. Problems may be escalated to higher levels of management as required.

Audit reports are distributed to appropriate management personnel and retained in accordance with applicable requirements.

Auditors receive training on audit standards and regulatory requirements and practices. Records are maintained by the User or Design Agency QA to document auditor qualification in accordance with established procedures.

9.19 REFERENCES

1. *Packaging and Transportation of Radioactive Materials*, Code of Federal Regulations, Title 10, Part 71, U. S. Nuclear Regulatory Commission, Washington, DC (November, 2005).

2. *Establishing Quality Assurance Programs for Packaging Used in the Transport of Radioactive Material*, Regulatory Guide 7.10, Rev. 2, U. S. Nuclear Regulatory Commission, Washington, DC (March 2005).

3. *Quality Assurance Program Requirements for Nuclear Facilities*, NQA-1-2004, American Society of Mechanical Engineers, New York, NY.

4. *Quality Assurance Manual*, WSRC-1Q, Westinghouse Savannah River Company, Aiken, SC (October, 2005).

5. *Quality Assurance Management Plan*, WSRC-RP-92-225, Rev 13, 2004, Westinghouse Savannah River Company, Aiken, SC (August 2004)

6. *Quality Assurance*. U. S. DOE Order 414.1C, U.S. Department of Energy, Washington, DC (June 2005).

7. *Packaging and Transportation Safety*, USDOE Order 460.1B, U. S. Department of Energy, Washington, DC (April 2003).

8. *Quality Assurance Requirements*, Code of Federal Regulations, Title 10, Part 830.120-122, U. S. Nuclear Regulatory Commission, Washington, DC (February 4, 2002).

9. Boiler and Pressure Vessel Code, Section III, *Rules for Construction of Nuclear Power Plant Components,* Division 1, Subsection NB, American Society of Mechanical Engineers, New York, NY (2005).

10. *Design Criteria for the Structural Analysis of Shipping Cask Containment Vessels*, Regulatory Guide 7.6, Rev. 1, U. S. Nuclear Regulatory Commission, Washington, DC, (March 1978).

11. F*abrication Criteria for Shipping Containers*, NUREG/CR-3854, Lawrence Livermore National Laboratory, Livermore, CA (March 1985).

12. *Recommended Welding Criteria For Use in the Fabrication of Shipping Containers for Radioactive Materials*, NUREG/CR-3019, Lawrence Livermore National Laboratory, Livermore, CA (March 1984).

This Page Intentionally Left Blank